

ASBMR 27th ANNUAL MEETING OFFICAL PROGRAM

Friday, September 23, 2005

Posters Open 5:15 pm – 7:00 pm
Exhibits Open 5:15 pm – 7:00 pm

9:30 am – 12:00 pm

Bone and Mineral Complications of
Chronic Kidney Disease (CKD)
Symposium
Delta Ballroom

12:00 noon – 1:00 pm

Meet-the-Professor Sessions
*Lincoln A, C, D, E &
Jackson A/B, C/D, E/F*

1:00 pm – 2:00 pm

Clinical Roundtable/Case Conference
Presidential Ballroom South

2:00 pm – 3:30 pm

Mini-Symposium A:
The Periosteum –
A Surface for All Seasons
Delta Ballroom

Mini-Symposium B:
Secondary Causes of Osteoporosis
Presidential Ballroom South

3:45 pm – 5:15 pm

Mini-Symposium C: Of Mice and Men:
Modeling Skeletal Disease in
Genetically Engineered Mice
Delta Ballroom

Mini-Symposium D: Stress Fractures
Presidential Ballroom South

5:15 pm – 7:00 pm

Welcome Reception & Plenary Poster
Session – *Ryman Exhibit Hall C*

7:00 pm – 8:00 pm

New Investigator/New Member/
First Time Attendee Reception
Washington B

Saturday, September 24, 2005

Posters Open 8:00 am – 6:00 pm
Exhibits Open 9:15 am – 4:30 pm

7:00 am – 8:00 am

New Investigator/New Member
Breakfast - *Governor's Ballroom C/D*

8:00 am – 8:10 am

Welcome & Announcements
Delta Ballroom

8:10 am – 9:10 am

Gerald Aurbach Memorial Lecture
Delta Ballroom

9:10 am – 9:25 am - *Delta Ballroom*

(9:10 am) William F. Neuman Award
Presentation
(9:15 am) Fuller Albright Award
Presentation
(9:20 am) Gideon A. Rodan Excellence in
Mentorship Award Presentation

9:25 am – 10:00 am

Break – *Ryman Exhibit Hall C*

10:00 am – 11:30 am

Plenary Orals
I Basic - *Presidential Ballroom South*
II Clinical/Translational - *Delta Ballroom*

11:30 am – 2:30 pm

Poster Session I – *Ryman Exhibit Hall C*
Odd: 11:30 am – 1:00 pm
Even: 1:00 pm – 2:30 pm

11:30 am – 12:30 pm

Meet-the-Professor Sessions
*Lincoln A, C, D, E &
Jackson A/B, C/D, E/F*

12:00 noon – 2:00 pm

Special Session for Allied Health
Professionals
Governor's Ballroom North

12:30 pm – 1:30 pm

Clinical Roundtable/Case Conference
Presidential Ballroom South

Saturday, September 24, 2005

(Continued)

12:30 pm – 2:00 pm

Grant Writing Workshop
Governor's Ballroom C/D

1:30 pm – 2:30 pm

Meet-the-Professor Sessions
*Lincoln A, C, D, E &
Jackson A/B, C/D, E/F*

2:30 pm – 4:00 pm

Concurrent Oral Sessions
1) Osteoblasts I
Presidential Ballroom South
2) Cartilage – *Governor's Ballroom C/D*
3) BMPs, TGF-beta, Other Growth
Factor and Cytokines
Presidential Ballroom A
4) Genetics of Bone and Mineral
Disorder *Presidential Ballroom B*
5) Osteoporosis Epidemiology
Delta Ballroom
6) Osteoporosis-Pathophysiology
Governor's Ballroom North

4:00 pm – 4:30 pm

Break – *Ryman Exhibit Hall C*

4:30 pm – 6:00 pm

Concurrent State-of-the-Art Lectures
A) (Basic) – Epigenetics
Presidential Ballroom South
B) (Clinical) – Absolute Risk
Delta Ballroom

6:00 pm – 7:00 pm

ASBMR Annual Business Meeting
Governor's Ballroom C/D

Sunday, September 25, 2005

Posters Open 8:00 am – 6:00 pm
Exhibits Open 9:30 am – 4:30 pm

7:00 am – 8:00 am

ASBMR Minority Breakfast
Washington B

8:00 am – 9:30 am

Plenary Symposium I
Bone and Its Vasculature
Delta Ballroom

8:00 am – 9:30 am

Clinical Half-Day Sessions
Presidential Ballroom South

9:30 am – 9:35 am

Presentation of Frederic C. Bartter
Award – *Delta Ballroom*

9:35 am – 10:00 am

Break - *Ryman Exhibit Hall C*

10:00 am – 11:30 am

Plenary Orals
I Basic - *Presidential Ballroom South*
II Clinical/Translational - *Delta Ballroom*

11:30 am – 2:30 pm

Poster Session II – *Ryman Exhibit Hall C*
Odd: 11:30 am – 1:00 pm
Even: 1:00 pm – 2:30 pm

11:30 am – 12:30 pm

The Art of Grant Reviewing
Jackson E/F

11:30 pm – 12:30 pm

Meet-the-Professor Sessions
*Lincoln A, C, D, E &
Jackson A/B, C/D*

12:00 pm – 2:00 pm

Clinical Half-Day Sessions
Presidential Ballroom South

12:30 pm – 2:00 pm

Biotechniques Workshop
Governor's Ballroom North

Sunday, September 25, 2005

(Continued)

12:30 pm -1:30 pm

The Role of Advocacy in
Musculoskeletal Research Funding:
Grassroots, NIH, Congress and
the Public
Governor's Ballroom C/D

1:30 pm – 2:30 pm

Meet-the-Professor Sessions
*Lincoln A, C, D, E &
Jackson A/B, C/D, E/F*

2:30 pm – 4:00 pm

Concurrent Oral Sessions
7) Osteoblasts II – *Governor's
Ballroom C/D*
8) Osteoclasts I – *Presidential
Ballroom A*
9) Osteoporosis – Epidemiology
Presidential Ballroom South
10) Osteoporosis Treatment
Delta Ballroom
11) Bone Acquisition & Pediatric Bone
Diseases – *Governor's Ballroom
North*
12) Mechanical Loading & Exercise
Presidential Ballroom B

4:00 pm – 4:30 pm

Break - *Ryman Exhibit Hall C*

4:30 pm – 6:00 pm

Concurrent State-of-the-Art Lectures
A) (Basic) - Embryonic Sources of
Skeletal Tissue – *Delta Ballroom*
B) (Clinical) - Bone Quality
Presidential Ballroom South

6:00 pm – 7:30pm

Women in Bone and Mineral Research
Event – *Washington B*

8:30 pm – 11:30pm

ASBMR Social Event
General Jackson Showboat

ASBMR 27th ANNUAL MEETING OFFICAL PROGRAM

Monday, September 26, 2005

Posters Open 8:00 am – 6:00 pm
Exhibits Open 9:30 am – 4:30 pm

5:30 am – 7:15 am

Fun Run/Walk
Two Rivers Park

8:00 am – 9:30 am

Plenary Symposium II
Phosphate: From Bench to Bedside
Delta Ballroom

9:30 am – 9:35 am

Presentation of Shirley Hohl Service
Award - *Delta Ballroom*

9:35 am – 10:00 am

Break – Ryman Exhibit Hall C

10:00 am – 11:30 am

Plenary Orals
I Basic - *Presidential Ballroom South*
II Clinical/Translational – *Delta Ballroom*

11:30 am – 2:30 pm

Poster Session III – *Ryman Exhibit Hall*
Odd: 11:30 am – 1:00 pm
Even: 1:00 pm – 2:30 pm

11:30 pm – 12:30 pm

Training and Career Development
Awards: Minding Your Fs and Ks
Jackson E/F

11:30 pm – 12:30 pm

Meet-the-Professor Sessions
*Lincoln A,C,D,E &
Jackson A/B, C/D*

12:30 pm – 2:00 pm

Career Options for Scientists Workshop
Presidential Ballroom B

12:30 – 1:30 pm

Clinical Roundtable/Case Conference
Presidential Ballroom South

Monday, September 26, 2005

(Continued)

1:00 pm – 2:00 pm

Meet-the-International Grant Writers
Session - *Canal A/B*

1:30 pm – 2:30 pm

Meet-the-Professor Sessions
*Lincoln A,C,D,E &
Jackson A/B, C/D, E/F*

2:30 pm – 4:00 pm

Concurrent Oral Sessions
13) Chondocyte/Osteoblasts
Bayou C/D
14) Steroid Hormones
Presidential Ballroom South
15) Cancer and Bone
Presidential Ballroom B
16) Bone Acquisition & Pediatric Bone
Diseases – *Presidential Ballroom A*
17) Osteoporosis – Epidemiology –
Delta Ballroom
18) Osteoporosis – Pathophysiology
Governor's Ballroom North

4:00 pm – 4:30 pm

Break – Ryman Exhibit Hall C

4:30 pm – 6:00 pm

Concurrent Oral Sessions
19) Osteoclasts II – *Governor's
Ballroom North*
20) Bone, Cartilage & Connective
Tissue Matrix – *Bayou C/D*
21) Peptide Calcitropic Hormones
Presidential Ballroom South
22) Other Disorders of Bone and
Mineral Metabolism
Presidential Ballroom A
23) Mechanical Loading & Exercising
Presidential Ballroom B
24) Osteoporosis Diagnosis &
Treatment – *Delta Ballroom*

Tuesday, Sept. 27, 2005

8:00 am – 9:00 am

Louis V. Avioli Memorial Lecture
Delta Ballroom

9:00 am – 9:05 am

Louis V. Avioli Memorial Award
Delta Ballroom

9:05 am – 9:30 am

Break – *Delta Lobby B*

9:30 am – 11:00 am

Concurrent Oral Sessions
25) Osteoblasts III – *Bayou A/B*
26) BMPs, TGF-beta, Other Growth
Factors and Cytokines & Others
Bayou E
27) Steroids/Hormones II – *Bayou C/D*
28) Genetics & Metabolic Bone
Disease – *Canal C/D*
29) Cancer & Bone – *Canal A/B*
30) Osteoporosis – Diagnosis and
Treatment – *Delta Ballroom*

11:30 am

ADJOURN

2005 ANCILLARY PROGRAM

Wednesday, September 21, 2005

The International Society for Clinical Densitometry (ISCD) – Sessions

7:30 am – 11:30 am

ISCD Bone Densitometry Course
General Session
Bayou E

11:30 am – 5:30 pm

ISCD Bone Densitometry - Clinician
Course Lectures
Jackson A/B

11:30 am – 5:30 pm

ISCD Bone Densitometry - Technologist
Course Lectures
Jackson C/D

Thursday, September 22, 2005

The International Society for Clinical Densitometry (ISCD) - Sessions

7:30 am – 11:15 am

ISCD Bone Densitometry – Clinician
Course Lectures
Jackson A/B

7:30 am – 11:45 am

ISCD Bone Densitometry –Technologist
Course Lectures
Jackson C/D

11:45 am – 2:00 pm

ISCD Bone Densitometry –
Clinician Exam
Jackson A/B

12:30 pm – 1:45 pm

ISCD Bone Densitometry –
Technologist Exam
Jackson C/D

1:00 pm – 5:45 pm

ISCD Vertebral Fracture Assessment
(VFA) Course
Tennessee Ballroom D/E

Friday, September 23, 2005

Working Groups

7:00 pm – 9:00 pm

Working Group on Rheumatic
Disease and Bone
Bayou C/D

7:00 pm – 9:30 pm

Muscle and Bone Working Group
Canal E

7:00 pm – 9:30 pm

In Vivo Working Group
Canal A/B

7:00 pm – 9:30 pm

Nutrition and Bone Health Working
Group
Canal C/D

7:00 pm – 10:00 pm

Vitamin D Working Group
Bayou E

7:15 pm – 10:00 pm

Working Group on Hormone-
Receptor Interactions
Bayou A/B

Industry-Supported Symposia

7:00 pm – 9:30 pm

Optimizing Outcomes for Patients
with Metabolic Bone Disease
Sponsored by Integrated
Communications Corp., and
Medical Education
Resources, Inc.
Supported by an educational grant
from Novartis Pharmaceuticals
Corporation
Tennessee Ballroom

7:00 pm – 9:30 pm

The Biology of Bone Loss:
Advancing the Clinical
Management of Osteoporosis
Sponsored by SciMed LLC and
Postgraduate Institute for
Medicine
Supported by an educational grant
from Merck & Co., Inc.
Presentation Ballroom North

7:00 pm – 9:30 pm

New and Future Clinical
Approaches to the Prevention
of Fractures
Sponsored by The Endocrine
Society
Supported by an educational grant
from Pfizer, Inc.
Governor's Ballroom North

Saturday, September 24, 2005

Working Groups

7:00 pm – 9:00 pm

Non-Invasive Assessment of
Trabecular Bone Microarchitecture
Working Group
Canal A/B

7:00 pm – 9:00 pm

Working Group on Musculoskeletal
Rehabilitation in Patients with
Osteoporosis
Bayou E

7:00 pm – 9:30 pm

Molecular Biology & Pathology of
Bone Working Group
Bayou A/B

7:00 pm – 9:30 pm

Working Group on Aging and the
Human Skeleton
Canal C/D

7:00 pm – 10:00 pm

Biochemical Markers of Bone
Turnover Working Group
Bayou C/D

Industry-Supported Symposia

7:00 pm – 10:00 pm

The RANK/RANKL/OPG Axis:
A New Therapeutic Target for the
Treatment and Prevention
of Bone Loss
Sponsored by Health Science
Center for Continuing
Medical Education
Supported by an education grant
from Amgen, Inc.
Tennessee Ballroom

7:00 pm – 10:00 pm

The Evolving Role of Vitamin D
Analog: Links between Bone
Metabolism, Cardiovascular Health,
and Long-Term Survival
Sponsored by the Albert Einstein
College of Medicine
Supported by an educational grant
from Abbott Laboratories
Presidential Ballroom North

2005 ANCILLARY PROGRAM

Sunday, September 25, 2005

Industry-Supported Symposia

6:00 am – 8:00 am

Parathyroid Hormone: A New Frontier in Bone Health

Sponsored by Postgraduate Institute for Medicine

Supported by an unrestricted educational grant from NPS

Pharmaceuticals
Tennessee Ballroom

8:30 pm – 11:30 pm

ASBMR SOCIAL EVENT

General Jackson Showboat
Tickets Required

Monday, September 26, 2005

5:30 am – 7:15 am

ASBMR FUN RUN/WALK

Supported by Novartis

Pharmaceuticals Corporation

Busing provided to Two Rivers Park

Working Groups

6:30 pm – 8:30 pm

Physical Activity and Falls Working Group

Bayou C/D

6:30 pm – 9:30 pm

Adult Bone and Mineral Working Group

Canal A/B

6:30 pm – 9:30 pm

Post Transplantation and Bone Disease Working Group

Bayou E

7:00 pm – 9:30 pm

Bone Remodeling and Stress Fracture Working Group

Canal C/D

7:00 pm – 10:00 pm

Pediatric Bone and Mineral Working Group

Bayou A/B

Monday, September 26, 2005 (Continued)

Industry-Supported Symposia

6:45 pm – 10:00 pm

Determinants of Fracture

Risk Reduction: From Bench to Bedside

Sponsored by Photosound

Communications Inc., and

Postgraduate Institute of Medicine

Supported by an unrestricted educational grant from The

Alliance for Better Bone Health

(Procter & Gamble

Pharmaceuticals

and Aventis)

Tennessee Ballroom

7:00 pm – 9:30 pm

Expanding the Options of

Bisphosphonate Therapy

Sponsored by Cerebrio and the

University of Kentucky

Supported by an educational grant

from Roche and

GlaxoSmithKline

Governor's Ballroom C/D

2005 Abstracts

Twenty-Seventh Annual Meeting of the American Society for Bone and Mineral Research

**Gaylord Opryland Resort and Convention Center
Nashville, Tennessee, USA
September 23-27, 2005**

The Journal of Bone and Mineral Research (ISSN: 0884-0431) provides a forum for papers of the highest quality pertaining to all areas of the biology and physiology of bone, the hormones that regulate bone and mineral metabolism and the pathophysiology and treatment of disorders of bone and mineral metabolism. All authored papers and editorial news and comments, opinions, findings, conclusions or recommendations in the *Journal* are those of the author(s) and do not necessarily reflect the views of the *Journal* and its publisher, nor does their publication imply any endorsement. *The Journal of Bone and Mineral Research* is the official journal of the American Society for Bone and Mineral Research and is published monthly plus a special issue in September by the American Society for Bone and Mineral Research, 2025 M Street, N.W., Suite 800, Washington, DC 20036-3309, USA. Address reprint/offprint inquiries to the Sheridan Press at US (717) 632-8448 x 8110. Periodicals postage paid in Washington, DC, and additional offices. POSTMASTER SEND ADDRESS CHANGES TO: *Journal of Bone and Mineral Research*, P.O. Box 2759, Durham, NC 27715, USA. 2005 Subscription Rates: U.S.: Personal \$495.00; Institutional: \$560.00; Canada/Mexico: Personal \$515.00; Institutional \$585.00; Overseas: Personal \$570.00; Institutional: \$605.00. Single issue \$50.00. Subscription term is January - December.

Claims for missing issues will be serviced at no charge if received within six months of issue date {journal@jbmr.org, or fax (US) 919-620-8465}. Duplicate copies cannot be sent to replace issues not delivered because of failure to notify publisher of change of address. Please notify ASBMR of new address six (6) weeks in advance of moving date. All subscriptions are payable in advance in U.S. funds drawn on a U.S. bank. If not fully satisfied, notify publisher for a refund on all unmailed issues.

Address advertising and commercial reprint inquiries to Mr. Steve Kavalgian, Mill River Media LLC, 141 Boston Post Rd. Old Lyme, CT 06371-1303, USA; (860) 434-6889 (phone); (860) 434-9744 (fax); kavalgian@adelphia.net (e-mail). Advertisements are subject to editorial approval.

No responsibility is assumed, and responsibility is hereby disclaimed, by the American Society for Bone and Mineral Research and the *Journal of Bone and Mineral Research* for any injury and/or damage to persons or property as a matter of products liability, negligence or otherwise, or from any use or operation of methods, products, instructions or ideas presented in the *Journal*. Independent verification of diagnosis and drug dosages should be made. Discussions, views and recommendations as to medical procedures, choice of drugs and drug dosages are the responsibility of the authors. Advertisers are responsible for compliance with requirements concerning statements of efficacy, approval, licensure, and availability.

The Journal of Bone and Mineral Research is a Journal Club™ selection. The *Journal* is indexed by Index Medicus, Current Contents/Life Science, CABS (Current Awareness in Biological Sciences), Excerpta Medica, Cambridge Scientific Abstracts, Chemical Abstracts, Reference Update, ScienceCitation Index, and Nuclear Medicine Literature Updating and Indexing Service. Copyright © 2005 by the American Society for Bone and Mineral Research. For permission to reproduce copyrighted materials from the *Journal*, send requests to the *Journal of Bone and Mineral Research*, P.O. Box 2759, Durham, NC 27715, USA; (919) 620-0681 (phone); (919) 620-8465 (fax). For libraries and other users registered with the Copyright Clearance Center, please contact the Copyright Clearance Center, 222 Rosewood Drive, Suite 910, Danvers, MA 01923, USA; www.copyright.com; (978) 750-8400 (phone); (978) 750-4470 (fax).



TABLE OF CONTENTS

General Information xv

WEDNESDAY, SEPTEMBER 21, 2005

Day-at-a-Glance xxviii

THURSDAY, SEPTEMBER 22, 2005

Day-at-a-Glance xxviii

FRIDAY, SEPTEMBER 23, 2005

Day-at-a-Glance xxix

SATURDAY, SEPTEMBER 24, 2005

Day-at-a-Glance xxx

SUNDAY, SEPTEMBER 25, 2005

Day-at-a-Glance xxxii

MONDAY, SEPTEMBER 26, 2005

Day-at-a-Glance xxxiv

TUESDAY, SEPTEMBER 27, 2005

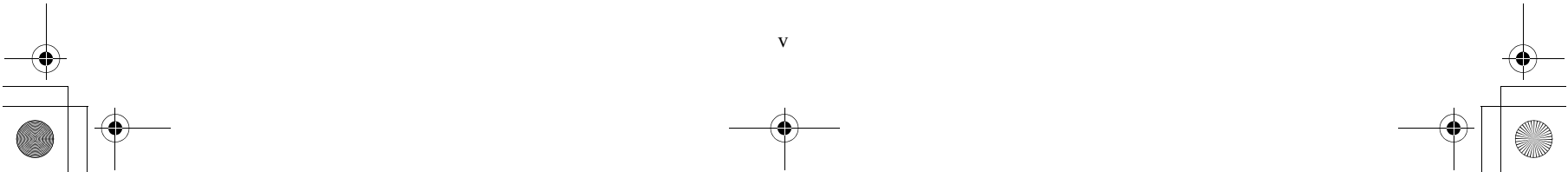
Day-at-a-Glance xxxvi

Abstracts Key xxxvii

Abstracts S2

Key Word Index S441

Author Index S491





Official Journal of the American Society for Bone and Mineral Research

Editor-in-Chief

John A Eisman
Sydney, Australia

Associate Editors

Sylvia Christakos
Newark, NJ, USA

Olof Johnell
Malmo, Sweden

Gerard Karsenty
Houston, TX, USA

Shigeaki Kato
Tokyo, Japan

Pamela Gehron Robey
Bethesda, MD, USA

G David Roodman
Pittsburgh, PA, USA

Clifford Rosen
Bangor, ME, USA

Andrew F Stewart
Pittsburgh, PA, USA

Rajesh V Thakker
Headington, Oxford, UK

Editors Emeritus

Marc K Drezner, Madison, WI, USA
Lawrence G Raisz, Farmington, CT, USA

Managing Editor Amber Williams, 3209 Guess Rd, Suite 201, Durham, NC 27705, USA, phone: (919) 620-0681, fax: (919) 620-8465, email: journal@jbmr.org

Editorial Board

Yousef Abu-Amer, *USA*
H Clarke Anderson, *USA*
John JB Anderson, *USA*
Troels T Andreassen, *Denmark*
Timothy R Arnett, *United Kingdom*
Paolo Bianco, *Italy*
Joseph P Bidwell, *USA*
Neil Binkley, *USA*
Brendan F Boyce, *USA*
Xu Cao, *USA*
Joseph Caverzasio, *Switzerland*
Marco Cecchini, *Switzerland*
Timothy Chambers, *United Kingdom*
Chantal Chenu, *United Kingdom*
Charles H Chesnut III, *USA*
Roberto Civitelli, *USA*
Juliet E Compston, *United Kingdom*
Steven R Cummings, *USA*
Hong-Wen Deng, *USA*
Colin Dunstan, *Australia*
Peter Ebeling, *Australia*
Thomas A Einhorn, *USA*
Ghada El-Hajj Fuleihan, *Lebanon*
Solomon Epstein, *USA*
David R Eyre, *USA*
Serge L Ferrari, *Switzerland*
Larry W Fisher, *USA*

Lorraine Fitzpatrick, *USA*
Tatiana Foroud, *USA*
Seiji Fukumoto, *Japan*
Edith M Gardiner, *Australia*
Harry K Genant, *USA*
Louis C Gerstenfeld, *USA*
Matthew T Gillespie, *Australia*
Susan L Greenspan, *USA*
Ted S Gross, *USA*
Theresa A Guise, *USA*
Geoffrey N Hendy, *Canada*
Janet M Hock, *USA*
Michael F Holick, *USA*
Keith A Hruska, *USA*
Kyoji Ikeda, *Japan*
Suzanne M Jan de Beur, *USA*
Teppo LN Järvinen, *Finland*
Harald Jüppner, *USA*
Sundeep Khosla, *USA*
Douglas P Kiel, *USA*
Robert F Klein, *USA*
Christopher S Kovacs, *Canada*
Elizabeth A Krall, *USA*
Paul H Krebsbach, *USA*
Nancy Krieger, *USA*
William Landis, *USA*

Nancy E Lane, *USA*
Craig B Langman, *USA*
Brendan Lee, *USA*
Mary B Leonard, *USA*
Jane B Lian, *USA*
Anne C Looker, *USA*
Toshio Matsumoto, *Japan*
Koichi Matsuo, *Japan*
Laurie K McCauley, *USA*
Ralph A Meyer Jr, *USA*
Leif Mosekilde, *Denmark*
Tally Naveh-Many, *Israel*
Tuan V Nguyen, *Australia*
Geoffrey C Nicholson, *Australia*
Riko Nishimura, *Japan*
Regis O'Keefe, *USA*
Lynne A Opperman, *USA*
Philip A Osdoby, *USA*
Roberto Pacifici, *USA*
A Michael Parfitt, *USA*
Anthony A Portale, *USA*
Richard L Prince, *Australia*
L Darryl Quarles, *USA*
Stuart H Ralston, *United Kingdom*
D Sudhaker Rao, *USA*
Robert R Recker, *USA*

Helmtrud I Roach, *United Kingdom*
F Patrick Ross, *USA*
Janet E Rubin, *USA*
Clinton T Rubin, *USA*
Isidro Salusky, *USA*
Philip N Sambrook, *Australia*
Ernestina Schipani, *USA*
Ego Seeman, *Australia*
Eileen M Shore, *USA*
Justin Silver, *Israel*
Stuart Silverman, *USA*
Frederick R Singer, *USA*
Ethel S Siris, *USA*
Timothy M Skerry, *United Kingdom*
Malcolm Snead, *USA*
Mary Fran Sowers, *USA*
Tim Spector, *United Kingdom*
Larry J Suva, *USA*
Naoyuki Takahashi, *Japan*
Sakae Tanaka, *Japan*
Steven L Teitelbaum, *USA*
Dwight A Towler, *USA*
Florence Tremollieres, *France*
Connie M Weaver, *USA*
Shlomo Wientroub, *Israel*
John J Wysolmerski, *USA*

AMERICAN SOCIETY FOR BONE AND MINERAL RESEARCH (ASBMR)

OFFICERS

President: Sylvia Christakos, Ph.D.
President-Elect: Elizabeth Shane, M.D.
Past-President: Robert A. Nissenson, Ph.D.
Secretary-Treasurer: Marc K. Drezner, M.D.

COUNCIL

Daniel Bikle, M.D., Ph.D.	<i>Term expires 2006</i>	Sundeeep Khosla, M.D.	<i>Term expires 2005</i>
Jane Cauley, Ph.D.	<i>Term expires 2006</i>	René Rizzoli, M.D.	<i>Term expires 2007</i>
John Eisman, M.B.B.S., Ph.D.	<i>Ex Officio</i>	Vicki Rosen, Ph.D.	<i>Term expires 2006</i>
Susan Greenspan, M.D.	<i>Term expires 2005</i>	Thomas Spelsberg, Ph.D.	<i>Term expires 2007</i>
Theresa Guise, M.D.	<i>Term expires 2007</i>	Gary Stein, Ph.D.	<i>Term expires 2005</i>

PAST PRESIDENTS

Louis V. Avioli, M.D.	<i>1979-1980</i>	Steven L. Teitelbaum, M.D.	<i>1992-1993</i>
Lawrence G. Raisz, M.D.	<i>1980-1981</i>	Henry M. Kronenberg, M.D.	<i>1993-1994</i>
Claude D. Arnaud, M.D.	<i>1981-1982</i>	Ernesto Canalis, M.D.	<i>1994-1995</i>
Stephen M. Krane, M.D.	<i>1982-1983</i>	John P. Bilezikian, M.D.	<i>1995-1996</i>
William A. Peck, M.D.	<i>1983-1984</i>	Gregory R. Mundy, M.D.	<i>1996-1997</i>
Paula H. Stern, Ph.D.	<i>1984-1985</i>	Michael Rosenblatt, M.D.	<i>1997-1998</i>
B. Lawrence Riggs, M.D.	<i>1985-1986</i>	Jane E. Aubin, Ph.D.	<i>1998-1999</i>
Norman H. Bell, M.D.	<i>1986-1987</i>	David Goltzman, M.D.	<i>1999-2000</i>
Gideon A. Rodan, M.D., Ph.D.	<i>1987-1988</i>	Robert Marcus, M.D.	<i>2000-2001</i>
John G. Haddad, Jr., M.D.	<i>1988-1989</i>	Robert R. Recker, M.D.	<i>2001-2002</i>
Armen H. Tashjian, Jr., M.D.	<i>1989-1990</i>	Clifford J. Rosen, M.D.	<i>2002-2003</i>
Frederick R. Singer, M.D.	<i>1990-1991</i>	Robert A. Nissenson, Ph.D.	<i>2003-2004</i>
Mark R. Haussler, Ph.D.	<i>1991-1992</i>		

PAST SECRETARY-TREASURERS

Norman H. Bell, M.D.	<i>1977-1985</i>	Steven R. Goldring, M.D.	<i>1997-2000</i>
Gregory R. Mundy, M.D.	<i>1985-1991</i>	Andrew F. Stewart, M.D.	<i>2000-2004</i>
Arnold J. Kahn, Ph.D.	<i>1991-1997</i>		

PAST COUNCILORS

Constantine Anast, M.D.	<i>1980-1982</i>	Hector F. DeLuca, Ph.D.	<i>1979-1980</i>
Claude D. Arnaud, M.D.	<i>1979-1980</i>	Marie Demay, M.D.	<i>2000-2003</i>
Andrew Arnold, M.D.	<i>1999-2002</i>	Richard Eastell, M.D., F.R.C.P.	<i>2000-2003</i>
Jane E. Aubin, Ph.D.	<i>1991-1994</i>	John Eisman, MBBS, Ph.D.	<i>1994-1997</i>
Roland Baron, D.D.S., Ph.D.	<i>1991-1994</i>	Murray J. Favus, M.D.	<i>1992-1995</i>
John P. Bilezikian, M.D.	<i>1987-1990</i>	David Feldman, M.D.	<i>1982-1986</i>
Dennis Black, Ph.D.	<i>2001-2004</i>	Lorraine A. Fitzpatrick, M.D.	<i>1998-2001</i>
Lynda F. Bonewald, Ph.D.	<i>1995-1998</i>	Francis Glorieux, M.D., Ph.D.	<i>1988-1991</i>
Arthur E. Broadus, M.D., Ph.D.	<i>1990-1993</i>	Julie Glowacki, Ph.D.	<i>1999-2002</i>
Ernesto Canalis, M.D.	<i>1989-1992</i>	Steven R. Goldring, M.D.	<i>1993-1996</i>
Janet M. Canterbury, M.D.	<i>1981-1984</i>	Ralph S. Goldsmith, M.D.	<i>1980-1983</i>
Sylvia Christakos, Ph.D.	<i>1989-1992</i>	David Goltzman, M.D.	<i>1984-1988</i>
Thomas L. Clemens, Ph.D.	<i>1998-2001</i>	Maxine Gowen, Ph.D.	<i>2000-2003</i>
Jack W. Coburn, M.D.	<i>1981-1984</i>	John G. Haddad, Jr., M.D.	<i>1982-1985</i>
David V. Cohn, Ph.D.	<i>1982-1985</i>	Mark R. Haussler, Ph.D.	<i>1982-1985</i>
Cary W. Cooper, Ph.D.	<i>1980-1981</i>	Hunter H. Heath III, M.D.	<i>1985-1988</i>
Steven R. Cummings, M.D.	<i>1996-1999</i>	Helen L. Henry, Ph.D.	<i>1985-1988</i>
Bess Dawson-Hughes, M.D.	<i>1996-1999</i>	Keith A. Hruska, M.D.	<i>1989-1992</i>

AMERICAN SOCIETY FOR BONE AND MINERAL RESEARCH (ASBMR)

PAST COUNCILORS (Continued)

Arnold J. Kahn, Ph.D.	1986-1989	Paul A. Price, Ph.D.	1986-1989
Frederick S. Kaplan, M.D.	1997-2000	Robert R. Recker, M.D.	1995-1998
Stephen M. Krane, M.D.	1979-1981	Pamela Gehron Robey, Ph.D.	1992-1995
Barbara E. Kream, M.D.	1985-1988	Gideon A. Rodan, M.D., Ph.D.	1984-1986
Henry M. Kronenberg, M.D.	1986-1989	Sevgi B. Rodan, Ph.D.	1990-1993
Jane B. Lian, Ph.D.	1991-1994	Michael Rosenblatt, M.D.	1988-1991
Barbara Lukert, M.D.	2002-2004	Elizabeth Shane, M.D.	1994-1997
Robert Marcus, M.D.	1995-1998, 1999-2002	Dolores M. Shoback, M.D.	1998-2001
T.J. Martin, M.D.	1987-1990	Ethel Siris, M.D.	1996-1999
Stephen Marx, M.D.	1983-1986	Eduardo Slatopolsky, M.D.	1980-1983
Toshio Matsumoto, M.D.	1999-2002	Paula H. Stern, Ph.D.	1980-1983
Gregory R. Mundy, M.D.	1983-1985, 1995-1997	Andrew F. Stewart, M.D.	1994-1997
Robert Nissenson, Ph.D.	1993-1996	Gordon J. Stewler, M.D.	1992-1995
Anthony W. Norman, Ph.D.	1980-1982	Larry Suva, Ph.D.	2001-2004
Philip A. Osdoby, Ph.D.	1997-2000	Armen H. Tashjian, Jr., M.D.	1979-1982
Susan M. Ott, M.D.	1988-1991	John D. Termine, Ph.D.	1984-1987
A. Michael Parfitt, M.D.	1990-1993	Robert Wasserman, Ph.D.	1984-1987
Nicola C. Partridge, Ph.D.	1993-1996	Glenda Wong, Ph.D.	1984-1987
William A. Peck, M.D.	1979-1981	Marian F. Young, Ph.D.	1997-2000
John T. Potts, Jr., M.D.	1979-1981		

ASBMR STAFF

Joan R. Goldberg, <i>Executive Director</i>	Bill Gaskill, <i>Accountant</i>
Karen R. Hasson, <i>Deputy Executive Director</i>	Melissa Huston, <i>Senior Convention Manager</i>
D. Douglas Fesler, <i>Associate Executive Director</i>	Cliff Pratt, <i>Registration Coordinator</i>
Gretchen Bretsch, <i>Project Manager</i>	Kelly Marks, <i>Exhibits Coordinator</i>
Yvette Dalka, <i>Program Manager</i>	Anne Whittaker, <i>Convention Assistant</i>
Earline Marshall, <i>Executive Assistant</i>	Brooke Hirsch, <i>Convention Assistant</i>
Amy Werner, <i>Program Coordinator</i>	Melissa Haynes, <i>Media Relations Manager</i>
Kimberly Seyran, <i>Senior Membership/Project Coordinator</i>	Adrienne Lea, <i>Publications Director</i>
Anna Camele, <i>Senior Membership/Marketing Assistant</i>	Amber Williams, <i>JBMR Managing Editor</i>
Rebecca Boulos, <i>Association Assistant</i>	David Allen, <i>Publications Specialist</i>
Kiley Thornton, <i>Association Assistant</i>	Matt Kilby, <i>Publications Assistant</i>

ASBMR BUSINESS OFFICE

2025 M Street, NW
Suite 800
Washington, DC 20036-3309
USA
Tel: (202) 367-1161
Fax: (202) 367-2161
E-mail: ASBMR@smithbucklin.com
Internet: <http://www.asbmr.org>

The Fuller Albright Award

Supported by an unrestricted educational grant from Amgen, Inc.

Michael F. Holick, M.D., Ph.D.	1980	Andrew Arnold, M.D.	1992
Mark R. Haussler, Ph.D.	1981	Pamela G. Robey, Ph.D.	1993
Stephen Marx, M.D.	1982	Roberto Civitelli, M.D.	1994
Gregory R. Mundy, M.D.	1982	Roberto Pacifici, M.D.	1995
Edward M. Brown, M.D.	1983	Clinton T. Rubin, Ph.D.	1996
Helen L. Henry, Ph.D.	1984	René St-Arnaud, Ph.D.	1997
Henry M. Kronenberg, M.D.	1985	Shigeaki Kato, Ph.D.	1998
Michael Rosenblatt, M.D.	1986	Theresa A. Guise, M.D.	1999
Michael P. Whyte, M.D.	1987	Dwight Towler, M.D., Ph.D.	2000
Rajiv Kumar, M.D.	1988	Charles H. Turner, M.D.	2001
Timothy Chambers, M.D.	1989	Nobuyuki Udagawa, M.D.	2002
Michael A. Levine, M.D.	1990	Patricia Ducey, Ph.D.	2003
Dean T. Yamaguchi, M.D., Ph.D.	1991	Hiroshi Takayanagi, Ph.D.	2004

The Louis V. Avioli Founders Award

Supported by an unrestricted educational grant from Merck & Co., Inc.

Stavros Manolagas, M.D., Ph.D.	2000	Edward Brown, M.D.	2003
Gerard Karsenty, M.D.	2001	Ernesto Canalis, M.D.	2004
Roland Baron, D.D.S., Ph.D.	2002		

The William F. Neuman Award

Supported by an unrestricted educational grant from Novartis Pharmaceuticals Corporation

Gerald D. Aurbach, M.D.	1981	Gideon A. Rodan, M.D., Ph.D.	1993
Paul L. Munson, Ph.D.	1982	Thomas John Martin, M.D., D.Sc.	1994
D. Harold Copp, M.D., Ph.D.	1983	Anthony W. Norman, Ph.D.	1995
Roy V. Talmage, Ph.D.	1984	Melvin Jacob Glimcher, M.D.	1996
Hector F. DeLuca, Ph.D.	1985	Tatsuo Suda, D.D.Sc., Ph.D.	1997
Lawrence G. Raisz, M.D.	1986	Steven L. Teitelbaum, M.D.	1998
John T. Potts, Jr., M.D.	1987	Gregory R. Mundy, M.D.	1999
Louis V. Avioli, M.D.	1988	R. Graham Russell, M.D.	2000
Stephen M. Krane, M.D.	1989	Harold M. Frost, M.D.	2001
Robert H. Wasserman, Ph.D.	1990	B. Lawrence Riggs, M.D.	2002
Claude D. Arnaud, M.D.	1991	Henry M. Kronenberg, M.D.	2003
Herbert A. Fleisch, M.D.	1992	Jane E. Aubin, Ph.D.	2004

The Frederic C. Bartter Award

Supported by an unrestricted educational grant from NPS Pharmaceuticals

Jack Coburn, M.D.	1986	C. Conrad Johnston, Jr., M.D.	1996
Constantine Anast, M.D.	1987	Robert Lindsay, MBChB, Ph.D.	1997
Charles Y.C. Pak, M.D.	1988	B.E. Christopher Nordin, M.D., Ph.D.	1998
Arthur E. Broadus, M.D., Ph.D.	1989	Pierre Meunier, M.D.	1999
B. Lawrence Riggs, M.D.	1990	John P. Bilezikian, M.D.	2000
Eduardo Slatopolsky, M.D.	1991	Joseph Melton, III, M.D.	2001
Norman H. Bell, M.D.	1992	Ego Seeman, M.D., F.R.A.C.P.	2002
Francis H. Glorieux, M.D., Ph.D.	1993	Robert R. Recker, M.D.	2003
Robert P. Heaney, M.D.	1994	Pierre Delmas, M.D., Ph.D.	2004
A. Michael Parfitt, M.D.	1995		

The Shirley Hohl Service Award

Supported by an unrestricted educational grant from Novartis Pharmaceuticals Corporation

Louis V. Avioli, M.D.	1997	Lawrence G. Raisz, M.D.	2001
Norman H. Bell, M.D.	1998	Nicola C. Partridge, Ph.D.	2002
Murray J. Favus, M.D.	1999	Marc K. Drezner, M.D.	2003
Arnold J. Kahn, Ph.D.	2000	Jane B. Lian, Ph.D.	2004

The Gideon A. Rodan Excellence in Mentorship Award

Supported by an unrestricted educational grant from Merck & Co., Inc.

Gideon A. Rodan, M.D., Ph.D.	2001	Webster S. S. Jee, Ph.D.	2003
Sylvia Christakos, Ph.D.	2002	Claude Arnaud, M.D.	2004

AMERICAN SOCIETY FOR BONE AND MINERAL RESEARCH (ASBMR)

2005 ASBMR YOUNG INVESTIGATOR AWARD RECIPIENTS

Co-Supported by educational grants from the Alliance for Better Bone Health (a collaboration between Procter & Gamble Pharmaceuticals and Aventis Pharmaceuticals, a member of the sanofi-aventis Group), Amgen, GlaxoSmithKline Consumer Healthcare, Merck & Co., Inc., Novartis Pharmaceuticals Corporation, NPS Pharmaceuticals, Roche and GlaxoSmithKline, and Wyeth Pharmaceuticals

J. Ignacio Aguirre, DVM, Ph.D.
Matthew R. Allen, Ph.D.
Laleh Ardesirpour, M.D.
Rebecca J. Barr, B.Sc., M.Sc., Ph.D.
Qian Chen, D.D.S.
Peiqi Chen, Ph.D.
Graziana Colaianne, Ph.D.
Timothy F. Day
Olivier Destaing, Ph.D.
Douglas J. DiGirolamo
Christine Donsante
Florent Elefteriou, Ph.D.
Emily G. Farrow, B.S.
Tripti Gaur, Ph.D.
Lindsay J. Gleghorn, B.Sc.
Kristen E. Govoni, Ph.D.
Xizhi Guo, Ph.D.

Atsuhiko Hikita, M.D.
Akio Hiraki, M.D., Ph.D.
Makoto Hirao, M.D.
Libby A. Kindle, Ph.D.
Shiva P. Kotha, Ph.D.
Takuo Kubota
Qingnan Li, Ph.D.
Mattias Lorentzon, M.D., Ph.D.
Heather Macdonald, BSc.
Naohiro Kawamura, M.D.
King Lun Kingston Mak, Ph.D.
Tobias Larsson, M.D., Ph.D.
Gwendolen Lorch, D.V.M., M.S.
Rhodri Martin, B.Sc.
Fumitaka Mizoguchi, M.D.
Roy Morello, Ph.D.
Amanda J. Notini, B.Sc.(Hons)

Yoshitomo Saita, M.D.
Taku Saito, M.D.
Rana Samadfam, Ph.D.
Leanne K. Saxon, Ph.D.
Claudine Woo Shinoff
Run Shen, M.S.
Kimberly S. Shimer, M.D.
Petra Simic, M.D., PhD
Alexandre Stephens, B.Sc. (Hons)
Farhan A. Syed, Ph.D.
Kiyoyuki Torigoe, M.D., Ph.D.
Akimi Ueda, D.D.S., Ph.D.
Antje Voss
Ilse S. Wicherts, M.Sc.
Qian Zhang, M.D.

2005 ASBMR MOST OUTSTANDING ABSTRACT AWARD

Supported by an unrestricted educational grant from NPS Pharmaceuticals

Xiaojun Wu, M.D., Ph.D.

2005 ASBMR AWARD FOR OUTSTANDING RESEARCH IN THE PATHOPHYSIOLOGY OF OSTEOPOROSIS

Supported by an unrestricted educational grant from Amgen, Inc.

Li Sun, M.D., Ph.D.

2005 ASBMR PRESIDENT'S BOOK AWARD

Supported by an unrestricted educational grant from Elsevier Science

Liesbeth Van Wesenbeeck, Ph.D

AMERICAN SOCIETY FOR BONE AND MINERAL RESEARCH (ASBMR)

2005 SCIENTIFIC PROGRAM COMMITTEE

President: Sylvia Christakos, Ph.D.
Program Co-Chair: Michael J. Econs, M.D.
Program Co-Chair: Pamela G. Robey, Ph.D.

John Adams, M.D.
 Roy Altman, M.D.
 Michael Amling, M.D.
 Gerald Atkins, Ph.D.
 Jane E. Aubin, Ph.D.
 Laura E. Bachrach, M.D.
 Zvi Bar-Shavit, Ph.D.
 Roland Baron, D.D.S., Ph.D.
 Teresita Bellido, Ph.D.
 Paolo Bianco, Ph.D.
 Joseph Bidwell, Ph.D.
 Daniel Bikle, M.D., Ph.D.
 Neal Binkley, M.D.
 Nicholas Bishop, M.D.
 Dennis Black, Ph.D.
 Robert Blank, M.D., Ph.D.
 Michael Bliziotis, M.D.
 Aubrey Blumsohn, M.D., Ph.D.
 Scott Boden, M.D.
 J.J. Body, M.D., Ph.D.
 Lynda Bonewald, Ph.D.
 Adele Boskey, Ph.D.
 Brendan Boyce, M.D.
 Maria Luisa Brandi, M.D., Ph.D.
 John Caminis, M.D.
 Ernesto Canalis, M.D.
 Xu Cao, Ph.D.
 Jane Cauley, Ph.D.
 Timothy Chambers, M.D.
 Roberto Civitelli, M.D.
 Thomas Clemens, Ph.D.
 Cyrus Cooper, D.M., F.R.C.P.,
 F.Med.Sci.
 Felicia Cosman, M.D.
 Peter Croucher, Ph.D.
 Steven Cummings, M.D.
 Sarah Dallas, Ph.D.
 Bess Dawson-Hughes, M.D.
 Pierre Delmas, M.D., Ph.D.
 Marie Demay, M.D.
 David Dempster, Ph.D.
 Linda Dimeglio, M.D.
 Marc Drezner, M.D.
 Hisham Drissi, Ph.D.
 Patricia Ducy, Ph.D.
 Colin Dunstan, Ph.D.
 Richard Eastell, M.D.
 Peter Ebeling, M.D., F.R.A.C.P.
 Ghada El-Hajj Fuleihan, M.D.
 Kristine Ensrud, M.D.
 Mary-Farach Carson, Ph.D.
 David Findlay, Ph.D.
 Larry Fisher, Ph.D.
 Lorraine Fitzpatrick, M.D.

Renny Franceschi, Ph.D.
 Robert Gagel, M.D.
 Tom Gardella, Ph.D.
 Edith Gardiner, Ph.D.
 Carol Gay, Ph.D.
 Louis Gerstenfeld, Ph.D.
 Matthew Gillespie, Ph.D.
 Francis Glorieux, M.D., Ph.D.
 Claus Glueer, Ph.D.
 David Goltzman, M.D.
 Catherine Gordon, M.D.
 Gail Greendale, M.D.
 Agamemnon Grigoriadis, Ph.D.
 Jerome Guicheaux, Ph.D.
 Theresa Guise, M.D.
 Kurt Hankenson, D.V.M., Ph.D.
 Janet Hock, Ph.D.
 Lorenz Hofbauer, M.D.
 Michael Holick, M.D., Ph.D.
 Ingrid Holm, M.D.
 Suzanne Jan de Beur, M.D.
 Robert Jilka, Ph.D.
 Olof Johnell, M.D.
 C. Conrad Johnston, M.D.
 Gerard Karsenty, M.D., Ph.D.
 Moustapha Kassem, M.D., Ph.D.
 Shigeaki Kato, Ph.D.
 Sundeep Khosla, M.D.
 Klaus Klaushofer, M.D.
 Robert Klein, M.D.
 Daniel Koller, Ph.D.
 Stravoula Kousteni, Ph.D.
 Christopher Kovacs, M.D.
 Elizabeth Krall, Ph.D., M.P.H.
 Barbara Kream, Ph.D.
 Peter Lakatos, M.D.
 Craig Langman, M.D.
 Beate Lanske, Ph.D.
 Meryl LeBoff, M.D.
 Beata Lecka-Czernik, Ph.D.
 Benjamin Leder, M.D.
 Michael Levine, M.D.
 E. Michael Lewiecki, M.D.,
 F.A.C.P.
 Jane Lian, Ph.D.
 Robert Lindsay, M.D., Ph.D.
 Nigel Loveridge, Ph.D.
 Karen Lyons, Ph.D.
 Paul MacDonald, Ph.D.
 Eleanor Mackie, D.V.M., Ph.D.
 Laurie McCauley, Ph.D.
 Michael McClung, M.D.
 L. Joseph Melton, M.D.
 Gregory Mundy, M.D.

Mark Nanes, M.D., Ph.D.
 Robert A. Nissenson, Ph.D.
 Masaki Noda, M.D., Ph.D.
 Lynne Opperman, Ph.D.
 Eric Orwoll, M.D.
 Philip Osdoby, Ph.D.
 Susan Ott, M.D.
 Roberto Pacifici, M.D.
 Munro Peacock, M.D.
 Steven Petak, M.D.
 John Pettifor, Ph.D.
 J. Wesley Pike, Ph.D.
 Carol Pilbeam, M.D., Ph.D.
 Anthony Portale, M.D.
 Charles Prince, Ph.D.
 Darryl Quarles, M.D.
 Lawrence G. Raisz, M.D.
 Stuart Ralston, M.D.
 Robert Recker, M.D.
 Jonathan R. Reeve, D.M., D.Sc.
 René Rizzoli, M.D.
 Trudy Roach, Ph.D.
 G. David Roodman, M.D., Ph.D.
 Clifford J. Rosen, M.D.
 Vicki Rosen, Ph.D.
 Patrick Ross, Ph.D.
 Clinton Rubin, Ph.D.
 Janet Rubin, M.D.
 Wayne Sampson, Ph.D.
 Ego Seeman, M.D.
 Peter Selby, M.D.
 Elizabeth Shane, M.D.
 Neil Sharkey, Ph.D.
 Caroline Silve, M.D., Ph.D.
 Justin Silver, M.D., Ph.D.
 Timothy Skerry, Ph.D.
 Thomas Spelsberg, Ph.D.
 Rene St-Arnaud, Ph.D.
 Andrew F. Stewart, M.D.
 Larry Suva, Ph.D.
 Pawel Szulc, M.D.
 Rajesh Thakker, M.D.
 Jon Tobias, M.D.
 Dwight Towler, M.D., Ph.D.
 Charles Turner, Ph.D.
 Andre Uitterlinden, Ph.D.
 Connie Weaver, Ph.D.
 Kristy Weber, M.D.
 Lee Weinstein, M.D.
 Kenneth White, Ph.D.
 Michael Whyte, M.D.
 Kristine Wren, Ph.D.
 Marian Young, Ph.D.
 Joseph Zmuda, Ph.D.

ADVOCACY COMMITTEE

Janet Rubin, M.D., *Chairperson*
 Jane E. Aubin, Ph.D., *Ex Officio*
 Bernard P. Halloran, Ph.D.
 Stephen E. Harris, Ph.D.
 Mary B. Leonard, M.D.
 Laura R. McCabe, Ph.D.
 G. David Roodman, M.D., Ph.D.
 Diane L. Schneider, M.D., MSc.
 Paula Stern, Ph.D., *Ex Officio*

ANCILLARY COMMITTEE

Fred S. Kaplan, M.D., *Chairperson*
 Elizabeth Barrett-Connor, Ph.D.
 Thomas L. Clemens, Ph.D.
 Barbara Lukert, M.D.
 Charles Turner, Ph.D.

ARCHIVES COMMITTEE

Frederick R. Singer, M.D., *Chairperson*
 Claude Arnaud, M.D., *Ad Hoc*
 Jane E. Aubin, Ph.D.
 Arnold J. Kahn, Ph.D., M.S.
 Lawrence G. Raisz, M.D.
 Paula H. Stern, Ph.D.
 Armen H. Tashjian, M.D.

EDUCATION COMMITTEE

Teresita M. Bellido, Ph.D., *Chairperson*
 Brendan Boyce, M.D.
 Maria Luisa Brandi, M.D., Ph.D.
 Jan M. Bruder, M.D.
 Christopher S. Kovacs, M.D., F.R.C.P.C., F.A.C.P.
 Benjamin Z. Leder, M.D.
 Susan M. Ott, M.D.
 Merry Jo Oursler, Ph.D., *Ad Hoc*
 Margaret Seton, M.D., *Ad Hoc*

ETHICS ADVISORY COMMITTEE

Julie Glowacki, Ph.D., *Chairperson*
 Thomas Clemens, Ph.D.
 David Goltzman, M.D., *Ad Hoc*
 Barbara Lukert, M.D.
 Robert Nissenson, Ph.D., *Ex Officio*
 Lawrence G. Raisz, M.D.
 Clifford J. Rosen, M.D.

FINANCE COMMITTEE

Marc K. Drezner, M.D., *Chairperson*
 Sylvia J. Christakos, Ph.D., *Ex Officio*
 Diane Cullen, Ph.D.
 Dolores Shoback, M.D.
 Elizabeth Shane, M.D., *Ex Officio*
 Timothy Skerry, Ph.D.

LOCAL ARRANGEMENTS COMMITTEE

Ronald Chandler
 Kelly J. McDermott
 Douglas P. Mortlock
 S. Bob Tanner, M.D.

MEMBERSHIP DEVELOPMENT COMMITTEE

Andre van Wijnen, Ph.D., *Chairperson*
 Peter Bodine, Ph.D.
 Patricia Collin-Osdoby, Ph.D.
 Ingrid Holm, M.D.
 Melissa Kacena, Ph.D.
 Hiroshi Kawaguchi, M.D.
 Xu Cao, Ph.D.
 Mone Zaidi, M.D.

NOMINATING COMMITTEE

Robert A. Nissenson, Ph.D., *Chairperson*
 Jane E. Aubin, Ph.D.
 Teresita Bellido, Ph.D.
 René Rizzoli, M.D.
 Vicki Rosen, Ph.D.
 Stuart L. Silverman, M.D.

PROFESSIONAL PRACTICE COMMITTEE

Stuart Silverman, M.D., *Chairperson*
 Robert Adler, M.D.
 Cyrus Cooper, M.A., D.M., F.R.C.P.
 Ghada El-Hajj Fuleihan, M.D.
 Catherine Gordon, M.D.
 Gillian Hawker, M.D., M.Sc.
 Meryl LeBoff, M.D.
 Richard Prince, M.D.
 Olof Johnell, M.D., *Ad Hoc*
 Laura Tosi, M.D., *Ad Hoc*

PUBLICATIONS COMMITTEE

Joseph Lorenzo, M.D., *Chairperson*
 Lynda Bonewald, Ph.D.
 Seiji Fukumoto, M.D., Ph.D.
 Douglas P. Kiel, M.D., MPH
 Stavroula Kousteni, Ph.D.
 John A. Eisman, Ph.D., *Ex Officio*
 Michael Econs, M.B.B.S., M.D., *Ad Hoc*
 Murray Favus, M.D., *Ex Officio*
 L. Darryl Quarles, M.D.
 Anna Teti, Ph.D.

PRIMER EDITORIAL BOARD

Murray J. Favus, M.D., *Chairperson*
 Sylvia Christakos, Ph.D.
 Steven R. Goldring, M.D.
 Teresa Guise, M.D.
 Michael F. Holick, M.D., Ph.D.
 Michael Kleerekoper, M.D.
 Suzanne Jan de Beur, M.D.
 Nancy Lane, M.D.
 Craig B. Langman, M.D.
 Pamela G. Robey, Ph.D.
 Clifford Rosen, M.D.
 Elizabeth Shane, M.D.
 Dolores M. Shoback, M.D.
 Andrew F. Stewart, M.D.
 Michael P. Whyte, M.D.

SCIENCE POLICY COMMITTEE

Philip Osdoby, Ph.D., *Chairperson*
 Matthew Gillespie, Ph.D.
 Sophie A. Jamal, M.D., Ph.D.
 Nancy Lane, M.D.
 Janet Rubin, M.D., *Ex Officio*
 Paula H. Stern, Ph.D., *Ex Officio*
 Stuart L. Silverman, M.D., *Ex Officio*

WOMEN IN BONE AND MINERAL RESEARCH COMMITTEE

Nicola Partridge, Ph.D., *Chairperson*
 Janine A. Danks, Ph.D.
 Deborah L. Galson, Ph.D.
 Carol C. Pilbeam, M.D., Ph.D.
 Shonni J. Silverberg, M.D.
 Jennifer J. Westendorf, Ph.D.

ASBMR REPRESENTATIVES TO FASEB

Jane E. Aubin, Ph.D.
FASEB Board
 Philip A. Osdoby, Ph.D.
Science Policy Committee
 Robert D. Blank, M.D., Ph.D.
Research Conferences Advisory Committee
 Jane B. Lian, Ph.D.
Excellence in Science Award Committee
 Dolores M. Shoback, M.D.
Finance Committee
 Paula Stern, Ph.D.
FASEB Board and Science Policy Committee
 Gloria Gronowicz, Ph.D.
Federal Funding Consensus Committee
 Bernard P. Halloran, Ph.D.
Federal Funding Consensus Committee
 Robert Civitelli, M.D.
FASEB Publications and Communications Committee

The ASBMR gratefully acknowledges the following companies and organizations for their support:

2005 SUPPORTERS

DIAMOND LEVEL SUPPORTER

Merck & Co., Inc.

PLATINUM LEVEL SUPPORTERS

Alliance for Better Bone Health (a collaboration between Procter & Gamble Pharmaceuticals
and Aventis Pharmaceuticals, a member of the sanofi-aventis Group)

Eli Lilly and Company

Roche and GlaxoSmithKline

GOLD LEVEL SUPPORTER

NPS Pharmaceuticals

SILVER LEVEL SUPPORTERS

Amgen, Inc.

Pfizer, Inc.

Novartis Pharmaceuticals Corporation

BRONZE LEVEL SUPPORTER

Abbott Pharmaceuticals

FRIEND LEVEL SUPPORTERS

Aastrom Bioscience

Aventis Pharmaceuticals

Elsevier Science

Genentech

GlaxoSmithKline Consumer Healthcare

Mission Pharmacal Company

National Dairy Council

The Paget Foundation for Paget's Disease of Bone and Other Diseases

Procter & Gamble Pharmaceuticals

Wyeth Pharmaceuticals

2005 EXHIBITORS*

Alliance for Better Bone Health
(a collaboration between Procter & Gamble
Pharmaceuticals and Aventis Pharmaceuticals, a
member of the sanofi-aventis Group)

ALPCO Diagnostics

Amgen

Bio-Imaging Technologies, Inc.

BIOQUANT Image Analysis Corporation

Cambrex

Charles River Laboratory, Pre-Clinical Services -
CTBR

Diagnostic Systems Laboratories, Inc.

DiaSorin

Duke Clinical Research Institute

Dyets, Inc.

Echo Medical Systems

Eli Lilly and Company

Elsevier (WB Saunders, Moby, Academic Press)

Faxitron X Ray Corporation

Federation of American Societies for Experimental
Biology

Genzyme

GE Healthcare

GlaxoSmithKline Consumer Healthcare

Hologic, Inc.

Humana Press

Hysitron, Inc.

Imaging Therapeutics, Inc.

Immuno-Biological Laboratories, Inc. (IBL-
America)

Immunodiagnostic Systems, Inc. (IDS)

Immutopics International

International Bone and Mineral Society (IBMS)

International Society for Clinical Densitometry
(ISCD)

Inverness Medical Innovations, Inc.

Jarrow Formulas, Inc.

Kamiya Biomedical Company

Kureha Special Laboratory Co., Ltd.

Linco Research

Merck U.S. Human Health

MicroMRI Inc.

Micro Photonics Inc.

Mindways Software, Inc.

Mission Pharmacal Company

National Institute of Diabetes and Digestive and
Kidney Diseases

National Kidney Foundation

National Osteoporosis Foundation

Nichols Institute Diagnostics

NIH Osteoporosis and Related Bone Disease -
National Resource Center

Nordic Bioscience Diagnostics A/S

Novartis Pharmaceuticals Corporation

Orthometrix

Osteometrics, Inc.

Pacific Biometrics, Inc. (PBI)

Pharmatest Services Ltd

Quidel Corporation

RATOC System Engineering Co., Ltd.

Roche and GlaxoSmithKline

Roche Diagnostics Corporation

Scanco U.S.A., Inc.

Scantibodies Clinical Laboratory

SkeleTech, Inc.

Skyscan

Springer

Synarc, Inc.

Wyeth Pharmaceuticals

*As of 8/01/05

GENERAL INFORMATION

ASBMR MEETING LOCATION

All ASBMR 27th Annual Meeting sessions will take place in the Gaylord Opryland Resort and Convention Center, unless otherwise stated. The Gaylord Opryland Resort and Convention Center is located at 2800 Opryland Drive, Nashville, Tennessee, USA.

AUDIO- AND VIDEOTAPING

ASBMR expects that attendees respect each presenter's willingness to provide free exchange of scientific information without the abridgement of his or her rights or privacy and without the unauthorized copying and use of the scientific data shared during his or her presentation. In addition, ASBMR expects that attendees will respect Exhibitors' desires not to have their products or booths photographed or videotaped.

The use of cameras, audio-taping devices, and videotaping equipment is strictly prohibited within all Oral Scientific Sessions, the Exhibit Halls, and the Poster Sessions without the express written permission of the ASBMR. Unauthorized use of the taping equipment may result in the confiscation of the equipment or the individual may be asked to leave the scientific session or Exhibit Hall. These rules are strictly enforced.

USE OF ASBMR NAME AND LOGO

ASBMR reserves the right to approve use of its name in all material disseminated to the media, public and professionals. ASBMR's name, meeting name, and meeting logo may not be used without permission. Use of the ASBMR logo is prohibited. Materials should be directed to ASBMR Executive Director Joan Goldberg. All ASBMR corporate supporters and exhibitors should share their media outreach plans with the ASBMR Executive Director before release.

No abstract presented at the ASBMR 27th Annual Meeting may be released to the press before its official presentation date and time. Press releases must be embargoed until one hour after the presentation.

ASBMR MEETING CONTENT AND EMBARGO POLICY

Abstracts submitted to the ASBMR 27th Annual Meeting are embargoed - that is, unavailable for public release in written, oral and electronic communications - until one hour after the abstract has been presented.

The ASBMR is sensitive to issues of commercial confidentiality and relevant aspects of the U.S. Securities and Exchange Commission (SEC) regulations. Therefore, the ASBMR reminds all readers that all must adhere to the U.S. Securities and Exchange Commission regulations and treat all scientific information as confidential until the embargo has been lifted - one hour after the abstract has been presented. Any reader of, or listener to, ASBMR Annual Meeting content may be viewed as an "insider" by the SEC due to knowledge of information included in abstracts, particularly clinical trial abstracts. SEC regulations may call for criminal penalties for using such information.

COPYRIGHT

Abstracts submitted to the ASBMR 27th Annual Meeting and published in the Abstracts supplement to the *Journal of Bone and Mineral Research* are copyrighted by the American Society for Bone and Mineral Research. Reproduction, distribution, or transmission of the abstracts in whole or in part, by electronic, mechanical or other means, or intended use, is prohibited without the express written permission of the American Society for Bone and Mineral Research. All inquiries regarding copyrighted material or reprint orders should be directed to Ms. Adrienne Lea, Director of Publications, American Society for Bone and Mineral Research, E-mail: adrienne@jbmr.org, Tel: (919) 620-0681; Fax: (919) 620-8465, Postal Address: 3209 Guess Road, Suite 201, Durham, NC 27705, USA.

DISCLAIMER

All authored abstracts, findings, conclusions, or recommendations contained herein are those of the author(s) and do not reflect the views of the American Society for Bone and Mineral Research or herein imply any endorsement. No responsibility is assumed, and responsibility is hereby disclaimed, by the American Society for Bone and Mineral Research for any injury and/or damage to persons or property as a matter of products liability, negligence or otherwise, or from any use or operation of methods, products, instructions, or ideas presented in the materials herein (2005 Abstracts). Independent verification of diagnosis and drug dosages should be made. Discussions, views and recommendations as to medical procedures, choice of drugs and drug dosages are the responsibility of the authors.

CONTINUING MEDICAL EDUCATION CREDITS

The Federation of American Societies for Experimental Biology (FASEB) is accredited by the Accreditation Council for Continuing Medical Education to sponsor continuing medical education for physicians. This activity has been planned and implemented in accordance with the Essential Areas and Policies of the Accreditation Council for Continuing Medical Education through the joint sponsorship of FASEB and the ASBMR.

Category I Continuing Medical Education (CME) credits toward the American Medical Association's (AMA) Physician Recognition Award will be offered at this meeting. FASEB designates this educational activity for a maximum of 40 category 1 credits. Each physician should claim only those credits that he or she actually spent in the activity. CME application forms will be available in the On-Site Program book, which will be distributed at the meeting. There is a \$45 application fee, payable to FASEB upon submission of the form.

For more information, please contact:

FASEB Office of Scientific Meetings and Conferences

Tel: (301) 634-7013

Fax: (301) 634-7007

E-mail: pmcgovern@faseb.org

Meeting Objective

The ASBMR 27th Annual Meeting is designed to allow members to present new developments in education, research and clinical practice related to bone and mineral metabolism. The program objectives include updating attendees on the recent advances in osteoporosis and other diseases of bone and mineral metabolism, vitamin D and other steroids, peptide calcitropic hormones, mechanical loading and exercise, bone acquisition and pediatric bone disease, cartilage and connective tissue matrix, and growth factors. As a result of their attendance, participants should have enhanced their knowledge of osteoporosis, other diseases of bone, basic bone biology and its correlation to mineral metabolism, as well as their ability to treat and care for their patients. Attendees should have developed a clearer understanding of the interrelationship among basic research, clinical research and patient care through the discussions that are expected to take place. The ASBMR 27th Annual Meeting program should produce an enhanced appreciation of the investigative, diagnostic and therapeutic aspects of metabolic bone disorders.

Target Audience

The program is designed for researchers, physicians, clinicians, and other allied health professionals with interests in endocrinology, physiology, cell biology, pathology, molecular biology, genetics, epidemiology, internal medicine, rheumatology, orthopedics, dentistry, nephrology, and pharmacology.

DISCLOSURE/CONFLICT OF INTEREST

The Federation of American Societies for Experimental Biology (FASEB) requires that audiences at FASEB-sponsored educational programs be informed of a presenter's (speaker, faculty, author, or contributor) academic and professional affiliations, and the disclosure of the existence of any significant financial interest or other relationship a presenter has with the manufacturer(s) of any commercial product(s) discussed in an educational presentation. This policy allows the listener/attendee to be fully knowledgeable in evaluating the information being presented. The Program will note those speakers who have disclosed relationships, including the nature of the relationship and the associated commercial entity.

All authors of submitted abstracts completed the disclosure statement in the online submission program. Invited speakers who are not required to submit an abstract received a form in the mail that they completed and returned.

Disclosure may include any relationship that may bias one's presentation or which, if known, could give the perception of bias. This includes relevant financial relationships of a spouse or partner. These situations may include, but are not limited to:

DISCLOSURE KEY

1. stock options or bond holdings in a for-profit corporation or self-directed pension plan
2. research grants
3. employment (full or part-time)
4. ownership or partnership
5. consulting fees or other remuneration
6. non-remunerative positions of influence such as officer, board member, trustee, or public spokesperson
7. receipt of royalties
8. speaker's bureau

For full-time employees of industry or government, the affiliation listed in the *2005 Abstracts* will constitute full disclosure.

Disclosures for invited speakers and abstract presenters are provided at the end of the session listing for invited speakers (see *On-Site Program* book) and directly after the body of an abstract for abstract submissions. If there is no conflict of interest or disclosure listed, this means that the invited speaker and/or abstract presenter indicated no conflicts to disclose.

The disclosure information will correspond to the key above. If disclosures are given, the company name, along with the respective disclosure relationship number will be listed (for example: Company Name, 2, 8.).

2005 ABSTRACTS BOOK

Supported by an unrestricted educational grant from Alliance for Better Bone Health (a collaboration between Procter & Gamble Pharmaceuticals and Aventis Pharmaceuticals, a member of the sanofi-aventis Group)

This *2005 Abstracts* book is distributed on-site at the Annual Meeting to all ASBMR members and non-member attendees. Non-member subscribers to *JBMR* will receive the *2005 Abstracts* book by mail. ASBMR members who do not attend the Annual Meeting will receive their copy of the *2005 Abstracts* book by mail following the meeting. The entire ASBMR Scientific Program (invited speaker sessions, lectures, and abstract-based oral and poster presentation information), as well as the 2005 Ancillary Program (Working Groups and Industry-Supported Symposia), are included in full detail in the On-Site Program book and on the ASBMR website at www.asbmr.org. **We encourage you to make use of the 2005 Abstracts On-line that is accessible via the ASBMR website at www.asbmr.org. A complimentary hard copy of the 2005 Abstracts book in PDF format will be available for download for all ASBMR members and pre-registered attendees via the ASBMR website as well.**

AWARD PRESENTATIONS

The following ASBMR Awards will be presented immediately following the morning Plenary Symposia and Plenary Lectures in the Delta Ballroom of the Gaylord Opryland Resort and Convention Center - the ASBMR Gideon A. Rodan Excellence in Mentorship Award, the Fuller Albright Award, the Louis V. Avioli Founders Award, the Frederic C. Bartter Award, the William F. Neuman Award, and the Shirley Hohl Service Award. Please refer to the schedule found in the inside cover of this book for award presentation times.

ASBMR VIRTUAL EXHIBIT HALL

The ASBMR Virtual Exhibit Hall (www.asbmr.org/LiveASBMRHall.com) showcases Exhibitors and their products, many of which are present at this year's ASBMR 27th Annual Meeting. Visitors to the ASBMR Virtual Exhibit Hall are able to learn more about Exhibitor's products and services, easily contact them for further information, and enjoy an Exhibit Hall experience at their leisure year-round.

CYBER CAFÉ

Supported by NPS Pharmaceuticals

The Cyber Café, located in the Exhibit Hall, has full Internet capability and enables attendees to search the Internet and check their email. The Cyber Café will be open during published Poster Hall hours.

NIH LOUNGE

Looking for another opportunity to ask U.S. National Institutes of Health and Center for Scientific Review staff about your grant proposal or idea? Plan to visit the Meet-the-NIH Lounge in the Ryman Chamber C of the Gaylord Opryland Resort and Convention Center and get your questions answered. Program staff from the National Institute and Musculoskeletal and Skin Diseases (NIAMS), the National Institute of Diabetes and Digestive and Kidney Diseases (NIDDK), the National Cancer Institute (NCI), the National Institute of Dental and Craniofacial Research (NIDCR), National Institute on Aging (NIA), Center for Scientific Review (CSR), National Institute of Child Health and Human Development (NICHD), and more will be on-hand, by appointment, to meet with you. Be sure to sign up for open time slots on-site.

YOUNG INVESTIGATOR LOUNGE

All Young Investigator Annual Meeting attendees are cordially invited to drop by the Young Investigator Lounge located in the Ryman Chamber B of the Gaylord Opryland Resort and Convention Center. Expand your network of colleagues and make new friends.

ASBMR HALF-DAY SYMPOSIUM: BONE AND MINERAL COMPLICATIONS OF CHRONIC KIDNEY DISEASE (CKD)

This session will be held on Friday, September 23, 2005, from 9:30 am to 12:00 noon, in the Delta Ballroom of the Gaylord Opryland Resort and Convention Center. Several issues of critical importance to clinicians and researchers in the field will be discussed.

RECEPTION FOR NEW INVESTIGATOR/NEW MEMBER/FIRST TIME ATTENDEES

Sponsored by the ASBMR Membership Development Committee

We are inviting new members and attendees who would like to become affiliated with the ASBMR for a special event which will follow the ASBMR Welcome Reception and Plenary Poster Session. The reception will be held in the Washington B room. The purpose of this social event is to assist attendees with opportunities to meet other recent attendees. The event has been organized to promote interactions among new and junior investigators. Beverages will be available at regular prices ("cash bar").

NEW INVESTIGATOR/NEW MEMBER BREAKFAST

*Sponsored by the ASBMR Membership Development Committee
Supported by an unrestricted educational grant from Merck & Co., Inc.*

The New Investigator/New Member Breakfast will be held on Saturday, September 24, 2005, from 7:00 am to 8:00 am, in the Governor's Ballroom C/D of the Gaylord Opryland Resort and Convention Center. New Investigators (those early in their research careers) and new ASBMR members are invited to join the ASBMR Council, the Membership Development Committee and colleagues for an informational breakfast. Highlights will include opening remarks by the President of ASBMR, Dr. Sylvia Christakos, and an overview of the program planning by the Program Chairs Drs. Michael Econs and Pamela Robey. Program Directors from U.S. NIH Institutes and Centers, along with ASBMR member senior and junior scientists, will be available for discussion at specially marked tables. Attendees should look for table signs advertising a specialty or NIH Institute or Center of Interest. Or attendees can make their own signs to join with colleagues who have similar interests. Breakfast will be provided.

SPECIAL SESSION FOR ALLIED HEALTH PROFESSIONALS

*Sponsored by the ASBMR Membership Development Committee
Supported by an educational grant from Amgen, Inc.*

This session will be held on Saturday, September 24, 2005, from 12:00 noon to 2:00 pm, in Governor's Ballroom North of the Gaylord Opryland Resort and Convention Center. This special session is of interest to allied health professionals, first time meeting attendees, individuals new to the field, nurses, clinical research study coordinators, physical therapists and/or those seeking guidance in navigating through the extensive ASBMR program. An overview of the ASBMR 27th Annual Meeting will be given along with lectures on "Nomenclature for Osteoporosis Drugs" and "AMG 162." There is no additional fee or registration required for this session, nor will food and beverages be served. However, you are welcome to purchase lunch from the concession area the Exhibit Hall (Ryman Hall C) in the Gaylord Opryland Resort and Convention Center.

GRANT WRITING WORKSHOP: TIPS ON GETTING FUNDED

Sponsored by the ASBMR Membership Development Committee

The Grant Writing Workshop will be held on Saturday, September 24, 2005, from 12:30 pm to 2:00 pm, in the Governor's Ballroom C/D of the Gaylord Opryland Resort and Convention Center. New investigators (those early in their research careers) and new members are invited to attend a workshop on the grant writing process, including advice on grantsmanship and the peer-review process. A panel discussion, based on questions and feedback from the audience, will be led by U.S. NIH representatives and experienced ASBMR members from academia, including an international representative. Funding source information and opportunities will be provided. This is a valuable opportunity for new investigators to gain helpful tips and information directly from these representatives and to become familiar with the different programs. There is no additional fee or registration required for this session, nor will food or beverages be served. However, attendees are welcome to purchase lunch from the concession area in the Exhibit Hall (Ryman Hall C) in the Gaylord Opryland Resort and Convention Center.

BIOTECHNIQUES WORKSHOP: BIOLUMINESCENT IMAGING

Sponsored by the ASBMR Education Committee

This session will take place on Sunday, September 25, 2005, from 12:30 pm to 2:00 pm, in the Governor's Ballroom North of the Gaylord Opryland Resort and Convention Center. There is no additional fee or registration required for this session, nor will food and beverages be served. However, you are welcome to purchase lunch from the concession area in the Exhibit Hall (Ryman Hall C) in the Gaylord Opryland Resort and Convention Center.

THE ART OF GRANT REVIEWING

Sponsored by the ASBMR U.S. Center for Scientific Review(CSR) Task Force

This session will take place on Sunday, September 25, 2005, from 11:30 am to 12:30 pm, in the Jackson E/F room of the Gaylord Opryland Resort and Convention Center. This session, intended for investigators who are at an early to mid-stage of their career, will address the U.S. National Institutes of Health (NIH) grant review process and will provide insight into the skills needed to serve as an effective grant reviewer. Through this session and other activities, the ASBMR U.S. Center for Scientific Review (CSR) Task Force hopes to increase the pool of experienced investigators who would be willing to serve on study sections and review different types of bone-related grants, including basic, translational and clinical grants. The discussion at this informal, interactive session will be led by a panel of CSR Program Directors and previous NIH Grant Study Section Chairs. There is no additional fee but registration is required for this session. Tickets can be obtained from the Meet-the-Professor ticket desk in the Delta Lobby B. Food and beverages will not be served. However, you are welcome to purchase lunch from the concession area in the Exhibit Hall (Ryman Hall C) in the Gaylord Opryland Resort and Convention Center.

CAREER OPTIONS FOR SCIENTISTS

Sponsored by the ASBMR Education Committee

The Career Options for Scientists Workshop will be held on Monday, September 26, 2005, from 12:30 pm to 2:00 pm, in the Presidential Ballroom B of the Gaylord Opryland Resort and Convention Center. This year's Career Options for Scientists Workshop is entitled "Perseverance Pays: Overcoming Nay Sayers to Get a Project on Track." While common, early career rejections and frustrations can be devastating to the morale and motivation of younger investigators. Three distinguished ASBMR members will give their perspective on how they have been able to overcome professional, personal, or career hurdles to complete important projects and advance professionally. This workshop targets basic scientists and clinical researchers in both academia and industry. It should be informative for attendees in all phases of their careers, but in particular for researchers who are in early phases of career development. There is no additional fee or registration required for this session, nor will food and beverages be served. However, you are welcome to purchase lunch from the concession area in the Exhibit Hall (Ryman Hall C) in the Gaylord Opryland Resort and Convention Center.

MEET-THE-INTERNATIONAL GRANT WRITERS

Sponsored by the ASBMR Membership Development Committee

This informal, interactive session is designed for international (non-U.S.) investigators seeking grant information and advice specific to their country or region. Attendees will have an opportunity to meet with grant writers from the various geographic areas identified including: Australia, Korea, Europe, Japan, United Kingdom, Central and South America. Information on international grant opportunities will be available. This session will be held on Monday, September 26, 2005, from 1:00 pm to 2:00 pm, in the Canal A/ B room. There is no additional fee or registration required for this session. Please note that food and beverages are not served. However, you are welcome to purchase lunch from the concession area in the Exhibit Hall (Ryman Hall C) the Gaylord Opryland Resort and Convention Center.

CLINICAL ROUNDTABLES/CLINICAL HALF-DAY

The Clinical Roundtable and Half-day sessions are informal sessions geared toward the practicing clinician, offering insight into treatment and diagnosis of bone diseases. These sessions will feature a focused discussion on topical issues of clinical relevance. The clinical roundtable on "What Is the Optimal Duration of Bisphosphonate Therapy?" and "Premenopausal Women with Low BMD" will be held on Friday, September 23, 2005, from 1:00 pm to 2:00 pm, in the Presidential Ballroom South of the Gaylord Opryland Resort and Conference Center. The session on "Acute Vertebral Fracture during a Seizure in a Patient on Long-Term Anticonvulsant Therapy - Is This Traumatic or Not?" and "Kidney Stones and Low Bone Mass" will be held on Saturday, September 24, 2005, from 12:30 pm to 1:30 pm, in the Presidential Ballroom South of the Gaylord Opryland Resort and Conference Center. The Clinical Half-Day sessions on "Steroid-Induced Osteoporosis" and Vertebroplasty/Kyphoplasty Point-Counterpoint: Pro and Con," will be held on Sunday, September 25, 2005 from 8:00 am to 9:30 am, in the Presidential Ballroom Sound of the Gaylord Opryland Resort and Convention Center. The Clinical Half-Day sessions on "Falls," "Vitamin D: Is There an Epidemic?" and "Pitfalls of Densitometry and Difficult Densitometry Cases" will be held on Sunday, September 25 2005, from 12:00 pm to 2:00 pm, in the Presidential Ballroom South of the Gaylord Opryland Resort and Conference Center. The session on "Osteogenesis Imperfecta (OI)" and "Bone Disease in Sick Children: What Standards Should Be Used?" will be held on Monday, September 26, 2005, from 12:30 pm to 1:30 pm, in the Presidential Ballroom South of the Gaylord Opryland Resort and Conference Center.

MEET-THE-PROFESSOR SESSIONS

The Meet-the-Professor Sessions are a series of informal sessions designed to provide an opportunity for meeting attendees to interact with experts in an intimate setting and discuss specific clinical and research topics. This year the Meet-the-Professor program has been expanded in order to increase the number of attendees who are able to participate in these sessions. The schedule allows for many Meet-the-Professor sessions to be given twice during the program.

Interested individuals must sign up on-site for the sessions. Tickets are extremely limited and are required for admission. If you are interested in attending one of these sessions, we encourage you to sign up at your earliest convenience on-site at the Registration Desk in the Delta B Lobby at the Gaylord Opryland Resort and Convention Center. There is no additional fee required for this session, nor will food and beverages be served. However, you are welcome to purchase lunch from the concession area in the Exhibit Hall (Ryman Hall C) in the Gaylord Opryland Resort and Convention Center.

ASBMR MINORITY BREAKFAST

Sponsored by the ASBMR Minority Task Force

Minority attendees - and those who want to help further minority participation in the bone and mineral research field and in the ASBMR - are invited to a complimentary breakfast with the ASBMR Minority Task Force. The Minority Breakfast will be held on Sunday, September 25, 2005, from 7:00 am to 8:00 am, in Washington B room of the Gaylord Opryland Resort and Convention Center. Participants can learn about minority research and travel grants and other career development programs as well as discuss concerns and recommendations for new initiatives. Space is limited to 50 attendees. There is no additional fee. However, you will need to register for the breakfast onsite at the ASBMR 27th Annual Meeting Meet-the-Professor Session Registration desk. All attendees will automatically be registered for a special drawing for free tickets to the ASBMR Social Event!

THE WOMEN IN BONE AND MINERAL RESEARCH EVENT

Sponsored by the ASBMR Women in Bone and Mineral Research Committee

Supported by a grant from Aastrom Biosciences, Inc.

The Women in Bone and Mineral Research Event will be held on Sunday, September 25, from 6:00 pm to 7:30 pm in the Washington B room in the Gaylord Opryland Resort and Convention Center. There is a \$35 registration fee (\$15 for students/trainees) for this event. Light hors d'oeuvres and soft drinks will be served. A cash bar will be available.

THE ROLE OF ADVOCACY IN MUSCULOSKELETAL RESEARCH FUNDING: GRASSROOTS, NIH, CONGRESS AND THE PUBLIC

Sponsored by the ASBMR Advocacy Committee

This session will provide a brief overview of the current political research funding climate in the U.S., and the strategies used in advocating for increased funding and grassroots advocacy. The Advocacy 101 session will be held on Sunday, September 25, 2005, from 12:30 pm to 1:30 pm in the Governor's Ballroom C/D in the Gaylord Opryland Resort and Convention Center. Speakers and panelists include the Bone Coalition's advocate on Capitol Hill, Washington, DC, USA, ASBMR's representative on the Federation of American Societies for Experimental Biology (FASEB) Board, and ASBMR's Advocacy Committee Chair and ASBMR's Executive Director. Attendees will learn about the ASBMR advocacy program and how scientists can become more effective research advocates around the world. Attendees will receive materials to assist in advocacy, including fact sheets and tips on successful advocacy approaches.

WELCOME RECEPTION AND PLENARY POSTER SESSION

Supported by an educational grant from Merck & Co., Inc.

On Friday, September 23, 2005, from 5:15 pm to 7:00 pm, attendees and registered guests are invited to attend the ASBMR Welcome Reception and Plenary Poster Session in Exhibit/Poster in Ryman Hall C of the Gaylord Opryland Resort and Convention Center. Simply display your badge for admission. Guests may purchase a badge for \$30 at registration, which will allow entrance to the Welcome Reception and Exhibit Hall.

ASBMR SOCIAL EVENT

On Sunday, September 25, 2005, from 8:30 pm to 11:30 pm, come cruise the Cumberland River with ASBMR aboard the General Jackson Showboat. The 300-foot-long General Jackson is an historic paddlewheel riverboat reminiscent of ones that cruised the Southern waterways in the 1800s. On board we'll enjoy light refreshments, drinks, music and, of course, a terrific dance band. The General Jackson boards across from the Gaylord Opryland Resort and Convention Center, but shuttle busing will be provided from the Presidential Portico from 8:15 pm - 9:00 pm. The boat sails promptly at 9:30 pm. Tickets are required for admission and must be purchased in advance for \$30. If available tickets remain, they will be sold on-site at the ASBMR Registration Desk in the Delta Lobby B of the Gaylord Opryland Resort and Convention Center. Don't be late! There are no refunds for those who miss the boat!

ASBMR FUN RUN/WALK

Supported by Novartis Pharmaceuticals Corporation

Delegates and guests of the ASBMR 27th Annual Meeting will have an opportunity to participate in a 5 Km Fun Run/Walk. Whether participants choose to walk or run, they will find this event a terrific way to begin a busy day. There is no cost to participate. Drinks and snacks will be provided. There will be busing provided to Two Rivers Park, where the Fun Run/Walk will be held from 5:30 am to 7:15 am on Monday, September 26, 2005. Meet the shuttle bus at the Presidential Portico outside the Presidential Lobby of the Gaylord Opryland Resort and Conference Center promptly at 5:30 am.

DINE-AROUND RESTAURANT RESERVATION SERVICE

Explore the fabulous hometown flavor of Music City! Or dine at one of Nashville's dozens of four-star restaurants. ASBMR will have a Restaurant Reservations Desk available in the ASBMR Registration Area in the Delta Lobby B of the Gaylord Opryland Resort and Convention Center. You can make reservations for your small group, or if you're dining alone, we can help you make a small group reservation with other ASBMR attendees. For Friday, Saturday and Monday evenings, ASBMR has set aside tables at a variety of restaurants in several of the city's hottest nightspots. We'll bus you from the Gaylord Opryland Resort and Convention Center to your restaurant. After dinner, enjoy the city's nightlife and hop on the bus to return to the hotel. The shuttle busing is complimentary. All meal and entertainment costs will be charged to individual diners and club visitors.

FREE ASBMR DOWNTOWN SHUTTLE BUS

ASBMR is providing free shuttle buses to downtown Nashville during the times below each evening. The buses will pickup at the Presidential Portico outside of the Presidential Lobby of the Gaylord Opryland Resort and Convention Center. The return shuttles will pickup at the same locations where you were dropped off downtown. Attendees using the restaurant reservation service will use the same shuttles. Stop by the Restaurant Reservations desk in Delta Lobby B during registration hours for more information.

Thursday, September 22	5:00 pm - 12:00 midnight - 1 Location: Downtown/Riverfront Park
Friday, September 23	7:00 pm - 12:00 midnight - 3 Locations: Downtown/Riverfront Park, Vanderbilt Area and West End/Hillsboro
Saturday, September 24	7:00 pm - 12:00 midnight - 3 Locations: Downtown/Riverfront Park, Vanderbilt Area and West End/Hillsboro
Sunday, September 25	6:00 pm - 12:00 midnight - 1 Location: Downtown/Riverfront Park
Monday, September 26	6:00 pm - 12:00 midnight - 3 Locations: Downtown/Riverfront Park, Vanderbilt Area and West End/Hillsboro

HOTEL SHUTTLES

ASBMR is not providing a shuttle bus from the GuestHouse International Inn, the Radisson Hotel at Opryland, the Fairfield Inn by Marriott, the Best Western Suites Near Opryland, the AmeriSuites, nor any of the hotels along Music Valley Drive. However, some of these properties have their own vans that will shuttle guests to the Gaylord Opryland Resort if the van is available. We encourage you to inquire at your specific hotel.

ASBMR is providing a shuttle from the Nashville Airport Marriott in the mornings and evenings. Additional shuttles may also be added for airport hotels within the official ASBMR block. Bus schedules will be provided in official ASBMR hotel lobbies as well as at the Information desk in Delta Lobby B at the Gaylord Opryland Resort.

REGISTRATION HOURS

All on-site registration will take place in the Delta Lobby B of the Gaylord Opryland Resort and Convention Center.

Thursday, September 22, 2005	9:00 am - 5:00 pm
Friday, September 23, 2005	7:00 am - 6:30 pm
Saturday, September 24, 2005	7:00 am - 5:30 pm
Sunday, September 25, 2005	7:00 am - 5:30 pm
Monday, September 26, 2005	7:30 am - 5:00 pm

EXHIBIT HALL HOURS

The Exhibit Hall is located in the Ryman Exhibit Hall C of the Gaylord Opryland Resort and Convention Center. For meeting attendees, lunch will be available for purchase in the hall during Exhibit hours

Friday, September 23, 2005	5:15 pm - 7:00 pm
Saturday, September 24, 2005	9:15 am - 4:30 pm
Sunday, September 25, 2005	9:30 am - 4:30 pm
Monday, September 26, 2005	9:30 am - 4:30 pm

ASBMR TELEPHONE NUMBERS

Management Office	Tel: (615) 458-0830
Registration Desk	Tel: (615) 458-0819
Media Office	Tel: (615) 458-0832
Media Office Fax	Fax: (615) 458-0816

SPEAKER READY ROOM

Supported by an unrestricted educational grant from Mission Pharmacal Company

Speakers must check into the Speaker Ready Room 24 hours in advance of their presentation. At that time, speakers may review their slides. The Speaker Ready Room is located in the Presidential Chamber A of the Gaylord Opryland Resort and Convention Center. Review of slides must occur at least 24 hours prior to your presentation. The Speaker Ready Room will be open during the following times:

Speaker Ready Room Hours

Thursday, September 22	12:00 noon – 5:00 pm
Friday, September 23	7:00 am – 5:30 pm
Saturday, September 24	7:00 am – 6:00 pm
Sunday, September 25	7:00 am – 5:30 pm
Monday, September 26	7:00 am – 5:30 pm
Tuesday, September 27	7:00 am – 11:00 am

SPEAKER LOUNGE

Supported by an unrestricted educational grant from the Alliance for Better Bone Health (a collaboration between Procter & Gamble Pharmaceuticals and Aventis Pharmaceuticals, a member of the sanofi-aventis Group)

The Speaker Lounge will be located in the Presidential Chamber B of the Gaylord Opryland Resort and Convention Center. The lounge provides a relaxing atmosphere for the oral presenters and invited speakers to rest, mingle with one another, and to catch up on office work. The room will be equipped with computers, fax, copier, phone/modem lines, snacks and beverages, sofas and chairs. The Speaker Lounge will be available from Friday, September 23 to Monday, September 26, from 7:00 am to 4:00 pm, and on Tuesday, September 27, from 7:00 am to 11:00 am.

POSTER SESSIONS

All poster sessions will be held in Ryman Hall C of the Gaylord Opryland Resort and Convention Center. Authors must be at their posters for 1½ hours of the designated poster sessions on Saturday through Monday and must be available to answer questions during this period. Authors of odd-numbered posters should be present from 11:30 am to 1:00 pm on their designated days. Authors of even-numbered posters should be present from 1:00 pm to 2:30 pm.

Poster numbers are listed in this 2005 Abstracts book prefixed with a letter that denotes the day of presentation, i.e., F (Friday), SA (Saturday), SU (Sunday), M (Monday). These letters are not posted on the boards. **Presenters should mount their posters on the board bearing their assigned numbers, disregarding the letter prefix. ASBMR accepts no liability for posters or poster materials and will not adjudicate disputes between abstract presenters.**

Plenary Poster presenters and Young Investigator Award recipients presenting posters should mount their posters on Friday, September 23, 2005, between 3:00 pm and 5:00 pm. Plenary Poster presenters and Young Investigator Award recipients presenting posters are expected to be present during the Welcome Reception and Plenary Poster Session on Friday, September 23, from 5:15 pm to 7:00 pm. Plenary Poster presenters and Young Investigator Award recipients presenting posters will follow the odd/even hours for presenters during Poster Session I on Saturday, September 24, 2005. Plenary Posters will remain posted until Saturday, September 24 at 6:00 pm. Young Investigator Award posters will remain posted for the duration of the meeting.

Please note that children 12 years of age and under will not be permitted in the poster area or the Exhibit Hall at any time.

Presenter Check-in:

Since only poster presenters are allowed in the Exhibit/Poster Hall during the below poster set-up hours, please go to the Poster Presenter Check-in Table to receive a security pass. The table will be located by the side entrance to Ryman Hall C2, which is accessed through Ryman Foyer B. To speed the check-in process, please have your poster board number ready.

**NOTE: Posters remaining after Poster Dismantling times will be discarded.
Young Investigator Award Posters remain up through Monday, September 26.**

Please adhere to these scheduled times to maximize interaction for other attendees:

POSTER PRESENTATION SCHEDULE

	Poster Set-Up	Posters Open	Authors Present	Dismantle Posters
Friday, Sept. 23 Welcome Reception/ Plenary Poster Session	3:00 - 5:00 pm	5:15 pm – 7:00 pm	5:15 - 7:00 pm Plenary Posters & YIA Award Posters	Do not dismantle.
Saturday, Sept. 24 Poster Session I	7:30 – 8:00 am	8:00 am – 6:00 pm	11:30 am - 1:00 pm for Odd # 1:00 pm - 2:30 pm for Even	6:00 – 6:30 pm Saturday Posters Plenary Posters
Sunday, Sept. 25 Poster Session II	7:30 – 8:00 am	8:00 am – 6:00 pm	11:30 am - 1:00 pm for Odd # 1:00 pm - 2:30 pm for Even #	6:00 – 6:30 pm Sunday Posters
Monday, Sept. 26 Poster Session III	7:30 – 8:00 am	8:00 am – 4:30 pm	11:30 am - 1:00 pm for Odd # 1:00 pm - 2:30 pm for Even #	4:30 – 5:00 pm Monday Posters YIA Award Posters

ASBMR MEMBERSHIP

The ASBMR Exhibit Booth is #213 (see Exhibit Hall map, pullout map #2) in the Ryman Exhibit Hall C. Come by and meet the ASBMR staff, pick up information about the Society, check out the online version of the Journal of Bone and Mineral Research, and order copies of the 5th Edition of the Primer on Metabolic Bone Diseases and Disorders of Mineral Metabolism.

The ASBMR Membership Counter is located in the Registration Area in the South Lobby and will be prepared to accept 2006 ASBMR membership renewal payments.

ASBMR JOB PLACEMENT SERVICE

The ASBMR Job Placement Service is easily accessible year-round online. You can access the most up-to-date job and candidate listings using the ASBMR Job Placement Service Website. Simply submit your resume or job announcement using the online forms at www.asbmr.org. After your forms are submitted and payment is received, you will be able to use your self-assigned login name and password to access the Online Placement Service database anytime you wish.

Employers enrolled in the service will be entitled to display unlimited job announcements online and onsite at the meeting on the bulletin board located in the Registration Area of the Delta Lobby B of the Gaylord Opryland Resort and Convention Center. In addition, employers will have access to candidates' Curricula Vitae.

Employers and candidates may request further information by accessing the ASBMR Online Job Placement Service at www.asbmr.org.

ASBMR MEDIA OFFICE

The ASBMR Media Office will be in operation during the ASBMR 27th Annual Meeting to facilitate media-related activities during the meeting. The Media Office will be located in the Governor's Chamber D room in the Gaylord Opryland Resort and Convention Center.

Media Office - Hours of Operation

Friday, September 23, 2005	9:00 am - 5:00 pm
Saturday, September 24, 2005	8:00 am - 5:00 pm
Sunday, September 25, 2005	8:00 am - 5:00 pm
Monday, September 26, 2005	8:00 am - 5:00 pm
Tuesday, September 27, 2005	8:00 am - 11:00 am

SPECIAL NOTICES — SAFETY TIPS

- Remove your convention badge outside the meeting sites. Do not wear your badge outside or advertise that you're a visitor and not familiar with your surroundings.
- Walk with another person rather than alone. Avoid alleys, walkways between buildings, and deserted parking lots.
- Remain alert, be aware of your surroundings, and carry your handbag in front of you.
- While in your hotel room, always lock your door. Know where emergency exits are in your hotel.
- Place any valuables in a hotel safety deposit box rather than leaving them in your room or carrying them with you.
- Keep a copy of your passport and travel papers in a safe place.

DOES THE ASBMR HAVE YOUR EMAIL ADDRESS?

Next year all important ASBMR Annual Meeting materials will be found on the ASBMR Website... and we will broadcast email to everyone on our correspondence list early notice of the Call for Abstracts, Preliminary Program, Registration and Housing information, Abstracts Online, and more! **So you don't miss out** on early notices and regular updates, please send all your contact information to the ASBMR, including your email address.

American Society for Bone and Mineral Research
2025 M Street, NW, Suite 800
Washington, DC 20036-3309, USA

Tel: (202) 367-1161
Fax: (202) 367-2161
E-mail: ASBMR@smithbucklin.com
Internet: www.asbmr.org

ANNUAL MEETING EVALUATION

The 2005 Annual Meeting Evaluation will be accessible online following the 27th Annual Meeting. An email will be sent to all meeting attendees who provided their email addresses at the time of registration. The email will provide a hyperlink to the online evaluation site. It will also be accessible via the ASBMR website at www.asbmr.org. We strongly encourage and welcome all attendees to provide us with feedback on the meeting. Your input is very important to us.

FUTURE ANNUAL MEETING DATES

September 15-19, 2006

ASBMR 28th Annual Meeting
Philadelphia, Pennsylvania, USA

September 16-20, 2007

ASBMR 29th Annual Meeting
Honolulu, Hawaii, USA

September 12-16, 2008

ASBMR 30th Annual Meeting
Montreal, Quebec, Canada

September 11-15, 2009

ASBMR 31st Annual Meeting
Denver, Colorado, USA

HOW THE PROGRAM WAS SELECTED

The 2005 ASBMR Program Co-Chairs and the President have spent close to two years in developing the scientific program for the 27th Annual Meeting. We very much appreciated the advice and suggestions of the previous Program Co-Chairs, Marie Demay, M.D., and Eric Orwoll, Ph.D., and Past-President Robert Nissenson, Ph.D., as we put the program together.

Dr. Ignarro Presents Aurbach Lecture

The basic format of the meeting, emphasizing short oral presentations and poster sessions, is the same as in past years. The meeting will begin with the Gerald D. Aurbach Memorial Lecture on Saturday, and we are very excited that Nobel Laureate Louis J. Ignarro, Ph.D., accepted our invitation to present our Society's most prestigious lecture.

Dr. Aubin Presents Avioli Lecture

The final day of the meeting will feature the Louis V. Avioli Memorial Lecture, to be presented this year by Jane E. Aubin, Ph.D. After considerable discussion with many ASBMR members, we selected topics for basic and clinical Mini-Symposia on Friday. Plenary Sessions on Saturday, Sunday and Monday, and State-of-the-Art Lectures on Saturday and Sunday, were selected by the Program Co-Chairs to cover emerging issues.

Program Features Innovations

There have been several changes in the 2005 program, however. One notable change is the expanded clinical sessions on Sunday. Also, based on the success of the clinical case conferences in 2004, the number of case conferences has been expanded from two to four sessions (Friday through Monday). To increase the opportunity for attendees to participate in the ever-popular Meet-the-Professor (MTP) sessions, we have greatly increased the number of MTP sessions available as well. Additionally, the number of Clinical MTPs has doubled and many faculty are giving two MTP sessions. Importantly, these changes have been made largely on the basis of participant survey results from the 2004 meeting. (The Program Committee carefully reviewed the 2004 survey results and took every comment into consideration.)

Handling Conflict of Interest

During the course of planning this year's meeting, the 2005 Program Committee and ASBMR staff experienced increased responsibilities in complying with the Updated Standards for Commercial Support of the U.S. Accreditation Council for Continuing Medical Education (ACCME). The ASBMR receives its Continuing Medical Education (CME) credits through the Federation of American Societies for Experimental Biology (FASEB), which is accredited by the ACCME. As the ability to provide CME for the ASBMR Annual Meeting is extremely important to the ASBMR, we have handled speaker potential conflicts of interest differently to comply with the updated standards. Current rules require not only disclosure of conflicts, but resolution of conflicts for all speakers, session chairs and Program Committee members. We would appreciate your comments on the post-meeting survey regarding how well these potential conflicts of interest were resolved.

Review and Selection of Abstracts, Awards

The categories for abstract submission were the same as in previous years, and authors were asked to identify up to three categories that best suited the content of their abstract. Each Program Co-Chair was responsible for reviewing abstracts self-identified as basic or translational/clinical. Slightly more than 1,800 abstracts were submitted, 41% basic and 59% translational/clinical, which is comparable to the distribution in 2004.

In consultation with the President, the Program Co-Chairs identified a Chair for each category and nine other reviewers. After abstract submission, the Co-Chairs reviewed all abstracts, and in some cases, reassigned them to other categories. The abstracts were reviewed "blindly" on a 5-point scale, and reviewers were instructed to refrain from reviewing abstracts in which they were in conflict. In addition, based on the ACCME's new requirements, reviewers were also asked to identify those abstracts in which commercial bias was evident. The scores were tabulated by Coe-Truman Technologies, ASBMR's abstract processing vendor; these scores were then used to select the oral program by the Program Co-Chairs and President, along with the President-Elect, Elizabeth Shane, M.D., and next year's Annual Meeting Co-Chairs, Andrew Arnold, Ph.D., and Susan Greenspan, M.D.

The over-arching principle in assembling the oral program was to select abstracts based on their scores, and then organize them into thematic sessions. The highest rated abstracts from the basic and translational/clinical (18 of each) submissions were selected for the plenary oral sessions. The next highest were selected for concurrent oral sessions; and highly ranked abstracts that were not selected for the oral program were assigned to the Plenary Poster Session on Friday evening. Slightly more than 12% of the submitted abstracts were assigned to the oral program, and each category had roughly similar representation on the oral program based on numbers of abstracts submitted, with only minor variation based on differences in the spread of scoring in the different categories.

This year, a separate "Late-Breaking" Abstract Session has not been designated in the program. This decision was made in consultation with Council, the Program Co-Chairs and the President. While there is an opportunity to submit late-breaking abstracts of broad interest where the findings were not available in time for submission by the regular abstract deadline, the abstract, if selected, will be assigned to a time slot at the end of a session that most closely matches its content. As stated in the Call for Abstracts, the merit of the late-breaking abstracts must reach or surpass the level of those selected for the regular oral program. Consequently, it is not known at the time of the Program Selection Meeting held in June whether or not abstracts that truly qualify will be submitted (Late-Breaking abstracts were due on July 20th). The time and location of any Late-Breaking Abstract that has been selected will be advertised, and an insert will be included in the ASBMR delegate bags.

The Society, assisted by corporate support, offers a number of awards, such as the ASBMR Young Investigator Award, the ASBMR Outstanding Abstract Award, the ASBMR Award for Outstanding Research in the Pathophysiology of Osteoporosis, and the ASBMR President's Book Award. As in previous years, these awardees have been selected based on abstract score and eligibility.

Thanks and Acknowledgments

We are extremely grateful to all of our colleagues and to the members who have provided us with a great deal of advice and many outstanding suggestions for speakers and topics. We also thank all of the scientific reviewers for the quality and timeliness of their efforts. And needless to say, not much would be possible without the support of the ASBMR Business Office Staff, Lizzy Koenst, (who left the ASBMR earlier in the year), Amy Werner, Yvette Dalka and Karen Hasson, and Judie Spalding of Coe-Truman Technologies (ASBMR's abstract processing vendor). It is because of all of the hard work and dedication of those involved that we feel that this is an outstanding scientific program. We hope that you enjoy it as much as we have putting it together!

Sincerely,

Sylvia Christakos, Ph.D., *President*

Pamela G. Robey, Ph.D., *Program Co-Chair*

Michael J. Econs, M.D., *Program Co-Chair*

WEDNESDAY, SEPTEMBER 21, 2005
DAY-AT-A-GLANCE

Time/Event/Location

All events will be held at the Gaylord Opryland Resort and Convention Center, unless otherwise noted.)

Ancillary Program - The International Society for Clinical Densitometry (ISCD)

7:30 am - 5:30 pm

ISCD Bone Densitometry - Clinician Course Lecture
Jackson A/B

7:30 am - 5:30 pm

ISCD Bone Densitometry - Technologist Course Lecture
Jackson C/D

THURSDAY, SEPTEMBER 22, 2005
DAY-AT-A-GLANCE

Time/Event/Location

(All events will be held at the Gaylord Opryland Resort and Convention Center, unless otherwise noted.)

9:00 am - 5:00 pm

ASBMR Registration
Delta Lobby B

Ancillary Program - The International Society for Clinical Densitometry (ISCD)

7:30 am - 11:15 am

ISCD Bone Densitometry - Clinician Course Lectures
Jackson A/B

7:30 am - 11:45 am

ISCD Bone Densitometry - Technologist Course Lectures
Jackson C/D

11:45 am - 2:00 pm

ISCD Bone Densitometry - Clinician Course Exam
Jackson A/B

12:30 pm - 1:45 pm

ISCD Bone Densitometry - Technologist Course Exam
Jackson C/D

1:00 pm - 5:45 pm

ISCD Vertebral Fracture Assessment (VFA) Course
Tennessee Ballroom D/E

FRIDAY, SEPTEMBER 23, 2005 DAY-AT-A-GLANCE

Time/Event/Location

(All events will be held at the Gaylord Opryland Resort and Convention Center, unless otherwise noted.)

7:00 am - 6:30 pm

Registration

Delta Lobby B

9:30 am - 12:00 noon

Bone and Mineral Complications of Chronic Kidney Disease (CKD) Symposium

Delta Ballroom

12:00 pm - 1:00 pm

Meet-the-Professor Sessions

Lincoln A, C, D, E & Jackson A/B, C/D, E/F

Ticket required. See ticket for room assignment.

1:00 pm - 2:00 pm

Clinical Roundtable/Case Conference: What Is the Optimal Duration of Bisphosphonate Therapy? Premenopausal Women with Low BMD

Presidential Ballroom South

2:00 pm - 3:30 pm

Mini-Symposium A: The Periosteum: A Surface for All Seasons

Delta Ballroom

2:00 pm - 3:30 pm

Mini-Symposium B: Secondary Causes of Osteoporosis

Presidential Ballroom South

3:45 pm - 5:15 pm

Mini-Symposium C: Of Mice and Men: Modeling Skeletal Disease in Genetically Engineered Mice

Delta Ballroom

3:45 pm - 5:15 pm

Mini-Symposium D: Stress Fractures

Presidential Ballroom South

5:15 pm - 7:00 pm

Welcome Reception and Plenary Poster Session

Ryman Exhibit Hall C

7:00 pm - 8:00 pm

New Investigator/New Member/First Time Attendee Reception

Washington B

Ancillary Program - Working Groups

7:00 pm - 9:30 pm

Muscle and Bone Working Group

Canal E

7:00 pm - 9:00 pm

Working Group on Rheumatic Disease and Bone

Bayou C/D

7:00 pm - 9:30 pm

In Vivo Working Group

Canal A/B

7:00 pm - 9:30 pm

Nutrition and Bone Health Working Group

Canal C/D

7:00 pm - 10:00 pm

Vitamin D Working Group

Bayou E

7:15 pm - 10:00 pm

Working Group on Hormone-Receptor Interactions

Bayou A/B

Ancillary Program - Industry-Supported Symposia (ISS)

7:00 pm - 9:30 pm

New and Future Clinical Approaches to the Prevention of Fractures

Governor's Ballroom North

7:00 pm - 9:30 pm

Optimizing Outcomes for Patients with Metabolic Bone Disease

Tennessee Ballroom

7:00 pm - 9:30 pm

The Biology of Bone Loss: Advancing the Clinical Management of Osteoporosis

Presidential Ballroom North

SATURDAY, SEPTEMBER 24, 2005

DAY-AT-A-GLANCE

Time/Event/Location

(All events will be held at the Gaylord Opryland Resort and Convention Center, unless otherwise noted.)

7:00 am - 8:00 am

New Investigator/New Member Breakfast
Governor's Ballroom C/D

7:00 am - 5:30 pm

Registration Open
Delta Lobby B

8:00 am - 6:00 pm

Posters Open
Ryman Exhibit Hall C

8:00 am - 8:10 am

Welcome and Announcements
Delta Ballroom

8:10 am - 9:10 am

Gerald D. Aurbach Memorial Lecture
Delta Ballroom

9:10 am - 9:15 am

Presentation of William F. Neuman Award
Delta Ballroom

9:15 am - 4:30 pm

Exhibits Open
Ryman Exhibit Hall C

9:15 am - 9:20 am

Presentation of Fuller Albright Award
Delta Ballroom

9:20 am - 9:25 am

Presentation of Gideon A. Rodan Excellence in Mentorship Award
Delta Ballroom

9:25 am - 10:00 am

Coffee Break
Ryman Exhibit Hall C

10:00 am - 11:30 am

Plenary Orals I - Basic (1001-1006)
Presidential Ballroom South

Plenary Orals II - Clinical/Translational (1007-1012)
Delta Ballroom

11:30 am - 2:30 pm

Poster Session I (Presentations SA001 - SA527)
11:30 am - 1:00 pm Odd numbers
1:00 pm - 2:30 pm Even numbers
Ryman Exhibit Hall C

11:30 pm - 12:30 pm

Meet-the-Professor Sessions

Lincoln A, C, D, E & Jackson A/B, C/D, E/F
Ticket required. See ticket for room assignment.

12:00 noon - 2:00 pm

Special Session for Allied Health Professionals
Governor's Ballroom North

12:30 pm - 1:30 pm

Clinical Roundtable/Case Conference: Acute Vertebral Fracture during a Seizure in a Patient on Long-Term Anticonvulsant Therapy - Is This Traumatic or Not? How Bad for Bone Are Seizure Meds? Kidney Stones and Low Bone Mass
Presidential Ballroom South

12:30 pm - 2:00 pm

Grant Writing Workshop: Tips on Getting Funded
Governor's Ballroom C/D

1:30 pm - 2:30 pm

Meet-the-Professor Sessions

Lincoln A, C, D, E & Jackson A/B, C/D, E/F
Ticket required. See ticket for room assignment.

2:30 pm - 4:00 pm

Concurrent Oral Sessions

- 1) Osteoblasts I (1013 - 1018)
Presidential Ballroom South
- 2) Cartilage (1019 - 1024)
Governor's Ballroom C/D
- 3) BMPs, TGF-beta, Other Growth Factors and Cytokines (1025 - 1030)
Presidential Ballroom A
- 4) Genetics of Bone and Mineral Disorders (1031 - 1036)
Presidential Ballroom B
- 5) Osteoporosis - Epidemiology (1037-1042)
Delta Ballroom
- 6) Osteoporosis - Pathophysiology (1043-1048)
Governor's Ballroom North

4:00 pm - 4:30 pm

Coffee Break
Ryman Exhibit Hall C

4:30 pm - 6:00 pm

State-of-the-Art Lectures A: Epigenetics
Presidential Ballroom South

4:30 pm - 6:00 pm

State-of-the-Art Lectures B: Absolute Risk
Delta Ballroom

6:00 pm - 7:00 pm

ASBMR Annual Business Meeting
Governor's Ballroom C/D

SATURDAY, SEPTEMBER 24, 2005 DAY-AT-A-GLANCE

Time/Event/Location

(All events will be held at the Gaylord Opryland Resort and Convention Center, unless otherwise noted.)

Ancillary Program - Working Groups

7:00 pm - 9:00 pm

**Non-Invasive Assessment of Trabecular Bone
Microarchitecture Working Group**
Canal A/B

7:00 pm - 9:00 pm

**Working Group on Musculoskeletal Rehabilitation in
Patients with Osteoporosis**
Bayou E

7:00 pm - 9:30 pm

Molecular Biology and Pathology of Bone Working Group
Bayou A/B

7:00 pm - 9:30 pm

Working Group on Aging and the Human Skeleton
Canal C/D

7:00 pm - 10:00 pm

Biochemical Markers of Bone Turnover Working Group
Bayou C/D

Ancillary Program - Industry-Supported Symposia (ISS)

7:00 pm - 10:00 pm

**The RANK/RANKL/OPG Axis: A New Therapeutic Target
for the Treatment and Prevention of Bone Loss**
Tennessee Ballroom

7:00 pm - 10:00 pm

**The Evolving Role of Vitamin D Analogs: Links between
Bone Metabolism, Cardiovascular Health, and Long-
Term Survival**
Presidential Ballroom North

SUNDAY, SEPTEMBER 25, 2005 DAY-AT-A-GLANCE

Ancillary Program - Industry-Supported Symposia (ISS)

6:00 am - 8:00 am

Parathyroid Hormone: A New Frontier in Bone Health
Tennessee Ballroom

7:00 am - 8:00 am

ASBMR Minority Breakfast
Washington B
Ticket Required

7:00 am - 5:30 pm

Registration Open
Delta Lobby B

8:00 am - 6:00 pm

Posters Open
Ryman Exhibit Hall C

8:00 am - 9:30 am

Plenary Symposium I: Bone and Its Vasculature
Delta Ballroom

8:00 am - 9:30 am

Clinical Half-Day Sessions:
Steroid-Induced Osteoporosis
Vertebroplasty/Kyphoplasty Point-Counterpoint: Pro and Con
Presidential Ballroom South

9:30 am - 4:30 pm

Exhibits Open
Ryman Exhibit Hall C

9:30 am - 9:35 am

Presentation of Frederic C. Bartter Award
Delta Ballroom

9:35 am - 10:00 am

Coffee Break
Ryman Exhibit Hall C

10:00 am - 11:30 am

Plenary Orals I - Basic (1049 - 1054)
Presidential Ballroom South

Plenary Orals II - Clinical/Translational (1055 - 1060)
Delta Ballroom

11:30 am - 2:30 pm

Poster Session II (Presentations SU001 - SU527)
11:30 am - 1:00 pm Odd numbers
1:00 pm - 2:30 pm Even numbers
Ryman Exhibit Hall C

11:30 pm - 12:30 pm

Meet-the-Professor Sessions
Lincoln A, C, D, E & Jackson A/B, C/D, E/F
Ticket Required. See ticket for room assignment.

11:30 am - 12:30 pm

Art of Grant Reviewing
Jackson E/F
Ticket Required

12:00 pm - 2:00 pm

Clinical Half Day Sessions:
Falls
Vitamin D: Is There an Epidemic?
Pitfalls of Densitometry and Difficult Densitometry Cases
Presidential Ballroom South

12:30 pm - 2:00 pm

Biotechniques Workshop on General and Molecular Imaging of Bone
Governor's Ballroom North

12:30 pm - 1:30 pm

The Role of Advocacy in Musculoskeletal Research Funding: Grassroots, NIH, Congress and the Public
Governor's Ballroom C/D

1:30 pm - 2:30 pm

Meet-the-Professor Sessions
Lincoln A, C, D, & Jackson A/B, C/D, E/F
Ticket Required. See ticket for room assignment.

1:30 pm - 2:30 pm

How to Pick a Mentor & Get Trained
Lincoln E
Ticket Required

2:30 pm - 4:00 pm

Concurrent Oral Sessions

7) Osteoblast II (1061-1066)
Governor's Ballroom C/D

8) Osteoclast I (1067-1072)
Presidential Ballroom A

9) Osteoporosis - Epidemiology (1073-1078)
Presidential Ballroom South

10) Osteoporosis Treatment (1079-1084)
Delta Ballroom

11) Bone Acquisition and Pediatric Bone Disease (1085-1090)
Governor's Ballroom North

12) Mechanical Loading and Exercise (1091-1096)
Presidential Ballroom B

4:00 pm - 4:30 pm

Coffee Break
Ryman Exhibit Hall C



SUNDAY, SEPTEMBER 25, 2005
DAY-AT-A-GLANCE

Time/Event/Location

(All events will be held at the Gaylord Opryland Resort and Convention Center, unless otherwise noted.)

4:30 pm - 6:00 pm

State-of-the-Art Lecture A: Embryonic Sources of Skeletal Tissue
Delta Ballroom

4:30 pm - 6:00 pm

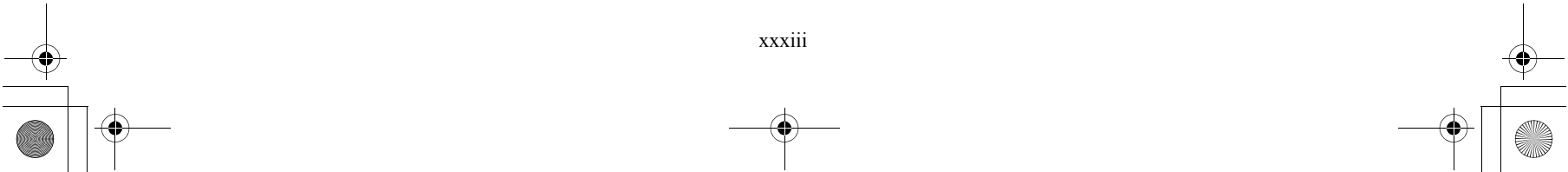
State-of-the-Art Lecture B: Bone Quality
Presidential Ballroom South

6:00 pm - 7:30 pm

Women in Bone and Mineral Research Event
Washington B
Ticket Required

8:30 pm - 11:30 pm

ASBMR Social Event
General Jackson Showboat
Ticket Required



MONDAY, SEPTEMBER 26, 2005

DAY-AT-A-GLANCE

Time/Event/Location

(All events will be held at the Gaylord Opryland Resort and Convention Center, unless otherwise noted.)

5:30 am - 7:15 am

ASBMR Fun Run/Walk

Two Rivers Park (Busing Provided)

7:30 AM - 5:00 PM

Registration Open

Delta Lobby B

8:00 am - 4:30 pm

Posters Open

Ryman Exhibit Hall C

8:00 am - 9:30 am

Plenary Symposium II: Phosphate: From Bench to Bedside

Delta Ballroom

9:30 am - 4:30 pm

Exhibits Open

Ryman Exhibit Hall C

9:30 am - 9:35 am

Presentation of Shirley Hohl Service Award

Delta Ballroom

9:35 am - 10:00 am

Coffee Break

Ryman Exhibit Hall C

10:00 am - 11:30 am

Plenary Oral I - Basic (1097-1102)

Presidential Ballroom South

Plenary Oral II - Clinical/Translational (1103-1108)

Delta Ballroom

11:30 pm - 12:30 pm

Meet-the-Professor Sessions

Lincoln A, C, D, E & Jackson A/B, C/D, E/F
Ticket Required. See ticket for room assignment.

11:30 pm - 12:30 pm

Training and Career Development Awards: Minding Your Fs and Ks

Jackson E/F
Ticket Required

11:30 am - 2:30 pm

Poster Session III (Presentations M001 - M5256)

11:30 am - 1:00 pm Odd numbers
1:00 pm - 2:30 pm Even numbers
Ryman Exhibit Hall C

12:30 pm - 2:00 pm

Career Options for Scientists Workshop

Presidential Ballroom B

12:30 pm - 1:30 pm

Clinical Roundtable/Case Conference: Osteogenesis Imperfecta (OI) Bone Disease in Sick Children

Presidential Ballroom South

1:00 pm - 2:00 pm

Meet-the-International Grant Writers Session

Canal A/B

1:30 pm - 2:30 pm

Meet-the-Professor Sessions

Lincoln A, C, D, E & Jackson A/B, C/D, E/F
Ticket required. See ticket for room assignment.

2:30 pm - 4:00 pm

Concurrent Oral Sessions

13) Chondocyte/Osteoblast (1109-1114)

Bayou C/D

14) Steroid Hormones (1115-1120)

Presidential Ballroom South

15) Cancer and Bone (1121-1126)

Presidential Ballroom B

16) Bone Acquisition and Pediatric Bone Disease (1127-1132)

Presidential Ballroom A

17) Osteoporosis - Epidemiology (1133-1138)

Delta Ballroom

18) Osteoporosis - Pathophysiology (1139-1144)

Governor's Ballroom North

4:30 pm - 4:30 pm

Coffee Break

Ryman Exhibit Hall C

4:30 pm - 6:00 pm

Concurrent Oral Sessions

19) Osteoclasts II (1145-1150)

Governor's Ballroom North

20) Bone, Cartilage & Connective Tissue Matrix (1151-1156)

Bayou C/D

21) Peptide Calcitropic Hormones (1157-1162)

Presidential Ballroom South

22) Other Disorders of Bone and Mineral Metabolism (1163-1168)

Presidential Ballroom A

23) Mechanical Loading and Exercise (1169-1174)

Presidential Ballroom B

MONDAY, SEPTEMBER 26, 2005
DAY-AT-A-GLANCE

Time/Event/Location
(All events will be held at the Gaylord Opryland Resort and Convention Center, unless otherwise noted.)

24) Osteoporosis Diagnosis & Treatment (1175-1180)
Delta Ballroom

Ancillary Program - Working Groups

6:30 pm - 8:30 pm
Physical Activity and Falls Working Group
Bayou C/D

6:30 pm - 9:30 pm
Adult Bone and Mineral Working Group
Canal A/B

6:30 pm - 9:30 pm
Post Transplantation Bone Disease Working Group
Bayou E

7:00 pm - 9:30 pm
Bone Remodeling and Stress Fracture Working Group
Canal C/D

7:00 pm - 10:00 pm
Pediatric Bone and Mineral Working Group
Bayou A/B

Ancillary Program - Industry-Supported Symposia (ISS)

6:45 pm - 10:00 pm
Determinants of Fracture Risk Reduction: From Bench to Bedside
Tennessee Ballroom

7:00 pm - 9:30 pm
Expanding the Options of Bisphosphonate Therapy
Governor's Ballroom C/D

TUESDAY, SEPTEMBER 27, 2005

DAY-AT-A-GLANCE

Time/Event/Location

(All events will be held at the Gaylord Opryland Resort and Convention Center, unless otherwise noted.)

8:00 am - 9:00 am

Louis V. Avioli Memorial Lecture

Delta Ballroom

9:00 am - 9:05 am

Presentation of Louis V. Avioli Founders Award

Delta Ballroom

9:05 am - 9:30 am

Coffee Break

Delta Lobby B

9:30 am - 11:30 am

Concurrent Oral Sessions

25) Osteoblasts III (1181-1188)

Bayou A/B

26) BMPs, TGF-beta, Other Growth Factors and Cytokines & Others (1189-1196)

Bayou E

27) Steroids/Hormones II (1197-1204)

Bayou C/D

28) Genetics and Metabolic Bone Disease (1205-1212)

Canal C/D

29) Cancer and Bone (1213-1220)

Canal A/B

30) Osteoporosis - Diagnosis & Treatment (1221-1228)

Delta Ballroom

11:30 am

Adjourn

ABSTRACT PRESENTATION KEY

Abstract Number	Session Type	Date	Presentation Time	Room
1001-1006	Plenary Oral I - Basic	Saturday, Sept. 24, 2005	10:00 - 11:30 am	Presidential Ballroom South
1007-1012	Plenary Oral II - Clinical	Saturday, Sept. 24, 2005	10:00 - 11:30 am	Delta Ballroom
1013-1018	Concurrent Oral 1	Saturday, Sept. 24, 2005	2:30 - 4:00 pm	Presidential Ballroom South
1019-1024	Concurrent Oral 2	Saturday, Sept. 24, 2005	2:30 - 4:00 pm	Governor's Ballroom C/D
1025-1030	Concurrent Oral 3	Saturday, Sept. 24, 2005	2:30 - 4:00 pm	Presidential Ballroom A
1031-1036	Concurrent Oral 4	Saturday, Sept. 24, 2005	2:30 - 4:00 pm	Presidential Ballroom B
1037-1042	Concurrent Oral 5	Saturday, Sept. 24, 2005	2:30 - 4:00 pm	Delta Ballroom
1043-1048	Concurrent Oral 6	Saturday, Sept. 24, 2005	2:30 - 4:00 pm	Governor's Ballroom North
1049-1054	Plenary Oral I - Basic	Sunday, Sept. 25, 2005	10:00 - 11:30 am	Presidential Ballroom South
1055-1060	Plenary Oral II - Clinical	Sunday, Sept. 25, 2005	10:00 - 11:30 am	Delta Ballroom
1061-1066	Concurrent Oral 7	Sunday, Sept. 25, 2005	2:30 - 4:00 pm	Governor's Ballroom C/D
1067-1072	Concurrent Oral 8	Sunday, Sept. 25, 2005	2:30 - 4:00 pm	Presidential Ballroom A
1073-1078	Concurrent Oral 9	Sunday, Sept. 25, 2005	2:30 - 4:00 pm	Presidential Ballroom South
1079-1084	Concurrent Oral 10	Sunday, Sept. 25, 2005	2:30 - 4:00 pm	Delta Ballroom
1085-1090	Concurrent Oral 11	Sunday, Sept. 25, 2005	2:30 - 4:00 pm	Governor's Ballroom North
1091-1096	Concurrent Oral 12	Sunday, Sept. 25, 2005	2:30 - 4:00 pm	Presidential Ballroom B
1097-1102	Plenary Oral - Basic	Monday, Sept. 26, 2005	10:00 - 11:30 am	Presidential Ballroom South
1103-1108	Plenary Oral - Clinical/Translational	Monday, Sept. 26, 2005	10:00 - 11:30 am	Delta Ballroom
1109-1114	Concurrent Oral 13	Monday, Sept. 26, 2005	2:30 - 4:00 pm	Bayou C/D
1115-1120	Concurrent Oral 14	Monday, Sept. 26, 2005	2:30 - 4:00 pm	Presidential Ballroom South
1121-1126	Concurrent Oral 15	Monday, Sept. 26, 2005	2:30 - 4:00 pm	Presidential Ballroom B
1127-1132	Concurrent Oral 16	Monday, Sept. 26, 2005	2:30 - 4:00 pm	Presidential Ballroom A
1133-1138	Concurrent Oral 17	Monday, Sept. 26, 2005	2:30 - 4:00 pm	Delta Ballroom

Abstract Number	Session Type	Date	Presentation Time	Room
1139-1144	Concurrent Oral 18	Monday, Sept. 26, 2005	2:30 - 4:00 pm	Governor's Ballroom North
1145-1150	Concurrent Oral 191	Monday, Sept. 26, 2005	4:30 - 6:00 pm	Governor's Ballroom North
1151-1156	Concurrent Oral 20	Monday, Sept. 26, 2005	4:30 - 6:00 pm	Bayou C/D
1157-1162	Concurrent Oral 21	Monday, Sept. 26, 2005	4:30 - 6:00 pm	Presidential Ballroom South
1163-1168	Concurrent Oral 22	Monday, Sept. 26, 2005	4:30 - 6:00 pm	Presidential Ballroom A
1169-1174	Concurrent Oral 23	Monday, Sept. 26, 2005	4:30 - 6:00 pm	Presidential Ballroom B
1175-1180	Concurrent Oral 24	Monday, Sept. 26, 2005	4:30 - 6:00 pm	Delta Ballroom
1181-1188	Concurrent Oral 25	Tuesday, Sept. 27, 2005	9:30 - 10:30 am	Bayou A/B
1189-1196	Concurrent Oral 26	Tuesday, Sept. 27, 2005	9:30 - 10:30 am	Bayou E
1197-1204	Concurrent Oral 27	Tuesday, Sept. 27, 2005	9:30 - 10:30 am	Rayopu C/D
1205-1212	Concurrent Oral 28	Tuesday, Sept. 27, 2005	9:30 - 10:30 am	Canal C/D
1213-1220	Concurrent Oral 29	Tuesday, Sept. 27, 2005	9:30 - 10:30 am	Canal A/B
1221-1228	Concurrent Oral 30	Tuesday, Sept. 27, 2005	9:30 - 10:30 am	Delta Ballroom
F002-F524	Plenary Posters	Friday, Sept. 23, 2005* Saturday, Sept. 24, 2005	Friday, 5:15 - 7:00 pm	Ryman Exhibit Hall C
SA001-SA527	Poster Session I	Saturday, Sept. 24, 2005	Odd: 11:30 am - 1:00 pm Even: 1:00 pm - 2:30 pm	Ryman Exhibit Hall C
SU001-SU527	Poster Session II	Sunday, Sept. 25, 2005	Odd: 11:30 am - 1:00 pm Even: 1:00 pm - 2:30 pm	Ryman Exhibit Hall C
M001-M525	Poster Session III	Monday, Sept. 26, 2005	Odd: 11:30 am - 1:00 pm Even: 1:00 pm - 2:30 pm	Ryman Exhibit Hall C
WG1-WG2	Vitamin D Working Group	Friday, Sept. 23, 2005	7:00 pm - 10:00 pm	Bayou E
WG3-WG8	Post Transplantation and Bone Disease Working Group	Monday, Sept. 26, 2005	6:30 pm - 9:30 pm	Bayou E
* (asterisk) by author's name denotes ASBMR non-membership				

DISCLOSURE/CONFLICT OF INTEREST

The Federation of American Societies for Experimental Biology (FASEB) requires that audiences at FASEB-sponsored educational programs be informed of a presenter's (speaker, faculty, author, or contributor) academic and professional affiliations, and the existence of any significant financial interest or other relationship a presenter has with the manufacturer(s) of any commercial product(s) discussed in an educational presentation. This policy allows the listener/attendee to be fully knowledgeable in evaluating the information being presented. The Program will note those speakers who have disclosed relationships, including the nature of the relationship and the associated commercial entity.

All authors of submitted abstracts completed the disclosure statement in the online submission program. Invited speakers who are not required to submit an abstract received a form in the mail that they completed and returned.

Disclosure may include any relationship that may bias one's presentation or which, if known, could give the perception of bias. These situations may include, but are not limited to:

DISCLOSURE KEY

1. stock options or bond holdings in a for-profit corporation or self-directed pension plan
2. research grants
3. employment (full or part-time)
4. ownership or partnership
5. consulting fees or other remuneration
6. non-remunerative positions of influence such as officer, board member, trustee, or public spokesperson
7. receipt of royalties
8. speaker's bureau

For full-time employees of industry or government, the affiliation listed in the *2005 Abstracts* will constitute full disclosure.

Disclosures for invited speakers and abstract presenters are provided at the end of the session listing for invited speakers and directly after the body of an abstract for abstract submissions. If there is no conflict of interest or disclosure listed, this means that the invited speaker and/or abstract presenter indicated no conflicts to disclose.

The disclosure information will correspond to the key above. If disclosures are given, the company name, along with the respective disclosure relationship number will be listed (for example: Company Name, 2, 8.).

**Key: 1001-1228 = Oral, F = Friday Plenary Poster, SA = Saturday Poster,
SU = Sunday Poster, M = Monday Poster, WG = Working Group Abstract
*(Asterisk) Denotes Non-ASBMR Membership**

1001

Dkk Proteins Control Osteoblast Function and Bone Formation both *In Vitro* and *In Vivo*. G. Rawadi^{*1}, S. Roman-Roman¹, K. Boulukos^{*2}, E. Morvan^{*3}, P. Martin^{*2}, S. Pinho^{*4}, P. Pognonec^{*2}, P. Clément-Lacroix^{*1}, C. Niehrs^{*4}, R. Baron⁵. ¹In Vitro Pharmacology, Prostrakan, Romainville, France, ²UMR CNRS 6548, Nice, France, ³Yale University, New Haven, CT, USA, ⁴DKFZ, Heidelberg, Germany, ⁵Prostrakan, Romainville, France.

The Wnt/ β -catenin signalling pathway has been demonstrated to play an essential role in bone biology. Loss of function mutations in the Wnt co-receptor LRP5, causes severe osteoporosis, while gain of function mutation in this same receptor leads to a high bone mass phenotype in both humans and mice. Wnt activity also regulates the expression and secretion of a number of Wnt-antagonizing proteins including Dickkopf (Dkks). We have investigated the effect of Dkk1, Dkk2 and Dkk3 on osteoblast differentiation and bone formation both *in vitro* and *in vivo* through a knockout. First, overexpression of Dkk1 and Dkk2 proteins in rat primary osteoblasts results in complete inhibition of mineralized nodule formation. These inhibitory effects on osteoblast differentiation were also confirmed by measuring the expression of osteoblast differentiation markers such as alkaline phosphate and osteocalcin. Interestingly, Dkk1 and 2 overexpression increased adipocyte differentiation in the same cultures, as observed by red-oil staining and PPAR γ expression. Unlike Dkk1 and 2, Dkk3 overexpression has no effect on osteoblast differentiation. Using purified recombinant murine Dkk proteins in MC3T3-E1 osteoblastic cells further supported our data. In fact, rmDkk1 inhibits spontaneous MC3T3-E1 cell mineralization as well as mineralization induced by the morphogenic proteins Sonic Hedgehog and BMP-2. In addition, rmDkk1 reduces alkaline phosphate expression in MC3T3-E1 cells. Our data clearly demonstrate that Dkk proteins are able to antagonize osteoblast differentiation and matrix mineralization *in vitro*. To analyze the role of Dkk1 *in vivo*, we generated *dkk1* knockout mice. While homozygous *dkk1*-deficient mice are embryonic lethal, heterozygous *dkk1* deficient mice are healthy, viable and develop normally. Importantly, structural, dynamic and cellular analysis of bone remodelling in *dkk1*^{-/-} mice showed a strong increase in bone mineral density, an increased trabecular number and enhanced osteoblast activity with a marked increase in the Bone Formation Rate. Osteoblast number was significantly higher in *dkk1*^{-/-} compared to wild type mice, whereas osteoclast number was not affected. We conclude that 1/ Dkk proteins, which antagonize the LRP5 and Wnt-dependent β -catenin pathway, regulate osteoblast differentiation, bone formation and bone mass *in vivo* and 2/ Heterozygous deletion of the gene encoding Dkk1 is sufficient to induce a high bone mass phenotype in mice.

Disclosures: **G. Rawadi**, None.

1002

Suppression of Dkk1 Is Not Essential for PTH-Mediated Activation of Canonical Wnt Signaling in Bone. J. Guo, E. Schipani, M. Liu^{*}, F. R. Bringhurst, H. M. Kronenberg. Endocrine Unit, Massachusetts General Hospital and Harvard Medical School, Boston, MA, USA.

Dkk1 acts as a negative regulator of canonical Wnt signaling by binding to and antagonizing activation of Lrp5/6. We have previously shown that PTH suppresses Dkk1 mRNA expression in osteoblasts *ex vivo* and that overexpression of Dkk1 leads to less trabecular bone *in vivo*. To explore whether the anabolic action of PTH on bone is mediated in part by canonical Wnt signaling, we examined the effect of overexpression of Dkk1 on the high bone mass caused by expression of a constitutively active PTHR in osteoblasts *in vivo*. Mice overexpressing Dkk1 under the control the mouse $\alpha 1(I)$ collagen promoter (Dkk1 mice) were mated to Jansen transgenic mice that express a constitutively active PTHR under the control of the same promoter as in Dkk1 mice. As reported previously, Dkk1 mice had low bone mass in the metaphyseal region, while Jansen mice exhibited overproduction of trabecular bone at 6 weeks of age. Interestingly, the increase in trabecular bone characteristic of the Jansen phenotype was partly prevented in mice that expressed both transgenes in the same time, as shown by histology. To determine the effect of overexpression of Dkk1 on canonical Wnt signaling in osteoblasts, Dkk1 mice were mated to TopGal reporter mice that carry a bacterial β -galactosidase transgene responsive to canonical Wnt signaling. We observed that Dkk1 overexpression leads to decreased Wnt signaling in osteoblasts. These osteoblasts exhibited lower levels of TopGal-associated β -galactosidase activity, and quantitative RT-PCR revealed lower levels of TopGal mRNA and lower levels of mRNA encoding Axin2, a Wnt-target gene, in bones from these mice. However, the continued expression of Dkk1 in these mice, which was not suppressed by PTH, did not block PTH's ability to activate Wnt signaling. When PTH was given to the Dkk1 mice for 24 hr, expression levels of TopGal and Axin2 mRNAs were significantly elevated (both >2-fold). Similar findings were observed in MC3T3 cells stably co-transfected with mouse PTHR and a Wnt/ β -catenin-dependent Topflash reporter gene. Reporter activity, determined by luciferase assay, in such stable cells was significantly suppressed by transient transfection with a mouse Dkk1 expression construct (50%) but was dramatically increased by PTH in a dose- and time-dependent manner. PTH still induced reporter activity despite the overexpression of Dkk1 in such stable cells. We conclude that PTH activates the Wnt pathway in bone, an action that may contribute to the anabolic action of PTH. Though PTH suppresses Dkk1 expression in osteoblasts, PTH still activates Wnt signaling even when Dkk1 expression is not suppressed in transgenic mice and cultured osteoblasts.

Disclosures: **J. Guo**, None.

1003

Hedgehog Signaling Interacts with Wnt/b-catenin Signaling in Controlling Endochondral Bone Formation and Synovial Joint Development. K. Mak^{*}, L. Garrett-Beal^{*}, Y. Yang^{*}. Genetic Disease Research Branch, NHGRI/NIH, Bethesda, MD, USA.

Chondrocyte and osteoblast differentiation and synovial joint formation are key aspects of endochondral skeletal development. We have shown previously that Wnt/b-catenin signaling is required for osteoblast and chondrocyte differentiation from mesenchyme progenitors, and it is also required for proper progression of chondrocyte hypertrophy. Indian hedgehog (Ihh) signaling is also required for endochondral bone formation and controls chondrocyte proliferation and hypertrophy by forming a negative feedback loop with parathyroid hormone related peptide (PTHrP). To test the genetic interaction of Wnt and Ihh-PTHrP signaling in both osteoblast differentiation and chondrocyte maturation, we have generated mouse embryos with disrupted Wnt and Ihh signaling in the skeletal system. The floxed alleles of Patched (Ptc) and Smoothened (Smo) which encode receptors of Hedgehog (Hh) ligand were used to upregulate or inactivate Ihh signaling respectively. We used two different floxed b-catenin (an obligatory component of canonical Wnt signaling) alleles, Catnb or CatnbEx3, to produce inactivated or constitutively activated b-catenin respectively. Col2a1-Cre mouse was used to specifically mutate Ptc, Smo and b-catenin in all chondrocytes and some osteoblasts. We have found that in Ptc^{-/-}; Col2a1-Cre mice, chondrocyte hypertrophy was significantly delayed whereas endochondral bone formation was greatly enhanced. Synovial joint fusion was observed, possibly due to Bone morphogenetic proteins (Bmps) upregulation. The Catnb^{-/-}; Col2a1-Cre mice showed delayed chondrocyte hypertrophy and diminished bone formation. Synovial joint fusion was observed in some areas. Interestingly, in the Ptc^{-/-}; Catnb^{-/-}; Col2a1-Cre double mutant embryo, bone formation was greatly diminished, similar to that observed in Catnb^{-/-}; Col2a1-Cre mutants, demonstrating that Hh signaling acts upstream of Wnt/b-catenin signaling in promoting osteoblast differentiation. In the cartilage of the double mutant embryo, however, delay of chondrocyte hypertrophy was more severe than either single mutant, indicating that Wnt/b-catenin and Ihh-PTHrP signaling act in parallel, but antagonistically with each other in controlling chondrocyte hypertrophy as the phenotypes of b-catenin loss of function mutants were enhanced by Ihh gain of function mutants. Lastly, synovial joint fusion was also greatly enhanced in the double mutant, indicating that Ihh signaling antagonizes with Wnt signaling in synovial joint induction too. The antagonistic activity of Ihh signaling is likely to be indirect due to Bmp-2, -4, -7 upregulation in the Ptc^{-/-}; Col2a1-Cre embryo.

Disclosures: **K. Mak**, None.

1004

Msx2 Enhances Bone Mass Via Canonical Wnt Signals. S. Cheng, J. Shao, N. Charlton-Kachigian^{*}, A. P. Loewy^{*}, J. M. Pingsterhaus^{*}, D. A. Towler. Div. of Bone and Mineral Diseases, Dept. of Med, Washington University School of Medicine, St. Louis, MO, USA.

Osteoblasts and adipocytes share a progenitor derived from the stromal cell lineage -- a progenitor possessing features of the pericytic microvascular smooth muscle cell. Since Msx2 promotes osteogenesis but suppresses adipogenic differentiation of vascular myofibroblasts, we studied effects of Msx2 on osteoblast physiology, implementing validated *in vitro* and *in vivo* models. In MC3T3-E1 osteoblasts and 10T1/2 mesenchymal cells, Msx2 stimulated proliferation via suppression of p27 and upregulation of cyclin D2. SFG-Msx2 transduced cells also expressed elevated levels of osterix (Osx), alkaline phosphatase (ALP), and bone sialoprotein (BSP) -- but not Runx2. ALP activity and Osx promoter activity (LUC reporter) were enhanced in cultures of SFG-Msx2 cells vs. SFG-LacZ controls, and Osx antisense oligonucleotide reduced Msx2 stimulation of ALP. Since canonical Wnts also stimulate bone formation, we examined the relationship between Msx2 and Wnt signaling. Msx2 upregulated multiple Wnt ligands, but down-regulated the expression of Dkk1, a Wnt inhibitor. β -catenin protein accumulation in Msx2 cells was increased, confirming activated canonical Wnt signaling. Moreover, β -Catenin accumulated to a greater extent in the nuclei in cells adjacent to EGFP-Msx2 transfected cells vs. EGFP controls. Using the TCF/LEF optimal promoter construct TOPFLASH, we identified that transcription supported from this Wnt-responsive reporter was increased 2 fold when co-cultured with SFG-Msx2 transduced cells vs. SFG-LacZ controls. Restoring Dkk1 activity with either SFG-Dkk1 retrovirus or Dkk1 treatment (a) diminished Msx2-dependent upregulation of ALP activity, (b) inhibited ALP, Osx, and BSP mRNA accumulation; (c) upregulated PPAR γ 2; and (d) reversed the adipostatic effect of Msx2. To confirm these observations *in vivo*, we studied CMV-Msx2 transgenic (Tg) mice, a model validated in studies of Msx2-dependent craniosynostosis. Msx2 Tg mice exhibited increased bone mineral density and decreased body fat accumulation as compared to non-transgenic sibs. Osteoblasts from Msx2 Tg expressed higher mRNA levels of ALP, Osx, and BSP, and exhibited increased matrix calcification. Msx2 Tg bone marrow cells displayed elevated osteogenesis and suppressed adipogenesis in histological assays. Finally, as compared to TOPGAL+ mice (Wnt signaling-LacZ reporter mouse), osteoblasts from Msx2Tg+; TOPGAL+ siblings exhibited 5-fold enhanced LacZ staining. Thus, Msx2 regulates mesenchymal cell fate and body composition. Canonical Wnt signals that upregulate Osx expression mediate in part Msx2 pro-osteogenic actions.

Disclosures: **S. Cheng**, None.

1005

Cartilage-Specific Over-Expression of Smurf2 Induces Osteoarthritis by Degradation of Phospho-Smad3. Q. Wu, Y. B. Lim*, K. Kim*, M. Zuscik, D. Chen, E. M. Schwarz, J. E. Puzas, R. J. O'Keefe, R. N. Rosier. Orthopaedics, University of Rochester, Rochester, NY, USA.

Articular cartilage in diarthrodial joints and nucleus pulposus of the intervertebral discs are tissues that are maintained by the activity of chondrocytes that facilitate matrix catabolism. During osteoarthritis (OA), the cartilage architecture in these tissues is degraded due to abnormal articular chondrocyte maturation. During the progression of OA, cartilaginous outgrowths and osteophytes are formed on the joint surface and periphery, which undergo endochondral ossification leading to further joint damage. Several lines of evidence have demonstrated that TGF- β signaling is essential to maintain articular cartilage by preventing articular chondrocyte from undergoing inappropriate terminal maturation. Supporting this idea, over-expression of Smurf2, an E3 ubiquitin ligase that targets Smad1 and Smad2 for the proteasome degradation, leads to reduced TGF- β signaling and accelerated chondrocyte maturation *in vitro*. We therefore hypothesized that over-expression of Smurf2 in cartilage *in vivo* will induce inappropriate chondrocyte maturation and cause OA. To test this hypothesis, we generated transgenic mice over-expressing Smurf2 under control of type II collagen promoter. We characterized the mice at 2, 4.5, and 6-8 months of age, and found an osteoarthritic phenotype in several diarthrodial joints and in the intervertebral disks. In the knee joints, the osteoarthritic changes included degenerated articular cartilage, chondro-osteophyte formation in periosteum, mineralization of the meniscus and ligaments, and sub-chondral sclerosis. The severity of these phenotypic changes progressed with aging. By 8 months, Smurf2 over-expressing mice had lost 80% of the articular cartilage in the knee, accompanied by severe clefting; chondrocyte cloning, hypertrophic differentiation and formation of marrow cavities within the meniscus and ligaments. To the mechanism of these phenotypes, we performed Smurf2 functional assays in chondrocytes derived from the neonatal mouse sternum. Among Smad1, Smad2 and Smad3 protein levels, only phospho-Smad3 is dramatically decreased in Smurf2-tg chondrocytes. Furthermore, this decrease can be partially rescued by application of a proteasome inhibitor, suggesting that Smurf2-mediated phospho-Smad3 degradation is proteasome dependent. Consistent with this data, TGF- β promoter activity is inhibited in Smurf2-tg chondrocytes, and the promoter responsive activity for BMP is similar in Smurf2-tg chondrocytes with that of WT. Thus, cartilage-specific overexpression of Smurf2-induced OA is mediated by degradation of phospho-Smad3.

Disclosures: Q. Wu, None.

1006

S100A1 and S100B, Transcriptional Target Molecules of SOX5, SOX6 and SOX9 (the SOX Trio), Inhibit Hypertrophic Differentiation and Calcification of Chondrocytes. T. Saito*, T. Ikeda, K. Nakamura, U. Chung, H. Kawaguchi. Sensory & Motor System Medicine, University of Tokyo, Tokyo, Japan.

SOX9 not only stimulates chondrogenic differentiation, but also suppresses hypertrophic differentiation and calcification of chondrocytes, and its co-activators SOX5 and SOX6 enhance these actions, so that the combination (the SOX trio) is reported to provide signals for the regeneration of permanent cartilage. To identify transcriptional targets of the SOX trio in the inhibition of the terminal differentiation of chondrocytes, we screened the target molecules of the SOX trio by a microarray analysis using human mesenchymal stem cells (hMSC) in which the SOX trio was adenovirally introduced. Compared to the LacZ-introduced control, 603 genes were up-regulated by the SOX trio, among which two homologous genes in the S100 family, S100A1 and S100B, showed very strong increases. Real-time RT-PCR analysis confirmed that expressions of S100A1 and S100B were strongly induced by the SOX trio introduction, while weakly by SOX9 alone, in hMSC, human dermal fibroblasts, and other non-chondrogenic cell lines. *In vivo* expressions of S100A1 and S100B were shown by *in situ* hybridization to be localized in the pre-hypertrophic chondrocytes of the mouse growth plate, following the expressions of the SOX trio. Luciferase-reporter assay identified the core enhancer elements of the SOX trio within 40 bp and 32 bp regions in the proximal promoters of S100A1 and S100B, respectively, both containing the paired HMG binding motif surrounded by GC rich sequences, which is a typical feature of SOX9 enhancers. These regions strongly and selectively responded to the SOX trio introduction depending on their repeat numbers, indicating that S100A1 and S100B are direct transcriptional targets of the trio. To further investigate the functional contribution of S100A1 and S100B to chondrocyte differentiation, these molecules or their siRNA were retrovirally introduced into mouse chondrogenic ATDC5 cells that underwent hypertrophic differentiation and calcification in the presence of insulin. Overexpression of S100A1 and/or S100B reduced type X collagen and osteocalcin mRNA levels, and ALP and Alizarin red stainings. In the meantime, silencing of S100A1 and S100B markedly accelerated these markers, e.g., the type X collagen mRNA level to more than 20-fold. We thus conclude that S100A1 and S100B, novel transcriptional target molecules of the SOX trio, inhibit hypertrophic differentiation and calcification of chondrocytes. Elucidation of the molecular network related to these signalings will much benefit the regenerative medicine of permanent cartilage.

Disclosures: T. Saito, None.

1007

Hypoxia and HIF-1 α Expression Enhance Osteolytic Bone Metastases in Breast Cancer. T. Hiraga¹, S. Kizaka-Kondoh², K. Hirota³, T. Yoneda¹.

¹Biochemistry, Osaka Univ Grad Sch Dent, Osaka, Japan, ²COE, Radiation Oncology, Kyoto Univ Grad Sch Med, Kyoto, Japan, ³Anesthesia, Kyoto Univ Grad Sch Med, Kyoto, Japan.

Hypoxia is a common feature of locally advanced solid tumors and is associated with malignant phenotype including resistance to anti-cancer therapies, recurrence, local invasiveness and distant metastasis. The transcription factor hypoxia-inducible factor-1 α (HIF-1 α) is a major regulator for cancer cells to adapt the hypoxia and is implicated in malignant progression of cancers. Hypoxia and HIF-1 α expression are correlated with poor survival in cancer patients. However, the role of hypoxia and HIF-1 α expression in bone metastasis has not been explored. Here, we studied whether hypoxia and HIF-1 α expression contribute to the development of bone metastases using an animal model of human breast cancer. The MDA-MB-231 human breast cancer cells metastasized to bone following intracardiac inoculation showed accumulation of a hypoxic marker pimonidazole. These hypoxic MDA-MB-231 cells also exhibited nuclear HIF-1 α expression. To verify the role of hypoxia in bone metastases, we tested the effects of the oxygen-dependent degradation domain of HIF-1 α fused with HIV-TAT protein transduction domain and caspase-3 (TAT-ODD-Casp3) on bone metastases. This fusion protein is shown to selectively induce apoptosis in hypoxic tumor cells. Intraperitoneal administration of TAT-ODD-Casp3 reduced bone metastases in a dose-dependent manner. We next examined the role of HIF-1 α in bone metastases by establishing MDA-MB-231 cells stably transfected with constitutively-active HIF-1 α cDNA (MDA/CA-HIF). Bone metastases of MDA/CA-HIF were significantly increased accompanied with elevated number of CD31-positive blood vessels. Since the progression of osteolytic bone metastasis is thought to be due to the uncoupling between osteoclastic bone resorption and osteoblastic bone formation, we examined the effects of hypoxia and HIF-1 α on the differentiation osteoblasts and osteoclasts. Hypoxia and CA-HIF overexpression markedly inhibited BMP2-induced osteoblastic differentiation and Runx2 expression in the pluripotent mesenchymal cells C3H10T1/2 and calcification in murine primary osteoblasts. On the other hand, hypoxia increased TRAP-positive osteoclast-like cell formation in spleen cell cultures in the presence of RANKL and M-CSF. In conclusion, these results suggest that tumor-associated hypoxia and HIF-1 α expression promote the progression of bone metastases in breast cancer. Our results also suggest that hypoxia and HIF-1 α play a role in the induction of osteolytic change in bone metastases through causing an uncoupling between bone resorption and formation.

Disclosures: T. Hiraga, None.

1008

Placental Calcium Transporter Gene (PMCA3) Expression Predicts Intra-Uterine Bone Mineral Accrual. R. Martin^{*1}, N. C. W. Harvey², S. R. Crozier^{*2}, M. K. Javaid², P. Taylor^{*3}, E. M. Dennison^{*2}, H. M. Inskip^{*2}, K. M. Godfrey^{*2}, C. Cooper², R. Lewis^{*1}. ¹Centre for the Developmental Origins of Health and Disease, University of Southampton, Southampton, United Kingdom, ²MRC Epidemiology Resource Centre, Southampton, United Kingdom, ³Medical Physics and Bioengineering, Southampton General Hospital, Southampton, United Kingdom.

Evidence is accruing that the intra-uterine environment has a persisting influence on childhood skeletal growth, and predicts fracture risk in later life. We have previously demonstrated that placental calcium transport, partly determined by maternal 25-(OH) vitamin D status, may underlie this phenomenon. The aim of this study was to explore the relationship between expression of calcium transporters in the human placenta, and neonatal bone mineral accrual in the offspring. Tissue samples from 70 human placentae were rapidly frozen in liquid nitrogen and stored at -70 °C. A quantitative real time polymerase chain reaction was used to measure the mRNA expression of PMCA isoforms 1, 3 and 4, using beta-actin as a control gene. Neonatal whole body bone area, mineral content and density (BA, BMC, BMD) were measured within 2 weeks of birth using a Lunar DPX DXA instrument. Linear regression methods were used to explore the relationship between PMCA expression and neonatal bone mass. Full ethical approval was granted for this study. After controlling for beta-actin expression, PMCA3 mRNA expression predicted BA (p=0.02), BMC (p=0.04) [Figure], placental weight (p=0.04) and birth weight (p=0.006) of the neonate. In a multivariate model, the relationship between placental PMCA3 expression and neonatal BMC was independent of maternal height, and pre-pregnant fat stores, parity and calcium intake (p=0.05). Thus expression of the placental calcium transporter PMCA3 predicts neonatal whole body bone mineral content. This association may explain, in part, the mechanism whereby a mother's 25(OH)-vitamin D stores influence her offspring's bone mass. Further elucidation of this process may allow development of novel therapeutic strategies to optimise childhood bone mineral accrual and thus reduce osteoporotic fractures in future generations.

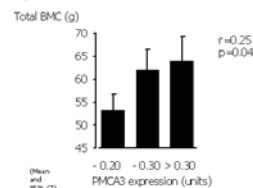


Figure: Neonatal whole body BMC (g) by thirds of PMCA3 expression, expressed relative to beta-actin (control).

Disclosures: R. Martin, None.

1009

A Comparison of Total Hip BMD as a Predictor of Fracture Risk: A Meta-Analysis. O. Johnell, J. A. Kanis, A. Oden*, H. Johansson*, C. Gluer, S. Fujiwara*, E. V. McCloskey, L. J. Melton, P. Delmas. Centre for Metabolic Bone Diseases, University of Sheffield, Sheffield, United Kingdom.

Meta-analyses of the predictive value of BMD on fracture risk have focussed on the use of DXA at the femoral neck. By contrast, many practice guidelines have favoured the use of total hip BMD, because of a smaller precision error. The aim of this study was to compare the performance characteristics of the two DXA sites. The hypothesis was that T-scores derived from either site would give comparable information on fracture risk. We studied 8,547 men and women from five prospective population-based cohorts, OPUS, Hiroshima, Sheffield, Rochester and OFELY with a total follow-up of 29,574 person years. The effect of BMD on fracture risk was examined using a Poisson model in each sex and cohort separately. The results of the different studies were then merged using weighted coefficients. BMD, both at the total hip and at the femoral neck, was a strong predictor of fractures in men and women and did not significantly differ, and the data were merged. For all fractures the risk ratio for 1 SD decrease of Z-score was 1.47 (1.36-1.58) for total hip vs 1.39 (1.28-1.50) for femoral neck. For all osteoporotic fractures the gradient of risk was 1.48 (1.36-1.61) vs 1.44 (1.33-1.57), respectively, and for hip fractures was 2.17 (1.81-2.61) vs 2.33 (1.92-2.84). There were no significant differences between the two hip measurements. In order to determine whether T-scores could be used interchangeably, we compared T-scores at the total hip and femoral neck using the NHANES database. When the Z-score was set a 0, T-scores at the two sites were fairly similar in women, but systematically lower at the femoral neck than at the total hip in men (Table).

Age	Men		Women	
	Femoral neck	Total hip	Femoral neck	Total hip
50	-0.21	0.40	-0.81	-0.51
55	-0.37	0.32	-0.98	-0.62
60	-0.51	0.14	-1.22	-0.93
65	-0.66	-0.04	-1.46	-1.22
70	-0.81	-0.21	-1.70	-1.50
75	-0.95	-0.38	-1.94	-1.79
80	-1.10	-0.55	-2.18	-2.07
85	-1.24	-0.72	-2.42	-2.36
90	-1.39	-0.89	-2.66	-2.64

We conclude that BMD measured at the total hip is a risk factor of substantial importance for fractures. The predictive ability was similar to measurement at the femoral neck. Whereas T-scores and Z-scores can be interchangeably used at the two BMD sites in women, this differs markedly in men. With this caveat, the two measurements can be used interchangeably in case finding models.

Disclosures: **J.A. Kanis**, None.

1010

Substantial Trabecular Bone Loss Occurs in Young Adult Women and Men: A Population-Based Longitudinal Study. B. L. Riggs¹, L. J. Melton², A. L. Oberg^{*3}, E. J. Atkinson^{*3}, S. Khosla¹. ¹Endocrinology, Mayo Clinic College of Medicine, Rochester, MN, USA, ²Clinical Epidemiology, Mayo Clinic College of Medicine, Rochester, MN, USA, ³Biostatistics, Mayo Clinic College of Medicine, Rochester, MN, USA.

Conventional wisdom holds that bone loss begins in women at menopause (due to sex steroid deficiency) and in men later in life (due to age-related factors). However, the possibility of earlier bone loss has not been assessed longitudinally in population-based studies using highly precise technology capable of distinguishing trabecular and cortical bone. Thus, in an age- and sex-stratified random population sample (n = 671), we made between 2- and 4-consecutive annual measurements of trabecular (trab) bone at distal radius (DR) and distal tibia (DT) and cortical (cort) bone at proximal radius (PR) and proximal tibia (PT) by peripheral quantitative computed tomography (pQCT, Densiscan, Scanco AG, CV 0.5%). We excluded from analysis 97 subjects receiving HRT, SERM, or bisphosphonate therapy. Both premenopausal women and young men had substantial rates of trabecular bone loss but minimal or no cortical bone loss until middle life whereas postmenopausal women and men older than 50 yrs had, as expected, substantial continuing cortical and trabecular bone loss (Table 1). Assessment of changes in volumetric BMD (vBMD) by decade in both sexes showed that substantial trabecular bone loss began in the third decade whereas substantial cortical bone loss did not begin until middle life. The decrease in cortical vBMD beginning in middle age is consistent with increases in bone turnover induced by menopause in women or by declining free sex steroids in men. However, the onset of substantial trabecular bone loss in both sexes soon after completion of pubertal growth at a time when sex steroids levels are, by definition, "normal" indicates that current paradigms on pathogenesis of osteoporosis are incomplete and that further study is required.

Table 1. Changes in vBMD in %/yr (mean ± SD)				
Group	DR-Trab	PR-Cort	DT-Trab	PT-Cort
Females				
Premenopausal	-0.67 ± 0.98**	-0.11 ± 0.51*	-0.53 ± 1.20**	-0.08 ± 0.44*
Postmenopausal	-1.08 ± 2.76**	-0.60 ± 0.77**	-0.61 ± 2.23*	-0.57 ± 0.91**
Males				
20-49 yrs	-0.66 ± 1.23**	-0.08 ± 0.37*	-0.68 ± 0.98**	-0.08 ± 0.37*
50+ yrs	-0.53 ± 1.19**	-0.38 ± 0.53**	-0.24 ± 0.65**	-0.22 ± 0.59**

For difference from zero: *P<0.05, **P<0.001

Disclosures: **B.L. Riggs**, None.

1011

A School Curriculum Based Exercise Program Increase Bone Mineral Accrual in Boys and Girls during Early Adolescence-Four Years Data from the POP-Study (Pediatric Osteoporosis Prevention Study) - a Prospective Controlled Intervention Study in 221 Children. C. Linden, P. Gardsell*, H. Ahlborg, M. Karlsson. Orthopaedics, University Hospital Malmö, Malmö, Sweden.

The longest reported prospective controlled intervention study with exercise in growing children which evaluate the accrual of bone mineral span 20 months. The purpose of this study was to evaluate the effect of an exercise intervention program within the school curriculum during the first school years, to catch also children not specifically interested in exercise, and to present the so far longest controlled follow-up data of exercise during growth. A population based cohort including 73 healthy Caucasian boys (aged 7.8 ± 0.6 at baseline) and 48 girls (aged 7.7 ± 0.6) in the only school in the Bunkeflo society outside Malmö, Sweden, were included in a school curriculum with 40 minutes physical activity every school day. One hundred healthy age and gender matched children (52 boys and 48 girls) in three nearby schools served as controls. These children were assigned to the general Swedish curriculum of physical activity in these grades (60-90 min/w). Bone mineral content (BMC; g) were measured with dual X-ray absorptiometry (DXA) at the lumbar spine (LS) and femoral neck (FN) before initiation of the intervention and then yearly for four years. The slope for each individual was estimated from the repeated measurements, and the annual changes calculated. Data is presented as mean ± SD. There were no differences in age, height, weight or BMC at baseline. In boys, the annual gain in BMC in the LS was greater in the intervention group in comparison with the controls during the 4 year follow-up, 7.0 ± 2.3 versus (vs.) 6.2 ± 1.5, p<0.05. In girls, a similar effect was seen in the LS 9.1 ± 4.1 vs. 7.1 ± 3.3 and in the FN 0.39 ± 0.20 vs. 0.29 ± 0.17, p < 0.01 respectively. The annual increase of the FN width (mm) was also greater in the intervention group, 1.23 ± 0.42 vs. 1.07 ± 0.49 in boys and 1.45 ± 0.91 vs. 1.03 ± 0.76 in girls, p < 0.05. The discrepancies remained after adjusting for differences in weight gain, height gain and pubertal development during the study, except for FN width in girls (p=0.08). A school based exercise program within the general curriculum during the first four school years seems to increase the accrual of bone mass and bone size. This is the first published intervention study that is population based and include the intervention within the school curriculum. Furthermore, it is so far the only intervention study that exceeds 20 months. Based on the data in this study it seems that increased time spent in physical education classes may increase peak bone mass and subsequently can be used as a prevention strategy for osteoporosis.

Disclosures: **C. Linden**, None.

1012

A 14-Year Longitudinal Study of the Relationship of Childhood Physical Activity to Adult Bone Mineral Content. A. D. G. Baxter-Jones*, C. A. Mundt*, R. L. Mirwald*, R. A. Faulkner, D. A. Bailey. College of Kinesiology, University of Saskatchewan, Saskatoon, SK, Canada.

The purpose of this study was to investigate longitudinally the influence of childhood physical activity on bone mineral content (BMC) measured during the third decade of life. We previously showed, in this cohort of children, that maturational and size adjusted total body and femoral neck BMC were greater in active boys and girls compared to their inactive peers, one year after the attainment of peak BMC velocity. In the present analysis we analyzed data from 82 females and 65 males, between the ages of 18.2 and 27.5 years, who were longitudinally assessed from 1991-1997 and re-assessed from 2002-2005. Subjects were from the University of Saskatchewan's Pediatric Bone Mineral Accrual Study. Physical activity and anthropometry were measured every 6 months during childhood and annually in adulthood. Dual-energy X-ray absorptiometry scans of the total body (TB), lumbar spine (LS), total hip (TH) and femoral neck (FN) (Hologic 2000, array mode) were collected annually. Ages at peak height velocity (PHV) and peak BMC velocity were identified using data collected over the growing years. A mean age- and gender-specific standardized activity (Z) score was calculated for each subject based on multiple yearly activity assessments. The childhood activity scores were used to identify active (top quartile), average (middle two quartiles), or inactive (bottom quartile) groups. Adult BMC values were averaged over a maximum of three years. At follow-up, the average age from PHV was 10.6 ± 3.4 years in females and 10.0 ± 2.2 years in males. Using two-way analysis of covariance (ANCOVA; covariates, years from PHV, average adult height and weight) for BMC, no significant interactions were found between sex and physical activity at any of the four sites (p>0.05). Significant gender and physical activity main effects were found for total body, total femoral hip, and femoral neck BMC (p<0.05). Lumbar spine BMC also showed a significant sex effect (p<0.05) however, there was no effect of physical activity at this site (p>0.05). We previously showed that the growing skeleton responded to increased everyday physical activity by increased bone mineral accrual. The present analysis suggests these changes persist into early adult life.

Disclosures: **A.D.G. Baxter-Jones**, None.

1013

Hoxa10: A BMP2-Responsive Gene Activates Runx2 and Regulates Osteogenesis. M. Q. Hassan*, R. Tare*, A. J. van Wijnen, J. L. Stein*, G. S. Stein, J. B. Lian. Department of Cell Biology and Cancer Center, University of Massachusetts Medical School, Worcester, MA, USA.

Homozygous mice targeted for disruption of the gene encoding Hoxa10, a member of the abdominal B class of homeobox proteins, show an anterior homeotic transformation of lumbar vertebrae and have severe fertility defects. Analysis of microarray gene profiles during BMP2 osteogenic induction of C2C12 myogenic cells identified Hoxa10 in a gene cluster together with Runx2, the transcription factor essential for bone formation. Because SMAD regulatory elements in the Runx2 gene have not been identified, we examined regulation of Runx2 by Hoxa10 as a mediator of BMP2 induced Runx2 gene expression. Hoxa10 binds specifically to the TTAT consensus core, rather than the classic ATTA homeodomain motif. Multiple putative TTAT motifs were identified within -1 kb of the Runx2 promoter. Overexpression of recombinant Hoxa10 protein in non-osseous and osteoblastic cells results in a 3-4 fold activation of Runx2. Deletion and site-directed mutagenesis studies confirmed a functional Hoxa10 site in the proximal promoter. By chromatin immunoprecipitation assay, we find that recruitment of Hoxa10 to the Runx2 promoter is maximal during the early stages of osteoblast differentiation from primary cells, and that Hoxa10 is not associated with the promoter in mature cells in a mineralized matrix. We next demonstrated the ability of Hoxa10 in MC3T3 cells to induce endogenous expression of markers of early osteoblast differentiation and observe that Runx2 and BSP mRNAs are increased by 2-3 fold within 24 hrs. The biological significance of this regulation was assessed in vivo. In situ immunohistochemistry of mouse bone sections confirmed the co-expression of Hoxa10 and Runx2 in long bone and vertebrae in hypertrophic chondrocytes and osteoblasts. These findings suggest Hoxa10 is linked to an early event in osteoblast differentiation. In conclusion, these studies identify Hoxa10 as a target of BMP2 signaling that results in activation of a lineage-specific transcription factor and other target genes. Thus, we propose that BMP2 induction of Hoxa10 and Hoxa10 activation of Runx2 are components of a regulatory cascade for the expression of genes promoting bone formation.

Disclosures: **M.Q. Hassan**, None.

1014

Involvement of Cbfb in the Cooperative Action of BMP and Runx2 Signaling on Osteogenic Differentiation. S. Ohba¹, T. Ikeda¹, F. Kugimiya¹, F. Yano¹, T. Fujita², T. Komori³, T. Ogasawara¹, K. Nakamura^{*1}, T. Takato^{*1}, H. Kawaguchi¹, U. Chung¹. ¹Univ. of Tokyo, Tokyo, Japan, ²Setsunan Univ., Osaka, Japan, ³Nagasaki Univ., Nagasaki, Japan.

Aiming at clinical application to bone regeneration, we previously developed a cell-based monitoring system for osteogenic differentiation, and found that the combination of BMP and Runx2 signalings induce this differentiation from various cell types including non-osteoblastic cells much more potently than either of them alone. We also showed that cell sheets of dermal fibroblasts stimulated by the combination, but not only one of them, induced bone formation in vivo in mouse critical-size bone defects. To learn the mechanism of the cooperative action of the two signalings, we investigated the involvement of Cbfb, a heterodimer partner of Runx2. Cultured calvarial cells derived from Cbfb-deficient mice failed to induce expression of ALP, osteopontin or osteocalcin as determined by real-time RT-PCR in response to infection of an adenovirus expressing constitutively active ALK6 and Runx2 (Ad-caALK6+Runx2), which was restored by an adenoviral reintroduction of Cbfb (Ad-Cbfb) to the level of the wild-type calvarial cell culture. To define the molecular interaction, we infected non-osteoblastic NIH3T3 cells with Ad-caALK6, Ad-Runx2, Ad-Cbfb or their combinations. Expression of osteocalcin mRNA was induced by Ad-caALK6+Runx2, but not by Ad-caALK6, Ad-Runx2, Ad-Cbfb, Ad-caALK6+Cbfb or Ad-Runx2+Cbfb, and the induction was enhanced by additional infection of Ad-Cbfb. Although Cbfb mRNA level was not altered by Ad-caALK6+Runx2, the protein level determined by immunoblot analysis was markedly increased by Ad-caALK6+Runx2 and Ad-Runx2 to the same extent. In the presence of lactacystin, a specific ubiquitin-proteasome inhibitor, the Cbfb protein level was increased without being affected by Ad-Runx2 or Ad-caALK6+Runx2, indicating that Runx2 protects Cbfb from being degraded by the ubiquitin-proteasome system. Although Runx2 and Cbfb were co-localized in the nucleus upon infection with Ad-caALK6+Runx2 or with Ad-Runx2 alone, immunoprecipitation analysis revealed that these two proteins bound to each other only upon infection with the former. In addition, chromatin immunoprecipitation analysis showed that Ad-caALK6+Runx2, but not Ad-Runx2, recruited Cbfb to the osteocalcin promoter (mOC-67/-471), whereas Runx2 was constantly recruited. These lines of results indicate that BMP and Runx2 signalings cooperatively induce osteogenic differentiation through regulation of Cbfb in the following ways: Runx2 increases the stability of the Cbfb protein; and BMP enhances formation of the Runx2-Cbfb complex and binding of the complex to the promoter.

Disclosures: **S. Ohba**, None.

1015

Reconstitution of Runx2/Cbfa1 Null Cells Identifies Runx2 Domains Required for Osteoblast Differentiation. J. Bae*, R. Narla*, S. Gutierrez*, J. Pratap, J. L. Stein*, J. B. Lian, G. S. Stein, A. Javed. Department of Cell Biology and Cancer Center, University of Massachusetts Medical School, Worcester, MA, USA.

While it is well established that Runx2/Cbfa1 promotes osteoblast differentiation, the specific regions of the Runx2 protein required for induction of the osteogenic lineage remain to be identified. We approached this question by characterizing gene expression profiles and osteogenic activity of calvarial derived cells from Runx2 null mice reconstituted with wild type (WT) or deletion mutants of Runx2. Absence of Runx2 activity in these cells was confirmed by both in situ immunofluorescence microscopy and western blot analysis. Culturing these cells for 3 weeks in the presence or absence of osteogenic media (β -glycerol phosphate and ascorbic acid) did not stimulate osteoblastic gene expression. However, infection with adenovirus expressing WT-Runx2 at the proliferation stage robustly induced the normal program of osteoblast differentiation. Early markers such as collagen type-I (Col-I) and alkaline phosphatase (AP) were induced (4-8 fold) at days 4 and 8. Genes representing mature osteoblast stages, Osteopontin (OP), Bone sialo protein (BSP), Runx2 and Osteocalcin (OC) were expressed in normal temporal order and were dramatically induced (18-36 fold) at later time points (days 8 and 12). Interestingly this pattern of gene expression was similar in cells infected with a mutant Runx2 protein that lacks 96 residues at the C-terminus (Runx2 Δ 432); thus, the Groucho repressor and the C-terminal activation domain are dispensable for Runx2 osteogenic activity. Upon infection with a Runx2 mutant in which a further 41 aa were deleted (Runx2 Δ 391), we find no osteoblast markers (AP, Col-I, OP, BSP, Runx2 and OC) were expressed and no osteogenic activity was observed. We note that the mutant Runx2 protein enters nucleus and can bind DNA and its expression was sustained through out the time course. Thus the 391-432 domain is a critical component of Runx2 osteogenic function. With the Runx2 null cell model, Runx2 and BMP2 dependent or independent events could be distinguished that can not be identified in other cell model systems because BMP2 strongly activate endogenous Runx2. Treatment of BMP2 alone could not induce the osteogenic program in these cells, while reconstitution of both BMP2 and Runx2 (WT or Δ 432) signals in these cells, results in a 20-40 fold increased expression of osteogenic genes. However, the Runx2 Δ 391 mutant with BMP2 fails to stimulate the normal osteoblast differentiation program. In conclusion, our studies demonstrate that: 1) the C-terminus of Runx2 is required to initiate the osteogenic differentiation program 2) BMP2 osteogenic activity requires Runx2.

Disclosures: **J. Bae**, None.

1016

Functional Switching of Runx2 by Cdk6 and Cdk4 in Regulation of Osteoblast Differentiation. T. Ogasawara¹, H. Chikuda¹, S. Ohba¹, D. Chikazu¹, M. Katagiri^{*1}, F. Yano¹, K. Nakamura¹, U. Chung¹, K. Hoshi¹, T. Takato^{*1}, H. Okayama^{*2}, H. Kawaguchi¹. ¹Sensory & Motor System Medicine, University of Tokyo, Tokyo, Japan, ²Biochemistry & Molecular Biology, University of Tokyo, Tokyo, Japan.

Because a temporal arrest in the G1 phase of the cell cycle is known to be a prerequisite for cell differentiation, this study investigated the involvement of cell cycle factors such as cyclins, cyclin-dependent kinases (Cdks) and Cdk inhibitors (CKIs) that critically influence osteoblast differentiation. Of the G1 cell cycle factors, Western blot and RT-PCR analyses in the presence and absence of proteasome inhibitors revealed that Cdk6 expression was most strongly down-regulated via transcriptional repression during differentiation of MC3T3-E1 cells and primary mouse calvarial osteoblasts induced by BMP-2. Overexpression of Cdk6 in MC3T3-E1 cells inhibited the BMP-2-induced alkaline phosphatase (ALP) activity and osteocalcin expression, while overexpression of dominant negative (dn)Cdk6 or silencing of Cdk6 through RNA interference stimulated the osteoblast differentiation. Immunoprecipitation assay showed that not only Cdk6, but also Cdk4, bound to Runx2 in MC3T3-E1 cells. Although the Cdk6-Runx2 complex was predominant over the Cdk4-Runx2 complex in the control culture, the BMP-2 treatment caused a marked decrease of the former and an increase of the latter. Cdk4-Runx2 complex was shown by chromatin immunoprecipitation analysis to bind to the osteocalcin promoter (mOC-67/471), while Cdk6-Runx2 complex did not. The Cdk6 overexpression did not alter the expression level or the subcellular localization of Runx2, but markedly reduced the Runx2 binding to mOC-67/471 in parallel with the differentiation inhibition. To further examine the involvement of Cdk4 and Cdk6 in the Runx2 function, these molecules were transfected to C3H10T1/2 cells which expressed little endogenous Runx2. The Cdk4 co-transfection enhanced osteocalcin and ALP expression induced by the Runx2 transfection, which was stimulated by the dnCdk6 transfection. These results indicate that Cdk6 inhibits promoter-binding and transcriptional activities of Runx2 by binding to Runx2 competitively, while Cdk4 acts as a transcriptional co-activator of Runx2. It is concluded that the down-regulation of Cdk6 expression by differentiation stimuli leads to the decrease in Cdk6-Runx2 complex and the increase in Cdk4-Runx2 complex, both causing enhancement of the Runx2 transcriptional activity. Hence, the present study is the first to shed light on novel roles of the Cdks that control a functional switching of Runx2 in the regulation of osteoblast differentiation.

Disclosures: **T. Ogasawara**, None.

1017

SOX9 Is a Potent Transcriptional Repressor for RUNX2 during Skeletogenesis. G. Zhou¹, E. Munivez^{*2}, Q. Zheng^{*1}, F. Elgin^{*1}, P. Fonseca^{*1}, Y. Chen^{*2}, E. Sebald^{*3}, D. Krakow^{*3}, B. Lee². ¹Dept. of Molecular and Human Genetics, Baylor College of Medicine, Houston, TX, USA, ²Dept. of Molecular and Human Genetics, Baylor College of Medicine, Howard Hughes Medical Institute, Houston, TX, USA, ³Dept. of Pediatrics, David Geffen School of Medicine at UCLA, Los Angeles, CA, USA.

Runx-domain transcription factor RUNX2 is essential for osteoblast differentiation and chondrocyte hypertrophy. However during mouse embryonic development it is also expressed early in mesenchymal condensations. Hence, antagonism of Runx2 is required to down regulate its expression and function in those condensates that are destined to differentiate into chondrocytes instead of osteoblast. But how this is achieved is still poorly understood. SOX9 is a HMG-box-containing transcriptional activator essential for chondrocyte condensation and cartilage formation. *SOX9* heterozygous mutations in humans cause severe skeletal malformation syndrome campomelic dysplasia. Since *Sox9* is expressed highly in chondrogenic mesenchymal cell condensations but absent in hypertrophic chondrocytes, we hypothesize that SOX9 also acts as a transcriptional repressor for osteoblast differentiation and chondrocyte hypertrophy via inhibition of RUNX2 activity. In this study, we demonstrate that SOX9 and RUNX2 directly interact with each other through their DNA binding domains. SOX9 decreased RUNX2 binding to its target sequence and severely repressed RUNX2 transactivation of its reporter constructs. To test the *in vivo* repressor function of SOX9 we have generated transgenic mice expressing *SOX9* in osteoblasts by utilizing a cell-type specific *Col1a1* promoter. The *Col1a1-SOX9* transgenic mice displayed generalized dwarfism. Von Kossa staining and alkaline phosphatase staining demonstrated that osteoblasts from transgenic mice were less active compared with wild-type mice. Expressions of osteoblast-related markers including *Runx2*, *Col1a1* were also downregulated in the long bones of transgenic mice as assayed by quantitative real-time RT-PCR. Furthermore, we correlated this observation in humans with campomelic dysplasia. Here, haploinsufficiency of SOX9 resulted in upregulation of a chondrocyte maturation marker *COL10A1*, a known transcriptional target of RUNX2. In summary, our results reveal a novel transcriptional repressor function of SOX9 during skeletogenesis. Understanding the interaction between these two key transcription factors will help us elucidate the transcriptional network governing cell fate commitment during skeletogenesis.

Disclosures: **G. Zhou**, None.

1018

TNF Inhibits Osteoblast Function by Increasing Runx2 Degradation through Smurf1 E3 Ligase. H. Kaneki, D. Chen, R. Guo^{*}, B. F. Boyce, L. Xing. University of Rochester, Rochester, NY, USA.

TNF and IL-1 stimulate osteoclastic bone resorption and inhibit osteoblastic bone formation, in part by inducing osteoblast (obl) apoptosis, but the molecular mechanisms by which they inhibit obl function are not well established. Ubiquitin-mediated proteasomal degradation has been implicated in the regulation of BMP and TGF- β signaling pathways in various cell types. The E3 ubiquitin ligase, Smad ubiquitin regulatory factor 1 (Smurf1), negatively regulates osteoblast differentiation by mediating proteasomal degradation of the BMP signaling proteins, Smads 1 and 5, and Runx2. To test the hypothesis that TNF or IL-1 inhibit obls by up-regulating Smurf1 E3 ligase and degrading these proteins, we first examined the effects of TNF and IL-1 on expression of Smurf1 in 2T3 and C2C12 obl precursor cells. TNF (7.5 ng/ml), but not IL-1 (1-20 ng/ml) increased expression of Smurf1 mRNA by 22 \pm 2-fold over control in a dose-dependent manner, an effect confirmed at the protein level by Western blotting. To determine if TNF or IL-1 induce Runx2 degradation, we transfected 2T3 and C2C12 cells with a FLAG-tagged Runx2 expression plasmid and treated them with TNF or IL-1. TNF, but not IL-1, significantly reduced transfected and endogenous Runx2 protein levels detected by anti-Flag and anti-Runx2 monoclonal antibodies, indicating that TNF induces Runx2 degradation. Proteasomal degradation of substrate proteins involves their ubiquitination. Therefore, we examined if ubiquitinated-Runx2 complexes could be detected in 2T3 cells treated with TNF. When Runx2 protein was immunoprecipitated, an ubiquitinated-Runx2 protein ladder was detected by Western blot in the presence of TNF. Treatment of cells with the proteasome inhibitor, MG-132, significantly increased TNF-induced Runx2 ubiquitination, indicating that TNF-induced Runx2 degradation is ubiquitin-proteasome-dependent. Next, to confirm if TNF-induced Runx2 degradation is Smurf1-dependent, we infected 2T3 cells with retrovirus expressing double stranded small interfering Smurf1 RNA to knock down expression of endogenous Smurf1. Smurf1 siRNA decreased TNF-induced Smurf1 expression by 92 % without changing the expression of other E3 ligases, such as Smurf2 and WWP1, and prevented TNF-induced Runx2 degradation. In addition, Smurf1 siRNA blocked TNF-induced inhibition of osteoblast marker gene expression (ALP 89 \pm 3 % vs. 45 \pm 2 %; Type I collagen 80 \pm 3 % vs. 35 \pm 2 %). In summary, TNF, but not IL-1, increases Smurf1 expression in osteoblasts and promotes ubiquitination and proteasomal degradation of Runx2 protein, which is blocked by Smurf1 siRNA. These findings indicate that TNF may inhibit bone formation by preventing BMP-mediated signaling in osteoblastic cells.

Disclosures: **H. Kaneki**, None.

1019

A Dual Role for Wnt in Chondrogenesis: Inhibition of Wnt/ β -Catenin Signaling by DKK1 Promotes Initial Chondrogenesis of Mesenchymal Stem Cell but Suppresses Chondrocyte Hypertrophy. G. Rawadi^{*}, Z. Yang^{*}, E. Susanto^{*}, R. Ee^{*}, H. Chan^{*}, Y. Liu^{*}, R. Baron. Prostrakan, Romainville, France.

The Wnt/ β -catenin pathway has recently been reported in the regulation of chondrogenesis and chondrocyte differentiation. Dickkopf (DKK) proteins are inhibitors of Wnt/ β -catenin signaling by antagonizing LDL-receptor related protein (LRP) 5 or 6 activity. The aim of this study was to investigate the effect of DKK1 on the differentiation process of murine limb bud-derived mesenchymal stem cells (MSC), to better understand the role of Wnt/ β -catenin pathway in cartilage development. Micromass culture of MSC isolated from limb buds of 11.5d murine embryos was used as an ex-vivo model of chondrogenesis differentiation in culture. Cultured MSC undergo initial condensation, chondrogenesis, followed by hypertrophy differentiation and terminal maturation forming calcified cartilage matrix. The effect of recombinant Wnt3a and DKK1 on chondrogenesis was assayed by alcian blue staining of matrix formation, real-time PCR analysis of chondrocyte markers expression, alkaline phosphatase (ALP) activity and alizarin red mineralization staining. Wnt3a treatment of MSC resulted in suppression of initial condensation in a dose-dependent manner as demonstrated by a reduction of matrix formation and mRNA expression of early chondrocyte markers, type II collagen and aggrecan. In contrast, treatment with Wnt3a potentiated hypertrophy differentiation in chondrocytes already engaged in maturation, with enhanced ALP activity as well as increased expression of ALP and type X collagen mRNA. The dual effect of Wnt3a was further supported by the use of a specific GSK3 β inhibitor, which mimics Wnt proteins and activates β -catenin signaling. In agreement with these observations, treatment of MSC with DKK1 enhanced the initial chondrogenesis process and significantly inhibited hypertrophy differentiation of matured chondrocytes. In addition, DKK1 antagonized the effect of exogenous Wnt3a on MSC differentiation; matrix formation suppressed by Wnt3a was reversed, and enhanced ALP activities inhibited. Finally, we analyzed the differentiation of MSC derived from both *Lrp5*^{-/-} and *Dkk1*^{-/-} mice and compared it to cells from wild-type littermate animals. The results confirmed that Wnt has a dual effect of chondrocytic differentiation. We conclude that early expression of Wnt3a retains mesenchymal stem cells in a pre-chondrocytic state whereas Wnt3a is later required for their differentiation into hypertrophic chondrocytes while the Wnt-signaling antagonist Dkk1 exerts opposite effects.

Disclosures: **G. Rawadi**, None.

1020

Canonical Wnt Signaling Mediates Chondrocyte Hypertrophy through the Runx 2 Transcription Factor. Y. Dong, E. M. Schwarz, R. J. O'keefe, H. M. Drissi. Orthopaedics, University of Rochester, Rochester, NY, USA.

Wnt secreted factors control limb morphogenesis in vivo. We investigated the molecular mechanisms underlying Wnt regulation of chondrocyte hypertrophy using the embryonic chick sternal chondrocyte model. RCAS viral over-expression Wnt8c and Wnt9a, upstream of β -catenin, up-regulated collagen X (colX) and Runx2 thereby inducing chondrocyte hypertrophy, while Wnt5a, which utilizes the calcium pathway, inhibited the expression of colX and has no effect on Runx2 transcripts. Furthermore, Wnt8c and Wnt 9a strongly inhibited the early chondrocyte phenotypic gene, collagen II (col2) and Wnt 5a over-expression significantly enhanced col2 expression in these cultures. BMP-2 enhanced canonical wnt8c- and wnt9a-induced chondrocyte hypertrophy while over-expression of wnt5a inhibited BMP-2 induction of colX. Similarly, TGF- β inhibited wnt8c- and wnt9a-induced expression of colX and Runx2, while it further potentiates the inhibitory effect of wnt5a on colX. Interestingly, both BMP-2 and TGF- β enhanced the expression of Col2 in wnt5a over-expressing cells. Over-expression of β -catenin mimics the effect of wnt8c and wnt9a by up-regulating Runx2, colX, and alkaline phosphatase mRNA levels while it inhibits col2 and Sox9 transcription. Thus our results indicate that activation of the canonical β -catenin wnt signaling pathway induces chondrocyte hypertrophy while the calcium pathway represses chondrocyte maturation. Our western blot analysis shows that β -catenin also induces the protein levels of Runx2 in chondrocytes. To determine the transcriptional mechanisms by which this canonical signaling regulated chondrocyte hypertrophy, we investigated the effects of β -catenin-TCF/LEF on Runx2 and type X collagen promoters which carry putative binding sites for TCF. Over-expression of TCF and β -catenin using deletion mutants of the Runx2 promoter shows that the proximal 128 base pairs of this promoter is responsible for the wnt-mediated induction of Runx2. Similarly, over-expression of β -catenin caused a significant transactivation of the ABC-640 and b2 chick type X collagen promoter. However mutant TCF binding site in Runx2 promoter -128 fragment leads a loss response of Runx2 promoter to β -catenin. Mutation of TCF binding site in type X collagen promoter however did not change its activity. Finally, gel shift assay analyses determined the functionality of the TCF/LEF binding sites on the Runx2 promoter. Altogether we demonstrate that Wnt/ β -catenin signaling induces chondrocyte maturation at least partly through activation of Runx2 gene expression.

Disclosures: **Y. Dong**, None.

1021

Activated Wnt Signaling in sFRP1 Null Mouse Alters Chondrocyte Differentiation *Ex Vivo*. T. Gaur^{*1}, L. Rich^{*2}, C. J. Lengner^{*1}, D. Ayers^{*2}, J. L. Stein^{*1}, G. S. Stein¹, P. V. N. Bodine³, B. S. Komm³, J. B. Lian¹. ¹Department of Cell Biology and Cancer Center, University of Massachusetts Medical School, Worcester, MA, USA, ²Department of Orthopedic Surgery, University of Massachusetts Medical School, Worcester, MA, USA, ³Women's Health Research Institute, Wyeth Research, Collegeville, PA, USA.

During chondrogenesis, mesenchymal cells condense and differentiate to a cartilage template for bone formation. Various Wnt proteins are implicated in positive and negative regulation of chondrocyte differentiation. Genetic ablation of sFRP1 (sFRP1 KO), an antagonist of Wnt signaling in mouse, promotes increased Wnt signaling and is characterized by a high bone mass phenotype in the adult. To examine chondrogenesis in these mice, we used mouse embryonic fibroblasts (MEFs) that undergo chondrocyte differentiation as micromass cultures and in the presence of BMP2, a regulator of chondrogenesis *in vivo*. We compared expression of marker genes during the chondrogenic differentiation time course (12 days) between WT and KO and with or without BMP2 treatment. In absence of BMP2, the levels of collagen type II are ~21 fold higher; collagen type X, a marker of chondrocyte hypertrophy is ~9 fold higher; and basal levels of Indian hedgehog, a marker for transition from chondrogenesis to osteogenesis is 3-5 fold higher in sFRP1 KO MEFs. These results demonstrate that sFRP1 KO MEFs could initiate chondrogenic differentiation in the absence of BMP2. In the presence of BMP2, the KO cells showed an increase in differentiation by alcian blue staining, consistent with the 12 fold higher expression of collagen II. However, Indian hedgehog was induced to ~160 fold in WT, but only 2 fold increase in KO and peak expression of collagen X and alkaline phosphatase is delayed in KO MEFs. These findings suggest a delay of *in vitro* terminal differentiation of hypertrophic chondrocytes in KO. This pattern of gene expression is consistent with the finding that sFRP1 is expressed at maximal levels from day 0 to 3, then suppressed during early differentiation when Collagen II is expressed in WT cells. sFRP1 is induced again at a late stage of hypertrophic chondrocytes and calcification (d9) when osteocalcin is expressed. Thus Wnt signaling is inhibited by sFRP1 prior to induction of chondrogenesis and at the hypertrophic stage. Our results suggest stage-specific roles of Wnt signaling during chondrogenesis which activates the initial recruitment of progenitor cells into the chondrocytic lineage. However, to reach the terminal differentiation of hypertrophic chondrocytes, attenuation of Wnt signaling is necessary. Thus, the sFRP1 KO model that exhibits constitutive Wnt signaling has identified key requirements for chondrogenesis.

Disclosures: **T. Gaur, None.**

1022

Retinoids Activate Collagen X Gene Expression in Prehypertrophic Chondrocytes both by Direct Transcriptional Activation and by Stimulation of BMP Signaling. S. L. Adams, L. Lassova^{*}, Z. Niu^{*}, E. B. Golden^{*}, A. J. Cohen^{*}. Biochemistry, School of Dental Medicine, University of Pennsylvania, Philadelphia, PA, USA.

During endochondral bone formation, chondrocytes undergo a terminal differentiation process characterized by hypertrophy and by production of type X collagen (Col X), a protein found only in hypertrophic cartilage. Retinoids stimulate chondrocyte maturation *in vitro* and are essential for endochondral bone formation *in vivo*, and clinical use of synthetic retinoids can cause premature growth plate closure and growth retardation. Despite the well-documented importance of retinoids in regulating endochondral bone formation, the molecular mechanisms by which they mediate this process are largely unknown. We show that retinoids act both by directly stimulating transcription of the Col X gene and by stimulating production of bone morphogenetic proteins (BMPs). We have defined the direct activation mechanism by analysis of wild-type and mutated fragments of the Col X promoter ligated to a luciferase reporter gene and by electrophoretic mobility shift assays (EMSAs). Our studies show that stimulation of the Col X promoter by retinoic acid (RA) requires a distal region of the promoter (nucleotides -2618 to -2594) containing two overlapping RA response elements (RAREs) that share a 6-nucleotide half-site. EMSAs using antibodies against various retinoic acid receptors (RARs) showed that RAR γ is the major receptor binding this compound RARE in cultured chondrocytes. Mutagenesis of the 6-nucleotide shared half-site abolished both RAREs, preventing binding of RAR γ and abrogating stimulation of the promoter by RA. Thus RA activation of Col X transcription occurs in part by direct activation of the RAR γ receptor, which acts as a ligand-activated transcription factor. However, the direct effects of retinoids on Col X transcription appear to be amplified by stimulation of BMP signaling. We used real-time polymerase chain reaction to show that RA induces a rapid ~30-fold stimulation of mRNAs encoding BMPs 2 and 6 and a lesser stimulation of BMP4 mRNA; BMPs were previously shown to stimulate Col X gene transcription. To determine the relative contributions of direct activation *versus* BMP-dependent activation of Col X by RA, we used a dominant-negative (DN) mutant of Smad 4, a constitutive component of the BMP signaling pathway; this mutant was shown previously to block BMP signaling (Lagna *et al.*, *Nature* **383**, 832-836, 1996). The DN Smad 4 decreased stimulation of the Col X promoter from 19 fold to 3.5 fold, indicating that RA stimulation of BMP signaling contributes significantly to transcriptional activation of the Col X promoter during chondrocyte maturation.

Disclosures: **S.L. Adams, None.**

1023

Constitutive Activation of MKK6 in Chondrocytes of Transgenic Mice Inhibits Proliferation and Delays Endochondral Ossification. R. Zhang^{*1}, S. Murakami², F. Coustry^{*1}, Y. Wang^{*1}, B. de Crombrughe^{*1}. ¹Molecular Genetics, UT MD Anderson Cancer Center, Houston, TX, USA, ²Orthopaedics, Case Western Reserve University, Cleveland, OH, USA.

To examine the role of the p38 MAPK pathway in endochondral ossification, we generated transgenic mice that express MKK6EE, a constitutively active mutant of MKK6, in chondrocytes. Four transgenic mouse lines showed a similar dwarf phenotype. Skeletal preparations showed shortened axial and appendicular skeletons. At 3 weeks of age, the average length of long bones was decreased by about 20-30% in transgenic mice. Histological examination of the growth plates of long bones revealed a reduced zone of hypertrophic chondrocytes and a delay in the formation of primary and secondary ossification centers. BrdU incorporation in growth-plate chondrocytes showed 43% and 58% reduction at postnatal days 9 and 21, respectively, indicating inhibition of proliferation. Consistent with these observations, *in situ* hybridization showed inhibition of positive regulators of proliferation, *Indian hedgehog*, *PTH/PTHrP* receptor, and *cyclin D1* and upregulation of a cell cycle inhibitor *p21* in chondrocytes of these mice. Since transgenic mice that express MKK6EE in chondrocytes showed phenotypes similar to those of mice that overexpress *SOX9* in chondrocytes, we examined Sox9 activity *in vivo* by generating mice harboring a Sox9-dependent reporter. We observed a 2-fold increase ($P < 0.05$) in the activity of this Sox9-dependent reporter in mice that express MKK6EE in chondrocytes without changes in Sox9 levels. Similarly, p38 signaling increased the transcriptional activity of Sox9 in COS7 cells and primary chondrocytes in transient transfection experiments. These observations are consistent with the notion that increased activity of Sox9 accounts at least in part for the phenotype caused by constitutive activation of MKK6 in chondrocytes. Activating mutations of FGFR3 cause the most common forms of human dwarfism, achondroplasia and thanatophoric dysplasia. Since p38 is activated by FGF in chondrocytes, it is possible that the anti-proliferative effects of Fgfr3 are at least in part mediated by p38. We previously generated transgenic mice that express a constitutively active mutant of MEK1 in chondrocytes. These mice showed an achondroplasia-like dwarf phenotype characterized by inhibition of hypertrophic chondrocyte differentiation; however, chondrocyte proliferation was not affected. Our observations strongly suggest that the ERK1/ERK2 and p38 MAPK pathways play distinct roles in endochondral ossification. We propose that both pathways contribute to the dwarfism caused by activating mutations in FGFR3 by different mechanisms.

Disclosures: **R. Zhang, None.**

1024

Hypoxia Promotes Cartilage Matrix Synthesis via p38 MAPKinase and Suppresses Terminal Differentiation via HDAC4. M. Hirao^{*}, N. Tamai^{*}, A. Myoui^{*}, N. Tsumaki^{*}, N. Araki^{*}, H. Yoshikawa. Dept. of Orthopaedics, Osaka University Graduate School of Medicine, Suita, Japan.

Cartilage is an avascular tissue that functions at a lower oxygen tension than do most other tissues. Under the hypothesis that oxygen tension plays an important role in chondrocyte differentiation and function, we investigated the influence of oxygen tension on chondrocyte biology using pluripotent mesenchymal cell line C3H10T1/2 and on endochondral ossification in 14.5E mice embryo forearm organ culture. 10T1/2 cells and embryo forearms were cultured in normoxia (O₂ 20%) or hypoxia (O₂ 5%) in the presence of rhBMP-2 (500ng/ml). 10T1/2 cells produced more abundant glycosaminoglycan (GAG) in hypoxia than in normoxia. In parallel, type II collagen (*Col2a1*) gene expression was elevated by hypoxia, while type X collagen (*Col10a1*) gene expression was suppressed. In organ cultures, hypoxia promoted cartilage matrix synthesis as estimated by the area stained by Safranin O and suppressed *Col10a1* expression by *in situ* hybridization. These data indicate that hypoxia promotes cartilage matrix synthesis and suppresses terminal differentiation. To elucidate the mechanisms, we overexpressed inhibitory Smad6 but it did not alter the GAG induction by hypoxia. Hypoxia promoted matrix synthesis even in organ culture of *Smad6* transgenic mice. In contrast, p38MAPK inhibitor, FR167653 as well as dominant-negative MKK3 abolished hypoxia-induced matrix synthesis both *in vitro* and in organ culture. However, FR167653 did not rescue the reduced *Col10a1* gene expression by hypoxia. These data suggest that hypoxia-induced cartilage matrix synthesis is mediated by p38MAPK pathway but the suppression of terminal differentiation is under the regulation of other molecules. Recently, it was reported that histone deacetylase 4 (HDAC4) controls chondrocyte hypertrophy by repressing *Runx2* gene expression and transcriptional activity. We found that in 10T1/2 cells, hypoxia reduced *Runx2* gene expression and increased HDAC4 protein expression in nuclear extract but that it did not alter Sox9 expression, phosphorylation and transcriptional activity. When *Runx2* activity was augmented by overexpressing wild-type *Runx2*, *Col10a1* gene expression was not suppressed by hypoxia. Inhibition of HDAC4 using siRNA caused up-regulation of *Runx2* gene expression and its transcriptional activity, and restored *Col10a1* gene expression down-regulated by hypoxia. These data strongly suggest that HDAC4 plays a key role in the regulation of chondrocyte terminal differentiation by oxygen tension. Collectively, our data indicate that hypoxia promotes cartilage matrix synthesis via p38 MAPK and suppresses terminal differentiation via HDAC4.

Disclosures: **M. Hirao, None.**

1025

Absence of BMP2 Results in Low Bone Mineral Density, Osteoarthritis, Spontaneous Fracture and Impaired Fracture Healing. K. Tsuji¹, B. D. Harfe^{*2}, K. Cox¹, M. Bouxsein³, L. Gerstenfeld⁴, A. Bandyopadhyay^{*5}, C. Tabin^{*5}, V. Rosen¹. ¹Oral and Developmental Biology, Harvard School of Dental Medicine, Boston, MA, USA, ²Department of Molecular Genetics and Microbiology, University of Florida College of Medicine, Gainesville, FL, USA, ³Beth Israel Daconess Medical Center, Boston, MA, USA, ⁴Boston University, Boston, MA, USA, ⁵Harvard Medical School, Boston, MA, USA.

Evaluating the importance of BMP2 in the skeleton is complicated by early embryonic lethality in mice lacking Bmp2, and by conservation of signaling pathways for osteogenic BMPs. To overcome these limitations, we established BMP2 conditional knockout mice (BMP2Prx1Cre) in which we inactivated Bmp2 only in the limb bud, effectively requiring the appendicular skeleton to form in the absence of BMP2. Here we report that BMP2Prx1Cre mice appear normal at birth but quickly develop pronounced defects in postnatal bone formation. At one week of age, the region specific expression of chondrocyte and osteoblast marker genes is conserved in limbs of BMP2Prx1Cre mice, but replacement of mineralized cartilage by bone and formation of secondary ossification centers are both significantly delayed. By week 2, the articular surfaces of the femur and tibia of BMP2Prx1Cre mice become increasingly fibrotic, and multiple spontaneous fractures are evident in femoral heads of BMP2Prx1Cre mice. At these sites, fracture callus formation is absent. As BMP2Prx1Cre mice age (17-28 weeks), they display significantly lower bone mineral density in appendicular skeletal elements compared to wild type and BMP2Prx1Cre heterozygous littermates. Spontaneous fractures that do not heal can be easily identified upon X-ray in these adult BMP2Prx1Cre mice. To test the bone repair capacity of adult BMP2Prx1Cre mice, we created transverse femur fractures in 30-week old mice and evaluated the time course of fracture repair. BMP2Prx1Cre mice showed no healing response at 10 or 21 days post fracture, in stark contrast to control mice where a robust healing response was evident by X-ray as early as day 10. Mice heterozygous for BMP2Prx1Cre showed an intermediate healing response, having little or no fracture callus on day 10, and a small callus on day 21. As a whole, our data are the first to indicate that locally produced BMP2 is absolutely required for normal postnatal bone formation and repair.

Disclosures: **K. Tsuji**, None.

1026

Targeted Deletion of BMP4 Causes Osteopenia in Adult Mice Supporting a Postnatal Role for BMP4 in Osteoblast Function and Bone Quality. D. Guo¹, W. Yang², M. Harris², J. Zhang¹, J. Feng¹, C. Anderson^{*3}, A. Lichtler⁴, B. Hogan^{*3}, H. Kullessa^{*6}, S. Liu^{*3}, L. Quarles^{*3}, B. Kream⁷, S. E. Harris². ¹Oral Biology, UMKC, Kansas City, MO, USA, ²Periodontics, UTHSCSA, San Antonio, TX, USA, ³Kansas U Medical Center, Kansas City, KS, USA, ⁴Genetics, U of Connecticut, Farmington, CT, USA, ⁵Genetics, Duke U, Durham, NC, USA, ⁶U of Vanderbilt, Nashville, TN, USA, ⁷Genetics and Developmental Biology, U of Connecticut Medical Center, Farmington, CT, USA.

In our previous study, a conditional knock-out mouse model was generated to determine the function of Bone morphogenetic protein 4 (BMP4) in postnatal development. BMP4 was successfully conditionally deleted (BMP4cKO) in osteoblasts by crossing 3.6kb collagen 1a1 promoter Cre transgenic mice with mice with one BMP4 floxed allele and one null allele. The resulting phenotypes showed incomplete penetrance and were sorted into three subtypes according to age at time of death. Type I (30%) were embryonic lethal. Type II showed severe osteopenia, small size, and prematurely died from hydronephrosis between 10 and 35 days after birth. Type III that constituted 65% survive beyond 35 days and show osteopenia with no hydronephrosis and normal kidney function as measured by BUN, calcium and phosphate. We have now focused on the skeletal changes in type III BMP4cKO with normal kidney function. Bones from adult (older than 2 months) BMP4 cKO were radiographed and compared to their sex-matched littermate controls with one copy of the normal BMP4 gene. Bone mineral density (BMD) in 9 month old BMP4 cKO were 7-18% lower than their control littermates, with significant changes observed in forelimbs, spine, calvaria and mandibles. The extent of BMD reduction was similar to the changes in 12-day-old and 1-month-old BMP4cKO, which were averaged from a combination of type II and III mutants. By both X-ray radiography and histology, the spines of BMP4 cKO show the greatest decreases in BMD in 9 month old animals, indicating a greater sensitivity of the vertebrae to BMP4 deletion. MicroCT analysis also showed similar reduction of cortical thickness, trabecular number and connectivity, and ratio of bone volume / total volume in the femurs from these 9 month old animals (n=3). Both type II (with hydronephrosis), and type III (without hydronephrosis) show this same bone phenotype, with the spine showing the most dramatic loss of bone. We have now confirmed the loss of BMP signaling in these adult BMP4 cKO mouse by reduced Osterix expression and other downstream genes of BMP signaling using in situ hybridization. Hydronephrosis is not responsible for the reduced BMD in BMP4 cKO, thus establishing BMP4 as an important direct contributor to bone quantity and quality in adult animals.

Disclosures: **D. Guo**, None.

1027

BMP-6 Restores Bone in Osteoporotic Aged Rats and, Unlike Estradiol and PTH, Restores Trabecular Bone in Ovariectomized BMP-6 Knockout Mice. P. Simic^{*}, J. Buljan-Culej^{*}, I. Orlic^{*}, F. Borovecki^{*}, S. Vukicevic. Laboratory for Mineralized Tissues, Zagreb Medical School, Zagreb, Croatia.

Bone morphogenetic proteins (BMPs) induce new bone formation when applied locally. However, there is no evidence that a recombinant BMP, given systematically, can restore bone in an osteoporotic rat model. Rats were ovariectomized at 6 months of age and the therapy started 6 months later. Total body, lumbar spine and hind limbs BMD was measured at 6 and 12 weeks period. Within three months, BMD in BMP-6 treated rats reached the values of sham treated animals at hind limbs and lumbar spine. BMP-6 was most effective at the lowest dose of 1 g/kg 3 times weekly. In vivo measurements were subsequently confirmed by ex vivo BMD values, by pQCT, μ CT and histomorphometry of distal femurs, and by biomechanical testing of long bones. In similar experiments BMP-7 was not effective, while estradiol was less effective, and did not have a synergistic effect with BMP-6. To further explore whether estradiol and PTH exerts their bone activity via BMP-6, Bmp-6 mutant and wild type mice were ovariectomized (OVX) and three weeks later treated for the next 6 weeks as follows: (1) sham, (2) OVX, (3) OVX + BMP-6 (10 μ g/kg i.v. 3xweek), (4) OVX + 17 β -estradiol (E2) (50 μ g/kg i.v. 3xweek) (5) OVX + PTH (75 μ g/kg s.c. 3xweek). As revealed by μ CT Bmp-6 $-/-$ sham animals had decreased BV/TV and trabecular number as compared to wild type sham mice. Unlike in wild type mice, OVX, estradiol and PTH therapy did not influence the BMD and trabecular bone volume in Bmp-6 $-/-$ mice. On the contrary, BMP-6 therapy increased BV/TV, trabecular number and trabecular thickness in Bmp-6 $-/-$ OVX mice to higher values than in sham animals. Gene expression profiling using femur mRNA of BMP-6 treated animals revealed significantly changed expression of extracellular matrix, cell cycle, growth factor/cytokine and transcription factor related genes, including procollagen type IX, fibronectin 1, IGF-1, EGF, cyclin D3, interleukins 12 and 17, respectively. Unlike estradiol and PTH, treatment with BMP-6 increased both osteoprotegerin and osteocalcin serum levels in wild type and Bmp-6 $-/-$ OVX mice. In conclusion, we demonstrate for the first time that systemically administered BMP-6 exerts both anti-resorptive and anabolic effects on restoring bone in aged OVX rats. Moreover, in OVX Bmp-6 $-/-$ mice BMP-6, but not estradiol and PTH, restores trabecular bone suggesting that both estradiol and PTH mediate at least partially their anabolic bone activity via BMP-6.

Disclosures: **S. Vukicevic**, None.

1028

SARAb Regulates BMP-Induced Gene Expression in Xenopus and Human Osteoblast Differentiation. W. Shi¹, C. Chang^{*2}, C. Sun^{*1}, J. Yang^{*1}, S. Nie^{*2}, J. Wang^{*1}, X. Li^{*1}, X. Cao¹. ¹Pathology, University of Alabama at Birmingham, Birmingham, AL, USA, ²Cell Biology, University of Alabama at Birmingham, Birmingham, AL, USA.

Signals of Transforming growth factor beta (TGF β) family are transduced by cytoplasmic Smad proteins. Smad Anchor for Receptor Activation (SARA) facilitates TGF β and activin/nodal signaling through recruitment of Smad2/3 to early endosomes to present them to the receptor complex. However, no similar protein has been identified for bone morphogenetic protein (BMP)/Smad1 pathway. In this study, a novel FYVE domain protein was found to bind specifically to Smad1 but not Smad2 and enhance Smad1 phosphorylation and nuclear localization upon BMP stimulation, and was therefore named SARAb. Expression of a small interfering RNA (siRNA) against SARAb results in decreased Smad1 phosphorylation. Disruption of the membrane-anchoring FYVE motif by a point mutation leads to reduction of BMP-responsive gene expression in cells. These data thus show for the first time that BMP signaling also requires a SARA-like molecule. Furthermore, it was demonstrate that similar to the Drosophila SARA, SARAb contains a protein phosphatase-binding motif, which functions to negatively modulate BMP signals through receptor dephosphorylation. Since BMPs play diverse roles during early Xenopus development, especially in embryonic dorsoventral patterning, to investigate whether SARAb can modulate BMP signaling *in vivo*, we examined the effect of SARAb overexpression on BMP-dependent endogenous mesodermal marker expression. We injected BMP4 RNA with or without RNAs encoding SARAb or SARAb mutants in animal poles of two-cell stage embryos and dissected animal caps from injected embryos at blastula stages 8.5-9. The caps were incubated to gastrula stages before total RNA was extracted for reverse transcription (RT)-PCR assay for marker gene expression. Injection of SARAb with mutant phosphatase binding domain (F872A) enhanced expression of BMP downstream genes including Xbra, Xhox3 and Xwnt8, further supporting the notion that recruitment of PP1c by SARAb for receptor dephosphorylation is a part of the negative feedback loop, and blockage of recruitment of PP1c enhances BMP *in vivo* function. More significantly, we observed that injection of SARAb FYVE(C735S) mutant or Smad binding domain Δ SBD mutant led to inhibition of the marker gene expression. Our data suggest that SARAb can modulate endogenous BMP-responsive gene transcription. Taken together, our results suggest that SARAb is an important component of the BMP signaling pathway and is capable of recruitment of R-Smads and negative feedback regulation of the BMP signals.

Disclosures: **W. Shi**, None.

1029

Sclerostin Inhibits BMP-Stimulated Bone Formation by Antagonizing Wnt Signaling. R. L. van Bezooijen¹, A. Visser^{*1}, G. van der Horst^{*1}, M. Karperien¹, S. E. Papapoulos¹, P. ten Dijke^{*2}, C. W. G. M. Löwik¹.

¹Endocrinology and Metabolic Diseases, Leiden University Medical Center, Leiden, The Netherlands, ²Molecular Cell Biology, Leiden University Medical Center, Leiden, The Netherlands.

Sclerosteosis is a rare skeletal dysplasia characterized by progressive bone thickening due to increased bone formation. It is caused by deficiency of the *SOST* gene product sclerostin, a negative regulator of bone formation secreted by osteocytes. The mechanism by which sclerostin inhibits bone formation is unclear. Sclerostin is a member of the DAN family of glycoproteins that share the capacity to antagonize BMP activity. Sclerostin binds BMPs and antagonizes their bone forming action without any preference for specific BMPs. Sclerostin's mechanism of action, however, is distinct from other BMP antagonists, since it does not antagonize direct BMP-induced responses such as Smad phosphorylation and BMP reporter construct, BRE-luc, activation. We have previously suggested two possible mechanisms by which sclerostin may antagonize BMP-stimulated bone formation. First, sclerostin may need a BMP inducible co-factor to antagonize BMP signaling. We tested this hypothesis and found that sclerostin did not antagonize BMP-stimulated BRE-luc activity after BMP pretreatment for 48 hours, a time period that should have facilitated production of a co-factor. Second, sclerostin may inhibit BMP-stimulated bone formation by antagonizing another yet unknown BMP-inducible growth factor. Wnts, for example, cooperate with BMPs to stimulate bone formation and other DAN family members also antagonize Wnt activity. We found that BMPs activated the Wnt reporter construct TBE-luc in mouse mesenchymal KS483 cells and sclerostin completely antagonized this action. Similarly, it antagonized TBE-luc activation by constitutive active BMP receptors Alk2 and Alk6, showing that in the absence of ligand-mediated BMP signaling sclerostin still inhibited Wnt signaling. Subsequently, we studied whether sclerostin antagonized Wnt-stimulated TBE-luc activity. Sclerostin indeed antagonized activation of TBE-luc by expression constructs for Wnt1, Wnt3, and Wnt3a. Remarkably, sclerostin did not antagonize recombinant human Wnt3a-induced TBE-luc activity. In conclusion, sclerostin does not antagonize early BMP signaling, but antagonizes BMP-stimulated Wnt signaling in osteoblastic cells. Furthermore, it antagonized Wnt1, Wnt3, and Wnt3a-induced signaling. These findings indicate that sclerostin, secreted by osteocytes, inhibits bone formation by antagonizing Wnt signaling in osteoblasts. High bone mass in sclerosteosis may, therefore, result from increased Wnt signaling due to the absence of sclerostin.

Disclosures: *R.L. van Bezooijen, None.*

1030

A Critical Point Mutation in the Runx2 Subnuclear Targeting Domain Abrogates Osteogenic Function by Blocking Integration of the BMP2 Signal. A. Javed, F. Afzal*, J. Bae*, S. Gutierrez*, S. K. Zaidi*, R. Devados*, M. Green*, A. J. van Wijnen, J. L. Stein*, G. S. Stein, J. B. Lian. Department of Cell Biology and Cancer Center, University of Massachusetts Medical School, Worcester, MA, USA.

The convergence of two regulatory pathways, BMP2 signaling and Runx2 transcriptional control, has been implicated as a requirement for bone formation *in vivo*. Genetic studies have shown that deletion of the Runx2 C-terminus which contains the Smad interacting domain (SMID) and the nuclear matrix targeting signal (NMTS) results in a complete loss of bone formation. We tested the hypothesis that Runx2 serves as a template for integration of the BMP signal by interacting with Smad. From a panel of nine point mutations within the SMID/NMTS domain of Runx2, we identified a critical triple mutant (tmRunx2) that abrogates Runx2-Smad physical association. This Runx2 mutant included a key tyrosine residue that is required for subnuclear targeting. Strikingly, mutation of this tyrosine alone did not affect formation of the Runx2-Smad complex. The tmRunx2, however, is deficient in its interactions with either BMP2 or TGF β responsive Smads and cannot integrate the BMP2/TGF β signal in promoter reporter assays. We next tested the ability of the wild type (WT) and tmRunx2 proteins to induce the program of osteoblast differentiation in a Runx2 null cell model. Cells were infected with WT and mutant Runx2 adenovirus and expression of a series of osteogenic markers was examined. The tmRunx2 exhibited a 30-40% reduction in activation of the COL-1, AP, OP, BSP, and OC marker genes compared to WT. Runx2 null cells are unresponsive to BMP2 treatment. When we examined integration of the BMP2 osteogenic signal by WT and mutant Runx2 proteins that retain Smad interaction, a robust induction of the osteoblast marker genes was observed. However, the tmRunx2 failed to activate the BMP2 induced osteogenic program. These studies demonstrate that the subnuclear targeting function and formation of a Smad-Runx2 osteogenic complex are functionally inseparable. Our results provide direct evidence for the role of nuclear architecture in organizing physiologically responsive BMP-Smad complexes as a mechanism that allows bone cell type-specific activity during osteogenesis.

Disclosures: *A. Javed, None.*

1031

Identification of Akp2 as a Gene that Regulates Peak Bone Mass in Mice. R. F. Klein, A. S. Carlos*, J. N. Kansagor*, D. A. Olson*, W. J. Wagoner*, E. A. Larson*, D. C. Dinulescu*, T. G. Munsey*, C. Vanek, D. L. Madison*, J. R. Lundblad*, J. K. Belknap*, E. S. Orwoll. Bone and Mineral Unit, Oregon Health & Science University, Portland, OR, USA.

The identification of genes underlying quantitative-trait loci (QTL) for complex diseases, such as osteoporosis, is a challenging and difficult task. We have previously identified a QTL on chromosome 4 (Chr 4) that is associated with variation in peak BMD in C57BL/6 (B6) and DBA/2 (D2) mice. Selective breeding was used to transfer the chromosomal fragment containing the Chr 4 QTL interval from D2 onto a B6 genetic background. Comparison of the resulting congenic (Cg) mouse strain with the background (Bgd) B6 strain established that a 65 megabase D2 genomic interval on Chr 4 in isolation confers increased peak whole body BMD (65.0 ± 0.6 mg/cm² vs. 61.2 ± 0.4 mg/cm², $p < 0.0001$) and femoral ultimate failure load (17.3 ± 0.8 N vs. 14.5 ± 0.5 N, $p < 0.01$). Examination of late pubertal animals (8-wk-old, when bone accrual rates are maximal) found serum alkaline phosphatase (ALP) activity reduced 43% (167 ± 8 U/L vs. 292 ± 11 U/L, $p < 0.0001$) in the B6 Bgd strain compared to the Cg strain but serum osteocalcin levels were similar. Bone histomorphometry revealed increased mineralizing surface, mineral apposition rates and bone formation rates in Cg mice when compared to the B6 Bgd mice. Sequencing of *Akp2* (which resides within the Chr 4 QTL and encodes ALP) identified an amino acid sequence variant at position 324 (B6 allele=Leu & D2 allele=Pro). This Pro residue is conserved in the homologous ALP genes of all vertebrates (human, rat, cow, dog, and cat) implicating an important functional role for this particular codon or region of the enzyme. Kinetic analysis of calvarial ALP from Chr 4 Cg and Bgd mice revealed no differences in enzymatic catalytic parameters. However, human osteoblastic U2OS cell cultures expressing the D2 ALP protein exhibited 50% more whole cell ALP activity, 70% more cell surface ALP activity and 4.8-fold more ALP activity in the conditioned medium compared to U2OS cell cultures expressing equivalent levels of the B6 ALP protein, suggesting that the B6 polymorphism may lead to aberrant intracellular processing and/or impaired cell surface localization of ALP. These results provide strong presumptive evidence that ALP is an important determinant of peak bone mass in laboratory mice. As the 1p36 chromosomal region harboring *TNSALP* (the human homolog of *Akp2*) has been linked to bone phenotypes relevant to osteoporosis in 3 different genome-wide linkage analyses, it is intriguing to consider that inherited differences in ALP activity may contribute to the natural variation in peak bone density and strength in human populations.

Disclosures: *R.F. Klein, Merck & Co. 8; Procter & Gamble 8; Sanofi Aventis 8; Eli Lilly 8.*

1032

The Role of the Trps1 Transcriptional Repressor in Endochondral Bone Formation. D. Napierala¹, K. Sam^{*2}, Q. Zheng^{*2}, G. Zhou², R. A. Shivdasani^{*3}, B. Lee¹. ¹Howard Hughes Medical Institute, Houston, TX, USA, ²Baylor College of Medicine, Houston, TX, USA, ³Dana-Farber Cancer Institute and Harvard Medical School, Boston, MA, USA.

Mutations in the *TRPS1* gene cause tricho-rhino-phalangeal syndrome (TRPS), a dominantly inherited skeletal dysplasia characterized by short stature, hip dysplasia, cone-shaped epiphyses, premature closure of growth plates, and distinctive craniofacial appearance. During mouse skeletal development *Trps1* is highly expressed in chondrogenic mesenchymal condensations, prehypertrophic chondrocytes and perichondrium. *Trps1* is a transcription repressor that contains nine zinc-fingers including GATA-type and Ikaros-type domains. To elucidate the role of *Trps1* in skeletogenesis, we analyzed *Trps1* mutant mice deleted for the GATA DNA-binding domain. Heterozygous mutant mice have normal appearance except of the craniofacial abnormalities with the shortening of the snout and a sloped down nose. Homozygous *Trps1* mutant mice die shortly after birth. Alcian blue and alizarin red staining of skeletons of new-born homozygous mutant mice demonstrated delayed ossification of vertebrae and sternum, and significantly reduced maxilla and mandible. Histological analysis of growth plates showed the elongation of prehypertrophic and hypertrophic chondrocytes zone and delay in endochondral ossification, which is more pronounced in homozygous mutant mice. To analyze the expression of genes involved in endochondral ossification, we performed quantitative real-time PCR on mRNA isolated from humerus of wild type and *Trps1* heterozygous mutant mice. This analysis showed dramatic increase of expression of chondrogenic markers - *col10a1* and *col2a1* as well as elevated expression of *Runx2*. *Runx2* is a key transcription factor involved in osteoblast differentiation and chondrocyte maturation. To test the potential interaction of *Trps1* and *Runx2*, we performed cotransfection studies in ROS17 and COS7 cell lines. In COS7 cells, *Trps1* strongly represses *Runx2* transactivation of the target 6xOSE reporter, which responds only to *Runx2* transactivation. The 6xOSE reporter is also down regulated in the presence of *Trps1* in ROS17 cells expressing high levels of endogenous *Runx2*. Moreover, the bone-related promoter of *Runx2* contains several potential GATA consensus sequences. *In vitro* analyses showed that *Trps1* forms complexes with each of these elements in COS7 but not in ROS17 cell lines. Our data suggest that *Trps1* regulates the cartilage to bone transition during endochondral ossification and that could be partially through inhibition of expression of the *Runx2* gene as well as *Runx2* protein function.

Disclosures: *D. Napierala, None.*

1033

A Knock-in Mouse Model for a Collagen Type X NC1 Domain Mutation Associated with Metaphyseal Chondrodysplasia Type Schmid (MCDS). M. H. Rajpar*, R. Eardley*, K. E. Kadler*, D. J. Thornton*, M. D. Briggs*, R. P. Boot-Handford*. Wellcome Trust Centre for Cell-Matrix Research, Faculty of Life Sciences, University of Manchester, Manchester, United Kingdom.

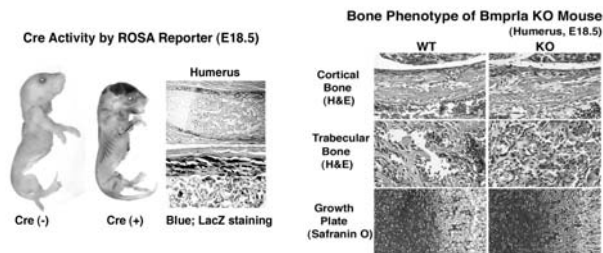
Metaphyseal chondrodysplasia type Schmid (MCDS) is an autosomal dominant disorder characterised by a shortened stature, waddling gait and *coxa vara*. Radiological findings include an irregular, widened growth plate and metaphyseal flaring. Numerous mutations in the collagen X gene (*COL10A1*) have been described in MCDS families, the majority of which are located in the C-terminal NC1 domain. Collagen X is synthesised by hypertrophic chondrocytes within the growth plate of developing bones. The disease mechanisms behind the pathology of MCDS remain controversial, with evidence for both a dominant interference effect, whereby the mutant protein interferes with the formation of normal homotrimers, and haploinsufficiency, where only 50% of the normal levels of collagen X are synthesised. Although a number of transgenic mouse *Col10a1* mutant models exist, there is currently no model which represents missense mutations causing the MCDS pathology in humans. We have utilised a gene targeting strategy to introduce the mouse equivalent of the MCDS N617K mutation into the mouse *Col10a1* gene. This mutation originally identified in an MCDS kindred, substitutes an asparagine residue for a lysine and is located on the outer surface of the NC1 homotrimer. A targeting construct containing the modified gene was integrated into the mouse genome using homologous recombination in R1 ES cells. Homologously recombined ES cells were identified, injected into blastocysts and implanted into pseudopregnant mice, resulting in high quality chimeric mice that have transmitted the mutation through the germline. Transgenic mice were analysed using x-ray imaging, monitoring of growth rate, bone measurements, skeletal preparations, histology, immunohistochemistry and RNA expression. Heterozygous offspring have no overt phenotype, displaying normal growth rates and fertility levels. Mice carrying two mutant alleles display a chondrodysplastic phenotype, characterised by reduced body weight and size, shortening of the long bones and dysplasia of the hip, and histologically, a disorganised growth plate. Expression of the mutant allele has been demonstrated by both RNA and immunohistochemical analyses. These results indicate that the mice carrying the N617K mutation have a phenotype reminiscent of that seen in the human condition, and will be used to investigate the disease mechanism underlying the pathology of MCDS.

Disclosures: **M.H. Rajpar**, None.

1034

Tamoxifen Induced Bone Morphological Protein Receptor 1A (*Bmpr1a*) Conditional Knockout Mice Display an Age-Dependent Phenotype in Long Bones Different from Calvariae. N. Kamiya*¹, L. Ye*², T. Kobayashi³, H. M. Kronenberg³, J. Feng², Y. Mishina*¹. ¹LRDT, NIEHS/NIH, Research Triangle Park, NC, USA, ²Oral Biology, School of Dentistry, University of Missouri-Kansas City, Kansas City, MO, USA, ³Endocrine Unit, Massachusetts General Hospital and Harvard Medical School, Boston, MA, USA.

Three type I receptors, BMPRIA(Alk3), BMPRIB(Alk6), and ActRI(ALK2), are responsible for signaling of the bone morphogenetic proteins. However, it is unclear what common and unique features these receptors share during bone development and remodeling. We previously rescued an early embryonic lethality of regular *Bmpr1a* KO mice in a later osteoblast-specific manner using Osteocalcin(Og2)-Cre and floxed *Bmpr1a* mice. The mutant mice showed reduced bone mass up to 3 months after birth, but bone mass was increased as they aged due to reduced bone resorption. To further investigate the age-dependent roles of BMPRIA in bone development and remodeling, the Cre-ERTM (a tamoxifen(TM) inducible Cre) mice were generated under the control of 3.2 kb type I collagen promoter. After TM injection into pregnant mice from day14 to day16, Cre activity was confirmed in osteoblasts and osteocytes in embryos at E18.5. A dramatic reduction of mineralization in long bone was observed in *Bmpr1a* CKO mice at E18.5. They showed thinner cortical and immature trabecular bone characters compared to littermates. The long bone cortex showed immature woven bone phenotype. On the other hand, calvaria of *Bmpr1a* CKO mice displayed a lamellar bone phenotype with large numbers of osteocytes at E18.5. Also, column formation of the growth plate was irregular. Interestingly, when TM was injected into newborn for three weeks, analysis of P21 showed more mature trabecular bone. Based on these observations, we propose that BMP signaling through BMPRIA is essential for early bone maturation and remodeling. Our results suggest that roles of BMPRIA are bone loci- and age-dependent, which may contribute to the diversity of bone shape and size.



Disclosures: **N. Kamiya**, None.

1035

Metabolic and Skeletal Consequences of a High Fat/Diabetogenic Diet on Bone Acquisition in a Congenic Mouse Strain with Altered Osteoblast Differentiation. C. Ackert-Bicknell, C. Marvin-Bivens*, J. Denegre*, L. Horton*, K. Shultz*, L. R. Donahue, W. Beamer, M. Boussein, C. Rosen. The Jackson Laboratory, Bar Harbor, ME, USA.

Congenic 6T mice were generated by backcrossing a 30 cM QTL region of Chr 6 from C3H/HeJ to C57BL/6(B6) 10 generations. Female 6T mice have low peak BMD, impaired bone formation due to decreased osteoblast (OB) differentiation, reduced liver and skeletal IGF-I, adipocyte infiltration in the marrow and liver, and more body fat vs B6. Three genes in the Chr6 QTL that can force a shift into the adipocyte lineage and alter OB differentiation show increased bone expression in 6T (i.e. *Klf15*, *Pparg*, *Alox 5*). To test their effect on bone acquisition, we fed either a reference (NIH31) diet (**RD**) or a high fat/sucrose diabetogenic diet (**HFD**) to female 6T and B6 mice post weaning for 13 wks. The diets consisted of the following: **RD**: protein:18%kcal, carbs: 71%kcal, Fat: 6%kcal, fiber: 5%; **HFD** protein:17% kcal, Carbs:51%kcal; Fat:32% kcal). At 16 wks, 6T mice fed **RD** had more hepatic fat droplets ($p<0.05$), lower vBMD ($p<0.01$), shorter femurs, decreased trabecular BV/TV ($p<0.01$), and reduced cortical thickness ($p<0.01$) vs B6 fed a **RD**. On a **RD**, 6T and B6 showed no differences in free fatty acids (FFA), calcium, triglycerides, (TG), insulin or glucose. But, on the **HFD** diet, B6 gained wt and increased body fat, had a rise in serum insulin ($p<0.05$), an elevated blood glucose (i.e. 200 mg/dL; $p<0.05$ vs **RD**), a decrease in IGF-I ($p<0.04$ vs **RD**) and greater free fatty acids. 6T mice on the **HFD** showed no change in body wt or fat, nor in any metabolic parameter (e.g. serum IGF-I, FFA,TG, serum insulin or glucose). In respect to bone, the **HFD** diet produced significant increases in trabecular BMD in 6T and B6 compared to the **RD** diet ($p<0.05$) such that 6T distal femoral BV/TV was fully rescued. On a **HFD** both strains had increases in periosteal circumference, while 6T had reduced femoral cortical BMD compared to **RD** fed 6T ($p<0.05$). B6 showed a significant reduction in femoral length on the **HFD** diet. In conclusion, 6T mice are protected from the insulin resistance/ diabetes syndrome in response to a **HFD** diet, a finding similar to the phenotype of the Pro12Ala mutation in the human *PPARG* gene. The **HFD** diet rescued the trabecular and periosteal, but not length or cortical phenotypes of 6T, without changing IGF-I. In the 6T mouse where OB differentiation is impaired and there is a shift into the adipocyte lineage, peak trabecular BMD can still be improved with a **HFD** diet. This suggests: 1) the OB and adipocyte differentiation programs *in vivo* are not mutually exclusive; 2) in 6T, the *Pparg* pathway is already activated;3) **HFD** diets can enhance peak BMD. Studies to identify the genes influencing acquisition of peak BMD and lineage allocation in 6T are ongoing.

Disclosures: **C. Ackert-Bicknell**, NIH AR45433 2.

1036

Different Epigenetic Variants of Pseudohypoparathyroidism Type-IB Are Associated with Distinct Mutations of *GNAS*. M. Bastepe¹, A. Linglart*¹, L. F. Fröhlich¹, H. Jüppner². ¹Endocrine Unit, Mass. General Hospital and Harvard Medical School, Boston, MA, USA, ²Endocrine Unit and Pediatric Nephrology Unit, Mass. General Hospital and Harvard Medical School, Boston, MA, USA.

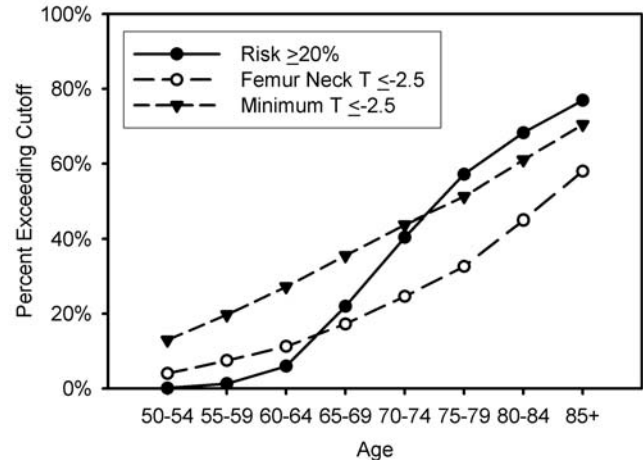
Pseudohypoparathyroidism type-Ib (PHP-Ib) is inherited only from maternal obligate carriers. The patients display genomic imprinting abnormalities of *GNAS*, including a loss of exon A/B methylation found in nearly all cases. We have previously identified, in multiple kindreds with autosomal dominant PHP-Ib (AD-PHP-Ib), a heterozygous 3-kb microdeletion in *STX16*, an apparently non-imprinted gene centromeric of *GNAS*. All the patients carrying this unique, maternally inherited 3-kb deletion show loss of exon A/B methylation without epigenetic defects at other *GNAS* differentially methylated regions (DMRs). Furthermore, in another AD-PHP-Ib kindred in whom affected individuals also display a loss of exon A/B methylation alone, we have identified a heterozygous 4.4-kb deletion within *STX16* that overlaps with the 3-kb deletion. Thus, in our cohort, 22 of the 23 patients who display isolated exon A/B defects carry mutations within *STX16*. In contrast, the remaining 21 sporadic and 2 familial PHP-Ib patients who show epigenetic defects at multiple *GNAS* DMRs, including exon A/B, do not appear to carry mutations within *STX16*. Recently, in the two familial cases with broad epigenetic defects, we have identified 4-kb and 4.7-kb deletions removing, in either case, the entire DMR containing exon NESP55 and exons 3 and 4 of its antisense transcript. After maternal transmission, each of the latter deletions causes loss of maternal *GNAS* imprints. However, similar large deletions at the NESP55 DMR have been excluded so far in all sporadic cases with broad methylation changes. Taken together, it appears that distinct genetic mutations lead to distinct epigenetic alterations within *GNAS*, which converge upon their phenotypic outcome, i.e. renal PTH-resistance. The latter is predicted to be affected by imprinting of exon A/B, which in turn determines expression of *Gsa* in renal proximal tubules. Based on the identified mutations, the region of overlap between the two *STX16* deletions (1.3 kb) likely contains a cis-acting element required for imprinting of maternal exon A/B, while the NESP55 DMR contains another cis-acting element required for imprinting of the entire maternal *GNAS* allele. The mutation(s) responsible for the *GNAS* defects in sporadic PHP-Ib cases remains to be determined. It may disrupt yet another imprinting control element, or alternatively, it is located in an entirely unlinked gene.

Disclosures: **M. Bastepe**, None.

1037

Comparison of Ten-Year Absolute Fracture Risk and WHO Risk Categorization in Menopausal Females. W. D. Leslie¹, K. Siminoski^{*2}, J. Brown^{*3}. ¹Faculty of Medicine, University of Manitoba, Winnipeg, MB, Canada, ²Dept. of Radiology, University of Alberta, Edmonton, AB, Canada, ³CHUL Research Centre, Laval University, Sainte-Foy, PQ, Canada.

There is increasing agreement that a risk-based approach to fracture risk assessment is preferable to risk categorization based upon bone mineral density (BMD) alone. How this might affect patient classification is unclear and needs to be clearly understood since there are large resource implications. We compared rates of high-risk classification in 17,053 women age 50 and older from a regional BMD program. This program maintains a large population-based database of clinical DXA results that has been previously described (JCD 2005;8:25-30). High-risk was designated according to 3 rules: femoral neck T-score ≤ -2.5 or below, minimum T-score (from L1-4, femoral neck, trochanter or total hip) ≤ -2.5 or below, or 10-year osteoporotic fracture risk (based upon age and femoral neck T-score) 20% or greater. The overall rates of high-risk categorization were 16.3%, 31.4%, and 20.3%, respectively ($P < 0.00001$ for all pairwise comparisons). 10-year fracture risk resulted in a lower rate of high-risk designation in women age 50-60, exceeded femoral neck categorization after age 65-69, and exceeded minimum site categorization after age 75-79. The overall rate of high-risk categorization with 10-year fracture risk 20% or above is slightly greater than with femoral neck BMD alone and much less than with a minimum T-score approach. Use of different risk cutoffs grossly over-classified (5%, 10%, 15%) or under-classified (25%, 30%) high-risk when compared with the conventional T-score based BMD thresholds. In conclusion, the use of 10-year fracture risk with a 20% high-risk threshold appropriately accentuates the age-related increase in fracture risk. Compared with BMD alone, its effect would be to de-emphasize risk in early menopausal women while emphasizing risk in older women.



Disclosures: *W.D. Leslie, None.*

1038

Long-Term Prediction of Incident Vertebral Fractures over 15 Years of Follow-Up: Data from the Study of Osteoporotic Fractures (SOF). M. C. Hochberg¹, L. Palermo^{*2}, J. Cauley³, K. Ensrud⁴, T. Hillier^{*5}, M. Nevitt⁶, S. R. Cummings⁶. ¹Medicine, University of Maryland, Baltimore, MD, USA, ²Epidemiology, University of California San Francisco, San Francisco, CA, USA, ³Epidemiology, University of Pittsburgh, Pittsburgh, PA, USA, ⁴Medicine, University of Minnesota, Minneapolis, MN, USA, ⁵Medicine, Kaiser Permanente Health System, Portland, OR, USA, ⁶Research, California Pacific Medical Center, San Francisco, CA, USA.

Prevalent vertebral fracture (VFX) is associated with an increased risk of incident VFX over a mean of 4 years; however, long-term predictors of incident VFX have not been examined. 2680 Caucasian women age 65 and above when they enrolled in SOF (mean [SD] 68.9 [3.3] years) had lateral lumbar and thoracic vertebral x-rays at baseline and a mean [SD] of 14.9 [0.7] years later (mean [SD] age 83.8 [3.3] years). Using vertebral morphometry, anterior (Ha), posterior (Hp) and mid-vertebral height (Hm) were measured. Prevalent VFX were considered present at baseline if any of the following ratios (Ha/Hp; Hm/Hp; Hp(i)/Hp(i-1) and Ha(i)/Ha(i-1); or Hp(i)/Hp(i+1) and Ha(i)/Ha(i+1)) was > 3 SDs below the "trimmed" mean. Incident VFX were defined as a decrease of at least 20% and 4mm in vertebral height at any level. Risk factors were measured at baseline except for bone mineral density (BMD) at the proximal femur; this was measured at the 1st follow-up visit 2 years after baseline. Multiple variable logistic regression analysis was used to estimate the odds ratio (95% confidence intervals) of incident VFX; all analyses were adjusted for baseline age and clinic. 492 (18.4%) of the 2680 women had an incident VFX during follow-up, including 164 (41.6%) of 394 with and 328 (14.3%) of 2286 without a prevalent VFX at baseline (aOR = 4.15 [95% CI: 3.28, 5.25], $P < .001$). Additional risk factors that were independently associated with incident VFX were included in the final multiple variable logistic regression model; results from this model are shown in the Table. There were no significant first-order interactions between prevalent VFX and any of these other risk factors. We conclude that having a prevalent VFX is associated with a 3 to 4-fold

increased risk of developing an incident VFX among long-term survivors even after 15 years. fractures. Older women with prevalent VFX should receive treatment to decrease their long-term risk of incident VFX.

Factors Associated with Incident VFX (adjusted for all other variables in the table)	
Variable	Odds Ratio (95% CI)
Prevalent VFX	3.21 (2.49, 4.14)
Age (per 5-years)	1.51 (1.29, 1.77)
Total Hip BMD (per SD)	1.65 (1.44, 1.88)
Nonspine Fx after age 50	1.40 (1.12, 1.76)
Fall in last 12 months	1.37 (1.09, 1.74)
Current smoker	1.44 (0.97, 2.14)
Body mass index (per SD)	0.89 (0.79, 1.01)

Disclosures: *M.C. Hochberg, None.*

1039

Osteoprotegerin Promoter Polymorphism, Bone Density and the Risk of Hip Fracture in Older Women. J. I. Oakley¹, J. M. Zmuda¹, S. P. Moffett¹, K. L. Stone², L. Y. Lui², J. Li^{*3}, J. A. Cauley¹, B. C. Taylor⁴, T. A. Hillier^{*5}, W. Browner^{*6}, M. C. Hochberg^{*7}, G. Peltz^{*8}, S. R. Cummings⁶. ¹Epidemiology, University of Pittsburgh, Pittsburgh, PA, USA, ²Epidemiology and Biostatistics, University of California, San Francisco, CA, USA, ³Human Genetics, Roche Molecular Systems, Alameda, CA, USA, ⁴General Internal Medicine, Veterans Affairs Medical Center, Minneapolis, MN, USA, ⁵Kaiser Permanente Center for Health Research Northwest/Hawaii, Portland, OR, USA, ⁶Research Institute, California Pacific Medical Center, San Francisco, CA, USA, ⁷Medicine and Epidemiology and Preventive Medicine, University of Maryland, Baltimore, MD, USA, ⁸Roche Biosciences, Palo Alto, CA, USA.

Osteoprotegerin (OPG) is a soluble decoy receptor that blocks osteoclastic bone resorption. We performed genetic association analyses of an A163G promoter polymorphism at the OPG locus, bone mineral density (BMD) and the risk of incident fracture among 6695 women aged 65 years and older in the prospective Study of Osteoporotic Fractures (SOF). We confirmed 700 incident hip (366 femoral neck, 334 intertrochanteric) and 510 incident wrist fractures by review of medical records during 13.6 years of follow-up (91,249 person-years). BMD was measured by DXA (Hologic QDR). The OPG polymorphism was genotyped in the context of a multiplex PCR followed by allele-specific SNP detection with immobilized oligonucleotide probes in linear arrays. Women who were homozygous for the less common G allele had significantly lower BMD at the total hip than those who were homozygous for the wild-type A allele (G/G: 0.74 ± 0.15 vs. A/A: 0.76 ± 0.13 ; $p = 0.009$). Similar reductions were observed for all sub-regions of the hip. Previous studies in the SOF cohort showed that family history of hip fracture predicts femoral neck but not intertrochanteric fractures. Thus, we analyzed the risk of these fractures separately by OPG genotype. Compared with A/A homozygotes, G/G homozygotes had an 82% greater risk of femoral neck fracture (RR: 1.82; 95% CI: 1.02-3.24) ($p = 0.04$). In contrast, the OPG polymorphism was not significantly associated with intertrochanteric fractures (RR: 0.86; 95% CI: 0.35-2.08). The association between OPG genotype and femoral neck fracture was attenuated and no longer statistically significant after adjusting for the lower femoral neck BMD in women with the G/G genotype (RR: 1.46; 95% CI: 0.82-2.61). There were no significant associations between OPG genotype and risk of wrist fracture. Older women with the G/G genotype of the OPG promoter polymorphism, or a closely linked allelic variant, may have a lower hip BMD and an increased risk of femoral neck fracture.

Disclosures: *J.I. Oakley, None.*

1040

Beta2 Adrenergic Receptor, Beta-Blockers and their Influence on Bone Mass in Humans: The Framingham Osteoporosis Study. S. Ferrarini¹, S. Demissie^{*2}, D. Karasik³, L. A. Cupples^{*4}, A. Imamovic^{*5}, J. Dupuis^{*4}, D. P. Kiel¹. ¹Geneva Univ Hosp, Geneva, Switzerland, ²BU Sch Pub Health & Prog Genom Applic, Boston, MA, USA, ³Hebrew SeniorLife, Boston, MA, USA, ⁴BU Sch Pub Health, Boston, MA, USA, ⁵BU Dept Neurol, Boston, MA, USA.

Beta 2 adrenergic receptors (ADRB2) regulate bone turnover. Beta-blockers (BB) increase bone mass in mice, and have been associated with higher BMD in postmenopausal women, but this association has not been confirmed. Whether ADRB2 signaling influences bone mass in humans remains uncertain. We examined the association of ADRB2 polymorphisms with BMD at the spine (LS), femoral neck (FN), and troch (FT) by DXA and their interaction with BB in 776 females and 740 males from the Framingham Offspring Cohort. Six SNPs, including two missense substitutions (Arg16Gly and Gln27Glu) affecting ADRB2 down-regulation, were determined within three ADRB2 LD regions. Main and interaction effects ANCOVA models were used to analyze BB and ADRB2 effects on BMD, adjusting for sex, age and estrogen (in women) (model 1), additionally for height and BMI (model 2), and for cardiovascular diseases (CVD, model 3). Mean age (\pm SD) was 61.3 ± 9.1 yrs. 274 women and men used BB, including 63 using non-beta1 selective beta-blockers (NSBB). In men and women together, BB users had higher BMD at all sites (BB, $P = 0.0004$ -0.017; NSBB, $P = 0.004$ -0.05, model 1). After adjusting for height and BMI, these effects remained significant only at LS (BB, $P = 0.04$; NSBB $P = 0.033$, model 2), but not after adjusting for CVD (model 3). In women, but not in men, associations with BMD were found for the T>C SNP in LD region 1, G>A SNP in LD region 3, and Gln27Glu and Arg16Gly SNPs in LD region 2. In females significant interactions with BB occurred for ADRB2 genotypes in LD regions 2 and 3.

ASBMR 27th Annual Meeting

P values for ADRB2 genotype associations and interactions with BB on BMD in women (model 2)				
	T>C Block 1	G>A Block 3	Gln27Glu Block 2	Arg16Gly Block 2
BMD	P assoc. P inter.	P assoc. P inter.	P assoc. P inter.	P assoc. P inter.
FN	0.058 ns	0.001 0.025	0.03 0.025	0.05 0.028
FT	0.035 ns	0.005 0.01	0.08 0.002	0.068 .0016
LS	0.037 ns	0.11 0.03	ns 0.088	ns 0.11

Further adjustment for CVD (model 3) did not alter these results. After excluding women on NSBB (n=31), haplotype analysis indicated that BMD and BUA decreased 1-3% at all sites per copy of the Arg16-Gln27 haplotype (freq 36%, p<0.05, model 3). In conclusion, evidence that ADRB2 genetic variation is associated with BMD in women supports a role of the adrenergic pathway in the regulation of bone mass in humans. Although doses of beta-blockers commonly used to treat CVD are unlikely to increase BMD overall, interactions between BB and ADRB2 polymorphisms suggest that BB might influence bone mass in distinct genotypic sub-groups.

Disclosures: **D.P. Kiel**, None.

1041

Sex Hormone Levels and Risk of Falling in Community-Dwelling Older Persons: A Prospective Study. **H. A. Bischoff-Ferrari¹, J. E. Orav², B. Dawson-Hughes³.** ¹Medicine, Brigham and Women's Hospital, Boston, MA, USA, ²Biostatistics, Harvard School of Public Health, Boston, MA, USA, ³Jean Mayer USDA Human Nutrition Research Center on Aging, Tufts University, Boston, MA, USA.

Background: Little is known how sex hormone levels affect the risk of falling in older persons. **Aim:** To prospectively assess the risk of falling in older men and women based on baseline sex hormone levels. **Methods:** 199 men and 246 women age 65 or older living at home were followed prospectively for 3 years after baseline assessment of estrone, estradiol, total testosterone, free testosterone, androstenedione, dihydroepiandrosterone (DHEA) and sex hormone binding globulin (SHBG). Falling at least once was the primary outcome using logistic regression analysis. All hormones were evaluated by gender, controlling for age, body mass index, baseline 25-hydroxyvitamin D levels, baseline physical activity, smoking, alcohol use, number of comorbid conditions, maximal follow-up and vitamin D plus calcium treatment. Testosterone and estrogen levels were also adjusted for SHBG. **Results:** In 3 years 49% of men and 57% of women suffered at least 1 fall. Men in the highest quartile of total testosterone (≥ 5.7 ng/ml) had a 78% decreased odds of falling compared to men in the lowest quartile with serum levels below 3.8 ng/ml (OR = 0.22; 95% CI [0.07,0.72]). Conversely, men in the top quartile of SHBG (≥ 65.5 ng/l) had a 3.9-fold increased odds of falling compared to those in the lowest quartile with serum levels below 41.1 ng/l (OR = 3.90; 95% CI [1.09,13.93]). Similar to men, women in the top quartile of testosterone levels (≥ 0.49 ng/ml) had a 66% decreased odds of falling compared to those in the lowest quartile with serum levels below 0.20 ng/ml (OR = 0.34; 95% CI [0.14,0.83]). While there was no effect of SHBG in women, women in the top quartile of DHEA (> 0.76 mcg/ml) had a 61% lower odds of falling compared to those in the lowest quartile with serum levels below 0.31 mcg/ml (OR = 0.39; 95% CI [0.16,0.93]). While there was a significant positive trend between higher testosterone levels and fall protection in both genders (men: p = 0.008; women: p = 0.03), there appeared to be a threshold effect with equally strong protection in the second, third and top quartile for SHBG in men and DHEA in women. Estrone, estradiol, free testosterone and androstenedione did not predict falling in men or women. **Conclusion:** Independent of other important risk factors of falling, higher total testosterone in both genders and higher DHEA levels in women appear to reduce the odds of falling by over 60%. On the other hand, high SHBG levels appear to increase the odds of falling in men almost 4-fold. Other sex hormones were not appreciably associated with falling in community-dwelling older persons.

Disclosures: **H.A. Bischoff-Ferrari**, None.

1042

Long Term Effects of a Randomised Controlled Trial (RCT) of Osteoporosis Screening on the Use of Medication and Fracture Risk. **R. J. Barr¹, A. Stewart¹, D. J. Torgerson², D. M. Reid¹.** ¹Medicine and Therapeutics, University of Aberdeen, Aberdeen, United Kingdom, ²Health Economics, University of York, York, United Kingdom.

Osteoporosis is a common condition occurring in 1 in 2 women but current management is unsatisfactory because it is generally not introduced until a major fracture has occurred. Population screening programmes are one means to identify menopausal women with low bone mineral density (BMD) and an elevated risk of future fracture but require to be proven effective in a RCT. In 1993 a random sample of 4800 women aged 45-54 years living within 32km of Aberdeen, Scotland, was selected from a primary health care register. Subjects were randomised in equal numbers to screening (active (A)) or no screening (inactive controls (C)). Only the active women were assessed and those found to be in the lowest quartile of BMD were suggested to consider HRT treatment and informed about other lifestyle factors to reduce fracture risk. Nine years after randomisation a follow-up questionnaire was mailed to both groups to assess the effect of screening on the uptake of treatment and on the incidence of fractures. Response rates after 9 years were C=56.8% and A=59.7%. No significant differences between the groups were observed in: age, weight, height or self-reported general health, nor in self-reported disease states with the exception of hyperparathyroidism (C=0.5% A=1.1%, p=0.05). 52.4% of the active

group reported taking HRT compared with 44.5% of the control group (p<0.001). No significant difference was observed in the mean duration of HRT use (C=86.0 months A=84.0 months p=0.58). Similarly the active subjects were significantly more likely to report current or past use of vitamin D, calcium, alendronate, etidronate or raloxifene than the control subjects (36.6% of the active group and 21.6% of the control group reporting to have taken some form of osteoporosis medication, excluding HRT, (p<0.001)). A significantly greater number of the active group not advised to take HRT at screening compared with the control group had taken HRT (49.7% vs 44.5%, p=0.017). This trend was repeated in the use of other osteoporosis medications. In a per protocol analysis of self-reported incident fractures a 23.7% reduction in fractures (of any site) in the active group was observed (RR=0.763 95%CI=0.579-1.006) which increased to 25.2% following adjustment for age, weight and height (RR =0.748, 95%CI=0.567-0.986). No significant difference was observed in the number of fallers (C=13.9% A=15.6%, p=0.202) or the rate of falls (C=0.28falls/year A=0.30falls/year, p=0.503). Screening for low bone density significantly increases the use of HRT and other treatment for osteoporosis and reduces fracture incidence.

Disclosures: **R.J. Barr**, None.

1043

FSH Directly Regulates Bone Mass: Implications for Understanding the Pathogenesis of Osteoporosis Due to Hypogonadism. **L. Sun¹, Z. Zhang^{*1}, Y. Peng^{*1}, I. Iqbal^{*1}, S. Zaidi^{*1}, D. J. Papachristou^{*2}, H. Zhou^{*1}, A. C. Sharrow^{*2}, B. B. Yaroslavskiy^{*2}, L. Zhu^{*1}, A. Zallone^{*3}, M. R. Sairam^{*4}, T. R. Kumar^{*5}, L. Cardoso-Landa^{*1}, M. B. Schaffler¹, B. S. Moonga^{*1}, H. C. Blair², M. Zaidi¹.** ¹Medicine, Mt. Sinai School of Medicine and the Bronx VA GRECC, New York, NY, USA, ²Medicine, University of Pittsburgh, Pittsburgh, PA, USA, ³Medicine, University of Bari, Bari, Italy, ⁴Medicine, Clinical Research Institute of Montreal, Montreal, ON, Canada, ⁵Medicine, University of Kansas, Kansas City, KS, USA.

Hypogonadal bone loss is thought to arise solely from declining estrogen. Nonetheless, due to a loss of estrogenic feedback, pituitary-derived serum FSH levels increase. Here we report that FSH (ligand) and FSH β receptor (FSHR) null mice have normal bone mass despite severe hypogonadism. Histomorphometry and micro-CT revealed that trabecular bone volume, cortical bone thickness and osteoclast resorption surfaces in null mice were not different from wild type littermates. Flow cytometry of bone marrow cells revealed no differences in osteoclast precursor populations. Together, the results establish that FSH is required for hypogonadal bone loss. Interestingly, bone mass was *increased* and osteoclast resorption surfaces decreased in haplo-insufficient FSH $\beta^{+/-}$ mice with intact ovarian function. This suggests that FSH acts on osteoclasts independently of estrogen. In parallel, we find that osteoclasts possess FSH receptors (FSHRs) coupled to the inhibitory G-protein, Gi; that FSH directly stimulates osteoclast formation, function and survival; and that these FSH-induced enhancements are Erk1/2- and Akt-mediated. Real time PCR, Western blotting, flow cytometry and confocal microscopy together revealed that FSHRs are present on both murine and human osteoclasts, but not on osteoblasts. FSH (3 to 100 ng/ml) stimulated RANK-L-induced osteoclast differentiation from hematopoietic stem cell precursors; no responses were observed with the related glycoprotein hormones LH and GnRH. FSH also stimulated Erk1/2 phosphorylation and c-fos nuclear translocation, both of which were pertussis toxin-inhibitable. In the pit assay, FSH (3 to 30 ng/ml) stimulated osteoclastic bone resorption; this likely resulted from the observed enhancements in actin ring formation (phalloidin staining) and acid secretion (lysotracker accumulation). Finally, FSH supported the survival of osteoclasts by enhancing Akt phosphorylation and reducing apoptosis (annexin V staining). Together, the results suggest that FSH, by stimulating osteoclastic bone resorption, contributes to the hypogonadal bone loss that has been attributed solely to declining estrogen. Potential therapeutic implications may eventually follow.

Disclosures: **L. Sun**, None.

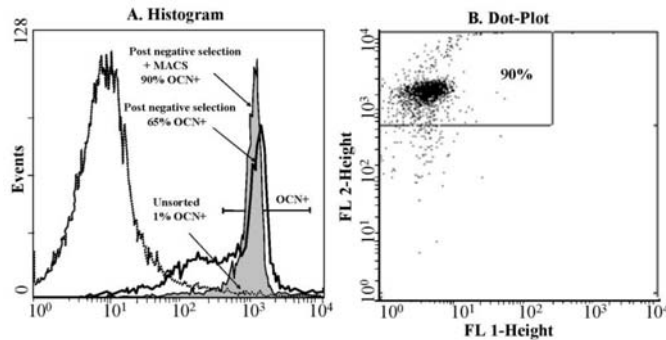
1044

Purification and Characterization of Circulating Osteoblast Lineage Cells: Expression of Type I Collagen mRNA Is a Key Difference between these and Adherent Bone Marrow Stromal Cells. **G. Z. Eghbali-Fatourehchi, S. Khosla.** Mayo Clinic, Rochester, MN, USA.

We recently reported on circulating osteoblastic cells in humans expressing osteocalcin (OCN) and/or bone alkaline phosphatase (BAP) (*NEJM, in press*). To further characterize these cells, we first tested for co-expression of OCN, BAP, RANKL, and the hematopoietic/endothelial progenitor marker, CD34. Using flow cytometry, we found that 57% of OCN+ cells were BAP+, whereas only 29% of BAP+ cells were OCN+. 51% and 62% of OCN+ and BAP+ cells, respectively, were CD34+, while 57% and 43% of each were RANKL+. To obtain highly purified populations of human OCN+ and BAP+ cells, we performed sequential negative selection (resulting in removal of cells expressing hematopoietic or myeloid markers) followed by magnetic cell sorting (MACS) using monoclonal antibodies to OCN or BAP. The Figure shows flow cytometry histograms of cell numbers vs. fluorescence intensity using the OCN antibody following each selection step for OCN+ cells (**A**). Cells isolated following this sequential enrichment were ~ 90% homogeneous for OCN or BAP expression (**B**). These highly purified circulating OCN+ and BAP+ cells were analyzed for gene expression in comparison with a well characterized, adherent human bone marrow stromal cell line (hMS 2-15 [JBMR 13:205, 1998]). OCN+ and BAP+ cells expressed similar levels of OCN mRNA and ~50 fold higher AP mRNA levels as compared to hMS 2-15 cells. By contrast, hMS 2-15 cells expressed 500 and 100 fold higher mRNA levels for type 1 collagen $\alpha 2$ (col1 $\alpha 2$) compared to BAP+ and OCN+ cells, respectively. The marked difference in col1 $\alpha 2$ mRNA

ASBMR 27th Annual Meeting

levels in adherent bone marrow stromal vs. circulating osteoblastic cells suggests that adherence to extracellular matrix may be necessary for maximal expression of collagen by the circulating osteoblastic non-adherent cells. Consistent with our data, a previous report (J Cell Biol 153:1133, 2001) has demonstrated high levels of collagen type I but absent AP expression in circulating adherent osteoblastic cells, although non-adherent circulating osteoblastic cells were not examined in that study. Finally, our method for obtaining highly purified osteoblast lineage cells from human blood should greatly facilitate studies examining changes in gene and/or protein expression in these cells in patients with osteoporosis and other metabolic bone disorders.



Disclosures: G.Z. Eghbali-Fatourechi, None.

1045

Spontaneous Fractures in the Mouse Mutant *Sfx* Are Caused by Deletion of Gulonolactone Oxidase (GULO) Gene, Causing Vitamin C Deficiency: Evidence that Vitamin C Is a Critical Determinant of ATP Synthesis in Differentiating Osteoblasts. S. Mohan¹, A. Kapoor^{*1}, A. Singgih^{*1}, Z. Zhang^{*1}, T. Taylor^{*1}, H. Yu^{*1}, R. Chadwick¹, Y. Chung^{*1}, L. Donahue^{*2}, G. Crawford^{*2}, C. Rosen^{*2}, J. E. Wergedal¹, D. J. Baylink¹. ¹JLP VAMC and LLU, Loma Linda, CA, USA, ²Jackson Labs, Bar Harbor, ME, USA.

To identify the genetic basis for osteoporotic fractures, we utilized a mouse model that develops spontaneous fractures (*sfx*) at an early age. After weaning, the *sfx/sfx* mice exhibited impaired somatic growth, reduced motility, *sfx* and died at 6-8 wks of age while *+sfx* mice were indistinguishable from *+/+* mice. Femur and tibial BMD were reduced by 30% in *sfx* mice at 5 wks of age. Histomorphometric analyses of bones from *sfx* mice revealed that mineral apposition rate was decreased by >80%, implying reduced osteoblast (OB) activity in *sfx* mice. The *sfx* gene was fine mapped to a 2MB region containing 30 genes in chr. 14. We have identified the GULO gene (38146 bp region), involved in the synthesis of ascorbic acid (AA), is responsible for the *sfx* phenotype as treatment of *sfx* mice with AA rescues the phenotype (Mohan et al., JBMR, in press). To identify the molecular pathways that contribute to impaired OB cell function, we performed a microarray analysis using 20,000 mouse oligo probes to identify genes differentially expressed in the bones of *sfx*. We found expression levels of several genes related to mitochondrial energy metabolism were severely compromised in the bones of *sfx* mice. We next used bone marrow stromal (BMS) cells derived from *sfx/sfx* mice as an *in vitro* model to test if AA deficiency influences ATP synthesis. We found that BMS cells derived from *sfx* mice are able to form mineralized nodules only when treated with AA which was associated with several-fold increase in the expression levels of collagen, ALP and osteocalcin and an 8-fold increase ($P<0.001$) in cellular ATP levels. Because of the established importance of glycerol 3-phosphate (G3P) shuttle in the generation of ATP, we evaluated if AA regulates G3P shuttle. Accordingly, we found that 24 h AA treatment caused a 3-fold ($P<0.01$) increase in expression of cytosolic G3P dehydrogenase (G3PD1) in BMS cells derived from *sfx* mice. The expression levels of G3PD1 but not G3PD2 increased by 20-fold during *in vitro* differentiation of BMS cells into OBs in the presence of AA. Conclusions: 1) The *sfx* mouse has a mutation of the GULO gene, which leads to AA deficiency, impaired OB cell function and fractures in the affected mice; 2) AA may be required for ATP production, OB differentiation via a G3P shuttle; and 3) Adequate vitamin C uptake may be critical in attaining and maintaining peak BMD in humans as they lack GULO gene and are therefore completely dependent on diet for vitamin C.

Disclosures: S. Mohan, None.

1046

Adipose Tissue Is a Negative Independent Predictor of Cortical Bone Size in Non-Weight Bearing Bones in Young Men; an Association Mediated by Leptin - The GOOD Study. M. Lorentzon, S. Movérare Skrtic, D. Mellström, C. Ohlsson. Center for Bone Research at the Sahlgrenska Academy, Departments of Internal Medicine and Geriatrics, Gothenburg University, Gothenburg, Sweden.

Adipose tissue (AT) is believed to exert a stimulatory effect on bone mass acquisition primarily due to increased mechanical loading on the bones. Due to the limitations of the DXA technique, the association between AT, leptin and volumetric BMD (vBMD) and size of the different bone compartments, i.e. cortical and trabecular bone, remains unknown. The aim of this study was to determine the role of AT and leptin as independent predictors of cortical bone size in weight bearing and non-weight bearing bones. We measured the cortical bone size and vBMD (at the diaphysis), trabecular vBMD (at the metaphysis) of the radius and tibia (pQCT), total body lean mass (DXA), total body AT (DXA), and serum

leptin levels in 1068 men (age 18.9±0.6 yrs) included in the Gothenburg Osteoporosis and Obesity Determinants (GOOD) study. A multiple linear regression model, including age, height, total body lean mass, present physical activity, calcium intake, smoking, and total body AT, was used to determine the independent predictors of cortical bone size as well as cortical and trabecular vBMD of the non weight bearing radius and the weight bearing tibia. Total body AT was a negative independent predictor of cortical bone size (cortical cross sectional area (CSA): $\beta=-0.09$, $p<0.001$, and periosteal circumference (PC): $\beta=-0.07$, $p<0.01$) of the radius but a positive independent predictor of the cortical bone size of the tibia (cortical CSA: $\beta=0.06$, $p<0.01$, and PC: $\beta=0.08$, $p<0.001$). When leptin was added to this multiple regression model, leptin was found to be a negative independent predictor of the cortical CSA of both the radius ($\beta=-0.07$, $p=0.04$) and tibia ($\beta=-0.06$, $p=0.048$). Serum leptin levels were not associated with cortical or trabecular vBMD of the radius or tibia. After adding leptin to the multiple linear regression model, total body AT was no longer a negative independent predictor of any parameter of cortical bone size of the radius, but was still a positive independent predictor of the cortical bone size of the tibia, suggesting that leptin is a mediator of the negative association between adipose tissue and cortical bone size of the non-weight bearing bone. The present findings suggest that AT exerts a positive effect on cortical bone size in bones subjected to mechanical loading, while it influences cortical bone size negatively in the non-weight bearing bone. Our data indicate that the negative role of AT on cortical bone size of the non-weight bearing bone is mediated via serum leptin levels.

Disclosures: S. Movérare Skrtic, None.

1047

Regulation of Bone Formation by Adiponectin through Autocrine/Paracrine and Endocrine Pathways. Y. Shinoda*, M. Yamaguchi*, N. Ogata, T. Akune, T. Kadowaki*, Y. Takeuchi, S. Fukumoto, K. Hoshi, U. Chung, K. Nakamura, H. Kawaguchi. Orthopaedic Surgery and Internal Medicine, University of Tokyo, Tokyo, Japan.

Accumulated evidence has shown that there is a common regulation of bone and adipose tissues. Leptin, a representative adipokine, has been reported to be a powerful inhibitor of bone formation. The present study investigated the regulation of bone metabolism by adiponectin, another representative adipokine, that is known to increase the sensitivity to insulin. We initially found by RT-PCR analysis that adiponectin and its receptors AdipoR1 and AdipoR2, but not leptin, were expressed in mouse calvarial primary osteoblasts (POB), M-CSF-dependent bone marrow macrophages, and osteoclasts, indicating that adiponectin can act on bone through an autocrine/paracrine pathway as well as an endocrine pathway. We then generated adiponectin-deficient (Ad-/-) mice and investigated the role of adiponectin in bone. These mice developed and grew normally, and showed no abnormality in bone mass or turnover as determined by radiological and histomorphometric analyses, implying an equivalent balance of the pathways above. In the cultures of POB derived from the Ad-/- mice, osteogenesis determined by ALP and Alizarin red stainings, but not osteoclastogenesis determined by TRAP staining, was markedly decreased compared to that in the wild-type culture, indicating a positive action of endogenous adiponectin through the autocrine/paracrine pathway on bone formation. To examine the endocrine action, we added recombinant adiponectin in the cultures of POB and marrow cells, and found that the direct action inhibited osteogenesis. However, in the presence of insulin or IGF-I, potent stimulators of bone formation, immunoprecipitation and immunoblotting analyses revealed that recombinant adiponectin enhanced the insulin/IGF-I-induced phosphorylation of IRS-1 and Akt, the main signaling molecules, suggesting indirect stimulation on bone formation. We then examined the endocrine action *in vivo* by generating transgenic mice that overexpressed adiponectin driven by the serum amyloid P component promoter, so that the expression was limited to the liver. The mice showed no abnormality in bone mass or turnover, possibly due to an equivalent balance of the direct and indirect actions of circulating adiponectin. The lines of results indicate that adiponectin regulates bone formation in three distinct pathways: a positive action through the autocrine/paracrine pathway by locally produced adiponectin, a negative action through the direct pathway by circulating adiponectin, and a positive action through the indirect pathway by circulating adiponectin that enhances the insulin/IGF-I signaling.

Disclosures: Y. Shinoda, None.

1048

Effects of Central Leptin Gene Therapy on Weight Reduction and Cancellous Bone Mass in Female Rats. U. T. Iwaniec, S. Boghossian*, M. G. Dube*, R. Torto*, R. R. Arzaga*, T. J. Wronski, S. P. Kalra*. University of Florida, Gainesville, FL, USA.

Obesity is one of the fastest-growing health problems worldwide, not only in adults but in children as well. Central leptin gene therapy (the delivery of the leptin gene into the hypothalamus for a sustained supply of the hormone in the brain) has the potential for long-term control of obesity as it has proven very effective in preventing age-associated increases in body weight in rats fed normal and high-fat diets. However, as hypothalamic administration of leptin has been shown to decrease bone mass in mice, osteopenia constitutes a potential adverse side-effect of leptin gene therapy. The objective of this study was to evaluate the effects of centrally administered, recombinant adeno-associated virus-leptin (rAAV-lep) gene therapy on bone in rapidly growing and sexually mature female Sprague-Dawley rats. Three-week old rats were implanted with cannulae in the 3rd ventricle and injected with either rAAV-lep (n=10) or rAAV-GFP (control vector encoding green fluorescent protein, n=10) and maintained on standard rat chow fed *ad lib* for 43 weeks. Proximal tibiae were then collected and processed for cancellous bone histomorphometry. rAAV-lep administration evoked a sustained decrease in body weight gain (33-35% lower in rAAV-lep than in rAAV-GFP rats) throughout the course of the experiment (Pediatr. Res. 52:189-98). At 43 weeks post-vector injection, cancellous bone

ASBMR 27th Annual Meeting

volume was 37% lower in rAAV-lep rats than in the rAAV-GFP rats (20±2.0% vs. 12.5±1.0%, mean±SE). In order to determine if similar changes were observed in sexually mature animals, 12-week old rats were implanted with cannulae and injected with either rAAV-lep or rAAV-GFP (4-6 rats/group). In the 1st experiment, the rats were maintained for 5 weeks, in the 2nd for 10 weeks, and in the 3rd for up to 86 weeks post-vector administration. Despite weight reductions of approximately 15% in rAAV-lep rats in comparison to rAAV-GFP rats at 5 and 10 weeks post-vector injection, significant differences in cancellous bone volume were not detected between the rAAV-lep and rAAV-GFP groups at either time point. In the 86-week study, a reduced body weight was maintained in the rAAV-lep in comparison to the rAAV-GFP rats for the duration of the experiment. However, significant differences in cancellous bone volume were likewise not detected between the two groups at termination of the study. We conclude that leptin gene therapy in rapidly growing rats results in sustained reductions in body weight as well as reduced peak bone mass. These data, however, suggest that increased hypothalamic leptin levels do not induce significant cancellous bone loss in adult female rats.

Disclosures: **U.T. Iwaniec**, None.

1049

Continuous PTH Treatment Causes Bone Loss through Upregulated T Cell Localization to the Bone Surfaces. X. Wu, W. Qian*, M. Ryan, K. Page*, X. Yang*, F. Grassi, N. Weitzmann, R. Pacifici. Emory University, Atlanta, GA, USA.

PTH is known to stimulate osteoclast (OC) formation and activity but the involved mechanism is unknown. We have investigated the novel hypothesis that continuous PTH treatment causes bone loss by inducing T cells to secrete osteoclastogenic cytokines. 10 week old WT Bl6 mice, T cell deficient nude mice and nude mice subjected to T cell reconstitution by adoptive transfer of WT T cells one week before the initiation of the study, were treated with hPTH1-34 (40 µg/kg/day) delivered by sc osmotic pumps for 4 weeks. Weekly BMD measurements by PIXImus revealed that PTH caused a significant bone loss in WT mice and (- 5.2 %, p<0.05) in T cell replete nude mice (- 5.7 %, p<0.05), but not in T cell deficient mice (- 0.4 %, p = ns). In contrast, no significant bone loss was observed in all groups of intact mice or mice treated with vehicle. PTH also caused a significant increase in serum levels of CTX, a marker of bone resorption in WT mice and (20.7 % compared to baseline) in T cell replete nude mice (96.0 %, compared to baseline), but not in T cell deficient mice (0.5 % compared to baseline). No changes in CTX were observed in control groups. In a second experiment in which mice were treated with hPTH1-34, 80 µg/kg/day for 2 weeks. T cell deficient nude mice were completely protected against the increase in bone resorption and the bone loss induced by PTH. Furthermore, measurements of cortical vertebral bone volume (CBV) by µCT in samples harvested at sacrificed revealed CBV to be 8.4 % lower in WT mice treated with PTH as compared to WT intact mice and WT mice treated with vehicle. In contrast, all groups of T cell deficient nude mice had similar CBV values. Thus, the catabolic effect of PTH is mediated by T cells. Staining of longitudinal diaphyseal bone sections for TRAP (an OC marker) and CD3 (a T cell marker) revealed that in control mice T cell were concentrated in the endosteal BM region. In vehicle treated mice the endosteal BM area occupied by T cells was 3 fold higher along OC covered endosteal surfaces than along naked surfaces, suggesting that T cells promote physiologic OC renewal. In contrast, after 2 weeks of PTH treatment, a time when new OC had already formed, the endosteal BM area occupied by T cells was only 1.4 fold higher along OC covered endosteal surfaces than along naked surfaces. These preliminary data suggest that T cells migrated to new areas where OC had yet to form. In summary, the finding that T cell mediates the catabolic effect of PTH on bone provides a new paradigm for T cells as an essential target of PTH in bone. The data also suggest that PTH induces bone loss by favoring the localization of T cells to endosteal surfaces available for remodeling.

Disclosures: **X. Wu**, None.

1050

Deletion of the Mid- and Carboxyl Regions of PTHrP Produces Growth Retardation and Early Senescence in Mice. D. Miao, H. Su*, B. He*, J. Gao, Q. Xia*, D. Goltzman, A. C. Karaplis. Medicine, McGill University, Montreal, PQ, Canada.

Previous studies have demonstrated the important biological role played by the NH₂-terminal end of PTHrP by interacting with the common PTH/PTHrP receptor. Other studies have suggested roles for the mid-region and carboxyl ends of the molecule in calcium and skeletal homeostasis. We and others have previously shown nuclear localization of PTHrP in multiple cell types and we previously identified a functional nucleolar localization sequence within the 87 to 107 region of the molecule. In the present study we examined the function of the mid- and carboxyl- regions ("C-terminal") of PTHrP *in vivo* by inserting a premature termination codon in the PTHrP gene and creating a "knock-in" (KI) mouse expressing PTHrP (1-84). Immunocytochemistry in mouse embryonic fibroblasts (MEFs) confirmed the absence of C-terminal PTHrP and the presence of N-terminal protein. Newborn PTHrP KI mice were morphologically normal but slightly smaller than wild-type littermates. Post-natally, however, KI mice failed to grow normally and developed an unstable gait, cachexia, reduced fat deposition, thin skin with hyperkeratosis of the epidermis, and osteoporosis. KI mice did not survive past 2 to 3 weeks of age. Serum calcium and PTH concentrations were normal. Skeletal growth retardation resulted from a reduction in both chondrocyte proliferation and differentiation and premature osteoporosis was caused by reduced osteoblastic bone formation in both trabecular and cortical bone associated with decreased expression of Cbfa1, alkaline phosphatase, type I collagen and osteocalcin. The proliferation of bone marrow cells was decreased in KI mice as demonstrated by BrdU incorporation and flow cytometry. Apoptotic cells in thymus and spleen were increased as demonstrated both by TUNEL assay and annexinV/propidium

iodide staining. Increased expression of the senescence marker β-galactosidase was observed in tubules of the renal cortex of KI mice and both MEFs and tissues demonstrated markedly increased expression of senescence-associated tumor suppressor genes such as p16^{INK4a}. These results indicate that the C-terminal region of PTHrP exerts an important role in stimulating cell proliferation and preventing apoptosis by regulating tumor suppressor genes such as p16^{INK4a} in a variety of tissues and that its absence produces a syndrome of early senescence.

Disclosures: **D. Miao**, None.

1051

Neurofibromin (Nf1) through its Expression in Osteoblasts, Controls Bone Formation and Bone Resorption. F. Elefteriou¹, D. M. Benson^{*2}, X. Liu^{*3}, L. Parada^{*2}, G. Karsenty³. ¹Cellular and Structural biology, UT Health Science Center at San Antonio, San Antonio, TX, USA, ²Center for Developmental Biology, University of Texas Southwestern Medical Center, Dallas, TX, USA, ³Molecular and Human Genetics, Baylor College of Medicine, Houston, TX, USA.

Type I Neurofibromatosis (NF1) is an autosomal dominant disease caused by loss of function mutations in the tumor suppressor gene *Nf1* and that affects multiple organs. Patients affected by NF1 display, among other pathological conditions, bone abnormalities that include macrocephaly, scoliosis/kyphosis, pectus excavatum, and tibial pseudoarthroses, suggesting that neurofibromin, the product of the *Nf1* gene, is involved in bone development and/or homeostasis. To address the role of *Nf1* in osteoblasts, we crossed mice bearing a floxed allele of *Nf1* with transgenic mice expressing *Cre-recombinase* under the control of the osteoblast-specific *alpha1(I) collagen* promoter fragment to generate a mouse model of osteoblast-specific *Nf1* deletion (*Nf1*_{ob}-deficient mice). *Nf1*_{ob}-deficient mice were born at a normal mendelian ratio without gross anatomical abnormalities, thus excluding that *Nf1* plays an important role during bone development. In contrast, histomorphometric analyses revealed that absence of *Nf1* in osteoblasts resulted in an increase in bone mass and osteoid surface and volume as a result of an increase in the bone formation rate. These bone abnormalities were not accompanied by any mineral ion abnormalities. In agreement with these observations, *Nf1*-deficient osteoblasts synthesized more collagen and formed larger colonies than wild type (WT) osteoblasts *in vitro*. Altogether, these results indicate that neurofibromin regulates osteoblast proliferation and functions and thereby bone mass. In addition, bone resorption parameters such as the number of differentiated osteoclasts and the elimination of urinary deoxypyridinoline were increased in *Nf1*_{ob}-deficient mice compared to WT mice. An osteoblast/osteoclast co-culture assay revealed that *Nf1*-deficient osteoblasts supported osteoclast differentiation markedly better than WT osteoblasts, indicating that *Nf1* deletion in osteoblasts is responsible for the increase in bone resorption observed in *Nf1*_{ob}-deficient mice. Molecular analyses by real-time PCR using isolated populations of WT and *Nf1*-deficient osteoblasts revealed that *Rankl* expression was significantly up-regulated in *Nf1*-deficient osteoblasts. Thus, osteoblast-specific deletion of *Nf1* reveals that neurofibromin is a potent regulator of both arms of bone remodeling. Ongoing studies aiming at identifying the signaling pathways downstream of *Nf1* in osteoblasts will be presented at the meeting.

Disclosures: **F. Elefteriou**, None.

1052

T-Cell Factor, Schnurri-2, Enhances Osteoblastic and Osteoclastic Function *In Vivo* as a Novel Transcriptional Modulator to Be Involved in Coupling in Bone Remodeling via its Link to BMP and RANKL Signaling. Y. Saita¹, T. Takagi^{*2}, K. Kitahara¹, M. Usui¹, Y. Ezura¹, K. Nakashima¹, H. Kurosawa^{*3}, S. Ishii^{*2}, M. Noda¹. ¹Molecular Pharmacology, 21st COE Program, Medical Research Institute, Tokyo Medical and Dental University, Tokyo, Japan, ²Laboratory of Molecular Genetics, RIKEN Tsukuba Institute, Ibaraki, Japan, ³Orthopedics, Juntendo University, School of Medicine, Tokyo, Japan.

Schnurri-2(Shn-2) is a large zinc finger protein, required for positive selection of thymocytes and for regulation of type 2 T helper cell differentiation via competitive binding to a consensus NFκB motif to inhibit promoter activity. Although immune systems and skeletal systems share critical signalings, little is known regarding the function of a Shn-2 in bone. Therefore we examine the function of Shn-2 in bone. Bone mineral density and bone mineral contents in long bones were significantly reduced in 12wk old Shn-2 knock out mice. Shn-2 deficiency also reduced cortical bone mass. The histomorphometrical analysis indicated Shn-2 deficiency suppressed mineral apposition rate and bone formation rate in cortical bone as well as cancellous bone. Furthermore RT-PCR analysis of the RNA taken from the long bone indicated that Shn-2 deficiency suppressed the levels of osterix as well as osteocalcin mRNA. Overexpression of Shn-2 in MC3T3E1 osteoblastic cells enhanced osteocalcin promoter activity. Interestingly Shn-2 enhanced the levels of a luciferase reporter expression via BMP response elements 12×GCCG as well as TGF-β response elements 3TP luciferase. In the presence of BMP or TGF-β, Shn-2 enhanced the GCCG or 3TP-luc activities more than BMP or TGF-β alone. TGF-β treatment enhanced Shn-2 gene expression in osteoblastic MC3T3E1 cells suggesting the presence of positive feedback. Similar to the suppression in osteoblastic activity in Shn-2 deficient mice, Shn-2 deficiency suppressed the number of osteoclasts *in vivo*. Osteoclastogenesis *in vitro* using bone marrow cells were also impaired in the absence of Shn-2. In RAW264.7 mouse monocytic cells, Shn-2 expresses at the basal state and treatment of RANKL enhanced the expression level of Shn-2. Thus, Shn-2 is an activator in both osteoblasts and osteoclasts. Interestingly trabecular bone volume was slightly increased in Shn-2 deficient mice, suggesting that reduction in osteoblastic activity

ASBMR 27th Annual Meeting

in Shn-2 deficient mice appears to be less than the reduction in osteoclastic activity. Overall, our data indicated that Shn-2 has the key role in the activation of both osteoblasts and osteoclasts and thus playing a pivotal role in each of the bone formation and bone resorption to be responsible for maintenance of coupling events in bone remodeling.

Disclosures: **Y. Saita**, None.

1053

The RUNX2 Transcription Factor Regulates Ribosomal RNA Gene Expression for Osteoblast Growth and Differentiation. **D. W. Young, M. Galindo*, X. Yang*, J. Underwood*, J. Pratap, J. L. Stein*, J. B. Lian, J. A. Nickerson*, A. J. van Wijnen, G. S. Stein.** Department of Cell Biology and Cancer Center, University of Massachusetts Medical School, Worcester, MA, USA.

Skeletal development as well as osteoblast cell growth and function require stringent control of ribosomal biogenesis. Genetic alterations that deregulate ribosome production (e.g., Treacher Collins Syndrome) result in craniofacial bone defects and growth retardation. Here we investigated whether ribosomal RNA biosynthesis is regulated by the bone-related RUNX2 transcription factor that controls the proliferative potential of osteoprecursors and osteogenic lineage commitment. We find that reduction of Runx2 levels in human Saos-2 cells by siRNA activates rRNA transcription, indicating that ribosomal gene production is indeed Runx2 responsive. Furthermore, a bioinformatics analysis reveals the presence of multiple Runx binding elements within regulatory regions of rRNA genes. We therefore performed chromatin immunoprecipitation (ChIP) analysis and establish that Runx2 directly associates with ribosomal RNA genes. Both immunofluorescence and immunoelectron microscopy reveal that a subset of Runx2 is localized to nucleoli where ribosomal genes reside and ribosomal biogenesis occurs. Interestingly, we find that during the mitotic silencing of gene expression Runx2 is localized at chromosomal foci that are associated with active chromatin at nucleolar organizing regions and co-localize with the RNA polymerase I transcription factor, Upstream Binding Factor (UBF1). Using cell synchronization strategies and ChIP assays, we demonstrate that the association of Runx2 with rDNA is a cell cycle regulated process that is modulated during the mitosis to G1 and G0/G1 transitions. Functional linkage between Runx2 and ribosomal gene expression is further established by enhanced ribosomal RNA synthesis in primary cells isolated from the calvarial tissue of Runx2 null mice compared with wild-type Runx2 counterparts. Notably, induction of Runx2 in uncommitted mesenchymal cells directly represses ribosomal biogenesis, and this repression of ribosomal gene expression by Runx2 is associated with cell growth inhibition and expression of osteoblast-specific genes. Taken together our findings establish that Runx2 not only controls osteoblast lineage commitment, but also acts as a suppressor of cell growth by inhibiting rRNA synthesis. Our findings elucidate a novel mechanism by which ribosomal biogenesis is coordinately controlled by the Runx2 transcription factor to support osteoblast differentiation and skeletal development.

Disclosures: **D.W. Young**, None.

1054

Fibronectin Serves as an Essential Template for Assembly of Multiple Bone Matrix Proteins, and Is Essential for TGF- β Deposition, Matrix Stability, and Normal Mineralization. **Q. Chen¹, P. Sivakumar¹, J. Zhao^{*1}, B. J. Rongish^{*2}, A. Czirok^{*2}, V. Dusevich^{*1}, M. R. Dallas^{*1}, D. M. Peters^{*3}, D. F. Mosher^{*3}, S. L. Dallas¹.** ¹Univ. of Missouri, Kansas City, MO, USA, ²Univ. of Kansas Med Cntr, Kansas City, KS, USA, ³Univ. of Wisconsin, Madison, WI, USA.

Fibronectin (FN) is an extracellular matrix (ECM) glycoprotein important for cell adhesion, migration and matrix assembly. Disruption of fibronectin in primary osteoblasts impairs mineralization. To gain further insight into the role of FN in bone, we have performed dynamic imaging of ECM assembly in living osteoblasts and have used fibroblasts from E6.5 FN-null embryos as a FN deficient cell model. When differentiated with BMP2, these cells express terminal osteoblast markers, yet fail to mineralize without addition of exogenous FN. We hypothesized that FN regulates mineralization by controlling assembly and stability of multiple bone ECM molecules. Immunostaining showed that type I collagen, fibrillin-1, latent TGF β binding protein 1 (LTBP1), decorin, biglycan and perlecan were initially colocalized with FN. Assembly of these ECM components was severely impaired in FN null cells, as shown by immunostaining, TEM and Western blotting, even though synthesis/secretion was unaffected. We also found an 80% reduction in TGF β 1 deposition into the ECM of FN null cells. Rescue experiments showed that mineralization, assembly of bone ECM components and TGF β deposition were rescued by full length FN but not by FN fragments that do not form fibrils, including a 160kDa RGD-containing fragment. This suggests that integrin signaling alone is insufficient to rescue these pathways. Although optimal mineralization occurred when FN was continually present, the critical period was between days 6 and 10. Dynamic imaging in living osteoblasts using fluorescent probes to ECM molecules showed that the ECM fibrillar networks were highly dynamic. Not only was FN required for initial assembly of these ECM proteins, but the continued presence of FN was required for their continued assembly and to maintain matrix stability. When FN null cells were grown on a preformed matrix or overlaid with a collagen gel, mineralization was rescued, suggesting that the key event for mineralization is collagen deposition. Sequential assembly of bone ECM components was suggested by studies with Mov13 cells lacking α 1(I) collagen. Assembly of fibrillin-1, LTBP1, perlecan and decorin was normal in these cells but biglycan was impaired. These data suggest that a major mechanism by which FN controls mineralization

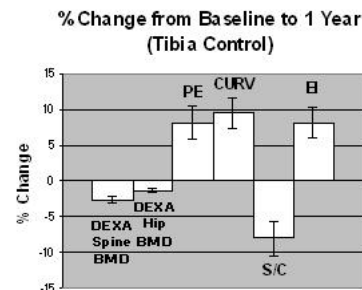
is by orchestrating the sequential assembly of multiple bone ECM components, maintaining ECM stability and regulating incorporation of growth factors, such as TGF β , into bone matrix.

Disclosures: **Q. Chen**, None.

1055

MRI Based Virtual Bone Biopsy Detects Large One-Year Changes in Trabecular Bone Architecture of Early Postmenopausal Women. **G. A. Ladinsky*, B. Vasilic*, A. M. Popescu*, B. Zemel*, A. C. Wright*, H. K. Song*, P. K. Saha*, H. Peachy*, P. J. Snyder*, F. W. Wehrli.** University of Pennsylvania, Philadelphia, PA, USA.

Estrogen depletion following menopause is accompanied by bone loss and architectural deterioration of trabecular bone (TB); hormone replacement therapy (HRT) protects against such bone loss. Here we provide an update on preliminary data from the first *in vivo* detection of such skeletal changes in an ongoing study involving early postmenopausal women, half of whom are getting HRT and half of whom are not (controls). Images of the distal radius and tibia were acquired by means of a MRI-based virtual bone biopsy at 137x137x410 μm^3 voxel size with bone volume fraction maps generated using subvoxel processing to yield a final voxel size of 62x62x103 μm^3 . These images were then binarized, skeletonized and subjected to 3D digital topological analysis (DTA). Skeletonization converts rods to curves and plates to surfaces. Parameters quantifying scale included BV/TV and Tb.Th while DTA parameters included the volume densities of curve voxels (CURV), surface voxels (SURF) and profile edges (PE, ends of structures intermediate between surfaces and curves) and composite parameters included the surface/curve ratio (S/C) and erosion index (EI, ratio of parameters expected to increase with osteoclastic resorption divided by those expected to decrease). Images were collected at baseline and 11-13 months with preliminary results presented for 29 control and 17 HRT subjects that afforded images of adequate quality. Scale parameters at the tibia were not significant while DTA parameters PE, CURV, S/C, EI provided highly significant changes ($P < 0.0001$ - 0.003) ranging from 8.0 to 9.5% in control subjects but little or no significant change was observed in the HRT group. Similarly, DEXA BMD in the spine (hip) decreased 2.7% (1.4%) in controls ($P < 0.0001$ - 0.001) (though less than DTA parameters) but not in HRT subjects. These findings, not previously observed *in vivo*, are consistent with the known protective effects of HRT ensuring maintenance of a more plate-like TB architecture. This work suggests that MRI-based *in vivo* micromorphometry of trabecular bone shows promise as a tool for monitoring osteoporosis treatment. (Sponsors: NIH R01AR41443, T32DK07006 & Novartis)



Disclosures: **G.A. Ladinsky**, Novartis 2; Micro-MRI 4.

1056

Finite Element Biomechanical Analysis of the PTH and Alendronate (PaTH) Study: PTH Increases Vertebral Strength by Altering both Average Density and Density Distribution. **D. M. Black¹, R. P. Crawford^{*2}, L. Palermo^{*3}, J. P. Bilezikian⁴, S. Greenspan⁵, T. M. Keaveny⁶.** ¹UC San Francisco, San Francisco, CA, USA, ²O.N. Diagnostics, LLC, Berkeley, CA, USA, ³Epidemiology and Biostatistics, UC San Francisco, San Francisco, CA, USA, ⁴Columbia University, New York, NY, USA, ⁵University of Pittsburgh, Pittsburgh, PA, USA, ⁶Mechanical Engineering and Bioengineering, UC Berkeley, Berkeley, CA, USA.

QCT-based finite element models biomechanically integrate all information in the QCT scans to provide measures of bone strength (Biomechanical CT or BCT). In this pilot study, we applied BCT to measure changes in vertebral strength in 20 randomly selected post-menopausal women treated with PTH (1-84) 100mcg sq daily for one year in the PaTH study, a randomized trial comparing PTH or alendronate alone and together. We also measured strength changes in the trabecular region by virtually "peeling away" the outer 2 mm of each vertebra (which includes the cortex), and also quantified the role of intra-vertebral density variation by virtually removing such variations. The results for areal spine BMD (DXA), volumetric density (QCT) and BCT are shown below. On average, PTH increased overall vertebral strength by almost 30% at one year. The strength of the trabecular region was increased by almost 50% more than overall vertebral strength. When all densitometric variations within each vertebra were virtually removed, vertebral strength increased by only 15%, about half the total increase in strength. Taken together, these results indicate that about half the overall increase in vertebral strength can be attributed to an *average* increase in bone density, and the remaining half of the effect is due to alterations in the *distribution* of bone density within the vertebra. This is the first study to use BCT clinically to investigate longitudinal changes in bone strength during treatment

for osteoporosis. BCT provides insight into the biomechanical implications not only of changes in overall bone density but also in changes in density distribution after PTH administration to human subjects. These biomechanical strength effects of the treatment are not appreciated by DXA or QCT alone.

	Baseline	12 Month	% Change
BMD L1-L4 (g/cm ²)	0.79 ± 0.12	0.84 ± 0.13	6.9 ± 5.0
QCT integral density (g/cm ³)	0.14 ± 0.02	0.16 ± 0.03	14.9 ± 13.0
QCT trabecular single slice (g/cm ³)	0.80 ± 0.02	0.10 ± 0.03	27.4 ± 28.4
BCT vertebral strength (N)	4521 ± 1042	5715 ± 1335	28.8 ± 25.9
BCT trabecular strength (N)	2234 ± 665	3084 ± 978	42.4 ± 38.2
BCT strength averaged-density (N)	3322 ± 523	3806 ± 600	15.4 ± 13.8

*all % changes (mean ± SD) were significant (baseline vs. 12 month, p<0.05).

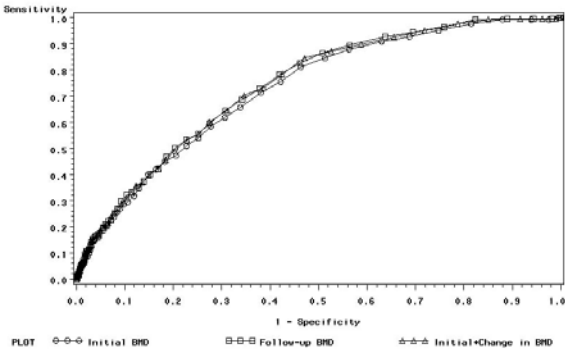
Disclosures: **D.M. Black**, NPS, Roche 5; Merck 8; Novartis 3.

1057

Bone Mineral Density (BMD) Measurement and Prediction of Fractures in Older Women: Is More Better? T. A. Hillier¹, K. L. Stone², J. R. Rizzo^{*1}, K. L. Pedula^{*1}, J. A. Cauley³, M. Hochberg⁴, S. R. Cummings². ¹Center for Health Research, Kaiser Permanente, Portland, OR, USA, ²San Francisco Coordinating Center, CPMC Research Institute and UCSF, San Francisco, CA, USA, ³U of Pittsburgh, Pittsburgh, PA, USA, ⁴U of Maryland, Baltimore, MD, USA.

Whether repeat BMD measurement adds additional benefit beyond the initial BMD measurement in prediction of non-traumatic fractures in older women is unknown. We measured total hip DXA BMD in 4,124 participants in the Study of Osteoporotic Fractures with a mean age of 72 years (SD 4) in 1989-90, and 8 years later (Hologic 1,000). We validated incident non-traumatic hip and non-spine fractures by radiology reports during 5 years of >98% follow-up. In addition, 2,193 of these women had lateral spine x-rays in 1991-2, then 6.5 years later. Incident spine fractures were defined morphometrically by >20% and at least 4 mm decrease in vertebral height at any level. We analyzed the association between fractures and (a) Initial (iBMD), (b) Follow-up BMD (fuBMD), (c) iBMD plus change between i and fu BMD (i+chgBMD). After the fuBMD measurement, 877 women suffered an incident non-traumatic non-spine fracture, 275 of which were hip fractures. In addition, 345 women developed a morphometric spine fracture. After adjustment for age and weight change, the risk of incident fracture was similar with either iBMD or fuBMD (per unit SD decrease in total hip) in prediction of non-spine (HR 1.5-1.6), spine (OR 1.7-1.8), or hip fracture (HR 2.0-2.2), p<0.001 for all models. Receiver-operator characteristic (ROC) curves revealed similar area under the curve (AUC) in fuBMD or i+chgBMD compared to initial BMD for non-spine fractures (0.65 for all models), spine fractures (0.67-0.68), or hip fractures (0.73-0.74; Figure). Further stratification by initial BMD group t-score (normal, osteopenic, osteoporotic) did not reveal much improvement in AUC for the repeat BMD measure compared to the initial BMD. Our results indicate, that for the average older post-menopausal woman age 65 or older, repeat BMD measurement may provide little additional benefit in predicting osteoporotic fractures beyond the initial BMD.

ROC Curve for BMD and Prediction of Hip Fracture in Older Women
adjusted for age and weight change



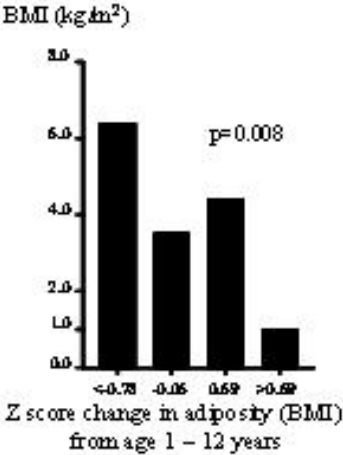
Disclosures: **T.A. Hillier**, None.

1058

Growth in Infancy and Childhood Predicts Hip Fracture Risk in Late Adulthood. M. K. Javaid¹, J. G. Eriksson^{*2}, T. Forsen^{*2}, E. Kajantie^{*2}, C. Osmond^{*1}, D. J. P. Barker^{*1}, C. Cooper¹. ¹Bone and Joint, MRC ERC Southampton, Southampton, United Kingdom, ²Diabetes and Genetic Epidemiology, The National Public Health Institute, Helsinki, Finland.

Peak bone mass has been shown to account for up to 60% of the variation in adult bone mass. We have previously demonstrated that poor late childhood growth predicts adult hip fracture. We now wish to further explore the relationship with early childhood growth and adult fracture risk, and test to what extent this is mediated by differences in proximal femoral densitometry. Maternity, school and welfare records were electronically linked with hospitalization and mortality records in Helsinki, Finland, and 8,760 individuals (4,130 women) born in the University Central Hospital Helsinki between 1934-1944 were identified. These individuals all had birth weight and length recorded as well as weight and height at varying intervals during infancy and while at school. Hip fractures were identified

from the hospitalization and mortality records using ICD-10 codes. In a sub-sample, 190 women with complete birth, infant and childhood records underwent DXA of the lumbar spine and proximal femur using a Hologic QDR 4500 DXA instrument. From the 8,760 individuals identified, 6,101 (2,825 women; mean age 56 yr (SD 4.4yrs) had regular measurements available enabling growth curves to be derived. From these individuals, 31 hip fractures were identified. Of the childhood predictors of fracture risk, the standard deviate (z) score change in indices of body build (years 1-12) were strongly associated with adult hip fracture risk. Thus those in the lowest quarter of the distribution of weight (BMI) gain (z score change <-0.78) had a 6.4 fold increase in hip fracture risk (p=0.008) compared with those in the highest quarter of this distribution (z score change >+0.69). The increased risk was present in both men and women. In the sub sample of 190 women who underwent bone mineral measurement, an equivalent change in BMI z-score during childhood was only associated with 0.11 SD decrease in aBMD and 0.33 SD decrease in bone area at the proximal femur. We have been able to demonstrate that poor growth during early childhood is associated with an increased risk in hip fracture; however, the mechanism for this appears to be explained only in part by the association between measures of early growth and adult bone size and areal density.



Disclosures: **M.K. Javaid**, None.

1059

Glutamine Repeat Mutations Define a New RUNX2 Related Syndrome with Decreased Femoral Neck BMD, Decreased Calcaneal Ultrasound and Increased Risk of Osteoporotic Fracture. A. Stephens^{*1}, J. Doecke^{*1}, S. H. Ralston², R. Prince³, G. C. Nicholson⁴, N. A. Morrison¹. ¹School of Medical Science, Griffith University, Gold Coast, Australia, ²Rheumatic Diseases Unit, University of Edinburgh, Edinburgh, United Kingdom, ³Department of Endocrinology and Diabetes, University of Western Australia, Perth, Australia, ⁴Department of Medicine, Geelong Hospital, University of Melbourne, Geelong, Australia.

RUNX2 is an essential transcription factor required for osteoblast differentiation and cartilage formation. Haplo-insufficiency of RUNX2 leads to cleidocranial dysplasia (CCD) a skeletal disorder characterized by gross skeletal dysgenesis. A notable feature of the RUNX2 protein is the polyglutamine and polyaniline (23Q/17A) domain coded by a repeat sequence. Such repeat sequences are subject to high mutation rates through strand slippage during replication. Since none of the known mutations causing CCD map in the glutamine repeat region, we hypothesised that Q-repeat mutations would exist at high frequency and may be related to a more subtle bone phenotype than the morphological abnormalities of CCD. We screened 3600 subjects derived from three normal populations for Q-repeat mutations. A total of 28 subjects were identified who were heterozygous for a wild type allele and were carriers of Q variants: (deletions 15Q, 16Q, 17Q, and extensions 30Q). 12 of the 28 Q variant carriers had osteoporotic fracture. BMD data were available for each of the populations and were expressed in the form of Z-scores around the appropriate age-adjusted mean. Collectively, Q-repeat variants presented with significantly decreased femoral neck BMD (p=0.0006) with an effect of -0.56SD in BMD attributable to a single copy of the Q-variant in the presence of a wild type allele. Broadband ultrasound attenuation (BUA) and speed of sound (SOS) measured in the calcaneus were available on 18 Q-variant subjects. Q-variants displayed significantly decreased BUA (p=0.006) with an effect of -0.65SD. To understand the mechanism via which the Q-repeat deletions and expansions were conferring decreased BMD and BUA, the transactivation function of the 16Q and 30Q alleles were analyzed using a RUNX2 reporter gene assay. 16Q and 30Q alleles were capable of transactivating target reporter plasmids but at levels significantly lower compared to wild type (23Q). Our analysis has identified a new class of functionally relevant RUNX2 variants in the Q repeat that influence BMD and fracture. Q-variants occur at the relatively high frequency ~0.8%, meaning that more than 2 million people in the US may be affected.

Disclosures: **A. Stephens**, None.

1060

Chronic High-Dose Glucocorticoids Are Associated with Increased Cortical Bone Mass and Minimal Trabecular Deficits in Children with Nephrotic Syndrome. M. B. Leonard, R. M. Herskovitz*, K. M. Howard, J. M. Burnham, B. S. Zemel. Pediatrics, The Children's Hospital of Philadelphia, Philadelphia, PA, USA.

Glucocorticoids (GC) suppress bone formation and impair growth. However, we recently reported that chronic high-dose GC therapy for childhood nephrotic syndrome (NS) was associated with increased whole body bone mineral content (BMC) and normal spine BMC, as measured by DXA (New Engl J Med, 2004). GC-induced obesity exerted a protective effect on BMC. The objective of this study was to use peripheral quantitative computed tomography (pQCT) to assess trabecular volumetric BMD (vBMD) and cortical dimensions in children treated with GC for NS. pQCT (Stratec XCT 2000) measurements of the tibia were obtained in 63 prevalent NS subjects (42M/21F) and 308 healthy controls (148M/160F), ages 5 to 21 yr. Trabecular vBMD was measured at the 3% distal site. Cortical BMC, periosteal (PERI) and endosteal (ENDO) circumferences, and cross-sectional moment of inertia (CSMI) were measured at the 38% mid-shaft. Height and BMI were converted to age and sex specific z-scores using national reference data. Sex-specific regression models were used to generate z-scores for trabecular vBMD relative to age and cortical measures relative to tibia length. NS subjects had lower height z-scores (-0.17 ± 0.81 vs. 0.23 ± 0.87 , $p < 0.01$) and higher BMI z-scores (0.88 ± 1.01 vs. 0.12 ± 0.89 , $p < 0.0001$), compared with controls. pQCT results are summarized in the Table. Trabecular vBMD was marginally lower in subjects with NS ($p = 0.08$); on average, vBMD was at the 40th percentile for age in NS. Cortical BMC, PERI and CSMI were all significantly greater in NS compared with controls (all $p < 0.001$). Adjustment for BMI z-score eliminated the group differences in cortical dimensions, e.g. adjusted mean CSMI z-score = 0.25 (95% CI: -0.4, 0.53, $p = 0.09$) in NS. After adjustment for BMI z-score, trabecular vBMD was significantly lower in NS (mean z-score: -0.43; 95% CI -0.73, -0.12, $p < 0.01$), compared with controls. These pQCT data confirm that GC therapy is associated with marginal deficits in trabecular vBMD and significantly greater cortical BMC, periosteal dimensions and CSMI in children with NS. The GC-induced obesity ameliorated trabecular vBMD deficits and was associated with greater cortical BMC and dimensions. GC-induced obesity may counteract the suppressive effects of GC on bone formation.

	pQCT Z-scores in Subjects with Nephrotic Syndrome and Healthy Controls				
	Trab vBMD	Cortical BMC	Cortical PERI	Cortical ENDO	Cortical CSMI
Controls	0.00 ± 1.03	0.00 ± 0.99	0.00 ± 1.03	0.00 ± 1.06	0.00 ± 1.02
NS	-0.27 ± 1.06	0.87 ± 1.27	0.51 ± 1.26	0.16 ± 0.84	0.55 ± 1.27
p-value	0.08	<0.0001	<0.001	0.24	<0.001

Disclosures: M.B. Leonard, None.

1061

Polycystin-1: A Novel Mechanosensor in Osteoblast/Osteocytes Coupled to Runx2. Z. Xiao*, S. Zhang*, J. Mahlios*, J. Calvet*, L. Bonewald*, L. Quarles*. ¹University of Kansas Medical Center, Kansas City, KS, USA, ²University of Missouri, Kansas City, MO, USA.

Osteocytes and osteoblasts are the key mechanotransducing cells in bone, but the molecular mechanisms mediating responses to mechanical strain are uncertain. Polycystin-1 (PC1), a transmembrane G-protein coupled receptor, functions as a putative flow-responsive mechanosensor complexed with polycystin-2 (PC2), a receptor-activated calcium channel, in renal epithelial cilia. Mutations of PKD1, the gene coding for PC1, cause autosomal dominant polycystic kidney disease (ADPKD). PC1 is also expressed in embryonic mesenchyme and neural crest tissues, which give rise to endochondral and intramembranous bone and mice lacking *Pkd1* have abnormal skeletogenesis. These observations raise the possibility that PC1 might be an important mechanosensor in the skeleton. To investigate the function of PC1 in bone, we evaluated *Pkd1*^{mlbe1} mice, which have an inactivating missense point mutation (T to G at 9248bp) that is embryonic lethal in homozygotes. Alizarin red and alcian blue staining of E14.5 and 15.5 *Pkd1*^{mlbe1} null embryos showed delayed calcification consistent with the reported role of PC1 in skeletal development. More importantly, we observed a 7% reduction in BMD of the femur as assessed by dual energy x-ray absorptiometry (DEXA) in 6-week-old *Pkd1*^{mlbe1} heterozygous mice, indicating that reduction of PC1 expression leads to osteopenia postnatally. To determine if PC1 and PC2 transcripts are expressed in osteoblasts and osteocytes, we performed RT-PCR with specific primers for PC1 and PC2 using RNA from MC3T3-E1 osteoblasts and MLO-Y4 osteocytes. We found that both PC1 and PC2 transcripts are highly expressed in both cell types. In addition, MC3T3-E1 and MLO-Y4 cells expressed transcripts for polaris, a protein present in cilia, consistent with the presence of cilia in osteoblasts/osteocytes. Activation of PC1 signaling can be achieved by overexpression of the C-terminus of PC1. To assess the function of PC1 on *Runx2* promoter activity in osteoblasts, we transiently co-transfected MC3T3-E1 osteoblasts with two mouse C-terminal PC1 constructs, PC1-LT containing the C-terminal 222 aa of PC1 or PC1-HT containing the C-terminal 193 aa of PC1 and the 1.4 kb *Runx2* P1 luciferase promoter/reporter construct. Overexpression of either PC1-LT or PC1-HT in this osteoblastic cell line resulted in a 3-4 fold increase of the P1 promoter activity of *Runx2*, an essential transcription factor controlling osteoblastogenesis. These findings suggest that PC1 is part of a mechanosensing complex in bone that allows osteoblasts/osteocytes to sense and transduce mechanical forces into anabolic cell signals leading to new bone formation.

Disclosures: Z. Xiao, None.

1062

Enhancement of Bone Formation by Small Molecule Compounds that Disrupt Dkk-LRP5/6 Interaction. P. Liu¹, Y. Zhang¹, X. Li^{2*}, J. Zheng^{3*}, D. Wu^{*1}. ¹University of Connecticut Health Center, Farmington, CT, USA, ²Enzo Biochem, Farmingdale, NY, USA, ³St. Jude Hospital, Memphis, TN, USA.

Both human and mouse genetic evidence indicates that the canonical Wnt signaling has an important role in bone formation. Our study of the mechanism underlying the high bone mass mutation of Wnt coreceptor LRP5 (G171V) suggests that this mutation reduces Dkk1-mediated antagonism. This finding allows us to hypothesize that disruption of the interaction between LRP5 and Wnt antagonist Dkk may lead to an increase in bone formation. To identify small molecules that can disrupt the interaction, we used an innovated approach that combines structural and molecular biology, "in silico" virtual screening, and biological assays. We first mapped the Dkk-binding domain on LRP5 by using site-directed mutagenesis. Based on the deduced structure of this Dkk-binding domain, computer-based "in silico" virtual screening of small molecule compound libraries was performed. The first-round screen yielded 50 candidate compounds, and we were able to obtain 17 of them for testing their ability to inhibit Dkk binding to LRP5. Three of the compounds showed inhibitory effects on Dkk binding, and they share a common structural core. A second-round screening for compounds that contain this basic structural core was then carried out. We obtained and tested 19 of top ranked compounds and found that one of them (IIC8) was able to reverse Dkk-mediated inhibition of Wnt signaling at low uM concentrations. The third-round virtual screening was carried out based on the structure of IIC8 and yielded a compound (IIC3) that can reverse Dkk-mediated antagonism of Wnt signaling at the high nM range. Both IIC8 and IIC3 are able to block the binding of Dkk1-AP to LRP5 or LRP6. To test their effects on bone formation, IIC8 and IIC3 were injected locally at mouse calvaria. Both compounds showed strong stimulatory effects on bone formation.

Disclosures: D. Wu, Enzo Biochem 1, 2, 8.

1063

Severely Reduced Bone Mass with Defective Osteoblastogenesis in N-Cadherin Heterozygous/Cadherin-11 Null Double Mutant Mice. C. Donsante*, A. Di Benedetto*, G. Mbalaviele, R. Civitelli. Bone and Mineral Diseases, Washington University in St. Louis, St. Louis, MO, USA.

We have previously shown that targeted expression of a dominant negative truncated form of N-cadherin (Ncad) delays acquisition of peak bone mass in mice and retards osteoblast differentiation. However, heterozygous *Ncad*^{+/−} mice are normal (homozygous loss of *Ncad* is embryonically lethal) and cadherin-11 (*Cad11*) null mice are only modestly osteopenic. To determine the specific roles of the two major osteoblast cadherins, we introduced an *Ncad* null allele in a *Cad11* null background to generate double *Ncad*^{+/−}/*Cad11*^{−/−} mutant mice. These mice are viable, although they are obtained at lower than expected Mendelian frequency. Whole body bone mineral density by DEXA was significantly lower in the double mutants relative to both wild type (wt) and *Cad11*^{−/−} mice, a difference detectable at 2 months and increasing with age ($-10.1 \pm 6.3\%$ and $-12.6 \pm 6.4\%$ vs. wt and *Cad11*^{−/−}, respectively at 6 months). *Ncad*^{+/−}/*Cad11*^{−/−} double mutants were also significantly smaller (body weight $-20.7 \pm 10.5\%$ and $-19.7 \pm 10.6\%$ vs. wt and *Cad11*^{−/−}) and had reduced percent body fat, after 2 months of age. Contact radiographs of isolated tibiae and femurs showed shorter length, rarefied trabecular pattern, cortical thinning and tubulation of diaphyses in *Ncad*^{+/−}/*Cad11*^{−/−} relative to wt mice; while *Cad11*^{−/−} bones were modestly osteopenic. Bone histomorphometry confirmed decreased bone mass (BV/TV: $14.6 \pm 4.8\%$ vs. $11.4 \pm 3.1\%$) and osteoblast surface (ObPm/BPm: $35.3 \pm 11.5\%$ vs. $14.8 \pm 7.2\%$) in the double mutants relative to wt mice, respectively, with no difference in osteoclast number. In vitro mineralization was reduced $>50\%$ in *Ncad*^{+/−}/*Cad11*^{−/−} relative to wt calvaria cells, but it was actually slightly more intense relative to *Cad11*^{−/−} osteoblasts. However, the number of colony forming units-fibroblasts isolated from the bone marrow of double mutants was reduced about 60% relative to both wt and *Cad11*^{−/−} cells, suggesting a decreased number of mesenchymal stem cells in the double mutants. Finally, in association with decreased cadherin abundance, total and nuclear β -catenin was significantly reduced in post-confluent *Ncad*^{+/−}/*Cad11*^{−/−} calvaria cells, and to a greater extent than in *Cad11*^{−/−} cells, relative to wt. Thus, single *Ncad* allele loss in a *Cad11* null background causes a far more severe osteopenic phenotype than either independent mutation, attended by defective osteoblastogenesis and reduced mesenchymal stem cell pool. *Ncad* and *Cad11* serve overlapping, though not identical roles in development of peak bone mass, in part via modulation of β -catenin abundance.

Disclosures: R. Civitelli, None.

1064

Canonical Wnt Signaling Controls Osteoblast or Chondrocyte Differentiation from Mesenchymal Progenitor Cells during Skeletogenesis. T. F. Day*, X. Guo*, L. Garrett-Beal*, Y. Yang*. National Human Genome Research Institute, Bethesda, MD, USA.

Vertebrate skeletal development starts from mesenchymal condensations, from which chondrocytes and osteoblasts are differentiated. During intramembranous ossification mesenchymal progenitor cells differentiate directly into osteoblasts, whereas in endochondral ossification they first differentiate into chondrocytes. Since we found that the β -catenin mediated canonical Wnt signaling activity is upregulated in early osteogenic condensations, we tested whether the canonical Wnt signaling controls osteoblast and chondrocyte differentiation from mesenchymal progenitors during vertebrate skeletal development. Mice with a floxed β -catenin allele (*catnby*) were crossed with *Dermo1-Cre* to ablate β -catenin in

mesenchymal condensations prior to osteoblast and chondrocyte differentiation. The *catnby^{fl/c}*; *Dermol-1-Cre* mouse embryos exhibited ectopic chondrocyte differentiation at the expense of osteoblasts where osteoblasts normally differentiate during both intramembranous and endochondral ossification. To further test the function of canonical Wnt signaling in osteoblast and chondrocyte differentiation, we isolated mesenchymal cells from the *catnby^{fl/c}* embryonic calvarium and limb buds at 12.5 dpc. Calvarial cells were cultured under osteogenic conditions whereas limb bud cells were used for micromass cultures. The cultures were infected by a *Cre*-adenovirus to inactivate β -catenin. Inactivation of β -catenin in calvarial cultures led to loss of bone nodules and ectopic cartilage nodule formation, while in micromass cultures cartilage nodule formation was greatly increased. These results indicate that the canonical Wnt signaling plays a decisive role in controlling chondrocyte versus osteoblast formation when mesenchymal progenitor cells differentiate. We then tested the interaction of Wnt/ β -catenin signaling with other signaling pathways mediated by PI3K, BMP2 and FGF, which also regulate chondrocyte and osteoblast differentiation. BMP2 promoted osteoblast differentiation in wild-type calvarial cultures as well as chondrocyte differentiation in β -catenin inactivated cultures, whereas the BMP antagonist Noggin inhibited both bone and chondrocyte nodule formation in wild-type and β -catenin inactivated cultures respectively. In addition, the PI3K inhibitor LY294002 and FGF8 not only inhibited osteoblast differentiation in wild-type cells, they also inhibited chondrocyte differentiation in cells with inactivated β -catenin. This data indicates that the BMP, PI3K, and FGF signaling pathways act independent of the canonical Wnt pathway in controlling osteoblast and chondrocyte differentiation.

Disclosures: **T.F. Day**, None.

1065

Adult Bone Marrow Derived Mesenchymal Stem Cell (MSC) Migration in Response to a Fracture Regeneration Cue. **K. S. Shimer^{*1}, B. Landis^{*2}, L. O'Rear^{*1}, S. Aakula^{*2}, L. Longobardi^{*1}, D. Jansen^{*3}, H. Moses^{*2}, A. Spagnoli¹.** ¹Pediatrics, Vanderbilt University Medical Center, Nashville, TN, USA, ²Vanderbilt University Medical Center, Nashville, TN, USA, ³Biomedical Engineering, Vanderbilt University, Nashville, TN, USA.

The *in vivo* regenerative ability of MSC is a fascinating but still poorly understood process. Our understanding of MSC recruitment into damaged tissues is minimal because of the limitations of the systems used for tracking the donor cells into the recipient. To determine the recruitment capacity of systemically administered MSC to a fracture repair site we engineered MSC with a luciferase reporter (MSC-luc) and tracked the MSC-luc migration using bioluminescence imaging (BLI). MSC were cultured from the bone marrow of syngeneic FVB WT mice and infected during the exponential growth phase with an Adenovirus-firefly luciferase-green fluorescent protein reporter (luc-GFP). Mice (age 8-12 weeks, n=3) tibias were pinned and fractured and MSC-luc-GFP were then injected into their tail veins. Fracture site was confirmed via CT imaging. Every day for a total of 7 days the mice were given an IP injection of luciferin followed by BLI. To quantify the MSC that migrated to the fracture site, we FACS sorted the MSC-luc-GFP positive cells. A serial dilution of MSC-luc-GFP were placed into a 6 well dish and BLI was performed after adding luciferin to each well to create a curve to correlate signal intensity with cell number. Due to the attenuating effects that tissues have on BLI signal intensity, a isotropic light-emitting bead was used to define an attenuation factor between *in vitro* and *in vivo* imaging signals. The skin over the fracture site was found to decrease the signal by 29.2%. When this attenuation factor was applied to our *in vivo* signal data and then correlated with the *in vitro* signal vs. cell number curve, we found that at least $4,787 \pm 389$ MSC ($p < 0.05$) migrated to the fracture site and was significant compared to the contralateral unfractured leg. Longitudinal migration patterns revealed that MSC resided in the lungs for one day then moved to liver and brain on day 2. MSC dispersed on day 3 with no foci other than the brain and by day 4 were shown to migrate to the fracture site, where they resided for the time study period. Our data provides critical information about the real time migrational pattern of MSC in response to a fracture repair cue. In particular, we found that MSC travel through the capillary beds of lung, liver and brain before being recruited to the fracture site. Understanding MSC migration will help delineate the actual MSC dose in real time that migrates to the sites of injury. Further studies will determine if the strength of these healed fractures through biomechanical testing.

Disclosures: **K.S. Shimer**, None.

1066

Administration of CD34-Positive Cells Contributes to Osteogenesis and Vasculogenesis for Functional Bone Healing. **T. Matsumoto¹, A. Kawamoto^{*1}, R. Kuroda^{*2}, M. Ishikawa^{*1}, H. Iwasaki^{*1}, S. Lee^{*2}, A. Oyamada^{*1}, K. Sadamoto^{*1}, M. Hori^{*1}, H. Nishimura^{*1}, S. Murasawa^{*1}, M. Kurosaka^{*2}, T. Asahara^{*1}.** ¹Stem Cell Translational Research, Kobe Institute of Biomedical Research and Innovation / RIKEN Center for Developmental Biology, Kobe, Japan, ²Department of Orthopedic Surgery, Kobe University Graduate School of Medicine, Kobe, Japan.

Recently, neovascularization has been reported to play a critical role in the process of fracture healing. Adult human peripheral blood CD34+ cells, an endothelial/hematopoietic progenitor cell-enriched cell population, also have been reported to differentiate into osteoblasts in vitro over a decade ago. However, therapeutic potential of CD34+ cells for fracture healing is still unknown. We performed a series of experiments to prove a reasonable hypothesis that functional fracture healing may be supported by osteogenesis and vasculogenesis via regenerative plasticity of CD34+ cells. Peripheral blood CD34+ cells were isolated from total mononuclear cells (MNCs) of adult human volunteers using a magnetic cell sorting system. PBS, 1×10^5 MNCs or 1×10^5 CD34+ cells were intravenously transplanted after creating femoral fracture with the periosteum cauterizing of nude rats

(n=12 in each group). Marked recruitment of CD34+ cells, not MNCs, labeled with Qdots were observed around fracture site by fluorescence microscopy at day seven. RT-PCR and immunohistochemical staining at the peri-fracture site demonstrated molecular and histological expression of human specific markers for endothelial cells (CD31, VE-cadherin) and osteoblasts (osteocalcin, collagen1A1) two weeks after CD34+ cell transplantation. Necropsy examination at week two disclosed augmentation of capillary density (CD34+, 1187.5 ± 79.3 ; MNC, 562.5 ± 36.6 ; PBS, $532.5 \pm 49.3/\text{mm}^2$ respectively. $P < 0.01$ for CD34+ vs MNC or PBS) and osteoblastic density (CD34+, 468.0 ± 25.3 ; MNC, 321.6 ± 28.8 ; PBS group, $141.6 \pm 14.0/\text{mm}^2$ respectively. $P < 0.01$ for CD34+ vs MNC or PBS). Frequency of fracture healing with the bridging callus assessed by radiological and histological examinations was 66% four weeks, and 100% eight weeks after CD34+ cell transplantation, while all fractures in other groups fell into nonunions at week eight. Biomechanical assessment by three point bending test at week eight revealed significantly functional healing by CD34+ cell transplantation compared to other groups. In conclusions, systemic administration of human peripheral blood CD34+ cells to immunodeficient rats subjected to femoral fracture induces osteogenesis as well as vasculogenesis in the peri-fracture zone and provides a favorable environment for bone healing and remodeling, followed by their functional recovery.

Disclosures: **T. Matsumoto**, None.

1067

Chondrocytes Support Osteoclast Formation by Expressing RANKL, a Process Controlled by $1\alpha, 25\text{-dihydroxyvitamin D}_3$. **R. Masuyama^{*}, L. Stockmans^{*}, S. Torrekens^{*}, K. Moermans^{*}, C. Maes^{*}, R. Bouillon, G. Carmeliet.** Laboratory of Experimental Medicine & Endocrinology, KUL, Leuven, Belgium.

$1\alpha, 25\text{-dihydroxyvitamin D}_3$ (VD) is required for normal mineral and bone metabolism mainly by regulating active intestinal calcium transport after weaning. The vitamin D receptor (VDR) is however already expressed during early endochondral bone development. To investigate the function of VD in this process we generated mice with chondrocyte-specific inactivation of VDR by mating $\text{VDR}^{\text{fllox/fllox}}$ to transgenic mice expressing Cre-recombinase under control of collagen 2 (Ovchinnikov *et al.* *Genesis*. 2000). As a result, VD treatment of cultured epiphyseal chondrocytes induced Cyp24 gene expression only in $\text{VDR}^{\text{fllox/fllox}}/\text{Col2Cre}^+$ cells ($p < 0.00005$, vs vehicle), but not in $\text{VDR}^{\text{fllox/fllox}}/\text{Col2Cre}^+$ chondrocytes. $\text{VDR}^{\text{fllox/fllox}}/\text{Col2Cre}^+$ mice were viable and showed normal growth. At 8 weeks, bone mass, measured by pQCT and histomorphometry, and dynamic bone parameters were similar between the genotypes. However, at pre-weaning stages (day15 and neonatal), histological analysis revealed an increased bone mass in $\text{VDR}^{\text{fllox/fllox}}/\text{Col2Cre}^+$ tibia ($p < 0.036$), which was associated with decreased osteoclast surface to bone surface at day15 ($p < 0.022$) and reduced osteoclast number at the growth plate in neonatal mice ($p < 0.019$) compared to $\text{VDR}^{\text{fllox/fllox}}/\text{Col2Cre}^+$ mice. In addition, the initial invasion of blood vessels and osteoclasts in embryonic day (E) 15.5 tibia was delayed in the $\text{VDR}^{\text{fllox/fllox}}/\text{Col2Cre}^+$ mice. Length of mineralization after culturing E15.5 metatarsals for 4 days was significantly smaller in $\text{VDR}^{\text{fllox/fllox}}/\text{Col2Cre}^+$ mice. These data suggest that VD regulates in chondrocytes the expression of genes involved in osteoclast formation. Accordingly, VD (10^{-8}M) treatment increased RANKL gene expression 40 fold in primary epiphyseal chondrocytes derived from $\text{VDR}^{\text{fllox/fllox}}/\text{Col2Cre}^+$ mice, whereas this effect was lacking in $\text{VDR}^{\text{fllox/fllox}}/\text{Col2Cre}^+$ chondrocytes. Furthermore, TRAP positive multinuclear cells were formed when primary $\text{VDR}^{\text{fllox/fllox}}/\text{Col2Cre}^+$ chondrocytes were cocultured with splenocytes derived from either genotype and treated with VD but not when $\text{VDR}^{\text{fllox/fllox}}/\text{Col2Cre}^+$ chondrocytes were used. In conclusion, VDR expression in chondrocytes contributes to timely osteoclast formation during early endochondral bone development by regulating RANKL expression.

Disclosures: **R. Masuyama**, None.

1068

A RANK Cytoplasmic Motif, PFQEP³⁶⁹⁻³⁷³, Plays a Predominant Role in Mediating Osteoclast Survival by Activating Akt and its Downstream Signaling Molecule AFX. **W. Liu^{*1}, S. Wang^{*1}, S. Wei^{*1}, L. Sun², X. Feng¹.**

¹Pathology, Univ. of Alabama at Birmingham, Birmingham, AL, USA,

²Medicine/Endocrinology, Mount Sinai school of Medicine, New York, NY, USA.

RANKL, a member of the TNF family, is a crucial cytokine regulating osteoclast formation, function and survival. RANKL exerts its effect by activating its receptor RANK, which recruits various intracellular signaling molecules via specific motifs in its cytoplasmic tail. Previously, we reported the identification of three functional RANK cytoplasmic motifs (Motif 1: PFQEP³⁶⁹⁻³⁷³; Motif 2: PVQEE^{T559-564} and Motif 3: PVQEEQ^{G604-609}) and demonstrated that Motif 2 and Motif 3 are more potent than Motif 1 in mediating osteoclast formation and function. In the present study, we examined the role of the three motifs in osteoclast survival. Our osteoclast survival assays demonstrated that Motif 1, in contrast to its minimal role in osteoclast formation and function, plays a predominant role in maintaining osteoclast survival. Moreover, while Motif 2 and Motif 3 are very potent in osteoclast formation and function, they exert a moderate effect on osteoclast survival. Given that RANKL has been shown to be able to activate Akt, which is a critical mediator of cell survival in a variety of cell types, we investigated the role of these motifs in activating Akt signaling pathway. Our data demonstrated that Motif 1, but not Motif 2 and Motif 3, is able to stimulate Akt activation (phosphorylation). Our previous study has shown that all three motifs are capable of activating NF- κ B, which is also a mediator of osteoclast survival. Thus, Motif 1 mediates osteoclast survival by activating both Akt and NF- κ B pathways while Motif 2 and Motif 3 do so by activating NF- κ B only. Since it has been established that Akt utilizes distinct downstream pathways

ASBMR 27th Annual Meeting

such as GSK3 β , FKHR, BAD and AFX to regulate cell survival, we then investigated which downstream signaling pathway(s) is activated by Akt to promote osteoclast survival. By using antibodies against phosphorylated GSK3 β , FKHR, BAD and AFX, we demonstrated that RANKL only stimulates AFX phosphorylation, indicating that the AFX pathway is the key pathway activated by Akt to modulate osteoclast survival. Taken together, we conclude that Motif 1 plays a predominant role in mediating osteoclast survival and Motif 1 does so by activating Akt and NF- κ B pathways. Moreover, Akt exerts its effect on osteoclast survival by activating its downstream signaling molecule AFX.

Disclosures: **W. Liu**, None.

1069

K63-Linked Polyubiquitin Chains Catalyzed by the E3 Ligase TRAF6 Are Required for RANK Signaling and Osteoclast Formation. **B. Lamothe***, **W. K. Webster***, **B. G. Darnay**. Experimental Therapeutics, University of Texas M.D. Anderson Cancer Center, Houston, TX, USA.

RANK plays a central role in the maintenance of the bone homeostasis by regulating the differentiation and activation of osteoclasts. The binding of RANKL to its receptor results in the recruitment of TRAF6, which activates the NF- κ B, JNK, p38, and MAPK pathways. The RING domain of TRAF6 is required for its ability to signal, most likely by functioning as an E3 ubiquitin ligase, which together with the ubiquitin conjugating enzyme complex Ubc13/Uev1A catalyzes the synthesis of a unique polyubiquitin chain linked through lysine-63 (K63). Thus, TRAF6-mediated polyubiquitination acts as a trigger to activate the stress kinase pathways. Here we present evidence that RANK induces rapid K63-linked ubiquitination of TRAF6, which is blocked by a catalytically inactive Ubc13. The ability of RANK to activate NF- κ B and JNK is abolished by ectopic expression of a RING finger mutant of TRAF6 devoid of autoubiquitination activity, or a catalytically inactive Ubc13. Previous studies indicated that the zinc finger protein A20, a protein known to interact with TRAF6 and RIP, prevents NF- κ B activation by TNF, IL-1, and LPS. Additionally, recent evidence suggests that A20 possess both E3 ubiquitin ligase activity and deubiquitinating activity. Similar to LPS, RANKL induced the rapid, transient upregulation of A20 in RAW264.7 cells. In addition, ectopic expression of A20 inhibited RANKL- and RANK-induced NF- κ B and JNK activation, which suggests that the deubiquitinating enzyme A20 tightly controls RANKL responses. To address the functional significance of the E3 ligase activity of TRAF6 in osteoclastogenesis, we infected RAW264.7 cells with a retrovirus that encodes for TRAF6 or the RING domain mutant of TRAF6. We observed that wild-type TRAF6, but not the RING domain mutant of TRAF6, caused RANKL-independent upregulation of NFATc1 and osteoclast differentiation. In addition, we have identified the lysines on TRAF6, which are involved for its auto-ubiquitination and are thus able to dissect the role of K63-linked polyubiquitin chain on TRAF6 and its ubiquitin ligase activity to activate downstream signaling pathways. To this end, we are actively pursuing the downstream targets of the E3 ligase activity of TRAF6 for K63-linked polyubiquitination, such as TAB2 and NEMO. The identification of TRAF6 substrates will provide the missing link by which ubiquitination initiates the activation of NF- κ B and JNK by RANKL. Thus, we present the first evidence that the E3 ligase activity of TRAF6 is required for RANK signaling and programming osteoclast progenitors to become fully differentiated and active osteoclasts.

Disclosures: **B. G. Darnay**, None.

1070

RANKL Induced iNOS/NO Acts as a Negative Feedback Inhibitor during Osteoclastogenesis via an NF- κ B and IFN- β /Stat1 Signaling Pathway. **H. Zheng**, **X. Yu**, **P. A. Collin-Osdoby**, **P. A. Osdoby**. Department of Biology, Washington University, St Louis, MO, USA.

RANKL is essential for osteoclast (OC) formation and binds RANK to trigger multiple signals (ERK, p38 MAPK, JNK, NF- κ B). We showed that RANKL also induces iNOS mRNA, protein and NO release during OC differentiation. Inhibitors of iNOS/NO augmented RANKL-induced OC formation and bone resorption, and OC development and resorption were greater in marrow cultures of iNOS $^{-/-}$ vs. iNOS $^{+/+}$ mice. Thus, NO is an autocrine negative feedback signal regulating RANKL-mediated OC development in murine RAW 264.7 and primary bone marrow cells. Here, we investigated signal mechanisms by which RANKL induces iNOS/NO to restrain OC formation using selective inhibitors, blocking antibodies, and marrow cells from normal, IFN receptor $^{-/-}$, or Stat1 $^{-/-}$ mice. Inhibitors of NF- κ B (PDTC), p38 MAPK (SB203580), or ERK1/2 (PD98059) blocked both OC formation and iNOS/NO induction in murine pre-OC, indicating they are required for both RANKL-induced OC formation and iNOS/NO negative feedback regulation. In contrast, JNK inhibition (SP600025) blocked only OC formation and RANKL activation of JNK was not needed for the NO negative feedback mechanism. Because IFN β was shown to be a RANKL-induced negative feedback signal during OC development, and IFN β can induce iNOS/NO in other cells, we investigated if RANKL induced IFN β and downstream phosphorylation of Stat-1 was involved in RANKL stimulated iNOS/NO and restrained OC formation. We found that: 1) RANKL induced IFN β (by 30') and P-Stat-1 (by 4 h), 2) RANKL stimulation of P-Stat-1 and iNOS/NO (but not IFN β) required new protein synthesis, was mimicked by exogenous IFN β and was inhibited by neutralizing Ab to IFN β thereby enhancing OC formation, and 3) NF- κ B inhibition blocked RANKL induced IFN β . Moreover, marrow cells from mice deficient in the IFN β receptor component IFNAR1 (IFNAR1 $^{-/-}$) or Stat1 $^{-/-}$ exhibited little iNOS/NO response to RANKL and generated more OC vs. marrow cells from IFNAR1 $^{+/+}$ or Stat1 $^{+/+}$ mice. These and other findings conclusively demonstrate that the novel autocrine negative feedback pathway triggered by RANKL during OC development involves NF- κ B activation, followed by IFN β induction, IFN-R signaling, P-Ser of Stat-1, and induction of iNOS mRNA, protein, and NO release. Specifically interfering with RANKL-mediated

IFN β or Stat-1 activation prevents iNOS/NO induction, enhances OC formation and bone resorption, and suggests a novel target for therapeutic intervention to diminish bone loss in skeletal pathologies characterized by elevated RANKL and OC bone resorption.

Disclosures: **H. Zheng**, None.

1071

SDF-1 Promotes the Transendothelial Migration of Circulating Human CD14 $^{+}$ Monocytes and Osteoclast (OC) Precursors, Resulting in Greater RANKL-Induced OC Formation and Bone Resorption. **L. Kindle**, **L. Rothe**, **M. Kriss***, **P. A. Osdoby**, **P. A. Collin-Osdoby**. Department of Biology, Washington University, St Louis, MO, USA.

OC precursors (pre-OC) of the monocytic lineage reside in the bone marrow and peripheral circulation, from which they may be recruited to sites for development and resorption of bone during normal skeletal remodeling or pathological bone erosion. A functional relationship exists between the bone microvasculature and areas of active resorption; however, little is known about how circulating pre-OC are recruited into bone and directed to sites for their OC differentiation and function. Chemokines are key signals regulating cell trafficking. SDF-1 is a chemokine highly produced by bone stromal and endothelial cells that acts as a normal homing signal for hematopoietic cells via their expression of the receptor CXCR4. SDF-1 is also highly produced by inflamed synovocytes in arthritic joints, and a selective CXCR4 antagonist inhibits OC numbers and bone loss in murine arthritis. Previously, we showed that SDF-1 chemoattracts pre-OC from human peripheral blood mononuclear cells (hPBMC), leading to greater RANKL-induced OC formation and bone resorption. Here, we investigated if SDF-1 is also important for pre-OC recruitment via stimulating their transendothelial migration (TEM) through a human microvascular endothelial cell (HMVEC) barrier using a transwell model. TEM of hPBMC into the lower chambers was increased > 2-fold by 10 nM SDF-1 and led to greater OC and resorption pit formation after M-CSF + RANKL culture of the migrated cells. SDF-1 stimulated TEM was inhibited (~65%) by HMVEC pretreatment with neutralizing antibodies to the key endothelial cell adhesion molecules ICAM-1, VCAM-1, and PECAM-1. HMVEC expressed modest SDF-1 mRNA and protein levels, and they efficiently took up and displayed on their surface exogenously supplied SDF-1 that stimulated hPBMC TEM. Because pre-OC derive from the CD14 $^{+}$ monocyte fraction of hPBMC, and CD14 $^{+}$ cells expressed modest CXCR4, we examined CD14 $^{+}$ TEM to SDF-1. Like hPBMC, CD14 $^{+}$ TEM was increased 2-fold by SDF-1 and led to 2-fold higher OC and bone pit formation after their M-CSF + RANKL culture. Furthermore, hPBMC that had undergone TEM to SDF-1 were enriched for pre-OC, suggesting preferential recruitment from the mixed hPBMC population. We conclude that SDF-1 may be a key signal provided by bone endothelial and stromal cells that has multiple roles in OC biology, including recruitment of circulating pre-OC through the endothelial barrier into the marrow and directing the chemotactic navigation of pre-OC to appropriate stromal sites for their differentiation and function during normal bone remodeling or pathological bone destruction.

Disclosures: **L. Kindle**, None.

1072

TNF Promotes Osteoclast Precursor Mobilization to the Blood by Inhibiting SDF-1 Production by Bone Marrow Stromal Cells. **Q. Zhang**, **Z. Yao**, **R. Guo***, **E. M. Schwarz**, **T. Bushnell***, **B. F. Boyce**, **L. Xing**. University of Rochester, Rochester, NY, USA.

Osteoclasts (ocls) differentiate from circulating ocl precursors (OCPs) and are essential effector cells for focal bone erosion in chronic inflammatory arthritis. TNF is a potent ocls stimulator that increases circulating OCPs numbers by enhancing their egress from the bone marrow. Stromal cell derived factor 1 (SDF-1) and its receptor, CXCR4, play a critical role controlling homing and mobilization of hematopoietic stem and progenitor cells, but it is not known if they serve this function in OCPs mobilization or if TNF might affect it. To investigate this question, we first examined the effect of TNF on expression of SDF-1 in stromal cells from TNF transgenic (TNF-Tg) arthritic and wt mice. Stromal cells from TNF-Tg mice expressed significantly lower SDF-1 than wt mice (0.4 \pm 0.1 vs 1 \pm 0.05 ng/ml, measured by ELISA). Administration of TNF to wt mice decreased marrow SDF-1 levels (0.2 \pm 0.03 ng/ml vs 0.74 \pm 0.07 in PBS-treated mice) and resulted in a 8-fold increase in blood OCPs (CD11b $^{+}$ /Gr-1 $^{-lo}$ cells: 2.6 \pm 0.2 \times 10E6/ml vs 0.3 \pm 0.02 \times 10E6/ml in PBS-treated mice). *In vitro*, TNF significantly lowered SDF-1 mRNA levels and protein production (2.4 \pm 0.8 ng/ml vs 6.9 \pm 0.9 ng/ml in PBS-treated cells) by ST2 stromal cells. To determine if OCPs express functional CXCR4, wt OCPs were cultured in a transwell/osteoclastogenesis assay. OCPs migrated toward an SDF-1 gradient in a dose-dependent manner and the cells that migrated differentiated with M-CSF and RANKL treatment into ocls (Trap +ve cells: 0 \pm 0/well in PBS-attracted cells vs 71 \pm 5 multinucleated cells/well and 118 \pm 15 mononucleated cells/well in SDF-1 (100ng/ml)-attracted cells). We observed no change in CXCR4 levels on OCPs from TNF-Tg mice or TNF-treated bone marrow OCPs. Pre-treatment of OCPs with TNF did not affect the rate of migration towards the SDF-1 gradient. To determine if TNF-mediated cell mobilization is specific for myeloid/occl precursors, the frequency of other cell types in the blood of TNF-Tg and wt mice was compared using combinations of cell surface markers. Except for the 8-fold increase in CD11b $^{+}$ /Gr-1 $^{-lo}$ myeloid/occl precursors, there was no alternation in the frequency of B220 $^{+}$ B cells, CD3 $^{+}$ T cells, or Lin-/Sca1 $^{+}$ /c-Kit $^{+}$ stem cells in TNF-Tg mice. In summary, TNF inhibits SDF-1 production by bone marrow stromal cells without affecting OCP migration or expression of CXCR4. Since stromal cells hold hematopoietic cells in the marrow by SDF-1/CXCR4 interaction, we propose that TNF promotes OCP egression to the blood stream and thus facilitates their subsequent mobilization in chronically inflamed joints by reducing bone marrow stromal expression of SDF-1.

Disclosures: **Q. Zhang**, None.

1073

Correlates of Femoral Neck Trabecular and Cortical Volumetric Bone Mineral Density (vBMD): The Osteoporotic Fractures in Men Study, **MrOS.** J. Cauley¹, T. Blackwell², J. M. Zmuda¹, D. C. Bauer², R. Fullman², K. E. Ensrud³, K. L. Stone², E. Barrett-Connor⁴, E. S. Orwoll⁵. ¹U of Pittsburgh, Pittsburgh, PA, USA, ²UCSF, San Francisco, CA, USA, ³U Minnesota, Minneapolis, MN, USA, ⁴UCSD, San Diego, CA, USA, ⁵Oregon Health & Science University, Portland, OR, USA.

Correlates of areal BMD (aBMD) are well established, but whether these same factors correlate with vBMD is unknown. The objective of the current cross-sectional analysis is to determine the correlates of femoral neck trabecular and cortical vBMD in 3,671 men, mean age 73.6y ± 5.9 and to compare them to those of aBMD. BMD was measured by QCT at 6 clinical centers; aBMD was measured by DXA. Demographic, history and lifestyle information was obtained by interview and height and weight by examination. All models were adjusted for clinic site, age, and race. To express the strength of the associations, % differences (95% CI) were calculated from multivariable linear regression models using the formula (beta * unit/mean BMD). Units were chosen to approximate 1 Standard Deviation (SD). Multivariable models explained 14%, 21%, and 20% of the overall variance in trabecular and cortical vBMD and aBMD, respectively. In general, the associations were stronger for trabecular than cortical vBMD, Table. Race and diabetes were the strongest positive predictors and history of non-trauma fracture, the strongest negative predictor. Past smoking, history of kidney stones, and corticosteroid use were associated with >5% lower trabecular vBMD and Parkinson's disease, >5% lower cortical vBMD. In general, the direction of the association of each characteristic with aBMD and vBMD were similar although the magnitude differed across variables. Identification of these correlates could help to identify men at risk for fracture and improve our understanding of fracture etiology.

Table: Multivariable Correlates of Femoral Neck aBMD and vBMD: % difference in BMD per unit (95% CI) in the characteristic

	Unit/ Referent	aBMD	Trabecular vBMD	Cortical vBMD
Age	5y	NS ⁺	-6.3 (-8.3, -4.3)	NS ⁺
Race	White			
Black		11.3 (8.9, 13.8)	31.8 (21.8, 41.8)	3.6 (1.8, 5.5)
Asian		NS	26.7 (15.3, 38.2)	NS
Weight	10kg	4.9 (4.3, 5.6)	2.9 (0.4, 5.5)	1.1 (0.7, 1.6)
Weight Change ⁺⁺	12.0 kg	-1.1 (-1.8, -0.4)	NS	NS
Height	7cm	-0.9 (-1.5, -0.2)	NS	NS
Height Change ⁺⁺	3cm	-1.0 (-1.5, -0.5)	-3.9 (-6.1, -1.7)	NS
Past Smoking	Yes	NS	-7.7 (-11.9, -3.5)	NS
Alcohol	6.7 dr/wk	1.2 (0.7, 1.7)	NS	0.5(0.1, 0.9)
Calcium Intake	589 mg/d	NS	3.0 (1.0, 5.1)	NS
Physical Activity (PACE)	68.2	0.8 (0.3, 1.3)	NS	NS
Non-Trauma Fracture	yes	-3.7 (-5.1, -2.3)	-14.1 (-19.8, -8.5)	-1.8 (-2.9, -0.8)
Maternal Fracture	yes	-1.4 (-2.7, -0.2)	NS	NS
Diabetes	yes	2.5 (0.8, 4.1)	11.9 (5.2, 18.5)	1.8 (0.6, 3.0)
Hypertension	yes	NS	5.4 (1.2, 9.6)	NS
Kidney Stones	yes	-2.2 (-3.7, -0.7)	-6.5 (-12.6, -0.5)	NS
Parkinson's	yes	NS	NS	-6.1 (-10.9, -1.2)
Corticosteroids	yes	NS	-12.3 (-21.3, -3.3)	NS
Tri-cyclic Antidepressants	yes	NS	NS	3.1 (0.2, 6.0)
Thyroid Hormone	Yes	NS	NS	-2.7 (-4.1, -1.2)
SSRI Antidepressants	yes	-3.7 (-6.8, -0.5)	NS	NS
Statin Use	yes	1.2 (0.03, 2.4)	NS	NS
COX-II Inhibitors	yes	3.1 (0.8, 5.4)	11.8 (2.5, 21.2)	NS
Chair Stands	3.23 sec	-0.7 (-1.2, -0.2)	NS	-0.6 (-1.0, -0.1)

⁺ Not significant in final multivariable model

⁺⁺ Change since age 25

Disclosures: **J. Cauley**, Merck 2, 8; Eli Lilly 2, 5; Pfizer 2, 5; Novartis 2, 5.

1074

Spinal Loading and Vertebral Strength: A Population-Based Study Using QCT. M. L. Bouxsein¹, B. L. Riggs², L. J. Melton², J. Muller*¹, E. J. Atkinson*², A. L. Oberg*², S. Khosla². ¹Orthopedic Surgery, Beth Israel Deaconess Medical Center, Boston, MA, USA, ²Mayo Clinic, Rochester, MN, USA.

Whereas spine BMD by DXA is widely used to predict vertebral fracture risk, approaches that incorporate better estimates of vertebral strength combined with spine loading may improve the identification of those at high risk for fracture. As a first step towards this goal, we studied an age-stratified sample of 375 women (W) and 325 men (M), aged 21 - 97 yrs. QCT was used to measure lumbar vertebral bone density (vBMD, mg/cm³) and cross-sectional area (CSA, cm²). Vertebral strength (VStr, Newtons, N) in compression was estimated from vBMD and CSA using engineering beam theory and in vitro mechanical testing data (Crawford et al, 2003). Individual height, weight and sex were incorporated into a biomechanical model to estimate the compressive load applied to the lumbar vertebra (VLoad, N) during bending forwards with a 10 kg weight in the hands. The factor of risk for fracture (Φ) was defined as VLoad/VStr (theoretically fracture occurs when Φ>1). **Results:** VStr was 22 to 54% higher in M than W at all ages (p<0.001), and declined over life significantly more in W (-40%) than in M (-25%, p=0.03). VLoad was on average 9% higher in M than W (p< 0.001). Thus, Φ was lower (ie, decreased risk of fracture) in M than W at all ages (-12.5% to -24.6%, p<0.001), and worsened with age more in W than M (+57% vs +35%, p = 0.006). The proportion of individuals in which fracture was predicted to occur increased with age, as Φ exceeded 1.0 in 8.2% and 1.6% of W and M below age 50, compared to 34.5% and 10.8%, respectively, above age 50.

Among those over age 50, persons with Φ > 1 were older, shorter (W only), had lower vBMD and VStr, and higher CSA (M only) and VLoad compared to those with Φ < 1 (p=0.03 - 0.001, Table). In conclusion, our findings, which represent the first population-based study incorporating estimates of vertebral strength and loads, demonstrate that 1) the age- and sex-differences in the 'factor of risk' mirror the reported prevalence of vertebral fracture, and 2) individuals at high risk for vertebral fracture have both lower vertebral strength and greater vertebral loads. These data provide strong rationale for future studies comparing DXA with Φ as predictors of fracture risk. Table 1. Characteristics of individuals over age 50 according to their "factor of risk" value.

	Women		Men	
	Φ < 1 (n=161)	Φ > 1 (n=85)	Φ < 1 (n=21)	Φ > 1 (n=173)
Age (yrs)	64.0 ± 10.3	72.8 ± 10.7 **	67.9 ± 11.6	78.0 ± 9.4 **
Ht (cm)	162 ± 7	160 ± 7 *	175 ± 7	176 ± 6
Wt (kg)	73.2 ± 15.2	74.4 ± 18.5	87.0 ± 15.7	88.2 ± 16.9
vBMD (mg/cm ³)	190 ± 38	138 ± 36 **	187 ± 42	116 ± 25 **
CSA (cm ²)	10.6 ± 1.4	10.7 ± 1.4	13.8 ± 2.0	14.8 ± 1.6 *
VStr (N)	4395 ± 830	3206 ± 869 **	5607 ± 1244	3759 ± 910 **
VLoad (N)	3354 ± 546	3910 ± 899 **	3823 ± 698	4350 ± 969 **
Φ	0.78 ± 0.13	1.25 ± 0.22 **	0.71 ± 0.15	1.18 ± 0.17 **

*, ** p < 0.05, 0.0001 vs Φ < 1 within sex

Disclosures: **M.L. Bouxsein**, None.

1075

Effects of Gender and Age on Bone Microstructure at the Wrist: A Population-Based *In Vivo* Bone Biopsy Study. S. Khosla, B. L. Riggs, A. L. Oberg*, E. J. Atkinson*, L. McDaniel*, J. M. Peterson*, L. J. Melton. Endocrine Research Unit, Mayo Clinic College of Medicine, Rochester, MN, USA.

Although changes in bone microstructure contribute to fracture risk independently of BMD, it has not heretofore been possible to assess this non-invasively in population-based studies. Thus, we used high resolution 3D-pQCT imaging (voxel size, 89 μm, Scanco AG) to define, in a random sample of women (F, n = 322) and men (M, n = 254) age 21 to 97 yrs, gender and age effects on bone microstructure at the wrist. Relative to young F (age 20-29 yrs, n = 17), young M (n = 18) had higher values for trabecular bone volume/tissue volume (BV/TV, by 26%, P = 0.002), trabecular thickness (TbTh, by 27%, P < 0.001), bone area (BA, by 50%, P < 0.001), and endocortical area (EnA, by 55%, P < 0.001), but similar values for trabecular number (TbN), trabecular separation (TbSp), and cortical thickness (CTh). Shown in the Table are the percent changes as a function of age (20-90 yrs), correlation with age (R), and comparisons of slopes (F vs. M) in these parameters.

Variable	Women		Men		P-value (F vs. M)
	% Ch	R	% Ch	R	
BV/TV	-27 ^c	-0.27 ^c	-25 ^c	-0.37 ^c	0.629
TbN	-14 ^{c, NL}	-0.29 ^c	+9 ^{NL}	-0.04	<0.001
TbTh	-14 ^{c, NL}	-0.22 ^c	-25 ^{c, NL}	-0.40 ^c	0.052
TbSp	+24 ^c	+0.30 ^c	-4 ^{b, NL}	+0.16 ^a	<0.001
BA	+11 ^b	+0.15 ^b	+13 ^b	+0.19 ^b	0.243
EnA	+26 ^c	+0.25 ^c	+22 ^c	+0.24 ^c	0.410
CTh	-52 ^{c, NL}	-0.58 ^c	-37 ^{c, NL}	-0.42 ^c	0.005

^aP < 0.05; ^bP < 0.01; ^cP < 0.001; NL, non-linear relationship with age.

More detailed analyses revealed that, whereas changes in TbN, TbTh, and TbSp were similar in F and M after age 50 yrs, there were clear differences in these changes in F vs. M aged 20-49 yrs. Thus, in M aged 20-49 yrs, TbN increased by 18% (P < 0.001), TbTh decreased by 28% (P < 0.001), and TbSp decreased by 12% (P < 0.001), consistent with a conversion of trabecular plates to rods, and these changes offset age-related decreases in TbN and increases in TbSp in M after age 50 yrs. By contrast, TbN and TbSp remained stable in F aged 20-49 yrs, and TbTh decreased by 13% (P = 0.02), with further decreases in TbN and TbTh and increases in TbSp after age 50 yrs, consistent with microstructural damage. Conclusions: 1) Relative to F, M begin adult life with a more plate-like, and thus stronger, trabecular microstructure; 2) This, combined with virtually no change over life in TbN or TbSp in M as compared to significant decreases in TbN and increases in TbSp in F likely contributes to lower life-long risk of fractures in M and to their virtual immunity to age-related increases in wrist (Colles') fractures; and 3) High resolution 3D-pQCT analyses of bone microstructure is a powerful new tool that will greatly enhance clinical assessment of fracture risk.

Disclosures: **S. Khosla**, None.

1076

The Effect of Cyclooxygenase-2 Inhibitors on Bone Mineral Density: Results from the CaMos Study. J. B. Richards*¹, L. Joseph*², D. Goltzman¹. ¹Endocrinology, McGill University, Montreal, PQ, Canada, ²Epidemiology and Biostatistics, McGill University, Montreal, PQ, Canada.

In animal models the inhibition of prostaglandin E2 production, through the use of cyclooxygenase-2 (COX-2) inhibitors, has been demonstrated to decrease load-induced bone formation but also to prevent menopause-associated bone loss. We hypothesized that COX-2 use would be associated with a lower bone mineral density (BMD) in men, but may conversely be associated with a higher BMD in post-menopausal women not using estrogen supplementation. To date the effect of COX-2 specific inhibitors on human bone mineral density has not been described. We tested these hypotheses using a multi-centered randomly selected population-based cohort of 1934 male (mean and [SD] 64.1 [13.6] years) and 4556 post-menopausal female (mean and [SD] 75.1 [6.3]) subjects. To test these hypotheses we used standard linear regression techniques. Compared to the rest of the

ASBMR 27th Annual Meeting

cohort, daily COX-2 users (males n=121, females n=337) were more likely to be older, have a higher body mass index (BMI), and carry a diagnosis of osteoarthritis or rheumatoid arthritis. When compared to non-users, men using daily COX-2 inhibitors had a lower BMD at all hip sites and a trend towards a lower BMD at lumbar spine. Females COX-2 users, not taking estrogen supplementation, were found to have a higher BMD than non-users. In the presence of exogenous estrogen this protective effect of COX-2 inhibitors was lost. These effects generally persisted after adjustment for confounders (age, BMI, number of ovulatory cycles (in females), calcium intake, previous fracture, osteoarthritis, rheumatoid arthritis, lupus, education level and centre). In addition, we found a linear relationship between COX-2 dose and these aforementioned effects. Our findings suggest that daily use of COX-2 inhibitors may decrease BMD in men, but conversely may increase BMD in women not using estrogen supplementation. These results support the hypotheses that COX-2 inhibition may prevent both load-induced bone formation and estrogen-withdrawal mediated bone loss. Men who previously used daily COX-2 inhibitors, who have other risk factors for low BMD, may benefit from BMD testing to assess their future fracture risk. COX-2 inhibition may however have utility in post-menopausal women if bone selective analogs can be developed.

Percent Change in BMD: COX-2 Users vs. Non-Users (95% CI) Adjusted Analysis			
BMD Site	Males	Females >65 years not using estrogen.	Females >65 years using estrogen.
Total Hip	-3.1 (-5.9, -0.26)	3.2 (0.39, 6.0)	-1.2 (-3.9, 1.5)
Lumbar Spine	-2.4 (-6.0, 1.1)	5.8 (2.4, 9.2)	4.4 (1.1, 7.7)
Trochanter	-4.2 (-7.6, -0.85)	3.4 (0.12, 6.6)	-1.2 (-4.2, 1.9)
Wards	-5.2 (-10.2, -0.2)	3.6 (-1.6, 8.9)	-0.18 (-5.0, 4.7)
Neck	-3.1 (-6.2, -0.04)	1.0 (-2.0, 3.97)	0.5 (-2.4, 3.4)

Disclosures: **J.B. Richards**, None.

1077

Time Trends in Mortality Following Hip Fracture. **A. B. Araujo¹, Y. Wang^{*2}, L. M. Brass^{*2}, H. M. Krumholz^{*2}, J. H. Lichtman^{*2}.** ¹New England Research Institutes, Watertown, MA, USA, ²Yale University School of Medicine, New Haven, CT, USA.

There are between 250,000-300,000 hip fractures in the U.S. annually. Nearly 20% of hip fracture patients die with one year of fracture. The impact of changes in population demographics, increasing hip fracture incidence, and advances in hip fracture management on post-fracture mortality outcomes is unclear since there are limited data on time trends in mortality among hip fracture patients. To address this issue, we obtained data for all U.S. Medicare fee-for-service claims for hip fracture (ICD-9-CM code: 820.0-820.9) between 1992 and 1999 to examine time trends in the 1-year mortality rate following hip fracture. Rates were estimated in the cohort overall and by age, gender, and race/ethnicity. Expected death rates were calculated for each year between 1992 and 1999 for each 5-year age, gender, race/ethnic group from National Center for Health Statistics data. Time trends in mortality following hip fracture were evaluated with Poisson regression, which yields estimates of the standardized mortality ratio (SMR) for fracture patients relative to the general population. Information on age, race/ethnicity (black, white, other), and gender was obtained from the Medicare Denominator File. A total of 1,929,797 qualifying hip fractures among patients 65 y or older were identified between 1992 and 1999. The mortality rate in the cohort overall was 20.5%, and rose significantly from 18.4% in 1992 to 22.8% in 1999. During the same period, the underlying mortality in the population increased 9.6%. As a result, the SMR increased from 2.01 to 2.29 (an increase of 13.5%) over the time period. The time trend in SMRs was more pronounced (p=.0039) among younger age groups but showed no variation (p=.9542) with gender-race/ethnic group. Changes in comorbidity and hospital length of stay did not explain the rise in SMRs. These findings are of great concern given the expected increase in the U.S. elderly population over the next few decades.

Disclosures: **A.B. Araujo**, None.

1078

Projections of Osteoporosis Fractures and Costs by Skeletal Site in the USA. **A. Tosteson¹, D. Solomon², A. B. King^{*3}, B. Dawson-Hughes⁴, R. Burge^{*3}, J. Wong^{*5}.** ¹Dartmouth College Medical School, Hanover, NH, USA, ²Division of Pharmacoepidemiology, Brigham and Women's Hospital, Boston, MA, USA, ³Procter & Gamble Pharmaceuticals, Mason, OH, USA, ⁴Tufts University, Boston, MA, USA, ⁵Tufts University School of Medicine, Boston, MA, USA.

Osteoporosis is characterized by a loss of bone strength, leading to an increased risk of fracture (Fx). In the United States, over 10 million people have osteoporosis, and an additional 34 million have osteopenia. Demographic changes and lifestyle factors may lead to increases in Fx and costs across multiple skeletal sites. The aims of the study were to estimate osteoporosis Fx incidence and costs by Fx type in the USA. A Fx incidence based Markov model of OP was used to estimate osteoporosis-related Fx and costs by skeletal site for the U.S. population aged 50-99 years. Fracture types included Hip, Vertebral, Forearm/wrist, Pelvic, and Other (non-pathologic clavicle, humerus, carpal, tibia, fibula, femur). Hip Fx incidence rates (ICD-9 820.xx, closed only; trauma cases excluded) were calculated from national hospital discharge data; clinical incidence rates for all other Fx types were obtained from published studies. Unit costs of Fxs were obtained from database estimates and from published studies. Annual Fxs and costs were projected through 2025

using U.S. Census Bureau population data. In 2005, total incident osteoporotic Fxs and related costs are predicted to exceed 2.05 million and \$16.9 billion, respectively, in the U.S. Non-vertebral Fxs account for 73% of total Fxs and 94% of costs. Hip Fxs comprise 14% of Fxs and 71% of costs in 2005. All other non-vertebral Fxs account for 59% of incident Fxs and 22% of costs. Incidence per 10,000 population (aged 50-99) is 77 for Other Fxs, 63 for Vertebral, 45 for Wrist, 34 for Hip, and 15 for Pelvic. Assuming no change, by 2025 total incident Fxs are predicted to increase by 48% to over 3 million, while costs grow to over \$25.2 B (49%).

Site	2005		2025	
	Fx (000s)(%)	\$Costs M (%)	Fx (000s) (% Growth)	\$Costs M (% Growth)
Vertebral	547 (27)	1,076 (6)	831 (52)	1,650 (53)
Hip	296 (14)	12,059 (71)	447 (51)	18,000 (49)
Wrist	397 (19)	535 (3)	571 (44)	757 (41)
Pelvic	135 (7)	873 (5)	210 (56)	1,401 (60)
Other	675 (33)	2,371 (14)	976 (45)	3,461 (46)
Total	2,050	16,915	3,036 (48)	25, 268 (49)

Projections for 2005 reveal that 73% of the 2.05 million clinical fractures and 94% of costs are non-vertebral. Fracture incidence and costs are expected to increase dramatically to over 3 million and \$25.2 billion per year by 2025 due to anticipated demographic changes. Osteoporosis intervention programs should consider the impact of fracture on the total skeleton, not only at vertebral and hip sites.

Disclosures: **A. Tosteson**, **Innovus Research**, **NPS Pharmaceuticals** 5.

1079

Effects of PTH Rechallenge 1 Year after the First PTH Course in Patients on Long-Term Alendronate. **F. Cosman, J. W. Nieves, M. Zion*, N. Barbuto*, R. Lindsay.** Clinical Research Center, Helen Hayes Hospital, West Haverstraw, NY, USA.

We performed a randomized clinical trial in 126 women, who had been treated for osteoporosis with alendronate for at least 1 year (mean 3.2 years) and assigned to remain on alendronate and receive daily PTH(1-34) 25 mcg/d, cyclic PTH(1-34) 25 mcg/d, given in 3 month on/3 month off cycles, or alendronate alone. After the active drug treatment period of 15 months, subjects were followed on continued alendronate for 12 subsequent months and then invited to participate in an observational extension protocol where all subjects were offered daily PTH(1-34) therapy for an additional 15 months. Of the 108 subjects who completed the original 15 month clinical trial, 82 completed the 12-month follow-up period and of those, 43 agreed to participate in the extension study. Here we present experience on the first 24 subjects, representing 13 subjects from the original daily PTH group and 11 subjects from the original cyclic PTH group. During the 12 month interval between the PTH challenge and the PTH rechallenge, biochemical indices returned to pre-PTH treatment baseline levels and there was no significant decline in BMD from the peak seen after the 15 month first PTH course. Since all subjects in both the original daily and cyclic PTH groups received the same PTH dose for the first 3 months, data from the PTH groups were combined for the 3-month biochemical bone turnover analyses. Also, as there were no significant differences in BMD response at 15 months between the daily and cyclic PTH groups during the first PTH challenge, the two PTH groups were pooled for the BMD analysis. Effects of PTH on bone turnover over the first 3 months of the PTH rechallenge were compared to the bone turnover effects of the first PTH challenge at the same time point. Effects of the PTH rechallenge on BMD of the lumbar spine at 15 months were compared to those seen at the same time during the first PTH challenge. Serum osteocalcin increased by 77.9±10% during the initial PTH challenge and by 75.6±23% during the PTH rechallenge at 3 months. Urine N-telopeptide increased by 102±52 % during the initial PTH challenge and by 124±55% during the PTH rechallenge at 3 months. Spine BMD increased by 5.3±1.2% during the first PTH challenge and by 4.3±0.7% during the PTH rechallenge at 15 months. The results suggest that, in patients on long-term ongoing alendronate therapy, rechallenge with PTH, after a 12 month interval off PTH, stimulates increases in bone formation, resorption and BMD similar to those seen during the first course of PTH administration. Patients who remain at high risk of fracture despite a first course of PTH therapy might benefit from a second discrete PTH course given 12 months later.

Disclosures: **F. Cosman**, **Merck** 5, 8; **Eli Lilly** 2, 5, 8; **NPS Pharmaceuticals** 5.

1080

Safety and Efficacy of PTH(1-84) at 18 and 24 Months in Women with Postmenopausal Osteoporosis Receiving Hormone Therapy: Results from the POWER Study. **L. Fogelman*¹, C. Christiansen*², T. Spector*³, W. Fraser*⁴, J. Fordham*⁵.** ¹Guy's, Kings and St Thomas' Hospital Medical School, London, United Kingdom, ²Center for Clinical and Basic Research, Ballerup, Denmark, ³St Thomas' Hospital, London, United Kingdom, ⁴Royal Liverpool University Hospital, London, United Kingdom, ⁵The James Cook University Hospital, London, United Kingdom.

PTH(1-84) reduces the incidence of vertebral fractures and increases BMD in women with postmenopausal osteoporosis. Adding PTH(1-84) to the therapeutic regimen of women with low BMD who are on stable HRT may provide additional benefits. The Prevention of Osteoporosis in Women on Estrogen Replacement (POWER) trial was a randomized, double-blind, placebo-controlled, multi-center study involving 180 women (mean age, 58.8 years; mean years postmenopausal, 12.6) with low BMD (LS T-scores ≤-2.0) who had received HRT for ≥6 months. Patients were randomized to daily injections of PTH(1-84) 100 µg/d + HRT (n=90) or HRT alone (n=90). Subjects received calcium (700-1050 mg/d) and vitamin D (800 IU/d). An increase in LS BMD was seen in both groups at Months 18 and 24; however, a statistically significant increase in subjects receiving

PTH(1-84) + HRT compared with HRT alone was seen at Months 18 (6.42%, p<0.001) and 24 (6.53%, p<0.001). In the PTH(1-84) + HRT group statistically significant increases over baseline of 7.9% and 8.6% (p<0.001) were seen at Months 18 and 24. At the femoral neck (FN), PTH(1-84) + HRT treatment resulted in a statistically significant increase in BMD of 2.27% relative to the increase observed with HRT alone (0.47%; p=0.024). There was a statistically significant increase in bone specific alkaline phosphatase (BSAP) of 97.7% at Month 12 and of 115.1% at Month 24 for PTH(1-84) when compared with placebo at Months 12 (18.5%, p=0.01) and 24 (28.7%, p=0.009). Similarly, a PTH(1-84)-associated increase in N-telopeptide (NTx) of 65.0% at Month 12 for PTH(1-84) compared with placebo (2.3%, p<0.0001) was maintained at Month 24 (69.2% vs 24.3%, p=0.0049). There was no significant change in these values in subjects on HRT alone. The incidence of vertebral and non-vertebral fractures in this study population was very low and the impact of PTH(1-84) on clinical fracture is difficult to assess. Adverse events (AEs) were similar in the HRT and PTH(1-84) + HRT groups; serious AEs occurred in 17.8% and 26.7% of subjects, respectively. Hypercalcemia was 2.2% and 14.4% respectively in the HRT and the PTH(1-84) + HRT groups. Combined PTH(1-84) + HRT therapy was associated with statistically significant increases in LS and FN BMD and other surrogates that indicate anabolic activity when compared to HRT alone. PTH(1-84) in combination with HRT was well tolerated and safe.

Disclosures: **I. Fogelman**, NPS Pharmaceuticals 2, 5.

1081

Risedronate and Alendronate Similarly Suppress Remodeling and Increase Microdamage in Beagles after 1 Year of Treatment at Clinical Doses. M. R. Allen¹, K. Iwata^{*1}, R. Phipps², D. B. Burr¹. ¹Anatomy & Cell Biology, Indiana University School of Medicine, Indianapolis, IN, USA, ²Procter and Gamble Pharmaceuticals, Inc., Mason, OH, USA.

One year of bisphosphonate treatment at 5-6x the post-menopausal osteoporosis (PMO) clinical dose suppresses cancellous bone remodeling by 90%, increases microdamage and reduces toughness in the lumbar vertebrae of normal beagles. The current study was designed to determine if bisphosphonates given at lower doses would result in lower levels of remodeling suppression and less microdamage accumulation. One-year-old female beagles were randomized into seven groups (n = 12/group) and treated daily for 1 year with oral doses of vehicle, risedronate (RIS; 0.05, 0.1, or 0.5 mg/kg/day) or alendronate (ALN; 0.1, 0.2, or 1.0 mg/kg/day). The 1:2 ratio of each of the three risedronate to alendronate doses was based on clinical dosing (= dose equivalents). The lower two doses of each compound correspond approximately to the daily PMO clinical dose on a mg/kg basis while the highest dose was 5-6x the clinical dose. Bone remodeling, microdamage, and mechanical properties of lumbar vertebrae were quantified. Cancellous bone activation frequency (Ac.f) was dose-dependently suppressed by RIS (p < 0.05) by -40%, -66%, and -84% compared to vehicle-treated animals. There was no dose-response in remodeling suppression for ALN; all three doses reduced Ac.f similarly (-65%, -71%, and 76%) compared to vehicle (p < 0.05). At the lowest dose-equivalent, RIS suppressed Ac.f significantly less than ALN; there was no difference at the other two dosing equivalents. Cancellous bone crack surface density (Cr.S.Dn) was significantly increased (3-4x) compared to controls with the lower 2 doses of each drug. The high dose of each drug increased Cr.S.Dn by >5x, significantly higher than lower doses. There was no difference in Cr.S.Dn between RIS and ALN at dose equivalents. The relationship between Ac.f and Cr.S.Dn was similar for both ALN and RIS (both r² = 0.22; p < 0.003). Both RIS and ALN significantly increased vertebral stiffness; there was no effect on other extrinsic or intrinsic mechanical properties. In summary: 1) risedronate dose-dependently suppressed cancellous bone remodeling while alendronate suppressed remodeling similarly at all three doses, 2) both RIS or ALN similarly increases microdamage accumulation (3-4x at PMO clinical dose levels and >5x at 5-6x clinical dose levels) without significant negative effects on mechanical properties.

Disclosures: **M.R. Allen**, Procter & Gamble 2; Merck 2.

1082

Sclerostin Monoclonal Antibody Treatment of Osteoporotic Rats Completely Reverses One Year of Ovariectomy-Induced Systemic Bone Loss. K. Warmington^{*1}, M. Ominsky¹, B. Bolon^{*2}, R. Cattley^{*1}, P. Stephens^{*3}, A. Lawson^{*3}, D. Lightwood^{*3}, V. Perkins^{*3}, H. Kirby^{*3}, A. Moore^{*3}, M. Robinson^{*3}, P. J. Kostenuik¹, W. S. Simonet¹, D. L. Lacey¹, C. Paszty¹. ¹Amgen Inc, Thousand Oaks, CA, USA, ²GEMpath Inc, Cedar City, UT, USA, ³Celltech R and D Ltd, Slough, United Kingdom.

Genetic data and gene expression analysis in humans and mice, along with pharmacological data generated in rodents, point at the secreted protein sclerostin as playing a key role in controlling bone mass throughout life. Sclerostin negatively regulates the anabolic output of the osteoblast lineage, and thus the absence of sclerostin results in increased bone formation and high bone mass. To explore the therapeutic potential of sclerostin as a target for the treatment of postmenopausal osteoporosis, 6 month-old female rats were ovariectomized (OVX), allowed to lose bone for 1 year, and were then treated with a sclerostin neutralizing monoclonal antibody (Mab). Bone mineral density (BMD) was determined *in vivo* by DXA and *ex vivo* by Micro-CT. Bone loss, at 1 year post-OVX, was similar at various skeletal sites with a ~ 12% decrease in BMD compared to age-matched, sham-operated controls. Five weeks of Mab treatment led to statistically significant increases in BMD in lumbar vertebrae (26 %), whole leg (16 %), femoral metaphysis (28 %) and femoral diaphysis (9%) compared to vehicle treated controls. These increases in BMD were similar to the increases seen in the PTH treated-group. Micro-CT analysis of the femur showed that sclerostin inhibition led to improved trabecular architecture [increased BV/TV (118%), BMD (64%), trabecular number (50%), trabecular

thickness (57%)] and cortical geometry [increased cortical thickness (26%) and decreased endosteal circumference (14%)]. At the five week timepoint, serum TRAP-5b (an osteoclast-specific resorption marker) was statistically significantly decreased in the Mab-treated rats (43 % vs vehicle). This decrease in TRAP-5b suggests that the sclerostin pathway, in addition to controlling osteoblasts, may also affect osteoclasts, perhaps by modulating osteoblast expressed OPG and RANKL levels. Gross observation, serum clinical chemistry, hematological analysis, and histopathological analysis revealed no abnormalities associated with pharmacological inhibition of sclerostin. In summary, very impressive increases in BMD were achieved in a rat model of post-menopausal osteoporosis (PMO) after five weeks of treatment with a sclerostin-neutralizing Mab. These data suggest that inhibition of sclerostin may be useful in humans for building bone in the clinical setting of PMO, even in cases where osteoporosis has progressed to the point where significant bone loss has already occurred.

Disclosures: **C. Paszty**, None.

1083

Effects of Parathyroid Hormone 1-84 on Cortical and Trabecular Bone at the Hip as Assessed by QCT: Results at 18 Months from the TOP Study. C. E. Bogado¹, J. R. Zanchetta¹, A. Mango^{*1}, A. L. Mathisen^{*2}, J. Fox^{*2}, M. K. Newman^{*2}. ¹Clinical Research, IDIM, Buenos Aires, Argentina, ²NPS Pharmaceuticals, Salt Lake City, UT, USA.

Treatment with PTH increases trabecular bone mineral density (BMD), but its effects on mixed trabecular and cortical bone sites, like the hip, are less well established. We used quantitative computed tomography (QCT) to assess the effects of treatment with parathyroid hormone 1-84 (PTH) on volumetric (v) trabecular (Tb), cortical (Ct) and integral (Int; Tb+Ct) BMD, bone mineral content (BMC) and bone volume (BV) at the total hip and femoral neck of postmenopausal women with osteoporosis. The QCT study consisted of 122 women from the TOP study (BMD T score ≤ -2.5 at the lumbar spine, total hip or femoral neck) who were randomly assigned to daily injections of PTH (100 µg; n=62) or placebo (n=60). The mean percent change from baseline for Placebo and PTH subjects is shown in the Table below.

	Total Hip			Femoral Neck		
	Placebo	PTH	p-value	Placebo	PTH	p-value
vTbBMD	-0.21	4.99	<0.001	-0.42	4.11	0.006
vTbBMC	-1.06	2.91	0.003	-2.56	7.80	0.003
TbBV	-0.83	-1.29	0.604	-1.46	3.34	0.074
vCtBMD	3.25	-1.41	0.001	1.22	-0.91	0.278
vCtBMC	-4.74	0.04	0.040	1.74	8.22	0.116
CtBV	-7.17	1.83	0.003	0.01	11.17	0.043
vIntBMD	-0.21	4.50	<0.001	1.37	3.37	0.178
vIntBMC	-1.06	2.91	0.003	0.23	7.25	0.032
IntBV	-0.83	-2.10	0.258	-1.61	4.26	0.041

The increase in vTbBMD at total hip and femoral neck in PTH-treated subjects was due primarily to an increase in vTbBMC; there was no significant change in TbBV at either site. In contrast, CtBV increased significantly in the PTH group at both hip regions. However, because the increase in vCtBMC was smaller than the increase in bone volume, there was a decrease in vCtBMD that was significant at the total hip, but not at the femoral neck. To our knowledge this is the first placebo controlled study of the effects of PTH treatment on vBMD at the hip using QCT. Daily administration of PTH for 18 months increases integral and volumetric trabecular BMD and BMC, and cortical bone volume. We found only a modest decrease in volumetric cortical BMD, which was not significant at the femoral neck region. These results are consistent with changes observed in PTH-treated osteopenic rhesus monkeys in which increases in integral vBMD and vBMC at these regions translated into significant increases in bone strength.

Disclosures: **C.E. Bogado**, NPS Pharmaceuticals 5.

1084

The Effects of Strontium Ranelate on Bone Remodeling and Bone Safety Assessed by Histomorphometry in Patients with Postmenopausal Osteoporosis. M. E. Arlot, P. Delmas, B. Burt-Pichat^{*}, J. P. Roux^{*}, N. Portero^{*}, P. J. Meunier. INSERM Unit 403, C. Bernard University, Lyon, France.

Strontium ranelate (SR), a novel antiosteoporotic drug, has been found in pre-clinical studies to stimulate bone formation and to decrease bone resorption, rebalancing bone turnover toward formation. As shown in the SOTI and TROPOS clinical studies, SR 2g/day is safe and effective in postmenopausal women with osteoporosis in reducing the risk of fractures (vertebral -41% and hip in osteoporotic women aged 74 years or more -36%). The objectives of our study on transiliac bone biopsies were a) to assess the mechanism of action of strontium ranelate at the cell or bone tissue level and b) to evaluate bone safety. Transiliac bone biopsies were obtained in a subset of the SOTI, TROPOS and STRATOS patients at baseline, 1, 2, 3, 4 or 5 years from the start of a treatment with either SR 2g/day or placebo. All patients received calcium and vitamin D supplementation. The analysis compared the pooled data from 1 to 5 years in patients treated with SR (treated; n: 49) with the pooled data from placebo plus baseline data obtained for patients in SR group (untreated; n: 87). Histomorphometric parameters were measured at both cancellous, endosteal and cortical envelopes. The positive effects of SR on bone formation were confirmed by a significant higher osteoblastic surfaces (Ob.S/BS) in treated as compared to untreated (+38%; p=0.047) and by a significant greater Mineral Apposition Rate (MAR) in cancellous and cortical bone (+8%; p=0.008, +11%; p=0.033, respectively). At the tissue level, there was no significant change in activation frequency. The effects on resorption consisted of a trend towards lower endosteal eroded surfaces, endosteal and cancellous osteoclast surfaces and osteoclast number (-14, -6%, -9%, -9%, NS, respectively.). With

the higher Ob.S/BS in treated, it was expected to also observe higher osteoclast surfaces, which was not the case, confirming the dual mode of action of SR. In terms of safety parameters, the cancellous osteoid thickness was found to be significantly lower in treated ($p=0.007$), the MAR was significantly higher in treated with no change in osteoid volume and mineralization lag time. These results demonstrate that primary mineralization rate is not impaired, but on the contrary stimulated by SR. All these findings indicate the stimulating effects of strontium ranelate on the osteoblastic population and MAR and a moderate decrease in bone resorption. They are in agreement with the increase of biochemical markers of formation and the decrease of those of resorption shown in clinical studies and confirm the dual mode of action of strontium ranelate, rebalancing the bone metabolism in favor of formation.

Disclosures: **M.E. Arlot**, Servier 5.

1085

SHP2 Mutations that Cause Noonan Syndrome May Lead to Disorganized Chondrogenesis. **N. Namba**¹, **K. Takahashi**^{*1}, **E. Ogura**^{*2}, **M. Kawai**^{*1}, **S. Kogaki**^{*1}, **H. Tanaka**², **K. Ozono**¹. ¹Pediatrics, Osaka University Graduate School of Medicine, Suita, Osaka, Japan, ²Pediatrics, Okayama University Graduate School of Medicine and Dentistry, Okayama, Japan.

Noonan syndrome (NS) is an autosomal dominant disorder characterized by unusual facial features, proportionate short stature, skeletal anomalies, and congenital heart defects. Recently, mutations in the *PTPN11* gene, which encodes the protein tyrosine phosphatase SHP2, have been reported to account for approximately 50% of NS. SHP-2 is a ubiquitously expressed protein composed of 2 amino-terminus SH2 domains (N-SH2 and C-SH2) followed by a protein tyrosine phosphatase (PTP) domain. Though the identified mutations have been postulated as gain-of-function changes, we have reported that this may not necessarily be the case. We have now extended our study to 4 other mutants. COS-1 cells were transfected with WT or mutant SHP2 and tested for phosphatase activity. While PTP activity was increased in D61N, E139D, and Y279C SHP2, it was lower than that of WT in Q510E SHP2. Deletion of the SH2 domains that allosterically inhibit the PTP domain had no effect suggesting that the Q510E mutation attenuates enzyme activity *per se* rather than affinity between the domains. To investigate how these changes in SHP2 function might affect chondrogenesis, we introduced WT, C459S (dominant negative), and two of the mutants, D61N and Q510E SHP2 into ATDC5 chondrogenic cells using adenoviral vectors. When BrdU incorporation was assayed in the presence of serum, mutations that decreased PTP activity diminished DNA synthesis. Interestingly, when the assay was done in serum/growth factor free conditions, mutant SHP2s upregulated DNA synthesis regardless of phosphatase activity, suggesting that adhesion-mediated signaling may be involved. Since fibroblast growth factors (FGFs) play a key role in chondrogenesis, we next evaluated FGF-2 (5 ng/ml) induced MAPK activity by immunoblotting and detection with anti-phospho-ERK1/2 and anti-ERK1/2 antibodies. Mutations associated with low PTP activity reduced ERK activation. We also examined cell spreading and actin organization since adhesion-mediated signaling could be altered as indicated above. Transfected cells were trypsinized and replated on coverslips for 60 min followed by staining with Alexa Fluor 546 phalloidin. D61N SHP2 induced cell spreading and stress fiber formation while the contrary occurred with Q510E SHP2. Taken together, these results suggest that SHP2 mutations perturb crosstalk between growth factor-mediated and adhesion-mediated signals, possibly leading to disorganized chondrogenesis.

Disclosures: **N. Namba**, None.

1086

Phenotypic Expression of a PTHR1 Null Mutation in Homozygous and Heterozygous States. **B. Gérard**^{*1}, **M. Vibert**^{*2}, **D. Menzies**^{*3}, **J. Ragage**^{*2}, **G. Bertrand**^{*1}, **D. Prie**^{*4}, **B. Grandchamp**^{*1}, **C. Silve**⁴. ¹Hôpital Bichat, Service de Biochimie Hormonale et Génétique, Paris, France, ²Hôpital Ste Croix, Metz, France, ³Centre de Pathologie, Metz, France, ⁴Faculté de Médecine Xavier Bichat, INSERM U426, Paris, France.

Blomstrand lethal chondrodysplasia (BLC) is a rare autosomal recessive disorder resulting from inactivating mutations in the PTH/PTHrP receptor (PTHR1) gene. Although the developmental defects in bone, tooth and breast have been characterized in detail, important aspects of the disease, including the cause of death, remain undefined, and no phenotypic abnormalities resulting from a heterozygous PTHR1 null mutation have been reported. Analysis of a new family with an inactivating mutation in PTHR1 has shed new light on these areas. PTHR1 gene analysis in the proband revealed the presence of a homozygous 10 kb deletion encompassing P2 and P3 promoter regions, the first translated exon and most of the first intron. This large deletion, which precludes PTHR1 transcription, was present in the heterozygous state in both parents. At delivery (29 weeks), the infant was severely hydropic, but had normal cardiac activity. Radiological and histological analysis of the skeleton confirmed the diagnosis of BLC. A striking reduction in bone marrow space was noted, due to the extreme shortness of the long bones and coarse and much widened trabeculae. Residual islands of haematopoietic tissue demonstrated erythroblastosis. Important extramedullary haematopoiesis in liver was present, and associated with hepatosiderosis. Iron deposition was lobular and diffuse, with a periportal to pericentral gradient, a feature reminiscent of dyserythropoiesis. Except for evidence of right ventricular hypertrophy, no cardiac defects were present. In view of recent evidence that both osteoblast differentiation and signalling through PTHR1 regulate the development of stromal and hematopoietic stem cells, the association of marrow dysplasia, extramedullary hematopoiesis and hepatosiderosis are consistent with the possibility that foetal anaemia resulting from abnormal erythropoiesis may contribute to the lethality of BLC. Both parents had hyperphosphatemia (mother: 1.45; father: 1.74; normal: 0.80-1.40 mM) and increased maximal renal phosphate reabsorption (1.6, and 1.8; respectively,

normal: 0.7-1.4 mM), despite serum PTH (bio intact 1-84) values that were normal or increased. Serum calcium concentration and urinary calcium excretion were normal. The failure of PTH to adequately inhibit phosphate reabsorption in the parents suggests that heterozygous inactivation of PTHR1 is sufficient to impair the PTH response of proximal renal tubular cells.

Disclosures: **C. Silve**, None.

1087

The Recovery of Bone Mass after Weaning in Mice Is Associated with Increased Rates of Bone Formation and Decreased Rates of Bone Resorption. **L. Ardeshirpour**, **J. N. VanHouten**^{*}, **P. R. Dann**^{*}, **J. J. Wysolmerski**. Internal Medicine (Endocrinology), Yale University, New Haven, CT, USA.

Mammalian reproduction triggers a remarkable cycle of skeletal catabolism and anabolism. Lactation is associated with the loss of significant amounts of bone, a deficit, which is fully repaired after weaning. In fact, the recovery of bone mass post weaning represents the most rapid accrual of bone during adult life. The purpose of this study was to characterize maternal bone and mineral metabolism upon weaning in mice. Twelve-week-old CD-1 mice were allowed to become pregnant and deliver. On day 12 of lactation, pups were removed to initiate weaning. Serial DEXA scans from mid-lactation to 4 weeks after weaning revealed a progressive increase in bone mineral density (BMD). Compared to mid-lactation, by 4 weeks post weaning, BMD increased by 37% in the spine, 27% in the femur and 25% in the whole body. Remarkably, BMD started to increase as early as 3 days post weaning and statistically significant differences were seen by day 7 at the spine, day 10 at the femur and day 14 when total body BMD was assessed. Histomorphometry revealed a trend towards increased trabecular volume and significant increases in trabecular thickness by day 28 post weaning. Levels of urinary collagen C-telopeptide (CTx) decreased and remained low during the post-weaning period, suggesting that the elevated rates of bone resorption seen during lactation are promptly suppressed after weaning. In contrast, plasma osteocalcin levels, which were already elevated during lactation, increased further at day 3 post weaning, suggesting that bone formation rates are augmented following weaning. Histomorphometry studies in trabecular bone confirmed these changes in biochemical markers. Osteoclast numbers declined significantly, immediately after weaning. Osteoblast numbers were variable, but dynamic histomorphometry revealed an increase in bone formation rates. Interestingly, the mice were hypercalcemic 3 days after weaning, but calcium levels returned to the normal range by 1 week. Circulating PTH and PTHrP levels did not change during this time. In conclusion, upon weaning, maternal bone density increases rapidly in mice. This is accompanied by a decrease in rates of bone resorption and an increase in rates of bone formation. These findings provide the basis for further investigation of the molecular mechanism underlying the transition from bone loss to bone gain following the cessation of suckling.

Disclosures: **L. Ardeshirpour**, None.

1088

The Effect of Pamidronate Discontinuation in Children and Adolescents with Moderate to Severe Osteogenesis Imperfecta. **F. Rauch**, **C. Land**, **C. Munns**, **R. Travers**, **F. Glorieux**. Shriners Hospital, Montreal, PQ, Canada.

Treatment with cyclical intravenous pamidronate is beneficial to children and adolescents with moderate to severe forms of osteogenesis imperfecta (OI). However, it is unclear at present how long the therapeutic effect persists after treatment discontinuation. In this study we therefore followed the course of 42 OI pediatric patients (19 girls) in the two years after stopping pamidronate. They had received the drug for an average duration of 5.1 years and were 13.2±5.0 years (mean±SD) old when treatment was discontinued. Expressed as a percentage of the result expected in age- and sex-matched healthy subjects, the bone resorption marker urinary NTx/creatinine increased from 45±21% to 72±33% during the first two years after pamidronate was stopped ($P < 0.001$ by ANOVA). However, NTx/creatinine at the two-year time point was still significantly lower than in healthy subjects or in untreated OI patients of the same age ($P < 0.001$). Lumbar spine bone mineral content increased by 12% in the two years following pamidronate discontinuation, whereas volumetric bone mineral density (vBMD) remained unchanged. Expressed as a percentage of the result expected in age- and sex-matched healthy subjects, lumbar spine vBMD decreased from 101±13% to 96±12% ($P = 0.02$). The study population sustained a total of 27 radiologically confirmed lower extremity fractures during the last two years of pamidronate treatment, whereas 18 such fractures occurred in the two years after discontinuation of therapy. These observations suggest that bone turnover recovers slowly after pamidronate is discontinued but is still suppressed after a drug-free interval of two years. Lumbar spine vBMD is maintained and fracture incidence does not increase within two years after stopping treatment.

Disclosures: **F. Rauch**, None.

1089

Bone Mineral Density of Relatives of Individuals with Osteogenesis Imperfecta. L. A. DiMeglio¹, L. Ford^{*2}, C. McClintock^{*2}, M. Peacock².¹Pediatrics, Section of Pediatric Endocrinology, Indiana University, Indianapolis, IN, USA, ²Medicine, Indiana University, Indianapolis, IN, USA.

Most cases of Osteogenesis Imperfecta (OI) are attributable to mutations in the genes for type I collagen (COL1A1 or COL1A2). Severe cases are often due to missense mutations that result in an abnormal collagen that interferes with the formation of collagen triple helices whereas mild cases are generally due to "null" mutations that reduce the amount of collagen produced. However, phenotype has wide variability and the relationship between genotype and phenotype is poor, even in family members with the same mutation. The reasons for this phenotypic variability remain uncharacterized. A striking phenotype in OI is decreased Bone Mineral Density (BMD). To examine if BMD is a potential marker for OI in families, we measured BMD in 70 relatives (45 parents, 21 siblings, 4 children) of 29 index patients with OI. 43 relatives had a first-degree family member with mild OI (Type I); 27 had relatives with severe OI (Type III or IV). Three parents and one daughter of individuals with Type I OI had an established diagnosis of OI. Relatives ranged in age from 5 to 69 years, with a mean age of 33 years. Relatives of individuals with Type I OI had lower mean BMD Z-scores of the lumbar spine than those with Type III OI (-0.56 v. 0.32, p<0.02), and trended toward lower total body Z-scores (0.03 v. 0.64, p<0.07) and lower femoral neck z-scores (-0.46 v. 0.18, p<0.07). These relationships were maintained even when the data from the 4 individuals with known OI were excluded. Six parents had total body z-scores of > +2. Surprisingly, 5 of these parents had children with severe OI. Although there was no correlation between the total body z-scores of index patients and of their relatives for type I patients (p=0.3), there was a strong **negative** correlation between total body z-scores of individuals with severe OI and those of their relatives (r = -0.62, p<0.05), indicating that affected individuals with severe OI had relatives with high bone mineral densities. Since type I OI is often inherited in an autosomal dominant fashion, one would anticipate as many as 50% of relatives would also carry an abnormal collagen gene. Mean BMDs that are low for age in these relatives, therefore, as we have documented, would be expected. Type III and IV OI are believed to be predominately sporadic mutations. The cluster of parents with high BMDs with children with severe OI, and the negative correlation between family members' BMDs and probands' BMDs are, therefore, unexpected and as of yet unexplained. The results suggest that in subjects with severe OI there are interactions between the genetic defects in collagen genes and genes that promote high bone mass.

Disclosures: **L.A. DiMeglio**, None.

1090

Effects of Pamidronate on Bone Modeling, Bone Remodeling and Degree of Mineralization of Bone from Children with Osteogenesis Imperfecta. G. Boivin¹, P. Chavassieux¹, V. Forin^{*2}, G. Pinto^{*3}, P. J. Meunier¹. ¹INSERM Unité 403, Faculty of Medicine R. Laennec, University C. Bernard Lyon1, Lyon, France, ²Hospital Trousseau, Paris, France, ³Hospital Necker, Paris, France.

Osteogenesis imperfecta (OI) is characterized by a bone fragility with a low bone mass, an alteration of the trabecular connectivity and a frequent increased bone remodeling (Rauch et al. 2000 Bone 26 :581-9). Treatment with bisphosphonates has been proposed. Intravenous pamidronate leads to increase bone mass and decrease bone remodeling in children with OI (Rauch et al. 2002 J Clin Invest 110:1293-99). The degree of mineralization, rarely measured was increased in untreated OI (Boyde et al. 1999 Calcif Tissue Int 64:185-90) and normal after pamidronate (Weber et al. 2004 J Bone Miner Res 19 suppl. 1:S99). Our purpose was to evaluate, using bone histomorphometry and quantitative microradiography, the effects of pamidronate in iliac bone biopsies from 38 children (17 boys and 21 girls, 10 ± 5 yrs old) with OI (type I, III ou IV) treated for 2 years (IV cumulative dose of 9 mg/kg/yr before the age of 3 years and 8.5 mg/kg/yr after this age), and daily supplementation in vitamin D (1200 UI) and calcium (250-500 mg). Compared to age-matched controls (Glorieux et al. 2000 Bone 26:103-9) untreated OI showed significant (p<0.0001) decreased cortical thickness, BV/TV and trabecular number, and increased trabecular separation. Bone turnover appeared significantly augmented (activation frequency : +77%, p<0.001) with increase in osteoid parameters, a delay in the mineralization without defect of primary mineralization. After 2 years of pamidronate, bone mass (cortical thickness +55%, p=0.008, BV/TV +59%) was increased with an improvement of trabecular connectivity. Bone remodeling was significantly (p<0.05) decreased (mineralizing surfaces, activation frequency). After pamidronate, the mean degree of mineralization was slightly increased (+4.6%). Compared to adult controls (Boivin & Meunier 2002 Calcif Tissue Int 70:503-11), degree of mineralization of bone was slightly decreased in untreated OI. In conclusion, these results confirm the decrease of bone remodeling and a positive bone tissue balance of modeling after 2 years of pamidronate in children with OI. The augmentation of BMD (+66%, p<0.001) in OI after pamidronate (Forin et al. Joint Bone Spine in press) is due to a strong increase in bone mass associated with a slight improvement of the degree of mineralization.

Disclosures: **G. Boivin**, None.

1091

Role of Estrogen Receptor Beta in Mechanotransduction. L. K. Saxon^{*}, A. G. Robling, C. H. Turner. Orthopaedic Research, Indiana University, Indianapolis, IN, USA.

Animal studies and longitudinal observations of women show that estrogen suppresses periosteal bone formation and continues to do so when combined with exercise. The discovery of estrogen receptors (ER) α and β have aided understanding of how estrogen and mechanical loading influence cortical bone formation. We hypothesized that the antagonistic effect of estrogen on the periosteum, when combined with mechanical loading, is due to signaling through ER β . To investigate this 60 male and 60 female WT and ER $\beta^{-/-}$ mice were randomly assigned to either high, moderate or low mechanical loaded groups. The right ulnae of each mouse were subjected to in vivo loading for 60 cycles/day using a 2 Hz haversine waveform, for 3 consecutive days. Fluorochrome labels were injected 2 and 7 days after beginning loading and mice were sacrificed on day 12. Strain gauges were used to measure the mechanical strain applied per load on the medial periosteal surface of the loaded ulna from a subgroup of mice from each group. Differences between periosteal bone formation rate (BFR/BS $\mu\text{m}^3/\mu\text{m}^2$ per year) in the loaded (right) versus nonloaded (left) ulna were measured using standard bone histomorphometry. Bone formation induced by mechanical loading was not different among the male WT and ER $\beta^{-/-}$ mice. In contrast, a difference in rBFR/BS was apparent between female WT and ER $\beta^{-/-}$ mice; periosteal bone formation was 5 times greater in female ER $\beta^{-/-}$ mice compared to WT for the same mechanical strain (p<0.05). These data suggest that removal of ER β signaling makes long bones more sensitive to mechanical loading. The results appear to support our hypothesis that estrogen inhibits exercise-induced periosteal bone formation via a signaling pathway that activates ER β . Because differences in loading responsiveness was detected in female ER $\beta^{-/-}$ and WT mice, but not in the male mice, it appears as though the ligand needs to be present for ER β to be activated and potentially decrease the osteogenic response to mechanical loading. In conclusion, we found that female mice with a null mutation of ER β formed more periosteal bone in response to mechanical loading. These results suggest that ER β signaling suppresses periosteal bone formation.

Disclosures: **L.K. Saxon**, None.

1092

Osteocyte Apoptosis and the Loss of Bone Mineral and Strength Induced by Tail Suspension in Mice Is Entirely Caused by Reduced Mechanical Strains, whereas Osteoblast Apoptosis Is Due to Endogenous Glucocorticoid Actions. J. Aguirre, L. Plotkin, K. Vyas^{*}, S. Stewart^{*}, C. O'Brien, A. Parfitt, R. Weinstein, S. Manolagas, T. Bellido. Endocrinology, University of Arkansas for Medical Sciences, Little Rock, AR, USA.

Mechanical stimulation of osteocytic cells in vitro prevents their apoptosis via an integrin/Src/FAK signaling pathway leading to ERK activation. Conversely, reduction of mechanical forces in vivo increases the prevalence of osteocyte apoptosis; and this event precedes temporally, and is spatially associated with, osteoclast-mediated resorption and the loss of mineral and strength induced by tail suspension in mice. Unloading also induces an early increase in osteoblast apoptosis, which is associated with reduced osteoblast number and osteoid perimeter reflecting decreased bone formation. The bone fragility induced by administration of glucocorticoids to mice and humans is also accompanied by an increased prevalence of osteocyte and osteoblast apoptosis; and skeletal unloading by tail suspension has been shown to increase endogenous corticosterone in mice and rats. To determine the potential contribution of endogenous glucocorticoid action to the bone changes induced by unloading, we tail-suspended transgenic mice overexpressing 11 β -hydroxysteroid dehydrogenase type 2 under the control of the murine osteocalcin promoter (OG2-11 β -HSD2 mice) (n=10-12/group). This genetic manipulation deflects glucocorticoid action in osteoblasts and osteocytes by a pre-receptor mechanism involving conversion of biological active glucocorticoids to their inert 11-keto metabolites. We found that tail suspension induced a similar increase in the prevalence of cortical and cancellous osteocyte apoptosis in OG2-11 β -HSD2 mice compared to wild type littermates after 7 days, which remained elevated up to 28 days. Likewise, the increased osteoclast number and the decreased cortical width, spinal BMD and vertebral strength found after 28 days of unloading were similar in bone of transgenic and wild type mice. Remarkably, the increase in apoptotic osteoblasts and the decrease in serum osteocalcin observed at 7 days in wild type mice were abrogated in OG2-11 β -HSD2 mice. These findings indicate that the early increase in osteoblast apoptosis and reduced bone formation induced by tail suspension is due to the action of endogenous glucocorticoids. On the other hand, the increase in osteocyte apoptosis followed by loss of BMD and strength is entirely due to reduced mechanical loading confirming that physiological levels of strains maintain osteocyte viability.

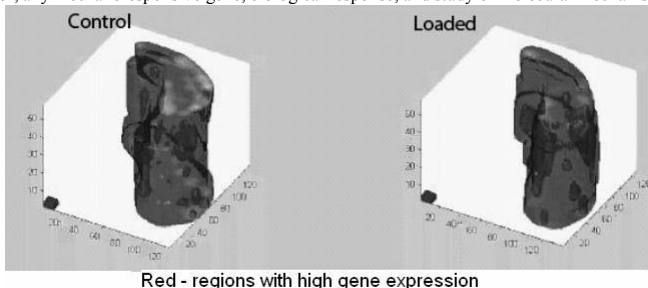
Disclosures: **J. Aguirre**, None.

1093

A 3D Model of Osteocyte Gene Expression in Response to Mechanical Loading - Correlation of DMP1 Gene Expression in Osteocytes with Local Strain. S. Kotha^{*1}, S. Gidla^{*1}, J. Gluhak-Heinrich², M. Schaffler^{*3}, S. Harris⁴, L. Bonewald¹. ¹Oral Biology, Univ of Missouri, Kansas City, MO, USA, ²Univ of Texas Health Science Center, San Antonio, TX, USA, ³Mount Sinai School of Medicine, New York, NY, USA, ⁴UTHSCSA, San Antonio, TX, USA.

The osteocyte is thought to act as a mechanotransducer, translating strain signals into a biological response. It is not known if osteocytes respond as a population or individually in response to local strains. In this study, mRNA expression of Dentin Matrix Protein 1

(DMP1), a mechanically responsive gene highly expressed in osteocytes, was used as a readout to characterize this response. The goal of this study was to generate a 3-dimensional model based on finite element analysis (FEA), correlating gene expression in osteocytes to their local strain environment. FEA was conducted on ulnae from 6 month old female Sprague Dawley rats and validated by strain gage measurements. Right ulnae were loaded at 4Hz, 20N until 30% loss in whole bone stiffness. Left ulnae served as contralateral controls. DMP1 expression was assayed 2 days after loading by quantitative in situ hybridization using P³² labeled RNA probes. Gene expression was evaluated in seven transverse sections, spaced 0.75mm apart at the ulnar mid-shaft. Gene expression in osteocytes was correlated to local (continuum level) strains as determined from FEA. DMP1 expression in loaded ulnae was 2 fold higher than controls. Within bone sections, the pattern of gene expression per osteocyte was highly correlated to local strain magnitude in both loaded (DMP1: $r^2=0.72$; $p<0.02$) and control (DMP1: $r^2=0.61$; $p<0.03$) ulnae, regardless of whether strains were tensile or compressive. Our 3D model of gene expression showed that the longitudinal pattern of DMP1 gene expression (i.e. along the length of the ulna) was also correlated to peak compressive strain in both the loaded (DMP1: $r^2=0.65$; $p<0.02$) and control (DMP1: $r^2=0.63$; $p<0.03$) ulnae. The highest expression of DMP1 occurred in locations where new bone formation is predicted. **Together, these data suggest that osteocytes can respond globally (i.e. as a population) to increased strain, and that the response of individual osteocytes is also correlated with its local strain environment.** Refinements to this 3D model will allow incorporation of, any mechanoresponsive gene, biological response, and study of molecular mechanisms.



Disclosures: **S. Kotha**, None.

1094

Repetitions of Mechanical Loading Potentiate Bone Cellular Responses by a Mechanism Involving NMDA Type Glutamate Receptors. **E. A. Bowe***, **T. M. Skerry**. Department of Medicine, University of Sheffield, Sheffield, United Kingdom.

It has been shown that mechanical loading is a more potent stimulus to bone if instead of a single daily period of loading, the same number of cycles are divided into shorter separate loadings. This suggests that bone cells have the ability to memorise effects of loading and to modify their responses to subsequent loads in accordance with previous load history. Such a system functions in the CNS, where synaptic plasticity, the ability of previous synaptic events to potentiate or depress subsequent responses, underlies learning and memory. Specifically, Long Term Potentiation (LTP) involves interactions between different glutamate receptors and post-synaptic proteins at the synapse. Previously we have shown that the necessary components for LTP are expressed by osteoblasts, and are involved in responses to loading. The studies reported here were to determine whether a previous loading event potentiates bone cell responses to subsequent load and if so, whether an LTP like mechanism was involved. We loaded ROS 17/2.8 cells cyclically using a four point bending device (peak strain 3400 $\mu\epsilon$ at 1Hz) for one or two 10 minute loading periods, 1 hour apart, with or without the competitive NMDA type glutamate receptor antagonist AP-5 (50M). Before the second loading period, AP5 was thoroughly washed off the cells. Cells were harvested 10 minutes after the last load for mRNA analysis. Real time RT-PCR was performed to measure changes in cFOS, JUNB and FOS-1 expression, which are immediate early genes involved in differentiation. A single 10 minute period of cyclic strain caused a significant increase in cFOS mRNA ($p<0.001$) that was unaffected by the presence of AP-5. Cells that experienced two intervals of strain showed a further significant ($p<0.004$) increase in cFOS expression compared with cells loaded once. This increased response to a second loading period was abolished when AP5 was present for either one or both of the loading periods, in which case cFOS levels were then not different from cells that had experienced just one period of strain. Equivalent changes were not detected in JUNB or FOS-1 mRNA. In cells subjected to one or two fluid flow regimens with and without AP-5, there was no difference between one and two flow periods, whether AP-5 was added or not. These data provide compelling evidence that the potentiation induced *in vivo* by divided loading events occurs *in vitro*, and that its mechanism involves NMDA receptor-mediated signalling. This suggests that an LTP-like process is functional in bone. Since it is known that in the CNS, LTP is enhanced by estrogen, subtle changes in bone's LTP could account for post-menopausal reductions in the osteogenic effects of habitual activity.

Disclosures: **E.A. Bowe**, None.

1095

Potential Role of $\alpha 5$ Integrin as a Mechanosensor in the Opening of Hemichannels for the Release of Prostaglandin in Response to Mechanical Stress. **P. P. Cherian¹, A. J. Siller-Jackson^{*1}, S. Burra¹, S. Gu^{*1}, L. F. Bonewald², E. Sprague^{*3}, J. X. Jiang¹**. ¹Biochemistry, University of Texas Health Science Center, San Antonio, TX, USA, ²Oral Biology, School of Dentistry, University of Missouri, Kansas City, MO, USA, ³Radiology, University of Texas Health Science Center, San Antonio, TX, USA.

Mechanosensing osteocytes express large amounts of the gap junction-forming protein, connexin (Cx) 43, yet gap junctions are only active at the small tips of their dendritic processes, suggesting another function for Cx43. Previous studies have shown that both primary osteocytes and the osteocyte-like MLO-Y4 cells respond to fluid flow shear stress (FFSS) by releasing intracellular prostaglandin E₂ (PGE₂). MLO-Y4 cells were exposed to FFSS at 16 dynes/cm² in the absence and presence of the gap junction inhibitors 18 β -glycyrrhetic acid (β -GA) and carbenoxolone, and Cx43 antisense. We observed that cells plated at lower densities release more PGE₂ than cells plated at higher densities (>20X) in response to FFSS. This response was significantly reduced by Cx43 antisense and by β -GA and carbenoxolone, even in cells without physical contact. Inhibitors of other channels, such as the purinergic receptor P2X₇ and the prostaglandin transporter PGT, had no effect on PGE₂ release. These results suggest that Cx43-hemichannels are involved in the release of PGE₂ in response to FFSS. Indeed, FFSS induced the opening of hemichannels in primary osteocytes and MLO-Y4 cells, and this opening was inhibited by an antibody specific for Cx43-hemichannels. To identify the potential mechanosensor responsible for the opening of hemichannels, immunolocalization of tethering molecules was examined. Co-localization of Cx43 was observed with $\alpha 5$ integrin, but not with vinculin, paxillin, or focal adhesions. Cx43 and $\alpha 5$ integrin co-localized not only on the cell surface, but also throughout the cell body and cell processes, becoming more prominent in flow conditions. With FFSS, Cx43 protein migrates to the plasma membrane with an increase in hexameric forms of Cx43 on the cell surface as Cx43 located at the cell surface was more resistant to Triton-X-100 extraction with FFSS, suggesting the formation of detergent-insoluble protein plaques, similar to previously reported for gap junctional plaques. Together, these results suggest FFSS induces the translocation and assembly of Cx43 in the membrane surface along with $\alpha 5$ integrin and that un-apposed hemichannels formed by Cx43 serve as a novel portal for the release of prostaglandin in response to mechanical strain.

Disclosures: **J.X. Jiang**, None.

1096

Identification of Transient Receptor Potential Vanilloid 4 (TRPV4) to Be Mechanosensitive Channel that Mediates Bone Loss Due to Unloading. **F. Mizoguchi^{*1}, A. Mizuno^{*2}, H. Kondo¹, Y. Ezura¹, K. Nakashima¹, M. Suzuki^{*2}, N. Miyasaka^{*3}, M. Noda¹**. ¹Molecular Pharmacology, Medical Research Institute, Tokyo Medical and Dental University, Tokyo, Japan, ²Department of Pharmacology, Jichi Medical School, Tochigi, Japan, ³Department of Medicine and Rheumatology, Tokyo Medical and Dental University, Tokyo, Japan.

Mechanosensing is one of the major determination paths for biological events. Transient receptor potential vanilloid 4 (TRPV4) is a Ca²⁺ permeable nonselective cation channel and it has been implicated in Ca²⁺ dependent signal transduction in several tissues, including brain, vascular endothelium and skin. TRPV4 has been suggested to be a channel that plays a role to sense heat, hyposmolality and pressure. Recently, TRPA1, a family member of TRP, was found to be mechanosensitive transduction channel in vertebral hair cells (Nature 2004). Mechanical stress also plays an important role in the maintenance of bone mass, as exemplified by the rapid loss of bone due to unloading in bed ridden patients to lead to osteoporosis. Such rapid events could be mediated by ionic movements through channels. In endothelial cells, cation channels have been suggested to sense shear stress. However, it has not been yet fully understood how bone senses the mechanical stress as no definite mechanosensitive cation channel has been discovered in bone. We examined whether TRPV4 is a sensor of mechanical stress in bone and if it is involved in the bone loss by using TRPV4^{-/-} mice subjected to tail suspension, a model of unloading. Unloading for two weeks by tail suspension resulted in reduction in the secondarily trabecular bone volume in wild type by about 40% as reported previously. In sharp contrast, there were no decreases in TRPV4^{-/-} mice subjected to tail suspension. Body weight at the end point of two weeks of tails suspension was comparable between loaded mice and tail-suspended mice regardless of the genotype. As we usually see that primary spongiosa is a sensitive site for unloading, we also measured trabecular bone mass in this area. The height of the primary spongiosa was reduced by about 40% in wild type mice. Again TRPV4 deficiency blocked such suppression in the height of the primary spongiosa even after two weeks tail suspension. These results indicate that TRPV4 serves a mechanosensitive channel in bone as it was identified in hair cells and this would be one of the important mechanisms that regulate bone homeostasis.

Disclosures: **F. Mizoguchi**, None.

1097

Ablation of the Androgen Receptor in Mineralizing Osteoblasts Results in Late-Onset Loss of Trabecular Bone. A. J. Notini^{*1}, J. F. McManus^{*1}, A. J. Moore^{*2}, M. L. Bouxsein³, V. Glatt^{*3}, B. E. Kream⁴, H. A. Morris², J. D. Zajac¹, R. A. Davey¹. ¹Medicine, University of Melbourne, Austin Health, Heidelberg, Australia, ²Hanson Institute, Adelaide, Australia, ³Beth Israel Deaconess Medical Center and Harvard Medical School, Boston, MA, USA, ⁴Medicine, University of Connecticut Health Center, Farmington, CT, USA.

Androgens stimulate bone formation and help maintain bone mass. However, the mechanisms by which androgens act on bone remain poorly defined. The aim of this study was to investigate the role of the androgen receptor (AR) in osteoblasts using osteoblast-selective AR knockout (ob-ARKO) mice. Mice with a floxed exon 3 of the AR gene were bred with Col 2.3-Cre transgenic mice, in which Cre recombinase is expressed in mineralizing osteoblasts. The skeletal phenotype of male ob-ARKO mice was assessed by histomorphometry and quantitative microcomputed tomography (microCT) at 6-, 12- and 32-weeks of age (n=8 per group). Wild-type, AR floxed and Col 2.3-Cre male littermates were used as controls. Data were analyzed by one-way ANOVA and Tukey's Post Hoc Test. Ob-ARKO males had normal body weight and femur length compared to controls. MicroCT analysis of the 5th lumbar vertebral body demonstrated that ob-ARKO mice had a decrease in trabecular number (Tb.N)(p<0.01) and an increase in trabecular thickness (Tb.Th)(p<0.05) compared to control mice at 12- and 32-weeks of age, suggesting increased bone turnover. This resulted in a reduction in trabecular bone volume (BV/TV)(p<0.05) in ob-ARKO mice compared to controls at 32-weeks of age. The effects observed in ob-ARKO mice were accompanied by a reduction in connectivity density (p<0.01) and an increase in trabecular separation (Tb.Sp)(p<0.01) compared to control mice at 12- and 32-weeks of age, suggesting a reduction in bone quality. MicroCT analysis of the distal femoral metaphysis also demonstrated a reduction in Tb.N (p<0.05), connectivity density (p<0.01) and an increase in Tb.Sp (p<0.05) in ob-ARKO mice compared to controls at 32-weeks (but not 12-weeks) of age. There was no effect on cortical thickness in ob-ARKO mice. We are currently performing dynamic histomorphometry, and measuring bone turnover markers and hormone levels in urine and serum samples collected from ob-ARKO and control mice. In summary, these findings demonstrate that inactivation of the AR, specifically in mineralizing osteoblasts in mice, results in increased bone turnover and decreased structural integrity of the bone, leading to a reduction in trabecular BV/TV in the vertebra at 32-weeks of age. Our data provides evidence of a role for androgens in the maintenance of trabecular bone volume directly via the AR in mineralizing osteoblasts.

Disclosures: A.J. Notini, None.

1098

Estrogens Control the Birth and Apoptosis of Bone Cells in Mice in Which ER α Cannot Interact with DNA (ER $\alpha^{\text{NERKI/}}$). S. Kousteni, M. Almeida, L. Han, A. Warren^{*}, V. Lowe^{*}, S. C. Manolagas. Div. Endocrinol., Center for Osteoporosis and Metabolic Bone Diseases, Central Arkansas Veterans Healthcare System, Univ. Arkansas Med. Sci., Little Rock, AR, USA.

Studies with 4-estren-3 α ,17 β -diol (estren), a synthetic ligand of the ER α or the AR that simulates the nongenotropic effects of estrogens on osteoblast/osteocyte apoptosis but has minimal effects on classical transcription, have suggested that the classical genotropic actions of sex steroid receptors are dispensable for their bone protective effects, but essential for their effects on reproductive tissues. To test this hypothesis directly, a knock-in mouse model in which one endogenous ER α allele has been replaced by a mutant form of ER α which lacks DNA binding activity and classical ERE-mediated transcription (ER α^{NERKI} ; Jakacka et al., Mol Endo 16:2188, 2002) was crossed with a heterozygote knock-out mouse model of the ER α gene (Dupont et al., Development 127:4277, 2000). We anticipated that the progeny of such a cross, designated ER $\alpha^{\text{NERKI/}}$, should allow signaling of the ER α only through non-ERE pathways. We report that, as compared to 3 month-old wt control mice, ER $\alpha^{\text{NERKI/}}$ mice of the same age had an atrophic uterus (weighing 4-fold less) and much lower mRNA expression (3-fold) of the ERE-dependent Complement 3 (C3) gene, as measured by Real-time PCR. Further, ovariectomy (ovx) reduced uterine weight in the wt control but not in the ER $\alpha^{\text{NERKI/}}$; and E₂ replacement administered by daily subcutaneous injections (30 ng/g) for 5 days was effective in restoring uterine weight in the wt control but not in the ovx ER $\alpha^{\text{NERKI/}}$ mice. However, 1 h following injection of E₂ to either wt controls or ER $\alpha^{\text{NERKI/}}$ mice we detected (by Western Blot analysis) an increase in the phosphorylation of ERK and the ERK-regulated transcription factors Elk-1 and C/EBP β in vertebral lysates from both types of mice. On the other hand, 1 h treatment of ovx ER $\alpha^{\text{NERKI/}}$ mice with E₂ induced phosphorylation of Smad1, 5 and 8, but this effect was absent in the wt controls. Osteoclastogenesis assayed in *ex vivo* bone marrow cultures was upregulated in both wt and ER $\alpha^{\text{NERKI/}}$ ovx mice. Moreover, in *ex vivo* bone marrow and calvaria cell cultures derived from the ER $\alpha^{\text{NERKI/}}$ mice E₂ (10⁻⁸ M) increased apoptosis of mature osteoclasts and protected calvaria-derived osteoblastic cells from etoposide-induced apoptosis, as effectively as in wt controls. We conclude that estrogens do indeed regulate the birth and death of bone cells via ERE independent mechanisms; and kinase-mediated (nongenotropic) actions of the ER, in the absence of perhaps counter regulatory classical ERE-mediated actions, may activate signaling pathways that promote osteoblast commitment and differentiation.

Disclosures: S. Kousteni, Nuvios, Inc. 1, 2, 5.

1099

The 1,25-Dihydroxyvitamin D/Vitamin D Receptor System Is Required for the Catabolic Effect of PTH but not its Anabolic Action. R. Samadfam, D. Miao, Q. Xia^{*}, G. N. Hendy, D. Goltzman. Calcium lab, McGill, Montral, PQ, Canada.

PTH administered intermittently is known to have an "anabolic" effect, i.e., to increase bone formation whereas continuous infusion of PTH produces predominantly a bone resorptive or "catabolic" response. We examined the effect of the 1,25-dihydroxyvitamin D [1,25(OH)₂D₃]/vitamin D receptor (VDR) system on these responses by administering PTH to wild-type mice, to mice with targeted deletion of the 1 α (OH)ase enzyme [1 α (OH)ase^{-/-}], and to mice with targeted deletion of the VDR [VDR^{-/-}]. Mice were maintained on a "rescue" diet high in calcium (2%), phosphorus (1.25%) and lactose (20%) from after weaning to 2 months of age. We and others have previously shown that mice on this diet exhibit normal serum PTH, calcium and phosphorus concentrations. We have also reported that 1 α (OH)ase^{-/-} and VDR^{-/-} animals on this diet exhibit reduced bone formation and trabecular bone volume suggesting a requirement for the vitamin D system for baseline bone formation. To examine the effect of deficiency of the vitamin D system on the anabolic effect of PTH, we treated animals with either vehicle, PTH (1-34) 80 μ g/kg per day or PTH 80 μ g/kg three times a day for 8 weeks. PTH 80 μ g/kg once daily produced an increase in bone density in both wild-type and mutant mice and PTH 80 μ g/kg three times a day produced an even more robust effect. Histologic analysis demonstrated increases in trabecular bone and in osteoblast numbers. The response was slightly less in mutant mice than in wild-type mice reflecting the requirements for the 1,25(OH)₂D₃ for baseline bone formation. We then examined the catabolic effect of PTH in wild-type and mutant mice by infusing PTH (1-34) 140 μ g/kg/day for 2 weeks using Alzet osmotic minipumps. The continuous infusion of PTH resulted in a significant decrease in bone density which was evident as early as one week after infusion into wild-type animals. In contrast infusion of PTH into mutant mice increased bone density, particularly in the lumbar spine and increased trabecular bone volume. The data indicate that the 1,25(OH)₂D₃/VDR system is not required for the anabolic effect of PTH but that the catabolic effect of PTH may be significantly dampened by reduced 1,25(OH)₂D₃/VDR activity. The catabolic action of PTH may therefore be dependent on an intact 1,25(OH)₂D₃/VDR system and may be converted to an anabolic action by modulating this system.

Disclosures: R. Samadfam, None.

1100

The Pituitary Hormone, FSH, Directly Enhances Osteoclast Formation and Survival. Z. Zhang^{*1}, L. Sun¹, Y. Peng^{*1}, J. Iqbal^{*1}, S. Zaidi^{*1}, D. J. Papachristou^{*2}, H. Zhou^{*1}, A. C. Sharrow^{*2}, B. B. Yaroslavskiy^{*2}, L. Zhu^{*1}, A. Zallone³, M. R. Sairam^{*4}, T. R. Kumar^{*5}, L. Cardoso-Landa^{*1}, M. B. Schaffler¹, B. S. Moonga^{*1}, H. C. Blair², M. Zaidi¹. ¹Medicine, Mt. Sinai School of Medicine and the Bronx VA GRECC, New York, NY, USA, ²Medicine, University of Pittsburgh, Pittsburgh, PA, USA, ³Medicine, University of Bari, Bari, Italy, ⁴Medicine, Clinical Research Institute of Montreal, Montreal, ON, Canada, ⁵Medicine, University of Kansas, Kansas City, KS, USA.

Post-menopausal bone loss is accompanied not only by declining estrogen, but also by elevated FSH levels. Nonetheless, a direct effect of FSH on bone cells has never been investigated. Here, we report for the first time that FSH directly stimulates the formation and survival of osteoclasts. We find that RANK-L-induced osteoclast formation from either bone marrow or RAW cell precursors is enhanced significantly in the presence of FSH at levels found in circulation (3 to 100 ng/ml). This was paralleled by a significant increase in the expression of the osteoclast differentiation markers TRAP, calcitonin receptor and VEGF α . These effects were strongly potentiated when the FSH receptor (FSHR) was over-expressed in adenovirus-infected RAW cells, and were lost in FSHR null osteoclast precursors; together the results establish that FSH effects are mediated *via* an osteoclastic FSHR. The effects of FSH on osteoclastogenesis remained intact in TSH receptor (TSHR) null cells, ruling out cross-reactivity between FSH and the TSHR, which is also present on the osteoclast. In parallel studies, FSH promoted the survival of osteoclast precursors and mature osteoclasts. In RAW264.7 cells, effects of FSH on early apoptosis were demonstrated by the dose-dependent reduction in the camptothecin-induced annexin V^{high}/PI^{low} cell population. In the absence of RANK-L and M-CSF, FSH caused a concentration-dependent increase in the number of surviving mature osteoclasts generated from bone marrow or RAW264.7 cells. Finally, FSH enhanced the phosphorylation of Akt1, a key anti-apoptotic kinase, as well as the MAP kinases Erk1 and Erk2 at 30 and 60 minutes post stimulation. This was paralleled by an increased nuclear localization of c-fos at 30 minutes. Consistent with a role for c-fos in mediating the osteoclastogenic and anti-apoptotic actions of FSH, basal c-fos levels were reduced in FSHR null osteoclasts compared with wild type cells. We conclude therefore that FSH acts directly on osteoclasts to promote their formation and survival. Increased circulating FSH levels accompanying ovarian failure may thus contribute to the bone loss that has been attributed traditionally to declining estrogen.

Disclosures: Z. Zhang, None.

1101

Glucocorticoid Induced Osteoporosis Requires the Glucocorticoid Receptor in Osteoblasts and Does Not Depend on DNA Binding of the Receptor. J. Tuckermann¹, A. F. Schilling², M. Priemel^{*2}, B. Stride^{*3}, M. Kirilov^{*3}, T. Wintermantel^{*3}, F. Tronche^{*4}, M. Amling², G. Schuetz^{*3}. ¹Tissue Specific Hormone Action, Institute of Molecular Biotechnology, Jena, Germany, ²Experimental Trauma Surgery, Hamburg University School of Medicine, Hamburg, Germany, ³Molecular Biology of the Cell I, German Cancer Research Centre, Heidelberg, Germany, ⁴Collège de France, Paris, France.

Osteoporosis is a severe adverse effect observed during glucocorticoid therapy. The physiological mechanism remains poorly understood. Glucocorticoids (GC) could influence bone homeostasis by lowering calcium levels, impact on the release of sex hormones and on hormones of the growth axis or by acting directly on bone cells. GC exert their effects by binding to the glucocorticoid receptor (GR) which in turn regulates gene expression by binding to GC responsible elements in the promoter region of target genes or by interacting with and thus interfering with other transcription factors. To address the cellular and molecular role of GR function in GC induced osteoporosis we analyzed the effect of GC on bone in mice with osteoblast specific and DNA binding deficient GR mutations. For the osteoblast specific deletion of the GR we generated transgenic mice carrying the cre recombinase gene under the control of regulatory sequences of the runx2 gene. In runx2-cre mice cre expression and recombination of loxP-sites occurs in cells of the osteoblastic lineage. These mice were crossed with GRloxP mice (GR^{runx2cre}). To study the DNA binding independent function of the GR we investigated the mechanism of GC induced osteoporosis in function selective GR mutant mice (GR^{dim}). In wildtype mice prednisolone treatment for two weeks strongly inhibited the bone formation leading to lower bone mass. In contrast in GR^{runx2cre} mice bone formation was not affected by prednisolone treatment and thus bone mass was maintained. This indicates that GC action on bone is mediated by direct effects of the GR in osteoblasts. To determine, if this action depends on DNA binding of the GR, we treated GR^{dim} mice with prednisolone. These mice responded to GC with a strong inhibition of bone formation. This results in a low bone mass phenotype, which was similar to that what we observed in wildtype mice. In summary, GC exert their bone deleterious effects primarily via the glucocorticoid receptor in osteoblasts and the DNA binding function of the GR is not required. These results define the critical cell type and provide insights into the molecular mechanism of GC induced osteoporosis. They could help to design GC therapies with less bone related adverse effects.

Disclosures: J. Tuckermann, None.

1102

Lack of Oxytocin in KO Mice Results in a Denser Appendicular Skeleton. Role of the Hormone as Autocrine-Paracrine Enhancer of Osteoblast and Osteoclast Activity. G. Colaianni^{*1}, R. Tamma^{*1}, N. Patano^{*1}, C. Camerino^{*1}, G. Montemurro^{*1}, M. Strippoli^{*1}, A. Di Benedetto^{*1}, S. Colucci^{*1}, M. Grano^{*1}, L. Sun^{*2}, M. Zaidi², A. Zallone¹. ¹Human Anatomy and Histology, University of Bari, Bari, Italy, ²Mount Sinai Medical School, New York, NY, USA.

Oxytocin (OT) is a well known hypothalamic hormone, whose effects in recent years have been demonstrated to be more widespread than previously believed. Oxytocin receptors (OTRs) are expressed by osteoblasts, mature osteoclasts and by their precursors. Here we show that oxytocin is an estrogen-controlled autocrine-paracrine short life peptide that turns on cell activity in bone, stimulating pulses of bone resorption and formation. OTRs are up-modulated by an estradiol pre-treatment. As simultaneous result, RNA for oxytocin also becomes evident in osteoblasts and osteoclasts, indicating local synthesis of the hormone. The effects of estrogen stimulation are reversed after 12-24 hours. OTR stimulation elicits in both cell kinds calcium increase and ERK activation within 5' from OT treatment, back to basal levels after 20'. OT strongly stimulates proliferation in growing osteoblast cultures and in blood-derived macrophage population. In more differentiated osteoblasts OT, as seen by Western Blot and RT-PCR, reduces the expression of osteoprotegerin and induces a RANK-L increase. This effect is reversed after 24 hours. Osteoclastogenesis is strongly enhanced: in the presence of MCSF and RANK-L, OT added to the medium gives rise to a higher number of TRAP-positive cells. By real time PCR a significant increase of Cathepsin K and Beta-3 expression is evident. Bone resorption activity is, however, decreased by 40% in the first 48 hour after OT stimulation, but is thereafter back to control levels. All together these results indicate that the Oxytocin acts as an estrogen-mediated switch that keeps up bone cell activity, stimulating proliferation of both cell kinds. Oxytocin KO mice have been generated and, while normally developed at birth, mature mice show a denser appendicular skeleton and a reduced mineralization of the skull. This preliminary observation can suggest that the overall effect in vivo of the lack of oxytocin is a reduced bone turnover, resulting in a reduced resorption of vertebrae and long bones and insufficient formation in the skull. Experiments with KO cells are under way. Oxytocin role can be relevant in particular during the final period of pregnancy and after parturition when a high level of circulating calcium is necessary for the mineralization of the baby skeleton and for lactation, and could also be an important switch that keeps high the bone turnover level.

Disclosures: G. Colaianni, None.

1103

Mutations in the PLEKHM1 Gene Cause Autosomal Recessive Osteopetrosis in Rat and Human. L. Van Wesenbeeck^{*1}, P. R. Odgren², A. Frattini^{*3}, P. Moens^{*4}, C. MacKay^{*2}, E. Van Hul^{*1}, J. Timmermans^{*5}, R. Jacobs^{*4}, B. Peruzzi^{*6}, A. Teti⁶, A. Villa³, W. Van Hul¹. ¹Center of Medical Genetics, University of Antwerp, Wilrijk, Belgium, ²Department of Cell Biology, University of Massachusetts Medical School, Worcester, MA, USA, ³Istituto di Tecnologie Biomediche Avanzate, Segrate, Italy, ⁴Pediatric Orthopaedics, Catholic University of Leuven, Leuven, Belgium, ⁵Laboratory of Cell Biology and Histology, University of Antwerp, Antwerp, Belgium, ⁶Department of Experimental Medicine, University of L'Aquila, L'Aquila, Italy.

The osteopetroses are a genetically heterogeneous group of bone disorders characterized by a reduction in bone resorption resulting in an overall increase in skeletal mass. Several forms have been described in both human and animals. The incisors absent (ia) rat displays a generalized skeletal sclerosis and a delay in tooth eruption due to numerous dysfunctional osteoclasts. In order to elucidate the gene responsible for the osteopetrotic phenotype of the ia rat, we previously performed segregation analysis and delineated a 4.7 cM region on rat chromosome 10q32.1, in which the disease-causing gene is located (Van Wesenbeeck et al, 2004). Sequencing analysis of the genes located in this interval resulted in the identification of a deletion of 1 nucleotide in the plekhm1 gene in ia rats, resulting in a frameshift mutation followed by additional unrelated amino acids and a premature stopcodon. We also performed mutation analysis of the entire coding sequence of the PLEKHM1 gene in patients diagnosed with various forms of osteopetrosis and identified a splice site mutation in the human PLEKHM1 gene in 1 family diagnosed with the intermediate type of osteopetrosis associated with chondrolysis of the hip. Expression analysis demonstrated that the plekhm1 gene is ubiquitously expressed. Immunohistochemistry experiments clearly show the expression of the plekhm1 protein in bone tissue. We also performed GFP fluorescence experiments and showed that the plekhm1 protein is localized intracellularly. So far, the role of the plekhm1 protein in bone metabolism has not been elucidated. However, the presence of a RUN and a Pleckstrin Homology domain suggests that the plekhm1 protein is linked to small GTPase signaling. Indeed, it has been shown that several members of the small GTPase superfamily play a role in osteoclast functioning (Coxon et al 2003). These findings implicate for the first time that the plekhm1 protein has a role in osteoclast functioning and, more generally, in the bone resorption process.

Disclosures: L. Van Wesenbeeck, None.

1104

Analysis of the Biochemical Mechanisms for the Endocrine Actions of FGF23. X. YU¹, O. A. Ibrahimji^{*2}, R. Goetz^{*2}, F. Zhang^{*3}, S. I. Davis^{*1}, H. J. Garringer¹, R. J. Linhardt^{*3}, D. M. Ornitz^{*4}, M. Mohammadi^{*2}, K. E. White¹. ¹Indiana University School of Medicine, Indianapolis, IN, USA, ²New York University School of Medicine, New York, NY, USA, ³Rensselaer Polytechnic Institute, Troy, NY, USA, ⁴Washington University Medical School, St. Louis, MO, USA.

Studies aimed at understanding the pathophysiology of several human disorders have collectively revealed that fibroblast growth factor-23 (FGF23) is a physiological regulator of renal phosphate reabsorption and vitamin D production. FGF23 is largely produced in bone, and unlike other FGFs, which are paracrine and autocrine factors, circulates in the bloodstream to the kidney where it ultimately acts within the proximal tubule to control mineral metabolism. Presently, it is unknown which of the seven principal FGF receptors (FGFRs) transmits FGF23 biological activity. Herein, we performed surface plasmon resonance (SPR) to comprehensively characterize FGF23 receptor binding specificity. We found that FGF23 specifically bound the 'c' splice isoforms of FGFR1-3 as well as FGFR4 with affinities of 200-700 nM, but did not bind the FGFR1-3 'b' splice forms. To provide biological evidence for the binding specificity of FGF23, we used an FGFR-based mitogenic assay. Consistent with our SPR data, in the presence of heparin, a glycosaminoglycan (GAG) cofactor required for FGF activation of FGFRs, FGF23 only activated FGFR1c (235% of control), 2c (243%), 3c (294%), and 4 (318%). The fact that FGF23 possesses modest receptor affinity and endocrine action led us to hypothesize that FGF23 may exhibit preferences for subsets of GAGs to produce biological activity within target tissues. We therefore assayed a library of in-house prepared GAGs for the ability to promote FGF23 activity. Of significance, highly sulfated and longer GAG species, with specific chemical backbones, were capable of synergizing dose-dependent FGF23 activity. Using opossum kidney (OK) cells, a model for kidney proximal tubule cells, FGF23 inhibited sodium-phosphate cotransporter Npt2a mRNA expression in a dose and time dependent manner. Removal of cell surface GAGs abolished the effects of FGF23, and only exogenous highly sulfated GAG was capable of restoring FGF23 activity, suggesting that OK cells naturally express specific GAGs permissive for FGF23 action. Based upon these results, we propose that the unique endocrine actions of FGF23 involve escape from FGF23-producing cells, circulation to the kidney, and signaling through multiple FGFRs in the presence of specific, highly sulfated GAGs. Our biochemical findings provide important insights into the molecular mechanisms by which dysregulated FGF23 signaling leads to disorders of hyper- and hypophosphatemia.

Disclosures: X. Yu, None.

1105

Osteoblasts Are the Physiologically Relevant Site of *PHEX/Phex* Mutation in X-Linked Hypophosphatemia (XLH). B. Yuan¹, M. Takaiwa¹, T. L. Clemens², M. K. Drezner¹. ¹University of Wisconsin, Madison, WI, USA, ²University of Alabama, Birmingham, AL, USA.

Cloning of the *PHEX* gene from the *HYP* region of Xp22.1 in patients with XLH and identification of *PHEX/Phex* mutations in >2/3 of affected patients tested and in *hyp*-mice established that defects in *PHEX/Phex* underlie XLH. However, although *PHEX/Phex* expression occurs primarily in cells of the osteoblast lineage, increased osteoblast specific *Phex* expression in transgenic *hyp*-mice fails to rescue the disease phenotype, including abnormal renal phosphate transport and hypophosphatemia. Despite contrary physiological evidence, including secretion of putative phosphate transport inhibitory activity by *hyp*-mouse osteoblasts *in vitro*, these data suggest abnormal *Phex* expression at sites other than bone/osteoblasts underlies XLH. To definitively explore this paradox, we created mice with global *Phex* knockout (*Phex*^{-/-}) and conditional osteocalcin (OC) promoted inactivation of *Phex* in osteoblasts (*OC-Cre-Phex*^{fllox/fllox}) to establish if abnormal *Phex* in osteoblasts alone may underlie the *HYP* phenotype. We found *Phex*^{-/-} mice exhibit ubiquitous absence of the *Phex* gene in tissues such as brain, lung, muscle, bone, kidney and heart. In contrast, *OC-Cre-Phex*^{fllox/fllox} mice have absence of the *Phex* gene only in bone. Subsequently, we compared biochemistries of normal, *hyp*-, *Phex*^{-/-} and *OC-Cre-Phex*^{fllox/fllox} mice. Serum calcium was similar in *Phex*^{-/-} (8.3±0.4 mg/dl), *OC-Cre-Phex*^{fllox/fllox} (7.9±0.1 mg/dl) and *hyp*-mice (8.3±0.1 mg/dl) and insignificantly different from that in normal mice (8.4±0.1 mg/dl). In contrast, serum phosphorus in *Phex*^{-/-} (3.3±0.2 mg/dl), *OC-Cre-Phex*^{fllox/fllox} (3.5±0.2 mg/dl) and *hyp*-mice (4.1±0.2 mg/dl) was significantly less (p<0.01) than in normal mice (7.1±0.4 mg/dl), albeit *hyp*-mice had a significantly greater (p<0.05) level than the knockouts. More importantly, the renal brush border membrane phosphate transport in *Phex*^{-/-} (146.8±10.9 pmol/mg protein/10s) and *OC-Cre-Phex*^{fllox/fllox} mice (134.3±8.6 pmol/mg protein/10s) was comparable and significantly less (p<0.001) than in normal mice (246.7±13.8 pmol/mg protein/10s) but no different than in *hyp*-mice (120.7±10.4 pmol/mg protein/10s). The abnormal renal phosphate transport in the *Phex*^{-/-} and *OC-Cre-Phex*^{fllox/fllox} mice occurred due to increased bone production (>7 fold) and serum levels of FGF-23 and consequent decreased kidney membrane Npt2 protein, a mechanism identical to that in *hyp*-mice. These data provide compelling evidence that aberrant *Phex* function in osteoblasts alone is sufficient to underlie the biochemical phenotype in *hyp*-mice, establishing osteoblasts as the physiologically relevant gene mutation site in XLH.

Disclosures: B. Yuan, None.

1106

Homozygous Loss-of-Function Mutation in the Renal Sodium-Phosphate Co-Transporter NaPi-IIc (SLC34A3) Leads to Isolated Renal Phosphate-Wasting in a Large Consanguineous Kindred with Hereditary Hypophosphatemic Rickets with Hypercalciuria. C. Bergwitz¹, N. M. Roslin², J. C. Loredó-Osti², M. Tieder³, H. Abu-Zahra¹, M. Fujiwara², K. Morgan², H. S. Tenenhouse², H. Jüppner¹. ¹Endocrine Unit, Massachusetts General Hospital, Boston, MA, USA, ²Research Institute of the McGill University Health Centre, McGill University, Montreal, PQ, Canada, ³Tel Aviv University, Tel Aviv, Israel.

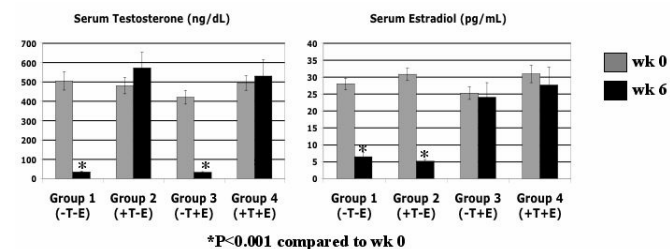
Hereditary hypophosphatemic rickets with hypercalciuria (HHRH) is an autosomal recessive disorder. Affected individuals show renal phosphate (Pi)-wasting leading to rickets/osteomalacia, but contrary to patients with XLH or ADHR, HHRH individuals show elevated 1,25(OH)2D3 leading to absorptive hypercalciuria. We performed a genome-wide linkage scan using genomic DNA from a consanguineous Bedouin kindred with HHRH (Tieder et. al. 1985) and showed that 8 of 10 affected individuals were homozygous at marker D9S1838; all parents were heterozygous. The two affected individuals, heterozygous at D9S1838, became homozygous at marker D9S1826, while three other HHRH patients were now recombinant, making it likely that the genetic defect leading to HHRH resides between markers D9S1826 and D9S1838. A novel microsatellite marker, CB9 (Chr9:137208898), showed homozygosity for all affected individuals, but heterozygosity for all available parents, indicating linkage to chromosome region 9q34. SLC34A3, which encodes the type IIc sodium-Pi co-transporter, NaPi-IIc, was an obvious candidate gene, since it is normally expressed in the brush border membrane of proximal tubular cells, where most filtered Pi is reabsorbed. Nucleotide sequence analysis of SLC34A3 (13 exons and introns) revealed a homozygous frameshift mutation, c.227delC. This mutation disrupts a StuI site which allowed us to independently confirm this homozygous mutation in all affected individuals while all available parents were heterozygous; the mutation was, furthermore, absent in 94 chromosomes from healthy controls. The c.227delC mutation is predicted to cause complete loss of function of NaPi-IIc, and as such is the first description of a genetic defect in humans leading to a primary impairment in renal Pi reabsorption. Our findings, furthermore, emphasize the importance of NaPi-IIc in humans since lack of functional NaPi-IIc protein in patients with HHRH results in severe renal Pi-wasting, leading to hypophosphatemia, an up-regulation of the renal 1-alpha hydroxylase, elevated serum 1,25(OH)2D concentrations and absorptive hypercalciuria.

Disclosures: C. Bergwitz, None.

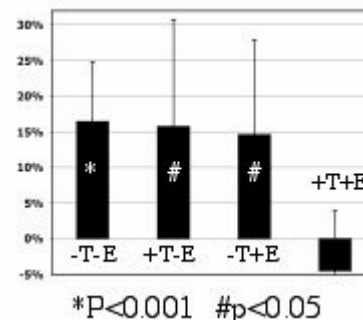
1107

Effects of Selective Testosterone and Estradiol Withdrawal on Skeletal Sensitivity to Parathyroid Hormone in Men. B. Z. Leder¹, J. S. Finkelstein¹, M. Miller^{*1}, S. Comeaux^{*1}, R. Cohen^{*1}, H. Lee^{*2}. ¹Endocrine, Massachusetts General Hospital, Boston, MA, USA, ²Biostatistics, Massachusetts General Hospital, Boston, MA, USA.

Gonadal steroid withdrawal increases bone turnover and causes bone loss in men, but the underlying mechanisms are not yet defined. We previously reported that gonadal steroid deprivation increases the skeletal sensitivity to the bone resorbing properties of PTH in men but it is not known if this effect is mediated by the absence of androgens, estrogens, or both. To make this determination, we randomized 58 men (age 20-45) to receive combinations of a GnRH analog, aromatase inhibitor, and hormone add-back therapy to produce the following groups: Group 1 (testosterone (T) and estradiol (E) deficient, n=16), Group 2 (T sufficient but E deficient, n=12), Group 3 (T deficient but E sufficient, n=14), and group 4 (T and E sufficient, n=16). 24-hour PTH infusions were performed before and 6 wk after hormonal manipulation. Serum NTX and OC were measured every 6 hours during the PTH infusions. The changes in gonadal steroid levels in each group are shown below.



Mean (SD) NTX levels measured prior to PTH infusion did not change in the eugonadal group but increased by 24% (17%) in group 1 (-T-E, P<0.001), by 16% (20%) in group 2 (+T-E, P=0.011), and by 11% (22%) in group 3 (-T+E, P=0.045). Serum NTX increased during PTH infusions in all groups at all time points (P<0.001). In the eugonadal group, the increase in PTH was the same at wk 0 and wk 6, whereas in all the other groups, the PTH-induced increase in serum NTX was greater at wk 6 compared to wk 0 (see figure).



Serum OC fell during PTH infusions in all groups and at all time points (P<0.001), but no differences were observed between wk 0 and wk 6 in any group. We conclude that the selective suppression of testosterone, estradiol, or both increases the skeletal responsiveness to the bone resorbing effects of PTH in men. Moreover, there does not appear to be a large additive effect of combined hormonal deprivation compared to the withdrawal of each hormone individually.

Disclosures: B.Z. Leder, None.

1108

The Leptin Receptor Strongly Influences Bone Structure and Strength: Results from a Genome-Wide Screen in Rats. C. H. Turner¹, I. Alam¹, Q. Sun¹, J. Li², R. K. Fuchs², H. J. Edenberg^{*3}, D. L. Koller⁴, T. Foroud⁴, M. J. Econs⁴. ¹Biomedical Engineering, Indiana University, Indianapolis, IN, USA, ²Anatomy, Indiana University, Indianapolis, IN, USA, ³Biochemistry, Indiana University, Indianapolis, IN, USA, ⁴Molecular Genetics, Indiana University, Indianapolis, IN, USA.

Previously, we identified two inbred strains of rats which differ greatly in bone mass and strength. These rat strains, F344 and LEW, were used to map quantitative trait loci (QTL) for skeletal phenotypes. A genome-wide screen was conducted on a 2nd filial (F2) population of 595 rats derived from F344 and LEW progenitors. The screen identified a QTL on chromosome (Chr) 5 that affected femoral and vertebral bone strength. At the Chr 5 locus, rats homozygous for F344 alleles had 8% greater femoral strength, 12% greater femoral moment of inertia, and 4% greater vertebral cross-section, than rats homozygous for LEW alleles. We subsequently extracted RNA from femurs from 4 wk old rats, and analyzed gene expression using the Affymetrix U34 rat genome array. Of the 31,099 putative genes on the array, 20,028 were expressed in the rat femur. Six genes on Chr 5 were differentially expressed in F344 compared to LEW, including the leptin receptor (*Lepr*). Real time PCR analysis confirmed that *Lepr* was expressed 11-fold higher (p<0.0001) in F344 femurs compared to LEW femurs. To test whether *Lepr* is linked to bone strength parameters, we genotyped the 595 rats in our F2 population using a

ASBMR 27th Annual Meeting

microsatellite marker that falls within an intronic region of the *Lepr* gene (D5Wox39). We found that variation at D5Wox39 explained 7.8% to 8.4% of the total variance in femoral structure and strength and that this marker accounted for the entire variance explained by the Chr 5 QTL. We then examined the effect of inactivating the *Lepr* in rats using the Zucker fa/fa rat model, which has an inactivating mutation of *Lepr*. At 5 months of age, Zucker fa/fa rats had bones with reduced cross-sectional size and strength. Zucker fa/fa rats had 17% lower femoral strength, 12% lower femoral moment of inertia, 41% lower vertebral strength, 17% lower vertebral cross-section, and 37% lower vertebral areal BMD ($p < 0.0001$ for all tests), compared to lean controls (fa/Fa or Fa/Fa). Consequently, lack of a functioning *Lepr* in Zucker fa/fa rats negatively affected bone strength and structure. In our F2 population, rats with F344 alleles had higher expression of *Lepr* and greater bone strength compared to rats with LEW alleles. Our observations suggest a positive association between *Lepr* expression and bone strength. In addition, polymorphisms in the *Lepr* appear to exert strong influences on femoral and vertebral structure and strength.

Disclosures: C.H. Turner, None.

1109

Competitive Recruitment of β -catenin by BMP-2 to Smad-Containing Complexes from Tcf/Lef-Dependent Transcriptional Machinery. V. Salazar*, R. Civitelli, G. Mbalaviele. Bone and Mineral Diseases, Washington University in St. Louis, St. Louis, MO, USA.

β -catenin is necessary for bone development and maintenance. We have previously shown that stabilized β -catenin synergizes with BMP-2 in inducing osteogenic differentiation from uncommitted, multipotent C3H10T1/2 cells. We studied the mechanisms of this interaction using 3 constitutively stabilized β -catenin mutants, *mutGSK3* (all 4 deactivating phosphorylation sites mutated to alanine), $\Delta N90$ and $\Delta N151$ (N-terminal truncation), which were retrovirally transduced into C3H10T1/2 cells. While all these mutants stimulated Tcf/Lef transcription, though with different potency [*mutGSK3* > ($\Delta N90$ $\Delta N151$)], only *mutGSK3* or $\Delta N90$, but not $\Delta N151$, were able to stimulate alkaline phosphatase activity in C3H10T1/2 cells in the absence of BMP-2 (6-, 6-, 1.5-fold stimulation, respectively). However, all mutants synergized with BMP-2 for alkaline phosphatase induction (10-, 10-, 4-fold stimulation by *mutGSK3*, $\Delta N90$ and $\Delta N151$, respectively). Nonetheless, even in the absence of exogenous BMP-2, the specific inhibitor of BMPs, Noggin, dose-dependently inhibited alkaline phosphatase activity induced by constitutively active β -catenin mutants, implying that endogenously produced BMPs participate in and are required for β -catenin osteogenic activity. We also detected rapid dephosphorylation of endogenous β -catenin within 10 minutes of BMP-2 exposure, an event required for transcriptional activity. Co-immunoprecipitation demonstrated a dramatic increase of β -catenin/Smad4 association upon BMP-2 stimulation, coincident with β -catenin and Smad4 nuclear translocation, indicating β -catenin participation in Smad-containing complexes. Interestingly, neither did BMP-2 activate a Tcf/Lef reporter system (TOPflash), nor did active β -catenin mutants transactivate a Smad binding element (SBE-Luc). However, when the endogenous canonical β -catenin signaling was activated by lithium chloride (a GSK3 inhibitor), TOPflash activity was reduced >75% in the presence of BMP-2. Conversely, lithium chloride almost completely prevented BMP-2 activation of SBE-Luc. Furthermore, a constitutively stabilized but transcriptionally defective C-terminus truncated β -catenin mutant abrogated SBE-Luc stimulation by BMP-2 (100-600 ng/ml), and decreased >80% BMP-2 induction of alkaline phosphatase. Thus, BMP-2 competitively recruits β -catenin to Smad-containing transcriptional complexes, at the expense of Tcf/Lef transcriptional machinery. These results demonstrate that β -catenin osteogenic action proceeds via novel, "non-canonical" mechanisms.

Disclosures: V. Salazar, None.

1110

Beta-Catenin Promotes Growth Plate Chondrocyte Differentiation and Maturation. M. Chen, Y. Yan, Y. Dong, H. Drissi, D. Chen, R. J. O'Keefe. Orthopaedics, University of Rochester, Rochester, NY, USA.

Chondrocyte maturation is a multi-step process essential for endochondral bone formation. Several growth factors regulate chondrocyte differentiation, including BMPs and Wnts. Wnt signaling was investigated in cartilage tissues and cells obtained from TopGal transgenic mice, which have the beta-catenin-responsive 3XTCF element driving the lacZ transgene. LacZ staining was present in 14.5 and 16.5 dpc embryos and in new born (P4) TopGal transgenic mice in proliferating and hypertrophic chondrocytes. To investigate the role of Wnt/beta-catenin signaling in chondrocyte differentiation, primary mouse sternal chondrocytes were isolated from neonatal TopGal mice. Treatment with Wnt3a increased the expressions of *BMP-2* (2-fold), *BMP-4* (2-fold) and *colX* (3-fold) after 3 days of exposure. While BMP-2 did not alter lacZ activity in chondrocytes derived from TopGal transgenic mice, it stimulated *colX*, *MMP13*, *alkaline phosphatase* and *VEGF*. To determine the role of Wnt3a/beta-catenin on chondrocyte maturation, C5.18 chondrocytes were transfected with beta-catenin expression plasmid or treated with recombinant Wnt3a. Wnt3a and beta-catenin stimulated the BMP reporter, 12XSBE-Luc, by 2.5 and 5-fold, respectively, and induced the expression of *colX*. Addition of noggin completely blocked the Wnt3a and beta-catenin-*colX* induction and BMP reporter activity. These results demonstrate that Wnt/beta-catenin induces chondrocyte differentiation in a BMP signaling-dependent manner. Experiments demonstrated expression of the natural intracellular inhibitor of beta-catenin signaling, inhibitor of beta-catenin/TCF4 (ICAT) in chondrocytes. ICAT over-expression in C5.18 chondrocytes reduced beta-catenin-induced Top-flash activity (60%). Transgenic mice targeting the ICAT transgene to cartilage using the 1.0kb type II collagen promoter (Col2-Flag-ICAT) were developed. Seven Col2-ICAT founder mice were identified and two independent transgenic lines produced and transgene expression was observed in cartilage tissues. Radiograph analysis showed retarded limb development with Col2-ICAT transgenic mice being 20-50% smaller than littermate

controls. While 2-week-old wild-type mice had a well-developed secondary epiphyseal centers of ossification, chondrocyte maturation was completely absent in the epiphysis of Col2-ICAT transgenic mice, demonstrating a marked delay in chondrocyte maturation. The growth plate demonstrated thickening of the proliferating region and reduced width of the hypertrophic chondrocyte region. These results demonstrate that beta-catenin signaling induces BMP signaling and is required for chondrocyte maturation.

Disclosures: M. Chen, None.

1111

Deletion of DMP1 Results in Osteomalacia and Abnormalities in the Osteocyte Lacuno-Canalicular System - Rescue by Re-expression of DMP1 in the Osteoblast Lineage but not by High Phosphate Diet. Y. Lu¹, H. F. Rios¹, D. Nicoletta², S. Kotha¹, S. Zhang^{*1}, Y. Xie^{*1}, L. Ye¹, J. D. Eick¹, L. Bonewald¹, J. Q. Feng¹. ¹Oral Biology, School of Dentistry, UMKC, Kansas City, MO, USA, ²Mech and Matls Engr, SW Res Ins., San Antonio, TX, USA.

Deletion of Dentin Matrix Protein 1 (DMP1) results in a severe osteomalacia-like phenotype, with a dramatic increase in osteoid seam thickness. Mineralization is defective as evidenced by diffuse fluorochrome labeling throughout the matrix. By immunogold labeling and immunostaining, DMP1 was shown to be highly expressed in osteocytes in normal bone and to localize specifically along the walls of the canaliculi. To gain further insights into the mechanisms for these osteocyte and mineralization abnormalities, the osteocyte lacuno-canalicular system in wild type and *Dmp1* KO mice was analyzed using procion red injection, atomic force microscopy, TEM, backscatter SEM, and resin casted SEM techniques. These experiments showed that the osteocyte lacunae in *Dmp1* KO mice, in both the long bones and alveolar bone, were twice as large, rounded and less ellipsoid compared to lacunae in wild-type mice. The osteocyte canaliculi in these KO mice were disorganized, reduced in number with loss of the lamina limitans, resulting in collapse of the canalicular space. Dendrite membrane surfaces appeared buckled and ridged. To distinguish from other conditions of osteomalacia such as Vitamin D resistant rickets, and to determine whether DMP1 functions in a local or systemic manner, a diet enriched in calcium, phosphorus, and lactose was fed to *Dmp1* KO mice from weaning until two months of age. In contrast to several other models of osteomalacia, including 25 hydroxyvitamin D 1 α hydroxylase KO and VDR KO mice, this diet failed to rescue the mineralization defect in *Dmp1* KO mice. To determine if re-expression of DMP1 in the osteoblast lineage would rescue the KO phenotype, 5 independent transgenic lines overexpressing DMP1 driven by a 3.6 kb rat type I α 1 collagen promoter were generated for crossing with *Dmp1* KO mice. Re-expression of DMP1 using this promoter rescued the phenotype by 1 month of age. High DMP1 protein expression was confirmed in both osteoblasts and in osteocyte canaliculi in the rescued mice. Interestingly, no phenotype was observed when DMP1 was overexpressed on a normal background. Together these data show that DMP1 is an extracellular matrix protein essential for establishment of normal osteocyte and lacuno-canalicular morphology. These findings identify DMP1 as a critical local regulator of mineral incorporation into osteoid and highlight its unique role in the molecular pathway for mineralization in bone.

Disclosures: Y. Lu, None.

1112

Overexpression of the Zinc Transporter ZIP1 Induces an Osteogenic Phenotype in Mesenchymal Stem Cells. A. Gupta, M. A. Khadeer^{*}, S. N. Sahu^{*}, G. Bai^{*}. Biomedical Sciences, University of Maryland, Baltimore, MD, USA.

Zinc (Zn) is an essential trace element that is involved in diverse metabolic and signaling pathways. Zn deficiency is associated with retardation of bone growth. Zn is relatively abundant in bone, and can be detected as free/loosely-bound Zn ions in both osteoid and in matrix vesicles produced by osteoblasts. Zn is thought to exert a direct effect on bone mineralization by its action on nucleation and mineral growth. Zn is also an important component of alkaline phosphatase (ALP) and several metalloproteases. Previous *in vitro* studies have suggested a direct effect of Zn on both proliferation and differentiation of osteoblast-like cells. However, the mechanisms for uptake of Zn into osteoblasts have not been examined in detail. Several families of Zn transporters have previously been characterized in mammalian cells, which function in either uptake, intracellular sequestration or efflux of Zn. The Zrt/Irt-like protein (ZIP) family of transporters mediates uptake of Zn into most mammalian cells, whereas the cation diffusion family (CDF) of transporters is involved primarily in Zn efflux. In the current study, we have examined Zn transport in osteoprogenitor cells, and have attempted to define a functional role for a Zn transport mechanism in osteogenic differentiation. We have identified at least two Zn transporters in both human mesenchymal stem cells and osteoblastic cells, namely the ubiquitous Zn transporter, ZIP1 and LIV-1, previously characterized to be expressed in breast cancer. The subcellular localization of both these Zn transporters suggested both plasma membrane and diffuse cytoplasmic distribution. During the process of osteogenic differentiation of pleuripotent mesenchymal stem cells, both Zn uptake and the expression of ZIP1 were increased. Adenoviral-mediated overexpression of ZIP1 in mesenchymal stem cells resulted in manifestation of an osteogenic phenotype in the absence of osteogenic culture conditions. The induction of an osteogenic lineage was associated with increased expression of osteopontin, Cbfa1/Runx2, bone sialoprotein, and collagen type I. A siRNA-mediated reduction of ZIP1 protein expression in mesenchymal stem cells caused decreased Zn uptake, and inhibition of osteoblastic differentiation under osteogenic culture conditions. Finally, following overexpression of ZIP1 in mesenchymal stem cells, DNA microarray analysis revealed differential regulation of genes associated with proliferation of osteoprogenitor cells and osteoblast differentiation. In conclusion, these studies provide important insights into the role of a plasma membrane Zn transporter in initiation of an osteogenic lineage from mesenchymal stem cells.

Disclosures: A. Gupta, None.

1113

Parathyroid Hormone Regulation of Notch Signaling during Osteoblastic Maturation. L. M. Bevelock*, X. Li*, C. Boumah, N. C. Partridge. Physiology & Biophysics, UMDNJ - Robert Wood Johnson Medical School, Piscataway, NJ, USA.

The Notch signaling pathway plays a critical role in many cell differentiation processes. Our laboratory first identified that parathyroid hormone (PTH) increased the expression of Jagged1, a ligand of the Notch signaling pathway, in UMR 106-01 osteoblastic cells. We hypothesized that Jagged1 stimulates the proliferation of preosteoblasts, while inhibiting their further differentiation, overall resulting in bone growth. The objective of this study was to characterize the regulation of Jagged1 by PTH both *in vitro* and *in vivo* and to determine the effect of Jagged1 stimulation on osteoblastic proliferation and maturation. Parathyroid hormone (1-34, 10^{-8} M) treatment of UMR 106-01 osteoblastic cells increased Jagged1 mRNA expression eightfold 2 h after treatment, as determined by real-time RT-PCR. The increase in Jagged1 mRNA persisted for 8 h of PTH treatment. This increase in Jagged1 mRNA expression translated into increased Jagged1 protein expression. We also found that injections of hPTH(1-34; 8 ug/100g) daily for 5 d in three-month old female rats increased Jagged1 mRNA levels fourfold in the femoral metaphyses. These results demonstrate that PTH increases Jagged1 mRNA levels both *in vitro* and *in vivo*. The upregulation of Jagged1 by PTH in osteoblastic cells is a primary response since it does not require *de novo* protein synthesis. The PKA inhibitor, H-89, abolished PTH's stimulation of Jagged1 mRNA, while the PKC inhibitor, GF109203X, mildly inhibited PTH's stimulation of Jagged1 mRNA, demonstrating that PTH's stimulation of Jagged1 mRNA occurs primarily via the PKA pathway. To stimulate Notch signaling, Jagged1 protein was immobilized on cell culture dishes upon which rat primary calvarial osteoblasts were grown. Cell cycle analyses demonstrated that Jagged1 stimulated proliferation of rat primary calvarial osteoblasts; 20.7% of proliferating calvarial osteoblasts treated with Jagged1 entered the cell cycle, compared to 16.0% of the control cells ($p=0.0002$). Jagged1 treatment strongly inhibited expression of mRNAs for matrix metalloproteinase-13, alkaline phosphatase, osteocalcin and Runx2 by 7-, 3-, 120-, and 7-fold, respectively, in differentiating primary osteoblasts. These results suggest that Jagged1 stimulates proliferation of osteoblasts, while inhibiting their further differentiation. PTH stimulation of Jagged1 on the mature osteoblast may result in increased signaling by Jagged1 to preosteoblasts through Notch to increase their proliferation and suspend their differentiation, resulting in overall bone growth. The increase in the preosteoblast pool may be one mechanism by which intermittent injection of PTH increases bone mass.

Disclosures: L.M. Bevelock, None.

1114

Adipocytes in Δ FosB Overexpressing Mice Accumulate Less Fat Independent of the Osteoblast Phenotype. G. C. Rowe*¹, L. Neff*², W. Horne*², R. Baron*². ¹MCDB, Yale University, New Haven, CT, USA, ²Orthopaedics, Yale School of Medicine, New Haven, CT, USA.

Osteoblasts and adipocytes share a common mesenchymal precursor and several observations have suggested an inverse relationship between differentiation in the two lineages. Overexpression of Δ FosB, a naturally occurring alternative splice form of the FosB transcription factor, upregulates osteoblast differentiation and bone formation, leading to osteosclerosis. In vivo, the expression of Δ FosB under the control of the enolase 2 promoter (NSE) results in both an increase in bone mass and a decrease in adipose tissue mass, supporting the hypothesis of an inverse relationship between the two cell lineages. However, further studies have shown that the bone mass increase was independent of the fat phenotype, since no difference in adipose mass occurred when Δ FosB was expressed under the control of the osteoblast-specific osteocalcin promoter (OG2). To determine if the decreased fat mass was due to a decrease in the number of adipocytes that differentiate from mesenchymal precursors or to a decrease in the ability of adipocytes to accumulate fat, resulting in a decrease in adipocyte size, we compared epididymal fat pads from the NSE- Δ FosB and OG2- Δ FosB mice. However, the adipocytes within the epididymal fat pads of the NSE- Δ FosB were significantly smaller than those of the control littermates. Detailed analysis of the adipose tissue revealed that the decrease in adipose mass was directly proportional to the decrease in cell size. To determine if this decrease in adipocyte size was restricted to the epididymal fat, we examined the subcutaneous fat from the skin in the abdominal region. The size of the subcutaneous adipocytes was also reduced in the NSE- Δ FosB mice, giving rise to a thinner skin, that was due solely to the decrease in adipocyte size and not to differences in the epidermal or dermal layers. These differences in adipocyte cell size were absent in the OG2- Δ FosB mice, reinforcing the observation that the osteoblastic phenotype is independent of the adipocytic phenotype. Thus, the results indicate that decreased adipocyte size may, at least in part, explain the reduced fat mass observed in the Δ FosB mice and confirm that this decrease in fat is indeed independent of the increased bone. We conclude from this study and from the analysis of the OG2- Δ FosB mice that the enhancement of osteoblast differentiation by Δ FosB does not hamper the differentiation of mesenchymal cells into the adipocytes, making it unlikely that the decrease in fat observed in these animals is due to increased osteoblast differentiation. Instead, these results suggest a direct and osteoblast-independent effect of Δ FosB on the ability of individual adipocytes to accumulate lipids.

Disclosures: G.C. Rowe, None.

1115

Increased Thymic T Cell Output Accounts for 50% of the Acute Bone Loss Induced by Ovariectomy. M. Robbie Ryan, W. Qian*, M. N. Weitzmann, R. Pacifici. Endocrinology, Metabolism and Lipids, Emory University, Atlanta, GA, USA.

Ovariectomy (ovx) induced bone loss is prevented by neutralization of IL-7, an estrogen regulated factor required for T lymphopoiesis and T cell homeostasis. Previous studies have revealed that ovx induced IL-7 causes bone loss by increasing the size of T cell pool producing the osteoclastogenic cytokine TNF. One mechanism by which ovx stimulates T lymphopoiesis is an IL-7 dependent increase in thymic T cell output, but the relative contribution of the thymus to ovx induced bone loss remained unclear. To determine if the IL-7 dependent expansion of T cells that occurs following ovx is due to an expansion of the existing T cell pool or due to *de novo* T cell production in the thymus, thymectomies (THX) were performed. Eleven-week-old C57BL6/J mice were either sham THX or THX, and one week later were ovx or sham operated and treated with neutralizing IL-7 antibody M25 or with irrelevant antibody for 4 weeks. Total body bone mineral density measurements by DEXA showed that THX/ovx mice lost ~50% less bone than sham THX/ovx mice. Furthermore, *in vivo* IL-7 neutralization completely prevented bone loss both in euthymic and THX ovx mice. These findings demonstrate that neutralizing IL-7 prevents bone loss due to both the thymic dependent and independent mechanisms of ovx induced bone loss. FACS analysis revealed that while ovx induced a significant increase in both the number of CD4+ T cells and in the number of activated (CD4+CD69+ and CD4+CD25+) T cells in the BM of THX mice, ovx caused a 5 fold higher change in sham THX/ovx mice. Similarly, there was a significant increase in the number of CD4+TNF+ T cells in the BM following ovx, but this was 3 fold lower than the sham THX/ovx group. The induction of T cell activation and TNF production was completely prevented by IL-7 neutralization. *In vivo* BrdU proliferation studies revealed a significant reduction in the number of proliferating naïve T cells in the THX/ovx group, whereas proliferation of memory T cells following ovx remained elevated. Together this data indicates that *de novo* T cell production contributes to approximately 50% of the T cell pool involved in ovx induced bone loss. Furthermore, this data indicates that even in the absence of the thymus, the peripheral T cell pool is able to expand and produce TNF in response to IL-7 and estrogen deficiency. Thus, the disruption of both T cell and bone homeostasis induced by ovx is mediated by IL-7 and due to both the thymic and extra thymic effects of this cytokine. We conclude that IL-7 is a pivotal upstream target through which estrogen regulates immune functions critical for bone homeostasis. Modulation of either IL-7 activity or thymic function may thus represent a novel therapeutic approach for osteoporosis.

Disclosures: M. Robbie Ryan, None.

1116

The Estrogen Receptors (ER α and ER β) Play an Essential Role in Osteocyte Mechanotransduction: Requirement of Membrane Localization and Caveolin-1, but not DNA Binding. J. Aguirre, L. Plotkin, K. Vyas*, S. Kousteni, C. O'Brien, S. Manolagas, T. Bellido. Endocrinology, University of Arkansas for Medical Sciences, Little Rock, AR, USA.

Mechanical stimulation prevents osteocyte apoptosis via a mechanism that requires activation of ERKs. However, cells lacking both ER α and β can not exhibit the ERK-activating effect of mechanical stimulation. Because of evidence that the ligand binding domain (E) of ER α is sufficient to mediate estrogen-dependent anti-apoptosis via an extranuclear non-genotropic mechanism, we investigated here whether ER α , ER β , as well as their respective E domains are sufficient to mediate ERK activation induced by mechanical stimuli; and, whether the subcellular localization of the receptors alters this response. Expression of ER α and ER β was knocked-down in MLO-Y4 osteocytic cells by small interference RNAs for the receptors, followed by rescue with wild type or ER mutants, along with ERK2 fused to a fluorescent protein to allow quantification of nuclear ERK accumulation. Receptor silencing and expression of receptor mutants were confirmed by Western blotting and real time PCR, respectively. Cultures were then subjected to biaxial stretching using a Flexercell Strain Unit (10 min at 5% elongation). Cells in which endogenous ER α and ER β were silenced fail to exhibit nuclear ERK2 accumulation induced by mechanical stimulation by mechanical stimulation, whereas cells silenced for the non-essential protein lamin A/C remained responsive. Stretch-induced nuclear ERK2 accumulation was recovered in ER α /ER β -silenced cells by transfecting ER α , ER β , as well as E α or E β ; or by transfecting an ER α mutant (L525A) which does not bind estrogens. In addition, the response to stretching in ER α /ER β -silenced cells was recovered by transfecting E α targeted to the plasma membrane, but not by E α targeted to the nucleus. Furthermore, transfection of an ER α mutant that exhibits decreased localization at the plasma membrane (S522A), or an unpalmitoylable ER α mutant with impaired plasma membrane localization and inability to interact with caveolin-1 (C447A), failed to confer ERK activation in response to stretching. These findings indicate that: a) both ER α and ER β are able to mediate the ERK-activating function of mechanical stimulation; b) the ligand binding domain of each receptor is sufficient to confer responsiveness to mechanical stimuli, albeit in a ligand-independent fashion; and c) both plasma membrane localization of the ER α and its interaction with caveolin-1 are required for mechanotransduction.

Disclosures: T. Bellido, NuVios 1, 5.

1117

Smad4 Induce Apoptosis by Inducing Bim Alternative Splicing as an ER α Cofactor. Q. N. Li, L. Wu*, D. Oelschlager*, C. Stockard*, W. Grizzle*, N. Wang*, M. Wan, H. Chen*, X. Cao. Pathology, University of Alabama at Birmingham, Birmingham, AL, USA.

Estrogens regulate differentiation and maintenance of reproductive, skeletal, cardiovascular and neural tissues by activating their estrogen receptors (ERs). Antiestrogen compounds such as SERMs regulate ER function by recruiting different co-factors. To examine their molecular mechanisms, we have identified that Smad4, a common signal transducer in BMP/TGF- β signaling, functions as a transcription ER α corepressor, and antiestrogen ligands, not by β -estradiol, induce the interaction of endogenous ER α with Smad4. To examine the function of the interaction, we examined the effect of Smad4 on apoptosis in 2 ER α positive (ER α +) cell lines (MCF-7 and T47D) and 2 ER α negative (ER α -) cell lines (MDA-231 and -468), and the results showed that Smad4 induced apoptosis only in ER α cells and not in ER α - cells. Western blot data demonstrated that Smad4 induces proapoptosis marker expression including Bim, Bax and Cytochrome c release in ER α cells. Bim is the BH3-only protein resides upstream in the apoptosis pathway. We found that Smad4 induces expression three alternative spliced isoforms at both protein and mRNA levels, and splice variants of human Bim mRNA were confirmed with DNA sequence analysis. The spliced short form Bim, the most potent inducer, is sufficient to induce apoptosis. These results indicate that Smad4 induces apoptosis in ER α cell by induction of Bim splicing. To further confirm that ER α is required, we expressed ER α siRNA in MCF-7 cells, which significantly reduced Smad4-induced Bax expression, Cytochrome c release and apoptosis. Smad4 was able to induce apoptosis in MDA-231 cells with acquired ER α expression. Finally, we examined the mechanism of Smad4-induced apoptosis *in vivo*. MCF-7 and MDA-231 cells were transfected with Smad4 or GFP, and were inoculated in nude mice. The tumor sizes of MCF-7 cells with Smad4 are only one tenth of those expressing GFP, and Tunnel assays showed apoptosis positive cells were significantly induced in Smad4 tumor xenograft compared with its GFP control. Whereas in MDA-231, tumor sizes in Smad4 transfected cells are not significantly different from GFP cells. Western blot and immunohistochemical staining of the tumor xenografts for apoptotic biomarkers showed that Smad4 expression induced pro-apoptosis expression including Bim, Bax and Cytochrome c release, but induction of these pro-apoptotic markers was not observed in nude mice bearing MDA-231 tumor xenografts. In summary, we characterized a novel mechanism that Smad4, an ER α cofactor, induces apoptosis by induction of Bim slicing, which may help to understand the diverse biological function of estrogen and serve as a potential drug target.

Disclosures: Q.N. Li, None.

1118

Regulation of Vitamin D Receptor Subcellular Trafficking. J. Barsony¹, K. Prufer*². ¹National Institutes of Health and Georgetown University, Bethesda, MD, USA, ²Department of Biological Sciences, Louisiana State University, Baton Rouge, LA, USA.

Previously we demonstrated that the vitamin D receptor (VDR) rapidly shuttles between the cytoplasm and the nucleus, and that the kinetics of nuclear import and export are influenced by the ligand, calcitriol. To elucidate the mechanisms of VDR trafficking, we continue to define segments of VDR that interact with the nuclear import receptors (nuclear localization sequence, NLS) and nuclear export receptors (NES) using mutational analysis. Moreover, we seek to understand the physiological importance and regulation of VDR trafficking in osteoblasts and osteoclasts. Confocal microscopy showed steady-state localization of VDR, and fluorescence recovery after photobleaching (FRAP) experiments indicated the kinetics of nuclear import and export. Deletion analysis and site-directed mutagenesis targeted potential NLSs of GFP-VDR to evaluate direct nuclear import, targeted leucine-rich regions to identify an interaction site for the crm-1 export receptor, and targeted coactivator, corepressor, and heat shock protein 70 (hsp70) binding regions to evaluate the influence of these protein partners on VDR nuclear import and export. Transcriptional activities of wild type and mutant receptors were assessed by luciferase reporter assays. Mutation of the R54 of VDR to glutamic acid abolished nuclear import, whereas mutation of R54 to glycine allowed import, suggesting that this NLS interacts with importin beta. A deletion preventing hsp70 binding precluded hormone-dependent nuclear accumulation of GFP-VDR, as did mutations in the AF-2 region preventing coactivator binding. We identified the N-CoR binding site of VDR by homology analysis and found that a mutation in this region (I242R) inhibits Crm-1 mediated VDR export. The crm-1 mediated export of NCoR required the binding of HDAC3, which has a well-defined NES. Taken together with the finding that the crm-1 inhibitor leptomycin B only prevents the export of unliganded VDR, these data indicate that the export of the unliganded VDR is indirect, requires assembly of the corepressor complex in the cytoplasm. TOR signaling regulates protein synthesis and cell proliferation, therefore nutrient deprivation and treatment with a specific TOR inhibitor, rapamycin, have profound effects on osteoblast functions. We found that nutrient deprivation or rapamycin facilitated calcitriol-induced nuclear import of GFP-VDR and increased transcriptional activities of VDR in ROS17/2.8 osteoblastic cells. Our findings provide new insight into the mechanisms of VDR subcellular trafficking and reveal the regulation of VDR import and transcriptional activities by the nutrient sensing TOR signaling pathway.

Disclosures: J. Barsony, None.

1119

Several Nuclear Hormone Receptors Interact with DNA-PK in Common to Exert nVDRE-mediated Transcriptional Inhibition of the PTHrP Gene. T. Okazaki, T. Fujita. Endocrine unit, Internal Medicine, University of Tokyo school of Medicine, Tokyo, Japan.

We reported that both 1,25(OH)₂ vitaminD₃ (abbreviated as D3) and 17 β estradiol (E2) repressed PTHrP expression in human breast cancer MCF7 cells. We proposed that recruitment of HDAC2 (histone deacetylase2) as well as the catalytic subunit of DNA-dependent protein kinase (DNA-PKcs) to the chromatinized nVDRE, a half site of DR-3 type DNA element in the PTHrP promoter region, is required in this process. On the assumption that the mechanism of gene inhibition by the liganded nuclear hormone receptors is somewhat conserved, we examined whether other nuclear hormones affect PTHrP gene expression. Here, by using RT-PCR, we report that dexamethasone, progesterone and dihydrotestosterone inhibit transcription of the endogenous PTHrP as well nVDRE-containing reporter genes by 40~70% in MCF7 cells. Such inhibition was recognized as early as 2h after administration of 10 nM of each hormone and lasted at least 12h, which was similar to the repression by D3 and E2. Chromatin immunoprecipitation (ChIP) assay revealed that each hormone, respectively, recruited HDAC2 as well as DNA-PKcs to the nVDRE DNA element in a sequence-specific manner. DNA-PKcs remained tethered to the nVDRE region at least for 12h since its first appearance 30min after hormone treatment. Then, we found that transcriptional repression of the PTHrP gene by each hormone was abrogated by the treatment of the cells with inhibitors of either HDAC (trichostatin A) or DNA-PKcs (high concentration of wortmannin). Introduction of the regulatory subunit of DNA-PK, p70 Ku antigen, in the anti-sense orientation into MCF7 cells decreased the amount of Ku70 protein by about 50%. In these cells, transcriptional repression of the endogenous PTHrP as well nVDRE-containing reporter genes by these nuclear hormones was almost completely abrogated. As expected, ChIP assay revealed that hormone-dependent recruitment of DNA-PKcs to the chromatinized nVDRE was also inhibited in these cells. So far, we were able to confirm hormone-dependent interaction between DNA-PK and VDR/ER α /R, respectively, by using IP (immunoprecipitation)-Western assay. The effects of other nuclear hormone receptor ligands such as triiodothyronine, all-trans/9-cis retinoic acids and troglitazone are currently under investigation. Taken together, we raise a possibility that in order to exert nVDRE-mediated gene inhibition, several nuclear hormones utilize conserved transcriptional machinery in which the interaction between nuclear hormone receptors and DNA-PK plays crucial roles.

Disclosures: T. Okazaki, None.

1120

PTH/Forskolin Induces Selective VDR DNA Binding to the Osteopontin Gene Promoter in the Absence of 1,25(OH)2D3 and Suppresses the Gene's Transcriptional Output. S. Kim, N. K. Shevde, J. W. Pike. Biochemistry, University of Wisconsin- Madison, Madison, WI, USA.

The vitamin D receptor (VDR) is a transcription factor that mediates the actions of 1,25-dihydroxyvitamin D₃ (1,25(OH)2D3) through association with target genes. Historical as well as more recent chromatin immunoprecipitation studies (ChIP) support the idea that this process is initiated through a ligand-dependent VDR activation event. This event promotes the formation of VDR/RXR heterodimers as well as subsequent DNA binding to specific regulatory elements located within the promoter regions of vitamin D responsive genes. The bound VDR/RXR then serves to recruit coregulatory complexes necessary for downstream transcriptional activation. In the present series of experiments, we explored the possibility that VDR might also impact the activity of target genes in the absence of 1,25(OH)2D3, particularly under conditions that might modulate either the level or the activity of the unliganded VDR. Of the many agents that regulate the VDR gene, perhaps the most profound is PTH and/or forskolin. Indeed, we show that the treatment of mouse MC3T3-E1 cells with forskolin leads to both a rapid and dose-dependent increase in VDR mRNA and a dramatic 8-fold increase in VDR protein. That this effect of PTH/forskolin could impact the activity of vitamin D target genes was supported by the interesting observation using ChIP analysis that forskolin treatment selectively increased the association of the VDR with the osteopontin gene promoter but not that for Cyp24 in intact cells. Surprisingly, forskolin-induced VDR binding was not accompanied by co-localization of RXR, although the recruitment of this VDR partner was observed upon treatment with 1,25(OH)2D3. The absence of RXR suggested the possibility that unliganded VDR might function to suppress rather than to induce osteopontin transcription. To explore this, we treated calvarial osteoblasts derived from either wildtype or VDR-null mice with forskolin for periods up to 24 hours and assessed OPN mRNA abundance using RT-PCR. Forskolin suppressed OPN gene expression in a time-dependent fashion in wildtype calvarial cells but not in those from VDR-null mice. These results suggest that factors such as forskolin (and PTH) can induce the binding of unliganded VDR to at least one vitamin D target gene (OPN). In the absence of RXR, however, VDR appears capable of suppressing rather than inducing gene expression. Further studies will be required to assess the nature of the VDR suppressing unit, and to determine whether OPN gene binding is due to VDR upregulation or to a PKA-induced modification.

Disclosures: S. Kim, None.

1121

Role of Acid-Sensing TRPV1 in Bone Pain Associated with Cancer Colonization in Bone. H. Wakabayashi^{*1}, S. Wakisaka^{*2}, T. Hiraga¹, T. Sakurai^{*1}, M. Tominaga^{*3}, T. Yoneda¹. ¹Biochem, Osaka Univ, Suita, Japan, ²Oral Anat, Osaka Univ, Suita, Japan, ³Okazaki Inst Integrat Biosci, NINS, Okazaki, Japan.

Bone pain is one of the major complications that affects QOL of cancer patients with bone metastases. Although the precise mechanism of bone pain is still unclear, the widely-known clinical observations that specific inhibitors of bone resorption bisphosphonates (BPs) reduce bone pain suggest a potential role of osteoclasts that play a central role in bone metastases. Osteoclasts dissolve bone minerals by releasing protons through the vacuolar type proton pump (V-H+-ATPase), thereby inducing acidosis, which is a well-known cause of pain. Recent studies have shown that acidosis directly activates the transient receptor potential channel-vanilloid subfamily member 1 (TRPV1) that converts pain signals into electrochemical signals and transduces them to the central nervous system. Here, we studied the role of TRPV1 in the induction of bone pain associated with cancer colonization in bone. Histological examination showed that TRPV1 was expressed together with calcitonin gene-related protein (CGRP)-positive sensory neurons in periosteum, cortical bone and bone marrow and dorsal root ganglion (DRG). To study the role of TRPV1, we established an animal model of cancer-induced bone pain by inoculating the Lewis lung cancer cells into tibiae in syngeneic wild-type (WT) and TRPV1-deficient (TRPV1^{-/-}) mice. In WT mice, tumor-inoculated tibiae showed hyperalgesia, decreased grip force and increased flinching compared with control tibiae, suggesting increased bone pain. The BP alendronate significantly reduced the hyperalgesia, increased grip force and decreased flinching. A specific inhibitor of the V-H+-ATPase bafilomycin A1 also showed the identical effects, suggesting a critical role of protons released by osteoclasts in bone pain. TRPV1-immunoreactive fibers were increased in tumor-inoculated bone compared with control bones. In contrast to WT mice, there were no differences in the hyperalgesia and grip force between bones with and without cancer cells in TRPV1^{-/-} mice. Flinching of tumor-inoculated hind-limbs in TRPV1^{-/-} mice was significantly less than WT mice. Number of c-Fos immunoreactive neurons in spinal dorsal horn (laminae I/II, L3-5) was greater in WT mice than TRPV1^{-/-} mice. Consistent with these in vivo results, the F-11 rat DRG-like cells transfected with TRPV1 showed elevated and sustained c-Fos expression in response to acid. In conclusion, our results suggest that TRPV1 activation in the sensory neurons innervating bone by the acidic microenvironment created by bone-resorbing osteoclasts plays a critical role in cancer-induced bone pain.

Disclosures: **H. Wakabayashi**, None.

1122

Ral Activation Promotes Prostate Cancer Metastasis to Bone. J. Yin, M. Chock^{*}, M. Oberst^{*}, Y. Ward^{*}, K. Kelly^{*}. National Institute of Health/ National Cancer Institute, Bethesda, MD, USA.

Ras activation has been linked to the progression of many cancer types including prostate cancer. To determine if Ras plays a causal role in prostate cancer metastasis and the contribution of Ras effector pathways to the development of metastasis, we expressed oncogenic RasV12 and effector domain mutants in a human prostate cancer cell line DU145 and assessed their metastatic ability in a mouse metastasis model. Our experiments show that, following intracardiac injection, DU145 expressing oncogenic RasV12 metastasized to multiple organs including bone, brain and adrenal glands. Mice bearing DU145/RasV12 cells developed metastasis within 6-8 week. However, mice bearing DU145 empty vector control cells rarely developed metastases even with extended observation time (3 months). Ras activates multiple pathways; three well characterized Ras downstream pathways are Raf-MEK, phosphatidylinositol-3 kinase (PI3K) and Ral guanine nucleotide exchange factors (RalGEFs). We further investigated the contribution of these pathways to the development of metastasis using Ras effector domain mutants that specifically activate one of the pathways. Ras12VS35, Ras12VC40 and Ras12VG37 activate Raf-MEK pathway, PI3K pathway, and RalGEFs pathways respectively. We found that each downstream pathway produced a distinct metastatic phenotype in our mouse model. DU145 cells expressing Ras12V35S and Ras12V40C produced mainly brain metastasis and very few bone metastases. However, DU145/Ras12V37G caused mainly bone metastasis. The bone metastases in this model involve long bones and spine, and are osteolytic with osteoblastic components. Since bone is the major metastatic site of prostate cancer, we focused on the major downstream pathway of Ras12V37G, the RalGEFs. To determine if RalGEFs mediate the development of bone metastasis, RlfCAAX, a RalGEF that constitutively activates the Ral pathway, was expressed in DU145 cells. Mice inoculated with DU145/RlfCAAX expressing cells developed long bone and spine metastases in 6 weeks. Furthermore, blocking the RalGEF pathway by expressing a dominant negative RalB protein (RalBN28) in DU145/Ras12V37G inhibited the development of metastasis and increased the survival rate compared with DU145/Ras12V37G alone. These results suggest that Ras activation promotes bone metastasis by activating the Ral pathway. Prostate cancer metastasis is a multi-step and multi-factor process, and our findings indicate that activation of Ras may play a major role in promoting prostate cancer metastasis. Furthermore, specific activation of the RalGEF pathway promotes the development bone metastasis.

Disclosures: **J. Yin**, None.

1123

Targeting Myeloma Bone Marrow Microenvironment by GammadeltaT Cells. M. Abe, T. Hara^{*}, H. Shibata^{*}, T. Hashimoto^{*}, S. Ozaki^{*}, S. Kido, D. Inoue, T. Matsumoto. Department of Medicine and Bioregulatory Sciences, University of Tokushima Graduate School of Medicine, Tokushima, Japan.

Multiple myeloma (MM) is characterized by devastating bone destruction and immune suppression leading to tumor escape and susceptibility to infection. MM develops and expands in a manner dependent on bone marrow (BM) microenvironment. We and others have demonstrated a vicious cycle between tumor expansion and bone destruction based on complex cellular interaction between MM cells and the BM microenvironment, providing a rationale for therapeutic strategies targeting the MM BM microenvironment. Aminobisphosphonate (N-BP), a potent anti-resorptive agent, can be recognized by human gammadeltaT cell receptors, and has a potential to expand gammadeltaT cells, which exert potent anti-myeloma effects. Although clinical application of gammadeltaT cells is underway in MM, their impact on BM microenvironment is unknown. In the present study, we explored the effects of the gammadeltaT cells on bone cells as well as co-cultures of MM cells and bone cells. GammadeltaT cells were expanded (30- to 100-fold increase) from peripheral blood mononuclear cells (PBMC) upon stimulation with N-BP (1micromM) and IL-2 for 2 weeks. The gammadeltaT cells added exogenously were found to densely adhere to PBMC-derived preOCs and OCs as well as RPMI8226 MM cells and destroy them more than a half. Of note, the gammadeltaT cells almost completely annihilated them within 12 hours in the presence of N-BP and IL-2. Cytotoxic effects of N-BP and IL-2 were not significant. Interestingly, the gammadeltaT cells showed only minor effects on the viability of normal lymphocytes and BM stromal cells at day 4 and the colony formation of hematopoietic progenitor cells (BFU-E and CFU-GM). Thus, OC lineage cells as well as MM cells are highly susceptible to gammadeltaT cells in an N-BP-inducible fashion. As we previously reported, growth and survival of MM cells and their resistance to anti-cancer agents are potentially enhanced by co-existing OCs, plus MM cells support OC survival. GammadeltaT cells also exerted potent cytotoxic effects on both RPMI8226 cells and OCs in the presence of N-BP and IL-2 even in the co-culture settings. Furthermore, gammadeltaT cells migrated towards factors derived from the tumor bone lesions, osteopontin and MIP-1alpha, produced mainly by the BM microenvironment (especially OCs) and MM cells, respectively. These results suggest that gammadeltaT cells expanded by N-BP and IL-2 are able to target MM cells and OCs in the MM BM microenvironment, thereby inhibiting tumor expansion along with bone destruction. Therefore, gammadeltaT cells may provide a novel and promising therapeutic approach against MM.

Disclosures: **M. Abe**, None.

1124

Dkk1 Modulates Osteoclastogenesis and Bone Resorption: Implications for Myeloma Bone Disease. B. O. Oyajobi¹, A. Gupta^{*1}, A. Flores^{*2}, C. Wideman^{*1}, C. Shipman¹, G. R. Mundy¹, I. R. Garrett². ¹Univ Texas Hlth Sci Ctr, San Antonio, TX, USA, ²OsteoScreen, San Antonio, TX, USA.

The two current concepts of myeloma bone disease are of (i) localized osteolysis; (ii) generalized osteopenia with bone loss adjacent to 'nests' of tumor cells. In the murine 5TGM1 model of myeloma bone disease, we find localized osteolysis together with generalized osteopenia, determined by histomorphometry and bone scintigraphy (99mTc-MDP uptake), distinct from tumor cells. Similar preliminary data consistent with a generalized suppression of bone formation have been suggested in human studies. Although the mechanism underlying the generalized osteopenia in myeloma is unknown, it is likely to involve a circulating mediator. Our notion is that Dkk1, a circulating antagonist of canonical Wnt signaling overexpressed in patients with myeloma bone disease (Tian et al., 2003), plays an important role in this generalized osteopenia. Transgenic mice overexpressing Dkk1 exhibit an osteopenic phenotype. We hypothesize that, in addition to its effects on bone formation, Dkk1 also affects osteoclastogenesis, acting to uncouple bone resorption from formation. To test this hypothesis, we examined (i) effects of Dkk1 in ex vivo bone organ cultures that reflect 'coupling'; (ii) effects of Dkk1 and Wnt-3a (to activate Wnt signaling) on osteoclastogenesis in vitro. In neonatal mouse calvarial cultures, Dkk1 (100ng/ml) strongly inhibited new bone formation stimulated by a combination of BMP-2 and Wnt-3a. Exposure of calvariae to IL-1alpha (0.1nM) for 24 hrs stimulates osteoclastic bone resorption over a 4 day period, which is then followed by a wave of new bone formation from day 4 through day 7, assessed histomorphometrically. Dkk1 dose-dependently abrogated the IL-1-induced new bone formation assessed morphologically. Next, we examined the effect of Dkk1 in mouse whole bone marrow cultures in which 1,25(OH)2D3 robustly induces formation of TRAP+ multinucleated osteoclasts (Ocl). Ocl formation was significantly augmented in the presence of Dkk1 (100-500 ng/ml). In contrast, Wnt-3a (10-100ng/ml) inhibited Ocl formation dose-dependently. More importantly, Dkk1 reversed the inhibitory effect of Wnt-3a, inducing Ocl formation 3-fold greater than in the presence of D3 alone. Together, our data indicates that Dkk1 has the potential to promote osteoclastogenesis while concomitantly blocking bone formation. In myeloma patients with elevated Dkk1 levels, this would exacerbate the local bone disease and potentially be responsible for the generalized osteopenia. Therapeutic strategies aimed at reducing Dkk1 expression in the tumoral bone microenvironment, such as proteasome inhibition, would be beneficial in such patients.

Disclosures: **B.O. Oyajobi**, OsteoScreen 5.

1125

Blocking DKK1 Activity in Primary Myeloma-Bearing SCID-rab Mice Is Associated with Increased Osteoblast Activity and Bone Formation, and Inhibition of Tumor Growth. S. Yaccoby*, F. Zhan*, B. Barlogie, J. D. Shaughnessy*. Myeloma Institute for Research and Therapy, University of Arkansas for Medical Sciences, Little Rock, AR, USA.

We have previously demonstrated that multiple myeloma (MM) cells produce DKK1 and that DKK1 inhibits differentiation of osteoblast precursors in vitro (Tian et al. *NEJM* 2003). This is thought to result in an uncoupling process that may lead to induction of lytic bone destruction in MM. The aim of this study was to test the role of DKK1 in our novel SCID-rab model for primary MM. In this system rabbit bones were implanted S.C. in unconditioned SCID mice. Following 6 weeks, primary MM cells were injected directly into the implanted bone. MM cells from >85% of patients (n>50) were successfully engrafted, grew exclusively in the implanted bone and produce typical disease manifestations including increased osteoclast activity, reduced osteoblast numbers and induction of osteolytic bone disease (Yata & Yaccoby, *Leukemia* 2004). In this study, SCID-rab mice were engrafted with MM cell-expressing DKK1 (assessed by global gene expression profiling) from 7 patients. Following establishment of MM growth, as monitored by weekly measurement of human monoclonal immunoglobulins in mice sera and radiographically, mice were injected subcutaneously into the surrounding area of the implanted bone with neutralizing antibody (AB) against DKK1 (polyclonal AB: n=4, 50 µg/injection/2 days; monoclonal AB: n=3, 100 µg/injection/day) or vehicle, for 4-6 weeks. Whereas bone mineral density (BMD) in control mice was reduced by 3.4%±3.3% from pre-treatment levels, BMD in mice treated with anti-DKK1 was increased by 8.8%±6.8% from pre-treatment levels (p<0.04). The bone anabolic effect of DKK1 could also be visualized on x-ray radiographs. Histological examination revealed that myelomatous bones of anti-DKK1-treated mice had increased numbers of osteocalcin-expressing osteoblasts (45±5 vs. 16±2 per mm bone in controls, p<0.02) and reduced number of multinucleated TRAP-expressing osteoclasts (5±3 vs. 13±2 per mm bone in controls, p<0.004). Whereas in control mice tumor burden was increased in all experiments, anti-DKK1 treatment was associated with reduced tumor growth from pre-treatment levels in 4 of 7 experiments. Overall, tumor burden in control and anti-DKK1-treated mice was increased by 373%±141% and 162%±62% from pre-treatment levels, respectively (p<0.02). We conclude that DKK1 is a key player in myeloma bone disease and that blocking DKK1 activity in myelomatous bones reduces osteolytic bone resorption, increases bone formation and helps control myeloma progression. Our data also suggest that anti-DKK1 treatment may be useful for treating osteoporosis.

Disclosures: **S. Yaccoby**, None.

1126

TGF-Beta Stimulates IL-6, PDGF-AA, and VEGF in Renal Cell Carcinoma Bone Metastasis. M. Doucet*, S. Kominsky, D. Nell*, K. Weber. Department of Orthopaedic Surgery, Johns Hopkins University, Baltimore, MD, USA.

TGF-β is a multifunctional cytokine, which has potent growth promoting effects on advanced cancers. We have shown that TGF-βRI and TGF-βRII are expressed in human RCC bone metastasis and are functional in human bone-derived RCC cell lines (RBM-IT4, RMB23, RBM21A, RBM17C). Since bone is the most abundant repository for TGF-β in the human body, we examined whether TGF-β plays a role in promoting the growth of RCC bone metastasis. We generated transgenic RBM1-IT4 cells stably expressing a dominant-negative (DN) TGF-βRII. RBM1-IT4, empty vector control cells, and two clones (DN1 and DN2) that showed a 46% reduction in TGF-β signaling were injected into the tibiae of athymic nude mice. Digital radiography showed that mice injected with DN2 cells had a significantly decreased incidence of bone lesions (p<0.05) and osteolysis (p<0.001) relative to parental cells while those injected with DN1 cells had no detectable lesions (p<0.001). Further, tumor growth, assessed by tumor weight and H&E staining, was significantly decreased in mice injected with DN1 and DN2 cells compared to parental cells (p<0.05). Since TGF-β treatment of RBM1-IT4 cells had no effect on cell proliferation as determined by MTT assay, we examined the ability of TGF-β to induce cytokines involved in cell growth, angiogenesis, and bone resorption. TGF-β stimulated increased secretion of IL-6 (x = 2.3-fold), VEGF (x = 1.3-fold), and PDGF-AA (x = 1.8-fold) from bone-derived RCC cells as determined by ELISA. Correspondingly, IHC analysis showed that IL-6, VEGF, and PDGF-AA were expressed in 8/9, 18/18, and 2/2 cases of human RCC bone metastasis. TGF-β-induced production of other growth promoting and bone resorptive factors, such as IL-8, TNF-α, and IL-1β was not observed. IL-6 is a multifunctional cytokine that has the ability to regulate cell proliferation and bone resorption. We found that IL-6 receptor (gp80) mRNA was expressed in 13/13 cases of human RCC bone metastasis and 4/4 bone-derived RCC cell lines. Further, gp80 protein expression was found in 16/16 cases of human RCC bone metastasis and RBM1-IT4 tumors established in the mouse tibia by IHC analysis. IL-6 treatment of bone-derived RCC cell lines stimulated STAT3, JNK, PI3K, and ERK signal transduction pathways by Western analysis. Interestingly, IL-6 stimulation of bone-derived RCC cells increased SMAD2/3 phosphorylation in response to TGF-β as determined by Western analysis, suggesting the possible potentiation of TGF-β signaling by IL-6. Taken together, these data suggest that TGF-β may play a substantial role in promoting the growth of RCC bone metastases and concomitant bone destruction, possibly involving the induction of cytokines IL-6, VEGF, and PDGF-AA.

Disclosures: **M. Doucet**, None.

1127

Determinants of Bone Geometry, Density and Strength in Growing Bone. H. M. Macdonald*¹, S. A. Kontulainen², M. A. Petit³, H. A. McKay². ¹Human Kinetics, University of British Columbia, Vancouver, BC, Canada, ²Orthopaedics, University of British Columbia, Vancouver, BC, Canada, ³Kinesiology, University of Minnesota, Minneapolis, MN, USA.

The determinants of bone mass as measured by DXA have been studied extensively in children. Less is known about the influence of body and muscle size, maturity, ethnicity, physical activity and calcium intake on the 3-dimensional properties of bone during growth. Thus, our objective was to use pQCT to identify determinants of bone geometry, density and strength at 3 sites of the tibia in boys and girls. We measured height, tibial length and weight of 440 children (225 boys, 215 girls) aged 9-11 years (Tanner stage I-III). Ethnicity, physical activity and calcium intake were determined by questionnaire. We used pQCT (XCT-2000) to measure total bone cross-sectional area (ToA, mm²) and total density (ToD, mg/cm³) at the distal tibia (8%) with which we calculated a bone strength index (BSI, mm³) as [ToA * (ToD)²]. We measured ToA, cortical area (CoA, mm²), cortical density (CoD, mg/cm³) and strength-strain index (SSI, mm³) at two shaft sites [midshaft (50%), proximal two-thirds (66%)] and muscle cross-sectional area (MCSA, cm²) at the 66% site. We used multiple regression to identify significant predictors of bone outcomes. Compared to girls, boys were significantly heavier (37.9 vs 36.1 kg, p < 0.05) and had greater MCSA (34.3 vs 33.1 cm², p < 0.05). Boys were also more physically active and had a higher calcium intake. All bone outcomes were 5-15% greater for boys (p < 0.05) except CoD which was not significantly different between sexes. For boys and girls, leg length explained the most variance in bone geometry and strength at the distal and shaft sites (20-64%) and was a weak predictor of density at all sites (1-6%). After adjusting for leg length, MCSA accounted for 13-20% of the variance in ToA, ToD and BSI at the distal tibia, 9-17% of the variance in ToA, CoA and SSI at both shaft sites and only 2-5% of the variance in CoD. Physical activity explained 5-8% of the variance in ToD and BSI at the distal site in both sexes and 1-2% of the variance in ToA, CoA and SSI at the shaft sites in boys only. Calcium was a weak predictor (1-4%) of ToD and BSI at the distal site and CoA, CoD and SSI at the shaft sites in boys only. Ethnicity explained less than 2% of the variance in ToA and CoA at the midshaft in girls only (Caucasian > Asian) and maturity was not a significant determinant of bone outcomes in either sex. Our data suggest that body size and MCSA explain most of the variance in tibial bone geometry, strength and total density but not cortical density in boys and girls. Higher physical activity levels and calcium intake among boys may explain why these factors influenced bone outcomes to a larger extent in boys.

Disclosures: **H.M. Macdonald**, None.

1128

RANKL Inhibition Decreases Femoral Head Deformity Following Ischemic Necrosis of the Femoral Head in Immature Pigs. S. Morgan-Bagley*¹, P. Kostenuik², H. Kim¹. ¹Shriners Hospital for Children, Tampa, FL, USA, ²Metabolic Disorders Research, Amgen, Inc., Thousand Oaks, CA, USA.

Legg-Calve-Perthes disease is a common pediatric hip disorder caused by ischemic necrosis of the femoral head. Osteoclastic bone resorption during the repair process has been shown to result in a flattening of the infarcted head that often leads to premature osteoarthritis. OPG is a soluble decoy receptor that inhibits osteoclastogenesis and bone resorption by neutralizing RANKL, a TNF member that is critical for osteoclast formation, function and survival. The therapeutic potential of RANKL inhibitors to inhibit bone resorption and preserve the structural integrity of the femoral head following ischemic necrosis has not been investigated. The purpose of this study was to investigate the effectiveness of recombinant OPG-Fc in the prevention of femoral head deformity in a large animal model of ischemic necrosis. In 10 piglets, ischemic necrosis was surgically induced by placing a ligature around the femoral neck. Two weeks later, OPG-Fc or PBS was administered subcutaneously to 5 animals per group for 6 wks. The animals were euthanized at 8 wks. Radiographic and histomorphometric assessments were performed on the femoral head. Western blot analysis for OPG and RANKL was performed on the bone from distal femoral condyle. The antiresorptive effects of OPG-Fc were monitored by measuring serum NTx. Radiographic assessment showed significantly greater preservation of the femoral head in the OPG-Fc group compared to PBS control (p=0.03). Epiphyseal quotient, the ratio of epiphyseal height to diameter, was significantly higher in the OPG group (0.39 ± 0.05) vs PBS controls (0.24 ± 0.06). Histomorphometry revealed a significant decrease in the number of osteoclasts (p<0.0001) present in the OPG group (1.8 ± 2.2/mm²) vs PBS controls (35.6 ± 6.7/mm²). Femoral epiphyseal bone volume (BV/TV) was significantly higher in the OPG group (16.5 ± 2.1) vs PBS controls (1.3 ± 2.6, p<0.0001). The area of fibrovascular tissue where all trabecular bone had been resorbed was significantly reduced by OPG (p<0.001 vs PBS controls). Western blot analysis showed an increase in OPG and a decrease in RANKL in the OPG group compared to saline group. Serum NTx levels were reduced by 93% in the OPG group vs. saline controls (p=0.01 and 0.005 at 3 and 8wks respectively). To our knowledge, this is the first study to demonstrate the efficacy of recombinant OPG-Fc in pigs. These data are also the first to show that RANKL inhibition prevents femoral head deformity following ischemic necrosis. RANKL inhibitors may therefore represent a novel and promising therapeutic approach to inhibit bone resorption and thereby preserve the structural integrity of infarcted bone.

Disclosures: **S. Morgan-Bagley**, None.

1129

Age at Pubertal Growth Spurt Is a Strong Independent Predictor of Both Trabecular and Cortical BMD in Young Adult Swedish Men - *The GOOD Study*. J. M. Kindblom, M. Lorentzon, E. Norjavaara*, Å. Hellqvist*, S. Nilsson*, D. Mellström, C. Ohlsson. Center for Bone Research at the Sahlgrenska Academy, Department of Internal Medicine, Gothenburg University, Gothenburg, Sweden.

A large part of adult bone mass is acquired during puberty. However, the role of the time of pubertal growth spurt for adult bone mass is unclear. The aim of the present study was to investigate the influence of age at pubertal growth spurt for adult cortical and trabecular bone mass. Detailed growth charts from birth up to 18-20 years of age were available for 549 men participating in the Gothenburg Osteoporosis and Obesity Determinants (*GOOD*) study. Peak Height Velocity (PHV; occurring two years after the initiation of puberty) was calculated using the infancy-childhood-pubertal growth model. The time of PHV was then correlated with cortical and trabecular bone phenotypes analysed at 18-20 years of age, using peripheral quantitative computerized tomography (pQCT). Environmental factors were assessed through questionnaires. The independent predictive role of time for PHV was assessed through linear regression, including time of PHV, age at pQCT analyses, height, weight, calcium intake, smoking and physical activity. Trabecular BMD, measured, in the distal metaphyseal area of the tibia revealed that time of PHV was a strong negative predictor of trabecular BMD ($\beta = -0.187$, $p < 0.0001$). Cortical bone analyses in the diaphyseal region of the tibia showed that time of PHV was an independent strong negative predictor of cortical BMD ($\beta = -0.337$, $p < 0.0001$) and a positive predictor of cortical endosteal circumference ($\beta = 0.213$, $p = 0.006$). Cortical periosteal circumference remained unchanged. We next compared the subjects with early puberty (EP, the 15% with earliest PHV, 12.0 ± 0.4 years of age) with those with late puberty (LP, the 15% with latest PHV, 15.2 ± 0.5 years of age). Subjects with EP had higher trabecular ($9.8 \pm 1.3\%$, $p < 0.001$) and cortical BMD ($1.9 \pm 0.2\%$, $p < 0.001$) than those with LP. Moreover, subjects with EP had decreased endosteal circumference ($-5.7 \pm 1.2\%$, $p = 0.003$) but unchanged periosteal circumference ($-1.8 \pm 0.7\%$, NS) compared with those with LP. Thus, the time of puberty is a strong independent predictor of both trabecular and cortical BMD in young Swedish men and subjects with LP displayed an endosteal cortical expansion. Our study indicates that late puberty might be a risk factor for the development of low bone mass later in adult life. Further studies are required to determine if time of puberty is a determinant of trabecular and cortical BMD in elderly men.

Disclosures: J.M. Kindblom, None.

1130

Children with Bone Fragility Fractures Have Reduced Bone Mineral Areal Density at the Forearm and Hip and Higher Percent Body Fat. S. L. Mobley*, E. Ha*, J. D. Landoll*, N. E. Badenhop-Stevens*, A. Clairmont*, P. Goel*, V. Matkovic*. ¹Bone and Mineral Metabolism Laboratory, The Ohio State University, Columbus, OH, USA, ²Department of Statistics, The Ohio State University, Columbus, OH, USA.

Bone fragility fractures in children are very common during the pubertal growth spurt. We previously showed a reduced volumetric bone mineral density of the radius in children with distal forearm fracture due to low to moderate trauma (Landoll et al. J Bone Min Res 19:S87, 2004). We now present anthropometry data as well as bone mineral areal density measurements at several skeletal regions of interest in a group of children with (N=458) and without (N=398) forearm fracture (60% males, 40% females). Bone mineral areal density of the proximal and distal radius, hip, spine, and total body were measured by DXA (GE-Lunar DPX-IQ). For case subjects, measurements of the forearm were made on the non-fractured arm. For control subjects, measurements were made on the matching (dominant vs. non-dominant) arm. The results of the measurements are presented in the table.

Variable	Fracture group Mean (\pm SE)	Control group Mean (\pm SE)	Significance P
Age	11.3 (0.1)	11.3 (0.1)	0.755
Height cm	149.7 (0.7)	149.0 (0.7)	0.510
Weight kg	47.4 (0.8)	44.5 (0.8)	0.011
Body fat kg	11.687 (0.449)	9.476 (0.387)	0.0002
% Body Fat	24.0 (0.5)	21.0 (0.5)	0.0001
TBBMC kg	1.634 (0.030)	1.598 (0.030)	0.393
Spine BMD g/cm ²	0.83 (0.007)	0.84 (0.009)	0.269
Femur neck BMD g/cm ²	0.86 (0.007)	0.89 (0.008)	0.0001
Femur trochanter BMD g/cm ²	0.75 (0.006)	0.78 (0.007)	0.015
Proximal radius BMD g/cm ²	0.522 (0.004)	0.531 (0.004)	0.112
Distal radius BMD g/cm ²	0.299 (0.003)	0.308 (0.003)	0.031

The above results show bone deficits in children with bone fragility fracture, not only at the forearm but also at the hip. The above results may be important in the view of rising obesity in children as well as fracture rate.

Disclosures: V. Matkovic, None.

1131

Fractures in Puberty - Causes and Implications in Old Age. M. Suuriniemi*, H. Suominen¹, H. Kröger², S. Cheng¹. ¹Univ. JKL, Jyväskylä, Finland, ²Univ. KU, Kuopio, Finland.

The aetiology of the large increase in the incidence of arm fractures during puberty and their relationship to the risk of osteoporosis in older age are unclear. The purpose of this study was to investigate the differences in bone properties and metabolism between girls with and without fractures during their early pubertal period. The subjects were 258 healthy 10-13-yr-old girls with Tanner stage I-III. Bone properties of the total body, total proximal femur, femoral neck, lumbar spine, distal radius, tibia shaft, and calcaneus were measured using different bone assessment modalities (dual-energy X-ray absorptiometry, peripheral quantitative computed tomography, scanning calcaneal ultrasonometry, and axial transmission ultrasonometry). Also, serum growth hormone, insulin-like growth factor-1, insulin-like growth factor-binding protein-3, estradiol, testosterone, sex hormone-binding globulin, leptin, parathyroid hormone, 25-hydroxyvitamin D, aminoterminal propeptide of type I collagen, osteocalcin, bone-specific alkaline phosphatase, and tartrate-resistant acid phosphatase isoenzyme 5b were analysed. Dietary intakes, physical activity, family history of osteoporosis, and fracture history were determined by questionnaires. The fractures were further confirmed by medical records including X-ray photographs. The fractures occurred during ages 10-13-yr and not caused by severe trauma were included in the analysis. Our results showed that each of the 11 fractures concerned the arm; 6 of them occurred 2-12 months before and 5 of them 2-19 months after the bone assessments. Girls with fractures had significantly larger cross-sectional area (269 ± 22 vs 225 ± 43 mm², $p = 0.001$) but smaller volumetric bone mineral density (242 ± 32 vs 290 ± 36 mg/cm³, $p < 0.001$) of the radius, as well as higher activity of the bone-specific alkaline phosphatase (147 ± 47 vs 119 ± 33 U/L, $p = 0.012$), than girls without a fracture history. No differences were found between girls who fractured before and those who fractured after the bone assessments. Noteworthy, the fractured girls also had 4.8 times higher relative risk of having a family member with osteoporosis ($p = 0.015$), compared to their non-fractured counterparts. These findings suggest that the increased incidence of arm fractures during the adolescent growth spurt may be accounted for the inability of mineral accrual to keep pace with the great increase in bone size of the arm. Furthermore, the fractured girls may share some common genetic factors with their family members, which predispose them to high bone turnover, posing complications on the bone modeling and remodeling. Pubertal fractures should thus be considered as a true risk for future postmenopausal osteoporosis.

Disclosures: M. Suuriniemi, None.

1132

Bone Mass at the Lumbar Spine in Young Adults: Late Effects of Very Low Birth Weight. C. M. Smith¹, N. P. Wright*, J. Wales*, C. MacKenzie*, R. Primhak*, R. Eastell¹. ¹Academic Unit of Bone Metabolism, University of Sheffield, Sheffield, United Kingdom, ²Sheffield Children's Hospital, Sheffield, United Kingdom, ³Dept of Child Health, University of Sheffield, Sheffield, United Kingdom.

A low peak bone mass (PBM) is an established risk factor for fracture in later life. Prepubertal children who were born with very low birth weight (<1500g, VLBW) have reduced bone mass compared to children born at full term. However, this reduced mass appears to be appropriate for their reduced body size, suggesting no reduction in bone strength during childhood. The effect of VLBW on PBM is unknown. A low bone mass in this population may become increasingly important as more VLBW infants survive into adulthood. PA lumbar spine bone mass was measured, using dual energy x-ray absorptiometry (Hologic Discovery), in 62 young men and women (age 21 -25 years); 36 born VLBW, 26 normal birth weight controls (C). There were 20 and 18 women, and 16 and 8 men in the VLBW and C groups respectively. Bone volume (BV) and volumetric bone density (bone mineral apparent density, BMAD) were estimated, using Carter's method (1997). Standard deviations scores (SDS), adjusted for age, height and weight, were calculated. The VLBW and C groups were compared using unpaired t-tests. Height and weight were not significantly different between the VLBW and C groups. Lumbar spine bone mineral density (BMD) was significantly reduced in the VLBW group. Mean (SD) BMD ZSc (Hologic output, adjusted for age only) was -0.68 (0.95) and -0.09 (0.99), $p = 0.02$, in the VLBW and C groups respectively. There were no differences in BV SDS. BMAD SDS (mean, SD) was reduced in the VLBW group (-0.49 (0.93), $p = 0.04$). PBM is reduced in VLBW young adults. This deficit is the result of reduced volumetric density, whereas bone size is normal. The deficit is still apparent after adjusting for differences in body size. Previous studies have suggested that VLBW children have reduced bone mass that is appropriate for bone and body size. We speculate that our results may suggest a deviation from normal bone mass accrual during puberty in VLBW individuals, which results in bones of normal size, but of reduced density. This reduced PBM may have implications for future fracture risk in VLBW individuals.

Disclosures: C.M. Smith, None.

1133

High Bone Turnover Predicts Mortality in the Frail Elderly: A Prospective Cohort Study. C. Chen^{*1}, P. Sambrook¹, L. March^{*1}, I. Cameron^{*1}, R. Cumming^{*2}, J. Simpson^{*2}, M. Seibel³. ¹Institute of Bone & Joint Research, University of Sydney, Sydney, Australia, ²School of Public Health, University of Sydney, Sydney, Australia, ³ANZAC institute, University of Sydney, Sydney, Australia.

Osteoporotic fractures are associated with accelerated bone turnover and excess mortality. In a prospective cohort study of 1112 elderly subjects, we assessed whether the rate of bone turnover is a direct predictor of mortality. Baseline data from elderly subjects (mean +/- SD age: 86 +/- 6.9 yrs; 21% male) living in residential care facilities were analysed. Parameters included: age, gender, co-morbidity, incident hip fractures, serum aminoterminal propeptide of type I collagen (PINP), carboxyterminal telopeptide of type I collagen (CTX), intact parathyroid hormone (PTH), serum 25 hydroxyvitamin D (25OHD). Serum calcium, phosphate and creatinine were measured in a randomly selected subgroup of 448 subjects (40%). Over a median follow-up of 817 (range: 4 - 2028) days, a total of 559 (50.3%) subjects died. In univariate analyses, time to death was significantly (p< 0.05) associated with age (HR 1.62, per 10 yrs), gender (HR 1.33, male vs. female), comorbidity (HR 0.31, mild vs. severe illness), hip fracture (HR 2.26, yes vs no), log serum creatinine (HR 1.67), log PTH (HR 1.29), log CTX (HR 1.50) and log PINP (HR 1.32). These associations remained unchanged when adjusted for serum creatinine levels. Mortality rates/ person/ year continuously increased with increasing serum CTX or PINP concentrations (highest quintile vs. lowest quintile, CTX: 32.4 vs 16.5%, PINP: 30.5 vs. 20.0%). In multivariate analyses adjusting for age, gender, comorbidity, 25OHD, PTH and hip fracture status, both bone turnover markers remained significantly associated with all cause time to death: log CTX, HR 1.27 (95%CI 1.11-1.47, p<0.001), log PINP, HR 1.21 (95%CI 1.06-1.39, p= 0.007). For individual causes of death, bone turnover markers were associated with deaths from cardiac and cerebrovascular causes, but not infections. We conclude that in the frail elderly, high bone turnover predicts death independent of age, gender, comorbidity, renal function, serum PTH levels and hip fracture status.

Disclosures: **M. Seibel**, None.

1134

Vitamin D Deficiency and Neuromuscular Performance in the Longitudinal Aging Study Amsterdam (LASA). I. S. Wicherts^{*1}, N. M. Schoor Van^{*1}, A. J. P. Boeke^{*1}, P. Lips². ¹EMGO, VU University Medical Center, Amsterdam, The Netherlands, ²Endocrinology, VU University Medical Center, Amsterdam, The Netherlands.

Vitamin D deficiency is common in the elderly. Recently vitamin D deficiency has been implicated as a cause of decreased physical performance and falls. The aim of this study was to determine whether lower serum 25-hydroxyvitamin D (25(OH)D) is associated with lower neuromuscular performance. The study was done within the framework of the Longitudinal Aging Study Amsterdam (LASA), a follow-up study in a representative sample of the older Dutch population which started in 1992. Subjects were 656 men and 695 women aged 65 years or older on January 1, 1996 (mean age ± SD: 75.5 ± 6.6 yr). In 1995-1996, data were collected on physical performance and vitamin D status. Neuromuscular performance was measured by the sum of the following tasks: 5 chair stands, a walking test and tandem stand, each scored in seconds and classified from 1 to 4 points according to quartiles of the distribution. The total performance score, representing muscle strength and balance, ranged from 0 to 12. Multivariate regression analysis, adjusted for age, gender and Conclusions:body mass index (BMI), was used to examine the association between vitamin D status and neuromuscular performance. Serum 25(OH)D (mean ± SD) was 53.3 ± 24.0 nmol/l. Serum 25(OH)D was ≤ 25nmol/l in 152 (11.3%) persons, 25-50 nmol/l in 486 (36.0%) persons, 50 -75 nmol/l in 449 (33.2%) persons, and > 75 nmol/l in 232 (17.2%) persons. Scores on chair stands, walking test and tandem stand each showed significant improvement with increasing serum 25(OH)D (P<0.001). The total performance score was 4.9 when 25(OH)D ≤25nmol/l, 6.82 when 25(OH)D was 25- 50 nmol/l, 8.10 when 25(OH)D was 50- 75 nmol/l and 8.72 when 25(OH)D > 75 nmol/l. The change in total performance score with increasing serum 25(OH)D was significant for all steps. When adjusting for age, gender and BMI, the performance score increased significantly with serum 25(OH)D up till 50 nmol/l (P< 0.005). In conclusion, a low serum 25(OH)D was significantly associated with lower neuromuscular performance up to a threshold of 50 nmol/l.

Disclosures: **I.S. Wicherts**, None.

1135

Ethnic Diversity in Volumetric Bone Density and Geometry in Older Men: The Osteoporotic Fractures in Men Study (MrOS). J. M. Zmuda¹, B. K. S. Chan^{*2}, L. M. Marshall^{*2}, J. A. Cauley¹, T. F. Lang³, K. E. Ensrud⁴, C. E. Lewis^{*5}, M. L. Stefanick^{*6}, E. Barrett-Conner^{*7}, E. S. Orwoll⁸. ¹Epidemiology, University of Pittsburgh, Pittsburgh, PA, USA, ²Oregon Health and Science University, Portland, OR, USA, ³University of California, San Francisco, CA, USA, ⁴VAMC and University of Minnesota, Minneapolis, MN, USA, ⁵University of Alabama, Birmingham, AL, USA, ⁶Stanford University, Palo Alto, CA, USA, ⁷University of California, San Diego, CA, USA, ⁸Oregon Health and Sciences University, Portland, OR, USA.

Bone mineral density (BMD) is not the only determinant of bone strength and fracture risk. The structural geometric properties of bone, such as the size, thickness, shape and spatial distribution of bone mass, also influences bone strength. Ethnic differences in bone geometry may have important effects on fracture epidemiology, but remain poorly defined. To address this, we characterized volumetric BMD (vBMD) and cross-sectional area (CSA) in 3,158 men aged 65+ from 6 geographic regions in the US who are enrolled in the Osteoporotic Fractures in Men Study (MrOS). Race/ethnicity was self-reported. BMD (g/cm³) and CSA (cm²) were derived from volumetric quantitative computed tomography scans of the femoral neck (FN) and lumbar spine (LS). Analyses were adjusted for age, height, weight and geographic area. Ethnic differences in vBMD were apparent in both the trabecular and cortical bone compartments at both skeletal regions (Table). FN and LS vBMD were greatest in African Americans (AA). FN and LS CSA were lowest in AA and greatest in Caucasians (CA). These ethnic differences in vBMD and geometry might contribute to at least some of the ethnic difference in hip and vertebral fracture epidemiology.

Femoral and Vertebral BMD and Geometry by Ethnicity				
Ethnic Group	CA	AA	AS	HA
No. of men	2786	168	117	87
FN Cortical BMD	.524	.541	.520	.525
FN Trabecular BMD	.069	.094	.093	.079
FN CSA	12.7	12.3	12.5	12.6
LS Trabecular BMD	.109	.140	.117	.113
LS CSA	11.9	11.1	11.7	11.7

All p<0.01 for differences by ethnic group adjusted for age, weight, height, geographic region. CA, Caucasian American; AA, African American; AS, Asian American; HA, Hispanic American;

Disclosures: **J.M. Zmuda**, None.

1136

Fracture in Childhood and Adolescence: a New Risk Factor for Osteoporosis? S. L. Ferrari, T. Chevalley, J. Bonjour, R. Rizzoli. Div. of Bone Diseases, Geneva University Hospital, Geneva, Switzerland.

Traumatic fractures affect nearly one out of two children, with a peak incidence concomitant to peak height velocity (PHV). Its has been hypothesized that bone fragility at that age results from a transient deficit in bone mineral accrual relative to bone size. Whether a low bone mass persists beyond the period of PHV however remains unknown. Bone mineral content (BMC) was longitudinally assessed by DXA at both fractured and non-fractured sites in a cohort of 125 females who were followed over 8.5 yrs, from pre-puberty to pubertal maturity (mean age ± sem, 16.4 ± 0.1 yrs). During this period, 58 fractures occurred in 41/125 girls (cumulative incidence, 46.4%), 48% of all fractures affecting the forearm and wrist. Girls with and without fractures had similar height, weight and BMI, as well as mean calcium intake (>900 mg/d), at all time points. Before puberty and at the time of PHV, BMC values at the proximal radius (33% Rad.) tended to be lower in those with fractures (p=0.066 by non-parametric tests). However, as these girls reached pubertal maturity, BMC at the ultradistal radius (UD Rad.), femur trochanter (FT) and lumbar spine (LS) were all significantly lower in girls with fractures, whereas BMC at femur neck (FN) and diaphysis (F.Dia) were not (Table).

	BMC (G)	BMC (G)	P VALUE (Mann-Whitney U)
	FRACTURES (41)	CONTROLS (84)	
LS	42.67 ±1.08	45.39 ± 0.85	0.020
FN	4.55 ± 0.09	4.69 ± 0.08	NS
FT	5.91 ± 0.15	6.36 ± 0.14	0.034
F. Dia	52.67 ± 1.25	51.49 ± 1.03	NS
UD Rad.	1.35 ± 0.04	1.44 ± 0.03	0.019
33% Rad.	1.81 ± 0.03	1.89 ± 0.03	NS

Moreover, compared to girls without fractures, BMC gain throughout puberty was significantly less in fractured girls at LS (-8.0%, p = 0.015) and UD Rad. (-12.0%, p = 0.006), and approached significance at FT (-8.4%, p = 0.064) and 33% Rad. (-6.0%, p = 0.09), without differences in height and weight gain. BMC values at all sites were highly correlated between pre-puberty and pubertal maturity (R=0.54 at FT to 0.81 at LS) and within-trait correlations between mature daughters and their mothers led to heritability estimates ranging 80%-90% for hip, spine and 33%Rad. BMC, but only 36% for UD Rad. BMC. In summary, female children with fractures have lower BMC gain and lower bone mineral mass when they reach pubertal maturity, particularly at sites containing predominantly trabecular bone. Taken together with the evidence of tracking for bone mass during growth and the strong contribution of genetic factors therein, these observations suggest that a history of fracture in childhood and adolescence may be a marker for genetically determined low peak bone mass and osteoporosis later in life.

Disclosures: **S.L. Ferrari**, None.

1137

High IGFBP-2 Levels Are Associated with an Increased Risk of Osteoporotic Fractures in Elderly Men. C. Meier¹, T. V. Nguyen², J. R. Center², M. J. Seibel¹, J. A. Eisman². ¹Bone Research Program, ANZAC Research Institute, University Sydney, Sydney, Australia, ²Bone and Mineral Research Program, Garvan Institute of Medical Research, St. Vincent's Hospital and UNSW, Sydney, Australia.

Serum IGFBP-2 levels increase with advancing age, are inversely associated with bone mineral density (BMD) and are positively correlated with bone resorption rates. We examined the relationship between serum IGFBP2 and fracture risk in community-dwelling men. This case-cohort control study included 139 men, aged 71 ± 5.3 yrs (mean±SD) who had been prospectively followed in the Dubbo Osteoporosis Epidemiology Study for a median of 6.3 yrs (range, 2-13 yrs). During this period, 38 men had incident low-trauma non-vertebral fractures (cases), while 101 men had no fractures (controls). Femoral neck BMD, markers of bone resorption (ICTP) and formation (PINP), and serum levels of IGF-I, IGFBP-2, IGFBP-3 were measured at baseline. In the entire sample, IGFBP-2 was negatively correlated with femoral neck BMD ($r = -0.21$; $p = 0.01$) and positively correlated with age ($r = 0.34$; $p < 0.001$). Men with a subsequent fracture had higher baseline IGFBP-2 levels and higher baseline ICTP levels than men without a fracture. There were no significant differences in IGF-I, IGFBP-3 between cases and controls. In univariate logistic regression analysis, increased fracture risk was associated with higher IGFBP-2 (odds ratio [OR] 1.9; 95%CI 1.3-2.9) or higher ICTP levels (OR 2.3; 95% CI 1.5-3.5). After adjusting for age and femoral neck BMD, the effect of IGFBP-2 remained statistically significant (OR 1.73; 95%CI: 1.1-2.7). However, with the introduction of ICTP, the OR associated with IGFBP-2 reduced to 1.4 (95% CI: 0.8-2.3). In conclusion, these results suggest that IGFBP-2 predicts fracture risk in men independent of BMD and age, and this association is possibly mediated through an association between IGFBP-2 and bone resorption.

Disclosures: C. Meier, None.

1138

Short-Term and Long-Term Absolute Risk of Fracture by Bone Mineral Density and Age in Women and Men. N. D. Nguyen, H. Alhborg, J. R. Center, J. A. Eisman, T. V. Nguyen. Bone and Mineral Research Program, Garvan Institute of Medical Research, Sydney, Australia.

Residual lifetime risk of fracture (RLRF) is a preferred absolute-risk approach of assessment fracture risk in an individual, because it takes into account the risk of mortality of the individual. Although bone mineral density (BMD) is the best predictor of fracture risk, the RLRF for various BMD levels is not known due to lack of long-term longitudinal data. The present study was undertaken to estimate the RLRF in elderly men and women by age and BMD level. A sample of 1358 women and 859 men aged 60+ years as at 1989 of Caucasian background who have participated in the Dubbo Osteoporosis Epidemiology Study were studied. The participants have been followed for 15 years (1989-2004), and all fractures were recorded and confirmed by X-ray and personal interview. Traumatic and pathological fractures and fractures of skull, cervical spinal or digits were excluded from the analysis. During the follow-up period, all-cause mortality was also recorded. Bone mineral density at the femoral neck was measured by dual energy X-ray absorptiometry (GE-LUNAR) at baseline. Short-term (10-year) and RLRF from the age of 50 were estimated by the survival analysis with left truncation using the Cox's proportional hazards model taking into account the competing risk of death. During the follow-up period, 496 women and 180 men had sustained at least one fracture, and 465 women and 374 men had died. After adjusting for the competing risk of death, the RLRF (from the age of 50) was 54% (95% CI: 48-59) in women and 32% (23-36) in men. In women, the 10-year risk of fracture increased from 16% (12-21) among those aged 60-69 yr to 49% (40-61) among those aged 80+. In men, the 10-year risk also increased from 11% (5-17) among those aged 60-69 yr to 26% (13-38) among those aged 80+. The risk of fracture, as expected, increased with reduced BMD levels. In women with BMD T-scores ≤ -2.5 , the 10-year and RLRF were 31% (19-44) and 71% (66-79), respectively; among men with the same BMD levels, the 10-year and RLRF risk of fracture was 30% (2-56) and 47% (35-77), respectively. For a given BMD level, the 10-year risk and RLRF also increased with advancing age, such that by the age of 70 and above, there was no significant difference in 10-year risk or RLRF between women with T-scores ≤ -2.5 . Thus, in Caucasian population, the residual lifetime risk of any fracture from the age 50 is 1 in 3 men and 1 in 2 women. The presence of low BMD increased the risk to 1 in 2 men and 7 in 10 women. These estimates provide a means to communicate the risk of fracture to an individual patient, and can be used to promote identification of high-risk individuals and target for treatment in the population.

Disclosures: N.D. Nguyen, None.

1139

Akt1 in Osteoblasts and Osteoclasts Contributes to the Maintenance of Bone Mass and Turnover. N. Kawamura, F. Kugimiya, R. Suzuki*, K. Tobe*, T. Kadowaki*, K. Nakamura, U. Chung, H. Kawaguchi. Orthopaedic Surgery and Metabolic Diseases, University of Tokyo, Tokyo, Japan.

The phosphoinositide-dependent serine-threonine protein kinase Akt has been proposed to be involved in regulation of bone metabolism in vitro. This study initially confirmed that Akt was phosphorylated in isolated mouse calvarial primary osteoblasts (POB) by stimulation of insulin / IGF-I or BMP-2, and in M-CSF-dependent bone marrow macrophages (BMM ϕ) and the BMM ϕ -derived mature osteoclasts by stimulation of M-

CSF. Among the three isoforms of Akt, Akt1 was shown to be most strongly expressed in the cells above by real-time RT-PCR. We then generated Akt1-deficient (-/-) mice and investigated the role of Akt1 in bone. Although Akt1 -/- mice developed normally without abnormalities of major organs except for 10-20% decrease in body size as compared to wild-type (+/+) littermates, they exhibited significant decreases in both trabecular and cortex bone volume at 4-16 weeks of age by bone densitometry, 3D- μ CT and pQCT analyses. Histomorphometric analysis of the proximal tibiae at 8 weeks revealed that parameters of both bone formation (Ob.S/BS, MAR & BFR/BS) and resorption (N.Oc/B.Pm & ES/BS) were lower in -/- mice than in +/+ mice. Cultured -/- POB showed markedly reduced differentiation and matrix synthesis determined by Alizarin red / von Kossa stainings and mRNA levels of osteogenesis markers such as COL1A1, ALP, BSP, osteopontin and osteocalcin. These decreases in -/- POB were restored to the +/+ POB levels by adenoviral reintroduction of Akt1. Runx2 adenovirally introduced into +/+ POB bound to and activated the osteocalcin promoter determined by chromatin immunoprecipitation and luciferase-reporter assays, respectively, both of which were markedly suppressed in -/- POB. After serum deprivation, cell survival rate was lower, and caspase-3 activity was higher in -/- POB than in +/+ POB; both were restored by Akt1 or Bcl-XL introduction. Osteoclastogenesis in co-culture of POB and bone marrow cells were reduced when either POB or marrow cells were derived from -/- mice. Furthermore, RANKL mRNA level in -/- POB, osteoclastogenesis from -/- BMM ϕ in the presence of soluble RANKL, and survival of the -/- BMM ϕ -derived mature osteoclasts were decreased. We conclude that Akt1 deficiency leads to low turnover osteopenia through dysfunctions of osteoblasts and osteoclasts: the former through decreased transcriptional activity of Runx2 and increased susceptibility to mitochondria-dependent apoptosis; and the latter through suppressed RANKL expression in osteoblasts and defects in differentiation / survival of osteoclastic cells. Akt1 was shown to play a pivotal role in the maintenance of bone mass and turnover.

Disclosures: N. Kawamura, None.

1140

The Pathogenesis of Age-Related Bone Loss in Mice Involves Increased Production of PPAR γ -Activating Oxidized Lipids Derived from the Lipoygenase Alox15. R. L. Jilka, R. A. Wynne*, X. Chen, S. Stewart*, L. Xu*, J. J. Thaden*, R. S. Weinstein, S. S. Manolagas. Depts. of Endo/Metab, Biostatistics, and Geriatrics, University of Arkansas for Medical Sciences, Center for Osteoporosis and Metabolic Bone Diseases, Central Arkansas Veterans Healthcare System, Little Rock, AR, USA.

Age-related bone loss is characterized by a decrease in osteoblast number, but the underlying mechanism is unknown. It was recently shown that the level of expression of the lipoygenase Alox15, and PPAR γ , are determinants of bone mass in mice; and that Alox15, as well as reactive oxygen species (ROS), oxidize polyunsaturated fatty acids to generate PPAR γ ligands. Moreover, activation of PPAR γ with rosiglitazone causes bone loss in mice associated with increased marrow adipocytes, reduced osteoblasts and bone formation rate, and increased osteoblast apoptosis. PPAR γ ligands also inhibited osteoblast differentiation and increased apoptosis of osteoblast progenitors. Therefore, we hypothesized that age-related bone loss is due at least in part to an increase in Alox15- and ROS-derived oxidized lipid ligands. Elsewhere in this meeting, we report that vertebral and femoral BMD declines by ~16% between 15 and 31 months of age in female C57BL/6 mice, and that this decline is associated with increased oxidative stress, increased osteoblast apoptosis and decreased bone formation rate. Here, we report that the bone content of oxidized lipid ligands of PPAR γ , including 12- and 15-HETE and 13-HODE, increased by ~2-fold with advancing age in these mice, as determined by mass spectrometry. Moreover, transcript levels of Alox15 and PPAR γ in bone increased progressively with age by 10-30 fold. The role of Alox15 was further examined using marrow cultures from 5-6 month old DBA/2 mice bearing an Alox15 allele characterized by high levels of expression, as compared to cells from C57BL/6 mice bearing the wild type allele or congenic DBA/2 mice bearing the C57BL/6 wild type allele. As expected, cells from DBA/2 mice exhibited a 30-50-fold increase in Alox15 expression, and this corresponded with a 2-fold reduction in osteocalcin expression as compared to wild type controls. Addition of the Alox15 substrates linoleic and arachidonic acid (20 μ M each) further reduced osteocalcin expression in cultures from DBA/2 mice, but had no effect on cultures from wild type controls. Taken together, these findings support the contention that PPAR γ is increasingly activated by lipid peroxidation products with advancing age, secondary to elevated levels of ROS and Alox15. This results in bone loss due to increased adipogenesis at the expense of osteoblasts, and increased apoptosis of osteoblasts and their progenitors.

Disclosures: R.L. Jilka, Nuvios, Inc. 1, 2, 5.

1141

Caspase-2 Deficient Mice Have an Age-Associated Increase in Osteoclastic Bone Resorption and Bone Turnover. Y. Zhang*, S. S. Padalecki, B. Grubbs*, B. Goins*, A. Soundararajan*, B. Story*, G. R. Mundy, B. A. Herman*. UT Health Science Center, San Antonio, TX, USA.

Caspase-2 is a cysteine protease that is an important regulator of apoptosis. Osteoclast apoptosis is a critical determinant of bone resorption, and drugs such as bisphosphonates that stimulate osteoclast apoptosis result in an inhibition of bone resorption. Accordingly, we examined the role of Caspase-2 in osteoclastic bone resorption and bone turnover using a genetic murine model lacking Caspase-2. A comparative study was performed on Caspase-2 deficient mice and wildtype mice over the course of their lifespan. Age-related phenotypes appeared earlier in the Caspase-2 null mice compared to wildtype mice, including an increase in kyphosis and a decrease in whole body bone mineral density

(BMD). We hypothesized that these differences were due to an increase in bone resorption and bone turnover in aged Caspase-2 deficient mice compared to wild-type controls. To characterize the age-related skeletal phenotype of Caspase-2 deficient mice, we performed BMD studies on these mice and controls. In addition, we performed ^{99m}Tc-MDP MicroSPECT to assess the state of bone turnover in Caspase-2 null and wildtype mice. Additionally, quantitative bone histomorphometry was performed on the spines of these mice to assess trabecular bone volume, osteoclast number and osteoblast number. In addition to a decrease in whole body BMD, Caspase-2 null mice also exhibited a significantly lower BMD of the femur compared to wildtype controls at 22-24 months of age. Quantitative region of interest measurements of ^{99m}Tc-MDP MicroSPECT studies of Caspase-2 deficient mice and wildtype mice showed a generalized increase in bone turnover in the Caspase-2 deficient mice. Biodistribution studies of ^{99m}Tc-MDP uptake performed at sacrifice on individual tissues confirmed this increase in bone turnover, particularly in the hind limbs of the Caspase-2 deficient mice. Histological analysis of the spines of Caspase-2 null mice revealed a significant decrease in trabecular bone volume and an increase in osteoclast number along the trabecular bone surface compared to wildtype controls. There was no difference in the number of osteoblasts per mm of bone surface. This work provides evidence for an in vivo physiological role for Caspase-2 in regulating bone resorption and bone turnover. Since the total body BMD decreased only in aged animals, these data support the hypothesis that Caspase-2 plays an important role in the regulation of osteoclastic bone resorption and bone turnover during aging and may be an important molecular target for the prevention of the increased bone turnover associated with age-related osteoporosis.

Disclosures: **Y. Zhang**, None.

1142

Elimination of Classical (ERE) ER α Signaling Causes Osteopenia and Deficits in Bone Mass Acquisition in Male Mice. **F. A. Syed, D. G. Fraser*, S. Khosla.** Endocrinology, Mayo Clinic College of Medicine, Rochester, MN, USA.

Estrogen receptor (ER α) mediates its effects either via the classical pathway requiring ERE binding or through non-classical, non-ERE pathways (e.g., AP-1 sites). Generation of mice with a wildtype ER α allele (ER α^+) and an ER α allele with a knock-in mutation abolishing the classical pathway [non-classical ER α knock-in, NERKI (Mol. Endo 16: 2188, 2002)] provides an opportunity to study the effects of this mutation on bone. Since heterozygous female mice are infertile, it is not possible to generate homozygous NERKI/NERKI mice. Therefore, ER α^+ /NERKI males were mated with ER α^+ /ERKO(-) females to generate ER α^+ /ER α^+ , ER α^+ /NERKI and ER α^+ /NERKI mice in the F1 generation. The ER α^+ /NERKI mice have one deleted ER α allele and a NERKI allele and signal exclusively through the non-classical pathway. We compared the in vivo bone phenotype of the ER α^+ /NERKI males to their ER α^+ /ER α^+ and ER α^+ /NERKI littermates at 6, 12, 20 and 25 weeks of age. Spine and femur BMD were assessed by DXA and tibial trabecular and cortical bone parameters were assessed by pQCT. ER α^+ /NERKI mice had reduced serum IGF-I levels and shorter bones. Spine and femur BMD were significantly reduced in both the ER α^+ /NERKI and ER α^+ /NERKI mice at all time points (P<0.01 and P<0.02 vs WT, respectively). In contrast to female NERKI mice of comparable age, the ER α^+ /NERKI and ER α^+ /NERKI mice had lower tibial trabecular BMD as compared to their ER α^+ /ER α^+ littermates at 12 weeks and this deficit was maintained at further time points. Cortical BMD and thickness at the tibial metaphysis and diaphysis were also significantly reduced in the ER α^+ /NERKI mice; the ER α^+ /NERKI mice also displayed a similar pattern except that at 20 and 25 weeks, their BMD at the metaphysis was not reduced. Periosteal circumference was significantly reduced in ER α^+ /NERKI and ER α^+ /NERKI mice (P<0.05 vs WT) at all time points, with the reduction being greater in the ER α^+ /NERKI mice (P<0.05 vs ER α^+ /NERKI). Endosteal circumferences were decreased in the ER α^+ /NERKI but not in the ER α^+ /NERKI male mice from 12 weeks of age onwards. This is in contrast to female ER α^+ /NERKI mice, where an increase in endosteal circumference was observed. Our results suggest that the attenuation or absence of classical ERE signaling leads to a reduction in both trabecular and cortical bone parameters and to a significant decrease in periosteal bone apposition which is offset by lower endosteal bone expansion in growing male ER α^+ /NERKI bones. These patterns of bone growth seem to be different from female ER α^+ /NERKI mice in which trabecular bone is maintained and there is increased endosteal bone expansion. These gender differences on the consequences of loss of ERE signaling require further study.

Disclosures: **F.A. Syed**, None.

1143

Estrogen Dependent Chromatin Remodeling at CIITA *In Vivo*: a Model for Estrogen Suppression of Inflammatory Bone-Wasting Genes. **E. Benasciutti¹, L. Oliva¹, W. Reith², S. Cenci¹.** ¹Dibit, San Raffaele Scientific Institute, Milan, Italy, ²University of Geneva Medical School, Geneva, Switzerland.

Estrogen (E)-mediated anti-inflammatory effects are crucial in bone homeostasis. Among bone-wasting factors, E suppresses inflammatory cytokines (IL-1 β , TNF α and IL-6) and the key immune regulator MHC class II transactivator (CIITA). While stimulation of target genes by E is well characterized and relies on chromatin remodeling to transactivate promoters, whether gene suppression by E occurs via chromatin dynamics has never been asked. We explored the mechanism by which E suppresses CIITA by chromatin immunoprecipitation (ChIP) and real time quantitative PCR on cross-linked samples of primary purified BMM from ovariectomized (ovx) and sham operated mice. We observed a profound hyperacetylation of histones H3 and H4 on the whole CIITA regulatory region, in conditions of E deficiency. Interestingly, within H3, promoter IV (the main CIITA inducible promoter) displays a selective hyperacetylation of lysine 9 (K9) and

hypermethylation of K4, two modifications known to direct gene expression. Furthermore, E-dependent histone hyperacetylation at pIV is not associated with increased recruitment of the coactivators CBP and p300, suggesting that a distinct E-regulated histone acetyltransferase, specific for H3, is required to modify chromatin structure at this site. To test whether histone acetylation plays a causal role in CIITA regulation by E, we tested the specific histone deacetylase inhibitor trichostatin A (TsA) on primary BMM. TsA significantly increased the capacity of IFN γ to induce MHCII expression in cells from sham mice to the level observed in those from ovx mice, suggesting a central role for histone acetylation in the regulatory effect of E on CIITA expression. ChIP for acetylated H3 and H4 in primary BMM revealed that E treatment *in vitro* directly suppresses IFN γ -induced histone acetylation at the CIITA regulatory region. Moreover, a dynamic analysis revealed that E suppresses the early induction of CIITA by IFN γ , mediated mainly by pIV, but not the sustained induction, operated by pI. Attesting to a central role of pIV in mediating E driven suppression of CIITA *in vivo*, we observed that pIV null BMM are resistant to E-operated CIITA suppression. Altogether, our data: (i) demonstrate that histone acetylation is causally involved in the mechanism by which E suppresses CIITA; (ii) describe an E-dependent histone code underlying CIITA overexpression; (iii) identify pIV as a key target of E-dependent CIITA suppression. Our data provide a framework for identifying molecular mediators whereby E suppresses inflammatory, bone wasting genes.

Disclosures: **E. Benasciutti**, None.

1144

Oxidative Stress Induced Dendritic Cell-Dependent T Cell Activation. A Novel Mechanism by Which Estrogen Deficiency Causes Bone Loss. **E. Grassi, M. Robbie-Ryan, W. Qian*, K. Page*, R. Pacifici.** Dep of Medicine, Division of Endocrinology, Metabolism and Lipids, Emory University, Atlanta, GA, USA.

Two novel mechanisms have recently been proposed to explain how estrogen (E) prevents bone loss. The finding that the anti oxidant N-Acetyl Cysteine (NAC) protects against ovariectomy (ovx)-induced bone loss have led to the hypothesis that the key effect of E is that of blocking the generation of reactive oxygen species (ROS), but the mechanism linking ROS to bone loss is still unclear. Studies in the nude mouse have shown that ovx causes bone loss by promoting T cell activation and the T cell production of osteoclastogenic factors through stimulation of antigen presentation (AP), but the involved mechanism is unknown. Among the cellular functions controlled by redox-signaling, is the maturation and activity of dendritic cells (DC), the most potent AP cells. Therefore, we asked whether ovx activates AP by promoting oxidative stress and weather activation of DC is the mechanism by which ROS cause bone loss. We found that ovx increases DC expression of MHCII molecule by 2 fold, and DC specific AP by 5 folds in the bone marrow (BM), while it had no effect in other lymphoid organs. When cocultured with T cells from intact donors, DC from the BM of ovx, but not sham operated, mice also increased T cell production of TNF and RANKL by 2-3 folds. Spleen or lymph nodes DC from all groups had no effects. To investigate the role of ROS in DC activation, 12-week old mice where ovx or sham operated and treated with NAC (100 mg/Kg/day i.p.) or vehicle for 4 weeks. We found that NAC treatment significantly protected against ovx-induced bone loss. Furthermore, NAC treatment also prevented 80% of the ovx-induced increase in DC mediated AP, thus leading to a 70% prevention (p<0.05) of the ovx induced increase in the number of BM activated CD4+ and CD8+ T cells. Furthermore, levels of TNF were strikingly regulated by NAC as the ovx-induced increase in both total BM TNF and T cell-secreted TNF was completely prevented by NAC treatment. We conclude that the mechanism by which oxidative stress causes bone loss in ovx mice is by inducing AP by DC, events which stimulate T cell activation and T cell TNF production. The data also show that ovx induces T cell activation by promoting a BM specific increase in the maturation and activity of DC with a mechanism involving increased ROS generation. Thus both oxidative stress and T cell activation are required for ovx to cause bone loss.

Disclosures: **F. Grassi**, None.

1145

Direct Measurement of Actin Dynamics Demonstrates that Actin Turnover Is Src Kinase-Dependent in Osteoclasts Podosomes. **O. Destaing^{*1}, A. Sanjay², W. Horne¹, P. De Camilli^{*3}, R. Baron¹.** ¹Cell biology, School of Medicine, New Haven, CT, USA, ²Temple university, Philadelphia, PA, USA, ³Howard Hughes Medical Institute, School of Medicine, New Haven, CT, USA.

Podosomes constitute a characteristic organization of actin that is essential for osteoclast (OC) attachment, migration and function. Confocal videomicroscopy and FRAP analysis have shown that podosomes contain a central column of actin which undergoes constant turnover at a rate of about 2-4 minutes. Moreover, the central column of F-actin is surrounded by a dynamic cloud of diffusely organized F-actin. The proto-oncogene c-Src is essential for bone resorption and for actin organization in OCs. Src-/- OCs do not form a peripheral ring of podosomes, have a defect in migration and fail to resorb bone efficiently. Although previous studies have suggested that Src deletion alters podosome assembly/disassembly and/or actin turnover, no study has explored the dynamics of the actin cytoskeleton organization in live Src-/- OCs. In this report, we used videomicroscopy of living OCs micro-injected with actin-GFP to address this question. After plating, Src-/- OCs formed few podosomes and the surrounding cloud of F-actin was decreased. In addition, Src-/- OCs failed to spread and presented an accumulation of dorsal ruffles. Also, Src-/- OCs plated on apatite collagen complex (ACC), a mineralized extracellular matrix coating mimicking the bone surface, failed to form a sealing zone or degrade the ACC. The podosome life span was markedly increased in the Src-/- OCs, while the rate of actin polymerization in the podosome core was decreased. Thus, Src controls both the formation

and disassembly of the F-actin core. Re-expression of avian Src or a constitutively activated form of Src (SrcY527F) induced the formation of numerous podosomes and the reappearance of the surrounding F-actin cloud and restored the dynamic characteristics of the podosome, confirming that the changes in podosome dynamics were a consequence of the lack of Src. Finally, we determined which domain of Src was necessary for the regulation of actin turnover at podosomes in OCs. The rescue of the altered actin organization in Src^{-/-} OCs required Src kinase activity, as the K295M (kinase dead) and K295M Y527F (kinase dead and fully open) mutants failed to rescue the actin dynamics phenotype. In contrast, deletion of either the SH2 or the SH3 domain, leaving intact their kinase activity, also rescued the Src^{-/-} OC phenotype, at least in part. This first direct confocal videomicroscopic analysis of actin turnover in Src^{-/-} OCs podosomes demonstrates that Src promotes osteoclast migration and bone resorption by regulating the assembly, actin polymerization and disassembly of podosomes.

Disclosures: *O. Destaing, None.*

1146

Impaired Recruitment of Csk into Lipid Rafts due to Decreased Cbp Expression Leads to Elevated c-Src Kinase Activity and Bone Resorption in Osteoclasts. T. Matsubara¹, F. Ikeda¹, K. Hata^{*1}, M. Okada^{*2}, R. Nishimura¹, T. Yoneda¹. ¹Biochem, Osaka Univ Grad Sch Dent, Osaka, Japan, ²Oncogene Res, Res Inst Microbial Disease, Osaka Univ, Osaka, Japan.

The tyrosine kinase c-Src, which plays an indispensable role in ruffled border formation and bone resorption, is constitutively increased in osteoclasts compared to other tissues and cells. The molecular mechanism underlying increased c-Src activity in osteoclasts is unknown. c-Src activity is negatively regulated by c-terminal c-Src kinase (Csk). Recently, Csk binding protein (Cbp) has been identified and shown to recruit Csk into lipid rafts where c-Src and cytoskeleton regulatory proteins also co-localize. The finding led us to examine whether Cbp is involved in elevated c-Src activity in osteoclasts. To approach this, we first examined the expression levels and subcellular localization of c-Src, Csk and Cbp in osteoclasts. Western blot analyses demonstrated that c-Src was expressed in a highly activated state in lipid rafts in osteoclasts. Of note, Csk expression was marginal in lipid rafts despite that overall cellular Csk expression was as high as other tissues and cells. Consistent with this, cellular Cbp expression was very low. These results suggest that low Cbp expression leads to reduced Csk recruitment to lipid rafts in osteoclasts. To examine this, we introduced Cbp into osteoclast-like cells formed in spleen cell cultures using the adenovirus technology. Cbp increased Csk recruitment to lipid rafts through a physical interaction between Csk and Cbp and suppressed c-Src activity in a dose-dependent manner. Furthermore, we found that introduction of Cbp markedly inhibited the formation of actin ring and resorption pits on dentine slices. These results suggest that the relationship between c-Src, Csk, and Cbp is critical to osteoclastic bone resorption. We next studied the regulatory mechanism of Cbp expression in osteoclasts. Undifferentiated RAW 264.7 cells expressed substantial levels of Cbp. Induction of osteoclastic differentiation of RAW 264.7 cells with soluble RANKL decreased Cbp expression. Furthermore, overexpression of TRAF6 and NFAT2 induced the osteoclastic differentiation of RAW264.7 cells with marked inhibition of Cbp expression. These results collectively suggest that activation of RANKL signaling regulates Cbp expression via TRAF6 and NFAT2 in association with osteoclastic differentiation. In conclusion, our results suggest that impaired recruitment of Csk to lipid rafts due to reduced Cbp expression leads to constitutively elevated c-Src activity in osteoclasts. They also suggest that Cbp expression in osteoclasts is modulated according to the state of RANKL-induced osteoclastic differentiation.

Disclosures: *T. Matsubara, None.*

1147

Osteoclast-Specific Inactivation of the Integrin-Linked Kinase (ILK) Inhibits Bone Resorption. T. Dossa^{*1}, A. Arabian¹, S. Dedhar^{*2}, G. D. Roodman³, R. St-Arnaud¹. ¹Genetics Unit, Shriners Hospital for Children, Montreal, PQ, Canada, ²Department of Biochemistry and Molecular Biology, University of British Columbia, Vancouver, BC, Canada, ³Bone Biology Center, University of Pittsburgh, Pittsburgh, PA, USA.

Bone resorption requires the adhesion of osteoclasts to extracellular matrix (ECM) components, a process mediated by the $\alpha_v\beta_3$ integrin. Following engagement with the ECM, integrin receptors signal via multiple downstream effectors, including the Integrin-Linked Kinase (ILK). In order to characterize the physiological role of ILK in bone resorption, we generated mice with an osteoclast-specific ILK gene ablation. Mice with one inactivated ILK allele (ILK^{+/-}) were mated with TRAP-Cre transgenic mice. Progeny from this cross (TRAP-Cre;ILK^{+/-}) was bred to mice homozygous for a floxed ILK allele (ILK^{fl/fl}) to yield mutant mice with ILK-deficient osteoclasts (TRAP-Cre;ILK^{-/-}). The mutant animals thus had one ILK allele inactivated in all tissues, and both alleles disrupted in osteoclasts. Mutant mice appeared phenotypically normal, but histomorphometric analysis of the proximal tibia revealed an increase in bone volume (24%) and trabecular thickness (44%). Osteoclastogenesis, assessed by TRAP staining of bone sections or in vitro cultures, was not affected. Indeed, osteoclast-specific ILK ablation was associated with an increase in osteoclast number both in vitro (12%) and in vivo (35%). Primary cultures of osteoclasts were generated on synthetic calcium phosphate discs and the mutant cells displayed a decrease in resorption activity (87%). We also measured decreased serum concentrations of the C-terminal telopeptide of collagen, a marker of osteoclastic activity, in mice with ILK-deficient osteoclasts. Our results show that ILK is important for the function, but not the differentiation, of osteoclasts. The characterization of the molecular mechanisms responsible for the observed phenotype will identify novel pathways regulating bone resorption.

Disclosures: *T. Dossa, None.*

1148

Extracellular Acidification Acts on Ovarian Cancer G Protein-Coupled Receptor 1 (OGR1) to Enhance Osteoclast Survival through an NFAT-Independent, Protein Kinase C-Dependent Pathway. A. Pereverzev^{*1}, S. V. Komarova², G. B. Tremblay³, S. J. Dixon¹, S. M. Sims^{*1}. ¹CIHR Group in Skeletal Development and Remodeling, University of Western Ontario, London, ON, Canada, ²Faculty of Dentistry, McGill University, Montreal, PQ, Canada, ³Alethia BioTherapeutics, Montreal, PQ, Canada.

For at least 85 years, acidosis has been recognized to have detrimental effects on the skeleton. We have recently reported that acidification and RANK ligand induce signals in osteoclasts that converge on the Ca/calcieneurin/NFAT pathway to stimulate resorption (Proc. Natl. Acad. Sci. USA 102: 2643-8, 2005). Moreover, expression of the proton sensing receptor OGR1 was strongly induced during *in vitro* osteoclastogenesis from RAW 264.7 cells, with corresponding increases in acid-induced elevation of cytosolic free Ca concentration ([Ca]_i). Here, we first assessed whether acid-induced elevation of [Ca]_i in osteoclasts is mediated by OGR1. [Ca]_i of fura-2-loaded osteoclasts was monitored by microspectrofluorimetry. Acid-induced rise of [Ca]_i was suppressed in osteoclast-like cells derived from RAW 264.7 cells in which OGR1 RNA was specifically depleted using siRNA. Moreover, acid-induced elevation of [Ca]_i in authentic rat osteoclasts was significantly inhibited by the OGR1 antagonist Cu. These data support an essential role for the proton sensing receptor OGR1 in mediating acid-induced Ca signaling in osteoclasts. Next, we examined effects of activation of OGR1 on osteoclast survival. Survival of authentic rat osteoclasts after 18 h was markedly enhanced by acidification of the culture medium, from 40 ± 10% at pH 7.6 to 83 ± 4% at pH 7.0. Osteoprotegerin had no effect on the enhanced survival induced by acidification, but inhibited that elicited by RANK ligand. Addition of Cu or chelation of intracellular Ca with BAPTA abolished the effect of acidification on survival, consistent with the involvement of OGR1. Surprisingly, inhibition of NFAT translocation with the cell-permeable peptide inhibitor 11R-VIVIT did not affect the increase in survival induced by acidification; however, it did significantly suppress the increase in survival induced by RANK ligand. On the other hand, the protein kinase C (PKC) inhibitor bisindolylmaleimide I, but not its inactive analog, abolished the effect of acidification on survival, implicating PKC signaling. Thus, extracellular acidification acts directly through OGR1 to enhance osteoclast survival through an NFAT-independent, PKC-dependent pathway. Increased osteoclast survival would contribute to bone loss in systemic acidosis and local acidosis associated with inflammatory and neoplastic bone diseases.

Disclosures: *S.J. Dixon, None.*

1149

Parathyroid Hormone Stimulates Osteoblastic Expression of Monocyte Chemotactic Protein-1 to Recruit Pre/Osteoclasts. X. Li^{*1}, L. Qin², N. Partridge¹. ¹Physiology & Biophysics, UMDNJ-Robert Wood Johnson Medical School and Graduate School of Biomedical Sciences, Piscataway, NJ, USA, ²Physiology & Biophysics, UMDNJ-Robert Wood Johnson Medical School, Piscataway, NJ, USA.

Parathyroid hormone (PTH) is the major hormone regulating bone remodeling via its actions on both bone formation and resorption. Inhibition of bone resorption blunts PTH's anabolic effects indicating that activated resorption is a prerequisite for the *in vivo* anabolic effect of PTH. The molecular basis of osteoclast activation involved in PTH's anabolic effects is not well deciphered. Since PTH signals via its receptor on osteoblasts, osteoclasts are impacted by PTH indirectly via osteoblasts. Microarray with Affymetrix Rat 230A chips of femoral metaphyseal RNA from 3-month-old female rats injected with hPTH (1-34) at 80ug/kg/d or vehicle for 14d identified a highly significant association between the stimulation of monocyte chemotactic protein-1 (MCP-1) and PTH's anabolic effect. The stimulation of MCP-1 by PTH was extraordinary both *in vivo* and *in vitro* and depended on the PKA pathway. Realtime RT-PCR showed that MCP-1's mRNA in RNA isolated from femora of rats injected with PTH for 1, 3, 7 or 14d increased to 32, 35, 54 or 224-fold respectively 1h after the last PTH injection, declining to basal levels within 2h. In UMR 106-01 cells, MCP-1 mRNA reached its peak (25-fold) at 90-min and MCP-1 protein was maximal in the cell media by ELISA, 2h after PTH treatment. We further confirmed MCP-1 stimulation is a dose-dependent primary response to PTH *in vitro*. MCP-1 is a potent chemokine for monocytes, and its *in vivo* expression pattern after PTH injection leads us to propose that MCP-1 recruits and activates pre/osteoclasts as part of PTH's anabolic effects. Studies with the mouse monocyte cell line RAW 264.7 showed that MCP-1 potently recruits osteoclastic monocyte precursors and facilitates RANKL-induced osteoclastogenesis. In the presence of RANKL, MCP-1 significantly increased TRAP mRNA (15-fold) and the number and size of TRAP-positive multinuclear osteoclasts in a dose dependent manner (increased by 15, 39 and 75% with 20, 50 and 100 ng/ml MCP-1 respectively). In chemotaxis experiments, both recombinant MCP-1 and conditioned media from UMR 106-01 cells treated with PTH for 2h had strong chemotactic effects on RAW cells and TRAP-positive multinuclear osteoclastic cells. Our model suggests that PTH-induced osteoblastic expression of MCP-1 is involved in osteoclast recruitment and differentiation at the stage of multinucleation of osteoclast precursors and provides a rationale for increased osteoclast activity in PTH's anabolic effects in addition to RANKL stimulation to initiate enhanced bone remodeling.

Disclosures: *X. Li, None.*

1150

Dynamin GTPase- and Src-Dependent Regulation of Pyk2 Phosphorylation in Osteoclasts. A. Bruzzaniti, L. Neff^{*}, W. Horne, R. Baron. Orthopaedics, Yale University School of Medicine, New Haven, CT, USA.

Signaling from the Pyk2-Src-Cbl protein complex is essential for the dynamics of podosomes, which mediate osteoclast (OC) attachment, migration and bone resorption. Accordingly, deletion of any of these genes leads to decreased OC motility, and to osteopetrosis in Src^{-/-} and Pyk2^{-/-} mice. While much is known about Pyk2-Src-Cbl complex assembly, the factors that promote the disassembly of this complex are unknown. We have previously shown that the GTPase Dynamin (Dyn) is localized to podosomes and interacts in a Src-sensitive manner with Cbl and is involved in podosome actin remodeling in OCs. Moreover, overexpression of the dominant-negative, GTP-binding mutant DynK44A slows actin turnover in podosomes and decreases bone resorption *in vitro*. Since Pyk2 is activated by Ca²⁺ mobilization following integrin engagement and has been implicated in cytoskeletal reorganization, we examined the potential interactions between Dyn and Pyk2. We report that Dyn colocalizes with Pyk2 in the podosome actin ring and forms a complex with Pyk2. The interaction of Dyn or DynK44A with Pyk2 involved the proline-rich domain of Dyn and the N-terminal region of Pyk2 but not the kinase activity of Pyk2. Importantly, phosphorylation of Pyk2 at Tyr402, a residue that is autophosphorylated upon Pyk2 activation and forms the binding site for the Src SH2-domain, was dramatically decreased by Dyn but not DynK44A. Although Dyn-Pyk2 complex formation was not dependent on Src's adaptor function, Src was required for the inhibition of Tyr402 phosphorylation by Dyn. Thus, once activated by integrin engagement via an increase in intracellular Ca²⁺, Pyk2 is autophosphorylated at Tyr402, recruiting and activating Src at attachment sites. Our study shows that Dyn is also recruited by Pyk2, possibly in the same Src- and Cbl-containing complex. Furthermore, the recruitment of Dyn leads to the Src- and Dyn GTPase-dependent decrease in the phosphorylation of Pyk2 at Tyr402, potentially leading to the dissociation of Src and/or decreased Src and Pyk2 kinase activities. In conclusion, we propose that a dynamic intermolecular interaction exists between Dyn and the Cbl-Src-Pyk2 complex which affects downstream signaling, leading to changes in podosome turnover and OC function.

Disclosures: **A. Bruzzaniti**, None.

1151

Aberrant Bone Formation in Mice Over-Expressing Specific VEGF Isoforms in Cartilage. C. Maes¹, J. J. Haigh^{*2}, A. Chan^{*2}, K. Haigh^{*2}, R. Bouillon³, G. Carmeliet⁴, A. Nagy^{*4}. ¹Legendo, K.U.Leuven, Leuven, Belgium, ²Vascular Cell Biology Unit, VIB, Ghent, Belgium, ³Legendo, K.U.Leuven, Leuven, Belgium, ⁴Samuel Lunenfeld Research Institute, Mount Sinai Hospital, Toronto, ON, Canada.

Previous loss-of-function studies revealed multiple roles of VEGF and its isoforms (VEGF120, 164 and 188) in bone development and repair. Accordingly, the potential use of VEGF in bone pathology is being explored. To determine the *in vivo* consequences of increased VEGF, we employed a gain-of-function approach. The 3 VEGF-isoforms were conditionally targeted to the Rosa-26 locus and over-expressed in collagen 2-expressing tissue. Q-RT-PCR verified that the total VEGF mRNA level was comparably upregulated, by 70-85%, in each of the mutants as compared to WT mice. Therefore, these models enable a direct comparison of the different isoforms on cartilage/bone formation. Skeletal staining of newborn mice showed that cartilage specific over-expression of VEGF164 or VEGF188, but not of VEGF120, impaired growth and resulted in short and misshapen limbs. To elucidate the mechanism, embryonic stages were investigated. In VEGF164 over-expressing mutants, no defects in cartilage development were observed by histomorphological analysis, BrdU marking, and collagen 2 and 10 *in situ* hybridization (ISH). However, the perichondrium was thickened with increased accumulation of TRAP+ cells and CD31+ blood vessels and strongly enhanced MMP-9 immunoreactivity. This was followed by premature and/or excessive invasion and erosion of the diaphyseal cartilage. Concomitantly, osteoblastogenesis seemed enhanced, as suggested by the presence of numerous BrdU+ cells in the perichondrium, strong Runx2 ISH signal, and increased osteocalcin staining. Yet, bone collar formation was severely impaired. In contrast, excessive bone formation occurred within the diaphysis, showing a dramatic re-orientation and increase of bony structures and blood vessels. This led to marked widening of the diaphyses and bowing of the long bones. A comparable phenotype was seen in VEGF188 over-expressing mice although it started later than in VEGF164 mutants, consistent with the more persistent localization of VEGF188 within the epiphysis, as revealed by ELISA. Notably, only VEGF164 mutants showed dramatic systemic edema, underscoring the importance of isoform selection for therapeutic use in terms of specificity and safety. Together, these findings reveal the capacity of VEGF to affect the coupling of bone collar formation and cartilage invasion during development and highlight the power of VEGF as a stimulator of bone formation. Importantly, our data show that application of VEGF, e.g. in fractures or osteoporosis, must be associated with careful monitoring of the new bone structure.

Disclosures: **C. Maes**, None.

1152

Chondrocyte-Specific Disruption of Insulin-Like Growth Factor (IGF)-I Expression Reduces Bone Density and Bone Size in Mice. K. E. Govoni¹, S. K. Lee^{*1}, Y. S. Chung^{*1}, R. R. Behringer^{*2}, J. E. Wergedal¹, D. J. Baylink¹, S. Mohan¹. ¹MDC, JLP VAMC, Loma Linda, CA, USA, ²MD Anderson Cancer CTR, Houston, TX, USA.

IGF-I is an important regulator of BMD and bone size, two important determinants of bone strength. IGF-I actions on bone are known to be mediated via endocrine and local autocrine/paracrine mechanisms. In mice in which liver production of IGF-I was disrupted, no changes in BMD or bone size were observed, suggesting that bone derived IGF-I may be more important than circulating IGF-I in regulating peak BMD and bone size. To test this hypothesis, we used the well established Cre-lox approach to disrupt IGF-I in chondrocytes. Type 2 α 1 collagen-Cre mice were crossed with IGF-I loxP mice to generate Cre+ (IGF-I disruption) or Cre- (control), loxP homozygous mice. Bone parameters were measured by DXA at 2, 4, 8, and 12 wks of age and pQCT at 12 wks. Cre and IGF-I expression were determined by real-time RT-PCR at 2 and 12 wks. Cre expression was greater in metaphysis and cartilage than diaphysis and calvaria tissue of Cre+ mice. Compared with Cre+ mice, IGF-I expression in Cre- mice was 1.7 and 2.0 fold greater in metaphysis and cartilage, respectively at 2 wks (P < 0.01) and 1.4 fold greater in the diaphysis at 12 wks (P < 0.05). A reduction (P < 0.05) in body length and skeletal parameters was observed in Cre+ mice at 4 wks and these deficits were maintained through 12 wks.

Age (weeks)	2	4	8	12
Body weight	105 \pm 6	93 \pm 5	90 \pm 4*	91 \pm 5*
Body length	100 \pm 3	93 \pm 2*	93 \pm 1*	93 \pm 1*
Total body BMC	109 \pm 10	86 \pm 4*	87 \pm 4*	89 \pm 3*
Total body BMD	101 \pm 2	95 \pm 1*	96 \pm 2*	95 \pm 1*
Total body bone area	106 \pm 8	90 \pm 3*	91 \pm 3*	94 \pm 2*

Values are % of Cre- mice (mean \pm SE); n = 16 mice per group (except 2 wks); * (P < 0.05)

Interestingly, bone size, measured by pQCT, was reduced 7% in both the vertebrae (P < 0.01) and femur (P < 0.05) of Cre+ mice at 12 wks. To investigate the role of chondrocyte derived IGF-I in mediating rapid bone accretion during puberty, we compared the rate of gain in skeletal parameters during this period. We found that gain in body length and total body BMC and BMD were reduced by 30%, 16%, 18%, respectively (P < 0.05), in Cre+ mice between 2 and 4 wks. Conclusions: 1) targeted disruption of IGF-I in chondrocytes results in decreased BMD, bone size, bone length, body weight, and IGF-I expression in bone, 2) chondrocyte derived IGF-I is involved, in part, in mediating rapid bone accretion that occurs during puberty, but not during the first 2 wks of postnatal growth, 3) our data are consistent with the hypothesis that bone derived IGF-I may be more critical than endocrine IGF-I for attainment of peak BMD and bone size in mice.

Disclosures: **K.E. Govoni**, None.

1153

Temporal Control of Gene Deletion in the Cartilage Using a Tamoxifen Inducible Cre Transgenic Mouse. M. J. Hilton, E. Long. Internal Medicine - Division of Bone and Mineral Diseases, Washington University School of Medicine - St. Louis, St. Louis, MO, USA.

Understanding of gene function in particular biological processes, such as specific stages of skeletal development, is often hampered by the early lethality or developmental arrest caused by gene deletion using conventional means. Here taking advantage of the Cre-loxP technology, we have created and characterized a Cre transgenic line that allows for temporal control of gene deletion in both the embryonic and postnatal skeleton. Specifically, the transgene expresses under the collagen a1 (II) (Col2a1) promoter/enhancer a tamoxifen (TM) activatable Cre recombinase (Col2Cre-TM). By crossing with the Rosa26LacZ reporter mice (R26R) which allowed for the expression of LacZ following Cre activation, we demonstrated that following intraperitoneal injections of TM at various time points, Cre activity was detected in distinct cell populations. In particular, early injection of TM at E8.5-E10.5 into the pregnant female resulted in Cre activity progressing through the limb cartilage elements in a proximal to distal fashion, reflecting the temporal activation of the Col2a1 promoter in the limb skeleton. Injection of TM at E11.5 showed strong Cre activity in chondrocytes, the perichondrium, as well as the joint capsules. Importantly, injections at E12.5 or later showed a near complete restriction of Cre activity to proliferating and prehypertrophic chondrocytes. Similarly, injection of TM in postnatal day 10 pups (P10) resulted in highly specific Cre activity in both the growth plate chondrocytes as well as the articular chondrocytes. Additionally, injection of TM at sub-threshold concentrations induced Cre activity within small clusters of chondrocytes (clones), which allowed for clonal analysis. Finally, in preliminary experiments, by removing Smoothed (Smo) at either E11.5 or P10 using the Col2Cre-TM line, we demonstrated a clear defect in chondrocyte development, consistent with the critical role of Ihh signaling in skeletal development. In summary, the Col2Cre-TM transgenic mouse line provides a useful tool in studying both embryonic and postnatal endochondral bone development.

Disclosures: **M.J. Hilton**, None.

1154

The Hedgehog Signaling Molecule Gli2 Regulates Both BMP-2 and PTHrP Expression in the Growth Plate. M. Zhao, J. A. Sterling*, M. Qiao*, B. O. Oyajobi, S. E. Harris, G. R. Mundy. Cellular and Structural Biology, University of Texas Health Science center at San Antonio, San Antonio, TX, USA.

Both PTHrP and BMP2 have been demonstrated to have important physiological roles in chondrocyte maturation at the growth plate. There clearly needs to be coordination between these growth regulatory cytokines at this site. We propose that the zinc finger protein, Gli2, which mediates Hedgehog (Hh) signaling, is responsible for this coordination. We have previously found that Gli2 is a powerful activator of BMP2 gene expression in osteoblasts. In an experiment using TMC23 cells, a clonal growth plate chondrocyte cell line, we found that these cells express all Gli family members, Gli1, Gli2 and Gli3, and the Ihh receptors, Ptc1, Ptc2 and Smo. We examined the effects of the Gli family on PTHrP expression and the chondrocytic phenotype in TMC23 cells, since these molecules mediate Hh signaling, and Ihh is known to influence PTHrP expression in growth plate chondrocytes. We found that Gli2 is the only member of the Gli family that markedly up-regulates PTHrP promoter activity, and this effect was dramatically diminished by Gli2 siRNA. Cytochemistry, RT-PCR and immunoassay have shown that overexpression of Gli2 in TMC23 cells elevated the synthesis of proteoglycans and the gene expression of Sox9 and collagen II. DNA analysis including EMSA indicated that the effect of Gli2 on the PTHrP promoter is likely indirect. We have also investigated the effects of Gli2 on BMP2 gene expression in chondrocytes. We found that overexpression of Gli2, but not Gli1 and Gli3, markedly enhances BMP2 promoter activity and BMP2 mRNA level in TMC23 cells determined by promoter reporter assay and real time PCR, which was largely blocked by Gli2 siRNA. Deletion studies and EMSA of the BMP2 promoter have demonstrated that three Gli binding sites in the promoter are required for the direct transactivation of Gli2. However, in a separate experiment, we found that the incubation of TMC23 cells with BMP2 did not affect PTHrP promoter activity, suggesting that Gli2 stimulates PTHrP expression in chondrocytes independent of its effect on the BMP2 pathway. Further, we examined the cartilage phenotype and the expression of BMP2 and PTHrP in Gli2 knockout mice. We found that Gli2^{-/-} mice, with lower bone mass, had severe cartilage defects including significantly expanded proliferating and hypertrophic zones of the growth plates, and both BMP2 and PTHrP expression were dramatically reduced in these areas. These findings suggest: Ihh mediates effects on chondrocytes through the signaling molecule Gli2; stimulation of Gli2 on expression of BMP2 and PTHrP are direct and indirect respectively; the effects of Gli2 on PTHrP are independent of the effects on BMP2.

Disclosures: **M. Zhao, None.**

1155

Dlx2 Stimulates the Murine Chondrocyte Maturation *In Vitro* and *In Vivo*. Y. Zhang^{*1}, M. Zuscik², D. Chen², R. Rosier², E. Schwarz², H. Drissi², R. O'Keefe². ¹Orthopaedics/Pathology and Laboratory Medicine, University of Rochester, Rochester, NY, USA, ²Orthopaedics, University of Rochester, Rochester, NY, USA.

Although BMP-2 strongly promotes chondrocyte maturation, the molecular mechanisms and downstream effectors of these events remain under investigation. *Dlx2* gene expression is induced by BMP-2 in immortalized human chondrocytes. *Dlx2* ^{-/-} mice have craniofacial and cartilage defects. However, comprehensive studies of the function of *Dlx2* during chondrocyte maturation have not been performed. In these studies, the function of *Dlx2* was examined *in vitro* in murine TMC-23 cells and in primary murine sternal chondrocyte (PSC) and *in vivo* by generating cartilage specific *Dlx2* transgenic mouse. Using real-time RT-PCR, the expressions of the *Dlx* genes (1-6) were examined after 24 and 48 hours of BMP-2 treatment in TMC-23 and PSC. While all *Dlx* genes are expressed, the highest baseline levels were observed for *Dlx2* and *Dlx5*. In TMC-23 cells, BMP-2 treatment for 24 hours caused induction in *Dlx1* (3-fold), *Dlx2* (8-fold), *Dlx5* (3-fold), and *Dlx6* (3-fold) compared to the control, and similar increases were maintained after 2 days of BMP-2 treatment. In PSC, BMP-2 stimulated *Dlx1* (3-fold) and *Dlx2* (2-fold) expressions at 24 hours, and induced *Dlx5* (3.5-fold) and *Dlx6* (3-fold) at 48 hours. Using pLenti vector, *Dlx2* was over-expressed in PSC. Three days after infection, *Dlx2* significantly promoted the expressions of *colX* (4 folds) and *osteocalcin* (5 folds), and repressed *col2* (2 folds). However, *Dlx2* had no effect on *VEGF*, *MMP9*, and *MMP13*. *Dlx2* over-expression also stimulated alkaline phosphatase activity (3-folds). A gain of function approach was used to determine if the *Dlx2* was directly involved *colX* induction. In 293T cells, *Dlx2* enhanced activity (3.5-fold) of the murine type X collagen promoter (4 kb). The type X collagen promoter contains two *Dlx2* consensus binding sequences at approximately -100 and at -1300 bp. Site-directed mutagenesis of the first TAAT motif significantly reduced reporter gene activity following *Dlx2* co-transfection. A 1.0kb *col2* promoter was used to drive *Dlx2* expression in cartilage tissues *in vivo*. Transgenic mice are significantly smaller than the wild type mice and have multiple skeletal malformations, including rib cage, spine, dental tissue, and craniofacial components. These results demonstrate that *Dlx2* is a downstream target of BMP signaling in chondrocytes, stimulates chondrocyte maturation, and induces expression of the type X collagen promoter.

Disclosures: **Y. Zhang, None.**

1156

Inactivation of Nek1 Protein Kinase Signaling in Kat2J Mice Leads to Skeletal Defects. S. L. Abboud¹, A. Singh^{*1}, K. Woodruff^{*1}, M. Roudier^{*2}, M. MacDougall^{*1}, D. Riley^{*1}, Y. Chen^{*1}. ¹University of Texas Health Science Center, VA Hospital, San Antonio, TX, USA, ²SkeleTech, Inc, Bothwell, WA, USA.

Nek1 was originally identified as a mammalian ortholog of never in mitosis A (NIMA), a protein kinase that controls mitosis and cell cycle progression in fungi. Mammalian Nek1 has dual serine-threonine and tyrosine kinase activity and is essential for responding to DNA damage and preventing aberrant apoptosis via the intrinsic mitochondrial pathway. We have discovered that Nek1 is normally expressed in growth plate cartilage, osteoblasts and osteocytes during murine postnatal development and declines with age. In the spontaneous mutant *kat2J/Nek1*^{-/-} mice, absence of Nek1 leads to dwarfism, facial dysmorphism and polycystic kidney disease. However, the precise biologic effect of Nek1 deficiency on skeletal tissues is unknown. To address this issue, the skeletal phenotype of *kat2J/Nek1*^{-/-} mice was analyzed. Mutant mice showed stunted growth 10 days after birth, were half the weight of wild type (wt) littermates and developed abnormal craniofacial features including rounded skull, shortened midface and malocclusion of the mandible. Compared to wt, *kat2J/Nek1*^{-/-} mice had skeletal defects characterized by altered chondrogenesis and osteogenesis. Radiographs of mutants at 3 weeks showed shortened long bones and an osteoporotic-like phenotype with decreased cortical thickness compared to wt. *Kat2J/Nek1*^{-/-} femurs by microCT showed a malformed epiphysis and distorted growth plate and, by pQCT, the bone mineral density was decreased. Histologic preparations and histomorphometry of femurs demonstrated a widened, less organized growth plate, decreased bone volume with few thin trabeculae and decreased osteoblasts in mutants compared to wt. Alizarin red and alcian blue staining also indicated defects in ossification as early as postnatal day 1. To determine whether skeletal changes in *kat2J/Nek1*^{-/-} were associated with altered cell survival, assays for apoptosis were performed. By TUNEL analysis, increased apoptosis was observed in growth plate chondrocytes of mutant mice. Bone marrow stromal/osteoblast cells isolated from mutants also showed increased apoptosis and loss of mitochondrial membrane potential, which were rescued by re-expression of wt Nek1 via an adenoviral vector. Results show for the first time that absence of Nek1 increases apoptosis within skeletal tissues and leads to defects in growing bone. Nek1 likely maintains cartilage/bone cell homeostasis and prevents aberrant apoptosis during the rapid phase of postnatal growth. Further elucidation of the downstream target molecules for Nek1 may provide unique strategies for enhancing skeletal growth and restoring bone loss.

Disclosures: **S.L. Abboud, None.**

1157

Interactions between PTHrP and BMP Signaling during Mammary Gland Development. J. R. Hens¹, P. R. Dann^{*1}, J. P. Zhang^{*1}, S. E. Harris^{*2}, J. J. Wysolmerski¹. ¹Internal Medicine, Yale University, New Haven, CT, USA, ²Periodontics, The University of Texas at San Antonio, San Antonio, TX, USA.

Parathyroid hormone-related protein (PTHrP) directs mesenchymal cell fate choices that are critical for the proper development of the embryonic mammary gland. In mice that lack PTHrP or its receptor, the mammary mesenchyme fails to develop and the morphogenesis of the mammary bud is arrested. In contrast, over-expression of PTHrP in keratinocytes in K14-PTHrP transgenic mice leads to the conversion of the ventral dermis to mammary mesenchyme. Our aims in this study were to understand how PTHrP modulates mesenchymal cell fate decisions and to discern why the effects of PTHrP over-expression are limited to the ventral surface of the embryo. Using a BMP-4/lac Z "knock-in" mouse, we found that prior to embryonic day 15 (e15), BMP-4 was strongly expressed in the ventral mesenchyme in a pattern approximating that portion of the ventral epidermis affected by PTHrP overexpression. Therefore, we examined whether changes in PTHrP expression in the embryonic mammary bud and epidermis altered mesenchymal BMP signaling. Wild-type (WT) embryos demonstrated intense nuclear staining for phospho-SMAD 1,5 and 8 in the mammary mesenchyme, suggesting that these cells were targets of BMP-signaling. Phospho-SMAD staining was reduced in PTHrP and PTH1R knockout mammary buds and was inappropriately present in the ventral dermis of K14-PTHrP embryos. We confirmed this change in BMP signaling by examining SMAD phosphorylation in WT and K14-PTHrP ventral skins by Western blot. We also examined whether PTHrP could modulate BMP signaling in mesenchymal cell lines *in vitro*. We treated C3H10T1/2 and C2C12 cells with BMP2 or BMP4 in the presence or absence of PTHrP and found that PTHrP augments SMAD phosphorylation in these cell lines. Finally, it has been shown that disruption of the gene encoding the homeobox transcription factor, *MSX2*, in mice partially phenocopies the mammary defects seen in PTHrP and PTH1R knockout mice. Given this observation and given the fact that *MSX2* is a BMP-responsive gene, we examined the expression of *MSX2* by *in situ* hybridization in our models of PTHrP over and under expression. In PTHrP and PTH1R knockout mice, *MSX2* expression was absent from mammary mesenchyme and in K14-PTHrP mice *MSX2* was ectopically expressed in the ventral dermis. These data suggest that PTHrP signaling alters mesenchymal cell fate in the mammary bud by modulating BMP signaling and inducing the expression of *MSX2*.

Disclosures: **J.R. Hens, None.**

1158

Nuclear Targeting of PTHrP and Cellular Proliferation: A Central Role for p27^{kip1} in Molecular Control of the Cell Cycle. N. M. Fiaschi-Taesch¹, K. R. Ubriani^{*1}, K. K. Takane^{*1}, B. M. Sicari^{*1}, B. Law^{*2}, A. F. Stewart¹.

¹Medicine, Endocrinology, University of Pittsburgh, Pittsburgh, PA, USA, ²Pharmacology, University of Florida, Gainesville, FL, USA.

Parathyroid hormone-related protein (PTHrP) contains a classical bipartite nuclear localization signal. Nuclear targeting of PTHrP has been associated with proliferation in osteoblasts, chondrocytes, breast and prostate cancer cells, and arterial vascular smooth muscle cells (VSMC). In the arterial wall, PTHrP is markedly upregulated in response to angioplasty, and is associated with arterial re-stenosis. Overexpression exacerbates arterial re-stenosis, and, conversely, knockout of the PTHrP gene is associated with deceleration of VSMC proliferation *in vivo*. The mechanism of nuclear PTHrP-induced cellular proliferation is therefore of interest in VSMC as well as in other cell types. Here, we explore the entire G1/S proteome in nuclear-targeted VSMC. Nuclear PTHrP is associated with an increase in phospho-pRb, and release of G1/S arrest. This pRb phosphorylation is associated with stable levels of cdk's 2, 4 and 6, the D cyclins, cyclins A and E, p15, p16, p18, p19 and p21. In striking contrast to the other members of the G1/S proteome, p27^{kip1} is markedly reduced, and this is associated with a dramatic increase in cdk-2/cyclin A/E kinase activity. Adenoviral replacement of p27^{kip1} normalizes proliferation rates, confirming that p27^{kip1} loss is responsible for the increase in VSMC proliferation in PTHrP-nuclear-targeted VSMC. p27^{kip1} mRNA levels are near normal in nuclear-PTHrP-expressing VSMC, suggesting that p27^{kip1} loss is regulated at the protein level. This was confirmed using the proteasome inhibitor, MG132, which resulted in normalization of p27^{kip1}. Cycloheximide degradation studies confirm that p27^{kip1} half-life is markedly reduced in nuclear-targeted PTHrP-expressing cells. Further, nuclear PTHrP overexpression leads to phosphorylation of p27^{kip1} on Thr¹⁸⁷, a well known signal for p27^{kip1} degradation. Finally, p27^{kip1} is known to be degraded by ubiquitination in other cell types, with cullin-1, skp-1 and skp-2 being critical members of the E3-ligase complex. Cullin-1 and skp-2, but not skp-1 are markedly upregulated in nuclear PTHrP-expressing cells, and are likely candidates for the mediators of nuclear targeted PTHrP-induced p27 degradation. The current observations define a novel "PTHrP-p27^{kip1} axis" that regulates cell cycle proliferation by nuclear-targeted PTHrP in VSMC and potentially other cell types as well. This axis is a potential target for therapeutic manipulation of the arterial response to injury, and possibly in cell types of skeletal origin as well.

Disclosures: **N.M. Fiaschi-Taesch, None.**

1159

Increased PTH Anabolic Effects in a Mouse Model Expressing a Phosphorylation-Deficient PTH/PTHrP Receptor (pdPTH1R). G. S. Bounoutas^{*}, H. Tawfeek^{*}, A. Abou-Samra. Endocrine, Massachusetts General Hospital, Boston, MA, USA.

In a variety of animal models it has been shown that intermittent PTH administration increases bone mineral density (BMD) whereas continuous PTH infusion decreases BMD. We have hypothesized that the differential anabolic responses of the two modalities of PTH administration may be secondary to their differential effects on PTH1R internalization and desensitization. We have recently described a pdPTH1R mouse model, in which a pdPTH1R was knocked into the locus of the PTH1R gene using homologous recombination, and have shown that this mouse model exhibits a sustained increase in plasma cyclic AMP level after subcutaneous PTH administration. In this study we used the pdPTH1R mouse model to examine the hypothesis that PTH1R phosphorylation is important for the anabolic response to intermittent PTH administration. We first backcrossed the pdPTH1R mouse into the C57/B6J background for 6 generations. Twelve-week-old WT and pdPTH1R male mice (7 mice per group) were injected 5 times/week with 40 g/kg PTH(1-34). Body weight, bone mineral density, and bone mineral content were measured at 2, 6, and 10 weeks. BMD increased over the experiment period by 3.1%±2.7 and 0.5%±3.3 in WT and pdPTH1R mice, respectively. Compared to vehicle-treated animals, PTH administration increased BMD by 6.2%±2.7 (p = 0.03) and 8.4%±2.8 (p = 0.0002) in WT and pdPTH1R mice, respectively. PTH administration resulted in a ~2-fold increase in the rate of BMD growth in WT mice and a ~16-fold increase in BMD growth in the pdPTH1R mice. The data thus show that PTH1R phosphorylation is not required for the anabolic effects of PTH, and that the bone anabolic effects of PTH is greater in pdPTH1R mice than in WT mice.

Disclosures: **G.S. Bounoutas, None.**

1160

NHMF1 Switches Extracellular Signal-Regulated Kinase Signaling by the PTH Receptor. B. Wang^{*1}, W. B. Sneddon¹, Y. Yang^{*1}, P. A. Friedman². ¹Dept. of Pharmacology, University of Pittsburgh School of Medicine, Pittsburgh, PA, USA, ²Dept. of Pharmacology and Medicine, University of Pittsburgh School of Medicine, Pittsburgh, PA, USA.

Parathyroid hormone (PTH) binds its cognate G-protein-coupled receptor (PTH1R) and results in several signaling events involving adenylyl cyclase/protein kinase A and phospholipase C/protein kinase C pathways. Many cellular effects of PTH depend on the activation of the mitogen-activated protein kinases (MAPK) ERK1 and ERK2 (ERK 1/2). Na/H exchange regulatory factor 1 (NHERF1) is a cytoplasmic protein that can regulate PTH-mediated PTH1R internalization in kidney tubule and osteoblastic cells and restore PTH-mediated increases of intracellular calcium in OKH cells. However, the effect of NHERF1 on PTH activation of ERK1/2 is unknown. The objective of the present study

was to determine if NHERF1 regulates PTH-dependent ERK1/2 activation. To address this problem, we engineered a cell system expressing the PTH1R, where NHERF1 could be induced. Chinese hamster ovary (CHO) cells, which have negligible endogenous PTH1R or NHERF1 expression, were stably transfected with pcDNA4-NHERF1, pcDNA6/TR and pcDNA3.1(+)-PTH1R-HA. Tetracycline (8-100 ng/ml) induced dose-dependent increases of NHERF1 expression. NHERF1 blocked PTH(1-34) (10⁻¹⁰-10⁻⁸ M)-induced ERK1/2 activity. NHERF1 also blocked PTH(7-34)-stimulated ERK1/2 activity. Different levels of NHERF1 induced by various concentrations of tetracycline in the CHO cell system blocked both PTH(1-34) and 7-34-induced ERK1/2 phosphorylation. The requirement for PDZ domain interaction between NHERF1 and the PTH1R for ERK1/2 stimulation was examined with a PTH1R containing a mutated PDZ recognition sequence. NHERF1 and wild-type or mutant PTH1R, where the terminal methionine 593 was replaced by alanine (M593A), were cotransfected in wild-type CHO cells. Stimulation of either wild-type or mutant receptor by PTH(1-34) (10⁻⁸ M) induced ERK1/2 phosphorylation. NHERF1 inhibited activation of ERK1/2 by wild-type PTH1R but had no effect on the mutant receptor. In conclusion, PTH(1-34) and 7-34 activate ERK1/2. NHERF1 blocks PTH1R-stimulated ERK1/2 activation by both PTH(1-34) and 7-34, thereby switching ERK signaling by the PTH receptor. This regulatory effect of NHERF1 depends on its binding to the carboxyl terminal PTH1R PDZ-binding domain.

Disclosures: **B. Wang, None.**

1161

Global Knock-Down of the Calcitonin Receptor (CTR) Results in Decreased Trabecular Bone Volume in Young Female Mice. R. A. Davey¹, J. F. McManus^{*1}, A. J. Moore^{*2}, M. W. S. Chiu^{*1}, A. M. Axell^{*1}, A. J. Notini^{*1}, H. A. Morris², D. M. Findlay³, J. D. Zajac¹. ¹Medicine, Austin Health, University of Melbourne, Heidelberg, Victoria, Australia, ²Hanson Institute, Adelaide, South Australia, Australia, ³Orthopaedics and Trauma, University of Adelaide, Adelaide, South Australia, Australia.

To investigate the physiological control of bone resorption and formation by calcitonin (CT), we have generated a global calcitonin receptor (CTR) knock-down (KD) mouse model using the Cre-loxP system. CTR-loxP mice were generated using embryonic stem cell technology. Exons 13 and 14 of the CTR, which encode the seventh transmembrane domain and C-terminus, were targeted for deletion. CTR KD mice were generated by breeding the CTR-loxP mice with CMV-Cre mice, which express Cre ubiquitously. We have demonstrated Cre-mediated deletion of exons 13 and 14 of the CTR in the bones of CTR KD mice and estimate the deletion to be greater than 90% at the mRNA level compared to controls using northern analysis. Male and female heterozygous (het) CTR-lox controls, het CTR KDs and homozygous (hom) CTR KDs were studied at 6, 12 and 24 weeks of age. Distal femora were prepared for quantitative histomorphometry using established resin embedding techniques. Trabecular bone volume (BV/TV %) was decreased in female hom CTR KD mice at 6 weeks of age (P<0.05) (hom CTR KD: 21.3 ± 2.4, het CTR-lox control: 34.5 ± 3.7, het CTR KD: 32.7 ± 2.8). This was associated with a decrease in trabecular number (P<0.05), while trabecular thickness and mineral apposition rate were unaffected, suggesting increased bone resorption. Osteoclast surface was unchanged in female hom CTR KDs suggesting that the increase in bone resorption observed in the hom CTR KD female mice may be a result of increased osteoclast activity and/or lifespan with no change in the number of osteoclasts. We are currently assessing the formation, activity and lifespan of osteoclasts derived from bone marrow cells of hom CTR KD mice *in vitro*. No changes were observed in serum calcium, serum total protein or intact PTH levels in female CTR KD mice. No changes in any of the bone histomorphometric variables were observed in hom CTR KD males at 6 weeks of age. Serum calcium however was decreased in male hom CTR KD mice compared to het CTR-lox controls and het CTR KDs (P<0.05), while serum total protein and intact PTH levels were unaffected. In conclusion, we have demonstrated that global knockdown of the CTR results in decreased trabecular bone volume in young female mice and that this bone loss is associated with increased bone resorption. These data suggest that the role calcitonin plays in regulating bone cell turnover is greater in young female mice than males.

Disclosures: **R.A. Davey, None.**

1162

Uncovering the Physiologic Function of Calcitonin Using Genetically Modified Mouse Models. A. Voss^{*1}, S. Liese^{*1}, M. Priemel¹, P. Catala-Lehnen^{*1}, A. F. Schilling¹, C. Mueldner^{*1}, M. Haberland^{*1}, J. M. Rueger^{*1}, R. B. Emeson^{*2}, R. F. Gagel³, T. Schinke¹, M. Amling¹. ¹Trauma Surgery, Hamburg University School of Medicine, Hamburg, Germany, ²Department of Pharmacology, Vanderbilt University School of Medicine, Nashville, TN, USA, ³Department of Endocrine Neoplasia and Hormonal Disorders, University of Texas, Houston, TX, USA.

The peptide hormone calcitonin (CT) is produced by thyroidal C-cells and is well known for its inhibitory action on bone-resorbing osteoclasts. However, the physiologic significance of this action is still under debate, since it was difficult to explain why thyroidectomy does not result in osteoporosis and why high circulating CT levels associated with medullary thyroid carcinoma fail to trigger osteopetrosis. Moreover, the high bone mass phenotype of three months old Calc1-deficient mice suggested a previously unknown physiologic function of CT as an inhibitor of bone formation. We have now extended this analysis to older Calc1-deficient mice and compared their phenotype to alpha-CGRP-deficient mice, since the loss of the Calc1 gene results in the lack of CT and alpha-CGRP. Consistent with our previous findings we observed a high bone mass phenotype of Calc1-deficient mice at several ages ranging from 3 to 18 months, whereas alpha-CGRP-deficient mice were osteopenic. Surprisingly, the high bone mass

phenotype of the *Calc1*-deficient mice at 12 months of age was accompanied by a specific increase of bone resorption parameters compared to wildtype controls (OcS/BS: 8.6 ± 1.5 % vs. 1.9 ± 0.6 %; urinary Dpd crosslinks (nM/nM creatinine): 41.7 ± 12.4 vs. 18.9 ± 7.7). Consistent with their high bone mass (BV/TV: 16.5 ± 1.6 % vs. 13.1 ± 1.0 %) we also observed an increased bone formation rate in *Calc1*-deficient mice compared to wildtype controls (BFR/BS ($\mu\text{m}^3/\mu\text{m}^2/\text{year}$): 135.1 ± 18.7 vs. 99.7 ± 17.8), despite the absence of alpha-CGRP that leads to decreased bone formation. These results demonstrate that *Calc1*-deficient mice develop a phenotype of high bone turnover with age. This severe phenotype is accompanied by hyperostotic lesions that were observed in more than 20 % of the *Calc1*-deficient mice at 12 months of age, but never in wildtype controls or in alpha-CGRP-deficient mice. Taken together, these data uncover a physiologic function of CT as a regulator of bone turnover affecting both bone resorption and bone formation. This dual action of CT may explain the conflicting results obtained by measuring bone densities in human patients with altered CT levels.

Disclosures: A. Voss, None.

1163

MEPE-ASARM-Peptide Associated Mineralization Defects in X-Linked Hypophosphatemic Rickets (hyp) Is Corrected by Protease-Inhibitors. P. S. N. Rowe¹, N. Matsumoto^{*2}, O. D. Jo^{*2}, R. N. J. Shih^{*2}, M. Roudier^{*1}, J. Harrison^{*1}, N. Yanagawa^{*2}. ¹University of Texas HSC, San Antonio, TX, USA, ²UCLA, Sulpveda, CA, USA.

MEPE and osteoblastic-proteases are elevated in the hyp-osteoblast. This leads to increased release of a small protease-resistant MEPE-peptide (ASARM-peptide), a potent inhibitor of mineralization and phosphate-uptake. Since our previous studies showed: (1) cathepsin-B cleaves MEPE releasing ASARM-peptide and (2) hyp-osteoblast cells hyper-secrete cathepsin-D, an activator of cathepsin-B, our aims were to: 1. Determine whether cathepsin-inhibitors correct the mineralization defect *in-vivo* (reduce peptide-release) and 2. Determine whether hyp-bone ASARM-peptide levels are elevated? Normal-littermates and hyp-mice (n=6) were subcutaneously injected once a day for 4 weeks with: 1. pepstatin (non-specific inhibitor of cathepsin-D), 2. CAO74 (specific inhibitor of cathepsin-B) and 3. vehicle. Animals were then sacrificed, bones removed and detailed histomorphometry, pQCT, uCT and immunohistochemistry (ASARM-antibodies) carried out. As expected, Goldner-staining of "vehicle-group" hyp-femurs revealed extensive regions of unmineralized-osteoid, widened epiphyses and disruption of the growth-plate. In contrast, hyp-animals treated with protease-inhibitors showed marked and significant improvement in all histomorphological parameters for endosteal/periosteal-bone and growth plate. The mineralization-apposition-rate (um/day), bone-formation-rate/ bone-surface referent (um³/um²/year) and mineralization-surface as a percentage of bone-surface (%) were normalized by protease-treatment. Moreover, the growth-plate-width (>42%, P=0.002), osteoid-thickness (>40%, P=0.002) and cortical-area (>40%, P=0.003) were significantly and markedly improved. Also, high-resolution pQCT density-maps of metaphyseal and diaphyseal regions confirmed major and significant increases of mineralized-bone in protease-inhibitor treated hyp-animals. This was confirmed further by uCT (figure 1).

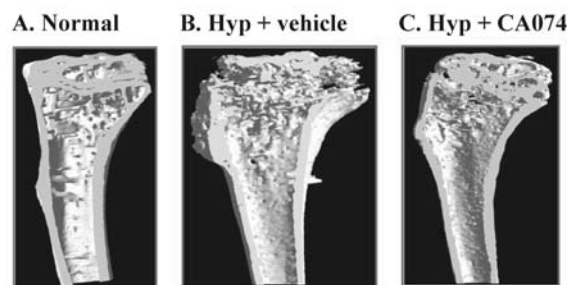


Figure 1: micro-computed-tomography (uCT) of tibiae.

Finally, the growth-plate and cortical-bone of hyp-femurs contained a massive accumulation of osteoblast-derived ASARM-peptide(s). Thus, *in-vivo* administration of cathepsin-inhibitors likely reduces ASARM-peptide release and improves bone-mineralization and architecture in hyp-mice.

Disclosures: P.S.N. Rowe, None.

1164

Vitamin D Dependent Functions of Fgf-23 In Vivo. D. Sitara¹, R. St-Arnaud², R. G. Erben³, M. S. Razzaque^{*1}, B. Lanske¹. ¹Oral & Developmental Biology, Harvard School of Dental Medicine, Boston, MA, USA, ²Genetics Unit, Shriners Hospital, Montreal, PQ, Canada, ³Dept. of Natural Sciences, University of Veterinary Medicine, Vienna, Austria.

FGF-23 has been identified as the circulating phosphaturic factor associated with renal phosphate wasting leading to rickets and osteomalacia, as found in patients with autosomal dominant hypophosphatemic rickets, oncogenic osteomalacia, and X-linked hypophosphatemia. We recently reported the generation of *Fgf-23* null animals resulting in a phenotype including growth retardation, severe hyperphosphatemia, increased serum ALP activity and 1,25(OH)₂D₃ concentrations, abnormal bone mineralization, and tissue calcifications. A similar phenotype has been reported in patients with familial tumor calcinosis, caused by inactivating mutations in the FGF-23 gene. In the current study we studied the expression of *Fgf-23* postnatally by *lacZ* staining of various adult tissues of *Hyp/Fgf-23*^{-/-} and *Hyp/Fgf-23*^{-/-} mice, and were able to detect strong signals in all bones.

We also investigated whether part of the abnormal *Fgf-23* null phenotype is due to the increased 1,25(OH)₂D₃ levels. Thus, we established a new mouse model in which we eliminated vitamin D dependent mechanisms in *Fgf-23* null mice by generating double mutant animals which were deficient for both *Fgf-23* and 1α (OH)ase, the enzyme that converts the inactive form of vitamin D to the active form. Our data demonstrate for the first time that deleting the 1α hydroxylase gene from *Fgf-23* null mice reverses the severe hyperphosphatemia to hypophosphatemia, suggesting that regulation of phosphate homeostasis by *Fgf-23* is at least partly vitamin D-dependent. In addition to the biochemical measurements, we performed routine histological analysis and analyzed the mineralization pattern of the long bones of *Fgf-23*^{-/-}, 1α (OH)ase^{-/-}, and *Fgf-23*^{-/-}/1α (OH)ase^{-/-} double mutant animals, by von Kossa staining on methylmetacrylate sections and Alizarin Red S staining on full body skeletons. Our findings suggest that *Fgf-23*^{-/-}/1α (OH)ase^{-/-} double mutant mice resemble the phenotype of 1α (OH)ase^{-/-} single knock-out animals as they exhibit ricketic appearance such as a wider growth plate with an expansion of hypertrophic chondrocytes, and a decrease in mineral deposition. Alizarin staining of all compound mutant skeletal elements clearly illustrated that the abnormal nodule formation previously observed in many *Fgf-23* null bones had completely disappeared indicating that 1,25(OH)₂D₃ must have caused these features. We are currently measuring proliferation and apoptosis rates and are evaluating the expression of skeletal marker genes by *in situ* hybridization.

Disclosures: D. Sitara, None.

1165

Structural Survey of FGF23. H. J. Garringer^{*}, S. I. Davis^{*}, T. E. M. Larsson, X. Yu, K. E. White. Medical and Molecular Genetics, Indiana University School of Medicine, Indianapolis, IN, USA.

Fibroblast growth factor-23 (FGF23) is a secreted factor required for normal phosphate and vitamin D metabolism. Our previous studies identified FGF23 mutations responsible for the heritable human disorders autosomal dominant hypophosphatemic rickets (ADHR) and tumoral calcinosis (TC) which alter the structure and processing of the encoded polypeptide. The objective of the present study was to isolate FGF23 domains central to its intracellular processing and secretion. In this regard, wild type and R176Q ADHR mutant FGF23s, were truncated by C-terminal deletions of 20, 38, and 52 residues, as well as by an N-terminal deletion of 25 residues. These truncated FGF23 species were transiently transfected into HEK293 cells and the conditioned media and cellular lysates were assessed for FGF23 expression. Western analyses of the media revealed the presence of all C-terminally truncated wild type and R176Q mutant FGF23s of the predicted sizes, whereas no signal was found in the corresponding lysates. Conversely, media from the cells transfected with the N-terminal deletion produced no FGF23 signal by Western analysis, whereas the corresponding lysates were positive. Although western analysis indicated that the N-terminally truncated FGF23 was retained within the cell, ELISA specific to the C-terminal domains of FGF23 showed that C-terminal protein fragments were present in the media, indicating that this mutant was cleaved by intracellular proteases and secreted. As expected, the C-terminally truncated proteins containing the R176Q mutation were more stable than their wild type counterparts. We recently demonstrated that an FGF23 mutation responsible for the TC phenotype, serine to glycine at residue 71 (S71G), results predominantly in the secretion of C-terminal FGF23 fragments. To understand substitutions tolerated at S71, we replaced S71 with corresponding residues conserved in other FGFs at the homologous position. A conserved threonine substitution (S71T) resulted in processing and secretion similar to wild type FGF23. In contrast, an asparagine substitution (S71N) resulted in complete intracellular retention of FGF23, and no secreted fragments. These findings indicate that S71N FGF23 is either resistant to, or not exposed to intracellular proteases, and does not enter the secretory pathway. In conclusion, our results indicate that the FGF23 C-terminus is not central to FGF23 processing. However, N-terminal domains of FGF23 are critical for processing, exemplified by the fact that the S71N mutant is capable of 'uncoupling' FGF23 production and secretion.

Disclosures: H.J. Garringer, None.

1166

Successful Transplantation of Infantile Hypophosphatasia Using Bone Fragments and Cultured Osteoblasts. R. Cahill^{*1}, S. Perlman^{*2}, S. Mumm³, W. H. McAlister^{*4}, M. P. Whyte⁵. ¹Pediatric Research Institute, St. Louis, MO, USA, ²All Children's Hospital, St. Petersburg, FL, USA, ³Division of Bone and Mineral Diseases, Washington University School of Medicine, St. Louis, MO, USA, ⁴St. Louis Children's Hospital, St. Louis, MO, USA, ⁵Center for Metabolic Bone Disease and Molecular Research, Shriners Hospitals for Children, St. Louis, MO, USA.

Hypophosphatasia (HPP) is a rare heritable form of rickets featuring deficiency of the "tissue non-specific" isoenzyme of alkaline phosphatase (TNSALP) due to deactivating mutation of the *TNSALP* gene. Infantile HPP (I-HPP) often leads to respiratory death in infancy. There is no established medical treatment. However, an 8-month-old with I-HPP who underwent bone marrow transplantation (BMT) in 1997 had temporary improvement of her skeleton and lasting clinical and radiographic improvement 13 months later after receiving marrow cells expanded *ex vivo*. We used a unique approach for a second patient with likely fatal I-HPP. She was admitted to the ICU at age 5 months with a typical presentation of I-HPP; failure to thrive, bone pain, hypercalcemia, low alkaline phosphatase (18 IU/L) and demonstrated progressive skeletal demineralization. She carried 2 *TNSALP* missense defects: G571A, Glu174Lys (usually associated with "childhood" HPP) and A1289G, Asn413Ser (unique). Reported preclinical studies to improve osteoprogenitor engraftment included placement of bone intraperitoneally or directly into

ASBMR 27th Annual Meeting

bone. Hence, at age 9 months, after a reduced conditioning regimen, she received T-cell depleted bone marrow from her HLA-mismatched (4/6) father and, 17 days later, donor bone fragments; 2 intraperitoneally and 2 near the iliac crest. On day +28, cultured osteoblast-like cells and additional bone marrow and T-cells from the donor were infused. At +3.5 months, bone pain improved, radiographic progression of demineralization halted, and new bone appeared. At 20 months pBMT, without any evidence of donor engraftment in the periphery, PCR of male marker SRY sequences was performed on patient bone marrow and adherent cells from a bone biopsy specimen. Evidence of donor cells (SRY+) was found only in cultured bone cells. Now, 6 years post-procedure, she is well but has small radiolucencies in long bones, normal growth plates, and bone mineral density resembling mild "childhood" HPP. We postulate that despite absence of peripheral engraftment or correction in biochemical changes of HPP, sufficient TNSALP activity from donor stromal cells in proximity to sites of mineralization largely reversed the clinical and radiographic features of I-HPP.

Disclosures: **R. Cahill**, None.

1167

Effect of Parathyroidectomy in Asymptomatic Primary Hyperparathyroidism: Preliminary Results of a Prospective Randomized Study. **E. Ambrogini**^{*1}, **L. Cianferotti**^{*1}, **E. Vignali**¹, **F. Cetani**¹, **A. Picone**^{*1}, **G. Viccica**^{*1}, **P. Miccoli**^{*2}, **A. Pinchera**^{*1}, **C. Marcocci**¹. ¹Endocrinology and Metabolism, University of Pisa, Pisa, Italy, ²Surgery, University of Pisa, Pisa, Italy.

Asymptomatic primary hyperparathyroidism (PHPT) is a disorder, usually not progressive, and therefore, according to the 1991 NIH Consensus Development Conference, most patients can be followed-up without parathyroidectomy (PTX). On the other hand there is evidence that also patients with mild PHPT can benefit from PTX. Aim of the present investigation was to compare in a 2-year, prospective, randomized study the effect of PTX vs no treatment in patients with asymptomatic PHPT. The primary endpoint was the change in lumbar spine bone mineral density (BMD). Secondary endpoints were: BMD changes at femur and distal radius, markers of bone turnover, quality of life (assessed by the SF-36 and SCL-90 questionnaires), echocardiography parameters, complication of surgery, and progression of the disease in the untreated group. Forty-nine patients (45 women and 4 men) with sporadic PHPT, who did not meet the NIH guidelines for PTX, have been enrolled so far: 24 underwent PTX and 25 were not treated. We report herein the results in 39 patients (19 treated with PTX and 20 untreated) who completed the one-year follow-up. At baseline the 2 groups were similar for age (63.0 ±7.4 vs 64.3 ±6.8 yrs), biochemical parameters (calcium, PTH, urinary calcium, renal function), vitamin D status and markers of bone turnover (B-ALP, osteocalcin, U-CTX, S-CTX), BMD at lumbar spine, total femur and distal radius. Patients were evaluated every 6 months. One patient had persistent PHPT after surgery and was excluded from the analysis. In the PTX-treated group lumbar spine and total femur BMD increased after one year by 4.4% and 1.6%, respectively, whereas in the untreated group they decreased by 1.6% and 2.8 %, respectively. The % changes were significantly different between the two groups (p=0.002 at both sites). No clinically meaningful changes in any of the SF-36 and SCL-90 scores were observed in the two groups during follow-up. Five of the 20 untreated patients (33 %) had *de novo* appearance of at least one of the NIH criteria for surgery: worsening of hypercalcemia (n=1), hypercalciuria (n=3), nephrolithiasis (n=1), cortical BMD below -2 Z-score (n=1) and clinical vertebral fracture (n=1). No complication of surgery were observed. In conclusion, our preliminary data suggest that PTX may be advantageously performed in patients with asymptomatic PHPT since treated patients had significantly improved BMD at lumbar spine and femur compared to untreated ones, and conservative follow-up was associated with a progression of the disease in about one third of patients.

Disclosures: **E. Ambrogini**, None.

1168

Prevalence of Vitamin D Depletion (-D) among Subjects Seeking Advice about Management of their Primary Hyperparathyroidism (PHPT). **N. Parikh**¹, **T. Eskridge**^{*1}, **J. Hill**^{*1}, **A. Bhan**^{*2}, **M. Honasoge**², **D. Rao**¹. ¹Bone & Mineral Research Laboratory, Henry Ford Hospital, Detroit, MI, USA, ²Bone & Mineral Metabolism, Henry Ford Hospital, Detroit, MI, USA.

There is growing concern about vitamin D depletion (-D) in the US population in general and in patients with bone and mineral disorders in particular. We reported a high prevalence of -D in a large cohort (>3500) of osteoporosis (OP) patients. Such information is lacking in PHPT patients. This is relevant because calcium (Ca) and vitamin D intakes are restricted based on intuition that it might aggravate hypercalcemia, but the rationale for such practice is not well founded. On the contrary, it may worsen the degree of HPT. Therefore, we assessed the prevalence of -D (serum 25-OHD ≤15 ng/ml) in all PHPT patients seen between Jan 2000-Dec 2004. We excluded patients with known causes for -D, and all non-whites and non-blacks. Serum Ca, creatinine (Cr), and PTH were measured in all patients. 559 PHPT patients were seen during the 5y; 456 women (72%); 296 whites (53%); mean age 65 ± 13y. In the entire cohort, the prevalence of -D was 28% (159/559) and 47% (263/559) with 25OHD ≤15 and ≤20 ng/ml cut-offs respectively; the rates remained relatively constant during the 5y by either criterion: 20, 33, 23, 24, and 21% and 45, 57, 47, 42, and 37% respectively and were higher than in OP patients. PTH correlated directly with Ca (r=0.34; p<0.001) and inversely with 25-OHD (r=-0.34; p<0.001) but not with age or Cr (data not shown). Serum 25-OHD was influenced by PTH and age, (multiple regression analysis; p<0.001 and =0.02 respectively), but not Ca or Cr. Based on the differences in slopes of PTH on 25-OHD between OP and PHPT cohorts, we found an effect of high PTH on 25-OHD level, most likely due to accelerated turnover leading to conditional -D in PHPT patients. Conclusions: In this largest study of its kind in the US,

we found unacceptably high prevalence of -D in unselected PHPT patients and an additional "stress" on vitamin D nutrition. Our findings have important clinical implications in medical and surgical management of PHPT. Since -D promotes adenoma growth and modifies disease expression, attention to Ca and vitamin D nutrition is essential in PHPT patients. The current pervasive practice of restricting Ca and vitamin D intake in PHPT patients is unwarranted: to paraphrase Fuller Albright...*for all practical purposes bone disease does not develop if the patient drinks milk sufficient to avoid negative Ca balance*. Finally, our findings in these 2 large cohorts imply that either the prevailing educational efforts are ineffective or the foods and supplements do not contain adequate amounts of vitamin D or both. The dichotomy between what is recommended and what is practiced needs urgent attention.

Disclosures: **D. Rao**, None.

1169

Inhibin A Reduces Bone but not Muscle Loss in Hindlimb Suspended Mice. **D. S. Perrien**¹, **N. S. Akel**¹, **L. J. Suva**¹, **E. Dupont-Versteegden**², **D. Gaddy**¹. ¹Department of Physiology and Biophysics and Center for Orthopaedic Research, UAMS, Little Rock, AR, USA, ²Department of Geriatrics, UAMS, Little Rock, AR, USA.

Inhibin A (InhA) overexpression protects mice from hypogonadal bone loss via a mechanism that stimulates osteoblast activity and possibly differentiation, without effects on bone resorption. Bone loss during disuse is thought to occur due to a reduction in bone formation suggesting anabolic agents such as InhA may prevent the ensuing osteopenia. In addition, myostatin, a potent suppressor of muscle mass, utilizes the Activin/TGFβ signaling pathways and hence may be antagonized by InhA. This led to the hypothesis that regulated InhA overexpression would prevent both bone and muscle atrophy in hindlimb suspended (HS) mice. This idea was tested using 6-month-old male mice harboring a Mifepirone (MFP)-inducible human InhA transgene. Mice were assigned to one of 3 treatment groups Con-Veh, HS-Veh, or HS-Inh (MFP-induced). At the time of suspension, a time release pellet containing MFP was subcutaneously implanted in all HS-Inh mice, while a placebo pellet was implanted in mice assigned to the Veh groups. HS mice were suspended by the tail at a 30° head-down angle while Con-Veh mice were individually housed in standard cages for three weeks. The volume and architecture of trabecular bone in the proximal tibial metaphysis was measured by *ex vivo* μCT. HS-Veh mice had significantly lower trabecular BV/TV (Con-Veh 0.175 ±0.069; HS-Veh 0.115 ±0.026; p<0.05) and deteriorated architectural properties including decreases in connectivity density, trabecular number and thickness and corresponding increase in separation (p<0.05 vs Con-Veh). In contrast, these measures were not significantly different between Con-Veh and HS-Inh mice. Moreover, the trabecular number in HS-Inh mice (5.28 ±0.36 mm⁻¹) was significantly greater than that of HS-Veh (4.68 ±0.51 mm⁻¹; p<0.05 vs HS-Inh) demonstrating that InhA overexpression reduced the loss of bone volume and prevented the decrease in trabecular number induced by HS. As expected, lower hindlimb muscle weight-to-body weight ratio (triceps sura) decreased with HS (Con-Veh 4.59±/-0.21 mg/g; HS-Veh 3.95±/-0.26; p<0.001) which was not prevented in InhA treated animals (HS-Inh 4.12±/-0.26; p<0.001 vs Con-Veh; NS vs. HS-Veh). Similar results were observed for the soleus muscle (Con-Veh 0.215 ±0.018 mg/g; HS-Veh 0.140 ±0.025 mg/g; p<0.001), while InhA overexpression had no effect on the atrophy (HS-Inh 0.143 ±0.011 mg/g; p<0.001 vs Con-Veh; NS vs. HS-Veh). Together these data demonstrate that InhA overexpression prevents bone, but not muscle loss during HS, further expanding its role as a potent bone anabolic agent.

Disclosures: **D.S. Perrien**, None.

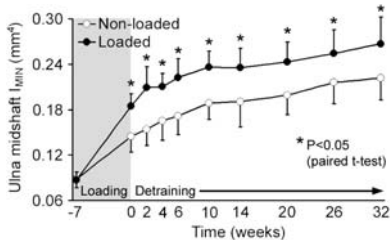
1170

Mechanical Loading during Growth Has Long-Term Benefits to Skeletal Health. **S. J. Warden**¹, **R. K. Fuchs**², **A. B. Castillo**³, **C. H. Turner**³. ¹Department of Physical Therapy, Indiana University, Indianapolis, IN, USA, ²Department of Anatomy and Cell Biology, Indiana University, Indianapolis, IN, USA, ³Department of Biomedical Engineering, Indiana University, Indianapolis, IN, USA.

A disparity exists between when the skeleton is most responsive to exercise (pre-puberty) and when it is most prone to low-trauma fracture (late adulthood). The aim of the current study was to investigate whether bone changes induced by mechanical loading during growth are preserved with subsequent long-term detraining in an animal model. The right forearms of 5-wk-old female Sprague-Dawley rats were mechanically loaded 3 days/wk for 7 wks using the ulna axial loading model. Left ulnas served as internal controls and were not loaded. Adaptation to the loading program was determined within-animal prior to and after the completion of the loading program using *in vivo* DXA and pQCT. Following completion of the loading program, animals were subsequently detrained (restricted to home-cage activity) for 32 weeks, during which time periodic *in vivo* measurements were performed. Mechanical loading induced significant adaptation of the ulna, without influencing longitudinal growth. Loaded (right) forearms had 4.0% and 4.2% greater aBMD and BMC on DXA than contralateral non-loaded (left) forearms, respectively (all P<0.01). Similarly, on pQCT the loaded ulnas had 5.3% and 4.3% greater BMC and cortical area than the contralateral ulnas, respectively (all P<0.02). The largest effect was observed for the minimum second moment of area (I_{MIN}) which was 27.8% greater in loaded ulnas (P<0.001). Each of these loading-induced changes were maintained during detraining (all P<0.05). In particular, all (100%) of the absolute difference in I_{MIN} between loaded and non-loaded ulnas was maintained with 32 wks detraining (see figure). This data indicates that mechanical loading during growth may have lasting benefits on the skeleton. Loading predominantly induced an adaptation in bone structure (increase in I_{MIN}). This change persisted for more than six months of detraining after only 7 wks of loading. I_{MIN}

ASBMR 27th Annual Meeting

represents the resistance to bending and is significantly correlated with bone strength in the rat ulna ($r^2=0.76$). Thus, our data suggests that exercise-induced loading during growth may have lasting benefits on bone strength.



Disclosures: *S.J. Warden, None.*

1171

Skeletal Recovery Following Long-Duration Spaceflight Missions as Predicted by Preflight and Postflight Dual X-ray Absorptiometry (DXA) Scans of 49 Crewmembers. J. D. Sibonga¹, H. J. Evans², H. Sung³, E. R. Spector⁴, V. S. Oganov³, A. V. Bakulin³, L. C. Shackelford⁴, A. D. LeBlanc¹. ¹Division Space Life Sciences, Universities Space Research Association, Houston, TX, USA, ²Wyle Laboratories, Houston, TX, USA, ³Institute of Biomedical Problems, Moscow, Russian Federation, ⁴NASA Johnson Space Center, Houston, TX, USA.

The weightless condition of spaceflight accelerates bone loss in crewmembers. At NASA Johnson Space Center (JSC), measurement of bone mineral density (BMD) by DXA is part of the astronaut medical evaluation requirements to monitor spaceflight effects on the skeleton. DXA scans performed before and after flight provide an opportunity to evaluate skeletal recovery in astronauts who return to a 1 g environment after long-duration spaceflight missions (4- 6 months). To increase the power of this analysis, the JSC lab was given access to BMD data of cosmonauts who served on the Russian MIR (n=22) and on the International Space Station (ISS) (n=8) together with data from 12 astronauts who served on ISS. We used BMD data from these 42 crewmembers to predict the skeletal response of 7 astronauts on the NASA MIR who provided multiple post-flight scans in a study of bone recovery. The deficit between pre- and postflight BMD, for every postflight scan performed on a crewmember, was plotted as a function of Days-after-Landing, as determined by the difference between landing date and the date of the postflight scan. The best fit of the data appeared to be an exponential function. A computed half-life, analogous to the decay of a radioisotope, was used to describe the number of days at which there was 50% recovery of bone lost during spaceflight. The "Recovery Half-lives" for lumbar spine, pelvis, total hip, femoral neck, trochanter and calcaneus were approximately six months. The fitted data from the multiple postflight scans of the 7 Mir astronauts fell within 95% confidence boundaries generated from the 42 international crewmembers indicating the predictive value of the original fitted data for skeletal recovery. In conclusion, the recovery half-lives for specific skeletal sites suggest that it will take more than 12 months before there is sufficient restoration of preflight BMD at these sites in crewmembers flown on missions of 4-6 months.

Disclosures: *J.D. Sibonga, None.*

1172

Recovery of Proximal Femoral Density and Geometry after Long-Duration Spaceflight. T. F. Lang¹, A. LeBlanc², H. Evans³, Y. Lu⁴.

¹Radiology, University of California, San Francisco, San Francisco, CA, USA, ²Life Sciences, Universities Space Research Association, Houston, TX, USA, ³Wyle Laboratories, Houston, TX, USA.

Bone atrophy is a well-known medical consequence of long-duration spaceflight. Recent studies have demonstrated the regional extent and compartmental distribution of this loss, but there is little information on skeletal recovery after prolonged weightlessness. To address this, we used volumetric quantitative computed tomography (vQCT) to measure changes, in crew of the International Space Station, of proximal femoral cortical and trabecular bone that occurred 12 months after flights lasting 4-7 months. 14 subjects were imaged with a helical vQCT protocol (80 kVp, 280 mAs 3mm slice thickness, pitch=1) at three time points: pre-flight, post-flight and 12 months after mission completion. In the total femur hip region, we measured integral volumetric BMD (iBMD), integral BMC (iBMC), integral tissue volume (iVOL), trabecular BMD (tBMD), cortical BMD (cBMD) and cortical volume (cVOL). As a bone size measure, we also quantified the minimum femoral neck cross-sectional area (minCSA). For each measure, we computed the mean percentage bone loss incurred over the flight, the mean percentage change during the recovery period, and the ratio of the 12 month post-mission measurement to preflight values. The paired t-test determined whether the inflight and postflight changes were non-zero, and whether the 12-month to pre-flight ratio was different from 1. Results are tabulated below for the hip. Total femur iBMC, but not iBMD or tBMD, recovered to its pre-flight value. Recovery of bone mass involved increases in both bone density and bone size. We found incomplete recovery of BMD in the hip in the year after long-duration spaceflight. As shown by increased minCSA and iVOL, the proximal femur appears to adapt to resumed load bearing by periosteal apposition.

	inflight (%)	postflight (%)	12mo/ preflight
iBMC	-10.6 **	9.1 **	0.97
iBMD	-9.5 **	3.9 *	0.94 ***
tBMD	-14.1 **	5.8 **	0.91 ***
cBMD	-2.6 **	0.4	0.97 *
iVOL	-1.3	6.7**	1.04 (p=0.09)
cVOL	-9.1 **	10.9 **	0.98
minCSA	0.03	2.7 *	1.03 *

*: p<0.05, **:0.001<p<0.01, ***:p<0.001

Disclosures: *T.F. Lang, None.*

1173

Femoral Osteocytes Are not Subject to Hypoxia in the Hindlimb Suspended Mouse. H. Y. Stevens, D. R. Meays*, J. A. Frangos. La Jolla Bioengineering Institute, La Jolla, CA, USA.

The enhancement of fluid flow in bone by means of mechanical loading induces an adaptive, osteogenic response. It is still unclear whether this remodeling activity is a result of increased shear stress *per se*, improved transport of chemical factors or streaming potentials generated at bone surfaces via fluid flow. The presence of high levels of osteocyte hypoxia, in an invasive avian ulna disuse model, relative to loaded control bone, would suggest that the supply of oxygen is limited in unloaded bone. This study investigated whether osteocytes in the non-invasive murine hindlimb suspension model of disuse osteopenia are subject to hypoxia. We measured levels of hypoxia in femora of mice that had been hindlimb-suspended (unloaded) or unsuspended (loaded) for 10 days (n = 7), and in the same animals observed the effect of increased IFF, via femoral vein ligation, on hypoxic fraction. In another group of animals, arterial occlusion was effected via femoral artery ligation and levels of hypoxia studied at day 1 and 4 (n = 3). Fluorescent immunolocalization of hypoxia inducible factor-1 alpha (HIF-1α) within osteocyte nuclei of midshaft cryostat sections, was used as an index of upregulation of hypoxia transcription factor. The fraction of osteocytes positive for HIF-1α was calculated from nine fields of view under the 40 X objective. Osteocyte viability and osteoclastic activity along bone surfaces were assessed in arterially-occluded bones by LDH and TRAP activity, respectively. Unloaded bone osteocytes were not hypoxic (1.2 ± 0.2 (% \pm S.E.M.)) when compared to loaded controls (1.6 ± 0.2 , $p = 0.3$) and increased IFF, via venous ligation, did not alter these levels significantly (unloaded 0.9 ± 0.2 ; loaded 1.3 ± 0.4 , $p = 0.3$). Arterially-occluded femora demonstrated a significant level of osteocyte hypoxia compared to sham-operated limbs at 1 day (occluded 11.8 ± 1.7 ; sham 3.7 ± 0.4 , $p < 0.05$) and 4 days after ligation (occluded 10.3 ± 2.0 ; sham 3.0 ± 1.0 , $p < 0.05$). However, TRAP activity was not elevated in the arterially-occluded hypoxic femur compared to the sham-operated limb, suggesting little association between hypoxic osteocyte occurrence and osteoclastic activity in this study. Assessment of LDH-positive osteocytes (viable cells) indicated that osteocyte death (approx 20%) had occurred in both femoral artery-occluded and sham-operated femora between day 1 and day 4, and therefore arterial ligation likely compromised blood supply to the contra-lateral limb. These results support the concept that osteocytes in unloaded bone are not oxygen- limited and that IFF-driven bone formation, seen in the hindlimb suspended mouse is not chemotransport-related but likely mediated by fluid shear stress itself.

Disclosures: *H.Y. Stevens, None.*

1174

MuRF1, which Induces Denervation-Dependent Protein Degradation in Muscle, Is Involved in Unloading-Induced Bone Loss. H. Kondo¹, H. Sorimachi², S. Takeda³, M. Noda¹. ¹Molecular Pharmacology, Medical Research Institute, 21st Century COE Program, Tokyo Medical and Dental University, Tokyo, Japan, ²Graduate School of Agricultural and Life Sciences, University of Tokyo, Tokyo, Japan, ³Molecular Therapy, National Institute of Neuroscience, Tokyo, Japan.

MuRF1 is a muscle RING finger protein which is involved in IKKB NFκB activation dependent muscle wasting induced by denervation (Cell 2004). Since MuRF1 is involved in muscle wasting and its expression is enhanced in the muscle of mice subjected to tail suspension (TS)(Science 2001), MuRF1 involvement in similar protein degradation in bone loss due to unloading was examined in this paper. We conducted TS using MuRF1 KO mice and wild type (WT) control mice. TS induced reduction in the weight of soleus muscle. However, MuRF1 deficiency totally prevented such loss of weight in soleus muscle. Bone mineral content (BMC) analysis indicated that BMC was significantly reduced in WT mice due to unloading. In contrast, MuRF1 deficiency suppressed such reduction in BMC. This was observed both in femora and tibiae. These data indicated that unloading induced osteopenic signals would be dependent on MuRF1. Cortical bone mass in the mid shaft of femur was reduced by TS in WT mice. Again in contrast, such reduction in the cortical bone mass in the femur was no longer observed even after TS in MuRF1 deficient mice. Similarly, the thickness of the cortical bone was reduced by TS in WT mice but the reduction was attenuated by MuRF1 deficiency. MuRF1 deficiency alone reduced about 30% of the cancellous bone volume compared to WT mice in loaded control groups. Unloading caused about 60% reduction cancellous bone volume (BV/TV) in WT mice. Compared to WT, TS-induced bone loss was reduced to about 30% in MuRF1 deficient mice. Thus the magnitude of TS-induced reduction in cancellous bone was reduced in MuRF1 deficient mice compared to WT ($p<0.05$). These data indicated that the ring finger protein, MuRF1, which is involved in protein degradation through ubiquitination in muscle, could affect bone mass at basal levels as well as bone loss due to unloading.

Disclosures: *H. Kondo, 21st Century COE Program 2.*

1175

Reduced Mineralization Density of Bone in Premenopausal Women with Idiopathic Osteoporosis. P. Roschger¹, I. Manjubala^{*2}, J. G. Hofstaetter¹, E. Shane³, M. A. Donovan^{*3}, J. Fleischer^{*3}, D. Dempster⁴, P. Fratzl^{*2}, K. Klaushofer¹. ¹Ludwig Boltzmann Institute of Osteology at the Hanusch Hospital of WGKK and AUVA Trauma Centre Meidling, 4th Medical Dept., Hanusch Hospital, Vienna, Austria, ²Max Planck Institute of Colloids and Interfaces, Dept. of Biomaterials, Potsdam, Germany, ³College of Physicians and Surgeons, Columbia University, New York, New York, NY, USA, ⁴Regional Bone Center, Helen Hayes Hospital, West Haverstraw, NY, USA.

The syndrome of idiopathic osteoporosis (IOP) is characterized by the development of fragility fractures in otherwise healthy, young individuals, in whom no contributing etiology can be identified. In a recent case-control study of premenopausal women with IOP (JCEM 2005 Epub doi: 10.1210/jc.2004-2042), we observed that the cases were characterized by lower spine bone mass (Z score +/-SD, -2.1 +/-1 vs 0.0 +/-0.8; p<0.05) and histomorphometric evidence of reduced bone formation (MS/BS 42% lower than controls; p=.02). Neither of these findings would be expected to result in such marked skeletal fragility in young subjects. However, the amount of mineral embedded in the collagenous matrix to form the collagen/mineral nano-composite of bone plays a pivotal role in defining its intrinsic mechanical properties (e.g. E-modulus). Therefore, we evaluated the integrity of the bone material itself. Using quantitative backscattered electron imaging (qBEI), the bone mineralization density distribution (BMDD) of trabecular bone in biopsies of patients with IOP (n=9) and age-matched healthy premenopausal women (n=15) was determined. The mean (CaMean) and typical (CaPeak) calcium content, the variation of calcium content (CaWidth) and the percentage of low mineralized matrix (CaLow) were measured to characterize the BMDD. A small but significant reduction in degree of mineralization in the cases (CaMean -3.0%, P<0.05 and CaPeak -2.7%, P<0.05) compared to the control group was detected, while the other BMDD parameters, CaWidth and CaLow, were not significantly different. The moderate decrease in mineralization density alone might not be sufficient to explain bone fragility. However, the decrease in mineralization was an unexpected finding with respect to the low bone turnover reported in the cases. One would have expected the contrary, namely an increase in degree of mineralization, because low bone turnover permits prolonged secondary mineralization in a larger number of bone packets, resulting in a higher mineral content. This finding suggests that in IOP, changes in the mineralization process itself might occur, which are most likely based on alterations of the organic matrix, and which, in turn, might contribute to increased fragility.

Disclosures: **P. Roschger**, None.

1176

Risk-Equivalent Z-Scores for DXA and Other Techniques Based on a Systematic Review. C. C. Glüer. Med. Physik, Klinik f. Diag. Radiologie, UK S-H, Kiel, Germany.

The WHO diagnostic T-Score criterion of -2.5 is not applicable to techniques other than DXA. There is a need for risk criteria that can be used across techniques and which are suited to define intervention criteria based on absolute fracture risk. An approach based on Z-Scores is presented. 1) Estimates of absolute and relative risk were compiled from SOF, EVOS/EPOS and the Rotterdam study. 2) Z-Score model. The most relevant predictors of fracture risk are age, bone mineral density (BMD) and prevalent vertebral fractures(prVFX). A factorial model of absolute risk using Z-Scores separates the impact of these three factors, described by relative risk (RR): AbsRisk=AbsRisk (woman age 70) x RR(age) x RR(Z-Score) x RR(prVFX). 3) Systematic review of gradients of risk for non-DXA techniques. Standardized risk or odds ratios per SD (sRR) derived from prospective studies or cross-sectional studies in which DXA was also measured, were accepted. Evidence was rated according to the Oxford Center for Evidence Based Medicine Criteria. 4) Risk equivalent Z-Scores for these techniques. In the factorial model, risk-equivalent Z-Scores for a non-DXA technique are given by: Z-Score(non-DXA) = ln(sRR(DXA)) / ln(sRR(non-DXA)) x Z-Score(DXA). For weighted combined risk of vertebral and hip fracture Z-Score intervention levels were calculated for 2 scenarios: a) absolute risk equivalent to current DXA T-score=-2.5 (WHO) and b) absolute risk fixed at level equivalent to DXA T-Score=-2.5 at age 70 (fixed). 1)&2) For a Western European woman aged 70 the absolute 10-year risk of hip fracture is 6.3% doubling every 6.3 years of age, with sRR = 2.4 for total femur BMD, and RR of 1.8 and 0.9 if vertebral fractures are present or absent; for vertebral fractures the absolute 10-year risk is 12.2% doubling every 8.1 years of age, with a gradient of risk of 1.9 for total femur BMD, RR of 3.3 and 0.8 if vertebral fractures are present or absent. 3) In the systematic review, 106 articles met the evidence criteria and 43 techniques/variables were graded. 4) The table lists Z-Score intervention levels for scenarios a) (WHO) and b) (fixed) along with level of evidence.

Method (level of evidence)	prVFX	WHO			fixed		
		60yrs	70yrs	80yrs	60yrs	70yrs	80yrs
DXA BMD tot. femur (A)	yes	0.4	0.6	0.7	-1.1	-0.7	-0.4
DXA BMD tot. femur (A)	?	-1.1	-0.7	-0.4	-2.0	-0.7	0.6
DXA BMD tot. femur (A)	no	-1.2	-0.9	-0.7	-2.2	-1.0	0.2
QUS calc Stiffn. Index (B)	?	-1.3	-0.9	-0.6	-2.3	-0.9	0.4

The model allows to estimate absolute risk and calculate intervention levels for different techniques and differently defined intervention levels in a consistent fashion. It can be expanded by interaction terms and more risk factors once robust data become available.

Disclosures: **C.C. Glüer**, None.

1177

Inadequate Vitamin D Status Despite Abundant Sun Exposure. N. Binkley¹, R. Novotny², D. Krueger¹, T. Kawahara-Baccus^{*1}, Y. G. Daida^{*2}, D. Gemar¹, G. Lensmeyer^{*3}, M. K. Drezner¹. ¹University of Wisconsin Osteoporosis Clinical Research Program, Madison, WI, USA, ²Human Nutrition, Food and Animal Sciences, University of Hawaii at Manoa, Honolulu, HI, USA, ³Laboratory Medicine, University of Wisconsin, Madison, WI, USA.

Lack of sun exposure is widely accepted as the cause of epidemic vitamin D inadequacy worldwide. However, a number of studies find that some individuals with seemingly adequate UV exposure have a low serum 25-hydroxyvitamin D (25OHD) concentration. Existing data are confounded by imprecision of the 25OHD assays employed and a lack of assurance that UV exposure was optimal. Therefore, we compared 25OHD status in a group of 100 adults in Honolulu, HI (latitude 21°) with self-reported habitually high sun exposure (3 or more hours, 5 days per week) to that in 174 adults in Madison, WI (latitude 43°), measuring 25OHD with a precise HPLC assay, the results of which correlate well with those obtained by tandem mass spectroscopy (r²=0.9). In the HI group, dietary vitamin D intake and sun exposure were determined by questionnaire and skin color by reflectance colorimetry. The HI population (33 women/67 men) and the WI population (94 women/80 men) had similar age (24.1±0.7 vs. 23.9±0.3 years) and BMI (23.5±0.4 vs. 23.1±0.2). Sun exposure of the HI adults was 21.4±1.5 hours/week. As anticipated, serum 25OHD was higher (p<0.001) in the HI than WI population (31.4±1.0 vs. 18.3±0.8 ng/ml). Surprisingly, the highest 25OHD concentrations were virtually identical in the HI (62.0 ng/ml) and WI (62.3 ng/ml) populations. Moreover, serum 25OHD concentration in the HI group was unrelated to hours of sun exposure or skin color. Additionally, the range of 25OHD levels in the HI population (12-62 ng/ml) broadly overlapped that of the WI population (5-62 ng/ml), suggesting that the vitamin D inadequacy undoubtedly present in the WI population likewise is manifest in the sun-exposed HI population. In fact, serum 25OHD was ≤20 ng/ml in 10% of the HI population, despite sun exposure without use of sunscreen of 23.1±4.9 (range 6-50) hours/week. These data suggest that variable responsivity to UVB radiation is evident among individuals, causing some to have inadequate vitamin D status despite abundant sun exposure. Though counter-intuitive, this possibility is evolutionarily feasible, as the high calcium intake of early humans may have allowed maintenance of optimal calcium balance despite seemingly inadequate vitamin D status. Finally, as the maximal 25OHD concentration produced by natural UV exposure appears to be ~65-70 ng/ml, clinicians prescribing high-dose vitamin D treatment are well-advised to avoid using such therapy in amounts or duration that increase serum 25OHD concentration above this range.

Disclosures: **N. Binkley**, Merck 2, 5, 8; Novartis 2, 5; Roche 8; Pfizer, Aventis, Mission, Eisai 2.

1178

Patients with Hip Fracture Exhibit Bone Micro-Architectural Deterioration Compared to Patients with Colle's Fracture as Assessed with In Vivo High Resolution 3D Micro-pQCT. European Advanced Detection of Bone Quality(ADOQ) Study. M. Zouch^{*}, B. Gerbay^{*}, T. Thomas, L. Vico, C. Alexandre. LBTO, INSERM 366, Saint-Etienne, France.

Osteoporosis is a bone fragility disease due to both low bone mineral density (BMD) and architectural deterioration. However, 3D architectural changes are poorly documented in fractured patients. Therefore, within the European ADOQ Study, we conducted a preliminary survey using a novel 3D pQCT device (XTreme CT, Scanco Medical, Zurich, Switzerland) in post-menopausal women with either hip fracture (HF, n=29; age: 76.1±12.5 yo), Colle's fracture (CF, n=15; age: 70.0±12.2 yo) or no fracture (C, n=30; age: 71.4±5.7 yo). No statistical significant difference in age was observed between the three groups. Measurements were performed up to 6 weeks after fracture. Total Hip BMD (H-BMD) was measured with DEXA (Delphi , QDR 4500, Hologic). Quantitative 3D densitometric parameters in mg/cm³ (Total Bone Density: D100, Cortical Density: DCort and Trabecular Density: DTrab) and qualitative micro-architectural parameters (Trabecular Bone Volume, BV/TV, %, Trabecular Number, Tb.N, /mm, Trabecular Thickness, Tb.Th, mm, Trabecular Separation, Tb.Sp, mm and Cortical Thickness, C.Th, mm) were analyzed at weight-bearing (distal tibia) and non weight-bearing (distal radius) sites. Results were adjusted for BMI since body weight was lower in the HF group. As expected, H-BMD and D100 were significantly reduced at both sites in HF and CF as compared to C. Surprisingly, in CF, we observed a significant decrease in radial DCort as compared to C (31.2±5.3 vs 36.9±6.3; p<0.05) while no cancellous microarchitectural differences were observed at both sites. In contrast, in HF, we observed a significant lower tibial DTrab (5.0±2.0 vs 6.4±1.8; p<0.01) and tibial BV/ TV (42±17.10⁻⁴ vs 53±15.10⁻⁴; p<0.01) as compared to C. In addition, architectural parameters were impaired, with higher Tb.Sp and lower C.Th than in C, at both the radial (467±261.10⁻⁴ vs 276±107.10⁻⁴; p<0.001 and 277±139.10⁻⁴ vs 344±85.10⁻⁴; p<0.05) and tibial sites (380±230.10⁻⁴ vs 231±53.10⁻⁴; p<0.001 and 248±137.10⁻⁴ vs 346±118.10⁻⁴; p<0.01), respectively. In conclusion, 3-D analysis suggests that CF are mainly related to local cortical low mineral density whereas HF are associated with a combination of both trabecular and cortical quantitative and qualitative damages occurring in both weight-bearing and non weight-bearing bones. Further studies are needed to understand the mechanisms leading to such differences which could explain the different responses to therapy observed in these peripheral sites.

Disclosures: **M. Zouch**, None.

1179

AAE581, a Novel Cathepsin K Inhibitor, Protects against Ovariectomy-Induced Bone Loss in Non-Human Primates, in Part by Stimulation of Periosteal Bone Formation. C. Jerome¹, M. Missbach^{*2}, R. Gamse^{*2}.
¹SkeleTech, Bothell, WA, USA, ²Novartis Institutes for BioMedical Research, Basel, Switzerland.

This study was designed to evaluate the effects of AAE581, a highly potent and specific small molecule inhibitor of the osteoclastic enzyme cathepsin K, on bone biomarkers, mass, strength, and histology in the ovariectomized non-human primate model of postmenopausal osteoporosis. Eighty ovariectomized female cynomolgus monkeys (*Macaca fascicularis*) were dosed orally twice daily with vehicle or AAE581 at 3, 10, or 30 mg/kg for 18 months. Twenty sham-ovariectomized animals (SHAM) received vehicle. Serum and urine samples for bone biomarker analysis, DXA measurements of spine and femur, and pQCT measurements of femur neck were collected at baseline and then at 3 or 6 month intervals. Vertebra, femur neck and mid-femur were subjected to biomechanical testing and histomorphometric analysis at 18 months. All groups were compared to ovariectomized control, with p<0.05 considered significant. Serum and urinary biomarkers of bone resorption and formation were significantly increased by ovariectomy. Medium and high doses of AAE581 reduced resorption markers (serum and urinary NTx) to sham levels or below, while maintaining elevation of formation markers (serum osteocalcin and BSAP) above SHAM. BMD and BMC of lumbar spine and femur were significantly lower in ovariectomized than in SHAM animals, and were significantly increased to levels comparable to (spine), or even greater than (femur) SHAM by all 3 doses of AAE581. Femoral neck total BMD was significantly increased to levels greater than SHAM by AAE581 treatment, due to improved BMD in both trabecular and cortical compartments. Vertebral maximum load and stiffness were significantly increased by high dose AAE581, vertebral ultimate strength and elastic modulus by medium and high doses. Vertebral and femoral midshaft BMC were significantly correlated to maximum load. Some (low dose) or most (medium and high dose) histomorphometric indices of bone turnover in vertebra and femoral neck were significantly decreased by AAE581. In contrast, periosteal bone formation rates were significantly increased at both sites by mid and high doses and in mid-femur by low and medium doses of AAE581. In conclusion, AAE581 improved bone mass and strength accompanied by the expected inhibition of bone turnover at most sites, and also had a unexpected stimulatory effect on periosteal bone formation.

Disclosures: C. Jerome, Novartis 2.

1180

Cyclic PTH Stimulates Bone Formation in the Murine Lumbar Vertebrae with A Magnitude Comparable to that Produced by Daily PTH. A. Iida-Klein¹, S. S. Lu¹, F. Cosman², D. W. Dempster¹, R. Lindsay². ¹Regional Bone Center, Helen Hayes Hospital, West Haverstraw, NY, USA, ²Clinical Research Center, Helen Hayes Hospital, West Haverstraw, NY, USA.

In humans, a regimen of repeated 3-month cycles of hPTH[1-34]-on and off (cyclic PTH) was found to be as effective as daily injections of hPTH[1-34] (daily PTH) in increasing vertebral bone mineral density (BMD) at 15 months (Cosman et al., ASBMR, 2003). In mice, an alternating one-week-on and off regimen of daily injections of hPTH[1-34] (cyclic PTH) has been shown to increase femoral BMD, strength and cortical width, as effectively as the daily PTH when improved BMD, strength and cortical width are calculated as a function of the amount of PTH administered (Iida-Klein et al., Endocrine Society, 2005). In order to further explore the potential of cyclical PTH administration, we performed histomorphometric analyses of vertebral bones from 20-week-old female C57BL/6 mice treated with the following regimens: 1) daily injections with vehicle for 7 weeks (control), 2) daily injections with hPTH[1-34] (40 µg/kg/day) for 7 weeks (daily PTH) and 3) daily injections with hPTH[1-34] (40 µg/kg/day) and vehicle alternating weekly for 7 weeks (cyclic PTH). Calcein (10 mg/kg) was injected at 10, 9, 3 and 2 days prior to euthanasia. Histomorphometry was performed on the cancellous and cortical bone of the 2nd lumbar vertebra. Cyclic PTH produced significant increases in BV/TV, trabecular width and number, trabecular osteoblast and osteoclast perimeters, cortical width, mineral apposition rate and bone formation rate, with magnitudes comparable to those of daily PTH (Table 1). Importantly, while the anabolic response was similar in magnitude with both regimens, the total amount of PTH delivered in the cyclic regimen was over 40 % less than that in the daily regimen. The current study supports the potential use of cyclic PTH regimens for the treatment of osteoporosis. Such an approach would have obvious financial benefits and may also improve adherence to PTH therapy.

Table 1 Histomorphometric Analyses of Vertebral Bones

	Unit	Lumbar Vertebra		
		Control	Daily PTH	Cyclic PTH
BV/TV	%	28.2 ± 1.0	46.4 ± 2.6 ^a	39.6 ± 1.8 ^a
Tb.Wi	µm	48.8 ± 2.5	54.1 ± 4.4	51.5 ± 2.8
Tb.N	# / mm ²	5.8 ± 0.3	8.8 ± 0.6 ^b	7.8 ± 0.4 ^b
Tb.OB.Pm	%	7.3 ± 0.8	13.9 ± 0.8 ^b	13.1 ± 0.7 ^b
Tb.OC.Pm	%	3.3 ± 0.3	6.0 ± 0.5 ^a	6.8 ± 0.5 ^a
Ct. Wi	µm	130 ± 9	181 ± 14 ^a	165 ± 9 ^a
Tb.MAR	µm/d	1.11 ± 0.04	1.38 ± 0.06 ^b	1.33 ± 0.05 ^b
Tb.BFR	µm ³ /mm ² /d	0.36 ± 0.03	0.60 ± 0.09 ^b	0.55 ± 0.05 ^a
Ec.MAR	µm/d	0.96 ± 0.17	1.29 ± 0.10	1.21 ± 0.17
Ec.BFR	µm ³ /mm ² /d	0.34 ± 0.06	0.52 ± 0.07	0.48 ± 0.09
Ps.MAR	µm/d	0.29 ± 0.07	0.53 ± 0.12	0.50 ± 0.10
Ps.BFR	µm ³ /mm ² /d	0.04 ± 0.02	0.13 ± 0.06	0.18 ± 0.06

a: p< 0.05, vs. control, b: p<0.01, vs. control

Disclosures: A. Iida-Klein, None.

1181

Skeletal Defects in Ringelschwanz Mutant Mice Reveal that Lrp6 Is Involved in Bone Resorption and Essential for Proper Bone Mass Acquisition. T. Kubota^{*1}, T. Michigami², C. Kokubu^{*3}, A. Suzuki^{*2}, N. Sakai^{*1}, S. Nakajima¹, K. Imai^{*4}, K. Ozono¹. ¹Department of Pediatrics, Osaka University Graduate School of Medicine, Osaka, Japan, ²Department of Environmental Medicine, Osaka Medical Center and Research Institute for Maternal and Child Health, Osaka, Japan, ³Center for Advanced Science and Innovation, Osaka University, Osaka, Japan, ⁴GSF-National Research Center for Environment and Health, Neuherberg, Germany.

Although accumulating studies have shown that low-density lipoprotein receptor-related protein 5 (LRP5) is a key regulator in bone homeostasis, the role of LRP6, another co-receptor for Wnt ligands, in bone metabolism has not been fully elucidated. Here, we present evidence that Lrp6 is involved in bone resorption and required for bone acquisition, using a mouse model with a hypomorphic allele of *Lrp6*. We previously reported that a novel spontaneous mutation *ringelschwanz* (*rs*) in the mouse was caused by a point mutation in *Lrp6*, leading to an amino acid substitution R886W. Homozygous *rs/rs* mice exhibited malformations of vertebral column and spina bifida in the lumbo-sacral region, oligodactyly, and delayed ossification of digits at birth. A genetic complementation test has revealed that *rs* is a hypomorphic *Lrp6* allele. Primary fibroblasts isolated from *rs/rs* mice could not efficiently transduce signals through the Wnt/β-catenin pathway. In the present study, we have further analyzed the bone phenotype in *rs/rs* mice. pQCT analyses on tibiae from 9 and 26-week-old mice revealed the decrease in trabecular density, cortical area, periosteal circumference and endosteal circumference in *rs/rs* mice in both sexes. Bone histomorphometry in 26-week-old female mice showed that bone volume and trabecular number were decreased in *rs/rs* compared with wild-type mice. Unexpectedly, eroded surface was increased in *rs/rs* mice. The cellular basis underlying this low bone mass phenotype in *rs/rs* mice was then studied using primary osteoblasts isolated from the calvariae. The *Rankl* mRNA expression level was markedly increased in osteoblasts from 7-week-old *rs/rs* mice, although it was unaltered in osteoblasts from neonatal *rs/rs* mice. There was no obvious difference in the expression levels of *Opg*, *Lrp6*, and *Lrp5*. The proliferation analyzed by MTS assay and the mineralization *in vitro* were not impaired in osteoblasts from 7-week-old *rs/rs* mice. In summary, *Lrp6* mutant *rs/rs* mice showed the low bone mass phenotype associated with increased bone resorption, and the *Rankl* mRNA expression level was markedly increased in *rs/rs* osteoblasts. These results indicate that Wnt signaling via Lrp6 is involved in bone resorption through osteoblasts.

Disclosures: T. Kubota, None.

1182

Caveolin-1 Deficient Mice Have Bigger Bones. J. Rubin¹, Z. Schwartz², K. Wong^{*2}, L. Wang^{*2}, M. Drab^{*3}, D. Smith^{*4}, H. Jo^{*4}, B. D. Boyan², T. Gross⁵. ¹Emory & VAMC, Decatur, GA, USA, ²Georgia Tech, Atlanta, GA, USA, ³Max Planck, Dresden, Germany, ⁴Emory Univ, Atlanta, GA, USA, ⁵Univ Washington, Seattle, WA, USA.

Caveolin-1 associates with signaling molecules in caveolae of the plasma membrane. It can be predicted that in the absence of caveolin-1 that many signaling pathways will be dysregulated. Caveolin-1 null mice in a C57/B6 background ("Cav-1 null") are viable and fertile, but smaller, leaner and have hyperproliferative lungs and vascular abnormalities. We evaluated the effect of caveolin-1 deficiency on the skeleton. Using micro-CT, we observed clear differences in both cortical and trabecular bone in the morphology of male Cav-1 null femurs by 6 wk of age through at least 9 wk compared to C57 wild type mice. At 7.5 wk, cortical bone area at the femoral mid-diaphysis was increased by 84% (p=0.0003) compared to wild type mice. The increased cortical bone area was achieved through a 44% increase in periosteal area (p=0.0016), which more than compensated for the 20% increase in endocortical area (p=0.06). Trabeculae of the distal femoral metaphysis and epiphysis of Cav-1 null mice demonstrated similar phenotypic alterations compared to wild type mice. Metaphyseal BV/TV was significantly elevated (metaphysis: 340% more than control, p=0.005), trabecular thickness increased (metaphysis: +34%, p=0.02), and trabecular spacing was diminished (metaphysis: -36%, p=0.004). Dynamic histomorphometry supported increased bone formation in both compartments, but also showed decreased trabecular MAR and BFR as well as cortical MAR (59, 52% and 32% of wt, all p<0.05). The skeletal phenotype implies that there has been increased bone formation due to either increased osteoblast proliferation or function; the decreased MAR at 7.5 wk, however, implies that the increased bone formation occurred at an earlier time or, less likely, that osteoclast activity is decreased. That still growing 7.5 wk Cav-1 null skeletons are ~25% larger than those of 16 wk C57 mice ensures a non-transient phenotype. Since the caveolin-1 scaffold can function to inactivate or damp incoming signals it is possible that an osteoprogenitor response to hormonal/mechanical stimuli is enhanced in its absence. Deciphering the etiology of the large bones in this transgenic will require evaluation at several time points, as well as generation of a bone specific Cav-1 knockout, since dysregulation of signaling networks in the global knockout may arise from non-skeletal sources.

Disclosures: J. Rubin, None.

1183

Overexpression of ZFP 521 (MC-33), a 30 Zinc-Finger Δ FosB-Interacting Protein, Induces an Increase in Bone Volume and Bone Formation Rates in Transgenic Mice. M. Wu*, F. Morvan*, J. Zhang*, L. Neff*, W. Philbrick*, W. C. Horne, R. Baron. Cell Biology, Yale University, New Haven, CT, USA.

A cell autonomous effect of overexpressed Δ FosB on osteoblast differentiation and bone formation leads to a severe and progressive osteosclerosis in transgenic mice. We previously identified ZFP 521 (formerly MC-33) as a novel Δ FosB-interacting protein in a yeast two-hybrid screen of an osteoblast library. ZFP 521 is a 180 kDa protein with 30 C2H2 Kruppel-like zinc fingers, which localizes to the nucleus. In adult mice, ZFP 521 was strongly expressed in brain, heart, lung, and skeletal muscle and at lower levels in fat, spleen, kidney and liver. ZFP 521 is expressed at high levels in primary calvarial osteoblasts. *In situ* hybridization studies demonstrated that ZFP 521 mRNA was expressed during bone development in mesenchymal condensations, in the preosteoblastic layers, and in the growth plate. *In vitro*, ZFP 521 mRNA was downregulated by osteogenic (BMP-2) or adipogenic agents (indomethacin, hydrocortisone and IBMX). Further, transient transfection of ZFP 521 into C3H10T1/2 and MC3T3-E1 cells suppressed the Δ 2 Δ FosB-induced increase in Runx2 expression, and stable overexpression in the same cells reduced alkaline phosphatase activity to background. In addition, ZFP 521 inhibited the activation of Runx2 and osteocalcin promoters by Runx2 in luciferase assays. In order to examine the *in vivo* role of ZFP 521, we generated transgenic mice that overexpressed ZFP 521 under the control of either the enolase 2 (NSE) or the osteocalcin (OG2) promoter. ZFP 521 overexpression *in vivo* resulted in a two-fold increase in bone volume with an increase in osteoblast number and osteoid volume. Dynamic bone formation parameters such as mineral apposition rate and bone formation rate were increased by three-fold. Von Kossa staining of *ex vivo* cultures of primary osteoblasts from OG2-ZFP 521-overexpressing mice demonstrated an increase in nodule formation and mineralization. In contrast, cultures of primary osteoblasts from NSE-ZFP 521 mice exhibited decreased nodule formation and mineralization. Given that 1/ The OG2 promoter is activated late in osteoblast differentiation; 2/ The exogenous NSE promoter is activated both early and late; 3/ Runx2 exerts opposite effects on early and late stages of osteoblast differentiation and 4/ ZFP 521 represses Runx2 transcriptional activity, we propose that ZFP 521 acts as a Runx2 repressor, inhibiting early stages of osteoblast differentiation while favoring osteoblast differentiation and bone formation when expressed during later stages.

Disclosures: **M. Wu**, None.

1184

The Transcription Factor EBF-1 Regulates Osteoblast and Adipocyte Development. D. G. T. Hesslein*¹, Y. Xi¹, S. Zhou*¹, C. M. Gundberg¹, R. Grosschedl^{*2}, J. A. Lorenzo³, D. G. Schatz*¹, M. C. Horowitz¹. ¹Yale University, Howard Hughes Medical Institute, New Haven, CT, USA, ²Max-Planck Institute, Freiburg, Germany, ³University of Connecticut, Farmington, CT, USA.

A regulatory network comprised of transcription factors control B cell fate specification. Two of these factors, PU.1 and Pax5, also regulate osteoclast development. Early B Cell Factor-1 (EBF-1) is another member of this network that has been shown to be essential for B cell differentiation. Interestingly, EBF-1^{-/-} mice are runted and have a reduced life span. We analyzed the bone phenotype of EBF-1 homozygous mutant (-/-) and wild-type (+/+) mice by histomorphometry and biochemistry. Spleen and bone marrow cells (BM) were used as sources of osteoclast precursors. Tibia from -/- mice had a striking increase in osteoblasts lining bone surfaces (>85%), at both 4 and 12 weeks of age (p<.01). Consistent with this was a 29% increase in osteoid thickness and a 185% increase in the bone formation rate (p<.001). This correlated with a 2 fold increase in serum osteocalcin (p<.001). However, *in vitro* proliferation and alkaline phosphatase activity of -/- osteoblasts did not differ from control. In contrast, osteoclast number was similar in 4 week-old +/+ and -/- mice; however, at 12 weeks the number of osteoclasts was more than twice that of controls (p<.0001). Culture of BM from 4 week-old -/- but not 12 week-old mice with M-CSF + RANKL consistently yielded less osteoclasts than controls. These data correlated with a 72% increase in bone volume at 12 weeks of age (p<.01). The most striking aspect of the EBF-1^{-/-} bones was the presence of adipocytes, which filled the marrow space. Unusually, adipocytes also filled the marrow space in the secondary center of ossification. Like the increased number of osteoblasts, the adipocytes in the marrow were present at both 4 and 12 weeks of age. Oil-red-O staining confirmed the increased fat deposition in BM smears. Increased adiposity was also seen histologically in the liver but not the spleen of -/- mice. Importantly, EBF-1 mRNA was expressed in pre-confluent, confluent and post confluent wild-type osteoblasts and in adipocytes. These data imply that the increased bone mass in mutant mice resulted from an increase in the number of osteoblasts and not from insufficient or defective osteoclasts. Loss of EBF-1 caused a pronounced, site-specific change in adipogenesis and fat deposition. Therefore, EBF-1^{-/-} mice may be a new model of lipodystrophy. The phenotype of EBF-1^{-/-} mice is distinct from that of either PU.1 or Pax5 deficient mice. The expression of EBF-1 in osteoblasts and in adipocytes and the distinct bone phenotype in EBF-1^{-/-} mice identifies EBF-1 as a novel regulator of osteoblast and adipocyte development.

Disclosures: **D.G.T. Hesslein**, None.

1185

The Homeoprotein Engrailed-1 Has Pleiotropic Functions in Calvarial Intramembranous Bone Formation. R. A. Deckelbaum¹, A. Majithia^{*1}, T. Booker^{*1}, J. E. Henderson², C. A. Loomis^{*1}. ¹Pathology, New York University, New York, NY, USA, ²Centre for Bone & Periodontal Research, McGill University, Montreal, PQ, Canada.

Recent studies have identified a growing number of homeodomain transcription factors as critical regulators of cranial intramembranous bone formation. Our unpublished observations have suggested a possible role for the homeoprotein Engrailed-1 (En1) in craniofacial development. In the present study we aimed to define the craniofacial expression of *En1* and investigate its regulatory functions during skull vault ossification. Using a *lacZ* reporter mouse strain, we show that *En1* expression initiates at embryonic day 11.5 (E11.5) within the skeletogenic mesenchyme of the primordial frontal and parietal bones, and subsequently expands into all facial and cranial vault mesenchyme. During overt osteogenesis (E14.5-E18.5) *En1* is expressed by calvarial osteoblasts and cells of the suture mesenchyme. Neonatal *En1*^{-/-} mice exhibit generalized calvarial bone hypoplasia and sutural patency, displaying prominent posterior-frontal foramina. Micro computerized tomography (microCT) analysis confirms that calvarial bones of *En1* mutants are osteopenic (BV/TV: Wt=3.460 ±0.4033, n=8; *En1*^{-/-}=2.205 ±0.3031, n=6; *p*=0.0301), exhibit increased trabecular spicule separation (Tb.Sp.: Wt=0.7007 ±0.05129, n=8; *En1*^{-/-}=0.8362 ±0.02945, n=6; *p*=0.0448), and show reduced osteoid mineralization. Assessment of osteogenic differentiation *in vivo* and in cultured calvarial osteoblasts indicates that *En1* regulates the onset of *osteopontin* and *osterix* expression and is later essential for the osteoblastic expression of *bone sialoprotein* and *osteocalcin*. In addition, BrdU incorporation analysis suggests a role for *En1* in regulating sutural osteoprogenitor proliferation. Ongoing studies are beginning to unravel a regulatory interplay between *En1* and the FGF/MAPK signaling pathway in osteoblasts. To examine the possibility that the calvarial osteopenia in *En1* mutants may result in part from increased bone resorption we performed histomorphometric analysis of TRAP⁺ osteoclasts. Significantly, we observed increased numbers of osteoclasts in *En1*^{-/-} calvariae that were also more widely distributed by comparison to their wt counterparts. Consistent with this observation, we show that *En1*-null osteoblasts upregulate the expression of receptor activator of NFκB ligand (RANKL) while maintaining normal *osteoprotegerin* expression. In summary, this study identifies *En1* as a novel cell-autonomous modulator of calvarial osteoblast differentiation, which also plays a non cell-autonomous role in regulating osteoclast recruitment and/or activation.

Disclosures: **R.A. Deckelbaum**, None.

1186

Regulation of Osteoblast Differentiation by Dlx5 in Transgenic Mice. H. Chin^{*1}, H. Li^{*1}, C. L. Wang^{*2}, A. C. Lichtler¹. ¹Genetics and Developmental Biology, University of Connecticut Health Center, Farmington, CT, USA, ²Transgenic Core Facility, Institute of Molecular Biology, Academia Sinica, Taipei, Taiwan Republic of China.

The *Dlx5* gene encodes a DNA-binding homeobox protein, which acts as a transcription factor and is expressed in many developing tissues. Previous studies have shown that *Dlx5* induces osteoblast differentiation *in vitro*, *Dlx5* knockout mice show delayed calvarial ossification, and that blocking *Dlx* gene signaling inhibits induction of many of the genes induced by BMPs in osteoblastic cells. These results indicate that activation of *Dlx5* is probably an important event for cells entering the osteogenesis pathway. To explore the role of *Dlx5* in regulating osteoblast differentiation *in vivo*, we generated transgenic mice over-expressing *Dlx5* using the bone-directed 1.7 kb and 3.6 kb rat type I collagen promoters. The 1.7 kb promoter drives expression primarily in differentiating osteoblasts, while the 3.6 kb promoter is expressed at earlier stages of osteoblast lineage progression, as well as other type I collagen expressing cells. Most *Coll(1.7)-Dlx5* mice die perinatally due to difficulties in breathing, and the survivors usually have generally mild phenotypes. The bones are generally well ossified, but are significantly malformed. On the other hand, *Coll(3.6)-Dlx5* mice are grossly smaller with severe bone phenotypes. *Coll(3.6)-Dlx5* mice usually suffer from malocclusion and twisted axial bones. Whole mount Alizarin Red and Alcian Blue staining of the mutant mice revealed multiple bone morphogenesis defects, including rib and vertebrae patterning abnormalities, craniofacial and long bone abnormalities, inner ear defects, and teeth problems. Comparing *Coll(3.6)-Dlx5* mice to the wildtype by histology, the trabecular bone is significantly reduced and the growth plate is less organized. In summary, our data demonstrate that overexpression of *Dlx5* significantly interferes with the development of axial bones, and can lead to a low bone mass phenotype in long bones. These bone phenotypes may be due to improper induction of osteoblast differentiation. Further analysis will focus on histology and histomorphometry, to evaluate the hypothesis that early expression of *Dlx5* causes premature induction of osteoblast differentiation leading to insufficient numbers of mature osteoblasts, while later expression of *Dlx5* promotes osteoblastic differentiation.

Disclosures: **H. Chin**, None.

1187

Smurf1 Mediates Runx2 Degradation through a Smad6-Dependent Mechanism. R. Shen, M. Chen, R. J. O'Keefe, D. Chen. Orthopaedics, University of Rochester, Rochester, NY, USA.

Runx2 is a bone-specific transcription factor that plays a critical role in bone development, postnatal bone formation, and chondrocyte maturation. In previous studies, we discovered that the E3 ubiquitin ligase Smurf1 mediates Runx2 degradation in an ubiquitin-proteasome-dependent manner. Over-expression of Smurf1 in osteoblasts inhibits osteoblast differentiation. In transgenic mice in which Smurf1 transgene is targeted to osteoblasts using the murine type I collagen promoter (2.3 kb), bone formation and osteoblast function are inhibited, demonstrating that Smurf1 plays an important regulatory role in osteoblast function and bone formation. In the present studies, we investigate the molecular mechanism by which Smurf1 mediates Runx2 degradation. Smurf1 is a Hect domain E3 ubiquitin ligase and interacts with the PY motif of substrate proteins. A conserved PY motif has been identified in all Runx family members. To determine if Smurf1 induces Runx2 degradation through direct binding to Runx2, we created a mutant Runx2 with a PY motif deletion and found that Smurf1 retained its activity to induce Runx2 degradation even when the PY motif of Runx2 is deleted. These results suggest that Smurf1 mediates Runx2 degradation through an indirect mechanism. It has been reported that Smurf1 interacts with Smads 1, 5, 6 and 7 and Smads 1 and 5 also interact with Runx2. We then determined if Smads 1 and 5 mediate Smurf1-induced Runx2 degradation and found that Smads 1 and 5 had no effect on Smurf1-induced Runx2 degradation. Although Smads 6 and 7 bind Smurf1 and co-localize with Smurf1 in the nucleus, it is not known if Smads 6 and 7 interact with Runx2 and mediate Runx2 degradation. We performed immunoprecipitation (IP) assays and found that Smad6 but not Smad7 interacts with Runx2. Smad6 enhances Smurf1-induced Runx2 ubiquitination and degradation in a dose-dependent manner and the effect of Smad6 on Runx2 degradation is completely abolished by the proteasome inhibitor PS-1, indicating that Smad6-mediated Runx2 degradation is ubiquitin-proteasome-dependent. These results demonstrate that Smurf1-mediated Runx2 degradation is Smad6-dependent and this degradation can serve as a negative regulatory mechanism for BMP-Smad-Runx2 signaling pathway.

Disclosures: **R. Shen**, None.

1188

Involvement of MT1-MMP and ADAM10 in RANKL Shedding. A. Hikita¹, I. Yana^{*2}, M. Seiki^{*2}, K. Nakamura¹, S. Tanaka¹. ¹Orthopaedic Surgery, The University of Tokyo, Tokyo, Japan, ²The Institute of Medical Science, The University of Tokyo, Tokyo, Japan.

Receptor activator of NF- κ B ligand (RANKL) is a member of tumor necrosis factor family cytokines, which plays essential roles in osteoclast differentiation and activation. RANKL is a type II integral transmembrane glycoprotein and known to undergo proteolytic release from the plasma membrane. Several proteinases such as tumor necrosis factor α converting enzyme (TACE), membrane-type1 matrix metalloproteinase (MT1-MMP) and a disintegrin and metalloproteinase (ADAM) 19 have been shown to possess RANKL shedding activity, but no definite RANKL sheddases have been identified yet. To identify molecules implicated in RANKL shedding, we developed an assay system using plasmids encoding SEAP (secreted placental alkaline phosphatase) fused with partial cDNA of mouse RANKL containing stalk region. The RANKL-SEAP plasmid was transfected into 293T cells together with various MMP and ADAM expression vectors, and the RANKL-shedding activity of these proteinases was detected as alkaline phosphatase activity in the supernatants. Among these proteinases, MT1-MMP and ADAM10 had relatively strong RANKL shedding activity. Soluble RANKL was recovered by osteoprotegerin-Fc, and subjected to Western blotting analysis with anti-RANKL antibody. Soluble RANKL was detected as two bands, suggesting that the cleavage occurred at two different sites. Introduction of RNA interference (RNAi) of MT1-MMP and ADAM10 resulted in the disappearance of the lower molecular weight band, and the reduction in the higher molecular weight band, respectively. Suppression of RANKL shedding with RNAi in osteoblasts resulted in an increase in the level of membrane-bound RANKL, and promoted osteoclastogenesis in co-cultures with spleen cells. In addition, osteoblastic cells obtained from MT1-MMP-deficient mice induced osteoclast differentiation in cocultures more efficiently than normal osteoblasts. In conclusion, at least two RANKL shedding enzymes with different cleavage sites exist, and MT1-MMP and ADAM10 are possible candidates of RANKL sheddase in osteoblastic cells. Further analyzing the role of these proteinases using knock-out mice will lead to clarification of the biological and pathological meaning of RANKL shedding in vivo.

Disclosures: **A. Hikita**, None.

1189

Osteoblast Specific Overexpression of Human Interleukin-7 Rescues the Bone Phenotype of Interleukin-7 Deficient Female Mice. S. Lee¹, J. Kalinowski^{*1}, D. J. Adams², H. L. Aguila^{*3}, J. A. Lorenzo¹. ¹Medicine, University of Connecticut Health Center, Farmington, CT, USA, ²Orthopaedic Surgery, University of Connecticut Health Center, Farmington, CT, USA, ³Immunology, University of Connecticut Health Center, Farmington, CT, USA.

Interleukin-7 (IL-7) is a potent stimulator of B and T lymphocytes and a direct inhibitor of *in vitro* osteoclastogenesis in murine bone marrow cultures. We previously reported that IL-7 deficient (KO) mice had significantly decreased trabecular bone mass and increased *in vitro* osteoclast (OCL) formation compared to wild type (WT) mice. To determine if the alteration in bone mass and osteoclast formation in KO mice can be rescued, we crossed

KO mice with mice that had targeted IL-7 production in osteoblasts (Tg). Tg mice contained a transgene, which used the rat 2.3 kb Col1A1 promoter to drive human IL-7 expression. We found an increase in early B cells (B220/IgM) in the bone marrow of Tg mice (WT = 21.3%, Tg = 48.9%), which is a known effect of IL-7. In contrast, KO mice had minimal bone marrow B-lymphopoiesis (KO=2.1%). However, KO mice that overexpress IL-7 in bone (KO/Tg) had normal early B cells development (KO/Tg=22.6%). To explore if the effect of IL-7 was limited only to bone, we examined the T cell populations in the thymus of these mice. Thymic cellularity was not affected by the IL-7 transgene but was decreased in KO mice (WT=19.0 \pm 0.82; Tg=14.5 \pm 1.50; KO=0.18 \pm 0.09; KO/Tg=0.17 \pm 0.18) confirming the specificity of IL-7 production in Tg mice. Micro-CT analyses of 8-9 week old male and female mice showed significant differences in trabecular bone mass only in KO females, which had a 24% decreased ($p<.05$) in this parameter (WT= 10.1 \pm 0.7%; KO=7.7 \pm 0.8%). KO/Tg mice had trabecular bone mass equivalent to that of WT (KO/Tg=9.6 \pm 0.6%). To investigate if locally produced IL-7 had effects on OCL formation *in vitro*, we cultured bone marrow cells from WT, KO and KO/Tg with M-CSF and RANKL for 4 days. Bone marrow cultures from KO mice showed increased osteoclast formation in cells from both males and females (45% to 51% increase, $p<.01$) compared to WT littermate cells. However, bone marrow cells from KO/Tg mice showed OCL formation both in males and females that was similar to that seen in WT cells (WT=293 \pm 9; KO=428 \pm 119; KO/Tg=288 \pm 13 in males, WT=201 \pm 8; KO=304 \pm 9; KO/Tg=194 \pm 11 in females). These findings demonstrate that targeted expression of IL-7 in osteoblasts rescues the bone phenotype of IL-7 KO mice. In addition, in KO mice bone mass differed from that of WT only in females. These results likely reflect both a direct inhibitory effects of IL-7 on osteoclastogenesis *in vivo* and gender-specific differences in responses to IL-7.

Disclosures: **S. Lee**, None.

1190

Cardiotrophin-1 Regulates Osteoclast Formation and Function in an Essential Manner Distinct from other gp130 Cytokines. N. A. Sims¹, J. M. W. Quinn², H. Saleh^{*2}, T. Martin². ¹Department of Medicine at St. Vincent's Hospital, The University of Melbourne, Fitzroy, Australia, ²St. Vincent's Institute, Fitzroy, Australia.

The gp130 family of cytokines, (IL-6, IL-11, CNTF, Oncostatin M, LIF and Cardiotrophin-1 (CT-1)) all signal by forming a receptor complex including the common gp130 receptor subunit. Previous work has shown that gp130 is required for normal osteoclastogenesis; in gp130 null mice there is a dramatic reduction in trabecular bone mass due to increased osteoclast generation *in vivo* and *in vitro*, which contrasts with the stimulatory effects of gp130 family members on cultured osteoclasts. Mice rendered null for IL-11R, IL-6 and LIF-R all have unique bone phenotypes, which suggest distinct signaling pathways induced by the cytokine-specific receptor complexes formed. In this study, we examined the skeletons of CT-1 null mice to determine its unique contribution to normal bone structure and bone cell function. In adult males, CT-1 null mice demonstrated a significant increase in trabecular bone volume measured by histomorphometry (increased by 229%) and trabecular BMD by pQCT (increased by 31%) compared with wild type controls. Histomorphometric markers of bone formation were unchanged by the CT-1 null mutation. The increase in bone mass was associated with an increased number of osteoclasts, and these were abnormally large. Osteoclast surface and number were approximately doubled and the amount of bone surface covered by each osteoclast was significantly elevated. However, these large osteoclasts appeared to be functionally impaired, suggested both by the increased bone mass, and by an increase in cartilage remnants within the trabecular bone of the CT-1 null mice. The increased osteoclastogenesis observed in CT-1 null mice appeared to be cell-lineage specific. Stimulation of CT-1 null bone marrow cultures with RANKL and M-CSF led to a significant elevation in osteoclast number in comparison with wild type marrow. As observed *in vivo*, the osteoclasts generated were larger, and with more nuclei than osteoclasts generated from wild type mice. This phenotype is distinct from knockouts of all other gp130 family members described to date. CT-1 is therefore essential for normal osteoclastogenesis and osteoclast function, and is unique in its actions on gp130 signaling. The high bone mass observed with CT-1 gene ablation in the presence of increased osteoclastogenesis suggests that inhibition of CT-1 signaling may provide a unique therapeutic target for inhibiting bone resorption.

Disclosures: **N.A. Sims**, None.

1191

Over-Expression of Dkk-1 in Osteoblasts Reduces Bone Mass but Does not Alter the Anabolic Response to Intermittent PTH Treatment in Mice. G. O. Yao, J. J. Wu^{*}, N. Troiano^{*}, M. Bartkiewicz, B. H. Sun, K. Insogna. Yale University, New Haven, CT, USA.

Gain-of-function mutations in LRP5 increase bone mass in part by conferring resistance to the inhibitory actions of Dkk-1. Increased expression of Dkk-1 by malignant plasma cells has been reported as the basis for reduced bone formation in multiple myeloma. These findings suggest that Dkk-1 suppresses bone formation *in vivo*. PTH is a potent anabolic agent, but the cellular mechanism by which it increases bone mass is unknown. We sought to determine if Dkk-1 and PTH interact in regulating bone mass. PTH treatment of primary murine osteoblasts for 24 hours reduced Dkk-1 expression by 90% as quantified by real-time PCR. To directly determine whether Dkk-1 modulates PTH's anabolic response *in vivo*, we engineered transgenic (TG) mice expressing murine Dkk-1 under the control of the 2.3-kb rat collagen alpha-1 promoter. We studied one of two transgenic lines in which Dkk-1 expression was increased 4- to 5-fold over endogenous levels. Using DEXA, we found that TG mice had significantly reduced bone mass (-7.3%), which was accompanied by reduced histomorphometric parameters of bone formation (reduced OV/TV, ObS/OS

and NoB/TAR). Trabecular thickness and number were significantly reduced and TbSp was increased as compared to control animals. Treatment of TG and wild-type (WT) littermates with 95 ng/g body-weight of h(1-34) PTH for 34 days resulted in comparable increases in bone mass at all skeletal sites. In the spine, bone mass increased by 9% in the PTH-treated WT mice and by 2% vehicle-treated WT mice. In TG mice the increases were 17%, and 4% respectively. PTH induced increases in bone density in the femur and the body as a whole were also comparable in TG and WT animals. We conclude that: (1) Continuous exposure to PTH *in vitro* suppresses Dkk-1 expression in primary murine osteoblasts. Whether this occurs with intermittent PTH treatment *in vivo* is under investigation. Since PTH has been reported to suppress the rat collagen 1 promoter *in vitro* it is possible that it also suppressed the transgene in our mice. (2) Over-expression of Dkk-1 in osteoblasts *in vivo* suppresses bone formation and reduces bone mass, consistent with the conclusion that Dkk-1 is an important negative regulator of bone mass. (3) The anabolic response to PTH is unaltered in TG mice that over-express Dkk-1 in osteoblasts. Whether this reflects the site of expression of Dkk-1 or the ability of intermittent PTH to circumvent or overcome the negative regulatory effects of Dkk-1 on bone anabolism is an important area for further study.

Disclosures: **G.Q. Yao**, None.

1192

Abnormal Axial Skeleton in TGF-Beta Type I Receptor-Deficient Mice. K. Torigoe^{*1}, M. Ishijima¹, T. Nakamura^{*1}, N. Haruyama^{*2}, A. B. Kulkarni^{*2}, S. Karlsson^{*3}, Y. Yamada^{*1}. ¹NIDCR, CDBRB, Molecular Biology Section, NIH, Bethesda, MD, USA, ²NIDCR, CDBRB, Functional Genomics Section, NIH, Bethesda, MD, USA, ³Molecular Medicine and Gene Therapy, Lund University, Lund, Sweden.

Transforming growth factor beta (TGF-β) initiates its diverse cellular responses during development and pathogenesis by binding to a specific cell surface complex consisting of TGF-β type I (TβRI/Alk5) and type II (TβRII) receptors, and activating downstream signaling through Smad and MAPK proteins. TGF-β has been implicated in the growth and differentiation of chondrocytes. For example, TGF-β transduces its signal through a MEK-ERK-Erk1 pathway to regulate chondrocyte proliferation. TGF-β induces aggrecan expression in chondrogenic cell lines. While TGF-β enhances chondrocyte proliferation, it inhibits the terminal differentiation of chondrocytes and helps them remain in the prehypertrophic stages. In response to TGF-β, ATF2 is phosphorylated via the activation of p38 MAP kinase. The phosphorylated ATF2 cooperates with Smad3 to inhibit the rate of chondrocyte maturation. To study the role of TGF-β signaling in cartilage development and disease, we have created cartilage-specific conditional knockout mice for TGF-β receptor type I by mating floxed-*TβRI* mice with *Col2a1cre* transgenic mice which express cre recombinase specific to cartilage under the control of the type II collagen promoter and enhancer. The conditional knockout mice with the cartilage-specific *TβRI* deficiency were perinatally lethal. We found that in the mutant mice, development of the axial cartilage in the spine and skull was impaired, while appendicular cartilage was relatively normal. The upper portion of the vertebrae was more severely disorganized and herniated than the lower portion. The formation of intervertebral disks was defective, and segmentation of the upper vertebrae was disrupted. Although chondrocytes were differentiated, histological staining indicated significantly reduced extracellular matrix and GAG (glycosaminoglycan) levels in mutant vertebral cartilage than wild-type cartilage. Perichondrium cells migrated into cartilage at the herniation site, suggesting a reduced strength of mutant cartilage. Mechanical force may cause the position-dependent and disproportionate abnormality of the vertebrae. Currently, the molecular mechanisms that cause axial skeleton defects are under investigation.

Disclosures: **K. Torigoe**, None.

1193

Temporal Deletion of the Hepatic IGF-I Gene at 4 weeks of Age Has a Dramatic Effect on Acquisition of Cortical and Trabecular Bone. S. Yakar¹, D. LeRoith¹, C. Rosen², M. Bouxsein². ¹NIDDK, Bethesda, MD, USA, ²The Jackson Laboratory, Bar Harbor, ME, USA.

Earlier studies established that circulating IGF-I was related to BMD. Using the *Cre-Lox P* technology, we generated liver-specific IGF-I gene deleted mice (LID) with a 75% reduction in circulating IGF-I, but no change in skeletal IGF-I expression. At 12 wks of age, LIDs had reduced: femur length, periosteal circumference, femoral cross sectional area and cortical thickness vs controls. Since peak cortical BMD is attained between 4-8 wks, we sought to determine how low circulating IGF-I during maximal bone accrual could affect trabecular and cortical compartments. We generated a tamoxifen (Tx) inducible LID mouse (i-LID/Cre) which carries two floxed alleles of the IGF-I gene and the Cre recombinase under the antitrypsin 1α promoter; this promoter can be induced by Tx injection. Control mice (i-LID) carry the floxed alleles of the IGF-I gene but do not express the Cre recombinase; hence injection of Tx should not lower serum IGF-I. Blood was drawn before Tx injections, at 4 wks and at 8 wks; bones and livers were harvested. Hepatic IGF-I mRNA was assessed by RNase protection assay to confirm IGF-I gene recombination in iLID/Cre injected with Tx. Serum IGF-I are noted:

Strain n	Tamoxifen	4 wk serum IGF-I	8 wk serum IGF-I p vs 4wk
i-LID 4	-	394±14 ng/ml	304±28.4 ng/ml p=0.10
i-LID +Tx 6	+	351±10 ng/ml	219±10 ng/ml p=0.05
i-LID/Cre+Tx 4	+	380±15 ng/ml	46.0±2.4 ng/ml p<0.0001

No differences in bone length were observed. Total mid-femoral cross-sectional area was greater in i-LID>i-LID+Tx >i-LID/Cre+Tx (p=0.007 and p=0.05 respectively). Cortical thickness was also lower in i-LID/Cre+Tx than the other two groups (p<0.02). Tx alone slightly reduced IGF-I and total cortical area. Surprisingly, femoral BV/

TV was ordered exactly the opposite of the cortical parameters: i-LID/Cre+Tx>i-LID>iLID+Tx; p<0.005; as such, there was a 40 % increase in trabecular BV/TV in i-LID/Cre+Tx mice vs controls (i-LID) treated with Tx. In sum, 1) temporal deletion of the liver IGF-I gene causes a marked decline in circulating IGF-I; 2) 4 wks after reducing serum but not skeletal IGF-I, there is a significant reduction in cortical bone area and thickness; and 3) trabecular bone volume fraction increases in response to very low serum IGF-I, a phenotype similar to IGF-I null mice. In conclusion, this unique system in which serum, but not skeletal IGF-I can be manipulated in mice, establishes the importance of circulating IGF-I during peak bone acquisition. The mechanism driving increased trabecular BMD in IGF-I deficient mice needs further study.

Disclosures: **C. Rosen**, NIH AR45433 2.

1194

Direct (IGF-1 Independent) Actions of Growth Hormone in Osteoblasts Identified through Cre/Lox Disruption of the IGF-1 Receptor. D. J. DiGirolamo^{*1}, A. Mukherjee^{*1}, Y. Wang^{*1}, X. Liu^{*1}, S. J. Frank^{*2}, T. L. Clemens¹. ¹Department of Pathology, University of Alabama at Birmingham, Birmingham, AL, USA, ²Department of Medicine, University of Alabama at Birmingham, Birmingham, AL, USA.

Growth hormone (GH) is one of the most important factors controlling bone growth and mass, yet the cellular targets and mechanisms of action of GH in bone remain unclear. The principal difficulty in studying GH action is the fact that GH stimulates insulin-like growth factor-1 (IGF-1) production, making it impossible to distinguish actions due to GH versus those resulting indirectly through IGF-1. To define *direct* actions of GH in bone, we utilized mice which lack the IGF-1 receptor (ΔIGF-1R) in osteoblasts, developed using Cre/Lox recombination. Growth hormone treatment of bone marrow stromal cells from wild type mice promoted the formation of CFU-OB and inhibited adipogenic markers, whereas stromal cells from ΔIGF-1R mice failed to differentiate normally. To examine signaling and function of GH in mature osteoblasts, calvarial osteoblasts from mice homozygous for the floxed IGF-1 allele (IGF-1^{lox/lox}) were infected with adenoviral vectors expressing Cre (Adeno-Cre). Knockdown of the IGF-1R mRNA (>90%) was accompanied by a near elimination of IGF-1 stimulated IRS-1 phosphorylation but retention of GH mediated JAK-2/STAT-5 phosphorylation. Growth hormone induced JAK-2/STAT-5 activation was consistently greater in osteoblasts with an intact IGF-1R, suggesting that although the receptor is not required for GH signaling, its presence may allow GH to activate its signaling pathways more effectively. To identify GH actions, we compared the effects of GH and IGF-1 on proliferation (MTT) and staurosporine induced apoptosis (TUNEL and Bax expression). In these studies, the ability of GH to increase osteoblast proliferation was abolished by removal of the IGF-1R, suggesting that GH increases osteoblast proliferation primarily by inducing IGF-1 production. In contrast, GH inhibited apoptosis even in cells lacking the IGF-1R, demonstrating that the anti-apoptotic actions of GH do not require IGF-1 signaling. However, the anti-apoptotic effect of GH was more pronounced in cells expressing the IGF-1R consistent with the idea that GHR and IGF-1R act in a synergistic fashion. In conclusion, these studies identify, for the first time, *direct* actions of GH on osteoblasts and validate a model system for further study of the GH/IGF-1 axis in bone.

Disclosures: **D.J. DiGirolamo**, None.

1195

Cooperative Signaling by Fibroblast Growth Factor Receptor 1 and 2 Is Required for Craniofacial Development. H. Kanazawa¹, K. Yu^{*1}, I. H. Hung^{*1}, A. Jacob^{*1}, J. M. Partanen^{*2}, D. M. Ornitz^{*1}. ¹Molecular Biology and Pharmacology, Washington University Medical School in St. Louis, St. Louis, MO, USA, ²Institute of Biotechnology, University of Helsinki, Helsinki, Finland.

Many craniosynostosis syndromes are caused by mutations in Fibroblast Growth Factor Receptors (FGFR) 1 and 2. In addition to craniofacial abnormalities, these patients often have short stature and malformations of the hands and feet. Although FGFR1 and FGFR2 each have important roles in skeletal development and are expressed in partially overlapping patterns, redundancy between these receptors is poorly defined. To address the combined affect of loss of function of both genes on craniofacial development, we have generated *Fgfr1/Fgfr2* double conditional knockout mice (DCKO) with *Dermo1*-cre and *Wnt1*-cre targeting alleles. *Dermo1*-cre DCKO mice have a much more severe phenotype than either single receptor conditional knockout. Significantly in *Dermo1*-cre DCKO mice, the frontal bones were much smaller and the sagittal suture was greatly expanded. These mice also had a hypoplastic squamous bone, missing tympanic rings, shortened or truncated zygomatic arch, and a shortened and malformed mandible. In contrast, temporal bones of DCKO mice were relatively normal. By whole mount in situ hybridization the expression level of *Osteopontin* in E16.5 and E.17.5 calvaria was elevated in *Dermo1*-cre DCKO in the frontal bone area compared to controls. These data suggested a specific role of FGFR1 and 2 signaling on cranial neural crest cells that contribute to cranial bones. Then thus generated *Wnt1*-cre DCKO mice to analyze the impact of FGFR 1 and 2 signaling on cranial neural crest cells. *Wnt1*-cre DCKO mice revealed a very dramatic phenotype: the frontal bone was very small, and the facial region was severely truncated. In conclusion, FGFR 1 and 2 signaling shows significant redundancy and preferentially affects cranial neural crest-derived cells.

Disclosures: **H. Kanazawa**, None.

1196

RANKL/RANK Expression Is Essential for TNF-Induced Joint Erosion and Inflammation *In Vivo*, but not for TNF-Induced Osteoclast Formation *In Vitro* where NF- κ B Expression Is Essential. L. Xing, Z. Yao, Q. Zhang, P. Li, E. Schwarz, B. Boyce. University of Rochester, Rochester, NY, USA.

Two major controversies regarding the RANKL/RANK pathway in TNF-mediated erosive bone loss are: 1) must osteoclast (ocl) precursors be primed by RANKL before TNF can induce them to form ocls; and 2) does this pathway regulate not only osteoclastogenesis, but also inflammation in TNF-induced arthritis? To address the first issue, we treated spleen cells from either RANKL^{-/-} or RANK^{-/-} mice with TNF and M-CSF and found that both formed numerous TRAP⁺ ocls (65 \pm 1 and 69 \pm 14/well, vs 90 \pm 12 from wt cells). These ocls expressed calcitonin receptors and resorbed bone slices (pits area: 0.52 \pm 0.02 and 0.6 \pm 0.1 mm² in TNF- vs 0 \pm 0 in PBS-treated cells). In contrast, TNF did not induce ocls from splenocytes from NF- κ B p50/p52^{-/-} mice, but when NFAT 1 or 2 was over-expressed in these cells by retroviral infection, ocls formed in response to TNF (61 \pm 5 and 71 \pm 17 ocls/well, for NFAT1 and 2, vs 0 \pm 0 for GFP-infected cells). To address the second issue, we crossed RANKL^{-/-} and RANK^{-/-} mice with TNF transgenic mice to generate RANKL^{-/-}/TNF and RANK^{-/-}/TNF hybrid mice. As expected, the RANKL^{-/-}/TNF (n=6) or RANK^{-/-}/TNF (n=3) mice had no ocls or joint erosion identified histologically, but surprisingly did not have joint inflammation (synovial membrane area: 0.03 \pm 0.02 mm² in RANKL^{-/-}/TNF vs 0.97 \pm 0.24 in TNF-Tg mice, vs 0 \pm 0 mm² in wt mice) after 4.5 month of age. In contrast, RANKL^{+/+}/TNF or RANK^{+/+}/TNF littermates all had joint inflammation and bone erosion. Serum TNF levels (by ELISA) were significantly decreased in RANKL/TNF hybrids compared to TNF-Tg mice (74 \pm 25.7 pg/ml vs 173 \pm 32, P<0.05). Consistent with this finding, RANK:Fc treatment of TNF-Tg mice (n=8) significantly reduced not only bone erosion, but also the joint inflammation area measured histologically: (0.15 \pm 0.13 mm² in RANK:Fc- vs 1.2 \pm 0.5 in PBS-treated mice) and blood TNF concentrations (47 \pm 2.5 pg/ml vs 85 \pm 5.3, P<0.05). In contrast, in the acute arthritis model induced by serum transfer, joint inflammation of similar severity developed in RANK^{-/-} mice as in wt littermates, despite the lack of ocls and bone erosion (n=3/genotype). We conclude that 1) TNF induces ocl formation from both RANKL and RANK knockout splenocytes *in vitro* through an NF- κ B/NFAT-dependent mechanism and 2) RANKL^{-/-}/TNF/or RANK^{-/-}/TNF hybrid mice do not have joint erosion or inflammation because the RANKL/RANK pathway is critical for TNF-induced joint inflammation, perhaps through regulation of TNF production by RANK expressing cells *in vivo*. Thus, inhibitors of RANKL may have efficacy in reducing inflammation in joints of patients with TNF-induced arthritis as well as inhibiting bone resorption.

Disclosures: **L. Xing**, None.

1197

Glucocorticoid Excess Disrupts the Canalicular Circulation: Potential Mechanism of the Disparity between Bone Density and Strength in Glucocorticoid-Induced Osteoporosis and Osteonecrosis. R. S. Weinstein, J. J. Goellner*, D. Jia, R. S. Shelton*, A. M. Parfitt, S. C. Manolagas. Div. of Endo/Metab, Center for Osteoporosis, Central Arkansas Veterans Healthcare System, Univ of Arkansas for Med Sci, Little Rock, AR, USA.

Patients treated with glucocorticoids suffer vertebral fractures in the presence of higher lumbar bone mineral density (BMD) than is found in patients with fractures due to postmenopausal osteoporosis, indicating that the adverse effects of glucocorticoids on bone may be due, in part, to abnormalities separate from the decline in bone mass. In addition to BMD, contributions to bone strength are also made by several other characteristics including bone size, architecture, osteocyte viability and the quality of the mineral, matrix and fluid phases. To investigate these other contributions, we examined *in vivo* spinal BMD by DEXA and *ex vivo* vertebral compression strength in adult mice receiving prednisolone pellets for 28 days compared to control mice implanted with placebo pellets. We found that the slope of the relationship between vertebral strength and spinal BMD in the control animals was significantly different from that in the prednisolone group, indicating a glucocorticoid-induced deterioration in bone quality similar to that found in patients with glucocorticoid-induced osteoporosis. Consistent with this resemblance, the prednisolone-treated mice developed a decreased rate of bone formation and an increased prevalence of osteoblast and osteocyte apoptosis, findings characteristic of glucocorticoid-induced osteoporosis. To determine the effects of the glucocorticoid excess on the fluid phase of bone, 0.3 mL of 1.6% procion red (a metabolically inert aqueous tracer, MW 300-400) was injected into a tail vein 2 hours before necropsy. In 5 μ m thin, longitudinal sections of undecalcified bone viewed under epifluorescent light, procion red was abundantly detected in the osteocytic lacunae and canaliculi of the mice receiving placebo pellets but was severely diminished in the animals receiving prednisolone. Interruption of the lacunocanalicular system would prevent delivery of nutrients and osteotrophic signals that are important to osteocyte survival. Therefore, disruption of the canalicular circulation could be a pathogenetic factor in glucocorticoid-induced osteocyte apoptosis. Furthermore, changes in the quality of the bone matrix and mineral that follow the decrease in canalicular circulation and increase in osteocyte apoptosis may be responsible for the disparity between bone density and strength in glucocorticoid-induced osteoporosis and osteonecrosis.

Disclosures: **R.S. Weinstein**, Nuvios 1, 2, 5; Merck 8; P & G, Novartis, Aventis, Roche 2.

1198

Androgen Receptor Transgenic Mice Have Decreased Body Fat, Reduced Adipogenesis and an Increased Osteoblast Differentiation Program. K. M. Wiren¹, A. S. Toombs^{*1}, A. M. Matsumoto², X. Zhang¹. ¹VA Medical Center and Oregon Health & Science University, Portland, OR, USA, ²VA Puget Sound Health Care System and University of Washington, Seattle, WA, USA.

The direct effects of androgen signaling on bone are demonstrated in transgenic mice with enhanced androgen sensitivity, using androgen receptor (AR) under the control of the 3.6-kb α 1(I)-collagen promoter (AR-tg). Male AR-tg mice show a complex anabolic bone phenotype with no change in circulating steroid levels. Since androgens are known to influence body composition, we hypothesized that targeted overexpression of AR in bone marrow stromal cells (MSCs) could alter lineage commitment to bone, fat and muscle. Body composition was analyzed by DXA, fat depot weights and adipogenesis in response to 5 α -dihydrotestosterone (DHT) in MSC cultures. Gene expression was evaluated with qRT-PCR analysis. Male AR-tg 6 month old mice showed significantly increased BMC/body weight ($P < 0.01$), percentage lean mass ($P < 0.001$) but reduced percentage fat mass ($P < 0.001$) by DXA. Fat pad dissection from male AR-tg versus littermate controls showed significantly reduced white adipose tissue in visceral ($P < 0.05$) and gonadal ($P < 0.01$) fat, with no effect in brown fat. AR-tg expression was targeted to bone, with the highest expression in calvaria but ~100-1000 fold lower in mature fat, muscle, skin, kidney, liver, and spleen. Fresh marrow isolates showed AR-tg expression; only males showed reduced PPARGamma expression. Since androgen is hypothesized to influence body composition through modulation of MSC lineage allocation, we investigated adipogenic differentiation in MSC cultures. MSC were grown to confluence, then switched to adipogenic media. AR-tg MSC DHT-treated cultures showed dramatic inhibition of adipogenesis assessed by Oil Red O staining, with greater inhibition of PPARGamma expression versus controls. M2-10B4 stromal cell cultures also showed reduced Oil Red O after DHT treatment. Conversely, osteoblast differentiation was enhanced assessed by alkaline phosphatase activity. Thus, male AR-tg mice have decreased adiposity, increased lean mass and increased osteoblast differentiation due to enhanced androgen signaling without systemic androgen treatment. These results are consistent with late-onset obesity observed in global AR null animals and provide *in vivo* confirmation of the hypothesis that AR in MSCs directs lineage allocation. Further analysis will be important to define the distinct contributions of androgens to the maintenance of healthy body composition, and may identify regulatory pathways responsible for the deleterious consequences of hypogonadism and aging on central fat accumulation, muscle weakness and declining bone mass.

Disclosures: **K.M. Wiren**, None.

1199

Estradiol Recovers Hepatic IGF-I Gene Expression in Growth Hormone Resistant Mice through Activation of the JAK-STAT Pathway. K. Venken^{*1}, F. Schuit^{*1}, L. Van Lommel^{*1}, K. Tsukamoto^{*1}, J. J. Kopchick^{*2}, K. Coschigano^{*2}, C. Ohlsson³, S. Movérare^{*3}, S. Boonen¹, R. Bouillon¹, D. Vanderschueren¹. ¹K.U.Leuven, Leuven, Belgium, ²Ohio University, Athens, OH, USA, ³Gothenburg University, Gothenburg, Sweden.

We previously observed that estradiol (E₂) therapy (0.03 μ g/day via subcutaneous implants) in orchidectomized (orx) male mice with disrupted growth hormone receptor (GHRKO) (6-10 weeks) increased hepatic and serum insulin-like growth factor-I (IGF-I). The E₂-induced increase in serum IGF-I was associated with a rescue of longitudinal and radial skeletal growth. The aim of this study was to investigate the molecular basis of the E₂-induced increase in hepatic IGF-I expression in GHRKO mice. Genome-wide mRNA expression profiles in the liver of orx GHRKO and orx wild-types (WT), treated with or without E₂, were studied using Affymetrix 430 2.0 arrays (45037 probesets). Our filtering strategy was based upon transcripts that were altered in orx GHRKO versus orx WT, and that showed an inverse change after E₂ treatment in orx GHRKO. IGF-I (represented by 4 probesets) and IGF binding protein, acid labile subunit (IGFBP, ALS) (1 probeset) mRNA expression was almost completely abolished in orx GHRKO (signal log ratio (SLR) -5.4 and -5.2 vs orx WT, resp., $P < 0.000001$), but was partly restored after E₂ therapy (SLR +4.4 and +3.8 vs orx GHRKO, resp., $P < 0.0005$). Interestingly, in the absence of the GHR, estrogen receptor alpha (2 probesets) and prolactin receptor (PrIR) (5 probesets) mRNA expression was significantly downregulated in orx GHRKO (SLR -1.6 and -3.9 vs orx WT, resp., $P < 0.0001$), indicating that GHR signaling is critical for the integrity of other major receptor signaling systems in the liver. Moreover, E₂ induced a full compensation for this multi-receptor deficit in GHRKO (SLR +2.1 and +4.0 vs orx GHRKO, resp., $P < 0.00005$). As the full recovery of PrIR expression suggested a compensation of a putative mechanism involving the JAK-STAT pathway, STAT5 activation (through phosphorylation) was measured. Phosphorylated STAT5, assessed by Western blotting, was significantly increased in E₂-treated GHRKO (+240% vs orx GHRKO), indicating that STAT5 activation contributed to the enhanced IGF-I gene expression. To date, GH is the only hormone known to induce hepatic IGF-I expression through activation of the JAK-STAT pathway. Here we demonstrate that, in the absence of a functional GHR, the JAK-STAT pathway is activated by estrogen, indicating a novel mechanism of stimulation of hepatic IGF-I production. Therefore, estrogen or estrogen-like compounds (e.g. SERMs) merit investigation as potential IGF-I secretagogues to restore serum IGF-I levels in GH/IGF-I deficient and/or GH resistant conditions.

Disclosures: **K. Venken**, None.

1200

Retinoblastoma-Binding Protein 1, a Novel Estrogen Receptor-Regulated Gene, Plays a Role in the Suppression of Osteoblastic Proliferation. D. G. Monroe¹, F. J. Secreto¹, M. Subramaniam¹, J. R. Hawse¹, B. J. Getz^{*1}, S. Khosla², T. C. Spelsberg¹. ¹Biochemistry and Molecular Biology, Mayo Clinic, Rochester, MN, USA, ²Endocrine Research Unit, Mayo Clinic, Rochester, MN, USA.

Estrogen (E2) is involved in mediating many important functions relevant to osteoblast cells (OBs). We and others have demonstrated that E2 inhibits cell proliferation by acting specifically through ER α and not ER β , in U2OS human osteosarcoma and hFOB cell lines. Using a combination of microarray and RT-PCR analysis of 2 hr E2-treated U2OS-ER α or-ER β cell lines, we identified retinoblastoma binding protein 1 (RBBP1) as a major E2-regulated gene. RBBP1 is a transcriptional repressor that functions by interacting with the retinoblastoma (Rb)/HDAC complex, important tumor suppressors involved in repressing E2F-dependent gene transcription, thus inhibiting cell proliferation. RBBP1 mRNA levels increase after 2hr of E2 treatment in both ER α - and ER β -expressing lines, however sustained increases in RBBP1 are only observed with ER α . We further demonstrate that E2-dependent regulation occurs in mouse primary calvarial OBs and in ER α -expressing Hs578T breast cancer cells, suggesting that E2 regulation of RBBP1 may be of more general importance in divergent tissues and animal species. Examination of the RBBP1 genomic sequence revealed an estrogen response element (ERE) within the first intron of RBBP1, which was confirmed to bind ERs using gel shift and chromatin immunoprecipitation assays. EREs were also discovered in the mouse and chicken genomic RBBP1 sequences, which also bind ERs, demonstrating an evolutionary conservation of RBBP1 regulation by E2. Furthermore, 35S-Met labeling/IP experiments in the ER α and ER β lines suggests that the Rb/HDAC corepressor complex exists at higher concentrations in the E2-treated ER α line compared to the ER β line. This suggests a model whereby a sustained increase in expression of RBBP1 through E2-bound ER α , stimulates the nucleation of the Rb/HDAC complex, thereby inhibiting cell proliferation. Flow cytometry analysis was performed to determine the extent of the G1 cell population in ER α and ER β lines. E2 treatment resulted in a significant increase (22%) of ER α cells in the G1 phase of the cell cycle, whereas no change was observed in ER β cells. We are currently examining siRNA knockdown of RBBP1 to determine whether RBBP1 is directly involved in suppression of E2- and ER α -dependent OB proliferation. These data support our hypothesis that RBBP1 is involved in ER α -specific decreases in cellular proliferation by stalling the cells in G1 of the cell cycle.

Disclosures: **D.G. Monroe**, None.

1201

SWI/SNF Chromatin Remodeling Complexes Cooperate with the Vitamin D Receptor and C/EBP Beta in the Regulation of 25-Hydroxyvitamin D₃ 24-Hydroxylase Transcription. Q. Shen^{*}, P. Dhawan^{*}, S. Christakos. Biochemistry and Molecular Biology, UMDNJ-New Jersey Medical School, Newark, NJ, USA.

The mammalian SWI/SNF related complexes facilitate gene transcription by remodeling chromatin using the energy of ATP hydrolysis. SWI/SNF is implicated in regulating differentiation as well as in transcriptional activation stimulated by estrogen, glucocorticoid and retinoic acid receptors. Each SWI/SNF complex contains one of two homologous ATPases, Brahma (Brm) and Brahma/related gene 1 (Brg-1). Little is known about their specialized functions and what role they may have in vitamin D receptor (VDR) mediated transcription. We demonstrate that SWI/SNF complexes contribute to transcriptional activation by VDR and cooperate with VDR and C/EBP beta in the regulation of 25-hydroxyvitamin D₃ 24-hydroxylase (24(OH)ase) transcription. In MC3T3-E1 osteoblastic cells that contain endogenous VDR, we found that the N-terminal region of Brg-1 (Brg-1-N) and mutant Brm, that can act as dominant negative inhibitors, significantly inhibited 1,25(OH)₂D₃ induction of 24(OH)ase transcription (3-6 fold). The effect was not specific for 24(OH)ase transcription since a similar inhibition of 1,25(OH)₂D₃ induced transcription was observed in MC3T3-E1 cells using the mouse osteopontin (OPN) promoter (-777/+79) or a construct containing multiple copies of the OPN vitamin D response element (VDRE) upstream of the minimal thymidine kinase (tk) promoter. Mutant Brm or Brg-1-N had no effect on the activity of the tk promoter. Using the Brm and Brg-1 deficient cell lines SW-13 and C33-A and the 24(OH)ase promoter, Brm was found to facilitate VDR mediated activation of 24(OH)ase transcription (4-7 fold) without being essential. In VDR transfected COS-7 cells, mutant Brm inhibited C/EBP beta enhancement of VDR mediated 24(OH)ase transcription, suggesting cooperativity between VDR, the SWI/SNF complex and C/EBP beta in regulating 24(OH)ase transcription. C/EBP beta enhancement of VDR mediated transcription was not observed using the OPN promoter, the VDRE tk promoter construct or the 24(OH)ase promoter with the C/EBP site mutated. GST pull down assays indicate that Brm associates with C/EBP beta and immunoprecipitation assays indicate that Brg-1 is capable of associating with VDR. Chromatin immunoprecipitation (ChIP) using MC3T3-E1 cells showed the association of SWI/SNF as well as C/EBP beta with the 24(OH)ase promoter. Together these studies reveal a role for SWI/SNF in VDR mediated transcription and suggest that the interaction between C/EBP beta and SWI/SNF may also be an important determinant in the C/EBP beta mediated enhancement of 24(OH)ase transcription.

Disclosures: **Q. Shen**, None.

1202

siRNA against 25-OHD₃ 1 α -Hydroxylase Inhibits Local Production of 1,25-(OH)₂D₃ and Prevents 25-OHD₃ Induced Growth Inhibition of Cancer Cells *In Vitro* and *In Vivo*. D. C. Huang¹, X. F. Yang^{*1}, J. S. Rhim^{*2}, R. L. Horst³, R. Kremer¹. ¹Department of Medicine, Royal Victoria Hospital and McGill University, Montreal, PQ, Canada, ²Center for Prostate Disease Research, Uniformed Services, University of the Health Sciences, Bethesda, MD, USA, ³USDA, Agriculture Research Service, National Animal Disease Center, Ames, IA, USA.

Extra-renal expression of the 1 α -hydroxylase enzyme which catalyzes the conversion of 25-hydroxyvitamin D₃ to 1 α , 25-dihydroxyvitamin D₃ may play an important autocrine/paracrine antiproliferative function. In the present study, we used a small interfering double-stranded RNA (siRNA) to knockdown 1 α -hydroxylase in two cancer cell lines previously shown to express this enzyme. A hairpin oligonucleotide sequence corresponding to the N-terminal region of the 1 α -hydroxylase gene was cloned into the siRNA vector. Transfection of this plasmid into the human amelanotic melanoma cell line A375 and the human prostate cancer cell lines FNC267B1-*ras* led to a dramatic decrease in the conversion of 25-OHD₃ to 1,25-(OH)₂D₃. We then examined the effect of substrate 25-OHD₃ on parameters of growth and differentiation in both 1 α -hydroxylase knockdown cell lines and compared them to the same parameters in the corresponding wild type control cell lines transfected with vector alone. Addition of 25-OHD₃ (10⁻⁶ M) to wild type cells inhibited growth by 28 \pm 5% in A375 cells (p<0.001) and by 36 \pm 6% in the human transformed prostate cell line FNC267B1 (p<0.001). In contrast, no significant growth inhibition was observed in both knockdown A375 and FNC267B1 cell lines in the presence of 25-OHD₃ (10⁻⁶ M). This growth inhibitory effect was further analyzed *in vivo* following subcutaneous injection of 1 α -hydroxylase knockdown or wild type cells in severely compromised immunodeficient (SCID) mice. Alzet osmotic mini-pump containing 25-OHD₃ were implanted two days before tumor cell transplantation to deliver a constant infusion of 25-OHD₃ (2000 pM/24h) or vehicle. Circulating 25-OHD₃ concentrations were at least 10 fold higher in 25-OHD₃ treated animals as compared to vehicle treated animals without significant changes in circulating calcium levels. A significant inhibition of tumor growth was observed in mice transplanted with wild type A375 or FNC267B1 control cells treated with 25-OHD₃ as compared to vehicle (p<0.001). In contrast no tumor reduction was observed in mice transplanted with siRNA knockdown cells. In summary our data demonstrate that local conversion of 25-OHD₃ to 1,25-(OH)₂D₃ inhibits tumor growth in both melanoma and prostate cancer cells. These data therefore suggest potential therapeutic cancer applications for the non-calcemic vitamin D precursor 25-OHD₃.

Disclosures: **D.C. Huang**, None.

1203

PTH and 1,25-Dihydroxyvitamin D₃ Each Independently Exert Skeletal Anabolic Effects and Improve Mineral Ion Homeostasis in Mice which Are Homozygous for both the 1 α -Hydroxylase and PTH Null Alleles. Y. Xue, A. C. Karaplis, G. N. Hendy, D. Goltzman, D. Miao. Medicine, McGill University, Montreal, PQ, Canada.

Parathyroid hormone (PTH) and 1,25-Dihydroxyvitamin D₃ (1,25-(OH)₂D₃) directly affect calcium and skeletal homeostasis, and each exerts important regulatory effects on the other. To identify whether PTH and 1,25-(OH)₂D₃ can exert skeletal effects and regulate mineral ion homeostasis in an independent manner *in vivo*, double knockout (double KO) mice, which are homozygous for both the 1 α -hydroxylase and PTH null alleles, were treated with vehicle or PTH 1-34 peptide (0.2 μ g) or 1,25-(OH)₂D₃ (0.02 μ g) per mouse per day subcutaneously starting from day 4 until 14 days of age. At day 14, we compared the PTH or 1,25-(OH)₂D₃ treated double KO mice to the vehicle-treated double KO mice and the vehicle-treated wild-type mice. Serum calcium rose from 1.23 \pm 0.03 mmol/L (43% of wild type) in untreated double KO mice to 2.08 \pm 0.04 mmol/L (73% of wild-type) and 1.97 \pm 0.05 mmol/L (69% of wild-type) in PTH- and 1,25-(OH)₂D₃-treated double KO mice, respectively. Messenger RNA and protein levels of the renal calcium transporters, TRPV5, calbindin-D_{28K}, calbindin-D_{9K} and NCX1 were down-regulated in the kidney of vehicle-treated double KO mice relative to wild-type, but were up-regulated by either PTH or 1,25-(OH)₂D₃ administration. Epiphyseal volume, chondrocyte proliferation and differentiation, and cartilaginous matrix mineralization were all increased after 10 days of exogenous PTH or 1,25-(OH)₂D₃ administration to the double KO mice, but the effect on the epiphysis was greater with 1,25-(OH)₂D₃. As a result of these positive effects long bone length increased with both treatments. The exogenous PTH and 1,25-(OH)₂D₃ administration also stimulated appositional osteoblastic bone formation at both trabeculae and cortices, in a manner independent of each other, however, the effect was greater with PTH. Treatment with PTH and 1,25-(OH)₂D₃ both increased osteoblast number and type I collagen deposition in bone matrix. Consistent with these observations, expression levels of the osteoblastic genes, Cbfa1, ALP, type I collagen and osteocalcin were all up-regulated following 10 days of PTH or 1,25-(OH)₂D₃ administration to the double KO mice. The number of TRAP positive osteoclasts in bone increased relative to the vehicle-treated double mutants but were still less in the PTH- or 1,25-(OH)₂D₃-treated double mutants than in vehicle-treated wild-type mice. These results indicate that PTH and 1,25-(OH)₂D₃ can increase serum calcium concentrations and exert skeletal anabolic effects independent of each other.

Disclosures: **Y. Xue**, None.

1204

Novel Regulation of 25-Hydroxyvitamin D₃ 24-Hydroxylase (24(OH)ase) Transcription by Glucocorticoids: Cooperative Effects of the Glucocorticoid Receptor, C/EBP beta and the Vitamin D Receptor in 24(OH)ase Transcription. P. Dhawan*, X. Peng*, S. Christakos. Biochemistry and Molecular Biology, UMDNJ-New Jersey Medical School, Newark, NJ, USA.

Glucocorticoid induced bone loss has been proposed to involve direct effects on bone cells as well as alterations in calcium absorption and excretion. Since vitamin D is important for the maintenance of calcium homeostasis, in the present study the effects of glucocorticoids on vitamin D metabolism through the expression of 24(OH)ase, an enzyme involved in the catabolism of 1,25(OH)₂D₃, were examined. Injection of 7 week old male vitamin D replete mice with dexamethasone (dex; 2mg/kg body weight for 5 days) resulted in a significant induction in 24(OH)ase mRNA in kidney (3.4 ± 0.4 fold), indicating a regulatory effect of glucocorticoids on vitamin D metabolism. Recent evidence has indicated cooperative effects between the transcriptional activator, C/EBP beta and the vitamin D receptor (VDR) in the regulation of 24(OH)ase transcription. In the presence of ligand bound VDR, C/EBP beta enhances 24(OH)ase transcription and this enhancement is mediated by a C/EBP binding site at -395/-388 in the 24(OH)ase promoter. Whether glucocorticoids can affect 24(OH)ase transcription is not known. Here we demonstrate for the first time a glucocorticoid receptor (GR) dependent enhancement of 1,25(OH)₂D₃ induced 24(OH)ase transcription. Transfection studies indicated that in the absence of 1,25(OH)₂D₃ activation, treatment with dex alone (10^{-8} M- 10^{-6} M) of GR transfected COS-7 cells did not affect 24(OH)ase transcription. However dex treatment of GR and VDR transfected COS-7 cells potentiated 1,25(OH)₂D₃ induced 24(OH)ase transcription (4-5 fold). In addition GR and dex treatment potentiated the C/EBP beta mediated enhancement of VDR mediated 24(OH)ase transcription (2-3 fold) and immunoprecipitation assays indicated that GR can interact with C/EBP beta. A glucocorticoid response element was not present in the rat 24(OH)ase promoter (-671/+74). Using the rat 24(OH)ase promoter (-671/+74) with the C/EBP beta site mutated, GR mediated potentiation of 1,25(OH)₂D₃ induced 24(OH)ase transcription was inhibited, suggesting functional cooperation between C/EBP beta and GR in the regulation of 24(OH)ase transcription. These findings indicate a novel mechanism whereby glucocorticoids can alter VDR mediated 24(OH)ase transcription through a functional interaction between GR and C/EBP beta that results in an enhanced ability of C/EBP beta to cooperate with VDR in the regulation of 24(OH)ase. In addition, these results suggest that glucocorticoid mediated alterations in vitamin D metabolism may contribute to glucocorticoid induced bone loss.

Disclosures: P. Dhawan, None.

1205

Abnormal Renal Phosphate Transport Underlies the Aberrantly Regulated 25-Hydroxyvitamin D-1 α -Hydroxylase (1-OHylase) Activity in Hyp-Mice. M. Takaiwa, B. Yuan, Y. Xing*, R. Achyutharao*, M. K. Drezner. University of Wisconsin, Madison, WI, USA.

Abnormal vitamin D metabolism in *hyp*-mice is due primarily to aberrant regulation of renal 1,25(OH)₂D production. We demonstrated that such defective regulation results from abnormal 1-OHylase mRNA translation in the cells of the proximal convoluted tubule. Hence, despite normal up-regulation of mRNA transcripts in *hyp*-mice in response to hypophosphatemia and PTH, these stimuli fail to substantially alter renal 1-OHylase protein content and consequently enzyme activity in the mutants. Whether this abnormality is due to a circulating phosphatonin (FGF-23) or to the direct/independent effects of abnormal phosphate transport in the renal proximal convoluted tubule, and the resultant changes in the intracellular milieu, remains unknown. Thus, to address the cause of the abnormal vitamin D metabolism, we created C57BL/6J transgenic (*KAP-Npt2*) mice and mated them with *hyp*-mice to produce transgenic *KAP-Npt2 hyp*-mice. Due to *Npt2* over-expression and enhanced renal Na⁺-dependent phosphate transport, the serum phosphorus concentration in the *KAP-Npt2 hyp*-mice (6.6 ± 0.7 mg/dl) was no different from normal (7.2 ± 0.6 mg/dl) but significantly greater ($p < 0.001$) than in *hyp*-mice (4.5 ± 0.4 mg/dl). Subsequently, we compared P- and PTH-stimulated 1-OHylase mRNA (RT-PCR), protein (Western) and enzyme activity in 8-12 week old male C57BL/6J normal and transgenic *KAP-Npt2 hyp*-mice. In concert with a normal serum phosphorus concentration under basal conditions, the *KAP-Npt2 hyp*-mice reset production of 1,25(OH)₂D and, unlike *hyp*-mice, exhibited normal abundance of 1-OHylase mRNA transcripts (1.3 ± 0.5 vs 1.0 ± 0.1 fold), as well as normal amounts of 1-OHylase protein (1.2 ± 0.5 vs 1.0 ± 0.1 fold) and enzyme activity (6.5 ± 0.5 vs 5.5 ± 0.3 fmoles/mg protein/min), consistent with normal 1-OHylase mRNA translation. Moreover, in response to PTH stimulation, the *KAP-Npt2 hyp*-mice displayed not only normal up-regulation of 1-OHylase mRNA transcripts (9.5 ± 0.3 vs 9.7 ± 0.5 fold), as in *hyp*-mice, but, in contrast, normal enhancement of 1-OHylase protein (1.6 ± 0.1 vs 1.6 ± 0.2 fold) and enzyme activity (13.0 ± 1.0 vs 14.9 ± 1.5 fmoles/mg protein/min), again consistent with normal mRNA translation. Normalization of vitamin D metabolism in the *KAP-Npt2 hyp*-mice occurred despite maintenance of an elevated serum FGF-23 level comparable to that in *hyp*-mice. These observations provide compelling evidence that the abnormal regulation of renal 1,25(OH)₂D production in *hyp*-mice is secondary to the direct effects of abnormal phosphate transport in the renal proximal tubule and undoubtedly resultant changes in the intracellular milieu that regulate mRNA translation.

Disclosures: M. Takaiwa, None.

1206

Osteoclasts from ADOl Patients Are Completely Normal *In Vitro* Indicating that Osteoblasts with a Aain of Function in LRP5 Loose their Ability to Support Osteoclastogenesis. K. Henriksen¹, J. Gram^{*2}, P. Hoegh-Andersen^{*1}, S. Schaller^{*1}, J. Bollerslev³, M. A. Karsdal¹. ¹Nordic Bioscience A/S, Herlev, Denmark, ²Ribe County Hospital, Esbjerg, Denmark, ³Department of Medical Endocrinology, National University Hospital, Oslo, Norway.

Patients harbouring mutations in the LRP5 protein have either Autosomal Dominant Osteopetrosis type I (ADOI) or Osteoporosis-Pseudoglioma Syndrome (OPPG), depending on whether the mutations lead to a gain or a loss of function. This proves that LRP5 is a central regulator of bone metabolism. Increased activity of LRP5 leads to increased osteoblast activity further leading to increased bone mass. ADOI patients have significantly reduced levels of osteoclasts, indicating that either LRP5 has a function in osteoclasts or that ADOI osteoblasts fail to support normal osteoclastogenesis. To investigate whether the defect in osteoclasts from ADOI patients is endo- or exogenous we isolated CD14+ monocytes from 5 patients with a T2531 mutation causing ADOI and from age and sex-matched controls and compared their ability to generate mature multinuclear resorbing osteoclasts, when treated with RANKL and M-CSF. We found that monocytes from ADOI patients differentiate into osteoclasts at the same rate as control monocytes. By comparison of expression of osteoclast markers, cathepsin K, TRACP, CIC-7 and MMP-9 by Western-blot, we found no differences between ADOI and control osteoclasts undergoing differentiation. In alignment, the ability of ADOI osteoclasts to form actin rings was not impaired. By immunolocalization of Cathepsin K, TRACP, MMP-9 and CIC-7, we found normal localization in gradients towards the resorption lacuna as expected. We investigated the ability of the ADOI osteoclasts to resorb bone and we found that they resorb bone as efficiently as their control counterparts as investigated by CTX-I collagen release from bone slices, and pit area measurements. In ADOI patients, we analysed the effect of the thyroid hormone T₃ *in vivo* to test whether the lowered number of osteoclasts had an effect on the induction of bone turnover, presented as increases compared to baseline values of osteocalcin and CTX-I in serum. We found that induction of bone formation was normal. In contrast, we found that the increase in bone resorption was reduced to 40% ($p < 0.05$) in ADOI patients compared to controls. In conclusion, LRP5 mutations do not affect osteoclast function *in vitro*. In contrast, osteoclast resorption *in vivo* is impaired. We speculate that ADOI mutations alter the osteoblastic phenotype towards a bone forming phenotype, and that these bone-forming osteoblasts possess a lower potential for supporting osteoclast function.

Disclosures: K. Henriksen, None.

1207

Expression of TAF_{II}-17 and IL-6 in Osteoclast (OCL) Precursors Is Sufficient for Formation of Pagetic-like OCL. N. Kurihara¹, K. Yamana^{*2}, G. D. Roodman¹. ¹Medicine-Hematology/Oncology, University of Pittsburgh, Pittsburgh, PA, USA, ²Bone and Calcium Metabolism, Teijin Institute for Bio-Medical Research, Tokyo, Japan, ³Medicine-Hematology/Oncology, University of Pittsburgh and VA Pittsburgh Healthcare System, Pittsburgh, PA, USA.

Osteoclasts (OCL) from patients with Paget's Disease (PD) differ from normal OCL. Pagetic OCL have increased nuclear number, hyper-sensitivity to 1,25-(OH)₂D₃ and RANKL, increased bone resorbing capacity and increased rate of OCL formation *in vitro*. However, the mechanism responsible for these abnormalities is unclear. Bone marrow cells from patients with PD express measles virus nucleocapsid protein (MVNP) transcripts, and expression of the MVNP gene in normal OCL precursors results in formation of OCL that express the abnormal characteristics of OCL from Paget's patients. Further, both OCL from PD patients and OCL precursors transduced with the MVNP gene also secrete large amounts of IL-6 and a VDR binding peptide, TAF_{II}-17. TAF_{II}-17 enhances the 1,25-(OH)₂D₃ responsivity of OCL precursors. We hypothesized that MVNP increased IL-6 production by OCL, which in turn upregulated expression of TAF_{II}-17, and enhanced 1,25-(OH)₂D₃ responsivity of pagetic OCL precursors. Therefore, we determined the capacity of TAF_{II}-17 to induce 1,25-(OH)₂D₃ hyper-responsivity and expression of a pagetic phenotype in normal OCL precursors *in vitro*. TAF_{II}-17 or MVNP was transfected into normal human marrow cells, which were then treated with 10^{-11} to 10^{-8} M 1,25-(OH)₂D₃, and the number and characteristics of the OCL formed were determined. TAF_{II}-17 transfected cells formed increased numbers of OCL that were hyper-responsive to 1,25-(OH)₂D₃, but did not demonstrate RANKL hyper-responsivity, increased numbers of nuclei per OCL or produce high levels of IL-6 (47 ± 1 pg/ml vs. 269 ± 11 pg/ml, TAF_{II}-17 vs. MVNP transfected cells). We then treated TAF_{II}-17 transduced OCL precursors with low concentrations of 1,25-(OH)₂D₃ and 100 pg/ml IL-6. TAF_{II}-17 transduced OCL precursors treated with IL-6 and 1,25-(OH)₂D₃ formed OCL that had increased numbers of nuclei per OCL, a markedly increased bone-resorbing capacity and increased responsivity to RANKL, similar to OCL formed by MVNP transduced OCL precursors. These results demonstrate that TAF_{II}-17 by itself can increase VDR mediated gene transcription and the sensitivity of OCL precursor cells to 1,25-(OH)₂D₃, but in addition, increased production of IL-6 by OCL precursors is required for formation of pagetic-like OCL.

Disclosures: G.D. Roodman, Novartis 8; Scios, Inc. 5; Merck 5.

1208

Differential Activity of Human RUNX2 P2 Promoter Alleles Associated with Deciles of BMD Show an Allele-Specific DNA-Protein Interaction in Osteoblast Nuclear Extracts. J. D. Doecke^{*1}, C. J. Day^{*1}, A. Stephens^{*1}, G. C. Nicholson², N. A. Morrison¹. ¹School of Medical Science, Griffith University, Gold Coast, Australia, ²Department of Medicine, Geelong Hospital, University of Melbourne, Geelong, Australia.

We hypothesized that by taking subjects from the extremes of a population, we would specifically find alleles related to the bone mineral density trait, if such alleles exist for any particular target gene. We tested this idea using RUNX2, the well known osteoblast transcription factor. From a population of 1300 subjects the age-weight adjusted femoral neck bone mineral density (BMD) was ranked and the upper and lower deciles taken to represent the adjusted extremes. After adjusting and ranking, the two groups (n=130 each) were not significantly different for age or weight. In these 260 subjects, we identified 19 allelic variations within the RUNX2 gene and promoter (P1 and P2), and characterized these novel variations with respect to BMD strata by genotype using dHPLC. A general linkage disequilibrium (LD) analysis of RUNX2 showed that LD drops off with physical distance, as expected. Within the P2 promoter were three polymorphic nucleotides for which the minor alleles were over represented in the upper decile of BMD. These alleles are in complete LD with each other and represent a haplotype block that is significantly associated with increased BMD. Constructs made from the "normal" and the "high BMD" alleles were cloned upstream of otherwise identical luciferase constructs. Despite there being only 3 nucleotide differences between the two constructs, when transfected into osteoblast-like cells the high BMD allele construct showed significantly greater P2 promoter activity than the normal allele. Comparative homology studies showed that the high BMD alleles were the major forms in other animals (dog, rat, mouse, chimp), suggesting that the human normal BMD alleles represent the evolutionary change. The rat sequence was identical to the human high BMD allele, permitting an analysis of DNA-protein interactions in the well characterized ROS17/2.8 rat osteoblast cell line. These data showed abundant nuclear factor binding to one the three polymorphic sites in the human normal BMD allele that does not occur in the high BMD allele (and rat sequence). The data suggest that the high BMD allele does not interact with a factor that otherwise binds strongly to the normal human allele. Since the high BMD allele had higher P2 promoter activity, the binding activity may be a repressor that limits the expression of the normal allele. In any event, the nuclear factor is a candidate for the allele-specific regulation of the RUNX2 promoter.

Disclosures: J.D. Doecke, None.

1209

PlexinD1, Is a Plexin Family Member Being Expressed in Central Nervous System and Endothelium, and Is Involved in the Skeletal Patterning in the Development of Bone. T. Kanda¹, Y. Yoshida^{*2}, K. Nakashima^{*1}, Y. Ezura¹, M. Noda¹. ¹Molecular Pharmacology, 21st COE program, Medical Research Institute, Tokyo medical and Dental University, Tokyo, Japan, ²Department of Biochemistry and Molecular Biophysics, Howard Hughes Medical Institute, Columbia University., New York, NY, USA.

Plexin family members are characterized by their large, single-pass transmembrane protein domain with homology to the scatter factor receptors encoded by MET gene. Plexins in the conjunction with the neuropilins are the receptors for semaphorins. These ligand-receptor signaling systems have been first identified to be involved in axonal guidance. In addition to the central nervous system, PlexinD1 is expressed in the endothelial cells. The signaling by semaphorin 3E and PlexinD1 controls the positioning of endothelial cells and the patterning of the developing vasculature in the mouse (Science 2005). As both the central nervous system and vascular systems are closely associated with the control of skeletal systems, we examined the effects of PlexinD1 deficiency on the skeletal development. PlexinD1 deficiency specifically altered the axial skeletal elements. Within the axial skeletal elements, vertebral body development was severely impaired and fragmentations or loss of the vertebral body was observed in PlexinD1-null mice. This was observed almost entirely from the caudal to rostral ends of the vertebral columns. Interestingly, although the vertebral body was fragmented, segmental pattern was intact and rib cages as well as the transverse processes was almost fully preserved. Therefore, PlexinD1 deficiency specifically affects the vertebral body formation. Although the fragmentation was occurring, the total body mineral density was not affected by the deficiency of PlexinD1. Interestingly, such of differences were specifically within the central axis since limb bones were more or less normal in PlexinD1 knockout mice. In order to access the role of PlexinD1 in adult bones in relationship to the osteogenesis, we have conducted bone marrow ablation experiments using adult wild type mice and heterozygous PlexinD1 knockout mice. Ablation causes new bone formation in the bone marrow within 10 days and the levels of newly formed bone at the growth plate area as well as bone marrow area were similar between the wild type and heterozygous knockout mice. These data indicated that PlexinD1 is specifically involved in the formation of precise patterning of vertebral body development of skeletal systems.

Disclosures: T. Kanda, None.

1210

Large Scale Prospective Meta-Analysis of BMD and Fracture in Relation to COL1A1 Sp1 Polymorphism: The GENOMOS Study. S. H. Ralston¹, A. G. Uitterlinden², S. Balcells^{*3}, M. L. Brandi⁴, A. H. Carey^{*5}, B. L. Langdahl⁶, R. Lorenc⁷, X. Nogues⁸, B. Obermayer-Pietsch⁹, J. Reeve¹⁰, D. M. Reid¹¹, H. A. Pols², N. M. van Schoor^{*12}, J. P. A. Ioannidis^{*13}. ¹University of Edinburgh, Edinburgh, United Kingdom, ²Erasmus University, Rotterdam, The Netherlands, ³University of Barcelona, Barcelona, Spain, ⁴University of Florence, Florence, Italy, ⁵Oxagen, Didcot, United Kingdom, ⁶University of Aarhus, Aarhus, Denmark, ⁷CMHI, Warsaw, Poland, ⁸Hospital del Mar, Barcelona, Spain, ⁹University of Graz, Graz, Austria, ¹⁰University of Cambridge, Cambridge, United Kingdom, ¹¹University of Aberdeen, Aberdeen, United Kingdom, ¹²Vrije Universiteit, Amsterdam, The Netherlands, ¹³Department of Hygiene and Epidemiology, University of Ioannina, Ioannina, Greece.

A Sp1 binding site polymorphism in COL1A1 has been suggested to be a genetic marker of osteoporosis. We conducted a prospective meta-analysis of individual level data from nine European centres and 26,242 study subjects in relation to spine and hip BMD and bone fractures. No between-centre heterogeneity was observed for any outcome in any genetic contrast (except modest heterogeneity for spine BMD) and Hardy Weinberg Equilibrium was met for all centres. There were no BMD differences in "GG" homozygotes vs. "GT" heterozygotes, but "TT" homozygotes had lower BMD than "GG" and "GT" at the spine (21 mg/cm² [95% CI, 0 to 41]; p=0.043) and hip (25 mg/cm² [16 to 34]; p<0.001). The BMD association was unaltered after adjustment for age, height, weight, HRT use and menopausal status. In the study group as whole, 6,498 subjects gave a history of bone fracture, of which 3,742 were considered low-trauma fractures. There were 2,380 vertebral fractures, and 2,550 incident fractures (403 incident vertebral fractures). The Sp1 polymorphism was not associated with fracture overall; odds ratio [95% CI] per T allele = 1.02 [0.96-1.08] or with prevalent vertebral fracture; odds ratio = 1.05 [0.93-1.19]. However, for incident vertebral fracture, Sp1 alleles were associated with risk in females; OR = 1.34 [1.04-1.73], (p=0.011) per copy of the T allele, independent of BMD, and unaltered in adjusted analyses. We conclude that the COL1A1 Sp1 polymorphism is associated with BMD and with incident vertebral fractures independent of BMD. No association with prevalent fractures was observed. The large sample size makes the study statistically robust, but the association we observed with BMD and fracture was modest illustrating that single genetic markers make a limited contribution to assessing fracture risk. Our study demonstrates the value of adequately powered studies in quantitating effects of common genetic variants on complex disease.

Disclosures: S.H. Ralston, Sequenom 7.

1211

Gene Search for Femoral Neck Cross-Sectional Geometry. D. H. Xiong, H. Shen^{*}, R. R. Recker, H. W. Deng. Osteoporosis Research Center, Creighton University, Omaha, NE, USA.

Bone geometry is a critical determinant of bone strength, which is highly heritable and is the ultimate intrinsic determinant of fracture risk. To search the underlying genes influencing bone geometry, we performed both genetic linkage and association analyses here. In 4,251 subjects from 471 pedigrees, we genotyped 410 microsatellite markers (~8.9 cM apart) across the whole human genome and performed linkage analyses for five bone geometry parameters at the femoral neck (FN): cross-sectional area (CSA), cortical thickness (CT), endocortical diameter (ED), sectional modulus (Z), and buckling ratio (BR). Significant linkage was found on chromosome 20q11 for CT (LOD = 4.07), 20q13 for BR (LOD = 3.49), and Xq25 for CT (LOD = 3.90). We also identified 13 suggestive linkage signals for the studied geometry traits. Interestingly, three genomic regions seem to be linked with multiple FN geometry traits such as 20q11-13 for CSA, BR and CT (LOD = 2.63, 3.49 and 4.07, respectively), 3q26-27 for CSA and CT (LOD = 2.01 and 2.09, respectively), and 1p12 for CT and CSA (LOD = 1.86 and 2.32, respectively). Given the significant linkage evidence and the exceptionally large sample size adopted, our data strongly support 20q11-13 as a promising region harboring FN geometry quantitative trait loci (QTLs). The association between the estrogen receptor alpha (ER-alpha) gene and FN geometry was tested due to the well-known important physiological effects of estrogen on bone mass and bone remodeling in both genders. We genotyped and tested seven single nucleotide polymorphisms (SNPs) and their haplotypes of the ER-alpha gene in relation to the FN bone geometry parameters in 405 Caucasian nuclear families. Significant association was detected between SNP4 (*rs1801132*) in exon 4 and ED in both single locus analyses ($P = 0.005$) and haplotype analyses ($P = 0.031$). Subjects carrying allele G at SNP 4 had 2.70% smaller ED than non-carriers (data were adjusted by age, sex, weight and height). In addition, SNP5 (*rs932477*) in intron 4 is associated with both CT and BR (single locus analyses: $P = 0.035$ and 0.041, respectively; haplotype analyses: $P = 0.010$ and 0.004, respectively). Similar patterns of association were shown in subgroup analyses stratified by sex, with no apparent sex-specific effects. In summary, we identified several highly significant genomic regions such as 20q11-13 that may contain major QTLs underlying variation in FN bone geometry and suggested that the ER-alpha gene may have modest genetic effects on variation in femoral neck geometry. This study represents an important step toward identifying genes underlying bone geometry (and thus bone quality) and ultimately the risk of osteoporotic fracture.

Disclosures: D.H. Xiong, None.

1212

Moving between Mouse and Humans to Identify a Candidate Gene on Chromosome 10 that Affects Serum IGF-I, Bone Turnover, and Bone Mineral Density. Y. Hsu¹, K. Delahunty^{*2}, T. Niu^{*1}, H. Terwedow^{*1}, J. Lorenzo³, B. Kream³, J. Brain^{*1}, W. Beamer², X. Xu¹, C. Rosen². ¹Population Genetics, Harvard Sch. of Public Health, BOSTON, MA, USA, ²The Jackson Laboratory, Bar Harbor, ME, USA, ³University of Connecticut Health Center, Farmington, CT, USA.

IGF-I is an important growth factor for skeletal remodeling. Several lines of evidence from mice inbred strains and humans suggest that serum IGF-I and BMD are related. We previously identified 4 QTL for the serum IGF-I in F2 mice derived from C3H x B6 crosses. Congenic mice were subsequently generated for two of these QTL (Chr 6 and 10). Those strains were found to have corresponding differences in IGF-I and volumetric BMD (vBMD) in females only. The Chr 10 congenic (10T) exhibited higher serum IGF-I, significantly greater skeletal IGF-I expression and 8% greater vBMD with evidence of increased turnover by histomorphometry versus B6. In vitro, 10T stromal cells showed greater AP staining, and had enhanced osteoclast generation after exposure to RANKL and mCSF versus B6 ($p < 0.01$). SNP block haplotyping using databases localized candidate genes to a <2cM region, very close to the IGF-I gene. To test whether polymorphisms in the IGF-I gene are associated with serum IGF-I and BMD in humans, we examined haplotype tagging SNPs using an extreme case control analysis derived from 13,000 Chinese men and women: 521 controls with extreme high hip BMD were matched with 519 extreme low hip BMD cases. Covariates were adjusted by gender- and menopause-specific regression for age, weight, physical activity, and smoking. We noted that serum IGF-I was negatively associated with total body and hip BMD in postmenopausal women ($p < 0.01$). The ORs for extreme low hip BMD were significantly associated with three LD SNPs (ORs ranging from 2.1-5.1, $p < 0.01$ - $p < 0.05$) for postmenopausal women. The SNP located in 3' UTR region was also significantly associated with low serum IGF-I but only in postmenopausal women ($p < 0.05$). Among women, there was a strong trend downwards in serum IGF-I concentrations related to the presence of osteoporosis; i.e. controls 104±5 ng/ml, Cases: 92±3, Osteoporosis by T-score: 86±3, Osteoporotic fractures: 80±7; $p < 0.01$. In summary, studies in congenic mice narrow the Chr 10 QTL to a region that includes the IGF-I gene. Studies in humans suggest that polymorphisms in the IGF-I gene are causally associated not only with expression of IGF-I but also with the acquisition of peak bone mass. Further subline analysis and haplotyping in the mouse will identify whether the 3'UTR region of the IGF-I gene is critical for regulating bone turnover and peptide expression. Moving between mouse and humans provides an ideal and complementary means for evaluating genomic function and its implications.

Disclosures: Y. Hsu, None.

1213

Combined Bisphosphonate and Endothelin A Receptor Antagonist Treatment More Effectively Reduces Prostate Cancer Growth in Bone than either Alone. K. S. Mohammad¹, C. McKenna^{*1}, A. Mison^{*1}, M. Niewolna^{*1}, R. Vessella^{*2}, E. Corey^{*2}, T. A. Guise¹. ¹Internal Medicine/Endocrinology, University of Virginia, Charlottesville, VA, USA, ²Urology, University of Washington Medical Center, Seattle, WA, USA.

Osteoblastic bone metastases are common in prostate cancer and cause significant morbidity. Endothelin-1 (ET-1) secreted by prostate cancers stimulates osteoblastic responses via the endothelin A receptor (ETAR). ETAR blockade reduces bone metastases in animal models as well as in men with prostate cancer. Osteoclastic bone resorption also contributes to the pathophysiology of osteoblastic metastases. Resorption markers are increased and bisphosphonate antiresorptive drugs reduce skeletal morbidity in patients with osteoblastic disease. We hypothesized that osteolysis contributes to skeletal morbidity in patients with prostate cancer, as much as pathologic bone formation. We used an animal model of osteoblastic prostate cancer to test the effect on tumor growth in bone of osteoblast inhibition with ETAR receptor antagonist (atrasentan) or osteoclast inhibition with bisphosphonate (zoledronic acid ZA), as single agents or in combination. Male nude mice were inoculated with LuCaP 23.1, a xenograft that secretes prostate specific antigen (PSA) and ET-1. Mice were treated with vehicle, atrasentan (20mg/kg/day), ZA (5ug/kg, 3X/week) or the combination, starting one week before tumor inoculation and continuing for 24 weeks. Tumor progression was followed by radiographs and serum PSA concentrations. Mice treated with atrasentan or ZA alone had less osteoblastic response on x-ray compared to vehicle ($p < 0.05$) but did not differ from each other. The combination of atrasentan and ZA was significantly more effective than vehicle or single treatments ($p < 0.01$). PSA concentrations were similar between the vehicle and single treatment groups but were significantly lower in mice treated with both atrasentan and ZA. Histomorphometric analysis of bone demonstrated markedly less tumor burden in bone ($p < 0.001$) as well as new bone area ($p < 0.05$) in mice treated with the combination of atrasentan and ZA compared with those treated with vehicle or ZA. Single agent treatment with atrasentan was associated with a greater reduction in tumor burden and new bone area than treatment with ZA alone. The data suggest that osteoblast and osteoclast activities cooperate to drive the progression of prostate cancer growth in bone. Thus, combination therapy targeting the two major bone cell types should be an effective treatment for osteoblastic bone metastases.

Disclosures: K.S. Mohammad, None.

1214

Reduced Bone and Lung Metastases of 4T1 Mouse Breast Cancer in Osteopontin Null Mice. A. Hiraki^{*}, N. Hashimoto^{*}, P. Williams^{*}, M. Bunegin^{*}, T. Yoneda. Division of Endocrinology, Department of Medicine, University of Texas Health Science Center at San Antonio, San Antonio, TX, USA.

A secreted phosphoglycoprotein osteopontin (OPN) is produced in various types of human cancers and has been implicated in tumorigenesis, local invasiveness and distant metastases. Recent studies have reported that tumor-produced OPN plays a role in bone metastases in human breast and prostate cancers. However the role of host-derived OPN in metastasis of these cancers to bone, in which OPN is abundant, and non-bone sites is unclear. It is also unclear whether OPN plays a specific role in bone metastases. To study these, we developed a syngeneic orthotopic model of metastasis in which inoculation of the 4T1 mouse breast cancer cells in mammary fat pad in female Balb/c mice caused metastases in bone and lung. The 4T1 cells were stably transfected with firefly luciferase cDNA (4T1/luc) for quantitative assessment of tumor burden. Western blot analyses showed that 4T1 cells produced substantial amounts of OPN. Introduction of an anti-sense-OPN cDNA in 4T1 cells (4T1/ASOPN/luc) markedly inhibited OPN production and reduced metastases to bone and lung compared to empty-vector-transfected 4T1 cells (4T1/EV/luc). These results show that tumor-produced OPN plays an important role in distant metastases in 4T1 breast cancer. To examine the role of host-derived OPN in distant metastasis, we inoculated 4T1/EV/luc and 4T1/ASOPN/luc into syngeneic female OPN-deficient (OPN^{-/-}) mice compared with wild-type (WT) mice. Tumor formation of 4T1/EV/luc and 4T1/ASOPN/luc at the orthotopic site did not differ between WT and OPN^{-/-} mice. In contrast, 4T1/EV/luc metastases to bone and lung were decreased in OPN^{-/-} mice compared with WT mice. Similarly, 4T1/ASOPN/luc metastases to bone and lung were also reduced in OPN^{-/-} mice. To understand the mechanism underlying reduced distant metastases in OPN^{-/-} mice, adherence, proliferation and apoptosis of 4T1 cells in plates coated with varying concentrations of OPN were examined. We found that the attachment and growth of 4T1/EV/luc and 4T1/ASOPN/luc cells in OPN-coated plates were greater than non-coated plates. The effects were dependent on OPN concentration. Furthermore, these cells displayed decreased apoptosis in OPN-coated plates. These results suggest that host-derived OPN contributes to the stimulation of arrest and colonization and protection from apoptosis of metastatic cancer cells in target organs. Taken together, our results using OPN^{-/-} mice suggest that not only tumor-derived but also host-derived OPN is critical to bone and lung metastases in breast cancer. The results also suggest that OPN plays an important role in non-bone metastases as well as bone metastases.

Disclosures: A. Hiraki, None.

1215

Inhibition of Epidermal Growth Factor Receptor Signaling Abrogates Humoral Hypercalcemia of Malignancy in a Mouse Model of Human Lung Squamous Cell Carcinoma. G. Lorch^{*1}, P. F. Koltz^{*2}, Y. M. Cho^{*2}, R. L. Konger^{*2}, K. S. Nadella^{*1}, J. L. Gilmore^{*2}, R. E. Toribio^{*1}, T. J. Rosol¹, J. Foley². ¹Veterinary Biosciences, The Ohio State University, Columbus, OH, USA, ²School of Medicine, Indiana University, Indianapolis, IN, USA.

Dysregulation of the erbB family of receptors and the epidermal growth-factor (EGF) family of peptide hormones plays an important role in the progression of human lung squamous cell carcinoma (SCC). Lung SCC is frequently associated with humoral hypercalcemia of malignancy (HHM) due to over production of parathyroid hormone-related protein (PTHrP). It has been reported that EGF induces PTHrP transcription through epidermal growth factor receptor (EGFR) signaling, likely involving the ras/Mek/Erk pathway in keratinocytes. The purpose of this study was to evaluate EGFRs' contribution to PTHrP expression and resulting HHM in the human lung SCC cell line, RWGT2. RWGT2 cells produce HHM when grown as a xenograft in nude mice. Using western blot analysis, we found that RWGT2 SCC express high levels of EGFR and moderate levels of erbB3. We identified that RWGT2 SCC produce the EGF-related growth factors amphiregulin, TGF- α and heparin binding-EGF by Q-RT-PCR. Amphiregulin mRNA levels were 1000-fold greater than the other two factors. To test the relationship between EGFR activity and PTHrP gene expression in RWGT2 SCC, we treated the cells for 6 hours with 1 μ M of EGFR tyrosine kinase inhibitors (TKI) PD153035 and ZD1839 (gefitinib) and measured PTHrP mRNA levels by Q-RT-PCR. Treatment with each TKI resulted in significant reductions (60%) of PTHrP/GAPDH mRNA ratios, suggesting that a substantial portion of PTHrP mRNA in RWGT2 cells was due to EGFR signaling. The *in vivo* relationship between EGFR and PTHrP gene expression was investigated using a xenograft RWGT2 HHM model. Hypercalcemic mice with total Ca²⁺ concentrations ≥ 12 mg/dl were treated with 200mg/kg of gefitinib for 3 consecutive 24-hour periods. Plasma calcium was measured at 6, 24, 52, and 78 hrs after the first treatment. Calcium concentrations were significantly reduced at all time points when compared to pretreatment and control values ($p < 0.05$). All gefitinib-treated HHM mice had normal calcium concentrations at 78 hrs. Plasma PTHrP concentrations in gefitinib-treated mice were significantly reduced (50%) when compared to untreated mice with RWGT2 xenografts at 78 hrs ($p < 0.05$). In conclusion, autocrine activation of PTHrP gene expression is mediated through the EGFR in this cell line. Moreover, inhibition of the EGFR pathway in an HHM model by administration of an anilinoquinazoline demonstrates for the first time that EGFR is a potential target for antihypercalcemic therapy in patients with lung SCC-associated HHM.

Disclosures: G. Lorch, NIH 2.

1216

SD-208, a Small Molecule Inhibitor of Transforming Growth Factor β Receptor I Kinase Reduces Breast Cancer Metastases to Bone and Improves Survival in a Mouse Model. E. G. Stebbins^{*1}, K. S. Mohammad², M. Niewolna^{*2}, C. R. McKenna^{*2}, A. P. Mison^{*2}, F. Schimmoller^{*1}, A. Murphy^{*1}, S. Chakravarty^{*1}, S. Dugar^{*1}, L. S. Higgins^{*1}, D. H. Wong^{*1}, T. A. Guise². ¹Scios, Inc., Fremont, CA, USA, ²Division of Endocrinology, University of Virginia, Charlottesville, VA, USA.

Breast cancer commonly metastasizes to and destroys bone to cause pain and fracture. Substantial data support central roles for bone-derived transforming growth factor-beta (TGF- β) and tumor-derived osteolytic factors such as parathyroid hormone related peptide (PTHrP) in a vicious cycle of local bone destruction in osteolytic metastases. TGF- β , stored in bone matrix and released in active form during osteoclastic resorption, stimulates PTHrP production by tumor cells. PTHrP in turn mediates bone destruction by stimulating osteoclasts. A dominant negative mutant of the type II TGF- β receptor inhibited TGF- β -induced PTHrP secretion *in vitro* and development of bone metastases in an MDA-MB-231 experimental metastasis model. These studies provided proof of principle to support a role for TGF- β blockade in the treatment of breast cancer bone metastases. SD-208, a small molecule inhibitor of TGF- β receptor I kinase (TGF-BRI), inhibits signaling downstream of the TGF- β receptor. The *in vivo* efficacy of SD-208 was evaluated in an experimental metastasis model using the breast carcinoma cell line MDA-MB-231. Pre-treating nude mice with SD-208 (0.3 and 1 mg/ml added to drinking water) reduced the rate of osteolytic bone destruction, as assessed by computerized image analysis of radiographs, and prolonged survival. In mice with established bone metastases, SD-208 (20 and 60 mg/kg po qd administered via oral gavage) reduced osteolytic lesion area and prolonged survival compared to vehicle control. To dissect the mechanism regulating these *in vivo* therapeutic benefits, the effects of SD-208 were analyzed in cultured MDA-MB-231 cells. SD-208 did not affect cell proliferation. However, SD-208 inhibited TGF- β -induced smad2/3 phosphorylation as well as decreased production of TGF- β -stimulation of osteolytic factors, IL-11, PTHrP, and growth promoting factor, connective tissue growth factor (CTGF). It also reduced TGF- β secretion from MDA-MB-231 cells, suggesting possible autocrine effects of TGF- β on the cancer cells. Taken together, these data indicate that therapeutic targeting of TGF- β may decrease the osteolytic bone metastases due to breast cancer by blocking tumor production of osteolytic and growth-promoting factors such as IL-11, PTHrP and CTGF.

Disclosures: E.G. Stebbins, Scios, Inc. 3.

1217

Inhibiting p62^{ZIP} Expression Decreases OCL Formation by Blocking the Effects of RANKL and TNF- α . N. Kurihara¹, T. Honjo¹, J. J. Windle², G. D. Roodman³. ¹Medicine/Hem-Onc, University of Pittsburgh, Pittsburgh, PA, USA, ²Human Genetics, Virginia Commonwealth Univ., Richmond, VA, USA, ³Medicine/Hem-Onc, University of Pittsburgh and VA Pittsburgh Healthcare System, Pittsburgh, PA, USA.

Osteolytic bone destruction occurs in up to 80% of patients with multiple myeloma (MM), and plays a critical role in promoting tumor growth. RANK ligand (RANKL), IL-6 and TNF- α production is increased in the marrow microenvironment in MM patients and have been implicated in this process. Recently, a new member of the RANKL signaling pathway, p62^{ZIP}, has been identified. p62^{ZIP} plays a critical role in NF- κ B activation induced by TNF- α , RANKL and IL-1 and is involved in multiple signaling pathways that can enhance tumor cell survival and bone destruction. It is our hypothesis that inhibiting p62^{ZIP} expression will profoundly diminish osteolytic bone destruction and myeloma growth by blocking the effects of RANKL and IL-6 produced in the tumor-bone microenvironment in response to TNF- α . Therefore, we used p62^{ZIP} $-/-$ mice to determine the role of p62^{ZIP} on OCL formation and the capacity of p62^{ZIP} stromal cells to support OCL formation by normal spleen cells treated with 1,25(OH)₂D₃ or PTHrP. Spleen or marrow cells from p62^{ZIP} $-/-$ and p62^{ZIP} $+/+$ mice were treated with RANKL or TNF- α to induce OCL formation and assess NF- κ B gene reporter activity. OCL formation and NF- κ B gene reporter activity in p62^{ZIP} $-/-$ mice were markedly decreased at low concentrations of RANKL and TNF- α compared to p62^{ZIP} $+/+$ OCL precursors. Expression of RANKL mRNA and protein in cultured marrow stromal cells from these mice showed that similar levels of RANKL mRNA were detected in both normal and p62^{ZIP} $-/-$ stromal cells treated with 1,25-(OH)₂D₃, or PTH-rp for 48 hours. Conditioned media from marrow stromal cells treated with vehicle (media alone), 1,25-(OH)₂D₃, PTH-rp, TNF- α or IL-6 for 7 days showed that 1,25-(OH)₂D₃ induced similar maximal RANKL levels in the conditioned media (1089 \pm 689 pg/ml for p62^{ZIP} $+/+$ and 1161 \pm 567 pg/ml for p62^{ZIP} $-/-$, mean \pm SD respectively). In contrast, in cultures treated with 100 pg/ml TNF- α , RANKL levels were significantly decreased in p62^{ZIP} $-/-$ stromal cell cultures (775 \pm 391 vs. 114 \pm 9 pg/ml, mean \pm SD). We then tested stromal cells from p62^{ZIP} $-/-$ mice for their capacity to support osteoclastogenesis by normal spleen CFU-blast. OCL formation was significantly decreased in cocultures of p62^{ZIP} $-/-$ stromal cells treated with PTH-rp, IL-6 and TNF- α . These results demonstrate that p62 plays an important role in OCL formation induced by inflammatory cytokines that are upregulated in the marrow microenvironment in patients with myeloma. They further suggest that blocking p62 signaling may markedly reduce OCL formation in myeloma patients.

Disclosures: N. Kurihara, None.

1218

Osteonecrosis of the Jaw in Patients Receiving Intravenous Bisphosphonate Therapy. A. O. Hoff, B. Toth*, K. Altundag*, V. Guarneri*, A. Nooka*, K. Desrouleaux*, M. Klein*, A. Adamus*, G. Sayegh*, A. Worthing*, R. F. Gagel, G. N. Hortobagyi*. University of Texas MD Anderson Cancer Center, Houston, TX, USA.

Advances in treatment modalities for metastatic bone disease (MBD) have resulted in a dramatic change in the outcome of cancer patients (pts). Part of this progress has occurred with the introduction of bisphosphonate (BP) therapy. Studies have shown that BPs significantly reduce the number and delay the onset of skeletal-related events such as fractures, cord compression and hypercalcemia. Although the efficacy of these drugs is well documented, there have been recent reports of osteonecrosis of the jaw (ONJ) occurring in pts receiving BP. This is a preliminary report of our 2239 patient records reviewed to date. To estimate the frequency, understand the clinical presentation and to identify risk factors for development of ONJ we have initiated a retrospective review of pts treated with intravenous (IV) BP at our Institution from January 1994 to December 31, 2003. A total of 4032 treated pts have been identified through the Pharmacy database. Patients diagnosed with ONJ at the dental oncology clinic are also reviewed. ONJ was defined as exposed non-healing bone with/without pain of at least 3-6 months duration. Among 2239 records reviewed to date, we have identified 29 pts with ONJ [estimated frequency (EF): 1.3%]. Fourteen of these pts have multiple myeloma (MM) (14/309, EF: 4.5%), 14 have metastatic breast carcinoma (MBC) (14/1147, EF 1.2%). One or more potential predisposing factors were identified in several pts: dental extraction prior to development of ONJ (12), mandibular exostosis (7), trauma (2), and periodontal disease (10). The time from starting BP therapy to the diagnosis of ONJ, defined as time to event (TTE), ranged from 4 to 65 months (mean TTE: 40 months). Thirteen patients were treated with pamidronate (PA) and zoledronic acid (ZA), 7 patients with ZA, 8 patients treated with PA and, 1 patient treated with alendronate and PA. The mean cumulative dose of PA was 2092 mg (range: 360-3610 mg), ZA was 53 mg (range: 28-96 mg). Pts were treated with aggressive oral hygiene, salicet or sodium bicarbonate oral rinse, debridement of necrotic bone and antibiotics when infection was detected. In conclusion, ONJ is a significant but relatively uncommon event observed in patients with MBC and MM treated with IV BP. The pathogenesis and etiology are still unclear but a combination of factors, possibly including chronic bisphosphonate therapy, exposure to extensive chemotherapy agents and steroids as well as a traumatic oral event, seem to be important in its evolution.

Disclosures: A.O. Hoff, Novartis 2, 5.

1219

Dickkopf's Are Expressed by Breast Cancer Cell Lines and Regulated by PTHrP. K. D. Hausler*. Bone, Joint and Cancer, St. Vincent's Institute, Melbourne, Australia.

Dickkopf (Dkk) proteins have been shown to bind to LRP-5 and prevent Wnt signalling, a pathway involved in bone formation. We have investigated the role of the Wnt pathway in breast cancer growth in bone using a candidate gene approach. We determined mRNA expression levels of secreted frizzled-related proteins (sFRP's), Dkk's and other Wnt pathway molecules using MCF-7 human breast cancer cell lines. MCF-7, vector control cell lines and several clonal cell lines overexpressing PTHrP, which induce greater osteolytic damage *in vivo* than parental MCF-7 cells, were found to express components of the Wnt pathway. Notably, the cell lines overexpressing PTHrP had increased Dkk-2 mRNA expression relative to vector control and parental MCF-7 cells. We investigated the association between Dkk-2 and PTHrP mRNA in MCF-7 cells using recombinant and synthetic peptides corresponding to various portions of PTHrP.C-terminal region of PTHrP (107-139aa), but not N-terminal sequences (1-34 and 1-108aa), were found to upregulate both Dkk-2 and Dkk-3 mRNA's 4-fold in MCF-7 and MCF-10A (mammary epithelial) cell lines. There was no effect of any fragments of PTHrP on Dkk-1 mRNA. We established that there is an active canonical Wnt signalling pathway present in MCF-7 cells by measuring translocation of β -catenin to the nucleus (immunocytochemistry) and activation of Tcf/Lef gene transcription (luciferase reporter) in the presence of either LiCl (GSK3 β inhibitor) or recombinant Wnt3a. To determine the effect of Dkks upon osteoclast formation, we used recombinant Dkk-1 and found that this inhibits osteoclast formation *in vitro*. sFRP-1, another inhibitor of the Wnt pathway, also inhibited osteoclast formation. Both sFRP-1 or Dkk-1 was able to dose dependently inhibit osteoclast formation in either osteoblast/bone marrow co-cultures, or RANKL+M-CSF-treated bone marrow cultures. The action of Dkk-1 and sFRP-1 to limit osteoclast formation may be explained by their ability to inhibit Wnt signaling (canonical, canonical and non-canonical respectively), suggesting that Wnt signaling is involved in osteoclastogenesis. Combined these data suggest that Dkk's produced by breast cancers may influence the proposed vicious cycle of destruction characteristic of breast cancer growth in bone in an autocrine manner, particularly since PTHrP, a driver of osteolysis, regulates expression of Dkk's. In addition, there may be paracrine actions of Dkk's on resident osteoclast and osteoblast cells.

Disclosures: K.D. Hausler, None.

1220

Inhibition of RhoA GTPase and p42/44 MAPKs Triggers Osteosarcoma Cell Apoptosis Independently of BMP-2 Signaling. O. Fromiguet^{*1}, S. Bouvet^{*1}, E. Hay^{*1}, A. Jacquet^{*2}, D. Modrowski¹, P. Auberger^{*2}, P. J. Marie¹.¹Laboratory of Osteoblast Biology and Pathology, Inserm U606, Paris, France, ²Faculty of Medicine Pasteur, Inserm U526, Nice, France.

Osteosarcoma is the most common primary bone tumor in young adults. Despite improved prognosis, resistance to chemotherapy remains responsible for failure of osteosarcoma treatment. The identification of signals that promote apoptosis in osteosarcoma cells may provide clues to develop new therapeutic strategies for chemoresistant osteosarcoma. We previously showed that BMP-2 induces apoptosis in human osteosarcoma cells through activation of BMP receptor IB (BMPR-IB). Here, we investigated whether statins that promote BMP-2 expression in osteoblasts, may induce human osteosarcoma cell apoptosis through activation of BMP signaling. Lipophilic statins (atorvastatin, simvastatin and cerivastatin, kindly provided by Bristol-Myers-Squibb, USA) strikingly induced caspases-dependent apoptosis in both BMPR-IB-expressing (SaOS2) and BMPR-IB-deficient (OHS4) human osteosarcoma cells, whereas the hydrophilic statin pravastatin had no effect. Statin-induced caspase-3 activity occurred earlier (7-24 h) than BMP-2 protein expression which increased at 72 h. The statin-induced apoptosis was not prevented by overexpression of noggin, a potent BMP antagonist and was not associated with increased Runx2, alkaline phosphatase and osteocalcin mRNA levels. The proapoptotic effect of statins was abolished by mevalonate and geranylgeranylpyrophosphate, but not farnesylpyrophosphate, indicating the involvement of small GTPases Rho proteins. Lipophilic statins rapidly induced RhoA cell membrane relocation to the cytosol and inactivation of RhoA activity with a time course consistent with activation of caspase-3, which implicates RhoA in human osteosarcoma cell death induced by statins. The inhibition of RhoA activity induced by statins resulted in decreased phosphorylation of the survival pathway p42/p44-MAPKs and decreased expression of the anti-apoptotic protein Bcl-2, whereas Bax, Bim and survivin were not affected. Constitutively active RhoA, but not wild type RhoA, rescued phospho-p42/p44-MAPKs and Bcl-2 levels and abolished statin-induced apoptosis, which establishes a key role for RhoA in controlling osteosarcoma cell apoptosis. The data provide the first evidence in osteosarcoma cells that inhibition of RhoA GTPase activity by statins is sufficient to induce irreversible apoptosis by a BMP-2-independent mechanism mediated by inhibition of the p42/p44-MAPKs-Bcl-2 survival pathway, and support the concept that osteosarcoma cell apoptosis can be induced independently of commitment to cell differentiation.

Disclosures: **P.J. Marie**, None.

1221

Influence of Estrogen Status and Alendronate on Periosteal Bone Formation in the Ilium of Adult Women. S. J. Bare^{*1}, S. Recker¹, R. Recker¹, D. Kimmel². ¹Creighton University, Omaha, NE, USA, ²Merck & Co., West Point, PA, USA.

The trabecular (Tb) envelope of transilial biopsy (TIBx) specimens is most often studied. TIBxs also contain periosteal [Ps] and endocortical [Ec] envelopes. The Ps and Ec envelopes may reflect unique hormonal/treatment effects on bone remodeling. Our purpose is to quantitate the influence of hormonal status change or alendronate (ALN) on the Ps and Ec envelopes of adult women. One unstained section from each of two levels of TIBx's of 42 healthy women (1-7yrs pre-menopause [peri] and at 1yr after last menses [post]); and 137 post-menopausal osteoporotic (PMO) women treated with placebo (PBO), ALN (10mg/d), hormone replacement (HRT), or HRT+ALN for 2yrs, was examined for: total (BS), and double (2XL)-fluorochrome labeled surface, and mineral apposition rate (MAR), in Ps and Ec envelopes. 2XL/BS was calculated omitting subjects lacking 2XL. Paired t-test was used for the first group (* P<.05; peri vs. post) (+ P<.05; Ps vs. Ec); two-factor ANOVA was used for the latter.

Table 1a Transmenopausal Women (N=42)				
Envelope	Surface (mm)	% with 2XL	2XL/BS (%)	MAR (µm/d)
Ps/Peri	30±4	14	1.24±1.15	0.76±0.26 (6)
Ps/Post	34±4	33*	1.14±1.14	0.99±0.47 (14)
Ec/Peri	34±5	91	6.12±4.64*	0.88±0.19 (38)
Ec/Post	38±4	93	5.65±4.00	0.97±0.22 (39)
Table 1b. Effect of HRT and ALN (N=137)				
Ps/PBO	30±9	38	1.36±1.06	0.86±0.36 (18)
Ps/ALN	32±6	29	0.75±0.58	0.86±0.35 (7)
Ps/HRT	28±10	16*	1.98±2.18	0.88±0.45 (5)
Ps/ALN+HRT	30±8	9*	0.28±0.19*	0.72±0.44 (3)
Ec/PBO	32±10	92	6.12±4.82	0.72±0.20 (44)
Ec/ALN	35±6	46*	2.03±1.84*	0.66±0.24 (11)
Ec/HRT	30±10	61*	3.68±3.92*	0.71±0.24 (19)
Ec/ALN+HRT	33±9	12**	1.26±1.31*	0.58±0.25 (4)

Based on 2XL/BS and percentage of subjects with 2XL, the Ps envelope had a much lower bone formation rate than the Ec envelope both peri- and post-menopause. The percentage of women with Ps 2XL doubled transmenopausally, without a change at the Ec envelope. 2XL/BS in each envelope was constant. In PMO biopsies the Ps envelope again had a lower percentage of subjects with 2XL and lower 2XL/BS than the Ec envelope. HRT reduced the percentage with 2XL at both envelopes, while ALN reduces that percentage only at the Ec envelope. Both HRT and ALN reduce 2XL/BS at the Ec envelope. **Conclusion:** The TIBx Ps envelope forms bone much more slowly than the Ec envelope. HRT slows bone formation at both envelopes, while ALN does so only at the Ec envelope. These data suggest that estrogen deficiency onset is accompanied by increased periosteal expansion. They further suggest that ALN permits periosteal expansion to continue unabated, while HRT inhibits it.

Disclosures: **S.J. Bare**, None.

1222

Preventing the First Vertebral Fracture in Postmenopausal Women with Low Bone Mass Using PTH(1-84): Results from the TOP Study. S. L. Greenspan^{*1}, H. G. Bone^{*2}, T. B. Marriott^{*3}, J. R. Zanchetta^{*4}, M. P. Ettinger^{*5}, D. A. Hanley^{*6}, M. K. Drezner^{*7}, P. D. Miller^{*8}.¹University of Pittsburgh, Osteoporosis Prevention and Treatment Center, Pittsburgh, PA, USA, ²Michigan Bone and Mineral Clinic, Detroit, MI, USA, ³NPS Pharmaceuticals, Salt Lake City, UT, USA, ⁴IDIM and USAL University, Buenos Aires, Argentina, ⁵The Regional Osteoporosis Center, Stuart, FL, USA, ⁶University of Calgary, Calgary, AB, Canada, ⁷University of Wisconsin Medical School, Madison, WI, USA, ⁸Colorado Center for Bone Research, Lakewood, CO, USA.

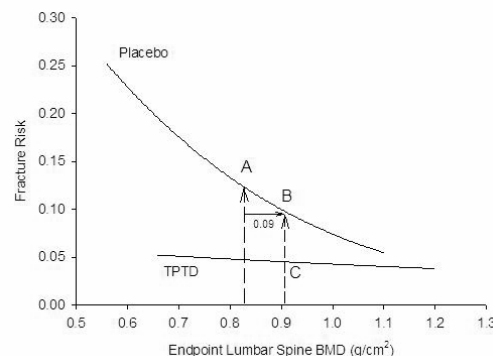
The occurrence of a first vertebral fracture may produce significant immediate morbidity, but clinical trials and population studies have also shown a vertebral fracture increases the risk of more vertebral fractures; these fractures have adverse implications for patients' long-term health. Reducing risk of first fracture in women with osteoporosis is an important goal. The Treatment of Osteoporosis with PTH (TOP) study, an 18-month, multinational, randomized, double-blind, placebo-controlled trial, assessed the effect of recombinant human PTH(1-84) on vertebral fracture incidence in postmenopausal women with osteoporosis. Analysis was by intent to treat (ITT), which included all randomized subjects with evaluable spine X-rays at 18 months. Subjects included postmenopausal women with low bone mass without (n=2056) and with (n=471) prevalent vertebral fracture (PVF) at baseline. Bone density criteria for entry without PVF were lumbar spine T-scores of ≤ -3.0 (age 45-54 years), or ≤ -2.5 (≥ 55 years). All subjects received calcium (700 mg/d) and vitamin D (400 IU/d) supplements. At 18 months, the incidence of vertebral fractures (total ITT) was 3.37% in placebo-treated subjects vs 1.32% in PTH(1-84)-treated subjects, a relative risk reduction (RRR) of 61%. In the ITT group without PVF, the incidence of new (first) vertebral fracture was 2.08% (placebo) and 0.67% (PTH(1-84)), a RRR of 68% (95% CI: 0.14-0.75, p=0.006). In the ITT group with a PVF, the incidence of new vertebral fracture was 8.94% (placebo) and 4.24% (PTH(1-84)), a 53% RRR (95% CI: 0.23-0.98, p=0.040). In general, PTH(1-84) therapy was well tolerated, with headache, dizziness, and nausea occurring with higher frequency in the PTH(1-84)-treated group than in the placebo-treated group. Although the incidence of hypercalcemia was higher (28.3% vs 4.7% in the placebo group), this led to discontinuation of therapy in only 0.5% of the PTH(1-84)-treated group (ITT). We conclude that PTH(1-84) therapy significantly reduces the incidence of vertebral fractures, and, in particular, significantly decreased the risk of first vertebral fracture in a population of postmenopausal women with osteoporosis defined by BMD.

Disclosures: **S.L. Greenspan**, NPS Pharmaceuticals 2, 5.

1223

Change in Bone Mineral Density (BMD) and Fracture Risk Reduction in Teriparatide-Treated Women with Osteoporosis. P. Chen^{*1}, P. D. Miller², P. D. Delmas³, D. A. Misurski^{*1}, J. H. Krege¹.¹Eli Lilly and Company, Indianapolis, IN, USA, ²Center for Bone Research, University of Colorado, Denver, CO, USA, ³Hopital Edouard Herriot, Claude Bernard University of Lyon, Lyon, France.

Changes in BMD account for a relatively small proportion of fracture risk reduction in patients treated with antiresorptive drugs.¹⁻³ The relationship between teriparatide (TPTD)-mediated increases in lumbar spine (LS) BMD and the risk of new vertebral fractures was assessed using data from the Fracture Prevention Trial. Postmenopausal women with osteoporosis (n=1637) were randomized to placebo or TPTD 20 or 40 mcg/day for a median 19 months.⁴ LS BMD was assessed at baseline and 18 months. Vertebral whose fracture status changed were removed from the present analysis. Baseline and endpoint lateral spine x-rays were assessed using a visual semiquantitative technique.⁵ Both baseline BMD and BMD change were contributors to fracture risk. The mean increase in TPTD-treated patients was 0.09 g/cm². This increase was similar across tertiles of baseline BMD. Fracture risk was assessed using a logistic regression model. Factors included in the model were endpoint BMD, treatment (pooled TPTD versus placebo), and treatment-by-BMD interaction. All were statistically significant (p < 0.05). Compared to placebo, fracture risk was lower in the TPTD group for all endpoint BMD values, and the absolute risk reduction was significantly different across the range of endpoint BMD values (Figure).



In the figure, A-B and A-C represent fracture risk reductions associated with a 0.09 g/cm² increase in BMD alone and in response to TPTD, respectively. The proportion of TPTD-

mediated fracture risk reduction attributable to the increase in BMD can be estimated by (A-B)/(A-C). For "A" values from 0.7 to 0.9 g/cm², the proportion of TPTD-mediated fracture risk reduction attributable to a 0.09 g/cm² increase in BMD ranged from 30 to 41%, respectively. The remainder of vertebral fracture risk reduction with TPTD was due to improvements in other non-BMD determinants of bone strength.

References

- ¹Sarkar S et al. J Bone Miner Res 2002;17:1-10
²Li et al. Stat Med 2001;20:3175-88
³Cummings et al. Am J Med 2002;112:281-289
⁴Neer et al. N Engl J Med 2001;344:1434-41
⁵Genant et al. J Bone Miner Res 1993;8:1137-48

Disclosures: **P. Chen**, Eli Lilly 3.

1224

Indications for Spinal Radiography in Postmenopausal Women. L. Ferrar¹, D. Felsenberg^{*2}, C. Roux^{*3}, D. M. Reid^{*4}, C. C. Gluer^{*5}, G. Armbricht^{*2}, T. Blenk^{*2}, R. Eastell⁶. ¹Division of Clinical Sciences (N), University of Sheffield, Sheffield, United Kingdom, ²Free University, Berlin, Germany, ³Descartes University, Paris, France, ⁴University of Aberdeen, Aberdeen, United Kingdom, ⁵University Hospital, Schleswig Holstein, Kiel, Germany, ⁶Division of Clinical Sciences (N), University of Sheffield, UK, Sheffield, United Kingdom.

Prevalent vertebral fracture is a powerful predictor of future fracture risk. The aim of this analysis was to evaluate a range of risk factors that could be used as indicators for referral for spinal radiography. The study subjects were postmenopausal women participating in a population-based study of osteoporosis (n = 2374). Vertebral fractures (VFs) were identified from spinal radiographs (vertebral height ratio < 0.80 and differential diagnosis by radiologist) in 378 women. Risk factors tested were older age (≥65 and ≥70 years), height (stature) loss ≥4 cm since age 25 years, history of low-trauma non-vertebral fracture (non-VF), bone mineral density (BMD) T score ≤-2.5 (spine or total hip) and corticosteroid use (≥5 mg/day for ≥6 months). These were tested individually for discrimination of women with VFs (chi-squared test), then together by logistic regression (with separate analyses for the 2 age thresholds). Receiver Operator Characteristic (ROC) analysis was used to evaluate the discrimination of women with VF by one or more of the significant risk factors from the logistic regression model. For individual risk factors, odds ratios for VF were 4.0 and 2.9 (T ≤-2.5 at hip and spine), 1.9 (history of non-VF), 1.9 and 1.8 (age ≥65 and ≥70 years), 1.6 (height loss ≥4 cm) and 0.9 (corticosteroid use). Significant risk factors from logistic regression were BMD T score ≤-2.5 (hip or spine), history of non-VF and age (≥65 or ≥70 years). Results for analysis of one or more significant risk factors are shown below in the table. Only 131 (35%) of women with VF would have been diagnosed with osteoporosis on the basis of BMD measurements alone.

	One or more significant risk factor		
	Age excluded	Including age ≥65 years	Including age ≥70 years
VF-positive [negative] (n)	211 [628]	304 [1262]	274 [1034]
Sensitivity [specificity] (%)	56 [69]	80 [37]	73 [48]
Positive predictive value	25.1	19.4	20.9
Odds ratio	1.6	2.4	2.5
Area under curve	0.62	0.59	0.60
95% CI	0.60, 0.64	0.57, 0.61	0.58, 0.62

We conclude that referral for VFA on the basis of axial BMD T score ≤ -2.5, history of low trauma non-vertebral fracture or age ≥65 years could identify around three-quarters of postmenopausal women with vertebral fracture.

Disclosures: **L. Ferrar**, None.

1225

GLP-2 Administration Attenuates Nocturnal Bone Resorption in Postmenopausal Women: A 14-Day Study. D. B. Henriksen¹, P. Alexandersen^{*2}, B. Hartmann¹, C. Adrian^{*1}, I. Byrjalsen^{*3}, J. J. Holst^{*4}. ¹Sanos Bioscience A/S, Herlev, Denmark, ²Center for Clinical and Basic Research A/S, Vejle, Denmark, ³Nordic Bioscience A/S, Herlev, Denmark, ⁴Medical Physiology, University of Copenhagen, Copenhagen, Denmark.

The gastrointestinal hormone, glucagon-like peptide-2 (GLP-2) has been suggested to be involved in an entero-osseous axis, which coordinates bone resorption in response to nutrient intake. We have located the GLP-2 receptor on osteoclasts and shown that GLP-2 exposure to osteoclasts in culture leads to a dose related reduction in bone resorption. Likewise, subcutaneous injection of GLP-2 in healthy postmenopausal women results in a dose related reduction in bone resorption as assessed by fragments derived from collagen type I, (CTX-I). Bone formation, as assessed by osteocalcin, was unaffected by the exogenous GLP-2 treatment. The objective of the study was to investigate whether the previously found single-dose effects of GLP-2 on the biochemical markers of bone turnover persist and are reproducible during continued daily administration. Nocturnal increase in bone resorption reflects the highest activity level of the osteoclasts. The current study was designed to evaluate the effect of exogenous GLP-2 on bone turnover in healthy postmenopausal women after one daily administration of GLP-2 at bedtime (10 p.m.) during a 2-week treatment period. This was a randomised, double-blind, placebo-controlled, parallel group, and dose-ranging study in 60 healthy postmenopausal women. Twenty subjects were randomised to each treatment group to receive treatment with daily doses of 1.6 or 3.2 mg of GLP-2, or placebo. We found an acute and sustained reduction of bone resorption after GLP-2 injection as compared to placebo for both 1.6 and 3.2 mg groups. This effect was similar at Day 1 and Day 14. The baseline normalised area under the curve (AUC_{0-6h}) for the 6-hour profile of s-CTX was highly statistically significant

different from placebo (P<0.0001) for both 1.6 and 3.2 mg GLP-2 groups and there were no statistically significant difference in the effect between Day 1 and Day 14. Thus, the effect seen at Day 1 was sustained after 14 days of treatment with GLP-2. Bone formation (osteocalcin) level was unaffected by treatment with GLP-2. The drug substance was well tolerated and none of the subjects developed antibodies against GLP-2. No serious adverse events were reported by the investigators, which could be attributed to the GLP-2 drug substance. In conclusion, these observations suggest that GLP-2 might be useful as a pharmacological agent for the un-coupling of the bone turnover processes. Further studies are warranted to determine the putative anti-osteoporotic effect of GLP-2.

Disclosures: **D.B. Henriksen**, None.

1226

RANKL Inhibition Improves Cortical Bone Geometry by Stimulating Periosteal Bone Formation in Orchiectomized Rats. X. Li, Z. Geng^{*}, S. Kaufman^{*}, H. L. Tan^{*}, S. Morony^{*}, M. Grisanti^{*}, K. Hoffmann^{*}, M. Ominsky, P. J. Kostenuik. Amgen, Thousand Oaks, CA, USA.

In cynomolgus monkeys, the RANKL inhibitor, OPG, increases cortical thickness and periosteal circumference. This periosteal expansion increases bone strength index by virtue of improvements in the cross-sectional moment of inertia (CSMI). The mechanism by which RANKL inhibition leads to cortical expansion is unclear. We examined the effects of OPG on cortical geometry and periosteal bone formation in a model of cortical osteopenia caused by androgen ablation. Three-month-old rats were either sham-operated (Sham) or orchiectomized (ORX). ORX rats were treated with PBS or OPG (10 mg/kg, twice/week SC, n=10-11/group) beginning immediately after the surgery. Periosteal and endocortical diameters at the femoral shaft were collected in a blinded manner from digital X-rays after 6 weeks of treatment. PBS-treated ORX rats had 9% and 12% decreases in periosteal and endocortical diameters, respectively (p<0.01 vs Shams). These changes resulted in a 27% decrease in CSMI (p<0.01 vs Shams). OPG-treated ORX rats had significantly greater periosteal (6%) and endocortical diameters (8%) than PBS-treated ORX rats. These OPG-induced changes led to a 16% increase in CSMI (p=0.06 vs PBS-ORX rats). Dynamic histomorphometry of the femoral shaft provided mechanistic insights into these geometric changes. Orchiectomy led to a significant (38%) reduction in periosteal bone formation rate (BFR) and a significant increase (133%) in endocortical BFR. These changes would contribute to reductions in periosteal and endocortical diameters. OPG caused a significant (33%) increase in periosteal BFR and a significant (142%) reduction in endocortical BFR. These changes returned periosteal and endocortical diameters in ORX rats to levels similar to Shams. OPG also caused significant improvements in cancellous bone. PBS-ORX rats had significant (67%) reductions in bone volume (BV/TV) at the distal femur. OPG treatment significantly reduced osteoclast surface by 67% and increased BV/TV by 107%. DXA showed that OPG increased distal femur BMD by 18% (p<0.05 vs PBS-ORX). In summary, androgen ablation in rats results in significant cortical and cancellous osteopenia. Cortical osteopenia was associated with reduced periosteal bone formation and a reduced CSMI. OPG treatment prevented these changes and restored cortical and cancellous bone mass to Sham levels. These data suggest that OPG improves cortical bone geometry and increases CSMI by stimulating periosteal apposition. RANKL inhibition therefore appears to be a promising therapeutic approach for preventing the loss of both cortical and trabecular bone after androgen ablation.

Disclosures: **X. Li**, Amgen 3.

1227

Age- and Dose Dependent Effects of Hormone Replacement Therapy on Fracture Risk on the Population Level. P. Vestergaard, L. Rejnmark, L. Mosekilde. The Osteoporosis Clinic, Aarhus Amtssygehus, Aarhus, Denmark.

Purpose: To assess the fracture preventive effects of hormone replacement therapy in different age groups and in different dosages in postmenopausal women. Methods: Population based case-control study. Cases were all women who sustained any fracture during the year 2000 in Denmark (n=64,548). For each case, three controls (n=193,641) matched on age were randomly drawn from the background population. Exposure was use of hormone replacement therapy (HRT) from 1996 to 2000. Adjustments were made for socio-economic factors, comorbidity, and use of other bone active drugs. The effect of HRT dose was examined by stratifying for average daily dose (DDD: defined daily dose). Results: A fracture reduction was only seen in women aged ≥50 years. A fracture risk reduction was seen in women using ≥0.3 DDD/day, i.e. in women using less than the recommended daily dose (1 DDD/day). The risk reduction for any fracture was larger in women aged ≥60 years (0.3-0.99 DDD/day: OR=0.77, 95% CI: 0.73-0.82, ≥1 DDD/day: OR=0.61, 95% CI: 0.56-0.67) than in women aged 50-59 years (0.3-0.99 DDD/day: OR=0.92, 95% CI: 0.85-0.99, ≥1 DDD/day: OR=0.77, 95% CI: 0.70-0.84). Larger risk reductions were seen for Colles' fractures (age 50-59 years: OR=0.64 for 0.3-0.99 DDD/day, and OR=0.57 for 1 ≥ DDD/day, age ≥60 years: OR=0.52 for 0.3-0.99 DDD/day, and OR=0.40 for ≥1 DDD/day). For hip fractures the risk reduction was as follows: age 50-59 years: OR=0.56 for 0.3-0.99 DDD/day, and OR=0.48 for ≥1 DDD/day, age ≥60 years: OR=0.77 for 0.3-0.99 DDD/day, and OR=0.64 for ≥1 DDD/day. Upon adjustment for socio-economic variables, comorbidity, and use of other bone active drugs, the risk reduction was even larger. Conclusions: Hormone replacement therapy poses a large fracture-reducing potential at population level even at dosages lower than usually recommended. This may be useful when trying to tailor estrogen-based therapies not associated with an increased risk of breast cancer and other adverse effects. The risk reduction was larger with advancing age for any fracture and Colles' fracture, while the opposite was the case for hip fractures. Differences in distribution of trabecular and cortical bone may be responsible for this.

Disclosures: **P. Vestergaard**, None.

1228

Connexin43 Is Required for a Full Osteoanabolic Response to Parathyroid Hormone. D. Chung¹, R. Civitelli². ¹Internal Medicine, Chonnam National University Med. Sch., Gwangju, Republic of Korea, ²Bone and Mineral Diseases, Washington University in St. Louis, St. Louis, MO, USA.

Parathyroid hormone (PTH) is currently used as anabolic therapy for osteoporosis, although its mechanism of action is not fully clarified. Previous in vitro work suggests that PTH action on bone cells requires connexin43 (Cx43) gap junctional communication. To test the role of Cx43 in PTH anabolic response we used mice with a selective osteoblast ablation of the Cx43 gene, obtained using a *Cx43^{flax}* allele and a 2.3 kb fragment of the $\alpha_1(I)$ collagen promoter to drive Cre in osteoblasts (Col-Cre). Adult (5- to 8-month-old) mice of three genotypes, *Cx43^{+/flax}* (wild type equivalent), *Cx43^{-flax}* (heterozygous equivalent) and *Col-Cre:Cx43^{-flax}* (conditional knockout) were injected subcutaneously (5 days a week for 4 weeks) with either vehicle (saline) or 40 μ g/kg b.w. PTH (1-34) (teriparatide, Eli-Lilly; n=12 or more per group). Untreated *Col-Cre:Cx43^{-flax}* mice develop low peak bone mass, attended by delayed osteoblast differentiation, and remain osteopenic with age. After 4 weeks of PTH treatment, whole body bone mineral content increased rapidly and progressively in the *Cx43^{-flax}* group (12.5 \pm 4.7% vs. baseline), an effect significantly attenuated in *Col-Cre:Cx43^{-flax}* mice (6.7 \pm 5.3%), whereas *Cx43^{-flax}* exhibited an intermediate response (9.3 \pm 4.6%). While this attenuated response was overcome by PTH 80 μ g/kg b.w. in *Cx43^{-flax}* mice, a full response was never obtained with higher doses of PTH in *Col-Cre:Cx43^{-flax}* mice. Attenuation of PTH anabolic action was associated with reduced mineral apposition rate in *Col-Cre:Cx43^{-flax}* relative to *Cx43^{-flax}* and *Cx43^{+/flax}* mice (tibia: 0.4 \pm 0.3, 1.5 \pm 0.2, 1.6 \pm 0.5 μ m/day; spine: 0.4 \pm 0.2, 1.2 \pm 0.1, 1.7 \pm 0.2 μ m/day, respectively). Other histomorphometric parameters of osteoblast activity were similarly reduced in osteoblast Cx43-deficient mice, whereas no evidence of increased osteoclast activity was noted in any genotypes. Regional DEXA analysis revealed that attenuation of PTH response in *Col-Cre:Cx43^{-flax}* mice was far more pronounced in the lumbar spine (primarily trabecular) than in the whole femur (primarily cortical). Consistent with these findings, 3-D vertebral bone mass by μ CT was lower in PTH treated *Col-Cre:Cx43^{-flax}* relative to *Cx43^{-flax}* and *Cx43^{+/flax}* mice (499.0 \pm 51.0, 517.6 \pm 32.6, and 561.6 \pm 46.3 g/cm³). In conclusion, lack of Cx43 in osteoblasts hinders the bone anabolic effect of PTH. This resistance is the consequence of failure to mount a full osteoblast response to the hormone, which is more apparent in trabecular than in cortical bone. Thus, osteoblast Cx43 has an instrumental role in the mechanism of PTH osteoanabolic action in vivo.

Disclosures: **D. Chung**, None.

F002

Paternal Skeletal Size Predicts Neonatal Bone Mineral Accrual. N. C. W. Harvey¹, M. K. Javaid¹, P. Taylor^{*2}, S. R. Crozier^{*1}, E. M. Dennison^{*1}, H. M. Inskip^{*1}, K. M. Godfrey^{*1}, C. Cooper¹. ¹MRC Epidemiology Resource Centre, Southampton, United Kingdom, ²Medical Physics and Bioengineering, Southampton General Hospital, Southampton, United Kingdom.

We have previously demonstrated that maternal body build and lifestyle factors predict neonatal bone mineral accrual. However, the paternal determinants of neonatal bone mass remain little known. In this study we explored the relationship between a father's bone mass and that of his offspring. 280 pregnancies were recruited from the Southampton Women's Survey, a unique, well established cohort of women, aged 20-34 years, who had been assessed before and during early and late pregnancy. The neonates underwent whole body DXA within 20 days of birth; at this time the fathers were invited to undergo a whole body DXA scan using an Hologic Discovery instrument. Multivariate regression methods were used to explore the parental determinants of neonatal bone mass. Full ethical approval was given for this study. After adjustment for the father's age, and the baby's gestational age, sex and age at DXA scan, there were highly significant positive associations between baby's whole body bone area (BA), bone mineral content (BMC), and bone mineral density (BMD), and the corresponding indices in the father (p=0.009, 0.001, 0.03 respectively- table 1). When mother's height, body composition (fat mass estimated from skin folds), smoking, and calcium intake were included in multivariate regression models of father's DXA indices, the associations for paternal variables remained statistically significant (BA: p=0.02, BMC: p=0.002, BMD: p=0.04). Thus father's skeletal size predicts skeletal size in the offspring, independently of the mother's body build and lifestyle. These data point to the importance of considering paternal genotype in studies exploring the developmental origins of adult osteoporotic fracture. Table 1

		BA	Baby BMC	BMD
Father	BA	0.15**	0.13*	-0.02
	BMC	0.20**	0.19**	0.07
	BMD	0.18**	0.18**	0.13*

** p<0.01, * p<0.05; Pearson correlation coefficients for paternal and neonatal DXA indices, adjusted for father's age, and baby's gestational age, sex and age at DXA.

Disclosures: **N.C.W. Harvey**, None.

F004

Effects of Skeletal and Sexual Maturation on Trabecular and Cortical Density of the Peripheral Skeleton. B. Zemel¹, H. Kalkwarf², M. Leonard¹, J. Shepherd³, S. Mahboubi^{*1}, M. Frederick^{*4}, K. Winer^{*5}. ¹Children's Hospital of Philadelphia, Philadelphia, PA, USA, ²Cincinnati Children's Medical Center, Cincinnati, OH, USA, ³University of California San Francisco, San Francisco, CA, USA, ⁴Clinical Trials & Survey Corporation, Baltimore, MD, USA, ⁵National Institute of Child Health and Human Development, Rockville, MD, USA.

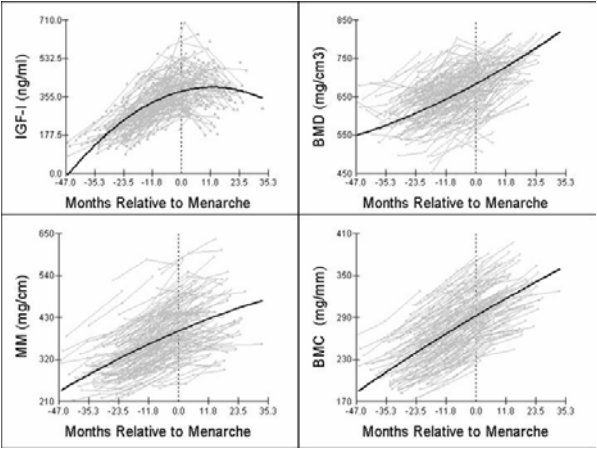
Determining the effects of maturational processes on bone density compartments is important for understanding the factors that influence the development of the adult skeleton. It may also reveal growth-related periods of vulnerability in healthy children. This study describes the relations between sexual and skeletal maturation and trabecular and cortical volumetric BMD (mg/cm³) in the distal radius and tibia, as measured by peripheral quantitative computed tomography in a subset healthy children, 6 to 17 years of age, from the multi-center Bone Mineral Density in Childhood Study. 159 children (43% black, 51% female) were evaluated at baseline and 12 months. Trabecular BMD was measured at the 3% radius and tibia sites. Cortical BMD was assessed at the 30% radius and 38% tibia sites. Bone age was evaluated by hand-wrist x-ray and sexual maturation by physical exam. Self-identified race was coded as black vs non-black. Mixed effects models were used to evaluate the effects of skeletal and sexual maturation on BMD. Polynomial terms were included to account for the distinct increase in cortical BMD that occurred at older ages. Overall, bone age was a better predictor of cortical BMD than chronological age. R² values for tibia cortical BMD increased from 0.19 to 0.31 for males and from 0.61 to 0.70 for females when bone age was used. R² values for radius cortical BMD increased from 0.37 to 0.40 for males and from 0.70 to 0.78 for females when bone age was used. Tibia cortical BMD models with bone age were improved by the addition of race for females (R²=0.76), and race and testes size for males (R²=0.45). Radius cortical BMD for males was best explained by bone age and race for males (R²=0.46), and for females, just by bone age. Radius trabecular BMD was best explained by testes size and black ethnicity for males (R²=0.06), and by race for females (R²=0.15). Tibia trabecular BMD was best explained by chronological age in males (R²=0.09) and breast stage and black ethnicity for females (R²=0.34). These findings demonstrate that (1) cortical BMD changes developmentally, with a rapid increase in late adolescence; (2) bone age is a better predictor of cortical BMD than chronological age; (3) skeletal maturation explains a greater amount of variance in BMD for females compared to males; and (4) the effects of puberty on trabecular and cortical BMD may be site and gender dependent.

Disclosures: **B. Zemel**, None.

F007

Bone Mass Accrual Is Modulated by IGF-I and Muscle Mass in Pubertal Girls: A Two Year Follow-Up Study. R. Zhao^{*1}, M. Alen^{*1}, A. Mahonen^{*2}, S. Sipilä^{*1}, T. Finni^{*1}, R. Wang^{*3}, U. Kujala^{*1}, S. Cheng¹. ¹Univ. of Jyväskylä, Jyväskylä, Finland, ²Univ. of Kuopio, Kuopio, Finland, ³Shanghai Institute of Physical Education, Shanghai, China.

The study aim was to investigate whether bone mass/density is associated with increased serum insulin-like growth factor-I (IGF-I) and muscle mass/size in 258 healthy Finnish girls (age 11-13 yrs). Bone cross-sectional area (BCSA), mineral content (BMC), density (BMD), muscle cross-sectional area (MCSA), and muscle mass (MM) were assessed using peripheral quantitative computed tomography (pQCT) at left lower leg (including fibula and tibia), and IGF-I by radioimmunoassay at the baseline, 12 months and 24 months. We found that IGF-I increased rapidly up to the menarche and decreased thereafter (hierarchical mode analysis taking into account growth). IGF-I correlated with BMC (r=0.29, p<0.001) and BMD (r=0.19, p=0.049) before menarche, but not after menarche (multilevel regression). The speed of growth of MCSA, MM, BCSA, and BMC tended to slow down after menarche, but BMD was continuously increased. BCSA and BMC correlated with MCSA and MM significantly both before (r=0.30, p<0.001; r=0.28, p=0.016, respectively) and after menarche (r=0.21, p=0.033; r=0.23, p=0.03, respectively). The effect of IGF-I on bone mass and density seems to be stronger prior to menarche, while muscle mass is associated with bone mass and size accrual during whole puberty.



Disclosures: **R. Zhao**, None.

F009

Sex Hormone-Related Polymorphisms as Predictors of Adult Stature in Swedish Men - The GOOD Study. M. Lorentzon, D. Mellström, C. Ohlsson. Center for Bone Research at the Sahlgrenska Academy, Departments of Internal Medicine and Geriatrics, Gothenburg University, Gothenburg, Sweden.

The regulation of longitudinal bone growth depends primarily on genetic factors, hormone status (thyroid hormones, GH/IGF-I and sex steroids), and environmental determinants such as nutrition. Androgens and estrogens are crucial for longitudinal bone growth and skeletal maturation in males. However, the relationship between polymorphisms in genes of the sex hormone system and adult stature remains unclear. The aim of the present study was to investigate the importance of sex hormone-related polymorphisms for the attainment of adult stature and skeletal proportions (the axial and appendicular skeleton) in 1068 men (age 18.9±0.6 yrs) included in the Gothenburg Osteoporosis and Obesity Determinants (GOOD) study. We investigated, in a systematic manner, 18 previously described sex hormone-related polymorphisms (1-5 polymorphisms in each gene; sex steroid synthesis - *aromatase/CYP19*, *CYP17*, *5-α-reductase*; sex steroid degradation - *CYP11A1*, *CYP11B1*, *COMT*; in the receptors for estrogens - *ERα* and *ERβ* and for androgens - *AR*; and in the sex hormone binding protein - *SHBG*). Two of these polymorphisms were clearly associated with final height: (1) the repeat sequence (CAG) polymorphism in the first exon of the AR and (2) the repeat sequence (TAAAA) polymorphism in the 5' promoter region of SHBG. The length of the tibia (appendicular skeletal site), sitting height (axial skeletal site) and final height were measured using standardized equipment. The (CAG)_n polymorphism in the AR and the (TAAAA)_n polymorphism in SHBG were determined using an ABI 3730 sequencer. The repeat number of the AR polymorphism has previously been shown to be inversely correlated to the AR activity. Our results reveal that the repeat number of the (CAG)_n polymorphism of the AR was inversely correlated to height (r= -0.07, p=0.02), sitting height (r= -0.07, p=0.04) and tibia length (r= -0.07, p=0.04), but not with serum sex hormone levels. The SHBG repeat polymorphism was clearly associated with serum levels of SHBG (r= -0.13, p<0.0001), total testosterone (r= -0.08, p=0.01) and with length of the tibia (r= -0.08, p=0.02), sitting height (r= -0.09, p<0.01) and adult stature (r= -0.08, p=0.02). Our results indicate that a high CAG repeat number in the AR (resulting in lower AR activity) or a high TAAAA repeat number of the SHBG gene (resulting in lower SHBG levels) negatively influences final height as a result of both reduced axial and appendicular skeletal growth. In conclusion, our screening of most of the known major sex-steroid-related polymorphisms, identified two genetic polymorphisms associated with final height in men.

Disclosures: **M. Lorentzon**, None.

F012

DLX5 Is Responsible for Cooperative Interactions between BMPs and RUNX2. M. Phimphilai^{*1}, H. Roca^{*2}, R. T. Franceschi³. ¹Biological Chemistry; Metabolism, Endocrinology and Diabetes, University of Michigan, Ann Arbor, MI, USA, ²Periodontics, Prevention and Geriatrics, University of Michigan, Ann Arbor, MI, USA, ³Periodontics, Prevention and Geriatrics; Biological Chemistry, University of Michigan, Ann Arbor, MI, USA.

BMPs are potent osteogenic factors that stimulate osteoblast differentiation and bone formation. BMPs are known to induce expression of RUNX2/CBFA1 and DLX5 transcription factors. Because overexpression of RUNX2 induces osteoblast-related genes and mineralization, as well as facilitates bone formation by non-osteoblast cell lines, it has been proposed that this factor mediates actions of BMPs in stimulating osteoblast differentiation. However, BMP treatment of calvarial-derived cells from *Cbfa1*-deficient mice still leads to modest induction of osteoblast markers suggesting that some actions of BMPs are independent of RUNX2 (Komori et al, 1997, Cell 89:755). Previous work from our laboratory showed that adenovirus-mediated overexpression of RUNX2 and BMP2 synergistically stimulated osteoblast differentiation. In this study, we examine this synergy in greater detail and explore downstream signaling events responsible for the complementary function between these two factors. BMP blocking antibodies and Noggin dramatically inhibited RUNX2-dependent induction of osteoblast differentiation markers (ALP, OCN and BSP). Moreover, recombinant human BMP2 synergistically enhanced RUNX2 actions. Our results indicate that BMP activity is necessary for RUNX2-dependent transcription and that RUNX2 and BMPs cooperatively interact to stimulate osteoblast differentiation. Interestingly, the ability of BMP2 to stimulate downstream signal transduction pathways (Smad 1,5,8 and p38, JNK and ERK MAPK pathways) was not affected by RUNX2. In contrast, BMP2 and RUNX2 synergistically induced DLX5 expression and this induction preceded induction of *Ocn* and *Bsp* genes. ChIP assays revealed that DLX5 preferentially associated with chromatin in the vicinity of RUNX2 binding sites in both *Bsp* and *Ocn* promoters only when both genes were transcriptionally active. A co-immunoprecipitation assay detected a physical interaction between RUNX2 and DLX5. Site-specific mutagenesis studies on the *Bsp* promoter demonstrated functional cooperativity between the RUNX2 site and adjacent DLX5 binding site in MC3T3-E1 cells. Taken together, our results suggest that DLX5 functions in concert with RUNX2. In conclusion, RUNX2 and BMPs cooperatively function in stimulating osteoblast differentiation and the orchestrated function between RUNX2 and DLX5 may lead to the functional cooperativity between these two factors.

Disclosures: **M. Phimphilai**, None.

F014

BMP Antagonist *Caf1*, which Suppresses BMP-Induced Bone Formation and MAR, Is Expressed in Chondrocytes, Ovary and Brain. K. Oikawa¹, T. Nakamura^{*2}, M. Usui¹, I. Ishikawa^{*3}, T. Yamamoto^{*2}, M. Noda¹. ¹Molecular Pharmacology, Tokyo Medical and Dental University, Tokyo, Japan, ²University of Tokyo, Tokyo, Japan, ³Periodontology, Tokyo Medical and Dental University, Tokyo, Japan.

Bone mass is determined based on the interactions among stimulators and suppressors for bone formation and bone resorption. *Caf1* (CCR4-associated factor 1) is a transcription factor (Nature Genetics, 2004) which associates with Tob. Tob antagonizes BMP actions *in vivo* (PNAS 2004, Cell 2000). Like Tob, *Caf1* suppressed BMP-induced bone formation *in vivo*, the levels of mineral apposition rate, bone formation rate, BMP-induced alkaline phosphatase expression *in vitro* and nodule formation activities *in vitro*. Moreover, *Caf1* deficiency preserved bone mass even after ovariectomy, indicating that *Caf1* is involved in bone mass determination as a BMP antagonist in adult bone in the ovariectomized mice. We have further examined the localization of the *Caf1* expression using LacZ makers in *Caf1* knockout mice and observed that *Caf1*(LacZ) expression in bone as well as the growth plate cartilage. Within the cartilaginous tissues, LacZ expression could be observed in articular chondrocytes as well as proliferating, prehypertrophic, and hypertrophic chondrocytes in long bone. LacZ expression in *Caf1* knockout mice was also observed in mandibular bone suggesting the role of *Caf1* in bone in oral tissue. Interestingly, *Caf1* was also highly expressed in brain especially in the cortical regions in embryos and adult mice. Since *Caf1* deficiency reduces bone loss due to ovariectomy, we tested whether *Caf1* is expressed in endocrine system. Although uterus weight was reduced similarly by ovariectomy in both wild type and *Caf1* knockout mice, *Caf1* (LacZ) was highly expressed in ovary. Within the ovary, *Caf1* (LacZ) is expressed at low levels in most of the cells. However, highest *Caf1* expression based on the LacZ staining was observed in oocytes. These data indicate that *Caf1* is involved in the adult bone mass determination by antagonizing BMP activities in osteoblastic cells while it is also expressed highly in chondrocytes as well as extraskeletal tissues including brain and ovary suggesting its multiple roles in the mediation of a neuronal and endocrine signaling that may be linked to bone signaling.

Disclosures: **K. Oikawa**, 21st COE Program 2; Core to Core Program 2.

F016

Vascular Calcification (VC) Stimulated by Chronic Kidney Disease (CKD) Is Reversible Linked to Stimulation of Skeletal Modeling. G. Saab^{*1}, S. Mathew^{*2}, L. Chaudhary², K. A. Hruska². ¹Internal Medicine, Washington University, St. Louis, MO, USA, ²Pediatrics, Washington University, St. Louis, MO, USA.

VC is an important cause of morbidity and mortality in CKD, for which no therapy is available. We have shown that CKD stimulates neointimal and medial VC in low density lipoprotein receptor deficient (LDLR^{-/-}) mice fed high fat/cholesterol diets over a 12 week course from 10 to 22 weeks of age. In the studies reported here, VC was allowed to develop for the 12 week period and treatment with BMP-7, 10 mcg/kg, or vehicle injected intraperitoneal once weekly from 22 to 28 weeks was begun. The hypothesis was that BMP-7 would reverse VC produced by CKD in this model. CKD was induced in 10 week old LDLR^{-/-} mice by cauterization of the right kidney followed by left nephrectomy, and animals were randomized into groups. One CKD group fed high fat/cholesterol was sacrificed at 22 weeks to determine baseline aortic calcification. At 28 weeks the aorta was removed, desiccated and calcium content determined using a cresolphthalein complexone method, (Sigma, St. Louis, MO). Renal function assessed by the serum BUN was 19±3mg/dl in wild type mice, 21±6 in sham operated mice, and similar between the CKD groups, 64±25mg/dl. In CKD high fat fed BMP-7 treated animals the serum PO4 was 10.1±0.02mg/dl before treatment and 6.2±0.02 at sacrifice. Ca, PTH, cholesterol and glucose levels were not affected by treatment. Skeletal histomorphometry revealed the adynamic bone disorder in the CKD high fat vehicle treated animals. Calcein labeled surfaces and adjusted apposition rates indicative of increased BMU's were stimulated by BMP-7 therapy. There was no increase in renal PO4 excretion. Finally, treatment with BMP-7 decreased aortic calcification in both the sham operated animals fed high fat and in animals with CKD by 40 and 45% respectively (p<0.05 for both). Groups of animals treated with CaCO3 to directly decrease the serum phosphorus were employed in the same protocol to further analyze the effect of serum phosphorus reduction. These groups demonstrated about 50% of the reduction in vascular calcification observed with the BMP-7 treatment. We conclude that there is a pathological link between abnormal bone mineralization and vascular calcification mediated in part by high phosphorus environments. By increasing skeletal deposition of phosphate, BMP-7 reduces serum PO4 which in turn inhibits vascular calcification. Thus, BMP-7 may represent a novel therapy for vascular calcification and renal osteodystrophy.

Disclosures: **G. Saab**, None.

F021

Osteoblastic Differentiation of Human Aortic Vascular Smooth Muscle Cells (VSMC) and Mineralization *In Vitro*. S. Mathew^{*}, T. Geurs^{*}, K. A. Hruska. Pediatrics, Washington University, St. Louis, MO, USA.

In patients with chronic kidney disease calcification of the aortic tunica media is associated with a high risk of adverse clinical events. Evidence has accumulated suggesting that vascular calcification (VC) is a regulated process akin to bone formation. Currently, no therapy is available for VC. Recently, we have shown that BMP-7 inhibits VC in a murine model of the metabolic syndrome and CKD with atherosclerosis and arteriosclerosis. Furthermore, a marker of the osteoblastic lineage, osteocalcin was inhibited by BMP-7 in the VSMC *in vivo*. Our central hypothesis is that BMP-7 will restore the differentiated phenotype of VSMC and inhibit calcification. To analyze the mechanism of BMP-7 action, we established a model of human calcifying VSMC obtained from the aortas of cadaver organ donors with atherosclerosis by increasing media phosphorus (Pi) from 1 to 2 mM. High Pi induced BMP-2, MSX2 and *Cbfa1* expression. Osterix and osteocalcin expression and matrix mineralization followed by days 7 to 14. The mineralization was due to hydroxyapatite nodules. High Pi decreased matrix Gla protein levels, along with markers of the contractile VSMC phenotype. Treatment with BMP-7 dose dependently prevented calcification by VSMC. *Cbfa1*, MSX2, Osterix and Osteocalcin expression were inhibited by BMP-7 in a similar dose response as mineralization. Matrix Gla protein levels were induced by BMP-7. The earliest osteoblast specific transcription factor, *Cbfa1*, was expressed and regulated by phosphorus and decreased with BMP-7. Since *Cbfa1*, MSX2 and osterix are critical transcription factors for bone formation as demonstrated by mice deficient in any of the three proteins *in vivo*, we conclude that the mechanism of BMP-7 action is through inhibition of osteoblastic specific gene transcription. This is the first demonstration that BMP-7 inhibits calcification stimulated by VSMC *in vitro* by inhibition of the calcifying cell phenotype through downregulation of osteoblast specific genes despite upregulation of the same transcriptional program in human bone marrow stromal cells.

Disclosures: **S. Mathew**, None.

F023

Mineral Nucleation within Biomineralization Foci Requires Serine Protease Activation of Bone Acidic Glycoprotein-75. N. T. Huffman^{*1}, D. Lovitch², R. J. Midura³, J. P. Gorski¹. ¹Molecular Biology and Oral Biology, Univ. of Missouri-Kansas City, Kansas City, MO, USA, ²Oral Biology, Univ. of Missouri-Kansas City, Kansas City, MO, USA, ³Biomedical Engineering, Cleveland Clinic and Foundation, Cleveland, OH, USA.

We have shown that nucleation of mineral crystals within developing primary bone and in common osteoblastic culture models occurs within supramolecular, extracellular, matrix vesicle containing complexes termed biomineralization foci (BMF). Proteomic analysis of laser captured BMF indicates specific enrichment of a 50 kDa fragment of bone acidic

ASBMR 27th Annual Meeting

glycoprotein-75 (BAG-75), which is also extractable from primary bone and present in serum. BAG-75 is a BMF biomarker. We hypothesized that proteolytic cleavage of BAG-75 into bioactive fragments may be required both for its uptake into BMF and its proposed function as an initiator of nucleation. To test this hypothesis, we first analyzed a series of protease inhibitors for their effect on mineralization in UMR 106 osteoblastic cultures. UMR cells mineralize rapidly over a 24 h culture period in the presence of β -glycerophosphate (BGP) (64 to 88 h after plating). Inhibitors were therefore present during the entire 24 h mineralization period. Of the inhibitors tested, only AEBSF [4-(2-aminoethyl)-benzenesulfonyl fluoride hydrochloride] (0.1-0.4 mM) was found to completely block mineralization, as determined by quantitation of Alizarin red S staining. Parallel studies with a cell proliferation assay demonstrate this was not due to an effect on viability. In contrast, 100 μ M antipain, 10 μ M E-64, 100 μ M elastatinal, 10 μ M GM 6001, 100 μ M leupeptin, 100 μ M Pefabloc PL or 3 μ g/ml aprotinin were all without effect. Although spherical BMF-like structures were visible by bright field microscopy in AEBSF-treated cultures, they failed to stain for BAG-75 suggesting a failure in uptake of BAG-75. This was not due to reduced synthesis of BAG-75 as an 8-fold increase in BAG-75 was detected in the culture media. In contrast, cell layer fractions from control BGP-treated cultures contained a 20 kDa fragment of BAG-75 which was absent from AEBSF-treated cultures. The size and bone sialoprotein content of BMF was also decreased by AEBSF. Direct fluorescent assays of total protease activity revealed about 10% of the activity in mineralizing UMR cultures was inhibitable by AEBSF. Our results demonstrate for the first time that initial nucleation of mineral within BMF can be blocked by serine protease inhibitor AEBSF. Mechanistically, AEBSF prevents BAG-75 fragmentation with the result that final assembly of BMF is inhibited. We hypothesize that mineralization within BMF is a sequential process requiring serine protease-catalyzed activation of BAG-75.

Disclosures: **N.T. Huffman**, None.

F028

CNP/Guanylyl Cyclase B (GC-B) System Regulates Endochondral Ossification - The Analysis of GC-B Null Mice. **Y. Komatsu**, **A. Yasoda***, **N. Tamura***, **Y. Nakatsuru***, **H. Arai***, **K. Nakao***. Department of Medicine and Clinical Science, Kyoto University Graduate School of Medicine, Kyoto, Japan.

C-type natriuretic peptide (CNP) regulates the endochondral ossification by binding guanylyl cyclase B (GC-B) expressed on the proliferative and prehypertrophic chondrocytes in the growth plate. We recently reported that the GC-B^{-/-} mice exhibit the dwarfism with short body length and extremities, exactly same as CNP^{-/-} mice. Furthermore, in the rare autosomal recessive genetic skeletal abnormality, known as acromesomelic dysplasia, type maroteaux, the missense mutations of GC-B were also reported. To investigate the function of CNP/GC-B system in endochondral ossification, we studied the interaction between CNP/GC-B system and FGFR-3, whose constitutive activation is responsible for achondroplasia, using GC-B^{-/-} mice. The naso-anal lengths of GC-B^{-/-} mice were 60 to 70% of wild type littermates at 4 to 10 weeks of age. Histologically, GC-B^{-/-} mice display striking narrowing of the growth plate of vertebrae and long bones. In situ hybridization revealed that both prehypertrophic and hypertrophic chondrocytes layers, expressing type II and type X collagens, respectively, were narrowed, but the normal columnar organization of the growth plate was maintained. The CNP-dependent production of cGMP was undetected in the tibia from GC-B^{-/-} mice. The 8-bromo-cGMP dose-dependently inhibited the induction of ERK phosphorylation induced by FGF18 without changing the level of FGFR-3, although it did not affect the phosphorylation of STAT-1 in the tibia from both GC-B^{-/-} mice and wild type littermates. CNP did not show any effect either on ERK or STAT-1 phosphorylation in those of GC-B^{-/-} mice. These results explain one of the molecular mechanisms of the growth stimulating action of CNP/GC-B system in the growth plate chondrocytes.

Disclosures: **Y. Komatsu**, None.

F030

A 300 bp of Mouse Col10a1 Distal Promoter Element Is Sufficient to Mediate Its High-level Tissue-Specific Expression in Hypertrophic Chondrocytes In Vivo. **Q. Zheng***¹, **B. Keller***¹, **G. Zhou**¹, **D. Napierala**², **Y. Chen***², **A. Parker***³, **B. Lee**². ¹Molecular and Human Genetics, Baylor College of Medicine, Houston, TX, USA, ²Howard Hughes Med. Inst., Houston, TX, USA, ³Respiratory and Inflammation Res. Area, Astrazeneca, Cheshire, United Kingdom.

Type X collagen gene (*Col10a1*) is specifically expressed in hypertrophic chondrocytes, the terminal stage of chondrocyte differentiation during cartilage development. Identification of the cis-regulatory element and its binding factors for tissue-specific mouse *Col10a1* expression in hypertrophic chondrocytes is thus essential for understanding the mechanisms that specify endochondral ossification and underlie the molecular pathogenesis of skeletal dysplasia. We have previously reported that 4kb *Col10a1* promoter containing Runx2 elements can specifically drive weak reporter gene (*LacZ*) expression in the lower hypertrophic zone of transgenic mice. Here we report generation of additional transgenic mouse lines harboring various *Col10a1* promoter/intronic fragment (Tg-10 kb) or distal *Col10a1* element (Tg-6kb and Tg-4.6kb) driving *LacZ* as reporter. High-level tissue-specific reporter expression was observed in these transgenic mice. These results correspond well with more recent mouse genetics study which demonstrated that 4.6 kb murine *Col10a1* promoter containing conserved enhancer (-4377 to -3865 bp) allows tissue-specific expression of *lacZ* reporter gene in hypertrophic cartilage in vivo. To clarify the contribution of this *Col10a1* distal element to its tissue-specific expression, transgenic mouse lines using two copies of the putative enhancer

element (-4.6 to -3.9 kb) upstream of the *Col10a1* basal promoter driving *LacZ* as reporter (Tg-2xEnh) have been established and showed similar tissue-specific expression pattern. More recently, we have generated transgenic founder mice carrying reporter construct containing four copies of highly conserved 300 bp fragments within the *Col10a1* distal promoter region (-4.3 kb to -4.0 kb) upstream of the same *Col10a1* basal promoter. These Tg-4x300 founder mice show similar tissue-specific reporter/*LacZ* expression pattern to that of the Tg-4.6 kb, Tg-6 kb, Tg-10 kb and Tg-2xEnh mice. These data together suggest that this 300 bp highly conserved element must contain the major enhancer sufficient for tissue-specific *Col10a1*/reporter expression throughout the hypertrophic zone. Further localization of the cis regulatory element within this region and its binding factors will ultimately help to identify possible signaling pathways relevant to skeletal development and therefore has the potential for therapeutic targets with preventive or curative value of related bone/cartilage disorders.

Disclosures: **Q. Zheng**, None.

F032

Runx1, 2 or 3 Regulates Chondrocyte Differentiation with Different Efficacy and Induction of Runx in Intervertebral Disk Leads to Disk Degeneration. **S. Takeda**¹, **J. Ozdemir***², **S. Sato***¹, **Y. Aso**³, **A. Kimura***³, **K. Shinomiya***¹, **G. Karsenty**². ¹Dept. of Orthopedics, 21COE, Tokyo Medical and Dental University, Tokyo, Japan, ²Dept. of Molecular and Human Genetics, Baylor College of Medicine, Houston, TX, USA, ³Dept. of Orthopedics, Tokyo Medical and Dental University, Tokyo, Japan.

Runx2 together with Runx3 has been shown to accelerate chondrocyte hypertrophy. However, it was uncertain if there is any difference in their ability inducing chondrocyte differentiation in vivo. To address that question, firstly we compared the expression of Runx2, 3 and the other member of Runx family Runx1 by in situ hybridization. Runx2 was expressed in prehypertrophic and hypertrophic chondrocytes strongly in the early stage of embryogenesis but declined thereafter. Runx3 was also expressed in prehypertrophic and hypertrophic chondrocytes and its expression level was unchanged throughout the embryogenesis. Runx1 was temporarily expressed in mesenchymal condensation. Secondly, we generated transgenic mice (tg) expressing Runx1, 2 or 3 in non-hypertrophic chondrocyte using α 1(II) collagen promoter. All Runx3 tg and most of the Runx2 tg died perinatally due to ectopic cartilage calcification. While, all Runx1 tg and some Runx2 tg survived and developed kyphosis and scoliosis by 3months. Histologically, intervertebral disk of Runx1 and Runx2 tg mice showed ectopic hypertrophic chondrocyte differentiation, characterized by type X collagen immunoreactivity. In human patients' intervertebral disk (IVD) degeneration, ectopic chondrocyte differentiation is documented. Therefore, we tested if weight loading, a most common cause of IVD degeneration, induces Runx expression, which may cause chondrocyte hypertrophy. Indeed, weight loading of the IVD by compression for a day significantly increased Runx expression. These results demonstrated that all of Runx genes control chondrocyte differentiation, albeit with different efficacy, and indicated that induction of Runx in IVD causes IVD degeneration.

Disclosures: **S. Takeda**, None.

F035

Chondrocyte-Specific Deletion of Indian Hedgehog (*Ihh*) in Postnatal Life. **Y. Maeda***¹, **M. Nguyen***², **S. Mackem***², **B. Lanske**¹. ¹Oral and Developmental Biology, Harvard School of Dental Medicine, Boston, MA, USA, ²National Cancer Institute, Bethesda, WA, USA.

Indian hedgehog (*Ihh*) has been shown to be essential for osteoblast differentiation and chondrocyte proliferation/differentiation during endochondral bone formation. *Ihh* null animals exhibit severe skeletal abnormalities and die early during midgestation or latest at birth. We recently discovered that targeted deletion of *Ihh* from only chondrocytes using the *cre/loxP* gene technology led to a similar abnormal phenotype with perinatal death. The early lethality of both animal models does not allow to study the physiological role of *Ihh* in endochondral bones in postnatal life. We, therefore, generated a new mouse model in which ablation of the *Ihh* gene from chondrocytes can be induced in a temporal-specific manner. To selectively ablate the *Ihh* gene from chondrocytes in the postnatal skeleton, floxed *Ihh* animals were mated with mice in which the *collagen type 2 (α1)* promoter drives a transgene coding for a fusion protein between *Cre* recombinase and an estrogen receptor with a point mutation in its ligand-binding domain (*ER**). This point mutation in the fusion protein (*CreER**) allows induction of *Cre* recombinase by tamoxifen (4-hydroxytamoxifen = 4-OHT), but not by estradiol. Injection of tamoxifen can, therefore, be used to induce ablation of the *Ihh* gene at any desired time point. We first tested and validated the consistent specificity and efficiency of postnatal *Cre* excision after tamoxifen injection in *Rosa26cre* indicator mice. A single dose of 2.0 mg 4-OHT was injected intraperitoneally (ip) into 2-week old (p14) *col2-CreER*-Rosa26* indicator mice. Mice were sacrificed at 1, 4, 7 and 14 days after 4-OHT injection and *lacZ* expression was examined by X-gal staining. Exposure to 4-OHT induced *Cre*-mediated recombination starting at 1 day after injection. Strong and specific *lacZ* staining was observed in growth plates of digits, long bones, ribs, vertebrates and tail, articular surfaces of long bones and palatal suture in the skull. Subsequently, we generated *col2CreER*-floxed Ihh* animals and injected them at p1 and p14 with 0.2 mg and 2.0 mg 4-OHT, respectively. We are currently analyzing the phenotype of these mutant animals to study the physiological role of *Ihh* in chondrocytes of the postnatal skeleton. These investigations provide a new system in which we can examine for the first time the functions of *Ihh* after birth.

Disclosures: **Y. Maeda**, None.

F039

HCN2 Ion Channels Regulate Bone Development, Mass and Strength. T. Notomi¹, A. Ludwig^{*2}, G. Reilly^{*3}, F. B. Hofmann^{*2}, T. M. Skerry¹. ¹School of Medicine & Biomedical Sciences, Univ. of Sheffield, Sheffield, United Kingdom, ²Dept. of Pharmacology and Toxicology, Technical Univ. of Munich, Munich, Germany, ³Dept. of Engineering Materials, Univ. of Sheffield, Sheffield, United Kingdom.

Hyperpolarization-activated cation currents (Ih) contribute to various physiological properties and functions in the Central Nervous System (CNS) and heart, including the generation of spontaneous rhythmic activity and setting of resting membrane potential. Recent reports also suggested that Ih affect synaptic transmission and Long-Term Potentiation (LTP) in the brain. Four subunits of the Hyperpolarization-activated and Cyclic Nucleotide gated nonselective cation channels (HCN), which generate Ih, have been cloned in the brain and heart. Since numerous neuronal signaling processes have been shown to have functions in bone, we investigated the expression and function of HCNs in the skeleton. Three HCN subtypes, HCN2, HCN3 and HCN4, were identified in whole murine bone (C3H, 12wk old) by RT-PCR and immunoblotting, qualitatively HCN2 was the most abundant. To investigate functions of HCN *in vitro*, mouse bone marrow cells (BMC) were cultured under osteogenic conditions in the presence or absence of the Ih inhibitor ZD7288 (50μM). Inhibition of Ih prevented the normal expression of all osteoblastic markers by BMCs, suggesting that HCNs is a key component in osteoblastic differentiation *in vitro*. To determine the physiological role of HCN, mice lacking the HCN2 gene were analyzed. In knockout mice, the body weight was reduced by 30-35% and femoral and tibial bone length and wet weight was significantly reduced compared to wild type (WT) mice (p<0.05). Peripheral computed tomography(pQCT) measurements showed that in the proximal tibia the trabecular bone mineral density (BMD) and area in HCN2^{-/-} mice were significantly less than that in WT mice (BMD, 266.4±23.3 vs. 366.8±17.3 mg/ccm; Area, 1.47±0.09 vs. 2.03±0.11 mm²; n=5, p<0.05). In the cortical area of mid-femur, both cortical bone BMD and area in HCN2^{-/-} mice was also significantly less than that in WT mice (BMD, 278.5±17.0 vs. 333.2±17.2 mg/ccm; Area, 0.80±0.03 vs. 1.04±0.02 mm²; n=5, p<0.05). Three point bending tests revealed that the HCN2 null mice had significantly reduced bone strength compared to WT mice (18.0±0.76 vs. 23.5±0.96 N; n=5, p<0.05) even after correction for bone weight (1.14±0.12 vs. 1.39±0.06 N/mg; n=5, p<0.05). These findings demonstrate a novel signaling pathway that impacts on bone architecture and strength. It is not yet clear whether this effect is due to a direct role of HCN2 in regulating cation currents in osteoblasts or some form of rhythmic activity or an effect mediated through other systems such as LTP.

Disclosures: **T. Notomi**, None.

F041

Wdr5, a BMP-2 Induced Gene, Interacts with Ihh and Wnt Signaling Pathways during Endochondral Bone Formation. F. Gori, L. Friedman^{*}, M. B. Demay. Endocrine Unit, Massachusetts General Hospital, Harvard Medical School, Boston, MA, USA.

Among the local signaling pathways known to play a role in endochondral bone formation is the BMP pathway. We identified a novel BMP-2-induced gene, named BIG-3 and recently renamed Wdr5, that is developmentally expressed in osteoblasts and chondrocytes and that dramatically accelerates the program of chondrocyte and osteoblast differentiation *in vitro*. To investigate whether Wdr5 has a functional role during endochondral bone formation, we generated transgenic mice overexpressing Wdr5 under the control of the 2.4-kb fragment of the mouse α (1) I collagen promoter. The targeted expression of Wdr5 to osteoblasts led to an overall bigger skeleton at embryonic day 14.5 compared to wild-type littermates. Histological analyses at 14.5 dpc demonstrated that the humeri of transgene positive embryos were longer than those isolated from wild type littermates. Interestingly, while no difference was observed in the length of the zone of proliferating chondrocytes, the hypertrophic layer was expanded in transgene positive embryos compared to wild type littermates. The expression domain of osteopontin, a marker of terminally differentiated chondrocytes was expanded and the expression of type I collagen was stronger and more extensive in the bone collar of humeri isolated from transgene positive embryos compared to wild type littermates, demonstrating accelerated chondrocyte differentiation and maturation of the bone collar, respectively. Using TOPGAL mice that express a TCF/ β -catenin-responsive β -galactosidase transgene, we showed that Wnt signaling was activated earlier in the osteoblasts of the bone collar of Wdr5 transgenic mice compared to wild type littermates. The expression of Ihh and its receptor Ptc-1 were also investigated to address the hypothesis that Wdr5 expressed in the bone collar interacts in a paracrine fashion with the Ihh signaling pathway in regulating chondrocyte differentiation. The expression levels and domains of Ihh and Ptc-1 were decreased in the humeri of transgene positive embryos compared to their wild type littermates. These findings indicate that Wdr5 plays a regulatory role in endochondral bone formation. Targeted overexpression of this novel protein to osteoblasts results in acceleration of osteoblast differentiation, likely mediated by the Wnt signaling pathway. The acceleration of chondrocyte differentiation and maturation suggests that Wdr5 expressed in the bone collar has paracrine actions on chondrocyte differentiation, likely mediated by the Ihh/PTHrP signaling pathway.

Disclosures: **F. Gori**, None.

F046

Tight Skin (Tsk) Mutant Mice Exhibit a Definitive Skeletal Phenotype. T. Barisic-Dujmovic^{*1}, I. Boban^{*1}, D. J. Adams^{*2}, S. H. Clark¹. ¹Genetics and Developmental Biology, University of Connecticut Health Center, Farmington, CT, USA, ²Department of Orthopedic Surgery, University of Connecticut Health Center, Farmington, CT, USA.

The tight skin (Tsk) mutation is an autosomal dominant located on mouse chromosome 2, and is associated with an intragenic duplication of the fibrillin 1 gene. Fibrillin 1 is an extracellular macromolecule, and it is known that fibrillin molecules join with each other to form structurally complex microfibrils. The Tsk phenotype includes a tightness of skin, lung emphysema, myocardial hypertrophy, enlarged skeleton and kyphosis. While the skin, lung and heart features of the Tsk mutation have been the subject of many studies the skeletal phenotype has largely been ignored. We have shown that Tsk mice have a bone phenotype similar to that of patients with Marfan syndrome (MFS). The clinical signs in Marfan syndrome are mainly musculoskeletal (thoracic malformations, spinal abnormalities, tall stature), ocular and cardiovascular (aorta aneurysm, aortic dissection). Despite the fact that mutations in the fibrillin 1 gene have been identified in many Marfan patients, the pathogenesis of Marfan syndrome is not understood. Similar to Marfan patients, Tsk mice display spinal abnormalities and have decreased bone mineral density. In addition Tsk mice have significantly longer bodies and femurs. To further assess the Tsk bone phenotype we used μ CT imaging analysis of femurs from Tsk versus normal 2 and 4-month old mice. Cortical and trabecular bone volume were significantly decreased (13% and 39%, respectively) in Tsk femurs. Trabecular thickness, number, connectivity, and surface area were significantly lower in Tsk mice, with an increase in trabecular spacing. Based on these observations we hypothesized that osteoblast differentiation might be impaired in Tsk mice and that this impairment could be associated with a decrease in the expression of bone differentiation markers. To examine this hypothesis marrow stromal cultures (MSC) from Tsk and normal mice were evaluated, showing decreased expression of osteocalcin in Tsk MSC. Staining with xylenol orange for mineral revealed decreased numbers of mineralized nodules in MSC from Tsk mice. Further MSC cultures were analyzed using an osteoblast specific marker pOBCol2.3GFP. These data showed a decreased number of GFP positive nodules in Tsk compared to normal. Taken together, these results suggest that fibrillin 1 as an important factor in osteoblast differentiation. Moreover, since transforming growth factor β (TGF- β) has been implicated in the pathogenesis of both MFS and the Tsk mutation, Tsk mice provide a good model to study interactions between fibrillin 1 glycoprotein and TGF- β .

Disclosures: **T. Barisic-Dujmovic**, None.

F048

Wnt/ β -Catenin Signaling Play Pivotal Roles in Synovial Joint Induction and Chondrocyte Maturation. X. Guo^{*}, T. F. Day^{*}, X. Jiang^{*}, L. Garrett-Beal^{*}, L. Topol^{*}, Y. Yang^{*}. Genetic Disease Research Branch, NIH/National Human Genome Research Institute, Bethesda, MD, USA.

Wnt signaling is one of the key signaling pathways in regulating skeletal development. To understand the molecular and cellular mechanism of Wnt signaling, we have used molecular genetic approaches to dissect the role of β -catenin-mediated canonical Wnt signaling *in vivo* in two important skeletal development processes: synovial joint induction and endochondral bone formation. We have generated a floxed allele of β -catenin mutant mouse, *Catnby*^{fl/c} which allows us to block the canonical Wnt signaling in a tissue-specific manner by crossing the *Catnby*^{fl/c} mice with *Col2a1-Cre* or *Dermo1-Cre* mice. Cre activity is detected in all chondrocytes and some osteoblasts in *Col2a1-Cre* mice whereas in *Dermo1-Cre* mice, Cre activity is detected in early mesenchymal condensations prior to chondrocyte or osteoblast differentiation. We found previously that some *Wnts* such as *Wnt14* signals through the canonical Wnt pathway in regulating skeletal development. Removal of β -catenin in *Catnby*^{fl/c}; *Dermo1-Cre* mice embryos resulted in synovial joint fusion, ectopical chondrocyte differentiation and diminished osteoblast differentiation. Conversely, in *Col2a1-Wnt14* transgenic embryos, synovial joint is ectopically induced, chondrocyte differentiation is inhibited and osteoblast differentiation is enhanced. These results demonstrate that the Wnt/ β -catenin signaling is necessary and sufficient for synovial joint induction and plays a pivotal role in endochondral bone formation. Interestingly, Wnt signaling appears to be required at different developmental stages for endochondral ossification. In the early mesenchymal condensation, Wnt signaling inhibits chondrocyte differentiation, but is required for osteoblast differentiation. In the differentiated chondrocytes, Wnt signaling promotes chondrocyte maturation. The onset of chondrocyte hypertrophy is normal in both *Catnby*^{fl/c}; *Col2a1-Cre* and *Catnby*^{fl/c}; *Dermo1-Cre* mice. However, the progression to the most mature chondrocytes which express *VEGF*, *MMP13* and *MMP9*, is significantly delayed in these mice. Conversely, in some *Col2a1-Wnt14* transgenic line where initial chondrocyte differentiation is not inhibited, expression domains of *VEGF*, *MMP13* and *MMP9* are greatly expanded. These data indicate that Wnt/ β -catenin signaling promotes endochondral bone formation through distinct mechanisms at different developmental stages: at early stage, it is required for osteoblast to differentiate from mesenchymal progenitor cells and later in hypertrophic chondrocytes, it promotes endochondral ossification by promoting the final maturation of hypertrophic chondrocytes.

Disclosures: **X. Guo**, None.

F051

Altered Sensory Sensitivities in Osteocalcin Null Mutant Mice. P. Buckendahl, Y. K. Kim*, L. A. Pohorecky*. Center of Alcohol Studies, Rutgers University, Piscataway, NJ, USA.

Osteocalcin (OC) is a small, extracellular mineral-binding protein synthesized almost exclusively by osteoblasts and deposited along with bone mineral during formation. OC synthesis is regulated by glucocorticoids (GC) as well as numerous other hormones. A relatively consistent amount of newly synthesized OC is released to circulation (pOC), influenced not only by bone formation but also by physical and environmental stimuli such as those that increase GC and decrease plasma Ca^{++} . Acutely stressful stimuli (fear, isoflurane anesthesia, restraint immobilization) in humans, monkeys, and rats increase pOC within minutes, while pain (surgery), cold exposure, or anxiety (anticipation of surgery, novel environment, mild restraint) more slowly decrease pOC over periods of hours to days. These responses may be related to GC or to as yet undetermined sympathetic neural factors. OC has been immunolocalized to nociceptive cells of rat dorsal root ganglia and in taste sensors in glossopharyngeal ganglia. Because these responses generally also involve mobilization of Ca^{++} , and because of the affinity of OC for Ca^{++} , we hypothesized that it could be involved in sensing or modulating sensory stimuli. To begin to confirm this hypothesis, we compared OC null mutant (KO, n=9) and wild-type C57BL/6 (WT, n=9) mice, progeny of heterozygous littermate parents. Unlike WT, KO mice have no OC in plasma or bone. We tested behavior in the open field (\pm EtOH), thermal sensitivity ($52.5^\circ C \pm$ EtOH), paw sensitivity to Von Frey fibers (0.16 to 2 g force), and light/dark exploration. Basic open field locomotion and center/periphery preference did not differ between KO and WT. However, following EtOH injection (1 g/kg i.p.), mice differed significantly in relation to light intensity, with WT spending more time in lower light intensity areas than KO. WT also spent more time in the dark side of a light/dark box than did KO. Although WT and KO did not differ in response to hot plate test, WT were more sensitive to Von Frey fibers. The apparent contradiction in the latter findings may relate to differences in pain/touch receptors in the paw and associated ganglia. These findings suggest a novel and unique involvement of OC in sensory responses. Whether that results from pOC or from in situ synthesis remains to be determined.

Disclosures: **P. Buckendahl**, None.

F053

Crtap Is Required for Prolyl 3-Hydroxylation of Fibrillar Collagens and Loss of its Function Causes Severe Kyphoscoliosis and Osteoporosis in Mice. R. Morello*¹, T. K. Bertin*¹, Y. Chen*¹, P. Castagnola*², D. R. Eyre*³, B. F. Boyce*⁴, B. Lee*⁵. ¹Molecular and Human Genetics, Baylor College of Medicine, Houston, TX, USA, ²National Institute for Cancer Research, Genoa, Italy, ³University of Washington, Seattle, WA, USA, ⁴University of Rochester Medical Center, Rochester, NY, USA, ⁵Howard Hughes Medical Institute, Houston, TX, USA.

Recently we described the isolation and characterization of a novel protein, Crtap, differentially expressed in chicken hypertrophic chondrocytes compared to proliferating chondrocytes in vitro. We isolated the mouse ortholog and demonstrated its expression in chondrocytes, osteoblasts and osteoclasts by in situ hybridization and RT-PCR. To understand its function, we generated mutant mice by homologous recombination. Heterozygous Crtap^{+/} mice were asymptomatic. Crtap null mice were generated and northern hybridization analysis of total embryo RNA confirmed the absence of Crtap mRNA. The null mice are born viable at the expected Mendelian ratios and, although smaller, they show no obvious abnormalities at birth. However, by 3-4 months of age they begin to develop a moderate kyphosis that becomes pronounced at 6 months of age. Faxitron analyses confirmed the deformity of the spine at the thoracic level and, most importantly, it revealed severe generalized osteoporosis affecting both cortical and trabecular bone. Histological analysis confirmed the severe osteoporosis and showed abnormal proliferating chondrocytes in the growth plate. Bone histomorphometry demonstrated approximately 50% decrease of axial and appendicular BV/TV compared to wild type mice, normal osteoblast and osteoclast numbers, but low mineral apposition and bone formation rates. Importantly, Crtap null mice have defective osteoid formation. Moreover, because Vranka JA et. al (2004) showed that Crtap co-purifies with prolyl 3-hydroxylase, we analyzed tryptic digested, cyanogens bromide derived peptides from types I and II collagen isolated from Crtap null mice tissues using tandem mass spectrometry. Interestingly, the single prolyl 3-hydroxylation modification known to exist in these collagen chains was completely absent. The altered post-translation modification of fibrillar collagens together with defective osteoid formation suggest a critical role of prolyl 3-hydroxylation for proper bone matrix formation and point to a key role for Crtap during skeletal development and bone mass acquisition. Moreover, these data point to a novel pathophysiologic mechanism leading to a new type of collagenopathy perhaps in the osteogenesis imperfecta spectrum of disorders.

Disclosures: **R. Morello**, None.

F057

Expression of Mechanosensitive, Prochondrogenic Genes: A Link between Mechanical Stimulation and Tissue Differentiation. M. Tagil*¹, R. Rajani*², P. Bahra*², X. Cao*², D. Fischer*², R. Thompson*², J. Astrand*¹, P. Aspenberg*³, K. Hankenson*². ¹Dep of Orthopedics, Lund University Hospital, Lund, Sweden, ²University of Michigan, Ann Arbor, MI, USA, ³Dep of Orthopedics, Linköping University Hospital, Linköping, Sweden.

Introduction We have developed an experimental bone chamber model in the rat. When hydrostatic pressure is applied, cartilage forms while bone forms without mechanical stimulation. To better understand chondroinduction secondary to mechanical load, we investigated morphologic changes at early time points following load, and used gene expression analysis to determine mechanosensitive genes. **Material and Methods** *Surgery:* Four groups of four Sprague Dawley rats had a non-loaded chamber implanted in one leg and a loaded chamber in the other. The tissue inside the loaded chamber was loaded by 2 MPa, in three second cycles, twenty times, twice a day. *Morphological analysis:* The rats were euthanized after 1, 3, 5 and 7 days of loading/non loading. Specimens were scanned using microCT and bone volume fraction and bone length were measured. The specimens were stained with H&E or safranin-O/fast green. *Gene expression analysis:* Another 12 male rats at each time point were operated, loaded and harvested at 1, 3, 5, or 7 days. RNA was harvested using Qiagen RNeasy. Affymetrix rat expression array 230 2.0 was hybridized with the eight samples and fluorescence signal detected. Microarray data was examined for genes exhibiting a minimum two-fold change in loaded vs unloaded specimens. DNA-Chip Analyzer (dCHIP) Software was used to filter genes showing a minimum 2.3 fold change in loaded vs unloaded specimens. To validate the array data, RNA was reverse transcribed and analyzed using qPCR. **Results** By d5, cartilage is evident in the mesenchyme overlying the bone, and by d7 has started to undergo endochondral ossification. The 20 most prevalent genes for unloaded and loaded specimens showed strong agreement. In addition to ribosomal proteins, hexokinase, and the cytoskeleton components beta-actin and vimentin, a number of genes related to bone formation were in the top 20, including collagens type I, III, and V, BSP1, osteopontin, and osteocalcin. Overall, over 2000 genes showed increased expression in loaded vs unloaded specimens at one of the days. **Discussion** Loading induced chondrogenic genes, as noted by increases in type II collagen, WISP2, and TSP4 on d5 and d7, as well, as a significant 5-fold induction of type X collagen on d7. Genes that may be associated with mechanoresponsiveness that leads to chondrogenesis are revealed by changes in d1 and d3 expression. Two likely candidates are cytokine receptor-like factor 3 (CRL3) and aldose reductase-like protein.

Disclosures: **M. Tagil**, None.

F062

Action of Prostaglandin E2 (PGE2) via EP4 Receptor Is Critical for Osteolysis due to Bone Metastasis of Cancer. M. Takita*¹, M. Inada*¹, T. Maruyama*², C. Miyaura*¹. ¹Biotechnology and Life Science, Tokyo University of Agriculture and Technology, Tokyo, Japan, ²Ono Pharmaceutical Co. Ltd., Osaka, Japan.

Bone metastasis of cancer induces osteolysis with increased bone resorption, but the mechanism of bone loss due to the presence of cancer cells is not fully understood. We have found that prostaglandin E2 (PGE2) acts mainly on EP4 receptor, one of the PGE receptor subtypes (EP1, EP2, EP3 and EP4), in osteoblasts to induce the receptor activator of NF- κ B ligand (RANKL) expression to stimulate bone resorption. Expression of cyclooxygenase-2 (COX-2) and RANKL mRNA was elevated in bone with cancer metastasis, but the roles of PGE2 and its receptor EP4 in bone metastasis are not clear up to the present. In this study, we made a model of osteolytic bone metastasis by injecting mouse malignant melanoma B16 cells into the left heart ventricle of C57BL/6 mice and examined the effects of EP4 antagonist, a selective inhibitor of EP4 receptor, on bone loss due to cancer metastasis. When mice were injected with B16 cells from the left heart ventricle, metastatic regions accompanying severe bone loss were detected in femurs and tibiae 12 days after the injection. Bone mineral density (BMD) in the femur with metastasis was significantly decreased because of the enhancement of bone resorption compared with that in the control femur without metastasis. We measured the level of PGE2 in bone marrow supernatant collected from femurs with or without metastasis, and found that PGE2 in bone marrow from the femur with metastasis was elevated compared with that in the control. When EP4 antagonist was orally administered to C57BL/6 mice injected with B16 cells, osteolysis due to bone metastasis in femurs was suppressed, and the decrease in BMD was restored to the control level. In vitro, cell-to-cell contact between fixed-B16 cells and osteoblasts induced the expression of RANKL in osteoblasts. Adding fixed-B16 cells to the cocultures of bone marrow cells and osteoblasts induced osteoclast formation without any bone-resorbing factor, suggesting that cell-to-cell interaction between osteoblasts and tumor cells could induce osteoclastogenesis and osteolysis in bone with cancer metastasis. PGE2 produced by host osteoblasts after contact with cancer cells may induce bone resorption by mechanisms via EP4 receptor expressed in osteoblasts. Therefore, EP4 antagonist may be a candidate for therapy for cancer accompanied by bone metastasis.

Disclosures: **C. Miyaura**, None.

F066

TGF- β Stimulation of PTHrP Expression in Breast Cancer Cells Is Regulated by Gli2. J. A. Sterling, L. Z. Sun*, B. Grubbs*, M. Zhao, B. O. Oyajobi, S. S. Padalecki, G. R. Mundy. Cellular and Structural Biology, UTHSCSA, San Antonio, TX, USA.

Some cancer cells, particularly squamous cell carcinomas, express parathyroid hormone-related peptide (PTHrP) in large amounts, and as a consequence cause increased bone resorption and hypercalcemia. Others, such as breast cancers, express PTHrP in the bone metastatic site as a consequence of stimulation of the cancer cells by bone-derived TGF- β . To understand why some cancer cells over-express PTHrP, we investigated the notion that cancer cells may hijack the Hedgehog (Hh) signaling pathway which regulates PTHrP expression physiologically in the growth plate. We have found that the Hh signaling molecule Gli2 enhances PTHrP expression in tumor cells that metastasize to bone. This stimulation is specific to Gli2, and not Gli1 and Gli3. Furthermore, we have found that several osteolytic and/or hypercalcemic human cancers which produce PTHrP also express Gli2, while 5 non-osteolytic cancers that do not produce PTHrP do not express Gli2. Mice inoculated via intracardiac injections with MDA-MB-231 breast cancer cells over-expressing Gli2 exhibited enhanced tumor induced osteolysis, as determined by histomorphometry and radiography, compared to empty vector control tumor bearing mice. These data indicate that Gli2 stimulates PTHrP and subsequent osteolysis in breast cancer that has metastasized to bone. To determine if Gli2-stimulated PTHrP expression is dependent on TGF- β signaling in breast cancer bone metastases, we utilized MDA-MB-231 cells stably transfected with a dominant negative TGF- β receptor type II (dnRII) and thus without intact TGF- β signaling. We found Gli2 was able to stimulate PTHrP promoter activity in these cells. In addition, using PTHrP luciferase constructs with the Smad binding site mutated, Gli2 also stimulated PTHrP promoter activity. Thus, TGF- β signaling is not required for Gli2 stimulation of PTHrP. To determine if TGF- β regulates Gli2 expression, MDA-MB-231 and MDA-MB-435 breast cancer cells were treated with TGF- β . TGF- β stimulated Gli2 protein expression by Western blot after only 30 min of treatment. By real-time PCR Gli2 expression was induced approximately 3-fold. These data indicate that Gli2 is regulated downstream of TGF- β , suggesting that the TGF- β -mediated increase in PTHrP production is mediated through Gli2. These data suggest Gli2 as a molecular target for drugs in metastatic breast cancer, and that inhibiting Gli2 expression in breast tumors that have metastasized to bone may disrupt the vicious cycle of TGF- β stimulation of PTHrP in advanced breast cancer.

Disclosures: J.A. Sterling, None.

F068

c-Src Inhibition Decreases Breast Cancer-Induced Lethality and Incidence of Metastases in Nude Mice. C. Di Giacinto*¹, D. Fortunati*¹, I. Recchia*¹, A. Angelucci*¹, M. Susa*², D. Fabbro*², A. Teti*¹, N. Rucci*¹. ¹Department of Experimental Medicine, University of L'Aquila, L'Aquila, Italy, ²Novartis Pharma, Basel, Switzerland.

We investigated the involvement of c-Src in the development of breast cancer metastases. Balb-c nu/nu mice were intracardiacally injected with the human breast cancer cells MDA (MDAMB231), or with MDA cells stably transfected with c-Src wild type (MDASrc^{WT}) or c-Src kinase-dead dominant negative (MDASrc^{DN}) constructs. Similar progression and incidence of cachexia and mortality was observed in animals injected with MDA or MDASrc^{WT} cells. In contrast, neither cachexia nor lethality was noticed in mice injected with MDASrc^{DN} cells. X-ray analysis showed 57% and 71% incidence of bone metastases in MDA- and in MDASrc^{WT} cell-injected mice, respectively, while in MDASrc^{DN} cell-injected mice the onset of bone metastases was delayed, reaching only 25% at the end of experiment. In the latter, the incidence of soft tissue lesions was also reduced (MDA/MDASrc^{WT} 85%, MDASrc^{DN} 25%). In subcutaneous xenografts, tumor weight was increased in MDASrc^{WT} (0.54 g \pm 0.068) and decreased in MDASrc^{DN} (0.15 g \pm 0.04) relative to MDA cells (0.34 g \pm 0.034) and the expression of the proliferation marker Ki67 changed accordingly (MDASrc^{WT} 15%, MDASrc^{DN} 2%, MDA 4%). MDA cell-injected mice were treated with 100 mg/kg/day of the c-Src inhibitor CGP76030, and showed an analogous reduction in cachexia, lethality and soft tissue metastases vs control animals. In untreated mice, osteolytic lesions appeared earlier, progressively increasing up to 57% incidence, while in treated mice the incidence was again 25%. In vitro, c-Src inhibition caused a concentration- and time-dependent reduction of MDA cell proliferation, adhesion, spreading and migration. Furthermore, it significantly inhibited bone marrow osteoclast formation and bone resorption. Treatment with c-Src inhibitor reduced osteoblast proliferation and increased the expression of alkaline phosphatase and of the osteoclast inhibitory cytokines GM-CSF and IL-12. Accordingly, IL-12 levels were reduced after osteoblast treatment with conditioned media (CM) from MDASrc^{WT}. Treatment of bone marrow cultures with CM from MDASrc^{WT} and MDASrc^{DN} cells stimulated osteoclast differentiation and increased endothelial cell activity to a similar extent as the MDA CM, suggesting that paracrine factors directly affecting these cell types are not altered. c-Src inhibitor treatment did not directly affect endothelial cell migration or invasion. In conclusion, we demonstrated a role for c-Src in the development of *in vivo* metastases, and identified a potential therapeutic target which could also reduce cachexia and lethality.

Disclosures: C. Di Giacinto, None.

F070

Prostate Cancer Cells Promote Osteoblastic Bone Metastases through Wnts. C. L. Hall¹, A. Bafico*², S. Aaronson*², E. T. Keller¹. ¹Urology, University of Michigan, Ann Arbor, MI, USA, ²Oncological Sciences, Mount Sinai School of Medicine, New York, NY, USA.

Prostate cancer (CaP) produces painful osteoblastic bone metastases through unknown mechanisms. CaP cells are known to produce a variety of potentially osteoblastic factors; however, identification of an osteoblastic factor using an *in vivo* CaP cell model has not been demonstrated to date. Wnts are a family of proteins that are necessary for bone development and are antagonized by endogenous proteins including Dickkopf-1 (DKK-1). We therefore examined whether CaP cells mediate osteoblastic activity through Wnts using DKK-1 as a tool to modify Wnt function. A variety of Wnt mRNAs were found to be expressed in CaP cell lines and Wnt mRNA expression was increased in primary CaP compared to non-neoplastic prostate tissue. In addition, osteolytic PC-3 cells expressed abundant message for the Wnt inhibitor DKK-1. To determine whether DKK-1 expression masked Wnt osteoblastic activity, osteolytic PC-3 cells were transfected with shRNA to DKK-1. Decreasing DKK-1 enabled PC-3 cells to induce osteoblastic activity, including alkaline phosphatase production and mineralization, in murine bone marrow stromal cells. Another CaP cell line, C4-2B, induces osteoblastic lesions *in vivo*. To determine if Wnts contribute to C4-2B's ability to induce osteoblastic lesions, C4-2B cells were transfected with a DKK-1 expression vector to block Wnt activity. The cells were then injected in the tibiae of mice and allowed to grow for 12 weeks. The expression of DKK-1 converted the C4-2B cells from an osteoblastic to a highly osteolytic tumor. Taken together, these data demonstrate that Wnts contribute to the mechanism through which CaP induces osteoblastic activity.

Disclosures: C.L. Hall, None.

F072

Bone Resorption Sites: Targets for Skeletal Colonization by Tumor Cells? R. J. Majeska¹, L. J. Silbert*¹, I. H. Gelman*², M. B. Schaffler¹. ¹Leni and Peter W. May Department of Orthopaedics, Mount Sinai School of Medicine, New York, NY, USA, ²Roswell Park Cancer Institute, Buffalo, NY, USA.

Bone is a preferred site for prostate cancer (CaP) metastasis. Once tumor cells enter bone from the circulation, development of metastatic lesions is facilitated locally by growth/survival factors produced or released from matrix during bone resorption. However, it is not clear whether bone resorption or formation may also target the initial tissue colonization of bone by tumor cells. Here we tested the hypothesis that CaP cells in the circulation preferentially colonize bone near sites of ongoing formation and resorption. A human prostate cell line (LNCaP) was transfected to express GFP constitutively (LNCaP-GFP), and highly expressing cells were selected by flow cytometric sorting. Under IACUC-approved protocols, young male nude mice were treated for 6 days with the bisphosphonate risedronate (RIS, 0.2 mg/kg, sc) to inhibit bone resorption or with PBS vehicle. One day later, mice received 105 LNCaP-GFP cells in 0.1 ml by iv (tail) or intracardiac injection. After 24, 48 or 72h, animals were euthanized and proximal tibiae fixed in fresh 4% buffered paraformaldehyde, decalcified with EDTA and processed for histology. The distance between each fluorescent tumor cell and the nearest bone surface was measured, and the surfaces were characterized as either forming, resorbing or quiescent by standard histological criteria. We found that 24h after injection in control mice, 54% of all tumor cells were closest to active surfaces (24% forming, 30% resorbing), while 46% were nearest to quiescent surfaces; by contrast, forming, resorbing and quiescent surfaces accounted for 16%, 25% and 58% of total bone surfaces, respectively. This indicates preferential localization of tumor cells near sites of tissue activity. Similar distributions were seen at 48 and 72h post-injection. In addition, over 91% of cells near forming and resorbing sites were within 25 μ m of bone surfaces, while only 56% of cells were this close to quiescent surfaces. When bone resorption was suppressed with RIS, almost no tumor cells were seen near active or inactive resorption sites; however, total tumor cells per section also declined from 4.2 \pm 0.9 to 2.0 \pm 0.6 in RIS-treated animals. In summary, these data indicate that the initial colonization of skeletal tissues in mice by circulating prostate cancer cells appears to occur preferentially near sites of active bone formation/resorption. The findings also raise the possibility that factors produced locally near sites of resorption may have more widespread effects on the earliest stages of tumor cell invasion in bone.

Disclosures: R.J. Majeska, None.

F074

Non-Isomerised C-Telopeptides of Type I Collagen (α CTX): A Sensitive Indicator of Metastatic Bone Disease. D. Leeming*¹, M. Koizumi*², B. Li*¹, I. Byrjalsen*¹, L. Tanko*³, P. Qvist¹, C. Christiansen³. ¹Nordic Bioscience, Herlev, Denmark, ²Cancer Institute Hospital, Tokyo, Japan, ³Centre for Clinical & Basic Research, Ballerup, Denmark.

Purpose: To investigate the usefulness of measurement of urinary α CTX (C-telopeptide of type I collagen) for detection of metastatic bone disease of different origin, and the pathogenic role of the OPG/RANKL system. Methods: Participants were 161 cancer patients; 90 breast cancer (45 with bone metastasis), 29 lung cancer (15 with bone metastases), and 42 prostate cancer (17 with bone metastases). Presence of bone metastases was determined by Tc99m scintigraphy and the skeletal involvement was graded according to the Soloway score; 1: <6 metastases, 2: 6-20 metastases, 3: >20 metastases but no super-scan, 4: superscan (i.e. >75% of ribs, vertebrae and pelvic being affected). For control purposes, 309 subjects without history or presence of cancer disease

ASBMR 27th Annual Meeting

were also included. Urine samples were collected and assessed for α CTX (Nordic Bioscience Diagnostics). Serum samples were analyzed for circulating OPG and RANKL (Immunodiagnostic AG). Results: Cancer patients with bone metastases revealed significantly increased levels of α CTX compared with cancer patients without bone metastases. There was a significant association between number of metastases and α CTX levels ($r=0.39$, $p=0.001$). Furthermore, as shown in Fig. 1, α CTX increased with the severity of skeletal involvement as expressed in Soloway score. Presence of bone metastases was associated with increased level of α CTX for all cancer types (Fig 2). Serum OPG, RANKL, OPG/RANKL measurements indicated no significant differences between cancer patients with and without bone metastases, and there were no association between the level of these bone regulatory factors and number of bone metastases. RANKL/OPG ratios were significantly elevated in patients with diagnosed cancer compared with controls, independent of cancer-type. Conclusions: α CTX could be a convenient indicator of the presence and extent of metastatic bone involvement in cancer patients. The accelerated bone resorption seems to involve OPG secretion from tumor cells, yet the RANKL/OPG ratio offers little information regarding skeletal involvement.

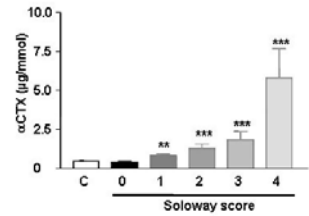


Figure 1. Means of α CTX in C:controls (white) and cancer patients without (black) and with (grey) bone metastases.

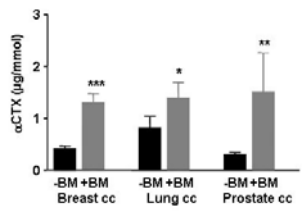


Figure 2. Means of α CTX in cancer patients without (black) and with (grey) bone metastases (analysis stratified for cancer type).

Disclosures: **D. Leeming**, Nordic Bioscience 3.

F077

Site-Discordance of Osteoporosis Categorization in Menopausal Females. W. D. Leslie. Faculty of Medicine, University of Manitoba, Winnipeg, MB, Canada.

The modest correlation in bone mineral density (BMD) between different measurement sites inevitably leads to potential discordance in classifying patients based upon the conventional cutoff T-score ≤ -2.5 . Some groups recommend patient diagnosis based upon lowest site (ISCD), while others recommend a hip site (IOF). The number of osteoporotic sites may also be important as some groups have reported that this correlates with fracture risk. Our objective was to describe the pattern of site-discordance in a large population-based database of clinical DXA results from a regional BMD program (JCD 2005;8:25-30). Analysis was based upon 17,053 women age 50 and older with complete measurements of L1-4, femoral neck, trochanter and total hip. We calculated the number of sites with T-score ≤ -2.5 , T-score mean, range (max-min) and discordance index (difference between lowest site and mean of the 3 remaining sites). Of 5,350 patients osteoporotic by ISCD (at least one site with T ≤ -2.5), almost half (2,530 [47%]) were abnormal at only a single site. Most of these (1,650 of 2,530 [65%]) were abnormal at L1-4 only and would be classified non-osteoporotic by IOF. The range and discordance index were highest for a single abnormal site ($P<0.00001$), suggested that the low value may be an outlier. The expected early spinal bone loss did not adequately account for single-site discordance (mean age 66 ± 8 for abnormal L1-4 vs. 68 ± 10 for abnormal hip). Age correlated only weakly with T-score range or discordance index ($r^2\leq 0.01$). In conclusion, site-discordance is common and markedly affects patient categorization when different diagnostic criteria are used. Fracture outcomes data are needed to see if a single abnormal site improves or degrades the gradient of risk for fracture.

# Sites T ≤ -2.5	Mean T (SE)	Range T (SE)	Discordance Index (SE)
0 (N=11,703)	-0.79 (.01)	1.25 (.01)	0.82 (.01)
1 (N=2,530)	-2.00 (.01)	1.56 (.01)	1.22 (.01)
2 (N=920)	-2.49 (.01)	1.20 (.02)	0.83 (.02)
3 (N=770)	-2.77 (.01)	1.33 (.03)	0.78 (.02)
4 (N=1,130)	-3.30 (.01)	0.92 (.02)	0.71 (.02)

Disclosures: **W.D. Leslie**, None.

F079

The Cross Section Geometry of The Femoral Neck. L. Yang*, E. V. McCloskey, R. Eastell. Bone Metabolism Group, University of Sheffield, Sheffield, United Kingdom.

The calculation of biomechanical properties of the femoral neck (FN) from DXA is based on the assumption that it is circular in cross-section (CS). A recent study (Seeman et al, M099, ASBMR Annual Meeting, 2004) showed that the FN was ellipsoid in CS. The purpose of this study was to obtain a detailed description of the CS geometry of the FN along its axis. We evaluated the baseline-visit CT scans of both proximal femurs of 27 women (mean age 81, range 65 to 86 yr) with osteoporosis who were recruited at a single centre participating in the HORIZON Study. Additional slices were generated by linear interpolation of the CT number so the voxel size was reduced from $0.96\times 0.96\times 3$ to $0.96\times 0.96\times 1$ mm. The images were segmented by semi-automatic intensity thresholding and the CT number converted to vBMD using a phantom. A voxel was considered full of bone tissue if $vBMD\geq 1.05$ g/cm³ and cortical if $vBMD>0.5025$ g/cm³. The FN axis line was placed manually and the neck CS defined along the axis at 1.5 mm intervals.

Nonlinear least-square regression was used to fit the CS to a circle and an ellipse. All the parameters were normalised along the length from the femoral head centre to the distal neck using cubic spline interpolation, and their mean and SD calculated. From the femoral head centre to distal FN the CS geometrical area, bone area, moment of inertia and modulus decreased and then increased. The lowest mean value for geometrical area was 7.1 ± 0.8 cm² (at 65% FN length) and for the bone area was 1.4 ± 0.2 cm² (40% to 60% FN length). The mean modulus about the anterior-posterior (AP) and medial-inferior to lateral-superior (MI-LS) axes were lowest at 38% (670 ± 169 mm⁴) and 54% (666 ± 143 mm⁴) FN length respectively. The CS shapes fitted better to an ellipse than to a circle for all CSs. The principal axes of the ellipse were not parallel to the anatomical axes in the distal half of the FN, they were increasingly internally rotated and reached a plateau of 23° at 80% FN length. From 5% to 45% FN length, the MI-LS axis was the short axis of the ellipse, significantly ($p<0.05$) shorter than the AP axis, but the difference was small. From 60% FN length onwards, the MI-LS axis was significantly ($p<0.05$) and increasingly longer than the AP axis, over 20% longer from 80% FN length onwards. The circularity assumption lead to a significant ($p<0.05$) under-estimation of the average vBMD in CS in the distal half of the FN, less than 80% of the actual vBMD from 65% FN length onwards. Cortical bone was found only in the CSs of the distal half FN and this could be due to the partial volume effect. In conclusion, the FN is ellipsoid in CS, and the ellipsoid size and orientation change along the FN axis. The circularity assumption can lead to large errors in estimating CS biomechanical properties, especially in the distal half of the FN.

Disclosures: **L. Yang**, None.

F081

Fracture Risk Assessment Using a Local versus an International Reference Database. A. Arabi¹, R. Baddoura², H. Awada^{*2}, N. J. Khoury^{*3}, S. Haddad^{*4}, G. Ayoub^{*2}, G. El-Hajjuleihan¹. ¹Internal Medicine, American University of Beirut, Beirut, Lebanon, ²Rheumatology, Saint Joseph University, Beirut, Lebanon, ³Diagnostic Radiology, American University of Beirut, Beirut, Lebanon, ⁴Radiology, Saint Joseph University, Beirut, Lebanon.

Dual-energy X-ray absorptiometry (DXA) is the accepted method for measurement of bone mineral density (BMD). The IOF recommends the measurement of hip BMD, using the universal NHANES reference database. However, in many countries local databases are used without validation of such an approach. The aim of this study was to assess the ability of BMD measurements, using the WHO criteria (T-score ≤ -2.5), to identify subjects with prevalent vertebral fractures, using either the local or the NHANES databases. 460 non-Western Caucasian subjects, aged 65-85 years, were randomly recruited from a large metropolitan area, based on geographical maps. BMD at the hip were measured by DXA, using Hologic device. Local and Western derived T-score were calculated, using gender matched local or NHANES databases¹⁻². Lateral radiographs of the thoraco-lumbar spine were assessed using the semi-quantitative method of Genant³. Mild fractures were excluded. The sensitivity, specificity, PPV, NPV and area under the ROC, of BMD measurements to identify subjects with vertebral fracture, were computed using STATA v7. 56 women (19%) and 18 (12%) men had at least one vertebral fracture. When the Western database was used, 33% of women and 23% of men had osteoporosis at the hip. When the Local database was used, these percentages were 13% and 2% respectively.

	women N=301		Men N=159	
	Western	Local	Western	Local
Sensitivity	52	25	38	11
Specificity	71	89	79	99
PPV	30	35	20	66
NPV	86	83	90	89
ROC	0.61	0.57	0.59	0.55

In both genders, the sensitivity and the area under the ROC for detecting patients with prevalent vertebral fractures were higher when the Western database was used, but the NPP and the PPV did not differ between the 2 databases. Similar results were obtained when the analyses were done in the overall group (data not shown) Our study suggests that the use of a local database decreases the ability of DXA to identify subjects with prevalent vertebral fractures. It validates the IOF recommendation favoring the use of universal standardized databases, over local database⁴.

1- Bone 2002, 31: 520-528.

2- Osteoporos Int 1995, 5:389-409.

3- JBMR 1993, 8:1137-48.

4- Osteoporos Int 1997, 7:390-406.

F084

Importance of the AP Spine View for the Reliability and Accuracy of Vertebral Fracture Assessment Compared to Radiography. J. T. Schousboe¹, K. E. Wilson², C. R. DeBold^{*1}. ¹Park Nicollet Clinic & Institute, Minneapolis, MN, USA, ²Hologic, Inc., Bedford, MA, USA.

Prevalent radiographic vertebral deformity is a powerful risk factor for incident fractures, yet the majority of these deformities are clinically unapparent. Imaging of the spine with a densitometer (vertebral fracture assessment, VFA) can detect these deformities, but the utility of the AP view in VFA and how scoliosis affects the performance of VFA is not fully established. To estimate the effect of scoliosis on the accuracy of VFA compared to x-ray and the utility of the AP view, we obtained lateral thoracic and lumbar spine radiographs and AP and lateral VFA images on 203 women age 65 and older who had been referred for bone densitometry. Both sets of images were evaluated for prevalent vertebral deformity consistent with fracture according to the

ASBMR 27th Annual Meeting

semiquantitative method of Genant. by two readers blinded to each other's readings. Each reader was also blinded to his own x-ray readings when evaluating VFA's. Reader 2 (JTS) evaluated the AP image for scoliosis. Considering all 203 participants, sensitivity of VFA for those with one or more grade 2 or 3 vertebral deformity was 63% for reader 1 (CRD) and 78% for reader 2. However, if subjects with moderate or severe scoliosis as graded by the VFA AP view were excluded (14 of 205), the sensitivity for those with grade 2 or 3 deformities was 87% for reader 1 and 93% for reader 2. A strategy of AP and lateral VFA followed by selective radiography in those with a grade 2 deformity (for confirmation) or those with moderate or severe scoliosis on the AP view showed excellent agreement with x-ray, as shown in the following table for reader 1 (values for reader 2 in parentheses).

	Radiography Negative	Radiography Positive	Totals
Absorptiometry Strategy Negative	185 (188)	2 (1)	187 (189)
Absorptiometry Strategy Positive	2 (1)	14 (13)	16 (14)
Totals	187 (189)	16 (14)	203

The kappa statistic for agreement between the two strategies was 0.864 (95% CI 0.794 - 0.934) for reader 1 and 0.923 (95% CI 0.853 - 0.993) for reader 2. The VFA strategy would require follow-up radiographs for 26 (12.8%) according to reader 1 and for 25 (12.3%) according to reader 2. VFA can detect those with grade 2 or 3 radiographic vertebral deformity very accurately, especially if the AP view is also obtained and follow-up radiographs are obtained for those with scoliosis and no obvious grade 3 fracture.

Disclosures: **J.T. Schousboe**, Hologic, Inc. 2.

F086

Trabecular and Cortical Bone Structure in Glutocorticoid-Steroid Induced Osteoporosis. **B. Hyun**^{*1}, **G. Blumenkrantz**^{*1}, **D. C. Newitt**¹, **S. Majumdar**¹, **N. Lane**². ¹MQIR, Department of Radiology, UCSF, San Francisco, CA, USA, ²Department of Medicine, UCD, Davis, CA, USA.

Subjects treated with glucocorticoids (GCs) fracture at higher bone mass than postmenopausal osteoporotic (PMO) women. Since GCs increase bone resorption and decrease bone formation, we hypothesize that changes that alter trabecular architecture with GC use differ from the PMO state. The purpose of this study was to evaluate trabecular bone (TB) and cortical bone (CB) structure in the distal radius using high-resolution MRI in subjects with GC induced bone loss (n = 13, mean age 53.4 ± 14.4 yrs, mean GC dose 6.7 mg/day, for 5 yrs.) compared to PMO fracture group (n=27, mean age 59.2 ± 3.2 yrs)(1). Methods: HR-MR images were obtained at 1.5 T (GE) using a gradient echo sequence at a spatial resolution of 156 x 156 x 500 µm. Trabecular and cortical regions of the distal radius were segmented, and bone measurements were calculated using semi-automatic in-house developed routines written in IDL (RSI, Boulder, CO). The TB region was segmented into bone and marrow components and measures such as App BV/TV (volume fraction), App TbN (trabecular number), App TbTh (trabecular thickness), and App TbSp (trabecular spacing) were calculated. TB measurements were calculated from the segmented trabecular regions and then averaged over two 5 mm slabs starting 7 mm from the endplate. The CB volume and average thickness was measured and also normalized for bone size in a 10 mm region 20 mm from the endplate. Results: The mean trabecular structure measures are shown in Table 1. When a subset (n = 8, mean age = 48.9 ± 15.2 yrs) was compared to the PMO subjects, the GC group had lower App BV/TV (-18.1%) App TbN (-3.3%), App TbTh (-15.8%), and higher trabecular spacing (+13.9%) in a 5 mm region that was 7 mm from the endplate. In the next 5 mm consecutive region, 12 mm from endplate, the GC group had lower App BV/TV (-23.2%), App TbN (-5.9%), App TbTh (-19.4%), and higher TbSp (+15.1%) than the PMO fracture group. Cortical volumes and thicknesses of the GC group were on average larger, 7.9% and 21.5% respectively, than the PMO group. These results suggest that GCs do alter TB architecture more than PMO state. However, CB appears less involved with low doses of GCs. Additional analysis to determine whether GCs alter CB and TB structure both at the hip and calcaneus is underway.

		GCS Induced Osteoporosis	Post-Menopausal Osteoporotic Fracture (1)	p value
Averaged 5 mm region 7 mm from the endplate	App BV/TV	0.300 ± 0.049	0.366 ± 0.042	<0.001
	App TbN	1.604 ± 0.156	1.659 ± 0.177	0.325
	App TbSp	0.444 ± 0.078	0.390 ± 0.072	0.046
	App TbTh	0.186 ± 0.016	0.221 ± 0.053	<1.5E-06
	App BV/TV	0.273 ± 0.058	0.355 ± 0.053	<0.003
Averaged 5 mm region 12 mm from the endplate	App TbN	1.502 ± 0.208	1.596 ± 0.260	0.229
	App TbSp	0.503 ± 0.129	0.437 ± 0.020	0.215
	App TbTh	0.180 ± 0.018	0.223 ± 0.020	<2.0E-07

References:

(1) Proceedings of 25th ASBMR, Presentation #SA361

Disclosures: **B. Hyun**, None.

F088

Role of Cortical Shell in Vertebral Strength Assessment. **S. K. Eswaran**^{*1}, **A. Gupta**^{*1}, **M. F. Adams**^{*2}, **T. M. Keaveny**¹. ¹Mechanical Engineering, University of California at Berkeley, Berkeley, CA, USA, ²Columbia University, New York, NY, USA.

One key issue in clinical non-invasive strength and fracture risk assessment for the spine is the relative biomechanical roles of the cortical shell vs. trabecular bone, an issue that remains poorly understood. To gain new insight into this issue, we developed high-resolution micro-CT based finite element models at 60-µm spatial resolution for 13 cadaveric thoracic vertebrae (age range: 54-87 years, 74.6±9.4 years). The shell was explicitly identified using custom image-processing routines, and three sets of models were

analyzed under uniform compressive loading using high-performance supercomputers: the intact vertebral body; a "no-shell" model in which the shell was virtually removed; and a "shell-only" model, consisting of only the removed shell. From this, we could extract the relative biomechanical roles of the cortical shell and trabecular bone. Results indicated that the shell mass fraction (cortical shell mass divided by total mass) ranged from 21%-39%, indicating that the shell represents a substantial portion of the bone material in the vertebral body even though the average shell thickness was only 0.38±0.06 mm. As expected, the maximum load taken by the shell in a vertebra occurred at the narrowest section of the vertebra, and across vertebra, this varied between 41%-66%. The maximum load taken by the trabecular bone within a vertebra, which typically occurs close to the endplates, ranged across vertebrae from 68%-92%. The reduction in vertebral stiffness due to the virtual removal of the shell ranged from 38%-68%, and depended more on the shell mass fraction (R²=0.93, p<0.0001) than on trabecular bone volume fraction (R²=0.42, p<0.02). Taken together, these findings establish that the biomechanical role of the thin cortical shell in the vertebral body is substantial, and is maximum at the mid-section where the vertebra is narrowest. The role of the trabecular bone can also be substantial and is greatest near the endplates. It follows then that non-invasive densitometric assays of vertebral strength should include measures of both cortical and trabecular bone density. If trabecular bone density alone is to be monitored, the most relevant regions for sampling are near the endplates and not at the center since it is precisely in the central section that the trabecular bone has least influence on overall structural behavior.

Disclosures: **S.K. Eswaran**, None.

F090

Predicting Hip Fracture in a Sub-Group of Subjects from the Study of Osteoporotic Fractures Using Automated Structural Measurements of Proximal Femur in Pelvic Radiographs. **D. Steines**^{*1}, **C. Arnaud**¹, **S. Liew**¹, **R. Vargas-Voracek**¹, **D. C. Bauer**², **S. R. Cummings**², **P. Hess**¹. ¹Imaging Therapeutics, Foster City, CA, USA, ²S.F. Coordinating Center, CPMC Research Institute and UC San Francisco, San Francisco, CA, USA.

Factors other than bone mineral density (BMD), such as trabecular structure (TS) and cortical bone thinning (CBT), contribute to fracture. We analyzed whether fracture cases could be differentiated from controls without fracture using automated TS and CBT surrogate measurements of proximal femur from pelvic radiographs using novel imaging analysis technology. Examples of such measurements include the density of micro-structure in principal tensile regions and measurement of the shaft and neck cortical bone thickness and width. Pelvic radiographs from a subgroup of 400 women participating in the Study of Osteoporotic Fractures (SOF) were used in the analysis. A sample of 108 prevalent controls at end of follow-up and 97 hip fracture subjects with radiographs performed close to the time of fracture were chosen based on available BMD measurements as well as minimum acceptable image quality and patient positioning as graded by two different observers. TS and CBT measurements were combined into two separate micro and macro classification indexes respectively using likelihood ratios. The classification performance of each of these indices and in combination with body mass index (BMI) and BMD was evaluated using receiver operating characteristic (ROC) curves with a leave-one-out cross-validation scheme. The corresponding areas under the ROC curves and mean values with 25%, 50% and 75% percentiles for the parameters from control and fracture cases are summarized in the table below.

Parameters Analyzed	Area Under ROC Curve (%)	Sensitivity at 80% Specificity (%)	Control Cases Mean Value (1 st , 2 nd and 3 rd quartiles)	Fracture Cases Mean Value (1 st , 2 nd and 3 rd quartiles)	p-value t-test for difference in means
(Macro+Micro)+BMD	88	80	NA	NA	NA
(Macro+Micro) index	86	76	5.29 (-1.18,4.61,10.5)	-8.47 (-11.11,-6.8,-2.32)	<0.001
BMD	81	68	0.8 (0.72,0.80,0.89)	0.64 (0.57,0.64,0.7)	<0.001
Macro index only	74	53	3.17 (-0.17,0.91,3.75)	-0.18 (-2.4,-0.8,0.74)	0.0252
Micro index only	73	52	-0.37 (-2.86,-0.29,2.5)	-5.74 (-8.7,-3.57,-1.7)	<0.001
BMI	60	28	26.48 (23.0,26.3,29.5)	24.85 (22.2,24.4,27.1)	0.0046

The combined macro and micro structural measurements had a higher AUC than BMD alone (86% vs. 81%, p-value<0.001). The best performance (AUC=88%) was obtained when macro and micro indexes were combined with BMD suggesting the presence of added complementary information. Further optimization and generalization verification of these results is needed using a broader population sample since only prevalent controls were considered. Nonetheless, these results indicate that this new technology has the potential of improving the prediction of hip fracture risk based on classification of macro and micro-structural measurements from standard pelvic radiographs.

Disclosures: **D. Steines**, None.

F093

Prediction of Non-Vertebral Fracture Risk in 5201 Postmenopausal Women by Quantitative Ultrasound of the Calcaneus: 36-Month Final Results from the ECOSAP Prospective Study. A. Díez-Pérez¹, J. González-Macías², J. Vila^{*3}, F. Gómez-Martín^{*4}, T. Guerrero^{*5}, G. Rodríguez-Roca^{*6}, J. J. Montero^{*7}, M. A. Fortea^{*8}, I. Nieto^{*9}, P. Arqueros^{*10}, F. Marín¹¹. ¹Dept. Internal Medicine, H. del Mar, Barcelona, Spain, ²Dept. Internal Medicine,, H.U. Valdecilla, Santander, Spain, ³IMIM, Barcelona, Spain, ⁴C.S. Guayaba, Madrid, Spain, ⁵C.S. Fuensanta, Sevilla, Spain, ⁶C.S. Puebla de Montalbán, Madrid, Spain, ⁷A.B.S. Ronda Prim, Mataró, Spain, ⁸C.S. Campanar, Valencia, Spain, ⁹C.S. Rochapea, Navarra, Spain, ¹⁰C.S. Ciudad Jardín, Almería, Spain, ¹¹Medical Research, Eli Lilly and Company, Madrid, Spain.

Several prospective studies have shown that bone quantitative ultrasound (QUS) variables are predictive of osteoporotic fractures with a similar magnitude to DXA. ECOSAP is a 3-year prospective study to evaluate the ability of calcaneus QUS and several clinical risk factors of osteoporosis and fractures to predict the non-vertebral fracture risk in women ≥ 65 years. 5201 women aged 72.3 ± 3.5 years (mean \pm SD) were assessed with a Sahara® equipment. Women were selected using non-probabilistic sampling of consecutive cases regardless of the reason for consultation in 58 Primary Care Centers across Spain. At baseline, 1042 women (20.1%) presented a history of fragility fracture in adulthood (>35 years). We report here the final study results. 4453 women (87.3%) have completed the 36-month final visit, with a total follow-up of 15,282 women/years. A total of 369 non-vertebral fragility fractures in 317 women were reported. A Cox proportional hazard regression analysis with non-vertebral fractures as the dependent variable was performed. Independent variables included were all those with a p-value < 0.15 . The final model consisted of age, history of falls, prevalent fractures, and family history of fractures. The hazard rates (and 95% CI) per SD decrease of each QUS parameter after adjusting for them are shown in the Table.

Type of fracture (number)	All non-vertebral (n=317)	Forearm (n=111)	Hip (n=52)	Humerus (n=51)
BUA	1.34 (1.18;1.52)	1.33 (1.08;1.65)	1.67 (1.22;2.30)	1.33 (0.98;1.81)
SOS	1.21 (1.09;1.34)	1.30 (1.12;1.50)	1.25 (0.99;1.57)	1.19 (0.90;1.55)
QUI	1.32 (1.17;1.50)	1.48 (1.19;1.84)	1.50 (1.08;2.08)	1.33 (0.97;1.82)
Estimated heel BMD	1.33 (1.17;1.51)	1.48 (1.19;1.85)	1.54 (1.11;2.14)	1.35 (0.98;1.86)
Estimated heel BMD (T-score)	1.30 (1.16;1.47)	1.44 (1.17;1.76)	1.56 (1.14;2.13)	1.35 (1.00;1.82)

The 3-year final results of the ECOSAP study show that QUS of the heel is a predictor of overall non-vertebral osteoporotic fractures, and of hip, forearm and humerus in a cohort of elderly Spanish women included regardless their bone mass status.

Disclosures: **F. Marín**, Eli Lilly and Company 3.

F096

A Model to Predict Hip Fracture in Elderly Women by Using Clinical Factors and QUS: The Combined “SEMOF + EPIDOS” Prospective Cohort. D. Hans¹, C. Durosier^{*1}, A. M. Schott^{*2}, C. Ruffieux^{*3}, P. J. Meunier⁴, R. Rizzoli⁵, J. Cornuz^{*3}, M. A. Krieg³. ¹Nuclear Medicine, Geneva University Hospital, Geneva - 14, Switzerland, ²Medical Information, Hospices Civils of Lyon, Lyon, France, ³Outpatient Clinic, Lausanne University Hospital, Lausanne, Switzerland, ⁴Inserm U 403, Edouard Herriot Hospital,, Lyon, France, ⁵Bone Diseases, Geneva University Hospital, Geneva - 14, Switzerland.

A European report deplores that only a marginal percentage of women at high risk of osteoporotic fracture are diagnosed. Studies have shown that heel bone ultrasound (HBU) could be useful as a pre-screening method. The SEMOF study group recently demonstrated that the association between QUS with other risk factors improved the prediction of women at high risk for non vertebral fractures. The aim of our study is to develop a mega model combining EPIDOS and SEMOF to predict hip fracture using a simple score. We built a data base “EPIMOF” (12960 women aged 70 to 97 years) by grouping the SEMOF (Swiss) and EPIDOS (French) prospective multi-centre cohorts. At baseline, all the women had been measured by the HBU Achilles+ (GE-Lunar), and examined for their risks for osteoporosis thanks to questionnaires. During a mean follow-up period of 3.2 ± 0.9 years (\pm SD), 307 women reported a hip fracture. While all clinical and QUS factors were tested using a Cox model, only significant ones were used in the building of a score of risk. The principle of this score is based on the coefficients of the Cox model to give a weight to each independent predictor. We fixed the score threshold corresponding to a “high risk” of hip fracture so that the specificity was 80% and the score threshold corresponding to a “low risk” so that the sensitivity was 80%. The independent predictors of hip fracture we kept to calculate the score of risk are the following : stiffness index (SI, in 3 classes), age (in classes), fracture history and weight (more or less than 59 kg). 53.4 % of the women who reported a fracture were at high risk at baseline and 57.7 % of the women who didn't report a fracture were at low risk at baseline. Concerning SI alone, the corresponding percentages were 57.3% and 23%, respectively. 6.3 % of the women who were at high risk at baseline reported a hip fracture and 99.1 % of the women who were at low risk at baseline didn't report a fracture. Concerning SI alone, the corresponding percentages were 4.8 % and 99.2 %, respectively. In conclusion, associating heel bone ultrasound with clinical risk factors clearly improve the detection of elderly women at low risk of hip fracture. The score allows to exclude women at low risk with more assurance. Current cost-effective analysis is underway to further validate such an approach for pre-screening.

Disclosures: **D. Hans**, Synarc 1.

F100

Five-Year Change in Bone Mineral Density Is Heritable in Mexican Americans: The San Antonio Family Osteoporosis Study. J. R. Shaffer^{*1}, C. M. Kammerer¹, J. Bruder^{*2}, R. L. Bauer^{*2}, B. D. Mitchell³. ¹U. Pittsburgh Grad. School Public Health, Pittsburgh, PA, USA, ²U. Texas Health Science Center, San Antonio, TX, USA, ³U. Maryland School of Medicine, Baltimore, MD, USA.

Acquisition of peak bone mass and subsequent rate of bone loss predict risk of osteoporosis. While numerous studies have documented the high heritability of peak bone mass acquisition, the genetic contribution to bone loss is largely unknown. We investigated the extent to which genes and environmental factors influence change in hip, spine, and radius bone mineral density (BMD) over time using data on 18 extended Mexican American families comprising 261 females, and 167 males, ages 18 to 78. DXA measurements of areal BMD of the hip, spine and radius were obtained at two time points, baseline and follow-up (3 to 7 years later, median = 5.5 years) and used to determine one-year change in BMD. Then, using maximum likelihood methods, we estimated the heritability of baseline BMD, follow-up BMD, and one-year change, after controlling for the effects of age, sex, and BMI. As expected, the proportion of variation due to genetic effects, the residual heritability, was significant and similar at baseline and follow-up, respectively, for hip (0.58 ± 0.10 vs. 0.51 ± 0.11), spine (0.54 ± 0.11 vs. 0.56 ± 0.11), and radius (0.26 ± 0.09 vs. 0.29 ± 0.10). Because most bone loss takes place later in life, we estimated heritability of BMD change in a subset of 176 individuals who were > 45 years of age at baseline. BMD decreased in these older individuals by an average of 0.0135, 0.005, and 0.003 g/cm² per five years, respectively, at hip, spine, and radius. Residual heritability of the one-year change in BMD at these sites, respectively, was 0.39 ± 0.20 ($p = 0.009$), 0.46 ± 0.22 ($p = 0.007$), and 0.45 ± 0.25 ($p = 0.02$). Thus, genetic factors may account for up to 40% of the variability in BMD change, whereas the variance explained collectively by age, sex, and BMI was about 30% for the spine, and $< 5\%$ for hip, and radius. While other unknown factors are also important, our estimates show that variation in one-year change of BMD, like peak BMD, is largely due to genetic factors. To the best of our knowledge, this is the first study to demonstrate the heritability of change in BMD, identifying the additional role of genetic factors affecting longitudinal loss of BMD in conjunction with those affecting acquisition of peak BMD. Furthermore, the magnitude of the heritability of BMD change indicates that subsequent linkage analyses to locate genes that affect BMD loss should be fruitful.

Disclosures: **J.R. Shaffer**, None.

F102

CAST Chromosome 1 QTL Is Complex and Contains Three BMD Loci and One Bone Size Locus: Evidence from Subcongenic Lines. B. Edderkaoui¹, D. J. Baylink², W. G. Beamer^{*3}, K. L. Shultz^{*3}, N. Dunn^{*1}, J. E. Wergedal², S. Mohan². ¹JLP VAMC, Loma Linda, CA, USA, ²JLP VAMC and LLU, Loma Linda, CA, USA, ³Jackson Labs, Bar Harbor, MI, USA.

BMD is an important component of bone strength and a recognized predictor of risk for osteoporotic fracture. Elucidating the genetic basis for BMD variation could lead to identification of potential preventive measures against developing osteoporosis. Genome wide-linkage analysis using C57BL/6J(B6)-CAST/EiJ (CAST) intercross revealed the presence of quantitative trait locus (QTL) responsible for BMD variations in Chr 1. Our goal was to delineate the chromosome interval harboring this QTL by using subcongenic lines of mice. The B6.CAST-IT congenic line, which carries the CAST segment covering the whole QTL region in Chr 1, was previously generated to confirm the effect of this QTL on femoral vBMD (Beamer et al., 2003). Ten subcongenic lines were generated after several backcrossing of the initial B6-CAST-IT congenic with the B6 mice. 16-week-old female mice were characterized. Three sublines carrying non-overlapping CAST segments showed significant change of femoral vBMD compared to B6 control mice. This provided evidence for the presence of 3 genes within the initial QTL capable of regulating BMD independently. Phenotypic characterization of the remaining sublines, which carried overlapping regions, confirmed the presence of at least three loci (BMD1-1, BMD1-2 and BMD1-3) responsible for vBMD variation in Chr 1 QTL. Sublines carrying CAST segment that covered the first two loci (BMD1-1 and BMD1-2) showed significantly greater femur vBMD (5-12%) compared to B6 mice. However, sublines carrying *cast* alleles within BMD1-3 locus showed significantly reduced femur vBMD compared to B6 mice (6%). Correlation analysis showed that femur vBMD phenotype had a strong negative correlation with endosteal perimeter ($r = -0.8$; $P = 0.003$), and a strong positive correlation with cortical thickness among the ten sublines ($r = 0.97$; $P < 0.001$). These data provide evidence that the three genes in Chr 1 may influence the vBMD phenotype by affecting endocortical bone formation and/or bone resorption. In addition to the vBMD loci, the proximal region of BMD1-2 locus contains bone size (BS) QTL. The significantly greater periosteal in the two sublines covering this region was lost after adjustment for body weight (BW). In contrast, none of the vBMD QTL was affected by BW adjustment. In Conclusion: 1) the initial vBMD QTL in Chr 1 is the result of three separate QTLs which affect vBMD both positively and negatively. 2) The three loci influence femur vBMD primarily by increasing or reducing the endosteal perimeter. 3) A genetic locus associated with BW and BS phenotypes was found within the BMD QTL in Chr 1.

Disclosures: **B. Edderkaoui**, None.

F104

An Update on N-Ethyl-N-Nitrosourea (ENU) Induced Mutation Screen for Musculoskeletal Phenotypes in Mouse. A. Srivastava, S. Mohan, D. J. Baylink. JLP VAMC and LLU, Loma Linda, CA, USA.

Chemical mutagenesis followed by screening for abnormal phenotypes in the mouse holds great promise as a method for revealing gene function. Earlier, we have described a mouse N-ethyl-N-nitrosourea (ENU) mutagenesis program incorporating a genome-wide screen of one-generation dominant (F1) as well as three-generation recessive (F3) recessive mutations affecting musculoskeletal disorders in mouse model. Abnormal phenotypes are identified as ± 2 -3SD units different from control mice. The mutant mice were progeny tested to determine whether their abnormality is inheritable with a bimodal segregation of offspring in expected 1:1 or 1:3 Mendelian ratios, in dominant and recessive screens, respectively. We have screened approximately 2000 F1 and F3 mice. We observed more than 60 quantitative phenodeviants in primary screen, confirmed more than 30 phenodeviants in secondary screen, and tested approximately 30 phenodeviants for inheritable phenotypes. So far six musculoskeletal phenodeviants have been confirmed in multiple litters and are currently undergoing positional cloning.

Mutant Mouse ID	Genetic Screen	Major Phenotype	# Affected Mice (# of Progeny Screened)
917	Dominant	10-13% Lower total body bone area in males, females not affected	68 (165)
12137	Dominant	11-12% Higher Total Body Bone Density (BMD) and 12-14% Higher Bone Mineral Content (BMC)	56 (132)
12184	Dominant	11-14% Higher BMD, 15-20% Higher Trabecular BMD at Proximal Femur & Lumbar Vertebrae	45 (102)
B24	Recessive	13-14% Higher BMD and 14-15% Higher BMC	29 (86)
B29	Recessive	20-30% Low Bone Markers and 8-10% Higher Total Body BMD	6 (30)
B54	Recessive	9-14% Higher BMD, 14% Higher BMC	26 (85)

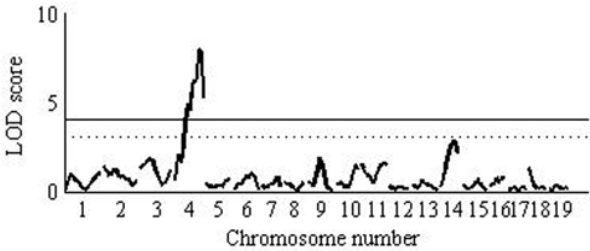
We have identified chromosomal location of a bone size mutant (ID 917) to a proximal region (12 cM) of chromosome 4. A high bone density mutant (ID12184) shows major locus on distal Chr 4 that regulates bone density. In conclusion, this program has identified mutants with significant differences in BMD, BMC and bone size, which would facilitate future discovery of major gene(s) that regulate BMD and other relevant skeletal phenotypes. In addition, the larger phenotypic variations in the mutant mice compared to QTL effects (~5%) and the availability of mutant mice for phenotypic characterization and gene expression without the need to develop congenic mice would increase the efficiency of gene identification process.

Disclosures: **A. Srivastava, None.**

F106

Mapping an ENU Mutant with High Bone Density Reveals a Major Locus on Distal Region of Chromosome 4. A. Srivastava, S. Mohan, V. Chest*, J.E. Wergedal, D. J. Baylink*. JLP VAMC and LLU, Loma Linda, CA, USA.

Using ENU mutagenesis approach to reveal gene function, we have identified a mutant with increased bone density in a dominant screen in C57BL/6J (B6) mice. Data from 16-week old progeny produced (total number of pups n=102) from this mutant mice showed that mean total body bone mineral density (BMD) was 9-13% higher ($p<0.001$, n=45) and total body bone mineral content (BMC) was 10-14% higher ($p<0.01$), as compared to age and sex matched wild type (WT) controls. The total body bone area was not significantly affected. In addition to bone density, the lean body mass determined by DEXA was 8-17% higher in mutant progeny. Volumetric bone density measured in tibia and femur by pQCT was 4-7% higher at midshaft region, as compared to WT mice. To determine the chromosomal location of the ENU mutation, we bred mutant B6 mice with C3H/HeJ (C3H) mice in an intercross breeding to generate 137 B6C3H F2 mice for a low-resolution (using 66 markers) QTL mapping. Body weight adjusted total body bone density and total body bone mineral content determined by DEXA were used as phenotypes. Data from female (n=67) and male (n=70) C3HB6 F2 mice were combined for QTL analysis. Interval mapping of BMD indicated a major peak with LOD score of 8.1 (genome wide significance value $p<0.00001$) on Chr 4 (70 cM). Similarly, interval mapping of BMC trait indicated a major peak with LOD score of 4.6 ($p=0.000024$) on Chr 4 (55 cM). In conclusion, we report identification and characterization of an ENU mutant with approximately 10% higher bone density, and QTL mapping of mutant mice indicates locus on distal Chr 4 that regulates bone density. Further studies on positional cloning will reveal the mutant gene that contributes to higher bone density in mutant B6 mice.



Disclosures: **A. Srivastava, None.**

F110

Isolation of a Gene Affecting Bone Mass on Rat Chromosome 4 Using Congenic Rats. I. Alam¹, L. Lumeng^{*2}, L. G. Carr^{*2}, C. H. Turner¹.

¹Orthopaedic Surgery, Indiana University Purdue University Indianapolis, Indianapolis, IN, USA, ²Medicine, Indiana University Purdue University Indianapolis, Indianapolis, IN, USA.

Several epidemiological studies showed an association between moderate alcohol intake and elevated bone mineral density. It is possible that gene regulating bone mass co-segregate with genes regulating the alcohol preference trait. Previously, we determined bone mass and strength phenotypes in three different alcohol-preferring rat lines. We observed that alcohol-preferring (P) rats have significantly higher bone mass and strength compared to alcohol-non-preferring (NP) rats, both in long bones and lumbar vertebra. Genetic mapping in P/NP rats has identified a major quantitative trait locus (QTL) on chromosome (Chr) 4 for alcohol preference. Also, a QTL linked to bone structure was identified at the same location, which suggests Chr 4 QTL harbor genes regulating both bone mass and alcohol preference. To further study the effects of the Chr 4 QTL, we created reciprocal congenic strains (P.NP and N.P.P) by introgressing the Chr 4 QTL region of one inbred strain (donor) into the genetic background of another inbred strain (recipient). Bone phenotypes, i.e. bone mineral content (BMC) by DXA and volumetric bone mineral density (vBMD) by pQCT, in P/NP and P.NP/NP.P rats at 3 months were measured in long bones and lumbar vertebrae. P.NP rats had significantly lower (4 - 10%, $p<0.05$) normalized BMC (BMC/body weight) in the femur, tibia, and lumbar 1-6 vertebrae compared to P rats. Also, P.NP had significantly lower (14 - 17%, $p<0.0005$) total and trabecular vBMD at proximal tibia. The cortical vBMD at tibial midshaft did not differ between these rats, suggesting that the low BMD phenotype was due mostly to reduced trabecular bone. These results indicate that transfer of the QTL region of Chr 4 from NP rats to P rats significantly decreases bone mass in these congenic rats, suggesting that the Chr 4 QTL harbors a gene or genes that affect bone mass. The most likely candidate gene in this region is neuropeptide Y (NPY). The P.NP rats had decreased bone mineral density, increased body weight, and decreased alcohol preference, which are all associated with increased production of NPY. Our results suggest that some genes regulating bone mass do co-segregate with the genes affecting alcohol preference in congenic P.NP rats. Consequently, congenic P.NP rat model will be a valuable model for identifying some novel genes regulating bone biology.

Disclosures: **I. Alam, None.**

F112

Genetic Architecture of Bone Strength Related Traits in Weight-Bearing versus Non-Weight-Bearing Bones: The Tobago Family Study. X. Wang^{*1}, C. M. Kammerer¹, V. Wheeler^{*2}, A. L. Patrick^{*2}, J. A. Cauley^{*1}, C. H. Bunker^{*1}, J. M. Zmuda¹. ¹U. of Pittsburgh, School of Public Health, Pittsburgh, PA, USA, ²Tobago Health Studies Office, Tobago, Trinidad and Tobago.

Populations of African ancestry have lower osteoporotic fracture risk than other ethnic groups, but the number of affected individuals is expected to increase dramatically in the future due to demographic changes and the number of African individuals at increased risk. In sharp contrast to our understanding of osteoporosis in Caucasians, there is a paucity of information about skeletal health in non-white populations, and particularly among those of African heritage. Using preliminary data on 238 women and 166 men aged 18 and older (mean 43 years old) from 8 large, multigenerational Afro-Caribbean families with a mean family size >50 individuals (range from 21 to 112), we dissected the genetic architecture of bone strength related phenotypes measured by peripheral quantitative computed tomography (pQCT) (including cortical and trabecular volumetric BMD, endosteal and periosteal circumferences, and cortical thickness for the distal and proximal tibia and non-dominant radius). Heritabilities were estimated after accounting for age, gender and their interaction. The majority of measured traits were moderately to highly heritable (H2r, 20% to 71%). H2r estimates were several-fold higher for trabecular than cortical BMD at both the radius and tibia (0.66 \pm 0.10 versus 0.25 \pm 0.09 for radius and 0.71 \pm 0.10 versus 0.33 \pm 0.09 for tibia). The genetic correlation (r_g) between trabecular BMD at the radius and tibia (0.86 \pm 0.05) was high and similar to that for cortical BMD at these regions (0.87 \pm 0.08) indicating that common genes may regulate cortical and trabecular volumetric BMD between different anatomical sites. However, the genetic correlation between cortical and trabecular BMD in the radius (or in the tibia) was not significantly different from 0 (0.31 \pm 0.20 for both). We provide the first comprehensive genetic epidemiologic analysis of bone strength related traits measured by pQCT in human families and the first analysis of these traits in extended families of African heritage. The low genetic correlation between trabecular and cortical BMD implies that linkage analyses should reveal different genes influencing each of these bone traits.

Disclosures: **X. Wang, None.**

F114

Genetic and Gender Regulation of Femoral Density and Size in Congenic Strains for Mouse Distal Chromosome 1. W. G. Beamer, K. L. Shultz, K. M. Delahunty*, L. G. Horton*, H. F. Coombs*, C. L. Ackert-Bicknell, L. R. Donahue, C. J. Rosen. The Jackson Laboratory, Bar Harbor, ME, USA.

Genetic analyses of F2 females from C57BL/6J (B6) and C3H/HeJ (C3H) inbred strains revealed at least 8 QTL for femoral vBMD measured by pQCT. Chromosome (Chr) 1 showed the highest LOD score and accounted for the largest fraction of vBMD variation. A B6.C3H-1T congenic strain carrying a large genomic segment from C3H confirmed the QTL presence. Nested congenic sublines were developed from the 1T congenic to

ASBMR 27th Annual Meeting

accurately map bone regulatory loci and test for possible gender differences. Femurs were isolated from groups (18-35) of 4 mo old female and male B6 progenitor and congenic mice homozygous for segments of distal Chr 1. Data acquired by SA Plus pQCT instrument included total femoral mineral and volume, metaphyseal trabecular mineral and volume, mid-diaphyseal cortical thickness, plus endosteal and periosteal perimeters. Body weights and femur lengths differed among the sublines, thus bone data were adjusted for effects of body mass and skeletal size prior to statistical comparisons with B6 data. Six of 14 congenic sublines span the most distal 22 Mb region of Chr 1 with informative overlapping sequences. Comparison of subline bone parameters with B6 in the region from 169.93-172.01 Mb showed: 1) reduced trabecular vBMD in females and increased trabecular vBMD in males; 2) unchanged femoral length in females but reduced in males. Comparison of bone parameters in the region from 173.54-177.51 Mb showed: 1) females increased total femoral vBMD, mineral, volume, and both endosteal and periosteal perimeters; 2) males had unchanged femoral vBMD and decreased total mineral; 3) female femoral length was unchanged but reduced in males. Body weight declined for both sexes in chromosomal regions proximal and distal to, but not within, the 173.54-177.51 Mb region carrying the female vBMD regulation. PIXImus DEXA data showed the BMC for total body and lumbar spine confirmed the pQCT data for total mineral in females and males for the 173.54-177.51 Mb region. Whole bone mRNA was examined for gene expression by the Affymetrix 430 v2 chip. There are 115 genes in the distal 22 Mb region, 13 of which were differentially expressed. There are 14 genes in the 173.54Mb-177.42Mb region containing the QTL regulating increased female vBMD, four of which were differentially expressed, two were up-regulated (*Irf202b*, *Irf203*) and 2 were down-regulated (*Spn1*, *Fmn2*). These alterations in gene expression are being tested by real time PCR for validation in independent bone samples. These data confirm sex specific pathways for acquisition of peak bone mass, reveal compartment specific effects, and imply caution is warranted when generalizing findings across gender.

Disclosures: *W.G. Beamer, None.*

F116

Molecular Basis of Heritable Forms of Osteoarthritis. L. J. Gleghorn^{*1}, R. Ramesar^{*2}, P. Beighton^{*2}, G. Wallis^{*1}. ¹Faculty of Life Sciences, University of Manchester, Manchester, United Kingdom, ²Department of Human Genetics, University of Cape Town, Cape Town, South Africa.

Osteoarthritis (OA) is a common, painful, debilitating disease that results in the progressive degeneration of the articular cartilage of synovial joints. Spondyloepiphyseal dysplasia - type Kimberley (SEDK) is a rare heritable skeletal dysplasia characterised by short stature, a stocky build and severe premature OA. This autosomal dominant disorder has been identified in a multi-generation family in South Africa. The aim of this study was to elucidate the molecular basis of SEDK in this family in order to gain an insight into the aetiology and pathogenesis of similar and more common forms of OA. Genetic linkage analysis was used to refine the SEDK disease locus to a 7cM region of chromosome 15q26.1. Candidate genes for the disorder were identified within this region on the basis of function and expression and then screened for mutations by direct sequencing. Screening of the aggrecan gene (*AGC1*), that encodes a major structural component of cartilage, identified a 1 bp insertion in the sequence of exon 12 that segregated with the disorder in the SEDK family. This mutation causes a frameshift plus a premature termination codon that predicts the synthesis of a truncated aggrecan core protein containing an abnormal sequence of 213 amino acids and lacking functionally important C terminal domains. This is the first *AGC1* mutation identified to cause a human disorder. *AGC1* mutations have however been identified to cause lethal recessive forms of skeletal dysplasia in the mouse and chick. Collectively these *AGC1* mutations establish an important role for aggrecan in both skeletogenesis and cartilage homeostasis. It is likely therefore that *AGC1* mutations cause as yet uncharacterized human forms of early onset osteoarthritis and studies to identify such mutations are underway. Further, studies are will be carried out to examine the molecular consequences of *AGC1* mutations on normal development and disease processes.

Disclosures: *L.J. Gleghorn, None.*

F120

LRP 6 Variants Determine Fracture Risk in Elderly Men. J. van Meurs^{*1}, M. Jhamai^{*1}, A. Hofman^{*2}, J. van Leeuwen¹, H. Pols¹, A. Uitterlinden¹. ¹Internal Medicine, Erasmus MC, Rotterdam, The Netherlands, ²Epidemiology, Erasmus MC, Rotterdam, The Netherlands.

Recent work identified Wnt-signaling to control postnatal bone formation, with a pivotal role for the Wnt co-receptor LRP5. A closely related homologue of LRP5, LRP6, is also capable to act as a co-receptor for Wnt ligands and was recently shown to be important in bone metabolism in mice (Kokubu et al, Development 2004). We here studied association of an amino-acid variant of the LRP6 gene (Ile1062Val) with bone parameters and fracture risk in 6373 participants of a large prospective population-based cohort of elderly subjects. In addition, we studied interaction between Ile1062Val and LRP5 Ala1330Val, which has previously been implicated in osteoporosis, and the Arg324Gly variation in secreted frizzled related protein 3 (sFRP3) that was found previously to influence the ability to antagonize Wnt-signaling (Loughlin et al, PNAS 2004) and reduce the vertebral fracture risk in older women (Zmuda et al, ASBMR 2003). In men, carriage of the Val-allele (f=20%) of the Ile1062V polymorphism in LRP6 was associated with increased height (p=0.04) and increased vertebral body size (p=0.01). Male carriers of the Val-allele of the LRP6 polymorphism had a 60% increased risk (p=0.01) for fragility fractures. We found an additive effect of the LRP6 and LRP5 variants with respect to fracture risk. While male carriers of a single LRP6 or LRP5 risk allele had a fracture risk of 1.5, carriers of both risk alleles had a 2.4 times increased risk (p=0.004) for fragility fractures compared to the reference group. A similar trend was seen in women, however

not reaching significance. In addition, we found a very significant interaction between the LRP6 and sFRP-3 variants. Either LRP6 or sFRP-3 risk allele carriers had 50% increased risk, while double risk allele carriers had a trend towards lower risk (p interaction term=0.06 for males and 0.002 in females) All the relations were independent of age, height, weight or BMD. In conclusion, in men the V-1062 variant of the LRP6-gene is associated with frame-size and fracture risk. An additive effect was seen for fracture risk between the LRP5 and 6 variants, while the sFRP-3 variant interacts with the LRP6 variant to reduce fracture risk. The Ile1062Val polymorphism in LRP6 lies within a domain that is predicted to form a structure resembling a propeller with 6 blades. These domains have been implicated in binding of Wnts and Wnt-inhibitors. Alignment of close homologues of LRP6 showed a strong evolutionary conservation of the 1062 Isoleucine, which is strong evidence for functional importance of this residue. Further experiments are needed to elucidate the effects of this variant on function of the LRP6-protein.

Disclosures: *J. van Meurs, None.*

F122

Haplotype Polymorphisms of the Calcium-Sensing Receptor Gene and their Association with the Renal Stone Phenotype in Primary Hyperparathyroidism. A. Scillitani^{*1}, V. Guarnieri^{*1}, C. Battista^{*1}, S. De Geronimo^{*2}, L. Muscarella^{*1}, I. Chiodini^{*1}, M. Cignarelli^{*3}, S. Minisola², E. Bertoldo^{*4}, C. Francucci^{*5}, N. Malavolta^{*6}, A. Piovesan^{*7}, L. D'Agruma^{*1}, D. Cole⁸. ¹Casa Sollievo Sofferenza, San Giovanni Rotondo, Italy, ²Un, Roma, Italy, ³Un, FG, Italy, ⁴Un, VR, Italy, ⁵Un, AN, Italy, ⁶Un, Bo, Italy, ⁷Un, TO, Italy, ⁸University, Toronto, ON, Canada.

Three clustered SNPs in exon 7 of the *CASR* gene (A986S, R990G, Q1011E) have been associated with variation in extracellular calcium levels in Caucasian populations, both individually and in haplotype combination. Looking for parallel associations in primary hyperparathyroidism (PHPT), we recruited 237 subjects with well-characterized sporadic PHPT [41 males 57 ± 15 yr (M ± SD) and 196 females age 58 ± 13 yr] for comparison with 433 controls recruited from a blood donor clinic. In all subjects, we measured serum calcium, albumin, PTH and in PHPT subjects we measured calcium/creatinine clearance (Cl_{Ca}/Cl_{Cr}), BMD by DEXA at spine and femur, and assessed kidney stones by ultrasonography. In all subjects, the 3 *CASR* SNPs were genotyped by direct sequencing. Frequencies of the four different haplotypes (ARQ, SRQ, AGQ, ARE) we observed did not deviate from that expected with Hardy-Weinberg equilibrium. The SRQ haplotype was significantly more common in patients (125/474 or 26.4% of chromosomes) than in controls (170/866 or 19.6% of chromosomes), without significant differences in the other haplotypes (χ^2 = 8.39 p = 0.038). SRQ frequency showed a significant trend with disease status (F = 7.48 p = 0.006), when SRQ copy number was assessed, consistent with a co-dominant effect. There was no significant association between *CASR* haplotype and BMD. There was a significant association of haplotype with the kidney stone phenotype (χ^2 = 15.2 p = 0.0017). In the stone- former sub-group, the SRQ haplotype was underrepresented (50/242 or 20.7% of chromosomes vs 66/210 or 31.4% of non-stoneformer chromosomes) and the AGQ overrepresented (6.6% vs 0.95% of non-stoneformer chromosomes). The association between renal stones in PHPT and presence of AGQ haplotype was significant (χ^2 = 9.73 p = 0.002) and robust to logistic regression analysis that corrected for age, sex, PTH and Cl_{Ca}/Cl_{Cr} (p = 0.015). PHPT subjects bearing at least one copy of the AGQ haplotype had an odds ratio of 3.8 (95% confidence interval: 1.29-11.2) for the presence of stones. Our data indicate that SRQ haplotype is significantly associated with PHPT and that AGQ haplotype within the PHPT patient population is significantly associated with renal stones in PHPT. Patients bearing this haplotype have a 3.8-fold increased risk for this complication, suggesting that it may be a useful predictor of clinical outcome

Disclosures: *A. Scillitani, None.*

F125

Contribution of Microsomal Prostaglandin E Synthase-1 (mPGES-1) in Fracture Healing and Osteoarthritis. K. Yamakawa¹, S. Kamekura¹, M. Murakami^{*2}, I. Kudo^{*2}, S. Uematsu^{*3}, S. Akira^{*3}, K. Nakamura^{*1}, H. Kawaguchi¹. ¹Orthopaedic Surgery, Univ. of Tokyo, Tokyo, Japan, ²Showa Univ., Tokyo, Japan, ³Osaka Univ., Osaka, Japan.

Among three isozymes of prostaglandin E synthase (PGES), the terminal enzyme in the biosynthesis of PGE₂ that shows anabolic and catabolic regulation of bone and cartilage metabolism, only microsomal PGES-1 (mPGES-1) is the inducible enzyme functionally coupled with cyclooxygenase (COX)-2. We previously reported that mPGES-1 deficient (-/-) mice showed less sensitivity to pain, lower inflammation, and less inflammatory bone resorption with no effect on physiological condition. This study further investigated the involvement of PGES in two skeletal pathological conditions, bone fracture healing and osteoarthritis (OA), using mouse experimental models. As the fracture model, a transverse osteotomy was created at the tibia in 8-week-old male -/- and the wild-type (+/+) littermates (n=10 / genotype). X-ray analysis of +/+ mice showed that callus formation was detected at 1 week and all fractures were united with bony bridging by 3 weeks after the surgery. Among the three PGES isozymes, only mPGES-1 was shown to be up-regulated following the osteotomy in the callus cartilage and periosteum in +/+ mice by real-time RT-PCR and immunohistochemical analyses. In contrast, 5 out of 10 -/- mice remained in a nonunion state at 3 weeks and the other 5 showed much weaker union with smaller callus: the average volume and mineral content was about half those of +/+ callus. Histologically, the number of both mesenchymal cells and chondrocytes associated with intramembranous and endochondral ossification, respectively, were markedly decreased in the -/- callus at 1 week, while type X collagen- or TUNEL-positive chondrocytes were normally visible. These defects were restored to the +/+ levels by injection of an adenovirus vector carrying the mPGES-1 gene into the fracture site 2 days after the surgery. OA was induced by

medial ligament transection and meniscectomy in the knee joints of 8-week-old male mice. Although the three isozymes of PGES were immunohistochemically detected in the joint cartilage of +/+ mice, the expressions did not change during OA progression. Both cartilage destruction and osteophyte formation were similar in +/+ and -/- mice during 14 weeks of observation. We thus conclude that mPGES-1 notably contributes to fracture healing by inducing cell proliferation at the early stage, but not to OA pathogenesis. An inhibitor of mPGES-1 is expected to be a highly selective agent against several disorders, and might replace COX-2 inhibitors whose fatal adverse events have recently been pointed out; however, it should be cautiously applied to patients with bone fracture.

Disclosures: **K. Yamakawa**, None.

F127

Prevention of Osteoporosis in Ovariectomized Mice Deficient in Platelet-Activating Factor Receptor (PAF): The Autocrine/Paracrine Action of PAF on Osteoclasts not via Osteoblasts. H. Hikiji¹, S. Ishii^{*2}, H. Shindou^{*2}, T. Takato^{*1}, T. Shimizu^{*2}. ¹Oral and Maxillofacial Surgery, University of Tokyo, Bunkyo-ku, Tokyo, Japan, ²Biochemistry and Molecular Biology, University of Tokyo, Bunkyo-ku, Tokyo, Japan.

Platelet-activating factor (PAF, 1-O-alkyl-2-acetyl-*sn*-glycero-3-phosphocholine) is a potent phospholipid mediator with various biological activities including platelet activation via activation of a G protein-coupled PAF receptor. PAF is produced in diseases associated with bone resorption such as gingival inflammation or arthritis. However, little is known about the functions of PAF in bone metabolism. We used PAF receptor-deficient mice to define the role of PAF in the process of bone resorption following ovariectomy, a model of postmenopausal osteoporosis. Dual X-ray absorptiometry and histomorphometry clarified that bone resorption was markedly attenuated in PAF receptor-deficient mice, indicating that PAF links estrogen depletion and osteoporosis in vivo. Osteoclasts had higher activity of acetyl-CoA:lyso-PAF acetyltransferase, an important enzyme for PAF biosynthesis, than osteoblasts. TNF- α /IL-1 β increased the enzyme activity in osteoclasts. Northern blot analysis revealed that osteoclasts, but not osteoblasts, expressed the PAF receptor mRNA. Consistently, PAF raised the [Ca²⁺]_i level in osteoclasts but not in osteoblasts. PAF receptor stimulation prolonged the survival of osteoclasts in vitro. Furthermore, the treatment of osteoclasts with a PAF receptor antagonist, WEB2086, reduced the survival rate and the Ca resorption activity. We also obtained similar results with osteoclasts from PAF receptor-deficient mice. In the organ culture study, bone resorption in dissected calvariae was significantly suppressed by the PAF receptor antagonist treatment and the genetic PAF receptor deficiency. Taken together, our results suggest that through the inflammatory cytokines, estrogen depletion enhances PAF production as a unique autocrine/paracrine factor for osteoclast functions. Inhibition of PAF function might develop a new strategy to prevent postmenopausal bone loss, without disturbing actions of osteoblasts.

Disclosures: **H. Hikiji**, None.

F129

Smad1 Inhibits the Prostate Cancer Cell Growth as an Androgen Receptor Co-Repressor Induced by Prostate-Derived Factor (PDF). T. Qiu^{*}, X. Shen^{*}, X. Cao. Pathology, University of Alabama at Birmingham, Birmingham, AL, USA.

Prostate-derived factor (PDF) is a member of the TGF- β /BMP superfamily that is expressed specifically in prostate and placenta. The expression of PDF is androgen-dependent. Subcutaneous implantation of recombinant PDF induced cartilage formation and the early stages of endochondral bone formation, indicating that PDF has a functional relationship to the bone morphogenetic protein (BMP). However, little is known about PDF signaling and its function. Here we report that for the first time Smad1 acts as androgen receptor (AR) co-repressor and PDF induces the interaction between AR and Smad1 by stimulating phosphorylation of BMP specific Smad1, not TGF- β Smads, indicating that PDF's activity is similar to BMPs. To investigate function of Smad1 as the AR transcriptional co-repressor, we examined the effects of phosphorylated Smad1 on prostate cell growth. We found that induction of Smad1 phosphorylation by constitutive BMPRI receptor (ALK6) inhibited the growth of AR⁺ LNCaP cells, but not AR⁻ PC3 cells with cell proliferation assays. Interestingly, siRNA AR abolished the inhibition in LNCaP cells, and stably expression of AR in PC3 resumed Smad1 ability in inhibition of cell growth, indicating that Smad1-mediated inhibition is AR dependent. We then examined the potential interaction of Smad1 with AR in immunoprecipitation assay. Our results demonstrated that PDF/BMP or ALK6 induced interaction between endogenous Smad1 and AR. Noggin and mutation of Smad1 phosphorylation site (G419S) blocked the interaction. To directly visualize the Smad1-AR association in vivo, we employed yellow fluorescent protein-based protein-fragment complementation assays. The Smad1 was observed coupling with AR and accumulating in nuclei of the living cells upon androgen or PDF/BMP stimulation. Finally, we examined the effect of Smad1 on AR DNA binding activity in gel shift and chromatin immunoprecipitation assays. We found that Smad1 and AR formed complexes on the androgen response DNA element. Smad1 is recruited by AR to the endogenous prostate-specific antigen (PSA) promoter and represses the PSA expression at both mRNA and protein levels. PSA is an important clinical diagnostic marker for prostate tumor progression. Thus, we characterized a novel mechanism in which Smad1, induced by PDF/BMP, inhibits prostate cell growth by balancing androgen mitogenic activity. Our findings provide a BMP/Smad1 based potential therapeutic target for the treatment of prostate cancer, and improve anti-androgen treatment for prostate patients.

Disclosures: **T. Qiu**, None.

F131

Inhibition of Bone Formation by Activated T Lymphocytes Is Partly Mediated through Interferon- γ . S. Varghese¹, N. Wyzga^{*2}, F. Sylvester^{*2}.

¹Saint Francis Hospital and Medical Center, Hartford, CT, USA, ²Connecticut Children's Medical Center, Hartford, CT, USA.

Osteopenia is common among patients suffering from inflammatory diseases. Since activation of T lymphocytes occurs in inflammatory diseases, we hypothesized that factors produced by activated T cells may decrease bone formation. We isolated T lymphocytes from 5-wk-old C57BL/6J male mice and activated them in vitro by culturing in the presence of anti-CD3 ϵ and -CD28 antibodies for 4 to 7 days. T cell conditioned medium (TCM) was collected and used as a source of activated T cell-derived factors. Bone marrow stromal cells, a source of osteoblast precursors, were harvested from femurs of 5- to 7-wk-old C57BL/6J male mice and cultured for 10 days to allow settling of adherent cells and colony formation. Stromal cells were then cultured under osteoblastogenic conditions and treated with up to 10% resting or activated TCM for 1 to 3 wks. Bone formation was assessed by measuring mineralized nodule formation and markers of the osteoblast phenotype alkaline phosphatase and osteocalcin. Bone formation occurred in stromal cells exposed to resting TCM whereas it was inhibited in cultures exposed to activated TCM. Activated T cells secreted 6 to 450 ng/ml of interferon-gamma (IFN- γ) (n = 6), and varying levels of IFN- γ in TCM suggested different degrees of T cell activation. We tested the direct effects of IFN- γ in stromal cells and found that IFN- γ inhibited bone formation at >0.5 ng/ml. Therefore, we postulated that the inhibitory effects of activated T cells on bone formation are mediated through IFN- γ . To test the role of IFN- γ in mediating the T cell effects on bone formation, we either blocked IFN- γ in activated TCM with an IFN- γ neutralizing antibody prior to testing TCM in stromal cells from wild-type mice or directly tested activated TCM in stromal cells from IFN- γ receptor null mice. The inhibitory effect on bone formation by a TCM, obtained from a modestly activated T cell preparation containing 6 ng/ml of IFN- γ and tested at 10%, was obliterated in stromal cells from IFN- γ receptor null mice. However, the inhibitory effect on bone formation by a TCM, obtained from a highly activated T cell preparation containing ~450 ng/ml of IFN- γ and tested at 1%, persisted even after blocking the IFN- γ effect suggesting that additional T cell factors that can inhibit bone formation may also be present in TCM from highly activated T cells. From these observations, we conclude that IFN- γ partly mediates the inhibitory effects of activated T cells on bone formation, although other factors are also involved. The inhibitory effects of T cell-derived factors, particularly IFN- γ , on bone formation may contribute to bone loss associated with inflammatory diseases.

Disclosures: **S. Varghese**, None.

F133

A Dishevelled-Smad1 Interaction Links Wnt/ β -catenin and BMP Signaling Pathways in Osteoblast Progenitors. Z. Liu^{*}, Y. Tang^{*}, D. J. DiGirolamo^{*}, X. Cao, T. L. Clemens. Department of Pathology, University of Alabama at Birmingham, Birmingham, AL, USA.

Genetic evidence from both humans and mice suggest that the Wnt/ β -catenin and BMP signaling pathways are essential for osteoblast development and differentiation. Upon binding of the Wnt ligands, activated Frizzled receptors then signal through Dishevelled (Dvl) which in turn stabilizes β -catenin and promotes nuclear translocation. In addition, previous studies suggest that BMPs, acting through Smads, can antagonize Wnt signaling to slow proliferation and promote osteoblast differentiation. In this study, we investigated the mechanisms responsible for crosstalk between Wnt/ β -catenin and BMP-Smad signaling pathways. We first tested for interactions in 293T cells transfected with individual Smads (1-8) and Wnt pathway components using immunoprecipitation assays. These studies revealed a specific interaction between Smad1 and Dvl-1 which was dependent on the presence of Wnt3a or BMP-2. Under unstimulated conditions, Smad1 and Dvl-1 were co-immunoprecipitated. Addition of BMP-2 transiently disrupted the Smad1/Dvl-1 interaction with re-assembly occurring within 5h. In contrast, when cells were exposed to both Wnt3a and BMP-2, there was an enhanced accumulation of the Smad-Dvl complex over the same time course. This suggested that BMP signaling might restrict β -catenin activation through binding of Smad1 to Dvl-1. Consistent with this observation, in the absence of BMP-2, the Wnt3a induced disassembly of Smad1 and Dvl-1 coincided temporally with nuclear accumulation of β -catenin, whereas, stimulation of cells with both ligands resulted in decreased nuclear β -catenin levels. To assess the functional consequences of this interaction, we measured the activity of a Wnt responsive luciferase reporter (Topflash) in C3H10T1/2 and ST2 cells transfected with Smad1 and Dvl-1. Treatment with Wnt3a, but not BMP-2, stimulated luciferase activity, whereas co-stimulation with both Wnt3a and BMP-2 markedly reduced reporter activity. Furthermore, in C3H10T1/2 cells, Wnt3a induced proliferation was markedly attenuated by co-treatment with BMP-2. In conclusion, these results provide a potential mechanism whereby BMP-2 antagonizes Wnt signaling in osteoblast progenitors by promoting an interaction between Smad1 and Dvl-1 which restricts β -catenin activation.

Disclosures: **Z. Liu**, None.

F135

Tumor Expression of RANKL and BMPs Influences the Formation of Metastatic Lung Cancer in Bone. A. Conduah^{*1}, B. T. Feeley^{*1}, N. Q. Liu^{*1}, S. Dubanett^{*2}, W. C. Dougall^{*3}, J. R. Lieberman¹. ¹Orthopaedic Surgery, UCLA, Los Angeles, CA, USA, ²Internal Medicine, UCLA, Los Angeles, CA, USA, ³Amgen, Seattle, WA, USA.

The formation of a metastatic lesion in bone is a multi-step process and the cytokines expressed by tumor cell lines determine the type of metastatic lesion formed. The human non-small-cell-lung cancer (NSCLC) cell line A549 which produces a mixed osteoblastic and osteolytic lesion was used in this study. Using RT-PCR we determined that A549 cells produce mRNA for the production of cytokines that influence the formation of osteoblastic lesions (BMP-2, -4, and -6) and osteolytic lesions (RANKL, IL-6, and TNF- α). The purpose of this study was to determine if blockade of osteoclast activity (RANK:Fc) and BMP expression (Noggin) would result in a reduction of the formation of a mixed bone lesion in a murine model of metastasis. We examined our treatments in an intra-tibial injection model. There were 5 treatment groups each consisting of 10 SCID mice. Animals were treated with either A549 cells alone (Group I), A549 cells plus RANK:Fc (Group II), A549 cells transduced with vector that over expressed noggin (Group III), A549 cells and both RANK:Fc and noggin over expression (Group IV), and A549 cells transduced with an empty vector to control for viral transduction. Tumor size calculation, radiographic analyses, and histomorphometric analysis were performed at 4 and 8 weeks. Animals in Groups II and III had significantly smaller tumor volumes compared to controls ($p < 0.01$) and combination treatment (Group IV) led to the smallest tumor volume. Furthermore, treatment with A549 cells alone led to a mixed osteolytic/osteoblastic lesion, overexpression of noggin (Group III) led to a smaller, predominantly lytic lesion, treatment with RANK:Fc (Group II) led to an even smaller, predominantly blastic lesion, and combination treatment led to no visible lesion (Figure 1). In conclusion, we have demonstrated that a lung cancer cell line that induces a mixed bone lesion which secretes factors that stimulate both osteoclast (RANKL) and osteoblast (BMP) activity. When only one of these pathways was blocked the other lesion type became predominant. When both pathways were blocked lesion formation was significantly inhibited. These findings suggest that multi-modal therapy may be necessary to successfully treat metastatic bone disease.

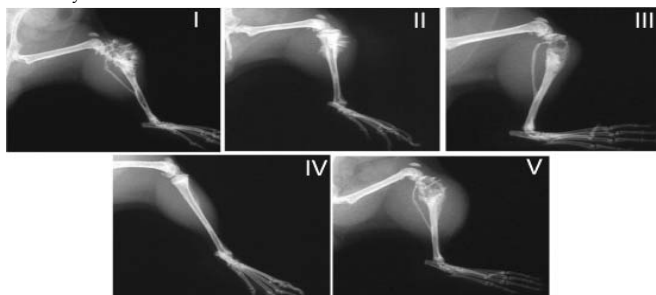


Figure 1. Radiographs of mice tibias at 8 weeks after intra tibial injection. Group I-A549 cells alone. Group II-A549 cells+RANK:Fc. Group III-A549 cells+Noggin. Group IV A54 cells+RANK:Fc+Noggin. Group V-A549 cells +empty vector.

Disclosures: **A. Conduah**, None.

F138

Osteoglophonic Dysplasia Defines Novel Roles for FGFR1 in Bone Formation and Mass. E. G. Farrow^{*1}, T. E. M. Larsson¹, S. I. Davis^{*1}, X. Yu¹, E. Imel^{*2}, M. J. Econs², A. C. Lichtler³, P. Pitukcheewanont^{*4}, L. Mascarenhas^{*4}, Y. Gutierrez^{*4}, K. Condon^{*5}, D. B. Burr⁵, J. K. Hartsfield^{*6}, P. Beighton^{*7}, K. E. White¹. ¹Med. and Molec. Genetics, Indiana Univ. Schl. of Med., Indianapolis, IN, USA, ²Medicine, Indiana Univ. Schl. of Med., Indianapolis, IN, USA, ³Univ. of Connecticut Health Center, West Hartford, CT, USA, ⁴USC Keck Schl. of Med., Los Angeles, CA, USA, ⁵Anat. & Cell Biol., Indiana Univ. Schl. of Med., Indianapolis, IN, USA, ⁶Dept. Oral Facial Devel., Indiana Univ. Schl. of Dentistry, Indianapolis, IN, USA, ⁷Univ. of Cape Town Med. Schl., Cape Town, South Africa.

The Fibroblast growth factors (FGFs) and their receptors (FGFRs) are central for many skeletal processes. Osteoglophonic dysplasia (OD, OMIM #166250) is a 'crossover' disorder that possesses phenotypes associated with activating FGFR1 and FGFR2 mutations, such as craniosynostosis, as well as with FGFR3 mutations, such as dwarfism. OD patients also present with non-ossifying metaphyseal bone lesions, and some patients have increased levels of FGF23, which inversely correlate with serum phosphate concentrations. We previously discovered that activating mutations in highly conserved residues (Y374C, N330I, and C381R) comprising the ligand binding and transmembrane domains of FGFR1 lead to OD. The patients with the Y374C and the C381R mutations had severe disease courses. We have identified two additional OD patients that have the N330I (ligand binding domain) and C381R (transmembrane domain) mutations. Besides craniosynostosis and dwarfism, both C381R patients have high metaphyseal lesional burden, giant cell granuloma of the gingiva, and hypophosphatemia with elevated serum FGF23 levels (110 and 250 pg/ml, normal mean 28 pg/ml). To gain insight into FGFR1 function in the skeleton, we expressed FGFR1 carrying the Y374C OD mutation under the regulation of the osteoblast-specific 2.3 kb type I ($\alpha 1$) collagen promoter in a transgenic mouse model. A severely affected founder mouse was produced, but it expired prior to mating. This animal had low trabecular (299 vs 344 mg/cm³) and cortical (1333 vs 1415 mg/cm³) BMD, as determined by pQCT in the proximal tibiae.

Radiographic analyses revealed severe, generalized osteopenia, and histological analyses demonstrated widened metaphyses with irregularities of the trabeculae, and decreased cortical thickness. In summary, we have confirmed that OD is caused by mutations in FGFR1, and expressing an OD FGFR1 mutant in osteoblasts results in low BMD and disturbed skeletal structure. Taken together, our results demonstrate that FGFR1 has critical functions in both cranial and long bone development, and that continuous activation of FGFR1 in osteoblasts may be a negative regulator of BMD.

Disclosures: **K.E. White**, None.

F140

Characterization of FGF23/VDR Double Deficient Mice. T. Shimada^{*1}, H. Hasegawa^{*1}, I. Urakawa^{*1}, Y. Yamazaki^{*1}, J. Yasutake^{*1}, K. Oono^{*1}, T. Fujita², S. Fukumoto², T. Yamashita¹. ¹Pharmaceutical Research Laboratories, KIRIN Brewery, Takasaki, Gunma, Japan, ²Department of Internal Medicine, The University of Tokyo Hospital, Tokyo, Japan.

The findings that FGF23 null mice demonstrated abnormal elevations in serum phosphate and 1,25-dihydroxyvitamin D₃ (1,25D) concentrations supported a significant role of FGF23 in the phosphate and vitamin D metabolism. However, FGF23 null mice also exhibited other multiple defects such as abnormal glucose and lipid metabolism, growth retardation, histological changes in some organs including bone, and impaired renal function. These abnormal phenotypes still leave two possibilities; they were caused by the absence of undefined roles of FGF23 or secondary by sustained high serum phosphate or 1,25D levels. In our preliminary study, feeding with low phosphate diet decreased serum phosphate level, but did not affect most other defects in FGF23 null mice. Therefore, hyperphosphatemia itself is not a likely cause for those severe phenotypes. To evaluate the contribution of excess 1,25D action in FGF23 null mice to their abnormal phenotypes, we developed FGF23/VDR double deficient mice (*Fgf23^{-/-}Vdr^{-/-}*). The phenotypes of the mice with double heterozygous targeted alleles for *Fgf23* and *Vdr* genes were completely normal. In contrast, the gross appearance of double KO mice was closely similar to that of VDR KO mice. Severe growth retardation observed in FGF23 KO disappeared in double KO (FGF23 KO; <10 g B.W. vs. double KO; >20g B.W.). Double KO mice showed almost normal life span maintaining normal serum BUN levels, while FGF23 KO suffered from short life span due to impaired renal failure. Serum glucose and cholesterol levels were also normal in double KO. Serum parameters for mineral metabolism of double KO were almost same as those in VDR KO mice characterized by low phosphate and calcium, and extremely high 1,25D and PTH levels. Bone histology of double KO mice demonstrated typical features of rickets as observed in VDR KO mice. However, the ratio of osteoblast surface/bone surface in double KO was much less than that in VDR KO mice and rather similar to that of FGF23 KO mice. Since the previous studies reported that the recombinant FGF23 functioned in VDR KO mice, FGF23 seems to regulate serum phosphate and vitamin D levels via VDR-independent action. However, the conserved phenotypic similarity between FGF23/VDR double KO mice and VDR KO mice indicates that excess 1,25D action caused other multiple defects in FGF23 KO except for the decreased number of osteoblasts.

Disclosures: **T. Shimada**, KIRIN Brewery CO., LTD. 3.

F142

Endogenous FGF2 Is Critically Important in PTH Induction of Bcl2, Phosphorylation of CREB and Runx2 Nuclear Accumulation in Osteoblasts. D. Agas^{*1}, M. G. Sabbieti^{*1}, L. Xiao², T. Naganawa³, M. M. Hurley². ¹Morf. and Comp. Biochem. Sciences, University of Camerino, Camerino, Italy, ²Medicine, University of Connecticut Health Center, Farmington, CT, USA.

PTH and FGF2 both stimulate bone formation through possible mechanisms including enhanced differentiation of osteoblast (OB) precursors, increased activity of existing OB and reduced OB apoptosis. PTH increases FGF receptor-1 and FGF2 expression in OBs and the anabolic response to PTH is significantly reduced in *Fgf2*^{-/-} mice. The goal of this study was to examine whether candidate factors implicated in the anabolic response to PTH were modulated in *Fgf2*^{-/-} OBs. PTH and FGF2 prolong OB lifespan by increasing the survival gene Bcl-2 and decreasing the pro-apoptotic gene Bax. Runx2, which is absolutely required for differentiation of OB precursors and modulates the activity of mature OBs, is regulated by both PTH and FGF2. To assess the role of Bcl2/Bax and Runx2 in the reduced anabolic response to PTH in *Fgf2*^{-/-} mice, these factors were measured by Western blot analysis and immunohistochemistry in cultured bone marrow stromal OBs from *Fgf2*^{+/+} and *Fgf2*^{-/-} mice. PTH induced a 2.6-fold increase in the Bcl2/Bax protein ratio in *Fgf2*^{+/+} but not *Fgf2*^{-/-} OBs. PTH increased Bcl2 in *Fgf2*^{-/-} OB after FGF2 pre-treatment. Western blot analysis showed that PTH increased Runx2 protein expression in *Fgf2*^{+/+} but not *Fgf2*^{-/-} OBs. Treatment with FGF2 restored the PTH responses in *Fgf2*^{-/-} OBs. In contrast to PTH, forskolin treatment induced a marked increase in Runx2 protein in both *Fgf2*^{+/+} and *Fgf2*^{-/-} OBs. By immunohistochemistry, FGF2 increased nuclear localization of Runx2 in OBs of both genotypes but PTH treatment induced nuclear accumulation of Runx2 only in *Fgf2*^{+/+} OBs. PTH and FGF2 act via activation of the protein kinase A and cAMP response element binding proteins (PKA/CREBs) as well as mitogen activated protein kinase (MAPK/ERK1/2) pathways to regulate Runx2 expression. Western blot analysis showed that PTH produced a similar increase in phospho-ERK1/2 levels in *Fgf2*^{+/+} and *Fgf2*^{-/-} OBs. However, PTH increased phospho-CREB levels in *Fgf2*^{+/+} but not *Fgf2*^{-/-} OBs. These data suggest that endogenous FGF2 is important in PTH effects on phospho-CREB, Bcl-2 and Runx2 levels as well as nuclear accumulation of Runx2. Reduced expression of these factors may contribute to the reduced anabolic response to PTH in the *Fgf2*^{-/-} mice. Our results strongly indicate that the anabolic PTH effect is dependent in part on FGF2 expression.

Disclosures: **D. Agas**, None.

F149

The Effects of PAPP-A Deletion on the Murine Skeleton. S. J. Tanner, C. A. Conover. Endocrine Research Unit, Mayo Clinic, Rochester, MN, USA.

The insulin-like growth factors (IGFs) are of undisputed importance in bone physiology. The effects of IGFs on bone cells are numerous and include stimulation of proliferation, increased expression of type I collagen, and suppression of osteoblast apoptosis. IGF activity is modulated by a number of regulatory molecules, including the six IGF binding proteins (IGFBPs 1-6). All of the binding proteins are expressed by bone cells *in vitro*, although IGFBP-4 is especially abundant in bone and inhibits IGF-I from interacting with its receptor. The binding proteins themselves are subject to regulation, thought mainly to be accomplished through proteolysis. In the case of IGFBP-4, this function is performed by pregnancy-associated plasma protein-A (PAPP-A), which cleaves IGFBP-4 at a single site mid-molecule, thereby increasing the local bioavailability of previously bound IGF-I. Recent work in our lab has resulted in the generation of a PAPP-A knockout (KO) mouse. Because PAPP-A is highly expressed by osteoblasts *in vivo* and *in vitro*, we are testing the hypothesis that deletion of PAPP-A has a negative impact on bone cell function and bone quality. Peripheral quantitative computed tomography (pQCT) was performed on the femoral midshaft of PAPP-A KO and wild-type (WT) littermates aged 1, 2, 4, 6, and 12 months of age. At this sampling site, the 1-month-old KO animals had a bone mineral density (BMD) that was not different from that of WT (500 ± 4.2 vs. 507 ± 31.3 mg/ccm for KO vs. WT, mean \pm SE, N=3/group); however, by 2 months of age, KO BMD was significantly less ($p < 0.05$) than WT (594 ± 15.7 vs. 642 ± 22.4 mg/ccm for KO vs. WT, N=4-6/group). This difference appeared to be maintained at 4, 6, and 12 months of age, suggesting that PAPP-A exerts its greatest influence on bone development during the transition into puberty. Histomorphometric data from 2-month-old mice indicate that the KO animals had significantly ($p < 0.05$) suppressed bone formation rates at both endocortical (5.24 ± 0.53 vs. 7.82 ± 0.76 $\mu\text{m}^2/\text{d}$ for KO vs. WT, N=4-5/group) and cancellous (0.80 ± 0.08 vs. 1.06 ± 0.04 $\mu\text{m}^2/\text{d}$ for KO vs. WT, N=4-5/group) surfaces relative to WT controls. Taken together, these preliminary data indicate an early role for PAPP-A in the acquisition of peak bone mass in the murine skeleton. Our ongoing analyses will provide a more complete picture of the IGF-I signaling system, and PAPP-A in particular, in bone development and maintenance.

Disclosures: **S.J. Tanner, None.**

F154

Jab1 regulates SCF $^{\beta\text{-TrCP1}}$ mediated Smad4 Protein Degradation in TGF- β /BMP Signaling. M. Wan, J. Huang*, Y. Tang*, C. Lu*, N. Wang*, X. Cao. Pathology, University of Alabama at Birmingham, Birmingham, AL, USA.

TGF- β superfamily of cytokines exerts a wide variety of biological activities, in particular, the regulation of skeletal development and bone development and remodeling. Smad4 is the common mediator shared in the TGF- β /BMP signaling pathways. Thus, the regulation of Smad4 protein steady state level is an important means of modulating TGF- β /BMP function. Previously, we identified that SCF $^{\beta\text{-TrCP1}}$, an E3 ubiquitin ligase complex containing F-box protein $\beta\text{-TrCP1}$, as a critical determinant for the protein degradation of Smad4. Jun Activation Binding protein (Jab1), another Smad4 protein degradation regulator, regulates SCF $^{\beta\text{-TrCP1}}$ -mediated Smad4 protein degradation. However, the detailed mechanism of this event is not clear. Here we found that $\beta\text{-TrCP1}$ interacts with Smad4 protein at its MH1 plus Linker region. Sequence analysis of the Smad4 MH1 region revealed a motif: DLSGLTLQS, which is similar to the consensus sequence DSG β XS (S-S motif) within common $\beta\text{-TrCP1}$ substrates. To determine whether $\beta\text{-TrCP1}$ -Smad4 interaction is mediated by this motif, we generated two Smad4 mutation constructs by either replacing two serine residues with alanine (S-S mutation) or deletion of this motif (S-S deletion). The $\beta\text{-TrCP1}$ -Smad4 binding was significantly decreased with either S-S mutation or S-S deletion. We then investigated how Jab1 regulates $\beta\text{-TrCP1}$ -Smad4 binding. Jab1 overexpression significantly enhanced the interaction between $\beta\text{-TrCP1}$ and Smad4, whereas Jab1 siRNA reduced the interaction. It has been shown that Jab1-associated protein kinase(s) phosphorylates protein substrates for their degradation such as p53. We therefore examined whether Jab1 regulates $\beta\text{-TrCP1}$ -Smad4 interaction through phosphorylation. Both Curcumin and Emolin, two inhibitors of Jab1-associated protein kinase(s), significantly reduced the interaction between $\beta\text{-TrCP1}$ and Smad4, indicating that Jab1-mediated phosphorylation of Smad4 is required for Smad4 recognition by $\beta\text{-TrCP1}$. Finally, we examined whether Jab1 and SCF $^{\beta\text{-TrCP1}}$ down-regulate TGF- β -mediated gene transcription. TGF- β response reporter plasmids, (SBE) 4-luc, and ARE-luc were cotransfected with SCF components and/or Jab1 plasmids in Mv1Lu cells. Expression of either SCF or Jab1 inhibits TGF- β -induced transcriptional activity, and expression of both enhanced the inhibition. In summary, we find that SCF $^{\beta\text{-TrCP1}}$ is the E3 ligase of Smad4, and Jab1 regulates the interaction between $\beta\text{-TrCP1}$ and Smad4 by phosphorylation of Smad4 S-S motif for SCF $^{\beta\text{-TrCP1}}$ -mediated Smad4 protein degradation. These findings revealed a novel mechanism that Jab1 controls the TGF- β /BMP activity by regulating Smad4 protein degradation.

Disclosures: **M. Wan, None.**

F156

Regulation of Matrix Metalloproteinases by TGF-Beta in Renal Cell Carcinoma Bone Metastasis. S. L. Kominsky, M. Doucet*, D. Nell*, K. Weber. Department of Orthopaedic Surgery, Johns Hopkins Medical Institute, Baltimore, MD, USA.

Matrix metalloproteinases (MMPs) are best known for their role in facilitating the invasion and migration of cancer cells through the ECM; however, MMPs also play a role in regulating cell growth and angiogenesis. While the role of MMPs in primary tumors has been extensively studied, their role in the colonization and growth of tumor cells at secondary sites has not been well defined. It is believed that degradation of the unmineralized bone matrix is necessary for the initiation of bone resorption, providing osteoclasts access to the mineralized bone surface. Due to their ability to degrade type I collagen, the major collagen constituent of unmineralized bone matrix, MMPs -1, -2, -8, -13, and -14 may play a role in bone resorption. Renal cell carcinoma (RCC)-derived bone metastases are predominantly osteolytic and exhibit extensive vascularization. Surprisingly, the specific mechanisms of RCC interaction with bone have been scarcely studied despite the inability to prevent or eliminate bone metastasis. We have shown that TGF- β , an abundant growth factor in the bone microenvironment, is essential for human bone-derived RCC cell growth following intratibial injection in nude mice. Interestingly, we have found that TGF- β increases the expression and activation of MMPs in human bone-derived RCC cell lines that cause lytic lesions in the nude mouse tibia (RBM1-IT4, RBM23), versus cell lines incapable of growing in the murine bone environment (RBM21A, RBM17C), despite equivalent activation of TGF- β signaling. Treatment with TGF- β resulted in the increased mRNA expression of MMPs -1, -2, -13, -14 by RT-PCR beginning as early as 3 hours following treatment. Correspondingly, protein expression of both the latent and active forms of MMPs -1, -2, and -13 was increased following treatment with TGF- β for a period of 72 hours, as determined by Western analysis of conditioned media. TGF- β -induced increases in MMP -1, -2, and -13 activity was confirmed by gelatin zymography analysis. Although TGF- β had no detectable effect on MMP-9 mRNA expression, gelatin zymography analysis showed an increase in the active form of MMP-9. Concordant with *in vitro* studies, IHC analysis revealed that MMPs -2, -9, and -13 were expressed *in vivo* following injection of RBM1-IT4 cells into the nude mouse tibia. Further, MMP-2 and -13 were expressed in 8/10 and 12/13 human RCC bone metastasis tissues, respectively, by IHC analysis. These data show that TGF- β can increase the expression and activation of MMPs involved in the degradation of type I collagen and angiogenesis, and suggest their potential involvement in RCC tumor growth and bone destruction.

Disclosures: **S.L. Kominsky, None.**

F160

Conditional Deletion of the TGF- β Type II Receptor (T β RII) in Prx-1 Expressing Cells Results in Defects in the Appendicular Skeleton and Calvaria. K. S. Shimer*¹, L. O'Rear*¹, R. Chandler*², S. Aakula*², L. Longobardi*¹, D. Mortlock*², A. Chytil*², H. Moses*², A. Spagnoli¹.

¹Pediatrics, Vanderbilt University Medical Center, Nashville, TN, USA,

²Vanderbilt University Medical Center, Nashville, TN, USA.

Studying the role of TGF- β signaling in developing cartilage is difficult secondary to the early embryonic lethality associated with T β RII knock-out. To address the role of TGF- β signaling in limb bud, joint and calvaria development we conditionally inactivated the T β RII in Prx-1 expressing cells by using a cre-loxP system. Prx-1 is a paired-related homeobox gene that plays a central role in regulating the growth of skeletal primordia. *Prx1-Cre* mice carry a cre-reporter gene under a PRX-1 enhancer that drives Cre expression in the limb buds and a subset of calvaria mesenchymal cells starting around embryonic day (E) 9.5. To generate *Tgfb β 2^{Prx1KO}* we mated *Prx1-Cre* mice with homozygous *Tgfb β 2^{lox/lox}* mice in which the TGF- β binding site of T β RII is floxed. On *Tgfb β 2^{Prx1KO}* and heterozygous *Tgfb β 2^{lox/+}* Cre negative (control) mice at P0, histomorphometric staining was performed using Hematoxylin & Eosin, Alcian Blue and Alizarin Red staining. We have generated homozygous *Tgfb β 2^{Prx1KO}* mice that are deficient in T β RII in limb bud primordia and a subset of calvaria mesenchymal cells. *Tgfb β 2^{Prx1KO}* are smaller than controls. The *Tgfb β 2^{Prx1KO}* birth weight is 1.03 ± 0.06 grams and 1.96 ± 0.13 grams for controls $p = 0.0003$. Length at birth for *Tgfb β 2^{Prx1KO}* is 2.60 ± 0.14 cm vs 3.58 ± 0.15 cm in controls $p = 0.0005$. They display a lack of small joint formation with minimal ossification centers of the phalanges, brachydactyly, bent metatarses, carpal/tarsal synostosis with rudimentary bones and rhizomelic limbs with dysplastic metaphyses. Furthermore, *Tgfb β 2^{Prx1KO}* mice showed minimal parietal and occipital bone formation, intracranial bleeding and died within hours of birth. Our data provides critical information regarding mechanisms of skeletal development and indicates that TGF- β signaling plays an essential role in skeletogenesis. In particular, we found that TGF- β is critical for small joint formation, calvaria formation and endochondrial growth as indicated by rhizomelic limbs with dysplastic metaphyses. Understanding the role of TGF- β in osteochondrogenesis will shed further light in the pathophysiologic mechanisms underlying osteochondrodysplasias and degenerative cartilage diseases.

Disclosures: **K.S. Shimer, None.**

F166

Mechanical Inhibition of RANKL Expression Is Regulated by H-Ras-GTPase in a Lipid Raft Dependent Manner. J. Rubin¹, T. C. Murphy^{*1}, J. Rahnert^{*1}, M. S. Nanes¹, E. M. Greenfield², H. Jo^{*3}, X. Fan¹. ¹Medicine, Emory University and VAMC, Decatur, GA, USA, ²Orthopaedics, Case Western Reserve University, Cleveland, OH, USA, ³Biomedical Engineering, Emory University, Atlanta, GA, USA.

Mechanical input is well known to regulate bone remodeling yet the molecular events involved in mechanical signal transduction are poorly understood. We here investigate proximal events leading to the ERK1/2 activation that is required for mechanical repression of RANKL expression, the factor that controls local recruitment of osteoclasts. Primary murine bone stromal cells were subjected to a regimen of dynamic mechanical strain via substrate deformation (1-2%, 10 cpm). Mechanical strain was shown to activate Ras-GTPase within 2 minutes, in particular the H-Ras isoform. Pharmacological inhibition of H-Ras function using a farnesyl transferase I inhibitor added 24 hour prior to application of the strain regimen prevented mechanical activation of H-Ras as well as the downstream mechanorepression of RANKL analyzed the next day by semi-quantitative RT-PCR. To further confirm the role of H-Ras in mechanorepression of RANKL, we generated Ras-isoform specific siRNA. Silencing of H-Ras, but not K-Ras, abrogated strain effects on RANKL expression. H-Ras specific inhibition of mechanorepression of RANKL was also demonstrated in a murine pre-osteoblast cell line which was generated from a T-Ag expressing mouse (CIMC-4 cell line); K-Ras silencing has no effect. H-Ras is known to be targeted to lipid raft microdomains by virtue of its post-transcriptional modifications. We asked whether H-Ras activation required its presence in the lipid raft: cholesterol depletion of rafts using cyclodextrin prevented mechanical activation of H-Ras. Using a non-detergent method to separate lipid raft microdomains from other membrane and cytosolic components, we found that after activation by mechanical strain, H-Ras was displaced out of the lipid raft domain. That the mechanical repression of RANKL requires activation of H-Ras, a specific isoform of Ras-GTP residing in the lipid raft microdomain, suggests that spatial arrangements are critical for generation of specific downstream events in response to mechanical signals. By partitioning signals this way, cells may be able to generate different downstream responses through seemingly similar signaling cascades.

Disclosures: **J. Rubin**, None.

F168

Mechanically Induced DMP1 and MEPE Expression in Osteocytes: Correlation to Mechanical Strain, Osteogenic Response and Gene Expression Threshold. J. Gluhak-Heinrich^{*1}, W. Yang^{*2}, L. F. Bonewald³, A. G. Robling^{*4}, C. H. Turner^{*4}, S. E. Harris⁵. ¹Orthodontics, UTHSCSA, San Antonio, TX, USA, ²Periodontics, UTHSCSA, San Antonio, TX, USA, ³Oral Biology, UMKC, Kansas City, MO, USA, ⁴Orthopedics, Indiana University Medical School, Indianapolis, IN, USA.

Dentin matrix protein (DMP) and matrix extracellular phosphoglycoprotein (MEPE) are selectively expressed in osteocytes and may modulate mineralization within the osteocyte canalicular system. By altering the osteocyte microenvironment, they may change how the osteocyte responds to mechanical loading. We have previously shown increased gene expression of DMP1 and MEPE after mechanically loading of bone. We now present the spatial and temporal correlation between DMP1 and MEPE expression, mechanical strain, and new bone formation in the mouse ulna subject to axial loading. Ulnae from 4-month-old C57BL/6 mice were loaded with a single 30-second bout of dynamic loading (2.4N peak load, and 2Hz). DMP1 and MEPE mRNA expression was analyzed with quantitative *in situ* hybridization 1, 2 and 24 hours after loading. Each data set consisted of expression patterns at 7 locations along the proximal-distal axis of the ulna. 1 and 2 hours after loading we find 2-3 fold increases in DMP1 expression in osteocytes. At these early times there was no significant change in MEPE expression either by Northern analysis or *in situ* hybridization. 24 hours after loading, we found a significant 3-10 fold increase in DMP1 and MEPE expression in osteocytes. The regions of maximum expression of both genes were on the medial and lateral sides of the ulna and correlated to the estimated mechanical strains. Along the longitudinal axis, expression of both DMP1 and MEPE mRNA was highest 2 mm distal to the mid-shaft (the location of greatest mechanical strain) and highest in osteocytes closer to periosteal and endosteal surfaces (locations of new bone formation). We developed a 3D model for DMP1 and MEPE expression along the mouse ulna. From these data, we determined the Gene Expression Threshold (GET), or minimum level of strain required to activate either MEPE or DMP1. The DMP1 gene had a lower GET and was activated earlier (1 hr) than MEPE gene (24 hr). Thus, gene expression in osteocytes correlated with predicted local strains that in turn were correlated to new bone formation measured using histomorphometry. Both DMP1 and MEPE proteins are found concentrated in the canalicular and lacunar walls surrounding the osteocyte cell body and cell process. These proteins most likely play key roles in local mineralization within the canalicular, lacunar system, and throughout the bone matrix. Mechanical loading appears to regulate expression of these genes and may modulate local mineralization.

Disclosures: **J. Gluhak-Heinrich**, None.

F170

Parathyroid Hormone Receptor Signaling Abrogates or Reverses Mechanical Unloading-Induced Signaling in Transgenic Mice Expressing Osteoblast-Specific Constitutively Active PTH/PTHrP Receptor. N. Ono¹, L. Calvi², E. Schipani², H. M. Kronenberg², K. Soma^{*3}, M. Noda¹. ¹Molecular Pharmacology, 21st COE Program, Medical Research Institute, Tokyo Medical and Dental University, Tokyo, Japan, ²Endocrine Unit, MGH, Harvard Medical School, Boston, MA, USA, ³Orthodontic Science, Tokyo Medical and Dental University, Tokyo, Japan.

Although unloading causes severe bone loss, the mechanisms underlying such events have not yet been fully understood. Unloading could be modulated by extracellular matrix proteins such as osteopontin and intracellular signaling molecules such as MAPK, and these modulators may be shared in hormonal signaling. The intermittent treatment of parathyroid hormone (PTH), a major regulator of calcium homeostasis, could result in the increase in bone mass, phenomenologically resembling what bone could respond to mechanical stimuli. In order to understand the signaling events in unloading-induced bone loss, we subjected the transgenic mice expressing osteoblast-specific constitutively active PTH/PTHrP receptor to tail suspension. In the primary trabeculae, unloading reduced trabecular BV/TV of wild-type (WT) by 50%, whereas NO REDUCTION was observed in transgenic mice (TG). In the secondary trabeculae, BV/TV was 2.5-fold higher in TG compared to WT as reported previously. BV/TV was reduced in WT by about 50%, whereas BARELY ALTERED in TG due to unloading. In terms of BMD of the whole bone, WT yielded statistically significant reduction after tail suspension. Though there was moderate suppression of BMD due to unloading in TG, the difference was not statistically significant, suggesting that the whole bone structure would be quite insensitive to unloading under constitutively active PTH signaling. Deoxypyridinoline (Dpyd) excretion into urine in TG was about 3 times higher than WT among loaded mice. Interestingly, unloading enhanced Dpyd excretion in WT, but suppressed it in TG. Thus these data indicated that unloading induced-signaling could be interfered by the presence of constitutively active PTH receptor signaling. Further reversal phenomena were observed in TRAP positive cell development in culture in the presence of vitaminD and dexamethasone to induce osteoclast-like cell formation. Unloading suppressed the levels of TRAP positive cell development in TG, contrasting with unaltered levels in WT. These data indicated that PTH receptor signaling crosses with the signals induced by unloading, either abrogating or reversing the effects of unloading induced-events.

Disclosures: **N. Ono**, None.

F172

The Climbing Exercise Prevents Trabecular Bone Loss with Highly Expressed mRNA of Estrogen Receptor alpha in Bone Cells after Ovariectomy in Mice. N. Nakura^{*}, T. Mori, N. Okimoto, A. Sakai, T. Nakamura. Orthopaedics, University of occupational environmental health Japan, Fukuoka, Japan.

To investigate the effect of climbing exercise on trabecular bone turnover, bone marrow cell development and gene expression for bone cells in ovariectomized mice, 100 C57BL/6J mice, 8 weeks of age, were assigned to baseline control and 3 groups: ground control group (sham), ovariectomized ground control group (OVX) and ovariectomized climbing exercise group (OVX+Ex). The mice of each group were sacrificed at 2, 4 and 8 weeks after the treatment. OVX+Ex mice were housed in a 100-cm tower cage and had to climb up to drink water toward a bottle placed at the top. We obtained bilateral femurs and tibias to evaluate bone mineral density (BMD) by DXA, trabecular bone turnover by histomorphometry, and mRNA expression in bone cells by real-time RT-PCR. At 8 weeks, BMD of the left femur in OVX significantly decreased compared with that in sham. BMD in OVX+Ex was maintained to the same level of that in sham throughout the experimental period. The trabecular bone volume (BV/TV) of the proximal tibia in OVX decreased compared with that in sham, but that in OVX+Ex was significantly increased compared with that in OVX and maintained to the same level of that in sham at 4 and 8 weeks. At 4 weeks, the osteoclasts surface (Oc.S/BS) and osteoclast number (Oc.N/BS) in OVX increased compared with those in sham, but those in OVX+Ex were restored to the same levels of those in sham. At 8 weeks, bone formation rate (BFR/BS) of periosteal surface and the mineralizing surface (MS/BS) in OVX+Ex increased compared with those in OVX. At 8 weeks, climbing exercise showed the significant increases in parameters of bone formation including BFR/BS and MS/BS compared with those in OVX. Quantitative RT-PCR using whole bone of femur revealed that at 8 weeks, estrogen receptor alpha (ERalpha) mRNA expression in OVX+Ex significantly increased compared with that in OVX. In conclusion, our results indicate that the climbing exercise prevents trabecular bone loss in ovariectomized mice. The climbing exercise reduced bone resorption in ovariectomized mice initially, and increased in bone formation finally. This subsequent increase in bone formation parameter after climbing exercise seems to be associated with highly expressed mRNA of ERalpha in bone cells.

Disclosures: **N. Nakura**, None.

F174

Nucleocytoplasmic Cas Interacting Zinc Finger Protein (CIZ) Acts as a Conversion Sensor for both Mechanical and Estrogenic Signaling in the Process of Disuse and Ovariectomy Induced Bone Loss. K. Hino¹, T. Nakamoto^{2*}, M. Morinobu³, H. Yamamoto³, H. Hirai^{2*}, M. Noda¹.

¹Molecular Pharmacology, Tokyo Medical and Dental University, Tokyo, Japan, ²Dept of Hematology and Oncology, University of Tokyo, Tokyo, Japan, ³Orthopedics, Ehime University, Ehime, Japan.

Postmenopausal osteoporosis and disuse-induced osteopenia are two major causes to increase risk of fractures in most of the aged population. The mechanisms underlying sensing of mechanical stress in bone is largely unknown. CIZ binds to p130 Cas which localizes at cell adhesion complex and translocates into nuclei to modulate transcription via acting through (G/C)AAAAA located in the promoter regions of MMP genes and antagonizes against BMP(MCB2000, JEM2005). We tested our hypothesis that mechanical stress signaling would be mediated by such nucleocytoplasmic shuttling proteins which would link signals from the cell adhesion site to nuclear events, and that such mechanosensitive signaling could be converged with estrogenic signaling. Unloading (tail suspension ;TS) reduced cancellous bone volume in WT mice by about 40%. In contrast CIZ deficient mice did not exhibit such reduction in cancellous bone mass due to TS. This was not limited to cancellous bone since bone loss due to TS in cortical midshaft and epiphyseal area was also blocked by CIZ deficiency. Mineralized nodule formation in the culture of bone marrow cells taken out from the bone of mice subjected to TS was suppressed by about 40% in WT mice. CIZ deficiency almost totally blocked such reduction in nodule formation induced by TS. Histomorphometric analysis revealed that tail suspension suppressed the levels of MAR and such suppression by TS of MAR was reduced by CIZ deficiency. Similarly, in WT mice TS reduction in BFR was suppressed in CIZ deficient mice. Marginal increase in Oc.S and Oc.N was observed at end point of TS in WT mice, but neither WT nor CIZ deficient mice indicated difference in the levels of Oc.S and Oc.N by unloading. Similarly, systemic bone resorption parameters such as deoxypyridinoline excretion were similar between WT and CIZ deficient mice regardless of loading or unloading condition suggesting that CIZ mediates mechanical signaling specifically in osteoblastic but not osteoclastic side in the animals subjected to unloading. To test whether estrogenic signaling is also mediated by the presence of CIZ, the animals were subjected to ovariectomy(OVX). OVX reduced cancellous bone mass in WT mice. In contrast, OVX failed to reduce bone mass in the absence of CIZ. These data indicated that nucleocytoplasmic shuttling protein, CIZ, acts as a mechanosensor as well as a sensing molecule for estrogenic signaling, and plays a pivotal role in the maintenance of bone mass.

Disclosures: K. Hino, None.

F176

Beta-Blockade Mitigates Bone Loss with Hindlimb Unloading. K. Baek^{*}, S. A. Bloomfield. Health and kinesiology, Texas A&M, College station, TX, USA.

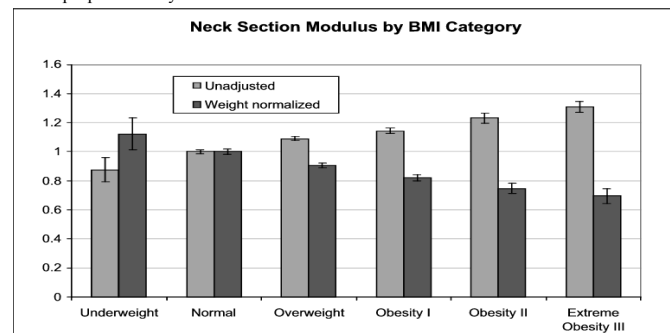
Leptin may be a candidate responsible for linking energy metabolism to bone mass and also may play a role in bone loss during hindlimb unloading(HU). In previous work, we have observed that serum leptin decreases more in rats exposed to HU than to food restriction; this may be due to SNS activation of β -adrenoreceptors inhibiting release of leptin from adipose. Our objective was to test whether β -blockade or administration of a leptin analog would attenuate bone loss with HU. Male, 6-mo-old Sprague-Dawley rats were randomized into six groups (n=10 each): 3 groups of HU rats treated with vehicle (HU-V), leptin analog (HU-L;Ly355101, Lilly), or β -blocker(HU- β ;DL-propanolol ,Sigma) via osmotic pump during 28d HU, and 3 groups of cage activity controls treated with the same 3 agents and pair-fed to HU rats (CC-V, CC-L and CC- β , respectively). On day 0 and 28, peripheral computed tomography (Stratec XCT Research M) assessed bone mineral density (BMD). Proximal tibiae metaphyses were analyzed by standard histomorphometry for mineral apposition rate (MAR), bone formation rate (BFR), and forming and resorbing surfaces. All animal procedures were approved by Texas A&M University Laboratory Animal Care Committee. Although all groups lost their body weight (BW) at first week, by day 28 all groups except HU- β gained BW compared to initial BW (p<0.05). The 11% decline in total BMD observed in HU-V was attenuated in HU- β rats (7%) and HU-L rats (5%) (p<0.05). The 20% decline in trabecular BMD observed in HU-V group was attenuated in HU- β rats (11 %) and HU-L rats (10%) (p<0.05). MAR in HU-L & HU- β was significantly greater than in HU-V (2.04 & 1.96 vs 1.27, respectively; p<0.05). Percent forming surface in HU-L & HU- β tended to be greater than in HU-V (7.90 & 6.54 vs 4.39, respectively; p< 0.09). Percent resorbing surface in HU-L & HU- β was significantly lower than in HU-V (4.31 & 3.03 vs 12.70, respectively; p<0.0001). No significant differences in histomorphometric values were observed among CC-L, CC- β and CC-V. The decrease in serum leptin (by ELISA, Crystal Chem) was significantly less in HU- β (-25%) and in HU-L (-31%) than in HU-V (-62%)(p<0.05) and did not correlate well with changes in body weight. We conclude that β -blockade is as effective as leptin analog administration in mitigating bone loss with HU through both stimulation of osteoblastic activity and suppression of osteoclastic activity, perhaps by disinhibition of leptin release from adipose.

Disclosures: K. Baek, None.

F179

Relative to Body Weight, Obesity Reduces Femoral Neck Structural Strength in Women among the Women's Health Initiative Observational Study. T. J. Beck¹, J. Cauley², C. E. Lewis³, A. LaCroix⁴, T. Bassford⁵, D. A. Nelson⁶, S. Going⁵, D. Sherrill⁵, T. Lohman⁵, R. D. Jackson⁷, M. LeBoff⁸, E. Outwater⁸, Z. Wang⁹, G. Wu⁵, N. Wright⁵, S. Nicholas⁵, Z. Chen³. ¹Johns Hopkins U., Baltimore, MD, USA, ²U. of Pittsburgh, Pittsburgh, PA, USA, ³U. of AL, Birmingham, AL, USA, ⁴Fred Huch. Canc. Res. Ctr., Seattle, WA, USA, ⁵U. of AZ, Tuscon, AZ, USA, ⁶Wayne St. U., Detroit, MI, USA, ⁷OH State U., Columbus, OH, USA, ⁸Harvard U., Boston, MA, USA, ⁹Columbia U., New York, NY, USA.

The obese have higher BMD so most assume that their bones are relatively stronger. However data in children indicate that femur structure scales with lean mass not body weight, suggesting that muscle forces stimulate bone adaptation. To determine the relationship between body weight and hip structural strength in postmenopausal women, we used the Hip Structure Analysis (HSA) program to examine femoral neck BMD and cross-sectional geometry in a substudy of 1410 women in the Women's Health Initiative Observational Study. Women (50-79 yr at baseline) were partitioned into categories of body mass index (BMI in kg/m²): underweight (<18.5, n=15), normal (18.5-24.9 n=483), overweight (25-29.9, n=497), obese I (30-34.9, n=248) obese II (35-39.9 N = 94) and extremely obese III (>=40, n=73). Femur neck BMD, bone cross-sectional area (CSA), outer diameter and section modulus (Z, an index of bending strength) were compared between BMI categories before and after normalizing to individual body weight. Although outer diameter did not, BMD, CSA, and Z were higher with higher BMI; each category differed from all others (p<0.05). After scaling to body weight, the trend with BMI reversed so that BMD, CSA outer diameter and section modulus were lower with higher BMI category, (p<0.05 vs. any group). The Figure plots mean Z values (95%CI) by category scaled to those with normal BMI, with and without normalization to body weight. Bending strength increases with BMI but less than the increase in weight. The same pattern is evident in CSA (axial strength) and BMD. We conclude that as a proportion of body weight, femur strength is reduced with greater obesity. It is unknown whether obesity makes fractures more likely; fat padding reduces impacts in certain fractures. Nevertheless traumatic forces that cause fractures are a function of body weight and femurs of the obese are disproportionately weaker in relation to those forces.



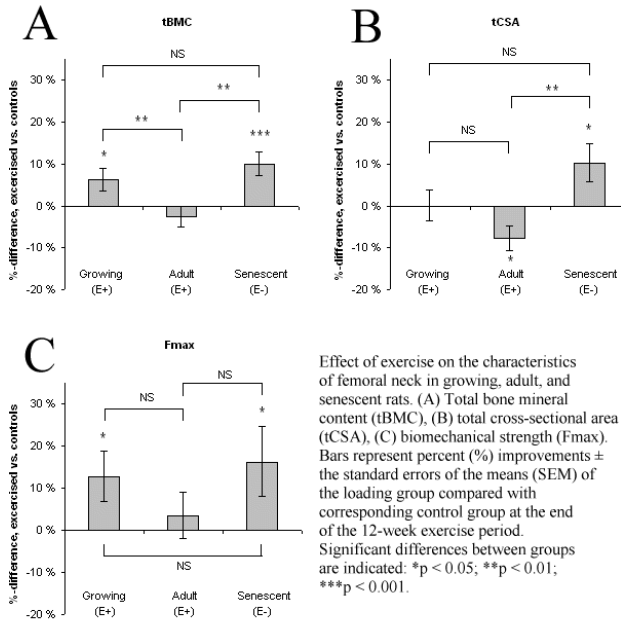
Disclosures: T.J. Beck, None.

F181

Estrogen-Withdrawal Increases the Mechanosensitivity of Bones to Loading. I. Pajamäki¹, O. Leppänen¹, J. Jokihaara¹, H. Sievänen², P. Kannus², T. L. N. Järvinen¹. ¹Department of Orthopaedics and Traumatology, University of Tampere, Tampere, Finland, ²UKK Institute, Tampere, Finland.

Estrogen, the primary non-mechanical regulator of female bones, has been suggested to enhance the mechanosensitivity of bones to loading. In this virtually life-long experiment, we evaluated whether the estrogen-status of the rats modulates the skeletal responsiveness to loading. A total of 105 growing [5-17-week-old, normal estrous cycle (E+)], adult [47-59-week-old, normal estrous cycle (E+)] and senescent [90-102-week-old, menopausal (E-)] female Sprague-Dawley rats were used. At entry, rats were randomly assigned into 6 groups; 3 control groups (n=15/group) and 3 exercise groups (n=20/group). In the exercise groups, rats were subjected to an identical, 12-week period of progressive treadmill training. At each time point, a comprehensive structural analysis of the femoral neck was performed (peripheral quantitative computed tomography and mechanical testing). The menopausal status of the senescent rats was confirmed by microscopic examination of the ovaries and uterus (the absence of functional follicles in the ovaries and uterine atrophy denoting the menopausal status) in age-matched control rats prior to the execution of the exercise period. In comparison to their age-matched controls, twelve weeks of treadmill training resulted in significant increases in femoral neck total bone mineral content (tBMC) in growing (E+) and senescent (E-) rats (A in figure below). In addition, a significant exercise-induced increase in the total cross-sectional area of the femoral neck (tCSA) was observed in senescent (E-) rats (B in fig.). These changes resulted in significantly increased breaking load of the femoral neck (F_{max}) in growing (E+) and senescent (E-) rats (C in fig.). In contrast, no exercise-induced benefits were observed in femoral neck parameters in the adult (E+) rats. In conclusion, these findings are in perfect agreement with both experimental and clinical studies, as we observed an estrogen-induced packing of mechanically excess mineral into fertile (adult) female skeleton, and consequent damping of the mechanosensitivity of these bones. At menopause, this extra

“bone stock” was shed, and consequently, the mechanosensitivity of bones to loading was regained.



Disclosures: I. Pajamäki, None.

F183

Novel Mechanoresponsive BMD and Bone Size QTL Identified in a Genome Wide Linkage Study Involving C57BL/6J-C3H/HeJ Intercross. C. Kesavan, S. Mohan, H. Yu*, S. Oberholtzer*, J. E. Wergedal, D. J. Baylink. JLP VAMC and LLU, Loma Linda, CA, USA.

Previously, we demonstrated that 2 wks of 4-point bending caused a dramatic 15% increase in volumetric BMD (vBMD) in the tibia of C57BL/6J (B6) but not C3H/HeJ (C3H) mice. To identify the genetic loci that contribute to variation in BMD response to mechanical loading (ML), we performed a genome wide linkage study in the B6-C3H mice intercross. The left tibiae of 329 B6-C3H F2 female mice at 10 wk age were subjected to 9 N cyclic load at 2Hz for 36 cycles daily for 2 wks while right tibia was used as unloaded control. Two days after the last loading, vBMD and bone size (periosteal circ.) were measured by pQCT. ML- induced changes ([loaded-unloaded/unloaded] X 100) in vBMD (-5 to +15%) and bone size (-5 to +20%) in the B6-C3H F2 mice showed normal distributions consistent with the complex traits controlled by several genes. % change in BMD or bone size in the F2 mice of loaded bones did not correlate with body wt, suggesting that variation in bone anabolic response to ML is independent of body size. Genome-wide search using 110 microsatellite markers with 15 cM intervals in the F2 mice revealed the following ML QTLs for BMD and bone size phenotypes (% change in loaded vs unloaded bone) using MAPQTL program (a=P<0.01; b=P<0.05):

Phenotype	Locus	LOD Score	% Variation
vBMD	D1Mit113	3.4 ^a	4.7
vBMD	D8Mit88	4.2 ^a	5.8
vBMD	D9Mit336	2.5 ^b	3.5
Bone Size	D8Mit49	3.0 ^b	4.1
Bone Size	D9Mit97	2.8 ^b	3.9
Bone Size	D11Mit333	2.6 ^b	3.6
Bone Size	D18Mit64	2.8 ^b	3.5

We found that ML BMD QTL for chr. 8 and 9 and bone size QTL for chr. 8 and 18 could not be detected using phenotype data from unloaded bones, suggesting that these QTLs are unique to ML phenotypes. Furthermore, chromosome 8 BMD QTL has not been reported for BMD in any other inbred strain crosses. Conclusions: 1) Our study provides the first demonstration of chromosomal location of genetic loci affecting variation in skeletal anabolic response to ML in the B6-C3H intercross. 2) Only 15 % of the genetic variation was accounted for by the identified ML QTL suggesting additional QTL or interactions exist. 3) Future identification of the genes responsible for the ML QTL should lead to improved understanding of molecular pathways for ML-induced skeletal anabolic response.

Disclosures: C. Kesavan, None.

F185

Bone Fluid Flow Induced By Skeletal Muscle Dynamics and its Role in Bone Adaptation. Y. Qin, H. Lam*, L. Orzechowski*, Y. Xia. Biomedical Engineering, SUNY Stony Brook, Stony Brook, NY, USA.

Skeletal muscle dynamics appears to retard disuse osteopenia. Exercise increase blood flow to the skeletal tissues, i.e., bone and muscle. To further elucidate the mechanism of muscle dynamics initiated bone remodeling, we propose that muscle dynamics generated by physiologic contraction can induce fluid flow and enhance perfusion in bone, which may act as a mediator in initiating and regulating osteonal adaptation. While we have previous shown that applying dynamic intramedullary pressure (ImP) stimulated new bone formation and inhibit disuse resorption, the objectives for this work were to evaluate (a) the role of muscle dynamics induced ImP, (b) the response of cortical perfusion enhanced by muscle contraction, and (c) its role for in vivo bone adaptation. Total of twelve 9-month old rats were used in the perfusion and in vivo study (n=4 for perfusion, n=4 for in vivo experimental and n=4 for sham control). In the pressure and perfusion measurement, an electronic muscle stimulator was used to the skeletal muscle adjacent to the right femur and excited with frequencies of 1, 2.5, 3.5, 20, 25, 35, 45 and 60 Hz. Convective filtration in the intracortical capillary was evaluated using fluorescent microspheres. Under in vivo study, a hind limb suspension (HLS) rat model was developed to generate interstitial fluid flow in femur via dynamic muscle contraction. Daily fluid flow loading was administrated via a low magnitude muscle stimulator at frequency of 10 Hz, 5 min/day, for 3 weeks. Dynamic muscle contraction significantly generated fluid ImP, in which ImP increased on the order of 8+/-1.4 mmHg at 1 Hz, 8.7+/-0.5 mmHg at 2.5 Hz, 9.3+/-4.7 mmHg at 25 Hz, and 1.8+/-0.1 at 45 Hz, with baseline of 2 mmHg generated by heart beats. Fluorescent tracer indicated that the perfusion in experimental bone was 3x greater than in the control. In the in vivo results, histomorphometry analysis indicated significant trabecular bone remodeling, in which the ratio of labeled vs. bone surface (LS/BS) has more than 50% increase in the experimental distal femur compared to contralateral control. Double labels have shown in the experimental group, but not in the sham control, in which mineral deposition rate (MAR) was at 1.5 micron/day. These results suggest that dynamic contraction of muscle may generate hyper-tension in the skeletal nutrient vessel and induce ImP, and may substantially influence the fluid flow in bone. Physiologic and dynamic muscle contraction may serve as a non-invasive source for generating fluid flow in bone, which can trigger modeling and remodeling in bone. This may help to devise a biomechanical based intervention for treating osteoporosis, muscle atrophy, and accelerating fracture healing.

Disclosures: Y. Qin, None.

F187

A School Curriculum Based Exercise Program Increase Bone Mineral Accrual in Boys and Girls during Early Adolescence-Four Years Data from the POP-Study (Pediatric Osteoporosis Prevention Study) - a Prospective Controlled Intervention Study in 221 Children. C. Linden, P. Gardsell*, H. Ahlborg, M. Karlsson. Orthopaedics, University Hospital Malmö, Malmö, Sweden.

The longest reported prospective controlled intervention study with exercise in growing children which evaluate the accrual of bone mineral span 20 months. The purpose of this study was to evaluate the effect of an exercise intervention program within the school curriculum during the first school years, to catch also children not specifically interested in exercise, and to present the so far longest controlled follow-up data of exercise during growth. A population based cohort including 73 healthy Caucasian boys (aged 7.8 ± 0.6 at baseline) and 48 girls (aged 7.7 ± 0.6) in the only school in the Bunkeflo society outside Malmö, Sweden, were included in a school curriculum with 40 minutes physical activity every school day. One hundred healthy age and gender matched children (52 boys and 48 girls) in three nearby schools served as controls. These children were assigned to the general Swedish curriculum of physical activity in these grades (60-90 min/w). Bone mineral content (BMC; g) were measured with dual X-ray absorptiometry (DXA) at the lumbar spine (LS) and femoral neck (FN) before initiation of the intervention and then yearly for four years. The slope for each individual was estimated from the repeated measurements, and the annual changes calculated. Data is presented as mean ± SD. There were no differences in age, height, weight or BMC at baseline. In boys, the annual gain in BMC in the LS was greater in the intervention group in comparison with the controls during the 4 year follow-up, 7.0 ± 2.3 versus (vs.) 6.2 ± 1.5, p<0.05. In girls, a similar effect was seen in the LS 9.1 ± 4.1 vs. 7.1 ± 3.3 and in the FN 0.39 ± 0.20 vs. 0.29 ± 0.17, p < 0.01 respectively. The annual increase of the FN width (mm) was also greater in the intervention group, 1.23 ± 0.42 vs. 1.07 ± 0.49 in boys and 1.45 ± 0.91 vs. 1.03 ± 0.76 in girls, p < 0.05. The discrepancies remained after adjusting for differences in weight gain, height gain and pubertal development during the study, except for FN width in girls (p=0.08). A school based exercise program within the general curriculum during the first four school years seems to increase the accrual of bone mass and bone size. This is the first published intervention study that is population based and include the intervention within the school curriculum. Furthermore, it is so far the only intervention study that exceeds 20 months. Based on the data in this study it seems that increased time spent in physical education classes may increase peak bone mass and subsequently can be used as a prevention strategy for osteoporosis.

Disclosures: C. Linden, None.

F190

Cbl-Mediated Ubiquitination of alpha 5 Integrin Subunit Mediates Fibronectin-Dependent Osteoblast Detachment and Apoptosis Induced by FGFR-2 Activation. K. Kaabeche^{*1}, H. Guenou^{*1}, D. Bouvard^{*2}, N. Didelot^{*1}, A. Listrat^{*1}, P. J. Marie¹. ¹Laboratory of Osteoblast Biology and Pathology, Inserm U606, Paris, France, ²LEDAC, UMR CNRS/UJF 5538, La Tronche, France.

Fibroblast growth factor receptor (FGFR) signaling is an important mechanism regulating osteoblast function and osteogenesis. To gain further insight into the regulatory role of FGFR-2 signaling in osteoblasts, we investigated integrin-mediated attachment and cell survival in osteoblasts expressing activated FGFR-2. Human calvarial osteoblasts obtained from a patient with Apert syndrome (craniosynostosis) exhibiting a S252W FGFR-2 mutation showed reduced cell attachment on fibronectin in culture compared to control cells. This was associated with reduced expression of the alpha 5 integrin subunit which we found by immunohistochemistry to be expressed in human calvarial osteoblasts *in vivo*. Treatment with lactacystin, a potent inhibitor of proteasome, restored alpha 5 integrin levels in FGFR-2 mutant osteoblasts. Immunoprecipitation analysis showed that alpha 5 integrin interacts with both the E3 ubiquitin ligase Cbl and ubiquitin. Immunocytochemistry revealed that alpha 5 integrin colocalizes with FGFR-2 and Cbl at the leading edge in membrane ruffle regions in normal and mutant FGFR-2 osteoblasts. Transfection with the 70Z-Cbl mutant lacking the RING domain required for Cbl ubiquitin interaction, or with the G306E Cbl mutant that abolishes the binding ability of Cbl phosphotyrosine binding domain, restored alpha 5 integrin levels in FGFR-2 mutant osteoblasts. This suggests that Cbl-mediated ubiquitination plays an essential role in alpha 5 integrin proteasome degradation induced by FGFR-2 activation. Reduced alpha 5 integrin expression was associated with increased Bax/Bcl-2 ratio and increased caspase-9 and caspase-3 activities in FGFR-2 mutant osteoblasts. Forced expression of alpha 5 integrin rescued cell attachment and corrected both the Bax/Bcl-2 ratio and caspase-3 and caspase-9 activities in FGFR-2 mutant osteoblasts. We conclude that Cbl recruitment induced by FGFR-2 activation triggers alpha 5 integrin degradation by the proteasome, which results in reduced osteoblast attachment on fibronectin and caspase-dependent apoptosis. This identifies a functional role of the alpha 5 integrin subunit in the induction of apoptosis triggered by FGFR-2 activation in osteoblasts, and reveals a novel Cbl-dependent mechanism involved in the coordinated regulation of cell apoptosis induced by alpha 5 integrin degradation.

Disclosures: **P.J. Marie**, None.

F192

The Evidence that Bcl-2 Is Dispensable for the Anabolic Action of PTH in Bone. J. Yamashita^{*}, Y. P. Chun^{*}, N. S. Data, L. K. McCauley. School of Dentistry, University of Michigan, Ann Arbor, MI, USA.

It is well recognized that intermittent administration of PTH has anabolic actions in bone. The proposed mechanism of this action has focused on two theories. First, anabolic PTH may increase the proliferation of pre-osteoblasts and stimulate their maturation. Second, PTH may extend the life span of mineral-forming osteoblasts by suppressing apoptosis. Despite suggestive evidence, the exact mechanisms of PTH anabolic actions are unclear. *Bcl-2*, which plays a pivotal role in preventing apoptosis, has drawn special attention. It has been hypothesized that PTH stimulates *bcl-2* so that mature osteoblasts can survive longer, resulting in increased bone formation. In this study, we tested the hypothesis that the activation of *bcl-2* is essential for the anabolic action of PTH in bone. Calvarial osteoblasts and splenocytes were isolated from *bcl-2*^{+/+}, *bcl-2*^{-/-}, and *bcl-2*^{-/-} mice and their *bcl-2* expression verified. Proliferation and mineralization assays revealed that *bcl-2*^{-/-} osteoblasts were not significantly different from *bcl-2*^{+/+} and *bcl-2*^{-/-} osteoblasts. There was also no significant difference found between the genotypes in survival rate with etoposide-induced apoptosis in osteoblasts although primary *bcl-2*^{+/+} splenocytes displayed greater protection than *bcl-2*^{-/-}. To determine the role of *bcl-2* in bone formation, two *in vivo* approaches were utilized. The first approach involved a novel implant system where vertebrae (vossicles) from neonatal *bcl-2*^{+/+}, *bcl-2*^{-/-}, or *bcl-2*^{-/-} mice were implanted to immunodeficient mice and PTH (80µg/kg/day) was administered daily for 3 weeks. The second approach was daily administration of PTH (50µg/kg/day) to *bcl-2*^{+/+}, *bcl-2*^{-/-}, and *bcl-2*^{-/-} mice from day-4 to day-13 of age. Histomorphometric and statistical analyses indicated that regardless of the genotype the vossicles responded similarly to PTH with substantially increased bone area when compared to vehicle-control groups ($p < 0.001$). Similarly, in the intact mice of PTH-administered groups there was increased metaphyseal trabecular bone area in the tibiae regardless of the genotype. In summary, there were no major differences detected in the osteoblast activity between *bcl-2*^{+/+} and *bcl-2*^{-/-} *in vivo* or *in vitro*. Our results indicate that, contrary to previous suggestions, *bcl-2* is dispensable in osteoblasts for the anabolic action of PTH.

Disclosures: **J. Yamashita**, None.

F194

Transgenic Expression of Human Bcl-2 in Osteoblasts Promotes Differentiation but Inhibits Bone Formation in Ex Vivo Calvarial Osteoblast Cultures. W. Zhang, A. G. Pantschenko^{*}, M. McCarthy^{*}, G. Gronowicz. Orthopedic Surgery, Uconn Health Center, Farmington, CT, USA.

Apoptosis is important in regulating bone homeostasis and turnover, and Bcl-2 is a key regulator of apoptosis in osteoblasts. In this study, we examined the role of Bcl-2 on the proliferation, differentiation, mineralization and apoptosis of murine transgenic osteoblasts. A Col2.3Bcl-2 transgenic mouse line was generated with 1.8 kb human Bcl-2

(hBcl-2) cDNA driven by the 2.3 kb rat Col1a1 promoter, so that hBcl-2 was expressed in mature osteoblasts. Animal use was approved by the Center for Laboratory Animal Care at UCHC. Calvarial osteoblasts were isolated from neonatal wild-type (+/+) and transgenic (tg/+) littermates by sequential digestion and cultured in DMEM with 10% FBS. For differentiation, the media was changed to α -MEM and supplemented with 50µg/ml ascorbic acid and 4mM β -glycerophosphate. hBcl-2 transcript and protein expression were detected by real-time PCR and Western blot. Culture doubling time was determined over 9 days for cells grown in DMEM by fluorometric DNA analysis. Acridine orange/ ethidium bromide staining and TUNEL were used to study apoptosis. The transcripts of type I collagen (Col1a1), bone sialoprotein (BSP) and osteocalcin (OC) were measured by Northern blot at days 14, 21, 28 and 35. Mineralization was determined by measuring calcium content and alizarin red staining. All assays were repeated at least 3 times. hBcl-2 expression increased during differentiation to over 100-fold more than endogenous mouse Bcl-2 without an effect on mouse Bcl-2 expression. There was no significant difference in the population doubling time between +/+ and tg/+ osteoblasts. The transgene was functional as indicated by the inhibition of apoptosis in tg/+ but not +/+ osteoblasts in response to 1 to 1000 nM corticosterone. Col2.3Bcl-2 promoted differentiation as indicated by the stronger expression of bone matrix markers in the tg/+ cells, especially BSP and OC. Tg/+ osteoblasts produced significantly less mineralization than +/+ on days 14, 21, and 28 with 47% less calcification on day 28. Alizarin red staining was also decreased in tg/+ cells. Apoptosis was found primarily in the mineralized nodules as shown by TUNEL, and it was decreased in tg/+ cultures on days 14, 21, 28 with 34% less apoptosis on day 28 than the +/+. In conclusion, overexpression of hBcl-2 protected osteoblasts from glucocorticoid-induced apoptosis and promoted their differentiation, but had no effect on endogenous mouse Bcl-2 or the proliferation of osteoblasts. Importantly, overexpression of hBcl-2 impaired mineral deposition and decreased apoptosis, suggesting that apoptosis is essential for osteoblast mineralization *in vitro*.

Disclosures: **W. Zhang**, None.

F197

Parathyroid Hormone Increases Osteoblastic Jagged1 through Protein Kinase A (PKA) Activation. J. M. Weber^{*}, S. R. Forsythe^{*}, C. A. Christianson^{*}, L. M. Calvi. Medicine, Endocrine Division, University of Rochester School of Medicine, Rochester, NY, USA.

In the bone marrow, osteoblastic cells have been shown to be an important component of the hematopoietic stem cell (HSC) niche. We demonstrated that activation of the PTH Receptor (PTH1R) in osteoblastic cells expands HSCs. Activation of the Notch signaling pathway was necessary to mediate the PTH-induced expansion of HSC. This pathway, through cell-cell interactions plays a fundamental role in HSC self-renewal. In particular, stromal cell expression of the Notch ligand Jagged1 has been shown to be sufficient for HSC expansion *in vitro*. To explore PTH regulation of Jagged1, we studied mice treated with intermittent PTH (1-34). In untreated adult mice, immunohistochemical analysis of the long bones showed low levels of Jagged1 protein in endosteal osteoblasts at both the metaphysis and diaphysis. In contrast, no Jagged1 was found in periosteal osteoblasts. As early as 5 days after PTH treatment, endosteal osteoblastic Jagged1 levels were increased compared to vehicle-treated animals. To study the molecular mechanisms involved in PTH regulation of osteoblastic Jagged1, we utilized rat osteosarcoma UMR106 cells, known to express the PTH1R. Jagged1 expression was increased in a time and dose-dependent fashion when measured by realtime PCR in RNA from UMR106 cells treated with PTH compared with vehicle. Western blot analysis with two distinct anti-Jagged1 antibodies confirmed the PTH-dependent increase in Jagged1 protein. In osteoblasts, PTH(1-34) is known to activate both the adenylate cyclase (AC) and the protein kinase C (PKC) signaling cascades downstream of the PTH1R. We independently determined the effect of activating either pathway on Jagged1. Forskolin, an AC activator, dramatically increased Jagged1 expression and protein. In addition, we could reproduce the Jagged1 increase in mRNA using PTH(1-31), which predominantly activates PKA downstream of AC. Moreover, PKA stimulation with cell-permeable cAMP analogues dibutyryl-cAMP and 8-bromo-cAMP stimulated Jagged1. Treatment with PTH (1-34) in the presence of the PKA inhibitor H89 inhibited the PTH-dependent Jagged1 increase. In contrast, Jagged1 levels were not increased by treatment with PTH(13-34), which predominantly activates PKC, or PMA, a PKC activator. In summary, osteoblastic cell treatment with PTH increases expression of the Notch ligand Jagged1 through activation of the AC/PKA signaling pathway downstream of the PTH1R. Further definition of the molecular mechanisms underlying osteoblastic PTH-dependent modulation of Jagged1 and its role in the PTH-induced enhanced osteoblastic support of HSC is likely to provide targets for manipulation of the HSC niche.

Disclosures: **J.M. Weber**, None.

F199

HB954, an Orphan 7 Transmembrane Receptor, Is Expressed at High Levels in Bone. J. R. Connor¹, C. A. Watson^{*2}, C. Hanning^{*1}, S. Hoffman^{*1}, P. Liang^{*1}, D. Rickard^{*1}, P. Hegde^{*3}, E. Docherty^{*3}, A. Morrison^{*3}, G. Hagger^{*2}, J. Minnion^{*2}, S. Kumar¹. ¹Musculoskeletal Diseases, GlaxoSmithKline, Collegeville, PA, USA, ²Discovery Research, GlaxoSmithKline, Collegeville, PA, USA, ³Genetics Research, GlaxoSmithKline, Collegeville, PA, USA.

HB954 was identified as an orphan 7 transmembrane receptor expressed at high levels in bone. The purpose of this study was to investigate the role of HB954 in bone formation and remodeling. Expression of HB954 mRNA was analyzed by TaqMan using standard techniques against a variety of human tissues and by *in situ* hybridization using 35S labeled riboprobes on cryostat sections of human osteoclastoma. Serial sections were stained for alkaline phosphatase. Human mesenchymal stem cells were differentiated to osteoblasts, adipocytes or chondrocytes by the supplier (Clonetics, Walkersville, MD) and

ASBMR 27th Annual Meeting

the RNA, harvested at time points up to 21 days, was analyzed for differential gene expression by transcriptome analysis using Affymetrix Chip technology. Human tissues were obtained with informed consent and with the approval of the institutional review board. Finally, 9 week old HB954 knockout (129ola/C57Bl/6) mice were examined for bone phenotype by histomorphometry following double calcein labeling and by microCT analysis. All procedures were performed in accordance with protocols approved by the GSK Institutional Animal Care and Use Committee. HB954 mRNA was expressed at high levels (15,000 copies of HB954 mRNA per ng mRNA pool) in bone compared to a variety of other tissues including liver, brain, adipose, cartilage and bone marrow by TaqMan analysis. In human osteoclastoma, HB954 mRNA was detected at high levels by in situ hybridization in osteoblasts on bone surfaces and in alkaline phosphatase positive areas of bone formation. During the time course of differentiation of human mesenchymal stem cells to osteoblasts, adipocytes or chondrocytes, HB954 was significantly and specifically upregulated at early time points in osteoblasts but downregulated in adipocytes and chondrocytes. In HB954 knockout mice, histomorphometric analysis demonstrated increased bone volume in knockout versus wild types due to increased and thickened trabeculae, increased modeling and decreased resorption. MicroCT analysis of the proximal tibia demonstrated trends toward increased bone volume per total volume, increased trabecular number and thickness, and increased connectivity density. In summary, the unique and high expression of HB954 in osteoblasts suggests a role in bone formation or remodeling. The observation of strong trends toward increased bone mass in the HB954 knockouts provides additional support for a role for this receptor in bone formation.

Disclosures: **J.R. Connor**, None.

F202

Modulation of Runx2 Expression Effects Bone Parameters *In Vitro* and *In Vivo*. **C. A. Frolík¹, A. G. Geiser^{*1}, G. Krishnan¹, C. D. Jones^{*1}, K. A. Houck^{*1}, E. C. Black^{*1}, L. M. Helvering^{*1}, T. L. Moore^{*1}, H. A. Bullock^{*1}, R. J. S. Galvin¹, L. Ma¹, M. Sato¹, R. C. Smith^{*1}, P. Ducy², G. Karsenty³.** ¹Lilly Research Laboratories, Eli Lilly and Company, Indianapolis, IN, USA, ²Cell Biology, Baylor College of Medicine, Houston, TX, USA, ³Molecular and Human Genetics, Baylor College of Medicine, Houston, TX, USA.

Runx2, an osteoblast-specific transcription factor, is essential for osteoblast differentiation. Compounds that modulate Runx2 expression or activity could have important effects on bone. LSN509010 was identified as a compound that increased Runx2 mRNA expression in C3H10T1/2 cells and also enhanced the transcription of a luciferase reporter plasmid containing the Runx2 binding element (OSE). In C2C12 and C3H10T1/2 cells, LSN509010 increased alkaline phosphatase activity, an effect that was dependent on BMP in C2C12 cells and amplified by BMP in C3H10T1/2 cells. The compound increased mineralization of cartilage rudiments maintained in organ culture and this increase was diminished by an antisense oligonucleotide to Runx2. LSN509010 also decreased osteoclast differentiation as determined in both osteoblast supported and osteoblast independent models. Since analogs of retinoic acid also increased alkaline phosphatase activity in C3H10T1/2 cells, LSN509010 was examined for retinoid-like activity. LSN509010 activated the DR5 retinoic acid response element in a transient transfection assay and a retinoic acid receptor (RAR) pan-antagonist blocked the response to retinoic acid analogs and LSN509010 in C3H10T1/2 and C2C12 cells. However, in the metatarsal assay, 13-cis-retinoic acid had a detrimental effect, not observed with LY509010, which was reversed by the RAR pan-antagonist. Finally, in vivo, LSN509010 increased bone volume in an intraosseous infusion model and increased femoral midshaft bone mineral density in a delayed dosing ovariectomized rat model. These findings suggest that modulation of Runx2 expression may lead to positive bone effects in vivo.

Disclosures: **C.A. Frolík**, Eli Lilly and Company 3.

F204

Multiple Histone Deacetylases and Histone Deacetylase Inhibitors Influence Runx2 Activities and Osteoblast Maturation. **E. D. Jensen^{*1}, T. M. Schroeder^{*1}, X. Li^{*1}, J. J. Westendorf².** ¹University of Minnesota, Minneapolis, MN, USA, ²Orthopaedic Surgery, University of Minnesota, Minneapolis, MN, USA.

Runx2 (Cbfa-1/ AML-3) is a key transcriptional regulator of bone and chondrocyte development, and influences cancer-associated bone disease. Runx2 acts as both a context-dependent activator and repressor of transcription. These opposing activities are mediated by interactions between Runx2 and a variety of co-activators and co-repressors, including p300/ CBP, YAP, Groucho/TLE, and histone deacetylases, notably HDAC3, HDAC4 and HDAC6. Histone deacetylases are recruited to promoters by transcription factors and repress gene expression by catalyzing the removal of acetyl groups from histones and other proteins, therein altering chromatin structure. HDAC Inhibitors (HDIs) are currently in phase I and II clinical cancer trials, but their effects on bone formation are not well characterized. In the current study, we show that Runx2 colocalizes and/or co-precipitates with the class II histone deacetylases, HDAC7, HDAC9-related protein (HDRP), and HDAC10. Multiple domains of Runx2 are required for these interactions. HDAC7, but not HDRP or HDAC10, attenuated the ability of Runx2 to activate the osteocalcin promoter. As we previously demonstrated with HDAC3 and HDAC6, HDAC7 and HDRP are expressed with Runx2 in a number of mesenchymal and osteoid tissue culture cell lines. General inhibition of HDAC activity by multiple small molecule HDIs accelerated mineralization of osteoblast cultures and increased alkaline phosphatase production by

calvarial organ cultures without affecting osteoblast viability. Together our data suggest that general HDAC activity regulates osteoblast maturation and bone formation, but each HDAC may regulate Runx2 target genes in specific ways.

Disclosures: **J.J. Westendorf**, None.

F206

C/EBP Homologous Protein (CHOP, Ddit3) Overexpression Inhibits Osteoblastic Function and Causes Severe Osteopenia. **R. C. Pereira^{*}, L. Stadmeier^{*}, D. Smith^{*}, E. Canalis.** Research, Saint Francis Hospital and Medical Center, Hartford, CT, USA.

CCAAT/enhancer binding proteins (C/EBPs) are transcription factors with important roles in cell differentiation and function. C/EBP homologous protein (CHOP) is a nuclear protein that forms heterodimers with C/EBPs and with members of the cyclic AMP response element binding protein/activator of transcription factor family. Studies in *chop* null mice revealed that CHOP is necessary to maintain normal bone mass, and CHOP overexpression *in vitro* accelerates osteoblastogenesis by enhancing BMP/Smad signaling. However, the effects of CHOP overexpression on osteoblastic cell fate and function *in vivo* are not known. To evaluate the role of CHOP expression in skeletal cell function, we created transgenic mice overexpressing CHOP under the control of a 3.6 kilobase (kb) fragment of the rat type I collagen promoter or of a 3.9 kb fragment of the human osteocalcin promoter. One month old homozygous CHOP overexpressing mice were compared to wild type littermates and their skeletal phenotypes defined by radiological and histomorphometric analyses. The skeletal phenotype of type I collagen and osteocalcin CHOP transgenics was similar, but type I collagen CHOP transgenics displayed lower body weight. Contact radiography did not reveal radiological abnormalities in CHOP transgenics, except for cortical thinning. Bone mineral density (BMD) was reduced, particularly in type I collagen CHOP transgenics, which exhibited a 10 to 20% reduction in femoral BMD. Bone histomorphometry confirmed that CHOP transgenics had severe osteopenia and trabecular bone volume/total volume was reduced by 30 to 50% in both lines. The decrease was secondary to a reduction in trabecular number. CHOP transgenics exhibited normal number of osteoblasts and osteoclasts/perimeter, and normal osteoblast and osteoclast surfaces. Bone eroded surface was not affected, indicating normal bone resorption. Dynamic histomorphometry revealed a marked decrease in bone mineral apposition rate of 35 to 60% in both transgenic lines, indicating that the trabecular bone loss was secondary to impaired osteoblastic function. Since type I collagen is expressed in undifferentiated cells, the normal osteoblast number suggests that osteoblast differentiation was not affected. In conclusion, although CHOP is necessary to maintain bone mass *in vivo*, its overexpression inhibits bone formation, causing severe osteopenia. The mechanism may involve CHOP dimerization with transcription factors required for the maintenance of osteoblastic function.

Disclosures: **R.C. Pereira**, None.

F208

Dominant-Negative Odd-Skipped Related 2 Impaired Parietal Bone Formation. **S. Kawai^{*1}, T. Yoneda², A. Amano^{*1}.** ¹Department of Oral Frontier Biology, Osaka University Graduate School of Dentistry, Suita-Osaka, Japan, ²Department of Biochemistry, Osaka University Graduate School of Dentistry, Suita-Osaka, Japan.

The drosophila pair-rule gene Odd-skipped encodes a zinc finger transcription factor required for accurate segment formation in the embryonic development. Mammalian homologues, odd-skipped related 1 (Osr1) and odd-skipped related 2 (Osr2), were subsequently cloned from both mice and humans. Mouse Osr1 has been shown to share a 65% homology with Osr2 and 100% homology in zinc finger domain. Osr1 is expressed in the intermediate mesoderm, limb, lung, and branchial arch of fetuses, as well as adult colon, small intestine, prostate, and testis tissues. While, Osr2 is preferentially expressed in the mesonephric vesicles, mandibular mesenchyme, and limb mesenchyme of fetuses. The function of Osr2 in the bone is not fully understood though Osr2 is expressed during limb development. To analyze the function of Osr2 in bone development, transgenic mice were generated using dominant negative Osr2 driven by a 5kb mouse Osr2 gene promoter (Osr2ΔN Tg). The genotype was confirmed by PCR of tail genome using transgene-specific primers. The growth was significantly retarded in Osr2ΔN Tg compared with wild type mice. At 2 weeks after birth, soft X-ray analysis of transgenic mice revealed markedly increased radiolucency compared with the wild type. Judged by skeletons of newborn mice stained with alcian blue and alizarin red those intensities of skull and skeletal elements of Osr2ΔN Tg were apparently reduced. Morphologically, calvaria of Osr2ΔN Tg composed of markedly thinner parietal bones and less number of osteoblastic cells on parietal bone surfaces, which indicates delayed intramembranous ossification. RT-PCR analysis revealed that expressions of osteoblast marker genes were significantly reduced or scarcely detected in primary osteoblastic cells of Osr2ΔN Tg, those included alkaline phosphatase, osteocalcin, Runx2, and osterix. These findings indicate that Osr2 play an important role during the process of parietal bone formation.

Disclosures: **S. Kawai**, None.

F210

Mandibular Phenotype of p20C/EBP β Transgenic Mice: Reduced Alveolar Bone Mass and Site-Specific Dentin Dysplasia. T. Savage^{*1}, D. J. Adams^{*2}, M. Mina^{*3}, J. R. Harrison^{*1}. ¹Orthodontics, University of Connecticut Health Center, Farmington, CT, USA, ²Orthopaedics, University of Connecticut Health Center, Farmington, CT, USA, ³Pediatric Dentistry, University of Connecticut Health Center, Farmington, CT, USA.

CCAAT enhancer binding proteins (C/EBP) comprise a family of basic-leucine zipper transcription factors that regulate cellular differentiation and function. To determine the role of C/EBP transcription factors in osteoblasts and odontoblasts, we generated a transgenic (TG) mouse model with Col1a1 (Col3.6) promoter-targeted expression of a FLAG-tagged dominant negative C/EBP isoform, p20C/EBP β (formerly LIP). Two of the four transgenic lines presented with a gross tooth phenotype manifested by incisor breakage, overgrowth and malocclusion. Histological examination revealed that the amount of alveolar bone was greatly reduced in TG compared to wild type (WT) mice. By microCT, the bone volume fraction of the mandible was reduced at the level of the first (WT 86 \pm 1%, TG 62 \pm 4%) and third (WT 79 \pm 1%, TG 57 \pm 4%) molars, demonstrating a severe mandibular osteopenia. The lingual dentin morphology of TG incisors differed dramatically. Labial dentin (enamel side) showed normal thickness and tubular structure, whereas the lingual dentin was thinner (25-30% of WT at the alveolar crest) with an amorphous globular structure characteristic of dentin dysplasia. FLAG immunostaining was seen in both lingual and labial odontoblasts, indicating that the site-specific defect was not due to a lack of labial transgene expression. Northern blot analysis demonstrated reduced osteocalcin expression in TG mandibles, while bone sialoprotein was increased, consistent with prior results in calvariae and long bones. Dental sialophosphoprotein (DSPP), a marker of the odontoblast lineage whose absence causes dentin dysplasia, was reduced in TG mice. By fluorescence microscopy, Col2.3-GFP, a marker of the odontoblast lineage, was expressed in both labial and lingual odontoblasts, although GFP-marked lingual odontoblasts appeared to be more flattened than WT cells. Moreover, GFP-positive processes in the lingual dentin tubules were truncated and less organized than those in WT dentin. By *in situ* hybridization, DSPP was expressed in TG lingual odontoblasts, but the signal appeared to be less intense than that seen in WT odontoblasts. These data suggest that C/EBP transcription factors may be involved in the regulation of both osteogenesis and odontogenesis. The differential effect of the p20C/EBP β transgene on distinct odontoblast populations suggests cellular heterogeneity within the lineage reflecting cell autonomous differences or the effects of local signals.

Disclosures: **J.R. Harrison, None.**

F212

Runx2 Association with Microtubules: A Potential Role in Nucleo-Cytoplasmic Shuttling. S. M. Pockwinse^{*1}, A. Rajgopal^{*1}, D. W. Young¹, K. A. Mujeeb^{*1}, A. Javed¹, J. B. Lian¹, A. J. van Wijnen¹, J. L. Stein^{*1}, S. J. Duxsey^{*2}, G. S. Stein¹. ¹Department of Cell Biology and Cancer Center, University of Massachusetts Medical School, Worcester, MA, USA, ²Program in Molecular Medicine, University of Massachusetts Medical School, Worcester, MA, USA.

Transcriptional activity of Runx2, a key factor in bone formation, is modulated by co-regulatory factors, including SMAD 2,3,4 and HDAC 6 that have been shown to associate with microtubules. We pursued biochemical and *in situ* studies to investigate whether Runx2 interacts with microtubules. We find that soluble α tubulin co-immunoprecipitates with Runx2 while a control IgG does not precipitate tubulin. We next performed microtubule co-sedimentation assays with or without taxol (Paclitaxel), a chemotherapeutic agent that stabilizes microtubules. Lysates from Runx2 expressing cells were incubated with taxol stabilized microtubules and centrifuged through a sucrose cushion. The pellet (microtubules) and supernatant fractions were examined for the presence of Runx2 by western blot analysis. We observed that the amount of pelleted Runx2 increases with increasing amounts of polymerized microtubules. Furthermore, if microtubules were depolymerized with nocodazole, Runx2 was not found in the pelleted fraction. These results indicate that Runx2 associates with microtubules. We identified a specific domain of Runx2 that interacts with microtubules. Using the co-sedimentation assay, we show that full-length and N-terminus (1-361) Runx2, but not the C-terminus (323-528), bind to and are pelleted with taxol-stabilized microtubules. Thus, there is a specific interaction between the Runx2 N-terminus and microtubules. Morphological analysis using immunofluorescence shows that Runx2 redistributes from the nucleus to the cytoplasm when microtubules are stabilized with taxol. Quantitation using the linescan function of the Metamorph software program confirms that nuclear Runx2 decreases in taxol treated cells with a concomitant increase in cytoplasmic levels. By confocal microscopy the taxol induced cytoplasmic Runx2 appears to be linearly arranged and associated with microtubules. To understand the potential significance of the Runx2-microtubule interactions, we blocked nuclear export using leptomycin B prior to taxol treatment. Under these conditions, Runx2 did not redistribute from nucleus to cytoplasm. Taken together, these data show that Runx2 associates with microtubules and shuttles between the nucleus and cytoplasm. We propose that nuclear-cytoplasmic shuttling may represent a mechanism for regulation of Runx2 transcriptional activity.

Disclosures: **S.M. Pockwinse, None.**

F214

Functional Study of a Unique Polyglutamine Stretch in RUNX2. P. M. Fonseca^{*1}, G. Zhou¹, Y. Chen^{*1}, B. Lee². ¹Molecular Human Genetics, Baylor College of Medicine, Houston, TX, USA, ²Howard Hughes Medical Institute, Chevy Chase, MD, USA.

RUNX2 is a non-redundant transcriptional activator involved in osteoblast differentiation and chondrocyte maturation. It contains a unique N-terminal polyglutamine-alanine (QA) domain consisting of a stretch of 23 residues of glutamine and 17 residues of alanine. Mutations in RUNX2 cause an inherited skeletal malformation syndrome, cleidocranial dysplasia (CCD). Until now, only one expansion in the alanine tract has been reported in an individual with CCD, while shortenings of the tract are benign polymorphic variants. Polyglutamine expansions are known to cause several neurodegenerative diseases, but the function of the QA tract in RUNX2 is still unclear. In this study, we generated a series of mutant forms of RUNX2 with a deleted (7QE2A-RUNX2) or expanded (72QE23A-RUNX2) QA domain. *In vitro* studies show that 7QE2A-RUNX2 results in reduced transactivation capacity of a reporter gene, while expansions only reduce transactivation when they exceed 70 repeats. Mice over expressing 7QE2A-RUNX2 under the osteoblast-specific action of promoter Col1a1 present short stature at birth. Skeletal preparations revealed delayed closure of fontanel while clavicles appeared normal. Preliminary radiographic analysis of a transgenic mouse suggests lower bone mass. Transgenic mice also show absence of upper teeth and overgrown lower teeth with malocclusion. Interestingly, a fragment containing only the QA domain exhibited a dominant-negative effect on full-length RUNX2 in RUNX2 transactivation assay in ROS17 cells. To test this *in vivo*, we also generated transgenic mice over expressing only the QA domain in osteoblasts. One of the founders was about half the size of the non-transgenic littermates and died prematurely, also showing lower bone density. We are in progress of analyzing the transgenic mice by histology, RNA *in situ* hybridization and real-time RT-PCR. The analysis of these different transgenic mice will lead to a better understanding of the function of the QA tract in RUNX2.

Disclosures: **P.M. Fonseca, None.**

F218

Activation of Small G-Protein Rap1 Increases Bone Mass. A. Ueda^{*}, T. Hiraga, T. Yoneda. Biochem, Osaka Univ Grad Sch of Dent, Osaka, Japan.

Small G-Proteins such as Ras, Rho and Rab have been shown to play a variety of roles in bone metabolism. Ras stimulates osteoblast differentiation and prolongs osteoclast survival. Rho and Rab are reported to promote the formation of actin ring and ruffled border, respectively. The small G-protein Rap1, which is a family member of Ras and originally identified as a natural antagonist of Ras, has been implicated in cell attachment and proliferation. However, the role of Rap1 in bone metabolism has not been explored. To approach this, we firstly studied bones of mice deficient in SPA-1 gene, which specifically inactivates Rap1. Histomorphometrical examination demonstrated significant increase in trabecular bone volume and decrease in osteoclast number in SPA-1-deficient (SPA-1^{-/-}) mice compared with wild-type (WT) mice. Furthermore, calcein double-labeling experiments revealed that bone formation rate was significantly increased in SPA-1^{-/-} mice. Western blot analyses showed that Rap1 was expressed in both osteoblasts and osteoclasts obtained from WT and SPA-1^{-/-} mice at equivalent levels. Ral-GDS pull-down assay showed that Rap1 was markedly activated in osteoclasts and osteoblasts of SPA-1^{-/-} mice compared with those of WT mice. These results collectively suggest that Rap1 activation is involved in the regulation of bone mass. To further understand the role of Rap1 in bone, we examined the effects of Rap1 on osteoblast differentiation *in vitro* using the multipotent mesenchymal cell line C3H10T1/2. BMP2 increased Rap1 activity along with osteoblastic differentiation of C3H10T1/2 cells. SPA-1 overexpression in C3H10T1/2 cells by retrovirus system suppressed BMP2-induced osteoblast differentiation. In contrast, overexpression of Epac, which specifically activates Rap1, enhanced osteoblastogenic effects of BMP2. In addition, Epac significantly increased the proliferation of C3H10T1/2 cells, whereas SPA-1 decreased it. We next examined whether Rap1 plays a role in osteoclast differentiation. TRAP-positive multinucleated osteoclast-like cell formation induced by soluble RANKL and M-CSF was significantly reduced in SPA-1^{-/-} mice-derived spleen cell cultures. RT-PCR analysis showed that OPG expression was elevated in SPA-1^{-/-} marrow stromal cells, suggesting that Rap1 activation negatively regulates osteoclast differentiation. On the other hand, actin ring formation, which is critical to osteoclastic bone resorption, was not affected in SPA-1^{-/-} osteoclast-like cells. In conclusion, our results suggest that Rap1 activation increases bone mass by promoting osteoblast differentiation and inhibiting osteoclast formation. Rap1 may be an important small G-protein in the regulation of bone metabolism.

Disclosures: **A. Ueda, None.**

F220

The Blunting of the Bone Anabolic Response to PTH Observed after Frequently Dosed Bisphosphonates in Rats May Be Explained by Inhibition of Farnesyl Diphosphate Synthase in Osteoblasts. J. A. Gasser, P. Ingold^{*}, A. Rebmann^{*}, M. Susa. Musculoskeletal Diseases, Novartis Institutes for Biomedical Research, Basel, Switzerland.

Chronic exposure to the bisphosphonate (BP) alendronate (ALN) has been shown to blunt the bone anabolic response to parathyroid hormone (PTH) in rats (Gasser, J Musculoskel Neuron Interact, 1:53, 2000) and human (Finkelstein, NEJM, 349:1216, 2003). We aimed to investigate the potential mechanism behind the BP-PTH interaction and determine whether a single BP injection exerted a different effect than chronic ALN.

ASBMR 27th Annual Meeting

Skeletally mature 16-month-old Wistar rats were treated with ALN (28µg/kg s.c. twice per week) or vehicle for 16 weeks before starting daily s.c.-injections of 100µg/kg hPTH(1-38) 5 times per week. The anabolic response was monitored by serial quantitative computed tomography (pQCT) and mechanical properties. The response to PTH was significantly blunted in the femur and tibia of ALN-pretreated rats; pQCT measurements indicated a 2-week delay. In addition, ALN-pretreated rats did not develop the full anabolic response observed in vehicle-pretreated rats over time. In pursuit of a potential mechanism, equipotent therapeutic doses of the BPs ALN (200µg/kg) and zoledronic acid (ZOL; 32µg/kg) were administered as single i.v. injections. A 10 times higher dose of ZOL (322µg/kg) was also administered. Daily s.c. PTH(1-34) treatment (40µg/kg, 5x/week) was initiated 24h later and continued for 6 weeks. Serial measurements of BMD, cortical and trabecular architecture in the proximal tibia metaphysis by pQCT (XCT Research) and *in vivo* microCT (vivaCT40) indicated a normal bone anabolic response in all cortical and cancellous structural parameters in ALN and ZOL treated animals, including those given the supra-pharmacological dose of ZOL. PTH is able to activate flat bone lining cells into cuboid, collagen-synthesizing osteoblasts (Obs) within 6 hours of administration. Our data suggest that chronic BP exposure may reduce the ability of PTH to activate bone lining cells into matrix-secreting Obs, a crucial step in the early bone anabolic response to PTH. In contrast, single i.v. injection of BP (even 10 times therapeutic dose) did not impair the response to PTH in rats. Single i.v. and chronic BP dosing result in a very different exposure pattern of bone cells to BP. Although Obs are not generally considered to be a target for BP inhibition, chronic dosing may be sufficient to exert a cumulative, direct inhibitory effect on the anabolic response of Obs to PTH. As in osteoclasts, inhibition of FPP-synthase by BP may reduce protein prenylation in Obs and thus disrupt cytoskeletal function, thereby preventing the shape change required for the activation of bone lining cells.

Disclosures: **J.A. Gasser**, Novartis Pharma AG 3.

F222

TGF-β Regulates CNC Proliferation and Differentiation during Frontal Bone Development. **T. Sasaki**, **Y. Ito***, **S. Chou***, **P. Bringas, Jr***, **K. Oka***, **M. M. Urata***, **H. C. Slavkin***, **Y. Chai***. Center for Craniofacial Molecular Biology, School of Dentistry University of Southern California, Los Angeles, CA, USA.

The murine frontal bone derives entirely from the cranial neural crest during calvarial morphogenesis. TGF-β signaling can induce premature suture obliteration in cultured fetal rat calvaria and plays an important regulatory role in postnatal calvarial development. It is not known, however, what the functional significance of TGF-β signaling is in regulating the fate of cranial neural crest (CNC) cells during frontal bone development. We show that mice with *Tgfb2* conditional gene ablation in the neural crest have severe frontal bone defect with complete phenotype penetrance. Importantly, loss of *Tgfb2* does not affect the migration of CNC cells during frontal bone development. TGF-β IIR is specifically required for proliferation and terminal differentiation of the osteoprogenitor cells in the CNC-derived frontal bone anlagen on the side of the developing skull while the orbital surface portion of the frontal bone forms despite the cell proliferation defect, inferring a differential requirement for TGF-β signaling during the development of different regions of the frontal bone. At the molecular level, TGF-β signaling regulates the expression of *Twist*, which may then differentially regulate the expression of *Fgfr* and *Dlx5* to control osteoprogenitor proliferation and differentiation, respectively. This study reveals the TGF-β signaling cascade that regulates the development of the CNC-derived frontal bone and provides a model for investigating abnormal CNC development.

Disclosures: **T. Sasaki**, None.

F225

Enhanced Bone Mass in Mice Lacking G Protein-Coupled Receptor Kinases. **L. Wang***, **R. F. Spurney**. Medicine, Duke University Medical Center, Durham, NC, USA.

G-protein coupled receptor (GPCR) systems are important regulators of bone remodeling. Studies from this laboratory suggest that the osseous effects of GPCR systems in bone are modulated by the rate of receptor desensitization. This desensitization is largely mediated by phosphorylation of GPCR proteins by a family of enzymes termed GRKs. In this regard, we previously found that: 1. Targeted overexpression of GRK2 in osteoblasts promotes bone loss (Am J Physiol 288:E826-834, 2005), and 2. Expression of a peptide GRK inhibitor in osteoblasts enhances bone mass (J Clin Invest 109:1361-1371, 2002). To further investigate the role of GRKs in regulating bone formation *in vivo*, we measured bone mineral content (BMC) and bone mineral density (BMD) in mice in which individual GRK genes had been disrupted by homologous recombination. Because homozygous disruption of GRK2 is lethal, studies using these animals were restricted to heterozygous mice (GRK2+/-). As shown in the table below, whole body BMC and BMD at 6 weeks of age was not altered by disruption of individual GRK genes. Because both GRK2 and GRK3 are likely to play important roles in regulating GPCR responsiveness in bone (J Clin Invest 109:1361-1371, 2002), we bred GRK2+/- and GRK3-/- mice to create mice lacking GRK3 and heterozygous for disruption of the GRK2 gene (GRK2+/-GRK3-/-). In GRK2+/-GRK3-/- mutant (MT) mice, both BMC (316 ± 6.8mg [WT] vs 361 ± 1.2mg [MT]; P=0.0018) and BMD (38.5 ± 4.8 mg/cm2 [WT] vs 41.8 ± 0.4 mg/cm2 (MT); P=0.0055)

were significantly increased compared to WT animals. Taken together, these data suggest that GRK2 and GRK3 have overlapping effects in osseous tissues and that both GRK2 and GRK3 play key roles in modulating GPCR responsiveness in bone.

	GRK knockout mice	
	BMC (mg)	BMD(mg/cm2)
Wild type (WT)	308 Å± 7.9	39.1 Å± 0.6
GRK2+/-	327 Å± 19	38.9 Å± 0.9
GRK3-/-	315 Å± 6.3	39.2 Å± 0.4
GRK4-/-	347 Å± 17	40.8 Å± 1.4
GRK5-/-	not done	not done
GRK6-/-	337 Å± 13	40.2 Å± 7.7

Disclosures: **R.F. Spurney**, None.

F227

Phosphatidylinositol 3 Kinase (PI 3 K)-Dependent Erk1/2 Activation Represents A Novel Mechanism of Statin-Induced BMP-2 Expression and Osteoblast Differentiation. **N. Ghosh-Choudhury**. Pathology, University of Texas Health Science Center at San Antonio and South Texas Veterans Health Care System, San Antonio, TX, USA.

Statins, inhibitors of HMG CoA reductase, stimulate expression of BMP-2 resulting in new bone formation. We have previously reported requirement of Erk1/2 and PI 3 K for BMP-2-induced growth and differentiation of osteoblasts. We investigated the signaling mechanism involving these two central pathways in BMP-2 expression in response to statins in 2T3 mouse osteoblasts. Simvastatin and lovastatin (referred as “statins” hereafter), but not pravastatin, increased BMP-2 promoter activity. Statins activated Erk1/2 MAPK in a time-dependent manner with optimal activation at 5 minutes as judged by activation-specific phospho-Erk1/2 immunoblotting and immunocomplex kinase assays, respectively. In contrast, statins had no effect on two other MAP kinases, JNK and p38. To examine the functional consequences of Erk1/2, its phosphorylation-dependent transactivation of Elk-1 transcription factor was examined. Statins stimulated transactivation of Elk-1 as determined by a reporter transfection assay in 2T3 cells. U0126, an inhibitor of MEK, blocked statin-induced Erk1/2 activation, resulting in significant attenuation of Elk-1-transactivation. Presence of GTP-bound Ras is essential for increase in Erk1/2 activity. Therefore, the effect of statin on Ras-GTP formation was determined using a pull down assay with Ras binding domain of Raf fused to glutathione S-transferase (GST-RBD). In this assay, only activated GTP-bound Ras interacts with GST-RBD. Statins increased formation of Ras-GTP in a time-dependent manner with optimal activation at 5 minutes similar to the activation pattern of Erk1/2 described above. These data for the first time indicate activation of Ras-Erk1/2 signaling in statin-induced BMP-2 expression. We have previously shown involvement of PI 3 K and its target Akt in BMP-2 expression and osteoblast differentiation. Ly294002, an inhibitor of PI 3 K, blocked statin-induced lipid kinase activity, resulting in attenuation of Erk1/2 activity. Adenovirus-mediated expression of dominant negative Akt prevented Erk1/2 activity in response to statins. Expression of both dominant negative PI 3 K and Akt kinase prevented statin-induced BMP-2 transcription. Also, the tumor suppressor protein PTEN, which inactivates PI 3 K signaling, inhibited expression of BMP-2 in response to statins. Furthermore, dominant negative Erk2 blocked BMP-2 expression. Together, these data provide the first evidence for a novel mechanism involving a cross-talk between PI 3 K and MAPK signal relay for statin-induced BMP-2 expression necessary for osteoblast differentiation.

Disclosures: **N. Ghosh-Choudhury**, None.

F229

Haploinsufficiency of Beta-Catenin Results in Reduced Bone Mass. **P. Maye***, **A. C. Lichtler¹**, **B. Kream²**, **D. Rowe¹**. ¹Genetics & Developmental Biology, University of Connecticut Health Center, Farmington, CT, USA, ²Endocrinology, University of Connecticut Health Center, Farmington, CT, USA.

Biochemical studies have shown that signaling through either LRP5 or LRP6 can activate the Wnt/beta-catenin signaling pathway, suggesting a functional redundancy exists between these two co-receptors. Surprisingly, recent genetic studies have shown that both LRP5 and LRP6 are required for proper bone formation and LRP5/6 compound mutants have an even greater deficiency in bone formation. This strongly suggests that in order to maintain normal levels of bone, extremely high levels of Wnt/beta-catenin signaling are required. Therefore, we hypothesized that mice deficient for one copy of the beta-catenin gene should result in lower bone mass and might serve as a model to study the effects of reduced levels of canonical Wnt signaling on bone formation, which may be analogous to complete loss of LRP5. We report that bone from both beta-catenin germline heterozygous mice and beta catenin heterozygous mice, that were conditionally inactivated by a 3.6KB Collagen Type I promoter driving Cre recombinase, have reduced bone mass compared to their wild-type littermate controls. Additionally, bone marrow stromal cell cultures derived from beta-catenin heterozygous animals exhibit limited growth and mineralization. In addition, heterozygous stromal cell cultures can be rescued by treatment with lithium chloride, a GSK3-Beta inhibitor. Thus, mice haploinsufficient for beta catenin or tissue restricted deficient via conditional inactivation, reveal a significant bone deficiency, demonstrating that beta catenin gene dosage is crucial for normal levels of bone formation. We speculate that mice haploinsufficient for beta-catenin will be a useful animal model to study osteoporosis.

Disclosures: **P. Maye**, None.

F232

Treatment of Young Male Monkeys for 12 Months With a Highly Potent Inhibitor of Cathepsin K Inhibits Bone Resorption, and Increases Bone Mineral Density and Strength. S. Kumar¹, S. Rehm¹, R. Boyce¹, J. Birmingham¹, G. Stroup¹, C. Jerome², P. Weir¹. ¹GlaxoSmithKline, King of Prussia, PA, USA, ²SkeleTech, Bothell, WA, USA.

Cathepsin K is a cysteine protease that is highly and selectively expressed in osteoclasts, and likely plays a key role in osteoclast-mediated bone resorption. SB-462795 is a potent inhibitor of human cathepsin K, L and V (K_i = 41, 68 and 53 pM, respectively), with 39-300 fold selectivity over other cathepsins. This study evaluated the pharmacological and toxicological effects of SB-462795 in monkeys, in which the enzyme is identical to the human form. Four groups of eight, 3-5 year-old, male, cynomolgus monkeys received vehicle or SB-462795 at 3, 30, or 1000 mg/kg/day by daily gavage for 52 weeks. Bone biomarkers and bone density (BMD, by DEXA and pQCT) were measured periodically; bone biomechanical testing, bone histomorphometry, gross and histopathologic evaluations were performed terminally. The compound was well tolerated at all doses, with no evidence of significant toxicity. Systemic drug exposure was only approximately 4-fold higher at 1000 mg/kg/day than at 30 mg/kg/day. Compared with pre-treatment values, treatment at 30 or 1000 mg/kg/day had significant and comparable effects to reduce cartilage and bone resorption biomarkers. At Week 52 at 30 or 1000 mg/kg/day, respectively, urinary Type II Collagen /Creatinine (UCRT) ratios were 79% and 74% lower and N-Telopeptide /UCRT ratios were 65% and 73% lower. There was also a decrease in one bone formation marker (Bone-specific Alkaline Phosphatase, activity 35% and 43% lower, respectively, at 30 or 1000 mg/kg/day in Week 52) but not another (Osteocalcin). BMD was significantly increased in lumbar spine, femur neck, and distal radius (predominantly trabecular bone), and in mid-femur and proximal radius (predominantly cortical bone). Of special interest was that mid-femur exhibited a dose-dependent decrease in medullary cavity area, consistent with positive bone balance on endocortical surfaces, and increased total area, consistent with stimulation of bone formation on the periosteal surface. Upon biomechanical testing, maximum load was significantly increased by 42% and 49%, respectively, at 30 and 1000 mg/kg/day in lumbar vertebrae. Histomorphometric data (LV2 and mid-femur) showed significantly decreased activation on all endosteal surfaces, consistent with a reduction in bone turnover in animals treated at 30 and 1000 mg/kg/day. Overall, SB-462795 appears to increase bone strength in young male monkeys by decreasing bone turnover and improving the balance between bone resorption and formation. The drug did not exhibit any toxicity nor compromise bone quality even at the highest dose tested (1000 mg/kg/day).

Disclosures: **S. Kumar**, GlaxoSmithKline 3.

F234

Cathepsin K Knockout Mice Lose Bone Following Ovariectomy. S. J. Hoffman, P. Liang, C. A. Capriotti, J. A. Vasko-Moser, S. Kumar, G. Stroup. GlaxoSmithKline, King of Prussia, PA, USA.

Cathepsin K is a cysteine protease that plays an essential role in osteoclast-mediated degradation of the organic matrix of bone. Knockout of the enzyme in mice as well as lack of functional enzyme in the human condition, pycnodysostosis, results in osteopetrosis. In the current study, changes in bone mass were evaluated in cathepsin K knockout mice following ovariectomy (Ovx). Wild-type (WT) and cathepsin K knockout (KO) mice underwent Ovx or sham-surgery at 4 months of age and groups of animals were sacrificed at 4 and 8 weeks post-surgery. In vivo analysis by peripheral Quantitative Computed Tomography (pQCT) was performed at the proximal metaphysis of the tibia. Dynamic histomorphometry and micro-computed tomography (micro-CT) of the trabecular bone of the tibial proximal metaphysis were also performed. Histological assessment at baseline showed that KO mice had 4.6-fold greater trabecular bone volume than their WT counterparts. This finding was corroborated by pQCT evaluation which showed a 53% increase in total BMC in the KO animals. Eight weeks after Ovx, KO animals had lost 0.24 mm² (51%) of trabecular bone compared to 0.1 mm² (67%) in the WT animals. Ovx KO animals had significantly lower Tb.Th (33%) and Tb.N (22%) and higher Tb.Sp (52%) than KO sham animals. WT Ovx animals showed relatively no change in Tb.Th but a small non-significant decrease in Tb.N (39%) and an increase in Tb.Sp (15%). Analysis by pQCT showed a significant decrease in vBMD in Ovx KO and WT animals compared to sham controls. Levels of plasma osteocalcin were similar in WT and KO mice at 4 months of age and increased significantly with ovariectomy. However, plasma levels of C-telopeptide of collagen I (CTX), a resorption biomarker, were significantly higher in KO mice (33.4 ng/mL) than WT mice (7.5 ng/mL) at baseline. Following ovariectomy, CTX levels were significantly higher in KO Ovx animals relative to sham controls at weeks 4 and 8. However, there was no significant change in this marker following ovariectomy in WT animals. Collectively, the histology and BMD data show clearly that bone loss occurs in cathepsin K-deficient mice. This suggests that proteinases other than cathepsin K can compensate and play a role in estrogen-deficient bone loss in aged mice, and that cathepsin K plays more of a developmental role in bone turnover in mice. These data are contrary to the pronounced anti-resorptive effects of cathepsin K inhibitors in estrogen deficient monkeys.

Disclosures: **S.J. Hoffman**, GlaxoSmithKline 3.

F236

Histomorphometric and Biochemical Evidence for a Cortical Bone-Forming Effect of a Cathepsin K Inhibitor in Ovariectomized Cynomolgus Monkeys. G. Stroup¹, C. Jerome², D. S. Yamashita¹, S. Kumar¹.

¹GlaxoSmithKline, King of Prussia, PA, USA, ²SkeleTech, Bothell, WA, USA.

Cathepsin K has been shown to play an important role in bone matrix degradation during osteoclastic bone resorption. We studied the effects of SB-462795, a novel, potent inhibitor of cathepsins K, L and V, on biochemical markers and histomorphometric measures of bone turnover at several sites in aged ovariectomized female monkeys following oral delivery. After collection of baseline data, adult female cynomolgus monkeys were randomized to 6 groups of 20 each, of which one was sham-ovariectomized (Sham) and the remainder ovariectomized (Ovx). Ovx animals were treated with vehicle, SB-462795 at 1, 3, or 10 mg/kg/d by gavage, or oral vehicle plus alendronate at 0.05 mg/kg by IV injection once every 2 weeks for 9 months. SB-462795 dose-dependently decreased urinary excretion of collagen-N-telopeptide. Significant reductions were observed between 1 week and 2 months at doses of 1 and 3 mg/kg/d, and for the entire duration of the study starting at week 1 at 10 mg/kg/d. Significant reduction of this biomarker by alendronate treatment was not observed until week 3 and continued to month 9. SB-462795 at 10 mg/kg/d decreased bone formation markers to a lesser extent than the bone resorption markers, and significantly increased serum osteocalcin from 3 to 9 months (1mg/kg/d) and at month 9 (3 mg/kg/d). In contrast, robust decreases in bone formation markers occurred with alendronate treatment. This suggests that SB-462795 may inhibit bone turnover while providing a more favorable balance of resorption and formation compared to a bisphosphonate. Histomorphometry data revealed a dose-dependent reduction in both bone resorption and formation parameters at cancellous sites (lumbar vertebra and femoral neck) with SB-462795 treatment and a similar reduction due to alendronate treatment. However, a stimulatory effect on femur periosteal bone was observed with SB-462795 treatment. This effect was significant (P<0.1) at the low dose only but was of similar magnitude at all three doses (Ps.BFR/BV increased 150%, 217% and 167% at 1, 3 and 10 mg/kg/d respectively, relative to Ovx). In contrast the impact of alendronate was an increase of only 17%. Furthermore, a significant increase in endosteal turnover, which was inversely related to dose level, was observed with SB-462795. Endosteal porosity and BFR were significantly higher at 1mg/kg/d than Ovx. At 10 mg/kg/d there was generally no difference relative to Ovx. These findings suggest that SB-462795 significantly differs from alendronate in that it may have classic anti-resorptive effects in cancellous bone, and a novel, beneficial, stimulatory effect on cortical bone.

Disclosures: **G. Stroup**, GlaxoSmithKline 3.

F242

Osteopetrosis in Oxidized LDL Receptor (SR-A) Knockout Mice. W. J. S. de Villier^{*1}, B. Garvy^{*2}, T. R. Nagy^{*3}, F. F. Safadi⁴, H. H. Malluche¹, M. C. Faugere^{*1}, J. P. Williams¹. ¹Internal Medicine, University of Kentucky, Lexington, KY, USA, ²Microbiology and Immunology, University of Kentucky, Lexington, KY, USA, ³Nutrition Sciences, University of Alabama at Birmingham, Birmingham, AL, USA, ⁴Anatomy and Cell Biology, Temple University School of Medicine, Philadelphia, PA, USA.

The Class A Scavenger Receptor (SR-A), or oxidized low density lipoprotein (LDL) receptor, is predominantly expressed by macrophages and is primarily involved in uptake of oxidized LDL. SR-A is also important in macrophage attachment which is mediated via a G protein coupled mechanism. Osteoclasts are monocyte/macrophage derived and disruption of cell attachment inhibits osteoclast development, therefore we evaluated the effect of SR-A deletion on bone remodeling. All comparisons reported are for animals at 4 weeks of age. SR-AI/II was eliminated by homologous recombination on a 129SvJ background. Knockout (KO) animals are larger than wildtype (WT). WT females average 11.2 +/- 0.9 g, while the KOs weigh 20.8 +/- 0.4 g. Body composition analyses were performed with a GE-Lunar PIXImus densitometer. Total lean and fat body mass were greater in KO animals for both sexes, but there was no significant difference in the percentage of lean and fat body mass between WT and KO, indicating that the KO animals are proportionally larger. However, bone mineral density (BMD) and content (BMC) are both significantly greater in the KO compared to WT animals (p< .0002 and p< .002, respectively). MicroCT analysis (Scanco) confirmed that total volume, bone volume as well as trabecular number and thickness were all significantly greater in KO mice. Furthermore, as expected with the increased bone volume, trabecular separation was greater in WT mice. Histomorphometric analysis of cellular and dynamic parameters of bone from KO and WT mice were measured at standardized sites under the growth plate in the femoral metaphysis using the semi-automatic method (Osteoplan II, Kontron, Munich). Analysis indicates a complex phenotype with a hypertrophied growth plate and a trend toward increased adiposity in the bone marrow of KO animals (p< .07). Significantly, there was also an approximate 50% reduction in osteoclast number compared to the WT mice that was independent of sex. Furthermore, there were no differences in osteoblast number or surface area between male and female WT and KO animals. In vitro osteoclast differentiation experiments with marrow macrophages from WT and KOs were problematic due to poor cell attachment of the KO derived macrophages. The phenotype observed upon deletion of the macrophage oxidized LDL receptor (SR-A) suggests novel roles for this receptor protein in animal growth/development and bone remodeling.

Disclosures: **J.P. Williams**, None.

F244

Syk, Src and avb3 Integrin Form a Complex Which Regulates the Osteoclast Cytoskeleton. W. Zou, H. Kitaura, Y. Liu*, F. P. Ross, S. L. Teitelbaum. Department of Pathology, Washington University School of Medicine, St. Louis, MO, USA.

$\alpha_v\beta_3$ integrin engagement in the osteoclast leads to cytoskeletal reorganization and activates a signaling cascade critical for bone resorption. c-Src transduces $\alpha_v\beta_3$ signaling and is essential for actin-ring formation and bone resorption, but the potential role of another non-receptor tyrosine kinase, Syk, has not been elucidated. We find that Syk deficiency does not affect osteoclast differentiation but disrupts the cytoskeleton, as formation of actin rings and bone resorption are completely arrested when the cells are maintained on dentin. These defects are normalized by retroviral-mediated Syk expression in Syk^{-/-} osteoclasts. We next asked if Syk modulation of the osteoclast cytoskeleton involves c-Src and/or the $\alpha_v\beta_3$ integrin. In co-immunoprecipitation experiments, Syk and c-Src associate with each other and both bind the cytoplasmic tail of the β_3 integrin subunit in a matrix adhesion-dependent manner. Consistent with integrin modulation of the complex, association between Syk and c-Src in β_3 integrin^{-/-} osteoclasts is dramatically reduced as compared to wild type, although expression of these tyrosine kinases is unaltered. Further confirming the central role of the integrin, its reconstitution in β_3 ^{-/-} osteoclasts rescues Syk and c-Src association. Binding of c-Src to $\alpha_v\beta_3$ does not occur in Syk^{-/-} osteoclasts but conversely, Syk continues to associate with the integrin in c-Src^{-/-} osteoclasts. On the other hand, Src family inhibitors or the absence of c-Src in osteoclasts arrests $\alpha_v\beta_3$ -induced Syk phosphorylation and c-Src/Syk association. Finally, Syk activates Vav3, an event essential for integrin-mediated organization of the osteoclast cytoskeleton. These findings establish a model in which $\alpha_v\beta_3$ -mediated organization of osteoclast cytoskeleton involves recruitment of Syk to the activated integrin, leading to a tri-molecular complex involving $\alpha_v\beta_3$ and the two kinases. Activated c-Src phosphorylates Syk which, in turn, activates Vav3, the Rho-family guanine nucleotide exchange factor. Thus, Syk is critical for $\alpha_v\beta_3$ mediated signals which prompt cytoskeletal organization in the osteoclast.

Disclosures: **W. Zou, None.**

F247

Marrow Stromal Cells Modulate the Contributions of Macrophages and T-cells to TNF-alpha Induced Osteoclastogenesis *In Vivo*. H. Kitaura, S. Wei*, P. Zhou, S. Takeshita, H. Kim, D. V. Novack, F. P. Ross, S. L. Teitelbaum. Department of Pathology, Washington University School of Medicine, St. Louis, MO, USA.

Bone marrow macrophages (BMMs), stromal cells and T-cells participate in TNF-induced osteoclastogenesis and therefore, the periarticular osteolysis attending inflammatory arthritis. Hence, our purpose was to determine the in vivo contribution of each cell type, as a direct or indirect TNF target, in the osteoclastogenic process. To this end we first generated chimeric mice using wild type (WT) or TNF receptor deficient (TNFR^{-/-}) marrow, both immunodepleted of T-cells and stromal cells. Following lethal irradiation of WT or TNFR^{-/-} mice to eliminate native marrow while retaining native stromal cells, the animals were reciprocally transplanted with the BMM-containing samples (i.e. WT > TNFR^{-/-}; TNFR^{-/-} > WT). As controls, similarly-treated WT marrow was transplanted into WT mice (WT > WT) and TNFR^{-/-} marrow into TNFR^{-/-} mice (TNFR^{-/-} > TNFR^{-/-}). Each group was administered increasing doses of TNF. The number of osteoclast was increased in a dose dependent manner. The number of osteoclasts in TNFR^{-/-} > WT is less than WT > WT chimeras confirming that TNF directly induces BMMs to undergo osteoclast differentiation. However, the reduction of osteoclast number in TNFR^{-/-} > WT is less than in WT > TNFR^{-/-} indicating that while both BMMs and stromal cells participate as direct cytokine targets in TNF-induced osteoclastogenesis, stromal cells are dominant. TNF increases the number of BMMs in TNFR^{-/-} > WT and WT > WT but not WT > TNFR^{-/-} mice. This suggests that the mechanism by which stromal cells mediate inflammatory osteoclastogenesis involves M-CSF. Confirming this hypothesis, administration of a mAb to the M-CSF receptor, c-fms, completely blocks osteoclastogenesis and bone erosion induced by TNF administration or inflammatory arthritis. Documenting that T-cells participate in TNF-simulated bone resorption, injection of the cytokine into mice immunodepleted of these lymphocytes, blunts TNF's osteoclastogenic effect (p<.01). On the other hand, reconstituting naïve TNFR^{-/-} mice with purified WT T-cells does not increase osteoclast number in response to TNF. Thus while T-cells participate in TNF-induced osteoclastogenesis they are not direct targets of the cytokine. We conclude that marrow stromal cells are central to TNF-mediated osteoclast recruitment by modulating the contributions of osteoclast precursors and T-cells. Our data also establish M-CSF or its receptor as potential therapeutic targets in inflammatory osteolysis.

Disclosures: **H. Kitaura, None.**

F249

MCP-1 Induces Super Abundant NFATc1 Expression and Results in TRAP+ Multinuclear Cells with Calcitonin Receptor Expression, but these Fail to Resorb Bone and Are Not Osteoclasts. M. S. Kim*, C. J. Day*, C. L. Magno*, S. R. J. Stephens*, N. A. Morrison. School of Medical Science, Griffith University, Gold Coast, Australia.

Monocyte chemoattractant protein 1 (MCP-1) is a CC chemokine that is induced by RANKL in human osteoclasts. MCP-1 enhances osteoclast formation in the presence of RANKL. In the absence of RANKL, treatment of human monocytes with MCP-1 and M-CSF results in TRAP+ multinucleated cells that are positive for calcitonin receptor and a number of other osteoclast markers. These cells look like osteoclasts and express a large range of osteoclast marker genes including a much greater abundance of NFATc1 compared to authentic osteoclasts induced by RANKL. The purpose of this study was to investigate the pathways of action of MCP-1 in osteoclast formation using osteoclasts derived in vitro from human peripheral blood mononuclear cells (PBMC). Human osteoclasts differentiate from PBMC in the presence of RANKL and M-CSF. Osteoclast formation mediated by RANKL was inhibited by both p38MAPK and ERK1/2 antagonists (SB203580 and U0126, respectively). PBMC treated with RANKL and SB203580 were small with a 2-3 nuclei, whereas U0126 treatment resulted in mononuclear cells. In marked contrast, MCP-1 mediated formation of TRAP+ multinucleated cells was only suppressed by the ERK1/2 antagonist (U0126), while SB203580 had no effect. In the presence of RANKL, MCP-1 rescued osteoclast formation from suppression by SB203580 (the p38MAPK antagonist), but could not rescue the effects of U0126 (the ERK1/2 antagonist). These data show that the formation of authentic osteoclasts requires both the p38MAPK and ERK1/2 pathways, and that blockade of p38MAPK can be circumvented by MCP-1. Furthermore, the formation of TRAP+ multinuclear cells induced by MCP-1 requires only the ERK1/2 pathway. Excess NFATc1 (noted in MCP-1 treated cells), is not sufficient for the formation of bone resorbing osteoclasts, although it is associated with cells that have the appearance of osteoclasts and express many genes in common. Despite high NFATc1 mRNA and nuclear NFATc1, the MCP-1 induced TRAP+ multinucleated cells are negative for bone resorption and cannot be called osteoclasts. Therefore, high NFATc1 expression does not automatically make an osteoclast, but is associated with multinucleation and TRAP positive status but not bone resorption. We propose that the MCP-1 induced TRAP+ multinuclear cells represent an ERK1/2 dependent stage in osteoclast differentiation, after NFATc1 induction and cellular fusion, but prior to the development of bone resorption activity.

Disclosures: **M.S. Kim, None.**

F251

Interleukin (IL)-12 Mediates the Anti-Osteoclastogenic Effect of CpG-oligodeoxynucleotides. A. Amcheslavsky*, Z. Bar-Shavit. Experimental Medicine and Cancer Research, Hebrew University Faculty of Medicine, Jerusalem, Israel.

Bacterial DNA activates the innate immune system via interactions with Toll-like receptor 9 (TLR9). This receptor recognizes CpG-oligodeoxynucleotides (CpG-ODNs) mimicking the CpG dinucleotides in certain sequence contexts characterizing bacterial DNA. Pathogen-derived molecules which activate different TLRs on bone cells are considered responsible for bacteria-induced pathological bone loss. Most studies show increased osteoclast differentiation by TLR ligands. In recent years, however, it was found that activation of TLRs in early osteoclast precursors (OCPs) results in inhibition of RANKL-induced osteoclast differentiation. The objective of the present study is to identify the mechanism leading to this inhibitory effect of a TLR ligand. Since both RANKL-RANK and CpG-ODN-TLR9 interactions result in the synthesis of the pro-osteoclastogenic cytokine TNF- α , we hypothesized that CpG-ODN (but not RANKL) in addition induces the synthesis of an anti-osteoclastogenic factor. Control OCPs and cells treated with RANKL, CpG-ODN or their combination were studied using DNA arrays (GEArray Q Series Mouse NF- κ B Signaling Pathway Gene Array, MM-016, SuperArray). We found marked increase in the established osteoclastogenesis inhibitor IL-12 mRNA levels in OCPs treated with CpG-ODN and CpG-ODN+RANKL, but not in OCPs treated with RANKL alone. Detailed northern and western analyses confirmed that addition of CpG-ODN to OCPs induces an increase in IL-12 mRNA and protein levels. No such effect was observed with RANKL. Moreover, using ELISA we showed that IL-12 is released from OCPs in response to CpG-ODN (but not in response to RANKL). In correlation with these findings, IL-12 inhibited RANKL-induced osteoclast differentiation and specific anti-IL-12-antibodies inhibited the anti-osteoclastogenic effect of CpG-ODN. In conclusion, activation of TLR9 by its ligand, CpG-ODN, results in synthesis and release of IL-12 opposing RANKL-induced osteoclast differentiation.

Disclosures: **A. Amcheslavsky, None.**

F253

Placental Growth Factor Is a Positive Regulator of Bone Remodeling. L. Coenegrachts*, S. Torrekens*, R. Van Looveren*, P. Carmeliet*, R. Bouillon¹, G. Carmeliet¹. ¹Laboratory of Experimental Medicine and Endocrinology, KU Leuven, Leuven, Belgium, ²The Center for Transgene Technology and Gene Therapy, Flanders Interuniversity Institute for Biotechnology, K.U. Leuven, Leuven, Belgium.

Vascular endothelial growth factor (VEGF) is critical for bone development and fracture repair. Placental growth factor (PlGF), a VEGF homologue, was shown to be involved in bone loss associated with arthritis, suggesting a role in pathological bone

metabolism. Therefore, we investigated the role of PIGF in different models of remodeling comparing wild type (WT) and PIGF deficient (PIGF^{-/-}) mice. PIGF^{-/-} mice are viable, fertile and do not display any developmental abnormalities. However, with older age, bone turnover is decreased compared to WT mice, as evidenced by a significant decrease of the mineral apposition rate (MAR; -49%) and bone formation rate (BFR; -62%) in 20-week old mice, without manifest effect on bone mass. This is reflected by reduced serum osteocalcin levels (-40%) and urinary excretion of collagen cross-links (-15%). In addition, differentiation of osteoclasts and formation of osteoblast colony-forming units *in vitro* was significantly decreased in PIGF^{-/-} cultures. Secondly, four weeks of skeletal unloading by tail suspension -a model of low turnover rate- induced severe bone loss (-51% of trabecular bone volume (TBV); p<0.05) in 16-week old WT mice with manifest decrease in MAR (-56%) and BFR (-65%) (p<0.01). In contrast, PIGF^{-/-} mice showed a non-significant loss in TBV (-25%) without any changes in MAR and BFR. Thirdly, in the model of glucocorticoid induced osteoporosis, administration of prednisolone (2.1 mg/kg/d) during four weeks to 16-week old WT mice decreased TBV by 41% and trabecular density by 35% (pQCT analysis) (p<0.05). In PIGF^{-/-} mice only a 25% decrease of TBV and a 21% decrease in trabecular density was found. Furthermore, pregnancy followed by a lactation period of three weeks decreased trabecular density more in WT mice (-68%; p<0.001) than in PIGF^{-/-} mice (-47%; p<0.01). In addition, cortical thickness decreased only in WT mice (-10%; p<0.01), suggesting cortical resorption in WT but not in PIGF^{-/-} mice. Finally, when a high turnover rate was induced by ovariectomy, 10-week old WT and PIGF^{-/-} mice showed a similar decrease in trabecular density after two and four weeks. In conclusion, deficiency of PIGF results in low bone turnover due to decreased osteoclast formation and differentiation of osteoprogenitors. Consequently, decreased bone loss is observed in PIGF deficient mice in osteoporosis models with a low turnover rate.

Disclosures: **L. Coenegrachts, None.**

F258

DC-STAMP Is Essential for Cell-Cell Fusion of Macrophage Lineage Cells and Is Regulated by Ap-1 and NFAT. M. Yagi^{*1}, T. Miyamoto¹, N. Hosogane^{*1}, N. Fujita^{*1}, K. Morita^{*1}, K. Ninomiya^{*1}, T. Suzuki^{*1}, K. Matsuo², Y. Toyama^{*1}, T. Suda^{*3}. ¹Orthopaedics, Keio University School of Medicine, Tokyo, Japan, ²Microbiology and Immunology, Keio University School of Medicine, Tokyo, Japan, ³Cell Differentiation, Keio University School of Medicine, Tokyo, Japan.

DC-STAMP (Dendritic Cell Specific Transmembrane Protein) is a seven transmembrane protein, which is highly expressed in osteoclasts in the presence of M-CSF and RANKL. As we described last ASBMR meeting, multinucleated osteoclasts do not formed in DC-STAMP deficient mice, indicating that DC-STAMP is essential for osteoclast fusion. Here, we analyzed the function of DC-STAMP in macrophage fusion and how DC-STAMP is transcriptionally regulated in the macrophage and osteoclast lineages. Foreign body giant cells (FBGCs) are known to form via fusion of mononuclear precursors. In DC-STAMP deficient mice, formation of FBGCs in response to implants was abrogated. Furthermore, FBGC formation by macrophages was abrogated in cells derived from DC-STAMP deficient mice under all culture conditions tested, namely in the presence of IL-3 plus IL-4, GM-CSF plus IL-4, as well as GM-CSF plus RANKL. Therefore, DC-STAMP is essential for macrophage fusion as well. In order to analyze the regulation of DC-STAMP gene expression by transcriptional factors, we cloned 4-kb and 0.2-kb fragments of the 5' flanking region of DC-STAMP. RANKL, IL-3 plus IL-4 activated both of the DC-STAMP reporter constructs 10-fold higher than promoter-less control. Thus, the 0.2-kb promoter is sufficient for inducing DC-STAMP expression. The 0.2-kb promoter region of the mouse DC-STAMP gene contains two potential AP-1 sites and three putative NFAT binding sites. The promoter was activated by RANKL, IL-3 plus IL-4, or overexpression of c-Fos or NFAT. Consistently the construct containing mutated AP-1 or NFAT consensus binding sites were not activated in osteoclastogenesis and FBGC formation. Moreover, DC-STAMP was not induced in cells derived from c-Fos deficient mice even in the presence of M-CSF and RANKL. However, in contrast to the complete inhibition of osteoclastogenesis, FBGCs were formed in cells derived from c-Fos deficient mice. Thus, while c-Fos and NFAT are essential transcriptional factors for DC-STAMP expression during osteoclast formation, these transcriptional factors are not essential for FBGC formation, suggesting that other AP-1 family members might substitute for c-Fos in macrophages. These data demonstrate that DC-STAMP is essential for cell-cell fusion not only in osteoclastogenesis, but also in macrophage fusion. However, macrophage fusion appears less dependent on c-Fos and NFATc1 than osteoclast fusion.

Disclosures: **M. Yagi, None.**

F260

Highly Potent Analogs of 1 α ,25-Dihydroxy Vitamin D₃ Induce Osteoclastogenesis and Hypercalcemia in Osteopetrotic op/op Mice, but not in Osteoclast-Absent c-fos Deficient Mice. M. Sato^{*1}, Y. Nakamichi², N. Sato^{*3}, M. Nakamura⁴, T. Ninomiya^{*2}, H. Nakamura⁵, M. Shimizu^{*6}, H. Ozawa^{*2}, N. Takahashi², N. Udagawa⁴. ¹Graduate School of Oral Medicine, Matsumoto Dental Univ., Shiojiri, Japan, ²Institute for Oral Science, Matsumoto Dental Univ., Shiojiri, Japan, ³Department of Periodontology, Aichi Gakuin Univ., Nagoya, Japan, ⁴Biochemistry, Matsumoto Dental Univ., Shiojiri, Japan, ⁵Department of Oral Histology, Matsumoto Dental Univ., Shiojiri, Japan, ⁶Laboratory of Medical Chemistry, Tokyo Medical and Dental Univ., Tokyo, Japan.

2-methylene-19-nor-(20S)-1 α ,25-dihydroxyvitamin D₃ (2MD), an analog of 1 α ,25-dihydroxyvitamin D₃ (1,25D₃), has been shown to strongly induce bone formation both *in vitro* and *in vivo*. We have synthesized five new substituents at C-2 position of 2MD (2MD

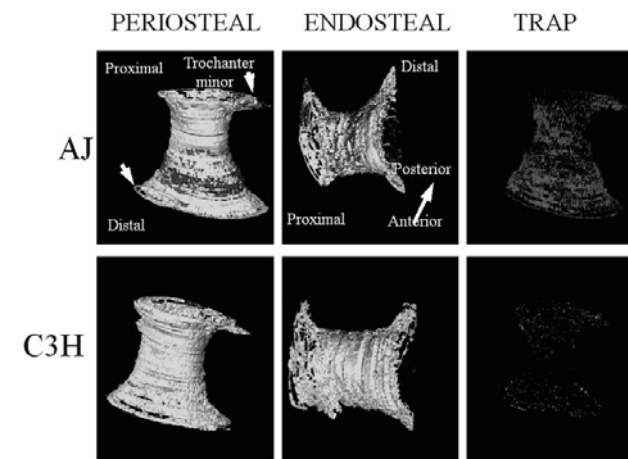
analogs) and five new 22-oxa compounds of these 2MD analogs (2MD 22-oxa analogs), and examined their activities in stimulation of osteoclastogenesis and induction of hypercalcemia. 2MD analogs were 100 times as potent as those of 1,25D₃ in stimulation of osteoclast formation *in vitro* and in induction of receptor activator of NF κ B ligand (RANKL), 25-hydroxyvitamin D₃-24 hydroxylase and osteopontin mRNA expression in osteoblasts in culture. The osteoclast inducing activities of 2MD 22-oxa analogs were much lower than those of 2MD analogs. Osteoprotegerin knockout (OPG^{-/-}) mice exhibited extremely high concentrations of serum RANKL. To evaluate the effects of 2MD analogs on serum RANKL levels, the same amounts of 2MD analogs and 1,25D₃ were daily administered into OPG^{-/-} mice for 2 days. Elevation of serum concentrations of RANKL and calcium was much greater in 2MD analog-treated mice than in 1,25D₃-treated mice. RANKL mRNA expression was increased in bone but not in thymus or spleen in both 2MD analog-treated and 1,25D₃-treated mice. Surprisingly, when 2 MD analogs were administered into macrophage colony-stimulating factor (M-CSF) deficient op/op mice, many osteoclasts appeared in bone tissues and hypercalcemia was induced in the mice with 2 days. In contrast, administration of 2MD analogs into c-fos deficient mice failed to induce osteoclastogenesis and hypercalcemia. These results suggest (1) that osteoclastic bone resorption is indispensable for hypercalcemic action of vitamin D₃, and (2) that 2MD analogs induce osteoclastogenesis even in the absence of M-CSF *in vivo*.

Disclosures: **M. Sato, None.**

F262

Genetic Variability in Osteoclast Activity and 3-Dimensional Spatial Distribution Within 14 Day Post Birth Femurs. S. Stapleton¹, D. Malouf^{*1}, D. Hindson^{*1}, K. J. Jepsen², C. Price², L. C. Gerstenfeld¹. ¹Orthopaedic Surgery, Boston University School of Medicine, Boston, MA, USA, ²Department of Orthopaedics, Mount Sinai School of Medicine, New York, NY, USA.

Numerous studies have shown that variation in bone morphology in different inbred strains of mice is genetically determined. The genetic variation is reflected in different rates of formation and resorption on endosteal vs. periosteal surfaces; the relative amount and location of cellular activities thus determining the relationship between bone size and the mechanical demands imposed by weight bearing during growth. A quantitative measure of osteoclast numbers and their 3-dimensional spatial distribution were assessed in A/J, C57BL/6J (B6), and C3H/HeJ (C3H) strains of mice. Transverse serial sections were taken at 100 micron increments along the length of femurs from 14 day mice and stained for osteoclast activity. Serial sections were arranged in stacks and the 3-D spatial distribution of osteoclasts within the femurs was reconstructed (AJ and C3H are presented). Renderings of the bone in differing longitudinal planes, or for TRAP activity alone, were examined. Moving distally along the femur revealed an approximate 50/50 distribution of TRAP staining on both endosteal and periosteal surfaces within AJ and B6 femurs, but no discernable pattern for C3H. The AJ strain, which has the smallest bone mass, had the highest level of TRAP activity with the majority of the enzyme activity seen either on the periosteal or opposing endosteal surfaces (compare the distribution of the pattern of dark grey coloring that denotes areas of TRAP activity). For the B6 strain, which had the next highest level, a pattern similar to AJ resulted, but with less staining visualized on the bone surfaces. Interestingly, this strain has the thinnest cortices and largest medullary space. TRAP staining in the C3H animals was almost unobservable when viewed in the reconstructions and this strain has both the thickest cortices and highest bone mass. These data demonstrate profound differences, in both the quantity and spatial characteristics of osteoclastic activities, in different strains of inbred mice. This suggested that both these features of cellular activity are relatable to spatial geometry and overall mass of a bone and are genetically regulated.



Disclosures: **S. Stapleton, None.**

F264

NF-κB p65 Subunit Is Critical for the Osteoclastogenic Effect of RANKL. C. Mena, A. Abdoulaziz*, J. Lebovitz*, C. Froelich*, S. Sprague. Medicine, Evanston Northwestern Healthcare, Evanston, IL, USA.

NF-κB is a key transcription factor in osteoclast (OC) biology and mediates the effect and the expression of major osteoclastogenic factors such as RANKL, IL-1, and TNF-α. However, the critical subunits involved in differentiation are not yet well defined. In mammals, NF-κB exists as homodimers and heterodimers composed of combinations of different subunits, NF-κB1 (p50/p105), NF-κB2 (p52/p100), p65, cRel, and RelB. The role of p50 and p52 in OC formation has been demonstrated *in vivo*. However, since these subunits are deficient in transcription activity, p65 or other subunits (RelB, c-Rel) should provide such a function and therefore, the p50 or p52 are necessary to form the complex resulting in nuclear DNA binding capacity. Last year, we presented studies which demonstrated that IκB mutant, that prevents nuclear translocation of p65 subunits, blocks OC formation. Therefore, the role of p65 in mediating the effect of RANKL in OC differentiation was now examined. Since p65 deletion gene is embryonic lethal, we developed OC precursors (RAW 264.7 cells) expressing a dominant negative c-terminal truncation of p65 (p65RHD) where amino acids (332-550) have been deleted. This mutant lacks the transactivation domain but retains the capacity of dimerization with other subunits and DNA binding as shown by gel shift assay and reporter gene using luciferase in response to RANKL and TNF-α. Furthermore, OC precursor stable cell line over-expressing the p65RHD is resistant to the development of mature OCs following RANKL stimulation compared to WT cells. Moreover, the addition of TAT-p65RHD to bone marrow cells stimulated with RANKL and M-CSF blocks OC formation in a dose dependent manner. This effect was not due to a blockade at the fusion step of OC precursors but rather to a deviation into OC differentiation as assessed by analyzing the expression of the OC markers, calcitonin receptor and β-integrin. Further analysis also demonstrated that the absence of p65 activity does not alter the OC precursor proliferation, RANK receptor expression or the capacity to respond to RANKL as measured by IκB degradation. In summary, these data demonstrate, for the first time, that p65 subunit is essential for OC differentiation. Thus, NF-κB activity requires either p65/p50 or p65/p52 as complex for successful osteoclastogenesis in response to RANKL. In conclusion, these results highlight the importance role of p65 as a key factor in NF-κB activity during bone resorption.

Disclosures: **C. Mena**, None.

F266

Col3.6 Promoter Drives the Expression of GFP in the Osteoclastic Lineage. I. Boban*¹, K. Prior*², C. Jacquin*², T. Barisic-Dujmovic*¹, S. H. Clark¹, H. L. Aguila². ¹Genetics and Developmental Biology, University of Connecticut Health Center, Farmington, CT, USA, ²Center for Immunotherapy, University of Connecticut Health Center, Farmington, CT, USA.

The type I collagen promoter has been used to develop transgene constructs that are useful to mark different stages of osteoblastic differentiation. The Col3.6 promoter has been shown to be active in preosteoblasts and osteoblasts. However, it is not specific for bone and can drive expression in other collagen producing cells. In contrast, expression from the Col2.3 promoter is restricted to osteoblasts and osteocytes. To evaluate the existence of circulating skeletal progenitor cells, a parabiosis model was developed in which Col3.6GFP transgenic mice were surgically joined with mice bearing a Col2.3 ΔTK transgene. After common circulation was established, parabiotic pairs were treated with ganciclovir (GCV). In single Col2.3 ΔTK mice this treatment induces ablation of osteoblasts and destruction of bone marrow (BM). However, in the Col2.3 ΔTK parabiont BM destruction was not observed suggesting a transfer of cells between parabionts. To evaluate the engraftment, stromal cell cultures were initiated with BM isolated from both parabionts. Cultures from Col2.3ΔTK parabionts did not display mineralized colonies co-expressing GFP suggesting that in this model, osteoblast progenitor cells did not circulate and engraft in the Col2.3 ΔTK parabiont. In contrast, scattered GFP positive clusters were observed that included large cells with morphology similar to osteoclast like cells (OCL). These OCL were also TRAP positive. As osteoclasts are of hematopoietic origin, purified hematopoietic stem cells were isolated from Col 3.6GFP mice. These purified cells (Lineage⁻ Sca-1⁺ c-kit⁺) were transplanted into GCV treated Col2.3ΔTK mice. Thirty days after transplantation, bone histology from these mice showed GFP positive cells around trabecular bone and on the endosteum and periosteum surfaces. Cultures of BM cells under osteoclast differentiation conditions showed OCL expressing GFP. To exclude the possibility that OCL were generated by fusion between GFP cells in the donor with osteoclast progenitors from the host, osteoclast progenitor cells [(B220, CD3, Mac-1)⁻ c-fms⁺] were purified from Col3.6GFP, Col2.3GFP and C57BL/6 mice and cultured under osteoclast differentiation conditions. OCL were generated in all the cultures, but only the OCL from Col3.6GFP mice were positive for GFP. Further RT-PCR showed that OCL did not express collagen, indicating that the Col3.6 promoter contains elements that are active during osteoclastogenesis. Thus caution should be used when utilizing this promoter in the study of mesenchymal progenitor cells.

Disclosures: **I. Boban**, None.

F270

Rac-2 Knockout Mice Have Increased Bone Mass and Osteoclasts with Reduced Resorptive Activity. T. Itokawa*, M. Zhu*, N. Troiano*, K. Insogna. Internal Medicine /Endocrinology, Yale University School of Medicine, New Haven, CT, USA.

Work from several laboratories has underscored the importance of the Rho family of small GTPases in regulating osteoclast motility and resorption. Recent work in macrophages has suggested a role for Rac-2 in targeting activated β-3 integrins in macrophages. To explore the potential role of Rac-2 in osteoclast biology we examined the bone phenotype of Rac-2 knockout mice. These mice, were of normal size and had normal tooth structure. However histomorphometric analysis (Table) demonstrated increased bone mass with normal to high-normal numbers of osteoclasts. Osteoblast number and function was normal. Increased bone density in the setting of high-normal osteoclast number and normal osteoblast function suggests defective osteoclast resorptive capacity as the basis for this skeletal abnormality. We examined the phenotypic appearance of isolated mature osteoclasts from Rac-2 wild-type mice and were unable to detect any differences in actin cytoskeletal architecture. Survival of mature osteoclasts prepared from wild-type and Rac-2 k/o mice was no different when cells were cultured in alpha MEM supplemented with 10% FCS. To quantify resorptive activity, mature osteoclasts were prepared by co-culturing osteoblasts and bone marrow from Rac-2 k/o mice on collagen gels and replating mature osteoclasts onto Osteologic® discs. Resorptive surface was quantified using Image J software. Basal resorptive activity was significantly attenuated in cells prepared from Rac-2 knockout mice. Specifically, the resorptive activity of Rac-2 k/o osteoclasts was reduced by 59% when compared to the resorptive activity of wild-type osteoclasts. We conclude that osteoclast function is defective in Rac-2 knockout mice resulting in an increased bone mass in these animals. Defective integrin targeting may be one mechanism for reduced resorptive activity of these cells.

	BV/TV	NOc/TAR	NOb/TAR	ObS/BS	OS/BS
Rac-2 k/o	25.6 ±2.02	130 ±24.4	901 ±151	16.9 ±2.70	25.6±7.5
Wild-type	19.5 ±0.72	99.6 ±14.3	791 ±58.0	17.1 ±0.96	19.0±2.68
p-value	0.05	NS	NS	NS	NS

Disclosures: **T. Itokawa**, None.

F275

Cloning and Characterization of the Annexin II Receptor. G. Lu¹, H. Maeda*², S. V. Reddy³, N. Kurihara¹, G. D. Roodman⁴. ¹Medicine/Hem-Onc, University of Pittsburgh, Pittsburgh, PA, USA, ²Oral Rehabilitation, Kyushu University Hospital, Kyushu, Japan, ³Dept. of Pediatrics, Medical University of South Carolina, Charleston, SC, USA, ⁴Medicine/Hem-Onc, University of Pittsburgh and VA Pittsburgh Healthcare System, Pittsburgh, PA, USA.

Annexin II (AX2) is a heterotetramer, consisting of two p11 and two p36 kDa subunits that is produced by osteoclasts (OCL) and increases OCL formation. AX2 indirectly stimulates OCL formation by inducing production of granulocyte-macrophage colony-stimulating factor (GM-CSF) and RANK ligand (RANKL). We have shown that biotinylated AX2 binds to normal primary human marrow stromal cells and the Paget's marrow-derived PSV10 stromal cell line. ¹²⁵I-labeled AX2 binding assays with PSV10 cells demonstrated that there was a single class of receptors with a K_d of 5.79 nM and B_{max} and 2.13 x 10⁵ receptors per cell. AX3 or AX5 did not bind the receptor. We then screened a human marrow cDNA expression library for a putative AX2 receptor since no annexin receptor had been previously identified. We identified a cDNA clone that encoded a 26-kDa protein that when expressed in HEK 293 cells, bound the p11 subunit to the cell surface. Further, chemical cross-linking (DTME) of biotinylated AX2 with intact PSV10 cells identified a 50 kDa band on Western blot analysis that reacted with both an anti-p11 antibody and streptavidin, but not an anti-p36 antibody. Western blot analysis of lysates from PSV 10 cells that had bound AX2 and been immunoprecipitated with an anti-p11 antibody detected a 26-kDa (without DTME) or a 50-kDa (with DTME) band respectively. When the putative AX2 receptor was over-expressed in HEK 293 cells and cell lysates immunoprecipitated with an anti-p11 antibody, similar results were observed. In addition, a rabbit polyclonal antibody raised against the putative AX2 receptor also recognized the 26-kDa protein band detected in PSV10 cells, as well as in HEK 293 cells transiently expressing the AX2 receptor cDNA clone. Further, treatment of human primary marrow stromal cells and marrow-derived PSV10 cells with the AX2 receptor antibody in the absence of AX2 modestly increased expression of GM-CSF and RANKL mRNA by RT-PCR in a dose-dependent manner. Importantly, the AX2 receptor antibody blocked the stimulatory effects of AX2 but not 1,25-(OH)₂D₃ on the OCL formation in human marrow culture in a dose-dependent manner. Thus we have identified the first surface receptor for an annexin and showed that it mediates the effects of AX2 on OCL formation. Identification of the AX2 receptor should permit further characterization of the role AX2 plays in normal and pathologic OCL formation and to identify small molecules that induce or block signaling by this receptor.

Disclosures: **G. Lu**, None.

F277

Delineation of TRAF2, 5, and 6 in RANKL Signaling and Osteoclastogenesis by the Use of Decoy Peptides. A. T. Poblentz^{*1}, S. Singh^{*2}, B. G. Darnay^{*1}. ¹Experimental Therapeutics, University of Texas M.D. Anderson Cancer Center, Houston, TX, USA, ²Imgenex Corporation, San Diego, CA, USA.

Osteoclastogenesis plays a central role in the development and maintenance of normal bone tissue, which requires osteoblastic matrix deposition and osteoclastic resorption to be closely coordinated. Interference with the process of osteoclastogenesis alters the kinetics of bone remodeling resulting in abnormal bone development. The osteoclast is the pivotal cell in the degradation of the bone matrix and stimulation of osteoclastic bone resorption is associated with a wide variety of human diseases. RANK and its ligand (RANKL) are essential mediators of osteoclastogenesis. RANK signals through TRAF molecules and activates the NF- κ B and MAP kinase pathways. We have previously identified a unique TRAF6-binding motif in RANK, which is distinct from other TRAFs. Furthermore, a peptide from RANK (residues 342-349) has been co-crystallized with the TRAF-C domain of TRAF6 and its structure indicates distinct molecular interactions. As TRAF6 is a critical adaptor molecule in RANK signal transduction, we previously developed cell-permeable TRAF6 decoy peptides (T6DP), which specifically target the interaction of TRAF6 with RANK and demonstrated that T6DPs inhibit RANKL-mediated signaling and osteoclast differentiation of RAW264.7 cells and primary mouse bone marrow derived monocytes (BMM). We earlier utilized a long leader peptide for the internalization of T6DP, since then we have employed the use of a palmitic acid linkage at the N-terminus of the peptides to allow for internalization. Through N- and C-terminal deletions, we have defined the sequence RKIPTDEY as a minimal scaffold for TRAF6 binding and inhibition of RANKL-mediated osteoclastogenesis. Furthermore, T6DPs effectively blocked activation of NF- κ B and JNK by RANKL. Additionally, we also demonstrated that TRAF6 is required in the first 24 hours of RANKL treatment for proper osteoclastogenesis. In an effort to identify the role of TRAF2 and TRAF5 in osteoclastogenesis, we utilized the same strategy as above and generated TRAF2/5 decoy peptides. Preliminary results indicate that blocking the interaction of TRAF2/5 with RANK had no effect on RANKL-mediated osteoclastogenesis. Thus, disruption of at least the TRAF6-RANK interaction may prove useful as a novel target for the development of therapeutic agents for osteolytic diseases.

Disclosures: **B.G. Darnay**, None.

F279

Cbl Downregulates Osteoclast Activity through Tyrosine Kinase-Binding Domain-Dependent Interactions. C. Itzstein¹, A. Sanjay², L. Neff^{*1}, W. Horne¹, R. Baron¹. ¹Yale University, New Haven, CT, USA, ²Temple University, Philadelphia, PA, USA.

Cbl is a major target of Src kinase in osteoclasts (OCs). Cbl^{-/-} OCs exhibit reduced *in vitro* and *in vivo* motility, and Cbl forms a tri-molecular complex with Pyk2 and Src downstream of integrins that is necessary for normal OC activity. Structurally, the N-terminal half of Cbl includes a phosphotyrosine-binding domain (designated TKB) and a RING domain required for the ubiquitin ligase activity of Cbl, while the C-terminal half contains several proline-rich motifs and regulatory tyrosines that interact with SH3 and SH2 protein-binding domains, respectively. Cbl downregulates non-receptor and receptor tyrosine kinases (N/RTKs), including Src and the EGF receptor (EGFR), interacting with them via its TKB domain and/or motifs in the C-terminal half. The contributions of these two interactions were analyzed by examining the effects of disabling or deleting Cbl binding domains on the association of Cbl with Src and the EGFR and also on *in vitro* bone resorption. HEK293 cells were co-transfected with constitutively active Src and myc-tagged 1/ wild-type (WT) Cbl, 2/ full-length Cbl with a disabled TKB domain (CblG306E), 3/ v-Cbl, which consists of only the TKB domain, 4/ v-CblG306E, 5/ 70Z-Cbl, which lacks ubiquitin ligase activity due to a deletion in the linker and RING domain, or 6/ the C-terminal half of Cbl (Cbl-CT), which lacks the TKB and RING domains. WT Cbl, v-Cbl, 70Z-Cbl and Cbl-CT all bound active Src, showing that both the TKB domain and C-terminal half motifs of Cbl independently mediate the Cbl-Src interaction. Despite the TKB-null mutation, CblG306E also bound Src, confirming that the Cbl-CT motifs are sufficient for binding. In contrast, v-CblG306E failed to bind Src, showing that phosphotyrosine-binding activity is required for the TKB domain-Src interaction. Similar results were obtained for Cbl binding to activated EGFR, confirming that N/RTKs interact with both regions of Cbl. To compare the roles of Cbl's binding domains in OC activity, the Cbl constructs were expressed in murine OCLs using the adenovirus system, and their effects on *in vitro* bone resorption was analyzed. WT Cbl, CblG306E, v-CblG306E and Cbl-CT had no effect on pit formation. In contrast, v-Cbl and 70Z-Cbl increased pit formation by 110% (p<0.05) and by 35% (p<0.05), respectively. Interestingly, v-Cbl, 70Z-Cbl and Cbl-CT all lack a functional RING domain, while only v-Cbl and 70Z-Cbl, which have functional TKB domains, stimulated bone resorption. Thus, the TKB-dependent targeting of the RING domain-dependent ubiquitin ligase activity of Cbl appears to be essential for a negative-feedback mechanism that decreases OC activity through down regulation of tyrosine kinases.

Disclosures: **C. Itzstein**, None.

F282

NEMO Integrates Cytokine-Induced Osteoclastogenesis. Y. Abu-Amer, S. Dai^{*}. Orthopaedics and Cell Biology & Physiology, Washington University School of Medicine, Saint Louis, MO, USA.

The transcription factor NF- κ B is considered central component mediating osteoclastogenesis and inflammatory responses that lead to bone erosion transmitted by RANKL and inflammatory cytokines, respectively. This notion is supported by the requirement of p50/p52 NF- κ B subunits for osteoclast formation. Initial RANKL binding to its cognate receptor triggers ample signaling events, notably recruitment of the adaptor protein TRAF6 and several tyrosine and serine/threonine kinase to RANK cytoplasmic domain. These steps are followed by series of constructive ubiquitination events culminating with poly-ubiquitination of I κ B Kinase- γ (also known as NEMO). NEMO is assumed to undergo polymerization and acts as a scaffold platform to recruit dimers of IKK α and IKK β to the kinase complex. This conformational proximity permits IKK cross-autophosphorylation leading to activation of the kinase complex, phosphorylation of the NF- κ B-inhibitory protein and activation of this transcription factor. We hypothesized that attenuation of NEMO oligomerization following cytokine stimulation of osteoclast precursors may disrupt formation of the IKK complex and thus inhibit basal (RANKL) and TNF-induced osteoclastogenesis. This hypothesis is supported by previous findings indicating that small decoy peptides targeting domain interaction between NEMO and IKK α/β successfully block osteoclastogenesis *in vitro* and focal bone erosion *in vivo*. In this study we utilized peptide sequences derived from the NEMO coiled-coil (CC2) and leucine zipper (LZ) domains, documented as the sequences required for NEMO oligomerization. These peptides were fused to PTD of HIV1-tat domain to enable cellular transduction. Using co-immunoprecipitation studies, we show that PTD-CC2 and PTD-LZ bind to NEMO. This interaction appears to destabilize NEMO as it degrades rapidly within one hour. Furthermore, we show that these NEMO-derived peptides attenuate activation of IKK β in a manner similar to that accomplished with NEMO-binding peptide. Most importantly, we provide evidence that PTD-CC2 and PTD-LZ are potent inhibitors of RANKL and TNF-induced osteoclastogenesis. In summary, it appears that NEMO-derived peptides designed to interfere with NEMO oligomerization, destabilize NEMO expression, attenuate cytokine-induced IKK β activation, and arrest osteoclastogenesis. Thus, NEMO-derived CC2 and LZ peptides provide a promising tool to inhibit osteoclastogenesis.

Disclosures: **Y. Abu-Amer**, None.

F286

Cx43-/floxOCN^{Cre} Mice Lacking Cx43 in Osteoblasts and Osteocytes Exhibit Normal Bone Accrual and Adult Peak Bone Mass. L. Plotkin, J. Aguirre, K. Vyas^{*}, S. Stewart^{*}, R. Weinstein, S. Manolagas, T. Bellido. Endocrinology, University of Arkansas for Medical Sciences, Little Rock, AR, USA.

Connexin (Cx) 43 is the major gap junction protein expressed in osteoblasts and osteocytes. Reduced Cx43 function in osteoblastic cells *in vitro* or its deletion in mice results in osteoblast dysfunction and delayed ossification. Furthermore, Cx43 expression and channels or hemichannels formed by Cx43 are required for at least some of the effects of bisphosphonates, PTH and mechanical stimulation on osteoblasts and osteocytes. Cx43 deletion in mice results in perinatal lethality precluding their study beyond birth. To determine the relevance of Cx43 function in osteoblastic cells in the adult skeleton, we generated mice deficient in Cx43 specifically in osteoblasts and osteocytes using the Cre/LoxP technology. Mice heterozygous for Cx43 (Cx43^{+/-}) were mated with mice expressing Cre recombinase driven by the human osteocalcin promoter (OCN^{Cre}). The resulting Cx43^{+/-};OCN^{Cre} were bred with mice expressing "floxed" Cx43 (fl). Calvaria cells derived from Cx43^{-/-};fl^{Cre} and Cx43^{-/-}fl expressed about 50% less Cx43 mRNA than Cx43^{+/+};fl^{Cre} or Cx43^{+/+}fl cells. In addition, 21 days of culture under differentiating conditions reduced Cx43 expression in Cx43^{-/-};fl^{Cre} calvaria cells to 20% of that of Cx43^{-/-}fl, whereas osteocalcin mRNA increased by 1,000 fold in both cell types. These results confirm the deletion of Cx43 by the Cre recombinase only in osteocalcin expressing cells. No differences were found in the weight of the animals or in the bone phenotype. Thus, global, spinal and hindlimb BMD measured by DEXA were similar in all four genotypes. This contrasts with previous evidence showing that Cx43^{-/-};fl^{Cre} mice in which Cre was driven by the murine osteocalcin promoter have lower global BMD compared to Cx43^{-/-}fl mice. In addition, we found no differences in vertebral bone geometry among animals of all genotypes. However, the femurs of Cx43^{-/-};fl^{Cre} mice had higher bone and bone marrow diameters at the midshaft and increased moment of inertia, but the cortical area was not different from Cx43^{-/-}fl mice. Thus, deletion of Cx43 in cells of the osteoblastic lineage does not affect bone accrual, suggesting that activation of Cx43 by endogenous ligands is not required to reach adult peak bone mass. However, these results do not exclude the possibility that Cx43 could be required for the maintenance of bone mass and strength under certain challenges, such as lack of mechanical stimulation or bisphosphonate administration.

Disclosures: **L. Plotkin**, None.

F289

Transgenic Expression of the Diphtheria Toxin Receptor, Otherwise Known as Heparin-Binding EGF-Like Growth Factor, in Osteoblasts and Osteocytes Reduces Bone Mass and Strength. C. A. O'Brien, Q. Fu, L. I. Plotkin, T. Bellido, J. J. Goellner*, R. L. Jilka, R. S. Weinstein, S. C. Manolagas. Endo/Metab, Center for Osteoporosis & Metabolic Bone Diseases, Central Arkansas Veterans Healthcare System, Univ. Arkansas for Med. Sciences, Little Rock, AR, USA.

The goal of these studies was to determine the role of apoptosis of mature osteoblasts and osteocytes in the control of bone mass and strength. To accomplish this, we sought to create a transgenic mouse in which these non-dividing cells can be specifically and conditionally ablated in vivo by administration of diphtheria toxin (DT). Wildtype mice are resistant to DT since the murine homologue of the primate diphtheria toxin receptor (DTR), also known as heparin-binding EGF-like growth factor (HB-EGF), does not effectively bind DT. Transgenic mice were created with a construct consisting of the monkey DTR inserted downstream from the human osteocalcin promoter (OCN). Nine transgenic founders were obtained and 7 of these were smaller than wildtype littermates and displayed abnormal or waddling gait. Three of these mice died after weaning. Three of the remaining mice were not fertile and had low BMD and shortened limbs. Two of the remaining lines were fertile and indistinguishable from wildtype littermates. Adherent bone marrow cells from these 2 lines were not sensitive to DT in vitro indicating that DTR expression in these mice was extremely low. The remaining affected founder was fertile and transgene mRNA was highly expressed and detected only in bone. Limbs in these mice were shorter than wildtype littermates and spinal and hindlimb BMD were reduced. Consistent with the low BMD, vertebral compression strength was reduced in transgenic mice compared to wildtype littermates. DT eliminated transgene mRNA expression in primary bone marrow cells from these mice indicating that DTR levels were sufficient to confer DT-induced cell death in this line of mice. Overexpression of the monkey DTR in the osteocyte cell line MLO-Y4 conferred sensitivity to DT, but also elevated apoptosis even in the absence of DT. The latter result suggests the possibility that the bone phenotype of the OCN-DTR mice involves an increase in apoptosis of osteoblasts and/or osteocytes. The presence of a bone phenotype in OCN-DTR mice in the absence of DT indicates that this approach is not suitable for studies requiring conditional ablation of mature osteoblasts and osteocytes. Use of inducible caspase 3 activation rather than DTR to induce cell death may circumvent the problems associated with OCN promoter-driven DTR expression. Nonetheless, these results demonstrate that HB-EGF is a negative regulator of bone mass and strength possibly via control of osteoblast and/or osteocyte survival.

Disclosures: **C.A. O'Brien**, None.

F293

Fracture Risk Assessment, Is T-Score Misleading? A. Hoiseth. Sentrum Røntgeninstitutt, Oslo, Norway.

T-scores give discordance in patient classification. Given a linear rate of bone loss and normally distributed parameters at all age groups, the proportion of cases below a given T-score is given by the ratio “rate of loss”/“range of dispersion at baseline”. This ratio for total spine BMD is, compared to the same ratio for total hip BMD, as 2.7 to 1. Thus, a substantially larger number of cases will be defined as having osteoporosis by spine BMD than by hip BMD. However, while the loss seems linear for hip BMD, spine BMD is curvilinear. Furthermore, the original Holgic reference values show an increased range of dispersion by age, indicating a between individuals non-linear rate of loss. Using total hip and -spine BMD measured in 38.840 females (mean age 61.6 years; range 10-95; SD 11.5), the actual age dependent variation in BMD was determined and the frequency of osteoporosis classification assessed. From the age of 47 years the rate of reduced total hip BMD was linear (~0.004g/cm²/year). In the spine it was linear between age 40 and 65 (~0.008 g/cm²/year). After age 65 there was an insignificant further loss. The SD of the dispersion was fairly constant in all age groups, but with a significant positive skewness for spine BMD after age 65 (skewness~0.8). At age 62 18% were classified as having osteoporosis by hip BMD and 32% by the spine; at age 67 the corresponding values were 22% and 43%; the difference between hip and spine was smaller at higher age, thus at age 77 the same values were 43% and 48% respectively. At age 67 years 41% were classified as having osteoporosis, 10% by both hip and spine BMD, 3% by hip BMD and 28% by spine BMD only. The same vales were 45%, 18%, 5% and 22% at age 77. In a subgroup of 8.307 patients with fracture history, risk ratios (RR) for having had more than 2 fractures was 2.8 for osteoporosis defined both by combined hip and spine and by hip only. RR was 2 for spine only. The RR for a hip fracture was 6.7 for hip BMD and 2.9 for spine BMD. RR for a spine fracture was 1.5 for hip BMD and 2 for spine BMD. In comparison, with a cut-off at Z-score -1 approximately 20% of patients were defined as having osteoporosis with a RR of at least 8 for hip fractures. Based on T-scores a substantial discordance between classification of osteoporosis was seen. Due to nonlinear age dependent reduction and a positive skewness of spine BMD, this discordance became less by age. However, as many as 50% of all may by time be defined as having osteoporosis and at age 70 spine BMD alone will account for more than 50% of the cases. Furthermore, a comparatively large number of low fracture risk patients seem to be defined as having osteoporosis by this approach. The T-score definition for osteoporosis may not give cost effective medical fracture intervention. It is suggested that the T-score should be replaced by the age adjusted Z-score.

Disclosures: **A. Hoiseth**, None.

F297

Bone Mineral Density (BMD) Predicts Incident Vertebral Fractures: Fifteen Years of Follow-Up. J. A. Cauley¹, L. Lui², L. Palermo², M. C. Hochberg³, K. E. Ensrud⁴, T. Hillier*⁵, S. R. Cummings⁶. ¹U of Pittsburgh, Pittsburgh, PA, USA, ²U of California, San Francisco, CA, USA, ³U of Maryland, Balitmore, MD, USA, ⁴VA Medical Center & U of Minnesota, Minneapolis, MN, USA, ⁵Kaiser Center for Health Research, Portland, OR, USA, ⁶UCSF & SFCC, CPMC Research Institute, San Francisco, CA, USA.

Low BMD predicts incident vertebral fractures over 4-5 years but the long term prediction of fractures is unknown. To test the hypothesis that low BMD predicts incident vertebral fractures over 15 years, we studied 2,680 Caucasian women age 65 years or older when they enrolled in the Study of Osteoporotic Fractures. All women had lateral lumbar and thoracic vertebral x-rays at baseline and an average of 15 years later. Using vertebral morphometry, anterior (Ha), posterior (Hp) and mid-vertebral height (Hm) were measured and 3 ratios formed (Ha/Hp; Hm/Hp, (Hp_(i)/Hp_(i-1)) and Ha_(i)/Ha_(i-1)), or (Hp_(i)/Hp_(i-1)) and Ha_(i)/Ha_(i-1))) > 3 SDs. Prevalent vertebral fractures were considered present at baseline if any ratio was > 3 SDs below the expected mean. Incident vertebral fractures were defined as ≥ 20% and at least 4mm decrease in vertebral height at any level. BMD was measured in the distal and proximal radius and calcaneus at baseline using single photon absorptiometry (Osteonalyzer). BMD of the proximal femur and lumbar spine was measured by DXA at the first follow-up visit 2 years later (Hologic, Inc). Logistic regression analysis was used to calculate the odds ratio (95% confidence intervals) of vertebral fracture per 1 standard deviation (SD) decrease in BMD after adjustment for baseline age and clinic. 492 (18.4%) of these women experienced an incident vertebral fracture during the 15-year follow-up. The odds ratios ranged from 1.46 to 2.16 for each SD decrease in BMD in prediction of incident vertebral fractures 15 years later (Table). There were no significant differences among BMD sites in the prediction of fracture. The association of low BMD and incident vertebral fracture was similar in women with and without a prevalent vertebral fracture at baseline (Table) and in women < age 70 vs. ≥ age 70 at baseline (data not shown). We conclude that a single measurement of BMD predicts vertebral fracture risk even after 15 years. Repeat BMD testing for the purpose of predicting vertebral fracture among women age 65 or older may not be indicated.

Table: Odds Ratio (95% CI) of vertebral fracture per 1 SD Decrease in BMD.

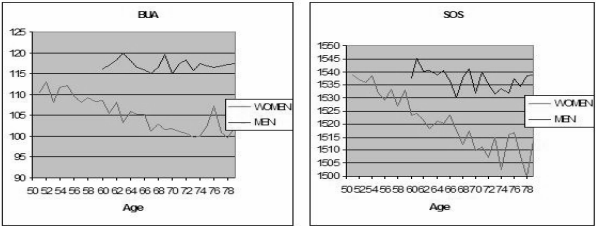
BMD Site	All Women (n=2,680)	Prevalent Vertebral Yes (n=394)	Fracture at Baseline No (N=2,286)
Calcaneus	1.74 (1.54, 1.96)	1.61 (1.26, 2.07)	1.58 (1.38, 1.82)
Distal Radius	1.58 (1.41, 1.77)	1.33 (1.07, 1.66)	1.52 (1.33, 1.74)
Proximal Radius	1.46 (1.31, .63)	1.41 (1.13, 1.76)	1.36 (1.20, 1.54)
Total Hip	1.83 (1.62, 2.07)	1.88 (1.45, 2.45)	1.60 (1.39, 1.84)
Femoral Neck	1.78 (1.57, 2.02)	1.51 (1.18, 1.92)	1.66 (1.44, 1.93)
Lumbar Spine	2.16 (1.89, 2.46)	1.96 (1.50, 2.55)	1.99 (1.71, 2.32)

Disclosures: **J.A. Cauley**, Merck 2, 8; Eli Lilly 2, 5; Pfizer 2, 5; Novartis 2, 5.

F301

Normative Data for Ultrasound Measurement of the Calcaneus within Italian Males and Females: The ESOPPO Study. S. Maggi*¹, M. Noale*¹, S. Adami², O. Di Munno*³, P. Filippini⁴, S. Giannini⁵, G. Isaia⁶, L. Sinigaglia*⁷, D. de Feo⁸, G. Crepaldi¹. ¹CNR Aging Center, Padova, Italy, ²Rheumatology, Valeggio Hospital, Verona, Italy, ³Rheumatology, Pisa University, Pisa, Italy, ⁴Internal Medicine, Umbertide Hospital, Perugia, Italy, ⁵Internal Medicine, Padova University, Padova, Italy, ⁶Internal Medicine, Torino University, Torino, Italy, ⁷Rheumatology, Gaetano Pini, Milano, Italy, ⁸Procter & Gamble, Rome, Italy.

The purpose of this study was to generate normative data for Italian females aged 40-79 and males aged 60-79 years participating in the Epidemiologic Study On the Prevalence of Osteoporosis (ESOPPO), using the Lunar Achilles Express (Lunar Co, Madison, USA). The ESOPPO is a cross-sectional study aiming at assessing risk of osteoporosis and fracture in a cohort of Italians, representative of the general population. The overall study population is represented by a random sample of 11,011 women and 4,981 men. All participants were administered a questionnaire on the most relevant risk factors for osteoporosis, that allowed us to apply the following exclusion criteria: corticosteroids use, menopause before the age of 45 years, ovariectomy, breast-feeding in the previous year, use of hormone replacement therapy, a previous osteoporotic fracture. Other information available included smoking status, BMI, wine and coffee consumption, physical exercise, daily calcium intake, weight at 25 years, family history of fracture, bed-ridden status for 2+ months, milk consumption up to 25 years, age at menarche, amenorrhea for 6+ months, drugs consumption, hysterectomy, estrogens use, abortions, pregnancy. Average decreases of 8 % in BUA (111 at 50 years of age vs 102 at 79 years) and 2% in SOS (1539 vs 1512) for females, while no significant changes with age in males have been detected. These data show lower values for women and a decline at a greater rate than in men.



Disclosures: **S. Maggi**, None.

F306

The Net Acid-Producing American Diet Adversely Affects Whole Body and Hip Bone Density Assessed Cross-Sectionally in Older Individuals. S. Perry^{*1}, F. A. Tyllavsky¹, K. A. Ryder^{*2}, J. Cauley³, J. Lee^{*4}, S. Pope^{*5}, T. Harris^{*6}, A. Sebastian^{*7}, D. E. Sellmeyer⁷. ¹Preventive Medicine, University of Tennessee Health Science Center, Memphis, TN, USA, ²Medicine, University of Tennessee Health Science Center, Memphis, TN, USA, ³Epidemiology, University of Pittsburgh, Pittsburgh, PA, USA, ⁴Epidemiology, University of North Carolina Chapel Hill, Chapel Hill, NC, USA, ⁵Epidemiology, University of Arkansas, Little Rock, AR, USA, ⁶Natioal Institute on Aging, Bethesda, MD, USA, ⁷University of California San Francisco, San Francisco, CA, USA.

Net dietary acid loads purportedly adversely affect skeletal health in older individuals. This study used nutrient data from a food frequency questionnaire (FFQ) to estimate renal net acid excretion (RNAE) an index of diet net acid load, and related it to systemic acid-base status and bone mineral density (BMD). We obtained values for dietary intake of kilocalories, protein, phosphorus, calcium, magnesium and potassium using an interviewer administered FFQ to participants in the Health Aging and Body Composition study. The community-based sample of 1520 comprised a majority of white (63.6%) and male (53.6%) participants, with a mean age of 73.5 years at baseline. We estimated RNAE dietary mineral and protein-sulfur intake and the net organic acid production (calculated from anthropometric data as urinary excretion of organic anions proportional to body surface area). We measured BMD of the whole body and hip by dual-energy X-ray absorptiometry (4500A, Hologic, Inc.) In multivariate regression analysis, BMD of both whole body and hip was associated negatively with RNAE/ kg of body weight, (p<0.0001). BMD declined with increasing values of RNAE; i.e, the greater the diet net acid load, the lower the BMD. By quartile of RNAE/kg of body weight:

	1 (Lowest)	2	3	4 (Highest)
¹ Whole Body BMD	1.112*	1.107*	1.097	1.082
¹ Total Hip BMD	0.910*	0.921*	0.900*	0.858
RNAE, meq/day	24.1	37.7	45.0	54.9

¹Adjusted for race, gender, clinical site, tobacco use, hypertension, diabetes, urine creatinine, estrogen use and kilocaloric intake. * p<0.0001 compared to highest quartile

We conclude that estimates of diet net acid load from anthropometric data plus FFQ-derived diet nutrient composition data predict the degree of diet-dependent metabolic acidosis and bone mineral density in a large scale epidemiological study of older Americans. The findings reveal that, in older Americans, greater diet net acid loads associate with greater degrees of metabolic acidosis and lower bone densities of whole body and hip. It remains undetermined whether losses of BMD in relation to the size of diet net acid load occur progressively over time.

Disclosures: *F.A. Tyllavsky, None.*

F309

Low Plasma Vitamin B12 Is Associated with Increased Hip Fracture Risk in Elderly Men and Women: The Framingham Study. R. R. McLean¹, P. F. Jacques^{*2}, J. Selhub^{*2}, L. Fredman^{*3}, E. J. Samelson⁴, D. P. Kiel⁴, L. A. Cupples^{*3}, M. T. Hannan⁴. ¹Hebrew SeniorLife, Boston, MA, USA, ²USDA HNRC, Tufts Univ, Boston, MA, USA, ³BU Sch of Public Health, Boston, MA, USA, ⁴Hebrew SeniorLife & Harv Med Sch, Boston, MA, USA.

Recent studies suggest plasma homocysteine concentration (tHcy) is associated with hip fracture (HFx) risk among elders. There is, however, little evidence that homocysteine directly affects bone and it has been hypothesized that tHcy may instead be a marker for the true causal factor. This factor may be low vitamin B12 which contributes to elevations in tHcy and is associated with bone density. We examined the association between plasma vitamin B12 concentration and HFx risk in men and women in the Framingham Study original cohort. Non-fasting blood samples were drawn from 375 men and 529 women (mean age 76 yr, range 67-96) in 1988-89 and plasma vitamin B12 (pmol/L) was measured by radioimmunoassay (RIA). Using the cutoff at which individuals are at a risk of vitamin B12 deficiency participants were classified as having normal (≥258 pmol/L) or low (<258 pmol/L) B12. Incident HFxs were ascertained from time of blood draw through December 2001. Sex- and age-adjusted incidence rates of HFx were calculated for B12 groups. Cox proportional hazards regression was used to calculate the hazard ratio (HR) and 95% confidence interval (CI) estimating the relative risk of HFx for low versus normal B12, adjusting for baseline measures: gender, age (yr), height (in), weight (lbs), smoking (cig/d), alcohol consumption (oz/wk), caffeine intake (>2 cup/d: y/n) and physical activity index. To determine any residual effect of B12 after accounting for any tHcy effect an additional regression was performed adjusting for tHcy status as defined by a common cut point for hyperhomocysteinemia (>14 μmol/L: y/n). The prevalence of low B12 was 41%. Mean follow-up time was 9.9 yr for the normal B12 group and 9.4 yr for the low B12 group, with 51 and 40 HFxs occurring for each group, respectively. Sex- and age-adjusted HFx incidence rates (95% CI) for the normal and low B12 groups were 9.1 (6.6, 11.6) and 12.5 (8.6, 16.4) per 1000 person-yrs, respectively. Participants with low B12 had a 39% multivariable adjusted increased risk of HFx compared to those with normal B12 (HR=1.39; 95% CI: 0.91, 2.13). After accounting for tHcy there remained a residual association between B12 and HFx (HR=1.29; 95% CI: 0.83, 1.99). Although neither effect measure was statistically significant, these findings suggest plasma vitamin B12 may be an independent and potentially modifiable risk factor for HFx among older persons. Further work is needed to evaluate how interrelations among components of homocysteine metabolism (including folate, vitamin B6) impact HFx.

Disclosures: *R.R. McLean, None.*

F313

Indications for VFA in Densitometry Patients. T. J. Vokes¹, D. Gillen^{*2}, J. Lovett^{*1}. ¹Medicine/Endocrinology, University of Chicago, Chicago, IL, USA, ²Department of Statistics, University of California, Irvine, Irvine, CA, USA.

Vertebral Fracture Assessment (VFA) is a new method for detecting vertebral fractures on the densitometer, usually performed with BMD measurement. It is presently unclear which patients should have VFA examination at the time of their densitometry visit. We evaluated the association of vertebral fractures seen on VFA with several factors (see table) associated with risk of vertebral fractures in population studies. 423 women aged 19-94 years (mean 64±13) who were referred for routine densitometry at the University of Chicago and agreed to participate in the study had VFA imaging and BMD measurement at the lumbar spine and the femoral neck using Prodigy (GE medical systems), and filled out an osteoporosis risk factors questionnaire. Presence of fractures was ascertained using Genant's semiquantitative method with the percent deformation confirmed using built in morphometry software. Fractures were present in 103 subjects (24%). The association of a given risk factor with probability of having a fracture was described using the relative risk of fracture as a summary measure. Confidence intervals and p-values for the relative risk were calculated based upon the normal approximation to the binomial distribution. Significant correlates of the risk of vertebral fracture in the sample included age greater than 65, self reported height loss > 4cm, history of peripheral osteoporotic fractures as an adult, and osteoporosis at hip or spine. History of steroid use was not found to be significantly associated with the risk of vertebral fracture. All of the factors noted above maintained a significant independent effect after adjustment for age. When 12 subjects with mild (grade 1) fractures or 49 women younger than 50 were excluded from the analysis the relative risk was numerically higher for all risk factors (data not shown). We conclude that the above risk factors, alone or in combination, may be reasonable indications to perform VFA in densitometry patients.

Risk factor	RR (95% CI)	p value	Frequ. in F (sensitivity)	Frequ. in N (specificity)
Age>65	2.99 (1.99-4.50)	<0.001	78/103 (76%)	138/320 (57%)
Height loss >4cm	2.86 (1.66-4.93)	<0.001	34/73 (47%)	60/257 (77%)
Peripheral Fx	1.7 (1.20-2.40)	0.003	41/96 (43%)	84/314 (73%)
T-score<-2.5 at hip	2.0 (1.40-2.87)	<0.001	63/99 (64%)	131/317 (59%)
T-score<-2.5 at spine	1.44 (1.03-2.01)	0.035	46/102 (45%)	107/319 (66%)
Steroid use	1.36 (0.87-2.13)	0.192	16/101 (16%)	41/319 (87%)
Any risk factor	6.16 (2-18.85)	<0.001	100/103 (97%)	257/320 (20%)

F- patients with vertebral fracture; N- no vertebral fractures

Disclosures: *T.J. Vokes, Merck 2, 8; Aventis 8.*

F315

Do Prevalent Radiographic Vertebral Fractures and prior Non-Spine Fractures Continue to Confer an Increased Risk of Incident Hip Fracture after 10 Years of Follow-Up? J. T. Schousboe¹, H. A. Fink², L. Lui^{*3}, B. C. Taylor², M. C. Nevitt³, K. E. Ensrud². ¹Park Nicollet Clinic & University of Minnesota, Minneapolis, MN, USA, ²VAMC & University of Minnesota, Minneapolis, MN, USA, ³SOF Coordinating Center, UCSF, San Francisco, CA, USA.

While a history of prior fractures is an independent predictor of incident hip fracture (HF), it is unclear whether this is so for prior fractures that occurred in the distant past. We used data from the Study of Osteoporotic Fractures (SOF), a large prospective cohort study of women age ≥ 65, to examine the associations of prevalent radiographic vertebral fractures (RVF) and self-reported prior non-spine fracture (NSF) ascertained at SOF exam 1 with incident HF occurring during three approximate follow-up time periods; 0-4 years after exam 1, 4-10 years after exam 1, and >10 years after exam 1. Cox regression was used to assess age-adjusted, age and hip BMD-adjusted, and multivariable-adjusted hazard ratios for incident HF in those with the predictor fracture (RVF or NSF) at baseline versus those without the predictor fracture at baseline. For each analysis, those with incident HF between exam 1 and the start of the follow-up period were excluded.

Table: Hazard Ratios (95% CI) for Incident HF Associated With Predictor Fracture^a by Follow-up Period

Predictor Fracture	Follow-up Period After Exam 1 (Number of Incident HF)		
	4 yrs ^b (102)	4 to 10 yrs ^c (328)	>10 yrs (317)
RVF at Exam 1	1.74 (1.13 - 2.69)	1.69 (1.33 - 2.15)	1.16 (0.88 - 1.53)
NSF Before Exam 1	1.46 (0.97 - 2.20)	1.28 (1.02 - 1.60)	1.20 (0.96 - 1.51)

^aAdjusted for age, hip BMD, body mass index, falls in the prior 12 months, walking speed; models with RVF as predictor also adjusted for history of HF prior to exam 1

^bMean follow-up time 3.7 years after exam 1

^cFollow-up period from mean 3.7 years after exam 1 to mean 10.2 years after exam 1

Prior self-reported NSF and prevalent RVF are associated with an increased risk of hip fracture for up to 10 years after ascertainment of NSF and RVF status, but these associations appear to wane with additional follow-up time beyond 10 years.

Disclosures: *J.T. Schousboe, Hologic, Inc. 2.*

F317

Osteoporosis Fractures and Costs by Race/Ethnicity and Gender in the USA. R. Burge^{*1}, A. King^{*1}, D. Solomon^{*2}, A. Tosteson^{*3}, J. Wong^{*4}, B. Dawson-Hughes⁵. ¹Proctor & Gamble, Cincinnati, OH, USA, ²Brigham & Women's Hospital, Boston, MA, USA, ³Dartmouth College, Lebanon, NH, USA, ⁴Tufts Univ-NEMC, Boston, MA, USA, ⁵Tufts University, Boston, MA, USA.

Osteoporosis leads to increased fracture risk throughout the skeleton. The disease has been thoroughly studied in white women but not across race/ethnicity groups and for men. The aim was to estimate osteoporosis fracture incidence and costs by race/ethnicity and gender in the USA. A Markov model of the natural history of osteoporosis was used to estimate fractures & costs in 2005 for men and women aged 50-99 years, by race/ethnicity (U.S. Census Bureau categories: White, Black, Hispanic, Other [Asian/Pacific Islander, Native American, other]). Hip fracture incidence rates were calculated from national hospital discharge data; clinical incidence rates for all other fracture types were obtained from published data. Mean costs per fracture were based on hospital discharge data analyses & estimates from the literature. Annual fractures & costs by race/ethnicity and gender were projected to 2025, & were based on population estimates. Predicted total incident fractures in 2005 were over 2.05 mil., and costs were \$16.9 bil. Whites accounted for 86% of fractures and 88% of costs. Fracture incidence per 10,000 (age 50-99), by race/ethnicity, was 260, 127, 160, and 165 for White, Black, Hispanic, and Other populations, respectively. Women incurred 71% of total fractures, with an incidence of 342 per 10,000; men had an incidence rate of 170 per 10,000.

Race	2005		2025	
	Fx (000s) (%)	\$ Costs M (%)	Fx (000s) (%)	\$ Costs M (%)
White	1,768 (86)	14,951 (88)	2,399 (79)	20,547 (81)
Non-White	283 (14)	1,964 (12)	637 (21)	4,721 (19)
Black	107 (5)	709 (4)	185 (6)	1,268 (5)
Hisp	103 (5)	754 (4)	268 (9)	2,071 (8)
Other	72 (4)	502 (3)	185 (6)	1,381 (5)
Gender				
Female	1,456 (71)	12,797 (76)	2,110 (70)	18,571 (73)
Male	595 (29)	4,119 (24)	925 (30)	6,698 (27)
Total	2,050	16,915	3,036	25,268

Assuming constant treatment patterns, total incident fractures are predicted to increase by 48% to over 3 million by 2025. Shares of annual fractures & costs for Black, Hispanic and Other grow to 21% and 19%, respectively. Hispanics have the highest fracture & costs in 2025 among these groups. The most rapid growth in fractures & costs (2005-2025) is projected for Hispanics (175%) and the Other race/ethnicity group (175%). The proportion of fractures & costs in 2025 for men rises slightly to 30% & 27%, respectively. Over 2 million clinical fractures with costs over \$16.9 B are predicted for 2005. By 2025, fracture incidence is expected to rise dramatically among Black, Hispanic and Other populations, especially for Hispanic and Other. Diagnosis and treatment need to increase greatly to offset projected societal burden of osteoporosis in all segments of the aging population.

Disclosures: **B. Dawson-Hughes**, None.

F319

The Association of High Sensitivity C-Reactive Protein Levels with Fracture Risk in Postmenopausal Women: Geelong Osteoporosis Study. J. A. Pasco¹, M. A. Kotowicz¹, M. J. Henry^{*1}, H. Spilbury^{*2}, G. C. Nicholson¹, J. Box^{*2}, H. G. Schneider². ¹Clinical & Biomedical Sciences: Barwon Health, The University of Melbourne, Geelong, Australia, ²Alfred Pathology Service, Prahran, Australia.

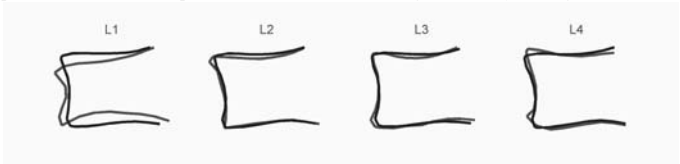
Reduced bone mass and increased risk of fracture are common among patients with inflammatory diseases. Furthermore, mediators of inflammation like IL-6 or TNF α have been shown to stimulate bone resorption. Systemic inflammation may be implicated in the pathophysiology of osteoporosis. We therefore tested the association between serum high sensitivity C-reactive protein (hsCRP) levels and risk of fracture in 744 postmenopausal women randomly-selected from the community and enrolled in the Geelong Osteoporosis Study, 1994-7. Baseline hsCRP levels were measured using a high-sensitivity immunoturbimetric assay; BMD was also measured at baseline. Fractures were identified from radiological reports. Subjects were followed longitudinally until the end of 2002, or until sustaining a fracture, death, or migration from the study region. Multivariable Cox proportional hazards regression was used to determine the association between hsCRP and fracture. 126 fractures were sustained during 4013 person-years of follow-up. Median hsCRP concentration was 2.5 mg/L (IQR 1.3-4.9). After adjusting for potential confounders, women with hsCRP in the highest quartile (≥ 4.9 mg/L) had a 1.6-fold (95%CI 1.1-2.4) greater risk of fracture than the lower quartiles pooled, independent of BMD. Both increased hsCRP and increased bone deficits contributed to increased fracture risk. Using hsCRP quartiles 1-3 and normal hip BMD (T-score > -1.0) as the referent group, women in the highest hsCRP quartile and with low BMD (T-score < -2.5) had the highest adjusted fracture risk (RR=9.1; 95%CI 3.6-23). Elevating hsCRP from quartiles 1-3 into the highest quartile was equivalent to increasing the fracture risk normally associated with osteopenia to that of osteoporosis. A similar pattern was observed for BMD measured at the spine. Circulating hsCRP is an independent predictor of fracture risk in postmenopausal women. These results may implicate systemic inflammation as a factor in the pathophysiology of osteoporosis. hsCRP may be a useful assay to predict fracture risk in conjunction with BMD.

Disclosures: **J.A. Pasco**, None.

F321

Initial Experience with a New Computerized Method for Clinical Assessment of Vertebral Deformations. M. T. Lund^{*1}, L. B. Tankó², M. de Bruijne^{*1}, M. Nielsen^{*1}, C. Christiansen². ¹Technical University of Copenhagen, Copenhagen S, Denmark, ²Center for Clinical and Basic Research, Ballerup, Denmark.

Currently, the diagnosis of a vertebral fracture in clinical trials relies on a 20% decrease in body height of a vertebra as measured on digitized lateral X-rays. Due to the categorical nature of this study parameter, clinical trials continue to demand a large number of participants and long follow-up time. The aim of the present study was to obtain initial experience with a novel computerized technique taking into account morphometric alterations over the full shape of the vertebra. The proposed method incorporates two key features: 1) A measure of fracture is based on changes in the shape of the vertebral body 2) The changes are quantified with reference to a predicted normal shape of the respective vertebra, incorporating data on the biological variation of intact vertebrae. The present analysis was based on 91 randomly chosen radiographs of the lumbar spine (L1-L4). Radiographs were digitalized and subsequently annotated with pre-defined landmarks. The statistical models of the normal vertebral shape were derived from a dataset of unfractured vertebrae to predict the normal shape of one vertebra from the shape of adjacent vertebrae (regularized multiple linear regression/ridge regression). The regression model accurately predicts the shape of the intact vertebra. In 95 % of the cases was the prediction error $< 5\%$ of the mean vertebral height with an average prediction error of 2.7% (< 0.8 mm). The obtained prediction accuracy is close to the maximum that can be expected with the current model. The prediction error gives the deviation from the expected intact shape and can therefore be directly used to assess the degree of abnormality for each vertebra. Presence of fracture had a mean prediction error of 11.7%. An example of fracture with reference to predicted normal shape is shown in Figure 1. In conclusion, this novel computerized technique carries notable potentials for the quantitative monitoring of vertebral deformations. Accurate measures of the changes in vertebral shape might provide us with continuous measures of vertebral deformation, which in turn could decrease number of patients and/or follow-up time in clinical trials assessing the efficacy of drug candidates.



Disclosures: **M.T. Lund**, None.

F323

Large Scale Analysis of the VDR Translation Start Site Polymorphism and Fracture in Older Women. S. P. Moffett¹, J. M. Zmuda¹, J. A. Cauley¹, K. L. Stone², L. Lui², K. E. Ensrud³, T. A. Hillier⁴, M. C. Hochberg^{*5}, G. Peltz^{*6}, S. R. Cummings⁷. ¹Epidemiology, Univ of Pittsburgh, Pittsburgh, PA, USA, ²Univ of California, San Francisco, CA, USA, ³Veterans Affairs Med Center, Minneapolis, MN, USA, ⁴Kaiser Permanente Center for Health Research Northwest/Hawaii, Portland, OR, USA, ⁵Univ of Maryland School of Med, Baltimore, MD, USA, ⁶Roche Molecular Systems, Palo Alto, CA, USA, ⁷Epidemiology, California Pacific Med Center, Pittsburgh, PA, USA.

The Vitamin D Receptor (VDR) is a nuclear receptor that regulates bone formation and resorption. A common C to T polymorphism in exon 2 of the VDR gene introduces a translation start site and a protein that differs in length by 3 amino acids (T=427aa, C=424aa; rs10735810). We conducted genetic association analyses of this polymorphism, bone mineral density (BMD) and fracture in 6680 women aged ≥ 65 years. BMD was measured using single-photon (wrist) or dual-energy X-ray (hip, spine) absorptiometry. Incident fractures were confirmed by physician adjudication of radiology reports. There were 2,532 incident fractures (excluding vertebral and traumatic fractures) during 13.6 years of follow-up including 509 wrist and 703 hip fractures. While no association was found between the VDR start codon polymorphism and either hip or spine BMD, women with the C/C genotype had significantly lower distal radius BMD compared to those with the T/T genotype (CC=0.358, CT=0.361, TT=0.369, p-value=0.003), an association not altered by adjusting for potential confounders. The C/C genotype was also associated with increased risk of non-spine, non-traumatic fracture (RR: 1.18; 95% C.I.: 1.04, 1.33; p=0.009) and wrist fracture (RR: 1.33; 95% C.I.: 1.01, 1.75; p=0.04) compared to the T/T genotype in age-adjusted models. Further adjustments for potential confounding factors had little effect on these associations while adjustments for distal radius BMD only slightly attenuated the associations. The VDR start codon polymorphism was not associated with hip fracture (RR: 0.94; 95% C.I.: 0.76, 1.19; p=0.64). The population attributable risk (PAR) of the C/C genotype for incident fractures was 6.1%. The PAR for established risk factors for fracture were: low hip BMD (PAR=16.3%), maternal history of fracture (PAR=5.1%), low body weight (PAR=5.3%), corticosteroid use (PAR=1.3%), and smoking (PAR=1.6%). The common and potentially functional translation start site polymorphism in the VDR gene confers a modestly increased relative risk of fracture among older Caucasian American women. However, the high frequency of this variant translates to a population attributable risk that is similar to or greater than several established risk factors for fracture.

Disclosures: **S.P. Moffett**, None.

F325

Differences in Site-Specific Fracture Risk among Older Women with Discordant Results for Osteoporosis at Hip and Spine. H. Fink¹, S. Litwack-Harrison^{*2}, B. Taylor¹, K. Ensrud¹, J. Schousboe³, K. Stone², D. Black², S. Cummings². ¹VA Medical Center, Minneapolis, MN, USA, ²SF Coordinating Center, CPMC Research Institute and UCSF, SF, CA, USA, ³Park Nicollet Clinic, Minneapolis, MN, USA.

T-score values for BMD of the hip and spine often disagree. Specifically, some women have a T-score ≤ 2.5 at one site but not the other. The value of this pattern for future risk of fractures (fx) is not known. To describe the patterns of fx when hip and spine BMD T-scores differ, we analyzed data from the Study of Osteoporotic Fractures (SOF), a prospective cohort study of women aged ≥ 65 years. At the 2nd SOF exam, women underwent BMD measurement at both hip and spine by DEXA (QDR 1000, Hologic, Inc.). "Osteoporosis" was defined separately at the femoral neck (FN) and lumbar spine (LS) as T-score ≤ -2.5 . For the present analyses, the 7761 women ($>99\%$) who also provided prospective fracture follow-up data were categorized as osteoporotic at FN only (n=702), at LS only (n=1341), at both FN and LS (n=1225), or at neither site (n=4493). Incident hip fx occurring after the 2nd SOF exam were validated by x-ray reports. Incident radiographic spine fx were defined morphometrically by $\geq 20\%$ and at least 4 mm decrease in vertebral height at any level in women who completed spine films at the 3rd and 8th SOF exams (mean interval 11.3 yrs). After adjusting for age and weight, for each of these categories of osteoporosis we calculated hazard ratios (HR) for prediction of hip fractures, and odds ratios (OR) for prediction of incident spine fractures. Of 7761 women followed for hip fx, 832 (10.7%) experienced an incident hip fx during 11.2 years of follow-up. Of 2364 women with repeat spine films, 375 (15.9%) experienced an incident radiographic spine fx. Women with T-scores ≤ -2.5 at the FN, but not the LS, had a substantially increased risk of hip, but not vertebral fx. Conversely, those with T-scores ≤ -2.5 at the LS but not the hip had a substantially increased risk of vertebral, but not hip fx. Women who have T-scores ≤ -2.5 at both sites have a substantially increased risk of both types of fx.

Table 1. Risk of hip and vertebral fracture by pattern of BMD T-score

Osteoporosis (T ≤ -2.5) at:	BMD, mean g/ cm ² (SD)		Incident fx rate, n/ 1000 person-yr	Cumulative fx rate, n/ 1000 person-yr	Incident fx risk*	
	FN	Spine			Hip, OR (95%CI)	Spine, OR (95%CI)
FN only	.53 (.04)	.87 (.09)	23.7	14.4	3.0 (2.4-3.7)	1.5 (0.9-2.5)
LS only	.64 (.06)	.70 (.06)	7.6	21.5	1.2 (0.95-1.5)	2.8 (2.1-3.8)
FN and LS	.51 (.04)	.66 (.07)	21.3	27.9	2.8 (2.3-3.3)	4.0 (2.9-5.6)
Neither	.71 (.09)	.95 (.13)	6.1	9.2	1.0 (referent)	1.0 (referent)

*Adjusted for age and weight

We conclude, that with respect to hip and spine, BMD T-score ≤ -2.5 at one site but not the other increases risk of fracture at that site, but does not significantly increase risk of fracture at the other site.

Disclosures: **H. Fink**, None.

F327

Hip Fractures in Women - Secular Trends Over 30 Years. H. G. Ahlborg, O. Johnell, M. K. Karlsson. Department of Orthopaedics, Malmö, Sweden.

Osteoporosis and its consequence of hip fracture represent a major public health problem among elderly women. Although the incidence of hip fractures has been reported to dramatically increase worldwide during the last decades, its not clear whether these findings are the result of an increasing prevalence of osteoporosis and/or an increasing proportion of elderly women in the population. This study was designed to characterize secular trends in the incidence of hip fractures within a female population with a stable prevalence of osteoporosis during the last three decades (1). All hip fractures, which occurred in the female population of Malmö aged 50 years or older, in the time between 1967-68, 1974-75, 1980-85, 1987-95 and 1999-2001, were identified at the Department of Diagnostic Radiology and Department of Orthopaedics. Demographic data were drawn from the yearbook of Local Statistics, which includes the annually number of inhabitants in Malmö by gender and one-year age groups between 1967 and 2001. The incidence of hip fracture was calculated and expressed as the number of hip fractures per 10,000 women per year. In the calculation of the age-adjusted fracture incidence, age adjustment was done by direct standardisation with the mean population between 1967 and 2001 as the standard population. Time-trend analysis was done by linear regression analysis. During the 23-year observation period from 1967 to 2001, altogether 1,136,435 person-years were generated and 8,059 hip fractures were registered in the target population. The annual number of hip fractures increased by 132% from 189 in 1967 to 439 in 2001. As the number of women aged 50 years or more in the population only slightly increased during the observation period, the crude incidence of hip fractures increased by 110% from 40 in 1967 to 84 in 2001. The overall trend in crude incidence between 1967 and 2001 was increasing (1.58 per 10,000 women per year; 95 percent confidence interval, 1.17 to 1.99), whereas the age-adjusted incidence was found to be stable over the same period (0.22 per 10,000 women per year; 95 percent confidence interval, -0.16 to 0.60). When the trend in the age-adjusted incidence was compared to the trend in the crude incidence, it was estimated that the proportion of variance of the trend in the crude incidence explained by demographic changes in the population was 69 percent. These data suggests that the increased crude incidence of hip fractures in elderly women is more likely to be attributable to demographic changes in the population, than to secular deterioration in bone mineral density.

Reference: (1) Prevalence of Low Bone Mass in Women - Secular Trends Over 30 Years. H. G. Ahlborg, O. Johnell, T. L. N. Järvinen, M. K. Karlsson. *JBMR* 2004;19(suppl1):S49.

Disclosures: **H.G. Ahlborg**, None.

F331

5yr Outcomes of a Program Offering Routine Assessment and Treatment of Osteoporosis after Fracture in Patients Over 50yr: Refracture Rates and Mortality. A. R. McLellan¹, M. Fraser^{*1}, A. Reece^{*2}. ¹Division of Cardiovascular Sciences & Medicine, Western Infirmary, Glasgow, United Kingdom, ²Department of Orthopaedic Surgery, Western Infirmary, Glasgow, United Kingdom.

Although secondary prevention of fractures (fx) using treatments for osteoporosis is endorsed by national guidelines, this is seldom achieved. The Fracture Liaison Service (FLS) offers routine assessment & treatment, where necessary, for fx secondary prevention (FxSP) to all women & men ≥ 50 yr presenting to our orthopaedic and A&E services with a new fx at any site. We describe mortality after fx and the characteristics of those who refractured (refx) during the first 5yr of the FLS. Our aim is to inform progress in developing services to achieve optimal FxSP. In the first 5yr of the FLS, 6137 patients with 6755 fx (97% were non-vertebral fx) were offered assessment &/or treatment for FxSP; 79% accepted & 21% declined. 15.9% of 6137 patients died. Mortality increased with age, was higher in men (O.R.(95%CI).2.11(1.83to2.44) and was higher after fx of hip(2.7(1.81to2.60)) & humerus(1.30(1.03to1.64)) compared to fx of radius/ulna, ankle & hand/foot. Depending on the patients' health status and willingness to be assessed, the FLS triaged fx cases into 6 groups among which mortality ranged from 6.7% (in patients who were fully assessed incl.DXA) to 38.2% (in those who had been assessed previously, and were usually on treatment). The refx rate in the first 5yr, among the 6137 patients was 8.8%. Refx were commoner in women (9.5% v 6.1%) but were more rapid in men: by 1 month after fx, 12% of male refx v 6% of female refx had occurred(p=0.02). Those with refx were older (74.6 v 72yr) and had lower BMD (LS T-score(mean(SD),-2.34(1.34)v-1.95(1.39),p=0.0001). Refx rates varied from 6% after fx of ankle or hand/foot, to 14% after vertebral fx. 10% of those with hip fx sustained a refx. Refx risk increased with higher cumulative past fx history; for each past fx ≥ 50 yr, risk of refx increased by 1.62(1.43to1.82) (p=0.0001). 31% of refx in the first 5yr of the FLS occurred within 6 months of the original fx; it is doubtful if treatments for osteoporosis will have impacted on these early, non-vertebral refx. Routine delivery of interventions for FxSP can be achieved in patients with new fx through services such as the FLS: intervention requires participation of the patients but can be tailored to their health status. While deployment of treatments with proven efficacy in reducing the incidence of osteoporotic fx is an essential component of the interventions offered by the FLS, this in itself may not be sufficient; if early refx are to be prevented, it may also be necessary to address non-skeletal risk factors for fracture such as those that determine risk of falling.

Disclosures: **A.R. McLellan**, None.

F334

Rates of Fracture after Stroke in International Population-Based Cohorts. C. W. Shinoff^{*1}, S. Sidney^{*2}, O. Johnell^{*3}, S. C. Johnston^{*4}, T. P. van Staag^{*5}, C. Cooper^{*5}, H. E. Whitson^{*6}, K. W. Lyles^{*6}, S. R. Cummings¹. ¹San Francisco Coordinating Center, San Francisco, CA, USA, ²Kaiser Division of Research, Oakland, CA, USA, ³Department of Orthopaedics, Malmö University Hospital, Malmö, Sweden, ⁴University of California San Francisco, San Francisco, CA, USA, ⁵University of Southampton School of Medicine, Southampton, United Kingdom, ⁶Duke University and VA Medical Centers, Durham, NC, USA.

About 700,000 people have a first or recurrent stroke every year in the United States. There may be increased risk for hospitalized hip fracture after stroke, but the risk of other types of fracture is not known. The objective of this study was to estimate rates of non-spine fracture after stroke in population-based cohorts, stratified by age and gender. We analyzed data from four large populations: Northern California Kaiser-Permanente patients; Study of Osteoporotic Fractures (SOF) participants; Swedish National Registry; General Practice Research Database (GPRD) from the U.K. Complete data were available for fractures treated in ambulatory care. Each cohort was analyzed separately, for rates of hip and non-spine fracture, within 1 and 2 years of stroke. The number of stroke patients were: Kaiser, 11,286; SOF, 1,554; Sweden, 15,858; GPRD, 5,114. The fracture rates were highest among those aged 70 and over. In the Kaiser cohort, non-spine fracture incidence in the first year after stroke was: 5.1 per 100 person-years for women <70 years compared to 8.2 for women over 70 years. In those aged 70 and over, the fracture rates were higher in women than men.(TABLE) In the Kaiser cohort, the rate of post-stroke fracture among Caucasians was higher than in other race/ethnic groups. Among women, fractures occurred at higher rate during the first year after stroke. Risk of hip fracture in the first year after stroke in women was higher in the Swedish cohort (6.2 per 100 person-years) than in the other cohorts (Kaiser, 2.5; SOF, 1.7; GPRD, 1.4). The risk of fracture in the first year after stroke is very high, with rates of hip fracture greater than in any other defined clinical population. The rates of non-spine fracture among those age 70 and over were about 6 to 7 times higher than the annual rate in the general U.S. population over the age of 70 (1% women and .5% men). Strategies to reduce this risk should be developed.

Disclosures: **C.W. Shinoff**, None.

F338

Differences in Hip Bone Mineral Density and Body Composition in a Multi-Ethnic Cohort of Older Men. Y. Sheu^{*1}, J. M. Zmuda¹, J. A. Cauley^{*1}, C. H. Bunker^{*1}, A. L. Patrick^{*2}, V. W. Wheeler^{*2}, E. Barrett-Connor^{*3}, M. L. Stefanick^{*4}, H. A. Fink^{*5}, C. E. Lewis^{*6}, L. M. Marshall^{*7}, E. S. Orwoll^{*7}.

¹Department of Epidemiology, Graduate School of Public Health, University of Pittsburgh, Pittsburgh, PA, USA, ²The Tobago Health Studies Office, Scarborough, Trinidad and Tobago, ³University of California, San Diego, CA, USA, ⁴Stanford Center for Research and Disease Control, Palo Alto, CA, USA, ⁵VA Medical Center & University of Minnesota, Minneapolis, MN, USA, ⁶University of Alabama at Birmingham, Birmingham, AL, USA, ⁷Oregon Health & Sciences University, Portland, OR, USA.

Compared with women, little is known about osteoporosis in men, particularly among non-white men. Thus, we have begun to characterize ethnic differences in bone mineral density (BMD) and bone mineral apparent density (BMAD) in a multi-ethnic cohort of older men. We hypothesized that there are major ethnic differences in BMD and BMAD that are independent of ethnic differences in body size and composition. The sample consisted of 5,475 men aged 65 to 80 years (mean=71.5) from the Osteoporotic Fractures in Men (MrOS) and Tobago Bone Health Studies (4,584 Caucasians; 230 African Americans; 180 Asian Americans; and 481 Afro-Caribbeans). Femoral neck BMD and BMAD, total body fat mass, total body fat percentage and appendicular lean body mass were measured by dual-energy X-ray absorptiometry (Hologic QDR 4500). Body size, body composition, BMD and BMAD were significantly different across the ethnic groups (Table; all p<0.001). Height was greatest in Caucasians and lowest in Asians. Men of African origin had greater appendicular lean mass, BMD and BMAD compared with other ethnic groups. BMD and BMAD were 1 standard deviation (SD) greater in Afro-Caribbeans compared with Caucasians and Asians and 1/3 SD higher than in African Americans. BMD and BMAD differences were independent of differences in body size and body composition. Caucasian and Asian American men have considerably lower hip BMD and BMAD than men of African ancestry. These differences are not explained by ethnic differences in body size or body composition. Further studies are needed to identify the factors contributing to the ethnic differences in bone health among older men.

	Afro-Caribbean	African American	Caucasian	Asian
Height (cm) ^a	171.6 (6.3)	174.0 (7.2)	175.0 (6.5)	167.0 (5.9)
Body Fat (%) ^b	20.9 (6.1)	25.1 (5.5)	26.3 (5.4)	24.2 (4.8)
Appendicular Lean Mass (kg) ^b	28.8 (4.2)	26.7 (4.5)	24.6 (3.3)	23.0 (2.6)
BMD (g/cm ³) ^c	.92 (.14)	.87 (.15)	.79 (.13)	.80 (.11)
BMAD (g/cm ³) ^c	.17 (.03)	.16(.03)	.14 (.03)	.14 (.02)

Values are mean (SD). ^aAdjusted for age; ^bAdjusted for age, height; ^cAdjusted for age, height, total body lean and fat mass.

Disclosures: Y. Sheu, None.

F341

Characterization of Genomic Variation at the Wnt10b Locus: Novel Association of Wnt10b Genotypes with Bone Density in a Multi-Ethnic Sample of Older Men. J. I. Oakley¹, S. P. Moffett¹, L. M. Yerges^{*1}, C. S. Nestlerode^{*1}, V. W. Wheeler^{*2}, A. L. Patrick^{*2}, C. H. Bunker^{*1}, J. M. Zmuda¹. ¹Epidemiology, University of Pittsburgh, Pittsburgh, PA, USA, ²Tobago Health Studies Office, Scarborough, Trinidad and Tobago.

Wnts comprise a family of secreted growth factors that regulate developmental processes. Recently, activation of the Wnt signaling pathway by Wnt10b was shown to stimulate osteoblastogenesis and bone formation in transgenic mice. To further evaluate the role of Wnt10b in bone mass regulation in humans, we resequenced about 8 kb of the *Wnt10b* gene region including 2.5 kb upstream of the transcriptional start site, the 5' and 3' untranslated regions (UTRs), the entire coding sequence, most of the introns including a highly conserved region in intron 3, and ~1 kb downstream of the 3'UTR in 192 individuals (96 African, 96 Caucasian). We identified 26 single nucleotide polymorphisms (SNPs) in the Caucasian and 20 SNPs in the African samples for a total of 38 unique SNPs with minor allele frequency ≥0.01. The majority of the 38 SNPs (79%) were not present in NCBI dbSNP database (build 124) whereas 11 of the 19 SNPs reported in dbSNP (58%) were not confirmed by our analysis. We genotyped 7 of the 8 common SNPs across the *Wnt10b* gene region in 260 Caucasian and 1001 Afro-Caribbean men aged 40 years and older using the TaqMan genotyping platform. We analyzed the relationship between genotypes at these 7 polymorphic sites and whole body and proximal femur bone mineral density (BMD) measured by DXA. Among Caucasians, a T to G polymorphism in a predicted exon splice enhancer site in the 3' UTR was significantly associated with whole body BMD (GG=1.13±0.13; GT + TT=1.18±0.11; P=0.01). Hip BMD was also significantly associated with this polymorphism in Caucasians (GG=0.91±0.19; GT + TT=0.96±0.14; P=0.04). The GG genotype was less common among Afro-Caribbeans than Caucasians (2% vs. 16%), but also tended to be associated with lower whole body BMD in this population (GG=1.22 ±0.12; GT + TT=1.26±0.12; P=0.09). A synonymous G to A variant in a predicted exon splice enhancer site in exon 5 was also associated with whole body BMD among Caucasians (AA=1.14±0.13; GA + GG=1.18±0.11; P=0.01) but not among the Afro-Caribbeans (AA=1.25 ±0.12; GA + GG=1.26 ±0.12; P=0.40). The variant in the 3' UTR and the variant in exon 5 were in high linkage disequilibrium in both the Afro-Caribbean (D'=1.00) and Caucasian men (D'=0.992). The present analysis suggests that Wnt10b may be a novel genetic element in the regulation of BMD variation within and between ethnic groups.

Disclosures: J.I. Oakley, None.

F345

Beta Blockers Reduce the Prevalence of Fracture: Influence on Bone Mineral Density, Bone Geometry and Microarchitecture. N. Bonnet^{*1}, C. Gadois^{*1}, G. Lemineur^{*2}, E. Lespessailles¹, D. Courteix¹, L. Benhamou¹.

¹U658Inserm & ATOSEP, Université d'Orléans, ORLEANS, France, ²Medical imaging, D3A medical system, ORLEANS, France.

Animal data suggest that bone remodeling is under β-adrenergic control via the sympathetic nervous system. The purpose of this cross-sectional study was to assess the prevalence of non traumatic fractures in post-menopausal women under β blockers treatment, versus controls and to evaluate the BMD, bone geometry and trabecular bone microarchitecture. We evaluated the association between β blockers use and bone status in a post menopausal women population from the age of 41 to 96 (mean 65.2 ± 9.3). We have investigated a group of 944 women - 131 were taking β blockers. From the controls, we have extracted 252 age-matched women. Proximal femur DXA scans were analyzed using a hip analysis program (Hologic) to calculate the subperiosteal width, cortical thickness, bone cross-sectional area (CSA), bone cross-sectional moment of inertia, buckling ratio and section modulus (Z) at the neck and femoral shaft. Trabecular porosity was assessed by the technique described by Beck T.J. et al. (2000) at the neck region. Bone microarchitecture was investigated by fractal analysis of texture on calcaneus radiographs in a subgroup of 43 subjects. Vertebral fractures were diagnosed by vertebral deformity on radiographs. Fracture odds ratio under β blockers was 0.58 (95% CI, 0.12-0.70). β blockers use was associated with a higher BMD at the total hip (+3.7%, p < 0.05), neck (+5%, p < 0.05) and trochanter (+4.6%, p < 0.05). No significant difference was observed on L1-L4 BMD. Proximal femur scans revealed significantly higher CSA (+5.4%, p < 0.05), cortical thickness (+5.2%, p < 0.05) and lower trabecular porosity (-1.0%, p < 0.05), buckling ratio (-4.3%, p < 0.05) at the neck under β blockers. It was noticed that femoral shaft geometry did not significantly differ under β blockers. Medication use and lifestyle factors indicated no association between β blockers and smoking, alcohol use, physical activity, calcium supplementation, antidepressants, statins, corticosteroids and estrogen therapies. The Hmean parameter, was significantly higher in the β blockers group (0.625 versus 0.610 in controls, p<0.05), reflecting a better trabecular microarchitectural organization. Our data suggest that current use of β blockers is associated with a reduction of osteoporotic fractures, higher BMD, better femoral neck geometry. Furthermore, preliminary results suggest benefic effects of βblockers on trabecular micrarchitecture. β blockers are widely used for the management of cardiovascular diseases and may have the dual benefit of also reducing bone fragility.

Disclosures: N. Bonnet, None.

F347

Risk Factors for Falls in Older Adults with Diabetes. A. V. Schwartz¹, E. Vittinghoff^{*1}, D. E. Sellmeyer¹, N. De Rekeneire^{*2}, K. R. Feingold^{*1}, M. C. Nevitt¹, E. S. Strotmeyer³, H. E. Resnick^{*4}, R. L. Short^{*5}, J. A. Cauley¹, K. A. Faulkner³, S. R. Cummings⁶, T. B. Harris^{*2}. ¹Epidemiology and Biostatistics, UCSF, San Francisco, CA, USA, ²National Institute on Aging, Bethesda, MD, USA, ³University of Pittsburgh, Pittsburgh, PA, USA, ⁴Medstar Research Institute, Hyattsville, MD, USA, ⁵University of Tennessee, Memphis, TN, USA, ⁶California Pacific Medical Center, San Francisco, CA, USA.

Older adults with type 2 diabetes mellitus (DM) are more likely to fall but little is known about risk factors for falls in this population. We examined glycemic control and other risk factors for falls in older DM adults who participated in the Health, Aging, and Body Composition Study of 3,075 white and black, well-functioning men and women age 70-79 years. Of 2,940 participants with baseline data on DM, 719 (24%) participants had DM, defined by self-report, use of hypoglycemic medication, or an elevated fasting glucose (≥ 126 mg/dl) or 2-hour glucose (≥ 200 mg/dl). Hemoglobin A_{1c} (A1C) was measured at baseline (Y1) and Y4, vision (visual acuity, contrast sensitivity, stereopsis) at Y3, and peripheral nerve function (light touch discrimination, vibration threshold, peroneal nerve conduction velocity and amplitude) at Y4. Weight was measured annually. At baseline, mean weight was 80.7 kg (SD 14.9), mean A1C was 7.6% (SD 1.6), and 16% reported insulin use. Participants reported the number of falls in the previous year at each annual clinic visit. Falling was evaluated over five years of follow-up using ordinal logistic models. In unadjusted models, older age, weight loss, insulin use, reduced light touch discrimination, poor nerve conduction amplitude, poor visual acuity, and poor contrast sensitivity were associated with an increased fall risk. In models adjusted for age, gender, race, and variables in the table, the odds ratio (OR) for more frequent falls in those with poor glycemic control (A1C ≥ 9%) compared with A1C<9% was 1.36 (95% CI: 0.94, 1.99); older age, weight loss and poor nerve conduction amplitude were associated with increased fall risk (Table).

Adjusted OR for more frequent falls in older DM adults		
	OR	(95% CI)
A1C (≥9% vs <9%)	1.36	(0.94, 1.99)
Peroneal nerve stimulation amplitude (worst quartile vs all others)	1.50	(1.06, 2.11)
Contrast sensitivity (worst quartile vs all others)	1.38	(0.96, 1.99)
Insulin use (yes)	1.42	(0.99, 2.04)
Weight change: Stable weight (<2 kg/yr)	1.00	Reference
Weight loss (≥2 kg/yr)	1.44	(1.15, 1.81)
Weight gain (≥2 kg/yr)	1.17	(0.93, 1.47)

Our results suggest that poor glycemic control and its long-term complications (poor peripheral nerve function and vision) are associated with increased fall risk. Weight loss, a marker of frailty in the elderly, was a risk factor for falls even in this overweight population.

Disclosures: A.V. Schwartz, None.

F349

What Is the Optimal Level of Serum 25-Hydroxyvitamin D for Bone Health in Older People? Results from the Longitudinal Aging Study Amsterdam. P. Lips¹, S. M. F. Pluijm^{*2}, J. H. Smit^{*3}, N. M. van Schoor^{*3}.

¹Endocrinology, VU University Medical Center, Amsterdam, The Netherlands, ²Public Health, Erasmus University Medical Center, Rotterdam, The Netherlands, ³EMGO Institute, VU University Medical Center, Amsterdam, The Netherlands.

Vitamin D deficiency is common in the elderly. It causes secondary hyperparathyroidism, increased bone turnover and bone loss. Serum 25-hydroxyvitamin D (25(OH)D) may influence these variables up to a threshold concentration, which may be between 50 and 80 nmol/l. The aim of this study was to assess the threshold serum 25(OH)D with regard to serum parathyroid hormone (PTH) concentration, bone ultrasound parameters and bone turnover markers in the healthy elderly Dutch population. The study was done in the framework of the Longitudinal Aging Study Amsterdam (LASA), a longitudinal study in a representative sample of the older Dutch population. Blood and urine samples were obtained, and ultrasound measurements were performed in 1319 community-dwelling men (643) and women (676), aged 65 years and older on January 1, 1996. Serum 25(OH)D was measured by competitive protein binding assay. Serum PTH, serum osteocalcin and urinary deoxypyridinolin (DPD) were measured by radioimmunological methods. Ultrasound variables were measured in the heel with the CUBA Clinical instrument. Serum 25(OH)D was < 12.5 nmol/l in 1.6 %, < 25 nmol/l in 11.5 %, < 50 nmol/l in 48.4 %, < 75 nmol/l in 82.4 % and > 75 nmol/l in 17.6 % of the respondents. Mean serum PTH decreased gradually from 4.8 pmol/l when serum 25(OH)D < 12.5 nmol/l to 2.7 pmol/l when serum 25(OH)D > 75 nmol/l. This decrease was very significant up to the last step (50-75 vs > 75 nmol/l) after correction for age and sex. Serum osteocalcin decreased from 2.6 nmol/l when serum 25(OH)D < 12.5 nmol/l to 2.1 nmol/l when serum 25(OH)D > 75 nmol/l, but this decrease was not significant after correction for age and sex. Urinary deoxypyridinolin/creatinine decreased from 7.3 nmol/mmol when serum 25(OH)D < 12.5 nmol/l to 5.0 nmol/mmol when serum 25(OH)D > 75 nmol/l, being significant up till 25 nmol/l after correction for age and sex. Broadband ultrasound attenuation increased from 61.9 dB/MHz when serum 25(OH)D < 12.5 nmol/l to 74.8 dB/MHz when serum 25(OH)D > 75 nmol/l, but this was not significant after correction for age and sex. Speed of sound increased from 1603 m/s when serum 25(OH)D < 12.5 nmol/l to 1638 m/s when serum 25(OH)D > 75 nmol/l. This increase was significant up till 50 nmol/l after correction for age and sex. Results were similar in men and women. In conclusion, bone health in older men and women may improve when serum 25(OH)D is raised over 50 nmol/l, and probably even over 75 nmol/l.

Disclosures: **P. Lips**, Eli Lilly and Co 2, 5; Merck and Co 2, 5; Aventis 2; Wyeth 2, 5.

F351

Low Vitamin D Level as a Risk Factor for Fractures in Community-Dwelling Older People. N. M. Van Schoor^{*1}, S. M. F. Pluijm^{*2}, J. H. Smit^{*3}, N. Kuchuk^{*4}, P. Lips¹. ¹EMGO Institute, VU University Medical Center, Amsterdam, The Netherlands, ²Department of Public Health, Erasmus University Medical Center, Rotterdam, The Netherlands, ³Department of Sociology and Social Gerontology, Vrije Universiteit, Amsterdam, The Netherlands, ⁴Department of Endocrinology, VU University Medical Center, Amsterdam, The Netherlands.

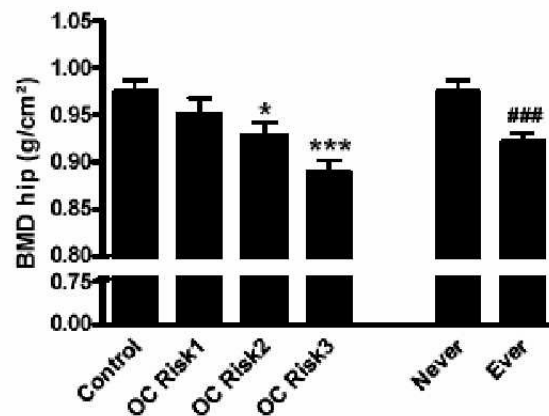
Vitamin D deficiency and insufficiency are very common in elderly people. The objective of this study is to examine whether a low vitamin D level is independently related to fractures. The study was conducted among 1320 community-dwelling older people (65 years or older on January 1, 1996) of the Longitudinal Aging Study Amsterdam (LASA). Serum 25(OH)D was measured by competitive protein binding assay in 1995/96. Fractures were prospectively assessed by a fall calendar between 1995/96 and 1998/99, and retrospectively between 1998/99 and 2001/02. Fractures were verified by the general practitioner or hospital. Of our population, 11.3% had a serum 25(OH)D below 25 nmol/l, and 48.4% had a value below 50 nmol/l. Furthermore, 132 persons (9.8%) had one or more fractures, of which 115 persons (8.5%) had one or more osteoporotic fractures (excluding head, foot, toe, hand and finger fractures, and fractures caused by traffic accidents). Different thresholds of serum 25(OH)D were examined with a threshold of 30 nmol/l giving the largest effects. Persons with a serum 25(OH)D equal to or below 30 nmol/l had a 1.69 times higher risk for osteoporotic fractures than persons with a value larger than 30 nmol/l (95% CI: 1.08-2.65). An interaction effect with age was found (p=0.02). Therefore, further results were presented separately for persons aged 65-75 years at baseline (n=656) and for persons aged 75-89 years at baseline (n=664). In the youngest age group, 8.2% had a serum 25(OH)D below 30 nmol/l (35.2% below 50 nmol/l) and 7.2% had one or more osteoporotic fractures. In the oldest age group, 27.0% had a serum 25(OH)D below 30 nmol/l (61.4% below 50 nmol/l) and 10.2% had one or more osteoporotic fractures. In the univariate analyses, a serum 25(OH)D equal to or below 30 nmol/l was significantly related to osteoporotic fractures (OR=3.45; 95% CI: 1.61-7.40) in the youngest age group, and not in the oldest age group (OR=1.09; 95% CI: 0.62-1.92). After adjustment for sex, body mass index and seven major chronic diseases, a serum 25(OH)D equal to or below 30 nmol/l was significantly related to osteoporotic fractures (OR=3.28; 95% BI: 1.41-7.62) in the youngest age group. In conclusion, in our study, a serum 25(OH)D below 30 nmol/l is a risk factor for osteoporotic fractures during six year of follow-up in persons aged 65-75 years at baseline, independent of sex, body mass index and chronic disease.

Disclosures: **N. M. Van Schoor**, None.

F353

Influence of Oral Contraceptive Use on Parameters of Bone Mass and Geometry in Young Women. M. Hartard¹, C. Kleinmond^{*1}, M. Wiseman^{*2}, E. R. Weissenbacher^{*3}, R. Erben⁴. ¹Faculty of Sport Science, AG-MSI, Technische Universitaet Muenchen, Munich, Germany, ²Leibniz Data Processing Center, Bavarian Academy of Sciences, Munich, Germany, ³Department of Gynecology and Obstetrics, Ludwig Maximilians Universitaet, Munich, Germany, ⁴Institute of Animal Physiology, Ludwig Maximilians Universitaet, Munich, Germany.

It was the aim of this retrospective analyze to examine the influences of low dosed oral contraceptives (OC) on parameters of bone mass and geometry in 261 young women aged 18 to 24 years. Hip (Fig.1) and lumbar spine bone mineral density (BMD) were evaluated by DXA (Norland XR 26 Mark II). Parameters of tibial bone mineral content (BMC), bone geometry and volumetric BMD were assessed by pQCT (XCT-2000 of STRATEC) at shank levels of 4% and 38%. The women were allocated into "Ever" (> 0.5 years OCuse) or "Never" OC users (<=0.5 years OCuse) and based on the results of multiple regression analysis we classified subjects into 4 groups: 1) subjects with 3 years after menarche (OC Risk1) 3) subjects with total OC use of > 2 years and start of OC use > 3 years after menarche, or total use of less than 2 years but start of OC use within 3 years after menarche, respectively (OC Risk2) and 4) women with total OC use for more than 2 years and OC initiation within 3 years after menarche (OC Risk 3). Statistical differences between 4 groups were evaluated by one-way analysis of variance (ANOVA), followed by Dunnett's multiple comparison test. An unpaired t-test was used between "Ever" and "Never" users. Women in the OC Risk 3 group were characterized by 9% lower hip areal BMD, 5% lower spine areal BMD, 5 - 6% lower distal tibial total and trabecular volumetric BMD, and 6% lower total BMC at the tibial shaft relative to control subjects (<= 6 months of OC use). In addition, women who had ever used OCs for more than 6 months had lower bone mass at the hip, distal tibia, and tibial shaft, despite similar height, weight, BMI, hours of exercise, and calcium intake compared with never users (<= 6 months of OC use). At the tibial shaft, OC use was associated with reduced periosteal apposition and medullary expansion. We conclude that OC use was associated with a decreased bone mass at all regions observed and obviously with influences on bone geometry of distal tibia in this group of young women.



Disclosures: **M. Hartard**, None.

F356

Prevalent Fractures, Low Bone Mineral Density and Ageing Are Associated with Greater Histomorphometric Indicators of Microdamage Accumulation in Postmenopausal Women. J. J. Stepan¹, D. B. Burr², I. Pavo³, A. Sipos³, D. Michalska^{*1}, J. Li², H. Petto^{*3}, M. Westmore², D. Michalsky^{*1}, M. Sato³, H. Dobnig⁴. ¹Department of Internal Medicine 3, Charles University, Faculty of Medicine, Prague, Czech Republic, ²Department of Anatomy and Cell Biology, Indiana University School of Medicine, Indianapolis, IN, USA, ³Lilly Research Laboratories, Indianapolis, IN, USA, ⁴Department of Internal Medicine, Medical University Graz, Graz, Austria.

This is the first exploratory investigation of the relationship between risk factors for fracture and microdamage accumulation in a clinical trial. We report baseline data from an ongoing open-label, uncontrolled two-center clinical trial. Sixty-six postmenopausal women with osteoporosis (mean age of 68.0 years, BMD T-score of -1.7 at total hip and -2.8 at lumbar spine; 62% with prevalent fractures) were recruited. Thirty-eight had been treated previously with alendronate (ALN) 10 mg/day-70 mg/week (mean duration 63.6 months) while twenty-eight were treatment naïve (TN). BMD, biochemical markers of bone turnover and transiliac bone biopsies (N=55) were analyzed at baseline. No overall differences in crack density (CrDn; ALN: 1.46 #/mm², 95%CI 0.8-2.1; TN: 0.95 #/mm², 95% CI 0.3-1.6, P=0.26) and crack surface density (Cr.S.Dn; ALN: 70.5 µm/mm², 95% CI 37-104; TN: 43.5 µm/mm², 95% CI 18-69, P=0.2) were detected between ALN and TN patients. The presence of prevalent fractures was significantly correlated with greater CrDn (r=0.30, P=0.025) and Cr.S.Dn (r=0.33, P=0.013). Among ALN patients, lower total hip BMD was associated with higher CrDn (r=-0.45, P=0.017) and Cr.S.Dn (r=-0.49, P=0.008) and increased age was also associated with higher CrDn (r=0.52, P=0.005) and Cr.S.Dn (r=0.52, P=0.005). These associations were not evident in TN subjects. We found no significant associations between biochemical and histomorphometric markers of bone

turnover and microdamage accumulation. Although patient demographics were similar, Cr.Dn and Cr.S.Dn were different between the two centers ($P<0.01$), apparently due to different techniques applied for bone biopsy sampling. At Center I ($N=41$) with lower values and variability, ALN patients had significantly more total microdamage (Cr.S.Dn of $44\text{ }\mu\text{m}/\text{mm}^2$, 95%CI 28-60) than TN patients ($25\text{ }\mu\text{m}/\text{mm}^2$, 95%CI 16-35, $P=0.046$). This difference remained significant after adjustment for age, prevalent fractures and total hip BMD ($P=0.031$). We conclude that increased microdamage accumulation occurs in older patients, those with low BMD and those with prevalent fractures. These associations appear more pronounced in ALN-treated patients. Microdamage characteristics may also depend on biopsy sampling technique.

Disclosures: **J.J. Stepan**, Eli Lilly & Co. 2, 8.

F358

Trans-Menopausal Changes in the Trabecular Bone Structure. **M. P. Akhter**, **B. L. McGuckin***, **T. D. Howard***, **S. P. Bare***, **K. M. Davies***, **J. M. Lappe**, **R. R. Recker**. Medicine, Creighton University, Omaha, NE, USA.

Post-menopausal osteoporosis is a disease of elderly women, that is characterized by atraumatic fractures of various skeletal sites. The overall hypothesis for this analysis is that the variables describing trabecular bone micro-architecture will be affected by change in hormonal status of women just prior to, and early after, last menses, and that volumetric bone mass, density, and trabecular structure will decline significantly. The study was designed to capture true longitudinal transmenopausal changes in three-dimensional (3D) trabecular bone architecture. Currently, minimal data exist regarding trabecular bone volumetric structure, mass, and density in human transilial bone biopsies that are obtained before and after menopause. Fifty-one transilial biopsies specimens were obtained on entry (pre-menopausal and >age 46), and at 12 months past the last menstrual period. Bone architecture was quantified using standard histomorphometric (histo) and micro-computed tomography (m-CT-40, Scanco) techniques. Embedded bone biopsies were scanned at 30-micron resolution such that the volume of interest was similar as in the two dimensional (2D) histomorphometric analyses. Simple regression analyses were done to determine the relationship between variables measured by 2D histo and 3D micro-CT. In addition, paired t-tests were used to compare pre- and post-menopausal bone structure data from each technique. There was good correlation between the structural variables measured by 2D histo and the 3D micro-CT. The correlation (r) ranged from 0.5 to 0.69 between the standard histo and the micro-CT measured variables (BV/TV, trabecular thickness and spacing). BV/TV showed highest correlation ($r=0.69$) between 2D histo and the 3D micro-CT. Most of the variables (from both histo and micro-CT) either showed the declining trends ($P=0.065$) (BV/TV histo) or were significantly decreased (BV/TV 3D micro-CT, trabecular number) in bone structure in post-menopausal women (Table). In addition, both trabecular spacing and the structure model index increased in the post-menopausal women suggesting the thinning of trabeculae (Table). These data suggest that 3D micro-CT measurements are comparable to standard histo measurements, and that most of the structural measurements are sensitive to hormonal status (pre- and post-menopausal) in women.

Trabecular Bone Structure			
Mean \pm SD	Pre	Post	
BV/TV % (2D Histo)	23.2 \pm 5.5	21.6 \pm 4.6 ^b	
BV/TV % (3D micro-CT)	28.3 \pm 7.1	24.9 \pm 7.4 ^a	
Trabecular number/mm (3D micro-CT)	1.8 \pm 0.4	1.7 \pm 0.2 ^a	
Trabecular spacing mm (3D micro-CT)	0.54 \pm 0.07	0.57 \pm 0.06 ^a	
Structure model index (3D micro-CT)	0.23 \pm 0.6	0.50 \pm 0.6 ^a	

^aP <0.05; ^b P <0.1 as compared to Pre by paired student's t test

Disclosures: **M.P. Akhter**, None.

F360

Non Invasive Measurement of Trabecular Architecture by 3D-pQCT Discriminates Osteopenic Women With and Without Fractures. **S. Boutroy***¹, **M. L. Bouxsein**², **F. Munoz***¹, **P. D. Delmas**¹. ¹INSERM Research Unit 403 and Claude Bernard University of Lyon, Lyon, France, ²Orthopedic Biomechanics Laboratory, Beth Israel Deaconess Medical, Boston, MA, USA.

Assessment of trabecular (Tb) architecture may enhance the prediction of fracture risk and improve monitoring of treatment response. A new high-resolution 3D-pQCT system permits *in vivo* assessment of Tb architecture and volumetric BMD (vBMD) at the distal radius and tibia with a voxel size of $82\text{ }\mu\text{m}^3$. Our aim was to evaluate the clinical performance of this 3D-pQCT system. We determined the short-term reproducibility (CV) of density and architecture parameters by measuring 8 healthy volunteers 3 times each. We also compared 3D-pQCT measurements in 108 healthy premenopausal (preM) and 148 postmenopausal (postM) women (w), classified by femoral neck or spine BMD as osteopenic (n=113) or osteoporotic (n=35). Furthermore, we compared DXA and 3D-pQCT values in postM osteopenic w with (n=42) and without prior fracture history (n=71). The precision of 3D-pQCT measurements was similar at both sites, with a CV of 0.5 to 1.3% for total, Tb and cortical vBMD, and 2.3 to 3.1% for Tb architecture. Bone density and architecture differed significantly between preM and postM w, and between postM osteopenic and osteoporotic w at both sites. For example, postM w had lower vBMD (11 to 37%), Tb number (12 to 23%) and cortical thickness (28 to 41%) and more heterogenous Tb distribution (53 to 83%) than preM w. Osteoporotic w had lower vBMD (5 to 18%), cortical thickness (15 to 18%) and Tb number (8.5 to 10%) than osteopenic w. Furthermore, although their spine and hip BMD did not differ, osteopenic w with a prior fracture history had lower total density, Tb density, number, separation and more heterogeneous Tb distribution at the radius compared to osteopenic w with no fracture history. There was no difference at the tibia between the two groups. In summary, 3D-pQCT is promising to assess Tb architecture at peripheral sites, with its excellent

reproducibility and ability to detect age- and disease-related changes. 3D-pQCT of the radius - but not hip and spine DXA - could differentiate osteopenic w with and without fracture history, suggesting that it might detect early architectural damage and therefore might be useful for assessing fracture risk in postM w. These preliminary and cross-sectional data should be validated prospectively.

Mean values at the distal radius of postmenopausal osteopenic women with and without history of fracture (mean \pm SD)

	Osteopenic women without fracture (n = 66)	Osteopenic women with fracture (n = 40)	p-value
Total density (mg HA/cm ³)	263 \pm 61	238 \pm 60	0.037
Cortical density (mg HA/cm ³)	813 \pm 80	789 \pm 81	ns
Trabecular density (mg HA/cm ³)	129 \pm 35	114 \pm 35	0.031
Trabecular number (mm ⁻¹)	1.49 \pm 0.28	1.37 \pm 0.29	0.046
Trabecular thickness (μm)	72 \pm 10	68 \pm 13	ns
Trabecular separation (μm)	630 \pm 174	700 \pm 200	0.034
Distribution of trabeculae (mm)	0.32 \pm 0.18	0.38 \pm 0.22	0.023
Cortical thickness (μm)	592 \pm 171	537 \pm 172	ns

ns: non significant

Disclosures: **S. Boutroy**, None.

F362

In Vivo Analysis of Vertebral Microstructure for Evaluation of Fracture Risk. **M. Ito**¹, **K. Ikeda**², **M. Uetani**^{*3}, **H. Orimo**^{*4}. ¹Radiology, Nagasaki University, Nagasaki, Japan, ²Bone and Joint Disease, National Center for Geriatrics and Gerontology, Aichi, Japan, ³Radiology, Nagasaki University, nagasaki, Japan, ⁴Health Science University, Tokyo, Japan.

Bone mineral density (BMD) measurement by dual X-ray absorptiometry (DXA) alone has limitations in predicting fracture, and methods for clinical assessment of bone quality, including microstructure, are awaited. The present study was undertaken to examine the applicability of multidetector row computed tomography (MDCT) for clinical assessment of fracture risk. We first evaluated the relationship of microstructure parameters (obtained by MDCT) with ultimate load (as determined by compression test), using 4 femoral head specimens obtained during surgery. A significant correlation with ultimate load was obtained for apparent bone volume fraction (app BV/TV) ($p<0.05$), structure model index (SMI) ($p<0.05$) and app Tb.N ($p<0.05$). We then analyzed vertebral microstructure in 82 postmenopausal women (55-76 years old), including 39 women with and 43 without a recent vertebral fracture. Microstructure indices obtained by MDCT scanning revealed much higher relative risk for prevalent vertebral fracture (odds ratio: 16.0 for SMI, 13.6 for app BV/TV, and 13.1 for Euler's number) than did spinal BMD obtained by DXA (odds ratio: 4.8). MDCT can provide volumetric BMD values, which also revealed high association with fracture (odds ratio: 12.7). Microstructure parameters (especially SMI), when combined with BMD, gave even higher odds ratio than did those of single microstructure alone. This is the first *in vivo* imaging and analysis of vertebral micro-architecture by MDCT, and microstructure parameters, together with volumetric BMD obtained at the same time, may be useful for clinical assessment of fracture risk.

Disclosures: **M. Ito**, None.

F365

Synergistic Induction of Osteoblastic 11 β -Hydroxysteroid Dehydrogenase Type 1 by Inflammatory Cytokines and Glucocorticoids: A Novel Mechanism for Glucocorticoid-Induced Bone Disease. **M. S. Cooper**, **K. Kaur***, **R. Hardy***, **C. D. Buckley***, **P. M. Stewart***, **M. Hewison**. Division of Medical Sciences, University of Birmingham, Birmingham, United Kingdom.

When used to treat inflammatory disease therapeutic glucocorticoids cause rapid bone loss. However clinical studies suggest that in patients without inflammation glucocorticoids have little impact on the skeleton. The mechanism by which inflammation magnifies the effects of glucocorticoids is unknown. We have proposed that intracellular glucocorticoid generation (inactive cortisone/prednisone to active cortisol/prednisolone conversion) via the 11 β -hydroxysteroid dehydrogenase type 1 (11 β -HSD1) enzyme determines the clinical effects of glucocorticoids on bone. In healthy subjects the effect of prednisolone on bone formation markers is predicted by measures of 11 β -HSD1 activity. We have now examined the hypothesis that the modifying effect of inflammation is due to increased local glucocorticoid generation in human osteoblasts. In MG63 osteosarcoma cells and primary osteoblasts IL-1 β and TNF α potently induced 11 β -HSD1 expression and activity (100 to 200-fold) whereas DEX treatment only mildly increased expression (10 to 50-fold). However, when combined with IL-1 β or TNF α , DEX synergistically induced 11 β -HSD1 expression and activity (1500-fold). Similar induction was also seen in primary cultures of human fibroblasts from bone marrow and synovium. This effect was specific for 11 β -HSD1 with DEX inhibiting the cytokine induction of other genes such as OPG and COX-2. Glucocorticoid receptor α and β , and H6PDH (11 β -HSD1 cofactor generating enzyme) expression were unchanged. Time course and actinomycin D studies showed that the synergistic effect of cytokines and glucocorticoids on 11 β -HSD1 expression is transcriptional. However subsequent promoter-reporter analyses indicated that DEX and cortisol act to suppress IL-1/TNF α -induced luciferase activity, suggesting a novel mechanism for synergistic induction of 11 β -HSD1 gene promoter activity. In response to

inflammation 11 β -HSD1 activity increases in osteoblasts. This effect is magnified by glucocorticoid treatment. Inflammatory cytokine/glucocorticoid synergism of 11 β -HSD1 induction is a potential mechanism to explain the modifying effect of inflammation on glucocorticoid-induced bone loss.

Disclosures: **M.S. Cooper**, None.

F367

Glucocorticoids Act Directly on Osteoclasts to Increase Their Lifespan and Reduce Bone Density. **D. Jia, C. A. O'Brien, A. M. Parfitt, S. C. Manolagas, R. S. Weinstein.** Div of Endo/Metab, Center for Osteoporosis, Central Arkansas Veterans Healthcare System, Univ of Arkansas for Med Sci, Little Rock, AR, USA.

Whether the negative impact of excess glucocorticoids on the skeleton is due to direct effects on bone cells, indirect effects on extraskeletal tissues, or both is unknown. To determine the contribution of direct effects of glucocorticoids on osteoclasts *in vivo*, we blocked glucocorticoid action on these cells via transgenic expression of 11 β -hydroxysteroid dehydrogenase type 2 (11 β -HSD2), an enzyme that inactivates glucocorticoids. Osteoclast-specific expression was achieved by insertion of the 11 β -HSD2 cDNA downstream from the tartrate-resistant acid phosphatase (TRAP) promoter. The transgene did not affect normal bone development or turnover as demonstrated by identical bone density, strength, and histomorphometry in adult transgenic and wildtype animals. Osteoclast precursor-enriched bone marrow cells from either genotype formed TRAP-positive multinucleated osteoclasts *in vitro* following 5 days of treatment with the receptor activator of NF- κ B ligand (RANKL) and macrophage-colony stimulating factor (M-CSF). Baseline apoptosis, assayed by caspase-3 activity, was reduced by glucocorticoids in cultures of wildtype osteoclasts but this effect was greatly attenuated in osteoclasts from the transgenic animals. Furthermore, the ability of glucocorticoids to prevent alendronate-induced osteoclast apoptosis in wildtype cells was abrogated in osteoclasts taken from the TRAP-11 β -HSD2 mice. In wild type mice, administration of excess glucocorticoids for 7 days induced more than a four-fold loss of spinal BMD when compared with placebo. Strikingly, the glucocorticoid-induced loss of BMD was completely abrogated in the TRAP-11 β -HSD2 mice. These results provide the first *in vivo* evidence that the glucocorticoid-induced prolongation of osteoclast lifespan is indeed the result of direct actions of glucocorticoids on these cells. Furthermore, these results confirm that the early, rapid loss of bone characteristic of glucocorticoid-induced osteoporosis results from direct glucocorticoid action on osteoclasts, rather than through secondary hypogonadism or hyperparathyroidism.

Disclosures: **D. Jia**, None.

F370

CD40 Ligand Prevents Glucocorticoid-Induced Bone Loss by Increasing Bone Formation, Decreasing Bone Resorption and Inhibiting Osteocyte Apoptosis. **W. Yao¹, G. Balooch², R. Nalla^{3*}, M. Guive^{4*}, J. Kinney³, L. Bonewald⁴, N. Lane¹.** ¹Medicine, UCDMC, Sacramento, CA, USA, ²UCSF, San Francisco, CA, USA, ³Lawrence Berkeley National Laboratory, Berkeley, CA, USA, ⁴University of Missouri at Kansas City School of Dentistry, Kansas City, MO, USA.

Glucocorticoid (GC) excess has been proposed to occur through GC inhibition of bone formation, elevation of bone resorption and apoptosis of osteoblasts and osteocytes. CD40L is a known survival ligand for osteoblast and osteocytes (Ahuja et al, JBMR, 2003). We conducted this study to assess the effects of CD40L on an *in vivo* model of GC bone loss in which 4 mo. old Swiss-Webster mice were treated for 21 days with placebo (PL), GC (1.4mg slow release prednisolone pellet) or GC + CD40L (50 μ g/mouse, sc, 2X/wk (Amgen, Thousand Oaks, CA). Urine and serum samples were collected to measure bone turnover markers. At sacrifice, the 5th LVB were used for μ CT scans and then processed for bone histomorphometry. Compression tests were performed on the 4th lumbar vertebrae and 3-point bending tests were performed on the right tibiae. **Results:** Compared to the placebo treated mice, BV/TV, Tb.N and Tb.Th were lowered by 54%, 42%, 9% (p<0.05), respectively, in the GC treated animals. These changes were accompanied by increased bone resorption (DPD/Cr, sRANKL, Oc.S), decreased bone formation (osteocalcin, MAR, BFR) and increased apoptotic osteocytes (p<0.05). CD40L treatment not only prevented GC-induced bone loss, but appeared to increase Tb.Th by preventing GC induced bone resorption and apoptotic osteocytes. Lumbar compression and 3-point bending tests revealed significant decreases in compression modulus, stiffness and energy to failure in GC-treated animals compared to PL group (p<0.05) while GC + CD40L group had significant increased energy to failure compared to PL. **Conclusions:** Our results indicate that CD40L treatment can prevent GCs induced deterioration of both bone structure and mechanical properties most likely by sustaining osteoblast activity and osteocyte survival while simultaneously preventing elevated osteoclast activity. Therefore, CD40L appears to be an attractive agent for the treatment of bone loss due to glucocorticoid excess. The mechanism for CD40L's ability to resist GC induced changes in osteoblast activity and osteocyte survival is currently under investigation.

Group	BV/TV (%)	Tb.N (1/mm)	Tb.Th (μ m)	DPD/Cr (nM/mM)	sRANKL (ng/ml)	Osteocalcin (ng/ml)	BFR/BS (μ m ³ /mm ³ /d)	Osteocyte Apop. (%)
1. PL	21.9 \pm 0.4	24.9 \pm 3.5	4.4 \pm 0.5	30.6 \pm 7.4	1.5 \pm 2.0	89.3 \pm 11.3	0.24 \pm 0.05	7.3 \pm 1.0
2. GC	10.1 \pm 0.9*	14.4 \pm 8.0*	4.0 \pm 0.8*	57.2 \pm 14.8*	6.0 \pm 3.8*	67.2 \pm 8.8*	0.05 \pm 0.01*	22.9 \pm 4.2*
3. GC+ CD40L	24.8 \pm 5.7	25.9 \pm 7.8	5.5 \pm 1.2	24.5 \pm 9.8	1.6 \pm 1.0	89.2 \pm 12.2	0.20 \pm 0.09	5.2 \pm 1.4

Disclosures: **W. Yao**, None.

F374

Estradiol Therapy Inhibits *In Vitro* Osteoclastogenesis and RANKL Expression in the Bone Marrow of Postmenopausal Women. **H. Kaneko^{*1}, P. Taxel², K. Lee², Y. Toyama^{*1}, H. L. Aguila^{*2}, L. G. Raisz², J. A. Lorenzo².** ¹Orthopedics, Keio University School of Medicine, Tokyo, Japan, ²Medicine, University of CT Health Center, Farmington, CT, USA.

Estrogen deficiency at menopause increases osteoclast (OCL) formation and bone resorption, predisposing women to osteoporosis. We examined *in vitro* OCL formation in cultured bone marrow cells from 3 premenopausal and 8 postmenopausal women before (B) and after (A) 3 weeks of estrogen (E) therapy (1 mg/day of micronized 17 beta estradiol). Subjects were postmenopausal and had not received E for at least 1 year. Bone marrow mononuclear (BMM) cells were prepared from bone marrow aspirates by ficoll-hypaque density gradient separation. OCL formation was stimulated with MCSF (30 ng/ml) and varying concentrations of RANKL for 14 days in 48 well plates. OCL were identified as TRAP positive multinucleated cells. We also examined the effects of E on the percentage of B-lymphocytes (CD-19+ cells) and cells expressing RANKL protein in uncultured bone marrow using flow cytometry and an anti-CD-19 or two anti-RANKL monoclonal antibodies (Ab) in 5 of the postmenopausal women and 3 premenopausal controls. Initial characterization of the bone marrow used forward/side light scatter to identify the granulocyte-enriched (R1) and the lymphocyte/monocyte-enriched (R2) subpopulations. Baseline bone mineral density in subjects, measured by DEXA, ranged from a T score of 1.6 to -3.1 in the lumbar spine and 0.3 to -1.8 in the femur. RANKL (3-100 ng/ml) produced a dose-dependent increase in OC formation and E therapy significantly (p<0.01) inhibited OCL formation by 33 to 50% (OCL/well for RANKL 3 ng/ml B= 102 \pm 25, A= 51 \pm 20; for RANKL 30 ng/ml B= 338 \pm 29, A= 216 \pm 19; for RANKL 100 ng/ml B= 442 \pm 53, A= 283 \pm 21, values are mean \pm SEM). Treatment with E did not affect the percentage of CD-19+ B-lymphocytes in the total marrow but did increase CD-19+ cells in R2 and decrease CD-19+ cells in R1. Anti- RANKL Ab binding was generally low (typically 0.2-3.5% of cells in R1 and 0.7-4.3 % of cells in R2 prior to E). There was no effect of E on the percentage of cells binding the anti-RANKL Ab in the R1 fraction. However, in the R2 fraction E treatment decreased the percentage of cells binding anti-RANKL Ab by 68 \pm 9% (p<0.01). These results demonstrate that 3 weeks of *in vivo* E treatment decreases the ability of human bone marrow cells to form OCL *in vitro*. Changes in the osteoclastic potential of bone marrow cells are likely involved in the ability of estrogen to regulate bone mass and influence the development of osteoporosis.

Disclosures: **P. Taxel**, None.

F376

FSH as a Direct Regulator of Bone Degradation in the Human. **B. B. Yaroslavskiy^{*1}, A. C. Sharrow^{*1}, D. J. Papachristou^{*1}, M. Virji^{*1}, L. Sun^{*2}, Z. Zhang^{*2}, Y. Peng^{*2}, J. Iqbal^{*2}, S. Zaidi^{*2}, H. Zhou^{*2}, L. L. Zhu^{*2}, B. S. Moonga^{*2}, M. Zaidi², H. C. Blair¹.** ¹Pathology, University of Pittsburgh, Pittsburgh, PA, USA, ²Mount Sinai Bone Program and Orthopedics Research Laboratories, Mount Sinai School of Medicine, New York, NY, USA.

It has long been an issue how estrogen can function as a sole regulator for sex-related effects on bone turnover. Complex schemes are required to explain how estrogen, mainly via ER α , can accomplish a wide variety of regulatory activities in hypogonadal men and women. We found a direct relationship of FSH to organic anions, phosphate or lactate, in early menopausal women. This is consistent with bone loss on estrogen withdrawal. However, these data were also compatible with a new hypothesis, that the glycoprotein hormone FSH may directly regulate bone turnover. A precedent, direct skeletal effects of the related glycoprotein hormone TSH, traditionally thought to affect only thyroxine production, was recently reported [Cell 115: 151, 2003]. Affymetrix screening of human CD14+ cells and osteoclasts produced using RANKL and CSF-1 revealed that osteoclasts but not CD14+ cells expressed the FSH receptor (FSHR). PCR confirmed FSHR mRNA in osteoclasts. Western blots showed FSHR protein in human osteoclasts, matching a granulosa cell line positive control. Based on rapid bone loss in early menopausal women with very high FSH (> 100 IU/l) and very low estrogen, we posited further that the osteoclast, and possibly some types of macrophages, are activated directly by FSH, augmenting estrogen effects which predominately reduces osteoclast formation via a nongenomic mechanism, while ER α is downregulated in the mature osteoclast [J Biol Chem 280: 13720, 2005]. We tested whether FSH promoted osteoclastic survival or activity. FSH gave a concentration-dependent increase in osteoclast number and pit formation at 14-21 d, with peak response at 30 ng/ml (equivalent to FSH at ~100 IU/l), and no resorption over control in GnRH or LH controls. In addition, with FSH treatment at short to intermediate times (2-18 h), osteoclasts on nonresorbable substrate showed reduced spread area, while attachment structures including podosomes and the actin ring appeared to be enhanced, in keeping with effects of FSH on motility and activity. Attached cell area was increased by addition of pertussis toxin (PTX), suggesting that effects of FSH are primarily mediated by a Gi pathway, although multiple regulatory pathways may be involved. Downstream, phosphorylation of the survival factor Akt, often modified by motility and adhesion factors, was increased by FSH with prolonged activity (to 18 h), which was reduced to ~control levels by PTX. We conclude that FSH directly stimulates human osteoclast activity and survival.

Disclosures: **H.C. Blair**, None.

F381

Alendronate Prevents Bone Loss in Men on Androgen Deprivation Therapy for Prostate Cancer. S. L. Greenspan¹, J. M. Wagner¹, J. B. Nelson^{*2}, N. M. Resnick^{*1}, R. A. Parker^{*3}. ¹Medicine, University of Pittsburgh, Pittsburgh, PA, USA, ²Urology, University of Pittsburgh, Pittsburgh, PA, USA, ³Center for Biostatistics in AIDS Research, Harvard School of Public Health, Pittsburgh, PA, USA.

Prostate cancer is the most common visceral malignancy and the second leading cause of cancer death in men. Androgen deprivation therapy (ADT) is the cornerstone of treatment for more advanced disease and is utilized as preventive therapy for recurrence of prostate cancer. Because chronic ADT often results in bone loss, we postulated that this loss could be reversed with a once weekly oral bisphosphonate. To address these hypotheses, we enrolled 112 men with nonmetastatic prostate cancer (mean age 71.5±8.4 years) who were on ADT for at least 6 months in an NIH-funded, 2-year, double-blind, placebo-controlled, randomized, partial cross-over clinical trial. Participants were randomized to alendronate 70 mg once weekly or placebo, and received appropriate calcium and vitamin D supplementation. This abstract reports the analysis of the primary endpoint results after one year of therapy. Only 9% of men had normal bone mass by World Health Organization criteria at the hip and spine (39% had osteoporosis; 52% had osteopenia). In men on alendronate therapy, bone mass increased significantly at the spine and hip (see Table). In contrast, men on placebo had significant decreases of bone mass at the spine, hip, and forearm. There were significant differences between the two treatment groups at all skeletal sites. Therapy was well-tolerated with no between-group differences in adverse events. In summary, less than 10% of men with nonmetastatic prostate cancer on ADT had a normal BMD. After 12 months on ADT, the placebo-treated men had significant additional bone loss; men treated with once weekly oral alendronate had significant gains. Since most men remain on ADT indefinitely, it is important to assess bone mass and consider measures to prevent bone loss.

	Percent Change in BMD at 12 Months			
	Spine	Total Hip	Femoral Neck	One-Third Distal Radius
Alendronate	3.7±0.4+	0.7±0.3+	1.5±0.5+	-0.7±0.3+
Placebo	-1.3±0.6+	-0.7±0.3+	-0.6±0.4	-1.8±0.4+
Difference++	4.9 (3.5-6.4)***	1.5 (0.6-2.4)**	2.1 (0.9-3.3)**	1.1 (0.0-2.2)*

+P < 0.05 change from baseline; * P < 0.05, ** P < 0.01, *** P < 0.001 change in active vs. placebo group; || mean±SEM; ++ mean (95% CI)

Disclosures: **S.L. Greenspan, Merck & Co., Inc. 2, 5, 8.**

F387

Direct Inhibitory, and T Cell Mediated Stimulatory Effects on Osteoclastogenesis Determine the Net Activity of IFN γ on Bone *In Vivo*. Y. Gao, M. Robbie-Ryan, K. Page*, W. Qian*, X. Yang*, M. N. Weitzmann, R. Pacifici. Division of Endocrinology, Metabolism and Lipids, Emory University School of Medicine, Atlanta, GA, USA.

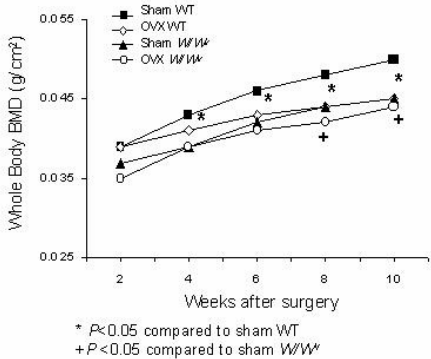
IFN γ has been implicated in the bone loss induced by ovariectomy (ovx) and inflammation, but its role remains controversial as IFN γ was shown both to inhibit and stimulate osteoclast (OC) formation and bone loss. rIFN γ blocked OC formation in monocyte cultures, confirming that it poses a direct anti-osteoclastogenic activity. Next, antigen presenting cells (APC) were pretreated with rIFN γ and cocultured with T cells to induce antigen presentation (AP) driven T cell activation. Pretreatment of APC with rIFN γ markedly increased TNF, RANKL and IFN γ levels in APC/T cell culture media (CM), demonstrating that IFN γ activates T cells via AP. When added to cultures of IFN γ R-/- monocytes, rIFN γ pretreated APC/T cell CM increased osteoclastogenesis 2 fold more than control CM. In contrast, rIFN γ pretreated APC/T CM and control CM caused equal OC formation in cultures of WT monocytes. Thus, IFN γ represses OC by targeting monocytes, but stimulates OC by indirectly activating T cells via APC. To determine the effects of IFN γ in vivo, WT, nude, and nude mice reconstituted with WT T cells were injected IP with rIFN γ (10⁶ IU/kg, twice a week, for 3 weeks). rIFN γ induced significant bone loss in WT mice (-7.2 %) and nude mice transferred with WT T cells (-9.3 %), but not in nude mice (+1.1 %). rIFN γ also caused a 2-3 fold increase in bone resorption, AP and TNF and RANKL production in T cell replete, but not T cell deficient mice. Thus, in healthy T cell replete mice the net effect of IFN γ is that of increasing bone loss. Next, we examined the role of IFN γ in 3 models of bone loss: ovx, which causes mild T cell activation through AP, LPS treatment, which causes maximal T cell activation through TLR-4, and blunted TGF β signaling in T cells, which activates T cells both directly and through AP. We found that ovx caused significant T cell activation and bone loss in WT but not in IFN γ R-/- mice. In contrast, LPS induced more severe bone loss in IFN γ R-/- mice than in WT mice. To investigate the role of IFN γ in conditions of blunted TGF β signaling in T cells, we adoptively transferred into nude mice T cells insensitive to TGF β (CD4dnTGF β IIIR), T cells lacking both TGF β signaling and IFN γ (CD4dnTGF β IIIR/IFN γ -/-), and WT T cells. Recipients of CD4dnTGF β IIIR T cells sustained a bone loss 2 fold greater than hosts of CD4dnTGF β IIIR/IFN γ -/- T cells, while recipients of WT T cells had no bone loss. We conclude that IFN γ directly blocks OC formation but indirectly stimulates osteoclastogenesis through AP induced T cell activation. The net effect of IFN γ on bone resorption in vivo depends on the pattern of T cell activation induced by specific disease states.

Disclosures: **Y. Gao, None.**

F389

Mast Cell Deficient Mice Delay the Development of Osteopenia after Ovariectomy. S. Lotinun¹, G. L. Evans^{*2}, R. T. Turner¹. ¹Department of Nutrition and Exercise Sciences, Oregon State University, Corvallis, OR, USA, ²Department of Orthopedics, Mayo Clinic, Rochester, MN, USA.

Mast cells produce and secrete proinflammatory cytokines implicated in post-menopausal bone loss and might provide a critical cellular link between estrogen deficiency and increased bone turnover. Mice carrying mutations at the dominant white spotting (*W*) locus coding for the *c-Kit* tyrosine kinase receptor have greatly reduced numbers of tissue mast cells. We utilized mast cell deficient mice, WBB6F1/J-*Kit^WKit^{W-v}* (*W/W^v*) to examine the functional role of mast cell as a mediator of ovariectomy (OVX) associated bone loss. Four-week-old female *W/W^v* mice and wild type (WT) littermates were ovariectomized. Bone mineral density (BMD) and bone mineral content (BMC) of whole body, tibia, femur and lumbar vertebrae were measured at 2, 4, 6, 8 and 10 weeks after OVX using PIXImus small animal densitometer and bone histomorphometry was analyzed at 15 weeks of age. Compared to WT, *W/W^v* mice had significant decreases in BMD in whole body, tibia, femur and lumbar vertebrae, largely due to a reduction in BMC. Histomorphometry indicated that the cross-sectional, cortical and marrow area of cortical bone were smaller in *W/W^v* mice. There was no change in double-labeled surface, mineral apposition rate and bone formation rate in cortical bone. Cancellous bone formation rate was suppressed in *W/W^v* mice compared with WT controls. Four weeks after OVX, a significant reduction in BMD and BMC was observed in all bones of WT. However, mice deficient in mast cells reduced response to OVX, so that by six weeks following OVX, there was no significant difference in BMD and BMC between OVX WT and OVX *W/W^v* mice. Histomorphometric analysis of cortical and cancellous bone of tibiae indicated less bone mass in OVX WT but not OVX *W/W^v* mice when compared to corresponding controls. Cancellous bone volume was reduced by 56% in OVX WT compared with WT controls whereas a slight decrease was observed in OVX *W/W^v* mice. In addition, OVX increased osteoblast surface by 6 fold and osteoclast surface by 2.4 fold in cancellous bone of WT controls but no differences were observed in *W/W^v* mice. Compared to WT, mast cell deficient mice have a lower peak bone mass and are resistant to OVX induced bone loss. These findings suggest that mast cells or *c-Kit* signaling contributes to normal bone growth and turnover and bone loss after OVX.



Disclosures: **S. Lotinun, None.**

F391

Association between Oxidative Stress and Bone and Mineral Metabolism. K. Baek*, M. Kang, S. Shim*, H. Tae*, J. Han, H. Kim*, K. Lee*. St.Mary's Hospital, The Catholic University of Korea, Seoul, Republic of Korea.

Reactive oxygen species (ROS), such as superoxide and hydrogen peroxide, can cause damage to DNA, protein and lipids. Oxidative stress has been implicated in a wide variety of disease processes, including atherosclerosis, diabetes, neurodegenerative disorders and process of aging. Recently, it has been also suggested that oxidative stress is causally associated with pathogenesis of osteoporosis. In this study, we investigated the association between the marker of oxidative stress and either the bone turnover markers and bone mineral density (BMD). We also examined the effects of hydrogen peroxide (H₂O₂) on the formation of osteoclasts in human bone marrow cell culture. Oxidative stress was evaluated in serum by measurement of 8-hydroxy-2-deoxyguanosine (8-OHdG) in 135 postmenopausal subjects (68.2 ± 4.9 years, BMI 24.4 ± 2.8). Women who had taken drugs which affect bone metabolism and who had past history of smoking were excluded. The biochemical markers of bone formation (osteocalcin) and resorption (ICTP) were measured from the same specimen. BMD of lumbar spine, and hip were measured by dual energy X-ray absorptiometry. In multivariate linear regression analyses, the 8-OHdG levels were negatively associated with BMD of lumbar spine, total proximal femur, femoral neck, and trochanter and positively associated with the ICTP levels. Odds ratio(OR) of the 8-OHdG for osteoporosis in lumbar spine and osteoporosis and/or osteopenia in total proximal femur were 1.70 (1.20-2.39, p=0.003) and 1.36 (0.97-1.91, p=0.043), respectively. OR for increased bone resorption was 4.22 (1.44-7.72, p=0.009) in the highest 8-OHdG quantile. In vitro bone marrow cell cultures, H₂O₂ caused a concentration-dependent activation of TRAP positive multinucleated giant cells. H₂O₂ also increased area of pits per dentin slice. RT-PCR measurements of RANKL, OPG, and M-CSF mRNA expression in primary human osteoblasts culture showed that H₂O₂ stimulated the expression of M-CSF and also increased the RANKL/OPG ratio. These findings suggest that oxidative stress is associated with increased bone resorption and low bone mass in healthy women.

Disclosures: **K. Baek, None.**

F393

Central Nervous Control of Bone Loss in Response to Unloading Is Mediated via Ventromedial Hypothalamus (VMH). K. Hino^{*1}, A. Nifuji¹, K. Nakashima¹, H. Yamamoto^{*2}, M. Noda¹. ¹Molecular Pharmacology, Tokyo Medical and Dental University, Tokyo, Japan, ²Orthopedics, Ehime University, Matsuyama, Japan.

Disuse osteoporosis has been major causes for the fracture risk. However, the mechanisms underlying such unloading induced bone loss have not been fully understood. We hypothesize that ventromedial hypothalamus (VMH) would be the center for the central nervous control of bone loss due to unloading. To test this hypothesis, mice were treated with gold thioglucose (GTG), a compound that destroys neurons in ventromedial hypothalamus (VMH) and were subjected to tail suspension (TS). In GTG-treated mice, GTG treatment was conducted by injection of GTG at 4weeks old. This mice were used at age of 10weeks. Unloading for two weeks reduced trabecular bone volume in saline-treated mice. GTG-treated mice revealed 31% reduction in the basal trabecular bone volume. In contrast to saline-treated mice, TS no longer suppressed the levels of bone volume in GTG-treated mice. Such GTG inhibition of bone loss was not limited to femur as it was observed in vertebral cancellous bone. In terms of cortical bone, bone mass was reduced by TS in saline-treated mice and GTG treatment alone preserved most of the bone mass (6% reduction). In GTG mice, TS failed to suppress cortical bone volume. TS suppressed mineral apposition rate (MAR) by 24% in saline-treated mice. GTG treatment alone reduced MAR by 23%. However, TS again failed to suppress MAR in GTG mice. Similarly, mineralizing surface as well as bone formation rate was all suppressed by TS in saline-treated mice but not in GTG-treated mice. No difference was observed in terms of TS effect on osteoclast surface as well as osteoclast number in either saline or GTG-treated mice. Mineralized nodule formation was suppressed in saline-treated mice by TS but not in GTG treated mice, indicating that the effect of destruction in VMH would be observed at least at cellular levels. Regarding the GTG prevention of TS-induced bone loss, one of the possibility was that bone volume was a at the far bottom level where further suppression may be no longer observed. To test such possibility, we conducted orchidectomy (ORX). In saline-treated mice, ORX suppressed bone mass by 62%. GTG-treatment alone reduced trabecular bone volume by 31%. However, ORX reduced bone volume further by 51% in GTG-treated mice. This is in contrast to the GTG blockage of the bone loss due to TS. Even in the presence of ORX-induced bone loss, additional TS further reduced bone mass in the absence of GTG treatment, but not in the presence of GTG treatment. Thus, VMH neuron plays the central role in specifically mediating the bone loss due to TS. These data indicate that VMH neuron plays a pivotal role in mediating unloading-induced bone loss.

Disclosures: **K. Hino**, None.

F395

Ovariectomy Increase the Formation of T Cell Niches at the Resorption Surfaces. F. Grassi, K. Page^{*}, W. Qian^{*}, M. N. Weitzmann, R. Pacifici. Dep of Medicine, Division of Endocrinology, Metabolism and Lipids, Emory University, Atlanta, GA, USA.

It has been reported that T cell produced cytokines are pivotal for stimulating osteoclast (OC) formation and inducing bone loss after ovariectomy (ovx). The mechanism by which ovx augments remodeling is unknown, but it could be that T cell regulate the spatial distribution of remodeling units by secreting factors in discrete niches of the bone marrow (BM). We thus asked whether T cells localize in the proximity of bone surfaces in order to induce OC formation, and whether estrogen regulates the spatial distribution of T cells. Mice were sacrificed 4 weeks after ovx or sham operation and longitudinal sections of femurs and tibiae were immunostained for TRAP (an OC marker) and CD3 (a T cell marker). Video imaging was utilized to delineate the BM area localized within 60 µm from the endosteal surface, which was arbitrarily defined as endosteal BM area. The rest of the BM was defined as central BM. We then analyzed the number of OC and T cells in the total, central and endosteal BM areas. We determined the endosteal BM areas to be 23.6 % of the total BM area. If T cells were randomly distributed then ~ 23.6 % of the T cells should fall within the endosteal BM. We found that the spatial distribution of T cells was not random ($p < 0.05$) and under estrogenic control. In fact, sham mice had 44 ± 2.6 % of their T cells in the endosteal region while ovx mice had 56.4 ± 3.8 % ($p < 0.05$). Attesting to specificity, analysis of total BM cells revealed that the observed BM area occupied by BM cells was identical to the predicted values in both sham and ovx mice. Thus, contrary to T cells, total BM cells are randomly distributed. Next, we asked whether the T cells colocalize with OC. To this aim, we divided cortical endosteal surfaces in segments of 0.3 mm and sorted it according to the surface size covered by OC. In OC poor endosteal areas (OC surface $\leq 10\%$ of total bone surface) T cells occupied 1.8 ± 0.2 % of the area. In OC intermediate area (OC surface equal to 10 - 30 % of total bone surface) T cells occupied 2.85 ± 0.39 % of the area, while OC rich areas (OC surface ≥ 30 % of total bone surface) T cells occupied 5.62 ± 0.85 % of the area. Furthermore, the T cell/OC ratio was equal in sham and ovx mice. These findings demonstrate that T cells are found in greater abundance in close proximity to OC. In summary, we show that T cells forms niches in the proximity of remodeling bone surfaces and that ovx increase the localization of T cell nearby areas of active resorption. These data support the hypothesis that T cells activate the resorption of specific bone areas through their accumulation in specially defined endosteal areas.

Disclosures: **F. Grassi**, None.

F397

Arrestins Selectively Regulate the Inhibitory Effects of Adrenergic Agonists on Bone and Fat. D. Pierroz¹, E. Bianchi^{*1}, D. Manen^{*1}, R. Rizzoli¹, M. L. Bouxsein², S. L. Ferrari¹. ¹Div. of Bone Diseases, Geneva University Hospital, Geneva, Switzerland, ²Orthopedic Biomechanics Lab., Beth Israel Deaconess Med. Center and Harvard Med. School, Boston, MA, USA.

Stimulation of $\beta 2$ adrenergic receptors ($\beta 2AR$) expressed in osteoblasts has been reported to decrease trabecular bone volume. Cytoplasmic arrestins (Barr) play a central role in the desensitization of $\beta 2AR$ -mediated signaling in vitro, and we previously found that Barr2 KO mice have low bone mass and micro-architecture. We hypothesized that these skeletal alterations could reflect poor regulation of adrenergic activity in bone in absence of Barr2. For this purpose, 6-wk-old male wild-type (WT) and Barr2 KO mice were treated with isoproterenol (ISO, 10mg/kg/d), a non-specific βAR agonist, or vehicle (VEH) (n=4-6/group). Total body (TB), spine (Sp.) and femur (Fem.) BMD, and % fat were evaluated by pDXA after 0, 4 and 8 wks, whereas trabecular (Tb) and cortical (Cort.) micro-architecture at the distal and mid-femur was evaluated after 8 wks by mCT. TB, Sp. and Fem. BMD were significantly lower in KO than WT mice ($p=0.002-0.014$ by repeated measures ANOVA), although these differences were observed only in the VEH group. Indeed, ISO significantly decreased TB and Fem. BMD after 4 and 8 wks in WT ($p<0.05$) but not in KO (Pinteraction <0.05), and decreased Sp. BMD more prominently in WT (-24%) than KO (-12%) after 8 wks (Pinter= 0.05). Hence, after ISO treatment, BMD became as low in WT as in KO mice. In contrast, percentage fat mass did not differ between KO and WT mice and was significantly decreased by ISO ($p=0.02$) in both KO and WT (Pinter=ns). In the femur, Tb. BV/TV and Tb. Number, cort. cross-sectional area, bone area, marrow area and cort. thickness were significantly lower in KO than WT ($p=0.003-0.029$ by 2F-ANOVA), but again these differences were observed only in VEH groups. Indeed, ISO-induced inhibition of bone architecture was more prominent and/or significant in WT than KO (Pinter= $0.008-0.10$). Quantitative RT-PCR showed that arrestins were similarly expressed in bone and fat. However, only $\beta 2AR$ was expressed in bone, whereas in fat, $\beta 3AR$ was more prominently expressed than $\beta 2AR$ and $\beta 1AR$. These results indicate that inhibition of bone mass and architecture by adrenergic agonists is blunted in absence of Barrestin2 and suggest that skeletal alterations in Barr2 KO mice may reflect improper regulation of adrenergic activity in bone. In contrast, adrenergic effects on fat are independent of Barr2, consistent with the fact that they are primarily mediated by the $\beta 3AR$ which does not interact with arrestins. Hence, interactions between βAR and arrestins selectively regulate the inhibitory effects of adrenergic stimulation on bone and fat.

Disclosures: **D. Pierroz**, None.

F399

PPAR Antagonist Prevents Type I Diabetic Bone Adiposity and Bone Loss. S. Botolin^{*}, L. R. McCabe. Physiology, Michigan State University, East Lansing, MI, USA.

Diabetes type I is associated with an increased risk for osteoporosis. Correspondingly, we demonstrated that streptozotocin induced type I diabetes in mice is associated with significant bone loss marked by suppressed osteoblast maturation (reduced osteocalcin mRNA levels and mineralization). A second component of the skeletal response to type I diabetes involves an induction of marrow adiposity marked by increased tibial PPARgamma2 (PPARg2) and aP2 mRNA levels. The purpose of this study is to test if prevention of cellular progression toward an adipocyte-like phenotype will ameliorate diabetic bone loss. Methods: Streptozotocin-induced adult diabetic mice were treated with vehicle or a PPARg antagonist. At 5, 14, 21, and 28 days post-induction of diabetes, tibias, serum, femoral fat pads and livers were harvested from control, control plus PPARg antagonist, diabetic and diabetic plus PPARg antagonist treated mice. Tibias were analyzed for bone mineral density (by uCT), histomorphometry (adiposity) and mRNA levels of osteoblast and adipose markers. Serum glucose, triglycerides and osmolality were also determined. Results: While untreated diabetic tibias showed a dramatic loss in bone mineral density and an increase in adiposity compared to controls, treatment with a PPARg antagonist prevented the diabetes-induced changes. These findings were supported by gene expression and morphometric analyses. Specifically, diabetic mice receiving PPARg antagonist treatment exhibited tibial PPARg2, aP2 and resistin mRNA levels that were no longer significantly different from controls. Treated mice also exhibited diminished bone loss. Interestingly, serum triglyceride levels were decreased in diabetic mice treated with the PPARg antagonist when compared with untreated diabetic mice. Conclusions: PPARg antagonist treatment rescues the osteoporotic phenotype and osteogenic gene expression, while inhibiting the adipogenic phenotype and gene expression in diabetic mouse tibias. These findings demonstrate a relationship between adiposity and bone loss, and suggest that bone adiposity plays an active role in the regulation of bone mineral density.

Disclosures: **S. Botolin**, None.

F401

Decreased Defense against Reactive Oxygen Species: A Common Pathogenetic Mechanism of the Effects of Aging and Estrogen Deficiency on Bone. S. C. Manolagas, M. Almeida, L. Han, R. Weinstein, R. Jilka, T. Bellido, C. O'Brien, S. Kousteni. Div. Endocrinol., Center for Osteoporosis and Metabolic Bone Diseases, Central Arkansas Veterans Healthcare System, Univ. Arkansas Med. Sci., Little Rock, AR, USA.

The molecular and cellular mechanisms of the adverse effects of aging on bone and the extent to which estrogen deficiency contributes to the age-related bone loss are unknown. Nonetheless, recent evidence indicates that the pro-apoptotic effects of estrogens on

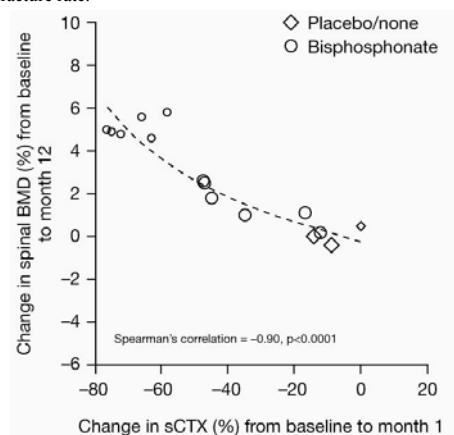
osteoclasts and their ability to suppress osteoclastogenesis as well as their anti-apoptotic effect on osteoblasts are mediated via cytoplasmic kinases and require non-protein thiols, such as glutathione. Based on this and mounting evidence that increased levels of reactive oxygen species (ROS) represent a major mechanism of aging and age-related diseases, we have searched for a mechanistic link among aging, ROS, estrogens, cytoplasmic kinases, and the birth and death of bone cells. We report that female C57BL/6 mice lose bone strength and mass progressively between the ages of 8 and 31 months. Importantly, the loss of strength is detectable 9 months before the loss of BMD, and is correlated with aging independently of BMD. These changes are temporally associated with increased osteoblast apoptosis; decreased glutathione reductase (GSR) activity; increased levels of ROS in the bone marrow; and a corresponding increase (in lysates from vertebrae) in the phosphorylation of Ser36 of the p66^{abc} adapter protein, which is part of a signal transduction pathway that is activated by increased intracellular ROS and leads to apoptosis. In line with these findings, H₂O₂ stimulated the phosphorylation of p66^{abc} in OB-6 osteoblastic cells, and this effect was suppressed by 10⁻⁸ M of E₂ or estren. In addition both compounds rapidly inhibited H₂O₂-induced expression of ATF4 - a substrate of Rsk2 and an integral component of a negative feedback pathway controlling amino acid import leading to synthesis of glutathione. Importantly, p66^{abc} phosphorylation increased 5 d following ovx in wild type controls as well as ER α ^{NERKL} mice in which the ER α is incapable of DNA binding strongly suggesting that p66^{abc} phosphorylation is negatively regulated by estrogens *in vivo*, and that this effect is mediated via a nongenotropic mechanism of ER α action. Based on these results we hypothesize that increased ROS levels with advancing age is a fundamental mechanism of the age-dependent decline of bone strength and mass, and loss of estrogens exaggerates the adverse effects of aging on bone by decreasing defense against ROS, thereby, contributing perpetually to the loss of bone mass and strength that persists for decades after menopause, and is associated with old age.

Disclosures: *S.C. Manolagas*, Nuvios, Inc. 1, 2, 5; Proctor and Gamble Pharmaceuticals 8; Eli Lilly and Company 5, 8.

F404

Relating Increases in Bone Mineral Density and Fracture Risk Reduction with Early Suppression in Biomarkers of Bone Turnover: A Literature-Based Meta-Analysis of Bisphosphonate Treatments. *M. Crane*^{*1}, *T. Davis*^{*2}, *R. Kaldate*^{*3}, *C. Black*^{*1}, *R. Davies*^{*1}, *V. Devas*^{*1}, *W. Williams*^{*1}.
¹GlaxoSmithKline, Collegeville, PA, USA, ²ClinForce, RTP, NC, USA, ³Smith Hanley, New York, NY, USA.

The relationship between bisphosphonate-related suppression of bone turnover markers and corresponding increases in bone mineral density (BMD) and fracture risk reduction is unclear. This meta-analysis further explores the nature of these relationships. Data on vertebral fracture rates, spine BMD and five biomarkers were obtained from 85 studies identified by a literature search. Spearman's correlations were computed to assess the strength of the associations. Linear regression on log-transformed values was used to model the changes from baseline in BMD at 6 and 12 months as functions of change from baseline in biomarkers at 1, 3 and 6 months, respectively. A nonlinear cumulative risk model was used to relate vertebral fracture rates over 24 to 36 month time periods with biomarker changes as factors. For each biomarker, the correlation with BMD showed a moderate to strong association (r : 0.63 to 0.90). In particular the association was strong for changes at 3 and 6 months in bone specific alkaline phosphatase (BSAP), osteocalcin (OC) and uNTX, and at 1, 3, and 6 months for uCTX and sCTX. Of particular interest is that correlation was highest ($r=0.90$) for the month 1 assessment of sCTX (**Figure**). Linear regression in all cases showed a positive association between BMD gains and biomarker suppression. The analysis for modeling the fracture risk rate, although based on fewer studies than the BMD analysis reported above, indicated that lower fracture rates were significantly ($p<0.05$) associated with greater decreases from baseline for OC, uCTX and uNTX. However, the confidence intervals for odds ratios were too wide for quantitative prediction in most cases. In summary, a strong relationship is present between BMD gains and early suppression in each biomarker, especially at month 1 for markers of bone resorption. This result suggests that studies of duration as short as one month may be sufficient for estimating the effect of a bisphosphonate on resorption. Lower vertebral fracture rates are also significantly associated with early suppression in most biomarkers. However, our results are not sufficient to suggest the use of biomarkers as surrogate markers for fracture rate.

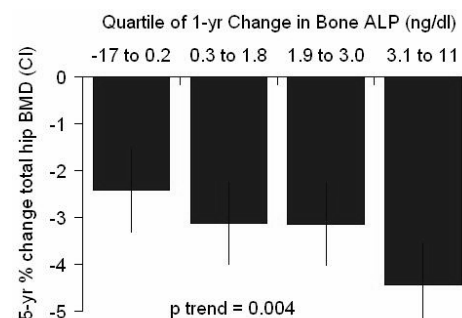


Disclosures: *M. Crane*, GlaxoSmithKline 3.

F406

Increased Turnover after Discontinuing Alendronate Predicts Bone Loss over 5 Years: The FLEX Study. *D. C. Bauer*¹, *A. Schwartz*¹, *M. C. Hochberg*², *A. C. Santora*³, *L. Palermo*^{*1}, *D. M. Black*¹. ¹Epidemiology and Biostatistics, UCSF, San Francisco, CA, USA, ²Medicine, University of Maryland, Baltimore, MD, USA, ³Merck Research Laboratory, Rahway, NJ, USA.

Bone turnover increases after discontinuation of alendronate therapy, but the relationship between short-term changes in turnover and long-term skeletal outcomes is unknown. The effects of discontinuation of alendronate on bone turnover markers, bone loss, and fracture were investigated in the FIT Long-Term Extension (FLEX) Trial among women who had previously used alendronate for an average of 5 years but received placebo in FLEX. Among the 1099 FLEX subjects who had previously received alendronate (ALN) during the Fracture Intervention Trial (FIT), 437 (40%) were randomized to receive placebo for an additional 5 years. Hip BMD was measured at FLEX baseline and at yearly visits. Clinical fractures were centrally adjudicated by review of x-ray reports or radiographs, and morphometric vertebral fractures were detected on paired radiographs obtained at baseline and after 5 years. Serum Bone ALP (Ostase, Hybritech) and urine NTX/Cr (Ostex) were measured at the FLEX baseline visit and after 1 year. Among placebo-treated women in FLEX, the mean (SD) age at baseline was 73.7 (5.9), mean (SD) total hip BMD was 0.72 (0.09), and geometric mean (SD) levels of Bone ALP and NTX were 9.1 (3.4) ng/ml, 19.6 (12.9) nmol/mmol Cr, respectively. After 1 year of placebo, Bone ALP and NTX increased by 17.1% (95% CI: 14.2, 20.1) and 23.3% (95% CI: 17.3, 29.6), respectively. Greater 1-year absolute increases in Bone ALP were associated with greater hip bone loss over 5 years (Figure); results were similar for NTX (p trend = 0.03). Relationships between change in turnover and incident non-spine fracture ($n=82$) were inconsistent, perhaps due to small numbers, but there was a trend towards a larger increase in NTX among those with non-spine fracture compared to those without fracture (35.2% vs. 20.7%, $p=0.075$). In summary, among postmenopausal women that discontinue long-term alendronate therapy, short-term increases in bone turnover are associated with higher rates of bone loss over 5 years. Additional studies are needed to determine if increased turnover after discontinuing alendronate is associated with increased fracture risk.



Disclosures: *D.C. Bauer*, Merck 2; SmithKline 2.

F408

Human Farnesyl Diphosphate Synthase (FDPS): Crystal Structure and Molecular Interactions with Nitrogen-Containing Bisphosphonates. *K. Kavanagh*^{*1}, *K. Guo*^{*1}, *X. Wu*^{*1}, *S. Knapp*^{*1}, *F. H. Ebetino*², *J. E. Dunford*³, *M. J. Rogers*³, *R. G. G. Russell*⁴, *U. Oppermann*^{*1}. ¹Structural Genomics Consortium, Botnar Research Centre, University of Oxford, OXFORD, United Kingdom, ²Procter & Gamble Pharmaceuticals, Mason, OH, USA, ³Bone Research Group, Institute of Medical Sciences, University of Aberdeen, Aberdeen, United Kingdom, ⁴Nuffield Dept Orthopaedic Surgery, Botnar Research Centre, University of Oxford, OXFORD, United Kingdom.

Farnesyl diphosphate synthase (FDPS) is a key regulatory enzyme in the mevalonate pathway that produces sterols and isoprenoid lipids. FDPS is now known to be the major molecular target of nitrogen-containing bisphosphonates (N-BPs), and the consequent inhibition of prenylation of several GTPases by N-BPs in osteoclasts leads to disruption of their resorptive activity and survival. The active site of FDPS contains two substrate-binding sites (for GPP/DMAPP, geranyl pyrophosphate/dimethyl allyl pyrophosphate, and for IPP, isopentenyl pyrophosphate), but the precise way in which BPs act on FDPS remains unresolved. Previous modeling and kinetic studies have indicated that N-BPs might inhibit the binding of both substrates. We report here for the first time the crystal structure of human FDPS. In order to define the molecular interactions, human FDPS was co-crystallized with the potent N-BP, risidronate. The 2.0Å structure of human FDPS in complex with Mg²⁺ and the tight-binding inhibitor, risidronate (K_d: 160 nM), shows the binding mode for this important class of inhibitors. Risidronate occupies the chain-elongation site as predicted, but not the IPP site. Two aspartate clusters chelate the Mg²⁺ ions that mediate ligand binding and are involved in catalysis. However, contrary to predictions suggesting two inhibitor-binding sites on FDPS, current studies using isothermal titration calorimetry (ITC), revised kinetic analysis, as well as the crystal structure itself, indicate a one-to-one stoichiometry, with risidronate being a strong inhibitor of the binding of the GPP substrate (IC₅₀: 10.3±0.07nM). The ITC experiments reveal that bisphosphonate binding to FDPS is predominantly entropy driven. These results

will further the understanding of structure-activity relationships among N-BPs and FDPS, and will enable optimization of their pharmacological potential.



Human FDPS in complex with risedronate

Disclosures: **R.G.G. Russell**, Procter & Gamble Pharmaceuticals 2, 5.

F410

Efficacy of Intravenous Ibandronate Injections in Postmenopausal Osteoporosis: 1-Year Findings from DIVA. M. Bolognese¹, D. M. Reid², B. Langdahl³, C. Hughes^{*4}, P. Ward^{*4}, D. Masanaukaite^{*4}, W. P. Olszynski⁵. ¹Bethesda Health Research, Bethesda, MD, USA, ²University of Aberdeen, Aberdeen, United Kingdom, ³Århus Amtssygehus, Århus, Denmark, ⁴F. Hoffmann-La Roche Ltd, Basel, Switzerland, ⁵Midtown Medical Center, Saskatoon, SK, Canada.

Intravenous (i.v.) bisphosphonate injections may provide a useful alternative for women with postmenopausal osteoporosis (PMO) who are unable to use or tolerate oral bisphosphonates. Ibandronate (Boniva), a potent, nitrogen-containing bisphosphonate, can be administered with extended dosing intervals, either orally or by rapid (15-30 seconds) i.v. injection. DIVA, a double-blind, double-dummy, phase III study involving 1,395 women (aged 55-80 years; ≥5 years postmenopause) with PMO (lumbar spine [L2-L4] BMD T-score <-2.5 and ≥-5), is ongoing to establish the optimal i.v. ibandronate dose regimen. In this study, participants are receiving either 2mg every 2 months (q2mo) or 3mg every 3 months (q3mo) i.v. ibandronate injections or an active comparator regimen of proven efficacy (2.5mg daily oral ibandronate; 3-year vertebral fracture risk reduction: 52%). Daily calcium (500mg) and vitamin D (400IU) supplements are also provided. One-year results demonstrated lumbar spine BMD increases (primary study endpoint) of 5.1%, 4.8% and 3.8% in the q2mo, q3mo and daily groups, respectively. Versus the established daily regimen, both i.v. regimens were proven statistically non-inferior (1% margin) and superior (p<0.001). Increases in total hip, femoral neck and trochanter BMD were also larger in both i.v. arms than the oral arm. At 1 year, residual levels of the biochemical marker of bone resorption serum CTX were decreased substantially in all treatment arms: -64.6% in the q2mo group, -58.6% in the q3mo group and -62.6% in the daily group. In conclusion, i.v. ibandronate injections are at least as effective in increasing BMD as a daily oral regimen with proven antifracture efficacy in women with PMO. A pre-planned 2-year analysis will further explore the efficacy and safety of these regimens. I.v. ibandronate injections are likely to be of significant utility for women in whom oral bisphosphonates cannot be used.

Disclosures: **M. Bolognese**, GlaxoSmithKline 2; F. Hoffmann-La Roche Ltd 2.

F412

Alendronate Has an Anabolic Effect on Bone through the Differentiation of Mesenchymal Stem Cells. G. Duque¹, D. Rivas^{*2}. ¹Medicine/Geriatrics, McGill University, Montreal, PQ, Canada, ²Center Bloomfield for Research in Aging, McGill University, Montreal, PQ, Canada.

Introduction: Alendronate has demonstrated its effectiveness in preventing bone loss in post-menopausal patients through the regulation of osteoclastic activity. However, it has also proven to be effective in elderly populations where instead of high osteoclastic activity the predominant mechanism of bone loss is the ineffective differentiation of mesenchymal stem cells (MSC) with a subsequent deficit in osteoblastogenesis. The aim of this study is to determine the effect of alendronate on bone MSC differentiation which may suggest a potential anabolic effect of Alendronate in bone. **Hypothesis:** The effect seen in the Alendronate treatment of senile osteoporosis is explained by its anabolic effect either by the inhibition of the adipogenic or the stimulation of osteogenic differentiation of MSCs. **Methodology:** Human MSCs (BioWhittaker) were plated at a density of 5 x 10⁵ cells per well in 150 cm² dishes containing mesenchymal stem cell growth medium. After the cells reached 60% confluence, medium was replaced with MSC growth medium, adipogenic or osteogenic medium with and without vitamin D (10⁻⁸ M) and supplemented with Alendronate at increasing concentrations (10^{-10M} to 10^{-7M}). Untreated differentiating MSCs were used as control. The drugs were present in the cultures for 21 days of both osteogenic and adipogenic stimulation. Alkaline phosphatase (ALP), oil red O and Alizarin red staining were performed at timed intervals (week 1, 2 and 3). Additionally, the expression of Cbfa1 and PPARγ2 was also measured in protein extracts. **Results:** We found that

Alendronate has a significant effect on ALP activity (p<0.01), on MSC proliferation (p<0.001), and on cell-mediated mineralization (p<0.01). This effect was highly significant at 10^{-8M} of Alendronate and was potentiated by the presence of vitamin D in the medium (p<0.001). Additionally, the expression of Cbfa1 quantified by densitometry was significantly increased in MSC treated with both Alendronate alone (p<0.01) and Alendronate+vitamin D (p<0.001) as compared to vitamin D alone or non-treated cells. Finally, PPARγ2 expression was only reduced in MSC in adipogenic medium containing both Alendronate and vitamin D. This effect was associated with a lower number of lipid droplets. **Conclusion:** This study shows a potential anabolic effect of alendronate on bone through the stimulation of osteogenic differentiation of MSC. Additionally, this effect is also potentiated by the addition of vitamin D to the Alendronate-treated cells. Finally, a potential inhibitory effect of Alendronate in bone marrow adipogenesis was also seen when combined with vitamin D

Disclosures: **G. Duque**, Merck USA 2; Procter and Gamble Canada 2.

F414

Influence of Alendronate on Periosteal and Endocortical Bone formation in the Ilium of Osteoporotic Women. S. Bare^{*1}, S. Recker¹, R. Recker¹, D. Kimmel². ¹Creighton University, Omaha, NE, USA, ²Molecular Endocrinology, Merck & Co., West Point, PA, USA.

Alendronate (ALN) increases bone mineral density (BMD), reduces bone resorption markers, and reduces hip and vertebral fracture risk in post-menopausal osteoporotic women. Our purpose is to document the bone envelope-specific effects of ALN in humans using transilial biopsy specimens (TIBx). Post-menopausal osteoporotic women with T-scores <-2 were treated for 1-2yrs with Placebo (PBO), 1, 2.5, or 5mg/d ALN orally. TIBx were obtained from 137 subjects at the end of treatment following double fluorochrome (Fl) labeling. The specimens were examined for total surface (BS), single (1XL), and double (2XL)-Fl labeled surface, and mineral apposition rate (MAR) in periosteal (Ps) and endocortical (Ec) envelopes. 2XL/BS was calculated omitted those individuals without 2XL. Kruskal-Wallis ANOVA with Student-Neuman Keuls post-hoc testing (P<0.05, *, P<0.001, **) was applied to all endpoints for each envelope.

Osteoporotic Women treated with Alendronate					
Envelope (Group)	Surface (mm)	% with 2XL	% with Any Label	2XL/BS (%)	MAR (µm/d) (N)
Ps(PBO)	30±9	39	77	1.35±0.99	0.80±0.34 (15)
Ps(1mg/d)	31±8	34	81	0.96±0.78	0.77±0.46 (11)
Ps(2.5mg/d)	28±8	31	83	1.27±1.26	0.79±0.39 (11)
Ps(5mg/d)	29±8	31	62	2.06±1.53	0.71±0.16 (9)
Ec(PBO)	33±9	92	97	6.11±4.74	0.73±0.21 (36)
Ec(1mg/d)	34±9	78	91	3.40±3.12*	0.82±0.38 (25)
Ec(2.5mg/d)	31±9	63*	77*	2.50±1.91*	0.78±0.34 (22)
Ec(5mg/d)	32±8	28**	59*	3.24±3.20*	0.70±0.08 (8)

The percentage of PBO subjects with Ps 2XL was ~40%, vs. ~90% with Ec 2XL. 2.5 and 5mg/d ALN reduced the percentage of subjects with Ec 2XL by 32-70%. Ec 2XL/BS was decreased by all ALN doses. In contrast, ALN had no significant effect on either Ps envelope population labeling percentage or 2XL/BS. The Ec results were similar to those for the trabecular envelope (data not shown). **Conclusion:** Quantitative analysis of the TIBx can reveal differences in the way various bone envelopes behave during treatment with bone active agents. The Ps envelope has a much lower, perhaps 10-fold, rate of bone formation than the Ec envelope. The Ec, but not the Ps, envelope responds to ALN by decreasing its rate of bone formation. The Ps envelope of osteoporotic women has a low, but measurable level of bone formation that is not affected by ALN. These data suggest that ALN positively affects cortical bone by permitting customary periosteal expansion, while slowing the rate of Ec bone remodeling, an action that slows bone loss, from the Ec surface.

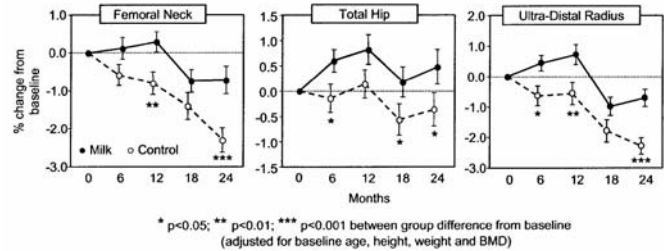
Disclosures: **D. Kimmel**, Merck & Co. 3.

F419

Calcium and Vitamin D₃ Fortified Milk Reduces Bone Loss at Clinically Relevant Skeletal Sites in Older Men: A 2-year Randomised Controlled Trial. R. M. Daly, M. Brown*, S. Bass, S. Kukuljan*, C. Nowson*. School of Exercise and Nutrition Sciences, Deakin University, Melbourne, Australia.

Osteoporosis and its related problems are now recognised as an increasing public health problem in men. This highlights the importance of identifying lifestyle interventions that are effective at maintaining bone mass and bone strength in men. The aim of this study was to examine the effect of milk fortified with additional calcium (milk minerals, 1000 mg/d of Ca) and vitamin D₃ (800 IU/d) on BMD, geometry and strength in men aged over 50 yrs. This was a 2 yr RCT in which 167 men were randomly assigned to receive either 400 mls of low fat (<1%) UHT fortified milk per day or to a control group receiving no additional milk. aBMD was assessed every 6 mths by DXA; L1-L3 trabecular vBMD and mid-femur total, cortical and medullary area, and cortical vBMD were assessed at baseline and 24 mths by QCT (n=110). Data were analysed using pooled time series regression analysis for longitudinal data with random effect models. Baseline characteristics between the groups were no different. Mean (±SD) dietary Ca intake at baseline was 941 ± 387 mg/d and mean serum 25(OH)D was 77 ± 23 nmol/L. A total of 149 men completed the study, and compliance with the fortified milk averaged 88%. At the FN, total hip and UD radius, the loss in aBMD was 0.9% to 1.6% less in the milk compared to control group (Figure). No differences were detected for L2-L4 aBMD after 24 mths. Both groups experienced a similar and significant reduction in L1-L3 trabecular vBMD [milk 2.5%; control 2.4%, both p<0.05]. In contrast, the reduction in mid-femur cortical vBMD was less in the milk compared to control group [1.5% vs 2.5%, interaction p=0.06]. Mid femur medullary area remained unchanged in the milk group [-0.04 ± 2.6%] but increased by 0.85 ± 2.9% [p=0.06] in controls [interaction, p=0.12]. Serum 25(OH)D levels increased and PTH

decreased in the milk relative to control group after 12 mths [net difference 25(OH)D 29.0%; PTH -17.4%, both $p<0.001$]. These differences remained after 24 mths. Body weight remained unchanged in both groups. In conclusion, supplementing the diet of men aged over 50 with 400 mls of low fat milk fortified with calcium and vitamin D₃ may represent a simple, inexpensive and effective strategy to increase dietary calcium and vitamin D levels to stop or slow age-related bone loss at clinically important skeletal sites.



Disclosures: **R.M. Daly**, None.

F425

Effects of Raloxifene or Alendronate on Fracture Risk Reduction: Results from the EVA (Evista®/Alendronate Comparison) Trial. **R. Recker¹, D. Kendler², C. Recknor³, T. Rooney⁴, E. M. Lewiecki⁵, W. H. Utian^{*6}, J. Cauley⁷, J. Lorraine^{*8}, Y. Ou^{*8}, P. M. Kulkarni^{*8}, L. Plouffe^{*8}, J. L. Stock⁸.** ¹Creighton Univ., Omaha, NE, USA, ²Osteoporosis Research Centre, Vancouver, BC, Canada, ³United Osteoporosis Center, Gainesville, GA, USA, ⁴Mercy Arthritis & Osteoporosis Center, Des Moines, IA, USA, ⁵New Mexico Clinical Research & Osteoporosis Center, Albuquerque, NM, USA, ⁶Rapid Medical Research, Cleveland, OH, USA, ⁷University of Pittsburgh, Pittsburgh, PA, USA, ⁸Eli Lilly, Indianapolis, IN, USA.

EVA is the first head-to-head, double-blind, randomized trial designed to compare 2 osteoporosis therapies for fracture risk reduction efficacy. The original protocol planned to treat 3000 postmenopausal women [50-80 yr old, femoral neck BMD NHANES T-score ≥ -4.0 to ≤ -2.5 , no prevalent vertebral fractures (VF), no prior bone-active agent use] with raloxifene 60 mg/d (RLX) or alendronate 10 mg/d (ALN) for 5 yr. The primary endpoint was the number of women with ≥ 1 new osteoporotic VF or nonvertebral fracture (NVF), assessed by a central reader. EVA was stopped early, due to difficulty in finding treatment-naïve women to meet enrollment goals within the planned timeline, resulting in insufficient power to show noninferiority of RLX to ALN. Analyses of fractures (Table), except VF, were based upon 1412 of the 1423 women randomized (mean age 66 yr). After 312 ± 254 (mean \pm SD) days, fracture risks were not different between groups (Table), except for moderate/severe VF, a pre-specified endpoint, which occurred in fewer women in the RLX group. BMD increases at 2 yr differed from baseline and between groups ($P<0.05$), at the lumbar spine (ALN 5.4%, RLX 2.5%), femoral neck (ALN 3.9%, RLX 2.3%), and total hip (ALN 3.9%, RLX 1.8%). Similar numbers of women in each group had ≥ 1 adverse event (AE) and discontinued due to an AE. The only AEs that differed between groups were colonoscopy, diarrhea, and nausea (each $P<0.05$); each was more common with ALN. In the RLX group, 1 woman had a pulmonary embolism, 1 in the ALN group had a deep venous thrombosis, and 1 in each group developed breast cancer. In summary, these limited data show no between-group differences in overall fracture risk. There are significant BMD changes between groups. Safety profiles are as expected from trial and post-marketing reports.

Type of Fracture	Women with ≥ 1 New Fracture, n(%)		
	ALN (N=713)	RLX (N=699)	ALN vs. RLX RR (95% CI) or P-Value ^a
Vertebral or Nonvertebral	22 (3.1)	20 (2.9)	1.08 (0.60, 1.95)
Vertebral ^b	8 (3.1)	5 (1.9)	1.63 (0.57, 5.70)
-Moderate/ Severe Vertebral ^b	4 (1.6)	0	P=0.04
-Clinical Vertebral	3 (0.4)	0	P=0.10
Nonvertebral	14 (2.0)	15 (2.2)	0.92 (0.45, 1.86)
-Nonvertebral-Six ^c	11 (1.5)	10 (1.4)	1.08 (0.47, 2.46)
-Hip	1 (0.1)	2 (0.3)	0.49 (0.04, 3.77)
-Wrist	6 (0.8)	8 (1.1)	0.74 (0.27, 2.02)

^a Exact unconditional test

^b ALN n=255; RLX n=259

^c Clavicle, humerus, wrist, pelvis, hip, leg

Disclosures: **R. Recker**, Eli Lilly 2, 5; Merck 2, 5.

F429

Lasofloxifene Increased BMD of the Spine and Hip and Decreased Bone Turnover Markers in Postmenopausal Women With Low or Normal BMD. **M. McClung¹, E. Siris^{*2}, S. Cummings³, H. Bone⁴, R. Recker⁵, P. Delmas⁶, J. Zanchetta^{*7}, M. Lewiecki⁸, C. Zerbin^{*9}, S. Miller^{*10}, K. Wolter¹¹, J. Proulx¹¹, R. Brunell^{*11}, D. Radecki¹¹.** ¹Oregon Osteoporosis Center, Portland, OR, USA, ²NY Presbyterian Hosp-Columbia Univ, New York, NY, USA, ³San Francisco Coordinating Ctr, San Francisco, CA, USA, ⁴Michigan Bone and Mineral Clinic, Detroit, MI, USA, ⁵Creighton Univ, Omaha, NE, USA, ⁶Univ Claude Bernard, Lyon, France, ⁷Instituto de Investigaciones Metabolicas, Buenos Aires, Argentina, ⁸New Mexico Clinical Research & Osteoporosis Ctr, Albuquerque, NM, USA, ⁹Hospital Helopolis, Sao Paulo, Brazil, ¹⁰SAM Clinical Research Center, San Antonio, TX, USA, ¹¹Pfizer Global Research and Development, New London, CT, USA.

Increased bone mineral density (BMD) and reduced bone turnover markers have been reported in Phase 2 trials with lasofloxifene, a new SERM. We report the pooled results from two identical Phase 3, double-blind trials. 1907 postmenopausal women (lumbar spine T-score 0 to -2.5) were randomized to lasofloxifene 0.025 mg/d, 0.25 mg/d, or 0.5 mg/d or placebo (PBO) daily for 2 years. They also received daily calcium and vitamin D. The primary endpoint, change in L1-L4 lumbar spine BMD at 2 years, was evaluated using an *a priori* fixed sequence multiple comparisons procedure on data pooled from both studies. At 2 years, patients treated with 0.025 mg/d, 0.25 mg/d, or 0.5 mg/d lasofloxifene had a significant increase in lumbar spine BMD from baseline: 1.5%, 2.3%, and 2.3%, respectively ($p \leq 0.001$) compared with a decrease of 0.7% with placebo. All 3 lasofloxifene doses significantly increased BMD of the total hip and its subcomponents ($p \leq 0.001$ vs. PBO). Lasofloxifene significantly increased BMD of the lumbar spine and total hip for all 3 doses at 6 and 12 months. At 6 and 24 months, lasofloxifene groups exhibited significant decreases in bone turnover markers vs. PBO. Median percent changes from baseline at 6 m for 0.025 mg/d, 0.25 mg/d and 0.5 mg/d lasofloxifene (underlined) and PBO respectively were osteocalcin: -9.40%, -22.5%, -20.8%, 5.71%; CTX: -37.5, -49.9%, -50.9%, -0.43; and PINP: -30.0%, -40.5%, -40.5%, -4.6% ($p \leq 0.001$). Bone biopsies in lasofloxifene-treated subjects showed bone of normal quality. Overall, lasofloxifene was generally safe and well-tolerated. Adverse events often reported included hot flushes, leg cramps, and increased vaginal moisture. In postmenopausal women with low or normal BMD, lasofloxifene treatment significantly increased lumbar spine and hip BMD and decreased bone turnover markers, with beneficial changes observed as early as 6 months. Lasofloxifene may be an appropriate therapy for the prevention of bone loss in postmenopausal women.

Disclosures: **M. McClung**, Pfizer 2.

F433

Intermittent Administration of Human Parathyroid Hormone Enhances Bone Formation and Bone Union at the Site of Cancellous Bone Osteotomy in Normal and Ovariectomized Rats. **K. Nozaka, N. Miyakoshi, Y. Kasukawa, S. Maekawa, H. Noguchi, E. Itoi.** Orthopedic Surgery, Akita University School of Medicine, Akita, Japan.

Intermittent administration of human parathyroid hormone (hPTH) has been reported to promote bone formation acting on osteoblasts and their precursor cells. The hPTH treatment also has been shown to enhance fracture healing and callus formation on cortical bone in animals. However, little is known about the effects of hPTH on cancellous bone healing. Therefore, the purposes of this study were: 1) to evaluate whether intermittent administration of hPTH enhances bone formation and bone union at the site of cancellous bone osteotomy; and 2) to elucidate the mechanisms of hPTH effects on bone marrow cells at and around the site of osteotomy. Following a cancellous bone osteotomy performed at the left proximal tibia in seven-month-old Wistar rats with ovariectomy (OVX) or sham-operation, hPTH (1-34) (100 μ g/kg) or its vehicle was administered subcutaneously once a week for 4 weeks. One week after the final administration, bilateral tibiae were harvested for decalcified histologic sections. The right tibiae were used as a non-operated control. In addition to the conventional bone histomorphometry, the adipocyte volume (AV/MV; %) and the number of adipocyte per marrow volume (N.A/MV; /mm²) were measured to evaluate the amount of fat tissue in bone marrow. The percentages of proliferating cell nuclear antigen (PCNA) positive cells in bone marrow cells were also evaluated. hPTH treatment decreased AV/MV and N.A/MV in the OVX group, and increased 1) bone formation and volume both in the sham-operated and OVX groups, 2) the percentage of PCNA positive cells both in the sham-operated and OVX groups, 3) PCNA positive cells at the osteotomy site more than non-osteotomy site in the OVX group, and 4) bone union rate both in the sham-operated and OVX groups. These results suggested that: 1) the hPTH treatment increased osteoblastogenesis and decreased adipocytogenesis at the site of cancellous bone osteotomy; and 2) hPTH might have a selective action in promoting bone union at the site of cancellous bone osteotomy. We conclude that intermittent administration of hPTH enhances bone formation and bone union at the site of cancellous bone osteotomy by, at least in part, a local regulation of bone formation in normal and OVX rats.

Disclosures: **K. Nozaka**, None.

F435

Treatment of Postmenopausal Osteoporotic Women with Parathyroid Hormone 1-84 for 18 Months Improves Trabecular Bone Architecture: A Study of Iliac Crest Biopsies Using Micro-Computed Tomography. D. W. Dempster^{*1}, I. A. Moreau^{*2}, A. Varela^{*2}, S. Y. Smith^{*2}, L. G. Ste-Marie^{*3}, J. Fox^{*4}, M. K. Newman^{*4}, R. R. Recker^{*5}. ¹Helen Hayes Hospital, West Haverstraw, NY, USA, ²CTBR, Senneville, PQ, Canada, ³Centre de Recherche du CHUM - Hospital Saint-Luc, Montreal, PQ, Canada, ⁴NPS Pharmaceuticals, Salt Lake City, UT, USA, ⁵Creighton University, Omaha, NE, USA.

Iliac crest biopsies were obtained from postmenopausal osteoporotic women enrolled in the TOP Study after 18 months of daily sc injections of placebo or 100 µg parathyroid hormone 1-84 (PTH). All subjects received daily treatment with calcium (700 mg) and vitamin D (400 IU). There were no significant differences between groups in age, weight, bone turnover markers, or spine and hip bone mineral density at baseline. Recently we reported (ASBMR, 2004) results of quantitative histomorphometry in these biopsies. Relative to placebo-treated subjects, cancellous bone volume (Cn.BV/TV), was 48% higher in subjects treated with PTH. This increase could be accounted for by increases in trabecular number (Tb.N) (24%) and thickness (Tb.Th) (17%) which resulted in a 21% decrease in trabecular separation (Tb.Sp). Prior to sectioning for histomorphometry, the biopsies (n = 8 / group) were subjected to micro-computed tomography (Micro-CT 20, Scanco Medical, AG). The values for trabecular structure obtained by µCT were very similar to those obtained by histomorphometry. Compared to placebo-treated subjects, mean Cn.BV/TV was 45% higher in PTH-treated subjects (PTH = 23.3% ± 2.0 vs placebo = 16.1% ± 1.4; *P* = 0.036). The higher Cn.BV/TV was the result of 12% and 17% increases, in mean Tb.N (PTH = 1.40/mm ± 0.06, placebo = 1.25/mm ± 0.04; *P* = 0.093) and mean Tb.Th (PTH = 186 µm ± 12, placebo = 159 µm ± 11; *P* = 0.128), respectively, with a 10% lower mean Tb.Sp (PTH = 696 µm ± 27, placebo = 771 µm ± 23; *P* = 0.036). Importantly, mean connectivity density (Conn.D) was 22% higher (PTH = 4.81/mm³ ± 0.34, placebo = 3.93/mm³ ± 0.52; *P* = 0.074). The mean structure model index (SMI) was also significantly lower (55%) in PTH-treated subjects relative to placebo-treated subjects (0.49 ± 0.25 vs 1.09 ± 0.16, respectively; *P* = 0.046), indicating a better connected trabecular architecture with a more plate-like structure, both indicative of a stronger bone. In conclusion, relative to placebo, treatment of osteoporotic women for 18 months with PTH resulted in marked increases in Cn.BV/TV, improved trabecular connectivity and a more plate-like structure. Structural variables obtained by µCT and bone histomorphometry were remarkably similar. All of these results are consistent with an increase in bone strength and the marked reduction in vertebral fracture incidence observed in the TOP Study.

Disclosures: **D.W. Dempster**, Merck / sanofi-aventis 6; Eli-Lilly / Procter & Gamble 5, 6; GlaxoSmithKline / Roche / NPS Pharmaceuticals 5.

F437

Changes in Osteoblast, Chondrocyte, and Adipocyte Lineages Mediate the Bone Anabolic Actions of PTH and Small Molecule GSK3 Inhibitor. N. H. Kulkarni^{*1}, T. Wei^{*1}, A. Kumar^{*1}, E. Dow^{*1}, T. Stewart^{*1}, J. Shou^{*1}, M. N'Cho^{*1}, D. L. Halladay^{*1}, T. Engler^{*1}, T. J. Martin², H. U. Bryant¹, Y. L. Ma¹, M. Liu^{*1}, J. E. onyia¹. ¹Lilly Research Labs, Greenfield, IN, USA, ²SVMRI, Fitzroy, Victoria, Australia.

Parathyroid hormone (PTH) and an orally bioavailable small molecule glycogen synthase kinase3 (GSK3) α/β dual inhibitor 603281-31-8, administered once daily increase bone formation *in vivo*. The cellular basis for the anabolic effects has been shown largely to impact cells of osteoblast lineage. The present study was designed to decipher molecular mechanisms behind the anabolic phenotype of PTH and 603281-31-8 in an osteopenic rat model using whole genome array profiling and pathway mapping. Female 6-month old rats were ovariectomized (Ovx) and permitted to lose bone for one month, followed by treatment with PTH (1-38) at 10 µg/kg/d sc or 603281-31-8 at 3 mg/kg/d po for 60 days. Twenty-four hr after the last treatment, RNA was isolated from distal femur metaphysis and subjected to gene expression analysis. Differentially expressed genes (*p* < 0.05) were subjected to pathway analysis to delineate relevant functional processes involved in skeletal biology. Genes involved in biological pathways such as morphogenesis, cell growth, differentiation, apoptosis, and extracellular matrix were significantly altered by Ovx and the treatments. Analysis of morphogenesis genes showed an overrepresentation of genes involved in osteogenesis/bone remodeling, chondrogenesis/cartilage condensation and adipogenesis. A striking finding (confirmed by Real-Time PCR) was that Ovx substantially decreased the markers of osteogenesis (Collagen α₁ (I), α₁(V), osteocalcin, BSP, osteonectin, osteopontin, matrix gla protein) and of chondrogenesis (Collagenα₁ (II), Collagen (X), aggrecan1, COMP, Cdrap) and increased markers of adipogenesis (PPARγ, LPL, leptin, CEBPA, Adipsin, FABP4, SREBF1, ADFP, caveolin 1, PEPCK). PTH and the GSK3 inhibitor reversed these effects, albeit at different levels. Overall, PTH was more efficacious at regulating these markers, with normalization to control or below control levels. Additionally, in intact animals, the inhibitory effects of PTH on the adipogenic markers tested so far were evident after 1-to-5 days of treatment. These results suggest that the anabolic actions of PTH and 603281-31-8 *in vivo* involve effects on other mesenchymal lineages (chondrocytes & adipocytes). The changes in cartilage markers in bone suggest an ongoing biosynthetic turnover of cartilage, but may also reflect progressive bone formation as a result of endochondral ossification. The decrease in adipogenesis markers by these anabolic agents might be a requirement for their stimulation of bone formation.

Disclosures: **N.H. Kulkarni**, None.

F440

Pamidronate Treatment Affects Metaphyseal Modeling in Children with Osteogenesis Imperfecta. C. Land, F. Rauch, F. Glorieux. Shriners Hospital for Children, McGill University, Montreal, PQ, Canada.

Cyclical intravenous therapy with pamidronate is of clinical benefit in children and adolescents with moderate to severe osteogenesis imperfecta (OI). However, recent case reports show that this medication has the potential to interfere with femoral metaphyseal modeling (shaping). In this study we elucidated the effects of pamidronate on the shape of the growing distal femur. We compared radiographs from 55 children with moderate to severe OI (mean age 6.5 years, range 2.2 -15.3 years; 29 girls) who had received between 2 and 4 years of pamidronate therapy (annual dose 9 mg/kg) and 55 untreated OI patients who were matched for age, sex and OI type. Distal femoral metaphyseal width (MW) was measured at a site whose distance to the growth plate corresponded to half of growth plate width (GPW). Metaphyseal index (MI) was calculated as the ratio between MW and GPW (Ward et al., Bone, in press). Even though the treatment and control groups had similar GPW, the two groups differed significantly with regard to MW (Table). Consequently MI was higher in treated patients, indicating a significant effect of pamidronate on metaphyseal modeling. This shows that pamidronate interferes with the process of periosteal resorption that is normally responsible for shaping the distal femoral metaphysis. However, at present, there is no evidence that this radiological adverse event is of clinical significance.

Variable	n	Pamidronate	n	Untreated	P value
GPW type I	8	5.91±0.92	8	6.02±0.92	0.81
GPW type III	18	3.93±1.00	18	3.66±1.64	0.54
GPW type IV	29	5.16±1.24	29	5.10±1.61	0.88
MW type I	8	4.26±0.53	8	3.19±0.55	<0.001
MW type III	18	2.82±0.69	18	1.94±0.42	<0.001
MW type IV	29	3.65±0.75	29	2.88±0.62	<0.001
MI type I	8	0.73±0.07	8	0.53±0.07	<0.001
MI type III	18	0.72±0.10	18	0.60±0.18	<0.02
MI type IV	29	0.72±0.08	29	0.58±0.08	<0.001

Values are mean±SD. GPW and MW are given in cm.

Disclosures: **C. Land**, None.

F442

FGF23 Mutants Causing Familial Ttumoral Calcinosis Are Differentially Processed. T. E. M. Larsson¹, S. S. Davis^{*1}, H. J. Garringer^{*1}, S. D. Mooney^{*1}, M. S. Draman^{*2}, M. J. Cullen^{*2}, K. E. White¹. ¹Medical and Molecular Genetics, Indiana University School of Medicine, Indianapolis, IN, USA, ²Endocrinology, Trinity College, Dublin Medical School, Dublin, Ireland.

Familial tumoral calcinosis (TC) is a heritable disorder characterized by high serum Pi, normal or elevated serum 1,25(OH)₂D₃, and ectopic periarticular and/or vascular calcifications. We, and others, have previously identified two recessive mutations in *Fibroblast growth factor-23 (FGF23)*, serine 71/glycine (S71G) and serine 129/phenylalanine (S129F), as causative for TC. Our reported S71G TC patients had markedly elevated C-terminal serum FGF23 levels (>3000 RU/mL, (ref: 50±55 RU/mL)), however low-normal intact FGF23 levels. Therefore, the goal of our study was to understand the pathophysiology of these FGF23 TC mutations. Studies of the entire FGF23 S71G kindred revealed that heterozygous carriers (S/G, n=5) had elevated serum FGF23 C-terminal fragments compared to wt (S/S, n=6) family members (74.1±5.5 vs. 54.6±4.7 RU/mL, *P* < 0.025), whereas intact FGF23 levels were not different. Carriers also presented with normal serum Pi and 1,25(OH)₂D₃, and displayed no evident disease phenotype. To understand the differential processing of FGF23 in TC patients, we transiently expressed the S71G and S129F mutants in HEK293 cells. FGF23 ELISA and Western analyses of conditioned media and cell lysates revealed increased proteolytic cleavage of FGF23, and a limited secretion of intact FGF23, parallel observations with the serum FGF23 profiles of our TC patients. Furthermore, expressing S71G and S129F FGF23s, in tandem with the known ADHR mutations that disrupt the furin-like protease RXXR motif, rescued FGF23 secretion by stabilizing the intact polypeptides. This finding was supported by similar sensitivity of these mutants to trypsin digests. Finally, S71G, but not the S129F mutant FGF23, is secreted by cells when incubated at low temperature (29°C), indicating that S71G mutant FGF23 protein structure may be in part corrected by cellular chaperones under these conditions. In summary, carriers for the S71G mutation have normal phenotypes, and FGF23 mutations causing TC lead to increased intracellular proteolysis of FGF23. Moreover, furin-like proteases play an important role in TC and may act as intracellular "quality control monitors", thus more efficiently processing FGF23s with improper folding or post-translational modification. Our findings provide new insights into the role of FGF23 in TC, as well as in Pi and vitamin D metabolism.

Disclosures: **T.E.M. Larsson**, None.

F444

A Homozygous S129P Missense Mutation in FGF-23 Causes Tumoral Calcinosis with Hyperphosphatemia. C. Bergwitz¹, S. Banerjee^{*1}, H. Abu-Zahra^{*1}, H. Kaji², T. Sugimoto³, K. Chihara², A. Miyauchi⁴, H. Jüppner¹.

¹Endocrine Unit, Massachusetts General Hospital, Boston, MA, USA,

²Department of Endocrinology/Metabolism, Kobe University, Kobe, Japan,

³Department of Endocrinology/Metabolism, Shimane University Medical School, Shimane, Japan, ⁴Department of Medicine, National Hyogo-Chuo Hospital, Sanda-shi, Japan.

Familial tumoral calcinosis with hyperphosphatemia (FTC) is an autosomal recessive disorder that can be caused by homozygous mutations in either *GALNT3* or *FGF23*. We analyzed the three exons encoding FGF23 and all intron/exon borders in genomic DNA of a previously reported individual affected by FTC [Yamaguchi 1995, Bone 16(4):247S]; serum phosphate 7.0 mg/dl (2.5-4.5), 1,25(OH)₂-D 44 pg/ml (15-60), %TRP 98.8% (85-96), Tmp/GFR 2.7 (0.8-1.35) and C-terminal FGF23 20233 RU/ml (50±51), intact FGF23 38 pg/ml (15-60). PTH and serum calcium were normal. We identified a homozygous nucleotide change c.385T>C in *FGF23* exon 2 that changes codon 129 from serine to proline (S129P). A different mutation in this codon (S129F) was previously reported in another case of FTC [Araya et al. 2004, JBMR 19:S41]. The patient's unaffected mother and normal controls are currently being analyzed. For functional analysis the S129P mutation, as well as two previously reported *FGF23* mutations, S71G and S129F, were introduced into an expression plasmid encoding human (h) FGF23 to yield [P129]hFGF23, [F129]hFGF23, and [G71]hFGF23; these plasmids were expressed in COS-7 and HEK293 cells. Medium and cell lysate were subjected to Western blot analysis using affinity purified anti-hFGF23(59-68) and anti-hFGF23(206-222) antibodies generated in goats (Immupotops). Lysates of HEK293 cells expressing wild-type FGF23 (WT-FGF23) revealed a 27 kDa band representing the intact and a 32 kDa band that presumably represents an intact, possibly modified form of FGF23. The 32 kDa peptide was efficiently secreted into the medium, along with N- and C-terminal fragments. Lysates from cells expressing [P129]hFGF23 revealed the 27 kDa intact molecule, but lacked the modified 32 kDa form. Only small amounts of N- and C-terminal fragments appeared in the medium, while intact FGF23 was undetectable. This suggests that P129 may prevent modification of [P129]hFGF23, thereby limiting the secretion of the intact protein into the medium. To determine whether the apparent lack of modification of [P129]hFGF23 is due to a lack of O-linked glycosylation, we currently determine whether WT-FGF23 undergoes such a modification at one or several of the conserved serine residues.

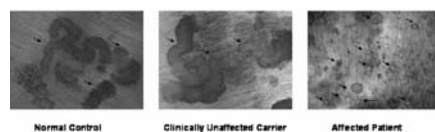
Disclosures: C. Bergwitz, None.

F446

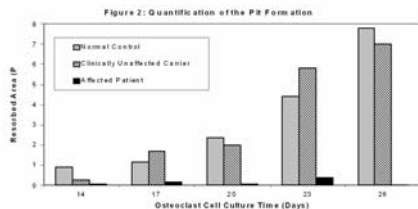
Determination of Carrier Status in ADO2: An In Vitro Study of Clinically Unaffected Gene Carriers. K. Chu^{*}, R. Snyder^{*}, M. J. Econs. Medicine, Indiana University School of Medicine, Indianapolis, IN, USA.

Autosomal dominant osteopetrosis type II (ADO2) is a heritable osteosclerotic disorder that results from heterozygous mutations in the *CICN7* gene. However, of those individuals with a *CICN7* mutation, 1/3 are asymptomatic carriers. Disease severity in the remaining 2/3 is highly variable. The most severely affected manifest multiple fractures, osteomyelitis, visual loss and, occasionally, bone marrow failure. There is no genotype/ phenotype correlation and families frequently have both carriers and severely affected individuals. To determine whether the carrier status results from the bone micro environment (i.e. secretion of cytokines, hormonal environment, and condition of the other bone cells) or is intrinsic to the osteoclasts, we performed in vitro osteoclast cell culture in affected patients, carriers and normal controls (n=5 in each group). Subjects were matched for age, sex and ethnicity. Human peripheral blood mononuclear cells were isolated by magnetic beads and differentiated into osteoclasts by stimulation with hRANK-L and hM-CSF. Cell fusion, F-

Figure 1: Pit Formation of the Osteoclasts (23 days after in vitro culture)



Arrows point to the pits



actin ring formation, TRAP activity, cell acidic microenvironment analysis were investigated and no significant difference was found between the three groups. However, osteoclasts from the carrier and normal groups generated more extensive and continuous resorption pits compared to the affected groups, which had rare and restricted pits (figure 1). Moreover, the pits from the carrier and the normal groups formed much earlier and extended much more rapidly than the pits from the affected groups (figure 2). There were no significant differences between the carrier and normal groups at any time point. In conclusion, osteoclasts from the carriers, in contrast to those from the affected individuals (who had the same *CICN7* mutations) function normally in cell culture. This finding supports the hypothesis that intrinsic osteoclast factors determine whether an individual with a *CICN7* mutation becomes an affected patient or an asymptomatic carrier. Further understanding of this mechanism is likely to lead to the development of new approaches for the treatment of affected patients.

Disclosures: K. Chu, None.

F450

Caveolin-1 Deficient Mice Exhibit Sexually Dimorphic Changes in Bone Phenotype: Micro-CT and Biomechanical and Biomechanical Analysis. H. Yao^{*1}, Z. Schwartz¹, H. Jo^{*2}, J. Rubin², R. E. Guldberg^{*1}, K. Wong^{*1}, L. Wang¹, B. D. Boyan¹. ¹Georgia Institute of Technology, Atlanta, GA, USA, ²Emory University Medical School, Atlanta, GA, USA.

Caveolae are plasma membrane invaginations that play an important role in numerous cellular processes including transport and signaling. Mice lacking caveolin-1 (Cav-1), the major scaffolding protein in caveolae, exhibit vascular dysfunction and pulmonary defects, and endothelial cells from these Cav-1^{-/-} mice have altered response to mechanical strain. Recent studies have shown that estrogen receptors traffic into and out of caveolae via Cav-1 in response to estrogen, suggesting that mechanically-sensitive bone might also exhibit a Cav-1^{-/-} phenotype and that it might be sex-specific. To test this, we evaluated the phenotypic consequences of knocking out the Cav-1 gene in bone. Cav-1^{-/-} and C57BL/6 wild-type male and female 8-week-old mice were used for these studies. A total of 32 femora (8 mice per genotype per sex) were scanned using micro-CT to obtain high-resolution images of the trabecular bone in the distal femur, as well as cortical bone in the mid-diaphysis. After scanning, the femora were tested to destruction in four-point bending at the mid-diaphysis. Morphologic parameters for trabecular and cortical bone as well as structural and material properties of cortical bone were determined. The Cav-1^{-/-} mice displayed enlarged growth plates for both male (18% increase in height) and female (93.1% increase in height) groups. The bone volume fraction, as well as trabecular thickness, in the metaphysis were significantly increased in the Cav-1^{-/-} mice, especially in the female group. In contrast, trabecular bone mineral densities in the metaphysis for knockout mice were slightly lower than the wild-type in both male and female groups. While the Cav-1^{-/-} mice had thicker cortical bone and higher maximum load in the mid-diaphysis, the value of the elastic modulus in the male Cav-1^{-/-} mice was lower than the wild-type counterpart. Interestingly, the values of elastic modulus in Cav-1^{-/-} female mice and both wild type groups were similar. Overall, the absence of Cav-1 increased bone tissue formation. Knocking out Cav-1 reduced bone quality in male animals based on elastic modulus, but not in female animals. Our results confirmed that Cav-1 is needed for normal bone physiology, and suggest that the absence of Cav-1 causes sexually dimorphic changes. The increase size of the growth plate in the Cav-1^{-/-} mice, particularly in female bones, may be related to the altered microarchitecture observed in the metaphysis.

Disclosures: H. Yao, None.

F453

Reduced 25-Hydroxyvitamin D₃-1alpha-Hydroxylase Activity Impacts Negatively on the Secondary Hyperparathyroidism Arising from FGF23 Overexpression. H. Fu^{*}, X. Bai^{*}, D. Miao^{*}, J. Gao^{*}, D. Goltzman, A. C. Karaplis. McGill University, Montreal, PQ, Canada.

Fibroblast growth factor 23 (FGF23) is a recently characterized protein likely involved in the regulation of serum phosphate homeostasis. We have previously generated transgenic mice expressing and secreting from the liver human FGF23(R176Q), a mutant form that fails to be degraded by furin proteases (Tg). High circulating levels of FGF23 were associated with disturbances in the regulation of phosphate and vitamin D metabolism as well as calcium homeostasis and elevated PTH levels due to secondary hyperparathyroidism may have also contributed to renal phosphate wasting. We and others have also previously reported a mouse model deficient in 1,25(OH)₂D₃ by targeted ablation of the 25-hydroxyvitamin D₃-1alpha-hydroxylase gene (K.O.). After weaning, mice that were fed a regular mouse chow, developed secondary hyperparathyroidism, retarded growth, and the skeletal abnormalities characteristic of rickets. To further investigate the role of secondary hyperparathyroidism and the 1-alpha hydroxylase enzyme in the biochemical alterations associated with FGF23 overexpression, the FGF23(R176Q) transgene was crossed into the K.O. background (Tg/K.O.). Post weaning these mice, relative to Tg mice, when fed a regular diet (1% Ca, 0.67% P), exhibited profound growth retardation and early demise by 2 months of age. In the Tg/K.O. mice relative to the Tg animals, serum levels of calcium decreased slightly while PTH levels increased dramatically and serum phosphorus and renal phosphate threshold diminished significantly from the already low levels seen in the Tg mice. Alkaline phosphatase activity was dramatically increased and bone volume and osteoid volume rose markedly above the high levels already seen in the Tg mice. When these animals were fed a rescue diet (2% Ca, 1.25% P, 20% lactose) post weaning, near-normal growth and survival were observed in both Tg and Tg/K.O. models, and much less pronounced changes in serum calcium, phosphorus, PTH, and alkaline phosphatase activity were seen compared to mice on a regular diet. Although serum phosphorus remained low, bone volume decreased and mineralization was markedly improved in both Tg and Tg/K.O. mice. In summary, our findings show that 1-alpha hydroxylase activity can play a pivotal role in modifying the biochemical and skeletal changes arising from FGF23 overexpression. Our findings also add further support to the premise that secondary hyperparathyroidism is an integral component of this disturbed state and that elevated PTH levels contribute to the renal phosphate wasting and to increased bone formation thereby potentiating the osteomalacia associated with this deranged state.

Disclosures: A.C. Karaplis, None.

F457

Adult Hypophosphatasia Treated with Teriparatide. C. L. Deal¹, M. P. Whyte². ¹Cleveland Clinic, Cleveland, OH, USA, ²Research Center, Shriners Hospitals for Children, St. Louis, MO, USA.

We report the first case of hypophosphatasia (HPP) treated with teriparatide (rhPTH 1-34, TPTD). HPP features low circulating alkaline phosphatase (ALP) activity from deactivating mutation of the gene encoding the “tissue nonspecific” isoenzyme of ALP (TNSALP). Extracellular accumulation of inorganic pyrophosphate (PPi) impairs skeletal mineralization causing rickets in children and osteomalacia in adults. There is no established medical therapy. Adult HPP typically presents with poorly-healing metatarsal stress fractures (MTSF) and unhealing femoral pseudofractures (FPF). At age 54, our patient had a painful MTSF with delayed healing over 7 months. Two MTSFs occurred 2 years later and did not heal. A FPF ensued. Pain occurred at fracture sites. Serum ALP ranged from 10-24 IU/L (40-150 nl) and bone-specific ALP was 6 IU/L (12-31 nl). Other biochemical studies were unremarkable except for two further features of HPP: elevated serum inorganic phosphate (Pi) level of 5.1 mg/dl and vitamin B6 concentration of 603 ug/L. DXA of the lumbar spine and total hip showed Z-scores of +2.9 and +1.5, respectively. Treatment was begun at age 56 with 20 mcg TPTD. After 2 mo, pain improved 50% and 90% in thigh and foot. After 4 mo, no fracture site was painful. Therapy was discontinued briefly when NTX rose and OC fell. X-rays of the feet showed significant healing after 4 mo in 2 MTSFs and delayed healing with exuberant callus in 1 MTSF (no callus was present 9 mo after MTSF prior to TPTD treatment). The FPF appeared completely healed after 9 mo. A marked reduction in chondrocalcinosis in the symphysis pubis was seen after 9 mo of TPTD. Sequential biochemical studies, including improved serum ALP activity, are below. Ours is the first report of HPP treated with TPTD. Complete pain relief at fracture sites occurred after 2 mo; MTSP and FPF healed. Biochemical studies documented increased ALP, NTX, and OC suggesting restoration of bone remodeling, but without hypercalcemia. Little change in circulating vitamin B6 levels suggested a focal (skeletal) effect from TPTD treatment. TPTD may engender clinical improvement and fracture healing in adult HPP due to enhanced osteoblast production of TNSALP and/or phosphaturia lowering (at mineralization sites) extracellular Pi levels which act as a competitive inhibitor of TNSALP.

	4/04 (start Rx)	6/04	8/04 (stop Rx)	11/04 (resume Rx)	2/05	Normal Range
ALP (IU/L)	24	37	43	39	38	40-150
NTX (nMmM Cr)	26	35	93	72	122	14-75
OC (ng/ml)	3	8.2	5.3	2.8	6.7	< 7.2
Pi (mg/dl)	5.1	5.2	4.3	4.4		2.5-4.5
vit B6 (ug/L)	603	1478	787	911	565	18-175

Disclosures: **C.L. Deal**, None.

F459

Phosphate Depletion and Hypophosphatemia Directly Regulate FGF-23 Expression. M. Takaiwa¹, B. Yuan¹, H. Tanaka², R. Kumar³, M. K. Drezner¹. ¹University of Wisconsin, Madison, WI, USA, ²Okayama University, Okayama, Japan, ³Mayo Clinic, Rochester, MN, USA.

Regulation of phosphate homeostasis is a complex process, likely involving both conventional hormones, such as parathyroid hormone and 1,25-dihydroxyvitamin D, as well as recently discovered novel factors, FGF-23 and sFRP-4. The integrated counter-regulatory effects of oral phosphate intake and serum phosphorus levels on these hormonal/metabolic factors remain incompletely defined. Thus, in the present study we sought to elucidate the effects of oral phosphate depletion and consequent hypophosphatemia on renal expression of sFRP-4 and 25-hydroxyvitamin D-1 α -hydroxylase and bone expression of FGF-23. We fed C57BL/6J mice, 8-12 weeks of age, a standard (Pi 1.0%, Ca 0.95%, Vitamin D 4.5 IU/g) or Pi depleted diet (Pi 0.02%, Ca 0.95%, Vitamin D 4.5 IU/g) for 3 days and quantified expression of the respective genes by real-time PCR using ABI 7000 (Applied Biosystems). We extended these observations by evaluating the protein abundance (Westerns) of renal 25-hydroxyvitamin D-1 α -hydroxylase and sFRP and the circulating levels of FGF-23 (ELISA). After 3 days of phosphate depletion, the serum phosphorus level in the treated mice decreased significantly (p<0.001) from 6.6 \pm 0.3 to 4.2 \pm 0.1 mg/dl. In concert, FGF-23 gene expression significantly (p< 0.05) decreased (30%), resulting in a concordant 70% decrement in the circulating levels of this protein. In contrast, renal expression of sFRP-4 and protein abundance did not change in response to the hypophosphatemic challenge. However, not unexpectedly, in response to the hypophosphatemia, renal 25-hydroxyvitamin D-1 α -hydroxylase gene expression increased (1.0 \pm 0.05 vs. 2.4 \pm 0.3 fold), as did the protein content (1.0 \pm 0.07 vs 1.49 \pm 0.15 fold). Since previous observations (J Biol Chem 2005; 280:2543-9) indicate 1,25(OH) $_2$ D dose dependently increases serum FGF-23 levels, our data suggest that phosphate depletion and hypophosphatemia attenuate these effects and independently regulate FGF-23 production. To confirm that the phosphate effects were independent and direct, we examined *in vitro* the effects of phosphate on FGF-23 gene expression in the mouse mesenchymal cell line ST-2. We found that phosphate significantly increased FGF-23 gene expression in a dose dependent manner, consistent with the diminished FGF-23 observed in response to hypophosphatemia. These results indicate that phosphate depletion and hypophosphatemia directly counter-regulate FGF-23 production and consequently circulating levels, suggesting that FGF-23 and the osteoblasts producing this factor may directly participate in a feedback loop regulating phosphate homeostasis.

Disclosures: **M. Takaiwa**, None.

F461

AC-100, a Fragment of MEPE, Promotes New Dentin Formation in both Direct and Indirect Pulp Capping Models in Beagle Dogs. M. Lazarov¹, C. Middleton-Hardie¹, M. Shih^{*2}, A. Negron^{*2}, V. Kiklevich^{*3}, M. Powers^{*3}, D. Rosen¹. ¹Research and Development, Acologix, Inc, Hayward, CA, USA, ²Skeletech, Bothell, WA, USA, ³Department of Veterinary Clinical Sciences, Washington State University, Pullman, WA, USA.

MEPE, a protein originally cloned from tumors associated with hypophosphatemic osteomalacia, is expressed primarily in normal human bone and odontoblast cells. AC-100 (Dentonin), a central 23-amino acid fragment of MEPE, contains motifs that are important in regulating cellular activities in the bone and dentin microenvironment. In vivo studies indicate that AC-100 is able to stimulate new dentin and bone formation in teeth and bone respectively. Unlike BMPs, no bone or dentin formation has been observed locally following subcutaneous administration of AC-100. Here we report that AC-100 stimulates new dentin formation in both direct and indirect pulp capping models in dogs. **Methods:** Deep class V preparations were made with or without penetrating the pulp cavity of the maxillary teeth in Beagle dogs. Each tooth was treated with AC-100 or with negative control (saline) or positive control (Dycal). Animals were sacrificed and teeth were analyzed histologically. **Results:** In the indirect pulp capping portion of the study at 3 days post surgery the saline or Dycal treated teeth showed an inflammatory response in the pulp tissue. Application of AC-100 completely abolished the pulp inflammation and dose-dependently decreased the number of apoptotic cells in the pulp. At 28 days post surgery the saline-treated teeth showed little new dentin formation while application of AC-100 induced a dose-dependent stimulation of dentin growth comparable to and better than Dycal. Considerably better results were obtained employing a multiple-dose application schedule. In the direct pulp capping portion of the study at 56 days the teeth that were sealed using saline showed no dentin bridge formation in 4 out of 5 dogs, while application of 200 μ g of AC-100 stimulated complete bridging of the defects in 3 out of 5 dogs. **Conclusion:** AC-100 stimulates new dentin growth and dentin bridge formation in both direct and indirect pulp capping studies in dogs in a dose and application method dependent manner. Importantly, the mechanism of action of AC-100 is notably different from the mechanism of the dentin stimulating agents available for clinical use at present. The currently approved agents stimulate dentin growth through non-physiologic irritation of the pulp tissue. In contrast, AC-100 achieves its activity by producing new dentin, while exhibiting reduced inflammatory and apoptotic activities locally.

Disclosures: **M. Lazarov**, Acologix, Inc 3.

F464

Measles Virus Nucleocapsid Protein Increases TNF- α Induced Osteoclast Differentiation. T. Honjo¹, N. Kurihara¹, J. J. Windle², G. D. Roodman³. ¹Medicine/Hem-Onc, University of Pittsburgh, Pittsburgh, PA, USA, ²Human Genetics, Virginia Commonwealth Univ., Richmond, VA, USA, ³Medicine/Hem-Onc, University of Pittsburgh and VA Pittsburgh Healthcare System, Pittsburgh, PA, USA.

Osteoclasts (OCL) from Paget's patients (PD) are abnormal and contain Measles Virus Nucleocapsid Protein (MVNP) transcripts. Furthermore, human OCL precursors transfected with MVNP demonstrate many features of pagetic OCL. We previously reported that OCL precursors from patients with Paget's disease or normal OCL precursors transfected with MVNP are hyperresponsive to RANKL and 1,25-(OH) $_2$ D $_3$. We determined if MVNP could also increase TNF- α responsivity of OCL precursors. To test this hypothesis, we used normal human bone marrow transfected with MVNP and OCL precursors from transgenic mice with MVNP targeted to the OCL lineage using the TRAP promoter (TRAP/MVNP). NIH3T3 cells transfected with MVNP or empty vector (EV) were also used as surrogate for OCL precursors and to further examine the NF- κ B pathway. Marrow cultures from TRAP-MVNP mice formed markedly increased numbers of OCL that were hyper-nucleated compared to wild type OCL. OCL precursors from TRAP/MVNP mice formed OCL at lower concentrations of 1,25-(OH) $_2$ D $_3$ and TNF- α than those required for normal marrow cultures. Western blot analysis and real time PCR showed treatment of MVNP-transfected human CFU-GM cells or TRAP/MVNP OCL precursors with TNF- α increased both p62 and TRAF2 expression levels approximately 200%, and increased IKK- γ 1.3-fold compared to results with EV-transfected cells. IKK- γ is an important regulator of NF- κ B signaling induced by TNF- α , and is absolutely required for IKK activation by TNF- α . We then determined if these effects resulted in enhanced NF- κ B signaling. Basal NF- κ B in MVNP-transfected human CFU-GM and TRAP/MVNP mouse OCL precursors was increased 2-fold compared to EV-transfected cells and wild type OCL precursors, and was increased 2.7-fold when MVNP-transfected cells and TRAP/MVNP OCL precursors were treated with TNF- α . Furthermore, a 7-fold increase in basal NF- κ B reporter gene activity was seen in MVNP-transfected NIH3T3 cells compared to EV-transfected cells. TNF- α also increased (by 350%) the phosphorylation of IKK- γ within 15 minutes after addition of TNF- α in MVNP-transfected NIH3T3 cells compared with EV-transfected cells. These results demonstrate that MVNP increases TNF- α induced OCL differentiation and activation by increasing NF- κ B signaling through increased expression of p62, TRAF2 and IKK- γ . These results suggest that MVNP's effects on TNF- α signaling may contribute to the increased OCL formation in PD.

Disclosures: **T. Honjo**, None.

F470

Stunted Growth and Altered Bone Phenotype in IL-6 Transgenic Mice. N. Rucci¹, E. Spica¹, C. Di Giacinto¹, A. Del Fattore^{*1}, R. Paro^{*1}, S. Berni^{*2}, P. Ballanti^{*2}, M. Vivarelli^{*3}, F. Muratori^{*3}, F. De Benedetti^{*3}, A. Teti¹.

¹Department of Experimental Medicine, University of L'Aquila, L'Aquila, Italy, ²Department of Experimental Medicine and Pathology, University of Rome "La Sapienza", Rome, Italy, ³Ospedale Bambino Gesù, Rome, Italy.

Osteoporosis and stunted growth are common complications of chronic inflammation in children. IL-6 is a pro-inflammatory cytokine which increases in inflammatory diseases. We observed that the skeleton of NSE/hIL6-transgenic mice (TG) expressing high circulating levels of hIL-6 from birth was smaller than wild type (WT), with decreased longitudinal growth and mineralization. In these mice, trabecular bone was reduced, with increased osteoclast- and decreased osteoblast-number and -surface. Cortical bone was thinner, with increased endosteal osteoclast number, and showed halved periosteal and abrogated endosteal apposition. Calvarial and endochondral developments were delayed and growth plate thickness was reduced. In vivo, increment of urinary DPD excretion and low serum levels of osteocalcin demonstrated increased bone resorption, and decreased osteoblast activity, respectively, which correlated with body weight in TG but not in WT mice. A 4-fold higher number of TRAcP positive mononuclear precursors was observed in TG bone marrow that originated a 1.6-fold higher number of mature multinucleated osteoclasts, with an average 4.14 ± 0.29 nuclei/cell. Calvarial osteoblasts from TG mice showed decreased proliferation, ALP activity and mineralized nodules, which were also reduced in WT osteoblasts treated with rhIL-6. TG osteoblasts demonstrated no changes in Runx-2 and ALP transcripts versus WT cells, with no modulation of these genes in rhIL-6-treated WT osteoblasts. In contrast, the osteocalcin and collagen-1a2 mRNAs were down-regulated in TG osteoblasts and in WT osteoblasts treated with rhIL-6 compared to untreated WT cells, indicating that osteoblast function rather than differentiation was impaired by IL-6. Mouse IL-6 transcript was increased in TG osteoblasts, and treatment with exogenous rhIL-6 induced the expression of endogenous mouse IL-6 in the WT osteoblasts. These results underscore the effects of IL-6 on skeletal tissues and provide a novel standpoint to explain the uncoupling of osteoclast/osteoblast activity and the growth defect in juvenile chronic inflammatory diseases.

Disclosures: **N. Rucci**, None.

F472

Prevalence of Orthopedic Complications in Overweight Children and Adolescents: A Multi-Dimensional Cross-Sectional Analysis. E. D. Taylor^{*}, M. Tanofsky-Kraft^{*}, D. Adler-Wailes^{*}, K. Calis^{*}, S. Ghorbani^{*}, M. Mirch^{*}, K. Theim^{*}, S. Brady^{*}, J. A. Yanovski^{*}. National Institute of Child Health and Human Development - Unit on Growth and Obesity, National Institutes of Health, Bethesda, MD, USA.

Overweight in children 6-17 y has increased 3-fold in the United States since the 1970's, with the Centers for Disease Control now finding more than 15% of US children and adolescents are overweight (BMI $\geq 95^{\text{th}}$ percentile for age and sex). Previous studies have described debilitating orthopedic complications of excess weight in overweight adult populations. However, few prospective data are available that quantify the prevalence of weight-related orthopedic conditions in a sample of otherwise healthy overweight children. This study compared the prevalence of orthopedic diagnoses and musculoskeletal conditions in overweight (OW) and non-overweight (NOW) children. Subjects were 227 OW (mean age $12.6 \pm 2.7y$) and 128 NOW (mean age $11.8 \pm 2.9y$) children and adolescents enrolled in pediatric clinical studies at the National Institutes of Health in Bethesda, Maryland between 1996 and 2004. A *medical chart review* documented pertinent orthopedic past medical history and general physical exam findings related to musculoskeletal complaints. *Questionnaire data* from 183 subjects who completed "The Impact of Weight on Quality of Life - adolescent version" (IWQOL-A) questionnaire were also reviewed to study the effects of excess adiposity on the "Mobility" subscale score. To examine systematically the effects of overweight on *lower extremity alignment*, bilateral metaphyseal-diaphyseal angle (MDA) measurements were obtained from 260 subjects who underwent whole body dual-energy x-ray absorptiometry (DEXA) scanning. The prevalence of reported fractures was significantly greater in OW than NOW children (13.1 vs. 3.9%, $p = 0.0053$). The prevalence of any reported musculoskeletal discomfort was also greater in OW than NOW children (12.6 vs. 3.9%, $p = 0.0073$). In the OW group, the most common musculoskeletal joint complaint was knee pain (6.3 vs. 2.3%, $p = 0.10$). OW children and adolescents reported greater impairment in mobility than their NOW counterparts (mobility score 17.0 vs. 11.6, $p < 0.001$). Bilateral MDA measurements showed greater degree of valgus alignment in the OW group compared to the NOW group for both the right (6.5 vs. 5.2°, $p < 0.05$) and left (7.2 vs. 4.8°, $p < 0.05$) lower extremities. In conclusion, reported fractures, musculoskeletal discomfort, impaired mobility, and valgus lower extremity alignment are more prevalent in OW than NOW children and adolescents. Future studies should explore role of overweight on bone quality and the severity of joint abnormalities in the pediatric population.

Disclosures: **E.D. Taylor**, Foundation for the NIH and Pfizer Pharmaceuticals Group 2.

F474

Homozygosity for TNSALP Mutation C1348T (Arg433Cys) Causes Infantile Hypophosphatasia Manifesting Transient Disease Correction and Variably Lethal Outcome in a Black Kindred. M. P. Whyte¹, K. Essmyer^{*1}, M. Geimer^{*2}, S. Mumm². ¹Center for Metabolic Bone Disease and Molecular Research, Shriners Hospitals for Children, St. Louis, MO, USA, ²Division of Bone and Mineral Diseases, Washington University School of Medicine, St. Louis, MO, USA.

Hypophosphatasia (HPP) features low circulating alkaline phosphatase (ALP) activity (hypophosphatasemia) from deactivating mutation of the gene encoding the "tissue nonspecific" isoenzyme of ALP (TNSALP) and is associated with a remarkable range of disease severity. Extracellular accumulation of inorganic pyrophosphate (PPi), one of several TNSALP substrates and an inhibitor of hydroxyapatite crystal nucleation, impairs skeletal mineralization causing rickets or osteomalacia. There is no established medical therapy. Here, we characterize HPP prevalence in blacks and determine the molecular basis for variably lethal and transiently reversible infantile HPP in a black kindred. A report in 1986 details temporary correction of severe HPP in this black family where "infantile" HPP was fatal in two of three patients representing two sibships. At this time, the improvement in one patient followed efforts to increase TNSALP activity endogenously and suggested upregulation of the *TNSALP* gene. Here, we assessed 29 years' experience to document HPP's prevalence in blacks and identified this kindred's *TNSALP* defect. Ethnicity was known for 119 HPP families studied directly and race was ascertained for an additional 159 of 235 consultand HPP families worldwide. Only this family was black. Homozygosity for *TNSALP* missense mutation C1384T(Arg433Cys) accounted for their infantile HPP. The *TNSALP* promoter was intact. Modeling of TNSALP(433Cys) indicated compromise of the enzyme's catalytic site. We find that HPP is especially rare in blacks. Homozygous *TNSALP*(C1348T) causes variably lethal and transiently reversible HPP in this black kindred. The mutation has been reported to cause severe HPP in whites. Although not fully understood, HPP manifestations from homozygous TNSALP(433Cys) can correct, perhaps with clues for HPP's phenotypic variation and treatment.

Disclosures: **M.P. Whyte**, None.

F476

Retention, Distribution, and Effects of Intra-Osseously Administered Ibandronate in the Infarcted Femoral Head. S. Athavale^{*1}, J. Aya-Ay^{*1}, F. Bauss², H. Kim¹. ¹Shriners Hospital for Children, Tampa, FL, USA, ²Roche Diagnostic GmbH, Penzberg, Germany.

Legg-Calve-Perthes disease (LCPD) is a juvenile form of osteonecrosis of the femoral head (FH), which can lead to FH deformity and premature osteoarthritis. Ibandronate (IB), a new potent bisphosphonate, has been shown to prevent FH deformity in a large animal model of LCPD when administered parenterally. However, since LCPD is a localized hip disorder, there is a need to explore the therapeutic potential of local, intra-osseous injection of IB to prevent FH deformity. This route has the advantage of avoiding systemic distribution of the drug in the immature skeleton for a localized condition. The purpose of this study was to determine the retention, distribution, and effects of intra-osseous injection of IB in the infarcted head. Ischemic necrosis was induced in 12 piglets by placing a ligature tightly around the femoral neck. A repeat arthrotomy was performed 1 wk later to inject 1ml of ¹⁴C-IB (56ug/ml) directly into the head. The heads were retrieved at 48h, 3 and 7wks after the injection. The amount of ¹⁴C-IB retained in the infarcted head was determined using liquid scintillation analysis. The distribution of ¹⁴C-IB within the head was determined using autoradiography. Liquid scintillation analysis showed 660 folds higher radioactivity level in the infarcted heads compared to the control heads with 29.5% retention of the radioactivity at 7wks. Autoradiographic assessment revealed diffuse distribution of ¹⁴C-IB in 2/4 heads and with anterior only distribution in the other 2/4 heads at 48h. Histological assessment showed extensive revascularization of the infarcted heads at 7wks with preservation of trabecular bone in some areas. During the study period, the femora grew 4.7cm (51% increase) and the animals gained 12.1kg (175% increase), indicating a rapid growth and bone turnover. To our knowledge, this is the first study that has investigated the therapeutic potential of local intra-osseous injection of bisphosphonate in the context of ischemic osteonecrosis. In addition to limiting the delivery of the drug to the target tissue, local injection has the advantage of bypassing the need for having restored blood flow to the infarcted head for the delivery of the drug. Our study shows that a single intra-osseous injection of IB can be retained within the infarcted head for at least 7wks in this rapidly growing animal model. This route of administration did not hinder revascularization of the infarcted head and preserved some portions of the head. Further improvements in the injection technique may allow more even distribution of IB within the femoral head and enhance the protective effect of IB on preserving the trabecular framework.

Disclosures: **S. Athavale**, Roche Diagnostic 2.

F479

Role of Ezrin in the Parathyroid Hormone-Mediated Downregulation of Sodium-Dependent Phosphate Transporter (NaPi-IIa) in Opossum Kidney Cells. Y. Taketani, K. Nashiki^{*}, A. Nakamura^{*}, N. Sawada^{*}, H. Yamamoto, H. Arai, E. Takeda. Department of Clinical Nutrition, University of Tokushima Graduate School, Tokushima, Japan.

Type IIa sodium-dependent phosphate (Pi) transporter (NaPi-IIa) carries out rate-limiting step of renal Pi reabsorption. Parathyroid hormone (PTH), a potent inhibitor for the Pi reabsorption, is rapidly involved in endocytosis of NaPi-IIa from apical membrane

ASBMR 27th Annual Meeting

to inhibit Pi transport immediately. We have reported that PTH mediated-phosphorylation of common substrates for both PKA and PKC in the membrane microdomains would be important for the downregulation of NaPi-IIa. We also found that ezrin, a member of ERM (ezrin-radixin-moesin) protein family, was a specific substrate for PKA and PKC in response to PTH. To understand the role of ezrin in the downregulation of NaPi-IIa, we investigated the phosphorylation of ezrin in response to PTH and the effect of dominant-negative ezrin on the downregulation of NaPi-IIa by PTH using OK-N2 cells (opossum kidney cells stably expressing NaPi-IIa). Go6978 (PKC-inhibitor) and H-89 (PKA-inhibitor) inhibited both PTH-mediated phosphorylation of ezrin and downregulation of NaPi-IIa. However, PTH did not affect the phosphorylation of ezrin at Thr567. Other phosphorylation site(s) must be important for the downregulation of NaPi-IIa. Since it has been known that ezrin can bind to NaPi-IIa via NHERF-1/EBP50 at N-terminal part, and also bind to cytoskeletal actin at C-terminal part, we expressed the dominant-negative ezrin (N-terminal half of ezrin) in OK-N2 cells. Overexpression of dominant-negative ezrin not only decreased apical targeting of NaPi-IIa, but also inhibited the PTH-mediated NaPi-IIa downregulation. Therefore, phosphorylation of ezrin by PTH may modulate the supermolecular complex of NaPi-IIa/NHERF-1/ezrin/actin targeted to the apical membrane, and may be trigger for NaPi-IIa endocytosis. Ezrin may be a key molecule for the hormonal regulation and apical targeting of NaPi-IIa in renal proximal tubular cells.

Disclosures: **Y. Taketani**, None.

F481

Signaling Selective PTH (1-34) Analogs Accelerate Bone Formation. **D. Yang¹, M. Bouxsein², R. Chiusaroli^{*1}, E. Schipani¹, P. Pajevic¹, J. Guo¹, R. Singh^{*1}, F. R. Bringham¹.** ¹Endocrine Unit, Massachusetts General Hospital & Harvard Medical School, Boston, MA, USA, ²Orthopedic Biomechanics, Beth Israel Deaconess Medical Center, Boston, MA, USA.

PTH regulates osteoblastic function by activating PTH/PTHrP receptors (PTH1Rs), which trigger several signaling pathways in parallel, including adenylyl cyclase (AC)/PKA and PKCs via both PLC-dependent and PLC-independent mechanisms. These signaling functions have been mapped to distinct domains within PTH(1-34). To study PTH1R signaling pathways that mediate regulation of bone formation, two analogs with restricted patterns of PTH1R signaling were synthesized. [G1,R19]hPTH(1-28), which lacks the 29-34 domain of hPTH(1-34) required for PLC-independent PKC activation and incorporates a Ser1 to Gly1 mutation that blocks PLC activation (the Arg19 change restores binding affinity otherwise lost by the C-terminal truncation), stimulates only cAMP/PKA signaling. [G1,R19]hPTH(1-34), with the 29-34 domain, was shown to activate cAMP/PKA and PLC-independent PKC. Doses of these peptides equipotent to 40 mg/kg hPTH(1-34) in acutely elevating blood cAMP 10 min after s.c. injection were administered to female C57BL mice 5 days/week for 4 weeks. Retesting of the blood cAMP responses after 4 weeks showed that acute AC activation was not altered by the preceding PTH treatment. Human PTH(1-34) increased total body BMD (PIXImus) and total femur BMD (4 weeks), which was mimicked by [G1,R19]hPTH(1-34) (a similar trend seen with [G1,R19]hPTH(1-28) was not significant). Micro-CT showed that all three analogs increased bone volume of the distal femur, T5 vertebra, and femur mid-shaft thickness, whereas [G1,R19]hPTH(1-34) was more potent in enhancing the microstructure of trabecular bone (as shown by ConnD and SMI). We conclude that the PLC signaling pathway is not required for PTH(1-34) to exert an anabolic effect on bone metabolism and that stimulation of cAMP/PKA alone, as demonstrated by the selective analog [G1,R19]hPTH(1-28), can increase bone formation with intermittent treatment. The PLC-independent PKC signaling pathway could play a role in the anabolic response by augmenting trabecular bone microstructure.

Disclosures: **D. Yang**, None.

F483

PTH Mediates Early Stem Cell Recruitment during Fracture Repair. **G. L. Barnes, S. Kakar^{*}, L. C. Gerstenfeld, T. A. Einhorn.** Orthopaedic Surgery, Boston University Medical Center, Boston, MA, USA.

Parathyroid hormone (PTH) is the first FDA approved systemic anabolic factor that has been shown to increase bone mass in osteoporotic patients. There is an increasing awareness that the anabolic activity of PTH may have additional applications in Orthopaedics. Several studies have recently reported on the enhanced healing of fractures treated with systemically administered PTH. However, the molecular mechanisms by which either enhanced healing or regain of bone mass in osteoporotic conditions is achieved remain elusive. The majority of research to date has focused on the role of PTH in modulating osteoblast function in the context of coupled remodeling. While this may be an important component of PTH mediated enhanced bone formation, alternate mechanisms may exist in fracture repair that occurs through an endochondral process dependent on early chondrogenic events. In order to define the stages of fracture repair enhanced by PTH treatment we analyzed the tissue, cellular, and molecular effects of PTH treatment (40 µg/Kg, PTH 1-34) during bone healing in a murine femoral fracture model. Radiographically, we observe that PTH treatment lead to increased mineralization of the fracture callus by day 10 and an earlier bridging of the fracture site. Histological analysis demonstrated that PTH increased the rate of cartilage recruitment, the total quantity of cartilage and its rate of hypertrophic maturation. Molecular analysis confirmed these observations showing that PTH treated fractures expressed Col2A1 and Col10A1 on average two days earlier than in vehicle treated animals. The earlier induction of cartilage hypertrophy was accompanied by an earlier induction of matrix metalloproteinases, specifically MMP9, associated with cartilage turnover and callus vascularization, critical steps in the endochondral repair process. Analysis of regulatory molecules associated with these early chondrogenic events demonstrated that PTH treatment lead to enhanced and earlier expression of Wnts-4 and -5b both shown in previous studies to be important regulators of chondrogenesis

proliferation and maturation. Together these results support the conclusion that PTH treatment enhanced fracture healing in part by inducing nascent mesenchymal cell recruitment into the chondrogenic lineage and by enhancing the subsequent maturation and expansion of these cells through a Wnt mediated mechanism. Finally these results suggest that PTH may have efficacy as a therapeutic to enhance fracture healing over a very short time course of systemic treatment.

Disclosures: **G.L. Barnes**, Lilly 2, 5.

F486

Calcium Transport into Milk Is Impaired in Deafwaddler Mice. **J. N. VanHouten^{*1}, M. C. Neville^{*2}, J. J. Wysolmerski¹.** ¹Endocrinology, Yale University, New Haven, CT, USA, ²Physiology, University of Colorado, Denver, CO, USA.

Milk production requires the transport of large amounts of calcium across the mammary epithelium. Prior work had suggested that, within mammary epithelial cells, calcium is transported into the Golgi apparatus where it becomes associated with casein micelles and enters milk via the secretory pathway. In order to define the molecules involved in transepithelial calcium transport in breast tissue, we performed a microarray analysis examining the transition between pregnancy and lactation in normal mice. This analysis demonstrated that plasma membrane calcium ATPase 2 (PMCA2) is the most abundant calcium transporter expressed in the mammary gland during lactation. Quantitative real-time RT-PCR demonstrated a 30-fold induction of PMCA2 mRNA levels in the mammary gland during the transition from pregnancy to lactation. Immunofluorescence and immunoelectron microscopy demonstrated that PMCA2 is located exclusively on the apical plasma membrane of mammary epithelial cells during lactation. Deafwaddler mice have neurological and inner ear defects due to loss-of-function mutations in the PMCA2 gene (Atp2b2). The dfw mutation is a single bp substitution resulting in reduced activity of the transporter, while the dfw-2J mutation is a 2 bp deletion that is functionally null. We analyzed milk calcium concentrations and maternal calcium metabolism in heterozygous and homozygous dfw and dfw-2J mice and wild type controls. Dfw-2J homozygotes showed a 75% reduction in milk calcium, while the heterozygous dfw-2J and homozygous dfw mice displayed lesser reductions in milk calcium concentrations. These results confirm that PMCA2 is necessary for the normal transport of calcium into milk. Furthermore, our data suggest that, in contrast to the generally accepted paradigm, a significant portion of the calcium in milk is transported from the cytoplasm directly across the apical membrane of mammary epithelial cells. We have previously found that the calcium-sensing receptor (CaR) regulates calcium transport into milk. Since the CaR has been shown to regulate PMCA activity in MDCK cells, we are currently examining the possibility that CaR signaling regulates PMCA2 activity in lactating mammary cells.

Disclosures: **J.N. VanHouten**, None.

F489

Phenylalanine-34 of Parathyroid Hormone Modulates Regulation of PTH(7-34)-Induced Type I PTH Receptor (PTH1R) Internalization by the Sodium/Proton Exchanger Regulatory Factor Type I (NHERF1/EBP50). **W. B. Sneddon.** Pharmacology, University of Pittsburgh School of Medicine, Pittsburgh, PA, USA.

Internalization of the Parathyroid Hormone Type I Receptor (PTH1R) is regulated in a cell- and ligand-specific manner. We previously demonstrated that the presence or absence of the sodium/proton exchanger regulatory factor type I (NHERF1; EBP50) is pivotal in determining the range of peptides that internalize the PTH1R. PTH(7-34) and PTHrP(7-34), which bind to, but do not activate the PTH1R, internalize the PTH1R 80% after 15 min in kidney distal tubule (DT) cells, where NHERF1 is not expressed. Introduction of NHERF1 into distal tubule cells blocks PTH(7-34)-, but not PTHrP(7-34)-induced PTH1R internalization. To delineate the sequences within PTH that confer NHERF1-sensitivity to PTH1R internalization, a series of chimeric PTH/PTHrP fragments were synthesized and tested for their ability to induce PTH1R internalization. PTH1R internalization was measured by real time confocal fluorescence microscopy of mouse DT cells stably expressing 10⁶ EGFP-tagged PTH1R/cell. PTHrP sequences in the C terminal of PTH(7-34) abolished NHERF1 sensitivity for PTH1R internalization. PTH(7-21)/PTHrP(22-34), PTH(7-32)/PTHrP(33-34) and PTH(7-33)/PTHrP(34) at 1 µM each internalized the PTH1R 50-70% in a NHERF1-independent manner. When the C terminus of PTHrP was replaced with homologous amino acids from PTH, NHERF1 inhibited PTH1R internalization. These experiments implicated position 34 (F in PTH, A in PTHrP) as being critical in determining the role of NHERF1 in PTH1R internalization. None of the chimeric peptides tested above activated the PTH1R but effectively competed for 1 nM PTH(1-34) in cyclic AMP assays. In the absence of NHERF1, PTHrP(7-21)/PTH(22-34) competed with an EC₅₀ of 0.1 nM, as compared with 100 nM for PTH(7-21)/PTHrP(22-34). In the presence of NHERF1, however, both PTHrP(7-21)/PTH(22-34) and PTH(7-21)/PTHrP(22-34) had comparable EC₅₀s (200 nM and 800 nM, respectively). Chimeric peptides substituted in the 32-34 positions competed for PTH(1-34) with EC₅₀s in the 100-1000 nM range and these values were not affected by the presence of NHERF1. Therefore, the sequences responsible for the NHERF1 sensitivity of PTH1R binding, in contrast to internalization, lie in the region of PTH(22-31). We conclude, therefore, that position 34 in PTH dictates NHERF1-dependent PTH1R internalization by non-activating PTH peptides and could provide a target for developing agents that can nonselectively downregulate the PTH1R.

Disclosures: **W.B. Sneddon**, None.

F491

Human XL α s (hXL α s) Functions as a Powerful α Stimulatory G Protein Subunit. A. Linglart^{*1}, M. J. Mahon¹, T. Dean^{*1}, T. J. Gardella¹, G. N. Hendy², H. Jüppner¹, M. Bastepe¹. ¹Endocrine Unit, Mass. Gen. Hosp. and Harvard Medical School, Boston, MA, USA, ²Depts. of Medicine, Physiology, and Human Genetics, McGill University and Royal Victoria Hosp., Montreal, PQ, Canada.

XL α s and the G protein α stimulatory subunit (G α) differ by their N-termini but share their C-terminal domains encoded by exons 2-13 of *GNAS*. G α is, in most tissues, biallelically expressed, whereas XL α s expression occurs only from the paternal allele. We have previously shown that hXL α s can mediate cAMP formation after agonist stimulation of G protein coupled receptors in cells that endogenously lack G α s and XL α s (Gnas^{E2-/-} cells). Moreover, loss of function mutations of *GNAS* alter receptor mediated cAMP generation through G α s and hXL α s, suggesting that hXL α s might be involved in phenotypes of diseases caused by paternally inherited mutations of *GNAS*, such as Albright's osteodystrophy and progressive osseous heteroplasia. To confirm that hXL α s functions as a component of the G protein, we characterized hXL α s signaling function in Gnas^{E2-/-} and COS-7 cells. Transduction of Gnas^{E2-/-} cells with an adenoviral vector encoding hXL α s, followed by confocal immunofluorescence microscopy with a hXL α s-specific antibody, determined that hXL α s localizes to both the cell membrane and the transGolgi network. In membrane binding assays, cotransduction of Gnas^{E2-/-} cells with the human PTH receptor (PTHr1) and G α s or hXL α s fully recovered receptor binding of PTH(1-15) analog, which, in contrast to PTH(1-34), completely failed to bind PTHr1 expressed alone in Gnas^{E2-/-} cells. Through the use of metal affinity chromatography, hXL α s could be co-purified and co-precipitated with the G β ₁ γ ₂ subunits from membranes of COS-7 cells triply transduced with hXL α s, His₆-tagged G β and G γ ₂. These data indicate that hXL α s localizes to the cell membrane and interacts with PTHr1 and the G β ₁ γ ₂ subunits. In addition, transduction of increasing amounts of G α s or hXL α s in Gnas^{E2-/-} cells showed a 2-fold greater cAMP generation in hXL α s transduced cells, both during the basal state and following endogenous β adrenergic receptor stimulation. Northern blot, quantitative RT-PCR and Western-blot analysis confirmed the greater efficiency of hXL α s in stimulating adenylyl cyclase, showing a 3 to 5-fold lower expression of hXL α s mRNA and protein compared to G α s in transduced Gnas^{E2-/-} cells. Interestingly, PTH(1-34) treatment induced similar levels of G α s and hXL α s dependent cAMP formation. In conclusion, we showed that hXL α s can mediate signaling as a stimulatory G protein, and that it might be more efficient than G α s in a receptor selective manner. Further studies are required to elucidate the function of hXL α s and its involvement in disease pathogenesis.

Disclosures: **A. Linglart**, None.

F496

Adipogenesis Is Enhanced in Bone Marrow Stromal Cells Lacking the Vitamin D Receptor. L. Cianferotti, M. B. Demay. Endocrine Unit, Massachusetts General Hospital Harvard Medical School, Boston, MA, USA.

The bone marrow contains multipotential mesenchymal stem cells (BMSCs) that are able to differentiate into multiple cell lineages including myocytes, chondrocytes, osteoblasts, and adipocytes. It has been demonstrated in a variety of bone marrow stromal cell models, either cell lines or primary cultures, that the differentiation into these lineages can be influenced by hormones and local growth factors. Factors that promote osteoblastic differentiation are generally considered to be inhibitory for adipocyte differentiation and vice versa. BMSCs are known to be target cells for the biologically active metabolite of vitamin D, 1,25-dihydroxyvitamin D (1,25D). The effects of 1,25D on osteoblastic and adipocytic cell differentiation are conflicting and they depend upon the species of origin as well as on the type and maturational stage of the cells. In primary cultures of murine BMSCs, 1,25D has been shown to inhibit adipocyte differentiation. To determine whether the ablation of the vitamin D receptor (VDR) results in an increased adipocytic commitment, the pattern of adipocytic differentiation in BMSC, isolated from VDR-null mice, was evaluated. BMSCs were harvested by flushing femora and tibiae from 17 day old wild-type and VDR knockout mice according to a standard protocol and seeded at a cell density of 4x10⁵ cells/cm². After 2h incubation at 37°C in 7% CO₂, humidified air the nonadherent cells were removed and fresh supplemented DMEM was added. Then cells were cultured until 80% confluent and then exposed to adipogenic agonists (0.5 mM methylisobutyl-xanthine, 0.5 μ M hydrocortisone and 60 μ M indomethacin, MHI) and/or 10⁻⁸ M 1,25D for 3 days. Cells treated with DMEM were used as controls. Cultures were harvested 10 days after the addition of the adipogenic agonists. Differentiation was assessed on fixed cultures with Oil Red O and alkaline phosphatase staining. The absence of the VDR did not alter the number of osteogenic or adipogenic foci under basal conditions. However, MHI induction resulted in an increased number of adipogenic foci in the VDR-null cultures relative to the MHI-treated wild-type cultures. While MHI treatment alone did not alter the number of osteogenic foci in the wild-type or VDR-null cultures, co-treatment with 1,25D and MHI blocked the effects of MHI on adipogenic differentiation in the wild-type cultures. Treatment with 1,25D alone did not alter the number of adipogenic foci, however, dramatically decreased the number of osteogenic foci in the wild-type cultures. These findings demonstrate that the absence of the VDR enhances adipogenesis and support a direct effect of 1,25D on differentiation of BMSCs.

Disclosures: **L. Cianferotti**, None.

F499

Phosphorylation of the Human Retinoid X Receptor Prevents Vitamin D-Dependent Nucleocytoplasmic Trafficking. L. Nguyen-Yamamoto¹, S. Laporte^{*1}, S. Mader^{*2}, M. Marcoritto^{*1}, D. C. Huang¹, R. Kremer¹. ¹Medicine, McGill University Health Center, Montreal, PQ, Canada, ²Biochemistry, University of Montreal, Montreal, PQ, Canada.

In previous studies we demonstrated that resistance to the action of 1,25 dihydroxyvitamin D₃ (1,25(OH)₂D₃) occurs in *ras*-transformed human keratinocytes (HPK1A-*Ras*) cells due to phosphorylation of the heterodimeric partner of the vitamin D receptor (VDR), the retinoid X receptor (RXR α), at serine 260, through the mitogen-activated protein kinase (MAP kinase) cascade (Solomom C *et al.* 1999). In the present study, we further explored the mechanism responsible for this resistance by examining the consequences of human (h) RXR α phosphorylation on nuclear/cytoplasmic distribution of the receptor following its induction by 1,25(OH)₂D₃ in the presence or absence of the MAP kinase inhibitor, U0126 (Promega). Nucleocytoplasmic trafficking of hRXR α was visualized using green fluorescent protein labeled hRXR α (GFP-hRXR α), generated using pGFP-CMV topaz into which the hRXR α cDNA was inserted. This plasmid was then transiently transfected into immortalized human keratinocytes (HPK1A) or *ras*-transformed human keratinocytes (HPK1A-*ras*) in the presence or absence of 10uM of U0126. Cells were treated with or without 10⁻⁷M of 1,25(OH)₂D₃ for 1; 1.5; 2; 24 and 48 hr and GFP-hRXR α distribution was assessed by confocal microscopy. In the absence of 1,25(OH)₂D₃, GFP-hRXR α distribution was predominantly cytoplasmic in both HPK1A and HPK1A-*Ras* cells. In HPK1A cells GFP-hRXR α reorganization occurred rapidly in a time dependent manner after 1,25(OH)₂D₃ treatment. Two hours after addition of 1,25(OH)₂D₃, GFP-hRXR α moved from the cytoplasm to the perinuclear region forming a visible ring around the nucleus and then rapidly penetrating the nuclear compartment. In contrast cytoplasmic transport towards the nucleus was delayed for at least 24 h in *ras*-transformed keratinocytes. Addition of 10 uM U0126 restored GFP-hRXR α movements in response to 1,25(OH)₂D₃ in *ras*-transformed cells but did not alter nucleocytoplasmic trafficking in HPK1A cells. Similar results were observed using a non-phosphorylatable hRXR α mutant (Ala 260hRXR α). These results therefore demonstrate that RXR phosphorylation delays its nuclear translocation and may explain the attenuated VDR-mediated transactivation and resistance to the growth inhibitory action of 1,25(OH)₂D₃ observed in *ras*-transformed keratinocytes.

Disclosures: **L. Nguyen-Yamamoto**, None.

F505

Nongenomic Estrogen Signalling Regulates Osteoclast Formation via An Adaptor Protein, BCAR1, that also Modifies Breast Cancer Progression. L. J. Robinson^{*}, A. C. Sharrow^{*}, V. Garcia Palacios, J. Xue^{*}, H. C. Blair. Pathology, University of Pittsburgh and Veteran's Affairs Medical Center, Pittsburgh, PA, USA.

It was discovered in trials of synthetic estrogen receptor modulators (SERMs) for osteoporosis that these compounds also modify breast cancer progression. Effects vary with agent. Some SERMs such as daidzein closely mimic estrogen effects and may increase risk, while others such as raloxifene or tamoxifen dramatically lower cancer risk. Despite their importance to osteoporosis and neoplasia, the mechanisms of estrogen and SERM activity remain poorly understood. We recently reported that estrogen and SERMs regulate osteoclast differentiation via non-genomic rapid effects (~15 min) on NF- κ B [J Biol Chem 280:13720, 2005]. Estrogen effects include interference with Map-kinase activation, but time course data show that the earliest effects are on NF- κ B activation. Here we show that a gene identified in breast cancer antiestrogen resistance, BCAR1, is a key element in nongenomic estrogen signaling in osteoclast differentiation. BCAR1 is an adaptor protein, the human homolog of murine p130Cas. Immunoprecipitation of ER α from murine Raw264.7 cells or human CD14 monocytes co-precipitated BCAR1. This occurred even after 18h in 10 nM estradiol. Thus, even at high estrogen activity a significant portion of the estrogen-bound ER α is cytoplasmic and capable of nongenomic interactions. The association of BCAR1 with ER α was greatly enhanced by short exposures to estrogen (5-15 minutes), and formation of the ER α -BCAR1 complex was further enhanced by concurrent RANKL stimulation. The antiestrogen ICI182780 abolished BCAR1 pull-down; tamoxifen had intermediate effects, with less marked stimulation of BCAR1 coprecipitation and no enhancement by RANKL. The estrogen-ER-BCAR1 complex might interfere with NF- κ B signaling through effects on Src or other tyrosine kinases, direct interactions with upstream signaling proteins such as trafs, or by the inhibition of I κ B degradation, which was observed following estrogen stimulation. The effects of RANKL on ER α -BCAR association, however, suggest that structural stabilization of the intermediate adaptor protein complex is also involved. Probing these complexes for traf6 showed variable association, with precipitation of traf 6 increasing by about 70% at 5 min in estradiol + RANKL, with ~half this effect in estradiol, relative to control, and with differences decreasing to undetectable levels by 15 min. We conclude that estrogen and SERMs, via BCAR1, regulate RANKL signalling. A similar nongenomic mechanism may thus regulate growth and survival in breast epithelium, and probably contributes to the effects of SERMs on breast cancer incidence.

Disclosures: **L.J. Robinson**, None.

F507

Inhibition of Glucocorticoid Signaling by Overexpression of 11beta HSD2 in Mature Osteoblasts Inhibits Nodule Formation and Increases Adipogenesis *In Vitro*. H. Zhou, K. Brennan*, Y. Zheng*, C. R. Dunstan, M. J. Seibel. Bone Research Program, ANZAC Research Institute, Sydney, Australia.

Transgenic (tg) expression of 11beta-hydroxysteroid dehydrogenase type 2 (HSD2), a glucocorticoid (GC) inactivating enzyme, under the control of a 2.3Kb collagen type 1 promoter (Col2.3-HSD2) abrogates intracellular GC signalling in mature osteoblasts, as demonstrated by Sher et al. (1). To characterise the phenotypic and functional properties of osteoblasts overexpressing Col2.3-HSD2, primary osteoblast cultures were generated from the calvaria of 1-day-old tg mice and wildtype (WT) littermates. Col2.3-HSD2 tg cultures developed 50% fewer nodules compared to WT after 2 weeks culture in the presence of 10 nM corticosterone, ascorbate and beta-glycerophosphate. Alkaline phosphatase (ALP) activity was decreased from day 3 in Col2.3-HSD2 tg cultures. At the same time, a significant increase in adipocyte numbers was observed in the cultures from Col2.3-HSD2 tg mice, suggesting a shift in lineage commitment from osteoblast to adipocyte. RNA was isolated at days 1, 3 and 7 of cultures. Quantitative RT-PCR revealed that mRNA for HSD2 was only detected in Col2.3-HSD2 tg mice with increased expression levels observed from day 3 to day 7, indicating that the number of mature osteoblasts was increasing during culture. At day 1, mRNA for Runx2, ALP, and osteocalcin were expressed at low but similar levels in cells from both Col2.3-HSD2 tg and WT. These mRNA levels remained low after 3 days in cells cultured from Col2.3-HSD2 tg mice, while they increased concurrently with osteoblast differentiation in the WT culture. Conversely, mRNA expression of the adipogenic transcription factors C/EBP alpha and PPAR gamma was increased at day 3 in Col2.3-HSD2 tg cultures but not in WT cultures. These results indicate that disruption of GC signalling in mature osteoblasts impairs early osteoblast differentiation and promotes adipogenic differentiation. This suggests the existence of a GC regulated paracrine signal between mature osteoblasts and their mesenchymal precursors that influences lineage commitment.

(1) Endocrinology 145:922-9, 2004. The authors would like to thank Prof B Kream for kindly providing the transgenic animals.

Disclosures: **H. Zhou, None.**

F509

Genetic Evidence of Androgen Receptor Function in Osteoclasts. T. Nakamura¹, T. Watanabe^{*1}, Y. Nakamichi¹, Y. Azuma², K. Yoshimura^{*1}, T. Matsumoto^{*1}, T. Fukuda^{*1}, E. Ochiai^{*1}, D. Metzger^{*3}, P. Chambon^{*3}, T. Sato^{*1}, S. Kato¹. ¹Institute of Molecular and Cellular Biosciences, The University of Tokyo/ ERATO, JST, Tokyo, Japan, ²Pharmaceutical Discovery Research Laboratories, Teijin Pharma Limited, Tokyo, Japan, ³Institut de Genetique et de Biologie Moleculaire et Cellulaire, CNRS/INSERM/ULP, College de France, Strasbourg, France.

Anabolic action of androgens in bone has been well described to increase BMD and bone mass. Such androgen action is believed to mediate nuclear androgen receptor (AR), and in fact, ablation of AR in male mice resulted in loss of BMD with high bone turnover. Androgen appears to suppress bone resorption (Kawano. H et al., PNAS, 100, 9416-9421, 2003). However, primary target cells of such androgen actions in bones have not yet been defined, though AR expression is detectable in osteoblasts, but not in osteoclasts. To directly examine physiological impact of AR in osteoclasts, we used a Cre/loxP system to disrupt AR gene in osteoclasts. First, we established Cathepsin K-Cre knock-in mice as an osteoclast-specific Cre expression Tg mice line. To generate osteoclast-specific ARKO (Oc-ARKO) mice, we then crossed the Cathepsin K-Cre mice with floxed AR mice. The Oc-ARKO mice had normal appearance, with no difference from the WT mice in the growth rate, gonad development and circulating hormone levels. However, 3D-micro CT analysis of distal femora from Oc-ARKO mice showed marked decrease of trabecular bone volume. Furthermore, histomorphometric analysis of the lumbar spine showed significantly increased number of osteoclasts with enhancement of the other bone resorption parameters compared with control mice. Reflecting increased bone resorption, the levels of urinary deoxypyridinoline was increased. Importantly, the bone formation parameters were also increased in Oc-ARKO mice. Thus, from the present findings all together, it is likely that anabolic action of androgens is exerted by suppression of bone resorption through AR at least in part in osteoclasts.

Disclosures: **T. Nakamura, None.**

F511

Loss of ER α Signaling via EREs Is Associated with Differential Effects on Total Body vs. Marrow Fat. F. A. Syed, U. I. L. Moedder, D. G. Fraser*, S. Khosla. Endocrinology, Mayo Clinic College of Medicine, Rochester, MN, USA.

Estrogen receptor α (ER α) is known to play an important role in both bone and adipose tissue. We have previously demonstrated that mice with a deleted ER α allele on one chromosome and a knock-in of a mutant ER α that cannot bind EREs on the other chromosome (ER α -NERKI) have a paradoxical response to ovariectomy (ovx) and E replacement in cortical bone (JBMR vol.19 :S339, 2004). In the present study, we examined consequences of loss of classical ER α signaling (via EREs) on total body and marrow fat in female mice. As assessed by DXA, ER α -NERKI mice had lower total body bone mineral density (BMD) (by 16%) but higher total body percent fat (by 56%) as compared to their wild type (WT) littermates ($P < 0.01$ for all comparisons), despite having similar body weights. By contrast, while trabecular bone volume/total volume (BV/TV) in

the tibial metaphysis was similar in female ER α -NERKI and WT mice, ER α -NERKI mice had a marked (~10-fold) reduction in bone marrow adipocyte number and volume per tissue area ($P < 0.001$). Moreover, whereas WT female mice had an increase in percent total body fat following ovx (of +257%), ER α -NERKI showed the opposite trend (decrease of 68%, $P < 0.01$ for a treatment x genotype interaction by ANOVA), reminiscent of the paradoxical responses to ovx in cortical bone we previously observed in ER α -NERKI mice. Again, in contrast to this paradoxical response to ovx in ER α -NERKI mice for total body fat, the bone marrow adipocyte parameters increased comparably following ovx in the ER α -NERKI and WT mice ($P = 0.575$ and $P = 0.394$ for a treatment x genotype interaction by ANOVA for adipocyte number and volume respectively). Collectively, these findings demonstrate that loss of classical ERE signaling has very different consequences for total body vs. marrow fat. The preservation of trabecular BV/TV and marked deficit in bone marrow adipocyte number and volume in the ER α -NERKI suggests a fundamental defect either in the mesenchymal precursors to these cells and/or in bone marrow adipocyte differentiation that is not evident in non-marrow adipocytes. Defining further the mechanism(s) of these site-specific differences in estrogen regulation of bone marrow vs. non-marrow adipocytes should provide novel insights into estrogen regulation of adipocytes at different sites as well as into estrogen effects on mesenchymal precursor cells and on adipocyte/osteoblast differentiation.

Disclosures: **F.A. Syed, None.**

F513

Gain Bones by Cutting off Fat. X. Shi¹, X. Cao², X. Shen^{*2}. ¹Institute of Molecular Medicine and Genetics, Medical College of Georgia, Augusta, GA, USA, ²Pathology, University of Alabama at Birmingham, Birmingham, AL, USA.

Bone marrow mesenchymal stem/progenitor cells (MSCs) can differentiate into multiple cell lineages. Accumulating evidence has shown that the osteoblast and adipocyte are two dominant lineages and that the commitment of MSCs toward these two pathways is reciprocal, i.e., when adipocyte pathway is blocked, the MSCs enter osteoblast pathway. CCAAT/enhancer-binding protein-alpha (C/EBP α), an important adipogenic factor, is also a potent inhibitor of cell proliferation. C/EBP α arrests cell proliferation by interacting with cyclin-dependent kinases (Cdk2/4) and disrupting their association with cyclins. We have found that glucocorticoid-induced leucine zipper (GILZ), a recently identified transcription factor whose expression is induced by glucocorticoid (GC), blocks adipocyte differentiation. To investigate the molecular mechanisms by which GILZ inhibits adipocyte differentiation, we examined the effects of GILZ on C/EBP α expression and the possible involvement of GILZ in C/EBP α -mediated cell cycle arrest. We found, in co-immunoprecipitation assays, that GILZ physically interacts with C/EBP α but not Cdk2, however, GILZ disrupts the interaction between C/EBP α and Cdk2, suggesting that the disruption of C/EBP α and Cdk2 interaction by GILZ is responsible for GILZ-mediated inhibition of adipocyte differentiation. The mRNA level and the promoter activity of C/EBP α were also inhibited by GILZ as shown by real-time RT-PCR and promoter-luciferase analyses, respectively. Because C/EBP α can bind to its own promoter and autoregulate its expression, we also examined whether GILZ affects the binding of C/EBP α to its own promoter region. Chromatin immunoprecipitation (ChIP) assay showed that C/EBP α binds to its own promoter in the region between nucleotides -109 to -245 covering a well-characterized C/EBP binding site (-176 to -203). Treatment of the cells with dexamethasone, which induces GILZ expression, inhibited the DNA-binding activity of C/EBP α . Interestingly, the expression of C/EBP α -beta and -delta, which also bind to this C/EBP binding site, was not affected as demonstrated by real-time RT-PCR and immunohistological staining experiments. These studies reveal a novel mechanism of transcriptional regulation of adipocyte differentiation and suggest a possibility of increasing new bone formation by inhibiting fat formation.

Disclosures: **X. Shi, None.**

F515

Androgen Action on Cortical Bone Surfaces Requires a Functional Androgen Receptor: Evidence from the Androgen Receptor Knock-out Mouse Model. K. Venken*, K. De Gendt*, S. Boonen, R. Bouillon, L. Swinnen*, G. Verhoeven*, D. Vanderschueren. K.U.Leuven, Leuven, Belgium.

Males develop wider bones than females during puberty. It remains uncertain to what extent this extra periosteal expansion in males is mediated by the androgen receptor (AR). The aim of the present study was to determine whether androgen action on male cortical bone modeling depends on activation of the AR or, alternatively, on aromatisation of androgens into estrogens. To this end, 3-week-old AR knock-out mice (ARKO) and corresponding male WT mice were either sham-operated (sham) or orchidectomized (orx). Orx mice were treated with either vehicle, testosterone (T) (1.5 μ g/day via subcutaneous implants) or T plus aromatase inhibitor (AI) (anastrozole, 10 mg/kg/day p.o.). At 8 weeks of age, endocortical and periosteal growth of the mid-femoral shaft was assessed by dynamic histomorphometry. Periosteal osteoblast number and activity were decreased in sham ARKO mice compared to sham WT, as reflected by a significantly reduced periosteal mineralizing perimeter (Min. Pm.) (-56%, $P < 0.001$) and mineral apposition rate (MAR) (-32%, $P < 0.05$). As a result, the periosteal bone formation rate (BFR) ($P < 0.05$) was reduced to more than 50% in ARKO mice ($P < 0.05$), associated with a decreased periosteal perimeter (-14%, $P < 0.0005$) and cross-sectional area (-13%, $P = 0.0001$). Moreover, the endocortical MAR and BFR were significantly increased in sham ARKO mice (+72% and +110% vs sham WT, respectively, $P < 0.05$), concomitant with a decreased endocortical perimeter (-5%, $P = 0.01$) and medullary area (-9%, $P < 0.005$). Furthermore, administration of T to orx WT mice significantly increased the periosteal Min. Pm. (+141% vs orx WT, $P < 0.0001$) and BFR (+163%, $P < 0.005$), resulting in an increased periosteal perimeter (+10%, $P < 0.0001$) and cortical thickness (+47%, $P < 0.0001$). Interestingly, administration

ASBMR 27th Annual Meeting

of T plus AI partly reduced the effects of T on the periosteal Min. Pm. (-25%, $P<0.0001$ vs WT orx + T) and BFR (-34%, $P<0.005$), resulting in a thinner cortex (-7%, $P<0.0001$) and smaller periosteal perimeter (-9%, $P<0.0001$). In contrast, the periosteal and endocortical bone surface of ARKO mice remained completely unresponsive to either T or T plus AI. Therefore, AR-mediated androgen action is clearly important for cortical bone growth in male mice; however, part of the androgen effect on the periosteal bone surface is also explained by aromatisation of androgens to estrogens. Moreover, this effect of aromatisation is only observed in the presence of a functional AR. We conclude that the AR is critically involved in cortical bone modeling and differentially regulates endocortical and periosteal growth, with suppressive versus stimulatory effects, respectively.

Disclosures: **K. Venken**, None.

F518

Recruitment of Vitamin D and Estrogen Hormone-Specific Modifiers to Chromatin. **H. Chen**, **M. Hewison**, **L. Nguyen***, **J. S. Adams**. Endocrinology/Medicine, Burns and Allen Research Institute and Division of Endocrinology, Cedars-Sinai Medical Center, David Geffen School of Medicine at UC, Los Angeles, CA, USA.

Heterogeneous nuclear ribonucleoproteins (hnRNPs) are naturally-occurring nucleic acid binding proteins. Generally recognized for their ability to regulate mRNA processing and splicing, hnRNPs can also compete *in trans* with sterol/steroid hormone receptor dimers for their cognate *cis* response elements in the promoters of hormone-regulated genes. In this mode the hnRNPs act predominantly as dominant-negative inhibitors of transactivation. When relatively over-expressed in either subhuman or human primate cells, these hnRNPs can cause hormone resistance *in vivo*. Here we employed chromatin immunoprecipitation (ChIP) studies to visualize the temporal recruitment and assembly of two such endogenous, dominant-negative-acting hnRNPs, one a human vitamin D response element binding protein (VDRE-BP) and another a primate estrogen response element binding protein (ERE-BP), as well as competitive vitamin D receptor (VDR) and estrogen receptor α (ER) on native VDR-VDRE- and ER-ERE-responsive promoters. The time course of interaction of ligand-activated VDR and ER with the VDRE in the 24-hydroxylase promoter and ERE in the cathepsin D promoter, respectively, was monitored in control (wild-type) cells as well as in those naturally over-expressing the VDRE-BP and ERE-BP cell lines. Cells were treated without or with 10 nM 17 β -estradiol (E2) or 1,25-dihydroxyvitamin D₃ (1,25-D) for 15, 30, 45, 60, 75, 90, 120 and 165 min before disruption and ChIP with anti-VDR, -ER, -hnRNP antibody or with nonspecific IgG followed by VDRE and ERE amplification by PCR. In control cells, lacking substantial amounts of the VDRE-BP and ERE-BP, the VDRE and ERE were relatively unoccupied by the VDR and ER in the absence of added hormone. Hormone exposure led to maximum recruitment of VDR and ER to the promoter as early as 15 min and an "on-off" cycling interval of 60 min for both the VDR-VDRE and ER-ERE. The VDR-VDRE and ER-ERE interaction in hnRNP over-expressing cells was characteristically altered from the wild-type, control situation: 1] before ligand exposure the response elements were already occupied by the VDRE-BP and ERE-BP; and 2] after hormone exposure there was a quantitative decrease and temporal delay in VDR and ER recruitment to the promoter as well as prolongation of the receptor-response element "on-off" cycle. Taken together, these data indicate that hnRNPs can legislate vitamin D- and estrogen-resistance by virtue of their persistent presence on the VDRE and ERE, respectively, blocking 1,25-D-VDR and E2-ER-driven transactivation.

Disclosures: **H. Chen**, None.

F520

Antiresorptive Effects of Calcitriol Are Independent of Parathyroid Hormone Secretion in Rats. **R. G. Erben**¹, **M. Herber**^{*2}, **K. Weber**^{*2}.

¹University of Veterinary Medicine, Institute of Pathophysiology, Vienna, Austria, ²University of Munich, Institute of Animal Physiology, Munich, Germany.

It is unclear at present whether the antiresorptive effects of vitamin D analogs *in vivo* are mediated through a suppression of parathyroid hormone (PTH) secretion or through a direct antiresorptive action on bone. In the current experiment, we examined the skeletal effects of calcitriol administration in sham-operated (SHAM) rats, parathyroidectomized (PTX) rats, and PTX rats supplemented with physiological doses of rPTH(1-34). Seventy-two female 6-month-old Fischer 344 rats were either PTX or sham-operated. The success of PTX was confirmed by measurement of ionized blood calcium 2 days after surgery. Subsequently, half of the PTX rats received subcutaneously implanted osmotic minipumps delivering 8 μ g rPTH(1-34) per kg body weight per day. This dose of rPTH(1-34) was found to normalize hypocalcemia and serum PTH in PTX rats in preliminary experiments. All other rats received minipumps delivering vehicle. Beginning the day after implantation of the minipumps, groups of SHAM, PTX, and PTH-supplemented PTX rats (n = 8 each) received vehicle, 0.05, or 0.1 μ g calcitriol/kg/day orally via the diet. Preliminary experiments had shown that the antiresorptive and bone anabolic effect of calcitriol is most pronounced when the drug is administered orally via the diet. All animals were killed 2 weeks after the start of the experiment. PTX resulted in hypocalcemia, and very low, but detectable immunoreactive serum PTH levels, 17 days postsurgery. Supplementation of PTX rats with rPTH(1-34) resulted in complete normalization of circulating PTH and serum calcium levels. Calcitriol administration increased serum calcium in PTX and rPTH(1-34)-supplemented PTX rats, but not in SHAM rats. However, all calcitriol-treated rats were hypercalciuric, independent of circulating PTH levels. Vertebral bone formation rate increased dose-dependently in calcitriol-treated rats, especially in PTX rats. Interestingly, the most pronounced decrease in urinary collagen cross-link excretion induced by calcitriol was found in rPTH(1-34)-supplemented PTX rats, showing that the

antiresorptive effects of calcitriol occurs in the presence of constant, physiological levels of PTH. Thus, the antiresorptive effects of calcitriol *in vivo* are not solely mediated through suppression of PTH secretion.

Disclosures: **R.G. Erben**, ClinTrialsBioResearch 5; Schering 5; Procter&Gamble 2.

F524

Clinical Relevance of Determining Vit-D by Fractionating 25-hydroxy-Vit-D into 25-hydroxy-Vit-D2 and 25-hydroxy-Vit-D3. **R. J. Singh**, Dept. of Laboratory Medicine and Pathology, Mayo Clinic, Rochester, MN, USA.

Introduction: Measurement of 25 OH vitamin D provides the single best assessment of vitamin D nutritional status. Vitamin D is an essential component in the regulation of calcium and bone metabolism. Vitamin D (calciferol) is a term used to include both cholecalciferol D3 and ergocalciferol D2. Both of these compounds are transported to the liver where they are hydroxylated to produce 25-hydroxyvitamin D. D2 and D3 are both used to supplement vitamin D deficient patients. Decreased levels may be due to dietary deficiency, mal-absorption, liver disease and in patients receiving medications that accelerate vitamin D metabolism. In addition Vitamin D levels vary widely with age and geographic region. **Materials and Methods:** LC-MS/MS method: Deuterated stable isotope (d3-25-hydroxyvitamin D) is added to a 0.2-mL plasma sample as internal standard. 25-Hydroxyvitamin D2, D3, and the internal standard are extracted using acetonitrile precipitation. The extracts are then further purified online and analyzed by LC-MS/MS using multiple reaction monitoring. 25-OH-VitD2 and 25-OH-VitD3 are quantified individually and a sum was used for correlation studies. Interassay CVs were less than 15% at various D2 and D3 levels. Sensitivity is set at 2 ng/mL for D3 based on interassay CV of 12.9% at 1.7 ng/mL. Sensitivity was 4 ng/mL for D2 based on interassay CV of 14.0% at 4.2 ng/mL. 100 patient samples submitted for 25 OH Vit-D analysis were used for the method comparison studies with the Diasorin RIA, LIAISON® (DiaSorin, Inc, Stillwater, MN) and the Nichols Advantage. **Results and Conclusions:** Quantification of 25 OH vitamin D with 100 patient samples by liquid chromatography-tandem mass spectrometry resulted in individual values for D2 and D3. The combined total values of 25 OH vitamin D were then compared to the values from immunoassays. Comparison of the LC-MS/MS method to the RIA (LC-MS-MC = 0.91(RIA) + 5.4 ng/mL (r=0.93)) and the LIA (LC-MS/MS method = 1.02(LIA) + 2.0 ng/mL (r=0.90)) yielded acceptable correlations in the range from 7-150 ng/mL, but poor correlation to another immunoassay due to under detection of 25-OH D2. In Conclusion the LC-MS/MS method which is considered to be a gold standard method for the measurement of 25 OH vitamin D is now widely available for clinical use and has several advantages over the immunoassays.

Disclosures: **R.J. Singh**, None.

SA001

Determinants of Bone Mineral Density in Female Adolescents. Z. Harel^{*1}, M. Gold^{*2}, B. Cromer³, A. Bruner^{*4}, M. Stager^{*3}, L. Bachrach⁵, P. Hertweck^{*6}, A. Nelson^{*7}, D. Nelson⁸, S. Coupey^{*9}. ¹Hasbro Children's Hospital and Brown University, Providence, RI, USA, ²Children's Hospital of Pittsburgh, Pittsburgh, PA, USA, ³Metro-Health Medical Center, Cleveland, OH, USA, ⁴Johns Hopkins University School of Medicine, Baltimore, MD, USA, ⁵Stanford University School of Medicine, Stanford, CA, USA, ⁶University of Louisville, Louisville, KY, USA, ⁷David Geffen School of Medicine at UCLA, Torrance, CA, USA, ⁸Wayne State University School of Medicine, Detroit, MI, USA, ⁹Children's Hospital at Montefiore, New York, NY, USA.

During adolescence, bone formation prevails over resorption, resulting in accumulation of 40% of peak bone mass. We examined several factors that may affect bone mass accrual during this critical period. The population comprised 389 healthy postmenarchal adolescent girls aged 11-18 years, who were recruited into a prospective, IRB-approved, ongoing study of the effect of depot medroxyprogesterone acetate (Depo-Provera® 150 mg) on bone health in adolescents. Healthcare providers collected demographic, reproductive health, and lifestyle data, and performed a complete physical examination. Body mass index (BMI) was calculated. Prior to study initiation, bone mineral density (BMD) at the lumbar spine, total hip, and femoral neck was measured by dual-energy X-ray absorptiometry (DXA), and markers of bone metabolism (serum osteocalcin, bone-specific alkaline phosphatase [AP], and urinary N-telopeptide [uNTX]) were measured. Potential associations between baseline BMD values and other parameters were assessed by analysis of variance and Pearson's correlation coefficients (PCC). Subjects enrolled in the study had mean [±SD (range)] chronological age 14.9 ±1.7 (11-18) years, gynecologic age 39.9 ±23.0 (0.5-119) months post menarche, and BMI 23.5 ±4.6 (16.0-42.2) kg/m². Ethnic distribution was African American 46%, Caucasian 35%, and other races 19%; 9.3% had previously been pregnant. Positive correlations were observed between lumbar spine BMD and chronological age, gynecologic age, and BMI (PCC 0.301, 0.349, 0.371, respectively). Average total hip and femoral neck BMDs were significantly higher (p=0.0028 and p=0.0060, respectively) in African Americans than in other participants. Smoking and alcohol use were not associated with significant differences in BMD. Negative correlations were observed between lumbar spine BMD and both uNTX (PCC -0.406) and AP (PCC -0.363) levels. Our data indicate that chronological age, gynecologic age, BMI, and race are independent determinants of BMD in adolescents. Serum AP and uNTX levels are inversely associated with BMD values in this age group.

Disclosures: **Z. Harel**, Pfizer/Pharmacia, Merck, Ortho-McNeil 2.

SA002

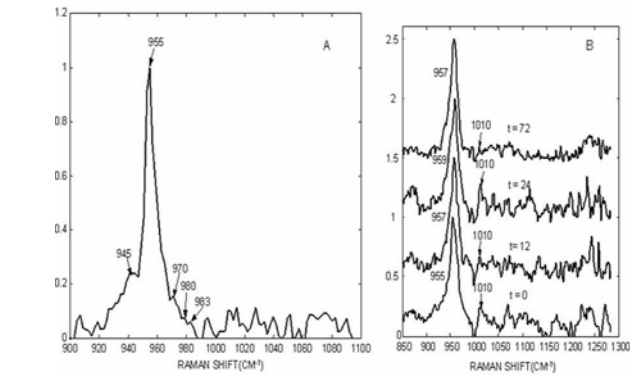
See Friday Plenary number F002.

SA003

Octacalcium Phosphate(OCP) and Other Transient Mineral Species Are Observed in Mouse Sutures during Normal Development and Craniosynostosis. V. Popescu^{*1}, N. J. Crane^{*1}, M. D. Morris^{*1}, M. A. Ignelzi Jr², P. Steenhuis^{*2}. ¹Chemistry Department, University of Michigan, Ann Arbor, MI, USA, ²Department of Orthodontics and Pediatric Dentistry, University of Michigan, Ann Arbor, MI, USA.

We have studied early mineralization of calvarial tissue from fetal day 18.5 B6CBA F1/J wild-type mice bone cultured in serum free media for up to 3 days. Specimens were treated with FGF2-soaked heparin acrylic beads to mimic craniosynostosis. Control specimens received beads containing only the culture medium. Tissue specimens were analyzed using Raman microspectroscopy at intervals of several hours. At each time point multiple spectra were obtained and multivariate curve resolution was used to obtain the spectra of mineral species and to estimate the relative amounts of minerals. During the first 24 h of both normal and accelerated mineralization we observed a transient intermediate similar to OCP, and a highly disorder calcium phosphate, similar to amorphous calcium phosphate (ACP), postulated precursors of bone mineral. We also observed normal bone mineral. For the OCP-like material, the P-O stretch was found at 955 cm⁻¹ and there was an additional HPO₄-2 P-O stretch at 1010-1014 cm⁻¹, as expected for OCP. Additionally a broad band was found at 945 cm⁻¹, characteristic of disordered calcium phosphate or ACP. Bone mineral, P-O stretch 957-962 cm⁻¹, was found at all time points. This is the first observation of non-apatitic early mineral in bone tissue. ACP and OCP have been detected as carbonated apatite precursors in inorganic model systems, but not in bone tissue itself. Detection of the same intermediates in normal and accelerated mineralization is further confirmation that craniosynostotic mineralization follows the same chemistry as normal mineralization, but at a more rapid rate.

Assignments for the Raman Bands of the Tissue Components		
Raman shift (cm-1)	Band Assignment	Component
945 cm-1	phosphate, P-O	ACP, disordered mineral
955 cm-1	phosphate, P-O	OCP
1010-1014 cm-1	monohydrogen phosphate, P-O	OCP
957-962 cm-1	phosphate, P-O bone mineral	carbonated apatite



Disclosures: **V. Popescu**, NIH R01 AR047969, R29DE011530, P30 AR046024 2.

SA004

See Friday Plenary number F004.

SA005

Determinants of Total Body and Forearm Bone Mass in Chinese Postmenarcheal Girls. K. Zhu^{*1}, H. Greenfield^{*1}, O. Zhang^{*1}, L. H. Foo^{*1}, G. S. Ma^{*2}, C. T. Cowell³, D. R. Fraser^{*1}. ¹Faculty of Veterinary Science, University of Sydney, Sydney, Australia, ²Institute for Nutrition and Food Safety, Chinese Center for Disease Control and Prevention, Beijing, China, ³Institute of Endocrinology and Diabetes, Children's Hospital at Westmead, Westmead, Australia.

The aim of this study was to evaluate the relationship between bone mass and weight, height, bone age, pubertal development, dietary intakes, physical activity and vitamin D status in Chinese postmenarcheal girls. The study subjects were 175 girls aged 15 ± 0.4 years from 17 schools in Beijing, who were in the control group of a milk intervention trial. Bone mineral content (BMC) and density (BMD) and bone area (BA) of total body and distal and proximal forearm were assessed by dual-energy X-ray absorptiometry (Norland XR-36). Dietary intakes were evaluated by two 3-day food records and physical activity by a questionnaire of past-year activity. Serum 25(OH)D concentrations were determined by radioimmunoassay (DiaSorin) in fasting blood samples obtained in late winter. This study was carried out with the approval of the ethics committees of the University of Sydney, Australia and the Institute for Nutrition and Food Safety, China. BMC and BMD of both total body and forearm were positively correlated with weight, height, bone age, Tanner stage of breast and pubic hair development, physical activity level, milk intake, total months of menstruation, and serum 25(OH)D concentration (P<0.05). The relationships between these variables and bone mass were further evaluated in multiple regression models. Corresponding BA was the most important predictor of total body and forearm BMC and accounted for 39.0-60.4% of the variation. Body weight entered all the regression models as the most important predictor of BMD (explaining 17.2 - 41.7% of the variation) and the second most important predictor of BMC (explaining 7.8-13.8% of the variation). The only other variable entering the regression models for total body BMC and BMD was milk intake, which accounted for 2.8-6.0% of the variation. Other significant predictors of proximal and distal forearm BMC and BMD were bone age (explaining 3-10.9% of the variation), serum 25(OH)D concentration (explaining 1.0-2.3% of the variation), and milk intake (for proximal forearm only, explaining 3.2-6.1% of the variation). The study results indicated that milk intake and vitamin D status were important determinants of bone mass in Chinese postmenarcheal girls. Increasing milk intake and improving vitamin D status may have beneficial effects on peak bone mass attainment in this population.

Disclosures: **K. Zhu**, None.

SA006

Age at Pubertal Growth Spurt Is a Predictor of Final Height as a Result of Affected Appendicular but not Axial Skeletal Growth - The GOOD Study. S. H. Windahl¹, J. M. Kindblom¹, M. Lorentzon¹, E. Norjavaara^{*2}, A. Hellqvist^{*3}, S. Nilsson^{*3}, D. Mellström¹, C. Ohlsson¹. ¹Center for Bone Research at the Sahlgrenska Academy, Departments of Internal Medicine and Geriatrics, Gothenburg University, Gothenburg, Sweden, ²Institute for the Health of Women and Children, Gothenburg University, Gothenburg, Sweden, ³Swegene Bioinformatics, Gothenburg University, Gothenburg, Sweden.

The control of linear growth is complex and depends on a number of factors including nutrition and hormones. Pharmacological manipulation of pubertal onset has been used to modulate final height in girls. However, the role of age at pubertal onset for final height in boys is unclear. A problem with assessments of growth is that most sets of height growth reference values are based on cross sectional studies. The aim with the current study was to investigate the importance of age at pubertal growth spurt for final height and body

proportions in a large well characterized cohort of young men. Detailed growth charts from birth up to 18-20 years of age were available for 549 men participating in the Gothenburg Osteoporosis and Obesity Determinants (GOOD) study. These growth charts were analysed using the infancy-childhood-pubertal growth model and used for the calculation of peak height velocity (PHV), occurring two years after the initiation of puberty. The time of PHV was then correlated with measurements of final height as well as upper (axial skeleton, sitting height) and lower (appendicular skeleton, height-sitting height) segments. Measurements of height, upper and lower segment at young adult age revealed that age at pubertal growth spurt was a strong positive predictor for final height ($\beta = 0.128$, $p = 0.003$) and a strong negative predictor for the ratio between upper and lower segment ($\beta = -0.213$, $p < 0.001$). We next compared the subjects with early puberty (EP, the 15% with earliest PHV, 12.0 ± 0.4 years of age) with those with late puberty (LP, the 15% with latest PHV, 15.2 ± 0.5 years of age). The positive association of age at PHV with final height was reflected by increased length of the lower segment ($+2.5 \pm 0.6$ cm over EP, $p = 0.002$) but unaltered sitting height (-0.4 ± 0.4 cm over EP, NS) in subjects with LP compared with EP. Consequently, the ratio between the upper and lower segment was reduced ($-3.31 \pm 0.81\%$, $p < 0.001$). We have determined PHV for 549 young Swedish men using longitudinal growth curves. Our results demonstrate that age at the pubertal growth spurt is a strong positive predictor of final height, reflecting increased appendicular but not axial skeletal growth in subjects with LP.

Disclosures: *S.H. Windahl, None.*

SA007

See Friday Plenary number F007.

SA008

A Randomised Controlled Trial (RCT) of Calcium Supplementation in School-Children and Gymnasts. *K. A. Ward¹, S. A. Roberts^{*1}, S. A. New^{*2}, J. E. Adams¹, M. Z. Mughal³.* ¹University of Manchester, Manchester, United Kingdom, ²University of Surrey, Guildford, United Kingdom, ³Central Manchester and Manchester Children's University Hospitals NHS Trust, Manchester, United Kingdom.

The adaptation of bone to exercise has been shown to be modified by calcium. The aim of this double-blind RCT was to investigate whether there was a differential response to calcium supplementation in elite gymnasts (G, 15 hours exercise/ week) and school children (controls; C 7 hours exercise/ week). The primary hypothesis was that G who took calcium supplements would have greater increases in cortical and trabecular bone mineral density (CtBMD, TrBMD) at the radius (R) and tibia (T). Secondary outcomes were changes in bone geometry at the R, T and lumbar spine and total body measurements. Children were randomised to 12 months daily supplementation of 500g calcium carbonate (CalcichewTM, Shire Pharmaceuticals) or placebo. Outcome measures were taken using peripheral quantitative computed tomography (pQCT) (distal and diaphyseal R and T) and dual energy X-ray absorptiometry (DXA) (lumbar spine and whole body). Eighty-six subjects (49 females) participated in the RCT (44G: 42C) and 75 subjects completed the trial (45 females, 39G: 36C). Data were analysed by analysis of covariance adjusting for baseline value, age, height, gender and puberty, and delay between baseline measurement and start of intervention. The primary analysis was for a calcium-exercise interaction; a pooled calcium effect with no interaction was also tested. The primary outcome measures are given in the table and expressed as a ratio of calcium: placebo.

Variable	Controls	Gymnasts	Pooled effect P	Interaction P
T CtBMD	1.00 (0.99, 1.01)	1.01 (1.00, 1.02)	0.357	0.207
T TrBMD	1.05 (1.00, 1.09)	0.98 (0.94, 1.02)	0.370	0.035
R CtBMD	1.01 (0.98, 1.01)	0.99 (0.98, 1.01)	0.250	0.675
R TrBMD	1.07 (0.99, 1.15)	0.96 (0.89, 1.03)	0.663	0.053

Results are presented as ratios (95% CI) For all other secondary outcomes at R, T, spine and whole body no significant interactions were found. In conclusion, there was no beneficial effect of calcium in gymnasts who already consume their recommended nutrient intake (800mg/day) for calcium. The interaction between calcium and exercise may only occur in children who do not participate in regular sports at the beginning of the intervention. We speculate that G have already adapted their bones (geometry and density) to the demands imposed upon them by the loading they are subjected to during gymnastics and do not require extra calcium supplementation.

Disclosures: *K.A. Ward, None.*

SA009

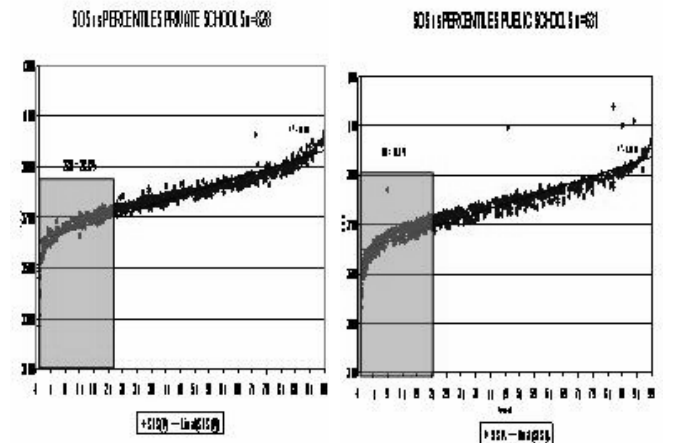
See Friday Plenary number F009.

SA010

A Novel Strategy to Study Healthy Elementary School Communities in Mexico City Focused in Osteoporosis Prevention at Different Socio Economical Levels; Invest in your Bones Program. *A. F. Goribar*, L. De Villafranca*, A. Cabra*, J. A. Tamayo*.* International Osteoporosis Foundation, Comité Mexicano para Prevención de la Osteoporosis, Mexico, Mexico.

The purpose of this study was to develop a strategy to obtain the participation of the whole school community, named: school master, teachers, parents and students in our long term program, and to define if there is a difference in bone development between two socio

economical environments (SE) public; lower C, (Pu) and private; middle B+ to high A, (Pi). The first phase objectives are: education, sensitization, teachers and students measuring their bone status, parents knowing the results of their own kids. Three motivational conferences: to the teachers coupled by SOS attenuation at the forearm and tibia: their own bones, parents and students given by their teachers coupled to a school activity. We got an informed consent to measure SOS in the kids Sunlight omniscense 8000S, height, weight & BMI were recorded. 3 Pu and 3 Pi schools participated. We included a total of 1459 students, 828 from Pi, 631 from Pu centers, over 95% of total population. Aged 6 to 12 years, 748 male, 711 female. As seen in the graphs 52.1% of the total population is below the 25th percentile of SOS, irrespectively of BMI, age & sex. A significant difference was also found between Pu vs Pr; 41.3% of Pu vs. 28.8% of Pi students were below the 25th percentile. This novel approach demonstrates that school community is quite sensitive to this strategy, irrespectively of their SE. Almost the total of the teachers and student population participated in the program. A key factor is the combination of a well designed conference to the teachers and parents, coupled with a direct measurement of the teachers own bones. The students interest was boosted by the educational activity and they knowing their own bone status. SOS measurements showed a significant deficiency in the development status of the bones in 52.1% of these healthy student populations. A significant influence of SE was also demonstrated.



Disclosures: *J.A. Tamayo, None.*

SA011

Molecular Dissection of BMP Signaling Pathways in Control and Fibrodysplasia Ossificans Progressiva Lymphoblastoid Cells. *J. L. Fiori*, P. C. Billings*, F. S. Kaplan, E. M. Shore.* Orthopaedic Surgery, University of Pennsylvania School of Medicine, Philadelphia, PA, USA.

Fibrodysplasia ossificans progressiva (FOP) is a rare genetic disease characterized by progressive heterotopic ossification and congenital malformation of the great toes. Perivascular accumulation of lymphocytes with subsequent infiltration and death of skeletal muscle are the earliest histopathological findings. Although the molecular mechanisms giving rise to this condition have not been fully elucidated, we have hypothesized that defects in the bone morphogenetic protein (BMP) signaling pathway play an important role in FOP pathophysiology. Previously, we demonstrated that BMP4 is overexpressed and BMP4 antagonists are underexpressed in FOP lymphoblastoid cells (LCLs). Also, the BMP receptor type IA (BMPRIA) is elevated 6-fold on the surface of FOP cells compared with controls. BMP receptors activate at least two downstream pathways; the canonical Smad pathway and the p38 MAPK pathway. In this study, we investigated the BMP signaling pathways and transcriptional targets in control and FOP LCLs. Basal mRNA levels of the early BMP response genes ID1 and ID3 were similar in control and FOP LCLs. However, in the presence of BMP4, levels of ID1 and ID3 in FOP cells were at least 2-fold higher than control cells. Although the Smad pathway has been described as the major transducer of BMP signaling in most reported cell types, we detected very low levels of Smad1 mRNA and protein in cultured LCLs as well as in primary B cells and found no upregulation of MSX2, a BMP-Smad specific target gene, following BMP4 treatment of control and FOP cells. When control LCLs were transfected with a Smad1 expression construct, treatment with BMP4 resulted in the induction of ID1, ID3, and MSX2. In contrast, MSX2 expression was not observed in cells transfected with Smad6 (inhibitory Smad) and treated with BMP4. Therefore, LCLs do not normally activate the Smad pathway in response to BMP4, but have the ability to utilize this pathway if the necessary components are provided. BMP induction of ID1 and ID3 is reported to be mediated through both Smad and p38 MAPK pathways. We determined that expression of ID1 and ID3 was specifically blocked by SB203580, a p38 MAPK inhibitor, in control and FOP cells, suggesting that these genes are downstream targets of the BMP-p38 MAPK pathway. We conclude that Smad mediated signaling is not a significant pathway in human lymphoblasts and that p38 MAPK may be a key mediator of BMP in these cells. Differences in the BMP-p38 MAPK signaling pathway between control and FOP LCLs may provide an opportunity to identify therapeutic targets for this disabling disease.

Disclosures: *J.L. Fiori, None.*

SA012

See Friday Plenary number F012.

SA013

Expression of Bone Morphogenetic Proteins and their Receptors in the Bone Marrow Megakaryocytes of Mice Genetically Impaired for GATA-1 Expression (GATA-1^{low} Mice): a Possible Role in Osteosclerosis. R. Garimella¹, M. A. Kacena², S. Tague*¹, M. C. Horowitz², H. Clarke Anderson¹. ¹University of Kansas Medical Center, Kansas City, KS, USA, ²Yale University School of Medicine, New Haven, CT, USA.

Bone marrow megakaryocytes contain various growth factors implicated in the process of bone remodeling and repair, such as bone morphogenetic proteins (BMPs), transforming growth factor- β (TGF- β), platelet derived growth factor (PDGF), osteocalcin (OC), osteopontin (OPN), osteoprotegrin (OPG), and vascular endothelial growth factor (VEGF). To date, only BMPs have been shown to induce new bone formation, in vivo. GATA-1 is a zinc finger transcription factor that plays an important role in erythroid and megakaryocyte differentiation. Low level expression of GATA-1 in mice results in excessive accumulation of immature megakaryocytes in the spleen and bone marrow, a reduction in blood platelets, and a striking increase in bone (osteosclerosis). The bone marrow in GATA-1^{low} mice contains elevated levels of TGF- β 1, PDGF, VEGF and osteocalcin compared to normal mice. The hypotheses of our current study are (1) that the megakaryocytes in the bone marrow of GATA-1^{low} mice contribute to the osteosclerosis by stimulating bone formation via the expression of BMPs, which can upregulate osteoblast proliferation and differentiation and (2) that the osteosclerosis, seen in GATA-1^{low} mice, is not due to reduced osteoclast activity. Immunohistochemistry was performed to localize the expression of BMPs and their receptors in 5 μ m paraffin embedded, decalcified, and paraformaldehyde (4 %) fixed tibia and spleen sections from twelve month-old GATA-1 wild-type and GATA-1^{low} mice, using polyclonal goat-anti-human BMP-2, 4, 6, 7, BMPR-IA, and BMPR-II antibodies. Marrow megakaryocytes of GATA-1 wild-type and GATA-1^{low} mice showed moderate to intense staining for BMP-2, BMP-4, BMP-6, BMP-7, BMPR-IA and BMPR-II, while splenic megakaryocytes showed no BMP-immunostaining. Overall, BMP expression in the bone marrow of GATA-1^{low} mice was more than that seen in controls, owing to an increased number of megakaryocytes and osteoblasts. To ascertain that the osteosclerosis seen in GATA-1^{low} mice is not due to reduced osteoclast activity, we performed TRAP staining and morphometry, and found that the number of TRAP⁺ osteoclasts was more in GATA-1^{low} mice than in controls. These findings demonstrate the presence of significant amounts of BMP-2, BMP-4, BMP-6, BMP-7, along with their receptors, in bone marrow megakaryocytes, which may, in part, be responsible for the stimulation of osteoblastic activity and resulting osteosclerosis seen in GATA-1^{low} mice.

Disclosures: **R. Garimella**, None.

SA014

See Friday Plenary number F014.

SA015

Ectopic Bone Formation in Response to BMP2 as Compared to DBM Shows Both Similar and Unique Profiles of Transcriptional Expression. J. L. Fitch¹, K. T. S. Palomares*², K. Behnam*³, D. Knaack*³, T. A. Einhorn¹, L. C. Gerstenfeld¹. ¹Orthopaedic Surgery, Boston University School of Medicine, Boston, MA, USA, ²Biomedical Engineering, Boston University College of Engineering, Boston, MA, USA, ³Osteotech, Inc., Eatontown, NJ, USA.

Demineralized bone matrix (DBM) is capable of inducing *de novo* cartilage and bone at extraskeletal sites. Bone morphogenetic proteins (BMPs) have been ascribed to primarily be responsible for the bioactivity of DBM. However, the bone matrix contains other morphogens, cytokines and mitogens that play a role in skeletal cell differentiation. This study compared the bioactivities associated with DBM and BMP2 by using active DBM, heat inactivated DBM and heat inactivated DBM conjugated to rhBMP2 that were implanted intramuscularly in nude rats over a 28 day time course. Transcriptional profiling of ~600 known skeletal tissue-associated genes was performed using a custom made 50nt oligo-nucleotide microarray. The mean expression values obtained for individual genes within the entire data set were used as the reference for that gene's expression and the transcriptional activity of a given gene was only considered if it was 1.5 fold greater or lesser than the reference. Using hierarchical clustering, separate groups of genes were identified as being uniquely induced by BMP2 or active DBM. While the expression data indicated that active DBM and BMP2 both induce osteogenesis via endochondral differentiation, conjugating BMP2 to DBM's osteoconductive matrix resulted in more rapid and robust differentiation. Selective genes that showed increased expression by both DBM and BMP-2 included osteocalcin (*oc*), bone sialoprotein (*bsp*), ras homolog gene family member b (*arhb*) and matrix metalloproteinases (*mmp*) 9 and 13. In addition to genes that were upregulated due to either treatment, we identified subset of genes that were uniquely upregulated as a result of DBM treatment alone. These included *bmp3*, nuclear hormone receptor co-activator interacting factor 1 (*nif1*), cartilage-derived retinoic acid-sensitive protein (*cd-rap*) and chloride intracellular channel 4 (*cltc4*). Our results indicate that the bioactivity of DBM is more complex than that a single BMP (BMP-2). Because other BMPs are known to be found in DBM the current data does not discriminate if this more complex inductive activity is due to these activities or other morphogenetic factors.

Disclosures: **J.L. Fitch**, Osteotech, Inc. 2.

SA016

See Friday Plenary number F016.

SA017

Adenosine 3', 5'-Cyclic Monophosphate (cAMP) Enhances Bone Morphogenetic Protein (BMP) Activities through the Suppression of Smad6 Expression in Osteoprogenitor Cells. R. Sugama*, T. Koike, Y. Imai*, C. Nomura*, K. Takaoka. Department of Orthopaedic Surgery, Osaka City University Medical School, Osaka, Japan.

Bone morphogenetic proteins (BMPs) present potent osteogenic activities. In considering efficacious use of the BMPs, a basic important problem is low responsiveness of human mesenchymal cells to the BMP. In order to overcome the problem, additional agents or methods that intensify the BMP activity would be desired. Phosphodiesterase inhibitor, Pentoxifyline (PeTx), facilitates BMP activities but the precise mechanisms are currently unknown. We have hypothesized that elevation of intracellular cAMP level might intensify BMP signaling with interference to negative feed back mechanism. The purpose of this study is to elucidate the changes in mRNA expression of inhibitory Smad (Smad6) and in phosphorylated receptor-regulated Smads levels by cAMP and BMP-4 in osteogenic ST2 cells. PeTx alone had no effect on ALP activity in ST2 cells. In contrast, PeTx enhanced BMP-4-induced ALP activities in a dose-dependent manner. Intracellular level of cAMP increased about 7 times in 15 minutes after the addition of PeTx (0.9 mM). There was no additive effect on the level of cAMP by simultaneous addition of BMP-4 and PeTx. The effect of PeTx to enhance BMP action was mimicked by dbcAMP. In ST2 cells, Smad6 mRNA expression was increased by BMP-4 treatment. Quantitative real-time RT-PCR of the Smad6 mRNA expression treated with or without BMP-4 (300 ng/ml) and various doses of dbcAMP (100 to 2000 μ M) revealed that dbcAMP reduced the BMP-4 induced Smad6 expression in a dose-dependent manner. Same result was obtained by Northern blotting. Phosphorylation of Smad1/5/8 after BMP-4 stimulation started from 1 hour later and became undetectable after day 3. Addition of dbcAMP did not exhibit significant effects on phosphorylation of Smad1/5/8 at 1 hour or 24 hour time points after treatments but maintained the phosphorylated Smad1/5/8 until day 5. These results indicate that elevated intracellular cAMP might enhance BMP signaling by suppressing Smad6 induction and prolonging intracellular BMP signaling. We concluded that the suppression of BMP-4 induced Smad6 expression would be one of the mechanisms for enhanced BMP action by PeTx and dbcAMP treatments. Manipulation of the BMP signaling loop may also provide a new insight to enhance efficacy of BMP-mediated local new bone formation for the treatment of damaged bone.

Disclosures: **R. Sugama**, None.

SA018

rhBMP-2 Enhances Bone Formation in a Biodegradable Scaffold. T. E. Hefferan, E. Jabbari*, A. Florschutz*, R. M. Mardones*, L. Lu*, B. L. Currier*, M. J. Yaszemski*. Dept of Orthopedics, Mayo Clinic College of Medicine, Rochester, MN, USA.

In the United States approximately 1 million patients per year require bone grafting procedures to repair skeletal defects. Current grafting options include the use of either autologous or allograft bone, metals, ceramics or bone cements, each of which have drawbacks. Synthetic biodegradable polymers have characteristics which could facilitate the repair of these defects. Therefore we investigated skeletal repair using a poly(propylene fumarate) (PPF) scaffold in conjunction with an osteogenic agent, rhBMP-2 (kindly provided by Wyeth), to induce bone formation in a critical size defect animal model. A 5 mm defect was generated in the femur of male Sprague-Dawley rats. Twelve animals were assigned to a treatment group and the defect was filled with either: PPF scaffold, PPF scaffold coated with rhBMP-2 (20 μ g/ml), PPF scaffold with rhBMP-2 (25 μ g/200mg) loaded microspheres or PPF scaffold with vehicle loaded microspheres. Poly(DL-lactic-co-glycolic acid) microspheres were embedded in the scaffold in order to examine the effect of encapsulation on the bone-forming activity of rhBMP-2. Scaffolds were harvested at 3, 6 and 12 weeks and bone mineral density (BMD) was measured using PIXImus DEXA (GE Healthcare). After determining the BMD, the scaffolds were processed for histology and stained with Goldners-Trichrome to evaluate mineralized tissue formation. At 3 weeks all scaffolds had similar BMD. At 6 weeks the scaffolds coated with rhBMP-2 had a significantly higher BMD (0.236 ± 0.014 g/cm²) compared to the PPF control scaffold (0.155 ± 0.018 g/cm²) ($p < 0.05$). Also at 12 weeks the BMD of the rhBMP-2 coated scaffolds was significantly greater than the PPF control scaffold (0.294 ± 0.01 vs. 0.194 ± 0.03 g/cm²) $p < 0.01$. Two-way ANOVA showed borderline significance ($p = 0.055$) for the effect of the scaffold, while the effect of time was highly significant ($p = 0.0001$). In fact, the BMD was greater at 12 weeks compared to 3 weeks for the PPF scaffold with vehicle microspheres ($p < 0.01$), PPF scaffold with rhBMP-2 microspheres ($p < 0.01$) and PPF scaffold coated with rhBMP-2 ($p < 0.01$). In addition, Goldners staining showed adding rhBMP-2 to the scaffold resulted in better integration between the scaffold and the surrounding bone. The scaffolds without rhBMP-2 had less mineralization and more fibrous tissue. In conclusion, rhBMP-2 enhances bone formation in PPF scaffolds as shown by increased BMD and mineralization. Therefore, combining rhBMP-2 with a synthetic biodegradable polymer holds promise for the treatment of skeletal defects.

Disclosures: **T.E. Hefferan**, None.

SA019

Proteomic Analysis of Bone Biomineralization Foci Isolated by Laser Capture Microscopy from Osteoblast Cultures. J. P. Gorski, N. T. Huffman*, H. Wright*. Oral Biology, Univ. of Missouri-Kansas City, Kansas City, MO, USA.

Biomineralization foci (BMF) are recently identified extracellular sites of mineral crystal nucleation in common osteoblastic culture models and in developing bone. Supramolecular complexes of 10-100 microns in diameter, BMF contain matrix vesicles and other membrane limited vesicles up to 900 nm in diameter. BMF are also enriched in bone acidic glycoprotein-75 (BAG-75), a phosphoprotein restricted to developing embryonic and primary bone, and, in bone sialoprotein. The goal of our study was to develop a method to isolate BMF and to begin to characterize their proteome in order to understand the underlying mineralization mechanism. UMR-106-01 osteoblastic cells were seeded at 4.8×10^5 cells/ml and grown on glass slides. Using a standardized protocol, cultures reach confluency by 64 h after plating. BGP (7 mM beta-glycerolphosphate) was added at 64 h and the location of mineral deposits scored 24 h later after fixation and staining with Alizarin red S dye (ARS). On culture slides, all specific ARS staining was associated with BMF. ARS-positive BMF were then isolated by laser capture microscopy (LCM) using an Arcturus Pix IIe microscope. BMF from several culture slides and different "caps" were pooled (2500-3000 BMF/preparation), extracted, and decalcified in 4 M guanidine HCl containing 0.5 M EDTA and protease inhibitors. Entire culture slides containing cells and BMF were also processed similarly and used as a total cell layer control. Extracts were subjected to one-dimensional SDS PAGE and either stained with Sypro Ruby or immunoblotted onto membranes and subjected to chemiluminescent detection. Also, stained bands were cut out, trypsinized, and subjected to mass spectrometric peptide mapping. Compared with the total cell layer, BMF were preferentially enriched in BAG-75 and bone sialoprotein, however, BMF exclusively contain a 50 kDa fragment rather than the 75 kDa BAG-75 precursor form. In contrast, fetuin and albumin from serum, and mitochondrial marker aspartate amino transferase were preferentially enriched in the total cell layer. Mass fingerprinting studies identified synaptotagmin VII (27% coverage) and immunoblotting studies confirmed its assignment as a 58,000 molecular weight component of BMF. The latter is thought to function in vesicular transport/secretion and may play a role in BMF assembly. Our study indicates that LCM can be used to isolate sufficient quantities of mineral containing BMF for proteomic and functional studies. The absence of fetuin from laser microscope captured BMF suggests the latter structures act as a barrier to mineralization inhibitors and provide a protected environment within which active mineral nucleation can occur.

Disclosures: J.P. Gorski, None.

SA020

Calcification versus Ossification - Histologic Features of Calcific Deposits of the Shoulder. C. Bartl*, P. Magosch*, S. Lichtenberg*, P. Habermeyer*, R. Bartl*. ¹Dep. of Sportorthopaedics, Technical University, Munich, Germany, ²Shoulder and Elbow Surgery, ATOS Clinic, Heidelberg, Germany, ³Bavarian Osteoporosis Center, LMU, Munich, Germany.

The pathogenesis of Calcifying Tendinitis (CT) is still not well established. A high percentage of patients describe persistent complaints after conservative or shock wave therapy of deposits around the shoulder. Prognostic factors for outcome could not yet be identified. The purpose of this study was to evaluate the histologic nature of the calcific deposits and their correlation with radiologic findings. 83 shoulders (79 patients) with a radiologically confirmed deposit were prospectively scheduled for arthroscopic shoulder surgery. Preoperatively the deposits were graded as fluffy (I) or sharply demarcated (2) on standard radiographs. After arthroscopic removal of the deposits biopsies were embedded in methylmethacrylate. Sections were stained (Giemsa-, Gomori- and Ladewig-stain) and also immunohistology (Monoclonal anti-human macrophage antibodies -CD 68- and monoclonal endothel antibodies -CD 34-, DAKO) as well as analysis of collagen types (Polyclonal antibodies to collagen type I, II, III, Acris) was performed. Three distinct histologic stages (HS) of the deposits could be identified

Stage I: Calcification n=24(29%)

Stage II: Fibrotic Organisation n=7(8%)

Stage III: Ossification n=52(63%)

No significant correlation between the preoperative radiologic appearance and the histologic stage of the deposits could be identified >Basic histology and immunohistology revealed the presence of bone specific cells in all stage III deposits: Osteoclasts (CD 68, Giemsa), Osteocytes (Giemsa, Ladewig) and woven bone (Gomori). Also collagen type I proof was positive in over 90% of the cases. Stage I deposits consist only of a calcific mass divided by fibrous strands with no cells between. Stage II deposits show high vascularisation and a positive collagen III proof. In this study three definite histologic stages of deposits were identified that have not been described previously in Calcifying Tendinitis of the shoulder. The stage of ossification and not the classical calcific deposit (I) represents the major part of the cases. We underline the hypothesis that CT is an active cell-mediated tissue process which leads to fibrotic organisation and finally to production of primitive bone ('fibro-osseous metaplasia') in a high number of cases. The significance of histologic stages of the deposits for pathogenesis and treatment of Calcifying Tendinitis of the shoulder must be evaluated in further studies.

Disclosures: C. Bartl, None.

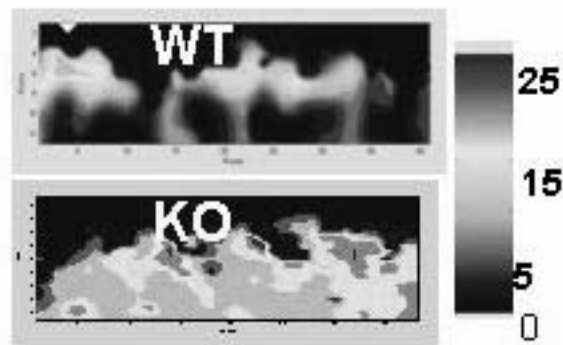
SA021

See Friday Plenary number F021.

SA022

An Unexpected Phenotype in Cathepsin K Deficiency. A. L. Boskey¹, L. Spevak*, E. Pourmand*, B. D. Gelb*, M. B. Schlaffler². ¹Research Division, Hospital for Special Surgery, New York, NY, USA, ²Orthopaedics, Mount Sinai School of Medicine, New York, NY, USA.

Cathepsin K (catK) is a cysteine protease with collagenolytic and proteoglycan degradative activities that is involved in osteoclast action, and is thought to be modify growth plate (GP) proteoglycans. Patients lacking catK activity show osteosclerosis and dwarfism, suggesting a role for CatK in endochondral ossification (EO). To define the role of catK in EO we asked if catK plays a direct or indirect (osteoclast-mediated) role in modulating GP matrix structure. CatK knockout (KO) mice have thicker bones and more numerous trabeculae but increased numbers of osteoclasts relative to age-matched wild type (WT) controls. The calcified cartilage and trabecular bone (just below GP) was characterized using infrared imaging (FTIRI) in 10 wk old KO and age, background, and sex-matched WT mice. Since proteoglycan aggregates (PGA) inhibit GP calcification we predicted that the KO in which PGA degradation would be limited would have decreased mineral content, mineral crystal size, carbonate/phosphate ratio, and collagen maturity as determined by FTIRI. Contrary to expectation, the KO GP had significantly increased mineral/matrix ratio (figure), increased collagen cross-link ratio, and no significant changes in mineral properties. The GP findings either indicate the failure of osteoclasts (whose functions depend on catK) to remodel the cartilage as it calcifies, an upregulation of another degradative enzyme in the absence of cathepsin K, an alteration in vascular invasion (facilitating calcification), or the possibility that the in vivo function of the enzyme does not match that observed in vitro. Parallel to these studies we added a broad spectrum cathepsin inhibitor (inhibitor III, Calbiochem) at 0-0.05 uM to calcifying chick limb-bud chondrocyte micro-mass cultures after the initiation of calcification. In this system there was a similar unexpected increase in calcification when the activity of the cathepsins was blocked. Since there is no osteoclast remodeling in this culture system, clearly there are effects on mineralization associated with matrix formation or endochondral ossification when cathepsin activity is limited. Thus, in the growth plate, catK may act as a mineralization inhibitor via matrix modification in ways we do not yet understand.



Disclosures: A.L. Boskey, None.

SA023

See Friday Plenary number F023.

SA024

Integrin Alpha Is Indispensable for Ligaments to Resist Mechanical Stress-Induced Mineralization. F. Takizawa*, T. Yoshizawa¹, S. Maruyama*, F. Iizawa*, A. Matsuda*, O. Ishibashi¹, T. Saku*, H. Yoshie*, U. Mayer*, H. Kawashima¹. ¹Cell Biology and Molecular Pharmacology, Niigata University, Niigata, Japan, ²Oral Pathology, Niigata University, Niigata, Japan, ³Periodontology, Niigata University, Niigata, Japan, ⁴Wellcome Trust Center for Cell-Matrix Research, University of Manchester, Manchester, United Kingdom.

Mechanical stress (MS) promotes differentiation and maturation of osteoblasts and increases bone density and strength. In contrast, ligaments never mineralize in vivo despite constant exposure to intermittent MS. This led us to hypothesize that ligaments have a mechanism by which mineralization is prevented against MS. However, studies dealing with the response of ligament cells to MS are scarce and controversial, because there has been no established cell line available. To circumvent this problem, we have recently established a cell line, designated PDL-L2, from mouse periodontal ligament (PDL). This cell line has an early differentiation stage osteogenic character, but does not mineralize in vitro in medium favoring osteogenic mineralization despite expression of a significant amount of alkaline phosphatase and Runx2. Using this cell line, we examined how ligament cells respond to MS. MS induced sequential activation of FAK, ERK1/2, Runx and osteocalcin (OCN) production, and eventual mineralization in MC3T3E1 cells, but failed to induce any of these effects in PDL-L2 cells. Although details of mechanotransduction signaling pathways are not elucidated yet, accumulating evidence indicates that cells sense MS through integrins. cDNA microarray and RT-PCR demonstrated that integrin $\alpha 7$ was abundantly expressed in PDL-L2 but not in MC3T3E1 cells. This was also confirmed at protein level by western blot and immunoprecipitation

analysis. In addition, in situ hybridization analysis demonstrated that integrin $\alpha 7$ was abundantly expressed in PDL cells but not in adjacent osteoblasts. Since both cell lines similarly express integrins $\alpha 5$, $\alpha 2$ and $\beta 1$, we reasoned that the presence of integrin $\alpha 7$ might alter the mechanotransduction signal pathway. Indeed, when expression of integrin $\alpha 7$ in PDL-L2 was reduced by means of RNAi, MS induced sequential activation of FAK, ERK1/2, Runx2 and OCN production, leading to mineralization in a similar manner observed in MC3T3-E1 cells. Moreover, integrin $\alpha 7$ KO mice developed ectopic mineralization in the PDL. These data clearly demonstrate that ligaments have a mechanism to resist MS-induced mineralization, in which integrin $\alpha 7$ is indispensable. Failure of this mechanism may be involved in the development of ossification of the posterior longitudinal ligaments of the spine.

Disclosures: **F. Takizawa**, None.

SA025

HtrA1 Regulates the Deposition of a Mineralized Matrix by Osteoblasts. K. D. Hadfield^{*1}, C. Farrington Rock^{*2}, S. L. Dallas³, L. Sudre^{*1}, G. A. Wallis^{*1}, R. P. Boot-Handford^{*1}, A. E. Canfield^{*1}. ¹Wellcome Trust Centre for Cell-Matrix Research, The University of Manchester, Manchester, United Kingdom, ²Cedars-Sinai Medical Center, Los Angeles, CA, USA, ³University of Missouri, Kansas City, MO, USA.

HtrA1 is a secreted multi-domain protein with proven serine protease activity. There is increasing evidence to suggest that this protein plays a role in regulating skeletal development and pathology. First, HtrA1 is expressed in developing skeletal elements. Second, HtrA1 inhibits signalling mediated by TGF β -family members. Third, HtrA1 is elevated in human osteoarthritic cartilage compared to controls. Finally, we have shown that HtrA1 is up-regulated as pericytes undergo osteogenic differentiation and mineralization. The purpose of this study was to investigate the role of HtrA1 in regulating matrix calcification and to identify which domains are essential for its activity. HtrA1 was markedly up-regulated in post-confluent cultures of the 2T3 murine osteoblast cell line and the growth plate chondrocyte ATDC5 cell line, just prior to calcification and was then down-regulated as matrix calcification occurred. The functional role of HtrA1 in osteoblast differentiation and matrix calcification was investigated using two complimentary approaches. First, a full-length HtrA1 expression plasmid was generated and transfected into 2T3 cells to generate stable over-expressing clones. These clones showed delayed mineralization relative to controls as determined by Alizarin red staining and ⁴⁵Ca incorporation. Furthermore, preliminary results have shown that high expression of HtrA1 negates BMP-2-induced mineralization of these cells. Second, recombinant full-length HtrA1 (rhHtrA1) and a series of domain-specific deletion constructs have been produced using a mammalian expression system. The protease activity of these proteins was confirmed by their ability to degrade β -casein. These proteins were added back to 2T3 cells and their effects on matrix mineralization determined. We report that rhHtrA1 decreases the extent of mineralization in 2T3 cells compared to controls. Finally, we tested the hypothesis that HtrA1 degrades specific matrix proteins, the loss of which is associated with matrix calcification. Accordingly, rhHtrA1 was found to degrade both recombinant decorin and matrix Gla protein (MGP). Furthermore, we demonstrated that both the protease domain and the PDZ domain were necessary for the degradation of MGP, whereas the PDZ domain was not essential for the degradation of decorin. Taken together, these results suggest that HtrA1 may regulate matrix calcification either via the inhibition of BMP-2 signalling and/or via the degradation of specific matrix proteins.

Disclosures: **K.D. Hadfield**, None.

SA026

The Elastic Lamellae of Devitalized Rat Aortas Calcify Rapidly When Incubated in Serum: Implications for the Pathogenesis of Vascular Calcification. P. A. Price, W. S. Chan^{*}, M. K. Williamson. Biology, University of California, San Diego, La Jolla, CA, USA.

The present studies show for the first time that EDTA-extracted, devitalized rat aortas calcify rapidly when incubated at 37°C in rat serum or plasma. This serum-induced artery calcification begins with numerous calcification foci in the elastic lamellae of the artery media, the same location seen for calcification in the arteries of patients with uremia and diabetes, and in the matrix Gla protein (MGP)-deficient rodent. The elastic lamellae of devitalized aortas also calcify when incubated in human serum for 6 days at 37°C, but only if serum phosphate is first raised from the normal 1mM level in human serum to 2mM or greater (the level normally found in rats). It is of interest to note that elevated serum phosphate is a strong predictor of medial artery calcification in uremic patients. Devitalized aortas also calcify when incubated in DMEM containing as little as 1.5% rat serum, but not when incubated in DMEM alone. Since the addition of 1.5% serum has a trivial impact on the ionic composition of DMEM, the probable explanation for this effect is that serum contains an agent that induces artery calcification. Living aortas do not calcify when incubated in DMEM containing serum, which suggests that vascular cells normally prevent the serum-induced calcification of the artery media *in vivo*. This hypothesis is supported by the observation that the living rat aortas secrete the calcification inhibitor MGP into culture medium at a rate of 3 μ g/aorta/day over the course of these experiments. The serum factor that initiates calcification of elastic lamellae in devitalized arteries has the same potency, size, and protease sensitivity as the serum factor recently shown to initiate the re-calcification of the type 1 collagen matrix of demineralized bone (J. Biol. Chem. (2004) 279:19169-80). If one serum calcification factor is indeed responsible for initiating calcification of collagen and elastin matrices, it could help to explain how agents that act specifically on bone, such as alendronate, ibandronate, and osteoprotegerin, are able to potently inhibit artery calcification in the rat (J. Biol. Chem. (2004) 279: 1594-1600).

Disclosures: **P.A. Price**, None.

SA027

Histone Deacetylase Inhibitors: New Strategy for the Management of Rheumatoid Arthritis. H. S. Lin^{*}, C. Y. Hu^{*}, H. Y. Chan^{*}, Y. Y. Liew^{*}, H. P. Huang^{*}, L. Lepescheux^{*}, E. Bastianelli^{*}, R. Baron, P. Clement-Lacroix, G. Rawadi. ProStrakan, Romainville, France.

Bone destruction is a characteristic feature of rheumatoid arthritis (RA) and constitutes a major cause of progressive disability. Bone loss involves osteoclasts, which are responsible for periarticular joint destruction, and are induced by a first step inflammatory process. Osteoclastogenesis secondary to the inflammatory process is evident in animal models of RA such as collagen-induced arthritis (CIA). It has been shown that synovial cells in CIA and RA release several inflammatory cytokines and treatment of CIA with anti-inflammatory agent blocks osteoclastogenesis, thereby preventing focal bone destruction. MS-275 and suberoylanilide hydroxamic acid (SAHA) are two histone deacetylase inhibitors (HDACi), a class of compounds known to have anti-inflammatory properties. In the present study, the anti-rheumatoid arthritis effects of MS-275 and SAHA were tested in two rodent collagen induced arthritis models. Animals were treated with SAHA or MS-275 and monitored 2-3 times per week for paw swelling. On day 36 after induction, the arthritis bearing mice had maximal clinical score. The clinical score of SAHA (50 or 5 mg/kg) and low dose of MS-275 (3 mg/kg) treated mice was about 30% and 60%, respectively lower than the clinical score in the vehicle group; while high dose MS-275 (10 mg/kg) treated mice had no significant clinical symptom of arthritis. Similar results were also observed in rats and MS-275 (3 mg/kg) could even completely prevent the onset of swelling of both paws in rats. At two weeks after onset of arthritis, the hind paws were evaluated using radiography and histology; while left tibia was analyzed with tomograph micro-CT. Radiological observation indicated HDACi treated animal had less or even no bone destruction; while the control animals suffered from serious bone erosion. Histopathologic analyses indicated the preventive effect of HDACi in structural joint damage. The protective effects of HDACi in bone loss associated with CIA were also documented. The anti-RA effects of the tested HDACi appeared to be dose dependent. These findings demonstrate that HDACi have powerful anti-inflammatory effects leading to bone protection in arthritis. In conclusion, HDACi could be a new strategy for the management of RA.

Disclosures: **P. Clement-Lacroix**, None.

SA028

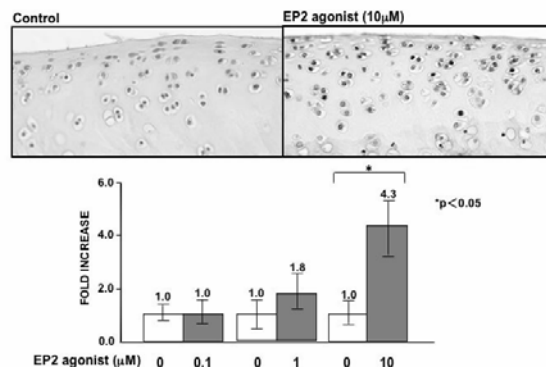
See Friday Plenary number F028.

SA029

PGE2 Signal through EP2 Promotes the Growth of Articular Chondrocytes. T. Aoyama¹, B. Liang^{*2}, T. Matsusaki^{*2}, T. Nakayama^{*2}, T. Nakamura², J. Toguchida¹. ¹Department of Tissue Regeneration, Institute for Frontier Medical Sciences, Kyoto University, Kyoto, Japan, ²Department of Orthopedic Surgery, Kyoto University, Kyoto, Japan.

Prostaglandin E2 (PGE2) exhibits pleiotropic effects in various types of tissue through four types of receptor, EP1-4. The role of PGE2 in the metabolism of articular cartilage is still a matter of debate. We examined the expression of EPs and effect of agonists for each EP on articular chondrocytes. Immunohistochemical and RT-PCR analyses revealed that chondrocytes in human articular cartilage expressed EP2 and EP3 with less intensity, whereas EP1 and EP4 were not detected in any cells. A chondrocyte cell line, MMA2, was established from articular cartilage of p53-/- mice and used to analyze the effects of agonists for each EP, which were provided by Ono Pharmaceutical Co. MMA2 expressed EP2 as well as primary cultured chondrocytes, and the treatment with EP2 agonist increased the level of intracellular cAMP in a concentration-dependent manner, suggesting a functional role for EP2 in MMA2. Molecules downstream of the PGE2 signal through EP2 in MMA2 were investigated by gene-expression profiling before and after the treatment with EP2 agonist (1 μ M) using a cDNA microarray. 22 genes were isolated as up-regulated by the treatment of EP2 agonist, including several growth-promoting and apoptosis-protecting genes such as the cyclinD1, fibronectin, integrin $\alpha 5$, AP2 α , and 14-3-3 γ genes. The up-regulation of these genes by the EP2 agonist was confirmed in human articular chondrocytes by quantitative mRNA analysis, suggesting a growth-promoting effect of the EP2 agonist on normal articular chondrocytes. The cellular incorporation of BrdU by primary human articular chondrocytes was decreased by the treatment with indomethacin (5 μ M) and increased by EP2 agonist (1 μ M). Growth promoting effect of EP2 agonist for articular chondrocytes was further analyzed in organ culture of rat femora, and the proportion of PCNA-positive cells was significantly increased after a 14-day incubation with EP2 agonist (Fig.1). These results suggested that the EP2 agonist was able to exert growth-promoting effects on cells surrounded by cartilage matrix, and combined with suitable drug-delivery systems, EP2 agonist is a promising therapeutic compound for the treatment of degenerative cartilage diseases.

Fig.1 Cell Proliferation was Promoted by EP2 Agonist :PCNA Staining in Organ Culture of Rat Femur



Disclosures: **T. Aoyama**, None.

SA030

See Friday Plenary number F030.

SA031

Wnt Signaling in Human and Bovine Articular Chondrocytes. K. E. Yates, S. Shortkroff*. Orthopedic Research, Brigham and Women's Hospital, Boston, MA, USA.

The Wnt signaling network is one of the major regulators of embryonic skeletal development. After birth, Wnts continue to function in osteoblast differentiation and bone density. Whether Wnts are similarly active in cartilage, however, is less clear. In this study, we hypothesized that Wnt signals regulate chondrocyte function. Human articular chondrocytes were isolated from cartilage discarded during total knee replacement surgeries for treatment of osteoarthritis. Bovine articular chondrocytes were isolated from shoulders of young calves. Gene expression of Wnt pathway components was measured by cDNA array (Superarray, Inc.) and by RT-PCR. Proteoglycan content was evaluated by Alcian blue staining of monolayer cultures. Conditioned media were prepared from L and LWnt3a cells (American Type Culture Collection). Whole cell lysates and nuclear extracts were prepared using a commercially available kit (ActiveMotif, Inc). Western blots were probed with anti-β-catenin (Santa Cruz Biologicals) and anti-histone H4 antibodies (Upstate Biotechnology). Human articular chondrocytes (n=3) were found to express high levels of b-CATENIN, AXIN2, and FRZB mRNAs. The AXIN2 protein is induced in response to Wnt signals and acts as a negative feedback inhibitor; FRZB competes with Wnt proteins for receptors. The presence of those components in hACs, therefore, was indicative of active Wnt/b-catenin signaling in those cells. RT-PCR confirmed expression of several Wnt mRNAs in hACs that are known to transduce signals via the canonical b-catenin pathway (*WNT7a*, *WNT10b*, *WNT14*). Moreover, treatment of bACs with Wnt3a induced stabilization of b-catenin in a similar time-frame as in control L cells (maximal response within 3h). *In vitro* aging/de-differentiation of bACs by cell passaging also stabilized b-catenin in bACs, prior to the expected decrease in matrix proteoglycan. B-catenin levels were not altered in primary cultures that achieved confluence. Those results suggested that the loss of chondrocyte phenotype in passaged bACs was associated with an increase in Wnt signaling via the canonical b-catenin pathway. It was surprising, therefore, that addition of the Wnt antagonist lithium chloride (LiCl) did not mimic the effect of *in vitro* aging on proteoglycan synthesis by bACs. Immunoblot analyses showed that b-catenin was not stabilized in bACs by short term (up to 6 h) or extended exposure (48 h) to 5 mM LiCl. Moreover, b-catenin was not stabilized after 48 h exposure to increasing amounts of LiCl (5, 10, and 20 mM). The mechanism underlying this resistance to LiCl in bACs is not known. Nevertheless, our data indicate that the Wnt/b-catenin signaling pathway is active, and actively modulated, in articular chondrocytes

Disclosures: **K.E. Yates**, None.

SA032

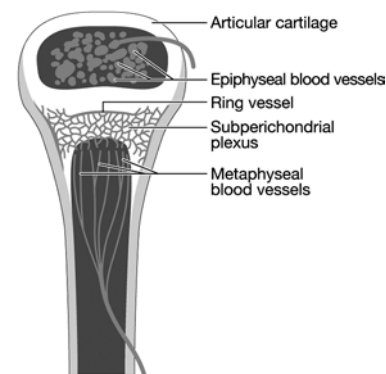
See Friday Plenary number F032.

SA033

In Vivo Delivery of Fluoresceinated Dextran to the Murine Growth Plate: Imaging of Three Vascular Routes by Multiphoton Microscopy. C. Farnum*¹, M. Lenox*¹, W. Zipfel*², W. Horton*³, R. Williams*². ¹Biomedical Sciences, Cornell University, Ithaca, NY, USA, ²Applied and Engineering Physics, Cornell University, Ithaca, NY, USA, ³Shriners Hospital for Children, Portland, OR, USA.

Bone elongation by endochondral ossification occurs through the differentiation cascade of chondrocytes of cartilaginous growth plates. Molecules from the systemic vasculature reach the growth plate from three different directions: epiphyseal, metaphyseal and via a ring

vessel and plexus associated with the perichondrium. This study is an analysis of the real-time dynamics of entrance of fluoresceinated tracers of different molecular weights into the growth plate from the systemic vasculature, and tests the hypothesis that molecular weight is a key variable in the determination of both the directionality and the extent of tracer movement into the growth plate. Multiphoton microscopy was used for direct in vivo imaging of the murine proximal tibial growth plate in anesthetized 4-5 week old transgenic mice with green fluorescent protein linked to the collagen II promoter. Mice were given an intracardiac injection of either fluorescein (332.3 Da) or fluoresceinated dextrans of 3, 10, 40, 70 kDa, singly or sequentially. For each tracer, directionality and rate of arrival, together with extent of movement within the growth plate, were imaged in real time. For each image series, fluorescence data were summed transversely across the growth plate. Arrival time was defined as the first time at which the position-specific fluorescence reach one half of its 5-minute value. The amount of tracer entering compared with that available in the vasculature varied with molecular weight, falling off significantly from fluorescein to dextrans of 3 kDa and 10 kDa, while 40 kDa and 70 kDa dextrans did not enter. Rate of entrance and potential directionality of entrance from the systemic injection did not appear to differ for fluorescein and the 3 kDa and 10 kDa dextrans. The potential for movement within the growth plate was equally permissive from either the metaphyseal or the epiphyseal side. These results have implications for understanding paracrine and systemic regulation of growth plate chondrocyte differentiation, as well as variables associated with effective drug delivery to the growth plate.



Disclosures: **C. Farnum**, None.

SA034

Thyroid Hormone (T3) Realizes Ideal Redifferentiation of Dedifferentiated Chondrocytes in Cooperation with BMP-2 and Insulin. K. Hoshi, G. Liu*, T. Ogasawara, Y. Asawa*, U. Chung, T. Takato*, K. Nakamura, H. Kawaguchi. The University of Tokyo, Graduate School of Medicine, Tokyo, Japan.

Chondrocytes isolated from donor cartilage should be made to proliferate in vitro, for the application in cartilage tissue engineering. However, decrease in the matrix synthesis of collagen type II (col2) and increase in collagen type I (col1) inevitably occur during the proliferation culture, termed dedifferentiation. 3D culture or hydrostatic pressure had been reported to induce redifferentiation of the dedifferentiated chondrocytes. For a more effective induction, we attempted to optimize combinations of soluble factors that are certificated for medical use, in the present study. We used human dedifferentiated chondrocytes originating from ears, ribs and joints. The combinational effects of 12 soluble factors (FGF-2, BMP-2, IGF-I, insulin, etc.) on the PG accumulation were examined using the analysis of variance in fractional factorial design. As a result, the combination of BMP-2 and insulin (BI) most significantly enhanced the PG accumulation. BI also promoted the expression of col2 and decreased that of col1 compared with the control containing no factors. However, BI also increased the expression of collagen type X (col10) that may induce endochondral ossification, suggesting a disadvantage to regenerate permanent cartilage. When we examined the third factor, the addition of thyroid hormone (T3) to BI (BIT) increased the expression col2 more effectively and unpredictably decreased col10 to the level of the control, because T3 had been known to enhance the hypertrophy of chondrocytes and their expression of col10. These effects of BI or BIT were reproducibly seen in chondrocytes of both hyaline and elastic cartilage. Histological and biochemical findings from the in vitro and in vivo regenerated cartilage stimulated by BIT confirmed the abundant PG and col2 content, compared with that in the control, while the compression strength was superior in BIT, being almost equivalent to that of the native cartilage. Regarding the molecular mechanisms, BI stimulated the phosphorylation of both Smad 1/5/8 and Akt, while it also enhanced the expression of Runx2. On the other hand, T3 added to BI induced the partial inhibition of both the Akt phosphorylation and Runx2 upregulation. When the Akt inhibitor was used instead of T3, the expression of col2 was promoted, compared with that in BI, while those of Runx2 and col10 decreased, corresponding to those seen in BIT. In conclusion, the addition of T3 to BI produces the ideal effects on the regeneration of permanent cartilage through the partial inhibition of the Akt activation, proposing a novel and practical technique for cartilage tissue engineering.

Disclosures: **K. Hoshi**, None.

SA035

See Friday Plenary number F035.

SA036

Prospective Study of Indian Hedgehog and Parathyroid Related-Peptide Expressions in the Rat Growth Plate during Recovery of Growth Retardation.

V. Pelletier*, V. Lascau-Coman*, N. Dion, G. Mailhot*, J. L. Petit*, C. Deschênes*, M. Gascon-Barré, L. G. Ste-Marie. Saint-Luc Hospital, CHUM Research Centre, Montréal, PQ, Canada.

Previously, we demonstrated that rats fed with D and Ca depleted diet (D-Ca-) present growth retardation. When D-Ca- rats were repleted with a high Ca content diet (Ca⁺) during 14 days (d), there was a partial reversion of growth retardation with a rate of weight gain equal to 50% of normal rats. In addition, when D-Ca- were repleted with a low Ca repletion diet (Ca⁺_{0.5}) growth rate was improved reaching 80% of normal rats. To characterize the dynamic changes occurring at the tibial growth plate (GP) during the 14d of repletion with the high or low Ca diets, we performed undecalcified bone morphometry on proximal tibia taken from rats sacrificed at 0, 3, 7 and 14d after the repletion diets. No significant differences for the GP thickness was observed between D-Ca-, Ca⁺ and Ca⁺_{0.5} at 0, 3 and 7d. However at 14d, the Ca⁺ rats showed a markedly enlarged GP compared to D-Ca- (1210 ±440µm and 449 ±55µm, respectively; p=0,002) while Ca⁺_{0.5} had intermediary GP thickness (680 ±186µm) which was not significantly different from D-Ca- and Ca⁺. To further study the endochondral ossification occurring in these animals, we performed immunohistochemistry of Indian Hedgehog (Ihh) and parathyroid hormone related-peptide (PTHrP), 2 proteins involved in proliferation and maturation of GP chondrocytes. In Ca⁺ rats as early as 3d of repletion, levels of Ihh and PTHrP were increased higher than in D-Ca- and Ca⁺_{0.5} and continued to increase up to 14d. In the Ca⁺_{0.5} rats at 3d, the expression level of both proteins were found to be similar to D-Ca- and then increased by 7d and 14d but at a lower intensity than Ca⁺ rats. During the study period, serum phosphorus did not significantly change in D-Ca- and Ca⁺_{0.5} (3,45 ±0,2mM and 3,03 ±0,4mM, respectively) whereas in Ca⁺, it fell significantly to 1,19 ±0,36mM (p<0,001) after 3d and remained at these low levels at 14d (0,63 ±0,22mM). The Ca⁺_{0.5} rats which had the best growth recovery, showed an increased expression of Ihh and PTHrP without an enlarged GP. Although Ca⁺ rats presented a markedly increased expressions of Ihh and PTHrP, they had a lesser growth recovery as they developed a rachitic GP. It is interesting to note that in this group the over-expression of Ihh and PTHrP as the hypophosphatemia preceded the onset of GP widening. Taken together, these results show that the mechanism of catch up growth is related to the increase of Ihh and PTHrP expressions however, the early development of hypophosphatemia in Ca⁺ rats induces rickets which impedes the growth recovery.

Disclosures: V. Lascau-Coman, None.

SA037

IL-1-Induced Chondrocyte Death Mediated by iNOS and NADPH Oxidase. R. Yasuhara*¹, Y. Miyamoto*¹, A. Yamada*¹, M. Takami¹, T. Suzawa¹, T. Akaike*², T. Akuta*², R. Kamijo¹. ¹Biochemistry, Showa University, Tokyo, Japan, ²Microbiology, Kumamoto University, Kumamoto, Japan.

IL-1 (interleukin-1) acts as a key mediator of the degeneration of articular cartilage in RA (rheumatoid arthritis) and OA (osteoarthritis), where chondrocyte death is observed. It is still controversial, however, whether IL-1 induces chondrocyte death. In the present study, the viability of mouse chondrocyte-like ATDC5 cells was reduced by the treatment with IL-1β for 48 h or longer. IL-1β augmented the expression of the catalytic subunit of NADPH oxidase, gp91^{phox}, as well as inducible NO synthase in ATDC5 cells. Generation of nitrated guanosine and tyrosine suggested the formation of reactive nitrogen species including ONOO⁻ (peroxynitrite), a reaction product of NO and O₂⁻ in ATDC5 cells and rat primary chondrocytes treated with IL-1β. Death of ATDC5 cells after IL-1β treatment was prevented by an NADPH oxidase inhibitor, AEBSE, an NO synthase inhibitor L-NAME, and a ONOO⁻ scavenger uric acid. The viability of ATDC5 cells was reduced by a ONOO⁻ generator SIN-1, but not by NO or S-nitrosoglutathione. Disruption of mitochondrial membrane potential and ATP deprivation were observed in IL-1β-treated ATDC5 cells. Both of which were restored by L-NAME, AEBSE or uric acid. On the other hand, any morphological or biochemical sign indicating apoptosis was not observed in these cells. These results suggest that the death of chondrocyte-like ATDC5 cells was mediated at least in part by mitochondrial dysfunction and energy depletion through ONOO⁻ formation after IL-1β treatment.

Disclosures: R. Yasuhara, None.

SA038

Regulation of Thrombospondin-2 Expression during Marrow Stromal Cell Differentiation. H. Shitaye*, M. Frohm*, J. Miller, K. D. Hankenson. Orthopaedic Surgery, University of Michigan, Ann Arbor, MI, USA.

Marrow stromal cells (MSC) are precursors that give rise to osteoblasts, adipocytes and chondrocytes. Various growth factors regulate differentiation of MSC; however, the role of the extracellular matrix (ECM) in regulating differentiation is relatively unexplored. Thrombospondin-2 (TSP2) is an ECM protein that is highly expressed in bone, cartilage, and the developing skeleton. Studies using knock out mice and TSP2-null primary cells have revealed that TSP2 plays an important role in MSC function. For this study, we determined whether TSP2 expression is altered during MSC differentiation and elucidated molecular mechanisms that regulate TSP2 expression. ST2 cells (murine MSC line) were induced to undergo either osteogenic (BMP2, β-glycerol phosphate, ascorbate) or adipogenic (either methyl-isobutyl-xanthine, dexamethasone, and insulin (MDI) or troglitazone (TZD)) differentiation and TSP2 mRNA and protein levels were measured 1, 3, 6, 9 and 12 days post-induction. In osteo-induced cells, TSP2 mRNA and protein levels

increased by ~ 6 fold relative to un-induced controls. In cells induced to undergo adipogenic differentiation with MDI, TSP2 mRNA level decreased to ~20% of un-induced controls by day 3 of the induction protocol and returned to control levels when switched to insulin alone. TZD induced cells showed no decrease in TSP2 expression despite accumulating similar levels of lipid as MDI induced cells suggesting that TSP2 down-regulation occurs prior to PPARγ induction. We next investigated mechanisms that may be involved in TSP2 down-regulation by MDI induction. We first determined which component of the MDI is responsible for TSP2 down regulation by treating cells with different combinations of IBMX, dexamethasone, and insulin and found that IBMX caused the greatest decrease in TSP2 expression. IBMX is a phosphodiesterase inhibitor that increases cAMP levels which in turn activates cAMP dependent Protein Kinase A (PKA). In order to determine whether this pathway is involved in regulating TSP2 expression, we treated cells with 8-Br cAMP (a cAMP analog), forskolin (a PKA activator), and H89 (a PKA inhibitor) alone and in combination with IBMX. Treatment with any of these compounds alone had little effect on TSP2 expression but both 8-Br-cAMP and forskolin acted synergistically with IBMX to inhibit TSP2 expression. Furthermore, inhibition of PKA with H89 abolished the negative effect of IBMX indicating that down-regulation of TSP2 expression is PKA dependent. Further work will be directed toward identifying cis-acting factors involved in regulating TSP2 expression, as well as characterizing mechanisms involved in TSP2 up-regulation during osteoblast differentiation.

Disclosures: H. Shitaye, None.

SA039

See Friday Plenary number F039.

SA040

Absence of Skeletal Abnormalities in Mice Lacking the Osteoblast-Specific Phosphatase OST-PTP. J. Ahn*¹, R. Dacquin*¹, E. Olmsted-Davis*², G. Karsenty¹. ¹Molecular and Human Genetics, Baylor College of Medicine, Houston, TX, USA, ²Pediatrics, Baylor College of Medicine, Houston, TX, USA.

OST-PTP (osteotesticular protein tyrosine phosphatase) is a receptor-like tyrosine phosphatase expressed in sertoli cells and in osteoblasts during development and after birth. In bone OST-PTP is more abundant in periosteal osteoblasts. In an effort to identify a function for this molecule during skeletal development and/or bone remodeling we generated mice lacking OST-PTP only in differentiated osteoblasts through homologous recombination in embryonic stem (ES) cells. To that end we generated a floxed allele of *Ost-ptp* and crossed these mice with transgenic mice expressing Cre recombinase under the control of the osteoblast-specific fragment of the *α1(I) collagen* promoter. The efficiency and cell-specificity of recombination at the *Ost-ptp* locus in osteoblasts was approximately 70% and no recombination was observed in other cell types. Mice lacking OST-PTP only in osteoblasts mutant were born at the expected mendelian ratio had normal life expectancy and did not display any overt phenotypic abnormality. Alizarin red/ alcian blue staining of skeletal preparations of wild type and OST-PTP^{ob}^{-/-} embryos did not show any abnormalities in skeletal development. Likewise, histological and histomorphometric analyses performed in 3 month-old mice failed to detect any bone mass abnormality in OST-PTP^{ob}^{-/-} mice. Experiments are in progress to determine whether OST-PTP is required for mechano-transduction in the entire animal. In summary the inactivation of OST-PTP failed to identify a function for this protein in the skeleton.

Disclosures: J. Ahn, None.

SA041

See Friday Plenary number F041.

SA042

Identification and Characterization of the Mustang Gene Promoter. C. Liu*, M. Hadjiargyrou. Biomedical Engineering, SUNY at Stony Brook, Stony Brook, NY, USA.

We previously identified Mustang, a novel gene that is exclusively expressed in cells of the musculoskeletal system. While Mustang expression is almost undetectable in intact bone (except in periosteum osteoprogenitor cells and articular cartilage), it is robustly upregulated during bone regeneration in osteoblasts and proliferating chondrocytes. In contrast, its expression in adult skeletal muscle is abundant. In vitro experiments also revealed that Mustang expression coincides with osteoblast and chondrocyte proliferation and myocyte differentiation. As such, Mustang represents a unique “marker” for these cells and thus identifying its tissue specific transcriptional regulation would enable us to characterize its functional significance in the musculoskeletal system. To accomplish this, we isolated and characterized a 1512bp mouse genomic clone corresponding to the 5'-flanking region of the gene. Bioinformatic analysis of this putative promoter identified a transcription start site (TSS), a TATA box, and transcription factor binding sites, including four AP-1 (activator protein-1) and two AP-2 sites. The overall Mustang promoter activity, as monitored by luciferase assays in myogenic (C2C12), chondrogenic (RCJ3.15) and osteogenic (MC3T3) cells, was found to be significantly higher than in non-Mustang expressing cells (COS-7 and HeLa), even reaching levels above those of the control SV40 promoter. Further, the contribution of each of the AP-1 and AP-2 sites was determined with serially deleted promoter constructs in transfected C2C12 cells. Our data indicate that only two of the four AP-1 sites (those closest to the TSS) are required for transcriptional

activation, as their deletion dramatically decreases luciferase activity (~75%) as compared to the full length fragment. In contrast deletion of both AP-2 sites, results in a very small decrease (~12.5%) in luciferase activity, thus indicating that these sites contribute weakly to the transcriptional activation of Mustang. We further characterized the binding subunits of the AP-1 site by electrophoretic mobility shift assay (EMSA) and identified that in both proliferating and differentiating C2C12 cells, c-Fos, Fra-2 and JunD were the only AP-1 members responsible for transcriptional activation. Therefore, given its unique cell specificity and transcriptional strength, the Mustang promoter appears to be a suitable candidate for utilization in cell lineage studies via the use of transgenic mice and could unveil cellular mechanisms responsible for musculoskeletal development and regeneration.

Disclosures: **M. Hadjiargyrou**, None.

SA043

Gene Expression of Passaged Human Articular Chondrocytes. Z. Lin^{*1}, J. Xu¹, J. Fitzgerald^{*2}, D. Wood^{*1}, M. H. Zheng¹. ¹Department of Orthopaedic Surgery, Univerisity of Western Australia, Nedlands, WA, Australia, ²Biological Engineering Division, Massachusetts Institute of Technology, Cambridge, MA, USA.

Autologous chondrocyte implantation (ACI) relies on the use of cultured cell *in vitro*, and the biosynthetic profile of cultured chondrocytes has been shown to be altered during the *in vitro* expansion. This study investigated the gene expression profile of chondrocyte associated genes during serially passaged human articular chondrocytes. Several clusters of genes were selected for these studies. These include extracellular matrix proteins (aggrecan, type I collagen, type II collagen, Type X collagen, fibromodulin, fibronectin, and link protein), matrix proteinases (MMP-1, MMP-3, MMP-9, MMP-13, ADAMTS-4 and ADAMTS-5), proteinase inhibitors (TIMP-1, TIMP-2 and TIMP-3), cytokines (IL-1 β , TGF β , TNF α , and IGF-1), transcription factors (Sox-9, c-fos and c-jun), and intercellular signaling (COX-2, MAPk1, and NOS2). Quantitative Real-time PCR was employed measure mRNA levels. A clustering analysis using Euclidean distance was done to further classify the gene expression pattern. Our results showed that with increasing passage numbers, matrix protein aggrecan, type II collagen and fibromodulin decreased their gene expression, whereas fibronectin and link protein increased expression. Matrix proteinases, MMP3, 9, 13 and ADAMTS-4, 5, showed a decreased expression pattern during subculture especially when cultured to sixth passages, whilst the expression of proteinase inhibitors (TIMP1, 2, 3) remained constant. Cytokine IL-1 has an increasing expression trend in serial cultured chondrocytes. No significant alternation was found on the expression levels of TNF- α , TGF- β , IGF-1 and transcription factors, Sox-9, c-fos and c-jun. These results suggest that with the increase of passage numbers, the chondrocyte gene expression profile is altered at various degrees, though the gene expression level of transcription factors which contribute to the hyaline cartilage regeneration are unchanged. This information might be useful for the future development of efficient approaches for the cultivation of human articular chondrocytes for ACI.

Disclosures: **Z. Lin**, None.

SA044

Effect of Weigh Reduction on the Quality of Life of Patients with Osteoarthritis and Obesity . C. Lee^{*1}, H. Lee^{*1}, S. Bae^{*2}, W. Choi^{*2}. ¹Department of Internal Medicine, Hanyang University Guri Hospital, Guri,, Republic of Korea., ²Department of Internal Medicine, Hanyang University Hospital, Seoul, Republic of Korea.

This study was to exam the effect of weigh reduction on the quality of life of patients with osteoarthritis and obesity. The participants of this study were 15 women with osteoarthritis and obesity who visited the Hanyang University Hospital Rheumatology Department. Data were collected for 2 years from 2003 to 2004. Weight, height, abdominal circumference, and BMI were measured before and after obesity therapy program which consisted of medical and behavior therapy. And also KWOMAC(Korean Western Ontario and McMaster Universities) and KSF-36 (Korean Medical Outcomes Study 36-Item Short Form) were used as a Health-related quality of life instrument. In use of KWOMAC, total KWOMAC score before and after treatment showed no significant change (34.00 \pm 16.52 (10~60) vs 27.13 \pm 24.71(10~49)) but pain showed significant change (6.50 \pm 3.38(1~11) vs 5.13 \pm 3.27(1~10), P <0.05). In use of KSF-36, Global score before and after treatment showed no significant change (49.43 \pm 5.25(38.8~56.4) vs 57.62 \pm 8.10(50.3~65.8)) but bodily pain (36.25 \pm 21.34(30~70) vs 33.75 \pm 13.03(20~50), P <0.05) and mental health(47.50 \pm 20.33 (16~84) vs 62.00 \pm 10.69 (48~80), P <0.05) showed significant changes. In conclusion, according to the result of this study, in treatment of patients with osteoarthritis and obesity, weigh reduction improved the quality of life. .

Table 1. Korean Western Ontario and McMaster Universities (KWOMAC) scores before and after treatment

	Before	After	P value
Pain	6.50 \pm 3.38	5.13 \pm 3.27	<0.05
Stiffness	3.50 \pm 2.20	2.13 \pm 1.81	NS
Function	24.00 \pm 13.01	19.88 \pm 8.77	NS
Total KWOMAC score	34.00 \pm 16.52	27.13 \pm 24.71	NS

Table 2. Korean Medical Outcomes Study 36-Item Short Form (KSF-36) scores before and after treatment

	Before	After	P value
Global	49.43 \pm 5.25	57.62 \pm 8.10	NS
Physical function	45.63 \pm 18.21	57.50 \pm 16.04	NS
Social function	53.13 \pm 5.79	43.75 \pm 13.36	NS
Role-physical	50.00 \pm 29.88	68.75 \pm 39.53	NS
Mental health	47.50 \pm 20.33	62.00 \pm 10.69	<0.05
Bodily pain	36.25 \pm 21.34	33.75 \pm 13.03	<0.05
General health	55.00 \pm 14.14	55.63 \pm 7.76	NS

Disclosures: **C. Lee**, None

SA045

Markers for Early Implant Performance Correlating with Bonding Strength between Titanium Implants and Bone. M. Monje^{*}, S. Lamolle^{*}, J. E. Ellingsen^{*}, H. J. Rønold^{*}, S. P. Lyngstadaas^{*}. Oral Research Laboratory, Institute for Clinical Dentistry., University of Oslo, Oslo, Norway.

Previous *in vivo* studies have shown that tensile testing using coin shaped titanium implants is a suitable method for direct *in situ* measurement of the attachment strength between implant and cortical bone. Using this model, we investigated the correlation between bone bonding strength and several bone markers to evaluate the progress of bone healing and implant performance. Titanium coins with a diameter of 6.25 mm and a height of 1.95 mm were blasted with titanium dioxide (TiO₂) particles with a size between 106 and 180 μ m, and placed into the cortical bone of the proximal tibia of 46 New Zealand White rabbits, 4 implants in each animal. After a healing time period of 4 weeks, animals were sacrificed, and the tibial bone with implants exposed placed in a pull-out test machine. During the pull-out test, implants were stressed with an increasing force perpendicular to the test surface, at constant speed, until detaching from the bone. A load versus time plot was recorded. After implant detachment, bone fluid from the implant site was collected for ALP activity analysis. Total protein and RNA was isolated from tissue attached to the extracted implants. Gene expression of bone marker genes (osteocalcin, collagen type I, runx2, IGF-1) and housekeeping genes (18S rRNA, GAPDH and β -actin) was analyzed using real-time RT-PCR. To obtain further data on the quality of the new bone formed at the implant interface, x-ray analyses were performed to measure the relative content of calcium, phosphor and carbon. Correlations between pull-out force and ALP activity, relative mineral content, total protein, and expression of bone marker genes, were assessed by Pearson's correlation coefficient. After 4 weeks of healing time, the pull-out force needed to detach the implants from the tibial cortical bone was found to be positively correlated to the relative mineral content (p=0.013) and negatively correlated to the total protein (p=0.003), indicating that at this stage, the increase in mineral content associated with bone bonding strength was accompanied by a decrease in the organic constituents. Also ALP activity in the bone fluid was negatively correlated to the pull-out force (p=0.019), pointing to a delayed healing in implants with low pull-out values and primary mineralization still ongoing. Finally, a positive correlation was observed between the pull-out force and the expression of osteocalcin (p=0.005), IGF-1 (p=0.015), runx2 (p=0.043) and collagen I (p=0.064). These results suggest that the evaluation of these markers might be important in the assessment of new implant surfaces for rapid bone healing and improved implant performance.

Disclosures: **M. Monjo**, None.

SA046

See Friday Plenary number F046

SA047

Anti-Depressants, Depressing Effects on Bone? B. I. Gustafsson^{*1}, E. Waarsing^{*2}, K. Stunes^{*1}, L. Thommesen^{*1}, H. Waldum^{*1}, H. van Leeuwen^{*2}, U. Syversen¹, H. Weinans^{*2}, I. Westbroek^{*2}. ¹NTNU, Trondheim, Norway, ²Erasmus MC, Rotterdam, The Netherlands.

Recently more evidence became available about the effects of serotonin on bone metabolism. Earlier we demonstrated functional serotonin receptors in osteoblasts and osteocytes. Furthermore, the serotonin transporter (5-HTT) has also been shown in bone cells, and disruption of 5-HTT results in decreased bone quality. Recently, the use of Selective Serotonin Reuptake Inhibitors (SSRIs) and their effects on bone metabolism, has been under debate. In the current study, we have studied the effects of the SSRI, fluoxetine, on mouse osteoblasts (OB) and human osteoclasts (OC) *in vitro* as well as investigated the effect of long-term fluoxetine use on bone metabolism in rats. Our *in vitro* data show that OC activity was increased by 30 \pm 8% when adding fluoxetine concentrations up to 1 μ M, higher concentrations resulted in an inhibition of OC activity, but was not toxic. Proliferation of OB was not affected in the lower concentration range (\leq 0.1 μ M), however it was inhibited at higher concentrations (>1 μ M), and RANKL release was increased, while OPG release was decreased at all concentrations (\leq 10 μ M), again indicating a possible stimulation of OC activity. Three month-old female Sprague-Dawley rats were treated orally with fluoxetine for 6 months (5 mg/kg/day). BMD was determined by means of DXA, and bone architecture was investigated in detail using μ CT scanning of right femurs. Left femurs were used for mechanical experiments. Total body BMD was significantly decreased in growing rats treated with doses of fluoxetine that are within therapeutical range. μ CT analysis showed that bone architecture of the metaphysis of the femur was significantly changed by fluoxetine treatment. Cortical bone volume was decreased, marrow cavity was increased, and trabecular thickness was decreased when treated with fluoxetine. These results imply that endosteal resorption was increased in fluoxetine treated animals, which is consistent with our *in vitro* data. Furthermore, three-point bending experiments showed that mechanical properties of the bone tissue were altered by fluoxetine. Stress and Youngs modulus were decreased in the fluoxetine group, indicating changes in quality of the bone tissue. Geometry (cross-sectional moment of inertia) however was non-significantly increased, resulting in similar bone strength. In conclusion, we demonstrate that, fluoxetine stimulates osteoclastic activity *in vitro* and most probably *in vivo* as well. Furthermore, we also show decreased quality of bone tissue in fluoxetine treated rats.

Disclosures: **I. Westbroek**, None.

SA048

See Friday Plenary number F048.

SA049

Mineralization and Bone Turnover at the Human Femoral Mid-Shaft. H. M. Goldman¹, B. P. George^{*2}, C. D. L. Thomas^{*3}, J. G. Clement^{*3}.
¹Neurobiology & Anatomy, Drexel University College of Medicine, Philadelphia, PA, USA, ²Drexel University College of Medicine, Philadelphia, PA, USA, ³Oral Anatomy and Surgery Unit, School of Dental Science, University of Melbourne, Melbourne, Australia.

Previous research has demonstrated distinct regional variability in the degree of bone mineralization at the Human mid-shaft femur (Goldman et al., J Anat 2003). As bone formed by secondary remodeling was not examined separately from primary bone in that study, it was not possible to determine whether this variability was due to regional differences in the amount of remodeling (number of poorly mineralized Haversian Systems) or in the amount of bone modeling (periosteal or endosteal apposition). Further study of such variation in mineralization density and bone turnover is important for enhancing our understanding of the bone aging process, and resultant bone quality. Entire cross-sections (N=37 adults, divided into three age groups with roughly equal sex distribution) were imaged using backscattered electron microscopy. The percentage area of low mineralization bone (gray levels <96 within a 0-255 range) was calculated for each of 16 sectors located radially around the bone cortex. This measure of 'new bone formation' included regions of secondarily remodeled bone and any bone of periosteal apposition. Within a sub-sample of young (N= 5) and old (N =6) individuals, osteons with low mineralization were counted within postero-medial and antero-lateral cortices. Regions of primary circumferential bone (regardless of degree of mineralization) were then manually traced (utilizing polarized light microscopy images of same field of view areas) to determine a percentage area of non-remodeled bone cortex. In the younger age group, the antero-lateral cortex had a significantly higher percentage of newly formed bone relative to the postero-medial cortex (p < 0.01). Similar results were found in the older age group (p < 0.05). Middle and older age groups had significantly higher proportions of newly formed bone than the younger age group (p < 0.001). Within younger individuals of the sub-sample, an average of 89% fewer new remodeling events were observed on the postero-medial cortex relative to the antero-lateral cortex. The former also contained a significantly higher proportion of primary bone, most of which was highly mineralized. The older group was more heterogeneous, but the postero-medial cortex still contained an average of 15% fewer new remodeling events. These data suggest that regional differences in bone turnover rates lead to long lasting effects on the distribution and quantity of primary versus secondary tissue types that is reflected in bone's mineralization density distribution.

Disclosures: **H.M. Goldman**, None.**SA050**

Impact of Glucose-dependent Insulinotropic Receptor Knockout on Mouse Behavior. K. H. Ding¹, O. Zhong¹, D. Xie¹, J. Duan^{*2}, C. Baile^{*3}, H. Chen^{*4}, M. Della-Fera^{*2}, A. Mulloy¹, W. Bollag^{*1}, R. Gujral^{*1}, W. Curl^{*5}, C. M. Isaacs⁶.
¹Medicine, Medical College of Georgia, Augusta, GA, USA, ²Agricultural Biotechnology, University of Georgia, Athens, GA, USA, ³Agricultural Biotechnology, University of Georgia, Augusta, GA, USA, ⁴Neurological Surgery, University of Florida, Gainesville, FL, USA, ⁵Orthopedic Surgery, Medical College of Georgia, Augusta, GA, USA, ⁶Medicine and Orthopedic Surgery, Medical College of Georgia and the Augusta VA Hospital, Augusta, GA, USA.

We have previously reported that a rise in glucose-dependent insulinotropic peptide (GIP), an enteric hormone released from endocrine cells in the proximal small intestine in response to nutrient intake, increases osteoblastic activity and subsequently bone mass. We have also reported that GIP receptor knockout mice have lower bone mass than controls. However, as these GIPR KO mice age they develop compensatory mechanisms involving increased secretion of hormones (particularly leptin) that ameliorate the impact of GIP receptor loss on bone mass. Since both leptin and GIP may have central nervous system effects on feeding behavior we examined the impact of GIP receptor knockout on mouse behavior. At four months of age standardized mouse behavior testing revealed that GIP receptor knockout mice had significantly increased open field locomotor activity (Distance traveled (cm): 784.6±67.3 vs. 996.2±52.3, Control vs. GIPR KO, Means±SEM, p<0.02), decreased tail flick latency (7.0±0.04 vs. 5.6±0.3 seconds, Control vs. GIPR KO, Means±SEM, p<0.01) and increased open arm entries in the Elevated Plus-Maze (10.6±1.3 vs. 16.9±1.9 % open arm entries, Means±SEM control vs. GIPR KO p<0.01). These data were consistent with GIPR KO mice having an increased activity level compared to control mice. In an effort to define the underlying mechanisms, hypothalamic mRNA from GIPR KO and control mice was analyzed by microfluidic analysis. Compared to Control mice, GIPR KO mice were found to have a significant (greater than two-fold, p<0.01) increase in mRNA expression of CART (cocaine and amphetamine regulated transcript) a neuropeptide involved in feeding behavior and recently shown to play a role in mediating CNS leptin effects on bone mass. Taken together, these data demonstrate that GIP has significant central nervous system effects and that compensatory changes in bone mass observed in aging GIPR KO mice may be in part mediated by leptin-induced changes in CART.

Disclosures: **K.H. Ding**, None.**SA051**

See Friday Plenary number F051.

SA052

The C-Terminal of Matrix Gla Protein Binds Vitronectin. S. K. Nishimoto, M. Nishimoto^{*}. Molecular Sciences, University of Tennessee, Health Science Center, Memphis, TN, USA.

Matrix Gla Protein (MGP) is an essential inhibitor of calcification. Loss of MGP results in Keutel Syndrome with patients suffering from cartilage calcification and arterial stenosis. Mice lacking MGP have extensive cartilage and vascular calcification that leads to perinatal death. The molecular basis for its calcification inhibitory activity is not yet determined. Mechanisms suggested include binding to calcified deposits, regulation of BMPs/TGF- β , and interaction with fetuin/calcium complexes. Additional activities and functions may exist for MGP. This is supported by high MGP synthesis during organ development and high MGP synthesis by many types of cancer. It is possible that MGP acts as to modulate cell-matrix interactions of migrating cells. A matricellular role for MGP predicts that it binds to selected matrix proteins in order to alter cellular interactions with matrix. The purpose is to prove that vitronectin interacts with MGP, to determine the MGP region involved in binding, and suggest a role for MGP-vitronectin interactions in embryonic development. Methods: Protein interactions are assayed by gel overlays with labeled vitronectin or MGP, and elution peak shifts on gel filtration. The binding of vitronectin to MGP or MGP peptides is determined by nitrocellulose filter binding assay. MGP and vitronectin are localized using polyclonal anti-MGP and monoclonal anti-vitronectin antibodies in paraffin embedded embryonic kidney. Results: Vitronectin binding is saturable and consistent with a single class of binding sites. MGP binds to vitronectin but not collagen, fibromodulin, heparin, osteocalcin, chondroitin sulfate, laminin, ovalbumin or albumin. MGP binds vitronectin by a naturally occurring MGP C-terminus, peptide 61-77. MGP and the 61-77 MGP peptide also bind fibronectin. MGP and vitronectin focally co-localize in embryonic kidney. Co-localization *in vivo* suggests that MGP-vitronectin binding may modify cell interactions with vitronectin. Thus MGP is proposed to cause cells to migrate or adhere differently. MGP may augment the capacity of cells to migrate during processes such as embryonic development, wound repair, or tumor cell metastasis. Conclusions: The current study demonstrates MGP binds vitronectin via a C-terminal region that is highly conserved. Co-localization of MGP and vitronectin suggests that the binding is physiologically relevant during elevated MGP synthesis in the embryonic kidney.

Disclosures: **S.K. Nishimoto**, None.**SA053**

See Friday Plenary number F053.

SA054

A Tendon Specific Angiogenesis Inhibitor, Soluble ChM1L Regulates Hypovascularity of Tendon. K. Yamana^{*}, Y. Nakayama^{*}, Y. Takahashi^{*}, H. Wada^{*}, Y. Yamanaka^{*}, Y. Kasahara^{*}, H. Mitsuhashi^{*}, S. Kondo^{*}, T. Kamimura^{*}, Y. Azuma. Teijin Institute for Bio-medical Research, Hino, Tokyo, Japan.

Tendon is typically characterized as hypovascular dense connective tissue that attach muscle to bone. In contrast to cartilage, a hypovascular tissue as well as tendon, little is known about the mechanisms of tendon tissue generation and maintenance of hypovascularity in tendon. Cartilage includes several endogenous angiogenesis inhibitors such as Chondromodulin-I (ChM-I), a secreted glycoprotein specifically expressed in cartilage. However, no existence of tendon-specific angiogenesis inhibitor has been reported. We have recently discovered ChM1L, a type II transmembrane glycoprotein, which is expressed in tendon and has high homology to ChM-I. We hypothesized that ChM1L is a key regulatory molecule that is involved in hypovascularity of tendon. To evaluate this hypothesis, we examined, (1) specificity of ChM1L mRNA expression by real-time PCR, (2) processing of ChM1L protein, and (3) anti-angiogenic activity of ChM1L protein *in vitro* and *in vivo*. ChM1L mRNA was preferentially expressed in mouse Achilles tendon and tenocytes by real-time PCR, compared to other 9 tissues and 5 cell lines. Immunoblot analysis revealed that soluble form of ChM1L protein (sChM1L) was detected in mouse Achilles tendon, and culture medium of COS7 and 293T cells transfected with transmembrane form of ChM1L expression vector. N-terminal sequencing and deglycosylation analysis revealed that sChM1L was secreted as non-glycosylated protein following cleavage at potential processing site, R-H-A-R. Processing of ChM1L was abrogated by furin inhibitor, golgi-disturbing agent (Brefeldin A), and deletion or mutation of R-H-A-R. Purified recombinant furin cleaved the transmembrane form of ChM1L protein. Recombinant sChM1L protein produced in E. coli inhibited DNA synthesis of endothelial cells *in vitro* induced by FGF-2, VEGF, HGF, or FBS, whereas sChM1L didn't inhibit DNA synthesis of fibroblasts. Moreover, sChM1L inhibited migration and tube formation of endothelial cells. Furthermore, sChM1L inhibited angiogenesis *in vivo* by the directed *in vivo* angiogenesis assay. In mouse tumor models using B16-F10 melanoma or Lewis lung carcinoma cells, sChM1L inhibited tumor growth, and this effect correlated with a low density of blood vessels in the tumors of sChM1L-treated mice. Taken together, these results indicate that sChM1L is a tendon specific angiogenesis inhibitor, which is secreted by furin-mediated processing in the trans-golgi network and may play an important role in the maintenance of vascularity in tendon.

Disclosures: **K. Yamana**, None.

SA055

Ca2+/Calmodulin-Dependent Protein Kinase II (CaM kinase II) Phosphorylation of Ets2 in a Mechanotransduction Pathway of Cranial Morphogenesis. J. L. Borke¹, J. R. Chen^{*2}, C. S. Chew^{*3}, J. C. Yu^{*4}, T. T. Wu^{*5}, N. N. Do^{*1}, X. W. Hou^{*6}. ¹Oral Biology and Maxillofacial Pathology, Medical College of Georgia, Augusta, GA, USA, ²I-Shou University, Kaohsiung, Taiwan Republic of China, ³Cell Biology and Anatomy, Medical College of Georgia, Augusta, GA, USA, ⁴Surgery, Medical College of Georgia, Augusta, GA, USA, ⁵Savannah River National Laboratory, Aiken, SC, USA, ⁶Stomatology, Third Hospital of Hebei Medical University, ShiJiaZhuang, China.

Our studies introduce a novel mechanism of mechanotransduction with an Ets family member as the key intermediate linking stretch-induced changes in cell membrane permeability to changes in cranial morphogenesis. Our data suggests that as intracellular Ca++ increases, CaM kinase II phosphorylates Ets2 changing its affinity for binding sites in the promoter regions of target genes important for cranial morphogenesis. This pathway is significant for mechanotransduction because Ca++-dependent phosphorylation of Ets2 could be initiated by Ca++ influx after cell stretching. We performed immunohistochemistry on 1 day old rat calvaria with anti-Ets2 antibodies and showed localization of Ets2 in the nuclei of cells of the forming cranial sutures and bone. We isolated mRNA and protein from bone-suture-bone explants of rat coronal sutures in organ culture with and without stretching. We prepared Western blots using Ets2 antibody in the presence and absence of a phosphorylation inhibitor. This study shows that the MW of Ets2 is increased by loading in the absence but not the presence of phosphorylation inhibitor. Bacterially expressed 1 -70 Ets2 protein was phosphorylated by CaM kinase II in the presence of γ -32P ATP. The identity of phosphorylated Ets2 was confirmed by subsequent Western blot analysis using anti-Ets2 antibody. Examination of the promoter region of several important target genes in bone development including BMP2&6, osteocalcin, osteonectin, osteopontin, and Tbx2, reveals putative binding sites for Ets2. Competition between the promoter of one of these target genes (Tbx2) and antibody to Ets2 promotes up-regulation of this gene. Electrophoretic mobility shift assay (EMSA) results show antibody competition with two nuclear extracts for binding to labeled probes representing Ets2 binding sequence in the Tbx2 promoter. Taken together, these findings suggest that the influx of Ca++ promotes Ca++-dependent phosphorylation of Ets2 and release of Ets2 from binding to the promoter region of genes important for bone development and cranial morphogenesis.

Disclosures: J.L. Borke, None.

SA056

Mapping the Mechanical Environment Surrounding Loaded Titanium Implants Using a Novel FEA/Histology Technique. X. W. Hou^{*1}, N. N. Do^{*2}, J. L. Borke³. ¹Stomatology, Third Hospital of Hebei Medical University, ShiJiaZhuang, China, ²Oral Biology and Maxillofacial Pathology, Medical College of Georgia, Augusta, GA, USA, ³Oral Biology and Maxillofacial Pathology, Medical College of Georgia, Augusta, GA, USA.

Finite element analysis (FEA) is a well established computer based analysis method used to predict the stress and strain characteristics of objects under applied mechanical loading. We present a novel use of the FEA technique to map the load environment in histological sections of bone surrounding mechanically loaded titanium implants. For this study we used paraffin embedded tissue sections of bone surrounding 1mm x 3mm titanium micro-screws (implants) installed in retired breeder rat maxilla following extraction of the maxillary first molar. Radiographs of implant sites were prepared after installation and again prior to sacrifice. Tissues were decalcified and sections of the maxilla containing the implants were processed for immunohistochemistry using antibodies to bone marker proteins. Stained sections were imported into the WinTopo program (SoftSoft.net, Biggleswade, Bedfordshire, UK), which transforms and saves the images in the "dxf" file format. In this format, FEA can be performed on the images using the J.L. Analyzer 9.0 FEA program (AutoFEA Engineering Software Technology Inc., Norwalk, California, USA). For our studies we created 2D models containing between 2000 and 4000 nodes incorporating published values for the modulus of elasticity and Poisson's ratio of composite bone and titanium with an applied load of 5N corresponding to a physiological bite force in rats. Comparisons were made to archived tissues surrounding human implants. The resulting stress maps created for each section were combined with the immunohistochemistry by image overlay to characterize the load environment, tissue characteristics, and protein expression in each tissue. Results show that sites of high compressive load correlate with sites of osteoclastic bone resorption, and sites of high shear stress correlate with the expression of bone formation markers. This novel technique offers a useful method for correlating the mechanical environment to the localization of cellular changes and sites of altered gene and protein expression in histological sections.

Disclosures: X.W. Hou, None.

SA057

See Friday Plenary number F057.

SA058

Contribution of the Advanced Glycation End Product Pentosidine to Compressive Biomechanical Properties of Human Lumbar Vertebrae. S. Viguet-Carrin^{*1}, J. P. Roux^{*1}, M. E. Arlot¹, E. Gineyts^{*1}, F. Duboeuf^{*1}, Z. Merabet^{*1}, M. L. Bouxsein², P. D. Delmas¹. ¹INSERM Unit 403, C. Bernard University, Lyon, France, ²Orthopaedic Biomechanics Laboratory, Beth Israel Deaconess Medical Center and Harvard Medical School, Boston, MA, USA.

Collagen structure is believed to play an important role in bone strength. Yet, few studies have analyzed the contribution to bone strength of posttranslational modifications of type I collagen independent of bone density. Thus, the aim of this study was to analyze the relative contributions of bone density, and both enzymatic and non-enzymatic crosslinks (advanced glycation end products) of type I collagen to the biomechanical properties of human vertebrae. Nineteen L3 vertebrae (age 26-93; 10 males, 9 females) were collected after necropsy. Bone mineral density (BMD) of the vertebral body was measured by lateral DXA. Compressive stiffness, failure load and work to fracture (energy absorbed) were directly measured and the apparent elastic modulus, ultimate strength and toughness were estimated by correcting the load-displacement data by the minimal cross-sectional area of the vertebral body. After mechanical testing, the concentration of both enzymatic pyridinoline (PYD), deoxypyridinoline (DPD) and the non-enzymatic crosslinks pentosidine (PEN) were analyzed by reversed-phase HPLC on trabecular and cortical bone separately and normalized to the hydroxyproline content. BMD was significantly positively correlated with stiffness ($r^2 = 0.74$; $p < 0.0001$), failure load ($r^2 = 0.69$; $p < 0.0001$) and work to fracture ($r^2 = 0.44$; $p = 0.003$). The trabecular concentrations of PEN -but not of PYD nor DPD- contributed to the failure load and work to fracture over and above BMD (multiple $R^2 = 0.82$ and 0.67 respectively, $p < 0.0001$ for both), but not to the prediction of stiffness. Similarly, ultimate stress and estimated toughness were better explained by BMD + PEN (multiple $R^2 = 0.66$ $p = 0.0002$ and $r^2 = 0.55$ $p = 0.002$ respectively) than by BMD alone ($r^2 = 0.52$ and $r^2 = 0.31$ respectively). In summary: 1) the concentration of collagen crosslinks did not contribute to bone stiffness and estimated elastic modulus, properties that are reported to depend mainly on bone mineral content; 2) the concentration of PEN in trabecular bone contributed independently of BMD to failure load and work to fracture of human lumbar vertebrae. We conclude that the impact of PEN on skeletal fragility deserves more attention.

Disclosures: S. Viguet-Carrin, INSERM Lilly contract 2.

SA059

Chronic Monitoring of Telemetered Bone Marrow Pressure in the Rodent. D. R. Meays^{*}, H. Y. Stevens, J. A. Frangos. La Jolla Bioengineering Institute, La Jolla, CA, USA.

It has been previously observed that venous ligation of the canine hindlimb increased venous pressure immediately but that the pressure decreased after several weeks due to deployment of collateral blood vessels¹. We previously showed, however, that venous ligation leads to prolonged increases in intramedullary pressure (IMP) in the rat. In this study we investigated the continuous measurement of IMP in the alert and unanesthetized rat using telemetry. This unique application of telemetry allowed us to measure IMP in both unsuspended and hindlimb suspended rats over the course of 21 days. Pressure transducers were implanted into the bone marrow cavity by inserting a 0.4 mm \varnothing catheter tip through a hole drilled distal to the femoral head, the hole sealed with bone cement and the transmitter secured onto the peritoneal wall. With the receiver placed under the animal's cage, telemetered pressure data was collected. Pressure readings were recorded in the early morning when the animal was awake and grooming. Intramedullary pressures, in limbs of animals subjected to femoral vein ligation or sham-operation, were recorded for the period of hindlimb suspension. This pressure was maintained throughout the suspension period of 21 days. The amplitude of the cardiac-induced pulsations was 0.8 mm Hg with a frequency of 1 Hz. We optimized the implantation of a vascular occluder cuff around the iliac vein in the hindlimb-suspended rat model to test the effects of increases in intra-osseous pressure of an intermittent nature and varying duration as opposed to a permanent ligation. In previous studies an intermittent occlusion of 30 min per day for 3 weeks was shown to increase tibial weight relative to controls. The contra-lateral vein had the same size cuff placed around it but was not occluded during the study. Preocclusion IMP was recorded as 10.5 mm Hg and this consistently rose to 15 mm Hg upon each occlusion on the same animal. Blood flow resulting from the iliac vein occlusion was monitored using an ultrasonic micro-flow probe, with flow in the artery reaching zero upon occlusion and climbing to normal levels of 1.2 ml/min after occlusion. The permanent occlusion of the femoral vein in rats caused an elevated and persistent intra-osseous pressure. Similarly, the transient occlusion of the iliac vein of the rat via an occluder cuff caused a consistent increase in IMP and a decreased blood flow in the femoral vein, both of which reverted back to normal once the occlusion was released.

¹ Lilley, AD *et al.* J Bone Joint Surg AM 1970; 52: 515-20.

Disclosures: D.R. Meays, None.

SA060

Elevated Serum FGF23 Concentrations in Plasma Cell Dyscrasias. I. J. Stewart^{*1}, C. Roddie^{*2}, A. Gill^{*2}, A. Clarkson^{*2}, M. Mirams^{*1}, A. E. Nelson^{*1}, L. Coyle^{*2}, C. Ward^{*2}, P. Clifton-Bligh^{*2}, B. G. Robinson^{*1}, R. S. Mason³, R. J. Clifton-Bligh^{*1}. ¹Kolling Institute of Medical Research, Sydney, Australia, ²Royal North Shore Hospital, Sydney, Australia, ³The University of Sydney, Sydney, Australia.

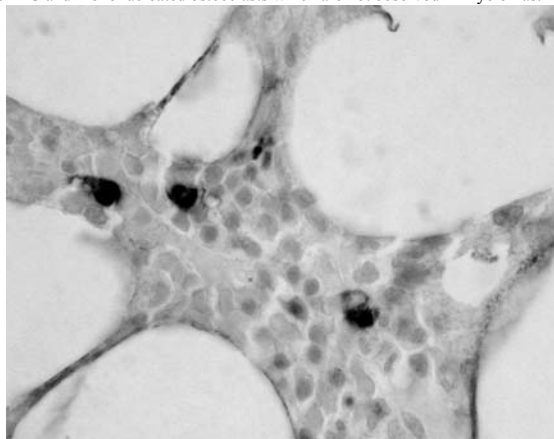
Fibroblast growth factor 23 (FGF23) is now recognized as a key regulator of phosphate metabolism. The syndrome of tumour-induced osteomalacia (TIO) is typically associated with mesenchymal tumours and elevated serum FGF23 concentrations. TIO is less commonly associated with non-mesenchymal tumours and serum FGF23 has not yet been studied in these cases. We identified an elevated serum FGF23 concentration (161 RU/mL) in one patient with small B-cell lymphoma and hypophosphatemia, prompting us to examine serum FGF23 in other patients with B-cell neoplasms. Serum FGF23 concentrations measured using the FGF23 C-terminal ELISA (Immunotopics, CA) in 26 normal controls was 23 ± 11 RU/mL (mean \pm SD). Serum FGF23 levels were elevated in 5/16 patients with myeloma (57, 83, 83, 89, 1111 RU/mL), 3/18 patients with monoclonal gammopathy of uncertain significance (MGUS) (81, 123, 177 RU/mL), and 1/12 patients with chronic lymphocytic leukaemia (249 RU/mL). In myeloma and MGUS patients, serum FGF23 concentrations were significantly and positively associated with serum paraprotein and beta-2 microglobulin concentrations ($p = 0.0006$). Hypophosphatemia was not observed even in those patients with elevated FGF23, and a weak positive correlation was noted between serum FGF23 and phosphate concentrations ($p = 0.03$). Dysplastic plasma cells in bone marrow biopsy samples showed intense FGF23 expression in a perinuclear distribution, a pattern also typical for FGF23 localisation in mesenchymal tumours. Our findings contribute to an expanding literature regarding abnormal FGF/FGF receptor-signalling in myeloma. The absence of hypophosphatemia in these cases suggests either that FGF23 produced by dysplastic B-cells lacks systemic bioactivity or that other factors contribute to maintain serum phosphate.

Disclosures: I.J. Stewart, None.

SA061

Are Bone Marrow Dendritic Cells a Major Key in the Understanding of Monoclonal Gammopathies (MGUS)? N. Josselin^{*1}, M. Rousset^{*1}, N. Ifrah^{*1}, M. F. Basle^{*1}, R. Bataille^{*2}, M. Audran¹, D. Chappard¹. ¹Faculté de Médecine, INSERM, EMI0335-LHEA, Angers, France, ²INSERM, U601, Nantes, France.

MGUS represents the common manifestation of multiple disorders and normal variants; it can represent an early stage of malignant disorders like B lymphoma or myeloma. Dendritic cells (DC) are specialized cells having a leading part in different development stages of B lymphocytes. DC originate from the same stem cell than osteoclasts and under particular culture conditions (M-CSF, IL-6), immature DC can differentiate into osteoclasts. Plasma cells induce an overexpression of RANKL in stromal cells in myeloma patients leading to osteoclastogenesis. It was hypothesized that DC genesis might also be increased in MGUS. Only few studies have been interested in the link existing between DC and MGUS. Bone and bone marrow biopsies were performed in 94 patients. Four normal control cases were similarly processed. Biopsy specimens were embedded in methacrylates. Stainings for histomorphometry were done with Goldner trichrome and TRAcP identification of osteoclasts. Bone marrow dendritic cells were detected using an antibody directed against the S-100 protein. For each patient, the number of bone marrow dendritic cells (20 consecutive fields) was compared to histomorphometric results and diagnosis. According to histopathological criteria, patients were classified into MGUS (44 cases), myeloma (44 cases), B lymphomas (6 cases). The average number of bone marrow DC was significantly higher in B lymphomas than in myeloma ($p=0.0003$; 24.4 ± 11.4 vs 5.1 ± 0.9), MGUS ($p=0.003$; 8.5 ± 1.2) and control cases (0.75 ± 0.25). The osteoclastic surfaces were higher in myeloma compared to B lymphoma ($p=0.002$; 23.3 ± 2.3 vs 10.1 ± 2.3) and MGUS ($p<0.0001$; 12.4 ± 1.3). DC were often mixed with B lymphoma cells (66.7 % of B lymphomas). Moreover, B lymphomas were frequently associated with mononucleated osteoclasts. There was no significant correlation between the number of dendritic cells and osteoclast parameters. DC appeared significantly increased in MGUS and especially in B lymphomas. It is likely that different cytokine networks are involved in myeloma and B lymphomas. This can favor the genesis of DC and mononucleated osteoclasts which are not observed in myelomas.



Disclosures: N. Josselin, None.

SA062

See Friday Plenary number F062.

SA063

Interaction of Metastatic Melanoma Cells and Osteoblasts Induces Collagenase 3 (Mmp13), a Potent Regulator of Bone Resorption. M. Inada¹, M. Takita^{*1}, S. M. Krane², C. Miyaura¹. ¹Biotechnology and Life Science, Tokyo University of Agriculture and Technology, Tokyo, Japan, ²Center for Immunology, Allergy and Immunology, Massachusetts General Hospital, Harvard Medical School, Boston, MA, USA.

Mmp13 is a key molecule produced by osteoblasts in inflammatory bone resorption. Recently we reported that Mmp13 deficient mice (Mmp13^{-/-}) exhibit an abnormal phenotype in cartilage and bone suggesting that Mmp13 is important for cartilage development and bone remodeling. It has also been suggested that Mmp13 invasion and metastases in a variety of malignant tumors. Here we examine whether Mmp13 is produced by cancer cells or osteoblasts/stromal cells in bone metastases. Malignant melanoma cells (B16) were suspended in PBS and injected into the left ventricle of C57Bl6 mice with a 27-gauge needle under anaesthesia. B16-injected mice were sacrificed at 12 days after injection and left femur was prepared for paraffin sectioning for tartrate-resistant acid phosphatase (TRAP) staining. The right femur was removed for measurement of bone mineral density (BMD) by DEXA to evaluate B16 induced bone resorption. Metastatic colonization in distal femurs was assessed by the black color of the melanoma. Histomorphometry showed suppressed BV/TV and Tb.th and increased Tb.sp in B16-injected mice indicating that cancer metastasis clearly increased bone resorption. DEXA confirmed B16-induced bone resorption in distal femurs. TRAP staining showed increased numbers of osteoclasts located close to cancer cells. When bone marrow cells and osteoblasts were co-cultured on fixed B16 cells, TRAP+ multinucleated osteoclasts were formed. When osteoblasts were cultured on fixed B16 cells, levels of Mmp13 and receptor activator of NF-kb ligand (Rankl) were increased. Mmp13 production was suppressed by treatment with a p38 MAP kinase inhibitor in a dose-dependent manner, suggesting that induction of Mmp13 in osteoblasts is regulated by cell-cell contact with B16 cells, mediated through the MAP kinase pathway. Thus, induction of Rankl and Mmp13 by contact of B16 cells with osteoblasts can promote osteoclastic bone resorption and soft tissue collagenolysis generating space in bone for cancer cell proliferation at sites of melanoma metastasis.

Disclosures: M. Inada, None.

SA064

Cells of the Bone Marrow Microenvironment Protect Myeloma Cells from Apoptosis Induced by TRAIL but not by Agonists of TRAIL Death Receptors. R. M. Locklin^{*1}, P. I. Croucher², R. G. G. Russell¹, C. M. Shipman^{*3}. ¹Institute of Musculoskeletal Sciences, Botnar Research Centre, University of Oxford, Oxford, United Kingdom, ²Division of Clinical Sciences, University of Sheffield Medical School, Sheffield, United Kingdom, ³University of Texas Health Science Center at San Antonio, San Antonio, TX, USA.

Myeloma cells grow preferentially in the bone marrow where their interactions with bone marrow stromal cells (BMSCs), osteoblasts (Obs) and osteoclasts are crucial for myeloma growth and the development of osteolytic bone disease. Osteoprotegerin (OPG) is secreted by BMSCs and Obs and functions as a soluble decoy receptor for both RANKL, thus inhibiting bone resorption, and TNF-related apoptosis-inducing ligand (TRAIL). TRAIL is produced by activated T-cells and is thought to mediate immune system anti-tumour activity by inducing tumour cell apoptosis. It binds to four membrane-bound receptors; death-inducing receptors DR4 and DR5 and decoy receptors DcR1 and DcR2. OPG also binds to TRAIL and we have previously shown that OPG released from MG63 osteoblast-like cells can inhibit TRAIL-induced apoptosis of myeloma cells. We hypothesise that OPG produced by cells of the bone marrow microenvironment may protect myeloma cells against TRAIL-induced apoptosis. This study aimed to determine whether BMSCs and Obs can protect myeloma cells against apoptosis induced by TRAIL or TRAIL receptor agonists using co-cultures of myeloma cells with primary human BMSCs, MG63 osteoblast-like cells or the normal osteoblast-like hPOB-tert cell line. The TRAIL-sensitive human myeloma cell lines NCI H929 and RPMI 8226 expressed both DR4 and DR5 on the cell surface. TRAIL or agonist antibodies to DR4 or DR5 induced apoptosis of myeloma cells in a dose- and time-dependent manner. In contrast to TRAIL, apoptosis induced by these agonists was not blocked by rhOPG or by media conditioned by osteoblast-like cells. Using dual colour flow cytometry, we demonstrated that myeloma cells are protected from TRAIL-induced apoptosis by co-culture with MG63 cells, hPOB-tert cells, or primary normal human BMSCs. In contrast, the induction of myeloma cell apoptosis by the agonist to DR5 was not blocked by these co-cultures. Cell surface TRAIL receptor expression was not regulated by TRAIL, rhOPG, osteoblast-like cell conditioned media or co-culture with osteoblastic cells. Our study demonstrates that cells of the bone marrow microenvironment protect myeloma cells against TRAIL-induced apoptosis. Specific agonist antibodies to active apoptosis-inducing TRAIL receptors are not inhibited by BMSCs or Obs and thus offer an alternative possibility for specific anti-myeloma therapy.

Disclosures: C.M. Shipman, None.

SA065

Antitumor Efficacy of the RANK Ligand Inhibitor OPG-Fc in the MDA-231 Breast Cancer and PC3 Prostate Cancer Experimental Osteolytic Metastases Models. R. Miller*, J. Jones*, M. Tometsko*, A. Armstrong*, N. Zhang*, J. Leal*, E. Trueblood*, W. Dougall. Amgen Inc., Seattle, WA, USA.

Bone metastases are a frequent complication of cancer and are commonly observed in patients with advanced breast and prostate cancer. In lytic bone metastases, tumor cells interact with the bone microenvironment to induce osteoclastogenesis, leading to bone destruction. RANK ligand (RANKL) is essential for osteoclast differentiation, function, and survival. Tumor cell-mediated osteolysis is thought to occur ultimately via induction of RANKL within the bone stroma, and inhibition of RANKL in animal models of breast cancer metastases blocks tumor-induced osteolysis and prevents the increase in bony tumor burden (Morony et al., 2001). The aims of this study were to define the mechanisms of the antitumor effect of RANKL inhibition on skeletal metastases and to test if similar effects are observed in both breast and prostate cancer-induced osteolysis. We first examined the effects of the RANK ligand inhibitor OPG-Fc on tumor-induced osteolysis and tumor burden in mice inoculated with MDA-MB-231 breast cancer cells. At 14 days post-inoculation, tumor-bearing mice received OPG-Fc subcutaneously (3 mg/kg, 3x/week). Radiographic analysis on day 28 indicated that OPG-Fc treatment prevented the progression of tumor-induced osteolysis. Serological, histological, and histomorphometric analyses also revealed that OPG-Fc treatment eliminated mature and immature osteoclasts, reduced tumor-induced bone resorption, and reduced osseous tumor burden. Comparable results were obtained after OPG-Fc treatment of mice with established skeletal PC3 prostate tumors and osteolytic lesions. To examine the potential mechanisms underlying the reduction in tumor burden, levels of proliferation and apoptosis markers in established breast tumors, taken from mice treated with OPG-Fc over 5 days, were analyzed by immunostaining. Short-term OPG-Fc treatment substantially reduced tumor cell histone H3 phosphorylation and increased activated caspase-3. Increased activated caspase-3 and decreased phospho-histone H3 levels were also observed in MDA-MB-231 skeletal tumors after combined treatment with OPG-Fc and the cytotoxic agent cytoxin. These data suggest that RANKL inhibition effectively blocks pathologic osteolysis induced by either breast cancer or prostate cancer cells in osteolytic metastases models. The significant reduction in skeletal tumor burden observed after OPG-Fc treatment appears to be due to a reduction in the growth rate and survival of tumor cells, indicating that RANKL inhibition may reduce tumor proliferation and increase tumor cell apoptosis within bone.

Disclosures: **R. Miller**, Amgen Inc. 3.

SA066

See Friday Plenary number F066.

SA067

Receptor Activator of NF-kappaB Ligand Influences Malignant Activities of Metastatic Breast Cancer Cells. M. R. Ray*¹, A. L. Allan*¹, A. B. Tuck*², A. F. Chambers*². ¹Department of Oncology, London Regional Cancer Program, London, ON, Canada, ²Departments of Pathology & Oncology, University of Western Ontario, London, ON, Canada.

Development of metastatic breast cancer can have devastating consequences that result in decreased quality of living and loss of life. Bone is amongst the most common sites for breast cancer metastasis, and factors in the bone microenvironment are thought to have a role in the metastatic process. Receptor activator of NF-kappaB (RANK) and its ligand, RANKL, are abundant in the bone microenvironment and have a crucial role in normal bone homeostasis. Activation of RANK by RANKL initiates differentiation of osteoclast precursors, through activation of NF-kappaB and AP-1 transcription factors, and gives rise to mature, multi-nucleated osteoclasts that are responsible for bone resorption. However, an emerging role for the RANK/RANKL signaling pathway has recently been described for normal development of the mammary epithelium in lactating mice. Therefore, to evaluate the role of RANK activity in breast cancer progression, *in vitro* responses to RANKL have been assessed for three breast epithelial carcinoma cell lines that have varying degrees of metastatic abilities: MDA-MB-435, -231 and -468. All three cell lines are tumorigenic in mice. However, MDA-MB-435 and -231 cells are highly metastatic, while MDA-MB-468 cells are non-metastatic. Initial Western blot experiments were carried out to determine RANK expression, and all three cell lines were found to express the RANK receptor. Therefore, cellular activities including adhesion to matrix proteins, proliferation, adhesion to bone marrow endothelial cells (BMECs) and motility were determined in the presence or absence of RANKL. Presence of RANKL significantly enhanced growth rates of the metastatic MDA-MB-435 and -231 cells, but did not alter the growth rate of non-metastatic MDA-MB-468 cells. RANKL also significantly enhanced adhesion of MDA-MB-231 cells to extracellular matrix proteins, but did not alter adhesion to BMECs for any of the three cell lines. Finally, RANKL may act as a chemoattractant to draw the metastatic breast cancer cells into the bone. The results described here suggest that RANKL influences behaviour of metastatic breast cancer cells, possibly by differential regulation of NF-kappaB and AP-1 transcription factors, and may encourage development of breast cancer metastases in bone.

Disclosures: **M.R. Ray**, None.

SA068

See Friday Plenary number F068.

SA069

***In Vivo* Imaging of Metastatic Osteolytic Prostate Cancer Lesions: Inhibition of BMPs and RANKL Decreases Tumor Formation.** B. T. Feeley¹, A. H. Conduah*¹, K. Roth*¹, N. Liu*¹, J. Huard*², J. R. Lieberman¹. ¹Orthopaedic Surgery, University of California, Los Angeles, Los Angeles, CA, USA, ²Department of Molecular Genetics & Biochemistry; Department of Orthopaedic Surgery, University of Pittsburgh, Pittsburgh, PA, USA.

Introduction: Most prostate cancer metastases to bone are osteoblastic, but some lesions are mixed or purely lytic. In addition, it is hypothesized that osteolytic activity, governed by the RANK-RANKL pathway, is necessary for the development of osteoblastic lesions. We have previously shown that overexpression of noggin with a retroviral vector (RN) inhibits the growth of osteolytic and osteoblastic metastatic prostate cancer lesions, and that treatment with RANK-Fc, a soluble inhibitor of the RANK-RANKL pathway, also inhibits the development of osteolytic lesions. In this study, we sought to determine the effects of inhibiting both osteolytic and osteoblastic pathways on the formation of metastatic osteolytic lesions. We used *in vivo* charged coupled device (CCD) imaging to follow tumor burden following implantation of osteolytic cells. **Methods:** SCID mice were treated with 1x10⁵ PC-3 cells in an intratibial injection model of metastasis. Group I: PC-3 cells transduced with a lentivirus encoding the luciferase (Lenti-Luc) reporter gene; Group II: PC-3 cells transduced with Lenti-Luc+RN; Group III: PC-3 cells+Lenti-Luc and treated twice weekly with RANK-Fc; and Group IV: PC-3 cells+Lenti-Luc+RN, treated with RANK-Fc. Radiographs and CCD images were obtained every 10 days for 50 days. **Results:** Tumor size was significantly smaller at 50 days in all treatment groups vs. PC-3 cells (Table I). Radiographic and histologic analysis confirmed smaller tumor size at each timepoint. CCD imaging demonstrated that animals treated with PC-3 cells (Group I) had an exponentially increasing signal at each timepoint. Groups II, III, and IV all had decreased signal intensity compared to Group I at 20, 30, 40, and 50 days (p<0.05 at these timepoints vs. Group I), although no significant difference between the groups was noted (Table I). **Discussion:** Our data confirms that treatment with RANK-Fc and RetroNog inhibit two key pathways in the formation of osteolytic metastatic prostate cancer lesions. *In vivo* CCD imaging is a successful technique to follow the progression of metastatic lesions in bone, and can also be used to follow treatment of these lesions *in vivo*.

	Summary of Data			
	PC-3	PC-3+RN	PC-3+RANK-Fc	PC-3+RN+RANK-Fc
Tumor Size at 50 days	18.1 ± 4.2 mm	12.4 ± 3.3mm*	9.3 ± 1.9mm*	8.1 ± 2.1mm*
CCD signal intensity (photons/sec) at 50 days	9.3x10 ¹⁰	6.5x10 ⁷	6.7x10 ⁵	4.5x10 ⁵

Disclosures: **B.T. Feeley**, None.

SA070

See Friday Plenary number F070.

SA071

Bone-Residing Breast Cancers Show Differential Gene Expression of Metastasis-Related Genes Compared to Orthotopic Tumors in a Mouse Model of Human Breast Cancer Metastasis to Human Bone. K. Anderson*¹, C. Kuperwasser*², M. Rosenblatt¹. ¹Physiology, Tufts University School of Medicine and Molecular Oncology Research Institute, Boston, MA, USA, ²Anatomy, Tufts University School of Medicine and Molecular Oncology Research Institute, Boston, MA, USA.

Over half of all patients with advanced breast cancer develop bone metastasis, a virtually incurable condition. Metastasis to bone results in increased morbidity, producing pain, pathological fractures, nerve compression, and hypercalcemia. There are few agents specific for treating bone metastasis; advancement in this area requires a better understanding of the process by which breast cancer metastasizes. We aim to understand the mechanisms of breast cancer osteotropism, and determine how specific stromal environments influence gene expression in order to favor the establishment of secondary colonies of breast cancer cells. To mimic all of the steps in the natural progression of human breast cancer, we implanted human bone grafts (freshly obtained from total hip surgery) subcutaneously into immunodeficient mice. Two subclones of human breast cancer cell lines SUM-159 and SUM-1315 were generated by serial passaging in human bone. These cells exhibit increased growth in bone compared to the parental cell lines, producing osteolytic lesions. These "bone-specific" subclones show increased migration toward bone stromal cells *in vitro*, and increased propensity to form bone metastasis *in vivo*. The stable expression of a luciferase/GFP fusion gene in both the parental and bone-passaged subclones enables us to image and monitor xenografted tumor cells *in vivo*. Using this model, we show that, after intracardiac injection, human breast cancer cells preferentially colonize and proliferate in the implanted human bone grafts compared to the mouse skeleton. In order to identify genes associated with tumors growing in bone, we performed transcriptional profiling using cDNA microarrays highlighting genes differentially expressed in bone-residing versus mammary fat pad-residing (orthotopic) tumors. We found expression of genes associated with different aspects of metastasis, such as regulation of extracellular matrix remodeling, migration, angiogenesis, and apoptosis in and different stromal environments. Among the genes observed to be up and down-regulated, several have been implicated in the development of metastasis and decreased survival in women with breast cancer.

Disclosures: **K. Anderson**, None.

SA072

See Friday Plenary number F072.

SA073

Similar Reductions in Bone Turnover Markers with Oral Ibandronate and Intravenous (I.V.) Zoledronic Acid for Bone Metastases from Breast Cancer: Phase III Trial Results. J. Body¹, M. Lichinitser^{*2}, S. Tjulandin^{*2}, P. Garnero^{*3}, B. Bergström^{*4}. ¹Université Libre de Bruxelles, Institut Jules Bordet, Belgium, Belgium, ²Centre of RAMS, NN Blokhin Russian Cancer Research, Moscow, Russian Federation, ³Synarc, Lyon, France, ⁴Hoffmann-La Roche Inc., Nutley, NJ, USA.

Bone markers are useful surrogates of clinical response to antiresorptive therapy in metastatic bone disease. Suppression of these markers correlates with a reduction in skeletal-related events and metastatic bone pain. This head-to-head trial examined the effect of oral ibandronate and i.v. zoledronic acid on markers of bone resorption and formation. In this multicenter, randomized, open-label, parallel group study, advanced breast cancer patients with at least one confirmed osteolytic or mixed bone lesion received oral ibandronate 50mg/day (n=114) or a 15-minute infusion of i.v. zoledronic acid 4mg (n=110) every 4 weeks for 12 weeks. Eligibility criteria included: ≥18 years of age; life expectancy ≥6 months, WHO Performance Status of 0, 1 or 2; serum creatinine ≤3.0 mg/dL. The primary endpoint was the mean percentage change in cross-linked C-terminal telopeptide of type I collagen in serum (S-CTX) at Week 12. Bone specific alkaline phosphatase (BAP), the amino-terminal procollagen propeptides of type I collagen (PINP), and osteocalcin (OC) were also measured. Mean percentage changes from baseline at Week 12 are shown in Table 1. These results show that once-daily oral ibandronate suppresses tumor-induced bone resorption as effectively as i.v. zoledronic acid infused every 4 weeks. Oral ibandronate was non-inferior to zoledronic acid for the primary endpoint S-CTX, with similar effects on serum levels of BAP, PINP and OC.

Table 1. Mean % change from baseline at Week 12 (95% CI).		
	Oral ibandronate 50mg	I.v. zoledronic acid 4mg
S-CTX	-77% (-82% to -73%)	-75% (-82% to -67%)
BAP	-35% (-43% to -28%)	-32% (-47% to -17%)
PINP	-48% (-56% to -40%)	-42% (-55% to -29%)
OC	-35% (-40% to -30%)	-34% (-45% to -22%)

Disclosures: **J. Body**, F. Hoffmann-La Roche Ltd 5, 8; Novartis 5.

SA074

See Friday Plenary number F074.

SA075

Sequence- and Dose-Dependent Synergistic Effects of Acute and Long Term Ibandronate Exposure in Combination with Single and Fractionated Ionizing Radiation Doses on Human Breast Cancer Cell Growth Inhibition. F. Journe¹, N. Magne^{*2}, C. Chaboteaux^{*1}, E. Kinnaert^{*3}, P. Van Houtte^{*2}, J. Body¹. ¹Laboratory of Endocrinology and Bone Diseases, Institut Jules Bordet, Bruxelles, Belgium, ²Department of Radiotherapy, Institut Jules Bordet, Bruxelles, Belgium, ³LOCE, Institut Jules Bordet, Bruxelles, Belgium.

Breast cancer cells commonly colonize the skeleton and stimulate osteoclast-mediated bone resorption. Bisphosphonates have therefore emerged as a rational approach for the management of bone metastases. *In vitro* studies have shown that they inhibit proliferation and induce apoptosis of cancer cells. Radiotherapy is also a highly effective treatment for bone metastases. Experimental studies reveal that ionizing radiation (RX) may alter cancer cell functions and induce apoptosis. The objectives of our study were to examine the cytotoxic effects resulting from various combinations of ibandronate (Iban) and RX on MCF-7 and MDA-MB-231 breast cancer cell lines. In an acute bisphosphonate exposure scheme (48h), single radiation doses (1, 4, 8 and 12 Gy) were given before, at halftime of, or after Iban incubation (30 to 200 µM for MCF-7 cells, 100 to 200 µM for MDA-MB-231 cells). In a chronic Iban exposure scheme (5 weeks), the single RX doses were applied at the end of Iban exposure (1 to 30 µM for both cell lines); the highest single radiation doses (8 and 12 Gy) were also compared with fractionated RX doses (4x2 and 4x3 Gy). The combination of acute Iban with RX led to synergistic effects for the ER-negative cell line (MDA-MB-231), whatever the doses and the sequences used. In contrast, for the ER-positive cell line (MCF-7), synergistic effects were only observed with low doses of Iban (30 µM), whatever the RX doses and the sequences used; synergy was more marked when Iban followed RX. Only additive effects were observed with higher Iban concentrations (100 and 200 µM). After long term Iban exposure, high single RX doses (8 and 12 Gy), and even more the corresponding fractionated RX doses (4x2 and 4x3 Gy), induced synergistic effects with Iban on MDA-MB-231 cells, while low single RX doses (1 and 4 Gy) showed additive effects, whatever the Iban concentrations used. By contrast, synergy was only detected for MCF-7 cells with low Iban concentrations (1 and 3 µM), whatever the RX doses used. In conclusion, these *in vitro* data reveal that the combination of Iban with ionizing radiation could exert synergistic effects on the inhibition of breast cancer cells growth, and indicate that sequencing is of importance, especially on ER-positive cells. Our data might provide a rationale for an optimal design of clinical protocols associating bisphosphonate administration and radiotherapy.

Disclosures: **F. Journe**, Roche Diagnostics GmbH (Mannheim, Germany) 2.

SA076

Single vs Dual Femur Monitoring with DXA. C. Simonelli, M. Schoeller^{*}. Osteoporosis Care Services, HealthEast Clinics, Woodbury, MN, USA.

Dual energy x-ray absorptiometry (DXA) is a widely accepted method to monitor patients under treatment for osteoporosis to determine whether therapy has prevented further bone loss and reduced future fracture risk. Evaluation of treatment efficacy is related directly to measurement precision error; the smaller the precision error, the smaller the biological change that can be detected. Monitoring the effects of antiresorptive drugs is generally done at the spine and proximal femur, with larger changes seen at the spine due to the higher proportion of cancellous bone. In older patients, the spine measurement may be compromised due to osteophytes and other degenerative changes. We compared measurements of single femur, dual femur, and spine for evaluation of treatment efficacy. We measured bone mineral density (BMD) with DXA (Lunar Prodigy, GE Healthcare) at the spine (L1-L4) and bilateral proximal femur in 96 postmenopausal women (mean age 62.1 ± 9.2 years) on antiresorptive therapy. Changes in BMD were evaluated after an average of 1.2 years of therapy. Femur results were reported for left total femur (TF), right TF, and dual TF (average of left and right). There was no significant difference in average BMD change (1.3% increase) between left TF and dual TF (p=0.80), or between right TF and dual TF (p=0.70). There was a slightly larger gain at the spine (1.6%). Using 95% confidence level and this center's measured precision error, the least significant change was determined to be 2.8% for single TF, 2.1% for dual TF, and 3.4% for spine. Significant BMD changes were seen in 24% of women for single TF, 33% for dual TF, and 31% for spine. There was a biologically significant decrease in BMD in 5% of women for single TF, 6% for dual TF, and 10% for spine. About 40% of the women who had a positive or negative significant change at dual TF did not have a significant change, positive or negative respectively, at the spine. We conclude that a) the average change in BMD for single total femur and dual total femur was equivalent in this treatment group, b) the number of patients with a positive biologically significant change was somewhat higher (albeit not significantly) for dual femur than single femur or spine, and c) about 40% of patients with a significant change at the dual total femur did not have a corresponding significant change at the spine.

	Left Total Femur	Right Total Femur	Dual Total Femur	Spine
CV	1.0%	1.0%	0.8%	1.2%
Least Significant Change	2.8%	2.8%	2.1%	3.4%
Average Change	1.3%	1.3%	1.3%	1.6%
% with Significant + Change	24%*	22%*	33%*	31%*
% with Significant - Change	5%	5%	6%	10%
% Significant + Change Femur Only	39%	57%	47%	
% Significant - Change Femur Only	40%	20%	33%	

* p=0.08 single vs. dual femur; p=0.14 single femur vs. spine; p=0.76 dual femur vs. spine

Disclosures: **C. Simonelli**, None.

SA077

See Friday Plenary number F077.

SA078

Prediction of Vertebral Fracture Risk by Radiographic Absorptiometry and Quantitative Ultrasound in Japanese Women. Y. Abe, K. Aoyagi. Department of Public Health, Nagasaki University Graduate School of Biomedical Sciences, Nagasaki, Japan.

The purpose of this study was to explore the ability of radiographic absorptiometry (RA) and quantitative ultrasound (QUS) to predict fracture risk prospectively among 367 Japanese women ages 42 to 91 years (mean age = 67.6, SD = 9.2 years); average follow-up was 3.4 years. Bone measurements were performed at baseline using RA for metacarpal bone and QUS for calcaneus (stiffness index). Lateral spine radiographs were obtained at baseline and at follow-up. Radiographic vertebral deformities at baseline were assessed by quantitative morphometry, defined as vertebral heights more than 3 SD below the normal mean. An incident vertebral fracture was defined as a decrease of more than 20 % in vertebral heights on subsequent films. The prospective associations of vertebral fractures with vertebral deformities and bone measurements at baseline were examined using logistic regression, adjusting for age. Presence of one or more vertebral deformities was strongly associated with subsequent vertebral fracture risk. The age-adjusted odds ratio was 3.19 (95% confidence interval [CI]: 1.70 to 5.99). Metacarpal bone mineral density (BMD) measured using RA had a significant prospective association with incident vertebral fractures. The age-adjusted odds ratio (corresponding to 1 SD decrease in bone mass) was 1.88 (95% CI: 1.35 to 2.61). Stiffness index of calcaneus also significantly predicted future vertebral fracture risk, with age-adjusted odds ratio of 1.44 (95%CI: 1.05 to 1.98). When adjusting for the presence of vertebral deformities as well as age, metacarpal BMD had a significant association with future vertebral fracture risk, but stiffness index did not. The age-adjusted odds ratios were 1.78 (95%CI: 1.27 to 2.48) for metacarpal BMD and 1.28 (95%CI: 0.92 to 1.77) for stiffness index. Our results suggest that the presence of previous vertebral deformities was a strong predictor for subsequent fractures. In addition, both metacarpal RA and calcaneal QUS are significant predictors of vertebral fractures. We reported earlier that metacarpal RA and calcaneal QUS had significant associations with the presence of vertebral deformities. Although dual X-ray absorptiometry at axial sites is currently considered necessary for diagnosing osteoporosis, these convenient techniques, with relatively low cost and portability, could be promising alternatives for assessing fracture risk.

Disclosures: **Y. Abe**, None.

SA079

See Friday Plenary number F079.

SA080

Peripheral Quantitative Computed Tomography at the Tibia in Individuals with SCI: Reproducibility and Methodological Considerations. L. M. Giangregorio¹, C. Gordon², J. Bugaresti³. ¹Spinal Cord Rehab Program, Toronto Rehabilitation Institute, Toronto, ON, Canada, ²Department of Radiology, McMaster University, Hamilton, ON, Canada, ³Department of Medicine, McMaster University, Hamilton, ON, Canada.

The present study investigated the reproducibility and utility of BMD and bone geometry measurements at the tibia in individuals with spinal cord injury (SCI) using peripheral quantitative computed tomography (pQCT). It was hypothesized that issues such as spasticity, contractures, and low BMD might influence the utility and precision of this technique in the SCI population. Nine individuals with SCI were recruited to participate in the study. Spasticity prevented positioning and scanning of one participant. Of the remaining 8 participants, the average age was 41 years and the average years post injury was 13. Six individuals had cervical lesions and two had lesions at T10. pQCT scans were performed twice at the ultra-distal tibia (4% site) and two-thirds tibia (66% of tibia length, measuring proximally from distal end), with repositioning between sets of scans. Trabecular BMD (mg/cm³) was evaluated at the 4% site. The analysis threshold for trabecular bone was set at 200mg/cm³ due to low BMD values in some patients. At the 66% site, total and cortical BMD, bone area (cm²), and strength-strain indices (SSI - polar, x, and y) were evaluated. For each outcome, the root mean squared coefficient of variation (RMSCV) was calculated. The average (±SD) trabecular BMD at the 4% site was 100.6±47.9 mg/cm³, and the RMSCV for trabecular BMD at this site was 2.6%. At the 66% site, the RMSCVs for total BMD, cortical BMD and bone area were 1.59%, 1.55% and 1.73% respectively. The RMSCV for polar SSI was 1.89%, and for SSIx and SSIy the RMSCVs were 3.97% and 3.06%, respectively. For individuals with limited mobility (i.e. complete cervical lesions), two technicians were required for positioning of the limb in the scanner. pQCT is a valuable tool for assessing volumetric BMD and bone geometry at the tibia in SCI as it does not require the patient to transfer out of a wheelchair. However, methodological issues such as spasticity and low BMD can influence proper positioning and analysis. Further, the RMSCV for trabecular BMD was high relative to the average BMD value in this group, and may limit the ability to detect change in this variable. Further study of the reproducibility and utility of this technique a larger number of individuals with SCI is warranted.

Disclosures: L.M. Giangregorio, None.**SA081**

See Friday Plenary number F081.

SA082

A New Method of Measurement of Mandibular Bone Mineral Density and Correlations with Dental Clinical Findings. Y. Takaishi^{*1}, T. Ikeo^{*2}, H. Morii³, M. Takeda^{*4}, K. Hide^{*5}, T. Arai^{*4}, K. Nonaka^{*6}. ¹Takaishi Dental Clinic, Himeji, Japan, ²Osaka Dental University, Osaka, Japan, ³Emeritus Professor, Osaka City University, Osaka, Japan, ⁴Furuno Electric Co., Ltd., Nishinomiya, Japan, ⁵Furuno Electric Co., Ltd, Nishinomiya, Japan, ⁶Elk Corporation, Tokyo, Japan.

While alveolar bones have been supposed to be affected by the process of osteoporosis as a systemic disease, it is important to evaluate how is bone mineral density (BMD) of alveolar bones from standpoint of both dental and medical practice. Forty post-menopausal Japanese women with the mean age 59.4±5.6(SD) years were studied with the written consent for the study. Twenty women were in their fifties and the rest in their sixties. Many methods of measurement of BMD of alveolar bones have been proposed, but the root area of mandibular first premolar was selected for measurement of BMD in the present study. A definite area of the root of the mandibular first premolar was divided into squares for measurement of brightness of each square from the soft ware developed by us. The distribution curve of brightness of each square was obtained and the mean value was calculated for each patient. Lumbar spine BMD was measured by Hologic QDR 4500W and the speed of sound (SOS) of calcaneus by quantitative ultrasound (QUS) by CM-100 (Furuno Electric, Co, Nihonmiya). Age-related significant decrease of alveolar BMD was demonstrated. There were significant correlations between alveolar BMD and lumbar spine BMD and between alveolar BMD and calcaneus SOS. Dentist made dental clinical observations including the depth of pockets, mobility of teeth and alveolar bone resorption by the method of Schei. Biochemical parameters of bone turnover were measured including bone alkaline phosphatase (BAP) and urinary deoxypyridinoline (DPD). Lumbar spine BMD showed significant negative correlation with BAP but the coefficient correlations between alveolar BMD and calcaneus BMD and BAP did not reach significant level. Multivariate analysis of factors in relation to dental clinical findings (attachment level) showed significant contributions of age, BAP, urinary DPD, urinary calcium/creatinine and calcaneus SOS. In conclusion, analysis of bone density at the root of mandibular first premolar could be an indicator of bone loss in patients with osteoporosis and periodontal diseases. There was an age-related bone loss from this

method of measurement of alveolar BMD. However, it seemed that many factors may contribute to the bone loss in alveolar bones in addition to risk factors which may contribute to the pathogenesis of systemic osteoporosis.

Disclosures: Y. Takaishi, None.**SA083**

Use of MRI of the Distal Radius to Assess Qualitative and Quantitative Aspects of Cortical Bone In Postmenopausal Women. D. C. Newitt¹, B. Hyun^{*1}, D. M. Black¹, C. J. Rosen², S. Majumdar¹. ¹UCSF, San Francisco, CA, USA, ²St Joseph Hospital, Bangor, ME, USA.

The purpose of this study was to use high resolution (HR) MRI to evaluate cortical shell geometry of the distal radius in post-menopausal women. We evaluated baseline wrist MRI scans from 41 post-menopausal women (age = 59 ± 6, range 46 to 69 yrs) enrolled in the POWR (PTR Once Weekly Research) study. Subjects were non-osteoporotic (spine BMD T-score > -2.5), with femoral neck DXA BMD T-score between -1 and -2. A Siemens 1.5T Symphony scanner with a dedicated wrist coil was used to acquire high resolution (.16 x .16 x 2 mm³) axial images of the distal radius using a 3D gradient echo sequence. The images were evaluated for focal signal areas within the cortex. A semi-automated program was used to segment the cortex from soft tissues, and cortical volume and mean cortical thickness were evaluated from 2 to 3cm proximal to the distal radius endplate. Figure 1 shows mean cortical thickness v. age, indicating a small trend to decreasing thickness with increasing age (.009mm/yr, r=0.31). Ultra-distal BMD (by DXA) was weakly correlated with cortical thickness (r=0.52) and volume (r=0.49). In 34 of 41 subjects there was no visible MR signal from the cortex, indicating little or no soft tissue in this region, while 7 subjects showed varying degrees of apparently fatty signal inclusions. Figure 2 shows a representative image from a subject with significant fat inclusions (white arrow) within the cortex. These results demonstrate that geometry of the distal radius cortex, and by extension other extremity bones, can be measured with HR MRI. In addition, focal areas of cortical porosity can be evaluated. In combination with previously demonstrated trabecular structure evaluation, HR MRI provides a tool for non-invasive evaluation of bone geometry and structure in vivo, which is unique in not requiring ionizing radiation.

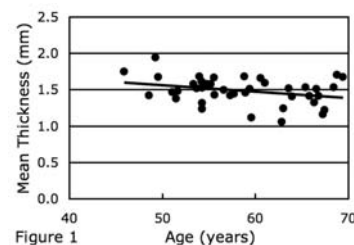
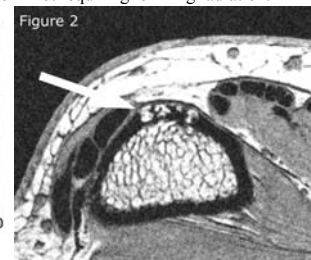


Figure 1

Disclosures: D.C. Newitt, None.**SA084**

See Friday Plenary number F084.

SA085

Assessment of Trabecular Bone Structure with Magnetic Resonance T₂ Relaxation Time. Y. Akvol^{*1}, F. Canturk^{*1}, G. Alayli^{*1}, D. Durmus^{*1}, B. Diren^{*2}. ¹Physical Medicine and Rehabilitation, Medical Faculty, Samsun, Turkey, ²Radiology, Medical Faculty, Samsun, Turkey.

This study was planned to investigate the utility of magnetic resonance imaging (MR), dual energy x-ray absorptiometry (DEXA) and ultrasound measurements in the assessment of osteoporosis quantitatively. The study group consisted of 31 osteoporotic postmenopausal women (age range 45-72 years) and control group consisted of 31 healthy postmenopausal women (age range 48-70 years). DEXA measurements were performed at lumbar vertebrae (L₂, L₃, L₄) and at femur (femoral neck, intertrochanteric region, wards triangle). The ultrasound parameters broadband ultrasound attenuation (BUA), speed of sound (SOS) and stiffness were measured in the calcaneus. The MR T₂ relaxation time (T₂ RT) measurements were performed at L₃ vertebrae and calcaneus. The results of MR imaging, DEXA and US measurements of the study and control groups were compared with each other. T₂ RT of osteoporotic patients were significantly higher than healthy controls (p<0.001). Although there was no correlation between T₂ RT and age, there was a moderate negative correlation between T₂ RT and weight, body mass index, menopause age. As postmenopausal period got longer T₂ RT values increased. A strong negative correlation was determined between bone mineral density (BMD) measured by DEXA and T₂ RT. There was a moderate negative correlation between T₂ RT and US measurements (BUA, SOS, and Stiffness). US measurement of study group were significantly higher than the control group (p<0.001). A moderate correlation was determined between US measurements and DEXA measurements. Since, prolonged T₂ RT in the osteoporotic patients indicates low bone quality; it seems to be possible to discriminate postmenopausal osteoporotic and healthy women with MR T₂ RT which assess trabecular bone structure.

Disclosures: F. Canturk, None.

SA086

See Friday Plenary number F086

SA087

Changes in the Geometry of the Proximal Femur throughout Life. L. Del Rio, S. Di Gregorio, J. Rosales*, M. Garcia*, M. Ramiro*, L. Castro*. CETIR Centre Medic, Barcelona, Spain.

Bone strength is related to bone mineral density (BMD), distribution of density, and macro and micro-structural factors. It is known that both bone geometry and BMD change in the growing skeleton, and that BMD decreases in the aging population. However, it is not clear how bone geometry changes with aging. Geometry of the proximal femur is of particular interest due to the clinical importance of hip fracture. We measured proximal femur geometry in a 1611 healthy subjects (1273 females and 338 males) between the ages of 10 and 78 years. Dual-energy x-ray absorptiometry (DXA) scans of the femur scans were performed with the Lunar Prodigy (GE Healthcare). Hip axis length (HAL), femur neck length (D2), cross-sectional area (CSA), cross-sectional moment of inertia (CSMI), neck-shaft angle (θ), and other parameters were measured using the Hip Strength Analysis program. During the period of skeletal growth, females had significantly longer D2 and larger θ compared to males. At young adulthood, HAL, CSA, CSMI, and D2 were higher in men than women. No significant difference in θ was observed with age (grouped by decade) from young adulthood until age 50 years, although femur neck width and θ decreased in both sexes with age. Neck-shaft angle decreased significantly, $p<0.0001$, in men (6.0 degrees) and women (3.4 degrees) between the ages of 10 and 78 years. A small but significant increase in CSA with age was observed in both sexes after young adulthood. Femur neck width and length were larger in adult men than women. HAL increased from childhood to adulthood, reaching the maximum value at ages 30-40 years, after which HAL remained constant. We conclude that significant changes in femur geometry, that may impact the risk of hip fracture, occur throughout life.

Disclosures: **L. Del Rio**, None.

SA088

See Friday Plenary number F088

SA089

Dental X-Rays Identify Women with Low Hip and Spine BMD. S. Liew¹, D. Steines^{*1}, M. Jeffcoat^{*2}, G. Adams^{*1}, P. Lang^{*1}, C. Arnaud¹. ¹Imaging Therapeutics, Foster City, CA, USA, ²University of Alabama, Birmingham, AL, USA.

It is estimated that less than 30% of postmenopausal women in the US with osteoporosis have been diagnosed. While numerous diagnostic technologies exist, the cost effectiveness in utilizing these techniques for mass screening is still debatable. We have developed an automated computer based technique to estimate the bone mineral density of hip and spine using digitized, calibrated, periapical dental x-rays. In a prospective optimization trial to develop this technology, hip and spine DXA BMD were measured in 48 postmenopausal women, and each had 2 periapical x-rays of the anterior mandible taken. The group had a mean spine BMD T-score of -1.4 (sd=1.5), mean hip BMD T-score of -1.8 (sd=1.3), mean age of 60.5 (sd=14.5), and a mean BMI of 23.9 (sd=5.1). Dental x-rays were taken with a phantom embedded in the film holder. They were digitized using a desktop scanner and analyzed using an algorithm that measures the bone density as well as a number of parameters that characterize the mandibular trabecular pattern. A composite parameter, the mandibular index (MI), was developed from these measurements. MI correlates with spine DXA BMD ($r=0.66, p<0.001$). This correlation coincides with the correlation of spine BMD with hip BMD ($r=0.66, p<0.001$) in this study. MI also correlated with hip BMD ($r=0.57, p<0.001$). We applied a leave-one-out cross validation process to identify patients with T-score ≤ -2.5 of hip or/and spine BMD. ROC curves showed that the MI can provide sensitivity of 81% (95% CI 59-94%, AUC=0.88) with 80% specificity. Age and BMI given the same specificity provided a sensitivity of 39% (95% CI 14.5-69.2%, AUC=0.70). T-score cutoffs of less than or equal to -2, -1.5 and -1 achieved sensitivity levels of 74%, 64%, and 57% respectively using MI. These results suggest that MI measurements correlate with hip and spine BMD to a similar degree as spine with hip BMD and can be more accurate than age and BMI in identifying women with osteoporosis. MI measurements do not require expensive capital equipment and can be employed during patient's routine dental exams to screen for osteoporosis. A prospective study is in progress to establish the population reference values and to further validate the technique.

Disclosures: **S. Liew**, None.

SA090

See Friday Plenary number F090.

SA091

Anabolic Changes in Vertebral Trabecular Microstructure in Osteoporotic Postmenopausal Women Treated for 2 years with Human Parathyroid Hormone Fragment (hPTH 1-34) as Determined by a New, Automated Noninvasive Imaging Technology that Uses Ordinary Lateral Spine Radiographs. C. Arnaud¹, S. Liew¹, D. Steines^{*1}, R. Vargas-Voracek¹, S. Sanchez^{*2}, P. Hess¹. ¹Imaging Therapeutics, Foster City, CA, USA, ²University of California San Francisco, San Francisco, CA, USA.

Until recently, quantitative assessment of trabecular structure required either bone biopsy followed by microscopy or 3-dimensional micro computed tomography (3D μ CT). Non-invasive options include the use of expensive capital equipment such as magnetic resonance imaging (MRI) of peripheral bones. We developed a new, noninvasive, 2D automated image analysis technology that uses ordinary radiographs that can measure surrogate trabecular parameters comparable to those measured by 3D μ CT. In general, it involves x-ray digitization, identification of regions of interest, background subtraction, and trabecular pattern extraction. Parameters of trabecular structures are measured using computer algorithms. In previous work, we applied this novel technology to ordinary radiographs of cores of proximal cadaveric femora showing that 2D measurements of trabecular structure correlate well with 3D μ CT measurements. Those 2D measurements also correlate with biomechanical failure loads applied to those cores as well to whole proximal femora (JBMR; Abst # 1218, Abst # 107; 18 Suppl 2; 2003). We applied the same technology to in-vivo lateral vertebral radiographs obtained in a previously performed study of the effect of hPTH (1-34) on the bone density of estrogen treated postmenopausal osteoporotic women (JBMR; Abst #1019; 14 suppl 1; 1999). The results are summarized below.

Structural Parameter	PTH (n=24)		Placebo (n=27)	
	% Change Between Baseline and 2 Yrs	t-test p value	% Change Between Baseline and 2 Yrs	t-test p value
L5 # Trabecular Fragments	-14%	0.00005	+5.8%	0.30371
L5 Area ratio (bone/total)	+1.7%	0.00087	+0.6%	0.39795
L5 Inter-connectivity Index	+35%	0.00074	+3.4%	0.75119
L5 Network Length	+23.1%	0.00004	-0.9%	0.88123

The 2D trabecular parameters shown above demonstrated highly significant changes from baseline in the PTH group whereas none of the corresponding parameters changed significantly in the placebo group. The results indicate that hPTH (1-34) dramatically reduces trabecular fragmentation, while increasing the trabecular bone/area ratio, the interconnectivity index and the trabecular network length. These changes are consistent with those shown in PTH treated subjects reported previously by others using 3D μ CT and provides strong evidence that noninvasive vertebral x-ray 2D image analysis can play a major role in the future, noninvasive, clinical evaluation of bone structure.

Disclosures: **C. Arnaud**, None.

SA092

Relationship between Quantitative Ultrasound of the Calcaneus and Mortality in Postmenopausal Women: A 3-Year Prospective Study. J. González-Macías¹, J. Vila^{*2}, S. Tojeiro^{*3}, M. Turégano^{*4}, J. A. Castro^{*5}, M. R. González^{*6}, E. de la Figuera^{*7}, M. Borge^{*8}, B. García-López^{*9}, M. B. Brun^{*10}, F. Marín^{*11}. ¹Dept. Internal Medicine, H.U. Valdecilla, Santander, Spain, ²IMIM, Barcelona, Spain, ³C.S. San Fernando, Madrid, Spain, ⁴C.S. Zona Centro, Cáceres, Spain, ⁵C.S. Cartuja-Almanjayar, Granada, Spain, ⁶C.S. Salvador Pau, Valencia, Spain, ⁷C.S. Delicias Sur, Zaragoza, Spain, ⁸C.S. Arturo Eyres Sur, Valladolid, Spain, ⁹C.S. San Andrés, Murcia, Spain, ¹⁰C.A.P. Moncada i Reixac, Barcelona, Spain, ¹¹Medical Research, Eli Lilly, Madrid, Spain.

Several studies have reported the association of low bone mineral density measured with dual-energy absorption densitometry (DXA), with an increased mortality risk. A recent study has also demonstrated that low quantitative bone ultrasound (QUS) values are associated with an increased mortality (Bauer et al. Osteoporos Int 2002). ECOSAP is a 3-year prospective cohort study to test the ability of calcaneus QUS and several clinical risk factors of osteoporosis and fractures, to predict the non-vertebral fracture risk in 5201 women aged ≥ 65 years. The aim of the present analysis was to test the relationship of QUS with mortality in the ECOSAP cohort. Women were selected using non-probabilistic sampling of consecutive cases regardless of the reason for consultation in 58 Primary Care Centers (PCC) in Spain. All women [aged 72.3 ± 5.3 years (mean \pm SD)] were assessed with a Sahara® equipment, and completed a health questionnaire. They were followed for up to 3 years with regular visits to the PCCs every 6 months. The physician recorded if the patient died and the cause of death. Cox proportional hazard regression model was designed to estimate the Hazard Rate (HR) of all-cause mortality per one standard deviation reduction in QUS parameters. One hundred (1.9%) women died during a median of 36.1 months of follow-up, for a total of 15,281 patient-years. Women who died were on average older and more likely to report a history of hearing or sight problems, chronic pulmonary obstructive disease (CPOD), diabetes mellitus (DM), and treatment with thyroxine or antiarrhythmics. After adjustment for age, none of the QUS variables showed statistically significant differences between the patients who died and the survivors. Final multivariate model for the best-fitted QUS variable (SOS) included age (HR: 1.11; 1.07-1.15), sight/hearing problems (HR: 2.70; 1.58-4.64), thyroxine therapy (HR: 3.60; IC: 1.65-7.83), DM (HR: 2.24; 1.31-3.82); CPOD (HR: 3.30; 1.60-6.84). SOS was marginally non-significant: (HR:1.19; 0.97-1.45)($p=0.094$). In conclusion, we did not observe a relationship between QUS and mortality in postmenopausal women in the ECOSAP study.

Disclosures: **J. González-Macías**, None.

SA093

See Friday Plenary number F093.

SA094

Do Axial Transmission Ultrasound Measurements of Bone Differ According to Ambient Temperature? A. S. Khan*, K. Brooke-Wavell, G. Havenith*. Human Sciences, Loughborough University, Leicestershire, United Kingdom.

The study examined whether axial transmission ultrasound measurements of bone vary according to ambient temperature and concomitant changes in tissue temperature. Ten healthy volunteers (5 men, 5 women) spent 20 minutes acclimatising in an environmentally controlled chamber at each of three ambient temperatures: 10, 20 and 30 °C, whilst wearing standard light clothing. Speed of sound (SOS) was then measured at the radius, tibia, proximal phalanx of digit III and metatarsal V using a Sunlight Omnisense device. Skin temperature was measured at the dorsal surface of the hand. Participants gave written informed consent for all procedures, which have been approved by the University Ethical Advisory Committee. Skin temperature varied significantly according to environmental temperature (table). Radial and tibial SOS did not differ in the different conditions. Phalangeal SOS decreased with increasing temperature, being 3% lower at 30 than 10 °C. Metatarsal SOS also differed significantly according to temperature by ≤2%.

Table: Skin temperature and SOS according to ambient temperature: mean (standard error)

Ambient temperature (°C)	10	20	30	
Skin temperature (°C)	24.1 (0.2)	30.3 (0.2)	33.7 (0.6)	*
Radius SOS (m/s)	4161 (48)	4172 (24)	4147 (30)	
Tibia SOS (m/s)	3942 (23)	4002 (32)	3931 (20)	
Phalanx SOS (m/s)	4037 (54)	3989 (56)	3907 (63)	*
Metatarsal SOS (m/s)	3503 (81)	3574 (82)	3525 (103)	*

*Differ according to ambient temperature: p<0.05
Speed of sound at the radius and tibia did not differ according to ambient temperatures covering the range that might be encountered in most laboratory or field situations. At the extremity sites (phalanx and metatarsal) some small but statistically significant variation according to ambient temperature was observed, possibly related to alterations in tissue temperature. Extremes of ambient temperature may influence axial transmission ultrasound measurements of bone at the extremities although not at radius and tibia.

Disclosures: **K. Brooke-Wavell**, None.

SA095

Evaluation of a New Multi-Site Quantitative Ultrasound Device in Childhood and Puberty - Precision and Normative Data for Caucasian Girls. A. Oldenburg*, O. Bock, D. Felsenberg. Centre for Muscle and Bone Research, Charite - Campus Benjamin Franklin, Berlin, Germany.

Quantitative Ultrasound (QUS) is a promising tool for bone health assessment in children, although there is uncertainty about the exact bone-entity measured by this technique. The aim of this study was to evaluate in-vitro- and in-vivo-precision and to acquire normative data for the Sunlight Omnisense™ in girls between 7 and 18 yrs of age. The study was conducted in 335 healthy Caucasian girls, mean age 12.6 years (range 7-18 yrs) - after institutional review board approval and in accordance with the Declaration of Helsinki. Anthropometric data, menarche and Tanner stages of breast and pubes were recorded. Ultrasound measurements, obtaining maximum speed of sound (SOS), have been performed at distal radius, mid-shaft tibia and proximal phalanx of the 3rd finger using Sunlight Omnisense™, a new multi-site QUS device. In-vitro-precision (phantom) of 0.25% and 0.28% was determined by daily measurements. The in-vivo-short-term precision was 0.41% (radius), 0.36% (tibia) and 0.45% (phalanx). In-vivo-long-term precision was 0.85% (radius), 1.47% (tibia) und 0.67% (phalanx). Reference values of SOS have been calculated for radius, tibia, and phalanges for girls in the age from 7 to 18 yrs. Age group related SOS values - mean (standard deviation/SD) - range at the distal radius from 3719.63 m/s (90.73) to 4001.40 m/s (69.87) with an annual increase of 26.50 m/s (3.14), at the tibia from 3517.38 m/s (144.00) to 3819.17 m/s (99.62) with an annual increase of 32.68 m/s (4.19) and at the phalanx from 3823.21 m/s (214.82) to 4028.60 m/s (126.43) m/s with an annual increase of 16.12 m/s (5.40). During puberty, mostly between the age of 13 and 14 yrs, SOS is increasing significantly (p < 0.001), but at radius and tibia only. SOS values at tibia and radius differ significantly (p < 0.001) between the grouped Tanner stages 1-3 and 4-5. SOS correlates positively and significantly with age and pubertal stages. With this study normative data for the Sunlight Omnisense™ device were established for Caucasian girls aged 7-18 yrs, as a prerequisite for evidence based use of the technique in a female paediatric population.

Disclosures: **A. Oldenburg**, None.

SA096

See Friday Plenary number F096.

SA097

Multisite Ultrasound and Vertebral Deformity: Findings from the Canadian Multicentre Osteoporosis Study (CaMOS). W. P. Olszynski¹, G. Ioannidis², J. P. Brown³, D. A. Hanley⁴, J. D. Adachi², K. S. Davison³. ¹Medicine, University of Saskatchewan, Saskatoon, SK, Canada, ²Medicine, McMaster University, Hamilton, ON, Canada, ³Medicine, University of Laval, Ste. Foy, PQ, Canada, ⁴Medicine, University of Calgary, Calgary, AB, Canada.

The use of multisite ultrasound to assess fracture risk is an attractive technology due to its simplicity of use, lack of ionizing radiation, low capital cost, and portability. It has been hypothesized that the qualitative ultrasound assesses the architectural properties of bone, such as stiffness, trabecular connectivity, and cortical porosity, rather than density. This investigation used a subset of the Canadian Multicentre Osteoporosis Study (CaMOS) dataset to cross-sectionally assess the association between ultrasound (speed of sound) at the distal radius, phalanx or tibia and vertebral deformity (>3 SD lower than population mean in anterior, middle, or posterior vertebral height) in women aged 50 years or greater. Data from Saskatoon, Quebec, St. John's, Calgary and Hamilton were used in this analysis. A Sunlight OmniSense Multisite Ultrasound (Israel) was used for all ultrasound assessments and all ultrasound data was collected at year 5 of CaMOS. A general linear model analysis was used to assess the association between ultrasound measures at all sites and vertebral deformity risk with correction for height, weight, age, and CaMOS centre. Following a radiograph of the spine at year 5 of CaMOS, 744 women (74.4%) were found to have no vertebral deformity, whereas 256 women had a vertebral deformity (25.6%). Women without a vertebral deformity had higher ultrasound measurements at the distal radius by 30.2 m/s (95% CI: 5.5, 55.1), at the tibia by 32.3 m/s (95% CI: 9.6, 55.0), and at the phalanx by 10.6 m/s (95% CI: -20.8, 42.0; NS). This analysis has shown that the Sunlight OmniSense Multisite Ultrasound has the ability to discriminate between women with or without vertebral deformity whether used at the distal radius or tibia, but not the phalanx, site. Since the data analysis for vertebral deformities and non-vertebral fractures in CaMOS is ongoing and soon to be completed, updated analyses investigating the use of Sunlight OmniSense Multisite Ultrasound for discriminating between those with a risk for both vertebral deformity and non-vertebral fracture will be reported at the meeting.

Disclosures: **W.P. Olszynski**, None.

SA098

Map of the Heel BUA May Provide Additional Information on Longitudinal Changes in Skeletal Integrity. R. K. Bhattacharya¹, J. Goll^{*2}, K. T. Vujevich^{*1}, D. L. Medich^{*1}, S. M. Sereika^{*1}, S. L. Greenspan¹. ¹Endocrinology, University of Pittsburgh, Pittsburgh, PA, USA, ²Quidel, Mountainview, CA, CA, USA.

Although bone mass accounts for 50-70% of the variance of fracture risk, other factors such as bone geometry, bone turnover, and biochemical indices also contribute. Traditionally, calcaneal ultrasound measures bone mass by broadband ultrasound attenuation (BUA). The QUS-2 Ultrasonometer (Quidel Corp., Mountainview, CA) reports BUA, averaged over a cross-sectional area of the calcaneus of about 1 cm². In addition, it measures "maps" of BUA values at discrete locations in a 2-dimensional grid on the heel, at a resolution of a few millimeters. These maps show substantial heterogeneity and biological diversity. We have previously described four ultrasound-derived topographical maps of the heel and found that the maps were associated with hip and spine bone mineral density as well as weight and body mass index. To determine whether longitudinal changes in BUA, bone mass, or biochemical markers were associated with the three-dimensional maps of the heel, we examined these variables in 88 early postmenopausal women previously naive to treatments that affect bone mineral metabolism. The age range was 40-60 (mean age 50). The maps were blindly assigned groups A-D based on certain topological features or shapes that were observed. Subjects were followed for 6 month. Percent changes in subgroup D's BUA measurements were significantly correlated with the 6-month percent decrease in osteocalcin. There was a borderline trend for significance for subgroup D's BUA percent changes and increase in PA spine and trochanteric bone mineral density (Table). We conclude that these maps may help identify a subgroup of patients who have early changes in spine and trochanteric bone density - areas rich in trabecular bone. Further studies are needed to determine the clinical utility of these findings. Table below describes the Spearman correlations between percent change in BUA QUS-2 and measures of BMD over a 6 month period.

Correlations of 6 Month Changes in BUA with Change in Bone Mineral Density or Bone Markers				
6-Month Change	BUA Group A	BUA Group B	BUA Group C	BUA Group D
PA spine	.084	.343	-.018	.397**
Trochanter	.246	-.206	-.066	.430*
Total hip	-.242	-.071	.088	.168
Femoral neck	.094	.038	-.093	-.084
Osteocalcin	.061	-.170	-.223	-.519***
NTx	-.084	.056	.151	.131

*P=0.058, **P=0.083, ***P=0.019

Disclosures: **R.K. Bhattacharya**, Proctor and Gamble 2, 8; Sanofi Aventis 8; GSK Roche 8.

SA099

LRP5 Impacts not only Bone Mass but also Bone Modelling and Shaft Thickness. A. Saarinen^{*1}, W. G. Cole^{*2}, E. B. Sochett³, E. Marttinen^{*4}, A. E. Lehesjoki^{*1}, O. Makitie⁴. ¹Department of Medical Genetics, Folkhalsan Institute of Genetics, University of Helsinki, Helsinki, Finland, ²Orthopaedic Surgery, The Hospital for Sick Children, University of Toronto, Toronto, ON, Canada, ³Pediatric Endocrinology, The Hospital for Sick Children, University of Toronto, Toronto, ON, Canada, ⁴Metabolic Bone Clinic, The Hospital for Children and Adolescents, University of Helsinki, Helsinki, Finland.

Osteoporosis-pseudoglioma syndrome (OPPG) is an autosomal recessive condition characterized by blindness and osteoporosis. OPPG is caused by homozygous mutations in the *LRP5* gene encoding the LDL Receptor-Related Protein 5. Heterozygous *LRP5* mutations have been associated with childhood onset primary osteoporosis characterized by recurrent fractures, even in the absence of low bone density. In order to gain more understanding on the impact of *LRP5* mutations on human skeletal development we have assessed characteristics of bone health, including fracture history, bone mineral density (BMD, Hologic Discovery A) and radiographs, in two patients with OPPG and in three related carriers of the same *LRP5* mutation. The R570W mutation, previously reported by Gong et al. (2001), was identified by direct sequencing of PCR amplified exon 8 of the *LRP5* gene. Two adult siblings (Patients 1 and 2) with OPPG were homozygous, and two healthy daughters (Patients 3 and 4) and an aunt (Patient 5) of Patient 2 were heterozygous for the mutation. The patients with OPPG had severe osteoporosis and multiple compression fractures. The adolescent carriers of the mutation were healthy and had had no fractures. In contrast, the 85 year old aunt had a history of several peripheral fractures at adult age. The radiographs of the homozygotes showed in addition to multiple compression fractures, severe generalized osteopenia with very thin and bowed long bones and abnormally wide metaphyseal ends of the tubular bones. The carriers had no compression fractures but abnormally thin tubular bones with overubulation of the metaphyseal ends.

Parameter	Patient 1	Patient 2	Patient 3	Patient 4	Patient 5
LRP5 mutation	Homozygous	Homozygous	Heterozygous	Heterozygous	Heterozygous
Age / Sex	58 / F	52 / M	19 / F	15 / F	85 / F
Vision	Blind	Blind	Normal	Normal	Normal
Peripheral fractures	++	++	-	-	+++
Lumbar spine BMD Z-score	-4.1	-3.3	-0.7	-0.3	NA
Femoral neck BMD Z-score	-4.8	-1.3	-0.3	-0.8	NA

These observations suggest that in addition to its impact on bone mass accrual *LRP5* has a role in bone modelling. Findings in the heterozygotes suggest that despite normal bone density these individuals may be more prone to fracture at adult age because of the abnormally thin bone shafts and lack of normal modelling of the tubular bones.

Disclosures: **O. Makitie**, None.

SA100

See Friday Plenary number F100.

SA101

Genetic Diversity of Skeletal Ontogeny Is Recapitulated during Fracture Healing. K. J. Jepsen¹, C. Price¹, P. Nasser^{*1}, M. Alapatt^{*2}, S. N. Stapleton², L. Silkman^{*2}, S. Kakar², T. A. Einhorn², L. C. Gerstenfeld². ¹Department of Orthopaedics, Mount Sinai School of Medicine, New York, NY, USA, ²Orthopaedic Surgery, Boston University Medical Center, Boston, MA, USA.

Microarchitecture (microCT) and mechanical properties (torque to failure) were examined over 35 days of fracture healing in A/J, C57BL/6J (B6), and C3H/HeJ (C3H) inbred strains of mice. These studies demonstrated that the major architectural characteristics of bone quality (moment of inertia, cortical area, trabecular volume), which varied significantly among the strains, were recapitulated during fracture healing. The strain having the highest pre-fracture strength (C3H) however regained this property the slowest. Both micro-CT analysis and the temporal expression patterns of cartilage versus bone mRNAs demonstrated very slow (≥ 2 wk delay) cartilage resorption for C3H compared to B6. This was due to the slower transit of C3H bones through the endochondral phase. Furthermore, this slower transit time could be related to genetic variability in the rate of endochondral maturation based on the 5-7 day difference in times of peak chondrocyte hypertrophy based on Col10A1 expression. Quantitative analysis of the expression of both cartilage and bone extracellular matrix mRNAs showed a direct correlation between the total anabolic activity of a given strain of mouse and the overall volume of bone tissue formed such that (C3H>B6>AJ). Examination of 14 day post birth growth plates demonstrated similar temporal patterns of endochondral progression with the AJ and B6 mouse strains showing substantially advanced stages of maturation as compared to C3H that lagged behind. These data suggested that the genetic elements, which control the primary structural attributes of bone quality are recapitulated during fracture healing and can be easily assessed in the temporal window of fracture healing. These data indicate that the basic temporal and quantitative attributes of endochondral bone formation during fracture healing are genetically regulated. Finally, we show that the rate of bone healing is not simply related to variability in bone quality but is also controlled by other factors associated with genetic variability intrinsic to endochondral bone formation.

Disclosures: **L.C. Gerstenfeld**, None.

SA102

See Friday Plenary number F102.

SA103

The Effects of Ovariectomy on Bone Quality of *Hrk*-Deficient Mice. L. M. Wise¹, B. Sukhu^{*1}, A. Benito^{*2}, G. Nunez^{*2}, A. Jurisicova^{*1}, M. D. Grynpas¹. ¹Samuel Lunenfeld Research Institute, University of Toronto, Toronto, ON, Canada, ²Department of Pathology & Comprehensive Cancer Center, University of Michigan Medical School, Ann Arbor, MI, USA.

Hrk and *Bax* are pro-apoptotic members of the *Bcl-2* gene family. Aged *Bax*-deficient mice exhibit a phenotype in ovarian reserve, which subsequently impacts on bone quality. We have previously shown that young *Hrk*-knockout (KO) mice also display alteration of bone quality, likely caused by increased osteoblast survival. Given the known relationship between *Hrk* and *Bax*, and the observed ovarian reserve phenotype in *Bax*-KO mice, the effect of ovariectomy on *Hrk*-KO is the focus of this work. Groups of KO (n=9) and WT (n=13) mice were ovariectomized (OVX) at 3 months of age, aged further for 3 extra months, and compared to intact age-matched control KO (n=10) and WT (n=12) females. Dual energy x-ray absorptiometry was performed on all mice to determine bone mineral density (BMD). Structural and turnover parameters were evaluated using histomorphometry on sections of undecalcified distal femora. To evaluate mechanical properties, 3-point bending, torsion testing and femoral neck fracture were performed on the femora, while unilateral compression was performed on the 5th lumbar vertebrae. The expected reduction in overall BMD due to OVX was observed in both WT (-6%) and KO (-8%) mice. However, bone mineral content in KO mice was unaffected due to OVX whereas the WT showed a 10% decrease. Structural and turnover parameters were also largely unaffected by OVX in KO mice, while WT mice experienced a significant reduction in both trabecular bone volume (-29%) and trabecular number (-27%). Mechanical tests on femora indicate that although the OVX reduced some mechanical properties in both WT and KO mice, KO cortical bone was significantly more affected by the OVX (for example, bending toughness; -58% versus -33% in WT). Vertebral compression showed similarly reduced mechanical properties in trabecular bone due to OVX in both WT and KO mice. Although both WT and KO mice experienced a similar reduction in BMD, the OVX did not cause a reduction in absolute mineral content in KO mice. Further, the OVX did not cause the expected structural effects on KO trabecular bone. By contrast, the mechanical properties of KO cortical bone were significantly more affected by OVX. Thus, the decreased mechanical integrity is likely due to the inherent material properties of bone; while more mineral may be present, it perhaps may not be properly packed within the organic matrix. As such, bone material properties will be further evaluated using back-scattered electron imaging and x-ray diffraction techniques.

Disclosures: **L.M. Wise**, None.

SA104

See Friday Plenary number F104.

SA105

Detecting BMD and Bone Size QTL Using a Cross of MRL and CAST Inbred Strains of Mice Both of Which Exhibit High BMD. H. Yu¹, S. Mohan¹, B. Edderkaoui¹, G. Masinde^{*1}, J. E. Wergedal¹, W. Beamer², D. J. Baylink¹. ¹JLP VAMC and LLU, Loma Linda, CA, USA, ²Jackson Labs, Bar Harbor, ME, USA.

Previous studies to identify genetic loci involved in BMD regulation involved the use of inbred strains of mice with high BMD and low BMD for generating F₂ mice. We have used a similar strategy and identified several BMD QTL using crosses involving high BMD CAST/EiJ (CAST) and low BMD C57BL/6J (B6) as well as high BMD MRL/MpJ (MRL) and low BMD SJL/J (SJL) mice. The identified QTL were contributed not only by alleles from a high BMD parent strain but also by alleles from a low BMD parent strain. In this study, we tested the hypothesis that novel QTL can be identified using a cross of two inbred strains of mouse (MRL and CAST), both of which exhibit high BMD. To this end, we generated 328 MRL X CAST F₂ (171 female and 157 male) mice and measured femur BMD and periosteal perimeter (Ppm, a measure of bone size) using pQCT. Whole genome genotyping was performed using 86 microsatellite markers at 10 - 15 cM intervals. QTL analysis was carried out using the interval mapping and permutation test options of MapQTL.

Phenotype	Marker	Position (cM)	LOD Score (P)	Source
BMD	D10Mit31	36	3.44 (<0.05)	CAST
BMD	D15Mit115	24	2.66 (<0.05)	MRL
P.Pm	D2Mit411	77.6	2.97 (<0.05)	MRL
P.Pm	D9Mit336	35	3.46 (<0.01)	MRL
P.Pm	D19Mit17	43	2.18 (<0.05)	MRL

Comparison of identified QTL in this cross with those obtained in earlier B6 X CAST and MRL X SJL crosses revealed the following: 1) The major BMD QTL on chromosome (chr) 1 detected using B6 X CAST or MRL X SJL crosses could not be found using an intercross between MRL X CAST, suggesting that this locus may be present in the both high BMD strains. 2) A new BMD QTL on chr 10 was identified in the MRL X CAST cross that was not present in either MRL X SJL or B6 X CAST crosses, indicating that novel QTL could be identified under different genetic backgrounds. 3) The Chr 2 and 9 QTL for bone size were similar to those detected in MRL X SJL cross, but Chr 19 bone size QTL was new. In conclusion: 1) our data demonstrate the utility of crosses involving two inbred strains of mice both of which exhibit similar phenotype in identification of novel QTL for a phenotype of

interest; and 2) the QTL data generated from various inbred strain crosses should be used in the future identification of candidate gene using SNP haplotype analysis or other techniques once the genomes of various inbred strains of mice are fully sequenced.

Disclosures: **H. Yu**, None.

SA106

see Friday Plenary number F106.

SA107

Verification and Fine Mapping of a Chromosome X QTL that Influences Femoral Cross-sectional Geometry and Bending Strength in Mice. **R. F. Klein, D. C. Dinulescu*, E. A. Larson*, T. G. Munsey*, J. N. Kansagor*, C. Vanek, D. A. Olson*, J. K. Belknap*, E. S. Orwoll.** Bone and Mineral Unit, Oregon Health & Science University, Portland, OR, USA.

Size and shape are critical determinants of the mechanical properties of skeletal elements and are highly heritable. In previous studies, using an F_2 intercross between C57BL/6J (B6) and DBA/2J (D2) mouse strains, we have described 4 quantitative trait loci (QTL) that contribute to natural variation in femoral cross-sectional moment of inertia (CSMI) - a composite biomechanical measure of the size, shape and distribution of bone mass around the longitudinal axis of the femur. One of these QTL resides within chromosome X (Chr X) and contributes a substantial proportion of the geometric and biomechanical variation between B6 and D2 femora. Selective breeding was used to transfer the chromosomal fragment containing the Chr X QTL interval from a B6 onto a D2 genetic background. Comparison of the resulting congenic mouse strain with the background D2 strain established that a 150 megabase (Mb) B6 genomic interval of Chr X in isolation confers increased mid-shaft femoral CSMI ($0.085 \pm 0.002 \text{ mm}^2$ vs. $0.075 \pm 0.002 \text{ mm}^2$, $p < 0.0001$). In order to confirm and narrow the location of CSMI QTL gene(s), we developed 4 subcongenic lines that contain different regions that provided overlapping coverage of the Chr X QTL region. Phenotypic analyses indicated that 20-week-old congenic mice bearing a 60 Mb region of B6 genomic material between *DXMit144* and *DXMit117* exhibited 16% greater ($p < 0.0001$) CSMI compared to control D2 mice. There were no differences in the QTL effect or position between males and females. Consistent with the increased CSMI, these Chr X congenic mice also showed a 5% increase ($p < 0.005$) in femoral cortical area, 17% increase ($p < 0.005$) in femoral marrow area and 6% increase ($p < 0.005$) in femoral ultimate failure load compared to control mice. The improved femoral cross-sectional geometry and resistance to bending of the congenic mice was not accompanied by changes in body weight, whole body BMD, femoral length or cortical thickness. Our data, using interval-specific congenic mice bred by introgressing a chromosomal region from the B6 donor strain into the D2 strain of contrasting phenotype, offer potentially much more precise QTL localization by establishing definitive limits for the Chr X region containing a femoral CSMI QTL. Ultimately, these congenic strains will provide an invaluable resource for further defining specific aspects of genetic architecture (e.g., mode of inheritance, gene order, gene-gene and gene-environment interactions, etc.) and for in depth studies of the mechanisms by which the Chr X QTL gene (or genes) affect skeletal development.

Disclosures: **R.F. Klein**, Merck & Co. 8; Sanofi-Aventis 8; Procter & Gamble 8; Eli Lilly 8.

SA108

Analysis of Global Expression of *MEN1* Gene Expression by Ribozymes and siRNAs in Cultured Cells. **A. Falchetti, E. Luzi*, I. Tognarini*, F. Marini*, G. Galli*, A. Carossino*, L. Masi, M. Brandi.** Internal Medicine, University of Florence, Florence, Italy.

Multiple endocrine neoplasia type 1 (MEN1) is characterized by the occurrence of tumors of the parathyroids, endocrine pancreas, and the anterior pituitary, including more than 20 other endocrine and nonendocrine tumor combinations. *MEN1* gene, a tumor suppressor gene encodes a protein, menin, with a molecular mass of 67 kDa. Loss of heterozygosity (LOH) at 11q13 has been found in MEN1 tumors, but also in sporadic pituitary tumors and in 30-70% of sporadic parathyroids and endocrine pancreas tumors, a subset of those with LOH at 11q13 exhibiting mutations in the *MEN1* gene. MEN1 mRNA and protein are expressed in all normal studied tissues, leaving the basis for endocrine predominance of neoplasia unexplained. Mutations in the *MEN1* gene frequently predict protein truncation possibly leading to inactivated function consistent with the idea of a tumor suppressor gene as mouse models further support. It has been shown that menin interacts with AP-1 transcription factor JunD, Smad3 and inhibits NF κ B-mediated transactivation. Moreover, it has been shown that menin also interacts with p53, nm23, GFAP, the 32-kDa subunit of REPA, and nonmuscle myosin II-A heavy chain. Menin uncouples Elk-1, JunD, and c-Jun phosphorylation from MAPK activation. Furthermore, overexpression of menin suppresses insulin-induced AP-1 activity in CHO-IR cells, expressing high levels of insulin receptor, and c-Fos induction at the transcriptional level. However, the effects of *MEN1* in human neuroendocrine cells and its role in gene regulation remain elusive. We begun to study the role of *MEN1* gene, its mRNA and menin protein in the global gene expression network in fibroblasts from MEN1 patients both with heterozygote truncating mutation of gene and from healthy individuals. Preliminary data show that no differences exist in protein expression in both affected and unaffected subjects, suggesting that the wild-type allele could compensate for a similar level of menin expression. Currently, we have designed specific ribozymes and siRNAs against different target along MEN1 mRNA in order to downregulate the wild-type allele and to obtain informations on the MEN1 mRNA gene transcription regulation levels.

Disclosures: **E. Luzi**, None.

SA109

High-Throughput Functional and Morphological Phenotyping of 2,000 Murine Femora. **G. H. van Lenthe¹, T. Kohler^{*1}, R. Voide^{*1}, L. R. Donahue², R. Müller¹.** ¹Institute for Biomedical Engineering, ETH and University Zurich, Zurich, Switzerland, ²The Jackson Laboratories, Bar Harbor, ME, USA.

The gold standard to determine bone strength is experimental biomechanics. However, it has its limitations, as it is a destructive test, laborious, and prone to errors, especially when testing small bones. Therefore, we recently used microstructural finite element analysis to determine bone strength directly from bone structure. We have applied this technique to femora of two murine growth-hormone (GH) deficient inbred strains (B6-*lit/lit* and C3H-*lit/lit*), and to their wild-type counterparts (B6-*lit/+* and C3H-*lit/+*). We found that GH had a sex-specific action on bone strength (Fig. 1), increasing strength more in males than in females. To further investigate the genetics causing the non-GH related differences in bone strength, an F2 population of 2,000 mice was produced based on the two GH-deficient parental strains.

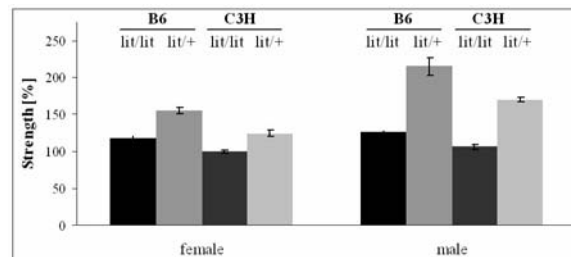


Figure 1: Femoral neck strength for two growth-hormone deficient inbred strains of mice, and of their wild-type counterparts

At four months of age, all 2,000 femora were μ CT scanned using a 20 μ m resolution. After automated alignment, microstructural finite element models were automatically created from which strength was calculated. In addition, morphometric parameters were calculated for different volumes of interest: whole bone, distal metaphysis, and femoral neck. As expected, we found large variations between femora and most parameters had a Gaussian distribution. On average, males had stronger femora than females. Interestingly, bone strength was not highly correlated to bone mass, but to femoral neck volume. We showed that high-throughput characterization of murine femora is now possible, allowing scanning, morphometric and functional analysis of 70 femora per day. The functional and morphological data obtained in this study, in combination with data on genomic markers that has been acquired for all 2,000 mice, will allow us to locate genetic loci for bone volume and other architectural parameters. Even more so, it will allow us to locate genetic loci for bone strength directly, rather than the fore-mentioned surrogate markers of bone strength.

Disclosures: **G.H. van Lenthe**, None.

SA110

See Friday Plenary number F110.

SA111

Test of Linkage and Association of 14 Genetic Loci with Bone Size. **H. Lau^{*1}, M. Ng^{*1}, L. Jin¹, A. Paterson^{*2}, P. Sham^{*3}, K. Luk^{*4}, V. Chan^{*1}, A. Kung¹.** ¹Medicine, The University of Hong Kong, Hong Kong, China, ²Program in Genetics and Genomic Biology, University of Toronto, Toronto, ON, Canada, ³Genome Research Centre, The University of Hong Kong, Hong Kong, China, ⁴Department of Orthopaedic Surgery & Traumatology, The University of Hong Kong, Hong Kong, China.

Bone size is an important independent contributor to bone strength, a determinant of osteoporotic fracture. To evaluate the genetic determinants of bone size, linkage and/or association of 14 polymorphic loci of 8 candidate genes were studied in 177 southern Chinese pedigrees of 674 subjects (567 females and 107 males). Four skeletal sites were studied, including the L1-4 lumbar spine, trochanter, femoral neck and total hip region. Age, sex, height and weight were included as covariates in the analysis. The candidate genes studied include estrogen receptor alpha (ER α) and beta (ER β), calcium sensing receptor (CASR), vitamin D receptor (VDR), collagen type I α 1 (COL1A1), LDL receptor-related protein 5 (LRP5), transforming growth factor β 1 (TGF β), and parathyroid hormone receptor 1 (PTH1R). Multi-point variance component linkage analysis was performed using the MERLIN program. Linkage was observed between D14S1026 genotypes of ER β with total hip area; CASR genotypes with femoral neck bone area; 266A/G, 2220C/T and 3989C/T genotypes of LRP5 with total hip bone area. Association of bone size was determined using the quantitative transmission disequilibrium test (QTDT). After covariates adjustment, total family association revealed significant association of D14S1026 genotypes of ER β with spine, trochanter and total hip bone area; D3S1289 genotypes with femoral neck, trochanter and hip region bone area; and CASR genotype with femoral neck and total hip bone area. These results were also seen when only the females were studied. In addition, 2T/C of VDR was associated with spine bone area in all subjects while 266A/G of LRP5 was associated with total hip bone area when the females were analysed separately. When all subjects were analysed, significant within-family association was detected between D14S1026 genotypes of ER β with spine bone area. Overall, these data suggested ER β , CASR and LRP5 are important candidate genes for determining bone size variation. In addition, VDR gene and D3S1289 may also contribute to bone size variation.

Disclosures: **L. Jin**, None.

SA112

See Friday Plenary number F112.

SA113

Genetic Effects on Bone Loss in Peri- and Post-Menopausal Women: A Longitudinal Twin Study. J. MAKOVEY^{*1}, V. Naganathan², T. V. Nguyen³, P. Sambrook¹. ¹Department of Rheumatology, Institute of Bone and Joint Research, Royal North Shore Hospital, University of Sydney, Sydney, Australia, ²Centre for Education and Research on Ageing, Concord Hospital, University of Sydney, Sydney, Australia, ³Bone and Mineral Research Program,, Garvan Institute of Medical Research, Sydney, Australia.

Cross-sectional twin and family studies have shown that bone density variance is mainly under genetic influences. The relative magnitude of genetic and environmental components on bone loss variance however is not clear. The aim of this study was to assess the heritability of bone loss in peri- and post-menopausal women. A sample of 176 pairs of twins (88 MZ and 88 DZ), (mean age 57 years (range: 45 - 57)) were seen. Each individual had base line BMD measurements at lumbar spine and the femoral neck measured by a HOLOGIC QDR-4500W bone densitometer and a repeat measure, on average 3.9 years (range: 1 - 7.5 years) later. Change in BMD (dBMD) was expressed as percent gain or loss per year. Intraclass correlation coefficients in dBMD were calculated for MZ and DZ pairs. Genetic model-fitting analysis was used to partition the total variance of dBMD into three components: genetic component (G), common environmental component shared by the twins (C), and specific environmental component, including measurement error (E). The index of heritability was estimated as the ratio of genetic variance over total variance. The mean (\pm SD) of annual change in BMD was -0.42 ± 1.4 at the lumbar spine and -0.31 ± 1.28 at the femoral neck. There was no significant difference in rate of bone loss between MZ and DZ twins. At the lumbar spine the intraclass correlation in MZ twins (0.39) was significantly higher than in DZ twins (0.19). However, at the femoral neck the intraclass correlation was low in both MZ twins (0.09) and DZ twins (0.00). Results of genetic model-fitting analysis indicated that the index of heritability for dBMD at the lumbar spine was 0.4. There was, however, no significant genetic effect on dBMD at the femoral neck. These data suggest that although genetic effects on bone loss with ageing are less pronounced than those on peak bone mass, they still account for approximately 40% of the between-individuals variation in bone loss at the lumbar spine in pre- and post-menopausal women.

Disclosures: **J. Makovey**, None.

SA114

See Friday Plenary number F114.

SA115

Lean Mass Plays a Significant and Sex-Specific Role in Resemblance for Femoral Neck Bone Mineral Density in Parent-Offspring Pairs. H. Blain^{*1}, A. Vuillemin^{*2}, E. Le Bihan^{*3}, F. Guillemin^{*2}, P. Jouanny^{*4}, E. Blotman⁵, C. Jeandel^{*1}. ¹Department of Internal Medicine and Gériatrics, Centre Antonin Balmes, Montpellier, France, ²Department of Clinical Epidemiology, Henri Poincaré University, Nancy, France, ³Department of Clinical Epidemiology,, Henri Poincaré University, Nancy, France, ⁴Department of Internal Medicine and Gériatrics, University Hospital, Rennes, France, ⁵Department of Rheumatology, University Hospital, Montpellier, France.

The aim of the present study was to examine the respective influence of heritable anthropometric factors on familial association in femoral neck bone mineral density (FN BMD) in a healthy community-dwelling sample constituted of 173 parent-child pairs, including 86 mother-daughter, 32 mother-son, 32 father-daughter, and 23 father-son pairs from 128 families. Pearson's correlations were used to examine parent-offspring associations in FN BMD and other factors. Multivariate regressions were performed in a Bayesian frame. Heritability (h^2) is defined as the regression coefficient of the mean of the parent's BMD. After adjustment for parents and children's age, smoking habits, calcium and alcohol intake, physical activity, as well as menopause and hormonal replacement therapy, if relevant, heritability estimates for FN BMD were found to be significant in father-daughter ($h^2 = 0.68$), mother-daughter ($h^2 = 0.40$), and in mother-son pairs ($h^2 = 0.23$), but not significant in father-son pairs. The lean mass of mothers and sons was not intercorrelated, but adjustment for the lean mass of the sons dramatically enhanced FN BMD h^2 in mother-son pairs (from 0.23 to 0.61). The lean mass of mothers and daughters was strongly intercorrelated, and adjustment for the lean mass of the daughters strongly reduced the FN BMD h^2 (from 0.40 to 0.23). Adjustment for fat mass and height of children did not affect the heritability estimates. In conclusion, anthropometric parameters are not involved in the heritability of FN BMD in father-daughter pairs or in the lack of heritability of FN BMD in father-son pairs. Lean mass resemblance between mothers and daughters plays a important role in the significant FN BMD heritability in mother-daughter pairs. Lean mass, which is not significantly correlated in mother-son pairs, plays a significant role in the heritability of FN BMD in mother-son pairs, suggesting that a low FN BMD has to be sought in sons of women with low FN BMD, particularly if the lean mass of sons and mothers is low.

Disclosures: **H. Blain**, None.

SA116

See Friday Plenary number F116.

SA117

Relationships between Quantitative Ultrasound and Vitamin D Receptor Gene in a Geographical Isolated Population From Lampedusa Island. C. Cepollaro¹, A. Falchetti¹, C. Sferrazza², A. Gozzini^{*1}, L. Masi¹, N. Napoli², G. Di Fede^{*2}, V. Cannone^{*2}, G. Cusumano^{*2}, M. C. Pandolfo^{*2}, G. B. Rini², A. Tanini¹, M. L. Brandi¹. ¹Department of Internal Medicine, University of Florence, Florence, Italy, ²Department of Internal Medicine, University of Palermo, Palermo, Italy.

Quantitative ultrasound (QUS) has been proposed as an alternative method for non invasive assessment of bone status, as it reflects both bone mass and qualitative aspects of bone. QUS may predict the risk of fracture independent of bone density. It has been suggested that heritability estimates of the QUS parameters are comparable with those of bone mineral density (BMD). However, in contrast to the many reports using BMD, genetic studies using QUS measurements are extremely rare. Several candidate genes have been proposed to be involved in the pathogenesis of osteoporosis, such as vitamin D receptor (*VDR*) gene. Genetic dissection of a multifactorial disease, such as osteoporosis, has taken advantage by several analytical models; one of the most promising genetic approach in complex diseases is represented by isolated population studies. The aim of our study was to investigate the association between QUS and polymorphism of VDR in a geographical isolated population from Lampedusa Island. Total population of Lampedusa consists of 5908 individuals with 2867 women. We analyzed 424 women (14,8% of total female population), 277 postmenopausal and 147 non-menopausal, for *VDR-FokI* genotypes. Allelic frequencies determined by *VDR-FokI* polymorphism were equal to 49% for the F allele and 51% for the f allele. Thus, *FF*, *Ff* and *ff* genotypes frequencies were 33,17 %, 32,69%, 33,89%, respectively. QUS at calcaneus were obtained in the study population by DTU-one (Osteometer Meditech, Hawthorn, CA, USA). Measurements were made at the right calcaneus, unless foot deformity or oedema precluded measurement in which cases the left heel was used. In order to assess the precision, two consecutive measurements were made in 30 healthy women, repositioning the foot between each measurement. The precision error was 0.4% and 1.2% for SOS and BUA, respectively. ANCOVA analysis was performed to evaluate the association of genotypes with ultrasound parameters (SOS and BUA). After adjustment for potential confounders (age, height, weight, YSM, calcium intake), SOS and BUA showed a significant relationship with *FOKI* genotypes ($p < 0.001$). In particular, women with *ff* genotype exhibited a significant lower SOS and BUA, when compared to *Ff* and *FF* genotypes. The strong association that we have found between *FOKI VDR* polymorphism and QUS parameters may suggest that such polymorphism could be associated not only with bone mineral content, but also with bone quality.

Disclosures: **C. Cepollaro**, None.

SA118

Identification of Gain Function Mutation in the Calcium-Sensing Receptor in an Italian Family with Autosomal Dominant Hypocalcemia. L. Masi¹, G. Leoncini^{*1}, E. Procopio^{*2}, A. Amedei^{*1}, A. Falchetti¹, R. Imbriaco^{*1}, R. Livi^{*1}, A. Tanini¹, M. L. Brandi¹. ¹Department of Internal Medicine, University of Florence, Florence, Italy, ²Department of Pediatric, University of Florence, Florence, Italy.

The calcium sensing receptor (CaR) was first identified in the parathyroid cells and was later found to be expressed in the kidney and other tissues. The human CaR gene encodes a polypeptide of 1078 amino acids. Inactivating mutations in the CaR gene are responsible of an elevation in extracellular calcium, leading to mild moderate hypercalcemia and relative hypocalciuria called Familial Hypocalciuric Hypocalcemic (FHH). Conversely, activating mutations in the CaR gene are associated with reverse phenotype, autosomal dominant hypocalcemic (ADH) and a sporadic hypoparathyroidism. So far, about 20 activating mutations in the CaR gene have been identified. Recently a Ser⁸²⁰Phe mutation in the CaR has been described in Japanese family. In the present study we described an Italian family affected by ADH in whom a CaR mutation was identified. The proband was a girl 13 year old affected by a mild hypocalcemia and hypercalciuria with normal range value of PTH. She underwent a computed tomographic examination of the brain because of headache which showed the presence of calcificatin of the basal ganglia. In addition a juvenile hypertension was present in the proband. Baseline biochemical data of the family members showed a mild hypocalcemia and hypertension in the mather and two of four uncles. Genomic DNA of all subjects was extracted from white blood cells with standard procedure. In the proband, all protein-coding exons (exons 2-7) of the CaR gene were amplified by PCR with standard procedures using primer pairs as described in the literature. Nucleotide sequences of both strands of the PCR products were determined by direct sequencing with a DNA kit and an automated DNA sequencer (ABI PRISM 3100, Perkin-Elmer Corp). A Ser⁸²⁰Phe activating mutation of the CaR was found. In summary, we have idenfied the Ser⁸²⁰Phe activating mutation in a Italian family affected by Hypertension and ADH.

Disclosures: **L. Masi**, None.

SA119

Polymorphisms of the Growth Hormone Receptor, Growth Hormone Secretagogue Receptor and Growth Hormone Releasing Hormone Genes Are Associated with Bone Mass: The Hertfordshire Cohort Study. E. M. Dennison^{*1}, H. E. Syddall^{*1}, I. N. M. Day^{*2}, T. R. Gaunt^{*2}, S. Rodriguez^{*2}, C. Cooper¹. ¹MRC Epidemiology Resource Centre, University of Southampton, Southampton, United Kingdom, ²Human Genetics Division, University of Southampton, Southampton, United Kingdom.

We have previously demonstrated relationships between single nucleotide polymorphisms in the growth hormone gene and adult bone mass in a UK population. Here we report associations between polymorphisms of the growth hormone receptor, growth hormone secretagogue receptor and growth hormone releasing hormone genes with bone mass in an extension to the original study. Four hundred and ninety eight men and 468 women aged 59-71 years living in Hertfordshire, UK were recruited. A lifestyle questionnaire was administered and bone mass at the lumbar spine and femoral neck measured using a Hologic QDR 4500 instrument. DNA was obtained from whole blood samples using standard extraction techniques. Single nucleotide variants in the growth hormone receptor gene (coded GGHRV12), the growth hormone secretagogue receptor gene (coded GGHSRV02), and the growth hormone releasing hormone gene (coded GGHRHV10) were analysed. Ethical approval was obtained, and the study conducted in accordance with the Declaration of Helsinki. Among men, GGHRHV10 12 heterozygotes had higher bone mineral content (BMC) and bone mineral density (BMD) at the total femur than GGHRHV10 11 homozygotes (test for trend BMC p=0.02, BMD p=0.12, fully adjusted for age, social class, body mass index, physical activity, calcium intake, cigarette and alcohol consumption). Similar relationships were observed in women at the lumbar spine (mean BMC lumbar spine GGHRHV10 11 genotype = 56.9g, GGHRHV10 12 genotype = 68.4g, p<0.001, fully adjusted; mean BMD lumbar spine GGHRHV10 11 genotype = 0.96g/cm², GGHRHV10 12 genotype = 1.10 g/cm², p<0.001 fully adjusted). Among men, individuals of genotype GGHRV12 22 had higher BMC and BMD at the lumbar spine than those of GGHRV12 11 or GGHRV12 12 genotype (test for trend BMC p=0.05; BMD p=0.03, fully adjusted). No such relationships were observed among women. Finally, among men, individuals of genotype GGHSRV02 22 had lower BMC and BMD at the lumbar spine than those of GGHSRV02 11 or GGHSRV02 12 genotype (test for trend BMC p=0.09, BMD p=0.12, fully adjusted). Again, no such relationships were observed among women. We have demonstrated relationships between polymorphisms of the growth hormone receptor, growth hormone secretagogue receptor and growth hormone releasing hormone genes with bone mass in a UK cohort that varied according to sex; we hypothesize that this sexual dimorphism may reflect a greater effect of genotype on peak bone mass than bone loss.

Disclosures: **E.M. Dennison**, None.

SA120

See Friday Plenary number F120.

SA121

Intron 1 Polymorphism (A/C) of *FDPS* Gene: A New Genetic Marker for N-BPs Therapy Response? S. Carbonell Sala^{*}, A. Falchetti, V. Martineti^{*}, F. Marini^{*}, F. Del Monte^{*}, L. Masi, N. Fossi^{*}, A. Amedej^{*}, F. Franceschelli^{*}, A. Tanini, M. Brandi. Internal Medicine, University of Florence, Florence, Italy.

Bisphosphonates (BPs) are potent inhibitors of the bone osteoclast-mediated resorption. They are usually divided in two main pharmacological classes: those who inhibit protein prenylation (amino-bisphosphonates, N-BPs) and those who are metabolized to ATP analogues (not N-BPs). Recent studies have found that N-BPs can specifically inhibit some enzymes of the intracellular mevalonate pathway required for prenylation, post-translation lipid modification of different signaling proteins (small GTPases). Their inactivation could therefore explain at least in part the cellular effects of BPs. However, the existence of not responders to N-BPs therapy, the variability on therapy response and the tendency to develop adverse events remain to be determined. The aim of this project is the polymorphism analysis of farnesyl pyrophosphate-synthase (*FDPS*) gene to assess genetic aspects of N-BPs response. We evaluated the genotype distribution for A/C polymorphism, located on intron 1 of *FDPS* gene, in Italian population. Our findings show that A allele frequency is 0.82, while C allele frequency is 0.18, with an heterozygosity index of 0.2981 (χ^2 Test p=0.29). As it was already showed for other genes involved in bone metabolism, also these *FDPS* genotypes distribution data are opposed to the ones described in Japanese population. The polymorphism information content of this marker is informative (PIC=0.29). Our future goal is to perform a case-control study with patients involved on clinic trials with N-BPs, searching the eventual correlation between polymorphism and therapy response, in order to early identify the subjects that could benefit BPs therapy, and patients genetically susceptible to develop adverse events.

Disclosures: **S. Carbonell Sala**, None.

SA122

See Friday Plenary number F122.

SA123

Polymorphisms of VDR, COL1A1 and ESR1 Genes and Bone Mineral Density in Men in Polish Population - The EPOLOS Study. M. Kruk^{*1}, M. Jaworski^{*1}, J. Lukaszewicz^{*2}, E. Karczmarewicz^{*1}, P. Bilinski^{*3}, E. Czerwinski^{*4}, A. Lewinski^{*5}, E. Marcinowska-Suchowierska^{*6}, A. Milewicz^{*7}, M. Spaczynski^{*8}, A. G. Uitterlinden⁹, R. S. Lorenc¹. ¹Dept. of Bioch. and Exp. Med., The Children's Memorial Health Institute, Warsaw, Poland, ²Dept. of Bioch., Pharm. Div., Medical Academy, Warsaw, Poland, ³Clinic of Orthopaedy and Traum., The Rydygier Medical University, Bydgoszcz, Poland, ⁴Dept. of Orth., Jagiellonian University, Cracow, Poland, ⁵Dept. of Thyroidology, Clinical Hospital No 3, Lodz, Poland, ⁶Dept. of Int. Med., The Orłowski Hospital, Warsaw, Poland, ⁷Endocrinology and Diabetology, University of Medicine, Wrocław, Poland, ⁸Dept. of Gynecology, The Marcinkowski University, Poznan, Poland, ⁹Dept. of Internal Medicine, Erasmus MC, Rotterdam, The Netherlands.

The aim of this study was to verify if polymorphisms of VDR, COL1A1 and ESR1 genes are accompanied by variation in BMD at different measurement sites in a large Polish cohort of men. The study group comprised 532, adult males (age range 20-80 years), randomly selected in 7 centres from the Polish population. DNA was isolated from peripheral blood with using Gentra Isolation Kits. Polymorphisms were evaluated with RFLP technique, and determined by restrictive enzymes: BsmI (VDR), Van91I (COL1A1, Sp1 binding site polymorphism), and PvuII and XbaI simultaneously (ESR1). BMD of the Femoral Neck, Trochanter, Total Hip and Lumbar Spine L2-L4 were evaluated by DXA (Lunar DPX-L). Subjects with systemic disorders were excluded for the statistical examination (ANOVA). The frequency of VDR genotypes was [bb] 37%, [Bb] 40.6%, [BB] 22.4% with allele (b) 57.2%, allele (B) 42.8%. The frequency of COL1A1 genotypes was [GG] 65.9%, [GT] 30.7%, [TT] 3.4% with allele (G) 81.2%, allele (T) 18.8%. The frequency of ESR1 genotypes was [px.px] 23.6%, [px.PX] 37.5%, [PX,PX] 16.3%, [PX,Px] 9.6%, [Px,px] 12.1%, [Px,Px] 0.9%, with haplotypes px (1) =48.4%, PX (2)=39.8%, Px (3)=11.8%, pX (4) haplotype was not found. There was no observed association between the VDR BsmI variation and BMD values for any site. For COL1A1 gene an association between Sp1 binding site polymorphism and BMD in femoral neck was found. Carriers of the G allele had 8.4% higher BMD values (p<0.03, normalized for age,) compared to [TT] non-carriers. Analysis of ESR1 gene polymorphisms showed that carriers of the PX (2) haplotype have 3.6% higher BMD values for Total Hip (p<0.04) and 4.6% for Trochanter (p<0.01), both normalized for age. None of investigated polymorphisms was associated with BMD at the Lumbar Spine. We conclude that the COL1A1 Sp1 G allele and the ESR1 haplotype 2 (PX) allele are associated with higher BMD in men from the Polish population, at several hip locations, but not at the lumbar spine.

Disclosures: **M. Kruk**, None.

SA124

Lysophosphatidic Acid Stimulates the Motility of MC3T3-E1 Osteoblastic Cells. J. S. Fotos^{*1}, D. S. Galileo^{*1}, N. J. Karin². ¹Biological Sciences, University of Delaware, Newark, DE, USA, ²Biological Sciences Division, Pacific Northwest National Laboratory, Richland, WA, USA.

Lysophosphatidic acid (LPA), a bioactive lipid generated by degranulating platelets during blood clot formation, is postulated to regulate angiogenesis and wound healing. LPA has growth factor-like actions on a variety of cell types but little is known about its potential role as a regulator of bone cell function. We previously reported that LPA is a potent Ca²⁺ signaling agonist in MC3T3-E1 cells, and that this signaling was blocked by pertussis toxin, consistent with a requirement for G protein-coupled receptors (GPCR) in LPA function. LPA has been shown to enhance the migration of endothelial and cancer cells but it is not known if this lipid can alter osteoblast motility. We used quantitative time-lapse video micrography to analyze the migration of MC3T3-E1 cells after linear wounds were introduced into cell monolayers. LPA-treated cells refilled the wounds to a much greater extent than control osteoblasts, exhibiting a two-fold increase in the average migration distance per cell. Lipid treatment also elicited substantial changes in cell shape and actin cytoskeletal structure. LPA-treated cells contained fewer stress fibers and possessed long membrane processes that were enriched in F-actin. RT-PCR analysis showed that MC3T3-E1 cells express all four known LPA-specific GPCR (LPA₁-LPA₄) with a relative mRNA abundance of LPA₁ > LPA₂ > LPA₄ >> LPA₃. LPA-induced increases in osteoblast motility were antagonized by both pertussis toxin and Ki16425, a subtype-specific blocker of LPA₁ and LPA₃. In parallel with its effect on osteoblast migration, Ki16425 also inhibited LPA-induced Ca²⁺ signaling in a dose-dependent manner. Alendronate, which inhibited the LPA-induced migration of ovarian cancer cells, had no effect on the ability of LPA to stimulate osteoblast motility. Our data show that LPA stimulates osteoblast motility via a mechanism that is linked to GPCR, particularly LPA₁, and possibly Ca²⁺ signaling. We postulate that LPA is among the platelet-derived factors that promote osteoblast migration during bone fracture healing.

Disclosures: **N.J. Karin**, None.

SA125

See Friday Plenary number F125.

SA126

Expression and Regulation of CCN Genes in Murine Osteoblasts. M. S. Parisi*, E. Gazzero, S. Rydzziel, E. Canalis. Research, Saint Francis Hospital and Medical Center, Hartford, CT, USA.

Members of the CCN family of genes include cysteine-rich 61 (CYR61), connective tissue growth factor (CTGF), nephroblastoma overexpressed (NOV), and Wnt-induced secreted proteins (WISP) 1, 2 and 3. CCN proteins are related to the insulin-like growth factor binding proteins (IGFBP), and to antagonists of Wnt and bone morphogenetic proteins (BMP), but their function in skeletal tissue is unknown. In an initial effort to assess the role of CCN proteins in the skeleton, we examined the expression and regulation of CCN genes in primary cultures of murine osteoblasts treated with transforming growth factor β (TGF β), BMP-2 and cortisol. Northern blot analysis revealed the presence of CYR61, CTGF, NOV and WISP 1 and 2 transcripts in murine osteoblasts. WISP 3 transcripts were not detected. Continuous treatment of osteoblasts with TGF β at 2 nM and BMP-2 at 3.3 nM caused a time-dependent increase in CYR61, CTGF and WISP 1 and 2 mRNA levels. TGF β treatment decreased NOV transcripts. The stimulatory effect was observed after 2 to 6 h of exposure to TGF β or BMP-2, whereas the decrease in NOV mRNA caused by TGF β occurred after 24 h. Treatment with cortisol at 1 μ M for 2 to 6 h increased CYR61 and CTGF after 2 to 6 h, WISP 2 mRNA levels after 24 h, and decreased WISP-1 mRNA levels after 24 to 48 h, but had no effect on NOV expression. In accordance with the results obtained by Northern blot analysis, Western blot analysis of conditioned medium from osteoblast cultures showed that TGF β /BMP-2 increased the protein levels of CYR61, CTGF and WISP 1 and TGF β decreases NOV protein levels. Cortisol increased CYR61 and CTGF. Nuclear run-on assays performed on nuclei from osteoblasts treated for 2 to 6 h revealed that BMP-2 and TGF β enhanced CYR61, CTGF, and WISP 1 and 2 transcription. Suppression of NOV transcription could not be detected due to low control levels. Cortisol increased CYR61 and CTGF and decreased WISP 1 gene transcription. In conclusion, five of the six known CCN genes are expressed by osteoblasts and their expression is regulated by transcriptional mechanisms by TGF β , BMP-2 and cortisol. Consequently, CCN genes could mediate selected actions of TGF β , BMP-2 and cortisol on osteoblastic differentiation and function.

Disclosures: **M.S. Parisi**, None.

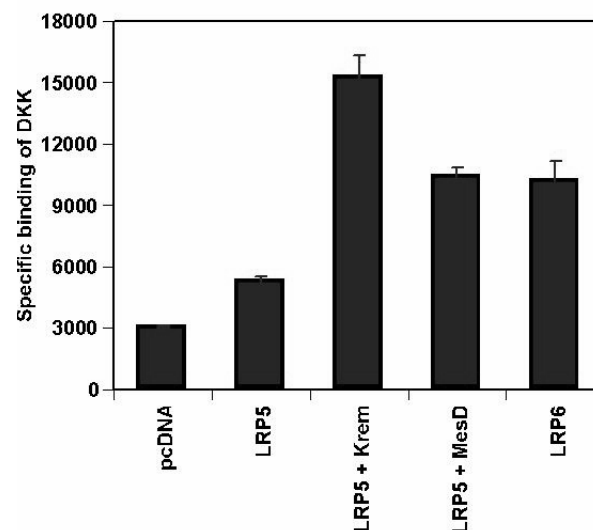
SA127

See Friday Plenary number F127.

SA128

Kremen-2 and MesD Each Enhance Binding of DKK1 to Cells Over-Expressing LRP5 in a Radioactive Binding Assay. R. J. Murrills¹, J. J. Matteo^{*1}, P. J. Yaworsky², B. M. Bhat¹, F. J. Bex¹. ¹Women's Health & Bone, Wyeth Research, Collegeville, PA, USA, ²Biological Technologies, Wyeth Research, Cambridge, MA, USA.

Wnt signaling plays a critical role in the proliferation and differentiation of osteoblasts, and involves the interaction of numerous proteins in a complex and sometimes poorly understood manner. DKK1 antagonizes Wnt signaling by binding to LRP5/6, a co-receptor for frizzled, in addition to other proteins such as Kremen. Kremen reportedly forms a ternary complex with LRP5/6 and DKK leading to internalization and depletion of surface receptors, enhancing the negative effect of DKK upon Wnt signaling. MesD is thought to function as a chaperone protein, guiding LRP5/6 proteins to the cell surface. We have investigated the effects of co-transfecting Kremen-2 or MesD on the binding of DKK1 to LRP5 and LRP6 using a whole cell binding assay. 293 cells were seeded in 48-well plates and transfected with pcDNA, LRP5 or LRP6, with or without Kremen-2 or the chaperone protein MesD. Transfected cells were rinsed and exposed to 0.4nM ¹²⁵I-labeled purified DKK1 for 3h at room temperature; non-specific binding was determined using an excess of cold DKK1. Cells transfected with pcDNA alone showed moderate binding of DKK1, consistent with the known expression of LRP5/LRP6 in 293 cells. When LRP5 was transfected alone, there was at best a modest increase in the total counts, relative to pcDNA, which contrasted with a robust increase in binding when LRP6 was transfected alone. Co-transfection of Kremen-2 and LRP5 resulted in a marked, apparently synergistic increase in the total amount of radioligand bound, which could be blocked dose-dependently by co-incubation with cold DKK1. Similarly, co-transfection of the chaperone protein MesD with LRP5 also resulted in an apparently synergistic increase in binding.



Our data suggest that (1) LRP6 binds DKK1 more strongly than LRP5 (2) Binding of DKK1 to cells expressing LRP5 can be increased either by co-transfecting kremen-2 or MesD. Further studies to control for LRP5/6 internalization or cellular redistribution will provide additional support.

Disclosures: **R.J. Murrills**, None.

SA129

See Friday Plenary number F129.

SA130

Temporal Expression of Lrp5/6, Dkk1 and Other Wnt-Signaling Components in Embryonic, Growing, and Adult Mouse Bone. W. G. Richards^{*1}, J. Pretorius^{*2}, J. Li³, D. L. Lacey¹, W. S. Simonet¹, C. Paszty¹.

¹Metabolic Disorders, Amgen, Thousand Oaks, CA, USA, ²Pathology, Amgen, Thousand Oaks, CA, USA, ³Licensing, Amgen, Thousand Oaks, CA, USA.

Gain-of-function and loss-of-function mutations in the Wnt co-receptor Lrp5 result in high and low bone mass respectively in primates and rodents. In addition, alterations in other components of the canonical Wnt signaling pathway result in increased or decreased bone mass depending upon whether Wnt signaling is activated or repressed. To strengthen our understanding of how members of the canonical Wnt signaling pathway contribute to bone mass, we used *in situ* hybridization to study the expression of the Wnt co-receptors Lrp5, Lrp6 and other modulators of Wnt signaling, Dkk1, Dkk2, Dkk3, Wif-1 and Sfrp4, during embryogenesis and in bone isolated from adolescent and adult mice. Expression of both Lrp5 and Lrp6 were detected as early as e12.5 in cartilage primordium from areas of developing bone. Lrp6, Wif-1 and Sfrp4 were observed in several tissues in the developing embryo, including bone. Dkk1 was also expressed in several regions from e11.5 to e15.5, with expression in bone first noted at e15.5. However, unlike the other molecules studied, Dkk1 expression became more restricted to bone as the embryo developed. Postnatally, in growing and adult mice Dkk1 expression was detected primarily in bone, whereas the other modulators of Wnt signaling, with the exception of Dkk2, were detected in various tissues, including bone. In the adult mouse Lrp6 expression was confined primarily to cells of epithelial origin and only limited expression was detected in adult bone. Lrp5 was more widely expressed than Lrp6 or Dkk1 in growing and adult bone. Both Lrp5 and Dkk1 expression co-localized to osteoblasts underlying the growth plate. Dkk1 expression was also detected in osteocytes within adult bone. Periosteal expression of Sfrp4 and Dkk3 were observed, whereas no expression of Dkk2 was seen in bone. Wif-1 was detected in osteoblasts and endosteal lining cells in marrow spaces throughout adult bone. Overall, the expression of these Wnt signaling components supports their role in regulating development and growth of mouse bone. For instance, the progressively restricted expression of Dkk1 to bone implies that it plays a prominent role in regulating Wnt signaling during bone development and growth. In addition, the more pronounced expression of Lrp5 compared to Lrp6 in adult bone, suggests that Lrp5 plays a more prominent role as a mediator of canonical Wnt signaling in adult mouse bone.

Disclosures: **W.G. Richards**, None.

SA131

See Friday Plenary number F131.

SA132

Reduced Bone Loss by Docosahexaenoic Acid (DHA) than Eicosapentaenoic Acid (EPA) in Ovariectomized Mice. M. M. Rahman*, A. Bhattacharya*, J. Banu, G. Fernandes*. Med/Clinical Immunology & Rheumatology, University of Texas Health Science Center at San Antonio, San Antonio, TX, USA.

Estrogen deficiency predisposes women to develop postmenopausal osteoporosis which is characterized by progressive loss of bone leading to increased risk of fractures. Recently, omega-3 fatty acids have been found to decrease bone loss in ovariectomized (OVX) mice. However, a comparative study between DHA and EPA enriched fatty acids on postmenopausal bone loss has not yet been investigated. In this study, 2 months old OVX and sham operated mice (5 mice per group) were fed 10% corn oil (CO) or 10% fish oil with either 50% EPA and 5% DHA (50/5) or 5% EPA and 50% DHA (5/50). After 12 weeks on diet, bone mineral density (BMD) was analyzed by DEXA. The data revealed that ovariectomy induced bone loss in the femur, tibia and lumbar vertebrae was significantly less in mice on 5/50 diet when compared to those on 50/5 and CO diets. To elucidate the mechanism by which DHA protects bone loss in OVX mice when compared to EPA, we carried out in vitro studies using RAW 264.7 cells. Two different concentrations (50 μ M and 100 μ M) of DHA or EPA were used. We found that DHA significantly inhibited the receptor activator of NF- κ B ligand (RANKL) stimulated multinucleated TRAP-positive cells formation in a dose dependent manner when compared to EPA or linoleic acid (LA). RANKL stimulated TNF- α production in RAW cells was also significantly decreased with DHA when compared to EPA and LA. By reverse transcription-polymerase chain reaction (RT-PCR) analysis, osteoclast-specific mRNA expression of cathepsin K, calcitonin receptor (CTR) and MMP-9 was also found to be significantly reduced with DHA when compared to EPA and LA. Moreover, bone resorption assay using calcium phosphate coated plate showed dramatic inhibition of RANKL stimulated pit formation of RAW cells treated with DHA when compared to EPA and LA. Thus DHA appears to be the most beneficial ω -3 fatty acid in preventing osteoclast activation and bone resorption. In summary, this study suggests that concentrated DHA ω -3 fatty acid is more efficient in reducing ovariectomy-induced bone loss than EPA.

Disclosures: **G. Fernandes**, None.

SA133

See Friday Plenary number F133.

SA134

Enamel Matrix Derivative Induces Osteoprotegerin Production by Human Osteoblasts. C. Galli*¹, G. M. Macaluso*¹, M. Pedrazzoni², R. Vescovini*², P. Sansoni*², R. Delsignore*¹, G. Passeri². ¹Chair of Periodontology, Univ. of Parma, Parma, Italy, ²Dep. Internal Medicine, Univ. of Parma, Parma, Italy.

Skeletal regeneration techniques increasingly rely on the use of exogenous molecules able to enhance bone tissue formation in pathological or traumatic defects. Enamel Matrix Derivative (EMD) from porcine tooth germs has been largely used to promote tooth ligament regeneration within periodontal pockets. Recent evidence suggests that EMD may contribute to induce osteoblasts' growth and differentiation. The present study aims to investigate EMD effects on growth, differentiation and bone balance markers in osteoblastic cells, in particular focusing on local factors relevant for bone remodeling, such as OPG and RANK-L. Cells were derived from bone specimen harvested from a healthy donor operated for mandibular reduction. These osteoblasts were producing osteocalcin and ALP, and were CD44 positive. Cells were cultured in the absence or in the presence of EMD at concentration of 20 and 50 μ g/ml. Cell growth was measured by MTT assay at day 3, 6 and 9 of culture, ALP activity, osteocalcin, OPG, and RANK-L production were assayed at week 1, 2 and 3. Bone nodules formation was detected by alizarin red staining in parallel cultures after 3 weeks. Our results show that cell growth was significantly increased by EMD as compared to control at all 3 time points ($p < 0.05$ at days 3 and 6, $p < 0.001$ at day 9) and differentiation markers were enhanced in 50 μ g/ml EMD treated cultures at week 2 and 3 (ALP $p < 0.01$ and osteocalcin $p < 0.05$). Supernatants from 50 μ g/ml EMD treated cultures showed a significantly higher amount of OPG at week 1, 2 and 3 ($p < 0.01$), while RANK-L was significantly decreased at week 3 ($p < 0.001$). Mineralized nodules number and dimension were higher in the 50 μ g/ml EMD treated cultures ($p < 0.01$) as compared to control. Our findings suggest that EMD is able to enhance osteoblastic cell growth and expression of differentiation markers. Moreover, EMD is able to create a favorable osteogenic microenvironment by enhancing OPG production, decreasing RANK-L release and promoting bone mineralized nodule formation. EMD can therefore be considered a promising tool for alveolar bone regeneration.

Disclosures: **C. Galli**, None.

SA135

See Friday Plenary number F135.

SA136

Effects of Aging on Angiogenic Response Following Ischemic Necrosis of the Femoral Head. H. Bian¹, L. Gerstenfeld^{*2}, T. A. Einhorn^{*2}, H. Kim¹. ¹Shriners Hospital For Children, Tampa, FL, USA, ²Boston University Medical Center, Boston, MA, USA.

Clinical studies show that the healing time and the extent of repair following ischemic necrosis of the femoral head (INFH) vary considerably depending on the age of onset. In patients near skeletal maturity and adults, the healing time is prolonged and the extent of repair is decreased compared to children with INFH. We hypothesize that revascularization of the femoral head following ischemic necrosis is impaired as a function of age, and that impaired revascularization is associated with an age-dependent reduction in the expression of a key angiogenic factor, VEGF and its transcription factor, HIF-1 α . The purpose of this study was to determine the effects of aging on VEGF and HIF-1 α expression using a large animal model of INFH and a cartilage explant model of hypoxia. For the animal study, 4 young pigs (4 wks old) and 4 "adolescent" pigs (6 months old) were surgically induced with INFH by placing a ligature tightly around the right femoral neck. The epiphyseal cartilage from the infarcted and normal femoral heads was assessed at 24h and 1 wk after the operation for VEGF and HIF-1 α expression using RNase protection assay (RPA). For the in vitro study, cartilage explants (5 x 5 x 1mm thick) were incubated in DMEM without serum and placed into a hypoxia chamber containing 1% O₂, 5% CO₂ and 94% N₂. The explants were assessed at 2 to 24h using RPA and western blot analysis. In the in vivo study, VEGF expression was reduced in the older animals at 24 h and 1 wk after the induction of ischemia, compared to the younger animals. In addition, the relative response rate was decreased in the older animals. The baseline HIF-1 α expression was lower in the older animals compared to the younger animals. However, HIF-1 α level did not change with ischemia in both age groups. Explant studies showed similar results with decreased VEGF expression in the explants from the older animals at 2 to 24h after hypoxia. HIF-1 α mRNA and protein levels were also decreased in the explants from the older animals. These findings support the hypothesis that there is an age-dependent reduction in VEGF and HIF-1 α expression following ischemia, which may explain impaired revascularization and repair seen in the adolescent and adult patients with INFH.

Disclosures: **H. Bian**, None.

SA137

Prior Intra-Arterial Injection of Mesenchymal Stem Cells Does not Enhance the Osteogenic Effects of Basic Fibroblast Growth Factor in Aged Ovariectomized Rats. U. T. Iwaniec¹, K. Moore^{*2}, M. F. Rivera^{*1}, S. M. Vanegas^{*1}, N. N. Teoh^{*1}, T. J. Wronski¹. ¹Physiological Sciences, University of Florida, Gainesville, FL, USA, ²Animal Sciences, University of Florida, Gainesville, FL, USA.

Previous studies have shown that the efficacy of PTH is limited in aged ovariectomized (OVX) rats with severe cancellous osteopenia due to lack of adequate numbers of bone spicules to serve as templates for new bone formation. Basic fibroblast growth factor (bFGF) may be useful in overcoming this limitation by its ability to induce formation of osteoid spicules within bone marrow. However, bFGF also has a diminished osteogenic effect in aged OVX rats, presumably due to an age-related decline in the population of mesenchymal stem cells (MSCs) that serve as targets for the growth factor. Therefore, the goal of this study was to determine whether prior treatment of aged OVX rats with MSCs would enhance the bone anabolic effects of bFGF. MSCs were harvested from the femoral bone marrow of relatively young OVX rats, expanded in culture, and cryogenically preserved for future use. Baseline (BSL) OVX and sham-operated rats were sacrificed at one year post-surgery (15 months old). Other groups of aged OVX rats were injected in their right femoral arteries with MSCs (2x10⁶ cells/kg body weight) or culture medium alone. These animals were then injected SC with bFGF (1 mg/kg) at 4 hours after intra-arterial injection of MSCs. The bFGF treatments were continued daily for a period of 3 weeks. The right proximal tibiae were then collected and processed for quantitative bone histomorphometry. Data are expressed as mean \pm SD and analyzed using the Kruskal-Wallis test followed by a non-parametric post-hoc test. In aged OVX rats injected intra-arterially with culture medium alone, treatment with bFGF induced an 11-fold increase in osteoid surface and a 7.5-fold increase in osteoblast surface compared to BSL OVX rats (69.3 \pm 24.5% vs. 6.1 \pm 3.9% and 49.2 \pm 20.0% vs. 6.5 \pm 4.0%, respectively). Osteoid volume was also markedly increased by bFGF treatment (7.9 \pm 5.7% vs. 0.1 \pm 0.1%). In aged OVX rats injected intra-arterially with MSCs, bFGF treatment induced a 14-fold increase in osteoid surface (88.0 \pm 9.0%), a 9.5-fold increase in osteoblast surface (61.6 \pm 14.8%), and a marked increase in osteoid volume (10.4 \pm 6.6%) compared to BSL OVX rats. However, the mean values for this group were not significantly different from those of bFGF-treated OVX rats previously injected with culture medium alone. Osteoclast surface was markedly decreased in both bFGF-treated groups compared to BSL OVX rats. In summary, our results indicate that prior intra-arterial injection of MSCs does not enhance the bone anabolic effects of bFGF in the proximal tibia of aged OVX rats.

Disclosures: **U. T. Iwaniec**, None.

SA138

See Friday Plenary number F138.

SA139

Adenovirus-Mediated Overexpression of FGF23 Suppresses Osteoblast Development and Matrix Mineralization in Fetal Rat Calvaria Cell Cultures. H. Wang^{*1}, R. Yamamoto^{*2}, K. Tanne^{*2}, J. E. Aubin³, N. Maeda^{*1}, Y. Yoshiko¹. ¹Oral Growth and Developmental Biology, Hiroshima University Graduate School of Biomedical Sciences, Hiroshima, Japan, ²Orthodontics and Craniofacial Developmental Biology, Hiroshima University Graduate School of Biomedical Sciences, Hiroshima, Japan, ³Molecular and Medical Genetics, University of Toronto, Toronto, ON, Canada.

FGF23 has been identified as a mediator of such hypophosphatemic diseases as autosomal dominant hypophosphatemic rickets, tumor-induced osteomalacia and possibly X-linked hypophosphatemic rickets. In skeletal tissue, mineralization defects are seen in FGF23-deficient hyperphosphatemic mice as well as in genetically-engineered hypophosphatemic mice overexpressing FGF23. Recent and growing evidence strongly suggests that FGF23 plays a central role in phosphate (Pi) homeostasis, predominantly through its effects on renal vitamin D metabolism and phosphate reabsorption. However, the FGF23 gene is widely expressed in multiple tissues including bone and cartilage, suggesting that the polypeptide may elicit at least some of its effects via other cell/tissue-specific effects. Taken together with our data that FGF23 mRNA is differentially expressed during osteoblast development and downregulated when osteoid nodules are induced to mineralize with β -glycerophosphate (β GP) in the fetal rat calvaria (RC) cell culture model, we speculated that FGF23 may act as a local factor on bone formation. To further address this possibility, we constructed recombinant adenovirus-human FGF23 (AV-FGF23) by using the Adeno-XTM expression system and assessed the effects of FGF23 overexpression during osteoblast development and matrix mineralization in the RC model. Infection of proliferating cells with AV-FGF23 did not affect cell growth as compared to cells infected with control AV (AV-c). However, we found that cells overexpressing FGF23 made fewer and smaller nodules than control cultures with a parallel decrease in levels of osteoblast differentiation marker mRNAs. Furthermore, FGF23 overexpression inhibited osteoid nodule mineralization in the presence of β -glycerophosphate. Concomitant with these phenotypic changes in AV-FGF23- vs. AV-c-infected RC cells, overexpression of FGF23 decreased NaPi uptake in RC cells. Thus, we conclude that FGF23 may act as a negative regulator of osteoblast development and matrix mineralization independently of its systemic effects on Pi homeostasis.

Disclosures: H. Wang, None.

SA140

See Friday Plenary number F140.

SA141

A Novel Recessive Mutation in Fibroblast Growth Factor-23 (FGF-23) Causes a Tumoral Calcinosis. L. Masi¹, A. Gozzini^{*1}, S. Carbonell^{*1}, A. Amedei^{*1}, A. Falchetti¹, R. Capanna^{*2}, A. Tanini¹, M. L. Brandi¹. ¹Department of Internal Medicine, University of Florence, Florence, Italy, ²Department of Orthopaedic, University of Florence, Florence, Italy.

Tumoral calcinosis (TC) is a rare genetic disorder characterized by periarticular cystic and solid tumors calcifications. Biochemical markers of disorder include hyperphosphatemia and an elevated serum of calcitriol concentration in every patients. The hyperphosphatemia results form an increase in capacity of renal tubular phosphate reabsorption. The identification of phosphonin family hormones suggest that mutations of these molecules could be involved in the pathogenesis of TC. One of these molecules is represented by FGF-23. The TC phenotype is similar to that described in the FGF-23 knockout mice. In the present study we described a new FGF-23 mutation in a subject affected by TC. A Caucasian women (years 67) was examined for a history of ectopic calcification. Biochemical exams showed and hyperphosphatemia and hyperphosphaturia with normal value of PTH and 1-25 (OH)₂ D₃. The patient presented a big shoulder calcification and also a calcification of femoral artery. We expanded the family tree through detailed family histories, which importantly revealed that parents were consanguineous. Hystologically the mass was characterized by calcium deposition and granulomatous reaction around the mass. Genomic DNA was extracted from blood collected from the patient, her daughter and her grandchild by standard procedure. DNA was not available from her parents. All three FGF-23 coding exons, as well as conserved splice sites, were amplified by standard PCR procedure. Nucleotide sequences were determined by direct sequencing with a DNA kit and an automated DNA sequencer (ABI PRISM 3100 - Perkin-Elmer Corp). We discovered a new homozygous codon 41, His/Gln (CAC-CAA) substitution in exon 1 of FGF-23 gene in the affected patient. A heterozygous substitution was present in the daughter. No mutation were found in the two children. FGF-23 gene mutation was not found in the SNP database (www.ncbi.nih.gov/snp). In summary, a recessive mutation in FGF 23 causes TC. Understanding the functional significance and molecular physiology of this novel mutation will reveal critical information regarding the role of FGF-23 in states of normal and of disorder of phosphate homeostasis.

Disclosures: L. Masi, None.

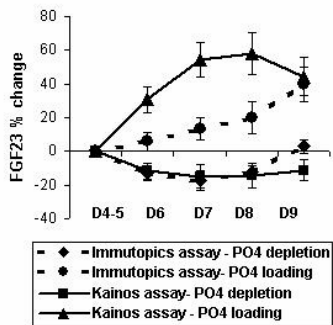
SA142

See Friday Plenary number F142.

SA143

1st vs. 2nd Generation Assays in Detecting Changes in Blood FGF-23 with Dietary Phosphate. S. M. Burnett, S. Gunawardene^{*}, F. R. Bringhurst, H. Jueppner, J. S. Finkelstein. Endocrine Unit, Massachusetts General Hospital, Boston, MA, USA.

Fibroblast growth factor 23 (FGF23) is elevated in phosphate (PO₄) wasting disorders. Serum PO₄ levels are elevated in the FGF23 KO mouse suggesting that FGF23 plays a physiologic role in PO₄ regulation. To examine the effects of dietary PO₄ on FGF23 in humans, we randomly assigned 66 healthy subjects, age 18-45, to either a low or high PO₄ diet for 4 days, after a 4 day control diet. During deprivation, dietary PO₄ was 0.5g daily and subjects consumed PO₄ binders QID. During PO₄ loading, subjects consumed 2.5g PO₄ daily from diet and supplements. Blood FGF23 was measured using both a 1st generation immunometric assay detecting intact and C-terminal FGF23 (*Immutopics*), and a 2nd generation immunometric assay detecting only intact FGF23 (*Kainos*). Data are presented as mean \pm SD. PO₄ loading increased 24 hour urine PO₄ excretion and FePO₄ (p<0.01). PO₄ deprivation decreased 24 hour urine PO₄ excretion and FePO₄ (p<0.01). Changes in FGF23 differed markedly in the 2 assays.



With PO₄ loading, the 2nd generation assay detected earlier and greater increases in FGF23 from 35 \pm 9 to 50 \pm 16 pg/mL (p< 0.01), an overall increase of ~ 60%; while the 1st generation assay detected a smaller increase in FGF23 from 57 \pm 31 to 74 \pm 52 RU/mL (p<0.01), an overall increase of ~ 30%. With PO₄ deprivation, the 2nd generation assay detected a ~ 20% sustained decrease in FGF23 from 37 \pm 13 to 31 \pm 10 pg/mL (p<0.01); while the 1st generation assay detected a transient fall in FGF23, the levels then returned to baseline, 58 \pm 31 vs. 56 \pm 32 RU/mL (p=0.13). There was weak correlation between the assays (r=0.26). The 2nd generation assay better detected correlations between FGF23 and PO₄ indices. These preliminary data suggest that physiologic changes in FGF23 are better detected using a 2nd generation assay that only measures intact FGF23, than using an assay which detects both intact FGF23 and C-terminal fragments.

R coefficients	Correlation Analysis of FGF23 vs. PO4 indices			
	Blood PO ₄	24 hour urine PO ₄	FePO ₄	1,25 (OH) ₂ vitamin D
2 nd generation FGF23 assay	0.37	0.45	0.28	-0.26
1 st generation FGF23 assay	0.07	0.18	0.05	0.01

Disclosures: S.M. Burnett, None.

SA144

Vitamin D₃ but not PTH Regulates Fgf23 Gene Transcription in Osteoblasts. S. Liu, W. Tang^{*}, J. Zhou^{*}, L. D. Quarles. Internal Medicine/The Kidney Institute, University of Kansas Medical Center, Kansas City, KS, USA.

FGF23 is a hormone that inhibits sodium-dependent phosphate re-absorption and 1 α -hydroxylase activity in the kidney resulting in phosphaturia and diminished 1,25-dihydroxyvitamin D₃ (1,25(OH)₂D₃) production. Recently, we have demonstrated that FGF23 is expressed in osteoblasts and may act as a counter-regulatory hormone for 1,25(OH)₂D₃-mediated increases in gastrointestinal phosphate absorption. In the current study, we further explored the mechanisms of 1,25(OH)₂D₃ regulation of Fgf23 gene transcription and evaluated the effects of PTH on FGF23 production. Serum Fgf23 concentrations were measured in adult mice 4, 8, 24 hours after IP injections of 1,25(OH)₂D₃ at a dosage of 100 ng/kg body weight or PTH1-34 at a dosage of 80 μ g/kg body weight. PTH administration had no significant effect on serum Fgf23 levels over 24 hours. In contrast, 1,25(OH)₂D₃ increased serum Fgf23 levels (mean \pm SEM) from a baseline value of 90.6 \pm 8.1 pg/ml to 141.0 \pm 6.9 pg/ml (p<0.01) at 4 hours, reaching a peak concentration of 213.8 \pm 14.6 pg/ml at 8 hours (p<0.01). 1,25(OH)₂D₃ treatment resulted in a decrease in serum PTH levels from 37.6 \pm 7.6 to 19.1 \pm 1.8 pg/ml (mean \pm SEM; p<0.05) at 8 hours and no changes in serum calcium or phosphate levels. We also observed a 4-fold increase of Fgf23 transcripts by real-time RT-PCR in calvaria isolated from mice 8 hours after injection of 1,25 (OH)₂D₃. In addition, we demonstrated that 1,25(OH)₂D₃ added to the culture medium increases Fgf23 mRNA levels in ROS17/2.8 osteoblasts. Promoter/reporter construct analysis of the murine *Fgf23* 5'-flanking region in ROS17/2.8 osteoblasts demonstrated the ability of 1,25(OH)₂D₃ to stimulate promoter activity in a dose dependent manner. The stimulatory effect was localized to a region between -1300 and -1260 bp upstream of Fgf23 translation start site. Sequence analysis of this region did not show a typical vitamin D response element (VDRE). Our data suggest that 1,25(OH)₂D₃ stimulates the production of FGF23 by osteoblasts through non-classical mechanisms. This novel regulation of FGF23 production in osteoblasts by 1,25(OH)₂D₃ provides further evidence for a bone-kidney axis regulating systemic phosphate homeostasis.

Disclosures: S. Liu, None.

SA145

Effects of R-FB, a Unique Nonsteroidal Anti-Inflammatory Drug (NSAID), on COX2-Mediated Inhibition of Insulin-like Growth Factor Binding Protein-6 (BP6) Transcription. S. L. Hall, J. C. Felt*, T. A. Linkhart, D. D. Strong. Musculoskeletal Disease Center, LLVAHCS, LLU, Loma Linda, CA, USA.

NSAIDs reduce prostaglandin (PG) synthesis by inhibiting cyclooxygenase-1 and -2 (COX2) enzymes. NSAIDs have anti-inflammatory and anti-nociceptive effects and may decrease Alzheimer's dementia and cancer risk, but side effects such as gastrointestinal (GI) damage and cardiac risk, limit their use. NSAIDs also produce detrimental bone effects such as ↓ fracture healing, ↓ osteogenesis, and ↑ bone resorption. These skeletal effects may be due to inhibition of COX2 which has been proposed to mediate increased bone formation in response to mechanical loading and fracture repair. PGs promote osteoblast (ob) differentiation and survival, and stimulate bone formation, *in vivo*. Consistent with these data, we previously showed that overexpression of COX2 decreased transcription of BP6 (a potent, constitutively expressed inhibitor of ob differentiation), suggesting that some COX2 skeletal effects may be mediated via BP6 expression. In this study, we used BP6 transcriptional regulation by COX2 as an endpoint to compare if different NSAIDs act by similar or different mechanisms. Flurbiprofen (FB), a nonselective NSAID, exists as a racemic mixture of R- and S-enantiomers (R-FB and S-FB) with minimal stereo-inversion in humans. R-FB efficacy is similar to other NSAIDs but data suggests it acts by modulating transcription factors rather than by COX inhibition, and it is not GI-toxic. The effects of R-FB and other NSAIDs on BP6 promoter activity were assessed in the presence and absence of COX2 overexpression. We cotransfected human ob-like osteosarcoma cells with a Luciferase reporter construct containing 158 bps of BP6 proximal promoter and a COX2 expression vector incubated with and without IC50 doses of several NSAIDs. Luciferase and protein content were determined 24 hrs after transfection. In the absence of NSAIDs, COX2 overexpression reduced BP6 promoter activity by 55% ($p < 0.0002$). At low (anti-inflammatory) and intermediate (neuroprotective) doses, the COX2 effect was attenuated or abolished by several NSAIDs (ibuprofen, diclofenac, celecoxib, Dup697) but not by R-FB ($p < 0.0004$). Reversal of the COX2 effect by R-FB was observed only at high (anti-tumor) doses. In summary, at low and intermediate doses COX2 inhibition of BP6 promoter activity was reversed by treatment with NSAIDs that inhibit PG synthesis, but not by R-FB. These data are consistent with reports that R-FB acts by alternative mechanism(s) and that COX2 transcriptional effects are mediated by PG production. Furthermore, in light of its lack of effect on COX2 activity, further study into the potential of R-FB as a "bone safe" NSAID is warranted.

Disclosures: S.L. Hall, None.

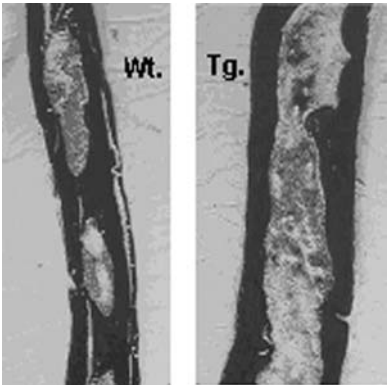
SA146

Transgenic Mice Overexpressing Pregnancy-Associated Plasma Protein (PAPP)-A, an IGFBP Protease, in Osteoblasts Exhibit a Dramatic Increase in Bone Accretion. X. Qin¹, J. E. Wergedal¹, M. Rehage^{*2}, K. Tran^{*2}, J. Newton^{*2}, D. J. Baylink¹, S. Mohan¹. ¹JLP VAMC and LLU, Loma Linda, CA, USA, ²JLP VAMC, Loma Linda, CA, USA.

IGFs play an important role in the regulation of peak bone mass. The actions of IGF in bone are modulated by IGFBPs which are in turn regulated by IGFBP proteases. Based on *in vitro* studies that osteoblasts (OBs) produce an IGFBP specific protease, PAPP-A, which degrades inhibitory IGFBPs and thereby releases IGFs for biological action, we hypothesized that transgenic overexpression of PAPP-A in OBs should exert anabolic effects on bone *in vivo*. To test this hypothesis, we generated human PAPP-A construct driven by rat type I collagen promoter and tested the efficacy of this construct in MG63 and HEPG2 cells *in vitro*. We found that active recombinant PAPP-A (FLAG tagged) with the expected molecular mass was detected in the conditioned medium of MG63 but not HepG2 liver cells. We next generated transgenic founders and confirmed expression of PAPP-A transgene by RT-PCR analysis. Femurs of female mice from 3 litters of F1 generation (10 transgenic and 5 wild type) at 3 months were analyzed by pQCT (Table).

Parameter	% of wild type (Mean±SEM)
Length	106±0.8*
BMC	127±9.4*
Bone area	125±7.1**
Peri. Circ.	128±4.5**
Endo. Circ	112±1.5*

*= $p < 0.05$; **= $p < 0.01$



Consistent with the increased bone accretion in femurs, calvaria thickness and skull BMD measured by DXA at 6 months were increased by $43 \pm 7.7\%$ ($n=3$, $p < 0.01$) and $20 \pm 5.8\%$ ($n=3$, $p < 0.05$), respectively. Histological analysis of calvaria suggests that the increase in cortical thickness is caused by increased amount of osteoid indicating new bone formation (Figure). *In vivo* DXA analysis of a second founder also revealed an increase in skull BMD. Conclusions: 1) Transgenic mice overexpressing PAPP-A exhibit a dramatic increase in BMC and bone size phenotypes at multiple sites; 2) Modulation of local IGF actions by upregulating PAPP-A expression and/or activity could provide a therapeutic opportunity to treat bone disorders.

Disclosures: X. Qin, None.

SA147

The Role of IGF-I Signaling in Regulating Osteoclastogenesis. Y. Wang, S. Nishida, H. Z. ElAlieh*, E. C. Buxton*, R. K. Long*, B. P. Halloran, D. D. Bikle. Endocrine Unit, University of California, San Francisco, VA Medical Center, San Francisco, CA, USA.

Although insulin-like growth factor-I (IGF-I) has been clearly identified as an important growth factor in regulating osteoblast proliferation and function, information regarding its role in osteoclastogenesis is limited and conflicting. Our study was designed to analyze the role of IGF-I in modulating osteoclastogenesis using mice homozygous for targeted ablation of the IGF-I gene (IGF-I^{-/-}). To determine the effects of IGF-I on osteoclasts, wild-type (IGF-I^{+/+}) mice were treated with IGF-I or vehicle. The number of osteoclasts in IGF-I treated mice increased 1.5 fold compared to vehicle treated mice. In contrast, the number of osteoclasts in the IGF-I^{-/-} mice were 76% of that observed in the IGF-I^{+/+} mice. To clarify the mechanism by which IGF-I regulates osteoclastogenesis, we cultured osteoclast precursors from IGF-I^{+/+} mice and IGF-I^{-/-} mice for six days in the presence of RANKL and M-CSF. The number of osteoclasts (3 or more nuclei) observed in the culture from IGF-I^{-/-} mice was significantly less (55%) than that from the IGF-I^{+/+} mice. When IGF-I^{-/-} osteoblasts and IGF-I^{+/+} osteoclasts were co-cultured, the number of osteoclasts formed was only 11% of that from co-cultures of IGF-I^{+/+} osteoblasts and osteoclasts. When IGF-I^{+/+} osteoblasts and IGF-I^{-/-} osteoclasts were co-cultured, the number of osteoclasts formed was 48 % of that observed in co-cultures of IGF-I^{+/+} osteoblasts and osteoclasts. To investigate if the RANKL/RANK signaling pathway was involved in this process, mRNA levels of RANKL and RANK were measured in bone tissue (marrow removed) using real-time PCR. In IGF-I^{-/-} mice, mRNA levels of RANKL and RANK were 55% and 33% of that in IGF-I^{+/+} mice, respectively. To evaluate if IGF-I could rescue the abnormal osteoclastogenesis in IGF-I^{-/-} mice, 10 ng/ml of IGF-I was added to the osteoclast precursor cultures. IGF-I increased the size (735 nuclei/ 100 osteoclasts), number (2.6 fold) and function (2.7 fold increase in resorption area in dentine) of osteoclasts in cultures from IGF-I^{+/+} mice, with lesser effects in cultures from IGF-I^{-/-} mice (400 nuclei/ 100 osteoclasts, and 2.0 fold increase in osteoclast number). In summary, our results indicate that IGF-I increases the size, number and function of osteoclasts. IGF-I is required for the normal interaction between the osteoblast and osteoclast via its regulation of RANKL and RANK expression. The role of osteoblasts in stimulating osteoclastogenesis is more impacted by lack of IGF-I than the ability of osteoclast precursors to respond to osteoblastic stimulation, although both osteoblasts and osteoclast precursors appear to function subnormally in the absence of IGF-I.

Disclosures: Y. Wang, None.

SA148

Non-canonical Wnt 11 Transcriptionally Suppresses Expression of Insulin-like Growth Factor Binding Protein-6, an Inhibitor of Osteoblast Differentiation. C. Strohbach*, T. A. Linkhart¹, S. Mohan¹, Y. Shi^{*2}, C. Glackin³, D. D. Strong¹. ¹Research 151, VA Loma Linda Healthcare System, Loma Linda, CA, USA, ²Neurosciences, City of Hope, Beckman Research Institute, Duarte, CA, USA, ³Molecular Medicine, City of Hope, Beckman Research Institute, Duarte, CA, USA.

IGFBP-6 (BP-6) overexpression decreases osteoblast (Ob) marker gene expression and binds to LMP-1, a nuclear protein that increases Ob differentiation. Based on these findings, we propose the hypothesis that osteoregulatory agents may mediate their effects on Ob differentiation in part by regulating BP-6 expression. As a means to test this hypothesis, we first measured BP-6 expression changes during Ob differentiation in a mineralizing MC3T3-E1 mouse Ob model system. Differentiation was induced with media containing β -glycerophosphate and ascorbic acid for 21 days. RNA was isolated at days 0, 3, 7, 14, and 21. Differentiation was confirmed by Von Kossa and Alizarin Red staining and mRNA measurement of osteocalcin. Using real-time PCR, we found that BP-6 mRNA levels progressively decreased (2-4 fold) as differentiation proceeded. We next tested the effects of Wnt 1 and Wnt 11 on BP-6 expression based on findings that 1) Wnt1 and Wnt 11 are expressed by osteoblasts, 2) non-canonical Wnt11 inhibits Twist expression and stimulates Ob differentiation, 3) functional LEF/TCF elements responsive to β -catenin reside in the BP-6 promoter and 4) canonical Wnt 1 and non-canonical Wnt 11 interact to regulate proliferation and differentiation in other mesenchymal tissues. Accordingly, we found that Wnt1 mRNA was constitutively expressed at low levels throughout MC3T3 cell differentiation, while Wnt11 mRNA expression was markedly upregulated early in differentiating cultures (4-fold increase at day 3). We next tested the ability of Wnt1 and Wnt11 to regulate BP-6 promoter activity. MC3T3 cells were co-transfected with a reporter vector containing 1.7 kb of the BP-6 promoter linked to luciferase, together with either Wnt1, Wnt11, or constitutively active β -catenin expression vectors in the presence or absence of LEF expression vector. Active β -catenin expression dose-dependently stimulated BP-6 promoter activity up to 2.4-fold in the presence of LEF and Wnt1 dose-dependently stimulated BP-6 promoter activity up to 20-fold in the presence of LEF. By

ASBMR 27th Annual Meeting

contrast, Wnt11 dose-dependently reduced basal BP-6 promoter activity up to 8.5-fold and this inhibition was reversed by addition of LEF. In conclusion, differential effects of Wnt1 and Wnt11 on BP-6 transcription may be mediated via β -catenin dependent and independent pathways. Wnt 11 may stimulate osteoblast differentiation in part by suppression of BP-6 at the transcriptional level.

Disclosures: **C. Strohhach**, None.

SA149

See Friday Plenary number F149.

SA150

Effects of 24-Months of Gymnastics Training on Insulin-Like Growth Factors in Prepubertal Females. **R. A. Gildea***¹, **E. M. Laing**¹, **D. B. Hall**^{*2}, **C. M. Modlesky**³, **T. J. Beck**⁴, **A. R. Wilson**^{*1}, **C. A. Baile**^{*1}, **R. D. Lewis**¹.

¹Department of Foods & Nutrition, The University of Georgia, Athens, GA, USA, ²Department of Statistics, The University of Georgia, Athens, GA, USA,

³Department of Health, Nutrition and Exercise Science, University of Delaware, Newark, DE, USA, ⁴Department of Radiology, Johns Hopkins Medical Institute, Baltimore, MD, USA.

The positive bone response to high impact loading exercise, such as gymnastics, in children may be partially mediated by insulin-like growth factors (IGFs). The present study was conducted to investigate the effects of 24-months of recreational artistic gymnastics participation on bone and plasma growth factors in 142 prepubertal females, 4-8 years of age. Gymnasts (GYM; n = 64) and controls (CON; n = 78) were not participating in organized activities prior to enrolling in the study. Bone area (BA), BMC and areal BMD (aBMD) of the total body, lumbar spine (LS), total proximal femur (TPF), and the forearm were determined using DXA (Hologic, QDR 1000-W), and structural properties of bone including BMD, cross sectional area (CSA) and section modulus (Z) of the intertrochanteric (IT) and shaft regions of the TPF using the hip structural analysis (HSA) program. Insulin-like growth factor-I (IGF-I), and IGF binding protein-3 (IGFBP-3) were determined using a chemiluminescent assay (IMMULITE®, DPC). Using ANCOVA, log values of IGF-I, IGFBP-3 and IGF-I/IGFBP-3 increased in GYM ($p < 0.02$ for all measures) and CON ($p < 0.0001$ for all measures) by 24-months, and the increases were similar between groups. In GYM, changes in log IGFs were not correlated with bone measures. In CON, the 24-month change in log IGF-I was positively correlated with TPF BMC and aBMD (partial $r = 0.28$ and 0.28 respectively, $p < 0.03$) and LS BA, BMC and aBMD (partial $r = 0.25$, 0.33 and 0.31 respectively, $p < 0.05$) when controlling for baseline age and height. When GYM and CON were combined, there were positive correlations between the 24-month change in log IGF-I and IT CSA and Z (partial $r = 0.20$ and 0.24 respectively, $p < 0.04$) and shaft Z (partial $r = 0.24$, $p < 0.01$) when controlling for baseline age and height. Significant negative correlations were observed between hours of gymnastics participation and the 24-month change in log values for IGF-I, IGFBP-3 and IGF-I/IGFBP-3 ($r = -0.46$, -0.38 and -0.38 respectively, $p < 0.01$). The discrepancy between GYM and CON with respect to the IGFs and bone correlations is not fully understood, however, may be related to the degree of variability in gymnastics participation.

Disclosures: **R.A. Gildea**, None.

SA151

Effect of IGF-I on Chondrogenic Differentiation of Mouse Bone Marrow Derived Mesenchymal Stem Cells. **S. Aakula**^{*1}, **L. Longobardi**^{*2}, **L. O'Rear**^{*2}, **K. Shimer**^{*2}, **W. A. Horton**^{*3}, **A. Spagnoli**². ¹General Surgery, Vanderbilt University, Nashville, TN, USA, ²Pediatrics, Vanderbilt University, Nashville, TN, USA, ³Research Center, Shriners Hospital for Children, Portland, OR, USA.

Chondrogenesis is initiated by the migration of chondroprogenitors to the future bone sites, where they undergo condensation, proliferation and differentiation. Bone marrow (BM) contains mesenchymal stem cells (MSC) that express a chondrogenic potential when cultured in high density pellets with TGF β . The role of IGF-I in the chondrogenic potential of MSC is poorly understood. In our study we evaluated the effect of IGF-I on chondrogenic pellet differentiation, alone or in combination with TGF β , analyzing the expression of different chondrocyte markers. MSC were isolated from long bones of 4-week old transgenic mice in which the expression of GFP is controlled by the murine type II collagen promoter/enhancer (Col2-GFP) to produce a fluorescent reporter for chondrogenic differentiation. MSC were immunodepleted of CD34, CD45 and CD11b positive hematopoietic cells and induced to form high density chondrogenic pellets by culturing them in serum- and insulin-free defined medium. To assess chondrocyte differentiation, pellets from Col2-GFP and WT-FVB mice were cultured for 7 days with or without des-IGF-I (100ng/ml) and/or TGF β (10 ng/ml). GFP expression was visualized by confocal microscopy. Total RNA, isolated from 20 pellets for each condition, was reversed transcribed and cDNAs were analyzed by quantitative real time PCR for the expression of type II collagen and Sox-9. IGF-I, similarly to TGF β , was able to drive the expression of collagen II in viable Col2-GFP chondrogenic pellets, as determined by the increase in GFP expression. To confirm this result, we analyzed the expression of chondrocyte markers in WT-MSC pellets by quantitative real time PCR. After normalization for the housekeeping gene GAPDH, we found that IGF-I, as well as TGF β , determined an increase in the expression of collagen II (119 ± 23 fold for IGF-I and 40 ± 0.9 fold for TGF β) compared to untreated control (1 ± 0.59 ; n=3; $p < 0.05$). We also found that IGF-I, similarly to TGF β , induced expression of Sox-9 (5.7 ± 1.5 fold for IGF-I and 4 ± 1.7 fold for TGF β) compared

to untreated control (1 ± 0.35 ; $p < 0.05$). IGF-I effect on the expression of collagen II and Sox-9 was additive to the TGF β action (326 ± 16 fold for collagen II and 18.7 ± 4.7 fold for Sox-9 vs respective untreated controls; n=3; $p < 0.05$). Our data indicate that IGF-I plays a major chondroinductive role in BM derived MSC. IGF-I effect is comparable and additive to TGF β action. Understanding the role of IGF-I in MSC chondrogenesis provides critical information to optimize the use of MSC in cartilage diseases.

Disclosures: **S. Aakula**, None.

SA152

IGF Signaling in the Growth Plate Early Regeneration after Irradiation. **Y. Wang**^{*1}, **J. A. Horton**^{*1}, **J. A. Strauss**^{*1}, **C. E. Farnum**^{*2}, **T. A. Damron**^{*1}.

¹Orthopedic surgery, SUNY upstate medical university, Syracuse, NY, USA,

²Department of Biomedocal Sciences, Cornell University, Ithaca, NY, USA.

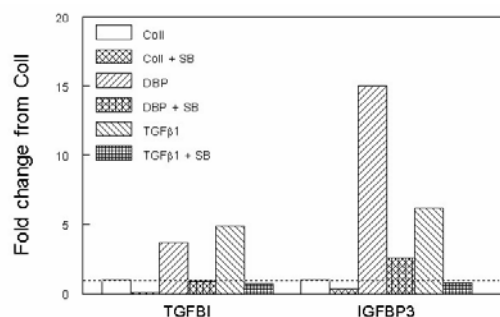
Radiotherapy plays an important role in the treatment of specific childhood malignant neoplasms. However, radiation-induced growth arrest is a major adverse consequence of radiotherapy in children. Potential treatments to minimize this complication require a better understanding the effect of radiation on growth factors involved in growth plate regeneration after radiotherapy. The insulin like growth factor (IGF) pathway has been widely investigated in musculoskeletal studies. IGF-I stimulates proliferation of chondrocytes in the growth plate proliferative zone. IGF-I has also been shown to stimulate osteoblast proliferation, matrix protein synthesis, and bone formation. In addition, skeletal expression of IGF-I is critical for bone cell differentiation. IGF-II is highly expressed in growth plate reserve and proliferative zones, where it serves an anti-apoptosis function. Our initial work examining histomorphometry, and immunohistochemistry after a single fraction model in the five week old rat has shown initiation of growth plate regeneration by 2 weeks. We combined cDNA microarray and laser capture microdissection to study the effect of radiation on growth factors in growth plate. In situ hybridization was used to confirm the microarray findings. Microarray data show that IGFII expression increased 8.3 fold in the PZ and 2.3 fold HZ and IGF1R increased 2.4 fold in the HZ at one week after irradiation. In addition, growth hormone receptor (GhR) increased in both zones at one week after irradiation. Both of these changes precede increases in parathyroid like hormone related protein (PTHrP), fibroblastic growth factor (FGF), bone morphogenetic protein (BMP), and transforming growth factor β (TGF β) at a transcriptional level. In this study, we focused on early recovery response at one week and late radio-recovery at two weeks. At the early time point, IGF1R, IGFII, and GhR were increased in IGF pathways after irradiation while showing an injury response at two weeks which indicated that IGF pathway play an significant role in the early radio-recovery response. Our studies suggested that the potential for recovery following growth plate injury is driven by IGF primarily and by PTHrP, BMP, FGF, and TGF β secondarily, resulting initially in accumulation of matrix followed closely by appearance of regenerative proliferative clones, the restoration of which is directly related to reduction of limb length discrepancy.

Disclosures: **Y. Wang**, None.

SA153

Demineralized Bone Activates Wnt Signaling in Human Dermal Fibroblasts: The Role of TGFbeta/Smad Signaling. **S. Zhou**, **J. Glowacki**. Orthopedic Surgery, Brigham and Women's Hospital, Boston, MA, USA.

Demineralized bone powder (DBP) induces chondro/osteogenic differentiation of human dermal fibroblasts (hDFs) in three-dimensional culture, but the initiating mechanisms have not been identified. Our previous data showed that, although BMP-2 was originally isolated as a putative active factor in DBP, rhBMP-2 alone and DBP do not affect all the same genes or in the same ways in hDFs [JBMR, 19(10):1732-41, 2004] and that TGF- β , in cooperation with Wnt signal, promotes chondrocyte differentiation in human marrow stromal cells [JBMR 19(3):463-470, 2004]. In this study, we tested the hypotheses that DBP would affect expression of Wnt signaling genes and that DBP's effects would require TGF β /Smad pathway. An induction model was used in which hDFs were cultured with and without DBP in a porous collagen sponge. Effects of DBP and TGF- β 1 (10 ng/ml) were compared by microarray, RT-PCR, and Western blot analysis of selected genes in the TGF β /Smad and Wnt signaling pathways. At day 3, DBP and TGF- β 1 have similar effects on TGF β /Smad target gene *TGFB1*, *PAT-1*, and *IGFBP3* expression in hDFs in 3D collagen sponges. A specific inhibitor (SB431542, 10 μ M) of TGF β type I receptor (ALK-5) antagonized the stimulation by DBP and TGF- β 1 on *TGFB1*, *IGFBP3*, *ID3* gene expression. This is evidence that DBP activates TGF β /Smad signaling in hDFs. To compare the effects of DBP and TGF- β 1 on Wnt signaling, we used RT-PCR and Wnt signal pathway microarray analysis. The results showed that DBP and TGF- β 1 have similar effects on Wnt signals; both stabilized intracellular Wnt signal molecule β -catenin proteins (Western blot), upregulated Wnt4, 5a, 7b, 10b, 11, 14, 16b and downregulated 2b, 5b gene expression (RT-PCR) in hDFs. Other Wnts were either not modulated by DBP or TGF- β 1, or were undetectable in hDFs. The effects of DBP on Wnt gene expression requires TGF β signaling because SB431542 inhibited the stimulation of DBP on Wnt7b. In conclusion, this study verified that Demineralized Bone modulates expression of Wnt signaling genes and that DBP's effects require TGF β /Smad pathway in hDFs. These and previous data indicate that multiple signaling pathways are involved in DBPchondro/osteoinduced target human dermal fibroblasts (hDFs) *in vitro*. One of the pathways involves the modulation of Wnt signals through TGF β /Smad.



Disclosures: **S. Zhou**, None.

SA154

See Friday Plenary number F154.

SA155

A Novel Large Latent Complex of TGFb Is Produced by Hypertrophic Chondrocytes. **A. Selim**¹, **P. M. Mattioli***², **V. L. Scheinfeld***², **M. D'Angelo**².

¹Endocrine Unit, Massachusetts General Hospital, Boston, MA, USA,

²Department of Anatomy and Center for the Study of Chronic Diseases of Aging, Philadelphia College of Osteopathic Medicine, Philadelphia, PA, USA.

Chondrocytes produce transforming growth factor beta (TGFb) and store it in their matrix in a large latent complex (LLC) that includes latent TGFb binding protein (LTBP). Large quantities of activated TGFb are produced as a result of hypertrophy in chondrocytes and collagenase 3 (MMP-13) is involved in the activation of TGFb from its latent complexes. In this study, tibial hypertrophic chondrocytes were isolated from day 19 chicks, immunoprecipitated with antiserum to LTBP1 and MMP-13 and immunoblotted with antiserum to TGFb. Immunoblots contained bands of immunoreactivity corresponding to a novel 250 kDa LLC, the 60kDa bLAP N-terminus fragment of TGFb and the 25kDa homodimer of TGFb. Thus, the novel LLC for TGFb produced by hypertrophic chondrocytes includes MMP-13. An alternatively spliced, short form of LTBP 1 has been identified whose N-terminus plays a role in tissue transglutaminase-dependent TGFb activation mechanism. To determine the involvement of our novel LLC in more efficient activation of TGFb, we designed primers to differentiate the long form of LTBP from the short form. Reverse-transcription PCR of total RNA isolated from serum-free alginate cultures revealed that early hypertrophic chondrocytes produce both the long and short forms of LTBP, but the late hypertrophic chondrocytes only produce LTBP short. Therefore, as a chondrocyte nears terminal differentiation, LTBPshort is preferentially produced suggesting that chondrocytes shift to a more easily activated form of the LLC. Since the protease sensitive hinge region on LTBPshort is the target for LLC release by enzymes studied to date, it is plausible that association of MMP-13 to LTBPshort places the metalloproteinase in a position for more efficient activation of the chondrocyte-unique TGFb LLC. Through our own bioinformatics assessment based on previously published models of the TGFb LLC, we are suggesting that the hemopexin domain of MMP-13 interacts with EGF-CA domains of LTBPshort in such an orientation that the peptidase domain of MMP-13 lies in close proximity to the linker region of LTBPshort. This orientation is supported by existence of candidate amino acids in the linker region of LTBPshort, Gly-Ile bonds at positions 807/808 and 819/820, that are known to interact with the peptidase domain of MMP-13. The association of MMP-13 with LLC points to a novel storage and activation process for chondrocyte-produced TGFb that would allow for local and rapid control of release and activation of TGFb from matrix storage.

Disclosures: **M. D'Angelo**, None.

SA156

See Friday Plenary number F156.

SA157

TGF-Beta Signaling in Early Limb Chondrogenesis. **H. Seo***, **S. Dong***, **R. Serra**. Cell Biololgy, University of Alabama at Birmingham, Birmingham, AL, USA.

Chondrogenesis is the first step for endochondral bone formation. It begins with the condensation of mesenchymal cells. During this process, condensing cells begin to form and deposit an extracellular matrix (ECM) that is a characteristic for cartilage. Type II collagen (Col2a) is one of the ECM molecules known as a specific marker of chondrogenesis. Previously, many studies have implicated TGF-b as an essential regulator of chondrogenic differentiation and Col2a expression in mesenchymal cells through unknown mechanisms. Another essential factor for chondrogenesis is Sox9, a transcription factor that regulates Col2a1 expression. Studies in mice showed that Sox9 haploinsufficiency results in lethal skeletal malformations including campomelic dysplasia. To determine the role of TGF-b signaling in chondrogenesis and Sox9 function, we generated an adenovirus vector that expresses a truncated, dominant-negative form of the TGF-b type II receptor (DNIIR). When DNIIR was expressed in C3H10T1/2 cells or

mouse embryonic limb bud cell before condensation, Sox9 protein and mRNA levels were remarkably down-regulated and cartilage nodule formation was inhibited. In contrast, exogenous addition of TGF-b to limb bud cells resulted in an increase in the level of phosphorylated Sox9 without alterations in total protein or mRNA levels. These results suggest a model in which TGF-b signaling is required for chondrogenesis via regulation of Sox9 activation. To further understand the role of TGF-b signaling on chondrogenesis, mice that express the cre recombinase under the control of the Prx1-promoter were crossed with mice in which both alleles of the TGF-b type II receptor were surround with LoxP sites. We propose this conditional knockout of TGF-b type II receptor will explain the overall role of TGF-b signaling on early chondrogenesis in the limb.

Disclosures: **R. Serra**, None.

SA158

Yeast-2-Hybrid Analysis Identifies Novel Protein Interactions with TGFβ Inducible Early Gene-1. **J. R. Hawse**¹, **M. Subramaniam**¹, **M. Oursler**², **B. A. Davies***¹, **B. J. Bellin***¹, **B. F. Horazdovsky***¹, **T. C. Spelsberg**¹. ¹Biochemistry and Molecular Biology, Mayo Clinic, Rochester, MN, USA, ²Endocrine Research Unit, Mayo Clinic, Rochester, MN, USA.

TGFβ inducible early gene-1 (TIEG) is a member of the Krüppel-like transcription factor family that was originally identified and characterized in human osteoblasts. TIEG is known to regulate the expression of a number of genes and plays an important role in mediating TGFβ effects in cells by enhancing the Smad signaling pathway. In order to elucidate the manner by which TIEG functions, we have utilized yeast-2-hybrid assays to identify specific proteins with which TIEG interacts. A Matchmaker System 3 yeast-2-hybrid kit (Clontech) was used to identify potential protein-protein interactions with TIEG. Screening of clones was conducted using high stringency selection plates to decrease the potential for identifying false-positives. Sequencing analysis of yeast colonies identified 28 unique genes that potentially interact with the human TIEG protein including the previously identified seven in absentia homologue 1 gene as well as the co-repressor, mSin3a, interferon regulatory factor 2 binding protein, actin binding double zinc-finger protein, apolipoprotein D, and the mitochondrial inner membrane preprotein translocase TIM17a, to name a few. GST pull-downs and co-immunoprecipitation assays are ongoing to further confirm the interactions between TIEG and the identified proteins of interest. Previous studies have shown that the TIEG family of proteins is capable of interacting with mSin3a through an alpha-helical repression motif. Our laboratory has also demonstrated that TIEG down-regulates Smad-7 expression by binding to a GC rich sequence upstream of the promoter. Since mSin3a was identified as a TIEG-1 interacting protein, we are currently performing chromatin immunoprecipitation assays on the Smad-7 promoter to determine if the mSin3a-histone deacetylase complex is recruited by TIEG to repress Smad-7 gene expression. Experiments are also currently underway to purify the human TIEG protein for subsequent use in protein array studies which will allow us to determine if TIEG is capable of interacting with over 1800 known human proteins. Identification of specific proteins via the above mentioned methods is an essential first step in the determination of how TIEG functions as a transcription factor and the mechanisms by which it elicits its effects on cell signaling, growth and function.

Disclosures: **J.R. Hawse**, None.

SA159

Effect of Recombinant Human Transforming Growth Factor-beta2 Dose on Bone Formation in Rat Femur Titanium Implant Model. **K. Sena***, **A. S. Virdi**, **D. R. Sumner**. Anatomy & Cell Biology, Rush University Medical Center, Chicago, IL, USA.

Growth factors such as transforming growth factor-beta (TGF-β) and bone morphogenetic proteins (BMP) have been shown to enhance bone repair and implant fixation in a number of animal models. Recently, we reported that application of recombinant human transforming growth factor-beta2 (rhTGF-β2) enhances peri-implant bone volume and bone-implant contact in a rat model where treatment with 10 μg TGF-β2 showed the greatest effect and lower doses (0.1 and 1 μg) were not effective. To further investigate this effect and to establish an optimal dose for future studies, present experiment evaluated the effect of three concentrations of rhTGF-β2 spanning across 10 μg dose on bone regeneration and mechanical fixation in the same model. The study was approved by the local Institutional Animal Care and Use Committee. Four groups (13 animals per group, 52 animals total) received unilateral femoral implantation of hydroxyapatite/tricalcium phosphate coated titanium (Ti/HATCP) implants. Three groups consisted of rats implanted with 1 of 3 doses of rhTGF-β2 (5, 10, 20 μg) loaded on to the implants. Implants in the control groups were treated with buffer only. Four weeks post-surgery, all implanted femurs were analyzed by micro computed tomography (μCT). Ten samples from each group were subjected to mechanical pull-out test to measure the strength of fixation of the implant. The remaining 3 specimens were embedded in plastic resin and sectioned for routine histology. From the μCT data, five comparable regions were selected along the length of the implant. The scanned sections were contoured to exclude the implant and bone volume per total volume (BV/TV) was calculated for region between the endocortical perimeter and the implant (diaphyseal sites). Compared to control, all rhTGF-β2-treated groups had significantly higher BV/TV than the control group (p < 0.001). These findings are consistent with our previous studies which demonstrated enhanced peri-implant bone volume with 10 μg of rhTGF-β2. Bone-implant contact didn't show difference between control and 5, 10 μg treated groups, however 20 μg group had less contact than the control. The mechanical pull-out tests showed decrease in strength in the rhTGF-β2 treated groups and this difference was significant between all rhTGF-β2-treated groups and the control group. Thus, while rhTGF-β2 was able to enhance bone formation (BV/TV), the relative lack of bone-implant contact depressed the strength of fixation, suggesting that the location as well as the amount of bone regeneration is important.

Disclosures: **K. Sena**, None.

SA160

See Friday Plenary number F160.

SA161

Isolation and Identification of Serum Factor(s) as BMP-4, which Inhibits Myogenesis and Induces Osteoblast Differentiation. K. Kodaira^{*1}, T. Katagiri², M. Goto^{*1}, A. Tomoyasu^{*1}, M. Namiki^{*3}, R. Kamijo³, K. Higashio^{*1}, T. Suda⁴. ¹Fuji Gotemba Research Labs, Chugai Pharmaceutical co., Ltd., Shizuoka, Japan, ²Division of Pathophysiology, Saitama Medical School, Research Center for Genomic Medicine, Hidaka-shi, Saitama, Japan, ³Department of Biochemistry School of Dentistry, Showa University, Tokyo, Japan, ⁴Saitama Medical School, Research Center for Genomic Medicine, Hidaka-shi, Saitama, Japan.

Unknown serum factor(s) regulates proliferation, differentiation and function of various types of cells. Fetal bovine serum (FBS) stimulates osteoblast differentiation and inhibits myogenic differentiation in vitro. We found that treatment of myogenic cells with FBS for 1 h induced expression of Id1, one of the early responsive genes for BMP signaling, via a 29 bp BMP-responsive element. FBS induced phosphorylation of Smad1/5/8 and their DNA-binding to the BMP-responsive element in the Id1 gene. Furthermore, inhibition of BMP signaling by expressing either dominant-negative BMP receptor (dnBMPR), noggin, or I-Smad similarly induced marked enhancement of myogenic differentiation even in the presence of a high concentration of FBS. Addition of recombinant dnBMPR or noggin to the osteoblast cultures suppressed dose-dependently osteoblast maturation in the presence of FBS, suggesting that the responsible factor(s) in FBS for inducing Id1 expression and regulating myogenic and osteoblast differentiation is a common BMP-like activity. We attempted to isolate the ALP-inducing activity of FBS by a series of column chromatography from 5 L of FBS. Finally, we obtained an active band with an apparent molecular weight of about 33kDa on SDS-PAGE under non-reducing conditions, and its activity was abolished under reducing conditions. After in gel-digestion of the band with trypsin, a fragment of the BMP-4 protein identical to both human and mouse sequences was detected by liquid chromatography-tandem mass spectrometry (LC-MS/MS). Furthermore, we found that the ALP-inducing activity of serum was high, but its specific activity was gradually decreased on the purification process. Interestingly, the ALP-inducing activity in serum was always eluted in a fraction larger than 100kDa by molecular sieving chromatography. To our knowledge, this is the first report to isolate and to unequivocally identify a serum factor(s) as BMP-4. The present study also suggests that the formation of a large complex comprised BMP-4 and other molecules potentiates its biological activity in serum.

Disclosures: **T. Katagiri**, Chugai Pharmaceutical Co., Ltd. 2.

SA162

Osteoblastic Expression of Transforming Growth Factor (TGF)- β 1 Is Increased in Osteoarthritic Patients and Reduced in the Elderly. C. G. Eriksen^{*1}, H. J. Olsen^{*1}, L. B. Husted¹, K. Søballe^{*2}, B. L. Langdahl¹. ¹Endocrinology, Aarhus University Hospital, Aarhus Sygehus, Aarhus C, Denmark, ²Orthopedics, Aarhus University Hospital, Aarhus Sygehus, Aarhus C, Denmark.

Osteoporosis and osteoarthritis are both very common diseases. Osteoporosis is defined as reduced BMD whereas osteoarthritis is associated with increased BMD. Likewise it is known, that BMD declines after peak bone mass is reached. We hypothesised, that these different phenotypes are caused by differences in osteoblastic expression of Transforming Growth factor (TGF- β 1), Receptor activator of NF- κ B (RANKL), Osteoprotegerin (OPG) and Interleukin (IL)-6. The four genes were chosen because they are expressed by osteoblasts and are involved in control of osteoblast and osteoclast activity; Standardized bone biopsies have been obtained from the femoral neck from 22 osteoporotic and 21 osteoarthritic patients during surgery for hemi- or total hip replacement. From 18 patients, 15 healthy age matched controls and 15 young individuals bone marrow aspirations from crista iliaca posterior were obtained. Osteoblasts and osteoblast precursor cells from bone biopsies and bone marrow aspirations were cultured until confluency. The quantitative gene expression analyses were carried out on the basis of Trizol/phenol isolated mRNA by using SYBR Green real-time PCR technique. The relative expression of the genes of interest (TGF- β 1, RANKL, OPG, and IL-6) is calculated in relation to three carefully selected housekeeping genes for each comparison. Osteoblasts from osteoarthritic bone marrow expressed more TGF- β 1 than osteoblasts from healthy age matched controls ($p < 0.05$). There were no significant differences in the relative expression of RANKL, OPG, IL-6 and the ratio RANKL/OPG between the two groups. The more mature osteoblasts from osteoarthritic bone biopsies expressed more TGF- β 1 ($p < 0.01$) and RANKL ($p < 0.001$) than the more immature osteoblasts obtained from bone marrow. OPG expression was not different and the ratio RANKL/OPG was higher in the more mature osteoblasts ($p < 0.01$). There was no difference in the relative expression IL-6. Osteoblasts obtained from bone marrow from healthy young individuals expressed more TGF- β 1 and OPG ($p < 0.05$) and less IL-6 ($p < 0.05$) than healthy elderly individuals. There was no difference in expression of RANKL between the two groups, however, the ratio RANKL/OPG tended to be reduced ($p = 0.08$). In conclusion, we have demonstrated that osteoblasts from young individuals express more TGF- β 1 and OPG and less IL-6, favouring bone formation over bone resorption. Furthermore, osteoblasts from osteoarthritic bone express higher levels of TGF- β 1 compared to age-matched controls.

Disclosures: **C.G. Eriksen**, None.

SA163

TGF-Beta Signaling Regulates the Mechanical Properties and Composition of Bone Matrix. G. Balooch^{*1}, G. W. Marshall^{*1}, M. Balooch^{*1}, S. J. Marshall^{*1}, R. O. Ritchie^{*2}, R. K. Nalla^{*2}, R. Derynck^{*1}, T. Alliston¹. ¹University of California, San Francisco, San Francisco, CA, USA, ²Lawrence Berkeley National Laboratory, Berkeley, CA, USA.

The ability of bone to resist fracture is determined by the bone mass and architecture, and the mechanical properties and composition of the bone matrix. Several signaling pathways, including estrogen, parathyroid hormone, and TGF- β , have been implicated in the control of bone mass and architecture. Presumably bone matrix mechanical properties are highly regulated; however, the regulators themselves remain unknown. TGF- β inhibits terminal osteoblast differentiation by binding its cell-surface receptor and activating Smad3 to regulate transcription of genes required for osteoblast differentiation. We hypothesized that TGF- β regulates mechanical properties and composition of bone matrix - including elastic modulus, fracture toughness, and bone mineral concentration (BMC). Existing transgenic mouse models show altered TGF- β signaling, from 16-fold (D4 mice) and 2.5-fold (D5 mice) over-expression of TGF- β in bone, to decreased TGF- β signaling due to osteoblast expression of a dominant negative TGF- β receptor (E1 mice) and targeted deletion of the Smad3 gene (Smad3+/- and -/- mice). Bones from these mice were evaluated using atomic force microscopy and elastic modulus mapping to measure elastic modulus (E), three-point bending to measure fracture toughness, and synchrotron x-ray tomography (XTM) to measure BMC. Mice with elevated TGF- β signaling (D4, D5) had up to 23% reduced E ($p < .001$) while mice in which TGF- β signaling was impaired (E1, Smad3+/-, and Smad3-/-) had up to 54% increased E ($p < .001$) compared to WT littermates. Histomorphometric, x-ray, XTM, and 3-D XTM reconstruction analyses showed that Smad3+/- bone, like E1 bone, possessed increased BV/TV, 48% increased cortical thickness ($p < .001$), and 53% increased BMC ($p < .01$) relative to WT. Osteopenic Smad3-/- mice had reduced BMC, likely secondary to systemic effects of Smad3 loss. In addition to elevated E and BMC, Smad3+/- mice also had elevated fracture toughness, similar to E1 mice that also had partially reduced TGF- β signaling, albeit through a different mechanism. Therefore, partial reduction of TGF- β signaling in bone is sufficient to produce bone with increased cortical thickness, structural bone parameters, mineral content and local mechanical properties, enabling these bones to better resist fracture. Our results suggest that a reduction of TGF- β signaling may be considered as a therapeutic target to treat bone disorders. We will investigate the effect on bone matrix properties of TGF- β RI kinase inhibitors, currently being considered for treatment of cancer metastases.

Disclosures: **G. Balooch**, None.

SA164

TGF-Beta1 Regulation of ATF-3 and its Target Genes in Bone Metastasizing Breast Cancer Cells. N. Selvamurugan¹, S. Kwok^{*1}, S. R. Rittling^{*2}, M. Reiss^{*3}, N. C. Partridge¹. ¹Physiology and Biophysics, UMDNJ-Robert Wood Johnson Medical School, Piscataway, NJ, USA, ²Rutgers University, Piscataway, NJ, USA, ³The Cancer Institute of New Jersey, New Brunswick, NJ, USA.

Transforming growth factor- β 1 (TGF- β 1) is the most potent known growth inhibitor for normal epithelial cells. In breast tissue, loss of this TGF- β 1 anti-proliferative response favors tumor formation. Moreover, in breast cancer cells, TGF- β 1 is a crucial molecule for stimulation of invasion and formation of bone metastases. The molecular mechanisms of how TGF- β 1 mediates these effects have yet to be completely determined. We have found that the transcription factor, activating transcription factor-3 (ATF-3) is strongly stimulated and its level is sustained by TGF- β 1 in highly invasive and metastatic human breast cancer (MDA-MB231) and mouse mammary pad tumor cells (r3T), in contrast to the transient stimulation and repression of ATF-3 by TGF- β 1 in non-cancerous cells. ATF-3 is also expressed in human primary breast tumors. Overexpression of ATF-3 increased normal human mammary epithelial cell (MCF-10A) number and DNA synthesis. Since TGF- β 1 stimulates and sustains expression of ATF-3 in breast cancer cells and ATF-3 increases cell proliferation in normal human mammary epithelial cells, we next determined whether knockdown of ATF-3 expression in breast cancer cells has any effect on expression of cell cycle genes. TGF- β 1 stimulated expression of cyclin A1, -B1, -D1, and -E in these cells while knockdown of ATF-3 with siRNA resulted in a decreased expression of only cyclin A1 in both control and TGF- β 1-stimulated MDA-MB231 cells. Since MDA-MB231 cells are highly invasive and metastatic in nature and TGF- β 1 stimulates matrix metalloproteinase-13 (MMP-13; collagenase-3; an invasive and metastatic gene), we next determined whether MMP-13 is a target gene for ATF-3. Transient transfection of ATF-3 siRNA reduced both the control and TGF- β 1-stimulated MMP-13 promoter activity in MDA-MB231 cells. To determine whether ATF-3 associates with the MMP-13 promoter, chromatin immunoprecipitation was carried out using an ATF-3 antibody and PCR amplification of DNA fragments corresponding to the TGF- β -responsive region of the MMP-13 promoter. The results identified *in vivo* the presence of ATF-3 protein on the MMP-13 promoter, and a shift and an increased binding of this protein from the AP-1 site to the RD/Runx binding site by TGF- β 1 in MDA-MB231 cells. Thus, we are the first to identify the TGF- β 1-regulation of ATF-3 and its target genes, cyclin A1 and MMP-13 in bone metastasizing breast cancer cells. The dysregulation of ATF-3 by TGF- β 1 in breast cancer cells may be key to the subsequent metastasis of these cells to bone.

Disclosures: **N. Selvamurugan**, None.

SA165

Baseline Bone Morphology and Cell Activity May Predict the Degree of Disuse Osteopenia. M. E. Squire¹, A. Brazin*¹, L. R. Donahue², C. Rubin¹, S. Judex¹. ¹Biomedical Engineering, SUNY Stony Brook, Stony Brook, NY, USA, ²The Jackson Laboratory, Bar Harbor, ME, USA.

The removal of functional loading rapidly decreases trabecular bone quantity within weight-bearing bones. Using male and female F1 crossbreds (BALB/cByJ x C3H/HeJ), we previously demonstrated that the deleterious effects of unloading (3 wk) on trabecular bone quantity were gender-dependent and that the magnitude of the effect varied across anatomic sites within a bone (metaphysis vs. epiphysis) and across distinct bones (femur vs. tibia). Here we tested the hypothesis that the gender- and site-specific mechanosensitivity demonstrated in the F1 skeleton can be predicted by differences in baseline indices of bone morphology and/or variations in bone's formative and resorptive activities. Micro-computed tomography (12µm) determined the ratio of bone surface to bone volume (BS/BV) and bone volume fraction (BV/TV) in the trabecular metaphyseal and epiphyseal regions of the distal femur and proximal tibia harvested from adult (4 mo) male and female (n=10 each) F1 mice. In these same regions of bones from a second set of F1 mice (n=10 per gender), histomorphometry was used to assess indices of bone formation (MS/BS, MAR) while resorptive activity (Oc.S/BS) was determined by staining for tartrate resistant acid phosphatase (TRAP). Across the four regions, linear regressions tested the relation between baseline BS/BV, BV/TV, MS/BS, MAR, Oc.S/BS and the relative loss in BV/TV after 3 wk of disuse. The results revealed a correlation between baseline BS/BV and percent bone loss across the four regions in both females ($r^2=0.99$, $p<0.01$) and males ($r^2=0.86$, $p<0.07$), suggesting that a greater ratio of BS/BV may result in greater bone loss. Baseline BV/TV and percent bone loss were inverse correlated in both females and males ($r^2=0.97$, $p<0.02$ and $r^2=0.86$, $p=0.07$), suggesting that less bone is lost from regions that have greater baseline bone quantity. This inverse relation between bone quantity and bone loss has been previously demonstrated within the skeleton of female BALB/cByJ and across skeletons from second generation BALB/cByJ x C3H/HeJ mice. Results from the current study also revealed that, in females, disuse-induced bone loss was correlated to MAR ($r^2=0.78$, $p=0.11$), whereas in males this loss was correlated to MS/BS ($r^2=0.70$, $p=0.16$), suggesting gender differences in baseline predictors of skeletal mechanosensitivity. Oc.S/BS was not correlated to relative bone loss in either females ($r^2=0.15$) or males ($r^2=0.36$). Taken together, the results suggest that, in the absence of genetic factors, baseline bone morphology and indices of bone formation may explain, in part, the gender- and site-specific sensitivity of the skeleton to unloading.

Disclosures: **M.E. Squire**, None.

SA166

See Friday Plenary number F166.

SA167

Mechanical Loading Alters RANKL and OPG Expression in MC3T3-E1 Cells. H. Lee¹, D. KIM¹, J. A. Karmin*¹, S. Lee*¹, J. Yang*², F. Y. LEE¹.

¹Center for Orthopaedic Research, Columbia University, New York, NY, USA,

²Anesthesiology, Columbia University, New York, NY, USA.

Bone adapts to mechanical loading to maintain its structural and functional integrity. However, the underlying molecular mechanisms by which bone cells respond to various mechanical environments are not fully understood. Osteoblasts play a pivotal role in bone formation and the regulation of osteoclastogenesis by generating RANKL (receptor activator of nuclear factor kappa B ligand) and OPG (osteoprotegerin). The balanced action of RANKL and OPG may be one of the key factors in the regulation of bone remodeling. However, the biochemical responses of these molecules to mechanical loading have yet to be studied in depth. In the present study, therefore, we used following two experimental paradigms to verify the aforementioned issue. Murine RANKL cDNA with HA and V5His tags at its N and C-terminal regions, respectively, were transfected into MC3T3-E1 pre-osteoblast cells cultured in 6-well bioflex culture plates. Then the cells were bi-equiaxially stretched (0, 0.5, 1, 2.5, and 5% strains) at a frequency of 1 Hz for 15 minutes once a day for 7 consecutive days using a Flexcell 4000 with a Tension Plus Control Unit. To detect secreted soluble RANKL-V5 in the conditioned medium, a Talon pull down assay was performed in conjunction with immunoblotting. Meanwhile, *in vitro* mechanical loading to bone cells in a direct manner do not truly represent *in vivo* condition. Furthermore, fluid shear stress generated by enforced fluid flow in lacunae-canalliculi porosities in response to mechanical loading may govern osteoclastogenesis via regulation of the expressions of RANKL and OPG from osteoblast. Thus 0, 1, 5, and 10 dynes/cm² at 0.5 Hz of shear stresses were applied to MC3T3-E1 cells which were grown in a monolayer on the cover slide for 15 min using a STREAMER™ system. We found that membrane-bound RANKL protein increased while the level of secreted RANKL-V5His protein decreased as mechanical strain increases. We also found that RANKL and OPG protein expressions increased in a fluid shear stress-dependent manner, and the RANKL/OPG ratio decreased as the intensity of fluid shear stress increased. RANKL/OPG ratio also found to be decreased as duration of shear stress increased. Taken together, mechanical loading may be a key initiator of bone remodeling by modulating the balance of RANKL and OPG expression.

Disclosures: **F.Y. Lee**, None.

SA168

See Friday Plenary number F168.

SA169

Fluid Flow Regulation of the 3'-Untranslated Region of Cyclooxygenase-2 in MC3T3-E1 Cells. M. Mehrotra, O. Voznesensky*, M. Saegusa*, C. Pilbeam. Dept. of Medicine, University of Connecticut Health Center, Farmington, CT, USA.

Mechanical strains may be transduced into biochemical signals by generating interstitial fluid flow (FF) within the mineralized bone matrix. FF induces expression of cyclooxygenase-2 (COX-2), the major enzyme involved in prostaglandin production, in osteoblasts. The COX-2 3'-untranslated region (3'-UTR) contains multiple copies of the adenosine and uridine (AU)-rich elements known to influence mRNA stability by interacting with specific RNA binding proteins. It is likely that, in addition to regulating transcription of COX-2 mRNA, FF also regulates stability of COX-2 mRNA via the 3'-UTR. We stably transfected MC3T3-E1 cells with the entire mouse COX-2 3'-UTR (1-2232 bp), cloned into pGL3 firefly luciferase vector, or with the vector only to examine effects of the COX-2 3'-UTR on luciferase protein and mRNA stability. In static culture, luciferase activity and mRNA (measured by real time qPCR) were >3-fold higher in cells carrying the full 3'-UTR than in vector only cells, suggesting mRNA stabilization by the full 3'-UTR in the absence of FF. In cells subjected to 30 min of pulsatile FF and then returned to static culture (post FF culture), the induction of COX-2 mRNA peaked at 2 h post FF and remained elevated for more than 4 h. The luciferase mRNA level in cells with the full COX-2 3'-UTR was decreased relative to vector only cells at 1 h post FF but subsequently increased 2-fold at 4 h post FF, suggesting that the 3'-UTR destabilized mRNA initially after FF but subsequently increased stabilization in post FF static culture. When cells were subjected to 30 min of FF and then treated with the transcription inhibitor actinomycin (ACT) as they were placed into static culture, luciferase mRNA levels in cells with the full COX-2 3'-UTR decreased more slowly (30% over 4 h) than levels in vector only cells (70% over 4 h) and were always higher than levels in vector only cells, suggesting that ACT might prevent transcription of a destabilizing factor interacting with the COX-2 3'-UTR. Destabilization of COX-2 mRNA may be associated with tristetraprolin, a zinc finger protein that can bind to AU-rich elements in the 3'-UTR of COX-2. Tristetraprolin was highly expressed in MC3T3-E1 cells under no flow conditions, and FF for 30 min increased mRNA expression 3.5-fold. However, in post-FF cultures, tristetraprolin mRNA expression decreased, falling to 1/5 of the level in no flow cells by 4 h of post-FF culture. These studies suggest that the full COX-2 3'-UTR enhances mRNA stability in static culture following briefly applied FF. We speculate that regulation of tristetraprolin expression by FF is one of the factors involved in this effect.

Disclosures: **M. Mehrotra**, None.

SA170

See Friday Plenary number F170.

SA171

Model Microgravity Decreases Osteoblastogenesis of Human Mesenchymal Stem Cells by Upregulation of Nitric Oxide Synthase 2 and Hypoxia Inducible Factor 1 alpha. K. Fulzele*, V. E. Meyers*, J. M. McDonald, M. Zayzafoon. The Department of Pathology, The University of Alabama at Birmingham, Birmingham, AL, USA.

The lack of gravitational stimulus during space travel or lack of mechanical environment during disuse and aging negatively affects osteoblastogenesis resulting in skeletal abnormalities such as osteopenia, decreased bone formation, decreased mineralization and reduced bone strength. We have previously demonstrate that modeled microgravity (MMG) inhibits osteoblastogenesis and induces adipogenesis of human mesenchymal stem cells (hMSC) by disrupting the actin cytoskeleton and inhibiting the small GTPase, RhoA. Increasing expression of inducible nitric oxide synthase (NOS2) and hypoxia inducible factor-1α (HIF-1α) are known to be associated with early adipocytic commitment and differentiation. The purpose of this study is to examine the effects of MMG on the expression of NOS2 and HIF-1α to elucidate the mechanism by which MMG suppresses osteoblastogenesis. Mesenchymal stem cells cultured in MMG acutely induce NOS2 protein expression within 1 hour and reaches plateau within 6 hours. Intracellular nitric oxide, measured by fluorescence staining with 4, 5-diaminofluorescein (DAF-2), increases to a maximal concentration after 6 hours of culture in MMG. Furthermore HIF-1α protein expression is rapidly induced after 30 minutes of MMG and returns to basal levels by 6 hours. In addition, electromotility shift assay demonstrates that MMG increases the DNA-binding activity of the hypoxia response element. These results were not due to hypoxia as MMG does not alter the pH, pO₂ and pCO₂ compared to gravity cultured cells, measured using a Radiometer ABL 715 blood gas analyzer. Selective inhibition of NOS2 activity by 1400W partially restored actin cytoskeletal stress fibers and reduced intracellular lipid accumulation in hMSC after 7 days of culture in MMG. Taken together, these results suggest a novel mechanism whereby MMG results in cytoskeletal disruption, reduced osteoblastogenesis and enhanced adipogenesis of hMSC by normoxic upregulation of HIF-1α and NOS2. Our work suggests that the inhibition of NOS2 activity may prove to be a novel countermeasure to rescue osteoblastogenesis in spaceflight-induced bone loss.

Disclosures: **K. Fulzele**, None.

SA172

See Friday Plenary number F172.

SA173

The Role of PKC-induced Cytoskeleton Rearrangement in Parathyroid Hormone Enhanced $[Ca^{2+}]_i$ Response to Mechanical Stimulation in Osteoblasts. J. Zhang*, Y. P. Formin, R. L. Duncan. Orthopaedic Surgery, Indiana University School of Medicine, Indianapolis, IN, USA.

A rapid increase in intracellular free Ca^{2+} ($[Ca^{2+}]_i$) is the earliest measured response to mechanical stimulation in osteoblasts. We have shown that parathyroid hormone (PTH) significantly enhances this mechanical-induced response by altering ion channel kinetics. While the PTH-induced changes in channel kinetics appear to be the result of protein kinase A (PKA) activation, we have found that PTH produces rearrangement of the actin cytoskeleton that, in turn, sensitizes the mechanosensitive cation-selective channel (MSCC) to respond to mechanical stimulation. Although previous data do not implicate PKC activation in the PTH augmentation of the $[Ca^{2+}]_i$ response to fluid shear, we have recently found that PKC activation can enhance the $[Ca^{2+}]_i$ response to mechanical load in a time dependent manner. Here we postulate that activation of PKC by PTH can increase the $[Ca^{2+}]_i$ response to mechanical loading by changing the actin organization. Using MC3T3-E1 preosteoblastic cells loaded with fura-2, we found that pre-incubation with 50nM PTH for 10min produced a 4.5 fold increase in the peak $[Ca^{2+}]_i$. Further, addition of 1 μ M GF109203X (a general PKC inhibitor) for 10 min prior to PTH treatment significantly reduced the peak $[Ca^{2+}]_i$ response to hypotonic challenge. Addition of 4 β -phorbol 12-myristate 13-acetate (PMA; 1 μ M) did not increase the $[Ca^{2+}]_i$ above that of PTH treatment alone. These data suggested that the PTH enhanced $[Ca^{2+}]_i$ response to mechanical stimulation at least partially involved the activation of PKC pathway. We found that only PKC α exhibited translocation from cytoplasm to plasma membrane region during hypotonic challenge. Inhibition of PKC α activation with the PKC α -specific inhibitor, Go6976, attenuated the hypotonic-induced $[Ca^{2+}]_i$ response, while specific inhibition of PKC with LY379196 did not. Treatment of MC3T3-E1 cells with 50nM PTH for 30min significantly disrupted the actin cytoskeleton and decreased the amount of stress fibers. Similar effects were observed with 1 μ M PMA. Pretreatment with either the general PKC inhibitor, GFX, or Go6976 ablated the PTH effect on the actin cytoskeleton while PKC β inhibitor LY379196 failed to do so. These data indicate that PTH alters the actin cytoskeleton through PKC α activation, thereby enhancing the $[Ca^{2+}]_i$ response to mechanical stimulation by altering the kinetics of the MSCC.

Disclosures: **J. Zhang**, None.

SA174

See Friday Plenary number F174.

SA175

Ski Inhibits TGF- β Signaling and Accelerates Hypertrophic Differentiation in Chondrocytes. K. Kim*, M. Pirri*, Q. Wu, R. N. Rosier, M. J. Zuscik. Orthopaedics, University of Rochester, Rochester, NY, USA.

It is well established that TGF- β signaling, which potently inhibits chondrocyte maturation, is required for maintenance of articular cartilage and regulation of the hypertrophic program during endochondral ossification. The seminal *in vivo* findings that support this idea derive from mouse models that display loss of TGF- β signaling, which display accelerated chondrocyte maturation in both articular and growth plate cartilages. Thus, endogenous negative regulation of the TGF- β signaling cascade likely plays a central role in the modulation of chondrocyte differentiation during skeletal development and repair processes. One such inhibitor of this cascade is Ski, a transcriptional co-repressor that links Smads to histone deacetylase, leading to blockade of target gene expression that would normally be induced by Smad-containing transcriptional complexes. Regarding specificity, Ski is known to inhibit TGF- β signaling via a strong interaction with Smads 2, 3 and 4 while BMP signaling is unaffected due to Ski's weak interaction with Smads 1 and 5. We hypothesize that due to the central regulatory role of TGF- β /Smad signaling in chondrocytes, inhibition of signaling by Ski is an important regulatory event in chondrocyte differentiation. As such, we predict that Ski-induced loss of signaling on this axis will lead to accelerated maturation of chondrocytes. We tested this hypothesis in the chick upper sternal chondrocyte (USC) model by assessing Ski expression and signaling function and by examining the phenotypic impact of Ski gain-of-function. Establishing that Ski is up-regulated as chondrocytes progress toward terminal maturity, the Ski mRNA expression pattern mirrors that of type X collagen during a six day time course. Suggesting that this up-regulation leads to reduced TGF- β signaling, over-expression of Ski in USCs completely abolishes both basal and TGF- β -stimulated signaling on the P3TP-luciferase reporter. The mechanism of this inhibition in USCs was determined via immunoprecipitation/western blot experiments which indicated that following TGF- β treatment, Ski specifically associates with phospho-Smad2 and to a lesser extent with phospho-Smad3 and Smad4. Finally, demonstrating a regulatory role, Ski over-expression leads to accelerated maturation in USCs, evidenced by increased type X collagen mRNA expression and enhanced alkaline phosphatase activity. Taken together, these results suggest that Ski participates in regulation of chondrocyte maturation through its inhibition of TGF- β signaling. Dis-regulation of the expression/function of Ski may therefore have ramifications in developmental and repair processes in the skeleton.

Disclosures: **K. Kim**, None.

SA176

See Friday Plenary number F176.

SA177

Quantitatively Profiling the Expression of P2Y Purinergic Receptors in Human Bone Related Cells and Their Intracellular Calcium Responses to Oscillatory Fluid Flow. Y. Gu*, C. M. Davis*, H. J. Donahue, J. You. Orthopaedics & Rehabilitation, The Pennsylvania State University College of Medicine, Hershey, PA, USA.

Substantial evidence has indicated that extracellular nucleotides signaling through P2Y purinergic receptors play an important role in the regulation of bone metabolism. To date, five major human P2Y purinergic receptors (P2Y1, P2Y2, P2Y4, P2Y6, and P2Y11) have been cloned. We hypothesize that different expression patterns/levels of P2Y purinergic receptors in bone cells may affect the ability of the cells to perceive and respond to changes in their extracellular milieu, both physical and chemical (hormonal). The aims of this study were to quantitatively profile the mRNA levels of five subtypes of P2Y receptors expressed in different human bone related cells, and to examine intracellular calcium (Ca^{2+}) mobilization responses to oscillatory fluid flow induced by mechanical loading. We first employed real time RT-PCR to profile the mRNA expression levels of five subtypes of P2Y receptors in different human bone related cells, including hFOB and MG-63 cell lines, human mesenchymal stem cells, and primary human osteoblastic cells from osteoporotic patients and non-osteoporotic patients. Our results demonstrated that bone cells expressed different P2Y receptor mRNA levels at different stages or in different bone cell lines. However, the profile of P2Y receptor mRNA expression levels for osteoblastic cells from osteoporotic patients was consistent with the profile in osteoblastic cells from non-osteoporotic patients. Secondly, we utilized fluorescent imaging techniques to quantify Ca^{2+} mobilization in response to oscillatory fluid flow. Similar to our P2Y profile results, there was no statistically significant difference in oscillatory fluid flow-induced Ca^{2+} mobilization between osteoblastic cells from osteoporotic patients and those from non-osteoporotic patients. However, the percentage of hFOB cells responding with an increase in $[Ca^{2+}]_i$ to oscillatory fluid flow was significantly ($p < 0.05$) less than that in MG-63 cells, human mesenchymal stem cells or primary human osteoblastic cells. After examining the sum of mRNA copy numbers of all subtypes of P2Y receptors, we found that the sum of all P2Y mRNA copy number was positively correlated with the percentage of cells responding to fluid flow with an increase in $[Ca^{2+}]_i$, suggesting that P2Y receptors play an important role in bone cell responses to fluid flow.

Disclosures: **J. You**, None.

SA178

Influence of Different Loading Modalities on Non-Weight Bearing and Weight Bearing Bone Structure. R. Nikander*¹, H. Sievänen*¹, A. Heinonen*², P. Kannus*¹. ¹UKK Institute, Tampere, Finland, ²Health, University of Jyväskylä, Jyväskylä, Finland.

Bone structure is known to adapt to the specific loading environment it regularly experiences. In this cross-sectional study of 113 young adult female athletes, representing volleyball, hurdling, racket-playing, soccer, and swimming, and their 30 non-athletic counterparts, we measured with pQCT the total bone mineral content, total area, cortical wall thickness, trabecular and cortical density, and polar section modulus at weight bearing tibia and at non-weight bearing radius and humerus. Our goal was to deepen the present, mostly DXA-based information (e.g. Nikander et al. JBMR 2005;20:520-528) on the influence of external loading modalities and internal joint moments on bone structure. In the tibia, substantial sport-specific skeletal benefits, swimming excluded, were observed (e.g. from racket players' 27% to hurdlers' 44% higher distal tibia section moduli). Estimated joint moment and loading modality explained ($p < 0.05$) from 29% to 50%, and from 8% to 25% of the variation in most bone variables, respectively. In the upper extremities, sports activity, the swimming included, was associated with clear benefits in bone variables (e.g. from swimmers' 19% to volleyballers' 27% higher humeral shaft section modulus). In contrast to tibia, only the estimated joint moment was clearly associated ($p < 0.05$) with structural characteristics, accounting for 6% to 26% of the variation in bone variables at shaft sites, but not at the distal site. Regardless of site, impact loading was clearly associated with strong bone structures, but the role of dynamic muscle activity and consequent joint moments became quite distinct in the upper extremities. It is thus obvious that different loading components dominate the specific skeletal adaptation in weight bearing and non-weight bearing bones.

Disclosures: **R. Nikander**, None.

SA179

See Friday Plenary number F179.

SA180

Loading Frequency-Dependent Enhancement of Bone Formation in Mouse Tibia with Knee-Loading Modality. P. Zhang*¹, S. M. Tanaka*², H. Jiang*³, M. Su*¹, H. Yokota*³. ¹Anatomy and Cell Biology, Indiana University School of Medicine, Indianapolis, IN, USA, ²Natural Science and Technology, Kanazawa University, Ishikawa, Japan, ³Biomedical Engineering, Indiana University Purdue University Indianapolis, Indianapolis, IN, USA.

The aim of the current study was to examine the role of mechanical loads applied to the tibial epiphysis underneath the knee. The specific question was whether this knee loading would present frequency-dependent enhancement of bone formation in the diaphysis without inducing *in situ* deformation of cortical bone. Twenty-four female C57/BL/6 mice

(~ 14 weeks old) were divided into three groups for three loading frequencies (5, 10 or 15 Hz, N = 8), and the loads with a peak-to-peak force of 0.5 N were applied to the left knee in the lateral-medial direction using a custom-made piezoelectric loader. Loads were given for 3 min per day for 3 consecutive days, and the right tibia was used as non-loading control. Mice were given an intraperitoneal injection of calcein at 30 µg/g body mass on days 2 and 6 after the last loading, and they were sacrificed 13 days after the last loading. The histomorphometric data such as mineralizing surface (MS/BS), mineral apposition rate (MAR), and bone formation rate (BFR/BS) were determined at two cross-sections, 25% (~ 4 mm) and 50% (~ 8 mm) distal to the knee. The results clearly showed frequency-dependent loading effects. First, the tibial cross-sectional area at 25% was significantly increased by the loading at 5 and 10 Hz ($p < 0.05$). Second, bone formation was enhanced on the periosteal surface, and the loading at 5 Hz resulted in a significant increase in the morphometric parameters ($p < 0.01$ for MS/BS; and $p < 0.001$ for MAR and BFR/BS). These parameters were elevated similarly at 10 Hz ($p < 0.05$ for MS/BS; and $p < 0.01$ for MAR and BFR/BS). Third, among the periosteal surfaces, bone formation was most effective in the medial surface with the loading at 5 and 10 Hz. In the section at 50%, the tibial cross-sectional area was significantly increased by the loading at 5 Hz ($p < 0.01$). On the periosteal surface, the loading at 5 Hz resulted in a significant increase in the morphometric parameters ($p < 0.05$ for MAR; $p < 0.01$ for MS/BS; and $p < 0.001$ for BFR/BS). In all measurements, no statistical difference was observed by the loading at 15 Hz. The strain in the tibia *ex vivo* ~ 4 mm and ~ 8 mm distant from the loading site (N = 4) was < 50 µstrains with the described knee-loading modality. Therefore, our results support that bone formation can be enhanced without *in situ* deformation. In summary, we demonstrate that the knee loading modality is an effective means to enhance bone formation in the tibial periosteum and the enhancement is maximized with the loading frequency at 5 Hz.

Disclosures: **P. Zhang**, None.

SA181

See Friday Plenary number F181.

SA182

Augmentation of Bone Gains during the Anabolic Post-Lactation Recovery Period Utilizing a Rat Bipodal Stance Model. J.E. Shea¹, S.L. Doody^{*1}, P.A. Eisenman^{*2}, S.C. Miller¹. ¹Radiobiology, University of Utah, Salt Lake City, UT, USA, ²Exercise and Sport Science, University of Utah, Salt Lake City, UT, USA.

There are profound changes in maternal metabolism and mineral homeostasis to meet the requirements of milk production during lactation, with bone loss occurring during lactation in all species studied. This catabolism during lactation is compensated by a marked anabolic phase that rebuilds skeletal structure and mineral stores after lactation. We sought to determine the influence of skeletal loading on cancellous bone during the post-lactation recovery period, utilizing a rat bipodal stance model. Established breeder rats were divided into three groups. The first, a baseline group (Base; n = 8) was taken at parturition. The second group of rats (n = 8) was maintained through lactation and a 6-week recovery period after weaning in normal cages (Rec). While, the third group (n = 8) was maintained in a raised cage through lactation and a 6-week recovery period after weaning (Rec-RC). The raised cage set-up requires the rats to stand on their hind legs to obtain food and water. The animals were given flourochrome markers 2 and 10 days prior to necropsy. Bone mineral content (BMC), bone mineral density (BMD), percent cancellous bone and cancellous bone formation indices were measured. The data are presented as the mean ± standard deviation. The femoral BMD of animals housed in raised cages (0.179 ± 0.008) was 9% higher than Base (0.163 ± 0.01) and 6% higher than Rec (0.169 ± 0.007). While, the femoral BMC of Rec-RC (0.467 ± 0.034) was statistically higher than Base (0.417 ± 0.034) but not Rec (0.438 ± 0.028). There were no differences between the Base and Rec groups in terms of BMD or BMC. However, the percent bone (BV/TV) in the proximal tibia, as determined by morphometry, was 20% higher in Rec-RC (24 ± 4) than Base (19 ± 7) and 17% higher than Rec (20 ± 3). There were no differences between the three groups in terms of the following bone formation indices: percent double labeled surface, mineral apposition rate, and bone formation rate. The data show that a relatively modest skeletal loading regimen significantly augmented increases in cancellous bone mass and density during the post-lactation anabolic period. An increase in skeletal loading (e.g. a reasonable exercise program) during this period may represent a unique opportunity to actually increase skeletal mass and strength in the adult female skeleton. This differs from other, non-pharmacological interventions that, at best, act to minimize loss of mass and strength with age. A greater bone mass in the adult female skeleton may provide an increased margin of protection against the development of osteoporosis and fractures later in life.

Disclosures: **J.E. Shea**, None.

SA183

See Friday Plenary number F183.

SA184

Three-Point Bending of Rat Femoral Midshaft in the Primary Loading Direction, the Mediolateral Plane - Introduction and Validation of a Novel Biomechanical Testing Protocol. O. Leppänen¹, H. Sievänen^{*2}, T. L. N. Järvinen³. ¹Medical School, University of Tampere, Tampere, Finland, ²Bone Research Group, UKK-institute, Tampere, Finland, ³Department of Orthopaedics and Traumatology, University of Tampere, Tampere, Finland.

Bones adapt their strength according to the incident loading. In the rat femoral midshaft, the principal direction of loading is in the medial and lateral plane. For obvious anatomical and subsequent practical reasons, three-point bending of rat femoral diaphysis has always been carried out in the anteroposterior direction. Therefore, to determine the mechanical properties of the femoral shaft in the apparent primary loading direction, we developed a test protocol that allows biomechanical testing of rat femoral midshaft in the mediolateral plane. This protocol was then validated by determining the repeatabilities (root-mean-square coefficient of variation, CV_{ms}) of bone strength, stiffness, and energy absorption (toughness). Thirty-eight pairs of Sprague-Dawley rat femora with a large variance in size were excised and subjected to a comprehensive structural analysis. All bones underwent peripheral quantitative computed tomography (pQCT) scanning of femoral midshaft, followed by the mediolateral three-point bending of the diaphysis. The repeatabilities (CV_{ms}) of the densitometric and mechanical parameters were determined by comparing the data from the ipsilateral and contralateral femora. On 37 pairs of femora, the testing was successful with a very constant failure mechanism; the failure taking place in the exact midshaft and the fracture line being perpendicular to the long axis of the bone without signs of torsion. The protocol showed excellent repeatability as the CV_{ms} of the structural strength, stiffness, and energy absorption were 3.8%, 6.6%, and 14.5%, respectively. The CV_{ms} for structural strength and stiffness in the mediolateral three-point bending were almost identical to the repeatabilities of the pQCT variables, indicating that the error of the method was minimal. However, the test showed considerably poorer repeatabilities for the energy absorption. In conclusion, we have introduced a new testing method for the determination of the structural strength of the rat femoral midshaft in mediolateral direction, the apparent principal loading direction of the bone site. This protocol was shown to be highly repeatable in terms of structural strength and stiffness.

Disclosures: **O. Leppänen**, None.

SA185

See Friday Plenary number F185.

SA186

Effects of Long-Term Tennis Playing on Bone Gross Geometry at the Distal Radius: A Quantitative Magnetic Resonance Imaging Study. G. Ducher^{*1}, S. Mème^{*2}, C. Magni^{*3}, J. Viala^{*3}, C. Chappard¹, D. Courteix¹, C. Benhamou¹. ¹Faculty of Sport Sciences & Inserm, EA 3895 & U658, Orleans, France, ²CNRS, Centre de Biophysique Moléculaire - UPR 4301, Orleans, France, ³Hopital of Orleans, Orleans, France.

The purpose of this study was to characterize the geometric changes of the dominant radius in response to long-term tennis playing using magnetic resonance imaging (MRI). Twenty competitive tennis players (10 men and 10 women, age: 23.1 ± 4.7 years, with 14.3 ± 3.4 years of practice), were recruited. Axial slices were obtained on both distal radii with a spin-echo sequence (TR: 645 ms, TE: 20 ms, pixel size: 195×195 µm, slice thickness: 2 mm) using a 1.5 T MR device. Six contiguous slices were analysed, covering 1.2 cm of the distal radius, starting 1.8 cm far from the articular surface between the radius and the lunatum. The total bone area, cortical area, endocortical area and muscle area were manually defined on each slice. Volumetric measurements were calculated as the summed products of measured areas and slice thickness over the region of interest. Bone mineral content (BMC) was derived from the DXA scan of the distal radius in order to match the region of interest scanned by MRI. Volumetric bone mineral density (BMD) was calculated as the quotient of DXA-derived BMC on the MRI-derived total bone volume. The comparison between the dominant and nondominant radius was performed by a parametric paired t-test. Significant relative side-to-side differences (p<0.0001) were found in muscle volume (+9.7%), BMC (+13.5%), total bone volume (+10.3%) and endocortical volume (+20.6%) but not in cortical volume (+2.6%, ns). The asymmetry in total bone volume explained 75% of the variance of the BMC asymmetry (p<0.0001). Volumetric BMD was slightly higher on the dominant side (+3.3%, p<0.05). On both sides, muscle volume was related to all bone parameters, except volumetric BMD (r=0.48-0.83, p<0.05-0.0001). The asymmetry in muscle volume did not correlate with any of the asymmetries in bone parameters. BMC was still greater on the dominant side after adjusting for muscle volume, whereas the side-to-side differences in bone geometric parameters disappeared. This study indicates that the greater BMC induced by long-term tennis playing at the dominant distal radius is mainly due to increased bone size, improving mechanical strength. Cortical volume is not significantly increased, except in the one-handed backhand players. The muscular volume and strength appeared to play a role in the bone response to loading. However, muscle and bone asymmetries were not correlated, suggesting that other stimuli, directly applied to the radius, may also stimulate bone mineral accrual.

Disclosures: **C. Benhamou**, None.

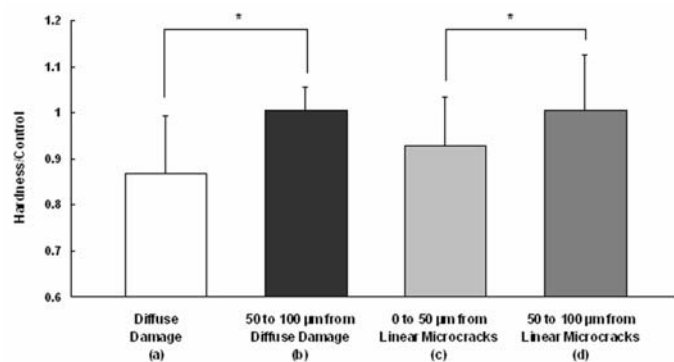
SA187

See Friday Plenary number F187.

SA188

Diffuse Damage Causes a Greater Loss of Local Material Properties of Cortical Bone than Linear Microcracks. T. Diab*, D. Vashishth*. Biomedical Engineering, Rensselaer Polytechnic Institute, Troy, NY, USA.

Historically, only bone mass has been considered to predict fracture risk but several recent studies have shown that other factors, including accumulation of microdamage may affect bone quality and contribute to bone fragility [Burr *et al.*, J Biomech 1998]. *In vivo*, microdamage occurs in the form of linear microcracks and diffuse damage. Evidence is beginning to emerge that different damage morphologies may affect bone quality differently [Diab and Vashishth, Bone In press], however, limited information exists on the effects of damage morphologies on local bone tissue properties. In this study, seven rectangular beams were wet machined from the anterior quadrant of bovine tibiae, and subjected to a four-point bending fatigue loading [Physiological conditions, 5000 μ strain]. Following fatigue loading, mechanical assessment of damage was done by microindentation based measurements of the local tissue hardness. Target areas of interest included a) diffuse damage region, b) 50 to 100 μ m zone surrounding diffuse damage, c) 0 to 50 μ m zone surrounding linear microcracks, and d) 50 to 100 μ m zone surrounding linear microcracks. For statistical analyses, data were examined using an ANOVA test. The results demonstrate that compared to controls, diffuse damage (Region a) and 0 to 50 μ m zone surrounding linear microcracks (Region c) show a significant drop in hardness ($p < 0.05$). The percentage of hardness loss was, however, distinct. Region (a) lost 83% more hardness than region (c). Based on these results we conclude that linear microcracks and diffuse damage affect the local bone properties differently. Linear microcracks are associated with 50 μ m zone that is softer than the surrounding bone tissue. The magnitude of local hardness loss due to a linear microcrack is, however, limited and is 83% less than the local hardness loss caused by the formation of diffuse damage. Based on evidence from engineering materials it is argued that greater softening of the local tissue properties will cause a greater dissipation of external applied energy and prevent a catastrophic fracture. Age-related modifications in bone quality, that alter the propensity of human bone to form diffuse damage over linear microcracks [Diab and Vashishth, Trans. ORS 2005], would therefore increase its propensity to fracture.



Acknowledgements: NIH grant AR49635

Disclosures: **T. Diab**, None.

SA189

The Role of Caspase3 in Bone Metabolism. H. Amano¹, K. Takahashi^{*2}, S. Niida³, S. Yamada^{*1}. ¹Pharmacology, School of Dentistry, Showa University, Tokyo, Japan, ²Physiological Chemistry, School of Pharmaceutical Science, Showa University, Tokyo, Japan, ³Dept of Bone and Joint Disease, National Center for Geriatrics and Gerontology, Obu, Japan.

Apoptosis is defined as programmed cell death, which is characterized by cell contraction and fragmentation, and nuclear aggregation and fragmentation. Various types of molecular signaling control Apoptosis. Caspase3, a type of cysteine protease, can be activated by stimulus, leading to degradation of a broad range of intracellular substances such as PARP and to induction of apoptosis. Approximately one-half of osteoblasts involved in bone formation undergo apoptosis during the process of transformation into osteocytes when embedded within the bone. In addition, osteoclasts are known to enter apoptosis away from the bone surface after bone resorption. Apoptosis in bone-related cells is considered an essential metabolic system in bone structure; moreover, Caspase3 may play a significant role in this process. We investigated the role of Caspase3 via utility of mice carrying a Caspase3 gene deficiency. Following completion of visual observation and x-ray photography of mouse skulls (8 weeks of age), skullcaps from mice with the gene deficiency exhibited quaquaversal (dome-like) formation characterized by an obtuse angle between the eye-ear plane and the anteroposterior diameter of the occipital skull-base in comparison with the wild type; consequently, growth suppression of the skull was apparent. Moreover, in mice with the gene deficiency, increased membranous ossification and mandibular prognathism were detected with increasing age. Newborn tibias, following fixation as tissue sections by conventional fixation, were decalcified, embedded in paraffin and observed under the microscope after TRAP staining for osteoclast counting; decreased osteoclast number was evident in mice with the gene deficiency. To investigate whether this decrease was a consequence of reduction of osteoblast support, osteoblasts were adjusted from calvaria and OPG mRNA expression was evaluated. Mice with the gene deficiency displayed elevated osteoblast OPG mRNA expression in comparison to the wild type. Increased calcification in osteoblasts carrying the gene deficiency was also demonstrated *in vitro*. This study confirmed abnormal skull formation with increased bone formation and resorption in mice lacking the

Caspase3 gene, which controls apoptosis. Caspase3 gene maintains a delicate balance between bone formation and bone resorption; moreover, it adjusts normal skull development via control of apoptosis in osteoblasts and osteoclasts.

Disclosures: **H. Amano**, None.

SA190

See Friday Plenary number F190.

SA191

Actions of PTH on Cell Proliferation and Apoptosis in Osteoprogenitor Cells From Mouse Calvarial Cultures Expressing a GFP Reporter. Y. Wang, Y. Liu^{*}, D. W. Rowe. University of Connecticut Health Center, Farmington, CT, USA.

Previously we have shown that early transient parathyroid hormone (PTH) treatment increases subsequent bone nodule formation in primary calvarial osteoblast cultures and this anabolic effect is not associated with an increase in total DNA content. To understand how this transient PTH treatment contributes to an anabolic outcome, we investigated the actions of PTH during and immediately after treatment of osteoblast cultures expressing stage-specific green fluorescent protein (GFP). Calvarial osteoblasts isolated from mice transgenic for pOBCol3.6GFP, which is activated in the preosteoblast stage, were cultured with 25 nM PTH for 7 days. Flow cytometry was then used to examine the effects of PTH on cell proliferation and apoptosis between GFP(+) and GFP(-) populations in the pre- and post-confluent cultures. Proliferating cells were labeled with BrdU and detected by fluorescent APC-conjugated anti-BrdU. Cell cycle was analyzed with flow cytometry using fluorescence of GFP, APC (for BrdU), and 7-AAD (for total DNA content). Results showed that in pre-confluent cultures, PTH caused a significant decrease in the percentage of cells in S phase, with a corresponding increase of cells in G0/G1 and G2+M phases in both GFP(+) and GFP(-) populations. However, there was no significant difference in the percentage of cells in S phase between GFP(+) and GFP(-) populations in the PTH-treated cultures. In contrast to its inhibitory effect in the pre-confluent cultures, PTH did not affect the percentage of cells in S phase once the cultures reached confluence. To measure apoptosis, apoptotic cells were detected by the binding of APC-conjugated annexin V. PTH significantly reduced the incidence of apoptosis in pre-confluent cultures. This reduction resulted solely from the decrease of apoptosis in the GFP(-) population, indicating PTH treatment increases the survival of GFP(-) cells in pre-confluent cultures. However, PTH treatment did not significantly alter the occurrence of apoptosis in post-confluent cultures. In conclusion, PTH reduced the percentage of cells in the S phase of the cell cycle in pre-confluent cultures, but this effect was lost once confluence was reached. In addition, PTH inhibited apoptosis in pre-confluent but not post-confluent cultures, and this effect was restricted to the GFP(-) population. We interpret this data to reflect one manifestation of PTH action on multipotential osteoprogenitor cells. PTH appears to enhance the progenitor population to commit to an osteogenic fate and this action results in a higher proportion of cells that achieve full osteoblast differentiation.

Disclosures: **Y. Wang**, None.

SA192

See Friday Plenary number F192.

SA193

The Experiment Study of Osteocalcin Promoter A20 Fusion Gene Inhibiting Osteoblast Apoptosis. Y. Qin^{*}, Z. Zhang, J. He^{*}. Center for Osteoporosis, Shanghai sixth hospital, Shanghai Jiaotong University, Shanghai, China.

To investigate that A20 protects mice osteoblast against apoptosis *in vitro*. At first the osteocalcin-A20 chimeric gene (OC-A20) was constructed by fusing a segment of the mouse osteocalcin promoter with a human A20 complementary DNA. MC3T3-E1 cells was transferred stably with vector OC-A20, and A20 mRNA and A20 protein expression were detected by RT-PCR and Western blotting. MC3T3-E1 cells, mouse embryo fibroblast NIH3T3 cells and human embryo kidney epithelial 293 cells were transiently transferred with OC-A20 gene. We didn't found that A20 mRNA expression in NIH3T3 and 293 cells. When OC-A20 or pcDNA3 transfer MC3T3-E1 cells were cultured in the presence of TNF- α for 8 h, cell apoptosis increased in pcDNA3 transfer cells compared with OC-A20-transfer cells by FACS. When the percentage of apoptosis were detected by TUNEL, we also found that the apoptosis increased in pcDNA3 group than OC-A20 group ($P < 0.001$). Simultaneously, cell apoptosis was determined by DNA gel electrophoresis. The results showed that DNA ladder was detected in pcDNA3-transferred group, OC-A20-transfer MC3T3-E1 cells had only one trace. In the study, osteocalcin promoter and A20 fusion gene was constructed successfully at first. Through MC3T3-E1, NIH3T3 and 293 cells transferred with OC-A20 gene, we confirmed that OC promoter A20 fusion gene was specific expression in MC3T3-E1 cells. It is the first time that efficacy of A20 protects MC3T3-E1 cells against TNF- α induced apoptosis was verified by FACS, TUNEL and DNA Ladder. Then OC-A20 transgenic mice were generated.

Disclosures: **Y. Qin**, None.

SA194

See Friday Plenary number F194.

SA195

Transcriptional Activation of Cyclin D1 Promoter by PTHrP Contributes to Cell Cycle Progression in Proliferating Osteoblasts. N. S. Datta, C. Chen*, L. K. McCauley. Perio/Prev/Geriatrics, University of Michigan, Ann Aror, MI, USA.

PTHrP has been implicated in the control of bone cell turnover but the mechanisms underlying its effect on osteoblast proliferation and differentiation have not been clearly defined. Cyclin D1 is a key regulator of G1 progression of the cell cycle. Our previous studies demonstrated that PTHrP signaling through cyclin D1 plays a role in the regulation of cell cycle progression in differentiating osteoblasts, which correlated with changes in the expressions of cyclin D1, CDK1 and JunB. In this report to define the mechanism by which PTHrP regulates osteoblast proliferation, we first investigated the expression of cyclin D1 by western blot analysis. Mouse calvarial MC3T3 cells were synchronized by serum starvation and induced with 0.1 μ M PTHrP for 2-24h. Results showed sustained expression of cyclin D1 protein in these cells with PTHrP treatment. Performing cyclin D1 promoter/ luciferase assays PTHrP significantly up-regulated cyclin D1 expression at the transcriptional level. Using a series of cyclin D1 promoter mutants (provided by RG Pestell and F Beier), luciferase assays revealed that regulation of PTHrP involved both AP-1 and CRE sites which were necessary but not sufficient alone for PTHrP mediated cyclin D1 activity. However, using both AP-1 and CRE mutants completely abolished the PTHrP effect of cyclin D1. Our studies also suggested that regulation of cyclin D1 protein accumulation is likely at the level of post-transcriptional or post-translational control(s). Finally, a moderate increase of CDK1 and sustained expressions of cyclins E and A proteins following PTHrP induction in proliferating cells was observed. Interestingly, PTHrP regulation did not seem to involve Jun B in proliferating MC3T3 osteoblasts. Together, these studies suggested a differential regulation of PTHrP in the cell cycle machinery of osteoblasts indicating that the action of PTHrP is developmental stage specific. While inhibition of cyclin D1 induced osteoblastic cell growth arrest in differentiated stage, the induction of cyclin D1 expression by PTHrP may be critical for continuous cell cycle progression in proliferating osteoblasts contributing to bone cell turnover.

Disclosures: **N.S. Datta**, None.

SA196

Interaction of the PGE₂ and JNK/p38 MAPK Signaling Pathways in Osteoblast-Adipocyte Fate Choices of Bipotential Progenitor Cells in Rat Calvaria Cell Cultures. T. Minamizaki*¹, Y. Yoshiko², K. Kozai*¹, J. E. Aubin³, N. Meada*². ¹Department of Pediatric Dentistry, Hiroshima University Graduate School of Biomedical Sciences, Hiroshima, Japan, ²Department of Oral Growth and Developmental Biology, Hiroshima University Graduate School of Biomedical Sciences, Hiroshima, Japan, ³Department of Molecular and Medical Genetics, Faculty of Medicine, University of Toronto, Toronto, ON, Canada.

Prostaglandin E₂ (PGE₂) is a well-known effective modulator of bone metabolism, with evidence from both hormone injections and recent experimental animal models that PGE₂ is, in particular, a powerful systemic and local anabolic agent. The anabolic effects of PGE₂ may be mediated, at least in part, by recruitment of new osteoblasts from their precursor cells via an EP2 and EP4 receptor-mediated cAMP-PKC signaling pathway. To address this further, we injected PGE₂, EP2 (EP2A) or EP4 (EP4A) agonists over the sagittal suture of the calvariae of newborn rats; in each case, the number of BrdU-labeled cells close to the newly formed bone was increased. Using the fetal rat calvaria (RC) cell culture model and pulse treatment protocols, we established that PGE₂ elicits its osteogenic stimulatory effects by acting on alkaline phosphatase-negative and/or positive precursor cells (osteoprogenitor cells) rather than pre-osteoblasts or mature osteoblasts. Given evidence for bipotential progenitors in RC cultures, we next asked whether the progenitor cell targets of PGE₂ may be bipotential osteo-adipocyte precursors. PGE₂ significantly increased the number of mineralized nodules, while concomitantly stimulating formation of a few adipocyte colonies. Similarly, Jun N-terminal kinase (JNK) (Dicumarol) and p38 map kinase (SB203580) inhibitors slightly but significantly increased adipocyte number in the RC model; both Dicumarol and SB203580 also increased levels of PPAR γ ₂ and adipocyte marker mRNAs. Notably, combined treatment of RC cells with EP agonists and MAPK inhibitors robustly increased these adipogenic parameters. SB203580 but not Dicumarol also inhibited both basal and EP agonist-induced osteoblast differentiation. ERK inhibitors (U0126) were ineffective in these experiments. Thus, we conclude that the JNK/p38 MAPK signaling pathway may interact with the EP2/EP4-mediated PGE₂ pathway to regulate osteoblast-adipocyte fate choices of bipotential precursors.

Disclosures: **T. Minamizaki**, None.

SA197

See Friday Plenary number F197.

SA198

Vitamin K-Dependent Gamma-Glutamyl Carboxylase Activity of Vitamin K Compounds in Liver and Bone. T. Okano, K. Nakagawa*. Department of Hygienic Sciences, Kobe Pharmaceutical University, Kobe, Japan.

Vitamin K is a cofactor for gamma-glutamyl carboxylase (GGCX), an enzyme catalyzing the post-translational modification of glutamyl residues (Glu) to gamma-carboxyglutamyl (Gla) residues in some proteins. In bone, osteocalcin, which has three Gla residues, is thought to be involved in the regulation of mineralization. Vitamin K compounds share a common chemical structure consisting of a naphthoquinone nucleus capable of redox cycling. Vitamin K1 (phyloquinone; PK) has a long phytol side-chain, whereas vitamin K2 has an unsaturated side-chain composed 1-13 isoprene unit. Menaquinone-4 (MK-4), a vitamin K2, possesses a significant pharmacological activity on bone formation and is used as a medication for osteoporosis in Japan. MK-4 enhanced the accumulation of Gla osteocalcin and the osteocalcin synthesis in cultured osteoblasts. The vitamin K-dependent gamma-carboxylation system consists of integral membrane proteins located in the endoplasmic reticulum membrane and includes the GGCX and warfarin-sensitive enzyme vitamin K 2,3-epoxide reductase (VKOR), which provides GGCX with reduced vitamin K cofactor. The endoplasmic reticulum chaperone protein calumenin is associated with GGCX and inhibits its activity. In the present study, we have examined the effects of PK and MK-4 on GGCX, VKOR, calumenin and osteocalcin mRNA expression and GGCX activity in hepatocyte and osteoblast cells. We used the cell lines derived from hepatocellular carcinoma (HepG2) and osteoblast (MG-63) cells. MK-4 was found to induce growth arrest in these cells tested. We also examined the co-factor activity of PK and MK-4 for the GGCX of microsomes from mouse liver, HepG2 or MG-63 cells. Co-factor activity of PK for GGCX was significantly weaker than that of MK-4. Moreover, GGCX, VKOR, calumenin mRNA expression in HepG2 and MG-63 cells were altered by the treatment with MK-4. However, PK and MK-4 did not affect the osteocalcin mRNA expression and vitamin D-dependent transcriptional activity on a human osteocalcin gene promoter in transfected MG-63 cells. In conclusion, these results indicate that molecular targets of PK and MK-4 in liver and bone may be side-chain structure-specific for the vitamin K molecule.

Disclosures: **T. Okano**, None.

SA199

See Friday Plenary number F199.

SA200

Smoke Exposure Alters the Bone Response to Estrogen Deficiency. D. M. Cullen, R. Kumar*, G. Alvarez*, M. P. Akhter. Osteoporosis Research, Creighton University, Omaha, NE, USA.

Smoking is associated with decreased bone mass and greater fracture risk in human epidemiology studies. The purpose of this study was to examine the interaction of ovariectomy and smoke exposure on bone remodeling in rats. We know that estrogen deficiency results in increased osteoclast and osteoblast activation and have seen the same pattern with smoke exposure. However, smoke exposure may suppress osteoblast formation rates. Adult (4 mo old, 266 (22) g) female Sprague-Dawley rats were randomized to four groups of 12 rats (sham or ovariectomized, and control or smoke exposed). Rats were exposure to a mixture of mainstream and sidestream cigarette smoke for 12 weeks at 2 hrs/d weekdays and 1 hr weekends at a concentration of 100 total suspended particles /mm³. The ovariectomized rats were pair fed to match body weight in sham rats. There was no smoke effect on body weight. Calcein was injected to label mineralization, the proximal tibia was processed undecalcified, and sections measured for bone volume (BV/TV, %), osteoclast surface (Oc.S/BV, um²/ um³), mineralizing surface (MS/BS, %), mineral apposition rate (MAR, um²/d), and bone formation rate (BFR/BV, %/ day). A two factor General Linear Model was used to test for effects due to Ovariectomy (Ovx) or Smoke and the interaction of these factors. Planned comparisons were used to test differences between individual groups (Table). We found that Ovariectomy decreased cancellous BV/TV (P<0.001) consistent with the activation of osteoclasts (P=0.006). Smoke did not alter BV/TV, but tended to increase osteoclasts (P=0.065). Compared to Nonsmoking-Sham rats both Ovariectomy and Smoke exposure treatments independently resulted in greater MS/BS, MAR, and BFR. However, there was an interaction between Smoke and Ovariectomy such that smoke exposure partially suppressed these formation measures in the ovariectomized rats. We conclude that smoke exposure stimulates cancellous bone remodeling as measured by osteoclast surface, but suppresses the formation phase of remodeling as measured by osteoblast activation (MS/BS) and osteoblast work (MAR, BFR). In women the effects of estrogen deficiency or menopause on bone loss, due to increased remodeling may be magnified in smokers in osteoblast function is suppressed.

Variable	Control		Smoke		Interact
	Sham	Ovx	Sham	Ovx	
BV/TV	31.6 (11.7)	9.3 (3.3) ^a	30.3 (8.8)	7.8 (2.6) ^a	NS
Oc.S/BV	22 (18)	57 (43) ^a	45 (49)	81 (45) ^a	NS
MS/BS	21 (12)	43 (9) ^a	33 (13) ^b	34 (10) ^b	0.002
MAR	0.68 (0.09)	0.83 (0.14) ^a	0.85 (0.08) ^b	0.72 (0.11) ^{ab}	0.001
BFR/BV	5.7 (3.4)	13.6 (4.0) ^a	8.9 (3.8) ^b	9.7 (3.2) ^b	0.002
mean (S.D.), ^a Ovx vs. sham, ^b Smoke vs. control					

Disclosures: **D.M. Cullen**, None.

SA201

Involvement of p300/CBP in Regulation of Id1 Promoter Activity by Wnt3a and Bone Morphogenetic Protein 2 in Osteoblastic Differentiation. A. Nakashima^{*1}, T. Katagiri², H. Takaku^{*3}, A. Minagawa^{*3}, M. Nashimoto^{*3}, M. Tamura¹. ¹Department of Biochemistry and Molecular Biology, Graduate School of Dental Medicine, Hokkaido University, Sapporo, Japan, ²Division of Pathophysiology, Research Center for Genomic Medicine, Saitama Medical School, Hidaka, Japan, ³Department of Applied Life Sciences, Niigata University of Pharmacy and Applied Life Sciences, Niigata, Japan.

It has been shown that loss of function of the Wnt co-receptor, LRP5, in both humans and mice leads to decreased bone formation and bone mass, and a point mutation in this gene results in high bone mass, indicating the crucial role that Wnt/LRP5 signaling plays in bone formation. However, the exact signaling mechanisms by which Wnt members regulate bone formation remain to be elucidated. Previously, we showed that the Id1 mRNA level induced by bone morphogenetic protein (BMP)2 was decreased by Wnt3a in C2C12 cells. This suppression is mediated by a 29-bp GC rich region of the BMP2-responsive element (BRE) of the human Id1 gene promoter and an interaction between Smad1/4 and β -catenin was identified and found to be crucial for Wnt-mediated suppression of the BMP2 response. In this study, we investigated whether a transcriptional co-activator is involved in regulation of transcription by Smad and β -catenin in osteoblast differentiation and functional cross-talk of Wnt and BMP2 signaling. p300, originally described as a protein which co-precipitated with adenovirus E1A, enhanced the BMP2-induced transactivation of IdWT4F-luc, a BMP2 responsive reporter. A dominant-negative form of p300 did not alter this promoter activity. Moreover, overexpression of p300 diminished Wnt-mediated suppression of the BMP2 response in Id1 gene promoter activity. These results identify the involvement of p300 in Id1 expression mediated by Wnt/ β -catenin signaling, and is the first study to demonstrate the presence of a coactivator by which Wnt/LRP5 regulates the BMP2-response in osteoblastic differentiation.

Disclosures: **A. Nakashima**, None.

SA202

See Friday Plenary number F202.

SA203

Mouse RANKL Gene Transcription Is Reversibly Suppressed by CpG Methylation of its Promoter Region. R. Kitazawa, K. Mori^{*}, T. Kondo, S. Kitazawa. Division of Molecular Pathology, Kobe University Graduate School of Medicine, Kobe, Japan.

The mouse RANKL gene promoter contains Runx2-binding sites, a vitamin D responsive element (VDRE) shared by CRE, and two CpG clustering regions: one around the transcription and translation start sites (-65/+350) and the other downstream of the VDRE (-920/-800). To clarify the epigenetic regulation of the RANKL gene, we analyzed the genomic DNA of the two subpopulations of ST2 cells: P9 which express RANKL and support osteoclastogenesis in response to vitamin D and P16 which do not, and found a higher frequency of CpG methylation of the -65/+350 region in P16 than in P9. Since VDR expression assessed by Western blotting and the specific binding to VDRE oligonucleotide assessed by EMSA were detected to an equal extent in P9 and P16, deterioration of the VDR signal was negated. By ChIP assay using anti-H3, -H4 antibodies and pairs of primers designed to amplify -950/-680 (containing VDRE) and -250/+10 (containing the transcription start site), histone acetylation in response to vitamin D occurred in P9 but not in P16, suggesting that CpG methylation in -65/+350 affects DNA acetylation. The effect of in vitro methylation on RANKL gene promoter was then analyzed. Promoter construct pGL3-1005 containing VDRE was methylated with SssI methylase (as pGL3-m1005) and transfected into P9 and P16. In both P9 and P16 the steady-state activity of pGL3-m1005 was 20% of that of pGL3-1005; pGL3-m1005 did not respond to vitamin D, whereas pGL3-1005 did. The effects of demethylating agent 5-Aza-dC on RANKL expression and osteoclastogenesis in the coculture were also analyzed. Assessed by quantitative RT-PCR and Western blotting, the expression of RANKL mRNA and protein in response to vitamin D was significantly restored in P16 by 5-Aza-dC treatment; by immunohistochemistry, RANKL protein expression was heterogeneously restored in P16. Furthermore, 5-Aza-dC treatment partially restored osteoclastogenesis in P16 cells. Our data suggest that CpG methylation of the promoter may reversibly suppress RANKL gene activation by vitamin D. The epigenetic mechanism may cause the heterogeneity and diversity of stromal/osteoblastic cells in response to bone-resorbing stimuli.

Disclosures: **R. Kitazawa**, None.

SA204

See Friday Plenary number F204.

SA205

Histone Deacetylase (HDAC) Inhibitors Induce the TCF/LEF-Driven Luciferase and Have Similar Effects on HDAC Activity in Nuclear Extracts from Bone and HeLa Cells. A. Regmi^{*}, D. L. Halladay^{*}, L. V. Hale^{*}, C. A. Frolik, E. C. Black^{*}, R. J. S. Galvin. Musculoskeletal Research, Eli Lilly and Company, Indianapolis, IN, USA.

Previous studies have provided evidence that HDACs repress TCF mediated gene transcriptional activity (Brantjes et al. Nucleic Acids Res 2001 29:1410-9; Levanon et al. PNAS USA 1998 95:11590-5). The present study was conducted to profile HDACs 1-11 mRNA expression in human bone and osteoblast-like cells and to evaluate the effects of HDAC inhibitors in bone cells. HDAC mRNA from human bone (53 and 85 years old donor), human osteosarcoma (SaOS-2) cells and human primary osteoblasts (hOB, L. X. Bi, Univ Texas Medical Branch) was profiled using Taqman analysis. HDACs 1-11 mRNA was present in both SaOS-2 cells and hOB at similar levels. HDACs 1-11 mRNA was expressed in human bone with the exceptions of the 85-year old donor, which did not have detectable HDAC4 mRNA and HDAC5 mRNA, which was present in low abundance in both donors. The effects of various HDAC inhibitors (Trichostatin A, MS-275, M-344, Scriptaid, Oxamflatin, Valproic Acid) on HDAC activity in nuclear extracts from mouse pluripotent cells (C3H10T1/2), SaOS-2 cells and human epithelial (HeLa) cells were evaluated. Splitomycin, a sirtulin inhibitor was used as a negative control. The compounds were also tested in a rat osteoblast cell line (UMR-106) stably transfected with the TCF/LEF-driven luciferase. There was no difference in the HDAC inhibitory activity when comparing nuclear extracts from the three cell types. Trichostatin A, Oxamflatin and M-344 had IC₅₀ in the range of 10-100 nM and MS-275, Scriptaid and Valproic Acid had IC₅₀ in the range of 0.13 - 250 μ M. All HDAC inhibitors also up regulated the TCF/LEF-driven luciferase in a concentration dependent manner. One HDAC inhibitor (M-344) was tested in a C3H10T1/2 cell differentiation assay and it increased alkaline phosphatase activity in a concentration dependent manner. In summary, bone cells contain mRNA for HDACs 1-11. A comparison of nuclear extracts between bone and epithelial cells did not show differences between HDAC activities in the presence of inhibitors. HDAC inhibitors up regulated TCF/LEF-driven luciferase in bone cells and an HDAC inhibitor induced osteoblast differentiation in C3H10T1/2 cells. Although further studies are necessary to clarify the role of HDAC inhibitors in the Wnt-induced signaling pathway, these studies do further support a role for HDACs in TCF-induced effects.

Disclosures: **A. Regmi**, Eli Lilly and Company 3.

SA206

See Friday Plenary number F206.

SA207

Compounds that Activate Runx2-Dependent Reporter Gene, Induce Osteocalcin and Enhance Osteoblast Differentiation Cause Bone Loss *In Vivo*. M. Susa, C. Halleux, D. Rohner^{*}, D. Packert Jensen^{*}, R. Vuille^{*}, F. Natt^{*}, T. Buhl¹^{*}, R. Lattmann^{*}, J. A. Gasser. Novartis Institutes for BioMedical Research, Basel, Switzerland.

Runx2, a master gene regulator of osteogenesis, is necessary for bone formation during development. Runx2 type II isoform (Osf2) expression was claimed to be sufficient for osteoblastic differentiation. However, data from cell culture do not support sufficiency of mere Runx2 expression for osteoblast differentiation. We sought to identify compounds that stimulate Runx2 activity in osteoblasts in order to study Runx2 role in vitro and in adult rodents in vivo. Pre-osteoblastic MC3T3-E1 cells were stably transfected with OSE2-Luciferase reporter gene, containing multimeric OSE2 response element for Runx2, derived from the osteocalcin promoter. High throughput compound screen with selected MC3T3-1b cell line resulted in one major class of activating compounds: amino thiazoles, which were inactive in several other reporter gene cell lines, but stimulated Runx2-dependent OSE2 activity in transient co-transfections. Compounds induced stably transfected OSE2-Luciferase up to 7-fold and Runx2 target gene osteocalcin up to 60-fold. In the presence of low doses of osteogenic stimulus, they could also enhance mineralization of MC3T3-1b cells up to 6-fold. However, compound concentration causing stable osteocalcin induction only transiently stimulated other osteoblast marker genes and was associated with osteoblast-selective apoptosis. Down-regulation of Runx2 type II isoform by anti-sense oligonucleotides did not reduce OSE2 activity, suggesting a role for other Runx2 isoforms, in agreement with Runx2 type II-specific knockout data (1). Structure-activity relationship studies of about 1,000 compounds indicated that osteoblast stimulation can be dissociated from OSE2 activation. One compound with acceptable bioavailability was tested in vivo in a 4-week intact rat model. The compound apparently induced an osteoclast-mediated loss of cancellous bone. It inhibited osteoclasts in vitro, but induced several osteoclastogenic cytokines in osteoblasts, most prominently TGF- β and IL-11. We conclude that Runx2 type II can be dissociated from OSE2 activation and that OSE2 activation can be dissociated from osteoblast stimulation. Runx2-activating amino thiazole compounds cause uncoordinated osteoblast gene activation, associated with osteoblast apoptosis and production of osteoclastogenic cytokines. In agreement with these data, a dominant effect in vivo was a loss of bone. Compounds from amino thiazole class could be of further use in vitro in osteoblast and osteoclast research and in vivo as inducers of bone loss.

1. Xiao et al., J. Biol. Chem. 2004; 279:20307-13.

Disclosures: **M. Susa**, None.

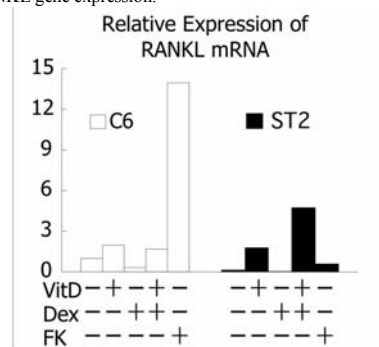
SA208

See Friday Plenary number F208.

SA209

Runx2 Modulates RANKL Expression by Repressing Its Steady-state Level in Mouse Osteoblastic/ Stromal Cells. K. Mori^{*1}, R. Kitazawa¹, T. Kondo¹, A. Yamaguchi², S. Kitazawa¹. ¹Division of Molecular Pathology, Kobe university Graduate School of Medicine, Kobe, Japan, ²Department of Oral Pathology, Tokyo Medical and Dental University, Tokyo, Japan.

Runx2, an essential transcription factor for bone formation, is also known to modulate osteoclastogenesis. In mouse RANKL gene, besides two putative Runx2 binding sites (-210, -195) in the basic promoter region, the Runx2 binding site located as far as 74 kb upstream from the transcription starting site plays critical roles in regulating the gene (Q. Fu et al. ASBMR 2004). We investigated the role of Runx2 in RANKL gene expression in mouse stromal cell line ST2 and in Runx2 ^{-/-} mouse-derived mesenchymal cell line C6. C6 and ST2 cells were cultured with or without 1 α ,25(OH)₂D₃ (VitD) and Dexamethasone (Dex) for 24 hours, then the expression of RANKL, OPG and Runx2 was quantified by realtime RT-PCR. Steady-state RANKL mRNA expression was higher in C6 cells than in ST2 cells. Conversely, with the Tet-On system, when the expression of Runx2 mRNA was restored in C6 cells, RANKL mRNA expression decreased to 70% of its steady-state expression level, suggesting that Runx2 has a repressive effect on the steady-state expression of the RANKL gene. In C6 cells, RANKL mRNA expression increased 2-fold by VitD treatment, but decreased to 32% by Dex treatment. Moreover, in contrast to the 38-fold increase of RANKL expression in ST2 cells by VitD and Dex treatment, C6 cells did not demonstrate such superinduction. On the other hand, administration of Folskolin (FK) resulted in a 14-fold increase of RANKL mRNA expression in C6 cells, suggesting that the induction of RANKL gene expression by protein kinase A signaling is mostly independent of Runx2. Reflecting the modest increase of RANKL expression by steroids, in the coculture system using C6 cells and normal mouse bone marrow macrophages, TRAP-positive multinucleated giant cells were induced with VitD treatment alone, and their number increased further by treatment with both VitD and Dex. We therefore speculate that Runx2 expression is crucial in repressing the steady-state expression of RANKL gene and thereby playing an important role in modulating RANKL gene expression.



Disclosures: **K. Mori**, None.

SA210

See Friday Plenary number F210.

SA211

Prenatal Onset of Osteosclerosis in Fra1 Transgenic Mice. T. Yamaguchi^{*1}, T. Nishiwaki^{*1}, Y. Toyama^{*1}, K. Matsuo². ¹Department of Orthopedic Surgery, Keio University School of Medicine, Tokyo, Japan, ²Department of Microbiology and Immunology, Keio University School of Medicine, Tokyo, Japan.

Fra1 is a component of the dimeric transcription factor AP-1. Fra1 transgenic (Tg) mice develop osteosclerosis, which is due to cell-autonomous enhancement of osteoblastic bone formation. Osteosclerosis in Fra1 Tg mice is reported to begin by four weeks of age, and progress over several months until the bone marrow cavity is occluded. However, the age of onset and pathogenesis of the osteosclerosis is unknown. To reveal the age of onset, we used an *in vivo* computed tomography scanner (LaTheta; Aloka, Japan). Tibial bone mineral density (BMD) of Fra1 Tg mice and wild-type littermates at various ages (n=15, each genotype) was measured twice a week over the course of three weeks under anesthesia. In addition, 16.5 d.p.c. embryos were isolated and tibial BMD was measured by the CT scanner, and mineralized areas were quantified on histological sections after von Kossa stain. *In vivo* analysis revealed higher BMD in Fra1 Tg mice as early as three days after birth. Consistently, von Kossa stain showed a larger proportion of mineralized area in three day-old Fra1 Tg tibiae than wild-type controls (n=8, each genotype), suggesting that osteosclerosis has an earlier onset. Prenatal analysis using tibiae isolated at 16.5 d.p.c. demonstrated increased BMD in Fra1 Tg embryos (wild-type n=12, Fra1 Tg n=8). Furthermore, von Kossa stain showed a larger proportion of mineralized area in 16.5 d.p.c. Fra1 Tg tibiae (n=7) than wild-type controls (n=11). Finally, Alizarin red- and Alcian blue-stained skeletal preparations of 15.5 d.p.c. embryos showed that development of bone and cartilage in Fra1 Tg mice and wild-type was indistinguishable. Therefore, while the ossification in Fra1 Tg mice starts at approximately the same time as in wild-type mice, once ossification has begun, elevated bone formation results in osteosclerosis in Fra1 Tg mice. We conclude that osteosclerosis in Fra1 Tg mice starts before birth. This rationalizes comparative biochemical analysis of pre- or neonatal bones prior to osteosclerotic structural alterations to reveal the pathogenesis of enhanced bone formation in Fra1 Tg mice.

Disclosures: **T. Yamaguchi**, None.

SA212

See Friday Plenary number F212.

SA213

Human Endothelial Cells Inhibit MSC Differentiation into Mature Osteoblasts *In Vitro* by Interfering with Osterix Expression. T. R. Meury^{*}, M. Alini^{*}. Cell Biology & Biochemistry, AO-Research Institute, Davos-Platz, Switzerland.

Several cell types have the capacity to influence the differentiation/commitment of mesenchymal stem cells (MSC) into a certain lineage. In this study, we were interested in the influence of endothelial cells (EC) on dexamethasone-induced differentiation of MSC into mature osteoblasts. We therefore performed co-cultures (indirect contact, conditioned medium) of human umbilical vein endothelial cells and mesenchymal stem cells (isolated from human bone marrow aspirates) for up to 28 days in osteogenic medium (OM), containing dexamethasone, beta-glycerophosphate and ascorbic acid. Typical osteoblastic markers were analyzed, including calcium-incorporation, ALP activity and gene expression using real-time RT-PCR. As expected, osteogenic medium induced an osteoblastic phenotype in MSC, as shown by high calcium-incorporation and ALP activity as well as elevated expression of osteoblastic marker genes encoding for extracellular matrix components like type 1 collagen, bone sialoprotein, osteonectin or MMP-13. The osteoblastic transcription factors Runx2 and Osterix (Osx) were also up regulated by OM. Co-cultures of MSC with EC in OM clearly down regulated calcium incorporation, ALP activity and gene expression of extracellular matrix proteins. Interestingly, the transcription factor Runx2 was not affected by EC, but Osx was significantly down regulated. There was no influence of EC on the expression of other mesenchymal transcription factors like the chondrocytic marker Sox9 or the adipocytic marker PPAR-gamma. This suggests, that EC are able to arrest final osteoblastic differentiation of MSC at a pre-osteoblastic stage by interfering with Osx expression. The fact that Runx2 as well as Sox9 and PPAR-gamma were not affected hints, that the inhibition takes place at a later stage than the Runx2-driven osteo-chondro-bipotent precursor stage, and that by this inhibition, the MSC are not driven to a chondrogenic or adipogenic phenotype. Fibroblast- or chondrocyte-conditioned medium did not have this effect on MSC differentiation, indicating that the inhibitory effect we observed was EC-specific. In conclusion, we have shown that EC specifically have an inhibitory effect on dexamethasone-induced MSC differentiation *in vitro* by suppressing Osx expression.

Disclosures: **T.R. Meury**, None.

SA214

See Friday Plenary number F214.

SA215

Molecular Phenotyping of Cell Lines from Osteoblastic Lineage Using Real-Time PCR TaqMan Low Density Arrays. C. Halleux^{*}, T. Grabenstaetter^{*}, N. Luong-Nguyen^{*}, D. Rohner^{*}, M. Susa. Musculoskeletal Diseases, Novartis Institutes for BioMedical Research, Basel, Switzerland.

Several mouse osteoblastic cell lines at various stages of osteoblastic differentiation are available for *in vitro* studies. Comparative molecular characterization of these cell lines, which would better define their phenotype and enable a more informed decision on their use, has not yet been done. Here we used a novel, advanced application of real-time PCR, the TaqMan Low Density Arrays, to simultaneously and quantitatively measure mRNA levels for 24 osteoblast markers in three murine cell lines: pluripotent C3H10T1/2 cells, stromal, osteoclast-supporting ST2 cells, pre-osteoblastic MC3T3-E1 cells, and in the most mature primary mouse calvarial osteoblasts. Cells were treated with osteogenic stimulus (ascorbic acid, beta-glycerophosphate and 1000 ng/ml BMP-2) or with 25 ng/ml TGF-beta1 for 1 and 3 days. We focused on upregulated genes. All four cell cultures displayed high levels of collagen type I alpha 1 and alpha 2 chain (Ct values of 15-19), whose expression are characteristic for osteoblastic cell lines. In all four cultures, BMP-2 or TGF-b1 stimulated expression of Dlx5 and TCF7, suggesting that initial events in BMP and Wnt signaling are not dependent on stage of osteoblastic differentiation. Primary osteoblasts, MC3T3-E1 and, to a lesser degree, ST2 cells, but not C3H10T1/2 cells showed a strong response of classical osteoblast markers alkaline phosphatase, bone sialoprotein and osteocalcin to BMP-2 stimulation. MC3T3-E1, ST2 and C3H10T1/2, but not primary cells responded well to BMP-2 or TGF-b1 with induction of Notch target gene hey1, osteogenic AP-1 component fra-1, fibromodulin and TGF-b1, suggesting that more mature cells lose responsiveness to these factors. MC3T3-E1 and ST2 cells, but not primary osteoblasts nor C3H10T1/2 induced well transcription factors Mx2, Osx, Smad6, c-fos and Id2. In MC3T3-E1, ST2 and C3H10T1/2 cells integrin alpha 2 chain was induced, pointing to the importance of collagen signaling in pre-osteoblastic, stromal and pluripotent cells. In MC3T3 cells, BMP-2 induced well PTH receptor and moderately osteomodulin and in ST2 cells, TGF-b1 increased OPG. We conclude that molecular phenotyping confirms the place of these cellular models in osteoblast lineage and reveals more details than previously known. This fast, reliable and quantitative method enables quick profiling of cells with respect to osteoblast-related genes and may find application in assessing effects of compounds on osteoblasts *in vitro*, as well as in profiling of osteoblast status in mouse bone *ex vivo*.

Disclosures: **C. Halleux**, None.

SA216

Expression of Periostin in Human Normal Tissue and Fibrous Dysplasia.

T. Kashima¹, K. Shimazu^{*2}, T. Nishiyama^{*2}, M. Shimazaki^{*2}, I. Kii^{*2}, M. Fukayama^{*1}, A. E. Grigoriadis³, A. Kudo². ¹Pathology, University of Tokyo, Tokyo, Japan, ²Biological Information, Tokyo Institute of Technology, Yokohama, Japan, ³Craniofacial development, King's College London, Guy's hospital, London, United Kingdom.

Periostin is a 90 kDa secreted protein which was originally cloned from murine osteoblast-like MC3T3-E1 cells. It is specifically expressed in the periodontal ligament and the periosteum in adult mice and is thought to function as a mechanosensor in the remodeling of the periodontal ligament. To examine further the tissue distribution and cellular pattern of periostin expression in human, a polyclonal anti-serum against human periostin was raised and used for immunohistochemistry (IHC). Initial screening of various normal and pathological samples was examined using a tissue microarray. Periostin was strongly localized not only to the periodontal ligament, the periosteum and surface of the articular cartilage, but also to the endocardium, the valves, the wall of the arteries and arterioles, where mechanical stress is normally occurring. Veins were negative for immunoreactivity, further supporting the hypothesis that periostin acts as a mechanosensor. As a marker of osteoblastic differentiation, periostin is also highly expressed at sites of intramembranous ossification in fetal calvaria but not in mature osteoblasts lining surfaces of trabecular bone. We therefore also examined fibrous dysplasia (FD) since the histology of FD is thought to resemble intramembranous ossification and collagen fibers in the periodontal ligament known as "Sharpey's fibers". We examined 40 cases of monoostotic FD, aged from 3 to 60 years old. In all FD cases, periostin was strongly positive in fibroblastic cells which were attached perpendicularly to woven bone, but bone matrix itself was negative. Finally, since it has been well documented that the c-Fos protooncogene is upregulated by mutation of the Gs alpha unit in FD patients, we speculated that periostin expression might be controlled by c-Fos. To investigate this, the expression of periostin in murine osteosarcomas arising in c-fos transgenic mice were also examined by in situ hybridization and IHC. Interestingly, periostin was expressed in immature lining osteoblastic tumor cells but not in fibroblastic tumor cells. Further, expression analyses employing previously established MC3T3-E1 cells which conditionally overexpress c-fos are now in progress. Taken together, these data suggest that periostin is expressed in mesenchymal tissues subjected to mechanical stress, and may have a role in skeletal pathologies.

Disclosures: **T. Kashima**, Grants-in-aid from the Ministry of Education, Culture, Sports, Science and Technology of Japan 2.

SA217

TRAIL and TNF α Regulate Human Osteocyte-Osteon Structure by Removal of Gap-Junctions via Proteasomal Degradation with a Probable β -Catenin Downstream Mechanism. A. C. Sharrow^{*}, Y. Li, A. Micsenyi^{*}, C. W. Borysenko^{*}, T. Lehmann^{*}, A. Wells^{*}, S. E. Kalla^{*}, V. García Palacios, S. P. Monga^{*}, H. C. Blair. Pathology, University of Pittsburgh and Pittsburgh VA Medical Center, Pittsburgh, PA, USA.

Osteoblasts express Death Receptor-5 (TRAIL-R2) and TNFR1 (P55) but resist apoptosis when exposed to their ligands. Osteoblasts function in multicellular units, osteons, organized by connexin43 (CX43) connexons, elaborate protein complexes that have intricate interactions with adaptor and regulatory proteins including β -catenin, a key component of the Wnt pathway. TRAIL or TNF α decreased intracellular connections in serum starved human MG63 cells and in nontransformed osteoblasts; RANKL and IL-1 controls were unaffected. Microinjection of lucifer yellow showed that serum starvation promoted connected cell groups, but TRAIL eliminated these almost entirely in MG63 and mature osteoblasts; immature osteoblasts responded similarly but only to TNF α . Western blots and immune localization of CX43 showed dramatic reduction by TRAIL or TNF α depending on cell differentiation state. Doublet-discrimination flow cytometry of MG63 showed cell shape changes and was consistent with decreased connectivity in response to TRAIL. If CX43 is separated from the connexon, β -Catenin, in other organ systems, undergoes nuclear localization and initiates events including CX43 mRNA synthesis and G2M cell cycle arrest. Real-time PCR showed that CX43 transcription in MG63 increased after TRAIL treatment that reduced CX43 protein, and TRAIL decreased MG63 S phase by 80% with a parallel increase in G2. After removal of TRAIL, cells re-established connections and expressed alkaline phosphatase, but cell number did not increase as in controls, suggesting that TRAIL can terminate proliferation. In MG63 the proteasomal inhibitor lactacystin eliminated CX43 reduction after TRAIL or TNF α , although 24 h serum starved cells had reduced CX43 and β -catenin. A decline in β -catenin occurred with or without lactacystin. This suggests that non-proteasomal mechanisms degrade β -catenin and that dissociation of CX43- β -catenin complexes does not require CX43 degradation. We conclude that TRAIL or TNF α , via DR5 or TNFR1, regulate osteoblast CX43 redistribution and degradation. Downstream events can arrest cell division and alter protein expression, and are probably mediated by β -catenin redistribution and activation. Thus TRAIL and TNF α receptors are late regulators of multicellular structure, with secondary effects on cell cycle and expression of proteins. Early β -catenin activation and nuclear localization after TRAIL or TNF α activation may be crucial thus defining a novel mechanism that regulates osteon structure.

Disclosures: **A.C. Sharrow**, None.

SA218

See Friday Plenary number F218.

SA219

Culture of Marrow Derived Mesenchymal Stem Cells in 3-Dimensional Matrices Made by Marrow Stromal Cells Promotes Retention of the Stem Cell Phenotype. X. Chen, S. C. Manolagas, R. L. Jilka. Center for Osteoporosis and Metabolic Bone Diseases, University of Arkansas for Medical Sciences, Little Rock, AR, USA.

Mesenchymal stem cells (MSCs) both replicate to produce identical daughter stem cells and differentiate into diverse cell types including osteoblasts. However, MSCs lose their unique properties and exhibit senescence-associated growth arrest when grown in standard 2-dimensional (2D) culture systems, thereby impairing investigation of their behavior and limiting their therapeutic potential. In other tissues, the extracellular matrix (ECM) forms part of the specialized niche that controls stem cell behavior. Therefore, we hypothesized that an appropriate ECM is required for studying MSCs in vitro. To test this hypothesis, we quantified the adhesion, differentiation, and BMP-2 responsiveness of murine MSCs cultured on cell-free 3D matrices made by cultured murine marrow stromal cells, as compared to uncoated plastic, or plastic coated with type I collagen or fibronectin. These matrices were ~100 μ m thick as determined by confocal and electron microscopy, and contained collagen as well as osteonectin, biglycan, and decorin. The distribution and content of these proteins was unaffected by removal of cells with 0.5% Triton-100 and 20 mM NH₄OH. 3D matrices promoted attachment and proliferation of MSCs as reflected by a >2-fold increase in the number and size of fibroblastic colonies arising from these progenitors (CFU-F). Compared to 2D systems, cells cultured in 3D matrices under basal conditions secreted 5-fold less osteocalcin. Addition of ascorbate-2-phosphate increased osteocalcin secretion in all cultures at day 15 and 25, but absolute levels remain 2-3-fold lower in 3D cultures. Previous studies of ours showed that osteoblastogenesis in 2D cultures depends on endogenous production of BMP-2/4; and that BMP-4 binds to the ECM. Therefore, we suspected that the retardation of osteoblastogenesis in 3D cultures reflected retention of the undifferentiated phenotype of MSCs due to sequestration of endogenous BMP-2/4, rather than loss of osteogenic capacity. Consistent with this, addition of BMP-2 (10 -100 ng/ml) at day 10 to cells cultured in 3D matrices dose-dependently stimulated expression of alkaline phosphatase activity (2-fold) and osteocalcin secretion (5-fold). In contrast, MSCs cultured on 2D systems failed to respond to exogenous BMP-2. Indeed, this is the first report of a response of murine marrow-derived MSCs to low concentrations of BMP-2. These findings indicate that, as in other stem cell niches, the ECM plays an essential role in the control of MSC behavior, perhaps by regulating exposure of cells to pro-differentiating growth factors such as BMPs.

Disclosures: **X. Chen**, None.

SA220

See Friday Plenary number F220.

SA221

1 α ,25-Dihydroxyvitamin D₃ and Wnt Pathway Effects on Proliferation and Differentiation of Osteoblastic Cells. Y. Shi^{*1}, J. A. Eisman¹, E. M. Gardiner².

¹Bone and Mineral Research Program, Garvan Institute of Medical Research, Sydney, Australia, ²School of Medicine, University of Queensland, Brisbane, Australia.

Active hormonal vitamin D, 1 α ,25-dihydroxyvitamin D₃ [1,25D₃], induces osteoblastic cell cycle arrest and matrix mineralization. The Wnt pathway regulates cell proliferation and differentiation in development and disease, with many reports linking the Wnt pathway to osteoblast differentiation and bone mass. Lithium chloride (LiCl) mimics activation of the canonical Wnt pathway by stabilizing β -catenin, which complexes with other transcription factors to regulate gene expression. Here, the effects of continuous treatment with 1,25D₃ and/or LiCl initiated at various stages of proliferation and differentiation were investigated in pre-osteoblastic MC3T3-E1 cultures. Cell proliferation was measured by BrdU incorporation, mineralized nodules were detected by Von Kossa staining, and gene expression was evaluated by quantitative RT-PCR. Initiating 1,25D₃ or LiCl treatment in subconfluent cultures (Day 1) inhibited cell proliferation in a dose-response manner and combining 1,25D₃ plus LiCl treatment had an additive effect, markedly reducing proliferation and mineralized nodule number and size. Treatment of matrix-forming cultures (Day 6) with 1,25D₃ or LiCl also reduced mineralized nodule number and size, but treatment with either agent after mineralization onset (Day 13) reduced nodule size but not number. Runx2 expression was not altered 24 hours after either LiCl or 1,25D₃ at any time point. 1,25D₃, but not LiCl, treatment at Day 1 was associated with decreased twist 1 expression. In contrast, LiCl treatment at Day 6 was associated with decreased osterix expression level, whereas 1,25D₃ had no effect on this gene. Thus, the Wnt pathway appeared to regulate osteoblastogenesis in pre- and post-confluent MC3T3-E1 cultures but was less active after onset of mineralization. In contrast, 1,25D₃ had effects at all culture stages, and the Wnt and vitamin D regulatory pathways were additive in pre-mineralizing cultures. Thus, although 1,25D₃ and LiCl had similar effects on differentiation of these osteogenic cultures, their underlying molecular mechanisms are distinct and additive, providing a basis for physiological interactions between these two bone anabolic pathways.

Disclosures: **Y. Shi**, None.

SA222

See Friday Plenary number F222.

SA223

N-Acetylcysteine Stimulates Mineralized Nodule Formation in Mouse Calvarial Osteoblasts. J. H. Jun*, M. Song*, S. Lee*, K. M. Woo*, G. S. Kim*, J. H. Baek, Department of Pharmacology and Dental Therapeutics, School of Dentistry, Seoul National University, Seoul, Republic of Korea.

N-acetylcysteine (NAC) is a precursor of glutathione and has oxygen radical-scavenging properties. The effectiveness of NAC administration in the prevention of several diseases induced by reactive oxygen species has been reported. Recent report showed that NAC prevented bone resorption in ovariectomized mice, suggesting the possibility of NAC as a therapeutic agent for osteoporosis. Thus we examined the effect of NAC on bone formation, the other side of bone remodeling. Long-term treatment of NAC increased the mineralized nodule formation in primary cultured mouse calvarial osteoblasts. In accordance with this stimulatory effect, NAC significantly enhanced the mRNA expression of osteoblast differentiation associated genes such as alkaline phosphatase, osteocalcin, bone sialoprotein, and osterix. NAC increased the expression of bone morphogenetic protein-2, -4, -7 and transforming growth factor-beta. While glutathione showed similar stimulatory effects, caffeic acid phenethyl ester, a strong phenolic antioxidant, did not stimulate osteoblast differentiation, suggesting that the osteogenic effect of NAC needs thiol group. Taken together, these results suggest that NAC might exert potent anti-osteoporotic effect by stimulating bone formation as well as by inhibiting bone resorption.

Disclosures: **J.H. Jun**, None.

SA224

Omega-3 Fatty Acids Inhibit *In Vitro* Vascular Calcification via the p38-MAPK Pathway. M. Abedin*, J. Lim*, D. Park*, T. Tang*, L. L. Demer, Y. Tintut, Medicine, UCLA, Los Angeles, CA, USA.

Fish oil supplementation improves outcome in coronary artery disease and evidence suggests a reduction of vascular calcification in an animal model. However, the mechanism of their action on vascular calcification is not fully understood. In this report, we identify the intracellular signaling pathways, through which omega-3 fatty acids, active ingredients of fish oil, inhibit vascular calcification. Eicosapentanoic acid (EPA) or docosahexanoic acid (DHA) inhibited alkaline phosphatase (ALP) activity and mineralization of calcifying vascular cells, a subpopulation of bovine aortic medial cells that undergo osteoblastic differentiation and form calcified matrix in vitro. Western blot analysis showed that DHA activated p38-MAPK but not ERK or Akt. Co-treatment of DHA with an inhibitor of p38-MAPK, reversed the DHA inhibitory effects on ALP activity. Pretreatment with DHA also inhibited the ALP activity and mineralization induced by the inflammatory cytokine, IL-6. DHA and anisomycin, a p38-MAPK activator, partially attenuated STAT-3 activation induced by IL-6. These results suggest that omega-3 fatty acids inhibit vascular calcification by stimulating the p38-MAPK pathway.

Disclosures: **L.L. Demer**, None.

SA225

See Friday Plenary number F225.

SA226

BMP-2 Activates β -Catenin Signaling in Osteoblasts. Y. Yan, Y. Lim*, M. Chen*, R. J. O'Keefe, D. Chen, Orthopaedics, University of Rochester, Rochester, NY, USA.

Recent studies demonstrate that BMP-2 has a synergistic effect with β -catenin to promote osteoblast differentiation. To determine the molecular mechanism of the interaction between BMP-2 and β -catenin, experiments were performed to assess the effect of BMP-2 on β -catenin signaling in 2T3 and MC3T3 osteoblasts. BMP-2 increased protein levels of the non-phosphorylated active form of β -catenin in a dose-dependent (10-200 ng/ml) and time-specific (24 h treatment) manner on Western blots. Consistent with this finding, BMP-2 induced β -catenin nuclear translocation (immunostaining) and enhanced protein levels of nuclear β -catenin (Western blot) in osteoblasts. BMP-2 activated β -catenin signaling by regulating the expression and activity of three critical molecules in the β -catenin signaling pathway: 1) BMP-2 inhibited Kremen-1 mRNA expression in a dose-dependent manner in 2T3 cells; 2) BMP-2 stimulated Lrp5 mRNA expression (over 2-fold, Northern blot) in 2T3 cells; and 3) BMP-2 inhibited β -TrCP protein expression (Western blot) in a dose-dependent manner. Maximal concentrations of BMP-2 nearly abolished β -TrCP expression in osteoblasts. β -TrCP is an E3 ubiquitin ligase in the SCF ^{β -TrCP} protein complex and induces β -catenin degradation in a dose-dependent manner in osteoblasts. Thus, the effects of BMP-2 on each of these genes would tend to enhance β -catenin signaling. β -catenin-deficient osteoblasts were used to further assess the importance of β -catenin signaling downstream of BMP-2. Primary osteoblasts isolated from β -catenin-loxP mice and infected with Cre recombinase-expressing adenovirus (AdCMV-Cre) had deletion of the β -catenin gene. In these cells, osteoblast proliferation (BrdU labeling, ~40% reduction) and expression of cyclin D1 protein were decreased and ALP activity and expression of osteoblast marker genes such as type I collagen, osteopontin and osteocalcin were inhibited 45-70% compared with control osteoblasts isolated from β -catenin-loxP mice and infected with AdCMV-GFP. BMP-2-induced osteoblast marker gene expression (type I collagen and osteopontin) and mineralized bone nodule formation were

significantly inhibited in β -catenin-deficient osteoblasts. Altogether the findings show that BMP-2 regulates the expression of genes controlling β -catenin signaling and that enhanced β -catenin signaling plays a critical role in BMP-2-induced osteoblast differentiation.

Disclosures: **Y. Yan**, None.

SA227

See Friday Plenary number F227.

SA228

Beta-Catenin Regulates NFAT Signaling Pathway in Osteoblasts. H. Yeo*, J. M. McDonald, M. Zayzafoon, The Department of Pathology, The University of Alabama at Birmingham, Birmingham, AL, USA.

The Nuclear Factor of Activated T cells (NFAT) is a family of transcription factors that regulates gene expression and differentiation of several cells, including osteoclasts. We have previously shown that NFAT, specifically NFATc1, negatively regulates osteoblast differentiation by inhibiting Fra-2 expression. Wnt/ β -catenin signaling is another important regulator of bone formation and osteoblast differentiation. Crosstalk between NFAT and Wnt/ β -catenin signaling has been previously reported but never examined in osteoblasts. The purpose of this study is to examine the relationship between NFATc1 and β -catenin during osteoblast differentiation. These studies were performed using a murine clonal osteogenic cell line, MC3T3-E1, and a mouse pluripotent mesenchymal stem cell line, C3h10T1/2. Here we show by Western blot analysis that the protein expression of both NFATc1 and β -catenin increases during osteoblast proliferation and early differentiation and decreases during mineralization, while the gene expression of both NFATc1 and β -catenin, as determined by RT-PCR remains unchanged, suggesting a post-transcriptional regulatory mechanism. Inhibition of proteasomic degradation in osteoblasts by MG132, a proteasome inhibitor, increases, dose- and time- dependently, the levels of NFATc1 and β -catenin. To elucidate the direct role of β -catenin in NFATc1 activity, we silenced β -catenin in osteoblasts using siRNA. Here we demonstrate by Western blotting and luciferase assay that the silencing of β -catenin decreases NFATc1 protein expression and NFAT transactivation. Furthermore, β -catenin siRNA decreases NFAT DNA-binding activity, as demonstrated by electrophoretic mobility shift assay. Treatment with MG132, while silencing β -catenin, rescues the decrease in NFATc1 protein expression and transactivation suggesting that NFATc1 is protected from proteasomic degradation by β -catenin. Finally, we show by immunoprecipitation and by three-dimensional computer based binding models that NFATc1 physically interacts with β -catenin. Taken together, our results suggest that during early osteoblast differentiation β -catenin and NFATc1 bind resulting in protection of NFATc1 from proteasomic degradation.

Disclosures: **H. Yeo**, None.

SA229

See Friday Plenary number F229.

SA230

Intercellular Junctions, Phosphatidylinositol Signaling and Osteoblast Differentiation. A. R. Guntur*¹, M. C. Naski². ¹Biochemistry, University of Texas Health Science Center at San Antonio, San Antonio, TX, USA, ²Pathology and Biochemistry, University of Texas Health Science Center at San Antonio, San Antonio, TX, USA.

Bone synthesis requires synchronous osteoblast differentiation and vectoral secretion of bone matrix. At sites of rapid bone synthesis osteoblasts form a tightly opposed layer of cells that secrete matrix toward the bone surface. We hypothesize that these cells synchronize their differentiation through activation of signaling cascades that are regulated by intercellular contact. To test this hypothesis we studied the assembly of intercellular junctions in MC3T3E1 osteoblasts. Immunofluorescence localization showed that intercellular contact leads to calcium dependent assembly of adherens junctions containing N-cadherin, β -catenin and p120. Interestingly, the tight junction protein zonula occludens-1 was also targeted to intercellular contacts. Significantly, the assembly of those junctions coincided with the activation of the phosphatidylinositol 3- kinase signaling pathway. This was demonstrated by increased phosphorylation of PTEN at Ser380 and a concomitant activation AKT through phosphorylation at Ser 473 and inactivation of glycogen synthase kinase3 β via phosphorylation at Ser9. The assembly of intercellular junctions and activation of phosphatidylinositol 3-kinase signaling also coincided with osteoblast differentiation as evidenced by 1) the induction of osterix, an essential osteoblast transcription factor and 2) increased expression of the osteoblast matrix genes osteoglycin and osteomodulin. We conclude that osteoblast differentiation is coupled to adherens junction assembly and activation of phosphatidylinositol 3-kinase signaling.

Disclosures: **A.R. Guntur**, None.

SA231

A Highly Potent Inhibitor of Cathepsin K Inhibits Bone Resorption both *In Vitro* and in Acute Model of Bone Resorption *In Vivo* in Monkeys. S. Kumar, L. Dare, J. A. Vasko-Moser, S. M. Hwang, T. Tomaszek, D. S. Yamashita, R. W. Marquis, H. Oh, J. U. Jeong, D. F. Veber, M. Gowen, G. Stroup. GlaxoSmithKline, King of Prussia, PA, USA.

Cathepsin K (catK) is a cysteine protease that is highly and selectively expressed in osteoclasts. Substantial evidence indicates that catK plays a key role in osteoclast-mediated bone resorption and that its pharmacological inhibition should result in inhibition of bone resorption *in vivo*. We have identified SB-462795, a potent inhibitor of human cathepsins K, L and V ($K_i = 41, 68$ and 53 pM, respectively) that exhibits 39-300 fold selectivity over other cathepsins. SB-462795 inhibited catK activity in sections of human osteoclastoma with an $IC_{50} \sim 45$ nM and inhibited human osteoclast-mediated bone resorption with an $IC_{50} \sim 20$ nM. The anti-resorptive potential of SB-462795 was evaluated in normal and Ovx female monkeys. Serum levels of the C- and N-terminal telopeptides of Type I collagen (CTX and NTx respectively) and urinary levels of NTx were monitored as biomarkers of bone resorption and serum osteocalcin was measured as a marker of bone formation. Subcutaneous (12 mg/kg) and oral (3, 10, 30 mg/kg) administration of SB-462795 to medically OVX (treatment with GnRHa) female monkeys clearly inhibited bone resorption as measured by inhibition of bone resorption markers in serum and urine. A single subcutaneous dose of 12 mg/kg resulted in a ~ 70 and $\sim 78\%$ inhibition of serum CTx at 1.5 and 72 hours, respectively. Similarly, oral dosing at 10 and 30 mg/kg also resulted in approximately 50% reduction in urinary NTx in the first 24 hours. The maximal effect in normal female monkeys was achieved after a single oral dose of 10 mg/kg where $\sim 38\%$ reduction in urinary NTx was observed for 48 hours. In these studies SB-462795 did not have a substantial impact on osteocalcin, a bone formation marker. Repeat oral administration of SB-462795 at 3 mg/kg to normal female monkeys for 5 days resulted in a progressive inhibition of resorption that was maximal on Day 5 (57%). After termination of dosing, both serum and urinary NTx returned to near control levels within 48 hours. In summary, both *in vitro* and *in vivo* data indicate that SB-462795 potentially inhibits human catK in osteoclasts, resulting in bone resorption inhibition both *in vitro* and in the monkey *in vivo*. *In vivo* bone resorption inhibition was measurable very rapidly after compound administration using validated markers of bone resorption, suggesting that SB-462795 will be effective at inhibiting the elevated bone resorption seen in post-menopausal osteoporosis. Furthermore, activity can be rapidly monitored by biochemical markers of bone resorption, suggesting that measurement of these markers should prove beneficial in monitoring clinical efficacy.

Disclosures: **S. Kumar**, GlaxoSmithKline 3.

SA232

See Friday Plenary number F232.

SA233

Bone Loss Following Ovariectomy in Cathepsin K Knockout Mice Is Attenuated by a Broad-Spectrum Matrix Metalloproteinase Inhibitor. S. J. Hoffman, P. Liang, C. A. Capriotti, J. A. Vasko-Moser, S. Kumar, G. B. Stroup. GlaxoSmithKline, King of Prussia, PA, USA.

Cathepsin K (catK), a cysteine protease, plays an essential role in osteoclast mediated degradation of bone organic matrix. Knockout of the enzyme in mice and lack of functional enzyme in the human condition pycnodysostosis result in osteopetrosis. Recent evidence suggests that proteinases other than catK play a role in bone loss following ovariectomy in aged mice and that catK may play more of a developmental role in bone turnover in this species. Prinomastat (AG3340) is a broad-spectrum, synthetic, nonpeptide, matrix metalloproteinase (MMP) inhibitor with selective inhibitory activity against MMPs 2, 9, 3, and membrane type-MMP1. In this study, effects of Prinomastat on bone were evaluated in catK deficient mice following ovariectomy (Ovx). Four month old catK deficient mice were randomized based on body weight into the following groups: baseline; sham + vehicle (acidified water, pH2.5) bid po; Ovx + vehicle bid po; Ovx + Prinomastat at 10 mg/kg bid po; and Ovx + Prinomastat at 30 mg/kg bid po. Baseline groups received no treatment or surgery and were euthanized on day 0. Dosing was initiated on day 1 post-surgery and continued for 8 weeks. Primary measures were histomorphometry of the proximal tibia and mid-femur and micro-computed tomography (micro-CT) of the 3rd lumbar vertebrae. Following Ovx, %Tb.Ar in the proximal tibia was significantly reduced relative to sham control animals. Prinomastat treatment resulted in 19% (ns) and 52% ($p=0.05$) protection of this loss at 10 and 30 mg/kg, respectively, and dose-dependent trends toward greater trabecular thickness and number, although these changes were not significant compared to Ovx controls. No significant effects due to Ovx or treatment were observed on bone formation or resorption rates (% eroded perimeter). MicroCT analysis of trabecular bone in the 3rd lumbar vertebrae showed lower BV/TV in Ovx (0.30) versus sham (0.34) mice (ns). Prinomastat treatment resulted in a higher BV/TV, 0.32 (ns) and 0.38 ($p<0.05$) at 10 and 30 mg/kg, respectively, than in Ovx control animals. Gains in BV/TV were due to increased Tb.Th and TB.N. The high dose of Prinomastat also significantly reduced the Structure Model Index (-0.26 vs. -1.49 for the Ovx and Prinomastat 30 mg/kg groups, respectively, $p < 0.01$) suggesting that Prinomastat treatment results in a more mechanically stable structure. In conclusion, Prinomastat prevented Ovx-induced trabecular bone loss. Contrary to the pronounced anti-resorptive effects of catK inhibitors in estrogen deficient monkeys, these data suggest that MMPs compensate and play a major role in trabecular bone turnover following ovariectomy in catK deficient mice.

Disclosures: **S.J. Hoffman**, GlaxoSmithKline 3.

SA234

See Friday Plenary number F234.

SA235

SB-462795, a Cathepsin Inhibitor, Prevents the Loss of Bone Mass at Several Sites in Ovariectomized Cynomolgus Monkeys. G. Stroup¹, C. Jerome², D. S. Yamashita¹, S. Kumar¹. ¹GlaxoSmithKline, King of Prussia, PA, USA, ²SkeleTech, Bothell, WA, USA.

Cathepsin K has been shown to play an important role in bone matrix degradation during osteoclastic bone resorption. We tested the ability of SB-462795, a novel, potent inhibitor of cathepsins K, L and V, to prevent loss of bone mass at several sites in aged ovariectomized (Ovx) female monkeys following oral delivery, and compared SB-462795 to IV alendronate. After collection of baseline data, adult female cynomolgus monkeys were randomized to 6 groups of 20 each, of which one was sham-ovariectomized (Sham) and the remainder Ovx. Ovx animals were treated with vehicle, SB-462795 at 1, 3, or 10 mg/kg/d by gavage, or oral vehicle plus alendronate at 0.05 mg/kg by IV injection once every 2 weeks for 9 months. All statistical comparisons are with Ovx, vehicle-treated animals. DXA analysis showed a significant ($p<0.001$) difference in aBMD between Sham and Ovx groups at the lumbar spine and proximal and distal femur after 9 months. Animals treated with SB-462795 had dose-dependent improvement in aBMD at the lumbar spine and proximal and distal femur. Protection from the relative loss of aBMD was observed with the high dose of SB-462795 at all three sites. At the distal femur SB-462795 prevented 73% of the loss in aBMD ($p<0.01$) while alendronate showed a non-significant 23% protection ($p>0.1$). At the proximal femur the level of protection by the two agents was 35% and 34%, respectively ($p < 0.1$). At the lumbar spine, SB-462795 protected 42% ($p<0.1$) while alendronate protected 100% ($p<0.001$) of the loss in aBMD. Femoral neck analysis using pQCT showed a similar level of protection of total vBMD by SB-462795 (58%, $p<0.05$) and alendronate (51%), but the latter was not statistically significant ($p>0.1$). Total BMC was significantly improved by SB-462795 (40%, $p<0.05$) but not by alendronate (24%, $p>0.1$). Both agents had a similar, positive effect on trabecular vBMD and BMC. Ovariectomy caused a 0.9% decrease in cortical area at the femoral neck. Treatment with SB-462795 at the high dose increased cortical area by 6.7% ($p<0.1$). A non-significant 2% increase in cortical area was observed with alendronate treatment. SB-462795 significantly improved cortical BMC (56% protection, $p<0.05$) but alendronate did not (25% protection, $p>0.1$). In conclusion, SB-462795 significantly prevented bone loss at several sites in Ovx monkeys. Femoral neck pQCT analysis indicated that, compared to alendronate, SB-462795 had a similar effect on trabecular bone but a more positive effect on cortical bone at this site. These data suggest site-specific differences in activity between bisphosphonates and cathepsin inhibitors that could potentially translate into differential efficacy.

Disclosures: **G. Stroup**, GlaxoSmithKline 3.

SA236

See Friday Plenary number F236

SA237

Matrix Metalloproteases from Cells of the Osteoclastic Lineage Resorb Demineralized Collagen in the Absence of Cathepsin K Activity. K. Henriksen¹, M. G. Sørensen^{*1}, R. H. Nielsen^{*1}, M. H. Dziegielel^{*2}, S. Schaller^{*1}, M. A. Karsdal¹. ¹Nordic Bioscience A/S, Herlev, Denmark, ²HS Blodbank, National University Hospital, Copenhagen, Denmark.

Loss of activity of the cystein protease cathepsin K leads to the disease pycnodysostosis, a disease characterized by defective osteoclastic degradation of type I collagen without impairment of dissolution of the inorganic phase of bone. Recent evidence suggest that degradation of the organic matrix takes place in the cathepsin K deficient individuals, however the molecular rational for this remains to be investigated. To investigate the osteoclastic proteolytic "machinery", we isolated CD14 positive monocytes from peripheral blood from humans, and cultured them in the presence of 25ng/ml RANKL and M-CSF to induce osteoclastogenesis. Mature osteoclasts were seeded on normal cortical calcified bone slices or bone slices decalcified with EDTA and cultured in the presence or absence of either the cystein protease inhibitor E64 or the Matrix Metalloproteinase (MMP) inhibitor GM6001 alone or in combination. We found that E64 completely blocked the release of the C-terminal crosslinked telopeptide of type I collagen (CTX) on calcified bone, as expected. In alignment GM6001 only inhibited the CTX release by 10-15%, confirming that the main protease involved in bone degradation under normal circumstances is Cathepsin K. In sharp contrast, when decalcified bone was used, MMP activity was responsible for 70-80% of the CTX fragments in face of 20-30% arising from Cathepsin K activity. To further investigate the release of extracellular matrix protease generated collagen fragments, we tested the release of the carboxyterminal telopeptide of type I collagen (ICTP), on both normal and decalcified bone in the presence and absence of protease inhibitors. On calcified bone, the release of ICTP was detected only when cathepsin K was inhibited. In addition, the release of ICTP in the presence of E64 was dose-dependently inhibited by GM6001, confirming that MMPs from cells of the osteoclastic lineage can release this fragment. On the decalcified bones, the ICTP fragment was released by the osteoclasts in the absence of inhibitors, and the release could be completely abrogated by the addition of GM6001, further confirming that MMPs are

ASBMR 27th Annual Meeting

important for the degradation of the decalcified bones. In conclusion, we have shown that MMPs are likely to play a role in the compensation for the loss of cathepsin K activity in the function of human osteoclasts.

Disclosures: **K. Henriksen**, None.

SA238

Tropomyosin Isoforms Localize to Distinct Microfilament Populations in Osteoclasts. **B. McMichael**^{*1}, **P. Kotadiya**^{*1}, **L. S. Holliday**², **B. S. Lee**¹.

¹Physiology and Cell Biology, The Ohio State University, Columbus, OH, USA, ²Orthodontics, University of Florida, Gainesville, FL, USA.

Osteoclasts are highly motile cells that transiently adopt a polarized phenotype during bone resorption. Because of the fluidity in cell shape associated with these processes, osteoclasts possess a dynamic cytoskeleton that contains specialized actin structures involved in motility (podosomes) and attachment during bone resorption (an F-actin ring surrounding the ruffled membrane). Here we have examined osteoclasts for the expression and distribution of tropomyosins, which are actin-binding proteins that regulate the stability of microfilaments and regulate their access to other proteins such as gelsolin, cofilin, Arp2/3, and myosins. Through Western analysis, immunocytochemistry, and RT-PCR, we assayed for the presence of 16 nonmuscle, nonbrain tropomyosin isoforms, and detected 6 that were expressed at moderate to high levels. Several of these were up-regulated during osteoclast differentiation. Immunocytochemical analysis showed that the isoforms were localized to distinct F-actin pools. One of these, Tm-4, co-localized with the actin core of podosomes, in addition to the peripheral and dorsal microfilaments of actin rings. Two similar tropomyosins, Tm-5a and -5b, were up-regulated during osteoclast differentiation, and associated with peripheral structures of podosomes instead of the actin core, but had a distribution similar to Tm-4 in actin rings. Tms -2 and -3, which are not expressed in macrophages, were expressed at moderate levels in osteoclasts. These were more generally distributed through the cells than other isoforms, but showed some enrichment near regions of podosomes. They also were intercalated loosely into the dorsal microfilaments of actin rings. These results demonstrate that tropomyosin isoforms are involved in the attachment structures of osteoclasts, and are likely to play specific roles in regulation of critical microfilament pools.

Disclosures: **B. McMichael**, None.

SA239

Suppression of Nonmuscle Myosin IIA in Differentiating Osteoclast Cultures Affects Cell Adherence and Multinucleation. **B. McMichael**^{*1}, **P. Kotadiya**^{*1}, **R. B. Wysolmerski**^{*2}, **B. S. Lee**¹. ¹Physiology and Cell Biology, The Ohio State University, Columbus, OH, USA, ²Pathology, St. Louis University, St. Louis, MO, USA.

We previously demonstrated that the nonmuscle myosin isoform IIA is associated with attachment structures of osteoclasts. This motor protein co-localizes with the actin core of podosomes and with the actin ring surrounding the ruffled border of polarized osteoclasts (the sealing zone). To define potential roles of myosin IIA in cell adhesion, we suppressed its expression via RNA interference technology. RAW 264.7 macrophages were induced to differentiate into osteoclasts by addition of RANKL, and were transfected with siRNAs when osteoclast formation first became evident (about day 4 of culture). Both inhibition of the corresponding mRNA and an altered cellular phenotype were demonstrable by two days following introduction of siRNAs. siRNA-treated cells that were lifted from their surface and re-plated demonstrated a diminished capacity to attach to either glass or bone substrates. Further, siRNA-treated cells were much larger in diameter and contained significantly greater numbers of nuclei than mock-treated cells. Finally, siRNA-treated cells generated dramatically more F-actin rings than mock-treated cells on bone. These results suggest that myosin IIA is required for appropriate attachment of osteoclasts, and may exert a suppressive effect on motility (affecting the extent of cell fusion) and sealing zone formation.

Disclosures: **B. McMichael**, None.

SA240

Osteoclasts and Mother Of Pearl Resorption: *In Vivo* and *In Vitro* Studies. **D. Duplat**^{*1}, **A. Chabadel**^{*2}, **M. Gallet**^{*3}, **O. Delattre**^{*4}, **S. Berland**^{*1}, **L. Bédouet**^{*1}, **C. Milet**^{*1}, **M. Brazier**³, **S. Kamel**^{*3}, **P. Jurdic**², **E. Lopez**^{*1}. ¹DMPA, Muséum National d'Histoire Naturelle, Paris, France, ²LBMC, ENS-Lyon, Lyon, France, ³UMRO, Faculté de Pharmacie, Amiens, France, ⁴Service Orthopédie, CHRU, Fort de France, France.

The nacre, mother-of-pearl, from the shell of the oyster *Pinctada margaritifera* is composed of calcium carbonate crystallized in aragonite tablets forming a lamellar structure. Our previous studies have demonstrated that the nacre exhibited biological activity on bone stem cells and osteoblasts and induced bone formation. Since bone remodelling is a balance between resorption by osteoclasts and new bone formation by osteoblasts, we wonder what happens when osteoclasts meets nacre? *In vitro* and *in vivo* studies were performed to consider mammalian osteoclasts in the nacre resorbing process. *In vivo* studies were performed on 14 sheep femurs implanted with raw nacre for 3 to 9 months. The femurs containing the implants were dissected out and subjected to histological study and morphometry to assess the changes that had occurred at the bone and nacre interface. Raw nacre implants persist even after 9 months of implantation into bone tissue in sheep. However the nacre surface undergoes a limited biodegradation process, smooth-surfaced nacre implants were seen to become microporous after implantation. The nacre surface resorption process was investigated using *in vitro* studies.

CD14 cells (osteoclast precursors) were experimentally differentiated and osteoclasts isolated from 10 days old rabbit long bones were both seeded on nacre slices. Osteoclasts on nacre were observed for adhesion and resorption by Scanning Electron Microscopy. The osteoclast cytoskeleton organization was analysed on osteoclast precursors isolated from 6 weeks old mouse spleen seeded on nacre slices. The *in situ* cell localization of F-actin and vinculin was investigated using confocal microscopy to point out adhesion and resorption activities. Osteoclasts from human, rabbit and mouse can adhere and resorb nacre. However the setting of the sealing zone and consequently the osteoclast activity depend on the orientation of the aragonite tablets facing the osteoclasts as shown by *in vitro* studies. It arises that nacre *in vivo* can also be subjected to resorption by osteoclast activity. In that case, the size and shape of the nacre are key factors in determining the nacre implant biodegradation rate and kinetics by osteoclasts.

Disclosures: **D. Duplat**, None.

SA241

Guanylyl Cyclase and cGMP-Dependent Protein Kinase I Induce Calcium and Calpain-Dependent Cytoskeletal Rearrangement in Osteoclasts, but Calcium Signals Are not Sufficient to Initiate Motility. **B. B. Yaroslavskiy**^{*}, **S. E. Kalla**^{*}, **A. C. Sharrow**^{*}, **H. C. Blair**. Pathology and of Cell Biology and Physiology, University of Pittsburgh, and Veteran's Affairs Medical Center, Pittsburgh, PA, USA.

Osteoclasts are highly regulated motile cells. Motility and survival respond to signals including the CSF-1, via fms, and nitric oxide (NO). Osteoclast survival is regulated by NO-generated free radicals, but at moderate NO activity, cGMP generation by the NO-dependent guanylyl cyclase is the predominant osteoclast NO regulatory mechanism. Downstream, the cGMP-dependent protein kinase I (PKG I) induces motility via phosphorylation of the adaptor protein VASP. VASP directs the NO signal to the podosomal complex that is also regulated by other motility signals, and regulates detachment. However, VASP phosphorylation by PKG I is insufficient for motility. We observed by Ca²⁺ imaging of human osteoclasts that, after NO/cGMP activation, Ca²⁺ currents occur at the detachment (trailing edge). This suggested Ca²⁺-activated proteinase activity. Gene screening showed that osteoclasts express the Ca²⁺-activated proteinases, M- and μ -calpain, the latter commonly active in cytoskeletal rearrangement for motility after Y-kinase receptor stimulation. Zymography and fluorescent calpain substrates *in situ* showed that μ -calpain was consumed after PKG I activation, and motility was blocked by calpain inhibitors. In contrast, Ca²⁺-induced contraction was caused by ionomycin at sublethal concentrations or by 20 mM supernatant Ca²⁺, but Ca²⁺ was insufficient to initiate detachment, indicating that upstream signals with direct effects on attachment structures are also required. Sequential fluo3 imaging to showed that Ca²⁺ increases and cell contraction were concurrent. NO increased src tyrosine phosphorylation, but surprisingly the PI-3-kinase/p-Akt pathway did not appear to be activated, in contrast to expectations based on post-Y-kinase receptor mechanisms. In ionomycin plus NO, osteoclasts detached, while after NO synthase inhibitors or PKG I inhibitors, cells shrank ~20% in ionomycin but did not detach. In no case was motility induced by artificial Ca²⁺ fluxes, which caused cells to retract symmetrically, while calcium fluxes by dual wavelength ratio imaging in NO treated osteoclasts were asymmetrical and occurred at attachments. We conclude that NO-induced motility requires Ca²⁺ fluxes related to detachment, that p-src is probably an intermediate, and that downstream Ca²⁺ signals function in cytoskeletal rearrangement whether motility is initiated by NO or other mechanisms such as integrin or Y-kinase receptors. On the other hand, Ca²⁺ currents alone are insufficient to initiate motility.

Disclosures: **B.B. Yaroslavskiy**, None.

SA242

See Friday Plenary number F242.

SA243

$\alpha_9\beta_1$ Integrin Signaling Is Required for Normal Osteoclast Activity. **H. Rao**¹, **V. Garcia Palacios**¹, **D. Sheppard**^{*2}, **J. Anderson**^{*1}, **K. Patrene**^{*1}, **S. J. Choi**³, **H. C. Blair**⁴, **G. D. Roodman**¹. ¹Medicine-Hematology/Oncology, University of Pittsburgh, Pittsburgh, PA, USA, ²Medicine, University of California at San Francisco, San Francisco, CA, USA, ³National Institute of Dental and Craniofacial Research, Bethesda, MD, USA, ⁴Pathology, University of Pittsburgh, Pittsburgh, PA, USA.

Recently, we found that $\alpha_9\beta_1$, a previously unknown integrin expressed on osteoclasts (OCL) and OCL precursors, is a receptor for a disintegrin and metalloproteinase (ADAM) 8. ADAM8 is a novel stimulator of OCL differentiation whose disintegrin domain mediates its effects on OCL formation. ADAM8 does not bind $\alpha_9\beta_1$ integrin. To access $\alpha_9\beta_1$ integrin regulates osteoclastogenesis and bone resorption, we measured OCL formation in bone marrow cultures and performed bone histomorphometry on vertebrae from 7 day old α_9 knockout (-/-) and wild type (WT) mice. α_9 -/- mice die of chylothorax at about 10 days of age. Normal numbers of OCLs formed in α_9 -/- marrow cultures, but the OCLs were smaller and more contracted compared to WT. Analysis of the bone resorption capacity and cytoskeleton of α_9 -/- OCLs formed *in vitro* showed they formed fewer resorption pits and failed to form normal actin rings compared to WT. Importantly, treatment of bone marrow cultures from β_3 integrin -/- mice with ADAM8, partially rescued the abnormal OCL cytoskeletal of the β_3 -/- OCL. ADAM8 treatment of α_9 -/- bone marrow cultures failed to rescue the abnormal α_9 -/- OCL cytoskeleton. Histologic analysis of α_9 -/- vertebrae showed thickened trabecular regions and retained cartilage within vertebral bodies of α_9 -/- mice. Three dimensional μ qCT analysis of α_9 -/- vertebrae also

showed a significant increase in trabecular bone volume/ total tissue volume (WT=16%±1.6; -/-= 20%±4.1; p=0.04), and a tendency of decreased trabecular separation (p=0.06) compared to WT mice. These results suggested that $\alpha_v\beta_1$ is required for normal OCL activity. We then determined how $\alpha_v\beta_1$ might signal in OCL. Previous reports showed that the α_v integrin cytoplasmic domain binds to paxillin in Chinese Hamster Ovary cells. OCLs express paxillin which is phosphorylated on multiple tyrosine and serine residues in response to cell adhesion, and /or exposure to various soluble growth factors and cytokines. Therefore, we determine if α_v integrin transduced signals through paxillin. Serum starved OCL precursors from WT and α_v -/- were exposed to ADAM8 or vehicle for 10 to 30 minutes. Immunoblot analysis showed transient tyrosine phosphorylation (pY118) of paxillin after 10 min of ADAM8 stimulation of WT, but not α_v -/- OCL. These results support an important role for $\alpha_v\beta_1$ integrin in OCL formation and function that is independent of $\alpha_v\beta_3$ activity.

Disclosures: **H. Rao**, None.

SA244

See Friday Plenary number F244.

SA245

Actin Assembly Induced by Cortactin Is Essential for Osteoclast to Resorb Bone. **R. Faccio**¹, **S. Tehrani**^{*2}, **J. A. Cooper**^{*2}. ¹Department of Orthopaedic Surgery, Washington University, St. Louis, MO, USA, ²Department of Cell Biology, Washington University, St. Louis, MO, USA.

Osteoclasts are essential for bone dynamics and calcium homeostasis in vertebrates. Osteoclasts form a tight seal on the bone surface, onto which they secrete acid and resorb bone. The sealing zone contains actin filaments and is presumed to assemble from podosomes, which also contain actin. Cortactin, a c-Src substrate, promotes Arp2/3-mediated actin assembly, is expressed in osteoclasts, and localizes to podosomes. We found that cortactin expression went from undetectable to substantial levels during osteoclast differentiation. To address the role of cortactin and actin assembly in osteoclasts, we depleted cortactin in osteoclasts by RNA interference. Cortactin-depleted osteoclasts had no podosomes, failed to make sealing zones, and did not resorb bone. The cells were normal in other respects, such as size, shape, motility and differentiation markers. We found that cortactin localizes to the nascent podosome, followed by actin assembly. Thus, cortactin has a critical role in osteoclast function related to regulation of podosomes and sealing zones formation, via Arp2/3-mediated actin assembly at the sealing zone.

Disclosures: **R. Faccio**, None.

SA246

Thyrotropin (TSH) Differentially Regulates TNF α Expression in Osteoclast and Osteoblast Progenitors. **H. Hase**^{*1}, **L. Liu**^{*1}, **A. Brebene**^{*1}, **Y. Peng**^{*1}, **H. Amano**², **E. Abe**¹. ¹Medicine, Mt. Sinai School of Medicine, New York, NY, USA, ²Pharmacology, Showa University School of Dentistry, Tokyo, Japan.

We have provided evidence that thyrotropin (TSH) inhibits bone remodeling and TSH receptor (TSHR) null mice exhibit an osteoporotic phenotype resulting from enhanced osteoclastogenesis and osteoblastogenesis. Our preliminary studies indicated that the enhanced osteoclastogenesis in the TSHR null mice is due to upregulated expression of TNF α and TNF receptor (TNFR) type I and II. TNF α is known to enhance osteoclast but suppress osteoblast differentiation. We therefore examined the mechanisms by which RANK-L and inflammatory cytokines upregulate TNF α and TNFR, and whether the overexpression of TSHR or caTSHR (constitutively active form of TSHR) in osteoclast and osteoblast progenitors affects TNF α expression and cell differentiation. TSHR expression is temporally upregulated during osteoclast and osteoblast differentiation. RANK-L and certain inflammatory cytokines such as IL-1 α /TNF α , lipopolysaccharide (LPS) and phorbol 12-myristate 13-acetate (PMA) enhanced TNF α expression in bone marrow macrophages (CD11b⁺) and RAW-C3 cell cultures, and these enhanced expression levels were suppressed by treatment with TSH. Overexpression of TSHR and caTSHR in bone marrow macrophages and RAW-C3 cells suppressed TNF α expression under basal and also RANK-L-stimulated conditions. As expected, the effective dose of TSH in osteoclast inhibition was lowered in cells overexpressing TSHR. Interestingly, RANK-L-induced osteoclast formation was completely abolished in cells overexpressing caTSHR. We next examined the effects of cytokines and TSH on TNF α expression and cell differentiation in osteoblasts. TSH itself significantly enhanced TNF α expression in bone marrow stromal cells (CD106⁺) and calvarial osteoblasts. Overexpression of TSHR and caTSHR in OB6 cells and calvarial osteoblasts also exhibited enhanced TNF α expression without the addition of TSH. In addition, the cells overexpressing caTSHR exhibited inhibition of BMP4-dependent osteoblast differentiation. These results suggest that TNF α plays a critical role in the inhibition of osteoclast and osteoblast differentiation induced by TSH and that the TNF α regulatory mechanisms are likely to be distinct in osteoclast and osteoblast progenitors.

Disclosures: **H. Hase**, None.

SA247

See Friday Plenary number F247.

SA248

Treatment of Bone Cancer in Mice Transgenic for Cytosine Deaminase Regulated by the TRAP Promoter. **M. Ramnaraine**, **W. Pan**^{*}, **J. M. Donohue**^{*}, **C. M. Lynch**^{*}, **D. Clohisy**. Orthopaedic Surgery, University of Minnesota, Minneapolis, MN, USA.

In this investigation we describe an osteoclast-mediated, tumor-targeted gene therapy which affects osteoclasts and cancer cells. Using the cytosine deaminase (CD)/5 fluorocytosine (5FC) prodrug system, we demonstrate effectiveness *in vitro* and *in vivo*. Osteoclast-specific delivery was achieved using a transgenic mouse containing the CD gene regulated by the tartrate-resistant acid phosphatase promoter (Tg/TRAP-CD). In this system, 5FC treatment of CD-expressing osteoclasts caused direct killing of osteoclasts and bystander killing of cancer cells. *In vitro*, osteoclasts from BM of Tg/TRAP-CT or WT mice were exposed to 5FC, resulting in a dose-dependent decrease in osteoclast number in all Tg/TRAP/CD (p < 0.001) compared to WT osteoclast cultures. Co-culture of Tg/TRAP-CD or WT osteoclasts with tumor cell lines showed reduction in sarcoma and breast cancer cells in Tg/TRAP-CD co-culture systems (p < 0.001) but not systems of tumor cells co-cultured with WT BM. *In vivo*, Tg/TRAP-CD mice received osteolytic bone sarcoma that after 5FC treatment resulted in elimination of tumor (p < 0.001) and reduction in osteoclast number. These studies provide the basis for developing a treatment for primary or metastatic bone cancers which would simultaneously kill tumor cells and eliminate osteoclast-mediated bone destruction.

Disclosures: **D. Clohisy**, None.

SA249

See Friday Plenary number F249.

SA250

IL-12 and IL-18 Require IFN- γ and GM-CSF Signaling, and Are Essential for Normal Bone Remodeling and Bone Mass. **N. A. Sims**¹, **D. Mirosa**^{*2}, **J. M. W. Quinn**², **N. J. Horwood**^{*2}, **M. J. Smyth**^{*3}, **M. T. Gillespie**^{*2}. ¹Dept of Medicine, The University of Melbourne, Fitzroy, Australia, ²Bone, Joint and Cancer Group, St Vincent's Institute, Fitzroy, Australia, ³Peter MacCallum Cancer Research Institute, Melbourne, Australia.

Interleukin-18 (IL-18) is a pleiotropic factor that shares structural features with IL-1 and functional activities with IL-12. IL-18 is expressed by osteoblasts and has been reported to inhibit *in vitro* osteoclast formation by acting upon T cells to promote GM-CSF production. In addition to its ability to enhance GM-CSF production, it also increases IFN- γ , another osteoclast inhibitor. Like IL-18, IL-12 is also an inhibitor of osteoclast formation as a result of its actions on T lymphocytes. When combined, IL-12 and IL-18 are powerful synergistic inhibitors of osteoclast formation. As IL-12 and IL-18 both increase IFN- γ and GM-CSF production we examined the contribution of IFN- γ and GM-CSF in the IL-12 and IL-18 responses. *In in vitro* osteoclast formation assays, a neutralising antibody to GM-CSF demonstrated that IL-18 acted through GM-CSF alone, but this antibody only partially rescued IL-12-induced osteoclast formation. Similarly, a neutralising IFN- γ antibody partially rescued IL-12-induced osteoclast formation, and combination of both GM-CSF and IFN- γ neutralising antibodies provided 50% rescue of the IL-12-induced osteoclast formation. However, the combination of GM-CSF and IFN- γ neutralising antibodies completely rescued osteoclast formation from inhibitory synergistic doses of IL-12- and IL-18, demonstrating a requirement for both GM-CSF and IFN- γ for the action of these two interleukins at synergistic doses, but implicating another inhibitor in response to IL-12 alone. Since both IL-12 and IL-18 are expressed in bone, we investigated their involvement in normal bone development, growth, and remodeling, by performing histomorphometric analyses of mice deficient in IL-12, in IL-18, and in both IL-12 and IL-18. No gross skeletal abnormalities were evident in these mice. Histomorphometry revealed an ageing-related osteopenia in each of these knockout mice. While only the IL-18 null mice demonstrated a significant reduction in trabecular bone volume at 10 weeks of age, by 6 months of age, in all three knockouts, both trabecular bone volume and trabecular number were approximately half that of wild type controls. Notably, the phenotype was not more severe in mice deficient in both IL-12 and IL-18 compared to the single IL-12 or IL-18 null mice. These results underscore a central role of IL-12 and IL-18, as well as T lymphocytes, in normal skeletal development.

Disclosures: **N.A. Sims**, None.

SA251

See Friday Plenary number F251.

SA252

Expression and Regulation of Resistin in Osteoblasts and Osteoclasts Indicate a Role in Bone Metabolism. K. Stunes^{*1}, L. Thommesen^{*2}, M. Monjo^{*3}, K. Grøsvik^{*1}, M. Tamburstuen^{*3}, E. Kjøbli^{*2}, S. Lyngstadaas^{*3}, J. Reseland^{*3}, U. Syversen¹. ¹Department of Cancer Research and Molecular Medicine, Norwegian University of Science and Technology, Trondheim, Norway, ²Sør-Trøndelag University College, Faculty of Medical Technology and Food Science, Trondheim, Norway, ³Oral Research Laboratory, Institute for Clinical Dentistry, University of Oslo, Oslo, Norway.

Recent studies have indicated that hormones from adipose tissue possess several biological functions. Leptin and adiponectin have previously been shown to be expressed and regulated in bone cells. In the present study we explore the role of resistin in bone metabolism, using murine preosteoblasts and osteoclasts (MC3T3-E1, RAW 264.7) and primary human bone marrow stem cells, osteoblasts and osteoclasts as model systems. We find that resistin is expressed in the murine osteoclast RAW 264.7 and preosteoblast MC3T3-E1 cell lines, in primary human bone marrow stem cells and in differentiated human osteoblasts. The expression of resistin mRNA in RAW 264.7 is regulated through PKC and PKA-dependent mechanisms. Recombinant resistin enhanced the proliferation of preosteoblasts, and the alkaline phosphatase activity in the medium, as well as the expression of collagen mRNA in osteoblasts. Resistin also enhances the number of differentiated osteoclasts. In RAW 264.7 cells transfected with NF- κ B reporter plasmid, resistin increased the promoter activity. In addition to the direct effect on osteoclasts, resistin increased the OPG to RANKL ratio and the secretion of IL-6 from osteoblasts, indicating an indirect effect on osteoclast differentiation and activity. Taken together our results indicate that resistin is involved in bone remodelling via paracrine and/or autocrine mechanisms.

Disclosures: **K. Stunes**, None.

SA253

See Friday Plenary F253.

SA254

TNF Induces Oscillatory and Combinatorial Transcription Factor-DNA Binding: A Requirement for Sustained Gene Expression. J. Iqbal^{*}, M. Zaidi. Medicine, Mt. Sinai School of Medicine and the Bronx VA GRECC, New York, NY, USA.

It has been shown recently that the activation and nuclear translocation of the NF- κ B subunit p65 occurs in cycles.^{1,2} Nonetheless, it is thought that NF- κ B must persistently bind to DNA to induce gene expression. Here, we show for the first time that TNF induces oscillations in NF- κ B binding to DNA; that this oscillatory binding is combinatorial; and that the persistence of such oscillations results in sustained gene expression. We analyzed the binding of both NF- κ B and c-jun transcription factors to the promoters of target genes, CD38 (an ADP-ribosyl cyclase) and I κ B α (an NF- κ B inhibitor). Using a combination of chromatin immunoprecipitation (ChIP) assays and real-time PCR, we quantified transcription factor-DNA binding at 15 minute intervals for 7 hours. TNF application to primary bone marrow macrophages resulted in NF- κ B recruitment to target promoters with a periodicity of ~3 hours and sustained binding amplitudes. Mathematical modeling suggested that both periodicity and sustained amplitudes arise from the large cytoplasmic-to-nuclear volume of primary macrophages. We also found that c-jun binding to the CD38 promoter was oscillatory with a temporal sequence that overlapped substantially with p65 and p50. To confirm this overlap, we re-ChIPed the CD38 promoter at 0 and 3 hrs post-TNF. TNF induced several combinatorial patterns of binding; for example, p65, p50 and c-jun bound simultaneously with the co-activator Brg-1. In contrast to the CD38 promoter, p65 was the only major oscillatory protein for the I κ B α promoter; this substantiates previous findings indicating that p65 is necessary and sufficient for I κ B α up-regulation.³ We next explored transcription factor-DNA binding in response to RANK-L, a member of the TNF superfamily that induces similar signaling pathways to TNF, but with distinct effects on gene transcription. Notably, we found that both CD38 and I κ B α mRNA levels were persistently elevated with TNF, but only transiently with RANK-L. This difference was consistent with a single wave of p65, p50 and c-jun binding to target promoters post RANK-L, but with a failure of this binding to oscillate. The results show that oscillatory transcription factor-DNA binding is critical for assembling combinatorial complexes required for cytokine-induced gene expression. Furthermore, differences in the expression of genes induced by closely related cytokines could be explained by their ability to sustain these oscillations.¹Hoffman, A. (2002) Science 298: 1241-5; ²Nelson, D.E. (2004) Science 306: 704-8; ³Hoffman, A. (2003) EMBO J. 22: 5530-9.

Disclosures: **J. Iqbal**, None.

SA255

c-Fos/NFAT1- or 2-Mediated Osteoclastogenesis Requires NF- κ B p50/p52 Expression. Z. Yao¹, K. Matsuo², R. Nishimura³, L. Xing¹, B. Boyce¹. ¹University of Rochester Medical Center, Rochester, NY, USA, ²Keio University, Tokyo, Japan, ³Osaka University, Osaka, Japan.

Expression of the transcription factors, NF- κ B, c-Fos, and NFAT, in cells in the osteoclast (ocl) lineage is essential for differentiation of ocl precursors to mature ocls. However, the relationship among NF- κ B, c-Fos and NFAT during ocl precursor differentiation is unknown. To study this issue, we used NF- κ B p50/p52 double knockout

(dKO) and wild-type (wt) splenocytes and a retrovirus gene transfer approach. First, we examined the temporal expression pattern of c-Fos and NFATs1-4, using real time PCR during RANKL-mediated osteoclastogenesis from wt splenocytes. RANKL increased c-Fos mRNA expression in M-CSF-dependent splenic ocl precursors at 8 hrs. This peaked at 24 hrs, prior to multi-nucleated ocl formation, and declined when mature ocls began to form at 48 hrs. In contrast, expression of NFAT1 and 2 mRNA paralleled ocl formation, being up-regulated at 48 hrs, peaking at 72 hrs when mature ocl numbers were highest and decreasing at 96 hrs when ocls were dying off. NFAT3 expression did not change and NFAT4 levels were very low. Next, we examined the effect of RANKL on c-Fos and NFAT expression in NF- κ B dKO cells: RANKL failed to induce c-Fos or NFAT up-regulation. c-Fos over-expression rescued RANKL-mediated osteoclast formation and NFAT2 protein expression in NF- κ B dKO cells, but did not induce ocls by itself. In contrast, NFAT1 or NFAT2 retrovirus infection alone, unlike c-Fos or NF- κ B p50 and p52 over-expression, induced small numbers of TRAP+ ocls from dKO cells. Addition of RANKL or IL-1 induced more ocls (61 \pm 5 and 124 \pm 15 /well, respectively, for NFAT1; and 149 \pm 31 and 145 \pm 34 for NFAT2, vs 0 \pm 0 for GFP-infected cells). Furthermore, NFAT1 or NFAT2 over-expression alone induced numerous mononucleated TRAP+ cells. Finally, over-expression of NFAT1 or NFAT2 plus IL-1 induced ocl formation from wt splenocytes in the absence of RANKL (21 \pm 3 in NFAT1-, 97 \pm 18 in NFAT2-, vs 0 \pm 0 in GFP-infected cells). In summary, 1) NF- κ B p50 and p52 expression is required in ocl precursors for RANKL-induced c-Fos and NFAT1 or 2 expression, and c-Fos precedes NFAT expression; 2) NFAT1 or 2 can substitute for NF- κ B, inducing ocl formation from NF- κ B dKO splenocytes alone or along with IL-1, independent of RANKL; and 3) cytokines, including RANKL and IL-1, are indispensable for ocl formation induced by c-Fos, but not by NFATs from NF- κ B dKO splenocytes. We propose a "temporal" model in which NF- κ B increases c-Fos expression in ocl precursors, which results in induction of NFATs1 and 2 and differentiation of TRAP+ cells. Cytokines promote the translocation of these over-expressed transcription factors to ocl nuclei and subsequent ocl maturation.

Disclosures: **Z. Yao**, None.

SA256

RANK Deficiency in the Hematopoietic Compartment Alters the Development of Osteoclasts but not Other Hematopoietic Lineages. C. Jacquin¹, S. K. Lee², J. A. Lorenzo², H. L. Aguila^{*1}. ¹Department of Immunology, UConn Health Center, Farmington, CT, USA, ²Department of Medicine, UConn Health Center, Farmington, CT, USA.

Interactions of RANKL and RANK play a crucial role in the development of both normal bone and hematopoietic tissues. RANK and RANKL deficient mice display a severe osteopetrotic phenotype due to the lack of mature osteoclasts. In addition, these mice demonstrate alterations in the organization of peripheral lymphoid organs and in the development of T and B lymphocytes. To determine whether the hematopoietic abnormalities observed in RANK deficient (RANK^{-/-}) mice are cell autonomous or due to a defective bone microenvironment, we generated bone marrow (BM) chimeric mice by transplanting unfractionated splenocytes from 3-4 week old RANK^{-/-} neonates in a C57BL/6 background (or unfractionated BM cells from wild-type (WT) littermates as control) into lethally irradiated 9-10 week old WT C57BL/6 mice, which were congenic for the CD45 allelic marker. Animals were allowed to recover for at least 11 weeks. Completeness of engraftment, as assessed by flow cytometry, was typically >90%. Flow cytometric analysis of multiple hematopoietic organs showed no significant differences in the development of T, B, dendritic or natural killer cells between RANK^{-/-}→WT and WT→WT chimeras. We also assessed the bone mineral density of tibias and femurs of individual mice from RANK^{-/-}→WT and WT→WT chimeras using DEXA and micro-CT at weeks 11, 17 and 26 post transplantation and found that both groups maintain a similar bone marrow volume at all three time points. Finally, we determined the ability of total BM preparations from both groups (11 weeks post-transplant) to form osteoclast-like cells (OCLs) *in vitro* in the presence of M-CSF and RANKL. Total BM preparations (5,000 or 75,000 cells per well) from individual mice of both groups were plated for 4 or 8 days with 30ng/ml of M-CSF and RANKL. In the WT→WT chimeras, OCLs formed readily (427 \pm 46 OCLs per 5,000 plated cells in 4-day cultures), in contrast, BM preparations from RANK^{-/-}→WT were very inefficient at forming OCLs *in vitro* (7 \pm 4 OCLs per 75,000 plated cells in 8-day cultures). In conclusion, we find that the hematopoietic abnormalities observed in RANK^{-/-} mice were not present in the RANK^{-/-}→WT chimeras, which unlike RANK^{-/-} mice have a bone marrow cavity. This data suggests that the defects in immune cells in RANK^{-/-} mice are due to their lack of a BM microenvironment. The only deficiency that we observed in RANK^{-/-}→WT chimeras was a defect in osteoclast development. RANK^{-/-}→WT chimeras likely maintain their bone marrow cavity because of decreased turnover in this model.

Disclosures: **C. Jacquin**, None.

SA257

NFATc1 Mediates RANKL Induction of the β 3 Integrin in Osteoclasts. T. N. Crotti, M. R. Flannery^{*}, J. D. Fleming^{*}, S. R. Goldring, K. P. McHugh. Rheumatology and Orthopaedics, BIDMC and Harvard Medical School, Boston, MA, USA.

NFATc1 is a RANKL-induced transcriptional mediator of osteoclast (OC) differentiation, however, the specific molecular targets of NFATc1 have not been identified. The present study was undertaken to determine the role of NFATc1 in RANKL-induced transcription of the β 3 integrin gene. Alignment of the human (h) and mouse (m) β 3 integrin promoters identifies a region (m promoter -1260 to -1350) displaying 89% sequence homology, with several conserved transcription factor binding sites, including the only conserved NFAT/AP1 site. To define the role of NFATc1 in RANKL-induction of the β 3 gene, truncated promoter/reporter constructs were transfected into RAW264 cells.

The full-length (1350 bp) promoter was induced > 10 fold by RANKL treatment. Deletion of the 5' putative NFATc1 binding site (to -1084) reduced RANKL induction to < 2.5 fold. Further evidence implicating NFATc1 in $\beta 3$ gene regulation was provided by the observation that transduction with a TAT dominant-negative NFATc1 (TAT-dnNFATc1) blocked RANKL induction of the full-length h $\beta 3$ promoter. We have shown that transduction with this construct dose-dependently blocked expression of the $\beta 3$ integrin (as measured by QPCR) and the formation of TRAP positive multinuclear cells in RANKL-treated mouse macrophages. In addition, transactivation of the $\beta 3$ promoter by cotransfection with NFATc1 resulted in induction of >100 fold. Additionally, transactivation by NFATc1 was dose-dependent. Transactivation by NFATc1 was abolished by deletion of the m $\beta 3$ promoter to -1084. Direct binding of NFAT to the m $\beta 3$ promoter was demonstrated using EMSA. A 21 bp probe (-1164 to -1185 from the TSS) of the m $\beta 3$ gene, bound to NFATc1 in nuclear extracts from Jurkat cells, mouse OCs, and RAW264 cells. Specificity of the shifted bands was determined by competition with consensus NFAT probes. Oligos containing a mutant NFAT site failed to compete. Supershift with anti-NFATc1 identified the shifted complex as NFATc1. Consensus AP-1 sites are not present in this oligo and therefore NFAT binding to the promoter is independent of AP-1. PU.1 was also found to bind to this oligo, as demonstrated by competition with consensus oligos and by supershift with anti-PU.1. Interestingly, PU.1 binding was lost upon mutation of the NFAT binding site indicating requisite NFATc1 binding for PU.1 binding. Furthermore, mutation of the NFAT sites in the h $\beta 3$ promoter blocked both RANKL induction and NFATc1 transactivation. Our results provide direct evidence that the $\beta 3$ integrin gene is a specific target of NFATc1 during RANKL-induced OC differentiation and that these effects are mediated through direct binding of NFATc1 to specific sites in the $\beta 3$ integrin gene promoter.

Disclosures: T.N. Crotti, None.

SA258

See Friday Plenary number F258.

SA259

RANK Expression in Normal and Malignant Haemopoietic Cells: A Monoclonal Antibody Study. G. J. Atkins¹, P. Kostakis^{*2}, C. Vincent^{*1}, A. N. Farrugia^{*2}, D. M. Findlay¹, A. Evdokiou^{*1}, A. C. W. Zannettino^{*2}.

¹Orthopaedics, University of Adelaide, Adelaide, Australia, ²Haematology, Institute of Medical and Veterinary Science, Adelaide, Australia.

The expression of RANK has been shown to be a prerequisite in order for osteoclast precursors (preOC) to differentiate into functional osteoclasts (OC). Although attributed to the monocytoid lineage, the true nature of the preOC in vivo has remained enigmatic. Also, although it is widely accepted that preOC are bone marrow derived cells and that they circulate in the peripheral blood, the stage at which these cells express RANK has not been adequately studied in the human. We tested a panel of murine monoclonal antibodies (MAbs; kindly supplied by J.P. Houchins, R&D Systems, MN) raised against full length recombinant human RANK, for reactivity by flow cytometry with normal human peripheral blood and bone marrow mononuclear cells (PBMC and BMMC, respectively), Giant Cell Tumour cells (GCT), as a confirmed source of preOC and mature OC, and various cell lines. RANK immunoreactivity in BMMC was observed with subpopulations of CD19+ B-cells, CD56+CD3+ NK cells and CD14+ monocytes. Similar reactivity was observed in PBMC, suggesting that RANK-expressing preOC circulate in the periphery. Positive selection of the RANK+ cells by magnet activated cell sorting (MACS) yielded a distinctive population of viable cells, some of which had large cytoplasmic to nuclear ratios. However, exposure of these cells to recombinant RANKL/M-CSF did not yield functional OC. In contrast, positive selection using a CD14 MAb yielded a population of monocytes that readily differentiated into OC. A possible explanation for the failure of RANK+CD14+ cells to differentiate into OC may be antagonism between the RANK MAb used and recombinant RANKL, for RANK receptors on these cells. Consistent with this, we observed differential effects of RANK MAbs when added to OC-forming assays from CD14+ PBMC precursors; one MAb, designated R24, profoundly inhibited the formation of functional OC, whereas others either did not influence OC formation or appeared to enhance RANKL-mediated OC formation. Furthermore, R24, but not other RANK MAbs, inhibited the resorbing activity of GCT cells in a dose-dependent manner. The specificity of the MAbs used was confirmed by western blot and immunoprecipitation. Our results indicate that RANK+ preOC are represented in the marrow and circulate in the periphery, potentially forming a pool of cells able to respond rapidly to RANKL. However, positive selection of preOC using RANK MAbs may developmentally and functionally inhibit these cells.

Disclosures: G.J. Atkins, None.

SA260

See Friday Plenary number F260.

SA261

Strength of TRAF6 Signaling Determines Osteoclastogenesis. Y. Kadono¹, F. Okada^{*2}, Y. Choi³. ¹Orthopaedic Surgery, University of Tokyo, Faculty of Medicine, Tokyo, Japan, ²Pahtology and Laboratory Medicine, University of Pennsylvania School of Medicine, Philadelphia, PA, USA, ³Pathology and Laboratory Medicine, University of Pennsylvania School of Medicine, Philadelphia, PA, USA.

Only the RANK has been shown to induce osteoclastogenesis in vivo, even though other immune receptors, including CD40 and IL-1R/Toll-like receptor, utilizing TRAF6 to activate overlapping signaling cascades. To clarify whether qualitative or quantitative differences exist between the TRAF6-mediated signals induced by TRANCE and by other ligand-receptor pairs, we first transduced RANK mutants that have mutations in TRAF6 binding sites not to bind TRAF6 into bone marrow macrophages (BMMs), and tested for their capacity to induce osteoclastogenesis. RANK with a single mutation, E342A, E375A or E449A (mutation in 1st, 2nd, or 3rd binding site, respectively), as well as wild type (WT), could successfully induce osteoclastogenesis. RANK mutants bearing two mutations, E342/449A or E375/449A, also induced osteoclastogenesis, but both E342/375A and the triple mutant failed to induce osteoclastogenesis. These results demonstrate that either the 1st or 2nd TRAF6 binding site has a greater capability of inducing osteoclastogenesis than the 3rd site and that at least one of the two membrane-proximal TRAF6 binding sites is required for optimal osteoclastogenesis. We hypothesize that when stronger stimuli are given by overexpression, CD40 can initiate osteoclast differentiation. When we overexpressed WT CD40 and stimulated with anti-CD40, TRAP(+) cells were formed, although most were mononuclear. To enhance the differentiation of TRAP(+) cells by CD40, WT CD40-overexpressing BMMs were treated with TGF-beta, a known costimulatory molecule for osteoclastogenesis. In the presence of TGF-beta, CD40-induced p38 kinase activation was enhanced, and bone-resorbing osteoclasts were formed. This CD40-induced osteoclastogenesis was not inhibited by a soluble form of RANK, which completely inhibited TRANCE-induced osteoclastogenesis. When CD40 mutants containing increased numbers of TRAF6-binding sites in the cytoplasmic tails were transduced, stimulation through these modified CD40 showed a dose-dependent increase in the recruitment of TRAF6, the activation of p38 kinase, and more pronounced osteoclastogenesis. Moreover, precursors overexpressing TRAF6 differentiate into osteoclasts in the absence of additional signals from any stimuli. Our results suggest that differences in the osteoclastogenesis-inducing capacity of TRANCE-R versus other TRAF6-associated receptors may in part stem from a quantitative difference in the TRAF6-mediated signals.

Disclosures: Y. Kadono, None.

SA262

See Friday Plenary number F262.

SA263

The Role of Calpain in RANKL-Supported Osteoclastogenesis. F. Y. Lee, D. Kim, J. A. Karmin*, S. Chang*, M. Fujisawa*, L. U. Bigliani*, T. A. Blaine*, H. Lee. Center for Orthopaedic Research, Columbia University, New York, NY, USA.

To clarify the role of calpain in RANKL (receptor activator of NF- κ B ligand)-supported osteoclastogenesis, RANKL-induced calpain activation was examined using murine RAW 264.7 cells and bone marrow-derived monocytes/macrophages (BMMs) α -spectrinolysis and *in vitro* osteoclastogenesis in conjunction with calpain inhibitors were performed to determine whether calpain is involved in RANKL-supported osteoclastogenesis in these cell types. We then verified those calpain species that play a key role in RANKL-supported osteoclastogenesis using immunoblotting. Finally, changes in calpain activity in response to RANKL were assessed using a calpain activity assay kit. We found that calpain activity increases in a RANKL-dependent manner and that μ -calpain, rather than m-calpain, is activated during RANKL-supported osteoclastogenesis in RAW 264.7 cells and BMMs. Cell permeable calpain inhibitors, such as calpastatin and calpeptin, were sufficient to suppress RANKL-supported osteoclastogenesis based on decreased expression of osteoclastogenic markers, including cathepsin K, MMP9 (matrix metalloproteinase 9), and the generation of TRAP (tartrate resistant acid phosphatase) positive-multinucleated cells in both cell types. Calpain inhibitors also suppressed NF- κ B (Nuclear Factor-Kappa B) activation via inhibition of the cleavage of I κ B α (inhibitor of NF- κ B) in RAW 264.7 cells. Lastly, μ -calpain overexpression in RAW 264.7 cells clearly augmented RANKL-supported osteoclastogenesis, thereby implicating its critical role in this process. Taken together, our findings suggest that calpain is essential to the regulation of RANKL-supported osteoclastogenesis.

Disclosures: H. Lee, None.

SA264

See Friday Plenary number F264.

SA265

Chemotactic Recruitment of Osteoclast Precursors by SDF-1 Is Enhanced by TGF β Elevation of CXCR4 or Suppressed by IFN- α Inhibition of CXCR4. X. Yu, P. A. Collin-Osdoby, P. A. Osdoby. Department of Biology, Washington University, St Louis, MO, USA.

Directed cell migration is essential for osteoclast precursors (pre-OC) in the circulation or bone marrow to navigate to sites for their expansion, differentiation, and bone resorption in skeletal development, bone remodeling, or pathological conditions exhibiting bone loss. SDF-1 and its unique chemokine receptor, CXCR4, critically regulate many important processes including hematopoietic cell homing to bone marrow and chemoattraction of metastatic, inflammatory, or other cells to particular tissues. SDF-1 is produced by stromal and endothelial cells in normal bone, and by inflamed synoviocytes in arthritic joints. Previously, we showed that SDF-1 induces murine pre-OC chemotaxis, MMP-9 expression and activity, and MMP-9 dependent transcollagen migration. Here, we investigated mechanisms mediating and regulating these key processes using RAW 264.7 or bone marrow cells. MMP-9 mRNA and activity were raised by SDF-1 in a dose- and time-dependent manner, and this occurred via signaling pathways involving NF- κ B, PI3K, and p38 MAPK, but not ERK $\frac{1}{2}$ or JNK. Because TGF β 1 is highly expressed in bone, increased in pathological conditions associated with bone loss, and it elevates CXCR4 in some cell types, we investigated if TGF β 1 affected CXCR4 expression and SDF-1 responses in pre-OCs. Both CXCR4 mRNA and protein were dose- and time-dependently increased in RAW and marrow cells by TGF β 1, with maximal effects at 10^{-9} M and 24-48 h, and via a SMAD3 pathway. Moreover, pre-treatment (20 h) of pre-OCs with TGF β 1 to increase CXCR4 led to enhanced chemotactic and intracellular signaling responses to SDF-1, as reflected in a greater sensitivity to low SDF-1 levels, higher peak chemotactic response, and stronger P-Akt and P-Src signals by SDF-1. In contrast, IFN- γ reduced both basal and TGF β 1 stimulated CXCR4 levels and corresponding basal (50%) and TGF β 1 stimulated (100%) chemotaxis to SDF-1. TGF β , CXCR4 and SDF-1 are all increased in rheumatoid arthritis, and a selective CXCR4 antagonist inhibits OC-mediated bone loss in murine arthritis. Thus, SDF-1 promotion of pre-OC chemotaxis, MMP-9 production, and transmatrix migration may contribute to OC formation and bone resorption in both normal and inflammatory states. Moreover, TGF β stimulated CXCR4 and SDF-1 responses in pre-OCs could amplify these processes and significantly enhance the abnormal influx and localized development of bone-resorbing OCs at inflamed arthritic sites. Conversely, IFN- γ downregulation of CXCR4 and SDF-1 responses may extend the routes by which IFN- γ interferes with OC formation and bone resorption, by inhibiting recruitment and localized accumulation of pre-OCs.

Disclosures: **X. Yu**, None.

SA266

See Friday Plenary number F266.

SA267

RANKL Activates NFATc1, Induces Autoregulation and Promotes Accumulation of this Transcription Factor on Osteoclast Target Genes. J. A. Fretz*, N. K. Shevde, J. W. Pike. Biochemistry, University of Wisconsin-Madison, Madison, WI, USA.

Osteoclasts are large multinucleated, bone resorbing cells that are formed from hematopoietic precursors in response to M-CSF and RANKL. While RANKL activates a number of signal transduction pathways and stimulates numerous transcription factors, recent studies have highlighted the requirement for NFATc1 in the processes of differentiation and activation as well as survival. In view of the critical nature of NFATc1 in osteoclastogenesis, we explored the process by which NFATc1 is induced in response to RANKL, the role of this factor in the activation of key osteoclast target genes and its essentiality in osteoclast formation using mouse bone marrow monocytes (BMMs) and the RAW264.7 cell line. Although NFATc1 is present in osteoclast precursors, it is rapidly upregulated in response to RANKL treatment at both the mRNA levels and protein level. Actinomycin D studies in both BMMs and RAW264.7 cells support a predominantly transcriptional upregulation of NFATc1, although the half-life of induced NFATc1 mRNA is slightly increased. RANKL induction of NFATc1 mRNA is facilitated by the ability of NFATc1 to autoregulate its own expression. Accordingly, ChIP analysis has revealed a selective and time-dependent increase in the binding of NFATc1 to NFATc1 P1, the promoter responsible for production of the NFATc1A isoform. Additional factors activated by RANKL and which bind to the NFATc1 promoter include c-fos, junB, p300 and RNA pol II. Regardless of mechanism, NFATc1 upregulation is essential to osteoclast formation as siRNA knockdown of NFATc1 results in a substantial diminution in osteoclast formation. The central role of NFATc1 in osteoclast function also suggests that this factor is likely to induce key osteoclastogenic genes including TRAP, MMP-9, cathepsin K and the calcitonin receptor (CTR). Indeed, ChIP analysis revealed an accumulation of NFATc1 on these genes as well. NFATc1 binding was also accompanied on these genes by additional transcription factors including components of AP-1 and C/EBP β as well as the coactivator p300. Interestingly, while the binding of NFATc1 to TRAP occurred early (12 hours) following induction, association of NFATc1 to the CTR gene occurred much later (48 hours). This observation suggests that an additional factor produced by mature osteoclasts may be essential for CTR regulation. In conclusion, our studies highlight details of the mechanisms by which RANKL induces NFATc1 in osteoclasts as well as mechanisms integral to NFATc1-induced expression of genes responsible for the osteoclast phenotype.

Disclosures: **J.A. Fretz**, None.

SA268

Interleukin-3 Inhibits Osteoclastogenesis By Irreversible Down-Regulation of RANK Expression. S. M. Khapli*, S. D. Yogesha*, M. R. Wani. National Center for Cell Science, Pune, India.

Interleukin-3 (IL-3), a cytokine secreted by activated T lymphocytes, stimulates the proliferation, differentiation, and survival of pluripotent hemopoietic stem cells. Recently, it is shown that IL-3 inhibits receptor activator of NF- κ B ligand (RANKL) induced osteoclast differentiation by prevention of RANKL-induced NF- κ B signaling, and diverts the cells to the macrophage lineage. In this study, we investigated that IL-3 significantly inhibits RANKL-induced c-Jun N-terminal kinase (JNK) activation. In addition, IL-3 down-regulates expression of c-Fos and nuclear factor of activated T-cells, cytoplasmic 1 (NFATc1) transcription factors induced by RANKL. Furthermore, IL-3 dose not alter expression of TNF receptor-associated factor 6 (TRAF6) but significantly down-regulates RANK expression posttranscriptionally. Interestingly, the inhibitory effect of IL-3 on RANK expression was irreversible. Thus, our results reveal that IL-3 inhibits RANKL-induced osteoclastogenesis by irreversible down-regulation RANK expression, and inhibits important signaling molecules involved in RANKL-induced osteoclastogenesis.

Disclosures: **M.R. Wani**, None.

SA269

Glucose-Dependent Insulinotropic Peptide Receptors Are Present in Osteoclastic Cells and Modulate Osteoclastic Activity. Q. Zhong¹, K. Ding¹, B. Kang², W. Bollag^{*1}, W. Curl^{*2}, K. Insogna³, C. M. Isaacs⁴. ¹Medicine, Medical College of Georgia, Augusta, GA, USA, ²Orthopedic Surgery, Medical College of Georgia, Augusta, GA, USA, ³Medicine, Yale University School of Medicine, New Haven, CT, USA, ⁴Medicine and Orthopedic Surgery, Medical College of Georgia and the Augusta VA Hospital, Augusta, GA, USA.

We have previously shown that receptors for glucose-dependent insulinotropic peptide, a hormone secreted from endocrine cells in the small intestine in response to nutrient intake, are present in osteoblastic cells and that activation of these receptors leads to an increase in collagen type I synthesis and alkaline phosphatase activity. However, in vivo experiments with GIP had suggested that GIP also had antiresorptive effects. To further evaluate this possibility primary rat osteoclasts were isolated and examined for GIP receptor expression. GIP receptor mRNA was found to be strongly expressed in isolated osteoclasts by Northern blotting. GIPR protein could also be identified in osteoclasts by Western blotting and in intact rat bone by immunocytochemistry using a polyclonal antibody against the GIP receptor. Using a fetal long bone resorption assay to assess the functional effects of GIP on osteoclastic activity we found that GIP dose dependently and completely inhibited PTH-induced bone resorption. Fetal long bone resorption assay: (PTH 10 nM: 2.3+0.4 vs GIP 10 nM: 1.5+0.2 and GIP 50 nM: 0.5+0.1 45Ca²⁺ release fold/control+SEM, p<0.01). Taken together, these data demonstrate that functional GIP receptors are present in osteoclasts and support a role for GIP in nutrient-induced inhibition of bone breakdown.

Disclosures: **Q. Zhong**, None.

SA270

See Friday Plenary F270.

SA271

Role of RAGE in Regulating Osteoclast Function and Bone Mass. Z. Zhou¹, A. Bierhaus^{*2}, P. Nawroth^{*2}, D. M. Stern^{*3}, W. Xiong¹. ¹IMMAG, Medical College of Georgia, Augusta, GA, USA, ²Department of Medicine I, University of Heidelberg, Heidelberg, Germany, ³Dean's Office, Medical College of Georgia, Augusta, GA, USA.

The receptor for advanced glycation end products (RAGE) is a receptor for multiple ligands including advanced glycation end products (AGEs), S100/calgranulins, A-beta, and HMGB1. Activation of RAGE is implicated in the pathogenesis of diabetic complications and neural degenerative diseases. However, the exact role of RAGE in bone remodeling is largely unknown. We demonstrate that mice lacking RAGE showed increased bone mass and bone mineral density (BMD) in vivo. This appeared to correlate well with the defects of osteoclast function cultured in vitro. RAGE mutant osteoclasts exhibited disrupted actin cytoskeletal organization and reduced bone resorptive activity. These results suggest that a defect of osteoclastic cell adhesion and function may contribute to the osteopetrotic phenotype in RAGE knockout mice, and demonstrate a requirement of RAGE in osteoclast function.

Disclosures: **Z. Zhou**, None.

SA272

The Role of Phosphoaminoacids in Osteoclastic Bone Resorption. Z. Unnisa*, C. Janeiro*, R. Bizios*, D. Vashishth*. Biomedical Engineering, Rensselaer Polytechnic Institute, Troy, NY, USA.

Bone resorption by osteoclasts involves the solubilization of mineral and hydrolysis of collagen. Osteopontin (OPN), present on the bone surface, mediates the attachment of osteoclasts to bone via the $\alpha_v\beta_3$ receptor on the cell membrane and interruption of this integrin mediated adhesion results in inhibition of bone resorption *in vivo* [1]. Since these specific phosphoproteins are exposed to TRAP during bone resorption, modifications in their phosphate content could result in altered bone resorption. Previous studies show that altered OPN phosphate moieties modify osteoclastic bone resorption [2]. Here we investigated the role of phosphorylated amino acids present in the cement line in bone resorption. Transverse slices were obtained from 17 human tibiae (34 to 89 yr). The immunoassay of the bone slices were performed by selecting antibodies specific to phosphoamino acid residues. After staining with the primary antibody, the slices were stained with a FITC-conjugate, secondary antibody. Bone slices were divided into seven groups depending on the antibody used (Table 1). Human osteoclast precursor cells (Cambrex Poietics™) were cultured on bone slices (10,000 precursor cells per bone slice) for 14 days. The bones slices were cleaned of osteoclasts, stained with toluidine blue, and quantified for resorption area (mm²). The results (Fig. 1) demonstrate that TRAP enzyme has the least specificity toward phosphothreonine as indicated by highest amount of resorption. Bone resorption was totally inhibited in groups V and VII. Based on these results we conclude that the phosphotyrosine domains are important in the resorption functions of osteoclasts. Specifically there is a SH2 (src Homology) binding domain in osteoclasts that recognizes the phosphotyrosine residues present at the cement line and initiates the signals required for resorption.

[1]Yamamoto M, et al (1994) *EMBO J* 13:1189-6.
[2]Ek-Rylander, B, et al. (1994) *J Biol Chem*. 269: 14853-6.
Acknowledgements: NIH Grant AR49635

Table 1			
Group	Antiphosphoserine	Antiphosphotyrosine	Antiphosphothreonine
I	X		
II		X	
III			X
IV	X	X	
V		X	X
VI	X		X
VII	X	X	X

Disclosures: **D. Vashishth**, None.

SA273

Molecular Aspects of Polyphosphoinositides in Osteoclast Migration. M. A. Chellaiah. Department of Biomedical Sciences, University of Maryland, Dental School, Baltimore, MD, USA.

Introduction: Phosphoinositides interact with several proteins in osteoclasts (OCs) and arbitrate a wide range of functions. We have previously demonstrated that both PI 4, 5 P2 (PIP2) and PI 3, 4, 5 P2 (PIP3) play active roles in actin cytoskeletal organization by their binding to proteins such as, gelsolin and WASP. This binding regulates podosomes assembly/disassembly and actin ring formation. PIP2 also binds to ezrin, radixin, and moesin (ERM) proteins and controls ERM activity in a variety of cell systems. The aim of this work is to gain an understanding of the mechanism by which PIP2 synthesis and its binding to ERM proteins coordinate CD44 surface expression and osteoclast motility. Results: We have recently demonstrated the relationship between the Rho signaling pathway and PIP2 interaction with WASP. Hence, we analyzed whether a similar mechanism exists in the interaction of PIP2 with ERM proteins. Transduction of TAT-fused constitutively active (CA) RhoVal14 into OCs increased phosphatidylinositol 4-phosphate (PI4P) 5-kinase activity and enhanced cellular levels of PIP2. The effects of RhoVal14 transduction simulate the effects of OPN in OCs. Neomycin (a competitor of PIP2 binding), the Rho inhibitor C3 transferase as well as Rho kinase inhibitor Y27632 reversed OPN or RhoVal14 effect. More over, OCs treated as above or expressing CA-Src by adenoviral infection have demonstrated an increase in PIP2 but not PIP3 association with ERM. Dominant negative Src or Rho Asn19 had no effect on PIP2 binding to ERM. An increase in phosphorylation and PIP2 binding of ERM proteins augment ERM/CD44 interaction and surface expression of CD44. PKC inhibitor staurosporin had no effect on OPN-induced phosphorylation or PIP2 binding of ERM proteins whereas Rho and Rho kinase inhibitors diminished the above-mentioned effects. SiRNA to ezrin not only blocked CD44/ERM/actin complex formation but also surface expression of CD44. OPN or RhoVal14-induced migration is blocked in OCs treated with neomycin, C3 transferase, Y27632, or SiRNA to ezrin in migration analyses. Conclusions: The increased levels of PIP2 in OCs subjected to above-mentioned treatments can be attributed to increased activity of PI4P 5 kinase which is located downstream from the Rho/Rho kinase-dependent pathway. ERM protein is dynamically regulated under these conditions and it may take part in CD44 surface expression. Although our understanding of the signaling mechanism of CD44 surface expression and osteoclast motility is limited, we believe our studies outlined above will provide new insights on these cellular processes.

Disclosures: **M.A. Chellaiah**, None.

SA274

MKK6-p38 MAPK Signaling Augments Osteoclast Survival. T. Yamashita¹, Y. Kobayashi¹, S. Tanaka², N. Udagawa³, N. Takahashi¹. ¹Institute for Oral Science, Matsumoto Dental University, Nagano, Japan, ²Dept of Orthopedic Surgery, University of Tokyo, Tokyo, Japan, ³Dept of Biochemistry, Matsumoto Dental University, Nagano, Japan.

Previously we reported that p38 MAP kinase (p38 MAPK) was essential for osteoclast differentiation. On the other hand, the survival and activation of osteoclasts were not affected by SB203580, a specific inhibitor for p38MAPK. Osteoclastogenic factors like RANKL, TNF and LPS activate MAPK signaling. To clarify the role of p38 MAPK signaling in osteoclast function, we measured activities of protein kinases involved in p38 MAPK signaling pathway using Western blot analysis. We also determined whether phosphorylation of p38 MAPK modulates osteoclast function using adenovirus-mediated gene transfer. Although osteoclasts expressed p38 MAPK protein at the level equivalent to that of bone marrow macrophages (BMM), phosphorylation of p38 MAPK was induced by LPS in BMM but not in osteoclasts. Other signals such as NF-kappaB and JNK were activated in response to LPS in osteoclasts. MKK3 and MKK6 are shown to selectively phosphorylate p38 MAPK. Then, we analyzed MKK3 and MKK6 in osteoclasts. Although MKK3 and MKK6 were expressed in osteoclasts as well as in BMM, the phosphorylation of MKK3/6 in osteoclasts was not increased by the treatment with LPS. Thus, the phosphorylation of MKK3/6 was depressed in osteoclasts, even JNK-MAP kinase signaling was activated in response to LPS. In order to force-induce phosphorylation of p38 MAPK, osteoclasts were adenovirally transduced with a constitutively active form of MKK6 (MKK6CA) or control LacZ. Western blot analysis showed that phosphorylation of p38 MAPK was observed in osteoclasts transduced with MKK6CA. Osteoclasts overexpressing MKK6CA significantly survived at 24 hours after purification when compared with LacZ-expressed osteoclasts (MKK6CA: 301 ± 31 vs. LacZ: 113 ± 25 TRAP(+) multinuclear cells/well). The survival activity of MKK6CA-expressing osteoclasts evaluated at 48 hours was as high as that of IL-1-treated LacZ-control cells (MKK6CA alone: 114 ± 18; LacZ plus IL-1: 87 ± 14; LacZ alone: 8 ± 2 TRAP(+)MNCs/well). The number of MKK6CA-expressing osteoclasts was reduced one third by the treatment with SB203580, so that p38 MAPK activation might contribute to MKK6CA-induced osteoclast survival. Real-time PCR analysis revealed that overexpression of MKK6CA in osteoclasts did not enhance expression of pro-inflammatory cytokines such as IL-1, TNF and IL-6. These results suggest that mature osteoclasts keep own p38 MAPK signaling in an inactive state to abort their survival. Signaling molecules involved in the p38 MAPK pathway would be novel targets to modulate osteoclast differentiation but not osteoclast function.

Disclosures: **T. Yamashita**, None.

SA275

See Friday Plenary number F275.

SA276

The Tec Kinases: Bmx and Btk Play Distinct Regulatory Roles in Osteoclast Differentiation. L. Danks*, B. M. Foxwell*, N. J. Horwood. The Kennedy Institute of Rheumatology, Imperial College, London, United Kingdom.

Src is a cytoplasmic non-receptor tyrosine kinase which is essential for the differentiation of functional osteoclasts. Src kinases regulate the activation of a closely related family known as the Tec kinases which include: Bmx, Btk, Itk/Tsk, Txk/Rlk and Tec. Despite the regulation of Tec kinases by Src, the direct involvement of the Tec kinase family members in osteoclast formation has not been previously described. In this study the function of the Tec kinases; Bone marrow tyrosine kinase gene in chromosome X (Bmx) and Bruton's tyrosine kinase (Btk) was examined by assessing adenoviral over-expression of these signalling proteins on human osteoclast differentiation *in vitro*. Human peripheral blood monocytes were treated with 100 ng/ml M-CSF for 72 hours (hrs). These cells were seeded onto either plastic or matrix (dentine or hydroxyapatite) substrates. Adenoviruses were developed encoding green fluorescent protein (GFP) with either wild type Bmx, kinase-deficient Bmx, wild-type Btk or kinase-deficient Btk. Adenoviruses encoding GFP alone or empty adenoviruses were used as additional controls. The cultures were infected +/- adenoviruses for 2 hrs, washed and incubated in RPMI (10% FBS) with M-CSF 25ng/ml and RANKL 20ng/ml for either 7 days or 21 days. Cultures were assessed for evidence of osteoclast differentiation (TRAP) and osteoclast activation (lacunar pit formation). Western blot analysis revealed that Bmx and Btk are constitutively expressed in osteoclasts formed during 21 days of culture. Bmx over-expression significantly inhibited the formation of TRAP multinucleated cells (MNCs) on plastic and also inhibited the formation of lacunar resorption pits on dentine. Btk over-expression had no effect on the formation of TRAP MNCs but significantly inhibited the lacunar resorbing activity of these cells. Btk may be involved in cytoskeletal reorganization, attachment to matrix and cell motility, this was therefore analysed by actin bundle fluorescent staining and time-lapse microscopy. There was no evidence to suggest that over-expression of Btk or Bmx affected cytoskeletal architecture or cell motility during osteoclast differentiation. Quantitative PCR is being carried out in order to characterise further the effect of Btk over-expression in the regulation of genes involved in osteoclast differentiation (i.e. c-fms, RANK) and those involved in resorption activity (cathepsin K e.t.c). These results suggest that Bmx and Btk signalling molecules have distinct regulatory roles in osteoclast differentiation and activation and may provide insight to the development of specific gene therapies for complex diseases involving bone destruction.

Disclosures: **L. Danks**, None.

SA277

See Friday Plenary number F277.

SA278

FHL2 Inhibits the Activated Osteoclast in a TRAF6 Dependent Manner. S. Bai¹, H. Kitaura¹, H. Zhao¹, J. Chen^{*2}, J. M. Muller^{*3}, R. Schule^{*4}, B. Darnay^{*5}, D. Novack¹, F. Ross¹, S. L. Teitelbaum¹. ¹Washington University School of Medicine, St. Louis, MO, USA, ²Medicine, University of California at San Diego, La Jolla, CA, USA, ³Universit t-Frauenklinik und Zentrum fur Klinische Forschung, Freiburg, Germany, ⁴Universit t-Frauenklinik und Zentrum fur Klinische Forschung, Freiburg, Germany, ⁵the University of Texas, Houston, TX, USA.

TRAF6 associates with the cytoplasmic domain of RANK, an event central to normal osteoclastogenesis. We discovered that TRAF6 also interacts with FHL2, a LIM domain only protein which functions as a transcriptional co-activator or co-repressor in a cell type specific manner. FHL2 mRNA and protein are undetectable in marrow macrophages and increase *parri passu* with osteoclast differentiation, in vitro. FHL2 inhibits TRAF6-induced NF- κ B activity in wild type osteoclast precursors and, in keeping with its role as a suppressor of TRAF6-mediated RANK signaling, TRAF6/RANK association is enhanced in FHL2 KO pre-osteoclasts. FHL2 overexpression further delays RANKL-induced osteoclast formation, I κ B- α phosphorylation and cytoskeletal organization. Interestingly, osteoclast-residing FHL2 is not detectable in naive wild type mice, in vivo, but is abundant in those treated with RANK ligand (RANKL) and following induction of inflammatory arthritis. Reflecting increased RANKL sensitivity, osteoclasts generated from FHL2-/- mice reach maturation and optimally organize their cytoskeleton earlier than their wild type counterparts. As a consequence, FHL2-/- osteoclasts are hyper-resorptive and mice lacking the protein undergo enhanced RANKL-stimulated bone loss. FHL2 is, therefore, an anti-osteoclastogenic molecule exerting its effect by attenuating TRAF6-mediated RANK signaling.

Disclosures: **S. Bai**, None.

SA279

See Friday Plenary number F279.

SA280

TGF-Beta Promotes Osteoclast Survival through Activation of Smad Independent Signaling. A. Gingery¹, M. C. Wilkes^{*2}, E. B. Leof^{*2}, M. J. Qursler³. ¹Biochemistry and Molecular Biology, University of Minnesota, Duluth, MN, USA, ²Thoracic Disease Research Unit, Mayo Clinic College of Medicine, Rochester, MN, USA, ³Endocrine Research Unit, Mayo Clinic College of Medicine, Duluth, MN, USA.

Increased osteoclast (OC) numbers are evident in many pathological bone conditions, causing elevated bone degradation. This results in the release of active Transforming Growth Factor beta (TGF-beta), which has diverse effects on bone metabolism. Thus, it is critical to understand the roles of TGF-beta in OCs. Using co-cultures of OC precursors and the ST2 stromal cell line, we have investigated the impacts of differentiation in the presence of TGF-beta on OC survival. Once the ST2 cells are removed from mature cultures, TGF-beta-induced OC apoptosis when TGF-beta is withdrawn at a higher rate than OCs with continued TGF-beta treatment. In contrast, OCs that differentiate in the absence of TGF-beta apoptosis when TGF-beta is added to mature cells. Thus, OCs that differentiate in the presence of TGF-beta become dependent on TGF-beta for survival. To further investigate the mechanism by which TGF-beta promotes OC survival, we have explored candidate TGF-beta signaling pathways for evidence of survival involvement. TGF-beta signaling involves both Smad-dependent and Smad-independent pathways. Here we report studies of the respective roles of these two signaling pathways in TGF-beta-mediated survival of OCs differentiated in the presence of TGF-beta. Using an adenoviral expression system, we infected mature TGF-beta-induced OCs with a dominant negative Smad3 expression construct or an empty expression vector for 24 hours. Expression of dominant negative Smad3, which interferes with TGF-beta-induced Smad signaling, did not block the ability of TGF-beta to promote OC survival. These data indicate that TGF-beta-mediated survival was independent of the Smad signaling pathway. To assess the role of Smad-independent signaling, we investigated activation of the PAK2/c-Abl and MEK/ERK signaling pathway components as they can be activated by TGF-beta independently of Smad signaling and their activation can support cell survival. We compared activation levels in both TGF-beta-induced OCs and OCs differentiated without TGF-beta treatment. Interestingly, activation of the PAK2/c-Abl pathway but not the MEK/ERK pathway was higher in TGF-beta-induced OCs. We conclude from these data that TGF-beta-mediated OC survival signaling is Smad independent and may result from signaling through the PAK2/c-Abl pathway.

Disclosures: **A. Gingery**, None.

SA281

Interaction between C-TAK1 and MITF during Osteoclast Differentiation. S. Murphy^{*}, K. Mansky. Diagnostic and Surgical Science, University of Minnesota, Minneapolis, MN, USA.

The severe osteopetrotic phenotype in microphthalmia (mi) mutant mice is caused by a defect in the terminal differentiation of osteoclasts. Immature mononuclear osteoclasts are present in the mi/mi mice, but these do not fuse or form ruffled borders. Thus the products of the MITF gene, the basic helix-loop-helix zipper (bHLHzip) factor MITF, and the closely related bHLHzip factor TFE3 have been shown to be critical regulators of osteoclast differentiation. Because MITF appears to be important for differentiation of osteoclasts, we are interested in proteins that interact with MITF. Using a yeast two-hybrid system, we identified several proteins that interact with the amino terminal region of MITF. One of the proteins we identified was Cdc25C-associated kinase 1 (C-TAK1). We have been able to verify by GST pull down assay and by co-immunoprecipitation that MITF and C-TAK1 can interact with each other. C-TAK1 is a member of the EMK/MARK/Par1 kinase family and was first cloned based on its ability to associate with and phosphorylate Cdc25C. For all the known substrates of C-TAK1, the serine residue phosphorylated by C-TAK1 serves as a 14-3-3 binding site. 14-3-3 proteins have been shown to modulate the nuclear/cytoplasmic shuttling of numerous proteins. We are currently mapping the serine residue in Mitf that is phosphorylated by C-TAK1. When osteoclasts are stimulated with M-CSF, we have observed in nuclear extracts and are confirming by immunofluorescence that MITF moves from the cytoplasm to the nucleus. To understand the mechanism of MITF shuttling in osteoclasts, we are currently demonstrating that MITF and 14-3-3 proteins can interact and that the interaction is dependent upon C-TAK1 phosphorylation. It has been shown upon stimulation of osteoclasts with M-CSF that Erk1/2 phosphorylates MITF and TFE3. We hypothesize that C-TAK1 interacts with MITF in the cytoplasm of osteoclasts and upon M-CSF stimulation MITF is phosphorylated by ERK1/2 and is shuttled into the nucleus where MITF activates genes necessary for osteoclast survival such as Bcl-2.

Disclosures: **K. Mansky**, None.

SA282

See Friday Plenary number F282.

SA283

Gap Junction Channels Mediate Signals Necessary for RANKL-Induced Osteoclastogenesis. S. Matemba^{*1}, A. Johansson^{*2}, A. Lie^{*1}, M. Ransj ¹. ¹Oral Cell Biology, Odontology, Ume , Sweden, ²Periodontology, Odontology, Ume , Sweden.

Many studies have demonstrated that interactions between osteoblasts/stromal cells and osteoclast precursors play a central role in osteoclastogenesis and osteoclast function. Gap junction intercellular channels provides a direct pathway for cellular crosstalk and allows adjacent cells to exchange second messengers, ions and cellular metabolites. In osteoblasts, gap junction protein connexin 43 (Cx43), is associated with expression of genes critical for bone formation and phenotypic markers of mature osteoblasts. However, the knowledge of gap junction intercellular communication in osteoclast differentiation and function is fragmentary. We have recently published that mouse bone marrow cultures and micro isolated osteoclasts express Cx43 mRNA (Ransj  et al BBRC, 2003). We here report that RAW 264.7 cells express Cx43 mRNA and immunostaining for Cx43 protein. Functional gap junctions in bone marrow cells and in RAW 264.7 cells were demonstrated by scrape loading and flow cytometry dye transfer techniques. Carbenoxolone (CBX), a pharmacological inhibitor of gap junctions, clearly impaired the dye transfer between bone marrow cells and RAW 264.7 cells. CBX caused a dose dependent significant inhibition of dye transfer and TRAP-positive multinucleated cells formed in 7-8 day mouse marrow cultures stimulated by PTH, forskolin, Vit D₃ and PGE₂. Furthermore, RANKL-stimulated osteoclastogenesis in marrow cultures and in RAW 264.7 cells was significantly inhibited by CBX. Quantitative real-time PCR analysis demonstrated that CBX down regulated the expression of osteoclast phenotypic markers but did not have any significant effects on RANK, RANKL or OPG. However, NFAT2 mRNA in RANKL-stimulated marrow cultures was clearly down regulated by CBX. Taken together, our data indicate that gap junction-mediated signals are critical in osteoclastogenesis and furthermore, our results suggest that the interaction is downstream RANKL.

Disclosures: **M. Ransj **, None.

SA284

Microstructural Compositional Changes Associated with Osteocyte Lacunae Detected Using Raman Imaging. J. Ling^{*1}, M. Miller^{*1}, D. Moravits^{*1}, J. Lankford^{*1}, L. Bonewald², D. Nicoletta¹. ¹Southwest Research Institute, San Antonio, TX, USA, ²Oral Biology, School of Dentistry, University of Missouri-Kansas City, Kansas City, MO, USA.

Previous studies have shown that matrix deformation associated with osteocyte lacunae is significantly greater than macroscopic bone deformation suggesting that osteocytes embedded within lacunae experience significantly higher strains than previously assumed. Determining the matrix composition and how the local micro-structural environment around osteocyte lacunae is altered due to stress is essential towards understanding how strains are transmitted from the surrounding bone matrix to osteocytes. Bone is predominantly a composite of type I collagen fibers and carbonated calcium phosphate

mineral particles. Previous studies have shown that bone mineral crystallinity can be inferred from the width of the phosphate vibrational Raman band at 960 cm^{-1} . Also, the peak location of this band shifts towards higher frequencies in bone matrix under compression and lower frequencies under tension. The objective of this study was to apply Raman imaging to investigate the composition of bone matrix in and around osteocyte lacunae and changes to the matrix microstructural composition around and within lacunae in response to mechanical strain. Human femoral cortical bone was milled into a 3x3x30 mm beam specimen and polished using silicon carbide papers followed by refinement with progressive diamond slurries (from 6 micron down to 0.25 micron). The specimen was loaded using three-point bending in a custom microscopy load frame that operates within the Raman imaging microscope (Renishaw 2000). Three direct Raman images at 952, 960, and 968 cm^{-1} bands were recorded for lacunae located at the tension side of the specimen. As the specimen was loaded to approximately 2000 microstrain on the tension side of the beam, the Raman phosphate vibrational band (960 cm^{-1}) shifted to higher frequencies on one side of the lacuna and towards lower frequencies on the opposite side, indicating that the lacuna is subjected to a complex strain field. Furthermore, the 960 cm^{-1} peak bandwidth was higher for the matrix material within the lacunae as compared to bone matrix material surrounding the lacunae. This change in crystallinity became more pronounced as the bone specimen was deformed. This information indicates that the bone mineral within the osteocyte lacuna is less crystalline compared to the surrounding bone matrix and that the degree of crystallinity decreases as the lacunae undergoes increasing deformation.

Disclosures: **D. Nicoletta**, None.

SA285

The Chemokine, MCP-3, Is Produced by Osteocytes and Protects against Glucocorticoid-Induced Apoptosis. **Y. Kitase¹, S. Ko², J. Gluhak-Heinrich³, S. E. Harris³, L. F. Bonewald¹.** ¹Oral Biology, UMKC, Kansas City, MO, USA, ²Kangnung National University, College of Dentistry, Kangnung, Republic of Korea, ³Periodontics and Cellular and Structural Biology, U of Texas Health Science Center at San Antonio, San Antonio, TX, USA.

The monocyte chemoattractant proteins, MCPs, were so named for their capacity to induce chemotaxis of monocytes during inflammation. This chemotactic property was thought to be their principal function. We found that MLO-Y4 osteocyte-like cells produce MCP-3 (20ng/ml/10⁴ cells or 500X compared to 2T3 osteoblasts) and MCP1 (40X). This osteocyte model also expresses the receptor for this chemokine, CCR2. *In vitro*, MCP3 is regulated by fluid flow shear stress at 16 dynes/cm² increasing 3-4 fold and *in vivo*, using *in situ* hybridization, MCP-3 was found to increase in osteocytes near the surface of alveolar bone and to dramatically increase in periodontal ligament cells in response to tooth movement. Conditioned media from MLO-Y4 cells (10%) stimulates osteoclast precursor (Raw264.7 or MOCP-5) chemotaxis, however, chemotaxis could not be abrogated by neutralizing antibody to MCP3 (10ug/ml). Recombinant MCP-3 (1~100ng/ml) only modestly stimulated Raw264.7 chemotaxis compared to MLO-Y4 conditioned media and had no effect on MOCP-5 chemotaxis suggesting another function for MCP-3. Recently, several studies have shown protective effects by members of this family. MCP-1 has been shown to be produced by osteoblasts and indirectly increases osteoblast number (Posner et al, Bone, 1997) and protects neurons and astrocytes from apoptosis (Eugenin et al, J Neurochem, 2003). RANTES, a related chemokine, promotes osteoblast survival (Yano et al, Endocrinol. 2005). We have found that MCP-3 (100 ng/ml) will block apoptosis of MLO-Y4 cells due to dexamethasone (10⁻⁶ M) and etoposide (50uM) using both the nuclear fragmentation and the trypan blue exclusion assay. These studies suggest that MCP-3 is produced by osteocytes in response to mechanical strain and that a major function may be not only to recruit osteoclast precursors, but to protect osteocytes against cell death. This study also has important implications for the treatment of glucocorticoid induced osteoporosis.

Disclosures: **Y. Kitase**, None.

SA286

See Friday Plenary number F286.

SA287

A Proposed Function for E11 in Osteoblast to Osteocyte Differentiation and Mineralization. **C. Barragan-Adjemian, D. Guo, J. Rosser*, L. Bonewald.** Oral Biology, University Missouri Kansas City, Kansas City, MO, USA.

E11 is the earliest osteocyte-specific antigen expressed as the osteoblast becomes embedded in osteoid and changes shape to a dendritic morphology. This membrane protein is also found in other cell types that express cytoplasmic extensions and form a barrier with fluid such as kidney podocytes or with air as in type II alveolar lung cells. As osteocytes are in contact with bone fluid and express extensive dendritic networks, it was hypothesized that E11 is responsible for one or both of these functions. To determine the function of E11 in bone cells, MLO-A5 cells were used as a model of late osteoblasts/early osteocytes and MLO-Y4 cells as a model of early osteocytes. MLO-A5 cells express low levels of E11 that increase with time in culture coinciding with the generation of dendritic processes at 3-4 days, maximizes by 9 days when sheets of mineral form and begins to decrease after 12 days of culture. This *in vitro* expression recapitulates *in vivo* expression in bone where E11 appears as the late osteoblast embeds in osteoid, is highest in the osteoid-osteocyte and is reduced in expression in the mature osteocyte surrounded by mineral. The MLO-Y4 cells express very high levels of E11 (100 fold) compared to confluent MLO-A5 cells. To inhibit E11 expression in order to determine function, such a dendrite formation, siRNA was designed. Sequences used include 66-87, 165-185 and 397-

417. It was found that a combination of all three siRNAs at 25nM would inhibit E11 expression 80% in MLO-A5 cells and 84% in MLO-Y4 cells. Unfortunately, several commercial transfection vehicles [Transit-ko (Mirus), Lipofectamine 2000 (Invitrogen), Silent (Bio-Rad)] were found to dramatically change cell morphology making assessment of changes in dendricity in MLO-Y4 cells impossible. Vehicle effects were also found on mineralization by MLO-A5 cells. The vehicle Lipofectamine plus (Invitrogen) was found to have no effects on either parameter. Preliminary experiments on MLO-A5 cells at five days of culture after two 24 hr exposures to siRNA suggest that siRNA inhibits mineralization. These cells have been shown to produce 20-50nm mineralized spherical structures as they generate dendritic processes, responsible for initiation of mineralization in these cultures. Experiments are underway to determine if blocking dendrite formation will block the generation of these mineralizing structures.

Disclosures: **C. Barragan-Adjemian**, None.

SA288

Proteomic Comparison of Osteoblasts and Osteocytes Reveal Unique Protein Expression Patterns. **D. Guo¹, J. Guthrie*², J. Zhao*¹, L. Barragan*¹, S. Harris³, L. Bonewald¹.** ¹UMKC, Kansas City, MO, USA, ²Midwest Res. Inst., Kansas City, MO, USA, ³UTHSCSA, San Antonio, TX, USA.

Genome-scale molecular profiling is used to examine global patterns of transcription in cell systems. However, mRNA does not always correlate with corresponding protein abundance, nor with post-translational modifications. Our hypothesis for these studies was that osteocyte proteomic expression will reflect osteocyte function. Total cell lysates of MC3T3 and 2T3 osteoblast cells and MLO-Y4 osteocyte-like cells were applied to 2D gels, analyzed by PDQuest, and differentially expressed spots excised for protein identification using mass spectrometry. Comparison of the protein expression profiles between the two osteoblast-like cells, showed only a 1-2% difference while comparison between MC3T3 and MLO-Y4 cells showed a 25% difference in expressed proteins. 80% of 69 spots were identified; 20 only detectable in MLO-Y4, 27 at least two fold greater in MLO-Y4 compared to MC3T3, 15 only expressed in MC3T3 and 7 two fold greater in MC3T3 compared to MLO-Y4. Direction of change in protein expression generally correlated with gene expression except for vimentin and lamin A where different forms were expressed between MLO-Y4 and MC3T3. Tubulin $\alpha 6$ was only present in osteoblasts while tubulin $\alpha 3$ was only present in MLO-Y4 cells. Collagen $\alpha 1$ and 2 were only observed in the osteoblasts. Three proteins with greater expression in MLO-Y4 osteocytes compared to osteoblasts, were chosen for *in vivo* validation because of a potential role in osteocyte function. These include; Cap G (macrophage capping protein P24452), destrin (Q9ROP5), and Hypoxia up-regulated factor ORP150 (NP_067370), expressed 14, 5, and 62X greater respectively in MLO-Y4 cells compared to the osteoblast cells and 3 and 5X higher in the gene arrays (ORP150 was not on the array). Cap G and destrin are involved in cytoskeletal rearrangement and therefore may play a role in dendrite formation. CapG is a member of the gelsolin family responsible for capping the barbed ends of actin filaments and destrin, also known as actin depolymerizing factor, is essential in regulating actin filament turnover by severing and enhancing depolymerization of actin filaments. ORP150 is important in neuronal survival in glutamate toxicity and oxygen deprivation and therefore could play a role in osteocyte survival. Immunostaining of murine bone showed that destrin is highly expressed in the embedding osteocyte compared to osteoblasts or mature osteocytes. Staining for the other two proteins are in progress. Comparison of differences in the proteome of osteocytes with osteoblasts should provide considerable insight into the various molecules and pathways responsible for osteocyte function.

Disclosures: **D. Guo**, None.

SA289

See Friday Plenary number F289.

SA290

Surface Area/Volume Relationships of Secondary Osteons in Equine Radii: Implications for Regional Variations in Convective Nutrient Delivery. **S. M. Sorenson*, G. Clark*, J. Hoopes*, W. E. Anderson*, K. Taylor*, J. G. Skedros*.** Univ. Utah Dept. Orthop. Surg., SLC, UT, USA.

In human ribs, positive correlations have been reported between osteon area (On.Ar) and Haversian canal area (Hc.Ar), perimeter (Hc.Pm), and osteocyte lacunae number/osteon (Lc.N/On). Hc.Ar and Hc.Pm also increase with increasing Lc.N/On [Qiu et al. 2003 Anat. Rec]. These data imply a coordination between the Haversian canal and osteocytes that may be dependent on nutrient delivery. However, it is unclear if these associations broadly apply in other mammals. Additionally, these relationships may not exist in bones where there are large regional variations in strain gradients and trans-cortical fluid flow. For example, these relationships may differ in bones that receive a non-uniform strain distribution [e.g., tension (T), compression (C), and shear (S)]. We examined 2,350 secondary osteons to evaluate relationships between Hc.Ar, Hc.Pm, On.Ar, and Lc.N/On in a bone that habitually experiences non-uniform strains (hence large regional variations in strain gradients and fluid flow). 50X backscattered electron images were obtained from 10 equine radii at mid-diaphysis in cranial "T", caudal "C", and medial/lateral "neutral axis; S" cortices. Sections were also examined in circularly polarized light to determine if osteon morphotypes differ in these regions. Results showed that the T, C, and S cortices exhibited similar correlations despite having variations in strain gradients: moderate-to-high positive correlations between On.Ar and Hc.Ar, Hc.Pm, and Lc.N/On; low positive correlations between Lc.N/On and Hc.Ar and Hc.Pm (Table). The largest surface-to-volume ratios (Hc.Pm/B.Ar) occurred in neutral axis (NA) regions where strain gradients are highest (p<0.001 vs. T & C). Additionally, the NA regions had significantly lower Lc.N/On than

the other regions ($p<0.05$). These results may reflect more efficient nutrient transport across NA regions. However, a potentially confounding factor in studies that deem lacuno-canalicular geometries as similar among *all* secondary osteons is that osteons with alternating lamellar organization are prevalent in the "C" and "S" cortices while the "T" cortex consists mostly of parallel-fibered osteons. Lacuno-canalicular geometries, hence conduits for convective fluid flow, might differ between these two osteon morphotypes.

	Correlation Coefficients (r values)	
	On.Ar Cranial "T"; Caudal "C"; M/L "S"	Lc.N/On Cranial "T"; Caudal "C"; M/L "S"
Hc.Ar	0.46; 0.55; 0.49	0.36; 0.37; 0.37
Hc.Pm	0.49; 0.53; 0.52	0.36; 0.36; 0.40
Lc.N/On	0.79; 0.78; 0.80	ALL P values are ≤ 0.0001

T= Tension; C= Compression; S= Shear [Medial (M) and Lateral (L) Cortices]

Disclosures: *S.M. Sorenson, None.*

SA291

Gene Expression Signatures of the Mouse MLO-Y4 Osteocyte Cell Model: Pathway and Gene Set Enrichment Analysis. W. Yang¹, M. A. Harris¹, D. Guo², L. F. Bonewald², S. E. Harris¹. ¹Dept. of Periodontics, University of Texas Health Science Center at San Antonio, San Antonio, TX, USA, ²Dept. of Oral biology, University of Missouri at Kansas City, Kansas City, MO, USA.

The MLO-Y4 mouse osteocyte cell model is widely used to study osteocyte biology *in vitro*. Few markers for osteocytes are recognized and the gene expression patterns and signaling pathways of osteocytes are not well defined. Identifying gene expression sets and signaling pathways should provide information concerning osteocyte function. Therefore, we investigated gene expression patterns of MLO-Y4 cells at low and high density for comparison to 2T3 osteoblast cells at subconfluent and confluent stages of osteoblast differentiation. After hybridization using Clontech Mouse 5K Microarray, gene expression intensity was quantified and statistically analyzed using triplicate experiments, classified using standard clustering algorithms and functionally organized using DAVID-EASE, a program that explore biological themes of microarray results. Northern analysis was performed to validate expression of key genes. From a data set of 181 genes highly overexpressed in MLO-Y4 osteocytes compared to osteoblasts, we built pathway maps to model the pathways that reflect the MLO-Y4 osteocyte gene expression signature. This signature was then compared to a variety of public gene sets characteristic of bone cells such as osteoblasts, osteoclasts, and a variety of other cell types such as macrophages using Gene Set Enrichment Analysis (GSEA). From the pathway analysis, MLO-Y4 osteocyte cells have patterns of expression that reflect activation of acute and defense response pathways, the TGF β pathway, the interferon activated pathway, and other closely related immune response pathways. As the cells are selected for their dendritic morphology, they have a set of genes that are involved in formation of cell processes or dendrites such as E11, SPPI, CD44, LAMA5. Several genes that inhibit apoptosis are also in the 181 MLO-Y4 gene set, such as Myc, Bag3. From the GSEA analysis, the MLO-Y4 181 gene set has high enrichment scores with other osteoblast differentiation models such as Col1 α 1 promoter-GFP selected osteoprogenitor maturation profiles, but is not enriched in macrophage, osteoclasts, APC dendritic cells, T cells, B cells. The MLO-Y4 selective gene expression signature can now serve as a basis for further comparison with primary isolated osteocytes and for characterizing osteocyte responses to mechanical signaling.

Disclosures: *W. Yang, None.*

SA292

Heel and Hip Bone Densitometry in Postmenopausal Women with Hip Fractures. J. D. McCrea, T. Hewer*. North Cumbria Osteoporosis Service, North Cumbria Acute Hospitals NHS Trust, Whitehaven, Cumbria, CA28 8JG, United Kingdom.

Reduced heel bone mineral density (BMD) is a risk factor for hip fracture yet there is scant information on heel BMD in patients with hip fractures and no consensus on the levels of reduced heel BMD at which treatment might be indicated. The aim of this study was to compare heel BMD results in postmenopausal female patients with recent hip fractures with those from 429 elderly community dwelling ladies studied previously. All postmenopausal women with low trauma hip fractures requiring surgery admitted to the West Cumberland Hospital in 2004 were included (n=120). After discharge, hip and heel BMD scanning was performed using Lunar Prodigy and Pixi scanners (GE Medical Systems) following our standard protocol. Thirty patients (25%) died prior to scanning and a further 43 (36%) did not attend leaving 47 patients (39%) who were scanned (9 heel only, 5 hip only, 33 both sites). Mean \pm SD results were: total hip BMD = 0.647 ± 0.132 g/cm², T-score = -2.94 ± 1.10 ; heel BMD = 0.323 ± 0.10 g/cm², T-score = -2.19 ± 1.22 . Results for the hip fracture and community dwelling patients are compared below:

Mean \pm SD	Community dwelling patients		Hip fracture patients (n = 47)
	Heel T > - 1.6 (n=301)	Heel T \leq - 1.6 (n=128)	
Age (years)	72.0 \pm 5.3	74.7 \pm 6.0	79.2 \pm 8.2 ^{<0.001}
Weight (kg)	71.5 \pm 14.3	58.4 \pm 11.0	54.3 \pm 12.0 ^{0.036}
Osteoporosis Screening Tool [OST]	- 0.12 \pm 3.23	-3.21 \pm 2.69	- 5.28 \pm 2.66 ^{<0.001}
Heel BMD (g/cm ²)	0.496 \pm 0.08	0.312 \pm 0.05	0.323 \pm 0.10 ^{NS}

Statistical comparisons (independent samples t tests) between hip fracture patients and patients with heel T \leq -1.6 are as in the table; for all comparisons between hip fracture patients and patients with heel T > - 1.6 p was < 0.001. 89% of patients scanned were advised to start antiresorptive treatment. Of the 33 patients with both hip and heel BMD results, 22 had hip T-scores \leq -2.5, 19 had heel T-scores \leq -1.6 and 17 had heel T scores \leq -2.0. This latter device specific figure (90% sensitivity & specificity for hip/spine osteoporosis) was adopted following the 2005 UK National Osteoporosis Society (NOS)

Position Statement on peripheral DXA. These results from a small group of patients indicate no significant difference between heel BMD in hip fracture patients and the subgroup of primary care patients who had T-scores \leq -1.6 in our previous community study. Adopting the device specific threshold, however, would have excluded 34% of the community dwelling ladies from treatment which may not be appropriate since BMD is a continuously distributed variable. We conclude that in the absence of central dxa, measurement of heel BMD with the Lunar Pixi, may offer a potentially valuable therapeutic intervention level for elderly women at risk for low trauma hip fractures.

Disclosures: *J.D. McCrea, John McCrea 2, 8.*

SA293

See Friday Plenary number F293.

SA294

Failure to Motivate Orthopedic Surgeons and Neurologists to Refer High Risk Patients for DEXA Exam. D. R. Mandel, P. L. Scott*, J. A. Holmes*. David R. Mandel, MD, Inc., Mayfield Village, OH, USA.

Osteoporosis patients with important clinical risk factors are often not evaluated in a timely way with bone mineral density (BMD) studies for possible medical therapy. Two large groups at risk are those who have had recent fragility fractures and those who have had a hemiplegic stroke. We initiated a study to educate local orthopedic surgeons and neurologists about these high risk patients. They were provided newsletters and medical articles about the benefits of BMD studies. At educational conferences we invited 40 orthopedic surgeons and 20 neurologists to refer at least 6 patients over a 3-month period of time who had a fragility fracture or a hemiplegic stroke in the past year. Each physician was provided with 6 vouchers which would enable their patients to receive a free DEXA BMD study. Results of the study would then be sent to both referring physicians and the patient's primary care physician. Only two patients were referred for BMD during the first 3 months. A follow-up letter informing the referring physicians of the small number of referrals was sent. Additional medical information and articles were also sent to encourage and motivate them. The study was continued for an additional 3 months with no additional patients referred. These results would indicate that physicians who come in contact with patients at risk for fracture do not refer for BMD studies. Additional study is required to understand what factors encourage and impede physicians to refer their patients who are at high risk for fracture.

Disclosures: *D.R. Mandel, The Alliance for Better Bone Health, P&GP Pharmaceuticals.,Sanofi-Aventis Pharmaceuticals 2.*

SA295

Fracture Patients Have Low Bone Mineral Density. A Consecutive Study of 239 Patients. J. Åstrand*, M. Tägil*, K. G. Thorgren*. Orthopaedic department, Lund University, Lund, Sweden.

Purpose: We screened fracture patients at our orthopaedic department for osteoporosis during one year to evaluate a relatively simple routine and identify patients with low BMD that might benefit from treatment. **Methods:** We included all patients between 50-75 years of age visiting our department with a distal radius-, proximal humerus-, vertebrae- or hip fracture from 1 November 2002 to 1 November 2003. A nurse identified patients who recieved a questionnaire concerning riskfactors for osteoporosis and were admitted for a DEXA-scan. Results of the scan were then evaluated together with the questionnaire and the diagnosis "normal", "osteopenia" or "osteoporosis" was established. **Results:** A total of 338 patients (84 males) were contacted, 87 hip fractures (38 males), 196 distal radius fractures (36 males), 27 vertebral fractures (5 males) and 28 with proximal humerus fractures (5 males). 99 patients were excluded: 33 were considered to have had high-energy fractures, 8 could not participate due to illnesses (1), dementia (4), poor language skills (2) or living far away (1). 28 did not want to participate or did not respond to the questionnaire. In total, only 13 patients were already examined and under treatment for osteoporosis. 256 patients were referred for a DEXA-scan (54 males). 16 patients never showed up at the DEXA-scan (3 males) and one woman died. Consequently, 239 patients (51 males) underwent DEXA scans. Of these, 13 % had a normal bone mineral density (< -1 S.D.), 45 % had osteopenia (-1 - 2.5 S.D.) and 42 % had osteoporosis (< -2.5 S.D.). **Conclusions:** In this study, fracture patients between 50-75 years of age had low bone mineral density and needed further investigations and treatment. If patients with low BMD are identified already after their first fracture, treatment can prevent or postpone subsequent fragility fractures. These patients appear at the orthopaedic clinic and orthopaedic surgeons have the opportunity not only to treat the fracture but also identify patients most at risk for future fractures. We organized our routine screening in a low resource demanding way using a team with a doctor, nurse and a secretary.

Disclosures: *J. Åstrand, None.*

SA296

Intake of ACE Inhibitor Is Associated with Greater BMD in Older Chinese. T. Kwok^{*1}, H. Lynn², W. Samuel^{*3}. ¹Medicine & Therapeutics, The Chinese University of Hong Kong, New Territories, Hong Kong Special Administrative Region of China, ²School of Public Health, The Chinese University of Hong Kong, New Territories, Hong Kong Special Administrative Region of China, ³Community and Family Medicine, The Chinese University of Hong Kong, New Territories, Hong Kong Special Administrative Region of China.

A cross-sectional study of 1,958 Chinese men and 1,929 women was used to explore the association between ACE inhibitor use and bone mineral density (BMD). The participants were aged 65 years and above, and were recruited using a combination of private solicitation and public advertising from community centers, housing estates, and the general community in Hong Kong. Demographic, medical, and lifestyle information were obtained from face to face interviews using standardized questionnaire, and physical examination measurements include anthropometry, tibial and brachial systolic blood pressures, and total hip and lumbar spine (L1 - L4) BMD. In multiple regression analyses, after adjusting for weight and age, ACE inhibitor use was associated with higher femoral neck and lumbar spine BMD ($p < 0.05$) among females, and higher femoral neck, total hip, and lumbar spine BMD ($p < 0.01$) among males. When further adjustments were made for thiazide, beta-blocker, corticosteroid use, height, history of diabetes, heart disease, presence of atherosclerosis, cigarette smoking, physical activity, and calcium supplement, ACE inhibitor use was associated with higher femoral neck BMD ($+0.014 \text{ g/cm}^2$, $p = 0.035$) in women, and higher femoral neck ($+0.015 \text{ g/cm}^2$, $p = 0.014$), total hip ($+0.016 \text{ g/cm}^2$, $p = 0.021$), and lumbar spine ($+0.045 \text{ g/cm}^2$, $p < 0.001$) BMD in men. This study demonstrates for the first time that ACE inhibitor use is associated with higher BMD among older Chinese, with the relationship seemingly stronger in men compared to women.

Disclosures: **T. Kwok**, None.

SA297

See Friday Plenary number F297.

SA298

The Postmenopausal Women with Consistently Accelerated Bone Turnover Achieve Lower BMD at Years beyond 10 Years Since Menopause. I. Gorai¹, Y. Uchiyama^{*2}, H. Yamauchi^{*2}, K. Kurasawa^{*2}, O. Chaki², F. Hirahara^{*2}, Y. Ji^{*3}. ¹Obstetrics and Gynecology, International University of Health and Welfare Atami Hospital, Atami, Japan, ²Obstetrics and Gynecology, Yokohama City University School of Medicine, Yokohama, Japan, ³Biostatistics Pfizer Global R&D Tokyo Laboratory, Pfizer Japan, Tokyo, Japan.

We assessed factors influencing bone mineral density (BMD) and bone loss by measuring bone markers and hormone levels in 257 postmenopausal Japanese women (60.0 ± 5.7 yr) who had been followed for eight years. Vertebral BMD was measured every year using DXA, and bone markers and sex steroid hormones were determined at the start of the study. Based on WHO diagnostic criteria, 10.1% of the subjects had osteoporosis, 84.4% had osteopenia, and 5.5% were normal. In cross-sectional study BMD decreased markedly within 10 years since menopause (YSM) and slightly thereafter, which makes a multiple linear regression analysis by separate models. In $YSM \leq 10$, increases in age and YSM showed inverse associations with BMD (g/cm^2) (0.030 and 0.055 decrease/a yr increase, respectively) and effects of YSM on BMD seem to be independent of age. Elevated NTX levels had negative associations with BMD ($r = -0.1999$, $P = 0.0158$). In $YSM > 10$, an increase in age showed an inverse association with BMD (0.041 decrease/a yr increase), however, YSM had no independent effect on bone density. Elevated levels of NOC showed an inverse correlation with BMD. The other bone markers showed non-significant inverse associations with BMD. DHEA values correlated with L-BMD ($r = 0.2062$, $P = 0.0395$). In both groups, BMD increased linearly with body weight (Wt) (0.017 and 0.022 increase/1kg increase, respectively). In longitudinal study stratification of YSM showed differences in rate in bone loss with each quartile (Q1: $YSM \leq 5$, Q2: $5 < YSM \leq 10$, Q3+Q4: $YSM > 10$), making the analysis by three separate models. In $YSM \leq 5$, NOC, total DPD and NTX inversely significantly correlated with BMD and significant correlations were lost after adjustment for ages, YSM and Wt. In $5 < YSM \leq 10$, there were significant correlations between total DPD, free DPD and NTX, and bone density, and PYR, total DPD and free DPD significantly correlated with BMD after adjustment for ages, YSM and Wt ($r = -0.223$, $P = 0.050$, $r = -0.300$, $P = 0.008$ and $r = -0.297$, $P = 0.011$, respectively). In $YSM > 10$, we could not find any correlations between each bone marker and BMD both before and after adjustment for ages, YSM and Wt. Each sex steroid hormone level did not correlate with BMD in three groups. The results suggest that postmenopausal women with consistently accelerated bone turnover achieve lower BMD at years beyond 10YSM whereas the effects of raised bone marker levels do not take its effects in early postmenopause.

Disclosures: **I. Gorai**, None.

SA299

Social Position in Pregnancy Is Related to Bone Mass in Childhood by Opposing Actions on Height and Weight. E. M. Clark^{*1}, A. R. Ness^{*1}, J. R. Tobias². ¹Community Based Medicine, University of Bristol, Bristol, United Kingdom, ²Clinical Science at South Bristol, University of Bristol, Bristol, United Kingdom.

Evidence that social factors influence skeletal growth raises the possibility that bone mass acquisition in childhood is socially determined. To clarify the role of social factors in bone mass acquisition in childhood, we investigated relationships between these variables in the Avon Longitudinal Study of Parents and Children (ALSPAC). Details on the parents' housing tenure, highest achieved educational qualifications, and fathers' occupation were collected during pregnancy. These measures of social position were linked to DXA results obtained at aged 9.9 years in 6702 children. Linear regression analyses were carried out after adjusting for age and gender. As previously found, measures of social position were positively related to height and negatively related to weight of the children at aged 9.9 years ($P < 0.001$). Measures of social position were unrelated to total body BMC in analyses adjusted for age and gender. However, after adjusting for height, a strong negative association was observed between BMC and all measures of parental social position ($P < 0.001$). After adjusting for weight as well as height, an association between social position and BMC and bone area was no longer observed. In further analyses, we found that adjusting for fat mass of the child led to similar results to those obtained with weight. Finally, we examined whether the associations between social position in pregnancy and bone mass in childhood varied between weight bearing and non-weight bearing sites. In analyses that were adjusted for height alone, social position was found to exert an equivalent negative influence on BMC at the upper limbs, lower limbs and trunk ($P < 0.001$). Adjusting for regional fat mass attenuated this negative influence of social position at the trunk ($P = 0.45$) and lower limbs ($P = 0.23$), whereas a modest effect persisted at the upper limbs ($P = 0.046$). In conclusion, social position in childhood appears to be positively related to bone mass acquisition in childhood as a consequence of enhanced longitudinal growth. However, this influence is counteracted by the tendency for increased fat deposition in those from a lower social position to increase bone area, presumably reflecting the stimulation of appositional bone growth. Furthermore, our observation that adjusting for regional fat mass attenuated the association between social position and BMC to a greater extent at the lower compared to upper limb is consistent with the possibility that fat mass influences periosteal apposition through increased mechanical loading.

Disclosures: **E.M. Clark**, None.

SA300

Self-rated Health, Forearm BMD and Bone Loss in Men and Women, a Longitudinal Study. The Health Study of Nord-Trøndelag (HUNT), Norway. S. Forsmo^{*}, S. E. Lilleeng^{*}, A. Langhammer^{*}. Dept. of Public Health and General Practice, Norwegian University of Science and Technology, Trondheim, Norway.

Several studies have shown that self-rated health represents a good predictor of morbidity and mortality. Less is known whether self-reported health status and longitudinal change in self-reported health correlate with bone mineral density (BMD) and bone loss. The aim of this study was to investigate the association between perceived health status, its change and forearm BMD and bone loss in a non-selected sample of adult men and women. In 1995-97 all citizens aged > 19 years (about 92,000) in the county of Nord-Trøndelag were invited to a multipurpose health survey (HUNT). Totally 18265 individuals were invited to forearm bone densitometry, and among them a 5% random population sample with 2779 (60%) men and women meeting. In 2001, 4.6 years after the first screening, follow-up densitometry was performed, and 1734 (62%) men and women from the 5%-sample attended. Mean age at baseline and at follow-up was 50.1 (range 20-85) and 54.6 years (range 24-89), respectively. BMD measurements were performed by single X-ray absorptiometry (Osteometer DTX 100) at the distal and ultradistal non-dominant forearm provided no previous fracture. Subjective health status was rated in four categories (1: poor, 2: not so good, 3: good and 4: very good) based on identical questions at baseline and follow-up. At follow-up 30% women and 22% men rated their health as poor or not so good ($p < 0.001$). Change in self-rated health status between baseline and follow-up was categorised as deteriorated, unchanged and improved. No statistically significant difference was found between the sexes for change in health status, in about two-third there was no change, deterioration in 18% and improvement 16%. In linear (men) and quadratic (women) regression models, a strong and positive association was found for self-rated health status and BMD (distal and ultradistal radius), adjusted for age and body weight. Statistically significant bone loss was found in both men and women older than 40 years at baseline. Bone loss was more pronounced at ultradistal than distal site until the age of 60 years in women and 65 years in men. The association between change in self-rated health and bone loss was assessed in linear and polynomial regression models in men and women < 80 years adjusting for age, body weight and interval of measurements. A statistically significant association was found at ultradistal radius in men ($p < 0.05$), somewhat weaker ($p < 0.1$) at distal forearm indicating that improvement in self-rated health status is followed by reduced bone loss and vice-versa. No statistically significant association could be found in women.

Disclosures: **S. Forsmo**, None.

SA301

See Friday Plenary number F301.

SA302

Valproic Acid Effects on Bone Mineral Density in Juvenile Sprague-Dawley Rats. B. L. Gracious¹, E. Puzas^{*2}, E. M. Healy^{*3}, J. Livingston-Carr^{*4}.
¹Psychiatry, University of Rochester, Rochester, NY, USA, ²Orthopedics, University of Rochester, Rochester, NY, USA, ³Orthopedics, University of Massachusetts, Worcester, MA, USA, ⁴Psychiatry, Beth Israel Hospital, New York, NY, USA.

FDA-approved for the treatment of acute mania in adults, valproic acid (VPA) is increasingly used as a first-line mood stabilizer for children and adolescents with bipolar disorder. Several cross-sectional studies have found decreased bone mineral density associated with VPA in children and adults with epilepsy(1-4). As children may be an especially vulnerable population to develop future osteoporosis if bone mineralization is suppressed during development, this study was undertaken to explore the usefulness of an animal model in attempts to understand if VPA has a direct effect on bone mineral density (BMD). Ninety-eight Sprague-Dawley rats (49 male and 49 female) were gavaged daily with VPA at 300mg/kg/day versus sham gavage beginning at 7 weeks of age for up to 8 weeks. Cohorts of 7 male and female rats in each group were sacrificed via CO inhalation at four time points: zero, 2, 4, and 8 weeks. Serum samples for valproate levels were obtained and DEXA was performed to determine bone density and bone mineral content (BMC). Utilizing a "best fit" model including quadratic factors duration and weight as covariates, BMDfemur, BMDspine, BMCfemur, BMCspine were compared for fixed weight. Significant decreases in BMCspine at 2 and 8 weeks were present (respective p<0.0001 and p<0.008). Significant decreases were also seen in log[BMDfemur]at 4 and 8 weeks duration (p<0.0000 and p<0.02). Preliminary evidence suggests that VPA reduces BMCspine and logBMDfemur in juvenile Sprague-Dawley rats. Potential mechanisms include direct inhibition of osteoclast and osteoblast activity altering bone resorption and mineralization, resulting in alterations in bone remodeling at a crucial stage of bone development. Replications of this work and additional human studies examining effects of VPA on BMD and BMC in humans across the life cycle are needed.
1 Kafali G et al. Effect of antiepileptic drugs on bone mineral density in children between ages 6 and 12 years. Clin Pediatr 1999, 38:93-98.
2 Sato Y et al. Decreased bone mass and increased bone turnover with valproate therapy in adults with epilepsy. Neurology 2001, 57:445-449.
3 Sheth RD et al. Effect of carbamazepine and valproate on bone mineral density. J Pediatr 1995;127:256-62.
4 Guo Y et al. Long-term valproate and lamotrigine treatment may be a marker for reduced growth and bone mass in children with epilepsy. Epilepsia 2001; 42(9):1141-1147.

Disclosures: **B.L. Gracious**, None.

SA303

Erythropoietin Is an Independent Predictor of Bone Mineral Density in Elderly Men - Mr OS Sweden. D. Mellstrom¹, H. Nilsson-Ehle^{*2}, E. Orwoll³, O. Ljunggren⁴, O. Johnell⁵, C. Ohlsson⁶.
¹Center for Bone Research at the Sahlgrenska Academy, Sahlgrenska academy University of Goteborg, Gothenborg, Sweden, ²Dep of Internal Medicine and Hematology., Sahlgrenska academy, University of Goteborg, Gothenborg, Sweden, ³Bone and Mineral Unit, Oregon Health and Sciences University Portland, Portland, OR, USA, ⁴Dep of Medical Sciences, University of Uppsala, Uppsala, Sweden, ⁵Dep of Orthopedics, Malmoe General Hospital, Malmoe, Sweden, ⁶Center for Bone Research at the Sahlgrenska Academy and Division of Clinical Pharmacology, Sahlgrenska academy, University of Goteborg., Gothenborg, Sweden.

The osteoclast is known to be derived from the haematopoietic stem cell and transplantation of maternal blood marrow leads to normal bone mineral density (BMD) and Hemoglobin (Hb) in children with osteopetrosis. Studies indicate that erythropoietin (EPO) might be a growth factor for malignant cells but also for normal prostate cells. It is not investigated if EPO regulates bone mass. The aim of the present study was to investigate if erythropoietin is associated with BMD in a community based population sample of elderly men in Göteborg, Sweden (n = 1000, Men age 75,2) Mr OS. **Methods:** Hemoglobin and an extended hematological examination was analysed in all 1000 men between 70 - 80 years of age. Blood sample were drawn from the antecubital vein after 10 hours fasting and non-smoking in the morning. EPO was analysed with an ELISA method (Quantikine IVD, R&D systems, Inc, Minneapolis) in a sub sample of 487 men. BMD was measured with a Hologic 4500 A DXA. **Results:** Mean EPO was 11.0 (6.9) IU/L. EPO correlated, as expected, to blood Hb (r = -0,328 P <0.01). Height, weight, age, physical activity, smoking, calcium intake and Hb were included in regression models for BMD. EPO was an independent predictor of Hip total BMD (β=0.092, P= 0.027), trochanter BMD (β=0.113, P<0.01) but not of spine BMD. EPO was not correlated to age but to body composition (lean mass r = 0,12, P = 0.012; fat mass r = 0.14, P = 0.003). In conclusion we found an independent correlation between Hip BMD and EPO, indicating that EPO might be a growth factor regulating bone mass.

Disclosures: **D. Mellstrom**, None.

SA304

Smoking Is an Independent Risk Factor for Decreased Physical Performance in Elderly Women. P. B. Rapuri¹, J. C. Gallagher¹, L. M. Smith^{*2}.
¹Bone Metabolism, Creighton University, Omaha, NE, USA, ²Department of Preventive and Societal Medicine, University of Nebraska Medical Center, Omaha, NE, USA.

Smoking is associated with increased fracture rate and may be a risk factor for declining physical function with age. In elderly women aged 65-77 years who participated in the STOP IT osteoporosis trial, previously we reported that smoking is associated with lower bone mineral density, lower calcium absorption, lower serum 25hydroxy vitamin D (25OHD) levels, secondary hyperparathyroidism and increased bone resorption. In present study in same population, we examined the association of smoking with physical performance measures of muscle function. Timed rise (time to rise from a chair 3 times as quickly as possible), timed walk over 5 meters at normal speed and grip strength (Hand Dynamometer in 90° of shoulder flexion) were compared between smokers and non smokers. We also compared physical performance tests between non, past and current smokers and in light (<1 pack/day) and heavy smokers (>1 pack/day). Data were analyzed using SAS. Significant associations were found between smoking status, age and total body fat. ANCOVA was used to compare physical performance variables while adjusting for confounding variables, age, BMI, calcium and caffeine intake and total body fat. Compared to nonsmokers, current smokers were slower on timed rise and timed walk tests and had decreased grip strength. The effect of current smoking on physical performance measures is equivalent to an age related decline in performance tests of 7-11 years. Smokers compared to non-smokers had significantly higher sex hormone binding globulin (SHBG) and lower serum 25OHD levels. Smokers compared to nonsmokers also had lower serum total estradiol, bioavailable estradiol and bioavailable testosterone, though the differences were not statistically significant. The interaction between smoking and 25OHD or SHBG were not significant. Compared to current smokers, past smokers and women who never smoked had better physical performance measures. There was no significant association between quantity of smoking and physical performance measures. The results suggest that current smoking is an independent risk factor for decreased physical performance in elderly women.

	Effect of Smoking on Physical Performance Measures		
	Non Smokers (n=268)	Past Smokers (n=163)	Current Smokers (n=56)
Timed rise (sec)	8.72±0.23	8.61±0.20	9.52±0.53*†
Timed walk normal (sec)	4.80±0.06	4.85±0.09	5.24±0.19*†
Timed walk fast (sec)	3.40±0.04	3.46±0.07	3.66±0.15*†
Grip Strength Right (kg)	25.18±0.27	25.18±0.35	23.84±0.58*†
serum 25OHD (ng/ml)	31.7±0.61	31.6±0.75	28.6±1.9*
serum bioavailable estradiol (pg/ml)	3.71±0.13	3.50±0.20	2.82±0.21
serum SHBG (nmol/L)	139.4±3.9	143.0±5.8	197.4±12.2*†

Data reported as unadjusted means±SEM. p values are from adjusted data. *p<0.05 vs non and †p<0.05 vs past smokers.

Disclosures: **P.B. Rapuri**, None.

SA305

Vitamin D Insufficiency in South Indian Rural and Urban Population. C. V.Harinarayan¹, U. V.Prasad¹, T. Ramalakshmi^{*1}, E. G.T.V.Kumar^{*1}, P. V.L.N.Srinivasarao^{*2}, P. R.Parthasarathy^{*3}, C. R.Surendranath^{*1}, M. M.Suchitra^{*2}.
¹Endocrinology and Metabolism, Sri Venkateswara Institute of Medical Sciences, Tirupati, India, ²Biochemistry, Sri Venkateswara Institute of Medical Sciences, Tirupati, India, ³Biochemistry, SV University, Tirupati, India.

To study the prevalence of dietary calcium intake and vitamin D status of south Indian rural and urban population. Urban (n=943) and rural (n=205) population were studied for their dietary intake of calcium(DC), phosphorous and phytate/calcium ratio. Serum calcium (SC), phosphorous(SP), alkaline phosphatase (SAP) levels, 25(OH)D and parathormone(PTH) levels were measured. The dietary calcium, phosphorous (mg/day) and phytate/calcium ratio of urban population was 307±51; 653±104; 0.5±0.1 and rural population was 267±30; 488±68; 0.8±0.1 respectively. The SC, SP (mg/dl), SAP (IU/L), 25(OH)D (ng/ml) and parathormone levels (pmol/l) of the urban population are 9.7±0.5; 3.6±0.7; 81±31; 16.7±8.4; 28±17 and that of rural population was 10±0.7; 2.9±0.5; 64±26;21.4±7.1; 29±10 respectively. The rural population had significantly (p<0.001) higher 25(OH)D levels, SC and lower SAP, DC than the urban population. The distribution of varying degree of 25(OH)D levels in the population are shown in table:

Parameter	Age yrs	n	Percentage of population with 25(OH)D levels		
			< 10 ng/ml	10.1-20 ng/ml	>20.1 ng/ml
Urban WG	46±13	943	21	52	27
Rural WG	43±14	205	2.5	53.5	44
Males WG	46±16	243	3	51	46
Females WG	46±13	905	21.4	53	25.6
Urban Males	47±17	134	6	56.7	37.3
Urban Females	46±13	809	23.5	51.2	25.3
Rural Males	45±15	109	NIL	44	56
Rural Females	41±14	96	5.2	64.6	30.2

WG - whole group

In urban population, PTH correlated negatively with 25(OH)D levels (r-0.13;p<0.001),SC(r-0.13;p<0.001)and SP (r-0.01;p<0.01). 25(OH)D levels correlated positively with SC(r 0.13;p<0.001). In rural population, PTH correlated negatively with 25(OH)D (r-0.24;p<0.002), DC(r-0.4;p<0.001) and positively with SAP(r0.3;p<0.001). 25(OH)D levels correlated positively with DC(r0.3;p<0.001) and negatively with SAP (r-0.22;p<0.002). The DC intake of the whole group is inadequate compared to the

Recommended Daily allowances of national guidelines. Around 30% of urban population and 50% of rural males have normal 25(OH)D levels. About 50% of the urban and rural population had 25(OH)D insufficiency. 21% of urban women and 5% of rural women had 25(OH)D deficiency. 25(OH)D deficiency and insufficiency is more common in urban female. The dietary calcium and 25(OH)D insufficiency could reflect fallaciously as osteopenia in BMD measurements. There is an urgent need to enrich the diet with calcium and supplement vitamin D with monitored food fortification programs in the country.

Disclosures: *C. V. harinarayan, None.*

SA306

See Friday Plenary number F306.

SA307

Vitamin D Status and Bone Health in Female Army Recruits. J. P. Greeves^{*1}, C. K. Wickes^{*1}, W. D. Fraser². ¹Centre for Human Sciences, QinetiQ Ltd, Farnborough, United Kingdom, ²Department of Clinical Chemistry, University of Liverpool, Liverpool, United Kingdom.

Vitamin D deficiency can lead to secondary hyperparathyroidism and bone loss, and may be associated with stress fracture risk during military training. This study aimed to establish Vitamin D status and its effect on bone health, in UK female Army recruits. Thirty five female Caucasian recruits age [mean(1SD)], 20.4 (2.9) y; body mass, 61.9 (7.2) kg; height, 1.64 (0.06) m, starting Army Phase 1 training between the months of October and February, volunteered to take part. Bone mineral density (BMD) at the lumbar spine, hip, and whole body; ultrasound speed of sound at the calcaneum (cSOS) and tibia (tSOS); and bone markers (plasma β -CTX, PINP, Bone ALP, urine free PYD and DPD) were measured during week one of training. Serum parathyroid hormone (sPTH); markers of nutritional status; and information on lifestyle factors, were also obtained. Vitamin D status was determined by HPLC measurement of total serum 25-hydroxyvitamin D (25(OH)D) concentration, and categorised as: Normal (>20 ng·ml⁻¹); Insufficient (<20 ng·ml⁻¹); Deficient (<15 ng·ml⁻¹); and Severely Deficient (<10 ng·ml⁻¹). The data were analysed using a One-Way ANOVA and a Bonferroni test. Total serum 25(OH)D was below the normal range in 17 (51%) subjects on entry to training. 5 (14%) subjects were Insufficient; 7 (20%) Deficient; and 6 (17%) Severely Deficient. Age, body mass, and height did not differ between subjects grouped by Vitamin D status ($P>0.05$). sPTH negatively correlated with serum 25(OH)D concentration ($r = -0.57$; $P<0.01$). Differences in tSOS, markers of bone resorption (β CTX) and bone formation (PINP, Bone ALP) are shown in Table 1. No differences in BMD, cSOS, or urinary pyridinolines (UPYD, UfDPD), were found ($P>0.05$). We found reduced cortical, but not trabecular bone, and increased bone turnover in female Army recruits when 25(OH)D concentration was below 15 ng·ml⁻¹. These findings suggest that Vitamin D deficiency may increase the risk of stress fracture injury during Phase 1 training, particularly at the tibia. The benefit of Vitamin D supplementation in preventing further bone loss and reducing the risk of stress fracture injury in female recruits should be determined.

Table 1: Mean (1SD) values for tSOS, and markers of bone turnover between groups				
	Normal	Insufficient	Deficient	Severely Deficient
tSOS (m·s ⁻¹)	4038 (82)	4028 (66)	3903 (71) ^a	3910 (134) ^a
-CTX (μ g·l ⁻¹)	0.51 (0.19)	0.61 (0.26)	0.82 (0.27) ^a	0.62 (0.24)
PINP (μ g·l ⁻¹)	51.8 (20.1)	70.8 (37.9)	97.1 (30.2) ^a	100.0 (53.0) ^a
Bone ALP(U·l ⁻¹)	16.2 (2.8)	16.4 (5.9)	19.3 (2.3)	27.7 (10.4) ^{b,c,d}

^{a,b} different from Normal ($P<0.05$, $P<0.01$, respectively)

^{c,d} different from Insufficient ($P<0.01$) and Deficient ($P<0.05$) groups, respectively

Disclosures: *J.P. Greeves, None.*

SA308

Lycopene Consumption Significantly Reduces Biomarkers of Oxidative Stress and Bone Resorption in Postmenopausal Women. E. S. Collins^{*1}, A. V. Rao^{*2}, R. G. Josse¹, T. M. Murray¹, L. G. Rao¹. ¹Medicine/Division of Endocrinology & Metabolism, St. Michael's Hospital, Toronto, ON, Canada, ²Medicine and Nutritional Science, University of Toronto, Toronto, ON, Canada.

Lycopene is an antioxidant known to counteract the damage caused by reactive oxygen species (ROS) in states of oxidative stress. Although demonstrated to be beneficial in reducing age-related chronic diseases, the effect of lycopene in osteoporosis has not yet been investigated. We examined the relationship between lycopene and oxidative stress parameters and bone turnover markers in 33 postmenopausal women aged 50-60 who completed seven-day estimated food records prior to giving fasting blood samples. Serum samples were used to measure serum lycopene, the oxidative stress markers lipid peroxidation and protein thiols, and the turnover markers bone alkaline phosphatase (BAP) and cross-linked N-telopeptides of Type I Collagen (NTx). Average daily intake of lycopene was determined from the dietary records. The serum lycopene per kilogram body weight of the participants was grouped into quartiles and correlated with the above serum parameters using one-way ANOVA and the Newman-Keuls post test. The average serum lycopene for each group was as follows (nM/kg): group 1; 1.1 \pm 0.2, group 2; 2.6 \pm 0.1, group 3; 4.0 \pm 0.2 and group 4; 8.1 \pm 0.6. The groups did not differ significantly in age or body mass index (BMI). There was a significant direct correlation between dietary intake and serum lycopene (ANOVA $p<0.005$). Higher serum lycopene was found to be associated with a lower NTx (ANOVA $p<0.005$) and protein oxidation (expressed as protein thiols) (ANOVA $p<0.05$). There was a trend towards a negative correlation between serum lycopene and BAP and lipid peroxidation. A synergistic effect between lycopene and

vitamin C on bone resorption was demonstrated with the following observation: participants who consumed more than 500 mg/day of vitamin C demonstrated a significant, inverse correlation between serum lycopene per kilogram body weight and NTx ($r = -0.68$, $p<0.05$). This effect was not seen in participants who consumed less than 500 milligrams per day (mg/day) of vitamin C. In conclusion, these results support our hypothesis that in postmenopausal women dietary lycopene is readily absorbed and is effective in reducing oxidative stress and bone turnover markers, an effect that may be enhanced with vitamin C use. Our data suggest that lycopene may be a candidate agent for the prevention of osteoporosis.

Disclosures: *E.S. Collins, None.*

SA309

See Friday Plenary number F309.

SA310

Physical Activity and Dietary Calcium Intake in Older Women Improve Geometric Indices of Bone Strength. M. K. Nurzenski^{*1}, N. K. Briffa¹, R. L. Price², B. Khoo^{*2}, A. Devine³, T. J. Beck⁴, R. L. Prince³. ¹School of Physiotherapy, Curtin University of Technology, Perth, Australia, ²Medical Technology and Physics, Sir Charles Gairdner Hospital, Perth, Australia, ³School of Medicine and Pharmacology, University of Western Australia, Perth, Australia, ⁴Dept Radiology, Johns Hopkins University, Baltimore, MA, USA.

In a population-based study of elderly women it has been shown that those in the highest tertile of physical activity (PA) and the highest two tertiles of dietary calcium intake (CI) had 4.4 to 6.4% higher hip BMD. The effects of these two lifestyle factors on geometric indices of bone strength have now been examined in 1010 women from the same cohort. Baseline PA and CI were assessed by validated questionnaires, and one year DXA scans (Hologic 4500A) were analysed using hip structural analysis software (v3). Section modulus (Z), an index of bending resistance, cross-sectional area (CSA), an index of axial bone strength and subperiosteal width (SPW) were measured at the femoral neck (NN), intertrochanter (IT) and femoral shaft (S) sites. These data were divided into tertiles of PA and CI and the results compared using ANCOVA (SPSS v11.5) with correction for age, BMI and treatment (calcium/placebo). PA showed a significant dose response effect on CSA and Z at all hip sites ($p<0.004$) and SPW at S ($p=0.03$). CSA of the two higher tertiles was 4.8, 3.7 and 3% higher than the lowest tertile at the NN, IT and S sites, respectively. Z was 4.9, 4.9 and 3% higher at these sites. SPW was 0.8% higher at the S. For CI, there was a dose response effect for CSA and Z at the IT and S regions ($p<0.05$). CSA of the highest tertile was 2.7 and 2.6% higher than the lower two tertiles at these sites. Z was 4.1 and 2.2% higher at these sites. These effects were additive such that the women ($n=241$) with PA levels in the upper two tertiles and CI in the upper tertile had higher CSA (NN 6.5%, IT 6.1%, S 5.3%) and Z (NN 6.6%, IT 3.8%, S 4.9%). These data suggest that lifestyle factors favourably influence bone structure as well as bone density. This supports the use of population-based lifestyle interventions to improve femoral axial strength and bending resistance to those levels already achieved by around one quarter of the population.

Disclosures: *R.L. Prince, None.*

SA311

Socioeconomic Status Is a Significant Predictor of Hip Fracture Rates in California 1996 to 2000. S. L. Silverman¹, D. Zingmond^{*2}. ¹Cedars-Sinai Medical Center, David Geffen School of Medicine UCLA, Beverly Hills, CA, USA, ²David Geffen School of Medicine UCLA, Los Angeles, CA, USA.

Purpose: Hip fracture is a significant source of morbidity and mortality. Prior research has identified gender and race as significant factors influencing hip fracture incidence. The impact of socioeconomic status (SES) on hip fracture has been little studied in the general population. **Methods:** Using inpatient discharge abstracts from the California Office of Statewide Health Planning and Development (OSHPD)'s inpatient discharge database (PDD), all patients of age 50 years and older hospitalized in California with acute hip fracture and repair were identified by zip code between 1995 and 2000. Population estimates, income estimates, and place of residence (rural vs urban) by zip code tabulation area (ZCTA) were obtained from the U.S. Census. Poisson regression analyses were performed comparing impact of SES (income by decile by zip code) on hip fracture rates accounting for potential confounders - race, gender, age, and rural residence. **Results:** Between 1996 and 2000, a total of 116,919 persons were admitted with hip fracture out of a population of 8,144,469 persons. 74% were female. 61% were in those 80 years and older and 28% in those 70 to 79 years old. 85% were non-Latino whites (NLW). NLW were 87% of persons in those 80 years and older, but 79% in those 50 to 59 years old. Mean per capita income by ZCTA was \$25.0K, but was higher for NLW (\$25.8K) than blacks (\$17.8K), Latinos (\$18.0K), Asians (\$24.1K), and others (\$23.8K). Mean rural residence (by ZCTA) was 4%. In Poisson regression analyses, compared to the lowest income decile higher income decile predicts lower incidence rate ratio (IRR) of fracture (highest income decile - IRR 0.79, 95% Confidence Interval (CI): 0.77 to 0.82) adjusting for other confounders. Adjusted IRR (AIRR) ranges between 0.79 and 0.85 for the 6 highest deciles (all $P<0.01$). Rural residence predicted lower rate of hip fracture (AIRR 0.85, 95% CI: 0.82 to 0.87). Being male, non-White, or younger predicted lower fracture rates. Similar findings were found when analyses were stratified within race. **Conclusions:** Risk of hip fracture is the confluence of multiple factors. The impact of higher SES independent of other demographic characteristics may reflect nutritional status as well access to BMD measurement and medications for osteoporosis that might decrease hip fracture incidence.

Further research to identify the factors mediating the impact of SES on fracture is needed. Acknowledgement: This study was supported by an unrestricted educational grant from Merck & Co, Inc.

Disclosures: *S.L. Silverman, None.*

SA312

Effectiveness of Osteoporosis Care Pathways for Hospital Patients with Fragility Fractures. *N. Kolatkar¹, M. S. LeBoff¹, M. B. Harris*², J. Glowacki².* ¹Medicine, Brigham and Women's Hospital, Boston, MA, USA, ²Orthopedic Surgery, Brigham and Women's Hospital, Boston, MA, USA.

Hip fracture survivors have a 2 to 5-fold increased risk for subsequent fragility fractures. Worldwide, however, less than 27% of hip fracture patients receive post-fracture evaluation and therapy. We previously implemented a computer-assisted care pathway comprising discharge recommendations for a multivitamin, calcium/vitamin D supplements, and an outpatient endocrinology appointment for osteoporosis evaluation. In 2004, we added recommendations for the admitting orthopedic surgeon: initiation of daily calcium carbonate with vitamin D (1000 mg elemental calcium, 200 IU cholecalciferol) and a multivitamin (400 IU cholecalciferol), orders for serum calcium, albumin, and 25-hydroxyvitamin D [25(OH)D; Diasorin RIA: normal 20-57 ng/ml], and endocrinology consultation. To evaluate the effectiveness of these guidelines, we reviewed medical records of all patients aged ≥ 50 years with a fragility fracture of the hip or femur admitted to Brigham and Women's Hospital between August 1 and December 31, 2004 (N=57). For this abstract, effectiveness of the surgeon-driven admission guideline was defined by measurement of serum 25(OH)D during the hospital admission; effectiveness of the discharge guideline was defined by a discharge prescription for calcium and/or multivitamin. Age (mean ± SD) at the time of fracture was 77.5 ± 11.1 years; 42/57 (74%) of patients were women. Serum 25(OH)D was measured in 19/57 (33%) patients; this was considered sub-optimal effectiveness of the admission guidelines. Median serum 25(OH)D level was 19.0 ng/ml; 16/19 patients (84%) were vitamin D-insufficient [serum 25(OH)D <32 ng/ml]. Seven primary orthopedic surgeons cared for the patients. Sub-analysis revealed that of the two surgeons who cared for the most patients, one (a co-author of the admission guideline) ordered serum 25(OH)D for 9/20 (46%) patients, while the other (who was not given specific reminders) ordered it for 1/11 (9%) (p=0.055). 38/57 (67%) were discharged on calcium and/or vitamin D. This analysis suggests that the pre-existing computer-assisted discharge guideline was twice as effective as the newly added surgeon-driven admission guideline (p=0.0007). In sum, effectiveness of guidelines was associated with surgeon reinforcement and familiarity. The prevalence of vitamin D-insufficiency stresses the importance of assessing vitamin D status in patients with fragility fractures. This pilot study highlights the use of care pathways in the implementation of practice guidelines for hospital patients with fragility fractures, and suggests that reinforcement of guidelines can improve patient care.

Disclosures: *N. Kolatkar, None.*

SA313

See Friday Plenary number F313.

SA314

The Association of Height Loss and New Vertebral Deformity over 1-Year: Results from the Horizon Pivotal Fracture Trial with Zoledronic Acid. *J. Zhang*¹, J. Caminis¹, P. Mesenbrink*¹, T. Rosario-Jansen¹, M. Flood*¹, K. Tong*¹, S. Farneth*², D. M. Black².* ¹Novartis Pharmaceutical, East Hanover, NJ, USA, ²University of California, San Francisco, San Francisco, CA, USA.

Vertebral deformity is often associated with height loss, but the extent to which short-term height loss might be a useful marker of vertebral deformity is unknown. We used data from the HORIZON PFT (Pivotal Fracture Trial) to examine this association in greater depth. The HORIZON PFT is a multi-national, randomized, double-blind, placebo-controlled clinical trial designed to evaluate the potential of zoledronic acid in reducing the risk of both hip and vertebral fracture in postmenopausal women age 65-89 with osteoporosis. Since the study is still in progress and remains blinded, we combined data from both treatment groups to examine the association between measured height loss over 1-year and new vertebral deformity. Approximately 46% patients had height assessed by stadiometer, and only these patients are included in this analysis. Incidence of new vertebral deformity assessment was based on morphometry and defined by at least 20% and 4 mm decrease in any vertebral height with a confirmation by semi-quantitative reading. A total of 2762 osteoporotic postmenopausal women with 1-year information on vertebral deformity and height measured by stadiometer are included in the analysis. The relationship of height loss over 1-year to new vertebral deformity is summarized in Table 1. The association between height loss over 1-year and new vertebral deformity remains statistically significant, even after adjustment for other risk factors including age, height loss from age 25 to baseline, baseline total hip BMD, and baseline prevalent vertebral deformity.

Table 1. The relationship of height loss over-1 year to new vertebral deformity

Height loss (cm)	Percentage with new vertebral deformity % (n / N)	Odds ratio	95% CI
No loss	0.7% (8 / 1220)	1	
0 < loss ≤1	2.3% (30 / 1283)	3.6	1.7, 7.9
1 < loss ≤2	9.1% (15 / 164)	15.3	6.4, 36.6
2 < loss ≤3	16.3% (8 / 49)	29.6	10.6, 82.7
loss > 3	15.2% (7 / 46)	27.2	9.4, 78.7

Overall, our results show that the probability of having a vertebral deformity over 1 year increases significantly with height loss as measured by stadiometer. We conclude that over 1 year there is a strong association of height loss with occurrence of new vertebral deformity. These data suggest that measured height loss, even over a short period, may be useful, particularly in conjunction with other risk factors such as history of vertebral fracture, in predicting morphometric vertebral fracture

Disclosures: *J. Zhang, Novartis Pharmaceutical 3.*

SA315

See Friday Plenary number F315.

SA316

Frequency of Vertebral Fractures and Radiological Signs of Osteoarthritis in Postmenopausal Women Admitted to Internal Medicine. *J. del Pino¹, A. López-Bernus*¹, M. García-Martín*², P. L. Álvarez-Álvarez*³, V. del Villar*⁴, J. Sánchez-Navarro*⁵, M. Valiente*⁶, A. Fuertes*¹, P. Martínez-Hernández*⁷, L. Carpio*⁸, C. Garcés*⁸.* ¹Clínico, Salamanca, Spain, ²Barco de Valdeorras, Orense, Spain, ³NS Reyes, Burgos, Spain, ⁴General, Soria, Spain, ⁵Rio Carrión, Palencia, Spain, ⁶S Pau i S Tecla, Tarragona, Spain, ⁷NSa Reyes, Tenerife, Spain, ⁸Lilly, Madrid, Spain.

Osteoporosis and osteoarthritis are prevalent diseases that usually go unrecognized. Both entities may be inversely related. The aim of this study was to assess the frequency of vertebral fractures and radiological signs of osteoarthritis in postmenopausal women admitted to Internal Medicine (IM). Women aged 55-80 years admitted to IM in 20 hospitals were consecutively included in 7 months. Inclusion criteria were: not admitted for osteoporosis, and lateral chest radiograph routinely performed. After being trained by a radiologist expert, each investigator evaluated X-ray films. Fracture was a diminution in vertebral height ≥ 25% (Genant's grades 2 and 3), and patients were classified as having or not fracture. Evaluated signs of osteoarthritis were presence of osteophytes (spondylosis), spondylolisthesis, and joint space narrowing (JSN). Mean (SD) age, prevalence of vertebral fracture, and frequency of each radiological sign of osteoarthritis were recorded. Frequency of osteoarthritis signs was calculated separately in women with and without vertebral fractures. 689 patients were included; age 71.3 (6.6) years. 30.7% [CI 95% 27.3-34.2] (n=212) had any vertebral fracture. Frequency of each radiological osteoarthritis sign in the total cohort and in the groups of patients with and without vertebral fractures is expressed in table 1.

Table 1: Frequency of osteoarthritis signs in total cohort and in patients with and without vertebral fractures

		Total (N=690)	With VF(N=212)	Without VF(N=478)
Osteophytes	NA	46 (6.7%)	24 (11.3%)	22 (4.6%)
	Yes	213 (30.9%)	75 (35.4%)	138 (28.9%)
	No	430 (62.4%)	113 (53.3%)	318 (66.5%)
Spondylolisthesis	NA	53 (7.7%)	22 (10.4%)	31 (6.5%)
	Yes	22 (3.2%)	11 (5.2%)	11 (2.3%)
	No	615 (89.1%)	179 (84.4%)	436 (91.2%)
JSN	NA	41 (5.9%)	18 (8.5%)	23 (4.8%)
	Yes	212 (30.8%)	98 (46.2%)	114 (23.9%)
	No	437 (63.3%)	96 (45.3%)	341 (71.3%)

NA: Data not available, because either radiological technique or other reasons; VF= vertebral fracture

In summary, postmenopausal women admitted to the internal medicine department for reasons not related to osteoporosis have a high frequency of radiological vertebral fractures. In these women there is also a high prevalence of osteoarthritis signs. Women with vertebral fractures have a trend to present a higher frequency of radiological osteoarthritis signs.

Disclosures: *J. del Pino, None.*

SA317

See Friday Plenary number F317.

SA318

Prevalence of Vitamin D Deficiency in Scottish Adults with Non-Vertebral Fragility Fractures. *S. J. Gallacher¹, C. McQuillan*¹, M. Harkness*¹, A. P. Gallagher¹, E. Finlay*².* ¹Medical Unit, Southern General Hospital, Glasgow, United Kingdom, ²Department of Biochemistry, Southern General Hospital, Glasgow, United Kingdom.

Fracture risk and vitamin D deficiency increase with age. Recent guidelines emphasise the importance of calcium and vitamin D supplements in fracture prevention. It is however unclear whether vitamin D deficiency is a risk factor in the majority of fracture patients and whether there is a difference in the degree of vitamin D deficiency amongst different fracture types. Results of serum 25-hydroxy vitamin D were reviewed for 661 consecutive patients (median age 82.4; range 56.6 to 100.2 years) presenting with hip fracture to our unit over a four year period. A further 50 patients (median age 66.5; range 50.6 to 83.8 years) presenting to our Fracture Liaison Service with a variety of non-vertebral fracture types who had DXA proven osteoporosis (lowest T-score spine or hip < -2.5; median -2.8; range -2.5 to -5.2) were also assessed (hip = 13, upper limb fractures = 27, lower limb fractures + others = 10). Vitamin D was measured using a chemiluminescence assay with a lower limit of detection of

15nmol/l (Nichols Institute Diagnostics). Results <15nmol/l were assigned a value of 15nmol/l for analysis purposes. No agreed international consensus exists for a diagnostic serum level of vitamin D deficiency. This work reviews a number of different thresholds ranging from 30-70nmol/l. With respect to the hip fracture patients mean (±SD) vitamin D level was 24.6±17.6nmol/l (10.3ng/ml). 97.8% of these patients had a vitamin D level below 70nmol/l (~30ng/ml), 91.7% patients had a level below 50nmol/l (~20ng/ml) and 74.7% patients had a level below 30nmol/l (~10mg/ml). No seasonal or gender differences were noted. For the prospective osteoporotic non-vertebral fracture patients mean (±SD) vitamin D level was 44.1±25.3nmol/l (18.4ng/ml). 82% of these patients had a vitamin D level below 70nmol/l (~30ng/ml), 72% patients had a level below 50nmol/l (~20ng/ml) and 24.0% patients had a level below 30nmol/l. (~10ng/ml). Numbers in the prospective group are not large enough for detailed statistical analysis but mean vitamin D levels were 34.5nmol/l (hip fractures) versus 48.2nmol/l (non-hip fractures). This study confirms the near universal prevalence of vitamin D deficiency in our population with a particularly high prevalence among hip fracture patients regardless of whether a 50 or 70nmol/l cut-off is used. This illustrates that vitamin D deficiency represents a significant correctable risk factor for fragility fracture in our population and is a particular issue for the very elderly. This observed prevalence of deficiency appears higher than that seen in some other parts of the world.

Disclosures: **S.J. Gallacher**, None.

SA319

See Friday Plenary number F319.

SA320

Detection of Prevalent Vertebral Fractures Using Historical Height Loss: Comparison of Tallest Recalled Height and Armspan for Determining Height Loss. **K. Siminoski¹, K. Lee^{*2}, H. Jen^{*2}, R. Warshawski^{*2}.** ¹Radiology and Medicine, University of Alberta, Edmonton, AB, Canada, ²Radiology, University of Alberta, Edmonton, AB, Canada.

Historical height loss (HHL) determined as the difference between the tallest recalled (TRH) height and current measured height (MH) has moderate accuracy in detecting the presence of vertebral fractures. One way to avoid potential error in recall of TRH might be to replace it with armspan (AS) as a marker of tallest stature. In this study, we have compared the clinical accuracy of HHL determined using tallest recalled height (HHLtrh) versus HHL determined using armspan (HHLas). Subjects were women referred for specialist assessment of osteoporosis (n=287; average age 52 yrs; range: 18-92 years). MH was assessed using a wall-mounted stadiometer and AS was determined using a wall-mounted horizontal anthropometer. Vertebral morphometry was performed on all subjects from T4 to L4. Prevalent vertebral fracture was defined as a vertebral height ratio < 0.80. One or more fractures were present in 30.0%; the average number of fractures among those with fractures was 2.3. HHLtrh was correlated with the presence of prevalent vertebral fractures (r = 0.563; p<0.0001) as was HHLas (r = 0.224, p<0.0001). The areas under the ROC curves for detection of vertebral fractures were 0.72 (95% CI, 0.65-0.78) for HHLtrh and 0.58 (95% CI, 0.51-0.65) for HHLas. The likelihood ratio for HHLtrh of 6-8 cm was 14.0 while it was 1.4 for HHLas. For height loss >8 cm, the likelihood ratio was 21.0 for HHLtrh but only 1.8 for HHLas. At an HHL threshold of > 6 cm, sensitivity, specificity, positive predictive value and negative predictive values were greater for HHLtrh than for HHLas (see Table). These results show that even with the errors intrinsic to recall of height, HHL determined using tallest recalled height is superior to HHL calculated using armspan for detection of prevalent vertebral fractures in postmenopausal women. The use of armspan should be limited to those cases where tallest recalled height is not available.

HHL TYPE	Comparison of TRH and AS using HHL > 6 cm			
	Sensitivity	Specificity	PPV	NPV
HHLtrh	24	99	88	75
HHLas	19	96	40	72

HHLtrh = tallest recalled height minus measured height

HHLas = armspan minus measured height

PPV = positive predictive value

NPV = negative predictive value

Disclosures: **K. Siminoski**, None.

SA321

See Friday Plenary number F321.

SA322

Can the Spinal Curvature Irregularity Index (SCII) also Predict Vertebral Fractures in Italian Women. **D. Diacinti¹, N. Schaaf^{*2}, E. D'Erasmo^{*1}, R. Del Fiacco^{*1}, S. Minisola^{*3}, G. Mazzuoli^{*3}.** ¹Departm. of Clinical Sciences, University "La sapienza", Rome, Italy, ²K.U., Leuven, Belgium, ³Department of Clinical Sciences, University "La Sapienza" Rome, Rome, Italy.

Detection and diagnosis of vertebral fractures (VFs) are very important in all stages of osteoporosis. Radiographs or DXA vertebral fracture assessment (VFA) images of thoracolumbar spine are therefore an important tool in the clinical evaluation of osteoporosis. However, diagnosing VFs still can be difficult. There is often no clear distinction between a structural failure and the normal anatomic variation in anterior, middle and posterior height of the vertebrae. The aim of this multicentric study is to determine if the SCII can also identify vertebral deformities in Italian women. The SCII is the integrated average of the

vertebral heights (VHs) over the thoracolumbar spine to give a quantitative estimate of the regularity of the spinal curvature (Zebaze et. al. (2004): JBMR, 19; 1099-1104). A large SCII is presumed to correlate with the presence of vertebral deformities. The study was performed with 569 Italian women, aged 28-89 yrs. from 4 different Italian centra. VHs were obtained from VFA (Lunar Prodigy, GE Healthcare). ROC analysis and logistic regression was performed using Minitab. SCII was transformed to ln (SCII) for normality. T-test was used to compare average transformed SCII. 40 women out of the 569 studied subjects had a vertebral deformity. The average SCII was significantly higher for subjects with one or more deformities: 13,40% compared to those without deformities 4,34% (p < 0,001). SCII increases significantly with increasing numbers of vertebral deformities. We conclude that the Spinal Curvature Irregularity Index clearly distinguishes between subjects with and without vertebral deformities also in an Italian population.

Disclosures: **D. Diacinti**, None.

SA323

See Friday Plenary number F323.

SA324

Evaluation of a New Vertebral Fracture Assessment Method (CADfx) versus Conventional Radiography. **F. E. Massari^{*}, M. O. Cachizumba^{*}, S. Gonçalves^{*}, R. A. Gallo^{*}, R. G. Agüero^{*}, F. D. Silveira^{*}, O. Gear^{*}, M. V. Freixá^{*}, M. Bruno^{*}, E. A. Stenglein^{*}, A. Kñallesvsky^{*}, A. Arias^{*}, C. Lombas^{*}, M. B. Zanchetta^{*}, J. R. Zanchetta.** IDIM, Buenos Aires, Argentina.

Objective: To evaluate the capacity to detect vertebral fractures through an Hologic Densitometer Automatic Computer Aided Detection Program (CADfx) and compare it to Conventional Radiography. Material and Methods: We selected a stratified sample of 362 caucasic women from a database with a previous dorsolumbar radiography who were participating in an osteoporosis detection campaign with DXA. This sample was split into 2 groups, one of 161 women with some vertebral fractures and another one of 201 women without vertebral fractures. Subsequently, for this study we performed new conventional dorsal and lumbar radiographies and an Instant Visual Assessment (IVA) of the dorsolumbar spine (T4 to L4). Due to a lesser subjectivity of the method, we performed a semiquantitative analysis (Genant's Method) of all dorsal and lumbar spine radiographies, in order to detect the presence of vertebral fractures. This analysis was carried out by a specialist in bone radiology and it was considered a gold standard method. All the images obtained by the IVA method were automatically analysed with the CADfx program (Hologic Discovery A Densitometer). For technical reasons 30 patients were excluded (15 of each group). All these analyses were blind to the physicians as regards to the previous diagnosis of vertebral fractures. A comparison between methods was done on a per vertebra basis in a double entry table, defining the sensitivity and specificity of the CADfx program and its predictive values. A statistical analysis of the subgroups was done based on the segments of vertebral spine assessed (T4-T7; T8-T12; L1-L4). Results: The CADfx program showed a sensitivity of 62.5% and a specificity of 92.1%; with a positive predictive value of 33.6% and negative predictive of 97.5%. When we subdivided the spine analysis by regions we observed an increase of the specificity (96.8%) in fracture detection of the lumbar area. Conclusion: Due to the speed of the method (12 seconds), its innocuousness and its acceptable negative predictive value, this method could be considered as a screening tool to discard vertebral fractures.

Disclosures: **J.R. Zanchetta**, None.

SA325

See Friday Plenary number F325.

SA326

Incidence of Femoral Neck Fracture in Okinawa, Japan. **H. Arakaki, I. Owan, H. Kudo^{*}, H. Horizono^{*}, F. Kanaya^{*}.** Orthopedic Surgery, University of the Ryukyus, Okinawa, Japan.

The occurrence of femoral neck fracture is increasing throughout the world. Hip fractures in aged populations are associated with considerable morbidity and high economic cost. We surveyed the rate of femoral neck fracture occurred in Okinawa in the year 2004, and compared with the same survey which was conducted in 1989. The purpose of this study was to investigate whether the occurrence rate of femoral neck fracture increases year by year. Okinawa prefecture is located in southwest part of Japan with a population of 1.2 million. The number of hip fracture in 1989 was 502 (103 men and 399 women), but which was increased to 977 (183 men and 794 women) in 2004(Table 1). The average age of patients in 2004 was 81.3 years old, and the average hospital stay was 52 days. 86% were treated operatively. The mortality rate at the discharge was only 0.25%. The subtotal of age-specific incidences of hip fracture by the method of Lewinnek is 44.8 in 1989 and 41.0 in 2004. The number of hip fracture was increased year by year, but age-specific incidence rate has not been changed in 15 years.

Table 1. Number of hip fracture by age group			
Age Group	Men	Women	Total
50-59	14	21	35
60-69	30	45	75
70-79	48	164	212
80-89	69	352	421
90-99	18	175	193
100-109	1	14	15
Total	183	794	977

Disclosures: **H. Arakaki**, None.

SA327

See Friday Plenary number F327.

SA328

The Association between Homocysteine Levels and Markers of Bone Metabolism, Bone Density and Fractures. P. Gerdhem¹, K. Ivaska^{*2}, A. Isaksson^{*3}, K. Pettersson^{*2}, K. Vaananen², K. Akesson¹, K. J. Obrant¹. ¹Dep of Orthopedics, Malmö University Hospital, Malmö, Sweden, ²Institute of Biomedicine, Dep of Anatomy and Dep of Biotechnology, University of Turku, Turku, Finland, ³Clinical Biochemistry, Lund University Hospital, Lund, Sweden.

Recently the association between high serum homocysteine (Hcy) levels and an increased risk of fracture has been described. The causal relationship between Hcy levels and fracture risk is not clear. We examined the association between Hcy levels, bone metabolism and fractures. Hcy levels were measured in 996 women, all 75 years old (range 75.0-75.9). Biochemical markers of bone metabolism (serum tartrate resistant acid phosphatase 5b, serum cross-linking telopeptide of type I collagen (CTX), urine and serum osteocalcin, urine deoxypyridinoline, serum bone-specific alkaline phosphatase), parathyroid hormone, 25-hydroxy vitamin D and bone density were measured at baseline. Fractures and mortality during a mean follow-up of 4.6 years were recorded. High Hcy levels correlated to high serum CTX ($r=0.19$, $p<0.001$), parathyroid hormone ($r=0.16$, $p<0.001$), serum osteocalcin ($r=0.15$, $p<0.001$) and plasma creatinine ($r=0.36$, $p<0.001$). The correlations between Hcy and the other biochemical markers of bone turnover and hormones were low ($r=0.09$ or less). During the follow-up 163 women sustained at least one fracture (including 46 vertebral, 39 hip and 35 wrist fractures). With each unit increase of the natural-log transformed (ln) Hcy levels vertebral fracture risk increased (odds ratio 2.21; 95% CI 1.002-4.86). The inclusion of creatinine in the logistic regression increased the OR to 2.57 (1.13-5.84). When femoral neck DXA, smoking status or walking speed were included in the logistic regression the association between ln Hcy and vertebral fractures decreased and was no longer significant. An increase of ln Hcy was not associated with a risk increase for any type of fracture, hip or wrist fracture. The correlations between Hcy and bone density measurements (DXA and ultrasound) were low or non-significant. During follow-up, women in the highest homocysteine quartile had a 1.9 times higher mortality rate (95% CI 1.13-3.21) than women in the lowest homocysteine quartile. The association between Hcy and vertebral fractures could to some extent be explained by an association to bone metabolism, especially collagen degradation. However, in this study the association between fractures and Hcy levels were weak or non-significant and were affected by other fracture predictors, such as bone density and walking speed. The increased mortality among women with high homocysteine levels indicates that high homocysteine may be a marker of frailty.

Disclosures: **P. Gerdhem**, None.

SA329

Incidence and Risk Factors for Low Trauma Fractures in Men with Prostate Cancer. H. G. Ahlborg¹, N. D. Nguyen², J. R. Center², J. A. Eisman², T. V. Nguyen². ¹Department of Orthopaedics, Malmö University Hospital, Malmö, Sweden, ²Bone and Mineral Research Program, Garvan Institute of Medical Research, Sydney, Australia.

Low bone mineral density (BMD) is a well-known risk factor for fracture in men. Moreover, non-skeletal risk factors, such as postural instability, have been identified to be significant predictors of fracture. However, the relative importance of these risk factors among men with prostate cancer has so far not been examined. This study was aimed at determining the risk of low trauma fracture in men with prostate cancer, and to characterize the association between potentially risk factors and fracture risk. From the prospective, population-based Dubbo Osteoporosis Epidemiology Study, 43 men were identified to have been diagnosed with prostate cancer; among whom, 20 received and 23 did not receive androgen deprivation therapy (ADT). Low trauma fractures were ascertained and compared with expected numbers in the study population and expressed as standard incidence ratio (SIR). Bone mineral density at the femoral neck (FNBMD) as well as postural instability was measured, and life-style factors were recorded in 29 of the subjects prior to the diagnosis of prostate cancer. Potential risk factors were assessed with a log-binomial model and expressed as risk ratios. During the 313 person-years of follow-up, 15 (35%) men sustained at least one low trauma fracture after the diagnosis of prostate cancer. Overall, fracture risk was increased (SIR 3.1, 95% CI 1.8-5.2) predominately among men with ADT (SIR 5.8, 95% CI 2.6-11.0). FNBMD in men with prostate cancer were 0.4 SD higher than in the underlying population ($P<0.05$). Additionally, a 1 SD lower FNBMD was associated with a risk ratio of 1.7 (95% CI 1.0-2.8), and a 1 SD higher rate of FNBMD loss with a risk ratio of 1.6 (95% CI 1.0-2.2) for fracture. These results suggest that men with prostate cancer, particularly those treated with ADT have an increased risk of sustaining a low trauma fracture. Although the average BMD in men with prostate cancer prior to treatment seems to be higher than expected, a low BMD prior to treatment or increased rate of bone loss after initiating of treatment is each a significant predictor of fracture.

Disclosures: **H.G. Ahlborg**, None.

SA330

Clinical Vertebral Fracture Outcomes: Medical Resource Utilization and Costs in the First Year Following the Fracture. J. Simon¹, N. N. Borisov^{*2}, R. Sheer^{*2}, M. Steinbuch^{*2}. ¹The George Washington University, Washington, DC, USA, ²Procter & Gamble Pharmaceuticals, Inc, Mason, OH, USA.

This study evaluated medical outcomes of a clinical vertebral fracture in the first year following the fracture, in a managed care setting, utilizing an integrated administrative, medical and pharmacy claims database. A retrospective cohort study was conducted among women (aged 45+) with a new vertebral fracture (non-trauma) that was verified by a diagnostic code and a record of a radiologic exam, between July 1, 2000 and June 30, 2003. The cohort was followed for 12 months after the vertebral fracture to identify medical resource utilization and direct medical cost related only to the vertebral fracture. The cost was defined as the cost of outpatient, inpatient and long-term medical care. Vertebral fracture related prescription drug costs such as the cost of analgesics, NSAIDs, and opiate agonists was also included. Medical cost for hospitalized and non-hospitalized patients was assessed first to reflect the inpatient hospital proportion of clinical cases in the total cost of the vertebral fracture. All costs were adjusted to 2004 dollar terms using Medical Care Services component of Consumer Price Index. A total of 4,634 women were identified with a new clinical vertebral fracture. The mean age was 76 years. Twenty two percent of women ($n=1,024$) were admitted to a hospital for their vertebral fracture, of which 20% ($n=202$) were discharged to long-term care. The average hospital length of stay was 7 days. After the discharge, 69% of hospitalized women continued fracture-related outpatient care. Fifty-nine percent of women with a vertebral fracture ($n=2,745$) were prescribed analgesics, NSAIDs, or opiate agonists within 15 days of their fracture, with an average 5 scripts per patient during the 1 year follow-up. The average cost of a vertebral fracture among hospitalized women during the follow-up was \$2,687 per patient, and among non-hospitalized women was \$593. The weighted average cost of the vertebral fracture was estimated at \$1,056 per patient during the follow-up. Inpatient care cost was 47% (\$498 per patient), outpatient cost was 29% (\$303 per patient), prescription drugs cost was 14% (\$149 per patient), and long-term care cost was 10% (\$107 per patient) of the weighted average cost. Nineteen percent of women with a vertebral fracture sustained a subsequent fracture within 1 year (10% vertebral and 9% non-vertebral). Vertebral fractures create a burden to patients and the health care system in terms of both medical resource utilization and direct medical costs. This suggests that therapies with rapid reduction in fracture risk may offer important cost benefit to health care payers, providers and patients.

Disclosures: **N.N. Borisov**, Procter & Gamble 1, 3.

SA331

See Friday Plenary number F331.

SA332

Risk of Hip Fracture in Elderly Women Is Defined by Physical Fitness First, by Nutrition Second. D. Chabane^{*1}, M. Krieg^{*1}, D. Ruffieux^{*1}, J. Cornuz^{*1}, P. Burckhardt¹, T. SEMOF-group^{*2}. ¹University, Lausanne, Switzerland, ²Switzerland.

Low calcium and protein intake, muscular weakness and propensity to fall are risk factors for osteoporotic fractures. The prospective SEMOF study (Swiss Evaluation of the Methods of the Osteoporotic Fracture risk) on 7788 women over 70 yrs (follow-up 3.5 years) compared the incidence of fractures and falls with the intake of calcium and protein as dairy products (4 questions: nb of portions of milk (2 dl), yogurt (180 g), soft cheese (20g), hard cheese (20g); calculations with PRODI 4.5[®]), with the chair-test and grip-strength (Dynamometer Jamar[®]), and with questions concerning fitness. They allowed to calculate:

1. Score for risk of fall 0-5 (5 questions: getting up in the night, dizziness and instability, difficulties in raising from chair, use of canes etc, resting on furnitures while walking at home). >1 = high risk.
2. Score of mobility 0-6 (6 questions : level of activity, walking outdoors, use of stairs, getting in and out of cars, crossing a street, use of public transport systems). <5 = unsatisfactory.
3. General score of inactivity 0 -2 (high risk on score 1 + unsatisfactory on score 2). Statistics with Stata 8.1[®].

The functional tests were corrected for age and BMI. T-Test for parametric, Mann-Withney for non-parametric variables. Anova when $N>2$.

Score for risk of fall : 0 - 1 - 2 - 3 - 4 - 5:

Incidence of falls (%): 26-30-37-42-54-61

Score of mobility: 0 - 1 - 2 - 3 - 4 - 5 - 6:

Incidence of falls (%): 51-42-36-43-40-31-36

For all differencies $p < 0.001$. Fall incidence increased ($> 30\%$), when score for risk of fall > 1 . Unsatisfactory mobility when score < 5 .

General score of inactivity 0-----1-----2

Incidence of falls-----28%---36%-----46%

Calcium/dairy products-- 494(276)-- 484(275)--489 (288)

(mg/day) (SD)

Proteins (g/day)(SD)--- 14.5 (8.0)--- 14.3 (8.0) -14.5 (8.3)

Chair test : Number----5221-----1663-----802

Normal-----98%*-----87%*-----53%*

Grip strength: Number --2976-----920-----476

Result (kg) (SD) -----20.8 (5.2)*- 19.1 (5.4)*-17.2 (5.3)*

Hip fracture incidence ---3.0-----4.4-----9.7

(per 10'000 women)

All fractures incidence ----27.8----- 34.2----- 46.7**

**) *p*=0.015 diff. from group 1

These scores of risk for fall and of mobility correlated with the incidence of falls in the follow-up. Women with a high inactivity score had more falls and more fractures, but had no lower calcium- and protein-intake in form of dairy products. Women with fractures differed from women without fractures in their scores (sign.), but not in their intakes. Only among the women with a high inactivity score, low intake was associated with higher fracture incidence.

Disclosures: **P. Burckhardt**, None.

SA333

Characteristics of Vertebroplasty Patients: An Analysis of Claims Data from A Large Not-For-Profit Healthcare Insurer. **A. S. Mudano**^{*1}, **J. Bian**^{*1}, **M. Elkins**^{*1}, **D. Briggs**^{*2}, **A. Neal**^{*2}, **J. Cope**^{*3}, **T. Gross**^{*3}, **D. McGunagle**^{*3}, **J. Graham**^{*3}, **A. Ferriter**^{*3}, **K. G. Saag**¹. ¹Center for Education and Research on Therapeutics of Musculoskeletal Disorders, University of Alabama at Birmingham, Birmingham, AL, USA, ²Health Management, Blue Cross and Blue Shield of Alabama, Birmingham, AL, USA, ³Office of Surveillance and Biometrics, Center for Devices and Radiological Health, Food and Drug Administration, Rockville, MD, USA.

Background: Vertebroplasty, a medical procedure that typically involves the injection of methymethacrylate directly into a vertebral body, is used to relieve pain associated with vertebral compression fracture (VCF) and other vertebral pathologic states. Despite its approval by the FDA, growing utilization, and coverage by insurers, there has been little evidence of the common reasons for its use as well as characteristics of patients receiving and physicians performing this procedure. **Objectives:** To examine the utilization patterns and patient/provider characteristics of vertebroplasty in a large population-based cohort. **Methods:** Using administrative claims data from a large regional health insurer with over 3 million enrollees, we used CPT-4 codes to identify a cohort of patients receiving at least one vertebroplasty from January 2003 to June 2004. In order to develop a longitudinal profile of this cohort, we retrieved all claims for these patients from January 2001 to December 2004. ICD-9 diagnosis codes were used to determine likely reasons for this procedure. In addition, we also examined other patient and provider characteristics. **Results:** We identified a total of 121 patients who received 135 separate vertebroplasty procedures. Among the patients, 63% were women. Seventeen percent of the patients were under age 50, and 15% were age 65 or older (mean age of 58 ± 10 years). Thirteen patients (11%) received multiple vertebroplasties. The main indications for a vertebroplasty at the date of a procedure were pathological fracture of vertebrae (56%) and VCF (20%). Of the 121 patients, 58 patients (48%) had a history of VCF, and 44 patients (36%) had a bone cancer diagnosis (just over half of these patients had at least one oncology visit). Radiologists performed half of all procedures, followed by orthopedic surgeons (30%) and neurosurgeons (10%). The average number of vertebroplasty procedures increased by 25% after September 1, 2003, the date the insurer began to reimburse for this procedure for VCF. **Conclusions:** Although vertebroplasty was used infrequently in this large privately-insured population, its utilization has been increasing. Additional research is underway to assess the long-term impact of vertebroplasty on post-vertebroplasty recurrent VCFs.

Disclosures: **A.S. Mudano**, None.

SA334

See Friday Plenary number F334.

SA335

Recognizing Osteoporosis and its Consequences in Quebec (ROCQ): The Care Gap Following a Fragility Fracture. **J. P. Brown**^{*1}, **L. Bessette**¹, **M. Beaulieu**^{*2}, **M. Baranci**^{*3}, **S. Jean**^{*1}, **K. S. Davison**¹, **L. G. Ste-Marie**⁴. ¹Laval University, Sainte-Foy, PQ, Canada, ²Merck Frosst Canada, Montreal, PQ, Canada, ³sanofi-aventis Pharma, Montreal, PQ, Canada, ⁴University of Montreal, Montreal, PQ, Canada.

The objective of this analysis is to evaluate the diagnostic and treatment rates of osteoporosis 6 months following a fragility fracture in women 50 years and over participating in a patient health-management programme (ROCQ). ROCQ is a prospective cohort study involving 18 centers in three socio-sanitary regions in the province of Quebec (Canada). At phase 1, women with fragility and traumatic fractures are recruited during their visit to a cast or outpatient clinic and contacted by phone to answer a short questionnaire to identify the specific circumstances of their fracture. During the first phone contact, there is no reference about the possible association between the fracture and osteoporosis, and no investigation nor intervention is proposed. Six months after the fracture event, women are contacted for a second time by phone (phase 2) to evaluate the diagnostic and treatment rates of osteoporosis (bisphosphonates, raloxifene, nasal calcitonin or teriparatide). After 18 months, 926 women (mean age: 63.4 years) have completed phase 1. A total of 752 (81%) sustained a fragility fracture and 174 (19%) sustained a traumatic fracture. Eighty-six percent of women recruited with a fragility fracture were 75 years of age or less. The age distribution between fragility and traumatic fractures was similar. To date, 338 participants with a fragility fracture have completed the questionnaire at phase 2 and 50 (15%) out of these 338 women were already on treatment for osteoporosis at the time of their fracture. Of those with no treatment (288) at phase 1, 52 (18%) initiated pharmacological therapy in the 6-month period following their fracture. At phase 2, 79 (27%) of participants either received a diagnosis of osteoporosis or were on treatment. In ROCQ, 81% of fractures were considered related to osteoporosis while the

literature estimates that 70% of the fractures in those over age 45 are attributable to osteoporosis (1). Despite the availability of diagnostic modalities and effective treatments for osteoporosis, there is a substantial care gap (73%) in the management of this disease. The proportion of fragility fractures is higher than expected and the management of osteoporosis is not optimal. The information from this programme may improve post-fracture diagnosis and treatment of osteoporosis in Quebec. (1) Iskrant AP, Smith RW Jr. Osteoporosis in women 45 years and over related to subsequent fracture. Public Health Rep 1969;84:33-8.

Disclosures: **J.P. Brown**, Merck Frosst Canada 2, 5, 8; Alliance (Sanofi-Aventis and P&G Pharmaceuticals) 2, 5, 8; Eli Lilly Canada 2, 5, 8; Novartis Pharma 2, 5, 8.

SA336

LRP5 Genetic Variants Influence Bone Mineral Density in Men. **M. A. Koay**¹, **S. Yeung**^{*2}, **M. A. Brown**¹, **P. R. Ebeling**³. ¹Botnar Research Centre, University of Oxford, Oxford, United Kingdom, ²Diabetes and Endocrinology, The Royal Melbourne Hospital, Parkville, Australia. ³Diabetes and Endocrinology and Medicine, The Royal Melbourne Hospital, Parkville, Australia.

Background: Osteoporosis in men is a poorly recognized condition. The NHANES III survey reported the prevalence of hip osteoporosis was 3-6% in men aged > 50 years. One third of all hip fractures and one fifth of vertebral fractures occur in men. There is increasing evidence that genetic factors underlying BMD and osteoporosis risk operate in a sex-specific manner. A leading genetic candidate in BMD regulation is the *LRP5* gene. **Hypothesis:** We propose that *LRP5* gene polymorphisms modulate BMD and fracture risk in men. **Methods:** Two cohorts were recruited. The first cohort comprised men with a history of spinal fractures (n = 78, age 22 to 88 years) and healthy, fracture-naïve men (n=65, age 21 to 80 years). The second cohort comprised 56 families of men with osteoporosis and fragility fractures. Lumbar spine, proximal femur and total body BMD and total body bone mineral content (TBBMC) were measured by DXA. Genomic DNA was obtained for determination of *LRP5* genotypes. *LRP5* allele, genotype and haplotype frequencies in control and fracture populations were compared using contingency table analysis. Association of *LRP5* gene polymorphisms and bone mass indices within families were assessed by QTDT (assuming additive interactions between un-measured environmental and polygenic factors). **Results:** *LRP5* allele, genotype or haplotypes were expressed at similar frequencies in men with and without fragility fractures, indicating that *LRP5* polymorphisms were not associated with fracture risk in our cohort. Instead QTDT analysis of families of osteoporotic men with fractures identified association between the coding C135242T (F549F) polymorphism in exon 8 and FN BMD Z-score (*p* = 0.026). Restricting analysis to men did not significantly reduce the strength of this association (*p* = 0.048). Within families, a trend towards association between height and the C165215T (A1330V) *LRP5* polymorphism in exon 18 was noted (*p* = 0.062 in the entire family cohort, *p* = 0.092 men-only analysis). No evidence of linkage between *LRP5* polymorphisms and bone mass nor height was observed. **Conclusions:** Positive association between the F549F *LRP5* polymorphism and femoral neck BMD, and a trend towards association between the A1330V *LRP5* polymorphism and height were noted in families of men with osteoporosis and fragility fractures. No single *LRP5* polymorphism was predictive of fracture risk. This study confirms previous work, which has demonstrated that *LRP5* gene polymorphisms modulate BMD in men.

Disclosures: **M.A. Koay**, None.

SA337

Calcification of Abdominal Aorta and Osteoporosis. **S. Yaturu**¹, **J. F. Bridges**^{*2}, **B. A. Bryant**^{*3}. ¹Endocrinology, VAMC/LSUHSC, Shreveport, LA, USA, ²Nutrition, VAMC, Shreveport, LA, USA, ³Endocrinology, VAMC, Shreveport, LA, USA.

Calcification is a common feature of atherosclerotic plaques. Coronary calcification and aortic calcification positively correlate with each other. Osteoporosis and Atherosclerotic heart disease are common in elderly people. There is accumulating evidence that osteoporosis is associated with both atherosclerosis and vascular calcification. Bone mineral density (BMD) measured at the lumbar spine in those over 70 years of age may be falsely elevated due to aortic calcification and structural changes within the spine such as osteophytes, osteochondrosis and facet sclerosis. BMD at radius is the proposed alternate site when AP spine data is unreliable. Since spine has more trabecular bone and radius has more trabecular bone, we hypothesized that we there is a need for alternate site to measure. We analyzed the bone mineral density results of 50 subjects with abdominal aortic calcification (AAC), with a mean age of 73. Atherosclerosis, either coronary artery and or peripheral vascular disease is prevalent in 80% of the subjects. The BMD at lateral spine correlates with % abdominal fat (r = 0.46). Though 8 subjects had fragile hip fractures, BMD at 33%radius were within normal range.

Site	BMD	Osteoporosis (%)	Osteopenia	Normal
AP spine	1.181	4	29	67
Lateral Spine	0.578	51	31	18
Hip	0.904	16	51	33
Radius	0.727	9	36	55

In conclusion, AAC was associated with increased abdominal fat, abnormal lipid parameters and decreased bone mineral density. BMD at AP spine in subjects with aortic calcification is unreliable and the lateral spine and hip are better alternatives than the 33% radius.

Disclosures: **S. Yaturu**, VAMC 3.

SA338

See Friday Plenary number F338.

SA339

Men with Hip Fractures Are Younger, Sicker and More Likely to Die. S. L. Silverman¹, D. Zingmond^{*2}. ¹Medicine and Rheumatology, Cedars-Sinai Medical Center, David Geffen School of Medicine UCLA, Beverly Hills, CA, USA, ²Medicine, David Geffen School of Medicine UCLA, Los Angeles, CA, USA.

Purpose: To compare demographics, length of stay, and short and long-term mortality in men and women with hip fracture in California 1991-2001. Methods: Using inpatient discharge abstracts from the California Office of Statewide Planning and Development (OSHPD)'s inpatient discharge database (PDD), all patients hospitalized in California with acute hip fracture and repair were identified between 1991 and 2001. Out of hospital death was ascertained by linkage to the state death registry through 2001. Results: There were fewer hip fractures in men than women (67,680 vs 183,311). Men with hip fractures were younger (mean age 74 vs 81, median age 74 vs 81). Men were more likely minority (17% vs 13% non-Caucasian). Men were sicker (mean Charlson index 1.2 vs 1.0) The percent admitted from SNF were similar (9% of men and 10% of women); however, men stayed longer in hospital (7.3 vs 6.5 days; were more likely to be discharged to home (17% vs 9.5%); and less likely to be discharged to SNF (61% vs 72%). Men were more likely to die in hospital (3.4% vs 1.9%) and more likely to have pulmonary embolism or other cardiovascular complication. Mortality was greater in men at 30 d (9.9% vs 5.6%); 60 d (13.6% vs 8.2%); 180 d (21.2% vs 13.7%) and 365d (27.6% vs 19.0%). Conclusions: Men with hip fractures in the last decade in California were younger, sicker and more likely to die in hospital and long-term. Men with hip fracture should be identified as being at high risk for increased morbidity and mortality. Acknowledgement: This research was supported by an unrestrsicted educational grant from the Alliance for Better Bone Health

Disclosures: *S.L. Silverman, None.*

SA340

Referral Patterns for Men to an Osteoporosis Scanning Service from Family Practitioners. A. D. Khan^{*}, G. M. Blake, I. Fogelman. Guy's King's and St Thomas' School of Medicine, London, United Kingdom.

The aim of this study was to investigate the reasons why General Practitioners (GPs) refer men for a bone densitometry examination and the relationship between patients' bone mineral density (BMD) and their clinical risk factors for osteoporosis. A total of 253 male patients referred between January 1998 and December 2004 were identified. Referral letters were reviewed and classified according to the indication for performing a BMD examination. Patients completed a questionnaire that was used to identify risk factors for osteoporosis. Spine and hip BMD scans were performed on a Hologic QDR4500A and interpreted using T- and Z-scores calculated from the manufacturer's reference range for the spine and the NHANES range for the hip. The 253 men (mean age 62.2 y; age range 25 to 91 y) comprised 2.8% of all GP referrals during the 7-year period. The percentage of men increased slightly from 2.4% in 1997 to 3.0% in 2004. The most common reasons for referral were: corticosteroid use (33%); radiographic evidence of osteopenia (19%); back pain (19%); follow-up of a previous scan (14%); recent fracture (12%). The most common risk factors identified on the questionnaire were: corticosteroid use (43%); alcohol intake (> 10 units a week) (35%); current smoking habit (27%); family history of osteoporosis (26%); previous fracture (23%). Forty-three men (17%) had a T-score of -2.5 or less at the spine, 29 (12%) at the femoral neck, and 16 (6%) at the total hip. Multi-variant regression analysis was used to examine the relationship between patients' Z-scores and their clinical risk factors for osteoporosis. For spine Z-score the statistically significant risk factors were: current smoking habit (Z -score decrement = -0.96, p <0.001), previous fracture: (Z -score decrement = -0.72, p = 0.008), and low BMI (< 20): (Z -score decrement = -1.13, p = 0.019). A history of osteoarthritis was associated with increased Z-score (Z-score increment = +1.11, p = 0.001). The same three factors (current smoker, previous fracture, low BMI) were also associated with statistically significant reduction in Z-score at the femoral neck and total hip. Former smokers were indistinguishable from men who had never smoked. In conclusion, only 3% of patients referred by GPs to an osteoporosis screening service were men. The indications given for referral were generally similar to those for women. Three clinical risk factors (current smoker, previous fracture and low BMI) were particularly associated with low Z-scores.

Disclosures: *G.M. Blake, None.*

SA341

See Friday Plenary number F341.

SA342

Vertebral Fractures in Patients with Chronic Obstructive Pulmonary Disease. Is Bone Mineral Density a Good Predictor? E. Casado^{*1}, M. Larrosa^{*1}, M. Gallego^{*2}, E. Naval^{*2}, A. Gómez^{*1}, J. Gratacòs^{*1}. ¹Rheumatology, Hospital Sabadell, Sabadell, Spain, ²Pneumology, Hospital Sabadell, Sabadell, Spain.

The aim of the study was to evaluate the prevalence of vertebral fractures in male patients with chronic obstructive pulmonary disease (COPD) and to assess the usefulness of dual-energy x-ray absorptiometry (DEXA) to predict vertebral fractures in these patients. A transversal study was conducted. All consecutive male patients with COPD who were visited in a 6-month period both in a Pneumology out-patient clinic and primary care were included. Conventional DEXA (lumbar spine and total femur) and thoracic and lumbar x-ray films were performed in all patients. The diagnosis of osteoporosis was established by bone mineral density (BMD) according to the WHO criteria (T-score ≤-2,5 in any of the explored region). A vertebral fracture was considered when the height of vertebral body was decreased at least 20% in any edge. The severity of COPD was established according to the American Thoracic Society (mild FEV₁>50%; moderated FEV₁ 35-50%; severe FEV₁<35%). 99 male patients with COPD were included. Mean age was 67±8 years. COPD was moderated to severe in 60% of patients. Using the WHO criteria 27 patients had osteoporosis (prevalence 28%). 32/94 patients (34%) had vertebral fractures. 10/27 patients (38%) had vertebral fractures in the group of osteoporosis by DEXA, and 22/67 (32%) in the group without osteoporosis. Using the thoracic and lumbar spine x-ray as a gold standard, the presence of osteoporosis by DEXA had a sensitivity of 31%, an specificity of 72% and a negative predictive value of 67%. The prevalence of vertebral fractures in patients with COPD was 34% in our series. The BMD by DEXA does not seem to be a useful tool to predict vertebral fractures in these patients, since 32% of patients without osteoporosis had vertebral fractures.

Disclosures: *E. Casado, None.*

SA343

Neuromuscular Function and Risk of Fractures in Older Men. K. Ensrud¹, R. Fullman², L. Marshall³, H. Fink¹, B. Chan³, J. Cauley⁴, S. Cummings², E. Orwoll³. ¹VAMC & U of MN, Minneapolis, MN, USA, ²UCSF & CPMC, San Francisco, CA, USA, ³OHSU, Portland, OR, USA, ⁴U of Pittsburgh, Pittsburgh, PA, USA.

Because men have higher peak bone mass than women and are less likely to experience rapid bone loss due to gonadal insufficiency, factors that increase propensity to falls such as impairment in neuromuscular function may be strong determinants of fracture (fx) risk in older men. To test the hypothesis that men with severe impairment in NMF are at increased risk of fx independent of bone mineral density (BMD), we performed measures of dynamic leg strength (ability and time to rise from a chair 5 times without using the arms), leg power (Nottingham Power Rig), dynamic balance (narrow walk speed) and femoral neck BMD at baseline in 5588 older men (mean age 73.6 yrs) enrolled in the MrOS cohort who were then followed prospectively for fxs. Each measure of NMF was first expressed as a categorical variable with 5 levels (first group comprised of those unable to complete measure and the remaining men divided into 4 groups of equal size) and then as a dichotomous variable (unable vs. able to complete measure). During an average follow-up of 3.7 yrs, 240 men (4%) experienced ≥1 non-spine fx, including 40 (0.6%) who suffered a first hip fx. After controlling for multiple potential confounders including BMD and fall history, men with severe impairment in NMF (as defined by inability to complete a given measure of NMF) were at increased risk of non-spine fx, including hip fx (table). When models for non-spine fx and hip fx included all 3 measures of NMF, inability to rise from a chair remained strongly associated with risk of fx, including hip fx. The relationship between each measure of NMF and non-spine fx was not entirely accounted for by an increased of hip fx; this was especially true for narrow walk where men unable to complete the narrow walk had a 1.9-fold (95%CI 1.2-2.8) increased risk of non-spine non-hip fx.

Unable to complete given measure of NMF (%)	Relative Risk of Outcome in Those Unable vs. Able*	
	Non-spine Fx RH (95% CI)	Hip Fx RH (95%CI)
Chair Stand (2.8%)	2.3 (1.3-3.8)	3.2 (1.3-7.6)
Leg Power (3.0%)	1.7 (1.0-3.1)	3.0 (1.1-8.0)
Narrow walk (8.8%)	1.7 (1.1-2.4)	1.2 (0.5-2.6)

*adjusted for age, clinic, health status, smoking status, physical activity, medical conditions, fall history, body weight and femoral neck BMD; models for non-spine fx also adjusted for race
Severe impairment in NMF in older men may be useful in a clinical setting to identify older men at high risk of fxs. Our findings suggest that inability to rise from a chair is most strongly associated with risk of hip fx, while inability to complete narrow walk is most strongly related to risk of other non-spine fxs.

Disclosures: *R. Fullman, None.*

SA344

Osteoporosis in Coumadin Clinic. K. E. Greenwald^{*}, A. Wilson^{*}, M. White-Greenwald. Desert Medical Advances, Palm Desert, CA, USA.

Vitamin K is an essential cofactor required for synthesis of bone matrix. We evaluated osteoporosis in 110 consecutive patients in a coumadin clinic, both men and women all over age 55, collecting data for height, weight, and bone mineral density by ultrasound of the calcaneus (Hologic Sahara). The broadband ultrasound attenuation units (BUA) have been shown previously to have 96% correlation with DEXA by using absolute fracture risk

(Arth& Rheum 48:92; 2003). Background information regarding medical history and concomitant medication was collected by interview and questionnaire. Time on coumadin ranged from 6 months to 20 years. Data was collected on a control cohort of patients with similar heart disease not on coumadin (chosen as a comparison group matched by sex, age, weight, use of alcohol or cigarettes, race, and economic background.) Patients with cancer or metabolic bone disease were excluded from this analysis. Less than 5% of patients were on any therapy for osteoporosis and these small numbers did not affect the statistical results. For men (n=62), the average age was 76 (SD 7), weight 185 lbs (SD 26), and we found the average BUA 70.3 (SD 20.5) with coumadin patients, and BUA 82.3 (SD 19.3) for men not on coumadin. There was no difference in baseline characteristics for the two populations. The difference in BMD was statistically significant p<0.02, and became more significant with age (evaluating groups in five year increments). For women (n=48), the average age was 76 (SD 7.2), weight 151 lbs (SD 33), and we found the average BUA 68.1 (SD 3.4) with coumadin patients, and BUA 73.6 (SD 3.1) for women not on coumadin. There was no difference in baseline characteristics for the two populations. The difference in BMD was highly significant, p<0.00001, and became more dramatic with age (evaluating groups in five year increments). With osteoporosis defined by absolute risk (red zone of high risk) , the relative risk of osteoporosis was 1.6 (CI 0.012,2.86) for patients taking prolonged warfarin therapy. This was significant for men, women, and for the group as a whole.

	Bone Density (* significant)	
	Men	Women
+ Coumadin	N=45	N=31
BUA	70.3*	68.1*
Control	N=17	N=17
BUA	82.3	73.6

Disclosures: *K.E. Greenwald, None.*

SA345

See Friday Plenary number F345.

SA346

Serum Levels of 1,25-Dihydroxy Vitamin D in Persons of Norwegian and Pakistani Origin Living in Oslo, Norway: The Oslo Health Study. K. Holvik¹, H.E. Meyer¹, R. Selmer^{*2}, A.J. Søgaard^{*2}, J.A. Falch^{*3}, E. Haug^{*3}. ¹Department of General Practice and Community Medicine, University of Oslo, Oslo, Norway, ²Norwegian Institute of Public Health, Oslo, Norway, ³Center of Endocrinology, Aker University Hospital, Oslo, Norway.

Higher or similar serum levels of the active vitamin D hormone (s-1,25(OH)₂D) in spite of low serum levels of 25-hydroxy vitamin D (s-25(OH)D) have been observed in African American subjects when compared to Caucasians. Also, one study from the US observed elevated s-1,25(OH)₂D levels in vitamin D-deficient Asian Indian immigrants compared to Caucasians, suggesting a compensatory mechanism in the vitamin D endocrine system. We have previously shown that although ethnic Pakistanis living in Oslo had a very high prevalence of secondary hyperparathyroidism (low s-25(OH)D and high serum parathyroid hormone) compared to ethnic Norwegians¹, the two ethnic groups had similar bone turnover² and bone mineral density³. The objective of the present study was to investigate s-1,25(OH)₂D in Norwegians and Pakistanis. We measured s-1,25(OH)₂D, s-25(OH)D and s-PTH in a subgroup of Norwegians and Pakistanis participating in the large cross-sectional Oslo Health Study 2000-2001. We here present results for 560 Norwegian men and women aged 45-60 years and 160 Pakistani men and women aged 30-60 years. Mean (95% CI) s-1,25(OH)₂D was 123.2 (120.4, 126.0) pmol/l in Norwegians and 93.5 (88.2, 98.7) pmol/l in Pakistanis (p<0.0005). Serum levels were similar in men and women within each ethnic group, and they did not vary with age. Adjustment for s-25(OH)D and s-PTH attenuated the ethnic difference although it was still significant with a mean difference of -9.1 (-17.0, -1.2) pmol/l (p=0.024). We conclude that Pakistani men and women living in Oslo have lower s-1,25(OH)₂D levels compared to ethnic Norwegians. This could partly, but not exclusively, be attributable to vitamin D deficiency.

¹ Meyer HE, Falch JA, Søgaard AJ, Haug E (2004) Bone 35:412-417

² Holvik K, Meyer HE, Falch JA, Søgaard AJ, Haug E (2004) JBMR 19;Suppl 1:S167 [abstract]

³ Alver K, Meyer HE, Falch JA, Søgaard AJ (2004) Osteoporosis Int Sep 9 [Epub ahead of print]

Disclosures: *K. Holvik, None.*

SA347

See Friday Plenary number F347.

SA348

A Structural Microsimulation Generates Type I and Type II Osteoporosis from Estrogen Deficiency. D. J. Vanness¹, A. N. A. Tosteson², S. E. Gabriel^{*3}, S. Khosla⁴, L. J. Melton, III⁵. ¹Department of Population Health Sciences, University of Wisconsin Medical School, Madison, WI, USA, ²Department of Medicine and Department of Community and Family Medicine, Dartmouth Medical School, Lebanon, NH, USA, ³Department of Health Sciences Research, Mayo Clinic College of Medicine, Rochester, MN, USA, ⁴Division of Endocrinology, Mayo Clinic College of Medicine, Rochester, MN, USA, ⁵Department of Population Health Sciences, Mayo Clinic College of Medicine, Rochester, MN, USA.

Structural microsimulations (i.e., use of mathematical equations to model the biological processes giving rise to osteoporotic fracture at the individual level) hold potential to be a powerful, theory-based tool for integrating evidence, generating testable hypotheses and evaluating the likely impact of osteoporosis interventions. We have developed a first-generation structural microsimulation in which a bone remodeling process serves both to maintain calcium homeostasis and preserve a constant level of sensed strain. A penalized optimization algorithm varies PTH levels, and consequently rates of excess resorption, to equilibrate supply of and demand for the pool of extracellular calcium. In the simulation, reductions in circulating estrogen at menopause reduce levels of sensed strain, triggering an increase in resorption and an excess supply of extracellular calcium, which in turn induces lower PTH and increased calcium excretion. Resulting changes in bone mass, quality and architecture increase both sensed and actual strain, ultimately resolving the first phase of osteoporosis (type I). In the simulation, long-term suppression of estrogen reduces both gastrointestinal calcium absorption and conversion of vitamin D to its metabolically active forms, thus reducing both the supply of extracellular calcium and promoting excess PTH secretion. The resulting secondary hyperparathyroidism induces a second phase of excess bone resorption that does not resolve over time (type II). Further reductions in bone mass, quality and architecture reduce the bone's work-to-failure, resulting in higher rates of fracture from traumatic loads as simulated by draws from an extreme-value distribution. The next steps in simulation development involve "calibration" of model parameters such that simulated data closely matches both cross-sectional and longitudinal empirical observations and "external validation" through replication of clinical trial data not used in the calibration process. Planned future applications of the simulation include both societal level health program evaluation and decision tools meant to improve the clinical care of individuals at risk of osteoporotic fracture.

Disclosures: *D.J. Vanness, None.*

SA349

See Friday Plenary number F349.

SA350

Heel Bone Ultrasounds and Resorption Markers as Independent Predictors of Non Vertebral Rracture: a Nested Case-Control Study. M. Krieg¹, W. Riesen^{*2}, M. Kraenzlin³, P. Burckhardt¹, J. Cornuz^{*1}. ¹Outpatient Clinic, University Hospital, Lausanne, Switzerland, ²State Hospital, St-Gall, Switzerland, ³Endocrinology, University Hospital, Basel, Switzerland.

It has been shown that heel bone ultrasounds (QUS) and resorption markers (RM) predict osteoporotic fracture independently of hip DXA in elderly women. However, only limited data are available on the combination of QUS and RM as a screening strategy. SEMOF is a multicenter cohort study of risk factors for non vertebral fracture in 7062 Swiss women aged 70 yrs or older, recruited from population-based listings. All the women were assessed by QUS (Sahara, Hologic), and gave a 2nd fasting urine sample for RM. During a mean follow-up of 2.8 years, 349 women reported a hip, forearm, or proximal humerus low trauma fracture. To assess the predictive power of RM, 250 fractured women and 250 controls (matched for age, BMI, center, and follow-up duration) were randomly selected and included in a nested case-control study. Total pyridinolines (PYD) and deoxypyridinoline (DPD) were measured by high performance liquid chromatography, and corrected by creatinine excretion. From the 500 selected women, 406 urine samples were analysable at the end of the study. 38 women were excluded because they were under HRT or antiresorptive therapy. Finally, 368 women (195 cases, 173 controls) were included in this analyse, mean age 76 yrs and BMI 25 kg/m2. Medians of the different variables were used as cutoffs (66 U for Sahara QUI, 73 nmol/mmol Cr for PYD, 13.9 nmol/mmol Cr for DPD). Associations of the variables with incident fractures were expressed as OR (95% CI) by logistic regression. AUC (95% CI) were also calculated in order to compare the power of the different variables. In conclusion, heel bone ultrasound, pyridinolines and deoxypyridinolines predict osteoporotic non vertebral fracture at the same magnitude in elderly women. Combining a resorption marker with a heel QUS measurement improve the prediction of patient at high risk of fracture.

	Low QUI	High PYD	Low QUI +High PYD	Low QUI +High DPD
OR (95% CI)	2.4 (1.6, 3.7)	1.9 (1.3, 2.9)	3.7 (2.1, 6.5)	3.3 (1.8, 5.9)
AUC (95% CI)	0.65 (0.60, 0.71)	0.62 (0.56, 0.68)	0.70 (0.63, 0.77)	0.68 (0.60, 0.76)

Disclosures: *M. Krieg, None.*

SA351

See Friday Plenary number F351.

SA352

Is DXA a Useful Tool for Assessing Skeletal Muscle Mass in Older Women? Z. Chen¹, Z. Wang^{*2}, E. Outwater^{*1}, S. Heymsfield^{*2}, D. Sherrill^{*1}, T. Lohman^{*1}, A. LaCroix^{*3}, S. Nicholas^{*1}, G. Wu^{*1}, N. Wright^{*1}, L. Arendell^{*1}, C. Moll^{*1}, G. Caire^{*1}, D. A. Nelson^{*4}, M. Punyanitya^{*2}, J. Cauley⁵, C. E. Lewis⁶, T. Beck⁷, R. Jackson^{*8}, M. LeBoff^{*9}, T. Bassford^{*1}, S. Going^{*1}.
¹University of Arizona, Tucson, AZ, USA, ²Columbia University, New York, NY, USA, ³Fred Hutchinson Cancer Research Center, Seattle, WA, USA, ⁴Wayne State University, Detroit, MI, USA, ⁵University of Pittsburgh, Pittsburgh, PA, USA, ⁶University of Alabama at Birmingham, Birmingham, AL, USA, ⁷Johns Hopkins University, Baltimore, MD, USA, ⁸Ohio State University, Columbus, OH, USA, ⁹Harvard Medical School, Boston, MA, USA.

Skeletal muscle mass (SMM), especially leg muscle, may have direct impact on risk of fall and fracture. Dual-energy x-ray absorptiometry (DXA) measures both bone mineral density and soft tissues and it has been widely used in osteoporosis screening, management and research. Although a method for predicting SMM by DXA measurements has been developed in a previous study, whether DXA can be used to estimate total body and regional SMM in the elderly remains to be studied. Using SMM measurements from magnetic resonance imaging (MRI) as the gold standard for SMM, we examined the utility of DXA-derived measurements in predicting SMM. Postmenopausal women (N = 39) who were 71.3± 6.1 years old, from an ancillary study of the Women's Health Initiative, had total body scans on both MRI (5x GE Signa, 10 mm per slice and 40 mm between slices) and DXA (Hologic Inc, QDR 4500w). DXA analyses were conducted on total and regional body composition from the whole body scans. MRI scans were analyzed using image analysis software (TomoVision Inc, Montreal, Canada). Linear regression analysis was used to study the linear association between MRI-derived SMM and DXA-derived body composition. We found that DXA-derived lean soft tissue mass was highly correlated with MRI-derived SMM (R² was 0.607, 0.822 and 0.812 for total body, whole leg and upper leg, respectively). Adding age and % body fat from DXA increased R² in the regression models (**Table 1**). In conclusion, DXA-derived body composition measurements are highly correlated with MRI-derived SMM in older women. The DXA measurements and age provide a better prediction for SMM of the leg than of the total body.

Table 1. Regression Models for Predicting MRI-derived SMM

Models	Regression coefficient	SE	P-value	R ²
Total Body				
Lean soft tissue mass (kg)	0.407	0.053	0.000	0.706
Age (year)	-0.173	0.053	0.002	
% Body fat (%)	-0.024	0.051	0.628	
Whole Leg				
Lean soft tissue mass (kg)	0.581	0.038	0.000	0.877
Age (year)	-0.035	0.014	0.016	
% Body fat (%)	-0.019	0.007	0.014	
Upper Leg				
Lean soft tissue mass (kg)	0.611	0.038	0.000	0.890
Age (year)	-0.025	0.010	0.018	
% Body fat (%)	-0.020	0.005	0.001	

Disclosures: **Z. Chen**, None.

SA353

See Friday Plenary number F353.

SA354

Osteoporosis Treatment in the Home Health Care Setting: A Window of Opportunity? J. R. Curtis¹, T. Bryant^{*2}, Y. Kim^{*3}, D. Scott^{*2}, M. Rousculp^{*4}, K. G. Saag¹. ¹Division of Rheumatology, University of Alabama at Birmingham, Birmingham, AL, USA, ²Alacare, Inc., Birmingham, AL, USA, ³Division of Preventive Medicine, University of Alabama at Birmingham, Birmingham, AL, USA, ⁴Eli Lilly & Co., Indianapolis, IN, USA.

Purpose Hospitalized fracture patients commonly receive structured home health services upon discharge. However, patterns and predictors of osteoporosis treatment in home health care settings are largely unknown. **Methods** Electronic medical records of a statewide home health agency (~7000 pts/yr) identified patients at high risk for new fracture based on prior fracture, osteoporosis dx, stroke, or glucocorticoid use. Linked medication data was used to compare use of osteoporosis Rx between groups. **Results** We identified 1742 unique high risk patients referred for home health services during 1/03 - 12/04. Potentially overlapping comorbidities of interest included prior fracture of any type (n = 364), hip fracture (n = 78), glucocorticoid use (n = 961), osteoporosis dx (n = 351), and stroke (n = 289). Patients were 71% female, 88% white, 11% Black, mean ± SD age 77 ± 12 yrs, and 95% Medicare enrollees. One-fourth of individuals had impaired decision-making capacity when referred. Individuals were taking a mean of 13 ± 7 concurrent medications. Home health services were provided for a mean of 84 ± 118 days per episode. Ninety-one percent of services were provided in a private residence; 48% of recipients received >1 episode of home health care. Sixteen percent (16%) died or were discharged to hospice, and 11% were readmitted to the hospital at the end of the episode of care. Rates of non-estrogen prescription osteoporosis Rx and calcium ± Vitamin D supplements are shown (Table) and were different between groups for non-estrogen osteoporosis prescription Rx (p < 0.001), calcium ± Vitamin D (p < 0.001), and the combined endpoint (p < 0.001). **Conclusions** Similar to results from both community and nursing home osteoporosis prevention studies, rates of both prescription and non-prescription osteoporosis treatment in home health care settings were relatively low, even among high

risk patients. In light of potential difficulties in initiating certain osteoporosis treatments in hospitalized patients, home health care may be an appropriate setting to target intervention efforts aimed at improving quality of osteoporosis care for high risk patients.

Comorbidity	N (%)	Non-estrogen	Calcium ±	Prescription Rx or
		Prescription Rx	Vitamin D	Calcium ± Vitamin D
		N (%)	N (%)	N (%)
Hip Fracture	71 (4)	13 (18)	15 (21)	23 (32)
Non-hip Fracture	252 (14)	46 (18)	62 (25)	85 (34)
Glucocorticoid use	871 (49)	184 (21)	167 (19)	271 (31)
Stroke	259 (15)	5 (2)	7 (3)	12 (5)
Any combination of Fracture, Glucocorticoid use, and Stroke	61 (4)	16 (26)	7 (11)	23 (38)
Osteoporosis Dx	228 (13)	113 (50)	86 (38)	145 (64)
All unique patients	1764	346 (20)	323 (18)	514 (29)

Disclosures: **J.R. Curtis**, None.

SA355

Differential Bone Histomorphometric Characters of the Mandible and Femur in Senescence-Accelerated Mice (SAMP6 and SAMP8), Murine Models for Senile Osteoporosis and Temporomandibular Joint Osteoarthritis. T. Matsuura, Y. Daigo^{*}, Y. Goto^{*}, M. Katafuchi^{*}, K. Tokutomi^{*}, T. Tsuzuki^{*}, H. Sato^{*}. Oral Rehabilitation, Fukuoka Dental College, Fukuoka, Japan.

To characterize the potential status of oral bone with senile osteoporosis (OP) and temporomandibular joint osteoarthritis (TMJOA), we performed histomorphometric analysis of the mandible and femur in three strains of senescence-accelerated mice, SAMP6 as a senile OP model, SAMP8 as a TMJOA model, and SAMR1 as a control. A total of 36 male mice at 2 and 4 months of age were used. Six left mandibles and femurs for each strain and age were examined by histomorphometrical analysis. The analysis of the femur was performed in the distal metaphysis for cortical and trabecular bone assessments, while that of the mandible was in the mandibular ramus for cortical bone assessment and in the alveolar bone for trabecular bone assessment. The cortical bone was assessed by cortical thickness index (CTI) and the trabecular bone was assessed by bone area (B.Ar/T.Ar), trabecular width (Tb.Wi), trabecular number (Tb.N), trabecular separation (Tb.Sp), osteoblast perimeter (N.Ob/B.Pm), and osteoclast perimeter (N.Oc/B.Pm). The experimental protocol was approved by the Ethical Committee for Animal Experiments in our institute. Compared with SAMR1, SAMP6 showed smaller values of B.Ar/T.Ar and Tb.Wi in the femur and mandible at 2 months of age. At 4 months of age, this strain kept the smaller values of these indices and furthermore showed smaller value of CTI in the two bones, larger values of Tb.N and Tb.Sp in the femur, and larger value of Tb.Sp in the mandible. On the contrary, SAMP8 showed larger value of CTI in the two bones at 2 months of age and kept them in the mandible but not in the femur at 4 months of age. This strain did not show smaller bone mass in the trabecular bone. Interestingly, SAMP6 exhibited a smaller value of N.Ob/B.Pm in the femur but not in the mandible at 4 months of age, while SAMP8 did show a smaller value of N.Oc/B.Pm in the mandible but not in the femur at 2 and 4 months of age. Collectively, the mandibles of SAMP6 showed osteoporotic features in structure without a decline in osteoblast numbers, while that of SAMP8 did show the thickening of the cortical bone with a decrease in osteoclast numbers. The mandibles in senile OP and before the onset of TMJOA attack appear to show histologic differences from each other, and specific features different from the femur.

Disclosures: **T. Matsuura**, None.

SA356

See Friday Plenary number F356.

SA357

Soluble RANKL Has Detrimental Effects on Cortical and Trabecular Bone Volume, Mineralization and Bone Strength in Mice. Y. Y. Yuan¹, A. G. Lau^{*1}, P. J. Kostenuik², S. Morony², S. Adamu², F. Asuncion², T. A. Bateman¹.
¹Bioengineering Department, Clemson University, Clemson, SC, USA, ²Metabolic Disorders, Amgen Inc., Thousand Oaks, CA, USA.

RANKL is an essential mediator of osteoclast formation, activation and survival. Preclinical studies have shown that RANKL inhibition significantly improves bone density and strength at both cortical and trabecular sites. RANKL inhibitors have also been shown to improve cortical geometry in rodents and primates. Cortical structural and material properties are important determinants of bone strength. We hypothesized that the direct injection of soluble RANKL will cause detrimental effects on bone geometry and density and therefore degrade strength. Ten-week-old C57BL/6J female mice (n=12) were injected twice daily (SC) with human recombinant RANKL (0.4 or 2 mg/kg/day) or vehicle (VEH) for 10 days. Mice treated with high-dose RANKL exhibited significant weight loss (11% vs. VEH, p<0.001) and hypercalcemia. Low dose RANKL did not cause significant hypercalcemia or weight loss. Bone turnover was greatly accelerated by RANKL, as evidenced by 83.8% and 49.2% increases in serum TRAP-5b levels (p<0.05 vs. VEH), 3-4-fold increases in alkaline phosphatase in mice treated with low- and high-dose RANKL, respectively (p<0.001 vs. VEH). Both doses of RANKL caused substantial catabolism of both cortical and trabecular bone. Dry and ash weights were used to determine the % mineral content (%Min) of the femoral diaphysis (cortical bone) and the proximal femoral metaphysis (mixed cortical and trabecular bone). Both doses of RANKL caused significant reductions in %Min at both sites (p<0.05 vs. VEH). MicroCT analysis of the proximal tibial metaphysis revealed a profound loss of trabecular bone in RANKL-treated mice.

Trabecular bone density was reduced by 85% with both doses of RANKL ($p < 0.001$ vs. VEH). Cortical bone geometry and strength were also negatively influenced by RANKL. MicroCT analysis of an 8 mm section of the femoral diaphysis showed that both doses of RANKL significantly reduced cortical bone volume (10-13% vs VEH, $p < 0.001$). Biomechanical testing confirmed that RANKL directly reduces bone strength. Three-point bending of the femoral diaphysis showed that both doses of RANKL caused significant reductions in maximum bending load (19-25% lower than VEH, $p < 0.001$). These data demonstrate for the first time that soluble RANKL administration has direct catabolic effects on both trabecular and cortical bone. These catabolic effects included reductions in bone volume and mineral density, and a significant decrease in bone strength. Inhibition of RANKL is therefore a logical and promising approach for improving cortical and trabecular bone mass and strength.

Disclosures: **Y.Y. Yuan**, Amgen Inc. 2.

SA358

See Friday Plenary number F358.

SA359

Longitudinal Assessment of Bone Architecture in Women - Relation to Hormonal Status, Bone Turnover Markers (BTM) and Fracture Risk. The OFELY Study. **P. Szulc**, **F. Duboeuf***, **E. Sornay-Rendu***, **F. Munoz***, **P. D. Delmas**. INSERM 403, Hopital E. Herriot, Lyon, France.

Longitudinal data on age-related changes in bone architecture in women and their relation to the fracture risk are scarce. We studied age-related changes of bone architecture at the third distal radius measured annually by QDR Hologic 2000 in 535 women aged 31-89 from the OFELY cohort. In 53 women, 71 incident fragility fractures occurred during the follow-up (7.1±2.5 years). Before the menopause, areal bone mineral density (aBMD) and cortical thickness decreased due to centrifugal displacement of the constant amount of bone mineral assessed by cross-sectional area (CSA). After the menopause, decrement in CSA and cortical thinning resulted in the decrease of estimated bending strength despite continuous periosteal expansion. In 72 women, these changes were significantly reduced by the hormone replacement therapy. In postmenopausal women, elevated serum levels of BTM (osteocalcin, β -CTX-I) at baseline were associated with accelerated decrease in CSA and cortical thinning but not with periosteal expansion. Low values of external diameter, CSA, cortical thickness and section modulus were associated with increased risk of incident fracture (O.R. = 1.46 - 1.99 per 1 SD decrease, $p < 0.01$ -0.0001). Bone width and section modulus remained predictive of fractures after adjustment for aBMD (O.R. = 1.63 and 1.74 per 1 SD decrease, respectively, $p < 0.0001$). In summary, our longitudinal data show age-related changes of bone architecture and estimated bending strength at the distal radius that vary according to the hormonal status. Elevated BTM are associated with accelerated bone mineral loss and cortical thinning. Low bone width and section modulus were predictive of incident fractures independently of aBMD.

Disclosures: **P. Szulc**, None.

SA360

See Friday Plenary number F360.

SA361

Latent Hypothyroidism Is Related to Lower Heel QUS in Postmenopausal Japanese Women. **S. Sekiguchi**, **M. Nagata***, **K. Nishiwaki-Yasuda**, **Y. Ono***, **K. Inagaki***, **T. Matsumoto***, **S. Imamura***, **H. Kakizawa***, **N. Hayakawa***, **N. Oda***, **A. Suzuki**, **M. Itoh***. Division of Endocrinology, Fujita Health University, Toyoake Aichi, Japan.

In untreated hypothyroidism, histomorphometric studies have disclosed a decreased bone turnover in both trabecular and cortical bones with an increased cortical thickness. Recent findings suggest that thyroid stimulating hormone (TSH) is a negative regulator of skeletal remodeling by reducing both differentiation of osteoblasts and formation of osteoclasts. In addition, increased fracture risk in untreated hypothyroid patients has been reported to begin up to 8 years before diagnosis. The aim of the present study was to investigate the bone quality by using the heel QUS in the patients with latent hypothyroidism. Subjects were outpatients without any past or present history of thyroid disease. Among 210 postmenopausal women, 23 subjects of 33 patients (Hypo), who had elevated serum TSH level (TSH > 4 μ U/ml) with normal serum free T4 (FT4) levels, agreed to join to this study. We also randomly selected 24 control subjects (Cont) from 176 postmenopausal patients with normal thyroid status. Calcaneus osteo sono assessment indices (OSI) of right feet were measured using the ultrasound bone densitometry AOS-100 (Aloka Co., Japan). Serum TSH levels in Hypo patients (5.31 ± 1.3 μ U/ml) were higher than those in Cont patients (2.05 ± 1.1 μ U/ml), but there was no significant difference of FT4 levels (Cont 1.33 ± 0.15 ng/dl; Hypo 1.19 ± 0.17 ng/dl). OSI in Hypo subjects (Mean \pm SD, 2.138 ± 0.152) were significantly lower than those in Cont subjects (Mean \pm SD, 2.347 ± 0.243) (Student's *t*-test, $p < 0.001$). Simple regression statistical analysis showed that OSI decreased according to the increase of serum TSH level ($R = 0.415$, $n = 47$, $P < 0.037$). In addition, multiple regression analysis showed that serum TSH level more than 4 μ U/ml was associated with the decrease of OSI. These results suggest that latent hypothyroidism affects the structure of bone, resulting in the elevation of fracture risk.

Disclosures: **S. Sekiguchi**, None.

SA362

See Friday Plenary number F362.

SA363

Remodeling Cavities and Stress Risers: A Biomechanical Study on Cancellous Bone Strength. **C. J. Hernandez**, **A. Gupta***, **T. M. Keaveney**. Orthopaedic Biomechanics Laboratory, Department of Mechanical Engineering, University of California, Berkeley, CA, USA.

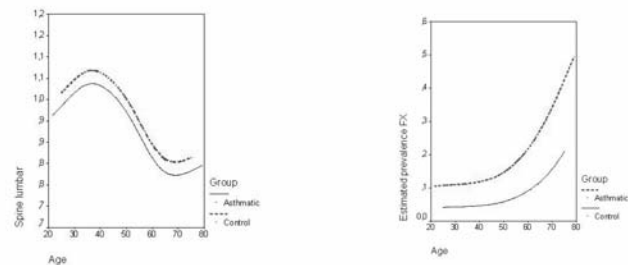
Bone turnover has been implicated as an aspect of bone quality. One proposed mechanism for this effect is the possibility that remodeling cavities can act as stress risers, substantially altering the strength of cancellous bone with only small changes in bone mass. This mechanism does not require disconnection of trabeculae and thus is independent of connectivity. In this study we tested this theory, namely, that geometric effects associated with remodeling cavities can alter cancellous bone strength more than would be expected from the associated loss of bone mass. Cubes of cancellous bone (5mm in each dimension) were derived from micro-computed tomography based images (22 m resolution) of vertebral bone from 10 female and 7 male donors (aged 54-90 years). Remodeling cavities (88 m in depth) were added at random to the cancellous bone surface using an algorithm that prevented trabeculae from being disconnected. Cavities were added until a total of 6% of the initial bone mass was removed. Each image was then converted into a high-resolution finite element model to compute elastic modulus (stiffness) and strength of the cube in compression. These models included both material and geometric non-linearities, and can be considered surrogates for actual biomechanical testing. Results indicated that addition of cavities reduced compressive elastic modulus in each sample by $18.4 \pm 2.6\%$ (mean \pm SD) and strength by $22.2 \pm 4.4\%$. After accounting for differences in bone volume fraction, elastic modulus and strength were typically 11% ($p = 0.10$) and 15% ($p = 0.08$) lower when cavities were present, but these changes did not reach statistical significance. Overall, the changes reported here represent an upper bound on expected effects since the assumed cavity depth was high. These results suggest two possibilities. First, that there is no appreciable stress riser effect - independent of bone mass. Or second, that stress riser effects are manifested either by cavities that occur exclusively in regions of high stress (van der Linden et al. 2001) (as opposed to random placement studied here), or, under more complex apparent loading conditions than studied here. Further study is therefore recommended to elucidate this potentially important aspect of bone quality.

Disclosures: **C.J. Hernandez**, None.

SA364

Inhaled Steroids Decrease Bone Mineral Density and Increase the Risk of Fractures: Data from the GIUMO Study Group. **M. Sosa**, **P. Saavedra***, & the GIUMO Study*. Medicine, University of Las Palmas de GC, Las Palmas de Gran Canaria, Spain.

Background: Although the negative effect of systemic steroids on bone is well documented, there is not clear evidence about the possible adverse effects of inhaled steroids on bone metabolism and fractures. **Design:** Cross-sectional study performed on 105 women suffering from bronchial asthma treated with inhaled steroids and 133 controls. Bone mineral density (BMD) was measured either by quantitative ultrasound (QUS) at the calcaneus or by dual x-ray absorptiometry (DXA) both at the lumbar spine and proximal femur. **Results:** Patients suffering from bronchial asthma showed no statistically significant changes in BMD measured by DXA or QUS compared to controls. However, the age-adjusted mean at the lumbar spine was of borderline significance ($p = 0.098$), being the 96%CI for the difference of means (-0.006 ; 0.067) and the upper bound for the percentage of diminution of 6.8%. A higher prevalence of fractures was found in the group of women with bronchial asthma, with an age-adjusted odds ratio of 2.79 (95% CI = 1.19 ; 6.54). **Conclusions:** Inhaled steroids do not seem to decrease BMD, but they are associated with an increased risk of fracture in women.



Disclosures: **M. Sosa**, None.

SA365

See Friday Plenary number F365.

SA366

The Participation of Endogenous Parathyroid Hormone in Pathogenesis of Glucocorticoid-Induced Osteoporosis. M. Yamauchi¹, T. Yamaguchi¹, S. Yano¹, H. Kajii², K. Chihara^{*2}, T. Sugimoto¹. ¹Department of Endocrinology, Metabolism and Hematological Oncology, Shimane University School of Medicine, Izumo, Japan, ²Division of Endocrinology/Metabolism, Neurology and Hematology/Oncology, Kobe University Graduate School of Medicine, Kobe, Japan.

It is the current recognition that the participation of secondary hyperparathyroidism is minor in the pathogenesis of glucocorticoid (GC)-induced osteoporosis (GIO). However, the role of endogenous PTH in the regulation of bone resorption by GC treatment remains unclear. We examined the effect of endogenous PTH on bone in patients with long-term GC therapy, and also investigated the effects of dexamethasone (Dex) on PTH-induced osteoclast differentiation *in vitro*. One hundred and seventy-four female patients with GC-treatment for more than 6 months were participated in this study (mean: age 47yr, daily dose of prednisolone 10mg, treatment duration 84months). Postmenopausal subjects were ninety. The serum levels of intact PTH and osteocalcin (OC), and urinary level of deoxypyridinoline (DPD) were measured (mean: 35pg/ml, 4.2ng/ml, 6.9nM/nMcr, respectively). BMD measurements were performed by DXA at the lumbar spine, femoral neck and distal one third of radius (mean: 0.857g/cm² [Zscore -0.440], 0.660[-0.387], 0.616[0.662], respectively). We assessed the architectural parameters of cortical bone by pQCT. Forty women had vertebral fractures (VFr). PTH levels exhibited positive correlation with DPD but not OC levels. Endocortical circumference was positively correlated with PTH levels. BMD at any site as well as cortical bone area and cortical thickness had negative correlations with PTH levels. PTH levels were significantly higher in women with VFr than in those without ones. These results suggest some participation of endogenous PTH in GIO. In unfractionated mouse bone cell cultures, Dex increased PTH/PTHrP receptor mRNA expression by Northern blot analysis and PTH-stimulated cAMP accumulation. Moreover, pretreatment with Dex significantly augmented PTH-induced osteoclast differentiation in a concentration-dependent manner. These findings suggest that GC enhances the sensitivity of bone to endogenous PTH, resulting in relatively accelerated bone resorption. In conclusion, our study showed that endogenous PTH was associated with bone resorption marker, BMD values, cortical thinning and the presence of VFr in GC-treated patients, and that GC augmented PTH-stimulated osteoclast differentiation. Our findings suggest that endogenous PTH, although within the normal range, partly participates in the pathogenesis of GIO presumably via acceleration of bone resorption.

Disclosures: **M. Yamauchi**, None.

SA367

See Friday Plenary number F367.

SA368

Importance of Age in Rate of Incident Fractures in Glucocorticoid-Induced Osteoporosis. I. Tanaka, H. Oshima. Department of Laboratory Medicine, Fujita Health University School of Medicine, Toyoake, Japan.

[Objective] It has been appreciated that glucocorticoid causes osteoporosis, however, the correlation between age and incidence of fractures has not been established. In this study, we tried to clarify the importance of age in glucocorticoid-induced osteoporosis. [Subjects & Methods] 165 patients (143 females and 22 males) with connective tissue diseases under glucocorticoid therapy were enrolled in this study. The means of age, daily glucocorticoid dosage (prednisolone equivalent), and total glucocorticoid dosage were 50 years old, 8.3mg/day, and 22.8g, respectively. Bone mineral density (BMD) at the lumbar spine was measured at the baseline and after two years with dual-energy X-ray absorptiometry. [Results] 1) The rates of incident fractures were 23.5% [45-49 years old], 60% [55-59 years], 71.4% [65-69 years], and 100% [75-79 years]. 2) There was no threshold of age that evoked new fractures. 3) The rate of incident fractures in patients over 65 years old was high (more than 60%). 4) In the group of patients over 65 years old, incident fracture was 33% (with daily doses ≤5mg of prednisolone), 50% (BMD≥80%), and 60% (without prevalent fractures). [Conclusion] 1) These results suggested that age was an important risk factor for incident fracture in patients with glucocorticoid-induced osteoporosis. 2) Fracture risk in patients over 65 years old was high, regardless of the lack of other risk factors. 3) Patients over 65 years old with glucocorticoid-induced osteoporosis should be treated for preventing osteoporotic fracture.

Disclosures: **I. Tanaka**, None.

SA369

Bone Mass and Turnover Is Normalized after Successful Treatment of Adult Patients with Endogenous Cushing's Syndrome: A 6-Year Prospective Study. C. Kristo^{*}, R. Jemtland^{*}, T. Ueland^{*}, K. Godang^{*}, J. Bollerslev. Medical Dept., Section of Endocrinology, Rikshospitalet University Hospital, Oslo, Norway.

Endogeneous Cushing's syndrome (CS) is associated with bone loss and an increased risk of fractures. However, the long-term outcome of treatment on bone health has not been adequately clarified. We followed 33 patients with active CS prospectively before and two times after treatment (mean follow-up 33 (n=25) and 71 months (n=18), respectively). The patients were compared to age-, sex-, BMI-matched controls, also followed longitudinally. Bone mineral indices (BMD, BMC, bone area) were evaluated at the lumbar spine (LS),

femoral neck (FN), and total body (TB) by DXA. Biochemical markers of bone turnover were assessed by measuring serum levels of osteocalcin and CTX-1. At baseline BMD at the LS, FN and TB was reduced by 14.8% ($P<0.001$), 15.7% ($P<0.001$), and 9.2% ($P<0.001$), respectively, in CS vs. controls. Serum osteocalcin was markedly reduced ($P=0.014$) and CTX increased ($P=0.012$), without correlation between the markers, indicating uncoupling of bone turnover. At the first follow up, BMD was increased in LS (7.9%, $P<0.001$) and FN (3.5%, $P=0.003$) compared to baseline and a positive correlation between increased BMD and time was demonstrated (LS ($r=0.59$; $P=0.002$) and FN ($r=0.52$; $P=0.007$)). This was paralleled by an increase in osteocalcin (275%, $P<0.001$) and the biochemical markers became correlated ($r=0.92$, $P<0.001$) indicating restoration of coupling. TB which predominantly represents cortical bone did not increase significantly before the second follow-up. At this time point, BMD Z-scores were normalized in all three compartments. In conclusions, these observations demonstrate that uncoupling of bone remodeling most likely explains the serious bone loss in active CS, and that treatment is followed by synchronization of bone remodeling and a successive normalization of bone mass, first evident at predominantly trabecular, later at cortical sites (in the order $LS>FN>TB$).

Disclosures: **C. Kristo**, None.

SA370

See Friday Plenary number F370.

SA371

Serum Osteoprotegerin Levels Are Increased in Patients with Cushing's Syndrome: A Case-Control Study. A. Dovio^{*}, B. Allasino^{*}, M. Ventura^{*}, L. Saba^{*}, M. Terzolo^{*}, A. Angeli. Dept. of Clinical and Biological Sciences, University of Turin, Orbassano-Turin, Italy.

Osteoprotegerin (OPG) plays a key-role in bone, immune and vascular systems. *In vitro*, glucocorticoids inhibit OPG expression in different cell types. *In vivo*, short-term glucocorticoids administration reduces serum OPG concentrations, while long-term glucocorticoid excess is associated with increased levels. Few data are available on serum OPG levels in Cushing's syndrome (CS). The aim of the present study was to assess serum OPG levels in patients with CS and age- and sex-matched controls, and to analyse correlations between serum OPG and clinical and hormonal variables. We studied 38 patients with CS (male/female 17/21, age (median, range) 55, 23-80 years). Twenty-seven of them had an ACTH-dependent syndrome (21 with Cushing's disease, 6 with ectopic ACTH hypersecretion). Eleven had an adrenal-dependent syndrome (9 with adrenal adenoma, 2 with adrenal carcinoma). 38 healthy subjects, mostly blood donors, served as controls (male/female 16/22, age 55, 22-79 years). Serum OPG concentrations were measured by an ELISA developed in our laboratory using commercially available reagents (OPG DuoSet, R&D Systems, Abingdon, UK). Serum OPG levels were higher in CS patients than in controls (1287, 403-4162 vs. 820, 349-2207 pg/ml, $p < 0.001$), and positively correlated with age in controls but not in CS patients. In the overall group of CS patients, OPG levels positively correlated with serum cortisol at 08:00 and 24:00. No significant correlation was found between serum OPG, on the one hand, and disease duration, bone turnover markers and BMD parameters, on the other one. Due to our previous findings that patients with Cushing's disease have BMD values higher than patients with adrenal adenoma, we searched for differences in serum OPG between these groups. Serum OPG levels were higher in Cushing's disease than in adrenal adenoma patients (1387, 827-2479 vs. 1059, 509-1250 pg/ml, $p < 0.02$); notably, the two groups were comparable for age and serum and 24-h urinary cortisol levels, but expectedly differed for ACTH and DHEA-sulphate levels; consistently with previous results, lumbar and femur BMD values were higher in Cushing's disease than in adrenal adenoma patients. In conclusion, OPG levels are increased in CS patients versus age- and sex-matched controls. In CS patients they positively correlate with serum cortisol and are higher in Cushing's disease than in adrenal adenoma patients. Whether this difference is linked to the greater bone loss observed in adrenal adenoma with respect to Cushing's disease patients remains to be elucidated.

Disclosures: **A. Dovio**, Novartis 2; Procter&Gamble 2.

SA372

Primary- and Secondary Prophylaxis to the Use of Systemic Glucocorticoid in Primary Health Care. B. R. Nielsen^{*}, N. R. Jorgensen, P. Schwarz. Osteoporosis Research Unit, Dep. of Clinical Biochemistry 339, Copenhagen University Hospital Hvidovre, Hvidovre, Denmark.

Our knowledge of glucocorticoid (GC) induced osteoporosis has increased significantly during the last years, but little information has been published regarding how primary care physicians handles prophylaxis of the condition. The question is, do GC patients receive primary- and secondary prophylaxis. Questionnaire was sent to all 3.617 family doctors in Denmark. We received responds from 1,000 family doctors, among these 535 questionnaires were evaluable representing 1,265,797 citizens corresponding to 23.4% of the Danish population. *Patients in actual treatment*; 303 (56,6%) of the responding physicians recommended calcium + vitamin D for their patients already in GC treatment without DXA of hip and spine or X-ray of the spine. Among the 303 9.9% recommend calcium + vitamin D from GC dosage > 7.5 mg, 27.1% from dosage 7.5 mg, 34.7% from dosage 5 mg and 28.1% from dosage 2.5 mg. Furthermore, we asked by which length of treatment the doctors gave there recommendation. 21.5% began after 1 month of treatment, 65.0% began after 3 months of treatment, whereas 6.0% began after 6 months. Further, 7.3% did not use length of treatment as parameter for starting prophylaxis. Among the doctors (232, 43,4%) who did not begin primary prophylaxis without DXA or X-ray

investigation, 65.1% made decision and began prophylaxis after DXA-scanning of hip or spine in case T-score was below -1, 78.4% began prophylaxis after DXA with a T-score below -2.5. Finally, 80.6% initiated prophylaxis after X-ray verifying vertebral fracture alone or with or without low T-score. *New patients, expected to start long term treatment of GC:* 23 of 535 (4.3%) doctors took routinely X-ray of the spine. 256 (47.9%) forwarded the patients for DXA of hip and spine. 18 (3.4%) did both investigations, whereas 274 (51.2%) did not perform any evaluation at all. 52 (9.7%) recommend calcium + vitamin D + bisphosphonate from the first GC prescription without DXA of hip and spine or X-ray of the spine, while 483 (90.3%) asked for DXA or X-ray before treatment. 138 (25.8%) began the treatment at a T-score of -1, whereas 303 (56.6%) began at T-score -2.5. Only 282 (52.7%) began treatment although X-ray showed vertebral fracture. In conclusion, our increased knowledge of GC side effects on bone and the increased risk of osteoporosis has not yet increased the use of calcium + vitamin D for primary prophylaxis in GC-induced osteoporosis in primary health care.

Disclosures: **B.R. Nielsen**, None.

SA373

Progesterone Is Rapidly Inactivated in Human Osteoblasts. M. S. Cooper¹, K. Kaur^{*1}, W. Arlt^{*1}, P. M. Stewart^{*1}, M. Hewison¹, M. Quinkler^{*2}. ¹Division of Medical Sciences, University of Birmingham, Birmingham, United Kingdom, ²Department of Clinical Endocrinology, Charite Campus Mitte, Berlin, Germany.

Progestogenic compounds have been proposed as treatments for osteoporosis. Progesterone receptors are expressed in osteoblasts and progestogens have anabolic effects in vitro. Clinical studies however have failed to show bone related effects with most progesterone preparations. The reason for this discrepancy is not known. We hypothesise that pre-receptor progesterone metabolising enzymes have a major impact on progesterone action in bone and have therefore investigated the metabolism of progesterone in primary cultures of human osteoblasts and MG-63 osteosarcoma cells. Primary osteoblasts were generated from trabecular bone obtained from 7 patients undergoing knee replacement surgery. Sub-confluent monolayers were incubated in triplicate for 16h with 4-¹⁴C-progesterone tracer and 50 nM unlabeled progesterone (to mimic luteal phase concentrations). After incubation, steroids were extracted with dichloromethane and two-dimensional thin-layer chromatography (TLC) used for identification. Steroid conversion was measured using a BioRad Molecular Imager. In parallel, RNA was extracted and RT-PCR analysis carried out to identify progesterone metabolizing enzymes. Intensive progesterone metabolism was observed in all primary cultures (up to 40%) with the specific activity being 2.3±0.3 pmol/mg protein/h. The two major products were the inactive 20 α -dihydro-progesterone and 5 α -dihydro-progesterone. Correspondingly, high expression of the enzymes responsible for these reactions, AKR1C1 and 5-reductase type 1, was observed using RT-PCR. The A-ring reduced metabolites, 3 α ,5 α - and 3 β ,5 α -tetrahydro-progesterone and their 20-reduced products were also detected along with mRNA for enzymes catalyzing these reactions; AKR1C2, 3 β -HSD type 1 and hydroxysteroid-epimerase. Whereas expression and activity of most enzymes were similar in osteoblasts from all subjects the expression of 5 α -reductase type 1 varied considerably. Expression of metabolizing enzymes also differed between primary osteoblasts and MG-63 cells. Total progesterone metabolism and the activity of specific pathways were unaffected by pre-incubation with 100 nM dexamethasone or estradiol for 72h. Human osteoblasts rapidly convert progesterone to inactive metabolites at an intracellular level. This effect may explain the lack of anabolism with progestones in vivo and suggests that synthetic progestones that are unable to be inactivated by osteoblasts may be more efficacious.

Disclosures: **M.S. Cooper**, None.

SA374

See Friday Plenary number F374.

SA375

Ovariectomy Decreases Trabecular Bone Mass in T-Lymphocyte Deficient Mice. S. K. Lee¹, Y. Kadono^{*2}, B. Koczon-Jaremk^{*1}, Y. Choi^{*2}, J. A. Lorenzo¹. ¹Endocrinology, University of Connecticut Health Center, Farmington, CT, USA, ²Pathology & Laboratory Medicine, University of Pennsylvania School of Medicine, Philadelphia, PA, USA.

Previous studies failed to demonstrate decreases in femoral bone mass with ovariectomy (OVX) in nude mice, which lack T-lymphocytes because they have a defect in thymic development. We examined OVX-induced bone loss in two T-lymphocyte deficient (TLD) mouse models, nude mice and alpha-beta T-cell receptor null ($\alpha\beta$ T null) mice. All mice were 5-6 weeks at the start of the studies, in a pure C57BL/6 background and examined either at 4 weeks (nude) or 8 weeks ($\alpha\beta$ T null) post- OVX. Bone mass was determined by DEXA, μ -CT and histomorphometry (histo) in sham-operated (SHAM) or OVX mice. Wild type (WT) C57BL/6 mice were controls. In WT and nude mice DEXA demonstrated significant femoral and vertebral OVX-induced bone loss in WT (7-11% P<0.05) but not nudes. However, the effects of OVX on bone mass in nude mice were complex. μ -CT demonstrated that OVX induced a similar loss of trabecular bone mass (TBM) in WT and nude mice (41-45% in femurs and 21-28% in vertebrae, p<0.05 for all). Unexpectedly, OVX had dissimilar effects on femoral cortical bone mass (CBM) in WT and nudes. In WT mice OVX caused a 7% decrease in femoral CBM (p=.05) but had no effect in nudes. Histo confirmed the μ -CT results and demonstrated significant OVX-induced TBM loss in the femurs of both WT and nudes (44-48%, p<0.05) but CBM loss was only seen in WT femurs (22%, P<0.05). Concordantly, osteoclasts (Oc) activity

measured as Oc area in femoral trabecular bone was increased similarly by OVX in both WT and nude femurs (37-57%, p<0.05), suggesting the OVX-induced TBM loss resulted from increased resorption. In WT and T null mice OVX decreased both vertebral and tibial bone mass (5-10%, p<0.05) as measured by DEXA. However, in femurs DEXA measured decreases in bone mass only in WT (p<0.05). By μ -CT, OVX decreased TBM in WT and $\alpha\beta$ T null mice equally (35-37%) in both femurs and tibia (p<0.05 for all). OVX also induced cortical bone loss in the tibias but not femurs of both WT and $\alpha\beta$ T null mice. In additional studies we failed to find differences in the number of T-lymphocytes or cells expressing the cytokine TNF- α in the bone marrow of WT OVX mice compared to WT SHAM. These results demonstrate that both WT and TLD mice lose TBM after OVX. However, unlike WT mice, CBM changes in TLD mice are bone specific and seem resistant to the effects of OVX. This latter effect likely explains the inability of DEXA to detect OVX induced bone loss in the femurs of TLD mice since this assay predominantly measures cortical bone mass. It appears that T-lymphocyte loss has no effect on OVX-induced TBM loss. The effects of OVX on CBM are variable and dependent on the model examined.

Disclosures: **S.K. Lee**, None.

SA376

See Friday Plenary number F376.

SA377

Mechanical Properties of Tibia in High Level Spinal Cord Injured (SCI) Men Are Decreased in Comparison to Low Level SCI. Y. Dionyssiotis^{*1}, G. Trovas², P. Raptou^{*2}, A. Galanos^{*2}, G. Kiniklis^{*2}, K. Petropoulou^{*1}, G. P. Lyritis². ¹2nd Rehabilitation Department National Rehabilitation Center, Athens, Greece, ²Laboratory of Research Musculoskeletal System, Athens, Greece.

The effects of Spinal Cord Injury (SCI) on bone in paralyzed areas are well documented but there are few data regarding the importance of the Level of Injury (LoI) in the decrease of mechanical strength in paralyzed legs. Peripheral quantitative computed tomography (pQCT) permits to assess cortical and trabecular bone density separately and evaluates the geometrical properties of long bones non-invasively. Twenty four men were included in this study: 16 had complete SCI in chronic stage (>1.5 yrs) separated as follows: Group A [eight men, high paraplegia: T4-T7 level, mean age: 26.8 yrs, Duration of Paralysis (DoP): 6.3 yrs] and group B [eight men, low paraplegia: T8-T12 level, mean age: 37 yrs, DoP: 4.3 yrs] in comparison with eight healthy men (group C) of similar age, height, and weight. None of the subjects was given bone acting drugs. All subjects underwent pQCT (STRATEC XCT-3000) of the left tibia. Bone parameters were measured at 4%: Bone Mass Density (BMD) trabecular (BMD trb), BMD total (BMD tot), at 14%: Stress Strain Index (SSI Pol 2), at 38%: BMD cortical (BMD crt), Cortical Thickness (THI crt), Stress Strain Index tibia (SSIPol 3) of the distal end of the tibia and the muscle cross-sectional area (Bone/Muscle Area ratio) was measured at the junction of the proximal third with the middle third of the tibia (at 66% site). Stress-strain index (SSI) parameter obtained multiplying the volumetric cortical density by section modulus, which is derived from the moment of inertia and also takes into account the eccentricity of bone material, was calculated at the 14% and at the 38% site. Results were analyzed with ANOVA. Compared to control (group C) SCI patients had significantly decreased BMD (p-value< 0.0005 for control group vs T4≤LoI≤T7 group and vs T8≤LoI≤T12 group), indicating severe bone loss after injury. Concerning the LoI, SSI difference between 14% and 38% sites (DSSI₂₋₃) was significantly increased in group B (321.41 ± 145.3) in comparison to A (122.76±145.2) (p=0.03). These differences between group A and group B in SSI despite the similarity in BMD maybe attributed to differences in loading. Results indicate that the LoI, possibly through differences in mechanical loading, adversely affect the bone strength in high risk fracture sites of the paralyzed lower extremities like the distal tibia. These findings give to the clinician additional informations about the risk of fracture in SCI patients.

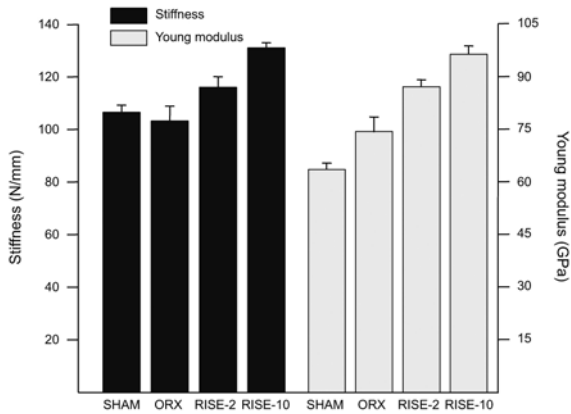
Disclosures: **Y. Dionyssiotis**, None.

SA378

Biomechanical Properties of Bones from Orchidectomized-Rats Treated with Two Doses of Risedronate. G. Mabillean^{*}, G. Brochier^{*}, H. Libouban^{*}, M. Moreau^{*}, E. Legrand, M. F. Baslé^{*}, D. Chappard. Faculté de Médecine, INSERM, EMI 0335-LHEA, Angers, France.

Orchidectomy (ORX) reduces cortical and cancellous bone mass in adult rats by inducing a high turnover in trabecular bone, an increase in cortical porosity and a decrease in periosteal apposition. Bisphosphonates are useful treatments in high turn-over osteoporosis. Risedronate (RISE) is capable of preserving bone mass in the rat following ovariectomy (OVX) or ORX. 48 adult rats were randomized in 4 groups (6 rats/group): SHAM, ORX and ORX treated with a s.c. injection of RISE (2 or 10 μ g/kg/D). Rats were sacrificed at 4 and 16 weeks post-ORX. Radius were dissected and radiographed to measure the outer diameter and the cortical thickness. Biomechanical characteristics were obtained by 3-point bending method. The ulnas of SHAM and RISE-10 rats were reduced in powder to look at the organization of hydroxyapatite crystal networks by electron microscopy. Cortical thickness and radius diameter were strongly influenced by ORX with a decrease of resp. 23.5% and 13.6% at 4w and 26.56% and 6.8% at 16w. RISE-2 or RISE-10 rats had a cortical thickness and radius diameter similar to SHAM rats at 4w. However, at 16w, the 2 μ g dose appeared insufficient to preserve radius diameter at the level of SHAM. At 4w post ORX, stiffness was reduced in ORX and RISE-10 vs SHAM rats.

However, when Young modulus (stiffness corrected by the cross-sectional moment of inertia) was considered, a significantly higher value was obtained in ORX than in SHAM or RISE rats. Ultimate stress was significantly higher for ORX than SHAM and RISE rats. At 16w post-ORX, Young modulus of ORX was higher than SHAM but smaller than RISE rats. RISE-10 rats had a significantly higher modulus than RISE-2 rats and a tendency to a less deformation on 3-point bending. No significant difference of ultimate stress was noted among all groups whereas toughness was significantly higher in ORX than in SHAM or RISE-10. RISE did not influence the organization of the hydroxyapatite crystal networks. OVX induces cortical thinning but does not inhibit bone expansion, thus reducing Young modulus. On the contrary, ORX depress periosteal apposition, reduces cortical thickness and bone diameter leading to an increase in Young modulus. It is likely that morphometric characteristics must be used to derive biomechanical parameters. RISE significantly increases Young modulus.



Stiffness and Young modulus at 16w post ORX

Disclosures: **D. Chappard**, None.

SA379

Osteocyte Density from Iliac Cancellous Bone Biopsy in Males with Idiopathic Osteoporosis. **M. Ciria¹, L. Perez-Edo¹, J. Blanch¹, M. Mariño², S. Serrano², X. Garcia-Miguel³, A. Diez-Perez³, J. Carbonell¹.**
¹Rheumatology, Institut Municipal d'Assistència Sanitària, Barcelona, Spain,
²Pathology, Institut Municipal d'Assistència Sanitària, Barcelona, Spain,
³Internal Medicine, Institut Municipal d'Assistència Sanitària, Barcelona, Spain.

In postmenopausal osteoporotic women with vertebral fractures have fewer osteocytes than controls. This fact may contribute to high bone fragility in this type of osteoporosis. There fore, some studies have that idiopathic male osteoporosis (IMO) is characterized by a decrease of bone formation. This fact could be shown a decrease of osteocytes in cancellous bone biopsy. The purpose of the present study is to examine the density of osteocytes in cancellous bone biopsies of male idiopathic osteoporotic subjects and in age-matched healthy controls. We compare 22 men with densitometric osteoporosis (Hologic QDR 1000, Waltham, Mass) defined as T-score values below -2.5 SD in lumbar spine or in femoral neck, with unknown cause of osteoporosis and normocalciuria. Control group included 14 healthy men. Bone iliac biopsy was done after men informed consent was signed. Sections (5 micrometers thick) of bone biopsy were processed with Goldner's trichrome. The number of osteocyte-occupied lacunae (stained) and empty lacunae (unstained) were selected. The number of total lacunae was obtained by adding both parameters. Results are expressed per bone area (/mm2) and percent osteocyte-occupied lacunae (osteocytes / total lacunae x100). This parameters were examined to < 25 micrometers and > 45 micrometers from the surface to find any difference between the recent and old mineralized bone. Results: Osteocyte density was similar in idiopathic osteoporotic men and in the control group, in new and old mineralized bone. Empty lacunae were higher in osteoporotic cancellous bone biopsy. The difference obtained only marginally significance in the old mineralized bone. Total lacunae density was similar in the two groups. The percent of osteocyte-occupied lacunae was lower in idiopathic male osteoporotic sample. (Table 1). Conclusions: In our sample, idiopathic osteoporotic men showed a increased number of empty lacunae. The osteocyte-occupied lacunae were lower in the older mineralized bone (> 45 micrometers). These facts could be reflecting an accelerated mortality of osteocytes in these patients.

	Osteocytes density		
	Idiopathic masculine osteoporosis	Controls	p
Osteocyte density	132.11 (45.27)	130.95 (39.16)	0.937
Empty lacunae < 25 micras	4.62 (6.16)	2.01 (2.38)	0.14
Empty lacunae > 45 micras	37.7 (23.4)	24.9 (11.3)	0.067
Empty lacunae (total)	42.32 (25.58)	27.3 (11.3)	0.046
Total lacunae density	139.52 (54.89)	128.69 (43.4)	0.54
Osteocyte / total lacunae < 25 micras	88.53 (13.9)	92.45 (9.42)	0.36
Osteocyte / total lacunae >45 micras	73.23 (10.97)	80.21 (7.36)	0.044

Disclosures: **M. Ciria**, None.

SA380

Osteoporosis in Men: Value of Laboratory Testing. **C. S. Ryan^{*}, V. I. Petkov, R. A. Adler.** Endocrinology, McGuire VAMC, Richmond, VA, USA.

Osteoporosis is well recognized in women, but a fracture is often the first sign of bone fragility in men. Studies in women with idiopathic osteoporosis suggest that most laboratory evaluation is unhelpful. However, men are more likely to have underlying, possibly correctable causes. The purpose of this study was to compare the prevalence of risk factors, secondary causes and laboratory abnormalities in men with and without previously known causes for osteoporosis. We reviewed the charts of 160 men with osteoporosis diagnosed by bone mineral density (BMD) testing. Group I (n = 69) were referred without a specific diagnosis, and Group II (n = 91) had a known cause of osteoporosis in the consultation request. In addition to screening chemistries, 25 hydroxyvitamin D, testosterone, LH, FSH, TSH, and spot urinary calcium to creatinine ratio were measured. The two groups were similar in age, BMI, calcium and vitamin D intake, and BMD. In Group I, laboratory evaluation revealed a specific diagnosis in 45%, including hypogonadism (23%), vitamin D deficiency (16%), hypercalciuria (11%), subclinical hyperthyroidism (3%), and hyperparathyroidism (3%). In Group II, 38% of pts with steroid-induced osteoporosis had additional diagnoses discovered. Vitamin D deficiency was previously unrecognized in 20% of patients with a known cause for their osteoporosis. In both groups, risk factors for osteoporosis were commonly found including age >65, smoking, vitamin D insufficiency, and prior fracture. Four or more risk factors existed in over 50% of patients in both groups. Evaluation revealed a specific cause in about half of men with "idiopathic" osteoporosis. Among men who already carried a specific diagnosis, additional causes for osteoporosis were identified. Risk factors were common and multifactorial regardless of a specific cause. Some of these (such as smoking, vitamin D insufficiency) are amenable to treatment. In conclusion, contrary to reports about osteoporosis assessment in women, evaluation of men with osteoporosis will often provide useful information and aid in the management of their bone disease.

Disclosures: **C.S. Ryan**, None.

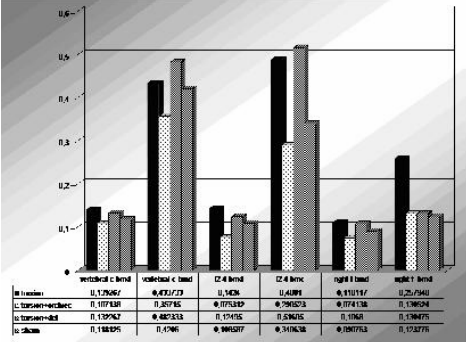
SA381

See Friday Plenary number F381

SA382

Bone Mineral Density and Bone Mineral Content in Rats with Testicular Torsion, Detorsion and Orchiectomy: Preliminary Results. **B. Tander^{*1}, F. Canturk^{*1}, U. Bicakci^{*2}, T. Basoglu^{*3}, B. Tander^{*2}.** ¹Physical Medicine and Rehabilitation, Medical Faculty, Samsun, Turkey, ²Pediatric Surgery, Medical Faculty, Samsun, Turkey, ³Nuclear Medicine, Medical Faculty, Samsun, Turkey.

Male osteoporosis is an increasingly considered problem among the current literature, but its etiologic factors are not clear yet. It is believed that, hypogonadism is an important factor related with osteoporosis. Testicular torsion is one of the leading cause of hypogonadism among the children. Its effect on the development of osteoporosis and bone mineral contents in the adulthood has not been investigated yet. We aimed to evaluate the bone mineral densities (BMD) and bone mineral contents (BMC) of adult rats of which testes were torsioned, detorsioned or removed in their childhood. Thirty-two prepubertal (35 days old) male Wistar albino rats were divided into four groups containing each 8 rats. Group 1 was a sham group and these rats underwent scrotal incision only. In group 2 rats (Torsion group), both testes were torsioned 720 degrees, and they were fixed to the scrotum. In group 3 (Torsion and detorsion group), the testes were detorsioned after 4 days of 720 degrees torsion. Group 4 rats (Torsion and Orchiectomy group) underwent orchiectomy at the 4th day subsequent to 720 degrees of bilateral torsion. Three months after surgery, BMD and BMC of all rats were measured by Dual Energy X-ray Absorptiometry (DEXA) the vertebral column, right femoral neck and lumbar region (L2-L4), then all of the rats were killed. Table 1 shows the values of the BMD and BMC measurements of the study groups. We found the lowest values of BMD and BMC in all regions in rats with torsion and orchiectomy. However, there were no statistically significant difference between the groups. We can preliminary conclude that testicular torsion in the pediatric rats do not seem to affect the BMD and BMC of the vertebral column and femoral neck in the adulthood. Definitive conclusion of this study could not be reported in this presentation due to the lack of, still continuing, histological and biochemical sample evaluation.



Disclosures: **F. Canturk**, None.

SA383

Bone Mineral Density and Bone Markers in Men with Coeliac Disease and Idiopathic Vertebral Fracture. M. W. J. Davie, S. Evans*, D. Powell*, D. Powell*, C. Sharp*, M. Worsfold*. Charles Salt Centre, Robert Jones and Agnes Hunt Hospital, Oswestry, United Kingdom.

Coeliac disease (CD) in men may be associated with osteopenia and secondary hyperparathyroidism, though frequently PTH is within the normal range. Bone turnover has usually been studied in female patients and results have been equivocal. We have studied male patients thus avoiding complications of varying estradiol status. We measured bone markers and bone density (BMD) in 43 men with CD, 43 with untreated idiopathic vertebral osteoporosis (IVF) and 37 healthy men (normals), all matched for age (range 30-79yr). BMD was measured by Hologic QDR4500A at L2-4, femoral neck and whole body (WBBMD) and serum bone-specific alkaline phosphatase (BSAP), iPINP and CrossLaps (CTx), and urine NTx/Cr by commercial assays. Comparisons (paired) and correlations were assessed by nonparametric methods. Studies were passed by the local ethics committee. In men with CD, BSAP (+44%, p<0.01) and iPINP (+35%, p=0.09) were raised compared with normals, and BSAP was 25% higher than in IVF (p<0.01). BSAP in IVF was 15% higher than in normals (p=0.06). Compared with normals serum CTx was elevated in patients with IVF (p<0.05) but not with CD. NTx/Cr and iPINP were not raised in either IVF or CD. CD patients had lower BMD than normals (WBBMD = -9.2% p<0.01) but BMD at all sites was lowest in IVF (WBBMD = -12.8%, p<0.01 vs normals; and p<0.05 vs CD). In normals NTx/Cr and CTx (r=0.79) and iPINP and NTx/Cr (r=0.47) were correlated, but iPINP and BSAP were not correlated. In CD and IVF, in contrast, iPINP correlated with BSAP (r=0.71 and r=0.64 respectively). NTx/Cr was not associated with CTx in either disease group. No bone marker correlated with BMD in normals. Correlations between bone markers and BMD were seen only in CD and in IVF. In CD patients BMD L2-4 correlated with iPINP (r= -0.436), and IVF subjects showed correlations between CTx and WBBMD (r=-0.49) and femoral neck (r=-0.43). No association between markers and BMD was seen in normals. BSAP and probably iPINP are raised more in CD than in IVF, despite a smaller loss of bone density. In contrast, in IVF only CTx is raised. This contrasting pattern suggests a different bone disease process in CD, consistent with an osteomalacia-like mechanism related to calcium malabsorption. Measurement of several markers may be valuable in the investigation of low BMD in an individual patient.

Disclosures: *M.W.J. Davie, None.*

SA384

Estrogen as a Determinant of Femoral Neck Bone Strength in Elderly Men. S. J. A. G. Goemaere¹, H. Zmierzczak*¹, I. Vanpottelbergh*¹, K. Toye*¹, D. Debaecker*², T. J. Beck³, J. Kaufman¹. ¹Unit for Osteoporosis and Metabolic Bone Disease, Ghent University Hospital, Ghent, Belgium, ²Department of Public Health, Ghent University Hospital, Ghent, Belgium, ³Department of Radiology, John Hopkins University, Baltimore, MD, USA.

Bone geometry is a determinant of fracture risk. How changing bone geometry contributes to age-related increase in fracture risk is less well explained. We investigated the role of sex-steroids in elderly men. Elderly men from a population list of a Flemish town were invited to participate in a longitudinal study on aging and bone loss after obtaining informed consent. Subjects with diseases or medications affecting the bone status were excluded. The present analysis pertains to DXA at the hip (Hologic QDR1000+) at start and after 4 years. BMD and geometry at the narrow neck were evaluated by using the hip structural analysis (HSA) software. The following parameters (and their %CV) were obtained: BMD (3.2%), Cross Sectional Area (CSA;3.2%), Width (W;1.9%), Endocortical Diameter (End Cort;2.1%), Average Cortical Thickness (AvgCortex;3.5%), Cross Sectional Moment of Inertia (CSMI; 4.9%), Section Modulus (Sect Mod; 4.3%) and the Buckling Ratio (BR; 5.2%). Fasting serum samples were obtained at baseline for total and bio-available testosterone (T), estradiol (E₂) and SHBG levels. Statistical significant differences are indicated by * p<0.05 or ** p<0.01. From the 269 participants 147 follow-up data were obtained. Age was 76.0y ± 4.2 and BMI was 26.1 kg/m² ± 3.6. In cross-sectional analysis for bioT and (bio)E₂ significant positive correlations were observed with BMD, CSA, Sect Mod and AvgCortex and negative correlations with W, End Cort and BR; no associations with CSMI were observed. Longitudinal data provided significant mean decreases of BMD (-0.6%) and AvgCortex (-0.7%); and significant increases of CSMI (+1.3%), W (+1.0%), End Cort (+1.1%) and BR (1.8%). No significant changes over 4 years were observed for CSA and Sect Mod. The associations between sex-steroids and longitudinal parameters are listed in the table below (age and BMI adjusted pearson correlations). SHBG was not associated with the any of the bone geometry parameters.

	T	BioT	E ₂	BioE ₂
%Δ BMD	0.13	0.01	0.22**	0.13
%Δ CSA	0.07	-0.04	0.17*	0.10
%Δ W	-0.11	-0.07	-0.10	-0.07
%Δ Sect Mod	-0.01	-0.08	0.21**	0.17*
%Δ End Dia	-0.12	-0.07	-0.12	-0.08
%Δ AvgCortex	0.12	-0.01	0.21**	0.13
%Δ BR	-0.14	-0.03	-0.22**	-0.14

The present longitudinal study provides evidence suggesting a predominant contribution of E₂ compared to T, for the maintenance of the biomechanical competence at the femoral neck in elderly men.

Disclosures: *S.J.A.G. Goemaere, None.*

SA385

A Novel Relationship between Estrogen and Leptin Levels in Men with Idiopathic Osteoporosis. E. S. Kurland¹, A. Peck*¹, D. J. McMahon¹, J. P. Bilezikian². ¹Department of Medicine, Columbia University, New York, NY, USA, ²Department of Medicine and Pharmacology, Columbia University, New York, NY, USA.

Idiopathic osteoporosis in men (IO) is a disorder of low bone formation. We have previously reported low E2 and lower BMI in a cohort of 44 men with IO (PT) compared with healthy controls (CO). Evidence linking bone mass, body weight and gonadal steroid regulation to the common pathway of the adipocyte hormone leptin prompted us to measure leptin levels in our PT. Plasma collected after an overnight fast for 30/44 PT and 41/44 CO was analyzed for leptin with values of 6.4 ± 0.9 and 5.4 ± 0.4 ng/mL in PT and CO, respectively (NS). Pearson correlation coefficients between leptin and BMI, T, BioT, E2, BioE2, SHBG, and IGF-I, revealed positive correlation between leptin and BMI in PT and CO respectively (r= 0.7 and 0.5; p <0.0001 and <0.01). An inverse correlation was noted for leptin and E2 or BioE2 in PT only (r= -0.4, p< 0.05; r in CO = -0.03, p = NS) with a trend to significance for the difference in r-value between PT and CO (p =0.08). To examine the effect of either E2 or BMI on difference in leptin between groups, we created tertiles of each variable, and then compared leptin levels between PT and CO by tertile of the ranked variable. Mean BMI tertiles were: 21.5 (range 16-23.3), 24.7 (23.6-25.6) and 27.8 (25.7-32.2) kg/m² for 1st, 2nd and 3rd tertiles, respectively. E2 tertiles were 16.3 (range 9.1-20.2), 22.8 (20.6-25), and 29.8 (25.3-47.4) pg/mL for 1st, 2nd and 3rd tertiles, respectively. Leptin values, in ng/mL ranked by E2 tertile were as follows:

	1 st tertile	2 nd tertile	3 rd tertile
#PT/CO	14/ 9	8/ 15	8/ 17
Leptin ng/mL PT	8.3 ± 1.7	6.2 ± 1.8	4.7 ± 0.9
Leptin ng/mL CO	5.8 ± 0.9	5.5 ± 0.6	5.1 ± 0.8

Leptin values, in ng/mL ranked by BMI tertile were 3.4 ± 0.5, 7.5 ± 1.5 and 10.3 ± 2.0 for PT compared with 3.4 ± 0.5, 5.5 ± 0.5, and 6.4 ± 0.9 for CO. Using ANOVA to test whether leptin differed between groups when ranked for E2 and controlling for BMI revealed a significant difference between groups (p< 0.01). In specific, the lowest E2 tertile of patients had a significantly higher leptin level than any of the 3 tertiles of CO (p <0.05 for all comparisons). In contrast, when ranked by BMI, groups do not differ significantly for leptin levels with or without controlling for E2 (p= NS). In summary, men with IO have higher leptin levels than controls when ranked by E2 tertiles, with leptin levels decreasing with increasing levels of E2. These data provide new insights into the relationship between leptin and estradiol in IO, a model of low bone formation.

Disclosures: *J.P. Bilezikian, None.*

SA386

Osteoblastic and Osteocytic Cells Express the Rate-Limiting Enzyme for Serotonin Synthesis and Contain Measurable Serotonin Content. M. M. Bliziotis¹, J. Hashimoto*², X. Zhang², A. Eshleman*³, K. Wiren⁴. ¹Medicine, Oregon Health and Science University/Portland VAMC, Portland, OR, USA, ²Behavioral Neurosciences, Oregon Health and Science University, Portland, OR, USA, ³Psychiatry, Oregon Health and Science University/Portland VAMC, Portland, OR, USA, ⁴Behavioral Neurosciences and Medicine, Oregon Health and Science University/Portland VAMC, Portland, OR, USA.

Neurotransmitter regulation of bone physiology is manifested by the osteopenic phenotype seen in serotonin transporter knockout mice. The serotonin transporter and serotonin receptors have been identified in both osteoblasts and osteocytes. The origin of the serotonin ligand that binds to cognate receptors and transporters in bone cells is unknown. Serotonergic nerves have not been identified in bone. Bone cells could synthesize serotonin, making the ligand effects autocrine/paracrine in nature. We investigated this hypothesis by 1) assessing expression of the initial and rate limiting enzyme in serotonin synthesis, tryptophan hydroxylase (TPH), and 2) measurement of serotonin content in osteoblastic and osteocytic cells. To assess TPH expression in bone cells, we performed semiquantitative RT-PCR using primers for the TPH1 isoenzyme (expressed in non-brain tissues such as gut, spleen and thymus). PCR was carried out for 40 cycles. We analyzed osteoblastic (ROS 17/2.8, MC3T3-E1, UMR 106) and osteocytic (MLO-Y4) cells; B14 rat medullary raphe cells and COS-7 cells were positive and negative controls, respectively. All osteocytic and osteoblastic cells lines analyzed express mRNA for TPH1, and thus have the capability for serotonin synthesis. No amplified products were observed in COS-7 cells, which do not have detectable TPH enzyme activity. TPH protein expression was evaluated with immunoblots using an antibody against recombinant rabbit tryptophan hydroxylase. ROS 17/2.8 and MLO-Y4 cells showed the expected 55 kDa band, while COS-7 cells did not. We next analyzed serotonin content from the same cells with an ELISA assay (Research Diagnostics, Inc.). Analysis was carried out on cell pellets from subconfluent cultures of B14, MLO-Y4, and MC3T3-E1 cells grown in serum free medium for 24 (n=3) or 72 (n=2) hours. The B14 cells contain approximately 50-100 pg serotonin per mg protein. In concert with our findings from the PCR studies of TPH1 expression, the MC3T3 cell line also contained serotonin at levels that exceeded the B14 cells. MLO-Y4 cells showed serotonin content roughly equal to B14 cells, and COS-7 cells had no detectable serotonin. We conclude that osteoblasts and osteocytes are capable of serotonin synthesis, and thus may produce paracrine/autocrine effects through this neurotransmitter on bone cells.

Disclosures: *M.M. Bliziotis, None.*

SA387

See Friday Plenary number F387.

SA388

Osteoprotegerin Gene Expression in the Liver of Patients with Primary Biliary Cirrhosis. Lack of Association with Elevated Circulating Levels. A. Enjuanes^{*1}, N. Guanabens¹, L. Alvarez¹, L. Caballeria^{*2}, M. Martinez de Osaba^{*1}, P. Peris¹, A. Monegal^{*1}, A. Pares^{*2}. ¹Metabolic Bone Diseases Unit, Hospital Clinic, IDIBAPS, Barcelona, Spain, ²Liver Unit, Hospital Clinic, IDIBAPS, Barcelona, Spain.

Osteoprotegerin (OPG), a decoy receptor of the nuclear factor kappa B ligand (RANKL), regulates bone resorption by preventing RANK and RANKL binding. OPG is produced by numerous cell types and a variety of tissues and their expression pattern targets three main biological systems: the osteoarticular, immune and vascular systems. In a previous study we have described high serum OPG levels in patients with primary biliary cirrhosis (PBC), which were associated with the severity of liver damage and unrelated to bone remodeling or osteoporosis. The aim of this study has been to assess if the OPG mRNA gene expression in the liver correlates with serum levels of OPG and with the severity of liver disease. Circulating OPG levels were measured by ELISA in sera from 58 patients with PBC and in a control group of 20 healthy females. Total RNA was prepared from 15 human liver samples (4 normal and 11 PBC), and reverse transcription reaction was performed using 1 µg of total RNA. In a first step, PCR reactions for OPG, tyrosine aminotransferase (TAT) and β-actin was performed in all samples. TAT was used as a hepatocyte phenotype control and β-actin as gene expression control. cDNA obtained from cultured human primary osteoblasts was used as a positive control of OPG expression and osteocalcin gene expression was used to show osteoblast phenotype. In a second step, transcript levels of osteoprotegerin were evaluated by Real-Time PCR. Results were expressed as OPG versus β-actin expression (OPG relative gene expression). Serum OPG levels were significantly higher in PBC (5.5 ± 0.2 pM/l) than in controls (2.9 ± 0.2 pM/l, $p < 0.0001$). Circulating OPG was associated with the severity of liver disease defined by higher bilirubin levels (< 1.2 mg/dl) (6.6 ± 0.6 vs 5.2 ± 0.2 pM/l, $p = 0.02$) and by the Mayo score above 4 (5.9 ± 0.3 vs 4.9 ± 0.2 pM/l, $p = 0.02$). OPG transcripts were observed in all normal and PBC liver samples. No significant differences in the quantitative OPG gene expression was observed between patients (1.9 ± 0.2) and controls (2.3 ± 0.2). In these 11 PBC patients the OPG serum levels were significantly higher (5.4 ± 0.2 pM/l) than in controls ($p < 0.001$). No correlation was found between circulating OPG and their respective transcripts in the liver of PBC patients. In conclusion, the high circulating OPG levels observed in patients with PBC are associated with the severity of liver disease, but not with their gene expression in the liver.

Disclosures: *N. Guanabens, Novartis 5.*

SA389

See Friday Plenary number F389.

SA390

Bone Mineral Density Changes and Bone Turnover in Thyroid Carcinoma Patients Treated with Supraphysiologic Doses of Thyroxine. I. Karner^{*1}, S. Sijanovic^{*2}, Z. Hrgovic^{*3}, D. Bucovic^{*4}, A. Klobucar^{*5}, K. Usadel^{*6}, W. J. Fassbender⁷. ¹Dept. of Gynaecology and Obstetrics, Clinical Hospital Osijek, Osijek, Croatia, ²Dept. of Nuclear Medicine, Radiation Protection and Pathophysiology, Clinical Hospital Osijek, Osijek, Croatia, ³Institute for Medical Research and Occupational Health, Zagreb, Croatia, ⁴Department of Gynaecology and Obstetrics, Clinical Hospital Osijek, Osijek, Croatia, ⁵Dept. of Gynaecology and Obstetrics, General Hospital Sveti Duh, Zagreb, Croatia, ⁶Endokrinologikum Frankfurt, Frankfurt am Main, Germany, ⁷Dept. of Internal Medicine, Hospital zum Hl. Geist Kempen, Kempen/Ndrh., Germany.

The aim of this one-year prospective study was to determine whether longterm thyroxine treatment is a risk factor for elevated bone turnover, loss of bone mass and subsequent development of osteoporosis. Premenopausal women (N=19), and men (N=9) suffering from differentiated thyroid gland carcinoma in the mean age of 39.0 ± 8.0 years and 41.8 ± 10.0 years were investigated. All of them had undergone a total thyroidectomy and subsequent thyroxine therapy. The duration of the TSH-suppressive therapy prior to the beginning of our study was 9.4 ± 6.4 years in the female and 8.1 ± 6.0 years in the male group. The prospective observation was performed by dual X-ray absorptiometry (DXA) at the spine and the femoral neck and by single-photon absorptiometry (SPA) at the distal radius. Laboratory testings included thyroid hormones T3, T4 and TSH, serum calcium, phosphate and PTH, and urinary calcium and phosphate from spontaneous and 24-hour urine samples. Markers of bone formation (osteocalcin, alkaline phosphatase and PICP) and resorption (Ca/Cr and ICTP) were determined. Statistically significant loss of bone mass was observed only on the distal radius in males ($p < 0.05$). At the lumbar spine and femoral neck, only a minor bone loss was registered in a small number of patients. Almost 50 % of the females showed values above the reference range. In more than 30 % of the females, and smaller number of male patients, ICTP values ranged above the reference range, corresponding to elevated bone turnover. These two variables exhibited a slight correlation with bone density at the measured skeletal areas, mostly considering the male group. The results are a proof that accelerated bone turnover and subsequent bone loss occurs during TSH-suppressive thyroxine therapy. In future prospective studies a

prolonged time of observation will be necessary, as well as to increase the number of studied patients, in order to better assess the relative risk of osteoporosis in patients undergoing TSH-suppressive treatment more precisely.

Disclosures: *W.J. Fassbender, None.*

SA391

See Friday Plenary number F391.

SA392

Lumbar BMD as the Major Factor Determining Increased Prevalence of Vertebral Fractures in Monoclonal Gammopathy of Undetermined Significance (MGUS). J. Pepe^{*1}, M. T. Petrucci^{*2}, I. Nofroni^{*3}, D. Diacinti^{*1}, S. Piemonte^{*1}, E. Romagnoli^{*1}, E. D'Erasmo^{*1}, S. Minisola¹. ¹Dpt of Clinical Sciences, University of Rome, Rome, Italy, ²Dpt of Haematology, University of Rome, Rome, Italy, ³Dpt of Experimental Medicine and Clinical Pathology, University of Rome, Rome, Italy.

This study was carried out to investigate the relative contribution of bone mass and turnover to the skeletal fragility reported in MGUS patients. We studied 65 consecutive postmenopausal MGUS patients attending our Institution for routine follow-up; they were divided on the basis of the presence or absence of at least one mild vertebral fracture. Patients with fractures (Fx, n=34) were significantly older (62.8 ± 6.0 yrs), with long-standing disease (8.8 ± 7.1 yrs) in respect to MGUS patients without fractures (NFx, n=31; 59.7 ± 5.0 yrs, $p < 0.05$ and 5.8 ± 4.1 yrs, $p < 0.05$, respectively). Lumbar spine (L = 0.811 ± 0.14 g/cm² vs 0.956 ± 0.12), femoral neck (0.660 ± 0.09 vs 0.747 ± 0.10) and total femoral BMD (0.788 ± 0.11 vs 0.884 ± 0.11) were significantly lower (all $p < 0.001$) in Fx-MGUS compared to NFx. Mean serum osteocalcin levels were lower (6.70 ± 2.5 ng/mL vs 7.3 ± 3.0) and mean serum β-CTX levels were higher (0.92 ± 0.32 ng/mL vs 0.76 ± 0.38) in Fx compared to NFx, albeit these differences did not reach statistical significance. However, the RANKL/OPG ratio was significantly higher in Fx compared to NFx (0.092 ± 0.018 vs 0.082 ± 0.020 ; $p < 0.05$). ROC curves analysis identified L-BMD as the variable that predicted vertebral fracture (area under the curve 0.817; C.I. 0.713-0.921), better than other parameters (age, years since diagnosis, monoclonal component, biochemical parameters, BMD measurements of the hip). At the value of L-BMD of 0.900 g/cm², the sensitivity was 76.5 % and the specificity 63.3%; considering the prevalence (52 %) of vertebral fractures in our patients, the positive predictive value was 70.3% and the negative predictive value was 70.4%. Corresponding figures for a cut off of 0.850 g/cm² were: 67.6, 80.0, 79.3, and 68.6%. Our investigation emphasizes the role L-BMD measurement as the most important surrogate for predicting axial strength in MGUS patients. The skeletal fragility might be favored by the uncoupling of the two processes of bone remodeling, as revealed by the high OPG/RANKL ratio of patients with fractures.

Disclosures: *S. Minisola, None.*

SA393

See Friday Plenary number F393.

SA394

Surface Specific Effects of Thiazolidinedione Darglitazone on Bone in Mice. M. Li, Y. Li*, H. A. Simmons, D. R. Healy*, B. Robinson*, L. C. Pan, H. Z. Ke, T. A. Brown. Cardiovascular and Metabolic Diseases, Pfizer Global Research and Development, Groton, CT, USA.

It has been hypothesized that a class of thiazolidinedione drugs (TZD), which are used for treatment of Type 2 diabetics, can increase adipogenesis at the expense of osteogenesis, leading to bone loss. However, the reported skeletal effects of rosiglitazone and troglitazone are varied and their effect on cortical bone is unknown. In this study, we examined the changes in both cancellous and cortical bone of 8-month-old male mice treated with darglitazone (Darg) at 10 mg/kg/d by dosing the compound in a food admixture for 8 weeks. Histomorphometric measurements of lumbar vertebral body, a cancellous bone site, showed a significant decrease in trabecular volume (-25%), number (-13%) and thickness (-13%), and an increase in trabecular separation (+23%) in the mice treated with Darg compared with controls. In addition, mineralizing surface and tissue-volume based bone formation rate were significantly lower, whereas osteoclast surface and number were significantly higher in Darg-treated mice. Furthermore, percent fat area and number of fat cells in bone marrow were significantly increased by 1339% and 457%, respectively, in Darg-treated mice. These data indicated that Darg enhanced adipogenesis and bone resorption and suppressed bone formation in lumbar vertebral cancellous bone in mice. To assess the effects of Darg on cortical bone, pQCT and histomorphometric analyses were performed on the femoral diaphysis. The mice treated with Darg had a significant decrease in total bone content (-10%), total bone density (-10%) and cortical thickness (-8%) and an increase in endocortical circumference (+5%) accompanied with an unchanged periosteal circumference and total bone area. Consistent with pQCT data, histomorphometric measurement showed a decrease in cortical bone area (-11%) and an increase in marrow area (+13%) with unchanged total tissue area. These data indicated that Darg caused bone loss on the endocortical surface that is adjacent to bone marrow. Interestingly, periosteal mineralizing surface, mineral apposition rate and bone formation rate were significantly increased by 32%, 23%, and 55%, respectively, in Darg-treated mice compared with controls. It is unclear whether the increased periosteal bone formation is compensatory or a direct effect of Darg. In summary, Darg, like the TZD rosiglitazone,

caused cancellous bone loss by increasing bone resorption and decreasing bone formation. Our data for the first time showed that Darg induced cortical bone loss on the endocortical surface but increased bone formation on the periosteal surface. These data reveal surface specific effects of the TZD Darg on bone.

Disclosures: **M. Li**, Pfizer Inc. 3.

SA395

See Friday Plenary number F395.

SA396

Parathyroid Hormone-Related Peptide Is a Candidate Stomach-Derived ECL-Cell Hormone. **N. Andersson¹, S. Movérare Skrtić¹, R. Håkanson², C. Ohlsson¹.** ¹Center for Bone Research at the Sahlgrenska Academy, Department of Internal Medicine, Gothenburg University, Gothenburg, Sweden, ²Department of Experimental Medical Science, Division of Cellular and Molecular Pharmacology, Lund University, Lund, Sweden.

A large part of all endocrine cells in the body are located within the gastrointestinal tract and it is suggested that endocrine signals from the stomach are of importance for the regulation of bone mass, supported by that gastrectomy (Gx) results in bone loss. The mechanism behind the Gx-evoked bone loss is unknown. We and others have demonstrated that the Gx-evoked bone loss reflects the lack of a factor expressed in the fundus part of the stomach. The existence of an osteotropic hormone (referred to as gastrocalcitonin) in the ECL cells of the gastric mucosa has been suggested. The aim of the study was to obtain a gene expression fingerprint of the gastric ECL cells in order to identify the anticipated ECL-cell hormone. Global gene (45.167 genes/probe sets) expression analysis of mouse stomach was performed in order to identify the ECL-cell peptide/protein. Specific functional activation of the ECL cell population (omeprazole-induced hypergastrinaemia) was used as a tool to generate a specific gene expression fingerprint of the ECL cells. The proposed fingerprint includes 14 genes, among them six known to be expressed by ECL cells (= positive controls), and some novel ones, which are likely to be ECL-cell-related. The known ECL-cell-related genes are those encoding histidine decarboxylase, chromogranin A and B, vesicular monoamine transporter 2, synaptophysin and the cholecystokinin-B receptor. In addition, the fingerprint included five genes, which might be peptide hormones or involved in the process of secretion. Interestingly, parathyroid hormone-related peptide (*PTHrP*) was identified as a candidate ECL-cell peptide hormone. *PTHrP* is of particular interest as a candidate ECL-cell hormone as it is (i) induced by gastrin (ii) a recognized peptide hormone, (iii) known to regulate Ca²⁺ homeostasis and bone mass and (iv) expressed by gastric endocrine tumours. The origin and the physiological role of circulating *PTHrP* in healthy adult individuals are unknown. We propose that *PTHrP* is secreted by the ECL cells in the stomach in response to gastrin and that it contributes to the regulation of calcium deposition in bone and the maintenance of normal bone mass (by securing appropriate calcium deposition into bone). However, additional studies are required to determine if *PTHrP* is the osteotropic hormone (gastrocalcitonin) thought to be produced in the gastric ECL cells.

Disclosures: **N. Andersson**, None.

SA397

See Friday Plenary number F397.

SA398

Radiation Affects the Micro-Architecture of Bone. **S. A. Hamilton^{*1}, M. J. Pecaut^{*2}, D. S. Gridley^{*2}, A. Obenaus^{*2}, T. A. Bateman¹.** ¹Department of Bioengineering, Clemson University, Clemson, SC, USA, ²Department of Radiation Medicine, Loma Linda University and Medical Center, Loma Linda, CA, USA.

According to the National Institutes of Health about one half of cancer patients receive radiation therapy. Radiation therapy uses ionizing radiation to kill cancer cells and shrink tumors. While precautions are taken to prevent damage to adjacent cells, radiation therapy still damages healthy cells. As advances in treatment increase the length of post-treatment survival, understanding any secondary effects of treatment is progressively more important. For example, presence of two key cytokines for bone metabolism, interleukin-1 beta and tumor necrosis factor alpha, have been shown to be elevated by proton radiation in pediatric patients undergoing radiation for brain tumors. It is hypothesized that expression of these cytokines by therapeutic radiation, gamma and proton, will activate osteoclastic bone resorption and cause a deficit in bone microarchitecture. Female C57BL/6 mice ten weeks of age were irradiated with proton (n=10) and gamma rays (n=10) (2 Gray (Gy)) and sacrificed 110 days post-exposure. The proximal tibia was analyzed using microcomputed tomography (MicroCT- Scanco USA). Results indicated significant losses in trabecular density and connectivity for both proton and gamma sources. The 2 Gy gamma group had a significantly lower trabecular density of 33% (p = 0.02) and connectivity density of 65% (p = 0.03) than the control group (n=10). The 2 Gy proton group also had a significantly higher trabecular density of 42% (p = 0.01) and connectivity density of 70% (p = 0.02) than the control group. The loss of trabecular connectivity results in a decrease of loading in the struts. These data demonstrate that bone loss and eventually osteoporosis may be a secondary effect of radiation therapy for cancer treatment, and needs to be considered as survival rates continue to improve. This finding could be particularly critical for younger

patients as peak bone mass is achieved by age thirty. If radiation therapy is given during this time period, it is feasible that peak bone mass could be adversely affected which may yield a higher susceptibility to osteoporosis and therefore a greater fracture risk.

Disclosures: **S.A. Hamilton**, None.

SA399

See Friday Plenary number F399.

SA400

Comparison of Lumbar Bone Mineral Density in Korean Women with or without Metabolic Syndrome. **S. K. Lee¹, H. W. Baik^{*2}, K. H. Lee^{*2}, J. Y. Kim^{*2}, H. J. Kim^{*3}, K. J. Ahn^{*3}, K. S. Park^{*3}.** ¹Biochemistry/Internal Medicine, Eulji University School of Medicine, Daejeon, Republic of Korea, ²Biochemistry, Eulji University School of Medicine, Daejeon, Republic of Korea, ³Internal Medicine, Eulji University School of Medicine, Daejeon, Republic of Korea.

Various studies have shown that higher body mass index (BMI) is a protective factor for bone mineral density (BMD), but there is a race-dependent effect of BMI on BMD. The metabolic syndrome encompasses a set of central obesity, insulin resistance, hypertension, high triglycerides and low HDL-cholesterol and several abnormalities. Little is known about the association between metabolic syndrome and BMD. In this cross-sectional study, we investigated the associations of metabolic syndrome, serum fasting insulin level, homeostasis model assessment-insulin resistance (HOMA-IR), and lumbar BMD in healthy, pre-menopausal (n=50; 43±7 years) and post-menopausal (n=58; 60±6 years) women with normal BMD or osteopenic or osteoporotic but otherwise normal, visiting Eulji University Hospital at Korea. The metabolic syndrome was defined by Adult Treatment Panel III and World Health Organization diagnostic criteria with slight modification of waist circumference. BMD (g/cm²) was determined at the lumbar spine (L₁-L₄) with dual-energy X-ray absorptiometry scanner. Frequency of osteoporosis was 2% in premenopausal women and 48% in postmenopausal women in this study participants. Frequency of metabolic syndrome was 14% in premenopausal women and 34% in postmenopausal women. Frequency of osteoporosis and metabolic syndrome was increased after menopause. Lumbar BMD (0.862±0.156 vs. 0.765±0.162, p<0.05), serum fasting insulin level (7.75±4.98 vs. 5.21±4.16 mIU/L, p<0.05) and HOMA-IR (1.916±1.286 vs. 1.176±1.016, p<0.05) were increased in subjects with metabolic syndrome, compared to those without metabolic syndrome among postmenopausal women, but not among premenopausal women. These results implicated that insulin resistance in metabolic syndrome would not occur in bone and higher insulin levels might play a role in maintaining bone mineral density after menopause. In conclusion, subjects with metabolic syndrome have higher lumbar BMD, serum fasting insulin level and HOMA-IR, compared to those without metabolic syndrome in postmenopausal Korean women.

Disclosures: **S.K. Lee**, None.

SA401

See Friday Plenary number F401.

SA402

Serum Osteoprotegerin in Patients with Anorexia Nervosa. **J. M. Olmos^{*1}, J. Menéndez-Arango^{*2}, C. Valero^{*1}, J. L. Hernández^{*1}, J. Martínez^{*1}, C. Lozano-Tonkin³, J. González-Macias¹.** ¹Medicina Interna, Hospital Universitario M. Valdecilla, Santander, Spain, ²Psiquiatría, Hospital Universitario M. Valdecilla, Santander, Spain, ³Medicina Interna, Hospital Clínico San Carlos, Madrid, Spain.

Objectives: To evaluate serum levels of osteoprotegerin (OPG) in patients with anorexia nervosa (AN) and in healthy controls, and to investigate the relationship of OPG levels with bone mineral density (BMD) and several nutritional factors. **Patients and methods:** We studied 64 Spanish females aged 15-36 yr. (26±7 yr.) with different stages of AN (DSM-IV criteria). Mean body mass index (BMI) was 19±3 kg/m². Serum OPG levels were measured by EIA, and leptin concentration by IRMA. Bone mineral density (BMD) and body composition (lean body mass, fat body mass, and % fat mass) were determined by DEXA (Hologic QDR-4500). 39 healthy women (28±8 yr) with a normal BMI (22±3 Kg/m²) formed the control group. **Results:** Patients with AN had a lower fat mass, lean body mass, and BMD at lumbar spine (LS), femoral neck (FN) and total hip (TH) than controls. OPG levels were similar in patients and controls. BMD was negatively correlated with leptin, BMI, lean and fat body mass in anorectic patients. No correlation was seen between OPG and BMD. However, patients with poor nutritional status (BMI<18,5 Kg/m²) had lower BMD and higher OPG values than recovered patients (Table)

	OPG	Z (LS)	Z (FN)	Z (TH)
BMI <18,5 (n:23)	62±24	-1.6±1.1	-1.7±0.9	-1.8±1.0
BMI >18,5 (n:41)	51±16	-0.9±1.0	-0.9±0.9	-0.8±0.8
p	0.05	0.05	0.01	0.01

Conclusions: OPG values were normal in patients with AN. However, anorectic patients with poor nutritional status had higher serum OPG levels and lower BMD than recovered patients.

Disclosures: **J.M. Olmos**, None.

SA403

Simulation Model Suggests Risedronate Surpasses Strontium Ranelate in Clinical Benefits and Cost Savings for Treating Postmenopausal Women with Established Osteoporosis: The Case of Germany. A. A. Kurth^{*1}, M. K. Pasquale^{*2}, R. T. Burge^{*2}, A. Lyssy^{*3}, R. Saadi^{*4}. ¹Orthopaedic Oncology Service and Bone Metabolism, University Hospital Frankfurt, Frankfurt, Germany, ²Epidemiology & Pharmacoeconomics, P&G Pharmaceuticals, Mason, OH, USA, ³Customer Business Development, P&G Pharmaceuticals - Germany, Damstadt, Germany, ⁴Oncology & Bone/Arthritis, Global Health Outcomes & Market Access, Sanofi-Aventis Pharmaceuticals, Bridgewater, NJ, USA.

Bisphosphonates have demonstrated efficacy in the prevention of osteoporotic fractures and have been considered first-line therapy to date. Strontium ranelate, a new chemical entity in the treatment of osteoporosis, was launched in Germany in October 2004 and is being introduced in most other European markets throughout 2005. This study compares risedronate to strontium ranelate in terms of treatment effect on fracture reduction and overall cost-effectiveness for a population of postmenopausal osteoporotic (PMO) women in Germany. The comparison is based on a previously validated Markov model of the natural history of osteoporosis (Tosteson, 2001). The model simulates treatment scenarios for risedronate and strontium ranelate using as a base case a population of 70-74 year-old PMO women with a prevalent vertebral fracture and BMD T-Score <-2.5. It simulates outcomes for five years of treatment and observation time, as approved by the German Osteoporosis Treatment Guidelines for the prevention of vertebral and hip fractures. Efficacy data for risedronate is taken from Reginster, Minne, Sorensen et. al. (2000) for the reduction in the relative risk of vertebral fractures (49%) and from McClung, Geusens, Miller et. al. (2001) for the reduction in relative risk of hip fractures (60%). For strontium ranelate the efficacy measures used are 41% for vertebral fracture risk reduction (Meunier, Roux, Seeman et. al., 2004) and 36% for hip fracture risk reduction (Reginster, Seeman, Vernejoul et. al., 2005). Other model inputs include fracture incidence rates, relative risk of fracture due to risk factors, health utilities, and costs of fracture treatment and prevention. The analysis is run using German epidemiological and cost data from published sources. In a cohort of 70-74 year-old patients with prevalent vertebral fractures in Germany (EPOS 2002), the model predicts that five years of treatment with risedronate would result in 5491 fewer vertebral and hip fractures and a cost savings of €114 million in comparison to strontium ranelate. These results suggest that treatment with risedronate would have both a clinical and economic benefit.

Disclosures: **A.A. Kurth**, P&G Pharmaceuticals 5; Roche Pharmaceuticals 5.

SA404

See Friday Plenary number F404.

SA405

Treatment-Related Changes in BMD Are not Associated with the Occurrence of a Fragility Fracture While on Risedronate Therapy. R. Lindsay¹, S. Magowan², P. Miller³, J. D. Adachi⁴, I. Barton^{*5}, D. Felsenberg⁶, N. B. Watts⁷. ¹Helen Hayes Hospital, West Haverstraw, NY, USA, ²P&G Pharmaceuticals, Mason, OH, USA, ³Colorado Center for Bone Research, Lakewood, CO, USA, ⁴McMaster University, Hamilton, ON, Canada, ⁵P&G Pharmaceuticals, Egham, United Kingdom, ⁶University Hospital Benjamin Franklin, Berlin, Germany, ⁷University of Cincinnati, Cincinnati, OH, USA.

There is a paucity of data addressing the risk determinants for fracture while actually on osteoporosis treatment. This valuable information would be helpful in identifying the higher risk patient. This analysis was designed to determine the effect of different parameters associated with the occurrence of an osteoporotic fracture (vertebral & nonvertebral) while taking risedronate 5 mg/day. The analysis specifically examined 4,324 postmenopausal women randomized to receive risedronate 5 mg/day in the risedronate phase III placebo-controlled fracture endpoint trials over a 3 year period (VERT-MN, VERT-NA and HIP). Women who sustained fragility fractures (F+ group) were compared to women who remained fracture free (F- group). These two groups of women were analyzed to determine the significance of the following parameters to fracture occurrence while on therapy: baseline LS & FN BMD, body mass index (BMI), prevalent vertebral fractures (PVF), and LS & FN BMD percent change from baseline over 3 years. Descriptive statistics were summarized for each fracture group and formally compared using the Wilcoxon Rank Sum test. Over 3 years 523 postmenopausal women sustained a fragility fracture and 3801 women remained fracture-free while on risedronate 5 mg/day therapy. There was a significant difference in baseline BMD scores, prevalent vertebral fracture status and BMI between women who did or did not sustain a fracture during treatment. (Table 1). Changes in lumbar spine or femoral neck BMD during treatment, however, were not different between patients who did or did not suffer from a fragility fracture during treatment.

PARAMETER (Median)	Patients with Fractures (F+) (n=523)	Patients without Fractures (F-) (n=3801)	p-value F(+) v F(-)
Baseline LS T-score	-3.0	-2.6	0.005
Baseline FN T-score	-2.8	-2.6	<0.001
Baseline PVFs	2.0	1.0	<0.001
Baseline BMI (kg/m2)	24.6	25.0	0.020
LS % BMD Change	5.4%	5.1%	0.359
FN % BMD Change	1.6%	1.8%	0.298

Of the investigated parameters, well-established risk factors for fracture such as low BMD, low BMI and prevalent vertebral fracture status allowed a differentiation between patients who did or did not fracture during treatment. Change in BMD with treatment was no different in patients who sustained a fracture compared with those who remained fracture free.

Disclosures: **R. Lindsay**, None.

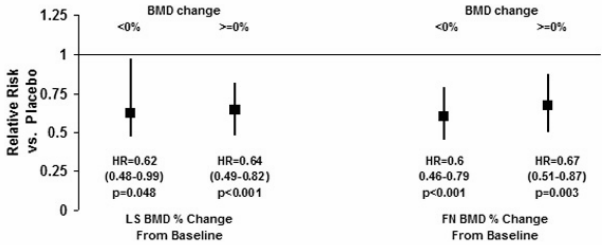
SA406

See Friday Plenary number F406.

SA407

Risedronate Demonstrates Efficacy to Reduce Fragility Fractures Independent of Treatment-Related BMD Changes. N. B. Watts¹, S. Magowan², J. P. Brown³, P. D. Miller⁴, I. P. Barton^{*5}. ¹University of Cincinnati, Cincinnati, OH, USA, ²Procter & Gamble Pharmaceuticals, Cincinnati, OH, USA, ³Laval University, Ste-Foy, PQ, Canada, ⁴CCBR, Lakewood, CO, USA, ⁵Procter & Gamble Pharmaceuticals, Egham, United Kingdom.

Risedronate 5 mg/day has previously demonstrated fracture efficacy independent of baseline BMD status. There is controversy in the literature if fracture efficacy is also independent of BMD changes experienced over the duration of therapy. This analysis was designed to determine the efficacy of risedronate 5 mg/day in reducing the risk of fragility fractures (vertebral and non-vertebral) in postmenopausal women who either gained or lost BMD over the duration of treatment. The analysis included 2,846 postmenopausal women (placebo N=1418, risedronate N=1428) enrolled in the risedronate phase III 3-year placebo-controlled fracture endpoint trials (VERT-MN & NA, HIP) who had lumbar spine (LS) and/or femoral neck (FN) BMD data available at baseline and post-baseline (3 years or last observation). The efficacy of risedronate in reducing fracture risk was estimated by the Hazard Ratio (HR) within each BMD group using a Cox regression model, stratified by clinical trial. The two groups were similar with regard to clinically important baseline characteristics; age, BMI, prevalent vertebral fracture status, and baseline LS and FN BMD. Antifracture efficacy was statistically significant vs. placebo whether there was gain or loss of BMD at the lumbar spine or the femoral neck (fig 1) and magnitude of antifracture efficacy of risedronate 5 mg/day vs placebo was similar in women whether there was gain or loss of BMD either at the LS or FN (treatment-by-BMD interactions p>0.6). This study demonstrates that risedronate is efficacious in the reduction of osteoporotic fractures regardless of whether there is a loss or gain in BMD over the duration of treatment as compared to placebo. As pointed out in recent studies, the mechanisms by which agents like risedronate reduce skeletal fragility are complex and only partly reflected in BMD changes.



Disclosures: **N.B. Watts**, Procter and Gamble Pharmaceuticals 2, 5; Amgen 2, 5; Merck & Co., Inc. 2, 5; Eli Lilly 2, 5.

SA408

See Friday Plenary number F408.

SA409

Bisphosphonates Suppress Periosteal Osteoblast Activity in Rat Femur and Tibia. K. Iwata^{*}. Anatomy and Cell Biology, Indiana University School of Medicine, Indianapolis, IN, USA.

Bisphosphonates (BPs) suppress bone resorption by inducing apoptosis of mature osteoclasts and by inhibiting differentiation of osteoclast precursors. In a coupled remodeling system, this will reduce bone formation at the level of the individual remodeling unit. The direct influence of BPs on osteoblasts in vivo is unknown. In vitro they have been shown to inhibit osteoblast apoptosis at low concentrations (potentially leading to increased bone formation), and to induce apoptosis or cell death at high concentrations. In this study we determined the effect of BPs on osteoblast activity on the periosteal surfaces of long bones in rats, where formation is not spatially coupled to resorption at least at the level of the BMU. We administered risedronate (RIS) or alendronate (ALN) to 6-month-old female Sprague-Dawley rats. Control rats (CNT; n=9) were given a daily subcutaneous (sc) injection of saline vehicle. Six groups of rats were injected sc daily for 17 days with RIS at doses of 0.05 µg/kg (RIS-low; n=9), 0.5 µg/kg (RIS-mid; n=9) or 5 µg/kg (RIS-high; n=9); or with ALN at doses of 0.1 µg/kg (ALN-low; n=9), 1.0 µg/kg (ALN-mid; n=8), or 10 µg/kg (ALN-high; n=9). All animals were double labeled with calcein (1-5-1-3), and dynamic histomorphometry was performed on the endosteal and periosteal surfaces of the tibia and femur. Both BPs at all doses significantly

reduced periosteal mineral apposition rate (MAR) in the femur (21-40% vs CNT, $p<0.05$) and in the tibia (41-52% vs. CNT, $p<0.01$, Fig1). In the tibia but not in the femur this resulted in a significant ($p<0.05$) reduction in periosteal bone formation rate (BFR/BS) in all groups. There were no significant differences in MAR on the endosteal surfaces of either femur or tibia, although BFR/BS was significantly reduced in the femur in some dose groups. These results show that in rats, BPs can suppress MAR on periosteal surfaces that are modeling in formation mode. This may indicate a direct effect on osteoblast activity and suppression of bone formation independently of bone resorption, but an indirect effect dependent on suppression of resorption at remote sites (e.g., endosteal surface) cannot be excluded.

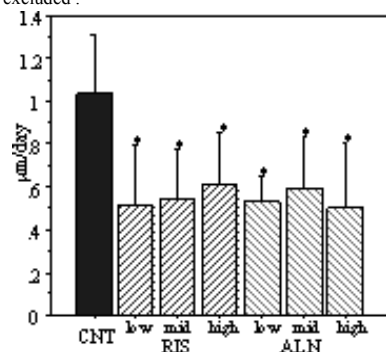


Fig1. MAR of tibial diaphyseal periosteal surface ; $p<0.01$ vs CNT

Disclosures: **K. Iwata**, Procter and Gamble Pharmaceuticals, Inc. 2.

SA410

See Friday Plenary number F410.

SA411

Non-Vertebral Fracture Reduction in Osteoporotic Women Using a Composite Measure of Baseline Fracture Risk. **D. E. Black¹, C. E. Barr^{*2}, S. Papapoulos³.** ¹Epidemiology and Biostatistics, UCSF, San Francisco, CA, USA, ²Roche Laboratories, Nutley, NJ, USA, ³Department of Endocrinology, Leiden University Medical Center, Leiden, Netherlands Antilles.

Recent approaches to identify osteoporotic women at higher risk of fracture have focused on estimating absolute fracture risk using composite algorithms that include clinical risk factors in addition to bone mineral density (BMD)¹. The observational Study of Osteoporosis Fractures (SOF)² developed such a predictive risk index; however, this approach has yet to be applied in a clinical trial setting. The BONE trial³ demonstrated significant reductions in vertebral fractures with ibandronate across the full study population as well as non-vertebral fracture (NVF) risk reduction in the subgroup of women with femoral neck BMD T-scores below -3.0. Using data from the BONE study, we examined a composite risk measure and its utility in assessing ibandronate efficacy for NVF reduction. The predicted 5-year risk of NVF was estimated using an equation, adapted from the SOF study, incorporating baseline age, lumbar spine BMD, and history of fracture as predictors. Clinical NVFs (clavicle, humerus, wrist, pelvis, hip, and leg) were collected as adverse events, confirmed radiologically, and excluded if due to accident/trauma. Two alternative categorizations of risk were explored: (a) population tertiles, based on dividing the study population into equal thirds, and (b) absolute risk categories (low/medium/high) based on the predicted NVF risk. Treatment effects were compared across these risk definitions. The observed number of NVFs across the study population was lower than predicted by this algorithm, especially in low risk groups. We found a significant interaction ($p=0.006$) between baseline risk of NVF and treatment effect. When defined by population tertiles, there was a 20% risk reduction ($p=0.293$) among patients in the high risk tertile (predicted 5 year NVF risk >20.4%). When defined by baseline absolute risk, a statistically significant 45% risk reduction was evident in the high risk group (risk >32.9%, $p=0.028$). Limitations of this analysis include the relatively low overall NVF rate (and consequent small number of fractures) as well as the post-hoc nature of the categories. These results underscore the value of composite measures of fracture risk as a clinical tool. They also provide evidence that ibandronate reduces NVF risk in a select group of high-risk women defined by a broader range of clinically relevant factors.

1. Kanis et al. Osteoporosis Int. 2002, Jul;13(7):527-36.
2. Black et al, Osteoporosis Int, 2001, 12, 519-528
3. Chestnut et al, J Bone Miner Res, 2004, 19, 1241-1249

Disclosures: **D.E. Black**, Novartis 2; Roche 5; Merck 8; GSK 5.

SA412

See Friday Plenary number F412.

SA413

Alendronate Treatment in Women with Impaired Renal Function: An Analysis of the Fracture Intervention Trial. **S. A. Jamal¹, D. C. Bauer², K. Ensrud³, J. A. Cauley⁴, M. Hochberg⁵, A. Ishani^{*3}, S. R. Cummings².**

¹Medicine, University of Toronto, Toronto, ON, Canada, ²S.F. Coordinating Center, CPMC Research Institute, and UC San Francisco, San Francisco, CA, USA, ³University of Minneapolis, Minneapolis, MN, USA, ⁴Medicine, University of Pittsburgh, Pittsburgh, PA, USA, ⁵University of Maryland, Baltimore, MD, USA.

Alendronate is cleared by the kidney and may have sustained effects on bone in subjects with impaired renal function. We hypothesized that as renal function decreased alendronate treatment would result in greater increases in bone mineral density (BMD) and greater decreases in fractures. We studied women participating in the Fracture Intervention Trial (FIT) a randomized controlled trial of alendronate or placebo (n= 6458). Women with serum creatinine above 112 mmol/L, serum parathyroid hormone (PTH) above 85 ng/L in isolation, or serum PTH above 65 ng/L in combination with abnormal serum calcium, alkaline phosphatase or phosphate, were excluded from FIT. We estimated baseline creatinine clearance (CrCl) using the Cockcroft Gault Formula. 581(9%) participants had severely reduced CrCl (<30 ml/min). Alendronate increased BMD regardless of CrCl; women with reduced CrCl had a 5.63% (95% CI: 4.75 to 6.51) increase in total hip BMD compared with 4.80% (95% CI: 4.57 to 5.03) among women with normal to moderate renal dysfunction (interaction p value = 0.04). There was no significant interaction for the increase in spine BMD (interaction p value = 0.75). The absolute changes in hip and spine BMD were similar by CrCl status with no evidence of a treatment effect (interaction p values 0.49 for hip and 0.54 for spine). Treatment with alendronate reduced the risk of clinical fractures to a similar degree in those with (OR: 0.78, 95% CI: 0.51 to 1.21) and without reduced renal function (OR: 0.80, 95% CI: 0.70 to 0.93; P-value for interaction = 0.89). Similarly, treatment with alendronate reduced the risk of morphometric spine fractures to a similar degree in those with (OR: 0.72, 95% CI: 0.31 to 1.7) and without reduced renal function (OR: 0.50, 95% CI: 0.32 to 0.76; P-value for interaction = 0.44). Limiting our fracture analyses to women with osteoporosis (by BMD T scores) did not substantially change our results (interaction p value for clinical fracture: 0.56 and interaction p value for spine fracture 0.54). A limitation of this analysis was that it post hoc analysis and we did not have direct measures of the glomerular filtration rate. Further, there was limited power for fracture analyses. Alendronate has similar effects on hip and spine BMD and reduction in risk of nonspine and spine fractures regardless of renal function as estimated by creatinine clearance.

Disclosures: **S.A. Jamal**, None.

SA414

See Friday Plenary number F414.

SA415

Re-Establishment of Normal Cancellous Bone Turnover Does not Differ Following the withdrawal of Alendronate or Risedronate Treatment in Ovariectomized Rats. **R. K. Fuchs, D. B. Burr.** Anatomy and Cell Biology, Indiana University Medical School, Indianapolis, IN, USA.

Bisphosphonates induce osteoclast apoptosis to decrease bone turnover and reduce bone loss due to estrogen-deficiency. Two commonly used bisphosphonates (alendronate [ALN] and risedronate [RIS]) have different skeletal pharmacokinetics. It has been suggested that ALN has a longer terminal half-life (10 years in humans) than RIS (20 days in humans). Given the potentially longer skeletal half-life of ALN, normal rates of bone remodeling may be expected to take longer to re-establish following its withdrawal than with equivalent doses of risedronate. The objective of this study was to determine the time required to re-establish normal bone turnover following the discontinuation of ALN and RIS. Female Sprague-Dawley rats (n=210) were ovariectomized (ovx) and starting 6 wks post ovx were treated 3x/wk for 8 wks with either vehicle, ALN (2.4μg/kg), low-dose RIS (1.2 μg/kg), or high-dose RIS (2.4 μg/kg) via subcutaneous injection. Doses were based on clinical dose levels (on an oral mg/kg basis) and on doses known to inhibit bone loss in ovx rats. Animals (10/group) were sacrificed at 0, 4, 8, 12 and 16 wks after treatment withdrawal. Histomorphometry was performed on tibial metaphysis, and pQCT and DXA scanning on distal femur. At the end of treatment (0 wk withdrawal), bone turnover within the proximal tibial metaphysis was significantly suppressed in all drug treated animals. This was evidenced by significant reductions in bone formation rate (BFR/BS; $P<0.05$) and mineralizing surface (MS/BS; $P<0.05$), and lack of double label. BFR/BS and MS/BS began to increase gradually in all drug-treated animals within as little as 4 wks after withdrawal, but remained significantly lower than vehicle-treated animals ($P<0.05$). Sixteen weeks after treatment withdrawal, BFR/BS and MS/BS in drug-treated animals returned to levels found in vehicle-treated animals. There were no significant differences between ALN and RIS in the rate at which bone turnover returned to baseline levels following treatment withdrawal. The histological data from the tibia were supported by the gradual but significant decline in bone mineral content of the distal femur during withdrawal in drug-treated animals ($P<0.05$), as assessed by pQCT and DXA, and a similar return to levels found in vehicle-treated controls by 16 wks after treatment withdrawal. We conclude that despite different clinical biological half-lives of ALN and RIS, the rate of return to untreated bone turnover rates after treatment discontinuation was similar in ovx rats.

Disclosures: **R.K. Fuchs**, Procter & Gamble Pharmaceuticals, Inc. 2.

SA416

Zinc Supplements Accelerate the Increase of IGF-I in Response to Protein Supplements and Decrease Bone Resorption. A. Rodondi*, P. Ammann, R. Rizzoli. Department of rehabilitation and geriatrics, Division of bone diseases, Geneva, Switzerland.

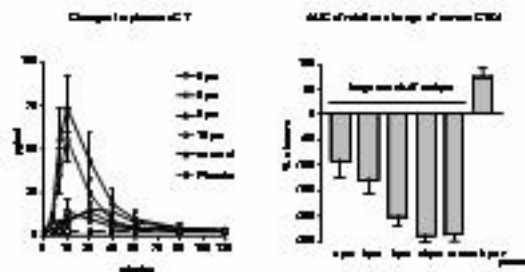
Protein undernutrition is frequently encountered in elderly. It is associated with decreased bone formation and increased bone resorption, together with lower IGF-I levels. Previous clinical and preclinical studies have demonstrated the favorable effect of aminoacids supplements on bone turnover and mineral density. On the other hand, dietary zinc supplement positively influences IGF-I production in zinc-depleted patients. To evaluate the possible additive effects of zinc and aminoacids supplements on serum IGF-I and bone turnover, we randomized 61 frail elderly with a mini nutritional assessment score between 17 and 24 (corresponding to a failure to thrive) into a daily oral protein supplement containing 15g whey protein, 5g essential aminoacids and 550mg calcium with or without 30 mg/day of zinc for 4 weeks on a double-blind trial. Fasting serum IGF-I ($\mu\text{g/l}$), IGF-BP3 ($\mu\text{g/l}$), Osteocalcin ($\mu\text{g/l}$) and CrossLapsTM (ng/ml) were measured at baseline, and after 1, 2 and 4 weeks of protein/zinc supplementation. Functional performance was assessed by an activity of daily living (ADL) score. At baseline, mean age was 83.6 ± 1.3 (x \pm SEM) and 86.4 ± 1.3 (NS), serum IGF-I 82.6 ± 9.0 and 73.3 ± 8.3 (NS), and albumin 31.0 ± 0.8 and 30.4 ± 0.8 (NS) in the zinc supplemented group and the controls, respectively. During essential aminoacids/whey protein supplements, serum IGF-I increased and reached a maximal of +40% by 2 weeks. Zinc accelerated this increase with changes of $+48.3 \pm 14.3^*$ vs $+22.4 \pm 4.7\%$ (*, $p < 0.05$) by 1 week, in the zinc supplemented group and the controls, respectively. IGF-I/IGF-BP3 ratio, taken as a reflection of IGF-I bioactivity, increased by $+37.3 \pm 10.7^*$ vs $13.1 \pm 3.4\%$ after one week. Zinc significantly decreased serum CrossLapsTM ($-10.3 \pm 4.9^*$ vs $+3.9 \pm 4.7\%$) already by 1 week. Osteocalcin increased in both groups ($+16.4 \pm 7.0$ and $+21.5 \pm 9.0\%$) irrespective of zinc supplements. ADL score significantly increased more in response to zinc in the subgroup of patients with baseline albumin lower than the mean ($+25.7 \pm 8.1^*$ vs $+11.9 \pm 6.5\%$). In conclusion, zinc supplement accelerated IGF-I response to essential amino acids/whey protein supplement and decreased bone resorption together with an increase in bone formation, in elderly. These results suggest that zinc supplements should thus be considered during protein repletion of undernourished elderly.

Disclosures: **A. Rodondi**, None.

SA417

Morning and Evening Dosing of Oral Salmon Calcitonin (SM021): The Influence of Food Intake on the Bioavailability and Efficacy of the Evening Dose. L. B. Tankó, I. Byrjalsen, B. J. Riis*, A. Moelgaard*, C. Christiansen. CCBR A/S, Ballerup, Denmark.

The aim of the study was to investigate the influence of food intake on the bioavailability and efficacy of salmon calcitonin (CT) in healthy postmenopausal women. The study was a single-blind, randomized, partly placebo controlled study. Participants were 36 postmenopausal women 62-74 years old, who were randomly assigned to one of 18 different treatment schedule involving 3 consecutive visits with at least 48 hours in between. This protocol resulted in 12 measurements of each response elicited by the following dosing regimes: 1) 0.8 mg CT at 10 pm followed by meal at 10:10 pm, 2) meal at 9 pm followed by 0.8 mg CT at 10 pm, 3) meal at 8 pm followed by 0.8 mg CT at 10 pm, 4) meal at 6 pm followed by 0.8 mg CT at 10 pm, 5) 0.8 mg CT at 10 pm but no meal 6) meal at 8 pm + placebo. Study parameters were the changes in plasma CT and bone turnover markers (serum and urinary C-terminal telopeptide of collagen type I, CTX I, and serum levels of osteocalcin, OC). For comparison of morning and evening benefits under fasting conditions, CTX I responses during fasting conditions elicited by 0.8 mg CT given at 8:00 am were also investigated. Postprandial intake of 0.8 mg CT at 10 pm was associated with decreased peak plasma concentrations of CT compared with peak concentrations associated with the same oral dose taken 10 min before meal or in the fasting state (Fig. 1). Furthermore, CT intake at 10 pm elicited smaller (Fig. 2) and shorter-lasting relative decreases in CTX I when administered after food intake. However, the AUC characterizing the 4-hour response elicited by 0.8 mg CT taken in the fasting state was comparable with that elicited by CT taken 10 min before food intake (group C vs. G, Fig. 2). Furthermore, the AUC of 4-hour CTX I responses elicited by preprandial dosing of 0.8 mg CT in the morning hours was comparable with that obtained by the same dose taken in the evening hours (253 ± 16 vs. $237 \pm 36\%$ x hours). Salmon CT did not exert significant effects on osteocalcin, independent of the relative time of drug intake. In conclusion, postprandial dosing may limit the bioavailability of oral sCT. However, the rapid absorption to the plasma suggests that maximal benefits in terms of inhibiting the nocturnal rise in bone resorption can be achieved if dosing occurs before evening meal.



Disclosures: **L.B. Tankó**, None.

SA418

Influence of Two Different Calcium and Vitamin D Dose on Parathyroid Hormone Secretion among Women over the Age of 65. M. T. Tuppurainen¹, M. H. Komulainen^{*2}, R. Honkanen¹, H. J. Kröger¹, E. M. Alhava^{*3}. ¹Bone and Cartilage Research Unit, Kuopio University, Kuopio, Finland, ²Obstetrics and Gynecology, Kuopio University Hospital, Kuopio, Finland, ³Department of Surgery, Kuopio University, Kuopio, Finland.

Calcium and vitamin D supplementation have been shown to reduce secondary hyperparathyroidism and play a protective role in age-related osteoporosis. In order to define the optimal regimen of calcium and vitamin D supplementation to produce the maximal inhibition of parathyroid -hormone (PTH) secretion, we compared the administration of a calcium-vitamin D supplement as a single morning dose with the administration of two divided doses at 8 -hour intervals among 30 healthy women over the age of 65 from OSTPRE- Fracture Prevention Study. This was an open, crossover study, where the sequence of administration of the two regimens was randomised. The two regimens were: treatment A, two calcium (500mg) + vitamin D3 (400IU) tablets (Calcichew- D3 Forte®, Leiras Nycomed) once a day in the morning during breakfast, treatment B; one calcium+ vitamin D tablet twice a day at 8 hours interval, first during breakfast and second during lunch. Venous blood samples were drawn for analysis prior to the study drug intake and every hour 11 hours after the first dose. RMANOVA was used for statistical analysis. During the first time interval (0-480 minutes) the PTH levels decreased rapidly until 120 minutes and then started gradually to increase until 480 minutes. However, the PTH levels did not rise back to their baseline level. When outlying observations were removed there were no statistically significant differences between the treatment groups in the PTH levels. During the second time interval (480-660 minutes) there was a statistically significant difference in the PTH levels between the treatment groups with the group B having lower PTH levels after the second administration. Both treatment groups seemed to have similar lowering effects on PTH levels during the first administration, but after the second administration the B- group lowered the PTH levels while in the A group the PTH levels continued to increase. Both treatment groups seemed to have similar effects on S-calcium levels during the first administration, but after the second administration the B- group had higher S-calcium levels than the A- group. In conclusion, by administering calcium and vitamin D in two separate doses, the secretion of PTH is decreased more effectively than by single daily dosing. Twice a day dosing may provide more effective protection against secondary hyperparathyroidism, bone resorption and may offer more fracture prevention than single dosing among elderly women.

Disclosures: **M.T. Tuppurainen**, None.

SA419

See Friday Plenary number F419.

SA420

Inulin and Fructo-Oligosaccharides Differ in their Ability to Enhance both the Bone Mineral Density and the Mucosal Levels of 9-kDa Calcium Binding Proteins in Rats. D. H. Manicourt*, A. Nzeusseu Toukap*, J. P. Devogelaer. Rheumatology Unit, St-Luc University Hospital, Brussels, Belgium.

The increase in BMD observed in growing rats fed with chicory fructans can be related, at least partly, to an increase in calcium absorption in the colon. It is generally believed that products of the colonic fermentation of fructans improve calcium absorption by increasing the solubility of calcium salts by lowering the luminal pH and by inducing hypertrophy of cecal walls, but direct effects such as an increase in the levels of calcium binding proteins (CaBPs) in the mucosal cells of the large bowel cannot be excluded. Therefore, for a 3-month time period, 3 groups of 13 six-week-old male rats each received either the standard AO4 diet (CTL group), the standard diet containing 5% inulin (INU group) or the standard containing 5% chicory oligofructose (OLF group). At sacrifice, rats of the 2 fructan groups both had a similar median cecal wall weight (1.5 g) that was significantly higher than that of the CTL group (0.9 g; $p < 0.001$). Mucosal proteins were subjected to Western blots and semi-quantification of blots probed with anti- 9-kDa-Calbindin antibodies showed that the levels of this CaBP was increased by a factor of 2 in the OLF group and by a factor of 3 in the INU group. Surprisingly, a monoclonal anti-28-kDa-Calbindin antibody detected a signal at the expected molecular weight in all specimens; further, when compared to the CTL group, the signal intensity was increased by a factor of 3 in the OLF group and by a factor of 5 in the INU group. Tibia and the third lumbar vertebra (L-3) stripped off adherent tissues were analyzed by using pQCT (Research SA+, Stratec, Germany). In both L3 and proximal tibia, the BMD of cancellous bone was significantly increased by INU (0.27 versus 0.23 and 0.33 versus 0.22 g/cm³, respectively; $p < 0.001$) and to a lower extent by OLF (0.26 and 0.28 g/cm³; $p < 0.05$). Further, inulin but not OLF, enhanced the BMD of cortical bone in both L-3 (0.98 versus 0.93 g/cm³; $p < 0.01$) and tibia (0.88 versus 0.83 g/cm³; $p < 0.01$). In conclusion, although inulin and OLF both have a positive effect of the BMD of the axial and peripheral skeleton of growing rats, the stronger effect of inulin cannot be related to an increase in the exchange surface area of the gut, as assessed by the cecal wall weight, but is likely to be related, at least partly, to a strongest increase in the mucosal levels of the 9 kDa and 28 kDa calcium binding proteins which both contribute to intestinal calcium absorption.

Disclosures: **J.P. Devogelaer**, Work supported by an institutional grant of Cosucra group, Warcoing, Belgium 2.

SA421

Effect on Bone Turnover and BMD of Low Dose Oral Silicon as an Adjunct to Calcium/Vitamin D3 in a Randomized, Placebo-Controlled Trial. T. D. Spector¹, M. R. Calomme², S. Anderson^{*1}, R. Swaminathan^{*1}, R. Jugdaohsingh^{*1}, D. A. Vanden Berghe^{*2}, J. J. Powell^{*3}. ¹St Thomas' Hospital, London, United Kingdom, ²Faculty of Pharmaceutical Sciences, University of Antwerp, Antwerp, Belgium, ³MRC Human Nutrition Research, Cambridge, United Kingdom.

Mounting evidence supports a physiological role for silicon (Si) as orthosilicic acid (OSA; Si(OH)₄) in bone formation. Mechanisms are unclear but collagen synthesis and improved mineralization have been demonstrated in cellular and animal models. Human data are lacking so here we have investigated the effect of low dose oral silicon on markers of bone turnover and BMD in a randomized, placebo-controlled trial. Over 12 months, 114 women (mean age: 61 y) out of 184 randomized (T score spine < -1) completed the study and received, daily, 1000 mg Ca and 800 IU cholecalciferol (Vit D3) ± Si as choline-stabilized orthosilicic acid (ch-OSA). Three different Si doses were used (Table) which, in this population, would typically increase dietary Si intakes by 12.5, 25 and 50%. In all groups, there was wide variation in the changes to bone markers at 6 and 12 months compared to baseline (Table) so covariate analysis was used to adjust for baseline values. Overall, there was a trend for Si to confer some additional benefit to Ca & VitD3, especially for markers of bone formation (Table), but only PINP was significant by ANCOVA: LSD post-hoc analysis indicated significance at 12 months for the 6 and 12 mg Si dose (p < 0.05 vs placebo) where there was also a trend for a corresponding increase in the bone resorption marker, collagen type I C-terminal telopeptide (data not shown).

Change in Markers of Bone Formation vs Baseline (% , mean ± SD)

Calcium/Vit D3 plus:		Placebo	3 mg Si	6 mg Si	12 mg Si
Serum Marker	Change at	n = 30	n = 26	n = 28	n = 30
PINP	6 mo	-12.9 ± 17.5	-8.92 ± 26.2	-11.3 ± 21.8	-9.03 ± 21.7
	12 mo	-19.9 ± 24.7	-15.9 ± 26.6	-0.88 ± 27.6*	-7.42 ± 20.7*
BAP	6 mo	-11.6 ± 16.6	-2.40 ± 20	-5.44 ± 12.8	-3.31 ± 15.5
	12 mo	-12.0 ± 20	-5.28 ± 15.5	-7.27 ± 16.6	-5.69 ± 17.3
Osteocalcin	6 mo	-4.62 ± 31.4	-3.36 ± 33.6	-7.24 ± 18.6	-3.65 ± 20.4
	12 mo	-15.0 ± 23.6	-6.08 ± 54.5	-12.4 ± 18.2	-7.79 ± 26.4

BAP = bone specific alkaline phosphatase. PINP = procollagen type I N-terminal propeptide. *p< 0.05 vs placebo (ANCOVA). BMD in the spine did not change significantly. Subgroup analysis (femur T score < -1) however was significant for the 6 mg dose at the femoral neck (t-test). This study suggests that combined therapy of ch-OSA plus Ca/vit D3 is a safe, well tolerated treatment that has a potentially beneficial effect on bone turnover, especially bone collagen, and possibly the femoral BMD compared to Ca/vit D3 alone. We acknowledge support of the National Osteoporosis Society and Bio Minerals n.v.

Disclosures: M.R. Calomme, Bio Minerals n.v. 2.

SA422

Effects of Calcium Supplementation on Body Composition and Fat Distribution in Korean Obese Postmenopausal Women. D. Kim*, Y. Rhee, C. Ahn*, B. Cha*, K. Kim*, H. Lee*, S. Lim. Internal Medicine, College of Medicine, Yonsei Univ., Seoul, Republic of Korea.

Backgrounds and aims According to National Health and Nutrition survey reported in 2002, daily dietary calcium consumption was unexpectedly low and tended to decrease gradually with increasing intake of protein especially in postmenopausal women. In this context, we hypothesized that low calcium intake at baseline would increase susceptibility to effects of calcium supplementation in view of a threshold effect. Thus, the aim of this study was to investigate the efficacy of elementary calcium on serum lipids, body composition and fat distribution, and insulin sensitivity and to identify the factors affecting weight change during calcium supplementation in Korean obese postmenopausal women. **Subjects and methods** Forty-four obese postmenopausal women (age=60±8.8years, BMI=29±4.6kg/m²) received a daily dose of 300mg calcium in addition to basal dietary calcium (400±200 mg per day) for 48 weeks. Lipid profiles, whole-body dual X-ray absorptiometry, fat Computed Tomography, and HOMA-IR scores were assessed at baseline and after 48 weeks. According to calcium intake at baseline, subjects were divided into low CA group (moderate-to-severe calcium deficiency, calcium intake <400 mg per day) and high CA group (mild calcium deficiency, calcium intake > 400mg per day). Calcium intake was assessed by calculating average amount of dietary calcium on the basis of 72-h diet diary. **Results** After 48 weeks, body weight decreased by 3.0±0.3kg (P<0.05). Total body fat (by 2.0±0.2%, P<0.05 and by 2.1±0.2kg, P<0.01), and areas of abdominal visceral fat and mid-thigh low-density muscle decreased (P<0.01). Serum triglyceride and 25-(OH) vitamin D levels decreased (P<0.05 in each case). Serum insulin and HOMA-IR scores showed a tendency to decrease (P=0.06 and p=0.05, respectively). Low CA group was more obese than high CA group at the time of entry. Low CA group achieved more weight and fat loss and improvement of insulin sensitivity after 48-week calcium supplementation than high CA group. **Conclusions** We confirmed that calcium supplementation induces body weight and fat loss with favorable changes of fat distribution (reduced abdominal visceral fat and low-density muscle), directing toward improvement of insulin sensitivity. We found adiposity and calcium intake at baseline may partially determine the magnitude of the response to calcium supplementation. In the presence of moderate calcium deficiency, Korean obese postmenopausal women may benefit from calcium supplementation for favorable changes of serum lipids and body composition.

Disclosures: D. Kim, None.

SA423

The Effect of Phytoestrogens on Intestinal Calcium Absorption. L. E. Ryan¹, D. L. Habash^{*2}, K. A. Foland^{*3}, H. N. Nagaraja^{*2}, R. D. Jackson¹. ¹Division of Endocrinology, Diabetes and Metabolism, The Ohio State University, Columbus, OH, USA, ²General Clinical Research Center, The Ohio State University, Columbus, OH, USA, ³Department of Geological Sciences, The Ohio State University, Columbus, OH, USA.

One of the mechanisms by which estrogen improves bone strength is its positive effect on intestinal calcium absorption efficiency. Phytoestrogens have emerged as a possible alternative to hormone therapy for protection against osteoporosis. Using a dual-isotope method in a pre-/post- design, we have evaluated the effect of high-dose dietary phytoestrogens (90mg/day of genistein + daidzein) on intestinal calcium absorption in postmenopausal women. Eleven participants were included in the study; their average age was 57 years (range 53 - 60) and time since menopause ranged from 1-9 years. For three months, during the Ohio winter season, the women ingested the soy or placebo protein (average 36gm protein/d), incorporated into muffins. One participant terminated the study after eight weeks secondary to nausea and constipation; the other ten women tolerated the protein well. All data will be presented in an intention-to-treat analysis. All subjects met the adherence criteria based upon urinary phytoestrogen levels and frequent muffin counts. From baseline to the end of the dietary intervention at 12 weeks the urinary daidzein increased from 0.06 µmol/L to 8.27 µmol/L, genistein 0.20 to 3.17 µmol/L, and equol 0.56 to 10.08 µmol/L, while those in the placebo group did not differ. Total dietary protein intake increased 12.9% from an average of 82.4gm/d to 92.9gm/d, and daily calcium intake increased by 49.7% from an average of 980mg/d to 1467mg/d. Fiber and vitamin D intake did not change with dietary intervention and was within the adequate intake (AI) range for each. The peak of intestinal calcium absorption at baseline and at three months was consistently reached, in each participant, between 3-4 hours after ingestion of the oral Ca42. A small but statistically insignificant increase in intestinal calcium absorption was noted in the group taking soy protein. In summary, although phytoestrogen levels significantly increased with dietary intervention, we found no correlation between ingestion of high dose phytoestrogens and peak intestinal calcium absorption.

Disclosures: L.E. Ryan, None.

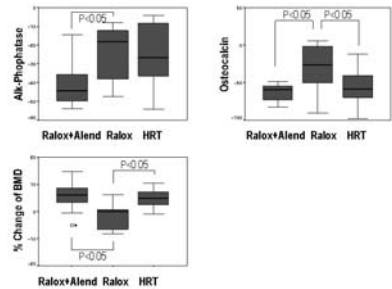
SA424

Effects of Raloxifene on Lumbar BMD and Bone Markers in Postmenopausal Osteoporotic Korean Women. I. Joo*, T. Bae*, H. Oh*. Family Medicine, Sungkyunkwan University, Seoul, Republic of Korea.

To determine the effects of Raloxifene on BMD and markers of bone turnover , we evaluated 68 postmenopausal osteoporotic Korean women who visited the Osteoporosis clinic in Samsung Cheil Hospital & Women's Health Care Center stratified in three groups ; raloxifene+alendronate(N=20), raloxifene(N=18), HRT(etradiol 2.0mg)(N=20). BMD at lumbar spine and markers of bone turnover(osteocalcin, alkaline phosphatase) were measured in the beginning and after 1-year treatment. BMD did not increase significantly in raloxifene alone group. However raloxifene with alendronate in combination and HRT groups showed the significant increase of BMD compared with raloxifene alone. All of three groups showed significant decrease of bone turnover markers such as osteocalcin and alkaline phosphatase. Serum levels of osteocalcin was significantly decreased in raloxifene with alendronate in combination and HRT groups compared with raloxifene alone. Raloxifene with alendronate in combination showed significant decrease of alkaline phosphatase level. In postmenopausal osteoporotic Korean women, treatment with raloxifene alone did not show significant increase in lumbar BMD. However, it decreased bone turnover markers not so much as raloxifene with alendronate in combination or HRT. Raloxifene might have an preventive effects on losing BMD in postmenopausal osteoporotic Korean women.

Variables	Baseline characteristics of the Subjects			
	Raloxifene with Alendronate(n=27)	Raloxifene Only(n=18)	HRT(n=23)	Total(n=68)
Age	61.4±6.9	57.5±8.3	56.1±7.2	58.6±7.1
Height	156.5±5.9	154.6±3.1	154.4±4.7	155.3±4.9
Weight	60.6±7.8	57.5±5.9	53.5±4.7	57.4±7.0
BMI	24.7±2.3	24.1±2.2	22.4±1.7	23.8±2.3
Spinal BMD	0.726±0.039	0.746±0.041	0.740±0.038	0.736±0.040
Osteocalcin	6.7±2.6	7.8±2.6	6.9±2.1	7.0±2.4
Total alkaline phosphatase	81.3±33.4	80.7±13.4	85.3±23.2	82.5±25.7

Figure 1. Changes of BMD & Bone turnover markers in post-menopausal osteoporotic Korean women After 1-Yr Treatment



Disclosures: H. Oh, None.

SA425

See Friday Plenary number F425.

SA426

3 Year-Follow-Up of Bone Mineral Density after a Randomised Trial of 12-Month Treatment with a GnRH Agonist (leuporelin 3.75 mg) Associated with 2 Options of Steroidal “Add-Back” Regimens in Patients with Endometriosis. C. Roux¹, C. Lucas^{*2}, K. Briot^{*1}, S. Kolta¹, J. Fechtenbaum¹, H. Fernandez^{*3}, ¹Rheumatology, Cochin University Hospital, Paris, France, ²Medical, Laboratoires Takeda, Puteaux, France, ³Gynaecology, Antoine Bécélère University Hospital, Clamart, France.

We previously compared, in a 12-month double-blind trial involving 78 patients with symptomatic endometriosis, the efficacy and safety of 2 add-back regimens associated with leuporelin acetate 3.75 mg: promegestone 0.5 mg (P) plus either placebo (PL) or estradiol 2 mg (E) per day (Hum Reprod. 2004 19: 1465-71). The BMD decrease was significantly more pronounced in the PL-group: $-6.1 \pm 3.7\%$ (n=30) versus $-1.9 \pm 3.1\%$ (n=29) in E-group (p<0.0001). Here, we report the post-treatment effects on a 3-year follow-up (FU). Methods: patients with a significant decrease of BMD at the end of the 12-month therapeutic period (> 2.8% from baseline at the L2-L4 vertebral site, related to the precision method) had an annual BMD (central analysis of scans; quality control 3 times/week on a spine phantom) until recovery or during 3 years. No patient received anti-osteoporotic drug during follow-up. Results: among the 59 patients assessed at the end of the trial, 36 (26 PL-group, 10 E-group) had a significant BMD decrease from baseline: 9 were lost for BMD FU while 2 (all PL-group) were excluded because their agonist treatment was prolonged off-protocol. Finally, 25 patients (19 PL- group, 6 E-group) had at least one BMD measurement during the 3-year follow-up: 8/21 (38%) patients recovered by 1 year, 16/24 (67%) by 2 years and 18/25 (72%) by 3 years (14/19 PL group, 4/6 E-group) with a mean delay until recovery of 19.3 ± 8 months (median 18.7). Bone loss during treatment was a determinant of the delay until recovery (p<0.05). Changes of BMD at the end of the treatment phase, after 1, 2 and 3 year FU (cumulated data) were:

	Post-treatment N = 25	12 month FU N = 21	24 month FU N = 24	36 month FU N = 25
Changes from baseline Mean % \pm SD	-6.61 \pm 2.9	-3.16 \pm 2.6	-2.20 \pm 2.2	-2.04 \pm 2.2
Changes from baseline Median %	-6.01	-3.48	-1.81	-1.81
Changes from post-treatment Median %	—	+3.39	+4.33	+4.65

In conclusion, majority of patients receiving a one-year treatment regimen combining leuporelin 3.75 mg plus P-E recovered spontaneously their baseline BMD within 3 years (out of 29, 2 didn't and 4 were lost for FU) while 5 out of 30 didn't recover in the P-PL add-back group (5 lost for FU, 2 not interpretable). In case a significant bone loss occurs during treatment, recovery is reached within 2 year in 2/3 women.

Disclosures: **K. Briot**, None.

SA427

Pharmacological Actions of a Selective Estrogen Receptor β (ER β) Agonist in Ovariectomized Rats. G. Krishnan¹, Q. Q. Zeng^{*1}, R. L. Cain^{*1}, J. Oskins^{*1}, K. Chen^{*1}, B. Norman^{*2}, T. I. Richardson^{*2}, D. A. Dodge^{*2}, C. Montrose-Rafizadeh^{*3}, B. C. Yaden^{*1}, S. Cockerham^{*3}, C. Frolik¹, M. Sato¹, H. U. Bryant¹, Y. L. Ma¹. ¹Endocrine Research, Eli Lilly and Company, Indianapolis, IN, USA, ²Discovery Chemistry, Eli Lilly and Company, Indianapolis, IN, USA, ³Lead Optimization Biology, Eli Lilly and Company, Indianapolis, IN, USA.

The key role of estrogen in the regulation of skeletal growth and maintenance of bone mass has been demonstrated in human and animal models. Studies demonstrated that mice lacking ER β show increased cortical bone in adolescent females and protection against age-related trabecular bone loss in aged females (Windahl et al, JCI, 1999, JBMR 2001). Therefore, it was important to evaluate the effects of an ER agonist in an estrogen deficient skeleton. The aim for this study was to examine the pharmacological effects of LSN500307, a tissue-selective ER β agonist in ovariectomized (Ovx) rats. LSN500307 had high affinity binding to the hER β (Ki=0.19 nM) -and hER α (Ki=2.7 nM) receptors, and induced alkaline phosphatase activity in Ishikawa cells EC₅₀=78 nM. In addition, it was found to reduce prostate weight in 12-week-old male CD-1 mice in a dose-dependent manner (ED₅₀ = 0.05 mg/Kg/day). We orally dosed 6 months old ovariectomized (Ovx) rats with 0.1, 0.3, 1 and 3mg/kg/d LSN500307 starting at 1 week post surgery for 5 weeks. LSN500307 prevented ovx-induced increases in body weight and serum cholesterol in a dose dependent manner, with similar efficacy to ethynyl- estradiol (EE, 0.1mg/kg/d) at a 1mg/kg dose. LSN 500307 also dose dependently maintained the uterine wet weight in Ovx rats. The uterine wet weight at 3mg/kg dose was 2.5 fold higher than Ovx but it was 50% less than Sham controls. Quantitative computed tomographic analyses of femur showed that LSN500307 did not affect bone mineral content at any dose in distal femur metaphysis and mid femur but had significantly higher bone mineral density at 1 and 3 mg/kg/d doses in distal femur metaphysis when compared to Ovx control. Similar results were seen in cortical bone site of mid femur. Our data suggest that a novel ER β agonist LSN500307 has positive effects on body weight and neutral/positive effects on bone in Ovx rats.

Disclosures: **G. Krishnan**, Eli Lilly Company 3.

SA428

Extraskelatal Effects of Lasofoxifene on Postmenopausal Women. M. Davidson¹, A. Moffett^{*2}, F. Welty^{*3}, J. Simon^{*4}, M. Bolognese⁵, N. deMelo⁶, K. Wolter⁷, J. Proulx⁷, D. Radecki⁷. ¹Rush University Medical Center, Chicago, IL, USA, ²OB-GYN Associates of Mid-Florida, Leesburg, FL, USA, ³Beth Israel Deaconess Medical Ctr, Boston, MA, USA, ⁴Women's Health Research Ctr, Laurel, MD, USA, ⁵The Bethesda Health Research Ctr, Bethesda, MD, USA, ⁶Instituto de Saude e Bem-Estar da Mulher, Sao Paulo, Brazil, ⁷Pfizer Global R&D, New London, CT, USA.

Lasofoxifene, a next-generation selective estrogen receptor modulator that prevents bone loss, interacts with the estrogen receptor differently in various tissues. It was important to determine the effects of lasofoxifene on extraskelatal targets i.e. breast, vagina, brain, and cardiovascular system. In 2 identical, phase 3, double-blind trials, 1907 postmenopausal women were randomized to lasofoxifene 0.025 mg/d, 0.25 mg/d, or 0.5 mg/d or placebo (PBO) daily, plus calcium and vitamin D. Changes in signs and self-assessed symptoms of vaginal atrophy (VA), cognitive function, and lipids were periodically analyzed over 24 months (mos). Neither breast density nor breast pain increased in the lasofoxifene groups. Vaginal pH and the maturation index were improved at 12 and 24 mos in all 3 lasofoxifene groups. At 24 mos, lasofoxifene subjects had significantly lower percentages of parabasal cells and significantly higher percentages of immediate cells and superficial cells versus PBO (p 0.004). There was a significant improvement in vaginal pH at 12 and 24 mos for all doses of lasofoxifene versus PBO (p<0.001). Cognitive function and mood, examined in a subset of subjects (n=267), showed no significant differences in the lasofoxifene groups versus PBO except a lower CESD-10 depression score at 12 mos in the 0.025 mg group (p=0.017) and a lower Digits Forward score at 24 m (p=0.026), neither clinically meaningful. At 12 mos, all lasofoxifene doses significantly decreased median LDL-C, total cholesterol (TC), TC/HDL-C ratio, apolipoprotein B100 (apo B-100), apo B-100/apolipoprotein A1 (apo A1) ratio, hs-C-Reactive Protein and lipoprotein (a) versus PBO. There was a beneficial effect on apo A1, a small decrease in HDL-C in one lasofoxifene group, and a 0.5 to 7.3% increase in median triglyceride levels. At 24 mos, fibrinogen levels significantly decreased from baseline for all lasofoxifene groups versus PBO. Adverse events often reported during lasofoxifene treatment included hot flushes, leg cramps and increased vaginal moisture. Lasofoxifene had no effect on breast density. VA parameters (pH and maturation index) were improved with lasofoxifene treatment. Cognitive function and mood were not affected. Lasofoxifene had a favorable effect on lipid and lipoprotein levels and established biomarkers of CV risk.

Disclosures: **M. Davidson**, Pfizer 2.

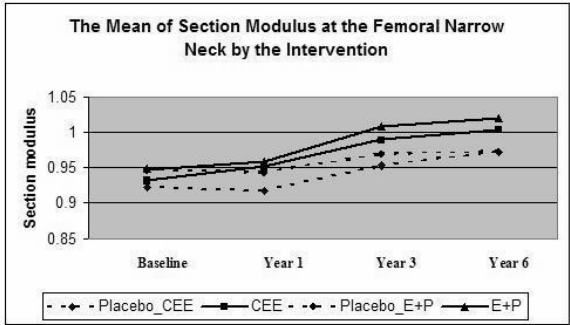
SA429

See Friday Plenary number F429.

SA430

Hormone Interventions Lead to Favorable Changes in Hip Geometric Structure ---Results from the Hormone Trials in the Women's Health Initiative (WHI). Z. Chen¹, C. E. Lewis², J. Cauley³, A. LaCroix^{*4}, T. Beck⁵, D. Nelson⁶, S. Green^{*1}, D. Sherrill^{*1}, T. Lohman^{*1}, R. Jackson^{*7}, M. LeBoff^{*8}, G. Wu^{*1}, N. Wright^{*1}, S. Nicholas^{*1}, L. Arendell^{*1}, E. Outwater^{*1}, Z. Wang^{*9}, S. Heymsfield^{*9}, T. Bassford^{*1}. ¹University of Arizona, Tucson, AZ, USA, ²University of Alabama at Birmingham, Birmingham, AL, USA, ³University of Pittsburgh, Pittsburgh, PA, USA, ⁴Fred Hutchinson Cancer Research Center, Seattle, WA, USA, ⁵Johns Hopkins University, Baltimore, MD, USA, ⁶Wayne State University, Detroit, MI, USA, ⁷Ohio State University, Columbus, OH, USA, ⁸Harvard Medical School, Boston, MA, USA, ⁹Columbia University, New York, NY, USA.

Loss of bone mechanical strength underlies osteoporotic fragility fractures and an effective therapy should demonstrably improve either the structural geometry or bone tissue strength. We hypothesized that hormone interventions among postmenopausal women significantly improve the structural geometry of the proximal femur. Study participants were a subgroup of women (one WHI clinical center) from the WHI randomized controlled hormone intervention trials: either conjugated equine estrogen only (CEE) or estrogen plus progestin (E+P), who were 50 to 79 years old at baseline and were followed up to 6 years. Bone densitometry, including scans at the hip, were conducted by dual-energy x-ray absorptiometry (DXA) at baseline, year1, year 3 and year 6. Hip structural analyses (HSA) on the DXA hip scans were conducted using the BECK HSA program. Mixed effect models with the intent-to-treat analysis approach were used. There were no differences in hip geometric measurements at baseline between the intervention and the placebo group in the CEE trial (N_{placebo} = 97, N_{CEE} = 87) or in the E+P trial (N_{placebo} = 114, N_{E+P} = 124). Statistically significant treatment benefits (p<0.05) of hormone interventions on hip strength were observed as early as one year after the starting of the intervention: Section Modulus (a measure of maximum bending stress) was preserved (figure 1), Buckling Ratio (a index of cortical instability under compression) was reduced by hormone interventions. In conclusion, hormone interventions led to favorable changes in femur cross-sectional geometry, which may help to explain the reduced fracture risk observed in hormone interventions.



Disclosures: **Z. Chen**, None.

SA431

Bazedoxifene Prevents Ovariectomy-Induced Bone Loss in the Cynomolgus Monkey. **S. Y. Smith¹, D. Minck^{*2}, J. Jolette^{*1}, L. Chouinard¹, C. H. Turner³, B. Komm⁴.** ¹Charles River Laboratories Preclinical Services/CTBR, Senneville, PQ, Canada, ²Wyeth Research, Chazy, NY, USA, ³Indiana University, Indianapolis, IN, USA, ⁴Wyeth Research, Collegeville, PA, USA.

Bazedoxifene (BZA) is a selective estrogen receptor modulator (SERM) currently in phase III development for the prevention and treatment of osteoporosis. The purposes of this study were to determine the efficacy of BZA after 18 months of treatment on bone mass, strength and architecture, and to evaluate effects on plasma lipids and reproductive tract histology, in surgically-induced postmenopausal monkeys. Ovariectomized (OVX) animals (18/group) were administered control article or BZA by daily oral gavage at 0.2, 0.5, 1, 5, or 25 mg/kg/day. A sham-operated control group was administered control article. Blood and/or urine were evaluated for markers of bone turnover (bone specific alkaline phosphatase, osteocalcin, serum C-telopeptide and urinary N-telopeptide), and serum lipids. BMD was determined *in vivo* by DXA for the lumbar spine and proximal femur, and by pQCT at the proximal tibia. Soft tissues were examined histologically, and histomorphometric analysis and biomechanical testing were performed on bones. Administration of BZA for 18 months to OVX animals had no meaningful effect on serum calcium, cholesterol, HDLC or triglycerides and showed no uterotrophic effect at any dose level. BZA partially prevented the OVX-induced rise in biochemical markers of bone turnover at all dose levels. The highest dose levels of BZA generally maintained BMD at pre-OVX levels at all sites evaluated, but most notably at the lumbar spine. BZA treatment partially prevented the OVX-induced accelerated bone remodeling in cortical bone with variable effects on indices of cancellous bone turnover. There were no deleterious effects of BZA on bone mineralization or structural parameters. BZA treatment up to 25 mg/kg/day for 18 months had no adverse effect on biomechanical strength parameters at the femur, femoral neck or lumbar spine. Bone strength parameters were significantly correlated with bone mass at the femur diaphysis, femoral neck and lumbar vertebrae. In conclusion, BZA treatment of OVX monkeys at dose levels up to 25 mg/kg/day for 18 months resulted in the partial preservation of bone mass as determined by bone densitometry. This was achieved by significant reductions in OVX-induced increases in bone turnover, evaluated by biochemical markers and histomorphometric indices in cancellous and cortical bone. BZA was well tolerated and was not associated with any adverse effects on plasma lipids or reproductive tract histology. Importantly, treatment with BZA did not adversely affect any measures of bone strength at the skeletal sites evaluated.

Disclosures: **B. Komm**, None.

SA432

Response of BMD and Back Pain to 12 Months of Teriparatide (rhPTH 1-34) in Patients with and without Prior Antiresorptive Treatment: One-Year Interim Results from the EUROFORS Study. **H. Minne¹, M. Audran^{*2}, E. Simoes^{*3}, B. Obermayer-Pietsch⁴, G. Sigurdsson^{*5}, T. Nicholson^{*6}, F. Marin⁶, T. N. Nickelsen⁶.** ¹Klinik Fuerstenhof, Bad Pyrmont, Germany, ²Centre Hosp. Universitaire, Angers, France, ³Inst. Portugues de Reumatologia, Lisbon, Portugal, ⁴Med. Univ.-Klinik, Graz, Austria, ⁵Landspítallinn Univ. Hospital, Reykjavik, Iceland, ⁶Eli Lilly & Company, Windlesham, United Kingdom.

EUROFORS is an ongoing prospective, randomized trial, designed to investigate various sequential treatments of teriparatide over 2 years in postmenopausal women with established osteoporosis. In year 1, all patients received open-label teriparatide 20 µg/d and supplements of 500 mg/d calcium and 400-800 IU/d vitamin D. For the 1-year analysis, we pre-defined 3 subgroups: (1) Osteoporosis treatment-naïve patients, patients with (2) adequate or (3) inadequate clinical outcome to prior antiresorptive (AR) therapy, with the latter defined as: (a) sustaining ≥1 new clinical fragility fracture(s) despite prescription of AR therapy during the 12 months prior to fracture; (b) T-score ≤ -3.0 SD or (c) BMD decrease ≥3.5% at lumbar spine (LS), total hip (TH) or femoral neck (FN) ≥2 years after initiating AR therapy. In 87.7% of pre-treated patients (groups 2 and 3 combined), a bisphosphonate (BP) was used preceding the study for a mean of 33.5 months. There were 159 early study discontinuations during year 1 (18.4%), 50 for adverse events and 31 for patients' decisions associated with the medication or injection device. The best adherence was seen in Group 3. In the total cohort, BMD showed a statistically significant increase from baseline at the LS and FN, and a reversal of the transient 0.5% loss after 6 months at

the TH. The Table lists the results by subgroup [% change, mean(SD); *<.05, **<.01, ***<.001]. Twenty patients (2.6%) showed a LS BMD loss of >3.5%, while 531 (68.3%) had an increase by >3.5%. Back pain, self-assessed by the patients on a 100 mm visual analog scale, decreased by a mean of 11.5 mm (p<0.001) in the total cohort. The proportion of patients with a clinically relevant pain improvement (defined as a decrease of ≥15 mm) was largest in those with severe pain at baseline (defined as a score >60 mm). We conclude that 12 months of treatment with teriparatide is well tolerated and associated with a BMD increase at the lumbar spine and femoral neck and a decrease in back pain.

Group (n)	LS	TH	FN
1 (184)	+7.7 (5.3)***	+1.5 (3.8)***	+1.5 (5.2)***
2 (177)	+6.9 (5.7)***	+0.4 (4.6)	+0.7 (5.7)
3 (416)	+5.9 (5.8)***	-0.4 (4.2)*	+0.3 (5.6)
Total (777)	+6.6 (5.7)***	+0.2 (4.3)	+0.7 (5.5)**

Disclosures: **T.N. Nickelsen**, **F. Marin**, **T. Nicholson**, **T. Nickelsen** 3; **H. Minne**, **M. Audran**, **E. Simoes**, **B. Obermayer-Pietsch**, **G. Sigurdsson** 2, 8.

SA433

See Friday Plenary number F433.

SA434

Increased Focal Uptake of Tc-99m Labelled MDP on Bone Scan Suggestive of Hyperostosis Frontalis Interna in a Patient Being Treated with Teriparatide. **G. C. Lim^{*}, W. S. Wafa^{*}, A. M. Moses.** Department of Medicine- Endocrinology, Diabetes and Metabolism, SUNY Upstate Medical University, Syracuse, NY, USA.

An 86-year-old woman with history of nontraumatic fractures including the right hip, wrists, and a thoracic vertebra was referred to our bone clinic because she continued to develop nontraumatic fractures even while taking alendronate for 5 years. Baseline lab tests showed a normal serum calcium, phosphorus, PTH, 25-hydroxy vitamin D and 24-hour urinary calcium. Serum alkaline phosphatase (SAP) was 116 U/L (36-126). T-score of the left total hip was -3.4 and Z-score was -1.1. Her lumbar spine bone density was factitiously elevated. She was then started on teriparatide. After being on teriparatide for 4 or 5 months, she developed increasingly severe dull headaches over the vertex and right frontoparietal areas of the skull. Follow-up SAP was 155 U/L. A bone specific alkaline phosphatase (BSAP) was 38 ng/ml (12-23). A bone scan showed a diffusely increased uptake in the skull which was not present 20 months before teriparatide was initiated. Routine radiographs and CT were more suggestive of hyperostosis frontalis interna than Paget's disease. Bone biopsy could not be obtained. On the basis of the lab and radiologic findings, teriparatide was discontinued. The patient noted immediate improvement in the frequency and severity of her headaches. Six weeks after discontinuing teriparatide, SAP was 134 U/L and BSAP was 37 ng/ml. Bone turnover markers are expected to increase during teriparatide treatment and this increase may correlate with improvement in bone density. However, there are no clear guidelines to alert the physician when to consider the development of other bone diseases such as Paget's disease, hyperostosis frontalis interna or even osteosarcoma. In summary, we present a case that raises a concern about when an elevation of turnover marker during teriparatide therapy should warrant radiologic evaluation. Follow-up bone turnover markers and bone scan on our patient will be made available at the meeting.

Disclosures: **G.C. Lim**, None.

SA435

See Friday Plenary number F435.

SA436

Bone Mass, Cortical Bone Histomorphometry and Trabecular Bone 3D-Microarchitecture in Ovariectomized Rats Treated with Intermittent PTH Administration. **S. Gomez^{*1}, C. de la Piedra^{*2}, M. Montero^{*2}, S. Luna^{*1}, D. Sarasa^{*1}, V. Crespo^{*3}, J. Garcia^{*3}, M. Diaz-Curiel^{*4}.** ¹Anatomic Pathology, Cadiz University, Cadiz, Spain, ²Fisiopatologia Osea, Fundacion Jimenez Diaz, Madrid, Spain, ³Histology, Granada University, Granada, Spain, ⁴Medicina Interna, Fundacion Jimenez Diaz, Madrid, Spain.

Bone formation response in long bones produced by intermittent PTH-treatment (4x10⁻⁶ g/Kg/day) was studied in ovariectomized rats under two perspectives: PTH was administered immediately after ovariectomy or in ovariectomized rats after a 6 months period of bone loss. 122 female rats 9 months old, 86 ovariectomized (OVX) and 38 Sham, were used. Rats were separated in two groups for experiments A and B. In experiment A, rats 11.5 months old were sacrificed and named Sham 1 (n=10); OVX 1 (n=10), and OVX+PTH 1 (n=10, PTH treatment for 2.5m). In experiment B, 2 subgroups 15 months old were sacrificed: Sham 2 (n=12), OVX 2(n=12), and 3 more 17.5 months old: Sham 3(n=16), OVX 3 (n=10), and OVX+PTH 3 (n=12, PTH treatment for the last 2.5m). Bone mineral density (BMD) was determined in the whole femur by DEXA using a Hologic QDR-100 TM (S/N 277). Bone morphometry (cortical bone area, bone marrow area, cortical bone thickness) was performed in 20µm thick ground sections of tibia diaphysis stained with von Kossa. Bone trabecular 3D-microarchitecture was studied using

ASBMR 27th Annual Meeting

stereoscopic optical microscopy and scanning electron microscopy (FEI Quanta 200) in anorganic 0.5mm thick tibia sections and apparent trabecular bone area was calculated. Data are summarized in the next table.

	FEMUR BMD g/cm2	TIBIA CORTICAL BONE AREA mm2	TIBIA BONE MARROW AREA mm2	TIBIA CORTICAL BONE THICKNESS µm	TIBIA APPARENT TRABECULAR AREA mm2
SHAM 1 11.5m	0.293±0.016	3.98±0.33	1.19±0.23	229±15	18.24±3.30
OVX 1 11.5m (2.5m)	0.284±0.012	3.99±0.16	1.38±0.21	219±11	14.44±3.33
OVX+PTH 1 11.5m (2.5m+2.5m)	0.324±0.016	4.70±0.32	1.53±0.30	244±19	20.06±3.28
SHAM 2 15m	n.d	3.98±0.33	1.41±0.26	210±12	15.09±2.85
OVX 2 15m (6m)	n.d	3.54±0.33	1.58±0.32	197±13	6.51±1.91
SHAM 3 17.5m	0.320±0.014	4.03±0.45	1.43±0.25	220±18	18.06±3.90
OVX 3 17.5m (8.5m)	0.255±0.002	3.93±0.31	1.59±0.33	215±13	7.51±2.04
OVX+PTH 3 17.5m (8.5m+2.5m)	0.279±0.005	4.13±0.34	1.31±0.28	236±14	7.92±2.07

Though an overall anabolic action of PTH was verified in long bones in both experiments, there are some differences. Cortical and trabecular bone formation was apparent in the first experiment. On the other hand, in the second experiment, when bone loss was established after a 6 month period of ovariectomy, only cortical bone responded considerably. In conclusion, PTH treatment results were conditioned by previous bone mass, bone microarchitecture, and presumably bone turnover status.

Disclosures: **S. Gomez**, None.

SA437

See Friday Plenary number F437.

SA438

Factors Associated with Patient Compliance to Teriparatide: Study Addendum to the DANCE Observational Study. M. D. Rousculp¹, M. Brod^{*2}, P. Chen^{*3}, R. B. Wagman³. ¹Health Outcomes, Eli Lilly and Company, Duluth, GA, USA, ²The Brod Group, San Francisco, CA, USA, ³US Medical, Eli Lilly and Company, Indianapolis, IN, USA.

The World Health Organization identifies compliance to therapy as a primary determinant in treatment success. The National Osteoporosis Foundation's guide for physicians further emphasizes that osteoporosis requires lifelong management and that physicians should encourage patients to be compliant to therapy. Although previous studies have examined compliance with osteoporosis therapies, there is interest in understanding potential factors barriers for an injectable osteoporosis therapy. In a retrospective study of community-based pharmacy claims records, persistency with therapy was relatively higher for patients initiating teriparatide than with patients initiating an oral, anti-resorptive therapy (64.6% vs. 59.9% at 60 days). To further identify potential factors associated with non-compliance with teriparatide, a qualitative study was conducted, including both community-based physicians who prescribed teriparatide and their patients. The results from this study indicated that compliance to therapy involves a dynamic relationship among physicians, patients, drug characteristics and health systems. The factors associated with compliance, and its relative importance, were different for short-term and long-term compliance as well as for adherence and persistence to treatment. Based on this qualitative study, a series of patient-administered surveys were created to be a part of the third phase of the Direct Assessment of Non-vertebral fractures in Community Experience (DANCE) study. The surveys are to be completed at baseline, at the first follow-up visit, and at the first annual follow-up visit. The baseline survey is intended to understand the subject's perception of their severity of disease, expectation of therapy, and concern over treatment modality. The second survey queries the patient's perception of availability of training and support for use of the FORTEO pen, therapy adherence, and persistence shortly after the therapy initiation visit. The third survey asks patients about perception of treatment modality, therapy training and support, therapy affordability, and therapy adherence and persistence one year after initiation of therapy. The data gathered via the surveys should provide better insight on the dynamic nature of compliance and as such could assist clinicians and researchers in identify potential interventions for improving both adherence and persistence to an injectable osteoporosis therapy.

Disclosures: **M.D. Rousculp**, Eli Lilly and Company 1, 3.

SA439

A Novel LRP5 Mutation in the Osteoporosis Pseudoglioma Syndrome. R. Levasseur¹, Y. Allanore^{*2}, M. Abi Fadel^{*3}, M. Varret^{*3}, C. Cormier², A. Kahan^{*2}, C. Boileau^{*3}. ¹Rheumatology, Angers teaching hospital, Angers, France, ²Rheumatology A Department, Cochin Hospital Paris 5 University, Paris, France, ³Inserm U 383, Necker Hospital Paris 5 University,, Paris, France.

Osteoporosis pseudoglioma syndrome (OPPG) is a rare autosomal recessive disorder caused by inactivating mutations in LRP5 (Low density lipoprotein receptor-related protein 5) localized in 11q13.4. This pediatric syndrome includes early-onset blindness

with severe osteoporosis and sometimes other clinical features (1). To date, only 12 mutations have been described in OPPG. Here we report a case of OPPG in a 19 year-old boy with a new LRP5 mutation. This patient is from a consanguineous family of Tunisian origin, has already had 8 fractures in childhood (tibias) and surgery for inter-auricular communication. Clinical examination showed a short stature (1.32m for 42 kg), hypotonia, lower limbs deformities and blindness with microphthalmia. The DXA (Hologic QDR1000, Waltham, MA) results are a lumbar BMD of 0.409 g/cm² and a lumbar Z-score of - 4.3. Calcemia, calciuria, phosphatemia, phosphaturia, intact PTH, 25OHVitD are normal. Mutation analysis of the LRP5 gene revealed a homozygous 5-base pair insertion (1048_1049insGGACA) in exon 5. This would cause a frame shift at amino acid 334 (R334fsX51) and lead to the appearance of a stop codon 51 amino acid downstream. Cell. The protein would lack 1231 amino acids and the co-receptor would not be fonctionnal. The treatment of this severe osteoporosis includes regular perfusion of pamidronate with no new fracture. This new case of OPPG emphasizes the major role of LRP5 in bone accrual and eye development (2).

(1) Levasseur R, Lacombe D, de Vernejoul MC. LRP5 : the gene mutated in Osteoporosis-pseudoglioma syndrome and the high bone mass phenotype. Joint Bone Spine 2005;72(3):207-14.

(2) Gong Y, Slee RB, Fukai N, Rawadi G, Roman-Roman S, Reginato AM et al. LDL receptor-related protein 5 (LRP5) affects bone accrual and eye development. Cell. 2001;107(4):513-23.

Disclosures: **R. Levasseur**, None.

SA440

See Friday Plenary number F440.

SA441

Variable Structure of Osteogenesis Imperfecta Bone. F. Shapiro, E. Flynn^{*}. Department of Orthopedic Surgery, Children's Hospital Boston, Boston, MA, USA.

This study assessed the histologic structure of osteogenesis imperfecta (OI) bone obtained from human long bone diaphyses. Bone samples were obtained from 30 patients, 4 at post-mortem study from Type II OI and 26 from patients undergoing osteotomy with Types I, III, and IV OI. Tissue underwent paraffin or plastic embedding, staining with hematoxylin and eosin or toluidine blue, and examination by light microscopy (LM) and polarizing LM. Assessments included: osteocyte cellularity in relation to matrix structure (woven or lamellar), the proportions and appearances of woven and lamellar bone where both were present simultaneously, and the structure of lamellar tissue deposition. The LM structure of normal diaphyseal bone from embryo onwards includes all woven bone (grade I), combinations of woven and lamellar bone (grade II), and all lamellar bone (grade III) progressing towards compact Haversian (osteonal) conformation. OI bone showed a non-mature pattern but developed along the normal pathway of woven and lamellar although the lamellar pattern differed from the normal in all but the mildest instances. The more tissue there was deposited, the more mature the tissue deposition pattern. The grading system applied to the OI bone follows. Grade I: woven bone only. This was seen in Type II OI (4 cases) as discontinuous spicules of woven bone. Grade II: both woven and lamellar bone, in 3 groupings. In Types II and IV OI (25 cases) the full spectrum of Grade II was seen: Grade IIa (woven bone greater in amount than lamellar bone)--only traces of lamellae on the woven scaffold, insufficient to promote osteonal synthesis; Grade IIb (woven and lamellar bone equal in amount)--allowing for beginning osteonal formation; and Grade IIc (lamellar bone greater in amount than woven bone)--leading to increased osteonal formation and compaction. Grade III: lamellar bone only, in 2 groupings; grade IIIa (partially compacted, forming osteonal systems) and grade IIIb (fully compacted lamellar osteonal bone). In Type I OI (1 case) normal appearing lamellar osteonal bone was present with slightly diminished compaction. All Grade II specimens had a mosaic structure: woven bone accumulations on which were deposited lamellar tissue and the lamellar tissue itself characterized by blocks of shortened, discontinuous, and multipplanar accumulations. Bone tissue compaction increased from Grade I to Grade IIIb. This study revealed the considerable variability in the structure of OI bone but also the tendency to develop a progression towards the normal. This categorization can be applied to all variants of OI bone, allowing for a qualitative and quantitative assessment of several structural variables, each of which is important in determining OI bone strength.

Disclosures: **F. Shapiro**, None.

SA442

See Friday Plenary number F442.

SA443

Treatment of Osteogenesis Imperfecta Type I with Weekly Alendronate. R. C. Gensure, T. Ponnappakkam^{*}. Pediatrics, Ochsner Clinic Foundation, New Orleans, LA, USA.

Treatment of severe forms of osteogenesis imperfecta (OI) (type III/IV) has been revolutionized by the report that cyclical administration of intravenous pamidronate results in significant increases in bone density and reduction in fracture rates (Glorieux F, et. al., NEJM, 1998). While children with OI type 1 have a much milder disease, the increased fracture rate and pain from microfractures results in significant morbidity and limitation on physical activity. Cyclical administration of IV pamidronate, and more recently daily administration of alendronate (Dimeglio LA, et. al., J Pediatr Endocrinol Metab 2005),

ASBMR 27th Annual Meeting

have been shown to be efficacious in the treatment of OI type I. To avoid complications of IV therapy and improve compliance over daily dosing, we treated four patients (ages 5-6) with OI type I with weekly oral alendronate (1 mg/kg/wk) and assessed the effects on bone mineral density after 6 months therapy. Each patient showed reduction in markers of bone turnover and improvement in bone mineral density z-score over the treatment period (Z-score increased by 1.08 +/- 0.35, p<0.05). None of the patients had any fractures during treatment. There were no incidents of esophagitis, and growth rates remained normal (growth velocity 7.6 +/- 1.0 cm/yr). While not formally assessed, all patients described a marked reduction in pain and increased physical activity while on treatment. Interestingly, one of the patients who had ankle films to evaluate for possible fracture showed transverse lines on the fibula similar to those described after cyclical pamidronate administration. For patients with milder forms of osteogenesis imperfecta, treatment with a simplified regimen of weekly oral alendronate provided an acceptable alternative to intravenous therapy.

Disclosures: **R.C. Gensure**, None.

SA444

See Friday Plenary number F444.

SA445

Bone Mineral Density in Patients with Myelomeningocele. G. Luisetto^{*1}, V. Camozzi^{*1}, G. de Eccher^{*2}, E. Bertossi^{*2}, B. Disarò^{*2}, A. Marucco^{*2}, P. Drigo^{*2}. ¹Dept. of Surgical and Gastroenterological Science, University of Padua, Padua, Italy, ²Dept. of Pediatrics, University of Padua, Padua, Italy.

Myelomeningocele (MMC) is a relatively frequent disease with a prevalence of 1/1000 newborns. The lower limbs motor deficiency of the patients with MMC prevents the normal bone growth and increases the risk of fracture. Although the fractures represent a main clinical problem, there is a little information about bone status in these patients. Purposes of this study are: 1) to establish the diagnostic significance of two different methods employed to evaluate bone status: Dual-energy X ray absorptiometry (DXA) and Quantitative Ultrasound technique (QUS); 2) to correlate BMD at spine and femur with the level of injury and the degree of motor deficiency. Sixty one patients, 27 females and 34 male, (mean age \pm SD: 15 \pm 6.2 years) have been studied. The level of injury was above L3 in 19 subjects, between L4-S1 in 25, and below S1 in 17. Regarding motor deficiency, patients were divided into three groups: completely unable to walk (NW, N=15, age = 18.7 \pm 6.2 years), partially walking (PW; N= 17, age 15.0 \pm 6.1), and able to walk (W; N=29, age = 16 \pm 6.8). Anthropometric variables, daily calcium intake, common laboratory parameters of bone and mineral metabolism, as well as DXA and QUS parameters have been assessed in each patient. BMD was measured using a Hologic QDR 4500 C densitometer (Waltham, Mass, USA) and values were expressed as BMD Z-Score at lumbar spine and proximal epiphysis of the left femur. QUS parameters have been measured at the proximal phalanges of the finger 2 to 5 of both hands with a DBM Sonic Profile device (Igea, Carpi, Italy). Results are expressed as amplitude-dependent speed of sound (AD-SOS). All DXA values were lower than reference normal values at both spine and femur. W patients showed spine Z-score higher than that of PW, and the latter showed spine Z-score higher than NW. (W: -1.04 \pm 1.89; PW: -1.26 \pm 1.26; NW: -2.17 \pm 1.86. ANOVA: p<0.01). At femoral level, PW patients showed BMD lower than that found in the other two groups of patients (Femoral neck BMD Z-score, PW: -2.65 \pm 1.13; NW: -1.66 \pm 1.49; W: -1.31 \pm 1.40; ANOVA: p<0.01). Patients with injury below S1 showed BMD values significantly higher than those found in the other two groups (p<0.05). QUS parameters, as well as laboratory variables did not differ among the groups. In conclusion, our findings show that the ability of walking doesn't have a significant influence on BMD in patients suffering from myelomeningocele. BMD is lower in the denervated sites, suggesting a pivot role of nervous system in the skeletal trophism, independent of motility. The lower BMD explains, at least in part, the high number of fractures at the lower limbs in these patients.

Disclosures: **G. Luisetto**, None.

SA446

See Friday Plenary number F446.

SA447

Safety and Efficacy of the Use of Zoledronic Acid (AZ) in Children with Osteogenesis Imperfecta - Preliminary Data. E. Ribeiro^{*}, G. Saraiva^{*}, S. Maeda^{*}, A. Castaldoni^{*}, M. Lazaretti-Castro. Endocrinology, Universidade Federal de São Paulo, Sao Paulo, Brazil.

Osteogenesis imperfecta (OI) is a genetic disorder of increased bone fragility and low bone mass. Severity varies widely, ranging from intrauterine fractures and perinatal lethality to very mild forms without fractures. The diagnostic clinical of OI is based mainly on signs and symptoms: blue sclera, dentinogenesis imperfecta, hyper laxity of ligaments and skin, hearing impairment. The most widely used classification of OI is by Silience and col with four clinical types. Recently three additional groups were described: Type I, II, III, IV, V, VII and VII. Clinical treatment with pamidronate has show to be safe and efficient to reduce fracture and improve the life quality in OI patients. The ZA is the most powerful available bisphosphonate and has a faster time of IV infusion than pamidronate. This possibility makes a great difference mainly for children, reducing the time of hospitalization and the costs of treatment. Its efficacy and safety in children with OI, however, has not yet been tested.AIM: To verify the safety and efficacy of ZA during one

year treatment in children with OI type III and IV. METHODS: Nine children were selected to participate of a research protocol to receive ZA (Zometa™ from Novartis), in a dose of 0.4 \pm 0.08mg/kg/year in a 30 minutes IV infusion every three to four months. Five patients have finished one year of treatment and the remaining, still under treatment; have received at least two infusions. Before each infusion, blood was collected for total and ionized calcium, alkaline phosphatase, phosphate, CTX and osteocalcin in serum, intact PTH, renal and hepatic function and hemogram. Bone Mineral density (BMD) at lumbar spine and total body were measured at the baseline and at the end of the study. RESULTS: Out of 9 patients (7 boys, 2 girls), 5 had type IV and 4 type III. The average age was the 5.1 \pm 2.8 years (from 1.6 to 9.4). The adverse events were: fever (n=9), nausea (n=5), and vomiting (n=2) during the 24 hours following the first infusion. Except for one patient with anemia at baseline, all had normal laboratory until the end of the study. From baseline to the end of treatment, spine BMD increased significantly (0.310 \pm 0.073 to 0.462 \pm 0.019mg/cm², respectively, p<0.016) and total body BMD almost reached significance (0.672 \pm 0.126 to 0.758 \pm 0.064mg/cm², p<0.059). CONCLUSION: ZA infusion was safe and efficient in increasing BMD in our group of children with OI. Due to its fast procedure, it is more convenient for children. However, a ZA effect on fracture risk, in despite to be likely, still has to be proved.

Disclosures: **M. Lazaretti-Castro**, None.

SA448

Bone Loss in Mice after Spinal Cord Injury; an Histomorphometrical, Biomechanical and Densitometrical Study. S. Picard¹, J. P. Brown¹, J. Frenette^{*2}, S. Jean^{*1}, P. A. Guertin^{*3}. ¹Rheumatology and Immunology Research Department, CHUL Research Center, Laval University, Sainte-Foy, PQ, Canada, ²Department of Rehabilitation, Laval University, Sainte-Foy, PQ, Canada, ³Neuroscience Research Center, CHUL Research Center, Laval University, Sainte-Foy, PQ, Canada.

Mechanical loading in daily life helps maintain bone strength. Conversely, immobilization activates osteoclast recruitment and depresses osteoblast activity, resulting in an unbalance in bone metabolism and significant bone losses. Although bone density loss after spinal cord injury is well-documented in humans, there is a lack of data with quantitative histology measurements after spinal cord injury in animal models. This study reports the development of a model of spinal cord injury in mice for which histomorphometric, biomechanic and bone mineral density (BMD) measurements were performed at fixed delays post-spinalization. At 10, 15, and 30 days post-spinal cord transection (low-thoracic level), left femoral bones were processed, paraffin embedded, and stained with Masson's trichrome procedures. Histomorphomeric analyses were performed with a NOVA Prime, Bioquant's image analysis system for primary bone morphometric parameters. The right femoral was preserved within humid condition at -20°C prior densitometrical and biomechanical testing. There was a marked decrease in bone volume (-25 %, p 0,0217), trabecular thickness (-12 %, p 0,0397) but no significative change for trabecular number (16 % p 0,0933) and trabecular separation (+ 25 %, p 0,0775). Results using three-point bending testing indicated a 23,7% p:0,035 decrease in elastic force with a rapid decrease, although non-significant, of total strength one month post-transection. BMD measurements using dual energy x-ray absorption (DEXA) revealed a significant 15% decrease of bone mineral contents. The complementary assessment methods shall help describe the overall changes in bone morphometry, strength, and mineral content occurring after spinal cord injury in paraplegic mice. Results obtained with this model may contribute to the development of new pharmacological approaches to prevent or reverse severe bone problems associated with complete immobilization.

Disclosures: **S. Picard**, None.

SA449

Predictors of Bone Mineral Density in Patients on Antiepileptic Drugs. L. Dib^{*1}, M. A. Mikati^{*2}, B. Yamout^{*1}, R. Sawaya^{*1}, G. El-Haji Fuleihan¹. ¹Internal Medicine, American University of Beirut, Beirut, Lebanon, ²Pediatrics, American University of Beirut, Beirut, Lebanon.

Use of antiepileptic drugs (AEDs) is associated with metabolic bone disease. Bone density in epileptic patients can be affected by seizure duration, 25(OH) vitamin D levels[25(OH)D], type of seizure and possibly type or mode of therapy. Characteristics of ambulatory subjects on AED therapy for at least 6 months and their relationship to bone mineral density (BMD) and content (BMC) were studied. The adult group included 106 subjects; 57 women/49 men, age 29.7 \pm 10.5 years, duration of AED therapy 11.9 \pm 10.2 years, mean 25(OH)D 14.9 \pm 9 ng/ml. The pediatric group included 88 subjects, 45 boys/43 girls, age 13.0 \pm 2 years, duration of AED therapy 4.7 \pm 4 years, mean 25(OH)D 18.5 \pm 8 ng/ml. In adults, but not in children, 25(OH)D levels and bone density at the spine and hip were significantly lower than that of age, gender matched controls using both the Western database, as well as the local database ¹ (p<0.04). Around 50% of overall subjects had low 25(OH)D levels, but vitamin D levels did not correlate with BMD in either age group. In adults only, duration of AED therapy negatively correlated with BMD at the trochanter (r=-0.23, p<0.05). Total duration of phenytoin use (current and previous) negatively correlated with total hip, femoral neck and trochanter BMD, R= 0.3-0.39, p<0.05. Similarly, in adult women the negative correlations varied between 0.5-0.7 at lumbar spine, total hip, femoral neck, and trochanter BMD, p< 0.05. Such correlations were not detected with the use of phenobarbital, carbamazepine, or with the non-enzyme-inducing AEDs. Similar bivariate analyses in children did not reveal any significant correlations. Linear regression analyses adjusting for age, weight and duration of therapy revealed a significant negative effect of enzyme-inducing AEDs on BMD in the adult group at the LS (p=0.04), FN (p=0.036) and an almost significant negative effect at the trochanter (p=0.07). In the pediatric group, there

was a significant negative effect of polypharmacy on subtotal BMD ($p=0.04$), and a similar negative effect on subtotal BMC in girls ($p=0.024$). In conclusion, ambulatory adults but not children on chronic AEDs had low BMD compared to age, gender and ethnic-matched controls. Vitamin D levels, in the range noted, were not correlated to BMD/BMC at any site. In adults, cumulative phenytoin use (past and current) and the use enzyme-inducing drugs were significant negative predictors of BMD. Polypharmacy adversely affected BMD in children.

1. El-Hajj Fuleihan G. Bone 2002; 31:520-528.

Disclosures: **G. El-Hajj Fuleihan**, None.

SA450

See Friday Plenary number F450.

SA451

The Importance of Fibroblast Growth Ractor-23 in Regulating the Phosphate Homeostasis in the Hyperphosphatemic Situation as in Untreated Graves' Disease. Y. Rhee¹, S. Park^{*1}, S. Kang^{*1}, S. Park^{*1}, D. Kim^{*1}, S. Lee^{*1}, Y. Kim², S. Lim¹. ¹Internal Medicine, College of Medicine, Yonsei Univ., Seoul, Republic of Korea, ²Internal Medicine, National Health Insurance Corporation Ilsan Hospital, Kyungki, Republic of Korea.

Fibroblast growth factor-23(FGF-23) is one of the phosphatonins that regulate phosphate homeostasis, have been discovered through studies of phosphate-wasting disorders such as X-linked hypophosphatemia, autosomal dominant hypophosphatemic rickets and oncogenic osteomalacia. The key role of the calcium and phosphate homeostasis was always assigned to parathyroid hormone and vitamin D axis. However, to identify the role of FGF-23 in the mineral metabolism, we selected the patient with hyperthyroidism which usually accompany with the elevated calcium and phosphate. The study group comprised 44 patients with or without Graves' disease. There were 23 patients with biochemically and radiologically proven Graves' disease (GD) blood sample taken before starting the anti-thyroid drug. The control group was composed of 21 people who were proven to be euthyroid without any diseases affecting mineral metabolism. Plasma FGF-23, calcium, phosphate, parathyroid hormone (PTH), 25-hydroxyvitamin D (25(OH)D) and bone turnover markers were compared between these groups. Plasma FGF-23 assay was to detect the intact form. (Immuopics, USA) As expected, the calcium and phosphate in the GD were significantly higher with elevated free T4. ($P < 0.05$) The bone turnover markers - osteocalcin and serum C-telopeptide were significantly elevated respectively in the GD group(13.3 +/- 4.9 ng/mL vs. 43.7 +/- 7.9 ng/mL and 0.38+/-0.44 vs. 1.13+/-0.67, $P<0.05$)) In the GD group, the serum FGF-23 level was significantly higher ($P < 0.05$) than in the control group (62.3 +/- 89.0 ng/L vs. 41.4 +/- 3.6 ng/L). However, there was no significantly lowered PTH in the GD group with surprisingly lower 25(OH)D level(12.5 ng/mL in GD) which would have affected the PTH level. Serum FGF-23 levels were positively correlated with serum phosphate levels ($r=0.457$, $P < 0.05$) and with free T4 levels ($r=0.393$, $P < 0.05$). The significant positive correlation between serum levels of phosphate and FGF-23 and the compensatory increase in GD group indicate that FGF-23 is an important regulator of serum phosphate homeostasis.

Disclosures: **Y. Rhee**, None.

SA452

Epidermal Nevus Syndrome with Focal Bone Defects and Hypophosphatemic Rickets: FGF23, GNASI, and Skeletal Histology Evaluation. D. Wenkert¹, S. L. Teitelbaum², W. H. McAlister^{*3}, F. H. Gannon⁴, S. Mumm⁵, M. P. Whyte¹. ¹Center for Metabolic Bone Disease and Molecular Research, Shriners Hospitals for Children, St. Louis, MO, USA, ²Department of Pathology, Washington University School of Medicine, St. Louis, MO, USA, ³Department of Pediatric Radiology, Mallinckrodt Institute of Radiology, St. Louis Children's Hospital, St. Louis, MO, USA, ⁴Armed Forces Institute of Pathology, Washington, DC, USA, ⁵Division of Bone and Mineral Diseases, Washington University School of Medicine, St. Louis, MO, USA.

Epidermal nevus syndrome (ENS) is a rare, sporadic condition sometimes associated with focal bone defects and renal phosphate (Pi) wasting causing hypophosphatemic rickets (HR) and weakness. The etiology of ENS is unknown. One such patient (#2, submitted) leads us to report 2 additional cases listed below in descending order of the degree of skin and bone involvement. In each, HR and weakness responded to treatment with 1,25(OH)₂D₃ and Pi supplementation as extensive removal of nevi was also performed. In DNA isolated from nevi of the first 2 patients and peripheral WBCs of all 3, no *GNASI* mutation was found. *Patient 1*, first evaluated at age 3, had predominately right-sided skin but bilateral focal bone lesions. Weakness was profound if she stopped medical therapy. She died at age 26 from pneumonia complicating severe skeletal disease. Histology of femoral bone at age 12 years showed a patchy area of fibrous dysplasia (FD) seen radiographically despite normal gross appearance. However, FD was not detected 14 years later at limited autopsy. Serum FGF23 at age 21 yrs was > 2,470 (63 +/- 33 (SD)). *Patient 2*, a 20-year-old, was referred at age 15 years with x-rays changes reminiscent of FD ipsilateral to his nevi. Bone from his affected and unaffected iliac crests revealed osteomalacia and decreased numbers of trabeculae, but no FD. His FGF23 level was elevated at 215. *Patient 3*, an 11-year-old, was referred at age 3 with schizencephaly, temporal lobe atrophy, seizures, and x-ray changes suggestive of FD limited to his skull. Bone biopsies were not obtained. His FGF23 level was normal at 90. Histologic evaluation of the extensive focal bone defects in our most severely affected patient showed at least one patchy area of FD. Serum FGF23 levels seemed to reflect the extent of skin involvement and extent of focal bone defects. The third patient despite having the lowest

FGF23 and the least skin and bone involvement had neurological findings of ENS. Many features of ENS are suggestive of McCune Albright syndrome (skin involvement, FD, HR, sometimes precocious puberty) yet our evaluation of *GNASI* was unremarkable. Studies of *GNASI* in dysplastic bone were not performed.

Disclosures: **D. Wenkert**, None.

SA453

See Friday Plenary number F453.

SA454

Cinacalcet Is Associated with Decreased Serum FGF-23 and Improved Phosphorous Homeostasis in Patients with Tumor-Induced Osteomalacia. J. L. Geller^{*1}, C. Cutler^{*2}, M. H. Kelly^{*2}, J. S. Adams¹, M. T. Collins². ¹Burns and Allen Research Institute, Division of Endocrinology, Cedars-Sinai Medical Center, David Geffen School of Medicine at UCLA, Los Angeles, CA, USA, ²Craniofacial and Skeletal Diseases Branch, NIDCR, NIH, DHHS, Bethesda, MD, USA.

FGF-23 is a circulating peptide hormone, which plays a key role in mineral homeostasis by inhibiting renal phosphorus reabsorption and the formation of 1,25-dihydroxyvitamin D (1,25-D). Tumor-induced osteomalacia (TIO) is an acquired syndrome of hypophosphatemic osteomalacia often caused by tumoral production of FGF-23. Patients exhibit hypophosphatemia, hyperphosphaturia, low or inappropriately normal 1,25-D levels and osteomalacia. Tumors are notoriously difficult to localize and medical therapy, consisting of large doses of oral phosphorous and 1,25-D, is often required. We have previously shown (Gupta et al. JCEM 89:4489, 2004) that high circulating levels of FGF-23 in patients with hypoparathyroidism were unable to bring about significant phosphaturia, suggesting that parathyroid hormone (PTH) is downstream of FGF-23 in the phosphaturic response. Therefore, we proposed that induction of (relative) hypoparathyroidism with the calcium sensing receptor agonist, cinacalcet, might improve phosphorous balance in TIO. Two patients with bone pain, pathological fractures, hypophosphatemia, phosphaturia, low serum 1,25-D and elevated serum FGF-23 were evaluated (Table 1). In both cases, despite extensive diagnostic studies, the source of FGF-23 remained elusive. Both were treated with a regimen of high dose oral calcitriol and phosphorus, which was poorly tolerated due to diarrhea. Treatment with cinacalcet at 30 mg daily was initiated. Serial measurements of serum FGF-23, (Kainos, Tokyo, Japan), calcium, phosphorus, iPTH and urine tubular reabsorption of phosphorus (TRP) were obtained.

Table 1. Response to cinacalcet in two patients with TIO

Patient	& cinacalcet	time post	FGF-23 pg/ml	Serum		iPTH pg/ml	Urine		Daily Rx K-Phos neutral mg/day
				Ca mg/dl	Phos mg/dl		TRP %		
1	0 hour		3625	9.7	2.2	29	66		1500
1	24 hours		2836	8.6	3.2	12	73		1500
1	4 weeks		2290	8.1	3.0	11	64		750
2	0 hour		190	9.1	1.9	24.1	48		2000
2	4 hours		178	8.9	2.5	11.2	82		2000
2	24 hours		73	8.7	2.1	25.5	64		2000
2	4 weeks		--	8.9	2.2	21.0	68		0

Initiation of cinacalcet resulted in 37% and 62% decrease in serum FGF-23 levels by 24 hours in both subjects, which was accompanied by an increase in TRP and serum phosphorus, and an eventual (4 weeks) decrease or elimination of oral phosphate supplementation. Via its ability to diminish PTH-directed phosphaturia, or by decreasing serum FGF-23, cinacalcet may prove to be an effective adjuvant in the medical management of FGF-23-mediated TIO.

Disclosures: **J.L. Geller**, None.

SA455

Secreted Frizzled Related Protein-4 Reduces Sodium-Phosphate Co-transporter Abundance and Activity in Proximal Tubule Cells. T. Berndt^{*1}, T. Craig^{*1}, B. Bielez^{*2}, P. Tebben¹, D. Bacic^{*2}, C. Wagner^{*2}, S. O'Brien^{*3}, S. Schiavi³, J. Biber^{*2}, H. Murer^{*2}, R. Kumar¹. ¹Nephrology Research, Department of Medicine, Biochemistry and Molecular Biology, Mayo College of Medicine, Rochester, MN, USA, ²Institute of Physiology, University of Zurich, Zurich, Switzerland, ³Receptor Ligand Therapeutics, Genzyme Corporation, Framingham, MA, USA.

The phosphatonin, secreted frizzled related protein (sFRP-4), a protein over-expressed in tumors associated with renal phosphate wasting, induces phosphaturia and inhibits 25-hydroxyvitamin D 1 α -hydroxylase activity that is normally induced in response to a hypophosphatemic stimulus. To determine the mechanism by which sFRP-4 acutely alters renal phosphate (Pi) transport, we examined the effect of intravenous infusion of sFRP-4 (n=10), vehicle (n=7), or PTH (n=7) on renal brush border membrane (BBMV) Na⁺-dependent Pi uptake and the abundance and localization of the major Na⁺-Pi Ila co-transporter in the proximal tubule and in opossum kidney cells. As reported earlier, short-term infusion of sFRP-4 (0.3 μ g/kg/Hr) significantly increased the fractional excretion of Pi (FE Pi) from 10 \pm 2 to 25 \pm 5% ($P<0.05$) and decreased β -catenin concentrations in the kidney. PTH infusion (8 μ g/kg/Hr) increased the FE Pi from 11 \pm 2 to 33 \pm 5% ($P<0.05$). The increase in FE Pi with sFRP-4 infusion was associated with a 21.9 \pm 3.4 % decrease in BBMV Na⁺-dependent Pi uptake ($P<0.001$) compared with a 39.5 \pm 2.1 % inhibition of Na⁺-dependent Pi transport in renal BBMV induced by PTH ($P<0.001$). The decrease in BBMV Na⁺-Pi uptake induced by sFRP-4 was associated with a 30.7 \pm 4.8 % decrease in Na⁺-Pi Ila

ASBMR 27th Annual Meeting

co-transporter protein abundance ($P < 0.01$) as assessed by Western blotting methods compared to a 45.4 ± 8.8 % decrease induced by PTH ($P < 0.001$). In opossum kidney cells, sFRP-4 significantly reduced surface expression of a heterologous Na⁺-Pi IIa co-transporter. We conclude that sFRP-4 increases renal Pi excretion by reducing Na⁺-Pi IIa transporter abundance in the brush border of proximal tubule through enhanced internalization of the protein.

Disclosures: **T. Berndt**, None.

SA456

Fibroblast Growth Factor-23 Is Regulated by 1,25-Dihydroxyvitamin D. M. T. Collins¹, J. R. Lindsay^{*2}, A. Jain^{*3}, M. H. Kelly^{*4}, C. M. Cutler^{*1}, L. S. Weinstein⁵, L. Jie^{*5}, N. S. Fedarko⁶, K. K. Winer^{*7}. ¹CSDB/NIDCR, National Institutes of Health, Bethesda, MD, USA, ²PREB/NICHD, National Institutes of Health, Bethesda, MD, USA, ³GCRC, Johns Hopkins, Baltimore, MD, USA, ⁴Nursing and Patient Care Services, National Institutes of Health, Bethesda, MD, USA, ⁵MDB/NIDDK, National Institutes of Health, Bethesda, MD, USA, ⁶Division of Geriatric Medicine, Department of Medicine, Johns Hopkins University, Baltimore, MD, USA, ⁷NICHD, National Institutes of Health, Bethesda, MD, USA.

FGF-23 is a recently described hormone that has been demonstrated to be involved in the regulation of phosphate and vitamin D metabolism. The physiologic role of FGF-23 in mineral metabolism and how serum FGF-23 levels are regulated have yet to be elucidated. Three patients with mineral metabolism defects that allowed for the investigation of the regulation of FGF-23 were studied. Patient 1 had post-surgical hypoparathyroidism and Munchausen's syndrome and consumed a pharmacologic dose of calcitriol. Patient 2 had post-surgical hypoparathyroidism and fibrous dysplasia of bone. She was treated with increasing doses of calcitriol followed by synthetic PTH 1-34. Patient 3 had pseudohypoparathyroidism type 1B and tertiary hyperparathyroidism. She underwent parathyroidectomy, which was followed by the development of hungry bone syndrome and hypocalcemia requiring treatment with calcitriol. Serum FGF-23 (Immutopics, San Clemente, CA) and serum and urine levels of mineral metabolites were measured in all 3 patients. Patient 1 had an acute and marked increase in serum FGF-23 (70 to 670 RU/ml, normal range 18-108) within 24 hours in response to high-dose calcitriol administration. Patient 2 demonstrated stepwise increases in serum FGF-23 from 117 to 824 RU/ml in response to increasing serum levels of 1,25-dihydroxyvitamin D (1,25-D). Finally, prior to parathyroidectomy, while hypercalcemic, euphosphatemic, with low levels of 1,25-D (10 pg/ml, normal 22-67), and very high serum PTH (863.7 pg/ml, normal 6.0-40.0), patient 3 had high serum FGF-23 levels (217 RU/ml). Following surgery, while hypocalcemic, euphosphatemic and with high serum levels of serum 1,25-D (140 pg/ml), FGF-23 levels were higher than preoperative levels (305 RU/ml). In the absence of PTH or a PTH effect, marked elevations of FGF-23 were not associated with a marked lowering of serum phosphorus or increases in phosphorus excretion. Serum FGF-23 is regulated by serum 1,25-D, but its phosphaturic effect may be diminished in the absence of PTH.

Disclosures: **M.T. Collins**, None.

SA457

See Friday Plenary number F457.

SA458

The Kidneys of X-Linked Hypophosphatemic (Hyp) Mice Have Altered mRNA Expression of Many Membrane Transporters Besides Phosphate. M. H. Meyer, R. A. Meyer. Department of Orthopaedic Surgery, Carolinas Medical Center, Charlotte, NC, USA.

X-linked hypophosphatemia is characterized by decreased renal reabsorption of phosphate, low plasma phosphate, and rachitic and osteomalacic bone disease. No other defects in the kidney are known to exist. To explore the impact of this mutation further, kidneys from five-week-old mice, normal and *Hyp* (hemizygous male and heterozygous female), were collected, and RNA was extracted and hybridized to Affymetrix Mouse 430A and 430B microarrays with probe sets for over 40,000 genes. The RNA for each array was pooled from three mice. A total of 24 arrays, six for each genotype and gender, were done. The data were transferred to an Excel spreadsheet, formulas for factorial analysis of variance were added, and the formulas were copied to all genes. GenMAPP (www.genmapp.org) was used to identify transport-related genes with a significant main effect of genotype (normal vs. *Hyp*). RNA levels for all phosphate transporters were significantly decreased ($P < 0.001$) in the *Hyp* mice. In addition, mRNA for the sulfate transporter, *slc13a1*, increased 2 fold ($P < 0.001$) in *Hyp*. mRNA for the chloride transporter, *slc12a3*, increased over 50% ($P < 0.001$). mRNA for organic anion transporters (OAT) also changed with a 16% decrease in OAT1 (*slc22a6*, $P < 0.001$), a 50% increase in OAT2 (*slc22a7*, $P < 0.01$), a 50% decrease in OATP1 (*slc01a1*, $P < 0.001$, only expressed in males), and a 33% decrease in females for *slc13a3* ($P < 0.01$). The organic cation transporter, *slc22-like 2* (*slc22a2*), also had a 33% decrease ($P < 0.001$) in the *Hyp* mice. mRNA for the sodium/potassium transporting ATPase, alpha 2 polypeptide, *atp1a2*, has four probe sets on the arrays, and all increased 2 to 8 fold ($P < 0.001$), while the thiazide-sensitive NaCl transporter, *slc12a3*, increased 50% ($P < 0.001$) in the *Hyp* mice. Changes in mRNA for glucose transporters were mixed with the low affinity sodium-dependent glucose transporter, *slc5a2*, decreasing 33% in *Hyp* mice ($P < 0.001$), along with smaller decreases in the facilitated glucose transporter, *slc2a2* ($P < 0.001$). mRNA for the high affinity sodium/glucose transporter, *slc5a1* increased 50% ($P < 0.001$), along with a smaller increase in the insulin-responsive facilitated glucose transporter *slc2a4* ($P < 0.01$). In

summary, the *Hyp* mutation causes changes in the mRNA expression of transporters in the kidney other than for phosphate. This suggests a broader metabolic effect of the *Hyp* mutation. (Supported in part by the NIH, DK064049.)

Disclosures: **R.A. Meyer**, None.

SA459

See Friday Plenary number F459.

SA460

Sensitivity of FGF23 Measurements in Tumor Induced Osteomalacia. E. A. Imel^{*1}, M. Peacock¹, P. Pitukcheewanont^{*2}, H. J. Heller^{*3}, L. M. Ward⁴, D. Shulman^{*5}, M. Kassem^{*6}, P. Rackoff^{*7}, M. Zimering^{*8}, A. Dalkin^{*9}, E. Drobney^{*10}, G. Colussi^{*11}, J. Shaker^{*12}, E. H. Hoogendorn^{*13}, M. J. Econs¹. ¹Indiana U, Indianapolis, IN, USA, ²USC, Los Angeles, CA, USA, ³UT SW Med Ctr, Dallas, TX, USA, ⁴U of Ottawa, Ottawa, ON, Canada, ⁵USF, St. Petersburg, FL, USA, ⁶U Hosp of Odense, Odense, Denmark, ⁷Beth Israel Hosp, NY, NY, USA, ⁸Dept of VA, New Jersey Hlth Care System, Lyons, NJ, USA, ⁹UVA Hlth System, Charlottesville, VA, USA, ¹⁰Medical College of Wisconsin, Milwaukee, WI, USA, ¹¹Circolo & Fondazione Macchi Hosp, Varese, Italy, ¹²St Luke's Med Ctr, Milwaukee, WI, USA, ¹³U Hosp at Radboud,, Nijmegen, Netherlands Antilles.

Tumor induced osteomalacia (TIO) is a paraneoplastic syndrome consisting of hypophosphatemia, hyperphosphaturia, inappropriately normal or low calcitriol concentrations and osteomalacia. Fibroblast growth factor 23 (FGF23) is mutated in autosomal dominant hypophosphatemic rickets, and elevated in patients with X-linked hypophosphatemic rickets and TIO. We measured plasma FGF23 levels by three ELISA assays in 22 patients with clinical presentation of TIO. Samples were assessed for plasma FGF23 levels and compared for sensitivity to the diagnosis of TIO and to serum phosphate levels. Diagnosis of TIO was based on clinical history of new onset hypophosphatemia and renal phosphate wasting, with bone pain and weakness. The sensitivity for TIO for the C-terminal (C-term) assay was 73%, for the Immutopics Intact assay 45%, and for the Kainos assay 86%. FGF23 was undetectable in 22% of cases by Immutopics Intact assay. In 13 cases we obtained tissue confirmation of TIO, and another had a nonresectable brain tumor. In the patients with confirmed tumors the sensitivity increased to 93% for the C-term assay, 100% by Kainos assay, and 57% for the Immutopics Intact assay. There was an inverse correlation between FGF23 levels and phosphorous levels with R² values for C-term, Immutopics Intact and Kainos assays of 0.23, 0.24 and 0.30 respectively. Nine patients had repeat FGF23 levels tested after tumor removal. FGF23 levels assessed by C-term assay and Kainos assay declined after surgery in 7 of 9 patients ($p = 0.04$). One patient had a tumor that was not fully resectable. The other had renal insufficiency and lower Kainos assay values after surgery, but continued to have elevated results on the C-term assay. Patients with TIO overexpress FGF23. Two assays had good sensitivity for TIO. Normal concentrations of FGF23 in some TIO patients may indicate that sensitivity is not optimal for any currently available assay, that other phosphaturic factors are responsible for the syndrome in some patients, or like many other endocrine tumors, the tumors are partially responsive to the metabolic state of the patient.

Disclosures: **E.A. Imel**, None.

SA461

See Friday Plenary number F461.

SA462

MEPE Is Overexpressed in Osteocytes of the DMP1 (Dentin Matrix Protein 1) Null Mouse, Contributing to the Hypophosphatemia and Osteomalacia. S. E. Harris¹, J. Gluhak-Heinrich², M. A. Harris¹, W. Yang¹, P. S. N. Rowe³, Y. Xie^{*4}, H. Rios^{*4}, S. Zhang^{*4}, M. D. McKee^{*5}, L. F. Bonewald⁴, J. Q. Feng⁴. ¹Dept. of Periodontics and Cellular and Structural Biol, University of Texas Health Science Center at San Antonio Health Science Center, San Antonio, TX, USA, ²Dept. of Orthodontics, University of Texas Health Science Center at San Antonio Health Science Center, San Antonio, TX, USA, ³Dept. of Periodontics, University of Texas Health Science Center at San Antonio Health Science Center, San Antonio, TX, USA, ⁴Dept. of Oral Biology, U. of Missouri at Kansas City, Kansas City, MO, USA, ⁵McGill University, Montreal, PQ, Canada.

DMP1 and Spp1 are localized in the canalicular and lacunar walls, as is MEPE protein. Previously we showed that DMP1 null mice display hypophosphatemia (30%), and excess woven bone with large amount of osteoid, similar to the *Hyp* mice and X-linked hypophosphatemic rickets in humans. Phex gene mutations are the major cause of *Hyp* phenotype, resulting in overexpression of MEPE, a gene predominately expressed in mature osteocytes. MEPE gene is also extremely sensitive to mechanical stimulation in osteocytes. Loads at low as 2.4N at 60 cycle at 2Hz (30sec) can stimulate osteocyte specific MEPE expression 3-10 fold at 24hr after loading. We now studied MEPE expression, with the hypothesis that osteocytes in the DMP1 null are overstimulated at basal load levels compared to wild-type mice. Bones of the DMP1 null mice are less stiff and may receive more strain for a given load. We mapped MEPE expression at the midshaft, both distally

ASBMR 27th Annual Meeting

and proximally at 1mm intervals, in the ulnae of control and DMP1 null mice. By quantitative in situ hybridization we found that MEPE expression is elevated 3-8 fold near the mid-shaft and distally in the DMP1 knock-out mice compared to control. This supports the hypothesis the osteocytes are overstimulated in the DMP1 null mice compared to control. With a 3D model we clearly visualized changes of these MEPE expression patterns. The overexpression of MEPE will most likely lead to production of excess ASARM peptide that will contribute to the hypophosphatemia and osteomalacia of the DMP1 null mouse.

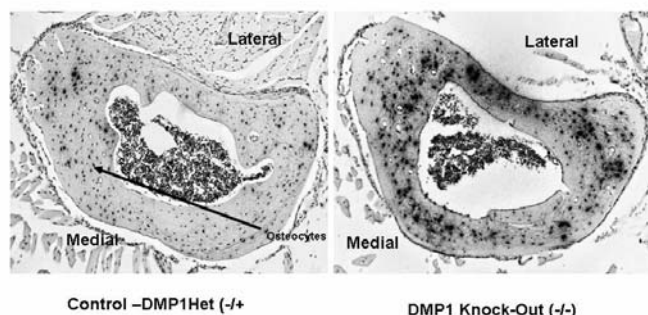


Figure 1. MEPE mRNA expression in osteocytes of the ulna in DMP1 knock-out mice is increased 3-8 fold with selective increased expression on the Lateral and Medial sides and just distal to the mid-shaft.

Disclosures: **S.E. Harris**, None.

SA463

Safety and Efficacy of a Single 4 mg Infusion of Zoledronic Acid in the Treatment of Paget's Disease of Bone. **G. Guardia¹, A. Al-Shoha², V. Reddy¹, Y. Bernardo¹, D. Rao¹.** ¹Bone & Mineral Metabolism, Henry Ford Hospital, Detroit, MI, USA, ²Internal Medicine, Henry Ford Hospital, Detroit, MI, USA.

Paget's disease of bone is the third most common metabolic bone disease after osteoporosis and renal osteodystrophy. Over the past 20 years, several treatment modalities have been used including oral and IV bisphosphonates. Zoledronic acid is a potent third generation bisphosphonate, which inhibits bone resorption after a single 4 mg intravenous infusion. We report our experience with 26 patients with Paget's disease of bone treated with Zoledronic acid between the years 2003 and 2004. Mean age was 75.9 ± 9.6 years; 42% were men, 58% were white, and 61% had polyostotic disease. Zoledronic acid was the initial treatment in 3 of the 26 patients. Mean \pm SD pre-treatment values for the relevant measurements were as follows: serum Alkaline Phosphatase (AP) 174 ± 111 IU/L, bone specific AP (BSAP) 86 ± 79 IU/L, urine N-telopeptide (NTx) 142 ± 134 nM/mM, serum calcium (Ca) 9.6 ± 0.4 mg/dl and serum creatinine (Cr) 1.0 ± 0.3 mg/dl. One month after a single 4 mg infusion of Zoledronic acid, the mean AP fell to 102 ± 43 IU/L (a 41.3 % decline), BSAP fell to 46 ± 20 IU/L (46.9 % decline) and NTx fell to 30 ± 32 nM/mM (78.5 % decline; $p < 0.001$). At 6 months, mean AP fell to 87 ± 37 IU/L (a 50 % decline; $p = 0.003$), mean BSAP fell to 26 ± 10 IU/L (70% decline; $p = 0.006$) and mean uNTx fell to 36 ± 30 nM/mM (74.5 % decline; $p < 0.001$). At 1 year, the mean NTx was still low at 38 ± 25 nM/mM (73.5 % decline; $p < 0.001$), not significantly different from the one and six month values. No significant change from baseline was noted in either serum Ca or Cr at 6 months. Response defined as 50% decrease or normalization in AP at 6 months was achieved in 53% of patients. NTx normalized in 86% and 90% of the patients at 6 months and 1 year after treatment respectively. In conclusion, Zoledronic acid is a safe and effective treatment for patients with both mono and polyostotic Paget's disease of bone.

Disclosures: **G. Guardia**, None.

SA464

See Friday Plenary number F464.

SA465

Economic Evaluation of Long Term Management Strategies for Paget's Disease of Bone. **M. Al¹, M. Groot¹, C. Galani², A. Engbersen².** ¹Institute for Medical Technology Assessment, Erasmus MC, Rotterdam, The Netherlands, ²Novartis Pharma AG, Basel, Switzerland.

In two pivotal registration trials, zoledronic acid (5 mg one time infusion) has been shown to be superior to risedronate (30 mg/day orally for 2 months) in terms of response rates, time to response and duration of response in the treatment of Paget's disease of bone (PDB). The aim of this study was to estimate the cost-effectiveness of zoledronic acid (ZOL) relative to risedronate (RIS), applied to the Dutch situation from a societal perspective. A decision tree was developed to estimate costs and effects of ZOL versus RIS over a period of 2 years. The tree consists of 4 half-year cycles and 4 possible health states, i.e. response, non-response, relapse and no relapse. Response was defined as SAP normalisation (SAP=serum alkaline phosphatase) and relapse as an increase in SAP of at least 50% from the measurement at 6 months and to at least 1.25 times the upper normal limit. Effectiveness was defined as time in response. All probabilities and the time-to-response were derived from the trial data. Based on information from local experts (physicians), resource use was defined for all 4 health states. It was assumed that both non-

response and a relapse would trigger re-treatment. All direct medical costs and travel costs were included, while costs due to production losses were assumed to be negligible. All costs and effects were discounted by 4%, in accordance with Dutch pharmacoeconomic guidelines. To address uncertainty around the outcomes, a probabilistic sensitivity analysis was performed, in which all parameters were varied simultaneously in 2,500 consecutive simulations. Probabilities were varied within 95% CI limits and costs were varied $\pm 20\%$. Using this model, it was estimated that over 24 months, 19.6 months are spent with normalized SAP levels in the ZOL group, versus 13.2 in the RIS group, leading to an incremental effectiveness of 6.4 months in response. The average numbers of treatments per year are estimated at 0.58 in the ZOL group and 0.94 in the RIS group. The costs in the ZOL group were lower (EUR 891) than in the RIS group (EUR 1217), leading to savings of € 326, mainly due to the smaller average number of treatments per year. Our probabilistic sensitivity analysis showed that ZOL is the dominant strategy with both increased time in response and a reduction in costs in 100% of the simulations. In conclusion, treatment of PDB with ZOL is more effective than treatment with RIS with a reduction in costs of treatment. Therefore, ZOL offers a dominant alternative to RIS for the treatment of PDB in the Netherlands.

Disclosures: **A. Engbersen**, Novartis Pharma AG 3.

SA466

Costs of Treating Paget's Disease in a Privately Insured Population. **B. Briesacher¹, D. Orwig², M. Seton³, M. Omar⁴, K. Kristijan⁴.** ¹Division of Geriatric Medicine, University of Massachusetts Medical School, Worcester, MA, USA, ²Department of Epidemiology and Preventive Medicine, University of Maryland School of Medicine, Baltimore, MD, USA, ³New England Registry for Paget's Disease of Bone, Massachusetts General Hospital, Boston, MA, USA, ⁴Novartis Pharmaceuticals Corporation, East Hanover, NJ, USA.

This retrospective observational study was designed to assess treatment costs for patients with Paget's disease of bone (PDB) compared to those of matched controls (MC) as a surrogate marker for the burden of disease. Epidemiological research and clinical reviews detailing the complications of Paget's disease since its initial description by Sir James Paget in 1876, served as the basis for the radiographs, laboratory tests and selected conditions examined in this study. Using 2001-2002 MarketScan Research databases, we linked medical claims, prescription records, and encounter data on 2.8 million active or retired employees to create a longitudinal panel with 24 months of observation. Patients with PDB were identified by ICD-9 code 731.0. The MC was identified through an exact match procedure using gender, age and risk adjustment score based on the DCG/HCC classification system. This analysis extracted all diagnostic and expenditure records for the sample and calculated the prevalence of 22 conditions potentially linked to PDB and their related costs. The prevalence of co-morbidities and health care costs were compared in PDB and MC, and differences tested using chi-square and t-tests. We identified 244 persons with PDB and 244 matched comparators (MC). The average age was 72.7 years; 50.8% were female. Significant differences in co-morbidities detected between PDB patients and MC ($p < 0.05$) were as follows: pathological fractures (4.9% vs. 0.4%), heart murmurs (3.3% vs. 0.4%), fractures of femur other than neck (2.9% vs. 0.4%), spinal stenosis (2.5% vs. 0.4%), hypercalcemia (1.6% vs. 0.4%), and bone neoplasms (7.8% vs. 2.5%), respectively. Biannual per patient outpatient costs were significantly higher in PDB patients (PDB \$9301 vs. MC \$6339, $p < 0.05$). There is a significant difference in morbidity in persons with PDB compared to MC as expressed in the complications measured and the excess costs detected in this analysis. This is the first study to examine the burden of PDB in this way. Future research should assess the impact of drug therapy to slow the progression of PDB, and the consequent morbidity and economic impact on patients' lives.

Disclosures: **B. Briesacher**, Novartis Pharmaceuticals Corporation 5.

SA467

Elevated Serum High Molecular Weight Kininogen in Patients with Paget's Disease of Bone. **E. Tsuruga¹, S. Rao², S. V. Reddy¹.** ¹Children's Research Institute, Medical University of South Carolina, Charleston, SC, USA, ²Bone and Mineral Metabolism, Henry Ford Hospital, Detroit, MI, USA.

Paget's disease of bone (PD) is a chronic focal skeletal disorder characterized by excessive bone resorption followed by abundant new bone formation, with eventual replacement of normal bone marrow by vascular and fibrous tissue. Enhanced levels of IL-6, M-CSF and endothelin-1 have been associated with PD, implicated in its pathogenesis and indicator of disease activity. RANK ligand (RANKL), a critical osteoclastogenic factor that is expressed on marrow stromal/osteoblast cells is upregulated in areas involved with PD. We have recently demonstrated that heat shock factor-2 (HSF-2) is a downstream target of fibroblast growth factor-2 (FGF-2) to induce RANKL expression in stromal/preosteoblast cells. These data suggest that heat shock proteins/heat shock factors may play an important role in bone remodeling. To further identify serum factors that are over-expressed in patients with PD, we performed 2D gel electrophoresis and mass spectrometric analysis of serum from patients. We identified increased serum levels of high molecular weight glycosylated kininogen (KNG) in a patient with PD compared to normal serum. Western blot analysis of serum samples (6 μ g total protein) from three PD patients further identified two to five-fold increase in levels of KNG heavy chain (63 kDa) compared to five normal subjects. However, there was no significant change in the serum levels KNG light chain (58 kDa) expression in these patients. We then examined the effects of KNG on human bone marrow derived stromal cells (SAKA-T cells). Treatment of SAKA-T cells with recombinant KNG (25 ng/ml) for 24 hr period resulted in a five-fold increase in the levels of phospho-HSP-27 and a three-fold increase in ERK1/2 phosphorylation in these cells. However, SAKA-T cells stimulated with KNG in the

presence of ERK activation inhibitor peptide-1 (25 µM) which binds to ERK2 and prevents interaction with MEK did not significantly affect the levels of phospho-HSP-27. These data suggest that KNG may play an important role in modulating stromal/preosteoblastic cell proliferation/differentiation. These results may implicate a potential pathophysiologic role for KNG in the progression of pagetic lesions in patients with PD.

Disclosures: *S.V. Reddy, None.*

SA468

Hypocalcemia as a Presenting Feature of Celiac Disease in a Patient with DiGeorge Syndrome. L. M. Gelfand^{*1}, L. A. DiMeglio². ¹Departments of Medicine and Pediatrics, Endocrinology and Pediatric Endocrinology, Indiana University School of Medicine, Indianapolis, IN, USA, ²Pediatric Endocrinology, Indiana University School of Medicine, Indianapolis, IN, USA.

DiGeorge syndrome is a genetic disorder, resulting from deletions on chromosome 22q11.2. DiGeorge is often associated with hypocalcemia in the neonatal period that resolves by the end of the first year of life, however, hypocalcemia may present in older patients under conditions of physiological stress or illness. Celiac Disease (CD) is an autoimmune malabsorption disorder that results in villous atrophy of the small intestinal mucosa after exposure to gluten-containing foods. Even though the incidence of autoimmune conditions such as juvenile rheumatoid arthritis, Graves' disease, and hemolytic anemia is increased in DiGeorge syndrome, only one case of CD has been reported to date, with no reported cases of CD presenting with hypocalcemia in DiGeorge patients. Here we describe a first case of a child with DiGeorge syndrome who presented with hypocalcemia due to CD. A 5 1/2 -year-old white female with DiGeorge syndrome presented to her pediatrician with short stature and weekly emesis. Her past medical history was complicated by a congenital heart disease requiring surgical correction, multiple infections requiring hospitalizations, asthma, and iron deficiency anemia. She had not had episodes of neonatal hypocalcemia. Her height was 100.2 cm (< 3rd percentile for age), and weight 15 kg (< 3rd percentile). Her abdomen was distended. Chvostek and Trousseau signs were absent. Her calcium was 6.5 mg/dL (8.5-10.5), phosphorus 4.5 mg/dL (3.4-5.5), and intact PTH 54 pg/mL (10-65). 25-hydroxy-vitamin D level was 19 ng/mL (20-57). She had a microcytic hypochromic anemia with hemoglobin of 9.0 g/dL (11.5-14.5). She was diagnosed with partial hypoparathyroidism due to DiGeorge syndrome and started on calcitriol and calcium supplementations. Celiac antibodies were evaluated, and tissue transglutaminase (tTG) antibody was positive. Endoscopic evaluation with small bowel biopsies was consistent with diagnosis of CD. A gluten free diet was initiated upon making diagnosis of CD with a marked improvement in the energy level, resolution of abdominal distension, and improved growth velocity and weight gain. Within four months she was weaned off calcitriol. By six months of gluten-free diet her calcium supplementation was decreased to 30 mg/kg of elemental calcium. In conclusion, we present a case where malabsorption caused by CD unmasked partial hypoparathyroidism in a patient with DiGeorge syndrome. Therefore, new hypocalcemia in previously stable patients with DiGeorge syndrome should prompt an evaluation for Celiac Disease.

Disclosures: *L.M. Gelfand, None.*

SA469

Insulin-like Growth Factor -1 (IGF-1), It's Binding Proteins, and Bone Turnover in Adolescent Girls with Type 1 Diabetes. M. A. Murray¹, D. McClain^{*2}, L. J. Moyer-Mileur¹. ¹Pediatrics, University of Utah, Salt Lake City, UT, USA, ²Internal Medicine, University of Utah, Salt Lake City, UT, USA.

Background: Children and adolescents with Type 1 diabetes (Type 1 DM) are at risk for decreased bone mass. We have reported significantly lower bone mass and mineral acquisition at axial and peripheral sites measured by densitometry in adolescents with Type 1 DM when compared to a non-diabetic reference population. (*J Ped*s 2004;145:662-9.) Growth hormone (GH) and its mediators (IGF-1 and -2) and binding proteins (BP1 &-5), promote skeletal growth and mineral acquisition. Pubertal diabetics have an altered GH-IGF axis. **Hypothesis:** *Suppression of the insulin-like growth factor type 1 (IGF-1) response to GH or alterations in IGF-1 BPs (↑BP-1, BP-4; ↓BP-5) decreases osteoblast recruitment and bone matrix mineralization and increases collagen degradation.* **Purpose:** To compare bone metabolism in adolescents with Type 1 diabetes mellitus and matched controls. **Design:** Girls age 12-15 y (n=5) with Type 1 DM and healthy age, maturation-matched controls (n=5) were recruited and admitted overnight to the GCRC. Following consumption of a standardized meal, blood and urine samples were collected hourly (2300 to 0800). GH, IGF-1, IGFBPs (-1,-3,-4,-5), bone-specific alkaline phosphatase (BAP), and urine pyridinium to deoxypyridinium crosslinks ratio (Pyr/Dpyd) were measured and area under the curve (AUC) determined for GH, IGF-1, and BP-1. Statistical analysis included t-test, regression and ANCOVA. **Results:** Age, Tanner stage, body weight and height, and physical activity levels were similar between groups. Type 1 DM girls had significantly greater GH and BP-1AUC, BP-5, and Pyr/Dpyd values (*p* ≤0.04) while IGF-1AUC was higher in controls (*p*=0.003) (Table 1). BP-3, -4, and BAP values were not significant. **Conclusions:** Our results suggest: 1) diminished IGF-1 bioavailability secondary to hepatic resistance to GH or sequestering by BP-1 and 2) collagen degradation greater than bone mineralization in adolescents girls with Type 1 DM. These preliminary findings may support our hypothesis that alterations in the GH/IGF axis decreases osteoblast recruitment

and matrix mineralization limiting pubertal bone mineral acquisition. Additional studies are needed to further characterize mechanisms of bone growth and mineralization in adolescents with Type 1 DM.

Table 1. IGF-1, IGF-BPs and Bone Turnover (Mean (+/-sd); *p<0.04)		
	Type 1 DM	Control
GH AUC	59.4 (33.9)*	32.9 (16.5)
IGF-1 AUC	2822 (947)	3709 (517)*
BP-1 AUC	314 (130)*	184 (111)
BP-4 ng/mL	552 (350)	581 (363)
BP-5 ng/mL	288 (43)*	223 (23)
Pyr/Dpyd nmol/L	0.30 (0.02)*	0.24 (0.01)

Disclosures: *M.A. Murray, None.*

SA470

See Friday Plenary number F470.

SA471

Bone Density in Children with Early Classical Congenital Adrenal Hyperplasia. A. Fleischman^{*}, J. Ringelheim^{*}, H. A. Feldman^{*}, C. M. Gordon. Children's Hospital Boston, Harvard Medical School, Boston, MA, USA.

Classic congenital adrenal hyperplasia (CAH), a deficiency of 21-hydroxylase, causes increased secretion of cortisol and aldosterone precursors that are diverted to androgens. Full suppression is usually not possible, and individuals are exposed to chronic glucocorticoids, and a mildly hyperandrogenic milieu. Therefore, children with CAH are at risk for glucocorticoid induced osteopenia. The goal of this study was to evaluate bone mineral density (BMD) in children with CAH to test the hypothesis that a hyperandrogenic state and altered body composition may provide skeletal protection. Thirteen subjects, ages 8 to 20 years from the endocrinology program of a tertiary care pediatric referral center, were evaluated with adrenal steroids, urine and serum bone markers, and a dual-energy absorptiometry (DXA) measurement for body composition, bone mineral content (BMC), and areal BMD of the hip, spine and total body using a Hologic 4500 scanner. The subjects received an average glucocorticoid dose of 14.4 mg/m2/day hydrocortisone equivalent (range 7.1-29.4). The protocol was approved by the local IRB.

DXA results				
	Minimum	Maximum	Mean	Std. Deviation
Age	8.1	20.3	12.3	4.5
Z score:				
Total Body	-1.2	1.9	.6	.9
Hip	-1.4	2.2	.8	1.1
Spine	-1.5	2.5	.7	1.1

11/13 (85%, 95% CI 55-98%) participants had a BMD at or above the mean for age. The 2 participants with age-adjusted BMD <-1 standard deviation (SD) were the oldest and on the highest glucocorticoid doses (>20 mg/m2/day). Eight participants (62%) had Z-scores > +1 SD, with 2 (15%) > +2 SD. The total body BMD Z-scores were negatively correlated with the glucocorticoid dose in mg/m2/day (Spearman *r*= -0.63, *p*=0.02) or mg/kg/day (*r*=-0.66, *p*=0.01). Body mass index percentile, DXA- derived fat mass, weight in kilograms, and serum adrenal steroid concentrations showed no correlation with age-adjusted areal BMD. In summary, these children with CAH and life-long glucocorticoid supplementation had normal or above normal BMD, except for those with the highest dose and duration of therapy. In this model, glucocorticoids had the expected negative effect on BMD. However, the normal mean BMD supports the presence of a protective factor which is apparently not fat mass accumulation or measurable adrenal steroids. Contributory factors may include other alterations in body composition, androgen effect or disease specific modulators.

Disclosures: *A. Fleischman, Pfizer, Inc. 2.*

SA472

See Friday Plenary number F472.

SA473

Bone Cross-Sectional Geometry in Adolescents with Anorexia Nervosa: A Hip Structural Analysis Study. A. D. DiVasta^{*1}, T. J. Beck², H. A. Feldman^{*3}, M. S. LeBoff^{*4}, C. M. Gordon⁵. ¹Adolescent Medicine, Children's Hospital, Boston, MA, USA, ²Radiology, Johns Hopkins University, Baltimore, MD, USA, ³Clinical Research Program, Children's Hospital, Boston, MA, USA, ⁴Endocrine/Hypertension, Brigham & Women's Hospital, Boston, MA, USA, ⁵Adolescent Medicine/Endocrinology, Children's Hospital, Boston, MA, USA.

Low bone mass and fractures are well-established complications of anorexia nervosa (AN). However, changes in bone geometry and strength may occur independently of changes in bone mineral density (BMD), and may be a better predictor of fracture risk. The purpose of this study was to determine the relationships among areal BMD, anthropometric measurements, and parameters of hip cross-sectional geometry in adolescents with AN. Baseline BMD measurements of the hip and spine were obtained in 88 young women with AN by dual x-ray absorptiometry (DXA) (Hologic 4500 Elite). We used the Hip Structural Analysis (HSA) Program to determine BMD, cross-sectional area (CSA), cross-sectional moment of inertia (CSMI), and section modulus (Z) at the femoral neck and femoral shaft regions. Height and weight were determined by standard procedures, and lean body and fat

mass measured by DXA. The protocol was approved by the local committee on clinical investigation. T-tests were used to compare study mean values to age- and gender-based normative data [Penn State Young Women's Health study]. Femoral neck BMD (mean \pm SD, 0.86 ± 0.15 g/cm²) was significantly lower than age-based normal values ($p < .001$); femoral shaft BMD (1.4 ± 0.15 g/cm²) was not. The hip BMD Z-score (-0.63 ± 0.89 , range -2.7 to 1.5) and lumbar spine BMD Z-score (-1.09 ± 0.88 , range -3.1 to 0.8) were also significantly below normal. Both height and weight were positively correlated with parameters of bone strength, as assessed by femoral neck CSA and Z (Pearson $r = 0.41$ – 0.56 , $p < .001$). Total hip BMD was correlated with femoral neck Z ($r = 0.45$, $p < .001$) and CSA ($r = 0.81$, $p < .001$). While lean body mass was correlated with femoral neck HSA variables ($p < .001$), body fat was not. In summary, in this sample of adolescent girls with AN, spinal bone density was more significantly compromised than that of the hip, indicating a larger deficit within trabecular bone. Anthropometric measures were correlated with variables of hip structural geometry. The hip structural variables were strongly correlated with standard areal BMD measurements by DXA. Lean tissue was predictive of bone strength, suggesting a beneficial effect of muscle on bone. The positive correlation between BMD and variables of hip structural geometry suggests that bone strength is also compromised in these patients.

Disclosures: **A.D. DiVasta**, None.

SA474

See Friday Plenary number F474.

SA475

Bone Mineral Density (BMD) in 5-8 Year Olds Who Were Treated with Corticosteroids (CS) for Chronic Lung Disease (CLD) of Prematurity. J. A. Eelloo^{*1}, S. A. Roberts^{*2}, A. J. B. Emmerson^{*1}, K. A. Ward², J. E. Adams², M. Z. Mughal¹. ¹Central Manchester & Manchester Childrens University Hospitals NHS Trust, Manchester, United Kingdom, ²The University of Manchester, Manchester, United Kingdom.

The adverse short-term effects of CS on growth and bone mineralisation in preterm infants are well known. However, it is not known whether these effects persist throughout childhood. We hypothesised that BMD would be reduced in pre-pubertal children who had received CS for the treatment of CLD. A group of 51, 5-8 year old children (32 male) born at < 34 weeks gestation took part in the study. BMD of the lumbar spine (LS) was measured using dual energy x-ray absorptiometry and the data expressed as LS bone mineral apparent density (LS BMAD; g/cm³). Volumetric total (vtotBMD; mg/mm³) and trabecular (vtrabBMD; mg/mm³) BMD of the distal radius was measured using peripheral quantitative computed tomography. Height and weight were measured at the time of bone densitometry and transformed into Z scores using the U.K reference data. All bone data was transformed into Z scores using the Manchester normative reference data ($n = 420$). Z scores for each of the variables were compared to zero using an independent samples t-test. Children treated with CS had a mean (SD) gestation of 26.73 (2.86) weeks, the control group 29.94 (2.17) weeks. The mean (SD) birth weight (g) in the children treated with CS was 1061.93 (529.43) and in the control group 1356.97 (451.59).

	Mean (SD) Z score		t-test (P =)	
	Steroids (n=15)	Controls (n=36)	Steroids	Controls
Height	-0.43 (1.24)	-0.09 (1.48)	0.20	0.73
Weight	-0.74 (0.96)	0.22 (1.58)	0.01	0.40
vtotBMD	0.32 (0.94)	0.60 (1.03)	0.21	0.001
vtrabBMD	0.13 (1.31)	0.24 (1.06)	0.71	0.18
LS BMAD	-1.42 (1.05)	-0.74 (0.90)	<0.0001	<0.0001

Children who received CS during the neonatal period were lighter compared with UK reference data. The distal radial vtotBMD was higher in the controls compared with the reference data. In both the groups the LS BMAD was lower compared with the reference data but the deficit was greater in the CS group. This greater deficit in the LS BMAD might be due to the effect of CS or being born on average 2-3 weeks earlier and approximately 300 grams lighter than the controls.

Disclosures: **M.Z. Mughal**, None.

SA476

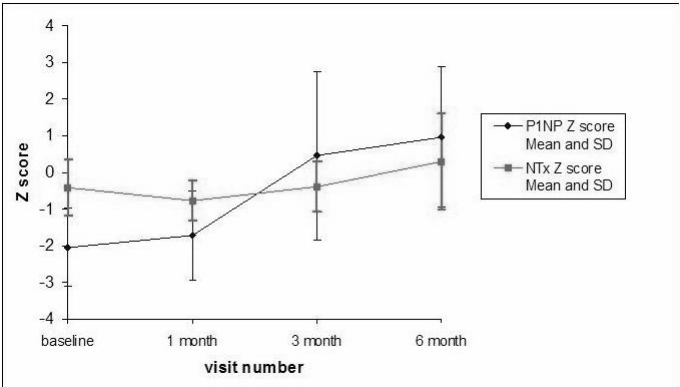
See Friday Plenary number F476.

SA477

Altered Bone Turnover in Children with Crohn Disease. M. Harpavat¹, Q. Dang^{*2}, D. Keljo^{*}, S. Greenspan². ¹Pediatrics, University of Pittsburgh, Pittsburgh, PA, USA, ²Medicine, University of Pittsburgh, Pittsburgh, PA, USA.

Bone turnover increases during childhood growth and development and can be altered in children with Crohn Disease (CD). This change has been attributed to corticosteroid use. This longitudinal study was designed to evaluate associations between markers of bone

turnover and bone mass in childhood CD. 22 otherwise healthy, steroid naïve children newly diagnosed with CD were studied. After baseline data were obtained, all children were started on corticosteroids (equivalent to 2mg/kg prednisone) which were stopped by 4 months. Biochemical markers of bone formation (serum PINP) and resorption (urine NTx) were measured at baseline, one, 3, and 6 months from initiation of therapy. Age and gender adjusted Z scores were calculated. Bone mineral content (BMC) and bone mineral density (BMD) of the total body (TB) and lumbar spine (LS) were obtained by DXA (Lunar Prodigy) at baseline, 6, and 12 months. 13 of the 22 children were male. Mean age was 12.3 years (range 5.5-16.7 years). CD patients had significantly reduced mean PINP Z scores at baseline (-2.05 ± 1.1 ; $p < .001$). By 6 months mean PINP Z scores had significantly increased above normal range (0.97 ± 1.9 ; $p = 0.03$, figure). Mean NTx Z scores at baseline were slightly reduced (-0.41 ± 0.77 ; $p = 0.02$) and remained stable through 3 months but returned to normal by 6 months. The percent increase in PINP from baseline to 6 months positively correlated with the percent increase in LS BMC from baseline to 6 months ($r = 0.59$, $p < .01$) and 12 months ($r = 0.48$, $p = 0.02$). The percent increase in PINP from baseline to 6 months positively correlated with the percent increase in LS BMD from baseline to 6 months ($r = 0.50$, $p = 0.02$) and 12 months ($r = 0.64$, $p < .01$). No significant correlations were found between changes in NTx and changes in TB or LS BMC or BMD. In summary, steroid naïve children newly diagnosed with CD have decreased bone formation. Despite corticosteroid use, bone formation increased over time and changes in mean PINP Z scores correlated positively with changes in BMC and BMD of the LS. Bone resorption changed minimally. We conclude the improvement in bone mass in children treated for CD may be explained by the increase in bone formation, with minimal change in bone resorption.



Disclosures: **M. Harpavat**, None.

SA478

Implication of G Beta-Gamma Proteins and c-SRC Tyrosine Kinase in PTH-Induced Signal Transduction in Rat Intestinal Cells. C. Gentili^{*}, R. Boland^{*}, A. Russo de Boland^{*}. Biologia, Bioquímica & Farmacia, Universidad Nacional del Sur, Bahia Blanca, Argentina.

PTH interacts in target tissues with a G protein-coupled receptor (GPCR) localized in the plasma membrane. Although activation of GPCR can elicit rapid stimulation of cellular protein tyrosine phosphorylation, the mechanism by which G proteins activate protein-tyrosine kinases is not completely understood. In the present work we demonstrated that PTH rapidly increases the activity of non-receptor tyrosine kinase c-Src in rat intestinal cells (enterocytes). The response is biphasic, the early phase is fast and transient, peaking at 30 sec (+120 %), while the second phase progressively increases up to 5 min (+220%). The hormone activates c-Src in intestinal cells through fast changes in the tyrosine phosphorylation of the enzyme. The first event in the activation of c-Src is the dephosphorylation of Tyr 527 (that happens at few seconds of PTH treatment), followed by a second event of activation with phosphorylation at Tyr 416 (+2 fold, 5 min). Removal of external Ca²⁺ (EGTA 0.5 mM) and chelation of intracellular Ca²⁺ with BAPTA (5μM) suppressed Tyr 416 phosphorylation and Tyr 527 dephosphorylation, indicating that Ca²⁺ is an upstream activator of c-Src in enterocytes stimulated with PTH. The G-protein subunits, Gas and Gβ, are associated with c-Src in basal conditions and this association increases two-three fold in cells treated with PTH. Sequestration of Gβ subunits abolished hormone-dependent c-Src Tyr 416 phosphorylation and ERK1/ERK2 activation. The results of this work show that PTH activates c-Src in intestinal cells through conformational changes via G proteins and calcium-dependent modulation of tyrosine phosphorylation of the enzyme and that PTH receptor activation leads via Gβγ-c-Src to the phosphorylation of the MAP kinases ERK1 and ERK2.

Disclosures: **A. Russo de Boland**, None.

SA479

See Friday Plenary number F479.

SA480

Distinct Conformations of the Parathyroid Hormone Receptor Mediate G Protein and β -Arrestin Dependent Activation of ERK1/2. D. Gesty-Palmer¹, E. Reiter^{*2}, R. F. Spurney³, L. M. Luttrell^{*4}, R. J. Lefkowitz^{*5}. ¹Endocrinology and Metabolism, Duke University Medical Center and The Geriatrics Research, Education and Clinical Center, Durham Veterans Affairs Medical Center, Durham, NC, USA, ²Medicine, Duke University Medical Center, Durham, NC, USA, ³Nephrology, Duke University Medical Center, Durham, NC, USA, ⁴Medicine and Biochemistry, Medical University of South Carolina, Charleston, SC, USA, ⁵Medicine and Biochemistry, The Howard Hughes Medical Institute Duke University Medical Center, Durham, NC, USA.

Parathyroid hormone (PTH) regulates calcium homeostasis *via* the type I PTH/PTHrP-related protein receptor (PTH1R). The purpose of the present study was to identify the contributions of distinct signaling mechanisms to PTH-stimulated activation of the mitogen-activated protein kinases (MAPK) ERK1/2. In HEK293 cells transiently transfected with hPTH1R, PTH stimulated a dose-dependent increase in ERK activity. The time course of ERK1/2 activation was biphasic with an early peak followed by a significant period of sustained ERK1/2 activation. Pretreatment of HEK293 cells with the PKA inhibitor H89 and the PKC inhibitor GF109203X (GFX), individually or in combination blocked the early component of PTH-stimulated ERK activity. These inhibitors of second messenger dependent kinases had little effect on the later phase of PTH-stimulated ERK1/2 phosphorylation. This later phase of ERK1/2 activation, however, was blocked by depletion of cellular β -arrestin 2 or β -arrestin 1 by small interfering RNA. Further, we found that stimulation of hPTH1R with a PTH analogue, (D-Trp¹², Tyr³⁴)-PTH(7-34), previously characterized as an inverse agonist for cAMP generation fails to activate classical heterotrimeric G protein signaling but does lead to receptor recruitment of β -arrestin 1 and 2 and activation of ERK1/2. This G protein-independent activation of ERK1/2 is abolished by depletion of cellular β -arrestin 2 or β -arrestin 1. It is concluded that PTH stimulates ERK1/2 through several distinct signal transduction pathways: an early G protein dependent pathway mediated by PKA and PKC and a late pathway independent of G proteins mediated through β -arrestin. Moreover these findings imply the existence of distinct active conformations for hPTH1R responsible for the two pathways, which can be stimulated by unique ligands. Such ligands may have distinct and valuable therapeutic properties.

Disclosures: **D. Gesty-Palmer**, None.

SA481

See Friday Plenary number F481.

SA482

Effects of Genetic Background on Phenotype of Cyclooxygenase-2 Knockout Mice. M. Xu, S. Choudhary, O. Gao^{*}, O. S. Voznesensky^{*}, D. J. Adams, L. G. Raisz, C. C. Pilbeam. Dept. of Medicine, University of Connecticut Health Center, Farmington, CT, USA.

The phenotype of a gene knockout (KO) may depend on the genetic background in which it is expressed. Previous comparison of cyclooxygenase-2 (COX-2) KO and wild type (WT) mice was reported in a C57Bl/6x129 background. A mixed background was necessary since few KO mice could be generated in an increasingly pure C57Bl/6 background. In the C57Bl/6x129 background, COX-2 KO mice died 4-5 times faster than WT mice after weaning, secondary to renal failure. Some surviving KO mice with renal failure had marked secondary hyperparathyroidism with low serum calcium, high serum phosphorus and PTH levels greater than 1000 ng/dl. In C57Bl/6x129 COX-2 KO mice with intact renal function, there was still a trend toward elevated PTH levels but serum calcium levels were normal or increased, serum phosphorus levels were normal, and 1,25-dihydroxyvitamin D₃ levels were elevated 2-fold, suggesting primary hyperparathyroidism. We have begun to characterize calcium metabolism and bone phenotype in COX-2 WT, heterozygous (HET), and KO mice in an outbred CD-1 background. Experimental mice are the offspring of COX-2 HET mice that have been backcrossed into the CD-1 background more than 9 generations. In the CD-1 background, there is no increased mortality in COX-2 KO mice after weaning. In CD-1 male mice analyzed at 5 mo of age, weights were 10% lower in KO mice (n=11) than in WT (n=12) or HET (n=14) mice. Serum creatinine and serum calcium did not differ among WT, HET and KO mice. However, PTH levels were variably elevated (p<0.05) in the 5-mo old male KO mice. The mean (\pm SD) PTH level in the KO mice was 114 \pm 130 ng/dl, compared to 30 \pm 23 ng/dl and 28 \pm 15 ng/dl in WT and HET mice, respectively. In the KO mice, 6/11 had PTH levels above 60 ng/dl. In 3.5 mo old CD-1 female mice, WT (n=11) and KO (n=8) mice had similar weights, serum creatinine and serum calcium. The mean PTH level in the KO females was only 1.5-fold greater (p<0.05) than that in WT females. In 9 mo old CD-1 mice (n=4-7 per group), KO mice had similar serum creatinine and calcium levels as WT and HET mice. In males, but not females, the mean PTH level was 2.5-fold greater (p<0.05) than that of WT or HET mice. These preliminary studies indicate that COX-2 KO mice in a CD-1 background do not have the increased mortality secondary to renal failure seen in KO mice in C57Bl/6x129 background. However, significant numbers of CD-1 COX-2 KO mice, especially male KO mice, have increased PTH levels with normal serum calcium levels. We speculate that the absence of COX-2 associated prostaglandins in KO mice may down regulate the sensitivity of calcium sensing pathways.

Disclosures: **M. Xu**, None.

SA483

See Friday Plenary number F483.

SA484

Predicting Bone Biomarker Response to PTH(1-34) Dosing in Rats with a Mathematical Model for the Remodeling Cycle. L. Potter¹, G. Stroup², D. Rickard², J. Vasko-Moser^{*2}, S. M. Hwang^{*2}, B. Votta², Z. Wu^{*2}, F. Tobin^{*3}. ¹Scientific Computing & Mathematical Modeling, GlaxoSmithKline, Research Triangle Park, NC, USA, ²GlaxoSmithKline, Collegeville, PA, USA, ³GlaxoSmithKline, King of Prussia, PA, USA.

A mathematical model has been developed for the bone remodeling cycle in rats that predicts the bone biomarker response to dosing with PTH(1-34). The model describes the kinetics of osteoblast and osteoclast maturation and activity, while incorporating only the key biological features necessary to capture the effects of PTH dosing on bone remodeling and biomarkers. Model components include the proliferation, differentiation and apoptosis of osteoblasts and osteoclasts, the kinetics of bone formation and resorption, osteoblast-osteoclast interactions via the RANK/RANKL/OPG pathway, PTH receptor kinetics, and the effects of PTH signaling on bone formation and resorption. Bone formation and resorption biomarker levels are predicted through a correlation with model-simulated active osteoblasts and osteoclasts, respectively. Model parameters associated with PTH receptor kinetics were calibrated using *in vitro* PTH(1-34) radioligand binding data in membrane fractions from HEK-293 cells transfected with type 1 PTH/PTHrP receptor. Other parameters were calibrated in comparison with *in vivo* plasma osteocalcin and urinary deoxypyridinoline data from intact female rats dosed with PTH(1-34). The model captures the observed behavior that small doses given daily result in greater bone formation than larger doses given weekly. Moreover, the model is able to predict the range of variability in biomarker response to PTH(1-34) dosing expected across a population. Using Monte Carlo simulations with both day-to-day and population variability in PTH(1-34) pharmacokinetics, the model predicts greater variability in the resorption biomarker response than the formation response. This mathematical model is a powerful tool that can help design optimal PTH dosing regimens across a population of patients.

Disclosures: **L. Potter**, GlaxoSmithKline 3.

SA485

Identification of a Novel Activating Mutation in the Calcium Sensing Receptor Gene Supports the Physiological Relevance of the Venus Flytrap Module. C. Silve¹, C. Petrel^{*2}, C. Leroy^{*1}, E. Mallet^{*3}, H. Bruel^{*4}, D. Rognan^{*5}, M. Ruat^{*2}. ¹Faculté de Médecine Xavier Bichat, INSERM U426, Paris, France, ²Institut de Neurobiologie, CNRS UPR9040, Gif sur Yvette, France, ³Hôpital Charles Nicolle, Rouen, France, ⁴Groupe Hospitalier Le Havre, Le Havre, France, ⁵UMR7081, Illkirch, France.

Class III G-protein coupled receptors (GPCRs), which include metabotropic glutamate receptors (mGluRs) and the Ca²⁺ sensing receptor (CaSR), are characterized by a long extracellular aminoterminal domain called a Venus flytrap module (VFTM) containing the ligand binding pocket, as demonstrated for mGluRs. Pathophysiological relevance of the VFTM remains to be ascertained, in part because no mutation associated with genetic disease has been identified in the mGluR binding site. Identification of a novel CaSR activating mutation, E297D, associated with autosomal dominant hypocalcemia (ADH), provides clinical evidence for the pathophysiological relevance of GPCR class III VFTM. E297 is structurally homologous to a D conserved in all VFTM mGluRs, and is essential for agonist binding and proper mGluR activation. Interestingly, replacement of the same glutamate by lysine (E297K) results in a loss of function of CaSR, a mutation previously observed in familial hypocalciuric hypercalcemia (FHH). Functional characterisation of the mutant receptors expressed in HEK-293 cells indicated that the E297D mutant was left-shifted in Ca²⁺ sensitivity compared to the wild-type receptor (EC₅₀ = 2.53 \pm 0.18 mM vs 3.75 \pm 0.22 mM, mean \pm SEM, n=4, p<0.001), whereas the E297K mutation was accompanied by a loss in Ca²⁺ sensitivity. A model of the CaSR VFTM was constructed based on mGluR1 crystal structure and on alignment between mGluRs and CaSR amino-acid sequences, which allowed us to predict potential residues involved in the calcium binding site. These residues, which include E297, are localized within the cleft of the two lobes thought to form the VFTM. The enhanced Ca²⁺ sensitivity of E297D mutant can be explained by a lower desolvation energy ($\Delta\Delta G_{\text{desolv}}$ = -4.53 kcal.mol⁻¹), which would favour stabilization of closed VFTMs by Ca²⁺ and subsequent CaSR activation. In the E297K mutant, the lysine 297 side chain ammonium exactly occupies the Ca²⁺ binding area and would keep the VFTMs closed, thus preventing Ca²⁺ binding. The clinical observation that the E297D and E297K mutations are respectively responsible for ADH and FHH and our *in vitro* data characterising their biochemical effects, are in agreement with the model, thereby supporting the physiological relevance of the VFTMs in the activation of receptors stimulated by the binding of small ligands in their extracellular domain.

Disclosures: **C. Silve**, None.

SA486

See Friday Plenary number F486.

SA487

The Calcium-sensing Receptor (CASR) Dimerizes in the Endoplasmic Reticulum: Biochemical and Biophysical Characterization of CASR Mutants Retained Intracellularly. S. Pidasheva*, M. Grant*, L. Canaff, U. Kumar*, G. N. Hendy. Medicine, McGill University, Montreal, PQ, Canada.

The calcium-sensing receptor (CASR) belongs to group C of the G protein-coupled receptor superfamily. The CASR exists at the plasma membrane as a homodimer. Although other members of group C have been shown to be constitutive homodimers it has not been precisely documented at which point in the biosynthetic pathway the CASR dimerizes. To address this issue we have made a biochemical and biophysical analysis of wild-type and mutant CASRs (harboring R66H, R66C or N538X inactivating mutations identified in familial hypocalciuric hypercalcemia/neonatal severe hyperparathyroid patients) that were transiently expressed in human embryonic kidney (HEK) 293 cells. By a trans-reporting assay (measuring MAP kinase activity) and an aequorin assay (measuring intracellular calcium release), all mutants were shown to be markedly deficient in cell signaling in response to increases in the extracellular CASR ligands, calcium and gadolinium, relative to wild-type. By immunoblot analysis of cell extracts, all mutants, although as well-expressed as wild-type, lacked mature glycosylation, indicating impaired trafficking from the endoplasmic reticulum (ER). In addition, whereas dimerized forms of wild-type, R66H and R66C mutants were present, none was observed with the truncated N583X mutant. By immunofluorescent confocal microscopy of nonpermeabilized cells, while strong staining at the plasma membrane was observed for the wild-type, little or no staining was seen for the mutants. In permeabilized cells strong perinuclear staining was observed for both wild-type and mutants. By fluorescent confocal microscopy using two different fluorophors, one for the CASR and the other for markers of the ER or Golgi apparatus, the mutant CASRs were localized within the ER but not the Golgi apparatus. By the use of the photobleaching fluorescence resonance energy transfer (pbFRET) method, it was demonstrated that the wild-type, R66H and R66C mutants were dimerized in the ER whereas the N583X mutant was not. Hence, CASR dimerization in the ER occurs as an early event and is likely to be necessary (but is not sufficient) for exit of the receptor from the ER and trafficking to the cell surface.

Disclosures: **S. Pidasheva**, None.

SA488

Intracellular Localization of Mutant PTH/PTHrP Receptors in Cultured Osteoblasts. J. Shimomura*¹, N. Amizuka², T. Kojima^{*2}, T. Maeda^{*2}, D. Goltzman³, A. Karaplis⁴, S. Shimooka^{*1}. ¹Pediatric Dentistry, School of Dentistry at Niigata, The Nippon Dental University, Niigata, Japan, ²Division of Oral Anatomy, Niigata University, Niigata, Japan, ³Calcium Research laboratory, Royal Victoria Hospital, McGill University, Montreal, PQ, Canada, ⁴Lady Davis Institute for Medical Research, Jewish General Hospital, McGill University, Montreal, PQ, Canada.

Mutations of the PTH/PTHrP receptor (PTH-R) have been discovered in Blomstrand's lethal chondrodysplasia (PTH-R^{P132L}) and Jansen type metaphyseal chondrodysplasia (PTH-R^{H223R}). Congenital deformities in these chondrodysplasia syndromes appear to be attributable to altered signal transduction linked to the receptor with diminished signal transduction in the Blomstrand lesion and constitutive signal transduction in the Jansen mutation. In the present study, we examined the possibility that mutations of these receptors result in abnormal intracellular localization and transport of the PTH-R proteins. MC3T3-E1 cells were transfected with pAlter-Max expression vectors containing cDNAs encoding rat wild-type PTH-R, and mutated PTH-Rs identical to those causing Blomstrand type and Jansen type chondrodysplasias. The cellular localization of these receptor-proteins was examined by immunofluorescence and immunoelectron microscopy. MC3T3-E1 cells transfected with the wild-type PTH-R cDNA displayed receptor immunoreactivity mainly on the cell surface, and partially in the region of Golgi apparatus. In contrast, the PTH-R protein carrying the Blomstrand type mutation was barely detectable on the cell surface. Instead, some mutant PTH-R was concentrated in the endoplasmic reticulum (ER), and some was present in the peripheral cytoplasm adjacent to the ER in the transfected cells. The Jansen type mutant PTH-R protein was localized mainly on the cell surface, but a minor amount was dispersed in the cytoplasm around the ER. The abnormal accumulation of the Jansen type mutant receptor in the ER and peripheral cytoplasm was therefore rare compared to that of the Blomstrand type mutation. Taken together, the findings show that wild-type PTH-R protein can be quickly transported to the Golgi apparatus and the cell surface after translation in the ER. Most of the Jansen receptor also appears to be incorporated in the cell membrane. In contrast, the Blomstrand type mutant PTH-R accumulates in the ER after translation, or leaks from the ER to the cytoplasmic region. Thus, skeletal deformities of Blomstrand's chondrodysplasia may result, at least in part, from receptor accumulation in the ER by cellular mechanisms of "quality control".

Disclosures: **J. Shimomura**, None.

SA489

See Friday Plenary number F489.

SA490

TIP39/Parathyroid Hormone Receptor 2 Signaling Inhibits Chondrocyte Proliferation and Differentiation by Negatively Regulating Sox9 Gene Expression. D. Panda¹, H. Juppner², D. Goltzman¹, A. C. Karaplis¹. ¹Medicine, McGill University, Montreal, PQ, Canada, ²Endocrine Unit, Massachusetts General Hospital, Boston, MA, USA.

TIP39 is the extended member of the parathyroid hormone super family that exerts its function by interacting with its specific receptor, parathyroid hormone receptor 2 (PTHr2). PTHr2 is highly expressed in thyroid cartilage, which persists as hyaline cartilage, while its expression in growth plate cartilage chondrocytes is restricted to certain cell populations. To investigate the role of G-protein mediated TIP39/PTHr2 signaling in chondrocyte biology, we first generated stably transfected CFK2 chondrocytic cells overexpressing PTHr2. Clones expressing PTHr2 were selected which demonstrated both G418 resistance and expression of the PTHr2 transcript by northern blotting. TIP39 (10⁻⁷M) treatment of CFK2 cells stably transfected with PTHr2 inhibited their proliferation in culture. In addition, TIP39 treatment of PTHr2-expressing CFK2 cells restricted cells at the G0/G1 phase of the cell cycle. The inhibition of proliferation and cell cycle restriction were tightly associated with decreases in the expression of cyclin dependent kinases, CDK2 and CDK4, while p21, an inhibitor of CDKs, was upregulated. Moreover, TIP39 down-regulated expression of the differentiation markers (alkaline phosphatase activity, proteoglycan, type II, and type X collagen) in CFK2 cells. Transcription of *Sox9*, the master regulator of cartilage development, was dramatically reduced in TIP39 treated cells. *Sox9* gene promoter activity as measured by luciferase reporter analysis was also severely impaired following TIP39 treatment. In summary our results show that TIP39/PTHr2 signaling regulates the proliferation and differentiation of chondrocytes by down-regulating the expression of the master transcriptional regulator Sox9, and therefore illustrate the functional significance of the parathyroid hormone family member TIP39 in chondrocyte biology.

Disclosures: **A.C. Karaplis**, None.

SA491

See Friday Plenary F491.

SA492

Development of a Novel Cell-Scanning System (Cell Track) for Expression Cloning of The Carboxyl-Terminal Parathyroid Hormone Receptor (CPTHr). A. Selim¹, B. McKenna^{*2}, S. El-Difrawy^{*2}, H. Juppner¹, P. Divieti¹, D. Ehrlich^{*2}, R. Bringham¹. ¹Endocrine Unit, MGH, Boston, MA, USA, ²White Head Institute, MIT, Boston, MA, USA.

Parathyroid hormone (PTH), an 84-amino-acid polypeptide, is a major systemic regulator of calcium homeostasis and bone remodeling and elicits its classical functions by activating PTH/PTHrP receptors (PTHrRs) on target cells. Carboxyl (C) fragments of PTH, secreted by the parathyroids in a calcium-dependent manner or generated by PTH proteolysis in the liver, circulate in blood at concentrations much higher than intact PTH(1-84) but cannot activate PTHrRs. Receptors specific for C-PTH fragments (CPTHrRs), distinct from PTHrRs, are expressed by bone cells, especially osteocytes, in which they may regulate intercellular communication and cell survival. Cloning of the CPTHr receptor is essential for characterization of its function(s) and mechanism of action(s). We are using an expression cloning approach to clone the CPTHr receptor. Expression cloning requires a highly sensitive, specific and rapid technique for detecting receptor expression in single cells transfected with pools of the cDNA library of interest. We have tested the sensitivity of a novel cell scanning system, "Cell Track", adapted from an instrument originally designed for analysis of multiplexed short tandem repeat DNA. The system supports a glass microdevice with 16 parallel channels, each of 20 cm effective length, and double-T cross injectors. A high-speed rotatory confocal line scanner with four-color detector enables detection of single-cell fluorescence(s) and was specially designed to accommodate the high elution rates on the microdevice. To examine the sensitivity of the Cell Track system, we tested samples in which 0.1% of cells (osteocytes) expressed CPTHrRs and were pre-bound to biotinylated human [Bio85, Tyr34]PTH (23-84) and then reacted with fluorescent streptavidin (Texas Red). The remaining cells in these samples (99.9%) were COS-7 cells that are known not to express CPTHrRs. The Cell Track System reliably detected the cells expressing CPTHr in these samples (0.1%), displaying data as images of single positive cells with corresponding fluorescent signal intensity. No signal was detected in control samples consisting of COS-7 cells alone. The Cell Track System, which is adaptable for analysis of 384 samples simultaneously, provides rapid, reliable and highly sensitive detection and promises to facilitate CPTHr expression cloning and other applications requiring analysis of low-frequency subpopulations of cells identifiable by fluorescent markers.

Disclosures: **A. Selim**, None.

SA493

The Receptor for Carboxyl-Terminal Parathyroid Hormone Regulates Osteocyte Cytoskeleton through Calcium Influx Dependent Mechanisms.

A. A. Selim, G. Suliman*, H. Juppner, J. Potts, R. Bringham, P. Divieti.
Endocrine unit, MGH, Boston, MA, USA.

Parathyroid hormone (PTH), an 84-amino-acid polypeptide, is a major systemic regulator of calcium homeostasis and bone remodeling and elicits its classical functions by activating PTH/PTHrP receptors (PTHRs) on target cells. Carboxyl (C) fragments of PTH, secreted by the parathyroids in a calcium-dependent manner or generated by PTH proteolysis in the liver, circulate in blood at concentrations much higher than intact PTH(1-84) but cannot activate PTHR. Receptors specific for C-PTH fragments (CPTHRs), distinct from PTHR, are expressed by bone cells, especially osteocytes, in which they may regulate intercellular communication and cell survival. Activation of CPTHRs previously was reported to modify intracellular calcium within chondrocytes. Our laboratory previously examined calcium signaling in several cell lines that express CPTHRs including osteocytes, ROS 17/2.8 osteosarcoma cells and RAW 264.7 myelomonocytic cells. Signaling studies demonstrated that CPTH induces voltage-sensitive calcium channel (VSCC) dependent calcium influx in the previously mentioned cells. Since calcium is a major regulator of the cytoskeleton, we examined the effect of CPTH-dependent calcium influx on cytoskeletal structure in the PTHR1-null osteocyte cell line (OC-59). OC-59 cells were treated with 100 nM CPTH (53-84) for 2 or 10 minutes and then examined by immuno-fluorescent staining of cytoskeletal components (actin and vinculin). OC-59 cells treated with 100 nM PTH(53-84) for 10 minutes demonstrated marked actin and vinculin condensations compared to cells treated with vehicles or cells treated with PTH(53-84) for only 2 minutes. The specificity of the cytoskeletal changes in response to CPTH treatment was examined by treating cells with the mutant CPTH analog, [Ala⁵⁵⁻⁵⁷]PTH(53-84), which does not bind to CPTHRs nor induce a calcium signal in OC-59 cells. [Ala⁵⁵⁻⁵⁷]PTH(53-84) failed to induce any cytoskeletal changes in OC-59 cells treated for 10 minutes. Similar results were observed using PTH 1-34, which does not bind to or activate CPTHRs. The role of calcium influx in cytoskeletal changes induced by CPTH treatment was examined by blocking calcium influx using gadolinium chloride (GdCl). PTH(53-84) failed to induce cytoskeletal changes in OC-59 cells pretreated with GdCl (1 and 10 μ M). In our previous calcium studies, GdCl completely inhibited the calcium signal in response to CPTH treatment. Collectively these data suggested that calcium signals induced by CPTHRs may play an important role in regulation of osteocyte cytoskeletal assembly and structure.

Disclosures: A.A. Selim, None.

SA494

1,25(OH)2D3 Regulates Vascular Invasion in Long Bone Development during Embryonal Period. K. Hasegawa*¹, Y. Seino², S. Kato*³, H. Tanaka¹.

¹Department of Pediatrics, Okayama university graduate school of medicine & Dentistry, Okayama city, Japan, ²Department of Pediatrics, Osaka Kosei Nenkin Hospital, Okayama city, Japan, ³Tokyo University, Tokyo, Japan.

Vitamin D has been thought as an important factor in bone formation. We have shown that Vitamin D receptor Knock Out mice (VDRKO) clearly showed increased membranous bone formation in bone transplantation experiment, in bone organ culture system, and in fetal skeletal development. These results led us to the idea that 1,25(OH)2D3 (D3) directly suppresses bone formation. But the underling mechanism has not been fully understood. To clarify the roles of D3 in endochondral ossification, we analyzed the bone development focusing on the vascular invasion in long bone development during embryonal period. At first, we made skeletal preparation of Wild type mice (WT) and VDRKO during embryonal period. Then we determined when the diaphyseal ossification starts in long bones such as femur of WT and VDRKO. At p.c.d 14.5, we could identify diaphyseal ossification in VDRKO in contrast to Wt in which no bone collar was yet formed. Histology using von Kossa staining confirmed the same consequence. Because endochondral ossification starts with vascular invasion into the cartilage, we investigated the expression pattern of angiogenic factor such as vascular endothelial factor (VEGF), its receptors and PCAM-1 (CD31) as a vascular endothelial marker, by immunohistochemistry and we quantified expression of VEGF and VEGF receptor 2 (FLK) by real time PCR. As a result, FLK and PECAM-1 appeared earlier in VDRKO than WT. Thus we consider that D3 suppress vascular invasion into long bone via expression of FLK and PECAM-1 during embryonal period. From these results, we concluded that D3 suppresses endochondral bone formation by inhibiting the vascular invasion during long bone development.

Disclosures: K. Hasegawa, None.

SA495

Two New SNPs in the Human Vitamin D Receptor Promoter Switch Transcription Factor Binding, Change Promoter Activity and Are Associated with Growth in Female Adolescents. A. d'Alésio*¹, M. Garabedian¹, J. Sabatier*², G. Guaydier-Souquières*², C. Marcelli*², A. Lemaçon*¹, O. Walrant-Debray*¹, F. Jehan*¹.

¹Inserm U561, Paris, France, ²Service de Rhumatologie, Centre Hospitalier Universitaire, Caen, France.

We have hypothesized that clinical or biological features may also be associated with variations in the expression of vitamin D receptor (VDR) due to the presence of single-nucleotide polymorphisms (SNPs) in promoter regions. In the present work, we have identified two SNPs located -1521 bp (G/C) and -1012 bp (A/G) upstream of the transcriptional start site of the main human VDR gene promoter (hVDRp) so-called 1a-promoter. Genetic analysis evidenced two major haplotypes -1521G/-1012A and -1521C/-1012G and three main genotypes: homozygous for -1521G/-1012A (21.1%), homozygous

for -1521C/-1012G (17.3%), and heterozygous -1521CG/-1012GA (57.3%). Electrophoretic mobility shift assays (EMSA) and competition experiments showed that one-base change at either polymorphism site was sufficient to switch the nature of the transcription factor bound, using either nuclear extracts from renal HEK293, intestinal Caco-2 or fibroblastic COS-7 cells. Transfection experiments performed in HEK293 or COS-7 cell lines revealed that the hVDR promoter activity was nearly 2 fold higher with the -1521G/-1012A haplotype, as compared to the -1521C/-1012G haplotype. Association between VDRp genotype and several features (clinical, radiological, and biological) were studied in a cohort of 185 healthy adolescent girls (14.7 \pm 2.8 years; range: 11-22 years), enrolled for a 4-year survey. Results show no association between VDRp genotype and parameters of calcium metabolism (serum calcium, urinary calcium excretion, serum PTH, serum 1.25-(OH)₂D) or bone mineralisation (bone mineral density, bone age, serum osteocalcin, or serum alkaline phosphatase activity). However, in comparison with girls with a GG/AA genotype, girls with a CC/GG genotype had: (i) lower circulating levels of 25-dihydroxyvitamin D (p=0.006); (ii) lower serum IGF-1 levels (p=0.03) and (iii) smaller height (p<0.008) from 11 years of age up to adult height. The significant association between hVDRp genotype and height could be overridden by sufficient calcium intake during puberty (> 865 mg/day). In conclusion, genotype variations at the two hVDRp SNPs are likely to change transcription factor docking and VDR expression, and may influence linear growth before and during puberty, especially in girls with low calcium intakes.

Disclosures: F. Jehan, None.

SA496

See Friday Plenary number F496.

SA497

The Vitamin D Receptor Antagonist, (23S)-25-dehydro-1 α -hydroxyvitamin D₃-26,23-lactone, Blocks RANK Ligand Induced Osteoclast Formation. S. Ishizuka¹, N. Kurihara², G. D. Roodman³.

¹Bone and Calcium Metabolism, Teijin Institute for Bio-Medical Research, Tokyo, Japan, ²Medicine/Hem-Onc, University of Pittsburgh, Pittsburgh, PA, USA, ³Medicine/Hem-Onc, University of Pittsburgh and VA Pittsburgh Healthcare System, Pittsburgh, PA, USA.

We recently demonstrated that (23S)-25-dehydro-1 α -hydroxyvitamin D₃-26,23-lactone (TEI-9647), a vitamin D₃ receptor (VDR) antagonist, inhibited both normal and Paget's disease (PD) osteoclast (OCL) formation in response to 1 α ,25-(OH)₂D₃, and decreased the hypersensitivity of PD OCL precursors to 1 α ,25-(OH)₂D₃. Compounds such as TEI-9647 and its naturally occurring structural analogue, 23(S)25(R)-1 α ,25-(OH)₂D₃-26,23-lactone (1 α ,25-(OH)₂D₃-lactone), which is not a vitamin D antagonist, have unique binding properties that may allow them to interact with other proteins in addition to VDR. Therefore we determined if TEI-9647 blocked OCL formation induced by RANKL as well, since many of the effects of 1 α ,25-(OH)₂D₃ on OCL formation are mediated via induction of RANKL expression. Both TEI-9647 and 1 α ,25-(OH)₂D₃-26,23-lactone, dose-dependently (10⁻¹⁰M to 10⁻⁶M) blocked OCL formation induced not only by 10⁻¹⁰M of 1 α ,25-(OH)₂D₃ but also by 50ng/ml of RANKL in pagetic and normal bone marrow cultures. This inhibition was not due to toxicity of these compounds since 10⁻⁶ M concentrations of these compounds did not inhibit CFU-GM colony formation. Importantly, another VDR antagonist that is not a lactone, the 25-carboxylic ester analogue of 1 α , 25-(OH)₂D₃ (ZK-159222), dose-dependently blocked osteoclast formation induced by 1 α , 25-(OH)₂D₃, but did not block RANKL induced OCL formation. These data suggest TEI-9647 and its natural analogue have VDR independent effects on OCL formation. To confirm that VDR was not mediating their effects on OCL formation, we tested the capacity of these compounds to inhibit OCL formation by VDR-/- marrow cells. Both TEI-9647 and 1 α , 25-(OH)₂D₃-26, 23-lactone blocked osteoclast formation induced by RANKL in bone marrow cultures of VDR -/- mouse. In contrast, ZK159222 did not inhibit OCL formation induced by RANKL. These data suggest that TEI-9647 has two mechanisms of action to inhibit osteoclast formation: One is a VDR-mediated antagonistic action and the other is a VDR independent 1 α , 25-(OH)₂D₃-26, 23-lactone-like action. Thus TEI-9647 is a novel OCL inhibitor that blocks both VDR and RANKL-mediated OCL formation. These data suggest TEI-9647 may be useful for treating diseases associated with increased OCL activity such as osteoporosis, bone metastasis and PD.

Disclosures: S. Ishizuka, None.

SA498

Identification of Vitamin D Response Element Binding Proteins and Transcription Factors by Oligonucleotide Trapping. W. Lutz*, R. Kumar. Nephrology Research, Department of Medicine, Biochemistry and Molecular Biology, Mayo Clinic College of Medicine, Rochester, MN, USA.

DNA affinity chromatography is widely used for purification of transcription factors and other DNA binding proteins. A recently developed approach for transcription factor purification involves an oligonucleotide trapping method in which a decameric oligonucleotide coupled to a resin is used to capture a complex of transcription factors bound to a specific DNA element. We investigated the suitability of this oligonucleotide trapping method for identifying transcription factors recruited to an osteopontin vitamin D response element (OP-VDRE). A DNA template consisting of two OP-VDREs flanked by (GT)_n overhangs was incubated with nuclear extract protein prepared from rat osteosarcoma cells (ROS 17/2.8) which had been treated with 10⁻⁷ M 1,25(OH)₂D₃ for 6 hours. The DNA template and bound proteins were captured by applying mixture to a Sepharose resin to which the complementary oligonucleotide (CA)_n was covalently coupled. After washing the

ASBMR 27th Annual Meeting

resin template-bound proteins were eluted with 1M NaCl. Eluted proteins were identified by Western blotting and liquid chromatography mass spectrometry/mass spectrometry. For Western blotting, an aliquot of the eluant was applied to a 4-15% SDS-PAGE gel and separated proteins transferred to PVDF membranes. The following antibodies were used: anti-VDR (rabbit polyclonal), anti-RXR (rabbit polyclonal, sc-774, Santa Cruz Biotechnology, Santa Cruz, CA), anti-RNA polymerase II (rabbit polyclonal, sc-899, Santa Cruz Biotech.), anti-CREB-binding protein (rabbit polyclonal, sc-369, Santa Cruz Biotech.), anti-p300 (rabbit polyclonal, sc-584, Santa Cruz Biotech.), anti-SRC-1 (goat polyclonal, sc-6098, Santa Cruz Biotech.), anti-GRIP-1 (rabbit polyclonal, sc-8996, Santa Cruz Biotech.), anti-TRAP150 (goat polyclonal, sc-5378, Santa Cruz Biotech.), and TFIIA- γ (goat polyclonal, sc-5316, Santa Cruz Biotech.). The remainder of the eluant was analyzed by mass spectrometry following concentration on PVDF membrane, trypsin digestion and liquid chromatography. Western blotting identified the following proteins bound to the OP-VDRE: VDR, RXR, and GRIP-1. The following DNA-associated proteins were identified by mass spectrometry: nucleolin, cellular nucleic acid binding protein, nonhistone chromosomal protein HMG-17, histone H1.2, nucleophosmin, FUSE binding protein 2, and general transcription factor II-L. These results indicate that the oligonucleotide trapping method is a powerful method for identifying VDRE-binding proteins.

Disclosures: **W. Lutz**, None.

SA499

See Friday Plenary number F499.

SA500

1,25(OH)₂D₃ Induces Rapid Response in Growth Plate Chondrocytes and Osteoblasts through Its Membrane-Associated Binding Protein, ERp60. L. Wang, R. A. Chaudhri^{*}, K. L. Wong^{*}, Z. Schwartz, B. D. Boyan. Georgia Institute of Technology, Atlanta, GA, USA.

Steroid hormones act via traditional nuclear receptor mechanisms, as well as rapid non-genomic pathways by activating membrane associated protein kinases. 1,25-dihydroxyvitamin D₃ [1,25] activates the PKC α signaling pathway in prehypertrophic and upper hypertrophic zone (growth zone) growth plate chondrocytes via activation of phospholipase A₂ (PLA₂), cyclooxygenase-1 (Cox) and PLC. Factors that upregulate responsiveness to 1,25 in growth plate chondrocytes increase expression of PLA₂ activating protein (PLAA), suggesting that it links ERp60 to PLA₂. Antibodies to the N-terminal amino acid sequence of ERp60 (Ab100), a 1,25 binding protein present in chondrocyte and osteoblast plasma membranes, block the signaling cascade. Growth zone chondrocytes from VDR^{-/-} mice also respond to 1,25 with a rapid increase in PKC via the same PLC-dependent mechanism. To better understand the role of ERp60, we examined its tissue distribution in the tibial growth plate of VDR^{-/-} mice using immunohistochemistry and compared this to PLAA; we determined its subcellular localization and relationship to the caveolar scaffolding protein caveolin-1 and to the nVDR by confocal microscopy of rat growth zone cells; we assessed the relative contributions of the N and C terminals to the overall mechanism; and we examined response to 1,25 in osteoblast-like ROS 17/2.8 cells (stable) after silencing ERp60 expression with siRNA. Immunohistochemistry using Ab100 showed that ERp60 and PLAA were limited to the prehypertrophic and upper hypertrophic cell zones of the growth plate and to the metaphyseal osteoblasts, both of which are responsive to 1,25. Immunostain was absent from the resting zone, which lacks a rapid PKC response. ERp60 and caveolin-1 were present in the plasma membrane whereas the nVDR was primarily in the nuclei of growth zone cells. Ab100 and Ab101 (generated to the C-terminus of ERp60) both blocked PLC and PKC activation and downstream biological responses, suggesting that both termini are involved in the mechanism. Compared to scrambled siRNA treated cells, Erp60 siRNA significantly decreased the effect of 1,25 on PKC activity in ROS 17/2.8 cells. Additional studies showed that activation of PKC in ROS 17/2.8 cells was via PLC and Cox. In conclusion, 1,25 binding protein ERp60 and PLAA are present in 1,25-responsive chondrocytes and osteoblasts in vivo and in vitro, ERp60 and Cav-1 are present in the plasma membrane, and rapid PKC signaling requires functional activation of ERp60 signaling via PLC and COX.

Disclosures: **L. Wang**, None.

SA501

VDR Gene Polymorphism and Falls in the Elderly. H. A. Bischoff-Ferrari¹, M. Conzelman^{*2}, H. B. Staehelin^{*3}, R. Theiler^{*4}, P. Geusens⁵, W. Dick^{*6}.

¹Medicine, Brigham and Women's Hospital, Boston, MA, USA, ²Geriatrics, Felix Platter Spital, Basel, Switzerland, ³Geriatrics, University Basel, Basel, Switzerland, ⁴Rheumatology, Triemli Hospital, Zurich, Switzerland, ⁵Rheumatology, Limburg University Center, Diepenbeek, Belgium, ⁶Orthopedics, Basel University, Basel, Switzerland.

Background: The Vitamin D receptor (VDR) is present in muscle tissue. Thus its allelic variation may have an independent effect on falls. **Aim:** To study the role of the BsmI VDR polymorphism and baseline vitamin D status as predictors of falls. **Methods:** This is a 12-week prospective study including 117 frail elderly women in long-stay geriatric care (mean age 85 years; range 63-99). The rate of falls was the primary outcome of this analysis. We used Poisson regression to evaluate whether the VDR polymorphism is a determinant of the risk of falling controlling for age, sex, body mass index, intact PTH, baseline 25-hydroxyvitamin D, number of comorbid conditions, Folstein Mini Mental Status, vitamin D treatment and length of follow-up. **Results:** 66 falls occurred in 117 persons. Mean baseline 25-hydroxyvitamin D levels were 16.3 ng/ml (SD \pm 10.3). BsmI VDR alleles were distributed as follows: Bb = 56%, bb = 32% and BB = 12% of sample.

Controlling for all other covariates, the bb VDR genotype carried a 2-fold increased risk of falls compared to the heterozygote genotype (RR = 2.0; 95% CI [1.12,3.58]). The BB genotype did not carry an increased risk. Independent of the VDR and controlling for all other covariates, a 1 ng/ml higher baseline 25-hydroxyvitamin D serum level accounted for a 5% reduction of falls (95% CI [1% - 8%]). **Conclusion:** Elderly women carrying the bb VDR genotype had a 2-fold increased rate of falls. However, independent of the VDR genotype, a higher baseline 25-hydroxyvitamin D level reduced falls by 5% per 1 ng/ml.

Disclosures: **H.A. Bischoff-Ferrari**, None.

SA502

VDR Heterodimer Binding to the Human PTHSP1/NF-Y_{DIST} DNA Element and Suppression of SP1/NF-Y Transactivation. A. P. Alimov¹, O. K. Park-Sarge^{*2}, K. D. Sarge^{*3}, H. H. Malluche¹, N. J. Koszewski^{*1}. ¹Division Nephrology, Bone & Mineral Metabolism, University of Kentucky, Lexington, KY, USA, ²Dept. Physiology, University of Kentucky, Lexington, KY, USA, ³Dept. Molecular & Cellular Biochemistry, University of Kentucky, Lexington, KY, USA.

We previously identified a NF-Y binding site (NF-Y_{DIST}) unique to the human PTH (hPTH) promoter adjoining a Sp1 DNA element that is highly conserved in a variety of mammalian PTH promoters. We also showed that a second NF-Y element (NF-Y_{PROX}) is located ca. 30 bp downstream from the Sp1/NF-Y_{DIST} site in the hPTH promoter. NF-Y_{PROX} overlaps with the repressor DNA binding site for the vitamin D receptor (VDR) heterodimer complex and the two factors compete for DNA-binding in vitro. In the present study, addition of recombinant VDR heterodimer to nuclear extracts possessing NF-Y binding activity revealed that the VDR heterodimer also formed a distinct complex on the hPTH Sp1/NF-Y_{DIST} element and could compete with NF-Y for binding to this DNA element. The binding activity was specific for the heterodimer and interference footprint analysis indicated the sites of DNA contacted by the complex comprised an everted repeat. Cold competition analysis indicated VDR heterodimer binding to the hPTH Sp1/NF-Y_{DIST} site was weaker compared to the downstream VDRE/NF-Y_{PROX} element, and interactions with a contiguous DNA sequence containing both binding sites did not reveal evidence of cooperativity. Sp1 and NF-Y can synergistically enhance transcription from the hPTH promoter; however, co-expression of the VDR heterodimer complex resulted in strong 1,25(OH)₂D₃-dependent suppression (>80%) of Sp1/NF-Y synergistic transactivation. This suppressive capability was lost when transient expression of the wild-type VDR in the heterodimer complex was replaced by VDR mutants L417S or E420Q. Thus, synergistic transactivation of the hPTH promoter by Sp1/NF-Y complexes can be suppressed by 1,25(OH)₂D₃ and requires hormone interactions with an intact VDR AF-2 domain. The data suggest that VDR heterodimer binding to the hPTH Sp1/NF-Y_{DIST} element may be contributing to the overall suppression of enhanced promoter activity.

Disclosures: **A.P. Alimov**, None.

SA503

Elucidation of the Molecular Mechanism of Antagonism of 1 α ,25(OH)₂-vitamin D₃ (1,25D)/ Nuclear Vitamin D Receptor (VDR) Transactivation by its 25-dehydro-26,23-lactone Analogs. M. T. Mizwicki^{*1}, C. M. Bula^{*1}, J. E. Bishop¹, S. Ishizuka², A. W. Norman¹. ¹Biochem, UC, Riverside, CA, USA, ²Teijin Inst. for Bio-Medical Res., Tokyo, Japan.

One class of 1,25D-VDR genomic antagonists has a (23S)-25-dehydro-26,23-lactone (MK) side-chain. Here we will use computer modeling (CM), site-directed mutagenesis (SDM) and protease sensitivity (PSA) to show that the mechanism underlying MK antagonism is novel to the nuclear receptor (NR) field because destabilization of the activation helix (H12) results from a reduction, rather than an increase in the molecular volume of the synthetic NR ligand (1,25D: \sim 421; MK: \sim 402 Å³). Furthermore, analysis of the VDRwt-1,25D and MK models prompted the design of VDR mutants that made MK a more potent 1,25D/VDR antagonist or VDR agonist. Novel to the 1,25D-VDR complex, 1,25D's terminal side-chain CH₃ groups (C26/C27) are held in place by the 25-OH H-bonds to H305 and H397 so they make direct van der Waals (vdW) contacts with the VDR hydrophobic crown residues L227 (H3, Helix-3), L404 (H11), L414 (H12), and V418 (H12). The importance of proper intra- and intermolecular vdW contacts in this area was confirmed by 1,25D's genomic EC₅₀'s in VDRwt & V418L (\sim 1 nM); L404F/ V418L (\sim 7 nM); L404V & L414V (\sim 30 nM); V418A & L404V/ L414V (\sim 70 nM), L404V/ V418L (\sim 350 nM). Our CM protocol removes side-chain placement bias in the VDR by docking a representative conformer from each side-chain population cluster (Pop. A = 73%, Pop. B = 14%, Pop. C = 11%; MK: 63%, 5%, 31%), obtained from dot map calculations for ligand alone (Mizwicki *et al.* PNAS 101, 2004). CM of Pop. B and C MK and 1,25D conformers in the VDR showed that only for MK both Pop. B and C forms are able to bind the VDR with equivalent potential interaction energies (PI_E = -94.2 and -94.6 kcal/mol; 1,25D Pop. B = -107.9; C = -98.7 kcal/mol). The reduced MK selectivity is a consequence of its reduced molecular volume altering the way MK's planar lactone can form noncovalent bonds with the H305 imidazole. In all MK-VDRwt complexes MK lacks optimal vdW contacts with the hydrophobic crown residues, leading to H12 instability and antagonism. This mechanism was confirmed by: a) H305A and H305A/H397F convert MK into a superantagonist, b) H305F and H305F/H397F turn MK into a superagonist and c) formation of a MK-VDR covalent adduct with H397 only occurs when [MK] is \geq 10⁻⁵M (all verified by PSA). The proposed mechanism is consistent with the enhanced VDR affinity, antagonistic potency and PI_Es of 24R/S-CH₃-MK and 2 α ,24R/S(CH₃)₂-MK analogs. Collectively the data provides a more detailed understanding to VDR structure/function and may represent a new paradigm for sterol and/or protein based drug design (i.e. MK is an attractive compound for treating Paget's disease).

Disclosures: **M.T. Mizwicki**, None.

SA504

Raloxifene Treatment Modulates ER α Expression in Bone. N. Bravenboer, P. Holzmann*, P. Lips. Endocrinology, VU medical center, Amsterdam, The Netherlands.

Raloxifene is acting as an estrogen agonist in the skeleton, thereby maintaining bone mineral density (BMD) and preventing new vertebral fractures in postmenopausal women. Estrogen receptors (ERs) are proteins that mediate the action of estradiol and a series of natural and synthetic chemicals that mimic estradiol structure. Tissue specific distribution partly determines the response of tissues to estrogenic compounds. Both ER α and β are present in bone tissue in distinct patterns of expression, whereas ER α is predominantly expressed in cortical bone. We questioned whether raloxifene treatment has any effect on the expression of the ER α in bone. 24 postmenopausal women who participated in the MORE trial were biopsied twice, before and after two years of treatment with either placebo or raloxifene 60 or 120 mg/d. All women were provided supplemental calcium (500 mg/day) and vitamin D (400 IU/day). Immunohistochemical detection of ER α was performed on two sections per biopsy. Semi quantitative analysis of the sections was performed by a single investigator, who was blind for the therapy. Ordinal scores for amount of positive osteocytes and osteoblasts were tested using Mann Whitney and Wilcoxon signed rank test. In all biopsies, there was a distinct expression of ER α in some osteocytes in the spongiosa as well as in both cortices. Osteoblasts were rarely positive in both trabecular and cortical bone. Biopsies from the two dosage groups, raloxifene 60 and 120 mg/d, were not different with respect to amount of osteocytes, therefore data from these two groups were combined. The amount of positive osteocytes in trabecular bone decreased after two years raloxifene treatment, while it increased after two years placebo treatment (p=0.026). In cortical bone no differences were observed for the amount of positive osteocytes. Positive osteoblasts were present in 7/24 biopsies at baseline and in 1/10 after placebo treatment and in 2/14 after raloxifene treatment. Although in cortical bone no differences were found in the amount of positive osteocytes, the amount of osteocytes expressing ER α in the trabecular bone decreased after raloxifene treatment while it increased after placebo treatment.

Disclosures: *N. bravenboer, None.*

SA505

See Friday Plenary number F505.

SA506

ER Isoform Specific Regulation of TGF- β Inducible Early Gene-1 by Estrogen in Human Osteoblasts. J. R. Hawse¹, M. Subramaniam¹, D. G. Monroe¹, E. J. Secreto¹, K. Rasmussen*¹, S. Khosla², M. Oursler², T. C. Spelsberg¹. ¹Biochemistry and Molecular Biology, Mayo Clinic, Rochester, MN, USA, ²Endocrine Research Unit, Mayo Clinic, Rochester, MN, USA.

TGF- β inducible early gene-1 (TIEG) is a Krüppel-like transcription factor that plays an important role in mediating TGF- β effects in osteoblasts (OB) and other cells. We have previously shown that estrogen directly regulates the expression of TIEG in human OB. To define this regulation, we have utilized U2OS human osteosarcoma cell lines stably transfected with a doxycycline inducible estrogen receptor (ER) α or β construct. Cells were pretreated with doxycycline for 24 hours followed by treatment with 10 nM estrogen for 2 hours. Total RNA was isolated and real-time RT-PCR analysis was performed to examine the expression of TIEG mRNA. This analysis revealed an approximately 6-fold increase in TIEG in the ER β cell line with a minimal increase in the ER α cell line. Based on these results, studies were initiated to elucidate the molecular mechanisms of this ER isoform specific regulation. We have identified 2 potential estrogen regulatory elements (EREs) in the first intron of TIEG. One of these sites is a perfect half ERE while the other closely resembles the consensus ERE sequence. Electrophoretic mobility shift assays were performed using each of these sequences and revealed that both ER α and ER β were capable of binding to these sites. Cold competition assays, using a consensus ERE sequence, indicated that the TIEG half ERE bound both isoforms of the ER much stronger than that of the full-length ERE-like element. To further characterize these two sequences, we cloned an 850 base pair region of TIEG intron 1, spanning these two potential EREs, into a pGL₃ luciferase vector. This construct was transfected into U2OS cells and used to examine estrogen regulation of these sequences *in vivo*. Interestingly, these ERE-like sequences were capable of eliciting a 3-fold increase in luciferase activity following estrogen treatment only when co-transfected with the β isoform of the ER. These results clearly suggest that, although both isoforms of the ER are capable of binding to these ERE-like sequences, only the β isoform is capable of activating TIEG transcription. Chromatin immunoprecipitation assays are underway to verify the binding of both ER isoforms to these elements under *in vivo* conditions and to determine if ER co-regulators play a role in the ER β specificity of this element.

Disclosures: *J.R. Hawse, None.*

SA507

See Friday Plenary number F507.

SA508

Loss of Sex-Specific Difference in Bone Size in Leptin Knockout Mice. X. Wang*, C. H. Rundle, A. Srivastava*, J. Tesfai*, E. I. Davis*, J. E. Wergedal, K. H. W. Lau, S. Mohan, D. J. Baylink. MDC, J.L. Pettis VAMC, Loma Linda, CA, USA.

Leptin is an important mediator of body weight and bone metabolism. The obesity of leptin-deficient (*ob/ob*) mice facilitates the study of several fat-related effects of obesity, including hypogonadism. It is well known that the bones of male wild-type mice are larger than female wild-type mice and are the result of androgen actions. Because the effects of androgen and estrogen on bone are mediated in part by different molecular pathways, we asked the question if leptin deficiency exerts differential effects on the bones of male versus female mice. We therefore compared the bones of male and female leptin knockout mice (in C57BL/6 background) with the C57BL/6 wild-type control strain at 10 weeks of age. pQCT measurements in the femoral midshaft using an analysis threshold of 570-214 revealed that the large differences in the periosteal circumference (PC), endosteal circumference (EC) normally observed between male and female wild-type mice were reduced in male leptin knockout mice to values not significantly different from those of female leptin knockout mice (Table 1). The same was true for femur length. Total fat and body weight, as determined by DXA, were not significantly different between male and female leptin knockout mice (Table 1). PC, EC and femur length were not significantly different between female wild-type mice and female leptin mice (Table 1), indicating that the reduction of these parameters in leptin knockout male mice was caused by diminished androgen functions that could be attributed to hypogonadism in leptin knockout male mice. In conclusion, this study suggests that (1) the bone size determination depends on the action of leptin, and (2) the deficiency of leptin action may induce defects in the biological actions of androgen in male mice.

Table 1. C57BL/6-Leptin Knockout Mouse Comparison			
Parameter	C57BL/6 Male/Female (%)	Leptin KO Male/Female (%)	C57BL/6 Female/Leptin KO Female (%)
Femur PC	108.9*	100.0	101.5
Femur EC	110.0*	98.0	94.4
Body Weight	130.0*	101.1	41.3*
Fat	132.9*	95.9	11.4*

* p<0.006 by T-test

Disclosures: *X. Wang, None.*

SA509

See Friday Plenary F509.

SA510

Sex Steroids as Predictors of Bone Mineral Density, Bone Size and Prior Osteoporosis-Related Fractures in Elderly Swedish Men- *MrOS Sweden*. D. Mellström¹, A. Eriksson¹, M. Lorentzon¹, E. Orwoll², Ö. Ljunggren³, Ö. Johnell⁴, C. Ohlsson¹. ¹Center for Bone Research at the Sahlgrenska Academy, Departments of Internal Medicine and Geriatrics, Gothenburg University, Gothenburg, Sweden, ²Bone and Mineral Unit, Oregon Health and Sciences University, Portland, OR, USA, ³Department of Medical Sciences, University of Uppsala, Uppsala, Sweden, ⁴Department of Orthopaedics, Malmö General Hospital, Malmö, Sweden.

Osteoporosis-related fractures constitute a major health concern not only in women but also in men. Previous studies have indicated that serum levels of estradiol but not of testosterone are associated with bone mineral density (BMD) in elderly men. The aim of the present study was to investigate if levels of free estradiol (FE2) or free testosterone (FT) are associated with BMD, bone size and/or prior osteoporosis-related fractures in a large cohort of elderly Swedish men. In the Swedish part of the MrOS study (n= 3000, average age 75.4 years) bone parameters were measured using DXA and prior fractures after 50 years of age were estimated using standardized questionnaires. Serum levels of testosterone, estradiol and SHBG were measure and FT and FE2 were derived from the mass action equations. Height, weight, age, physical activity, smoking habits and calcium intake were included together with FE2 and FT in regression models for BMD. FE2 (β = 0.120, p<0.0001) but not FT (β = 0.003, NS) was an independent predictor of lumbar spine BMD. Both FE2 and FT were independent predictors of total body (FT β = 0.066, p< 0.001; FE2 β = 0.083, p< 0.001) and trochanter (FT β = 0.068, p< 0.01; FE2 β = 0.067, p< 0.01) BMD. FT (β = 0.041, p<0.01) but not FE2 (β = 0.023, NS) was an independent predictor of total body bone area. Both FT (β = -0.061, p= 0.001) and FE2 (β = -0.042, p= 0.023) were negative predictors of prior fractures after 50 years of age (n= 497 individuals with reported fracture). Similar results were seen when only fractures at the major osteoporosis-related sites (vertebrae, radius, hip and humerus) were counted (n= 187 individuals with reported fracture, FT β = -0.044, p = 0.018; FE2 β =-0.037, p = 0.046). In conclusion, FE2 is an independent predictor of BMD at most skeletal sites while FT only is an independent predictor of BMD at selected sites. In contrast, FT but not FE2 is an independent predictor of bone area. Both FT and FE2 are predictors of prior osteoporosis-related fractures.

Disclosures: *C. Ohlsson, None.*

SA511

See Friday Plenary F511.

SA512

A TAAAA Repeat Polymorphism in the SHBG Gene Is Associated with Hormone Levels and BMD in Elderly Swedish Men - *MrOS Sweden* . A. Eriksson¹, M. Lorentzon¹, E. Orwoll², Ö. Ljunggren³, O. Johnell⁴, D. Mellström¹, C. Ohlsson¹. ¹Center for Bone Research at the Sahlgrenska Academy, Departments of Internal Medicine and Geriatrics, Gothenburg University, Gothenburg, Sweden, ²Bone and Mineral Unit, Oregon Health and Sciences University, Portland, OR, USA, ³Department of Medical Sciences, Uppsala University, Uppsala, Sweden, ⁴Department of Orthopaedics, Malmö General Hospital, Malmö, Sweden.

Sex hormone binding globulin (SHBG) serves as a transporter of sex steroids in the blood, and thereby regulates free levels of estradiol and testosterone. Free sex steroids in turn regulate skeletal homeostasis. Furthermore, some studies have indicated that SHBG is an independent regulator of bone mineral density (BMD). Recently, a pentanucleotide repeat polymorphism (TAAAA)_n in the 5' promoter region of the SHBG gene has been characterized. The aim of the present study was to investigate if the TAAAA repeat polymorphism is associated with serum levels of SHBG and sex steroids, and BMD in a large cohort of elderly Swedish men. In the Swedish part of the MrOS study (n= 3000, average age 75.4 years) bone parameters were measured using DXA. Serum levels of testosterone, estradiol and SHBG were measured and free testosterone and free estradiol levels were derived from the mass action equations. The TAAAA repeat polymorphism was divided into long (>6 repeats = L) and short (6 repeats = S) variants. The SHBG repeat polymorphism was clearly associated with serum levels of SHBG (r= 0.114, p<0.0001), total testosterone (r=0.100, p<0.0001), free testosterone (r=0.057, p=0.007) and total estradiol (r= 0.065, p=0.002) but not with free estradiol levels (r= 0.032, p=0.12). Subjects with two short alleles had the highest levels of SHBG (SS 48.8 ± 2.0 nmol/l, SL 43.9 ± 0.7 nmol/l, LL 41.4 ± 0.6 nmol/l, p<0.0001), total testosterone (SS 19.2 ± 0.6 nmol/l, SL 17.3 ± 0.3 nmol/l, LL 16.0 ± 0.1 nmol/l, p=0.005) and total estradiol (SS 105.2 ± 3.0 pmol/l, SL 100.0 ± 1.4 pmol/l, LL 95.9 ± 1.1 pmol/l, p=0.005). We next investigated if the SHBG repeat polymorphism was an independent predictor of BMD. Height, weight, age, physical activity, smoking habits and calcium intake were included together with the SHBG repeat polymorphism in regression models for BMD. The SHBG repeat polymorphism was a significant independent predictor of trochanter BMD (β= -0.052, p=0.009) but not a significant predictor of lumbar spine BMD (β= -0.031, p=0.128). In conclusion, a TAAAA repeat polymorphism in the promoter region of the SHBG gene is associated with serum levels of SHBG and trochanter BMD in elderly men.

Disclosures: **A. Eriksson**, None.

SA513

See Friday Plenary number F513.

SA514

Phenolic Compounds in Safflower Seeds Reduce Bone Loss in Ovariectomized Rats. W. Lee^{*1}, Y. Bae^{*2}, J. Jin^{*1}, Y. Jung¹, S. Choi^{*3}, S. Cho^{*3}, I. Park¹, R. Park^{*1}, I. Kim^{*4}, S. Kim¹, J. Choi¹. ¹Biochemistry, Kyungpook National University, School of Medicine, Skeletal Diseases Genome Research Center, Daegu, Republic of Korea, ²Oral Anatomy, Kyungpook National University, School of Dentistry, Daegu, Republic of Korea, ³Food Science and Nutrition, Catholic University, Daegu, Republic of Korea, ⁴Biochemistry, Kyungpook National University, School of Medicine, Daegu, Republic of Korea.

We previously reported that safflower seeds attenuated bone loss in ovariectomized rats (Kim *et al.*, Calcif Tissue Int., 71:88-94, 2002). In the present study, we investigated whether the phenolic compounds in safflower seeds are responsible for the bone-protecting effects. Female Sprague-Dawley rats (12 week old) were subjected to bilateral ovariectomy (OVX) or sham surgery. Ovariectomized rats were randomly assigned to groups and either fed a diet containing powder of defatted safflower seeds (SP) or phenolic compounds extracted from safflower seeds (SE), or injected with 17β-estradiol (E₂). After 4 weeks, their proximal tibiae were processed for scanning electron microscopy and quantitative bone histomorphometry. In contrast to marked bone loss and marrow fat deposition of the OVX group, both SP and SE groups showed approximately 80% of the bone volume of the sham group and no increase in marrow adiposity. The amount of the osteoid bone, reflecting newly formed bone, increased to 170% of the sham level in the OVX group, but was maintained at almost the sham level both in the SP and SE groups. In an attempt to find out which phenolic compounds exert the beneficial effects, lignans, flavones and serotonin derivatives were isolated from SE and administered to ovariectomized rats. Each phenolic compound significantly reduced the OVX-induced trabecular bone loss, increase in osteoclast numbers and marrow adiposity in the proximal tibiae. The present data provide the first direct *in vivo* evidence that the mixture of phenolic compounds from safflower seeds reduces the bone turnover and bone loss caused by estrogen deficiency.

Disclosures: **J. Choi**, None.

SA515

See Friday Plenary number F515.

SA516

Follicle-Stimulating Hormone Receptor Deficiency in Female Mice Results in an Osteoporotic Phenotype Characterized by Impairment of Osteoblastic Bone Formation and Stimulation of Osteoclastic Bone Resorption. J. Gao¹, Y. Yang^{*2}, D. Miao¹, M. R. Sairam^{*2}, A. C. Karaplis¹, D. Goltzman¹. ¹Department of Medicine, McGill University, Montreal, PQ, Canada, ²Molecular Reproduction Research Laboratory, Clinical Research Institute of Montreal, Montreal, PQ, Canada.

Follicle-stimulating hormone receptor (FSHR) knockout mice display impaired ovarian follicular development and infertility in females. FSHR deficiency also causes marked bone loss; however, the mechanism whereby FSHR affects bone remodeling is unclear. In order to investigate whether the effect of FSH on bone is direct or indirect and whether the bone loss in FSHR deficient mice results from the impairment of osteoblastic bone formation or the stimulation of osteoclastic bone resorption, we examined the expression of the FSHR in skeletal tissues and the effect of FSHR deficiency on bone remodeling. We found that the FSHR was undetectable in skeletal tissues as demonstrated by RT-PCR. The skeletal phenotype was normal at 4 weeks of age in the female FSHR knockout mice. By 3 months of age, as determined by contact radiography, Pixmap densitometry, micro-CT and histomorphometric analysis, bone mineral density and trabecular bone volume were decreased significantly in the female FSHR knockout mice compared to their sex-matched wild type littermates. To determine whether the alterations of bone volume which were observed were associated with alterations of osteoblastic bone formation, we examined osteoblast number and osteoblast surface by histomorphometry and the alterations in expression of genes related to bone formation using RT-PCR. Both osteoblast number and surface were markedly diminished and expression of genes encoding Cbfa 1, alkaline phosphatase, type I collagen and osteocalcin were all reduced in bones of the female FSHR knockout mice. Following histochemical staining for tartrate resistant acid phosphatase (TRAP), osteoclast surface was quantified. The results showed that the osteoclast surface relative to the bone surface was increased significantly in the female FSHR knockout mice. The level of RANKL mRNA was not significantly increased but the level of OPG mRNA was reduced in bone of the mutants compared to wild-type bone. These results indicate that the effect of FSHR on bone is an indirect one that is likely mediated by sex hormones. FSHR deficiency therefore indirectly caused an osteoporotic phenotype associated with both the impairment of osteoblastic bone formation and the stimulation of osteoclastic bone resorption and which is only manifest after sexual maturation.

Disclosures: **J. Gao**, None.

SA517

Vitamin D Receptor Antagonist ZK 191784 Augments ApoA1 Gene Expression. K. R. Wehmeier^{*}, M. J. Haas^{*}, A. E. Beers^{*}, A. D. Mooradian^{*}. Division of Endocrinology, Department of Internal Medicine, Saint Louis University School of Medicine, St. Louis, MO, USA.

Studies of arteriosclerosis have used *in vivo* models of vascular calcification created by pharmacologic doses of vitamin D. Investigators have previously demonstrated that human high-density lipoprotein (HDL) inhibits the spontaneous osteogenic differentiation and mineralization of calcifying vascular cells *in vitro*. Members of the steroid receptor super family are known to alter the transcription of the major apoprotein of HDL, ApoA1. 1α,25-Dihydroxyvitamin D₃ was shown to reduce ApoA1 synthesis in our lab. Interventions that increase HDL cholesterol level significantly reduce the risk of coronary heart disease events. To investigate the effects of a vitamin D receptor (VDR) antagonist ZK 191784 (ZK) on ApoA1 gene expression in a human hepatoma cell line (HepG2), we assessed the effect of ZK on apoA1 synthesis and promoter activity. In HepG2 cells transfected with the apoA1 reporter gene construct pA1.474.CAT, ZK induced apoA1 promoter activity in a dose-dependent manner with a plateau at 10 μM. To determine the time course of ZK on apoA1 protein levels, HepG2 cells were incubated with 1 μM ZK for 0, 1, 3, 6, 12 and 24 hours, and apoA1 protein levels were measured by Western blotting. ApoA1 protein levels in the media were significantly increased only after 24 h. To quantify the effect of ZK dose on apoA1 protein levels, HepG2 cells were incubated with increasing amounts of ZK and after 24 h, apoA1 protein levels were measured by Western blot analysis. ApoA1 protein levels increased significantly at 10 nM, reaching a rapid plateau. To assess the effect of ZK on apoA1 promoter activity in the presence or absence of vitamin D (Table 1), HepG2 cells were transfected with the apoA1 reporter gene construct, and treated with ZK, and vitamin D (1α,25-dihydroxyvitamin D₃ 250 nM) for 24 h. ZK, in a time and dose dependent manner, relieved vitamin D mediated transcriptional repression. These studies suggest that VDR analogs may be important in the regulation of ApoA1 synthesis. Further studies are needed to define the implications of VDR ligands on cardiovascular risk.

Effect of ZK on apoA1 promoter activity in the presence or absence of vitamin D.

Conditions	CAT Activity (% Acetylation)	% Change (from control)	P (vs. Control)
Control	25.0 ± 0.8	--	--
ZK (0.02 nM)	24.8 ± 0.4	-0.8	N.S.
ZK (0.2 nM)	22.5 ± 1.6	-10.0	N.S.
ZK (2.0- nM)	30.1 ± 0.8	20.4	0.01
Vit. D (100 nM)	15.8 ± 0.7	-36.8	0.001
Vit. D + ZK (0.02 nM)	17.5 ± 1.2	-30.0	0.006
Vit. D + ZK (0.2 nM)	22.4 ± 1.0	-10.4	0.06
Vit. D + ZK (2.0 nM)	27.7 ± 1.0	10.8	N.S.

Disclosures: **K.R. Wehmeier**, None.

SA518

See Friday Plenary number F518.

SA519

The Effects of UV-B Light on Serum 25(OH)D in Humans. L. A. G. Armas*¹, R. P. Heaney¹, M. J. Barger-Lux*¹, C. Huerter*², R. Lund³.

¹Osteoporosis Research Center, Creighton University, Omaha, NE, USA,

²Dermatology, Creighton University, Omaha, NE, USA, ³Nephrology, Creighton University, Omaha, NE, USA.

We report results of work to quantify the relationship of skin color and 25(OH)D response to graded doses of UV-B light delivered by a light booth. The subjects (n=48, age 21-49 yr, females = 28, males = 20) were healthy indoor workers with limited non-solar sources of Vitamin D. They were divided into 5 treatment groups based on their self-reported susceptibility to tan or burn (Fitzpatrick skin types I-VI). Data were gathered from January through April. We determined BMI, 25(OH)D, Ca²⁺ and PTH at baseline. We used a portable skin colorimeter that utilizes the CIE L*a*b* color system to measure constitutive skin color of the upper inner arm and facultative skin color of the forearm. The subjects were exposed to UV-B light from a UV light booth 3 times a week for 4 weeks (12 treatments) in graded doses ranging from 40mJ to 80 mJ per treatment . 25(OH)D was drawn weekly during, and 4 weeks after, completion of UV-B treatment. There was a rise in 25(OH)D of 29.9 nmol/L (median; interquartile range 24.3-40.7) during the 4 weeks of UV-B treatment and a fall 4 weeks after UV-B treatment ceased of 3-14% from peak 25(OH)D levels. The L* values of exposed skin did not vary significantly throughout the treatment period. There was a significant correlation between L* readings (a continuous darker-to-lighter scale) of baseline facultative and constitutive skin color and 25(OH)D response per mJ of UV-B light given (r²=0.535, r²=0.551) (i.e. the lighter skinned subjects had a greater response). In conclusion, increase in 25(OH)D per mJ of UV-B exposure was related to the "L" value of skin at baseline. This increase in 25(OH)D was achieved without changing "L*" values (i.e. becoming darker).

Disclosures: **L.A.G. Armas**, None.

SA520

See Friday Plenary number F520.

SA521

Cellular Entry of Vitamin D Ligands Together with VDR Affinity Represent the Primary Determinants of Biological Potency. L. A. Zella, N. K. Shevde, J. W. Pike. Biochemistry, University of Wisconsin- Madison, Madison, WI, USA.

Vitamin D superagonists are analogs of 1,25-dihydroxyvitamin D₃ (1,25(OH)2D₃) that display biologic potencies inconsistent with their relative affinities for the vitamin D receptor (VDR). Mechanisms proposed to account for this interesting feature include differential cellular uptake, altered metabolism and the potential for these ligands to provoke unique VDR conformations capable of unusual coregulator interactions. To define the mechanism responsible for increased biologic potency, we evaluated the ability of three vitamin D superagonists, MC1288, KH1060 and 2MD as well as 1,25(OH)2D₃ to induce Cyp24, osteopontin (OPN) and RANKL gene expression in osteoblastic cells *in vitro*. Mouse MC3T3-E1 and/or ST2 cells were treated for 6 hrs with increasing concentrations of each ligand and isolated RNA was analyzed by RT-PCR. As expected, the vitamin D superagonists induced expression of the three target genes with potencies 2 logs greater than that for 1,25(OH)2D₃. Interestingly, however, despite a direct correlation between superagonist affinity for VDR and their ED₅₀'s, this relationship diverged for 1,25(OH)2D₃. This suggested the possibility that "restricted entry" of 1,25(OH)2D₃ might be solely responsible for the phenomenon of differential ligand potency. To test this, osteoblasts were treated with ligand in the absence of serum and isolated RNA subsequently analyzed for Cyp24, OPN and RANKL mRNA induction. Surprisingly, this maneuver increased the potency of 1,25(OH)2D₃ to a level fully equivalent to that of the superagonists. We then assessed whether the transcriptional effects of serum could be linked directly to VDR activation. We determined the capacity of tritiated 1,25(OH)2D₃ and 2MD to bind directly to the VDR in intact cells, the potency of each ligand to induce VDR protein upregulation, and the ability of ligands to promote VDR binding to endogenous Cyp24 and OPN gene promoters using chromatin immunoprecipitation. All studies were carried out in the presence and in the absence of serum. The results revealed that serum impacts each of these VDR-associated activities in a fashion identical to that observed for transcription. In a final experiment, we used serum derived from either wildtype and DBP-null mice to demonstrate that the decrease potency observed for 1,25(OH)2D₃ in the presence of serum was due exclusively to DBP. Our studies indicate that in the absence of catabolism, the primary determinants of vitamin D ligand potency are affinity for the VDR and affinity for serum component such as DBP. Our results do not support a molecular mechanism for potency that involves unusual interactions between the VDR and its coregulators on target genes.

Disclosures: **L.A. Zella**, None.

SA522

Measurement of Specific Vitamin D Binding Protein Capacity and Calculation of Free 1,25-Dihydroxyvitamin D (1,25D). D. Laurie*, M. Gardner*. R&D, IDS Ltd, Boldon, United Kingdom.

A purely mass measurement of vitamin D binding protein (DBP) could give an erroneously elevated indication of functionality if all the DBP can not bind vitamin D. The aim of the study was to demonstrate the utility of the newly developed IDS Vitamin D Binding Protein Capacity (DBPc) reagent pack (AA-36F1). DBPc levels were measured in normal, liver disease (LD) and third trimester pregnancy (3TP) sample groups. This was used with a total 1,25D measure to calculate a 'free' 1,25D level for samples. The IDS DBPc method involved saturating 20µL serum sample with excess 25D (500µL of 1200nM) at 37°C for 30min. Cold charcoal reagent (100µL) was added after 10min chilling on crushed ice. The mixture was incubated for a further 1hr on the ice to remove unbound or low affinity albumin bound 25D. After centrifugation, a proportion of the supernatant containing the high affinity DBP-bound 25D was measured using the IDS 25-hydroxyvitamin D RIA kit (AA-35F1). Samples (Biochemed, U.S.) were also assayed for total 1,25-dihydroxyvitamin D (1,25D), 25-hydroxyvitamin D (25D) (IDS RIA kits) and albumin (BCG Method, Thermoelectron). DBPc levels were significantly higher in the 3TP and lower in the LD groups compared to the normal group. Levels of total 1,25D followed the changes in DBPc levels. Free 1,25D levels calculated from total 1,25D and DBPc levels were higher in the 3TP group, despite the rise in DBPc values. Rises in DBPc, total and free 1,25D were also seen in the pregnancy compared to the normal group in the referenced study ⁽¹⁾. 25D and albumin levels were generally as expected for sample groups with the low 25D levels in the normal group probably a reflection of the season when samples were taken. This study shows that the 3 sample groups tested gave differing DBPc levels using the IDS DBPc reagent pack. From DBPc and total 1,25D measures, it is possible to calculate a potentially physiologically relevant level for 'free' 1,25D in these samples. The IDS DBPc Reagent Pack is effective in measurement of the specific binding capacity of DBP for vitamin D compounds in serum. This might provide a more meaningful indicator of the functionality of DBP in samples in relation to vitamin D physiology than a purely mass DBP measurement.

	Normal (n=60)	LD (n=20)	3TP (n=20)
DBPc (µM)	5.56 (+/-0.61)	4.35* (+/-0.79)	8.16* (+/-0.69)
Total 25D (nM)	34.8 (+/-13.8)	35.4 (+/-12.0)	69.5* (+/-17.4)
Total 1,25D (pM)	99.0 (+/-39.7)	43.8* (+/-20.5)	338* (+/-52.2)
Free 1,25D** (fM)	87.6 (+/-34.7)	50.7* (+/-27.1)	203* (+/-31.7)
Albumin (g/dL)	4.23 (+/-0.41)	1.94* (+/-0.11)	4.21 (+/-0.26)

Mean (+/ SD) * t-Test p<0.001 vs normal. **Free 1,25D (fM) = (Total 1,25D pM x 4.88)/DBPc ⁽¹⁾.

Ref ⁽¹⁾: Vieth 1994. Clin Chem 40: 435-441.

Disclosures: **D. Laurie**, None.

SA523

Development of a Rapid LC-Tandem MS Assay for Serum 25-Hydroxyvitamin D₂ and 25-Hydroxyvitamin D₃ and Comparison with Nichols Advantage, CPBA and HPLC Assays on Serum from Patients Treated with Pharmacological Doses of Vitamin D₂. D. P. Jamieson*¹, A. Zhang*¹, J. Mathieu*¹, R. Ray*¹, D. G. Kelling*², T. C. Chen¹, M. F. Holick¹.

¹Vitamin D Research Laboratory, Boston University School of Medicine, Boston, MA, USA. ²Diabetes Self-Care Program,, NorthEast Medical Center, Concord, NC, USA.

Serum assays for 25-hydroxyvitamin D [25(OH)D] are used to determine the vitamin D status of patients. These assays include radioimmunoassay, competitive protein binding assay (CPBA), and high performance liquid chromatographic assay (HPLC). To date there are only a few Tandem LC Mass Spectrometry (LC-MS/MS) assay methods for the determination of serum 25(OH)D, and most reported methods have low sensitivity and need extensive sample preparation. The LC-MS/MS assay we have developed measures both 25(OH)D₂ and 25(OH)D₃ and shows remarkable sensitivity and accuracy with a lower limit of quantification of 2 ng/ml and with coefficients of variance less than 10% over the range from 2 to 200 ng/ml, respectively. The rapid LC-MS/MS method utilizes a unique extraction procedure, and direct sample loading without the need for further sample preparation, allowing for a total analysis time of 6 minutes per sample. To determine the accuracy of the LC-MS/MS assay for detecting both 25(OH)D₂ and 25(OH)D₃, as compared to other methods, serum samples were obtained from 80 patients who were treated with pharmacologic doses of vitamin D₂ for a period of several months to years. Samples were analyzed by four different methods including: LC-MS/MS, HPLC, CPBA, and the Nichols Advantage System. For all of the vitamin D₂ treated patient samples, we were able to detect and quantify 25(OH)D₂ and 25(OH)D₃ by all four methods. A linear analysis shows no correlation between the levels of 25(OH)D₂ and under detection in the Nichols Advantage assay. This suggests that the discrepancy is more of a patient specific phenomenon and/or a result of possible metabolite interference.

Disclosures: **D.P. Jamieson**, None.

SA524

See Friday Plenary number F524.

SA525

Do Different Storage Conditions Affect the Measurement of Vitamin D Metabolites? J. L. Berry, P. L. Selby, M. Davies. Vitamin D Research Group, Medicine, Manchester Royal Infirmary, Manchester, United Kingdom.

Assays for vitamin D metabolites can be extremely variable. The UK Vitamin D External Quality Assessment Scheme (DEQAS) has shown that the coefficient of variation (CV) of vitamin D metabolite measurements can vary from 19-28% between laboratories. Many laboratories have specific requirements for storing samples before assay. For example, some insist that samples should be frozen immediately and sent frozen to the assay laboratory, others that samples can be sent unfrozen by first class post. We have examined different storage conditions to see whether this could account for some of the variation in measurement of vitamin D metabolites between laboratories. Whole blood or serum (separated within 30 min of sampling) were left at room temperature (RT) or placed in the fridge (4-6°C), serum was frozen at -20°C. Samples were assayed 1, 2 and 7 days post-sampling. A further serum sample was packaged and posted back to our own laboratory then frozen before assay. Whole blood was centrifuged immediately prior to assay. 25-hydroxyvitamin D (25OHD) was measured by HPLC and 1,25-dihydroxyvitamin D (1,25D) by in-house radioimmunoassay. An example from one sample is shown in table 1

Table 1 The effect of different storage conditions on the measurement of vitamin D metabolites

Sample	Storage conditions	Day 1		Day 2		Day 7	
		25OHD ng/ml	1,25D pg/ml	25OHD ng/ml	1,25D pg/ml	25OHD ng/ml	1,25D pg/ml
Serum	RT	8.2	41	8.3	39	8.6	34
	4°C	8.8	38	9.2	30	8.3	37
	-20°C	8.5	38	8.9	36	8.2	34
	By post			8.6	39		
	Freeze/Thaw 1			8.7	44		
	Freeze/Thaw 2					8.5	34
Whole Blood	RT	8.3	49	8.6	32	7.1	36
	4°C	8.9	36	8.4	40	8.3	35

Mean (±SD) 25OHD 8.5±0.4 ng/ml CV 5.1%; 1,25D 37±4 pg/ml CV 11.9%
Mean coefficient of variation from all samples with varying levels of vitamin D metabolites was 5.13±0.06% for 25OHD and 10.8 ±1.0% for 1,25D. This was not significantly different from the normal assay variation for control serum run on the same assays (4.5% for 25OHD and 12.3% for 1,25D). We conclude that different storage conditions do not account for the variation in vitamin D metabolite measurements between laboratories. Furthermore, samples do not need to be frozen before assay.

Disclosures: **J.L. Berry**, None.

SA526

Assessing Vitamin D Status; the Problem of Assay Variation. M. F. Holick¹, N. C. Binkley², D. Jamieson^{*1}, D. Baran³, R. A. Petruschke^{*3}, E. Chen^{*3}, A. E. de Papp³. ¹Boston University School of Medicine, Boston, MA, USA, ²University of Wisconsin, Madison, WI, USA, ³Merck & Co., Inc., West Point, PA, USA.

Vitamin D status is best assessed by measuring serum 25-hydroxyvitamin D [25(OH)D]. However, wide variations in commercially available 25(OH)D assay performance have been reported. We recently conducted an observational study to assess the prevalence of vitamin D inadequacy using the Nichols Advantage chemiluminescent system in 1536 North American postmenopausal women receiving osteoporosis therapy. Because of the reported variability in 25(OH)D measurements, we randomly selected a subset of 293 samples from this cohort and re-measured total 25(OH)D by Diasorin radioimmunoassay (RIA) and 25(OH)D₃ and D₂ using liquid chromatography- mass spectrometry (LC-MS).The mean (median) serum 25(OH)D was 30.2 (30) ng/mL using the Nichols Advantage system, 32.7(34) ng/mL using the Diasorin RIA and 29.6 (29.3) ng/mL using LC-MS. The mean (median) serum 25(OH)D₃ as measured by LC-MS was 3.9 (0.8) ng/mL. Significant correlation was found between all three assays for measurement of total 25(OH)D; r = 0.698 between Nichols Advantage and LC-MS, r = 0.789 between Diasorin and LC-MS, and r = 0.748 between Nichols Advantage and Diasorin. At lower serum concentrations, there was good agreement (kappa= 0.7-0.75) between the three assays for determining the prevalence of vitamin D deficiency (<15 ng/mL); 9.6% with Nichols Advantage, 8.2% with Diasorin and 9.9% with LC-MS. More moderate agreement (kappa= 0.49-0.57) was seen at higher cutpoints; the prevalence of vitamin D inadequacy (<30 ng/mL) was 49.2% with Nichols Advantage, 34.5% with Diasorin and 50.5% by LC-MS. Compared to LC-MS, the Diasorin RIA had greater specificity but less sensitivity than the Nichols Advantage system across all cutpoints of serum 25(OH)D concentrations. There was even greater variability among 16 patients in whom vitamin D₂ accounted for more than 50% of their serum 25(OH)D. These results suggest that commercially available 25(OH)D assays perform in a similar manner and are reasonably good for detecting vitamin D inadequacy in a population when compared to a more sensitive chromatographic method. This is likely due in part to the low intake of vitamin D₂ in the North American population. However, variation between assays may exist in individual patients and can be problematic in clinical practice.

Disclosures: **M.F. Holick**, Merck & Co., Inc. 2, 8.

SA527

Comparison of DiaSorin Immunoassay Methods with LC-MS/MS for the Measurement of 25-OH Vitamin D. J. A. Schmidt¹, J. S. Fenske^{*1}, K. A. Pieper^{*1}, K. J. Belisle^{*1}, M. Eastvold^{*2}, R. J. Singh^{*2}. ¹DiaSorin Inc, Stillwater, MN, USA, ²Laboratory Medicine & Pathology, Mayo Clinic and Foundation, Rochester, MN, USA.

Vitamin D is an essential component in the regulation of calcium and bone metabolism. Measurement of 25-OH vitamin D is used for the assessment of vitamin D nutritional status. Decreased levels may be seen in dietary deficiency, malabsorption and various disease states. The measurement of 25-OH Vitamin D is growing in importance with the recognition of the involvement of Vitamin D in autoimmune diseases, cancers, and cardiovascular disease as well as bone health. Because both D2 and D3 forms of the vitamin are used to supplement low levels of Vitamin D, and it is important both forms be measured to accurately assess Vitamin D sufficiency. The purpose of this study is to demonstrate the equivalence of immunoassays made by DiaSorin Inc. to LC-tandem mass spectrometry for the determination of 25-OH Vitamin D. Isotope dilution liquid chromatography -tandem mass spectrometry was used to measure 25-OH Vitamin D2 and 25-OH Vitamin D3 in 100 serum samples containing D2 and D3, or D3 alone. The sum of 25-OH Vitamin D2 and 25-OH Vitamin D3 was compared to 25-OH Vitamin D determined by 125-I RIA and by chemiluminescence immunoassay on LIAISON®. Both immunoassays are from DiaSorin Inc., and utilize the same rabbit polyclonal antibody. The immunoassay methods demonstrated good correlations to LC-MS/MS and clinical equivalence in the range from 7-150 ng/mL. Linear regression analysis gave the following equations: RIA = 0.91(LC-MS/MS) + 5.4 ng/mL (r=0.93) and LSN = 1.02(LC-MS/MS) + 2.0 ng/mL (r=0.90). These comparisons show that both the RIA and the LIAISON® methods measure 25-OH Vitamin D2 and 25-OH Vitamin D3 accurately, and that results determined by DiaSorin immunoassays compare very closely to the LC-MS/MS method, which is considered the “gold standard” method for the measurement of 25-OH Vitamin D.

Disclosures: **J.A. Schmidt**, None.

SU001

Age-Related Change of Spinal Bone Mineral Density and Accumulated Bone Loss Rate in Korean Women. H. Choi^{*1}, D. Lee^{*2}, B. Kim^{*3}. ¹Family Medicine, Eulji University Hospital, Daejeon, Republic of Korea, ²Family Medicine, Samsung Jeil Hospital, Seoul, Republic of Korea, ³Family Medicine, Ajou University Hospital, Suwon, Republic of Korea.

Objective: We investigated the age-related bone mineral density(BMD), accumulated bone loss rate(ABLR) and the prevalence of osteoporosis at lumbar spine in Korean women. Methods: Using dual energy X-ray absorptiometry(DEXA), lumbar spine BMD(L1-4) were measured in 3,988 pre- and postmenopausal women. We obtain corrected spinal BMD through spinal BMD devide by a square of height. Results : In early postmenopausal age group(51~55 years), the prevalence of osteoporosis was 20.1%, but after 60 years old, more than 60% of women were classified as osteoporosis. In correlation analysis, age was strongly associated negatively with spinal BMD and corrected spinal BMD($r=-0.61$, $r=-0.45$, $p<0.001$ respectively). After controlling weight and height, age was strongly associated negatively with spinal BMD and corrected spinal BMD($r=-0.54$, $r=-0.54$, $p<0.001$ respectively). When the data were analyzed by 5-year old age groups, the peak spinal BMD was at the age of 36-40 years, but the peak corrected spinal BMD was at the age of 41-45 years. The bone loss rate was the greatest in 51-55 years. In this age group, the accumulated bone loss rate was 8.5%. In the premenopausal women, the bone loss was not occurred significantly. Conclusion: We conclude that the physiological age was the most important factor that affect the rate of bone loss in women. And our data support the benefit of active intervention being initiated in the late perimenopausal period or as early as possible after the menopause in women identified as having low bone mass at that time.

Disclosures: **H. Choi**, Eulji University Hospital 3.

SU002

Middle-Aged Cycling Women Show Aging Effects on Androgens, Osteocalcin, and Hip Bone Density Prior to Menopause. J. L. Lukacs¹, M. Kleerekoper², R. Ansbacher^{*3}, V. Padmanabhan^{*3}, N. E. Reame^{*1}. ¹School of Nursing, University of Michigan, Ann Arbor, MI, USA, ²School of Medicine, Wayne State University, Detroit, MI, USA, ³School of Medicine, University of Michigan, Ann Arbor, MI, USA.

To distinguish age effects on bone turnover and mineral density we studied 3 groups of volunteers differing by age and menopause status: 21 cycling young (CY; mean age = 24.5 ± 0.8 yrs), 19 cycling older (CO; mean age 48.9 ± 0.5 yrs) and 19 postmenopausal (PM; mean age 49.0 ± 0.7 yrs, mean yrs PM 2.8 ± 0.5) women. Cycling women were assessed on menstrual cycle day 4 ± 1. Volunteers were not using oral contraceptives or hormone replacement. We assessed estradiol (E₂), testosterone (T), free T, bone turnover with bone alkaline phosphatase isoenzyme (BAP), osteocalcin (OC), and bone mineral density (BMD) at the lumbar spine (L1-L4) and total hip sites with DEXA. As expected CO women had similar estradiol (34 ± 5 vs 24 ± 3 pg/ml), but lower T (0.2 ± 0.02 vs 0.4 ± 0.03 ng/ml, $p < 0.0001$) and free T (0.5 ± 0.06 vs 0.9 ± 0.07 pg/ml, $p < 0.0001$) compared to CY. PM women had lower E₂ (7 ± 1 pg/ml) but T (0.2 ± 0.02 ng/ml) and free T (0.5 ± 0.08 pg/ml) did not differ from CO group ($p = NS$). CO women had lower OC, a marker of bone formation (3.8 ± 0.2 vs 5.7 ± 0.5 ng/ml, $p = 0.01$), plus lower total hip BMD (1.0038 ± 0.032 vs 1.1126 ± 0.030 gm/cm²), femoral neck BMD (0.9088 ± 0.032 vs 1.0743 ± 0.035 gm/cm²) and femoral shaft BMD (1.1879 ± 0.038 vs 1.3058 ± 0.031 gm/cm²) than the CY group. The rate of bone turnover was higher in PM women (BAP: 128.6 ± 6.6 vs 85.7 ± 5.7 U/L; OC 6.5 ± 0.6 vs 3.8 ± 0.2 ng/ml) compared to CO. Lower BMD at all sites, L1-L4 (-0.26), total hip (-0.5), femoral neck (-0.6), trochanter (-0.39), and shaft (-0.44) was associated with older age ($p < 0.05$). BMD at hip sites: total hip ($r = 0.323$), femoral neck ($r = 0.4$), trochanter ($r = 0.26$), shaft ($r = 0.28$) is positively associated with free T ($p \leq 0.05$); and femoral neck ($r = 0.32$, $p = 0.01$) with T. The data suggest that the age-related decline in androgens may be one factor in lower bone formation and bone density in the hip of mid-life premenopausal women, while the well known increase in rate of bone turnover is evident at menopause.

Disclosures: **J.L. Lukacs**, Supported by a Pfizer Postdoctoral Fellowship to J.L. Lukacs 2.

SU003

Age, Body Weight and a History of Fracture Are Major Predictors of Bone Mineral Density in both Asian Men and Women - Results from Mr and Ms Os Hong Kong, the First Cohort Study in Asians. E. Lau¹, P. Leung^{*2}, T. Kwok^{*3}, J. Woo^{*4}, E. Orwoll^{*5}, S. Cumming⁶. ¹Hong Kong Osteoporosis Center for Treatment and Research, Hong Kong, Hong Kong Special Administrative Region of China, ²Department of Orthopaedics and Traumatology, The Chinese University of Hong Kong, Hong Kong, Hong Kong Special Administrative Region of China, ³Medicine, The Chinese University of Hong Kong, Hong Kong, Hong Kong Special Administrative Region of China, ⁴Community and Family Medicine, The Chinese University of Hong Kong, Hong Kong, Hong Kong Special Administrative Region of China, ⁵Medicine, Oregon University of Health Sciences, Oregon, OR, USA, ⁶Coordinating Center, University California San Francisco, San Francisco, CA, USA.

Little is known about the determinants of bone mineral density in Asian men and women. Mr and Ms Os is the first cohort study designed to do so in Asians. Four thousand men and women aged 65 to 95 were interviewed using a standardized questionnaire. Various physical measurements were performed, and bone mineral density was measured by dual X-ray densitometry.

Predictor (unit)	Percentage change in BMD (g/cm ³)			
	Men		Women	
	Femoral Neck	Total Spine	Femoral Neck	Total Spine
Age (year)	-1.3	2	-3.6	0.4
Body weight (kg, per SD)	7.6	8.1	7.7	9.1
Fracture after 50 years (yes/no)	-1.1	-0.9	-1.7	-1.9
R ² for regression model	0.25	0.179	0.304	0.223

It can be seen that age, body weight and a history of fracture after 50 years accounted for 25% and 31% of the variation in femoral neck BMD in men and women respectively. Adding other variables such as cigarette smoking, and medical risk factors caused only very slight increase in the r². We conclude that age, body weight and a history of fracture were major predictors of BMD in Asian men and women, and these could be applied to identify subjects in whom BMD measurements are truly indicated.

Disclosures: **E. Lau**, None.

SU004

Osteoprotegerin and RANK-L in Extreme Longevity, and their Changes during the Aging Process. G. Passeri¹, C. Galli^{*1}, A. R. Telera^{*1}, R. Vescovini^{*1}, G. M. Macaluso^{*2}, R. Minelli^{*1}, R. Delsignore^{*1}, P. Sansoni^{*1}, M. Pedrazzoni¹. ¹Dep. Internal Medicine, Univ. of Parma, Parma, Italy, ²Chair of Periodontology, Univ. of Parma, Parma, Italy.

RANK-L and its decoy receptor Osteoprotegerin (OPG) are key regulators of bone resorption in vitro and in vivo, and their balance is therefore critical for modulation of osteoclastogenesis and bone remodeling. RANK-L is expressed by osteoblasts, bone marrow stromal cells and activated T lymphocytes, RANK is a transmembrane receptor in cells of osteoclastic lineage, and OPG is produced by osteoblasts. It has been recently demonstrated that bone remodeling, especially bone resorption, is active even in extreme longevity, and in particular in centenarians. We have here evaluated some parameters of bone metabolism, and in particular circulating OPG and RANK-L serum levels, in a group of 44 centenarians (average age 101±1.5 years, 37 females and 7 males, group 1) and in two other groups, averaging approximately 60 (18 females and 2 males, group 2) and 20 years of age (16 females and 4 males, group 3). Centenarians were showing features of secondary hyperparathyroidism, with elevated levels of PTH, serum CTX, significantly lower levels of serum calcium and phosphates, and elevated ALP as compared to the other two groups. Average serum creatinine was 1.2±0.55, 0.86±0.1 and 0.89±0.1 mg/dl, while creatinine clearance was 29, 78 and 95 ml/min in centenarians, 60 and 20 years old subjects respectively. OPG was significantly elevated in centenarians as compared to the other 2 groups ($p<0.001$). In 60 years old subjects OPG was slightly higher as compared to the youngest group. Circulating RANK-L resulted significantly elevated in 20 years old subjects as compared to the other 2 groups, while no differences were present between 60 years old subjects and centenarians. In conclusion our data confirm a condition of secondary hyperparathyroidism, already demonstrated in extreme longevity, and show an increment in OPG levels in centenarians. This can be considered as a possible, although insufficient, homeostatic mechanism able to limit bone loss. RANK-L serum level may reflect, at least in part, an age dependent different production by circulating T lymphocytes, without considering the membrane bound form expressed by cells of osteoblastic lineage. Therefore it may not mirror the real amount present and active in the bone microenvironment.

Disclosures: **G. Passeri**, None.

SU005

Association of Estrogen Receptor Beta Gene Polymorphisms and Rate of Bone Loss in Perimenopausal Women. J. Gu, B. Lai, V. Chan, A. Kung. Medicine, The University of HongKong, Queen Mary Hospital, HongKong, Hong Kong Special Administrative Region of China.

Estrogen deficiency associated with menopause is a major cause of osteoporosis in women. Understanding the pathogenesis of bone loss associated with menopause and early identification of perimenopausal women with rapid bone loss is an effective approach to

ASBMR 27th Annual Meeting

help reduce the increasing incidence of osteoporosis. To determine the role of estrogen receptor beta gene (ESR2) and rate of bone loss in perimenopausal women, we studied 12 single nucleotide polymorphisms (SNPs) encompassing the whole ESR2 gene in 269 Southern Chinese women aged 40-60 years (mean age 49.8± 3.6). Bone mineral density (BMD) was measured at a mean interval of 18months (range 12-24 months). The association and risk of rapid bone loss (3% per annum) with ESR2 SNP and SNP haplotype was assessed using chi-square test and logistic regression model. The results showed that allele C carriers at a SNP in the promoter region (nt -1213 TC) was associated with lower risk of rapid bone loss at both the spine and hip (lumbar spine OR=0.47, p=0.023, femoral neck OR=0.47, p=0.017, trochanter: OR=0.053, p=0.041 and total hip OR=0.41, p=0.005). When adjusted for age, height and body weight, all sites remained significant (lumbar spine: OR=0.47, p=0.023, femoral neck: OR=0.47, p=0.017; total hip: OR=0.41, p=0.005). Analysis of the haplotype data revealed similar findings as individual SNP analysis. In conclusion, SNP and SNP haplotype of ESR2 is associated with rate of bone loss in perimenopausal women and may be useful for predicting bone loss during early postmenopausal period.

Disclosures: **J. Gu**, None.

SU006

A Cross-Sectional Study of Changes in BMD and Bone Turnover Associated with Aging in 888 Volunteer Women in Their Early Adolescence to Middle and Advanced Age. **Y. Onoe¹, Y. Miyabara^{*1}, A. Harada^{*2}, R. Yoshikata^{*1}, M. Yoshida^{*1}, M. Mikumo^{*1}, T. Kuroda^{*1}, H. Okano¹, M. Kume^{*3}, H. Ohta¹.** ¹Obstetrics and Gynecology, Tokyo Women's University, Tokyo, Japan, ²Biostatistics, Tokyo University, Tokyo, Japan, ³Nursing, Tokyo Women's University, Tokyo, Japan.

Bone mineral density (BMD) in women is known to increase in their early adolescence and begin to decrease in their perimenopausal years, and after a certain decrease in BMD, they become eligible for the diagnosis of osteoporosis. While pharmacological interventions are commonly applied to established osteoporosis, there is no consensus regarding prophylaxis against osteoporosis. To establish such prophylactic strategies requires investigating changes in BMD associated with aging in women from adolescence onwards, and optimizing therapeutic interventions for each age group. A cross-sectional study in a broad range of women from early adolescence to middle and advanced age was therefore conducted to address this issue. This study was conducted in female volunteers aged 19 to 60 years. Women with conditions that affect BMD, as well as pregnant or breast-feeding women, were excluded from the study. The subjects were asked about their age and current menstrual status. Additionally, height, body weight, as well as serum calcium, phosphorus, albumin, intact-osteocalcin (OC), cross-linked N-telopeptide of type I collagen (NTX), and bone-alkaline phosphatase (BAP) were measured in these women. The BMD of the lumbar vertebrae 2 to 4 (L 2-4), as well as the total BMD of the proximal femur (BMD of the hip), was also measured in the subjects using QDR 4500. A total of 888 women (mean age, 27.3 ± 8.2) were enrolled in the study between October 2003 and August 2004. The BMD of the L2-4 was confirmed to remain at a certain level (mean: 1.00 ± 0.11 g/cm²) between the ages of 19 to 40, and then to tend to decrease thereafter. The total BMD of the hip (mean: 0.87 ± 0.10 g/cm²) was seen to decrease between the ages of 19 to 30, remain stable for a time, and then decrease again thereafter. During this observation period, of the bone metabolic markers examined, NTX was noted to decrease until age 30, and then to increase after age 45, while BAP was shown to decrease until age 25, and then to increase after the age of 48. Our study results indicate that BMD peaks in these women before age 19 and that changes in BMD associated with aging differ between the lumbar vertebrae and femur with the BMD of the femur seen to decrease earlier. The status of bone turnover during this period appears to be independent of changes in BMD, where the bone turnover tends to be lower in younger years, and after a time, begins to increase again, preceded by an increase in bone resorption markers.

Disclosures: **Y. Onoe**, None.

SU007

Osteoporosis of Ossicles and Hearing Loss in Mice. **K. Matsuo¹, M. Ito², K. Ogawa^{*3}, S. Kanzaki^{*3}.** ¹Department of Microbiology and Immunology, Keio University School of Medicine, Tokyo, Japan, ²Department of Radiology, Nagasaki University, Nagasaki, Japan, ³Department of Otolaryngology, Keio University School of Medicine, Tokyo, Japan.

Hearing loss and osteoporosis are both associated with aging, but whether osteoporosis can directly contribute to impaired auditory function is unclear. Mice lacking osteoprotegerin (OPG^{-/-} mice) develop osteoporosis due to enhanced differentiation of osteoclasts. We therefore isolated the three auditory ossicles, the malleus, incus, and stapes, from the middle ear cavity of adult OPG^{-/-} mice, and compared them with heterozygous controls. All three ossicles in OPG^{-/-} mice showed apparent thinning, especially at the malleal manubrium, malleal processus brevis, and stapedial arch. Furthermore, ossicles from OPG^{-/-} mice stained more extensively positive for tartrate-resistant acid phosphatase (TRAP) activity than those from heterozygous controls indicating elevated osteoclastic bone resorption of ossicles in OPG^{-/-} mice. Radiological analysis using micro CT (μCT40, Scanco Medical, Switzerland) showed that malleal bone thickness was decreased in OPG^{-/-} mice, corresponding to the decrease in tibial bone mineral density measured by quantitative CT (LaTheta, Aloka, Japan). To examine hearing sensitivity in OPG^{-/-} mice, we measured auditory brainstem response (ABR) at 6, 10 and 15 weeks of age. OPG^{-/-} mice showed progressive hearing loss over the frequency range tested (2-20 kHz). At 15 weeks, mutant mice were more than 20 decibels (dB) less sensitive than

wild-type controls at the highest frequency of 20 kHz. These data suggest that auditory ossicles are susceptible to bone resorption by osteoclasts and that osteoporosis may be a risk factor for conductive hearing loss.

Disclosures: **K. Matsuo**, None.

SU008

Bone Quality in Elderly Community-Dwelling Men Is Significantly Associated to Muscle Strength and to A Creatinine Clearance of Less than 65ml/min. **L. C. Dukas^{*}, E. Schacht, H. B. Stähelin^{*}.** Acute Geriatric Clinic, Kantonsspital Basel, Basel, Switzerland.

Few studies have investigated the association between muscle strength, life style and biometric factors and bone density in elderly men. Within a randomized controlled study we assessed in an observational survey in 188 independently living community-dwelling men, aged 70 years and older, the association between bone density and calcitropic hormones, creatinine clearance, muscle strength measured as grip strength and some demographic and life style variables. The t-score as measured with ultrasound of the calcaneus was used as measure of bone density. Serum concentrations of calcitropic hormones, grip strength, creatinine clearance (CrCl) and other variables were studied in multivariate controlled linear regression models with the t-score as the dependent variable and/or as dichotomous variables (i.e. CrCl < 65ml/min vs ≥65ml/min). The dependent variable t-score was analyzed as a continuous variable as well as in categories (t-score < -2.5 vs ≥-2.5 to -1 vs ≥-1). Calcitropic hormones (calcidiol, Calcitriol, iPTH) were in multivariate analyses not associated with the t-score as measured by US calcaneus. Decreasing BMI (p<.0001), decreasing CrCl (p=.0) and decreasing muscle strength (p=.032) were significantly associated with decreasing t-scores. Significantly more men with a t-score of <-2.5 had a CrCl of <65ml/min compared to men with higher t-scores (CrCl<65ml/min. and t-score <-2.5 vs ≥-2.5 to -1 vs ≥-1: 60% vs 37.5% vs 27.3%, p=0.034). Men with a t-score of <-2.5 had also significantly lower grip strength muscle strength performance as compared to men with higher t-scores (grip strength performance in kilopounds and t-score <-2.5 vs ≥-2.5 to -1 vs ≥-1: 0.60 ± 0.12kp vs 0.72 ± 0.15kp vs 0.78 ± 0.15kp, p=.004). The use of statins and history of polyarthrosis was inversely associated with lower t-score (p=.029, res. .024) In elderly community-dwelling men a CrCl of <65ml/min. is associated with a significant increased more than doubled risk of having a t-score of <-2.5. A t-score of <-2.5 was also associated with significantly reduced muscle strength. Since Calcitriol has been shown to significantly decrease with a CrCl of <65ml/min., it is highly probable that the decreasing bone density associated with a low CrCl and decreasing muscle strength is due to a common factor, decreasing serum levels of Calcitriol. Therefore, we hypothesize that the low CrCl associated decrease in bone density and muscle strength has to be treated with Calcitriol in order to prevent fall associated osteoporotic fractures.

Disclosures: **L.C. Dukas**, TEVA Pharmaceuticals Industries Ltd, Israel 2; Scientific Grant University Hospital Basel, Switzerland 2.

SU009

Bone Mass and BMC Changes among Pre- and Postmenopausal Women: a 10-y Follow-Up Study. **K. Uusi-Rasi, H. Sievänen^{*}, P. Kannus^{*}.** UKK Institute, Tampere, Finland.

This prospective, 10-year study evaluated bone mass and changes in BMC of due to exercise and calcium among pre- and postmenopausal women. At baseline, 265 healthy women were divided into groups based on their habitual level of physical activity (PA+ = > 20 min vigorous exercise > twice/wk; PA- = no vigorous exercise) and calcium intake (Ca+ = > 1200 mg/d; Ca- = < 800 mg/d). At 10-year follow-up, measurements were completed for 212 women (80% of the original sample), 102 premenopausal women (mean age 38 ± 2 yrs), and 110 elderly postmenopausal women (mean age 73 ± 2 yrs). Measurements were taken at the proximal femur by DXA. The baseline groups were maintained. Repeated measures ANCOVA was used to analyze the between-group differences in bone mass and in BMC changes, and regression analysis to find predictors of changes. For the postmenopausal women, BMC of the femoral neck averaged 4.9% (95% CI 0.1% to 9.9%) higher in the Ca+ group than in the Ca- group, and 6.8% (1.7% to 12.1%) higher in the PA+ group than in the PA- group. The corresponding differences at the trochanter were 2.2% (-2.5% to 7.1%) and 5.4% (0.4% to 10.6%) for Ca+ and PA+, respectively. For the premenopausal women, the observed BMC values were higher in the Ca+ and PA+ groups compared with Ca- and PA- groups, respectively, although the between-group differences were statistically significant at the trochanter only. In both age groups, BMC at the proximal femur declined similarly between the high and low physical activity groups. However, there was no significant difference in BMC decline between Ca-groups among postmenopausal women, but the premenopausal women with high calcium intake (Ca+) seemed to loose less bone mass than the Ca- group. The mean difference in BMC change at the femoral neck was 1.2% (-0.8% to 3.3%) and at the trochanter 3.8% (1.4% to 6.3%) in favour of the Ca+ group. Regression analysis showed that current breast feeding was a strong predictor of BMC decline at the femoral neck. This unique 10-year follow-up suggested that decrease in BMC occurred both among premenopausal and elderly postmenopausal women, but the initial between-group differences remained. High calcium intake seemed to retard the decrease in BMC at the proximal femur, especially among the premenopausal women.

Disclosures: **K. Uusi-Rasi**, None.

SU010

TGF- β Inducible Early Gene-1 Null Mice Display Weaker Bones with Ultra-Structural Defects Compared to Wild-Type Mice. S. F. Bensamoun¹, M. Subramaniam², J. R. Hawse², B. Ilharreborde^{*1}, D. Fraser^{*3}, M. Oursler³, P. Amadio^{*1}, K. N. An^{*1}, T. C. Spelsberg². ¹Orthopedic Research, Mayo Clinic, Rochester, MN, USA, ²Biochemistry and Molecular Biology, Mayo Clinic, Rochester, MN, USA, ³Endocrine Research Unit, Mayo Clinic, Rochester, MN, USA.

TGF- β inducible early gene-1 (TIEG) is a member of the Krüppel-like transcription factor family originally cloned from human osteoblasts. Previously, we have demonstrated that TIEG plays an important role as a transcriptional repressor involved in TGF β mediated Smad signaling. To elucidate the function of TIEG in skeletal development, we generated a TIEG knockout (KO) mouse. Osteoblasts isolated from TIEG KO mice display a reduced expression of osteoblast marker genes and defects in mineralization. We have further characterized the skeletal phenotype using mechanical tests (3-point bending) and morphological analyses (light microscopy, micro-CT and pQCT) on the femurs and vertebrae of these animals. The L5 vertebrae and femurs were removed from 7 wild-type, and 7 TIEG KO 3-month old C57 Black/129 female mice. A three-point bending test was performed with the left femur using a slow velocity (0.3mm/s) and load-displacement curves were used to measure the ultimate force. As seen in Table 1, the femurs of TIEG KO mice are significantly weaker when compared to wild-type controls. Cross sections (70 μ m) were cut in the mid-shaft of each right femur and polished. These sections indicate that the cortical thickness and area are significantly reduced in TIEG KO mice (Table 1). Micro-CT analysis (n=3; resolution= 5.99 μ m) was performed on the femoral head, vertebrae and lower metaphysis. Interestingly, there is a 42% increase in the femoral head trabecular separation in TIEG KO mice (Table 1). Trends of decreased cortical bone and vertebral bone volume were also observed in these animals. pQCT analysis of 25 tibias from 4-month old wild-type and TIEG KO mice revealed significant decreases in cortical area, thickness, content as well as periosteal and endosteal circumference (Table 1). These studies demonstrate that the loss of TIEG, in our TIEG null mouse model, results in a significant decrease in the size, strength and structure of long bones, supporting a role for this gene in bone modelling/remodelling.

Mechanical and morphological parameters of wild-type and TIEG knockout mice (*P<0.05)			
		Wild-Type	TIEG KO
Bending Test	Ultimate Force (N)	31.56 \pm 4.00	24.13 \pm 3.67 *
Light Microscopy	Femoral Cortical Surface (mm ²)	1.01 \pm 0.10	0.77 \pm 0.10 *
	Femoral Cortical Thickness (μ m)	231.61 \pm 37.72	177.89 \pm 27.4 *
Micro-CT	Femoral Head Trabecular Separation (%)	18.58 \pm 4.46	32.18 \pm 2.08 *
	Periosteal Circumference (mm)	4.26 \pm 0.24	4.04 \pm 0.26 *
pQCT	Endosteal Circumference (mm)	2.88 \pm 0.18	2.74 \pm 0.22 *
	Cortical Content (mg)	0.89 \pm 0.10	0.79 \pm 0.10 *

Disclosures: S.F. Bensamoun, None.

SU011

Use of ³H-Tetracycline to Assess the Effects of Ovariectomy Stabilization and Diet on Bone Resorption in Rats. J. M. K. Cheong^{*1}, N. S. Gunaratna^{*2}, G. P. McCabe^{*2}, C. M. Weaver¹. ¹Foods and Nutrition, Purdue University, West Lafayette, IN, USA, ²Statistics, Purdue University, West Lafayette, IN, USA.

Tritiated tetracycline (³H-TC) can be used to measure bone resorption (BR) in animal models. ³H-TC is absorbed and attached to the apatite of the bone structure and when bone turns over, the label is released into the urine providing a direct measure of BR. Our ultimate goal is to develop use of urinary ⁴¹Ca appearance from bone to directly measure BR in humans. Here we used this inexpensive rat model to understand timing of label incorporation and release when BR was manipulated by ovariectomy stabilization and dietary calcium (Ca). Sixty-four ovariectomized (ovx) 6-month old rats were randomized to 1 of 16 groups that differed in terms of (1) ovx stabilization (ovx non-stabilized (ON) or ovx stabilized (OS)), (2) dietary Ca (0.2% or 0.5% Ca), and (3) time of euthanasia (1 week, 1 month, 3 months, or 6 months post ³H-TC dose). The ON group received a single subcutaneous injection of 30 uCi of ³H-TC while ovariectomy was being stabilized while the OS group received the same dose after ovariectomy was stabilized for 3 months. Diet treatment was started at the time of dose. Total skeleton and 48-hour urine and feces were recovered and collected at 1 week, 1 month, 3 months, and 6 months post dose for the assessment of ³H-TC in urine and bone, Ca balance, and percent Ca retention. This study was approved by the Purdue animal care and use committee. Ca balance and Ca percent retention were higher in rats that were fed 0.5% Ca diet than rats fed 0.2% Ca diet. BR as assessed by urinary ³H-TC decreased over time for all time points, but the difference between 3 and 6 months post dose was no longer significant. There was an ovx stabilization effect on BR at 1 week post dose, as reflected by a higher urinary ³H-TC in OS rats. At one month post dose, we find that OS rats have lower values of urinary ³H-TC and that a 0.5% Ca diet leads to lower urinary ³H-TC for OS rats. However, we failed to detect any differences due to ovx stabilization or diet three months post dose or later although Ca balance was persistently higher on higher Ca intakes. We conclude that perturbations in BR by hormonal status and diet are transient effects and best measured in rats at 1 month (1 sigma in rats) post dose.

Disclosures: J.M.K. Cheong, None.

SU012

Aging Decreases the Responsiveness of Bone Marrow Stromal Cells to Insulin-Like Growth Factor-I (IGF-I) through Down-Regulation of IGF-I Signaling Pathways. J. J. Cao, P. S. Kurimoto^{*}, B. Boudignon^{*}, B. P. Halloran. Medicine, UCSF, San Francisco, CA, USA.

Bone development, growth and metabolism are tightly regulated. With advancing age, the osteoprogenitor pool diminishes, while the osteoclast progenitor pool increases and the balance between formation and resorption necessary to maintain bone mass is lost. Coincident with the changes in bone cell activity, the serum concentration of IGF-I decreases with age. Insulin-like growth factor-I (IGF-I) is abundant in bone and can stimulate osteoblast proliferation and promote bone formation. It has been suggested that decreases in serum IGF-I, alterations in IGF-I signaling or both may contribute to age-related bone loss. To determine the effect of IGF-I on bone in animals of different ages and how aging affects IGF-I signaling in bone cells, we examined the effect of IGF-I on bone *in vivo* and bone marrow stromal cells (BMSCs) cultured *in vitro* from 6 week (young), 6 month (adult), and 24 month (old) old mice. Aging markedly increased apoptosis and decreased proliferation of osteoblasts. With aging, the effect of IGF-I on cell proliferation is diminished. While IGF-I receptor expression increased at both the message and protein levels with aging, the phosphorylation of IGF-I receptor, ERK 1/2 (p44/42 MAPK), and Akt in cultured BMSCs was decreased in cells from mice of increasing age. When normalized to cell number, IGF-I binding sites (Scatchard analysis) in adult and old animals were reduced by approximately 75% of that in young. The receptor internalization was similar among all ages but the degree was less in adult and old animals when compared to young. These data suggest that the decrease in bone responsiveness to IGF-I is associated with decreases in IGF-I binding sites and intra-cellular signaling.

Disclosures: J.J. Cao, None.

SU013

The Impact of Feeding Orange on Bone Homeostasis in Orchidectomized Rat Model of Osteoporosis. F. Deyhim^{*1}, K. Garcia^{*1}, A. Villarreal^{*1}, K. Mandadi^{*2}, R. Rios^{*1}, B. S. Patil^{*3}. ¹Human Sciences, Texas A&M University-Kingsville, Kingsville, TX, USA, ²Department of Agronomy and Resource Sciences, Texas A&M University-Kingsville, Citrus Center, Kingsville, TX, USA, ³Vegetable and Fruit Improvement Center, Department of Horticultural Sciences, Texas A&M University, College Station, TX, USA.

Reactive oxidative species could be one of the factors causing osteoporosis. Citrus fruits are known to be a rich source of multitude bioactive compounds, antioxidants, vitamins, minerals and eating citrus fruits may potentially prevent osteoporosis. In a previous study, we observed that daily consumption of orange juice significantly increases 4th lumbar density in male osteoporotic rats. The current study evaluated whether feeding orange pulp in varied concentrations (2.5%, 5%, and 10%) impact 5th lumbar density, femoral density, femoral strength, and plasma antioxidant capacity in male rat model of osteoporosis. Forty-five retired breeder male rats were randomly divided into five treatment groups as follows: 1. Sham (control); 2. Orchidectomy (ORX); 3. ORX+2.5% powdered orange pulp/Kg diet; 4. ORX+5% powdered orange pulp/Kg diet; and 5. ORX+10% powdered orange pulp/Kg diet. The treatment diets were isocaloric and isonitrogenous with similar fiber content. After four months of feeding, all rats were sacrificed, blood was collected for measuring plasma antioxidant capacity while right femur and the 5th lumbar were separated to determine bone mineral density and femoral strength. Orchidectomy depressed (P<0.05) plasma antioxidant capacity in the ORX group while feeding orange pulp restored it to the level of the sham group. Orchidectomy decreased (P<0.05) femoral and 5th lumbar density, femoral strength, and significantly (P<0.05) shortened time induced femoral fracture in the ORX group while feeding orange pulp dose dependently increased (P<0.05) femoral and 5th lumbar density to the level of the sham group. Femoral strength and time induced femoral fracture were also significantly (P<0.05) increased with all orange pulp dosages compared to the ORX group. In conclusion, feeding orange pulp enhances bone density, bone strength, and delays time induced bone fracture. These effects may be mediated through increasing the plasma antioxidant capacity.

Disclosures: F. Deyhim, None.

SU014

Influence of Calcium Channel Antagonists on Estrogen-Regulated Bone Resorption. L. A. Ashley^{*}, D. L. Brown^{*}, S. G. Combs^{*}, D. A. Dillon^{*}, R. P. Filiatreau^{*}, J. L. Mack^{*}, E. D. Nickel^{*}, C. M. Pendleton^{*}, K. D. Trent^{*}, D. L. DeMoss. Biological Sciences, Morehead State University, Morehead, KY, USA.

Bone metabolism is invariably correlated with calcium transport indicating that calcium channels are a potential point of regulation for skeletal remodeling. Calcium channel antagonists are utilized therapeutically and experimentally to decrease the influx of calcium into cells by blocking voltage-regulated L-type calcium channels. Previous experimental evidence has suggested that calcium antagonists decrease osteoblastic activity, thus decreasing the activity of the bone forming cells at a time when bone formation is already exceeded by bone resorption, exacerbating the situation. Literature also reports a ten-year lag in the age-related rise in cardiovascular mortality in women as compared to men. Therefore, the established principle that bone formation decreases following the attainment of peak bone mass, illustrates the need for a more comprehensive understanding of the action calcium channel antagonists have on bone turnover and an improved understanding of the protective action estrogen exerts on skeletal mass.

Experimentation utilized female Brown Norway Rats six months of age to compare the effects of estrogen and the antagonists on blood pressure and bone turnover from both the amorphous and calcified compartments. In order to evaluate the positive or negative impact of estrogen and various calcium channel antagonists on bone loss, bone resorption parameters were compared between normal females, estrogen-deficient females, females receiving hormone replacement therapy, females receiving calcium channel antagonists (Diltiazem, Nifedipine, Verapamil), or females receiving a combination of the two agents. The models utilized to study bone turnover were the pharmacokinetic loss of the tracer H³-tetracycline, a compound deposited in the active mineralization front an freely released in urine and the measurement of various bone degradation markers (deoxypyridinoline, pyridinium, and helical peptide) in urine collected throughout the experimental period. Ovariectomized females display an increased turnover rate while those receiving hormone replacement therapy were not significantly different from controls. The physiologic mechanism by which these drugs elicit their action appears to be antagonistic to that of estrogen for the amorphous compartment while synergistic to that of estrogen for the calcified compartment. Data obtained suggest that calcium channel antagonists potentially elicit their actions through alternative mechanisms in each of these highly regulated calcium pools.

Disclosures: **L.A. Ashley**, None.

SU015

Degree of Mineralization in the Cortical Bone of Fibular Shaft Was Higher in Aged Male than in Female Patients. **T. Mashiba, S. Mori, N. Gomi*, Y. Kaji*, T. Manabe***. Orthopedic Surgery, Kagawa Medical University, Kagawa, Japan.

Objective We have reported that degree of mineralization in the cortical bone of fibular shaft was increased in female over 70 years old. In this study, the degree of mineralization in the fibular shaft was examined in aged male patients. Sexual difference of cortical bone mineralization between female and male were also evaluated. **Patients and Methods** Specimens for this study came from fibular mid-shafts of eleven men (60-75 y.o.) who underwent high tibial osteotomy for medial type osteoarthritis of the knee. The collected bones were stored frozen at -80°C until specimens were made. After thawing at room temperature, they were stained en-bloc with 1% basic fuchsin dissolved in ascending concentration of ethanol, defatted with xylene, and embedded in methyl methacrylate. A 125 µm-thick transverse ground section was made for the static histomorphometry and measurement of degree of mineralization of bone (DMB). For DMB measurement, quantitative contact microradiograph was taken and DMB at each osteon was calculated using a computerized microdensitometric method. Measured DMB parameters include mean osteonal DMB and the distribution of osteon based on DMB. Age related changes in static cortical histomorphometric parameters and DMB parameters were evaluated. **Results** Cortical structural parameters, mean DMB and DMB distribution did not significantly change with age in the fibular shaft of aged male patients. However, when comparing with data form women of almost same age, mean osteonal DMB was significantly higher in men than in women, and DMB distribution was located in narrower range. **Discussion** We have reported age related structural deterioration of cortical bone, such as bone marrow expansion, cortical thinning and increased cortical porosity and elevated DMB in the fibular shaft of aged women. However, these age related changes were not observed in aged men, indicating that skeletal aging changes after sixty years old is much slower in men than in women probably because of the gender difference of bone remodeling activity. Higher and homogenous DMB distribution in age men demonstrated in this study is compatible with very common findings that bone mineral density measured by DXA is higher in men than in women. This also suggests that because older osteon should have higher DMB, replacement of old into new osteon was suppressed by lower osteonal remodeling activity especially in aged men.

Disclosures: **T. Mashiba**, None.

SU016

The Role of Age and Body Size in Predicting the 3D Structure of Cortical Porosity at the Human Anterior Femoral Mid-Shaft. **D. M. L. Cooper***¹, **C. D. L. Thomas***², **J. G. Clement***², **B. Hallgrimsson**³. ¹Archaeology and Medical Science, University of Calgary, Calgary, AB, Canada, ²School of Dental Science, University of Melbourne, Melbourne, Australia, ³Cell Biology & Anatomy, University of Calgary, Calgary, AB, Canada.

The 3D structure of cortical bone porosity undergoes continuous change through the process of remodeling. The goal of the current study was to examine the roles of age and body size in predicting the 3D structure of cortical porosity (at the level of osteonal canals) and to assess whether these roles vary between the sexes. The sample included 79 individuals, 28 females and 51 males, spanning 18 to 92 years of age. The mean (+/- SD) ages for the males and females were 55.90 (+/- 20.21) years and 52.61 (+/- 23.56) years, respectively. Anterior femoral midshaft blocks, 5 mm wide and 8 mm long were micro-CT scanned at 7 µm isotropic resolution. Cylindrical volumes of interest, 3 mm in diameter and 3 mm long, adjacent to the periosteal surface, were isolated from the scan data for quantitative analysis of cortical porosity (CaV/TV), mean canal diameter (CaDm), canal number (CaN), mean canal separation (CaSp), and degree of anisotropy (DA). Height and weight were measured at autopsy. Stepwise multiple linear regression was employed to determine the combination of variables (height, weight, and age) that best predict the morphological parameters for each of the sexes. For males, all parameters were significantly predicted (p<0.05) by age alone, with adjusted r² values of 0.408, 0.275, 0.380, 0.430, and 0.090 for Log CaV/TV, Log CaDm, CaN, CaSp, and DA, respectively. Age was a significant predictor (p ≤0.001) for all parameters in females, however weight was also included in the predictive models for Log CaDm and DA, while height was included for CaN. The best fit adjusted r² values for females were 0.722, 0.682, 0.408,

0.525, and 0.440, respectively. The results indicated that 3D parameters of cortical porosity are better predicted for females and that, while age is the most important predictor for both sexes, body size plays a significant role in females. Further, this study revealed that cortical bone, which is generally regarded as more stable than trabecular bone, is extensively affected by systemic bone loss, even at a site as robust as the femoral midshaft.

Disclosures: **D.M.L. Cooper**, None.

SU017

Recovery of Skeletal Growth and Mineralization from Dietary Calcium Deficiency in Young Pigs. **A. J. Smiltneek***, **C. E. Pardo***, **D. K. Schneider***, **T. D. Crenshaw**. Animal Sciences, University of Wisconsin -Madison, Madison, WI, USA.

In earlier studies (J Bone Miner Res 18:S184) prepuberal pigs failed to recover skeletal mass following a period of dietary Ca deficiency. A limitation of the earlier study was that pigs were fed diets with Ca at minimum requirements during the recovery period. The objective of the current experiment was to determine the potential for recovery of skeletal mass in young pigs (initial wt. = 9.2 kg, age = 39 d) fed diets with 150% of Ca requirements following a period of Ca depletion. During the depletion period (4 wk), pigs were fed diets with either 150% (excess Ca, n=16) or 70% (deficient Ca, n=16) of the dietary calcium requirement. Subsequently, during a six week recovery period, pigs within each depletion period group were fed diets with excess (150 %) or deficient (70 %) Ca. Pigs were scanned at intervals throughout the trial using dual energy X-ray absorptiometry (DXA, GE Lunar Prodigy software version 8.10.027) using the pediatric scan mode. After a 4-wk depletion period, total body bone mineral content (BMC, g) was reduced (P ≤0.001) by 67% and bone mineral density (BMD, g/cm²) by 29% in pigs fed deficient vs excess Ca diets. During the recovery period, the change in BMC, g/d was the same within dietary Ca groups regardless of whether pigs were fed deficient or excess Ca during the depletion period. See Table below. However, the daily change in BMD during the recovery period was greater (P≤0.05) in pigs fed a deficient diet during the depletion period than that of pigs fed excessive Ca during the depletion period . The greater change in BMD implies a potential for recovery of bone mineralization following a period of deficiency if excess dietary Ca is provided.

Dietary Ca,	Results after 4 wk Depletion - 6 wk Recovery Periods			
	BMC, g	ΔBMC, g/d	ΔBMD, g/cm ²	BMD, g/cm ² /d
150-150	1792 ^a	27.1 ^a	1.14 ^a	0.008 ^b
150-70	1234 ^b	13.9 ^b	0.89 ^b	0.003 ^c
70-150	1388 ^b	27.9 ^a	1.01 ^a	0.011 ^a
70-70	688 ^c	10.8 ^b	0.71 ^b	0.004 ^c
Pooled SEM	57	1.03	0.02	0.0004

Variable superscripts within column differ, P≤0.05.

Disclosures: **T.D. Crenshaw**, None.

SU018

Atrovastatin Attenuates Cardiovascular Calcification and Osteoporosis in the Experimental Hypercholesterolemic LDLR-/- Mice. **N. M. Rajamannan**¹, **M. Subramaniam**², **F. Caira***¹, **S. Stock**¹, **A. Flores***¹, **J. Gocek***¹, **T. C. Spelsberg**². ¹Cardiology, Northwestern University, Chicago, IL, USA, ²Biochemistry and Molecular Biology, Mayo Clinic, Rochester, MN, USA.

Atherosclerosis and osteoporosis are the leading causes of morbidity and mortality in the aging population in the Unites States. Evidence indicates that hyperlipidemia plays a paradoxical role in these disease processes. However, the hyperlipidemic mechanisms of atherosclerotic calcification and decrease bone mass are not well understood. We have previously shown that cardiovascular calcification expresses an osteoblast phenotype in humans. We hypothesize that hyperlipidemia plays a role in cardiovascular calcification and osteoporosis. We propose to test this hypothesis in an experimental hypercholesterolemia model and further test if statins play a protective role in this process. LDLR-/- mice (n=60) were treated with Group I (n=20) normal diet, Group II (n=20) 1.25% chol diet (w/w), and Group III (n=20) 1.25% (w/w) chol diet+atorv to determine the development of calcification in the hearts and osteoporosis in the bones. The aortic valve and aortas (AVA) was examined for myofibroblast cell proliferation, calcification, and bone matrix markers by immunohistochemistry and RTPCR. Bone formation was assessed by micro Computed Tomography (microCT), calcein injection, osteocalcin, cbfa-1 and osteopontin expression. The cholesterol diet induced complex bone formations by microCT in the calcified AVA with an increase in cellular proliferation, osteopontin, osteocalcin and cbfa-1 expression. Atrovastatin reduced bone formation, cellular proliferation and cbfa-1 levels and calcification in the AVA. Ex vivo analysis of calcein label demonstrated an increase in calcein label (4+) in the hypercholesterolemia AVA and the periosteal femoral bone surface with attenuation of the calcein label (1+) with atorvastatin therapy in the the AVA and the femoral bones. (Calcein Scale =1-4, 4+=severe label, 1+=miminal label). Experimental hypercholesterolemia induces cardiovascular calcification and increased bone turnover which is attenuated by atorvastatin and mediated in part by an osteoblast pathway in the cardiovascular tissues. This model may have future implications in the treatment of cardiovascular calcification and osteoporosis with statin therapy.

%GAPDH	Osteocalcin and Cbfa-1 RNA expression in the AVA		
	Control	Chol	Chol+Atorvastatin
Osteocalcin	0.72	0.75	0.50
Cbfa-1	0	0.83	0.39

Disclosures: **N.M. Rajamannan**, None.

SU019

Age-Related Loss of Bone Strength in the Spine and Hindlimb of Mice Independently of BMD. A. Parfitt, R. Weinstein, T. Bellido, R. Jilka, C. O'Brien, J. Goellner, S. Kousteni, S. Stewart*, P. Roberson*, S. C. Manolagas. Div. Endocrinol. and Dept. Biostatistics, Center for Osteoporosis and Metabolic Bone Diseases, Central Arkansas Veterans Healthcare System, Univ. Arkansas Med. Sci., Little Rock, AR, USA.

Age is a far more critical determinant of fracture risk than BMD in humans. Heretofore, this was thought to be the result of changes in balance, visual acuity, and muscle mass, rather than changes in the strength of bone itself. In the studies reported herein, we have tested the hypothesis that there may be age-related factors associated with bone strength which are independent of BMD. To this end, we determined BMD of vertebrae and hindlimbs by DEXA and bone strength by vertebral compression and 3-point bending of femora of female C57BL/6 mice (an animal cohort maintained with support from the NIA at Harlan Inc.) at 8, 16, 25, and 31 months of age (n = 11-12 per group). We report that with advancing age these mice exhibit a progressive loss of bone strength and BMD in both the spine and hindlimbs. Most importantly, the loss of strength is detectable 9 months earlier than the loss of bone mass. Likelihood ratios comparing models with both age and site specific BMD as predictors of strength indicated that for each site (spine and hindlimbs) the two predictor model is significantly better than a model with age or BMD alone ($p < 0.001$), establishing that for both vertebrae and hindlimbs there is a statistically significant age-related impact on strength which is independent of the BMD contribution. In addition, cancellous osteoblast apoptosis increased by 48% in the 25 month old animals and by 99% in the 31 month old animals when compared with the 8 month old mice ($p < 0.001$ and < 0.0005 , respectively; by ANOVA); and cortical osteocyte apoptosis increased by 84% in the 25 month old animals when compared with the 8 month old animals ($p < 0.001$). Bone formation rate was decreased by 60% at both 25 and 31 months of age when compared with the 8 month old mice ($p < 0.02$); and it was inversely related to the prevalence of osteoblast apoptosis ($r = -0.46$, $p < 0.04$). These changes were temporally associated with a decrease in glutathione reductase activity and a corresponding increase in the levels of reactive oxygen species in the bone marrow, and an increase in the phosphorylation of the p66^{bac} in vertebrae - an adapter protein that is induced by oxidative stress and is an important determinant of lifespan in mammals. The temporal dissociation of strength and BMD decline with age in this model provides, for the first time, an opportunity to investigate experimentally the contribution of different qualitative influences on bone strength in a mammal.

Disclosures: **A. Parfitt**, None.

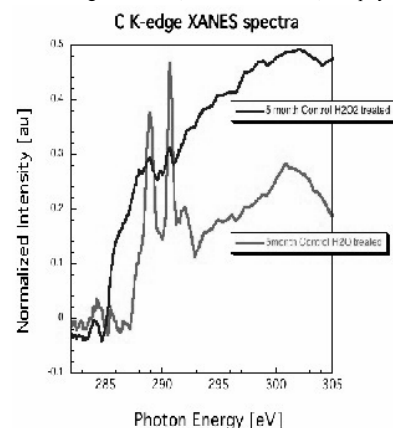
SU020

Spectromicroscopy Shows Oxidative Damage to Collagen. N. Saless¹, B. Frazer^{2*}, G. E. Lopez Franco¹, G. de Stasio^{2*}, S. Litscher^{1*}, R. D. Blank¹. ¹Medicine, University of Wisconsin, Madison, Madison, WI, USA, ²Synchrotron Radiation Center, University of Wisconsin, Madison, Madison, WI, USA.

A major effect of aging is the deteriorating bone quality. While multiple factors contribute to the greater fracture risk of the very old, old bone has poorer intrinsic quality than young bone. Collagen is the major protein of the bone and on the molecular scale; it plays a significant role in bone viscoelasticity. Conditions characterized by increased oxidative stress are also associated with skeletal fragility. Oxidative damage to the extracellular matrix of bone could account for some of the age-related deterioration of biomechanical performance. Exposure to oxidative stress *in vivo* allows physiologic adaptation to the altered mechanical properties of the bone matrix. In order to study the effects of oxidative damage to the bone matrix in isolation of such a response, we have developed an *ex vivo* protocol testing of paired bones from individual animals, thus eliminating bone mass, bone architecture, and physiological adaptation to an abnormality

as confounding factors in interpreting biomechanical performance. Further, we have established a spectromicroscopic assay of carbon bond energies that can spatial information that cannot be obtained biochemically. In pilot experiments, femora were excised from mice. One bone of each pair was incubated overnight in H₂O₂, and the other member of the pair in H₂O. The bones were then tested by 3-point bending to failure, under displacement control. The preliminary data demonstrate a trend toward reduction of post-yield deflection and energy to failure. Spectromicrographic analysis of bone powder (figure) demonstrates the loss of 2 signals, that we believe represent pyridinoline and deoxypyridinoline cross-links. Next steps in characterizing the nature and extent of biomechanical impairment arising from oxidative damage will be to titrate the time and concentration of oxidizing agents to mimic the degree and distribution of oxidative damage encountered in *in vivo* oxidative stress models.

Disclosures: **N. Saless**, None.



SU021

Influence of Bone Osteocalcin Level in Bone Loss Induced by Ovariectomy in Warfarin-Treated Rats. K. Hara, M. Kobayashi, Y. Akiyama. Applied Drug Research Department, Eisai Co., Ltd., Tokyo, Japan.

Introduction: We have established bone OC level-reduced rats by warfarin (WF) treatment over the long term. To test the function of OC in bones, the changes in bone parameters after OVX were compared between in WF-treated and normal rats. **Methods:** Female 4-week-old rats were divided into the intact (n=24) and WF treated groups (n=40). Warfarin was orally given to rats at 0.4mg/kg, 3 times a week for 16 weeks. Then, 8 rats in each group were sacrificed (pre) and the remaining WF-treated rats were further divided into 2 groups: the WF-discontinuing group and the WF-continuing group. Each group was divided into sham-operated and OVX groups (n=8) and the operation was performed. After 12 weeks, bone and plasma osteocalcin, bone parameters (pQCT), mechanical properties (three-bending test) in the femurs were measured. **Results:** After 16 weeks of WF treatment (pre), the ratio of γ -carboxyglutamyl (Gla)-OC to total-OC in plasma was 53% of that in the intact group, and OC level in the femoral diaphysis and metaphysis were 14% and 12%, respectively. There were no differences in bone mineral content (BMC) and bone strength between the intact and WF-treated groups. Twelve weeks after OVX, the ratios of Gla-OC to total-OC in plasma in the WF-discontinuing-sham and the WF-continuing-sham were 100% and 54% of that in the intact sham, respectively. Diaphysal and metaphysal OC levels in the WF-discontinuing-sham were 16% and 36%, and those in the WF-continuing-sham were 11% and 10%, respectively. In the intact group, OVX resulted in a decrease only in metaphysal bone mineral density (BMD), and in the WF-discontinuing group, decreases in metaphysal BMC, BMD and diaphysal BMD were observed. In the WF-continuing group, the parameters above-mentioned, and diaphysal BMD, area, cortical thickness and maximum load (bone strength) were decreased after OVX. Plasma total OC and urinary deoxypyridinoline levels in the OVX rats were both higher than in the sham rats in all groups. **Conclusion:** These data indicated that although low levels of OC in bone did not affect bone parameters directly, low level of OC in bone clearly influenced bone loss after ovariectomy. Therefore, bone OC levels may play an important role in maintaining BMC, BMD or bone strength when bone turnover increases.

Disclosures: **K. Hara**, None.

SU022

Osteoporosis and Calcification of Cardiovascular System. C. Woong Hwan*, S. Hong*. Endocrinology, internal medicine, hanyang university medical center, seoul, Republic of Korea.

Background: Cardiac valve calcification and arteriosclerosis were correlated with congestive heart failure, hypertension and coronary heart disease. And the incidences of these two diseases and osteoporosis were increased with ages. Few studies suggested the correlation of these two diseases and osteoporosis. We observed the correlations of two diseases and osteoporosis. **Method:** We selected 23 patients with cardiac valve calcification (Group A) and 32 controls with normal cardiac valve (Group B) from 164 patients (over 60 years olds) who were checked the echocardiography and the bone mineral density from may 2003 to September 2004. And we also studied the correlation of aortic calcification (n=24) and osteoporosis (n=38) by 3D-QCT in 62 patients. Chronic renal failure patients and calcium metabolic disorder patients were excluded. Cardiac valve calcifications were defined as three or more hyper-echogenic nodules on cardiac valves in parasternal short axis view or post acoustic shadows at the base of posterior leaf of mitral valve. And aortic calcifications were confirmed by CT films. We also checked body weights, serum calcium, phosphate, albumin, alkaline phosphate, and total cholesterol. **Result:** There was no difference of basic characteristics (ages, body weight, serum calcium, and alkaline phosphate) except total cholesterol (174.4±39.1 vs. 202.0±35.7 mg/dL; $P < 0.05$). The mean of bone mineral densities (T-score) were decreased in cardiac valve calcification group (L-spine -2.67±1.33 vs. -1.83±1.50; $p < 0.05$, Femur -3.38±0.91 vs. -2.11±1.00; < 0.001). The odds ratio of osteoporosis (T-score ≤ -2.5) for cardiac valve calcification is 7.92 (95% CI 2.28-27.4). And the odd ratio of valve calcification for femur Z-score was 1.13 (95% CI 1.05-1.22). And the mean BMD in patients with aortic calcification was significantly lower than the mean BMD in patients without aortic calcification. (61.3 vs 74.0, $p < 0.05$) **Conclusion:** Bone mineral density is correlated with valve calcification and vascular calcification. So the dictation of valve or vascular calcification indicates a high probability of osteoporosis.

Disclosures: **C. Woong Hwan**, None.

SU023

Histological Analysis on Altered Bone Matrix of Warfarin-Administered Rats. N. Amizuka¹, M. Li^{1*}, K. Hara², M. Kobayashi², Y. Akiyama², T. Maeda^{1*}. ¹Oral Biological Science, Niigata University, Niigata, Japan, ²Pharmacological Evaluation Section, Eisai Co., Ltd., Tokyo, Japan.

Bone mineral maturation seems to require the participation of osteocalcin. This prompted us to elucidate the ultrastructural role of gla-proteins in early stages of mineralization in bone by employing warfarin-administered rats. Male Wistar rats at 4-week-old, were administered warfarin (0.4 mg/kg, warfarin group), or Ringer's solution (control group), and fixed after 4, 8 and 12 weeks with an aldehyde solution. The extracted tibiae and femora were embedded in paraffin for alkaline phosphatase, osteocalcin and tartrate-resistant acid phosphatase histochemistry, as well as in epoxy resin for ultrastructural observation under transmission electron microscopy (TEM). After 4, 8 and 12 weeks, there were no apparent histological alterations in the warfarin group. Therefore, the warfarin administration at the dosage of 0.4 mg/kg appeared not to affect bone turnover. We next examined if warfarin could affect gla-proteins in bone matrix. The

intense osteocalcin-immunoreactivity at the control bone surface was in contrast to the extremely reduced immunoreactivity in the matching region of the warfarin group. We therefore investigated the ultrastructure of initial mineralization of metaphyseal trabeculae. Mineralized nodules, globular assembly of crystalline particles or ribbon-like structures were seen in the control osteoid. However, the warfarin administration gave rise to dispersed crystalline particles throughout the osteoid without showing typical mineralized nodules. Immunoelectron microscopy verified less association of osteocalcin with those scattered crystalline particles, whereas normal mineralized nodules in control rats accumulated osteocalcin. Thus, gla-proteins appear to play a pivotal role in the assembly of mineralized nodules, rather than affecting bone turnover.

Disclosures: **N. Amizuka**, None.

SU024

Mineralization of the Rachitic Growth Plate Despite Calcium Deprivation Leading to Hypocalcemia. N. Dion, G. Mailhot*, J. L. Petit*, C. Deschênes*, V. Lascau*, M. Gascon-Barré, L. G. Ste-Marie. Saint-Luc Hospital, CHUM Research Centre, Montréal, PQ, Canada.

Previously, our group used a non-rachitogenic rat model [vitamin D (D)depleted and low calcium (Ca) diet (D-Ca-)] to study endochondral ossification and bone mineralization defects. These rats had growth retardation, hyperosteoridosis and, high serum parathyroid hormone (HPTH) secondary to hypocalcemia and D depletion. When D-Ca- rats were repleted with a high Ca content diet (Ca⁺) for 14 days (d), serum Ca and PTH were normalized, hyperosteoridosis was partly corrected but severe hypophosphatemic rickets developed. When Ca⁺ rats were abruptly switched to the initial D-Ca- diet, they all died within 5d. When Ca⁺ rats were progressively repleted over a period of 11d there was also a very high mortality rate (80%) but the time-to-mortality curve shifted to the right with a survival rate of 20% after 14d. Surviving rats were found to have hypocalcemia similar to D-Ca-. To investigate at the bone level, the pathophysiological causes leading to the death of Ca⁺ rats during repletion we performed undecalcified bone morphometry on proximal tibiae taken from rats sacrificed after 3d of the rapid repletion (RR) or after 5, 8, 11 and 14d of the progressive repletion (PR). In RR compared to Ca⁺, Goldner's trichrome, Von Kossa and Alizarin red stainings showed a widened growth plate (GP) with matrix mineralization abnormally occurring within GP cartilage at the hypertrophic chondrocyte zone. During PR, rickets regressed progressively with the primary spongiosa getting enlarged. In addition, hyperosteoridosis returned, being at 14d of PR similar to D-Ca-. Detection of alkaline phosphatase and annexin II, two markers of matrix vesicles (MV) involved in GP mineralization, showed that RR and Ca⁺ had a high level of MV markers due to the accumulation of hypertrophic chondrocytes. In PR rats, MV markers decreased over time being at 14d, at similar levels of D-Ca-. Our data suggest that during Ca repletion, correction of hypophosphatemia in Ca⁺ allowed the return of mineralization at the rachitic GP and increased demand for Ca by the enlarged GP ensued (evidenced by significant matrix mineralization). The little amount of Ca absorbed from the Ca-D- diet associated with an incapacity of the bone to provide sufficient Ca (despite the return of secondary HPTH) could not meet the Ca demand from the GP. This caused a rapid and severe hypocalcemia leading to the death of these animals, most likely by arrhythmia. This hypothesis is further supported by the observation that rats in PR which had a more progressive fall in their serum Ca, exhibited a delay in death rate, a gradual involution of rickets and survival only in animals returning to the D-Ca- phenotype.

Disclosures: **N. Dion**, None.

SU025

The Mineralization of the Bone Matrix and the Elemental Mapping of Calcium, Phosphorus, and Magnesium in the Klotho Mouse. H. Suzuki*¹, N. Amizuka*², M. Noda*³, H. Ohshima*¹, T. Maeda*². ¹Department of Oral Biological Science, Niigata University, Division of Anatomy and Cell Biology of the Hard Tissue, Niigata, Japan, ²Department of Oral Biological Science, Niigata University, Division of Oral Anatomy, Niigata, Japan, ³Tokyo Medical and Dental University, Medical Research Institute, Tokyo, Japan.

The klotho gene-depleted mouse is known as an animal model for accelerated gerontic state, mimicking osteoporosis, skin atrophy, ectopic calcification, pulmonary emphysema and gonadal dysplasia. To elucidate the influence of klotho-deficiency on bone mineralization, we examined the ultra-structures of osteoblasts and bone matrices, as well as performed the elemental mapping of calcium, phosphorus and magnesium in bone. Under anesthesia, 5-week-old klotho-deficient mice (klotho^{-/-} mice) and their wild-type littermates were perfused with 4% paraformaldehyde. The tibiae and femora were processed for light and electron microscopic observation. Paraffin sections were subject to alkaline phosphatase (ALP) and tartrate resistant acid phosphatase (TRAP) histochemistry. Semi-thin and ultra-thin sections obtained from epoxy resin-embedded specimens were used for detecting mineralization, according to von Kossa's staining method, and for elemental mapping by electron probe micro-analyzer (EPMA), respectively. ALP-positive plump osteoblasts adjacent to the growth plate normally developed cell organelles in the klotho^{-/-} metaphyses. However, this was contrasting with the flattened osteoblasts covering the trabecular bone of the diaphyses, accompanied by small TRAP-positive osteoclasts. The wild-type mice displayed well-mineralized metaphyseal trabeculae parallel to the longitudinal axis of the bone. Alternatively, the klotho^{-/-} mice demonstrated a fine meshwork or patches of mineralized bone in the metaphyses, as well as large non-mineralized area in the diaphyseal bone. Consistently, EPMA verified sporadic distribution of the higher or lower concentrations of calcium and phosphorus in each trabecule. The distribution of magnesium, however, was almost uniform. Thus, the klotho-deficiency appears not only to reduce osteoblastic population, but also to disturb important osteoblastic functions, bone mineralization.

Disclosures: **H. Suzuki**, None.

SU026

Intracellular Signaling Mechanism of Vasopressin-Induced Na-Dependent Phosphate Transport Activity in Rat Aortic Smooth Muscle Cells. K. Nishiwaki-Yasuda¹, A. Suzuki¹, A. Kakita^{*2}, Y. Ono^{*1}, S. Sekiguchi¹, K. Inagaki^{*1}, T. Matsumoto^{*1}, S. Imamura^{*1}, H. Kakizawa^{*1}, N. Hayakawa^{*1}, N. Oda^{*1}, Y. Oiso^{*3}, M. Itoh^{*1}. ¹Division of Endocrinology, Fujita Health University, Toyoake Aichi, Japan, ²Department of Internal Medicine, Hekinan Municipal Hospital, Hekinan Aichi, Japan, ³Department of Metabolic Diseases, Nagoya University Graduate School of Medicine, Nagoya Aichi, Japan.

We investigated the effect of arginine vasopressin (AVP) on inorganic phosphate (Pi) transport, which has been reported to be involved in the mechanism of atherosclerosis, and its intracellular signaling mechanism in A-10 rat aortic vascular smooth muscle cells (VSMCs). AVP time- and dose-dependently stimulated Pi transport in A-10 cells. A protein kinase C (PKC) inhibitor calphostin C partially suppressed the stimulatory effect of AVP on Pi transport. AG1478, a selective inhibitor of EGFR tyrosine kinase, suppressed AVP-stimulated Pi-transport. The selective inhibitors of mitogen-activated protein (MAP) kinases, such as ERK and p38, did not affect AVP-induced Pi transport. Both LY294002 and wortmannin, phosphatidylinositol (PI) 3-kinase inhibitors, attenuated AVP-induced Pi transport. A selective inhibitor of S₆ kinase, rapamycin, reduced this effect of AVP, while Akt kinase inhibitor did not. In summary, these results suggest that AVP stimulates Na-dependent Pi transport activity in VSMCs. The mechanism responsible for this effect is not mediated by p38 or ERK MAP kinase, but involves activation of PKC, EGFR tyrosine kinase, PI 3-kinase and S₆ kinase. These findings seem to be important for the targeting the molecule responsible for the progress of atherosclerosis.

Disclosures: **K. Nishiwaki-Yasuda**, None.

SU027

Effects of Adrenalectomy and γ_2 -MSH Administration on Bone Histomorphometric Change in Leptin-Deficient Ob/Ob Mice. J. K. Yeh, J. F. Evans*, Q. T. Niu*, J. F. Aloia. Metabolism Laboratory, Winthrop-University Hospital, Mineola, NY, USA.

The hypothalamic-pituitary-adrenal axis may be associated with mechanisms involved in the regulation of bone formation and bone linear growth. This study was designed to investigate bone histomorphometric changes induced by adrenalectomy (ADX) in wild-type (W) and ob/ob (Ob) mice. Groups of 30 Ob, 30 W female 4-week old mice were each divided into 3 groups of 10 animals each as Sham-Ob, ADX-Ob, ADX- γ_2 -MSH-Ob, Sham-W, ADX-W, and ADX- γ_2 -MSH-W. All ADX animals were implanted subcutaneously (s.c.) with a pellet designed to deliver 2.4ug corticosterone per day over 21 days. The ADX- γ_2 -MSH treatment groups received 50ug/day acetyl-(lys⁰, Nle³)- γ_2 -MSH amide (γ_2 -MSH) s.c. over the 21 days. Calcein (8mg/kg) was injected at 10 and 3 days, respectively, before the end of the experimental period. The proximal tibial metaphases were processed undecalcified for quantitative bone histomorphometry. In comparison to Sham-W mice, Sham-Ob mice had shorter tibial length (16.19±0.30mm vs 16.92±0.11mm, P<0.05) without a significant difference in growth plate width (99.8±11.8um vs 96.2±14.1um). The trabecular bone volume (TV/BV, %) was lower in the Sham-Ob (8.99±2.46) than that of the Sham-W group (11.59±2.39). ADX resulted in a significant increase in tibial length of Ob mice (16.57±0.33mm, P<0.05), a non-significant increase in the W mice (17.1±0.27mm), and a significant decrease in TV/BV in Ob (5.63±1.2, P<0.05) and a decrease in W mice (6.04±1.46, P<0.05) as compared to the respective Sham group. The bone formation rate (BFR) was significantly higher in the ADX-Ob mice (51.9±12.7 mcm/day vs. 35.5±5.5, P<0.05) and non-significantly higher in the ADX-W mice (47.0±11.2 vs. 41.6±3.9, P=0.167) as compared to the respective Sham group. Although, γ_2 -MSH treatment to the ADX-mice resulted in no significant effect on the TV/BV or on the BFR in both groups, it resulted in an increase in the growth plate width (150.7±18.1um vs. 134.9±17.5, P=0.06) and a trend increase in the tibial length (16.83±0.29mm, vs. 16.57±0.33, P=0.078) of the ADX-Ob mice. In conclusion, elevated ACTH and depleted corticosterone after ADX enhances linear growth and bone turnover rate. Administration of the melanocortin-3-receptor specific agonist, γ_2 -MSH, to the ADX mice further enhances bone linear growth without affecting the bone turnover.

Disclosures: **J.K. Yeh**, None.

SU028

Strontiums Effect on Bone Ultrastructure in Rats: Insights from Laboratory Scanning Small Angle X-Ray Scattering (sSAXS). T. P. K. Hansen^{*1}, M. H. Büniger², F. Besenbacher^{*3}, B. Langdahl⁴, H. Oxlund⁵, J. S. Pedersen^{*6}, H. Birkedal^{*6}. ¹Interdisciplinary Nanoscience Center (iNANO), University of Aarhus, Aarhus, Denmark, ²Interdisciplinary Nanoscience Center (iNANO) & Dept of Endocrinology and Metabolism C, University of Aarhus, Aarhus, Denmark, ³Interdisciplinary Nanoscience Center (iNANO) & Dept of Physics and Astronomy, University of Aarhus, Aarhus, Denmark, ⁴Dept. of Endocrinology and Metabolism C, Aarhus Sygehus, Aarhus, Denmark, ⁵Dept. of Anatomy, University of Aarhus, Aarhus, Denmark, ⁶Interdisciplinary Nanoscience Center (iNANO) & Dept. of Chemistry, University of Aarhus, Aarhus, Denmark.

Strontium salts (containing Sr²⁺) have attracted strong interest as a possible anabolic drug for the treatment of osteoporosis. Sr is believed to be incorporated into the inorganic phase of bone by substituting Ca in the apatite crystal lattice. However, detailed knowledge about possible effects of Sr treatment on the ultrastructure of bone is still missing. In the

ASBMR 27th Annual Meeting

present work, scanning Small Angle X-ray Scattering (sSAXS) is used for studying the effects of a strontium treatment regime in a rat model. In bone the SAXS signal originates from differences in electron density between the mineral and organic phase and SAXS offers unique information about thickness, orientation and shape of the mineral particles. The effect of Sr on the treatment of ovariectomy induced osteoporosis was studied in 6 month old female Wistar rats. Animals were treated with 4 mmol SrCl₂ (aq)/kg/day or placebo in the drinking water for a period of 140 days. All rats were labelled with fluorochromes at days 7, 126 and 136. Four ~150 µm thick cross sections (-ov/-Sr, +ov/-Sr, -ov/+Sr and +ov/+Sr) of midshaft femur were studied in detail using fluorescence microscopy and scanning electron microscopy (SEM) including element mapping with energy dispersive X-ray analysis (EDAX) and sSAXS. The new bone, identified by fluorescence microscopy, was found to contain increased levels of Sr by EDAX analysis in the two +Sr animals. The SAXS survey scans, with a ~50 µm lateral resolution, revealed a large variation in the SAXS intensity in the central part of the individual sections, while they were more homogeneous toward the periost in agreement with current models of bone maturation. Qualitatively, the sSAXS results illustrated the osteoinductive behaviour of Sr as seen by comparison of survey scans of the four samples. Detailed SAXS investigations of selected regions were used to determine crystallite orientation, shape and thickness. We will compare +Sr and -Sr bone to bring to light any possible effects of Sr treatment on the crystallite properties and distribution.

Disclosures: **M.H. B nger**, None.

SU029

Lovastatin Microbead Scaffolds Stimulate Local Bone Formation. **G. Rossini***, **G. Gutierrez**, **G. Mundy**, **L. R. Garrett**. OsteoScreen, Ltd, San Antonio, TX, USA.

Statins are inhibitors of the enzyme HMG Co-A reductase, the rate-limiting step in hepatic cholesterol biosynthesis. It is now recognized statins produce a multitude of effects including potential benefits on bone formation which are unrelated to the lowering of serum cholesterol. Statins increase bone formation in vitro by increasing the expression of bone morphogenetic protein-2 (BMP-2), which acts as an autocrine-paracrine factor in osteoblast differentiation. Preclinical animal studies and in vitro studies have revealed the importance of the mode of administration of statins. When statins are administered locally, they markedly stimulate new bone formation^{1, 2}. Statins, therefore, represent the first small-molecular-weight BMP-like molecule that stimulates new bone formation locally. Our hypothesis is that the use of lovastatin impregnated microbead scaffolds made from biodegradable polymers will enhance fracture repair through both the osteoconductive properties of scinted-polymer-microbeads scaffolds and the osteoinductive capabilities of controlled lovastatin release. Microbeads of PLGA polymer containing lovastatin at 10mg/gm of polymer were made. The raw microbead/lovastatin product was developed for various scaffolds and matrices. 3D scaffolds were prepared by scinting beads together using either heat, microwaving or by proprietary chemical scinting. The resultant matrix scaffold structures were light, porous and showed excellent compressive strength when measured by constant loading rate (3 mm/min) in an MTS Q-test 5 mechanical test machine. Whereas, lovastatin injected over the calvaria of mice at 125ug/day for 5 days did stimulate new bone formation (new bone area 0.13±0.05mm²), the scaffolds releasing lovastatin at 5ug/day placed over the calvaria of mice, increased new bone area by over 400% (scaffold alone 0.06±0.005mm² and lovastatin scaffold 0.32±0.007mm²). Lovastatin in the serum of these mice was undetectable and no toxicity was evident at the site of implantation. Delivery of anabolic compounds, such as statins, by controlled release microbead scaffold technology provides an extremely effective treatment and repair of bone void defects. This simple but innovative approach has the potential to deliver lovastatin as well as other low-cost anabolic agents to fracture sites to significantly accelerate fracture repair, and has the added potential for use in a wide range of surgical environments.

1. Thylin MR, McConnell JC, Schmid MJ, et al. Effects of simvastatin gels on murine calvarial bone. J Periodontol 2002; 73:1141-8.
2. Wong RW, Rabie AB. Statin collagen grafts used to repair defects in the parietal bone of rabbits. Br J Oral Maxillofac Surg 2003; 41:244-8.

Disclosures: **I.R. Garrett**, Osteoscreen Ltd 1, 3.

SU030

Analgesic and Chondroprotective Effect of Risedronate in Osteoarthritis Assessed by Electroalgotmetry and Measurement of Collagen Type II Fragments in Urine. **T. Fujita¹**, **M. Ohue^{*1}**, **A. Miyauchi^{*2}**, **Y. Takagi^{*3}**.

¹Medicine, Katsuragi Hospital, Kishiwada, Japan, ²Medicine, National Hospital System Hyogo Chuo Hospital, Hyogo, Japan, ³National Hospital System Hyogo Chuo Hospital, Hyogo, Japan.

In order to evaluate the effect of risedronate on pain and cartilage metabolism in osteoarthritis, 233 patients with osteoarthritis of the knee were randomly divided into two groups. In Group RC, 2.5 mg risedronate and 900 mg calcium as active absorbable algal calcium (AACA) was given daily for 8 months, and only calcium was given in Group C during the same period. Pain on exercise was estimated by subjective visual rating scale (VRS) and electroalgotmetry (EAM) measuring skin impedance (General Devices, New Jersey) and fragments of cartilage-specific collagen type II in the second morning urine samples were measured before and during the administration (Nordic Bioscience Diagnostics, Copenhagen). Alleviation of pain induced by walking assessed by the fall of skin impedance was significantly more efficient in RC than in C after 4 month treatment (p=0.0179) and on overall comparison before and after supplementation (p=0.0084). Pain induction by knee bending and lying on bed in addition also gave similar finding (p=0.0088, and 0.0067). Urinary excretion of type II collagen fragments was significantly more pronounced in the third month (p=0.0089) and on overall comparison (p=0.0236).

Though the results of VRS and EAM pain evaluation generally correlated significantly, EAM (p=0.0153) but not VRS (p=0.6482) demonstrated a significantly more effective alleviation of exercise-induced pain by RC than C on overall comparison of pre-and post-treatment. Approximate synchronicity between electroalgotmetry pain alleviation and decrease of urinary collagen type II excretion due to cartilage destruction suggests a chondroprotective effect of risedronate leading to pain alleviation. Osteoarthritis characterized by increased cartilage Ca content, hardening, degeneration and wasting in response to physical stress is apparently caused by increased bone resorption induced by calcium deficiency and other causes, with consequent Ca entrance into cartilage. Chondroprotective effect of risedronate may be explained by its inhibition on bone resorption and Ca entrance into cartilage.

Disclosures: **T. Fujita**, None.

SU031

Circulating Chondrogenic Precursors. **S. A. Kuznetsov**, **M. H. Mankani**, **A. Leet**, **P. Gehron Robey**. Craniofacial and Skeletal Diseases Branch, National Institute of Dental and Craniofacial Research, Bethesda, MD, USA.

In cultures of human peripheral blood, macrophages and their derivatives can acquire notoriously diverse morphological and tinctorial phenotypes. Consequently, subsets of these cells frequently have been mistakenly identified as fibroblast-like cells, thus incorrectly suggesting an abundance of connective tissue progenitors in human blood. In fact, when rigorous criteria are applied (ability to form discrete colonies and to undergo multiple passages, precise immunophenotyping, capacity for bone formation upon in vivo transplantation, or display of other phenotypes), true connective tissue precursors are extremely scarce in human blood. Using a number of cell separation techniques and various culture conditions, we were able to identify just three donors out of 62 studied whose blood contained connective tissue colony-forming cells. Out of these three, one was a patient with multiple bone fractures, and another had been subjected to blood mobilization by G-CSF injections. In contrast, blood cells of several animal species, such as mouse, rabbit, and, in particular, guinea pig, demonstrate much more reproducible connective tissue colony formation. Based on this fact, we chose the guinea pig model to study the differentiation potential of adherent strains of circulating cells. Multicolony-derived strains (5 in total) consisted uniformly of spindle-shaped, fibroblast-like cells, positive for the markers of fibroblasts, osteogenic cells, and smooth muscle cells, and negative for the markers of endothelial cells, leukocytes, and macrophages. Following in vivo transplantation, one of the strains formed abundant bone, accompanied by adipocytes and hematopoiesis-supporting stroma, and formed abundant cartilage in pellet cultures in vitro. Out of 22 single colony-derived strains of various morphologies (6 spindle-shaped, fibroblast-like, 4 flat-shaped, fibroblast-like, 11 polygonal, 1 intermediate), only 5 spindle-shaped strains were able to proliferate extensively. None of these formed bone in vivo, while two did form cartilage in pellet cultures. Apparently, there are cells in guinea pig blood capable of both extensive proliferation and differentiation towards cartilage: circulating chondrogenic precursor cells. These cells lack osteogenic potential and therefore represent committed chondrogenic precursors. This is the first time that precursor cells with chondrogenic but not osteogenic potential have been identified. At the same time, our finding of a multicolony-derived strain capable of osteogenesis, chondrogenesis, and stromal tissue formation suggests that circulating multipotential skeletal stem cells do exist.

Disclosures: **S.A. Kuznetsov**, None.

SU032

Basic Calcium Phosphate Crystals Promotes Apoptosis in Bovine Articular Chondrocytes. **H. K. Fa^{*1}**, **B. Uzan^{*1}**, **C. Rey^{*2}**, **F. Liot  ^{*1}**.

¹Hospital Iariboisi  re, INSERM 606, Paris, France, ²CIRIMAT, UMR CNRS 5085, ENSIACET, Toulouse, France.

Basic calcium phosphate (BCP) crystals including octacalcium phosphate (OCP), carbapatite (CA) and hydroxyapatite (HA) are frequently found in articular fluid and are associated with a severe and destructive form of osteoarthritis (OA). These crystals have heterogeneous biological properties and induce different inflammatory responses as demonstrated *in vivo* and *in vitro* studies. Beside inflammatory cytokines and metalloproteases (MMPs) released after synovocyte stimulation, recent studies have demonstrated that BCP crystals directly activated chondrocytes to produce MMPs and nitric oxide. The aim of this study was to investigate the role of BCP crystals in articular chondrocytes apoptosis, a hallmark feature in OA. Sterile and pyrogen-free OCP, CA and HA crystals were characterized by X-ray diffraction and infrared spectroscopy. Primary bovine articular chondrocytes isolated from calf metatarsal phalangeal joints were cultured in monolayer condition for 7 days. To study apoptosis cells were then replated and cultured in serum-free medium for 4-48 hours. Apoptosis was assessed by caspase 3 activity, Hoechst staining and phosphatidylserine labelling with annexin V-FITC. Chondrocytes viability was evaluated with MTT assay. All three BCP crystals induced articular chondrocyte apoptosis : chromatin condensation and phosphatidylserine externalisation. Caspase 3 activity increased in a dose- and time-dependent fashion for each crystal and this was associated with a dose-dependent decrease in chondrocyte viability. Maximal caspase 3 activity was obtained with the low dose (50 µg/ml) for OCP (+400%) and CA (+400 %) crystals whereas a ten-fold higher dose (500 µg/ml) was necessary with HA crystals to achieve the same effect. Using a transwell system, BCP crystals did not induce caspase 3 activity indicating that BCP crystal-induced apoptosis was not secondary to calcium release. Furthermore, chelating extracellular calcium with EGTA or EDTA, or using a calcium-free medium increased caspase 3 activity as well. Finally caspase 3 activity was associated with increase Bax/Bcl-2 ratio and was markedly diminished in a dose-dependant fashion when chondrocytes were pre-incubated with caspase-8 (Z-IETD-FMK) and caspase-9 (Z-LEHD-FMK) inhibitors, suggesting the involvement of the 2 signal

pathways. Our data showed for the first time that BCP crystals directly promoted chondrocyte apoptosis. This further suggested that they might participate to cartilage destruction in crystal related-joint diseases.

Disclosures: **H.K. Ea**, None.

SU033

A New Thienindazole Derivative Promotes Chondrogenic Differentiation in a Sox9-Independent Manner without Inducing Hypertrophy. **F. Yano¹, S. Ohba¹, F. Kugimiya², T. Ikeda¹, N. Ogata¹, T. Ogasawara¹, T. Takato¹, K. Nakamura², H. Kawaguchi², U. Chung¹.** ¹Division of Tissue Engineering, Faculty of Medicine, University of Tokyo, Tokyo, Japan, ²Department of Sensory and Motor System Medicine, Faculty of Medicine, University of Tokyo, Tokyo, Japan.

Aiming at clinical application to cartilage regeneration, we established prechondrogenic ATDC5 cell lines stably expressing green fluorescent protein (GFP) under the control of the chondrocyte-specific fragment of the type II collagen promoter. Using these cells as a monitoring system of chondrogenic differentiation, we screened natural and synthetic compound libraries and discovered that a thienindazole derivative small compound T-198946 (TM) strongly induced GFP fluorescence in a period as short as 3 days. To clarify its molecular mechanism of action, we treated mouse embryonic stem cells (ESC), undifferentiated mesenchymal C3H10T1/2 cells and bone marrow-derived mesenchymal stromal cells (MSC) with TM and examined markers of chondrocyte differentiation. Real-time RT-PCR analysis revealed that TM treatment up-regulated expression of chondrogenic differentiation markers such as type II collagen, aggrecan and chondromodulin-1, but not that of hypertrophic differentiation markers such as type X collagen and osteopontin. Toluidine blue and Alcian blue stainings of C3H10T1/2 and MSC revealed that TM treatment increased cartilage matrix synthesis in a dose-dependent manner. Furthermore, TM treatment of dedifferentiated primary chondrocytes which were isolated from newborn mouse ribs and passaged three times led to restoration of mRNA expression of chondrogenic differentiation markers and synthesis of cartilage matrix, suggesting that TM promotes redifferentiation of dedifferentiated chondrocytes. Since Sox9 is required during sequential steps of chondrocyte differentiation, we investigated whether Sox9 and its cofactors Sox5 and Sox6 were involved in the action of TM. TM treatment of ESC, C3H10T1/2 and MSC did not significantly alter mRNA level, protein level or phosphorylation of Sox9, whereas it dramatically up-regulated mRNA expression of Sox5 and Sox6. TM treatment of Sox9-deficient ESC up-regulated expression of chondrogenic differentiation markers to the level comparable to that of wild-type ESC. These data suggest that TM induces chondrogenic differentiation in a Sox9-independent manner without inducing hypertrophy. TM may be useful for the regenerative medicine of permanent cartilage.

Disclosures: **F. Yano**, None.

SU034

Connective Tissue Growth Factor (CTGF/CCN2) Reinforces the Molecular Phenotype of Auricular Chondrocytes *In Vitro*. **T. Fujisawa^{*1}, K. Nakao^{*2}, T. Hattori^{*2}, S. Kubota^{*2}, T. Kuboki^{*1}, M. Takigawa².**

¹Department of Oral and Maxillofacial Rehabilitation, Okayama University Graduate School of Medicine, Dentistry and Pharmaceutical Sciences, Okayama, Japan, ²Department of Biochemistry and Molecular Dentistry, Okayama University Graduate School of Medicine, Dentistry and Pharmaceutical Sciences, Okayama, Japan.

Cartilage is an avascular tissue, so once damaged, hyaline and elastic cartilage have limited capacity for self-repair. However, recent advances in tissue engineering technology have brought significant progress in reconstruction of cartilage defects. It is well known that connective tissue growth factor (CTGF/CCN2) is a multifunctional growth factor for chondrocytes, and plays important roles in the control of the proliferation and differentiation of chondrocytes *in vitro*. We have previously reported that CTGF/CCN2 promotes all process of the endochondral ossification, such as cell proliferation, maturation and hypertrophy of growth cartilage cells, however, does not stimulate their hypertrophy or calcification of articular chondrocytes *in vitro*. These results indicate that CTGF/CCN2 may reinforce their own molecular phenotype of chondrocytes derived from different cartilage, such as growth cartilage and articular cartilage. Therefore, in this study, we tried to investigate the effects of CTGF/CCN2 on auricular chondrocytes. Rabbit primary auricular chondrocytes were isolated from their auricular cartilage by enzyme digestion and cultured in alpha-MEM containing 10% FBS. Chondrocytes were cultured in the presence or absence of 50 ng/ml recombinant human CTGF/CCN2. The effect of CTGF/CCN2 on the auricular chondrocytes proliferation was evaluated by MTS assay and [³H] thymidine incorporation, and the proteoglycan synthesis was determined by [³⁵S] sulfate incorporation. The mRNA level of *elastin* was evaluated by real-time PCR analysis, and the accumulation of elastin fibers were visualized by Victoria-blue stain. CTGF/CCN2 stimulated the proliferation of rabbit auricular chondrocytes slightly, DNA synthesis up to 1.8 times and proteoglycan synthesis up to 1.6 times. The gene expression of *elastin* after stimulation with CTGF/CCN2 was increased up to 2.5 fold in comparison with the control condition. In addition, the production of elastin fiber was slightly up-regulated by stimulation with CTGF/CCN2. This is the first report to show that CTGF/CCN2 promotes the phenotypes of the auricular chondrocytes such as *elastin* gene expression and elastin fiber accumulation, which suggests that CTGF/CCN2 may be useful for repair or reconstruction of elastic cartilage, e.g., auricular cartilage.

Disclosures: **T. Fujisawa**, None.

SU035

CTGF Acts as A Downstream Mediator of TGF- β 1 in Promoting Condensation And Regulating FN and Sox9 Expression in Mesenchymal Stem Cells. **J. J. Song¹, R. A. Aswad^{*1}, R. A. Kanaan^{*2}, M. C. Rico¹, T. A. Owen³, M. F. Barbe¹, F. F. Safadi¹, S. N. Popoff¹.** ¹Anatomy & Cell Biology, Temple University School of Medicine, Philadelphia, PA, USA, ²Orthopaedic Surgery, University of Pennsylvania, Philadelphia, PA, USA, ³Cardiovascular and Metabolic Diseases, Pfizer Global Research and Development-Groton Laboratories, Groton, CT, USA.

Condensation or the aggregation of mesenchymal stem cells (MSCs) precedes chondrocyte differentiation and is required for cartilage formation and subsequent skeletal development. CTGF is a matricellular protein that has been found to be expressed in condensations and the perichondrium by *in situ* hybridization studies. Since TGF- β 1 initiates the condensation of MSCs and CTGF is a downstream gene of TGF- β 1, this study examined whether CTGF mediates TGF- β 1-induced MSC condensation. In addition, the relationship between the expression of CTGF and Sox9, the master transcription factor required for chondrocyte differentiation, was examined. The expression of CTGF, TGF- β 1, Sox9, and FN was evaluated by immunohistochemical analysis of developing vertebrae in sections from mouse embryos at E10.5-E12.5. CTGF, TGF- β 1 and FN were co-expressed at high levels in condensations, while high levels of Sox9 expression were observed at a later time point in chondrocytes of developing vertebrae, at a time when CTGF expression had shifted to the perichondrium. To model condensation *in vitro*, micromass cultures of C3H10T1/2 mesenchymal stem cell-line (MSC) were used. TGF- β 1 stimulation initiated the condensation of MSCs and this effect was concomitant with the up-regulation of CTGF expression. To study the importance of CTGF in condensation, CTGF siRNA (siCTGF) and CTGF antisense oligonucleotide (antisense) were used to silence CTGF expression in TGF- β 1 stimulated cultures. Migration and proliferation assays were performed to evaluate the effects of CTGF silencing on MSCs; Western blot and quantitative Real Time RT-PCR analyses were performed to evaluate expression of CTGF, Sox9 and FN in these cultures. CTGF silencing by siCTGF and antisense showed that TGF- β 1-induced condensation of MSCs was CTGF dependent. In addition, the up-regulation of FN and suppression of Sox9 expression by TGF- β 1 were also found to be mediated by CTGF. The down-regulation of CTGF expression by siRNA significantly decreased the proliferation and rate of migration of MSCs, two events that play a crucial role in condensation. In conclusion, these results demonstrate that CTGF acts as a downstream mediator of TGF- β 1 in promoting condensation of MSCs (via proliferation and migration), and in regulating the expression of FN and Sox9 prior to their overt differentiation into chondrocytes.

Disclosures: **J.J. Song**, None.

SU036

Expression of Osteoclastogenesis-Related Molecules in Chondrocytes: *In Vivo* And *In Vitro* Evidence. **G. Mailhot, A. Mason-Savas*, C. A. Mackay*, P. R. Odgren.** Department of Cell Biology, University of Massachusetts Medical School, Worcester, MA, USA.

Commitment of mononuclear precursors to mature osteoclasts relies on two major and interdependent pathways: interaction of csf-1 with its receptor c-fms and binding of RANKL to its receptor RANK. Animals with inactivating mutations in either one of these pathways lack osteoclasts and are severely osteopetrotic. In addition, these osteoclast-deficient mutants display progressive postnatal growth plate dysplasia characterized by loss of columnar organization, increased thickness, decreased vascular invasion and reduced hypertrophic chondrocyte apoptosis. In order to better understand the involvement of osteoclastogenic molecules in postnatal growth plate physiology, *in vivo* and *in vitro* studies were carried out using laser microdissected growth plate chondrocytes and a well-characterized chondrocyte culture model. We investigated the presence and expression of these molecules along with others involved in growth plate function and regulation by quantitative PCR, *in situ* hybridization and immunohistochemistry. *In vivo* expression of collagen types II and X and aggrecan as well as parathyroid receptor 1, its ligand PTHrP, Patched and Indian hedgehog confirmed the phenotype of the dissected area. Expression of csf-1, RANKL and their receptors is largely confined to hypertrophic zone chondrocytes. Low levels of osteocalcin and TRAP expression excludes extensive bone tissue contamination. *In vitro* studies confirm the *in vivo* findings and showed that gene expression follows the course of chondrocyte differentiation. This study shows for the first time that osteoclastogenic molecules are expressed in laser-captured hypertrophic chondrocytes of the growth plate. These results may help explain the growth plate dysplasia in csf-1 or RANKL-related pathway knockout animals. Further studies comparing mutant and wild-type growth plates as well as investigations of signaling events should lead to a better understanding of the role of csf-1 and RANKL in chondrocyte differentiation.

Disclosures: **G. Mailhot**, None.

SU037

Regulators of G Protein Signaling (RGS) Regulate Chondrocyte Differentiation. C. T. G. Appleton*, C. G. James*, F. Beier. Physiology & Pharmacology, University of Western Ontario, London, ON, Canada.

RGS proteins are known to exhibit negative control of G protein signaling. Our goal was to characterize the functions of RGS (regulator of G-protein signaling) proteins during chondrocyte differentiation, a well-defined process in endochondral bone development. Initially, microarray analyses indicated differential expression of several *Rgs* genes during chondrogenic differentiation; we confirmed this using RT-PCR (James et al., in revision). To investigate biological roles played by the murine *Rgs* genes, we transfected the murine ATDC5 chondrogenic cell line with human *RGS2*, *RGS4*, *RGS5*, *RGS7*, or *RGS10* constructs to overexpress the RGS proteins. Using real time PCR, RT-PCR, alkaline phosphatase activity assays, and staining techniques we assessed changes in the chondrocyte differentiation program. Premature increases in Type II collagen expression were detected in clones overexpressing RGS2, RGS7, or RGS10. These same clones exhibited accelerated hypertrophic differentiation as demonstrated by increases in the hypertrophic chondrocyte marker genes Type X collagen and BSP (bone sialoprotein), and increased levels of alkaline phosphatase activity. FGFR3 and IHH expression was also altered due to RGS protein overexpression. In contrast, RGS4 and RGS5 overexpression accelerated the transition from the proliferative to the pre-hypertrophic chondrocyte, but had no effect on hypertrophic differentiation compared to vector-transfected controls. To investigate how RGS proteins regulate a specific G protein signaling pathway we measured cAMP production by ELISA after stimulation with 10^{-7} M PTHrP. Interestingly, RGS protein overexpression caused an increase in cAMP production in response to stimulation with PTHrP. Finally, preliminary studies using *Rgs2*^{-/-} mice suggest that RGS2 is required for skeletal growth and development. Histological and *in situ* hybridization studies are currently underway to investigate this phenotype in detail. These data show, for the first time, a role played by RGS proteins in chondrogenic differentiation. Identification of the signaling pathways and downstream targets regulated by RGS proteins will shed further light on the mechanisms controlling chondrocyte physiology and pathophysiology.

Disclosures: **C.T.G. Appleton**, None.

SU038

B-Raf Is Dispensable for Normal Endochondral Bone Development. S. Provot*, J. Paruch*¹, A. Chen*², A. Silva*², H. M. Kronenberg*¹. ¹Endocrine Unit, MGH - Harvard Medical School, Boston, MA, USA, ²Department of Neurobiology, UCLA - Brain Research Institute, Los Angeles, CA, USA.

Parathyroid hormone-related peptide (PTHrP) through its G protein-coupled PTHrP-receptor (PPR) is a positive regulator of chondrocyte proliferation and a negative regulator of chondrocyte maturation in endochondral bone development. We have previously demonstrated that these effects most likely involve cAMP-dependent signaling pathways. Because it has been suggested that the ability of cAMP to stimulate cell proliferation involves the MAPKKK B-Raf, we hypothesized that PPR's proliferative action in chondrocytes might be mediated by B-Raf. We observed *B-raf* expressed in proliferative but not hypertrophic chondrocytes, and conditionally inactivated this gene in cartilage, using a collagen II promoter-driven cre, and a floxed *B-raf* allele. Mice lacking B-Raf in cartilage are identical to wild-type mice. Histologic analysis of the *B-raf*-null growth plate showed no difference compared to control littermates, both in prenatal and postnatal animals. *In situ* hybridization analysis with various chondrogenic markers did not reveal any abnormal chondrocyte differentiation. We also found that *B-raf*-null chondrocytes have a similar proliferation rate to that of control littermates. Because B-Raf may have subtle effects in the growth plate, we looked for possible consequences of a lack of B-Raf in settings in which PTHrP signaling has been ectopically activated. Metatarsal explants treated acutely with PTHrP presented both a similar proliferation rate, and a similar delay of chondrocyte maturation, in presence or absence of B-Raf. We verified that B-Raf protein was efficiently removed from primary chondrocytes using Western blot. Lastly, we looked at the expression of the two other members of the Raf family in the growth plate, in order to see whether they could compensate for the lack of B-Raf. We found that *A-raf* is expressed in proliferative chondrocytes and its expression is unchanged in *B-raf*-null chondrocytes, whereas *C-raf* is only expressed in mature hypertrophic chondrocytes. Based on our results, we conclude that B-Raf is dispensable for normal growth plate development and that B-Raf alone is not responsible for PTHrP-induced chondrocyte proliferation. Because *A-raf* expression is identical to that of *B-raf* we speculate that A-Raf might play a redundant function with B-Raf in cartilage.

Disclosures: **S. Provot**, None.

SU039

How Do Hypertrophic Chondrocytes Die? Y. Ahmed*, L. Tatarczuch*, C. N. Pagel*, K. Alkhodair*, A. F. Clarke*, H. M. S. Davies, M. Mirams*, E. J. Mackie. School of Veterinary Science, University of Melbourne, Parkville, Victoria, Australia.

During endochondral ossification, chondrocytes in growth cartilage undergo hypertrophy then die by a process that is morphologically distinct from classical apoptosis but has not been well characterised. The aims of the current study were to document the morphology of dying hypertrophic chondrocytes in different anatomical locations throughout foetal and postnatal growth, and to develop a culture system for studying the molecular mechanisms of physiological death of these cells. Specimens of articular-epiphyseal and physeal growth cartilage (AEGC and PGC, respectively) were collected from the distal femur and distal tibia of horses during foetal and postnatal growth, and

examined by transmission electron microscopy. Two types of dying chondrocyte were observed, 'dark' and 'light' chondrocytes. Dark chondrocytes were characterised by a dark nucleus with small, irregular patches of condensed chromatin; their electron dense cytoplasm was gradually being extruded into the extracellular space. Light chondrocytes also contained a condensed nucleus but their cytoplasm and organelles appeared to be undergoing gradual disintegration within a preserved cellular membrane. The proportion of light chondrocytes was higher in foetal than postnatal specimens and greater in AEGC than in PGC. Chondrocytes were isolated by collagenase digestion from epiphyseal cartilage excised from foetal horses. These cells were centrifuged and grown as pellets for up to 28 days under a variety of conditions, then analysed by light and electron microscopy. By day 7, pellets cultured in 0.1% or 10% foetal calf serum (FCS) were organized into a cartilage-like tissue surrounded by a perichondrium-like layer of flattened cells, and contained hypertrophic chondrocytes resembling those seen *in vivo*. Some light chondrocytes were present at days 7 and 14; dark chondrocytes and a small number of apoptotic cells were present at all stages of culture. The addition of transforming growth factor- β to the culture medium resulted in an increase in the proportion of cells dying as dark chondrocytes. Triiodothyronine added to medium containing 0.1% FCS caused an increase in the proportion of cells dying as light chondrocytes, but had no effect in the presence of 10% FCS. Staurosporine, which induces apoptosis in a variety of cell types, increased the proportion of cells dying as dark chondrocytes, but did not induce apoptosis in pellet culture. This culture system will provide a useful model for studies on the mechanism of physiological death of hypertrophic chondrocytes.

Disclosures: **E.J. Mackie**, None.

SU040

Transient Receptor Potential Vanilloid 4 (TRPV4) Deficiency Alters Chondrocytic Column Formation during Endochondral Ossification in Mice. A. Mizuno*¹, N. Amizuka*², M. Li*², M. Suzuki*¹. ¹Molecular Pharmacology, Jichi Medical School, Tochigi, Japan, ²Division of Oral Anatomy, Center for Transdisciplinary Research, Niigata University, Niigata, Japan.

Mechanical stress including the gravity is generally believed to affect endochondral ossification. Transient receptor potential vanilloid 4, TRPV4, is a member of TRP family of calcium-permeable cation channels, which can respond to hypotonicity, moderate heat, acidic pH in neurons, keratinocytes, and endothelial cells. The previous investigation on TRPV4 deficient (TRPV4^{-/-}) mice have verified that this molecule serves as mechanosensor *in vivo*. The molecular mechanism of the mechanosensation is, however, still veiled in the research field of bone. The purpose of this study is to investigate the role of TRPV4 during bone development, by employing TRPV4^{-/-} mice. Immunohistochemical staining showed the TRPV4 channel in chondrocytes of the proliferative and the early stage of hypertrophic zones of the wild-type growth plate, consistent with the TRPV4 mRNA in cultured normal chondrocytes and osteoblasts. Furthermore, an electrophysiologic analysis verified the functional TRPV4 in the primary cultured chondrocytes, indicating that the channel on chondrocytes act as a mechanosensor during bone development. Tibiae of 4-week-old TRPV4^{-/-} mice showed the deformed chondrocytic columns and irregularly-shaped primary trabeculae. Staining of type X collagen, a hallmark of the hypertrophic zone, demonstrated the isolated islets of the hypertrophic chondrocytes in the mutant growth plate, indicating non-synchronous differentiation of some chondrocytes. No remarkable alterations were found in osteoblasts and osteoclasts, as well as CD31-positive vascular endothelial cells at the chondro-osseous junction in TRPV4^{-/-} mice. Therefore, the lack of TRPV4 appears to result in a failure of spatially-organized gradient of chondrocytic differentiation, giving rise to the malformation of chondrocytic columns in the growth plate. Electron microscopy furthermore demonstrated the cell nests of chondrocytes, which closely attached each other, as well as dispersed collagen fibrils in all directions, in the TRPV4^{-/-} mice, thereby, suggesting a defective cellular polarity associated with extracellular matrices. These results indicate that TRPV4 appears to be responsible for maintaining normal cellular polarity of chondrocytes, and consequently enable spatially-organized gradient of chondrocytic differentiation. Thus, it is likely that signaling linked to TRPV4 channels plays a crucial role in spatial orientation of chondrocytes during normal endochondral ossification.

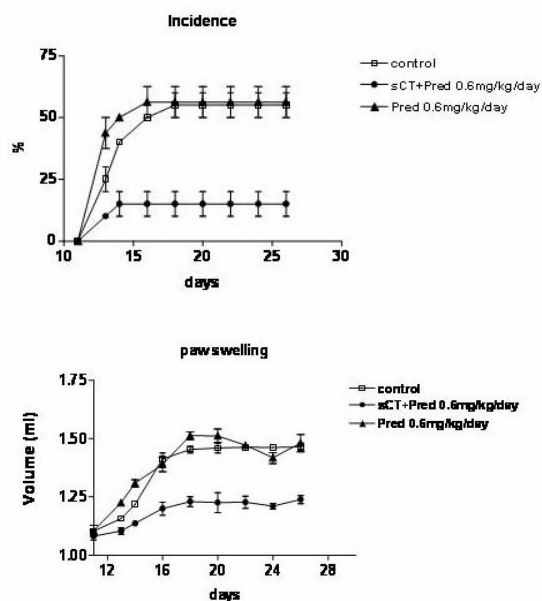
Disclosures: **A. Mizuno**, None.

SU041

Calcitonin Abolishes Collagen-Induced Arthritis. I. MacIntyre, L. Mancini*, M. Perretti*. William Harvey Research Institute, Queen Mary's School of Medicine and Dentistry, London, United Kingdom.

Female Lewis rats (150 \pm 20g) on a standard chow pellet diet were injected with bovine nasal collagen II (4 mg/ml) at the base of the tail. Arthritis developed at day 18 to 21. In preliminary experiments, calcitonin had a variable and modest anti-inflammatory effect. In further definitive and extensive experiments rats were given calcitonin (2 μ g/kg/day) alone and accompanied by prednisolone (3 mg/rat/day) and in a separate group prednisolone (0.6 mg/rat/day). Prednisolone alone (3 mg/rat/day) suppressed the arthritis while calcitonin alone had little effect in this experiment. However when administered with prednisolone (0.6 mg/rat/day) calcitonin completely abolished the arthritis as judged by paw swelling, incidence and clinical score. These results suggest that in the presence of the lesser prednisolone dosage (itself without effect) calcitonin has a marked anti-inflammatory effect. The synergistic effect of prednisolone might represent suppression of calcitonin receptor down-regulation but this remains to be established. These results might have implications for calcitonin in human subjects with rheumatoid arthritis.

ASBMR 27th Annual Meeting



Disclosures: **I. MacIntyre**, None.

SU042

Mechanisms of Parathyroid Hormone (PTH) Inhibition of Extracellular Signal-Regulated Kinases (ERK1/2) in Chondrocytic Cells. **L. P. Lai***, **J. Mitchell**. Pharmacology, University of Toronto, Toronto, ON, Canada.

Indian Hedgehog (Ihh) is produced by growth plate pre-hypertrophic chondrocytes, and is the master regulator of endochondral bone formation. It regulates the rate of proliferation and differentiation of growth plate chondrocytes as well as osteoblast differentiation. Previously, we have shown that parathyroid hormone (PTH) downregulates Ihh mRNA levels in a chondrocytic cell line, CFK-2, and this is mainly mediated by PTH inhibition of extracellular signal-regulated kinases (ERK1/2) activities (Lai, et al., *J. Cell. Physiol.* 203: p177, 2005). In this study, we investigated the mechanisms by which PTH inhibits ERK1/2 activities in CFK-2 cells. PTH (PTH (1-34)) decreased the phosphorylation levels of c-Raf at ser338 in both time (maximally in 5 min and sustained for 30 min) and concentration (from 10^{-11} to 10^{-7} M) dependent manner. Similarly, PTH was also able to decrease the phosphorylation levels of MEK1 with a similar time frame. On the other hand, PTH induced the expression of MAP kinase phosphatase 1 (MKP-1) in both time (detectable within 30 min and sustained for 90min) and concentration (from 10^{-11} to 10^{-7} M) dependent manner. These data showed that both PTH inhibition of the Raf-MEK pathway and PTH induction of MKP-1 expression can potentially mediate PTH inhibition of ERK1/2 activities in chondrocytes. To further elucidate the signaling pathway, we transiently transfected different mutant constructs in CFK-2 cells, and determined their effects on PTH inhibition of ERK1/2 activities. While a constitutively active mutant of c-Raf alleviated 50% of the PTH-dependent decrease of ERK1/2 phosphorylation, overexpression of the wild type, dominant negative mutant of MKP-1, or construct encoding the si-MKP-1 had no effect. These data demonstrated that PTH inhibition of ERK1/2 activities is mainly mediated by the Raf-MEK pathway. Furthermore, they suggested the central role of Raf-MEK-ERK signaling pathway in mediating PTH downregulation of Ihh in chondrocytes.

Disclosures: **L.P. Lai**, None.

SU043

Targeted *In Vivo* Measurements of Small Cartilage Defect Volumes in Knee Joint MRI's. **R. Vargas-Voracek¹**, **D. Steines^{*1}**, **J. Ryaby²**, **S. Liew¹**, **C. Arnaud¹**, **P. Hess¹**. ¹Imaging Therapeutics, Inc., Foster City, CA, USA, ²Orthologic, Corp, Tempe, AZ, USA.

There is clinical need for non-invasive imaging tools that are capable of detecting and evaluating cartilage defects as well as monitoring response to new cartilage repair therapies. Magnetic resonance imaging (MRI) has shown the greatest promise of all such tools motivating studies to determine whether it is accurate and reproducible enough to quantitatively measure the volume and thickness of cartilage tissue. Most work has focused on measurements of large cartilage volumes on *in-vitro* specimens without the effect of inter-scan or operator variability; the latter two effects being of practical clinical relevance. The purpose of this study is to obtain a quantitative assessment of the *in vivo* reproducibility of small and clinically relevant (up to 125mm diameter) cartilage defect measurements from MRI of the knee using image processing tools. We acquired sixteen baseline and short-term follow up knee-MRI scans in the sagittal and coronal planes from eight patients with three-dimensional spoiled gradient-echo (3D SPGR) sequences. The images were 256 by 256 pixels at 0.55mm by 0.55 mm pixel resolution and 1.5 mm slice spacing. Three operators with low, average and high skill levels segmented the cartilage regions from the images using image segmentation tools. Targeted defect volumes were selected and extracted randomly without overlap from the baseline segmented images. Baseline volumes were then compared

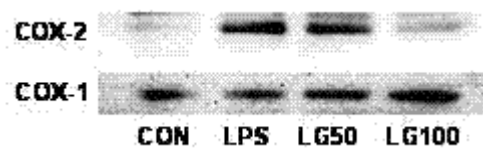
with volumes extracted from the same location in the corresponding follow-up images. Reproducibility was evaluated by comparing the defect volumes from baseline and follow-up scans through linear regression. For inter-scan reproducibility, results with 270 focal cartilage defect measurements show high measurement correlation (average R^2 of 0.95) between baseline and follow up scans. Intra and inter observer reproducibility showed consistent improvement with increased operator skill (R^2 (low) =0.95, R^2 (high) =0.99, average R^2 =0.96). In conclusion, we were able to quantitatively and reproducibly measure targeted small volumes from MRIs. Intra and inter observer reproducibility can be optimized and variability minimized by either increasing operator skill level or improving the automation of the segmentation process. The possibility for improving inter-scan reproducibility with higher MR scan resolution and 3D image processing algorithms further emphasizes the potential usefulness of MRI as a non-invasive tool for *in-vivo* quantitative assessment of cartilage disease, disease progression, and monitoring response to treatment.

Disclosures: **R. Vargas-Voracek**, None.

SU044

Naturally Occurring Selective Estrogen Receptor Modulators, Genistein, may Reduce the Production of Proinflammatory Molecules in Human Chondrocytes. **S. Hooshmand^{*1}**, **D. Y. Soung¹**, **S. V. Madhally^{*2}**, **L. Devareddy^{*1}**, **E. A. Lucas¹**, **B. H. Arimandi¹**. ¹Nutritional Sciences, Oklahoma State University, Stillwater, OK, USA, ²Chemical Engineering, Oklahoma State University, Stillwater, OK, USA.

Previously, we reported that cartilage is an estrogen receptor (ER) positive tissue and that mRNA levels of ER β increase in postmenopausal women with osteoarthritis. Based on our findings and those of other investigators, we hypothesize that local rather than circulating estrogen levels negatively affect chondrocyte metabolism and that selective estrogen receptor modulators (SERM) augment cartilage health. To test the latter part of our hypothesis, we have begun to explore the role of genistein, a naturally occurring SERM with high affinity to bind ER β , in inhibiting the lipopolysaccharide (LPS)-induced cyclooxygenase (COX)-2 but not COX-1 in human chondrocytes (HCH). Cells (PromoCell, Germany) were treated with three levels of genistein (0, 50, and 100 μ M). After one hour, the genistein-treated cells were stimulated by one μ g/mL LPS for six hours. Cells were then harvested and the cytosolic fraction was isolated for assessing COX-1 and COX-2 protein levels using Western blot. Our preliminary data indicate that the LPS-induced increase in COX-2 protein level is reduced by pretreatment of 100 μ M of genistein, whereas COX-1 protein level is not affected by genistein. These findings support our clinical study (Arimandi *et al. Phymed*, 11:567-575, 2004) that patients with osteoarthritis may benefit from consumption of soy isoflavones.



Disclosures: **B.H. Arimandi**, None.

SU045

Intact Caveolae and Caveolin-1 Are Required for $1\alpha,25(\text{OH})_2\text{D}_3$ Regulation of the Growth Plate. **B. D. Boyan^{*1}**, **L. Wang¹**, **K. Wong^{*1}**, **H. Yao^{*1}**, **R. E. Guldberg^{*1}**, **H. Jo^{*2}**, **Z. Schwartz¹**. ¹Georgia Institute of Technology, Atlanta, GA, USA, ²Emory University Medical School, Atlanta, GA, USA.

$1,25$ -dihydroxyvitamin D $_3$ [$1,25(\text{OH})_2\text{D}_3$] dependent PKC signaling in rat growth plate chondrocytes is mediated by a plasma membrane associated $1,25(\text{OH})_2\text{D}_3$ -binding protein, ERp60. Activation of PKC involves rapid increases in phospholipase A $_2$ and phospholipase C, both of which are found in lipid rafts/caveolae in many cells. Here, we examined the hypothesis that the caveolae microenvironment is required for ERp60 function and that caveolae play an important role in regulating growth plate physiology. Rat costochondral cartilage prehypertrophic/upper hypertrophic zone chondrocytes were examined for caveolae by transmission electron microscopy (TEM) and for caveolae proteins caveolin-1 (Cav-1), -2 and -3. TEM showed that the cells had caveolae and Western blots demonstrated that Cav-1, 2 and 3 were present. Resting zone chondrocytes, which do not exhibit a PKC response to $1,25(\text{OH})_2\text{D}_3$, also had Cav-1, 2 and 3 but their caveolae were fewer in number and were structurally larger. Confocal microscopy showed that ERp60 and Cav-1 were in the plasma membrane of growth zone cells, whereas the traditional nuclear vitamin D receptor (VDR) was found primarily in the nuclei. Beta-cyclodextrin (CD) was used to disrupt lipid rafts/caveolae and was found to block $1,25(\text{OH})_2\text{D}_3$'s stimulatory effects on PKC, alkaline phosphatase and [^{35}S]-sulfate incorporation. Growth plate chondrocytes from Cav-1 $^{-/-}$ mice did not respond to $1\alpha,25(\text{OH})_2\text{D}_3$, although wild type C57BL/6 cells exhibited $1,25(\text{OH})_2\text{D}_3$ -dependent increases in PKC, alkaline phosphatase, and proteoglycan production. Histology of tibial growth plates from 8-week-old male wild type and Cav-1 $^{-/-}$ mice showed marked differences. Cav-1 $^{-/-}$ growth plates were longer and had more hypertrophic cells in each column. Micro-CT analysis confirmed that the height of the growth plate was greater and showed that the cross-sectional area of the Cav-1 $^{-/-}$ growth plates was greater as well. These results indicate that the membrane mediated effects of $1,25(\text{OH})_2\text{D}_3$ via ERp60 require caveolae and Cav-1, and demonstrate the consequences of Cav-1 deficiency on growth plate physiology.

Disclosures: **B.D. Boyan**, None.

SU046

Expression of CaMK I β mRNA in Growth Plate Chondrocytes and Metaphysal Osteoblasts. M. E. Pedersen^{*1}, D. Fortunati¹, M. Nielsen^{*1}, S. H. Brorson^{*2}, O. P. Løseth^{*1}, L. S. H. Nissen-Meyer^{*1}, R. Paro^{*3}, A. Teti³, F. P. Reinholt², K. M. Gautvik⁴, R. Jemtland^{*5}. ¹Department of Biochemistry, Institute of Basic Medical Sciences, University of Oslo, Oslo, Norway, ²Institute of Pathology, National University Hospital, Oslo, Norway, ³Department of Experimental Medicine, University of L'Aquila, L'Aquila, Italy, ⁴Department of Biochemistry, Institute of Basic Medical Sciences University of Oslo, Ullevål University Hospital and Lovisenberg Hospital, Oslo, Norway, ⁵Endocrine Section, Dept. of Medicine, National University Hospital, Oslo, Norway.

The family of Ca²⁺/calmodulin-dependent protein kinases (CaM-kinases) are known to mediate many of the effects of Ca²⁺ as a second messenger in eukaryotic cells, which includes regulating signaling pathways involved in modulating various cellular functions such as proliferation, differentiation and gene expression. Our group has previously cloned CaMK I β , which belongs to the group of multifunctional CaM-kinases thought to be specifically enriched in the brain, from a hypothalamus subtraction cDNA library. In the present study, we characterized the localization of cells expressing mRNA for CaMK I β in mouse skeletal tissue *in vivo*, using *in situ* hybridization with digoxigenin labeled antisense RNA probes. We also assessed expression of CaMK I β mRNA in clonal and normal osteoblasts and chondrocytes of human and rodent origin by Real-Time PCR. *In situ* hybridization of whole embryos demonstrated that CaMK I β mRNA was most highly expressed in growth plate hypertrophic chondrocytes of long bones and also in hypertrophic chondrocytes of various other skeletal elements. In mouse hind limbs, expression of CaMK I β was sustained at similar high levels throughout the observation period (i.e. from embryonic day 16.5 until postnatal day 10). In addition, positive hybridization signals were detected in a subpopulation of cells with the appearance of osteoblasts situated along trabecular bone surfaces in the metaphysal region. Real-Time PCR of total RNA from primary mouse calvarial osteoblasts, rat UMR 106 osteosarcoma clonal cells and primary human chondrocytes derived from cartilage explants confirmed that CaMK I β is expressed in both chondrocytes and osteoblasts *in vitro*. Our data demonstrating unexpectedly high expression of CaMK I β in extraneural skeletal tissue, suggest a role for this protein in chondrocyte maturation and in osteoblast development.

Disclosures: **M.E. Pedersen**, None.

SU047

Premature Degenerative Joint Disease of the Knee in Mice Lacking Phosphoadenosine-Phosphosulfate Synthetase 2 Activity (Papss2): a Model of Human PAPSS2 Deficiency. A. F. Ford-Hutchinson^{*1}, Z. Ali^{*1}, R. A. Seerattan^{*2}, D. M. L. Cooper^{*3}, B. Hallgrímsson^{*4}, P. T. Salo^{*2}, F. R. Jirik^{*1}. ¹Biochemistry and Molecular Biology, University of Calgary, Calgary, AB, Canada, ²Surgery, University of Calgary, Calgary, AB, Canada, ³Archaeology and Medical Science, University of Calgary, Calgary, AB, Canada, ⁴Cell Biology and Anatomy, University of Calgary, Calgary, AB, Canada.

We investigated whether loss of Papss2 activity, a cause of degenerative joint disease in humans, would similarly lead to degenerative joint disease in mice. Murine brachymorphism (bm) results from an autosomal recessive mutation of the Papss2 gene that encodes 3'-phosphoadenosine 5'-phosphosulfate synthetase 2, one of the principal enzymes required for the sulfation of extracellular matrix molecules in cartilage and other tissues. A form of human spondylo-epimetaphyseal dysplasia has been identified in Pakistani kindred having a mutation of PAPSS2. These individuals have skeletal malformations, including short stature evident at birth, short bowed lower limbs (genu varum), brachydactyly, kyphoscoliosis (Ahmad, 1998). These individuals also demonstrate premature onset of degenerative joint disease. Animals homozygous for the Bm (Papss2) gene mutation on a C57BL/6 background were obtained from the Jackson Laboratory. Knee joints were analyzed by micro-computed tomography (micro-CT) analysis and histology. Compared to control 12-14 month old C57BL/6 mice that demonstrated minimal if any pathology, by 12 months both male and female brachymorph mice exhibited severe degenerative knee joint disease, with cartilage damage being most evident in the patello-femoral and medial compartments. Micro-CT imaging of Bm knees revealed skeletal malformations, including bowing of the fibula and tibia, bone remodeling of the patello-femoral groove, and variable remodeling of the tibial crest and tubercle. Whether brachymorph knee joint degeneration results primarily from a cartilage matrix abnormality (e.g. hyposulfation of proteoglycans), altered biomechanics associated with abnormal bone structure, abnormal muscle packing, or a combination of these features is not clear. The Bm mutant mouse thus represents a novel example of hereditary murine degenerative joint disease, and is also model of human PAPSS2 deficiency-associated arthrosis.

Disclosures: **A.F. Ford-Hutchinson**, None.

SU048

A Murine Epiphyseal Chondrocyte Model of ADAMTS 5- Mediated Aggrecanlysis. M. Stewart¹, A. J. Fosang^{*2}, C. B. Little^{*3}, J. D. Sandy^{*4}.

¹Veterinary Clinical Medicine, University of Illinois at Urbana-Champaign, Urbana, IL, USA, ²Paediatrics, University of Melbourne, Parkville, Australia, ³Raymond Purves Bone and Joint Research laboratories, University of Sydney, St Leonards, Australia, ⁴Shriners Hospital, Tampa, FL, USA.

This study assessed the utility of murine epiphyseal chondrocyte cultures for studying aggrecan synthesis and degradation. Distal femoral and proximal humeral epiphyses were collected from 4-day-old WT, NITEGE-null and ADAMTS-5-null mice. Chondrocytes were isolated by collagenase digestion and cultured as non-adherent aggregates in serum-free medium. Cultures were maintained for up to 12 days, with sample collections at 3-day intervals. GAG content in the pericellular and medium compartments was monitored by DMMB assays. Aggrecan expression and degradation were assessed by Western blot analyses of chondroitinase-treated lysates, using antibodies specific for the full-length protein and neopeptides created by ADAMTS activity. Expression of cartilage-linked ADAMTS genes (TSs 1, 4, 5, 8, 9 and 15) was determined by RT-PCR. Murine epiphyseal chondrocytes synthesized 60-80 ug GAG/million cells/3-days. Approximately 10% of total GAG was retained in the pericellular compartment while 90% was released into the medium. Aggrecan immunoblotting demonstrated spontaneous degradation of the full-length protein with neopeptide expression characteristic of ADAMTS activity. Chondrocytes from mice lacking the NITEGE motif were unable to cleave aggrecan in the amino-terminal interglobular domain, as expected, but exhibited an alternate aggrecanlysis profile. Epiphyseal chondrocytes expressed all six of the cartilage-linked ADAMTSs. However, chondrocytes isolated from mice lacking TS5 secreted full-length aggrecan with no evidence of aggrecan cleavage, indicating that aggrecan degradation in this model is dependent on TS5 activity. In conclusion, the neonatal murine epiphyseal chondrocyte model is a valuable tool for investigating aggrecan synthesis and turnover by ADAMTS proteases. Aggrecanase activity is an inherent property of the model, and does not require stimulation by retinoic acid or inflammatory cytokines. Comparisons of WT and KO chondrocytes emphasize the utility of this culture model for genetic and transgenic approaches to the investigation of aggrecan turnover. These analyses indicate that aggrecan cleavage by epiphyseal chondrocytes requires TS5 activity. Recent studies have shown the importance of TS5 in osteoarthritis. The epiphyseal model represents an ideal vehicle to investigate the pathways that regulate TS5 expression and activity, and test the efficacy of putative antagonists against this protease.

Disclosures: **M. Stewart**, None.

SU049

Insight into the Mechanisms of Bone Remodeling in Prostate Cancer Bone Metastasis. M. P. Roudier¹, C. Morissey^{*1}, L. M. Coleman^{*2}, L. D. True^{*3}, C. S. Higano^{*4}, P. S. Nelson^{*2}, S. M. Ott⁵, R. L. Vessella¹. ¹GU Cancer Research Lab, University of Washington, Seattle, WA, USA, ²Fred Hutchinson Cancer Research Center, University of Washington, Seattle, WA, USA, ³Pathology Dept, University of Washington, Seattle, WA, USA, ⁴Oncology Dept, University of Washington, Seattle, WA, USA, ⁵Medicine, Metabolism and Endocrinology, University of Washington, Seattle, WA, USA.

We collected bone samples from patients who died of PCa using a rapid autopsy procedure. Bone samples were submitted to bone histomorphometry and to gene expression profile analysis. Mean bone volume per biopsy was 30% and ranged from 3.72% to 72.60% (median 39.70%) of the total tissue volume. There is a wide variation of bone volume from one patient to another and from a biopsy to another in a given patient. Except in 2 patients (where mean bone volume was less than 20%), bone metastases were osteodense. In each bone biopsy, total bone consisted of lamellar bone, woven bone and osteoid. The volume of the lamellar trabecular bone, ranged from 0 % to 27.10% (median 9.4%) of the tissue volume. The volume of woven bone ranged from 0% to 70.3% (median 20%). There was woven bone formation in all patients. In 2 patients with osteolytic pattern, bone biopsies showed an osteoblastic remodeling with woven bone. Increased eroded surface (greater than 7% of the bone surface) was noted in 50% of the osteodense samples. Osteoclast number was increased and not correlated to bisphosphonate treatment. A SAM two-sample unpaired t-test comparing osteolytic metastases with osteoblastic metastases found no genes statistically different between the two groups. However, 347 genes were identified which exhibited >3 fold differences between the average ratios of the two groups and 6 genes were bone related. Among them, IGF-BP3 mRNA levels were higher in osteolytic than osteoblastic metastases. IGF-BP3 has been reported to influence bone remodeling. IGF-BP3 mRNA level decrease in osteoblastic prostate bone metastasis might induce a higher availability of IGF which in turn can increase osteoblast activity. These data suggest that CaP cells influence osteoblast activity by inducing a few known osteoblast signaling pathways. Inhibition of downstream targets should be investigated as it could result in inhibition of the CaP/Osteoblast interaction, which in turn might lead to the development of preventive agents and/or more effective therapies for advanced prostate cancer. The heterogeneity of prostate cancer bone metastases makes gene expression analyses much more difficult than those of the primary tumor.

Disclosures: **M.P. Roudier**, None.

SU050

Unanticipated Development of Cataract and Nephrotic Syndrome in Transgenic Rats Overexpressing Type III Na-Dependent Phosphate Transporter. A. Suzuki¹, K. Nishiwaki-Yasuda¹, J. Caverzasio², Y. Ono^{*1}, S. Sekiguchi¹, S. Nagao^{*3}, H. Takahashi^{*3}, M. Matsuyama^{*4}, K. Yan^{*5}, R. Kaneko^{*6}, M. Hirabayashi^{*6}, P. Ammann², R. Rizzoli², Y. Oiso^{*7}, M. Itoh^{*1}.

¹Division of Endocrinology, Fujita Health University, Toyoake, Japan, ²Service of Bone Diseases, University Hospital of Geneva, Geneva, Switzerland, ³Education and Research Center of Animal Models for Human Diseases, Fujita Health University, Toyoake, Japan, ⁴Department of Surgical Pathology, Fujita Health University, Toyoake, Japan, ⁵Department of Pediatrics, Kyorin University, Tokyo, Japan, ⁶National Institute of Physiological Sciences, Okazaki, Japan, ⁷Division of Metabolic Diseases, Nagoya University Graduate School of Medicine, Nagoya, Japan.

Type III sodium-dependent inorganic phosphate (Pi) transporter, Pit-1 (Glvrl-1), is a ubiquitous protein. Its expression was found to increase in a subpopulation of hypertrophic chondrocytes suggesting a role in bone development. The aim of the present study was to investigate the effect of Pit-1 overexpression on the development of different organs. Mouse Pit-1 gene was overexpressed under the control of CAG promoter in transgenic (Tg) rats. Na-dependent Pi transport was increased by 2.5-3 fold with no change in alanine uptake in primary cultured osteoblastic cells derived from calvaria of Tg compared with wild type (WT) animals. Skeletal development and body length were normal in Tg animals. Body weight was significantly decreased in Tg compared with WT rats, a difference that was more pronounced in male compared with female animals (8wks WT 378±42 g, Tg 296 ±30 g; 20wks control 551±50 g, Tg 441±30 g). An early onset of cataract development was observed after 2 to 8 wks of age. In addition, male Tg rats developed massive proteinuria at 20 wks of age (Tg 308±177 mg/day, WT 33±20 mg/day). This effect was associated with lower serum albumin levels (Tg 3.5±0.5 mg/day, WT 4.7±0.1 mg/day) and hyperlipidemia (Tg 237±99 mg/day, WT 99±14 mg/day). Proteinuria was detected at 3 months of age and glomerular deformity assessed by EM images already observed in kidneys of 8 weeks old Tg rats. Survival was much shorter in Tg rats with death already occurring between the 7 and 9 month of age. In conclusion, results presented in this study indicate that Pit-1 overexpression and high cellular Pi transport does not markedly influence skeletal development. However, it is associated with an early onset of cataract and alterations of the glomerular system leading to a nephrotic syndrome.

Disclosures: **A. Suzuki**, None.

SU051

Identification of the Genes Regulated by Extracellular Inorganic Phosphate in the Early Stage of Chondrocyte Differentiation. M. Kimata^{*1}, K. Tachikawa^{*1}, K. Ozono², T. Michigami¹. ¹Department of Environmental Medicine, Osaka Medical Center and Research Institute for Maternal and Child Health, Osaka, Japan, ²Department of Pediatrics, Osaka University Graduate School of Medicine, Osaka, Japan.

During endochondral bone formation, extracellular inorganic phosphate (Pi) as well as calcium plays important roles in mineralization and regulation of gene expression. In osteoblasts, it was reported that the expression level of osteopontin was increased in response to extracellular free Pi, suggesting that extracellular Pi might act as a signaling molecule on bone cells. Here we have attempted to identify the genes that respond to extracellular Pi in the early stage of chondrocyte differentiation. To address this issue, we utilized ATDC5 cells, a model for endochondral bone formation. ATDC5 cells were plated in the usual growth media, and 24 hours later, the medium was changed to those containing 1 mM or 10 mM Pi. After 24-hour incubation in 1 mM Pi or 10 mM Pi, total RNA was extracted and subjected to microarray analysis. There was no obvious difference in the viability of the cells between the two groups. The microarray analyses were performed three times, and the genes showing >1.5-fold increase or <0.66-fold decrease in expression on all the three microarrays were selected. Among 4285 genes, 15 genes showed at least 1.5-fold increase in expression when incubated in 10 mM Pi for 24 hours, while 98 genes exhibited <0.66-fold decrease. In the genes up-regulated in response to 10 mM Pi, 47% of them were classified in enzyme by functions, 7% structure, 13% transcription, and 7% apoptosis. On the other hand, in the genes down-regulated in response to 10 mM Pi, 35% of them were categorized in enzyme, 12% structure, 9% transcription, 1% cell cycle, and 4% transporter. The differential expressions of some genes identified were confirmed by reverse transcription-polymerase chain reaction (RT-PCR) analyses. The expression of alkaline phosphatase gene was markedly decreased when cultured in 10 mM Pi compared with the cells cultured in 1 mM Pi. Interestingly, the expressions of BMPs and TGF-β as well as collagens were also decreased within 24 hours in response to 10 mM Pi. The expression of type II collagen gene was also decreased, although a reporter assay demonstrated that the promoter activity of the gene was not suppressed in response to 10 mM Pi, suggesting that mechanism might be involved other than the direct action on the promoter activity. In summary, using ATDC5 cells of proliferation stage, we have identified some genes whose expression was altered in response to high concentration of extracellular Pi. The results suggest that chondrocytes of early stage might have a sensing system for extracellular Pi level.

Disclosures: **M. Kimata**, None.

SU052

Tracking the Osteoblast Lineage via the *In Vitro* Differentiation of Murine Embryonic Stem Cells. N. L. Woll^{*}, K. Dunham^{*}, C. Niyibizi^{*}, S. Bronson. Cellular and Molecular Physiology, Penn State College of Medicine, Hershey, PA, USA.

The process of bone formation can be observed in vitro, in the form of a mineralized nodule. Mesenchymal stem cells (MSCs), the immediate precursors to osteoprogenitors are found in the marrow, and likely in numerous other sites throughout the organism. Differentiation of these progenitors, when placed into culture under appropriate conditions, proceeds through characteristic stages of commitment, proliferation, matrix secretion and mineral deposition during a period of 3-4 weeks. We have developed an ESC-derived osteogenic culture system as a model of MSC commitment and differentiation. ESCs were allowed to form embryoid bodies (EBs). EBs were disrupted and plated at concentrations as low as 25 cells/cm². By 8 days post plating a significant percentage of the colonies had morphology characteristic of other types of osteogenic cultures. By three weeks in culture these colonies go on to form layered nodules. At 21 days cultures were fixed and stained using silver nitrate to identify mineralized colonies, and with methyl green to identify all other colony forming units. Generally 60% of the colonies are layered, mineralized nodules. We have isolated RNA from entire plates and individual colonies at different stages of the differentiation process and have used Quantitative Real Time PCR (QRT-PCR) to investigate the expression of genes characteristic of the osteoblast lineage as well as genes characteristic of other lineages and stem/progenitor cells. Runx2, Osterix, Type I Collagen and Osteocalcin are all transcriptionally upregulated by day 14 and continue to increase in expression out to 21 days. Twist1 and 2 both peak by approximately day 14 and are downregulated by 21 days in culture. Analysis of gene expression in the first week revealed that Brachyury, Twist2, Runx2 and Sox-9 are upregulated by day 4 of the osteogenic culture, with osterix expression increasing by day 7. QRT-PCR analysis of amplified RNA from individual colonies indicates that it is the morphologically osteogenic colonies that are expressing mRNA characteristic of the osteoblast lineage and allows us to further categorize colonies into hematopoietic, osteogenic, adipogenic, myogenic or a mixture of mesenchymal lineages. We have also investigated the impact of exposure to exogenous bone morphogenetic protein 2 (BMP-2) at various points in the differentiation process. Exogenous BMP2 added prior to day 5 of the osteogenic culture disrupts mesenchymal differentiation. We hypothesize that a critical decision point involving the mesenchymal lineages occurs somewhere between day 4 and day 5 of the osteogenic culture.

Disclosures: **N.L. Woll**, None.

SU053

Defining Embryonic Stem Cell Derived Therapeutic Osteogenic Populations. J. E. DeMarco^{*1}, J. D. Heaney^{*2}, N. L. Woll^{*1}, S. K. Bronson¹. ¹Cellular and Molecular Physiology, Penn State College of Medicine, Hershey, PA, USA, ²Case Western Reserve University, Cleveland, OH, USA.

We are initiating a new series of experiments to test the in vivo osteogenic capacity of our murine embryonic stem cell (ESC)-derived osteogenic cultures. Transfer of murine ESCs beneath the kidney capsule or subcutaneously results in a teratoma, reflecting the pluripotent differentiation capacity of embryo-derived stem cells. Conversely, mature osteoblasts while phenotypically stable have restricted proliferative potential and thus limited therapeutic capacity for degenerative, congenital or traumatic bone loss. The goal of these experiments is to determine where in the in vitro differentiation of ESCs to mature osteoblasts we can isolate and transfer a cell population with therapeutic capacity. Cells have been engineered to express EGFP in mature osteoblasts under control of the human osteocalcin gene regulatory sequences contained on a bacterial artificial chromosome (BAC). Progenitors derived from this ESC line will be used to assess the presence of mature, donor-derived osteoblasts in our transplants. Cells will be tested in three different contexts: loading in synthetic scaffolds with subsequent subcutaneous transfer, intravenous injection, and intramedullary injection, with the goal of narrowing down the window of time when cells from osteogenic cultures are capable of engrafting and synthesizing bone matrix. These experiments will provide critical proof of concept for the future use of human ESCs for osteogenic therapies.

Disclosures: **J.E. DeMarco**, None.

SU054

Expression of CD24 in Intravertebral Disk. N. Fujita^{*1}, T. Miyamoto¹, J. Imai^{*2}, N. Hosogane^{*3}, M. Yagi^{*1}, K. Morita^{*3}, K. Ninomiya^{*1}, T. Suzuki^{*1}, K. Chiba^{*3}, S. Watanabe^{*2}, Y. Toyama^{*3}, T. Suda^{*1}. ¹Cell Differentiation, Keio University School of Medicine, Shinjuku, Japan, ²Clinical Informatics, Tokyo Medical and Dental University, Bunkyo, Japan, ³Orthopaedics Surgery, Keio University School of Medicine, Shinjuku, Japan.

Low back pain is one of the most common diseases and constitutes a devastating economic burden on the individual and society. Degeneration of the intervertebral disc (IVD) based on aging is considered as a cause of low back pain, however, the molecular mechanism of IVD degeneration is still unclear. In order to reveal what molecules are expressed in annulus fibrosus (AF) and nucleus pulposus (NP), both of which are the component of IVD, we performed microarray analysis in independent tissues including AF and NP in adult rats. We identified that CD24 was highly expressed in NP compared with other tissues. CD24 is a cell surface glycosyl-phosphatidylinositol-anchored protein. It was reported to be expressed physiologically in pre-B cell, T cell, keratinocyte and renal tubular epithelium. The CD24 expression in NP and its tissue distribution was confirmed

ASBMR 27th Annual Meeting

by real-time PCR analysis and immunohistochemical analysis. The CD24 expression was also detected in notochord from which NP develops and its expression level was not changed in NP between 3 to 40 week old rats, although the expression of chondrogenic extracellular matrix proteins, type2 collagen and aggrecan were reduced as aging. CD24 expression was also detected in the hemiated NP as well as the remaining NP in the rat. These results suggested that CD24 is the useful marker to detect the NP and notochordal cells. CD24 was reported to function as a ligand of P-selectin and was expressed in wide variety of malignant tumors such as epithelial ovarian cancer, breast cancer and prostate cancer. We found that CD24 is also expressed in the human chordoma. Chordoma is the common primary malignant neoplasm of the skeleton and is considered to be a notochordal origin. Since the CD24 expression was not detected in chondrosarcomas, CD24 is a new diagnostic marker for chordoma to distinguish from chondrosarcoma. We propose that CD24 is a significant molecular marker for NP, including chordoma.

Disclosures: N. Fujita, None.

SU055

Enhanced Runx2 Expression Is Accompanied with Degenerative Changes in Canine Intervertebral Disc. H. Ito^{*1}, Y. Asou², S. Takeda³, Y. Hara^{*1}, Y. Nezu^{*1}, Y. Harada^{*1}, H. Haro^{*4}, H. Komori^{*2}, M. Tagawa^{*1}, K. Shinomiya^{*2}.

¹School of Veterinary Medicine, Nippon Veterinary and Animal Science University, Division of Veterinary Surgery, Tokyo, Japan, ²Tokyo Medical and Dental University, Department of Orthopaedic Surgery, Tokyo, Japan, ³Tokyo Medical and Dental University, Center of Excellence program for Frontier Research Program on Molecular Destruction and Reconstruction of, Tokyo, Japan, ⁴Graduate School of Medicine, University of Yamanashi, Department of Orthopaedic Surgery, Yamanashi, Japan.

Degeneration of the intervertebral disc (IVD) is an underlying etiology in many of spine disorders including intervertebral disc herniation (DH). However, the mechanisms for the degenerative process in the IVD are not well understood. Runx2 is a transcriptional factor that upregulates type X collagen and promotes hypertrophic differentiation of the chondrocyte, both of which are typically observed in degenerated IVD. Therefore, to understand the molecular mechanisms that lead to cartilage degeneration during the progression of disc degeneration, we have investigated the expression of the transcription factor Runx2 in intact or degenerated IVD. Tissue samples were surgically collected from the disc materials of canine disc herniation patients (dachshund, ages 4-7 years, 4-8kg). As control, annulus fibrosus (AF) and the nucleus pulposus (NP) from normal dogs were both collected from young, skeletally mature, beagle dogs (age 1-2 years, 10-12kg). Each sample was divided into two blocks, one for histological analysis, another for RT-PCR analysis. Histological analysis revealed that extruded NP from DH patients showed low proteoglycan content and abundant hypertrophic chondrocyte-like cells. Additionally, immunohistological analysis indicated that the expression of Type II collagen, an essential constituent of the healthy NP, was decreased, whereas the expression of type I and type X collagen, the markers of cartilage degeneration, were enhanced in NP from DH patients. To investigate the contribution of Runx2 in canine bone and cartilage metabolism, complete length of canine Runx2 cDNA sequence was determined with 3'- and 5'-rapid amplification of cDNA ends (RACE) procedure from canine bone tissue. Canine Runx2 cDNA showed over 97% conservation with human RUNX2. Interestingly, RT-PCR analysis demonstrated that Runx2 transcript was specifically expressed in the NP from DH patients, while no expression was detected in control. These results indicate that Runx2 was specifically expressed in herniated IVD, and may contribute to degenerative changes of the IVD.

Disclosures: H. Ito, None.

SU056

Betula Platyphylla var. Japonica Inhibits Interleukin-1 α Induced Cartilage Metabolism, Viability, and Morphology in Rabbit Articular Cartilage. D. Kim^{*1}, J. E. Huh^{*2}, Y. H. Baek^{*2}, J. D. Lee^{*2}, D. Y. Choi^{*2}, D. S. Park^{*2}, M. Yoo^{*3}. ¹Internal Medicine, Kyung Hee University Hospital, SEOUL, Republic of Korea, ²Oriental Medicine Research Center for Bone & Joint Disease, Kyung Hee University, SEOUL, Republic of Korea, ³Orthopedic Surgery, Kyung Hee University Hospital, SEOUL, Republic of Korea.

Articular cartilage is a potential target for drugs designed to inhibit the activity of matrix metalloproteinases (MMPs) to stop or slow the destruction of the proteoglycan and collagen in the cartilage extracellular matrix. Many cartilage protective agents have been developed from natural products. *Betula platyphylla* var. *japonica* (*B. platyphylla*), is one of these natural products, and is widely distributed in Korea, Japan, China, Sahalin, and Siberia. The bark of *B. platyphylla* has been used in folk medicine for the treatment of arthritis, cancer, nephritis, dermatitis, poisoning, and chronic bronchitis. The purpose of this study was to investigate the effects of *B. platyphylla* in inhibiting the release of glycosaminoglycan (GAG), the degradation of collagen, and MMP activity in rabbit articular cartilage explants. The cartilage-protective effects of *B. platyphylla* was evaluated by using GAG degradation assay, collagen degradation assay, colorimetric analysis of MMP activity, measurement of lactate dehydrogenase activity and histological analysis in rabbit cartilage explants culture. Interleukin-1 α (IL-1 α) rapidly induced GAG, but collagen was much less readily released from cartilage explants. *B. platyphylla* significantly inhibited GAG and collagen release in a concentration-dependent manner. *B. platyphylla* dose-dependently inhibited MMP-3 and MMP-13 expression and activities from IL-1 α -treated cartilage explants cultures when tested at concentrations ranging from 0.02 to 0.2 mg/ml. *B. platyphylla* had no harmful effect on chondrocytes viability or cartilage morphology in cartilage explants. Histological analysis indicated that *B. platyphylla* reduced the degradation of the cartilage matrix compared with that of IL-1 α -treated cartilage explants. These results indicate that *B. platyphylla* inhibits the

degradation of proteoglycan and collagen through the down-regulation of MMP-3 and MMP-13 activities without affecting the viability or morphology of IL-1 α -stimulated rabbit articular cartilage explants.

Disclosures: D. Kim, None.

SU057

Biological Effects of a Self-Setting Alpha-TCP on Osteogenesis in Combination with Dental Implant Placement. M. Nakadate^{*1}, N. Amizuka², S. Nomura^{*1}, T. Maeda^{*2}. ¹Division of Aging and Fixed Prosthodontics, Niigata University Graduate School of Medical and Dental Sciences, Niigata, Japan, ²Division of Oral anatomy, Niigata University Graduate School of Medical and Dental Sciences, Center for Transdisciplinary Research, Niigata, Japan.

This study aimed to evaluate the biological effects of a self-setting alpha-tricalcium phosphate (α -TCP) bone substitute on new bone formation in the concomitant presence of dental implants. 4-weeks-old male Wistar rats had their first and second maxillary molars removed, and dental implants were inserted in the healed extraction area after four weeks. Standardized bone defects surrounding the dental implants were filled with self-setting α -TCP for stabilization. The treated rats were perfused with an aldehyde solution at 1, 2, 4, and 8 weeks post-operatively, and the maxillae were processed for histochemical examination. Bone mineral density (BMD) was measured by peripheral quantitative computed analysis. Bone formation was assessed in two areas: (1) the interface between α -TCP and the implants, and (2) the surface of α -TCP corresponding to the previous alveolar ridge. At the α -TCP/implant interface, new bone formation was showed to progress from the cavity-bottom toward the alveolar ridge. Tartrate-resistant acid phosphatase (TRAPase)-reactive osteoclasts arrived into the narrow α -TCP/implant interface, followed by the migration of alkaline phosphatase (ALPase)-positive osteoblasts that covered thin new bone matrices. Osteopontin-reactive reversal lines on the α -TCP were observed in relation with the invading osteoclasts. On the surface of α -TCP corresponding to the previous alveolar ridge, consistent with the findings at the α -TCP/implant interface, osteoclastic resorption on α -TCP preceded ALPase-positive osteoblastic bone deposition. Moreover, the new formed bone appeared to share the features of compact rather than woven bone, as evidenced by the BMD values (874 \pm 140 and 918 \pm 104 mg/cm² at 4- and 8-weeks, respectively). Thus, bone deposition onto α -TCP was coupled with previous bone resorption, which may give rise to a tissue structure similar to that of compact bone, the gold standard for "bone quality". Our findings suggest that a self-setting α -TCP might be a reliable bone substitute when combined with dental implant placement.

Disclosures: M. Nakadate, None.

SU058

Enhancement of Osteogenesis on NaOH-Treated PLGA Scaffolds. W. Huang, J. Roostaean^{*}, S. David^{*}, K. Ishida^{*}, G. H. Rudkin^{*}, D. T. Yamaguchi, T. A. Miller^{*}. VA Medical Center of West Los Angeles, Los Angeles, CA, USA.

Chemical etching of scaffolds using NaOH could result in a more hydrophilic surface, increased surface area, altered porosity and pore size, and a greater degree of nanometer roughness. These features might provide a more favorable environment for proliferation and differentiation of bone marrow stromal cells. Treatment of PLGA with NaOH has been shown to enhance osteoblast and chondrocyte function. We assessed the effect of NaOH on osteogenic differentiation by studying rabbit bone marrow stromal cells and mouse pre-osteoblastic MC3T3-E1 cells. PLGA films or scaffolds were treated with 1 N NaOH for 10 minutes. Cells were cultured on NaOH treated PLGA film and scaffolds and their untreated counterparts. NaOH treatment significantly enhanced osteogenic differentiation in both cell types cultured in 3-D scaffolds as measured by increases in mRNA expression of osteocalcin, osteopontin, bone sialoprotein, and Type I collagen. Minimal effect by NaOH was observed on both cell types cultured on 2-D PLGA films. Secretion of alkaline phosphatase was also significantly higher in both cells cultured in treated scaffolds. NaOH treatment also enhanced mineralization of rabbit bone marrow stromal cells cultured in 3-D scaffolds as revealed by von Kossa staining. Treatment of PLGA films with NaOH, however, showed little effect on mineralization of bone marrow stromal cells. These results indicate pretreatment of scaffolds with NaOH stimulates osteogenic differentiation in both undifferentiated bone marrow stromal cells and partially differentiated pre-osteoblastic cells.

Disclosures: W. Huang, None.

SU059

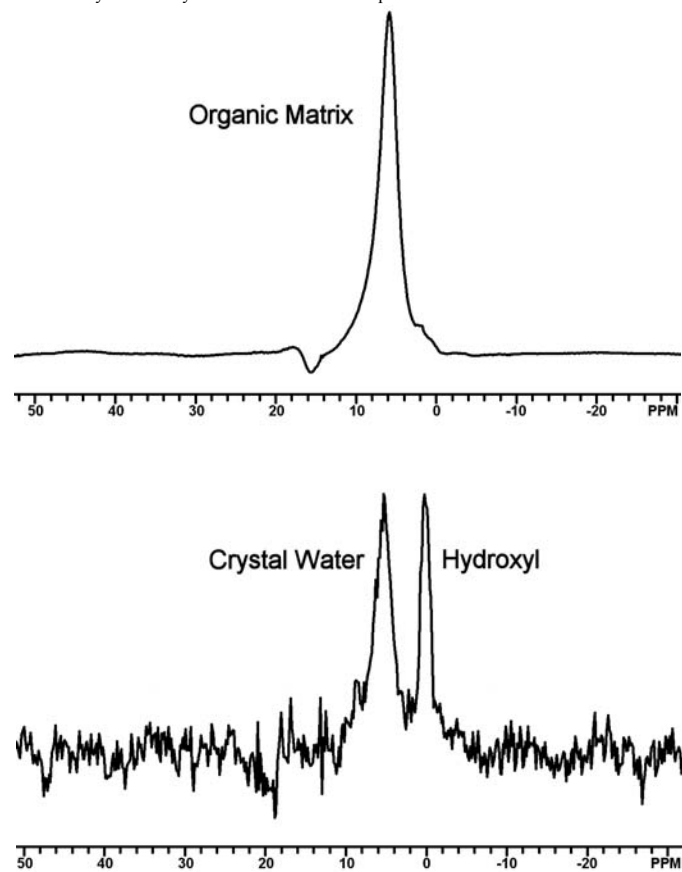
Hydroxyl Ions in Bone Mineral Observed By 1D ³¹P-¹H NMR Spectroscopy. Y. Wu¹, J. L. Ackerman^{*2}, L. Graham^{*1}, M. J. Glimcher¹.

¹Orthopaedic Surgery Department, Children's Hospital, Boston, MA, USA,

²Radiology Department, Massachusetts General Hospital, Boston, MA, USA.

Solid state NMR spectroscopy has recently proved extremely useful in helping to resolve the longstanding controversy over the hydroxyl ion content of bone mineral crystals. Previous 2D ¹H-³¹P heteronuclear correlation NMR methods have detected OH⁻ ion in bone mineral, but due to their two dimensional nature, these measurements are time consuming (about 24 hrs/spectrum). Here we demonstrate a novel one dimensional solid state ³¹P-¹H reverse cross polarization (CP) NMR method that substantially speeds up the measurement of structural OH⁻ ion in bone mineral. In the new method, polarization is transferred from ³¹P to ¹H, the reverse of conventional CP. Because the magnetization transfer rate is inversely proportional to the sixth power of the internuclear distance, only those signals arising from protons located within atomic distances of phosphorus will yield

signal, insuring that only mineral crystal proton signals are observed. Experiments were carried out on powdered synthetic HA (hydroxyapatite) and 27 week old chicken bone samples on a 600 Mz Bruker NMR spectrometer. Conventional single pulse proton spectra contain signals from all components of the sample (Fig. 1), but the crystal OH⁻ and water signals are obscured. Using the new technique (Fig. 2) the matrix signals are completely suppressed and the OH⁻ and interfacial/crystal water signals from the mineral are readily observed. Peak assignments were determined by comparing CP spectra of bone and HA, and further confirmed by experiments in which the CP contact was turned off, causing these peaks to disappear. One CP spectrum can be obtained in 3 hr for ~ 110 mg of bone specimen powder with good signal to noise ratio. This study further confirms the existence of OH⁻ in bone mineral crystals and demonstrates that the measurement time can be dramatically reduced by 1D ³¹P-¹H reverse CP experiments.



Disclosures: Y. Wu, None.

SU060

Oxandrolone Weakly Stimulates Osteoblast Differentiation. L. X. Bi, G. L. Klein, E. G. Mainous, W. L. Buford*, D. N. Herndon*. Depts. of Surgery, Pediatrics and Orthopaedics & Rehabilitation, The University of Texas Medical Branch and Shriners Hospitals for Children, Galveston, TX, USA.

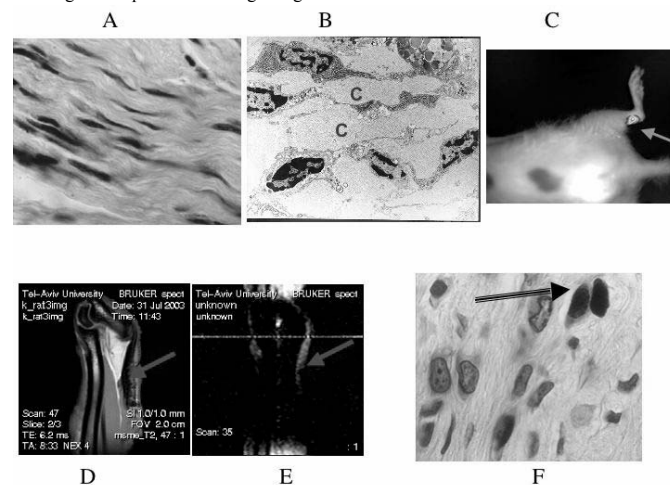
Previous studies have shown that Oxandrolone increases nuclear translocation of androgen receptor and stimulates collagen type I synthesis in vitro (Bi LX et al, JBMR 19: SU489 Suppl. 1, 2004), and in burned children increases lean body mass at 6 mo and bone mineral content at 1 yr post-burn (Murphy KD et al, Surgery 2004;136:219-224). In the present study, we examined expression of osteocalcin and alkaline phosphatase activity (ALP). Human osteoblast cells were cultured in a-minimum essential medium [a-MEM] and 10% fetal bovine serum with or without oxandrolone at the concentration of 5ug, 10ug and 15ug/ml, respectively, for 24 hr. The levels of ALP were assayed using a commercial kit. Expression of osteocalcin (polyclonal antibody, Santa Cruz Biotechnology, Inc. CA) was examined using immunoquantitative assay. ALP activities were elevated (11-20%, P<0.05) in oxandrolone-treated group, compared to control group. Expression of osteocalcin was increased (12-18%, P<0.05) after oxandrolone treatment. While there is a statistically significant increase in both osteocalcin and alkaline phosphatase following oxandrolone stimulation, the increase is small when compared to the magnitude of the dose given. These data suggest that the observed increases in bone mineral content with long-term oxandrolone therapy may be unrelated to direct effects of oxandrolone on osteoblasts.

Disclosures: L.X. Bi, None.

SU061

Neotendon Formation Induced by the Manipulation of Smad8 and BMP2 in Mesenchymal Stem Cells. A. Hoffmann*, G. Pelled*, G. Turgeman*, P. Eberle*, Y. Zilberman*, H. Shinar*, K. Keinan-Adamsky*, A. Winkel*, S. Shahab*, G. Navon*, G. Gross*, D. Gazit*. ¹Signaling and Gene Regulation, Gesellschafter Biotechnologische Forschung (GBF), Braunschweig, Germany, ²Skeletal Biotech Laboratory, Hebrew University of Jerusalem, Jerusalem, Israel, ³School of Chemistry, Tel Aviv University, Ramat Aviv, Tel Aviv, Israel.

Members of the Bone Morphogenetic Protein (BMP) family have been shown to have a role in tendon formation in vivo. To date, no specific Smad molecule has been identified to mediate such an effect in mesenchymal stem cells (MSCs). In this study, we defined a novel mechanism that mediates the differentiation of MSCs into tendon based on the expression of Smad8 and BMP2. Smad8 and BMP2 were co-transfected to MSCs. The in vitro phenotype of the engineered MSCs was evaluated using RT-PCR, histochemistry and morphology. In addition, the cells were implanted in vivo in ectopic sites and in tendon defects in order to assess their potential in tendon regeneration. 5 weeks post implantation the area of the implantation was isolated and analyzed. Cell survival in the implantation site was non-invasively and quantitatively demonstrated in vivo by the detection of Luciferase bioluminescence. Our results indicated a **tenocytic phenotype** of the engineered MSCs that over expressed the characteristic genes Six1, EphA4 and Scleraxis. Formation of tendon tissue in vivo was confirmed by the finding of dense connective tissue with parallel-organized fibers and spindle shaped cells (A). Electron microscopic analysis showed tightly packed collagen fibers (B). Moreover, we were also able to repair Achilles tendon defects with the engineered MSCs. Bioluminescence imaging monitored cell survival in the operated tendon, and immunohistochemical staining detected the labeled implanted cells in site (C & F). DQF MRI analysis proved that highly ordered collagen fibers were formed in the site of implantation as opposed to the control group (D, E). Since the expression of BMP2 is known to drive MSCs to osteogenic differentiation, we propose that the expression of Smad8 in MSCs induces an inhibition of the BMP2 signaling pathway, resulting in the differentiation of MSCs into tendon cells. This is the first study showing that a specific Smad signaling molecule is involved in tendon formation.



Disclosures: G. Pelled, The study is supported by FP-6 of the EU in the GENOSTEM consortium 2.

SU062

Connective Tissue Growth Factor (CTGF/CCN2) Enhanced Human Bone Marrow Stromal Cell Attachment In Vitro and Migration and Survival of the Cells in a Hydroxyapatite Scaffold In Vivo. M. ONO*, W. Sonoyama, K. Akiyama*, T. Fujisawa*, T. Nishida, M. Takigawa, T. Kuboki*. Okayama University Graduate School of Medicine, Dentistry and Pharmaceutical Sciences, Japan, Okayama, Japan.

For establishment of bone regeneration in a large scale, adhesion of osteogenic cells (e.g., bone marrow stromal cells: BMSC) to a scaffold, osteoblastic differentiation of the cells and angiogenesis into the scaffold would be necessary. We have previously reported that connective tissue growth factor (CTGF/CCN2) promotes osteoblasts proliferation and differentiation, as well as vascular endothelial cell migration. These results suggest a possibility that CTGF/CCN2 with autologous BMSC transplantation may be useful to accelerate bone formation and to overcome the hypoxia inside of the scaffold. Therefore, we investigated 1) effects of CTGF/CCN2 adsorption to hydroxyapatite (HA) disks on initial human bone marrow stromal cell (hBMSC) attachment in vitro, 2) effect of CTGF/CCN2 addition to a porous hydroxyapatite/hBMSCs hybrid on cells migration and survival of the hBMSCs inside of the hybrid in vivo. The hBMSCs were isolated from human iliac bone marrow of a volunteer and their multipotent (osteoblastic and adipogenic) differentiation abilities were confirmed. Recombinant human CTGF was adsorbed onto HA disks according to Shimo et al. Then the hBMSCs were seeded and allowed to attach onto CTGF-treated disks for 3 hours under a serum-free condition. Disks treated without CTGF were served as control. After removal of non-attached cells, the relative attached cell number was estimated by MTS assay. In addition, the hBMSCs were incubated with or without anti- α V β 3 integrin antibody for an hour prior to cell seeding, and the same cell-

attachment-assay was done. Mean value of four wells in each condition was calculated and statistically analyzed by one-way factorial ANOVA followed by Scheffe's multiple comparison tests. Next, hBMSCs were incubated to attach onto porous HA blocks (Pentax Co., Japan) for a week. The porous HA/hBMSCs hybrids were implanted subcutaneously in nude mice (4 week-old) with CTGF (1 μ g) or distilled water (control). The implants were harvested after 4 weeks for SEM observation. CTGF (100ng/ml) adsorption onto the HA disks significantly enhanced the cell attachment, while the anti-integrin-subunit antibody partially suppressed the enhancement. SEM observation supported that hBMSC-like cells migrated and survived inside of the porous HA scaffold with CTGF application, while without CTGF, no viable cells were observed inside of the scaffold. These results suggested that CTGF enhanced hBMSC attachment onto HA disks *in vitro*, and migration and survival of the cells inside of the HA scaffold *in vivo*.

Disclosures: **M. Ono**, None.

SU063

Effects of Ultrasound Stimulation on the Proliferation and Metabolism of Cementoblasts *In Vitro*. **D. A. Dalla-Bona¹, E. Tanaka^{*1}, H. Oka^{*2}, E. Yamano^{*1}, N. Kawai^{*1}, M. Miyauchi^{*2}, T. Takata², K. Tanne^{*1}.** ¹Department of Orthodontics and Craniofacial Developmental Biology, Hiroshima University

Graduate School of Biomedical Sciences, Hiroshima, Japan, ²Department of Oral Maxillofacial Pathology, Hiroshima University Graduate School of Biomedical Sciences, Hiroshima, Japan.

Root resorption is an adverse outcome of orthodontic tooth movement. Recently, it has been shown that ultrasound (US) stimulation accelerates repair of orthodontically induced root resorption in *in vivo* human study. However, the mechanism by which US achieves these outcomes is not clear. Cementoblast is one of the cells involved in root repair process. The aim of the present study was, thus, to evaluate the effect of US exposure on proliferation and metabolism of cementoblast *in vitro*. Cultured cementoblasts, mouse cementoblastic cell line (OCCM-30), received US exposure (frequency = 1 MHz; intensity = 100, 150 or 400mW/cm²) or sham exposure for 15 min per day for 4 days, and then assayed for cell proliferation and calcium concentration. Expression levels of osteocalcin (OCN), bone-sialoprotein (BSP), alkaline phosphatase (ALP) and osteopontin (OPN) were analyzed by real time-PCR. Furthermore, we investigated the effects of US exposure on the gene expression of interleukin-1 beta (IL-1B), interleukin-6 (IL-6), OPG and receptor activator of NF-kappa B ligand (RANKL). US exposure had no effect on cell proliferation. Calcium concentration was statistically increased (p<0.05) after US exposure at 100 or 150 mW/cm² compared with control. US exposure had no effect on transcripts for OPN, OCN and BSP. In contrast, ALP mRNA levels were significantly (p<0.05) increased by US stimulation with 150 mW/cm². Expression levels of IL-1 B, IL-6, OPG and RANKL were not significantly altered by US. These results demonstrate that US alters cementoblast function *in vitro* and may be an important candidate as a medical remedy to accelerate repair of root resorption.

Disclosures: **D.A. Dalla-Bona**, None.

SU064

Evaluation of the Efficacy of Vitamin D3 and its Metabolites to Prevent Thiram-Induced Growth Plate Dysplasia in Chickens. **N. C. Rath¹, W. E. Huff^{*1}, G. R. Huff^{*1}, R. L. Horst^{*2}.** ¹PPPSRU, USDA, ARS, Fayetteville, AR, USA, ²NADC, USDA, ARS, Ames, IA, USA.

Tibial dyschondroplasia (TD) is a metabolic disorder in rapidly growing broiler chickens and turkeys that is characterized by the failure of growth plate cartilage to be replaced by bone. Although the natural etiology of the disease is not understood, it has been suggested that diets supplemented with certain vitamin D metabolites could ameliorate TD in birds that were induced TD feeding Ca: P imbalanced diets. We have currently developed an experimental model of TD using tetramethyl thiram disulfide (thiram), a dithiocarbamate pesticide, which when included in the diet at a concentration of 100 ppm between 1-3 week of age induces TD in more than 90% of chickens. Using this model the objective of our study was to evaluate the ability of vitamin D₃ or its selective metabolites to prevent TD in chickens. Groups of broiler chickens were fed control or diets supplemented with vitamin D₃ or its different metabolites over and above the content of vitamin D₃ in the control diet. The study consisted of birds that were fed *ad libitum* (a) control non supplemented feed, (b) vitamin D₃, 4,000 IU cholecalciferol / kg, (c) HYDTM, a 25 (OH)₂ D₃, 63 μ g / kg, (d) low dose 1, 25 (OH)₂ D₃: 1 μ g / kg, and, (e) high dose 1, 25 (OH)₂ D₃: 5 μ g / kg, starting from day of hatch. On day 7 feed was withdrawn for a period of 12 h after which each group was divided into two sub groups of 25 birds each. One received its assigned diet while the other received the same diet containing 100 ppm thiram for a period of 48 h. At the end of experimental thiram feeding, all birds in each group received their assigned diets until the day of necropsy on day 15. The birds were weighed, bled prior to necropsy and the tibial growth plates were evaluated for TD index (incidence times severity score) (scores: 0= normal, 1= growth plate width increased more than 2 times, and 2= growth plate size increased more than 3 times). Some growth plates were processed for histological evaluations. In all birds that received thiram treatment, regardless of vitamin D treatment, the body weight was significantly reduced (p \leq 0.005) and the TD index remained high (\geq 1.7) as compared to \leq 0.2 in birds that did not receive thiram. Thiram caused chondrocyte apoptosis and blood capillary atrophy in the hypertrophic zone. It is concluded that extra supplementation of vitamin D or its metabolites do not protect birds against thiram-induced TD.

Disclosures: **N.C. Rath**, None.

SU065

Effects of Halogenated Hydrocarbons and Electromagnetic Field on Bone Tissue. **Z. Valkusz¹, L. Gáspár^{*1}, M. Radács^{*2}, A. Juhász^{*3}, A. Petri^{*4}, M. Gálfi^{*2}.** ¹Dept. of Endocrinology, University of Szeged, Szeged, Hungary, ²Environmental Protection Group, Faculty of Juhász Gyula Teacher Training College, Szeged, Hungary, ³Department of Psychiatry, University of Szeged, Szeged, Hungary, ⁴Department of Surgery, University of Szeged, Szeged, Hungary.

The formation and eventually the functionality of the osteocytes are determined by the modifications of extracellular environment. The structure of bone tissue is changed after hexa-chlorobenzene (HCB) or electromagnetic field (EMF) treatment. The chemical potential of HCB is low, because this agent has nonreactive activities. These facts can cause the main biological effects of HCB: eg. depuration into different organisms and can modify biological food cascades. The biological effects of EMF depend on its energy content, frequency, wave-length. Thus environmental effects (chemical and/or physical) play a very important role among the factors inducing osteoporosis. We have investigated how they effect the bone structure by extremely low doses (eld) of HCB diet, and of eld-EMF chronic treatment. Wistar rats (male, 100-250g/bw.) were treated orally with chlorobenzenes (HCB 0,5 μ g/bw. kg) for 30 and 60 days. We administered the compound through gastric tubes. The HCB pretreated rats were then exposed to eld EMF (50 mT, 60Hz) for further 30 days. The investigated were taken from the bone (femur) tissues of treated and control animals. Tissue structure and Ca²⁺ content of the bone, and liver function were estimated by determination of γ GT, SGOT, SGPT). Bone structure were investigated by morphometry. As a result of the chronic chlorobenzene treatment (60 days) showed significant changes in the femur. This modification of bone tissue consisted of significant change in the Ca²⁺ content of the bone matrices. After the combined treatment (HCB pretreating + eld-EMF exposition) femur samples showed no differences than that of the control animals. The eld-EMF alone has not caused significant changes according to the examined parameters. From our results we suppose that the EMF treatment can protect the degenerative effects of HCB on bone structure.

This work was supported by: ETT 61/2003 and ETT 270/2003.

Disclosures: **Z. Valkusz**, None.

SU066

gp130-Mediated Signaling Is Important for the Normal Morphogenesis of Meckel's Cartilage and Subsequent Mandibular Development. **J. W. Choi^{*1}, J. T. Kim^{*1}, J. Y. Choi², S. Y. Kim², E. K. Park², H. I. Shin¹.** ¹Oral Pathology, School of Dentistry, Kyungpook National University, Daegu, Republic of Korea, ²Skeletal Diseases Genome Research Center, Kyungpook National University, Daegu, Republic of Korea.

gp130-Mediated signaling is involved in both chondrogenesis and osteogenesis, but its direct role in the mechanism of embryonic Meckel's cartilage and associated mandibular development has not yet been elucidated. In this study, we examined the influence of gp130 ablation on the developing mandibular Meckel's cartilage by evaluating the morphological and histological changes as well as the gene expression patterns in developing embryonic *gp130*^{-/-} mice. The ablation of the gp130 gene showed no change in region-specific collagen mRNA expression except for a slight delay in its expression but caused shortened embryonic Meckel's cartilage, delayed hypertrophic chondrocyte maturation and subsequent bony replacement with characteristic bending of the intramandibular Meckel's cartilage. The bending of Meckel's cartilage leads to a narrow mandibular arch at the rostral area with poor cortical plate formation. These findings indicate that gp130-mediated signaling is important for the normal morphogenesis of Meckel's cartilage and subsequent mandibular development.

Disclosures: **H.I. Shin**, None.

SU067

Both Risedronate and PTH Maintain Bone Mechanical Properties and Matrix Composition in a Mouse Model of Glucocorticoid-Induced Osteoporosis. **G. Balooch^{*1}, W. Yao^{*2}, R. K. Nalla^{*3}, J. H. Kinney^{*1}, M. Balooch^{*1}, N. E. Lane².** ¹University of California, San Francisco, San Francisco, CA, USA, ²University of California, Davis, Davis, CA, USA, ³Lawrence Berkeley National Laboratory, Berkeley, CA, USA.

Glucocorticoid-induced osteoporosis (GIOP) commonly results from suppression of bone formation and enhancement of bone resorption, which alters bone structure and induces bone fragility. Bisphosphonates, acting as anti-resorptive agents, and anabolic agents, are effective therapies in the prevention and treatment of GIOP in clinical trials; however, the mechanism by which they increase bone strength is not yet clear. The purpose of this study was to assess if concurrent treatment of mice with GCs + Risedronate (RIS) or GCs + PTH would maintain bone mechanical properties (local and global) and bone mineral concentration (BMC) compared to GC treatment alone. Four groups of mice were randomized to placebo, GC (1.5mg/kg in a slow-release pellet that was s.c. implanted x 21 days), GC + RIS (5 μ g/kg, sc, 5X/wk) and GC + hPTH (1-34) (40 μ g/kg, sc, 5X/wk- and treated for 21 days). After sacrifice, the following procedures were done: microCT for trabecular microarchitecture and compression tests of 3rd LVB. The 4th LVB were processed for Elastic Modulus Mapping (EMM), a scanning probe microscopy-based technique that allows high resolution (15nm) mapping of elastic modulus (E) surrounding osteocyte lacunae. In addition, synchrotron x-ray tomography (XTM) analysis was performed on femurs to assess changes in BMC. Finally, EMM and XTM were performed

ASBMR 27th Annual Meeting

on iliac crest biopsies from GC and GC+RIS treated subjects. Treatment with GCs reduced BV/TV by 53% and both GC+RIS and GC+PTH treatment prevented loss of BV/TV. Compared to the PL group, E was reduced by 66% and 58% in GC-treated mice ($p<.001$) and humans ($p<.05$), respectively, along the trabeculae perimeter and surrounding the osteocyte lacunae; however, E was maintained with GC+ RIS and GC+ PTH groups. Compression tests of the LVB3 in mice treated with GC+ PTH and GC+RIS revealed a 62% and 88% increase in strength ($p<.001$), 64% and 61% increase in compression modulus ($p<.001$), and 51% and 39% increase in stiffness ($p<.01$), respectively, compared to PL mice. XTM analysis revealed a 45% and 31% reduction in BMC in the trabeculae of both GC-treated mouse ($p<.01$) and human bone ($p<.01$), respectively, while GC+RIS and GC+PTH treatment led to a 33% ($p<.01$) and 48% ($p<.01$) increase in BMC compared to PL, respectively. These results indicate that PTH and RIS treatments in the presence of GCs prevent the deterioration of BMC and both local and global mechanical properties. Therefore, these therapies appear to be effective means in reducing bone fragility in GC treated individuals.

Disclosures: **G. Balooch**, None.

SU068

Achieving Bone Augmentation with Hydroxyapatite and a Polyactic Acid Plate: A Histological Study in Rats. **T. Kojima**^{*1}, **N. Amizuka**², **C. Saito**^{*1}, **T. Maeda**^{*2}. ¹Division of Reconstructive Surgery for Oral and Maxillofacial Region, Niigata University Graduate School of Medical and Dental Sciences, Niigata, Japan, ²Division of Oral Anatomy, Niigata University Graduate School of Medical and Dental Sciences, Center for Transdisciplinary Research, Niigata University, Niigata, Japan.

One of the primary goals for bone augmentation is the establishment of compact bone with rigidity, toughness and strength—desirable bone quality—, in addition to the induction of new bone grown up to, or higher than the previous bone surface. We applied a polylactic acid (PLA) plate that is clinically used for osteosynthesis and hydroxyapatite (HA) as the grafting material to surgically-created bone defects, and then, evaluated the histological alterations. Standardized bone defects (ϕ 5mm) in rat calvariae were filled with a compound of atelo-collagen and authentic bovine HA, commercially available as Boneject[®], and then covered with a molded PLA plate (DeltaSystem[®]). The rats were fixed with an aldehyde solution at 1, 2, 4, 8 and 12 weeks post-operation, and the newly-formed bone in the defects was examined for alkaline phosphatase (ALP), tartrate resistant acid phosphatase (TRAP), osteopontin (OPN) and osteocalcin (OCN). One week after surgery, HA particles revealed OPN- and OCN-immunopositivity at their surfaces. At the bottom of the cavity, ALP-positive cells were found covering the HA particles, suggesting that bone proteins *i.e.*, OPN and OCN, may accumulate on HA-surfaces to affect osteoblastic migration and attachment. At 2 weeks, woven bone with many ALP-positive osteoblasts and osteocytes extended from the bottom of pre-existing bone, and surrounded the HA particles. At 4 weeks, the new bone attained at the level of the PLA plate, only separated by a thin fibrous layer without ALP-positivity. ALP-positive osteoblasts and TRAP-positive osteoclasts were abundantly localized at the surfaces of the new bone, indicative of bone remodeling. At 8 and 12 weeks, the new bone encompassing the HA particles increased in width and showed the histological profile of compact bone, which, therefore, seemed to satisfy, at least in part, preferable bone quality. Thus, the combination of HA and a PLA plate appears to promote desirable osteoconduction and bone remodeling, resulting on compact bone formation.

Disclosures: **T. Kojima**, None.

SU069

Implication of Connexin43 Gap Junctions in the Responsiveness of HIG-82 Cells to Interleukin1 Beta Treatment. **C. Niger**^{*}, **F. Lima**^{*}, **J. P. Stains**. Orthopaedics, University of Maryland School of Medicine, Baltimore, MD, USA.

Synovial inflammation is one of the changes observed in osteoarthritis (OA) pathophysiology. Current evidences attribute a key role to the matrix metalloproteinases (MMPs), which control the breakdown of the cartilage extracellular matrix, in OA disease progression. Previous studies have shown that cytokines such as interleukin-1 beta (IL1), produced by activated synoviocytes, up-regulate MMP gene expression. Recently, connexin43 (Cx43)-mediated gap junctional intercellular communication between synovial lining cells was also shown to contribute to the etiology of OA. Previously, we have reported that gap junctions play a critical role in regulating signaling and gene transcription in osteoblasts. Accordingly, we set out to examine the role of Cx43 gap junctions in synovial cell responses induced by IL1, to determine if an analogous process occurs in these cells. First, we have shown that treatment of HIG-82 rabbit synovial fibroblast cell line for 16 hours with 100 pg/ml IL1 stimulates Cx43 protein expression 1.6-fold, as determined by western blotting. Further, transient transfection of Cx43 in synovial fibroblasts results in an increase of MMP-1 (1.3-fold), MMP-13 (1.7-fold) and cyclooxygenase-2 (COX-2, 2.24-fold) gene expression by real time PCR, suggesting that gap junctional intercellular communication can mediate regulatory signals of these genes. However, the action of IL1 on Cx43-transfected cells is still under investigation. In addition to a direct effect of IL1 on Cx43 protein expression, we have shown that gap junctions further regulate signaling activated by IL1. IL1-treated HIG-82 cells activate extracellular signal regulated kinase (ERK) and treatment of the cells with the gap junction inhibitor glycylrrhettinic acid decreases the magnitude of the ERK activation, as determined by western blotting. Thus, we propose a model in which low grade inflammation present in the synovial fluid during OA induces Cx43 expression, which leads to up regulation of genes associated with cartilage destruction. Further, Cx43 may propagate and the downstream effects of IL1, as disruption of Cx43 gap junctional communication can

attenuate the effects of IL-1 β on HIG-82 cells. In conclusion, our results indicate that Cx43-mediated gap junctions enhance transcription of specific genes implicating in osteoarthritis pathophysiology and could represent a target for IL1 β action in promoting the progression of OA.

Disclosures: **C. Niger**, None.

SU070

Twist Gene Dosage may Contribute to Craniofacial Defects in Endothelin-A Receptor (*Ednra*) Mutant Mice. **M. Abe**, **D. E. Clouthier**^{*}. Department of Molecular, Cellular and Craniofacial Biology, Birth Defects Center, Univ. of Louisville, Louisville, KY, USA.

Much of the bone, cartilage, and connective tissue of face and neck is derived from cephalic neural crest cells (NCCs). Multiple signaling molecules are involved in the precise patterning and differentiation of NCCs, one of which is endothelin-1 (Edn1), whose binding to the endothelin-A receptor (Ednra) on neural crest cells induces multiple signaling cascades. Targeted inactivation of either *Edn1*^{-/-} or *Ednra*^{-/-} results in severe craniofacial defects in lower jaw and middle ear structures, including homeotic transformation of the mandible into an upper jaw-like structure. This correlates with changes in gene expression in the mandibular portion of the first arch (from which the lower jaw arises), including loss of distal gene expression involved in mandible development and an up-regulation of gene expression normally associated with more proximal arch gene expression. One gene whose expression is upregulated in *Ednra*^{-/-} embryos encodes the basic helix-loop-helix (bHLH) transcription factor Twist. A recent study shows that *Twist* and the bHLH molecule *Hand2* functionally antagonize each other in limb development. Since *Hand2* expression is down-regulated in *Ednra*^{-/-} embryos, it is possible that an upregulation of *Twist* in addition to loss of *Hand2* might contribute to the observed facial defects. To address this point, we crossed *Twist* mutant mice onto the *Ednra*^{-/-} background and then examined the phenotypic consequences. We find that midline clefting frequently observed in the lower jaw of E18.5 *Ednra*^{-/-} embryos is not present in E18.5 *Ednra*^{-/-}; *Twist*^{+/-} embryos. Further, tongue formation is partially rescued and soft tissue is more abundant around the lower incisors. These findings suggest that alterations in bHLH levels (and the types of heterodimers and homodimers subsequently formed) may play a role in the mis-patterning of NCCs observed in *Ednra*^{-/-} embryos.

Disclosures: **M. Abe**, None.

SU071

Hyaluronan Inhibits MMP-1 and -3 Productions Induced by IL-1 beta in Rheumatoid Synovial Fibroblast via ICAM-1. **T. Hiramitsu**^{*1}, **T. Yasuda**^{*2}, **H. Ito**¹, **M. Shimizu**^{*1}, **T. Nakamura**^{*1}. ¹Department of Orthopaedic Surgery, Kyoto University, Graduate School of Medicine, Kyoto, Japan, ²Department of Sports Medicine, Tenri University, Faculty of Health, Budo, and Sports Studies, Tenri, Japan.

In rheumatoid arthritis (RA), it is well known that rheumatoid synovial fibroblasts (RSFs) produce metalloproteinases (MMPs) stimulated by cytokines such as interleukin-1 β (IL-1 β), which causes joint destruction in those patients. As one of the treatments, it has been reported that hyaluronan (HA) injection into RA joints has clinically beneficial effects, but how it works remained to be clarified. We have previously shown that HA inhibits IL-1 β actions in RSFs via CD44, one of HA receptors, but that CD44 only mediates the HA effects partially, which led us to speculate that other receptors of HA do as well. Thus, we investigated whether HA affected matrix metalloproteinase (MMP) -1 and -3 productions induced by IL-1 β in RSFs and whether intercellular adhesion molecule-1 (ICAM-1), one of HA cell surface receptors, was involved in the HA effects. Human rheumatoid synovial tissues were obtained from patients with rheumatoid arthritis (RA) at total knee replacement surgery. RSFs were isolated from the rheumatoid synovial tissues by enzymatic digestion and were cultured in monolayer. RSFs of 3 - 7 passages were examined. The confluent cells were incubated for 48 hours with IL-1 β at 2 ng/ml, IL-1 β plus HA at the various concentrations, IL-1 β plus HA after the pretreatment of anti ICAM-1 antibody at the various concentrations, or without any treatment. MMP-1 and MMP-3 secretions were analyzed by immunoblotting of the conditioned media. Immunofluorescent cytochemistry was performed to evaluate HA binding to ICAM-1. MMP-1 and MMP-3 were markedly produced by 2 ng/ml IL-1 β stimulation, and HA at more than 2 mg/ml significantly inhibited MMP-1 and MMP-3 productions induced by IL-1 β in a dose dependent manner. Moreover the pretreatment with anti ICAM-1 antibody at 50 μ g/ml significantly attenuated HA effect for IL-1 β action on RSFs. Immunofluorescent cytochemistry demonstrated that, indeed, HA bound to RSFs, and that the pretreatment with anti ICAM-1 antibody partially prevented HA from binding to RSFs. It also showed that anti ICAM-1 antibody hardly bound to RSFs after the pretreatment with HA. Therefore HA bound to RSF, at least partially, via ICAM-1. Taken together, we conclude that HA suppresses IL-1 β action on RSFs via ICAM-1.

Disclosures: **H. Ito**, None.

SU072

Regulation of the Expression of MMP-13 by Reactive Oxygen Species in Chondrogenic ATDC5 Cells. K. Morita^{*1}, T. Miyamoto², H. Takaishi^{*1}, M. Yagi^{*2}, N. Fujita^{*2}, K. Ninomiya^{*2}, T. Suzuki^{*2}, Y. Toyama^{*1}, T. Suda^{*2}.

¹Orthopaedic Surgery, School of Medicine, Keio university, Tokyo, Japan, ²Cell Differentiation, School of Medicine, Keio university, Tokyo, Japan.

The matrix metalloproteinases (MMPs) are the extracellular matrix (ECM) degrading proteins, and play crucial roles in many pathological and physiological processes, including cell growth, differentiation, tissue remodeling and destruction. MMPs are consisted of 25 subtypes in vertebrates. Among them, MMP-13 (also known as collagenase-3) plays a central role of degrading proteoglycans and collagens of cartilage ECM, and it is reported to be involved in destruction of articular cartilage in osteoarthritis (OA) and rheumatoid arthritis (RA). Recently, it has been shown that reactive oxygen species (ROS) of joint fluid was increased in OA and RA. In this study we analyzed the induction of MMP-13 expression by ROS in chondrogenic ATDC5 cells. The expression of MMP-13 was upregulated by hydrogen peroxide (H2O2) and buthionine sulfoximine (BSO) as ROS in ATDC5 cells, and this induction was abolished by addition of anti-oxidant, N-acetylcysteine (NAC). To detect the intracellular signal transduction mechanism of this induction, phosphorylation of mitogen-activated protein kinase (MAPK), such as p38, extracellular signal-regulated kinase (ERK) 1/2 and c-Jun N-terminal kinase (JNK), by H2O2 was investigated. Phosphorylation of p38 and ERK1/2 were rapidly induced by H2O2, while JNK was not. The phosphorylation of p38 and ERK1/2 by H2O2 were inhibited by NAC, resulting in inhibition of the induction of MMP-13. Furthermore, MAPK specific inhibitors, SB203580 (p38 inhibitor) and U0126 (ERK inhibitor) inhibited the MMP-13 expression, while SP600125 (JNK inhibitor) did not, indicating that p38 and ERK1/2 pathways were involved in MMP-13 induction by ROS in chondrogenic ATDC5 cells. These results suggest that ROS might be involved in cartilage degradation of OA and RA by inducing MMP-13 expression via p38 and ERK1/2 pathways.

Disclosures: **K. Morita**, None.

SU073

Assembly and Reorganization of Bone Extracellular Matrix Proteins Imaged in Living Osteoblasts. P. Sivakumar¹, Q. Chen¹, B. J. Rongish^{*2}, A. Czirik^{*2}, V. P. Divakara^{*1}, V. Dusevich^{*1}, S. L. Dallas¹. ¹Univ. of Missouri, Kansas City, MO, USA, ²Univ. of Kansas Med Cntr, Kansas City, KS, USA.

Fibronectin (FN) is an extracellular matrix (ECM) glycoprotein critical for cell adhesion, migration and survival. Osteoblast-like cells lacking the gene for FN show impaired mineralization and fail to assemble multiple bone ECM components, including type I collagen (Col I), fibrillin-1, decorin, biglycan and latent TGF-beta binding protein-1 (LTBP1). To gain further insights into the mechanisms of assembly of FN and its spatial and temporal interactions with other bone ECM proteins, we have performed dynamic imaging in living osteoblasts using fluorescent probes for ECM components. We have also developed computational techniques to analyze cell and ECM fibril kinetics. Dual imaging of FN together with LTBP1 or Col I indicated that these proteins were initially co-assembled onto similar fibrils in the ECM of primary osteoblasts (FRC). These fibrils were highly elastic and continually underwent large dynamic movements in response to cell motion. Motile cells appeared to actively participate in ECM assembly by moving or shunting "globules" or "packets" of fibrillar material onto growing fibrils. The cells also reorganized the assembled ECM by shunting fibrillar material and/or exchanging material between fibrils. In mature FRC cultures, LTBP1 and Col I were found in fibrils that were distinct from FN, suggesting ECM reorganization or partitioning. These distinct fibrillar networks showed different dynamic properties in response to cell movement. A more detailed dynamic imaging analysis of FN assembly revealed that FN was initially incorporated onto the cell surface as small spots/patches, resembling focal adhesions, which then progressively coalesced to form fibrils. Individual fibrils received contributions from multiple cells. Pulse-chase analysis using alexa488-green followed by alexa555-red labeled FN showed that newly incorporated FN first assembled into spots/patches on the cell surface, which then redistributed to become co-localized with pre-existing fibrils. Quantitative analysis showed that redistribution was maximal after 12h and was inhibited by jasplakinolide, an actin destabilizing agent, suggesting that cell motility is critical for FN redistribution. Vector displacement mapping showed that the motions of cells and fibrils were significantly correlated. Our data suggest novel mechanisms by which motile cells may participate in the assembly and reorganization of bone ECM proteins and confirms a key role for FN in the assembly of Col I. These findings have important implications in normal bone physiology as well as diseases associated with defective collagen assembly.

Disclosures: **P. Sivakumar**, None.

SU074

Homocysteine Modification of Matrix Proteins - a Potential Mechanism of Osteoporosis and other Diseases of "Normal" Aging. C. Prince¹, C. Krumdieck^{*2}. ¹University of Alabama at Birmingham, Birmingham, AL, USA, ²Nutrition Sciences, University of Alabama at Birmingham, Birmingham, AL, USA.

Five years ago we recognized that several diseases common to late life (presbyopia, occlusive vascular disease, osteoporosis and cognitive decline) have parallels with manifestations of homocystinuria (ectopia lentis, occlusive vascular disease, osteoporosis, and mental retardation)(1). We proposed that these manifestations, which occur at a young age in homocystinuria (in which plasma homocysteine (Hcy) is often >100M), develop only after many years of exposure to moderately elevated levels of plasma Hcy. For example, osteoporosis is detectable by radiographs in 80% of untreated homocystinuric patients by age

30(2). Recently, Sato et al(3), among others, have shown that prolonged, moderately elevated Hcy (~20-30 M) is likely to have a causal role in the development of osteoporosis, and should, by extension, play a similar role in the other diseases of aging. Because of a lack of change in bone mineral density, Sato, et al.,(3) speculated that the mechanism underlying their observed association may involve interference in collagen crosslinking resulting in the formation of an altered bone matrix. Indeed, collagen crosslinking may be affected, but similarities in connective tissue pathologies of homocystinuria, Marfan syndrome, sulfite oxidase deficiency and molybdenum cofactor deficiency are informative as to mechanism of action. Marfan syndrome is caused by mutations in the fibrillin-1 gene that disrupt disulfide bonds in epidermal growth factor-like repeats of the fibrillin molecule, while Hcy has the capacity to break and rearrange disulfide bonds in similar protein domains (4). (Similarly, the sulfite anion, which accumulates in sulfite oxidase and molybdenum cofactor deficiencies, also reacts avidly with protein thiols breaking disulfide bridges). Thus, post-translational "homocysteinylolation" of fibrillin-1 and other disulfide rich proteins, with disruption of critical disulfide bonds, may play a causal role in many connective tissue disorders often associated with "normal" aging, including, but not limited to, osteoporosis. In support of this hypothesis, we have preliminary data which show that human adult bone matrix protein extracts release high levels of Hcy on reductive cleavage.

References

1. Krumdieck CL and Prince CW. *J Nutr.* 2000; 130:365S-368S.
2. Mudd SH, Skovby F, Levy HL, Pettigrew KD, Wilken B, Pyeritz RE, Andria G, Boers GH, Bromberg IL, Cerone R et al. *Am. J. Human Genet.* 1985; 37:1-31.
3. Sato Y, Honda Y, Iwamoto J, Kanoko T, Satoh K. *JAMA.* 2005; 293:1082-1088.
4. Hutchinson S, Aplin RT, Webb H, Kettle S, Timmermans J, Boers GH, Handford PA. *J Mol Biol.* 2005; 346:833-44.

Disclosures: **C. Prince**, None.

SU075

Non-Enzymatic Glycations of Bone Collagen Modify Osteoclastic Activity. U. Valcourt^{*}, B. Merle^{*}, E. Gineyts^{*}, P. D. Delmas, P. Garnero. INSERM Research Unit 403 - Hôpital E. Herriot, Lyon, France.

Type I collagen, the major organic component of the bone matrix, undergoes a series of enzymatic and non-enzymatic posttranslational modifications that are altered with ageing and osteoporosis. Among these, advanced glycation end products (AGEs), which are formed by a non-enzymatic reaction between amino groups of proteins and sugars, can modify both the biological properties of affected structural proteins and cellular activity, through their interaction with specific cell-membrane receptors including RAGE. Pentosidine -one of the most investigated AGEs- has been shown to markedly increase with age in human bone and to be associated with alterations of bone biomechanical properties, although the influence of AGEs on bone remodelling is unknown. The aim of our study was to investigate whether the bone content in AGEs modifies osteoclastic activity. We used an in vitro model of bone resorption based on the seeding of rabbit unfractionated bone cells enriched in osteoclasts on 3-month-old calf cortical bone or ivory slices incubated with or without ribose (0.2 M for 45 days), a mediator of AGEs formation. Bone resorption was evaluated by measuring the number and the area of the resorption cavities on the slices and the release in the culture media of the type I collagen degradation products, CTX and helical peptide (ELISA), and hydroxyproline (HPLC). The bone content of pentosidine in bone or ivory slices incubated with ribose was 0.75±0.1 mol/mol of collagen and not detectable in untreated specimens. When osteoclasts were cultured for 3 days on AGE-modified matrices, there was little variation of the total area of bone resorbed, whereas the number of pits increased (from +19% to +42%). Consequently, the area of bone resorbed per cavity was decreased (from -23% to -43%). At 8 days the total area of bone resorbed also decreased. Inhibition of bone resorption was also supported at 8 days by a marked and consistent reduction of the release of collagen fragments in the culture media as judged by CTX (average: -92%), helical peptide (-90%) and hydroxyproline (-68%) concentrations. The content of AGEs in bone matrix influences osteoclast-mediated bone resorption in vitro. These findings suggest that the extent of non-enzymatic posttranslational modifications of type I collagen could play a role in the alterations of bone remodelling associated with aging and metabolic bone diseases including osteoporosis. The molecular mechanisms by which AGEs modulate osteoclast activity remain to be determined.

Disclosures: **U. Valcourt**, None.

SU076

OA-Derived Peptides Stimulate Osteoblast Adhesion, Spreading, Migration and Differentiation. I. Arango-Hisijara^{*}, J. M. Reyes^{*}, J. LeGates^{*}, S. N. Popoff, F. F. Safadi. Anatomy and Cell Biology, Temple University School of Medicine, Philadelphia, PA, USA.

Osteoactivin (OA) plays an important role in the regulation of osteoblast differentiation and function. In a previous study, OA-derived peptides termed the OA-D peptide that has the RGD domain and the OA-E peptide that has glutamic acid (E) in the place of aspartic acid (D) stimulated osteoblast differentiation in an RGD-independent manner. In this study, we examined the role of both peptides as extracellular matrices on osteoblast adhesion, migration and differentiation. MC3T3-E1 osteoblast-like cells were plated on a polystyrene non-tissue culture plate coated with either peptides at various concentrations (5-20 µg/well), cells adhered to poly-L-lysine served as control, an adhesion assay was then performed. Both peptides stimulate osteoblast adhesion in a dose-dependent manner with more profound effect using the RGE peptide. These data suggest that OA stimulates osteoblast adhesion in an RGD-independent manner. We next examined the formation of focal adhesion in osteoblasts adhered to OA peptides. Cells were plated in dishes pre-coated with either OA-D or OA-E peptides and incubated at different time points (0-18 hours). The phosphorylated focal adhesion kinase (p-FAK) was evaluated by Western blot

analysis. p-FAK was increased reaching maximum at 2 hours in cells adhered to OA-E when compared to control. We next examined osteoblast migration in response to OA peptides. Cells were plated in chamber slides pre-coated with either peptide OA-D or OA-E, cells were then wounded with pipette tips and wound healing was evaluated. Osteoblasts migration was enhanced in cells adhered to OA peptides when compared to control. Osteoblast adhesion to OA peptides also stimulated the formation of focal adhesion and cytoskeletal re-organization as determined by immunofluorescent staining for vinculin and TRITC-conjugated phalloidan, respectively. These results indicate that OA derived peptides play a role in osteoblast spreading, formation of focal adhesion and actin cytoskeletal re-organization and migration. We next examined the effect of OA peptides as an extracellular matrix on osteoblast differentiation. Primary osteoblast cultures were plated in dishes pre-coated with OA peptides or Poly-L-Lysine and examined for their differentiation using alkaline phosphatase staining. Osteoblasts that adhered to OA-peptides differentiated faster than cells adhered to Poly-L-Lysine. Collectively, this might explain, in part, the role of OA-derived peptides in stimulating osteoblast differentiation and function.

Disclosures: **I. Arango-Hisijara**, None.

SU077

Periostin-Like-Factor: A Putative Anabolic Factor in Bone Formation. **S. Zhu***, **F. Safadi**, **J. Litvin***. Anatomy and cell Biology, Temple University, Philadelphia, PA, USA.

We have identified a new isoform of periostin, referred to as Periostin-like-factor (PLF). PLF was identified in the developing mouse heart. It is also expressed in bone and vascular smooth muscle cells. Our findings show that (1) PLF is a secreted protein, (2) PLF promotes and accelerates osteoblast differentiation in vitro and (3) PLF promotes bone formation in vivo. The effect of PLF over-expression in osteoblasts in vitro was assessed by alkaline phosphatase staining, von kossa staining to evaluate nodule formation and mineralization and by RT-PCR to evaluate the expression of osteoblast-specific differentiation markers. Over-expression of PLF in primary osteoblasts accelerated alkaline phosphatase expression and resulted in nodule formation after only eight days in culture. These findings were compared to those obtained from untreated cells or cells infected with control adenovirus expressing GFP or LacZ. In vivo, over-expression of PLF in the bone marrow cavity of six-week-old rats induced bone formation within the marrow cavity. Therefore, we conclude that PLF mediates osteoblast differentiation in vitro and bone formation in vivo.

Disclosures: **S. Zhu**, None.

SU078

CTGF-Derived Peptide (CTGF-P) Stimulates Osteoblast Adhesion, Spreading and Differentiation. **I. Arango-Hisijara***¹, **R. A. Kanaan***², **F. F. Safadi**¹, **S. N. Popoff**¹. ¹Anatomy and Cell Biology, Temple University School of Medicine, Philadelphia, PA, USA, ²Department of Orthopedics, University of Pennsylvania School of Medicine, Philadelphia, PA, USA.

Connective tissue growth factor (CTGF/CCN2) is a member of the CCN family of secreted proteins that regulates multiple cellular functions. In previous studies we showed that recombinant CTGF protein (rCTGF) stimulated osteoblast proliferation and differentiation in vitro, supported by the osteogenic effect in vivo. Our recent studies showed that the rCTGF stimulates osteoblast adhesion in a dose dependent manner, and that $\alpha v \beta 5$ integrin is the adhesion receptor for CTGF in osteoblasts. In this study, we examined the role of a C terminus CTGF-derived peptide (CTGF-P) in osteoblast adhesion, migration and differentiation. MC3T3-E1 osteoblast-like cells were plated in a polystyrene non-tissue culture plate coated with CTGF-P at various concentrations (2-50 $\mu g/well$), an adhesion assay was then performed. CTGF-P stimulated osteoblast adhesion in a dose-dependent manner. We next examined the formation of focal adhesion in osteoblasts adhered to CTGF-P. Cells were plated in dishes pre-coated with CTGF-P peptide or Poly-L-Lysine, as control, and incubated at different time points (0-30 minutes). The phosphorylated focal adhesion kinase (p-FAK) was evaluated by Western blot analysis. p-FAK was increased reaching maximum at 10 min in cells adhered to CTGF-P when compared to control. We next examined whether this adhesive property of CTGF is mediated through the extracellular signal regulated kinase (ERK) pathway, osteoblasts were plated in dishes pre-coated with CTGF-P and incubated at different time points (0-2 hours). The phosphorylated-ERK (p-ERK) was evaluated by Western blot analysis. p-ERK was increased reaching maximum at 1 hour in cells adhered to CTGF-P, suggesting that MAPK family is involved in regulating osteoblast adhesion to CTGF. Osteoblast adhesion to CTGF-P also stimulated the formation of focal adhesion and cytoskeletal re-organization determined by immunofluorescent staining for vinculin and TRITC-conjugated phalloidan, respectively. We next examined the effect of CTGF-P as an extracellular matrix on osteoblast differentiation. Primary osteoblast cultures were plated in dishes pre-coated with CTGF-P or Poly-L-Lysine and examined for their differentiation using alkaline phosphatase staining. Osteoblasts adhered to CTGF-P differentiated faster than cells adhered to Poly-L-Lysine. These results clearly show that CTGF-P plays a role in osteoblast adhesion and spreading through ERK signaling pathway and this might lead to enhance osteoblast differentiation.

Disclosures: **I. Arango-Hisijara**, None.

SU079

MicroRNA (miRNA) Binding Sites in the Osteonectin 3' Untranslated Region (UTR) Regulate Expression. **C. Kessler***, **A. M. Delany**. Center for Molecular Medicine, University of Connecticut Health Center, Farmington, CT, USA.

Abundant in bone, osteonectin or SPARC (secreted protein acidic and rich in cysteine) is a "matricellular" glycoprotein that functions more as a regulator of cell behavior than as structural component of the matrix. It is associated with conditions of active matrix remodeling and cellular stress in multiple organ systems ranging from skin, bone, muscle, brain, and adipose. Cells regulate their expression of osteonectin in response to normal and pathogenic stimuli, causing changes in cell behavior that are critical for biological response. However, the mechanisms regulating osteonectin are largely unknown. Modulation of osteonectin RNA stability is likely to play a key role in its regulation, and determinants of RNA stability are often found in the 3' UTR. We sought to define sequence motifs and trans-acting factors regulating osteonectin RNA stability in murine osteoblasts, using chimeric luciferase-osteonectin 3' UTR reporter constructs. The mouse osteonectin 3' UTR is ~1 kilobase, and use of the full length osteonectin 3' UTR as the 3' UTR for the luciferase gene (in the constitutive reporter pGL3-control) decreases luciferase activity by 90-95%. Insertion of the first 220 bases of the UTR (997-1217) 3' to luciferase has a similar effect, whereas insertion of the latter 831 bases of the osteonectin 3' UTR causes a 1.5 to 2 fold increase in luciferase activity. These data indicate that the proximal portion of the osteonectin 3' UTR contains a dominant motif for regulation of RNA stability and/or translation. This region of the UTR can form a stem-loop structure, and it demonstrates specific binding to osteoblast cytoplasmic proteins in RNA mobility shift assays. Further, it contains overlapping potential binding sites for miRNAs 29a, 29c, and 96, which are conserved across the mouse, human, rat, cow and dog osteonectin transcripts. miRNAs are a class of endogenous noncoding ~22 base RNAs that regulate gene expression by pairing with mRNAs and specifying cleavage or repression of translation. Deletion of the 27 base overlapping miRNA binding sites in the luciferase-osteonectin 3' UTR chimera increases activity by ~7 fold, verifying the regulatory nature of these sites. A second site in the proximal UTR, homologous to a well characterized SNP in the human osteonectin gene (human 998 G/C) and upstream of the miRNA sites, also has regulatory activity in our assays. In conclusion, we've defined a powerful regulatory motif in the proximal portion of the osteonectin 3' UTR, likely a target for miRNA regulation. We hypothesize that a specific array of miRNAs modulates osteonectin RNA stability and/or translation in normal differentiation and in disease states.

Disclosures: **A.M. Delany**, None.

SU080

Osteopontin Deficient Mice Show Delayed Healing during Distraction Osteogenesis. **Z. S. Alaql***¹, **K. A. Jacobsen**², **T. A. Finhorn**², **L. Gerstenfeld**², **R. S. Carvalho**¹. ¹Department of Orthodontics, Boston University School of Dental Medicine, Boston, MA, USA, ²Department of Orthopaedic Research Laboratory, Boston University School of Medicine, Boston, MA, USA.

Osteopontin (OPN) is a phosphoprotein found in the extracellular matrices of mineralized tissues and is believed to play a role in the remodeling of these matrices. OPN is also one of a limited number of genes that respond to mechanical strain. Distraction osteogenesis represents a unique *in vivo* surgical method of applied mechanical tension that induces new bone formation and therefore represents an ideal model to assess the multiple functional roles of osteopontin. Tibia distraction osteogenesis was carried out using a monolateral fixator on male transgenic mice lacking osteopontin (C57B1/6 OPN ^{-/-}) and their background strain (C57B1/6). The tibiae were harvested at defined times over a 31 day time course and bone formation was evaluated radiographically and by assessment of mRNA expression for matrix genes. In the absence of OPN bone repair failed to reach completion relative to the controls. Surprisingly, when bone repair began in the distraction gap in the OPN ^{-/-} mice it was initiated in the center of the gap while in the control bones bridging proceeded from the proximal and distal edges of the osteotomy. Assessment of the multiple mRNAs associated with osteoblastic activity (BSP, OC, Col1A1) all showed compensatory (30% to 115%) elevation of their expression in OPN ^{-/-} mice through out the time course relative to controls. Interestingly, multiple mRNAs encoding numerous matrix metalloproteinases (MMPS) that are associated with bone remodeling were also over-expressed (15%-45%) throughout the time course of distraction in the OPN deficient mice. These observations suggest a crucial role for OPN in this model of bone formation. They show that osteopontin plays a clear structural role in relating the spatial orientation of new trabecular bone formation. Furthermore, they suggest that insufficiencies in the expression of one matrix component lead to alteration in the expression of others and may affect the normal balance between bone formation and turnover.

Disclosures: **Z.S. Alaql**, None.

SU081

Wnt Induced Secreted Protein 1 (WISP-1) Splice Variants and Possible Relationship with BMP Signalling. **C. A. Inkson***, **S. Wadhwa***, **P. Gehron**, **Robey**, **M. F. Young**. NIDCR, NIH, Bethesda, MD, USA.

Wnt induced secreted protein 1 (WISP-1/CCN4) is a member of the cysteine rich CCN protein family, some of which members have been shown to modulate bone and joint development and repair. Expression of WISP-1 was recently identified in bone, and experiments by others implicated WISP-1 in the fracture healing process. We have now identified multiple splice variants of WISP-1 in human bone. RNA was collected from cultures of human trabecular bone cells and bone marrow stromal cells with differing degrees

ASBMR 27th Annual Meeting

of differentiation, and used for RT-PCR analysis of CCN family members. WISP-1 and connective tissue growth factor (CTGF/CCN2) had notably increased expression in the more mature trabecular bone cells, as judged by levels of bone sialoprotein (BSP) expression. Other WISPs (CCNs 5 and 6) had lower levels of expression in these samples. In contrast to full length WISP-1 which was constitutively expressed, we observed a smaller WISP-1 variant with up-regulated expression during osteoblastic differentiation. Sequence analysis revealed that the smaller variant corresponds to a previously reported oncogenic WISP-1va, which is a result of exon splicing. We performed gene and protein alignment of the WISP-1 variants with other CCN family members using the web based Clustalw (1.82) program. Both WISP-1 and WISP-1va were the most homologous to CTGF. However, WISP-1va protein is lacking the Von Willebrand factor type C-like domain (VWFC). This variable domain contains a cysteine rich (CR) consensus motif found in chordin-like molecules, and also holds the putative site of the BMP/TGF binding capacity of CTGF. We also analysed another cysteine rich region found at the c-terminal of CCN proteins. This motif is analogous to the cysteine knot region of other BMP antagonists such as noggin, twisted gastrulation (Tsg) and the Dan family. Both WISP-1 and WISP-1va possess the cysteine knot region, but do not resemble these BMP antagonists in any other way. Others have previously shown that overexpression of WISP-1 in osteoblast-like cells can exaggerate the effect of BMP-4 induced differentiation. However, little is known of the molecular mechanisms involved in this process. It is plausible that like CTGF, WISP-1 could modulate TGF- β 1 superfamily members and their functions in bone. In light of our observations of a WISP-1 variant lacking in the domain responsible for such putative activity, we hypothesize that that in addition to being a wnt inducible gene, alternative expression of WISP-1 variants may differentially regulate BMP induced osteoblastic differentiation.

Disclosures: **C.A. Inkson, None.**

SU082

Targeting and Immobilization of Bioactive Peptides on Mineralized Tooth Matrices. **J. Song***, **A. Wlodarska***, **H. Ko***, **W. Grzesik**. Anatomy, School of dental Medicine, Univ. Pennsylvania, Philadelphia, PA, USA.

The need to enhance healing and/or regenerate structurally and functionally competent tooth root cementum appears to be critically important for successful restoration of periodontal attachment. Since cementum deposition needs to be confined to the tooth root surface, there is a need for targeting and stably integrating biologically active molecules to this location. We have developed a new method for targeting and covalently binding synthetic peptides to the surface of mineralized biological matrices. This method utilizes poly-glutamic acid stretch ((pE))to target peptides to mineral and a glutamine-containing transglutaminase (TG) substrate sequence to allow formation of a covalent bond between the peptide and the organic matrix. In this study, as biologically active model molecule we have employed the integrin-binding motif, RGD. Using synthetic peptides containing TG substrate sequence, pE and RGD we have evaluated the effects of their immobilizing on tooth root dentin on the adhesion of human cementoblastic cell in vitro. Tooth root dentin was treated with synthetic peptides containing the TG substrate sequence, mineral binding motif (pE) and cell attachment motif RGD and the transglutaminase consensus motif (glutamine) and transglutaminase. Untreated dentin slices as well as slices treated with peptide or TG only were employed as controls. Prepared dentin substrates were used as a substrate for cell attachment assay employing Human Cementum-Derived Cells (HCDC), a model of cementoblastic cells for cell attachment assays throughout all experiments. The cementoblastic phenotype of the cellular strains used was confirmed during previous studies in an in vivo transplantation assay. HCDC were seeded onto dentin substrates and cell adhesion was evaluated quantitatively (cell number) and qualitatively (cell morphology) as a function of time and peptide concentration. Cementoblastic adhesion (both cell attachment and spreading) was significantly increased on the surface of dentin that contained covalently bound peptides compared to all controls. However, dentin treated with TG alone also showed an effect on cementoblastic attachment (an effect that was expected), although to a lesser degree. Cellular spreading was pronounced best on dentin with peptides immobilized on. These effects were dependent on the dose of the peptide employed. Transglutaminase-catalyzed covalent binding of bioactive peptides targeted to mineralized collagenous dentin matrix via the polyglutamate motif can be readily achieved. If further confirmed in an in vivo assay, it may be of clinical use in periodontal regeneration.

Disclosures: **J. Song, None.**

SU083

Involvement of RhoE and Regulator of G-protein Signaling Protein (RGS) 2 in the Response of Human Periodontal Ligament Cells to Mechanical Stress. **R. M. Santos de Araujo**, **Y. Oba**, **K. Moriyama**. Department of Orthodontics and Dentofacial Orthopedic, Institute of Health Biosciences, University of Tokushima, Tokushima, Japan.

The periodontal ligament (PDL) is thought to play a critical role as a transducer of mechanical signals into biological response including alveolar bone remodeling. However, the intracellular signaling pathways in the PDL cells in response to mechanical stress are still unclear. Using a cDNA microarray approach for gene expression induced in PDL cells under compressive force, we recently identified the monomeric G-protein RhoE and regulator of G-protein signaling protein (RGS) 2, which catalyzes the hydrolyzation of GTP (active form) to GDP (inactive form). The purpose of this study is to investigate the involvement of RhoE and RGS2 in the PDL cells under compressive force. Human PDL cells isolated from extracted premolars for orthodontic treatment were suspended into a collagen solution at a concentration of 1×10^6 cells/ml and the collagen gels were molded in 24-well plates. The gels containing PDL cells were transferred to 6-well culture plates with fresh media and then subjected to 6.0 g/cm² of compressive force for 1, 3, 6, 12, 24, 48 and 72 hours. The quantitative PCR and Western blotting analyses demonstrated that the expressions of RhoE and RGS2 were time-dependently increased by compressive force

compared with control groups. The compressive force also significantly increased the production of intracellular cAMP, which plays an important role in G protein signaling, in the PDL cells in a time-dependent manner. To examine the involvement of RGS2 in the cAMP production induced by compressive force, the cells were treated with dideoxyadenosine (DDA), an inhibitor of adenylyl cyclase activity, at 1, 10, and 20 μ M. Western blotting analysis showed that the RGS2 expression induced by compressive force was suppressed by DDA in a dose dependent manner. Transfection of PDL cells with antisense S-oligonucleotide (10 μ M) to RGS2 enhanced the intracellular cAMP production under compressive forces. These results suggest that RhoE and RGS2 participate in the cellular responses to mechanical stress mediating cAMP in PDL cells.

Disclosures: **R.M. Santos de Araujo, None.**

SU084

Contributions of Cortical and Trabecular Architecture to Biomechanical Properties of Human Vertebrae. **J. P. Roux***¹, **Z. Merabet***¹, **M. E. Arlot**¹, **F. Duboeuf***¹, **P. D. Delmas**¹, **M. L. Bouxsein**². ¹INSERM Unit 403, C. Bernard University, Lyon, France, ²Orthopedic Biomechanics Laboratory, Beth Israel Deaconess Medical Center and Harvard Medical School, Boston, MA, USA.

Vertebral fractures are common in elderly persons, yet the mechanisms of injury underlying these fractures remain obscure. Whereas there is clear evidence for a strong influence of the quantity of bone (i.e., bone mass or BMD) on the mechanical behavior of vertebrae, there are less data addressing the relative influence of cortical and trabecular microarchitecture. Thus, the aim of this study was to determine the relative contributions of bone mass, trabecular microarchitecture and cortical thickness to the mechanical behavior of human lumbar vertebrae. We obtained 19 L3 vertebrae (10 men and 9 women, aged 26 -93 yrs, and assessed BMD (g/cm²) of the vertebral body by lateral DXA; vBMD (g/cm³, as BMC / directly measured vertebral body volume); 3D trabecular microarchitecture (BV/TV, trabecular thickness, degree of anisotropy, and structure model index) and thickness of the anterior cortex by μ CT (35 μ m voxel size, Skyscan). Then, compressive stiffness and failure load were measured, and apparent modulus and ultimate strength computed using the minimal cross-sectional area of the vertebral body. Bivariate regression analysis showed that BMD was strongly correlated to compressive stiffness ($r=0.86$) and failure load ($r=0.82$). Except for trabecular thickness, all trabecular parameters ($r = 0.50$ - 0.76 , $p=0.03$ - 0.0002) and anterior cortex thickness ($r = 0.58$ - 0.65 , $p=0.01$ - 0.003) were also strongly correlated with mechanical behavior. The quantity of bone (ie; BV/TV, BMD or BMC) explained 42 to 74% of variability in mechanical properties. Trabecular architectural features were strongly correlated with BMD and BV/TV ($r = 0.58$ to 0.95), and thus did not improve prediction of mechanical properties over that provided by BMD. Conversely, anterior cortical thickness was not correlated with trabecular architecture and weakly with BMD ($r = 0.52$). Accordingly, the combination of BMD or BV/TV with anterior cortical thickness significantly improved the prediction of mechanical properties, with the combination explaining 58 to 80% of variability in mechanical properties. Our data imply that measurements of cortical thickness may enhance predictions of vertebral fragility, and that therapies which improve both vertebral cortical as well as trabecular bone properties may provide a greater reduction in fracture risk.

Disclosures: **J.P. Roux, INSERM-Lilly contract 2.**

SU085

Mechanical Significance of Human Mandibular Bone Structure Assessed by a Remodeling Simulation. **K. Tezuka**¹, **A. Kawaguchi**^{*2}, **A. Takahashi**^{*3}, **T. Takeda**^{*2}, **Y. Wada**^{*3}, **M. Kikuchi**^{*3}. ¹PRESTO, Graduate School of Medicine, Gifu University, Gifu, Japan, ²Graduate School of Medicine, Gifu University, Gifu, Japan, ³Department of Science and Technology, Tokyo University of Science, Noda, Japan.

Bone is continuously being remodeled by bone-forming osteoblasts and -resorbing osteoclasts. These 2 types of cells are tightly linked and adapt the shape of bone to the local stress. Wolff proposed a theory that the trabecular architecture of bone matches the stress trajectories. Additionally, computer-aided strategies have made it possible to calculate the stress distribution in bone tissue and investigate how bone remodeling can adapt the structure of bone to voluntary mechanical stress. Recently, we proposed a simple bone remodeling model, iBone, based on a reaction-diffusion system. We have applied this model to calculate structures of human mandibular bone adapted to various biting conditions. A three-dimensional 14-year old female mandible bone model consisting of approximately 1.4 million elements was used for the analysis. The locations and directions of muscles, and their forces were predicted from the CT images. Incisor, right or left group, and right or left molar biting conditions were simulated by fixing corresponding teeth. Considering the complexity of occlusion, we used comprehensive analysis approach to survey various biting conditions. Approximately 40 different loading conditions were tested. Remodeling simulation was performed by 10 sets of finite element analysis, reaction-diffusion calculation, and remodeling simulation for each loading condition. Simulations indicated that angles of the tooth movement had substantial effects on internal structure of the model bone. Fixing teeth in a plain allowing upper-forward movement caused significant stress in most part of the model, and produced internal structures similar to that of real bone. However, some locations, such as lingual side of mentum, did not bear significant stress in this condition. On the other hand, conditions allowing the tooth movement toward upper-backward direction caused stress accumulation at the lingual side of mentum and induced bone formation in this location. Very interestingly, the real bone structure looked like a sum of these different structures, and these results suggested that mandible bone seemed to have a sophisticated structure which can resist to a wide range of loading conditions. Combination of remodeling simulation with comprehensive

ASBMR 27th Annual Meeting

mechanical analysis may become a powerful tool to analyze structural significance of living bone, and potentially be used for medical diagnosis and treatment of various bone disorder based on the high-resolution CT images.

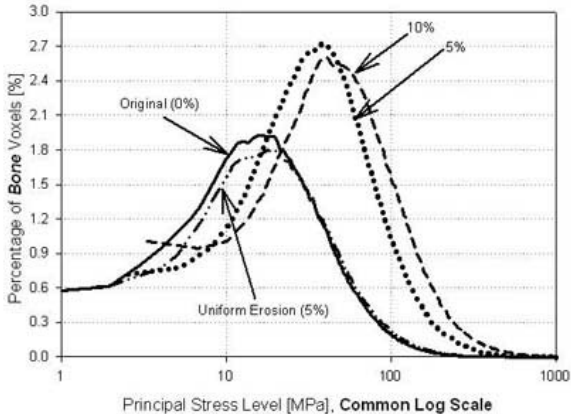
Disclosures: **K. Tezuka**, None.

SU086

Directed Bone Removal Causes Significant Changes in Biomechanical Properties Over Uniform Erosion. **H. Hong***, **G. Gross***, **B. Borah***, **R. Phipps**, **T. E. Dufresne***. P&G Pharmaceuticals, Mason, OH, USA.

Increased rates of bone turnover, as observed in many postmenopausal women, are associated with loss of bone mass, deterioration of trabecular architecture, decrease in mineralization and increase in local stress risers caused by osteoclastic resorption. These factors, among others, are determinants of bone quality and may compromise bone strength leading to increased risk of fracture. The objective of the study was to use finite element modeling (FEM) to investigate the effects of removing bone selectively from high stress regions compared to uniform surface erosion of the bone to test whether loss of specific localized regions would result in large changes in biomechanical integrity. FEM analysis was performed on a 3D μ CT image of a female iliac crest trabecular bone obtained with a Scanco μ CT40 scanner at 16 micron resolution over a 3.5 mm³ volume of interest. The brick elements of the bone were assigned a single material property of 18 GPa with a Poisson's Ratio of 0.3. A simple compression test along the long axis was performed with a fixed force of 18 N. The resulting stress distribution was calculated using the Scanco FEM solver. FEM analysis was then repeated under the following conditions: (a) the top 5% highest stressed voxels were removed [5% localized erosion,(5% LE)], (b) the top 10% of the highest stressed voxels were removed [10% localized erosion,(10% LE)] and (c) a 5% uniform erosion was performed towards the center of the original model data [5% uniform erosion,(5% UE)]. The results of this analysis are shown in Figure 1. The stress distribution of the 5% UE case is very similar to the original. However, in the 5% LE case, there was more heterogeneity, with an increased percentage of high stress voxels. As discussed by Weinans et al [1], this broader distribution can be considered to be a compromised architecture, with a larger percentage of elements approaching their failure threshold. The results of the 10% LE case indicates that the trend continues with higher levels of localized bone loss. This data suggests that directed bone loss in high stress regions can have deleterious effects on the biomechanical properties of bone. Therefore, preservation of trabecular bone with anti-resorptive therapies could have a larger impact on bone integrity than suggested by changes in BMD.

[1] Weinans H., Van Reithbergen B. Huiskes R., #813, 43rd ORS 1997



Disclosures: **T.E. Dufresne**, P&G Pharmaceuticals 3.

SU087

The Effects of Rowing Versus Running on Skeletal Homeostasis. **M. Walcott***¹, **K. E. Ackerman**², **S. Hurwitz**¹, **N. Glass**¹, **M. S. LeBoff**¹. ¹Medicine, Brigham and Women's Hospital, Boston, MA, USA, ²Internal Medicine, Hospital of the University of Pennsylvania, Philadelphia, PA, USA.

Attainment of peak bone mass is affected by exercise, nutrition, and reproductive function. To understand how to best maximize bone mass in young adulthood, we studied the effects of rowing versus running on skeletal homeostasis in 123 women between the ages of 18 and 32. Bone Mineral Density (BMD) by dual x-ray absorptiometry (hip, spine, whole body), bone turnover markers (osteocalcin, N-telopeptides) and serum 25 (OH) vitamin D were measured on 68 elite female rowers (Olympic and top collegiate) and 55 elite female distance runners (top collegiate and marathoners). In addition the athletes completed food frequency and athletic training questionnaires. The rowers were divided into two standard groups: openweight rowers (>130lbs, n=55) and lightweight rowers (<130lbs, n=13). The runners and rowers did not differ significantly in prevalence of amenorrhea, oral contraceptive use, or incidence of stress fractures. The lightweight rowers had equivalent body mass index as the runners (p=0.14). Although the caloric intake was the same, compared with runners, lightweight rowers consumed significantly fewer (p<0.05) vitamins and minerals including calcium, vitamin D, and B vitamins. The rowers had significantly higher bone density at the lumbar spine compared with the runners (p=0.0001). The runners had increased bone density at the hip compared with the lightweight rowers, but not at the lumbar spine. In addition, only the hip BMD was significantly different in openweight versus lightweight rowers.

	Runners n=55	Light Row n=13	Run vs Row p-value	Run vs L Row p-value
Fem. Neck BMD (g/cm2)	0.90±0.1*	0.78±0.2	0.91	0.02
Troch BMD (g/cm2)	0.80±0.1	0.73±0.1	0.52	0.02
Total Hip BMD (g/cm2)	1.06±0.1	0.98±0.1	0.32	0.02
L Spine BMD (g/cm2)	1.01±0.1	1.05±0.1	0.0001	0.39
Osteocalcin (ng/ml)	7.1±2.3	4.26±1.7	0.001	0.0001
NTX (nM BCE/mM Cr)	45.4 ±23.3	39.0±21.1	0.85	0.37
Vitamin D (ng/ml)	31.76±9.4	37.43±8.9	0.01	0.05

*mean ± stdev

Osteocalcin, N-Telopeptide, and serum vitamin D levels (DiaSorin RIA, Stillwater, MN) were normal in all groups, but differences were noted between groups. Osteocalcin levels were significantly lower in the lightweight rowers than the other groups, while that of the runners was significantly higher than any other group. Vitamin D was significantly lower in the runners than the rowers. Runners, whose sport provides repetitive impact on the hip, had higher BMD at the hip compared with lightweight rowers, who are comparable in size. Openweight and lightweight rowers, despite differences in size, had similar spine BMD, likely a result of the forces applied on their backs during rowing and possibly conferring long-term benefit in protection against spine fractures.

Disclosures: **M. Walcott**, None.

SU088

Differentiated Chondrogenic Cell Line ATDC5 Cells Up-regulates Type II, X Collagen and Aggrecan mRNA Expression in Response to Mechanical Strain. **H. Horizono***, **I. Owan**, **F. Kanaya***. Orthopedic Surgery, University of the Ryukyus, Okinawa, Japan.

Mechanical strain is an important factor to regulate chondrocyte proliferation and differentiation. Response of chondrocyte to mechanical strain could be differentiation dependent. Chondrogenic ATDC5 cells differentiate into hypertrophic chondrocytes in response to insulin, and regulates type II, X collagen, aggrecan, ALP, and PTH/PTHrP receptor mRNA expression. In the present study, we examined whether ATDC5 cells respond to mechanical strain in differentiation specific manner. ATDC5 cells were cultured on plastic plates at 1×10⁶ cell/plate in the medium of F12/DMEM containing 5% FBS and 10 μ g/ml insulin. ATDC5 cells were stained with toluidine-blue to observe the morphologic change. We utilized an in vitro cell loading system using four-point bending. The magnitude of strain was 4200 μ strain and the frequency was 0.5 Hz. To assess the effects of mechanical strain on ATDC5 cells, the expression of type II, X collgaen, aggrecan, ALP, and PTH/PTHrP receptor mRNAs were determined using northern blot analysis. Six to 24 hours after beginning of loading on day 4 through day 28, total RNA was extracted and hybridized with various cDNA probe. ATDC5 cells initiated chondrogenic differentiation as reported before. Type II collagen mRNA expression was firstly observed on day 4, type X collagen and aggrecan on day 14. The effects of mechanical strain were not observed on day 4 or 7, but mechanical strain up-regulates type II, X collagen, and aggrecan mRNA in a time-dependent manner thereafter. However, there were no increase in ALP and PTH/PTHrP receptor expression. These results indicate that differentiated, but not undifferentiated ATDC5 cells up-regulates type II, X collagen, and aggrecan transcripts in response to mechanical strain.

Disclosures: **H. Horizono**, None.

SU089

Prediction of Ultimate Stress in Femoral Cortical Bone by Quantitative Computed Tomography. **L. Duchemin***¹, **V. Bousson**^{*2}, **C. Raossanally***¹, **C. Bergot**^{*2}, **J. Laredo**², **W. Skalli**^{*1}, **D. Mitton**^{*1}. ¹Laboratoire de Biomécanique, ENSAM - UMR CNRS 8005, Paris, France, ²Laboratoire de Radiologie Expérimentale, CNRS UMR 7052, Paris, France.

The purpose of this study was to assess a relationship between QCT grey levels and ultimate mechanical properties of femoral cortical bone, in order to develop a personalized fracture risk predicting Finite Element model of the proximal femur. 13 human femoral mid-diaphysis segments were collected, within 10 days post-mortem, from 2 males and 11 females aged from 54 to 101 years (mean 81.8), cleaned of soft tissue and frozen at -20°C. Segments were investigated using a CT-scan device (Somatom Plus 4 Siemens - 140 kV, 139 mAs, 0.25 mm pixels, 1.25 mm slices thickness). Cylinders were divided in 4 quadrants (posterior, anterior, medial and lateral) and 3 cortical parallelepipedic samples were obtained from each quadrant, using a micrometric low speed diamond saw (BUELHER Isomet) : two for compression (about 3x3x5mm) and one for traction (about 3x3x25mm). The long axis of the specimens corresponded to the diaphyseal axis. After removal of unusable specimens, 87 compression and 46 traction specimens were considered. Mechanical testing was performed on a universal testing system (INSTRON 5500-R). Each sample was tested destructively at a displacement rate of 0.6 mm/min after a pre-loading, and a pre-conditioning process of 3 cycles. Ultimate stress value was calculated as the maximal load divided by the cross sectional area of the specimen, measured on each specimen using a caliper. Ultimate stress values ranged from 10 to 98 MPa (mean value 54 +/- 21 MPa) in traction and from 36 to 151 MPa (mean value 107 +/- 30 MPa) in compression. Significant correlations were found between ultimate stress values and CT-scan Hounsfield Units in traction (r = 0.75, p<0.001) and in compression (r = 0.85, p<0.001).Considering the old age of the donors and the high number of females, ultimate stress values obtained in this study are coherent with previous values found in the literature. Good correlations between CT-scan data and maximal stresses, obtained on a large number of specimens and donors, will be useful for the individual prediction of femoral fracture for the elderly patients.

Disclosures: **L. Duchemin**, None.

SU090

Low-Intensity Pulsed Ultrasound and New Bone Formation within Interconnected Porous Calcium Hydroxyapatite Ceramics. T. Iwai*, N. Tsumaki, J. Murai*, A. Myoui, H. Yoshikawa. Department of Orthopaedic Surgery, Osaka University Graduate School of Medicine, Suita, Japan.

Micromechanical strain caused by ultrasound transmission through the body can promote bone formation in a manner comparable to the bone responses to mechanical stress postulated by Wolff's law. Clinical investigations and animal studies have shown that low-intensity pulsed ultrasound (LIPU) accelerate repair process of pseudoarthroses, delayed unions, non-unions, and distraction gaps generated in hemicallotasis. Recently developed fully open interconnected porous calcium hydroxyapatite ceramics (IP-CHA) show good osteoconductivities by allowing cells to enter into the pores deeply. Although IP-CHA can be a bone graft substitute in a variety of clinical settings, newly formed bone within the pores often matures very slowly. The effects of LIPU on formation of new bone within the pores of IP-CHA was explored in this study. **Methods:** Because ultrasound produces micromechanical strain, there are possibilities that LIPU could weaken IP-CHA mechanically by introducing cracks on thin walls of IP-CHA. To examine these possibilities, we applied LIPU to IP-CHA immersed in water for 48 hours and performed compression tests. Then animal studies were done using New Zealand white rabbits. After drill holes of 4 mm in diameter were made in the femoral condyles of both limbs, size-matched cylindrical blocks of IP-CHA were implanted. The right limb was subjected to LIPU treatment for 20 minutes daily, while the left limb was untreated as the control. After 2 weeks of treatment, rabbits were sacrificed and IP-CHA implants were harvested. After scanning of implants by micro-CT, volumes of newly formed bone within IP-CHA were measured using image analysis software. **Results:** Mean compressive strength of IP-CHA immersed in water without LIPU application was 10.38 ± 0.90 Mpa (n = 12). That of IP-CHA receiving LIPU application for 48 hrs was 9.86 ± 0.77 Mpa (n = 12). There was not significant difference (P = 0.14), suggesting that LIPU application may not weaken IP-CHA itself. Following animal studies showed that mean volumes of the newly formed bone were 9.89 ± 5.05 (n = 3) for IP-CHA implants treated with LIPU and 19.21 ± 4.64 (n = 4) for those without LIPU treatment. These results suggest that LIPU application may substantially accelerate maturation of bone which is newly formed within the pores of IP-CHA. The use of LIPU in combination with IP-CHA may be one of options in treating bone defects.

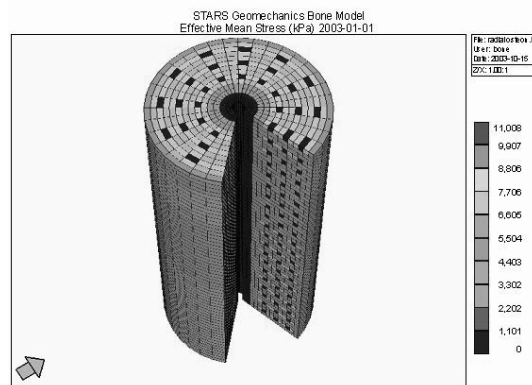
Disclosures: **T. Iwai**, Teijin 2.

SU091

Modeling Fluid Flow and Tracer Transport in Haversian Bone. G. C. Goulet*¹, N. Hamilton*¹, D. Coombe*², D. Tran*², R. Zernicke³. ¹Mechanical Engineering, University of Calgary, Calgary, AB, Canada, ²Computer Modelling Group, Calgary, AB, Canada, ³Mechanical Engineering & Faculties of Kinesiology and Medicine, University of Calgary, Calgary, AB, Canada.

Intrinsic fluid flow likely plays a major role in the initiation of bone adaptation, but the underlying mechanisms remain unclear (Knothe Tate, 2003). To better understand fluid flow characteristics in bone, a model was developed to recreate idealized fluid flow in cortical loaded bone at the osteonal level. This model was implemented in STARS, an advanced process fluid flow simulator that contains a coupled mechanical displacement simulator. Bone was modeled at the osteonal level with a radial grid to approximate an osteon. High porosity regions were added to simulate the presence of the Haversian canal at the center of the osteon and lacunae, in which osteocytes are encased within the solid bone matrix. Multiple cycles of 0.1% axial strain were applied at physiologically relevant frequencies (0.8 Hz - step loads). Interactive molecular transport was modeled with tracers with molecular weights equivalent to glucose and lactate, and placed initially in the Haversian canal and osteocyte lacunae, respectively. As the simulation progressed, the tracers were transported through the model by diffusion and load-induced convection. The possibility of osteocyte-induced glucose to lactate reactive conversion was considered. Immediately after compressive load application, fluid flowed from the high porosity regions into the low porosity bone matrix. Following that initial flow, the fluid flowed back from the solid matrix into the lacunae and Haversian canal. The largest load-induced fluid velocities were found in regions surrounding the modeled lacunae. If osteocytes triggered the remodeling process based on the cells sensing fluid flow (cf. Cowin & Weinbaum, 1998), then the model showed that the signal for load transduction was especially strong in their vicinity. The loading-enhanced fluid flow also had the effect of increasing the nutrient supply and waste removal potential to and from the osteocytes. Thus, these simulations provided evidence that cyclical loading could contribute to bone health by enhancing intrinsic fluid flow.

Cowin S and Weinbaum S (1998) *Am J Med Sci* 316 (3) 184-188
Knothe Tate M (2003) *J Biomech* 36, 1409-1424



Disclosures: **G.C. Goulet**, None.

SU092

Mechanobiological Regulation of Molecular Expression and Tissue Phenotype during Bone Healing. K. T. S. Palomares*¹, T. A. Einhorn², L. C. Gerstenfeld³, E. F. Morgan³. ¹Department of Biomedical Engineering, Boston University, Boston, MA, USA, ²Department of Orthopaedic Surgery, Boston University School of Medicine, Boston, MA, USA, ³Department of Aerospace and Mechanical Engineering, Boston University, Boston, MA, USA.

A growing body of evidence indicates that mechanical cues modulate the development and repair of skeletal tissues by regulating gene expression and cell differentiation. Several studies have shown that the mechanical environment plays a crucial role during the bone repair process which involves mechano-sensitive, pluripotent mesenchymal cells. The overall goal of this project was to purposefully modulate the bone repair process by using an applied, cyclic bending motion in order to promote cartilage, rather than bone formation. A mid-diaphyseal, transverse osteotomy was created in each of 64 (32 experimental and 32 control) rat femora and was stabilized with a custom-designed external fixator. Experimental animals were subjected to daily bending stimulation of the osteotomy gap; this stimulation consisted of 60° (±30°) of cyclic angular displacement applied at 1 Hz for 15 minutes daily for 1, 2 or 4 weeks following a 10-day latency period. Control animals were subjected to continuous rigid fixation. Tissue phenotypes and expression of specific mRNA levels were analyzed at each timepoint using histological analyses, ribonuclease protection assays, and cDNA microarrays. Statistical analyses included analyses of variance (ANOVA) and Tukey *post hoc* tests. Bending stimulation substantially altered the bone healing response at both tissue and molecular levels. Stimulated specimens exhibited an increase with time in the amount of cartilage present within and surrounding the osteotomy gap, whereas control specimens demonstrated complete bony bridging at 42 days. Molecular analyses revealed corresponding temporal alterations in the chondrogenic and osteogenic mRNA expression patterns. As compared to expression patterns in the control animals, expression of collagen types II and X persisted until later timepoints (days 17-24), the peak in the expression levels of osteopontin and osteocalcin occurred later (days 24-38), and the expression levels of bone morphogenetic protein-3, which has been shown to be down-regulated during bone formation, was higher at all timepoints. These results indicate that manipulation of the local mechanical environment can directly alter skeletal tissue repair, and they further suggest the potential of using applied mechanical stimulation to elucidate novel mechanisms of cartilage repair. Such insights into cartilage repair may substantially benefit treatment strategies for degenerative joint diseases such as osteoarthritis.

Disclosures: **K.T.S. Palomares**, None.

SU093

Directional Sensitivity of Rodent Long Bone Cortical Strength to Collagen Denaturation. M. Barrero*, L. Gubago*, D. J. Adams. Orthopaedic Surgery, University of Connecticut Health Center, Farmington, CT, USA.

The small size of rodent long bones precludes the application of most formal mechanical property testing techniques, requiring structural bending tests to measure cortical bone tissue strength in the longitudinal direction. Because whole bone tests exhibit variation and inaccuracy, alternative tests are desirable. We developed a test technique for measuring the circumferential strength of rodent diaphyseal cortex using open-ring specimens cut from multiple long bone cross-sections. The purpose of this study was to measure the longitudinal versus circumferential sensitivity of long bone cortical strength to thermally induced collagen denaturation. 50 diaphyseal open-ring specimens were cut from left and right femora (5 per femur) of 6 month old Sprague-Dawley rats. The radius was isolated for 3-point bend tests, and cross-section area moment of inertia was measured from microCT images. Control specimens were tested to establish baseline cortical strength in the circumferential (open-ring) and longitudinal directions (whole bone bending). Treatment specimens were subjected to controlled thermal denaturation of collagen prior to testing, using dry oven heat exposure for 4 hours at either 90°C (control for drying and rehydration) or 150°C (to break hydrogen bonds in calcified collagen). Cortical tissue strengths were compared between groups using unpaired t-tests. Whole bone tests demonstrated an average longitudinal cortical tissue strength of 199 ± 48 MPa, exhibiting 24% variation in the measurement. Collagen denaturation reduced longitudinal strength by 61.2% to 77 ± 55 MPa (p < 0.0001), but with 71% variation. Open-ring tests

ASBMR 27th Annual Meeting

demonstrated an average circumferential cortical tissue strength of 54 ± 13 MPa, exhibiting 23% variation. Collagen denaturation reduced circumferential strength by 43.3% to 31 ± 6 MPa ($p < 0.0001$), with only 21% variation. Cortical bone strength was reduced approximately 50% due to heat-induced collagen denaturation at 150°C , whereas others have found significant reductions in mechanical properties of bovine bone only when heated beyond 150°C for the same 4 hour exposure. Despite the predominant orientation of collagen, documented higher strength, and larger reduction in strength with collagen denaturation in the longitudinal direction, circumferential strength also was reduced substantially. Open-ring specimens demonstrated considerably less variation in strength measurements following collagen denaturation than whole bone bending tests. With the ability to obtain multiple specimens per long bone with relative ease, the opening test may provide increased statistical power for hypothesis testing in rodent skeletal research.

Disclosures: D.J. Adams, None.

SU094

Direct Effects of Bisphosphonates on Primary Bone Tumor Cells *In Vitro*.

U. C. Stumpf¹, S. Goettig², M. Schoenherr¹, C. Eberhardt¹, W. J. Fassbender³, R. Henschler², A. A. Kurth¹. ¹Orthopedic Surgery, University Hospital, Frankfurt, Germany, ²German Red Cross Blood Center, Institute of Transfusion Medicine and Immune Hematology, Frankfurt, Germany, ³Department of Internal Medicine, Hospital Zum Heiligen Geist, Kempen, Germany.

Regardless the survival rate of 80% there is still a significant number of non-responders to the chemotherapeutic treatment of osteo- and Ewing's sarcomas who develop metastasis and finally die. Bisphosphonates are known to induce apoptosis in different cell types such as osteoclasts and breast cancer cells. Direct effects of bisphosphonates on primary bone tumors are not resolved. Therefore we tested and compared the effects the bisphosphonates Clodronate (CL) and Ibandronate (IB) could have on human sarcoma cells in order to evaluate their different potency in vitro. Two human osteosarcoma cell lines (SAOS 2 and 791 TM HOS) and two human Ewing's sarcoma cell lines (RD-ES and TC 71) were treated with CL (2 mM, $1\text{mM} \cdot 10^{-7}\text{M}$) and IB ($10^{-3}\text{M} \cdot 10^{-7}\text{M}$) for 24, 48 and 72 h. Cell apoptosis was evaluated by fluorescent flow cytometric analysis: quantification via FACS and PI staining. After 72 h staining with trypan blue and cell counting of dead cells was done. CL-treated cultures of SAOS show after 72 h of incubation in a concentration 2 mM and 10^{-3}M 12,6 % and 8,7 % apoptotic cells, respectively. HOS cell cultures show already after 48h in the range of 2 mM and 10^{-3}M apoptosis <10 % of the cells, after 72 h and the concentration of 10^{-3}M there are 10-25 % apoptotic cells. Ewing's sarcoma cell cultures were evaluated after 72 h treated with CL: RD-ES cells show at 2mM 10-25 % apoptosis. TC-71 show at 2mM Clodronate < 10% of apoptosis. 10^{-3}M IB solution causes on SAOS cells after 48 h <10% and after 72 h 10-25% apoptotic cells. HOS cells show after 48 h in the range of 10^{-3}M 10-25 % and at 10^{-4}M < 10 % apoptotic cells; after 72 h in both concentrations of IB solution apoptotic cells increased to > 40 %. RDES cells which were incubated with IB showed at 10^{-3}M (5,1%) - 10^{-5}M (12,3 %) clear parts of the culture in s-phase of cell cycle. TC 71 show at concentration of 10^{-3}M and 10^{-4}M IB 10- 25 % and of 10^{-5}M and 10^{-6}M < 10 % of apoptotic cells, respectively. We could demonstrate that the bisphosphonates CL and IB have time- and dose-related direct effects on the investigated primary bone tumor cells. Both induce apoptosis and inhibition of cell proliferation in different ranges, but with IB a much better effect with lower concentration was found. If similar findings are observed in vivo, the use of IB may also be indicated as an adjuvant to existing chemotherapeutic protocols.

Disclosures: U.C. Stumpf, None.

SU095

Expression of RANKL, OPG, PTHrP and OCIL in Multiple Myeloma Are Influenced by the Tumor Cells' Proximity to Bone. V. Kartsogiannis¹, C. Ly¹, H. Zhou¹, O. Gallagher³, C. Buckle³, E. De Leenheer³, K. Vanderkerken⁴, K. W. Ng⁵, T. J. Martin¹, M. T. Gillespie¹, P. I. Croucher³.

¹Bone, Joint and Cancer Unit, St. Vincent's Institute, Fitzroy, VIC, Australia, ²Bone Biology Unit, ANZAC Research Institute, Concord, NSW, Australia, ³Academic Unit of Bone Biology, Division of Clinical Sciences, University of Sheffield Medical School, Sheffield, United Kingdom, ⁴Department of Hematology and Immunology, Free University Brussels, Brussels, Belgium, ⁵Department of Endocrinology, St. Vincent's Hospital, Fitzroy, VIC, Australia.

Multiple myeloma is characterized by the development of lytic bone lesions mediated by increased osteoclastic bone resorption. A number of molecules have been implicated in promoting the increase in osteoclastic resorption including RANKL and macrophage protein-1 alpha. While the RANKL/RANK/OPG system may indeed play a critical role in the osteolysis in myeloma, other molecules may also contribute. One novel family of osteoclast inhibitors, named OCILs (Osteoclast Inhibitory Lectins) may also be effective in altering the progression of multiple myeloma since they are effective in blocking RANKL-, TNF α -induced and TGF β -primed osteoclast formation. Using in situ hybridization and immunohistochemistry, mRNA and protein expression of OCIL was examined in the 5T2MM murine model of myeloma. OCIL was shown to be expressed by 5T2MM myeloma cells residing in bone. Approximately 80% of myeloma cells within the marrow cavity expressed OCIL. Myeloma cells residing closer to the growth plate, or those contained well within the bone environment, exhibited higher levels of OCIL mRNA and protein than the population of myeloma cells outside the bone. We therefore examined the mRNA and protein expression for other key factors in myeloma including RANKL, OPG and PTHrP. Similar to OCIL, the expression of each of these was elevated when myeloma cells were in proximity to bone but not outside of bone. OPG mRNA and protein were

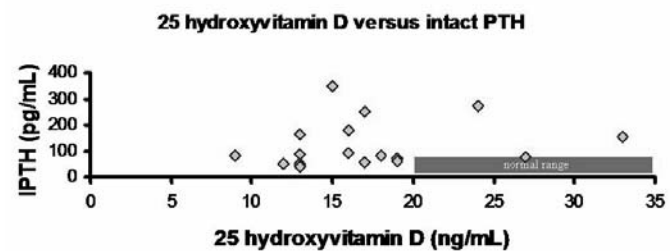
expressed in only a limited number of myeloma cells. Furthermore, quantitative RT-PCR analysis, also revealed a consistent expression of OCIL in the 5T2MM and 5T33MM myeloma cell lines as well as the murine bone marrow endothelial cell lines, STR10 and STR12. These results demonstrate that murine myeloma cells express OCIL and raise questions about the potential role of OCIL in the progression of myeloma as well as the role of the bone microenvironment to influence the expression of other candidate molecules (RANKL, OPG and PTHrP) in the development of osteolytic bone disease.

Disclosures: V. Kartsogiannis, None.

SU096

Vitamin D Deficiency Occurs with High Frequency in Acute Leukemia. M. E. Cabanillas, D. A. Thomas*, A. O. Hoff, M. C. Foudray*, G. N. Mattiuzzi*, H. M. Kantarjian*, C. Escalante*, R. F. Gagel. General Internal Medicine, MD Anderson Cancer Center, Houston, TX, USA.

Background: Acute lymphoblastic leukemia (ALL) and lymphoblastic lymphoma (LL) are conditions associated with rapid clonal expansion of cells of the B and T-cell lymphocytic lineage. In pediatric patients osteopenia and lytic bone abnormalities have been found with some frequency but prior reports have documented no abnormalities of parathyroid or vitamin D (VD) function. There has been no systematic evaluation of calcium metabolism in adults with this disorder. **Methods:** As part of a prospective study of bone loss in ALL & LL during chemotherapy with hyperCVAD, serum 25OHD3 (Quest Diagnostics), calcium (Ca^{++}) and bone density were measured. Most patients had intact PTH (iPTH) measurements. **Results:** Ten men and 13 women were prospectively evaluated in this updated report. Median age was 49 (r: 18-71). Seventeen pts had ALL, 6 had LL. Low 25OHD3 levels (<20ng/ml) were found in 15/23 (65%), while an additional 4/23 pts (17%) had low normal levels (20-25ng/ml). Evidence of secondary hyperparathyroidism (high iPTH [$>65\text{ pg/mL}$] and 25OHD3 $\leq 25\text{ng/mL}$) was seen in 11/17 (65%) of pts (see graph). Five of these pts had secondary hyperparathyroidism characterized by high iPTH levels with low ionized Ca^{++} . Baseline skeletal abnormalities were seen in 13/17 (93%) (osteopenia: 11/17, osteoporosis: 1/17, vertebral fracture: 1/17, lytic bone lesions: 1/17, and osteosclerosis: 2/17). Mean SD lumbar spine BMD T and Z scores were -0.6 (range -2.9-2.2) and -0.04 (range -2.7-3.5), respectively. Although these abnormalities occurred in both diseases, the pts with the most striking abnormalities had B-ALL. **Conclusions:** 1) Abnormalities of vitamin D and calcium metabolism occur in adult ALL and LL with surprising frequency, indicating that evaluation for this possibility should be performed routinely. 2) The etiology of these abnormalities is unclear and may be related to absorptive abnormalities in leukemic patients or inadequate UV exposure because of illness. 3) Vitamin D inhibits clonogenic growth of leukemic B-cells *in vitro* and is a differentiating agent in leukemic myeloid cell lines. It is therefore possible that VD deficiency may contribute to the pathogenesis of this neoplastic disorder.



Disclosures: M.E. Cabanillas, Procter and Gamble 2.

SU097

Evidence that Interferon Signaling Is Required for 2-ME-Mediated Osteosarcoma Cell Death. A. Maran¹, K. L. Shogren¹, M. Zhang¹, M. J. Yaszemski¹, R. T. Turner². ¹Orthopedic Research, Mayo Clinic, Rochester, MN, USA, ²Nutrition and Exercise Science, Oregon State University, Corvallis, OR, USA.

2-Methoxyestradiol (2-ME) is a metabolite of estradiol that leads to induction of interferon- β gene expression and apoptosis in human osteosarcoma cells. Interferons exert pleiotropic effects and have been shown to be involved in the anti-viral, anti-growth and anti-cancer activities in a number of systems through the stimulation of one or more responsive genes. However, no cause and effect relationship has been established between interferon signaling and 2ME-induced osteosarcoma cell death. Therefore, we have investigated the requirement of the interferon pathway for 2-ME-induced cell death in MG63 human osteosarcoma cells. 2-ME treatment induced interferon- β gene expression and increased interferon- β promoter-dependent reporter gene activity in osteosarcoma cells but not in normal primary human osteoblasts. Normal cells are resistant to 2-ME. In addition, 17 β -estradiol and metabolites (2-, 4- and 16 α -hydroxyestradiol), none of which induce cell death have no effect on interferon gene expression and promoter activity in MG63 cells. RNA-dependent protein kinase (PKR), a downstream mediator of interferon signaling, is induced in MG63 cells by 2ME. Blockage of the downstream signal through a dominant negative mutant interferon-regulated protein, PKR prevents 2-ME-mediated cytotoxicity. Taken together these data demonstrate a close association between induction of interferon signaling, induction of PKR and cell death in MG63 cells.

Disclosures: A. Maran, None.

SU098

Imaging Tumor Burden by [¹⁸F]FDG-PET and Osteoblast Activity by [^{99m}Tc]MDP-SPECT/CT in the 5TGM1 Mouse Model of Myeloma Bone Disease. B. O. Oyajobi¹, B. Goins^{*2}, A. Gupta^{*1}, C. Zavaleta^{*2}, B. Grubbs^{*1}, C. Wideman^{*1}, Z. Wang^{*2}, I. R. Garrett³, W. Phillips^{*2}, G. R. Mundy¹. ¹Cell & Structural Biology, Univ Texas Hlth Sci Ctr, San Antonio, TX, USA, ²Radiology, Univ Texas Hlth Sci Ctr, San Antonio, TX, USA, ³OsteoScreen Ltd, San Antonio, TX, USA.

The high morbidity and mortality rates associated with multiple myeloma (MM) are due to complications resulting from its effects on the skeleton. These complications including pathological fractures reflect, in part, tumor-induced osteolysis as well as failure of new bone formation. Lack of suitable preclinical models of MM bone disease that closely reflect changes seen in humans has hampered development of novel anti-myeloma agents. Standard histological techniques, which are the gold standards for monitoring tumor progression and osteoblast function, are labor-intensive and invasive and therefore limit the use of mouse models for rapidly assessing efficacy of new treatment modalities. To remedy these shortcomings, we have applied state-of-the-art small animal nuclear imaging modalities [positron emission tomography (PET) and single photon emission computed tomography (SPECT/CT)], similar to those utilized clinically, to the murine 5TGM1 myeloma bone disease model. PET scans performed using [¹⁸F]-fluorodeoxyglucose (FDG) provide functional measurements of tumor burden and preliminary studies demonstrate accumulation of FDG in tumors in the skeleton. To demonstrate the feasibility of using SPECT to assess osteoblast function in myeloma-bearing mice, we performed scintigraphic scans after administration of [^{99m}Tc]-hydroxymethylene diphosphonate (MDP) and found that overall skeletal uptake was reduced in tumor-bearing mice. Biodistribution studies confirmed that uptake was suppressed in all bones of 5TGM1-bearing mice in comparison to soft tissues from same mice or to bones of non-tumor bearing mice. Consistent with these findings, cancellous bone volumes and bone formation rates, determined by dynamic bone histomorphometry, are significantly reduced in the 5TGM1 model. These data suggest utility of (i) PET in real-time, longitudinal monitoring of tumor growth and spread or regression in response to therapy within skeletons of individual live animals; (ii) SPECT/CT in concurrent spatial localization of increased osteoblastic activity in response to investigative bone anabolic therapy. Together, these novel imaging capabilities increase the utility of the 5TGM1 model beyond what would otherwise be possible using two-dimensional radiography and bone histomorphometry, and should have a substantial impact not only on identifying novel anti-myeloma therapies, but also in studies to gain mechanistic insights to these therapies.

Disclosures: B.O. Oyajobi, Osteoscreen 5.

SU099

RANKL Expression Is Regulated in Oral Squamous Cell Carcinoma. E. Li^{*1}, M. Liu^{*1}, N. D'Silva^{*2}, K. L. Kirkwood¹. ¹Periodontics/Prevention/Geriatrics, University of Michigan, Ann Arbor, MI, USA, ²Oral Med/Path/Surgery, University of Michigan, Ann Arbor, MI, USA.

Invasion of oral squamous cell carcinoma (SCC) into bone is a result of osteoclastic activity. RANKL is a key cytokine involved in osteoclastogenesis and mediates bone invasion of a variety of malignant tumors. The purpose of the present study was to determine if established oral SCC cell lines express RANKL in response to osteotropic cytokines and hormones in vitro and in vivo. Several different oral SCC cell lines were treated with cytokines/hormones (IL-1 β , TNF α , IL-6/IL-6sR, PTH, or 1,25-di(OH)₂VitD₃) for 16-18 hours. Total RNA was isolated and RANKL expression was determined by real-time PCR (ABI 7900 Real-Time System). To determine if osteotropic cytokines/hormones affected RANKL proximal promoter function, UMSCC11B, an oral SCC cell line, was transfected with the human proximal promoter containing 1974-bp of 5'-flanking sequence of the RANKL gene in reporter plasmid, pGL3-Basic. Stable cell lines were established by co-transfection with the pcDNA3.1-neo. Luciferase (Luc) reporter activity was assessed following osteotropic cytokines/hormone cell treatment using a luminometer (Molecular Devices) with normalized total cytoplasmic protein. To determine if RANKL promoter activity in oral SCC was active in vivo, UMSCC11B-RANKL-Luc cells were injected into the tibia (1x10⁷ cells; n=6) or floor of the mouth (3 or 5 x10⁷ cells; n=3 each) of athymic (nu/nu SCID) mice. In vivo real-time RANKL promoter activity was assessed by bio-luminescence following intraperitoneal injection of D-luciferin substrate (Xenogen IVIS imaging system) over a 4 week period. Results from real-time PCR indicated UM-SCC -(11A and 22B) express RANKL mRNA upon TNF α stimulation whereas UMSCC 11B, 74A and 74B respond to IL-1 β , VitD₃, PTH, and IL-6. UMSCC11B cells stably transfected with -RANKL-Luc, exhibited a 2-3 fold increase in Luc activity following 18-hr treatment with VitD₃, PTH and IL-6, in agreement with real-time PCR results. In vivo RANKL promoter activation data from UMSCC11B-RANKL-Luc injected cells indicates that both the tibia and floor of the mouth model exhibit increased Luc activity over time in most animals injected. The data indicate that SCC tumors produce RANKL in response to osteotropic cytokines and hormones, consistent with the ability of SCC to invade bone through local extension of the tumor.

Disclosures: K.L. Kirkwood, None.

SU100

Alpha-Calmodulin Kinase II (α -CaMKII) Is Critical for Cell Cycle Progression in Osteosarcoma. V. Saini^{*1}, A. Zayzafoon^{*2}, G. P. Siegal^{*2}, J. M. McDonald², M. Zayzafoon². ¹The Department of Physiology and Biophysics, The University of Alabama at Birmingham, Birmingham, AL, USA, ²The Department of Pathology, The University of Alabama at Birmingham, Birmingham, AL, USA.

Osteosarcoma is the most frequent primary malignant bone tumor in children and adolescents and is characterized by its abnormal cell proliferation. Overexpression of *c-fos* and subsequent alterations in the cell cycle have been suggested to be involved in the neoplastic transformation of osteoblasts. We have previously shown that α -CaMKII is expressed in osteoblasts and regulates *c-fos* expression and osteoblast differentiation. In this study we examined the role of α -CaMKII in the growth and neoplastic progression of osteosarcoma. We used multiple well-characterized human osteosarcoma cell lines, HOS, SaOS-2, MG-63 as well as primary human osteosarcoma tissue derived from patients. Immunofluorescence and Western blotting analyses show that α -CaMKII is expressed in all osteosarcoma cell lines and in human tumor tissue tested. The phosphorylated form of α -CaMKII has distinctive punctate perinuclear localization. Pharmacologic inhibition of CaM and CaMKII by 10 μ M TFP and KN93, respectively, significantly reduced the mRNA levels of *c-fos*, the osteoblastic gene markers *alkaline phosphatase*, *collagen I*, *osteocalcin* and the metastatic marker *metalloproteinase-13*. TFP and KN93 treatment also inhibited proliferation (80%, P<0.01) of osteosarcoma cell lines as determined by an MTT assay and cell counting. Similarly, a dramatic decrease in the number and size of colonies formed by osteosarcoma cells grown in growth factor reduced Matrigel supplemented with 10 μ M TFP or KN93 was observed. The pharmacologic inhibition of CaMKII decreases levels of the cyclins, specifically cyclins D1, D2 and D3. This decrease is more pronounced in the nuclear fraction as compared to the cytoplasmic fraction indicating that the inhibition of CaMKII inhibits proliferation of osteosarcoma cells by decreasing the nuclear localization of cyclins. Taken together, our results demonstrate that the inhibition of α -CaMKII in osteosarcoma decreases proliferation by inhibiting the nuclear translocation of cyclin D and promoting cell cycle arrest.

Disclosures: V. Saini, None.

SU101

Inhibition of Primary Bone Tumor Cell Proliferation by a Hedgehog Pathway-Inhibitor. J. Warzecha^{*1}, C. Brünning^{*1}, S. Goettig^{*2}, R. Henschler^{*2}, A. A. Kurth^{*1}. ¹Orthopaedic Surgery, University Hospital Frankfurt, Frankfurt, Germany, ²Institute of Transfusion Medicine and Immune Hematology, University Hospital Frankfurt, Frankfurt, Germany.

Osteosarcomas (OS) and Chondrosarcomas (CS) are the most frequent primary malignant bone tumors in humans. Even though OS are chemosensitive, about 30% of patients remain poor responder and have a bad long term prognosis. In CS there is a resistance to conventional forms of treatment such as chemotherapy and radiation, resulting in a high recurrence rate. The Hedgehog (Hh) signalling pathway has been shown to regulate crucial pathways of proliferation and differentiation during embryonic development. Moreover, in adult tissues the Hedgehog (Hh) signalling pathway controls stem cell behaviour. There is evidence that uncontrolled activation of this pathway results in specific types of cancer. Furthermore in certain types of cancer - such as medulloblastoma -inhibition of Hh signalling is able to suppress tumour growth and induces apoptosis of neoplastic cells. We investigated whether the novel agent Cyclopamine causes growth inhibition in osteosarcoma and chondrosarcoma cells. Using different cell proliferation assays, including BrdU-incorporation and assessment of XXT metabolism, we are able to demonstrate that cyclopamine exhibits considerable in vitro efficacy against the chondrosarcoma cell line SW-1353 and the osteosarcoma cell line HOS. Assessment of the altered proliferative activity reveals a reduction of the cell count by 50% for SW 1353 and by 90% for HOS upon incubation with cyclopamine. In conclusion, our results provide first evidence for the important role of Hh-signalling in the proliferative activity of malignant osteochondrogenic tumor cells and distinguish Hh-inhibition by cyclopamine as a potential molecular target in the treatment of these tumors.

Disclosures: J. Warzecha, None.

SU102

Myeloma Cell-Derived MIP-1 Suppresses Dendritic Cell Maturation and Induces Aberrant Osteoclastogenesis from Immature Dendritic Cells. T. Hashimoto^{*1}, M. Abe¹, M. Hiasa^{*2}, J. Asano^{*1}, Y. Tanaka^{*1}, E. Sekimoto^{*1}, S. Ozaki^{*1}, S. Kido¹, D. Inoue¹, T. Matsumoto¹. ¹Department of Medicine and Bioregulatory Sciences, University of Tokushima Graduate School, Tokushima, Japan, ²Department of Orthodontics, University of Tokushima Graduate School, Tokushima, Japan.

Multiple myeloma (MM) is characterized by devastating bone destruction and immune suppression in which impaired dendritic cell (DC) function plays a role. We have demonstrated that MM cells reciprocally reduce myeloid DC formation along with enhanced osteoclast (OC) formation from their common progenitor, monocytes. MM-derived osteoclastogenic macrophage inflammatory protein (MIP) -1 α and β turned out to play critical roles in OC induction and suppression of myeloid DC differentiation from monocytes. We also found that CD83+ mature DC formation from immature DCs was almost completely suppressed by co-existing MM cells, suggesting suppression of DC function. Such immature DCs have also been shown to endow with the propensity to differentiate into OCs upon the stimulation with M-CSF and RANK ligand. In order to

ASBMR 27th Annual Meeting

further clarify the effects of MIP-1 as well as MM cells on DC differentiation and function, we first investigated the function of immature DCs after the treatment of TNF-alpha in the presence or absence of RPMI8226 cells or MIP-1. When thus treated DCs were irradiated and co-cultured with anti-CD3-treated autologous CD8+ T cells, interferon-gamma production from the T cells was substantially reduced by the DCs pretreated with MIP-1 or RPMI8226 cells, indicating defective function of these DCs. However, MIP-1 as well as MM conditioned media were able to induce the formation of TRAP+ - multinucleated cells from immature myeloid DCs in the presence of soluble RANK ligand, although MIP-1 or MM conditioned media alone showed only minor effects. Consistently, antibodies against MIP-1 alpha and beta in combination abrogated the MM conditioned media effects, suggesting an additional role for MM cell-derived MIP-1 in enhanced osteoclastogenesis in MM. From these results, MM cell-derived MIP-1 not only triggers the reciprocal induction of OC and myeloid DC differentiation from monocytes but also acts on immature DCs to suppress functional maturation of DCs and induce aberrant differentiation into OCs. Therefore, inhibition of MIP-1 actions may enhance anti-tumor immunity and protection against infection through restoration of impaired DC function along with prevention of bone destruction in MM.

Disclosures: **T. Hashimoto**, None.

SU103

Identifying Targets anti-Myeloma by Characterizing the Plasma Cell Specific Unfolded Protein Response. **L. Oliva**, **E. Benasciutti**, **R. Sitia***, **S. Cenci**. DiBiT, San Raffaele Scientific Institute, MILANO, Italy.

Multiple Myeloma (MM) is a frequent, severe, and still incurable hematological malignancy that originates from the clonal expansion of plasma cells and causes massive bone destruction. Recently, a new class of drugs, proteasome inhibitors (PI), proved effective in MM therapy, and are currently in phase 4 clinical trial. The anti-tumour effect of these drugs owes to their ability to prime apoptosis selectively in MM cells, via undetermined mechanisms. The normal counterpart of MM, plasma cells, the factories of soluble Ig, are subject to intense ER stress and rely on the adaptive unfolded protein response (UPR) for their differentiation and activity. PI induce a robust UPR, providing a framework to understand their peculiar efficacy on MM cells. To explore the molecular bases of such therapeutic effect, we first asked whether plasma cell differentiation confers apoptotic sensitivity to PI on different models (in vitro, from the murine inducible B lymphoma I.29μ+, and ex vivo, from primary mouse B cells). Our findings reveal that plasma cell differentiation generates apoptotic sensitivity to PI at late stages of differentiation, in correlation with Ig production and activation of a robust UPR activation. The selective toxicity of PI on plasma cells was then confirmed ex vivo in plasma cells from LPS-injected mice. Moreover, we found that PI treatment in vivo significantly reduces the title of circulating Ig in OVA-immunized mice. These data demonstrate that proteasomes regulate plasma cell lifespan and the resulting duration of the humoral response. The UPR is a key inducer of apoptosis in many diseases. To gain insights on the mechanisms that trigger death in plasma cells, we investigated the ordered unfolding of the B cell-specific UPR over time by assessing histone post-translational modifications and cofactor recruitment to UPR target genes by chromatin immunoprecipitation. Our data reveal that: 1) the plasma cell-specific UPR, unlike that induced by pharmacological ER stressors, is accompanied by profound chromatin remodelling at UPR genes (e.g. XBP-1, CHOP and BiP); 2) plasma cell differentiation activates a potentially protective heat shock response (HSR); 3) histone acetylation at target genes correlates with recruitment to gene promoters of the key UPR transcriptional coactivator XBP-1. Our findings link the molecular bases of sensitivity of MM to PI to the Ig-secreting phenotype, and reveal that chromatin remodelling is involved in the plasma cell UPR. Altogether, our data, by characterizing plasma cell differentiation, may help identify potential targets and design more specific therapeutic tools against MM.

Disclosures: **L. Oliva**, None.

SU104

SERMs-Induced Myeloma Cell Apoptosis: A Study of NF-κB Inhibition and Gene Expression Signature. **S. Olivier***¹, **P. Close***², **E. Castermans***³, **L. de Leval***⁴, **S. Tabruyn***⁵, **A. Chariot***², **M. Malaise***¹, **M. Merville***², **V. Bours***², **N. Franchimont***¹. ¹Rheumatology, University of Liège, Liège, Belgium, ²Clinical Chemistry and Human Genetics, University of Liège, Liège, Belgium, ³Hematology, University of Liège, Liège, Belgium, ⁴Pathology, University of Liège, Liège, Belgium, ⁵Molecular Biology and Genetic Engineering, University of Liège, Liège, Belgium.

As multiple myeloma (MM) remains associated with a poor prognosis, novel drugs affecting specific signalling pathways are needed. Osteolytic lesions remain a critical morbidity factor in MM and drugs that would target both myeloma cell growth and osteoclast development would be of great interest. The efficacy of selective estrogen receptor modulators for the treatment of MM and its associated bone lesions is not well documented. We demonstrated that two SERMs, raloxifene and tamoxifen, decreased JJN-3 myeloma cell viability and induced caspase-dependent apoptosis. Moreover, raloxifene inhibited constitutive NF-κB activation in myeloma cells by removing p65 from its binding sites through ERα interaction with p65. In contrast to myeloma cells, raloxifene had no effect on NF-κB activity in osteoblasts. Importantly, micro-array analysis showed that raloxifene treatment decreased the expression of known NF-κB-regulated genes involved in myeloma cell survival and myeloma bone disease (e.g. *c-myc*, *mip-1a*, *hgf*, *pac1*,...) and induced the expression of a subset of gene regulating cellular cycle (e.g. *p21*, *gadd34*, *cyclin G2*,...). As raloxifene inhibits *mip-1a* synthesis in JJN3 and *mip-1a* is a factor known to influence osteoclast development, raloxifene may be an interesting drug to test for the prevention or treatment of MM osteolytic lesions. In conclusion, raloxifene

induces myeloma cell apoptosis most likely by an NF-κB dependent mechanism. These findings also provide a transcriptional profile of raloxifene treatment on JJN-3 cells, therefore offering the framework for future studies of SERMs therapy in MM.

Disclosures: **N. Franchimont**, **Eli Lilly** and **Co.** 5.

SU105

Impaired Proteasomal Capacity and ER Stress as Therapeutic Targets against Multiple Myeloma. **S. Cenci***¹, **A. Mezghrani***¹, **P. Cascio***², **L. Oliva***¹, **A. Orsi***¹, **E. Ruffato***¹, **E. Pasqualetto***¹, **R. Sitia***¹. ¹DIBIT, San Raffaele Scientific Institute and University Vita-Salute San Raffaele, Milano, Italy, ²Dept. of Morphophysiology, University of Turin, Turin, Italy.

Multiple Myeloma (MM) is an aggressive, debilitating and deadly hematological malignancy, arising from the clonal expansion of plasma cells at multiple sites in the bone marrow. Recently, MM proved sensitive to a new class of drugs, proteasome inhibitors (PI), currently in phase 4 clinical trial. Understanding the molecular bases by which PI induce apoptosis selectively in MM cells promises to help identify novel molecular strategies to combat MM. We explored the mechanisms underlying sensitivity of MM to PI on plasma cells differentiated in vitro from the murine B lymphoma I.29μ+ and ex vivo from primary mouse B cells. We found that in both models apoptotic sensitivity to PI directly correlates with the Ig-synthetic load. Surprisingly, as apoptosis increases, the relative amount of proteasomal subunits and the resulting proteolytic activity decrease dramatically, thus denying the demand for a higher degradative capacity when antibody production becomes maximal. Pulse-chase assays confirmed that proteasomes are overloaded in differentiating plasma cells. The excessive load for the reduced proteolytic capacity causes accumulation of poly-ubiquitinated proteins and stabilization of endogenous proteasomal substrates such as the UPR mediator Xbp1, the NF-κB inhibitor Iκ-Bα, and the pro-apoptotic Bcl-2 relatives Bim and Bax, two proteins critical in limiting B lymphocyte lifespan and activity. Accumulation of these proteins critically exaggerates endoplasmic reticulum (ER) stress, thus predisposing plasma cells to apoptosis upon treatment with PI. Importantly, a similar scenario can be reproduced in HeLa cells, a non-B tumoral line, by driving Ig heavy chain over-expression under an inducible promoter, leading to proteasomal overload, apoptotic sensitivity to proteasome inhibitors, and eventually spontaneous apoptosis, establishing a cause-effect relationship between synthetic load and cell death. Our results unveil a novel developmental program enabling plasma cells to count the integral of produced Ig, linking death to protein production, thus ending the humoral immune response upon accomplishment of its goal. Based on our data, we propose that the high efficacy of PI against MM is due, to a significant extent, to overloading the cell's degradative capacity, a key component of the stress response, already challenged by misfolded chains generated as a side product of intense Ig synthesis. This model provides a framework for attempting to achieve tumour cell destruction through modulation of stress in MM.

Disclosures: **S. Cenci**, None.

SU106

Microarray Analysis of Differential Gene Expression in OSCC Cell Lines. **C. B. Knight***, **D. Richardson***, **M. MacDougall***, **M. Thornhill***. UTHSCSA Dental School, San Antonio, TX, USA.

Oral squamous cell carcinoma (OSCC) has a high rate of morbidity and mortality despite advances in treatments. Increases in OSCC death rates are primarily due to distant metastases (40-50%). While local control over the disease has improved, much work remains to elucidate the underlying mechanisms of primary invasion and distant spread in order to develop effective therapies for patients with advanced disease. Our laboratory evaluated multiple commercially available OSCC cell lines for their ability to bind and transmigrate across endothelial cells under physiological conditions of flow, *in vitro*. Two cell lines, SCC-4 and CAL-27, demonstrated dramatic differences in this ability. SCC-4 and CAL-27 were both derived from primary OSCC tumors on the tongue of male patients in their fifth decade of life. Interestingly, SCC-4 cells are incapable of binding and transmigrating through endothelial cells; in contrast, CAL-27 cells have the ability to tether and to transmigrate across endothelial cells under physiological conditions of flow, *in vitro*. Our hypothesis is that there are specific gene products in OSCC that enable these tumor cells to invade tissues within the oral cavity. Purpose: Our goal is to characterize differential gene expression patterns in SCC-4 and CAL-27 OSCC cell lines to identify potential regulators of tumor development and metastases. Methods: Differential gene expression was screened using Affymetrix human genome U133 gene array. To confirm these results, semi-quantitative reverse transcriptase polymerase chain reaction (SQ-RT-PCR) and quantitative real time PCR (QRT-PCR) were performed on selected transcripts. Results: 39,000 transcripts were tested, in triplicate, by gene array. 110 genes had statistically significant changes in expression levels in CAL-27 cells compared to SCC-4 cells. 76 genes were up-regulated and 38 genes were down-regulated. Dramatic increases in gene expression levels of S100A2, tumor associated calcium signal transducers 1 and 2 (TACSTD1 & 2), and plasminogen activator urokinase (PLAU) were detected. This data also confirmed increased gene expression of osteonectin (OSN) and tenascin-C(TNC) in CAL-27 cells. Each of these proteins is correlated with aggressive tumor phenotypes in various types of cancer. However, their precise role in invasion has yet to be determined. Conclusion: Microarray analysis of differential gene expression in OSCC cell lines exhibiting different abilities to transmigrate across endothelial cells, *in vitro*, is useful for identifying candidate biomarkers for aggressive OSCC tumors.

Disclosures: **C.B. Knight**, None.

SU107

Roles of Hepatocyte Growth Factor in Bone Metastasis of a Mouse Mammary Cancer Cell Line, BALB/c-MC. K. Ono¹, S. Kamiya^{*1}, T. Akatsu², N. Kugai^{*2}, M. Li^{*3}, N. Amizuka³, K. Matsumoto^{*4}, T. Nakamura^{*4}, S. Wada¹. ¹Department of Clinical sciences, Josai International University, Togane, Japan, ²Department of General Medicine, National Defense Medical College, Tokorozawa, Japan, ³Niigata University, Niigata, Japan, ⁴Osaka University, Suita, Japan.

Since several kinds of cancer metastasize to skeletal tissue, it has been recognized that bone microenvironment supports the growth of certain cancer cells. Once metastasize, some tumors stimulate osteoclastogenesis and expand in the hard tissue. Hepatocyte growth factor (HGF) is a molecule produced mainly by cells of mesenchymal origin, though the factor was also expressed by some cancer cells. In this study, we investigated the roles of HGF in bone metastasis using a mammary cancer cell line, BALB/c-MC. When mice were inoculated with BALB/c-MC, osteolytic lesions were recognized in tibiae as well as femur by histological examination and 3 D μ CT (Scanco μ CT40). Immunoreactivity for HGF was found in the stroma surrounding the metastatic lesions. CD31 (a marker of neovascularization)-positive blood vessels corresponded well to the loci showing HGF immunoreactivity. In contrast, expression of VEGF which is noted as a potent angiogenic factor for tumor neovascularization was not detected. To identify the cells of HGF production, we examined the secretion in the culture media. Concentration of HGF was elevated in osteoblasts (3.13 ± 0.25 ng/ml), while undetectable (< 0.4 ng/ml) in BALB/c-MC or bone marrow cells. The production of HGF by osteoblasts was significantly increased in response to PGE₂. Addition of HGF (10 ng/ml) to BALB/c-MC cultures increased the number of cells 2 times during 6 days of cultures. In the invasion chamber assay, addition of HGF into the bottom wells facilitated motility and invasive potency of BALB/c-MC. By western blot analysis, c-Met/HGF receptor was identified in BALB/c-MC. When BALB/c-MC was cocultured in the upper chamber with osteoblasts in the bottom half, the number of infiltrating BALB/c-MC was increased 3 times compared with that in the cultures without osteoblasts. Addition of 240 nM NK4, an inhibitor of HGF, abolished accelerated invasive potency of the cells. Based upon these in vitro findings, we suppose that in certain types of bone metastasis osteoblasts would decoy cancer cells from sinusoidal capillary into bone marrow space and facilitate tumor proliferation through the actions of HGF. These observations would provide a basis to recognize a developing process of skeletal metastasis and explore therapeutic procedure for management of the disease. Since NK4 completely abolished the enhanced invasive potency of cancer cells, HGF inhibitors could be an alternative to prevent progress of bone metastasis.

Disclosures: **K. Ono**, None.

SU108

Alendronate Prevents Femoral Neck Bone Loss in Postmenopausal Women with Breast Cancer Following Tamoxifen Withdrawal. J. Fleischer, A. Cohen, M. Johnson^{*}, L. Brown, A. Joe^{*}, D. J. McMahon, S. J. Silverberg. Medicine, Columbia University P & S, New York, NY, USA.

Postmenopausal women in the United States are at increased risk for both osteoporosis and breast cancer. Tamoxifen (TMX), a selective estrogen receptor modulator, has been used for many years to treat breast cancer. TMX has anti-estrogenic effects in the breast, but acts as an estrogen agonist in the skeleton, where it increases lumbar spine (LS) BMD and attenuates bone loss associated with the chemotherapy induced premature menopause. TMX is currently approved for 5 years of treatment. Since women withdrawn from estrogen experience a rapid decline in BMD, we hypothesized that women who stop taking TMX after 5 years would also experience this rapid decline. We therefore initiated a randomized, double blind, placebo controlled trial to determine whether alendronate 70 mg weekly prevents bone loss associated with the discontinuation of TMX. Eligible subjects were postmenopausal women with breast cancer who had no bone metastases. Patient accrual was limited by the introduction of aromatase inhibitors, which reduce estrogen levels and are now routinely begun in those discontinuing TMX at our center. After TMX withdrawal, 11 subjects (58 ± 8 [\pm SD] years old; 11 ± 7 years past menopause) were randomized to alendronate (ALN) or placebo (PLB) for 1 year along with calcium and vitamin D. T-scores were: LS -1.1 ± 1.2 ; total hip (TH) -0.4 ± 1.0 ; femoral neck (FN) -0.7 ± 1.0 ; and distal radius (DR) -0.3 ± 1.2 . There were no differences in age or baseline BMD measurements between groups. After one year, FN BMD decreased in patients on PLB, but were stable in those receiving ALN (ALN $+0.1\%$ vs. PLB -5.2% ; $p=0.02$). The effect on BMD did not differ by treatment at the LS (ALN: $+2.0\%$ vs. PLB: -1.6% ; $p=0.19$), the TH (ALN: $+0.48\%$ vs. PLB: -1.26% ; $p=0.36$), or DR (ALN: -1.4% vs. PLB: $+1.0\%$; $p=0.10$). In summary, TMX withdrawal was associated with a 5.2% decline in BMD at the femoral neck, which appeared to be prevented by weekly alendronate. This difference was evident despite the small sample size. These data suggest that in postmenopausal women with breast cancer completing TMX: 1) an evaluation of skeletal health is warranted; 2) bisphosphonate therapy may be an appropriate treatment to prevent bone loss. The current trend of placing patients on aromatase inhibitors following or even before TMX treatment raises even greater concern for the skeletal integrity of these at risk women.

Disclosures: **J. Fleischer**, None.

SU109

PTHrP Derived Peptides without Amino Termini Can Be Identified in Prostate Cells. L. Deftos¹, C. Chalberg^{*1}, T. Downs^{*2}, S. Tu^{*1}, D. W. Burton¹. ¹Medicine, Veterans Administration San Diego Healthcare System (VASDHS) and University of California, San Diego, San Diego, CA, USA, ²Surgery, VASDHS and UCSD, San Diego, CA, USA.

PTHrP is robustly expressed in prostate cancer, where its three isoforms may be processed into distinct peptides by endoproteolytic cleavage. The resulting peptides mediate unique biological effects, including growth regulation, tumor progression, and metastases. The PTHrP 1-34 peptide is the most biologically characterized form, but potential non-amino terminal peptides of PTHrP (NTPs) can independently exert biological effects. To identify the presence of prostatic NTPs, we used 2-site immunoassays, immunoaffinity chromatography, westerns, and mass spectrometry. We evaluated extracts of human prostate cell lines and DU 145 cells that were stably transformed with PTHrP1-141 and mutant PTHrP1-141(1-32 region deleted) expression plasmids by two-site PTHrP immunoassays specific for PTHrP1-141, 38-141 and 67-141. The wild type PC-3 and LNCaP cells expressed PTHrP38-141 and 67-141, but no 1-141 was detectable (P 38-141 > 1 -141 (pmol/ml), consistent with endoproteolytic processing events. As expected, the mutant PTHrP1-141(1-32 region deleted) cells expressed PTHrP38-141 and 67-141, but not the intact 1-141 ($P < 0.05$). We also evaluated fresh extracts of patient prostate cancer tissues and primary cultures using a similar approach. The two-site PTHrP immunoassays demonstrated significant increases ($P < 0.05$) in the expression for the 67-141 species compared to the 38-141 and 1-141 species in the prostate cancer tissues, 10, 8.5 and 0.5 pmol/ml, respectively. We further characterized the conditioned medium from DU 145 cells stably transformed with a PTHrP1-173 expression plasmid and profiled on a Ciphergen Protein G array pre-bound with anti-PTHrP. Several putative PTHrP processed peptides were identified in the secreted media using Time-of-Flight mass spectrometry. The masses of the identified PTHrP peptides from the Protein G array were 3144.9, 4109.4 and 5168.4 daltons, which are consistent with PTHrP15-40, 14-48 and 23-68, respectively. Taken together, these findings are supportive of the presence of non-amino terminal PTHrP peptides in prostate cancer cells and indicate endoproteolytic processing sites within the 1-37 and 38-64 regions of PTHrP that may or may not involve basic residues.

Disclosures: **D.W. Burton**, None.

SU110

Design, Syntheses and Biological Activities of Less Calcemic, Prohormone- and Hormone-like 19-Nor-Vitamin D₃ Analogs for Prostate Cancer Treatment. A. Kittaka^{*1}, M. Arai^{*1}, R. Tsutsumi^{*1}, T. Sakaki^{*2}, N. Urushino^{*3}, K. Inoue^{*3}, S. Ito^{*4}, K. Takeyama^{*4}, S. Kato⁴, M. F. Holick⁵, T. C. Chen⁵. ¹Faculty of Pharmaceutical Sciences, Teikyo University, Kanagawa, Japan, ²Faculty of Engineering, Toyama Prefectural University, Toyama, Japan, ³Graduate School of Agriculture, Kyoto University, Kyoto, Japan, ⁴The Institute of Molecular and Cellular Bioscience, University of Tokyo, Tokyo, Japan, ⁵Endocrinology, Boston University School of Medicine, Boston, MA, USA.

1 α ,25-Dihydroxyvitamin D₃ (1,25D) is known to inhibit the proliferation and invasiveness of prostate cancer cells. Furthermore, prostate cells possess 1 α -hydroxylase (1 α -OHase), and can convert 25-hydroxyvitamin D₃ (25D) to 1,25D to inhibit their proliferation. Since 25D and 19-nor-1,25D are known to be less calcemic than 1,25D when administered systemically, we were interested in knowing whether 19-nor-25D and 2-substituted analogs of 19-nor-1,25D would exert potent antiproliferative activity toward prostate cells and therefore could be used as chemopreventive agents without causing hypercalcemic side effects. Synthesis of 19-nor-25D and 2-substituted analogs of 19-nor-1,25D, including 2-allyl-, 2-propyl-, 2-hydroxypropyl-, and 2-phenylcarbamoyl, 3-deoxy-19-nor-1,25D were achieved by our new coupling method utilizing Julia-type olefination principle. In addition, a high-throughput analyzing system using a combination of fluorescence and micro-titer-plate has been developed to detect ligand-induced protein/protein interactions between vitamin D receptor (VDR) and coactivators (TIF2 or SRC-1). This system will be used to examine the selectivity of 2-substituted-19-nor-vitamin D₃ derivatives. Our results showed that 19-nor-25D had potent antiproliferative activity in prostate cells possessing high levels of 1 α -OHase activity (e.g., PZ-HPV-7), but not in those lacking the enzyme (e.g. LNCaP cells). Moreover, 19-nor-25D was shown to be hydroxylated at the 1 α position to form 19-nor-1,25D in a reconstituted cell-free system. The results suggest that 19-nor-25D must be converted to 19-nor-1,25D by endogenous 1 α -OHase before exerting its antiproliferative activity. Among the 2-substituted analogs of 19-nor-1,25D, we found that a substitution with 2-phenylcarbamoyl group eliminated the antiproliferative activity, whereas substitution with 2-allyl, 2-propyl and 2-hydroxypropyl groups maintained the antiproliferative potency. We conclude that 19-nor-25D and 2-substituted analogs of 19-nor-1,25D can be effective chemopreventive agents for prostate cancer.

Disclosures: **T.C. Chen**, None.

SU111

Osteocyte Stimulation of Chemotaxis and Invasiveness of Breast Cancer: A Proteomic Analysis. P. A. Veno¹, J. Zhao^{*1}, J. Guthrie^{*2}, S. Ko^{*1}, L. F. Bonewald¹, M. R. Dallas^{*1}, S. L. Dallas¹. ¹Univ. of Missouri, Kansas City, MO, USA, ²Midwest Research Institute, Kansas City, MO, USA.

Breast cancer frequently metastasizes to bone, causing bone destruction with complications of hypercalcemia, pain, fracture, and nerve compression. It is well established that osteoblasts and osteoclasts are critical for growth of breast cancer in the bone microenvironment and its associated bone destruction. However, even though osteocytes are the most abundant cells in bone, little is currently known concerning the potential role of osteocytes in breast cancer-associated bone disease. We hypothesized that osteocytes play an important role in breast cancer metastasis to bone and influence the behavior of the tumor in the bone metastatic site. To test this, we first examined the effects of conditioned media from the osteocyte-like cell line, MLO-Y4, on chemotaxis, invasiveness and proliferation of MDA-231 human breast cancer cells. Conditioned media from MLO-Y4 cells was chemotactic for MDA-231 cells and enhanced invasiveness as determined using the transwell migration assay and matrigel invasion chambers. MLO-Y4 conditioned media also stimulated production of matrix metalloproteinases 2 and 9 (MMP2 and MMP9) by MDA-231 cells, suggesting a role for these proteases in invasion. None of these effects were due to increased cancer cell numbers, as MLO-Y4 conditioned media had no effect on MDA-231 proliferation. To identify proteins and pathways that may mediate breast cancer cell responses to osteocyte-derived factors, a proteomics approach was used. Whole cell lysates from MDA-231 cells treated with 50% MLO-Y4 conditioned media for 24 hrs were compared to untreated control MDA-231 cultures by 2D gel electrophoresis. Differentially expressed protein spots were identified by peptide mass mapping with MALDI-TOF and/or by peptide sequencing (MS/MS). 19 differentially expressed or potentially modified protein spots were identified. One subset with increased expression included several proteins involved in cytoskeletal reorganization such as profilin, coactosin-like protein 1, GTP binding protein-rhoC, consistent with increased chemotaxis and invasion. Proteins involved in resistance to hypoxia and with angiogenesis, such as phosphoglycerate mutase and phosphoglycerate kinase, were also increased. Calcyclin, a calcium-binding protein that has been associated with malignant tumors, was also upregulated. This protein has been shown to act as a calcium sensor in osteoblasts and has been associated with bone formation. These data suggest that in addition to osteoblasts and osteoclasts, osteocytes may play an important role in the vicious cycle of cancer growth and bone destruction in metastatic lesions.

Disclosures: **P.A. Veno**, None.

SU112

Zoledronic Acid and PTH Increase Bone Mass and Mechanical Strength Following Radiation Therapy for Osteolytic Bone Metastases. S. A. Arrington¹, J. E. Schoonmaker^{*1}, K. A. Mann^{*1}, T. Sledz^{*2}, G. Willick^{*3}, T. A. Damron^{*1}, M. J. Allen¹. ¹Orthopedic Surgery, SUNY Upstate Medical University, Syracuse, NY, USA, ²Micro Photonics, Allentown, PA, USA, ³Biological Sciences, NRC, Ottawa, ON, Canada.

The specific aim of this study was to quantify the effects of a clinically proven bisphosphonate (zoledronic acid, ZA; Novartis Pharma AG, Basel) on bone mass, microarchitecture, and mechanical properties following radiation therapy for an osteolytic bone lesion. Additionally, we sought to determine if the beneficial effects of ZA could be further enhanced by concurrent use of an anabolic agent, PTH 1-34, following irradiation. The right distal femora of 22 female nude mice were injected with 1x10⁵ F10 human breast cancer cells. Mice were then divided into four groups: non-irradiated (0Gy, n=4), 20Gy only (20Gy, n=6), 20Gy plus ZA (ZA, n=6), and 20Gy plus PTH and ZA (PTH/ZA, n=6). The left non-operated limb of the 0Gy mice served as the control (n=4). Radiation therapy was administered to the right femur 3 weeks post-tumor inoculation. ZA (100µg/kg SC) was administered once weekly for 6 weeks starting three days before irradiation and PTH (80µg/kg SC) was administered 5 days a week for 4 weeks starting the day after irradiation. X-rays and DEXA scans were obtained at 3, 6 and 9 weeks post-tumor inoculation. Mice were euthanized at 9 weeks or earlier if severe lameness or pathology occurred. Hind limbs were explanted, scanned by micro-CT (10.46µm resolution) and mechanically tested through the intact knee joint. ANOVA and Fisher's PLSD were performed to analyze comparisons between groups. Bone mineral density significantly increased in both the ZA (19%, p=0.0109) and PTH/ZA (34%, p=0.0001) groups compared to treatment with 20Gy only. A 3-fold increase in fractional trabecular bone volume was measured in the PTH/ZA group compared to the 20Gy only group (p=0.003). Mechanical strength increased 115% in the ZA group (p=0.0133) and 92% in the PTH/ZA group (p=0.0645) compared to 20Gy only. Neither treatment with ZA or PTH/ZA completely restored mechanical strength to its normal value. These results clearly demonstrate that ZA used as an adjuvant to radiation leads to clinically relevant increases in mechanical strength. The combination of an anti-resorptive drug (ZA) along with an anabolic agent (PTH 1-34) as adjuvants to radiation therapy also significantly increase bone mass and trabecular bone volume. These results indicate that increased BMD and BV/TV do not restore the limb to its normal strength. Future work will include evaluation of bone quality and strength with altering the dosing and timing of adjuvant therapies.

Disclosures: **S.A. Arrington**, None.

SU113

Targeting Cathepsin K in Prostate Cancer Skeletal Metastasis *In Vivo*. Y. Lu¹, E. Keller², J. Dai², J. Escara-Wilke^{*2}, E. Corey³, Z. Yao^{*4}, J. Zimmermann^{*5}, J. Zhang¹. ¹Department of Medicine, University of Pittsburgh, Pittsburgh, PA, USA, ²Department of Urology, University of Michigan, Ann Arbor, MI, USA, ³Department of Urology, University of Washington, Seattle, WA, USA, ⁴Department of Immunology, Tianjin Medical University, Tianjin, China, ⁵Novartis Pharma Ltd, Basel, Switzerland.

Prostate cancer (CaP) frequently metastasizes to bone causing a mixture of osteoblastic and osteolytic lesions. The tumor invasion process is facilitated by proteolytic cascade involving multiple proteases, including matrix metalloproteinases (MMPs), serine proteases (uPA, plasmin), and cysteine proteases including cathepsin K (CatK). CatK degrades collagen I, and expresses predominantly in osteoclasts. Recently CatK expression has been shown in breast and prostate cancer cells. Importantly, its expression level is higher in CaP bone metastatic sites than primary tumor or normal prostate tissues. The role of CatK in CaP skeletal metastasis, however, has not been studied. In this study, we hypothesized that CatK contributes to CaP-induced osteoclast activity at bone metastatic sites, and inhibition of CatK by its selective inhibitor may prevent the CaP establishment and diminish the CaP progression in bone. Accordingly, we first confirmed the expression of CatK in LNCaP, C4-2B, and PC3 CaP cell lines. Then, we observed the inhibitory effect of CatK inhibitor on the CaP cell invasion suggesting the role of CaK in CaP tumor invasion. Finally, we injected C4-2B cells into the tibiae of SCID mice and then the animals (10 per group) received either vehicle or Cat K inhibitor (high or low dose) either at the time of tumor cells injection (tumor establishment model) or 4 weeks after tumor cells were injected (tumor progression model). In the tumor establishment model, CatK inhibitor significantly prevented the establishment of mixed osteolytic/osteoblastic tibia tumors as were observed in vehicle-treated animals; and in the progression model, CatK inhibitor diminished tumor-induced bone lesions, as demonstrated by radiograph, histology and bone histomorphometry. CatK inhibitor also decreased serum PSA levels in both animal models indicating decreased tumor burden. We concluded that CatK inhibitor is an effective drug to prevent the establishment and diminish progression of CaP growth in bone.

Disclosures: **Y. Lu**, None.

SU114

PTHrP Peptides Regulate Expression of Osteoblast Stimulating Factors by Prostate Cancer Cells. D. W. Burton, S. Tu^{*}, C. Chalberg^{*}, K. C. Smith^{*}, L. J. Deftos. Medicine, Veterans Administration San Diego Healthcare System and University of California, San Diego, CA, USA.

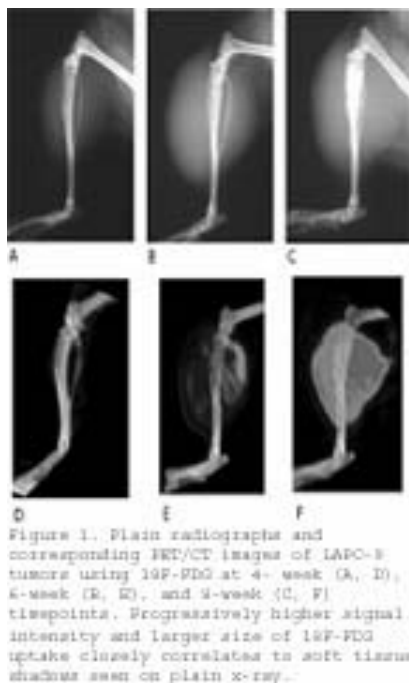
Prostate cancer metastasis to bone is associated with increased osteoblast activity. The osteoblastic phenotype of metastatic prostate cancer lesions results largely from the actions of several stimulatory factors produced by prostate cancer cells. Since PTHrP is robustly expressed by prostate cancer cells, we evaluated 7 human prostate cancer cell lines, including DU 145, LNCaP, PC-3, Dupro-1, PPC-1, 267B1 and 267B1-XR for changes in the expression of several prostate derived osteoblast regulating factors, including OPG, RANKL, TGF-beta, ornithine decarboxylase (ODC), IL-6 and IL-8, after treatment with PTHrP peptides and expression plasmids. In general, OPG expression was increased by treatment with PTHrP1-34 and 38-64, and was decreased by PTHrP109-138. PTHrP140-173 stimulated OPG levels in PC-3 and PPC-1 cells but inhibited OPG levels in Dupro-1 cells. RANKL expression was inhibited by PTHrP140-173 in most of the cell lines. PTHrP140-173 treatment increased IL-6 expression in 267B1 cells, but decreased the IL-8 levels in the 267B1 and LNCaP cells. We further studied the intracrine effects of PTHrP by transfecting the DU 145 cells with full-length PTHrP and mutant (without the 1-32 amino acid region) expression plasmids. Cells transfected with full-length PTHrP1-139, 1-141, and 1-173 stimulated RANK, RANKL, IL-6, IL-8 and ODC levels and inhibited OPG. Deletion of the 1-32 region from the PTHrP plasmids prevented the maximal increases in IL-6 and IL-8 expression levels, indicating that the 1-32 region was critical for these changes. Conversely, deletion of the 1-32 region had no significant effects on the increased RANK, RANKL and ODC levels compared to controls, indicating that a non-amino terminal PTHrP region was responsible for the increases. There were also differences in cytokine levels of the PTHrP1-173 transfected cells compared to the PTHrP1-139 and 1-141 transfected cells, indicating a biological function for the 140-173 region. It is evident that PTHrP and the peptides derived from its processing can have multiple and varying biological effects in different tissues and in different preparations of the same tissue. So careful studies are required to gain insight into the mechanisms that lead to the formation of bone lesions by prostate cancer cells, to understand the predilection of prostate cancer to spread to bone, and to develop of more effective therapies for advanced prostate cancer. Our studies also confirm the biological activities of non-amino terminal PTHrP forms.

Disclosures: **D.W. Burton**, None.

SU115

The Use of ^{18}F -FDG and ^{18}F -fluoride PET/CT Scans to Longitudinally Assess Biologic Behavior of Metastatic Osteolytic, Osteoblastic, and Mixed Lesions in a Prostate Cancer Model. W. Hsu, M. Jo*, B. T. Feeley, L. Krennek*, S. Gamradt*, D. Stout*, A. Chatziioannou*, J. R. Lieberman. Orthopaedic Surgery, UCLA Medical Center, Los Angeles, CA, USA.

Introduction The development of an imaging method that can assess the biologic activity of bone metastases *in vivo* would be advantageous in providing an objective assessment of the efficacy of different treatment modalities. The aim of our study was to evaluate the use of PET/CT scanning in the characterization of osteolytic, osteoblastic, and mixed cell prostate cancer lines in an established murine tibial injection model. **Materials and Methods** 1×10^5 cells of human prostate cancer cell lines PC-3, LAPC-9, and C42B were injected into the left tibia of 8-week old male SCID mice via a previously published protocol. Three animals were used for three consecutive time points for each cell line. Tail-vein injections using 250 uci of either ^{18}F -FDG and ^{18}F -fluoride ion tracer were then performed under a high-flow hood. All PET/CT images were analyzed using Amide®, Version 0.7.154. For ^{18}F -Fluoride ion and ^{18}F -FDG scans, regions of interest (ROIs) were drawn over the injected left tibia and contralateral control tibia using a standardized isocontour value for both sides. Lesion size was calculated by subtracting the size of right control tibial ROI from that of the left. **Results** ^{18}F -fluoride PET/CT scans detected greater uptake at consecutive time points for all cell lines. LAPC9 and PC-3 tumors exhibited greater bone turnover than C42B lesions. A progressively larger lesion was demonstrated by ^{18}F -fluoride scans for LAPC9 cells. In addition, a small lesion was measured using PET scan at the 4-wk time point that was undetectable using plain radiographs. ^{18}F -FDG PET/CT scans also demonstrated greater signal uptake for all cell lines at successive time points (figure 1). **Discussion** Our results indicate that using novel ROI drawing protocols and software analysis on PET/CT imaging, biologic activity, and osteoblastic and osteolytic lesion sizes can be detected at early time points and quantified longitudinally. This “real time” technique may prove to be superior to tumor burden measurements in the assessment of treatment modalities. Furthermore, by using *in vivo* imaging methods, the animals required for statistical power in further studies could be reduced.



Disclosures: W. Hsu, None.

SU116

The Utility of Measuring Non-Isomerised C-Telopeptides of Type I Collagen (α -CTX) for Early Detection of the Skeletal Metastasis in Patients with Diagnosed Breast or Prostate Cancer. D. Leeming*, M. Koizumi*, C. Christiansen³, P. Qvist¹, L. Tanko*, I. Byrjalsen*¹. ¹Nordic Bioscience, Herlev, Denmark, ²Cancer Institute Hospital, Tokyo, Japan, ³Centre for Clinical & Basic Research, Ballerup, Denmark.

Skeletal metastases represent a serious complication of carcinoma of the breast or prostate, with direct implications for pain, fracture and overall prognosis. Early detection of such metastases is a prerequisite of timely intervention aiming the prevention of such complications. To date, bone scintigraphy remains the method of choice for diagnosis and monitoring of bone metastases. Biochemical markers provide useful support in first-line diagnostic approach and surveillance of these patients. We evaluated a novel biochemical marker of bone resorption, i.e. the non-isomerised C-telopeptide of type I collagen (α -CTX), for the detection of osteolytic tumour activity and thus the presence of bone metastases in patients with breast and prostate cancer. Morning urine samples were

collected from 132 newly diagnosed cancer patients visiting the Cancer Institute Hospital, Tokyo, from October 2002 until April 2004. The study population included 90 women with breast cancer (45 with bone metastases) and 42 men with prostate cancer (17 with bone metastasis). Number of metastases was determined by scintigraphy, and those with >75% of their skeleton affected were excluded from the study (n=8). The urinary concentration of α -CTX was assessed by the ALPHA CrossLaps ELISA (Nordic Bioscience Diagnostics, Herlev, Denmark). The coefficient of long-term intra-individual variation in α -CTX was determined using fasting urine specimens from 115 generally healthy postmenopausal women collected at 4 consecutive time points over a two-year observation period. Regression analysis revealed a statistically significant correlation between α -CTX and the number of bone metastases ($r=0.64$, $p<0.0001$). Using this model, the average increases in α -CTX associated with the presence of one, two, or three skeletal metastases were estimated to be 37, 56 and 73%, respectively. Long-term intra-individual variation and least significant change (LSC) in the background population were estimated to be 20.4% and 40.0%, respectively. These initial observations suggest that measurement of α -CTX carries notable potentials for the early detection of skeletal involvement in patients with breast and prostate cancer. Longitudinal studies monitoring cancer patients with scintigraphy and biomarkers such as PSA and the herein introduced α -CTX are needed to define the relative utility of these diagnostic options for the early detection of skeletal metastases.

Disclosures: I. Byrjalsen, Nordic Bioscience 3.

SU117

Convergence of AR & BMP Signaling Pathways on β -catenin. K. H. Emami*, L. G. Brown*, K. D. Brubaker*, R. L. Vessella*, E. Corey¹. ¹Urology, University of Washington, Seattle, WA, USA, ²Bloomsburg University, Bloomsburg, WA, USA.

A major challenge in prostate cancer (CaP) research is understanding why CaP cells survive and proliferate in bone. Involvement of β -catenin as a coactivator modulated by androgen receptor (AR) as well as the BMP and Wnt signaling pathways, suggests involvement of a multiprotein signaling complexes in CaP growth in the bone environment. The objective of this study was to evaluate the effects of BMP-7 on the AR and Wnt (TCF/ β -catenin) signaling network. Our preliminary data have shown that β -catenin is present in the nuclei of LNCaP, C4-2 and LAPC4 cells, and associates with AR. Treatment with BMP-7 dramatically increased association between AR and β -catenin. Interactions of these transcription factors with Smad1, was also enhanced upon BMP-7 treatment which led to increased AR transcriptional activity in LNCaP cells. Overexpression of AR in PC-3 CaP cells along with nuclear β -cateninS33F led to a reduction in TCF/ β -catenin promoter activity. Similarly, abolishing AR expression in LNCaP cells led to increases in TCF/ β -catenin activity in these cells. Competition between TCF/ β -catenin and AR/ β -catenin pathways in CaP cells was further demonstrated by growing cells in an androgen-free environment. The activity of AR was low and the activity of TCF/ β -catenin pathway was the highest in the absence of the ligand (DHT), while in the presence of 1 nM DHT, AR activity was the highest and TCF/ β -catenin showed the lowest activity. Interestingly, the effect of BMP-7 on TCF/ β -catenin signaling was dependent on co-transfection of β -cateninS33F, suggesting that endogenous β -catenin is in association with AR as opposed to TCF-4 in CaP cells. TCF/ β -catenin transcriptional activity was undetectable in CaP cells and CaP cells treated with BMP-7. However overexpression of β -cateninS33F increased TCF/ β -catenin transcriptional activities and treatment with BMP-7 further increased these activities. In conclusion, our data show that BMP signaling can interact with both the AR and TCF/ β -catenin signaling pathways. We hypothesize that BMP-7 treatment enhances the AR or the TCF/ β -catenin pathway, depending on the β -catenin status of the cell. We speculate that in the bone environment BMPs play a role in adaptation and proliferation of CaP cells in bone by activation of the AR and Wnt pathways. Further investigation of the effects of BMPs on CaP cells is warranted to delineate the signal-transduction network alterations in CaP cells and to elucidate further the role of BMPs in CaP bone metastases.

Disclosures: E. Corey, None.

SU118

Does the Human Kallikrein Prostate Specific Antigen (PSA) Contribute to the Prostate Cancer Osteoblastic Response? J. S. Lai, E. Corey, L. G. Brown*, R. L. Vessella*. Urology, University of Washington, Seattle, WA, USA.

Metastatic prostate cancer has the propensity to elicit an osteoblastic response when in bone, in contrast to nearly all other tumors metastatic to bone which are mainly osteolytic. An obvious difference between prostate cancer and these other tumors is the expression of prostate associated serine proteases, including PSA. Our hypothesis is that PSA, as an active enzyme within the bone microenvironment, helps promote the osteoblastic response. We first blocked PSA proteolytic activity *in vivo*. LuCaP 23.1, a prostate cancer xenograft which produces high levels of PSA and causes an osteoblastic reaction in bone, and the neutralizing monoclonal antibody 17-1A3 developed by our laboratory were used in these experiments. Administration of 17-1A3 did not cause significant changes in bone mineral density or in trabecular bone volume. The percentage of free PSA was increased in animals treated with the 17-1A3 antibody, (26.11 ± 0.59 vs. 6.17 ± 0.80 , $P<0.0001$), suggesting that the antibody exhibited neutralizing activity. Interestingly, tumor volume was significantly lower in the 17-1A3-treated animals as determined by bone histomorphometry (26.05 ± 1.62 vs. 35.67 ± 3.51 , $P=0.031$). To further explore an association of PSA with the osteoblastic response, we overexpressed PSA in Chinese hamster ovary (CHO) cells using the Tet-on inducible system. *In vitro*, PSA-transfected CHO cells treated with tetracycline had up to 6 times higher levels of PSA when compared to LNCaP cells (161.97 ± 6.67 vs. 26.75 ± 0.825 ng/ml/ 10^5 cells, $P=0.0025$). When TREx-CHO/PSA cells were injected

subcutaneously, high serum PSA levels were observed in the induced animals (~1ng/ml/mm³ tumor), and the PSA expression did not affect tumor growth in this model. To evaluate the effects of PSA overexpression on bone, TReX-CHO/PSA cells were injected intra-tibially. Immunohistochemical and bone histomorphometric analyses of bone response and effects on tumors will be presented.

Disclosures: **J.S. Lai**, None.

SU119

Multiple Pathways Involved in the Interaction between Prostate Cancer Cells and Osteoblasts during Bone Metastases. **J. Wang***, **A. S. Levenson***, **J. C. Jarrett***, **R. L. Satcher**. Department of Orthopaedic Surgery, Northwestern University, Chicago, IL, USA.

The interaction between prostate cancer cells and osteoblasts is critical to progression of bone metastasis. The molecular mechanism on the bi-directional interaction is poorly understood through conventional co-culture methods, because they only allow soluble interaction but exclude physical contact. By using our novel heterotypic co-culture system, we previous found that both physical contact and soluble factors contributed to metastasis progression. This study is to investigate the signal pathways between prostate cancer cells and osteoblasts in bone metastases. In the heterotypic co-culture system, fluorescence-labeled prostate cancer cells were mixed and co-cultured with osteoblasts. Two types of cells were then re-separated through fluorescence-activated cell sorting. Gene expression profiles and kinase signaling were studied by using pathway-focused gene arrays, RT-PCR and Western blot. The results showed that extracellular protease were up-regulated in both prostate cancer cells and osteoblasts, including MMP-2, MMP-9, uPA and cathepsin K. The protease activation contributed to modification of extracellular matrix components and cell adhesion molecules, such as collagen III, collagen IV, collagen X, collagen XII, fibronectin, integrin α 1, integrin α 2 in prostate cancer cells and collagen VIII, collagen IX, VCAM-1 in osteoblasts. Some other bone matrix proteins (biglycan, decorin, osteopontin) were also modified during the interaction. TGF β -BMP superfamily pathway was activated in both types of cells. In prostate cancer cells, TGF β receptor 1 and downstream signal transduction molecule smad 9 were up-regulated. In contrast, TGF β receptor 1, TGF β receptor 3 and smad 6 were down-regulated in osteoblasts. In addition, colony-stimulating factors (CSF) were also involved in the interaction, including CSF1, CSF2 and CSF-1 receptor. MAP kinase signal transduction pathway was activated in prostate cancer cells. Among the cascade members, MMK4/JNKK1 was down-regulated while mta-1 and raf-1 were up-regulated. In conclusion, the interaction between prostate cancer cells and osteoblasts modified extracellular matrix protein/protease and growth factors. It in turn activated protein kinase signaling through various growth factors receptors and cell adhesion molecules. It suggested that multiple signal pathways were activated in prostate cancer bone metastasis. Blockage of various pathways simultaneously may be necessary to interfere the progression of tumor metastases.

Disclosures: **J. Wang**, None.

SU120

Enhanced Expression of E-selectin on Bone-Derived Vascular Endothelial Cells: Potential Role in Breast Cancer Metastasis. **C. V. Gay**, **L. A. Makuch***, **D. L. Geffel***, **D. M. Sosnoski***. Biochemistry and Molecular Biology, The Pennsylvania State University, University Park, PA, USA.

Breast cancer cells frequently metastasize to the ends of long bones, ribs and vertebrae, structures which contain a rich microvasculature in close juxtaposition to metabolically active trabecular bone surfaces. This study focuses on the effects of osteoblast secretions on the expression of surface adhesive proteins by skeletal vascular endothelial cells. Vascular endothelial cells were isolated from trabecular bone regions and from the central marrow cavity (which lacks trabecular bone) from long bones of 7 week old Swiss Webster mice. Both types of endothelial cells were placed in culture for 7 days, then exposed 24 hrs to conditioned media (CM) from MC3T3-E1 osteoblasts. CM from two different stages of osteoblast development were tested: (1) from immature MC3T3-E1 cells cultured 5-7 days and (2) from mature MC3T3-E1 cells cultured 28-30 days. The immature osteoblasts were in a state of rapid proliferation; the mature osteoblasts formed a matrix that mineralized. Following exposure to the conditioned media, the vascular cells were exposed to specific antibodies to p-selectin, e-selectin, ICAM-1 or VCAM-1, cell surface adhesive proteins to which breast cancer cells are known to bind. To visualize surface staining, fluorescent secondary antibody was applied followed by confocal microscopy. Of the four proteins evaluated, e-selectin was consistently found on more (~30%) cell surfaces of bone-derived vascular endothelial cells (BVECs) when exposed to the immature osteoblast CM. Vascular endothelial cells from marrow (MVECs) did not show this response to either immature CM or mature CM. RNA has been isolated from both BVECs and MVECs using Qiagen RNeasy; BVECs contained ~3-fold more total RNA than MVECs, an indication that BVECs are more metabolically active. Finally, secretions from immature and mature OBs were found to be chemotactic for a breast cancer cell line, MDA-MB-231, with the mature OB cell secretion being ~ 2-fold more effective as a chemoattractant. Collectively, these studies suggest that 1) the BVEC blood vessels near immature bone cells express more surface adhesive protein, i.e. e-selectin, that could enhance entrapment of breast cancer cells, and 2) once cancer cells have undergone extravasation into marrow adjacent to bone they could be attracted to nearby bone surfaces, particularly sites of bone formation where mature osteoblasts are found. This combination of factors may contribute to the uniqueness of bony sites and therefore to breast cancer cell adhesion and subsequent tumor growth.

Disclosures: **C.V. Gay**, None.

SU121

Effects of Alendronate on Bone Mineral Density in Men with Prostate Cancer Treated with Androgen Deprivation Therapy. **J. M. Bruder¹**, **D. Katselnik^{*1}**, **N. Wing^{*1}**, **J. Z. Ma^{*2}**. ¹Medicine, University of Texas HSC at SA, San Antonio, TX, USA, ²Psychiatry, University of Texas HSC at SA, San Antonio, TX, USA.

It is known that bone mineral density (BMD) is low in men with prostate cancer receiving androgen deprivation therapy (ADT). Recent studies have demonstrated the efficacy of intravenous bisphosphonates in preventing this bone loss, however, the effectiveness of oral bisphosphonates has not been studied in this population. Therefore we reviewed the charts of patients with prostate cancer receiving ADT referred from the VA Urology Clinic for BMD testing and identified 47 patients with baseline and follow up BMD measurements (mean \pm SD = 18 \pm 7 months). As part of routine care, all were receiving calcium supplements and a multivitamin. Twenty-two men (47%) were also receiving alendronate 70 mg po every week. BMDs were measured at the spine (L1-L4), total hip, trochanter, femoral neck, and radius. To account for the variability in recall, changes in BMD measurements were converted to percent change per year. The most significant difference between groups was seen at the femoral neck. There was a decrease of 2.17 \pm 0.7 % per year in the untreated patients but a 0.32 \pm 0.6 % increase per year in the alendronate treated patients (p 0.0086). Statistically significant differences (p<0.05) in the 2 groups were also seen at the L1-L4 spine (-1.29 \pm 0.7 % vs +1.41 \pm 0.7%), total hip (-0.94 \pm 0.6 % vs +0.97 \pm 0.5 %) trochanter (-2.01 \pm 0.7 % vs +0.79 \pm 0.8 %). In the four other sites measured at the radius (proximal, mid, ultra distal and total), there were no statistically significant differences (p > 0.05). These findings confirm that bone loss occurs in men receiving ADT at all sites measured. The use of alendronate can prevent bone loss at the spine and hip, but does not seem to have the same protective effect at the radius. Further study will be required to determine why the radius does not seem to adequately respond to alendronate therapy.

Disclosures: **J.M. Bruder**, Merck 5; Procter & Gamble 5.

SU122

Gene Expression Associated with Prostate Cancer Bone Metastasis. **C. Morrissey¹**, **L. M. Coleman^{*2}**, **M. P. Roudier^{*1}**, **E. Corey¹**, **T. S. Kim^{*2}**, **L. G. Brown^{*1}**, **J. Hahn^{*1}**, **C. S. Higano^{*1}**, **L. D. True^{*1}**, **P. S. Nelson^{*2}**, **R. L. Vessella^{*3}**. ¹Urology, University of Washington, Seattle, WA, USA, ²Fred Hutchinson Cancer Research Center, Seattle, WA, USA, ³Urology, University of Washington and Puget Sound VA Medical Center, Seattle, WA, USA.

One of the two major sites of metastases of prostate cancer is bone, but the mechanisms and key factors involved in the propensity of prostate cells to go to bone, proliferate in the bone environment and promote an osteoblastic response are not understood. Our objective is to elucidate phenotypic differences between soft-tissue metastases and bone metastases of prostate cancer. Soft tissue and bone metastasis samples were obtained from patients expiring from advanced prostate cancer within 2-6 hours of death under the auspices of our Rapid Autopsy Program. First, we grossly microdissected metastatic foci from frozen samples and performed expression analysis using a 7K Prostate Expression Data Base (PEDB) and 18k human cDNA microarray chips. Examples of phenotypic changes associated with bone metastases included altered expression of Factor XIIIa, EBP50 and Bone Sialoprotein. To minimize or eliminate the potential of contamination of tumor cells with stromal and bone cells we have mastered laser capture microdissection of tumor cells. cDNA array analysis of these samples showed that 65 genes were upregulated in bone metastases vs. non-osseous metastases, while 41 genes were down regulated (q-value < 1). We are now combining and comparing the cDNA array results from these 2 experiments. Because of the rate of false positive and false negative results from cDNA analyses we will validate the phenotypic changes in two ways. First, the immunohistochemical analyses of markers associated with bone metastases will be performed using a tissue microarray from 30 individuals containing prostate cancer metastases to lymph node (N=46), liver (N=19), and bone (N=104). Secondly, we will elucidate *in vitro* the potential of the bone environment to cause the phenotypic changes detected in patient specimens. In this model PC-3 and C4-2B cells are co-cultured with mouse osteoblasts (MC3T3-E1) at different stages of differentiation. Real-time PCR, immunohistochemistry and cDNA arrays will be used to evaluate altered gene expression of selected candidates. In conclusion we have resources and techniques in place to obtain critical information about key factors associated with the propensity of prostate cancer to metastasize to bone and to yield an osteoblastic response. Results of these validation studies will be presented.

Disclosures: **C. Morrissey**, None.

SU123

Morphological Study for a Mechanism of Osteolysis by the Human Breast Cancer Cell MDA-MB-231. **H. Nakamura^{*1}**, **T. Hiraga²**, **T. Ninomiya^{*3}**, **A. Hosoya^{*1}**, **M. Yamaki^{*3}**, **Y. Arai^{*3}**, **T. Yoneda²**, **H. Ozawa^{*3}**. ¹Oral Histology, Matsumoto Dental University, Shiojiri, Japan, ²Biochemistry, Osaka University Graduate School of Dentistry, Suita, Japan, ³Institute for Oral Science, Matsumoto Dental University, Shiojiri, Japan.

We investigated osteolytic bone metastasis induced by the human breast cancer cell MDA-MB-231 using morphological and immunohistochemical methods. To clarify the mechanism of osteolysis, we used an experimental animal model in which inoculation of MDA-MB-231 cells into the left cardiac ventricle of female nude mice causes osteolytic lesions in bone. Four weeks after the cell inoculation, metastatic tumor cells occupied bone marrow cavity and bone trabeculae were extensively destroyed. On the bone surfaces

facing tumor cells, there existed many TRAP- and cathepsin K-positive multinucleated osteoclasts. Of note, TRAP-positive mononuclear and multinuclear cells were also observed in the tumor nests. Immunohistochemical and electron microscopical examinations revealed that these TRAP-positive cells were in direct contact with RANKL-positive stromal cells. Furthermore, we found that MDA-MB-231 cells colonized in bone expressed PTHrP in their cytoplasm. This evidence suggests that tumor-producing PTHrP upregulates RANKL expression in bone marrow stromal cells, which in turn stimulates osteoclast differentiation, leading to the progression of osteolytic bone metastases. On the other hand, it has been reported that bone metastasis was reduced in osteopontin (OPN)-deficient mice. We also examined the localization of OPN, CD44 and hyaluronan in tumor nests. MDA-MB-231 cells showed CD44 -positive reactivity on their plasma membrane. OPN and hyaluronan, ligands for CD44, localized in the extracellular matrix around stromal cells and tumor cells. Immunoelectron microscopy demonstrated that OPN was localized in the Golgi apparatus of stromal cells and in the extracellular matrix between stromal cells and tumor cells. Western blotting using tumor lysate indicated that tumor nests contained OPN and CD44. These results suggest that CD44-OPN interaction may play an important role in initial step of metastasis in bone. RANK-RANKL interaction may be involved in the differentiation and activation of osteoclasts in osteolytic bone metastasis

Disclosures: **H. Nakamura**, None.

SU124

Repeatability and Sensitivity of Vertebral Morphometry Studies Using the Norland Scanner. **J.M. Wang¹, J.C. Liu^{*2}, T.V. Sanchez³.** ¹Research and Development, Norland--a CooperSurgical Company, Beijing, China, ²Department of Nuclear Medicine, PLA 304th Hospital, Beijing, China, ³Research and Development, Norland--a CooperSurgical Company, Socorro, NM, USA.

The use of DXA equipment to do vertebral morphometry assessments has generated recent interest in the community--this study examines the repeatability of Norland based vertebral morphometry studies and compares those studies to film based morphometry studies. Thirty subjects between 22 and 85 years of age underwent Lateral Spine X-ray Film studies and scans of the T8-L4 spine in lateral recumbancy using the Ruler Tool on Research Scan studies obtained on a Norland XR-36 fitted with Illuminatus software. Additionally, six of these subjects between 22 and 45 years of age undertook a total of four repeated DXA studies--with repositioning--to examine procedural repeatability. Examining the repeatability of DXA-measured anterior, mid and posterior vertebral body height ratios (A_h/P_h , M_h/P_h , P_h/A_h , M_h/A_h) showed repeatability was consistently below 4% for studies of the T8 to L4 region and compares well with the 5% repeatability reported in the literature. When the 1,080 anterior, mid and posterior vertebral body height ratios (A_h/P_h , M_h/P_h , P_h/A_h , M_h/A_h) measured by DXA were compared with morphometric study of Lateral Spine X-ray Film, results proved highly correlated ($r = 0.99$). Further, when--based on vertebral body height ratios--Lateral Spine X-ray Film demonstrated 11 subjects had evidence of deformity those subjects also showed indications of a deformity by DXA. In conclusion, this study demonstrates that vertebral morphometry studies done with the Norland system are repeatable and that those studies show strong agreement with Lateral Spine X-ray Film studies.

Disclosures: **J.M. Wang**, Norland--a CooperSurgical Company 3.

SU125

Fat Mass Loss in Obese Subjects Treated with Carnitine: A Whole Body DXA Evaluation. **C. V. Albanese¹, M. Danti^{*1}, I. Preziosa^{*2}, A. Laviano^{*2}, R. Passariello^{*1}.** ¹Department of Radiologic Science, Univerity of Rome, Rome, Italy, ²Departement of Clinical Medicine, Univerity of Rome, Rome, Italy.

Purpose: Carnitine (CAR) is involved in fatty acid oxidation and its supplementation may facilitate body weight (BW) loss in dieting obese patients. Similarly, calcium (Ca) supplementation appears to influence BW loss by increasing in fatty acid oxidation. We, therefore, hypothesised that CAR and/or Ca supplementation in dieting overweight/obese patients may boost BW loss. **Material and methods:** patients with a body mass index (BMI) ranging 25-35 were considered for the study for a period of six months. They were randomly assigned to 4 groups. Group 1: hypocaloric diet (4800 kJ/d for females and 5600 kJ/d for males; Ca: 900 mg/d); group 2: hypocaloric diet (isocaloric with group 1; Ca: 1500 mg/d); group 3: hypocaloric diet (isocaloric with group 1; Ca: 900 mg/d) + CAR 4g/d; group 4: hypocaloric diet (isocaloric with group 1; Ca: 1500 mg/d) + CAR 4g/d. BW and BMI were monthly measured. Results are expressed as mean \pm SD. Total and regional fat mass and lean mass was evaluated by whole body DXA. **Results:** At present, 44 patients have been enrolled and completed 3 months of follow-up. In all groups BW significantly decreased, and % BW vs. baseline is: 94.5 \pm 4.7 (Group 1; n=11), 94.4 \pm 3.1 (Group 2; n=11), 94.3 \pm 3.2 (Group 3; n=12), 94.3 \pm 3.2 (Group 4; n=10). The protocol also included analysis of body composition via DXA basal and at 6 months. However, the number of patients in each group who completed the 6-month follow-up does not allow statistical analysis. Thus, we pooled patients from groups 1 and 2 (no CAR) and compared their body composition analysis at 6 months with that of the pool of patients from groups 3 and 4 (CAR). Data analysis shows a trend toward increased fat mass loss in patients receiving CAR vs patients not supplemented (-4.7% vs -2.7%, respectively). By pooling patients from groups 2 and 4 (high Ca) and then comparing their body composition analysis with that of patients from groups 1 and 3 (normal Ca), Ca supplementation does not appear to induce any effect on fat mass loss (-3.2% vs -5%, respectively). **Conclusions:** CAR or Ca supplementation seem to enhance BW loss in dieting overweight/obese patients. The results also appear to suggest that CAR supplementation may facilitate fat mass loss. Whole body DXA was able to discriminate between total and regional fat and lean mass in such subjects with high degree of accuracy and diagnostic sensibility.

Disclosures: **C.V. Albanese**, None.

SU126

Allometric Scaling of Bone Mineral Content at Various Skeletal Sites in Boy and Girls: Accounting for Bone Size and other Confounding Variables. **M. Burrows^{*1}, J. R. Welsman^{*1}, D. Simpson^{*2}.** ¹Childrens Health and Exercise Research Centre, University of Exeter, Exeter, United Kingdom, ²Nuclear Medicine, Kent and Canterbury Hospital, Canterbury, United Kingdom.

There is debate regarding appropriate methods of controlling for bone size when interpreting bone mass in children. Traditionally bone mineral density is calculated by dividing bone mineral content (BMC) by projected bone area (A_p) but this may not accurately reflect bone volume at specific sites. In addition, bone size is not the only confounding variable associated with BMC. This study assessed the effects of age, sex, A_p and selected anthropometric variables on the interpretation of BMC in children, 38 boys and 94 girls (aged 10.5 \pm 3.7). BMC (g), body fat (%), and projected bone area (A_p, cm²) at the Femoral neck (FN), Trochanter (T) and Total body (TB) were measured using DEXA (GE Lunar, Prodigy). Stature (cms) and body mass (kg) were also recorded. Log-linear regression was used to examine whether age and selected anthropometric variables were predictors of BMC, alongside A_p across the skeletal sites in boys and girls. Significant predictors of FN BMC, T BMC and TB BMC in the boys and girls are shown in Tables 1 and 2 respectively. All coefficients for A_p were significantly different from that predicted by geometric similarity (1.5). In boys, the positive effect of body mass combined with the negative coefficient for body fat indicate that lean body mass is a key determinant of BMC alongside A_p. For girls body fatness was not associated with BMC at any site and the influence of other anthropometric predictors was not consistent across sites as seen in the boys. These results suggest that the predicted exponent of 1.5 does not hold true across skeletal sites and for accurate interpretation of BMC at different sites individual exponents need to be utilised in children. In addition, it may not be adequate to interpret BMC in children according to A_p alone.

Table 1. Log-linear regression results for the boys				
Dependent variable	Explanatory variables	Coefficient	SE	Sig.
Log _e FN BMC	Constant	-1.005	.285	.001
	Log _e body mass	.476	.105	.000
	Log _e body fat	-.153	.063	.021
	Log _e FN A _p	.587	.276	.042
Log _e T BMC	Constant	-1.168	.276	.000
	Log _e body mass	.289	.110	.013
	Log _e body fat	-.157	.072	.036
	Log _e T A _p	1.063	.092	.000
Log _e TBBMC	Constant	-.498	.542	.336
	Log _e body mass	.291	.100	.007
	Log _e body fat	-.103	.034	.005
	Log _e TB A _p	.952	.116	.000

Table 2. Log-linear regression results for the girls				
Dependent variable	Explanatory variables	Coefficient	SE	Sig.
Log _e FN BMC	Constant	-5.111	.773	.000
	Log _e stature	.891	.206	.000
	Log _e body mass	.204	.057	.001
	Log _e FN A _p	.709	.159	.000
Log _e T BMC	Constant	-1.609	.111	.000
	Log _e body mass	.212	.047	.000
	Log _e T A _p	1.172	.048	.000
Log _e TBBMC	Constant	-2.279	.509	.000
	Log _e TB A _p	1.307	.071	.000

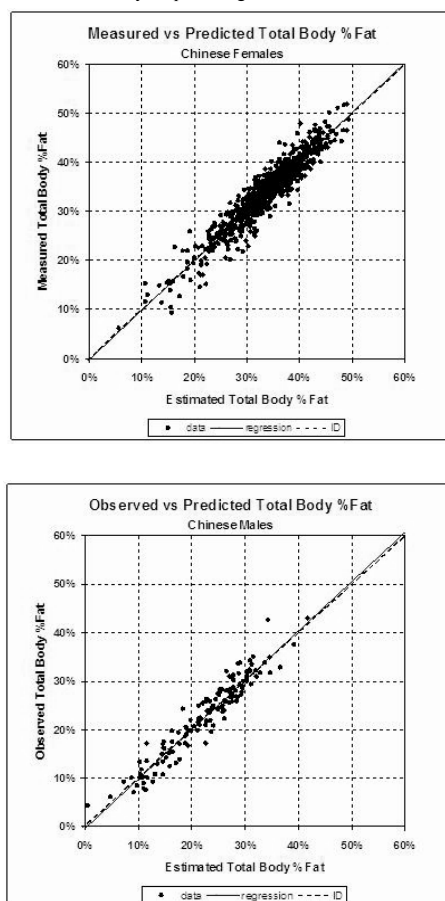
Disclosures: **M. Burrows**, None.

SU127

Assessment of Total Body Percent Fat from Spine and Femur DXA Measurements in Chinese Women and Men. **H. Xu^{*1}, Q. Zhou^{*2}, Y. Zhang^{*3}, J. Gong^{*1}, W. K. Wacker^{*4}, L. S. Weynand^{*4}, F. Chen^{*3}, K. G. Faulkner^{*}, S. Lin^{*3}.** ¹Nuclear Medicine, Ji Nan University 1st Hospital, Guangzhou, China, ²GE Healthcare, Shanghai, China, ³Peking Union Medical College Hospital, Peking Union Medical College, Chinese Academy of Medical Science, Beijing, China, ⁴GE Healthcare, Madison, WI, USA.

In the past, body composition studies with DXA have required total body scans to measure total body %fat. Recently, estimation of total body %fat from spine and femur DXA scans has been validated for American adult males and females (JBMR 2004;19; Suppl 1:S363). We determined whether regional body composition estimates from spine and femur DXA scans, along with height, weight and body mass index (BMI), in Chinese women and men could be used to predict total body %fat. We examined results from 748 female Chinese subjects (mean age 52 \pm 15; range 20-90 years), and 138 male Chinese subjects (mean age 52 \pm 17; range 20-84 years) whose spine, femur, and total body were measured concurrently with a Lunar Prodigy densitometer (GE Healthcare) at one of two centers. Regression models of female and male total body %fat as functions of BMI and spine and femur soft tissue thickness and %fat were developed. Five female subjects were excluded as statistical outliers; no male subjects were excluded. Strong correlation between measured and predicted total body %fat was observed ($r=0.95$ for females, $r=0.96$ for males). Regression of measured with predicted total body %fat gave a slope and intercept not significantly different from one and zero, respectively, for both females and males (Figures 1,2). The standard errors for the measured values are 2.3 %fat for females and 2.4 %fat for males. We conclude that data obtained from spine and femur scans, in combination with anthropometric information, provide a good estimate of total body fat and fat-free

body composition in the Chinese population. On systems that do not offer total body measurements, regional body composition information derived from spine and femur scans can be used to estimate total body fat percentage.



Disclosures: **H. Xu**, None.

SU128

Long-Term *In Vivo* QCT Scanning of Nasal Turbinates in Cynomolgus Monkeys. **A. Varela**, **I. A. Moreau***, **M. Sabourin***, **C. Chevrier***, **J. Jolette***, **S. Y. Smith**. Charles River Laboratories Preclinical Services•CTBR, Senneville, PQ, Canada.

The purpose of this study was to assess the long-term reproducibility of quantitative computed tomography (QCT) scanning of nasal turbinates (NT) in cynomolgus monkeys. It is important to precisely evaluate the safety of inhalation or intranasal administration of bone active drugs in chronic studies. QCT scanning also offers a unique opportunity to identify abnormalities for further histologic assessments that may go undetected. QCT scans were obtained of NT for 6 females aged 6 to 9 years, at baseline, 3, 6 and 9 months. For comparison, scans were obtained at larger and more traditional sites at mid L4 and the distal femur (metaphysis [met] and diaphysis [dia]). QCT NT scans were normally obtained posterior to the second premolar (anterior site) and mid first molar (posterior site). The pattern of the turbinates and sinuses, and the anatomy of the maxilla and orbits were used as landmarks for positioning. For analysis, separate regions of interest were placed manually around the left and right middle turbinate, inferior turbinate and nasal septum at each site. Precision was calculated for area as the coefficient of variation (%CV) over the 4 scanning occasions for each animal. CV% was also determined for BMC and BMD but these parameters were expected to be more variable in monkeys that may not have attained peak bone mass. There were no differences observed between right and left NT therefore both were included as separate observations for the purpose of assessing precision. The %CV for the NT (inferior, middle and septum) at anterior and posterior sites was similar for area and ranged from 3.7±1.4 to 7.6±6.6%. As expected, the CV% for BMC and BMD were more variable and ranged from 3.8±1.6 to 11.7±7.8%. In comparison, the overall %CV obtained for total area at the femur met was 3.3±2.0%, the dia was 2.2±2.7%, and mid L4 was 1.4±0.5%. Precision of NT scanning was acceptable but reflected the limitation of the equipment to detect low amounts of mineral in a small area. The area under evaluation for NT was: 15.8±3.5 to 22.7±6.9 mm², compared to larger areas at the femur: 126±20 mm² (met) and 39±4 mm² (dia), and L4: 117±17 mm². The amount of mineral (BMC) in the NT differed markedly from the other sites, contributing to the level of precision attainable: NT: 2.3±0.7 to 5.7±2.2 mg/mm; femur met: 64.3±10.2 mg/mm, dia: 49.6±5.2 mg/mm; L4: 52.6±8.8 mg/mm. QCT detected abnormalities of the NT which may otherwise have gone undetected, permitting a more complete histologic evaluation. The long-term reproducibility of *in vivo* QCT scanning of NT was considered acceptable supporting safety assessments at this site to monitor the chronic intranasal administration of bone active drugs.

Disclosures: **A. Varela**, None.

SU129

Osteoporosis in Chinese American Women: Determinants of Bone Mass. **M. Donovan**¹, **R. Babbar**², **A. Opatowsky**³, **F. Nabizadeh**⁴, **A. Rohira***⁵, **W. Chung***², **J. Chiang***², **A. Mediratta***², **D. McMahon**¹, **G. Liu***², **J. P. Bilezikian**¹. ¹Medicine, College of Physicians and Surgeons, Columbia University, New York, NY, USA, ²Medicine, NYU Downtown Hospital, New York, NY, USA, ³Medicine, Brigham and Women's Hospital, Boston, MA, USA, ⁴Obstetrics and Gynecology, NYU Downtown Hospital, New York, NY, USA, ⁵Medicine, Cabrini Medical Center, New York, NY, USA.

Asian women have lower bone mineral density (BMD) than Caucasian women. Chinese women, however, have a lower hip fracture rate than Caucasian women. The relationship between BMD and fracture risk, thus, may differ for Caucasian and Chinese women, which may have implications for diagnosis and treatment of osteoporosis (OP). The purpose of this study is 3-fold: (1) to identify determinants of BMD in Chinese American women; (2) to develop a referent BMD database among Chinese American women; (3) to compare these data to that of Caucasian women in the US. Four hundred Chinese American women, in New York City, age 20-90, are being recruited. Along with DXA of the total hip (TH) and lumbar spine (LS), demographic, familial, nutritional, and behavioral data are being obtained using a questionnaire. To date, 359 women have been recruited. In this cohort, 94 % are foreign born and mean (±SEM) age at emigration was 31±8 yrs. Mean residence in the US is 14.2±6 yrs. Mean BMI is 23.3±2 kg/m². Mean age of menarche and menopause are 13.6±1 and 50.1±4 yrs respectively. Mean # of pregnancies and live births are 2.3±1 and 1.6±1 respectively. Seventy-five percent engage in weekly physical activity. Among this cohort, 4.4% were ever-smokers with mean pack-yrs 38±26. Thirty five percent imbibe alcohol, consuming 14±2.5 grams of alcohol weekly. Daily calcium intake is 612±17 mg. Peak BMD (PBMD) in Chinese American women is lower at the TH (0.906±0.13 vs 0.942±0.12, p<.0001) and LS (1.013±0.13 vs 1.047±0.11, p<.0001) compared to Caucasian women. In contrast to Caucasian women who reach PBMD in the third decade, PBMD is not achieved until the fifth decade (ages 40-49). Determinants of BMD are being evaluated using multiple regression. When we used this newly established Chinese American database, the OP detection rate in our Chinese American cohort ≥age 50 was 51% lower than when we used the Hologic Caucasian database (p<.001). If fracture risk is considered in relation to peak BMD for a specific population, and not BMD in absolute terms (g/cm²), then use of a Caucasian reference for diagnosis of OP leads to an overestimate of fracture risk among Chinese Americans. These observations may explain discrepancies between T-scores and fracture incidence among Chinese Americans. This study provides a race and geographically-specific BMD database that has clinical relevance to a Chinese American population.

Disclosures: **M. Donovan**, None.

SU130

Co-Morbidity of Decreased Bone Mineral Density (BMD) and Increased Cholesterol Levels among Women Aged 65 Years and Older: Results from NHANES III. **J. P. Bilezikian**¹, **M. Davidson***², **S. Hendrix***³, **L. Liu***⁴, **M. Louie***⁵. ¹College of Physicians and Surgeons, Columbia University, New York, NY, USA, ²Rush University Medical Center, Chicago, IL, USA, ³Wayne State University Health Center, Detroit, MI, USA, ⁴Pfizer, Inc., New York, NY, USA, ⁵Weill Medical College of Cornell University, New York, NY, USA.

Low bone mineral density (BMD) is known to be prevalent among women aged 65 years and older, but the co-prevalence of low BMD and increased total and low density lipoprotein (LDL-C) cholesterol levels in this population has not been previously explored. The purpose of this study was to assess the co-prevalence of low BMD and high total and LDL-C cholesterol levels among women aged 65 years and older in the United States. We analyzed BMD and cholesterol data from the third National Health and Nutrition Examination Survey (NHANES III), conducted by the Centers for Disease Control (CDC) from 1988-1994. NHANES data are weighted to be representative nationally. All women aged 65 years and older who participated in the survey were identified for this study. Based on central BMD measurements, these women were classified into three groups as defined by World Health Organization (WHO) criteria for BMD T-scores: normal (>-1.0), osteopenic (-1.0 to -2.5), and osteoporotic (<-2.5). We also examined total and LDL-C cholesterol levels among the study cohort. Among the 19.0 million women aged 65 and older estimated from this national database, 9.6 million (50%) were found to be osteopenic, 3.9 million (21%) were found to be osteoporotic, and 5.5 million (29%) had normal BMD. Seventy-three percent of the osteopenic individuals had total cholesterol (TC) levels of 200mg/dl or greater and 63% had LDL-C levels of 130mg/dl or greater. Among women with osteoporosis, 63% had high TC and 53% had increased LDL-C levels. Among women with normal BMD, 78% had elevated TC and 61% had increased LDL-C. The NHANES III analysis indicates that greater than 70% of all American women aged 65 and older have either osteopenia or osteoporosis, and the majority of these women also have high total and LDL-C cholesterol levels. The fact that the percentage of normal subjects and osteopenic/osteoporotic subjects who have elevated TC and LDL-C is similar raises questions about the relationship between coronary artery disease and bone loss in postmenopausal women. Nevertheless, the presence of high TC and LDL-C amongst patients with osteopenia/osteoporosis presents a significant comorbidity profile that may have important clinical implications.

Disclosures: **J.P. Bilezikian**, Pfizer 2.

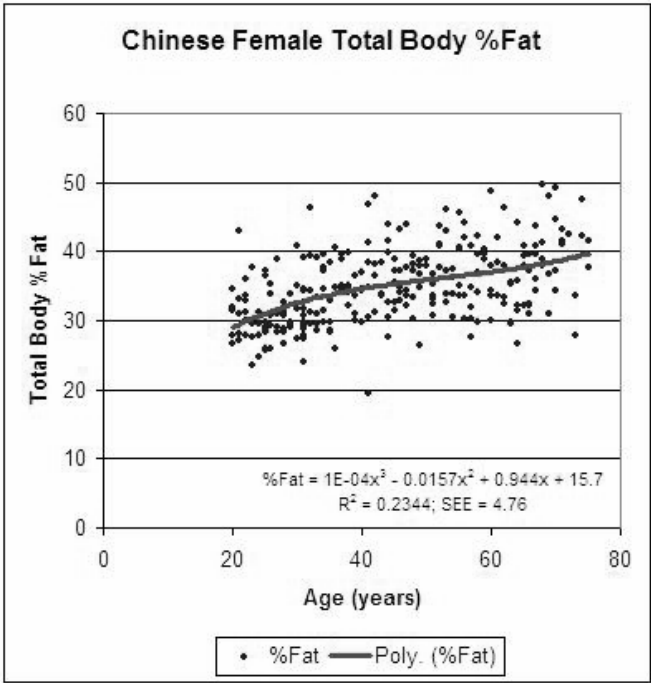
SU131

Body Composition Reference Values in Normal Chinese Women. S. Lin^{*1}, Q. Zhou^{*2}, Y. Chen^{*3}, X. Lin^{*4}, Q. Yang^{*3}, R. Chen^{*1}, H. S. Barden^{*5}, Y. Zhang^{*1}, F. Chen^{*1}, K. G. Faulkner⁵. ¹Obstetric and Gynecology, Peking Union Medical College Hospital, Peking Union Medical College, Chinese Academy of Medical Science, Beijing, China, ²GE Healthcare, Shanghai, China, ³Jinan Maternity And Child Care Hospital, Jinan, China, ⁴Guangdong Zhongshan Obstetric and Gynecology Hospital, Zhongshan, China, ⁵GE Healthcare, Madison, WI, USA.

Dual-energy X-ray absorptiometry (DXA) is used increasingly as a rapid, precise and accurate method for measurement of regional and total body composition in both clinical and research settings. Numerous clinical conditions affect body composition, including, obesity, eating disorders, malabsorption disorders, sex hormone disorders, growth hormone deficiency, diseases that cause muscle wasting and liver and heart disease. We measured body composition with DXA (GE Lunar Prodigy) in 268 normal Chinese females aged 20 to 75 years. In addition to the traditional measurements of total body bone mineral content (BMC), lean mass (LM), fat mass (FM), and %Fat, we measured android (waist) and gynoid (hip) %Fat.

Age (years)	n	Height (cm)	Weight (kg)	BMC (g)	Lean (g)	Fat (g)	%Fat	Android (%Fat)	Gynoid (%Fat)
20-29	53	160.4	54.2	2260	34723	16124	30.5	34.2	40.4
30-39	57	159.2	56.8	2328	35869	17527	33.4	36.8	40.9
40-49	50	159.9	61.2	2367	37021	20533	35.7	40.1	43.1
50-59	48	157.2	60.2	2134	35297	21249	36.9	43.9	44.0
60-69	45	155.6	58.6	1925	34947	19969	36.7	44.1	41.9
70-79	15	154.4	62.3	1927	35593	23329	40.3	45.1	44.0

Results showed LM and BMC peaked during the 5th decade, followed by a decline of 19% and 4% for BMC and LM, respectively by age 75 years. Total body FM and %Fat, as well as android and gynoid %Fat showed a general increase with age throughout the age range studied. FM increased 38.4% from young adult age (20-39 yr) values to age 70-79 years, while %Fat increased from 32% at young adult age to 40% at age 70-79 years. Total and regional fat measurements generally continued to increase with age, while lean mass and BMC peaked in the decade of 40-49 years in these Chinese women. Comparison of patients to an appropriate reference group is important because average body composition may vary substantially between populations.



Disclosures: **S. Lin**, None.

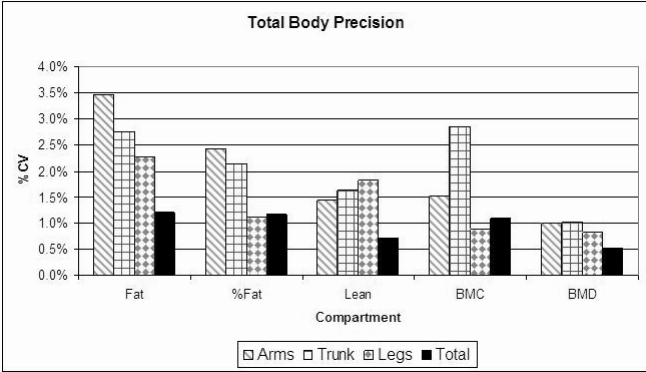
SU132

Precision of Total Body BMD and Body Composition Using the GE Lunar Prodigy Densitometer. R. Chen^{*1}, Q. Yang^{*2}, F. Chen^{*1}, Y. Chen^{*2}, S. Lin^{*1}. ¹Peking Union Medical College Hospital, Peking Union Medical College, Chinese Academy of Medical Science, Beijing, China, ²Jinan Maternity And Child Care Hospital, Jinan, China.

Total Body BMD and body composition measured with dual-energy x-ray absorptiometry (DXA) are utilized increasingly to evaluate a variety of clinical conditions, as well as for nutritional, exercise, and epidemiological research. Total body scans with DXA provide measurements of total body and regional body composition, including bone mineral content (BMC), bone mineral density (BMD), lean tissue mass (lean), fat tissue mass (fat), and % fat. Monitoring changes in BMD and body composition associated with disease and/or the effects of therapy contributes to a thorough patient evaluation.

Minimizing precision error allows detection of smaller changes in BMD and body composition. Ten volunteers were scanned with a GE Lunar Prodigy densitometer 5 times each day for 2 days, with the time interval between not exceeding 4 days. Subjects moved off and onto the scanner between each scan. Subjects fasted for at least 6 hours prior to each scan, and there were no known cases of illness that could have affected BMD or body composition over the short term. All scans were acquired and analyzed by the same experienced operator. Precision was calculated using the root-mean-square methodology. Total body precision was 1.2% for fat, 0.7% for lean, 1.2% for % fat, 1.1% for BMC and 0.5% for BMD. As expected, precision errors were generally greater at the regional (arms, legs, and trunk) measurement sites.

	Total Body Precision (% Coefficient of Variation)				
	Fat Mass	%Fat	Lean Mass	BMC	BMD
Arms	3.5	2.4	1.4	1.5	1.0
Legs	2.3	1.1	1.8	0.9	0.8
Trunk	2.7	2.1	1.6	2.8	1.0
Total	1.2	1.2	0.7	1.1	0.5



Disclosures: **R. Chen**, None.

SU133

The Advantage of Mechanical Response Tissue Analyzer in Detecting Decreased Mineralization of Cortical Bone versus DEXA and QUS. L. D. Moreno¹, C. Chan^{*2}, C. Wynnckvj^{*1}, S. Waldman^{*3}, M. Grynepas¹, A. Cheung². ¹SLRI, Mount Sinai Hospital, Toronto, ON, Canada, ²University Health Network, Toronto General Hospital, Toronto, ON, Canada, ³Department of Mechanical Engineering, Queen's University, Toronto, ON, Canada.

Dual energy absorptiometry (DEXA) and quantitative ultrasound (QUS) are the most commonly used technologies for evaluating fracture risk. However neither method provides a direct mechanical measurement of bone. A promising candidate for such a device is the Mechanical Response Tissue Analyzer (MRTA). The objective of our study was to investigate whether MRTA measurements of bone stiffness is a better tool in predicting bone quality change due to mineral loss, compared to DEXA and QUS. The emu was chosen as a new animal model for this study. Tibias of 24 male and female emus ages 2-5 years old, were used for the study. The ends of the bones were cut and the bone marrow removed. Bone mineral density (BMD), stiffness (EI) and the speed of sound (SOS) were measured for all the bones. Also determined was the flexural stiffness; bones were loaded in the elastic region in four-point bending at 0.04 mm/s using mechanical machine (Instron 8511). After the first set of measurements the bones were partially demineralized from the inside out. A pump was used to drive the fluid from the bottom to the top of the bones that were in the vertical position, and were kept moist with saline through out the demineralization process of the endocortical surface. After partial demineralization, BMD, EI, SOS and the flexural stiffness were again determined and compared with the values obtained before demineralization. The coefficient of correlation between the stiffness as determined mechanically and the measurements from the different devices are shown in the table below. From all the devices the ultrasound measurements showed the weakest correlation. After demineralization, DEXA measurements showed a decrease of 6.13% demineralization, the QUS showed a decrease of 1.24% in SOS, and the stiffness (EI) measured from the MRTA and the flexural stiffness showed an 11.73% and 11.78% decrease, respectively. From all the medical devices the MRTA measurements was the one that show the highest differences after partial demineralization. This study suggests that the MRTA has better discriminatory power than DEXA and QUS in determining decrease mineralization in cortical bone.

	BMD (DEXA)	SOS (QUS)	EI (MRTA)
Flexural stiffness (Instron)	0.83 (p<0.0001)	0.38 (p=0.07)	0.93 (p<0.0001)
EI (MRTA)	0.72 (p<0.0001)	0.34 (p=0.1)	
SOS (QUS)	0.51 (p<0.0001)		

Disclosures: **L.D. Moreno**, None.

SU134

The Effect of Precision on T-scores for Diagnosing Osteoporosis. K. G. Faulkner, L. S. Weynand*, W. K. Wacker*, H. S. Barden. GE Healthcare, Madison, WI, USA.

Effective use of serial DXA measurements for monitoring BMD change requires the minimization of precision error. However, even a single BMD result is subject to both offset (accuracy) errors and variability (precision) errors, which will influence the T-score and potential diagnosis of osteoporosis. In this investigation, we determined the influence of precision error on the T-score for the diagnosis of osteoporosis. Precision has been shown to depend on the experience of the operator, type of DXA system used, and the skeletal site measured. For this study, reported precision errors for expert DXA centers [1] and clinical DXA centers [2] were used. Using the Lunar Prodigy, expert precision error (g/cm²) in women (mean age 63 ± 9 years) was 0.010 at the L1-L4 spine, 0.013 at the femoral neck, and 0.008 for the total hip region (1). At clinical centers using the Lunar Prodigy, precision error in women (mean age 61± 10 years) was reported as 0.014 at the L1-L4 spine, 0.025 at the femoral neck, and 0.012 at the total hip (2). Assuming BMD is normally distributed, the 95% confidence interval (CI) for a single T-score measurement can be estimated using the following equation: 95% CI = T-score ± 1.96 (Precision/Population SD). Population SD from the reference database for the Lunar Prodigy is 0.12 g/cm² at the spine, femoral neck, and total hip. Using this model, the 95% CI for T-scores at each skeletal site are shown in Table 1.

Table 1: 95% CI for T-scores based on Expert and Clinical Precision

	Spine	Neck	Total Hip
Expert	±0.16	±0.21	±0.13
Clinical	±0.23	±0.41	±0.20

We conclude that clinical DXA T-scores have 95% confidence limits of ±0.2 at the spine and total hip and ±0.4 at the femoral neck. T-scores variations of ±0.2 or less at the spine or total hip and ±0.4 at the femoral neck should not be considered significant when diagnosing osteoporosis. Minimizing precision error can increase confidence in T-scores by reducing the confidence limits to less than ±0.2 at the spine and total femur and to ±0.2 at the femoral neck.

References:

1. Shepherd et al, WCO 2004
2. Weynand et al, ASBMR 2004

Disclosures: **K.G. Faulkner**, None.

SU135

Monitoring Antiresorptive Therapy with Dual Femur. P. K. Burke¹, G. N. Burke*¹, H. S. Barden², K. G. Faulkner². ¹Osteoporosis Diagnostic and Treatment Center, Richmond, VA, USA, ²GE Healthcare, Madison, WI, USA.

Monitoring patients with dual-energy x-ray absorptiometry (DXA) helps physicians assess treatment efficacy in preventing further bone loss and increased fracture risk. Minimizing DXA precision error reduces the least significant measurement change (LSC) required to detect a biological change in patient BMD. Larger increases in bone mineral density (BMD) with antiresorptive therapy are typically observed at the spine, compared to the femur, due to a higher proportion of high-turnover, cancellous bone at this site. However, spine assessment may be compromised in older patients due to osteophytes and other degenerative changes that occur with aging. We compared DXA measurements (Lunar Prodigy, GE Healthcare) of single femur, dual femur, and lumbar spine (L1-L4) for evaluation of treatment efficacy in 309 postmenopausal women (mean age of 65.8 ± 9.9 yrs) on antiresorptive therapy. Changes in BMD were evaluated after an average of 2.1 years of therapy. Femur results were reported for left femur neck (FN), total femur (TF), and dual TF. There was no significant difference in average BMD change (0.8% increase) between left TF and dual TF (p=0.63) or between FN and TF (p=0.82). A larger BMD increase (2.4%) was seen at the spine. Using this center's precision error and 95% confidence levels, the LSC was determined to be 3.9% for FN, 2.5% for single TF, 2.0% for dual TF, and 2.6% for spine. A significant increase in BMD was seen in 21% of subjects at FN, 27% at single TF, 31% at dual TF, and 48% at the spine. A significant decrease in BMD was observed in 9% of subjects at FN, 13% at single TF, 14% at dual TF, and 14% at the spine. About 77% of the women who had a significant positive or negative change at FN, TF or dual TF did not have a corresponding significant change at the spine. We conclude that a) there was no significant difference in the average BMD change for femur neck, single total and dual total femur after 2 years of antiresorptive therapy, b) the number of subjects with a significant positive change was larger (although, not significantly) for dual (n=97) than for single (n=84) total femur, c) more than 25% of patients with a significant positive change at the single or dual total femur did not show a significant positive change at the spine, and d) dual total femur identified an additional 51 subjects with a significant BMD change compared to measurement of spine alone.

	Left Neck	Left Total Femur	Dual Total Femur	Spine
CV (LSC)	1.40% (3.9%)	0.90% (2.5%)	0.72% (2.0%)	0.92% (2.6%)
Average BMD Change	0.8%	0.8%	0.8%	2.4%
Subjects (%) with Significant + Change	65 (21%)*	84 (27%)*	97 (31%)*	148 (48%)*
Subjects (%) with Significant - Change	27 (9%)	41 (13%)	42 (14%)	42 (14%)
Subjects (%) with Sig. + Change Femur Only	17 (26%)	22 (26%)	27 (28%)	
Subjects (%) with Sig. - Change Femur Only	14 (52%)	24 (59%)	24 (57%)	

* p=0.003 (neck vs dual total); p=0.25 (single total vs. dual total); p<0.0001 (single total vs. spine); p<0.0001 (dual total vs. spine)

Disclosures: **P.K. Burke**, None.

SU136

Changes in Total Body Composition with HIV Treatment. T. O. Chernova¹, H. S. Barden², N. I. Sazonova*¹. ¹Russian Academy of Medical Sciences, Moscow, Russian Federation, ²GE Healthcare, Madison, WI, USA.

Infection with the human immunodeficiency virus (HIV) is associated with a variety of metabolic and endocrine disorders, including progressive weight loss and hypogonadism that may affect body composition and bone density. Wasting syndrome associated with HIV infection results in loss of lean mass, and sometimes fat mass. Recently available highly active antiretroviral therapy (HAART) also is associated with alterations in body composition, fat distribution (lipodystrophy), and may be associated with osteopenia. Lipodystrophy is characterized by wasting of subcutaneous fat, peripheral fat loss, and accumulation of central or visceral fat. Dual-energy x-ray absorptiometry (DXA) allows study of total body and regional changes in soft tissue distribution, bone mineral content (BMC), and bone mineral density (BMD) in HIV-infected patients. We used DXA (Lunar Prodigy, GE Healthcare) to measure total body BMD and body composition in two small groups of Russian male subjects with HIV: Group 1 (n = 8, age 28.7 ± 10.1 yrs) measured at baseline; and Group 2 (n = 10, age 30.5 ± 4.2 yrs) measured at baseline and after treatment with HAART for 4 months. Expected BMD was determined by comparing results with Lunar Northern European reference data. Results showed slightly lower total body BMD than expected, with the largest deficits in the legs (-1.6%) in Group 1 and in the trunk (-5%) in group 2. The largest change with therapy for Group 2 occurred with fat mass, with average total body fat mass increasing 14%. This change appeared to be distributed evenly throughout the body. Total body lean mass showed a modest gain of 2%, while BMC and BMD both decreased overall by about 1%. We conclude that BMD was not substantially different from expected reference values at baseline and that BMC and BMD loss during the short therapy period of 4 months was minimal (~1%). The largest change with therapy was a surprising 14% increase in total body fat, evenly distributed among all regions of interest.

	Difference (%) from Expected BMD			
	Arms	Legs	Trunk	Total
Group 1 (n = 8)	2.4%	-1.6%	1.9%	-0.7%
Group 2 (n = 10)	-0.8%	-1.6%	-5.0%	-0.2%
Percent Change with Therapy				
Group 2				
BMC	-2.6%	-1.2%	-0.3%	-1.0%
Fat Mass	17.3%	14.0%	15.3%	14.3%
Lean Mass	-0.2%	2.7%	2.3%	2.1%
BMD	-2.7%	-1.8%	-0.2%	-1.2%

Disclosures: **T.O. Chernova**, None.

SU137

Poblational Screening with Accudexa. Relationship with Hip Frature Incidence. M. Ciria¹, M. Coll^{*1}, I. González^{*2}, J. Fernandez^{*3}, L. Perez-Edo¹, J. Blanch¹, P. Benito^{*1}, X. García-Miguel^{*1}. ¹Rheumatology, Institut Municipal d'Assistència Sanitària, Barcelona, Spain, ²Primary Care, Institut Català de Salut, Barcelona, Spain, ³Primary care, Institut Català de la Salut, Barcelona, Spain.

To assess the incidence of hip fracture in a poblational screening with ppheripheral densitometrical equipment (Accudexa) on medium phallanx and FRACTURE questionnaire, in comparison with a non-screened population. We performed a randomized, poblational-based prospective study. The universe were women higher than 65 years-old from an urban Primary Care unit. A randomized screening of half of the population was done, by their family physician in the Primary Care Unit. A structured questionnaire was done, including anthropometrical data, calcium intake, tobacco and alcohol habit, osteopenic drugs, age of menarchia and menopause, and previous use of antiresorptive drugs. The FRACTURE questionnaire was calculated without bone mineral density. A densitometrical study of the second phallanx of the non-dominating hand was done. Women with high risk of hip fracture were those with an Accudexa T-score < -2.5 SD or T-score <-1.6 SD and FRACTURE higher than 4 units. All women with high risk of hip fracture started therapy with risedronate once weekly. Patients with hip fractures being admitted in the reference hospital were compiled. Statistical analysis with Chi-square was done. Results: screening group: 1.650 women, screened: 789. Denied to enter in the study: 7%. Control group: 1990. Basal features of both groups were similar. Number of women identified as hip fracture high risk: 284 women. Hip fracture in first year: 14 (3 in screened group and 11 in control group, p=0.072). Hip fracture in second year: 13 (5 in screened group and 8 in control group, p=0.62). Four of the 8 women with hip fracture in the screening group declined their participation in the study and were not screened. Conclusions: The incidence of hip fracture in the screened population in the first year of following tends to be lower than the control group. This phenomenon disappears in the second year. Possibly, the change of incidence in the second year could be almost explained by a low compliance treatment. The Accudexa equipment, along with the FRACTURE questionnaire, helps to detect population with risk of hip fracture and to prescribe antiresorptive drugs if necessary.

Disclosures: **M. Ciria**, None.

SU138

Cross-Calibration of a Pencil-Beam and a Fan-Beam DXA (600 subjects): Identification of Factors Determining Differences between BMD Measurements. B. Sutter¹, O. Legrand^{*1}, G. Weryha². ¹Nuclear Medicine, Institut Calot, Berck sur Mer, France, ²Endocrinology, CHU, Vandoeuvre les Nancy, France.

Follow-up of individual patients who are receiving treatment for osteoporosis leads to difficulties when a newer model replaces an old DXA system. We report the results of an in vivo cross-calibration study performed between a HOLOGIC® QDR 1000/W pencil-beam and a HOLOGIC® 4500 ACCLAIM fan-beam Dual X-ray Absorptiometer. Phantom quality control measurements were comparable for the two devices (QDR 1000/W: 990.4 +/- 4.1 mg/cm²; ACCLAIM 989.2 +/- 2.5 mg/cm², 10 measurements). Lumbar spine and hip DXA scans were performed same day in 600 patients attending long-term BMD monitoring: female 512, male 88, age 62.0 +/- 10.0 years, Body Mass Index (BMI) 26.0 +/- 4.1 kg/m². Lumbar spine BMD measurements on the two systems agreed closely: r²=0.978. ACCLAIM values were 1.4 % higher than those on the QDR 1000/W (mean difference 11.7 +/- 22.3 mg/cm²). Difference correlated positively with age and negatively with bone density. On an other hand, the 121 subjects with a difference over 4% are significantly older, with a higher BMI and a lower BMD. Femoral neck and total BMD (586 subjects) also correlated closely between the two systems: r²=0.937 for femoral neck, r²=0.956 for total femur. We found an overestimation of BMD with ACCLAIM: +40.2 +/- 27.1 mg/cm² for femoral neck (+5.5%), +19.5 +/- 3.0 mg/cm² for Total femur (+2.8%). Difference positively correlated with BMI (femoral neck & Total femur) and BMD (Total femur). The 197 patients with a femoral neck BMD difference over 5% are significantly older, with a higher BMI and a lower BMD. In summary, despite a close correlation between the pencil beam and fan beam devices, we found an overestimation with fan beam measurements, especially for femoral (neck and total femur) which could not be predicted with quality phantom measurement. Additionally, difference significantly correlated with age, BMI, and BMD values.

Disclosures: **B. Sutter**, None.

SU139

Risk-Equivalent Cutoff Levels for DXA Measurements Based Exclusively on Total Femur. C. C. Glüer¹, R. Eastell², D. M. Reid³, C. Roux⁴, D. Felsenberg⁵. ¹UK SH, Kiel, Germany, ²University of Sheffield, Sheffield, United Kingdom, ³University of Aberdeen, Aberdeen, United Kingdom, ⁴René Descartes University, Paris, France, ⁵Charité, Berlin, Germany.

The current efforts to develop risk based intervention criteria for osteoporosis treatment requires the definition of cutoff levels at well defined levels of absolute fracture risk. Currently the WHO-criterion of a minimum T-Score < -2.5 for spine and total femur measurements is commonly used both for diagnosis and as an intervention threshold. To facilitate diagnosis and risk assessment the definition of cutoff levels based exclusively on total femur measurements has been proposed. We investigated which cutoff level would be risk-equivalent to the current WHO criterion if measurements were only carried out at a single site, the total femur. Gradients of risk for spine and hip fractures for DXA measurements at the spine and total femur are well established. The gradient of risk for the current approach can be estimated from population-based distributions of spine and hip results. Thus the relative risk for a minimum T-score of -2.5 can be calculated and subsequently the equivalent T-score for a total femur measurement can be derived. We used DXA data of 2374 women (age 55-79, mean age 67) examined in OPUS, a population based multi center study. The gradients of risk per standard deviation of the population variance (sRR) are 1.5 and 2.4 for hip fractures based on spine or total femur measurements respectively and 1.9 for spine fractures for either measurement site (Cummings, JAMA 2002). As gold standard we therefore calculated relative risk of hip fracture from total femur results; gold standard relative risk for spine fractures was calculated as the average of spine and total femur result. We then fitted the result of minimum T-Score of spine and total femur results to gold standard risk levels and observed sRR=2.0. A total femur measurement with its higher sRR of 2.4 reaches the risk level of T=-2.5 already at a T-Score of -2.0. Similarly, the -2.5 level for vertebral fractures for an sRR=1.8 is reached at a T-Score of -2.2 if measurements are only based on total femur results. Equal weighting of both results leads to a risk-equivalent threshold of -2.1 for total femur measurements. Levels of risk equivalency and prevalence equivalency vary with age. Prevalence of subjects below the two criteria was similar (15%) for women above age 65. We conclude, that for a typical population aged 55-79 a T-Score of -2.1 at the total femur is risk-equivalent to the current -2.5 T-Score criterion for DXA of the spine and the hip; the impact of age, however, may necessitate the use of Z-Score criteria which allow to separate density associated components of fracture risk from age effects.

Disclosures: **C.C. Glüer**, Eli Lilly & Company 2; Procter & Gamble Pharmaceuticals 2; Sanofi Aventis 2; Novartis 2.

SU140

Parity Influence on Femur Geometry. S. Di Gregorio^{*1}, L. M. Del Rio¹, S. N. Zeni², J. Rosales^{*1}. ¹Densitometria, Cetir Centre Medic, Barcelona, Spain, ²Sección Osteopatías Médicas, Hospital de Clínicas. UBA, Buenos Aires, Argentina.

Reproductive history could affect bone mass in postmenopausal population. We found in a previous study that hip fracture prevalence in multiparous women was lower than in nulliparous and is associated to a high bone mineral density (BMD). Although there are a general concern that hip fracture is related to proximal femur geometrical parameters, there are few data about the impact of parity on femur geometry. We recruited a total of 1074 postmenopausal women for the study (from 39 to 89 years). A standardized interview was employed to obtain information about life style, fracture prevalence and reproductive history.

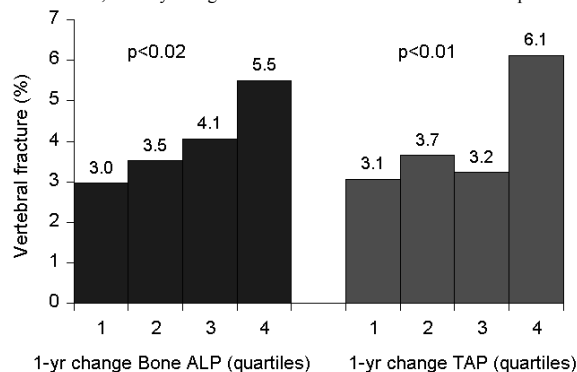
Patients were divided into four group according to the number of pregnancies: G0: 150 nulliparous (60 ±8 year), G1: 566 with one or two pregnancies (59±8 years), G2: 303 with three or four pregnancies (61 ±7years) and G3: 54 grand multiparous -five or more pregnancies- (63 ±8years). Femoral hip (total, neck and trochanter) was measured by DXA (GE-Lunar Prodigy V8.1). The bone status and femur geometry was assessed by using the femur strength analysis program (Lunar GE). Results: The first step analysis was performed comparing nulliparous vs all parous women independently of pregnancies number: there was statistical difference in body weight (61 vs 65 kg p < 0.0001) and in BMD at total hip (0.847 vs. 0.884 p<0.001) ; trochanter (0.658 vs. 0.686, p=0.006)and femoral neck (0.809 vs. 0.830, p=0.045). We didn't find differences between geometry parameters. When the impact of pregnancies number was taken into account the BMD results showed a similar tendency was observed in BMD areas. Sectional cross area (CSA) , (p=0.019), as well as the femoral neck angle (p=0.02) and length (p=0.01) were larger in women with one or two pregnancies (p=0.019; p=0.02 and p =.001 respectively . Pearson test showed a positive correlation between body weight and the following geometrical parameters: CSA: G0: R: 0.317 p <0.001; G1: R:0.345 p < 0.001; G2: R =.324 p <0.001; G 3: R: 0.413 p < 0.002 ; CSMI: G 0: 0.347: p 0.001; G1: R: 0.337; p 0.001; G2: R:0.427 p: < 0.001; G3: NS. Conclusion: pregnancy has an influence on proximal femur geometry and BMD, perhaps due to a macro-architectural adaptation that could affect biomechanical characterist of bone.

Disclosures: **S. Di Gregorio**, None.

SU141

The Effect of Alendronate on Bone Alkaline Phosphatase Vs. Total Alkaline Phosphatase: The Fracture Intervention Trial. D. C. Bauer¹, P. Garnero², L. Palermo^{*1}, P. Delmas³. ¹Epidemiology and Biostatistics, UCSF, San Francisco, CA, USA, ²Synarc, Lyon, France, ³INSERM 403, Lyon, France.

Among alendronate-treated women in the Fracture Intervention Trial (FIT), greater 1-year reductions in markers of bone turnover were associated with fewer spine and non-spine fractures (Bauer et al, JBMR, 2004). The utility of less specific skeletal biomarkers, such as total alkaline phosphatase, has not been reported. We measured both bone specific alkaline phosphatase (Bone ALP, Hybritech) and total alkaline phosphatase (TAP, Nichols) at baseline and after 1 year of alendronate (ALN), 5 mg/d, in 3044 participants in the Fracture Intervention Trial. TAP was measured as a component of routine "safety labs". Total hip BMD (Hologic) was measured at baseline and after a mean follow-up of 3.6 years. Among ALN-treated women, 252 women had non-spine fractures and 119 had incident vertebral fractures on paired lateral spine x-rays during follow-up. We used age-adjusted logistic and hazard models to examine the independent relationships between 1-year change in Bone ALP or TAP and subsequent spine and non-spine fracture. These analyses are by intention to treat, and are limited to ALN-treated subjects. At baseline, Bone ALP and TAP were modestly correlated (r=0.67). After 1 year of ALN, the mean (SD) change in Bone ALP was -4.8 (4.0) ng/ml (-32.6%), while the mean change in TAP was -14.0 (16.0) mg/dl (-15.3%). The correlations between the 1-year change in Bone ALP or TAP and long-term changes in hip BMD were similar (r=0.28 and r=0.24, respectively). Greater reductions in both Bone ALP and TAP were associated with fewer incident spine fractures (Figure, 4th quartile represents largest reductions). Each additional SD reduction in the 1-year absolute change in Bone ALP was associated with a 28% reduction (95% CI: 12%, 40%) in spine fracture risk, while each SD reduction in the change in TAP was associated with a 22% reduction (95% CI: 8%, 33%). One-year changes in Bone ALP were also associated with a reduced risk of non-spine fracture (RH per SD=0.84, CI: 0.74, 0.96), but 1-year changes in TAP were not (RH per SD=0.98, CI: 0.87, 1.10). We conclude that among ALN-treated women, 1-year changes in both Bone ALP and TAP are associated greater increases in BMD and fewer incident vertebral fractures, but only changes in Bone ALP are associated with non-spine fracture risk.



Disclosures: **D.C. Bauer**, Merck 2; P and G 2.

SU142

Serum Cathepsin K Levels Reflect Osteoclastic Activity in Women with Postmenopausal Osteoporosis and Patients with Paget's Disease. C. Meier¹, U. Meinhardt^{*2}, M. E. Kraenzlin¹, J. R. Greenfield^{*2}, T. V. Nguyen², C. R. Dunstan³, M. J. Seibel³. ¹Clinic for Endocrinology, University Hospital Basel, Switzerland, ²Garvan Institute of Medical Research, University of NSW, Sydney, Australia, ³ANZAC Research Institute, University of Sydney, Sydney, Australia.

Cathepsin K, a cysteine protease, plays an essential role in osteoclast-mediated collagen degradation. Recently, an immunoassay to quantify cathepsin K in serum has been developed. We assessed the usefulness of serum cathepsin K as a marker of bone turnover

in cross-sectional and longitudinal studies of patients with metabolic bone disease. The study cohort consisted of 40 healthy controls (13 premenopausal women [age, 30.6±6.6 yrs (mean±SD)]; 11 postmenopausal women [64.1±8.3 yrs]; 16 men [41.6±12.4 yrs]), 21 women with postmenopausal osteoporosis (66.1±7.9 yrs) and 10 patients with Paget's disease of bone (67.1±11.6 yrs). Patients were started on oral or intravenous bisphosphonate treatment and were followed prospectively over 6 months. Circulating cathepsin K levels were determined by a specific sandwich enzyme immunoassay (Biomedica, Austria). In addition, serum carboxyterminal cross-linked telopeptide of type I collagen (βCTX-I) and bone-specific alkaline phosphatase (BALP) were measured for comparison. Serum cathepsin K levels were similar in the three healthy control groups with a mean (±SD) level of 3.1 (±1.7) pmol/L. When compared to healthy controls, mean cathepsin K levels were significantly elevated in women with postmenopausal osteoporosis (11.3 ± 13.1 pmol/L, p=0.01) and in patients with Paget's disease of bone (6.2 ± 4.4 pmol/L, p=0.04). In postmenopausal osteoporotic women, both oral and intravenous bisphosphonate treatment resulted in a significant reduction in serum cathepsin K levels with a nadir at one month (-33.9 % vs. baseline; p=0.01) and stable suppression thereafter. The magnitude of these changes was intermediate to those seen with βCTX-I and BALP. In patients with mild Paget's disease (baseline BALP, 73.3±50.4 U/L), cathepsin K tended to decrease during bisphosphonate treatment (mean % change after one month: -30.3%). Serum cathepsin K levels appear to reflect osteoclastic activity in patients with postmenopausal osteoporosis and Paget's disease and may hold promise as a direct cellular marker of osteoclast activity.

Disclosures: **C. Meier**, None.

SU143

The Effect of Discontinuation of Long-Term Oral Low Dose Hormone Therapy to Skeletal and Metabolic Markers and Bone Mineral Density. J. Haapalahti¹, J. Heikkinen^{*2}, J. Ramberg^{*1}, J. Risteli³, R. Vaheri^{*4}. ¹R&D, Orion Diagnostica Oy, Oulu, Finland, ²Deaconess Institute, Oulu, Finland, ³Clinical Chemistry, University of Oulu, Oulu, Finland, ⁴Orion Group Orion Pharma, Espoo, Finland.

It has been earlier established that oral hormone replacement therapy (HRT) may modify levels of biochemical markers such as total testosterone (T), sensitive C-reactive protein (s-CRP) and intact aminoterminal propeptide of type I procollagen (PINP). The aim of this study was to elucidate the effect of discontinuation of long-term oral low dose hormone replacement on these biomarkers and lumbar spine bone mineral density (BMD). Serum samples taken from 35 healthy postmenopausal women (mean age at inclusion 55.9 years) were retrospectively analysed at baseline before starting HRT with a continuous-combined low-dose 1mg estradiol valerate/2.5mg medroxyprogesterone acetate product (Indivina®, Orion Pharma, Finland) from samples taken at 12-month and 108-month time points after treatment start and one year after discontinuation. T (nmol/l), PINP (microg/l) and s-CRP (mg/l) were measured using commercially available methods (Orion Diagnostica Oy, Espoo, Finland). For s-CRP 12-month analysis was not available. BMD was measured at the same time points using DEXA (g/cm²). At 12 months BMD was significantly increased (+2.4%, p<0.001) and PINP decreased (-29.5%, p=0.0012). At 108 months increase from baseline was found in T (+18.4%, p=0.012) and BMD (+9.5%, p<0.0001) and decrease in PINP (-22.7%, p=0.004). At one year after discontinuation of HRT BMD had significantly decreased from end-of-treatment values (-2.3%, p<0.001) and PINP had increased (+109%, p<0.0001). No change was found in s-CRP (p=0.672). When HRT-users were divided into subgroups of low and high bone turnover, based on PINP with cut-off of 40 microg/l at baseline, it was found that at 12 months increase in BMD and decrease in PINP were significant in "high bone turnover" group only (p<0.0001 for both). Discontinuation more strongly affected PINP levels in women with "low bone turnover" at baseline. It can be concluded that discontinuation of long-term oral low dose hormone replacement within one year restores mildly elevated levels of T to baseline level but does not affect s-CRP level, whereas BMD and PINP are clearly affected. Biochemical marker of bone turnover PINP shows theranostic potential in prediction of skeletal response to HRT at both initiation and discontinuation of oral HRT.

Disclosures: **J. Haapalahti**, Orion Diagnostica Oy 3.

SU144

Serum Cathepsin K Measurements: Repeatability, Intra-Subject and Postprandial Variability. U. J. Meinhardt^{*1}, C. Meier², T. V. Nguyen³, J. R. Greenfield^{*4}, C. R. Dunstan^{*5}, C. Kraenzlin², M. J. Seibel⁵. ¹Pituitary Research Unit, Garvan Institute of Medical Research, Sydney, Australia, ²University Hospital, Basel, Switzerland, ³Bone and Mineral Research Program, Garvan Institute of Medical Research, Sydney, Australia, ⁴Diabetes and Obesity Program, Garvan Institute of Medical Research, Sydney, Australia, ⁵University of Sydney, ANZAC Research Institute, Sydney, Australia.

Cathepsin K, a cysteine protease, plays a major role in bone matrix degradation. Recently, an enzyme-linked immunosorbant assay for cathepsin K measurement in serum and cell culture (Cathepsin K ELISA BI-20432, Biomedica, Austria) was developed using a polyclonal sheep antibody. In this study we assessed the repeatability and intra-subject and postprandial variability of cathepsin K measurements in human sera. Serum samples from nine healthy postmenopausal women aged 65.9 ± 6.5 years (mean ± SD) were collected a) in the fasting state on two occasions separated by 1 - 4 weeks, and b) 120, 240 and 360 minutes after a standard breakfast (1385 Kcal, 37g protein, 88g fat, 104g carbohydrate). Samples were kept frozen at - 20 °C up to 6 months and at - 80°C up to 12 months before being analysed in batch duplicates by a single investigator. Measurement of sera obtained on two separate occasions yielded mean (±SD) cathepsin K values of 3.20 ± 1.41 pmol/L and 2.65 ± 1.29 pmol/L, respectively, with no statistical difference between

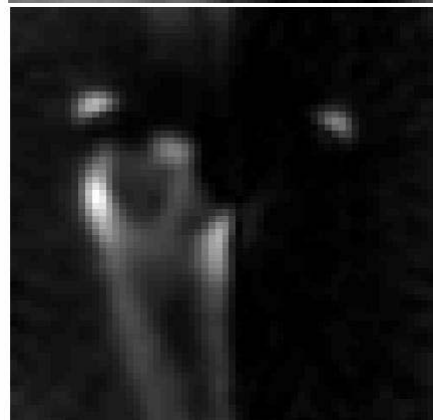
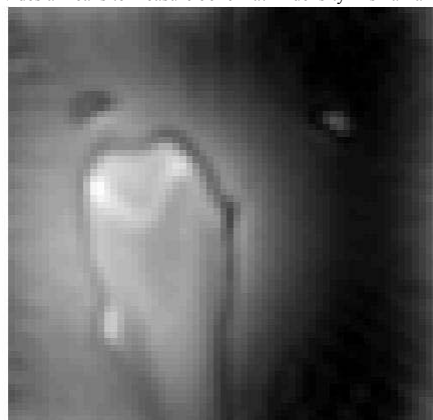
the two sets of data (p = 0.39). Mixed-effect analysis of variance suggested that the intra-subject variance of cathepsin K was 1.81 ± 0.90 pmol/L² of which biological and inter-assay variance accounted for 68 % (1.28 ± 0.87 pmol/L²) and analytical variance accounted for 32 % (0.58 ± 0.28 pmol/L²). The postprandial cathepsin K levels at baseline, 120, 240 and 360 minutes were 2.65 ± 1.29, 2.79 ± 1.07, 2.37 ± 1.00 and 2.75 ± 0.96 pmol/L, respectively; no statistically significant difference was observed between these results (p = 0.79). Cathepsin K levels did not appear to be affected by haemolysis of the blood sample (2.73 ± 1.15 vs. 2.28 ± 1.24 pmol/L, respectively, p= 0.12, n = 5). We conclude that serum cathepsin K levels as measured by the Biomedica assay show good intra-subject repeatability and low postprandial variability.

Disclosures: **C. Meier**, None.

SU145

Solid Bone Matrix of Rat Femur Imaged by Water and Fat Suppressed Proton Magnetic Resonance Imaging. Y. Wu^{*1}, J. L. Ackerman^{*2}, G. Dai^{*2}, D. A. Chelsler^{*2}, M. Hrovat^{*3}, B. D. Snyder^{*4}, A. Nazarian^{*4}, M. J. Glimcher¹. ¹Orthopaedic Surgery Department, Children's Hospital, Boston, MA, USA, ²Radiology Department, Massachusetts General Hospital, Boston, MA, USA, ³Mirtech, Inc, Boston, MA, USA, ⁴Orthopedic Biomechanics Lab, Beth Israel Deaconess Medical Center, Boston, MA, USA.

One of the crucial parameters to assess bone quality is the degree of bone mineralization (DM), conventionally defined as the weight of bone mineral in unit volume of bone matrix. A closely related definition of DM is the ratio of bone mineral density (BMD) divided by bone matrix density. Micro-CT (μCT) has gained popularity in bone and mineral research on small rat bone specimens (< 18 mm) due to its high spatial resolution, but as an X-ray based method, μCT of bone can only reflect the mineral content, not the solid matrix content (mostly collagen). Here we explore the feasibility of water and fat suppressed projection magnetic resonance imaging (WASPI) to image the solid matrix content of rat bone specimens, in order to determine matrix density. The MRI experiments were carried out with a 33 cm ID 4.7 T Bruker MR scanner and home made 1.5 cm ID RF coil. A typical measurement time for 1838 projections was 31 min, which yielded a 3D image data set of 64X64X64 with field of view: 20 mm and spatial resolution: 0.63 mm. Figure 1 shows one slice from the full 3D data set of the normal (no water or fat suppression) ¹H projection MR image of a rat femur, in which the soft tissue surrounding bone and the water and fat in the medullary cavity are shown clearly while the bone is dark. Figure 2 is the WASPI image of the same rat bone specimen. The signal from the medullary cavity (water and fat) has been largely suppressed, along with the water and fat signal inside bone tissues; the solid matrix is well visualized. In this study, the solid matrix of rat bone was imaged directly by MRI for the first time to the best of our knowledge. This method provides a means to measure bone matrix density in small animals.



Disclosures: **Y. Wu**, SkelScan, Inc 1.

SU146

Association of 13 Serum Biochemical Markers with Bone Metastases in Women with Breast Cancer. N. Voorzanger-Rousselot^{*1}, F. Juillet^{*1}, J. Zimmermann^{*2}, V. Cretet^{*1}, E. Mareau^{*1}, T. Kalebic^{*2}, P. Garnero¹. ¹Synarc, Lyon, France, ²Novartis Pharma, East Hanover, NJ, USA.

Background: Bone metastasis (M) is a frequent complication of breast cancer (BC). Diagnosis of M from BC is challenging and relies mainly on bone scintigraphy, which lacks specificity. Alternatively, serum biochemical markers may be useful to detect bone metastases, although when used alone, they lack sensitivity. The aim of this study was to analyze the value of combining systemic markers of bone turnover, inflammation, and angiogenesis to identify M from BC. **Patients and methods:** Eighteen women with BC and M (BC, M+, mean age: 56 yr), 19 women with BC and no M (BC, M-, mean age 52) and 15 healthy women (mean age 59 yr) were included. Thirteen serum markers were measured: bone alkaline phosphatase (BAP) and N-propeptide type I collagen (PINP) as markers of bone formation; CTX-I, ICTP as markers of bone resorption, tartrate resistant acid phosphatase 5b (TRAP5b) and osteoprotegerin (OPG) as markers of osteoclastic activity; matrix-metalloproteases (MMP), 2, 7 and 9, the tissue inhibitor of MMP (TIMP-1), IL-6, TGF β and VEGF. We performed backward multivariable analyses to identify independent markers which were then included in a discriminative model for classifying patients. **Results:** All bone turnover markers were higher in patients with BC M+ than in healthy women (p<0.01-0.0001) and patients with BC, M-(p<0.01-0.0001, except for CTX-I). OPG, MMP-2, 7, 9, TIMP-1 and VEGF were also significantly higher in BC, M+ than healthy women (p<0.01-0.0001) and BC, M- (p<0.05-0.0001 except OPG). Serum TGF β was decreased in BC, M+ compared to healthy women (p=0.05) and there was no difference between groups in IL-6 levels. Patients with BC, M- had similar levels than healthy women except for higher levels of CTX (p=0.001), MMP-2 and 9 (p=0.03). When each marker was considered individually, the diagnostic value was highest and similar for TRAP5b, MMP-2 and MMP-7, with 79-84% of patients being correctly classified. In multiple variable model, only ICTP, TRAP 5b, MMP-2 and 9, TGF β , and VEGF remained independently associated with bone metastases. This combination of markers correctly identified 94% of patients with and without bone metastases. **Conclusion:** Combination of serum markers of bone resorption, MMPs, growth and angiogenic factors improve the diagnosis of bone metastases from breast cancer.

Disclosures: **P. Garnero**, None.

SU147

Comparison of the Clinical Performance of Six Different Serum Tartrate-Resistant Acid Phosphatase Assays for Monitoring Alendronate Treatment. K. M. Fagerlund^{*1}, A. J. Jankila², H. Ylipahkala^{*1}, S. L. Alatalo^{*3}, L. T. Yam^{*2}, H. K. Väänänen^{*1}, J. M. Halleen^{*1}. ¹Institute of Biomedicine, Department of Anatomy, University of Turku, Turku, Finland, ²Veterans Affairs Medical Center, Louisville, KY, USA, ³Finnish Red Cross Blood Service, Helsinki, Finland, ⁴Pharmatest Service Ltd, Turku, Finland.

Two isoforms of tartrate-resistant acid phosphatase (TRACP) circulate in human blood, TRACP 5a derived from inflammatory macrophages and TRACP 5b derived from bone-resorbing osteoclasts. We have studied the clinical performance of six different serum TRACP assays and compared them with other commonly used markers of bone turnover, including serum CTX, PINP, BAP, OC and urinary DPD, for monitoring alendronate treatment. This double-blinded study included 137 healthy postmenopausal women that were randomly assigned into two groups, one receiving 5 mg alendronate daily (n = 70), and the other receiving placebo (n = 67). The TRACP assays were as follows: 1) A pH-selective in-house immunoassay measuring TRACP 5b activity (also available commercially as BoneTRAP® assay, SBA-Sciences, Oulu, Finland); 2) An immunoassay measuring total TRACP activity (TRAP5, Biovendor, Brno, Czech Republic); 3) An immunoassay using naphthol-ASBI-phosphate as a selective substrate for TRACP 5b (ASBI); 4) An immunoassay measuring TRACP 5a activity; 5) An immunoassay measuring total TRACP protein amount; 6) An immunoassay measuring TRACP 5a protein amount. All bone markers were assessed at baseline and at 3 months after start of treatment. Alendronate treatment decreased significantly serum TRACP measured by the BoneTRAP® assay, TRAP5 assay and ASBI assay, the largest decrease being observed with the BoneTRAP® assay. These three TRACP methods correlated significantly with the other bone markers measured, highest r-values being observed with the BoneTRAP® assay. TRACP protein, 5a activity and 5a protein were not affected by alendronate treatment and did not correlate with the other TRACP methods or with the other bone markers measured. Sensitivity, area under ROC curves and signal-to-noise ratio were higher for the BoneTRAP® assay than for the other TRACP methods. These results demonstrate that serum TRACP 5a is not associated with bone turnover and TRACP 5b specific methods should be used in assessing bone resorption.

Disclosures: **K.M. Fagerlund**, SBA-Sciences 5, 7.

SU148

The Type I Collagen Related Biochemical Markers of Bone Resorption, ICTP and CTX-Reflect Different Biological Pathways in Patients with Breast Cancer and Bone Metastases. P. Garnero¹, N. Voorzanger-Rousselot^{*1}, J. Zimmermann^{*2}, T. Kalebic^{*2}. ¹Synarc, Lyon, France, ²Novartis Pharma, East Hanover, NJ, USA.

Background: Bone resorption generates type I collagen fragments such as ICTP and CTX that can be quantified in serum using specific ELISAs. In vitro studies have shown that ICTP and CTX are released from bone matrix by different enzymatic pathways namely

matrix-metalloproteases (MMP) for ICTP and cathepsin K for CTX (JBMR, 2003). The aim of this study was to analyze the respective sensitivity of ICTP and CTX to detect bone metastases (BM) in patients with breast cancer (BC) and to analyze their association with circulating levels of MMPs and markers of osteoclastic activity. **Patients and methods:** Eighteen women with breast cancer and bone metastases (BC, M+, mean age: 56 yr), 19 women with BC and no bone metastases (BC, M-, mean age 52) and 15 healthy women (mean age 59 yr) were included. Serum levels of ICTP, CTX, MMP-2, MMP-7, MMP-9, TIMP-1, tartrate resistant acid phosphatase 5b (TRAP5b) and osteoprotegerin (OPG) were measured by specific ELISAs. **Results:** Serum ICTP was increased by a median 2 fold (p<0.0001) in patients with BC, M+ compared to both healthy women and patients with BC, M-. Serum CTX was increased by 8 fold in patients with BC, M+ compared to healthy women (p=0.004), and by 20% (p=0.08) compared to: BC, M-, MMP-2, MMP-7, MMP-9, TIMP-1 (p<0.01-0.0001), TRAP5b (p<0.005) and OPG (p0.07-0.001) were also higher in patients with BC, M+ compared to healthy women and patients with BC, M-. When all patients were analyzed together, ICTP strongly correlated with MMP-2 (r=0.60, p<0.0001), MMP-7 (r=0.67, p<0.001), TIMP-1 (r=0.60, p<0.0001) and to a lesser extent MMP-9 (p=0.27, p=0.05). In contrast serum CTX did not significantly correlated with MMPs, except slightly with MMP-7 (r=0.36, p=0.02) and TIMP-1 (r=0.42, p=0.004). Both ICTP and CTX correlated significantly with the markers of osteoclastic activity, TRAP 5b (r=0.66, p<0.0001 and r=0.47, p=0.006 for ICTP and CTX, respectively) and OPG (r=0.63, p<0.0001 and r=0.35, p=0.019). **Conclusion:** A significant increase in ICTP and CTX has been found associated with osteoclastic activity. Consistently with prior in vitro observations, circulating ICTP -but not CTX- correlates with MMPs driven type I collagen degradation. Osteolysis from breast cancer involved both MMPs and cathepsin K, mediated pathways which can be evaluated by serum ICTP and CTX, respectively

Disclosures: **P. Garnero**, None.

SU149

Lack of Hepatic Metabolism of C-Telopeptides of Type I Collagen. P. Qvist¹, K. Petersen^{*2}, J. Jespersen³, N. Vinberg^{*4}, C. Christiansen⁵. ¹Nordic Bioscience, Herlev, Denmark, ²Department of Obstetrics and Gynecology, Odense University Hospital, Odense, Denmark, ³Department of Clinical Biochemistry, University of Southern Denmark, Ribe, Denmark, ⁴Isotope Agency, Rigshospitalet, Copenhagen, Denmark, ⁵Centre for Clinical & Basic Research, Ballerup, Denmark.

Bone biochemical markers have been used in dynamic studies of bone metabolism, and for accurate interpretation of measured marker levels it is essential to have information of extra-skeletal metabolism. Therefore the objective of the present study was to investigate if the circulating C-telopeptides of type I collagen (CTX) was subject to hepatic extraction. Eight, non-obese females between 22 and 32 years of age without previous history of diabetes, arterial or venous thrombosis, or hepatic diseases, participated in the study. Under local anaesthesia and fluoroscopy, a pre-shaped F 7 catheter was inserted through the right femoral vein and the tip of the catheter located in a large right liver vein; a 15-cm F4 catheter was inserted into the femoral artery. A constant-rate infusion of Tc-99m mebrofenin was given intravenously through an arm-vein, approximately 20 MBq over 2.5 hours. In order to measure splanchnic plasma flow, four sets of samples from the artery and the liver vein were obtained at 20-min intervals after one hour of infusion. Simultaneously, samples were obtained for measurements of CTX and PINP. Plasma volume was calculated by injection of approximately 300 kBq I-125 albumine and subsequently obtaining serial arterial blood samples post injection. The study was performed while the participants were in the resting, fasting steady state, and therefore the volume of distribution, splanchnic plasma flow and extraction were assumed to be constant during the period of investigation. No change in plasma level of CTX could be detected over the liver. In contrast, PINP decreased from an average of 52.9 ng/ml in the artery to 42.4 ng/ml in the vein, corresponding to a 19.8% reduction. Therefore it can be concluded that C-telopeptides of type I collagen (CTX) is not subject to hepatic metabolism.

Disclosures: **P. Qvist**, Nordic Bioscience 3.

SU150

The Discovery of New Biomarkers for the Diagnosis of Osteoporosis: Is SELDI the Answer? S. Bhattacharyya^{*1}, E. Siegel^{*2}, S. Jennings^{*3}, S. Khosla⁴, L. J. Suva¹. ¹Department of Orthopaedic Surgery, Center for Orthopaedic Research, UAMS, Little Rock, AR, USA, ²Department of Biometry, UAMS, Little Rock, AR, USA, ³Department of Applied Science, University Arkansas at Little Rock, Little Rock, AR, USA, ⁴Endocrine Research Unit, Mayo Clinic College of Medicine, Rochester, MN, USA.

Proteomic pattern analysis leading to the discovery of novel biomarkers has emerged as an effective method for the early diagnosis of many diseases, such as ovarian, breast and pancreas cancer. However, there is little information regarding the utility of this approach for the diagnosis of diseases other than cancer. In this study surface enhanced laser desorption ionization time-of-flight (SELDI-TOF) mass spectrometry was used to screen for potential biomarkers in the serum of 58 postmenopausal women, clinically diagnosed with or without high bone turnover and osteoporosis. The diagnosis and follow-up of this disease is currently reliant on annual bone mineral density measurements and the measurement of unreliable biochemical markers. Accurate biochemical markers of skeletal activity would potentially provide a means of evaluating the skeleton and help in the diagnosis and follow-up of the disease. Serum samples from 28 osteoporotic and 30 age-matched unaffected women were fractionated based on charge (6 fractions) and SELDI spectra collected from each fraction of each patient, in duplicate, and in three molecular weight ranges, generating a total of 2436 spectra, with an average of 15,000 data points per spectra. All spectral data were normalized, standardized and subjected to multivariate statistical analysis and data mining procedures

ultimately leading to the detection of eight peaks (MW ranging from 3.1-7.1kDa) that optimally separated the two groups with a high degree of significance (p<0.05). In addition, multiple correlations of the diagnostic SELDI profiles from these patients with clinical parameters such as BMD and t-score strongly support the diagnostic significance of the identified SELDI peaks. This unique discriminatory profile represents a diagnostic fingerprint of the multiple biomarkers that distinguishes post-menopausal osteoporosis from normal post-menopausal, non-osteoporotic controls.

Disclosures: **S. Bhattacharyya**, None.

SU151

Potential Cost-Effective Use of Bone Turnover Markers to Select Osteopenic Post-Menopausal Women for Alendronate Therapy. **J. T. Schousboe¹, K. E. Ensrud², D. C. Bauer³, J. A. Nyman^{*4}, R. L. Kane^{*4}, L. J. Melton⁵.** ¹Park Nicollet Clinic & University of Minnesota, Minneapolis, MN, USA, ²VAMC & University of Minnesota, Minneapolis, MN, USA, ³UCSF, San Francisco, CA, USA, ⁴University of Minnesota, Minneapolis, MN, USA, ⁵Mayo Clinic, Rochester, MN, USA.

A substantial proportion of fractures (Fx) occur in post-menopausal women without osteoporosis (T-score ≤ -2.5). High bone turnover, a risk factor for incident Fx independent of bone density, may be useful in identifying osteopenic older women at increased fx risk who may derive a greater Fx risk reduction with alendronate therapy. We used a Markov model with 8 health states to estimate the cost-effectiveness of serum C-telopeptide (CTx) and tartrate resistant acid phosphatase (TRACP5b) to identify osteopenic (T-score -2.0) older post-menopausal women with high bone turnover and treat them with alendronate to prevent incident fractures. Fracture rates, Fx direct costs, and long-term care costs after hip Fx were derived from comprehensive population-based data of Rochester, MN. We compared 5 years of alendronate Rx to no initial Rx, included 5 years of additional alendronate Rx following an incident Fx for both strategies, and assumed a relative risk of vertebral Fx on alendronate Rx of 0.54 vs. No Rx for the base case analysis. We assumed relative risks of 1.53 and 1.0 for incident vertebral and non-vertebral Fx, respectively, for those in the top quartile of CTx vs. the bottom 3 quartiles, and relative risks of 2.21 and 1.54 for incident vertebral and non-vertebral Fx, respectively, for those in the top quartile of TRACP5b vs. the bottom 3 quartiles.

Table: Lifetime costs per quality adjusted life year (QALY) gained for a 70-year-old woman with a T-score of -2.0, by quartile of specific marker under different assumptions of non-vertebral Fx reduction benefit from alendronate(Aln).

Condition	Relative Risk of Non-Vertebral Fx, Aln Rx vs. No Rx		Serum CTx	Serum TRACP5b
Marker in Bottom 3 Quartiles	1.0		\$114, 370	\$131,866
Marker in Top Quartile	1.0		\$77,093	\$69,011
Marker in Top Quartile	0.8		\$50,660	\$40,613

If the societal willingness to pay (WTP) per QALY gained is \$100,000, obtaining a serum CTx or TRACP5b in post-menopausal women with a T-score of -2.0, followed by alendronate Rx for those in the top quartile, is cost-effective. If the societal WTP is only \$50,000 per QALY gained, this strategy is still cost-effective if alendronate lowers the risk of non-vertebral Fx in osteopenic women with high bone turnover by 20% or more.

Disclosures: **J.T. Schousboe**, Hologic, Inc. 2.

SU152

Validation of Cross-Linked N-Telopeptides of Type I Collagen (NTx) in Cynomolgus Monkey Serum. **J. Mayer^{*}, S. Desranleau^{*}, S. Y. Smith, P. Oldfield.** Charles River Laboratories Preclinical Services•CTBR, Senneville, PQ, Canada.

The assay to detect N-terminal telopeptides of type I collagen (NTx), which reflects the rate of bone resorption, was validated in cynomolgus monkey serum. The validation included parameters such as specificity, linearity, range of quantification, intra-assay precision and accuracy. In addition, the stability of NTx in cynomolgus monkey serum at 4°C, at room temperature, after three freeze and thaw cycles, and long-term storage stability at approximately -20°C was assessed.The NTx assay in serum is performed using the Osteomark NTx Serum ELISA kit (Wampole Laboratories). The wells of the plate are pre-coated with synthetic NTx antigen to which the conjugated antibody and diluted samples are added and incubated. The wells are washed followed by the addition of a chromogenic substrate, and after a further incubation period the reaction is stopped with sulfuric acid and the absorbance at 450 is measured. The lower limit of quantitation (LLOQ) of the assay is 2.85 BCE. The method has been shown to be specific for the determination of the NTx in cynomolgus monkey serum. Accuracy and precision are summarized as follows:

NTx (nM BCE)	Intra-Assay (n = 6)	
	CV (%)	Recovery (%)
2.85	14.5	105.1
6.34	7.8	97.3
9.51	4.1	106.8
15.84	3.3	105.3
31.69	1.1	100.0

NTx was shown to be stable in cynomolgus monkey serum after three freeze-thaw cycles, at room temperature for 4 hours, at 4°C for 22 hours and at -20°C for at least 63 days.The NTx ELISA assay in cynomolgus monkey serum in conjunction with other available markers of bone turnover in serum and urine, provides a comprehensive panel to monitor the response to ovariectomy procedures and/or treatments with bone active agents in this species.

Disclosures: **S.Y. Smith**, None.

SU153

Biomarker Discovery in Osteoarthritis. **S. Bhattacharyya^{*1}, E. Siegel^{*1}, D. M. Findlay², N. L. Fazzalari^{*3}, M. Chehade^{*2}, S. Neale^{*2}, G. Wittert^{*4}, L. J. Suva¹.** ¹Center for Orthopedic Research, University of Arkansas for Medical Sciences, Little Rock, AR, USA, ²Department of Orthopaedics and Trauma, University of Adelaide, Adelaide, Australia, ³Division of Tissue Pathology, Insititute of Medical and Veterinary Science, Adelaide, Australia, ⁴Department of Medicine and Florey Adelaide Male Aging Study, University of Adelaide, Adelaide, Australia.

Osteoarthritis (OA) is the most common joint disorder, producing pain and disability that leads eventually to the destruction of articular cartilage. Although many of the risk factors for OA have been defined (genetic factors, BMI, female sex), the etiology of this disease is poorly understood. Recent data, from examination of bone in OA, from MRI and from circulating bone markers, suggest a role for subchondral bone in initiation and progression of OA. Sensitive disease markers, which will permit diagnosis of OA during the early pre-radiologic stages, and which facilitate monitoring of disease progression, are urgently required. In this study, surface enhanced laser desorption/ionization time-of-flight-mass spectroscopy (SELDI TOF MS) was used to screen for specific serum biomarkers in end-stage OA patients presenting for hip replacement surgery. Serum samples from 31 OA patients (median age of 67 years) and 30 age-matched unaffected patients (median age of 64.5 years) were fractionated based on charge (6 fractions) and SELDI spectra were collected from fraction 1 of each patient, in triplicate, and in three molecular weight ranges [1.5-10 kDa(low), 6.5-30 kDa(mid) & 25-150 kDa(high)]. All spectral data were normalized, standardized and subjected to multivariate statistical analysis and data mining procedures, ultimately leading to the detection of a number of peaks that optimally separated the two groups. Multiple peaks were identified from each mass range and combined across all three mass ranges in each patient sample. Twenty-two specific peaks were identified that could discriminate between the two sample sets; 10 peaks (m/z 2-9 kDa), 7 peaks (m/z 7-16 kDa) and 5 peaks (m/z 31-71 kDa) were significantly different (p <0.05) between the two groups. This profile represents a diagnostic fingerprint of the multiple biomarkers that discriminates OA from normal controls. Ongoing analyses involve the correlation of the SELDI profile with patient characteristics. This study has potentially identified a panel of biomarkers that represents a diagnostic fingerprint of risk factors and/or predictors of OA progression, which we will now seek to validate in patients earlier in disease progression. The identification of validated biomarkers will greatly accelerate therapeutic development for this major public health concern.

Disclosures: **D.M. Findlay**, None.

SU154

Serum C-Terminal Telopeptide of Type I Collagen in Osteoporotic Patients with Vertebral and Hip Fracture. **S. B. Hong¹, E. Kim^{*1}, S. Han^{*2}, M. Nam^{*1}, K. Moon^{*3}, B. Lee^{*4}, Y. Kim^{*1}.** ¹Internal medicine, Inha University, Incheon, Republic of Korea, ²Emergency Medicine, Inha University, Incheon, Republic of Korea, ³Orthopedics, Inha University, Incheon, Republic of Korea, ⁴Gynecology, Inha University, Incheon, Republic of Korea.

Introduction: Bone quality including bone turnover rate have been identified important. Biochemical marker of bone turnover is useful in diagnosis and monitoring response to treatment. However high within-person variability complicate their use. We investigated whether the bone mineral density and bone turnover marker(serum C-terminal telopeptide;cTx and osteocalcin) were associated with fracture in the the patients with femur fracture and vertebral fracture, and also whether sampling time affect the level of cTx. Methods: From January 2004 to December 2004, we had enrolled prospectively 42 patients who visited the emergency department due to fragility fracture in the elderly. 30 patient diagnosed femur fracture(Fx) and 12, vertebral fracture(Vx). Bone mineral densities (BMD) of the lumbar spine and femur were examined. Total calcium, phosphate, alkaline phosphatase, osteocalcin, s-CTx were measured. The patients of femur fracture were divided into two subgroups according to the presence of vertebral fracture.Results: All BMDs of the patients showed osteoporosis. The CTx level increased in the morning than random sampling, but show correlation(r=0.63, p<0.01). The s-CTx levels were higher than control(p<0.05). The group of Fx with Vx was older than Fx only group, and had lower BMD. There were no significant differences in markers between the subgroups. But the incidence of trochanteric fracture was higher in Fx with Vx than Fx only group.Conclusion: Fx in the elderly was associated with osteoporosis, specially in Fx with Vx. The bone turnover markers and BMD are useful to know the degree of osteoporosis in Fx. so we suggest that they are helpful for planning of treatment and prevention of fragility fracture in the elderly.

Disclosures: **S.B. Hong**, None.

SU155

Effect of a Fracture on Bone Turnover Markers in Daily Clinical Practice. **E. van der Veer^{*}, K. Koerts^{*}, L. Wagenmakers^{*}, J. Hoving^{*}, J. Hegeman^{*}, J. Slaets^{*}, G. Willemssen^{*}, J. van Nieuwpoort^{*}, H. ten Duis^{*}, H. Kreeftenberg^{*}.** University Medical Center Groningen, GRONINGEN, The Netherlands.

Can we use bone markers to assess bone turnover when a fracture interferes with baseline values? An important goal of our Fracture- and Osteoporosis Clinic (FO) is case-finding by measuring BMD by DEXA in patients aged 50 years and older after presentation with a low energy fracture. Blood was drawn during the first visit and six weeks later, for osteocalcin, PINP and sCTx. The Z-score for these bone markers was

obtained by using a reference group (n=300) with normal BMD of lumbar spine and femur and normal vitamin-D levels. PINP and sCTX were raised at the day of fracture, mean Z-score 0.48 and 1.21 respectively. Levels above 2 SD were found in 14.6 % and 29.3 %. Not all patients visited the FO on the day of fracture, so we plotted the influence of fracture against time, see table. It is obvious that during the first week PINP and sCTX levels are hardly increased, thereafter they are significant higher. Osteocalcin levels were not significant influenced by the fracture.

Table. Mean of bone turnover markers of patients (n=326), sampled at their first visit in the Fracture policlinic

first visit at day after fracture	PINP				sCTX				Osteocalcin			
	s n	ug/ L	Zscor e	% patients > 2 SD	pg/ ml	Zscor e	% patients > 2 SD	ug/ L	Zscor e	% patients > 2 SD		
0	123	46,9	0,48	14,6%	310	1,21	29,3%	13,5	0,08	6,6%		
1 - 2	48	45,7	0,39	10,4%	304	1,14	25,0%	12,0	-0,33	7,0%		
3 - 4	40	47,4	0,62	20,0%	354	1,70	32,5%	14,6	0,49	10,8%		
5 - 7	33	47,5	0,62	18,2%	349	1,65	33,3%	12,2	-0,23	3,2%		
8 - 14	34	64,4	1,70	38,2%	380	2,02	41,2%	14,0	0,20	17,9%		
15 - 28	48	61,2	1,53	35,4%	405	2,30	35,4%	13,8	0,32	17,9%		

Paired t-tests between blood samples of the first and second visit showed that all bone markers increased. First visit samples of patients obtained after the first week were excluded. For PINP the change of the Z-score was from 0.50 to 1.88 SD (p < 0.0001), for sCTX from 1.50 to 2.04 SD (p< 0.001) and for osteocalcin from - 0.07 to 0.59 SD (p< 0.0001). The Z-score of PINP in osteoporotic patients increased more than in patients with normal or osteopenic BMD (2.23 SD vs 1.53 SD, p= 0.0359). *Conclusion:* During the first days after a fracture bone turnover markers reflect the situation before. In comparison with a healthy reference group collagen turnover markers were already elevated at the day of the fracture. Using the day of fracture as baseline PINP and sCTX were significantly increased at day 7, and osteocalcin at 6 weeks. PINP increase was highest in osteoporotic patients. It is recommended to use Z-scores for bone markers for follow up in individual fracture patients in daily clinical practice.

Disclosures: **E. van der Veer, None.**

SU156

Effect of Depot Medroxyprogesterone Acetate on Markers of Bone Turnover. **J. S. Walsh, R. Eastell, N. F. Peel.** Academic Unit of Bone Metabolism, University of Sheffield, Sheffield, United Kingdom.

We have previously shown that Depo-Provera (depot medroxyprogesterone acetate, DMPA) use is associated with a bone mineral density deficit at the spine and proximal femur in women who commence usage before age 20, but not in women who commence usage over age 34. This study aims to identify the effect of Depo-Provera on bone turnover, and whether it is age-specific. We measured serum procollagen type I amino-terminal propeptide (PINP) and urine collagen type I crosslinked N-telopeptide (NTx) in 200 women; 100 Depo-Provera users of more than 12 months duration, and 100 individually matched controls, ages 18-25 (Depo-Provera started before 20y) and 35-45 (Depo-Provera started after 34y). Controls were matched by age, postcode, height, body mass index and smoking habit. We included controls using the combined oral contraceptive as there is good evidence that it has no effect on bone density in estrogen-replete women. Paired t-test of log10 transformed data showed that both markers were higher in Depo-Provera users than their controls, and both markers were higher in the younger age group, consistent with active bone modelling.

	PINP mg/l			NTX/Cr nmol/mmol		
	DMPA users	controls	p value	DMPA users	controls	p value
18-25y	76.4	51.1	<0.001	58.9	50.0	0.007
35-45y	39.9	31.7	0.004	39.4	31.2	0.018

The differences between groups persisted when users of the combined oral contraceptive were excluded. We conclude that Depo-Provera increases bone turnover, associated with decreased bone density in younger users. This age-specific effect may be due to greater susceptibility of actively modelling and remodelling bone to estrogen deficiency.

Disclosures: **J.S. Walsh, None.**

SU157

Correlation between Serum and Salivary Concentration of Biochemical Markers of Bone Turnover. **S. N. Zeni.** Sección Osteopatías Médicas, Hospital de Clínicas, University of Buenos Aires, Buenos Aires, Argentina.

It has been suggested that periodontal disease is a typical early manifestation of osteoporosis; association between them was established in both humans and animals 30 years ago. Proper management of osteoporosis involves early diagnosis of the disease, which includes complementary tests such as assessment of biochemical markers of bone turnover. Currently, remodeling is assessed by serum and urinary biomarkers; however, there is little information concerning presence of these biomarkers in human saliva. The purpose of this study was to determinate whether salivary concentration of bone markers correlated with serum concentration. At the moment of the study 10 young non-pregnant healthy women (aged: 21±2 years) with a self-reported history of medical and dental care were recruited at the school of dentistry, Buenos Aires University, who volunteered for this purpose. In addition, 10 normal adult Wistar rats (300±5g) were studied. Fasting serum (s) and total saliva (sal) were analyzed for bone alkaline phosphatase (b-AL: UL/L) and Carboxy terminal telopeptide of collagen type I (CTX). The b-AL was assessed using a colorimetric method (Wiener Lab) after bone isoenzyme precipitation with wheat-germ lectin, and CTX was measured employing a commercial kit (Crosslaps one step and rat-CTX, respectively. Osteometer Bio Tech, Denmark). Although results were obtained from a small population, data suggest bone markers can be measured in saliva. Significant

correlation was observed between saliva and serum concentration of both markers (b-AL: 0.78 and CTX: 0.89). However, whereas sal b-AL was slightly lower (approximately two fold), sal CTX was ten fold lower than that of serum concentration. Although further studies are necessary, this correlation suggests that a simpler and less invasive method exists to assess bone turnover than measurement of serum or urine samples. Since dental visits are more often than medical check-ups, performing routine assay of salivary biomarkers of bone disease in conjunction with delivering routine dental care could allow earlier diagnosis of metabolic bone diseases. Grant M099 UBA.

	s b-AL	Rel s/sal	s CTX	s b-AL	Rel s/sal	s CTX
Rats	79±12	42±4	1.88±0.28	59.1±16.1	5.8±1.0	10.3±2.7
Women	74±17	49±2	1.71±0.27	32.0± 3.2	2.4±0.1	13.4±1.3

Disclosures: **S.N. Zeni, None.**

SU158

Reference Range for Bone Turnover Markers in Healthy Premenopausal Women; a Comparison of Oral Contraceptive Users and Non-Users. **A. E. de Papp¹, R. Kagan^{*2}, A. Buinewicz^{*1}, C. Mullen^{*1}, E. Chen^{*1}, M. P. Caulfield^{*3}, R. E. Reitz^{*3}.** ¹Merck & Co., Inc., West Point, PA, USA, ²Foundation for Osteoporosis Research and Education, Oakland, CA, USA, ³Quest Diagnostics Nichols Institute, San Juan Capistrano, CA, USA.

Biochemical markers (BCMs) of bone turnover reflect whole body bone resorption and formation activity. Commercial BCM assays are used in clinical trials and clinical practice to assess antiresorptive and anabolic efficacy. There are few published premenopausal BCM reference ranges using newer automated assays. A cross-sectional observational study was conducted of 237 healthy premenopausal women (119 combination oral contraceptive [OC] users and 118 non-OC users), with regular cyclic menses and normal bone density determined by central DEXA. A single fasting blood sample was obtained to assess serum chemistry, serum C-telopeptide (CTx) (ElecSys 1010/2010, Roche Diagnostics), serum bone-specific alkaline phosphatase (BSAP) (Access Ostase, Beckman Coulter, Inc.), and serum N-terminal propeptide of type 1 procollagen (PINP) (Orion Diagnostics). A second morning-void urine sample was collected for analysis of urine N-telopeptide of type 1 collagen (NTx) corrected for creatinine (Cr) (VITROS, Ortho-Clinical Diagnostics). Laboratory values were measured at a central laboratory (Quest Diagnostics). The mean subject age was 37 years (range 28-45), 77.6% were Caucasian. Among OC users, the mean duration of contraceptive use was 10 years. Mean (standard deviation, SD) BCM values among OC users were NTx, 19 (14.3) nmol/mmol; CTx, 251.0 (127.6) pg/mL; BSAP, 8.0 (2.8) µg/L; and PINP, 33.0 (13.7) µg/L. Among non-OC users, mean values were; NTx, 30.0 (16.4) nmol/mmol; CTx, 304.0 (137.0) pg/mL; BSAP, 9.8 (2.8) µg/L; and PINP, 45.0 (16.6) µg/L. Table reference ranges (geometric mean ± 2 SD) are based on log transformation with back transformation, except for NTx. Overall, BCM values in our study were generally consistent with those previously reported by the manufacturers for healthy premenopausal women. The mean values of all BCMs tested were significantly lower among OC users than nonusers. We believe that the values obtained from this well characterized population could represent reference ranges for these BCMs of bone turnover in premenopausal women. It is uncertain if these ranges are relevant to untreated or treated postmenopausal women.

Biomarker	OC Users		Non-OC Users	
	n	Reference Range	n	Reference Range
NTx (nmol/mmol)*	104	3 - 60	98	4 - 64
CTx (pg/mL)	82	80 - 614	96	113 - 675
BSAP (ug/L)	111	4.1 - 14.2	100	5.4 - 16.4
PINP (ug/L)	81	13 - 68	100	21-85

*Based on mid 95% range of normal values for NTx

Disclosures: **A.E. de Papp, Merck & Co., Inc. 1, 3.**

SU159

Levels of Biochemical Markers of Bone Turnover in Postmenopausal Osteoporotic Women: Comparison to a Premenopausal Reference Range. **M. C. Hochberg¹, D. Hosking^{*2}, H. Bone³, R. A. Petruschke^{*4}, M. Melton⁴, N. Verbruggen^{*4}, E. Chen^{*4}, A. E. de Papp⁴.** ¹University of Maryland School of Medicine, Baltimore, MD, USA, ²Nottingham City Hospital, Nottingham, United Kingdom, ³Michigan Bone and Mineral Clinic, Detroit, MI, USA, ⁴Merck & Co., Inc., West Point, PA, USA.

Biochemical markers (BCMs) of bone turnover are used in clinical practice and clinical trials to assess bone resorption and formation and treatment effects. Typically, BCM levels in postmenopausal women are higher than those in healthy premenopausal women, although differences have not been adequately characterized. A cross-sectional study in 237 healthy premenopausal women (mean age 37 years [range, 28-45 years]; 78% white), with regular cyclic menses and normal bone mineral density (BMD) evaluated BCMs using newer commercial assays. Reference ranges for BCMs were established from 98 non-oral contraceptive users. A fasting blood sample was obtained to assess serum C-telopeptide of type 1 collagen (CTx), bone specific alkaline phosphatase (BSAP), and serum N terminal propeptide of type 1 procollagen (PINP). Second morning void urine was collected to analyze urine N-telopeptide of type 1 collagen (NTx) corrected for creatinine (Cr). Data for serum CTx, BSAP, and PINP, and urine NTx in postmenopausal osteoporotic women (T-score ≤-2.0 at least one site) were obtained using pre-treatment samples from two clinical trials of identical design (Study 1 in USA, N=1053; Study 2 international, N=936). Study 1 patients had a mean age of 65 years (range 26-98) and averaged 19 years postmenopausal; mean total hip BMD T-score was -1.8. Study 2 patients had a mean age of 64 years (range 43-90) and averaged 17 years postmenopausal; mean total hip BMD T-score was -1.7. Results are shown in the Table. As expected,

ASBMR 27th Annual Meeting

postmenopausal median BCM values were higher than premenopausal medians. However, there was substantial overlap in the distributions; the majority of postmenopausal women had pretreatment BCM values that fell within the premenopausal range. In both untreated postmenopausal populations, the lower end of the 95% range fell below the lower end of the 95% range of premenopausal women for PINP and CTx. Further research is needed to determine whether there is an optimal target range for each BCM during antiresorptive therapy, or if alternative targets such as percent reduction from baseline might be preferable.

Biochemical Marker	Premenopausal (N=98) Median (95% range)	Postmenopausal Study 1 (N=1053) Median (95% range)	Postmenopausal Study 2 (N=936) Median (95% range)
NTX nmol/mmol	29.5 (4-64)	43 (18.0-103.0)	43 (14.0-101.0)
CTx pg/mL	273 (124-637)	364 (110-832)	389 (91-949)
BSAP ug/L	9.4 (5.9-16.9)	14.1 (6.8-29.4)	14.5 (7.2-29.2)
PINP ug/L	41.5 (23-93)	47.0 (19-102)	50.0 (20-104)

Ranges in table are 2.5 - 97.5 percentiles

Disclosures: **M.C. Hochberg**, Merck & Co., Inc. 2, 8.

SU160

Serum CTX and PINP by Roche Elecsys as Theranostics in the Treatment of Osteoporosis. **E. T. Leary¹**, **T. H. Carlson^{*1}**, **C. Wu^{*1}**, **T. K. Aggoune^{*1}**, **V. Luzzi^{*2}**, **A. P. Foster^{*3}**. ¹Pacific Biometrics, Inc., Seattle, WA, USA, ²Core Laboratory for Clinical Studies, Washington University, St. Louis, MO, USA, ³Roche Diagnostics, Indianapolis, IN, USA.

Theranostics are diagnostic companion products to therapeutics in predicting risks of disease, diagnosing disease, stratifying patients and monitoring therapeutic response. Emerging data from osteoporosis clinical trials suggest the value of bone markers in fracture risk prediction in addition to treatment monitoring. We investigated serum beta-CrossLaps (CTX), a bone resorption marker, and total serum N-terminal propeptide of type I procollagen (PINP), a bone formation marker, analyzed as a panel using the Elecsys 2010 immunoanalyzer (Roche Diagnostics, IN) for their robustness and performance as candidate theranostics. Sample stability and imprecision of CTX and PINP were previously reported. Total imprecision for CTX was <6% CV and <4.5% CV for PINP. CTX was stable in serum and heparin plasma for 8 hr at room temp, 1 d at 4° C; in K₃ EDTA plasma for 1 d at room temp and 7 d at -4° C. All sample types were stable for > 2 yr at -70° C. PINP was stable 1 d at room temp, 14 d at 4° C and >3yr at -70° C. Long term consistency in sample, assays and response to therapy was evaluated in 57 women with osteoporosis on antiresorptive therapy. Bone marker values measured immediately after 3 month-treatment period were compared with those measured after 3 years of sample storage at -70° C. Regression comparison of CTX measured 3 years apart was y = 0.85 x + 0.016, R² = 0.97. Regression comparison for PINP was y = 0.95 x - 6.53, R² = 0.98. % Change of CTX and PINP from baseline after 3 month of treatment in samples measured 3 yr apart was similar. Reference ranges in healthy individuals, age 25-83 years, without osteoporosis were determined in 273 Caucasian and 320 African American women, and 272 Caucasian and 281 African American men. Differences in reference ranges among subgroups based on age and ethnicity were small. Overall, African American women have greater CTX and PINP than Caucasian women (p<0.05).). In men, there was no difference for CTX between ages and ethnic groups. For PINP, an age dependency was observed in both Caucasian and African American men (p<0.05). In conclusion, serum CTX and PINP measured as a panel on the Roche Elecsys may be suitable as theranostics in the treatment of osteoporosis. The preferred sample type is EDTA plasma collected in the fasting state within a controlled time window to minimizes CTX variation. There is large overlap in reference values for CTX and PINP among subgroups. Establishing common reference ranges, based on the healthy state, that are independent of age and ethnic group, may be desirable.

Disclosures: **E.T. Leary**, None.

SU161

The Ratio of Osteoclast Activity/Osteoclast Number (CTX/TRACP 5b) Is a Useful Parameter in Rat Orchidectomy Model. **J. P. Rissanen¹**, **J. J. Reponen^{*1}**, **R. Hirsinummi^{*2}**, **L. Ravanti^{*2}**, **P. J. Kallio^{*2}**, **J. M. Halleen¹**. ¹Pharmatest Services Ltd, Turku, Finland, ²Orion Pharma, Turku, Finland.

C-terminal cross-linked telopeptides of type I collagen (CTX) are released from bone collagen during bone resorption, and serum CTX is a useful marker of osteoclast activity. It has been shown recently that serum tartrate-resistant acid phosphatase isoform 5b (TRACP 5b) reflects osteoclast number. We have studied the use of serum CTX and TRACP 5b in rat orchidectomy (ORX) model. Three-month old Sprague-Dawley rats were randomly divided into 3 groups (n = 12 in each group) according to body weight as follows: 1) Sham-operated rats receiving vehicle; 2) ORX rats receiving vehicle; 3) ORX rats receiving testosterone propionate (TP). TP was administered daily by subcutaneous injections at a dose of 0.6 mg/kg/day. Fasting blood samples were collected before the operation and at days 5, 14, 28 and 56 after the operation. Serum CTX (RatLaps®, Nordic Bioscience, Herlev, Denmark) and serum TRACP 5b (RatTRAP®, SBA-Sciences, Oulu, Finland) were measured using commercially available immunoassays. Prostate weight was significantly decreased by ORX and the decrease was completely prevented by TP, demonstrating that the operations and dosing were performed successfully. ORX increased serum CTX and decreased serum TRACP 5b values at all timepoints. TP increased TRACP 5b values to sham-level at all timepoints. However, serum CTX values were slightly decreased at day 5, slightly increased at day 14, not affected at day 28 and significantly decreased below the sham-level at day 56. A resorption index was calculated by dividing the CTX values by the TRACP 5b values, demonstrating the mean activity of a single osteoclast. ORX increased significantly the resorption index at all timepoints, the difference being most pronounced at

day 5. TP decreased significantly the resorption index towards the sham-level at all timepoints, the difference being most pronounced at day 56 when the values decreased substantially below the sham-level. These results suggest that ORX increased resorption at all timepoints as shown by the increased CTX values, and because of the bone loss caused by ORX, the absolute number of osteoclasts was decreased at all timepoints as shown by the decreased TRACP 5b values. TP prevented the decrease in osteoclast number at all timepoints, which resulted as an increase in bone resorption during the first 4 weeks. After that, TP substantially decreased bone resorption by other mechanisms than affecting osteoclast number. These results demonstrate that the resorption index (CTX/TRACP 5b) is a useful tool in rat ORX model, showing more significant effects than can be observed with either CTX or TRACP 5b alone.

Disclosures: **J.P. Rissanen**, None.

SU162

Stability of Tartrate-Resistant Acid Phosphatase Isoform 5b (TRACP 5b) in Human Serum Samples. **J. M. Halleen¹**, **L. Wahlberg^{*2}**, **P. Saloranta^{*2}**, **S. Rasi^{*2}**. ¹Pharmatest Services Ltd, Turku, Finland, ²SBA Sciences, Oulu, Finland.

Osteoclasts secrete tartrate-resistant acid phosphatase isoform 5b (TRACP 5b) into the blood circulation, and serum TRACP 5b is considered a useful marker of osteoclast number and bone resorption. Serum TRACP 5b activity is elevated in conditions of increased bone turnover and decreased during antiresorptive treatment. We have studied stability of TRACP 5b in human serum samples. A panel of 6 serum samples was stored at different conditions, and serum TRACP 5b activity was measured before and after the storage periods using the BoneTRAP®-assay (SBA-Sciences, Oulu, Finland). TRACP 5b activity was stable for 2 days both at 37°C and at room temperature (20 - 25°C), 3 days at 4°C, 1 month at -20°C and several years at -70°C. Several freeze-thaw cycles from -70°C performed at consecutive days showed no effect on TRACP 5b activity levels. However, a rapid decrease of serum TRACP 5b activity levels was detected during long-term storage of serum samples at -20°C and -70°C when one freeze-thaw cycle was performed before starting the storage period. Approximately 50% of the enzyme activity was lost already after 4 days storage at -20°C. We conclude that serum TRACP 5b activity is relatively stable when samples are incubated at temperatures of 4°C or above, allowing the performance of routine laboratory measurements to freshly collected samples without problems. Storage of serum samples at -20°C should be avoided for periods longer than one month. Long-term storage of serum samples should be performed at -70°C, where TRACP 5b activity is stable for several years. Although TRACP 5b activity survives several consecutive freeze-thaw cycles, long-term stability of the enzyme in frozen serum samples is decreased already after one freeze-thaw cycle. Extreme care should be used in cool transportation of frozen serum samples, and thawing of the samples during transportation should be avoided. It is recommended to send serum samples unfrozen at 4°C rather than frozen if it can not be guaranteed that the samples are not thawed during transportation.

Disclosures: **J.M. Halleen**, SBA Sciences 5, 7.

SU163

N-MID Osteocalcin Measured by Roche Elecsys Is a Stable Analyte. **E. T. Leary**, **C. Wu^{*}**, **M. K. McLaughlin^{*}**, **T. H. Carlson^{*}**. Pacific Biometrics, Inc., Seattle, WA, USA.

There is a lingering impression that analysis of osteocalcin (OC) is problematic because of OC instability in patient samples. This perception persists despite contrary data from assays that measure both the intact OC (amino acid 1-49) and the main N-terminal fragment (amino acid 1-43). We have demonstrated in a variety of studies that N-MID OC measured by the Elecsys analyzer (Roche Diagnostics, Indianapolis, IN) is stable (Leary, et al, Clin Chem 2000; 46:A145; Carlson, et al, Clin Chem 2004; 50:A109, Leary, et al, JBM 2004; 19:S240). The purpose of this work was to consolidate and extend information on N-MID OC stability using the Elecsys 2010. Imprecision and sample stability of OC were previously reported in different sample types including commercial control materials, human serum, heparinized plasma and EDTA plasma. Long term total imprecision was 5.7% CV in the 10 - 69 ng/mL range. Short-term OC stability was evaluated in all three sample types after 0, 4, 8, 24, 48, 72, 96, and 168 hours at room temperature and 4 °C. EDTA plasma was stable for at least 3 d and serum and heparin plasma stable for > 8 hr (recovery within 10%). In a separate study of six sera, OC recovery averaged 85.1% after 14 days at 4 °C. Long term OC stability was evaluated in paired sets of serum, heparinized plasma and EDTA plasma. Measurements made within 8 hr of sample collection and after 1, 3, 6, 12, 18 and 24 months of storage at -70 °C demonstrated recovery within 10% of baseline values at all time points. No trending was observed. Stability at -70 °C in all three sample types may be extended to 3 to 4 yr based on clinical samples reanalyzed after 3 years of storage (slope = 0.964, intercept = -0.699 and R² = 0.924) and renal dialysis patient samples (all 3 sample types) reanalyzed after 4 years of storage (slopes = 0.92 to 1.01, intercepts = 7.2 to +1.3 ; all R² >0.98). Stability of twice-thawed samples was evaluated in 21 frozen sera (4.2 to 134.6 ng/mL). After the initial analysis, the samples were refrozen and thawed for reanalysis after 3 months using same lot of reagents. Linear regression comparison gave slope = 1.00, intercept = -0.197 and R² = 0.991. In conclusion, OC measured by the Elecsys N-MID OC assay is a stable analyte and does not require special sample handling precaution. Furthermore, OC may be analyzed in twice-thawed samples and samples stored at -70 °C for up to 4 years.

Disclosures: **E.T. Leary**, None.

SU164

Bone Turnover Is Reduced at 18 Months after a Single Intravenous Dose of Zoledronic Acid. G. J. Paz-Filho^{*1}, C. A. M. Kulak¹, J. P. Bilezikian², M. J. Seibel³, V. Z. C. Borba¹. ¹Serviço de Endocrinologia e Metabologia da UFPR (SEMPR), Curitiba, Brazil, ²Department of Medicine, College of Physicians & Surgeons, Columbia University, New York, USA., New York, NY, USA, ³Internal medicine, ANZAC Research Institute, The University of Sydney, Sydney, Australia., Sidney, Australia.

Zoledronic acid (ZOL) is a highly potent bisphosphonate, which has been shown to inhibit bone resorption for up to 12 months after a single intravenous dose (1). The exact dosing period of this agent is yet unknown. In the present investigation we evaluated changes in bone turnover at 12 (T12) and 18 (T18) months after a single injection of 4 mg of ZOL (T0) in 29 patients (24 female; age 61.2 ± 15 years) with low BMD. Lumbar spine, femoral neck and total hip BMD as well as serum CTX-I, a bone resorption marker, and serum BALP, a bone formation marker, were measured concurrently. Results: Median CTX levels were 0.183 ng/ml at T0 (range: 0.01 - 0.69), 0.039 ng/ml (0.01 - 0.37) at T12 (p<0.001 vs. T0) and 0.108 ng/ml (0.012 - 0.42) at T18 (p>0.05 vs T0). There was no significant change in median BALP levels at any time point. The median percent increase in BMD (vs. T0) at the lumbar spine was 3.3% (-9.5 to +26.6) at T12 and 5.1% (-5.9 to +21.93) at T18. At the femoral neck, the corresponding changes were 2.1% (-4.7 to +83.3) and 0.13% (-6.8 to +116.2), and at the total hip 2.5% (-5.2 to +68.3) and 1.14% (-6.2 to +7.5), with p>0.05 in the same site, at T0, T12 and T18. Changes in hip BMD and serum CTX correlated inversely at T12 (r= -0.509, p=0.01), but no correlations were found between other skeletal sites and bone markers at T12 and T18. In conclusion, bone resorption rates, as assessed by serum CTX-I, were suppressed at 12 months and remained below baseline at 18 months after a single dose of 4mg zoledronate. The increase in BMD was most evident at 12 months. These results demonstrate that a single application of 4mg of ZOL inhibits bone resorption effectively for 12 months, with the effect still being observed at 18 months. Therefore, a dosing interval of 12-18 months may be appropriate in patients with low BMD to inhibit bone resorption.

(1) Reid I et al. NEJM Feb 2002

Disclosures: **G.J. Paz-Filho**, None.

SU165

41Ca and Accelerator Mass Spectrometry to Monitor Calcium Metabolism in End Stage Renal Disease Patients. R. L. Fitzgerald^{*1}, D. J. Hillegonds^{*2}, D. W. Burton^{*1}, T. L. Griffin^{*1}, S. Mullaney^{*1}, J. S. Vogel^{*2}, L. J. Deftos¹, D. A. Herold^{*1}. ¹VAMC/UCSD, San Diego, CA, USA, ²Lawrence Livermore National Laboratories, Livermore, CA, USA.

Background: Stable (⁴²Ca and ⁴⁴Ca) and short-lived radioactive isotopes (⁴⁵Ca and ⁴⁷Ca) of Ca have been used to study calcium metabolism for years. The advantage of combining a marker such as ⁴¹Ca (low noise) with a technique with attomole sensitivity, such as accelerator mass spectrometry, is that excellent signal/noise can be obtained from ng quantities of isotopes administered. Our hypothesis is that bones can be labeled *in vivo* with ⁴¹Ca and that after an equilibration period, the ratios of ⁴¹Ca/Ca in serum will indicate the status of bone resorption. We describe the development of an intravenous ⁴¹Ca dose suitable for humans, analytical method validation for measuring ⁴¹Ca /Ca isotope ratios in biological samples, and experiments with eight human volunteers dosed with 10 nCi of ⁴¹Ca. **Methods:** Using sterile techniques ⁴¹Ca was formulated and aliquotted into individual vials. The ⁴¹Ca doses were tested for sterility and endotoxins according to USP guidelines. Purity as checked by inductively coupled plasma mass spectrometry. Measurement of ⁴¹Ca /Ca ratios in serum were made by accelerator mass spectrometry after isolating calcium with three precipitation steps and a cation exchange column. Four healthy controls and four end stage renal disease patients on hemodialysis were dosed with 10 nCi of ⁴¹Ca and distribution kinetics were determined over 168 days. **Results:** The dosing solution was chemically and radiologically pure, contained < 0.1 endotoxin unit per mL (Eu/mL) and passed USP sterility tests. The analytical method for quantification of the ⁴¹Ca/Ca ratios was linear from 6 x 10⁻¹⁴ to 9.1 x 10⁻¹⁰. The run to run precision of the method was 3 % and 2 % at 9.1 x 10⁻¹¹ and 9.1 x 10⁻⁹ respectively. The area under the curve (AUC), representing the time course of ⁴¹Ca in the central compartment, was significantly less for end stage renal disease patients as compared with control subjects (p < 0.005). **Conclusions:** The calculated overall radiation dose commitment of 0.06 µSv for the first year following a 10 nCi dose of ⁴¹Ca is a factor 30,000 times smaller than the total dose from natural radiation. The biological risks associated with this low level radiation exposure are to small too quantify. The ⁴¹Ca dose was administered to eight volunteers without adverse effects. Accelerator mass spectrometry was used to measure isotope ratios that span 5 orders of magnitude with excellent precision in the range observed after administration of 10 nCi ⁴¹Ca. For the first time, we show that ⁴¹Ca can be used to monitor differences in bone turnover between normal subjects and ESRD patients.

Disclosures: **R.L. Fitzgerald**, None.

SU166

Prospective Evaluation of Risk of Vertebral Fractures Using Quantitative Ultrasound Measurements and Bone Mineral Density in a Population-Based Sample of Postmenopausal Women: Results of the Basel Osteoporosis Study. F. C. Hartl¹, H. Didier², R. Holländer^{*1}, M. Kraenzlin³, C. Gückel^{*4}, M. Krieg⁵, C. Buitrago^{*4}, R. Theiler^{*6}, A. Tyndall^{*1}. ¹Rheumatology, University, Basel, Switzerland, ²Nuclear Medicine Division, University, Geneva, Switzerland, ³Endocrinology, University, Basel, Switzerland, ⁴Radiology, University, Basel, Switzerland, ⁵Internal Medicine, University, Lausanne, Switzerland, ⁶Rheumatology, University, Zürich, Switzerland.

The aim of our study was to investigate the ability of quantitative ultrasound (QUS) and dual x-ray absorptiometry (DXA) to predict vertebral fractures in a population based sample of postmenopausal women. Five hundred women (age 65- 75 years) were prospectively followed for at least 3 years. Lateral spine x-rays in all subjects (lumbar and thoracic) at baseline and follow-up were used to assess incident vertebral fractures. In addition bone measurements using DXA at the spine and hip (GE-Lunar expert), QUS measurements at the calcaneus (GE-Lunar Achilles and Hologic Sahara) and the proximal phalanges (Igea Bone Profiler) were performed. Follow-up information was available for 433 women, representing 89% of subjects found eligible at baseline. Spine x-rays were reviewed for incident vertebral fractures (height loss of at least 20%) by 2 independent radiologists. Appropriate statistical analysis was done. A total of 24 individuals (5.5%) had documented incident vertebral fracture. Baseline characteristics between fracture group (n=24) and controls (n=409) were similar for age, weight and body mass index (BMI), but not for height (height controls: 159.8 cm, height fractured subjects: 157.3 cm, p=0.03). Mean values for the different bone measurements for the fracture group and controls were significantly different (p< 0.05) except for ultrasound measurements at the proximal phalanges (BP SOS p=0.21, BP UBPI p=0.29). Age and height adjusted relative risks (RR) for vertebral fracture are shown in table below with their respective 95% Confidence interval:

		RR	Min	max
Heel Achilles	BUA	1,82	1,1	2,9
	SOS	2,73	1,6	4,8
	Stiffness	2,37	1,4	4,0
Heel Sahara	BUA	2,25	1,3	3,8
	SOS	3,14	1,6	6,0
	Stiffness	2,86	1,6	5,3
Finger BP	SOS	1,08	0,7	1,6
	UBPI	0,98	0,6	1,5
Spine - BMD	L1-L4	2,11	1,2	3,6
	Neck	1,83	1,1	3,1
	Ward	2,31	1,3	4,1
Femur - BMD	Troch	1,46	0,9	2,3
	Total Hip	1,80	1,1	3,0

In conclusion, quantitative ultrasound measurements of the calcaneus are significant predictors of vertebral fracture equally well as DXA at lumbar spine, femoral neck and total hip. The predictive value of a bone measurement using Igea Bone Profiler at the proximal phalanges cannot be confirmed.

Disclosures: **F.C. Hartl**, Novartis Pharmaceuticals 3.

SU167

Differences in Bone Ultrasound between Infants and Children. S. Winder^{*}, G. Chan, T. McNaught^{*}. Pediatrics, University of Utah, Salt Lake City, UT, USA.

The growth and development of bones during the pediatric age period are important. It is the foundation of the highest calcium accretion in ones life. Optimizing the bone quality in infants may provide long time benefits and may be a prerequisite for the prevention of osteoporosis. The purpose of this study is to evaluate the bone quality of two different pediatric age groups. One hundred and twelve children aged from 4 months to 12 years were studied and stratified into a infant group (aged less than 3 years) and a school aged group (aged 5 to 12 years). Gender and anthropometric measurements were recorded. Dietary intake of calcium was evaluated in the school-aged group. The speed of sound (SOS) was measured using a commercially available bone sonometer (Sunlight Omnisense) at the midshaft tibia or distal 1/3 radius. Fifty males and 62 females were studied; 10 males and 12 females in the infant group, 40 males and 50 females in the other group. There was no difference in SOS between males and females in the infant group. In the school-aged group, SOS was greater in males than the females, 3605Å± 81 vs. 3567Å± 88 m/s (P=0.04). There was a non-linear relation between age and weight and SOS (r=0.3). However, only in the infant group there was a positive association of the midshaft SOS and their age(r=0.90, P<0.001) while in the school aged group there was no relationship between their age and SOS (r=0.15, NS). There was a non-linear relation between the midshaft SOS and calcium intake (P<0.01). There were no differences between males and females in their weight, height, or calcium intakes. In conclusion, the bone quality as measured by SOS in pediatric subjects is different and needs to be age-adjusted. This finding may have implications for nutritional interventions and bone assessment for children.

Disclosures: **S. Winder**, None.

SU168

Fracture Index Validation in a Population-Based Sample of Swiss Elderly Women Using a QUS Device. O. Lamy, M. Krieg*. Internal Medicine, University Hospital, Lausanne, Switzerland.

Background : Due to the magnitude of osteoporosis and its related morbidity and mortality, the identification of high risk individuals for fracture is essential. The Fracture Index (6 questions), an assessment tool with or without DEXA measurement, was shown to be predictive of hip fracture, as well as vertebral and nonvertebral fractures in postmenopausal women (D. Black et al. Osteoporosis Int 2001). The Swiss Evaluation of the Methods of Measurement of Osteoporotic Fracture Risk (SEMOF) study is a prospective multicenter study which compares 3 QUS devices for the assessment of fracture risk in a population-based sample of Swiss elderly women. The aim of the study was to validate the Fracture Index in the SEMOF study, including QUS in place of DEXA measurement. **Method :** Among the 7062 women age 70 years or older (75.2 ± 3.1), 607 clinical fractures were reported. According to the Fracture Index scoring, women were divided in quintiles. A linear increase of fracture risk was assumed during the follow-up (conservative approach). The follow-up duration varied from 953 to 1121 days, according to the quintile group and the type of fracture. **Results :** 495, 1679, 1264, 2276, and 1348 women were included respectively in quintile one to five. The total number of clinical fractures was 21, 88, 85, 205 and 208, respectively. The annualised incidence of clinical fracture per 1000 women increased from 14.1, 18.3, 23.7, 32.8, to 59.1 with the quintile one to five. The total number of hip fracture was 0, 9, 13, 25 and 43 corresponding to an annualised incidence per 1000 women of 0.0, 1.8, 0.8, 3.8, and 11.4. **Conclusion :** The Fracture Index is a very simple tool that identified women at high risk for fracture, and may defined a threshold for treatment. The use of QUS device in place of DEXA seem very attractive. The risk of fracture observed in our Swiss cohort was lower than in the SOF or EPIDOS studies. It may be in part explained by the shorter follow-up period or by the younger age of women. Another explanation may be the difference of fracture risk related to different population or country.

Disclosures: **O. Lamy**, None.

SU169

Quantitative Ultrasound (QUS) Measurements of the Calcaneus in a Portuguese Population: Normative Data. H. Canhao*¹, R. Ferreira*², L. Costa*², J. Romeu*³, J. Branco*⁴, H. Barros*². ¹Hygiene and Epidemiology,, University of Porto Medical School, Lisboa, Portugal, ²Hygiene and Epidemiology,, University of Porto Medical School, Porto, Portugal, ³Rheumatology, Hospital Santa Maria, Lisboa, Portugal, ⁴Rheumatology, Hospital Egas Moniz, Lisboa, Portugal.

Background: Quantitative Ultrasound (QUS) of the calcaneus is a safe and reliable method to evaluate skeletal status. However, few normative data were published and none for the Portuguese population. **Aims:** To estimate QUS parameters describing a representative sample of an adult Portuguese population. **Methods:** Cross-sectional evaluation of 1482 consecutive subjects (1010 females and 472 males), aged from 18 to 92 years, selected as part of the EpiPorto study, using random digits dialling, among the non-institutionalised population of Porto, Portugal. Information was obtained on demographic, social, clinical and behavioural characteristics using a standard protocol. Calcaneus QUS (Shara Clinical Sonometer, Hologic) parameters were obtained: Broadband Ultrasound Attenuation (BUA) and Speed of Sound (SOS), Qualitative Ultrasound Index (QUI) and Estimated Bone Mineral Density (EBMD). **Results:** Short-term in vivo precision was 5.5% for BUA and 0.4% for SOS, while in vitro precision was 3.23% for BUA and 0.15% for SOS. The table describes age and sex calcaneus QUS parameters. Significant sex differences were found after 39 years for BUA and after 59 for SOS. A significant age decrease was observed for every parameter, both in males and females. **Conclusion:** Our data are similar to others obtained in south European countries. These normative values are crucial since there are no previous Portuguese data and the method is increasingly used because of its safety, portability, low cost, simplicity, and capacity to reflect qualitative aspects of bone tissue.

Age / N (%)	BUA (Mean±SD)	SOS (Mean±SD)	QUI (Mean±SD)	EBMD (Mean±SD)
<29 / 116(11.5)	77±20	1564±35	102±21	0.571±0.135
30 - 39 / 149(14.8)	76±21	1558±35	99±21	0.550±0.133
40 - 49 / 206(20.4)	71±15	1557±28	96±17	0.536±0.106
50 - 59 / 222(22)	67±17	1548±27	91±17	0.502±0.107
60 - 69 / 165(16.3)	60±16	1539±28	84±17	0.458±0.107
>70 / 152(15)	55±16	1525±24	76±16	0.411±0.1
Total / 1010(100)	p=0.0001	p=0.0001	p=0.0001	p=0.0001
Age / N (%)	BUA (Mean±SD)	SOS (Mean±SD)	QUI (Mean±SD)	EBMD (Mean±SD)
<29 / 65(13.8)	81±23	1569±34	105±23	0.592±0.142
30 - 39 / 77(16.3)	79±20	1558±33	100±21	0.560±0.130
40 - 49 / 90(19.1)	78±18	1559±31	100±19	0.558±0.121
50 - 59 / 85(18.0)	73±15	1552±27	95±17	0.529±0.105
60 - 69 / 79(16.7)	71±18	1545±26	91±17	0.504±0.110
>70 / 76(16.1)	72±17	1547±26	93±17	0.514±0.107
Total / 472(100)	p=0.0638	p=0.0001	p=0.0021	p=0.0015

Disclosures: **H. Canhao**, POCTI/ESP/35769/2000 2.

SU170

Determinants of Bone Quantitative Ultrasound Parameters in an Adult Portuguese Population. H. Canhao*¹, R. Ferreira*², L. Costa*², J. Branco*³, H. Barros*². ¹Hygiene and Epidemiology, Rheumatology, University of Porto Medical School / Hospital Santa Maria, Lisboa, Portugal, ²Hygiene and Epidemiology,, University of Porto Medical School, Porto, Portugal, ³Rheumatology, Hospital Egas Moniz, Lisboa, Portugal.

Background: Quantitative Ultrasound (QUS) of the calcaneus is a safe and reliable method to evaluate skeletal status. However, few data are available on the determinants of QUS parameters. **Objectives:** To estimate the effect of demographic, social, behavioural and anthropometric factors in QUS parameters. **Methods:** Cross-sectional evaluation of 1482 consecutive subjects (1010 females and 472 males), aged 18 to 92 years, selected as part of the EpiPorto study, using random digit dialling, among the non-institutionalised population of Porto, Portugal. Information was obtained on demographic, social, clinical and behavioural characteristics using a standard protocol. Calcaneus QUS (Sahara Clinical Sonometer, Hologic) parameters were obtained: Broadband Ultrasound Attenuation (BUA, dB/MHz) and Speed of Sound (SOS, m/s), Quantitative Ultrasound Index (QUI) and Estimated Bone Mineral Density (EBMD g/cm²). Comparisons according to exposure levels were done using the Kruskal-Wallis test and the multivariate effect on QUS parameters was estimated by multivariate regression. **Results:** QUS values were significantly different in males and females (p<0.01) and analysis was performed separately by gender. In women, the multivariate model showed that age and duration of the reproductive period (years) were independent predictors of BUA and SOS. Education and body mass index (BMI, kg/m²) significantly influenced BUA level, and smoking status had an effect on SOS. Physical activity, energy, calcium, vitamin D and ethanol intake, age at menarche and number of pregnancies showed no significant effect on QUS parameters. In men, age was found to be significantly associated with BUA and SOS. The multivariate model showed that BMI and calcium intake were significant BUA determinants. SOS was also significantly associated with BMI, total caloric and calcium intake. Physical activity, vitamin D or alcohol intake had no significant effect on male QUS parameters. **Conclusion:** This study favours the hypothesis that BUA and SOS reflect specific bone characteristics influenced by a different set of independent determinants.

Disclosures: **H. Canhao**, FCT-POCTI/ESP/35769/2000 2.

SU171

Bone Surface Topology Mapping and its Role in Trabecular Bone Quality Assessment Using Scanning Confocal Ultrasound. Y. Xia, W. Lin*, Y. Qin. Biomedical Engineering, Stony Brook University, Stony Brook, NY, USA.

Quantitative ultrasound (QUS) measurement has been used for assessing bone quality, i.e., density and strength, non-invasively, in which ultrasound velocity (UV) is one of the primary acoustic properties that directly relates to bone quality evaluation. The calculation of UV requires the tissue thickness information in the pathway of wave propagation. It is extremely difficult to extract this information *in vivo*, because of (1) the irregular shape of human bone; (2) surrounded soft tissue around bone, e.g., at site of calcaneus and (3) hard to measure topology by direct measurement. The objective of this study was to identify 3D surface topology of bone for accurate calculation of UV. Scanning confocal ultrasound was performed at surface of bone, in which the reflected wave from surface was utilized to determine the 3-D topology at both medial and lateral sides. The thickness of bone, which is delineated by the bone surfaces, can be calculated from the distance between two bone surfaces. 25 human calcanei have been measured with the surface mapping technique. Wave

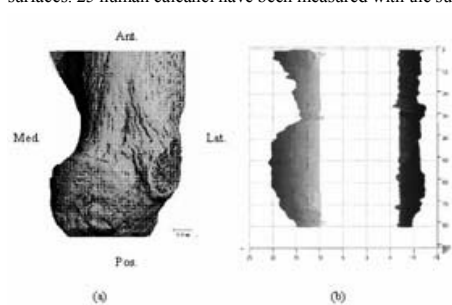


Fig 1 Bottom view of (a) calcaneus 3D surfaces measured by micro-CT with Medial (Med.), Lateral (Lat.), Anterior (Ant.) and Posterior (Pos.) positions as marked, and (b) 3D ultrasound reconstructed surfaces by surface mapping technique.

velocity was calculated from region of interesting (ROI) based on the thickness determined by this technique. To evaluate the accuracy of UV and its capability in predicting bone's density and strength properties, micro-CT (~20 micron resolution) and DEXA scanning was performed on intact calcaneus with parameters extracted from the similar ROI as UV calculation. Mechanical test was performed on the rectangular trabecular bone specimen extracted from the calcaneus. The irregular surfaces of calcaneus can be clearly depicted using surface mapping (Figure 1) and UV determined by using this new technique was highly correlated to bone mineral density (BMD) ($r = 0.75$), bone volume fraction (BV/TV) ($r=0.66$) and bone modulus ($r = 0.69$). This is higher than the prediction capability of UV without using this technique, corresponding correlation coefficients were $r=0.59$ for BMD, $r=0.46$ for BV/TV, and $r=0.58$ for modulus. These results suggest that surface topology mapping using scanning ultrasound is capable of determining calcaneus bone thickness accurately and hence enhancing the accuracy of UV measurement. It is a non-invasive method and no significant hardware modification is necessary, which have potentials and can be easily incorporated into future *in vivo* clinical application.

Disclosures: **Y. Xia**, None.

SU172

New Ultrasound Device for Bone Assessment. J. J. Kaufman¹, G. Luo^{*1}, R. S. Siffert^{*2}. ¹CyberLogic, Inc., New York, NY, USA, ²Department of Orthopedics, Mount Sinai School of Medicine, New York, NY, USA.

The objectives of this study were to design and fabricate a novel ultrasound device that estimates a new set of parameters - known as net time delay (*NTD*) and mean time duration (*MTD*) - and to examine in both computer simulations and clinically the relationship of the ultrasound parameters to bone mineral density (*BMD*) as determined with x-ray absorptiometry at the same anatomical site. The new device, known as the *QRT™ 2000* - for Quantitative Real-Time -- is entirely self-contained, portable, and handheld - being powered by 4 "AA" rechargeable batteries - and permits near real-time evaluation of the ultrasound parameters and their on-line display to the user. In the simulation study, 3D micro-CT images of 10 human calcaneal trabecular bone cores were further processed using morphological image processing to obtain 36 "samples" in various states of porosity and micro-architecture. Ultrasound simulations in through transmission along the medial-lateral direction of each core were carried out using computational software (*Wave3000 Pro*, CyberLogic, Inc.). A linear regression to estimate bone mass from the simulated values of the ultrasound parameters produced an R-squared value of 0.985. In a clinical IRB-approved study the *QRT™ 2000* was used to measure 85 adult women (age range: 21 - 82 years) at the heel. *BMD* at the calcaneus was measured at the same time using *DEXA* (*PIXI*, GE). A linear regression - using the *NTD*, age and weight associated with each subject produced an R-squared value of 0.78, equivalent to a linear correlation coefficient of 0.88, which represents a significant improvement over present ultrasound bone densitometers, but not nearly as good as the simulation results. Reasons for this have been identified (*viz.*, errors in distance measurement and lack of coincidence between the *DEXA* and ultrasound regions of interest) and a new device (*QRT™ 3500*) and experimental protocol to deal with these sources of error are being developed that should improve the accuracy of the ultrasound device over existing technology even more. In addition, an examination of the *MTD* parameter - which appears to be sensitive to both mass and architecture - is being carried out in conjunction with *NTD* measurements to determine if both parameters together may be used to more accurately estimate fracture risk than bone mass alone. Finally, the *QRT™* devices were designed to be manufactured at very low cost, and therefore should enable the significant expansion of quantitative ultrasound measurements to, for example, primary care physicians in this country and abroad, including for use in the developing world as well as in spaceflight. Acknowledgement: This research was supported by NIH (NIAMS) SBIR Grant No. 2 R44 AR45150.

Disclosures: **J.J. Kaufman**, CyberLogic, Inc. 4.

SU173

Quantitative Prediction of Bone Density and Strength in Human Calcanei Using a Scanning Confocal Acoustic Diagnostic System. Y. Qin¹, Y. Xia¹, W. Lin^{*1}, B. Gruber¹, S. Judex¹, C. Rubin¹. ¹Biomedical Engineering, SUNY Stony Brook, Stony Brook, NY, USA, ²Medicine, SUNY Stony Brook, Stony Brook, NY, USA.

Microgravity and aging induced osteopenia is a critical skeletal complication occurred particularly in the weight-supporting skeleton, which leads to osteoporosis and risk of fracture. Bone integrity is dependant not only on the mineral density, but also on the quality of bone which includes the strength and structural parameters. Advents in quantitative ultrasound (QUS) provide a potential method for evaluating both strength and density of bone. The object of this study was to integrate automatic region of interest (ROI) algorithm and using a Scanning Confocal Acoustic Diagnostic (SCAD or SCAN) system to non-invasively assess bone quality in human calcaneus trabecular region. An imaging pattern recognition algorithm is developed and integrated in a newly developed SCAD system. The method was designed for the selection of an irregular ROI in the ultrasound attenuation (ATT) images from calcaneus bone. When the ROI is automatically determined, broadband ultrasound attenuation (BUA), and ultrasound velocity (UV) for bone quality in the real body region were evaluated. Total of 36 human cadaver calcanei, age from 60 to 97 years old, were tested by SCAD, micro-CT and DEXA, as well as mechanical failure tests. The SCAD properties were then correlated to the bone mineral density (BMD), structural and strength parameters. Correlations between BMD and ultrasound parameters were significantly improved by using SCAD with the automatic ROI algorithm, yielding correlations between BMD (DEXA) and SCAD parameters as R2=0.83 (BUA), and R2=0.65 (UV). Correlations were significant between bone volume fraction and BUA, R2=0.75, and between volume fraction and UV, R2=0.54. SCAD parameters predicted the trabecular bone strength, in which correlation between BUA and elastic modulus was R2=0.54, and correlation between ultimate strength and BUA was R2=0.60. These data have suggested that scanning confocal ultrasound may provide potentials for in vivo bone quality prediction. It may be used for monitoring instant changes of both bone strength and density alteration, e.g., progressive bone loss and evaluation of treatment of osteopenia. High resolution bone acoustic images can be generated at particular sites, e.g., calcaneus, with automatic region of interest algorithm. Prediction of bone quality by imaging based ultrasound in density and strength assessment may ultimately provide a non-invasive modality for bone quality evaluation in space and on Earth.

Disclosures: **Y. Qin**, None.

SU174

Trait Loci Determining the Degree of Disuse Osteopenia. S. Judex¹, H. Chung^{*1}, S. Xu^{*1}, V. Guido^{*2}, A. Torab-Parhiz^{*1}, A. Li¹, C. Rubin¹, L. Donahue². ¹Stony Brook University, Stony Brook, NY, USA, ²The Jackson Laboratory, Bar Harbor, ME, USA.

The extent of disuse-related trabecular bone loss during space flight or bedrest is high, approaching declines in vBMD of up to 2.7% per month. In contrast to the uniformity of the newly imposed environment across individuals, including similarity in diet and length of daily exercise regimes, the degree of bone loss between individual astronauts is highly variable, indicating the influence of genetic factors. In an effort towards elucidating the genetic basis of bone's sensitivity to the loss of appropriate mechanical signals, here we subjected a genetically heterogeneous mouse population to simulated weightlessness and report preliminary data from the genetic and phenotypic analyses. Five hundred second generation (BALBxC3H) female mice (4mo), were subjected to 3wk of disuse (hindlimb suspension). The progenitor strains were selected based on their greatly different skeletal mechano-sensitivity. In each mouse, in-vivo microCT scanning quantified longitudinal changes in trabecular bone morphology and architecture of the distal femur over the 3wk of unloading. Upon sacrifice, DNA was extracted and regions with single nucleotide polymorphisms (SNP) were identified via allele typing. Map Manager QTX was used to regress variations in genotype to variations in the morphological response to disuse. Over 3-wk of disuse, trabecular bone volume fraction diminished on average by 52%±16% (p<0.0001) with losses ranging from 17%-83%. Trabecular bone architecture also deteriorated with unloading; connectivity density decreased on average by 54% (p<0.0001), and trabecular thickness by 17% (p<0.0001). The values for each trait were normally distributed, indicating that multiple loci are involved in defining the changes in bone quantity and micro-architecture to mechanical unloading. Because of the small number of mice used for this preliminary analysis (100), no QTL could be determined with statistical significance (p=0.0001). Nevertheless, a large number of QTL was suggested by the regression analyses when using a higher significance value. These preliminary data confirm the strong genetic influence on bone's susceptibility to unloading and suggest that this particular F2 double-cross is well suited to define the chromosomal regions that modulate the degree of bone loss induced by a catabolic mechanical stimulus. Identification of the QTL (and the responsible genes) may ultimately be used as a critical predictive sensor for disuse osteopenia, as a discovery tool for novel drug targets, and for the selection of individual countermeasures of bone loss.

Disclosures: **S. Judex**, None.

SU175

Genome Wide Linkage of Hip Geometry: Framingham Study. S. Demissie^{*1}, D. Karasik², S. Menn^{*2}, Y. L. Tsai^{*1}, L. A. Cupples^{*1}, T. J. Beck³, D. P. Kiel². ¹School Pub Health, Boston University, Boston, MA, USA, ²Research & Training, Hebrew SeniorLife, Boston, MA, USA, ³Radiology, Johns Hopkins University, Baltimore, MD, USA.

Femoral geometry contributes to bone strength and predicts hip fracture risk. The technique of hip structural analysis (HSA) expresses the bone mass data in a mechanically interpretable form so that genetic influences on mechanical properties might be directly evaluated. There has been only one previous genome-wide linkage analysis of femoral geometry in women only using plain radiographs. The purpose of this study was to evaluate heritability (h²) and to perform a whole-genome genetic linkage analysis of geometric indices of the proximal hip in men and women from extended pedigrees. Proximal femur scans from 1351 members of 326 pedigrees (mean age 67.8 (SD 12.8), range 31- 96 yrs) from the population-based Framingham Osteoporosis Study were analyzed. A set of 401 microsatellite markers were genotyped. Femur cross-sectional geometry was measured at 3 sites: the narrowest neck (NN), intertrochanteric (IT), and femoral shaft (S) regions. HSA provided measures of endosteal diameter (END, cm), subperiosteal width (WID, cm), cross-sectional area of bone (CSA, cm²) - a measure of axial strength, and section modulus (Z, cm³) - measure of bending strength. Bone geometric measures were adjusted for age, age², body mass index, height, and physical activity, in each sex and generation. Multipoint quantitative linkage analyses were performed for 4 indices at each of the 3 femoral regions using the maximum likelihood variance components method. A moderate to strong genetic influence was found for all indices, with h² values between 0.321 [NN_Z] and 0.567 [IT_END]. Multipoint linkage analysis revealed loci of suggestive linkage (LOD scores >=1.9) on chromosomes 3p, 4q, 12p, 13q, and 16p. The maximum LOD score was 3.1 for IT_END at 3p26.1. The same region provided LOD score 2.7 with IT_WID. Also, IT_END was also linked to 12p13 and IT_WID to 13q21 (both LOD=2.7). In general, both endosteal and subperiosteal diameters were linked to the same chromosomal regions: NN_END and NN_WID were linked to 16p12, with LODs>2.0. IT_CSA and SS_CSA were linked to a long region of 4q. In conclusion, these results suggest that measures of femoral bone geometry are heritable and linked to several autosomes. This represents an important step toward identifying genes contributing to geometric aspects of strength. Despite the limitation of HSA method is that it is based upon two-dimensional projections of complex three-dimensional anatomy, use of hip geometric traits may help clarify the genetic contributions to bone strength and osteoporotic fragility in the general population.

Disclosures: **D. Karasik**, None.

SU176

Admixture Mapping of Genes Underlying Peak Bone Mineral Density Variation in Humans. D. L. Koller^{*1}, M. Peacock², T. Foroud¹, M. J. Econs².

¹Medical and Molecular Genetics, Indiana University School of Medicine, Indianapolis, IN, USA, ²Medicine, Indiana University School of Medicine, Indianapolis, IN, USA.

Identification of genes underlying variability in peak bone mineral density (BMD) is an important goal in osteoporosis research. However, while progress has been made, the major fraction of the genetic variation in BMD remains unexplained. The study designs employed so far to identify these genes (polymorphisms within candidate genetic loci and linkage screens in humans and animals) have notable strengths as well as weaknesses. To overcome some of these weaknesses, we have applied a recently developed method, admixture mapping (McKeigue, 2005; Hoggart, 2004), to human peak BMD and genetic marker data. This method complements the three established study designs by providing much finer genetic resolution of linkage regions, directly testing large human chromosomal regions, and substantially narrowing critical genetic intervals before the identification of positional candidate loci is undertaken. Admixture mapping is applicable when a trait such as BMD is significantly different between ancestral populations, and when recent admixture between these populations (20 generations ago or less) results in individuals having varying degrees of genetic material from each of the ancestral groups. These conditions are met in the African-American population. Sizable chromosomal regions (2-3 cM) of African or European ancestry remain intact in African-Americans. The ancestry of these specific regions can be determined using genetic markers whose allele frequencies differ between the ancestral populations. Importantly, BMD and fracture risk also differ significantly between the European and West African populations. Given ancestrally informative markers, admixture mapping tests whether variability in BMD is predicted by variation in ancestry at the chromosomal position of interest. We have applied admixture mapping using the software package ADMIXMAP (O'Donnell, 2004) to a sample of 230 unrelated premenopausal African-American women, selected from a sibpair cohort. A 9 cM genome screen and spine BMD was obtained in each individual. A significant relationship between BMD and ancestry ($p < 0.02$) on chromosome 10p was found, and the genome screen markers on 10p provided adequate ancestry information. This is the same region where some evidence of linkage was found in our American white and African-American sample (LOD=1.8 at D10S1432). We anticipate that using additional informative markers, and increasing marker density from 9 cM to 2-3 cM, will enable the use of admixture mapping to effectively narrow linkage regions to a more manageable size for identification of genes.

Disclosures: **D.L. Koller**, None.

SU177

Genotype-by-Parity Effects on Bone Mineral Density in Pedigreed Baboons. L. M. Havill, J. Rogers^{*}, D. E. Newman^{*}, M. C. Mahaney. Genetics, Southwest Foundation for Biomedical Research, San Antonio, TX, USA.

The dramatic sex difference in osteoporosis (OP) prevalence requires explanation and may provide avenues for deciphering OP pathogenesis. The obvious sex-specificity of pregnancy and lactation have focused attention on possible effects of reproductive history on bone maintenance and turnover in women. While these events can result in transient changes in bone mineral density (BMD), studies of their long-term effects on BMD and fracture risk show inconsistent results. While these apparent inconsistencies may be due in part to differences in study design, the effects of genes on a woman's bone metabolism during pregnancy and lactation may also contribute to variation in the long-term effects of reproductive history on bone fragility. We tested the hypothesis that genotype interacts with reproductive history effects on BMD in a non-human primate model by analyzing genotype-by-parity (G×P) interaction effects on lumbar spine and forearm BMD in pedigreed adult baboons (N=676). We previously reported that BMD in these baboons is heritable and that increasing parity has a significant negative effect on BMD at all sites ($p < 0.0001$ to $p = 0.01$; 0.5% to 0.8% per pregnancy). Using maximum likelihood-based variance components methods developed to test for genotype-by-environment interactions, we modeled the additive genetic covariance for BMD in the baboon pedigrees as a function of parity. More specifically, we defined the additive genetic variance as an exponential decay function of parity. We modeled the genetic correlation between relative pairs similarly. Significant parity-dependent changes in the genetic variance and/or departures from complete pleiotropy (genetic correlation=1) between relatives as a function of parity were interpreted as evidence of G×P interaction. We simultaneously estimated the phenotype, BMD, as a linear function of these two G×P interaction terms and the mean effects of sex, age, weight, and parity. At no skeletal site in these baboons does the genetic correlation between BMD in relatives change significantly in a parity dependent manner; therefore, we conclude that the genes affecting BMD do not differ as a function of parity. However, because the estimated genetic variances in BMD at all skeletal sites do change significantly in a parity-dependent manner ($p < 0.00001$ to $p = 0.01$), we conclude that the magnitude of the effect of those genes is influenced by parity. This first formal test for genotype-by-parity interaction shows that at trabecular bone sites (spine and ultradistal radius) the effect of genes on BMD decreases with increasing parity. At cortical bone sites (diaphyseal radius and ulna) the effect of genes increases with increasing parity.

Disclosures: **L.M. Havill**, None.

SU178

Quantitative Trait Loci for Bone Mineral Density Identified by Genome-Wide Linkage Scan to Chromosomes 7q and 21q in Men from the Amish Family Osteoporosis Study. E. A. Streeten, J. R. O'Connell^{*}, D. J. McBride^{*}, T. I. Pollin^{*}, A. R. Shuldiner^{*}, B. D. Mitchell. Endocrinology, Diabetes and Nutrition, University of Maryland School of Medicine, Baltimore,, MD, USA.

Bone mineral density (BMD) is highly heritable, with genetic factors accounting for 50-70% of variation in adult BMD and up to 85% of variation in peak bone mass. The purpose of this study was to identify genes contributing to variation in BMD. We carried out a genome-wide scan among participants of the Amish Family Osteoporosis Study (AFOS), a study designed to identify genes that influence bone health. The Amish are a genetically closed population who descended from a relatively small number of founders. Importantly, most Amish follow a homogeneous lifestyle, rarely smoke or drink alcohol and prefer to avoid prescription medications. Our genome scan was carried out in 988 participants (mean age \pm SD = 50.2 ± 16.3 yrs, range 18-99 yrs) recruited from 50 large multigenerational families, including 4 having more than 100 members. BMD was measured at the spine, hip and radius using dual x-ray absorptiometry (DXA). Mean T scores in the participants were: spine (L1-4) -1.3 ± 1.4 , total hip -0.4 ± 1.2 , total wrist -0.2 ± 1.3 . Multipoint linkage analysis was carried out using 731 highly polymorphic microsatellite markers with average spacing of 5.4 cM. Sub-analyses were conducted in men (n = 386) and women (n=602). No significant QTLs related to BMD were identified in the study population as a whole (highest LOD = 2.11 for radius BMD at 3q26). On subgroup analysis of all men, we found significant evidence for QTLs influencing variation in both total hip (LOD = 3.83) and femoral neck (LOD = 3.09) BMD at 7q31 and for spine BMD at 21q22 (LOD = 3.19). For the women only subgroup, no significant QTLs related to BMD were identified (highest LOD = 2.11 for spine BMD at 1q21). Previous studies in mice have found a QTL for femur BMD at a mouse site syntenic to human 7q32 and in humans a QTL for trochanter BMD at 21q22. In conclusion, these results provide evidence for QTLs in men that influence hip BMD on chromosome 7q and spine BMD on 21q, replicating previous findings in mice and humans.

Disclosures: **E.A. Streeten**, Merck & Co. 2.

SU179

Genomic Regions Identified for BMD in an Exceptionally Large Sample by Considering Epistasis. P. Xiao, Y. F. Guo^{*}, R. R. Recker, H. W. Deng. Osteoporosis Research Center, Creighton University, Omaha, NE, USA.

Low bone mineral density (BMD) is an important risk factor for osteoporosis and under strong genetic control. Several whole genome scan (WGS) studies have been conducted for BMD in humans, resulting in largely inconsistent results so far. It is now recognized that small samples and thus lack of statistical power are an undisputable reason behind the inconsistent and none-robust results. No previous WGS for BMD considered epistatic effects, which usually underlie complex traits. In this study, an exceptionally large and powerful sample of 471 Caucasian families with 4,251 subjects was phenotyped and genotyped for 410 microsatellite markers throughout the human genome. WGS was conducted. In WGS analyses, a LOD score of 3.01 was achieved on 5q23 for wrist BMD. For spine and hip BMD, the highest LOD scores were obtained on 3p25 (LOD = 2.27) and 3q27 (LOD = 2.62), respectively. Another interesting suggestive linkage region on 2q32 was detected for spine BMD (LOD = 1.91), hip BMD (LOD = 2.17), and wrist BMD (LOD = 1.98). However, in further analyses that incorporated epistasis into the original WGS, quite interesting results emerged. When epistasis was considered with 3p25 for spine BMD, we identified highly significant results in two genomic regions that showed only suggestive linkage evidence or small LOD score in the original WGS. Specifically, the LOD score increased from 1.91 to 3.75 at 2q32, and increased from 1.35 to 3.29 at 11q23. This study highlights large sample and incorporation of epistasis in WGS in identifying QTLs for complex diseases.

Disclosures: **P. Xiao**, None.

SU180

Is There Evidence of Heritability of Hyperkyphosis in Older Women? D. M. Kado¹, L. Palermo^{*2}. ¹Medicine, University of California, Los Angeles, Los Angeles, CA, USA, ²Epidemiology and Biostatistics, University of California, San Francisco, San Francisco, CA, USA.

Hyperkyphosis, or an increased thoracic curvature, is often considered one of the undesirable consequences of osteoporosis. However, up to one half of those with the worst hyperkyphosis do not have vertebral fractures. Therefore, hyperkyphosis is likely a result of other important and possibly reversible causes. We hypothesized that compared to unaffected women, older women with hyperkyphosis would be more likely to have a family history of hyperkyphosis. Study participants were from the Study of Osteoporotic Fractures and included 611 women, aged 67 or older, who had their thoracic spinal curvature assessed using an architect's flexicurve during the second clinic visit. In addition to assessing morphometric vertebral fractures, spine and hip bone mineral density, and a family history of fractures, these women answered questions that inquired whether their natural mother and/or natural father had a history of a dowager's hump, or a spine that was stooped or bent forward. Of the original 611 women, 557 (91%) answered the question regarding family history. Of those, 17% reported that their mother had a dowager's hump and 5% reported that their father had a dowager's hump. Modeled continuously, there was a significant age-adjusted association between either having a mother or father's history of dowager's hump and worse degrees of kyphosis ($p = 0.001$). In multivariable models adjusted for age, spine or hip bone mineral density, and prevalent vertebral fracture, the

association between a positive family history of dowager's hump and worse degrees of kyphosis remained significant ($p = 0.009$). In similarly adjusted logistic models examining the odds of being in the highest quartile of kyphosis, reporting a father's history of dowager's hump was the strongest predictor (Odds ratio = 3.0; 95% CI: 1.2-7.3, $p = 0.015$). A positive family history of fracture was not associated with degree of kyphosis. While we cannot exclude the possibility of recall bias as a potential explanation for our study findings, these results present preliminary evidence that hyperkyphosis is a heritable condition that is not simply reflective of underlying osteoporosis.

Disclosures: **D.M. Kado, None.**

SU181

QTL for Bone and Body Composition Phenotypes Are Sex Specific in a Mouse Model of GH/IGF-I Deficiency. **L. Donahue, W. Beamer, K. Shultz*, J. Hurd*, V. Guido*, C. Rosen.** The Jackson Laboratory, Bar Harbor, ME, USA.

QTL analysis is a powerful tool for the discovery of regulatory genes for complex traits such as body composition and skeletal phenotypes. Crosses between inbred strains of mice provide QTL data and are contributing to new genetic insights regarding body morphology. Our QTL analysis has 2 goals: to identify genes that are independent of GH/IGF-I regulation, and to determine if these genes are sex specific. We are utilizing a spontaneous mouse mutation, *little*, with a non-functional GHRHR. A congenic strain was made by transferring the *little* mutation from the low BMD C57BL/6J (B6) to the high BMD C3H/HeJ (C3) strain. In both B6-*lit/lit* and C3.B6-*lit/lit* mice, circulating GH is undetectable, serum IGF-I is low, and femoral vBMD (pQCT), aBMD (PIXImus), femur length, and body mass are reduced compared to *lit/+* mice. Although C3.B6-*lit/lit* mice are of the same body weight and femur length as B6-*lit/lit* mice, C3.B6-*lit/lit* mice have higher aBMD and vBMD. Crosses between B6-*lit/lit* and C3.B6-*lit/lit* produced 1037 male and 1095 female F2 GH/IGF-I deficient mice, but segregating alleles from B6 and C3. Analyses of genome-wide data from 120 polymorphic markers (nearly 192,000 genotypes) revealed gender-specific and gender-independent regulatory loci for all phenotypes. Data show: 1) The best QTL for all phenotypes differs between sexes, per ex the best QTL for vBMD is on Chr 11 in females (F) and on Chr 1 in males (M); 2) The best QTL for one sex often has a significant (not necessarily the best) QTL for the other sex, per ex the QTL for vBMD on Chr 1 has a LOD score of 11.2 for males and 9.2 for females, but the best QTL for vBMD in females is on Chr 11 (LOD 12.6); 3) Some QTL have significant (but not the highest) LOD scores for sexes combined and for each individually, per ex all of the QTL for vBMD are significant for all 3 groups. We conclude that it is important to separate sexes when performing QTL analyses. Moreover, it is misleading to infer significance for a QTL in both sexes when it is found to be important in one or the other, or in sexes combined. In addition, the QTL for vBMD on Chrs 1,4, and 11 are in approximately the same location as those found in B6C3H +/- F2 mice; however the QTL on Chr 8 is unique to the GH/IGF-I deficient mice.

Disclosures: **L. Donahue, None.**

SU182

A Major QTL on Mouse Chromosome 12 That Regulates Bone Nanoindentation Property. **Y. Jiao*¹, Z. Fan*², H. Chiu*³, F. Jiao*¹, E. C. Eckstein*³, J. Rho*³, W. G. Beamer⁴, W. Gu¹.** ¹University of Tennessee Health Science Center, Memphis, TN, USA, ²Marquette Univ, Marquette, WI, USA, ³Univ. of Memphis, Memphis, TN, USA, ⁴The Jackson Laboratory, Bar Harbor, ME, USA.

It has speculated that regulate bone quality measured by nanoindentation technology represents a novel approach in our understanding of molecular mechanisms that control bone matrix properties. In this study, we measured bone quality of mouse tibiae by nanoindentation and three-point bending. We then mapped and compared quantitative trait loci (QTLs) detected by these two methods. 1) Mouse tibiae for age testing were from C3H/HeJ and for QTL mapping were from a F2 population derived from C57BL/6J and C3H/HeJ. Those tibiae were from the same population used for the analysis of QTLs of bone mineral density at The Jackson Laboratory. 2) For nanoindentation measurement, a Triboindenter (Hysitron, Inc. Minneapolis, MN) was used to conduct all indentation tests. The Oliver-Pharr method was used to determine the elastic modulus. 3) The bone strength of the same set of bones was tested for three-point bending using ISO 4049, with the support width adjustable to accommodate specimen sizes outside the scope of ISO 4049. 4) Genome scan was performed in The Jackson Laboratory using microsatellite markers. 5) QTL mapping was conducted using Map Manager QTX software. Analysis of data of nanoindentation obtained 683 F2 mice detected five QTLs on hardness and four on stiffness of the nanoindentation properties. 2). Analysis of data of three-point bending detected four QTLs of Elastic Modulus and 11 QTLs of Maximum Loading (hardness). 3) Most of the QTLs from three-point bending have been mapped on to the same locations of bone mineral density. QTL on Chr. 4 (60% influence) has the most impact on the bone strength measured by three-point bending. 4) The QTL on Chr. 12 (12% influence) has the most influence on nanoindentation property. While previously there is no bone related QTL reported on mouse Chr. 12, homologous region of this QTL on human Chr. 14q has been linked to peak bone mineral density at the hip. Our study suggests that nanoindentation has a great potential as a novel approach to improve our understanding of molecular mechanisms that control the matrix properties of bone.

Disclosures: **Y. Jiao, None.**

SU183

The Relationship between Interleukin-1 System Gene Polymorphism and Change in Bone Mineral Density after Hormone Replacement Therapy in Postmenopausal Korean Women. **J. KIM, D. Lee*, S. Ku*, B. Jee*, C. Suh*, S. Kim*, Y. Choi*, S. Moon*.** Dept. of Obstetrics & Gynecology, Seoul National University Hospital, Seoul, Republic of Korea.

The purposes of this study were to investigate the relationship between interleukin-1 (IL-1) system gene polymorphisms, and change in production of IL-1 by whole blood cells (WBCs), and bone mineral density (BMD) after hormone replacement therapy (HRT) in postmenopausal Korean women. The IL-1 α C-889T polymorphism, IL-1 β C-511T polymorphism and 86-base pair variable number tandem repeat (VNTR) polymorphism in the IL-1 receptor antagonist (IL-1ra) gene was analyzed by restriction fragment length polymorphism (REFLP), polymerase chain reaction-Genescan, and DNA sequencing in 206 postmenopausal Korean women receiving sequential HRT for 1 year. IL-1 α , IL-1 β , and IL-1ra produced by WBCs cultured with lipopolysaccharide for 2 days, and serum CrossLaps (CTX), and osteocalcin were measured using enzyme-linked immunosorbent assay (ELISA) and immunoassay respectively. BMD at the lumbar spine and proximal femur was determined by dual energy X-ray absorptiometry. The IL-1 system genotypes were not distributed differently between HRT-responders and HRT-nonresponders (women who lose more than 3 % of bone mass per year), and no differences in the annual percent change of BMD after HRT were noted among IL-1 system genotypes. After HRT, the production of IL-1 α by WBCs decreased but no changes in the production of other components of IL-1 system were noted. There were no differences in the 6 month changes of bone turnover markers and the production of IL-1 system components by WBCs and IL-1 β /IL-1ra ratio after HRT across IL-1 system genotypes. Except a negative correlation between IL-1 α with annual change of BMD at trochanter after HRT, the production of other components of IL-1 system by WBCs and their changes after HRT of 6 month did not correlated with annual change of BMD after HRT. In conclusion, the IL-1 system gene polymorphisms do not affect change in BMD, and change in the production of ILs by WBCs after HRT in postmenopausal Korean women.

Disclosures: **J. Kim, None.**

SU184

Influence of Genetic Factors Related to Estrogen Synthesis and Activity on Peak Bone Mass. **J. A. Riancho¹, C. Valero*¹, A. L. Zarrabeitia*¹, M. T. Zarrabeitia*², J. Gonzalez-Macias¹.** ¹Internal Medicine, Hospital U.M. Valdecilla, University Cantabria, Santander, Spain, ²Legal Medicine, University Cantabria, Santander, Spain.

Osteoporosis may result from an accelerated loss of bone mass with advancing age, or from an impaired accretion of bone during the growth period, which leads to an inadequate peak bone mass in early adulthood. Although the factors that actually determine peak bone mass are not well known, there is evidence that both heredity and estrogen activity are important in females as well as in males. Therefore we studied healthy individuals between 22 and 45 years of age (147 men, 194 women) and analysed the relationship between bone mineral density (BMD) and a number of frequent polymorphisms in genes related to estrogen metabolism and activity. They included a T/C SNP in the 5' region of the 17-hydroxylase gene; an A/G SNP in the 3' UTR of aromatase; a CA microsatellite in intron 6 of the estrogen receptor beta; and four polymorphisms of the estrogen receptor alpha (TA repeat in promoter; C/T and G/A SNPs in intron 1, and A/G SNP in exon 8). Areal BMD was higher in men than in women (spine: 1.048 \pm 0.120 vs. 1.034 \pm 0.112; hip: 0.907 \pm 0.131 vs. 0.822 \pm 0.104 g/cm², $p < 0.001$). Body weight was the single most influential factor on BMD in both sexes, explaining 8-9% of BMD variance. Among the genetic factors studied, a common CA repeat polymorphism in estrogen receptor beta showed a significant association to BMD in women ($p = 0.03$ at the spine, and 0.008 at the hip). The effect of estrogen receptor genotype persisted after adjustment by body weight, explaining a further 2-3% of BMD variance. Other polymorphisms did not show an independent association with BMD. These results suggest that body weight and some common allelic polymorphisms in estrogen receptor beta contribute to determining peak bone mass. However, they only explain a small proportion of the overall BMD variance. Therefore, other unidentified factors exerting a significant influence must exist.

Disclosures: **J.A. Riancho, None.**

SU185

Farnesyl Diphosphate Synthase (FDPS), a New SNP that Is Associated with BMD in Elderly Women. **M. Levy¹, R. E. Ferrell*², R. A. Parker*³, S. L. Greenspan¹.** ¹Medicine, University of Pittsburgh, Pittsburgh, PA, USA, ²Genetics and Pharmaceutical Sciences, University of Pittsburgh, Pittsburgh, PA, USA, ³Center for Biostatistics in AIDS Research, Harvard School of Public Health, Boston, MA, USA.

Previous studies have demonstrated single nucleotide polymorphisms (SNPs) in several candidate genes, including the estrogen receptor alpha gene and the vitamin D receptor gene, have a minimal impact on bone mass in postmenopausal women. Farnesyl diphosphate synthase (FDPS) is an enzyme involved in the mevalonate pathway in osteoclasts and is inhibited by nitrogen-containing bisphosphonates. We postulated that an FDPS SNP (rs2297480) may be associated with bone mineral density (BMD) and response to antiresorptive therapy. To test this hypothesis, we examined FDPS in addition to polymorphisms associated with the estrogen receptor alpha gene (ESR1: *PvuII* and *XbaI*), the vitamin D receptor gene (VDR: *BsmI* and *FokI*), and a lipoprotein-related protein 5 (LRP5: *A1330I*) polymorphism in elderly women who had completed a 3-year, double-

blind, placebo-controlled clinical trial of alendronate, hormone replacement, or combination antiresorptive therapy. As previously reported, bone mass increased significantly at all skeletal sites in women on active treatment. Our study found FDPS was associated with baseline BMD. Patients with AA genotypes had significantly higher BMD than those with either the CA or CC genotype (combined) at the spine ($P = 0.009$), hip ($P = 0.018$) and trochanter ($P = 0.010$). Each C allele decreased BMD by 0.036 g/cm^2 at the spine ($P = 0.029$), 0.021 g/cm^2 at the hip ($P = 0.064$), and 0.022 g/cm^2 at the trochanter ($P = 0.027$), after adjustment for age and body mass index. VDR, ESR1 and LRP5 SNPs were not associated with baseline BMD. None of the polymorphisms were related to change in BMD during treatment. We conclude that FDPS is related to baseline bone mass, but does not influence response to therapy. Further studies are needed to examine whether this polymorphism is related to fracture risk in addition to BMD.

FDPA Alleles (n)	Baseline BMD (g/cm ² , mean +/- SD)		
	Spine*	Total Hip	Trochanter*
AA (145)	0.906±0.166	0.802±0.118	0.614±0.101
CA (120)	0.858±0.160	0.772±0.123	0.588±0.102
CC (14)	0.850±0.146	0.754±0.144	0.563±0.118

* $P < 0.05$ difference across FDPS alleles

Disclosures: **M. Levy**, None.

SU186

Estrogen Receptor Beta Polymorphisms Predict Risks of Osteoporosis in Men and Women: A Linkage and Association Study. A. W. C. Kung¹, B. M. H. Lai¹, M. Y. M. Ng^{*1}, W. M. W. Cheung^{*1}, V. Chan^{*1}, P. C. Sham^{*2}.
¹Department of Medicine, The University of Hong Kong, Hong Kong, China,
²Genome Research Centre, The University of Hong Kong, Hong Kong, China.

Estrogen receptor beta is expressed in both osteoblast and osteoclast and estrogen receptor beta gene (ESR2) is likely to play a role in bone mass determination. We previously reported a weak association between a dinucleotide CA repeat polymorphism (D14S1046) in the intronic region of ESR2 with bone mineral density (BMD) in women. To evaluate the role of ESR2 in BMD determination and osteoporosis risk prediction in men and women, linkage and association approach were utilized by evaluating 1484 subjects from 306 extended southern Chinese pedigrees and 770 pairs of population-based case-control subjects. The cases were subjects with BMD Z score < -1.3 at either the spine or total hip region (equivalent to the lowest 10th percentile of the population) and the controls were subjects with BMD Z score $> +1$. Out of 11 SNPs, a SNP in the promoter region (nt -1068T→C) was in significant linkage disequilibrium with 21 CA repeats of D14S1046. Using Merlin program, 6 tagged SNPs were in linkage with spine BMD (LOD 1.50 to 1.67, $p=0.003$) and femoral neck BMD (LOD 1.21, $p=0.009$). Using quantitative trait disequilibrium test (QTDT), nt -1068T→C was found to be associated with hip BMD in women ($p=0.005$) but not in men in both total family association and within-family association testing. In the population-based study, nt -1068T→C was associated with 10% reduction in spine and hip BMD in men, 4% reduction in spine BMD in premenopausal women and 4-6% reduction in spine and hip BMD in postmenopausal women. Furthermore, this SNP was associated with higher risk of osteoporosis at the lumbar spine (male: odds ratio 3.4, female: odds ratio 2.8) and at the hip (male: odds ratio 1.9, female: odds ratio 2.9). SNP haplotype analysis provided similar results as individual SNP analysis. In conclusion, nt -1068T→C polymorphism of the ESR2 gene is associated with lower BMD and higher risk of osteoporosis in both males and females. This SNP may serve as a potential marker for assessing the risk of osteoporosis and identification of at risk subjects.

Disclosures: **A.W.C. Kung**, None.

SU187

A Deletion Polymorphism in the Gene for the Estrogen Receptor Alpha Coactivator RIZ1 Is Associated with BMD in Elderly Men - MrOS, Sweden. E. Grundberg^{*1}, O. Johnell², Ö. Ljunggren¹, D. Mellström³, E. Orwoll¹, C. Ohlsson³, H. Mallmin^{*3}, A. Kindmark¹, H. Brändström¹.
¹Department of Medical Sciences, Uppsala University, Uppsala, Sweden,
²Department of Orthopaedics, Malmö University hospital, Malmö, Sweden,
³Center for Bone Research, Department of Internal Medicine, The Sahlgrenska Academy at Göteborg University, Göteborg, Sweden, ⁴Department of Medicine, Oregon Health Sciences University, Portland, OR, USA,
⁵Department of Surgical Sciences, Uppsala University, Uppsala, Sweden.

Predisposition to osteoporosis is largely genetically determined. It is likely that the genetic risk consists of several common polymorphisms of genes that have weak effects individually, but major effects in concert. A novel candidate gene for BMD is the estrogen receptor-alpha (ERalpha) coactivator RIZ1 that strongly enhances ERalpha function. The gene contains a natural occurring deletion encoding a proline in exon 8. Previously, we have demonstrated that the deleted form of RIZ1 shows an impaired response in coactivating ERalpha in a ligand- and dose-dependent manner compared with the non-deleted form of RIZ1. In this study we examined the relationship between the deletion in the RIZ1 gene and BMD in 3000 Swedish elderly men, included in the Swedish part of the MrOs study. The study is population based and the participants were between 70 and 80 years old at inclusion. BMD was measured by dual x-ray absorptiometry (DXA). Serum levels of testosterone, estradiol and SHBG were measured using radio immuno assay and free estradiol levels were derived from the mass action equations. The genotypes for the RIZ1 polymorphism were named homozygous presence P704+, absence P704-, heterozygosity P704+/- of a proline at position 704. The genotype frequencies in the study population were P704+ 18%, P704 +/- 49% and P704- 33% which is in agreement with Hardy-Weinberg equilibrium. A significant association was observed between spine BMD

and RIZ1 genotype (ANOVA $p=0.024$). Multiple regression analysis was used to adjust the data for differences in weight, height, age, smoking, physical activity, total calcium intake and free estradiol levels, to define the relative contributions of independent variables to the variation of spine BMD. After adjustment, the RIZ1 genotype was an independent predictor of spine BMD in elderly men ($p=0.004$, $\beta=-0.06$).

Disclosures: **E. Grundberg**, None.

SU188

Dinucleotide CA Repeat Polymorphisms in ESR1 Gene Are Associated with Increased Risk of Low BMD and Osteoporotic Fractures. B. M. H. Lai^{*}, A. W. C. Kung. Medicine, The University of Hong Kong, Queen Mary Hospital, Hong Kong, China.

Studies of PvuII and XbaI polymorphisms of the estrogen receptor alpha (ESR1) gene have shown that these intronic polymorphisms may be associated with fracture risk, but their relation with bone mineral density (BMD) is controversial. We postulated that other polymorphic sites of ESR1 may be of importance in determining osteoporosis and fracture risk, such as the dinucleotide CA repeats polymorphism (D6S440) in intron 5 of the gene. To assess the role of D6S440 as a marker for predicting risk of low BMD and osteoporotic fractures, we studied 770 Southern Chinese case-control pairs (93 male, 677 female pairs). Cases were subjects with BMD Z scores < -1.28 at either the spine or hip (equivalent to lowest 10th percentile of the population), and controls were subjects with BMD T scores $> +1$. Among them, 88 perimenopausal women (aged 45-55years) were studied at 18 months to determine the association between the CA repeat and rate of bone loss. All subjects were followed prospectively for incidence of osteoporotic fractures. The results showed that allele size shorter than 18 CA repeats (CA <18) were associated with 6% reduction in hip BMD ($p<0.01$) and 3% reduction in lumbar spine BMD ($p<0.05$) in female but not male subjects. During the 18 month study period, peri-menopausal women carrying CA <18 demonstrated greater bone loss at the hip than those with CA >18 . (2.65% vs 0.468%, $p=0.01$). Postmenopausal women with CA <18 had a 5-fold increase in osteoporosis risk and a 2-fold increase in fracture risk at both the spine and hip ($p<0.01$). These results indicate that ESR1 CA repeats may be a useful diagnostic marker for osteoporosis and fracture risk assessment in peri- and postmenopausal women.

Disclosures: **B.M.H. Lai**, None.

SU189

A Polymorphism in the Gene Coding for Low-Density Lipoprotein Receptor-Related Protein-5 (LRP5) Is Associated with Peak Bone Mass in Men - Results from the Odense Androgen Study. K. Brixen¹, T. L. Nielsen^{*1}, K. Wraage^{*1}, L. Batum^{*2}, M. Andersen^{*1}, B. Abrahamsen¹. ¹Endocrinology, Odense University Hospital, Odense, Denmark, ²Clinical Biochemistry, Odense University Hospital, Odense, Denmark, ³Internal medicine, Roskilde County Hospital Koege, Odense, Denmark.

Twin studies have demonstrated that genetic factors account for 50-80% of the inter-individual variation in bone mineral density (BMD). The transmembrane protein LRP5 has been implicated in the adaptive response of bone to mechanical load and mutations in this gene are responsible for the rare conditions of "high bone mass phenotype" and the "osteoporosis pseudoglioma syndrome". Moreover, a number of common polymorphisms in this gene have also been reported to affect bone accretion in childhood, to increase the risk of osteoporosis, and susceptibility to osteoporotic fractures. We hypothesized that the 3989C>T polymorphism in exon 18 of the LRP5 gene is associated with peak bone mass in men. The Odense Androgen Study is a population-based, prospective, observational study on the inter-relationship between endocrine status, body composition, muscle function, and bone metabolism in young men. In brief, 3000 males aged 20-30 years were randomly selected from the civil registration database in Funen County, Denmark, and invited by mail to participate in the study. A total of 2042 men returned the questionnaire, 783 gave written informed consent to participate in the study, and data from 779 are presented here. Participants were genotyped using real-time PCR. BMD of the spine and hip was measured using a Hologic-4500a densitometer. A total of 589 of the participants had the CC, 170 the CT, and 20 the TT genotype, compatible with Hardy-Weinberg equilibrium ($\chi^2=0.13$, $p=0.93$). No association between genotypes and BMD was observed in the overall group. In physically active young men ($n=589$), however, BMD of the spine was significantly higher in CC genotype ($p=0.02$) than in the combined CT and TT genotypes. In sedentary young men ($n=190$) there was no significant effect of genotype on BMD ($p=0.26$). Using multiple regression analysis and adjusting for body mass index, smoking, chronic medication, and serum 25-hydroxy-vitamin-D, a significant relationship between the number of T alleles and BMD of the spine was found in the physically active men ($R=-0.21$, $p<0.05$). No such relationship could be demonstrated regarding BMD of the proximal femur or in the sedentary young men. We conclude that the CC polymorphism of the LRP5-gene is significantly associated with lumbar spine peak bone mass in physically active men. This gene-environment interaction provides support for LRP5 as a mediator of load-induced bone formation.

Disclosures: **K. Brixen**, None.

SU190

Q89R Polymorphism in the LDL Receptor-Related Protein 5 Gene Is Associated with Spine Osteoarthritis in Postmenopausal Japanese Women. T. Urano¹, M. Shiraki², K. Narusawa³, T. Usui^{*1}, T. Hosoi⁴, Y. Ouchi^{*1}, T. Nakamura³, S. Inoue¹. ¹Department of Geriatric Medicine, University of Tokyo, Tokyo, Japan, ²Research Institute and Practice for Involuntional Diseases, Nagano, Japan, ³Department of Orthopedic Surgery, University of Occupational and Environmental Health, School of Medicine, Kitakyushu, Japan, ⁴Tokyo Metropolitan Geriatric Medical Center, Tokyo, Japan.

Recent studies indicate that the appearance of osteoarthritis is influenced by genetic factors, physical loading, and other factors not yet identified. Association studies using various definitions of osteoarthritis have been performed, mainly investigating genes encoding structural proteins of the extracellular matrix of cartilage or genes that participate in the regulation of the bone and cartilage metabolism. Wnt- β -catenin signaling pathway regulates bone density through the low-density lipoprotein receptor-related protein 5 (LRP5), a receptor of this signaling. This pathway is also involved in cartilage development and homeostasis in vivo, suggesting that genetic variation in Wnt- β -catenin signaling genes may affect the pathogenesis of cartilage diseases, such as osteoarthritis. Therefore, we analyzed the association between a single nucleotide polymorphism causing amino-acid change (Q89R) in the LRP5 coding region and the severity of radiographically observable osteoarthritis of the spine. Ethical approval for the study was obtained from appropriate ethics committees, and informed consent was obtained from all subjects. For this purpose, we evaluated the presence of osteophytes, endplate sclerosis, and narrowing of disk spaces in 357 healthy postmenopausal Japanese women. Because only one of these subjects carried the RR genotype of the Q89R polymorphism, we compared those who carried the R allele (QR or RR) with those who did not (QQ). We found that subjects without the R allele (QQ; n = 321) had a significantly lower osteophyte formation score than did subjects bearing at least one R allele (QR + RR; n = 36) (7.80 vs 10.89, $p = 0.0019$ by analysis of covariance). On the other hand, the occurrence of disk narrowing and endplate sclerosis did not significantly differ in those with and without at least one R allele. Thus, we suggest that a genetic variation at the LRP5 gene locus is associated with spine osteoarthritis, in line with the involvement of the LRP5 gene in the bone and cartilage metabolism.

Disclosures: **T. Urano**, None.

SU191

Association of a Single Nucleotide Polymorphism in Low-Density Lipoprotein Receptor-Related Protein 5 (LRP5) Gene Promoter Region with Peak Bone Mineral Density: A Case-Control Study. C. L. Cheung, W. W. Ng^{*}, B. M. H. Lai^{*}, V. Chan^{*}, A. W. C. Kung. Department of Medicine, The University of Hong Kong, Hong Kong, Hong Kong Special Administrative Region of China.

Low-density lipoprotein receptor-related protein 5 (LRP5) is important for osteoblast differentiation and mutations of the gene are associated with both low and high bone mass syndromes. To determine the importance of LRP5 in determining peak bone mass acquisition in the general population, we performed a population-based case control study. 187 pairs of sex and age matched case-control pairs (mean 36.4, range 20-44 years) of southern Chinese in ethnicity were evaluated. Cases were subjects having a BMD Z score at either the hip or spine ≤ -1.28 , which is equivalent to the lowest 10th percentile of the population, and controls were subjects having a BMD Z score $Z \geq +1$. Mutations and single nucleotide polymorphisms (SNPs) were determined in 30 case-control pairs of subjects by sequencing 3000 bp in the promoter region, all the coding exons and 100bp upstream and downstream of the adjacent intronic regions. Using this gene-based approach, 8 SNPs with a minor allele frequency $>5\%$ were studied. BMD were adjusted for age, sex and body weight and height. The results showed that subjects bearing a variant T allele (TT and TC) at the C-864T polymorphism (rs682429) in the promoter region was significantly associated with lower BMD at the lumbar spine ($p = 0.006$), trochanter ($p = 0.016$) and total hip ($p = 0.014$). When the two sex were analyzed separately, this polymorphic site was associated with a reduction in BMD in men at all sites measured (lumbar spine -15.6%, $p = 0.01$, femoral neck -15.9 %, $p = 0.04$; trochanter -15.9%, $p = 0.04$ and total hip -15.1%, $p = 0.03$), and in women at the lumbar spine (-3.7%, $p = 0.03$). Haplotype TATGCCAC was associated with lower BMD in female at the lumbar spine ($p = 0.01$), femoral neck ($p = 0.003$), trochanter ($p = 0.002$) and total hip ($p = 0.001$). The C allele was associated with a 2.9 folds low risk of low BMD (Z score < -1.28) in whole population, and 2.6 folds low risk of low BMD in female. The C-864T polymorphic site is 2 bases adjacent to a consensus recognition site for the Elk-1 binding element. In conclusion, C-864T polymorphism of LRP5 is associated with low BMD in both young men and women, and may be a useful marker for predicting low peak bone mass.

Disclosures: **C.L. Cheung**, None.

SU192

Association of Vitamin D Receptor Start Codon and CDX-2 Polymorphism with the Effect of Calcium Supplementation on Bone Mineral Density in Postmenopausal Women. Z. Zhang, Y. Qin^{*}, J. He^{*}. Center for Osteoporosis, Shanghai Sixth Hospital, Shanghai Jiaotong University, Shanghai, China.

AIM To investigate the association of vitamin D receptor (VDR) gene start codon and CDX-2 polymorphism with the effect of calcium supplementation on bone mineral density (BMD) in postmenopausal women. **Methods** 200 Shanghai postmenopausal women of Han nationality were randomly divided into 2 groups of 100 women: high calcium group

(1000 mg element calcium and 400 units of vitamin D were given daily for 12 months) and low calcium group (300 mg element calcium and 300 units of vitamin D were given daily for 12 months). BMD and bone metabolism markers were measured before and after calcium supplementation. VDR gene start codon (Fok I) and CDX-2 polymorphisms were analyzed using polymerase chain reaction-restriction fragment length polymorphism (PCR-RFLP) and allele-specific multiplex PCR, respectively. **Results** 171 women completed 12-month study period. By the end of study, the lumbar spine BMD was increased by $0.90 \% \pm 2.90 \%$ ($P < 0.05$) and $1.31 \% \pm 3.40 \%$ ($P < 0.01$) in the high calcium group and low calcium group, respectively. The trochanter BMD was increased by $1.29 \% \pm 3.62 \%$ ($P < 0.05$) and $1.06 \% \pm 3.65 \%$ ($P < 0.01$) in the high calcium group and low calcium group, respectively. But the percent increase of BMD between groups was not significant difference. The serum ALP and PTH decreased by 14.0 % and 27.8 % respectively in the high calcium group, both significantly more than those in the low calcium group ($P < 0.01$ and $P < 0.05$, respectively). The frequencies distribution of Fok I and CDX-2 alleles were not deviation with Hardy-Weinberg equilibrium in study population. No significant difference in BMD between Fok I genotypes or CDX-2 genotypes was observed in two study groups. Moreover, after 12 months of calcium supplementation, there was no effect of an interaction between Fok I or CDX-2 polymorphism and calcium supplementation on BMD or bone metabolism markers either in high calcium group or low calcium group. **Conclusion** The calcium and vitamin D supplementation on postmenopausal women could reduce the loss of bone mass. No significant association was found between VDR gene Fok I or CDX-2 polymorphism and the effect of calcium supplementation on BMD and bone metabolism markers in postmenopausal Chinese women of Han nationality.

Disclosures: **J. He**, None.

SU193

Bone Architecture, Biomechanical Properties and their Relationships in Two Mice Strains. N. Bonnet^{*1}, A. Basillais^{*1}, H. Beaupied^{*1}, S. Pothion^{*2}, J. Bizot^{*2}, F. Trovero^{*2}, Y. Herault^{*3}, E. Lespesailles¹, D. Courteix^{*1}, L. Benhamou¹. ¹U658Inserm & ATOSEP, Université d'Orléans, Orléans, France, ²Key-obs, Orléans, France, ³CNRS FRE 2815, Orléans, France.

There is a growing interest in bone characterization of mice strains. The relationship between architecture and bone strength deserves to be detailed in each genetic mice. The aim of this study was to evaluate the relation between bone architecture and biomechanical properties in C3H/HeJ and CBA/H mice. Ten C3H and 10 CBA male mice were studied at an age of 14 weeks. The femur geometry was measured with a digital calliper. Trabecular bone microarchitecture was characterized by X-ray microcomputed tomography : on the distal femur metaphysis. The 2D slices obtained by μ CT were used to measure the cortical parameter at the mid diaphysis. Mechanical properties were obtained using three-point bending tests. C3H mice weighed 23.66 ± 2.23 g, and CBA mice 26.11 ± 2.54 g. Mid-diaphysis diameter was lower in C3H than in CBA (1.65 vs 1.74mm) whereas bone length was higher in C3H (14.47 vs 14.08mm). Compared to CBA, C3H mice had a significantly higher BV/TV (51%, $p < 0.001$); Tb.Th (13%, $p < 0.001$) and Tb.N (50%, $p < 0.006$). Structural model index indicated a significantly lower proportion of rod shape in C3H (SMI = 2.32) than in CBA (2.52; $p < 0.01$). C3H had a higher ultimate force (+38%, $p < 0.001$), stiffness (+22%, $p < 0.04$) and lower ultimate displacement (-29%, $p < 0.001$) than CBA. Multiple regression coefficient of ultimate displacement of the total mice indicated that Tb.N ($r = 0.77$), mid-diaphysis diameter ($r = 0.835$) and cortical/bone marrow ratio ($r = 0.84$) were the explicative factors ($p < 0.01$). The table gives the multiple regression coefficient of ultimate force for the total group and for each mice model. When studied in a global group of 20 mice the analysis indicate cortical width as the most explicative factor. But when considering each genetic mice model, the ultimate force is not explained by the same bone characteristics. C3H ultimate force was more dependent upon cortical width whereas CBA ultimate force was more dependent upon Tb.Th. Different studies have previously suggested that the genes which regulate BMD or architecture are different in genetic mice models. In addition to these genes differences, our data suggest that the link between the different bone properties are not the same in genetic mice models.

Multiple regression coefficient for ultimate force ($p < 0.01$)		
CBA and C3H mice (n=20)	CBA mice (n=10)	C3H mice (n=10)
C.width $r = 0.86$	Tb.Th $r = 0.99$	C.width $r = 0.55$
C/ B.marrow $r = 0.91$	Mid-diaphysis $\Phi r = 0.999$	Tb.Th $r = 0.81$
Tb.Th, length, SMI, Tb.N $r = 0.95$		

Disclosures: **N. Bonnet**, None.

SU194

Polymorphisms in the PPAR γ Gene Influence Bone Density in Humans. D. P. Kiel¹, S. Ferrari², L. A. Cupples^{*3}, D. Karasik¹, J. Dupuis^{*3}, C. J. Rosen⁴, A. Imamovic^{*5}, S. Demissie^{*6}. ¹Hebrew SeniorLife, Boston, MA, USA, ²Div Bone Dis, Geneva Univ Hosp, Geneva, Switzerland, ³BU Sch Pub Health, Boston, MA, USA, ⁴Maine Ctr Osteo, Bangor, ME, USA, ⁵BU Dept Neuro, Boston, MA, USA, ⁶BU Sch Pub Health & Prog Genom Applic, Boston, MA, USA.

PPAR γ is a key transcription factor for differentiation of mesenchymal progenitors into adipocytes. In turn PPAR γ gene haploinsufficiency promotes osteogenesis in mice. Allelic differences in the PPAR γ gene produce a senescent skeletal phenotype in the 6T congenic mouse. Since PPAR γ effects on bone in humans remains unknown, we studied the association between polymorphisms in this gene and BMD and BUA. Seven intronic/3'-transcr region, and 1 missense, exonic SNPs in the PPAR γ gene were genotyped in the Framingham Offspring Study (740 males, 776 females). Three sets of markers in high LD were identified (1) *rs1805192 missense* (exon 1) [$C > G$], *rs4684848* [$G > A$]; (2)

ASBMR 27th Annual Meeting

rs1151999[A>C], *rs709150[C>G]*, *rs1175544[C>T]*; (3) *rs1152004[T>C]*, *rs1175381[T>C]*, *rs1186464[A>G]*). Femoral neck (FN), troch (FT) and spine (LS) BMD was measured using a Lunar DPX-L and calcaneal BUA using a Hologic Sahara. Genotype and haplotype (for markers in LD) sex-specific associations with bone measures were analyzed using ANCOVA first adjusting for age and estrogen (women), then for BMI and height, and finally, diabetes (DM), as PPAR γ is associated with obesity and DM. Mean age (\pm SD) was 61.3 \pm 9.1 yrs. Women with the CC genotype of rs1805192 (minor allele (G) freq 12%) had higher FN, LS BMD, and BUA (p=0.01-0.045, age, estrogen adjusted) and the effect size remained unchanged across all models (p=0.009-0.093). Men with the CC genotype had lower FN and FT BMD (p=0.011-0.028, age adjusted) even with additional adjustments (p=0.008-0.028). Women with the C allele of rs1175381 in LD region 3 (allele freq 4%) had lower age- and estrogen-adjusted FN, FT, and LS BMD (p=0.045-0.077) and remained with additional adjustment (p=0.011-0.035). Haplotype analyses in LD regions 1 and 3 were similar. In contrast, whereas single SNPs in LD region 2 were not associated with BMD or BUA, women with the haplotype *rs1151999[A]-rs709150[C]-rs1175544[C]* (frequency 21%) had lower age- and estrogen-adjusted BMD at the FN (p=0.013). The effect size was slightly less after adjustment for all covariates (p=0.062). Similar findings in women were observed for the ACC haplotype at the FT (p=0.004-0.014), LS (p=0.01-0.05), and BUA (p<0.0001). On average, BMD decreased by 0.10-0.15 SD per copy of the ACC haplotype, equivalent to the effect of 3 yrs of age at FN and 8 yrs at LS. Polymorphisms in the PPAR γ gene are associated with BMD and BUA, particularly in women, independent of BMI and DM, supporting a direct role of PPAR γ on bone mass in humans.

Disclosures: **D.P. Kiel**, None.

SU195

Modest Association of Fibroblast Growth Factor Binding Protein 1 (FGFBP1) with Bone Mineral Density in Mexican Americans. N. Hoppman^{*1}, D. J. McBride¹, J. Bruder², R. L. Bauer², J. R. O'Connell^{*1}, C. M. Kammerer^{*3}, B. D. Mitchell¹. ¹Division of Endocrinology, Diabetes and Nutrition, University of Maryland School of Medicine, Baltimore, MD, USA, ²University of Texas Health Science Center, San Antonio, TX, USA, ³University of Pittsburgh Graduate School of Public Health, Pittsburgh, PA, USA.

The San Antonio Family Osteoporosis Study (SAFOS) was designed with the goal of identifying genes and environmental factors influencing bone mineral density (BMD) in Mexican Americans. In a set of 29 large Mexican American families, we previously detected strong evidence for linkage of forearm BMD, measured by DXA, to a region on chromosome 4p near D4S2639 (lod = 4.3). This region contains several strong candidate genes for bone metabolism, including fibroblast growth factor binding protein 1 (*FGFBP1*). *FGFBP1* is 234 amino acids in length and can bind fibroblast growth factor-2 (FGF2) and modulate its activities, one of which is to stimulate osteoblast replication. We sequenced both exons, the intron-exon boundaries, and approximately 2 kb of the 5' and 3' UTR regions of this gene in 40 Mexican American subjects who were selected for having high or low forearm BMD. We identified 9 SNPs, as well as a novel deletion mutation in exon 2 that resulted in a nonsense mutation at amino acid position 27. After genotyping these SNPs in 887 Mexican Americans, we tested for associations of BMD of the forearm, spine, and hip, following adjustment for age, sex, BMI, and family structure. Significant, albeit modest, associations (p < 0.05) were observed between forearm BMD and SNPs rs12503796 and rs732245 under an additive genetic model. Three additional SNPs showed modest associations (p < 0.05) with BMD at either the forearm, hip, or spine under a dominant genetic model. The nonsense mutation was observed in 5 individuals from the same family and was not associated with variation in BMD. These findings suggest that sequence variation in *FGFBP1* may have a modest effect on osteoporosis.

Disclosures: **N. Hoppman**, None.

SU196

Osteoblastic Bone Forming Capacity Is Stimulated *In Vitro* by Metformin, an Anti-diabetic Drug. C. Sedlinsky^{*1}, V. Castro^{*2}, A. D. McCarthy^{*2}, L. Schurman^{*1}, A. Blanco^{*1}, A. M. Cortizo^{*2}. ¹Centro de Endocrinología y Metabolismo, Hospital Frances, Buenos Aires, Argentina, ²Catedra de Bioquímica Patológica, Facultad de Ciencias Exactas, Universidad Nacional de La Plata, La Plata, Argentina.

Metformin, an oral anti-hyperglycaemic agent, is widely used in the management of type 2 Diabetes mellitus and metabolic syndrome, although its mechanism of action is incompletely known. Recently rosiglitazone, an anti-diabetic PPAR- γ agonist, has been shown to promote commitment of osteoprogenitor cells to the adipocyte lineage while inhibiting osteoblastogenesis. In the present study, we evaluated the effects of metformin on the growth and differentiation of osteoblasts in culture. In addition, we investigated its possible mechanism of action. Two osteoblast cell lines (MC3T3E1 and UMR106) were examined for the ability to progress in the presence of different doses of metformin. 24 hours of culture with 25-500 μ M metformin significantly increased the proliferation (crystal violet bioassay) of both cell lines (p<0.05-0.01). Cell differentiation (alkaline phosphatase activity and type-I collagen production) was also stimulated in a dose-dependent manner by 25-500 μ M metformin (p<0.05-0.02). Alizarin red staining of mineralised nodules was greatly increased by 200-500 μ M metformin (120-290% basal, p<0.05-0.01). We assessed the possible involvement of extracellular-signal regulated kinase (ERK) in metformin action on osteoblastic cells. ERK phosphorylation (western immunoblot) was transiently increased by 1 mM metformin after 5-15 minutes incubation, but decreased to basal levels after 90 minutes. A similar temporal pattern was observed for P-ERK evaluated by immunofluorescence. Additionally, a transient translocation of P-

ERK was observed from cytoplasm to nuclei, showing a peak after 15 minutes incubation with metformin. These results show for the first time a direct osteogenic effect of metformin on osteoblasts in culture. These potentially bone-preserving effects of metformin could be particularly relevant in a clinical setting, in view of the deleterious side effects which other anti-diabetic drugs have on bone.

Disclosures: **C. Sedlinsky**, None.

SU197

Inhibitory Effect of (-)-Epigallocatechin Gallate on Titanium Particle-Induced TNF- α Release through Inhibition of MAP Kinase and AP-1/NF- κ B In RAW264.7 Cells. J. Shan^{*1}, J. Park^{*2}, J. Hong^{*2}, T. Kim^{*2}, J. Choi³, E. Park², S. Kim⁴. ¹Skeletal Disease Genome Research Center, Kyungpook National University Hospital, Daegu, Republic of Korea, ²Skeletal Diseases Genome Research Center, Kyungpook National University Hospital, Daegu, Republic of Korea, ³Department of Biochemistry, Kyungpook National University, School of Medicine, Daegu, Republic of Korea, ⁴Department of Orthopedic Surgery, Kyungpook National University Hospital, Daegu, Republic of Korea.

Macrophage activation by particulate debris from orthopaedic implants triggers an inflammatory response that ultimately leads to periprosthetic bone resorption and implant failure. Tumor necrosis factor- α (TNF- α) has been identified as a critical cytokine involved in the response to the debris particles but the mechanisms underlying activation of TNF- α synthesis by titanium (Ti) particle are unclear. Moreover, there is no drug that can effectively treat aseptic loosening in patients. In the present study we demonstrate an inhibitory effect of EGCG, a major component of green tea, on Ti particle-induced TNF- α release in murine macrophage and its underlying mechanism. As previously shown, Ti particles stimulated TNF- α release with a time and dose dependent manner and treatment of EGCG substantially suppressed TNF- α release. Ti particle induced activation of ERK and JNK as well as degradation of I κ B and specific inhibitors of JNK (SP600125) and NF- κ B (MG132) dramatically inhibited Ti-stimulated TNF- α release, suggesting that JNK and NF-B pathways are primarily involved in Ti particle-induced TNF- α release and that EGCG may suppress Ti particle-induced activation of JNK and degradation of I κ B in macrophages. In fact EGCG dramatically inhibited activation of JNK, degradation of I κ B and transcriptional activation of AP-1 and NF- κ B. Taken together, these results demonstrated that Ti particles induced TNF- α release is at least in part mediated through JNK/AP-1 as well as NF-B pathways and EGCG has an inhibitory effect on Ti particle-induced TNF- α release. Therefore, EGCG may be a potential candidate compound in the prevention and treatment of osteolysis and bone loosening after total joint arthroplasty.

Disclosures: **S. Kim**, None.

SU198

Osteoformin Accelerates Repair of Fresh Fracture in Rats. L. X. Bi, E. G. Mainous^{*}, Y. Zeng^{*}, W. L. Buford^{*}. Depts. of Surgery and Orthopaedics & Rehabilitation, The University of Texas Medical Branch, Galveston, TX, USA.

Our previous studies have shown that Osteoformin (negatively charged polypeptide) increases activity of alkaline phosphatase, expression of type-I collagen and BMP-7 and bone mineralization by human preosteoblast cells (Bi LX et al, JBMR 18: S212 Suppl. 2, 2003) and negatively charged resins increase bone formation and accelerate bone defect healing in vivo. In order to investigate potential effect of osteoformin on experimental femoral fracture healing in young male rats, femurs in anesthetized rats were stabilized with intramedullary pins and subjected to closed midshaft transverse fracture by bending to failure. In experimental rats (6 rats/group), fracture (Fx) sites were injected with 100ug of Osteoformin dissolved in 0.1 ml Phosphate buffered saline (PBS) at day 1 and day 7 postop, in controls (6 rats/group), Fx sites received 0.1 ml PBS at the indicated time above. Between 2 and 4 weeks post-Fx, animals were sacrificed and the healing femurs were removed for radiography and histology. Both forms of analysis indicated that Osteoformin treatment advanced Fx repair. In the Osteoformin treated group, histological study showed that the fracture gap was completely filled with newly formed cartilaginous tissue and woven bone two weeks after treatment, and was entirely replaced by woven bone at three weeks. Newly formed bone was partially transitioned from woven bone to lamellar bone at four weeks. In contrast, the control group showed newly formed bone only at the fracture ends, while the center of the fracture site was filled with fibrous tissue two weeks after the fracture. Cartilaginous tissue was seen at three weeks and woven bone was formed four weeks after the fracture. Radiographic assessment showed that the Osteoformin treated fractures had evidence of mineralized callus and blurring of the fracture gap as early as two weeks after treatment. By three weeks, the fracture ends were bridged with newly formed bone. By four weeks, the fracture line was no longer visible and remodeling callus was observed. In the control group, new bone formed only at the fracture ends, and the fracture gap was visible two weeks after the fracture. Although the fracture gap was blurring, the fracture line was still seen four weeks after the fracture. We conclude that Osteoformin stimulates the differentiation of osteoblast cells in vitro and accelerates femoral fracture healing in vivo.

Disclosures: **L.X. Bi**, None.

SU199

Canonical Wnt Signaling and Twist1 Repress Chondrogenesis and Chondrocyte Gene Expression. M. C. Naski, M. I. Reinhold*, R. Kapadia*. Pathology, University of Texas Health Science Center at San Antonio, San Antonio, TX, USA.

Wnt signaling is essential for many developmental processes including skeletogenesis. To investigate the effects of Wnt signaling during chondrogenesis we studied the effects of Wnt on cultured chondrocytic cells and differentiating limb bud mesenchyme. Wnt3a strongly repressed chondrogenesis and chondrocyte gene expression. The expression of type II collagen and aggrecan was strongly repressed and the development of cartilage was similarly inhibited. Canonical Wnt signaling was responsible for the repression of differentiation, as evidenced by results showing that inhibition of glycogen synthase kinase 3 or expression of β -catenin caused similar repression of differentiation and cartilage gene expression. Significantly, we showed that the transcription repressor Twist1 was induced by canonical Wnt signaling. We hypothesized that Twist1 was responsible for the inhibition of chondrocyte gene expression. Consistent with this, adenoviral transduction of Twist1 strongly inhibited aggrecan and type II collagen gene expression. Moreover, shRNA knockdown of Twist1 transcript levels increased the expression of aggrecan and type II collagen. We inferred that Twist1 indirectly repressed the chondrocyte gene expression and interestingly Twist1 interfered with BMP2-induced expression of aggrecan and type II collagen expression. Additionally, knockdown of Twist1 augmented BMP2-induced aggrecan and type II collagen expression. These data support the conclusion that Twist1 contributes to the repression of chondrogenesis and chondrocyte gene expression resulting from canonical Wnt signaling. In addition these results support a model whereby Twist1 inhibits chondrogenesis by interfering with BMP-dependent signaling.

Disclosures: *M.C. Naski, None.*

SU200

Efficacy of CP-533,536 a Selective EP2 Agonist of Prostaglandin E₂ in Oblique Canine Tibial Osteotomy. F. Borovecki*¹, D. D. Thompson², S. Vukicevic¹, V. M. Paralkar². ¹Laboratory for Mineralized Tissues, Zagreb Medical School, Zagreb, Croatia, ²Pfizer Central Research, Pfizer Inc., Groton, CT, USA.

Previously we have shown that CP-533, 536, an EP2 selective PGE₂ agonist, stimulates local bone formation and enhance bone healing in animal models. However, bone quality and mode of healing of newly formed bone were not fully determined. In this study we tested different modes of administration of CP-533,536, in an oblique dog osteotomy model to stringently asses its ability to accelerate bone healing at different bone compartments in 40 dogs. Poly-(D,L-lactide-co-glycolide) (PLGH) matrix alone or CP-533,536 dissolved in PLGH was administered at the defect site, either as a single application in the middle of the defect or the dose was split into two applications at the opposite ends of the osteotomy. The animals were divided into 5 groups, namely: (1) control (0.1 ml PLGH), (2) 1 mg CP-533,536 in 0.1 ml PLGH (single), (3) 1 mg CP-533,536 in 0.1 ml PLGH (split), (4) 0.1 mg CP-533,536 in 0.01 ml PLGH (single), (5) 0.1 mg CP-533,536 in 0.01 ml PLGH (split). Radiographic analysis of *in vivo* and following termination at 10 weeks revealed accelerated healing of animals treated with CP-533,536. In particular, animals treated with a 1 mg of CP-533,536 exhibited 85% (7/8) rate of healing when compared to control, showing that a single application is sufficient to achieve the maximum efficacy. CT analysis showed that animals treated with 0.1 ml of PLGH exhibited no endosteal ossification, with most of the bone formed periosteally. In animals treated with a single application of CP-533,536 abundant callus formation could be observed, with pronounced osteogenesis in all bone compartments, including periosteum, endosteal surface and the cortical bone of the fractures site. Non-destructive four point bending tests revealed that animals treated with 1 mg of CP-533,536 in a single dose exhibited the highest stiffness index and the area ratio, with mean values 1.3 and 1.9 fold, respectively, higher than in control dogs. Histological assessment confirmed the CT analysis, with CP-533,536 achieving new bone formation in all bone compartments. Normal fracture healing pattern was observed in all dogs treated with CP-533,536. The results collectively demonstrate the ability of CP-533,536 to accelerate bone healing in a canine model of oblique tibial osteotomy achieving superior bone quality in a single dose administration.

SU201

Bone Marrow of Multiple Myeloma Patients Provides an Environment Favoring Osteoclastogenesis. A. Huston¹, A. Lokshin*¹, G. Anderson*¹, S. Primeaux*², J. Anderson*¹, N. Callander*³, G. D. Roodman¹, S. Lentzsch*¹. ¹Hem/Onc, Univ. of Pittsburgh, Pittsburgh, PA, USA, ²UT-Health Science Ctr., San Antonio, TX, USA, ³Comprehensive Cancer Ctr., Univ. of Wisconsin, Madison, WI, USA.

The pathogenesis of multiple myeloma (MM) is believed to occur as a multistep transformation process. In addition to genetic alterations in MM cells, the bone marrow (BM) microenvironment contributes to the progression of myeloma through cytokines promoting the growth of myeloma cells and osteoclastogenesis. This study's aim was to investigate which cytokines, in the BM microenvironment, contribute to progression of MM and osteolytic lesions. BM plasma samples were evaluated for their cytokine expression profiles from 40 patients with MM and 40 normal controls. Supernatants were analyzed for IL-1 α , IL-1 β , IL-2, IL-4, IL-5, IL-6, IL-7, IL-8, IL-10, IFN α , IFN γ , GM-CSF, TNF α , IL-12p40, IL-13, IL-15, IL-17, MCP-1, MIP-1 α , MIP-1 β , EOTAXIN, RANTES, IP-10, MIG, TNF-R1, TNF-R2, DR5, EGF, VEGF, FGF β , G-CSF, HGF, EGFR, FASL, FAS, and Kallikrein 8 by LabMAP technology (Luminex). Cytokines differing

significantly between MM patient and control samples are listed in Table 1. Specific trends included IL-1 α and IL-6, which appeared to fall following autologous stem cell transplantation. IL-1 α , IFN α and VEGF trended towards lower levels with lower stage disease. A significant up-regulation of cytokines supporting osteoclastogenesis (Table 1, asterisk) and the soluble receptor of TNF-R1 and TNF-R2 were also observed.

Table 1. Significantly regulated cytokines from MM patients compared to normal controls.

Up-Regulated	P-value	Up-Regulated	P-value	Up-Regulated	P-Value
IL-1 α	p<0.01	IL-15	p<0.01	TNF-R1	p<0.01
*IL-6	p=0.02	*IL-17	p<0.01	TNF-R2	p<0.01
*IL-7	p=0.04	*MIP-1 β	p=0.04	EGF	p<0.01
*IL-8	p<0.01	RANTES	p<0.01	VEGF	p<0.01
IFN α	p<0.01	IP-10	p<0.01	HGF	p<0.01
IL-12p40	p<0.01	MIG	p<0.01		
Down-Regulated					
IL-5	p<0.01				

Cytokine array analysis represents a powerful method for characterizing the microenvironment of MM. Our data shows that the bone marrow microenvironment in MM supports the growth of myeloma cells, angiogenesis, and osteoclastogenesis, through multiple cytokines simulating these processes. In contrast to prior studies using peripheral blood and individual ELISA kits, our results represent a more accurate reflection of the scope of cytokine dysregulation in the BM of MM patients. To our knowledge, this is the first time a comprehensive analysis of the cytokine regulation of MM patients and disseminated bone disease has been done. Therefore, it provides a framework for future areas of investigation in further defining the role of cytokines in the BM microenvironment of MM.

Disclosures: *A. Huston, None.*

SU202

In Vitro Osteogenic Response of Rat Bone Marrow Cells to bFGF and BMP-2 Treatments. M. Varkey*¹, C. Kucharski*¹, T. Haque*¹, W. Sebald*², H. Uludag³. ¹Department of Chemical & Materials Engineering, Faculty of Engineering, University of Alberta, Edmonton, AB, Canada, ²Theodor-Boveri-Institut für Biowissenschaften, Universität of Würzburg, Würzburg, Germany, ³Department of Chemical and Mat. Engineering, Dept. of Biomedical Engineering, Faculty of Medicine, University of Alberta, Edmonton, AB, Canada.

To explore the use of bFGF and BMP-2 for systemic therapy in osteoporosis, their *in vitro* effects on bone marrow cells (BMC) which are the primary target of growth factor therapy *in vivo*, were investigated. The osteogenic effects of bFGF and BMP-2 on BMC in culture were directly compared, and the effects of cell source (young and old rats) and duration of growth factor exposure on induced osteogenic parameters were evaluated. The relative potencies of these prototypical growth factors to achieve the desired osteogenic response in BMC were assessed by monitoring the changes in two well established osteogenic markers, alkaline phosphatase (ALP) activity and mineralization. BMC were obtained from young (8 weeks) and adult (34 weeks) female Sprague-Dawley rats by femoral aspiration, expanded *in vitro*, and exposed to osteogenic medium containing known concentrations of growth factors (0-50 ng/mL bFGF and 0-500 ng/mL BMP-2). The cells were treated with BMP-2 and bFGF either continuously for 3 weeks, or for a short duration of 1 week followed by 3 weeks of culture in osteogenic medium with no growth factors, and the osteogenic response was investigated in both cases. Cells were harvested after 1, 2 and 3 weeks of continuous growth factor treatment or after 1, 2 and 3 weeks of the removal of the growth factors, for the short growth factor treatment. Quantitative measures of DNA content, ALP activity and calcification were obtained, and the results statistically analyzed by ANOVA (p<0.05). Results suggested that both bFGF and BMP-2 were osteogenic and were capable of stimulating mineralization under select set of culture conditions, but significant differences in their effects were evident. Irrespective of the duration of exposure, a clear dose-response was consistently obtained for BMP-2, with progressively higher levels of mineralization upto 500 ng/mL. Interestingly, although bFGF effects were evident even at ~ 10 ng/mL, on continuous treatment, no significant effects on short-time exposure was observed. The extent of mineralization of BMC varied with the source of the cells, it being significantly lower for old rats than for young rats. Interestingly, a synergistic effect of lower doses of BMP-2 on bFGF responses was observed on BMC from the old rats, but not from the young rats. In conclusion, although bFGF was more potent for stimulating osteogenic parameters, BMP-2 effects were more lasting on the BMC.

Disclosures: *M. Varkey, None.*

SU203

ELR⁺ CXC Chemokine Secretion during Human Mesenchymal Stem Cell Osteogenic Differentiation Is Dependent on Dexamethasone. D. S. Bischoff*, N. S. Makhijani*, J. H. Zhu*, D. T. Yamaguchi. Research Service, VA Greater Los Angeles Healthcare System, Los Angeles, CA, USA.

The potential role of ELR⁺ CXC chemokines in early events in bone repair was studied using human mesenchymal stem cells (hMSCs). Inflammation, which occurs in the initial phase of tissue healing in general, is critical to bone repair. Release of cytokines from infiltrating immune cells and injured bone can lead to recruitment of MSCs to the region of repair. CXC chemokines bearing the glu-leu-arg (ELR) motif are also released by inflammatory cells and serve as angiogenic factors stimulating chemotaxis and proliferation of endothelial cells. hMSCs, induced to differentiate with osteogenic medium (OGM) containing ascorbate, β -glycerophosphate (β -GP), and dexamethasone (DEX), showed an increase in mRNA and protein secretion of the ELR⁺ CXC chemokines IL-8

and GRO α . At day 7, OGM induces significant increases in both IL-8 mRNA expression (65 ± 11 vs. 0.05 ± 0.01 relative units) and IL-8 secretion (9089 ± 494 vs. 79 ± 10 pg/ml). GRO α also had significant increases in mRNA expression (3.8 ± 1.1 vs. 0.18 ± 0.05) and protein secretion (12257 ± 865 vs. 18.5 ± 1.2 pg/ml). This increased expression/secretion is a result of DEX in the OGM. hMSCs cultured in media containing DEX alone had a relative expression level of IL-8 mRNA at 185 ± 0.15 ($P < 0.001$) at Day 10, significantly higher than cultures containing ascorbate alone (0.73 ± 0.25 ; $P > 0.05$), β -GP alone (2.5 ± 0.9 ; $P > 0.05$), or in non-OGM media (1.1 ± 0.15). IL-8 secreted into the media also increased from 212 ± 62 (non-OGM media) to 847 ± 78 pg/ml ($P < 0.001$) for DEX, whereas ascorbate (108 ± 31 ; $P > 0.05$), or β -GP-containing media (195 ± 55 ; $P > 0.05$) did not significantly alter protein levels. GRO α gave similar patterns of mRNA expression and protein secretion in the DEX-containing cultures. Experiments were conducted three times in triplicate. Values are mean \pm SD of one representative experiment. RNA interference by transient expression of IL-8 siRNA could inhibit expression of IL-8 as determined by real-time RT-PCR. This effect was short-lived and did not have any effect on alkaline phosphatase mRNA, a marker of osteogenic differentiation. To test the ability of IL-8 inhibition to affect later differentiation events, an adenovirus has been constructed that expresses the IL-8 siRNA providing long-term suppression of IL-8 production by hMSCs. Conclusions: 1) hMSCs are induced to produce CXC chemokines, IL-8 and GRO α , when stimulated towards osteogenic differentiation; 2) DEX is the component in OGM responsible for the stimulation of IL-8 and GRO α mRNA and protein; 3) short-term suppression of IL-8 production in hMSCs can be accomplished using siRNA technology.

Disclosures: **D.S. Bischoff**, None.

SU204

Nell-1 Induced Bone Formation, Fusion, and Regeneration. C. M. Cowan^{*1}, T. Aghaloo^{*2}, Y. Chou^{*1}, X. Zhang^{*2}, C. Soo^{*3}, B. Wu^{*1}, K. Ting². ¹Bioengineering, UCLA, Los Angeles, CA, USA, ²Dental and Craniofacial Research Institute, UCLA, Los Angeles, CA, USA, ³Divisions of Plastic and Reconstructive Surgery, USC, Los Angeles, CA, USA.

Researchers in the developing field of regenerative medicine have identified bone tissue engineering as an attractive translational target. The discovery of Nell-1 (a protein strongly expressed in neural tissues and containing EGF-like domains, type 1) in craniosynostosis presents a potential for bone growth in other acquired and congenital craniofacial deformities. The purpose of these studies was to further elucidate the ability of Nell-1 to accelerate bone regeneration within the calvaria. The methods for these experiments were as follows: biodegradable PLGA scaffolds were coated with 200 ng of recombinant rat (rr)Nell-1 or recombinant human bone morphogenetic protein-2 (rhBMP-2) and implanted into 3 mm full-thickness calvarial defects in Sprague-Dawley rats. All animals were handled in accordance with guidelines of the Chancellor's Animal Research Committee of the Office for Protection of Research Subjects at our institution. Rats were sacrificed after 1, 2, or 4 weeks and examined by microCT. Area quantifications were performed using software BioQuant. Ten micron thick paraffin-embedded sections were examined histologically. The data clearly demonstrate that after 4 weeks of healing, Nell-1 ($97\% \pm 3\%$) and BMP-2 ($93\% \pm 8\%$) implanted defects reached near 100% closure, while control ($54\% \pm 16\%$) defects were only minimally healed. Additionally, live imaging revealed increasing bone mineralization over a 12 week time period. Trichrome staining demonstrated mature bone within defects, while BSP indicated accelerated osteogenic differentiation. In conclusion, calvarial defect healing can be augmented by growth factors, as their delivery can provide the necessary environmental cues for cellular migration, proliferation, and differentiation; creating a suitable niche for bone regeneration. Nell-1 and BMP-2 are both known to induce bone formation *in vivo*; however, the transition from animal studies into clinical studies has been only mildly successful with BMP-2. The ability of Nell-1 and BMP-2 to accelerate bone formation may relate to their ability to influence cells out of a proliferative phase and into a differentiated phase. Nell-1's ability to accelerate calvarial bone regeneration, equivalent to BMP-2, may provide an alternative non-BMP-based paradigm for the study of calvarial bone healing and future tissue engineering studies. Thus, grafting Nell-1 coated scaffolds into calvarial defects has pharmacological value and reveals alternatives to currently accepted techniques for bone regeneration.

Disclosures: **C.M. Cowan**, None.

SU205

The Role of Adiponectin in Bone Remodeling. J. E. Reseland¹, M. V. Tamburstuen^{*1}, H. S. Berner^{*1}, A. K. Stunes^{*2}, G. Kvalheim^{*3}, L. Thommesen^{*4}, S. P. Lyngstadaas^{*1}, U. Syversen⁴. ¹Oral Research Laboratory, University of Oslo, Oslo, Norway, ²Department of Cancer Research and Molecular Medicine, University of Oslo/University of Science and Technology, Trondheim, Norway, ³Department of Oncology, The Norwegian Radium Hospital, Oslo, Norway, ⁴Department of Cancer Research and Molecular Medicine, University of Science and Technology, Trondheim, Norway.

We have previously demonstrated the expression of adiponectin in bone forming cells. Although recombinant adiponectin do stimulated osteoblast proliferation, the role of adiponectin in bone metabolism and maintenance remains largely unknown. We aim at describing the relationship between adiponectin and mechanical properties of bone, and characterizing possible autocrine and paracrine effects of adiponectin on osteoblasts and osteoclasts. Bone mineral density (BMD) was measured by DXA scanning in intact female Fisher-344 rats. Bone biomechanical data were recorded, and RNA was isolated from femur. The effect of adiponectin was tested on primary human osteoblasts, bone marrow stem cells, and osteoclasts (differentiated from peripheral mononuclear cells) from different donors, and on RAW 264.7 cells. There was no significant relationship between

plasma adiponectin levels, BMD and bone biomechanical properties observed in these rats. In contrast, the relative expression of adiponectin mRNA in femur correlated positively to ultimate bending moment, ultimate energy absorption and deflection. However, a negative correlation to bending stiffness was observed. When compared to untreated cells, recombinant adiponectin acutely stimulates adiponectin mRNA expression, as well as leptin mRNA expression and leptin secretion to the medium after 6 hours incubation. Recombinant adiponectin enhanced the differentiation of human peripheral monocytes into osteoclasts ($p < 0.004$) and activates ($p < 0.001$) the promoter of NF- κ B in transfected RAW 264.7 cells. Adiponectin stimulates proliferation, but only minor effects were observed on osteoblast differentiation and the expression of markers involved in osseoid mineralization. Based on our observations adiponectin may play a role in regulating elasticity and flexibility of the bones, by regulating recruitment and differentiated endpoint of cells involved in bone remodelling.

Disclosures: **J.E. Reseland**, None.

SU206

Early Response of Circulating Osteoprotegerin in Patients Treated with Zoledronic Acid. R. A. Hannon¹, D. Santini^{*2}, B. Vincenzi^{*2}, G. Tonini^{*2}, L. Holen^{*3}. ¹Academic Unit of Bone Metabolism, University of Sheffield, Sheffield, United Kingdom, ²Clinical Oncology, University Campus Bio-Medico, Rome, Italy, ³Clinical Oncology, University of Sheffield, Sheffield, United Kingdom.

Bisphosphonates, including zoledronic acid, have been shown to stimulate osteoprotegerin (OPG) expression in primary human osteoblasts¹. Early response of circulating OPG to bisphosphonates has not been observed *in vivo*. The aim of this study was to investigate the response, including the very early response, of plasma OPG and the bone resorption marker C terminal crosslinked telopeptides of Type I collagen (β CTX) to zoledronic acid in patients with metastatic bone disease. Twenty four patients (9 males, 15 females), aged 44-76 years (median age, 65), with advanced solid cancer and bone metastases, who had not been previously treated with bisphosphonate, were infused with a single infusion of 4mg zoledronic acid in 100 ml of 0.9% saline over a period of 15 minutes. Exclusion criteria were any steroid therapy, radiotherapy, chemotherapy or haemopoietic growth factors during the study or in the 4 weeks prior to the study. Blood samples were collected before 10.00 after an overnight fast at baseline, prior to infusion, and on days 1,2,7 and 21 after infusion. Plasma was stored at -80 deg C until analysis. Plasma levels of β CTX were measured by electrochemiluminescent assay (Roche Elecsys, Roche Diagnostics GmbH, Penzberg, Germany). Plasma levels of OPG were measured by ELISA (BioVendor Laboratory Medicine Inc, Brno, Czech Republic). All samples from an individual were measured in the same analytical batch. Table shows median change in OPG and β CTX

Day	OPG median % change from baseline (CI)	p*	β CTX median % change from baseline (CI)	p*
1	+12.8 (-8.6, +20.6)	0.057	-67.1 (-76.3, -52.4)	<0.0001
2	+11.6 (-1.5, +38.9)	0.010	-85.7 (-90.2, 78.2)	<0.0001
7	-2.6 (-7.2, +8.5)	0.900	-79.2 (-87.0, -67.4)	<0.0001
21	-2.7 (-13.6, +9.3)	0.807	-76.9 (-83.4, -35.0)	<0.0001

*Signed rank test vs baseline

At day 1, but not at the other timepoints, percentage change in OPG was inversely correlated with percentage change in β CTX ($r = -0.44$, $P < 0.05$). We conclude that the early response of plasma OPG to zoledronic acid may indicate a direct action of zoledronic acid on osteoblasts to stimulate OPG production which, in turn may contribute to the suppression of osteoclast activity and bone resorption.

¹Viereck V, Emons G, Lauck V et al. Biochem Biophys Res Commun 2002; 291:680-686

Disclosures: **R.A. Hannon**, None.

SU207

Interleukin-4 and Interleukin-13 Inhibit Osteoclast Formation and Bone Resorption by Increasing OPG and Decreasing RANKL and RANK in a STAT-6 Dependent Pathway. P. Palmqvist^{*1}, P. Lundberg^{*1}, E. Persson^{*1}, A. Johansson^{*2}, I. Lundgren^{*1}, A. Lie^{*1}, H. H. Conaway³, U. H. Lerner¹. ¹Department of Oral Cell Biology, Umeå University, Umeå, Sweden, ²Department of Periodontics, Umeå University, Umeå, Sweden, ³Department of Physiology and Biophysics, University of Arkansas for Medical Sciences, Little Rock, AR, USA.

Interleukin-4 (IL-4) and interleukin-13 (IL-13) are cytokines which inhibit bone resorption. In the present study we studied molecular mechanisms in osteoclasts and osteoblasts by which IL-4 and IL-13 inhibit bone resorption. We found that release of ⁴⁵Ca from cultured mouse calvarial bones stimulated by different cytokines, peptides and steroid hormones was inhibited by both IL-4 and IL-13. The effect could not be attributed to inhibition of prostaglandin formation since stimulation by several agonists, the effect of which was not inhibited by indomethacin, was inhibited by IL-4 and IL-13. IL-4 and IL-13 decreased receptor activator of nuclear factor- κ B ligand (RANKL) and RANK mRNA expression and increased osteoprotegerin (OPG) mRNA expression in mouse calvariae. In agreement with the mRNA data, IL-4 and IL-13 decreased RANKL protein and increased OPG protein in calvarial bones. In osteoblasts isolated from calvariae, both an increase in RANKL mRNA and a decrease in OPG mRNA and protein elicited by D3 were reversed by IL-4 and IL-13. IL-4 and IL-13 decreased the number of tartrate resistant acid phosphatase (TRAP) positive multinucleated cells and the mRNA expression of calcitonin receptor, TRAP and cathepsin K in mouse spleen cells and bone marrow macrophages (BMM) treated with M-CSF/RANKL. Inhibition of mRNA for RANK and the transcription factor NFAT2 was also noted in spleen cell cultures following treatment with

ASBMR 27th Annual Meeting

IL-4 and IL-13. In addition, RANK mRNA and formation of RANK protein were decreased by IL-4 and IL-13 in RAW 264.7 cells. Mouse calvarial osteoblasts and spleen cells expressed mRNA for the four proteins making up the IL-4 and IL-13 receptors and the expression levels were regulated by D3 and M-CSF/RANKL. The data indicate that IL-4 and IL-13 can inhibit osteoclast differentiation and bone resorption by affecting the RANKL/RANK/OPG system. In addition to activating receptors in osteoclasts and decreasing RANK formation, IL-4 and IL-13 activate receptors in osteoblasts, causing decreased RANKL formation and increased OPG formation. The effects of IL-4 and IL-13 on mRNA expression of RANKL and bone resorption in mouse calvarial bones as well as osteoclast formation in mouse spleen cell cultures were dependent on STAT6, since no effects were seen in cells from STAT6^{-/-} mice.

Disclosures: **P. Palmqvist**, None.

SU208

Activation of the Oncostatin M Receptor Results in Substantially More Effective Stimulation of Bone Resorption, RANKL and IL-6 mRNA Expression, and STAT3 Activation, Compared to the Leukemia Inhibitory Factor Receptor. **E. Persson***, **U. H. Lerner**. Oral Cell Biology, Umea University, UMEA, Sweden.

The members of the interleukin-6 (IL-6) family are pleiotropic cytokines, often inducing overlapping actions. In mouse tissues, murine and human leukemia inhibitory factor (mLIF and hLIF, respectively), and human oncostatin M (hOSM), all exert their effects through the LIF receptor (LIFR), whereas murine OSM (mOSM) signals through the OSM receptor (OSMR). In the present study, the effects of LIF and OSM on bone resorption, mRNA expression of IL-6, RANKL and OPG, as well as IL-6 promoter induction have been investigated. Both mLIF and mOSM concentration-dependently stimulated ⁴⁵Ca release in mouse calvarial bones, OSM being about 3-4 times more effective than LIF. Furthermore, treatment with mLIF or mOSM for 48 h resulted in increased IL-6 and RANKL mRNA expression in mouse calvarial osteoblasts, as assessed by PCR. The effects were concentration-dependent, with OSM being a substantially more effective stimulator of both IL-6 and RANKL mRNA expression. In contrast, neither mLIF nor mOSM caused any regulation of OPG mRNA expression in calvarial osteoblasts. In cells from the osteoblastic cell line MC3T3-E1 transfected with a fragment (-225 to +13) of the human IL-6 promoter coupled to a luciferase reporter, human and murine LIF and OSM all stimulated IL-6 promoter induction as assessed by luciferase activity. Treatment with mOSM resulted in about 10-fold higher luciferase activity compared to mLIF, hLIF, and hOSM. To investigate possible explanations for the differences between mOSM and mLIF, we studied the mRNA expression of LIFR and OSMR, and the activation of the transcription factor STAT3 that mediates the effects of both receptors. Murine OSM clearly increased the OSMR mRNA level in calvarial osteoblasts, and the effect was present from 1 h up to at least 72 h of incubation compared to control cells. Furthermore, the stimulatory effect was specific for OSM since incubation with IL-11, IL-6 + soluble IL-6R, PTH or vitamin D3 did not result in any regulation of OSMR mRNA levels. Treatment with LIF did not result in any regulation of neither OSMR nor LIFR mRNA levels. Incubation of calvarial osteoblasts with mLIF or mOSM resulted in activation of STAT3, OSM treatment resulting in a more prominent activation as assessed by Western blot for the phosphorylated form of STAT3. These data show that both LIF and OSM stimulate bone resorption in mouse calvariae, and that stimulation of IL-6 and RANKL expression are downstream effects of the LIF and OSM receptors. Signaling through the OSM receptor is substantially more effective, with specific autostimulation of the receptor by mOSM being one possible explanation.

Disclosures: **E. Persson**, None.

SU209

Regulation of SOST Expression by Osteotropic Factors in Calvaria Organ Culture. **H. Keller**, **H. Jeker***, **A. Studer***, **J. Wirsching***, **M. Kneissel**. Bone & Cartilage Unit, Novartis Institutes for BioMedical Research, Basel, Switzerland.

SOST is an osteocyte-expressed potent negative regulator of bone formation and a putative bone morphogenetic protein (BMP) antagonist. Recently, we have shown that SOST expression is regulated by parathyroid hormone (PTH) in bone. SOST was down-regulated during PTH-induced bone formation *in vivo*. Consistent with this finding, PTH suppressed SOST expression in calvaria organ culture *in vitro*. Now, we have further analyzed SOST regulation by various factors impacting on bone metabolism using quantitative real-time RT-PCR (qPCR) in calvaria culture, since this well established bone organ culture system offers a relevant model to study an osteocyte-expressed factor *in vitro*. Similarly to PTH, transforming growth factor β 1 (TGF β 1), basic fibroblast growth factor (bFGF), platelet-derived growth factor (PDGF) and vitamin D3 (VitD3) strongly reduced SOST expression in cultured calvaria of newborn mice after 24h treatment. In contrast and in line with published data, BMP-2, -5, -6, and -7 stimulated SOST expression several-fold. Steroid hormones and prostaglandin E2 (PGE2) did only weakly or not regulate SOST expression: dexamethasone and 17 β -estradiol weakly induced, while progesterone, dihydro-testosterone and PGE2 only marginally regulated SOST expression. The relatively minor impact of sex hormones on SOST expression in calvaria organ culture is in line with our observation that estrogen status has no impact on *in vivo* SOST expression in rats as opposed to regulation by PTH. We proceeded to analyze SOST expression during TGF β 1 or BMP-2 induced *in vitro* bone formation. Stimulation of bone formation was assessed by histology. In addition, expression of the bone formation marker genes alkaline phosphatase (ALP) and osteocalcin (OSC) was determined. Compared to freshly dissected calvaria, SOST expression decreased about 80% during the 24h pre-incubation period, but regained initial levels after three day culturing. TGF β 1 increasingly repressed SOST expression over the three day monitoring period. BMP-2 induced SOST

expression at day one, but the induction was lost at day three compared to control levels. ALP was not regulated by any treatment, but OSC was strongly decreased during pre-incubation by about 90% and in contrast to SOST expression continued to decrease in control cultures reaching about 100-fold down-regulation. TGF β 1 treatment led to almost complete extinction of OSC expression, while BMP-2 had no impact. In summary, calvaria organ culture experiments demonstrate differential regulation of SOST by TGF β 1, BMPs and other osteotropic factors providing further evidence for an important role of this osteocyte-expressed factor in bone metabolism.

Disclosures: **H. Keller**, None.

SU210

Leptin Inhibits Bone Formation and Controls Bone Mass not only in Rodents, but also in Sheep. **P. Pogoda***¹, **J. C. Schnell***¹, **M. Egermann***², **M. Priemel**¹, **A. F. Schilling**¹, **M. Alini***², **J. M. Rueger***¹, **S. Thorsten**¹, **E. Schneider***², **I. Clarke***³, **M. Amling**¹. ¹Trauma Surgery, Hamburg University School of Medicine, Hamburg, Germany, ²AO Research Institute, Davos, Switzerland, ³Department of Physiology, Monash University, Melbourne, Australia.

Genetic studies in mice have identified leptin as a potent inhibitor of bone formation acting through the central nervous system and unravelled the central nature of bone mass control and its disorders. Although these studies have radically enhanced our understanding of skeletal physiology as they have established a hypothalamic regulation of bone remodeling via the sympathetic nervous system, controversy remains about the physiological relevance of these observations as leptin's effect on bone after intracerebroventricular application have only been demonstrated in mice. In addition, the conflicting reports on bone mass in leptin-deficient ob/ob mice and leptin-deficient fa/fa rats have further questioned whether leptin has a role in regulating bone mass beyond rodents. To address this question we have treated ewe by long term intracerebroventricular application (icv) of leptin and analyzed the bone phenotype after a period of 3 month of treatment. Three groups of corriedale sheep (n=16) were compared (i) control entire (entire), (ii) ovx and icv application of cerebrospinal fluid (csf), and (iii) ovx and icv application of leptin (leptin). Analysis included histomorphometric characterization of iliac crest, spine and femur by histology and microcomputed tomography as well as measurement of bone turnover parameters in serum and urine. Indeed, central application of leptin decreased both bone formation by 70% and mineralizing surface (MS/BS 39.4 \pm 3.3% vs. 16.1 \pm 2.1%) significantly (p<0.01). While ovariectomy increased osteoclast indices and urinary crosslap excretion by 2- and 3-time respectively, serum parameters (bone alkaline phosphatase and osteocalcin) of osteoblast activity were significantly reduced by icv application of leptin (p<0.01). Consequently ewe treated with leptin were highly osteopenic (iliac crest BV/TV entire 22.7 \pm 1.3% vs. csf 18.9 \pm 2.4% vs. leptin 12.4 \pm 2.6%) after 3 month of treatment (p<0.01). Taken together, these data suggest that leptin controls bone formation via a hypothalamic relay leading to osteopenia in sheep. Most importantly however, they demonstrate that the central regulation of bone formation is not limited to rodents, but also found in large animals confirming that bone remodeling in vertebrates is centrally controlled.

Disclosures: **P. Pogoda**, None.

SU211

Relationships of Serum Leptin and Adiponectin Concentration with Bone Mineral Density in Korean Postmenopausal Women. **D. Byun**, **J. Mok***, **K. Lee***, **Y. Kim***, **H. Park***, **C. Kim***, **S. Kim***, **K. Suh***, **M. Yoo***. Endocrinology, Soonchunhyang University Hospital, Bucheon-si, Republic of Korea.

Overweight is associated with both higher fat mass and higher bone mineral density (BMD). Leptin is synthesized and secreted by adipocytes and serum concentrations are highly correlated with fat mass. It has been suggested that leptin levels may play a mediating role in maintaining bone mass. Unlike other adipokines such as leptin, adiponectin levels decrease in obesity. The purpose of this study was to investigate associations of serum leptin and adiponectin with BMD. We measured the bone markers, serum leptin, adiponectin level and bone mineral density (BMD) in 33 Korean postmenopausal women. Serum leptin level was significantly increasing associated with weight and body mass index (BMI) (r=0.69, p=0.0001 and r=0.78, p=0.0001 respectively), while serum adiponectin level was not changing. Serum leptin and adiponectin levels were not correlated with alkaline phosphatase level, urine N-telopeptide, lumbar BMD and femoral BMD. Only femoral BMD was decreased following by serum adiponectin levels but it was not significant (r=-0.31, p=0.08). These results suggested that serum leptin and adiponectin concentrations did not appear to affect directly BMD in Korean postmenopausal women.

Disclosures: **D. Byun**, None.

SU212

Bone Loss in the Femur but not the Spine Is Attenuated in Lactating Interleukin-1 Receptor 1 Deficient Mice. J. N. VanHouten^{*1}, J. Kalinowski^{*2}, J. J. Wysolmerski¹, J. A. Lorenzo². ¹Endocrinology, Yale University, New Haven, CT, USA, ²Medicine, University of Connecticut Health Center, Farmington, CT, USA.

Lactation is associated with the transient loss of significant amounts of bone from the maternal skeleton. Previous studies have shown that estrogen-deficiency is an important component of lactational bone loss in mice. Interleukin-1 (IL-1) is an inflammatory cytokine with osteoclastogenic properties. In addition, IL-1R1-/- mice, which lack the bioactive receptor for IL-1, are protected from the bone loss that occurs after ovariectomy. This finding suggests that IL-1 is an important mediator of the bone loss that occurs with estrogen deficiency. In order to examine if IL-1 might similarly contribute to bone loss during lactation, we first examined circulating levels of IL-1 α , IL-1 β , and IL-1ra in nulliparous and lactating wild-type mice. None of these cytokines was elevated during lactation, suggesting that any actions of IL-1 in this model would be autocrine or paracrine within the skeleton. To examine this possibility, we studied lactating IL-1R1-/- mice and wild-type (WT) littermate controls. Total body bone mineral density (BMD), spinal BMD and vertebral BMD were measured by DEXA. Mice were examined 3 and 10 days postpartum. Dams were of equivalent age and litter sizes were adjusted to be similar between groups. We found that lactation decreased total body and spine BMD at similar rates in IL-1R1-/- and WT mice. However, bone loss at the femur was attenuated in IL-1R1-/- mice as compared to controls. Femoral BMD in WT controls declined by 13.7 +/- 0.7 % between day 3 and 10 of lactation, while BMD declined by only 9.6 +/- 1.3 % (30% less) in the IL-1R1-/- dams (p<0.02). Circulating concentrations of biochemical markers of bone formation (osteocalcin) and bone resorption (urine CTX) were similar in WT and IL-1R1-/- mice, suggesting that rates of bone turnover were similar despite the loss of IL-1 signaling. Finally, levels of serum calcium, PTH, urine calcium and milk calcium were not significantly different in lactating IL-1R1-/- mice as compared to controls. These data demonstrate that IL-1 signaling has only minor, site-specific effects on bone loss induced by lactation in mice. Furthermore, these results suggest that the downstream mediators of bone loss due to lactation are fundamentally different than those that mediate the effects of estrogen withdrawal in ovariectomized mice.

Disclosures: **J.N. VanHouten**, None.

SU213

Long-Term Serotonin Administration Affects Cortical Bone Architecture and Increases Bone Mineral Density in Rats. B. I. Gustafsson^{*1}, L. Westbroek^{*1}, E. Waarsing^{*2}, L. Thommesen^{*1}, K. Stunes^{*1}, H. Waldum^{*1}, H. van Leeuwen^{*2}, H. Weinans^{*2}, U. Syversen¹. ¹Cancer Research and Molecular Medicine, NTNU, Trondheim, Norway, ²Internal Medicine and Orthopaedics, Erasmus MC, Rotterdam, The Netherlands.

Recently, more and more evidence is found for a control of bone mass by the central nervous system. Many studies indicate a role for the nervous system in embryonal skeletal development, during fracture healing, and during remodelling after insertion of implants. We have previously shown functional serotonin receptors in bone cells and a stimulatory effect of serotonin on proliferation of osteoblast precursor cells. In this study we investigated the effects of serotonin on bone metabolism *in vitro* and *in vivo*. Murine preosteoblasts (MC3T3-E1) were treated with serotonin and OPG and RANKL release were measured. We also investigated if osteoblasts and osteoclasts express tryptophan hydroxylase (Tph) mRNA. Two months old female Sprague-Dawley rats were treated with daily subcutaneous serotonin injections (5mg/kg) for 3 months. DXA scans were made after two and three months of treatment. We further investigated bone architecture and mechanical properties by μ CT and mechanical testing. Serotonin induced OPG and inhibited RANKL release from murine preosteoblasts. Murine osteoblasts as well as murine (RAW 264.7) and human osteoclasts expressed Tph, the rate-limiting enzyme in serotonin synthesis. Despite a significant decrease in body weight, total body BMD was significantly increased in the treated animals after two and three months. μ CT analysis of femurs after 3 months of treatment showed significantly increased cortical thickness, while trabecular bone volume was significantly decreased. Interestingly, the perimeter and cross-sectional moment of inertia (MOI), a proxy for geometrical bone strength, were the same in both groups. These data suggest a reduced endosteal bone resorption in serotonin treated animals. The mechanical testing showed that bone stiffness was increased in serotonin treated animals whereas the strength remained unchanged. In conclusion, serotonin treatment seems to decrease endosteal bone resorption, leading to an increase in BMD and cortical bone thickness, and a decrease in trabecular bone volume. These effects may be mediated through a serotonin induced increase in OPG/RANKL ratio. We also find that bone cells express Tph, indicating that they are capable to produce serotonin. Our study shows that serotonin has important effects on bone metabolism.

Disclosures: **B.I. Gustafsson**, None.

SU214

AC-100, a Fragment of MEPE, Promotes New Bone Formation via Enhanced PGE2 Production and Cell Binding to Matrix Proteins. C. A. Middleton-Hardie¹, S. Aswani^{*1}, D. M. Rosen¹, M. S. Shih^{*2}, R. Leininger^{*2}, M. Lazarov¹. ¹Acologix, Hayward, CA, USA, ²Skeletech, Bothell, WA, USA.

MEPE, a protein originally cloned from tumours associated with hypophosphatemic osteomalacia, increases renal phosphate excretion and is expressed in normal human bone and odontoblast cells. AC-100 (Dentonin), a central 23-amino acid fragment of MEPE, contains motifs important in regulating cell activities in the bone and dentin microenvironment and has demonstrated potent anabolic activity on osteoblast and odontoblast precursor cells *in vitro*. *In vivo* studies in rodents indicate AC-100 is able to stimulate new dentin formation in teeth, and bone formation at fracture healing sites. Previous studies have implicated COX2 involvement in AC-100 induced proliferation of hMSC cells (1). Here we report the activity of AC-100 is associated with induction of the bone anabolic factor PGE2, increased production of matrix proteins and upregulation of integrin binding. **Methods** Hemi-calvariae from neonatal mice were incubated in the presence of AC-100, BMP2 or media alone. AC-100 was added to the media daily for seven days. Samples of the conditioned media were collected on days 2 - 8 for analysis of anabolic factors. At day 8 the hemicalvariae were embedded in paraffin and sectioned. The sections were analysed using a qualitative scoring system for osteoblast surface, cell density and new bone growth (0-4). **Results** AC-100 significantly increased new bone formation, bone cell density and osteoblast surface with levels comparable to the BMP2 treated group. The optimum AC-100 dose was 10 μ g/mL. Analysis of the conditioned media samples showed that AC-100 potently induces PGE2 production in a dose dependent manner. The optimal AC-100 dose for new bone formation induced a 5-fold increase in PGE2 production. AC-100 also induced modest increases in TGF β -1 and fibronectin production but does not stimulate BMP2 production. Analysis of hMSC with the CytoMatrix Screen Kit (Chemicon) demonstrated that AC-100 not only induced the production of fibronectin but also increased the binding of hMSC to different matrices (laminin, fibronectin, vitronectin and collagen). This increased binding was accompanied by upregulation of β 1, β 2, β 3 and β 4 integrin binding but not β 6 or α V β 5 integrin binding as assayed by the Beta-integrin-mediated cell adhesion array (Chemicon). **Conclusion** This study indicates the bone anabolic activity of AC-100 is strongly connected to the induction of PGE2 production and the stimulation of cell binding to matrix proteins. These results reinforce the findings of previous studies where AC-100 has been shown to increase proliferation of hMSC cells via induction of COX2 (1).

(1) DE Nagel et al., J Cell Biochem 2004, 93(1107-14)

Disclosures: **C.A. Middleton-Hardie**, Acologix 3.

SU215

Intracellular Fate of Plasmid DNA and Non-Viral (Polymeric) Carriers in Bone Marrow Stromal Cells. H. Uludag^{*}, L. Farell^{*}, B. Acan^{*}, W. Hu^{*}, C. Kucharski^{*}. University of Alberta, Edmonton, AB, Canada.

Non-viral methods to transform Bone Marrow Stromal Cells (BMSC) are advantageous over the viral vectors, since non-viral carriers do not integrate into cellular genome, and they cannot transform the target cells. Polymeric non-viral vectors function by binding to a desired DNA sequence, condensing it into compact structures, and facilitating the uptake into the cells through the anionic cell-surface membrane. Little information is available about the intracellular fate of the delivered DNA and the polymeric carriers in BMSC. This study was conducted to investigate the fate of a plasmid DNA and polymeric carriers in rat BMSC. Towards this end, two cationic polymeric, poly-L-Lysine (PLL) and polyethyleneimine (PEI), were labelled with fluorescein isothiocyanate (FITC) and Alexafluor-350TM. A commercially-available plasmid DNA (pEGFP-N2) was also labelled with the same fluorescent markers and the cellular uptake of DNA in conjunction with unlabeled polymers were followed. BMSC were derived from Sprague-Dawley rats and used between passage 2 and 4 for growth on glass cover slips. Atomic force microscopy indicated plasmid/polymer complex formation with 50-200 nm size at the optimal plasmid:polymer ratios. The PEI and PLL polymers were both readily taken up by the cells, irrespective of the fluorescent label used on polymers. Flow-cytometry also confirmed the abundant uptake of the polymers. Close to 100% of the cells exhibited polymer uptake with 70-80% of the cells exhibiting polymer uptake in the nucleus for both PEI and PLL. DNA was also taken up by the cells (90-100% of BMSC), but nuclear localization of the DNA was significantly less (5-10%). These results indicated a strong ability of the cationic polymers to target to cellular nucleus, but the DNA payload appeared to be dissociated from the polymers intracellularly, and not targeted to nucleus. Understanding the mechanism(s) by which DNA transport to nucleus is impeded might provide superior carriers for genetic modification of bone marrow stromal cells.

Disclosures: **H. Uludag**, None.

SU216

Mechanical Strain Regulates Effectors of both Formation and Resorption in an Immortalized Osteoblast Cell Line. X. Fan¹, J. A. Rahner^{*1}, T. C. Murphy^{*1}, M. S. Nanes¹, E. M. Greenfield², J. Rubin¹. ¹Dept. of Medicine, Emory University/VA Medical Center, Decatur, GA, USA, ²Dept. of Orthopaedics, Case Western Reserve University, Cleveland, OH, USA.

Mechanical strain inhibits osteoclastogenesis by regulating osteoblast functions: we have shown that strain inhibits RANKL expression and increases eNOS and nitric oxide levels through ERK1/2 signaling in primary bone stromal cells. The primary stromal culture system, while contributing greatly to understanding of how the microenvironment regulates bone remodeling is limited in use for biochemical assays and studies of other

ASBMR 27th Annual Meeting

osteoprogenitor cell responses to mechanical strain: stromal cells proliferate poorly and loose aspects of the strain response after a relatively short time in culture. In this study, we used the established mouse osteoblast cell line, CIMC-4 cell, which was harvested from mouse calvaria conditionally immortalized by insertion of the gene coding for a temperature-sensitive mutant of SV40 large T antigen. The CIMC-4 line is known to support osteoclastogenesis. We characterized these cells showing that vitamin D induced RANKL expression and nitric oxide decreased the RANKL/OPG mRNA ratio. Osteoblast characteristics consistent with differentiation were studied: mineralizing medium as well as Wnt-3a conditioned medium enhanced alkaline phosphatase activity and osteocalcin secretion. This panel of responses was next studied to see if the cells were able to sense mechanical strain. We applied mechanical strain (0.5-2%, 10 cpm, equibiaxial) to the CIMC-4 cultures. Strain caused magnitude-dependent decreases in RANKL expression to less than 50% those of unstrained cultures. Overnight strains of 2% also increased osterix (OSX) and RUNX2 expression by nearly 2-fold as measured by RT-PCR. Importantly, the ERK1/2 inhibitor, PD98059, completely abrogated the strain effects bringing RANKL, OSX and RUNX2 gene expression completely back to control levels. This data indicates that the strain effects on CIMC-4 cells require activation of ERK1/2 pathway. Therefore, the CIMC-4 cell line is a useful alternative *in vitro* model which effectively recapitulates aspects of the primary stromal cells and adds an extended capacity to study osteoblast control of bone remodeling in a mechanically active environment.

Disclosures: **X. Fan, None.**

SU217

ATP Release Mediates Fluid Flow-Induced Proliferation of Human Mesenchymal Stem Cells. R. C. Riddle, A. F. Taylor*, H. J. Donahue. Orthopaedics, Pennsylvania State University College of Medicine, Hershey, PA, USA.

Accumulating evidence points to a role for ATP and purinergic signaling in bone cell mechanotransduction. Both osteocytes and osteoblasts have previously been shown to release ATP in response to mechanical stimulation and *in vivo* models illustrate that the expression of purinergic receptors is necessary for skeletal homeostasis. In these studies, we examined the effect of oscillatory fluid flow on the release of ATP and the effect of this signaling molecule on human mesenchymal stem cell proliferation. Exposing mesenchymal stem cells to fluid flow inducing a shear stress of 20dynes/cm² at 1Hz triggered a robust increase in ATP release compared to static controls (6.3±0.9nM to 0.3±0.1nM) without disrupting plasma membrane integrity. Concentrations of released ATP peaked within one minute of the initiation of fluid flow but remained elevated through 15 minutes of flow. As we and others have shown fluid flow to induce a proliferative response in human mesenchymal stem cells, we hypothesized that the release of ATP may be an important step in the mechanism by which biophysical signals regulate mesenchymal stem cell behavior. Two different approaches were utilized to test this hypothesis. Initially, cells were treated directly with physiologic concentrations of ATP ranging from 0 to 250µM to determine whether mesenchymal stem cells respond to ATP treatment with an increase in proliferation. We observed a dose-dependent increase in mesenchymal stem cell proliferation following ATP treatment, with 25µM ATP stimulating the greatest increase in proliferation (147.3±17.4% increase over untreated controls). Subsequently, cells were exposed to fluid flow in the presence of apyrase (10U/mL), an enzyme that degrades extracellular nucleotides, to determine whether ATP release is necessary for fluid flow-induced proliferation. Fluid flow inducing a shear stress of 20dynes/cm² stimulated a 109.9±18.8% increase in human mesenchymal stem cell proliferation over static controls. Treatment with apyrase completely abolished this response to fluid flow. These data provide strong evidence of a role for ATP in the biophysical regulation of mesenchymal stem cell behavior. Current efforts are focused on identifying the purinergic receptor responsible for this response as both P2Y2 and P2X7 isoforms have previously been implicated in bone cell mechanotransduction.

Disclosures: **R.C. Riddle, None.**

SU218

Enhanced Real-Time Ca²⁺ Oscillations Induced by Rest-Inserted Loading Predicts Sustained Osteoblastic Activity. B. J. Ausk*, T. S. Gross, S. Srinivasan. Orthopaedics, University of Washington, Seattle, WA, USA.

Inserting 10 s rest between each load cycle transforms low-magnitude loading events into potent osteogenic stimuli primarily via more sustained osteoblast function. To begin to explore mechanisms underlying the effectiveness of rest-inserted loading, we implemented a complimentary approach utilizing an agent based model of real-time Ca²⁺ signaling in osteocyte networks to generate hypotheses testable *in vivo*. In model simulations, we found that real-time Ca²⁺ oscillations induced by cyclic loading display a high-magnitude transient followed by low-level fluctuations while rest-inserted loading induced a series of secondary spikes following the initial transient. This phenomenon has also been observed when osteocytes were subject to oscillating fluid flow *in vitro*. We then employed a data mining approach to partition real-time Ca²⁺ oscillations induced in the model into two distinct components: initial activation and sustained activation. Initial activation was slightly but consistently increased by rest-inserted versus cyclic stimuli (19 ± 4%, range: 10 to 47%, n = 10; p = 0.02). In contrast, sustained activation was much more dramatically increased by rest-inserted versus cyclic stimuli (310 ± 150%, range: 60 to 1600%, n = 10; p = 0.04). Based on these emergent data and assuming that Ca²⁺ signaling in osteocytes scales to subsequent osteoblast function, we hypothesized that a single bout of rest-inserted loading would induce a more sustained osteoblast response than a single bout of cyclic loading. We examined this hypothesis by subjecting the right tibiae of 16-wk C57BL/6J mice to a single bout of cyclic or 10 s rest-inserted loading (1600 me, 50 cycles, n = 4 per group). The relative periosteal percent labeled surface (rLS) was quantified in loaded vs intact contralateral tibia at 5 d (alizarin) and 9 d (calcein) post-loading. In response to cyclic loading, rLS was increased by

5 d, but declined to near background levels by 9 d (13.6 ± 9 to 3.7 ± 6%, p=0.05). In contrast, rLS induced by rest-inserted loading was sustained through 9 d (d 5: 15.1 ± 13.9% vs d 9: 17.7 ± 9.9%). At 9 d, rLS was significantly enhanced by rest-inserted loading compared to cyclic loading (by 380%; p=0.03). These data, albeit preliminary, demonstrate that real-time cellular events initiated during a single bout of loading (order of seconds) potentially control distinct down-stream adaptations (over a week later). Importantly, the nonlinear analysis enabled by agent based modeling coupled with predictive validation via *in vivo* models should provide a unique framework to identify novel pathways underlying mechanotransduction function within bone.

Disclosures: **S. Srinivasan, The Whitaker Foundation 2.**

SU219

The Canonical Wnt Pathway Is Downstream to the BMP Signaling Pathway in Mediating Fluid Shear Stress-Induced Osteoblast Proliferation. S. Kapur, D. J. Baylink, K. H. W. Lau. Musculoskeletal Disease Center, J. L. Pettis Memorial VAMC, Loma Linda, CA, USA.

C57BL/6J (B6) inbred mice, but not C3H/HeJ (C3H) mice, responded to loading with an increase in bone formation. Our previous microarray study showed that genes of the Wnt, BMP/TGFβ, IGF-I, and Estrogen receptor (ER) pathways were upregulated in B6, but not in C3H, osteoblasts (Obs) 4 hrs after the 30-min steady shear strain of 20 dynes/cm², suggesting that the Ob mitogenic response to shear stress may involve these 4 pathways. Since there is abundant evidence for the involvement of IGF-I and ER pathways in shear stress-induced Ob mitogenic response, the present study focused on the potential role of and crosstalk between the Wnt and BMP pathways. Obs isolated from B6 mice were subjected to a 30-min steady shear stress at 20 dyne/cm². Cell proliferation was assessed by [³H]thymidine incorporation. Expression of genes of the Wnt and BMP pathways (normalized against β-actin) was measured with real-time PCR 4 hr after the stress. The stress significantly increased cell proliferation (by 2-fold, p<0.005) in B6 Obs but not in C3H Obs. It also significantly (p<0.05 for each) upregulated the expression of genes of the canonical Wnt pathway: Wnt1 (2.3-fold), Wnt3a (3.3-fold), β-catenin (3.4-fold), LEF-1 (2.8-fold), and Axin (3.5-fold) and that of the BMP pathway: BMPR (2.6-fold), BMP4 (1.7-fold), Necdin (1.4-fold), and DLX1 (1.6-fold), in B6 Obs. The upregulation of many of these genes was confirmed by immunoblots. This shear stress-induced Ob proliferation and BMPR expression was each completely abolished by the BMP pathway inhibitor, noggin (300 ng/ml), while it was only partially (~60%, p<0.002) blocked by endostatin (10 µg/ml), an inhibitor of the canonical Wnt pathway. The lack of a complete inhibition was not due to an incomplete blockage of the shear stress-induced upregulation of canonical Wnt pathway, since this dose of endostatin abolished the shear stress-mediated upregulation of β-catenin expression completely. To evaluate potential crosstalk between the canonical Wnt and BMP pathways, we examined the effect of the noggin pretreatment on shear stress-induced upregulation of genes of the canonical Wnt pathway. The shear stress-induced Wnt1, Wnt3a, and β-catenin expressions were completely blocked by the noggin pretreatment. The shear stress also upregulated Wnt5a expression (non-canonical Wnt pathway) by 1.7-fold (p<0.01), but noggin had no significant effect on the shear stress-induced Wnt5a expression. In conclusion, the canonical Wnt pathway is downstream to the BMP pathway in the shear stress-mediated Ob proliferation and the BMP pathway mediated the shear stress-induced Ob proliferation partially through the canonical Wnt pathway.

Disclosures: **K.H.W. Lau, None.**

SU220

MAPK and GSK Signaling Pathways Are Involved in the Mechanical Responses of Cementoblasts to Fluid Shear Stress. D. Liu, R. L. Duncan. Orthopaedic Surgery, Indiana University, Indianapolis, IN, USA.

External apical root resorption (EARR) occurs in 75-80% of patients undergoing orthodontic treatment and can be caused by multiple factors. However, the cellular and molecular mechanism of this process is unclear. Cementum, the shielding layer covering the dental root, bears a dynamic mechanical load during orthodontic tooth movement. Cementoblasts secrete the mineral matrix and ultimately become embedded in cementum. We hypothesize that cementoblasts actively respond to mechanical loading and play a pivotal role in the control of cementogenesis and remodeling of cementum. To determine whether cementoblasts respond to mechanical loading, OCCM.30 cells, an immortalized murine cementoblastic cell line (a gift from Somerman MJ, U. Washington, Seattle), were seeded onto glass slides coated with type I collagen (10µg/cm²) and grown in DMEM supplemented with 10% FBS and 2mM L-glutamine. Upon confluency, OCCM.30 cells were subjected to 12 dyn/cm² laminar fluid shear stress (FSS) for 30 minutes or 1 hour. Static controls were kept in the identical environment without flow. During flow, media samples were taken at 5 and 15 minutes to determine the release of ATP and PGE₂, respectively. Following application of FSS, OCCM.30 cells were post incubated for either 30 minutes or 6 hours to determine Cox-2 or osteopontin (OPN) production. FSS induced a rapid release of ATP in OCCM.30 cells, followed by increased PGE₂ release at 15 min. FSS also increased both Cox-2 and OPN production compared to static controls. We, and others, have shown that MAP kinases are rapidly phosphorylated by shear in osteoblasts. As in cementoblasts, both ERK1/2 and P38, but not JNK, were phosphorylated within 30 min by FSS. Glycogen Synthase Kinase (GSK)3β was also phosphorylated in cementoblasts in response to FSS within 1 hour. These data indicate that, like osteoblasts, cementoblasts are mechanosensitive, activating many of the same signaling pathways involved in the cellular responses to mechanical loading. Further, these results imply a potential role of cementoblasts in the adaptation of cementum to a mechanical environment.

Disclosures: **D. Liu, None.**

SU221

Reloading after Skeletal Unloading Restores Osteoblast Proliferation and IGF-I Responsiveness. S. Nishida¹, Y. Wang¹, R. K. Long^{*1}, E. C. Buxton^{*1}, A. Burghardt^{*2}, B. Boudignon¹, P. Kurimoto^{*1}, H. ElAlieh^{*1}, S. Majumdar², B. P. Halloran¹, D. D. Bikle¹. ¹Endocrine Research unit, Univ of California, Veterans Affairs Medical Center, San Francisco, San Francisco, CA, USA, ²Musculoskeletal and Quantitative Imaging Research Group, Univ of California San Francisco, San Francisco, CA, USA.

Skeletal unloading leads to decreased bone formation and decreased bone mass. These results can be explained in part by a failure of IGF-I to activate its signaling pathways in unloaded bone. To determine whether reloading restores IGF-I responsiveness we examined the response of unloaded (4 weeks hindlimb elevation), normally loaded, and reloaded (2 weeks normally loaded after 2 weeks unloaded) tibia and spine to IGF-I administration. The rats were given IGF-I (2.5 mg/kg/day) or vehicle by continuous infusion during the final 2 weeks of unloading, reloading, or normal loading. IGF-I treatment significantly increased the serum level of IGF-I in all animals to the same extent. Unloading and reloading did not affect the serum level of IGF-I in the vehicle-treated rats. We used micro CT to analyze bone mass and structure and BrdU incorporation to assess osteoprogenitor cell proliferation. Unloading decreased BV/TV by 25% in lumbar spine and 50% in proximal tibia compared to the control group with partial but not complete recovery in the reloaded group. This decrease in BV/TV was accompanied by a change in the Structure Model Index (SMI) of trabecular bone from a plate to a rod structure. IGF-I treatment did not alter these structural changes caused by unloading. Continued unloading resulted in a reduction in BrdU labeled osteoblasts and blocked the ability of IGF-I to stimulate osteoblast proliferation. However, the reloaded group, vehicle and IGF-I treated, demonstrated an increased number of BrdU labeled osteoblasts, and the reloading enhanced this response to IGF-I. These results indicate that reloading reverses the negative impact of skeletal unloading on osteoblast proliferation and IGF-I responsiveness.

Disclosures: **S. Nishida**, None.

SU222

Modeled Microgravity Inhibits Osteoblastogenesis through Downregulation of RhoA Activity and Subsequent Actin Cytoskeletal Disruption. E. C. Seales^{*}, V. E. Meyers^{*}, M. Zayzafoon, J. M. McDonald. Pathology, University of Alabama at Birmingham, Birmingham, AL, USA.

Low gravity spaceflight-induced bone loss results in part from decreased osteoblastic bone formation; however, the causative mechanisms directing reduced osteoblastogenesis during microgravity conditions remain unclear. Previously, utilizing a modeled microgravity (MMG) system developed by NASA, we demonstrated that culture for 7 days in MMG conditions causes an irreversible switch from an osteoblastic to an adipogenic phenotype in human mesenchymal stem cells (hMSCs). Intriguingly, reduced osteoblastogenesis during microgravity was associated with loss of actin stress fiber formation and dramatically reduced activation of RhoA, a small G protein which is required for integrin-mediated signaling, actin cytoskeletal organization, and lineage commitment in many different cell types. Given that downregulation of RhoA is also linked to adipogenesis, these findings suggested that MMG-induced downregulation of RhoA activity, and subsequent actin cytoskeletal disorganization, is a causative mechanism for failed osteoblastogenesis and subsequent bone loss during spaceflight. The aim of the present study is to determine if blockade of MMG-induced RhoA downregulation can restore osteoblastogenesis under microgravity conditions. Here we show that overexpression of constitutively-active RhoA (RhoA-V14) in hMSCs prevents MMG-induced loss of actin stress fiber formation and completely restores phosphorylation (and, hence, activation levels) of both the actin-severing protein cofilin and focal adhesion kinase. Furthermore, RhoA-V14 expression partially restored expression of osteoblastic markers including runt-related transcription factor 2, Type I collagen, and alkaline phosphatase, while simultaneously reducing expression of the adipocytic markers leptin and GLUT-4. Collectively, our findings suggest that microgravity-induced RhoA inactivation and subsequent actin cytoskeletal dysregulation shift the lineage commitment of hMSCs away from an osteoblastic to an adipogenic phenotype, resulting in bone loss during spaceflight. Ultimately, RhoA downregulation might play a causal role in both age and disuse-related bone loss as well since an osteoblastic-to-adipogenic lineage shift also occurs in these disorders.

Disclosures: **E.C. Seales**, None.

SU223

Mechanical Stimulation of Rat Bone: Micro-Array. C. M. A. Reijnders^{*1}, N. Bravenboer¹, H. Beek van^{*2}, M. A. Blankenstein^{*3}, P. Lips¹. ¹Endocrinology, VU University Medical Center, Amsterdam, The Netherlands, ²Molecular Cell Physiology, Free University, Amsterdam, The Netherlands, ³Clinical Chemistry, VU University Medical Center, Amsterdam, The Netherlands.

Mechanical loading plays an essential role in maintaining skeletal integrity. Bone modifies its structure throughout life in order to serve as a structural support¹. Little is known about the molecular mechanisms, which are involved in the translation of mechanical stimuli into bone formation described as osteogenic response. Various animal experiments have been designed to test the effect of mechanical stress on bone formation. The four-point bending apparatus produces controlled mechanical strains in the tibia of living rats. The aim of our study is to investigate which genes are involved in the osteogenic response after mechanical loading. DNA microarray provides a tool for identification of differentially expressed genes. Female 12-week-old Wistar rats (weight 225.2g ± 11.1g) were randomly assigned to two weight-matched groups: load (n=8) and sham (n=8). The right tibia underwent

“mediolateral” bending or sham-loading using the 4-point bending system^{2,3}. The left tibia served as contra-lateral controls. The rats were subjected to a single episode of loading comprising 300 cycles (2Hz) using a peak magnitude of 60N. After total RNA isolation, cDNA probes were generated and indirectly labelled with Fluorolink Cy3 or Cy5 dyes. Hybridization of 5K oligo rat arrays was performed. Quantification of the Cy3 and Cy5 intensities was processed with Bluefuse. Statistical analysis, micro-array-ANOVA, was performed with the statistical program R. Preliminary results show that 37 genes are differentially expressed as tested in a fixed model with lowess correction. We will perform gene set enrichment analysis to elucidate the role of these candidate genes.

References:

1. Lean et al. Am.J.Physiol (270) 1996
2. Turner et al. Bone (12) 1991
3. Forwoord et al. Bone (23) 1998

Disclosures: **C.M.A. Reijnders**, None.

SU224

Nuclear Factor of Activated T Cells (NFAT) Is a Mechanical Signal Transducer in MC3T3-E1 Osteoblast-Like Cells. D. KIM, S. Lee^{*}, J. A. Karmin^{*}, H. Minematsu^{*}, H. Lee, F. Y. Lee. Center for Orthopaedic Research, Columbia University, New York, NY, USA.

Bone adapts to mechanical environments, however, the underlying molecular mechanism by which osteoblast responds to physical forces are not fully understood. Although several studies have focused on the key roles of NFAT (nuclear factor of activated T cells) in T cells, cancer cells, kidney cells, cardiac muscle cells, the significance of NFAT in osteoblast in response to mechanical loading has never been studied. Here, we therefore hypothesized that mechanical loading activates calcineurin/NFAT which were known to regulate the transcriptions of various bone active cytokines and/or COX-2 (cyclooxygenase-2), one of proven final products of mechanical loading in osteoblasts. In order to verify our hypothesis, 5 dynes/cm² at 1 Hz of fluid shear stress for 15 min was directly applied to MC3T3-E1 pre-osteoblasts which were grown in a monolayer on the cover slide using a STREAMERTM system. After application of 3 hours of shear stress, cells were harvested and divided into cytoplasmic and nuclear fractions to identify the response of NFATc1 to fluid shear stress using immunoblotting. In addition, NFAT nuclear translocation in response to fluid shear stress was visualized under fluorescent microscopy with an ectopically expressed NFATc1-EGFP cDNA construct. We found that nuclear translocation of both endogenous and ectopically expressed NFATc1 were facilitated by fluid shear stress. We also found that calcineurin activity increased 1.8 times upon the application of fluid shear stress. Fluid shear stress caused 50% increase in COX-2 protein expression, and its increase was suppressed with VIVIT, a cell permeable NFAT activation inhibitor, judging from densitometry. NFATc1 overexpression also increased COX-2 protein expression compared to controls. Taken together, our data suggested that NFATc1 regulates COX-2 expression in response to fluid shear stress in MC3T3-E1 osteoblasts. Further studies will shed light on the role of NFATc1 in response to mechanical loading in the regulation of bone active cytokines and enhancement of bone health.

Disclosures: **F.Y. Lee**, None.

SU225

Shear Intensity-Dependent Regulation of Runx2 in MC3T3 Mouse Osteoblasts. Y. Huang^{*}, M. Su^{*}, H. Yokota. Anatomy and Cell Biology, Indiana University School of Medicine, Indianapolis, IN, USA.

A family of Runx transcription factors (also known as Cbfa and AML) is a lineage-specific regulator of gene expression in developmental pathways. Runx2 (Cbfa1) is known as a key transcription factor in the differentiation of osteoblasts and mesenchymal stem cells. The long-term objective of our research project is to elucidate the role of Runx2 in load-driven bone remodeling, and a specific aim of the current study was to investigate the transcriptional regulation of Runx2 in response to fluid shear. In our *in vitro* experiments, mouse osteoblasts (MC3T3 E1 cell line) were cultured in a three-dimensional porous type I collagen matrix (CollaCote, Sulzer Dental, Inc.) with and without fluid flow. The matrix dimension is 7 mm x 21 mm x 2 mm, and is composed of tubular collagen of 50 to 100 µm in diameter. A custom-made flow chamber, connected to a variable flow mini-pump, was used to induce flow at 0 to 10 ml/min through a 21 mm x 2 mm cross-section, and the flow treatment was applied for 3 min in the αMEM medium with 10% fetal bovine serum. Cells were harvested 1 hr and 3 hrs after the shear treatment, and total mRNA was isolated for RT-PCR. GAPDH was used as control. The mRNA expression data exhibited a unique transcriptional response of Runx2 isoforms. Three major Runx2 isoforms (types I, II, and III) are regulated either by P1 or P2 promoters. Our RT-PCR results show that the transcription driven by the distal P1 promoter was sensitive to fluid shear. However, the proximal P2 promoter was insensitive to fluid shear used in the current study. Interestingly, P1 promoter acted as a multi-stage toggle switch and the expression level altered depending on flow speed. The fluid flow at 5 ml/min upregulated Runx2 expression, while the flow at 1 and 10 ml/min downregulated its expression. Note that the expression of c-fos was upregulated at all flow speeds, and cox-2 mRNA level was elevated under shear at 5 and 10 ml/min. The observed multi-leveled regulation of Runx2 is somehow similar to the response of MMP-1 in other tissues such as chondrocytes, whose expression level was shear intensity dependent. Our results demonstrate for the first time that Runx2 mRNA expression is responsive to fluid shear, and indicate that a minimum shear threshold may exist to trigger load-driven osteogenesis. Consistent to our results, it is reported that the P1-derived type II isoform is bone specific, and the predominantly expressed isoform in non-osteoblastic cells is type I. A further analysis is required to elucidate the molecular mechanism underlying the observed multi-level expression pattern in osteoblast cells.

Disclosures: **Y. Huang**, None.

SU226

Homocysteine Enhances Apoptosis via ROS-Mediated Mitochondrial Pathway in Human Bone Marrow Stromal Cells: A Possible Mechanism for Homocysteine-Mediated Bone Loss. D. J. Kim^{*1}, O. S. Lee^{*2}, J. M. Koh¹, E. K. Park^{*3}, J. Y. Choi^{*3}, S. Y. Kim^{*3}, G. S. Kim¹. ¹Division of Endocrinology and Metabolism, Asan Medical Center, Seoul, Republic of Korea, ²Asan Institute for Life Sciences, Seoul, Republic of Korea, ³Skeletal Diseases Genome Research Center, Kyungpook National University Hospital, Daegu, Republic of Korea.

Several lines of evidence strongly suggest that high plasma homocysteine (Hcy) concentrations may weaken bone. However, the exact mechanism underlying this effect has not been elucidated. Previously, it has been shown that Hcy significantly reduced cell viability in many types of cells including vascular endothelial cells, and the rate of apoptosis of osteoblast-lineage cells is a critical determinant of bone formation. Therefore, we examined the possible effects of Hcy on apoptosis of osteoblast-lineage cells using primary human bone marrow stromal cell (hBMSC) and HS-5 cell line. Hcy significantly reduced cell viability and increased apoptosis by Cell Counting Kit-8 and analysis of cytoplasmic histone-associated DNA fragments. This cytotoxic effect was inhibited by z-VAD-fmk (z-Val-Ala-Asp-fluoromethylketone), a pan-caspase inhibitor, implicating that Hcy-induced apoptosis was caspase-dependent. Further investigation demonstrated that Hcy increased cytochrome C release into cytosol, and activated caspase-9 and caspase-3, but not caspase-8, indicating that Hcy induced apoptosis via mitochondrial pathway. In addition, immunoblotting showed that Hcy enhanced the phosphorylation of I κ B, but not of p38, ERK, and JNK. As expected I κ B inhibitor, PDTC (pyrrolidine dithiocarbamate), blocked Hcy-induced caspase-3 activation. Hcy also increased intracellular ROS and reduced total glutathione levels. And Pretreatment with N-acetylcysteine prevented Hcy-induced changes such as increased ROS, increased cytochrome C release, I κ B activation, and cell death. In summary, Hcy induced apoptosis via ROS mediated mitochondrial pathway in primary hBMSC and HS-5 cell line. To our knowledge, this is the first study demonstrating the direct detrimental effect of Hcy on bone cells.

Disclosures: **D.J. Kim**, None.

SU227

Heat Shock Protein 60 Induces Apoptosis via ROS-Mediated Mitochondrial Pathway and p38 Activation in Osteoblast-Lineage Cells; a Possible Mechanism of Estrogen Deficiency-Induced Bone Loss. J. M. Koh¹, O. S. Lee^{*2}, D. J. Kim^{*1}, E. K. Park^{*3}, J. Y. Choi^{*3}, S. Y. Kim^{*3}, G. S. Kim¹. ¹Division of Endocrinology and Metabolism, Asan Medical Center, Seoul, Republic of Korea, ²Asan Institute for Life Sciences, Seoul, Republic of Korea, ³Skeletal Diseases Genomic Research Center, Kyungpook National University Hospital, Daegu, Republic of Korea.

Postmenopausal osteoporosis is a heterogenous disorder characterized by an accelerated bone loss after natural or surgical menopause, resulting in increased risk of fractures. In spite of several decades of investigation, the mechanisms by which estrogen-deficiency induces bone loss remain complex and elusive. To identify proteins potentially involved in estrogen deficiency-induced osteoporosis, we conducted a proteomics-based analysis using ovariectomy and sham-op rat bones, and found that heat shock protein 60 (HSP60) was up regulated in bones of ovariectomized rats. ELISA assay also revealed that plasma HSP60 concentration was significantly higher in ovariectomized rats than in sham-operated rats, and in postmenopausal women (n=10) than in premenopausal women (n=10). To investigate whether HSP60 affect proliferation of osteoblast-lineage cells that is a critical determinant of bone formation, we examined its effects on cell viability and apoptosis in primary human bone marrow stromal cells (hBMSC), HS-5 hBMSC cell line, mouse calvarial osteoblasts and MC3T3 preosteoblast cell line. HSP60 significantly reduced cell viability, and increased caspase-dependent apoptosis, which were blocked by pretreatment with blocking antibodies for toll-like receptor 2 (TLR2) and TLR4. HSP60 activated caspase-3 and caspase-9, but not caspase-8, and increased the cytochrome c release into cytosol. In addition, immunoblotting showed that HSP60 activated p38, but not ERK, JNK and NF κ B, and that a p38 inhibitor, SB203580, abolished the HSP60-induced cell apoptosis. Further investigation demonstrated that HSP60 increased intracellular reactive oxygen species (ROS) levels and reduced total glutathione levels. Antioxidants, such as α -lipoic acid and N-acetylcysteine, completely prevented these HSP60-induced changes, such as reduced cell viability, increased apoptosis, activation of caspase-3, increased cytochrome c release and activation of p38. In summary, endogenous HSP60 was up regulated in estrogen deficient state and HSP60 induced apoptosis via ROS-mediated mitochondrial pathway and p38 activation in osteoblast-lineage cells. The up-regulation of HSP60 may have a critical role for the bone loss in estrogen deficient state.

Disclosures: **J.M. Koh**, None.

SU228

Control of Runx2 Activity in Proliferating Osteoblasts by Mitotic Phosphorylation and Postmitotic Dephosphorylation. A. Rajgopal^{*}, D. W. Young, A. Javed, J. L. Stein^{*}, J. B. Lian, A. J. van Wijnen, G. S. Stein. Department of Cell Biology and Cancer Center, University of Massachusetts Medical School, Worcester, MA, USA.

Skeletal development and osteoblast maturation require the osteogenic activity of the transcription factor Runx2, which controls both cell growth and differentiation in osteoblasts. One function of Runx2 we recently discovered is its ability to control the

expression of specific target genes as cells enter and exit mitosis during active proliferation. Western blot analysis of proteins from osteoblastic cells released from mitotic inhibition into early G1 show a phosphatase-sensitive shift in the mobility of Runx2 in SDS gels. Therefore, we addressed the hypothesis that post-translational modifications of Runx2 control its activity at mitosis. The slowly migrating form of Runx2 appears to be hyper-phosphorylated and is clearly immunoreactive with a CDK related phospho-epitope (detected by the MPM2 antibody) in mitotic cells but is below detection limits in asynchronous cells. The hyper-phosphorylated form of Runx2 is converted into a faster migrating putative hypo-phosphorylated form of Runx2 when cells complete mitosis. This conversion is inhibited by okadaic acid, an inhibitor of protein phosphatases PP1 and PP2A, but not by deltamethrin which affects PP2B. Thus, Runx2 is rapidly dephosphorylated after mitosis by a PP1 and/or PP2A dependent mechanism. Furthermore, mitotic phosphorylation of Runx2 protein is sensitive to the CDK inhibitors roscovitine and olomoucine, and is phosphorylated in vitro by the CDK1/cyclin B complex. These data together indicate that Runx2 is hyper-phosphorylated during mitosis, and suggest that post-mitotic regulation of Runx2 target genes involves the dynamic PP1/PP2A dependent dephosphorylation of S/T residues in Runx2 that are targeted by the CDK1/cyclin B kinase.

Disclosures: **A. Rajgopal**, None.

SU229

High Osteoblastic Activity in C3H/HeJ (C3H) Mice Compared to C57BL/6J (B6) Mice May Be Related to a Reduced Population Apoptosis in C3H Osteoblasts. M. H. C. Sheng, K. H. W. Lau, D. J. Baylink, J. E. Wergedal. Musculoskeletal Disease Center, J. L. Pettis Memorial VAMC, Loma Linda, CA, USA.

We have previously reported that the higher peak bone density in C3H mice compared to B6 mice was attributed to a greater bone formation (BF) rate that was due to an intrinsic, higher differentiation status and BF ability in C3H osteoblasts (Obs) compared to B6 Obs. In addition to an intrinsic, higher differentiation status and BF activity, C3H Obs also exhibited a significantly lower cell population apoptosis. Because recent studies indicate that cell population apoptosis may have a regulatory effect on Ob differentiation and/or BF activity, this study sought to test whether the higher differentiation status and BF ability in C3H Obs were inversely associated with their lower population apoptosis in vitro. Accordingly, we first measured the basal differentiation status [by measuring alkaline phosphatase (ALP) specific activity, and cbfa1, bmp2, bsp, type-I collagen, osteopontin, and osteocalcin gene expression (by real-time PCR)] and population apoptosis (measured by FACS) in Obs isolated from new-born and 6-week C3H and B6 mice (n = 6 each). C3H Obs at either age showed significantly greater ALP activity and Ob gene expression (p<0.05 for each) and a significantly lower cell population apoptosis (p<0.001). C3H Obs also showed a significantly higher bcl2 expression and a lower Caspase activity (with the Roche Caspase assay kit) (p<0.001 for each) than B6 Obs. These findings confirm our previous conclusion that C3H Obs had a higher basal differentiation status and a lower cell population apoptosis. To support a potential association between the differentiation status and the cell population apoptosis, we found a highly significant negative correlation between the log of the basal ALP activity and apoptosis (r=-0.574, p=0.012). We next perturbed cell population apoptosis of C3H and B6 Obs by treating these cells with a number of apoptosis enhancers (TNF, DEX, LPS, Etoposide) and inhibitors (PTH, IGF-I, TGF1, E₂) and then determined their ALP specific activity and insoluble collagen synthesis (an index of bone-forming activity). We again found significant negative correlations between ALP and apoptosis (r=-0.62, p<0.05) and between insoluble collagen synthesis and apoptosis (r =-0.46, p<0.05). In summary, these findings suggest a potential inverse relationship between cell population apoptosis and BF activity. Because the differentiation status depends on the cell life span, which is inversely proportional to apoptosis, these findings led us to conclude that the higher differentiation and/or BF activity of C3H Obs than B6 Obs may in part be due to a lower cell population apoptosis in C3H Obs.

Disclosures: **M.H.C. Sheng**, None.

SU230

Lactoferrin's Potent Anti-Apoptotic Effect in Osteoblasts Is not Mediated by LRP1. A. B. Grey, A. Zhu^{*}, K. E. Callon^{*}, M. Watson^{*}, I. R. Reid, J. Cornish. Medicine, University of Auckland, Auckland, New Zealand.

Previously we have demonstrated that lactoferrin is anabolic to bone. Lactoferrin, in vitro, stimulates osteoblastic cell proliferation and differentiation, stimulates primary chondrocyte proliferation as well as increasing bone formation in vivo. In addition, lactoferrin decreases osteoclastogenesis in mouse bone marrow cultures. We have also reported that the low density lipoprotein receptor-related protein (LRP) 1, mediates the mitogenic effects of lactoferrin in osteoblastic cells. In the present study, we have investigated lactoferrin's effects on osteoblastic cell apoptosis, using TUNEL, DNA fragmentation and colormetric methodology (Biocolor™). Lactoferrin inhibits osteoblast apoptosis induced by serum withdrawal by 70%. This effect is not sensitive to receptor associated protein (RAP), a specific LRP1 and LRP2 inhibitor, suggesting the cell survival signaling activated by lactoferrin is not mediated by LRP1. Furthermore, lactoferrin inhibition of cell apoptosis is demonstrated to a similar degree in LRP1 knockout fibroblast cell line (PEA13 cells) and the wild type fibroblast cell line (MEF-1 cells). Western blot analysis demonstrated that lactoferrin activates PI3K-dependent Akt phosphorylation in osteoblastic cells. This activation is also not RAP-sensitive. We then questioned whether lactoferrin's ability to promote osteoblast survival was acting through the PI3 kinase pathway, however, inhibition of apoptosis in osteoblasts by lactoferrin was not blocked by a PI3 kinase inhibitor, LY294002. We have earlier reported that lactoferrin's mitogenic activity on osteoblasts is involving the ERK pathway. However, the anti-apoptotic effect of lactoferrin in osteoblasts did not appear to be working via the ERK pathway as the MAP

kinase inhibitor U0216 did not block this effect. In conclusion, interestingly, these results indicate that lactoferrin acts through a diversity of pathways to effect multiple functions within the osteoblast. The mitogenic effect of lactoferrin is mediated by LRP1 and signals through the ERK pathway. However, the anti-apoptotic effects of lactoferrin in osteoblasts are not mediated by LRP1 and neither does it involve the PI3 kinase or ERK pathways.

Disclosures: **J. Cornish**, None.

SU231

Requirement of Protein Palmitoylation in Osteoblast Differentiation. W. Leong*, T. Zhou*, B. Li. Institute of Molecular and Cell Biology, Singapore, Singapore.

Protein modification plays a critical role in regulating protein function. Palmitoylation, a reversible lipid modification, has been demonstrated to control protein localization, protein-protein interaction, and protein trafficking. Ablation of an enzyme that catalyzes palmitoylation led to defects in mouse development and survival. Moreover, palmitoylation of hedgehog was found essential for bone development. In an attempt to understand the possible roles for protein palmitoylation in osteoblast differentiation, we used an inhibitor for palmitoyl transferase (PAT) and primary osteoblasts isolated from mice deficient for a palmitoyl transferase. Inhibition of PAT with an inhibitor was found to impede osteoblast differentiation, manifested by reduced expression of ALP and osteocalcin, and reduced bone mineralization in *in vitro* cultures. Yet osteoblast proliferation was not significantly affected by the inhibitor. Several proteins were found to be modified by palmitoylation during osteoblast differentiation. Data obtained with the PAT deficient osteoblasts and data on identification of the palmitoylated proteins will be presented.

Disclosures: **W. Leong**, None.

SU232

Decreased Bone Mineral Density in Adult Mice Heterozygous for the PTH-Regulated Transcription Factor Sox4 Is Associated with Suppressed Osteoblast Activity. L. S. H. Nissen-Meyer*¹, R. Paro*², M. E. Pedersen*¹, D. Fortunati*¹, S. Reppe*¹, V. T. Gautvik*¹, S. H. Brorson*³, A. Teti², F. P. Reinholt³, R. Jemtland*⁴, K. M. Gautvik⁵. ¹Dept. of Biochemistry, Institute of Basic Medical Sciences, University of Oslo, Oslo, Norway, ²Department of Experimental Medicine, University of L'Aquila, L'Aquila, Italy, ³Institute of Pathology, National University Hospital, Oslo, Norway, ⁴Endocrine Section, Dept. of Medicine, National University Hospital, Oslo, Norway, ⁵Dept. of Biochemistry, Institute for Basic Medical Sciences, University of Oslo, Ullevål University Hospital and Lovisenberg Hospital, Oslo, Norway.

Sox4 is a transcription factor crucial for normal development of the cardiovascular system. We have previously demonstrated expression of Sox4 mRNA in the embryonic cartilage growth plate, and its regulation via the PTH/PTH-rP receptor in osteoblast-like cells. Complete gene knockout induces intrauterine death, while *Sox4*^{+/-} animals have an apparently normal phenotype. We here present data suggesting a potential role for Sox4 in osteoblast regulation. We have examined longitudinal changes in bone mass indices in *Sox4*^{+/-} and wildtype (wt) mice, and characterized primary calvarial osteoblasts from *Sox4*^{+/-} and wt mice and their response to PTH stimulation *in vitro*. Male and female *Sox4*^{+/-} and wt mice were analysed by DEXA every 6-8 weeks (2-12 months). Epoxy-embedded tibiae were analyzed by light and electron microscopy. Osteoblast primary cultures were derived from 8-10 day-old mice. We evaluated cell differentiation, proliferation and mineralization, and the response to PTH-stimulation by intracellular cAMP measurements and c-fos expression. mRNAs typically expressed by osteoblasts were analysed by real-time PCR in unstimulated and PTH-stimulated cells. DEXA measurements of *Sox4*^{+/-} mice compared to sex- and age-matched controls revealed decreased peak bone mass in 6 months old males (-5.1%, p<0.05). This difference was later reduced (-2% and -0.8 % at 10 and 12 months). In female *Sox4*^{+/-} mice, BMD was decreased by 3.1% at 6 months (n.s.) and by 5.3 (p<0.01) and 4.1 % (n.s) at 10 and 12 months, respectively. In osteoblast cultures, *Sox4*^{+/-} cells incorporated only ~30% [³H]-thymidine (p <0.001) compared to wt, and the number of alkaline phosphatase-expressing cells and mineralized bone nodules appeared considerably decreased. Preliminary real-time PCR data indicated a lower expression of c-fos following PTH-stimulation of *Sox4*^{+/-} osteoblasts compared to wt. *Sox4*^{+/-} mice display reduced and delayed peak bone mass compared to wt. Our data show impaired proliferation and function of osteoblasts from *Sox4*^{+/-} mice, providing a possible explanation to these observations.

Disclosures: **L.S.H. Nissen-Meyer**, None.

SU233

Pueraria Thunbergiana Promotes Differentiation and Mineralization in Human Osteoblast-Like SaOS-2 Cells. D. Y. Kim*¹, J. E. Huh*², H. R. Yang*², Y. H. Baek*², J. D. Lee*², D. S. Park*², M. C. Yoo*³. ¹Internal Medicine, Kyung Hee University Hospital, SEOUL, Republic of Korea, ²Oriental Medicine Research Center for Bone & Joint Disease, Kyung Hee University, SEOUL, Republic of Korea, ³Orthopedic Surgery, Kyung Hee University Hospital, SEOUL, Republic of Korea.

The differentiation of osteoblasts is controlled by various growth factors and matrix proteins expressed in bone. *Pueraria thunbergiana* (*Pueraria T.*), the root of *Pueraria lobata* Ohwi, a wild creeper leguminous plants, is one of the earliest and most important

crude herbs used in oriental medicine. It has been reported that *Pueraria T.* prevents bone loss by growth hormone release in ovariectomized rats. The aim of this study was to identify the *Pueraria T.* that may induce the osteogenic activity in human osteoblast-like SaOS-2 cells. The osteogenic activity of *Pueraria T.* were evaluated by WST-8 assay, alkaline phosphatase (ALP) activity, RT-PCR analysis of vascular endothelial growth factor (VEGF), osteocalcin (OCN), osteopontin (OPN), type I collagen (Col I) mRNA, and ELISA or colorimetric analysis, and mineralization by Alizarin red staining in SaOS-2 cells. *Pueraria T.* had no effect on viability of osteoblastic cells, and dose dependently increased ALP activity. Treatment of the cells with *Pueraria T.* at 1 µg/ml increased VEGF mRNA synthesis at 3, 7, and 14 days of culture in a dose-dependent manner. Extracellular accumulation of proteins such as VEGF, and Col I was increased in a dose-dependent manner. Following treatment of the cells with 1 µg/ml *Pueraria T.* for 14 days of culture, the expression of OCN, OPN, and Col I mRNA was not affected by treatment with *Pueraria T.* at 3 and 7 days, but was markedly enhanced at 14 days of culture. OCN, OPN, and Col I mRNA expression showed a dose-dependent increase at 14 days of culture following *Pueraria T.* treatment compared to vehicle-treated cells. Also, *Pueraria T.* significantly induced mineralization in the culture of SaOS-2 cells. Calcified tissue formation was clearly observed after 14 days of culture with *Pueraria T.*, and the amount of mineralization increased in a dose-dependent manner. This study showed that *Pueraria T.* not affect on viability, but it enhanced ALP activity, VEGF, bone matrix proteins such as OCN, OPN and Col I, and mineralization in SaOS-2 cells. These results propose that *Pueraria T.* plays an important role in osteoblastic bone formation.

Disclosures: **D.Y. Kim**, None.

SU234

Effect of Statins on the *In Vitro* Differentiation of Human Bone Marrow Stromal Cells. K. László*, T. R. Meury*, M. Alini*. AO Research Institute, Davos, Switzerland.

Statins are inhibitors of 3-Hydroxy-3-Methylglutaryl Coenzyme A Reductase. They are known to decrease the amount of isoprenoids in the cell through the inhibition of mevalonate synthesis. Because of this statins are widely used in clinics to reduce the cholesterol level in blood. In addition, recent results suggest a possible role for statins in bone formation. The aim of this study was to evaluate the effect of three statins (lovastatin, simvastatin and pravastatin) on human bone marrow stromal cells (BMSC) differentiation into osteoblasts. The different statins were added to BMSCs and the differentiation process was followed by measuring different osteogenic markers (ALP, BMP-2, osterix and MMP-13). We also determined the DNA, ALP activity and Ca-45 incorporation into the mineralized matrix. Vital staining and apoptotic assays were also performed. In addition, BMSCs were cultured in osteogenic (containing dexamethasone as a positive control of the differentiation process) and non-osteogenic (without dexamethasone as a negative control) media. Our results show that at high concentrations (3 and 5 µM), lovastatin and simvastatin had a significant toxic effect on BMSCs, indicated by a drop in the DNA content and by a reduced number of adherent cells over time in culture. ALP gene expression was as well suppressed and no ALP activity could be measured. However, non-specific calcification was observed, indicating possible cells death. Interestingly, pravastatin showed no toxic effect at these concentrations, probably due to the lack of LST-1 anion transporter protein, which has been shown to be necessary for its internalization into hepatocytes. (D. Nakai et al., 2001) At lower concentrations (50 nM to 1 µM), statins did not show any adverse effect on BMSCs over three weeks of culture period, but at the same time, they also did not induce any osteogenic cell phenotype markers. Overall, these findings suggest that statins (lovastatin, simvastatin and pravastatin) do not play an essential role on human BMSCs differentiation into osteoblasts *in vitro*.

Disclosures: **K. László**, None.

SU235

Functional Interaction between PKA and BMP Signaling during Osteogenic Differentiation of Human Mesenchymal Stem Cells. R. Siddappa*¹, C. Gaspar*², R. Fodde*², C. van Blitterswijk*¹, J. de Boer¹.

¹Institute for Biomedical Technology, University of Twente, Prof Bronkhorstlaan 10D, 3723MB, Bilthoven, The Netherlands, ²Dept Of Pathology, Erasmus Medical Center, Rotterdam, The Netherlands.

We approach cell based bone tissue engineering by *in vitro* expansion and osteogenic differentiation of pluripotent human mesenchymal stem cells (hMSCs) isolated from bone marrow and subsequent seeding onto calcium phosphate ceramics. To optimise the osteogenic differentiation process we want to understand the molecular signalling pathways underlying differentiation of hMSCs into active osteoblast *in vitro* and *in vivo*. G protein coupled receptors (GPCR) are involved in bone formation. Therefore we investigated the role of GPCR signalling in hMSC osteogenesis. Short term PKA activation using cAMP or cholera toxin induced expression of the osteogenic markers alkaline phosphatase, osteocalcin, collagen type I and it enhanced *in vitro* mineralization. Inhibition of PKA signalling with H89 reversed the cAMP and cholera toxin induced effects. Micro array studies on 6 hours cAMP treated hMSCs showed an up regulation of BMP target genes Id1, Id2, Id4 and Smad6, which was further confirmed by quantitative PCR. The PKA induced expression of BMP target genes was not inhibited by cycloheximide treatment indicating direct activation of BMP target genes via cyclic AMP response element binding protein (CREB). Micro array studies further show that hMSCs treated with cAMP for 7 days displayed a strong expression of a number of growth factors and cytokines with known osteogenic activity, including BMP2. Since we observed induction of BMP2 upon PKA activation, we tested autocrine induction of BMP target genes using noggin (an inhibitor of BMP signalling). Noggin partially inhibited PKA induced expression of BMP target genes, but reduced the BMP2 induced expression to the basal level confirming the autocrine effect. A similar effect was observed in MG63, a

ASBMR 27th Annual Meeting

human osteosarcoma cell line. We conclude that PKA activation in hMSCs not only directs the cells into the osteogenic lineage by direct induction of BMP target genes but also induces the expression of BMPs and other bone inducing cytokines. We currently investigate whether PKA activated hMSCs can stimulate uncommitted progenitor cells into the osteogenic lineage using *in vitro* and *in vivo* models. The functional interaction between PKA and BMP signalling pathways can be further explored to augment current bone tissue engineering protocols.

Disclosures: *R. Siddappa, None.*

SU236

Identification and Functional Characterization of Fidgetin-Like 1 in MC3T3-E1 Cell. S. Kim^{*1}, S. Park^{*2}, S. Park^{*1}, J. An^{*1}, J. Byun^{*1}, D. Kim^{*2}, S. Lee^{*2}, Y. Rhee^{*2}, S. Lim^{*2}. ¹Brain Korea 21 Project for Medical Sciences, College of Medicine, Yonsei Univ., Seoul, Republic of Korea, ²Internal Medicine, College of Medicine, Yonsei Univ., Seoul, Republic of Korea.

The protein encoded by the fidgetin gene is a new member of the ATPases associated with diverse cellular activities (AAA proteins). The mouse fidget mutation is known to be associated with various skeletal abnormalities in affected mice. The purpose of this study was to determine the function of fidgetin-like 1, one of two closely related proteins, in osteoblast proliferation. We examined the effect of fidgetin-like 1 gene on proliferation, differentiation and apoptosis in MC3T3-E1 cells using flow cytometry, RT-PCR, cell proliferation assays (WST1 assay and FACS) and cell death assays (LDH assay and FACS). Microarray analysis revealed many genes up-regulated or down-regulated greater than twofold in MC3T3-E1 cells after cotreatment of bFGF and PTH compared to the genes regulated by bFGF alone (bFGF vs. bFGF + PTH). Fidgetin-like 1 is one of the genes up-regulated greater than twofold by cotreatment of bFGF and PTH. Fidgetin-like 1 encoding a polypeptide of 2,100 amino acids was obtained from a mouse muscle cell cDNA library. Expression of fidgetin-like 1 using RT-PCR analysis was increased by parathyroid hormone and bFGF, but decreased by bFGF only. Proliferation and apoptosis assay indicated that fidgetin-like 1 increased in osteoblast proliferation by promotion of S-phase, but osteoblast death was not affected by fidgetin-like 1 ($p < 0.01$). In addition, RT-PCR analysis revealed that fidgetin-like 1 was equally expressed at all developmental stages from embryo day(E) 8.5 to embryo day(E)17.5 in mouse embryonic cell. We propose that fidgetin-like 1, a member of the AAA family protein, may play a regulatory role in cell proliferation during embryonic development. Further analyses of fidgetin-like 1 will be required to identify additional mechanism concerned in cell proliferation.

Disclosures: *S. Kim, None.*

SU237

Altered Expression of Extracellular Matrix Genes in Demineralized Bone-Mediated Osteogenic Differentiation. S. Honsawek¹, L. Wolfinbarger². ¹Biochemistry, Faculty of Medicine, Chulalongkorn University, Bangkok, Thailand, ²LifeNet, Virginia Beach, VA, USA.

The osteoinductivity of bone-derived materials has been shown to play a crucial role in their ability to stimulate de novo bone formation. Demineralized bone matrices (DBM) have been used extensively for clinical repair of bone injuries and abnormalities, including nonunion fractures, bone cysts, and cranio-maxillofacial reconstructions. The objectives of this study were to determine whether DBM promote *in vitro* osteogenic differentiation of human periosteal cells and to identify genes whose expression was altered during osteogenesis. We illustrated that human periosteal cells cultured with DBM acquire the osteoblast phenotype and express alkaline phosphatase activity after 7 days. Macroarray analysis demonstrated altered expression of extracellular matrix genes during osteoinduction of human periosteal cells. DBM-treated periosteal cells revealed that biglycan was upregulated but collagen 14A1 was downregulated. Interestingly, TGF- β 1 involved in the enhancement of the formation of extracellular matrix and inhibition of matrix degradation was also upregulated, including its receptor, TGF- β RI following DBM treatment. In addition, reverse transcriptase-polymerase chain reaction (RT-PCR) analysis of selected genes at 0, 4, 7, 10, and 14 days showed different expression patterns for those extracellular matrix genes during osteogenesis. We found that biglycan was consistently upregulated whereas collagen 14A1 was downregulated and persisted for 14 days in DBM-induced osteogenic differentiation. Biglycan coding for extracellular matrix protein is a prominent osteoblastic marker that has previously been associated with the development and function of osteoblasts and has been shown to play an important role in the bone formation. In contrast, downregulation of the gene encoding for collagen14A1 might have implications during the process of bone development because collagen14A1 occurs in virtually every collagen I-containing tissue. Thus, the results of the present study suggest an induced osteoblast stage with a unique extracellular matrix gene expression that may contribute to a matrix supportive of osteogenesis by periosteal cells.

Disclosures: *S. Honsawek, None.*

SU238

Canonical Wnt Signaling Is Inhibited by Tumor Necrosis Factor- α . X. Lu, L. C. Gilbert, J. Rubin, M. S. Nanes. Department of Medicine, Division of Endocrinology, Emory University and VA Medical Center, Atlanta, GA, USA.

Wnt signaling is required for differentiation of osteoblasts (OB), skeletal development, and fracture repair. Evidence supporting a role for Wnts derives from inherited mutations of the Wnt co-receptor LRP5 in humans and transgenic modification of components of the wnt canonical signal pathway (LRP5, APC, β catenin). We have shown that the

inflammatory cytokine tumor necrosis factor- α (TNF) inhibits OB differentiation by a mechanism that includes inhibition of expression of the transcription factors Runx2 and Osx. These transcription factors are critical for commitment of precursor cells to the OB phenotype. We hypothesized that the mechanism of TNF action could include inhibition of wnt signaling. To test this, we studied the effect of TNF on wnt-stimulated expression of Osx mRNA, activity of the Osx and RUNX2 promoters, and on wnt activation of the β catenin-responsive reporter TOPFLASH. Transfection of C3H10T1/2 and MC3T3-E1 cells with a wnt-1 expression plasmid or treatment with conditioned medium from Lwnt3a cells increased Osx, Runx2, and TOPFLASH promoter activity 2, 19, and 9 fold, respectively. Simultaneous treatment with TNF inhibited the wnt-stimulated responses by 50%. Wnt-stimulated Osx mRNA, was also blocked by TNF. TNF inhibition of TOPFLASH suggested interference with the canonical wnt signaling pathway. Since Wnt stimulation promotes β catenin nuclear entry, we measured the effect of TNF on accumulation of β catenin in the nucleus of MC3T3-E1 cells by western analysis. TNF treatment inhibited β catenin nuclear content while simultaneously increasing the entry of free NF κ B. The level of RNA polymerase II, a control, was unchanged. Real Time RT-PCR did not reveal an effect of TNF on β catenin mRNA suggesting that TNF affected β catenin post-translationally, its transport into the nucleus, or its nuclear stability. To determine the signal pathway mediating TNF effects, specific inhibitors of MAPK were added prior to TNF treatment. TNF inhibition of wnt signaling and Osx promoter was abrogated by PD98059, a MEK1 inhibitor, but not by inhibitors of p38 or JNK. These results suggest that cytokine signal pathways may interact with the canonical Wnt pathway. Such an interaction could contribute to TNF inhibition of OB differentiation.

Disclosures: *X. Lu, None.*

SU239

High Concentration of Serum Low-Density-Lipoprotein Inhibits Maturation of Osteoblast, Decreases Trabecular and End-Cortical Bone Formation, and Results in Osteopenia in Apolipoprotein E Knock-Out Mice Fed with High-Fat Diet. H. Hirasawa^{*1}, S. Tanaka^{*1}, A. Sakai¹, M. Tsutsui^{*2}, H. Miyata^{*3}, M. Ito⁴, T. Nakamura¹. ¹Dept. of Orthopaedic Surgery, University of Occupational and Environmental Health, Kitakyushu, Japan, ²Dept. of Pharmacology, University of Occupational and Environmental Health, Kitakyushu, Japan, ³Laboratory Animal Reserch Center, University of Occupational and Environmental Health, Kitakyushu, Japan, ⁴Dept. of Radiology, Nagasaki University, Nagasaki, Japan.

Objective; To clarify whether high concentration of serum low-density-lipoprotein (LDL) regulates osteoblast differentiation and bone metabolism. Materials and Methods; 4-week-old male apolipoprotein E (apo-E) knock-out mice and littermates were given high-fat (groups ApoEHf and WildHf) or standard chaw (groups ApoES and WildS) for 12 weeks. At the age of 17 weeks, bilateral femurs, tibias, and lumbar vertebrae were harvested, and serum and urine for 24 hours before sacrifice were collected. Assessments; Concentration of serum LDL and urinary deoxypyridinoline (D-pyr) were measured. Micro-CT at lumbar vertebra was analyzed. Bone histomorphometry at diaphysis and distal metaphysis of femur, and proximal tibia was performed. mRNA expressions in cortical bone and bone marrow adherent cells of femur were examined using quantitative RT-PCR. Results; Serum LDL levels in ApoEHf were the highest among the four groups, and followed by ApoES, WildHf, and WildS. The values of urinary D-pyr were increased in WildHf and ApoEHf. Trabecular bone volume in lumbar vertebra and cortical bone area of femoral mid-shaft were significantly decreased in ApoEHf compared with those in the other three groups. Bone formation rate in trabecular bone in femoral metaphysis and endosteum of femoral mid-shaft were decreased in ApoEHf. The values of bone formation rate in these areas revealed significant negative-correlation with serum LDL levels ($R = -0.819$, -0.834). Osteocalcin mRNA expressions in cortical bone in ApoEHf were the lowest, and followed by ApoES, WildHf, and WildS, and also negatively correlated with serum LDL levels ($R = -0.761$). Type 1a collagen (Col1a1) mRNA in bone marrow adherent cells was increased in ApoEHf, but osteocalcin was not increased. The ratio of Col1a1 to osteocalcin mRNA in adherent cells had significant positive-correlation with p53 mRNA expression ($R = 0.849$). Osteoclast surface in trabecular bone and eroded surface in endosteum were significantly increased in ApoEHf and WildHf. Conclusion; Serum LDL was related to inhibition of osteoblast maturation. High-fat diet resulted in osteopenia in association with the increase of bone absorption in Apo-E knock-out mice fed with high-fat diet.

Disclosures: *H. Hirasawa, None.*

SU240

Effects of Bisphosphonates on UMR-106 Cells Depend upon their Cultural Milieu. R. W. Katz¹, Q. Sun², J. P. Bilezikian². ¹Oral Medicine, College of Dentistry, New York University, New York, NY, USA, ²Division of Endocrinology, College of Physicians and Surgeons, Columbia University, New York, NY, USA.

Bisphosphonates (BPs) have had a major impact on the management of osteoporosis and other metabolic bone diseases. Previously, we have shown that BPs affect signaling pathways utilized by parathyroid hormone and that osteoblast cultures exposed to BPs in solution exhibit a reduced accumulation of total DNA. In this study, we determined the effects of BPs on cell growth and whether their physical adherence to calcium phosphate coated discs (CPdiscs) would change their actions to influence osteoblast characteristics. The amount of cellular DNA obtained from UMR-106 cultures was decreased significantly, compared to control values, when the cells were exposed to BPs in solution at concentrations greater than 1 μ M. BPs were rendered adherent to CPdiscs by soaking them thoroughly before using them as a culture substrate for UMR-106 cells. Under these

ASBMR 27th Annual Meeting

conditions, BPs had a different effect, namely increasing total DNA at 1 uM. At this concentration in solution, BPs are associated with a reduction in total UMR-106 DNA. At higher concentrations, BPs on CPdiscs showed the same inhibitory effect on total DNA in UMR-106 cells as is seen with BPs in solution. To determine whether the inhibition of culture growth by BPs in solution was due to increased cell death, cell viability was examined by flow cytometry of propidium iodide exposed suspensions. Treatment with 100 uM BPs led to a 2-3 fold increase in the proportion of non-viable cells as compared to control cultures. Assessing cell proliferation through BrdU incorporation revealed no significant difference in DNA replication between control cultures and those exposed to 100 uM BPs. In summary, our results indicate that BPs affect osteoblast survival and cell accumulation *in vitro*; that there is a rather uniform inhibitory effect when UMR-106 cells are exposed to BPs in solution; but that when BPs are present on CP-discs, a direct stimulation can be observed at low concentrations. The effect of BPs appear to be directed towards cell viability, not cell proliferation. These results provide further evidence for a direct effect of BPs on osteoblasts, a heretofore unappreciated target cell for these compounds. Further studies are needed to understand by what mechanisms BPs affect osteoblast survival but the results reported here suggest that BPs adsorbed onto mineralized surfaces may affect osteoblast survival in a clinically significant manner.

Disclosures: **R.W. Katz**, Alliance for Better Bone Health 2; College of Physicians and Surgeons, Columbia University 5.

SU241

Inhibition of Osteoblast Differentiation by TNF Requires Mitogen Activated Protein Kinase. **L. C. Gilbert, X. Lu, J. Rubin, M. S. Nanes.** Department of Medicine, Division of Endocrinology, Emory University, Atlanta, GA, USA.

Commitment of pluripotent precursor cells to the osteoblast (OB) lineage requires expression of the essential transcription factors Runx2 and Osx. We have shown that the inflammatory cytokine tumor necrosis factor- α (TNF) inhibits OB differentiation at an early stage in lineage commitment. Low doses of TNF (0.5 ng/ml) inhibit expression of Runx2 and Osx without decreasing cell viability. Here we investigate the role of TNF-stimulated mitogen activated protein kinase (MAPK) in the inhibition of differentiation using specific inhibitors of MEK1 (PD98059), JNK (SP600125), or p38 kinase (SB203580). Experiments were done using MC3T3-E1 cells cultured in the presence of ascorbate and β glycerophosphate. MAPK inhibitors were added on day 3 of culture prior to TNF (10 ng/ml) and the inhibitors and TNF were removed on day 6. Differentiation was assessed by measuring the phenotypic markers alkaline phosphatase, osteocalcin, and mineralization by alizarin red staining. In addition, Osx mRNA and basal promoter activity were measured by Real Time RT-PCR and transient transfection of an Osx-luciferase promoter construct. TNF inhibited alkaline phosphatase activity, osteocalcin secretion, and mineralization of cells. RUNX2 and Osx mRNA and promoter activity were potentially inhibited by TNF. The MEK1 inhibitor abrogated TNF inhibition of alkaline phosphatase, osteocalcin, and mineralization in a dose dependent manner. These results were not observed using inhibitors of JNK or p38. The MEK1 inhibitor partially prevented TNF inhibition of Osx mRNA and Osx promoter activity but did not reverse TNF inhibition of RUNX2 mRNA or promoter activity. The dose of MEK1 inhibitor that restored the phenotypic markers of differentiation also blocked the rapid (5 and 10 minutes) TNF stimulated phosphorylation of ERK1/2 as seen on western analysis. Surprisingly, NF κ B expression stimulated Osx mRNA and promoter activity, excluding NF κ B as the mediator of TNF inhibition of Osx. These results show that TNF inhibition of OB differentiation requires activation of MAPK. The decrease in OB differentiation in the TNF excess states of inflammatory arthritis or estrogen deficiency could contribute to a blunted bone formation response.

Disclosures: **L.C. Gilbert**, None.

SU242

PPAR- γ 2 Nuclear Receptor Controls Multiple Regulatory Pathways of Osteoblast and Adipocyte Differentiation Including IGF-1 and TGF- β /BMP Signaling. **K. Shockley*¹, O. Lazarenko*², G. Churchill*¹, C. Ackert-Bicknell¹, C. Rosen¹, B. Lecka-Czernik².** ¹The Jackson Laboratories, Bar Harbor, ME, USA, ²Geriatrics, UAMS, Little Rock, AR, USA.

PPAR- γ 2 adipocyte-specific transcription factor controls marrow mesenchymal stem cell (mMSC) differentiation toward adipocytes and osteoblasts. *In vitro*, in a model of mMSC differentiation of U-33/ γ 2 cells, PPAR- γ 2 activated with a specific agonist and anti-diabetic drug rosiglitazone (R) acts as a positive regulator of adipocyte and a dominant negative regulator of osteoblast development. In animal models, PPAR- γ 2 activation with R leads to a significant bone loss. In order to determine the mechanisms by which PPAR- γ 2 exerts anti-osteoblastic effects in mMSC we have performed a high throughput analysis of gene expression using microarray containing 40,000 murine transcripts. An experiment factorial design 2x3x2 corresponded to two cell lines (U-33/ γ 2 - with, and U-33/c - without PPAR- γ 2), three time points of R treatment (2, 24, and 72 hr), and two independently performed experiments. The number of genes which expression was significantly affected in U-33/ γ 2 cells increased exponentially with a time of exposure to R resulting in 41 genes after 2 hr, 2,349 after 24 hr, and 6,501 after 72 hr ($q < 0.01$). None of the analyzed genes was affected by R in U-33/c cells indicating that effects seen in U-33/ γ 2 are specific for PPAR- γ 2. A pathway-specific correlation analysis identified several gene clusters, which function is essential for osteoblasts and adipocyte differentiation, and bone homeostasis. Significant changes in expression of cell proliferation and fatty acid metabolism regulators were among the earliest observed. These changes were followed by a suppression of osteoblast-specific gene markers essential for their development and function, among them transcriptional regulators such as Dlx5, Runx2, and Osterix. Most importantly, PPAR- γ 2 had a pleiotropic effect on the expression of members of several signaling pathways

controlling bone growth and remodeling, including IGF-1 and TGF- β /BMP. *Ex vivo* analysis of mMSC supported these findings and provided evidence that R-induced changes in the expression of cytokines, their receptors and cellular mediators of their activity corresponded to decreased functional activities of these pathways. In conclusion, our results clearly indicate that PPAR- γ 2 is a major regulator of mMSC differentiation. They also provide information about hierarchical interactions between different regulatory pathways and may ultimately lead to the identification of a "master" regulatory mechanism by which PPAR- γ 2 controls osteoblast differentiation.

Disclosures: **K. Shockley**, None.

SU243

Metabolic Regulation of Osteoblast Gene Expression and Differentiation. **G. D. Gibson*, B. Bieber*, R. Irwin*, R. W. Wiseman*, L. R. McCabe.** Departments of Physiology and Radiology, Michigan State University, East Lansing, MI, USA.

Osteoporosis can result from conditions that contribute to altered cellular metabolism such as age-related hormone deficiencies, limb disuse, and disease. This is particularly evident in diabetes type I where cells must adapt to conditions of hyperglycemia, hypertriglyceridemia and hypoinsulinemia. Moreover, differentiating osteoblasts undergo phenotypic changes in metabolism (Komarova, et al, 2000). Pre-osteoblasts display higher glycolytic activity, while mature osteoblasts exhibit increased mitochondrial oxidative phosphorylation. Based on these findings, we hypothesize that modulation of osteoblast metabolism alters osteoblast differentiation and gene expression. To test this hypothesis we treated MC3T3-E1 osteoblasts for 24 hours with inhibitors of glycolysis and in parallel experiments we also treated osteoblasts with inhibitors of oxidative phosphorylation. Glucose consumption, lactose production, cell viability, ATP and metabolite levels, and gene expression were measured. All treatments lead to significant changes in osteoblast gene expression. Irrespective of metabolic pathway manipulation, runx2 expression was suppressed in proliferating (day 3) and differentiating (day 14) osteoblasts. In contrast, alkaline phosphatase expression, a marker of osteoblast differentiation, was suppressed only by inhibition of oxidative phosphorylation and not by inhibition of glycolysis. These findings suggest that the metabolic fate of glucose may contribute to the regulation of osteoblast phenotype. The use of additional inhibitors and further monitoring of cellular metabolic status will help us to distinguish between specific effects of cellular ATP depletion and/or metabolic control of bone formation.

Disclosures: **L.R. McCabe**, None.

SU244

Analysis of Functional Knockdown of Rho Kinase Expression in Primary Osteoblasts by siRNA. **A. Danikas*¹, A. Coudert*¹, E. Gurzov*², M. Izquierdo*², A. E. Grigoriadis¹.** ¹Dept Craniofacial Development, King's College London, London, United Kingdom, ²Universidad Autonoma de Madrid, Madrid, Spain.

Rho family GTPases (Rho, Rac, cdc42) are molecular switches acting at the cell membrane which cycle between inactive, GDP-bound states, and active GTP-bound states. We have recently studied the role of the Rho GTPase in osteoblast differentiation using the unique bacterial protein toxin, Pasteurella Multocida Toxin (PMT). Addition of PMT to primary mouse calvarial osteoblasts results in cytoskeletal rearrangements and stress fibres due to activation of Rho and its downstream effector Rho kinase (ROCK). In primary calvarial cultures, PMT potently inhibited bone nodule formation as well as osteoblast marker gene expression and this inhibitory effect was reversed by addition of Rho and ROCK inhibitors. More importantly, addition of Rho/ROCK inhibitors alone to primary calvarial cultures stimulated bone nodule formation. These results suggested that the Rho/ROCK pathway is a critical determinant of osteoblast differentiation and bone formation. To investigate further the role of ROCK in osteoblast differentiation, we are using a retroviral strategy to generate functional siRNA produced intracellularly using the pSUPERretro vector. We first determined which ROCK isoform was expressed, and Western blot analysis determined that both ROCK1 and ROCK2 were expressed in primary osteoblasts. Sequences specific for both ROCK1 and ROCK2 were identified and cloned into pSUPERretro, and the resulting vectors, pRETROCK1 and pRETROCK2 were transfected into Phoenix packaging cells. High titre viral supernatant was subsequently used to infect primary osteoblasts and Western blot analysis demonstrated that ROCK1 or ROCK2 protein levels were selectively reduced. To investigate whether the silencing of ROCK was functional, we analyzed cytoskeletal rearrangements. Preliminary results showed that inhibition of ROCK activity abolished stress fibre formation in osteoblasts. These specific siRNAs are currently being used in differentiation studies and *ex vivo* bone cultures to determine the effects of reduced ROCK levels on bone formation and expression of osteoblast marker genes. This effect, achieved by alteration of endogenous ROCK levels, will provide further evidence of the key role of the Rho-ROCK pathway in osteoblast differentiation.

Disclosures: **A. Danikas**, None.

SU245

Comparative Study of Human Fetal Osteoblast Long-Term Growth Dynamics in a Compartmentalized Bioreactor. X. Liu^{*1}, A. Tabakovic^{*2}, D. Ravi^{*2}, E. A. Vogler^{*3}. ¹Bioengineering, Pennsylvania State University, University Park, PA, USA, ²Materials Science and Engineering, Pennsylvania State University, University Park, PA, USA, ³Bioengineering, Materials Science and Engineering, Pennsylvania State University, University Park, PA, USA.

Long-term (~30d) *in vitro* culturing of human fetal osteoblastic (hFOB 1.19, ATCC, CRL-11372) cells is studied in a compartmentalized bioreactor that employs the simultaneous cell-growth-and-dialysis principle¹ to confer extraordinarily stable culture environment that simulates the *in vivo* condition. hFOB growth dynamics, morphology, differentiation, and extracellular matrix (ECM) mineralization in the bioreactor are compared to that in conventional culture (tissue-culture grade polystyrene: TCPS) for 15 and 30 days. Results show that short-term cell adhesion and proliferation (assayed by hemacytometry) were relatively "slow (time-to-half-maximal adhesion)" and "low (percentage of inoculum)" in the bioreactor compared to relatively "fast" and "high" in TCPS. However, long-term cell densities (assayed by fluorescent staining) were approximately the same in the bioreactor and TCPS. Cells formed confluent, interconnecting multilayer at tissue-like density with distinct cytoplasmic processes and membranes in the bioreactor (relative to TCPS) as observed by SEM and TEM. Apoptosis (assayed by Terminal deoxynucleotidyl Transferase dUTP Nick End Labeling) for hFOB was 2~3x higher in TCPS compared to the bioreactor, possibly correlates with reduced production of insoluble ECM. Alkaline phosphatase (ALP) activity and Ca deposition were quantified with chromogenic assays, respectively. Significantly higher ALP level (6.6-fold) at day 15 and Ca content (1.7-fold) at day 30 in the bioreactor (relative to TCPS) indicate enhanced matrix mineralization due to increased osteoblast activity. Preliminary studies show that hFOB can sustain long-term *in vitro* culture in a compartmentalized bioreactor with superior cell performance relative to conventional culture. Thus, the bioreactor provides an ideal tool for assessing osteoblast-mediated mineralization *in vitro*, which is necessary toward both fuller understanding of bone pathology and development of advanced orthopedic biomaterials.

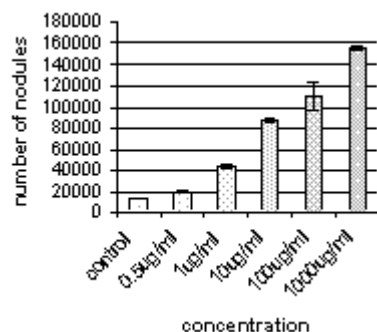
1. Vogler EA. A compartmentalized device for the culture of animal cells. *Biomater., Art. Cells, Art. Org.* 17(5):597-610, 1989.

Disclosures: X. Liu, None.

SU246

Polyphenol Extract from Dried Plum Dose-Dependently Increases Nodule Formation in MC3T3-E1 Osteoblast-Like Cells. L. L. Kamkar^{*1}, S. Hooshmand^{*1}, A. Soliman^{*1}, D. Y. Soung¹, J. K. Collins^{*2}, E. A. Lucas¹, S. V. Madhally^{*3}, B. H. Arjmandi¹. ¹Nutritional Sciences, Oklahoma State University, Stillwater, OK, USA, ²USDA ARS, South Central Agric. Lab, Lane, OK, USA, ³Chemical Engineering, Oklahoma State University, Stillwater, OK, USA.

Our earlier findings indicate that dried plum is highly effective in preventing and/or reversing ovarian hormone deficiency-associated bone loss in a rat model of osteoporosis. Additionally, our short-term clinical trial results showed that dried plum supplementation significantly increased indices of bone formation in postmenopausal women. However, the question remains as to what component(s) of dried plum modulate bone metabolism. The present study investigated the role of polyphenol extract from dried plum in increasing bone mineralization using MC3T3-E1 osteoblast-like cells. Cells were treated with various doses of polyphenols (0, 0.5, 1, 10, 100, 1000 µg/ml). Medium were collected every three days and analyzed for alkaline phosphatase (ALP) activity, a marker of bone formation. After 14 days, the mineralized nodules were characterized by Alizarin red staining. ALP activity was higher at days six and nine but not thereafter. The reduced ALP activity towards the end may signal the completion of mineralization. Figure shows that dried plum polyphenols dose-dependently increased mineralization without affecting cell viability. In summary, the present preliminary findings suggest that polyphenol extract from dried plum is efficacious in increasing bone formation.



Disclosures: B.H. Arjmandi, None.

SU247

Regulation of Osteoblast Differentiation by the Retinoid Signaling Pathway. A. V. Sampaio^{*1}, R. A. Chandraratna^{*2}, T. M. Underhill¹. ¹Cellular and Physiological Sciences, University of British Columbia, Vancouver, BC, Canada, ²Vitae Pharmaceuticals, Inc., Irvine, CA, USA.

The active metabolite of vitamin A, retinoic acid (RA), has profound effects on skeletal development and remodeling. RA operates in a stage-dependent manner during skeletogenesis and hyper- and hypovitaminosis-A both result in skeletal abnormalities. RA exerts its pleiotropic effects by modulating the activity of the nuclear receptors for RA (RARs), which are ligand-inducible transcription factors. The negative effects of supra or super physiological levels of RA on the skeleton have been known for more than 70 years; however, the precise mechanisms underlying these actions remains unresolved. Herein, using pharmacological and molecular approaches, we demonstrate that antagonism of the RAR signaling pathway potently induces bone formation in primary osteoblastic cultures derived from rat calvaria (RC). Further, antagonism of RAR-mediated signaling rescues bone formation in "osteogenic-challenged" cultures (cells that have been maintained for 2 weeks at sub-confluence prior to plating under differentiation conditions). Inhibition of RAR-mediated signaling in these cultures increases alkaline phosphatase activity and restores bone nodule formation as determined by von Kossa staining. In unchallenged cultures, quantitative PCR demonstrated that RAR antagonism leads to increased expression of *integrin binding sialoprotein (Ibsp)* and *bone gamma-carboxyglutamate protein (Bglap2)* by ~ 47-fold and ~ 8-fold, respectively, in comparison to 20-day vehicle-treated cultures. Further, under these conditions, *Runx2* expression exhibits a modest increase of ~ 1.5 fold, whereas *Sp7* expression is elevated ~ 11-fold. In contrast, treatment of unchallenged RC cultures with RA leads to a dose-dependent decrease in osteogenic activity and decreased expression of the aforementioned genes. In this regard, even physiological concentrations of RA (10 nM) were found to cause an appreciable decrease in bone nodule formation. To further address the role of endogenous RA in osteogenesis, we measured the expression and manipulated the activity of the genes involved in RA synthesis (*Aldh1a2*) and degradation (*Cyp26a1*). Both *Aldh1a2* and *Cyp26a1* were expressed throughout the culture period and inhibition of their activity with diethylaminobenzaldehyde or ketoconazole, stimulated and inhibited bone nodule formation, respectively. Together, these findings reveal novel and unexpected roles for retinoid signaling in regulating osteoblast differentiation--abrogation of retinoid signaling is required for expression of the osteoblast phenotype.

Disclosures: A.V. Sampaio, None.

SU248

Cell Cycle Regulation of Runx2 Activity Supports the Proliferative Stage of Osteoblast Growth and Differentiation in Osteoblasts. N. Teplyuk¹, M. Galindo^{*1}, X. Yang^{*1}, D. W. Young¹, H. Hovhannisyan^{*1}, M. Q. Hassan^{*1}, J. Pratap¹, J. Choi¹, M. Montecino², J. B. Lian¹, J. L. Stein^{*3}, G. S. Stein¹, A. J. van Wijnen¹. ¹Department of Cell Biology and Cancer Center, University of Massachusetts Medical School, Worcester, MA, USA, ²Department of Biochemistry, Kyungpook National University School of Medicine, Daegu, Republic of Korea, ³Departamento de Biología Molecular, Universidad de Concepcion, Concepcion, Chile.

Genetic defects that cause human bone abnormalities may be due to alterations in osteogenic lineage commitment, regulatory mechanisms that control osteoblast cell number and/or the subsequent development of cells into mature osteocytes. While the bone-related transcription factor Runx2 is well known to control bone cell differentiation and osteoblast function, we recently discovered a novel regulatory function for Runx2 as a suppressor of osteoblast proliferation. Here we analyzed how cells control the growth inhibitory function of Runx2 during progression of the mitotic cell division cycle. MC3T3 osteoblastic cells were synchronized at different cell cycle stages and analyzed in parallel for multiple parameters of gene expression including western blot analysis, quantitative PCR, run-on analysis, genomic footprinting, chromatin immunoprecipitations and reporter gene assays. When quiescent osteoblasts are stimulated to proliferate by serum growth factors, we find that the levels of Runx2 gene transcription, mRNA and protein are each downregulated as cells initially enter the cell cycle and progress toward the G1/S phase transition. Transcriptional modulation involves increased occupancy of an AP1 (c-Fos/c-Jun) element within a distal suppressor segment of the Runx2 P1 promoter. Transcription may account for decreased accumulation of Runx2 mRNA at the G1/S phase transition. However, our data also indicate that Runx2 protein is actively destabilized in late G1 by a proteasome dependent (i.e., MG132 sensitive) mechanism. As cells progress towards mitosis, Runx2 transcription resumes and mRNA accumulates during the G2/M phases of the cell cycle. However, Runx2 protein levels in G2/M remain low independent of MG132, suggesting translational rather than stability control of Runx2 protein. Following mitosis Runx2 protein levels are acutely upregulated in G1 concomitant with modulations in the expression of cell cycle related Runx2 target genes that may support the Runx2 dependent attenuation of cell growth in G1. We propose that Runx2 levels and function are controlled during the cell cycle by multiple gene regulatory mechanisms (e.g., transcription/ promoter occupancy, protein stability and mRNA translation) to modulate the proliferative potential of osteoblasts.

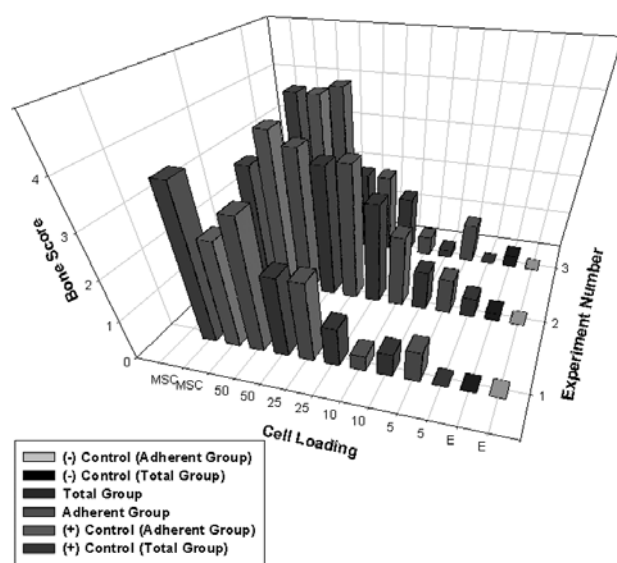
Disclosures: N. Teplyuk, None.

SU249

Optimizing Bone Marrow-Derived Osteogenic Progenitor Cell Expansion Using the RepliCell™ Bioreactor System. J. E. Dennis¹, K. Renshaw^{*2}, A. Awadallah^{*1}, K. Goltry^{*2}. ¹Biology, Case Western Reserve University, Cleveland, OH, USA, ²Astrom Biosciences, Inc., Ann Arbor, MI, USA.

The purpose of this study is to simplify and optimize the bioreactor process to produce osteogenic cells from human-derived bone marrow mononuclear cells (BMMNC). Human BMMNC aliquots were inoculated into AstromRepliCell® System (ARS) bioreactors and cultured for 12 days under different culture conditions, harvested, and combined with porous ceramics, implanted into SCID-17 mice, harvested 6 weeks later and evaluated for *in vivo* bone formation. Control Mesenchymal Stem Cells (MSCs) were obtained from the same donor, when possible, or were prepared from marrow obtained from University Hospitals of Cleveland (All procedures had Institutional Review Board approval) and were cultured under standard conditions. All RepliCell®-derived cells were evaluated for cells expressing Thy-1+, CD-166+, and CD-105+ cell surface markers by flow cytometry prior to *in vivo* osteogenesis assessment. The Total Cell Population (TCP) obtained by a standard trypsinization, and an Adherent Cell Population (ACP) obtained by trypsinization after non-adherent cell depletion were compared. TCPs and ACPs were tested at ceramic loading concentrations of 5, 10, 25, and 50 million cells per ml. Empty ceramics and MSC-loaded ceramics served as controls. A total of 12 mice were used in each experiment (N=6 for each TCP and ACP sample; N = 12 for negative and positive controls); implantation sites were randomized. Serial sections of implants were scored for bone on a scale of 0-5, under blinded conditions. The bone scores for ACP cells consistently showed higher bone scores than TCP cells (Figure 1). Next, TRC-1 medium (IMDM + 10% FBS, 10% horse serum, hydrocortisone, PIXY321 [an IL-3/GM-CSF fusion protein], erythropoietin, and flt3-ligand), and TRC-3 medium (TRC-1 without exogenous growth factors) were compared. The bone scores for the TRC-3 group (N=11, two donors) were consistently higher than those of the TRC-1 group. Based on these results, BMMNCs were cultured in TRC-3 and MSC conditions and compared side-by-side with the *in vivo* bone assay. The TRC-3 bone scores were indistinguishable from that of MSCs. In addition, flow cytometry data indicate that the *in vivo* bone scores correlate closely ($r^2 > 0.92$) with the cell surface markers Thy1, CD-166 and CD-105.

In Vivo Bone in Total and Adherent BMMNC Populations



Disclosures: J.E. Dennis, Astrom Biosciences, Inc. 2, 5.

SU250

Bone Anabolic Effects of Inhibin A Are Not Mediated by Direct Effects of FSH and LH on Bone Marrow Cells. N. S. Akel, D. S. Perrien, K. M. Nicks*, D. Gaddy. Physiology and Biophysics, University of Arkansas for Medical Sciences, Little Rock, AR, USA.

Inhibin A (InhA) overexpression protects mice from hypogonadal bone loss via a mechanism that stimulates osteoblast activity and possibly differentiation, without effects on bone resorption. InhA is a known suppressor of pituitary follicle stimulating hormone (FSH) secretion, which occurs in this InhA overexpression model, and changes in serum FSH have previously been correlated with increases in bone turnover in peri-menopausal women. Therefore, the goal of the current study was to determine if osteoblast progenitors are directly responsive to FSH, which might play a role in mediating the anabolic effects of InhA *in vivo*. Our bigenic *Glvp/InhA* mouse model of mifepristone (MFP)-induced InhA overexpression was used. Placebo or MFP pellets were inserted in 6-month old intact mice to induce InhA overexpression, and bone marrow cells harvested after 1, 2, 3, and 4 weeks of control or InhA overexpression, as confirmed by ELISA. *Ex vivo* bone marrow cultures were initiated and cells cultured in osteogenic medium with or without 10 ng/ml of the pituitary hormones FSH, or luteinizing hormone (LH). At 10 and 28 days of culture, cells

were harvested and stained and alkaline phosphatase positive (AP+) and Alizarin Red positive (CFU-OB) colonies determined, respectively. Following an initial suppression of AP+ colony development (45%) after 1 wk of *in vivo* InhA overexpression ($p < 0.05$), AP+ colonies were significantly increased in response to *in vivo* InhA overexpression for 2, 3, or 4 weeks ($p < 0.05$). AP+ colony formation in bone marrow cultures established from either placebo control animals or InhA overexpressing animals was unaffected by *in vitro* treatment with either FSH or LH. Similarly, InhA overexpression significantly increased *ex vivo* development of Alizarin Red + CFU-OB whereas FSH or LH treatment *in vitro* had no effect on CFU-OB development. To exclude the possibility that lack of FSH and LH responsiveness was unique to our InhA overexpression model, similar osteogenic bone marrow cultures were established from untreated adult Swiss-Webster mice. AP+ colony development was unaffected by treatment with either FSH or LH, compared with control osteogenic medium. Together, these data indicate that osteoblast progenitors are not direct targets of FSH or LH action, and suggest that the demonstrated anabolic effects of InhA are not mediated by direct action of pituitary FSH or LH on bone marrow progenitors. Instead, InhA anabolism may occur through increases in the commitment and/or proliferation of osteoblast progenitors.

Disclosures: D. Gaddy, None.

SU251

Expression and Localization of Osteoactivin in Alveolar Bone Regeneration in Post-Extraction Healing Sockets in Normal and Diabetic Rat Model. R. A. Aswad^{*1}, M. C. Rico¹, H. Devlin^{*2}, S. N. Popoff¹, E. F. Safadi¹. ¹Anatomy and Cell Biology, Temple University, Philadelphia, PA, USA, ²Restorative Dentistry, Temple University, School of Dentistry, Philadelphia, PA, USA.

Delayed healing and impaired alveolar bone regeneration in post-extraction sockets is one of the complications in patients with type I diabetes. In our laboratory we previously showed using a fracture repair model that OA was highly expressed at sites of active osteogenesis. Furthermore, osteoactivin (OA) is known to play a critical role in osteoblast differentiation and function. In this study we investigated the expression and localization of OA during healing of extracted teeth sockets in normal and streptozotocin-induced diabetic rat. One week after the induction of diabetes, animals underwent the extraction of first and second right maxillary molars. Animals were then sacrificed at three, five, seven and ten days post-extraction and sockets were harvested for qPCR and immunohistochemical (IHC) analyses. RNA expression of OA and bone-related genes including alkaline phosphatase, type I collagen, osteocalcin and osteopontin determined by qPCR was significantly decreased in the diabetic sockets compared to control. IHC analysis showed OA expression was localized in osteoprogenitor cells and differentiating osteoblasts within the socket and the expression level was decreased in diabetic compared to normal rats. To further examine the effect of glucose treatment on OA expression in osteoblasts, an *in vitro* study was undertaken to support our *in vivo* results. Primary osteoblast cultures were established and treated with and without different concentrations of D-glucose. Glucose-treated cultures showed an increase in alkaline phosphates staining, nodule formation and calcium deposition compared to control cultures. Glucose treatment also decreased OA mRNA and protein expression determined by qPCR and Western blot analyses and this reduction was associated with a decrease in osteoblast-related genes. In addition cultures treated with OA recombinant protein seemed to rescue the effect of glucose treatment on osteoblast differentiation markers. Future studies will examine the mechanism of action of glucose treatment regulation on OA expression and its relation to osteoblast differentiation and function.

Disclosures: R.A. Aswad, None.

SU252

***In Vitro* Proliferation and Differentiation Assays of Secreted Frizzled-Related Protein 3 (SFRP3) Transgenic Mice.** Y. Chung¹, H. Song^{*1}, E. Yu^{*1}, Y. Shen^{*1}, S. Ahn^{*1}, D. Kim^{*1}, K. Lee^{*1}, Y. Rhee^{*2}, S. Lim². ¹Endocrinology, Ajou University School of Medicine, Suwon, Republic of Korea, ²Endocrinology, Yonsei University College of Medicine, Seoul, Republic of Korea.

The authors reported previously that exogenous SFRP3 decreased proliferation and increased differentiation in osteoblast cell culture (J Bone Miner Res 19:1395-1402, 2004). Further studies with SFRP3 transgenic mice were conducted. Osteoblast-like cells were cultured from 12-week and 40-week-old transgenic mice. MTT assay was performed after 48 hrs of explant cell culture. Alkaline phosphatase activity was measured after 3 and 6 days of bone marrow stromal cell culture. Mineral nodules were counted after alizarin red-S stain with 30 days of bone marrow stromal cell culture with mineralization media including ascorbic acid and beta-glycerophosphate. There were no significant differences in cell numbers between 40-week-old wild and transgenic mice (0.110 vs. 0.098). Alkaline phosphatase activities were not significantly different between wild and transgenic mice of 12-week-old (50 vs. 54 mU/mg protein) and 40-week-old (448 vs. 541 mU/mg protein). Mineral nodule numbers were not different between 40-week-old wild and transgenic mice (45 vs. 43). *In vitro* cell proliferation and differentiation experiments of SFRP3 transgenic mice were not significantly different with wild mice of 12-week and 40-week-old age.

Disclosures: Y. Chung, None.

SU253

P2X7 Receptors Act through a Cell-autonomous and Cyclooxygenase-Dependent Mechanism to Stimulate Bone Formation. N. Panupinthu^{*1}, H. Z. Ke², S. M. Sims^{*1}, S. J. Dixon¹. ¹CIHR Group in Skeletal Development and Remodeling, University of Western Ontario, London, ON, Canada, ²Pfizer Global Research and Development, Groton, CT, USA.

Nucleotides are released in response to mechanical stimuli and can activate P2X7 receptors, ATP-gated ion channels present on osteoblasts, macrophages and osteoclasts. P2X7 receptor knockout (KO) mice display a skeletal phenotype involving decreased periosteal bone formation and increased trabecular bone resorption, but no change in longitudinal bone growth (Mol. Endocrinol. 17: 1356-67, 2003). Our purpose was to investigate the mechanism through which P2X7 receptors influence bone formation. Cells were isolated from the calvariae of newborn rats and mice by sequential collagenase digestion. Approximately 40% of cells in these osteoblast-enriched cultures were found to express functional P2X7 receptors using a pore formation assay. After reaching confluence, cultures were supplemented with ascorbic acid (50 µg/ml) and β-glycerophosphate (2 mM) to induce nodule formation. Cells expressing P2X7 receptors were found to be associated with bone nodules. Alkaline phosphatase (AP) activity and mineral deposition were quantified by digital image analysis. Mineralization in cultures of cells isolated from P2X7 KO mice was markedly reduced compared to wild-type (WT). At day 21, mineralized area in KO cells was approximately half that in WT, with no difference in AP-positive area. Furthermore, benzoylbenzoyl-ATP (BzATP, a relatively potent P2X7 receptor agonist, 100 µM) promoted mineralization in rat calvarial cell cultures (BzATP induced an 80% increase in mineralized area at day 21). Since BzATP activates several P2 receptors in addition to P2X7, we examined the effect of UTP, which activates a number of P2Y receptors but not P2X7. In contrast to BzATP, neither UTP (100 µM) nor inorganic phosphate (300 µM) affected mineralization at day 21. These data indicate that nucleotides act specifically via P2X7 receptors on osteoblastic cells to promote bone formation. Next we investigated underlying signaling pathways. We have shown previously that P2X7 receptors couple to activation of phospholipase A2, leading to dynamic membrane blebbing of undifferentiated calvarial cells. In rat calvarial cell cultures, inhibition of cyclooxygenases by ibuprofen (10 µM) abolished the stimulatory effect of BzATP on bone formation without affecting mineralization in control cultures. Taken together, these data establish that P2X7 receptors act through a cell-autonomous, cyclooxygenase-dependent mechanism to enhance bone formation. Thus, nucleotides released in response to mechanical stimuli may act through P2X7 receptors to stimulate osteogenesis.

Disclosures: N. Panupinthu, None.

SU254

Necessity of Immune Recognition and Control of a Human Organ Stem Cell Circulating in Blood as a Monocyte, in Order to Avoid Proliferating Diseases. Consequences in Term of Transplantation. M. Labat¹, G. Mouthon^{*2}, F. Escaig^{*2}, P. Boireau^{*3}. ¹Life Sciences, CNRS, Maisons-Alfort, France, ²Chimie Physique, ENVA, Maisons-Alfort, France, ³UMR 956, INRA/AFSSA/ENVA, Maisons-Alfort, France.

The aim is the study of the control circulating organ stem cells that are normally almost quiescent but may proliferate, migrate and differentiate in order to participate in tissue repair. Such powerful cells have to be tightly controlled in order to avoid fibrosis and/or malignancies. Organ stem cells are characterized by immunofluorescence and their destruction by phagocytic T lymphocytes (PTLs) is studied by time-lapse microcinematography. Organ stem cells circulate under the appearance of monocyte that constitutively express HLA-DR molecules. Spontaneous expression of neuronal markers favors a neural crest origin. Once they started to differentiate after the adhere to the support in vitro, they became both the activators and the targets of PTLs that penetrate and circulate inside these stem cells, under complete destruction of the latter. It is a beneficial exception to the principle of self-tolerance that avoids their accumulation out of a precise repair purpose. Contrarily, in disorders such as fibrosis and malignancies (chondrosarcoma), clones of organ stem cells proliferate indefinitely, escape destruction by PTLs and as a consequence, accumulate, giving rise to a 'tissue' that evokes the disorder of the patient. In vivo, this control probably takes place at the capillary-tissue interface. Failure in the control of circulating stem cells is involved in the early steps leading to fibrosis and malignancy. Therefore, in term of transplantation, to avoid such disorders, the host has to be able to control the grafted organ stem cells. Transplantation rules for stem cells differ from those for specialized cells: although they are not rejected when transplanted into a mismatching host, transplanted organ stem cells have to be of the same tissue type as the recipient, in order to allow their control.

This work was supported by a grant from Foundation Jérôme Lejeune.

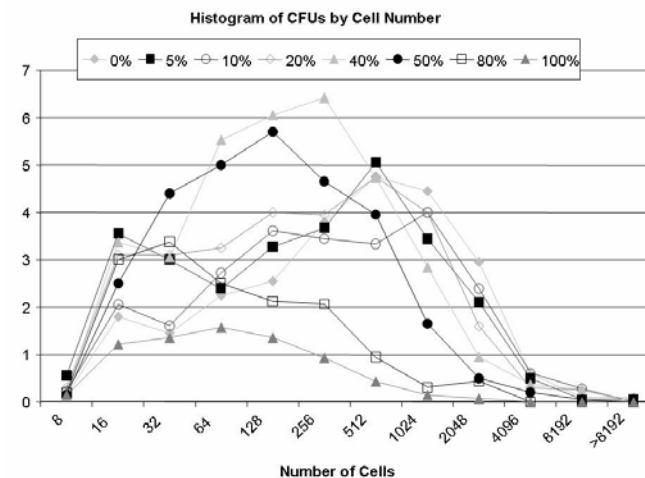
Disclosures: M. Labat, None.

SU255

Effects of Wnts on Colony Formation and Proliferation in Human Connective Tissue Progenitor Cells. R. Rakos^{*1}, C. Boehm^{*2}, J. Tao^{*2}, K. Powell^{*2}, G. F. Muschler³, S. Villarruel^{*2}. ¹Department of Biomedical Engineering, Cleveland Clinic Foundation and Hathaway Brown School, Cleveland, OH, USA, ²Biomedical Engineering, Cleveland Clinic Foundation, Cleveland, OH, USA, ³Orthopaedics and Biomedical Engineering, Cleveland Clinic Foundation, Cleveland, OH, USA.

Connective Tissue Progenitor cells (CTPs) are capable of developing into a variety of tissues including bone, cartilage, fat, and muscle. Optimal assay and use of CTPs in therapeutic applications requires improved characterization CTPs from human tissues and their response to mediators of proliferation and differentiation. Wnt signaling is an important regulator of these events. Wnt proteins bind to transmembrane Frizzled receptors, preventing GSK-3β driven phosphorylation of β-catenin and its subsequent degradation. Wnts: 6, 7a, 8b, and 10a are present in SW480 conditioned media. This study assessed the response of CTPs to these exogenous Wnts using a new quantitative colony-forming unit assay strategy. Human marrow-derived CTPs were cultured for 9-days, under increasing doses of SW480 conditioned media (CM) (0% to 100%). Colony formation as a cell level was assessed using quantitative image analysis of DAPI stained colonies. Large field of view (FOV) images (2x2cm²) were created using a digital camera/motorized microscope controlled by Metamorph. Image analysis algorithms were developed using C/C++ in a Motif X-Windows TM environment. In eleven patient donors, a total of 3,564 colonies containing 1,279,826 total cells were assayed. Colony formation and proliferation were both Wnts signaling dependent, but affected at different dose ranges. Maximum colony formation occurred at 40%CM, and was dramatically reduced at CM ≥ 80%. In contrast, proliferation (cells per colony) decreased progressively with increasing CM. CM ≥ 80% s produced a majority of small colonies (16-128 cells), whereas, 0%CM-20%CM primarily produced large (512-2048) cell colonies. Colony area also decreased 10-fold between 0%CM and 100%CM. These data demonstrate the robust potential for large FOV colony level quantitative image analysis in identifying independent effects of Wnt and other exogenous factors on CTP activation, proliferation, migration and differentiation.

Figure 1: Histogram of colony number by size (cell number) under increasing Wnt signaling environments.



Disclosures: R. Rakos, None.

SU256

The Effect of Secreted Frizzled-Related Protein 3 (sFRP3) Over-Expression on Bone Metabolism. Y. Rhee¹, S. Park^{*1}, J. Lee^{*1}, J. Byun^{*2}, Y. Chung³, S. Lim¹. ¹Internal Medicine, College of Medicine, Yonsei Univ., Seoul, Republic of Korea, ²Brain Korea 21 Project for Medical Sciences, College of Medicine, Yonsei Univ., Seoul, Republic of Korea, ³Internal Medicine, Ajou University School of Medicine, Suwon, Republic of Korea.

sFRP3 is known to have a strong influence on limb skeletogenesis. *In vitro* treatment of sFRP3 inhibited the proliferation of the primary cultured osteoblasts and surprisingly accelerated the differentiation of these cells. Therefore, to see the *in vivo* effect of sFRP3 over-expression, we generated sFRP3 transgenic mice. After testing the sFRP3 gene construct in vitro as to secreting the sFRP3 protein, the gene was integrated into C57BL/6 mice. The COL1A1 promoter (2.3kb) was used for the gene to be specifically expressed in the osteoblasts. The 3 generation with sFRP3 over-expression confirmed by PCR & Southern blot generation was bred. The mice with various ages from the most successfully bred generation were tested. The whole body densitometry by PIXIMUS (Lunar, USA) was compared (Figure 1). There was tendency of Tg mice to be in the lower level of BMD throughout the ages with no statistically significant differences between the wildtype and the Tg mice. Some of these mice were assessed by the microcomputed tomography (Skyscan) of L2 vertebrae without any differences between two groups. However, 20 male mice and 10 female mice which were grew for another 4 months showed an interesting change. There was significantly more increase in the BMD of the Tg female mice (11%) compared with Wt mice (6%) with no differences in the male mice group. Additional result of the response to the anabolic agent is being tested and will

be addressed. In conclusion, it seemed that sole over-expression of sFRP3 was not enough to see the effect of modifying the wnt pathway to find specific phenotype. However, according to an accelerated differentiation *in vitro* might well be adapted to interpret the higher increase in the gain of BMD during the normal growth period in the female sFRP3 Tg mice.

Disclosures: **Y. Rhee**, None.

SU257

Nitrogen-Containing Bisphosphonates Activate Purinergic Receptor Signalling and Induce the Expression of Hsp90/Hsp47 in Osteoblast Cell Lines. G. Tell^{*1}, M. Romanello^{*2}, N. Bivi^{*1}, A. Pines^{*2}, D. de Feo³, L. Moro^{*1}. ¹Biomedical Science and Technology, Udine University, Udine, Italy, ²Biochemistry, Center for the Study of Metabolic Bone Diseases, Trieste University, Trieste, Italy, ³Procter & Gamble, Rome, Italy.

The reduction in fracture risk with bisphosphonate (BP) treatment cannot be explained by the increase in BMD alone, and beneficial effects on other aspects of bone quality need to be considered. BPs prevent osteoblast apoptosis by a mechanism involving extracellular signal-regulated kinase (ERK) activation, but whether this has a role in BP effects on bone formation and bone quality *in vivo* is unclear. We investigated the hypothesis that this effect on osteoblasts is mediated through cellular membrane purinergic receptors, which based on recent data might provide a link to control of collagen structure and thus to bone quality. The existence of possible cross-talk between BPs and purinergic receptor signalling might be expected since both nucleotide triphosphates and BPs have a high negative charge. In previous work we demonstrated that in response to mechanical stress, osteoblasts release ATP via a non-lytic mechanism. In addition, extracellular nucleotides exert stimulatory effects on osteoblasts via the P2 family of membrane-bound receptors that comprise P2Y (G-protein-coupled) and P2X (ligand-gated ion channel) receptors, by acting on Egr-1 and Runx2 transcription factors (Pines et al. Biochem. J. 2003 373: 815-824; Costessi et al., Bone 2005 36 418-432). In this study in co-stimulatory experiments on different osteoblast-like cells (HOBIT, MG-63, ROS17/2.8, Saos-2), we found that purinergic signaling was activated by direct and indirect BP (10⁻⁷M) induction of ERKs phosphorylation. Both risedronate and alendronate significantly promoted non-lytic ATP extrusion. The BP-induced ERK-1/2 phosphorylation was partially blocked by pretreatment of the cells with the ATP/ADPase apyrase. In addition, BP-induced ERK phosphorylation was not seen in the ROS17/2.8 cell line not expressing P2Y1 and P2Y2 receptors, and was blocked by suramin. These data support a primary role for P2Y receptors in mediating the BP activation of ERK and ERK phosphorylation. The relevance of these observations is significant in light of recent data showing that the expression of chaperonin is a target of purinergic signalling. In fact, both Hsp90beta protein, which has a protective and mitogenic roles, and Hsp47 protein, which is strongly involved in the control of collagen folding and therefore on the quality of collagen fibril, are stimulated by BPs. Thus these data provide a new explanation for a molecular mechanism of BP action which may ultimately result in effects on bone quality.

Disclosures: **G. Tell**, None.

SU258

Activation of p38 MAP Kinase Mediates Induction of Prostaglandin Synthesis and Bone Resorption by Metabolic Acidosis. N. S. Krieger, K. LaPlante^{*}, J. Sullivan^{*}, D. A. Bushinsky. Medicine, University of Rochester, Rochester, NY, USA.

Chronic metabolic acidosis stimulates net calcium (Ca) efflux from bone by modulation of osteoblastic activity leading to stimulation of osteoclastic bone resorption. This acid-induced bone resorption is mediated, in large part, by stimulation of osteoblastic cyclooxygenase 2 (COX2) mRNA and subsequent prostaglandin E2 (PGE2) synthesis; however, the initial signaling pathway(s) activated by acidosis in the osteoblast are not known. Activation of p38 MAP kinase (p38) has been shown to regulate COX2 and subsequent PGE2 production. We utilized a specific inhibitor of p38, SB203580 (SB), to determine the role of p38 in acid-induced stimulation of PGE2 synthesis and bone resorption. We incubated neonatal mouse calvariae for 48 h in neutral pH (pH=7.45, [HCO3-] =24 mM, Ntl) or physiologically acid pH (pH=7.19, [HCO3-]=12 mM, Acid) medium in the absence or presence of 10 M SB. SB significantly inhibited the acid-induced increase in PGE2 production and net Ca efflux at both 24 and 48h (Table, below). P38 is activated by phosphorylation. To determine if there is also an increase in phosphorylated p38 (phos-p38) in response to acid, we measured changes in phos-p38 compared to total p38 levels in primary cells isolated from calvariae, which are almost exclusively osteoblasts. Cells were made quiescent by overnight incubation in Ntl medium in the absence of serum and then incubated in Ntl or Acid medium each containing 1% serum. Cells were lysed in the presence of phosphatase inhibitors followed by Western analysis using a specific antibody to phos-p38; blots were reprobbed with an antibody to total p38 to normalize data. Compared to incubation in Ntl medium, incubation in Acid led to a significant increase in the ratio of phos-p38 to total p38 within 1 min (Ntl= 100%+3; Acid = 139%+9, p<0.05). Thus acid-induced activation of p38 appears to be an integral signaling step leading to induction of COX2 mRNA and subsequent PGE2 production in the osteoblast, ultimately resulting in increased osteoclastic bone resorption.

@ 48h	Ntl	Acid	Ntl + SB	Acid + SB
Ca (nmol/bone)	113 +/- 55	658 +/- 78*	17 +/- 64+	392 +/- 57*+o
PGE2 (ng/ml)	0.7 +/- 0.8	2.4 +/- 0.8*	0.3 +/- 0.1+	0.5 +/- 0.2+
*p<0.05 vs Ntl	+p<0.05 vs Acid	op<0.05 vs Ntl + SB		

Disclosures: **N.S. Krieger**, None.

SU259

Differentiation Switch of Mesenchymal Stem Cells through Suppression of PPARgamma Function by NLK. I. Takada^{*}, M. Suzawa^{*}, S. Takezawa^{*}, Y. Yogiashi^{*}, Y. Mezaki^{*}, M. Igarashi^{*}, S. Kato. Nuclear signalling, Institute of Molecular and Cellular Bioscience, University of Tokyo, Tokyo, Japan.

Pluripotent mesenchymal stem cells in bone marrow differentiate into osteoblasts, adipocytes and the other cells. Balanced cytodifferentiation of stem cells is essential for the formation and maintenance of bone formation, however the mechanism of these differentiation switch is largely unknown. Recently, several factors controlling these cytodifferentiation have been identified. Among them, PPARgamma is known as a major inducer of adipogenesis. PPARgamma is a ligand-dependent nuclear receptor and activated by fatty acid derivatives and synthetic compounds such as the TZDs. In addition, several cytokine signals are known to modulate the transactivation function of PPARgamma in a ligand-independent manner. We previously found that TAK1-NIK/NFkappaB signaling activated by IL-1 or TNFalpha, strongly suppressed the ligand-dependent transactivation function of PPARgamma and inhibited adipogenesis of bone marrow mesenchymal stem cells (Suzawa, et al., Nat. Cell Biol. 2003, 224-230). Interestingly, PPARgamma ligand together with IL-1 or TNFalpha potentiate differentiation of ST2 cells into osteoblasts. These results raised the possibility that the transactivation function of PPARgamma might be suppressed by other signlaing molecules. To identify such factors, we examined the transcriptional activity of PPARgamma in ST2 cells using a reporter assay and found that NLK(Nemo Like Kinase), which is a MAP kinase like protein, suppressed the transactivation function of PPARgamma. NLK is activated by Wnt or TGFbeta through CaMKII-TAK1/TAB2 cascade and we confirmed that these signaling cascade also suppressed the PPARgamma function. We then elucidated molecular mechanism of this repression and found that the C-terminal region of NLK is required for repression activity. We have established the HeLa cells stably expressing Flag-NLK and purified a number of NLK interacting proteins from these cells. As a result, we identified NLK interacting proteins and found that histone modification played a significant role in the repression of PPARgamma function by NLK. Thus, we found that suppressive PPARgamma function by activated NLK is involved in differentiation switch of mesenchymal stem cells into osteoblastgenesis.

Disclosures: **I. Takada**, None.

SU260

Adenosine Receptor Expression by MC3T3-E1 Osteoblasts. J. M. Russell^{*}, H. P. Benton^{*}. VM:Anatomy, Physiology and Cell Biology, University of California, Davis, CA, USA.

Extracellular purine and pyrimidine nucleotides and nucleosides signal through two classes of purine receptors: P1 which primarily recognize adenosine and P2 which primarily recognize ATP and related molecules. Interest is growing in the role of ATP in bone metabolism via P2 receptors but the P1 receptor class has not yet been explored in bone cells. The purpose of this study was to determine whether osteoblast cells express members of the P1 purine receptor class (A1, A2a, A2b, A3) that bind adenosine. MC3T3-E1 (clone 14) cells were grown in alpha minimal essential medium with 10% FCS and antimicrobial agents. Total RNA was isolated (RNeasy mini kit, Qiagen, Inc) and P1 adenosine receptor transcripts were reverse transcribed and then amplified (ONestep RT-PCR, Qiagen). Receptor protein expression was investigated using receptor sub-type specific polyclonal antibodies (Abcam, Inc) for immunostaining of cells cultured on glass coverslips. Using gene specific primers for the A1, A2a and A2b receptor gene transcripts, RT-PCR produced a single band, as resolved by gel electrophoresis. Identity of each band was confirmed by sequencing. Using gene specific primers for the A3 receptor gene transcript, multiple bands were observed along with the expected product, suggesting the presence of multiple isoforms. By immunofluorescence, all four known adenosine receptor sub-types were identified on the osteoblast cell surface. The P2 receptors that recognize ATP are G protein-linked calcium mobilizing receptors whereas the P1 adenosine receptors are all linked to adenylate cyclase with the A2a and A2b receptors stimulating cAMP via Gs and the A1 and A3 receptors inhibiting cAMP via Gi, resulting in protein kinase A (PKA) activation or inhibition. It is well accepted that the cAMP-linked pathways, through which adenosine receptors are known to act, are essential for regulating bone metabolism. For example, PTH is a major player in the regulation of osteoblast function and many of the actions of this hormone are known to be PKA-dependent. Our results identifying adenosine receptors on osteoblasts indicate that manipulation of this class of receptors, using receptor specific agonists and antagonists, may represent a novel mechanism through which PKA-dependent osteoblast responses can be manipulated.

Disclosures: **H.P. Benton**, Centocor Inc 2.

SU261

Endothelin-1 Stimulates Bone Formation by Regulating Osteoblast Secretion of the Paracrine Regulators IL-6, Cyr61, CTGF and Dkk1. G. A. Clines, K. S. Mohammad, L. L. Wessner^{*}, J. M. Chirgwin, T. A. Guise. Internal Medicine, University of Virginia, Charlottesville, VA, USA.

Endothelin-1 (ET-1) secreted by breast and prostate cancers activates the endothelin A receptor (ETAR) on osteoblasts, leading to cellular proliferation and new bone formation. ETAR blockade inhibits osteoblastic responses and prevents the development of bone metastases in an animal model. This treatment also reduces progression of bone metastases in men with advanced prostate cancer. Targets of ET-1 action in osteoblasts were identified by gene microarray analysis of murine calvarial organ cultures and confirmed by real-time RT PCR of primary osteoblast cultures. We focused on secreted factors with potential

ASBMR 27th Annual Meeting

effects on bone. Transcripts for interleukin-6 (IL-6) and two related proteins, cysteine-rich protein 61 (Cyr61) and connective tissue growth factor (CTGF) were increased within one hour of ET-1 treatment. Messenger RNA for the Wnt inhibitor dickkopf homolog 1 (Dkk1) was decreased by 24 hours. These effects of ET-1 on osteoblast transcription were blocked by an antagonist selective for the ETAR receptor, but not by one selective for the endothelin B receptor. IL-6 has complex effects on bone, while CTGF is an established stimulator of osteoblast proliferation and bone formation. We concentrated on the less-understood roles of Dkk1 and Cyr61. Recombinant Dkk1 blocked ET-1-mediated increases in osteoblast numbers and new bone formation in calvarial organ cultures but did not suppress basal levels of new bone formation. Dkk1 also blocked the actions of two other osteoblast stimuli, insulin and BMP2. Conversely, Dkk1 neutralizing antibodies markedly increased osteoblast numbers and new bone formation. These data suggest that ET-1 acts on osteoblasts via a common Dkk1 inhibitory pathway through which multiple factors regulate new bone formation. Cyr61 and CTGF are expressed in the developing skeleton, but an action of Cyr61 on osteoblasts has not been reported. Human Cyr61 protein expressed under control of the CMV promoter was delivered to calvarial organ cultures by transduction with a lentiviral vector for 48 hours. Cyr61 lentivirus resulted in significant new bone formation (10,700 μm^2) equivalent to positive control, compared to control beta-galactosidase lentivirus or untreated control calvariae (5,200 μm^2) ($p < 0.01$). Our results suggest that ET-1 stimulates new bone formation by inducing osteoblast expression of paracrine factors. The negative regulator Dkk1 may be a common mediator of many bone anabolic agents, while Cyr61 and CTGF may be positive paracrine stimulators of bone in response to tumor-secreted ET-1.

Disclosures: **G.A. Clines**, None.

SU262

IGF-1 Stimulated beta3 Integrin Recruitment Is Associated with Potentiation of the IGF-1 Receptor. **R. K. Long***, **S. Nishida**, **D. D. Bikle**. Endocrine Unit, University of California, Veterans Affairs Medical Center, San Francisco, CA, USA.

Recent studies have demonstrated an interaction between the IGF-1 and integrin signaling pathways in osteoblasts. Skeletal unloading by hind limb suspension of rats causes IGF-1 resistance by blunting IGF-1 receptor phosphorylation following IGF-1 binding. Bone marrow stromal cells (BMSC) from these unloaded limbs demonstrate a decreased expression of the beta3 integrin subunit. Echistatin, an alphaVbeta3 integrin blocker, when added to BMSC, recapitulates the IGF-1 resistant state of unloading suggesting a role for alphaVbeta3 integrin in IGF-1 signaling in rats. The role of the beta3 integrin subunit in IGF-1 signaling of human osteoblasts was evaluated. Human fetal osteoblasts (ATCC hFOB 1.19) were grown to confluence. Cells were transitioned to a non-proliferative environment, serum free at 37 degree C, for various periods of time and treated with IGF-1 (100 ng/mL) or vehicle for 10 minutes. Binding of beta3 integrin subunit to the IGF-1 receptor and its activation by IGF-1 were evaluated by immunoprecipitation and immunoblotting. Activation of the hFOB IGF-1 receptor in response to IGF-1 treatment as assessed by its tyrosine phosphorylation increases as a function of time in culture in a non-proliferative environment. This increased activation of the IGF-1 receptor is accompanied by a coincidental increase in the amount of beta3 integrin subunit bound to the IGF-1 receptor. In addition, IGF-1 treatment further increased the amount of beta3 integrin subunit bound to the IGF-1 receptor. The correlation between increased intensity of IGF-1 receptor phosphorylation and increased amount of IGF-1 receptor bound beta3 integrin subunit suggests a regulatory role for the integrin subunit in IGF-1 signaling pathway in human osteoblasts. The increase in beta3 integrin binding to the IGF-1 receptor in response to IGF-1 illustrates an "inside-out" activation of integrin signaling. The binding of the beta3 integrin subunit in turn may potentiate the "outside-in" activation of the IGF-1 receptor by IGF-1.

Disclosures: **R.K. Long**, None.

SU263

Bone and Cartilage Stimulating Peptides (BCSP) "Superactivate" Osteoblast-Like Cell Lines to Increase Adhesion on Collagen Substrates. **J. W. Terryberry***, **J. Auluck**, **D. R. Sindrey**. Millenium Biologix Corp., Mississauga, ON, Canada.

Several collagen-derived fragments and peptides have been shown to exert various effects on cell migration, proliferation and differentiation. Some cryptic and exposed sequences in collagen I provide ligand binding sites for a spectrum of integrins, including $\alpha 1\beta 1$, $\alpha 2\beta 1$, $\alpha 9\beta 1$, $\alpha 11\beta 1$ and $\alpha 11\beta 3$. Bone and Cartilage Stimulating Peptides (BCSP™) are matricryptic peptides found in collagen I (procollagen 1A1 1156-1174). We compared their effects in a standardized cell adhesion assay to other non-overlapping sequences reported in the literature to exert effects on integrin binding and/or osteoblast-like cell adhesion. Peptides were tested for inhibitory or activating activity using collagen substrates coated onto microtiter plates, in conjunction with two human osteoblast cell lines: MG-63 ($\alpha 2\beta 1$ integrin-dominant) and SAOS-2 ($\alpha 1\beta 1$ integrin-dominant). Cumulative results indicated that BCSP-1, -12, and -21 caused significant ($p < 0.05$) increases in the adhesion of SAOS-2 cells to collagen at doses of 0.2-2.0 μM . Superactivation, defined as the ability of a ligand to promote receptor binding, was greatest for BCSP-1 and -12 ligands facilitating the binding of SAOS-2 cells to rat tail collagen I substrate. Less dramatic activating effects were seen with MG-63 suggesting that the BCSP sequence exhibits preferential partial agonist activation of $\alpha 1\beta 1$ integrin. Control peptides "P-15" (PepGen, procollagen 1A1 947-961) and KTTKS (procollagen 1A1 1430-1435) were without any activating or inhibitory effects on cell adhesion; whereas the $\alpha 2\beta 1$ integrin-binding sequence DGEA (procollagen 1A1 232-235) demonstrated significant inhibitory antagonistic effects at high doses ($> 100 \mu\text{M}$). A Newman-Keuls multiple comparisons test revealed that dose responses to all 3 BCSPs were significantly ($p < 0.001$)

different than that obtained for DGEA. Moreover, the RGD peptide GRGDSPK inhibited adhesion at doses $> 1 \mu\text{M}$, indicating that it too was a functional antagonist as opposed to BCSP's agonistic effect. These findings demonstrate that BCSP ligands have significant osteoinductive potential at physiological doses, whereby they activate osteoblast like cells to adhere to the extracellular matrix in what is likely to be an integrin-mediated allosteric mechanism. This is in contrast to the effects of DGEA and RGD peptides which act as integrin-binding competitive substrates rather than ligands that conformationally activate the receptor from a low affinity to a high affinity state. Further studies are in progress to determine the binding parameters of BCSPs to purified integrins and recombinant ligand-binding (inserted) domains.

Disclosures: **J.W. Terryberry**, Millenium Biologix Corp. 3.

SU264

Wnts Suppress Osteoclast Survival and Formation and Prevent Apoptosis of Uncommitted Osteoblast Progenitors and Osteoblasts by β -Catenin-Dependent as well as Independent Signaling Cascades Involving Src/ERK and PI3K/Akt. **M. Almeida**, **L. Han**, **A. Warren***, **T. Bellido**, **S. C. Manolagas**, **S. Kousteni**. Div. Endocrinol., Center for Osteoporosis and Metabolic Bone Diseases, Central Arkansas Veterans Healthcare System, Univ. Arkansas Med. Sci., Little Rock, AR, USA.

Murine models with mutations in LRP5 and secreted Frizzled-related protein-1 have revealed an involvement of Wnt signaling in the control of osteoblast apoptosis. Based on this, we examined the ability of canonical and non-canonical Wnts to affect the survival and/or formation of bone cells. We have found that in cultures of the uncommitted cell line C2C12, the pre-osteoblastic cell line MC3T3-E1, or the MLO-Y4 osteocytic cell line serum withdrawal from the culture medium or etoposide induced apoptosis within 6 hours, which could be reversed by the addition of purified Wnt3a protein or transfection of a Wnt1 expression plasmid. Importantly, MC3T3-E1 cells transfected with an expression plasmid for the non-canonical Wnt5a were also protected from apoptosis. In MC3T3-E1 cells, Wnt3a induced a rapid (within 2 min) and transient phosphorylation/nuclear accumulation of ERKs as well as phosphorylation of Akt. However, Dkk1, an inhibitor of Wnt signaling, did not affect Wnt3a-induced phosphorylation of ERKs or Akt indicating that the kinase-activating actions of Wnt3a do not involve LRP5 and canonical Wnt signaling. Further, the anti-apoptotic effects of both Wnt3a or Wnt5a was abrogated by dominant negative mutants of MEK, Src, PI3K, or Akt. On the other hand, transfection of MC3T3-E1 cells with Dkk1, axin or a dominant negative TCF, abrogated the anti-apoptotic effect of Wnt3a, but did not interfere with the effect of Wnt5a. Nonetheless, activation of canonical Wnt signaling by itself was not sufficient to promote survival as constitutive active β -catenin did not rescue cells from apoptosis. Further, Wnt3a induced phosphorylation of the GSK-3, and increased the expression of the anti-apoptotic protein Bcl-2 in MC3T3-E1 cells; both of these effects were inhibited by the MEK kinase-specific inhibitor PD98059. In contrast to its protective actions on osteoblast precursors and osteoblastic cells, Wnt3a promoted apoptosis of mature bone marrow-derived osteoclasts and suppressed osteoclastogenesis in the presence of 30 ng/ml RANKL and M-CSF. These results demonstrate that irrespective of their ability to activate the canonical pathway, Wnts prolong the survival of osteoblasts, osteocytes, and uncommitted osteoblast progenitors via activation of the Src/ERK and PI3K/Akt signaling cascades. Conversely, Wnt signaling promotes apoptosis of osteoclasts and suppresses osteoclast formation.

Disclosures: **M. Almeida**, None.

SU265

Modulation of Connexin43 Alters the Osteoblast Response to Serum, FGF2 and IGF1. **F. Lima***¹, **C. Niger***¹, **R. Civitelli**², **J.P. Stains**¹.

¹Orthopaedics, University of Maryland School of Medicine, Baltimore, MD, USA, ²Bone and Mineral Diseases, Washington University, St Louis, MO, USA.

Gap junctions composed of connexin43 (Cx43) are abundantly expressed in osteoblasts. Previously, we have shown that activation of extracellular signal regulated kinases (ERK) signaling is required for optimal elaboration of osteocalcin transcription, and that disruption of Cx43 function attenuates both ERK activation and osteocalcin gene transcription. Using highly Cx43-coupled ROS17/2.8 cells and moderately Cx43-coupled MC3T3 cells, we are investigating the molecular details of the influence of Cx43 on osteoblast transcription. In both cell lines, disruption of Cx43 function with chemical inhibitors or connexin45 (Cx45) overexpression followed by serum stimulation results in a ~50% attenuation of extracellular signal regulated kinase (ERK) activation and an attendant > 2 fold decrease in osteocalcin transcription. In contrast, transient overexpression of Cx43 in moderately coupled MC3T3 cells potentiates cellular response to serum stimulation both at the level of ERK activation (66%) and osteocalcin transcription (1.7 fold greater than mock transfected cells). To elucidate growth factors that may transmit signals via Cx43, we have begun to analyze signal transduction and gene transcription in response to treatment of osteoblasts with fibroblast growth factor 2 (FGF2) and insulin-like growth factor 1 (IGF1). Both FGF2 and IGF1 play a critical role in bone formation by regulating osteoblast gene expression. Treatment of MC3T3 cells with 5ng/ml FGF2 and 50ng/ml IGF1 increases phosphorylation of ERK as determined by western blotting, an effect that is attenuated by blocking Cx43 function. In addition, treatment of MC3T3 cells with FGF2 stimulates osteocalcin promoter activity 1.8-fold, as determined by luciferase activity. When Cx43 is overexpressed, the osteocalcin response to FGF2 is potentiated; resulting in a 2.7-fold stimulation, suggesting that Cx43 gap junctions amplify FGF2 activated signaling to affect cellular function. Disruption of Cx43 function by expression of Cx45 attenuates the action of FGF2 on osteocalcin transcription. However, the molecular details of the gap junction-influenced effects of FGF2 on osteocalcin

transcription are still under investigation. Similar to FGF2, overexpression of Cx43 enhances the IGF1-mediated increase in bone sialoprotein expression by >50%, an effect that is not observed when cells are transfected with Cx45. In total, our data reveal that Cx43 regulates signal transduction affecting the responsiveness of osteoblastic cells to growth factors, and gain or loss of function of Cx43 can potentiate and attenuate these responses, respectively.

Disclosures: **F. Lima**, None.

SU266

Ascorbic Acid Protects Osteoblast from ER Stress. Z. Zhao¹, G. Xiao¹, C. Ge^{*1}, D. Jiang^{*1}, R. J. Kaufman^{*2}, R. T. Franceschi³. ¹Department of Periodontics, Prevention, and Geriatrics, School of Dentistry, University of Michigan, Ann Arbor, MI, USA, ²Department of Biochemistry, School of Medicine, University of Michigan, Ann Arbor, MI, USA, ³Department of Periodontics, Prevention, and Geriatrics; Department of Biochemistry, University of Michigan, Ann Arbor, MI, USA.

The osteoblast is a major secretory cell responsible for production of collagen and other extracellular matrix (ECM) proteins of bone. The synthesis and secretion of this ECM is highly regulated in response to the dynamic changes occurring during skeletal development and remodeling. Ascorbic acid (AA) promotes collagen matrix production by stimulating procollagen hydroxylation and folding, which is necessary for proper ECM assembly. We previously showed that AA-dependent accumulation of a type I collagen matrix stimulates osteoblast differentiation in part by interacting with cells via $\alpha 2\beta 1$ integrins that subsequently stimulate MAP kinase activity and osteoblast-specific gene expression. However, AA may have other functions in osteoblasts related to regulation of the protein folding response. AA may alter matrix production by increasing rates of translation and processing of ECM proteins. The underlying mechanism coupling the synthesis and secretion of these proteins is still unclear. The endoplasmic reticulum (ER) serves as the site where all secretory proteins are folded and assembled. An imbalance between ER protein folding load and the ability to secrete the protein causes ER stress. Eukaryotic initiation factor 2 (eIF2) is involved in the early events of ER stress. ER stress leads to phosphorylation of the α -subunit of eIF2, thereby inhibiting the translation initiation. Here we demonstrated that AA promotes collagen synthesis by inhibition of ER stress. AA induced the dephosphorylation of eIF2 α as early as three hours after treatment. 3,4-dehydroproline, a specific collagen matrix synthesis inhibitor which inhibits collagen hydroxylation, blocks AA-induced dephosphorylation of eIF2 α . AA induced eIF2 α dephosphorylation is mediated by PERK, an eIF2 α kinase, in that AA treatment induced the dephosphorylation of PERK.

Disclosures: **Z. Zhao**, None.

SU267

Both Phosphatidylethanolamine and Phosphatidylcholine Are Hydrolyzed by Phospholipase D following Parathyroid Hormone Treatment of UMR-106 Cells. A. T. K. Singh¹, M. A. Frohman^{*2}, P. H. Stern¹. ¹Dept of Molecular Pharmacology & Biological Chemistry, Northwestern University Feinberg School of Medicine, Chicago, IL, USA, ²Pharmacology, Center for Developmental Genetics, Stony Brook, NY, USA.

Parathyroid hormone (PTH) activation of phospholipase D (PLD) has been identified as a signaling pathway for the hormone in normal osteoblasts and osteoblastic UMR-106 cells. PTH also stimulates phosphatidylcholine (PC) hydrolysis in the cells, although the effects on PLD were several fold greater than effects on PC hydrolysis. In other tissues phosphatidylethanolamine (PE) is also hydrolyzed by PLD. Differential sensitivities of PC and PE hydrolysis to stimulators have been reported. Studies were carried out (a) to determine if hydrolysis of PE is also activated by PTH, (b) to compare the time- and dose-dependence of the effects of PTH on the hydrolysis of the two phospholipids, and (c) to determine if PTH-stimulated PC and PE hydrolysis is mediated through PLD, since phospholipase C can also mediate hydrolysis of these phospholipids. UMR-106 cells were co-labeled with ³H-choline and ¹⁴C-ethanolamine and treated with PTH. ³H and ¹⁴C radioactivity released into the medium was determined by dual channel scintillation counting. The selectivity of radioactive labeling in the products (no significant ³H in ethanolamine and no significant ¹⁴C in choline fractions) was established by thin layer chromatography. PTH (10nM) stimulated PC and PE hydrolysis within 5 min, and the responses were sustained for at least 60 min. PTH (1-100nM) showed biphasic effects on PC hydrolysis, while its effects on PE hydrolysis plateaued at 10nM. The calcium ionophore ionomycin (1 μ M) and the PKC activator phorbol-12,13-dibutyrate (PDBu, 5-500nM) had similar effects to PTH to increase both PC and PE hydrolysis, although PTH effects on PC hydrolysis are not dependent on PKC. To test whether the PTH effects on PC and PE hydrolysis were mediated by PLD, UMR-106 cells were transfected (Lipofectamine Plus[®]) with dominant negative constructs of PLD1 and PLD2, using pcDNA3 as a control vector (48h transfection, 0.5 μ g DNA). The dominant negative constructs inhibited PTH-stimulated increases in PC or PE hydrolysis, suggesting the involvement of PLD in these effects of PTH. The findings indicate that PE is a phospholipid substrate for PTH actions in osteoblasts. The possibility of PE hydrolysis by PLD provides another PTH-stimulated signal that could provide differential regulation of osteoblast responses.

Disclosures: **A.T.K. Singh**, None.

SU268

Activation of PKCdelta Is Required in Wnt-Induced Osteogenesis. X. Tu^{*}, F. Long. Internal Medicine, Washington University in St. Louis, St. Louis, MO, USA.

Wnt signaling has been implicated in osteoblast development, however the underlying mechanism is not understood. By employing a proteomics approach in the mouse stromal cell line ST-2 cells, we identified that a specific substrate for protein kinase C, Myristoylated-Ala-Rich Kinase C Substrate (MARCKS), was markedly phosphorylated in the cytosol of cells stimulated with either Wnt3a conditioned medium or recombinant Wnt3a protein. Moreover, MARCKS phosphorylation induced by Wnt3a was dramatically inhibited by a PKC δ -specific drug, Rottlerin. Remarkably, Rottlerin completely inhibited Wnt3a-induced osteogenesis in ST-2 cells, as assayed by the expression of Alkaline Phosphatase (AP), Collagen I and Bone Sialoprotein (Bsp). Importantly, Rottlerin did not inhibit activation of the canonical pathway by Wnt3a, as neither the induction of a *lef-1-luc* reporter nor the stabilization of β -catenin was affected. Finally, immunostaining experiments demonstrated that recombinant Wnt3a recruited PKC δ to the cell membrane within 30 minutes, and in preliminary experiments siRNA knock-down of PKC δ markedly repressed osteoblast differentiation in ST-2 cells. In summary, these results demonstrate an essential role for PKC δ activation in Wnt-induced osteogenesis.

Disclosures: **X. Tu**, None.

SU269

BCA3 (Breast Cancer-Associated Gene-3) Is a Novel Rac-Interacting Protein in Osteoclasts. K. Yu, T. Itokawa, K. Insogna. Endocrinology, Yale University, New Haven, CT, USA.

Rac-1 is a member of the family of small GTPases with prominent effects on the actin cytoskeleton. In osteoclasts, Rac-1 is required for CSF-1-induced cytoskeletal remodeling. To explore other metabolic pathways in osteoclasts where Rac-1 plays a role, we undertook a yeast two-hybrid screen using the Clontec Matchmaker-3 system with wild-type Rac-1 as bait and a cDNA library prepared from osteoclast-like cells (OCLs) as prey. OCLs were prepared by co-culturing murine bone marrow and calvarial osteoblasts. RNA isolated from these cells was highly enriched for c-src, cathepsin K and calcitonin receptor transcripts. Five clones were identified in an initial mating assay screen of the OCL library, which contained 8.6X10⁵ transformants. A repeat Y2H screen confirmed three of the five clones as Rac-interacting proteins. One of these proved to be BCA3 (Breast Cancer-Associated Gene-3) (GenBank accession number AF512007), a protein previously identified as a primarily nuclear protein that contains SH2 and PDZ domain binding motifs as well as putative phosphorylation sites for PKC and PKA. The transcript for BCA3 was found to be highly expressed in OCLs. To determine if the Rac/BCA3 interaction was direct, the cDNA for BCA3 was translated and radiolabeled using rabbit reticulocyte lysates and ³⁵S-methionine. The radiolabeled protein was used in an *in vitro* pull down with GST-coupled Rac in the presence of ATP. GST-coupled Rac was able to efficiently pull down BCA3 under these conditions, confirming a direct interaction of BCA3 and Rac-1. Deletional analysis of BCA3 revealed that amino acids 76-125 were required for optimal binding of BCA3 to Rac-1. Confocal microscopy demonstrated co-localization of Rac-1 with BCA3 in mature murine osteoclasts using an antibody specific for murine BCA3. Despite the reported nuclear localization of BCA3, Rac-1 and BCA3 co-localized in cytoplasmic and perinuclear areas of osteoclasts. These are the first data demonstrating an interaction of BCA3 with another cellular protein and suggest a possible role for BCA3 in cytoskeletal remodeling. The osteoclast will provide an interesting and physiologically relevant model system in which to test this hypothesis.

Disclosures: **K. Yu**, None.

SU270

AAE581, a Potent and Highly Specific Cathepsin K Inhibitor, Prevents Bone Resorption after Oral Treatment in Rat and Monkey. M. Missbach¹, E. Altmann^{*1}, C. Betschart^{*2}, T. Buhl^{*1}, R. Gamse¹, J. A. Gasser¹, J. R. Green^{*1}, H. Ishihara^{*3}, C. Jerome⁴, M. Kometani^{*3}, M. Susa^{*1}, N. Teno^{*3}, K. Toriyama^{*3}, R. Lattmann^{*1}. ¹Musculoskeletal Diseases, Novartis Pharma AG, Basel, Switzerland, ²Novartis Pharma AG, Basel, Switzerland, ³Novartis Pharma KK, Tsukuba, Japan, ⁴SkeleTech, Bothell, WA, USA.

Cathepsin K has been shown to be highly expressed in osteoclasts and to play an essential role in bone matrix degradation. The effects of AAE581, a reversible inhibitor of cathepsin K on *in vitro* and *in vivo* assays of bone resorption have been examined. AAE581 inhibits cathepsin K with Ki values of 0.7 nM, 4.2 nM and 57 nM, in human, rabbit and rat, respectively. It is highly specific for the human enzyme with an IC50 of 2.5 nM for cathepsin K versus 7700 nM for cathepsin B, 9700 nM for cathepsin L and >10⁵000 nM for cathepsin S. However, for the rat enzymes a reduced specificity profile was detected. Cellular activity *in vitro* was demonstrated by the reduction of the total pit volume produced by rabbit osteoclasts on ivory slices with an IC50 of 16 \pm 0.9 nM (n=3). Bone matrix degradation by human osteoclasts was inhibited with an IC50 of 8.2 \pm 2.1 nM (n=3). *In vivo* activity on bone resorption was tested in ovariectomized rats treated orally with 50 mg/kg bid. AAE581 reduced urinary deoxypyridinoline excretion by 83% after 2 weeks of treatment. In a separate experiment with 100 mg/kg bid over 12 weeks, the ovariectomy-induced loss of cross-sectional BMD at the proximal tibia was prevented by 78% as measured by pQCT. To confirm the ~80-fold higher potency of AAE581 on the human/monkey over the rat enzyme, the compound was evaluated in cynomolgus monkeys rendered estrogen deficient by a depot GnRH agonist. After oral administration of 10 mg/kg bid two serum markers of bone resorption, CTx and NTx, were already at levels far

below those of the non-GnRH treated group at day 1. They remained suppressed throughout treatment over 4 weeks and returned to normal within less than 5 days after the end of dosing with AAE581. Even in intact cynomolgus monkeys, a significant, dose-dependent reduction of serum CTx and NTx compared to vehicle treated animals occurred starting as early as day 1 with an ED50 after 4 day treatment of about 1 mg/kg bid. In conclusion, AAE581 is a highly potent and specific cathepsin K inhibitor that effectively reduces bone resorption markers in rats and monkeys after oral dosing and protects from ovariectomy-induced BMD loss in rats. AAE581 is currently in clinical development for osteoporosis and related diseases with increased bone loss.

Disclosures: **M. Missbach**, Novartis Pharma AG 3.

SU271

Histochemical Examination on the Osteoclastic Function on the Microenvironment of Extracellular Matrices in Osteolytic Metastasis. **M. Li**^{*1}, **N. Amizuka**¹, **K. Takeuchi**^{*2}, **T. Maeda**^{*1}. ¹Division of Oral Anatomy, Niigata University Graduate School of Medical and Dental Sciences, Center for Transdisciplinary Research, Niigata University, Niigata, Japan, ²Division of Oral Anatomy, Niigata University Graduate School of Medical and Dental Sciences, Niigata, Japan.

We have examined the osteoclastic function on the microenvironment of extracellular matrices in osteolytic metastasis, by employing well-standardized lung cancer metastasis model of nude mice. Lung cancer cells (SBC-5) were injected into the left cardiac ventricle of 6-week-old nude mice under anesthesia. After confirming an obvious bone metastasis in femur and/or tibia by soft X-ray, the mice were perfused with 4% paraformaldehyde in 0.1 M phosphate buffer (PH 7.4). The metastasized femora and tibiae were processed for paraffin and epoxy-resin embedding. We performed histochemistry of alkaline phosphatase (ALP), osteopontin, CD44, cathepsin K and matrix metalloproteinase 9 (MMP-9) and tartrate resistant acid phosphates (TRAP), as well as transmission electron microscope (TEM) observation on paraffin and ultrathin epoxy-resin sections, respectively. Metastasized tumor nests were formed in the subcartilaginous region of the growth plate. TRAP-positive osteoclasts were found mainly in the ALP-positive osteoblastic layer covering bone surface, but were also localized in the ALP-negative stromal cell layer of the tumor nests. TRAP-positive osteoclasts showed immunoreactivity for CD44 that can bind to osteopontin. Meanwhile, osteopontin was distributed in the stromal tissue of tumor nests widely. Therefore, osteoclasts appeared to easily migrate into the stromal tissue of tumor nests, by attaching to osteopontin. Next, we examined the localization of cathepsin K and MMP-9 in osteoclasts. Osteoclasts adjacent to the bone surfaces were positive for both cathepsin K and MMP-9, whereas the osteoclasts in the stromal tissue of the tumor nests showed only MMP-9 immunoreactivity. Immunoelectron microscopy localized MMP-9 in the Golgi apparatus and vesicular structures in the baso-lateral cytoplasmic region of the osteoclasts in stromal tissue. In addition, vesicular structures positive for MMP-9 included fragmented extracellular fibrils. Therefore, it is likely that osteoclasts in stromal tissue of tumor nests synthesize MMP-9 and have an ability of digesting internalized extracellular fibrils. Thus, osteoclasts appeared to be involved in the alteration of extracellular matrices in the microenvironment of osteolytic metastasis.

Disclosures: **M. Li**, None.

SU272

A Possible Role for Cathepsin K as a Regulator of Tartrate-Resistant Acid Phosphatase in Osteoclasts. **H. Ylipahkala**^{*1}, **J. Vääräniemi**^{*1}, **K. M. Fagerlund**^{*1}, **J. Rissanen**², **S. L. Alatalo**^{*3}, **H. K. Väänänen**^{*1}, **J. M. Halleen**². ¹Anatomy, University of Turku, Institute of Biomedicine, Turku, Finland, ²Pharmatest Services Ltd, Turku, Finland, ³Finnish Red Cross, Blood Service, Helsinki, Finland.

Osteoclasts secrete tartrate-resistant acid phosphatase (TRACP) into the circulation as a highly active two-subunit form known as TRACP 5b. TRACP 5b is formed by cleaving the polypeptide chain of TRACP at a protease sensitive loop peptide. TRACP is capable of generating reactive oxygen species (ROS) that can destroy bone collagen. We have studied the possible role of cathepsin K in cleaving TRACP in osteoclasts. Confocal microscopy with specific antibodies revealed co-localization of TRACP and cathepsin K in transcytotic vesicles of resorbing osteoclasts. Using recombinant enzymes we were able to show that cleavage of TRACP by cathepsin K *in vitro* increased both the phosphatase activity and the ROS generating activity of TRACP. Addition of the cysteine protease inhibitor E64 into cultures of resorbing human osteoclasts dose-dependently decreased medium TRACP 5b activity levels, whereas total TRACP protein amount did not change, suggesting that the specific activity of secreted TRACP enzyme was decreased because of inhibition of cysteine proteases such as cathepsin K. C-terminal cross-linked telopeptides of type I collagen (CTX) is formed as a result of degradation of bone collagen by cathepsin K. Medium CTX was dose-dependently decreased by addition of E64, and medium CTX and TRACP 5b levels correlated significantly in the human osteoclast cultures. Because total TRACP protein amount did not change by addition of E64, it suggests that TRACP is secreted at a constant rate from osteoclasts despite of their resorption activity. This supports recent evidence suggesting that TRACP 5b would be a marker of osteoclast number rather than osteoclast activity. These results suggest that cathepsin K cleaves TRACP into the two-subunit TRACP 5b isoform with high specific activity in transcytotic vesicles of resorbing osteoclasts and that this TRACP 5b generates ROS that finalize degradation of bone matrix components in the transcytotic vesicles. TRACP 5b is released from the osteoclasts into the blood circulation at a constant rate, being a marker of osteoclast number in situations where cathepsin K activity is not modified.

Disclosures: **H. Ylipahkala**, None.

SU273

Trypsin-Cleavage Enhances the ROS Generating Activity of Human Recombinant Tartrate-Resistant Acid Phosphatase. **K. M. Fagerlund**^{*1}, **H. Ylipahkala**^{*1}, **S. L. Alatalo**^{*2}, **A. J. Janckila**³, **H. K. Väänänen**^{*1}, **J. M. Halleen**⁴. ¹Institute of Biomedicine, Department of Anatomy, University of Turku, Turku, Finland, ²Finnish Red Cross Blood Service, Helsinki, Finland, ³Veterans Affairs Medical Center, Louisville, KY, USA, ⁴Pharmatest Service Ltd, Turku, Finland.

Osteoclasts and macrophages express high amounts of tartrate-resistant acid phosphatase (TRACP). TRACP contains a redox-active iron that can catalyze generation of reactive oxygen species (ROS) and a loop-peptide that can be cleaved by proteases. We have studied the effects of proteolytic cleavage and reduction on the phosphatase and ROS generating activity of human recombinant TRACP produced in insect cells. The 35 kD monomeric native TRACP was cleaved by trypsin into two subunits of 23 and 16 kD that were linked together by a disulfide bridge. Ascorbate and β -mercaptoethanol were used as reducing agents. β -mercaptoethanol had no effect on the pH-optimum of the phosphatase activity measured using pNPP as substrate, but either trypsin-cleavage or reduction by ascorbate alone changed the pH-optimum from 5.4 to 6.2. Cleavage alone had no effect on k_{cat}/K_m but reduction of the cleaved form with β -mercaptoethanol increased k_{cat}/K_m approximately 5-fold. Ascorbate increased k_{cat}/K_m of both native and cleaved form approximately 5-fold. The cleaved high activity form was similar to osteoclast-derived serum TRACP 5b, and the monomeric low activity form was similar to macrophage-derived serum TRACP 5a. ROS generating activity was measured in the presence of ascorbate using hydrogen peroxide as substrate. Formation of ROS was monitored in the presence of coumarin-3-carboxylic acid, a non-fluorescent compound that is converted to a fluorescent product in the presence of ROS. Trypsin-cleavage increased the k_{cat}/K_m -value of the ROS generating activity by 2.5-fold, and the pH-optimum of both the cleaved and non-cleaved forms was 7.0. These results suggest that the osteoclast-derived TRACP 5b circulates in blood in an active cleaved form, and the macrophage-derived TRACP 5a in a less active non-cleaved form. The different effects of ascorbate and β -mercaptoethanol on the phosphatase activity suggest that these two reducing agents act differently. Cleavage of the polypeptide chain of TRACP may be an important regulator of both the phosphatase and the ROS generating activity of TRACP. The neutral pH-optimum of the ROS generating activity together with the acidic pH optimum of the phosphatase activity suggests that pH of the environment may be an important regulator for these two separate TRACP activities.

Disclosures: **K.M. Fagerlund**, None.

SU274

Changes in Serum Cathepsin k Levels in the Evaluation of Postmenopausal Women Treated with Alendronate. **R. Reyes-García**^{*1}, **D. Fernández-García**^{*1}, **G. Alonso**^{*1}, **P. Mezquita-Raya**^{*2}, **M. Ruiz-Requena**^{*3}, **M. Muñoz-Torres**¹. ¹Bone Metabolism Unit, Endocrinology Division, San Cecilio Hospital, Granada, Spain, ²Endocrinology Division, Torrecárdenas Hospital, Almería, Spain, ³Biochemistry Division, San Cecilio Hospital, Granada, Spain.

Cathepsin k is a member of the cysteine protease family that plays a critical role in osteoclast function and the degradation of protein components of the bone matrix. This protease cleaves both helicoidal and telopeptide regions of collagen type I, the major type of collagen in bone. Postmenopausal osteoporosis is characterized by an increase of bone resorption, resulting in a high turnover state that may be identified by measurements of biochemical markers. Alendronate therapy induce sharply reductions in bone remodelling but there is no data on serum Cathepsin K changes after this treatment. Our aim was to evaluate the performance of serum cathepsin K as a biochemical marker of bone resorption in women with postmenopausal osteoporosis before and after 3 months of treatment with alendronate and a control group of healthy premenopausal women. We selected 30 patients (64 \pm 7 years) with densitometric criteria of osteoporosis (T-score < 2.5 SD) that started alendronate treatment (70 mg/weekly). Serum samples were obtained at baseline and after 3 months for measurements of biochemical markers of bone remodelling. Serum cathepsin K levels were measured by ELISA (Biomedica Medizinprodukte GbH & Co KG Wien,Austria). The reference range was 0-300 pmol/l. The detection limit was 1.1 pmol/l, and the intra and inter-assay coefficients of variation (CV) were 4% and 6% respectively. The control group consisted of 12 nonselected healthy premenopausal women (26 \pm 3 years). We found increased levels of cathepsin K compared with the premenopausal control group (p<0.001). After 3 months of alendronate treatment cathepsin K decreased significantly (p<0.001). Baseline and 3 months levels were significantly correlated (r: 0.69; p<0.0001). We not found correlation between cathepsin levels, age or years since menopause. Baseline concentrations of cathepsin K and tartrate resistant acid phosphatase (TRAC) were significantly correlated (r: 0.35; p<0.045). Our data suggest that serum cathepsin K measurements seem to be a valuable parameter in the evaluation of women with osteoporosis treated with antiresorptives.

Disclosures: **R. Reyes-García**, None.

SU275

Tartrate-Resistant Acid Phosphatase Plays an Essential Role in Antigen Presentation by Dendritic Cells. E. Esfandiari^{*1}, C. R. Stokes^{*1}, M. Bailey^{*1}, T. M. Cox^{*2}, M. J. Evans^{*3}, A. R. Hayman¹. ¹School of Clinical Veterinary Science, University of Bristol, Langford, BS40 5DU, United Kingdom, ²Department of Medicine, University of Cambridge, Cambridge, CB2 2QQ, United Kingdom, ³School of Biosciences, University of Cardiff, Cardiff CF10 3US, United Kingdom.

Tartrate-resistant acid phosphatase (TRAP) is highly expressed by osteoclasts, activated macrophages and dendritic cells (DCs). DCs are the most potent antigen-presenting cell of the immune system, critically involved in the initiation of primary immune responses, graft rejection, T cell dependent humoral immune responses and autoimmune diseases such as rheumatoid arthritis (RA). RA is associated with Th 1 hyperactivation. Blood-derived human DCs matured by induction with LPS displayed a five-fold increase in TRAP activity compared with immature DCs suggesting a role for TRAP in the immune response. Osteopontin (OPN) has been shown to be a substrate for TRAP *in vivo*. OPN, also known as early T cell activating factor-1 (Eta-1) is a phosphorylated glycoprotein secreted by activated T lymphocytes and has been implicated in the pathogenesis of inflammatory arthritis. Our aim in this study was to investigate the significance of TRAP in dendritic cells. DCs were cultured from the bone marrow of TRAP deficient (KO) and wild-type (WT) mice and matured with LPS. The expression of MHCII and CD80 was significantly up-regulated in DCs from WT mice compared with DCs from KO mice. DCs from KO mice produced significantly higher amounts of IL10, but showed no significant differences in the production of IL12. The number of mature DCs in KO DC cultures were significantly less than in WT DC cultures. TRAP KO mice exhibited a defect in the expression of delayed hypersensitivity responses. Mice from both genotypes were sensitised and challenged with the contact sensitising agent picryl chloride. The response in KO mice was significantly reduced compared with WT. The ability of TRAP deficient mice to generate antigen-specific immune responses *in vivo* was investigated. Mice were immunised with ovalbumin. Ten days later T cells isolated from spleens of TRAP KO mice showed less proliferation than T cells isolated from the spleens of WT mice in response to OVA, suggesting that the antigen-specific priming of T cells was deficient in mice lacking TRAP. T cells from TRAP deficient mice produced less IFN- γ in response to OVA, however there was no difference in IL-4 production. KO mice produced reduced amounts of OVA-specific IgG2a after immunization with OVA. Differences in IgG1 OVA-specific levels were not significant. In conclusion TRAP has an essential role in the maturation of DCs. It is the Th1 pathway and not the Th 2 pathway that is affected in TRAP deficient mice.

Disclosures: A.R. Hayman, None.

SU276

A Potent and Orally Active Inhibitor of Cathepsin K Selectively Suppresses Bone Resorption without Affecting Bone Formation in Cynomolgus Monkeys. H. Yamada^{*}, Y. Ochi^{*}, N. Kawada^{*}, Y. Nakanishi^{*}, H. Mori^{*}, R. Kayasuga^{*}, A. Hatayama^{*}, K. Ohmoto^{*}, M. Tanaka^{*}, K. Kishikawa^{*}. Discovery Research Laboratories II, Ono Pharmaceutical Co., Ltd., Osaka, Japan.

Cathepsin K, a cysteine protease highly expressed in osteoclasts, is capable of degrading bone type I collagen. Recently, cathepsin K inhibitors have drawn much attention as novel therapeutic agents for treatment of elevated bone turnover including osteoporosis. We investigated anti-bone resorptive activities of cathepsin K inhibitor, compound A, in ovariectomized cynomolgus monkeys. *In vitro* studies showed that this compound potentially inhibited human cathepsin K with a K_i value of 0.10 nM. In addition, this compound concentration-dependently inhibited the release of C-terminal telopeptide of type I collagen (CTX) from bovine bone slices incubated with rabbit bone cells. In ovariectomized cynomolgus monkeys (>9 years old), this inhibitor was given orally once daily from next day of operation for 8 months at 3 dose levels (0.3, 3 and 30 mg/kg). As the bone resorption marker, serum CTX, urinary CTX, serum N-telopeptide of type I collagen (NTX), urinary NTX, urinary free deoxypyridinoline, and as the bone formation marker, serum Osteocalcin and serum bone alkaline phosphatase were measured to monitor bone turnover. The compound A strongly and immediately suppressed bone resorption markers dose-dependently without affecting bone formation markers. These results suggest that an orally active compound A specifically suppressed bone resorption in ovariectomized monkeys. We conclude that cathepsin K inhibitors have the therapeutic potential in primates, and that would be new ideal drugs for the osteoporosis therapy.

Disclosures: H. Yamada, None.

SU277

Cathepsin K-Deficient Mice Exhibit Pycnodysostosis Features due to Loss of Cathepsin K-Mediated Osteoclast Senescence for Bone Homeostasis. Y. P. Li¹, Y. Abe^{*1}, R. Isoda^{*1}, R. Moroi^{*1}, S. Yang^{*1}, J. Z. Shao^{*1}, E. Li^{*2}, W. Chen^{*1}. ¹The Forsyth Institute & Harvard School of Dental Medicine, Boston, MA, USA, ²Department of Medicine, Cardiovascular Research Center, Massachusetts General Hospital, Harvard Medical Medicine, Charlestown, MA, USA.

Osteoclast is a bone resorption cell and its numbers need to be precisely controlled to keep bone homeostasis. How osteoclast life is regulated is unclear. Pycnodysostosis resulted from *Cathepsin K* mutation that exhibited a unique phenotype characterized by short stature, wide cranial sutures, osteolysis and osteosclerosis due to bone homeostasis defect. To understand the role of *Cathepsin K* in pathogenesis of pycnodysostosis, we generated a novel *Cathepsin*

K knockout mouse strain. Surprisingly, osteoclast numbers in the *Cathepsin K*^{-/-} mice largely increased up to 15-fold high compared to that in wild-type, whereas extracellular acidification function was unaffected in *Cathepsin K*^{-/-} osteoclasts. This suggests that the large amounts of *Cathepsin K*^{-/-} osteoclasts with normal acidification ability and impaired bone matrix degradation function may be the cause of pycnodysostosis. We hypothesized that *Cathepsin K* may be involved in the regulation of osteoclast life. *Cathepsin K*^{-/-} OCLs grew 10-fold faster than wild-type osteoclasts and can continue for more than forty passages. Apoptosis was not detected in both *Cathepsin K*^{-/-} osteoclasts and wild-type osteoclasts *in vivo* or *in vitro* with conditional medium, indicating apoptosis may not be the major anti-osteoclast survival pathway in bone homeostasis. Notably, senescence was observed in 95% of wild-type osteoclasts, but was not detected in *Cathepsin K*^{-/-} osteoclasts. Our data showed that *Cathepsin K* regulates osteoclastic senescence by acting as a modulator of the p19, p53 and p21 senescence pathway. Forced expression of *Cathepsin K* in pre-osteoclast cell line, MOC-P-5, induces premature senescence. This is the first report that *Cathepsin K*-deficient mice exhibit unique pycnodysostosis features due to loss of *Cathepsin K*-mediated osteoclast senescence, and *Cathepsin K*-mediated p53 and p21 senescence pathway may be the major anti-osteoclast survival mechanism to control osteoclast life and bone homeostasis.

Disclosures: Y.P. Li, None.

SU278

Aquaporin 9 Plays a Role in Osteoclast Differentiation. R. Aharon^{*}, Z. Bar-Shavit. Experimental Medicine and Cancer Research, Hebrew University Faculty of Medicine, Jerusalem, Israel.

Aquaporins are water channels that selectively enhance the water permeability of the membrane. The distribution of mammalian aquaporins suggests their participation in a wide range of physiological events. Empirical evidence of a physiological role for aquaporins is emerging from studies in both mice and humans, and suggests that aquaporins are likely to play significant roles in human pathophysiology. Since osteoclast differentiation includes a dramatic increase in volume of the cell we hypothesize that aquaporin(s) is/are critical for the formation of the multinucleated osteoclast from its mononuclear precursor. For our studies we used two cell models, bone marrow macrophages (BMMs) and the murine macrophage-like cell line, RAW264.7, as osteoclast precursors. RANKL+M-CSF and RANKL were used to induce osteoclast differentiation in BMMs and RAW264.7 cells, respectively. We first used qualitative RT-PCR to examine which of the aquaporins are expressed in osteoclasts and in their precursor cells. Out of the ten aquaporins examined, only aquaporin 9 (AQP9) was expressed in the osteoclast lineage cells. Characterization of AQP9 revealed that it has a unique aqueous pore mediating in addition to water the passage of a wide variety of non-charged solutes. Quantitative real-time PCR analyses demonstrated higher AQP9 mRNA levels in RANKL-treated cells. Western analyses using specific antibodies revealed also a higher AQP9 level in RANKL-treated cells. Finally, we examined the effect of phloretin, an AQP9 inhibitor, on RANKL-induced osteoclast differentiation. Cells were incubated with RANKL for 5 days, and phloretin was added for the last two days, when most fusion occurs. A dramatic reduction in osteoclast number was observed in cultures containing phloretin. The inhibitor did not exhibit a significant effect on the number of mononuclear phagocytes in cultures not treated with RANKL. Our results suggest a role for AQP9 in osteoclast differentiation, and specifically in the fusion process.

Disclosures: R. Aharon, None.

SU279

Osteoclasts Produce Interferon Gamma: A Novel Autoregulation Mechanism of Osteoclastogenesis. S. Yang, Y. Z. Zhang^{*}, S. V. Reddy, W. Ries, L. L. Key. Pediatrics, Children's Research Institute, Medical Univ. of SC, Charleston, SC, USA.

Osteoclasts are multinucleated cells formed from hemopoietic cells, and their formation is tightly controlled by a network of cytokines produced in the bone microenvironment. While there are intensive efforts in recent years to understand the mechanisms of osteoclastogenesis by positive stimulators, very little attention has been given to negative regulatory mechanisms. Interferon gamma (IFN- γ), a systemic immune factor produced primarily by T and NK cells, inhibits osteoclastogenesis and bone resorption. In this study, we demonstrated that osteoclasts express IFN- γ by immunostaining and RT-PCR analysis. ELISA analysis showed that IFN- γ produced by osteoclasts reached 0.37 ng/ml, which is above the minimum dose (0.2 ng/ml) required to inhibit osteoclastogenesis. IFN- γ mediates its biological effects through the receptor. The presence of IFN- γ receptors in osteoclasts is demonstrated by their binding activity to ¹²⁵I-labeled IFN- γ . Scatchard plot analysis revealed that osteoclast progenitors have an average of 5300 IFN- γ receptor sites/cell. We have also identified that IFN- γ inhibits osteoclast precursor proliferation significantly. These data suggest that a negative feedback loop exists by which osteoclasts negatively control their own differentiation and formation by producing IFN- γ . Evidence that supports our study is obtained from the IFN- γ receptor null mice, which have a more rapid onset of arthritis and bone resorption, as more osteoclasts appeared in the IFN- γ receptor (-/-) mice than in wild type mice. IFN- γ failed to suppress osteoclastogenesis in bone marrow cell cultures derived from the IFN- γ receptor (-/-) mice. These data suggest that osteoclast formation in the IFN- γ receptor (-/-) mice lacks negative regulation when the IFN- γ signaling is interrupted. Without such negative control, more osteoclasts are formed and lead to excess bone resorption in the IFN- γ receptor (-/-) mice. Osteoclast-derived IFN- γ may be one of the major negative regulators of osteoclastogenesis in the bone microenvironment. This regulation may function more efficiently than the systemic source of IFN- γ , through paracrine and autocrine mechanisms. This negative regulation limits the number of osteoclasts during bone remodeling by a feed-back mechanism. Our study provides the novel concept that osteoclasts negatively control their own differentiation and formation by producing IFN- γ in the bone microenvironment.

Disclosures: S. Yang, None.

SU280

Menatetrenone (MK-4) Directly Inhibits Osteoclast Formation and Enhances the Inhibitory Effect of Aminobisphosphonates on Osteoclast Precursor Cell Differentiation. D. C. Ireland*, S. Bord, J. E. Compston. Department of Medicine, University of Cambridge, Cambridge, United Kingdom.

The aim of this study was to determine the direct effects of MK-4, alone and in combination with the aminobisphosphonate pamidronate (PAM), on human osteoclast formation and activity. MK-4 affects the γ -carboxylation of certain bone proteins and has effects on bone cells that appear to depend on its geranylgeranyl side chain. In a model of osteoclastogenesis and bone resorption, osteoclasts were generated on dentine slices and calcium phosphate films from human CD14⁺ blood cells cultured with macrophage colony stimulating factor and receptor activator of NF κ B ligand. Osteoclasts were identified by morphology, TRAP-staining and dentine resorption. Calcium phosphate films allowed the addition of compounds to mature, resorbing osteoclasts and quantification of resorption. MK-4, geranylgeraniol (GGOH) and PAM were added, alone and in combination, to cells, both at the outset to detect changes in osteoclast formation and to mature osteoclasts to detect changes in activity. Total cell proliferation was estimated by MTS assay and substrate resorption was quantified by image analysis of von Kossa stained calcium phosphate films. TUNEL staining was used to detect apoptosis. Four replicates were used for each group and results compared to carrier controls using Student's t-test. Compared to control alone, resorption, but not total cell proliferation, was significantly inhibited by 10⁻⁵M MK-4 (39% cf control), GGOH (33%) and PAM (14%) (p<0.05) when these compounds were added at the outset. Examination of the stained cells showed that decreased resorption was due to inhibition of osteoclast formation not inhibition of activity. Combinations of PAM with MK-4 or GGOH further decreased osteoclast formation. None of the cultures showed increased TUNEL staining compared to the controls. When compounds were added to cultures with mature osteoclasts, 10⁻⁵M MK-4, GGOH and PAM did not alter cell proliferation or substrate resorption but 10⁻⁴M PAM (32% cf control) and 10⁻⁴M PAM plus 10⁻⁵M MK-4 (no resorption) significantly decreased resorption (p<0.05) whereas 10⁻⁴M PAM plus 10⁻⁵M GGOH did not. In summary, MK-4 directly inhibited osteoclast formation from CD14⁺ precursors and enhanced the inhibitory effect of PAM without inducing apoptosis. Unlike GGOH, MK-4 was unable to reverse the antiresorptive effect of PAM on mature osteoclasts. The data suggest that MK-4 directly inhibits osteoclastogenesis and enhances the effects of pamidronate on osteoclast formation and activity.

Disclosures: **D.C. Ireland**, None.

SU281

Use of Acumen Explorer to Quantitate Calcitonin Receptor-Positive Mononucleated and Multinucleated Cells in Differentiating Cultures of Osteoclasts. R. J. S. Galvin, L. L. Burris*, T. Fuson*, A. Kriauciunas*. Musculoskeletal Team, Lilly Research Labs, Indianapolis, IN, USA.

The traditional method for quantifying the number of osteoclasts (OCs) is labor intensive, time consuming and highly subjective. *In vitro*, OCs differentiate unevenly across a well making it imperative to analyze the entire well. OCs are typically identified as multinucleated cells that stain positive for tartrate-resistant acid phosphatase or calcitonin receptor. Counting the number of mononuclear cells present in a differentiation culture is usually not practical and therefore is rarely done. The purpose of this study was to develop a novel assay using high content analysis to simultaneously quantify both multinucleated and mononucleated calcitonin-receptor positive cells in differentiating cultures of bone marrow cells. Murine bone marrow cells were isolated from male balb/c mice and cultured in the presence of rmM-CSF (25 ng/ml) and rh-RANKL (0.31-80 nM) in the presence or absence of TGF- β 1 (0.01- 10 ng/ml). On day 6, the cultures were fixed and stained with calcitonin receptor antiserum using a secondary Alexa Fluor 488 antibody for detection. The nuclei were counterstained with propidium iodide. The number of calcitonin-receptor positive mononucleated and multinucleated cells (OCs, two or more nuclei) per well were quantified using the Acumen Explorer. An argon laser was used to excite the sample and the emitted light was captured by one of four photomultiplier tubes. Multi-parametric analysis was used to exclude fluorescent artifacts. The Acumen Explorer allows for discrimination between the cell populations and also for more rapid data collection with acquisition and analysis taking approximately 15 minutes for a 96-well plate. RANKL induced a concentration-dependent increase in OC differentiation with an EC₅₀ of appropriately 5 nM and increased OC numbers approximately 350% at 10 nM RANKL. The mononucleated cell numbers were decreased by RANKL in a concentration-dependent manner with an approximately 25% decrease at 10 nM RANKL. TGF- β 1 enhanced OC differentiation in a concentration-dependent manner with a 430% increase at 10 ng/ml of TGF- β 1 and 1.5 nM RANKL. Under these conditions monucleated cell numbers were decreased by about 50%. Manual counting of OCs correlated (r²=0.98) with the counts generated with the Acumen Explorer. These results demonstrate that high content analysis using the Acumen Explorer can be used to monitor OC differentiation providing quantitative information on both osteoclast and mononucleated cell number.

Disclosures: **R.J.S. Galvin**, None.

SU282

Osteoclast Fusion Is Mediated by DC-STAMP, a Seven Transmembrane Receptor via its C-Terminus Domain. T. Miyamoto¹, M. Yagi^{*1}, N. Fujita^{*1}, K. Morita^{*1}, Y. Toyama^{*2}, T. Suda^{*1}. ¹Cell Differentiation, Keio University School of Medicine, Shinjuku, Japan, ²Orthopaedics, Keio University School of Medicine, Shinjuku, Japan.

Osteoclasts are bone resorbing cells, which play a pivotal role in bone remodeling. Osteoclasts form large multinuclear giant cells by cell fusion of mononuclear osteoclasts. While some osteoclast fusion mediating factors were reported, essential molecules remain unclear. Here we identify the dendritic cell-specific transmembrane protein (DC-STAMP), a putative seven transmembrane protein by DNA subtraction screen between multinuclear osteoclasts and mononuclear macrophages. DC-STAMP is highly expressed in osteoclasts, and thus the function in osteoclast formation was analyzed in DC-STAMP deficient mice. The targeting vector was constructed to insert an EGFP sequence into exon 2 such that EGFP was in-frame with amino acid Leu55 of DC-STAMP. Osteoclasts were identified as GFP-positive cells in vivo and in vitro in DC-STAMP-heterozygous mice. DC-STAMP-null mice were generated at Mendelian ratios, and osteoclastogenesis was analyzed in DC-SATMP homozygous mice. The transcription factors required for osteoclast differentiation such as c-Fos and NFATc1, or osteoclast maturation marker including TRAP, cathepsin K and bone resorbing activity were induced in osteoclast derived from DC-STAMP deficient mice as wild type osteoclast. However, the cell fusion of osteoclasts was completely abrogated in DC-STAMP deficient mice in vivo. The in vitro osteoclast multinucleation was not detected in the culture of bone marrow cells from DC-STAMP-deficient mouse in the presence of M-CSF and RANKL and was not rescued by a high-dose M-CSF or co-cultivation with osteoblasts. As osteoclast multinucleation was restored by retroviral expression of DC-STAMP, the loss of cell fusion is directly attributed to the lack of DC-STAMP. Interestingly, DC-SATMP-delta lacking a C-terminus putative cytoplasmic domain failed to rescue the cell fusion of DC-STAMP deficient osteoclast indicating that DC-SATMP is an essential protein for osteoclast cell fusion, and its C-terminus domain is required for cell fusion signaling of osteoclasts. We will discuss about the mechanism of cell fusion mediated by DC-STAMP.

Disclosures: **T. Miyamoto**, None.

SU283

Proteomic Study of Osteoblast Differentiation Using Isotope-Coded Affinity Tags And Maldi-Tof Analysis. Y. Zhang*, A. F. Taylor*, D. C. Genetos*, Z. Zhou*, B. A. Stanley*, H. J. Donahue. The Pennsylvania State University, Hershey, PA, USA.

The aim of this study was to identify the protein expression profile or “fingerprint” of differentiating human mesenchymal stem cells (hMSC) using the ICAT-MALDI-TOF-TOF approach, which permits the quantitation and identification of proteins, including lower-abundance proteins, membrane proteins, and highly charged proteins. hMSC and murine MC3T3-E1 were cultured in growth medium. Upon reaching 70-80% confluence cells were switched to differentiation medium for an additional 14 days. Proteins isolated from undifferentiated and differentiated hMSC/MC3T3-E1 were labeled on cysteine residues with either a “light” or a “heavy” ICAT reagent (mass difference of 9.03 atomic units), and then pooled together. The pooled ICAT-labeled proteins were separated on a 10% SDS-PAGE gel. Following electrophoresis, individual gel lanes were divided into 10 pieces and soaked in a trypsin solution. Peptides eluted from the gel pieces were then affinity purified and separated into 100 or more fractions using a nanoflow LC reverse-phase column which mixes the fractions with matrix and spots them onto MALDI plates. Peptide / matrix spots were analyzed by MALDI-TOF, and peak clusters differing by multiples of 9.03 Daltons, indicative of light-heavy ICAT labeled peptide pairs, were selected for further analysis. The relative levels of matched peptides from undifferentiated and differentiated cells were indicated by the relative areas of the light vs. heavy peaks in these pairs. The identity of peptides showing 30% or greater differences in peak areas was then determined by fragmenting the parent peaks and comparing the tandem ms/ms spectra generated to the theoretical ms/ms spectra of all known peptides having the parent peak mass. Alkaline phosphatase activity was increased dramatically in hMSC cells cultured for 14 days in osteogenic media, confirming that they had differentiated to osteoblastic cells. In total, we saw 607 and 2237 ICAT labeled peptide pairs in hMSC and MC3T3-E1 samples, respectively, at a signal/noise ratio of 25 or better (Table). The median values for pairs were 0.9857 and 0.9967, suggesting that there was no bias in the Light vs. Heavy ICAT label sampling. Our results demonstrate that an ICAT-based proteomic approach can be used as a method to generate protein “fingerprints” of osteoblast differentiation.

Cell	hMSC	MC3T3
Peptides pairs identified (S/N=25)	607	2237
Peptides pairs with difference more than 30%	442	1270
Protein matched (expression level difference>30% and C.I.>90%)	45	64
Up regulated proteins (>30%)	21	7
Down regulated proteins (>30%)	24	57

Disclosures: **Y. Zhang**, None.

SU284

CaMKII gamma Is the Sole Osteoclastic CaM Kinase Responsible for the Regulation of Osteoclastogenesis via Modulating RANK Signaling. C. Yao^{*1}, P. H. Stern², J. J. Mao³, L. Zhang¹. ¹Biomedical Sciences, University of Illinois at Chicago, Rockford, IL, USA, ²Molecular Pharmacology and Biological Chemistry, Northwestern University, Chicago, IL, USA, ³Orthodontics, University of Illinois at Chicago, Chicago, IL, USA.

Recently, Ca²⁺/calmodulin signaling has been recognized as a major regulator in osteoclastogenesis. Efforts have ensued to identify the downstream targets of this signaling pathway in the context of regulating osteoclastogenesis. Calcineurin-NFAT pathway has thus been identified as such a target. In this presentation, we describe the discovery of another novel downstream target, CaMKII γ , as the sole known CaMK expressed with significant amounts in bone marrow derived osteoclasts and their precursors. Other known CaMKs such as CaMKIV and CaMKII α , β , δ , are not detectable, while CaMKI is expressed at a negligible level. Furthermore, the expression of CaMKII γ is tightly correlated with the osteoclastogenic process, with a peak level on Day 3 of cell culturing. Osteoclastogenesis is halted by treatment with the CaMKII γ inhibitor, KN93, independently from apoptosis, with the IC₅₀ for osteoclastogenesis matching that for blocking CaMKII γ function. In addition, KN93 blocked RANK-NF κ B and RANK-Akt pathways in the osteoclast precursor cells. Collectively, these data indicate that CaMKII γ is a novel regulator of osteoclastogenesis via modulating RANK signals.

Disclosures: **L. Zhang, None.**

SU285

TIEG Expression in Osteoclast Precursors Suppresses Osteoclast Differentiation. L. Pederson^{*1}, M. Subramaniam², J. R. Hawse², T. C. Spelsberg², M. Oursler³. ¹Endocrinology/Metabolism & Internal Medicine, Mayo Clinic, Rochester, MN, USA, ²Biochemistry and Molecular Biology, Mayo Clinic, Rochester, MN, USA, ³Endocrinology, Mayo Clinic, Rochester, MN, USA.

We have shown that TGF- β Inducible Early Gene 1 (TIEG) plays an important role in osteoblast (OB) differentiation and OBs isolated from TIEG knockout mice are less efficient in supporting OC differentiation. Tibial bone histomorphometry of TIEG knockout mice exhibited increased OB numbers with no change in OC numbers. This study examines the effect of loss of TIEG on osteoclast (OC) differentiation. We have examined differentiation of M-CSF dependent nonadherent OC precursors from marrow and spleen in co-cultures with ST2 cells and following treatment with RANKL and M-CSF. In both models, loss of TIEG enhanced OC differentiation. The combination of increased numbers of OBs present in bones and increased ability of OC precursors to differentiate into mature OCs may result in a net effect of normal OC numbers in the bones of mice lacking TIEG. This is supported by increased OC differentiation when we increase the density of calvarial OBs in TIEG knockout co-cultures. The increased OC differentiation in the TIEG knockout models may be due to (a) the presence of more precursors or (b) an increased capacity of a similar number of precursors to differentiate. This was examined by identifying OC precursors using flow cytometry analysis of CD11b, c-fms, and/or RANK expression. We found no significant differences in the number of OC precursors between wild type and TIEG knockout spleen or marrow cells. Moreover, equal numbers of CD11b⁺ OC precursors were differentiated in the presence of M-CSF and RANKL. Compared to wild type, there was enhanced differentiation of TIEG knockout OC precursors, verifying that loss of TIEG increased the capacity of OC precursors to differentiate. Transfection with siRNA to block TIEG expression in wild type OC precursors resulted in enhanced differentiation, similar to TIEG knockout OC precursors. Conversely, using adenovirus delivery, restoration of TIEG expression in TIEG knockout OC precursors resulted in reduced OC differentiation. Thus, TIEG expression in OC precursors directly impacts OC differentiation. We examined known pathways important in OC differentiation. We found increased activation of the NF κ B pathway in knockout compared to wild type OC precursors, whereas activation levels of other pathways critical to OC were unchanged. In summary, TIEG expression in OC precursors directly affects OC differentiation, and loss of TIEG expression in OC precursors enhances OC differentiation through sustained activation of the NF κ B pathway.

Disclosures: **M. Oursler, None.**

SU286

Role of Sphingosine Kinase in RANKL-Induced Osteoclastogenesis. J. Ryu^{*}, H. Kim^{*}, K. Han^{*}, S. Lee^{*}, H. Kim. Dept of Cell and Developmental Biology Seoul National University Dental School, Seoul, Republic of Korea.

Osteoclasts are highly specialized multinucleated cells that differentiate from monocyte/macrophage lineage hematopoietic precursors. Two hematopoietic factors are both necessary for osteoclastogenesis, the TNF-related cytokine RANKL and the polypeptide growth factor M-CSF1. The mature, multinucleated osteoclast is activated by signals, which lead to initiation of bone remodeling. The differentiation and activation of osteoclast stimulate bone resorption, thereby contributing to the pathogenesis of rheumatoid arthritis, periodontitis, and bone metastases. Sphingosine kinase (SPHK) is an enzyme that catalyzes the phosphorylation of sphingosine to sphingosine-1-phosphate (S1P). Diverse external stimuli, particularly growth and survival factors and chemoattractants stimulate the sphingosine kinase to generate intracellular S1P. Sphingosine-1-phosphate is a bioactive lipid that regulates cell proliferation, differentiation, motility and survival. The discovery that S1P can bind to specific cell surface G protein-coupled receptors has led to the concept that S1P can function as an extracellular first messenger. The activation of the

small GTPase Rac and Rho has been linked to cytoskeletal rearrangements and motility. Other related signaling pathways include the activation of ERK and p38 MAP kinases, intracellular calcium mobilization, and activation of AKT. In this study, we evaluate the role of SPHK and its product, sphingosine-1-phosphate in RANKL-induced osteoclastogenesis. Knock-down of SPHK gene with siRNA increased phospho-p38 activation as well as RANKL-induced osteoclastogenesis. The overexpression of SPHK to bone marrow-derived macrophage cells and Raw cells reduced the formation of multinucleated osteoclasts. In addition, treatment of S1P into BMC-derived macrophage inhibited the formation of TRAP positive multinucleated osteoclastogenesis. These data demonstrate the important role of SPHK and its product S1P in RANKL-induced osteoclastogenesis.

Disclosures: **J. Ryu, None.**

SU287

EphrinB2 Is a Transcriptional Target Gene of NFATc1 during Osteoclast Formation. N. Irie^{*1}, C. Zhao^{*1}, T. Miyamoto², T. Suda^{*2}, K. Matsuo¹.

¹Department of Microbiology and Immunology, Keio University School of Medicine, Tokyo, Japan, ²Department of Cell Differentiation, Keio University School of Medicine, Tokyo, Japan.

Bone remodeling is delicately regulated at the level of differentiation and activation of osteoclasts and osteoblasts. Eph receptor tyrosine kinases and ephrin ligands have key roles in regulating migration and adhesion of cells in neuronal and vascular development. Both Ephs and ephrins are membrane-bound proteins which evoke bidirectional signaling upon interacting with each other. Last year, we reported that ephrinB2 (encoded by *Efnb2*) and EphB4 are expressed on osteoclasts and osteoblasts, respectively. Reverse signaling through ephrinB2 into osteoclast precursors suppresses osteoclast differentiation, while forward signaling through EphB4 enhances osteoblast differentiation. Expression of *Efnb2* in osteoclasts was initially identified by microarray analysis using osteoclast precursors isolated from mice lacking c-Fos (*Fos*^{-/-} mice). Although *Fos*^{-/-} precursors do not differentiate into osteoclasts, overexpression of a major c-Fos target gene, *Nfatc1*, rescued osteoclast differentiation and restored expression of *Efnb2*. We examined whether *Efnb2* could be a direct target gene of the transcription factor NFATc1. First, we transiently transfected *Efnb2* promoter-luciferase constructs into the osteoclast precursor cell line RAW264.7. The DNA fragment containing the 3.1-kb *Efnb2* sequence upstream of the translation initiation site responded to both RANKL treatment and overexpression of a constitutively-active form of NFAT. Next, we examined the seven putative NFAT sites in the mouse *Efnb2* promoter within the 3.1-kb upstream region. Electrophoresis mobility shift assays (EMSA) revealed one strong NFAT binding site (-2863 relative to ATG codon) and two adjacent weak sites. Furthermore, NFATc1 supershift was observed only with nuclear extracts from wild-type but not *Fos*^{-/-} osteoclastogenic cultures, which lack NFATc1. This demonstrates that NFATc1 binds to the -2863 site. These data suggest that the RANK-c-Fos-NFAT cascade activates not only osteoclastogenic genes, but also *Efnb2*, which encodes anti-osteoclastogenic molecule during osteoclast formation.

Disclosures: **N. Irie, None.**

SU288

Effects of Calcitonin on Osteoclast Formation and Gene Expression. S. Granholm^{*}, P. Lundberg^{*}, U. H. Lerner. Department of Oral Cell Biology, Umeå University, Umeå, Sweden.

Calcitonin (CT) was discovered in 1962 as an acute hypocalcemic hormone and this hypocalcemic effect has later been shown to be due to inhibition of bone resorption, caused by activation of calcitonin receptors (CTR) in mature osteoclasts. Studies on effects by CT on osteoclast differentiation are however limited. Here, the effects of CT on osteoclast formation and gene expression have been studied in cultured mouse spleen cells and mouse bone marrow macrophages (BMM). CT inhibited formation of tartrate resistant acid phosphatase positive multinucleated osteoclasts (TRAP⁺ MuOCL) in spleen cells and BMM, cultured in the presence of macrophage colony-stimulating factor (M-CSF) and receptor activator of NF- κ B ligand (RANKL), with half maximal effect at 10⁻¹² M of salmon CT. The effect was obtained also by adding CT during the last 24 h of the 96 h cultures. CT did not affect the mRNA expressions of RANK and c-fms, nor the mRNA expressions of c-Fos, c-Jun, NFAT2 or I κ B α . The increased mRNA expression of CT receptor (CTR) caused by M-CSF/RANKL was abolished by CT. In contrast, CT did not affect M-CSF/RANKL induced increase of the mRNA expressions of TRAP, cathepsin K, MMP-9, proton pump subunit Atp6i, chloride channel ClC-7, or the integrins α , and β ₃. CT induced inhibition of TRAP⁺ MuOCL formation was not associated with any decrease of total TRAP activity resulting in large number of TRAP⁺ mononucleated cells in CT treated cultures. Fusion of mononucleated osteoclast progenitor cells has been suggested to be controlled by the two ITAM harboring adaptor proteins DAP12 and FcR γ , forming complexes with several cell surface receptor proteins in the immunoglobulin-like superfamily. The critical role of these co-stimulatory signals has been demonstrated by the finding that *FcR γ /DAP12*^{-/-} mice are osteopetrotic and lack osteoclasts. CT did not affect the mRNA expression of DAP12 or FcR γ , nor were the mRNA expression of the receptors affected. It is concluded that CT is a potent inhibitor of osteoclast formation, caused by a direct effect on the osteoclast progenitor cells, and that this effect is not associated with decreased transcription of a variety of genes known to be important for osteoclast progenitor cell differentiation, fusion or function.

Disclosures: **S. Granholm, None.**

SU289

Comparison of Human and Bovine Bone Substrates in Human Osteoclast Cultures. J. P. Rissanen, S. Suutari^{*}, S. Ylönen^{*}, J. M. Halleen. Pharmatest Services Ltd, Turku, Finland.

Bovine bone and dentine slices are widely used substrates for *in vitro* osteoclast (OC) cultures. In order to perform effective and reliable antiresorptive drug screening assays, it would be advantageous to use human bone as substrate for human osteoclasts. We have compared the performance of human and bovine bone substrates in two different human OC assays, a 7-day OC differentiation assay and a 10-day OC activity assay. We cultured commercially available CD34-positive osteoclast precursor-cells (Cambrex, East Rutherford, NJ, USA) on bovine bone slices (obtained from Nordic Bioscience, Herlev, Denmark) or on human bone plates (OsteoAssayTM, Cambrex, East Rutherford, NJ, USA) in the presence of M-CSF and RANKL. Osteoprotegerin (OPG) was used as a reference inhibitor in the OC differentiation assay and the cysteine protease inhibitor E64 was used as a reference inhibitor in the OC activity assay. In the OC differentiation assay, OPG was added at day 0 and the cultures were stopped at day 7. Tartrate-resistant acid phosphatase isoform 5b (TRACP 5b) was measured from the culture medium collected at day 7 as an index of OC number using a commercially available immunoassay (BoneTRAP[®], SBA-Sciences, Oulu, Finland). In the OC activity assay, culture medium was replaced with fresh medium at day 7 and the formed OCs were allowed to resorb bone for an additional 3 days. At day 10, C-terminal cross-linked telopeptides of type I collagen (CTX) were measured from the culture medium as an index of osteoclast activity using a commercially available immunoassay (CrossLaps[®] for culture, Nordic Bioscience). Baseline cultures without added compounds were included in both OC assays. In the OC differentiation assay, OPG decreased dose-dependently OC number in both substrates. TRACP 5b values were substantially higher in the baseline cultures in bovine bone than in human bone, and the decrease caused by OPG was significantly larger in bovine bone than in human bone. However, there was also considerably more variability in the TRACP 5b values in bovine bone than in human bone. In the OC activity assay, E64 decreased significantly medium CTX values in both substrates and the values of baseline cultures were substantially higher in bovine bone than in human bone. We conclude that both the bovine bone slices and human bone plates are convenient and reliable substrates when studying the effects of antiresorptive agents on OC differentiation and activity.

Disclosures: **J.P. Rissanen**, None.

SU290

The Ratio of Osteoclast Activity/Osteoclast Number (CTX/TRACP 5b) Improves the Interpretation of the Effects of Anti-Resorptive Treatment in Human Osteoclast Cultures. J. P. Rissanen¹, S. Suutari^{*1}, S. Ylönen^{*1}, M. Baugh^{*2}, C. Long², J. M. Halleen¹. ¹Pharmatest Services Ltd, Turku, Finland, ²Organon Laboratories, Newhouse, United Kingdom.

C-terminal cross-linked telopeptides of type I collagen (CTX) are released from bone collagen during bone resorption, and serum CTX is a useful marker of osteoclast activity. It has been shown recently that serum tartrate-resistant acid phosphatase isoform 5b (TRACP 5b) reflects osteoclast number. We have studied the use of CTX and TRACP 5b as endpoint measurements in human osteoclast cultures. We cultured commercially available CD34-positive osteoclast precursor-cells (Cambrex, East Rutherford, NJ, USA) on bovine bone slices (obtained from Nordic Bioscience, Herlev, Denmark) for 7 days in the presence of M-CSF and RANKL, allowing their differentiation into bone-resorbing osteoclasts. At day 7, the culture medium was changed and test compounds were added. A baseline group without added compounds, a control group with the reference inhibitor E64 and groups with 7 different concentrations of two potential resorption inhibitors named as resorption inhibitors A and B were included in the study. The formed osteoclasts were cultured for an additional 3 days, allowing them to resorb bone in the presence of the test compounds. TRACP 5b was measured from the culture medium collected at day 7 as an index of osteoclast number using a commercially available immunoassay (BoneTRAP[®], SBA-Sciences, Oulu, Finland). At day 10, CTX was measured from the culture medium as an index of osteoclast activity during days 7-10 using a commercially available immunoassay (CrossLaps[®] for culture, Nordic Bioscience). The reference inhibitor E64 significantly decreased CTX in the medium. The second lowest test concentration of compound A as well as the two lowest test concentrations of compound B showed decreased CTX in the medium compared with baseline CTX levels. However, TRACP 5b values at day 7 were lower in these three groups, suggesting that the decreased CTX values at day 10 were due to the presence of lower number of osteoclasts in these groups before the addition of the test compounds. CTX values were divided by TRACP 5b values to obtain a resorption index calculated per osteoclast. The resorption index was dose-dependently decreased by both compounds A and B. These results suggest that the resorption index (CTX/TRACP 5b) is a useful endpoint measurement in human osteoclast cultures, preventing variable results caused by the presence of different number of osteoclasts in different test groups when studying the effects of test compounds on osteoclast activity.

Disclosures: **J.P. Rissanen**, None.

SU291

Adrenocorticotrophic Hormone Modulates Osteoclastic Cell Differentiation. S. Sridhar¹, Q. Zhong¹, C. M. Isaacs². ¹Medicine, Medical College of Georgia, Augusta, GA, USA, ²Medicine and Orthopedic Surgery, Medical College of Georgia and the Augusta VA Hospital, Augusta, GA, USA.

We have previously reported the presence of melanocortin receptors in osteoblastic and osteoclastic cells. Melanocortin receptors are activated by peptides derived from processing of a larger prohormone, pro-opiomelanocortin (POMC) which include hormones such as adrenocorticotrophic hormone (ACTH) and melanocyte stimulating hormone (MSH). We have also shown that POMC derived fragments such as ACTH can be synthesized and released from osteoclasts although what autocrine effect these fragments have on osteoclastic function is unknown. In an effort to define ACTH effects on osteoclast differentiation we utilized an osteoclast cell line RAW264.7. RAW cells were stimulated with 10 nM ACTH (1-24) and gene expression for the osteoclastic markers tartrate resistant acid phosphatase (TRAP), c-Fms and Cathepsin-k were measured sequentially over nine days by RT-PCR and quantitated by comparing to the housekeeping gene GAPDH. ACTH was not found to have any effect on c-fms expression. However, significantly increased expression of TRAP and cathepsin K was observed by the fifth day of exposure to ACTH. In contrast, in the absence of ACTH, expression of these markers was not evident in RAW cells until the seventh day of culture. Taken together these data demonstrate that ACTH facilitates the maturation of the osteoclastic cell line RAW264. into a more mature phenotype and suggests a novel autocrine mechanism for local regulation of bone resorption.

Disclosures: **S. Sridhar**, None.

SU292

A Central Role for Caspase 3 and Hydrogen Peroxide in RANKL-induced Osteoclast Differentiation. K. H. Szymczyk, T. A. Freeman^{*}, I. M. Shapiro, M. J. Steinbeck. Orthopaedic Surgery, Thomas Jefferson University, Philadelphia, PA, USA.

Recent studies indicate that caspase 3 plays a crucial role in events unrelated to programmed cell death, including cell cycle progression, cell activation, and cellular differentiation. To this end, we used pharmacological inhibitors specific for caspase 3 and created a permanent RNAi procaspase 3 clonal knockdown of RAW264.7 cells (RAWC3KD) to investigate the role of caspase 3 in RANKL-induced differentiation of osteoclasts. In the absence of stimulation, RAW264.7 cells contained measurable amounts of procaspase 3 that co-localized to lipid rafts within the plasma membrane and to the cytosol by immunofluorescent microscopy. Within 5 min of RANKL treatment, immunoreactive caspase 3 levels increased and co-localized to lipid raft regions. Since RANK co-localizes to lipid rafts, our results suggest a potential interaction between these two proteins. The increase in caspase 3 in response to RANKL occurred as early as 5 min, peaked at 15 min, and returned to baseline levels within 30 min. Western blot analysis confirmed early activation, and showed that procaspase 3 levels decreased as caspase 3 levels increased. Based on these spatio-temporal events, we evaluated the involvement of caspase 3 in early RANKL signaling. Our results demonstrate that in the absence of caspase 3, NF- κ B activation and nuclear translocation were defective, indicating that this enzyme plays a role in mediating early RANK signaling events. In addition, the increase in caspase 3 in RANKL treated cells was inhibited by pretreatment of cells with a NADPH-oxidase inhibitor. Conversely, caspase 3 levels increased in response to exogenous hydrogen peroxide, a reactive oxygen species shown by others to be important in RANKL-mediated signaling. Most compellingly, cells without active caspase 3 were TRAP negative and remained mononucleate. Our results point to a central role for caspase 3 and hydrogen peroxide in mediating osteoclast differentiation.

Disclosures: **K.H. Szymczyk**, None.

SU293

Relationship of Osteoclast Mitochondrial Mass and Potential to its Morphology and Function. S. J. Wimalawansa, C. S. Herath, J. Ghosh^{*}. Medicine, Robert Wood Johnson Medical School, New Brunswick, NJ, USA.

The molecular basis of age-related oxidative-stress associated imbalance in bone cell coupling is complex. These include enhanced osteoclast differentiation, life span, and increased bone resorption. We have developed methodologies to quantitate osteoclastic mitochondrial mass and potentials using a dual-color Florescent Activated Cell Sorting (FACS) method based on osteoclast marker RANK receptors (RANK-R) expression and osteoclast nuclear density. Bone marrow cells were cultured on glass cover slips to obtain over 98% pure osteoclast progenitors cells. Cells were harvested at 48, 72, 96 and 192 hrs, and their differentiation rates were analyzed on reference to their expression of RANK-R protein (immuno-labeling of RANK-R using goat-anti-mouse RANK-R Ab, and secondary labeling with Green fluorochrome Labeled-rabbit anti-goat IgG). RANK-R labeled cells were stained with Propidium Iodide for simultaneous analysis of nuclear density. Osteoclast formation rates were examined at same time points by counting multi-nucleated vs. mono nucleated cells on randomly selected 16 fields after staining with Hoechst nuclear stain in a fluorescence microscopy. This method accurately separates distinct sub-population of high nuclear density and RANK-R expressing mature osteoclast cells. Linearity of the method and its' simplicity allowed us to accurately measure the osteoclast cell differentiation rates per unit time (i.e., slope of the graph) in many situations. Using this methods we have analyzed osteoclast differentiation rates from bone marrow cells, osteoblast mediated regulation on osteoclasts, and rates of osteoclast differentiations and maturity. An example of differentiation rates of RANK-R expressing and high nuclear

ASBMR 27th Annual Meeting

density (multinucleated) osteoclasts by FACS method is shown in figure 1. Mitochondrial mass and potential are highly correlated with the osteoclastic cell maturation, morphology and cellular integrity, and its bone resorbing activity. This simple methodology can be adapted to further understand the role of osteoclasts in different disease status.

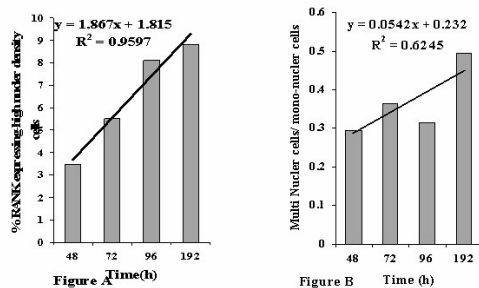


Figure A: Differentiation rates of RANK-R expressing & high nuclear density OCs by FACS method Figure B: Multi-nuclear OCs formation rate by nuclear counting.

Disclosures: **S.J. Wimalawansa**, Better Bone Health 5; Roche 8; Lily 8.

SU294

A Specific Requirement for the Microphthalmia Transcription Factor (Mitf) in Osteoclast Differentiation and Bone Development. **C. L. Hershey¹, Y. L. Lin², M. L. Boussein³, H. R. Widlund^{*1}, D. E. Fisher¹.** ¹Pediatric Oncology, Dana-Farber Cancer Institute, Boston, MA, USA, ²Oral Pathology, University of Kentucky, Lexington, KY, USA, ³Orthopedic Biomechanics, Beth Israel Deaconess Medical Center, Boston, MA, USA.

The Microphthalmia-associated transcription factor (Mitf) is a member of the MiT basic/helix-loop-helix/leucine zipper transcription factor family, which includes Mitf, Tfe3, Tfeb and Tfec. Dominant negative *Mitf* mutations (*Mitf^{microphthalmia}*) demonstrate that the MiT family is required for the differentiation and survival of osteoclasts, melanocytes, retinal pigment epithelium and mast cells. However, the requirement for individual family members is not known. Here we demonstrate a specific requirement for Mitf in osteoclast differentiation and bone development using a previously identified *Mitf*-null mouse, *Mitf^{trG-A-9}* (Hodgkinson et al., 1993). It is shown here that the *Mitf^{trG-A-9}/Mitf^{trG-A-9}* mice have a mild osteopetrosis. Histological analysis of femurs and tibiae from *Mitf^{trG-A-9}/Mitf^{trG-A-9}* mice reveals residual primary and secondary spongiosa compared to control littermates, indicating a defect in bone resorption. The increase in bone was visible in the majority (87%, n=47) of *Mitf^{trG-A-9}/Mitf^{trG-A-9}* mice examined but varied in severity and appeared to improve with age. Micro CT measurements indicate increased trabecular bone in the femurs and vertebrae of *Mitf^{trG-A-9}/Mitf^{trG-A-9}* mice compared to heterozygous controls, with significant differences in femoral (p<0.05) Tb.N, Tb.Sp and BMD and vertebral (p<0.001) bone volume fraction (BV/TV%), Tb.N and Tb.Sp. The micro CT, histology and X-ray evaluations of the *Mitf^{trG-A-9}/Mitf^{trG-A-9}* mice demonstrate they have a nearly solid block of bone below the growth plate in the femurs and tibia. In *in vitro* osteoclast differentiation assays, the *Mitf^{trG-A-9}/Mitf^{trG-A-9}* bone marrow and spleen had an impairment in the generation of multinucleated TRAP+ cells. The *Mitf^{trG-A-9}/Mitf^{trG-A-9}* cultures showed a decreased ability to resorb bone *in vitro* when grown on bovine cortical bone slices. We examined *in vitro* osteoclastogenesis in another recessive *Mitf* allele, *Mitf cloudy-eye* (*Mitf^{ce}*) and found the ability to generate bone-marrow derived osteoclasts was also diminished in the *Mitf^{ce}/Mitf^{ce}* mice. The results presented here indicate that loss of Mitf produces a bone phenotype that cannot be fully compensated for by other MiT family members, identifying a specific requirement for Mitf in osteoclastogenesis. This places Mitf among the transcription factors, including Pu.1, AP1, NFκB and NFATc1 that are fundamentally required for osteoclast differentiation and proper bone development.

Disclosures: **C.L. Hershey**, None.

SU295

RANKL Inhibition with Osteoprotegerin (OPG) Prevents Bone Loss but Does not Affect Immune Status in Arthritic Rats. **M. Stolina¹, S. Adamu^{*1}, D. Dwyer^{*1}, S. Middleton^{*1}, F. Asuncion^{*1}, M. Ominsky¹, G. Schett^{*2}, U. Feige^{*1}, P. Kostenuik¹, D. J. Zack^{*1}.** ¹Amgen Inc., Thousand Oaks, CA, USA, ²Div Rheum, Med Univ Vienna, Vienna, Austria.

Rheumatoid arthritis (RA) is an autoimmune disease characterized by inflamed joints, focal bone erosions, and periarticular osteopenia. Overproduction of receptor activator of NF-κB ligand (RANKL) is present at sites of erosion and is implicated in juxta-articular osteopenia. Rat adjuvant arthritis (AdA) is an immune-mediated, rapidly destructive disease characterized by the presence of RANKL-expressing activated T cells in the juxta-articular intramedullary space of bone. OPG, a RANKL inhibitor, prevents bone loss during the course of AdA. The role of RANKL inhibition on the inflammatory aspects of arthritis was evaluated by administering OPG during the course of AdA. AdA was induced in male Lewis rats using heat-killed mycobacteria in paraffin oil. AdA rats were treated subcutaneously every 3 days with placebo (PBS) or recombinant OPG-Fc (3 mg/kg) for 10 days beginning 4 days after disease onset, and sacrificed on day 14 after onset. Concentrations of RANKL and TRAP 5b (a bone resorption marker) were evaluated in terminal serum, as were PGE2 and pro-inflammatory cytokines (IL-1β, TNF-α, IL-6, KC/GRO, and MCP-1) associated with progression of inflammatory arthritis. Hind paw volume was measured by water plethysmography and BMD by DXA. Serum RANKL concentrations were 138% higher in AdA rats vs non-arthritic controls (p<0.01). RANKL

concentrations were significantly reduced to levels similar to non-arthritic controls (p<0.01) by OPG treatment. OPG also caused significant reduction in bone resorption, as shown by a 90% reduction in serum TRAP-5b (p<0.001 vs PBS-AdA rats). AdA rats had significantly lower ankle joint BMD (p<0.05 vs. non-arthritic controls), and OPG prevented this bone loss. Despite these potent antiresorptive effects, OPG had no apparent effect on the inflammatory component of arthritis. Hind paw volume in AdA rats was 100% greater than in non-arthritic controls (p<0.05); OPG had no effect on paw volume. AdA rats also had significantly greater serum levels of IL-1β, TNF-α, KC/GRO, IL-6, MCP-1 and PGE2 (2, 5, 2.5, 5, 2.5, and 4.5-fold greater than non-arthritic controls, respectively, p<0.05). OPG had no effect on serum concentrations of these pro-inflammatory cytokines. RANKL inhibition by OPG effectively prevented bone loss in arthritic rat paws. Despite clear evidence of systemic suppression of bone resorption and the presence of activated T cells expressing RANKL, OPG treatment did not influence any measured indicators of inflammation. These data suggest that RANKL plays an important role in bone resorption, but not in immune function.

Disclosures: **M. Stolina**, Amgen 3.

SU296

Lipid Rafts, Vacuolar H⁺-ATPases, and the Formation of the Ruffled Membranes of Osteoclasts. **L. S. Holliday, J. Zuo.** Orthodontics, University of Florida College of Dentistry, Gainesville, FL, USA.

Osteoclasts form ruffled membranes by transporting cytosolic vesicles to the plasma membrane. Subunit a3-containing vacuolar H⁺-ATPases (V-ATPases) are abundant components of ruffled membranes. Osteoclasts contain both the constitutively expressed a1 isoform of subunit a, and a3, which is upregulated during osteoclastogenesis. After extraction of osteoclasts with cold 1% Triton X-100, 92% of a1 remained soluble while 94% of a3 pelleted during centrifugation of extracts at 150 KXg for 60 minutes. Flotillin, a marker for lipid rafts, was also abundant in the detergent-insoluble pellet along with a3. Treatment of osteoclasts with methyl-β-cyclodextrin altered the distribution of a3 in subcellular fractions, and triggered disruption of the ruffled membranes of pre-activated osteoclasts. V-ATPases co-segregated with flotillin in lipid raft fractions isolated by density gradient centrifugation. Cholera toxin subunit (CTB), which detects ganglioside GM1, another marker of lipid rafts, stained the plasma membranes of unactivated, fixed, unpermeabilized, osteoclasts weakly. In contrast, CTB stained internal vesicular structures in these cells intensely, after they were permeabilized. Many of these internal vesicles were also stained with a polyclonal antibody against subunit E of V-ATPase. The ruffled membranes of resorbing osteoclasts were stained intensely by both CTB and the anti-E subunit antibody. These data suggest that integration of V-ATPases into lipid raft-rich vesicles plays a role in their transport to ruffled membranes, and that ruffled membranes, formed as these vesicles fuse with the plasma membrane, are rich in lipid rafts. The need for cholesterol for the formation of V-ATPase-containing lipid rafts may contribute to the profound sensitivity osteoclasts exhibit to inhibitors of farnesyl pyrophosphate synthase and HMG-CoA reductase.

Disclosures: **L.S. Holliday**, None.

SU297

Expression of the Zinc Transporter ZIP1 in Osteoclasts. **S. N. Sahu^{*}, M. A. Khadeer^{*}, G. Bai^{*}, A. Gupta.** Biomedical Sciences, University of Maryland, Baltimore, Baltimore, MD, USA.

Zinc has been demonstrated to be an essential trace element for normal skeletal growth, and zinc deficiency has been associated with retarded growth. Zinc has been implicated in bone mineralization through regulation of alkaline phosphatase and other metalloenzymes. Zinc is fairly abundant in bone. Zinc has been previously demonstrated to be a potent inhibitor of osteoclastogenesis and osteoclast function. The mechanisms for cellular uptake of zinc into osteoclasts have not been characterized. Intracellular zinc homeostasis is maintained by two distinct families of transporters, Zrt/Irt-like proteins (ZIP) and the cation diffusion facilitator (CDF) family. The ZIP family of transporters mediates uptake of zinc into cells, whereas the CDF family is involved in zinc efflux and intracellular sequestration. We have corroborated previous studies on the reduction of osteoclastogenesis in the presence of extracellular zinc in murine osteoclasts. The optimal concentration of extracellular ZnCl₂ supplementation of culture medium for significant inhibition (45-55%) of osteoclastogenesis was determined to be ~5-10 μM ZnCl₂. Using reverse transcriptase-polymerase chain reaction, a ZIP1 fragment of 230 bp from murine osteoclasts was amplified. The sequence homology between the human and murine ZIP1 transcripts revealed ~82% nucleotide identity. ZIP1 is a 324 amino acid protein with a predicted molecular mass of ~34 kD, but can be seen as a dimer, presumably because of a leucine zipper motif. In both the human osteoblast and murine osteoclast, the ZIP1 protein can be detected at ~68 kD. The protein levels of ZIP1 were not appreciably changed during the transition from pre-osteoclast precursors (between days 1-4 of culture) to multinucleated osteoclasts (between days 5-6 of culture). ZIP1 was both diffusely distributed throughout the cytoplasm and present at the plasma membrane. Following an adenoviral-mediated overexpression of ZIP1 in murine osteoclasts, ZIP1 was predominantly colocalized with actin at the sealing zone, and significantly inhibited osteoclast function, as assessed by *in vitro* assays for resorptive activity. Finally, overexpression of ZIP1 negatively impacted NF-κB binding activity in osteoclasts, as assessed by electrophoretic mobility shift assays. In conclusion, these data both corroborate previous studies on regulation of osteoclast formation and activity by zinc, and provide the first direct evidence for a zinc transporter negatively impacting osteoclast differentiation and activity.

Disclosures: **S.N. Sahu**, None.

SU298

Characterization of the Actin-Binding Activity of Subunit B of Vacuolar H⁺-ATPases. J. Zuo, S. Vergara^{*}, S. Chen^{*}, J. Jiang, M. KAKU^{*}, S. Kohno^{*}, Y. Gong^{*}, I. Hurst, H. Huang^{*}, L. Holliday. Orthodontics, University of Florida, Gainesville, FL, USA.

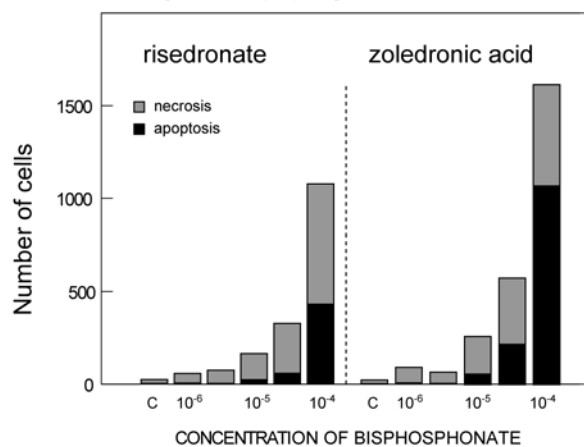
The B1 "kidney" and B2 "brain" isoforms of subunit B of vacuolar H⁺-ATPase (V-ATPase) have actin binding sites that mediate interactions between the intact enzyme and filamentous-actin. Osteoclasts express B2, but not B1. Adeno-associated virus vectors were used to transduce mouse osteoclasts with wild-type B1 or B1^{mut}, a full length B subunit that contained minor alterations that disrupted actin-binding activity. Immunoprecipitations suggested that both B1 and B1^{mut} assembled with endogenous V-ATPase subunits to form intact enzyme. Both B1 and B1^{mut} were localized like endogenous V-ATPase subunits in unactivated osteoclasts. Wild-type B1 associated with the actin cytoskeleton and was transported to ruffled membranes, domains of the plasma membrane of resorbing osteoclasts. In contrast, B1^{mut} failed to associate with the actin cytoskeleton and was not transported efficiently to ruffled membranes. Yeast subunit B also bound microfilaments with similar affinity as the mammalian B subunits, and competed with mammalian B subunits in vitro microfilament binding assays. Efforts are underway to disrupt the actin binding site in yeast subunit B to test to what extent the mutant, compared with wild type, rescues V-ATPase function when transduced into a B subunit null strain. These data show that the B1 isoform of B subunit contains the necessary information for targeting to the ruffled membranes of osteoclasts, even though it is not normally expressed in osteoclasts. The actin binding activity of B1 is involved in proper ruffled membrane targeting. Complimentary studies of the actin binding activity of yeast subunit B are ongoing.

Disclosures: **J. Zuo**, None.

SU299

In Vitro Effects of 5 Bisphosphonates on Apoptosis and Death of Macrophage-Like Cells. M. Moreau^{*}, P. Massin^{*}, M. F. Basle^{*}, D. Chappard. Faculté de Médecine, INSERM, EMI 0335-LHEA, Angers, France.

Bisphosphonates (BPs) inhibits bone resorption by reducing osteoclastic activity. This implies either a reduction of osteoclast number by cell death (apoptosis) or a reduce activity at the cell level, or by a combination of both effects. Pathophysiology of prostheses loosening is complex and implies an inflammatory reaction secondary to the phagocytosis of wear debris by macrophages with a secondary increased bone resorption by osteoclasts. It has been reported that BPs can inhibit proliferation and cause cell death in macrophages by induction of apoptosis and necrosis. We have used mouse macrophage-like J774.1 cells to evaluate the effects of 5 BPs. These cells can express TRAcP activity in vitro, like osteoclasts. Macrophage-like cells 5x10⁴ were cultured in 6-wells plates for 2 days. BPs (alendronate, pamidronate, etidronate, risedronate, zoledronic acid) were added in the medium at concentration of 10⁻⁶, 5x10⁻⁶, 10⁻⁵, 5x10⁻⁵ and 10⁻⁴M during 3 days. For each concentration, experiment was done in triplicate. Cells were washed and resuspended. The effects of BPs were measured by flow cytofluorometry using annexin V-FITC (apoptosis) and propidium iodide (necrosis) on 2000 cells per technique. Etidronate did not cause apoptosis or cell death at any concentration. Alendronate and pamidronate caused apoptosis and death only at very high concentration [10⁻⁴M]. On the contrary, apoptotic and dead cells were evidenced with risedronate or zoledronic acid at lower concentrations. These effects were dose-dependant and occurred when concentration reached [10⁻⁵M]. The number of apoptotic cells was higher with zoledronic acid. AminoBPs could be proposed as a countermeasure in aseptic loosening of joint prostheses.



Disclosures: **M. Moreau**, None.

SU300

Rapid Osteoclast Apoptosis at the End of Lactation in the Maternal Skeleton. B. M. Bowman, S. C. Miller. Radiobiology, University of Utah, Salt Lake City, UT, USA.

Lactation is a period of high turnover dominated by bone resorption to permit utilization of skeletal mineral for milk production. At weaning, however, there is a rapid transition to an anabolic phase that rebuilds skeletal mineral stores. Within several days after weaning there is a rapid expansion of the osteoblast population, with a substantial portion of the cells being derived from proliferating progenitors. The purpose of this study was to document this rapid reversal period and to correlate these events with changes in the endocrine milieu. Established breeder, Sprague-Dawley rats were assigned to 5 groups; 1) Day 10 of lactation, 2) Day 19 of lactation, 3) 1 day post-weaning, 4) 1 week post-weaning and 5) age-matched, non-mated, estrus cycling females. The litters were normalized and pups weaned on day 20 of lactation. Estrus status was determined by vaginal smears and at necropsy tissues were collected to determine bone cell populations, morphology and apoptosis. Sera were collected for measurements of estrogen (E), prolactin (PRL), PTH and calcitonin (CT). Through lactation the animals were continually in diestrus, consistent with low serum E levels. At Day 10 and 19, TRAP-positive osteoclasts were abundant and spread over much of the cancellous bone surface. There was little, if any, indication of osteoclast apoptosis during this period as determined by morphological criteria and ISOL-BrdU labeling of DNA fragmentation. By one day after weaning most of the osteoclasts had rounded up and were removed from bone surfaces. There were numerous TRAP-stained apoptotic fragments of osteoclasts in the bone marrow and osteoclast nuclei were observed with the ISOL-BrdU label in the marginalized chromatin. Interestingly, on the day after weaning, serum CT levels were over 6 times greater than those observed the day before weaning, 136 ± 40 pg/ml vs. 21 ± 7 pg/ml, respectively. The greatly increased CT levels were transient, and returned to about 15 ± 3 pg/ml within 6 days after weaning. E levels also increase shortly after weaning and by the second day, all animals showed estrus-positive vaginal smears. The physiological change initiated by weaning triggers a mechanism in the maternal skeleton for the rapid reduction in the osteoclast population by apoptosis. These rapid changes are associated with a marked increase in circulating CT as well as the re-initiation of estrus (with increased circulating E). These rapid changes in osteoclast morphology are consistent with known effects of CT. This study further demonstrates the well synchronized events and adaptations that occur in the maternal skeleton during and after the reproductive cycle and provides new insights into endocrine regulation of natural physiological cycles in skeletal tissues.

Disclosures: **B.M. Bowman**, None.

SU301

Suppressions of Phenytoin in the Bone Resorption and Production of PGE₂ Induced by LPS. M. Koide, S. Fujita^{*}, T. Sobue, N. Sato, M. Suzuki^{*}, Y. Ishihara^{*}, N. Yoshinari^{*}, K. Inagaki, T. Noguchi^{*}. Department of Periodontology, School of Dentistry Aichi-Gakuin University, Nagoya, Japan.

Phenytoin (Diphenylhydantoin, DPH) is often used a drug for seizure control. Gingival overgrowth is well known as an adverse effect and is characterized by increased proliferation of gingival fibroblasts and collagen synthesis. However, the effects of DPH on bone metabolism are still unclear. The purpose of this study is to examine the effect of DPH on bone resorption stimulated with lipopolysaccharide (LPS), as a bacterial pathogenic component *in vitro*. The effects of DPH stimulated with or without LPS which examined by mouse calvarial organ culture and osteoclast formation methods. DPH inhibited significant bone resorption and osteoclast formation induced by LPS. Moreover, RANKL mRNA expression examined in primary osteoblast (OB) cell by RT-PCR method. DPH did not affect RANKL mRNA expression in OB cell. We previously reported that the PGE₂ production is an important mediator for bone resorption induced by LPS. Therefore, the amount of PGE₂ measured in mouse calvarial organ and osteoclast formation culture supernatants by EIA method. DPH reduced the PGE₂ production stimulated with or without LPS in both culture supernatants. Furthermore, DPH inhibited bone resorption and osteoclast differentiation induced by LPS. Thus, it is suggested that DPH will have a possibly to protect an alveolar bone resorption induced by bacteria in periodontal disease.

Disclosures: **M. Koide**, The Ministry of Education, Culture, Sports, Science and Technology(No.16791323) 2; High-Tech Research Center Project, 2002-2006 2.

SU302

Osteopontin Deficiency Impairs Wear Debris-Induced Osteolysis. S. Shimizu^{*1}, Y. Asou², N. Okuda^{*3}, N. Kato⁴, S. R. Rittling⁵, K. Shinomiya^{*2}, T. Muneta^{*3}, D. T. Denhardt⁵, M. Noda⁴. Tokyo Medical and Dental University, Center of Excellence program for Frontier Research Program on Molecular Destruction and Reconstruction of Tooth and Bone, Tokyo, Japan, ²Tokyo Medical and Dental University, Department of Orthopaedic Surgery, Tokyo, Japan, ³Division of Bio-Matrix, Graduate School Tokyo Medical and Dental University, Section of Orthopaedic Surgery, Tokyo, Japan, ⁴Medical Research Institute, Tokyo Medical and Dental University, Department of Molecular Pharmacology, Tokyo, Japan, ⁵Rutgers University, Department of Cell Biology and Neuroscience, Piscataway, NJ, USA.

Periprosthetic osteolysis is the major complication following total joint replacement. Osteolysis reflects progressive generation of implant-derived wear particles that initiates a macrophage-mediated inflammatory response by resident macrophages, leading to osteoclast activation and bone resorption at the implant interface. To investigate molecular mechanisms underlying this clinically important event, we focused on osteopontin (OPN),

ASBMR 27th Annual Meeting

a cytokine and cell attachment protein. OPN is produced at high levels by macrophages in granulomas and is implicated in the mediation of inflammatory process and subsequent bone resorption by osteoclasts. The purpose of this study was to investigate the functions of OPN by previously established *in vivo* murine model of particle-induced osteolysis. OPN-deficient mice and wild-type littermates (1.5- to 3-month-old female mice), were anesthetized and the scalp incised longitudinally to expose the external cranial periosteum. The periosteum was elevated off the external cortex of the calvarium by sharp dissection. Thirty mg of commercially prepared titan particles were placed directly on the surface of the bone. Sham operation consisted of the entire procedure without particle implantation. Animals were sacrificed at 10 days, and each calvaria was excised, fixed, and decalcified. Frontal histological three sections of parietal bones with 200um intervals were picked up for each animal and evaluated immunohistologically. Whereas an inflammatory reaction was observed regardless of the genotypes, bone resorption area more than 400um away from sagittal suture was 50% decreased in OPN deficient mice compared with littermates. Histomorphological analysis indicated that osteoclast surface/bone surface was significantly reduced in OPN-deficient mice. Bone volume/tissue volume in vertebral body and urinal deoxypyridinoline was not affected by recipient genotypes after the particle implantation, indicated that general bone metabolism was not affected by OPN-deficiency. These results indicate that OPN plays a critical role in wear debris-induced osteolysis.

Disclosures: **S. Shimizu**, None.

SU303

Tartrate-Resistant Acid Phosphatase 5b Is a Marker of Osteoclast Number in Human Osteoclast Cultures. **H. Ylipahkala**^{*1}, **J. Rissanen**², **H. K. Väänänen**^{*1}, **J. M. Halleen**². ¹Anatomy, University of Turku, Institute of Biomedicine, Turku, Finland, ²Pharmatest Services Ltd, Turku, Finland.

Tartrate-resistant acid phosphatase 5b (TRACP 5b) is released into the blood circulation from osteoclasts, and serum TRACP 5b has proved to be useful marker of bone resorption. Recent evidence has suggested that serum TRACP 5b would be a marker of osteoclast number rather than osteoclast activity. We have studied the effects of osteoprotegerin (OPG), sodium azide, alendronate (ALN) and clodronate (CLN) on secretion of TRACP 5b from human osteoclasts *in vitro*. Human osteoclast precursor cells (PoieticsTM, Cambrex, East Rutherford, NJ, USA) were cultured on bovine bone slices for 9 days. OPG was added into the culture medium at day 0 and azide at day 7, whereas ALN and CLN were coated into the bone slices before starting the culture period. TRACP-positive multinucleated osteoclasts and apoptotic osteoclasts were counted under a microscope. Medium TRACP 5b activity was determined using an in-house immunoassay and medium C-terminal cross-linked telopeptides of type I collagen (CTX) using a commercial immunoassay (CrossLaps® for culture, Nordic Bioscience, Herlev, Denmark). OPG, azide, CLN and ALN inhibited bone resorption by decreasing the number of osteoclasts. Both medium TRACP 5b activity and medium CTX decreased dose-dependently by all four compounds. Medium TRACP 5b activity correlated with both medium CTX and osteoclast number, and the correlation was in all cases stronger with osteoclast number. Azide, CLN and ALN dose-dependently increased cell death and decreased medium TRACP 5b activity, suggesting that TRACP 5b is not released from dying osteoclasts as an active enzyme. We conclude that medium TRACP 5b activity reflects the number of osteoclasts in this human osteoclast culture system, and TRACP 5b is not released from dying cells as an active enzyme.

Disclosures: **H. Ylipahkala**, None.

SU304

RANKL Inhibition with AMG 162, a Fully Human MAb, Causes Sustained Suppression of Bone Resorption and Increased BMD in Knockin Mice Expressing Humanized RANKL. **P. J. Kostenuik**, **K. Warmington**^{*}, **M. Grisanti**^{*}, **S. Morony**^{*}, **Z. Geng**^{*}, **H. L. Tan**^{*}, **C. Christensen**^{*}, **J. Sullivan**^{*}, **H. Nguyen**^{*}, **S. Adamu**^{*}, **F. Asuncion**, **M. Ominsky**, **X. Li**, **J. McCabe**^{*}. Metabolic Disorders/Functional Genomics, Amgen Inc., Thousand Oaks, CA, USA.

RANKL plays an essential role in osteoclast formation, function, and survival. The RANKL inhibitor OPG-Fc suppresses bone resorption in postmenopausal women and in many animal models of bone disease. AMG 162, a fully human monoclonal antibody, is a RANKL inhibitor that increases BMD in postmenopausal women. AMG 162 does not neutralize rat or murine RANKL, which has hindered the direct comparison of AMG 162 and OPG-Fc in non-primate models. We therefore genetically engineered mice to express a chimeric form of RANKL that is neutralized by AMG 162. Knockin technology was used to replace the 5th exon of the murine RANKL gene with a hybrid exon containing a human coding region and a murine non-coding region. We compared the pharmacodynamic response of these mutant homozygous (huRANKL) mice to AMG 162 and huOPG-Fc. Male huRANKL mice (2-3 months old, 8/group) or normal wild type (WT) controls were treated with PBS or with AMG 162 or OPG-Fc (5 mg/kg, twice/week, SC) for 3 weeks. As expected, AMG 162 had no detectable pharmacologic effects in normal WT mice. In contrast, treatment of huRANKL mice with AMG 162 caused a significant increase in lumbar BMD (by DXA) from week 1 through week 3 ($p < 0.05$ vs PBS controls). OPG-Fc caused smaller, non-significant increases in BMD in huRANKL mice. The greater BMD response with AMG 162 was associated with more sustained suppression of bone resorption versus OPG-Fc. AMG 162 and OPG-Fc both caused rapid (24 h) and significant (75%) reductions in serum TRAP-5b. However, AMG 162 maintained this antiresorptive effect through day 21, while the antiresorptive effect of OPG-Fc was no longer apparent at day 21. Results in these young mice may have been influenced by their rapid growth, so the efficacy of AMG 162 was tested in aged (10 month old) female huRANKL mice. Mice were treated once/week with PBS or AMG 162 (2 or 10 mg/kg, SC) for 3 weeks. AMG 162 caused significant, dose-dependent reductions in serum TRAP-5b. Histomorphometric analysis of the proximal tibia showed that both doses of AMG 162 caused increased bone

volume and decreased osteoclast surface ($p < 0.05$ vs PBS controls). MicroCT analysis of lumbar vertebra showed that AMG 162 (10 mg/kg) increased bone volume and trabecular thickness ($p < 0.05$ vs PBS controls). In summary, huRANKL mice represent a novel non-primate system for testing the pharmacologic effects of AMG 162, a fully human RANKL monoclonal antibody. AMG 162 caused greater increases in BMD and more sustained suppression of bone resorption compared to OPG-Fc.

Disclosures: **P. J. Kostenuik**, Amgen 3.

SU305

Flavopiridol Inhibits Osteoblasts and Osteoclasts. **J. Nguemo-Djiometio**^{*1}, **W. Jaeger**^{*2}, **O. Hoffmann**¹. ¹Pharmacology and Toxicology, University of Vienna, Vienna, Austria, ²Clinical Pharmacy and Diagnostics, University of Vienna, Vienna, Austria.

Flavopiridol (FP) is a novel cyclin-dependent kinase inhibitor currently undergoing clinical development for the treatment of cancer. The aim of this study was to examine the effects of FP on osteoclast (OC) and osteoblast (OB) survival and function to determine whether this may be a potential treatment for tumour metastasis to bone. FP was evaluated in osteoclastogenesis using OC generated from spleen cells incubated with RANKL (25 ng/ml) and M-CSF (20 ng/ml). We assessed OC isolated from 4 day old New Zealand rabbits to test the effects on bone resorption and attachment. Primary cultures of mouse osteoblastic cells obtained by sequential collagenase/dispase digestion from calvaria of 1- to 2-day-old mice were used to investigate the effect of FP on cell viability and attachment. We stained OB and OC cytoskeleton with phalloidin-rhodamine and evaluated the actin content in OB under the fluorescence microscope. OB and the OC precursor cell line RAW 264.7 were evaluated for survival and apoptosis in the presence of FP using nuclear DAPI staining and the Celltiter96 Assay. FP inhibited bone resorption of mature rabbit OC by 100%, 50% and 25% at 10, 1, and 0.1 μ M, respectively. FP at doses greater than 0.1 μ M significantly decreased OC attachment to bovine bone slices. FP exerts its inhibitory effects at the NF- κ B level through inhibition of I κ B α phosphorylation resulting in inhibition of OC differentiation. Osteoclastogenesis was completely inhibited when FP was added to cultures at early time points (0-4 days), and was only inhibited by approximately 10% when cells were treated after 4-5 days of culture showing that early differentiation was affected. FP reduced OC and OB viability after 12 hours of *in vitro* FP treatment. FP inhibited OB and RAW 264.7 cell proliferation, it induced apoptosis in OB at high doses (10 μ M) and in RAW 264.7 cells at lower doses (1 μ M). At low FP doses (0.1 μ M), we observed altered cytoskeleton organization and stress fibers, which resulted in spindle-shaped OB. Taken together, these results demonstrate that FP inhibits both OB and OC. It affects differentiation, function and viability of OC and interferes with cytoskeletal organisation and survival of OB. The mechanism of action is not entirely clear, however, FP inhibits the activation of NF- κ B and therefore reduces the expression of genes that regulate OC differentiation and survival. FP may be a novel treatment approach for bone tumours and metastases.

Disclosures: **O. Hoffmann**, None.

SU306

A Computational Model Delineates Differences in Hydroxyapatite Binding Affinities of Bisphosphonates in Clinical Use. **F. H. Ebetino**¹, **B. L. Barnett**^{*2}, **R. G. G. Russell**³. ¹Procter & Gamble Pharmaceuticals, Mason, OH, USA, ²Dept of Chemistry, University of Cincinnati, Cincinnati, OH, USA, ³Institute for Musculoskeletal Sciences, Oxford University, Oxford, United Kingdom.

Differences in bone mineral binding affinities of clinically utilized bisphosphonates (BPs) have been described with a decreasing rank order of zoledronate>alendronate>ibandronate>risedronate>etidronate, (Nancollas et al, Bone, in press). Although all of these contain the central hydroxyl group, characteristic of high mineral affinity, significant differences in affinity among these drugs exist which may lead to differences in bone uptake and release. Work on early generation BPs demonstrated the importance of a tridentate binding mode to calcium in hydroxyapatite (HAP). In this current analysis, similar modeling on the HAP mineral surface with the nitrogen (N) - containing BPs allowed a computer-aided 3-D analysis of the potential orientation of the N functionality of these agents. Once a low energy conformation of each BP was oriented in this tridentate binding mode on the trigonal prismatic column of calcium atoms in HAP, the N side chain conformations of the BPs were examined for their interaction with the [001] surface. The 4-amino group of alendronate can form a strong N-H---O hydrogen bond (132°, 2.7Å N---O distance) to the labile 'OH oxygen on HAP, where carbonate and fluoride are known to substitute. The corresponding ring N of zoledronate can only form a weaker electrostatic interaction with this labile 'OH site. However it can form an additional strong hydrogen bond to a bifurcated network between two P-O oxygen atoms closely oriented within the crystal lattice including a 132° angle and a 2.7 Å N---O distance, explaining its high binding affinity. In the case of risendronate, steric hindrance of the pyridyl ring prevents its N from strong hydrogen bonds in either fashion and it may form only weaker electrostatic interactions, such as at the labile 'OH (N---O distance 3.0 Å, 102°) This affords weaker binding affinity compared to alendronate and zoledronate, but does lead to higher affinity than that of etidronate (which has no N functional group). Comparative modeling of other BPs further demonstrates this affinity/H-bonding correlation. For example, the higher affinity 2-pyridyl analog of risendronate, NE-58018, can form a strong N-H---O hydrogen bond (127°, 2.9Å N---O distance) to the labile 'OH and a strong bifurcated interaction at the P-O oxygen atoms. There is increasing evidence that the mechanism of action of each BP combines a differing ratio of biochemical activity vs bone mineral interaction, which can lead to different pharmacology and perhaps different bone quality over extended dosing periods.

Disclosures: **F. H. Ebetino**, Procter & Gamble Pharmaceuticals 3.

SU307

Cathepsin K siRNA Transfection Inhibits Bone Resorption in Primary Human Osteoclasts. C. I. Selinger*, C. J. Day*, N. A. Morrison. School of Medical Science, Griffith University, Gold Coast, Australia.

The ability to easily transfect siRNAs into mature human osteoclasts, while they are in the process of resorbing actual bone, would provide an extremely useful tool for the large scale analysis of target genes in osteoclasts. We have undertaken a study which outlines the effectiveness of 'diced' siRNA in primary human osteoclasts using a number of transfection reagents, the potency of diced siRNA and its ability to significantly diminish bone resorption. Highly specific human siRNA for Cathepsin K was generated using recombinant human Dicer RNase III. Six transfection reagents (SiLentFect, Oligofectamine, Lipofectamine, GeneSilencer, JetPEI and Fugene6) were tested for effectiveness of siRNA incorporation using quantitative PCR and their cellular toxicity was monitored. Fugene6 and Lipofectamine were found to be the most effective for siRNA incorporation with the least cytotoxic effects in primary human osteoclast cells. We found 25nM to be the most potent siRNA concentration which achieved a reduction in Cathepsin K expression of >91% using Fugene6 and Lipofectamine. Osteoclasts could be transfected directly on dentine slices. For this method, human osteoclasts were differentiated for 14 days in the presence of RANKL and M-CSF on collagen coated plates and resuspended with dissociation buffer, then purified by low g centrifugation through 20% serum in medium at 200 rpm for 5 minutes. Resulting giant cells were plated directly onto sperm whale dentine slices cultured in normal medium and transfected immediately. Osteoclastic bone resorption was then monitored quantitatively by pit formation. Using this assay osteoclast bone resorption was significantly inhibited by Cathepsin K siRNA. This was demonstrated by a reduction in bone resorption area (p=0.03) and pit number (p=0.03). We show siRNA generated using Dicer enzyme is a potent inhibitor of the osteoclast gene Cathepsin K, and significantly inhibits the ability of primary human osteoclasts to resorb bone. siRNA provides a ready means of testing novel target genes directly for the bone resorption phenotype using the best possible standard, electron microscopy of bone resorption pits on whale dentine. Further optimizing and scaling up this technique should permit the simultaneous analysis of the involvement in bone resorption of large numbers of gene targets.

Disclosures: **C.I. Selinger**, None.

SU308

Rosuvastatin Inhibits Bone Resorption *In Vitro* by Inhibiting Protein Prenylation, and Prevents Ovariectomy-Induced Bone Loss *In Vivo*. A. Hughes*, J. C. Crockett*, A. I. Idris*, R. J. van't Hof*, M. J. Rogers. Medicine and Therapeutics, University of Aberdeen, Aberdeen, United Kingdom.

Statins are highly effective drugs that inhibit HMG-CoA reductase activity, thereby reducing the biosynthesis of cholesterol via the mevalonate pathway. Inhibition of HMG-CoA reductase also reduces protein prenylation by reducing the synthesis of farnesyl- and geranylgeranyl-diphosphate, which account for many of the pleiotropic effects of statins. For example, we have previously shown that mevastatin is a potent inhibitor of osteoclast function *in vitro* by causing loss of prenylated small GTPases, although others have suggested that statins may have bone anabolic properties. We investigated the *in vitro* effects on osteoclasts of the hydrophilic statin rosuvastatin (RSV, Crestor) in comparison to cerivastatin/CER, pravastatin/PRA and simvastatin/SIM. All four statins (0.1 to 10 microM) prevented the prenylation of the small GTPase Rap1A in rabbit osteoclasts in a concentration-dependent manner (order of potency CER>SIM>RSV>PRA). These concentrations also significantly inhibited bone resorption in cultures of rabbit osteoclasts, with the same order of potency. Addition of mevalonic acid (100 microM) or geranylgeraniol (20 microM) at least partially restored protein prenylation and bone resorption from inhibition by all four statins, confirming that these agents inhibit bone resorption by inhibiting the mevalonate pathway. 20mg/kg RSV also inhibited prenylation in osteoclasts in neonatal rabbits *in vivo*, demonstrated by accumulation of unprenylated Rap1A in osteoclasts purified from long bones 24 hours after injection. The effects of statin treatment on ovariectomy (OVX)-induced bone loss were examined in 8-week old Balb-C mice. Groups of seven sham operated or OVX mice were injected intraperitoneally with RSV for three weeks, then changes in bone parameters were measured by pQCT and microCT in the proximal tibia. OVX caused an 11% decrease in cortical BMD and a 54% decrease in trabecular bone volume. RSV significantly prevented loss of cortical BMD (47% recovery from OVX-induced loss with 2 mg/kg/day RSV, p<0.002) and loss of trabecular bone volume (27% recovery from OVX-induced loss with 2 mg/kg/day RSV, p<0.05). Mineral apposition rate, assessed by calcein double labelling, was significantly decreased by RSV treatment in sham and OVX mice. In conclusion, RSV, like other statins, inhibits bone resorption *in vitro* by reducing protein prenylation in osteoclasts. RSV can also inhibit protein prenylation in osteoclasts *in vivo* and appears to prevent OVX-induced bone loss in mice, primarily by inhibiting bone resorption.

Disclosures: **A. Hughes**, AstraZeneca 2.

SU309

Resorbing Osteoclasts Increase the Availability of Mineral-Bound Bisphosphonates to Non-Resorbing Cells. F. P. Coxon*¹, K. Thompson*¹, F. H. Ebetino², M. J. Rogers¹. ¹Medicine & Therapeutics, University of Aberdeen, Aberdeen, United Kingdom, ²Procter & Gamble Pharmaceuticals, Mason, OH, USA.

Bisphosphonates (BPs) target to bone due to their high affinity for calcium ions. During resorption, BPs are released from the acidified bone surface and taken up by osteoclasts, where they act by inhibiting the prenylation of small GTPases essential for osteoclast function. We recently investigated whether osteoclasts are the only cells in the bone microenvironment that can internalize BPs from the bone surface, by using a fluorescent alendronate analogue (FL-ALN) and by examining changes in the prenylation of the small GTPase Rap1A following treatment of cells with risedronate (RIS). Non-resorbing osteoblasts, macrophages and tumour cells internalized small amounts of BP from bone surfaces, but it remained unclear whether this was sufficient to affect the function of these cells. In this study, we measured the number of J774 macrophages and MCF-7 breast cancer cells remaining on dentine discs pre-coated with RIS, after 48 or 72 hours of culture, respectively. J774 cells were more susceptible to inhibition of prenylation under these conditions than MCF-7 cells, presumably due to the higher endocytic activity of the macrophages. Whereas 100µM RIS in solution reduced viable cell number by 96% (J774 cells) and 45% (MCF-7 cells), culturing these cells on dentine discs pre-coated with 100µM RIS caused only a small reduction in viable cell number (9% for J774 cells; 12% for MCF-7 cells). When cells cultured on dentine were incubated continuously with RIS, an intermediate effect was found (36% and 24% respectively), presumably because only a proportion of RIS becomes bound to dentine and unavailable for uptake by the cells. However, these cultures were carried out in the absence of osteoclasts, and it is possible that BPs released from the surface of mineralized tissues by the resorptive activity of osteoclasts can then be internalized by other cells in the local microenvironment. To investigate this possibility, we used confocal microscopy to analyse the uptake of FL-ALN by J774 cells co-cultured with rabbit osteoclasts. J774 cells adjacent to resorbing osteoclasts frequently internalized more FL-ALN than J774 cells distant from osteoclasts, although it is unclear whether this FL-ALN had diffused through the sealing zone or passed through the osteoclasts by transcytosis. In addition, J774 cells occupying resorption pits that had been vacated by osteoclasts internalized more FL-ALN than those attached to unresorbed surfaces. These results indicate that BPs may have direct effects on non-resorbing cells such as tumour cells, particularly those that are in the vicinity of resorbing osteoclasts *in vivo*.

Disclosures: **F.P. Coxon**, None.

SU310

Osteoclasts Resorb Human Cortical Bone Anisotropically. C. Janeiro*, R. Bizios*, D. Vashishth*. Biomedical Engineering, Rensselaer Polytechnic Institute, Troy, NY, USA.

When *in vivo* osteoclastic resorption occurs, the cutting cones are led longitudinally by osteoclasts through the long bones. It is unknown how osteoclasts orient themselves to lead the basic multicellular unit [1,2]. The present *in vitro* study investigated the role of bone microstructural elements in directing osteoclastic bone resorption. Longitudinal and transverse slices (4mmx4mmx200-300µm, WxLxH), were obtained from 17 frozen human tibiae (Ages 34 to 89). Human osteoclast precursor cells (Cambrex Poietics™) were prepared per the manufacturer's instructions, and cultured on the human bone slices (10,000 precursor cells/bone slice) for 14 days. The osteoclastic phenotype was confirmed by cell multinuclearity, TRAP-positive staining, and the ability to resorb bone. The bone slices were cleaned of osteoclasts and stained with toluidine blue; the area and the number of resorption pits were measured. For each transverse slice, the resorption pits were categorized based on their interaction with a cement line. These interactions were classified as either Type I (the resorption area contacts a cement line but does not cross it) or Type II (the resorption area crosses a cement line) [4]. The number of resorption pits/mm² and average resorption pit surface area of the longitudinal and transverse slices, as well as the number of Type I and Type II interactions, were compared using parametric tests (MiniTab). The number of resorption pits formed on the longitudinal slices was significantly (p<0.01) greater than the number of resorption pits found on the transverse slices. The resorption pits found on the longitudinal slices were also significantly (p<0.01) larger than those found on the transverse slices. On the transverse slices, the number of Type I interactions was significantly (p<0.05) higher than the observed Type II interactions. Based on these results we conclude that microstructural element of bone, including the cement lines, may be involved in directing osteoclastic bone resorption. More importantly, a large proportion of the resorption pits did not cross the cement line, which is consistent with literature results [3,5] that showed that dephosphorylation of osteopontin (OPN) causes osteoclast detachment. The mechanism of this event may involve OPN, which is known to be present in high amounts in the cement line [4], and the propensity of osteoclasts to bind with OPN [5].

[1]Frost, HM, *Bone Remodeling Dynamics*, 1963.

[2]Doblaré, M, *et al, Eng Fracture Mechanics*, 71:1809-1840, 2004.

[3]Heinegard, D, *et al, Ann NY Acad Sci*, 760: 213-222, 1995.

[4]Sit, S, *et al, ORS Proceedings*, 2003.

[5]Burr, DB, *et al, J Biomechanics*, 21: 939-945, 1988.

Acknowledgments: NIH Grant AR049635

Disclosures: **C. Janeiro**, None.

SU311

Interferon- γ Regulation of Osteoclast Inhibitory Peptide-1 (OIP-1/hSca) Gene Promoter Activity. S. Srinivasan*, E. Tsuruga*, W. L. Ries, L. L. Key Jr., S. Yang, S. V. Reddy. Children's Research Institute, Medical University of South Carolina, Charleston, SC, USA.

Osteoclast formation and activity are regulated by autocrine/paracrine factors produced in the bone microenvironment. We have previously identified and characterized osteoclast inhibitory peptide-1 (OIP-1/hSca), a member of Ly-6 gene family. Immune cell products such as IFN- γ are potent inhibitors of osteoclast formation. We have previously shown that IFN- γ stimulates OIP-1/hSca expression in osteoclast precursor cells. However, IFN- γ modulates gene expression through complex regulatory mechanisms. To determine the molecular mechanisms that regulate OIP-1 gene expression in osteoclast precursor cells, we isolated and characterized the human OIP-1/hSca gene (2 Kb) promoter. IFN- γ treatment of RAW 264.7 cells transfected with an OIP-1 gene promoter-luciferase reporter plasmid demonstrated a significant (4 fold) enhancement of luciferase activity. Analysis of the OIP-1 gene promoter sequence identified a potential Stat-1 binding motif at -1625 to -1640 bp position relative to the transcription initiation site. We therefore examined Stat-1 regulation of OIP-1 gene promoter activity in response to IFN- γ treatment to osteoclast precursor cells. IFN- γ stimulation of RAW 264.7 cells transfected with OIP-1 gene (-1 to -1988 bp) promoter-luciferase reporter construct in the presence of Stat-1 inhibitor, fludarabine (50 μ M) abolished IFN- γ stimulated OIP-1 gene promoter activity. Electrophoretic mobility shift assay (EMSA) demonstrated activated Stat-1 binding to the OIP-1 gene promoter sequence. Antiphospho-Stat-1 antibody addition to the EMSA reaction abolished Stat-1 binding to the OIP-1 gene promoter region. Furthermore, nuclear extracts derived from fludarabine treated IFN- γ stimulated RAW 264.7 cells did not demonstrate binding to the Stat-1 consensus sequence present in the OIP-1 gene promoter. However, IFN- γ treatment did not stimulate the activity of a OIP-1 gene promoter deletion construct that lacked the Stat-1 binding region. These data suggest that IFN- γ regulates OIP-1 gene promoter activity in osteoclast precursor cells through a Stat-1 dependent signaling pathway.

Disclosures: **S. Srinivasan**, None.

SU312

Access to BMD Testing Is Weakly Associated with Osteoporosis Management. D. H. Solomon¹, J. Polinski^{*1}, C. Truppo^{*2}, C. Egan^{*2}, S. Jan^{*2}, M. Patel^{*2}, Y. Chen³, T. Weiss³, M. A. Brookhart^{*1}. ¹Division of Pharmacoepidemiology, Brigham and Women's Hospital, Boston, MA, USA, ²Horizon Blue Cross Blue Shield of New Jersey, Newark, NJ, USA, ³Merck, Whitehouse Station, NJ, USA.

Introduction: While sub-optimal management of osteoporosis has been well described, the correlates are not well understood. We assessed whether decreased access to BMD testing was related to lower rates of osteoporosis management in a large cohort of at-risk beneficiaries of Horizon Blue Cross Blue Shield of New Jersey (NJ). **Methods:** We identified 9639 at-risk beneficiaries, including women ≥ 65 years old (n = 8283), and men and women ≥ 45 years old with a fracture (n = 740) or taking chronic oral glucocorticoids (n = 616) during the period 2003-2004. Osteoporosis management measured by a BMD test and/or filled a prescription for a medicine used for osteoporosis was determined through insurance claims data. Two aspects of access were examined -- the number of persons ≥ 65 per DXA machine for each of the 21 counties in NJ and the driving time for each person to the nearest DXA machine. To assess the independent effects of these measures of access on osteoporosis management we constructed regression models that included patient variables such as age, prior fracture, and comorbid conditions. These models were constructed using Generalized Estimating Equations and accounted for the clustering at the county level. **Results:** Of 9639 at-risk subjects, we found that 3104 (32%) had undergone a BMD test, 2893 (30%) had filled a prescription for an osteoporosis medication, and 4364 (45%) had one or the other. Across the 21 counties of NJ, the percentage of at-risk patients who had a BMD test and/or medication for osteoporosis ranged from 38% to 52%. In a multivariate model adjusting for various patient factors, an increase of 1000 people per DXA machine was associated with a decrease in probability of 1.6% (p=0.01) of a patient being screened or treated for osteoporosis. However, driving times were not associated with screening or treatment. There was a reduced probability of being screened or treated for patients with more comorbidities, -1.6% (p<0.001) per condition. **Conclusion:** Access to BMD testing as measured by the number of persons ≥ 65 years old per DXA testing center appears to be a significant but relatively weak predictor of receiving BMD and/or medications for osteoporosis. However, driving times to DXA testing centers were not associated with osteoporosis management. These data suggest that increasing the number of BMD testing sites may only have a weak impact on improving the management rates for osteoporosis in a state like NJ.

Disclosures: **D.H. Solomon**, Merck 2; Procter & Gamble 2.

SU313

Diagnosed Osteoporosis: The Tip of the Iceberg. M. S. Anthony*, B. D. Bradbury*, J. A. Satia*. Epidemiology, Amgen Inc., Thousand Oaks, CA, USA.

Osteoporosis is a silent disease that is often undiagnosed until there is a bone fracture. This study was done to determine the prevalence of physician-diagnosed osteoporosis in U.S. men and women and relate this to osteoporosis prevalence determined by bone mineral density (BMD) measurement. Data were from the National Health and Nutrition Examination Surveys (NHANES) III (1988-1994) and IV (1999-2002) which were

designed to obtain a representative sample of the non-institutionalized, U.S. civilian population. Demographic data and self-reported physician diagnosis of osteoporosis were collected by questionnaire. Femoral BMD was measured using dual-energy X-ray absorptiometry. Classification of osteoporosis was based on total femur BMD (t-score<-2.5) using data for non-Hispanic white women as the referent. Prevalence of osteoporosis at hip+spine was projected from the NHANES III hip data. Age- and gender-specific hip osteoporosis prevalence estimates from NHANES were multiplied by gender-specific ratios of osteoporosis prevalence at hip+spine/hip from published reports. Weighting variables provided by NHANES were used to project to the U.S. population and prevalence estimates were calculated using "surveymeans" procedure in SAS (Cary, NC). The prevalence of osteoporosis and diagnosed osteoporosis increased with age and was higher in women than men. Prevalence of osteoporosis and diagnosed osteoporosis differed by racial group in women, with highest prevalence among non-Hispanic whites, lowest in non-Hispanic blacks, and intermediate in Hispanics (data not shown). The biggest discrepancy between prevalence of osteoporosis determined by BMD and self-reported, physician-diagnosed osteoporosis was in older men and women. Prevalence of osteoporosis projected to hip and spine may be an underestimate of the true osteoporosis prevalence; therefore, the discrepancy between physician-diagnosed and BMD-determined osteoporosis might be even greater. The recent Surgeon General report cited that about 10 million U.S. individuals over age 50 have osteoporosis at the hip. When projected to hip and spine, to reflect physician practice, osteoporosis prevalence is likely double that. Osteoporosis appears to be under-diagnosed by physicians, suggesting that a sizeable portion of the population may have unrecognized and untreated disease and is therefore at significant fracture risk.

Projected osteoporosis prevalence determined by BMD and physician-diagnosed osteoporosis prevalence

Age group	Females		Males	
	Hip+spine osteo prevalence	Diagnosed 1999-2002	Hip+spine osteo prevalence	Diagnosed 1999-2002
50-59	6.0%	7.8%	3.9%	1.2%
60-69	24.4%	15.5%	4.3%	2.2%
70-79	35.7%	23.3%	6.7%	2.7%
80+	62.3%	28.6%	11.6%	3.6%

Disclosures: **M.S. Anthony**, Amgen 3.

SU314

A Meta-Analysis of Relationships among Leptin, Fat Mass, Lean Mass, and Bone Mineral Density. C. Pongchaiyakul¹, N. D. Nguyen², V. Pisprasert^{*3}, T. V. Nguyen². ¹Division of Endocrinology and Metabolism, Department of Medicine, Khon Kaen University, Khon Kaen, Thailand, ²Bone and Mineral Research Program, Garvan Institute of Medical Research, Sydney, Australia, ³Division of Nutrition, Department of Medicine, Khon Kaen University, Khon Kaen, Thailand.

While the association between leptin and fat mass is well established, the association between leptin and bone mineral density (BMD) is not clear due to conflicting finding from observational studies. The present study was aimed at examining the inter-relationships among leptin, fat mass (FM), lean mass (LM) and BMD by a meta-analysis. A systematic search of literature (via PubMed and Medline search engines) was conducted to identify all published studies on the association among the variables. The publication was limited to English language. Only studies on post-menopausal women were included in the analysis. For each study, the correlation coefficients among the variables were manually extracted and tabulated in the SAS system for analysis. The DerSimon-Laird random-effects meta-analysis model was used to estimate the overall correlation coefficient and its 95% confidence interval. In total, 25 studies were identified from the literature, which involved 5803 post-menopausal women aged between 50 and 90 years. Results of the random-effects meta-analysis indicate that leptin was significantly correlated with FM (r=0.61; 95%CI: 0.55-0.67) and whole body BMD (r=0.13; 0.10-0.16). There was no significant correlation between leptin and femoral neck BMD (r=-0.04) or lumbar spine BMD (r=-0.03). Moreover, the correlation between LM and BMD (rLM) was consistently and significantly higher than that between FM and BMD (rFM): for whole body BMD: rLM=0.30 (95%CI: 0.24-0.36) vs. rFM=0.19 (0.13-0.25); for lumbar spine BMD: rLM=0.34 (0.30-0.39) vs. rFM=0.19 (0.19-0.29); and for femoral neck BMD: rLM=0.37 (0.32-0.43) vs. rFM=0.24 (0.17-0.29) for femoral neck. At the femoral neck, there were 99.4% chances that rLM>0.3, but there were only 0.9% chances for rFM>0.3. In each correlation analysis, there was a significant heterogeneity among studies. These results suggest that although leptin was highly correlated with fat mass, the effect of leptin on BMD was modest, accounting for around 1% of BMD variance. The modest leptin-BMD association was partly due to the fact that BMD was more likely to be correlated with lean mass rather than fat mass.

Disclosures: **C. Pongchaiyakul**, None.

SU315

Bone Loss Associated with Primary Biliary Cirrhosis in Japanese Women. K. Takaguchi^{*1}, T. Inaba^{*1}, K. Kita^{*1}, Y. Onoda^{*2}, H. Miyatake^{*3}, Y. Takei^{*4}, A. Satou^{*5}, M. Ando^{*6}, K. Kawamura^{*7}. ¹Department of Internal Medicine, Kagawa Prefectural Central Hospital, Takamatsu, Japan, ²Department of Surgery, Kagawa Prefectural Central Hospital, Takamatsu, Japan, ³Department of Internal Medicine, Hiroshima Municipal Hospital, Hiroshima, Japan, ⁴Department of Orthopaedics, Ritsurin Hospital, Takamatsu, Japan, ⁵Department of Internal Medicine, Kagawa Prefectural Saiseikai Hospital, Takamatsu, Japan, ⁶Department of Internal Medicine, Mitoyo General Hospital, Toyohama, Japan, ⁷Department of Health, Kibi International University, Takahashi, Japan.

Primary biliary cirrhosis (PBC) is a chronic cholestatic liver disease mostly occurred in women and associates increasing rate of bone loss and higher risk of fractures. The objective of this study was to investigate the pathogenesis of bone loss associated with PBC in postmenopausal Japanese women. Forty PBC Japanese female in- or out-patients who are already post-menopause and fifty age-matched post menopausal women without PBC living in Kagawa prefecture were investigated. Both PBC patients and the control group were examined their bone mineral density (BMD) with dual X-ray absorptiometry (QDR2000 or QDR4000, Toyo-Medic Inc.) at the lumbar spine. Osteoporosis or osteopenia were diagnosed according to their T-scores. The biological markers for bone metabolism and hepatic were evaluated in PBC group. No significant difference was observed in ages, BMD's and T-Score's between PBC group and control group. Numbers of patients diagnosed as osteopenia and osteoporosis in PBC group were 7 (17.5%) and 13 (32.5%), respectively. Those in control group were 13 (25.5%) and 5 (9.8%), respectively and the frequency of osteoporosis including osteopenia in PBC group was significantly higher than that in the control group (p<0.005). Serum levels of i-PTH, osteocalcin and 1,25(OH)₂D₃ in all patients were within the control levels. Negative association between BMD and serum osteocalcin was observed (p<0.05). PBC patients showed higher urinary NTX levels suggested the stimulated bone resorption in PBC patients with bone loss who were diagnosed as osteopenia or osteoporosis. No apparent relationship was confirmed between BMD and impaired absorption of vitamin D due to cholestasis which were reported in the literatures. No significant correlation between BMD and biological parameters of hepatic function such as γ-GTP, but a negative correlation was observed. This does not suggest that the reduced BMD was attributed to the impaired hepatic function. Further investigation should be required in severe chronic hepatitis patients in order to reveal the pathogenesis of bone loss in patients with lowered hepatic function such as PBC.

Disclosures: **K. Takaguchi**, None.

SU316

Growth- and Age-Related Deficit in Bone Mass in Women with Low Volumetric BMD: Insights from their Daughters. Y. Duan¹, P. Garnero², X. Wang^{*1}, P. Szulc², O. Borel^{*2}, S. Filardi^{*1}, P. D. Delmas², E. Seeman¹. ¹Endocrinology and Medicine, the University of Melbourne, Heidelberg, VIC, Australia, ²INSERM Unit 403, Hôpital Edouard Herriot, Lyon, France.

We measured remodelling markers, bone size, and volumetric BMD (vBMD) at the femoral neck (FN) in healthy postmenopausal women, women with spine or hip fractures and their premenopausal daughters to test the following hypotheses: (i) the deficit in vBMD in the mother will be due to low peak vBMD if the daughter has a deficit in vBMD and remodelling markers are normal; (ii) the deficit in vBMD will be due to high remodelling (and excess loss) if the daughter has normal vBMD and markers but mother has high remodelling markers. From our 300 mother-daughter pairs, we selected 70 postmenopausal mothers (mean age 69.3 yrs) with low FN vBMD (T < -1.5SD) with or without fractures and their 62 premenopausal daughters (mean age 40.0 yrs). We further divided mothers with low vBMD into those with higher remodelling markers (26 mothers and their 23 daughters) and mothers with low vBMD with normal and lower remodelling markers (44 mothers and their 39 daughters). We measured FN diameter and vBMD using dual energy x-ray absorptiometry. Serum osteocalcin and β-CTX were measured by Elecsys immunoassay analyser.

Trait Z-Scores (SD unit) in Premenopausal daughters

	FN Diameter	vBMD	Osteocalcin	β-CTX
Mother with low vBMD	0.31±0.10*	-0.66±0.08*	-0.02±0.15	-0.12±0.12
Mother with low vBMD & high marker	0.41±0.20*	-0.73±0.14*	0.42±0.30	-0.11±0.22
Mother with low vBMD & normal marker	0.25±0.11*	-0.63±0.11*	-0.27±0.16	-0.12±0.15

* p < 0.05 compared with zero

The daughters of mothers with low vBMD, irrespective of marker status, had high FN diameter, reduced vBMD and normal markers suggesting that the larger FN with low vBMD in mothers (data published and replicated here but not shown) originated during growth. Daughters of mothers with low vBMD and high markers had increased FN diameter, reduced vBMD and higher Z-score for osteocalcin, consistent with the view that the low vBMD in the mothers was also due to higher remodelling. In mothers with low vBMD and normal markers, their daughters also had increased FN diameter and reduced vBMD but the markers were normal. We infer that low vBMD in elderly women has its origins in growth and ageing and rational approaches to therapy may require understanding the heterogenous pathogenesis of bone fragility.

Disclosures: **Y. Duan**, None.

SU317

Factors that Affect Decision to Undergo a Bone Mineral Density Scan. A. Baheiraei¹, J. A. Eisman¹, N. A. Pocock², T. V. Nguyen¹. ¹Bone and Mineral Research Program, Garvan Institute of Medical Research, St Vincent's Hospital, University of New South Wales, Sydney, Australia, ²Nuclear Medicine, St Vincent's Hospital, University of New South Wales, Sydney, Australia.

Because bone mineral density (BMD) is a primary predictor of fracture risk, a BMD measurement to diagnose osteoporosis plays a key role in treatment decisions. However, several recent studies suggest that high-risk individuals are not being diagnosed or treated. The aim of the study was to investigate factors that could influence the decision to undergo a BMD measurement in a non-English speaking group in an English-speaking community. The study was designed as a cross-sectional investigation, in which 131 Iranian- Australian women aged 35 years or older (range: 35-77) participated in a study of osteoporosis knowledge and preventive behaviors. After obtaining informed consent, each woman completed a set of questionnaires from which data on socio-demographic, clinical characteristics and lifestyle factors were obtained. All women were offered a free BMD scan, which was measured at the lumbar spine and femoral neck by using DXA (GE-LUNAR, WI, USA). Only 90 women (or 69%) took up the offer to have a BMD measurement. Among these women, 13.3% were found to have osteoporosis (T-scores ≤ -2.5). In multivariate logistic regression analysis, the following factors were found to be independent predictors of accepting a BMD scan: a familial history of osteoporosis (odds ratio [OR] 2.7; 95% CI 1.1-8.0), higher knowledge of osteoporosis scores (OR 1.3; 1.1-1.5), perception of susceptibility to osteoporosis (OR 1.1; 1.0-1.2), and those with lower calcium intake (OR 1.0; 1.0-1.1) were less likely to accept the offer. These findings in a group with limited access to public media suggest that familial history of osteoporosis was the strongest predictor of BMD scan decision. However, other behavioral factors such as knowledge and perception of osteoporosis also influence a woman's decision to undergo a BMD measurement. These findings should help the development of multilingual educational programs designed to overcome the underdiagnosis and undertreatment in osteoporosis.

Disclosures: **A. Baheiraei**, None.

SU318

Gender Discrepancies in Bone Size and Bone Mineral Density. Data from the Copenhagen School Child Intervention Study (CoSCIS). H. Hasselstrom¹, M. K. Karlsson², S. E. Hansen^{*1}, V. Grønfeldt^{*1}, L. Andersen^{*1}. ¹Institute of Exercise and Sport Sciences, Copenhagen, Denmark, ²Clinical and Molecular Osteoporosis Research Unit, Department of Clinical Sciences, Lund University, Malmö University Hospital, SE-205 02 Malmö, Sweden.

The aim of this study was to provide gender specific normative data of peripheral bone mineral density (BMD) and bone size in children aged 6 to 8 years. A total of 368 boys and 326 girls with a mean age of 6.7 ± 0.4 years had their BMD (g/cm²) evaluated by a peripheral dual energy X ray absorbtometry (DXA) device in the distal forearm and os calcanei. Weight, height, skinfolds, the width of distal forearm and the femur condyles were also measured and body composition estimated from skinfolds measurements according to the Weststrate equation. The results show no difference between the boys and girls was found in calcaneus BMD whereas boys had 4.5% higher forearm BMD than girls (p<0.001). Boys also had 2.7% larger distal forearm width and 4.7% larger knee width (both p<0.0001, respectively). Calcaneus BMD correlated with weight (partial r = 0.50), fat free mass (FFM) (partial r = 0.50), fat mass (FM) (partial r = 0.45), percent body fat (partial r = 0.29) and knee width (partial r = 0.46), all p<0.0001. Adjusted for weight, no significant relationship remained while adjusted for FFM, the relations remained but all at lower level than in the unadjusted correlations. Forearm BMD correlated with weight (partial r = 0.37), FFM (partial r = 0.39), FM (partial r = 0.28), percent body fat (partial r = 0.14) and wrist width (partial r = 0.24), all p<0.0001. Adjusted for body weight and FFM separately, the relationship remained but at a lower level than the unadjusted correlations. Children measured in the spring had 3.5% greater calcaneus BMD than children measured in the winter (p<0.01). In conclusion. This study suggests that in children aged 6 to 8, boys have higher peripheral BMD and larger bone size than girls, a seasonal variation in BMD exists and body weight is the best predictor of calcaneus BMD whereas both body weight and FFM are similar good predictors of forearm BMD.

Disclosures: **H. Hasselstrom**, None.

SU319

Evaluation of Gender Differences in Long Bone Shape in Childhood. E. M. Clark^{*1}, J. H. Tobias². ¹Community Based Medicine, University of Bristol, Bristol, United Kingdom, ²Clinical Science at South Bristol, University of Bristol, Bristol, United Kingdom.

Recent studies indicate that cross sectional area of long bones is greater in boys compared to girls, reflecting more rapid appositional growth in the former. This is thought to contribute to the well-documented gender differences in bone strength and fracture risk. Whether the relative rates of appositional and longitudinal growth in childhood also differs between boys and girls, leading to gender differences in bone shape, is currently unclear due to difficulties in measuring other parameters such as long bone length. To test the hypothesis that overall shape of long bones differs between boys and girls as a result of gender-specific differences in the relative rates of longitudinal and appositional growth, we developed a novel technique for measuring long bone length, width, and aspect ratio (AR; length divided by width) from total body DXA scans. This technique was applied in 142

girls and 132 boys randomly selected from the Avon Longitudinal Study of Parents and Children (ALSPAC), a birth cohort study from the UK. The humerus was defined as a specific region of interest on total body scans obtained using a Lunar Prodigy at age 9.9 years, following which length, mean width and AR was derived (CV for humeral width = 2.0%, 95% CI 1.51 to 2.50). As expected, humeral width and length were positively correlated with age and height (P<0.01). Gender differences in these measures were subsequently examined by linear regression after adjustment for age and pubertal stage as assessed by self-completion Tanner questionnaires. We found that the humerus in boys compared to girls is shorter but wider, leading to a smaller aspect ratio (see Table). Therefore, as well as gender differences in cross-sectional area, boys and girls show significant differences in the relative rates of longitudinal and appositional growth, which translate into differences in overall bone shape. To the extent that AR is negatively correlated with skeletal strength, as predicted by bioengineering first principles, our results raise the possibility that differences in bone shape make a hitherto unrecognised contribution to gender differences in fracture rate. We are keen to explore this further in future studies.

Mean (SD) age and bone geometry of boys and girls, by linear regression adjusted for age and puberty

	Boys N=132 Mean (SD)	Girls N=142 Mean (SD)	P value
Age (years)	9.9 (0.35)	9.9 (0.36)	0.642
Humerus length (cm)	23.8 (1.6)	24.2 (1.6)	0.023
Humerus width (cm)	1.92 (0.17)	1.86 (0.17)	0.004
Humerus area (cm ²)	45.8 (5.7)	45.2 (5.6)	0.380
Aspect Ratio	12.5 (1.1)	13.1 (1.1)	<0.001

Disclosures: *E.M. Clark, None.*

SU320

Birthsize, Adult Size and Body Composition Effect on Bone Mass: The PROGRAM Study*. *PROGRAM= Programming Factors of Growth and Metabolism. A. S. Slingerland¹, A. A. Hellingman^{*1}, E. P. Krenning^{*2}, A. C. S. Hokken-Koelega^{*1}. ¹Dep. of Pediatrics, Erasmus Medical Centre, Rotterdam, The Netherlands, ²Dep. of Nuclear Medicine, Erasmus Medical Centre, Rotterdam, The Netherlands.

Low birth size, poor adult height gain and low adult body mass have independently shown to decrease BMD and increase osteoporosis and/or fracture risk in 60 year olds. For preventive measures or early intervention it is necessary to know whether in these populations, bone mass is already decreased at an early age-eg if peak bone mass has just been attained-and at which to aim: birth size, adult size or body composition. We assessed the effect of birth size, adult size and body composition on the total body as in Bone Mineral Content (BMC) and Bone Mineral Density (BMD) and on the lumbar spine as in BMD-LS and Bone Mineral Apparent Density (BMAD) in 167 healthy 18-23 year olds. They were divided into four unique groups as part of the PROGRAM-study: 1. Small for Gestational Age (SGA)-Short 2. SGA-Catch up 3. Appropriate for Gestational Age-Short and 4. AGA-Controls. We found BMC and BMD to be decreased in SGA-Short and AGA-Short but this difference disappeared once completely corrected for height as in BMAD. In multiple regression analyses across the groups, neither of the measures for bone mass related to birth size. Total body BMC and BMD were best predicted by Adult Weight, whereas Lumbar spine BMD and BMAD were best predicted by Lean Body Mass reflecting muscle mass. We conclude that in populations of low birth size or poor adult height gain, bone mass is not decreased once corrected for adult height, at least in young adulthood when peak bone mass has just been attained. Preventive measures or interventions should aim at body composition especially muscle mass to increase bone mass of lumbar spine.

Disclosures: *A.S. Slingerland, None.*

SU321

Better BonesWorkshop® Improves Knowledge, Confidence and Intention to Change Among Family Medicine Residents. M. M. Luckey¹, S. Albert^{*2}, C. Berry^{*3}. ¹Saint Barnabas Osteoporosis and Metabolic Bone Disease Center, Mount Sinai Medical Center, Livingston, NJ, USA, ²New York University, New York, NY, USA, ³New York University, Oregon Osteoporosis Center, New York, NY, USA.

Despite the availability of evidence-based guidelines, simple diagnostic tests and effective therapy, less than one-third of patients with osteoporosis are identified or treated. Intervention by primary care providers(PCPs) will be key to changing these statistics; however, most PCPs receive little formal training in metabolic bone disease and many lack the confidence and knowledge needed to make osteoporosis surveillance and treatment a routine part of primary care practice The *BetterBones Workshop*® was developed in collaboration with the Academy of Family Medicine Residency Directors and is a 1.5 day intensive, interactive, small-group, case-based osteoporosis workshop for family medicine residents. . Pre-and post-workshop demographics and knowledge were assessed by questionnaire and multiple choice tests in all. Participants in 2004 also answered questions regarding their level of confidence. From March 2003-December, 2004, 738 residents from 256 residency programs attended 20 *BetterBones* workshops. The workshop was well received by residents (overall rating 4.9 on a 5 point Likert scale) Knowledge-test scores increased from a baseline of 58 ± 14% pre-workshop to 88± 11% (mean±SD) immediately post-workshop (p<.0001). Compared to before the workshop: 99% felt"more comfortable ordering & using bone density tests"; 100% agreed that they were "more knowledgeable about how & when to treat osteoporosis" and 98% felt "very confident that I can identify & manage most patients with osteoporosis". 98 % indicated that they had learned something that would change their practice with 83% volunteering an intention to increase bone density testing and/or treatment among at least one high-risk group. These results indicate that an interactive, small-group osteoporosis workshop is highly effective in increasing

knowledge as well as confidence and the intention to increase diagnosis and treatment among primary care physicians in training. Additional studies to assess the impact of this workshop on objective measures of behavior are needed.

Disclosures: *M.M. Luckey, None.*

SU322

Rib Fracture as a Marker of Osteoporosis and Mortality in Men and in Women. M. Naves^{*}, J. B. Díaz-López^{*}, C. Gómez-Alonso, A. Rodríguez-Rebollar^{*}, J. B. Cannata-Andía. Bone and Mineral Research Unit, Hospital Universitario Central de Asturias, Oviedo, Spain.

It is well known that hip, spine and distal forearm fractures are important predictors for the risk of future fractures, however few studies have involved rib fracture as a marker of osteoporosis. The aim of this study was to find out the predictive value of rib fracture for risk of both osteoporotic fracture and rate of bone loss in a non-selected population. A likely association between prevalent rib fracture and mortality was also investigated. A cohort of 308 men and 316 women aged 50 years and over participated in this study. Subjects were invited to complete an interview-administered questionnaire which included questions about previous fractures including rib fracture. Prevalent and incident vertebral fractures, according to semi quantitative Genant method, were defined by means of two lateral dorsal and lumbar radiographs performed at baseline and again 4 years later. The rate of bone loss was obtained by lumbar and hip bone densitometry study performed at baseline and again 4 years later. The subjects were followed prospectively during 8 years by 4 postal questionnaires to determine the occurrence of non-vertebral osteoporotic fractures caused either spontaneously or after a fall from a maximum height equal to or below the upright position of the patient. The age and number of any previous fracture, excluding rib fractures, were higher in those subjects with previous rib fractures (n=29) compared with those without (71±7 vs 65±9 years old and 72 vs 41% respectively, p<0.001), 13.6% of subjects with previous rib fractures had incident osteoporotic fracture compared with 3.5% of those without (p<0.001). Logistic regression analysis after adjustment by age, sex and any previous fracture showed that previous rib fractures increased 4 times the risk of having an incident osteoporotic fracture (odds ratio [OR]=4.33; 95% Confidence Intervals [CI] 1.70, 11.01). After adjustment by age, sex and any previous fracture, the rate of bone loss at lumbar spine in patients with previous rib fracture was significantly higher than those without (-3.94±1.97 vs 0.05±0.28, p=0.006 in the univariate analysis and p=0.032 in the covariance analysis). Non-significant differences were found in femoral neck or in total hip. Also after adjustment by age, sex and any previous fracture, the presence of previous rib fractures was associated with an increase in mortality (Relative risk [RR] = 2.03; 95%CI 1.03, 4.12). In summary, previous rib fractures were an important risk factor for future osteoporotic fractures, rate of bone loss and mortality in both sexes, indicating that their presence should be always taken into account as independent marker of osteoporosis.

Disclosures: *M. Naves, None.*

SU323

Detection of Vertebral Fractures by Physical Examination: Comparison between Men and Women. K. Siminoski¹, K. Lee^{*2}, H. Jen^{*2}, R. Warshawski^{*2}. ¹Radiology and Medicine, University of Alberta, Edmonton, AB, Canada, ²Radiology, University of Alberta, Edmonton, AB, Canada.

Vertebral fractures are the most common fracture in osteoporosis and the lifetime vertebral fracture risk in men may be similar to the risk in women. We have previously described four physical examination maneuvers that can detect prevalent vertebral fractures in women. There has been little published data available on physical changes in men resulting from vertebral fractures, so in this study we have compared the performances of these four methods between the two sexes. Subjects were men (n = 326) and women (n = 824) referred for specialist assessment of osteoporosis (average age 52 +/- 17 years for men, 57 +/- 15 years for women). Vertebral morphometry was performed on all subjects from T4 to L4. Prevalent vertebral fracture was defined as a vertebral height ratio < 0.80. One or more fractures were present in 39.5% of men and 34.9% of women. Among those with fractures, the average number in men was 2.5 +/- 1.8 and the average number in women was 2.3 +/- 1.9. Height was measured using a Harpenden stadiometer, kyphosis angle using a digital inclinometer from T4 to T12. The four parameters that were compared were (i) historical height loss (HHL; tallest recalled height minus measured height) for detection of all thoracic and lumbar fractures; (ii) wall-occiput distance (WOD) for detection of thoracic fractures; (iii) kyphosis angle (KA) for detection of thoracic fractures; (iv) rib-pelvis distance (RPD) for detection of lumbar fractures. The area under the receiver operating characteristics curve for each maneuver wwas evaluated for its ability to detect fractures and 95% confidence intervals were determined. The AUCs ranged from 0.69 to 0.75 for women and 0.68 to 0.73 for men, falling in the range that is considered to represent good performance The confidence intervals overlapped between men and women for all four maneuvers. These data suggest that the four physical exam maneuvers (HHL, WOD, KA, and RPD) will be useful in men for detection of prevalent vertebral fractures. The thresholds to be used for clinical application will require further analysis and may differ from those in women.

Areas Under the ROC Curves for the Presence of Prevalent Vertebral Fractures

	HHL (cm) (95% CI)	WOD (cm) (95% CI)	KA (degrees) (95% CI)	RPD (fingerbreadths) (95% CI)
Men	0.68 (0.61-0.75)	0.71 (0.63-0.79)	0.73 (0.65-0.81)	0.72 (0.63-0.81)
Women	0.69 (0.64-0.74)	0.75 (0.68-0.82)	0.72 (0.65-0.79)	0.76 (0.71-0.81)

ROC = receiver operating characteristics curve, HHL = historical height loss, WOD = wall-occiput distance, KA = kyphosis angle, RPD = rib-pelvis distance

Disclosures: *K. Siminoski, None.*

SU324

Detection of Osteoporotic Vertebral Fractures: A Comparison of Radiographs and Sagittal CT Reformations. J. S. Bauer¹, D. Mueller^{*2}, A. Ambekar^{*1}, M. Dobritz^{*2}, M. Matsuura^{*3}, F. Eckstein^{*4}, E. J. Rummeny^{*2}, S. Majumdar¹, T. M. Link¹. ¹Radiology, University of California, San Francisco, CA, USA, ²Institut für Röntgendiagnostik, Technische Universität, München, Germany, ³Anatomy, Ludwig-Maximilian-Universität, München, Germany, ⁴Anatomy, Paracelsus Private University, Salzburg, Austria.

Purpose Vertebral fracture assessment is a major issue in diagnosing osteoporosis. Lateral radiographs are currently considered to be the standard technique for vertebral fracture assessment. With the advent of Multislice CT (MSCT) thinner axial sections are obtained routinely during standard CT exams and can serve as a basis for high quality sagittal reformations (SR) of the spine. The purpose of this study was to analyze, which slice thickness in axial CT-datasets is required to reliably identify these fractures as well as to compare lateral radiographs and SR in their performance to identify osteoporotic vertebral fractures. **Materials and Methods** Sixty-five vertebrae were harvested from 21 human cadaver spines in segments with three to four vertebrae each and examined with a 64 row MSCT scanner. Axial images of these specimens were acquired with a slice thickness of 0.6, 1, 2, 3 and 5 mm. SR were obtained using these datasets with the same slice thickness as the axial images. In addition the specimens were radiographed in a.p. and lateral orientation. Radiographs and CT reformations were graded by two radiologists separately according to the spinal fracture index (SFI) classification. These results were compared with the fracture status determined in consensus by two different radiologists based on all combined imaging findings and a pathological examination of the vertebrae. **Results** The level of agreement for the fracture grading in the CT reformations decreased with spatial resolution in the z-axis. Average κ for both readers showed good values for the 0.6, 1, 2 and 3 mm CT reformations ($\kappa=0.74, 0.72, 0.70$ and 0.61). It was moderate for plain films ($\kappa=0.51$) and fair for the 5mm protocol ($\kappa=0.34$). Specificity and sensitivity showed equal trends: In the standard radiographs both readers missed 18% of the fractures with a specificity of 90% and 83%, while in the 1mm SR less than 6% of the fractures were missed, with a specificity of 93% and 100% for the two radiologists, respectively. **Conclusion** Sagittal reformations based on thin section MSCT scans were superior compared to standard spine radiographs in grading and detecting osteoporotic vertebral fractures. For a reliable detection of vertebral fractures SR are, however, required that are based on axial images with a slice thickness of 3mm or less. The thinnest available slice thickness of the axial images performed best in fracture grading.

Disclosures: **J.S. Bauer**, None.

SU325

Knowledge Dissemination Strategies Translate into Improved Post-Fracture Osteoporosis Care. D. R. Cohen^{*}, D. A. Haaland^{*}, C. Kennedy, J. D. Adachi, N. Khaldi^{*}, A. Papaioannou. Department of Medicine, McMaster University, Hamilton, ON, Canada.

Osteoporosis is a major public health problem in Canada, and its prevalence is increasing. Osteoporosis greatly increases fracture risk, thus resulting in significant morbidity and mortality. These fractures, however, can be preventable with appropriate therapy. Current guidelines indicate that individuals who sustain a fragility fracture are at high risk for future fractures and require bone mineral densitometry (BMD) and pharmacologic therapy. There is, however, a recognized gap between guidelines and practice with regard to measurement of BMD and treatment of osteoporosis in individuals with fragility fractures. In Hamilton, Ontario, a prior observational study from April 1st, 1995 to March 31st, 1996 indicated very poor recognition of osteoporosis following discharge from an academic teaching hospital after a fragility hip fracture. Osteoporosis was noted in 2% of 141 patient charts, and only 18% had vitamin D or calcium recorded as discharge medications. No patient was discharged on a bisphosphonate. Since that time, osteoporosis education has been disseminated to the geriatric/rehabilitation consultation teams in Hamilton, in an effort to improve care. In this study, a retrospective chart review examined 342 charts of patients age 50 years or older, admitted with a fragility hip fracture to the orthopaedic services of two Hamilton, Ontario, teaching hospitals between March 1st, 2003 and April 30th, 2004. Three quarters of patients were women, with a mean age of 81 years. Twenty six percent and 33% had previous diagnoses of osteoporosis and fracture, respectively. On admission, 14%, 9%, and 18% of patients were on calcium, vitamin D and bisphosphonates, respectively. A new diagnosis of osteoporosis was made in 25% of patients. Thus, 49% of patients left hospital without a diagnosis of osteoporosis. BMD was suggested in 11%. On discharge, calcium, vitamin D and bisphosphonates were prescribed for 38%, 36% and 27% of patients, respectively. Thirty three percent of those with no prior diagnosis of osteoporosis were transferred to a geriatric/rehabilitation unit, while 67% were not. Of those that were transferred, 75% received a diagnosis of osteoporosis as compared with only 19% of those who were not transferred ($P<0.001$). We conclude that targeted dissemination of information is paramount to osteoporosis recognition and treatment in hospitalized patients with fragility fractures. While a care gap still exists, this study suggests that a multidisciplinary approach to osteoporosis, including consultation teams, osteoporosis education and standardized orders may be useful and warrants further study.

Disclosures: **D.R. Cohen**, None.

SU326

Fracture Frequency in Patients over 50 of Age in a Trauma Hospital in Mexico City. F. A. Cisneros, L. M. Muciño^{*}. Spine, HTOLV, Mexico, Mexico.

In the last 20 years, osteoporosis has been focusing on diagnosis and treatment. In the early years the objective was to improve the BMD, in recent years, however, with better knowledge in the pathology; the main objective is to prevent fractures. The objective of this revision is to learn about fracture frequency in a population over 50 and correlate with the diagnosis of osteoporosis, without a densitometry study to establish the diagnosis and trying to determine which fractures are in a compromised mechanical bone, and at the same time knowing that not all the injuries that happened were in an osteoporotic bone. We can also recognize the need of better resources in orthopedic hospitals to improve the diagnosis and treatment of this condition. **RESULTS.-** Throughout November and December 2004, we collected all the patients over 50, with a fracture of any bone, who came to the hospital emergency room. We found 509 patients with a traumatic injury and 511 fractures, 340 female (67%) and 169 males (33%). The most common lesion was distal radio cubital fracture with 118 patients (23% of the lesions), 98 female and 20 males, the average age for women was 68 years and for men, 62 years. 94% of the cases were treated conservatively. Hip fracture was the second most common lesion with 101 patients (20% of the cases). 68 females and 32 males, the average age for women was 76 years and for men, 74 years. 80% were treated surgically. Ankle, humeral and foot were the next injuries in frequency; all these 5 anatomical segments constituted 70% of the lesions. **CONCLUSIONS.** The most frequent fractures found were Colles and hip fractures, both constituted 43% of the cases. Women were affected twice than men. Treatment in patients over 50 is mainly conservative, exceptions are hip and ankle, both are frequent fractures in these patients. Because of the age, hip and femur, shoulder and humeral fractures occur in osteoporotic or mechanical incompetent bones. This means that we have to focus our efforts on treating these patients for osteoporosis.

Disclosures: **F.A. Cisneros**, None.

SU327

Increased Prevalence of Morphometric Vertebral Compression Deformities in Canadian Aboriginal Women: The First Nations Bone Health Study. W. D. Leslie¹, C. J. Metge², H. A. Weiler³, M. Doupe^{*1}, E. A. Salamon¹, P. Wood Steiman^{*4}. ¹Faculty of Medicine, University of Manitoba, Winnipeg, MB, Canada, ²Faculty of Pharmacy, University of Manitoba, Winnipeg, MB, Canada, ³Human Nutritional Sciences, University of Manitoba, Winnipeg, MB, Canada, ⁴Assembly of Manitoba Chiefs, Winnipeg, MB, Canada.

Canadian Aboriginal (First Nations) women are at increased fracture risk compared with the general population with over double the rate of clinical vertebral fractures (CMAJ 2004;171:869-73). The First Nations Bone Health Study (FNBHS) reported site-specific reductions in BMD among a random age-stratified (25-39, 40-59 and 60-75) sample of Aboriginal women compared with age-matched White women (JBMR 2004;19 Suppl 1:S288). The prevalence of vertebral morphometric deformities was assessed in the older subgroup (age 60-75) which included 43 Aboriginal and 49 White women with 1,183 analyzable thoraco-lumbar vertebrae (T4-L4) from lateral spine radiographs. Blinded vertebral morphometry was performed at the Canadian Multicentre Osteoporosis Study (CaMos) data centre using published methods derived from 9,424 subjects (Osteoporos Int 2000;11:680-7). Spinal morphometry was used to categorize any deformity using 3 standard deviations (SD) as a limit of normality (Grade 1 if 3-4 SD, Grade 2 if 4-5 SD, and Grade 3 if > 5 SD). Vertebral fractures were more common in the Aboriginals (16.3% vs 11.9%, $P<0.05$ Chi-square) with significantly higher vertebral fracture grades ($P<0.05$ Mann-Whitney). The odds ratio for morphometric fracture of 1.45 (95% CI 1.11-1.78) was less than the previously reported standardized incidence ratio for clinical fractures of 2.18 (95% CI 1.88-2.51), possibly reflecting differential ascertainment of subclinical vs. clinical fractures. Nonetheless, these data continue to demonstrate an important effect of Aboriginal ethnicity in terms of bone health with an excess burden of osteoporotic fractures.

	Prevalence of vertebral morphometric fractures	
	Aboriginal	White
Normal	468 (83.7)	550 (88.1%)
Grade 1	72 (12.9%)	59 (9.5%)
Grade 2	15 (2.7%)	9 (1.4%)
Grade 3	4 (0.7%)	6 (1.0%)
Any deformity	91 (16.3%)	74 (11.9%)

Disclosures: **W.D. Leslie**, None.

SU328

Low Sensitivity for Visual Recognition of Vertebral Compression Deformities: The First Nations Bone Health Study. W. D. Leslie¹, C. J. Metge², H. A. Weiler³, M. Doupe^{*1}, E. A. Salamon¹, P. Wood Steiman^{*4}. ¹Faculty of Medicine, University of Manitoba, Winnipeg, MB, Canada, ²Faculty of Pharmacy, University of Manitoba, Winnipeg, MB, Canada, ³Human Nutritional Sciences, University of Manitoba, Winnipeg, MB, Canada, ⁴Assembly of Manitoba Chiefs, Winnipeg, MB, Canada.

Under-recognition of vertebral fractures on routine x-rays is a global problem and leads to a missed opportunity for identifying high risk individuals (JBMR 2005;20:557-63). We hypothesized that radiologists reporting spine radiographs as part of an osteoporosis clinical research study would show a much higher level of fracture identification than in

routine clinical practice. The prevalence of vertebral morphometric deformities was assessed in 92 older women (age 60-75) from the First Nations Bone Health Study (FNBHS) which included 43 Aboriginal (First Nations) and 49 White women with 1,183 analyzable thoraco-lumbar vertebrae (T4-L4) from lateral radiographs. An initial clinical interpretation was provided by practicing radiologists aware that this was an osteoporosis clinical research study, with blinded vertebral morphometry performed at the Canadian Multicentre Osteoporosis Study (CaMos) data centre using published methods derived from 9,424 subjects (Osteoporos Int 2000;11:680-7). Spinal morphometry was used to categorize any deformity using 3 standard deviations (SD) as a limit of normality (Grade 1 if 3-4 SD, Grade 2 if 4-5 SD, and Grade 3 if > 5 SD). The clinical report was used to designate each vertebral level as definitely or possibly fractured. Overall, less than one in three morphometric fractures (52 of 165) was clinically reported to be definitely or possibly fractured despite the fact that the radiologists knew that this was a clinical research study being done to look for vertebral fractures. Although visual identification improved with more severe fracture grades, one-third of the grade 3 fractures were still missed. Specificity was also poor with one-half of the visual definite fractures showing normal morphometry and almost all of the visual possible fractures being morphometrically normal.

Comparison of vertebral fractures using visual and morphometric criteria			
	Visual definite	Visual possible	Visual combined
Normal (n=1018)	50 (4.9%)	16 (1.6%)	66 (6.5%)
Grade 1 (n=131)	30 (22.9%) ¹	1 (0.8%)	31 (23.7%)
Grade 2 (n=24)	13 (54.2%)	1 (4.2%)	14 (58.4%)
Grade 3 (n=10)	7 (70.0%)	0 (0.0%)	7 (70.0%)
Any deformity (n=165)	50 (30.3%)	2 (1.2%)	52 (31.4%)

Disclosures: **W.D. Leslie**, None.

SU329

Medical Risk Factors Contribute to the High Fracture Risk in Canadian Aboriginal Peoples. **W.D. Leslie¹, H.J. Prior^{*1}, S. Derksen^{*1}, C.J. Metge², L. L. Lix^{*1}.** ¹Faculty of Medicine, University of Manitoba, Winnipeg, MB, Canada, ²Faculty of Pharmacy, University of Manitoba, Winnipeg, MB, Canada.

Although Canadian Aboriginal (First Nations) peoples are known to be at high fracture risk, the factors contributing to this have not been well described. The role of diabetes mellitus, disease comorbidity, and substance abuse as defined from administrative health data were examined as possible explanatory variables. A retrospective, population-based matched cohort study of fracture rates was performed using Manitoba (Canada) administrative health data (1984-2003). The study cohort consisted of 27,952 registered Aboriginal adults and 83,856 controls (matched three to one for year of birth and gender). Diabetes, comorbidity (number of ambulatory diagnostic groups [ADGs]), substance abuse and post-inception fractures were based upon validated definitions. Poisson regression models of fracture rates, which included covariates of age, sex, income quintile and area of residence, were constructed to look at the statistical significance of candidate variables both in two-way interactions and main effects. Diabetes, multiple ADGs, and substance abuse were more common in the Aboriginal cohort (p<0.000001) and were strongly associated with increased fracture rates, but this effect was similar for the Aboriginal cohort and controls (p for interaction > 0.1). Longer duration of diabetes correlated with hip, spine, and wrist fractures but not craniofacial fractures, but this effect was greatly reduced after controlling for number of ADGs. In conclusion, higher rates of diabetes, comorbidity and substance abuse among Aboriginal people contribute to the higher rates of fracture. Ethnicity is still a significant risk factor for fracture after adjustment for these factors, suggesting additional unidentified risk factors in this high risk population.

	Odds ratio for fracture at various sites		
	Craniofacial	Hip-spine-wrist	Hip only
Aboriginal	3.67 (3.28-4.12)	2.01 (1.86-2.17)	2.09 (1.58-2.78)
Diabetes	0.76 (0.59-0.98)	1.09 (0.96-1.22)	1.44 (1.06-1.95)
Number of ADGs:			
None	Reference	Reference	Reference
1-2	1.21 (1.02-1.44)	1.16 (1.02-1.32)	0.95 (0.60-1.50)
3-5	1.60 (1.95-2.91)	1.47 (1.29-1.66)	1.05 (0.67-1.64)
6 or more	2.38 (1.95-2.91)	1.82 (1.58-2.09)	1.55 (0.97-2.46)
Substance abuse	2.04 (1.80-2.31)	1.72 (1.55-1.91)	2.06 (1.39-3.04)

Disclosures: **W.D. Leslie**, None.

SU330

What Is the Prevalence of Post-Menopausal Fragility Fracture? **E. Brankin¹, C. Mitchell^{*1}, R. Munro^{*1}, A. Gallagher².** ¹Lanarkshire Osteoporosis Service, NHS Lanarkshire, Coatbridge, United Kingdom, ²Medical Unit, Southern General Hospital, Glasgow, United Kingdom.

Literature review would suggest a prevalence of post-menopausal fragility fracture in the region of 15%. Recent reports have suggested this may be an underestimate and 1-2% higher results may be a more true reflection of fracture prevalence. As part of the Coatbridge Disease Management Programme, questionnaires were sent to 4045 ladies in the locality aged 65 or over to identify those who had already suffered a fragility fracture or those at risk of fracture, according to standard criteria. Responses were received from 2386 patients, a response rate of 59%. Of these 852 patients were identified as having already suffered a fragility fracture, and a further 1395 were identified as meriting an open access bone densitometry scan according to risk factor evaluation. The prevalence of fragility fracture in this patient population was therefore 21.1% (852/4045), a figure significantly higher than previously reported. As this particular study excluded those in nursing and residential homes the prevalence is likely to be even higher. Of the 41% who did not respond, surmising a prevalence rate of approximately that for those who did

respond, then an overall prevalence of ~30% could potentially be expected in this population. One might argue that those who did not respond may have lower prevalence rates, since if they had suffered a previous fracture they may be more motivated to respond, but by the same token they may not have responded because they had already been assessed and were on appropriate treatment. Even if the prevalence was half that of responders, this would still give an overall prevalence rate of the middle 20's %. We are currently contacting all those who did not initially respond to the programme to ascertain their fracture risk, but feel that this result is likely to reflect an underestimation of the scale of the problem which should be addressed by initiating programmes such as ours to identify and treat those with prevalent fracture who have previously slipped through the system before fracture liaison services were set up.

Disclosures: **E. Brankin**, MSD Ltd 2, 5; Alliance for Better Bone Health 2, 5; Roche Products Ltd 2, 5; Eli Lilly Ltd 2, 5.

SU331

Think Fracture! A Comparison between Standard Risk Factor Audit and Targeting Fragility Fracture in Identifying Patients with Osteoporosis. **E. Brankin¹, C. Mitchell^{*1}, R. Munro^{*1}, A. Gallagher².** ¹Lanarkshire Osteoporosis Service, NHS Lanarkshire, Coatbridge, United Kingdom, ²Medical Unit, Southern General Hospital, Glasgow, United Kingdom.

Running from 1998-2000, the Osteohealth Audit, performed within a family medicine setting, was designed to identify patients with osteoporosis, or at high risk of developing osteoporosis, in 125 general practices across the UK. Patients were identified for review and investigation according to identification of standard risk factors. From 2496 individuals who were subsequently scanned, bisphosphonate therapy was instituted in 615 (24.6%), Calcium & Vitamin D in 401 (16.1%) and HRT in 562 (22.5%). Following on from the Osteohealth Audit, as part of the Coatbridge Disease Management Programme, all ladies over 65 within the town (4045) were sent a postal questionnaire asking about prevalent postmenopausal fracture. 852 were identified as having already suffered from fracture (a prevalence of 21% - higher than previously reported in literature) and further 1395 identified as being at high risk. 1054 patients were subsequently scanned, 659 of those with fracture, and 395 patients were chosen from the 'routine' scanning waiting list based on standard risk factors alone. None of those scanned from the audit were under 65, thereby targeting only those at higher absolute risk as identified by age and fracture. Of those 659 with fracture in the age group 65-75, 49.3% were found to be osteoporotic and in the over 75s, 69.2% had osteoporosis. Of those 395 without fracture the prevalence of osteoporosis was substantially lower at 43% and 47.2% respectively for the two age groups as above. 62.7 % of those with previous fracture were subsequently prescribed an evidence based bisphosphonate plus Calcium/vitamin D compared to 48% of those who had never sustained a fracture. Identifying and treating post-menopausal women at highest absolute risk of osteoporosis, ie those with previous fracture, is a much more cost effective way of targeting management strategies in the secondary prevention of fracture.

Disclosures: **E. Brankin**, MSD Ltd 2, 5; Alliance for Better Bone Health 2, 5; Roche Products Ltd 2, 5; Eli Lilly Ltd 2, 5.

SU332

10 Year Hip Fracture Risk in Ireland 1995-2003. Are Changes in Life Expectancy Blunting the Effect of Intervention? **B. R. Whelan^{*1}, L. Brennan^{*2}, E. Falvey^{*1}, M. Daly^{*1}, F. Drummond^{*3}, F. Shanahan^{*3}, A. McGuinness^{*2}, M. G. Molloy^{*1}.** ¹Rheumatology, University College Cork, Cork, Ireland, ²Orthopaedics, Cork University Hospital, Cork, Ireland, ³Medicine, University College Cork, Cork, Ireland.

Introduction Hip Fracture is a significant public health problem worldwide and is the most serious consequence of Osteoporosis. Over the past 10 years there has been an increase in the screening for and treatment of osteoporosis. In this time there has also been an increase in life expectancy in Ireland. We undertook to examine the net effect of these changes on individual fracture risk using the endpoint of 10 year fracture risk. Methods All persons resident in Cork city and county who admitted to Cork University Hospital with a hip fracture between 1995-97 and 2001-03 were included. This is the only orthopaedic trauma centre for this area. Population statistics for this population were obtained from the Central Statistics Office in Ireland. Using published life tables for the time periods we calculated the 10 year fracture risk for both sexes at ages 50, 60, 70 and 80. Results There were 1101 fractures in 1.248 million person years from 1995-97 and 1168 fractures in 1.343 million person years from 2001-03. Male life expectancy increased by 1.5 years and female life expectancy increased by 1.3 years. There was a significant increase in the 10 year fracture risk for the over 80 year olds. Only in 70 year old females was fracture risk significantly reduced. (See Table) Discussion Screening for and treatment of osteoporosis in the 70 year old age group has had an impact on individual fracture risk. The strategies adopted have not had a beneficial impact in any other age group. The reasons for this require further investigation. The increase in life expectancy and decrease in mortality rate blunting the effect of screening and treatment. This is supported by increased fracture risk in the over 80 year olds where the effect of increasing life expectancy is greatest.

10 Year Fracture Risk (** denotes significant change)				
	Male		Female	
Age	1995-1997	2001-2003	1995-1997	2001-2003
50	0.38%	0.31%	0.34%	0.4%
60	0.93%	0.97%	1.56%	1.3%
70	2.56%	2.53%	6.09%	5.17% **
80	8.41%	9.94% **	18.13%	20.27% **

Disclosures: **B.R. Whelan**, None.

SU333

Application of the Norwegian Medicines Agency Osteoporosis Treatment Guidelines on Male and Female Patients with Wrist Fractures in Norway. G. Haugeberg^{*1}, C. G. Gjesdal^{*2}, H. C. Gulseth^{*3}. ¹Dept. of Rheumatology, Sorlandet Hospital, Kristiansand, Norway, ²Dept. of Rheumatology, Haukeland University Hospital, Bergen, Norway, ³Dept. of Rheumatology, Betanien Hospital, Skien, Norway.

Background: Norway is a high endemic area for osteoporotic fractures. Treatment guidelines has been given by the Norwegian Medicine Agency (NMA) to reduce fracture risk in patients with a high risk profile of future fractures. According to these guidelines treatment with bisphosphonates is considered as first choice and SERM or estrogens as second treatment choice. In the NMA guidelines patients with low energy fracture with reduced bone mass (T-score ≤ -2) is defined as a high risk group of future fractures. **Aim:** To explore the number of patients age 50 years or older with a low-energy wrist fracture in need for specific osteoporosis treatment according to the NMA osteoporosis treatment guidelines for fracture risk reduction. **Material and Method:** A total of 639 patients (84 men and 555 women) were recruited from three centres in Norway (Bergen: 272, Skien 239, Kristiansand 128) and data were collected from spring 2003 to December 2004. Bone density at left total hip and lumbar spine (L2-4) was measured using Lunar DXA machines following standardised procedures. Gender specific T-scores were assessed. In patients with left side hip replacement bone density measures of the right total hip was used. Patients with high energy trauma wrist fractures were excluded. **Results:** Mean age (\pm SD) was 65.3 years (\pm 10.4) among men and 69.3 (\pm 10.5) among women. Mean weight was 78.3 (\pm 14.7) and 66.9 kg (\pm 12.4) and height 176.1 (\pm 8.3) and 162.8 (\pm 6.4) among men and women, respectively. No major differences in age, weight and height, and hip and spine BMD was seen between the three centres. 99% of the females reported to be postmenopausal. The prevalence of patients with a previous fracture prior to the current wrist fracture was 59% in male and 55% in females. In the table below the prevalence of male and female patients recommended specific osteoporosis treatment according to the NMA osteoporosis treatment guidelines for fracture risk reduction are shown. **Conclusion:** Approximately every second male and female patients aged 50 years or older with low energy wrist fracture is in need of specific osteoporosis treatment applying the NMA treatment guidelines for fracture risk reduction.

T-score ≤ -2 SD	Men (n=84)	Women (n=555)
Spine L2-4 (n=627)	25 (29.8%)	237 (43.8%)
Total Hip (n=612)	25 (30.5%)	203 (38.4%)
Spine or Hip (n=639)	37 (44.0%)	307 (55.4%)

Disclosures: G. Haugeberg, None.

SU334

The Accuracy of Self-Report of Fractures in Older People; a Comparison of Questionnaire and Fracture Registry in the AGES Reykjavik Study. K. Siggeirsdottir^{*1}, T. Aspelund^{*1}, G. Eiriksdottir^{*1}, B. Mogensen^{*2}, M. Chang^{*1}, L. Launer^{*3}, T. Harris^{*3}, G. Sigurdsson⁴, B. Y. Jonsson^{*5}, V. Gudnason^{*1}. ¹Icelandic Heart Association, Kopavogur, Iceland, ²Department of Emergency Medicine, Landspítalinn University Hospital, Reykjavik, Iceland, ³NIA, Bethesda, MD, USA, ⁴Department of Endocrinology, Landspítalinn University Hospital, Reykjavik, Iceland, ⁵Department of Orthopaedics, Malmö University Hospital, Malmö, Sweden.

Epidemiological studies often need to rely on participants' self-report of health status to obtain information. It is therefore important to validate the accuracy of participant answers to questions. Participants from the Reykjavik study, a 35-yr prospective population study are being re-examined in the Age, Gene/Environment Susceptibility (AGES)-Reykjavik Study. For all participants in AGES, we developed a fracture registry (FR) based on an examination of all medical and radiographic records located in hospitals in Reykjavik and Akureyri. The accuracy of self-report (SR) of fractures of the wrist (WR), vertebrae (VT) and hip (HP), was evaluated in a subgroup of 2300 individuals (1324 women and 976 men). The mean age for both sexes was 76 years (range 66 - 95 years). All participants were administered the Mini Mental State Examination (MMSE) and Digit Symbol Substitution Test, (DSST); which together represent cognitive impairment defined as MMSE ≤ 23 and DSST ≤ 17 . Kappa statistics were calculated to determine agreement between SR and FR. Sensitivity (Sn), specificity (Sp), positive predictive value (PV), negative predictive value (NV) were also calculated (table).

	Fractures	FR %	SR %	Sn	Sp	PV	NV	Kappa
Men N = 970	Wrist *	6.7	7.1	0.56	0.96	0.53	0.97	0.51
	Vertebrae	3.8	3.9	0.44	0.98	0.43	0.98	0.41
	Hip*	1.9	1.1	0.17	0.99	0.27	0.98	0.20
Women N =1316	Wrist *	24.9	25.4	0.84	0.94	0.83	0.95	0.78
	Vertebrae	6.9	10.6	0.71	0.94	0.46	0.98	0.52
	Hip*	4.0	2.6	0.44	0.99	0.68	0.98	0.52

*Significant difference in kappa value between men and women, $p < 0.05$

SR of the fractures was available for 2286 individuals. Those who recall their fracture were fairly correct about the year it occurred as validated by the FR (spearman rank correlation= 0.85 for VT, 0.79 for WR). Those who were false negative (WR/VT/HP) were more likely to be cognitive impaired, $p=0.0008$, compared to those who were true positive. There was no evidence of cognitive impairment in those who were false positive, $p= 0.31$. Men answered consistently less reliably than women. SR is relatively accurate when ruling out fractures (good NV) but less accurate regarding PV, supporting the need for ascertainment of fractures based on radiographs and medical records in epidemiology research.

Disclosures: K. Siggeirsdottir, None.

SU335

Frailty and Risk of Falls and Fractures in Older Women. K. Ensrud¹, S. Ewing^{*2}, H. Fink¹, J. K. Tracy^{*3}, P. Cawthon², M. Hochberg³, J. Cauley⁴, P. Bowman^{*1}, K. Stone², S. Cummings². ¹VAMC & U of MN, Minneapolis, MN, USA, ²UCSF & CPMC, San Francisco, CA, USA, ³U of MD, Baltimore, MD, USA, ⁴U of Pittsburgh, Pittsburgh, PA, USA.

Although many factors are associated with frailty in older adults, weight loss and leg weakness often characterize this condition and are easily assessed in a clinical setting. To test the hypothesis that older women with frailty simply defined by the presence of both weight loss and leg weakness are at increased risk of falls and fractures (fxs), weight change and leg strength (ability to rise from a chair 5 times without using the arms) were measured at the 4th exam in a cohort of 6777 older women (mean age 76.8 yrs) enrolled in the Study of Osteoporotic Fractures who were then followed prospectively for falls and fxs, including hip fx. Weight loss was defined as a 5% or greater loss in body weight between baseline and 4th exams (5.7 yrs between exams) and leg weakness was defined as inability to rise from chair without arms. At the 4th exam, women were categorized as not frail (64%), weight loss only (24%), leg weakness only (7%) or frail (5%). During an average follow-up of 1 yr, 11% reported ≥ 2 falls (frequent falls), 33% experienced ≥ 1 non-spine fx (average follow-up 7.4 yrs) and 10% suffered a first hip fx (average follow-up 8.6 yrs). After controlling for multiple potential confounders, frail women were at increased risk of falls and fxs; in particular, frail women had a 2.7-fold increase in the odds of frequent falls and a 1.8-fold increase in the risk of hip fx. The relationship between frailty and non-spine fx was primarily due to an increased risk of hip fx.

	Relative Risk of Outcome*		
	Frequent Falls OR (95% CI)	Non-spine Fx RH (95%CI)	Hip Fx RH (95% CI)
Not frail	1.0 (referent)	1.0 (referent)	1.0 (referent)
Lost weight only	1.3 (1.1-1.6)	1.3 (1.1-1.4)	1.6 (1.4-2.0)
Leg weakness only	2.4 (1.8-3.1)	1.2 (1.0-1.5)	1.3 (0.9-1.8)
Frail	2.7 (1.9-3.9)	1.4 (1.1-1.8)	1.8 (1.2-2.6)

*adjusted for age, health status, smoking status, medical conditions, estrogen use, body mass index and femoral neck bone density

Frailty in older women simply defined by the presence of weight loss and leg weakness may be useful in a clinical setting to identify women at elevated risk of falls and hip fx.

Disclosures: K. Ensrud, None.

SU336

What Accounts for Lack of Osteoporosis Care Following Fracture? The Provider Perspective. A. N. A. Tosteson¹, B. Ettinger^{*2}, N. Gordon^{*3}, M. R. Grove^{*1}, L. H. Pearson^{*1}, G. T. Ray^{*3}, P. Silver^{*3}. ¹Dartmouth Medical School, Hanover, NH, USA, ²University of California San Francisco, San Francisco, CA, USA, ³Kaiser Permanente Medical Care Program, Oakland, CA, USA.

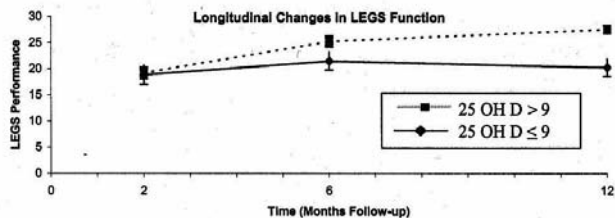
A new HEDIS measure for 2005, defined as osteoporosis work-up and/or treatment in the 6 months following fracture, will be used to evaluate the quality of osteoporosis care. Our objective was to identify physician-reported factors that correlate with post-fracture osteoporosis care in a large health maintenance organization. Primary care providers who had an office visit with a patient aged 60 or older in the 6 months following a hip, wrist, vertebral or humerus fracture received a patient-specific questionnaire regarding osteoporosis care. Using administrative data, we defined osteoporosis care as a filled osteoporosis prescription and/or a bone mineral density test in the 6 months post-fracture. Comparisons between patients with and without care were made using t-tests and chi-square tests. Multiple logistic regression analyses estimated the odds of osteoporosis care as a function of physician responses. Questionnaires for 669/922 patients were completed by 434 physicians (73% response). Mean patient age was 74 years and 72% were female. Osteoporosis care differed significantly by fracture type and patient gender (p-values < 0.001). Care was most prevalent following vertebral fracture (51%, 116/227) and least prevalent following humerus fracture (17%, 21/124). Care was more common in women (41%, 119/481) than in men (19%, 36/188). Physician-reported post-fracture osteoporosis counseling occurred for 287 patients of whom 60% received care. Absent counseling, care occurred in 16% (59/376) of patients. The most common reasons for lack of counseling were presence of more pressing comorbidities (57%) and physician unaware of fracture (23%). In multiple regression analyses, adjusted for fracture type, the odds of post-fracture care were significantly decreased by the following: male patient gender (OR: 0.30, 95%CI: 0.19, 0.49), physician report of comorbidities (OR: 0.20, 95%CI: 0.12, 0.33), physician unaware of fracture (OR: 0.19, 95%CI: 0.09,0.38), and physician assessment that osteoporosis treatment is not important or only somewhat important for the specific patient's overall health (OR: 0.39, 95%CI: 0.24, 0.62). Post-fracture osteoporosis care was evident in only a minority of patients. While information systems could improve fracture awareness, competing health concerns are likely to remain an important barrier to osteoporosis care in the primary care setting where physicians have limited time to attend to multiple health concerns. Other care pathways, such as a specialty clinic, warrant consideration.

Disclosures: A.N.A. Tosteson, NPS Pharmaceuticals 5; Innovus Research 5.

SU337

Vitamin D-Deficiency and Post-Fracture Changes in Lower Extremity Function and Falls in Women with Hip Fractures. M. S. LeBoff¹, W. Hawkes^{*2}, Y. Yahiro^{*3}, J. Glowacki¹, S. Hurwitz^{*1}, J. Magaziner². ¹Brigham & Women's Hospital, Boston, MA, USA, ²University of Maryland, Baltimore, MD, USA, ³Union Memorial Hospital, Baltimore, MD, USA.

To evaluate the prevalence of vitamin D deficiency in hip fracture patients and the association of vitamin D levels at the time of fracture with functional capacity after a fracture, we measured 25-hydroxyvitamin D levels (25-OHD) immediately post-fracture and lower extremity function, falls, and other parameters in the year following a hip fracture. In 110 community-dwelling women with hip fractures from Boston, MA (n=30) and the Baltimore Hip Studies, Baltimore MD (n= 80) recruited before 1998, the median 25-OHD levels measured by RIA (DiaSorin, Stillwater, Minn.), were 12.96 and 10.2 ng/ml, respectively. Vitamin D deficiency (defined as a 25-OH D level <15 ng/ml) was present in 66% of the women, with 38% having levels ≤ 9 ng/dl; 3.6% had vitamin D sufficiency with a 25-OHD level >32 ng/ml. In a subset of 61/80 women from Baltimore, post-fracture changes in a performance measure of the lower extremities (Lower Extremity Gain Scale:LEGS) a summary score of 9 tasks that focuses on lower extremity functioning were measured at 2, 6, and 12 months. Falls, grip strength, chair rise time, walking speed, balance, BMD, and lean and fat mass were also measured at these times. Compared to women with a 25-OHD level > 9 ng/ml, those with a 25-OHD level ≤ 9 ng/ml at time of fracture had a significantly worse composite LEGS performance (27.5 vs 20.2; $p<0.001$) at 1 year (Fig) and more falls (30.0% versus 51.5%; $p<0.05$). There were no differences between the 2 groups in grip strength, chair rise time, walking speed, balance, or body composition. These data show that vitamin D deficiency was present in 66% of women with hip fractures. Moreover, this is one of the first studies to reveal that very low concentrations of vitamin D at the time of fracture are associated with impaired lower extremity function a year following a hip fracture. Women with very low vitamin D levels at the time of a hip fracture also show increased falls possibly related to impaired muscle function. Prevention of vitamin D deficiency in the elderly may have important beneficial effects on lower extremity function without incurring excessive healthcare costs following hip fractures.



Disclosures: **M.S. LeBoff**, Novartis 2, 5; Procter and Gamble 5; Eli Lilly 2.

SU338

Personal-Fall History Predicts Non-Spine Fracture but not Spine Fracture. S. Fujiwara, N. Masunari^{*}. Clinical Studies, Radiation Effects Research Foundation, Hiroshima, Japan.

Many limb fractures develop as a result of falls among the elderly. Our previous report demonstrated that age, bone mineral density (BMD) and previous fracture are major predictors for hip and spine fracture, but we did not take into account history of personal falls. We examined the association of personal-fall history with risk of spine fracture or non-spine fracture among a cohort of 2,613 men and women (794 men and 1,819 women) aged 47 to 95 years old, who have been followed up by biennial health examinations. Follow-up averaged four years after baseline measurements of BMD using dual x-ray absorptiometry (QDR-2000, Hologic) and included a questionnaire survey on history of personal falls during the previous six months. Vertebral fracture was assessed using semi-quantitative methods, and information on non-spine fracture was obtained through interview by a trained nurse at the biennial health examinations. A total of 141 persons developed new vertebral fractures and 191 persons developed new non-spine fractures during the four-year follow-up period. Cox regression analysis was used. Incidence of personal falls in the previous six months increased with age: about 18% of men and 17% of women in their seventies reported that they had experienced more than one fall in the previous six months. Relative risk (RR) for vertebral fracture per 1SD decrease in spine BMD was 1.7 (95% Confidence Interval (CI) 1.2 - 2.7) for men and 1.6 (95%CI 1.4-2.0) for women, and RR for non-spine fracture per 1SD decrease in BMD was 1.3 (95% CI 0.9 - 1.8) for men and 1.4 (95%CI 1.1-1.7) for women. After adjustment for age, previous fracture, and baseline BMD, personal-fall history in the previous six months predicted non-spine fracture, but did not predict spine fracture. Personal-fall history was predictive for non-spine fracture with a relative risk of 3.6 (95% CI 1.7 - 7.5) after adjustment was made for age, previous fracture and spine BMD for men, and with a relative risk of 2.1 (95% CI 1.4 - 3.2) for women. In conclusion, personal-fall history is a strong predictor for non-spine fracture in the elderly. Strategies to prevent such falls would lead to a reduction of non-spine fracture in the elderly population.

Disclosures: **S. Fujiwara**, None.

SU339

Reduced Volumetric Bone Mineral Density and Geometric Properties in Hip Fracture Patients. A. Heinonen¹, T. Mikkola^{*1}, E. Portegijs^{*1}, R. Sakari-Rantala^{*1}, M. Kallinen^{*2}, I. Kiviranta^{*2}, S. Sipilä^{*1}. ¹Department of Health Sciences, University of Jyväskylä, Jyväskylä, Finland, ²Jyväskylä Central Hospital, Jyväskylä, Finland.

Existing literature provides ample human data on areal bone mineral density (aBMD), suggesting an injury of a limb leads to a decline in aBMD in the injured extremity resulting in a considerably side-to-side difference between affected and unaffected limb. However, little is known about the changes in bone geometric properties after considerable trauma such as hip fracture. The purpose of this study was to examine the side-to-side differences in volumetric bone mineral density (vBMD) and geometric properties of tibia in hip fracture patients, and to assess the determinants of the possible side-to-side differences in bone. Thirty-one 60-85- year old men and women with previous hip fracture, on average 34 months earlier, participated in this cross-sectional study. The bone scans were obtained from the distal tibia and tibial shaft of both lower limbs by pQCT (Stratec XCT 2000) to determine volumetric bone mineral density (vBMD) and bone geometry parameters. In addition, physical activity, leg extension strength and power, stair-climbing time and 10 m walking time were measured. Paired t-test and regression analysis were used in statistical analysis. Total density (-5.8%, $p<0.001$), trabecular density (-4.5%, $p=0.001$) and polar moment of inertia (-6.9%, $p<0.001$) were significantly lower in the distal tibia of the injured side compared to the uninjured side. In the tibial shaft of the injured side, total area (-3.5%; $p=0.004$), cortical area (-4.2%; $p=0.001$), and polar moment of inertia (-4.7%; $p=0.001$) were significantly lower than on the uninjured side. Time since injury had no association with the side-to-side differences in bone. Stair-climbing time and physical activity were associated with relative total area of tibial shaft ($R^2=0.61$) whereas stair-climbing time alone had an association with relative cortical area of tibial shaft ($R^2=0.27$). Hip fracture results in significantly reduced vBMD in distal tibia and deteriorated geometric properties in tibial shaft of the fractured limb. Physical activity and mobility seem to be of great importance for the good quality of bone geometry in older men and women with hip fracture history.

Disclosures: **A. Heinonen**, None.

SU340

Association of Wrist Fracture with Subsequent Hip, Spine, Rib, and Wrist or Forearm Fractures in Postmenopausal Women: Results from the National Osteoporosis Risk Assessment (NORA). E. Barrett-Connor¹, E. Siris², P. Miller³, S. Sajjan^{*4}, Y. Chen⁴. ¹Department of Family and Preventive Medicine, University of California, San Diego, La Jolla, CA, USA, ²Metabolic Bone Disease Program, Columbia University Medical Center, New York, NY, USA, ³Colorado Center for Bone Research, Lakewood, CO, USA, ⁴Outcomes Research and Management, Merck & Co., Inc, West Point, PA, USA.

Prior wrist fracture has been shown to be associated with an increased risk of future hip or vertebral fracture. Less is known about the increased risk of fracture for other fracture sites. We examine the relationship between prior wrist fractures and self-reported incident fractures at hip, spine, rib, and wrist or forearm during follow-up in postmenopausal women using data from NORA. Women were eligible for NORA if they were ≥ 50 years old, postmenopausal, had no diagnosis of osteoporosis and were not currently taking bone-specific medication (hormone therapy use was allowed). Current analysis included 158,940 women who responded to follow up surveys either 1 or 3 years post baseline and who had self-reported baseline information on prior wrist fractures occurring after age 45. Women who reported non-wrist fractures at baseline were excluded from the analysis. Absolute risks (per 1,000 person-year) for new fracture were calculated by summing fractures divided by person-years of follow-up. Relative risks for incident fracture were computed for women with prior wrist fracture (N=8665) compared to those with no prior fracture (N=150,275) using Cox proportional hazards model. Models were with and without bone mineral density (BMD), adjusted for covariates including age, ethnicity, health status, maternal history of fracture, education, weight, smoking status, use of hormone therapy, cortisone, or thyroid medication, use of alcohol, and exercise, age at menopause. A total of 4316 women reported 4728 incident fractures, including 697 hip, 669 spine, 1147 rib, 1726 wrist, and 469 forearm. Excess of future fracture (absolute and relative risks) is shown in Table. We concluded that prior wrist fracture is an important predictor of future wrist/forearm, hip, and rib fracture. Women presenting with a wrist fracture should be evaluated for appropriate management to prevent future fractures.

Fracture site	Absolute Risk (95% CI)		Adjusted Relative Risk (95% CI)	
	No Prior Fracture	Covariates	Covariates+BMD	Covariates+BMD
Hip	1.7 (1.5, 1.8)	1.9 (1.5, 2.3)	1.6 (1.3, 2.0)	1.6 (1.3, 2.0)
Spine	1.7 (1.6, 1.8)	1.3 (1.0, 1.6)	1.1 (0.9, 1.5)	1.1 (0.9, 1.5)
Rib	2.9 (2.7, 3.1)	1.6 (1.3, 2.0)	1.4 (1.2, 1.8)	1.4 (1.2, 1.8)
Wrist/Forearm	4.8 (4.5, 5.0)	3.5 (3.2, 4.0)	3.0 (2.7, 3.3)	3.0 (2.7, 3.3)

Disclosures: **E. Barrett-Connor**, Merck & Co., Inc, Eli Lilly, Pfizer Pharmaceuticals 5.

SU341

Incidence and Outcomes of Hip Fractures in Quebec, Canada, 1992-2002. S. N. Morin¹, M. Hudson^{*2}, H. Behloul^{*2}, L. Pilote^{*3}. ¹Dept of Medicine, McGill University Health Center, Montreal, PQ, Canada, ²Research Institute, McGill University Health Center, Montreal, PQ, Canada, ³Dept of Medicine and Research Institute, McGill University Health Center, Montreal, PQ, Canada.

The morbidity and mortality of osteoporotic hip fractures have a substantial impact on health care systems around the world. Increased awareness of osteoporosis and availability of potent therapies in the last decade may have an impact on incidence of hip fractures and their consequences. Our objectives are to describe recent trends in the incidence of hip fractures and post-hip fracture outcomes, and to evaluate the effect of independent co-morbidities on these endpoints. All patients aged 65 years and older admitted to hospital with a primary diagnosis of hip fracture between 1992 and 2002 were identified through the Quebec hospital discharge summary database. Fracture and re-fracture incidence rates (age and sex-adjusted for the Quebec population during the same period), 30-day and 1-year mortality rates were determined by gender and age group. We identified a number of co-morbidities and defined them using the Manitoba-Darhmouth Index. Logistic regression analyses were done to predict mortality after adjustment for co-morbidities. Overall, there were 50,251 incident hip fractures in 46,974 patients between 1992 and 2002. We identified 11,656 incident hip fractures for men (mean age [SD] 79.7 years [7.4]) and 38,595 for women (81.9 years [7.7]). Men had more associated co-morbidities; namely malignancy, cardiovascular (previous myocardial infarction, congestive heart failure and peripheral vascular diseases), renal and pulmonary diseases. Dementia and hypertension were more frequent in women. The overall annual age-adjusted incidence rates of hip fracture were stable over the study period: 667 fractures/ 100,000p-years for women and 289 fractures/ 100,000p-years for men. The age-specific incidence of hip fractures was also stable over time. The mortality rates were constant over time; being significantly higher in men than in women. After adjusting for age, co-morbidities and fiscal year, the 30-day and the 1-year mortality rates for men were twice that of women (OR 1.93, 95% CI 1.81, 2.05 and OR 1.91, 95% CI 1.81, 2.01, respectively). The higher mortality rate post hip fracture in men has previously been attributed to a higher prevalence of co-morbidities; whereas our findings indicate a two-fold increase in mortality rate even after adjusting for co-morbidities. We conclude that, despite widespread availability of diagnostic and therapeutic modalities for osteoporosis during the last decade, the incidence of hip fractures has not decreased and associated mortality rates have remained stable.

Disclosures: **S.N. Morin**, None.

SU342

Genetics and Remaining Lifetime Risk of Fracture: The Collagen I Alpha 1 Gene. T. V. Nguyen, N. D. Nguyen, J. R. Center, J. A. Eisman. Bone and Mineral Research Program, Garvan Institute of Medical Research, Sydney, Australia.

The association between genetic polymorphisms and fracture risk is commonly examined in a relative risk-based approach. However, given the time-invariant nature of the genetic information and age-related nature of fracture risk, a lifetime risk approach is more meaningful and appropriate. The present study examined the association between polymorphisms of the Collagen type I alpha 1 (COL1A1) and remaining lifetime risk of fracture in elderly men and women. COL1A1 genotypes (SS, Ss and ss) were determined in 698 women and 378 men aged 60+ years as at 1989 of Caucasian background, who have been followed for up to 15 years (1989-2004). During the follow-up period, low trauma, non-pathological fractures were recorded and confirmed by X-ray and personal interview. Femoral neck bone mineral density (FNBMD) was measured by dual energy X-ray absorptiometry (GE-LUNAR DXA) at baseline. An individual was classified as having "osteoporosis" if the individual's FNBMD T-scores was less than or equal to -2.5. Remaining lifetime risk of fracture (RLRF) from the age of 50 was estimated by the Cox's proportional hazards model, with adjustment for the competing risk of death. The proportion of individuals with SS, Ss and ss genotypes in the population of 64%, 31% and 5%, respectively, was consistent with Hardy-Weinberg equilibrium. After adjusting for competing death, the RLRF in women with ss genotype was 66% (95% CI: 45-92), significantly higher than those with SS (51%; 95% CI: 44- 58) or Ss genotype (47%; 95% CI: 38-56). The RLRF for women with osteoporosis was 65% (58-74), which was equivalent to those with ss genotype. Moreover, the RLRF for osteoporotic women with ss genotype was 94% (95% CI: 82-100). In men, there was no significant difference in RLRF between those with SS or Ss genotype (32%; 95% CI: 22-39) and ss (27%; 95% CI, 10-41). These data suggest that women with the COL1A1 ss genotype have a greater remaining lifetime risk of fracture. Their absolute risk was equivalent to that associated with osteoporotic BMD and additive to it. Although there appeared to be difference between men and women, the combination of COL1A1 genotypes and BMD measurement can potentially increase the accuracy of identifying high-risk individuals.

Disclosures: **T.V. Nguyen**, None.

SU343

Bone Loss and Weight Fluctuation Predict Mortality Risk in Elderly Men and Women. N. D. Nguyen, J. R. Center, J. A. Eisman, T. V. Nguyen. Bone and Mineral Research Program, Garvan Institute of Medical Research, Sydney, Australia.

Low bone mineral density (BMD) has been suggested as a risk factor for mortality in women. The present study examined the contribution of bone loss, weight loss and baseline BMD to the risk of all-cause mortality risk in both elderly men and women. Data from 1059 women and 644 men aged 60+ years as at 1989 of Caucasian background who have participated in the Dubbo Osteoporosis Epidemiology Study were analyzed. All-cause mortality was recorded annually between 1989 and 2004. Information of concomitant diseases, including cardiovascular diseases (CVD), all type cancer and type I/II diabetes mellitus was also recorded. Baseline femoral neck BMD (GE-LUNAR DXA) was measured between 1989 and 1992, and repeated approximately every two years afterwards. The rate of change in BMD was derived for each individual by the linear regression model. Weight fluctuation was assessed by the coefficient of variation in weight measurements during the 15-year follow-up. The association between each risk factor and mortality was assessed by the hazards ratio (HR) in a Cox's proportional hazards model after adjusting for age and concomitant diseases. During the follow-up period, 254 and 295 women died; a mortality incidence (per 1000 person-years) of 41.2 in men and 20.4 in women. In men, the annual rate of bone loss at the femoral neck was $0.4 \pm 1.2\%$ and $0.7 \pm 2.0\%$ for the surviving and deceased, respectively. In women, annually bone loss at femoral neck was $0.5 \pm 1.2\%$ and $0.9 \pm 2.6\%$ for the surviving and deceased, respectively. In both sexes, the weight fluctuation was higher in the deceased subjects than their surviving counterparts (4.2%/yr vs. 3.5%/yr, $p=0.0013$ in men and 5.3%/yr vs. 4.2%/yr, $p<0.0001$ in women). In both men and women, the following factors were independently significant predictors of mortality: bone loss (HR: 1.6; 95% CI, 1.0-2.4 in men and HR 1.6; 1.2-2.2 in women) and weight fluctuation (HR: 1.2; 1.0-1.3 in men, and HR: 1.1; 1.0-1.2 in women). Moreover, in women baseline femoral neck BMD (HR: 1.3; 1.1-1.5) and weight loss (HR: 1.2, 1.1-1.4) were additional independent predictors of mortality risk. Omitting the last weight measurement (before death) did not alter the results. These data suggest that in addition to low BMD, BMD loss and weight change were also significant predictors of all-cause mortality in elderly men and women, independent from age and concomitant diseases.

Disclosures: **N.D. Nguyen**, None.

SU344

Fall-Related Factors Predict Fracture Risk in Elderly Men and Women without Osteoporosis. T. V. Nguyen, N. D. Nguyen, J. R. Center, J. A. Eisman. Bone and Mineral Research Program, Garvan Institute of Medical Research, Sydney, Australia.

More than 50% of women with fracture do not have osteoporosis (defined as BMD T-scores being ≤ -2.5), yet risk factors for fracture in the non-osteoporosis group have not been well-documented. The aim of this study was to examine the contribution of non-BMD factors to low trauma fracture risk in elderly men and women without osteoporosis. Among women aged 60+ years who participated in the Dubbo Osteoporosis Epidemiology Study, 939 women and 719 men were found to have femoral neck BMD T-scores > -2.5 (non-osteoporosis). The women have been followed for up to 15 years (1989-2004), and during this period, the incidence of low trauma, non-pathological fracture was recorded and confirmed by X-ray and personal interview. Femoral neck BMD was also measured by dual energy X-ray absorptiometry (GE-LUNAR DXA) at baseline. Postural sway was measured by a swaymeter at baseline. During the follow-up period, 227 women and 103 men had sustained a fracture. The majority of fractures occurred at the vertebral (30%), hip (11%) and forearm and wrist (20%). The incidence of fracture (per 1000 person-years) was 23.5 for women and 14.3 for men. In the multivariate Cox's proportional hazards model, the following risk factors were significantly related to fracture risk: postural sway (HR: 1.2; 95% CI: 1.1-1.3 in women, and HR 1.3; 1.1-1.4 in men); fall in the previous 12 months (HR: 2.0, 1.1-3.5 in women and HR 2.3; 1.5-3.5 in men), and baseline femoral neck BMD (HR: 1.6, 1.5-2.6 in women and 1.3; 1.1-1.4 in men). Population attributable risk analysis suggested that an exposure to both highest tertile postural sway and fall accounted for 22% and 15% of any fracture in women and men, respectively. Thus, in non-osteoporotic women and men, the combination of low BMD, a history of fall, and postural instability could identify a subgroup of individuals with high-risk of fracture.

Disclosures: **T.V. Nguyen**, None.

SU345

Implementation of a Mandatory Osteoporosis Consultation in Patients with Low Intensity Hip Fracture. A. Q. Macasa^{*}, M. Spady^{*}, R. Quinet, J. Zakem^{*}, W. Davis^{*}, L. Serebro^{*}, Y. Menon^{*}. Rheumatology, Ochsner Clinic Foundation, New Orleans, LA, USA.

Osteoporosis remains an underdiagnosed and undertreated major health problem. The current treatment rate for patients who have experienced at least one osteoporotic fracture is 20 - 25%. In an attempt to improve this situation, the Rheumatology and Internal Medicine Departments of Ochsner Clinic Foundation implemented a mandatory osteoporosis consult as part of the admission orders for all patients admitted with a hip fracture. Methods: 65 patients were admitted with a low intensity hip fracture from June 2004 until March 2005. These patients were seen in the hospital after they had undergone hip fracture repair. They were screened for osteoporosis risk factors and were then advised appropriate treatment. 65 age matched controls admitted for low intensity hip fracture in

ASBMR 27th Annual Meeting

2003 served as our comparison group. Pearson chi-square test was used for statistical analysis. Results: Mean patient age was 80.9 (range: 54 - 99). Out of the 65 control patients, 16 (24%) were on treatment (calcium, Vitamin D, hormones or antiresorptive agents) before the hip fracture and 17 (28%) were on treatment post fracture repair. Out of the 65 cases, 29 (44%) patients were receiving osteoporosis treatment prior to hip fracture and 62 (94%) patients were receiving treatment post fracture repair. Conclusion: Improvement in osteoporosis management is achievable by several means. In our institution, we were successful in capturing and treating osteoporosis patients by putting an automatic consult for Rheumatology Department to see post hip fracture patients. The implementation of a mandatory osteoporosis consult resulted in a greater than 100% increase in treatment ($p = 0.0001$) compared to the control group.

Disclosures: **A.Q. Macasa**, None.

SU346

Cognitive Resemblance in Patients Suffering from Osteoporosis and their First Degree Relatives. **N. Kafri**^{*1}, **P. Werner**^{*1}, **I. Vered**². ¹Gerontology, Faculty of Social Welfare and Health Studies, University of Haifa, Haifa, Israel, ²Endocrinology, Sheba Medical Center, Tel Hashomer, Ramat Gan, Israel.

The importance of positive family history as a risk factor for osteoporosis has been widely documented. First-degree relatives of osteoporotic patients are regarded as a high-risk group for development of the disease, and engagement in preventive behaviors aimed at reducing the risk of bone loss and fractures is of utmost importance for them. Studies assessing other chronic diseases demonstrated that rates of adherence to preventive and screening behaviors among first-degree relatives are associated to their illness representations, i.e., to their health beliefs and cognitive representations regarding the disease. The aim of the present study was to assess and compare the illness representations among women suffering from osteoporosis and their first degree relatives. Fifty two dyads of osteoporotic women (mean age = 67.8 years; 98% menopausal, 46% have had an osteoporotic fracture), and their daughters (mean age = 40.9 years; 10% menopausal) participated in the study. Illness representations were assessed using an adapted version of the Illness Perception Questionnaire (Weiman, Petrie, Moss -Morris & Horne, 1996). Overall, although the daughters perceived the symptoms of the disease as more severe than the mothers, especially regarding bending of the back, weakness, and loss of height, the mothers perceived the disease as more permanent than the daughters. The mothers also perceived the outcomes of the disease as more serious than the daughters, particularly regarding the influence of the disease on their lives, and the financial outcomes of the disease. Compared to their daughters, the mothers perceived the disease as caused mainly by internal reasons such as inadequate diet, genetic reasons, life habits, and lack of physical activity, while the daughters tended to perceive external or chance causality. Our findings suggest that osteoporotic women and their daughters do not share similar beliefs regarding various aspects of the disease of the mother, such as the causes of the disease, its symptoms, chronicity and outcomes. These data also provide the foundation for future studies aimed at the development of interventions to increase adequate knowledge and awareness of the disease among relatives of individuals with osteoporosis.

Disclosures: **I. Vered**, None.

SU347

Bone Density and Fracture Risk in Women Who Are HIV Positive--Case Population-Based Control Study with Canadian Multicentre Osteoporosis Study. **J. C. Prior**¹, **D. Burdge**^{*2}, **E. Mann**^{*3}, **R. Milner**^{*3}. ¹Endocrinology/Medicine, U of British Columbia, Vancouver, BC, Canada, ²Infectious diseases / Oak Tree Clinic, U of British Columbia / Children & Women's Health Centre, Vancouver, BC, Canada, ³Oak Tree Clinic, Children & Women's Hospital, Vancouver, BC, Canada.

The purpose of this cross-sectional case control study is to determine whether women who are HIV positive (HIV+) are at increased risk for osteoporosis by bone mineral density (BMD) and lifetime fragility fractures. Cases are women participating in the Canadian Women's HIV Study (cases) who are on anti-retroviral therapy (ART+ n = 100) or not (ART- n = 38). Controls are women from the population-based Canadian Multicentre Osteoporosis Study (CaMOS) matched for age and geographic region. Hypotheses: 1) HIV+ women will have lower BMD related to illness, weight cycling, lifestyle differences and oligomenorrhea; 2) HIV+ women will have more fragility fractures. Methods included completion of the CaMOS interviewer-administered questionnaire in English or French. BMD data were adjusted to common spine and hip phantoms and reported as Hologic values. Cases and controls were matched within-region, by age ± 5 years in a ratio of 3 controls: 1 case. Results show that HIV+ women (n = 138) did not differ from CaMOS controls (n = 401) in age (37.7 versus 38), BMI (25.3 vs. 36.1), age at menarche (13.0 vs. 12.7), number of live births (1.5 vs. 1.9) or oral contraceptive use ≥ 3 mo. (82.4 vs. 81.3%). Cases' cigarette use was greater (4521 vs. 3594 lifetime packs), but alcohol intake, exercise and education were similar. There was no difference in a family history of osteoporosis (13.6 vs. 14.2%). Oligomenorrhea (≥ 3 skipped cycles) was greater in cases (29.4 vs. 15.4%; 95%CI -22, -6; OR 2.3). Lifetime weight cycling 20-lb occurred in 66% HIV+ vs. 43% controls (OR 2.6). Finally, fewer controls than HIV+ women had used glucocorticoid therapy (2.9% versus 8.1%, OR 2.9). Outcome measures showed L_{1-4} BMD was 1.0 ± 0.12 in HIV+ and 1.0 ± 0.14 g/cm² in controls (95% CI -.27, 0.27). Total hip BMD was 0.91 ± 0.15 vs. 0.93 ± 0.12 g/cm² (95%CI -0.005, 0.045) in HIV+ vs. controls. However, lifetime history of fragility fracture was significantly greater in HIV+ women. Low trauma fractures were reported by 26.1% of HIV+ vs. 17.3% control women (difference = 8.4%; 95%CI 16.6, 0.2, OR 1.7). This difference is important and current data do not adequately explain it. Conclusions from this population-based case:control study of HIV positive women are that, although being closely matched and

having similar bone density values, women who are HIV+ are at higher risk for fragility fractures. Hip structural analysis of all participants is planned, as is analysis of bone marker and vitamin D data in the HIV+ women.

Disclosures: **J.C. Prior**, None.

SU348

Inter-Relationships among Dietary Restraint, Subclinical Ovulatory Disturbances and BMD in Healthy Pre-Menopausal Women. **E. J. Waugh**^{*}, **G. A. Hawker**, **J. Polivy**^{*}. University of Toronto, Toronto, ON, Canada.

The aim of this study was to examine whether cognitive dietary restraint in young women was associated with lower BMD and whether this may be due to an association between dietary restraint and subclinical ovulatory disturbances, subsequent to increased cortisol. Participants were healthy Caucasian pre-menopausal women, aged 20-40 years (mean age 32.4 ± 4.6 y), recruited from the community for a two-year prospective cohort study. Women who reported irregular menstrual cycles, a history of an eating disorder, use of oral contraceptives or other medication or illness known to affect bone metabolism or menstrual function, were excluded. An average of 9.7 cycles per participant was monitored over the two-year time period using salivary progesterone measurements and ovulation detection kits. A single morning serum sample for estradiol, free testosterone and cortisol was collected once during days 3-5 of one menstrual cycle. The restraint subscale of the Three-Factor Eating Questionnaire was used to measure dietary restraint and women were categorized as high or low restrained eaters based on upper and lower tertiles of the baseline scores. Exercise was measured by the Baecke scale. Body composition and BMD (measured at the lumbar spine (L2-L4), femoral neck and total body) were determined by DEXA. Baseline values were used in this analysis. Of the 332 participants assessed at baseline, hormonal data was obtained for n=226 and these participants were included in this analysis. The group classified as high restrained eaters had significantly higher BMI's ($p=0.005$), lower percent lean mass ($p=0.008$) and exercised more ($p=0.01$). There was no significant difference in any hormone values between the two restraint groups. The mean luteal length did not differ between groups (13.6 vs 13.5 d for low and high restraint groups, respectively) and the number of women who had at least one anovulatory cycle and/or short luteal phase was similar (29 vs 28 women for low and high restraint groups, respectively). BMD at each of the 3 sites, adjusted for BMI and exercise, was not significantly different between the two restraint groups. Women with a mean luteal length of < 11 days had lower mean luteal progesterone ($p = 0.003$), a trend towards lower estradiol ($p = 0.07$) and had significantly lower total body BMD by 0.0245 g/cm² ($p = 0.047$) adjusted for BMI. In conclusion, dietary restraint was not associated with subclinical ovulatory disturbances, increased cortisol or lower BMD but a mean luteal phase length of < 11 days was associated with lower total body BMD in healthy pre-menopausal women.

Disclosures: **E.J. Waugh**, None.

SU349

Hyperaldosteronism as a Cause of Osteopenia in Cardiac Cachexia. **Z. XING**^{*1}, **V. S. Chhokar**^{*2}, **R. A. Smith**^{*1}, **S. K. Bhattacharya**^{*3}, **K. A. Hasty**^{*1}, **K. T. Weber**^{*2}. ¹Orthopaedic Surgery, University of Tennessee, Memphis, TN, USA, ²Department of Medicine, University of Tennessee, Memphis, TN, USA, ³Department of Surgery, University of Tennessee, Memphis, TN, USA.

Cardiac cachexia, a complication of congestive heart failure (CHF), is characterized by generalized loss of lean tissue, fat tissue, and bone tissue. Cachectic CHF patients have raised plasma levels of aldosterone¹. We hypothesize that hyperaldosteronism is the cause of bone loss in CHF patients. To test this hypothesis, we examined changes in bone in rats with hyperaldosteronism and the effect of spironolactone treatment. Male, 8-week-old SD rats were uninephrectomized and continuously received aldosterone (0.75 g/h) via a subdermal minipump together with 1% NaCl/ 0.4% KCl in drinking water and standard laboratory chow containing 1.13 % Calcium and 0.24% Magnesium. Some rats were also treated with spironolactone via gastric gavage (75mg/rat/day). Unoperated, untreated, age/gender-matched rats served as controls. Rats were euthanized 6 weeks after surgery. A 24-hour urine was collected prior to sacrifice while blood was collected at sacrifice. Concentrations of urine Calcium and plasma ionized Calcium were tested. Bone mineral density (BMD) was determined for femurs using a GE Lunar PIXImus2. A three-point bending test was performed to determine the flexure stress of rat femoral diaphyses. At 6 weeks, urine Calcium excretion was significantly increased in rats with hyperaldosteronism ($p<0.05$) along with marked decrease of plasma ionized Calcium levels ($p<0.05$). BMD of the femur was significantly decreased in these rats ($p<0.05$) along with a fall in bone strength compared with control rats ($p<0.05$). Spironolactone successfully reduced calcium loss and improved BMD and bone strength ($p>0.05$, compared with the control). Expansion of the extracellular volume is considered as the likely reason of increased urinary excretion of Calcium in hyperaldosteronism. Urinary loss of Calcium would stimulate PTH secretion, which then stimulates calcium release from the bone as well as reabsorption of calcium in renal tubules and intestinal absorption of calcium and phosphate via enhancing the synthesis of $1,25(\text{OH})_2\text{VitD}_3$. These early compensatory responses may not be sufficient to preserve plasma Calcium during prolonged hyperaldosteronism. This would represent a continuous stimulus to PTH secretion, thus resulting in progressive bone loss. Spironolactone, an aldosterone receptor antagonist, successfully reduced bone loss in our experiment, further demonstrating the role of aldosterone in bone loss and providing a potential treatment for osteopenia in cardiac cachexia patients.

Disclosures: **Z. Xing**, None.

SU350

The Association of Bone Mineral Density and Depression in Postmenopausal Korean Women. H. Kwak, S. Kim. Physical Medicine and Rehabilitation, Dong-A University College of Medicine, Busan, Republic of Korea.

Objective: To assess the impact of bone mineral density (BMD) on depressive symptom in postmenopausal women **Method:** We examined 20 ambulatory postmenopausal Korean women (mean age 66.5±8.7 years). The participants underwent BMD measurements using dual-energy X-ray absorptiometry of the lumbar spine and femoral neck and using quantitative ultrasound (QUS) of the left radius and left tibia. Beck's Anxiety Index (BAI) and Beck's Depression Index (BDI) were used as a questionnaire to assess the depressive symptom. Higher the score indicate more depressive. **Results:** Low BMD of lumbar spine was correlated with high score in BDI. **Conclusion:** In postmenopausal Korean women, BMD of lumbar spine has a major impact on depressive symptom.

Disclosures: **H. Kwak**, None.

SU351

Osteoporosis and Fall Risk in Patients with Fragility Fractures. P. P. Geusens¹, S. H. van Helden^{*2}, A. C. Nieuwenhuijzen-Kruseman^{*2}, G. Dinant^{*2}, E. Pijpers^{*2}, R. ten Broeke^{*2}, P. R. Brink^{*2}. ¹University Hospital & Limburg University Center, Belgium, Maastricht, The Netherlands, ²University Hospital, Maastricht, The Netherlands.

Low BMD and fall risk are well-documented risk factors for fractures. The prevalence of both risk factors has only scarcely been reported in the same population of patients with recent clinical fractures. *Methods* 261 consecutive patients (women and men of 50 years and older) admitted to the hospital with a recent clinical fracture were included and had extensive evaluation of bone mineral density (BMD) and fall risk (135 patients with fracture of the upper limb, 94 of the lower limb, 12 of the spine, 10 other and 10 multiple simultaneous fractures). Fractures after a car accident were excluded. BMD was measured in the spine and hip using DXA and expressed in gender-specific T-scores. Other evaluated risk factors included an ADL-score (the Groningen Activity Restriction Scale (GARS)), the Timed Get up and Go test (TGUGT), chair stand test, the four test balance scale and classic risk factors for fractures (Table). *Results* Osteoporosis in the spine or hip was present in 41% of the patients and osteopenia in 41%. The prevalence of other risk factors for fractures ranged from 2% (use of glucocorticoids) to 34% (osteoarthritis) (Table). Patients with classic osteoporotic fractures (clinical spine, humerus, forearm, femur or multiple fractures) (n=158) were older (70 vs. 64 years; p<0.001), had lower Z-score in the hip (-0.4 vs. +0.2; p<0.001), higher GARS (14.7 vs. 12.5, p<0.01), lower body weight (68 kg vs. 74 kg; p<0.01), more disturbed balance (standing on one leg timed: 13 sec vs. 20 sec; p<0.001) and lower hand grip strength (52 kg vs. 63 kg, p<0.05) than patients with other fractures. *Conclusions* Patients with clinical fractures had a wide spectrum of risks for fractures in terms of BMD and non-BMD related risks, including fall risk. Patients with classic osteoporotic fractures had lower BMD in the hip and more other risk factors for fractures and falls than patients with other fractures, including lower muscle strength. These results indicate that patients with clinical fractures should have attention for both osteoporosis and fall risk in order to target the right population with the right treatment.

Patient characteristics (n=261)	
Women (%)	74
Age (mean, SD)	67 (12)
Osteoporosis in spine or hip (%)	41
GARS (range: 0-4) >2 (%)	24
TGUGT (range: 5-70 seconds) >15 sec (%)	23
History of clinical vertebral fracture (%)	8
History of non-vertebral fracture (%)	16
Family history of hip fracture in mother (%)	22
Body weight <60 kg (%)	19
Severe immobility (%)	7
On glucocorticoids (%)	2
Disturbed balance (%)	25
Other fall during previous year (%)	26
Using >4 medications/day (%)	20
Osteoarthritis (%)	34
Urinary incontinence (%)	13

Disclosures: **P.P. Geusens**, None.

SU352

Influence of Endurance Training and Low Dose Oral Contraceptives on Parameters of Bone Mass and Geometry in Young Women. A. Kirchbichler^{*1}, C. Kleinmond^{*1}, M. Wiseman^{*2}, E. Preisinger³, E. R. Weissenbacher^{*4}, M. Hartard¹. ¹Faculty of Sport Science Technical University Munich, Working Group MusculoSkeletal Interactions, Munich, Germany, ²Bavaria Academy of Sciences, Leibniz Data Processing Center, Munich, Germany, ³Department Physical Medicine and Rehabilitation, Hospital Lainz, Vienna, Austria, ⁴Faculty of Medicine, Klinikum Grosshadern, Ludwig Maximilians Universität, Department of Gynecology and Obstetrics, Munich, Germany.

It was the aim of this retrospective analyze to examine the influences of low dosed oral contraceptives (OC) on parameters of bone mass and geometry in 48 young female endurance athletes, compared to 105 non-exercising young women. Women, aged 18 to 28

years, were separated into four groups according to the data on training history and OC use. Impact on bone was expected after 3 years of regular training with a minimum of three hours per week and an intake of OC for more than 3 years in women younger than 22, or in women, aged 22 - 28 years, when OC use was more than 50% of the time after menarche. Due to this classification, subjects were allocated into exercising OC users (EX-OC, n = 22) or exercising controls (EX-C, n = 26), and into non-exercising OC users (NEX-OC, n = 39) and non-exercising controls (NEX-C, n = 66). Cortical BMC and area, total area, and area of bone marrow were assessed by pQCT (XCT-2000, STRATEC) at distal tibia shank level 38% (diaphysis). Mean values of cortical content and area were lower in OC users compared to non-users, obviously more evident between the exercising OC users and the exercising controls. In addition, OC use was associated with a medullary expansion at tibial diaphysis. Data are given as mean values (SD) in the table; superscripted characters indicate significant differences (p < 0.05) between groups.

	EX-C	EX-OC	NEX-C	NEX-OC
Cortical BMC (mg/cm)	350.65 ^{abc} (46.37)	327.14 ^{bd} (49.93)	309.56 ^{ad} (33.58)	304.54 ^c (38.78)
Total Area (mm ²)	393.48 ^{ef} (53.03)	383.68 ^{eb} (48.35)	359.16 ^{eg} (40.07)	353.55 ^h (46.43)
Marrow (%)	21.44 ^{ij} (4.60)	24.60 ^{ij} (5.93)	23.87 (4.49)	23.76 ⁱ (4.78)
Cortical Area (mm ²)	300.19 ^{klm} (41.12)	279.37 ^{kn} (43.77)	263.44 ^{ln} (28.87)	259.39 ^m (33.26)

We conclude that OC use was associated with influences on parameters of bone mass and geometry at tibial diaphysis, obviously more evident in the exercising women under OC use.

Disclosures: **A. Kirchbichler**, None.

SU353

The Relationships between Dietary Intakes, Parental Fracture History, and Birth Status and Bone Mass of the School-Aged Children in Taiwan Assessed by Quantitative Ultrasound. Y. Lin¹, S. Tu^{*2}, W. Pan^{*3}. ¹Institute of Nutritional Science, Chung Shan Medical University, Taichung, Taiwan Republic of China, ²Center for Survey Research, Academia Sinica, Taipei, Taiwan Republic of China, ³Institute of Biomedical Sciences, Academia Sinica, Taipei, Taiwan Republic of China.

The Children Nutrition and Health Survey in Taiwan, 2001-2002 was carried out to evaluate the overall nutrition and health status of school children aged between 7 and 13 years. The survey was conducted using a multi-stage complex sampling scheme and was consisted of two phases including physical examination and questionnaire interview. Bone mass measured as broadband ultrasound attenuation (BUA, in dB/MHz) was taken at heel by quantitative ultrasound (CUBA Clinical, McCue), and the corresponding Z-score was calculated. The preliminary results have been previously reported. In the current analysis, 1161 boys and 992 girls who had complete questionnaire information with ultrasound bone scan were included. Statistical analyses were performed using SAS v8.2 and SUDAAN v8.0. All variables were weighted to represent the children population in Taiwan. In terms of dairy products consumption, there was a significant inverse correlation between frequency of cheese intake (0.25-17.5 slices/week) and BUA Z-score in girls (r²=0.22, p=0.009) but not in boys. No significant relationships between consumption of other dairy products and BUA Z-score were observed in these boys and girls. A weak but significant positive correlation also existed between the frequency of fresh fruits/juices intake (0.25-24.5 exchanges/week) and girls' BUA Z-score (r²=0.08, p=0.02). In addition, the frequency of soymilk drinking was negatively correlated to the BUA Z-score in girls (r²=0.15, p=0.001) and also in boys with less significance (r²=0.08, p=0.06). On the other hand, boys with paternal fracture history had higher BUA Z-score than those whose fathers did not previously fracture (p=0.055). Maternal history of fracture did not result in significant difference in BUA Z-score in both boys and girls. Girls who were born prematurely (before 38 weeks gestation) had significantly lower BUA Z-score than those born full-term (p=0.0013). Based on the data collected in this island-wide survey on the children in Taiwan, it appears that dietary intake of certain foods, including dairy, fruits, and/or soymilk, may be related to bone health status in the children. The gender difference in the relationships between paternal fracture history or birth status and BUA Z-score deserves further attention.

Disclosures: **Y. Lin**, None.

SU354

Impact on Quality of Life of Conditions that May Increase the Risk of Fractures in Women with Established Osteoporosis: A Matched Pair Analysis from the Osso Spanish Cohort. R. Pérez Cano^{*1}, C. Lozano², E. Muñoz^{*3}, D. Toledo^{*4}, A. Rodríguez-García^{*5}, I. Vesga^{*6}, A. Oteo^{*7}, R. Ramos^{*8}, E. Martín Forero^{*9}, C. Barbazán^{*10}, E. Martín Mola^{*11}, C. Garcés^{*3}. ¹H V Macarena, Sevilla, Spain, ²H Clínico, Madrid, Spain, ³Lilly, Madrid, Spain, ⁴H. Puerta del Mar, Cádiz, Spain, ⁵H Ramón y Cajal, Madrid, Spain, ⁶H Txarrigurrutxu, Vitoria, Spain, ⁷H Moratalaz, Madrid, Spain, ⁸Private, Sevilla, Spain, ⁹H V Salud, Toledo, Spain, ¹⁰H Xeral, Pontevedra, Spain, ¹¹H La Paz, Madrid, Spain.

The Observational Study on Severe Osteoporosis (OSSO) is a 12-month prospective, European study. The baseline analysis in Spain aimed to know the frequency of conditions that may increase the risk of fracture in established osteoporosis (OP) and their effect on quality of life (QoL) A non-probabilistic sampling of consecutive patients with postmenopausal established OP (BMD≤-2.5 and at least one fragility fracture) was performed in 64 OP outpatient clinics. Age, risk factors for OP and falls (BMI, menopause,

exercise, nulliparity, mother hip fracture, smoking, sight problems, steroids use), and disease data (earliest lumbar T score, years since first fracture, and current use of AR) were collected. We defined following criteria as potentially associated with higher risk for fractures: a) history of 2 or more fragility fractures and/or b) inadequate response to antiresorptives (AR). Inadequate response was defined: 1.new fragility fracture despite prescription of any OP drug for at least 12 months before fracture, 2.discontinuation of any OP drug due to compliance problems or side effects. QoL was assessed with QUALEFFO. Two matched groups were obtained from the cohort, one with 1 or more higher fracture risk criteria and a control group without any. Matching criteria were age, years since menopause and years on AR. Osteoporosis risk factors and QoL were compared between groups 846 women; 68.8 (7.7) years, were recruited. 330 did not present any criteria of higher risk for fracture. 370 (44% from total) had 2 or more fractures, 346 (41%) a new fragility fracture after a minimum of 12 months of AR therapy, and 103 (12%) history of AR discontinuation. 257 matched pairs were found. Most OP risk factors were not different between the 2 groups. QUALEFFO total score, and domains of physical function, social function and general health perception, showed significantly lower QoL in the group with any criteria for higher risk for fractures ($p<0.05$) In summary, prevalence of multiple fractures and fracture despite at least one year of continued AR treatment in established OP is very high. Patients with multiple fractures and/or any criterion of inadequate response to AR therapies as defined above, have a worse QoL than those with no one of these criteria.

Disclosures: **R. Pérez Cano, None.**

SU355

Risk Factors for Falling and Fracture in Older Women with Type 2 Diabetes. **S. Patel¹, K. Tweed^{*1}, S. Hyer^{*2}, A. Rodin^{*2}, S. Kerry^{*3}, J. Barron^{*4}.**
¹Dept of Rheumatology, St Helier University Hospital, Carshalton, United Kingdom, ²Dept of Endocrinology, St Helier University Hospital, Carshalton, United Kingdom, ³Dept of Community Health Sciences, St George's, University of London, London, United Kingdom, ⁴Dept of Clinical Chemistry, St Helier University Hospital, Carshalton, United Kingdom.

Type 2 diabetes mellitus (DM) is associated with increased risk of hip fracture despite patients with type 2 DM having normal to high BMD. This suggests that non-skeletal risk factors, such as increased fall risk, may be important in the aetiology of fractures in type 2 DM. The aim of this cross-sectional study was to determine risk factors for falling and fracture in older women with Type 2 DM. We recruited women 65 years or older from a Type 2 DM community based register. To date we have recruited 130 women with a mean age of 75 yrs (range 66 to 91), mean duration of DM 11 yrs (range 1 to 54), mean BMI 30 (range 20 to 52) and mean HbA1c of 7.6 (range 5.1 to 11.8). BMD was measured by DXA and quantitative ultrasound (heel). Mean BMD values were significantly higher than the manufacturer's reference range for all skeletal sites. Thus mean lumbar spine BMD Z score was + 1.61 ($p<0.001$), mean total hip BMD Z score was + 1.08 ($p<0.001$) and mean heel Stiffness Z score was + 0.48 ($p<0.001$). A history of one or more falls in the previous 12 months was given by 54 /130 (41.5 %) of the women. Those women with a history of falling had higher BMI compared to those without a history of falling (mean 31 versus 29 respectively ; $p=0.02$) and higher vibration perception threshold (mean 21.1 volts versus 17.6 volts respectively; $p=0.02$). We found no differences in duration of diabetes, HbA1c, visual acuity, capillary return, balance tests and lying and standing heart rate and blood pressure between women with and without a history of falling. A history of a previous low trauma fracture was given by 49/130 (38%) of the women. The fracture group tended to be older than the non-fracture group (mean age 75.8 years versus 73.6 years; $p=0.05$) but there were no differences in diabetes related factors. No differences were found in BMD measured by DXA between the fracture and non-fracture groups although Stiffness Z scores tended to be lower in the fracture group versus the non-fracture group (mean 0.31 versus 0.59 respectively; $p=0.15$). These preliminary findings suggest that both high BMI and reduced vibration sense have a role in contributing to increased risk of falling in women with Type 2 DM. No significant differences were found in the measured variables for differing fracture status.

Disclosures: **S. Patel, None.**

SU356

Menstrual Irregularity and Low Bone Mineral Density in Female High School Runners. **M. Barrack^{*1}, J. Nichols¹, M. Rauh^{*2}, K. Edwards^{*1}.**
¹Exercise and Nutrition Science, San Diego State University, San Diego, CA, USA, ²Public Health, San Diego State University, San Diego, CA, USA.

The purpose of this study was to determine the prevalence of and relationship between menstrual irregularity and low bone mineral density in high school cross-country athletes. One hundred forty two female high school cross country runners ages 13-18 (mean age 15.93 ± 1.22 y) were recruited from 12 high schools in southern California. Menstrual function was assessed by an interviewer-assisted self-report questionnaire. Menstrual irregularity was defined as fewer than 10 menses in the past year. Bone mineral density and mineral content (BMD/BMC) of the spine (L1-L4), proximal femur (total hip), and total body were assessed by dual energy x-ray absorptiometry (DXA; GE/Lunar DPX NT). The International Society for Clinical Densitometry (ISCD) and the World Health Organization (WHO) criteria of ≤ -2 or ≤ -1 SD, respectively, below age-matched reference data were used to classify athletes as having low BMD relative to age. The prevalence of menstrual irregularity was 25.7%, whereas 9.5% of the athletes met ISCD criteria for low BMD. However, using WHO criteria, 40.9% of the athletes had spine BMD values of 1SD or more below reference values. The number of menstrual cycles in the past year was positively associated with BMD at the spine ($r=0.26$, $p<0.01$), but not at the hip or total body. One-way analysis of covariance (controlling for body weight) indicated that athletes with menstrual irregularity had significantly lower BMD at the spine (1.03 ± 0.12 g/cm²)

compared to eumenorrheic athletes (1.12 ± 0.11 g/cm², $p<0.03$). These results indicate that female high school cross-country runners with menstrual irregularity have a greater risk of developing osteopenia/osteoporosis than their eumenorrheic peers. Screening for menstrual irregularity, and education to promote bone health in this population may be beneficial steps toward helping female athletes optimize bone mineral accrual during their adolescent years.

Disclosures: **M. Barrack, None.**

SU357

An Assessment Tool for Prediction of Non-Vertebral Fracture Risk in Postmenopausal Women. **c. roux¹, k. briot^{*1}, a. varbanov^{*2}, s. horlait^{*3}.**
¹Rheumatology, Cochin hospital, PARIS, France, ²Procter and Gamble, Cincinnati, OH, USA, ³Procter and Gamble, Neuilly sur seine, France.

Non-vertebral fractures are common and responsible for the greatest amount of morbidity, mortality and cost attributable to osteoporosis. The risk of these fractures may play a key role in therapeutic decision-making as discrepancies remain regarding the effect of treatments on non-vertebral (NV) fractures. The objective of this analysis was to design a risk assessment tool for NV fracture risk. 2548 osteoporotic postmenopausal women included in the placebo groups of the phase III fracture endpoint risedronate trials (VERT-MN, VERT NA & HIP Group 1) were included (mean age 72, mean femoral neck T score -2.53, 60% and 53% of patients with prevalent vertebral and NV fractures, respectively). During a follow-up of 3 years, 206 NV fractures were observed including 50 hip fractures. Baseline data on 14 parameters (age, height, weight, body mass index, years since menopause, femoral neck T score, serum 25OHD3, prevalent vertebral and NV fractures, current alcohol intake and smoking, current use of thiazide diuretics, history of breast cancer and rheumatoid arthritis) were included in a logistic regression analysis. Baseline factors significantly associated with NV fracture risk included: Prevalent NV fracture ($p=0.006$), no.of prevalent vertebral fractures ($p<0.001$), femoral neck T score ($p=0.034$), 25OHD3 ($p<0.001$), age ($p=0.019$) and height ($p=0.037$). The predicted NV fracture risk (probability) is given by the equation: risk = $\exp(x)/[1+\exp(x)]$, where, $x=-9.0733+0.0351*Age + 0.0240*Height - 0.2534*femoral\ neck\ T\ score - 0.0104*serum\ 25OHD3 + 0.1126*number\ of\ prevalent\ vertebral\ fractures - 0.2141*prevalent\ NV\ fractures$. Prevalent NV fractures are assigned a value of 1 if the woman has no previous NV fracture, and -1 otherwise. The ROC results were used to define a subgroup of women with high risk of NV fracture. The cut-off value of 0.082 (i.e. 8.2% NV fracture risk at baseline) corresponded to sensitivity of 62.6% and specificity of 62.3%. In the subgroup of women with high risk of NV fracture (N = 1013), the incidence of NV and vertebral fractures was 12.7% and 22.3%, respectively, i.e. 1.6 and 1.5 times higher than the average of the population. The use of six parameters easily assessable in clinical practice can help to define patients at high risk of non-vertebral fracture. As a number of compounds approved for the treatment of osteoporosis have no or little demonstrated effect against non-vertebral fractures the risk assessment tool may be useful for the selection of optimal treatments.

Disclosures: **C. Roux, None.**

SU358

Changes in Weight and Body Composition Are Associated with Bone Loss and Incident Vertebral Fracture in Women Over 50. **J. Finigan, D. M. Greenfield*, R. A. Hannon, A. Blumsohn, N. F. Peel, G. Jiang*, R. Eastell.**
 University of Sheffield, Sheffield, United Kingdom.

It has been observed that weight loss is associated with loss of bone density and with incident non-spine frailty fractures. It is unclear whether it is the loss of fat mass or of lean mass that is significant for bone loss or whether weight loss is related to the risk of vertebral fractures. We carried out a 10-year prospective study of a population-based group of 375 women, ages 50 to 85 years. At baseline we measured height, weight, bone mineral density (BMD) by DXA of the femoral neck and total body for body composition. Incident vertebral fractures were determined for subjects with 2 or more study visits (n=314) by a single radiologist from spinal radiographs at 0, 2, 5, 7 and 10 years. BMD measurements were repeated at these visits, and the annual percentage rate of bone loss at the femoral neck (FN) was calculated from a regression line. Only those subjects who attended for 5 or more years were included in the bone loss analysis (n=254). Weight and body composition changes were calculated as annual percentages of baseline values for all subjects with at least 2 visits. Neither height, weight, BMI, fat mass nor lean mass at baseline predicted the rate of change of hip bone density, but older age was associated with greater annual bone loss ($\rho=-0.16$, $p=0.012$). Rates of change in weight, fat mass and lean mass were all positively associated with rate of change of bone density ($r=0.41$, $r=0.32$, $r=0.38$ respectively, all $p<0.001$). By multiple linear regression, each of these was independent of age, and changes in fat mass and lean mass were independent of each other, with $p<0.001$ in each case. When subjects under or over age 65 (n=159, n=95) were analysed separately, the associations were similar in both analyses. By logistic regression, the rates of change of weight and fat mass were associated with incident vertebral fracture, with odds ratios of 1.66 (95% CI 1.13, 2.46) for weight change and 1.56 (1.05, 2.31) for fat change, for each SD decrease, but these were not independent of age. Change in lean mass was not associated with fracture. We have previously observed that a greater fat mass protects against vertebral fractures. When obese subjects (BMI>30, n=57) were excluded from the current analysis, the odds ratios for each SD decrease in weight change and fat change were 1.86 (1.20, 2.87) and 1.62 (1.07, 2.44), with both independent of age. We conclude that, regardless of baseline weight or body composition, weight loss is associated with greater bone loss, with changes in fat mass and lean mass making similar and independent contributions. Incident vertebral fractures, on the other hand, are associated with loss of weight and fat mass, but not lean mass, in non-obese subjects.

Disclosures: **J. Finigan, None.**

SU359

Epidemiology and Treatment Practices of Osteoporosis in Elderly Americans. M. A. Omar^{*1}, K. H. Kahler^{*1}, M. Edmonson^{*2}, K. Annunziata^{*2}. ¹Novartis Pharmaceuticals Corporation, East Hanover, NJ, USA, ²Consumer Health Sciences, East Hanover, NJ, USA.

Osteoporotic fractures are a major public health concern, resulting in substantial morbidity and mortality. The objective of this study was to determine the recent epidemiology of osteoporosis and related treatment practices of the elderly in the US. The study population consisted of respondents from the 2004 US National Health and Wellness Survey (NHWS). The NHWS is an annual cross-sectional survey of a nationally representative sample of the adult US population (≥ 18 years) that contains a broad range of health-related topics. The survey was fielded via the internet in June 2004 and completed by 40,730 US adults. Of all respondents who completed the NHWS, 3.8% reported being diagnosed with osteoporosis by a physician. Fifty percent of these were ≥ 65 years. Of the latter group, 93% were female, and about 11% were part of the workforce. Of the overall population ≥ 65 years (regardless of osteoporosis diagnosis), 20% reported having had ≥ 1 fracture(s) in the past. The proportion increased to 31% for all respondents diagnosed with osteoporosis. Of all NHWS respondents ≥ 65 years with past fracture(s), 38% had never had a bone mineral density scan, 19% had received a diagnosis of osteoporosis, and 12% were on prescription drug therapy for osteoporosis. Of the respondents ≥ 65 years who did not have a diagnosis of osteoporosis by a physician, 24% considered themselves at risk for the condition, while 59% reported taking no measures to prevent it. The results from this study suggest that under-treatment of osteoporosis in the elderly is an important concern. Patient education, adequate screening and appropriate treatment of those at risk for fractures may help reduce the clinical and economic burden of this disease.

Disclosures: **M.A. Omar**, Novartis Pharmaceuticals Corporation 3.

SU360

Overweight, but not Obesity, Is Associated with Higher Bone Mineral Density in Women Across the Age-Span. R. A. Brownbill, J. Z. Ilich. School of Allied Health, University of Connecticut, Storrs, CT, USA.

Studies show that weight loss causes reduction in bone mineral density (BMD), however, it is not clear whether and to what extent higher body weight might contribute to higher BMD in women across the age span. This study was conducted to determine if degree of overweight/obesity was related to BMD of various skeletal sites in 311 healthy Caucasian women of wide age range (18.6-88.6 y, mean \pm SD 49.3 \pm 20.3 y). Weight and height were measured in indoor clothing by standard methods and body mass index (BMI, kg/m²) was calculated. BMD and t-scores of the whole body, femur (neck, Ward's triangle, shaft, trochanter and total hip), lumbar spine and forearm were measured with Lunar DPX-MD densitometer. Subjects were classified according to their BMI as either normal weight (BMI<25 kg/m², n=141, age 50.6 \pm 19.8 y), overweight (BMI=25-29 kg/m², n=114, age 49.2 y), or obese (BMI>30 kg/m², n=56, age 47.1 y). ANCOVA, controlled for age, and pair-wise group comparisons with Bonferroni corrections were used to assess group differences in BMD and t-scores. Obese and overweight subjects had significantly higher BMD and t-scores for all skeletal sites (p<0.05) than normal-weight subjects. Whole body BMD for ascending BMI groups was 1.110 \pm 0.10, 1.163 \pm 0.11, and 1.193 \pm 0.10 g/cm², respectively, while hip t-scores were -0.92 \pm 1.28, -0.55 \pm 1.37, and -0.31 \pm 1.30, respectively. Although obese subjects had higher BMD than overweight subjects for most of the skeletal sites, results were not significant. The findings of this study indicate excess body weight is associated with higher BMD in women of wide age range, however, excess weight beyond BMI of 30 kg/m² is not associated with additional increase in BMD.

Disclosures: **J.Z. Ilich**, None.

SU361

Bone Turnover and Micro-Architecture in Premenopausal Women with Idiopathic Osteoporosis. J. Fleischer¹, M. Donovan¹, H. Zhou², D. McMahon¹, D. Dempster², R. Müller³, E. Shane¹. ¹Medicine, Columbia University P & S, New York, NY, USA, ²Regional Bone Center, Helen Hayes Hospital, West Haverstraw, NY, USA, ³ETH and University Zürich, Zürich, Switzerland.

Most young women with osteoporosis (OP) have an identifiable cause. Others have an idiopathic form (IOP) for which no cause can be found. To characterize histomorphometric features of IOP, 9 otherwise healthy premenopausal women who presented with OP and fragility fractures, underwent tetracycline-labeled transiliac bone biopsy. Secondary causes of OP were excluded. Compared to age and sex matched controls (n=18), significant differences in bone turnover were identified. Although osteoid thickness and surface did not differ, parameters that reflect bone formation were lower in IOP patients, wall width by 12% (p<0.01), mineral apposition rate by 18% (p<0.01), mineralizing surface by 42% (p \leq 0.02), bone formation rate by 52% (p<0.01) and activation frequency by 54% (p=0.07). Conversely, bone resorption variables were increased, including a markedly longer resorption period (p=0.02) and increased eroded surface (p=0.05). Despite abnormalities in bone turnover, structural parameters assessed by 2-dimensional (2D) histomorphometry, such as cancellous bone volume (BV/TV) and trabecular width (Tb.Wi), did not differ, although there was a trend toward lower trabecular number (Tb.N; 1.7 \pm .07 vs 1.9 \pm .05; \pm SEM; p=.12) and increased trabecular separation (Tb.Sp; 429 \pm 20 vs 388 \pm 17 μ m; p=.16) in women with IOP. To further assess microarchitecture, biopsies were analyzed by microCT. Consistent with 2D results, BV/TV and bone surface/bone volume (BS/BV) did not differ between groups (p=.59 and p=.46, respectively), but bone surface/total volume (BS/TV; 3.74 \pm .19 vs 4.34 \pm .13 1/mm; p=.01) was significantly lower in IOP subjects. Trabecular thickness (Tb.Th; 226 \pm 19 vs 194 \pm 10 μ m; p=.11) and Tb.Sp (551 \pm 27 vs 464

\pm 30 μ m; p=.06) tended to be higher and Tb.N tended to be lower (1.6 \pm .07 vs 2.3 \pm .49; p=.18) in IOP. Moreover, there was significantly greater (p<0.04) intra-individual variability in Tb.Th and Tb.Sp in IOP subjects than controls. In summary, women with IOP have evidence of increased bone resorption and decreased bone formation compared to controls. Microarchitectural changes were less pronounced, although with more sensitive micro-CT analysis, significant decreases in BS/TV, increases in Tb.Sp and evidence of structural heterogeneity were detected. The microCT data suggest abnormal bone remodeling in premenopausal women with IOP is associated with loss of whole trabecular elements, rather than thinning of individual trabeculae, changes that may ultimately lead to abnormal bone quality and increased fragility.

Disclosures: **J. Fleischer**, None.

SU362

Comparison of Male and Female Response to Regenerative Nerve Damage. A. M. Miesse^{*}, T. A. Bateman. Bioengineering, Clemson University, Clemson, SC, USA.

It is known that different modes of nerve damage cause osteoporosis. This decrease in bone mass coincides with the loss of muscle stimulation, resulting in a measurable increase of bone resorption local to the affected limb. This study was designed to examine a potentially different response to nerve damage-induced bone loss between male and female mice. Twenty-four C57BL/6J mice were used in this study. At surgery, all animals were 105 days old and assigned to one of two groups: Sciatic nerve crush male (MAL, n=12); and sciatic nerve crush female (FEM, n=12). The sciatic nerve was surgically exposed and then crushed flat with mosquito forceps midway between the sciatic notch and patella for 30 seconds. The left limb was used as a control. The mice were sacrificed two weeks post-surgery and the hindlimbs excised. These analyses were performed on the femora: bone mass, 3-point bending, and microCT (μ CT) of the diaphysis and epiphysis. For all comparisons, a t-test was performed comparing the right (surgical) limb to the left (non-surgery) limb within the MAL and FEM groups. The FEM group experienced an 8.0% (p<0.001) decrease in bone mass while the MAL group had a 6.3% (p=0.16) decrease. Yield strength was unchanged for both groups. Maximum strength decreased significantly for FEM (7.0%, p=0.02) but not for the MAL group (0.2%). Stiffness decreased significantly in both the FEM and MAL groups with mean decreases of 67% (p<0.001) and 32% (p<0.001), respectively. These data suggest that functionally FEM were more severely affected by the nerve damage compared to the MAL. Cortical diaphysis (9mm) was measured via μ CT in order to quantify the effects of nerve crush on cortical volume and moment of inertia. The cortical volume decreased in the FEM group by 4.4% (p=0.005) but there was no significant decrease in the MAL group (2.2%). This decrease in cortical volume coincides with a trend of a decrease in average maximum principle moment of inertia (I_{max}) for FEM. I_{max} was diminished 6.4% (p=0.06) for the FEM group, while MAL had no difference in I_{max} (-0.2%). Trabecular bone density was measured at both the proximal and distal ends to assess the effects of nerve damage at different regions. Neither group had significant differences in bone density at the distal end, but both experienced differences at the proximal end (FEM 16%, p=0.03; MAL p=0.009, 16%). These data demonstrate that male and female mice experience a difference in functional bone loss due to regenerative damage to the sciatic nerve. These differences are primarily manifested in cortical bone, resulting in greater changes in mechanical strength for female mice.

Disclosures: **A.M. Miesse**, None.

SU363

Loading Influences the Size, Shape and the Architecture of the Bone Rather than its Mass. R. M. Zebaze¹, A. Jones^{*2}, M. Knackstedt^{*2}, E. Seeman¹. ¹Endocrinology, Austin Health, Melbourne, Australia, ²Department of Applied Maths, RSPHysSE, Australian National University, Australia.

The structural basis of femoral neck (FN) strength was studied using high resolution micro-CT. Two hundred cross-sectional slices were analyzed in each of 13 postmortem specimens from Caucasian women aged 29 to 85. At the FN-shaft junction (a region mainly subjected to bending), the section modulus was highest, the FN had a large ellipsoid total cross-sectional area (T-CSA) with a supero-inferior long axis. The bone at this junction was largely cortical with greater thickness inferiorly than superiorly. Moving proximally along the FN, T-CSA decreased then increased becoming less ellipsoid and more circular; while the cortical mass diminished, trabecular mass increased so that bone mass (represented by bone area) from section to section was almost constant along the FN but the proportions of cortical and trabecular bone varied in a reciprocal fashion. From the FN-shaft junction to FN-femoral head junction, cortical bone mass decreased by $\sim 60\%$ (199.6 \pm 12.7 vs. 78.5 \pm 8.6 mm²), this was associated with a similar $\sim 60\%$ increase in trabecular bone mass (72.8 \pm 9.4 vs. 174.2 \pm 16.3mm²) towards the femoral neck-head junction, a region subjected to mainly compressive and shear stresses. From the FN-shaft junction to the neck-head junction, the section modulus decreased by 67% (1491 \pm 101.9 vs. 496 \pm 66.1mm³) while the coefficient of circularity (the degree to which the T-CSA approximates a circle) of the cross section increased from 59 to 87.5%. Thus, bone mass from slice to slice was relatively constant despite the change in T-CSA size and shape along the FN. Loading influences the structural and spatial organization of bone, but has little effect on its mass; adapting the size, shape and architecture to prevailing loads; ellipticity and cortical bone favours resistance bending, circularity and trabecular bone favours resistance to compression and shear stresses. The inability of bone to adapt its structural parameters (shape, relative distribution of cortical and trabecular bone) to prevailing loads may play an important role in the development of bone fragility. Understanding the mechanisms regulating these structural parameters independently of bone mass may be important in understanding the pathogenesis of bone fragility.

Disclosures: **R.M. Zebaze**, None.

SU364

The Disproportionately Shorter Femoral Neck Length in Chinese Contributes to Higher Hip Strength than in Caucasians. X. Wang^{*1}, Y. Duan¹, M. J. Henry^{*2}, E. Seeman¹. ¹Endocrinology and Medicine, Austin Health, the University of Melbourne, Heidelberg, VIC, Australia, ²Clinical and Biomedical Sciences, Barwon Health, the University of Melbourne, Geelong, Australia.

Racial differences in femoral neck (FN) traits are the result of differences in structure rather than differences in volumetric bone mineral density (vBMD) (Wang et al, in press). We hypothesized that the lower hip fracture rate in Chinese than Caucasians may be partly due to Chinese having shorter FN length, a trait that contributes to the higher hip strength than in Caucasians. We studied 821 healthy Chinese (540 females) and 1052 Caucasians (692 females) aged 18-93 years living in Melbourne. Trunk length and leg length were measured by anthropometry. Using DXA hip strength analysis program, we calculated safety factor (SF), an estimate of hip strength expressing the ratio of estimated failure stress in tension to applied tensile stress during walking. In both sexes, 85% of the shorter stature in Chinese than Caucasians was due to their shorter leg length. FN length was 6% shorter in Chinese than Caucasians after adjusting for their shorter stature. SF decreased with age in all subjects but was 5-10% higher in Chinese than in Caucasians. About 13% of the racial difference in SF was independently attributed to the racial difference in FN length. Comparing sexes, shorter standing height in women was equally due to shorter leg and trunk length in both races while FN length was 4-6% shorter in women than men after adjusting for age, standing height and weight. Young adult women and men had a similar SF in both races. There was also no sex difference in SF in elderly Caucasian women and men, but SF was 7.8% lower in elderly Chinese women than men ($p < 0.01$). We infer the disproportionately shorter leg length and the shorter FN length may partly account for the lower hip fracture rates in Chinese than Caucasians. However, women also have shorter leg length and FN length but fracture more often than men. Whether deleterious structural abnormalities in women overwhelm any protective effect remains to be determined.

Disclosures: **X. Wang**, None.

SU365

The Different Response to D-Galactose on Bone Tissue from Female and Male Rats. L. Cui, T. Wu^{*}, H. M. Luo^{*}. Pharmacology, Guangdong Medical College, Zhanjiang, China.

D-galactose is known to induce senescent animal models such as age-dependent cataractogenesis and brain senescence partially due to the oxidative damage and lipid peroxidation induced by D-galactose. Since osteoporosis is also involved in a senescent procedure, whether D-galactose induces bone loss is not being studied. The aim of current study was to examine the effects of D-galactose on rats bone tissue in order to duplicate D-galactose-induced bone loss as a senescent-related osteoporosis model. Fifty Sprague-Dawley rats at age of 3 months with half female and half male were divided into control, ovariectomized, orchietomized or treated with D-galactose at doses of 50, 100 and 200mg/kg/d for two months respectively. Double in vivo fluorochrome labeling was given. The undecalcified longitudinal proximal tibial metaphyseal sections were processed for bone histomorphometric analysis. The testicles and the ovaries were processed for observation under microscope. As the results, D-galactose at three doses decreased bone mass (% Tb.Ar) by 53.5%, 53.6% and 64.4% respectively in male rats (parallel to ORX which decreased by 62.4%), decreased bone formation parameter (BFR/BV) by 24.1%, 65.5% and 89.1% respectively in male rats (parallel to ORX which had no changes on BFR/BV). However, D-galactose has no effects on female rats of bone tissue while OVX rats had a marked decrease of bone mass by 75% with increase of bone formation indices. Comparing with control rats, the interstitial cells of testicles were sparse and the convoluted seminiferous tubules were vacuous in D-galactose treated male rats but no changes in ovaries of D-galactose treated female rats. Our study suggested that D-galactose can induced cancellous bone loss and inhibit bone formation rate but have no effects on female rats probably due to the different response of D-galactose to gonad gland, this indicate D-galactose-induced bone loss can be an model of man osteoporosis. The mechanism of D-galactose on bone tissue in different gender rats need further investigating.

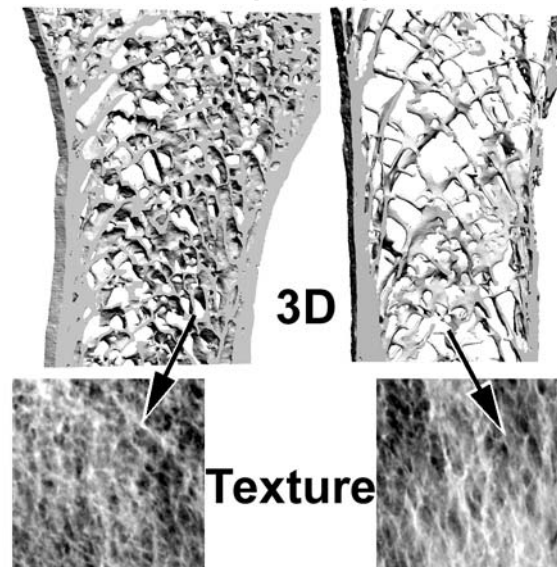
Disclosures: **L. Cui**, None.

SU366

Texture Analysis of X-Ray Radiographs Is Correlated with 3D Descriptors of Bone Microcomputed Tomography. P. Guggenbuhl¹, E. Bodic^{*2}, L. Hamel^{*2}, M. F. Basle^{*1}, D. Chappard¹. ¹INSERM, EMI 0335, ANGERS, France, ²Faculté Chirurgie Dentaire, Nantes, France.

Alteration of bone trabecular architecture is an independent predictor of fracture risk in osteoporosis. Until now, microarchitecture can only be measured on a bone biopsy, thus limiting microarchitecture analysis in routine clinical practice for osteoporosis. Texture analysis on X-ray images has been shown a suitable means to assess 2D microarchitecture. But, little is known on the relationships between 3D architecture and texture analysis. In this study, the anterosuperior part of the iliac bone was removed from twenty-four cadavers. Large samples were prepared and comprised the crest and a stripe of bone approximately 3cm in width and 5cm in height. These large specimens were used in order to preserve bone architecture; they also corresponded to the location used by histomorphometrists for the diagnosis of metabolic bone diseases on iliac crest biopsies. Bone samples were examined with a microcomputed tomograph for 3D microarchitecture (BV/TV, C.BV/C.TV, Tb.Pf, SMI, Tb.Th, Tb.N, Tb.Sp). (cf figure with 3D reconstructions

and corresponding textures). Texture analysis was done by several methods (skeletonization, run lengths, fractal techniques) from X-ray projection images. Significant correlations were found between bone mass parameters (BV/TV and C.BV/C.TV - which takes into account both cortical and trabecular bone) and other histomorphometric parameters (e.g., [BV/TV] /Tb.Pf, $r = -0.875$; /SMI, $r = -0.849$; /Tb.Th, $r = 0.6$; /Tb.N, $r = 0.824$; /Tb.Sp, $r = -0.856$) but no correlation was found with texture parameters. However, when specific descriptors of trabecular bone microarchitecture were used, several relationships with texture parameters were found ([Tb.N] /BOUND, $r = 0.628$; /VGLN, $r = 0.596$; / Fractal D, $r = 0.569$). When multiple correlations were used, the correlation coefficients were markedly improved with trabecular characteristics. X-ray texture analysis seemed to be a suitable approach for 2D bone microarchitecture assessment. Furthermore, there is a good correlation between texture analysis of X-ray radiographs and 3D bone microarchitecture assessed by microcomputed tomography.



Disclosures: **P. Guggenbuhl**, None.

SU367

Bone Turnover, Bone Mass, Size and Volumetric Density Differences between Young Adult and Senile Osteoporosis. D. Merlotti, L. Gennari, G. Martini, N. Dal Canto^{*}, V. De Paola, R. Nuti. Internal Medicine, Endocrine-Metabolic Sciences and Biochemistry, University of Siena, SIENA, Italy.

Although osteoporosis predominantly affects older postmenopausal women, low bone mineral density also occurs in men and younger women. While most young people with osteoporosis have an identifiable cause, others have an idiopathic form for which no etiology can be found. In order to better characterize the structural and metabolic basis of reduced bone mass in young adults, we measured bone turnover markers (bone alkaline phosphatase, BALP and serum crosslaps, CTX), areal bone mineral density (aBMD), bone volume and volumetric BMD (vBMD) by dual-energy X-ray absorptiometry in 70 adult males (32-49 yrs) and 30 premenopausal females with low bone mass (< 2 SD), in 100 age-matched healthy subjects, in 150 elderly men (59-85 yrs) and 150 postmenopausal women (55-70 yrs). Body weight was reduced in young adult and elderly osteoporotic subjects with respect to controls. Average BALP was within the normal reference range both in young and elderly males and was significantly decreased in young adult than in elderly osteoporotic men. CTX levels appeared significantly lower in young adult than in elderly osteoporotic men, while did not significantly differ from those in healthy age-matched controls. Similarly, young women with osteoporosis had reduced BALP and CTX levels than healthy and osteoporotic postmenopausal women. No major differences were observed in parathyroid hormone and 25 hydroxy-vitamin D even though a trend for decreased levels was observed in elderly subjects. Smaller aBMD and vBMD were observed between young adult osteoporotic males and age-matched controls as well as between elderly osteoporotic and non osteoporotic men, at both femoral and lumbar sites. When we considered bone size, only the bone volume at the spine was significantly reduced in young osteoporotics compared with controls. Moreover, bone volume at the spine was also significantly reduced when young osteoporotic males were compared to healthy elderly subjects. A similar but more pronounced deficit in vBMD and bone size was observed in premenopausal women with osteoporosis as compared to age-matched controls as well as in postmenopausal osteoporotic women compared to healthy osteoporotic women. Even though the pathogenesis of low bone mass in young men and women may be heterogeneous, these results suggest that a low bone turnover with a possible osteoblast dysfunction may be responsible of these forms of osteoporosis in both sexes. Moreover, the reported differences in bone size between elderly osteoporotic and non osteoporotic subjects may be accentuated in young adult idiopathic osteoporosis as compared to normal controls.

Disclosures: **D. Merlotti**, None.

SU368

Bone Formation in the Periosteal, Endocortical, and Trabecular Envelopes of the Ilium of Adult Women. S. Bare^{*1}, S. Recker^{*1}, R. Recker¹, D. Kimmel². ¹Creighton University, Omaha, NE, USA, ²Merck & Co., West Point, PA, USA.

Transilial biopsy (TIBx) specimens contain all bone envelopes (periosteal [Ps], Haversian, endocortical [Ec], and trabecular [Tb]); the Tb envelope is most frequently studied. Consistently orienting Haversian systems in TIBx sections is difficult. Though current therapeutic agents influence mainly the Tb and Ec envelopes, future ones may work elsewhere. Our purpose is to compare bone formation activity in the TIBx Ps and Ec envelopes to that of the Tb envelope. One unstained section from each of two levels of TIBx's from 55 untreated post-menopausal osteoporotic (PMO) women (16yrs post-menopause), 79 similar PMO alendronate (ALN)-treated (1-2yrs) women, and 42 women at one yr after last menses, were examined for total surface (BS), single (1XL), and double (2XL)-fluorochrome labeled surface, and mineral apposition rate (MAR) in Ps, Ec, and Tb envelopes. 2XL/BS was calculated omitted those individuals without 2XL. Differences were tested by Kruskal-Wallis ANOVA with Student Neuman-Keuls post-hoc analysis.

Ps, Ec, and Tb Envelopes of 55 Untreated PMO Women					
Env	Surface (mm)	% with 2XL	% with any Label	2X/BS (%)	MAR (µm/d)
Ps	29±10	38	70	1.59±1.36	0.88±0.33 (21)
Ec	31±10	90*	100	6.07±4.77*	0.73±0.19 (50)
Tb	79±26	98*	100	2.26±1.41	0.54±0.12 (54)
Ps Envelope (176 Post-Menopausal Women)					
-	29±9	33	73	1.43±1.26	0.79±0.35 (58)

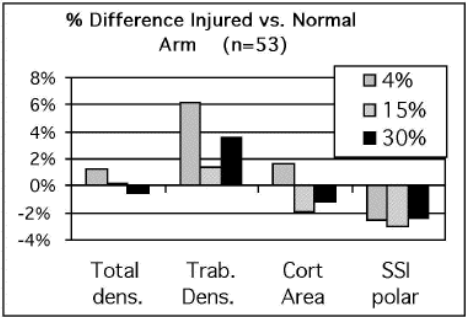
The Tb envelope of a TIBx of untreated PMO women presents ~3X as much surface as the Ps or Ec envelopes. 90-98% of subjects had 2XL at the Ec and Tb envelopes; only ~40% had 2XL at the Ps envelope. Ec 2XL/BS was 2-3X higher than in the Tb and Ps envelopes. While ALN subjects had less 2XL at the Tb and Ec envelopes than untreated subjects (data not shown), Ps labeling was not ALN sensitive (Bare et al., 2005 [two ASBMR Abstracts]). Thus, the frequency of Ps 2XL was confirmed in a group of 176 post-menopausal women. **Conclusion:** The TIBx Ps envelope of PMO women forms bone at a lower rate than do the Tb and Ec envelopes. Considering that only ~35% of subjects had Ps 2XL when 30mm of surface was studied and 2X/BS was ~25% of that at the Ec envelope, Ps bone formation seems to be about 10X lower than at the Ec envelope. The T envelope also has three times lower 2X/BS than the Ec envelope. Since ~65% of TIBxs showed no Ps 2XL, about four-fold additional Ps surface should be examined to improve the accuracy of bone formation assessment at the iliac Ps envelope.

Disclosures: S. Bare, None.

SU369

Structural and Density Changes following Injury to the Forearm Seen by Quantitative CT. J. A. Spadaro^{*}, C. Button^{*}, A. Pennella^{*}, W. H. Short^{*}. Orthopedic Surgery, Upstate Medical University, Syracuse, NY, USA.

Loss of bone density in the radius following fracture or surgery has been reported, but it is not entirely clear what gives rise to it. Losses appear rapidly (average 8-10% or more distally 2-4 months after injury). The aim was to characterize the early post-injury structural/quality changes in the bone that may not be reflected in conventional densitometry. We used baseline data from an NIH funded trial of electromagnetic treatment of post-injury osteopenia (the 'e-Bone study'). The distal radius was studied in 53 consecutive subjects (34 females, 19 males, median age 42, range 18-78) (Upstate IRBPHS #4812). Peripheral quantitative computed tomography (pQCT) scans (Norland-Stratec XCT-2000) were made about 6 weeks after either a distal radius fracture or carpal surgery, requiring cast or external fixation. Bilateral axial scans were made at the 4%, 15% and 30% sites of the forearm from the distal end and determined 4 key parameters: the average total density of the slice, the trabecular density, the cross-sectional area of the cortex and the structural strength index (SSI) (~polar moment of inertia). Data was expressed as the % difference from the contralateral (uninjured) arm. Results for the entire



group show the total density in the sections was unchanged on average, trabecular density was increased in the 4 % site (t-test, P<0.1)(Fig. 1). Cortical area was decreased at the 15% site and the structural strength index was decreased at all three test sites (P<0.05, 0.1). Changes were larger when subgroups were considered. The fracture subgroup had 12% increase in trabecular density at the 4% region and 2-5% decrease in cortical area and SSI at the more proximal sites. The surgery subgroup had only a 3% decrease in cortical area at the 4% site. Those whose non-dominant arm was injured had significant reductions (3-8%) in cortical area and SSI. We conclude that the pattern of these early changes following injury suggests an increase in trabecular bone associated with the distal radius fracture and decreases in cortical cross-sectional area and strength in all cases. These findings are consistent with endosteal resorption as an important part of the response to injury/disuse. pQCT provides an excellent insight into these changes.

Disclosures: J.A. Spadaro, None.

SU370

Characterization of the Age-Dependent Osteoporotic Phenotype in Sca-1/Ly6A Null Mice. C. Holmes^{*1}, T. S. Khan^{*1}, C. Owen^{*2}, M. D. Grynpas², W. L. Stanford^{*1}. ¹Institute of Biomaterials and Biomedical Engineering, University of Toronto, Toronto, ON, Canada, ²Samuel Lunenfeld Research Institute, Toronto, ON, Canada.

Stem cell antigen-1 (Sca-1/Ly6A) is an 18-kDa glycosyl phosphatidylinositol-anchored cell surface protein expressed by a variety of stem cell populations, including those of the blood, muscle, liver, and mammary epithelium. Previous studies involving Sca-1 knockout (KO) mice implicate that Sca-1 is required directly for the self-renewal of mesenchymal progenitor cells and indirectly for the regulation of osteoclast differentiation. Sca-1 KO mice undergo normal bone development but by 12 months of age exhibit dramatically decreased bone mass and bone brittleness characteristic of age-dependent osteoporosis. The objective of this study was to further characterize the cellular, mechanical, and microarchitectural bone phenotype of Sca-1 KO mice at earlier time points to increase our understanding of its initiation and progression. To achieve this, we carried out both in vitro and in vivo analyses of the bone phenotype of 13 nine-month old Sca-1 KO mice and compared it to that of 16 Sca-1 wild type (WT) age matched controls. Colony-forming unit fibroblast assays revealed that KO mice exhibit an 81.8 % reduction (p<0.01) in the number of total mesenchymal progenitors compared with WT controls; a decrease that was mirrored by a similar dramatic reduction in colony-forming unit osteoblast assays. Whole body bone mineral density (BMD) analysis indicated that the KO mice displayed a 5.7% (p<0.01) reduction in BMD compared to WT controls. This was paralleled by 4.0% (p<0.03) and 4.4% (p<0.02) decreases in femoral and spinal BMD, respectively. This suggests that the reduction in total mesenchymal progenitor cells had a negative impact on the BMD of both cortical and trabecular bones in Sca-1 KO mice. Although femoral neck fracture and three point bending tests revealed no statistically significant differences in stiffness between WT and KO femurs, Sca-1 KO femurs required a lower ultimate load (p<0.03), as well as failure load (p<0.03) in three point bending tests, and less energy for failure (p<0.01) than the WT controls in femoral neck fracture tests. These results reinforce our previous findings in 12-month old Sca-1 KO mice, indicating that Sca-1 plays a role in maintaining self-renewal of mesenchymal progenitor cells, which in turn are important in maintaining normal bone mass and mechanical properties with age in mice.

Disclosures: T.S. Khan, None.

SU371

Devastation of Skeletal Quality by Neuromuscular Degeneration. B. J. Lee^{*1}, S. Judex¹, G. A. Cox^{*2}, C. Rubin¹. ¹Biomedical Engineering, SUNY - Stony Brook, Stony Brook, NY, USA, ²The Jackson Laboratory, Bar Harbor, ME, USA.

A spontaneous autosomal recessive mutation in C57BL/6J mice, causing the degeneration of neuronal innervation of skeletal muscle fibers (Neuron, 1998), was used to study the skeletal consequences of neuromuscular degenerative disease (*nmd*). Comparing *nmd* and wild-type control (WT) at skeletal maturity (15-19wks of age, n=6 in each group), this study used microCT to determine how the reduction in locomotory activity caused by motor neuron dysfunction would influence cortical bone area (mm²), trabecular bone volume fraction (%), and trabecular connectivity density (1/mm³). These parameters of bone quality were evaluated at the diaphysis of the humerus and femur (cortical bone), and the metaphysis of the distal femur (trabecular bone). *nmd* mice were markedly less mobile and weighed 43% less (p<0.001) as compared to WT. This difference was paralleled by *nmd* mice having 41% less bone area (p=0.001) in the diaphyseal regions of the humerus, and 37% less bone area (p=0.001) in the diaphyseal regions of the femur. In the trabeculae of the metaphysis (table below), the *nmd* mice had 95% less bone area (p=0.002), 99% less connective density (p=0.003), and 91% less bone volume fraction (p=0.003) than WT.

comparison of bone quality parameters in trabecular bone				
	BA (mm ²)	BV/TV	Conn. D. (1/mm ³)	Body Mass (g)
WT	0.18	6%	148.5	25.6
<i>nmd</i>	0.009	0.5%	1.30	14.5
% difference	95%	91%	99%	43%
p value	0.002	0.002	0.003	<0.001

Neuromuscular dysfunction, as modeled by the *nmd* mice, occurs concurrently with a significant reduction in an array of parameters central to bone quality, with the largest consequences observed in the trabecular envelope. Of course, it is not yet clear if this reduction is caused by a systemic metabolic retardation of growth, as evidenced by the reduced body weight, elevated resorptive activity in bone tissue as permitted by diminished motor function, or some combination thereof. Nevertheless, these data imply that any pharmacologic or physical means of restoring bone quality, perhaps as an anabolic surrogate for functional activity, will result in a marked reduction in the risk of atraumatic fracture. *Work kindly supported by NIAAMS.*

Disclosures: B.J. Lee, None.

SU372

Ethnic Differences in Novel Markers of Bone Metabolism and Fracture Risk: The First Nations Bone Health Study. W. D. Leslie¹, J. Krahn^{*1}, C. N. Bernstein^{*1}, M. Sargent^{*1}, H. A. Weiler², C. J. Metge³, M. Doupe^{*1}, E. A. Salamon¹, P. Wood Steiman^{*4}. ¹Faculty of Medicine, University of Manitoba, Winnipeg, MB, Canada, ²Human Nutritional Sciences, University of Manitoba, Winnipeg, MB, Canada, ³Faculty of Pharmacy, University of Manitoba, Winnipeg, MB, Canada, ⁴Assembly of Manitoba Chiefs, Winnipeg, MB, Canada.

Canadian Aboriginal (First Nations) women are at increased fracture risk compared with the general population (CMAJ 2004;171:869-73). The First Nations Bone Health Study (FNBHS) reported site-specific reductions in BMD among a random age-stratified (25-39, 40-59 and 60-75) sample of Aboriginal women compared with age-matched White women, lower serum 25OHD values and higher PTH (JBMR 2004;19(Suppl 1):S288 and S423) but these were insufficient to account for the large difference in fracture rates. Therefore, we looked at novel markers of bone metabolism and fracture risk. Morning fasting serum samples were assessed for serum OPG, homocysteine, vitamin B12 (cobalamin) and folate. Mean serum OPG was significantly greater in Aboriginals, the group known to have higher fracture risk and lower BMD. This may imply a counter-regulatory response as has been described with other conditions that adversely affect bone metabolism (such as aging and inflammatory bowel disease). Although mean serum homocysteine was similar, there were significant reductions in both B12 and folate. OPG correlated negatively with BMD at 4 of 5 sites (heel, spine, hip, total body; P<0.05, r=-0.11 to -0.14) while homocysteine correlated negatively with BMD at the heel only (P=0.014, r=-0.12). This study demonstrates that novel factors involved in bone metabolism may be important in explaining ethnic differences in fracture rates independent of their effects on BMD.

	Biochemical analyses Aboriginal (N=250)	White (N=177)	P
OPG (pg/mL)	1.29 ± 0.63	1.03 ± 0.71	0.00014
Homocysteine (umol/L)	8.7 ± 3.1	8.9 ± 3.0	>0.2
B12 (pmol/L)	291 ± 160	339 ± 177	0.00350
Folate (nmol/L)	28.7 ± 8.2	32.2 ± 9.1	0.00006

Disclosures: **W.D. Leslie**, None.

SU373

Blood Homocysteine Is Correlated with Bone Mass and Bone Turnover Rate, not with Bone Size in Postmenopausal Women. B. Kim¹, B. Ahn^{*1}, J. Son^{*2}, H. Choi^{*3}, K. Kim^{*1}, S. Kim^{*4}, D. Lee⁵. ¹Family Practice and Community Health, Ajou School of Medicine, Suwon, Republic of Korea, ²Family Medicine, Eulji University School of Medicine, Suwon, Republic of Korea, ³Family Medicine, Eulji University School of Medicine, Daejeon, Republic of Korea, ⁴Family medicine, Sungkyunkwan University School of Medicine, Suwon, Republic of Korea, ⁵Family Medicine, Sungkyungkwan University School of Medicine, Suwon, Republic of Korea.

Hyperhomocysteinemia is related to fractures due to osteoporosis. We assessed the relation between blood homocystein and bone mass, size, bone turnover rate. This study included 2,670 postmenopausal women who underwent periodic health examination in ajou university health promotion center, from January 2002 to December 2003. Serum homocysteine, bone turnover marker and bone mineral density were measured. The age,osteocalcin,25-vit D,total lumbar BMD,total lumbar T- score,very low lumbar BMD,very low lombar T-score,femur neck BMD,femur neck T-score,femur trochanteric BMD and femur trochanteric T-score showed a significant correlation with the serum total homocysteine. However, after adjusting for age, the only osteocalcin is significantly correlated with the serum total homocysteine, At 3rd lumbar vertebra, the BMC,volumetric BMD and areal BMD showed a significant correlation with the serum total homocysteine but the bony size and the volume were not significant. Even after adjusting for age, the 3rd lumbar BMD is significantly correlated with the serum total homocysteine. Our study show that serum total homocysteine is correlated small but significantly with bone mass, bone turnover rate but not with bone size.

Disclosures: **B. Kim**, None.

SU374

Circulating Levels of OPG, Colia1 Polymorphism and Bone Mass in Healthy Postmenopausal Women. P. Mezquita-Raya^{*1}, D. Fernandez-Garcia^{*2}, M. de la Higuera^{*2}, G. Alonso^{*2}, J. M. Quesada³, G. Dorado^{*3}, E. Luque-Recio^{*3}, M. E. Ruiz Requena^{*4}, M. Muñoz-Torres². ¹Endocrinology, Torrecardenas Hospital, Almeria, Spain, ²Endocrinology, San Cecilio University Hospital, Granada, Spain, ³Endocrinology, Reina Sofia University Hospital, Cordoba, Spain, ⁴Biochemistry Division, San Cecilio University Hospital, Granada, Spain.

Background: Twin and family studies have suggested that BMD has a strong genetic component and is under polygenic control. Several candidate genes have generated considerable attention, although conflicting results have been published. Also, previous studies have revealed the critical role of the RANKL-OPG system on the regulation of bone resorption. To our knowledge no previous studies have investigated the links among genetic factors, serum OPG levels and bone mass in a population of postmenopausal women. **Aims:** To examine the relationship among circulating levels of OPG, COLIA1, VDR and ER genotypes and bone mineral density (BMD) in healthy postmenopausal women. **Subjects**

and Methods: We determined anthropometric parameters, serum OPG levels, the COLIA1 (MslI), VDR (BsmI, TaqI, FokI) and ER (Xba, Pvu) polymorphisms by PCR and BMD by dual X-ray absorptiometry in 134 ambulatory postmenopausal spanish women (61±7 yrs). **Results:** There were no significant differences in serum OPG levels or BMD according to VDR and ER genotypes. There was a strong overrepresentation of the "s" allele in osteoporotic women (p=0.003) and a significant association between serum OPG levels and COLIA1 polymorphism (SS[N=64]: 137±54 vs. Ss/ss[n=70]: 119±36; p=0.028). However, the association of serum OPG levels (OR: 3.2; CI95%: 1.3-7.6) and COLIA1 polymorphism (OR:2.8; CI95%: 1.2-6.6) with the osteoporotic densitometric criteria (T-score ≤-2.5) were significatively independent in the logistic regression model. **Conclusion:** these preliminary results show a significant relationship between serum OPG levels and COLIA1 polymorphism. However, the results of the logistic regression model suggest that these factors influence bone mass in an independent way.

Disclosures: **P. Mezquita-Raya**, None.

SU375

Reduced Bone Mineral Density in Male Patients with Untreated Graves' Disease. T. Majima^{*1}, Y. Komatsu², K. Doi^{*1}, M. Shigemoto^{*1}, C. Takagi^{*1}, K. Nakao^{*2}. ¹Endocrinology and Metabolism, Rakuwakai Otowa Hospital, Kyoto, Japan, ²Medicine and Clinical Science, Kyoto University Graduate School of Medicine, Kyoto, Japan.

Introduction Although it has been established that hyperthyroidism leads to a reduction in bone mineral density (BMD) with accelerated bone turnover promoting bone resorption in female patients, there is a dearth of data for male patients with hyperthyroidism. The purpose of this study was to evaluate bone mineral density and bone metabolism in male patients with Graves' disease. **Subjects and Methods** This study included 56 Japanese male patients with newly diagnosed Graves' disease (mean age 43.6±10.0 years, mean BMI 22.9±2.1 kg/m²), and 34 normal Japanese male control subjects of similar age (mean age 43.8±10.5 years) and body mass index (mean BMI 22.9±2.0 kg/m²). We used dual energy X-ray absorptiometry to measure BMD at sites with different cortical/cancellous bone ratios (lumbar spine (LS), femoral neck (FN), and distal radius (DR). **Results** In patients with Graves' disease, the levels of thyroid hormones were elevated (mean free triiodothyronine (FT3) 11.71±4.0 pg/ml, mean free thyroxine (FT4) 4.36±1.4 ng/dl), while thyroid-stimulating hormone (TSH) levels were suppressed below sensitivity. Urinary N-terminal telopeptide of type I collagen normalized by creatinine (U.NTx) and bone-specific alkaline phosphatase (BAP) levels of the GD patients were significantly higher than those of controls (p<0.0001 for both). At the LS and the DR, BMD and T scores were significantly lower for patients than for controls. At the FN, on the other hand, the same values were relatively, but not significantly, lower in patients than in controls. However, Z scores at all three sites were significantly lower for patients than for controls. The Z score at the DR was significantly lower than those at the LS and FN (p<0.0001 for both), whereas no marked difference in Z score was found between the LS and the FN. In addition, the Z-score at the DR, but not at the LS or the FN, correlated negatively with age, FT4, TSH receptor antibodies (TRAb), thyroid stimulating antibody (TSAb) and U.NTx. **Conclusion** These results indicate high prevalence of cortical bone loss in male patients with Graves' disease, especially in elderly patients. We conclude that BMD measurement is crucial in all Graves' patients regardless of their gender, and that the radial BMD as well as those in the LS and FN should be monitored to effectively prevent bone loss and subsequent fracture.

Disclosures: **T. Majima**, None.

SU376

Factors of Importance for the Age Related Increase in Fragility Fractures of the Hip. H. Christoffersen, S. N. Holmegaard^{*}. Orthopaedic, Hospital Nord / Thisted, Thisted, Denmark.

Age is a BMD-independent risk factor for fragility fracture (FF). In order to evaluate the influence of co morbidity we analyzed laboratory investigations for secondary osteoporosis (OPO) in 302 patients, 221 females (F) and 81 males (M), consecutively admitted due to FF of the hip (FFH). Mean age for F was 80.9 years, for M 77.6 years. One or more previous FF was present in 26% of F and in 29% of M. Laboratory tests comprised Haemoglobin (Hgb), Leucocytes (Leu), ESR, Sodium (Na), potassium (K), Calcium (Ca), phosphate (P), Creatinine (Cr), Albumin (Alb), Alkaline phosphatase (AP) and thyrotrophin (TSH). Considering the age and presence of fracture, limits for abnormality were set at Hgb < 7 mmol/L; Leu > 18 or < 3 /10⁹/L; ESR > 60 mm/h; Cr > 150 mmol/L and AP > 10% above the upper normal reference value. Normal reference values were used for the rest. The table shows number of patients with abnormal values expressed as percentage of the total number of patients investigated.

	Hgb	Leu	ESR	Na	K	Ca	P	Cr	Alb	AP	TSH
F	29,4	4,3	4,9	2,3	2,7	42,6	16,4	4,1	64,3	9,6	14,7
M	24,7	0,0	7,7	4,9	3,7	59,6	11,4	8,6	73,1	18,8	6,4

Most frequently encountered abnormal results were low Hgb, Ca and Alb, but other abnormalities were also found with high frequency. A significant correlation was observed between Alb and Hgb (F: p < 0.01, M: p < 0.05), Alb and Ca (p < 0.01) and Ca and Hgb (p = 0.011). Except for Hgb and TSH, M generally had more abnormal results than F. Surprisingly mean age for M was less than for F, though this was not statistically significant. Previously unrecognized elevation of ESR was rarely encountered. Since ESR seldom is of informative value and more time consuming than other laboratory tests it can be omitted in the screening procedure. Our results suggest that the age related increase in FFH is as much a sign of underlying disease and poor nutrition as of idiopathic OPO. This is supported by the observation that the mean age of males unexpectedly was lower than for females.

Disclosures: **H. Christoffersen**, None.

SU377

Chronic Mild Stress Induces Depression and Bone Loss in Mice: Pharmacological Attenuation by Anti-Depressant Therapy and Possible Involvement of the Sympathetic Nervous System and Hypothalamic-Pituitary-Adrenal Axis. A. Bajayo^{*1}, I. Goshen^{*2}, S. Feldman^{*3}, T. Kreisel^{*2}, V. Csernus^{*4}, J. Weidenfeld^{*5}, E. Shohami^{*6}, R. Yirmiya^{*2}, L. Bab¹. ¹Bone Laboratory, The Hebrew University of Jerusalem, Jerusalem, Israel, ²Department of Psychology, The Hebrew University of Jerusalem, Jerusalem, Israel, ³Bone Laboratory and Department of Pharmacology, The Hebrew University of Jerusalem, Jerusalem, Israel, ⁴Department of Anatomy, University Medical School Pécs, Jerusalem, Hungary, ⁵Department of Neurology, Hadassah University Hospital, Jerusalem, Israel, ⁶Department of Pharmacology, The Hebrew University of Jerusalem, Jerusalem, Israel.

In humans, osteoporosis is often accompanied by major depression. However, it is unclear whether bone loss and the associated morbidity and incapacitation induces depression or vice versa. To determine the cause-effect relationship in this case, we examined the bone status in mice subjected for five weeks to chronic mild stress (CMS), a model for depression in rodents. CMS-induced depression was confirmed by reduced sucrose consumption, an established indicator of anhedonia, and reduced social exploration. The CMS mice exhibited normal motility. Micro-computed tomographic measurements of femora and lumbar vertebrae showed a marked bone loss in CMS mice, reflected by a significant decrease in overall bone mass, in particular trabecular bone volume density (30% loss). A further histomorphometric analysis showed CMS-induced decreases in osteoblast number and bone formation rate and increased osteoclast number. While serum testosterone levels were similar in the CMS and control mice, serum corticosterone was almost twice higher under CMS. The anti-depressant drug imipramine, administered in the drinking water throughout the experimental period, attenuated both the depressive symptoms and bone loss. CMS mice responding to imipramine by increased sucrose preference had normal bone mass as compared to non-responders that displayed bone loss. The CMS-induced bone loss was blocked by propranolol, a β -adrenergic receptor antagonist. These results demonstrate that CMS induces bone loss in mice possibly via activation of the sympathetic nervous system and hypothalamic-pituitary-adrenal axis, and are consistent with a causal relationship between depression and bone loss in human osteoporosis.

Disclosures: **A. Bajayo**, None.

SU378

The Effects of Recombinant TSH on Bone Turnover Markers and Serum Osteoprotegerin and RANKL Levels. G. Martini¹, F. Pacini^{*2}, M. S. Campagna^{*1}, B. Franci^{*1}, A. Avanzati^{*1}, B. Lucani^{*1}, S. Salvadori^{*1}, L. Gennari¹, R. Valenti¹, V. De Paola¹, T. Pilli², R. Nuti¹. ¹Department of Internal Medicine, University of Siena, Siena, Italy, ²Endocrine Unit, University of Siena, Siena, Italy.

The only established biologic function of thyroid stimulating hormone (TSH) is to regulate the synthesis and secretion of thyroid hormone from thyroid follicle cells. Recently it has been found that TSH-receptors are present both in osteoclast and osteoblast and that TSH can modulate bone remodeling independently of thyroid hormones (T3 and T4). In mice TSH inhibits both osteoclast and osteoblast activity, while rhTSH administration in postmenopausal thyroidectomized women causes a rise in bone specific alkaline phosphatase (BSAP) and a decrease of C-telopeptide of Type-I collagen (CTX) without any change in Osteoprotegerin (OPG) serum levels. Moreover older women with low levels of TSH showed an high risk of vertebral and hip fractures. The aim of this study was to evaluate: 1) the role of TSH on bone remodeling both in men than women 2) the role of serum levels of Osteoprotegerin and RANKL regarding the effect of TSH on bone turnover. We studied 30 thyroidectomized patients affected by thyroid carcinoma on L-thyroxine therapy: 10 premenopausal women (aged 32.9 ± 7.6), 10 postmenopausal women (aged 67.2 ± 7.9) and 10 men (aged 49.5 ± 13.9). A blood sample was drawn from each patient at baseline and three and five days after the rhTSH administration (0.9 mg i.m. once daily for the first two days). Sera were assayed for thyroid function (TSH, fT3, fT4) and bone turnover: BSAP, osteocalcin (BGP), N-terminal propeptide of type-I procollagen (PINP) as markers of bone formation, and CTX as marker of bone resorption. Serum OPG and RANKL were assessed using a sandwich enzyme immunoassay (Osteoprotegerin and RANKL, Biomedica, Austria); precision intra and interassay was lower than 10%. In basal conditions serum TSH values were in low-normal range or suppressed with no differences between the three groups. Postmenopausal patients had significantly higher basal values of OPG and BSAP compared to premenopausal women and men. After the rhTSH administration, serum TSH values peaked at day 3, but we were not able to find any significant changes on bone turnover markers in all groups. Serum RANKL levels significantly increased after three days in postmenopausal patients and men returning to baseline values at day 5, while serum OPG levels did not change significantly. These preliminary data showed that TSH has not effect on bone markers; on the other hand the increase of RANKL could suggest an osteoblast activation which only later can lead to bone turnover adjustment.

SU379

Serum Brain Natriuretic Peptide (BNP) Correlates with OPG Levels and Influences Bone Mass and Body Segment Lengths in Elderly Subjects. L. Gennari, R. Valenti, A. Palazzuoli^{*}, B. Franci^{*}, S. Campagna^{*}, D. Merlotti, F. Valleggi^{*}, G. Martini, A. Calabrò^{*}, V. De Paola, A. Avanzati^{*}, B. Lucani^{*}, R. Nuti. Internal Medicine, Endocrine-Metabolic Sciences and Biochemistry, University of Siena, SIENA, Italy.

Natriuretic peptide family consists of 3 structurally related endogenous ligands, atrial, brain, and C-type natriuretic peptides (ANP, BNP, and CNP), and is thought to be involved in a variety of homeostatic processes, including longitudinal bone growth. BNP is a 32-aminoacid peptide that is markedly elevated in patients with congestive heart failure and acute coronary syndrome (ACS). Even though cardiac myocytes constitute the major source of BNP, this peptide is synthesized and released by bone marrow stromal cells at physiologically relevant levels in vitro. Moreover, BNP receptors have been described in osteoblasts and BNP knockout mice exhibit cardiac fibrosis and bone malformations. The aim of this study was to characterise the relationship between plasma BNP, bone mineral density (BMD), and bone turnover markers in 150 subjects. BNP levels significantly increased with age ($r = 0.25$; $p < 0.01$) both in males and females and were higher in postmenopausal than premenopausal women. Of interest, BNP highly correlated with OPG levels ($r = 0.85$; $p < 0.0001$) and total body BMD ($r = 0.30$, $p < 0.001$). Negative correlations between BNP and urinary calcium or phosphate excretion were also observed in both sexes. When subjects were grouped according to BNP quartiles, we observed significantly higher OPG levels and RANKL/OPG ratio in subjects within the high BNP quartile. No major differences were observed concerning bone alkaline phosphatase and serum CTX. Moreover, in postmenopausal women with BNP in the highest quartile, the average total body BMD was from 4% to 14% higher than in men in the other BNP quartiles ($p < 0.005$). A similar but not significant trend was observed in men. Sitting height measured by a stadiometer was significantly related to BNP levels ($r = 0.24$; $p < 0.05$). Finally, to further explore the relationship between OPG and BNP we evaluated their levels in 50 patients affected with ACS. A similar positive correlation between OPG and BNP was observed ($r = 0.38$; $p < 0.01$) and both markers significantly correlated with left ventricular systolic function and the severity of disease. These data confirm experimental observations demonstrating a skeletal effect of BNP and further support the reported link between bone and cardiovascular disorders.

Disclosures: **L. Gennari**, None.

SU380

Uncoupled Bone Remodeling in Hyperhomocysteinemia-Restoration by Folate Therapy Possibly Involving OPG/RANKL/RANK-Related Mechanisms. T. Ueland^{*}, P. Aukrust^{*}, L. Ose^{*}, J. Bollerslev, M. Nenseter^{*}, K. Holven^{*}. Rikshospitalet University Hospital, Oslo, Norway.

Background Osteoporosis is characterized by a combination of low bone mass and deterioration of the microarchitecture of bone, resulting in increased risk of fractures in the elderly. Critical for the bone remodeling process is the balance between the newly discovered OPG and RANKL, which mediate the effects of many upstream regulators of bone metabolism. Recently, an association between osteoporotic fractures and increased serum levels of homocysteine was demonstrated. **Purpose** To further elucidate the association between homocysteine and bone metabolism we hypothesized that subjects with hyperhomocysteinemia may display disturbances in bone turn-over and the OPG/RANK/RANKL axis. **Methods** This was investigated by measuring biochemical markers of bone turn-over (osteocalcin and CTX-1) and OPG in serum from 35 patients with hyperhomocysteinemia (age 47 ± 13 ; 20 men) as well as mRNA expression of RANK and RANKL in peripheral blood mononuclear cells (PBMC). The effect of intervention with folate was also assessed. Age- and sex-matched controls were analyzed in parallel. **Results** At baseline no disturbances in bone turn-over were found although OPG was higher and osteocalcin lower in patients. A strong correlation was observed between baseline osteocalcin and CTX-1 in controls ($r = 0.59$, $p < 0.001$), but not patients ($r = 0.20$, $p = \text{NS}$). Quantitative RT-PCR revealed that subjects with hyperhomocysteinemia had higher mRNA expression of both RANK and RANKL in PBMC compared to controls ($p < 0.05$). Following folate treatment a significant increase was observed for osteocalcin, while circulating osteoprotegerin decreased ($p < 0.05$). Furthermore, osteocalcin and CTX-1 were correlated ($r = 0.43$, $p < 0.05$) and mRNA levels of RANK and RANKL decreased following folate treatment ($p < 0.05$). **Conclusion** Our data suggest that patients with hyperhomocysteinemia are characterized by normal bone turn-over quantitatively, however the lack of correlation between bone markers may suggest a uncoupling of the remodeling process. Furthermore, the enhanced RANK/RANKL mRNA expression in circulating immune cells may indicate an increased pro-resorptive potential in these patients. Importantly, both RANK and RANKL were modulated, and the coupling process was restored by folate treatment suggesting that intervention aimed at lowering the serum homocysteine level may be a treatment option for reducing fracture rates.

Disclosures: **T. Ueland**, None.

SU381

Bone Loss following Ovariectomy Is Maintained in Absence of Adrenergic Receptor $\beta 1$ and $\beta 2$ Signaling. D. D. Pierroz¹, M. L. Boussein², P. Muzzin³, R. Rizzoli¹, S. L. Ferrari¹. ¹Rehabilitation and Geriatrics, Div of Bone Diseases, University Hospital, Geneva, Switzerland, ²Beth Israel Deaconess Medical Center, Orthopedic Biomechanics Laboratory, Boston, MA, USA, ³Cellular Physiology and Metabolism, Geneva University Hospital, Geneva, Switzerland.

Whether β -blockers may increase bone mass in post-menopausal women remains controversial. Compared to wild-type (WT) mice, $\beta 2$ -adrenergic receptor ($\beta 2$ AR) KO mice were reported to have greater trabecular (Tb) bone volume (BV/TV) by 6 months of age, and also following ovariectomy (OVX) during growth. However, intact $\beta 2$ AR KO mice apparently do not have greater BV/TV before 6 months of age nor do they have higher cortical bone volume. Moreover, we previously reported vertebral Tb BV/TV is not increased in growing and adult $\beta 1\beta 2$ adrenergic receptor ($\beta 1\beta 2$ AR) KO mice, and that bone mass and cortical microarchitecture are actually lower in these mice compared to WT. Therefore it remains unclear whether inhibition of adrenergic-mediated signaling may prevent OVX-induced bone loss in adults. For this purpose, 15-week-old $\beta 1\beta 2$ AR KO and WT mice were OVX and pair-fed to a non-OVX group (Sham) (n=7-10/group). Bone mineral density (BMD) was evaluated 0, 4 and 8 wks after OVX by pDXA, trabecular (Tb) and cortical (Cort.) micro-architecture at the distal and mid-femur after 8 wks by μ CT, and biochemical markers of bone turnover (TRAP5b and osteocalcin, OC) at 0, 4 and 8 wks. Adult $\beta 1\beta 2$ AR KO mice were confirmed to have lower total body (TB, -16%), spine (Sp, -21%) and femur (Fem, -26%) BMD compared to WT (p<0.0001 for all by repeated measures ANOVA). Compared to Sham, OVX significantly decreased TB and Sp BMD (p<0.001) and to a lesser extent Fem BMD (p=0.02) after 4 and 8 weeks, with a non-significant trend for greater decrease in WT (TB BMD: WT -6.8%, KO =-2.7%, ns; Sp BMD: WT -12.3%, KO -6.7%; Fem BMD: WT -7.3%, KO -5.4%). OVX also significantly decreased Tb BV/TV and Tb number (p<0.003) and increased Tb separation (p<0.0001) without changes in Tb thickness. These effects were more prominent in KO than WT (Pinteraction=0.04-0.005). Moreover, OVX significantly decreased Cort bone volume in KO (p=0.046 vs Sham), but not in WT. Osteocalcin levels were significantly lower in KO than WT (p=0.013 by repeated measures ANOVA) and were transiently increased 4 wks after OVX in both genotypes (p<0.0001), whereas TRAP5b did not significantly differ between WT and KO. Altogether these data indicate that non-selective inhibition of $\beta 1\beta 2$ adrenergic receptor signaling may not prevent increased bone remodeling nor bone loss due to estrogen deficiency.

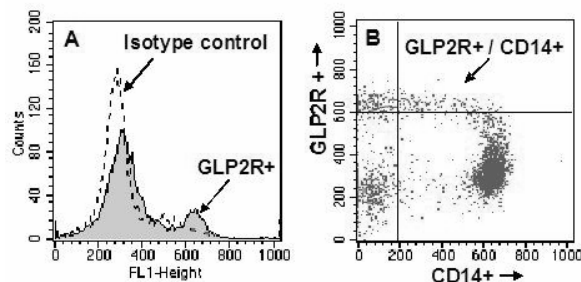
Disclosures: D.D. Pierroz, None.

SU382

Evidence that Gut Hormone Receptors Are Expressed on Circulating Peripheral Blood Cells. J. A. Clowes¹, J. Xiao², R. Eastell², S. Khosla¹.

¹Endocrine Research Unit, Mayo Clinic College of Medicine, Rochester, MN, USA, ²University of Sheffield, Sheffield, United Kingdom.

Recent studies have identified a nutrient regulated decrease in bone resorption. The mechanism for this effect is currently unclear. The intestinal hormone, glucagon-like polypeptide 2 (GLP2), has been shown to decrease bone resorption *in vivo*. In addition, leptin and ghrelin are expressed on peripheral blood mononuclear (PBMN) cells and are important hormones involved in regulating immune function and energy homeostasis. To investigate the potential mechanisms involved, we examined the expression of GLP2 receptors (GLP2R) on PBMN cells and determined the co-expression with osteoclast (OC) precursors using CD14, a monocyte marker, and RANK. Osteoblast (OB) precursors were characterized using an anti-osteocalcin (OCN) antibody. We also examined the co-expression of GLP2R with leptin receptor (ObR) and ghrelin receptor (GHS-R). We identified approximately 2% of PBMN cells in the circulation of adult humans that express GLP2R (A). The majority of the GLP2R+ cells co-expressed CD14 (B), but not RANK. A small but consistent percentage of GLP2R+ cells were OCN+, and none of these cells expressed T- or B-cell markers (CD-3 or -19, respectively). ObR was expressed on 1.8% of PBMN cells, but ObR did not co-localize with GLP2R+ cells, suggesting these are distinct populations. We were unable to identify GHS-R on PBMN cells. We conclude that GLP2R+cells circulate in small but significant numbers in the peripheral circulation. The co-expression of GLP2R with CD14, but not RANK, suggests potentially distinct subpopulations of OC precursors. The GLP2R+/OCN+ cells suggest a potential nutrient-induced role in differentiation of OB lineage cells. These findings need to be confirmed using bone marrow and functional studies are required. Clearly, however, these techniques represent a powerful new tool for investigating the effect of nutrition on the pathophysiology of osteoporosis and other metabolic bone diseases.



Disclosures: J.A. Clowes, None.

SU383

Immobilization Inhibits Sensory Neuropeptide Signaling in Bone at a Post-Junctional Level. W. S. Kingery¹, W. Yao¹, W. Zhao¹, X. Jia¹, T. Guo¹, T. Wei¹, D. Lindsey², C. Jacobs². ¹PM&R service (117), VAPAHCS, Palo Alto, CA, USA, ²RR&D Service, VAPAHCS, Palo Alto, CA, USA.

We recently observed that lesioning substance P (SP) and calcitonin gene-related peptide (CGRP) containing sensory neurons in rats caused a loss of trabecular bone integrity, an effect that we attributed to impaired sensory neurotransmitter signaling in bone. Immobilization also causes a loss of trabecular mass, structure, and strength, and in the current study we tested the hypothesis that these deleterious effects of immobilization could be due to impaired sensory neuropeptide signaling. The right hindlimbs of skeletally mature Sprague Dawley male rats were casted for 4 weeks. After 4 weeks immobilization there was no change in SP and CGRP gene expression in the sensory neurons innervating either hindlimb, but in trabecular bone there was a dramatic reduction in gene expression for the SP and CGRP receptors in the immobilized hindlimb, and to a lesser extent, the contralateral hindlimb. Electrically and SP evoked extravasation responses were impaired in both hindpaws, indicating a bilateral post-junctional inhibition of SP signaling after immobilization. Immunocytochemical and PCR studies demonstrated the presence of SP and CGRP receptors on osteoblasts and osteoclasts *in vitro*, while immunohistochemical studies in bone sections demonstrated SP and CGRP containing neurons innervating trabecular bone, evidence that sensory neuropeptides released in trabecular bone could have a direct effect on bone cells. Immobilization also caused a reduction in bone mineral density (by DXA scanning at 4 weeks after cast removal) in the of the ipsilateral, and to a lesser extent, contralateral distal femur. There was no effect on diaphyseal bone density in either limb. Microcomputed tomography (μ CT) in the distal femur demonstrated bilateral loss of trabecular bone volume and connectivity after unilateral immobilization. On biomechanical testing bone strength was also reduced bilaterally. These results support the hypothesis that the widespread osteoporotic effects of unilateral limb immobilization are a consequence of impaired neural-osseal signaling at the post-junctional level in the trabecular bone.

Disclosures: W.S. Kingery, None.

SU384

Chronic Inflammation-Induced Bone Loss and Coronary Artery Disease in Aged Rat Model. S. Y. Bu¹, M. R. Lerner², D. Morgan², K. Denson², M. S. Bronze³, S. A. Lightfoot⁴, D. J. Brackett², B. J. Smith².

¹Department of Nutritional Sciences, Oklahoma State University, Stillwater, OK, USA, ²Department of Surgery, University of Oklahoma Health Sciences Center, Oklahoma City, OK, USA, ³Department of Medicine, University of Oklahoma Health Sciences Center, Oklahoma City, OK, USA, ⁴Department of Pathology, University of Oklahoma Health Sciences Center, Oklahoma City, OK, USA.

Epidemiological evidence indicates a link exists between osteoporosis and cardiovascular disease. Inflammatory processes have been shown to play a pivotal role in both of these conditions. The purpose of this study is to assess the skeletal and cardiovascular changes in old animals in response to chronic inflammation. Eighteen-month old male Sprague Dawley rats (n=8/group) were implanted subcutaneously with time-release pellets designed to deliver either 33.3 μ g or 0 μ g of LPS/day for 90 days. Analysis of bone microarchitectural properties was performed using μ CT imaging on the proximal tibia and the tibia middiaphysis. Trichrome stains were used for histological examination of atherosclerotic fibrosis within the coronary arteries and arterioles. Although at the end of 90 days there was no significant change in bone volume (BV/TV) in the proximal tibial metaphysis, deleterious effects on trabecular number (TbN; p=0.0039) and separation (TbSp; p=0.0038) were observed in the LPS group. Trabecular thickness was also increased (p=0.0143) in response to chronic LPS. Furthermore, in the tibia midshaft, the LPS-treated group experienced an increase in cortical bone porosity (p=0.0377). In addition to these alterations in bone, trichrome staining indicated that chronic LPS administration increased fibrosis within the coronary arteries and arterioles. Additionally, infiltration of lymphocytes was observed which is consistent with coronary vascular disease. In conclusion, utilization of LPS time-release pellets appears to provide an *in vivo* model of chronic inflammation-induced bone loss and a potentially novel system to study concurrent development of osteopenia and vascular disease.

Disclosures: S.Y. Bu, None.

SU385

Urinary Calcium Loss, Independent of Calcium and Sodium Intake, Leads to Reduced Forearm Bone Mineral Density in Postmenopausal Women Over a 3-Year Period. J. Z. Ilich¹, R. A. Brownbill¹, T. V. West², A. H. N. Cillessen².

¹School of Allied Health, University of Connecticut, Storrs, CT, USA, ²Department of Psychology, University of Connecticut, Storrs, CT, USA.

It is well established in animals and humans of all age groups that dietary sodium (Na) decreases renal calcium (Ca) reabsorption leading to greater urinary Ca excretion. The positive association between dietary and urinary Ca in postmenopausal women has been established as well. However, the effect of increased urinary Ca excretion on BMD in this population is not clear. The purpose of this study was to evaluate effects of urinary Ca loss, controlling for dietary Ca and urinary Na, on forearm BMD in over 100 generally healthy, Caucasian, postmenopausal women enrolled in a 3-year longitudinal evaluation. After the baseline screening, half of the subjects were instructed to reduce their Na intake to about 1500 mg/day. The other half remained on a habitual Na intake of about 3000 mg/day. All subjects were given Ca (~600 mg/day) and vitamin D (~400 IU/day) supplements to bring

their total Ca intake at ~1300 mg/day. The average age at enrollment was 68.6±7.1y (mean±SD) and subjects' anthropometries, bone mass measurement, 24-h urine analyses and dietary and activity records were assessed every 6 months, totaling 7 evaluations. Data were analyzed using multilevel growth curve modeling to examine the changes over-time in bone variables of interest and their predictors. The following covariates were controlled for in all analyses: age, body mass index, total body fat and lean tissue, systolic blood pressure, physical activity, alcohol and caffeine consumption, as well as calcium, energy, protein, and vitamin D intake. Statistically significant linear and curvilinear effects were found for proximal radius and total forearm (ulna and radius at proximal and ultradistal sites) BMD. After controlling for all significant covariates, a main effect for age indicated that, as expected, it was negatively associated with BMD, $p < 0.001$. A main effect for Na indicated that higher urinary Na was associated with higher BMD, $p = 0.02$. However, this effect was modified by interactions with time and with urinary Ca. These interactions indicated that at all levels of Na intake, increased urinary calcium was associated with a curvilinear decrease in BMD over time, $p < 0.01$. Results also revealed a statistically significant lower forearm BMD in women with higher urinary Ca in both younger and older subjects, regardless of urinary Na. We conclude that higher urinary Ca, independent of Ca and Na intake, leads to loss of BMD over time in postmenopausal women. This effect might increase risk of developing osteoporosis in this population.

Disclosures: **J.Z. Ilich**, None.

SU386

The Rate that Family Physicians Prescribe Osteoporosis Medications to their Patients: Canadian Quality Circles (CQC) Project. **A. Hodsman¹, G. Ioannidis², A. Papaioannou², B. Kvern^{*3}, D. Johnstone^{*4}, C. Crowley⁴, J. D. Adachi².** ¹University of Western Ontario, London, ON, Canada, ²McMaster University, Hamilton, ON, Canada, ³University of Manitoba, Winnipeg, MB, Canada, ⁴Procter and Gamble Pharmaceuticals, Toronto, ON, Canada.

The CQC Pilot Project was designed to facilitate family physicians' adoption of the Osteoporosis Society of Canada (OSC) 2002 clinical practice guidelines for osteoporosis (OP) and included training, a first wave of data collection (wave 1), an educational intervention, a second wave of data collection, using different patients (wave 2), and strategy implementation. 52 physicians were recruited as members of 7 Quality Circles. Each wave of data collection consisted of recording OP risk factors, diagnosis and treatment information on separate patients via chart reviews and knowledge of their patients using the CQC data collection form. All patients were women 55 years of age and older and attended at least 2 visits to the member's practice in the previous 24 months. 1505 and 1359 patients comprised waves 1 and 2, respectively. Individual and QC data were collated in profiles and provided to the members. The QC's then met to discuss the profiles, identify and analyze problems, recommend solutions, and participate in an OP workshop. The primary focus of the workshop was to assess postmenopausal OP and risk factor identification. The second wave of data collection occurred after the intervention. Our analyses examined the rate that family physicians prescribe OP medications to their patients who had a prior osteoporotic fracture of the hip, wrist, or spine according to their BMD status. The OSC guidelines recommend treating those with a prior fracture in association with osteopenia (BMD T-score < -1.5). The medications examined were divided into two groups: Bisphosphonate Therapy (etidronate, alendronate, or risedronate) and Any Therapy (bisphosphonates, raloxifene, or hormone replacement therapy). A total of 139 patients from wave 1 and 129 from wave 2 had a prior fracture. The table shows the rate therapy was prescribe in these patients.

Table: Treatment Given For Patients with Fractures According to Their BMD Status (Wave 1, Wave 2)		
BMD T-score	Bisphosphonate Therapy	Any Therapy
Osteoporosis (≤ -2.5)	(87%, 88%)	(91%, 93%)
Osteopenia (≤ -1 to > -2.5)	(51%, 66%)	(56%, 72%)
Normal (> -1)	(9%, 29%)	(9%, 29%)
BMD not Tested	(27%, 30%)	(27%, 39%)

In conclusion, most patients with a fracture and BMD in the osteoporosis range were given therapy. More than a third of the patients did not receive therapy if they had a fracture and osteopenia. Future QC interventions should focus on the use of therapy in patients with fractures and osteopenia.

Disclosures: **A. Hodsman**, Merck 5; Lilly 5; Zelos Pharma 5; NPS 5.

SU387

The Evaluation of Process Factors Involved in Performing the Canadian Quality Circle (CQC) Pilot Project for the Care of Patients at Risk for Osteoporosis. **B. Kvern^{*1}, G. Ioannidis², A. Papaioannou², A. Hodsman³, D. Johnstone^{*4}, C. Crowley⁴, S. Glezer^{*5}, J. D. Adachi².** ¹University of Manitoba, Winnipeg, MB, Canada, ²McMaster University, Hamilton, ON, Canada, ³University of Western Ontario, London, ON, Canada, ⁴Procter and Gamble Pharmaceuticals, Toronto, ON, Canada, ⁵Sanofi-Aventis, Laval, PQ, Canada.

The CQC project was planned in two phases, the Pilot and the National study, to facilitate family physicians' adoption of the Osteoporosis Society of Canada 2002 clinical practice guidelines for osteoporosis. One specific aim of the Pilot was to examine the process factors involved to determine if a planned National study was feasible. Current analyses of the Pilot evaluated the success of the processes and physicians' self perceptions of the effectiveness of the study. During recruitment, 52 physicians from two provinces were recruited as members of 7 Quality Circles (QC). Members collected data at random on different patients during two waves (wave 1, wave 2) via chart reviews and the

completion of the CQC form that captures data on osteoporosis. Physicians were responsible to assess 30 patients during wave 1 and 30 during wave 2 using the CQC chart-audit form. Individual and QC data were collated in profiles and provided to the members. An individualized profile was only seen by the individual who collected the data from their own practice; data was compared to circle and the entire project sample. The QC then met to discuss the profiles and participate in an OP workshop. The primary focus of the workshop was to assess postmenopausal osteoporosis and risk factor identification. Wave 2 data collection occurred after the intervention and was used to provide feedback and to gauge overall progress. The evaluation process indicated that 96% of the circle members agreed that the format of the CQC meetings was conducive to learning, 98% agreed that the meetings permitted them to compare their profiles to their peers, and 98% felt that the information they learned was practical and could be immediately implemented in their practice. A total of 98% of participating physicians felt that the CQC initiative had either "some" or a "great deal" of influence on the manner in which they provided care to patients with or at a high risk of developing osteoporosis. In addition, 45% and 53% of physician respondents felt that their patients had benefited "a little" or "most definitely" from their involvement in the research, respectively. In conclusion, the use of QC is a feasible stepwise approach to education that provides the opportunity for physicians to systematically analyze patient-related problems and develop solutions to these problems.

Disclosures: **B. Kvern**, None.

SU388

Persistent Bisphosphonate Usage Reduces the Risk of Hospitalizations for Osteoporotic Fractures. **W. G. Goettsch^{*1}, F. Penning^{*1}, J. E. Erkens^{*1}, N. O. Lynch^{*2}, A. Novak^{*3}, R. M. C. Herings^{*1}.** ¹PHARMO Institute, Utrecht, The Netherlands, ²GSK, Greenford, United Kingdom, ³Roche Products Ltd, Woerden, The Netherlands.

Bisphosphonates are widely used to treat osteoporosis and have been proven to reduce the risk of osteoporotic fractures. However, suboptimal compliance and treatment discontinuation might lead to gradual loss of this effect. This study aimed to investigate the effect of persistent bisphosphonate usage on the risk for hospitalization due to osteoporotic fractures. The PHARMO database, which includes linked drug-dispensing records and hospital discharge records of more than one million subjects in defined areas in the Netherlands, was used to identify new female users of alendronate, etidronate or risedronate ≥50 years in the period Jan '96 - Jan '03. Persistence of treatment was determined by using episodes of bisphosphonate treatment based on the method of Catalan. Within the cohort a matched case control study was performed. Cases were selected on the basis of a first hospitalization for an osteoporotic fracture (index date). Controls were matched 10:1 to cases on month of inclusion in the cohort and were assigned a random index date. The association with risk for fractures was assessed for bisphosphonate use at the index date and for persistent bisphosphonate use before the index date. The study cohort included 8,845 new female bisphosphonate users; 334 patients (3.8%) were hospitalized for a fracture after inclusion in the cohort. 3280 controls were matched to the 334 cases. Bisphosphonate use at the index date significantly reduced the risk for osteoporotic fractures (RR 0.78; 95%CI 0.61-0.99, adjusted for age, previous fractures and co-medication). At least one year of persistent bisphosphonate usage reduced the risk for osteoporotic fractures even more evidently (adjusted RR 0.70; 95%CI 0.50-0.99). Patients who were persistent on their bisphosphonate treatment reduced their risk of hospitalization for osteoporotic fractures by 20-30%. The protective effect was highest (30%) in patients who used bisphosphonates consistently for more than one year. These results emphasize the importance of persistent bisphosphonate usage to obtain the maximal protective effect. Previous studies have demonstrated that persistence with bisphosphonates is higher with less frequent dosing regimens but still suboptimal. This study has demonstrated that improving persistence will result in reduced fracture rates.

Disclosures: **W.G. Goettsch**, Roche 2; GSK 2.

SU389

Alendronate 35mg Once-Weekly Treatment Increased Bone Mineral Density in Japanese Patients with Osteoporosis. **S. Uchida¹, T. Taniguchi^{*1}, T. Shimizu^{*1}, T. Kakikawa^{*1}, K. Okuyama^{*1}, M. Okaniwa^{*2}, H. Arizono^{*2}, K. Nagata^{*2}, A. Santora³, M. Shiraki⁴, M. Fukunaga⁵, T. Tomomitsu^{*3}, Y. Ohashi^{*6}, T. Nakamura⁷.** ¹Clinical Development Institute, Banyu Pharmaceutical Co., Ltd., Tokyo, Japan, ²Pharmaceutical Business Unit, Teijin Pharma Ltd., Tokyo, Japan, ³Merck Research Laboratories, Rahway, NJ, USA, ⁴Research Institute and Practice for Involutional Diseases, Nagano, Japan, ⁵Kawasaki Medical School, Okayama, Japan, ⁶Biostatistics, University of Tokyo, Tokyo, Japan, ⁷University of Occupational and Environmental Health, Kitakyushu, Japan.

The therapeutic equivalence of 70 mg alendronate (ALN) once weekly and 10 mg ALN daily was demonstrated in postmenopausal patients with osteoporosis (~96% Caucasians), based on percent changes in bone mineral density (BMD) and bone markers. However, the effects of 35 mg ALN once weekly have not been compared with those of 5 mg daily, the approved daily dose in Japanese patients with osteoporosis. The present study was carried out in a double-blind manner in a Japanese patient population with involutional osteoporosis, to compare the efficacy and safety of oral ALN 35 mg once-weekly to 5mg once-daily over a 52 week period. The primary efficacy endpoint was the percent change from baseline in lumbar spine (L1~L4) BMD after 52 weeks treatment. Three hundred twenty eight patients were randomized to ALN 5 mg once-daily (160 patients) or ALN 35 mg once-weekly (168 patients). The adjusted mean percent change from baseline in spine BMD after 52 weeks treatment was 5.8% and 6.4% in the once-daily group and the once-weekly group, respectively. The 95% confidence interval for the difference in spine BMD

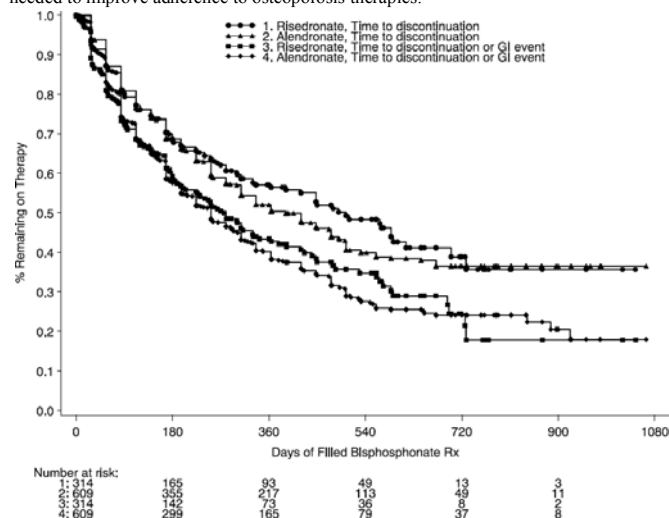
change between the two treatment groups was -0.31~1.48%, indicating that the two regimens are therapeutically equivalent, since it fell entirely within the predefined equivalence criterion ($\pm 1.5\%$). The time-course of the spine BMD increase was also similar for both regimens. When the results of this study were compared with the results from the earlier (primarily Caucasian) study, the percent changes from baseline in the L1~L4 BMD were similar. Mean changes in total hip BMD from baseline at 52 weeks were 2.8% and 3.0% in the once-daily group and the once-weekly group, respectively. In addition, the bone markers (urinary deoxypyridinoline, urinary Type-I collagen N-telopeptides and serum bone-specific alkaline phosphatase) were reduced to a similar level by either treatment throughout the treatment period. The tolerability and safety profiles were also similar between the treatment groups. These findings suggest that the efficacy and safety of ALN 35 mg once-weekly are similar to ALN 5 mg once daily in Japanese patients with osteoporosis.

Disclosures: S. Uchida, None.

SU390

Persistence and Adherence to Alendronate and Risedronate among Chronic Glucocorticoid Users. J. R. Curtis¹, A. O. Westfall^{*2}, J. J. Allison^{*3}, C. I. Kiefe^{*3}, K. G. Saag¹. ¹Division of Rheumatology, University of Alabama Birmingham, Birmingham, AL, USA, ²Department of Biostatistics, University of Alabama Birmingham, Birmingham, AL, USA, ³Division of Preventive Medicine, University of Alabama at Birmingham, Birmingham, AL, USA.

Purpose Adherence to oral bisphosphonates (BPs) is often suboptimal. Based on anecdotal data, we hypothesized differences between alendronate and risedronate in adherence and persistence among glucocorticoid (GC) users enrolled in managed care. **Methods** Using claims and pharmacy data from a U.S. managed care plan, we identified new alendronate or risedronate users (no BP Rx within 180 days) receiving 60+ GC days filling >1 BP Rx during 7/01 - 6/04. GI events, GI Rx, and NSAIDs prior to 1st BP and during 1/01-6/01 were examined to evaluate channeling (i.e. patients at high GI risk preferentially prescribed one drug over another). Adherence defined as BP days filled / (first BP fill date - last BP fill date). Persistence defined as ongoing BP Rx through 6/04 without discontinuing (> 180 day gap after last Rx). Survival analysis evaluated BP discontinuation (1- persistence) and a combined endpoint of (BP discontinuation or GI event). **Results** Of 1483 GC users filling ≥ 1 BP Rx, new alendronate (n = 609) and risedronate (n = 314) users filling >1 BP Rx had similar mean \pm SD age (54 \pm 13 yrs; sex (22% men), # of comorbidities (7 \pm 3); BMD (65%); fracture claims (12%), and prior NSAID Rx (50%). Alendronate users filled more days (353 \pm 254 vs. 316 \pm 228, p < 0.05) and more often received weekly BP (91% vs. 79%, p < 0.0001). Prior to 1st BP Rx, risedronate users were more likely to have a GI event (OR 1.40; 95% CI 1.04 - 1.88) or receive GI Rx (OR 1.41; 1.07 - 1.86), suggesting channeling. Alendronate and risedronate users had similar adherence (73 \pm 26%) and persistence (Figure). Factors associated with discontinuing BPs included age (hazard ratio 0.86, 95% CI 0.78 - 0.93 per 10yrs), BP days dispensed (0.91, 0.86 - 0.96 per 90 days), BMD test (0.82, 0.67 - 0.99), and comorbidity count (1.04, 1.00 - 1.07). **Conclusions** Despite adjustment for potential channeling, no difference in adherence or persistence between oral BPs was observed among chronic steroid users enrolled in managed care. At 2 years, > 50% of new users discontinued BP Rx. Alternate medications, new BP formulations, and new monitoring mechanisms are needed to improve adherence to osteoporosis therapies.



Disclosures: J.R. Curtis, None.

SU391

Consistent 60% Risk Reduction of New Vertebral Fractures in Men with Osteoporosis after the First and Second Year of Risedronate Therapy. J. D. Ringe, A. Dorst*, H. Faber*. Medizinische Klinik IV, Klinikum Leverkusen, University of Cologne, Leverkusen, Germany.

Background: Clinical studies in postmenopausal osteoporosis with risedronate have shown rapid reduction of vertebral and non-vertebral fractures. Vertebral fracture reduction during risedronate treatment was equally proved in glucocorticoid-induced osteoporosis and interestingly, the risk reduction observed in male and female subgroups was not different. **Purpose of the study:** To examine the effects of risedronate on vertebral fractures and mean changes in lumbar spine, femoral neck and total hip BMD only in men with primary and secondary osteoporosis. Secondary endpoints include non-vertebral fractures, height loss, pain, safety, and tolerability. **Patients and methods:** In this single center, open label, controlled prospective two year trial we enrolled 316 male patients with T-score values of lower than -2.5 SD at lumbar spine (LS) and lower than -2.0 SD at the femoral neck (FN) with or without prevalent vertebral fractures (vert.-fx). Patients in group A (n=158; 81 with, 77 without prevalent vert.-fx) received risedronate 5 mg plus calcium 1000 mg and 800 IU Vit. D daily. Group B comprised equally 158 men. Those with a prevalent vert.-fx (subgroup B1 n=81) were treated with alfacalcidol 1 μ g plus calcium 500 mg daily, whereas patients without prevalent vert.-fx (subgroup B2, n=77) were treated with 800 IU plain vitamin D plus calcium 1000 mg daily. BMD measurements and x-rays were performed at baseline and 12 and 24 months thereafter. **Results:** The LS-BMD increase after 12 and 24 months amounted to 4.7% and 6.5% resp. in risedronate patients compared with a mean resp. increases of 1.0% and 2.2% in controls (p<0.001). The mean changes at the total hip site were 2.7% and 4.4% for group A after the first and second year. For group B an average change of 0.4% was documented after one year and unchanged after the second (p< 0.001). In the first year 8 patients of group A and 20 of group B sustained new vert.-fx (risk reduction 60%). The cumulative patient numbers with new vert.-fx after 2 years were 14 and 35 in the resp. groups, i.e. an unchanged fracture reduction of 60% (Fisher's exact test 0.0026). **Conclusion:** Risedronate therapy in men with established primary or secondary osteoporosis consistently reduces the risk of new vertebral fractures by 60% over two years and significantly increases BMD at the lumbar spine and proximal femur.

Disclosures: J.D. Ringe, MSD, Roche, Sanofi-Aventis, Procter & Gamble Pharmaceuticals 5.

SU392

Alendronate 70 mg Once-Weekly Is More Effective and Has a Better Tolerability than Alendronate 10 mg Daily in the Treatment of Osteopenia Associated with Primary Biliary Cirrhosis. N. Guanabens¹, I. Vazquez^{*1}, L. Alvarez¹, F. Pons^{*1}, L. Caballeria^{*2}, D. Cerdà^{*1}, P. Peris¹, A. Monegal^{*1}, A. Pares^{*2}. ¹Metabolic Bone Diseases Unit, Hospital Clinic, IDIBAPS, Barcelona, Spain, ²Liver Unit, Hospital Clinic, IDIBAPS, Barcelona, Spain.

The treatment of osteoporosis in patients with primary biliary cirrhosis (PBC) has been poorly analyzed. We have described that alendronate 10 mg daily is more effective than cyclical etidronate for increasing bone mass in osteopenic patients with PBC. The objective of this study was to evaluate the efficacy and tolerability of once-weekly alendronate 70 mg compared with alendronate 10 mg daily on bone mineral density (BMD) and bone markers. 32 women with PBC (age: 63 \pm 2 years) were randomly assigned to receive 70 mg once-weekly (n=16) or 10 mg daily (n=16) for one year. BMD of the lumbar spine and proximal femur (DXA), liver function tests, 25-hydroxyvitamin D and bone markers (serum OC, bone ALP and PINP, and urinary NTX) were measured initially and every 6 months. At entry, women assigned to the two treatment groups were similar with respect to age, BMD and severity of cholestasis. All patients in the once-weekly group completed the 1-yr trial whilst only 10 of 16 patients in the daily group (in 4 patients because minor gastrointestinal events). 18 patients (62%) had osteoporosis by densitometric criteria and/or fragility fractures and the others met criteria of osteopenia. At month 12, there were significant increases in BMD at the spine (from 0.920 \pm 0.03 to 0.950 \pm 0.04 g/cm², p<0.01) and at the total hip (from 0.841 \pm 0.029 to 0.851 \pm 0.29 g/cm², p=0.02) in the once-weekly group, with no significant changes in the daily group (spine: from 0.890 \pm 0.03 to 0.901 \pm 0.03 g/cm², p=ns; total hip: from 0.842 \pm 0.03 to 839 \pm 0.04 g/cm², p.n.s). Both regimens induced early and significant reductions in bone markers, although NTX was only significantly reduced by 12 months in the once-weekly group (from 46.8 \pm 6.4 to 27.7 \pm 5.2 nM/mM, p<0.01). Compliance, monitored by % remaining pills, was 86 \pm 5% and 70 \pm 12% in the once-weekly and daily groups, respectively (p.n.s). Neither treatment impaired liver function or cholestasis. When patients were classified according to spine BMD changes at 12 months, those who maintained or experienced a loss of BMD (n=9) had higher bilirubin levels than patients who experienced gains in BMD (n=17) (1.2 \pm 0.2 vs 0.7 \pm 0.1 mg/dl, p<0.01) without significant differences in compliance, age or baseline BMD. These results suggest that once-weekly alendronate is more effective and has a better tolerability profile than daily dosing in the treatment of low bone mass in patients with PBC. The effects of alendronate on BMD are lower in patients with higher indices of cholestasis.

Disclosures: N. Guanabens, Novartis 5.

SU393

Effect of Alendronate on Cortical and Trabecular Bone of the Transilial Biopsy as Measured by Micro-CT. P. J. Masarachia¹, R. Recker², A. Santora³, P. Chavassieux^{*4}, M. Arlot^{*4}, D. Kimmel¹. ¹Molecular Endocrinology, Merck Research Laboratories, West Point, PA, USA, ²Osteoporosis Research Center, Creighton University, Omaha, NE, USA, ³Merck & Co., Whitehouse Station, NJ, USA, ⁴INSERM, Lyon, France.

The purpose of this study is to use micro-CT (m-ct) endpoints to compare cortical (Ct) and trabecular (Tb) bone microarchitecture (MA) of transilial biopsies obtained from postmenopausal osteoporotic women treated with alendronate (ALN, N=29) or PBO (N=59) for 2-3 years (Curr Med Res Opin 21:185-194 (2005)). M-CT variables obtained from scans at 19 µm resolution (GE Healthcare, Explore Locus SP, Explore MicroView V.2.0) included bone volume (BV/TV); trabecular thickness (TbTh); trabecular number (TbN); trabecular spacing (TbSp) [plate model]; trabecular thickness [fitting of maximum spheres] (TbTh-3D); Structure Model Index (SMI); Degree of Anisotropy (DA); and “purified” Euler number (PEuler#). Thickness of each cortex of each specimen was measured at four equidistant points in each of two planes separated by 2mm. The two cortices were of significantly different thickness (P<.0001). The thicker cortex (CtTk) and all thinner cortex (CtTn) from each sample were grouped. Mean thickness of the combined cortices was calculated (CtTh). T-test of means, based on treatment groups, was executed for all endpoints. All Tb m-ct endpoints were correlated to BV/TV (Pearson R).

Table 1.	Mean ± S.D.		
	ALN	PBO	P=
BV/TV (%)	19.6±6.3	16.0±6.6	0.017
TbTh (µm)	132±29	120±30	0.070
TbSp (µm)	580±181	705±260	0.034
TbN (#/mm)	1.47±0.31	1.30±0.33	0.022
TbTh-3D (µm)	192±46	171±50	0.063
SMI	1.12±0.57	1.30±0.73	0.251
DA	1.61±0.35	1.66±0.69	0.693
PEuler# (#/cc)	4.94±2.26	4.30±1.77	0.148
CtTh (mm)	0.896±0.299	0.865±0.242	0.626
CtTk (mm)	1.035±0.398	1.079±0.347	0.615
CtTn (mm)	0.745±0.274	0.651±0.218	0.100

As previously shown (CMRO), BV/TV and TbN were greater, and TbSp was less, in ALN than in PBO patients; TbTh tended to be greater. For 3D-specific m-ct algorithms, TbTh-3D also tended to be greater. However, SMI, DA, and PEuler# did not differ between groups. In addition, a trend for the thin cortex of the ALN group to be thicker than the thin cortex of the PBO group was found. TbTh-3D values were ~50% greater than TbTh, with high correlation (r = 0.924). BV/TV was highly correlated to TbTh (r = 0.82), TbSp (r = 0.71), TbN (r = 0.82), TbTh-3D (r = 0.61) and SMI (r = -0.75); moderately with PEuler# (r = 0.24) and CtTn (r = 0.28); and mildly with DA (r = -0.20). **Conclusion:** ALN treated patients have significantly higher bone volume and better Tb MA (plate method) than PBO patients. However, 3D-specific endpoints (SMI, DA, PEuler#) did not differ between ALN and PBO groups. Most Tb MA endpoints were solidly related to bone volume.

Disclosures: P.J. Masarachia, Merck & Co. 3.

SU394

Low Doses of Pamidronate for the Treatment of Osteoporosis in Children with Cerebral Palsy. H. Plotkin¹, M. Bruzoni^{*2}, S. Coughlin^{*3}, G. Lerner^{*3}, S. Allbery^{*3}, B. Schroeder^{*3}, K. Heldt^{*3}, L. Grovas^{*3}, R. Kreikemeier^{*3}. ¹Pediatrics, University of Nebraska Medical Center, Omaha, NE, USA, ²Surgery, University of Nebraska Medical Center, Omaha, NE, USA, ³Children's Hospital, Omaha, NE, USA.

Cerebral palsy (CP) is a non-progressive motor disorder resulting from a defect or lesion in the developing brain. It is the most common physical disability of childhood. Patients often have low bone density and fractures. Pamidronate treatment has been successfully tried in these patients at 9.0 mg/kg/year. This dose has caused retention of calcified cartilage within secondary spongiosa in children with OI. Higher doses have led to osteopetrosis in a patient, suggesting a dose-related effect. We have evaluated the effects of 4.12 mg/kg/yr of IV pamidronate on lumbar spine (LS) and femoral neck (FN) bone density in 25 children (age 3.5 to 17.9 years) with severe CP. IV Pamidronate (0.75 mg/kg/day for two days) was administered every 4 months. On the first day of treatment patients received 0.37 mg/kg, to minimize the acute phase reaction, and acetaminophen was administered every 6 hours during the first 2-day infusion. LS and FN BMD (DEXA, Hologic Delphi) was obtained at baseline, 4 months and 12 months. All patients had adequate calcium and vitamin D intakes for age. The study was approved by Children's Hospital IRB. FN BMD increased from 0.272 ±0.14 at baseline to 0.355 ±0.13 at 4 months (p=0.04), and to 0.386 ±0.12 at 12 months (p=0.01). Z-scores increased from -4.8 ±1.2 at baseline to -3.8 ±1.0 at 4 months (p NS) and -3.2 ±1.1 at 12 months (p=0.02). FN BMC increased from 0.9 ±0.6 at baseline to 1.6 ±0.5 at 12 months (p= 0.02) and FN area increased from 3.2 ±1.2 at baseline to 3.4 ±0.9 at 12 months (p= NS). LS BMD increased from 0.348 ±0.17 at baseline to 0.412 ±0.15 at 4 months (p NS), and to 0.485 ±0.16 at 12 months (p=0.02). Z-scores increased from -3.9 ±1.6 at baseline to -3.2 ±1.2at 4 months (p NS) and -2.3 ±1.5 at 12 months (p=0.03) LS BMC increased from 11.2 ±9.8 at baseline to 15.3 ±5.0 at 12 months (p=NS) and LS area increased from 23.4 ±13.7 at baseline to 31.3 ±3.1 at 12 months (p=NS). Femoral neck is more severely affected than lumbar spine in children with CP. Bone density should always be measured in more than one region in the pediatric population. Low doses of pamidronate are effective to increase bone mineral density in young patients with CP.

Disclosures: H. Plotkin, Novartis 2; Procter and Gamble 2.

SU395

Comparative Effects of Alendronate and Risedronate Treatment on Bone Mineral Density and Bone Resorption and New Incident Vertebral Fractures. T. Tsuchida¹, T. Kobayashi^{*2}, N. Konno^{*2}, M. Ogino^{*2}. ¹Orthopedic Surgery, Akita University School of Medicine, Akita, Japan, ²Orthopedic Surgery, Koto General Hospital, Akita, Japan.

The purpose of this study was to compare the effects of alendronate (ALN) and risedronate (RIS) treatment on bone mineral density (BMD) and bone resorption marker and incidence of vertebral fractures in patients with involutional osteoporosis. In this study, a total of 249 postmenopausal women with osteoporosis were randomized to receive either treatment with 5 mg/day of alendronate or 2.5 mg/day of risedronate for 12 months. Dual-energy x-ray absorptiometry (DXA) was used to measure patients' BMD (distal radius) at baseline and 12 months later. Lateral thoracic and lumbar spine radiographs were obtained at baseline and at 12 months to find new incident vertebral fractures. Urine N-telopeptides of type 1 collagen (NTx) corrected for creatinine level were measured at baseline and at 6 months. A significant increase in BMD (distal radius) was observed at 12 months after initiation of therapy in both ALN (1.6%) and RIS (1.1%) groups. However, the difference in percentage increase in BMD measurements was not statistically significant between the two groups. ALN produced a significantly greater mean reduction in urine NTx than did RIS (-51% vs -42%, p < 0.05) at 6 months. Incidence rates of patients who had at least one new vertebral fracture during the 12-months period were 7.9% for ALN and 9.4% for RIS. However, there was no statistically-significant difference between both groups. These results suggest that there are no differences in enhancing the BMD and in anti-vertebral fracture efficacy between the two agents, although ALN (5 mg) exhibited efficacy superior to that of RIS (2.5 mg) in suppression of bone resorption.

Disclosures: T. Tsuchida, None.

SU396

Long-Term Effects of I.V. Bisphosphonates after their Discontinuation in Pediatric Patients. K. M. Waterhouse^{*}, C. Haney^{*}, T. Srivastava^{*}, G. Colgan^{*}, U. S. Alon. Nephrology, Children's Mercy Hospital, Kansas City, MO, USA.

Purpose: To determine the long-term effects of bisphosphonates after their discontinuation in a pediatric patients cohort. Methods: Retrospective analysis of all 17 children with metabolic bone disorders, seen in our clinic, in which I.V. bisphosphonate therapy was discontinued for at least 12 months. Data of fracture rate, musculoskeletal pain, height (SDS), weight (SDS), DEXA's Z-scores of total body (T.B.) and spine L²⁻⁴, urine N-telopeptides (NTX), serum bone specific Alk. Phos. (BSAP) and osteocalcin were compared between (a) before treatment, (b) end of treatment, (c) at last follow-up visit, utilizing two-tailed paired T test. Results: Are shown in the Table below.

Long-term effects of I.V. bisphosphonate therapy in children (mean±SE)			
	Before Treatment	End of Treatment	Follow-up
Median Age (y)	7.6	9.6	11.0
Fractures (/y)	0.74 ± 0.21*	0.35 ± 0.11	0.31 ± 0.15
Height (SDS)	-1.78 ± 0.52	-1.43 ± 0.38	-1.23 ± 0.32
Weight (SDS)	-1.42 ± 0.57	-1.39 ± 0.50	-1.29 ± 0.59
DEXA T.B. (Z-score)	-1.24 ± 0.50*	-0.37 ± 0.44	0.23 ± 0.37
DEXA Spine (Z-score)	-1.65 ± 0.57*	-0.34 ± 0.56	0.31 ± 0.48*
NTX	684 ± 121*	192 ± 28	196 ± 27
BSAP	172 ± 51*	51 ± 8	55 ± 5
Osteocalcin	32 ± 5	15 ± 3*	34 ± 7

*P<0.05 in comparison to the two other periods. Three children had bone pain before treatment, 6 during treatment with bisphosphonates, and 0 at the last follow-up (Chi-square, P<0.05). Summary of Results: Treatment with I.V. bisphosphonates had no adverse effect on height or weight. There was a significant and sustained reduction in fracture rate and pain. Bone density showed a significant improvement with therapy which was maintained after its discontinuation, with further gain in the spine. Bone remodeling markers showed sustained effect of bisphosphonates, with potential recovery of osteocalcin levels. Conclusion: I.V. bisphosphonates continue to exert their effect for at least 17 months after their discontinuation. Further observations are required to evaluate long-term outcome with the potential in the future to lower therapeutic doses.

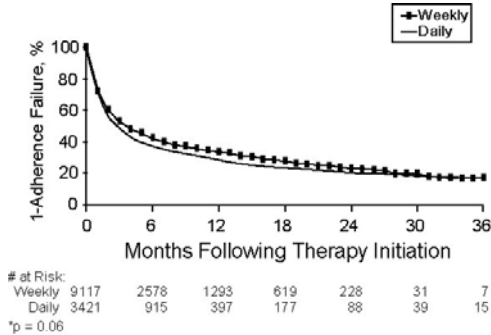
Disclosures: K.M. Waterhouse, None.

SU397

Adherence with Weekly Versus Daily Bisphosphonate Therapy among Women with Postmenopausal Osteoporosis. D. Weycker^{*1}, D. Macarios^{*2}, G. Oster^{*1}. ¹Policy Analysis Inc., Brookline, MA, USA, ²Amgen Inc., Thousand Oaks, CA, USA.

Adherence with daily bisphosphonate therapy is relatively poor; it is unknown whether it improves with less frequent (i.e., weekly) administration. Data were obtained from a medical claims database containing information from over 30 US health plans on 15 million lives annually. Study subjects consisted of all women aged ≥45 years with postmenopausal osteoporosis (PMO) who initiated bisphosphonate therapy between July 1998 and December 2003; those with secondary causes of osteoporosis were excluded. Subjects were stratified according to whether they received daily or weekly therapy, and adherence was assessed for each patient based on the ratio of the number of therapy-days to the number of calendar days over time (“adherence ratio”); adherence failure was defined as an adherence ratio <80%. Unadjusted “survival curves” describing time to

adherence failure were estimated for patients in each group using Kaplan-Meier methods. A Cox proportional hazards (PH) model was employed to examine the relationship between regimen and time to adherence failure, controlling for age, drug received, history of fracture, and other potential confounders. The study sample consisted of 12,538 women with PMO initiating weekly (n=9,117) or daily (n=3,421) bisphosphonate therapy. Weekly therapy patients were younger (mean age: 62 years vs. 67 years for daily therapy, p<0.01), and were less likely to be hospitalized during the six months prior to therapy initiation (5.5% vs. 6.9% respectively, p<0.01); history of fracture was similar (4.2% vs. 4.9%, p=0.06). By month 6 following therapy initiation, 57% of women receiving weekly therapy and 62% of those receiving daily therapy experienced adherence failure (Figure). In Cox PH regression, risk of adherence failure did not differ between women initiating weekly versus daily therapy (HR: 1.01, p=0.81); risk of adherence failure was higher among women aged ≥ 65 years (HR: 1.23, p<0.01) and was lower among those with a history of fracture (HR: 0.84, p<0.01). Adherence with weekly bisphosphonate therapy is poor, and appears to be no better than adherence with the daily regimen among women with PMO. Figure. Kaplan-Meier (unadjusted) estimates of time to adherence failure following therapy initiation*



Disclosures: D. Weycker, Amgen Inc. 5.

SU398

Calcium Supply in Women with Postmenopausal Osteoporosis on Bisphosphonate Therapy in Daily Practice. J. D. Ringe¹, G. Möller², B. C. Wick³. ¹Medizinische Klinik IV, Klinikum Leverkusen, Leverkusen, Germany, ²Medical Affairs, Procter&Gamble Pharmaceuticals-Germany GmbH, Weiterstadt, Germany, ³European Medical&Technical Affairs, Procter&Gamble Pharmaceuticals-Germany GmbH, Weiterstadt, Germany.

The objective of the study was to assess whether women with postmenopausal osteoporosis on bisphosphonate therapy have a sufficient calcium intake. 264 community-based physicians were asked to interview patients with postmenopausal osteoporosis on bisphosphonate therapy regarding their knowledge about the importance of calcium and their daily calcium intake using a questionnaire. The survey was conducted from July to September 2004. Questionnaires were analyzed from 726 patients. The importance of calcium for their osteoporosis therapy was rated as important or very important by 678 (93.4%) of the patients. Patients estimated their required daily calcium intake to be 1000 mg (median, 25% 500, 75% 1000); 75.5% believed that they take enough calcium per day. Calculation based on the reported intake of calcium-rich foods showed a median of 913.2 mg calcium per day (25% 466.7; 75% 1514.7). 157 (21.6%) patients reported that they take no additional calcium, and of these patients, 54.8% believed that they take sufficient calcium with their dairy products. A regular calcium supplement was considered too expensive by 17.8%, too cumbersome by 17.8%, and 16.6% admitted that they forget to take it. Although more than 90% of the women interviewed rated the intake of calcium for their osteoporosis therapy as important or very important, they underestimated their required calcium intake. The German Dachverband Osteologie (DVO) recommends 1500 mg daily calcium intake for women with postmenopausal osteoporosis (<http://www.lutherhaus.de/osteo/leitlinien-dvo/index.php>). Studies show that the daily calcium intake from food for women aged ≥ 50 years is below the recommended amount (DGE Report, 2000). Our results confirm these findings, identifying a deficit in daily calcium of 500-600 mg versus the required intake. More than 20% of patients took no supplemental calcium to reach the daily requirement. When asked for the reason, more than half considered extra calcium supplementation too expensive or too inconvenient. Osteoporosis therapy with bisphosphonates requires a sufficient calcium level. We conclude that a simplified way to supply calcium to patients on bisphosphonate therapy could ensure greater compliance to this evidence-based osteoporosis therapy and, thereby, could be more cost-effective.

Disclosures: J.D. Ringe, Procter&Gamble Pharmaceuticals 5.

SU399

Cbfa1/Runx2 Overexpressing Mice: A New Animal Model for Evaluation of Bisphosphonates Efficacy on Bone Quality, Bone Strength and Fractures. V. Geoffroy¹, R. Phipps², M. de Vernejoul¹. ¹INSERM U606, Paris Cedex, France, ²P & G Pharmaceuticals, Mason, OH, USA.

Mice overexpressing Cbfa1/runx2 specifically in cells of the osteoblastic lineage (cbfa1+) exhibit an increase in bone remodeling leading to severe osteopenia and spontaneous vertebral fractures after 1 mo of age (Geoffroy et al, MCB, 2002). The objective of the current study was to determine whether an anti-fracture effect could be

demonstrated in caudal vertebral fractures of this mouse model after therapy with the bisphosphonates risedronate (RIS) and alendronate (ALN). Five-wk old female Cbfa1 mice were randomized to receive RIS at 4 or 20 μ g/kg/wk (RIS4 and RIS20), or ALN at 4 or 20 μ g/kg/wk for 12 wk (ALN4 and ALN20). Cbfa1 and age- and background-matched wild type mice received vehicle as controls (VEH and WT groups, respectively). Only Cbfa1 mice exhibiting fewer than 3 fractures in the tail vertebrae at baseline were included in the study. We measured BMD of whole body (WB) and caudal vertebrae (CV) (PIXImus, Lunar, France) and the number of fractures in the caudal vertebrae (via X-ray; FAXITRON). Fractures were also scored for severity (0 to 3). Compared to WT VEH treated mice, Cbfa1 VEH treated mice had significantly lower BMD (19% in WB and 24% in CV) at end of 12-wk treatment period. RIS20 significantly increased BMD of WB (12%) and CV (12%) compared to Cbfa1 VEH controls (p<0.001). There was no significant effect on BMD in the other treatment groups. RIS20 significantly reduced (by 43%) the average number of new fractures compared to Cbfa1 VEH treated controls (3.13 \pm 0.42 vs 5.48 \pm 0.53 fractures/mouse). There was no significant effect on the number of fractures with RIS4 (-9%), or ALN4 and ALN20 (-9% and -10%, respectively). The fracture severity score per vertebrae was unchanged by treatment.

Group	Mean fractures	Severity	WB BMD	CV BMD
WT VEH	0	0	0.048	0.054
Cbfa1 VEH	5.48	1.41	0.039	0.041
ALN 4 μ g/kg/wk	5.00	1.44	0.040	0.041
ALN 20 μ g/kg/wk	4.91	1.58	0.039	0.042
RIS 4 μ g/kg/wk	5.00	1.52	0.038	0.042
RIS 20 μ g/kg/wk	3.13*	1.39	0.044**	0.046**

Values are means; *, p<0.01 and **, p<0.001 vs Cbfa1 VEH

In conclusion, we describe here a transgenic mouse model that allows for the first time the assessment of bone fragility and fractures in vivo. In this study RIS had a dose related effect, and at 20 μ g/kg/wk significantly increased vertebral BMD and reduced the occurrence of vertebral fractures. ALN at an equal dose had no significant effect. Further analyses are being performed to determine the roles of BMD, architecture, matrix composition and mechanical properties to this RIS-induced reduction in bone fragility.

Disclosures: V. Geoffroy, None.

SU400

Change in Bone Turnover Markers Following Discontinuation of Long-Term Alendronate in FLEX. A. V. Schwartz¹, D. C. Bauer¹, P. Garnero², A. C. Santora³, L. Palermo⁴, D. M. Black¹. ¹Epidemiology and Biostatistics, UCSF, San Francisco, CA, USA, ²Synarc, Lyons, France, ³Merck Research Laboratories, Rahway, NJ, USA.

Limited information is available on the response of bone turnover markers to alendronate (ALN) discontinuation after long-term use. Effects of discontinuation of ALN on bone turnover markers were investigated in the FIT Long-Term Extension (FLEX) Trial among women who had previously used ALN for an average of 5 years. 1099 women who had previously been randomized to receive ALN during the Fracture Intervention Trial (FIT) were re-randomized to receive placebo (40%), ALN 5 mg (30%) or 10 mg (30%) for an additional 5 years. Participants received a daily supplement of calcium (500 mg) and vitamin D (250 IU). At FLEX baseline, the mean duration of previous ALN was 5 years and 80% were still taking ALN. The mean age was 73.5 (8) years; total hip BMD 0.73 (0.09) g/cm² and t-score -1.8 (0.7); lumbar spine BMD 0.90 (0.14) g/cm² and t-score -1.6 (1.3). Samples were obtained at the FIT baseline visit before any ALN treatment and at FLEX baseline and 5-year visits. Only the FIT baseline visit was fasting. Bone ALP (Ostase, Hybritech) and U-NTX (Ostex) were assayed at different times over a period of 10 years at two commercial labs. To eliminate possible assay drift or lab differences, at the end of the study we also performed concurrent measurements of Bone ALP, PINP, and S-CTX at one specialized lab using stored serum specimens. Participants selected for concurrent measurements were compliant with the FLEX protocol. 41 participants had complete data available for the separate and concurrent assays. Bone Turnover Markers in Women Who Discontinued ALN (N=41)

Timing of assays	Marker	Geometric mean			% change FIT baseline to FLEX 5yr (95% CI)
		FIT baseline	FLEX baseline	FLEX 5 yr	
Separate	Bone ALP (ng/ml)	11.0	8.6	11.2	4.1 (-11, 22)
	U-NTX (nmol/mmol Cr)	57.8	16.4	23.5	-54.5 (-66, -38)
Concurrent	Bone ALP (ng/ml)	12.0	8.4	11.2	-6.9 (-17, 4.3)
	PINP (ng/ml)	52.9	23.2	38.2	-23.2 (-37, -6.0)
	S-CTX (pg/ml)	210	110	200	2.3 (-20, 31)

After an average of 5 years of ALN use followed by 5 years of placebo, there was little continuing effect of ALN on Bone ALP (in separate and concurrent assays) or S-CTX. PINP and U-NTX increased after discontinuation of ALN, but their levels remained below pre-treatment levels. The large difference between change in U-NTX (separate assays) and S-CTX (concurrent) may be due to assay drift in U-NTX measurements or possible biological differences between NTX and CTX. In conclusion, marker levels increased in women who discontinued ALN after long-term use and some, but not all, returned to pre-treatment levels, possibly because of biological differences in response to ALN discontinuation or to calcium supplementation.

Disclosures: A.V. Schwartz, Merck 2; Aventis 2; Procter & Gamble 2.

SU401

Bone after Cessation of Alendronate Use in Children with Fracturing Osteoporosis. C. B. Langman, A. L. Arwady*, H. Price. Pediatric Kidney Diseases, Northwestern University, Childrens Memorial Hospital, Chicago, IL, USA.

We report on bone mineral density (BMD), somatic growth, and bone markers in blood and urine in children with fracturing osteoporosis after cessation of a therapeutic course of oral alendronate. Forty-six consecutive children (23 girls, 23 boys) of normal growth for age (-0.6 Z score for height by chronologic age; -1.0; +1.0 [median; 25%ile; 75%ile]) and pubertal status were treated for 672 (513; 959) days with 70 or 35 mg/week oral alendronate, depending on body mass (≥30 kg, or below, respectively) for fracturing osteoporosis (88% with radiographically-confirmed fracture). No patients were growth-hormone or vitamin D deficient during or after alendronate therapy. Initial DXA Z-BMD in the L1-L4 spine = -1.8 (-2.4; -1.3), and at conclusion of therapy, the Δ Z BMD in the spine = +1.7 (+1; +2.2) differed (p 365 days of follow-up as of end of 2004, the most recent evaluation of BMD spine Z-score after 410 (373; 797) days of absence of alendronate use = -0.2 (-0.9; +0.33) did not differ from the value at the time of discontinuation of the drug. Height Z-score at this time = -0.5 (-1.1; +0.7) did not differ from either alendronate initiation or discontinuation time points. Urinary N-linked telopeptides (NTx) were reduced from 372 (184; 504) at initiation of alendronate to 105 (71; 221) at drug discontinuation (p < 10-3), and remained at 110 (77; 309) at most recent evaluation (p < 10-3), while serum bone-specific alkaline phosphatase activity (BsAP) was unchanged (median values at the 3 time points: 90; 128; 77; p = NS). During and after alendronate therapy, 4% of children sustained a fracture. In conclusion, alendronate therapy in children of normal growth with fracturing osteoporosis did not affect subsequent somatic growth while placing BMD of the lumbar spine into the normal range. Subsequently, BMD and growth have remained normal. Analysis of bone markers suggest a more profound effect of alendronate on remodeling than modeling space dynamics. Appropriate algorithms for the use of alendronate must take into account subsequent effects on bone after its discontinuation, and the data provided here lend support for its time-limited utility in children of normal growth but with fracturing osteoporosis.

Disclosures: **C.B. Langman**, Merck 5.

SU402

Characteristics Associated with Non-Persistence during Daily Therapy - Experience from the Placebo Wing of a Community-Based Clinical Trial. E. McCloskey¹, D. deTakats^{*1}, J. Orgee^{*1}, S. Aropuu^{*2}, T. Jalava^{*2}, J. Cliffe^{*1}, L. Reaney^{*1}, C. McGurk^{*1}, D. Charlesworth^{*1}, J. A. Kanis¹. ¹University of Sheffield, Sheffield, United Kingdom, ²Schering Oy, Helsinki, Finland.

Despite well-proven efficacy, long-term persistence with therapy for osteoporosis is reported to be poor, at least partly related to drug-specific adverse events. Other factors underlie poor persistence, however, and need to be identified and addressed to improve management strategies. For this reason, we compared the baseline characteristics of elderly women who persisted or failed to persist with placebo capsules throughout a 3-year double-blind study of daily oral clodronate (Bonafos®). Of 2248 women aged 75 years or more, recruited from the general community and unselected for osteoporosis, 706 (31%) failed to persist with the placebo capsules during a follow-up of at least 1000 days. The analysis excluded women who discontinued the capsules following hip fracture. Half of the women stopping treatment did so within the first 6 months and 71% had discontinued by one year. At baseline, the women who subsequently discontinued treatment were slightly but significantly older (79.8 vs. 79.1yrs, P<0.001) than women who persisted with treatment and they also had significantly lower total hip BMD (0.74 vs. 0.76gcm², P=0.003). BMI was similar in the two groups. Non-persistence was significantly associated with poor health as judged by increased reports of hospital admissions within the previous year (20.3 vs. 14.3%, P=0.002), increased out-patient attendances (34% vs. 25%, P<0.001) and lower health-related quality of life as judged by higher scores in all 5 dimensions of the Euroqol-5D questionnaire and lower self-rated health score on the Euroqol VAS (67 vs. 73, P<0.001). There were, however, no significant differences in reports of prior fractures in the two groups or the prevalence of vertebral fractures on spine images (15% vs. 14%, NS). Furthermore, despite poorer health as described above, non-persistence was not associated with an increased risk of incident hip fracture (RR 1.02, 95%CI 0.59-1.74). We conclude that extraskeletal health-related factors contribute to non-persistence with therapy in elderly women unselected for osteoporosis. Management strategies need to address these issues by either overcoming the influence of such factors (by contact, feedback etc) or through novel dosing regimens.

Disclosures: **E. McCloskey**, None.

SU403

Greater Adherence to Bisphosphonate Therapy Is Associated with Greater Fracture Risk Reduction in Postmenopausal Women. E. Siris¹, C. Rosen², S. Silverman³, T. Abbott⁴, C. Barr^{*5}, S. Harris⁶. ¹Department of Medicine, Columbia University College of Physicians and Surgeons, New York, NY, USA, ²Maine Center for Osteoporosis Research and Education, St. Joseph's Hospital, Bangor, ME, USA, ³Cedars-Sinai Medical Center, David Geffen School of Medicine UCLA, Beverly Hills, CA, USA, ⁴Thomson-Medstat, Philadelphia, PA, USA, ⁵Medical Affairs, Roche Laboratories Inc., Nutley, NJ, USA, ⁶Department of Metabolism and Endocrinology, University of California, San Francisco, San Francisco, CA, USA.

Purpose: The Medstat MarketScan® Research Databases encompass 6 million members, 45 employers, and 100 health plans, and include both managed care claims and Medicare claims. We have analyzed data from these large claims databases and investigated the association between refill compliance with bisphosphonate dosing regimens and fracture risk in women who had received a prescription for bisphosphonate therapy. *Methods:* Data were extracted from the Medstat MarketScan® Research Databases on 37,698 women ≥45 years of age who had received a first (index) prescription for alendronate or risedronate. The relationship between refill compliance and fracture risk was analyzed over 24 months following the index prescription. Exclusion criteria included Paget's disease of bone, cancer, HIV, and prior bisphosphonate therapy. Patients were categorized by the percent of time during which drug was available, based on number of prescription refills, to yield a Medication Possession Ratio (MPR). MPR was calculated as the sum of days' supply divided by the total follow-up period (24 months). A new occurrence of osteoporotic fracture was determined by a subset of ICD-9 codes. *Results:* The probability of fracture decreased with higher rates of refill compliance, with the greatest decline in fracture risk related to increases in MPR from 75% to 100%. For example, the fracture rate was 11.45% for women with 70% to 75% MPR versus 8.07% for those with 95% to 100% MPR. Overall, fracture risk was reduced by 19.6% over 24 months for women with ≥75% refill compliance and by 20.4% for women with ≥80% refill compliance compared to those with lower MPR. Comparable reductions in fracture risk were similarly associated with better adherence, a measure that includes persistence with medication over time, as well as refill compliance. *Conclusion:* Greater refill compliance was associated with a significantly lower fracture risk in women taking bisphosphonates. The largest decline in fracture risk occurred for compliance >75%. Strategies are needed to help women with osteoporosis increase their compliance to therapy.

Disclosures: **E. Siris**, Merck 2, 5, 8; Eli Lilly & Company 5, 8; Pfizer, Amgen, Novartis, and Procter & Gamble 5.

SU404

Oral Risedronate Treatment in Men with Osteoporosis: Study Design and Baseline Characteristics. S. Boonen^{*1}, D. Wenderoth², P. J. Schofield^{*3}, D. Cahall⁴, E. S. Orwoll^{*5}. ¹University Hospital Leuven, Leuven, Belgium, ²Procter & Gamble Pharmaceuticals, Schwalbach a. Ts., Germany, ³Procter & Gamble Pharmaceuticals, Mason, OH, USA, ⁴Sanofi-Aventis, Bridgewater, NJ, USA, ⁵Oregon Health and Sciences University and Veterans Administration Medical Center, Portland, OR, USA.

Epidemiological studies have shown that osteoporosis is a significant medical health issue facing men. If one uses the WHO suggested diagnostic threshold for women but uses male reference data (i.e., -2.5 SD below the peak bone mass reference standard for young men), it is estimated that 1-2 million men in the United States have osteoporosis and 8-13 million have osteopenia. More importantly, according to the EPOS study one-third of all vertebral fractures occur in men. In the United States and Northern Europe approximately 25% of all hip fractures occur in men, with men reaching the same incidence as women when they are 5-10 years older. Men have a higher mortality (31%) than women (17%) during the first year after a hip fracture. Risk factors for male osteoporosis include: history of a nontraumatic fracture, osteopenia, family history, excess alcohol consumption, tobacco use, and glucocorticoid use. A 24-month, double-blind, placebo-controlled multinational study with 35 mg weekly oral risedronate is ongoing. All patients are being supplemented with 1000 mg calcium and 400-500 IU of vitamin D. Male patients at least 30 years old, with a femoral neck BMD T-score ≤-2 and lumbar spine BMD T-score ≤-1, or with a femoral neck BMD T-score ≤-1 and lumbar spine BMD T-score ≤-2.5, were included. DXAs of the spine and hip are performed at screening, and months 6, 12, and 24; bone turnover markers (serum CTX and BAP and urine NTX) are performed at baseline, and months 3, 6, 12, and 24; spine radiographs are performed at screening, and months 12 and 24. Bone biopsies are performed in a subset of patients at month 24. 285 patients were randomized into the trial and 95% were Caucasian. Preliminary baseline characteristics for the patients that entered the study are presented in the table below.

Baseline Characteristics	
Age - (years) - n	285
Mean (SD)	60.5 (10.65)
Min-max	36 - 80
Lumbar Spine BMD T-score - n	282
Mean (SD)	-2.8 (0.79)
Femoral Neck BMD T-score - n	282
Mean (SD)	-2.1 (0.48)
Tobacco Use - n (%)	
Current	71 (25%)
Previous	114 (40%)
Never	100 (35%)
Alcohol Use - n (%)	
Current	160 (56%)
Previous	101 (35%)
Never	24 (8%)

Upon completion of the initial 24-month study, all eligible patients are being invited to continue in a 2-year, open-label extension where all patients will receive 35 mg risedronate weekly.

Disclosures: **S. Boonen**, Procter & Gamble Pharmaceuticals 2, 5.

SU405

Risedronate Demonstrates Favorable Safety Profile in Postmenopausal Osteoporosis over Wide Range of Serum Concentrations. **P. Miller¹, S. Magowan², I. Barton^{*2}, S. Boonen^{*3}.** ¹Colorado Center for Bone Research, Lakewood, CO, USA, ²Procter & Gamble Pharmaceuticals, Mason, OH, USA, ³Leuven University for Metabolic Bone Diseases, Leuven, Belgium.

Risedronate's serum steady state levels during therapy are determined by renal clearance (CrCl) of risedronate, the daily drug dose, and body weight. Therefore, studies of patients varying in CrCl and body weight provide useful information for clinicians. This analysis investigated the safety profile of risedronate over a wide range of drug serum concentrations in postmenopausal women. Patients who took at least one dose of daily risedronate (2.5 mg or 5 mg) in the risedronate phase III clinical trials investigating postmenopausal osteoporosis for up to 3 years were included. Because the serum drug concentration is inversely proportional to CrCl and body weight, and directly proportional to drug dose, these variables were incorporated for each patient to estimate a serum concentration ratio (SCR). The patient with the maximum combination of both CrCl and body weight, and receiving the lowest dose of risedronate (2.5 mg/day), was given an arbitrary value of 1. All other patient SCR values were calculated relative to this index case. Patients were then ranked according to SCR decile (1=lowest, 10=highest). For patients in each of these SCR deciles, the adverse event rate per 100 patient years and corresponding 95% confidence interval was calculated using a Poisson regression model. The analysis identified 9,606 postmenopausal women randomized to daily risedronate. Serum steady states ranged from an arbitrary value of 1 to 57 with a median of 7.9 (interquartile range from 5.3 to 11.9). The adverse event (AE) rate per 100 patient years for risedronate-treated patients (Table) was 323 (95% CI=318 to 328). There was no increase in the adverse event rate experienced over the deciles of serum concentration of risedronate. This analysis demonstrates that risedronate has an excellent safety profile across a wide spectrum of serum drug concentrations in postmenopausal women.

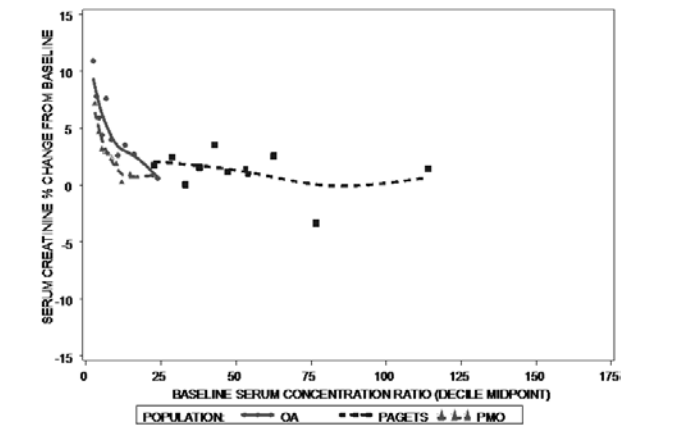
AE Rate (per 100 patient years) for Each Decile of Risedronate Baseline SCR			
Decile	SCR Midpoint	N	AE Rate/100 Yrs (95% CI)
1	2.9	960	344 (327, 362)
2	4.3	961	317 (300, 334)
3	5.3	961	322 (306, 340)
4	6.3	960	315 (299, 332)
5	7.4	961	309 (294, 326)
6	8.6	961	305 (290, 321)
7	10.1	960	341 (325, 359)
8	11.9	961	335 (319, 351)
9	14.7	961	316 (300, 332)
10	22.7	960	325 (309, 343)

Disclosures: **P. Miller**, Procter & Gamble Pharmaceuticals, Aventis 2, 5; Roche, Lilly, Merck, Novartis, Amgen, NPS 2, 5; Pfizer, Pharmacia 2.

SU406

Risedronate Demonstrates Favorable Renal Safety Over a Wide Range of Serum Concentrations. **P. Miller¹, S. Magowan², I. Barton^{*2}, J. Beary^{*2}, S. Boonen^{*3}.** ¹Colorado Center for Bone Research, Lakewood, CT, USA, ²Procter & Gamble Pharmaceuticals, Mason, OH, USA, ³Leuven University Center for Metabolic Bone Diseases, Leuven, Belgium.

Important factors that determine risedronate's serum steady state level include renal clearance of risedronate (CrCl), the daily drug dose, and volume of distribution (i.e. body weight). This analysis was designed to investigate the renal safety of risedronate over a wide range of drug steady state serum concentrations. Patients who took at least one dose of daily risedronate from the risedronate clinical trial programme (investigating postmenopausal osteoporosis, osteoarthritis and Paget's disease) were included. Serum drug concentration is inversely proportional to CrCl and body weight, and directly proportional to daily drug dose. These variables were incorporated for each patient to estimate a serum concentration ratio (SCR). The patient with the maximum combination of both CrCl and body weight and the lowest dose of risedronate (2.5 mg/day) was given an arbitrary value of 1. All other patient SCR values were calculated relative to this reference case. CrCl was estimated using the Cockcroft-Gault methodology. For each disease state, patients were ranked according to SCR decile. For these SCR deciles, the average of the maximum percent creatinine change from baseline was calculated. The analysis identified 11,193 patients who were randomized to risedronate in daily doses ranging from 2.5 to 30 mg/day: 9679 postmenopausal osteoporosis patients (2.5 mg/day=4833 and 5 mg/day=4846), 1237 osteoarthritis patients (5mg/day=628 and 15mg/day=609), 277 Paget's (30 mg/day). Risedronate SCR values (Figure) ranged from 1 to 175 with a median value of 8.1 (inter-quartile range=5.3 to 12.4). There was no observed deleterious change in renal function as a function of risedronate drug concentration over a range of 1 - 175 serum concentrations. This analysis suggests that risedronate over a range of SCR values from 1 to 175 has no deleterious effect on renal function. This is reassuring data for the clinician providing osteoporotic care to the elderly population with mild to moderate renal function.



Disclosures: **P. Miller**, Procter & Gamble Pharmaceuticals, Aventis 2, 5; Roche, Eli Lilly, Merck, Novartis, Amgen, NPS 2, 5; Pfizer, Pharmacia 2.

SU407

Fast Reduction of Bone Resorption with Risedronate Treatment within Two Weeks. **C. Günther¹, A. Kapner^{*1}, H. W. Schultis^{*2}, G. Moller³, O. Günther^{*1}, S. Günther^{*1}.** ¹Deutsches Zentrum für Osteoporose, Fachklinik Johannesbad, Bad Füssing, Germany, ²Gemeinschaftspraxis für Laboratoriumsmedizin und Mikrobiologie, Weiden, Germany, ³Dept. of Bone Pathology / Center for Biomechanics, Hamburg University School of Medicine, Hamburg, Germany.

The risk of a subsequent fracture after an osteoporotic fracture is highest immediately after the fracture event. Therefore, a very early intervention after fractures can avoid recurrent fractures. Risedronate 5 mg is an important antiresorptive drug in postmenopausal osteoporosis and reduces the risk of clinical vertebral and nonvertebral fractures in postmenopausal women with osteoporosis within 6 months. Short-term changes in bone turnover markers can prove fast onset of an antiresorptive therapy. Aim of this study is to determine how fast risedronate 35 mg once a week can reduce the bone turnover markers in patients with osteoporosis after treatment in clinical practice. 31 patients (26 women, 5 men, mean age 67 years) with a LWS BMD T-score < -2.5 and strong osteoporotic risk factors according to the German guidelines for osteoporosis (DVO) were enrolled. The patients were treated with calcium supplementation (800mg/d) and vitamin D (1000-1200 I.U./d) and received one dose of risedronate 35 mg per week. β -CTX levels were measured fasting in the morning at baseline and after 14 days of treatment using the Elecsys® β -CrossLaps test (Roche Diagnostics GmbH, Mannheim). Statistical analyses were determined by the sign-test. p<0.05 was considered statistically significant. β -CTX levels were significantly reduced by 42.1% (p<0.001) compared to baseline in osteoporotic patients two weeks after beginning treatment with risedronate 35 mg once a week. Risedronate 35 mg once a week significantly reduces bone resorption markers in osteoporotic patients as soon as two weeks after treatment. This fast reduction of bone resorption markers by risedronate 35 mg once a week is consistent with its fast reduction of vertebral and nonvertebral fractures in postmenopausal women with osteoporosis within 6 months. Treatment of postmenopausal osteoporosis with risedronate 35 mg once a week provides therefore an opportunity for early intervention in osteoporotic patients to avoid further osteoporotic fractures.

Disclosures: **G. Moller**, None.

SU408

Comparative Study of Bone Turnover and BMD Response to Treatment with Risedronate, Vitamin D, or Vitamin K in Japanese Osteoporosis Patients. **H. Iwata^{*}, S. Yamada^{*}, H. Takagi^{*}.** Rheumatology and Joint Replacement Center, Nagoya Kyoritsu Hospital, Nagoya, Japan.

The Japanese have the world's longest average life span (85 years for women, 78 years for men) and the elderly population of Japan is rapidly rising. Measures to counter diseases specific to the elderly, particularly osteoporosis, are important. We compared changes in bone turnover markers and bone mineral density (BMD) with the administration of risedronate (RIS) with those of vitamin D and vitamin K. Japanese patients with primary osteoporosis (6 men, 117 women) were enrolled at Nagoya Kyoritsu Hospital between May 2002 and May 2003 and were randomly assigned to one of three oral treatment groups: risedronate (Actonel®, RIS) 2.5 mg/d (n=37), vitamin D3 (Alfarol®, VD3) 1.5 μ g/d (n=45), vitamin K (Glakey®, VK2) 45 mg/d (n=41). The mean (SD, P-value vs RIS) changes in bone turnover markers and BMD from baseline to 48 weeks are shown in the table below:

Variables	% Changes from Baseline		
	RIS (SD)	VD3 (SD, P-value vs RIS)	VK2 (SD, P-value vs RIS)
Urinary NTX	-46.8 (17.7)	-0.01 (62.6, <0.001)	18.3 (55.7, <0.001)
Serum NTX	-44.8 (11.6)	-16.1 (70.1, 0.207)	-7.2 (23.8, 0.002)
Urinary DPD	-35.4 (29.5)	-5.7 (41.3, 0.004)	14.4 (60.6, 0.001)
Serum OC	-44.4 (31.2)	-27.8 (30.0, 0.049)	-6.8 (30.0, <0.001)
Serum BAP	-34.6 (19.9)	-25.9 (16.4, 0.083)	-4.1 (18.6, <0.001)
BMD	5.1 (3.9)	1.2 (4.6, 0.013)	1.0 (5.3, 0.008)

NTX=cross-linked N-telopeptides of type I collagen; DPD=deoxypyridinoline; OC=osteocalcin; BAP=bone alkaline phosphatase; BMD=bone mineral density. Beginning 4 weeks after the initiation of therapies, significant differences were observed for urinary and serum NTX, urinary DPD and serum OC with RIS compared to both VD3 and VK2. For serum BAP, similar decreases were observed for RIS and VD3; the decrease was greater for RIS compared with VK2. At 48 weeks, the BMD increase was significantly greater with RIS compared with VD3 or VK2. After These findings indicate that after 48 weeks of treatment in Japanese patients, risedronate was a more effective treatment for osteoporosis than VD3 or VK2.

Disclosures: **H. Iwata**, None.

SU409

Short-Term Monitoring of Bone Turnover Markers Improves Compliance in Postmenopausal Osteoporotic Patients under Antiresorptive Therapy.

O. Günther^{*1}, A. Kapner^{*1}, S. Günther^{*1}, H. W. Schultis^{*2}, C. Günther¹.

¹Deutsches Zentrum für Osteoporose, Fachklinik Johannesbad, Bad Füssing, Germany, ²Gemeinschaftspraxis für Laboratoriumsmedizin und Mikrobiologie, Weiden, Germany.

To control the onset of an antiresorptive therapy for treatment of postmenopausal osteoporosis bone turnover markers are usually measured 3-6 months after beginning treatment. We could recently show (Osteoporose & Rheuma aktuell 1/03, 12-13) that short-term monitoring of bone turnover markers as soon as 14 days after beginning antiresorptive treatment in patients with postmenopausal osteoporosis is a useful tool for proving the onset of treatment in rehabilitation. Aim of this study was to determine if short-term bone turnover marker monitoring can further improve long-term compliance in patients with postmenopausal osteoporosis on risedronate treatment. 31 patients (26 women, 5 men, mean age 67 years) with a LWS BMD T-score < -2.5 and strong risk factors according to the German guidelines for osteoporosis (DVO) were enrolled. The patients were treated with calcium supplementation (800mg/d) and vitamin D (1000-1200 I.U./d) and received one dose of risedronate 35 mg per week. β -CTX levels were measured fasting in the morning at baseline and after 14 days of treatment using the Elecsys® β -CrossLaps test (Roche Diagnostics GmbH, Mannheim). The results were discussed with the patients immediately after the measurement of bone turnover markers. To assess the compliance patients were called by telephone 12 months after first prescription. Compliance data could be collected from 83.9% of the 31 patients. 19.2% of this population stopped treatment with risedronate 35 mg once a week 4 weeks after the first prescription because the therapy was not continued by their family physicians. But 12 months after beginning of the risedronate treatment a great majority of the patients (80.8%) took their medication as prescribed. Short-term monitoring of bone turnover markers 14 days after beginning of bisphosphonate treatment can further improve long-term compliance in patients with postmenopausal osteoporosis on antiresorptive therapy and is therefore a great tool in rehabilitation medicine.

Disclosures: **C. Günther**, None.

SU410

Once-Monthly Oral Ibandronate Effectively Normalizes Biochemical Markers of Bone Resorption in Postmenopausal Osteoporosis: MOBILE 2-Year Analysis. P. D. Miller¹, D. L. Kendler², P. Garnero³, S. Silverman⁴, C. Hughes^{*5}, N. Mairon⁵, B. Bonvoisin⁵, C. Christiansen⁶. ¹Colorado Center for Bone Research, Lakewood, CO, USA, ²University of British Columbia, Vancouver, BC, Canada, ³INSERM Research Unit 403 and Synarc, Lyon, France, ⁴Cedars Sinai Medical Center, Los Angeles, CA, USA, ⁵F. Hoffmann-La Roche Ltd, Basel, Switzerland, ⁶Center for Clinical and Basic Research, Ballerup, Denmark.

When administered daily or weekly, oral bisphosphonates effectively normalize the elevated rate of bone resorption associated with postmenopausal osteoporosis (PMO). Ibandronate (Boniva) is a potent, nitrogen-containing bisphosphonate that can be effectively administered with extended dosing intervals.^{1,2} In MOBILE, an ongoing, randomized, double-blind, phase III study, the influence of once-monthly (50+50mg [single doses, consecutive days], 100mg [single day] and 150mg [single day]) and daily (2.5mg) oral ibandronate dosing schedules on bone turnover is being evaluated in 1,609 women (aged 55-80 years, \geq 5 years postmenopausal) with PMO (lumbar spine BMD T-score <-2.5 and \geq -5). Calcium (500mg) and vitamin D (400IU) supplements are provided. Median change (%) in the biochemical marker of bone resorption serum CTX (sCTX) was assessed as a secondary efficacy endpoint at 3, 6, 12 and 24 months. Values in the once-monthly arms were obtained by sampling at the end of the dosing interval. In all treatment arms, pronounced decreases in sCTX were observed at the 3 month time point, and were maintained for the duration of study (Table). At all time points, median decreases in sCTX with the 150mg once-monthly regimen were substantially greater than those with the daily and 100mg regimens (by 6.2-12.8% and 7.2-13.2%, respectively). These data demonstrate that the once-monthly ibandronate dosing schedule is similar to the daily dosing schedule in normalizing bone resorption, which has shown strong antifracture efficacy in a prior

placebo-controlled fracture study.^{1,2}

1. Chesnut CH, et al. J Bone Miner Res 2004;8:1241-9.

2. Delmas PD, et al. Osteoporos Int 2004;15:792-8.

	Median change (%; n) from baseline in sCTX.			
	2.5mg	50/50mg	100mg	150mg
Month 3	-53.6 (269)	-50.0 (278)	-53.2 (271)	-66.4 (276)
Month 6	-63.2 (270)	-60.8 (272)	-63.2 (274)	-73.4 (278)
Month 12	-67.3 (272)	-62.8 (276)	-66.7 (276)	-75.9 (267)
Month 24	-61.5 (221)	-56.1 (215)	-60.5 (211)	-67.7 (235)

Disclosures: **P.D. Miller**, **F. Hoffmann-La Roche Ltd**. 2, 5; **GlaxoSmithKline** 2, 5.

SU411

Bisphosphonate Augments PTH Effect on Trabecular Bone in Rats but Attenuates the Effect in Humans; How Relevant Is the Therapeutic OVX Model in Rat for Bisphosphonates? R. J. Arends^{*}, H. v. Oudheusden^{*}, A. G. H. Ederveen. Pharmacology, N.V. Organon, Oss, The Netherlands.

Osteoporosis can be therapeutically approached in two different ways; by use of anti-resorptive agents or by use of anabolic agents. Nowadays, anti-resorptive agents like bisphosphonates (BP), estrogens and SERMs are widely used to prevent menopause related bone loss. However, these treatments are only limited in preventing bone loss and do not restore the lost bone. Daily administration of parathyroid hormone (PTH) has been found to possess this anabolic quality and is therefore a promising agent to treat osteoporosis. However, stopping PTH treatment results in a rapid loss of newly gained bone. Preclinical studies have been described in literature to address the hypothesis that there may be an advantage in using PTH in combination with anti-resorptive agents. The results published so far are inconclusive, partially due to the large variety of different experimental set-ups used. In the present study, we evaluated the effect of PTH (16.5 μ g/kg.d.sc) alone, BP (10, 50, 100 μ g/kg.d.sc) or the combined treatment of PTH with BP on the bone mass and bone strength of ovariectomized female rats (OVX). Eighty-eight three-month-old female Wistar rats were ovariectomized and randomized in 11 groups (n=8). The animals were left untreated for two weeks to await development of moderate osteopenia. The sham-operated and the control OVX animals were treated with vehicle starting two weeks after surgery, while other groups received PTH, BP or a combination of PTH plus BP. All animals were sacrificed after 6 weeks of treatment. Both femurs were collected for bone mineral density measurement by pQCT and biomechanical testing by use of an indentation test, three-point bending test and cantilever bending test. In addition, the vertebral body L4 was dissected for a compression test. Our study demonstrated that treatment with either PTH or BP alone, or combined treatment of PTH with BP significantly restored the ovariectomy-induced loss of bone mass and trabecular bone strength in rats. Moreover, combined treatment of PTH with BP strongly augmented the effect of PTH alone. In conclusion, these preclinical in vivo data suggest that a bisphosphonate and PTH may act synergistically on bone mass and bone strength in rats thereby improving bone quality. This, however, is in contrast to recent clinical studies that failed to demonstrate any additive effect of the combined treatment of both agents on trabecular BMD in men and women. The fact that the above described results in rats are not in line with human data warrants carefulness in extrapolating these data to clinical outcome. Further animal studies to evaluate this discrepancy are ongoing.

Disclosures: **R.J. Arends**, **Akzo Nobel**, **N.V. Organon** 3.

SU412

Renal Tolerability of Ibandronate When Administered by Intravenous Injection: DIVA 1-Year Analysis. R. Civitelli¹, L. B. Tankó², V. Vyskocil³, C. Leigh^{*4}, P. Ward^{*4}, D. Masanaukaite^{*4}, R. R. Recker⁵. ¹Washington University School of Medicine, St Louis, MI, USA, ²CCBR, Ballerup, Denmark, ³University Hospital, Plzen, Czech Republic, ⁴F. Hoffmann-La Roche Ltd, Basel, Switzerland, ⁵Creighton University, Omaha, NE, USA.

Currently, intravenous (i.v.) bisphosphonates need to be administered as extended infusions to ensure renal tolerability. The ability to administer an intravenous bisphosphonate with a shorter dosing time without compromising renal function may be beneficial in some clinical situations. In prior clinical studies, ibandronate (Boniva), a potent, nitrogen-containing bisphosphonate, has demonstrated a favourable renal safety profile in women with postmenopausal osteoporosis (PMO) when administered as an i.v. injection. In the DIVA study, an ongoing, randomised, double-blind, double-dummy, phase III clinical trial, 2mg q2mo and 3mg q3mo i.v. ibandronate injections are being compared with an established 2.5mg daily oral ibandronate regimen in 1,395 women with PMO. In DIVA, renal safety parameters were assessed by continuously monitoring for renal adverse events (AEs), measuring serum creatinine concentrations and estimating creatinine clearance at baseline and every 4 and 3 months thereafter in the q2mo and q3mo treatment arms, respectively. Increases in serum creatinine concentrations were considered clinically important if they doubled during treatment or increased by >0.5mg/dl or >1mg/dl from baseline levels of <1.4mg/dl or >1.4mg/dl, respectively. In the 1-year safety analysis, baseline creatinine clearance was <90ml/min in all and <60ml/min in approximately half of the 1,382 women included. There were no reports of acute renal failure. Renal adverse events showed a low incidence, with no difference across all treatment groups (2%, 3% and 2% in the daily arm, q2mo arm and q3mo arm, respectively). Clinically important changes in serum creatinine occurred in only six participants (n=4 in the q2mo arm and n=2 in the q3mo arm), none of which were regarded as treatment-related, mostly due to the presence of concomitant conditions known to compromise kidney function. Only 14.2%, 14.1% and 17.4% of participants in the daily, q2mo and q3mo groups, respectively, showed any fall in creatinine clearance at any time point during the study. When administered as an

ASBMR 27th Annual Meeting

intermittent i.v. injection, ibandronate has a good renal safety profile in PMO, which is comparable to that of the established daily oral ibandronate regimen that has previously shown tolerability similar to placebo.

Disclosures: **R. Civitelli**, *F. Hoffmann-La Roche Ltd. 2; GlaxoSmithKline 2.*

SU413

Consistent Bone Mineral Density Gains with Intravenous Ibandronate Injections: Results from the DIVA Study. **R. Emkey¹, J. Halse², H. P. Kruse^{*3}, C. Hughes^{*4}, P. Ward^{*4}, D. Masanauskaitė^{*4}, R. R. Recker⁵.** ¹Radiant Research, Wyomissing, PA, USA, ²Osteoporoseklinikken, Oslo, Norway, ³Universitätsklinikum Hamburg-Eppendorf, Hamburg, Germany, ⁴F. Hoffmann-La Roche Ltd, Basel, Switzerland, ⁵Creighton University, Omaha, NE, USA.

DIVA is an ongoing randomized, double-blind, double-dummy, phase III, non-inferiority study. In this study, 2mg q2mo and 3mg q3mo intravenous (i.v.) ibandronate injections were at least as effective (for BMD endpoints) as an established 2.5mg daily oral ibandronate regimen (3-year vertebral fracture risk reduction: 52%) in 1,395 women with postmenopausal osteoporosis (PMO). In DIVA, a prospective analysis explored the influence of the following baseline patient characteristics on bone mineral density (BMD) gain: BMD T-score, prevalent fracture, and age (**Table**). Each subgroup comprised approximately 20% of the total study population. Although formal non-inferiority tests were not performed, spinal BMD gains in the i.v. groups were compared with the oral group using 95% confidence intervals (CI) in a post-hoc analysis. At 1 year, sizeable gains in lumbar spine BMD were observed in all patient subgroups, independent of the dosing route or schedule (**Table**). Increases in BMD were generally similar across the patient subgroups and between the i.v. regimens (**Table**). For each of the subgroups analysed, gains in lumbar spine BMD in the i.v. treatment arms were non-inferior (1% margin) to those observed in the daily arm (**Table**). In all study subgroups, i.v. ibandronate injections provided sizeable and comparable gains in lumbar spine BMD, which were at least as large as those observed with the established daily oral regimen. I.v. ibandronate injections have a consistent effect on BMD, regardless of baseline patient characteristics.

Table. Mean change (% , n) from baseline in lumbar spine BMD (plus 95% CI for difference versus daily) with i.v. ibandronate injection in the overall population and by patient subgroup.

	2.5mg daily oral	2mg q2mo i.v.	3mg q3mo i.v.
Overall population	3.8 [377]	5.1 [353] (0.76, 1.86)	4.8 [365] (0.49, 1.58)
Baseline BMD <-2.5 to ≥-3.0	3.4 [142]	4.4 [135] (0.14, 1.75)	4.3 [140] (0.03, 1.63)
Baseline BMD <-3.0 to ≥-3.5	3.9 [117]	4.8 [104] (-0.10, 1.89)	5.1 [118] (0.24, 2.18)
Baseline BMD <-3.5 to ≥-5.0	4.3 [118]	6.3 [114] (0.87, 3.03)	5.2 [107] (-0.21, 1.98)
No previous fracture*	3.7 [243]	5.0 [230] (0.61, 2.00)	4.7 [239] (0.34, 1.72)
Previous fracture*	4.0 [134]	5.3 [123] (0.42, 2.26)	5.0 [126] (0.16, 1.97)
Age <70 years	3.8 [268]	4.8 [227] (0.33, 1.67)	4.7 [256] (0.23, 1.53)
Age ≥70 years	3.9 [109]	5.8 [126] (0.89, 2.83)	5.3 [109] (0.38, 2.39)

*Since age 45

Disclosures: **R. Emkey**, *F. Hoffmann-La Roche Ltd 2, 5; GlaxoSmithKline 2, 5.*

SU414

Risedronate Inhibits Spontaneous Osteoclastogenesis from Peripheral Blood Mononuclear Cells in Post Menopausal Osteoporosis. **P. D'Amelio^{*1}, A. Grimaldi^{*1}, C. Tamone^{*1}, S. Di Bella¹, G. P. Pescarmona^{*2}, G. C. Isaia¹.**

¹Department of Internal Medicine, University of Torino, Torino, Italy, ²Department of Genetics, Biology and Biochemistry, University of Torino, Torino, Italy.

In our previous study we demonstrated an increased osteoclastogenesis from peripheral blood mononuclear cells (PBMC) in postmenopausal osteoporosis: the aim of this study is to evaluate a possible reduction of osteoclastogenesis in osteoporotic women after treatment with risedronate, and possible differences in osteoclasts formation in wells treated or not with vitamin D. Furthermore we will investigate possible effects of risedronate on the serum level of IL1 β, TNFα, IL6. 15 osteoporotic women and 13 controls were enrolled in the study. In all the subjects circulating PBMC were obtained with Ficoll-Pacque method. All cell incubations were performed in triplicate in 96 well/ plates (2 x 10⁵ cell/well) using the alpha minimal essential medium with or without 1,25-OH vitamin D₃ [10⁻⁸ M]. On the 10th day the cells were fixed and stained for Tartrate resistant acid phosphatase (TRAP) and for the expression of vitronectin receptor (VNR). In order to quantify the formation of TRAP+ and VNR+ multinucleated cells, the number of stained cells in each well was counted and identified as osteoclast. In all the subjects we measured the serum level of TNF α, IL-1β and IL-6 with ELISA method. All the patients received risedronate 5 mg/day for three months; after three months the patients were recalled and the above mentioned exams were repeated. After therapy there is an important decrease in the number of osteoclasts, the difference in osteoclasts number between wells treated or not with 1,25-OH vitamin D₃ was not significant before therapy, while after therapy 1,25-OH vitamin D₃ significantly reduced osteoclasts number (table). The

comparison between calcium, phosphorus, markers of bone turnover and levels of measured cytokines before and after therapy is not significant. In conclusion our data demonstrate that:

1. Osteoclast formation is significantly decreased by the administration of risedronate 5 mg/day for three months
2. The number of osteoclasts is reduced by the addition of vitamin D₃ *in vitro* only after treatment with risedronate *in vivo*.
3. Levels of TNFα , IL-1β and IL-6 are not significantly different in patients with respect to controls, and are not significantly modified by therapy

	Patients at baseline	Patients after therapy	p
Number of OC without 1,25-OH vitD ₃	50.23±30.97	20±24	0.008
Number of OC with 1,25-OH vitD ₃	37.44±26.44	5.11±11.4	0.000

Disclosures: **P. D'Amelio**, *None.*

SU415

Once-Monthly Oral Ibandronate Is Safe and Well Tolerated in Women with Postmenopausal Osteoporosis: MOBILE 2-Year Analysis. **E. M. Lewiecki¹, R. Emkey², S. Adami³, L. Rowell^{*4}, N. Mairon^{*5}, B. Bonvoisin⁴, D. Felsenberg⁶.** ¹New Mexico Clinical Research & Osteoporosis Center, Albuquerque, NM, USA, ²Radiant Research, Wyomissing, PA, USA, ³University of Verona, Verona, Italy, ⁴F. Hoffmann-La Roche Ltd, Basel, Switzerland, ⁵F. Hoffman-La Roche Ltd, Basel, Switzerland, ⁶Charité-University Medicine Berlin, Berlin, Germany.

Post-dose upper gastrointestinal adverse events (AEs) are a major reason for the discontinuation of oral bisphosphonates.^{1,2} An effective oral bisphosphonate that combines favorable safety with a reduction in the opportunity for post-dose AEs may improve adherence to therapy. When administered orally, the potent, nitrogen-containing bisphosphonate, ibandronate (Boniva), has shown a safety profile similar to placebo. In the MOBILE study, a favorable and comparable safety profile was observed at 1 year with once-monthly (50+50mg [single doses, consecutive days], 100mg [single day] and 150mg [single day]) and daily (2.5mg) oral ibandronate regimens in 1,609 women (aged 55-80 years; ≥5 years since menopause) with postmenopausal osteoporosis (PMO; lumbar spine BMD T-score <-2.5 and ≥-5). Safety and tolerability parameters were continuously monitored throughout 2 years of treatment. At 2 years, as at 1 year, once-monthly and daily oral ibandronate were well tolerated, with no meaningful differences between groups in the overall incidence of AEs (76.5-80.3%), treatment-related AEs (30.1-36.9%) or treatment-related AEs resulting in withdrawal (5.1-7.6%). Most serious AEs were considered unrelated to treatment, with the incidence and number of related serious AEs being very low over the 2-year study period (0.3-0.8%; n=8). No imbalance in the overall incidence of upper GI adverse events was observed across the daily (22.8%) and once-monthly (19.9-25.8%) treatment arms, with most events mild to moderate in intensity. The incidence of clinical fractures was comparable across the treatment arms. At 2 years, the safety profile of once-monthly and daily oral ibandronate in MOBILE was similar, and consistent with that reported at 1 year. Importantly, no tolerability disadvantage was observed with the 150mg once-monthly dose versus the 2.5mg daily dose and 100mg once-monthly dose.

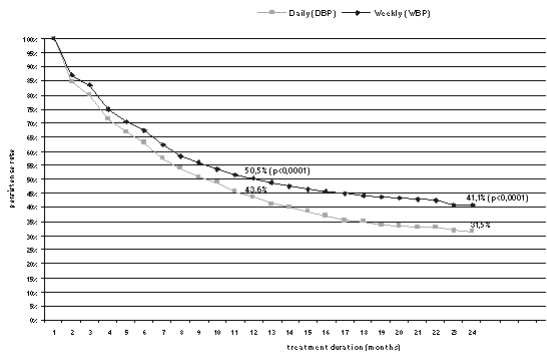
1. Tosteson AN, et al. Am J Med 2003;115:209-16.
2. Hamilton B, et al. Osteoporos Int 2003;14:259-62.

Disclosures: **E.M. Lewiecki**, *F. Hoffmann-La Roche Ltd 2, 5; GlaxoSmithKline 2, 5.*

SU416

Comparison of the Persistence of Daily and Weekly Bisphosphonates in French Female Patients Treated for Osteoporosis. **P. Fardellone^{*1}, A. F. Gaudin^{*2}, F. E. Cotte^{*2}, A. Lafuma^{*3}, C. Marchand^{*3}, A. El Hasnaoui^{*2}.** ¹CHU Nord, Amiens, France, ²GlaxoSmithKline, Marly le Roi, France, ³CEMKA - EVAL, Bourg la Reine, France.

The aim of this study was to compare the persistence of treatment with bisphosphonate (BP) according to their administration regimen. Persistence was assessed by the time to discontinuation of therapy. Two cohorts of female patients treated for osteoporosis with BP were retrospectively selected in a national computerized database representative of the French GPs prescriptions. Included women have consulted their GP at least twice a year for any reasons. The first cohort consisted of women whose treatment with daily BP (DBP) was first prescribed in 2000 or 2001 without prior treatment with SERMs or BP the previous year. Alendronate 5mg treatment was excluded because it is indicated in prevention of osteoporosis and etidronate was excluded because of its particular administration regimen. The second cohort included women with first weekly BP (WBP) treatment during the period 2002 and 2003. These periods were selected because in France, DBP were available from 2000 and WBP from October 2002 and this allowed us to have comparable cohorts. Duration of follow-up was as far as October 2002 for DBP cohort and October 2004 for WBP cohort. Survival analyses were performed in both cohorts using the end of treatment as endpoint. End of treatment was defined as the non-renewal of prescription 30 days after the length of the previous prescription. DBP cohort included 1,363 female patients, aged 69.7 years on average and WBP cohort included 3,969 patients, aged 69.7 years. Median duration of persistence was substantially higher in the WBP cohort than the DBP cohort during the 24 months of follow-up (391 days vs 301 days to discontinuation, respectively). The actuarial survival analysis curves below showed that after 12 months, 50.5% of women with the WBP regimen and 43.6% of women with the DBP regimen persisted with therapy. These rates decreased to 41.1% and 31.5% respectively at the end of 24 months. These results indicated that persistence differences between daily and weekly regimen appeared from three months and increased as far as two years of follow-up. Weekly regimen allowed a better persistence rate than daily regimen for the osteoporosis treatment but was still sub-optimal.



Disclosures: **A. El Hasnaoui**, Glaxo Smith Kline France 3.

SU417

Adherence to Bisphosphonate Therapy Is Associated with Decreased Nonvertebral Osteoporotic Fracture Risk. **S. Silverman**¹, **E. Siris**², **T. Abbott**³, **C. Barr**^{*4}, **S. Harris**⁵, **C. Rosen**⁶. ¹David Geffen School of Med UCLA, Beverly Hills, CA, USA, ²Columbia Univ Coll of Physicians and Surgeons, New York, NY, USA, ³Thomson-Medstat, Philadelphia, PA, USA, ⁴Roche Laboratories Inc., Nutley, NJ, USA, ⁵UCSF, San Francisco, CA, USA, ⁶St. Joseph's Hosp, Bangor, ME, USA.

Purpose: Nonvertebral fractures account for a substantial proportion of the morbidity and mortality associated with postmenopausal osteoporosis (PMO). One in 4 hip fracture patients dies within 1 year of the incidences.¹ The US Surgeon General emphasized the importance of treatment adherence to improve suboptimal clinical outcomes in PMO. The present study examines the association between adherence to newly prescribed bisphosphonate therapy and the risk of nonvertebral osteoporotic fractures, including hip and wrist, in postmenopausal women. **Methods:** A medical and pharmaceutical claims database (Medstat MarketScan®, covering 6 million lives) was analyzed to assess the relationship between adherence and the risk of nonvertebral fracture over 24 months in 37,698 women ≥45 years of age who received a first prescription for a bisphosphonate. Exclusion criteria included Paget's disease of bone, prior bisphosphonate use, prior cancer, or HIV infection. Two adherence measures based on claims data were evaluated: refill compliance (drug available ≥80% of the time) and persistence (no gaps in refills >30 days). **Results:** A total of 3,441 new nonvertebral fractures were reported during the study period. Of these, 1463 occurred at typical osteoporotic sites (734 hip and 732 wrist). Overall nonvertebral fracture risk was 25% lower in persistent versus nonpersistent subjects (*P*<.0001) and 21.2% lower in compliant vs poorly compliant subjects (*P*<.0001). Hip fracture risk was reduced by 33% among compliant subjects (*P*<.0001) and by 36% among persistent subjects (*P*<.0001). The risk of wrist fracture was reduced by 19% among persistent subjects (*P*=.0357) and by 13% among compliant subjects (*P*=.0596).

Influence of Adherence on Hip Fracture Risk (N=37,698)				
Adherence Status	n (%)	24-mo Hip Fracture Risk, %	% of Relative Risk Reduction	P value*
Compliant	16,350 (43)	1.5	33	<.0001
Noncompliant	21,348 (57)	2.3		
Persistent	7,113 (19)	1.3	36	<.0001
Nonpersistent	30,585 (81)	2.1		

*Fisher Exact Test

Conclusions: Adherence to bisphosphonate therapy is associated with a significant reduction in the risk of nonvertebral fracture, particularly hip and wrist, within 24 months of treatment initiation. Fewer nonvertebral fractures may minimize the morbidity and mortality associated with PMO.

1. NOF. *Osteoporosis Fast Facts 2004*. Available at: <http://www.nof.org/osteoporosis/diseasefacts.htm>.

Disclosures: **S. Silverman**, Merck, Procter & Gamble, Lilly, Novartis, Roche, and Kyphon 2, 5, 8; Wyeth 2, 5; Amgen 5; CompuMed 1.

SU418

Diet, Not Genotype, Affects Bone Size in Ovariectomized Estrogen Receptor Alpha Knockout Mice. **C. A. Peterson**, **N. Bagegni**^{*}. Nutritional Sciences, University of Missouri-Columbia, Columbia, MO, USA.

Several studies have shown beneficial effects of soy protein and soy isoflavones (IF) on bone during states of compromised estrogen status, yet the mechanisms are not yet fully elucidated. Using bones collected from a colon tumorigenesis experiment involving a unique estrogen receptor alpha knockout (ER-alpha KO) mouse model, we tested the following hypothesis: Ovariectomized (OVX), ER-alpha KO mice fed a soy protein diet with added IF will have greater bone mineral content (BMC) than those fed a soy protein diet without IF which in turn, will have greater BMC than mice fed a casein diet. Because IF have a purported greater affinity for the estrogen receptor beta in bone, we also hypothesized that there will be no significant difference in BMC between wild-type and ER-alpha KO mice. Mineral analysis of whole mouse tibias revealed significant diet effects, but no genotype effect. Consumption of soy protein with added IF resulted in greater bone weights and greater total tibia Ca than soy protein without IF or casein

controls; total tibia P and Mg were not different between soy groups, both of which were greater than casein. Furthermore, the *proportion* of Ca, Mg and P in bone remained rather constant regardless of diet. Our results support the observation that soy IF act through the ERB to affect bone growth and mineralization, while soy protein alone (without IF) appears to have limited effects.

Disclosures: **C.A. Peterson**, None.

SU419

Dietary Calcium Intake in Women with Early Postmenopausal Osteoporosis in Zurich Is Insufficient. **M. A. Dambacher**^{*1}, **M. Neff**^{*2}, **E. Brunner**^{*3}, **G. Moeller**⁴. ¹Dept. of Rheumatology and Rehabilitation, University Clinic Balgrist, REKO Südbaden-Südwürttemberg, Zürich, Switzerland, ²Center of Osteoporosis, Zürich, Switzerland, ³Dept. of Rheumatology and Rehabilitation, University Clinic Balgrist, Zürich, Switzerland, ⁴Medical Affairs, Procter & Gamble Pharmaceuticals-Germany GmbH, 65824 Schwalbach am Taunus, Germany.

Introduction: All large bisphosphonate trials have added calcium in amounts ranging from 500 to 1000 mg/day above individual dietary intake. Accordingly calcium supplements or calcium/vitamin D combinations are recommended today as co-medication to antiresorptive therapy in all recently published national or international guidelines on the care strategy for osteoporosis. In our experience general practitioners often disregard this important supplementation. Objective of this examination was to assess the dietary mean calcium intake of early postmenopausal osteoporotic (osteoporotic according to the WHO definition) women in Zurich. **Patients and Methods:** We assessed the daily calcium intake of 500 early postmenopausal osteoporotic (osteoporotic according to the WHO definition) women in Zurich. The calcium intake was determined by direct inquiry and calculated according to standardized tables (from Novartis and Roche). **Results:** Less than 3% of these 500 postmenopausal women (mean age: 58 years) reached the WHO recommendation for daily calcium intake for postmenopausal women which is 1300 mg. The mean daily calcium intake was 590 mg. **Conclusions:** There is an insufficient dietary mean calcium intake of the vast majority of early postmenopausal osteoporotic women in the (small big) town of Zurich. An additional calcium supplementation is highly recommended to achieve the recommended co-medication to antiresorptive therapies in all recently published national or international guidelines on the care strategy for osteoporosis. Integrated packaging that combined antiresorptive therapy with calcium (e.g., a bisphosphonate with calcium) could simplify and therefore improve current osteoporosis therapy.

Disclosures: **M.A. Dambacher**, None.

SU420

Effects of Vitamins B6 and K2 on Bone Mechanical Properties and Collagen Cross-Links in Spontaneously Diabetic WBN/Kob Rats. **M. Saito**, **S. Soshi**^{*}, **T. Tanaka**^{*}, **K. Fujii**^{*}. Orthopaedic Surgery, Jikei University School of Medicine, Tokyo, Japan.

Diabetes is associated with an increased risk of fracture, although type 2 diabetes is often characterized by normal bone mineral density (BMD). It is generally thought that latent vitamin B6 deficiency in diabetic patients is due to upregulated gluconeogenesis. Cross-links involves two different mechanisms, lysyl oxidase (LOX) mediated cross-links and non-enzymatic cross-linking (Advanced glycation end products; AGEs). LOX cross-links play important roles in the expression of proper physiologic function of collagen, whereas AGE accumulation has opposite effects. We recently demonstrated that low serum vitamin B6 was associated with a decrease in LOX-mediated cross-link and a sharp increase in AGEs (Pentosidine) cross-links, which correlated with bone fragility despite a lack of change in BMD in spontaneously diabetic WBN/Kob rats. Vitamin B6 is believed to act as both a coenzyme of LOX and as an inhibitor of AGE formation. In this study, we determined the effects of administration of vitamin B6 (pyridoxal 5-phosphate; PLP) or vitamin K2 (menatetrenone; MK-4) on bone mechanical properties and collagen LOX and AGE cross-link formation in male WBN/Kob rats. The onset of diabetes in these rats was observed at 12 months of age with mean fasting blood glucose levels of 493±119 mg/dl thereafter. Fourteen-month old male WBN/Kob rats were given either vehicle, PLP (250mg/kg bw/day) or MK-4 (50mg/kg bw/day) for 8 or 16 weeks. Low serum PLP levels were restored in the PLP-treated group. Femoral 3-point bending tests showed a significant increase in elastic modulus and toughness in rats treated with PLP or MK-4, despite no change in femoral BMD. The mechanical test results coincided with LOX and AGE cross-linking levels in bone collagen, such that the sum of LOX examined cross-linking components (DHLNL, HLNL, LNL, PYD, and DPD) was increased in the PLP (148%) and MK-4 (141%) groups over the vehicle-treated group. In contrast, Pentosidine levels were reduced in both PLP (49%)- and MK-4 (78%)-treated rats compared with the vehicle treated group. Bone collagen and serum intact osteocalcin levels were significantly greater in the MK-4 group than either the vehicle or PLP groups. These findings suggest that PLP stimulated not only LOX cross-link formation due to amelioration of the vitamin B6 deficiency, but also inhibited AGE cross-link formation in diabetic male rats. In contrast, MK-4 increased collagen accumulation in bone, suggesting that MK-4 improved the bone turnover rate without forming AGEs. These results indicate that both PLP and MK-4 increased collagen cross-link profiles and increased bone strength in diabetic osteopathy, but via different mechanisms.

Disclosures: **M. Saito**, None.

SU421

Bone Mineral Density (BMD) Evolution in Young Premenopausal Women with Idiopathic Osteoporosis. P. Peris¹, A. Monegal^{*2}, C. Moll^{*2}, J. Mundo^{*2}, A. Martinez^{*2}, S. Vidal^{*3}, F. Pons^{*3}, M. Martinez de Osaba^{*4}, N. Guañabens². ¹Rheumatology, IDIBAPS, Hospital Clinic, Barcelona, Spain, ²Rheumatology, Hospital Clinic, Barcelona, Spain, ³Nuclear Medicine, Hospital Clinic, Barcelona, Spain, ⁴Hormonal Laboratory, Hospital Clinic, Barcelona, Spain.

Idiopathic osteoporosis is one of the most frequent causes of osteoporosis in young premenopausal women. However, there are no data about the therapy and the spontaneous evolution of BMD in these patients. The aim of this study was to analyse the evolution of BMD in premenopausal women with idiopathic osteoporosis treated with calcium and vitamin D supplements. Methods: Retrospective study of 16 premenopausal women with idiopathic osteoporosis (aged 35.7±7 years) with a mean follow-up period of 4 years (1-7 years). BMD measurements at the lumbar spine and femoral neck (DXA) were obtained in all patients at baseline and yearly. All patients had one or more fragility fractures and/or a Z-score < -2 in the lumbar spine or femur. In all patients secondary causes of osteoporosis were excluded. In addition, serum Ca, P, total alkaline phosphatase (TAP), 25-OH vitamin D and PTH were determined as well as urinary calcium and hydroxyproline. Patients were treated with calcium (500mg/d) and vitamin D (400 UI) supplements and were advised to increase physical activity. Results: 25% of patients had associated fragility fractures and 50% had family history of osteoporosis. The mean calcium intake was 734±62 mg/day. The mean lumbar BMD at baseline was 0.909±0.04 g/cm² (Z-score -2.04±0.1), and in femur it was 0.766±0.06 g/cm² (Z-score -1.47±0.1). A significant increase in lumbar and femoral BMD was observed after 2 and 3 years of follow-up, respectively (1.9±1.9% mean increase in lumbar spine, p= 0.021, at 2 years) (5.6±4.5% mean increase in femur, p=0.04, at 3 years). Although no significant changes were observed in the other variables analysed (Ca, P, TAP, 25-OH vitamin D and PTH), the TAP values tended to increase at 2 years (122±46 vs 140±36 U/l, p=0.054). In addition, a negative correlation between baseline TAP serum values and lumbar BMD evolution at 2 years was observed (r=-0.748, p=0.013). No patient developed new skeletal fractures during the follow-up period. Conclusion: In young premenopausal women with idiopathic osteoporosis the conservative treatment with supplements of calcium and vitamin D associated with an increase of physical activity is associated with an increase in BMD without evidence of further skeletal fractures after more than 4 years of follow-up.

Disclosures: **P. Peris**, None.

SU422

Bisphosphonate Users Do not Purchase Enough Calcium to Ensure Sufficient Supplementation. B. Dawson-Hughes¹, M. P. Bradshaw^{*2}. ¹Bone Metabolism Lab, Tufts University, Boston, MA, USA, ²Procter & Gamble Pharmaceuticals, Mason, OH, USA.

The Surgeon General's Report on Bone Health suggests the average calcium intake of women 50 years and older is far below recommended levels for optimal bone health. The 1994-1996 Continuing Survey of Food Intakes by Individuals (CSFII) reports over 90% of women over 50 consume less than the dietary reference intake (DRI) of 1200 mg calcium. Recent NHANES data (2004) report average daily intake of 660 mg/day. This indicates a large percentage of the population will need dietary supplements to reach the DRI for calcium. Most postmenopausal osteoporotic women claim to understand calcium is a necessary part of osteoporosis treatment, but it is unknown how many actually take enough calcium supplements to meet the DRI of 1200 mg. This study analyzed calcium purchasing practices of current bisphosphonate users (Actonel® and/or Fosamax®) over a one-year period. 498 households of women who filled a prescription for either Actonel and/or Fosamax one year prior to and at least once during the current 52-week period were included in this study. These households were part of Information Resources Inc (IRI) RxPulse™ Patient Panel. This panel is a subset of IRI's Consumer Network Panel, a nationally representative set of 70,000 households that scan all their bar-coded purchases at home. Households within the RxPulse Patient Panel use their scanning device to record prescription information, including name of drug, strength and dose frequency, for each individual in their households. Data for supplement purchases included brand, calcium content (mg) and total tablet count. This panel provided a single source of data for bisphosphonate usage as well as total number of calcium supplement tablets (including Tums®) purchased. Panel data are weighted to match US demographics, and aggregate claimed purchases are verified through a comparison to store level scanner data. For this study, the supplement category was specifically examined and confirmed to fit within standard limits. 73% of bisphosphonate users' households did not purchase enough calcium supplements for them to take at least one tablet every day. Moreover, 40% of bisphosphonate users did not purchase any calcium supplements at all during the year. Calcium intake in osteoporotic women currently taking bisphosphonates is far below the recommended levels. Only about one in four patients currently taking a bisphosphonate purchases enough calcium to take one tablet every day. Providing osteoporotic women a convenient source of calcium with their osteoporosis treatment may help increase the percentage who actually take calcium on a regular basis, thereby improving the fracture risk reduction benefits of osteoporosis therapy.

Disclosures: **B. Dawson-Hughes**, P&G Pharmaceuticals, Aventis 5; Novartis 5; Eli Lilly 5; GSK-Roche 5.

SU423

No Effect of Vitamin K₁ Intake on Bone Mineral Density and Fracture Risk in Perimenopausal Women. L. Rejnmark¹, P. Vestergaard¹, P. Charles^{*1}, A. P. Hermann^{*2}, C. Brof^{*3}, P. Eiken^{*4}, L. Mosekilde¹. ¹Dept. of Endocrinology and Metabolism C, Aarhus Sygehus, Aarhus University Hospital, Aarhus, Denmark, ²Dept. of Endocrinology, Odense University Hospital, Odense, Denmark, ³The Osteoporosis Research Centre, Hvidovre Hospital, Hvidovre, Denmark, ⁴Dept. of Endocrinology and Clinical Physiology and Nuclear Medicine, Hilleroed Hospital, Hilleroed, Denmark.

Vitamin K functions as a cofactor in the posttranslational carboxylation of several bone proteins including, osteocalcin. In recent studies from the USA, a high vitamin K₁ intake has been associated an increased bone mineral density (BMD) and a decreased fracture risk. However, in the populations previously studied, the averages vitamin K₁ intake estimated by the food frequency method was approximately three times the recommended daily intake. We the present study, we investigated relations between vitamin K₁ intake and BMD and fracture risk in a European population. Within the Danish Osteoporosis Prevention Study (DOPS), including a population-based cohort of 2016 perimenopausal women, associations between vitamin K₁ intake and BMD was assessed at baseline and after 5-years of follow-up (cross sectional design). Moreover, associations between vitamin K₁ intake and 5- and 10-years changes in BMD were studied (follow up design). Finally, fracture risk was assessed in relation to vitamin K₁ intake (Nested case control design). In our cohort, dietary vitamin K₁ intake (0.6 µg/day) was close to the daily intake recommended by the FAO, but substantively lower than the intake reported in previously studied populations. Cross-sectional and longitudinal analyses showed no associations between intake of vitamin K₁ and BMD of the femoral neck or lumbar spine. Neither did BMD differ between those 5% who had the highest- and those 5% who had the lowest vitamin K₁ intake. During the 10-years of follow-up, 360 subjects sustained a fracture (cases). Compared to 1440 controls, logistic regression analyses revealed no difference in vitamin K₁ intake between cases and controls. Thus, in a Danish population, with an average vitamin K₁ intake close to the recommended daily intake, vitamin K₁ intake is not associated with effects on BMD or fracture risk.

Disclosures: **L. Rejnmark**, None.

SU424

DHEA Supplementation Does not Change Bone Turnover in Postmenopausal Osteopenic Women. M. R. Rubin, J. Slinex^{*}, M. Johnson^{*}, S. J. Silverberg. Columbia University College of Physicians & Surgeons, New York, NY, USA.

Dehydroepiandrosterone (DHEA) is an endogenous steroid that declines with age. On the basis of mainly anecdotal data, supplemental DHEA has become popular for putative anti-aging effects. Although DHEA administration has been associated with an increase in femoral neck BMD in postmenopausal women with normal BMD, no data exist on the effects of DHEA supplementation on skeletal metabolism in postmenopausal osteopenic women. We conducted a double-blind randomized placebo-controlled trial to investigate the effects of DHEA treatment on bone turnover in postmenopausal women with osteopenia. 37 postmenopausal women with osteopenia at the lumbar spine (LS) and/or total hip (TH) were randomized to 1 yr of DHEA (50 mg/d) or placebo (PLB). At baseline, the groups were well matched (mean ± SEM) in terms of age (DHEA: 63.2 ± 2 vs PLB: 62 ± 1 yrs; p=NS), time since menopause (DHEA: 10.3 ± 1 vs PLB: 11.5 ± 1 yrs; p=NS), LS T-score (DHEA: -1.2 ± 1 vs PLB: -1.8 ± 1; p= 0.1), TH T-score (DHEA -1.4 ± 1 vs PLB: -1.1 ± 1; p=NS), serum NTX (DHEA: 13.9 ± 1 vs PLB: 15.9 ± 2; nl range: 8.7-19.8 nmol BCE/liter; p=NS) and BSAP (DHEA: 27.4 ± 2 vs PLB: 26.4 ± 2 ng/ml; nl range: 8.0-16.6 ng/ml; p=NS). Osteocalcin was higher in the DHEA group at baseline (7.0 ± 1 vs 5.6 ± 1; nl range: 2.4-10.0 ng/ml; p = 0.006). Data are presented from an efficacy analysis of the subjects who continued in the study after the first baseline visit. 11 women (4 DHEA, 7 PLB) dropped out after the baseline visit, but they did not differ from the remaining 26 subjects (14 DHEA, 12 PLB) in terms of age, years since menopause, LS and TH BMD, serum NTX, BSAP or osteocalcin. After 1 year, there was no evidence of DHEA effect (assessed as % change) on levels of bone turnover markers (serum NTX-DHEA: -7.3 ± 9%; PLB: 4.2 ± 19%, p=NS; BSAP-DHEA: 1.8 ± 8%; PLB: -0.7 ± 8%, p=NS; or osteocalcin- DHEA: -9.6 ± 5%; PLB: 0.7± 8%, p=NS), nor did the rate of change in bone markers differ among the two groups. The time x treatment interaction was not significant (serum NTX: F(6,47) = 1.03, p =0.4; BSAP: F(6,42) = 0.97, p= 0.5; osteocalcin: F(6,69) = 2.0, p=0.08) in a mixed model analysis with fixed effect of treatment and random effects of time and subject, adjusted for the baseline difference in osteocalcin. In conclusion, this small, preliminary study suggests that DHEA supplementation does not significantly influence bone turnover in postmenopausal osteopenic women. Whether a larger study might detect smaller changes in bone turnover remains to be seen.

Disclosures: **M.R. Rubin**, None.

SU425

Vitamin K Treatment Reduces Undercarboxylated Osteocalcin but Does not Alter Bone Turnover or Density in Postmenopausal North American Women. J. M. Harke¹, D. Krueger¹, D. Gemar¹, M. Checovich¹, S. Zeldin^{*1}, J. Engelke^{*1}, R. Chappell^{*2}, J. Suttie^{*3}, N. Binkley¹. ¹University of Wisconsin Osteoporosis Clinical Research Program, Madison, WI, USA, ²Biostatistics and Medical Informatics, University of Wisconsin, Madison, WI, USA, ³Biochemistry, University of Wisconsin, Madison, WI, USA.

Prior data suggest that vitamin K may improve skeletal health by enhancing osteocalcin carboxylation. For example, low vitamin K status, as measured by elevated undercarboxylated osteocalcin concentration, is associated with increased osteoporotic fracture risk. Additionally, some studies find vitamin K treatment to reduce vertebral fracture risk. However, whether vitamin K plays a role in the skeletal health of North American women remains unclear. Moreover, it is possible that various K vitamers (phylloquinone [K1] and menatetrenone, [MK4]) have differing skeletal effects. The purpose of this study was to evaluate the effect of K1 or MK4 treatment on markers of skeletal turnover and bone density in non-osteoporotic postmenopausal North American women. As such, in this randomized, double-blind, placebo-controlled study, 381 women not meeting the National Osteoporosis Foundation criteria for receipt of osteoporosis medications received K1 (1 mg daily), MK4 (45 mg daily) or placebo for 12 months. All participants received calcium citrate with vitamin D₃ (315 mg/200 IU) twice daily for two months prior to randomization and for the study duration. Serum markers of bone turnover (bone specific alkaline phosphatase [BSAP] and n-telopeptide of type 1 collagen [NTx]) were measured at baseline, 1, 3, 6 and 12 months. Bone mineral density (BMD) of the lumbar spine and proximal femur was measured by dual-energy x-ray absorptiometry at baseline, 6 and 12 months. 176 women are included in this preliminary analysis, their mean age and spine BMD was 62.3 years and 1.188 g/cm². At baseline, the three treatment groups did not differ in age, albumin, creatinine, AST, BSAP, NTx, percent undercarboxylated osteocalcin or BMD. Median compliance with calcium supplements, K1 and MK4 treatment was 95%, 95% and 91% respectively. K1 and MK4 treatment reduced serum undercarboxylated osteocalcin by 72% and 74% respectively, averaged over all follow-up visits; the decreases were immediate and stable. No effect of either K1 or MK4 treatment was observed on BSAP or NTx. Moreover, no effect of K1 or MK4 on lumbar spine or total proximal femur BMD was demonstrated. This preliminary analysis does not support a role for vitamin K treatment in bone turnover or density among postmenopausal North American women receiving calcium and vitamin D supplementation.

Disclosures: **J.M. Harke, None.**

SU426

A Controlled Trial of the Effect of Milk Basic Protein (MBP) Supplementation on Bone Metabolism in Healthy Menopausal Women. A. Itabashi¹, S. Aoe^{*2}, Y. Toba^{*3}, Y. Takada^{*4}, T. Koyama^{*5}. ¹Central Clinical Laboratory, Saitama Medical School, Saimata, Japan, ²Department of Home Economics, Otsuma Women's University, Tokyo, Japan, ³Functional Products Business Development, Snow Brand Milk Products Co.,Ltd, Tokyo, Japan, ⁴Product Planning Department, Snow Brand Milk Products Co.,Ltd, Tokyo, Japan, ⁵Koyama Takao Clinic, Tokyo, Japan.

Milk has more beneficial effects on bone health than other food sources. Recent in vitro and in vivo studies have showed that milk whey protein, especially its basic protein fraction (milk basic protein, MBP), contains several components capable of promoting bone formation and inhibiting bone resorption. The object of this study was to examine the effect of MBP on bone metabolism of healthy menopausal women. Thirty-two healthy menopausal women were randomly assigned to treatment with either placebo or MBP (40 mg per day) for six months. The bone mineral density (BMD) of the lumbar vertebrae L2-L4 of each subject was measured by dual-energy x-ray absorptiometry (DXA) at the beginning of the study, and after six months of treatment. Serum and urine indexes of bone metabolism were measured at baseline, after three months, and at the end of the study. Daily intake of nutrients was monitored by a three-day food record at the beginning of the study, and after three and six months. Twenty-seven subjects who completed the study according to the protocol were included in the analysis. The mean rate of gain of lumbar BMD of women in the MBP group (1.21%) was significantly higher than for women in the placebo group (-0.66%, p=0.046). When compared with the placebo group, urinary cross-linked N-telopeptides of type-I collagen (a biochemical marker of bone resorption), adjusted for creatinine excretion, was significantly decreased in the MBP group at six months, but no significant difference in serum osteocalcin (a biochemical marker of bone formation) was observed between the two groups. The urinary NTx excretion was found to be related to serum osteocalcin in the MBP group at the 3 and 6 months. Daily MBP supplementation of 40 mg in women can significantly increase their BMD, independently of dietary intake of minerals and vitamins. These results suggested that MBP supplementation was effective in preventing bone loss in menopausal women, and that this improvement in BMD may be primarily mediated through inhibition of osteoclast-mediated bone resorption, while maintaining the balance of bone remodeling, by MBP supplementation.

Disclosures: **A. Itabashi, None.**

SU427

Safety and Bone Mineral Density Effects of Bread Fortified with 125 mcg Vitamin D₃/day in Romanian Nursing-Home Residents. V. Mocanu¹, P. A. Stitt^{*2}, A. Costan^{*3}, E. Zbranca^{*3}, V. Luca^{*1}, R. Vieth⁴. ¹Department of Pathophysiology, University of Medicine and Pharmacy, Iasi, Romania, ²Nutritional Resource Foundation, Madison, WI, USA, ³Endocrinology, University of Medicine and Pharmacy, Iasi, Romania, ⁴Pathology and Laboratory Medicine, Mount Sinai Hospital, Toronto, ON, Canada.

If older men and women maintain serum levels of 25(OH)D higher than the threshold of 75 nmol/L, they should be at lower risk of fracture (Dawson-Hughes et al, Osteoporosis Int. online Mar 2005). The European OPTIFORD Study proposes bread as a useful vehicle for vitamin D fortification. However, both groups propose vitamin D intakes of 25 mcg/d or less, which we regarded as unrealistically low for vitamin D deficient elderly. We carried out a single-arm trial to evaluate the safety and efficacy of vitamin D₃ bread fortification in 45 Romanian nursing residents (age 71.02±6.73 years). Their basal serum 25(OH)D in Dec 2003 was 28.5±10.3 nmol/L (11 ±4 ng/mL), and in 86% of them it was <40 nmol/L (<16 ng/mL). Each day, each resident consumed one bun whose dough had been enriched with 250 mcg of vitamin D₃ and 315 mg calcium. After baking, the vitamin D content averaged 125 mcg per 100-g bun. Serum calcium, parathyroid hormone, bone markers, 25(OH)D, urinary calcium/creatinine ratio and C-telopeptide were measured every 3rd month for 1-yr. At baseline and 12 mo, bone-mineral density (BMD) was measured at the hip, spine, and total body by dual-energy x-ray absorptiometry (Hologic Delfi A densitometer). After 12 mo, serum 25(OH)D levels were 125.6±38.8 (SD) nmol/L, but in 10% of subjects it was <75 nmol/L. The vitamin D and Ca-fortified bread lowered serum PTH (basal vs 12 mo: 64. ± 19 pg/ml vs 21.17±23.1 pg/ml; p=0.0001). At every follow-up, there were no changes in serum calcium (basal vs 12 mo: 2.29±0.15 mmol/L vs 2.29±0.15 mmol/L), urinary calcium (3.72±0.3 mmol/d vs. 3.16±0.3 mmol/l) or calcium/creatinine ratio (0.378 ± 0.18 mmol/mmol vs. 0.357±0.20 mmol/mmol). However, at 12 mo, there were significant increases in lumbar spine BMD (+4%, 0.831±0.128 g/cm² vs 0.863±0.146 g/cm²; p=0/037) and hip BMD (+24%, 0.734±0.126 g/cm² vs 0.907±0.156 g/cm²). The gain in BMD may be explained by mineralization of osteoid, and closure of the remodeling space because of sharply lower PTH concentrations that would have reduced bone remodeling. Fortification of bread with much more vitamin D than previously studied was safe and appears to be appropriate for sun-deprived nursing-home residents.

Disclosures: **R. Vieth, None.**

SU428

Daily, Weekly or Monthly Protocols to Reach the Desired Serum 25-Hydroxyvitamin D Concentration for the Elderly. S. Ish-Shalom¹, T. Salganik^{*2}, E. Segal^{*2}, B. Raz^{*2}, I. Bromberg^{*3}, R. Vieth³. ¹Calcium and Bone Unit, Rambam Medical Center, Haifa, Israel, ²Calcium and Bone Unit, Technion Faculty of Medicine, Haifa, Israel, ³Pathology and Laboratory Medicine, Mount Sinai Hospital, Toronto, ON, Canada.

A recent consensus about vitamin D₃ for prevention of hip fractures in the elderly stated that serum 25-hydroxyvitamin D (25(OH)D) concentrations should be higher than 30 ng/mL (75 nmol/L) (Dawson-Hughes et al, Osteopor Int. Mar 18, 2005). To achieve this goal, the consensus was that all elderly should be supplemented with 1000 IU/day. We investigated whether the 25(OH)D response to supplementation might differ when the same total dose of vitamin D was given daily, weekly or monthly. We randomly allocated 48 patients (age 81 ±8 SD yrs) to three different regimens of vitamin D supplementation; delivering the same total dose: 1500 IU/daily; 10500 IU/weekly; or 45000 IU/monthly as crystalline USP vitamin D₃ in USP ethanol (diluted so that mixing 1 mL into a drink delivered 1500 IU, 10500 IU or 45000 IU). Before starting, mean serum 25(OH)D of all subjects was 19 ±9 SD ng/mL, and in 95% of them it was < 30 ng/mL. At the end of the 8-week protocol, mean increases in 25(OH)D approached a plateau. Concentrations did not differ between dosing strategies (Table). The major difference was that the monthly protocol produced distinctive jumps in 25(OH)D during the week after each dose. After 8 wk, for all 48 subjects, mean serum 25(OH)D was 36 ±11 SD ng/mL. This was significantly higher than 30 ng/mL (p=0.001), yet in 35% of the subjects, serum 25(OH)D was < 30 ng/mL despite the intake of 1500 IU/day. We conclude that a dose of vitamin D₃ higher than 1500 IU/day is required to ensure that within 2 months, essentially all treated patients achieve serum 25(OH)D levels higher than the minimum concentration desired for fracture prevention.

Regimen	Increases in serum 25(OH)D ng/mL after 8 weeks of vitamin D3			
	N	25(OH)D Mean Increase	25(OH)D 2.5 percentile	25(OH)D 97.5 percentile
1500 IU/day	16	18	6	33
10500 IU/wk	17	13	7	20
45000 IU/mo	15	21	-2	40
Overall data	48	17	-2	40

Disclosures: **S. Ish-Shalom, None.**

SU429

Neutralization of the Acidogenic Western Diet With K Citrate Increases DXA BMD in Postmenopausal (PM) Osteopenic Women: Results of a DBRCT. S. Jehle^{*1}, A. Zanetti^{*1}, J. Muser^{*2}, H. N. Hulter³, R. Krapf[†].
¹Medicine, Kantonsspital Bruderholz, Bruderholz/Basel, Switzerland, ²Laboratory Medicine, Kantonsspital Bruderholz, Bruderholz/Basel, Switzerland, ³Genentech Inc, South San Francisco, CA, USA.

The effect of alterations in either acid or protein intake on bone mass remains controversial. Both net anabolic and catabolic (via chronic acid loads) effects on bone have been attributed to the high animal/grain protein content of the Western diet. There are no reported controlled trials on the effects of altered acid intake on bone mass in humans. In a single-center, prospective DBRCT, PM non-vegetarian osteopenic (T-score -1 to -4 at L2-L4) women (n = 161) were randomized 1:1 to receive either blinded 10 mmol of trivalent Kcitrate or KCl (30 mmol) p.o. daily in 3 div doses for 12 mos. All subjects received Ca 500 mg and D3 400 IU daily. The primary endpoint was DXA (Lunar DPXL) BMD % change, L2-L4 at mo 12. There were no significant baseline differences among the 2 groups with regard to BMD (all sites), 25-OHD, intact PTH, acid-base parameters, Ca, Pi or markers.

	Month 6		Month 12	
	%Δ KCl	%Δ K Cit	%Δ KCl	%Δ K Cit
L2-L4 BMD	-0.4	+0.5*	-1.0	+0.9#
THip BMD	-0.8	+0.2*	-1.5	+0.5#
FN BMD	-1.2	-0.3	-1.9	-0.5*
S BSAP	+9.2	+10.4	+5.9	+9.1
S osteocal	-9.1	-7.7	-6.8	-11.7
S Ctx	-12.1	-33.5	+37.6	+20.2
U Pyr/Cr	+0.5	-5.6	-3.8	-5.0
U DPD/Cr	+2.7	-6.4	-7.3	-10.3

* p<0.05, # p<0.001

%Δ BMD at L2-L4 was significantly higher in K Cit group by month 6 and differences increased progressively to mo 9 and 12. Bone marker changes showed a non-significant trend to decreased resorption and increased formation at mo 6 assessment. K Cit induced a sustained and significant reduction in urinary Ca and Pi excretion: U Ca/creat in Kcit at mo 6 was -0.065 (p = 0.033) and -0.073 at mo 12 (p = 0.040). In addition, the increases in Ucit excretion correlated directly and significantly with Δ%BMD at L2-L4, while the Δ net acid excretion (an estimate for endogenous acid production) correlated inversely and significantly with the %Δ L2-L4 BMD in a subset (N=22). In conclusion, Kcitrate - by neutralizing the dietary acid load - induced large (+1.9% net of control, L2-L4) mo 12 BMD increases, intermediate in magnitude between raloxifene and bisphos. The progressive BMD increases at mo 12 with small marker trends persisting only to mo 6 and the sustained effects on urinary Ca excretion suggest improved mineralization as part of the underlying mechanism, in addition to cellular mechanisms.

Disclosures: **R. Krapf**, None.

SU430

Polyphenolic Compounds in Dried Plum Enhance Bone Recovery Following Skeletal Unloading. E. A. Lancaster^{*1}, E. A. Lucas¹, J. Collins^{*2}, L. Howard^{*3}, N. O. Maness^{*4}, B. H. Arjmandi¹, B. J. Smith⁵. ¹Department of Nutritional Sciences, Oklahoma State University, Stillwater, OK, USA, ²South Central Agricultural Research Laboratory, USDA ARS, Lane, OK, USA, ³Department of Food Science, University of Arkansas, Fayetteville, AR, USA, ⁴Department of Horticulture and Landscape Architecture, Oklahoma State University, Stillwater, OK, USA, ⁵Department of Surgery, University of Oklahoma Health Sciences Center, Oklahoma City, OK, USA.

Dried plums have been used medicinally for many years, but recently have been shown to enhance the recovery of bone in osteopenic animal models. The aim of this study was to begin to investigate the bioactive components of dried plum, i.e. polyphenols and boron, on bone recovery following hindlimb unloading (HU). Fifty-four, 6-month-old, female Sprague Dawley rats were randomly assigned to either HU (5 groups) or ambulatory (AMB=1 group). Following 4 wks of HU and confirmation of bone loss by DXA, rats were returned to normal ambulation and treatments initiated: HU-control diet (HU-Con); HU-control diet with 15% (w/w) dried plum (HU-DP); or HU-control diet with a comparable dose of boron (HU-B) or polyphenol (HU-PP) extract to that found in dried plum. One HU group was fed control diet and received subcutaneous parathyroid injections (80 ug/kg body wt; 3 x wk) (HU-PTH) to serve as a positive control. Bone recovery of the 4th lumbar vertebrae (L4) was evaluated in terms of bone mineral density, trabecular microarchitecture, and bone strength. The recovery of L4 BMD in the HU-PP and HU-B animals was the same as that observed in the HU-DP and HU-PTH groups. Furthermore, the HU-PP had similar effects on trabecular bone volume (BV/TV), thickness (TbTh) and linear attenuation as the dried plum, but was not able to enhance recovery to that of the HU-PTH. While the HU-B group was statistically similar the HU-PP group on a number of microarchitectural parameters, it was not able to have the same effect as the dried plum. Bone strength of the L4 was increased in the HU-DP group, but the HU-PP and HU-B were not able to enhance overall bone strength. At the end of the 12 weeks no alterations in bone biomarkers were observed, but urinary calcium was elevated in HU-DP and HU-groups. We conclude that the extracted polyphenols account for large proportion of the effects observed with dried plum on trabecular bone and appear to be one of the primary bioactive components in dried plum.

Disclosures: **E.A. Lancaster**, None.

SU431

Sevelamer Prevents Bone Loss in Ovariectomized Rats. P. Simic^{*1}, S. Vukicevic¹, N. Draca^{*1}, A. Blair², S. Burke², K. T. Sampath². ¹Laboratory for Mineralized Tissues, Zagreb Medical School, Zagreb, Croatia, ²Drug Discovery and Development, Genzyme Corporation, Waltham, MA, USA.

In patients with chronic kidney diseases (CKD), hyperphosphatemia is associated with renal osteodystrophy, vascular and soft-tissue calcification, and mortality. In a randomized clinical trial, we recently reported that sevelamer hydrochloride (Renagel®), a non-calcium phosphate binder, is capable of reducing progressive coronary artery and aortic calcification and significantly increasing trabecular bone mineral density (BMD) in CKD (stage 5) patients as compared to calcium containing phosphate binders (acetate and carbonate salts) (Raggi P, et.al., JBMR., in press). In the present study, we examined whether sevelamer could also prevent and restore bone loss that follows ovariectomy in rats (an animal model of osteoporosis). Sprague Dawley rats were ovariectomized (OVX) at 6 months and the sevelamer therapy was started immediately (prevention model), and 3 months following OVX (restoration model). Six months old rats (n=96) were ovariectomized (OVX) and divided into following groups: (1) Sham; (2) Sham + sevelamer 3%; (3) OVX; (4) OVX + sevelamer 1%; (5) OVX + sevelamer 3%. Sevelamer was mixed with food immediately following OVX and therapy was continued for 25 weeks. The whole body, hind limbs and lumbar spine bone mineral density (BMD) was monitored by DEXA in vivo throughout the study. Ex vivo measurements of femur, tibia and lumbar spine were performed using DEXA, pQCT and µCT. At 4 and 8 weeks following administration, sevelamer (at both doses) significantly increased BMD at all measured sites. Although sevelamer did not maintain the increased BMD at later time intervals (above 20 wks), at 3% in OVX animals it progressively increased BMD of sham animals towards 20 weeks following administration which was maintained until the termination at week 25, and then confirmed by ex vivo measurement of BMD. In a restoration model, sevelamer (3%) was mixed with food and therapy started at 3 months following OVX and continued for another 12 weeks. Results show that Sevelamer increased BMD of hind limbs and lumbar spine for 8% and 5%, respectively thus restoring lost bone. These results suggest that sevelamer has a positive effect on bone mineral density by preventing bone loss and restoring bone volume in aged OVX rats.

Disclosures: **S. Vukicevic**, None.

SU432

Additive Bone Protective Effects of Fuctooligosaccharide and Soy Isoflavones. L. Devareddy^{*}, D. A. Khalil, D. Y. Soung, E. A. Lucas, S. C. Chai^{*}, K. Korlagunta^{*}, S. S. Mahajan^{*}, B. H. Arjmandi. Nutritional Sciences, Oklahoma State University, Stillwater, OK, USA.

We have previously reported that the addition of fructooligosaccharide (FOS), an indigestible fermentable polysaccharide, to soy protein (Soy) reverses the loss of BMD in ovariectomized (Ovx) osteopenic rats. In this study, we examined the effects of Soy, FOS, and their combination on microstructural properties of tibiae. For this, 60 nine-month old female Sprague-Dawley rats were either sham-operated (sham) or Ovx and then maintained for 90 days to establish bone loss. Thereafter, rats were divided into five groups (n=12; one Sham and four Ovx): Sham, Ovx (control), Soy, FOS+casein, and FOS+Soy. After 125 days of dietary treatment, rats were necropsied and bones were analyzed. Treatment effects on selected bone microstructural properties were assessed using microcomputed tomography (Scanco Medical). Below is a summary of our findings.

Measures	Sham	Ovx	Soy	FOS	FOS+Soy	P Value
BV/TV	0.111 ^a	0.069 ^b	0.061 ^b	0.069 ^b	0.075 ^c	0.0007
ConnD	20.1 ^a	5.7 ^b	5.3 ^b	6.1 ^b	8.1 ^b	<.0001
SMI	1.98 ^b	2.50 ^a	2.71 ^a	2.61 ^a	2.59 ^a	0.0003
TbN	2.03 ^a	1.54 ^{bc}	1.50 ^c	1.61 ^{bc}	1.81 ^{ab}	0.0003
TbTh	0.078 ^b	0.090 ^a	0.088 ^a	0.087 ^a	0.085 ^{ab}	0.0234
TbSp	0.507 ^c	0.668 ^a	0.691 ^a	0.634 ^{ab}	0.559 ^{bc}	0.0057

Data are mean (n=12). Values in a row that do not share the same superscript letters are significantly (P<0.05) different from each other. In terms of certain trabecular microstructural properties, the results of this study indicate that the combination of these two agents is better than either alone. FOS, in part, may enhance the bone protective effects of soy isoflavones by altering gut microflora that improves calcium and isoflavone bioavailability.

Disclosures: **B.H. Arjmandi**, None.

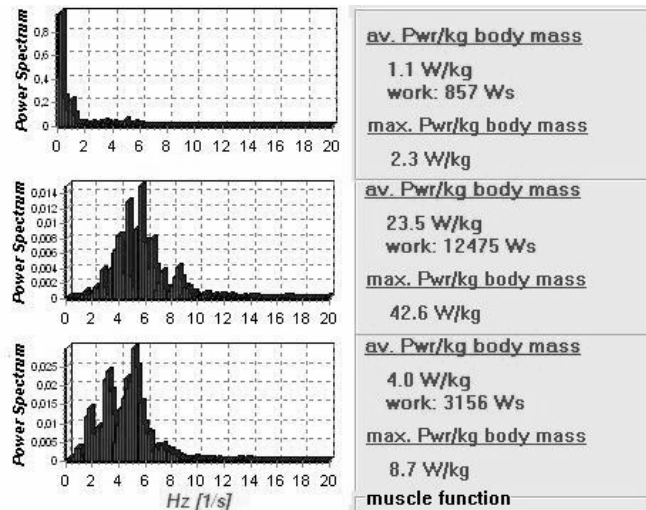
SU433

A Novel Method for Monitoring of Neuromuscular Function as a Potential Factor for Risk of Fall. P. Schneider, H. Haenscheid^{*}. Clinic for Nuclear Medicine, University of Wuerzburg, Wuerzburg, Germany.

According to epidemiological studies bone mineral density accounts for only 15% of fracture risk in elderly. The risk of fall, the primary factor leading to fracture depends largely on neuromuscular function. Therefore a method is required to directly assess the risk of fall instead of indirect questionnaire approaches. The device developed is capable of tracing force vectors during a provoked tandem stand test (TST) and tracing muscle force during a series of enforced knee-bends (KB), simulating the chair-rising test (CRT). During the measurement time the novel device assesses the forces and activation velocity (power) exhibited by the muscle groups essential for walking and balance. The time series is analysed and displayed as a power spectrum. Average power to maintain the gravity's center of body mass is calculated. The test can be repeated as one leg test, with eyes open or closed. Sensitivity is +/- 2N. Measurement time for the TST and KB test, the surrogate

for the CRT is e.g. 10 seconds each. The number of bends with maximum force is registered and the maximum power is calculated by analysis of the recorded time series. The methods show clear differences in muscle activation frequencies which are generally in a range of 0-20 Hz, and power, depending on training, age, disease or neurotropic drug status. There is an inverse relation between the individuals capability to maintain balance, the power to remain in the neutral center of gravity, leading to muscle fatigue. The balance and KB tests show considerable differences in muscle frequency and power, related to age, training status or drug intake in individuals. The figure shows a patient with vertebral osteoporosis (89 y., female, top), a soccer player (19 y., female, middle), and a patient on 20 mg prednisolon (54 y., female, bottom). The novel method described^o is able to monitor an individual's capability of keeping balance depending on different influences, to measure the muscle power required for the test, to display muscle activation frequencies and to measure gross and maximum muscle power during the KB test. Other than the classic stopwatch versions, the tests are digitally recorded and analysed. According to the bone mechanostat the results should be associated with bone health and fracture risk via the functional bone-muscle unit, which yet has to be studied longitudinally.

^opatent application filed



Disclosures: *P. Schneider, None.*

SU434

Recovery of Site-Specific Bone Loss in Amenorrheic Runners. M. E. Walcott^{*1}, K. E. Ackerman², N. Glass¹, M. S. LeBoff¹. ¹Medicine, Brigham and Women's Hospital, Boston, MA, USA, ²Internal Medicine, Hospital of the University of Pennsylvania, Philadelphia, PA, USA.

While amenorrhea has been shown to have detrimental effects on skeletal health, little is known about whether this process is reversible in amenorrheic athletes who develop normal menstrual function. To examine the skeletal impact of amenorrhea on bone mass, we measured metabolic markers of bone turnover and bone density in elite long distance runners (5k to ultra-marathons.) We enrolled 73 female runners ages 18-40 (mean 26.6±6.5) with and without amenorrhea and with no other secondary causes of low bone mass. Bone density was tested at the left hip, lumbar spine, and whole body by dual x-ray absorptiometry (DXA) and at the bilateral distal radii by peripheral quantitative computed tomography (pQCT). Participants were tested for n-telopeptides, osteocalcin, and 25 (OH) vitamin D and completed dietary intake and training questionnaires. Runners were classified as currently amenorrheic (Amen, n=18), currently eumenorrheic with a history of amenorrhea during adolescence (AdAmen n=15), or eumenorrheic (Eu n=40). The Eu and Amen groups reported 50% oral contraceptive use, while the AdAmen runners reported 92% oral contraceptive use. While 55-60% of the runners used multivitamin or calcium supplements, data from the dietary intake questionnaire indicated that 79.5% of runners, especially the Amen runners, were unable to meet daily calcium, vitamin D, and B vitamin intakes without supplementation. A significant difference was observed between the Amen and Eu athletes in the pQCT measured Bone Strength Index (p=0.02), at the lumbar spine (p<0.01), but not at the hip. Specifically, 50% (n=9) of the Amen athletes versus only 12.5% (n=5) of the Eu athletes had a Z-score < -1.0 S.D. at the lumbar spine. BMD at the lumbar spine in the AdAmen runners was significantly higher than the Amen runners, but was not significantly different from the Eu runners. In fact, AdAmen BMD at all locations was comparable to Eu BMD. All three groups showed similar, normal osteocalcin, N-telopeptide, and serum vitamin D levels. The BMD of runners who regain menstrual function after adolescence can recover to levels of eumenorrheic runners. In addition, BMD of the hip was protected from the effects of amenorrhea as a result of the site-specific force from running. Because 60% of the currently amenorrheic runners have had sustained amenorrhea for more than 8 years, these data suggest that the duration of amenorrhea, rather than age of occurrence, is a determining factor in skeletal health.

Disclosures: *M.E. Walcott, None.*

SU435

The Economic Implications of a Policy of Provision of Hip Protectors to Institutionalized Elderly in Ontario, Canada. A. M. Sawka¹, A. Gafni^{*2}, P. Boulos^{*1}, K. Beattie^{*3}, A. Papaioannou¹, A. Cranney⁴, D. A. Hanley⁵, J. D. Adachi¹, E. A. Papadimitropoulos⁶, L. Thabane^{*7}. ¹Medicine, McMaster University, Hamilton, ON, Canada, ²Centre for Health Economics and Policy Analysis, McMaster University, Hamilton, ON, Canada, ³Faculty of Health Sciences, McMaster University, Hamilton, ON, Canada, ⁴Medicine, University of Ottawa, Ottawa, ON, Canada, ⁵Medicine, University of Calgary, Calgary, AB, Canada, ⁶Eli Lilly and University of Toronto, Toronto, ON, Canada, ⁷Clinical Epidemiology and Biostatistics, McMaster University, Hamilton, ON, Canada.

Our objective was to determine whether a policy of provision of hip protectors to Ontario nursing home residents age 65 years and older could result in cost savings, stemming from reductions in initial hospitalizations for hip fracture. We conducted a cost analysis from a Ministry of Health perspective (one year cycle length). The anti-hip fracture efficacy of hip protectors in nursing home residents was based on a Bayesian meta-analysis of randomized controlled trials. We determined that at current prices of hip protectors, a strategy of provision of hip protectors to all elderly nursing home residents in the province could result in an overall mean cost savings of 3.6 million Canadian dollars in one year (95% credibility interval [CRI], -30.3 million, 39.4 million), with a probability of cost savings of 0.57. A strategy of provision of hip protectors to high risk elderly nursing home residents with osteoporosis or dementia would be expected to result in a mean overall cost savings of \$12.0 million (95% CRI -18.9 million, 44.8 million), with a probability of cost savings of 0.77. Provision of hip protectors to elderly nursing home residents without either dementia or osteoporosis is unlikely to result in cost savings. Decreasing the price of hip protectors would increase the magnitude and probability of cost savings in each scenario. In conclusion, the largest cost savings in acute hip fracture care are most likely to be achieved if hip protectors are only provided to high risk nursing home residents. Cost savings can be increased by negotiating a lower price for these devices.

Disclosures: *A.M. Sawka, None.*

SU436

A Meta-Analysis of Hip Protector Trials in Institutionalized Elderly Using a Bayesian Approach. A. M. Sawka¹, P. Boulos^{*1}, K. Beattie^{*2}, A. Papaioannou¹, A. Gafni^{*3}, A. Cranney⁴, D. A. Hanley⁵, J. D. Adachi¹, E. A. Papadimitropoulos⁶, L. Thabane^{*3}. ¹Medicine, McMaster University, Hamilton, ON, Canada, ²Faculty of Health Sciences, McMaster University, Hamilton, ON, Canada, ³Clinical Epidemiology and Biostatistics, McMaster University, Hamilton, ON, Canada, ⁴Medicine, University of Ottawa, Ottawa, ON, Canada, ⁵Medicine, University of Calgary, Calgary, AB, Canada, ⁶Eli Lilly and University of Toronto, Toronto, ON, Canada.

Objective: Our objective was to design a Bayesian random effects model for pooling hip fracture outcome data from cluster randomized trials (CRTs) and individually randomized trials (IRTs) of hip protectors in institutionalized elderly. Institutionalized elderly included residents of nursing homes, hostels, or residential group homes. A second analysis was conducted in trials of exclusively nursing home residents. **Study Design and Setting:** Eight electronic databases were searched; abstracts and full-text papers were reviewed in duplicate. The pooled mean odds ratio (OR) of a hip fracture in an individual allocated to hip protectors with 95% credibility interval (CRI) was calculated using a Bayesian random effects model. The uncertainty of model parameters (such as cluster size or the intra-cluster correlation coefficient) was modeled. Statistical adjustments were performed to account for the design effect of cluster randomized trials. **Results:** We included six trials of 6213 individuals (2 IRTs and 4 CRTs). The pooled OR of an institutionalized elderly individual (including residents of nursing homes, hostels, or residential group homes) sustaining one or more hip fractures with hip protector allocation was 0.56 (95% CRI 0.17, 1.06); the OR for hip fracture in trials of exclusively nursing home residents was 0.39 (0.06, 0.68). The model was robust in multiple sensitivity analyses in which alternative statistical assumptions were explored. **Conclusion:** Using a Bayesian approach to meta-analysis, we determined that hip protectors decrease the risk of hip fracture in elderly nursing home residents, but not in all institutionalized elderly.

Disclosures: *A.M. Sawka, None.*

SU437

Mechanical vs. Metabolic Component of Self-Reported Physical Activity and Bone Mineral Density in Postmenopausal Scottish Women. A. Mayroedi^{*1}, H. M. Macdonald¹, A. D. Stewart^{*2}, D. M. Reid¹. ¹School of Medicine, University of Aberdeen, Aberdeen, United Kingdom, ²School of Health Sciences, The Robert Gordon University, Aberdeen, United Kingdom.

Physical activity (PA) is an important risk factor for osteoporosis and associated fractures, but its assessment in epidemiological studies has always been a challenge. We have developed and validated a new self-administered bone-specific physical activity questionnaire (bsPAQ) using tri-axial accelerometers, which estimates both the metabolic and mechanical component of self-reported PA. Using the Aberdeen bsPAQ we aimed to assess the importance of mechanical vs. metabolic component of PA on BMD. A total of 1847 postmenopausal women from the North of Scotland Osteoporosis Study (NOSOS) who underwent bone densitometry in 2001-3 (mean ± SD age: 69.3 ± 5.5y) were contacted in 2004 and 68.7% (n = 1254) completed the bsPAQ. Median values for self-reported PA

(metabolic component) were 149.4 (IQR: 46.2) MET.h/wk and for peak scores (mechanical component) 4.5 (IQR: 2.0). After excluding women that were taking any medication or suffering from conditions likely to affect bone metabolism (n =148), we found that those in the highest tertile of PA (metabolic component) had a higher BMD at the lumbar spine (LS) (ANOVA p = 0.036), at the total right (RH) (ANOVA p = 0.001) and total left hip (LH) (ANOVA p <0.001) compared to women in the lowest tertile. Differences remained significant for hip BMD (ANCOVA RH p = 0.035 and LH p = 0.013), but not LS BMD (ANCOVA p = 0.164), after adjusting for important confounders (age, weight, height, smoking, HRT use, socio-economic status, energy adjusted calcium and vit D intake, alcohol consumption, family history of osteoporosis, seasonal variations, and time interval between BMD scan and PA assessment). Women in the highest tertile of the mechanical component of PA had a higher BMD at the total RH (ANOVA p = 0.038) and LH (ANOVA p = 0.002) compared to women in the lowest tertile. Differences remained significant after adjustment for confounders at LH (ANCOVA p = 0.017) but not at RH (ANCOVA p = 0.174). There were no differences across tertiles for LS BMD. Multiple regression analysis revealed that the mechanical component of PA explained 1.3% of the LH BMD variation (unstandardized β (SE): 0.007 (0.002)); the metabolic component explained a further 0.2% (β (SE): <0.001 (<0.001)). The corresponding values for RH BMD were 0.6% (β (SE): 0.005 (0.002)) and 0.2% (β (SE): < 0.001 (0.001)). Amongst older Scottish postmenopausal women PA seems to have a small but significant independent effect on current BMD, with the mechanical component explaining more of the BMD variation than the metabolic component, especially at the total hip site.

Disclosures: **A. Mavroeldi**, None.

SU438

Radiologic Evidence of Improvement in Thoracic Kyphosis in Osteoporosis and Osteopenia Using a Kypho-Orthosis Program. **S. M. Ali***, **M. Sinaki**. Physical Medicine and Rehabilitation, Mayo Clinic, Rochester, MN, USA.

Kyphosis in osteoporosis has detrimental effects, including a decrease in physical activity and respiratory function, gait and balance dysfunction, and a poor quality of life. In a previous study we reported that kyphosis in osteoporotic subjects can increase the risk of falls. Therefore, measures that improve kyphosis in this population are important in improving physical activity and quality of life and decreasing the risk of falls. The weighted kypho-orthosis is a device used to improve kyphosis by providing a gentle posterior/inferior back-force below the scapulae and by providing proprioceptive feedback. Our objective was to assess radiographic changes in osteopenic/osteoporotic individuals with kyphosis after intervention with a weighted kypho-orthosis. We examined radiographs of the thoracic spine in 22 patients (19 female and 3 male) with either osteopenia or osteoporosis who had been evaluated in an outpatient osteoporosis program at our multispecialty clinic. The study was performed with the approval of the institutional review board. The kypho-orthosis program included the use of a kypho-orthosis for ½ to 1 hour once or twice a day, along with shoulder retraction exercises. Radiographs were obtained at baseline and at follow-up visits with a range of 74 to 878 days (mean 318.4 days) between visits. The angle of thoracic kyphosis was measured using the Lippman-Cobb technique by a physiatry resident (SA). The thoracic curve was measured from the superior edge of T4 to the inferior edge of either T12 or the interference vertebra (the vertebra that comprises the caudal end of the curve). Height and weight were also obtained at baseline and follow up. The results showed subjects' age ranged from 38 to 90 years (mean 66.4 years). Thoracic kyphosis ranged from 42 to 87 degrees at baseline (mean 61.1 degrees) and from 28 to 85 degrees at follow up (mean 57.8 degrees) which was a statistically significant difference (p<0. 0280). This study showed that intervention with a weighted kypho-orthosis showed statistically significant radiologic improvement in thoracic kyphosis. Our study did not take into account the level of patient compliance. More in-depth studies are required with a larger number of subjects to further elucidate radiographic changes in osteoporotic individuals with kyphosis using this kypho-orthosis program.

Disclosures: **S.M. Ali**, None.

SU439

Effect of Low-Intensity Back Exercise on Quality of Life in Patients with Osteoporosis. **M. Hongo¹**, **E. Itoi¹**, **N. Miyakoshi¹**, **Y. Shimada^{*1}**, **M. Sinaki²**. ¹Department of Orthopedic Surgery, Akita University School of Medicine, Akita, Japan, ²Department of Physical Medicine and Rehabilitation, Mayo Clinic, Rochester, MN, USA.

We have demonstrated that back extensor strength is the most significant contributor to the spinal mobility and spinal mobility has strong effect on quality of life (QOL) in patients with osteoporosis. We also reported back strengthening exercise using a weighted backpack was effective for increasing back extensor strength and decreasing risk of vertebral fractures. However, the weighted back exercise needs to be prescribed on an individual basis according to musculoskeletal fragility in order to be safe. Therefore, an exercise program needs to be safe in intensity but exertional enough to be biomechanically challenging to be effective. The aim of this study was to determine the effects of low-intensity back strengthening exercises on back extensor strength, spinal mobility, and QOL. A total of 80 women with postmenopausal osteoporosis participated in the study. Initial screening excluded women with severe back pain, severe spinal deformity, and history of any known health problems. Average age was 67 years (range, 50-78 years). Participants were randomly assigned to a control group (n=38) or an exercise group (n=42). The study period was 4 months. Each subject in the exercise group was instructed to lie in a prone position with a pillow under the abdomen such that her spine was slightly flexed. Then, she was to lift the chest off the bed toward the neutral position for 5 seconds. Each contraction was repeated 10 times and each exercise was performed 5 times a week.

Isometric back extensor strength was measured using the specific dynamometer. Spinal range of motion between upper thoracic spine and sacrum was analyzed with Spinal Mouse®. Scores for the QOL was evaluated by the questionnaires which contained six domains. Back extensor strength significantly increased both in the exercise group (26%; p<0.0001) and in the control group (11%; p=0.01). There was no significant difference in back extensor strength at four month between the groups. Spinal range of motion did not significantly change in both groups. There was no significant difference in spinal range of motion between the groups. Scores for QOL increased in the exercise group (7%; p<0.0001), whereas it remained unchanged in the control group (0%). There was a significant difference in QOL score between the groups (p=0.036). Scores of the domain for the activities of daily living and general health in the exercise group improved significantly and greater than in the control group. In conclusion, low-intensity back strengthening exercise was effective in improving QOL and back extensor strength for patients with osteoporosis.

Disclosures: **M. Hongo**, None.

SU440

Nutritional Evaluation and Body Composition in Well-Trained Cyclists. **V. S. R. Penteado^{*1}**, **M. G. Santana^{*2}**, **S. V. Bertolino^{*3}**, **M. T. Mello^{*3}**, **M. M. Pinheiro^{*1}**, **V. L. Szejnfeld¹**. ¹Rheumatology Division, São Paulo Federal University, São Paulo, Brazil, ²Psychobiology Division, São Paulo Federal University, São Paulo, Brazil, ³Psychobiology Division, São Paulo Federal University, São Paulo, Brazil.

It is well established that cycling plays an important role on body composition. It increases muscle mass and decreases body fat. This sporting event is characterized by weight bearing with minimal strain and involves prone orientation for long and exhaustive trainings. There is little evidence demonstrating the impact of cycling on bone mass. Moreover, bone health and sporting performance in these athletes could be optimized by suitable nutritional support. Objectives: In this study we aimed to evaluate bone mineral density (BMD), body composition and nutritional aspects in well-trained cyclists. Methods: Thirty-six high performance cyclists (31 road and 5 mountain bike) and 15 health controls, matched for body mass index (BMI), age and race were invited to participate in the study. All the subjects answered a detailed questionnaire about risk factors to osteoporosis and fractures and had the kind and frequency of their physical activities recorded. The nutritional inquiry was performed by four days recording - macronutrients and micronutrients (calcium, phosphorus, magnesium, iron, zinc, vitamin A and C) intake was compared with specific dietary recommendations for each group (FAO/ OMS, 1995; DRI 2002; Williams & Devlin, 1998). Maximal rate of oxygen uptake kinetics test ($\dot{V}O_{2\max}$) and bone densitometry at lumbar spine, proximal femur and body total (DXA, GE-Lunar MD +) were performed in all subjects. Results: The athletes had significantly better $\dot{V}O_{2\max}$ results as compared to the control group (p<0.05). BMD measurements did not differ significantly between athletes and controls at all sites examined (total body, p = 0.15; lumbar spine, p = 0.71; femoral neck, p = 0.62). Total lean mass and skeletal muscle mass indexes were significantly higher in cyclists as compared to health controls (p = 0.001), while body fat was significantly lower in the athletes (p<0.05). Positive significant correlation was demonstrated between total and lumbar spine BMD measurements and lean mass (r = 0.6029, p <0.001) and body fat (r = 0.5730, p<0.001). Conclusions: Our results demonstrate that cycling has significant beneficial effects on body composition, however no relevant impact on bone mineral density could be demonstrated.

Disclosures: **V.S.R. Penteado**, None.

SU441

Prevention of Hip Fracture in Aged-Care Facilities with Increased Use of Hip Protectors in Japan. **T. Koike¹**, **Y. Orito^{*1}**, **H. Toyoda^{*1}**, **M. Tada^{*1}**, **R. Sugama^{*1}**, **S. Kobayashi^{*2}**, **K. Takaoka¹**. ¹Orthopaedic Surgery, Osaka City University Medical School, Osaka, Japan, ²Orthopaedic Surgery, Shinshu University Medical School, Nagano, Japan.

To assess the effects of an intervention program designed to increase use of hip protectors in frail elderly women in aged-care facilities, we developed a cluster randomization trial in Japan. Two hundred fifty aged-care facilities in seven prefectures in Japan were invited and 76 units agreed to participate. Low adherence rate with protectors is a problem. Adherence will be largely determined by the motivation and competence of staff in nursing homes. To reduce burdens on staff in intervention group, the nursing staff selected 5 residents from each home in protector group and 15 residents in control group according to predefined inclusion criteria: >65 years old, female, not bedridden, with risk factors for falls. Therefore, facilities were randomly allocated in a 1:3 ratio to control and protector group. To keep the motivation of staff in nursing homes, monthly newsletters, posters, illustrated books were provided for all facilities. Furthermore, members of research team visited and conducted staff in all 76 nursing homes every month. We provided three hip protectors per resident (Safehip, Teijin, Japan). Totally 614 residents (308; protector, 306; control) were enrolled and 21 residents (12; protector, 9; control) were excluded from analysis by bedridden, hospitalization and death at 10 months of follow up. At baseline level, there were no important differences between intervention and control groups in age, body height, body weight, arm span, grip strength, %fat, calcaneus SOS (CM-100, Elk, Japan) and cognition level (MMSE). Six hip fractures occurred in the intervention group while 17 occurred in the control group; (RR 0.35; 95% CI 0.14 to 0.86). Adherence with wearing protectors at least daytime was 87.5%. There were 450 falls during follow up with 268 in the intervention group (a mean of 0.91 falls per person) and 182 in the control group (a mean of 0.61 falls per person). Especially among residents who had hip fractures, a mean of falls per person in the intervention group was greater than

ASBMR 27th Annual Meeting

control group, 2.83 and 1.94, respectively. We evaluated the hardness of floors in all facilities by measuring the maximum acceleration during the impact of an eight pounds weight and could not find the differences between two groups. Furthermore, there were no differences in the number of staff, rate of hip fractures, rate of falls between the intervention and control facilities recent three years. We conclude the increase in use of hip protectors reduce the number of hip fractures in aged-care facilities.

Disclosures: **T. Koike**, None.

SU442

Resistance Training Using Mechanical Vibration as a New Form of Physical Exercise for Prevention of Osteoporosis. **C. Kleinmond**^{*1}, **F. E. Thomasius**², **S. Scharla**³, **M. Wiseman**^{*4}, **E. R. Weissenbacher**^{*5}, **M. Hartard**¹. ¹Faculty of Sport Science, AG-MSI, Technische Universitaet Muenchen, Munich, Germany, ²Osteoporosis Study Society, Frankfurt, Germany, ³Practice for internal medicine, Bad Reichenhall, Germany, ⁴Leibniz Data Processing Center, Bavarian Academy of Sciences, Munich, Germany, ⁵Department of Gynecology and Obstetrics, Faculty of Medicine, Klinikum Grosshadern, Ludwig Maximilians Universitaet, Munich, Germany.

High-frequency mechanical strain stimulates bone strength in animals. The effects of mechanical vibrations on the human skeleton however have rarely been examined, especially in postmenopausal women with a higher risk of osteoporosis. Therefore the aim of this randomized controlled 12 month long trial was to prove parameters of safety, bone mass, geometry and metabolism under vibration training (VRT) in comparison to conventional resistance training (CRT) in postmenopausal women. Hip and lumbar spine bone mineral density (BMD) were evaluated by DXA (Norland XR 26 Mark II). Tibial bone mineral content (BMC), bone geometry and volumetric BMD were assessed by pQCT (XCT-2000 of STRATEC) at shank levels of 4, 14 and 38%. 73 post- menopausal (mean age 56.04 ± 3.78) women were randomized to VRT (25 Hz, Galileo 2000®) or CTR. The training was performed twice weekly with an intensity of up to 50-60% (month 1-6) and 60-70% (month 7-12) of 1-RM in 2 sets each over the 12-month intervention time. 50% of each group decided to take a defined HRT (estradiol 2 mg, MPA 10 mg) half of the group did not receive HRT. After intervention there were no significant intergroup differences for parameters of safety, mean spinal or femoral BMD and tibial BMC, BMD and geometric parameters at all shank levels. In both groups we observed a significant increase of torque for the knee extension. Furthermore, the well-known bone sparing properties of HRT were shown in both groups, however, more significant under VRT. At the tibial shaft, HRT user showed higher values for cortical BMC at shank levels of 14% and 38% (14% HRT: 1.31% ± 1.49, Non-HRT: -1.17% ± 2.72, p = 0.016; 38% HRT: 2.21% ± 0.93, Non-HRT: -0.10% ± 1.72, p = 0.002). Smaller medullary areas were seen at 38% under VRT (HRT: -3.30% ± 2.19, Non-HRT: 0.26% ± 2.15, p = 0.003) possibly as a result of an increased endosteal apposition. We conclude that VRT was as safe and at least as effective as CTR. VRT was associated with a significant increase of bone mass in most regions and obviously influenced bone geometry at the distal tibia when in combination with HRT.

Disclosures: **C. Kleinmond**, None.

SU443

The Orthoses Spinomed and Spinomed Active Improve Posture, Trunk Muscle Strength and Quality of Life in Postmenopausal Women with Vertebral Fractures due to Osteoporosis: A Controlled, Randomized, and Prospective Clinical Trial. **M. Pfeifer**¹, **L. Kohlwey**^{*1}, **B. Begerow**^{*1}, **H. W. Minne**². ¹Institute of Clinical Osteology, Bad Pyrmont, Germany, ²Institute of Clinical Osteology and Clinic "DER FÜRSTENHOF", Bad Pyrmont, Germany.

Spinal orthoses may play an important role in the treatment of spinal fractures due to osteoporosis. So far, however, clinical trials addressing efficacy according to evidence-based medicine are rare. In a first pivotal study, an improvement in posture, trunk muscle strength, and quality of life after wearing the orthosis *Spinomed* has been demonstrated (Pfeifer M et al. 2004). In order to further improve compliance and increase overall acceptance and comfort, a new device has been developed: the initially used system with belts and Velcros has been integrated in a body, whereas the stabilizing back pad is fixed by textile strain elements at the spine. The back pad, which is easily deformable, may be adjusted to individual spinal deformities and is included in a pocket sewed on the back of the body (*Spinomed active*). One hundred and ten patients suffering from vertebral fractures and an angle of kyphosis of 60° and above were recruited via newspaper advertisements and invited to participate in this randomized, prospective clinical trial with the angle of kyphosis being the primary endpoint. Secondary endpoints include body height, trunk muscle strength, body sway, pain and limitations of daily living using standardized questionnaires. **Table 1** presents results after six months of treatment: both orthoses *Spinomed* and *Spinomed active* led to an improvement in posture, trunk muscle strength, and quality of life in patients suffering from osteoporotic vertebral fractures.

Especially *Spinomed active*, which is completely invisible below normal clothes is characterized by a very high compliance and acceptance among patients and thus comes very close to an ideal orthosis for the treatment of osteoporosis.

Table 1: Results After Six Months			
Parameter	Spinomed active ("Body", N=48)	Spinomed (N=31)	Controls (N=31)
Age (Years)	68.5 +/- 10.6	72.8 +/- 7.1	72.3 +/- 6.7
Baseline Vertebral Fractures (Number)	1.5 +/- 2.4	2.0 +/- 2.7	2.1 +/- 2.8
Angle of Kyphosis (Change in Degrees)	-6.2 +/- 5.3*	-7.9 +/- 4.9*	-1.6 +/- 5.5
Back Extensor Strength (Change in Newton)	+178 +/- 135*	+189 +/- 152*	+7 +/- 55
Body Sway (Change in mm)	-16.2 +/- 31.2*	-20.4 +/- 40.2*	-1.7 +/- 35.6
Vital Capacity (Change in %)	+5.6 +/- 18.9#	+6.1 +/- 20.5#	-9.9 +/- 16.1
Pain (Change in Score-Points)	-1.3 +/- 1.0*	-1.5 +/- 1.2*	+0.1 +/- 0.9
	*:p<0.01	#p<0.05	

Disclosures: **M. Pfeifer**, None.

SU444

Bone Safety Evaluation: Balance Domain Validation. **C. Recknor**¹, **S. Grant**^{*1}, **J. Empert**^{*2}, **F. Bride**^{*2}, **M. Shotwell**^{*2}, **B. Schell**^{*2}. ¹United Osteoporosis Centers, Gainesville, GA, USA, ²Brenau University, Gainesville, GA, USA.

Patients with osteoporosis present with a unique set of musculoskeletal concerns. The Bone Safety Evaluation© (BSE) is a performance-based assessment tool that is designed to address these unique concerns by assessing spinal compression forces, balance, strength and flexibility. Test properties of the BSE were studied in order to determine the clinical and research utility of this tool. Initial tool validation involved establishing inter-rater reliability. To strengthen this test property, scoring guidelines and standardized instructions were developed. Concurrent criterion-based validity was tested in two stages. First, a convenience sample of 42 patients (age range 63-88) with osteoporosis who were tested with the BSE and a subtest of a computerized assessment of balance: computerized dynamic posturography-sensory organization test (CDP-SOT) was examined retrospectively to determine if a correlation existed between the balance domain on the BSE and CDP-SOT. Then, a prospective study of 37 participants (age range 52-84) with and without osteoporosis was conducted comparing the same instruments and another balance assessment: Modified Clinical Test of Sensory Interaction and Balance (mCTSIB). Among four people scoring the BSE an ICC was found to be ICC=.994. A Pearson Product Moment correlation coefficient of .61 (p < .001) was found between the BSE balance domain and CDP-SOT on the retrospective study. In the prospective study, a Pearson Product Moment correlation coefficient of .62 p < .001 was found between the BSE balance domain and CDP-SOT when one outlier was removed and 45 p< .01 was found between the BSE balance domain and mCTSIB. Additionally, an independent samples t-test was calculated between participants with and without osteoporosis. Results showed no significant difference between these groups on CDP-SOT or mCTSIB, but the BSE detected a difference (df = 35), t = -3.0, p < .01 (two-tailed)). The BSE has good inter-rater reliability and concurrent criterion-related validity with mCTSIB prospectively and CDP-SOT retrospectively and prospectively. Interestingly, the BSE appears to detect a significant difference between balance scores in participants with and without osteoporosis when the other tools did not. This finding is likely related to the BSE characteristic of dynamic motion (i.e. lifting, climbing, squatting) not present in the other instruments. Further validation of the other domains (spinal compression, strength and flexibility) and dynamic balance characteristics is planned. The BSE is a promising tool that addresses the unique musculoskeletal concerns of the osteoporosis population.

Disclosures: **C. Recknor**, None.

SU445

Evaluation of Vibration as a Mechanical Stimulation of Bone in Osteoporosis. **A. C. A. Souza**^{*1}, **E. Dieter**^{*1}, **D. Barbieri**^{*2}, **R. Schneider**^{*1}. ¹Institute of Geriatrics, PUCRS University, Porto Alegre, Brazil, ²Dep of Bio Engineering, PUCRS University, Porto Alegre, Brazil.

From the premise that low frequency and high amplitude mechanical stimulus provide an osteogenic response in bone, we designed a study to observe this effect in the human skeleton by using a vibrating platform. The study was quantitative, experimental, and in a longitudinal perspective. It was approved by an Ethical Committee of the University as an experimental study for six months in order to evaluate the results in bone and possible side effects by the use of vibration. The subject sample was composed by 20 post menopausal women (59.9 ± 6.2 years) as an experimental group and 8 females (56.3±8.9) as control group. In both groups the diagnosis of osteoporosis were defined by DEXA. All subjects with history of osteoarthritis and osteoarthritis were excluded. The mechanical platform was developed in order to produce a frequency of 28,8 Hz with an acceleration of 0,2 G. The subjects in experimental group stand in relaxed orthostasis on vibrating platform for 15 minutes, three times a week, during six consecutive months. Bone mass of lumbar spine (L1 to L4), of femur, (neck, trochanter and total)and tibia (ultradistal, mid and 1/3) were measured before(BMD1) and at six months (BMD2) by using a Dual Energy X Ray Absorptiometry - QDR 4500 Acclaim, Hologic Inc USA. Statistical analysis, were performed by using a SPSS® 11,5; Excel 2000; descriptive Statistics; Student t test with p<0,05, one-tailed, and paired. At the end of the study, a consistent and significant increase in bone mineral density was seen in the 1/3 region tibia in the experimental group (BMD1 0,985 BMD2 1,005 p<0,03). An important and not expected finding was a significant bone loss in ultra-distal region of tibia in the experimental group (BMD1 0,711 ± 0,091 BMD2 0,655 ± 0,085 p<0,0014). Femur and lumbar spine showed no significant changes intra group in the period. Comparing experimental and control group, femur showed significant improvement in experimental group. This prospective clinical study disclosed that

mechanical stimulus can have osteogenic effect, however depending of the bone location and intensity of stimulus an opposite effect could happen as it was seen in ultradistal tibia. These results are important findings for future studies on the effect of vibration on bone and also in the study of the impact during exercise when used for the treatment of osteoporosis.

Disclosures: **A.C.A. Souza**, None.

SU446

The Pharmacokinetics (PK) of AMG 162 following Various Multiple Subcutaneous (SC) Dosing Regimens in Postmenopausal Women with Low Bone Mass. **M. C. Peterson**, **B. J. Stouch***, **S. W. Martin***. Amgen Inc., Thousand Oaks, CA, USA.

Receptor Activator of NF- κ B Ligand (RANKL) is essential for the differentiation, function, and survival of osteoclasts. The PK of AMG 162, a fully human monoclonal antibody to RANKL, was evaluated in a randomized, double-blind, placebo-controlled, multidose study of AMG 162 in the treatment of postmenopausal women with low bone mass (average T-score -2.2). Eight cohorts of approximately 40 women each received AMG 162 at the following dose levels and frequencies: placebo, 6 mg, 14 mg, or 30 mg every 3 months; or 14 mg, 60 mg, 100 mg, or 210 mg every 6 months. Serum levels of AMG 162 were quantified using a validated ELISA methodology. PK parameters were calculated by noncompartmental methods. Following SC administration, AMG 162 exhibited nonlinear clearance across the dose range investigated; increasing 1.4-fold as dose decreased from 30 to 6 mg every 3 months and increasing 2.6-fold as dose decreased from 210 to 14 mg every 6 months. Absorption was rapid and prolonged with serum levels (~70-80% of maximum) detectable within 72 hours of dosing, and maximum serum concentrations occurring between 3 and 29 days post-dose. Maximum observed concentrations generally increased linearly with dose and dosing frequencies. Following peak concentrations, serum levels generally declined in a linear fashion until reaching a concentration threshold below which concentrations fell more rapidly, producing a biphasic concentration-time curve. Over 12 months, AMG 162 did not accumulate appreciably at any dose or dosing frequencies investigated, and the PK did not change substantially following multiple dosing. Consistent with PK, AMG 162 produced rapid (within 72 hours), profound (>70% reduction), and sustained (up to 6 months) reductions in the levels of the bone resorption marker, serum C-telopeptide, that were dose-dependent and reproducible following multiple dosing. AMG 162 was safe and well tolerated in this study. Two patients exhibited transient non-neutralizing antibody responses to AMG 162 that did not appear to be influential on AMG 162 disposition. In conclusion, the multiple dose disposition and PK of AMG 162 was well characterized in postmenopausal women with low bone mass, and these results support infrequent dosing of AMG 162 in future studies.

Disclosures: **M.C. Peterson**, Amgen Inc. 3.

SU447

Safety, Effects on Markers of Bone Resorption and Pharmacokinetics of Cathepsin-K Inhibitor, AAE581, in Healthy Subjects. **S. K. Roy***¹, **G. Pillai***², **T. G. Woodworth***², **A. Skerjanec***¹, **W. C. J. Collins***². ¹Novartis Pharmaceutical Corporation, East Hanover, NJ, USA, ²Novartis Pharmaceutical Corporation, Basel, Switzerland.

AAE581 is a specific direct inhibitor of the cysteine protease cathepsin-K intended for the prevention and treatment of osteoporosis. A double-blind, placebo-controlled trial was designed to assess the safety, tolerability, effects on markers of bone resorption and pharmacokinetics of single ascending oral doses of AAE581 in healthy male and female subjects. Six dose levels were evaluated sequentially: 10 mg, 25 mg, 50 mg, 100 mg, 200 mg and 400 mg. In total, 44 subjects (25 males and 19 females) ranging in age from 18 to 45 years participated in the study: 32 received AAE581 and 12 placebo. The overall tolerability of AAE581 was good and no serious adverse events occurred. A dose-dependent suppression in biochemical markers of bone resorption (serum CTx and NTx), that is clearly discernible from circadian variation, was noted. At dose levels of ≥ 25 mg approximately 90% suppression was noted 6-12 hours post-dose. Pre-treatment biomarker concentrations were reached approx. 48 hours after single dose treatment. Experience with bisphosphonates indicates that, after drug administration biomarker concentrations decrease, reaching a nadir of 65 - 83% suppression at 1 month with a gradual recovery of the biomarker response over the next few months. In comparison, AAE581 clearly demonstrated a more rapid onset and offset of effect on the order of hours and days, respectively. AAE581 pharmacokinetics was characterized by rapid absorption across all doses, with t_{max} values ranging from 1.0 h to 2.25 h. The mean C_{max} and AUC values increased proportionally with increasing dose. AAE581 exhibited moderate plasma clearance with mean Cl/F values ranging from 39.4 ± 4.22 L/h (10 mg dose) to 29.6 ± 2.36 L/h (400 mg dose). The AAE581 mean $t_{1/2}$ ranged from 19.9 ± 1.95 (10 mg dose) to 11.7 ± 0.79 h (400 mg dose). Active metabolite, AEE325, mimicked the time course of the parent compound, but accounted for only 8 - 16.6% of the AAE581 systemic exposure across the dose range. The effect of food on AAE581 and AEE325 pharmacokinetics was evaluated in 5 subjects who received a 200 mg dose of AAE581. Prolongation of mean t_{max} from 1.80 h to 3.20 h, 19% decrease in C_{max} and 12% increase in AUC of AAE581 was observed in presence of food. These changes are not considered to be clinically relevant. These data show that AAE581, given as a single dose to a non-osteopenic population, is well tolerated and potentially decreases serum markers of bone resorption.

Disclosures: **S.K. Roy**, Novartis Pharmaceutical Corporation 1, 3.

SU448

The RANKL Inhibitor RANK-Fc Has Potent Antiresorptive Efficacy but Does not Affect Host Immune Responses to Influenza Infection. **R. E. Miller***, **D. Branstetter***, **J. Jones***, **L. Cowan***, **W. C. Dougall**. Amgen Inc., Seattle, WA, USA.

The receptor activator of NF- κ B (RANK) and its ligand (RANKL), a tumor necrosis factor (TNF) family cytokine, are essential for osteoclast differentiation and bone resorption. Osteoprotegerin (OPG) is the endogenous soluble receptor inhibitor of RANKL. We investigated whether RANKL inhibition by recombinant mouse RANK-Fc has similar anti-osteoclast efficacy to recombinant OPG-Fc. Since the RANKL pathway is implicated in mouse lymphocytic maturation and activation as well, we also tested if RANK-Fc would affect host immune resistance responses to influenza infection. The relative efficacy of RANK-Fc to OPG-Fc was tested in a Vitamin D hypercalcemia model. C57/BL6 mice received a single dose of 0, 10, 100, 500, or 1000 μ g RANK-Fc or 100 g OPG-Fc 2 hours pre-challenge on Day 0. Mice were sacrificed on Days 1, 2, 4, 6, 8, 12, 16, and 20 followed by analysis of serum markers and skeletal parameters. Single doses of ≥ 100 μ g RANK-Fc completely suppressed the elevation of serum calcium at Day 4 and later timepoints, similar to that observed with OPG-Fc. Both RANK-Fc and OPG-Fc suppressed the bone turnover marker, serum pyridinoline, at Day 4 and thereafter. At Day 6, both immature and mature osteoclasts were completely depleted by high doses (500 and 1000 μ g) of RANK-Fc or OPG-Fc 100 μ g. The effects of RANKL inhibition by RANK-Fc on immune parameters were tested in a mouse respiratory influenza virus host-resistance model. Treatment with dexamethasone, a known immunosuppressant, resulted in enhanced and prolonged virus infection and decreased virus-specific IgG levels. RANK-Fc (100 μ g or 500 μ g) had no deleterious effect on viral clearance or on the influenza-specific IgG response. In addition, RANK-Fc had no immunotoxicologic effects on the ability to acquire T-cell dependent antigen immunity, as measured by antibody-forming cell induction, or on the innate immune response, as measured by interleukin (IL)-1 β , TNF- α , or IL-6 induction in the lung. Viral clearance requires an intact immune system that produces cytokines and antibodies and stimulates the activities of natural killer cells, macrophages, and cytotoxic T-cells. Influenza virus is a T-dependent antigen; hence, formation of antibody to influenza virus requires functional T and B cells, and functional antigen presenting cells. Thus, RANKL inhibition by RANK-Fc, at doses shown to have antiresorptive efficacy, did not appear to inhibit host immune responses, suggesting that a RANKL inhibitor may be a safe and effective therapeutic for treating excess bone loss.

Disclosures: **R.E. Miller**, Amgen Inc. 3.

SU449

Identification of Small Molecule Stimulators of Osteoprotegerin Secretion. **S. Kim**¹, **S. Chang**^{*2}, **H. Sung**^{*2}, **Y. Kim**^{*2}, **S. Cho**^{*2}, **S. Ko**^{*3}. ¹OCT Inc. Dept. of Dental Pharmacology, Dankook University, Cheonan, Republic of Korea, ²OCT Inc., Cheonan, Republic of Korea, ³Dept. of Oral Biochemistry, Dankook University, Cheonan, Republic of Korea.

Osteoprotegerin (OPG) is a soluble member of the tumor necrosis factor receptor family, which regulates bone mass by inhibiting osteoclast differentiation and activation. Novel Small Molecule Stimulators of OPG secretion is currently under investigation for osteoporosis treatment. We used high-throughput screening for approximately 16,000 compounds of the Korea Chemical Bank to identify compounds that increase OPG secretion from osteoblastic cell. We found two compounds (O-1, O-2) significantly increased OPG secretion. Secretion of OPG, which was detected from MG63 cell by sandwich ELISA method, showed marked increases after treatment of compounds. Individually, a 1.5 to 2.0 fold increase in the OPG secretion level was observed at the concentration of 1-2 μ M compared with the control. Treatment of these compounds resulted in significant decreases in number of TRAP (+) multinucleated cells in total bone marrow cell culture. The inhibitory effect was dose-dependent. These results provide proof of the concept that these compounds can be applied to the treatment of osteoporosis. These hit compounds are under development as a candidate molecule for antiosteoporosis new drugs.

Disclosures: **S. Kim**, None.

SU450

Age-Associated Iron and Free-Radical Accumulation in Bone: Implications for Osteoporosis and a New Ttarget for Prevention and Treatment by Chelation. **G. Liu**, **P. Men***, **G. H. Kenner***, **S. C. Miller**. Radiology/Radiobiology, University of Utah, School of Medicine, Salt Lake City, UT, USA.

Iron is an essential nutrient, but it is also a powerful catalyst for auto-oxidation reactions creating harmful free radicals in cells and tissues. The body has developed numerous mechanisms to sequester iron and thus limit free radical production, but storage iron accumulates with age and is considered a primary catalyst in many free-radical associated diseases. The skeleton is no exception and skeletal disease is reported in iron overload conditions such as hemochromatosis and thalassemias. There is evidence that iron accumulation is inversely related to estrogen levels in women and we hypothesize that this may facilitate the development of osteoporosis in a variety of disease conditions. Using electron paramagnetic resonance spectroscopy (EPR) techniques, we have documented an increase in free iron and long-lived organic free radical accumulation in bone after menopause in women and following ovariectomy (Ovx) in rats. We sought to determine the ability of a novel amphipathic, orally administered transition metal chelator to mitigate changes in bone after ovariectomy in aged rats. The chelator, 1-N-docosyl-

triethylenetetramine-pentaacetic acid (C22TT), was given orally three times per week for 9 weeks beginning the day after Ovx. The free iron content of the bone from the untreated Ovx rats was about 22% greater than the sham-operated controls, as measured by EPR. The free iron in the bones from the C22TT-treated animals was about 60% of the untreated Ovx rats and about 73% of the sham controls. Importantly, the C22TT treatments significantly slowed the loss of bone mineral density (BMD) and cancellous bone volume by about 50% and also mitigated the deterioration of bone microstructure (from pQcT and microCT) after ovariectomy. Histomorphometric analyses show a significant reduction in cancellous bone eroded surface, with a trend ($p > 0.05$ but < 0.1) for greater cancellous bone formation rates. These results add further support to the somewhat controversial theory that age-associated iron accumulation in tissues increases the risk of a variety of diseases, including atherosclerosis, cancer, diabetes, dementia and others. This study suggests that skeletal diseases might now be added to this list. While there is evidence from other studies that free radical reduction does offer some skeletal protection, this study identifies a new target and a potential therapeutic strategy for the treatment of osteoporosis and perhaps other age-related diseases. Our findings may also help raise awareness about iron nutrition, iron supplements and Western diets that may be associated with excess iron intake and accumulation.

Disclosures: **G. Liu**, None.

SU451

RANKL Inhibition Increases Extrinsic Bone Strength and Maintains Intrinsic Bone Strength in Transgenic Rats that Continuously Overexpress a Secreted Osteoprotegerin Transgene. M. S. Ominsky¹, T. J. Corbin^{*2}, X. Li¹, S. Morony^{*1}, K. S. Warmington^{*1}, Z. Geng^{*1}, M. S. Grisanti^{*1}, H. L. Tan^{*1}, V. Shen^{*3}, B. Bolon^{*1}, J. McCabe^{*1}, P. J. Kostenuik¹. ¹Metabolic Disorders, Amgen Inc., Thousand Oaks, CA, USA, ²Functional Genomics, Amgen Inc., Thousand Oaks, CA, USA, ³Skeletech Inc., Bothell, WA, USA.

The optimal level of bone turnover suppression for fracture prevention is unknown. RANKL inhibition provides rapid and sustained reductions in bone turnover. The relationship between these changes and bone strength is unclear. We therefore created a new animal model of continuous turnover suppression to evaluate the relationships between bone turnover and bone strength. Transgenic rats were made to overexpress a soluble rat osteoprotegerin transgene (OPG-Tg) driven by a liver-specific (ApoE) promoter. OPG is the endogenous inhibitor of RANKL, a TNF family member that is critical for osteoclast formation, activation, and survival. Female OPG-Tg rats ($n = 10$) and age-matched wild-type (WT) controls ($n = 5$) were analyzed at 16, 20, 24 and 28 weeks of age. Dramatic and continuous suppression of bone turnover was demonstrated in OPG-Tg rats by 80%-90% reductions in serum TRAP-5b at each age ($p < 0.01$ vs WT controls). Histomorphometry of the lumbar vertebrae (LV) of 28-week-old OPG-Tg rats showed a 98% reduction in osteoclast surface and a 48% increase in bone volume (BV/TV) ($p < 0.01$ vs age-matched WT controls). DXA of the LV revealed significantly greater BMD in OPG-Tg rats at all ages (22%-30% greater than age-matched WT controls, $p < 0.01$). These changes were associated improvements in vertebral bone strength. Compression testing showed that the 5th LV of 28-week-old OPG-Tg rats could withstand a 2-fold greater maximum load and had 2.6-fold higher stiffness compared to age-matched WT controls ($p < 0.01$). These extrinsic parameters are influenced by bone size and density. Intrinsic parameters, such as ultimate strength, elastic modulus, and toughness, are normalized to bone mass (BV/TV) and are therefore indicative of bone matrix strength and quality. Continuous suppression of RANKL in OPG-Tg rats showed no significant differences in these intrinsic material properties compared to WT controls. These results show that profound and continuous suppression of bone turnover, via RANKL inhibition, results in improvements in vertebral bone mass and strength. No changes were observed in intrinsic bone strength, despite a 98% reduction in osteoclast surface. These data suggest that RANKL inhibition improves rat bone strength by increasing bone mass and maintaining normal bone tissue strength and quality.

Disclosures: **M.S. Ominsky**, Amgen 3.

SU452

RANKL Inhibition Improves Trabecular Architecture in Female Mice. M. S. Ominsky, X. Li, M. S. Grisanti^{*}, K. S. Warmington^{*}, H. L. Tan^{*}, P. J. Kostenuik. Metabolic Disorders, Amgen Inc., Thousand Oaks, CA, USA.

RANKL is the primary physiological mediator of osteoclast formation, function, and survival. RANKL inhibition leads to rapid, profound, and sustained suppression of bone resorption and increased bone mineral density (BMD). While BMD is an important component of strength in cancellous bone, the organization and mineralization of bone mass are important co-factors. Losses of trabecular number, thickness, plate-like structures, and connectivity are hallmarks of osteoporosis and may be associated with increased fracture risk, independent of reduced BMD. We used osteoprotegerin (OPG-Fc) to examine the effects of RANKL inhibition on BMD and trabecular architecture in 2-3 month old intact female mice. OPG-Fc was injected SC twice weekly for 3 weeks at 5 mg/kg ($n = 8$) while control animals ($n = 8$) received vehicle. Distal right femurs and lumbar vertebrae (L5) were Micro-CT-scanned ex-vivo (GEHC eXplore Locus SP) and reconstructed at 18 μ m isotropic voxel resolution. A region of trabecular bone was selected within the distal femur and vertebral body relative to anatomical landmarks and bone length, and analyzed for trabecular parameters. OPG-Fc treatment significantly increased bone mass, mineral density, and mineralization at both sites (Table 1). Trabecular architecture was improved as reflected in significant increases in trabecular thickness, number, connectivity, and decreased spacing. Structural Model Index was decreased 25% ($p < 0.01$) in the distal femur with OPG treatment, indicating a preservation of more plate-like structures. No group differences were found in degree of anisotropy, indicating that RANKL inhibition does not alter the normal trabecular orientation. The ability of OPG to

increase bone mass and mineralization, while improving aspects of trabecular architecture, suggests that RANKL inhibition results in improved bone quality.

Table 1: % Difference Between OPG- and Vehicle-treated Mice
[Significantly greater than vehicle-treated controls, * $p < 0.05$]

MicroCT Parameter	Distal Femur	Lumbar Vertebra
Trabecular BV/TV	+ 162*	+ 56*
Trabecular vBMD [mg/cm ³]	+ 54*	+ 36*
Trabecular Bone Matrix Mineral Density [mg/cm ³]	+ 14*	+ 5*
Trabecular Thickness	+ 13	+ 22*
Trabecular Number	+ 70*	+ 28*
Trabecular Spacing	- 40*	- 42
Trabecular Connectivity	+ 108*	+ 7

Disclosures: **M.S. Ominsky**, Amgen 3.

SU453

AMG 162, a Fully Human RANKL Antibody, Increases Bone Mass and Bone Strength in Cynomolgus Monkeys. J. Atkinson¹, P. Cranmer^{*1}, T. Saunders^{*1}, M. Niehaus^{*2}, S. Y. Smith³, A. Varela^{*3}, M. S. Ominsky¹, M. E. Cosenza^{*1}, P. J. Kostenuik¹. ¹Amgen Inc., Thousand Oaks, CA, USA, ²Covance Laboratories GmbH, Munster, Germany, ³CTBR, Montreal, PQ, Canada.

AMG 162 is a fully human monoclonal antibody that inhibits bone resorption by neutralizing RANK Ligand (RANKL). RANKL inhibition increases BMD in human and non-human primates, but the effects of AMG 162 on bone mass and strength have not been previously described. Male cynomolgus monkeys (4-5 years old) were treated with AMG 162 (50 mg/kg/mo, SC; $n = 8$) or vehicle (Veh; $n = 8$) for 1 year. Bone mass, mineral density, and strength were determined at 6 and 12 mos ($n = 3$), and following a 3-mo non-treatment recovery period ($n = 2$). Right femurs were analyzed by pQCT for bone mineral content (BMC) and geometry, and lumbar vertebrae (L3 & L4) were analyzed by DXA for BMC and bone mineral density (BMD). Bone strength was measured by destructive mechanical testing of the femoral diaphysis (3-point bending) and the vertebrae (compression). At the femoral diaphysis, 1 year of AMG 162 treatment resulted in significantly greater cortical area (26%) and cortical BMC (30%) ($p < 0.05$ vs Veh). These increases in bone mass were associated with a 40% increase in femur bending load ($p < 0.01$ vs Veh). Intrinsic strength parameters, which are normalized to femoral bone mass, were not significantly altered by AMG 162. At the lumbar vertebrae, 1 year of AMG 162 treatment resulted in significantly greater BMC (45%) and BMD (40%) ($p < 0.05$ vs Veh). These changes were associated with significant ($p < 0.05$ vs Veh) increases in maximum compressive load (101%), apparent strength (97%), and toughness (78%). When bone quality is normal, increases in bone mass should correlate positively with increases in bone strength. We combined all time points within each group to obtain regression analyses that compared bone mass and strength. At the femoral diaphysis, strong positive correlations were shown between maximum load and cortical BMC or cortical area ($r^2 \geq 0.84$ for both treatment groups, $p < 0.002$). In the vertebra, strong positive correlations were observed between maximum load and BMC ($r^2 \geq 0.74$ for both treatment groups; $p < 0.006$). These results show that AMG 162 increases bone mass at both trabecular and cortical sites in cynomolgus monkeys. Extrinsic bone strength increased in proportion to improvements in cortical area and BMC, while intrinsic bone strength was maintained by AMG 162. The strong positive correlation between cortical area and femur bending load confirms the important contribution of cortical geometry for bone strength. The ability of AMG 162 to improve bone density, cortical geometry, and strength suggests that RANKL inhibition is a promising therapeutic approach for reducing fractures.

Disclosures: **J. Atkinson**, Amgen 3.

SU454

Improved Delivery and Retention of Osteoprotegerin to Bone after Conjugation to a Bisphosphonate Drug. M. R. Doschak^{*1}, C. M. Kucharski^{*1}, J. E. I. Wright^{*1}, R. F. Zernicke², H. Uludag¹. ¹Chemical & Materials Engineering, University of Alberta, Edmonton, AB, Canada, ²Faculties of Kinesiology, Medicine & Engineering, University of Calgary, Calgary, AB, Canada.

The loss of bone mineral density (BMD) through up-regulated osteoclast-mediated resorption is of great clinical concern for many diseases of bone. The peptide factor osteoprotegerin (OPG) is known to block osteoclastogenesis and conserve BMD, however, high quantities of OPG need to be administered to elicit any therapeutic efficacy. The purpose of this study was to improve the specificity of OPG delivery to bone by the chemical conjugation of OPG to a "bone seeking" bisphosphonate (BP) carrier. We chemically conjugated recombinant human OPG monomer (20 kDa) to a bisphosphonate (thioBP) using the heterobifunctional cross-linker N-succinimidyl-3-(2-pyridyldithio) propionate (SPDP). The OPG-thioBP conjugate was characterized using high performance liquid chromatography (HPLC) and polyacrylamide gel electrophoresis (PAGE). The conjugate was then radiolabeled with I-125 and tested with hydroxyapatite (HA) powder 'in vitro' to assess the affinity for bone mineral. For all experimentation, the OPG-thioBP conjugate was compared against control OPG, that was incubated in the absence of the cross-linker. The conjugates were tested for improved targeting to bone 'in vivo' after radiolabeling and intravenous injection into rats, followed by pharmacokinetic (PK) evaluation of bones and soft tissues at 24 and 72 hr. Our HPLC results confirmed the chemical modification of the OPG-thioBP conjugate with increased retention on a C4 protein column prior to elution. PAGE also confirmed that the modified OPG-thioBP conjugate was not degraded, and ran as a single protein band at the expected molecular weight for OPG. HA binding experiments showed that the OPG-thioBP conjugate had a 10-fold greater affinity for bone mineral in a phosphate buffer and in the presence of donor serum, as compared to control OPG. PK evaluations 'in vivo' in the rat confirmed that the

uptake by bone of systemically injected radiolabeled OPG-thioBP conjugate was significantly increased (2-fold) over that of control OPG at the 24 hr time point. Furthermore, the significantly improved retention of the OPG-thioBP conjugate was confirmed at the 72 hr time point, whereas control OPG was barely detectable in bone. In conclusion, the systemic administration of BP-conjugated OPG resulted in the significantly improved targeted delivery, and retention of the peptide factor to bones 'in vivo' in the rat. Thus, peptide-BP conjugation targeting strategies showed significant therapeutic implication for use in osteopenic bone diseases, including osteoporosis and the arthritides.

Disclosures: **M.R. Doschak**, None.

SU455

Phase 2 Study of AMG 162 in Postmenopausal Women: Subanalyses and Supplemental Safety. **S. B. Cohen¹, E. M. Lewiecki², Y. Liu³, D. J. Zack^{*3}, L. A. Fitzpatrick³.** ¹Radiant Research, Dallas, TX, USA, ²New Mexico Clinical Res and Osteoporosis Cent, Albuquerque, NM, USA, ³Amgen Inc., Thousand Oaks, CA, USA.

AMG 162 is a fully human monoclonal (IgG₁) antibody that binds to RANK Ligand to inhibit osteoclast formation, function, and survival. We have previously reported that AMG 162 treatment for 1 year rapidly decreased markers of bone turnover and increased bone mineral density (BMD) at the spine (4.6%), total hip (3.6%), and distal 1/3 radius (1.3%; 60 mg 6-monthly dose) compared with placebo in a randomized, dose-ranging, phase 2 study in postmenopausal women with low bone mass. We hereby report BMD and bone turnover data analyzed by subgroups including baseline weight and lumbar spine T-score. Safety, including immune function, was assessed for overall treatment groups. Following 1 year of treatment, greater increases from baseline in lumbar spine BMD were observed in patients treated with AMG 162, 6-monthly, compared with placebo for each baseline weight subgroup (Table). AMG 162 treatment also reduced serum CTX levels regardless of baseline weight. An overall mean reduction in serum CTX of 62.6% ± 7.9% occurred in the AMG 162 60-mg, 6-monthly group compared with a mean change of 0.1% ± 5.9% in the placebo group. When analyzed by baseline T-score, lumbar spine BMD increased by 2.2% to 6.8% with AMG 162 treatment (6-monthly) for patients with T-score <-2.5 compared with changes of -1.1% for placebo and 5.0% for alendronate. The corresponding changes in patients with baseline T-score ≥-2.5 were 3.3% to 5.3% (AMG 162 6-monthly), -0.6% (placebo), and 4.5% (alendronate). Incidence of adverse events, including infections, was not different between AMG 162-treated patients overall and placebo or alendronate. Upper respiratory tract infection was the most common infection (13% placebo, 19% AMG 162, 17% alendronate). No significant differences in white blood cell or lymphocyte counts and no significant changes in T, B, or NK cell (CD3, CD4, CD8, CD19 and CD16/56) numbers occurred across all dose and treatment groups. Therefore, in this study AMG 162 treatment increased bone mass at the lumbar spine regardless of patient weight or bone density at baseline and may be an effective and well-tolerated treatment for osteoporosis.

Table. Percent Change from Baseline in Lumbar Spine BMD at 1 Year by Baseline Weight

Patient Weight Category (kg)	Placebo		AMG 162 (6 monthly dosing)							
	n	Mean (SE)	n	Mean (SE)	n	Mean (SE)	n	Mean (SE)	n	Mean (SE)
< 55	5	-2.14 (1.34)	8	2.06 (1.06)	5	6.09 (1.33)	3	8.06 (1.71)	9	5.36 (1.00)
55 - <65	14	-1.12 (0.80)	13	3.19 (0.83)	11	4.97 (0.91)	14	5.16 (0.79)	12	6.02 (0.86)
65 - <75	12	-0.29 (0.88)	16	3.68 (0.74)	9	3.85 (0.99)	11	4.95 (0.92)	8	4.95 (1.05)
75 - <85	5	1.15 (1.34)	4	2.82 (1.49)	8	4.30 (1.07)	6	5.35 (1.22)	8	3.60 (1.06)
≥ 85	3	-1.74 (1.74)	7	2.25 (1.12)	8	4.10 (1.06)	3	6.24 (1.72)	4	4.66 (1.50)
Unknown	1	-3.38 (2.97)								

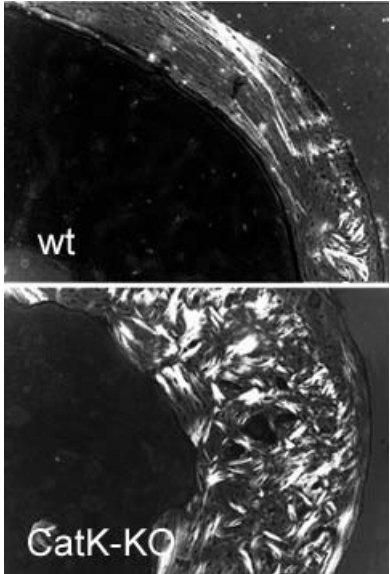
Disclosures: **S.B. Cohen**, Amgen Inc 5.

SU456

Cathepsin K Deficiency Results in Bone Fragility in Mice. **C. Y. Li^{*1}, B. D. Gelb^{*2}, K. J. Jepsen¹, M. B. Schaffler¹.** ¹Orthopaedics, Mount Sinai School of Medicine, New York, NY, USA, ²Pediatrics/Human Genetics, Mount Sinai School of Medicine, New York, NY, USA.

Cathepsin K (CatK)-deficiency has been shown to markedly impair osteoclastic function, leading to osteosclerosis in both humans and in mice. This osteosclerosis (pseudosclerosis) in humans has a significant bone fragility component, the bases of which are not understood. Bone strength in CatK-knockout (KO) mice was reported to be unchanged from normal mouse bone. However, the previous studies did not adequately characterize the overall fracture resistance of bones from CatK-KO mice. In order to address this issue, we examined the bone mechanical properties of CatK-deficient mice. Femoral mid-diaphyses from ten-week-old wild type (wt), heterozygous and homozygous mice were loaded to failure in four point-bending test using a servohydraulic material test system at a displacement rate of 0.05 mm/sec. Maximum load (ultimate force that the specimen sustained), stiffness (the slope of the initial, linear portion of the load-deformation curve), post-yield deflection (deflection at failure minus deflection at yield), and work-to-failure (the area under the load-deformation curve prior to failure) were determined. Cross-sectional architecture was assessed at the mid-diaphyses of contralateral limbs. Despite markedly (30%) increased cortical bone area in CatK-deficient mice, diaphyseal maximum load and stiffness did not differ significantly from wt bone, consistent with previous reports. However, CatK-deficient bones were dramatically impaired in their ability to resist fracture. They were more brittle (60% decrease in post-yield deflection), and work-to-fracture was reduced by nearly 40% compared to wild-type bones. Because CatK-KO morphology was not altered, the increased brittleness of CatK-

KO femurs must be a consequence of altered matrix construction. Analysis of femoral cross-sections by polarized light microscopy revealed that the predominantly organized (lamellar-like) matrix architecture of wt was severely altered in CatK-KO (Fig 1). Ongoing studies will test whether there are accompanying alterations in mineralization. These results indicated that the increased fragility associated with impaired osteoclast function results from a failure of modeling and remodeling to establish normal matrix architecture during growth and development.



Disclosures: **C.Y. Li**, None.

SU457

Treatment of Bone Loss after Renal Transplantation in Children: Alfacalcidol versus Calcitonin Therapy. **A. A. M. El-husseini.** Nephrology, Mansoura Urology and Nephrology Center, Mansoura, Egypt.

Background. Osteoporosis is a well-known complication of renal transplantation in children. We conducted a randomized trial comparing alfacalcidol with calcitonin for the treatment of bone loss. **Methods.** Among 59 young patients who received live related renal transplant and were subjected to dual energy x-ray absorptiometry (DEXA), 30 patients had low bone mineral density (BMD) (z-score < -1) were enrolled onto the study. Their mean age at time of transplantation was 13.5 ± 3.4 years and the mean duration after transplantation was 46 ± 32 months. Patients with low BMD were randomized into two equal homogeneous groups: group 1 received daily alfacalcidol 0.25 microg by mouth and group 2 received 200 IU /day nasal spray calcitonin. Every patient in both groups received daily 500-mg calcium carbonate supplements. Parameters of bone metabolism (intact parathyroid hormone, serum osteocalcin and urinary deoxypyridinoline) and BMD were assessed before and after the study period. Estimates of bone loss and the incidence of fractures among untreated patients were obtained from a reference group of 15 prospectively recruited patients who received renal transplants within the same period as the intervention groups. **Results.** At one year, the BMD at the lumbar spine had increased from -2.3 to -0.5 in the alfacalcidol group and from -2.3 to -1.0 in the calcitonin group while it was decrease from -2.2 to -2.5 in the reference group. Incidence of vertebral fractures did not differ significantly among the groups (13.3 percent in the calcitriol group, 6.7 percent in the calcitonin and the reference groups). Serum intact parathyroid hormone level decreased significantly in the alfacalcidol group compared with the calcitonin group (P = 0.042). Apart from transient hypercalcemia in 1 patient in the alfacalcidol group, no other significant adverse effects were noted. **Conclusion.** This study suggested the value of alfacalcidol and calcitonin agents in the treatment of osteopenia and osteoporosis in young renal transplant recipients. These therapies were safe, tolerable, simple to administer and potentially applicable to other renal transplant patients.

Disclosures: **A.A.M. El-husseini**, None.

SU458

Comparison of the Effects of Alfacalcidol to Vitamin D Plus Calcium in Spinal BMD in Postmenopausal Osteoporosis. **R. Nuti¹, G. Bianchi², M. L. Brandi³, R. Caudarella⁴, E. D'Erasmo^{*5}, C. Fiore⁶, G. Isaia⁷, G. Luisetto^{*8}, M. Muratore^{*9}, P. Oriente^{*10}, S. Ortolani¹¹.** ¹University of Siena, Siena, Italy, ²Ospedale La Colletta, Genoa, Italy, ³University of Florence, Florence, Italy, ⁴University of Bologna, Bologna, Italy, ⁵University La Sapienza, Rome, Italy, ⁶University of Catania, Catania, Italy, ⁷University of Turin, Turin, Italy, ⁸University of Padua, Padua, Italy, ⁹Presidio Ospedaliero G.Cascione - A.Galateo, Lecce, Italy, ¹⁰University of Naples, Naples, Italy, ¹¹Istituto Auxologico Italiano, Milan, Italy.

In a randomized multi-center double blind, double dummy parallel group study a comparison of the efficacy and safety of 1µg alfacalcidol to 880 IU vitamin D plus calcium carbonate (1 g calcium) once daily per os was performed on 148 postmenopausal

ASBMR 27th Annual Meeting

osteoporotic Caucasian patients with normal vitamin D serum levels for 18 months. BMD was measured at baseline, 12 and 18 months. Safety parameters were followed during the entire study period. Sixty-nine (90.8%) in the alfacalcidol group and 67 (93.1%) in the vitamin D group were included in the ITT analysis. Lumbar BMD in the alfacalcidol group increased by 0.017 (2.33%) and 0.021 g/cm² (2.87%) from baseline ($p < 0.001$) at 12 and 18 months, respectively, whereas in the vitamin D plus calcium group the increase was 0.005 g/cm² (0.70%) from baseline (N.S.) at both 12 and 18 months. The higher changes from baseline in the alfacalcidol group, as compared to the changes in the vitamin D plus calcium group at both 12 and 18 months, were found to be statistically significant ($P = 0.018$ and $P = 0.005$). A small increase of mean femoral BMD was achieved in both groups (N.S.). Adverse events were similar in both groups. No significant differences were noted between the groups in serum calcium. In conclusion, alfacalcidol was found to be superior in significantly increasing lumbar BMD as compared to vitamin D plus calcium while safety characteristics were found to be similar in both treatments.

Disclosures: **R. Nuti**, None.

SU459

BMD and Bone Markers in Patients with a Recent Low-Energy Fracture: Effect of Treatment with Vitamin D and Calcium. **M. F. Hitz¹, P. C. Eskildsen^{*2}, J. B. Jensen^{*1}**, ¹Osteoporosis and Bone Metabolic Unit, Copenhagen University Hospital Hvidovre, Hvidovre, Denmark, ²Medical Department, Roskilde University Hospital in Koge, Koge, Denmark.

The present study evaluate the effect of treatment with calcium and vitamin D for one year on Bone Mineral Density (BMD) and bone-markers in patients with a recent low energy fracture. The trial was double blinded with a prospective design. Patients with a fracture of the hip (LEF) or an upper-extremity-fracture (UEF) were randomly assigned to: 1000 mg CaCO₃+1000 IU cholecalciferol or placebo (200 IU cholecalciferol). Baseline visit was performed 14 days post-fracture for the LEF-group and 27 days post-fracture for the UEF-group. We measured BMD of the total hip (HBMD) and lumbar spine (LBMD) by Dual Energy X-ray Absorptiometry (DEXA) and physical performance by Timed Up and Go-test (TUG) at inclusion and after 12 months. Serum levels of vitamin 25-OH-D, parathyroid hormone (PTH), ICTP (crosslinked carboxyterminal telopeptide of type I collagen), osteocalcin and N-propeptides of collagen type I (PINP) were measured at baseline and 1, 3 and 12 months after inclusion. We included 122 patients (84% women) with a mean age of 70 years (SD = 11 years). 79 patients completed the study. For the LEF-group bone turnover increased to a maximum after 1 month and declined there after, osteocalcin levels increased throughout the study. Intervention significantly decreased bone turnover. PTH decreased in the intervention group ($p < 0.001$) but increased in the placebo group ($p < 0.001$). For the UEF-group bone-markers declined post-fracture and intervention reduced osteocalcin and ICTP levels significantly. No significant change was demonstrated for levels of PTH in either the intervention or the placebo group. LBMD increased significantly by 1.58% for patients below 70 years of age and reduced the BMD loss for patients older than 70 years regardless of fracture type. ICTP and ALBMD correlated with the results of TUG-test. We conclude that one-year intervention with 1000 mg CaCO₃ and 1000 IU cholecalciferol to patients with a recent low energy fracture reduced bone turnover, increased BMD in patients younger than 70 years of age and decreased the bone loss in older patients. Effects of treatment were related to physical performance.

Disclosures: **M.F. Hitz**, None.

SU460

Rapid Correction of Vitamin D Inadequacy in Nursing Home Residents. **S. Agrawal^{*}, D. Krueger, J. Engelke^{*}, R. Przybelski^{*}, N. Binkley**. University of Wisconsin Osteoporosis Clinical Research Program, Madison, WI, USA.

Approximately 1.6 million Americans currently reside in nursing homes (NH); a number expected to triple by 2030. Osteoporosis and vitamin D inadequacy are epidemic in this population. Vitamin D deficiency contributes to bone loss, muscle weakness, and increased falls risk; this deficiency combined with osteoporosis leads to a fracture incidence of approximately 10% annually among NH residents. However, approaches to rapidly correct vitamin D inadequacy among NH residents have received limited attention. This study evaluated the effect of oral high dose vitamin D₂ (ergocalciferol) on serum 25-hydroxyvitamin D (25OHD) status, markers of skeletal health and gait speed. This ongoing study examined 23 NH residents. Volunteers were assigned to receive vitamin D based upon serum 25OHD; those individuals with inadequacy (defined as a 25OHD < 25 ng/ml) received vitamin D₂ 50,000 IU, 3 times weekly for 4 weeks; the others received no change to their routine care. The investigative staff were blinded to treatment group assignment. Serum for 25OHD and other skeletal health measurements (bone specific alkaline phosphatase [BSAP], n-telopeptide of type I collagen [NTx], parathyroid hormone [PTH], and calcium) was obtained at baseline and at 4 weeks. Timed 4-meter walk tests were performed at baseline and at 4 weeks. Average subject age was 87.4 (range 75 to 99) years. There were no between group differences in age, gait speed, serum calcium, BSAP or NTx at baseline. Mean (SEM) total 25OHD concentration increased ($p < 0.0001$) from 16.6 (1.9) to 61.6 (5.0) ng/ml in the D₂ treated group and remained unchanged in the control group at 32.9 ng/ml. Serum 25OHD₃ remained stable in the control group, but declined ($p < 0.0001$) with D₂ treatment from 15.8 (2.0) to 9.4 (1.3) ng/ml over the 4 weeks of study. Mean serum calcium was 9.5 (0.1) and 9.6 (0.1) mg/dl at baseline and after 1 month of vitamin D₂. Hypercalcemia was not observed. Mean PTH concentration decreased ($p < 0.05$) from 48.7 (10.3) to 37.2 (8.3) pg/ml in the D₂ treated group and remained unchanged in the control group. No treatment-induced changes were observed in BSAP, NTx or gait speed. In conclusion, 4 weeks of high-dose oral vitamin D₂ supplementation safely increases serum 25OHD and reduces PTH concentrations. The absence of changes in bone turnover markers and gait speed likely reflects short study duration and small sample size.

It seems likely that rapid vitamin D repletion of NH residents would reduce fracture risk, however this supposition requires prospective study confirmation. As vitamin D₃ has recently been reported to be more potent than D₂, the observed reduction in 25OHD₃ following D₂ treatment is interesting and merits further evaluation.

Disclosures: **S. Agrawal**, None.

SU461

Long-Term Treatment Of Hypovitaminosis D. Calcidiol Or Cholecalciferol? **E. Casado^{*1}, M. Larrosa^{*1}, A. Gómez^{*1}, E. Fernández^{*1}, E. Berlanga^{*2}, J. Gratacòs^{*1}**, ¹Rheumatology, Hospital Sabadell, Sabadell, Spain, ²Laboratory, UDIAT. Coporació Sanitària Parc Taulí., Sabadell, Spain.

There are different vitamin D metabolites for the treatment of hypovitaminosis D. It is not well known which of them is more efficacious for the long-term treatment. In a previous publication (Rev Esp Reumatol 2003; 30:548-553) we proved that calcidiol 16.000UI/week for 4 weeks is a useful treatment regimen to normalize 25-OHD₃ levels in patients with vitamin D deficiency. The aim of the study was to compare the long-term efficacy of calcidiol vs cholecalciferol to maintain normal levels of 25-OHD₃ in patients with previously corrected hypovitaminosis D. In a longitudinal study (12 months of follow-up) 99 out-patients visited in our department were included. 88/99 female (89%), mean age 72±9.7 years (43-88). All of them had a hypovitaminosis D previously corrected with calcidiol (16.000UI/week for 4 weeks). The patients were randomised in two-arms of treatment: 63 p with calcidiol 16.000UI every 3 weeks and 36 p. with cholecalciferol 800UI/day. Daily 1-1.2 g of calcium was added in all the patients during the study. The following parameters: 25-OHD₃, PTH, Ca, P, ALP and 24-hour calciuria, were determined at baseline, 3, 6 and 12 months. Both groups of patients treated with calcidiol and cholecalciferol had a mean 25-OHD₃ serum levels within the normal range at 3, 6 and 12 months, but the calcidiol group achieved higher levels at 6 months (71±31 vs 44±18; $p = 0.000$) and 12 months (75±26 vs 48±23; $p = 0.001$). The percentage of patients with a successful treatment (25-OHD₃ within the normal range) was similar in both groups at 3 months, but this rate was higher in the calcidiol group at 6 months (93% calcidiol vs 86% colecalciferol $p = 0.004$) and 12 months (100% calcidiol vs 85% colecalciferol $p = 0.02$). There were not significant differences in PTH, Ca, P, ALP and 24-hour calciuria between the groups any time during follow-up. The proportion of patients who withdrew the treatment was similar in both groups: 30/63 (47.6%) treated with calcidiol and 15/36 (41.6%) with cholecalciferol. We concluded that both calcidiol (16.000 UI every 3 weeks) and cholecalciferol (800 UI/ day) are efficacious to maintain normal levels of 25-OHD₃, but these levels were higher with calcidiol. On long-term treatment (1 year) no patients with calcidiol had hypovitaminosis D. The withdrawal was high in both treatment regimens.

Disclosures: **E. Casado**, None.

SU462

Vitamin D Insufficiency Impairs the Effect of Alendronate for the Treatment of Osteoporosis in Postmenopausal Women. **M. Ishijima¹, M. Yamanaka^{*1}, Y. Sakamoto^{*1}, K. Kitahara¹, F. Enomoto^{*2}, M. Sawa^{*2}, M. Nozawa^{*1}, A. Tokita³, H. Kurosawa^{*1}**, ¹Orthopaedics, Juntendo University, School of Medicine, Tokyo, Japan, ²Orthopaedics, Juntendo Tokyo Koto Geriatric Medical Center, Tokyo, Japan, ³Pediatrics, Juntendo Univ. School of Medicine, Tokyo, Japan.

It has been reported that approximately five percents of alendronate (ALD) users for the treatment of osteoporosis did not increase in bone mineral density (BMD) of the spine. There is overwhelming evidence that vitamin D insufficiency (moderate vitamin D deficiency) is common in the elderly, not only in traditional risk groups but also in independent elderly or postmenopausal women with/without osteoporosis. The purpose of this study is to investigate whether ALD used for the treatment for osteoporosis could give full play to increase in BMD in case of the vitamin D insufficiency. A total of twenty-four Japanese postmenopausal women (aged 58 to 78, 65.6 in average) who were diagnosed as a primary osteoporosis were enrolled in this study. All the patients involved in this study took 5mg of ALD daily for one year. Lumbar spine BMD (L-BMD) was measured at first medical examination and every six months thereafter. Serum levels of 25-hydroxy vitaminD (s-25(OH)D), 1 α ,25-dehydroxy vitamin D₃ and intact-PTH were also measured at the first medical examination and every six months thereafter. Serum levels of bone specific alkaline phosphatase (BAP) and urinary levels of N-telopeptide (u-NTX), calcium and creatinine were measured at the first medical examination and every three months thereafter. This study was approved by our institutional research committee. We divided the patients for three groups by the s-25(OH)D during twelve months; <15ng/ml: Group A, 15~20ng/ml: Group B, >15ng/ml: Group C. While significant suppression of u-NTX excretion by ALD for one year was observed in Group B and C, such suppression of u-NTX excretion was not observed in Group A. Moreover, while the percent increase in L-BMD by ALD for one year was 5.7% and 8.4% in Group B and C, respectively, that was 1.4% in Group A. These differences of the percent increase in BMD by ALD for one year between Group A and B and Group A and C were statistically significant ($p < 0.01$), respectively. These results suggest that vitamin D insufficiency would be a one of the causes for the non-responder of ALD for the treatment of osteoporosis. Therefore, we have to pay more attention to vitamin D status of postmenopausal women in the treatment of osteoporosis. These efforts must be contributed to obtain a more adequate effect of ALD for the treatment of osteoporosis. In conclusion, the effect of ALD for the treatment of osteoporosis was impaired in postmenopausal women with vitamin D insufficiency.

Disclosures: **M. Ishijima**, None.

SU463

Relationship between Serum 25-hydroxy-Vitamin D Levels and Health-Related Quality of Life in Postmenopausal Women with Osteopenia. A. M. Cheung¹, B. Stewart^{*1}, G. Tomlinson^{*2}, H. Hu^{*1}, J. Scher^{*1}, R. Vieth^{*3}.
¹Osteoporosis Program and Department of Medicine, University Health Network and Mount Sinai Hospital, University of Toronto, Toronto, ON, Canada, ²Department of Medicine, University Health Network and Mount Sinai Hospital, University of Toronto, Toronto, ON, Canada, ³Department of Pathology & Laboratory Medicine, Mount Sinai Hospital, Toronto, ON, Canada.

Recent evidence suggests that vitamin D may affect wellbeing and mood. The objective of this study is to examine whether serum levels of 25-hydroxy-vitamin D are associated with health-related quality of life in postmenopausal women with osteopenia. We examined the baseline data obtained from the ECKO trial -- a 2-year single-centre double-blind placebo-controlled randomized trial investigating the effect of vitamin K supplementation on bone mineral density. Four hundred and forty-four postmenopausal women with osteopenia (lowest T-score between -1 and -2 in the lumbar spine (L1-L4), total hip, or femoral neck) completed the screening visit. Serum 25-hydroxyvitamin D levels were measured at the screening visit when each participant also completed a Medical Outcomes Survey 36-item short form questionnaire on health-related quality of life (SF-36). The SF-36 assesses nine health domains: physical functioning, role functioning - physical, bodily pain, general health, vitality, social functioning, role functioning - emotional, mental health, and reported health transition. After adjusting for seasonal variation, we performed regression analyses of serum 25-hydroxyvitamin D levels versus the various domains of the SF36. The mean serum 25-hydroxyvitamin D levels was 76.7 nmol/L (SD 25.2nmol/L). The mean scores for all domains of the SF-36 is approximately 100% of age-adjusted predicted mean scores in the general population. After adjusting for age and seasonal variation, we found that a higher serum 25-hydroxyvitamin D level is associated with higher scores for physical functioning ($r^2=0.04$, $p=0.002$), mental health ($r^2=0.05$, $p=0.05$) and overall health-related quality of life ($r^2=0.05$, $p=0.003$), although the effects are small. For an increase of 10nmol/L of serum 25-hydroxyvitamin D level, there is a 1 point, 0.5 point and 1point increase in score in physical functioning, mental health and overall health-related quality of life, respectively. Our results showed that higher 25-hydroxyvitamin D levels may be beneficial to health-related quality of life in postmenopausal women with osteopenia.

Disclosures: *A.M. Cheung, None.*

SU464

Incidence of Primary Hyperparathyroidism in Rochester, Minnesota, 1993-2001: An Update on the Changing Epidemiology of the Disease. R. A. Wermers, S. Khosla, E. J. Atkinson*, S. J. Achenbach*, A. L. Oberge*, C. S. Grant*, L. J. Melton. Endocrinology, Mayo Clinic, Rochester, MN, USA.

Automated serum calcium measurements were associated with a dramatic rise in primary hyperparathyroidism in the early 1970's, but a progressive decline in incidence thereafter was unexpected and suggested a fundamental change in the epidemiology of the disease. Our objective was to evaluate trends in the incidence of primary hyperparathyroidism since 1992. In this population-based descriptive study, Rochester, Minnesota residents who met defined diagnostic criteria for primary hyperparathyroidism from January 1993 through December 2001 were identified through the medical record linkage system of the Rochester Epidemiology Project and the Mayo Clinic Laboratory Information System. Changes in incidence rates were evaluate by Poisson regression. Altogether, 136 Rochester residents (94 women and 42 men) were newly identified with primary hyperparathyroidism in 1993-2001. Their mean age was 56 years, and 93% had definite disease. The overall age- and sex-adjusted (to 2000 U.S. whites) rate during this period was 21.6 per 100,000 person-years, which was less than the annual rate of 29.2 per 100,000 observed in 1983-1992 and 83 per 100,000 in July 1974-1982. The decline in incidence persisted despite improved case ascertainment through the Laboratory Information System. Although community incidence declined, the number of parathyroidectomies performed at our institution increased during the same period. Serum calcium was deleted from the automated chemistry panel in June 1996, but most subjects remained asymptomatic at diagnosis (95%) with mild hypercalcemia. The majority of subjects were observed (75%), and there was minimal impact on patient management from the 1990 NIH consensus conference on asymptomatic primary hyperparathyroidism. The lower incidence of primary hyperparathyroidism noted through 1992 has persisted in our community from 1993-2001, while parathyroidectomies at our institution remained high. Consequently, perceptions about incidence from referral centers may not reflect the true changing incidence. These data suggest that some underlying etiologic factor in addition to the introduction of automated serum calcium testing may have been responsible for the peak incidence in the 1970s.

Disclosures: *R.A. Wermers, Eli Lilly & Co. 2.*

SU465

Bone Quality Is Markedly Abnormal in Hypoparathyroidism. M. R. Rubin¹, D. W. Dempster², S. J. Silverberg¹, E. Shane¹, R. Müller³, H. Zhou², A. L. Boskey⁴, J. P. Bilezikian¹. ¹Columbia University College of P & S, New York, NY, USA, ²Regional Bone Center, Helen Hayes Hospital, West Haverstraw, NY, USA, ³ETH, Zurich, Switzerland, ⁴Hospital for Special Surgery, New York, NY, USA.

Hypoparathyroidism (HypoPT) is a disorder in which PTH is absent from the circulation. Whereas bone properties have been well described in disorders of PTH excess, virtually nothing is known about the quality of bone that is chronically deprived of PTH. We studied 6 women (52.5 ± 5 yr) with HypoPT (duration 21.2 ± 6 yrs; 4 postsurgery, 2 autoimmune). Bone mineral density was: lumbar spine 1.231 g/cm² (T-score, +1.7 ± 1), total hip 0.967 g/cm² (T-score +0.1 ± 1) and 1/3 distal radius 0.665 g/cm² (T-score, -0.5 ± 1). Iliac crest bone biopsies were performed on all subjects. 2-D histomorphometry was compared with 6 age-matched controls (C). In comparison to C, HypoPT bone was characterized by greater cortical width (1046 ± 236 vs 542 ± 159 µm, $p=0.002$) and cortical area (32.9 ± 15 vs 15.6 ± 3 %, $p=0.02$). Osteoid width (Lam#) was reduced in cancellous (2.8 vs 4.6, $p=0.02$), endocortical (1.5 vs 3.6, $p=0.001$) and intracortical (2.0 vs 3.7, $p=0.03$) envelopes. Osteoid perimeter (%) was reduced in cancellous (3.9 vs 9.5, $p=0.02$) and endocortical (4.6 vs 18.6, $p=0.01$) envelopes. Mineralized perimeter, mineral apposition rate, and bone formation rate were lower in HypoPT in both cancellous and endocortical envelopes. µCT was used to compare HypoPT biopsies with 52 C biopsies from human cadavers (20 females, 32 males; age: 24-92 yrs). Bone volume was significantly greater in HypoPT (BV/TV; 0.35 ± 0.1 vs 0.16 ± 0.1, $p=0.005$). Trabecular number (Tb.N.; 2.1 ± 0.8 vs 1.4 ± 0.3 1/mm) and trabecular thickness (Tb.Th; 0.21 ± 0.1 vs 0.15 ± 0.1 mm) were greater in HypoPT, while trabecular separation (Tb.Sp; 0.53 ± 0.1 vs 0.75 ± 0.2 mm) was lower in HypoPT. Estimation of the plate-rod characteristic (SMI) was significantly reduced in HypoPT (-0.82 ± 2.0 vs 1.15 ± 0.6, $p=0.001$). Connectivity Density was high (51.0 ± 35 1/mm³). 2-D (histomorphometry) and 3-D (µCT) parameters were significantly associated: BV/TV: $r=+.91$; ($p=.01$); Tb.Th. $r=+.94$ ($p<.01$), Tb.N $r=+.54$ ($p>.05$), Tb.Sp $r=+.82$ ($p<.05$). Fourier Transform Infrared Spectroscopic Imaging showed markedly increased crosslink ratio, consistent with increased mean bone age. These results show, for the first time using highly specific analytical techniques, that bone deficient in PTH is markedly abnormal. Increased bone density in HypoPT is associated with abnormal bone quality. How the administration of PTH can restore these abnormalities towards normal is the subject of ongoing research.

Disclosures: *M.R. Rubin, None.*

SU466

Markedly Elevated Bone Density in a Man with Longstanding Hypoparathyroidism. G. C. Lim^{*1}, M. Khosla^{*1}, J. A. Spadaro^{*2}, A. M. Moses¹. ¹Department of Medicine- Endocrinology, Diabetes and Metabolism, SUNY Upstate Medical University, Syracuse, NY, USA, ²Department of Orthopedic Surgery, SUNY Upstate Medical University, Syracuse, NY, USA.

An 85-year-old man was diagnosed with idiopathic hypoparathyroidism in1976 and since then we have maintained his serum calcium and phosphorus levels in the normal range on calcitriol 0.25 mcg bid and calcium carbonate 500 mg tid. No fractures or height loss. Expecting that his BMD might be above age matched controls due to chronic hypoparathyroidism, we obtained a DXA which revealed **remarkably dense bone**. DXA was repeated with a different machine and results were confirmed. Blood work showed low bone turnover markers. See details in Table 1.

Table1 Blood work	Recent Lab Results	Densitometry Sites	GE Lunar DPXIQ	Hologic QDR 4500
Calcium (8.4-10.3 mg/dl)	9.3		<u>L1-L4</u>	
		BMD(g/cm ²)	2.510	2.154
Phosphorus (2.5- 4.5 mg/dl)	3.7	T-Score	+10.6	+9.7
		Z-Score	+11.5	NA
BSAP (2-24 ng/ml)	10.0		<u>Total hip</u>	
		BMD(g/cm ²)	1.641	1.472
Osteocalcin (11.3-35.4 ng/ml)	9.5	T-Score	+4.2	+2.9
		Z-Score	+5.5	NA
Serum N-telopeptide (10.7- 22.9 nmol BCE /L)	9.3		<u>Distal 3rd radius</u>	
		BMD(g/cm ²)	0.852	NA
PTH (11-80 pg/ml)	<3	T-Score	-0.2	
		Z-Score	+1.2	
CK-BB* (0%)	0%		<u>Total Body</u>	
		BMD(g/cm ²)	1.577	NA
TartrateResistant Acid Phosphatase* (3.0-6.0 U/L)	7.0	T-Score	+4.5	
		Z-Score	+5.5	

*Elevated in osteopetrosis
Other tests including serum lead, copper, fluoride, PSA, H/H, SPEP, creatinine, 25-OHD & 1,25-OHD levels are all normal.

Routine radiographs were unremarkable except for a coarsening of the trabecular pattern in the spine. A peripheral quantitative CT of the ultra-distal radius showed a cortical cross-sectional area about 35% above young adult values and a 50% higher strength index (density adjusted cross-sectional polar moment of inertia). Our patient's radiological bone difference from normal are similar to those caused by teriparatide treatment of osteoporotic patients. However, his bone turnover markers are opposite from those caused by teriparatide. Unfortunately bone biopsy could not be obtained for further comparison. Laboratory testing ruled out other sclerosing bone disorders such as osteopetrosis. **In summary**, we report the highest bone density yet reported in

hypoparathyroidism. His low bone turnover markers could be explained by PTH hormone deficiency. Long standing hypoparathyroidism is the only apparent factor causing his marked increase in bone density. Whether or not this increased bone density translates to increase bone quality remains unknown but he has had no fractures by age 86 and the distal radius cortical area and structural strength were at or above young normal values. Since hypoparathyroidism can increase bone density and probably decrease risk of fracture, it is possible that suppression of the parathyroid glands using calcimimetics may in the future be a means of treating osteoporosis.

Disclosures: **GC. Lim**, None.

SU467

Low Bone Turnover in Hypoparathyroidism Can Be Restored to Normal by PTH Administration. **M. R. Rubin¹, J. Fleischer¹, M. J. Seibel², J. de Winter^{*2}, D. W. Dempster³, T. F. Lang⁴, E. Shane¹, S. J. Silverberg¹, J. P. Bilezikian¹.** ¹Columbia University College of P & S, New York, NY, USA, ²Bone Research Program, ANZAC Research Institute, University of Sydney, Concord NSW, Australia, ³Regional Bone Center, Helen Hayes Hospital, West Haverstraw, NY, USA, ⁴University of California San Francisco, San Francisco, CA, USA.

Hypoparathyroidism (HypoPT) is a disorder in which PTH is absent from the circulation. In addition to the biochemical manifestations of hypocalcemia and relative hypercalciuria, bone turnover is low. We sought to quantify bone turnover in HypoPT and to determine whether low bone turnover can be enhanced by PTH. We studied 6 women (52.5 ± 5 yr) with HypoPT (duration 21.2 ± 6 yrs; 4 postsurgical, 2 autoimmune). Baseline biochemistries were: serum calcium, 8.6 ± 0.4 mg/dl (nl 8.5-10.4); PTH, 7.6 ± 3 pg/ml (nl 10-65); urinary calcium, 248.7 ± 63 mg/l; serum phosphorus, 4.6 ± 1 mg/dl (nl 2.5-4.5); total alkaline phosphatase, 76.3 ± 10 IU/l (nl 33-96); 25-hydroxyvitamin D, 70.1 ± 25 ng/ml (nl 9-52); 1,25-dihydroxyvitamin D, 28.8 ± 4 pg/ml (nl 15-60). Baseline calcium supplementation ranged from 1-6 g/d (av.3 g/d); baseline calcitriol doses ranged from 0 to 1 ug/d (av. 0.5 ug/d). Baseline bone mineral density was: LS 1.231 g/cm² (T score +1.7 ± 1), TH 0.967 g/cm² (T score +0.1 ± 1) and 1/3 distal radius 0.665 g/cm² (T score -0.5 ± 1). By QCT, volumetric bone density was 53% above normal at the trabecular spine and 150% above normal at the trabecular hip. Biochemical markers of bone turnover, measured twice at baseline, were never elevated and in most cases were below the normal reference ranges: PINP (-2%), BSAP (+1.5%), osteocalcin (-65%), B-CTX (-62%) and TRAcP5b (-11%). PTH(1-84) was administered in an open-label, randomized design at 3 dosing regimens: 100 ug daily, 100 ug every other day, or 100 ug every third day. Bone turnover markers increased at 1 month. On the daily dose, PINP increased 173%, from baseline to almost 2 times above normal; on the every other day dose, it increased 49% to the mid- to high-normal range; on the every third day dose, it increased 38%, to the low-normal range. Serum calcium was maintained at a range of 8.5-10.0 mg/dl, permitting reductions in calcium supplementation by 25 ± 12% and in calcitriol supplementation by 31 ± 16%. We conclude that bone turnover is suppressed in a state of chronic PTH deprivation and that the administration of PTH improves bone turnover in the hypoparathyroid skeleton. The long-term effects of PTH replacement on skeletal dynamics in HypoPT remain to be seen but it is possible that the enhancement of these skeletal dynamics by PTH will be associated with improvements in other qualities of bone.

Disclosures: **M.R. Rubin**, None.

SU468

Differences in Accuracy of the Sestamibi Scanning between Severe and Mild Forms of Primary Hyperparathyroidism. **F. Bandeira, A. T. Corioloano*, L. Griz*, G. Caldas*, C. Bandeira*.** Endocrine Unit and Osteoporosis Research Center, Agamenon Magalhães Hospital/ SUS/ University of Pernambuco and Dilab Laboratories, Recife, Brazil.

The preoperative location of the parathyroids using Tc99m-sestamibi scanning is not yet established as a routine diagnostic procedure for primary hyperparathyroidism (PHPT), but the use of the technique is becoming increasingly common. A number of studies have demonstrated a variable degree of accuracy (70-98%) in asymptomatic patients. We evaluated the accuracy of this technique in 64 patients who underwent a scan between January 2000 and January 2005 according to the clinical manifestations of the disease. In 25 asymptomatic patients (Group I) 80% were females, mean age 66.75 ± 0.63 yr, mean serum Ca 10.98 ± 0.02 mg/dL, mean serum P 2.79 ± 0.29 mg/dL, mean PTH 135.45 ± 13.50 pg/mL, mean serum 25OHD 26.97 ± 4.13 ng/mL, urinary Ca 213.21 ± 42.7 mg, t score LS BMD -2.02 ± 0.15 %, t score FN BMD -2.03 ± 0.28 %, t score distal radius BMD -2.23 ± 0.74 %. In 18 nephrolithiasis patients without overt bone disease (Group II) 77.7% were females, mean age 55.8 ± 5.09 yr, mean serum Ca 11.32 ± 0.17 mg/dL, mean serum P 2.56 ± 0.47 mg/dL, mean PTH 165.85 ± 15.06 pg/mL, mean serum 25OHD 20.02 ± 0.56 ng/mL, urinary Ca 303.45 ± 58.9 mg, t score LS BMD -1.83 ± 0.85 %, t score FN BMD -1.81 ± 0.38 %, t score distal radius BMD -1.79 ± 0.04 %. In 21 patients with severe bone involvement / osteitis fibrosa cystica (Group III) 47.6% were females, mean age 38.7 ± 4.38 yr, mean serum Ca 13.35 ± 0.35 mg/dL, mean serum P 1.99 ± 0.29 mg/dL, mean PTH 579.6 ± 628.4 pg/mL, mean serum 25OHD 15.91 ± 1.11 ng/mL, urinary Ca 285.5 ± 67.1 mg, t score LS BMD -4.25 ± 0.24 %, t score FN BMD -5.44 ± 1.37 %, t score distal radius BMD -5.33 ± 0.69 %. Mean urinary NTX in groups I, II and III was 51.3 ± 6.4 nmol/mmol creatinine (9 patients), 154.1 ± 62.9 nmol/mmol creatinine (10 patients) and 501.5 ± 201 nmol/mmol creatinine (16 patients) respectively. Mean serum CTX in groups I, II and III was 752.6 ± 496.3 pg/mL (16 patients), 727.3 ± 220.4 pg/mL (8 patients) and 2210.2 ± 375.4 pg/mL (5 patients) respectively. Sestamibi scan was positive in 64% of patients in Group I, in 83.33 % of those in Group II and in 100% of those in Group III. From patients with severe bone disease, 70% already showed an increased uptake in the initial images,

compared with the other groups, in which the increase in uptake was seen only in the later images, as expected. Our data show a high degree of accuracy of Tc99m-sestamibi scanning, as locating procedure, in severe primary hyperparathyroidism.

Disclosures: **A.T. Corioloano**, None.

SU469

Can Biochemical Bone Markers, PTH or Ionized Calcium Predict Changes in Bone Mass after Parathyreodectomi in Patients with Primary Hyperparathyreoidism? **L. S. Stilgren*, L. Hegedüs*, K. Brixen, B. Abrahamsen.** Dept. of Endocrinology, Odense University Hospital, Odense C, Denmark.

In the last decade, the diagnosis of primary hyperparathyroidism (PHPT) is diagnosed increasingly early. While PTX is required in many patients, others may be treated conservatively and monitored for disease progression. To make this decision, it would be useful to identify the patients who will obtain the greatest increases in bone mass after surgery. We speculated that bone turnover markers could aid in identifying patients with greater disease intensity and thus particular skeletal benefit from PTX. The study comprised 24 patients (females/males=10/2), aged 52 to 75 years (median 60 years), with PHPT confirmed by elevation of plasma PTH (range 8- 44; median 16 pmol/l) and serum ionized calcium levels (range 1.33-1.82; median 1.49 mmol/l). None of the patients had renal disease or other conditions known to affect bone metabolism, or received bisphosphonates, glucocorticoids, or fluoride. Patients were investigated before and one year after successful PTX. Whole body BMC and BMD were measured using a Hologic 2000 DXA-scanner. Serum ionized calcium was normalized in all patients after surgery. During the first year after surgery, total BMC as well as BMD increased significantly by 5% and 2 %, respectively, while biochemical bone markers decreased. A significant, positive correlation was found between pre-operative serum PTH and ionized calcium on the one hand and the change in total BMC on the other hand. Similarly, pre-operative serum phosphate was negatively correlated to the change in total BMC. By contrast, bone turnover markers showed no relationship with the subsequent gain in BMC.

	Parathyroid hormone	Ionized calcium	Phosphate
	Rho	Rho	Rho
Total BMC before PTX	0.23	0.26	-0.23
Change in total BMC	0.67**	0.61**	-0.43*

* p<0.05; **p<0.005

	Alkaline phosphatase	Osteocalcin	PINP	PICP	Cross-links	U-NTX
	Rho	Rho	Rho	Rho	Rho	Rho
Total BMC before PTX	-0.44*	-0.33	-1.57*	-0.63*	-0.47*	-0.61*
Change in total BMC	-0.02	0.21	-0.15	-0.06	0.02	-0.1

* p<0.05

In this preliminary study we have shown pre-operative serum PTH, ionized calcium, and phosphate predict the change in total body BMC after parathyroidectomy. In contrast, biochemical bone markers had no value as severity markers.

Disclosures: **L.S. Stilgren**, None.

SU470

Normal Bone Mineralization Density Distribution (BMDD) in Hypoparathyroidism. **M. R. Rubin¹, D. W. Dempster², S. J. Silverberg¹, E. Shane¹, P. Roschger³, K. Klaushofer³, J. P. Bilezikian¹.** ¹Columbia University College of P & S, New York, NY, USA, ²Regional Bone Center, Helen Hayes Hospital, West Haverstraw, NY, USA, ³Hanusch Hospital of WGKK and AUA Trauma Centre Meidling, Ludwig Boltzmann Institute of Osteology, Vienna, Austria.

In Hypoparathyroidism (HypoPT), bone turnover is markedly reduced and bone mineral density (BMD) is increased. In states of low bone turnover induced by bisphosphonate therapy, along with increased BMD, uniformity of mineralization as reflected by bone mineralization density distribution (BMDD) is also enhanced. We investigated whether prolonged low turnover due to chronically deficient levels of parathyroid hormone in HypoPT would also be associated with a shift of BMDD towards increased mineralization. BMDD was assessed by backscattered electron imaging (qBEI) in iliac crest bone biopsies from 6 women (52.5 ± 5 yr) with HypoPT (duration 21.2 ± 6 yrs). Mean calcium content (CaMean), the variation of calcium content (CaWidth) and the percentage of low mineralized matrix (CaLow), as measured by qBEI, were used to characterize BMDD. The data were compared to 52 normal controls. While variability was present, the mean values for all mineralization parameters, including CaMean (HypoPT 22.3 ± 0.9 vs 22.2 ± 0.45), CaPeak (22.9 ± 0.93 vs 22.9 ± 0.39), CaWidth (3.29 ± 0.16 vs 3.35 ±0.34) and CaLow (4.38 ± 1.72 vs 4.96± 1.57) were all within control values in HypoPT. These results are in marked contrast to the expectation that an increase in mineralization density in HypoPT would be seen because of an association between low bone turnover and increased bone mineralization. However, these findings are consistent with other data indicating that mineralization is remarkably consistent among different skeletal sites, as a function of age, and between men and women and between races (Roschger P et al, *Bone* 32:316-323, 2003). There may well be a maximum, and perhaps optimum, extent of mineralization that is not exceeded even when bone turnover is reduced. Recent data with bisphosphonates also suggest a limit to which the degree of mineralization can be enhanced. These unique results are providing new insights into our understanding of HypoPT and are likely to have direct clinical relevance to prolonged antiresorptive therapy for osteoporosis.

Disclosures: **M.R. Rubin**, None.

SU471

Severe Hypercalcemia due to Thyrotoxicosis. S. Psarelis^{*1}, G. Trovas², S. Gazi^{*1}, N. Tsakalakos², K. Tempos^{*1}, G. P. Lyritis². ¹Reumatology, KAT Hospital, Athens, Greece, ²Laboratory for Research of the Musculoskeletal System, Athens, Greece.

Hypercalcemia might be associated with hyperthyroidism rarely. We present a 42 year-old black woman who referred to our department complaining for myalgias, arthralgias, polydipsia and polyuria. She had no history of previous serious illness and her symptoms began before two months but became severe the last two weeks. The physical examinations show generalized tendonitis, sinus tachycardia (120/min) and blood pressure 110/75 mmHg. Laboratory studies revealed : WBC 5450, (NEU 51%, LYM 38%), HCT 32, Hb10.4, MCV 74, PLT 333.000, RF(-), ANA(-), Anti-ENA(-) CRP<0.325, ESR 25, C₃ 170, C₄ 41 HBsAg (-), Anti-HCV(-), Anti-HIV(-), GLU 94, BUN 42, CREAT 0.7, SGOT 31, SGPT 23, BIL 0.5, GGT 24, Albumin 4.3, P 4.7, PTH 7.4, 25(OH)D₃ 17.1, Anti TG 16, P24h 371, CEA 0.5, CEA 0.5 , CA₁₂₅ 9.1, CA₁₉₋₉ 10.92, CA₁₅₋₃ 6.3, Serum protein electrophoresis was normal.

	8/2/05	25/2/05	28/03/05
TSH	0 (0.49-4.67)	0.06	0.06
T ₃	5.17 (0.58-1.59)	3.11	1.39
T ₄	22.95 (4.8-11)	15.9	5.8
AntiTPO	50.4 (<2.5)		
Ca	13.1 (8.5-10.2)	10.7	9.8
ALP	107 (40-104)	106	105
BALP	70 (11-30.6)		
Ca 24h	690 (100-300)		
Ca/Cr2h	0.45 (0.02-0.45)		
P/Cr	0.9 (0.3-0.6)		
Pyrilinks D/Cr	10.5 (3-7.4)		
NTX/Cr	79.9 (20-50)		

Chest Xrays and U/S abdomen: with normal findings, U/S of thyroid gland : Heterogenicity of parenchyma with the presence of multiple nodules. DPXL L₂-L₄ 1.229 g/cm² Tscore 0.2, Zscore -0.5.

After excluding primary hyperparathyroidism and other secondary causes of hypercalcemia, we started hydration with normal saline and administration of Furosemide for hypercalcemia and Carbimazol (5mg) 1x3 and Propanolol (40mg) ½ x3 for hyperthyroidism. Her hypercalcemia resolved completely after 11/2 month. Mild hypercalcemia usually can occur in up to 15 to 20 percent of patients with hyperthyroidism. Our case is unusual because the patient demonstrated a significant degree of hypercalcemia secondary to hyperthyroidism alone and we speculate a high bone turnover as reflected by increased bone markers as the putative pathophysiology of this thyroid bone disease and physicians should consider thyrotoxicosis in the differential diagnosis of hypercalcemia.

Disclosures: **S. Psarelis**, None.

SU472

Mutational Analysis of the PTH 3' Untranslated Region in Primary Hyperparathyroidism. J. Costa-Guda^{*1}, T. Naveh-Many², J. Silver², A. Arnold¹. ¹Molecular Medicine, University of Connecticut Health Center, Farmington, CT, USA, ²Minerva Center for Calcium and Bone Metabolism, Hadassah Hebrew University Medical Center, Jerusalem, Israel.

Sequence alterations in untranslated regions of genes are important contributors to human diseases, including hereditary thrombophilia, hereditary hyperferritinemia cataract and fragile X mental retardation syndromes. Recently, functional studies of the *PTH* gene 3' untranslated region (UTR) have highlighted it as a potential target for pathogenic mutations in patients with primary parathyroid disorders. Specifically, regulation of *PTH* gene expression by calcium and phosphate occurs post-transcriptionally, primarily through alteration of *PTH* mRNA stability (Naveh-Many, T., *et al*, FEBS Lett., 2002). Calcium and phosphate appear to influence the binding of proteins, including a known regulator of mRNA stability AUF1, in a sequence dependent manner to a specific *cis* element in the 3' untranslated region of *PTH* mRNA. Decreased serum calcium and increased phosphate lead to increased protein binding to *PTH* mRNA, resulting in increased stability. AUF1 stabilizes *PTH* mRNA *in vitro* and decreasing AUF1 decreases *PTH* secretion from cells transfected with the human *PTH* gene. Thus, the *PTH* 3'UTR has emerged as an important potential contributor to primary parathyroid dysfunction. Consequently, we sought to rigorously examine, by direct DNA sequencing, the *PTH* 3'-UTR in 21 parathyroid glands from 14 patients with primary parathyroid hyperplasia and 40 sporadic parathyroid adenomas from 40 patients. No alterations from the normal sequence were detected in any of the 61 samples examined. Based on the absence of identifiable DNA sequence alterations in these forms of primary hyperparathyroidism, it is unlikely that mutation of the *PTH* 3' UTR frequently contributes to their pathogenesis.

Disclosures: **J. Costa-Guda**, None.

SU473

Physical Activity and Nutrition Education Promotes Fitness and Bone Mineral Acquisition in Children with Acute Lymphoblastic Leukemia (ALL). L. J. Moyer-Mileur¹, H. Slater^{*1}, R. VanOrden^{*1}, C. Bruggers^{*2}. ¹Pediatrics, University of Utah, Salt Lake City, UT, USA, ²Pediatric Oncology/Hematology, University of Utah, Salt Lake City, UT, USA.

Background: Young adult survivors of childhood ALL are reported to have higher incidence of obesity and osteoporosis and their related complications. Altered nutrient intake and decreased physical activity in response to cancer therapies and their side effects, particularly corticosteroids, may be key factors for growth, body composition, and bone mineral acquisition alterations in children with ALL. **Purpose:** To compare growth, body composition, bone mineral acquisition, and fitness during 12-mos of maintenance therapy in children with ALL. **Design:** Children age 4-10 y with standard-risk ALL were recruited from the Pediatrics Oncology Program, Primary Children's Medical Center, Salt City, UT at the completion of induction therapy and randomized to a monthly physical activity and nutrition education program (EX, n=6, 3M/3F) or control (C, n=7, 4M/3F). Height, weight, fitness testing (aerobic endurance by PACER test, flexibility, and muscular strength), DEXA measurements of the femoral neck (FN) and lumbar spine (LS), pQCT cross-sections of the tibia, physical activity and dietary intake records, and bone alkaline phosphatase (BAP) and urine pyridinium cross-links (Pyd) samples are obtained at baseline, 6 and 12 months. Statistical analysis included t-test, regression, and MANCOVA. **Results:** Age, weight, height, body mass index (wt/hr²), body composition, and nutrient intakes were similar at baseline, 6, and 12 mos. EX children had dramatically improved aerobic endurance (201% ± 22% vs. 7% ± 33%, p=0.01) and flexibility (5%±12% EX vs. 1%±13%C, p=0.001) from baseline to 12M. FN and LS bone area, FN BMC, and tibia periosteal circumference 12mo gains were greater in C children while greater gains in LS BMC (g), FN and LS BMAD (g/cm³), and tibia cortical bone area (mm²), BMC (mg), thickness (mm), and bone strength index (BSI, mm³) were found in EX children (p≤0.04). Trabecular volumetric BMD (vBMD) values were similar for groups over 12 mos and significantly lower than references values (172 ± 36 mg/cm³ ALL vs. 235 ± 39 mg/cm³ REF, p=0.001). BAP values did not change while urine Pyd:creatinine values decreased in EX vs. C children (p=0.006) suggesting increased bone mineralization. **Conclusions:** This pilot work suggests that a monthly physical activity and nutrition education program during maintenance therapy promoted cardiovascular fitness and bone mineral acquisition in children with standard-risk ALL. Further longitudinal work is needed to determine whether lifestyle interventions will lower the risk of obesity and osteoporosis in later life.

Disclosures: **L.J. Moyer-Mileur**, None.

SU474

Polycystic Ovary Syndrome Is a State of Low Bone Resorption: A Study in Youth. J. G. Warren-Ulanch¹, S. Arslanian^{*1}, S. L. Greenspan². ¹Endocrinology, Children's Hospital of Pittsburgh, Pittsburgh, PA, USA, ²Endocrinology, University of Pittsburgh Medical Center, Pittsburgh, PA, USA.

Adults with polycystic ovary syndrome have normal bone turnover. Adolescence, a time of peak growth velocity and bone mineralization, is associated with high bone turnover. No studies have evaluated the bone turnover rates in adolescents with or without PCOS. To determine the impact of age, hormone levels, BMI, and glucose homeostasis on bone turnover, we examined these variables in fifteen obese (BMI>85%ile) females (6 African American) with PCOS and 10 obese females (5 African American) without PCOS. Bone formation was assessed by levels of aminoterminal propeptide of type 1 collagen (PINP), and bone resorption was assessed by levels of C-telopeptide of collagen cross-links (CTX) measured in plasma. Bone mass was evaluated with dual-energy x-ray absorptiometry (DXA). Those with PCOS had higher BMI (p=.004), and were more mature by Tanner stage (p=.024) than the controls. They had higher levels of estradiol, testosterone, and fasting insulin. No differences were noted in bone mass, but those with PCOS were found to have lower markers of both bone formation and bone resorption. (p<.001).

	BMI, Hormone levels, and Bone Turnover. Data are mean (SD).		
	PCOS	Controls	P
BMI (kg/m ²)	38.1 (5.7)	31.5 (4.1)	.004
Estradiol (pg/mL)	65.6 (51.5)	32.1 (45.6)	.014
Free Testosterone (pg/mL)	12.0 (8.7)	3.4 (3.0)	.001
Fasting Insulin (uU/mL)	52.7 (19.1)	37.8 (32.5)	.002
CTX (ng/mL)	1.39 (.63)	2.67 (.67)	<.001
PINP (ug/L)	245.5 (227.7)	458.4 (151.1)	.012

Using stepwise linear regression analysis to allow for weight, age, BMI, and Tanner stage, only age had a significant contribution to PINP (r²=56.5%, p<.001) and CTX (r²=32.2%, p=.03). After making this adjustment, PCOS did not significantly affect PINP, however, it accounted for 30.6% of the variance of CTX (p<.001). These values were not affected after further adjusting for testosterone, estradiol, IGF-1, or fasting insulin. In conclusion, we find that PCOS is a state of low bone resorption in obese adolescents, in the absence of changes in bone formation or bone mass. This is consistent with findings of preserved, if not elevated, bone mass in adults with PCOS. Further studies are needed to determine the etiology of the low bone resorption in this population.

Disclosures: **J.G. Warren-Ulanch**, None.

SU475

Growth Hormone as an Anabolic Agent in Burned Children. G. L. Klein¹, D. J. Sherrard², D. N. Herndon^{*3}. ¹Pediatrics, University of Texas Medical Branch, Galveston, TX, USA, ²Renal Dialysis, VA Medical Center and University of Washington School of Medicine, Seattle, WA, USA, ³Surgery, University of Texas Medical Branch and Shriners Burns Hospital, Galveston, TX, USA.

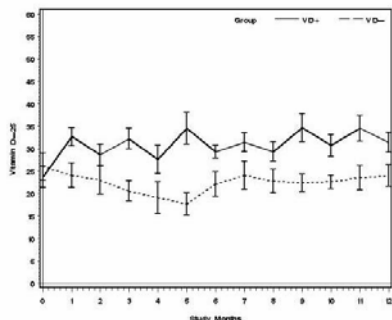
Children burned at least 40% total body surface area are catabolic with negative nitrogen balance and loss of muscle mass, lose a mean of 8% lumbar spine bone mineral content(BMC) by 2 mo and 3% total body BMC by 6 mo post-burn. Bone loss is due to glucocorticoid-related reduction in bone formation and excessive urinary Ca loss and results in an increased annual extrapolated age-and sex-related post-burn fracture incidence and a hypothetical reduction in peak bone mass. The aim of our study was to determine if treatment of burned children with an anabolic agent, recombinant human growth hormone (rHGH) or oxandrolone(ox) increases BMC, bone area(BA) and bone mineral density (BMD). We enrolled 28 children, ages 5-19 yr, 22M, 6F with burns of at least 40% body surface area and randomized them to an anabolic agent (rHGH, n=14, ox, n=2) or placebo (n=12) for 1 yr double-blinded. Bone densitometry (DEXA) and iliac crest bone biopsy were obtained at hospital discharge and at 1 yr and analyzed for changes in total body BMC, BA, lean body mass (LBM) and lumbar spine BMD Z scores. Compared to placebo, children receiving anabolics increased total body BMC (p=0.028) and BA(p<0.025) at 1 yr. Changes in BMC correlated with changes in BA, r=0.96, p<0.001. Changes in BMC per gram LBM did not differ between groups. Changes in lumbar spine BMD Z scores were also not different nor were changes in height. There was a trend toward increased LBM in the anabolic group. 130 +/- 44% vs 110 +/- 11% change from discharge (p=0.18). Thus anabolic agents increase BMC and BA in proportion to each other without gain in BMD. If BMD is a risk factor for fractures, anabolic agents are not optimal treatment. Future studies should ascertain whether BA (size) or BMD is more important as a risk factor following bone loss and whether the time needed to improve LBM is a factor in the delayed action of anabolic agents on bone.

Disclosures: **G.L. Klein**, None.

SU476

The Effect of Oral Cholecalciferol on Serum Concentrations of 25-Hydroxyvitamin D in HIV-Infected Children and Adolescents. S. M. Arpadi^{*1}, E. Shane¹, D. McMahon^{*1}, R. Lazell^{*2}, E. Abrams^{*3}, M. Bamji^{*4}, M. Purswani^{*5}, E. Engelson^{*6}, M. Horlick¹. ¹Columbia University, NY, NY, USA, ²St. Luke's-Roosevelt Hospital, NY, NY, USA, ³Harlem Hospital, NY, NY, USA, ⁴Metropolitan Hospital, NY, NY, USA, ⁵Bronx-Lebanon Hospital, Bronx, NY, USA, ⁶St. Luke's-Roosevelt Hospital, NY, NY, USA.

We have previously reported that bone mass is decreased in HIV-infected prepubertal children and that vitamin D deficiency and insufficiency are highly prevalent in HIV-infected children and adolescents living in New York City. To determine whether supplementation with vitamin D and calcium results in increased bone mass accrual, we have undertaken a 24 month randomized clinical trial. Here, we report the effect of the intervention (oral cholecalciferol, 100,000 IU every 2 months) on monthly serum 25-hydroxyvitamin D (25OHD) levels and serum and urine calcium during the first year of the trial. Perinatally HIV-infected children and adolescents, aged 6-16 yrs (mean 10.9±2.4), were randomly assigned to receive vitamin D and calcium (VD+; n=18) or placebo (VD-; n=19). Subjects with baseline serum 25OHD < 12 ng/ml were excluded. Dietary vitamin D and calcium were assessed by questionnaire (Block Kids Questionnaire, Berkeley, CA) at baseline and 1 year. Serum albumin-corrected calcium and spot urinary calcium/creatinine ratios (Uca/cr) were measured monthly. Subjects with spot Uca/cr ratios >0.25 were evaluated with 24-hour urinary calcium excretion (Uca). Monthly serum 25OHD levels for each individual were analyzed in batches by radioimmunoassay (Diasorin, Stillwater, MN). VD+ and VD- groups did not differ with respect to age, gender, dietary intake of vitamin D and calcium or baseline serum 25OHD. No episodes of hyper- or hypocalcemia, or hypercalciuria were detected. Mean monthly serum 25OHD levels (Figure 1), were significantly higher in the VD+ group, 32.1 ±8.7 vs. 23.0 ±9.6, p=0.004. In addition, mean serum 25OHD area-under-the-curve was higher in the VD+ than the VD- group, p<0.0001. We conclude that oral cholecalciferol (100,000 IU every 2 months) is safe and results in significant increases in serum 25OHD levels in HIV-infected children and adolescents. Whether this intervention improves bone mass accrual remains to be determined. Figure 1. Mean monthly serum 25OHD ± SD in HIV infected children receiving 100,000 IE of VD3 (solid line) and placebo (broken line).



Disclosures: **S.M. Arpadi**, None.

SU477

Peak Bone Mass after Childhood Acute Lymphoblastic Leukemia (ALL): Findings in 37 Adult Males. O. Makitie, J. P. Puutio^{*}, K. Jahnukainen^{*}, L. R. Viertomies^{*}, M. Henriksson^{*}, K. Vetteranta^{*}, M. A. Siimes^{*}. Hospital for Children and Adolescents, University of Helsinki, Helsinki, Finland.

Peak bone mass is attained by early adulthood. Controversy exists whether any chronic illness in childhood results in subnormal peak bone mass attainment or whether catch-up in the growth of bone mass takes place after recovery from the illness, ensuring normal bone mass by adult age. We have assessed bone health and its correlates in adult males about 25 years after they have survived childhood ALL. The ALL survivors had been treated at the Hospital for Children and Adolescents, University of Helsinki. Data on their previous medical history were collected from hospital records. The patients were prospectively assessed for bone mineral density (BMD) of the lumbar spine (L1-L4), femoral neck and whole body with dual-energy x-ray absorptiometry (DXA, Hologic Discovery A); the BMDs were transformed into T-scores using age- and sex-specific reference data for the equipment. Lateral spine images were obtained with the same equipment for vertebral morphology assessment. Laboratory investigations included serum Ca, Pi, ALP, PTH, 25-OH-vitamin D, testosterone and IGF-I. The present study comprised 37 males aged 26 - 39 yrs (median 30 yrs) who had been diagnosed with ALL at the median age of 4 yrs (1 - 15 yrs) and treated according to the Nordic treatment protocols. Of the patients, 30 (81%) had received CNS irradiation (18 - 26 Gy) and 11 (30%), testicular irradiation. The median height was 177 cm (-0.3 SDS, range from -2.4 to +2.4 SDS) and BMI 24 kg/m² (-0.7 SDS, from -2.1 to +2.2 SDS). The median BMD T-scores were for lumbar spine -0.7 (from -3.1 to +3.6), for femoral neck, -0.2 (from -2.2 to +2.1) and for whole body, -1.2 (from -2.4 to +2.2); the lumbar spine T-score was at or below -1.0 in 16 patients (43%). The T-scores for the lumbar spine and total body were significantly lower than normal (P=0.005 and P<0.0001). Compression fractures were recorded in 9 patients (24%). The median serum testosterone concentration was 14.4 nmol/L; it was below 10 nmol/L in 6 patients (16%). Altogether twelve patients (32%), 10 of whom had received testicular irradiation, had primary hypogonadism; 3 of them were not on replacement therapy. 25-OH-vitamin D concentration was below 38 nmol/L in 11 patients (30%). The results suggest that adult males who have survived childhood ALL have i) significantly reduced peak bone mass and ii) high frequency of spinal compression fractures. The low testosterone and vitamin D concentrations suggest that preventive measures of osteoporosis are often neglected.

Disclosures: **O. Makitie**, None.

SU478

Activated T Cells: Regulators of Bone Metabolism in Pediatric Crohn Disease? F. A. Sylvester¹, P. M. Davis^{*1}, N. Wyzga^{*2}, J. S. Hyams^{*1}, T. Lerer^{*1}. ¹Pediatric Gastroenterology, Connecticut Children's Medical Center, Hartford, CT, USA, ²Research, Saint Francis Hospital & Medical Center, Hartford, CT, USA.

Crohn disease, a chronic inflammatory condition of the gastrointestinal tract, is associated with osteopenia and T cell activation. Activated T cells are emerging as regulators of bone mass. We hypothesized that circulating activated T cells of patients with Crohn disease produce cytokines that modulate bone cell function. To examine this hypothesis, newly diagnosed children with Crohn disease (n =23, previously untreated) and healthy age- and sex-matched controls (n = 40) between 7-17 years of age (mean age 12.5 years) were invited to participate. After informed consent, we determined clinical severity and disease location in patients, bone age, bone mineral density of whole body and spine by DXA, laboratory markers of bone turnover, and the serum concentration of RANKL, INF- γ and OPG. We harvested circulating T cells and measured the *in vitro* production of these cytokines after activation. Results were expressed as mean \pm SD. Children with Crohn disease had decreased BMD Z scores compared to healthy children (-1.03 \pm 0.81 vs. -0.47 \pm 0.90, p < 0.05, corrected for bone age, lowest Z score at any site). Biochemical markers suggested a state of low bone turnover. Serum OPG (pmol/L) was higher in Crohn patients (mean \pm SD 4.24 \pm 1.73 vs. 3.3 \pm 1.00, p < 0.05), whereas serum RANKL (pmol/L) was lower (0.50 \pm 0.86 vs. 1.02 \pm 1.63, p < 0.05). INF- γ (ng/ μ g protein) released by activated T cells from Crohn patients *in vitro* was two-fold higher than in controls (20.03 \pm 26.39 vs. 9.76 \pm 14.10, p < 0.05). In summary, children with Crohn disease may have reduced BMD at the time of diagnosis, probably due to reduced bone turnover. This may be caused, at least in part, by INF- γ secreted by circulating activated T cells. Since osteoblast function appears to be decreased in children with Crohn disease at diagnosis, elevated serum OPG may be secreted by the inflamed intestine, and may contribute to reduce bone turnover by suppressing osteoclast formation and activity.

Disclosures: **F.A. Sylvester**, None.

SU479

The Vitamin D Ratio (P-1,25(OH)₂D / P-25OHD) Is Insufficient in Separating Familial Hypocalciuric Hypercalcemia (FHH) from Primary Hyperparathyroidism (PHPT). S. E. Christensen¹, P. H. Nissen^{*2}, B. Moosgaard^{*3}, P. Vestergaard¹, L. Heickendorff^{*2}, L. Mosekilde¹. ¹Dept. of Endocrinology and Metabolism, Aarhus University Hospital, Aarhus, Denmark, ²Dept. of Clinical Biochemistry, Aarhus University Hospital, Aarhus, Denmark, ³GCP Unit, Aarhus University Hospital, Aarhus, Denmark.

Clinically Primary Hyperparathyroidism (PHPT) is usually separated from Familial Hypocalciuric Hypercalcemia (FHH) by the calcium-creatinine clearance ratio (CCCR). Studies have shown reduced P-25OHD and high plasma P-1,25(OH)₂D in PHPT, whereas FHH has been characterized by normal P-25OHD and reduced P-1,25(OH)₂D. The ratio P-

1,25(OH)₂D / P-25OHD (D-ratio), which reflects the renal 1- α -hydroxylase activity, could be a diagnostic tool in separating FHH and PHPT. We wished to compare the D-ratio in FHH and PHPT and to test its discriminative power. Our material consisted of 49 patients with FHH, based on hypercalcemia (mean of 3 measurements) and mutation(s) in the calcium sensing receptor gene (CaSR-gene), who were compared with 160 patients with surgically verified PHPT. The FHH group was separated into two subgroups: subgroup I (n=27) included mutations with obvious effect on the FHH phenotype (R886W, C582F, C582Y, G509R, 1998 insT, S171N, G397R), subgroup II (n=22) included mutations with less effect on the FHH phenotype (R990G, A986S, Q1011E, 1732+16 T>C). All patients had a P-creatinine level < 150 μ mol/l. All sequenced DNA fragments were compared to reference sequences. As expected, P-PTH was higher in PHPT than in FHH (2p<0.001). P-25OHD was reduced in the PHPT group compared with the FHH group and subgroups I (2p<0.001) and II (2p<0.001). We found no significant differences between the PHPT group and the FHH groups with regard to P-1,25(OH)₂D and P-creatinine. The PHPT group had higher D-ratio (3.42 ± 2.01 (SD) μ mol/nmol) than the FHH group (2.10 ± 0.94 , 2p<0.001), and the subgroups I (2.12 ± 0.85 , 2p=0.001) and II (2.07 ± 1.06 , 2p=0.002). ROC curve analysis of the FHH group showed that D-Ratio < 1.60 was the best cut off value for separating FHH from PHPT, diagnostic sensitivity = 0.33, and diagnostic specificity = 0.88. The positive predictive value was 0.44 for D ratio < 1.60 compared with 0.92 for CCCR < 0.01 in the same material. In the FHH group the D-ratio was unrelated to P-PTH (2p=0.38) and P-creatinine (2p=0.75). In the PHPT group the D-ratio was positively correlated to PTH (r=0.17, 2p<0.04) and inversely correlated to P-creatinine (r=-0.21, 2p<0.01). The D-Ratio is insufficient in discriminating between FHH and PHPT. It is important also to consider calcium-creatinine clearance ratio, pedigree, mutations in the CaSR gene, P-PTH, and eventually ultrasound, and parathyroid scintigraphy.

Disclosures: **S.E. Christensen**, None.

SU480

Causes of Bone Loss in a Clinical Pediatric Population. **K. Vandenbulcke**^{*1}, **T. Chernova**², ¹Katholieke Universiteit, Leuven, Belgium, ²Russian Academy of Medical Sciences, Moscow, Russian Federation.

Although dual energy x-ray absorptiometry (DXA) is a fast, non-invasive, low-dose and highly reproducible method for the assessment of skeletal status in children, its application in clinical pediatric practice is not widespread. Numerous pathologies (growth hormone (GH) deficiency, AIDS, anorexia nervosa, diabetes) can influence the growth and mineralization of the pediatric skeleton. GE Healthcare provides enhanced pediatric software including spine and total body bone mineral density (BMD) measurements as well as tools to adjust for the child's body size (ratios of height for age, bone mineral content (BMC) for bone area, and bone area for height). In this study we evaluated the clinical value of DXA measurements in pediatric subjects. We reviewed all the pediatric patients who were referred to the clinic over the past four years. A total of 837 boys and girls ranging in age from 5 to 19 years were measured on the Lunar Prodigy (GE Healthcare) in this clinical practice. Of the total, 192 subjects were healthy, while 645 subjects had pathologies known to affect BMD. All children had either a spine scan or a total body scan, or both. Bone density values were compared to the pediatric reference population in the Lunar enCORE software. Follow-up measurements were performed in 176 children with low BMD at baseline.

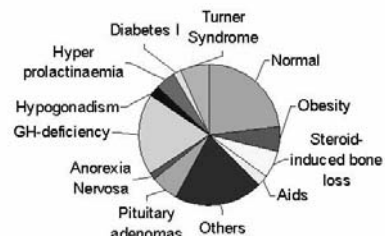


Figure 1: Different pathologies of children having a DXA skeletal assessment

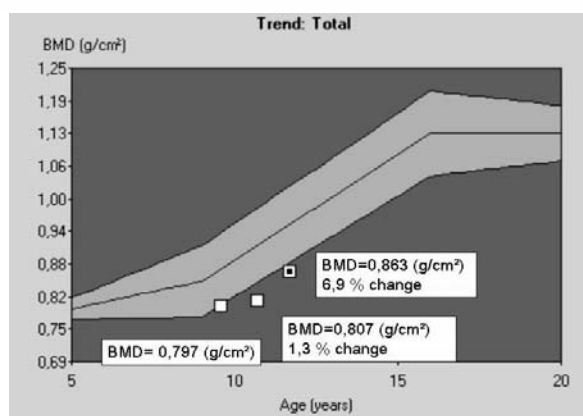


Figure 2: Baseline and follow-up values for a girl with anorexia nervosa

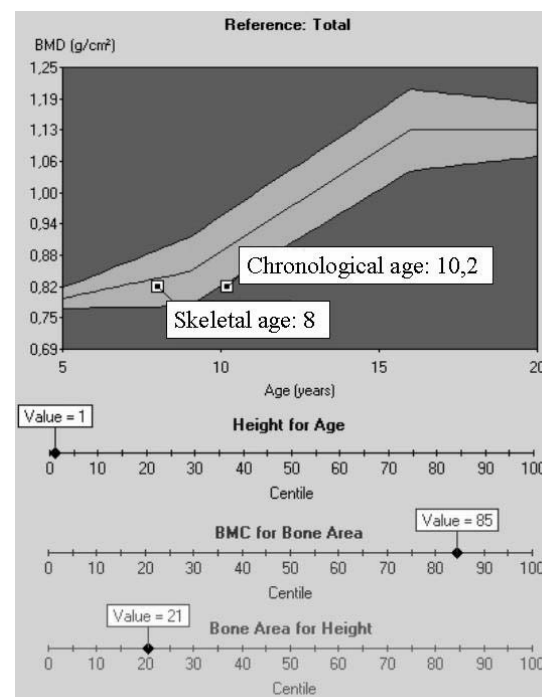
The primary pathologies affecting BMD found in this group were GH deficiency, Turner's syndrome, steroid-induced bone loss, and pituitary adenomas (Figure 1). With most pathologies children had lower bone area, BMC, and BMD when compared to the reference. In 176 of the measured 837 children follow-up scans were performed to check if their bone status improved in function of treatment and/or age. Figure 2 illustrates baseline and follow-up values for a girl with anorexia nervosa. In this study we illustrated that in many diseases occurring in children DXA measurements of the spine and total body allowed baseline and on-going assessment of the bone status of these children.

Disclosures: **K. Vandenbulcke**, None.

SU481

Improved Assessment of Bone Status in Children with the Lunar Pediatric Total Body Software. **H. Fors**^{*1}, **S. Valdimarsson**^{*1}, **K. Albertsson Wikland**^{*1}, **K. Vandenbulcke**^{*2}, ¹GP-GRC, Sahlgrenska Academy of Göteborg University, Göteborg, Sweden, ²Katholieke Universiteit, Leuven, Belgium.

Measurement of bone mineral density (BMD) in children has become important in clinical endocrinology. Dual-energy X-ray absorptiometry (DXA) is the method of choice to evaluate BMD in children, but the two-dimensional measurement is influenced by body size and can impact the accurate assessment of bone accrual in the growing skeleton. Children with growth abnormalities often show deficient BMD for chronological age, but this low BMD might be a reflection of skeletal size rather than poor mineralization. The Lunar pediatric software provides, in addition to BMD values, a number of tools to adjust for body size. In this study we wished to determine if these body size tools are of clinical value in the assessment of pediatric bone status. Forty-eight children (5-18 yrs, 17 girls), with growth hormone deficiency, had total body scans on the Lunar Prodigy (GE Healthcare). Skeletal age was determined by the Greulich-Pyle method. BMD plots against chronological age (CA) and skeletal age (SA), Z-scores for chronological age (ZCA), the subject's height for age, BMC for bone area (BMC/BA), and bone area for height were obtained with the enCORE software. Z-scores for skeletal age (ZSA) were calculated in the same way as the ZCA. Skeletal age in these subjects was on average 1.5 years (-4 to +0.5 range) younger than chronological age. The children had significantly lower total body BMD (p = 0.0005) when compared to normal children of the same chronological age (average ZCA = -0.2). However, their BMD was not significantly different than normal children of the same skeletal age (average ZSA = 0.5), illustrating that bone mineralisation might be underestimated when only BMD for chronological age is considered. Regression analyses of BMC/BA as a function of CA confirmed that the bone mineralisation of these children is generally normal for their bone area (bone size). Results from this small group of children with growth hormone deficiency demonstrate that adjustment of pediatric densitometry values for body size and skeletal age can be vital for appropriate clinical decisions. Bone mineralisation may be underestimated when only BMD for chronological age is considered.



Lunar total body results for a 10 year old girl with a growth hormone disorder

Disclosures: **H. Fors**, None.

SU482

Children with Osteogenesis Imperfecta Treated with Bisphosphonates Have Site-Specific Bone Responses to Therapy. R. K. Fuchs¹, M. Peacock², C. McClintock^{*2}, L. A. DiMeglio³. ¹Department of Anatomy and Cell Biology, Indiana University Medical School, Indianapolis, IN, USA, ²Department of Medicine, Indiana University Medical School, Indianapolis, IN, USA, ³Department of Pediatrics, Indiana University Medical School, Indianapolis, IN, USA.

Bisphosphonate therapies improve bone mass, reduce fractures, and improve physical function in children with Osteogenesis Imperfecta (OI). In addition to the primary defect in type I collagen, children with OI also have "disuse osteoporosis" because of fracture- and deformity-induced limitations in their mobility. To test if there were differing responses to bisphosphonate therapy in the arms and legs, we examined site-specific changes in bone mass in ambulatory and non-ambulatory children clinically diagnosed with OI and treated with bisphosphonates. Thirteen children between the ages of 5 and 13 were treated for 24 months with one of two bisphosphonates—intravenous pamidronate (n=7) [3 mg/kg over 3 days every 4 months] or oral alendronate (n=7) [1 mg/kg from a minimum of 10 mg to a maximum of 20 mg daily]. Three children had severe (Type III or IV) OI and 10 children had mild (Type I) OI. Nine children were ambulatory and 4 were non-ambulatory (minimal walking). No children had rods newly implanted during the treatment period. Bone mineral content (BMC; g) of the upper and lower limbs derived from total body DXA scans were evaluated at baseline, and after 24 months of bisphosphonate treatment. Both ambulatory and non-ambulatory children had significant increases in upper and lower limb BMC over 24 months of bisphosphonate treatment (both p<0.001 based on repeated measures ANOVA). However, ambulatory children were found to have greater absolute increases in mineral content of the lower limbs compared to non-ambulatory children (absolute Δ over 24 months: 263g vs 103g, respectively; p<0.02). In contrast, for the upper limbs there were no differences in mineral content accrual between the ambulatory and non-ambulatory children (absolute Δ over 24 months: 82g vs 53g, respectively). Additionally, the observed site-specific differences between ambulatory and non-ambulatory children were similar between those children receiving IV or oral bisphosphonate treatment. The greater increases in bone mass in the lower limbs may be due to site-specific effects of the bisphosphonates. Alternatively, the greater increases in mechanical loading of the legs in the ambulatory children may have contributed to the greater increases in lower limb bone mass.

Disclosures: **R.K. Fuchs, None.**

SU483

Decreased Bone Size and Density in Children with Turner Syndrome (TS) Prior to Growth Hormone Therapy. G. Costin^{*1}, P. Pitukcheewanont¹, D. Safani^{*1}, S. Rossmiller^{*1}, V. Gilsanz². ¹Endocrinology, Childrens Hospital Los Angeles, Los Angeles, CA, USA, ²Radiology, Childrens Hospital Los Angeles, USC Keck School of Medicine, Los Angeles, CA, USA.

Background: While some studies have reported decreased bone mineral density (BMD) in children with Turner syndrome (TS), others have found normal BMD values when compared to healthy controls. Most studies using dual-energy x-ray absorptiometry (DXA) to evaluate BMD have found that untreated prepubertal girls with TS have normal BMD. The purpose of this study was to compare bone size and density of children with TS to healthy age-, gender-, and ethnicity-matched controls using DXA and quantitative computed tomography (CT). **Subjects and Methods:** 23 prepubertal females, mean age of 11.93 ± 3.28 , with karyotype-proven TS had bone measurements obtained prior to growth hormone therapy. Whole body (WB) and spine bone measurements were obtained using DXA while spine and femoral bone measurements were obtained using CT. Subjects were matched with controls based on age, gender and ethnicity. **Statistics:** Paired Student's t-test was used to compare bone size and density measurements between children with TS and controls. Pearson's correlation was used to find associations between anthropometric measurements and bone size. **Results:** Children with TS were shorter (p<0.001), lighter (p<0.001) and had lower BMIs (p<0.05) than controls. Accordingly, bone area by CT (CBA of the femur and CSA of the spine and femur) and DXA (spine and whole body area) were lower in children with TS than in controls (ps<0.001). These areal bone measurements also correlated strongly with height in children with TS (ps<0.001). Both DXA- and CT-measured BMD of the spine were lower in children with TS compared to controls (ps<0.05). In addition, DXA-measured WB BMD (p<0.001) was lower in Turner children than in controls. The mean decreases in CT spine BD and DXA WB BMD were 14% and 13%, respectively. **Conclusion:** Cancellous bone size and density were lower in children with TS compared to controls. While the decreased bone size appears to be secondary to the smaller size of children with TS, the decreased bone density may be due to a chronic lack of estrogen.

Disclosures: **P. Pitukcheewanont, None.**

SU484

Performance of the Lunar Infant Total Body Software in Newborns and Preterm Infants. S. Di Gregorio^{*1}, L. Del Rio¹, P. Pludowski^{*2}, J. Czech-Kowalska^{*3}, A. Dobrzanska^{*3}, K. Vandembulcke^{*4}, R. Lorenc^{*2}. ¹Cetir Centre Medic. Densitometry Department., Barcelona, Spain, ²The children's memorial Health Institute, Warsaw, Poland, ³Department of Neonatology, The Childrens Memorial Health Institute, Warsaw, Poland, ⁴Katholieke Universiteit, Leuven, Belgium.

Different factors like environment, nutrition, hormonal status, diseases affect postnatal skeletal growth and mineralization in preterm infants. Compared to their term counterparts preterms have an increasing incidence of osteopenia and postnatal growth deficiency at the time of hospital discharge. Dual energy x-ray absorptiometry (DXA) is a non-invasive, low dose, fast, accurate and precise method in measuring bone mineralisation and has therefore become the method of choice to measure infants and preterm infants. Recently, GE Healthcare Lunar introduced a total body software dedicated to measure infants. In this study we wished to evaluate the performance of this software both in healthy newborns as well as in preterm infants. 33 healthy Spanish newborns (16 boys, 17 girls), between 8 and 28 days old were scanned with the infant total body software on the Lunar Prodigy (GE Healthcare). Their weight was between 2,4 and 4,3 kgs, their height ranged between 45 and 55cm. 16 Polish preterms (9 boys, 7 girls) were also scanned with the same software. Their weight at birth was between 0,6 and 1,2kg. On acquisition time they weighed between 2 and 4,2 kg and were between 2 and 4 months old. Their body size at acquisition was still rather small ranging from 42 to 50 cm. Acquisition times were around three minutes. The average total body bone mineral density (BMD) of the healthy newborns is 0,157 g/cm² and their average total body bone mineral content (BMC) is 119 g. There was no difference between girls and boys when total body bone mineral density and total body bone mineral content were compared with height and weight. The average total body BMD is 0,154 g/cm² of the polish preterms but their average total body BMC is remarkably low: 42 g. We conclude that the new Lunar infant total body software is a clinically valid, non-invasive, low dose and fast method for measuring bone mineralisation in infants.

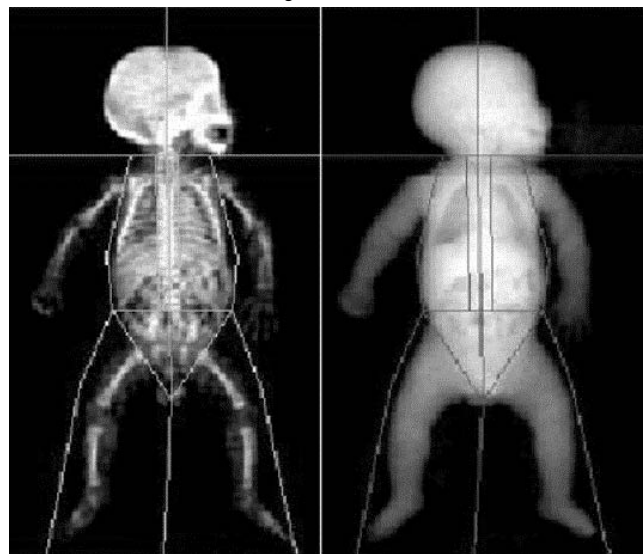


Figure: Total body scan of a 3 month old preterm boy. His weight was at birth 0,700 kg. At acquisition time his weight was 3,3kg and his height 47 cm.

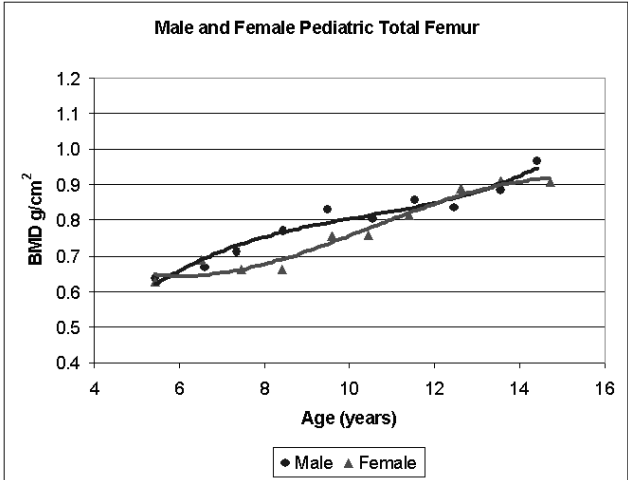
Disclosures: **S. Di Gregorio, None.**

SU485

Femur Densitometry with Adjustment for Body Size in Healthy German Children. K. Minas. Orthopädische Praxis, Papenburg, Germany.

Measurement of pediatric bone mineral density (BMD) of the proximal femur with dual-energy x-ray absorptiometry (DXA) is challenging due to the changing morphometry of the femur during aging. Dimensions of femur regions-of-interest (ROI) should automatically adjust to changes in the child's body size with aging. Pediatric femur software is now available for investigational use that automatically adjusts the neck ROI and total ROI based on the child's stature. Reference data based on this new software is currently being developed. We used the Lunar Prodigy (GE Healthcare) to measure the proximal femur in a sample of healthy, normal German boys (n = 143) and girls (n = 171) age 5 through 15 years. Scans were analyzed with Lunar enCORE software version 9.15, with automatic calculation of BMD values for the size-adjusted ROIs. For comparison, scans were also analyzed without the automatic ROI size adjustment. Results showed that total femur BMD values in boys were somewhat higher (5 to 15%) than girls from age 7 to 11 years, with less difference at younger and older ages. In about 15% of scans, automated analysis of the total femur region was incorrect unless the new software with size-adjusted ROIs was used. Automatic adjustment of the size of femur analysis regions for a child's

stature should allow better evaluation of the pediatric patient. Femur reference data for size-adjusted BMD values are important for appropriate interpretation of BMD in the growing pediatric skeleton.



Disclosures: **K. Minas**, None.

SU486

Reduced Bone Mineral Density in Patients with Early and Active Rheumatoid Arthritis. **W. F. Lems¹, J. Bijsterbosch^{*2}, J. de Vries Bouwstra^{*2}, Y. Goekoop-Ruiterman^{*2}, F. Breedveld^{*2}, R. Allaart^{*2}, B. Dijkmans¹.**

¹Rheumatology, Free University medical centre, Amsterdam, The Netherlands, ²Rheumatology, Leiden University medical centre, Leiden, The Netherlands.

Background Generalized osteoporosis is considered as an important extra-articular feature of rheumatoid arthritis (RA). The majority of studies designed to evaluate bone mineral density (BMD) in RA patients is conducted in patients with established RA. **Objective** To identify patients with osteoporosis and to evaluate possible risk factors for osteoporosis in a study population with early, active RA. **Patients and Methods** The BeSt study is a multi-centre randomized controlled trial designed to evaluate the effect of four different treatment strategies for early (symptom duration < 2 years) and active RA. In 342 patients baseline BMD measurements of the lumbar spine L1-L4 and total hip were performed by DXA. Between patients with (T-score <-2,5 at the hips or spine) and those without osteoporosis, clinical, demographic and radiological characteristics were compared using univariate and multivariate analysis. **Results** The population consisted of 240 women and 102 men with a mean age of 54.6 years. Osteoporosis was observed in 10.2% of the patients. Osteoporosis was found more often in rheumatoid factor (RF) positive patients, in patients with higher age, in postmenopausal women and in patients with low body mass index (BMI). No association was found between the presence of osteoporosis and symptom duration or disease activity measured by the DAS₄₄-score (table 1). Stepwise multiple logistic regression analysis showed that postmenopausal status and BMI were independent predictors of osteoporosis. **Conclusions** We found that osteoporosis is already present in a substantial proportion of patients with recent onset of active RA. In this population osteoporosis was predominantly related to classic risk factors as postmenopausal status and low BMI, but not to disease duration or disease activity. Thus, screening for osteoporosis might be also important in early RA, particularly since these patients might be at risk for additional bone loss, because of the disease (RA) and/or antirheumatic drugs (prednisone).

Table 1.

	Odds Ratio	95% Confidence Interval
Age	1.03	1.01-1.06
Symptom duration	1.01	1.00-1.01
DAS ₄₄ -score	0.76	0.52-1.12
Positive Rheumatoid Factor	2.39	1.01-5.66
Postmenopausal status	6.29	1.44-27.47
Body Mass Index	0.86	0.77-0.95

Disclosures: **W.F. Lems**, None.

SU487

Homocysteine Level, Bone Mineral Density and Fracture Risk in Systemic Lupus Erythematosus Women. **E. Y. Rhew¹, C. Lee¹, P. Eksarko^{*1}, A. R. Dyer^{*2}, R. M. Pope^{*1}, S. Spies^{*3}, R. Ramsey-Goldman¹.** ¹Rheumatology, Northwestern University, Chicago, IL, USA, ²Preventive Medicine, Northwestern University, Chicago, IL, USA, ³Nuclear Medicine, Northwestern University, Chicago, IL, USA.

Elevated homocysteine (HCY) is an independent risk factor for fractures (FXs) in the general population. Patients with systemic lupus erythematosus (SLE) are at increased risk for bone loss and FXs, but no data exist in SLE on the relationship between HCY and bone mineral density (BMD) or FXs. We examined the association of baseline HCY with BMD and the incidence of FXs in SLE. We assessed baseline HCY in SLE cases (n=100) and non-SLE controls (n=100) matched on age, race, and menopause status. All women received BMD measurements of at least one anatomic site (lumbar spine, hip or distal

forearm) at baseline by dual x-ray absorptiometry. BMD results were expressed as T-scores. Non-fasting serum HCY levels were measured using an enzyme immunoassay (Biorad) (intra-assay CV 5.2-7.3%; inter-assay CV 7.1-9.3%). We collected data on current smoking status; alcohol, caffeine, and total calcium (dietary and supplemental) intake; estrogen and corticosteroid (CS) use; height and weight; FXs at baseline; and new FXs occurring over 2 years of follow-up. Statistical analyses were performed using Student's t-test for paired values, Spearman's correlation and McNemar's test. IRB approval was obtained for this study. Mean HCY \pm SD was higher (p<0.001) in cases (9.98 \pm 3.8 μ mol/L) than controls (7.98 \pm 2.6 μ mol/L). Elevated HCY and older age were correlated in cases (r=0.219; p=0.028), but not in controls. In cases, there were no significant differences in HCY when stratified by race, menopause status, and estrogen or CS use. In controls, premenopausal women had notably lower mean HCY than menopausal women (mean 7.63 \pm 2.49 μ mol/L vs. 8.59 \pm 2.65 μ mol/L, p=0.016), but HCY did not differ based on race or estrogen use status. Baseline L-spine BMD T-scores were significantly lower in cases than controls (-0.73 vs. -0.20, p=0.003), whereas hip and distal forearm T-scores were comparable between the groups. However, there were no significant correlations between HCY and BMD T-scores at any site for both cases and controls. Cases sustained 14 new FXs, while controls experienced 4 new FXs over the 2 year follow-up period (p=0.021). Baseline HCY did not predict new FXs in either cases or controls. In conclusion, cases (women with SLE) have significantly greater baseline HCY, lower L-spine BMD T-scores, and a higher number of new FXs over 2 years as compared with controls. However, in cases and controls, HCY was not significantly associated with BMD T-scores at the L-spine, hip, or distal forearm, and baseline HCY measurement did not predict new FXs.

Disclosures: **E.Y. Rhew**, None.

SU488

Autoimmune IFN-Alpha Irreversibly Biases Myelopoiesis Towards Dendritic Cells and Depletes Osteoclast Precursors: A Central Mechanism for Non-Erosive Inflammatory Arthritis. **L. Ma^{*1}, H. Awad¹, C. Ritchlin^{*1}, R. J. O'Keefe¹, H. Drissi¹, A. Mathian^{*2}, J. Banchereau^{*2}, E. M. Schwarz^{*1}.** ¹Orthopaedics, University of Rochester, Rochester, NY, USA, ²Baylor Institute for Immunology Research, Dallas, TX, USA.

Introduction: Autoimmune arthropathies present in various forms. While rheumatoid arthritis (RA) is associated with erosive disease there are also non-erosive forms, which are most common in patients that have systemic lupus erythematosus (SLE). Here we investigate the effects of IFN α on myelopoiesis as a potential mechanism. **Methods:** NZBxNZW (lupus) TNF-Tg (arthritis) or Balb/c and B6 (control) mice were untreated, or received recombinant adenovirus containing an empty cassette (Ad-Nul) or IFN α (Ad-IFN). Osteoclast precursor (OCP) and dendritic cell precursor (pDC) populations in blood and spleen were evaluated by FACS using antibodies specific for CD11b and CD11c and by TRAP osteoclastogenesis assays. Tibias were also analyzed by micro-CT and histology. **Results:** IFN α was detected only in the serum of mice treated with Ad-IFN α . Only the NZBxNZW F1 mice (100%) developed lupus. No differences in osteoclast numbers were observed in any of the control groups (Balb/c untreated 70 \pm 8; Balb/c empty vector 73 \pm 9; NZBxNZW F1 untreated 73 \pm 7; NZBxNZW F1 empty vector 73 \pm 9). However, Balb/c mice treated with Ad-IFN α had a significant decrease in osteoclasts (26 \pm 6; p<0.002). The NZBxNZW F1 Ad-IFN α group had significantly lower osteoclast numbers than controls or Balb/c mice (4 \pm 2; p<0.005). Micro-CT analysis revealed that the untreated NZBxNZW F1 mice had a 1.5-fold increase in bone volume vs. Balb/c mice and that IFN significantly increased the bone volume in both strains over 2-fold (p<0.005). In the TNF-Tg experiments we found that Ad-IFN: 1) decreased CD11b⁺/CD11c⁺ OCP from 53.2% to 30.0% and increased CD11b⁺/CD11c⁺ pDC from 13.7% to 36.1% in PBMC, 2) decreased the osteoclastogenic potential of CD11b⁺/CD11c⁺ OCP down to that observed in untreated CD11b⁺/CD11c⁺ pDC, and 3) completely eliminated the osteoclastogenic potential of CD11b⁺/CD11c⁺ pDC. Discussion: The recent discoveries that: 1) SLE patients suffer from systemic IFN, and 2) IFN dominantly alters myelopoiesis away from osteoclastogenesis, provides a potential mechanism to explain the non-erosive lupus phenotype. The finding here that systemic IFN significantly reduces OCP frequency in the periphery and osteoclast numbers at sites of bone resorption in the absence of lupus documents the dominance of this cytokine. That similar effects are observed in animals that suffer from aggressive-erosive arthritis highlights the role of IFN during myelopoiesis.

Disclosures: **E.M. Schwarz**, None.

SU489

Botanical Extracts Isolated from Turmeric or Ginger Prevent Joint Swelling and Associated Joint Destruction in an Animal Model of Rheumatoid Arthritis. **J. L. Funk, J. A. Beischel^{*}, J. N. Oyarzo-Somoza^{*}, G. Chen^{*}, R. C. Lantz^{*}, A. M. Solvom^{*}, S. D. Jolad^{*}, B. N. Timmermann^{*}.** Arizona Center for Phytomedicine Research, University of Arizona, Tucson, AZ, USA.

PURPOSE: Dried ground rhizomes of turmeric and ginger, related herbs from the Zingiberaceae family that contain structurally similar phenolic compounds (i.e. curcuminoids and gingerols), have been used for centuries in Ayurvedic medicine to treat inflammation and are being viewed with increased interest in the "post-Vioxx era" for the treatment of arthritis. However, scientific data regarding the clinical efficacy of these chemically complex botanicals are lacking. Studies were therefore undertaken to test the effects of well-characterized extracts of turmeric or of ginger on joint inflammation and associated bone destruction in an animal model of rheumatoid arthritis. **METHODS:** Female Lewis rats were treated with: (1) vehicle alone; (2) botanical extract; (3) streptococcal cell wall (SCW) (25 mg/kg ip); or (4) SCW + botanical extract. Extracts tested include: (i) crude extract of turmeric dosed at 46 mg curcuminoids/kg/D (ii)

essential oil-free, curcuminoid fraction of turmeric dosed at 23-46 mg curcuminoids/kg/D (iii) crude extract of ginger dosed at 26 mg gingerols/kg/D, or (iv) essential oil-free, purified extract of ginger dosed at 26 mg gingerols/kg/D. Extracts were administered via intraperitoneal injection 5-7 days/week beginning 4 days prior to SCW injection and effects of treatment were monitored by clinical evaluation of joint swelling and *in vivo* or *ex vivo* measures of joint destruction. RESULTS: Treatment with crude or purified extracts of turmeric and ginger that contained curcuminoids or gingerols, respectively, profoundly inhibited joint swelling. Joint destruction, as measured by histologic assessment of cartilage destruction, periarticular accumulation of TRAP-positive osteoclasts, and decreases in periarticular BMD, was similarly prevented. Further evaluation of animals treated with the curcuminoid fraction of turmeric revealed an inhibition of NFκ-B activation in arthritic joints, as well as inhibition of *ex vivo* osteoclast formation stimulated by M-CSF and RANK-activating antibody. CONCLUSIONS: Extracts of turmeric or ginger containing phenolic compounds prevent inflammation and inflammation-associated joint destruction. At least part of the bone-protective effects of these complex botanical mixtures may be due to inhibition of RANK-mediated bone resorption. These complex botanicals may therefore also be of benefit in the treatment of other bone diseases associated with activation of the RANK pathway, including post-menopausal osteoporosis. (The NIH [P50 AT00474] supported this work).

Disclosures: **J.L. Funk**, None.

SU490

Baseline Bone Mineral Density (BMD) and Bone Turnover Markers (BTM) to Predict 2-Year Change in BMD in Systemic Lupus Erythematosus (SLE). C. Lee¹, O. Almagor^{*2}, D. D. Dunlop^{*2}, C. B. Langman³, H. Price^{*3}, S. Spies^{*4}, A. B. Chadha^{*1}, R. Ramsey-Goldman¹. ¹Rheumatology, Northwestern Univ., Chicago, IL, USA, ²Institute for Healthcare Studies, Northwestern Univ., Chicago, IL, USA, ³Pediatrics, Childrens Memorial Hospital, Chicago, IL, USA, ⁴Radiology, Northwestern Univ., Chicago, IL, USA.

We assessed the utility of baseline bone turnover markers (BTM) and BMD in predicting 2-year change in BMD at the hip, lumbar spine (LS), and distal forearm (DF) in women with SLE (cases) compared with matched controls. Cases (n=97) and controls (n=97) were matched on age, race, and menopause status. All had baseline and 2-year BMD measurements (Hip, LS, and/or DF) and baseline measurements of BTM: 1) osteocalcin (OC), 2) bone alkaline phosphatase (BAP), 3) urine N-telopeptide (U-NTX). Women completed a lifestyle questionnaire and medication survey. We assessed disease features of SLE, including disease duration, renal involvement, and the ACR/SLICC Damage Index (SDI), modified to exclude an osteoporosis/fracture item. Effect of baseline BMD and BTM to predict 2-year change in BMD was determined using multiple regression with generalized estimating equations to account for the matched case/control design. Cases and controls were comparable for age at study visit and body mass index (BMI), but cases were younger at menopause (see Table). Both groups were similar in the proportion using caffeine or alcohol, who currently smoked and used female hormones. Cases had mean SLE duration of 8.4 ±8.2 years, mean SDI of 1.07 ±1.7, 25.8% had SLE renal disease, 76.3% ever used corticosteroids (CS), and 47.4% were currently using CS with a dose equivalent to 8.7 ±10.6 mg/day of prednisone.

TABLE. Comparison of Cases and Controls

Characteristics	Cases (n=97)	Controls (n=97)	P value
Mean age at study visit ±SD	43.3 ±11.4	43.7 ±10.8	0.11
Mean body mass index (BMI) ±SD	26.9 ±7.3	26.1 ±6.0	0.39
Mean age at menopause in years ±SD	41.0 ±7.6	44.5 ±5.9	0.01
Mean total daily calcium intake (mg) ±SD	1201.3 ±680.4	959.6 ±603.6	0.004
Mean daily vitamin D intake (IU) ±SD	487.8 ±167.6	434.3 ±149.4	0.15
Proportion taken thiazide diuretics (%)	18.6%	5.2%	0.01
Baseline Mean BTM			
BAP (U/L)±SD	17.3 ±7.7	18.9 ±7.7	0.09
OC (ng/ml)±SD	8.2 ±7.7	8.5 ±6.6	0.71
U-NTX (nM/mM)±SD	35.3 ±37.9	32.7 ±16.5	0.67
2-year change in BMD (gm/cm²)			
Anatomical Site			
Hip ±SD	-0.011 ±0.04	-0.002 ±0.03	0.09
Spine ±SD	0.004 ±0.05	0.003 ±0.03	0.91
Distal Forearm ±SD	-0.012 ±0.03	-0.005 ±0.05	0.29

Cases had significantly more BMD loss at the hip (p=0.02) controlling for baseline BMD and BTM. Greater BMD loss at the DF was experienced by cases and increased with higher baseline values of BMD and U-NTX. Cases and control differences were not significant for spine BMD loss controlling for other factors. We conclude that women with SLE (cases) compared to those without SLE (controls) have comparable baseline BTM but greater BMD loss at the hip and DF. Higher baseline hip and DF BMD predicted greater future bone loss at each of these sites. Greater U-NTX predicted larger DF BMD loss controlling for BTM of bone formation.

Disclosures: **C. Lee**, None.

SU491

RANKL Protein Is Expressed at the Pannus-Bone Interface at Sites of Erosion in Rheumatoid Arthritis. A. R. Pettit¹, N. C. Walsh², C. Manning^{*2}, S. R. Goldring², E. M. Gravallese^{*2}. ¹Institute for Molecular Bioscience, University of Queensland, Brisbane, QLD, Australia, ²New England Baptist Bone and Joint Institute, Beth Israel Deaconess Medical Center/Harvard Institutes of Medicine, Boston, MA, USA.

Bone erosion is a characteristic feature of rheumatoid arthritis (RA) and is associated with significant morbidity and with poor prognosis. We previously reported the generation of inflammatory arthritis in the receptor activator of NF-κB ligand (RANKL)-/- mouse. Bone erosion was dramatically reduced in arthritic RANKL-/- mice, and osteoclast-like cells, abundant in erosions in arthritic control mice, were absent in arthritic RANKL-/- mice. These data support the hypothesis that RANKL is required for osteoclast generation in inflammatory arthritis. The expression of RANKL and its decoy receptor osteoprotegerin (OPG) has been reported in RA synovial soft tissues. However, the identification of RANKL, its receptor, receptor activator of NF-κB (RANK), and OPG protein expression in the RA bone microenvironment is essential to fully characterize their contribution to osteoclastogenesis and subsequent bone erosion in RA. Tissues from 20 orthopedic surgeries on RA patients fulfilling American College of Rheumatology criteria were collected as discarded materials, as approved by the Institutional Review Board. Average duration of RA was 16 yrs (range 4 - 31 yrs). Six tissue samples contained only synovium/tenosynovium remote from bone, 7 samples contained bone with adjacent synovium, and 7 samples contained both synovium remote from bone and bone with adjacent synovium. Immunohistochemistry was used to characterize RANKL, RANK, and OPG protein expression. RANKL expression in the bone microenvironment was confined to sites of osteoclast-mediated bone erosion at the pannus-bone interface and at sites of subchondral bone erosion. RANK expressing osteoclast precursor cells were also present in erosion sites and most multinucleated cells on bone expressed RANK. OPG expression was prominent in synovium remote from bone, particularly in cells of the synovial lining layer, but was minimal in the local bone microenvironment, especially at sites of bone erosion and RANKL expression. The results indicate that in the RA bone microenvironment the RANKL/OPG expression balance favors osteoclastogenesis. This is the first demonstration of RANKL, RANK and OPG protein expression at sites of RA focal bone erosion and provides additional strong support for the importance of RANKL and of osteoclasts in the process of bone erosion in inflammatory arthritis.

Disclosures: **A.R. Pettit**, None.

SU492

Relationship between Baseline Levels of Bone Mineral Density (BMD) and Measures of Calcium Homeostasis (MCH) with 2-Year Change in BMD in Systemic Lupus Erythematosus (SLE). C. Lee¹, O. Almagor^{*2}, D. D. Dunlop^{*2}, C. B. Langman³, H. Price^{*3}, S. Spies^{*4}, A. B. Chadha^{*1}, R. Ramsey-Goldman¹. ¹Rheumatology, Northwestern Univ., Chicago, IL, USA, ²Institute for Healthcare Studies, Northwestern Univ., Chicago, IL, USA, ³Pediatrics, Childrens Memorial Hospital, Chicago, IL, USA, ⁴Radiology, Northwestern Univ., Chicago, IL, USA.

We assessed the relationship of baseline measures of calcium homeostasis (MCH) and BMD to 2-year change in BMD at the hip, lumbar spine (LS), and distal forearm (DF) in women with SLE (cases) and matched controls. Cases (n=99) and controls (n=99) were matched on age, race and menopause status. All women had baseline and 2-year BMD (Hip, LS, and/or DF) and baseline measurements of MCH: 1) 25-hydroxyvitamin-D (25-OH-D) and 2) intact parathyroid hormone (PTH). All women completed a lifestyle questionnaire and medication survey. We evaluated SLE features, including disease duration, renal involvement, and the ACR/SLICC Damage Index (SDI), modified to exclude an osteoporosis/fracture item. Effect of baseline BMD and MCH to predict 2-year change in BMD was determined using multiple regression with generalized estimating equations (GEE) to account for the matched case/control design. Cases and controls had similar age at study visit and BMI, but cases were younger at menopause (see Table). Both groups were comparable in the proportion using caffeine or alcohol, who currently smoked and used female hormones. Cases had disease duration of 8.4 ±8.3 years, a mean SDI of 1.06 ±1.7, 26.3% had SLE renal disease, 75.8% ever used corticosteroids (CS), and 48.5% were currently using CS equivalent to 8.7 ±10.5 mg/day of prednisone.

TABLE. Comparison of Cases and Controls

Characteristics	Cases (n=99)	Controls (n=99)	P value
Mean age at study visit ±SD	43.5 ±11.4	44.0 ±10.8	0.08
Mean body mass index (BMI) ±SD	27.0 ±7.2	26.2 ±6.1	0.34
Mean age at menopause in years ±SD	41.3 ±7.8	44.5 ±5.8	0.02
Mean total daily calcium intake (mg) ±SD	1219.3 ±674.7	974.8 ±601.2	0.003
Mean daily vitamin D intake (IU) ±SD	495.2 ±172.4	443.2 ±157.3	0.15
Proportion taken thiazide diuretics (%)	18.2	5.1	0.01
Baseline Mean MCH			
25(OH)D (ng/ml) ±SD*	12.8 ±6.2	13.5 ±8.0	0.42
Intact PTH (pg/ml) ±SD**	28.6 ±21.5	28.0 ±26.7	0.86
2-year change in BMD (gm/cm²)			
Anatomical Site			
Hip ±SD	-0.013 ±0.04	-0.002 ±0.03	0.06
Lumbar Spine (LS) ±SD	0.002 ±0.05	0.004 ±0.03	0.73
Distal Forearm (DF) ±SD	-0.012 ±0.03	-0.005 ±0.05	0.28

*Reference range for 25(OH)D: (15 - 40 ng/mL)

**Reference range for Intact PTH: (15 - 55 pg/mL)

Cases and controls had similarly low 25(OH)D levels. Cases had more BMD loss at the hip (p=0.04) controlling for baseline BMD and MCH, and greater baseline hip BMD predicted BMD loss. Both groups had similar changes in LS and DF BMD controlling for baseline BMD and MCH. Higher baseline LS and DF BMD were predictive for BMD loss at the LS (p=0.01) and DF (p=0.002) in both groups. We conclude that women with (cases) and without (controls) SLE have low 25(OH)D and similar PTH levels at baseline. 25(OH)D and PTH are not predictive for future change in BMD in SLE. Women with SLE have greater bone loss at the hip, but not at the LS or DF controlling for 25(OH)D and PTH. Higher baseline BMD at any site was predictive for bone loss in both groups.

Disclosures: C. Lee, None.

SU493

Bisphosphonate(Alendronate) Decreases Osteoclastogenesis and Changes the Related Cytokine Expression from the Human Peripheral Blood Mononuclear Cells(PBMCs) *In Vitro*: The PBMCs from Patients with Rheumatoid Arthritis (RA) Respond to Bisphosphonates Differently from those of Normal Control. W. Park, S. Kwon*, S. Hong, J. Shin*. Medicine, IN-HA University Hospital, Incheon, Republic of Korea.

There have been many studies regarding the cytokine change and influence on inflammation by the alendronate, but they are conflicting in their results. Although the RA is osteoporosis prone inflammatory disease, there are few studies about the effect of alendronate on osteoclastogenesis from the PBMCs in these patients. Six normal control and 6 patients with definite RA who had not taken the bisphosphonates were selected. The culture of the human PBMC was done with M-CSF (25 ng/ml) containing RPMI-1640 media. After 3 weeks culture with alendronate at the concentration of 50 μM, TRAP stain was done for cytochemical assessment of osteoclast(OC) development and calcium phosphate nano crystal coated culture plate (OAAS™-04, Oscotec, Korea) was assessed for the osteoclastic resorption activity. After 24 hour incubation of PBMCs in the presence of alendronate 200 μM, real time RT-PCR was done to quantify the expression of the interleukin(IL)-1, tumor necrosis factor(TNF)-α, receptor activator of nuclear factor-kappaB (RANK), RANK-ligand (RANKL), interferon(IFN)-γ, TRAP, and cathepsin-K. At baseline, there was no significant difference of these cytokines mRNA expression in PBMCs between RA patients and normal control. After the incubation with alendronate, the increased mRNA expression of the IL-1, TNF-α, IFN-γ, RANKL, and decreased expression in TRAP mRNA from baseline was seen in control, but it was blunted in PBMC of the RA patients (Mann-Whitney U, 2-tailed significance < 0.05). The cathepsin-K expression was not changed in either group, but the RANK expression was decreased to 27% of the baseline in RA PBMC and to 16% in control group (no significant difference between groups). The TRAP positive adherent giant cell development and calcium phosphate plate resorption were almost completely inhibited throughout the 3 weeks culture in the presence of alendronate in both groups. The bisphosphonate acts on human PBMC to change the osteoclastogenesis related cytokine expression of them, inhibit the development of the osteoclast from them, and finally inhibit the osteoclastic activity of OC. The mechanism of anti-osteoporosis effect of the bisphosphonates in RA may be different from that of the normal population. The anti-absorptive effect of bisphosphonates may be blunted in patients with RA. Further study is needed to define whether the difference in response to bisphosphonate in RA patients is due to the disease itself, glucocorticoid, or other disease modifying drugs

Disclosures: W. Park, None.

SU494

Relationship of Serum Osteoprotegerin (OPG), Receptor Activator of Nuclear Factor Kappa-B Ligand (RANKL), and 2-Year Change in Bone Mineral Density (BMD) in Systemic Lupus Erythematosus (SLE). C. Lee¹, O. Almagor^{*2}, E. Y. Rhew¹, P. Eksarko^{*1}, K. McKinney^{*3}, A. B. Chadha^{*1}, D. D. Dunlop^{*2}, S. Spies^{*4}, R. M. Pope^{*1}, R. Ramsey-Goldman¹. ¹Rheumatology, Northwestern Univ., Chicago, IL, USA, ²Institute for Healthcare Studies, Northwestern Univ., Chicago, IL, USA, ³Univ. of Pennsylvania, Philadelphia, PA, USA, ⁴Radiology, Northwestern Univ., Chicago, IL, USA.

Our aim was to assess the relationship between baseline OPG, RANKL, and 2-year change in BMD at the hip, lumbar spine (LS), and distal forearm (DF) in women with SLE (cases) compared with controls. Cases (n=92) and controls (n=92) were matched on age, race, and menopause status. All had baseline and 2-year BMD (Hip, LS, and/or DF) and baseline serum OPG and RANKL measurements. Women completed a lifestyle questionnaire and medication survey. We assessed SLE features, including disease duration, renal involvement, and the ACR/SLICC Damage Index (SDI), modified to exclude an osteoporosis/fracture item. Effect of baseline BMD, OPG, and RANKL to predict 2-year change in BMD was determined using multiple regression with generalized estimating equations (GEE) to account for the matched case/control design. Cases and controls had similar age at study visit and BMI, but cases were younger at menopause (see Table). Both groups were similar in the proportion using caffeine or alcohol, who currently smoked and used female hormones. Cases had a mean age at SLE diagnosis ±SD of 35.2 ±12.4 years, disease duration of 8.1 ±7.8 years, a mean SDI of 1.03 ±1.7, 22.8% had SLE renal disease, 73.9% ever used corticosteroids (CS), and 42.4% were currently using CS with a current dose equivalent to 8.1 ±9.9 mg/day of prednisone.

TABLE. Comparison of Cases and Controls			
Characteristics	Cases (n=92)	Controls (n=92)	P value
Mean age at study visit in years ±SD	43.8 ±11.5	44.0 ±11.1	0.26
Mean body mass index (BMI) ±SD	27.0 ±7.2	25.7 ±6.1	0.13
Mean age at menopause in years ±SD	41.2 ±8.0	44.6 ±5.9	0.02
Mean total daily calcium intake (mg) ±SD	1224.4 ±700.3	1003.2 ±609.6	0.01
Mean daily vitamin D intake (IU) ±SD	500.0 ±175.4	443.2 ±157.3	0.12
Proportion taken thiazide diuretics (%)	18.5 %	4.4 %	0.008
Baseline serum OPG and RANKL			
Mean OPG (pg/ml) ±SD	88.5 ±47.8	81.3 ±38.1	0.24
Mean RANKL (pg/ml) ±SD	10.1 ±19.0	7.3 ±9.7	0.16
2-year change in BMD (gm/cm³)			
Anatomical Site			
Hip ±SD	-0.008 ±0.04	-0.006 ±0.03	0.75
Spine ±SD	0.003 ±0.05	0.002 ±0.03	0.88
Distal Forearm ±SD	-0.012 ±0.03	-0.006 ±0.05	0.38

Cases had similar 2-year changes in BMD as compared with controls at the hip (p=0.74), LS (p=0.87), and DF (p=0.34) controlling for baseline OPG and RANKL levels. Cases with higher baseline hip and LS BMD and greater baseline RANKL levels had more BMD losses at these sites controlling for OPG levels. Cases with higher baseline DF BMD also had greater BMD loss at this site. OPG was not predictive for bone loss at any site. We conclude that women with SLE (cases) compared with matched controls have similar OPG and RANKL levels and comparable hip, LS, and DF BMD at baseline. Women with SLE having higher baseline BMD experience more BMD loss over 2-years. Higher RANKL level is predictive for BMD loss at the hip and LS in SLE.

Disclosures: C. Lee, None.

SU495

Effects of Infliximab on Bone Turnover Markers in Patients with Rheumatoid Arthritis: Improvement of Bone Remodeling Balance and Differential Effects on Cathepsin K and Matrix-Metalloproteases Mediated Bone Resorption.T. Thomas¹, A. le Henanff^{*2}, F. Debiais³, A. Daragon⁴, C. Roux⁵, J. Sany^{*6}, D. Wendling⁷, C. Zarnitsky^{*8}, P. Ravaux^{*2}, P. Garner⁹. ¹Inserm 0366, University Hospital, St-Etienne, France, ²Hôpital Bichat, Paris, France, ³University Hospital, Poitiers, France, ⁴University Hospital, Rouen, France, ⁵Hôpital Cochin, Paris, France, ⁶University Hospital, Montpellier, France, ⁷University Hospital, Besançon, France, ⁸Groupe Hospitalier, Le Havre, France, ⁹Molecular Markers, Synarc, Lyon, France.

There is growing evidence that rheumatoid arthritis (RA) is associated with both systemic bone loss and subchondral bone erosion, a major feature of joint destruction, under the control of pro-inflammatory cytokines, including TNFα. Therefore, we tested the hypothesis that administration of infliximab, an anti-TNFα drug in the treatment of RA would modulate both systemic and local bone resorption and improve the balance of bone remodeling. We performed a prospective study of a multicentric cohort of 48 women, mean age 54.2±12.1 years old, with severe RA for 11.4±7.8 years, who started infliximab after failure of other disease-modifying antirheumatic drugs. We measured in the serum type I procollagen N-terminal propeptide (PINP), a marker of bone formation, C-terminal cross-linked telopeptide of type I collagen (CTX), a marker of cathepsin K-mediated bone collagen degradation and carboxyterminal cross-linked telopeptide of type I collagen (ICTP), an index of matrix-metalloprotease (MMP) mediated type I collagen degradation, at 0, 6, 22 and 54 weeks. Total hip and lumbar spine bone mineral density (BMD) was assessed at baseline, and after 6 and 12 months by DXA. No patient received bisphosphonates while 77% were under oral glucocorticoids. BMD remained stable over one year. Serum CTX levels rapidly decreased by 19% and 28% at week 6 and week 22, respectively (p<0.001 vs baseline), values returning to pre-treatment level at week 54. In contrast ICTP levels progressively declined with a maximal 25% decrease at week 54 (p<0.01). On the other hand, PINP levels remained stable over time, which lead to a 30 to 40% improvement in bone remodeling balance as assessed by the ratios of PINP/CTX and PINP/ICTP (p<0.05-0.001). In summary, the improvement in the formation/resorption marker ratio indicates beneficial bone effects of infliximab in patients with RA. The differences in the pattern of changes in CTX and ICTP may correspond to biological difference in response to infliximab, with CTX mainly reflecting effects on systemic cathepsin-K mediated bone resorption while ICTP effects on local MMP-mediated subchondral bone erosion.

Disclosures: T. Thomas, None.

SU496

PTH(1-34) Improves Spine Fusion Rate and Fusion Mass Volume. S. V. Bukata¹, E. A. Tomin^{*2}, A. Poynton^{*2}, J. A. Lane². ¹Orthopaedics, University of Rochester, Rochester, NY, USA, ²Orthopaedics, Hospital for Special Surgery, New York, NY, USA.

Up to 40% of lumbar fusions fail to heal despite current techniques. In humans and rats, parathyroid hormone (PTH) in low pulsatile doses leads to increased bone formation in fracture and nonfracture conditions. The effect of PTH on spine fusion is unknown. 44male New Zealand white rabbits underwent harvest of iliac crest autograft(1cc/side) and bilateral posterolateral spine fusion (L5-L6). Animals were divided into equal groups and starting post-operative day 4, half received daily subcutaneous injections of PTH(1-34) at 10mcg/kg/dose. Animals were sacrificed at 6 weeks. Animals had an x-ray of the bone grafting site immediately post-op and at the time of sacrifice. The L5-L6 vertebral segments were removed and analyzed by manual bending for fusion in the coronal, sagittal and torsional planes. All specimens were analyzed by faxitron radiograph and scored by 3

ASBMR 27th Annual Meeting

independent investigators for radiographic fusion and quantity of bone formation. All segments underwent fine cut (0.6mm) CT and volume analysis of the fusion mass. Representative specimens were fixed in parafin and plastic and stained to allow for analysis of new bone formation. Manual bending testing identified fusion in 30% of the control animals while 81% of animals treated with PTH fused (Chi-squared test=10.8, p<.001, Fisher exact test p<.002). Faxitron radiographic analysis of individual fusion sites showed 20% of control animal sites fused and 69% of sites in PTH treated animals fused (p<.001). Using a radiographic scoring system where 0 represented no bone formation and 5 represented full fusion, the average fusion mass score for control animals was 3.36 while the average fusion mass score for PTH treated animals was 4.51 (Chi-squared test= 29.4 , p<.001, Cohen's kappa statistic 0.76 with 83% agreement in interobserver scoring). Fine cut CT analysis and volume measurement demonstrated a 75% increase in bone formation in the PTH treated animals with an average mass of 3.5cc in control animals [range 2.25cc-5.40cc] and 6.1cc with PTH treatment [range 4.34cc-10.58cc] (p<.001). Median bone mass formation was 3.44cc for control and 6.03cc for PTH treatment. Histology showed increased mature bone mass and minimal cartilage in the PTH treated animals and total tissue formation correlated with the radiographic analysis for each group. Intermittent PTH administration increases the rate of spine fusion by 170% and the mass of bone formation by 75%. PTH is a potential treatment to improve the rate of spine fusion and improve the quantity of bone mass formed in the fusion. Histology shows that the maturity of the fusion mass is also improved with more mature bone formation and less cartilage with PTH treatment.

Disclosures: **S.V. Bukata**, None.

SU497

Role of Caveolin-1 and the Cytoskeleton in Extracellular Ca²⁺-Regulated PTH Release. **O. Kifor**^{*1}, **I. Kifor**^{*1}, **S. J. Quinn**^{*1}, **F. D. Moore**^{*2}, **R. R. Butters**^{*1}, **E. M. Brown**¹. ¹Endocrinology, Diabetes, and Hypertension, Brigham and Women's Hospital, Boston, MA, USA, ²Medicine and Surgery, Brigham and Women's Hospital, Boston, MA, USA.

Extracellular calcium is the principal physiological regulator of parathyroid hormone secretion. The calcium-sensing receptor mediates the effects of calcium on parathyroid hormone release, such that increasing levels of extracellular calcium inhibit parathyroid hormone secretion. The calcium-sensing receptor, along with various other signaling molecules, resides within caveolin-rich microdomains in parathyroid cells. In this study, we examined the role of caveolin-1 and the cytoskeleton in the regulation of parathyroid hormone secretion. Parathyroid hormone, calcium-sensing receptor, and chromogranin A co-localized with caveolin-1 at the apical secretory pole of parathyroid cells and were also recovered from Triton X-100-insoluble cholesterol/caveolin-1-rich microdomains. Immunocytochemical analysis demonstrated that high calcium caused caveolin-1 and F-actin to aggregate at the apical pole of the cells, and that depolymerization of F-actin with cytochalasin B or disruption of caveolae by depletion of cholesterol with methyl-β-cyclodextrin reduced the actin network and induced redistribution of actin/caveolin-1. Subcellular fractionation of parathyroid cells showed that parathyroid hormone, actin, chromogranin A, and caveolin-1 were present within the secretory granule fraction, and methyl-β-cyclodextrin treatment reduced the amounts of these proteins in secretory granules. Moreover, methyl-β-cyclodextrin and both of the two F-actin-severing compounds, latrunculin and cytochalasin B, significantly increased parathyroid hormone secretion, while the actin polymerizing agent, jasplakinolide, substantially inhibited parathyroid hormone secretion. Thus, we have demonstrated that in polarized parathyroid cells, caveolin-1-containing microdomains are required for secretory granule formation and for entry of parathyroid hormone into the regulated secretory pathway, and that assembly of a caveolin-1/actin network is required for inhibition of parathyroid hormone secretion by high calcium.

Disclosures: **S.J. Quinn**, None.

SU498

A Structure-Activity Relationship Study of PTH Analogs Modified in Position 5. **I. Woznica**^{*1}, **N. Tsomaia**^{*2}, **P. Ruchala**^{*1}, **B. E. Thomas**^{*1}, **D. F. Mierke**^{*2}, **M. Chorev**^{*3}, **R. V. Alexander**^{*4}, **J. Sueiras-Diaz**^{*4}, **C. Schteingart**^{*4}, **K. O. Akinsanya**^{*4}, **P. J. Riviere**^{*4}, **M. Rosenblatt**¹, **A. Wittelsberger**¹. ¹Department of Physiology, Tufts University School of Medicine, Boston, MA, USA, ²Departments of Chemistry and Molecular Pharmacology, Brown University, Providence, RI, USA, ³Laboratory for Translational Research, Harvard Medical School, Cambridge, MA, USA, ⁴Ferring Research Institute, San Diego, CA, USA.

Parathyroid hormone 1-34 (PTH) activates both PTH receptors 1 (PTHr1) and 2 (PTHr2), whereas PTH-related peptide 1-36 (PTHrP) only interacts with PTHr1. The residue in position 5 of PTH (Ile) and PTHrP (His) was found to be the major structural determinant of receptor specificity. Namely, it was shown that Ile⁵-containing PTHrP activates both PTHr1 and PTHr2 and that His⁵-containing PTH activates only PTHr1 [1]. To investigate the role of position 5 in receptor selectivity, we designed eight new PTH analogs containing phenylalanine, alicyclic, and aromatic, non-natural amino acids in position 5 with side-chains varying in hydrophobicity, ring size, and the presence of heteroatoms. Activities and binding affinities were determined for both PTHr1 and PTHr2, expressed stably on HEK293 cells (see Table). Two analogs, [Cpa⁵]PTH and [2''-PyAla⁵]PTH, were fully selective for PTHr1.

Analog	PTHr1 EC50 (nM)	PTHr2 EC50 (nM)	Ratio EC50 PTHr2/ PTHr1	Binding (IC50 PTHr1 [nM])
PTH*	0.33	13.6	41.2	6.1
[Chg ⁵]PTH	0.73	87.7	120.2	41.0
[Cha ⁵]PTH	6.87	21.1	3.1	440
[Cpa ⁵]PTH	5.03	no fit	selective	170
[Phe ⁵]PTH	7.15	28.5	4.0	410
[2''-PyAla ⁵]PTH	8.7	no fit	selective	230
[3''-PyAla ⁵]PTH	140.18	145.6	1.0	360
[4''-PyAla ⁵]PTH	212.97	no fit		530
[2-Nal ⁵]PTH	260.76	90.8	0.3	400

* based on sequence [Nle^{8,18}, 2-Nal²³, Tyr³⁴] hPTH (1-34)-NH₂.
Chg: cyclohexylglycine. Cha: cyclohexylalanine. Cpa: cyclopentylalanine. PyAla: pyridylalanine. Nal: naphthylalanine.
Molecular dynamics simulations of the ligand-receptor complex were carried out for each analog for both PTHr1 and PTHr2. The resulting models give insight into interactions occurring between the side-chain of residue 5 and receptor residues in its binding pocket. These atomic details help to more rationally explain certain differences in activities and receptor specificities: 1) the position 5 binding pocket of PTHr2 is smaller and less tolerant to substitutions than the one of PTHr1; 2) a coulombic interaction (such as with His) becomes advantageous in the PTHr1 binding pocket when residues larger than Ile⁵ are introduced. This is rationalized by the negative charge of receptor residue D421 at the entrance of the binding cavity.
[1] Behar, V., et al., Endocrinology 137:4217, 1996.
[2] Rolz, C., et al., Biochemistry 38:6397, 1999.

Disclosures: **I. Woznica**, None.

SU499

Intermittent vs. Continuous PTH Differentially Regulate Primary Response Gene Expression in a Gene, Dose and Time Dependent Manner. **C. E. Magyar**^{*}, **O. Bezouglaia**^{*}, **S. Tetradis**. School of Dentistry, UCLA, Los Angeles, CA, USA.

Intermittent and continuous PTH treatments have important and diverse effects on bone metabolism. Because the molecular mechanisms mediating PTH's effect are largely unknown, we examined how PTH pretreatment regulates induction of select primary response genes (PRG) in osteoblasts. Expression levels of Nurr1, Nurr77, c-fos, cox-2, IL-6 and RANKL were evaluated by real-time PCR of RNA isolated from primary mouse osteoblasts (POB). To compare the effect of intermittent vs continuous PTH exposure on PRG induction, POB were treated with 10 nM PTH for 0-4h. PTH was removed at 0.5, 1 or 2h and replaced by fresh media for the remainder of 4h. 0.5-1h PTH exposure was sufficient to induce maximal and transient expression, similar to continuous PTH, for all genes except RANKL. Continuous PTH exposure was necessary for sustained induction of RANKL mRNA levels. Given that both continuous and 1h PTH exposure resulted in similar PRG expression patterns, we investigated the effect of these PTH regimens on subsequent PTH-induced PRG expression. Continuous pretreatment with 10 nM PTH for 24h prevented subsequent PTH induced PRGs, but upregulated basal RANKL levels. POB pretreatment with 10 nM PTH for 1h followed by 23h in PTH-free media attenuated, but did not block, maximal PTH-induced Nurr1 and cox-2 and had no significant effect on c-fos, IL-6 and RANKL induction. The inhibition of PTH induced PRG by continuous PTH pretreatment was dose dependent. 50% inhibition was attained at approximately 0.1 nM and 95-100% inhibition by 1-10 nM PTH for all PRGs, except RANKL, where increased continuous PTH concentrations upregulated expression. PTH binding to its receptor activates cAMP-PKA, PKC and calcium signaling cascades. To elucidate the effect of PKA or PKC signaling in continuous PTH regulation of PRGs, POB were pretreated with 10 nM PTH, 10 μM forskolin (FSK), or 1 μM PMA for 24h and then treated with the same doses of PTH, FSK or PMA. FSK pretreatment completely blocked PTH induction of all PRGs except RANKL. However, PMA pretreatment attenuated PTH induction of c-fos and IL-6, but not of the other PRG. PTH pretreatment partially blunted FSK induced PRG expression. In conclusion, 0.5-1h PTH treatment is sufficient to elicit maximal and transient induction of all PRGs tested except RANKL. The duration and concentration of PTH pretreatment differentially regulated the ability of subsequent PTH to induce PRGs. This inhibition is primarily cAMP-PKA mediated. We hypothesize that the differences on PRG regulation might reflect the diverse effects of intermittent vs continuous PTH on osteoblastic function.

Disclosures: **C.E. Magyar**, None.

SU500

Rapid In Vivo Integrated Hormonal Responses to Alterations in Dietary Phosphate Intake. **S. Sommer**^{*}, **T. Berndt**^{*}, **R. Singh**, **R. Kumar**. Nephrology Research, Department of Medicine, Biochemistry and Molecular Biology, Mayo Clinic College of Medicine, Rochester, MN, USA.

The temporal and quantitative changes in serum/tissue concentrations of various peptide and sterol hormones in response to changes in dietary phosphorus intake are unknown. Male Sprague Dawley rats (n=45) were fed a normal phosphate diet (NPD) for 2 weeks. Rats were divided into 3 groups and fed either a low phosphate diet (LPD) (0.02%; n=15), NPD (0.6%; n=15) or high phosphate diet (HPD) (1.65%; n=15) for another 2 weeks. We measured plasma or blood ionized and total calcium (Ca), inorganic phosphorus (Pi), intact immunoreactive parathyroid hormone (iPTH), intact full-length fibroblast growth factor-23 (iFGF-23), and urinary Pi and creatinine on day 0 and again on days 1, 3, 7 and 14. Plasma 1,25-dihydroxyvitamin D concentrations were measured on days 1 and 14. On days 1 and 14, the rats were killed and renal tissue was harvested for assessment of

ASBMR 27th Annual Meeting

messenger RNA levels and protein expression of 25-hydroxyvitamin D 1 α -hydroxylase cytochrome P450 and secreted frizzled related protein 4 (sFRP 4). In the rats fed the LPD, there was a reduction in plasma Pi (NPD=2.27 mm/L; LPD=0.86 mm/L; p<0.0001) and an increase in ionized calcium concentrations (NPD=2.23 mEq/L; LPD=2.53 mEq/L; p=0.002) within 1 day. The excretion of urinary Pi (NPD=0.17 mm/24hr; LPD=0.006 mm/24hr; p<0.0001) showed a marked decrease on day 1 that was associated with a reduction in iPTH (NPD=52.7 pg/ml; LPD=5.36 pg/ml; p=0.0002) and iFGF-23 (NPD=292.7 pg/ml; LPD=106.4 pg/ml; p<0.0001) plasma concentrations. Similar changes in UVPi, iPTH and iFGF23 were observed at days 3, 7 and 14. There were no changes in sFRP4 in the renal tissue at day 14. In contrast, in rats fed a HPD, an increase in plasma Pi concentrations was not observed on days 1 through 14. There was a marked increase in the excretion of Pi in the urine (NPD=0.17 mm/24hr; HPD=2.22 mm/24hr; p<0.0001) within 1 day that remained elevated on days 3 to 14. Modest changes were observed in iPTH concentrations from day 1 to day 14 (HPD day 0=57.6 pg/ml; day 1=30.8 pg/ml, p=0.09; day 3=72.8 pg/ml, p=0.014; day 7=92.3 pg/ml, p=0.62; day 14=47.2 pg/ml, p=0.32; all values compared to NPD). There was a 2-fold increase in FGF-23 concentrations on day 1 (NPD=292.7 pg/ml; HPD=526.3 pg/ml; p<0.0001) and day 3 (NPD=190.1 pg/ml; HPD=361.9 pg/ml; p=0.0009). However, by day 7, iFGF23 concentrations were approximately 1.5-fold higher (NPD=253.8 pg/ml; HPD=395.8 pg/ml; p=0.0096) and only slightly elevated on day 14 (NPD=358.3 pg/ml; HPD=454.4 pg/ml; p=0.17). sFRP-4 in renal tissue assessed by Western blot analysis was increased at day 14. We conclude that iPTH, iFGF-23, and sFRP-4 are involved in the adaptation of low and high phosphate diets.

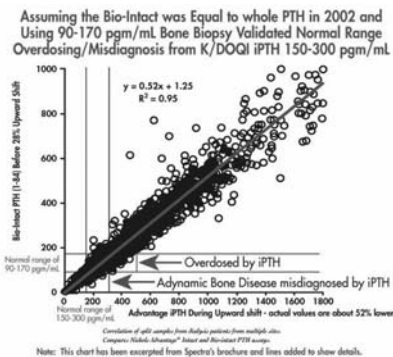
Disclosures: **S. Sommer**, None.

SU501

Estimate of Misdiagnosis of ABD and Potential Overdosing of Suppressive Therapy Resulting from the Use of the Intact PTH Assay Compared to the Specific 1-84 PTH Assay for ESRD Patients. **T. L. Cantor**¹, **A. Tokumoto**^{*2}.

¹President, Scantibodies Laboratory, Inc., Santee, CA, USA, ²Nephrology, San-in Rosai Hospital, Tottori, Japan.

The intact PTH assay is a measurement of both 1-84 PTH and 7-84 PTH. 7-84 PTH is secreted by the parathyroid gland and binds to PTH target cells and has been demonstrated to be a counter regulatory hormone compared to 1-84 PTH in that it is hypocalcemic, inhibitory of osteoblast & osteoclast formation, inhibitory of bone resorption, lowering of bone turnover, inhibitory of 1-84 PTH secretion, down regulating the PTH type 1 receptor (when NHERF1 is absent). The specific measurement of 1-84 PTH does not include the measurement of 7-84 PTH. It has been shown with bone biopsies and ROC curves by both Malluche et al and Tokumoto et al that the 1-84 PTH assay is more accurate than the intact PTH assay in predicting bone turnover in ESRD patients. Using bone biopsies it was also possible to determine the optimal range for bone turnover in these patients at 90-170 pg/ml. 150-300 pg/ml has been the range used for the intact PTH assay for normal bone turnover in ESRD patients. Using these 2 ranges and the 1-84 PTH assay range as the evaluation standard it was possible to estimate the number of adynamic bone disease ESRD patients misdiagnosed with the intact PTH assay and the number of patients that might be overdosed with PTH suppressive therapy for approximately 1000 ESRD patient specimens.



Disclosures: **T.L. Cantor**, Scantibodies 4.

SU502

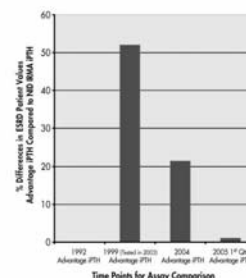
Changes in the Nichols Advantage iPTH Assay. **T. L. Cantor**¹, **S. Schibel**^{*2}, **Z. Yang**^{*3}.

¹President, Scantibodies Laboratory, Inc., Santee, CA, USA, ²Research and Development, Scantibodies Laboratory, Inc., Santee, CA, USA, ³Research and Development, Scantibodies Laboratory, Inc., Santee, CA, USA.

The Nichols IRMA intact PTH assay has been the standard used for research studies that have formed the basis for clinical practice guidelines. In particular the National Kidney Foundation's Kidney Disease Outcome Quality Initiative Clinical Practice Guidelines for Bone Metabolism and Disease in Chronic Kidney Disease (K/DOQI) have relied on 73 articles that used the Nichols IRMA iPTH assay. It is important to note that Nichols manufactures two types of intact PTH assays, the manual overnight, radioactive IRMA iPTH assay and a 37 minute, chemiluminescent automated version called the Advantage intact PTH assay. Not one of the 73 articles used by K/DOQI referenced the Advantage intact PTH assay. ESRD patient lab testing is centralized in the US. Virtually all ESRD patient lab specimens are tested at one of seven centralized laboratories. All of these 7 centralized laboratories use the Nichols Advantage PTH tests. These labs do not use the Nichols IRMA iPTH test on which K/DOQI is based. When the Advantage iPTH assay was

launched in 1992 patient specimen values matched those obtained using the Nichols IRMA iPTH assay. However, in 1999 there was an upward shift of approximately 52% for ESRD plasma specimens with some specimens measuring 2 or 3 times higher on the Advantage compared to the Nichols IRMA iPTH assay. In 2004 this upward shift observed in ESRD plasma specimens was reduced to approximately half and in 2005 this upward shift was eliminated. Also in 1999 there was a similar upward shift in Japan in a Nichols chemiluminescent iPTH assay, but in that case that upward shift was eliminated in Japan in the year 2000.

Changes in the Nichols Advantage iPTH Over Time



Disclosures: **T.L. Cantor**, Scantibodies 4.

SU503

PTH 1-84 More Effectively Induces Jagged-1 mRNA than Does PTH 1-34 in UMR 106-01 Osteoblastic Cells. **A. T. Pearman**, **B. L. Baker**, **N. E. Lloyd**^{*}, **J. Fox**. Pharmacology, NPS Pharmaceuticals, Salt Lake City, UT, USA.

Microarray and immunohistochemistry have shown that parathyroid hormone (PTH) 1-34 increases expression of the Notch receptor ligand, jagged-1 (jag-1) (Qin *et al.* and Calvi *et al.*, 2003). However, the effects of full length PTH (1-84) on relative jag-1 expression are unknown. Therefore, we determined the levels of jag-1 expression in UMR106-01 rat osteosarcoma cells treated with either PTH 1-84 or PTH 1-34 (1 nM) for 30 min to 24 hr. Northern blot analysis revealed that PTH 1-84 induction of jag-1 peaked at 16 hr while PTH 1-34 maximally induced jag-1 mRNA by 2-4 hr. Concentration-dependence experiments were then conducted for each peptide at their peak time points. Both PTH 1-84 and PTH 1-34 maximally induced jag-1 expression at 1 nM with peak jag-1 induction in response to PTH 1-84 significantly exceeding that of PTH 1-34. Both PTH peptides induced jag-1 independent of *de novo* protein synthesis as indicated by cycloheximide addition. Analysis of the jag-1 5'-UTR revealed a region similar to the enhancer A element. Enhancer A interacts with the Mod-1 protein complex consisting of fos related antigen 2 (fra-2) and the NF- κ B p50 subunit. A time course showed identical fra-2 induction in response to the peptides. However, concentration-response studies revealed that PTH 1-34 is significantly more potent than PTH 1-84 with regard to fra-2 mRNA induction. Specifically, 0.1 nM PTH 1-34 induced fra-2 while 1 nM PTH 1-84 was required for similar induction. Given that the relative efficacy of PTH 1-84 and PTH 1-34 is reversed for jag-1 and fra-2 expression and the presence of an enhancer-A-like region in the jag-1 5'-UTR, fra-2 may regulate PTH1R-mediated jag-1 expression as a subunit of the Mod-1 complex. Forskolin induced both fra-2 and jag-1 suggesting a cAMP-mediated mechanism. However, there was no difference in cAMP accumulation in response to the two PTH peptides. Alternatively, PTH 1-34 was a slightly more potent activator of protein kinase C (PKC) than was PTH 1-84. This suggests that PTH 1-84 and PTH 1-34 differentially modulate cAMP-mediated gene expression through differences in PKC activation. In summary, PTH 1-84 is a more efficacious inducer of jag-1 gene expression than PTH 1-34 although both events are independent of protein synthesis. Additionally, PTH 1-84 induces jag-1 at a later time point than does PTH 1-34. Furthermore, PTH 1-84 and PTH 1-34 induce fra-2 and PKC activation with reverse relative efficacy compared to jag-1 expression patterns. Based on these data, differential responses of fra-2 and PKC may participate in the mechanisms through which the PTH peptides induce jag-1 expression. These observations demonstrate unique differences between the effects of PTH 1-84 and PTH 1-34.

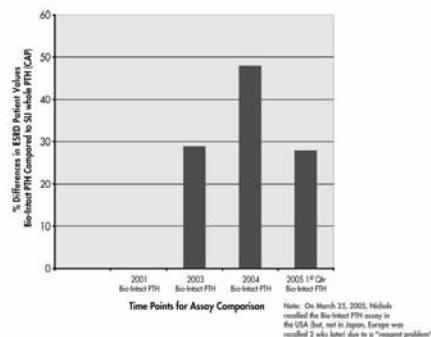
Disclosures: **A.T. Pearman**, None.

SU504

Changes in the Nichols Bio-Intact PTH Assay. T. L. Cantor¹, S. Scheibel^{1*2}, Z. Yang^{*2}. ¹President, Scantibodies Laboratory, Inc., Santee, CA, USA, ²Research and Development, Scantibodies Laboratory, Inc., Santee, CA, USA.

The Nichols Bio-Intact PTH assay was launched in 2001 and has been demonstrated to not measure 7-84 PTH which is a counter regulatory hormone compared to 1-84 PTH. Several studies (including those of our own) from 2001 to early 2003 used ESRD plasma specimens to demonstrate that the Bio-Intact PTH assay gave equivalent results compared to the Scantibodies 1-84 PTH or whole PTH (CAP) assay. However, in late 2003 we observed a 29% increase in the Bio-Intact PTH assay values compared to the Scantibodies whole PTH assay using ESRD plasma specimens. This same (28%) increase was also observed in 2005 for the same type of patient specimens.

Changes in the Nichols Bio-Intact PTH Assay Over Time



Disclosures: **T.L. Cantor**, Scantibodies 4.

SU505

Chondrosarcoma of the Right Hip in Association with Teriparatide. M. C. Spady^{*}, A. M. Macasa^{*}, J. Zakem^{*}, R. Quinet. Rheumatology, Ochsner Clinic Foundation, New Orleans, LA, USA.

We describe a 74-year old female with pre-existing polymyalgia rheumatica requiring low dose prednisone with a history of severe osteoporosis. Between 1996 to 2003 she sustained 17 osteoporotic fractures (including hip, lumbar spine, thoracic spine, and ribs) while on FDA approved treatment for osteoporosis. She was tried on and failed all FDA available antiresorptive agents to treat osteoporosis. She was then treated with teriparatide (Forteo) for 9.5-months. While on treatment she was found to have a grade III chondrosarcoma of the right femur. To date there is no other reported incident of chondrosarcoma or osteosarcoma and teriparatide use.

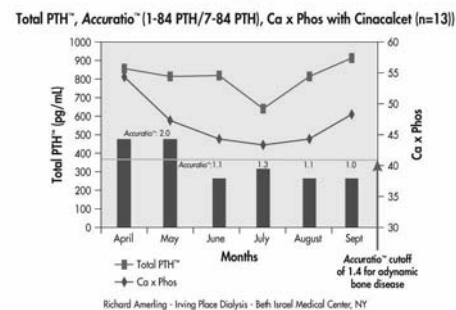
Disclosures: **M.C. Spady**, None.

SU506

Changes in Intact PTH, 1-84 PTH/7-84 PTH and the Calcium x Phosphate Product following 5 Months of Cinacalcet Therapy in 13 ESRD Patients. T. L. Cantor¹, R. Amerling^{*2}. ¹President, Scantibodies Laboratory, Inc., Santee, CA, USA, ²Division of Nephrology and Hypertension, Beth Israel Medical Center, New York, NY, USA.

Cinacalcet HCL (Sensipar) is a calcium sensing receptor stimulating agent (calcimimetic) that has been demonstrated to be effective in suppressing the level of both calcium and PTH in ESRD patients. The new pharmaceutical has been proposed as an alternative or adjunct therapy compared to the use of calcium supplements and vitamin D sterols with the advantage of eliminating hypercalcemia associated in some patients with the use of vitamin D sterols or calcium. Increased calcium and calcium x phosphate product have been demonstrated to be associated with increased mortality among ESRD patients. As with any PTH suppressant an accurate marker of parathyroid function and bone status is essential in order to guide therapy. The intact PTH assay has been demonstrated to be a measurement of 2 counter regulatory hormones, 1-84 PTH and 7-84 PTH with opposite biological actions. Both the intact PTH assay and the measurement of the 1-84 PTH/7-84 PTH ratio were assessed with bone biopsies for accuracy in predicting bone turnover in ESRD patients. It was found that the iPTH assay was 72% accurate whereas the 1-84 PTH/7-84 PTH assay was 94% accurate in predicting bone turnover in ESRD patients. 13 ESRD patients were placed on Cinacalcet (one 30 mg tablet per day) and their intact PTH, calcium x phosphate products and 1-84 PTH/7-84 PTH ratios were studied over 5 months. An overall lowering in the intact PTH value was not observed over the 5 months of study. However after the first 2 months of therapy the 1-84 PTH/7-84 PTH ratio decreased indicating a significant lowering of bone turnover. During the first 4 months there was a decrease in the calcium x phosphate product. However, following the 4th month there was a rise in the calcium x phosphate product. The changes in calcium x phosphate suggest that the bones may have entered into an adynamic bone disease status and were, therefore, unable to buffer calcium and phosphate, thus causing a rise in the serum calcium x phosphate product.

Effect of Cinacalcet (Sensipar™) on 13 Hemodialysis Patients



Disclosures: **T.L. Cantor**, Scantibodies 4.

SU507

Parathyroid Hormone Is also Mediating Osteoporosis in Hypersensitive Patients? M. R. G. Mascarenhas¹, J. Ferreira^{*1}, D. S. Pinto^{*2}, D. J. Duarte^{*2}, M. Bicho^{*1}. ¹Metabolism e Endocrinology Center (Genetics Lab), Lisbon's Faculty of Medicine, Lisboa, Portugal, ²Endocrinology, Diabetes and Metabolism Lisbon's Clinic, Lisboa, Portugal.

Aim Prospective and cross-sectional study in order to evaluate the bone mineral density (BMD) in hypertensive patients, females and males, and the intact parathyroid hormone (PTHi) blood levels and BMD relationships. **Methods** Bone mineral density (BMD, g/cm²) at the lumbar spine (L1-L4), at the proximal femur (femoral neck, trochanter and total) and at the distal forearm (total) and at the whole body were studied by using the radiological densitometer QDR Discovery W (Hologic, Inc.) in a group of 524 hypertensive patients. BMI (kg/m²) was also estimated. In this group 369 were women (mean age: 62 years, post-menopausal since 13.4 years⁹ and 155 males (56.7 years) The PTHi blood levels were measured in a subset of patients (n = 309). The T-scores of the BMD have also divided the patients in three subgroups: normal BMD (T-score > -1.0 SD), osteopenia and osteoporosis (T-score ≤ -2.5 SD), as compared with reference populations. The One-Way Anova test was used to differentiate the data, after descriptive analysis, with statistical difference for P < 0.05. **Results** In these **hypertensive patients, osteoporosis** was detected in 38,8% of the women and 19,0% of the males. **Hypertensive and osteoporotic patients**, both sexes, were the **oldest** (P < 0,05), the **leanest** (P < 0,05) and those with **shortest stature** (P < 0.05). However, PTHi was higher just in hypertensive and osteoporotic patients sub-groups, both women and men (P < 0.05). **Conclusions** The data of our study show that prevalence of osteoporosis is higher in the oldest, lowest weight and shortest stature hypertensive patients, as described for osteoporotic individuals with normal blood pressure. Finally, in hypertensive osteoporotic patients, the PTHi blood levels were higher, suggesting a potential role for PTHi in osteoporosis development and in high blood pressure mediation.

Disclosures: **M.R.G. Mascarenhas**, None.

SU508

Impact of Aromatic Versus Branched-Chain Amino Acids on Calcium Excretion, Absorption, and Bone Turnover - Potential Role of the Calcium Sensor Receptor. B. Dawson-Hughes, H. Rasmussen^{*}, S. S. Harris^{*}, G. Dallal^{*}. USDA Human Nutrition Research Center on Aging at Tufts University, Boston, MA, USA.

Aromatic amino acids (AAAs), but not branched-chain amino acids (B-CAAs), bind to the calcium sensor receptor (CaSR) in renal tissue and thus AAAs may have a greater calciuric action than B-CAAs (1). This study was done to determine and compare the effects of increasing intake of these two types of amino acids on urine calcium excretion (U_{Ca}), calcium absorption (CaAbs), serum parathyroid hormone (PTH), and biochemical markers of bone turnover in humans. Thirty men and women, age 51+, were placed on low-protein metabolic diets containing 0.5 g/kg/d of protein and including 0.027 moles of phenylalanine (phe), 0.023 moles of histidine (his), 0.070 moles of leucine (leu), and 0.046 moles of isoleucine (ileu) per 100 g of protein, for 24 days. On days 13-24, 15 subjects, selected randomly, received a 5-fold increase in gm-molar content of the two AAAs (phe and his) and the other 15 received a similar increase in B-CAAs (leu and ileu), mixed into their food. Bloods and 24-hr urines were collected on days 1, 13, and 24 and CaAbs (estimated from 4-hr increase in Ca excretion after a 600 mg Ca load) was assessed on days 13 and 24. Mean values on the low amino acid intakes (day 13) and changes (day 24-13) in U_{Ca}, CaAbs, urinary N-telopeptide (NTX), and serum osteocalcin were compared in the two groups. The groups did not differ significantly in mean age, BMI, or day 13 biochemical measures. The change (day 24-13) in U_{Ca} on AAAs differed from that on B-CAAs (0.252 ± 0.931 mmol/d vs -0.457 ± 0.808, respectively, P = 0.034). There was a trend toward a greater change in CaAbs in the AAA than the B-CAA group (0.172 ± 0.351 mmol vs -0.003 ± 0.173, respectively, P = 0.098). Although the difference in correlation coefficients did not achieve statistical significance (P=0.103) in this small sample, on day 24, U_{Ca} was significantly correlated with CaAbs in the AAA group (r = 0.715, P = 0.003) but not in the B-CAA group (r = 0.227, P = 0.416). Changes in serum PTH, serum osteocalcin, and urinary NTX did not differ significantly in the two groups. In conclusion,

AAAs promote UCa excretion more than B-RAAs, perhaps because they bind to renal CaSRs. The higher UCa excretion in the AAA group appears to result from increased calcium absorption rather than increased bone resorption.
(1) Conigrave AD. PNAS 2000;97:4814-9.

Disclosures: **B. Dawson-Hughes**, None.

SU509

Cinacalcet in a Case of Hypocalciuric Hypercalcemia with Recurrent Pancreatitis. P. Filippini¹, S. Cristallini^{*1}, A. Nicasì^{*1}, G. Pioda^{*2}. ¹ASL1 Umbria, Centro Regionale Osteoporosi e Malattie Metaboliche dello Scheletro, Umbertide - Perugia, Italy, ²Perugia, Polizia di Stato, Perugia, Italy.

Introduction. Inactivating mutations in CaSR gene has been reported as the cause of hypocalciuric hypercalcemia (HH) with inappropriate PTH serum levels. Calcimimetic agents, allosterical activators of CaSR, have been successfully tested in the treatment of primary, as well of secondary, hyperparathyroidism. We report the effect of the calcimimetic Cinacalcet on mineral metabolism in a patient affected with hypocalciuric hypercalcemia and recurrent acute pancreatitis. **Case report and methods.** A16 year-old male presented with mild hypercalcemia and acute pancreatitis at Perugia Regional Hospital. The patient had a cholecistectomy and initiated a treatment with ursodesossolic acid, which is still in use. After a second pancreatitis episode the patient was referred to our Centre. The patient's basal mineral metabolism parameters were assessed over 4 months using 4 different determinations. After basal investigations, cinacalcet 30 mg/day was started and administered for 15 days. On day 16, the dosage of cinacalcet was doubled to 30 mg twice daily (60 mg/day). **Results.** The Table shows the patient's mineral metabolism parameters before and during treatment with cinacalcet. sCa decreased from a mean value of 11.5 to 10.0 and to 9.2 mg/dL respectively with 30 and 60 mg/day cinacalcet administration. sCa++ decreased from 1.43 to 1.29 and 1.28 mmol/L respectively with 30 and 60 mg/day cinacalcet dosing. There was a parallel decrease in tubular reabsorption of Calcium (TmCa) and a decrease in urinary Ca/Cr ratio. Serum phosphate levels increased from a mean basal value of 2.8 to 4.2 and 3.9 mg/dL respectively with 30 and 60 mg/day cinacalcet dose, with a parallel increase in tubular reabsorption of phosphate (TmPO4). Cinacalcet was well tolerated and no changes were observed in pancreatic enzymes and other laboratory parameters except for the indices of mineral metabolism. **Conclusions.** The results of this case report shows that the calcimimetic cinacalcet, 30 mg twice daily, normalizes serum calcium in a patient affected with HH. This encouraging case shows the need to evaluate cinacalcet as a potential therapy for HH.

Disclosures: **P. Filippini**, None.

SU510

Expression and Functional Assessment of an Alternatively Spliced Extracellular Ca²⁺-Sensing Receptor in Growth Plate Chondrocytes. L. Rodriguez^{*}, C. Tu^{*}, T. Chen^{*}, Z. Cheng, D. Bikle, D. Shoback, W. Chang. Endocrine Research Unit, VAMC, Department of Medicine, University of California San Francisco, San Francisco, CA, USA.

Previous studies on extracellular Ca²⁺-sensing receptor (CaR)-knockout (CaR^{-/-}) mice indicate that insertion of a neomycin cassette into exon 5 of the mouse CaR gene blocks the expression of full-length CaRs, but it allows the expression of alternatively spliced CaRs [^{Exon5(-)}CaRs] missing exon 5. This shift in expression of the full-length CaR to the alternatively spliced CaR occurs in a number of tissues including growth plate chondrocytes (GPCs). We characterized the signaling and expression properties of the ^{Exon5(-)}CaRs and addressed whether CaR^{-/-} GPCs, that express ^{Exon5(-)}CaRs, remain responsive to changes in extracellular [Ca²⁺] ([Ca²⁺]_e). Expression of ^{Exon5(-)}CaR transcripts and protein in growth plates from CaR^{-/-} mice and cultured CaR^{-/-} GPCs was confirmed by RT-PCR and immunocytochemistry. In stably or transiently transfected CHO and HEK-293 cells, recombinant human ^{Exon5(-)}CaRs [^{Exon5(-)}hCaRs] failed to reach the cell-surface as determined by intact-cell ELISA and immunocytochemistry and was therefore unable to activate the PLC pathway in response to high [Ca²⁺]_e. Western analysis confirmed the expression of ample amounts of ^{Exon5(-)}hCaR protein in these cells. In contrast, ^{Exon5(+)}hCaRs trafficked normally to the cell surface when expressed in GPCs from either wild-type or CaR^{-/-} mice. Immunocytochemistry of growth plate sections and cultured GPCs from CaR^{-/-} mice showed cell-surface expression of endogenous CaR protein (judged to be ^{Exon5(-)}CaRs in CaR^{-/-} cells), suggesting that stable expression of ^{Exon5(-)}CaRs to the membrane requires a specific cellular context. In GPCs from CaR^{-/-} mice, raising [Ca²⁺]_e increased total InsP production with a potency comparable to that in GPCs from wild-type mice. Raising [Ca²⁺]_e also promoted the differentiation of CaR^{-/-} GPCs as indicated by decreased proteoglycan accumulation, increased mineral deposition, and altered gene expression indicative of advanced cell differentiation. Taken together, our data suggest that ^{Exon5(-)}CaRs may compensate for the loss of full-length CaRs in GPCs in CaR^{-/-} mice and perhaps in other tissues in a cell context that permits stable cell-surface expression of ^{Exon5(-)}CaRs.

Disclosures: **W. Chang**, None.

SU511

The Effects of Strontium Ranelate on Osteoclasts Are Calcium-Sensing Receptor Dependant. R. Mentaverri^{*1}, R. Mentaverri^{*2}, N. Chattopadhyay^{*1}, A. S. Lemaire-Hurtel^{*1}, S. Kamel^{*1}, M. Brazier^{*1}, E. M. Brown². ¹Université de Picardie Jules-Vernes, 80037 Amiens, France, ²Brigham and Women's Hospital, Boston MA 02115, MA, USA.

Strontium ranelate is a new compound available for the treatment of osteoporosis to reduce vertebral and hip fracture risk in postmenopausal women. Strontium ranelate stimulates bone formation and decreases bone resorption resulting in a rebalance of bone turnover in favor of bone formation. As with Ca, extracellular strontium, is a full agonist of the calcium sensing receptor (CaR). To date, there has been no direct proof of the role of the CaR in mediating the effects of strontium ranelate on osteoclasts (OC). The present study firstly used bone cells isolated from wild-type or CaR knock-out mice (as a negative control) to confirm CaR expression on OC, by immunohistochemistry and confocal microscopy. Secondly, we demonstrated the role of the CaR in strontium ranelate effects using mature rabbit OC: 1) Increasing strontium ranelate concentrations, up to 25 mM, stimulated OC apoptosis by 40% (Hoechst staining). Western blots analysis using antibodies to caspases 3 and 9 as well as specific caspases inhibitory peptides (Z-VAD-fmk, Z-LEHD-fmk), clearly demonstrated that the caspases cascade is involved in strontium ranelate-induced OC apoptosis. 2) For the first time, we have established with the immunocytochemical method¹, that increasing concentrations of strontium ranelate directly trigger a transient translocation of NFkB into OC nuclei. Temporal control of NFkB activity regulates the expression of numerous genes involved in cell survival as well as in cellular responses to inflammation and stress. This effect is maximal at 30 min, when 50% of OC showed a nuclear localization of NFkB. 3) Both strontium ranelate-induced NFkB nuclear translocation and OC apoptosis, were blocked by a phospholipase C inhibitor (U73122, 10µM), indicating that a G protein coupled receptor could mediate the effect of strontium ranelate on OC. 4) Moreover, in mature rabbit OC infected with a dominant negative form of CaR (rAAV technology), the strontium ranelate-induced NFkB nuclear translocation was abolished and the strontium ranelate-induced OC apoptosis was significantly reduced by 50% compared to β-galactosidase transfected cells (i.e. control infected cells). This approach unequivocally demonstrates that strontium ranelate acts at least in part through the CaR to enhance OC apoptosis, confirming several converging lines of evidence. Further studies are needed to further clarify the role played by NFkB signaling in these cellular events and whether this pathway is involved in mediating the effects of strontium ranelate on bone resorption.

¹Komarova, JBC 2003

Disclosures: **R. Mentaverri**, SERVIER 5.

SU512

Efficient Expression of the Extracellular Domain of the Calcium-Sensing Receptor in Insect Cells. T. Craig^{*1}, Z. Ryan^{*2}, J. Thompson^{*2}, R. Kumar¹.

¹Nephrology Research, Department of Medicine, Biochemistry and Molecular Biology, Mayo Clinic College of Medicine, Rochester, MN, USA, ²Department of Physiology and Biomedical Engineering, Mayo Clinic College of Medicine, Rochester, MN, USA.

The human Calcium-Sensing Receptor (CaSR) is a 1078-amino acid cell-surface G protein-coupled receptor involved in the fine sensing of serum calcium concentrations and is localized in tissues involved in calcium homeostasis including parathyroid gland, kidneys, thyroid C-cells, bones (osteoclasts, osteoblasts), intestines and in several tissues such as nerve terminals and oligodendrocytes without obvious roles in maintenance of extracellular calcium. The CaSR is composed of three domains: a large extracellular domain (ECD, amino acids (aa) 20-612), a seven-transmembrane-spanning segment (aa 613-867), and an cytoplasmic tail (aa 868-1078). The exact amino acid residues and molecular orientations which are responsible for Ca²⁺ binding, Ca²⁺ sensing, and signal transduction in response to changes in the serum Ca²⁺ concentrations are unknown. In order to examine the biophysical properties of the CaSR, we devised an efficient system for the expression of the CaSR in quantities sufficient for functional studies and x-ray crystallography. The c-DNAs coding for amino acids 20-610 (extracellular domain)(ECD), 536-610 (cysteine rich domain)(CRD) and 20-535 (extracellular domain without the cysteine rich domain)(ECD w/o CRD) were inserted into the pIB/V5-His insect vector. In place of the native secretory signal a melittin secretory signal was used, and was inserted 5' to the CaSR coding sequences. The orientation of the inserts and the DNA sequences thereof were verified by DNA sequencing. *Trichoplusia ni* (High Five) insect cells were stably transformed with pIB/V5-His-CaSR constructs. After Blasticidin S selection of adherent cells, the stably transformed cells were adapted to grow in suspension cultures. Shake cultures in 2L flask were grown for protein production. Secreted CaSR proteins were isolated from the conditioned media by ion exchange chromatography and Ni²⁺ chelate chromatography and analyzed by SDS-PAGE, Western blots, PNGase F deglycosylation and amino-terminal protein sequencing. CaSR constructs were readily expressed in low milligram amounts. The results demonstrate the utility of the insect expression system for production of properly folded, glycosylated CaSR protein constructs that contain disulfide bonds.

Disclosures: **T. Craig**, None.

SU513

Experimental Hypercalcemia in Horses Results in Hypomagnesemia, Hypokalemia, and Hyperphosphatemia with Increased Urinary Excretion of Electrolytes. R. E. Toribio, K. M. Rourke*, A. L. Levine*, C. W. Kohn*, T. J. Rosol. Veterinary Biosciences, The Ohio State University, Columbus, OH, USA.

Electrolyte disturbances are common in critically ill humans and animals. In critically ill horses, low serum ionized calcium (Ca²⁺) and ionized magnesium (Mg²⁺) concentrations are frequent. High serum Ca²⁺ is common in horses with chronic renal failure, hypercalcemia of malignancy, hyperparathyroidism, and vitamin D intoxication. There is evidence that the renal reabsorption of Ca²⁺ is also regulated by parathyroid hormone (PTH)-independent mechanisms, primarily by the calcium-sensing receptor (CaR) that affects the transepithelial transport of Ca²⁺ and Mg²⁺. Because extracellular Ca²⁺ can affect other electrolytes, the goals of this study were to evaluate the effects of experimental hypercalcemia on the serum concentrations of electrolytes and their urinary excretion in healthy horses. By the direct effects of Ca²⁺ on CaR, we speculated that hypercalcemia will result in hypomagnesemia and increase the urinary excretion of electrolytes. Hypercalcemia was induced in twelve healthy mares; six were infused with 23% calcium gluconate (G) for 120 min and six mares were infused with 10% calcium chloride (CaCl₂) for 120 min. Blood was collected to measure serum electrolytes, PTH, and insulin concentrations, and urine was collected to determine the fractional excretions of Ca²⁺ (FCa), Mg²⁺ (FMg), Na⁺ (FNa), Pi (FP), K⁺ (FK), and Cl⁻ (FCl). In hypercalcemic mares, serum Ca²⁺ increased 6.6±0.1 to 9.7±0.3 (G) and 6.4±0.1 to 10.2±0.10 mg/dL (CaCl₂); Mg²⁺ decreased 0.52±0.02 to 0.33±0.02 (G) and 0.51±0.02 to 0.32±0.02 mmol/L (CaCl₂); K⁺ decreased from 4.3±0.1 to 3.4±0.1 (G) and 4.2±0.2 to 3.6±0.2 mEq/L (CaCl₂), and Pi increased from 3.4±0.2 to 4.8±0.3 (G) and 2.9±0.2 to 4.1±0.4 mg/dL (CaCl₂). PTH decreased to very low concentrations. No changes in insulin concentrations were detected. FCa increased from 5.4±1.0 to 56.2±6.9% (G) and 5.4±1.1 to 47.7±6.4 % (CaCl₂); FMg from 23.5±2.4 to 55.0±4.5 (G) and 28.5±4.3 to 54.4±7.3 % (CaCl₂); FNa from 0.09±0.04 to 4.3±0.8 (G) and 0.03±0.003 to 4.8±0.8 % (CaCl₂); FK from 45.4±7.6 to 116.6±19 (G) and 38.4±1.5 to 89±8.3% (CaCl₂); FCl from 0.65±0.1 to 5.6±1.5% (G) and 0.7±0.1 to 9.3±1.6% (CaCl₂), and FP from 0.04±0.02 to 0.5±0.2 (G) and 0.14±0.06 to 0.81±0.3 % (CaCl₂). Urine specific gravity and osmolality decreased and urine output increased. In conclusion, hypercalcemia results in hypomagnesemia, hypokalemia, and hyperphosphatemia, increases the urinary excretion of Ca²⁺, Mg²⁺, K⁺, Na⁺, Pi, and Cl⁻, and has diuretic effects. This study has clinical implications as excessive administration of Ca²⁺ salts can further increase the waste of electrolytes, in particular of Mg²⁺.

Disclosures: R.E. Toribio, None.

SU514

Interleukin-6 Upregulates Transcription of the Calcium-Sensing Receptor Gene via Elements in both P1 and P2 Promoters. L. Canaff, G. N. Hendy. Medicine, McGill University, Montreal, PQ, Canada.

The calcium-sensing receptor (CASR), expressed in parathyroid gland, thyroid C-cells and kidney tubule critically regulates the blood calcium concentration. Increases in expression of the CASR in these tissues leads to hypocalcemia. Hypocalcemia is common in critically ill patients (such as those with burn injury or sepsis) in whom circulating levels of cytokines, such as interleukin-6 (IL-6) are markedly increased. We hypothesized that IL-6 upregulates expression of the CASR thereby reducing parathyroid hormone (PTH) secretion and renal calcium reabsorption and increasing calcitonin secretion. We first demonstrated by immunoblot analysis that the CASR protein was increased (~3 fold) in human thyroid C-cells (TT) stimulated with IL-6 (8ng/ml) for 16, 24 and 36 hours. The human CASR gene has two promoters (P1 and P2) yielding transcripts having alternative 5' untranslated regions (1A and 1B), but encoding the same receptor (exons 2-7). By run on assay of nuclear extracts of human proximal tubule kidney (HKC) and TT cells, it was shown that IL-6 stimulated CASR exon 1A, exon 1B and exon 2 transcripts >2 fold at 8 and 12 hours. The transcriptional activities of human CASR P1 and P2 promoter constructs driving a luciferase reporter gene were stimulated ~2-3 fold by IL-6 (relative to basal activity) after transient transfection into HKC and TT cells. The P1 construct contained 1439 bp of the promoter upstream of the transcription start site (+1), the 638 bp exon 1A and 242 bp of exon 2 before the ATG translation start site. Transfection of a series of P1 deletion constructs (-1439, -938, -701, -382 and -194) into HKC cells revealed that specific regions from -382 to -194 bp in the promoter and +197 to +206 bp of exon 1A (both of which have canonical STAT elements) mediated the induction of P1 by IL-6. The P2 construct contained 460 bp of the promoter upstream of the transcription start site (+1), the 259 bp exon 1B and 242 bp of exon 2 before the ATG translation start site. Transfection of a series of deletion constructs (-460, -341, +220) into HKC cells showed that the -341 to +220 region is required for IL-6 responsiveness. There are no STAT elements in the P2 promoter or exon 1B but potential AP-1 and SP1 elements (that have been implicated in IL-6 responsiveness of other genes) are present. In conclusion, elements in the CASR gene promoters mediate transcriptional upregulation by the proinflammatory cytokine, IL-6. This is likely to be important in contributing to the hypocalcemia of critically ill patients with burn injury or sepsis.

Disclosures: L. Canaff, None.

SU515

Extracellular Ca²⁺ Concentration Directly Regulates 1,25-Dihydroxyvitamin D Receptor (VDR) Level in Human Kidney, HK-2, Proximal Cells. A. Maiti^{*1}, A. Bajwa², M. J. Beckman². ¹Orthopaedic Surgery, Virginia Commonwealth University, Richmond, VA, USA, ²Biochemistry, Virginia Commonwealth University, Richmond, VA, USA.

The primary role of biologically active form of vitamin D, 1,25-dihydroxyvitamin D₃ (1,25(OH)₂D₃), is to regulate calcium (Ca) homeostasis, proliferation, differentiation and other cellular physiological processes. Many of the actions of 1,25(OH)₂D₃ are mediated by interaction with vitamin D receptor (VDR) a member of steroid/thyroid receptor superfamily of ligand regulated transcription factors. In renal proximal tubules, VDR is transiently decreased by parathyroid hormone (PTH) during times of hypocalcemia and returns to normal levels commensurate with the rise in serum Ca²⁺. These in vivo effects were mimicked in vitro using the human proximal kidney HK-2 cell line that expresses extracellular Ca sensing receptor (CaSR) endogenously. In these cells, PTH significantly decreased (p<0.05) VDR mRNA in a low Ca²⁺ (0.2 mM) medium, which led to a decrease in VDR protein. However, high extracellular calcium (3.2 mM) treatment triggered an increase in HK-2 cell VDR mRNA following 6 hrs of incubation and an increase in protein at 12 hrs in a manner consistent with CaSR activation. To better understand the hypothesis that transition from low to high serum calcium concentration is marked by an upward directional regulation of VDR by a mechanism that utilizes CaSR activation, HK-2 cells were treated with different doses of calcium for different time periods to study phosphorylated-ERK (pERK) activation and VDR by Western blot analysis. An increase in extra cellular calcium from 0.2 mM to a maximum of 4.2 mM increased the percentage of pERK/total ERK in HK-2 cells. A treatment of 3.2 mM Ca²⁺ in the medium caused rapid activation of pERK at 5 min, which remained elevated at 15 min and declined at 30 min. In addition, extracellular Ca²⁺ treatment dose-dependently activates VDR increases compared to low 0.2 mM Ca²⁺ in HK-2 cells. Past studies by our laboratory have explored the PTH-dependent down-regulation of VDR in renal proximal cells and demonstrated a possible counter regulatory role of Ca²⁺. The present study supports the concept of opposing regulation by Ca and PTH in effecting changes in renal proximal cell VDR. In conclusion, in renal proximal HK-2 cells, a normal level of VDR protein is partially dependent upon adequate extracellular Ca²⁺ in a range of 1.0-2.0 mM, and high extracellular Ca²⁺, ~3.2 mM, plays a modulating role to increase VDR protein, that is independent of PTH.

Disclosures: A. Maiti, None.

SU516

Identification of a Novel G-Protein Coupled Receptor with Calcium and Osteocalcin Sensing Properties. M. Pi¹, G. Ekema^{*2}, P. Faber^{*2}, P. D. Jackson^{*2}, K. Brunden^{*2}, J. J. Harrington^{*2}, L. D. Quarles¹. ¹Kidney Institute, Department of Medicine, KUMC, Kansas City, KS, USA, ²Athersys, Inc., Cleveland, OH, USA.

The extracellular calcium sensing receptor (CASR) plays an important role in the regulation of calcium homeostasis. CASR, which belongs to the C family of G-protein coupled receptors, is characterized by a long extracellular segment containing calcium binding domains and a 7-transmembrane (7-TM) region typical of GPCRs. Calcium sensing responses are also observed in tissues, such as bone, where the physiological role of CASR is not certain. There is evidence that bone expresses a distinct calcium sensing receptor in osteoblasts, called Ob.CASR, which has not yet been isolated and cloned. To identify if other Family C receptors are present in bone and sense extracellular calcium, we investigated a recently described orphan receptor belonging to this family. Alignment of this receptor with CASR revealed that two of the putative calcium binding residues in CASR (Ser-147 and Ser-169) are conserved in this receptor (Ser-149 and Ser-171). To test the response to extracellular cations, we transfected the full-length of this receptor into HEK-293 cells and evaluated the effects of a panel of cations to stimulate a co-transfected serum response element/reporter construct (SRE-luciferase), ERK activation and increments in intercellular calcium. Calcium, magnesium, strontium, aluminum, and gadolinium resulted in a dose-dependent stimulation of activity in HEK-293 cells, requiring concentrations that exceeded those needed to activate CASR. To examine the effects of calcium binding proteins in the bone milieu to modify the response of this receptor to extracellular calcium, we investigated the effects of osteocalcin, the most abundant calcium binding protein in bone, on the ability of calcium to activate this receptor in HEK-293 cells. Osteocalcin resulted in a dose-dependent stimulation of this receptor in the presence of calcium, but inhibited the calcium-dependent activation of CASR transfected into HEK-293 cells. Coexpression of either beta-arrestins 1 and 2, regulators of G protein signaling, RGS2 or RGS4, the RhoA inhibitor C3 toxin, and the dominant negative Galphaq(305-359) minigene, all inhibited cation-mediated activation of this receptor. Results from RT-PCR analyses showed that this receptor is expressed in mouse heart, brain, lung, liver, spleen, skeletal muscle, kidney, testis, epididymis, fat, bone, calvaria and the osteoblastic cell line MC3T3-E1. These data suggest that this is a novel calcium sensing receptor with unique properties that make it a strong candidate for Ob.CASR.

Disclosures: M. Pi, None.

SU517

DMPA-SC 104 Is Associated with Significantly Smaller Effects on Bone than Leuprolide Acetate in the Treatment of Endometriosis. J. Jain^{*1}, S. Kipersztok^{*2}. ¹Department of Obstetrics and Gynecology, Keck School of Medicine, University of Southern California, Los Angeles, CA, USA, ²Department of OB/GYN, University of Florida College of Medicine, Gainesville, FL, USA.

A clinical trial compared depot medroxyprogesterone acetate subcutaneous injection 104 mg/0.65 mL (DMPA-SC 104) with leuprolide acetate in patients with endometriosis. The primary safety endpoint was percent change in bone mineral density (BMD). This 18-month, evaluator-blinded, comparator-controlled trial was conducted in the United States and Canada. Premenopausal women aged 18 to 49 years with recently diagnosed, persistent, or recurrent endometriosis were randomized to 6 months' treatment with DMPA-SC 104 or leuprolide acetate 11.25 mg every 3 months and followed for an additional 12 months post-treatment. BMD assessment included percent change from baseline to months 6, 12, and 18. BMD data were available for 77 DMPA-SC 104 subjects and 98 leuprolide subjects at month 6; approximately 50 and 63 subjects, respectively, at month 12; and approximately 31 and 42 subjects, respectively, at month 18. As previously reported, DMPA-SC 104 was associated with significantly ($P<.001$) smaller median percent changes from baseline in total hip and lumbar spine BMD at month 6 compared with leuprolide. At month 12, the leuprolide group continued to show significant ($P<.001$) decreases in median percent change from baseline in both total hip and lumbar spine BMD, while the DMPA-SC 104 group did not. The median percent change from baseline was -0.25 in the DMPA-SC 104 group compared with -1.60 in the leuprolide group for total hip BMD ($P=.002$), and 0.00 versus -3.20, respectively, for lumbar spine BMD ($P<.001$) at month 12. For total hip BMD, most DMPA-SC 104 users had only small decreases from baseline to month 12 (48% of subjects had 0%-2.4% decreases; 10% of subjects had 2.5%-4.9% decreases; none had $\geq 5\%$ decreases), while more leuprolide users had larger decreases (34% of subjects had 0%-2.4% decreases; 25% of subjects had 2.5%-4.9% decreases; 14% of subjects had $\geq 5\%$ decreases). For lumbar spine BMD, more DMPA-SC 104 users had smaller decreases from baseline to month 12 (26% of subjects had 0%-2.4% decreases; 24% of subjects had 2.5%-4.9% decreases; 2% of subjects had $\geq 5\%$ decreases) while leuprolide users had larger decreases (27% of subjects had 0%-2.4% decreases; 37% of subjects had 2.5%-4.9% decreases; 22% of subjects had $\geq 5\%$ decreases). Results were similar at month 18. In this study, 6-month treatment with DMPA-SC 104 resulted in significantly less reduction in BMD compared with leuprolide. At month 12, BMD values were at or near baseline levels in the DMPA-SC 104 group but not in the leuprolide group.

Disclosures: **S. Kipersztok**, NIH, Merck, Wyeth, P&G 2; Merck, P&G, Wyeth 5; Merck, P&G, Wyeth 8; Johnson & Johnson, Lilly 1.

SU518

Expression and Subcellular Localization of 17 β -Estradiol Binding Proteins in C2C12 Cell Line. L. Milanesi^{*}, A. Russo de Boland^{*}, R. Boland^{*}. Biologia, Bioquímica & Farmacia, Universidad Nacional del Sur, Bahía Blanca, Argentina.

The classical cellular mechanism of 17 β -estradiol actions involves the steroid diffusion through the plasma membrane; its binding to a cytoplasmic/nuclear receptor (ER), and subsequent transcription and protein synthesis regulation. In addition to this mechanism, increasing evidence for non-genomic estrogen short-term effects in different cells types has been accumulated and led to hypothesize the existence of cell-surface resident receptor forms triggering membrane events. These cell- surface protein receptors have been detected in different cell lines (MCF-7, SHM, HT-29) and the expression of an estrogen binding protein and its effects on the development and function of human and bovine skeletal muscle was reported. The present study was focused to analyze the subcellular localization of ER binding proteins in C2C12 cells (a murine skeletal muscle cell line). By competition assays we have detected binding sites for [³H]17 β -estradiol in total homogenates. The subcellular localization of these binding sites was predominantly mitochondrial-microsomal. The sites were specific for the steroid hormone 17 β -estradiol, as progesterone was no effective to compete with the radioactive ligand. The nonsteroidal estrogenic and antiestrogenic compounds diethylstilbestrol, tamoxifen and ICI 182, 780 were as effective as 17 β -estradiol in competition studies. The protein nature of the estrogen binding sites was clearly indicated by their sensitivity to trypsin degradation. Specific antibodies against different domains of the classical ER (ER α) could reduce the specific radioligand binding. Immunohistochemical studies employing the same monoclonal antibodies detected the 67 kDa immunoreactive band expected for the ER α in nuclear and cytosolic fractions and, additionally, low molecular weight bands present in the mitochondrial and microsomal fractions. These reactive bands were able to bind the steroid hormone in Ligand blot assays. Also these studies showed a clear surface labeling of the macromolecular complexes E₂-BSA-FITC in non-permeabilized living cells. The characterization of these estrogen binding proteins and the signaling cascades activated thereby by the steroid hormone in skeletal muscle cells may provide information about molecular events implicated in alterations in muscle contractility and development which occur in menopause.

Disclosures: **R. Boland**, None.

SU519

Regulation of Mouse Osteoprotegerin Gene Expression by Glucocorticoids. T. Kondo¹, R. Kitazawa¹, A. Yamaguchi², S. Kitazawa¹. ¹Division of Molecular Pathology, Kobe University Graduate School of Medicine, Kobe, Japan, ²Department of Oral Restitution, Oral Pathology, Graduate School of Tokyo Medical and Dental University, Tokyo, Japan.

Increased bone fragility attributed to osteopenia is a serious side effect of glucocorticoid (GC) treatment. It is known that GC-induced bone loss is caused primarily by hypofunction and apoptosis of osteoblasts; an increase in bone resorption markers is concurrently observed during GC therapy, indicating that accelerated bone resorption also contributes to this loss. The mechanism whereby dexamethasone (Dex) stimulates osteoclastogenesis was explored by analyzing the effect of Dex on cis-acting elements of mouse osteoprotegerin (OPG) and on the c-Jun signaling pathway. Realtime RT-PCR analysis revealed that the steady-state transcription of the OPG gene in C6 cells, established from calvariae of *runx2*-deficient mice, was 7 times that in ST2 cells, suggesting that Runx2 itself may suppress steady-state OPG gene expression. Dex, however, reduced OPG expression to the same extent in both cells, indicating that the inhibitory effect of Dex on OPG expression is independent of Runx2; nevertheless Dex reduced the Runx2 expression in ST2. On the other hand, the amount of OPG protein secreted by ST2 was significantly decreased by Dex treatment. We have reported that mainly the c-Jun homodimer binds to the AP-1 binding site (-293/-287) in the mouse OPG promoter and maintains steady-state transcription of the OPG gene. Since the mutation of the AP-1 site negated Dex-driven OPG suppression, we focused on the mitogen-activated protein (MAP) kinase signaling cascade. Western blot analysis revealed that the amount of phospho-c-Jun protein (p-c-Jun) decreased 1hr after treatment of ST2 with Dex; correspondingly, the amount of the phosphorylated p46 isoform of Jun N-terminal kinase (JNK) decreased significantly after 30 min, whereas that of the p54 isoform decreased after 12 hr. The amount of phospho-SEK1 also decreased significantly after 30 min, whereas the amounts of phospho-ERK and p38 were constant. Among MAP kinase inhibitors (JNK inhibitor SP600125, ERK inhibitor PD98059 and p38 inhibitor SB203580), only the JNK inhibitor mimicked the inhibitory effect of Dex on the OPG promoter activity. These data suggest that Dex negatively regulates OPG by transrepressing the OPG gene through the AP-1 site via a reduction in the proportion of the p-c-Jun in a JNK-dependent manner; also the reduction is mediated mainly by the decrease in the p46 isoform of JNK. We speculate therefore that GCs per se promote osteoclastogenesis mostly by inhibiting OPG as the main target and partly by concurrently stimulating RANKL reciprocally, thereby enhancing bone resorption.

Disclosures: **T. Kondo**, None.

SU520

Osteoblast Targeted Overexpression of Hydroxysteroid Dehydrogenase Type 2 Induces Delayed Calvarial Development in Transgenic Mice. C. R. Dunstan, H. Zhou, K. Brennan^{*}, Y. Zheng^{*}, M. J. Seibel. Bone Research Program, ANZAC Research Institute, Sydney, Australia.

The effects of glucocorticoids on bone are still obscure. Transgenic (tg) expression of 11 beta hydroxysteroid dehydrogenase type 2 (HSD2), a glucocorticoid inactivating enzyme, under the control of a 2.3Kb collagen type I promoter abrogates intracellular glucocorticoid signalling in mature osteoblasts, as demonstrated by Sher et al. (1). We evaluated morphological changes in the calvaria and tibiae of wild-type (WT) and tg mice aged 1 day, 7 days and 6 weeks. Tg and WT littermates were assessed concurrently to avoid litter-to-litter variation. HSD2 mRNA and protein expression was present in the calvaria and the long bones of tg mice at these time points, but absent in WT mice. Skeletal expression of HSD1 was similar in WT and tg mice. Histomorphometry of 1 day old HSD2 tg mice revealed a distinct phenotype with incompletely formed calvaria. The amount and extent of bone was reduced by 33% relative to WT mice. Cartilage was present in all tg mice but almost completely absent in WT mice. In 7-day old mice, increased amounts of cartilage were present in the calvaria of tg animals, but the extent of bone was similar to WT mice, indicating a degree of recovery. Calvaria appeared normal at 6 weeks of age. The tibiae and femurs were similar in transgenic and wild type mice at all ages evaluated. These results indicate that in mice, glucocorticoid signalling in osteoblasts is required for normal development of the calvarial bone structures, but not of the long bones. Calvarial bones form by intramembranous bone formation above a cartilaginous template that is then removed after adjacent bone is formed without undergoing hypertrophy or mineralisation as occurs during endochondral bone formation of the long bones. Blocking of glucocorticoid signalling through the overexpression of HSD2 in mature osteoblasts results in a delay in bone formation and in cartilage removal in the calvaria. This may reflect a specific requirement for glucocorticoid signalling in the formation of intramembranous bone structures or may be specific for the calvaria.

(1) Endocrinology 145:922-9, 2004). The authors would like to thanks Prof B Kream for kindly providing the transgenic animals.

Disclosures: **C.R. Dunstan**, None.

SU521

Determinants of Aromatase Expression and Serum Estradiol Levels in Males. C. Swanson, M. Lorentzon, S. Movérare Skrtic, J. Brandberg*, L. Lonn*, C. Ohlsson. Center for Bone Research at the Sahlgrenska Academy, Dept. of Internal Medicine, Göteborg University, Göteborg, Sweden.

Serum levels of estradiol are of importance for the regulation of bone mass in males. Cyp 19 (aromatase) is responsible for the synthesis of estradiol, using testosterone as a precursor. Inactivation of the aromatase gene results in reduced bone mass in males. Thus, the aromatase activity is of importance for serum estradiol levels and bone mass in males. The major part of serum estradiol in males is believed to be fat-derived. The aims of the present study were (i) to elucidate the major determinants of serum estradiol in a large male clinical cohort (19-year-old men participating in *the GOOD study*, n=1068) and (ii) to investigate the hormonal regulation of the aromatase expression in white adipose tissue in male mice. In the clinical study, total body lean mass and fat mass were measured by DXA and fat distribution was analysed by cross sectional CT scans of the abdomen. In the mouse study, orchidectomized male mice were treated with vehicle, estradiol or DHT (not aromatizable, specifically activating the androgen receptor). Aromatase levels were analysed by qRT-PCR. Regression models including age, BMI, smoking, physical activity and serum testosterone levels as covariates demonstrated that BMI ($\beta = 0.129$, $p < 0.001$) and serum testosterone ($\beta = 0.37$, $p < 0.001$) are strong independent positive predictors of serum estradiol levels in men. Individuals in the highest quartile of serum estradiol levels had increased total fat mass (+46%, $p < 0.001$), serum levels of leptin (+55%, $p < 0.001$) and subcutaneous fat mass (+41%, $p < 0.05$) while the total lean mass and the intra abdominal visceral fat mass were unaltered compared with individuals in the lowest quartile of serum estradiol. These findings indicate that it is the subcutaneous and not the visceral fat mass that is responsible for the major part of the aromatase activity in fat mass in men. As serum testosterone levels were the strongest predictor of serum estradiol levels in men, we next wanted to investigate if the aromatase expression in white adipose tissue is regulated by androgen receptor stimulation in male mice. Orchidectomy resulted in a dramatic reduction of aromatase mRNA levels. DHT treatment clearly increased the aromatase expression compared with vehicle treated orchidectomized mice ($p < 0.001$). Estradiol treatment did not affect the aromatase levels. In conclusion, subcutaneous but not visceral fat mass is a strong determinant of serum estradiol levels and this might be due to higher aromatase activity in subcutaneous fat than in visceral fat. Furthermore, the aromatase mRNA levels in fat are strongly up-regulated by androgen receptor but not estrogen receptor stimulation.

Disclosures: **C. Swanson**, None.

SU522

5 α -Androstane-3 β ,7 β -diol in Urine Is an Independent Positive Predictor of Trabecular and Cortical Bone Mineral Density in Young Adult Swedish Men -The GOOD Study. L. Vandenput¹, M. Lorentzon¹, D. Mellström¹, J. Jakobsson^{*2}, A. Rane^{*2}, C. Ohlsson¹. ¹Center for Bone Research at the Sahlgrenska Academy, Departments of Internal Medicine and Geriatrics, Gothenburg University, Gothenburg, Sweden, ²Department of Laboratory Medicine, Karolinska Institute, Huddinge, Sweden.

Androgens and estrogens regulate skeletal growth and maturation in both males and females, but there is limited information on the relevance of (locally produced) sex steroid precursors and metabolites for bone mass and structure. Urinary levels of conjugated sex steroid metabolites are believed to be reliable markers of the total androgen and estrogen pool. Recently, the dihydrotestosterone metabolite 5 α -androstane-3 β ,17 β -diol (3 β Adiol) was reported to act as an estrogen receptor- β agonist in the prostate, while its role in bone is still unknown. To address this, we investigated the predictive role of urinary 3 β Adiol for bone density and size in young adult Swedish males (age 18.9 ± 0.6 years) at peak bone mass, included in the Gothenburg Osteoporosis and Obesity Determinants (GOOD) study. 3 β Adiol in urine was quantitated by GC-MS in 124 men. Serum levels of testosterone and estradiol were measured by RIA and corresponding serum free levels were calculated. Bone parameters were assessed using both DXA (total body, lumbar spine) and pQCT (tibia, radius). Regression models including age, height, weight, smoking, calcium intake and physical activity as covariates demonstrated that 3 β Adiol in urine is an independent positive predictor of areal BMD of the total body ($\beta = 0.18$, $p < 0.05$) and lumbar spine ($\beta = 0.25$, $p = 0.002$), as measured by DXA. pQCT analysis, separating cortical (diaphyseal) and trabecular (metaphyseal) bone, showed that urinary 3 β Adiol is significantly correlated with cortical volumetric BMD (vBMD) at both the tibia ($\beta = 0.28$, $p < 0.001$) and radius ($\beta = 0.33$, $p < 0.001$). In addition, trabecular vBMD of the tibia ($\beta = 0.29$, $p = 0.001$) and radius ($\beta = 0.17$, $p < 0.05$) were also positively associated with levels of 3 β Adiol in urine. Including serum free estradiol and free testosterone in the regression model did not change the predictive value of 3 β Adiol for any of these bone parameters. These findings demonstrate that urinary 3 β Adiol is a strong independent predictor of cortical and trabecular vBMD in young adult men and support the notion that local sex steroid metabolism is an important determinant of skeletal homeostasis. Therefore, 3 β Adiol in urine may be an interesting novel diagnostic marker for osteoporosis.

Disclosures: **L. Vandenput**, None.

SU523

Estradiol Regulates Gene Expressions of Osteoclast Cytoskeleton: A Microarray Study. D. Saintier^{*1}, N. Sevenet^{*2}, P. Manivet^{*2}, M. de Vernejoul¹, M. E. Cohen-Solal¹. ¹Hospital lariboisiere, INSERM 606, Paris, France, ²Hospital lariboisiere, IFR 139, Paris, France.

Estrogen deficiency in postmenopausal women is followed by enhanced bone resorption and bone loss. Estradiol is a potent inhibitor of bone number and activity. However the mechanisms by which estradiol inhibits osteoclastic resorption is not clearly known. To identify gene regulatory mechanisms that drive osteoclast differentiation and function in response to estradiol, we performed gene expression by microarray analysis of about 15 000 genes (CEA, Evry, France). We used RAW 264.7 monocyte cell line differentiated into osteoclasts in order to analyze changes in gene expression that occur after estradiol exposure. Total RNA was isolated from RAW cells cultured for 5 days with RANKL (30 ng/ml) and in the presence or absence of 17 β -estradiol (10^{-6} M). Hybridization were performed with the inverted labeling (flip/flop method). The RNA samples from each condition were subjected to oligonucleotide gene chips. The experiment was performed three times on two sets of RNA. Analysis was assessed using Image software (Biodiscovery, USA). Overall, in three experiments we found that estradiol consistently changed the expression of several genes with different levels of significance : 7 genes with p value <0.001, 38 with p value <0.005 and 77 with p value <0.01. Thirteen genes were continually up-regulated and 25 were continually down-regulated. Estradiol increases the expression of plakoglobin, a protein implicated to cell-cell adhesion in adherent junctions. We also observed changes in mRNA expression of genes involved in cytoskeleton reorganization. Genes of myosin 1D, an actin-based motor and Ckap1, a cytoskeletal-associated protein for microtubule folding, were significantly down-regulated. These latter suggest that estradiol might have a potential inhibitory role on actin contractility and microtubule polymerisation and therefore might result in a decreased cell migration and motility. In agreement with this result, we found that estradiol decreased actin polymerisation by phalloidin staining. Furthermore, estradiol inhibited the mRNA expression of Rps3a, a ribosomal protein involved in the inhibition of cell apoptosis. These data indicated a potential role of estradiol on cell-cell adhesion, cytoskeletal dynamics and apoptosis. In conclusion, the analysis using microarray showed that estradiol might regulate the expression of several genes implicated in osteoclast fusion, motility and survival. Moreover, the microarray may provide tools for further investigations in order to improve the understanding of the regulation of osteoclast function with estradiol.

Disclosures: **D. Saintier**, None.

SU524

SHBG Is an Independent Negative Predictors of Bone Mineral Density in Elderly Swedish Men- MrOS Sweden. M. Lindberg¹, A. Eriksson¹, E. Orwoll², Ö. Ljunggren³, O. Johnell⁴, D. Mellström¹, C. Ohlsson¹. ¹Center for Bone Research at the Sahlgrenska Academy, Department of Internal Medicine, Gothenburg University, Gothenburg, Sweden, ²Bone and Mineral Unit, Oregon Health and Sciences University, Portland, OR, USA, ³Department of Medical Sciences, University of Uppsala, Uppsala, Sweden, ⁴Department of Orthopaedics, Malmö General Hospital, Malmö, Sweden.

SHBG is an important determinant of bioavailable and free estradiol and testosterone. However, some studies have indicated that it also is an independent regulator of serum bone markers and bone mineral density (BMD). It has been suggested that SHBG exerts direct cellular functions by acting through a specific membrane receptor, and that this effect may be independent of estradiol and testosterone. The aim of the present study was to investigate if SHBG is an independent predictor of BMD in a large cohort of elderly Swedish men. In the Swedish part of the MrOS study (n= 3000, average age 75.4 years) bone parameters were measured using DXA. Serum levels of testosterone, estradiol and SHBG were measured and free testosterone and free estradiol were derived from the mass action equations. The independent role of SHBG as a predictor of skeletal parameters was evaluated in regression models including age, height, weight, physical activity, smoking habits, calcium intake, free testosterone, free estradiol and SHBG. SHBG was an independent negative predictor of total body ($\beta = -0.041$, $p = 0.02$), lumbar spine ($\beta = -0.045$, $p = 0.02$), trochanter ($\beta = -0.040$, $p = 0.03$) and femur neck ($\beta = -0.053$, $p = 0.005$) BMD. We next compared the subjects with high SHBG levels (h-SHBG, the 10% with highest SHBG levels) with those with low SHBG levels (l-SHBG, the 10% with the lowest SHBG levels). Subjects with l-SHBG had increased BMD in the lumbar spine (12.2 % over h-SHBG, $p < 0.001$), trochanter (8.9 % over h-SHBG, $p < 0.001$) and femur neck (8.8% over h-SHBG, $p < 0.001$) compared with subjects with h-SHBG. In conclusion, SHBG is an independent predictor of BMD in elderly Swedish men, supporting the notion that SHBG exerts effects on bone independent of estradiol and testosterone. The mechanism(s) of action for the estradiol/testosterone independent effects of SHBG remains to be elucidated.

Disclosures: **M. Lindberg**, None.

SU525

Longitudinal Follow-Up of Androgen Action on the Skeleton of the Growing SAMP6 Mouse Model: No Evidence for Blunting of Androgen Action. J. Ophoff^{*}, K. Venken^{*}, S. Boonen, E. Van Herck^{*}, R. Bouillon, D. Vanderschueren. KULeuven, Leuven, Belgium.

The SAMP6 mouse model (P6) is a well-characterized animal model of deficient peak bone mass acquisition and osteoporosis. Previous studies suggested that the P6 skeleton is also resistant to orchidectomy. However, bone effects of androgen replacement have never been evaluated in P6 and their respective SAMR1 (R1) controls. In this study, the non-

ASBMR 27th Annual Meeting

aromatisable androgen 5 α -dihydrotestosterone (DHT) was administered (45 μ g/day via subcutaneous implants) to orchidectomized male P6 and R1 mice at week 4 (start of puberty). Both bone resorption and formation markers (urinary deoxypyridinoline [DPD] and serum osteocalcin [oc]) and tibial bone mass (by *in vivo* pQCT) were measured every 4 weeks between 4-20 weeks of age. At baseline and endpoint serum osteoprotegerin (OPG) was evaluated. At the tibial diaphysis, DHT had similar bone anabolic effects in P6 and R1. DHT increased periosteal expansion more than endocortical expansion, resulting in thickening of the cortex (+7% in P6 and +4% in R1, respectively; $P < 0.001$). At the tibial metaphysis, DHT also induced a sustained increase of trabecular bone mineral density during the entire experimental period; this increase was significantly greater in P6 (+150% in P6 versus +68% in R1, $P < 0.001$), despite similar action of DHT on seminal vesicles in P6 and R1. In accordance with its bone sparing action on cancellous bone, DHT lowered oc and DPD in P6 (-47% and -59%, respectively, $P < 0.001$) and R1 (-53% and -60%, respectively, $P < 0.001$) during the entire experimental period. Moreover, DHT increased serum OPG (which was already higher in P6 than R1) in P6 (+63%, $P < 0.05$) but not in R1. In conclusion, DHT action on the skeleton is not impaired in growing P6. DHT has similar anabolic action on cortical bone in P6 compared to controls. In cancellous bone, on the other hand, DHT shows a stronger bone sparing effect in P6; this effect is consistent with an increase of OPG in this animal model of senile osteoporosis. The longitudinal follow-up of bone markers in combination with *in vivo* pQCT appears an interesting tool for the combined evaluation of cortical and cancellous bone acquisition during growth in animal models.

Disclosures: **J. Ophoff.** None.

SU526

Aromatase Inhibition Causes Lower Bone Density Than Ovariectomy in Mice, an Effect Prevented by Bisphosphonates. W. Kozlow¹, K. Mohammad¹, R. McKenna¹, N. Niewolna¹, L. Suva², C. Rosen³, T. A. Guise¹.
¹Internal Medicine, University of Virginia, Charlottesville, VA, USA,
²Orthopaedic Surgery, University of Arkansas, Little Rock, AR, USA, ³Jackson Laboratory, Bar Harbor, ME, USA.

Aromatase inhibitors (AIs), effective treatment for breast cancer, block estrogen synthesis by inhibiting the conversion of testosterone and androstenedione to estradiol and estrone. Increased bone resorption and decreased bone mineral density (BMD) are predicted consequences. We hypothesized that bisphosphonates (BPs) may prevent bone loss from AI therapy. We studied the effect of estrogen deficiency on bone remodeling in 4-week-old female nude mice that underwent ovariectomy (ovx) or sham surgery. Ovz and sham mice did not differ in BMD (assessed by DXA) or in histomorphometric assessment of trabecular bone volume. Next, to study the effect of AIs +/- BPs on bone remodeling, 4-week-old female nude mice were treated with letrozole (10 mcg/d), zoledronic acid (ZA) (5 mcg/kg twice weekly), letrozole (10 mcg/d) + ZA (5 mcg/kg twice weekly) or control. Mice treated with letrozole alone had lower BMD compared to control mice ($p < 0.0001$; total body, spine, femur and tibia). Mice treated with ZA alone had higher BMD compared to control mice ($p < 0.0001$; total body, spine, femur and tibia). Mice treated with letrozole plus ZA achieved the same BMD as mice treated with ZA alone at the spine and tibia, but had greater BMD than mice treated with ZA alone at the femur ($p < 0.0001$) and total body ($p < 0.0023$). MicroCT analysis of the proximal tibia showed no difference in bone volume (BV/TV), structural model index, or trabecular number, thickness or spacing in mice treated with letrozole alone compared to control. Treatment with ZA (+/- letrozole) resulted in a significant increase in BV/TV and trabecular number and thickness, and the structural model index indicated that the bone structure was unusually solid. Dynamic bone histomorphometry of the lumbar spine demonstrated decreased bone formation and mineral apposition rates in mice treated with letrozole, ZA or the combination compared to control. Serum testosterone concentrations were increased in mice treated with letrozole compared to control. Serum IGF-1 concentrations were similar in all groups. These data indicate that aromatase inhibition with letrozole caused lower BMD in female nude mice than that observed with ovx. The greater effect of AIs compared to ovx may be due to reduced adrenal androgen conversion to estrogen. ZA prevented AI-induced bone loss, but microCT and dynamic bone histomorphometry suggest reduced bone remodeling. BPs may be useful to prevent AI-induced bone loss, but further studies are needed to assess the effects of these treatments on bone quality.

Disclosures: **W. Kozlow.** None.

SU527

Estradiol Therapy in Murine Congenital Aromatase Deficiency Normalizes Serum IGF-I and Femoral Width but not Length. O. K. Oz¹, A. M. Thomas¹, G. Hirasawa¹, C. Rosen², E. R. Simpson³.
¹Radiology, UT Southwestern Medical Center at Dallas, Dallas, TX, USA, ²Maine Center for Osteoporosis Research, St. Joseph's Hospital, Bangor, ME, USA, ³Victorian Breast Cancer Consortium, Prince Henry's Institute of Medical Research, Clayton, Victoria, Australia.

Aromatase catalyzes the biosynthesis of estrogens from androgen precursors. We have shown previously that adult aromatase deficient male mice (ArKO) have significantly lower trabecular bone volume, low turnover, low serum IGF-I and significantly decreased femur length compared with Wt males. In the present study we sought to determine if estradiol therapy during puberty could normalize IGF-I levels and axial and appendicular skeletal growth. We followed and compared the growth of male ArKO mice, or ArKO mice treated with 20ug E2 3x/week subcutaneously in sesame oil, to their Wt littermates from age 3 weeks to 7 weeks. Nasal anal length (NAL) was used as an index of axial skeletal growth. Femur length and transverse mid-shaft diameter at the time of sacrifice were used as a measures of appendicular skeletal growth during puberty. Serum IGF-I

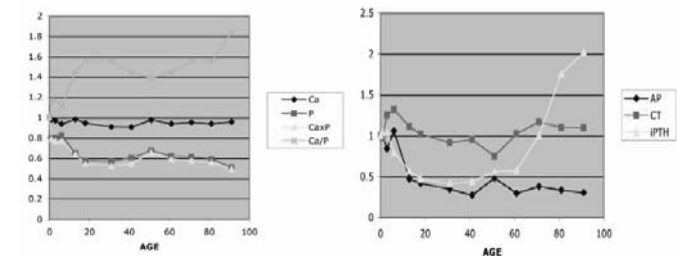
levels were measured by RIA. Compared to Wt littermates ArKO males showed shorter NAL beginning at 5 weeks ($p < 0.05$) of age and lower body weight. Placebo treated ArKO mice had shorter ($p < 0.05$) and narrower femurs ($p < 0.05$). Estradiol therapy normalized the mid-shaft diameter but worsened the femur length deficit. IGF-I serum levels in placebo treated male ArKO mice were lower than Wt males ($p < 0.001$). Estradiol treatment normalized serum IGF-I levels. Since hepatic IGF-I production is regulated by growth hormone signaling through the JAK/Stat pathway and inhibited by SOCS-2, we measured SOCS-2 levels in hepatic proteins of 7 week old animals. The placebo treated ArKO animals had lower SOCS-2 levels compared to Wt. Estradiol therapy raised the SOCS-2 expression to Wt levels. Despite this, serum IGF-I was normalized. These data show that the dose regimen of estradiol used was not sufficient to normalize appendicular skeletal growth despite normalization of IGF-I but was sufficient to normalize transverse mid-shaft diameter. Estradiol may regulate radial bone growth through IGF-I action. In previous work we have shown that femur length in ArKO males can be restored by treatment with rhIGF-I. Taken together, the data raise the question of whether estradiol and IGF-I might have opposing effects at the growth plate of animals in the age range of this study.

Disclosures: **O.K. Oz.** None.

M001

A Cross Sectional Survey of Age-Dependent Changes in Mineral Metabolism and Bone Turn-Over Markers in 461 Chinese Subjects Age 2 Month to 100 Years. B. H. Sun¹, W. J. Chu², H. Y. Zhang², K. L. Insogna¹.
¹Internal Medicine/Endocrinology, Yale University School of Medicine, New Haven, CT, USA, ²Laboratory Medicine, Beijing Ji Shui Tan Hospital, Beijing City, China.

Several studies have reported that the ratio of dietary calcium to dietary phosphorus is an independent predictor of bone mineral content (BMC) and bone mineral density (BMD). Effects on circulating levels of PTH, and a vitamin D-independent effect on intestinal calcium absorption have been suggested as possible mechanisms for this relationship. Although alterations in dietary calcium and phosphorus can effect circulating levels of these ions, little is known about the relationship of the serum calcium/phosphorus ratio (Ca/P) or the serum calcium-phosphorus product (CaxP) to age-dependent changes in mineral metabolism and bone turnover. To address this issue BMD and BMC as well as serum iPTH, calcitonin and Alk.Phos were measured, and their relationship to Ca/P and CaxP analyzed in 461 healthy Chinese subjects from age 2 months to 100 years. Subjects were divided into 13 age groups with 30-40 individuals in each group and equal proportions of each sex in each group. The data are summarized graphically below. We found that Ca/P was positively correlated with BMD before age of 40 (i.e. before attainment of peak bone mass) and negatively correlated with BMD after age of 40. Sex-dependent differences were found only for iPTH and only in the 41 to 50 and 71 to 80 age groups (data not shown). Alk. Phos. declined and iPTH rose in parallel with the change in Ca/P ratio. We conclude that the Ca/P ratio tracks with changes in bone anabolism, such as Alk Phos and with bone accretion in childhood and young adulthood. The divergence between Ca/P and bone mass in later adult life may reflect changing needs in these two minerals for optimal skeletal health or simply age-dependent changes in mineral homeostasis. These two possibilities are currently under investigation.



Disclosures: **B.H. Sun.** None.

M002

Flagellin Stimulate Osteoclast Formation by Increasing RANKL Expression in Osteoblasts. Z. Lee, H. Ha*, H. Kwak*, H. Kim*, J. Lee*, M. Kang*, H. Kim*. Cell and Developmental Biology, College of Dentistry, Seoul National University, Seoul, Republic of Korea.

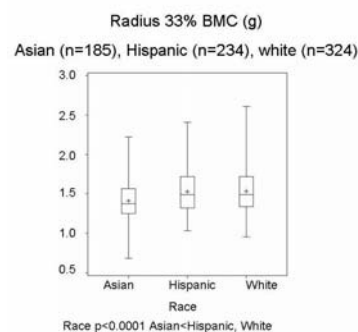
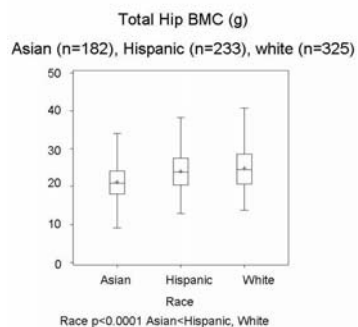
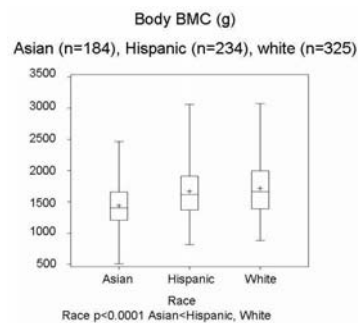
Stimulation of several Toll-like receptors (TLRs) has been shown to increase osteoclast formation in the co-cultures of osteoblasts and bone marrow cells. We investigated whether activation of TLR5 could modulate osteoclastogenesis. Flagellin, which act as a ligand of TLR5 stimulated osteoclast formation in co-cultures, and significantly increased the number of osteoclasts and the resorbed area in the calvarial bone of mice. Flagellin also stimulated the expressions of RANKL, TNF- α , IL-1, and M-CSF, known to stimulate osteoclastogenesis. Flagellin-induced osteoclastogenesis was blocked by addition of OPG, but not IL-1ra and anti-TNF Ab. In addition, flagellin had no effect on PGE₂ production in co-cultures. We also found that the activation of Erk pathway was involved in flagellin-induced RANKL expression in osteoblasts. However, treatment with flagellin from the beginning of the BMM cultures significantly inhibited RANKL-induced osteoclast formation by inhibiting expression level of c-Fos protein. Taken together, these results suggest that flagellin stimulate osteoclastogenesis via osteoblasts which overcome the inhibitory effect of flagellin on osteoclast precursors, as well as increasing RANKL induction.

Disclosures: **Z. Lee.** None.

M003

Bone Mineral and Predictors of Whole Body, Total Hip, and Lumbar Spine for 740 Early Pubertal White, Hispanic, and Asian Girls. C. M. Weaver¹, L. D. McCabe^{*1}, G. M. McCabe^{*1}, R. Novotny^{*2}, M. D. Van Loan³, S. B. Going⁴, C. Boushey^{*1}, D. A. Savaiano^{*1}, V. Matkovic⁵. ¹Purdue University, West Lafayette, IN, USA, ²University of Hawaii, Honolulu, HI, USA, ³University of California - Davis, Davis, CA, USA, ⁴University of Arizona, Tucson, AZ, USA, ⁵Ohio State University, Columbus, OH, USA.

To determine ethnic differences and predictors of bone mass in early pubertal girls, we recruited White, Hispanic, and Asian 6th grade girls across six states for a school-based educational intervention. Here we report baseline bone mineral content data (Figs 1-3) and developed models for predicting bone mineral content (BMC) for the whole body, 33% radius, total hip, and lumbar spine for 740 subjects. Multivariate analysis of variance indicated that there are differences in BMC among ethnic groups (Wilks' Lambda=0.926, $p<0.0001$). For each of the bone sites, the corresponding area was a strong predictor of BMC with correlations ranging from 0.78 to 0.98, confirming that larger subjects have more BMC. Detailed results for total body BMC, and radius 33% BMC were qualitatively similar. Ethnicity was not a significant predictor when added to the models that predict BMC with area. Models using anthropometric variables (height, weight, bitrochanteric width, waist depth, waist circumference, trunk length, forearm length) plus ethnic group to predict total body area, and radius 33% area explained 88%, and 32%, of the variability respectively. Final models included ethnic group, the anthropometric predictors of area, Tanner score, age, physical activity, and dairy calcium intake explained 85% and 64% of BMC respectively. Ethnic group was not a significant statistical predictor of BMC in these models. Significant positive associations of BMC were found with Tanner score and physical activity for both bone sites; and with age for total body BMC. For lumbar spine and total hip, 76% and 79% of the variability in area was explained by anthropometric variables. Final models predicted 79% and 77% of the variability in BMC. These models included statistically significant interactions of ethnicity with anthropometry variables. Significant positive associations of BMC were found with Tanner score, age, and dairy calcium for lumbar spine; Tanner score and physical activity for total hip. All analyses were controlled for study site.

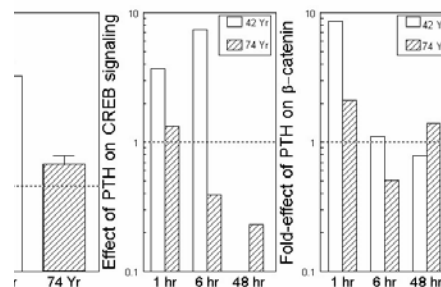


Disclosures: C.M. Weaver, USDA 2.

M004

Responses of Human Bone Marrow Stromal Cells to PTH Decrease with Age. S. Zhou, I. Amato*, J. Glowacki. Orthopedic Surgery, Brigham and Women's Hospital, Boston, MA, USA.

Studies with human and animal culture systems indicate that a sub-population of bone marrow stromal cells (hMSCs) has the potential to differentiate into osteoblasts. We and others showed that there is an age-related decline in the osteoblast potential of hMSCs. Parathyroid hormone (PTH), when applied intermittently, has osteoanabolic effects in a variety of systems. The ability of PTH to regulate gene expression in target cells is dependent upon activation of transcription factors involved in cascades stemming from PKA, such as cAMP response element binding protein (CREB), or β -catenin. In this study, we tested the hypothesis that the response of human marrow stromal cells to PTH decreases with age. Early passage hMSCs obtained from young (Y ; 34, 42 yr) and elderly (E ; 68-90) women were treated with PTH in MEM- α with 1% heat-inactivated FBS, 1% P/S supplemented with 10^{-8} M dexamethasone, 50 μ g/ml ascorbate phosphate, 5mM β -glyceraldehyde. Growth of cells, abundance of Senescence Associated β -galactosidase (SA β), and effects of PTH on alkaline phosphatase (ALK) activity, and Western immunoblots for activation of CREB and β -catenin were assessed. An additional 6 days was required for E cells to expand to the numbers reached by Y cells. There were 10-fold (± 2) more SA β -positive cells in E cultures than in Y . Osteoblast differentiation, measured by ALK activity, in E cultures was half that in Y . After 7 d, alkaline phosphatase (ALP) activity in a Y culture was stimulated by 10^{-8} M PTH to a magnitude twice that in E (Figure, Left). PTH activation of p-CREB and β -catenin was diminished in E (Figure, Center and Right). In sum, there are age-related decreases in human marrow stromal cell proliferation, differentiation into osteoblasts, and magnitude of stimulation of osteoblastogenesis by PTH. PTH signaling of p-CREB and β -catenin are diminished with age. Intrinsic alterations in signaling pathways may explain cellular and tissue aging.



Disclosures: S. Zhou, None.

M005

Effects of Local Administration of Recombinant Human IGF-I (hIGF-I) on New Bone Formation in an Aged-Mouse Model Using Distraction Osteogenesis. J. L. Fowlkes¹, L. Liu^{*2}, E. C. Wahl^{*1}, R. C. Bunn^{*1}, K. M. Thraill¹, C. K. Lumpkin¹. ¹Pediatrics, UAMS, Little Rock, AR, USA, ²Orthopaedics, UAMS, Little Rock, AR, USA.

Human and rodent research supports a primary role for insulin-like growth factor-I (IGF-I) in bone formation. IGF-I is involved in stimulating longitudinal bone growth and in enhancing bone formation. In mice, elimination of hepatic IGF-I affects bone formation only minimally, suggesting that paracrine/autocrine actions of IGF-I may play an essential role in bone homeostasis. To test this hypothesis, we designed a study using surgical distraction osteogenesis (DO) in aged mice (12-month CB57BL/6 male mice) who were distracted one day after surgery at 0.075 mm bid for 13 days. At the time of surgery, Alzet® Model 2002 mini-osmotic pumps were filled with either 1) PBS (vehicle; $n = 10$); 2) human IGF-I (hIGF-I; $n = 11$; delivery rate: 1 μ g/7 μ l/day); or 3) methylene blue ($n = 2$). Alzet pumps were inserted subcutaneously and infusion tubing was routed subcutaneously from the pump to the distraction site with the catheter outlet placed adjacent to the osteotomy. Continuous infusion of vehicle, hIGF-I or methylene blue occurred for the full 14 days. After DO, the mice were anesthetized, decapitated for blood collection, and the distracted tibiae were removed and fixed. DO gaps were assessed by X-ray analyses for new bone formation and blood was sampled to determine hIGF-I concentrations using a human-specific IGF-I ELISA. No hIGF-I was detected in the serum of hIGF-I treated or vehicle treated animals, attesting to the concept that local delivery of this growth factor can be achieved with little to no systemic spread. Methylene blue as tracer confirmed that the delivery modality was precise and efficient. Comparison of radiographs from vehicle versus hIGF-I treated animals showed that more calcified bone was present within the distraction gaps of hIGF-I treated versus vehicle-treated mice. Radiologic quantification of aligned distraction gaps revealed that vehicle-treated mice demonstrated 16.532 \pm 6.425 % new bone formation compared to the hIGF-I treated mice which displayed 45.178 \pm 8.152 % new bone formation ($p = 0.02$). These studies demonstrate that local hIGF-I can be effectively and successfully applied to the distraction gap using a subcutaneous osmotic minipump. Furthermore, local infusion of hIGF-I to the distraction gap was successful in producing a ~2-3 fold increase in new bone when compared to no hIGF-I, making it highly feasible to detect a local IGF-affect in this new bone formation model, without altering peripheral IGF-I concentrations.

Disclosures: J.L. Fowlkes, Pharmacia 2.

M006

Lean Mass, but not Fat Mass, Is a Significant Predictor of Peak BMC and BMD in Mice Fed a High-Fat Diet. M. Hamrick, C. Pennington*, C. Webb*, C. M. Isales. Medical College of Georgia, Augusta, GA, USA.

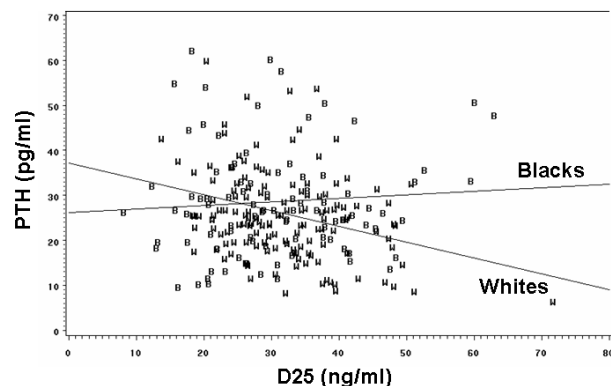
Body mass is known to be a significant predictor of bone strength, although it is unclear whether lean mass or fat mass is a more important determinant of peak bone mass (BMC) and density (BMD). We examined the effects of lean mass and fat mass on peak BMC and BMD by feeding normal (wild-type CD-1/ICR) mice and myostatin-deficient mice a high-fat (45 kcal %fat) diet for 8 weeks starting at two months of age. Mice lacking myostatin (GDF-8) have increased muscle mass compared to normal mice, and are also known to have less body fat than normal mice. Control mice of each genotype were fed standard chow (4 kcal %fat). Lean and fat mass, percent body fat, BMC, and BMD were analyzed using DEXA (PIXImus system). Serum insulin, leptin, and resistin levels were measured using a Luminex assay kit (Linco Research). Fat mass, percent body fat, and serum resistin levels increased significantly in normal and myostatin-deficient mice fed a high fat diet, whereas serum leptin increased significantly in normal mice but not in myostatin-deficient mice. Whole-body BMC decreased by approximately 10% in normal mice fed a high fat diet compared to mice on the control diet, whereas the high fat diet yielded a slight but non-significant increase in skeletal BMC and BMD in the myostatin-deficient mice. Coefficients of determination calculated from regression analyses within mice of each genotype (pooled control and high fat diet animals) indicate that lean body mass is a significant ($P < .05$) determinant of BMD and BMC in mice of each genotype whereas fat mass, serum leptin, serum insulin, and serum resistin were not significant predictors of BMD or BMC in either group. These data suggest that increasing lean mass early in life may be an effective strategy for increasing peak BMD and BMC, whereas fat mass and total body weight may be more important for maintaining bone mass and density after skeletal maturity.

Disclosures: **M. Hamrick**, None.

M007

Vitamin D Status and Calcium Absorption in Black and White Boys and Girls on a Range of Controlled Calcium Intakes. M. Braun¹, B. R. Martin¹, G. P. McCabe^{*2}, L. A. DiMeglio^{*3}, M. Peacock³, C. M. Weaver¹. ¹Foods & Nutrition, Purdue University, West Lafayette, IN, USA, ²Statistics, Purdue University, West Lafayette, IN, USA, ³Indiana University School of Medicine, Indianapolis, IN, USA.

The relationships among serum 25 and 1,25 vitamin D, serum levels of calcium regulating hormones and calcium absorption have been established in adults but not in children. These relationships were investigated in 236 adolescents during their pubertal growth spurt to determine whether similar relationships exist in children and whether they are affected by race and sex. Calcium balance studies were conducted in American white and black girls and boys, aged 11-15 years, on calcium intakes ranging from 760 to 2195 mg Ca/day for 3-week controlled feeding periods. In addition, dual stable isotope calcium tracer studies were conducted in a subset of individuals. All procedures were approved by the Purdue University and Indiana University School of Medicine Institutional Review Boards. Serum 1,25 D increased in response to a low calcium intake and apparent calcium absorption increased as 1,25 D increased. Serum parathyroid hormone (PTH) levels and 1,25 D were positively related. Serum 1,25 D was different between American whites and blacks ($p < .05$). Serum 25 D was different between racial groups ($p < .0001$) and between boys and girls ($p = 0.0010$). Serum 25 D was inversely related to PTH, however, the relationship varied with race (Figure 1). Relationships among serum 25 and 1,25 vitamin D, serum levels of calcium-regulating hormones and calcium absorption are similar in children as in adults, but in addition to racial differences known in adults, sex differences were found.



Disclosures: **M. Braun**, None.

M008

Defining the Serum Vitamin D Concentration Required for Maintenance and Buildup of Bone in Young Japanese Women. H. Ohta¹, Y. Onoe¹, Y. Miyabara^{*1}, A. Harada^{*2}, R. Yoshikata^{*1}, T. Kuroda^{*1}, H. Okano¹, N. Tsugawa^{*3}, T. Okano³, M. Kume^{*4}, S. Sasaki^{*5}. ¹Obstetrics and Gynecology, Tokyo Women's University, Tokyo, Japan, ²Biostatistics, Tokyo University, Tokyo, Japan, ³Hygienic Science, Kobe Pharmaceutical University, Kobe, Japan, ⁴Nursing, Tokyo Women's University, Tokyo, Japan, ⁵National Institute of Health and Nutrition, Tokyo, Japan.

Vitamin D is known to play as a important role in bone mineralization, and Vitamin D insufficiency is known to cause hyperparathyroidism, bone reduction and fracture in elderly people. In recent years, it is suggested that serum vitamin D levels are reduced in the elderly, and vitamin D supplementation is called for in these people. To develop a methodology for the prevention of osteoporosis, we examined serum 25OH-VD and PTH levels in young Japanese females, to elucidate the relationship between these variables and bone mineral density (BMD) in these subjects. Between October 2003 and April 2004, healthy female volunteers aged between 19 to 25 years who gave prior informed consent were recruited into the study. Those receiving treatment for any disease affecting bone mass, as well as pregnant or breast-feeding women, were excluded from the study. The subjects were asked about their age, current menstrual status, height, body weight, weight at birth, and as well as their gestational age. Biochemical variables examined in these subjects included the levels of serum calcium (Ca), phosphorus (P), intact-PTH, cross-linked N-telopeptide of type I collagen (NTX), and bone-alkaline phosphatase (BAP). The BMD of the lumbar vertebrae 2 to 4 (L 2-4), as well as the total BMD of the proximal femur (BMD of the hip) was also measured in the subjects using QDR 4500. A total of 293 subjects (mean age, 20.6 \pm 1.5) were enrolled in the study. The BMD of the L2-4 (mean, 1.00 \pm 0.11 g/cm²) and of the total hip (mean, 0.90 \pm 0.10 g/cm²) were confirmed to remain at a certain level between the ages of 19 to 25. The mean serum Ca and P levels were 9.50 \pm 0.33 mg/dl and 3.75 \pm 0.43 mg/dl, respectively. The mean serum 25OH-D and intact-PTH levels were 18.8 \pm 4.9 ng/ml and 22.0 \pm 7.4 pg/ml, respectively. During the entire observation period, serum Ca and P levels remained stable, while 25OH-VD levels were shown to significantly negatively correlate with intact-PTH levels. Furthermore, the subjects who had higher vitamin D levels (over 25 ng/ml) showed no increase in intact-PTH levels; however, they showed significantly higher BMD values than those with lower vitamin D values. Our study results indicate that reduced vitamin D levels lead to an increase in intact-PTH levels resulting in reduced BMD values even in young females; in contrast, higher vitamin D levels contribute toward higher BMD levels in these subjects.

Disclosures: **H. Ohta**, None.

M009

Impact of Nutrition and Exercise on Acquisition of Bone Mineral Density in Young Japanese Women. Y. Miyabara^{*1}, A. Harada^{*2}, Y. Onoe¹, R. Yoshikata^{*1}, M. Yoshida^{*1}, T. Kuroda^{*1}, H. Okano¹, M. Kume^{*3}, S. Sasaki^{*4}, H. Ohta¹. ¹Obstetrics and Gynecology, Tokyo Women's University, Tokyo, Japan, ²Biostatistics, Tokyo University, Tokyo, Japan, ³Nursing, Tokyo Women's University, Tokyo, Japan, ⁴National Institute of Health and Nutrition, Tokyo, Japan.

Acquisition of bone mineral density (BMD) in women in their early years is assumed to be crucial to the prevention of osteoporosis. Furthermore, observance of appropriate physical exercise and intake of necessary nutrients are assumed to play a key role in their early acquisition of BMD. A cross-sectional study was therefore conducted to identify which lifestyle habits might be definitive factors affecting the status of BMD in young Japanese women based on their background factors, nutritional intake, physical exercise, and BMD. Female volunteers aged 19 to 25 years of age were enrolled in this study and the subjects were asked about their age, weight at birth, and age at menarche; height, weight, serum Ca, P, ALB, intact-OC, NTX, BAP were also measured in these subjects. Furthermore, BMD of the lumbar vertebrae 2-4 (L2-4 BMD), as well as BMD of the proximal femur (hip BMD), was also measured in these subjects by using QDR4500. Additionally, all subjects were asked about their physical activity and nutritional intake using the Questionnaire on the Amount of Physical Activity developed by the JALS Physical Activity Working Group, Japan Atherosclerosis Society, and the self-administered Diet History Questionnaire (DHQ). The present study accrued 254 subjects over time between October 2003 and April 2004, and the data collected from these subjects were analyzed. The mean age of the subjects was 20.7 \pm 1.5 years old; the mean age at menarche, 11.9 \pm 1.2 years old; and the mean L2-4 and hip BMD, 1.00 \pm 0.11 and 0.90 \pm 0.10 ng/cm², respectively. Of the variables examined, height, weight, BMI, weight at birth, and intact-OC were found to be significantly correlated with the mean L2-4 and hip BMD values; total physical energy, prior exercise habits, of all physical activity-related variables examined, as well as cholesterol and phosphorus, of all DHQ variables examined, were significantly correlated with the L2-4 and hip BMD. Furthermore, multiple regression analysis of the data showed BMI, prior exercise habits, total physical energy, and total cholesterol intake to be definitive factors affecting the status of the L2-4 and hip BMD. Our study results suggest that self-control of BMI, regular physical activity, and cholesterol intake play a pivotal role in promoting the acquisition of BMD in women in their early years.

Disclosures: **Y. Miyabara**, None.

M010

Weight at the Age of Peak Bone Growth Affects Bone Mass in Japanese Adolescents but Birth Weight Does not. M. Iki¹, J. Tamaki^{*1}, Y. Ikeda^{*1}, A. Morita^{*1}, Y. Sato^{*2}, H. Naka^{*3}. ¹Department of Public Health, Kinki University School of Medicine, Osaka-Sayama, Japan, ²Department of Nutrition, Tenshi College, Sapporo, Japan, ³Department of Physical Education, Kyoto University of Education, Kyoto, Japan.

The birth weight has been suggested to affect adult bone mass in Caucasian women. Neonatal bone growth retardation may increase the risk of osteoporosis later in life. We tested whether this was the case in for Japanese persons or not, and investigated which weight measured during childhood had the greatest effect on bone mass. We examined 263 healthy Japanese boys and girls from the 4th to 6th grade of the elementary schools (11.2±0.9 years old) for height, weight and bone mineral density (BMD) at the spine and hip by DXA, and measured the same items for the same subjects 3 years after the baseline. The height and weight values for the subjects at birth and at health checkups for children of age 1.5 and 3 years were obtained from their Maternal and Child Health Handbook and values for those at the entry into elementary school (6 years old) and junior high school (12 years) were obtained from the medical records at the schools. The correlation coefficient between the weight at birth or at age 1.5 years and BMD at baseline or follow-up was not significant, regardless of sex and skeletal site. The correlations between weight at age 3 years and BMD at both skeletal sites and on both occasions were all significantly positive only in boys. The weight after age 3 years showed a significantly positive correlation with BMD. The correlation between the weight and BMD at follow-up was the strongest in boys, while the correlation between those at baseline was the strongest in girls. When the results were adjusted for age and weight at the time of bone measurement, all the correlations turned out to be insignificant in boys, but the correlations between weight at the entry into junior high school and BMD at follow-up were still significant in girls. We performed a multiple regression analysis for BMD at follow-up in girls using the age and weight at follow-up and weight at the entry into junior high school, in order to evaluate the relative importance of the weights at these 2 time points for BMD. A significant regression coefficient was given to the weight at the entry into junior high school but not for the weight at follow-up. The weight at birth or in infancy did not affect the BMD in the Japanese pupils and junior high-school students. The greatest effect on BMD in girls was observed for the weight at the upper grades of elementary school or at the entry into junior high school, which was around the age at peak bone growth. This finding suggests that weight around the age at peak bone growth may have a critical effect on the peak bone mass in women.

Disclosures: **M. Iki**, Japan Society for the Promotion of Science 2.

M011

Correlations among Age, Sex and Growth Variables for Bone Mineral Content and Bone Mineral Density Acquisition in Healthy Children from Central Italy . P. Caradonna¹, E. Ausili^{*2}, D. Rigante^{*2}. ¹Department of Internal Medicine, Università Cattolica Sacro Cuore, Rome, Italy, ²Department of Pediatric Sciences, Università Cattolica Sacro Cuore, Rome, Italy.

Aim: To evaluate cross-sectionally bone mineral content (BMC) and bone mineral density (BMD) in healthy Italian children and to find correlations with age, sex and growth variables. *Methods:* We have examined a cohort of 359 healthy children (187 males and 172 females, aged 3-14 years) recruited from the same Italian region in 1 year: demographic, anthropometric data and informations about physical activity and pubertal development were obtained. Total body (TB), lumbar spine (LS), femoral neck (FN) and body composition were assessed with dual-energy X-ray absorptiometry (Hologic QDR 2000). *Results:* No significant difference of TB-BMC annual increments was found for both sexes (b value: 107.5 in females, 113.5 in males). LS-BMD increased at the same rate in males and females until the age of 9 years (23 g/cm²/year); then females showed a significant greater annual increment (95 g/cm²) differently from males (24 g/cm²). When compared by gender, LS-BMD was higher in females older than 9 years. FN-BMD showed until the age of 9 years a mean annual increment of 26 g/cm² in males and 30 g/cm² in females; then the increment was 50 g/cm² in both sexes. When compared by gender, FN-BMD appeared higher in males than in females for all age groups. Stepwise multiple linear regression analysis (multivariate model) was performed using BMD as dependent variable. This model revealed that pubertal stage was the stronger predictor of LS-BMD increase in females rather than in males (respectively R = 0.837 and 0.738); if physical activity was considered, R improved only in the female sex (0.885). When other variables (BMI, father BMI, mother BMI, lean/fat mass, pubertal stages according Tanner) were introduced, the interaction of lean mass and pubic hair stage gave the best fit for females (R = 0.939), while the exclusive lean mass fitted in the model for males (R = 0.833). When FN-BMD was considered as dependent variable, only age was the stronger predictor of BMD increase both for males and females (respectively R = 0.663 and 0.810). If BMI and lean/fat mass were analyzed, the stronger predictor of FN-BMD increase was lean mass both in males and females (respectively R 0.817 and 0.900). *Conclusions:* Before puberty LS-BMD was equally distributed in both sexes; after puberty LS-BMD resulted significantly higher in females, due to minor dimensional development of female vertebrae. FN-BMD was higher in males at whatever age. In both sexes the stronger predictors for bone mass acquisition were pubic hair stage and lean mass at LS and only lean mass at FN.

Disclosures: **P. Caradonna**, None.

M012

Effect of Physical Activity in Elementary School on Bone Mineral Density in Japanese Children and Adolescents: A 3-Year Longitudinal Study. J. TAMAKI¹, M. Iki¹, A. Morita^{*1}, Y. Ikeda^{*1}, Y. Sato^{*2}, H. Naka^{*3}. ¹Public Health, Kinki University School of Medicine, Osaka-Sayama, Japan, ²Nutrition, Tenshi College, Sapporo, Japan, ³Physical Education, Kyoto University of Education, Kyoto, Japan.

It is recognized that physical activity during childhood plays an important role in determining peak bone mass. However, how the frequency and the duration of physical activity affect bone growth is not well known. We examined the effects on bone mineral density (BMD) at the baseline and 3-year later among Japanese children and adolescents. We studied 579 healthy children aged 10-16 y (283 boys, 296 girls) from a town in Japan in 2001, and conducted a follow-up (follow-up rate; 75.8%). At both surveys, we investigated the following. We measured their heights and weights, and BMDs at the spine and hip using dual-energy X-ray absorptiometry. A history of each child's physical activity in sport clubs from the elementary school (from age 6 y) was estimated, using a questionnaire administered by interviewers who were trained public health nurses in the town. The questionnaire asked the average active duration (hours) per each activity, the frequency per week, and the period taken participate in each sport club. The total time spent in sport clubs was calculated as the sum of each active duration multiplied by the frequency, and by the period. The Ethics Committee of Kinki University School of Medicine approved the studies. With multivariate analysis predicting BMDs at baseline among 579 children, the total time spent during elementary school (ages 6-12 y) was significantly and positively related with hip and lumbar BMD among pre-pubertal boys, and with hip BMD among post-pubertal boys and girls, respectively. The total time spent during junior high school (ages 13-15 y) was significantly and positively related with only lumbar BMD among pre-pubertal boys. Multivariate analysis adjusted for years after the onset of puberty, height, and weight to predict BMDs at 3-year follow-up showed that the total time spent during elementary school was significantly and positively related with hip and lumbar BMD among boys, and with lumbar BMD among girls. Similar analysis showed that the total time spent during junior high school was significantly and positively related with hip lumbar BMD among boys. Similar analysis predicting percent change of BMDs during 3 years showed that the time spent at elementary school during follow-up period was still significantly and positively related with lumbar and hip percent change of BMD among boys, and the time spent at high school was similarly related with hip and lumbar BMD among girls. Thus, the physical activity before age 13 may be especially important for child and adolescent bone growth.

Disclosures: **J. Tamaki**, Japan Society for the Promotion of Science, The Ministry of Education, Culture, Sports, Science and Technology, Japan 2.

M013

Eating Disorders and Amenorrhea Are Strong Predictors of Change in Bone Mass in Physically Active Young Females. J. W. Nieves, M. Zion*, J. Ruffing*, P. Garrett*, R. Lindsay, F. Cosman. Clinical Research Center, Helen Hayes Hospital, West Haverstraw, NY, USA.

Data concerning prospective changes in bone mass in a college-aged physically active population, as a function of diet, menstrual function and oral contraceptives use are limited. In a cohort of 91 females entering the US Military Academy (average age=19; 75 Caucasian, 9 Asian, 7 African American), we prospectively evaluated the relative importance of menstrual function, use of oral contraceptives (OC) or depot medroxyprogesterone acetate (DMPA), eating disorders and calcium intake on bone mass accrual over 4 years. Menstrual function and use of OC or DMPA were assessed annually by questionnaire. Menstrual function was assessed as number of cycles per year. Calcium intake was determined by annual food frequency questionnaires. Eating disorders were assessed by using 3 subscales of the Eating Disorder Inventory: EDI-A (anorexia); EDI-B (bulimic tendencies) and EDI-D (body dissatisfaction) and the final score was divided into quartiles. A Lunar Dual x-ray absorptiometry (DPX-IQ) was used to assess bone mineral density (BMD) at the lumbar spine and total hip at baseline and annually. Slopes of change in spine and hip BMD were determined in each cadet over 4 years. The average daily calcium intake was 1073±420 mg. The highest quartile of EDI for the 3 scales had a mean of 38.5 with a range of 25-57, a value equivalent to that representing sub-clinical eating disorders. The average change in BMD over the 4 years was +0.3±3.9% in the spine and -1.0±4.5% in the hip; gains in BMD occurred at the spine in 50% and at the hip in 36% of cadets. In univariate analyses, bone gain in the spine, but not hip, was significantly and positively related to number of menstrual cycles (p=0.037). Both spine and hip BMD change were inversely related to EDI score (p<0.03) and DMPA use (p=0.007). There was no significant relationship between change in BMD at the spine or hip and OC use or calcium intake, although the average calcium intake was high in these women. Those women with EDI scores in the highest quartile had average change in spine BMD of -0.99% and hip BMD of -2.59%, as compared to the rest of the cohort that had a change of +0.74% in the spine and no change in the hip, after controlling for number of menstrual cycles, use of DMPA or OC, BMI and race. Females with an average of 0-9 menstrual cycles/year, over the four years, had spine BMD loss of -1.19%, compared to women with normal cycles (≥10/year) who gained 0.87%, after controlling for EDI, BMI and race. There was the same trend at the hip (-2.26 vs -0.52 respectively; p=0.09). Both sub clinical eating disorders and infrequent menstrual function can have significant detrimental effects on bone gain in young athletic women.

Disclosures: **J.W. Nieves**, None.

M014

Bone Accretion Elongation and Metabolic Activity during Skeletal Growth in the Rat. J. A. Horton*, J. T. Bariteau*, R. M. Loomis*, T. A. Damron*. Orthopedic Surgery, SUNY Upstate Medical University, Syracuse, NY, USA.

Introduction: Due largely to advances in cancer treatment, a population of long term survivors of pediatric solid tumors has been identified who present with osteopenia and signs of precocious osteoporosis as young adults. While the etiology for this morbidity is multifactorial, age at which therapy was begun relative to the stage of skeletal maturity has been implicated as one of several factors of this late effect. Developing prophylactic strategies requires use of animal models to evaluate the efficacy of such methods. The purpose of this study was to identify periods of high skeletal metabolic activity, growth and mineral accretion in the growing rat to serve as a foundation for further study of this clinical morbidity. Methods: With institutional approval, 6 male and 6 female 21 day old Sprague Dawley rats were obtained. The rats were subjected to weekly *in vivo* bone densitometry, radiography, blood collections, and body weight measurement. DXA derived bone mineral content and density was determined for both femurs and lumbar vertebra using the Piximus2 densitometer. Tibial lengths were measured from digitized plain film radiographs. Serum levels of osteocalcin were measured by IRMA as an indicator of osteoblastic bone formation. Serum levels of tartrate resistant acid phosphatase 5b were measured by ELISA, as an indicator of osteoclastic resorption. Results: An early phase of exponential bone mineral accretion, elongation and body weight gain was identified through 10 weeks of age ($R^2 > 0.96$). An inflection toward less aggressive tibial elongation was seen from 10 to 20 weeks of age where decay in the exponential growth rate was evident. A similar decay pattern was seen for both femoral and lumbar mineral accrual, though the plateau in bone density was reached 3 weeks later than the asymptote of elongation. Serum analysis indicated that osteoclastic activity remained relatively constant throughout the time observed, while osteoblast activity declined 3 fold from high levels of formation during exponential growth to a static level upon plateau. Temporal patterns of growth were not different between sexes though males tended to be larger in tibial length and body weight beyond 5 weeks of age (t test, $p < 0.04$). Discussion: The plotted curves of these femoral and lumbar BMD, tibial length over time were found to conform to the Gompertzian model of growth ($R^2 > 0.93$). Body weight also followed a similar decay pattern, though the failure to reach an asymptotic plateau is likely due to extraskeletal gain rather than maturative skeletal growth. Metabolic activity in the young rat favored bone formation, with the decline in osteoblast activity corresponding to the plateau in femoral and lumbar BMD.

Disclosures: J.A. Horton, None.

M015

Determinants of Consolidation of Peak Bone Mass in Young Women - Bath Cohort Study. S. Venkatchalam¹, D. Elvins^{*2}, I. Reading^{*3}, A. K. Bhalla², C. Cooper³. ¹Rheumatology, Cannock Chase Hospital, Cannock, United Kingdom, ²Royal National Hospital for Rheumatic Diseases, Bath, United Kingdom, ³MRC Environmental Epidemiology Resource Centre, Southampton, United Kingdom.

We had earlier identified that infant growth and physical activity in childhood are important determinants of peak bone mass in women at the age of 21 years, in a cohort of young women from Bath, UK born in 1968-69. We aimed to identify the determinants of consolidation of peak bone mass in these young women at the age of 31 years. We traced 90 of 153 women from the initial cohort and assessed bone mineral density (BMD) at 31 years of age by DXA (Hologic QDR4500A). We ascertained lifestyle factors like calcium intake, physical activity, smoking and alcohol consumption by questionnaire. Data were analysed by multiple regression with changes in BMD as the dependent variable. The mean percentage gain in lumbar spine BMD between 21 and 31 years of age was 1.7(4.4) and in the total hip BMD was 1.1(4.6). Current weight and weight at 21 years of age were significantly associated with lumbar spine ($r = 0.28$, $r = 0.28$) and total hip ($r = 0.31$, $r = 0.32$) BMD. Only the lumbar spine BMD correlated with height at 21 and 31 years of age ($r = 0.26$, $r = 0.27$). Weight of the women at 21 years of age was associated with increase in BMD at both lumbar spine ($r = 0.30$) and total hip ($r = 0.42$). It also significantly predicted gain in BMD at 31 years at both the spine ($\beta = 0.179$, $p = 0.022$) and the hip ($\beta = 0.263$, $p = 0.001$). However, weight at birth and conditional weights at 1 year, 5 or 10 years did not predict gain in BMD. Weight at 1 year conditional on birth weight negatively predicted total hip BMD and BMAD (bone mineral apparent density) at 31 years ($p = 0.006$, $p = 0.007$). Walking was significantly associated with only the total hip BMD at 31 years but did not predict consolidation. Calcium intake, smoking or alcohol consumption failed to determine consolidation in the women. Parity was negatively associated with the change in BMD and BMAD only at the lumbar spine over the decade. Our longitudinal study shows continuing gain in BMD in the third decade at both the lumbar spine and the total hip in young women. Their weight at the age of 21 years was the only significant determinant of consolidation of peak bone mass.

Disclosures: S. Venkatchalam, None.

M016

Genetic and Maternal Determinants of Bone Mass at the Humerus in Newborns. V. De Paola¹, D. Merlotti¹, L. Gennari¹, A. Cadirni^{*1}, A. Calabrò^{*1}, G. Martini¹, E. Cervo^{*2}, G. Buonocore^{*2}, S. Gonnelli¹, N. Dal Canto^{*1}, A. Montagnani^{*1}, R. Nuti¹. ¹Internal Medicine, Endocrine-Metabolic Sciences and Biochemistry, University of Siena, SIENA, Italy, ²Department of Pediatrics, Obstetrics and Reproductive Medicine, University of Siena, SIENA, Italy.

Bone metabolism is strongly influenced by heredity and environmental factors. Although some studies have reported a relationship between several candidate polymorphic genes and bone mineral density in adults, little is known concerning the genetic factors influencing bone mass in children. Moreover the role of environmental and genetic factors during intrauterine or early postnatal life is actually unknown. The aim of this study was to evaluate the role of maternal environmental factors and of the translation initiation site (FokI) polymorphism in the vitamin D receptor gene (VDR) in 200 newborns and their mothers. Quantitative ultrasound (QUS) parameters at distal diaphysis of humerus were assessed within three days of birth by using a Bone Profiler (IGEA, Italy), after an appropriate modification of the calliper and software. Newborn's anthropometric data, such as weight, length, head circumference and APGAR score at 3rd and 5th minute after birth were also collected. Phalangeal QUS measurements were performed in all mothers. In all subjects the amplitude-dependent speed of sound (AD-SOS) and the bone transmission time (BTT) QUS parameters were evaluated. Maternal AD-SOS at phalanges significantly correlated with newborn QUS parameters at the humerus. Interestingly, the correlation was higher in mother-daughter pairs than in mother-son pairs. No gender specific differences in body height or weight were observed. In contrast, head circumference and BTT (but not AD-SOS) were significantly higher in male than female newborns. Moreover head circumference, birth weight and height and BTT were significantly and positively related to gestational age. None of the newborn QUS parameters was influenced by maternal smoking or calcium intake. In newborns, BTT showed a significant positive correlation with birth weight and head circumference. A trend approaching statistical significance was observed between maternal Fok I genotype and BTT at birth. By contrast, Fok I genotype in newborns did not significantly correlate with neonatal QUS or anthropometric measurements at birth. In conclusion, results from this study suggest that newborn bone mass is, at least in part, genetically determined and that gender related differences in QUS parameters may exist at birth. Fok I polymorphism at the VDR gene does not seem to play a major contribution in the determination of body weight and ultrasound bone parameters at birth.

Disclosures: V. De Paola, None.

M017

Is my Arm Broken? The Likelihood of Forearm Fracture According to Age, Gender and Race among Children Undergoing Conventional Radiologic Evaluation. H. J. Kalkwarf, T. Laor*, L. Tague*, A. Roy-Chaudhury*, D. Bianchi*, J. Bean*. Cincinnati Children's Hospital Medical Center, Cincinnati, OH, USA.

Forearm fractures are common among children and adolescents. However not all children who are injured and are evaluated for a suspected fracture have a radiographically evident bone fracture. Little information is available regarding the probability of fracture among the children referred for radiographic diagnosis. The objective of this study was to determine the probability of a radiologically evident fracture among children undergoing radiography based on the child's age, gender and race. To collect our sample, we performed weekly queries of the Radiology Information System at a large regional pediatric hospital to identify all consecutive children who underwent a radiograph of the forearm or wrist during initial evaluation. Over 29 months, we identified 2994 patients ages 6-16 years. We excluded radiographs obtained for follow-up of fracture, identification of foreign bodies, motor vehicle related-injuries, injury at multiple skeletal sites, genetic disorders and identified chronic diseases. Fracture cases were those in which a fracture was identified in the radiology report. Controls included those in which no fracture was clearly evident. The sample was 54.5% boys, 45.5% girls, 71.6% white, 25.5% black and 2.9% other races. The largest number of radiographic evaluations occurred at ages 12-13 years among boys and at ages 9-10 years among girls. Boys were more likely than girls to have a fracture identified in the radiology report (64.7% vs. 52.0%, $p < 0.0001$), and whites and other races were more likely than blacks to have had a fracture identified (62.2% and 61.4% vs. 49.5%, $p < 0.0001$). The likelihood of fracture decreased with age. Among boys the proportion fractured decreased from 83% (207/250) at ages 6-7 years to 42% (83/196) at ages 15-16 years ($p < 0.0001$), and a plateau was evident between 10-14 years of age. Among girls, the respective decrease in the proportion fractured was from 77% (190/246) to 21% (20/95) ($p < 0.0001$), with less evidence of a plateau at interim ages. The absolute number of fractures was greatest among boys 6, 12 and 13 years of age and among girls between 6-11 years of age. We conclude that: 1) the probability of a radiologically evident fracture among children evaluated decreases with age, is lower in girls than boys, and is lower in blacks than whites; 2) peaks in fracture occurrence at the onset of adolescence is apparent in boys but not girls. These data may underestimate fracture rates in the community, because as children age we speculate that they are more likely to seek injury-related orthopedic care at adult facilities.

Disclosures: H.J. Kalkwarf, None.

M018

Accretion of Bone Quantity and Quality in the Developing Murine Skeleton. S. Judex¹, W. Little^{*1}, C. Rubin¹, L. Donahue², L. Miller³. ¹SBU, Stony Brook, NY, USA, ²Jackson Labs, Bar Harbor, ME, USA, ³BNL, Upton, NY, USA.

To meet the mechanical challenges during early development, the skeleton requires the rapid accretion of bone quantity as well as bone quality. Here, we describe early bone development in the murine skeleton and tested the hypothesis that changes in a number of morphological, chemical, and mechanical bone properties are controlled interdependently. Tibiae of female BALB mice were harvested at 8 time points (n=4 each) distributed between birth and 40d of age. Tibiae of 15mo old mice served as fully mineralized control specimens. High-resolution microCT determined bone area and volumetric material density of the tibial mid-diaphysis. Chemical and mechanical properties of the same region were analyzed by high-resolution in situ synchrotron infrared spectroscopy and nano-indentation, including phosphate/protein content, carbonate/protein content, collagen cross-linking, and Young's modulus. Relations between morphological, chemical, and mechanical properties across different time points were tested by non-parametric rank correlations. Cortical bone area increased linearly (tau=0.87) by 30-fold over the first 40d of post-natal growth, reaching 60% of its adult (15mo) areal properties. Concomitantly, material density increased linearly (tau=0.88) by 46%. The phosphate/protein ratio in 40d old mice was 90% greater than in 1d old mice (tau = 0.70 for linearity) and 30% smaller than in 15mo old mice. In contrast, the carbonate/protein ratio showed a smaller (28%) and highly non-linear increase over the first 40d of life. Collagen cross-linking was not altered over time. Spatial variability in chemical properties across the mid-diaphysis was very high for the early time points and declined over time. Similarly to changes in bone area, Young's modulus increased dramatically with age and reached 87% of its adult value at 40d of age. Cortical bone area, volumetric mineral density, phosphate/protein ratio, and carbonate/protein ratio all showed significant correlations with the reduced elastic modulus (tau = 0.4-0.6). These data indicate that the mineralization of new bone during early skeletal development is at least one order of magnitude slower than during the later adolescent stages of growth. Considering that murine long bone development covers at least three distinct morphological stages during the first 40d of life, the linearity by which many of the morphological, chemical, and mechanical matrix properties are acquired is remarkable. Future more detailed analyses with these high-resolution in situ measurement techniques may provide insight into the chemical, cellular, and molecular factors by which bone modulates its quality and quantity.

Disclosures: *S. Judex, None.*

M019

Total Body Bone Mineral Content in Young Children: Influence of Head Bone Mineral Content. J. M. Eichenberger Gilmore^{*1}, S. M. Levy¹, T. A. Marshall^{*1}, E. M. Letuchy^{*2}, T. L. Burns^{*3}, K. F. Janz^{*4}, M. C. Willing², J. C. Torner^{*2}. ¹Preventive and Community Dentistry, University of Iowa, Iowa City, IA, USA, ²Epidemiology, University of Iowa, Iowa City, IA, USA, ³Program in Public Health Genetics, University of Iowa, Iowa City, IA, USA, ⁴Health and Sports Studies, University of Iowa, Iowa City, IA, USA, ⁵Pediatrics, University of Iowa, Iowa City, IA, USA.

Assessment of bone health in children requires acknowledgement of the contributions of bone mineral content (BMC) from various body compartments. Reference values are typically presented as age or body size adjusted values. An important consideration when evaluating these measures is the contribution of the head BMC during childhood growth. Our objective was to describe the contribution of head BMC relative to whole body BMC (WB BMC) and determine the change in contribution of head BMC over time among participants of the Iowa Fluoride Study. Analysis included 981 whole body scans (466 M, 515 F) of children age 4.5 - 10.5 years. Four hundred twelve children (192 M, 220 F) had baseline and 3 year follow-up scans. BMC was measured by DXA using a Hologic QDR-2000 (Waltham, MA) in the array-beam scanning mode (software version 5.60A). SAS MIXED procedure was used to compare WB BMC, head BMC, subtotal BMC (WB BMC - head BMC), and % head BMC for each age group (4.5-5.5 years, 5.5-6.5 years, 7.5-8.5 years, 8.5-9.5 years, and 9.5-10.5 years) incorporating correlations for observations on the same person. The contribution of head BMC decreased from 51% to 32% WB BMC from youngest to oldest (Table 1). Repeat scans revealed an increase in all body size parameters (height, weight, WB BMC, head BMC and subtotal BMC) with a 4.4% decrease in the contribution of head BMC per year (Table 2). The results suggest care must be used when comparing individual bone scan data to reference values. Further statistical interpretation of body compartment contributions to WB BMC is warranted.

Table 1. Least Square Means by Age Group.

Age group, years	n	WB BMC, gm		Head BMC, gm		Subtotal BMC, gm		% Head BMC	
		Mean	SE	Mean	SE	Mean	SE	Mean	SE
4.5-5.5	348	479	7	239	2	239	7	51.0	0.3
5.5-6.5	111	557	11	257	2	300	10	47.5	0.4
7.5-8.5	206	817	9	295	2	522	8	36.8	0.3
8.5-9.5	246	919	8	308	2	610	8	34.7	0.3
9.5-10.5	70	1023	15	317	3	707	14	31.6	0.5

Table 2. Change per Year for Repeated Observations (N = 412).

Variable	Mean	SD	Minimum	Maximum
Time between scans, year	3.4	0.6	2.1	5.5
Change per Year:				
Height, cm	6.4	0.7	3.2	8.8
Weight, kg	3.5	1.7	0.9	14.8
WB BMC, gm	112	30	56	244
Subtotal BMC, gm	95	29	43	229
Head BMC, gm	17	5	-1	37
% Head BMC	-4.4	-1.0	-7.8	-1.7

Disclosures: *J.M. Eichenberger Gilmore, None.*

M020

A Prospective Analysis of Geometric Changes in the Proximal Femur in Young Female Gymnasts. E. M. Laing¹, C. M. Modlesky², A. R. Wilson^{*1}, D. B. Hall^{*3}, T. J. Beck⁴, R. D. Lewis¹. ¹Foods and Nutrition, The University of Georgia, Athens, GA, USA, ²Health, Nutrition and Exercise Science, University of Delaware, Newark, DE, USA, ³Statistics, The University of Georgia, Athens, GA, USA, ⁴Radiology, Johns Hopkins Medical Institute, Baltimore, MD, USA.

Assessment of bone mineral accrual with exercise is limited because important changes in the geometric properties of bone may occur and go undetected. Changes in the strength indices of the intertrochanteric (IT) and shaft (S) regions of the proximal femur (PF) were examined in prepubertal females, 4-8 yrs of age, who selected to perform recreational gymnastics (GYM; n=65), nongymnastic activities, or no organized activity (CON; n=78). High-level gymnasts advancing to competition (HLG; n=9), low-level nonadvancing gymnasts (LLG; n=56) and CON were compared. Participants had essentially no lifetime history of organized athletic participation (<12 wks). Pubertal maturation was assessed annually by a physician. Non-dominant PF scans were obtained every 6-mo using DXA (Hologic QDR-1000W). BMD (g/cm²) and bone strength indices [cross sectional area (CSA; cm²) and section modulus (Z; cm³)] were calculated using the hip structural analysis program. Baseline differences between groups were determined using independent samples t-tests. Repeated measures ANCOVA (covariates: race, age, socio-economic status, initial strength value, calcium intake, height, weight and final breast stage) was used to assess changes over 4 consecutive 6-mo time periods. At baseline, GYM were shorter, lighter, and had lower IT Z compared with CON (p<.05), whereas HLG did not differ from LLG in any measure. Group x time interactions were found for S BMD (p=.098) and CSA (p=.035). Interactions between group and final breast stage were found for IT (p=.036) and S (p=.001) BMD, IT (p=.003) and S (p=.003) CSA and IT (p=.009) and S (p=.038) Z. In these cases significant differences between groups where GYM>CON were found in high maturational status subjects for IT BMD (p=.099), IT CSA (p=.010), IT Z (p=.019), S BMD (p<.025 at each measurement occasion), S CSA (p<.074 at each measurement occasion), and S Z (p=.032). HLG remained prepubertal throughout the study and showed no geometric differences in the PF compared to LLG or CON. These results indicate that recreational artistic gymnastics initiated in prepubertal females conferred moderate geometric structural benefits at the PF. GYM who advanced in pubertal stage at the conclusion of the study demonstrated the greatest strength benefits over time compared to CON.

Disclosures: *E.M. Laing, None.*

M021

Body Fatness and Bone Properties in Prepubertal Females: A Two Year Study. N. K. Pollock¹, E. M. Laing¹, A. R. Wilson^{*1}, C. M. Modlesky², T. J. Beck³, R. D. Lewis¹. ¹Foods and Nutrition, University of Georgia, Athens, GA, USA, ²Health, Nutrition and Exercise Science, University of Delaware, Newark, DE, USA, ³Radiology, Johns Hopkins Medical Institute, Baltimore, MD, USA.

Overweight and obese children are thought to be at high risk for skeletal fractures. Whether this is the result of poor bone mineral acquisition is equivocal. The purpose of this prospective study was to explore the effects of body fatness on changes in bone area (BA), BMC and femur geometry in prepubertal females. Fat mass (FM, kg), percent fat (%FAT), fat-free mass (FFM, kg), bone area (BA) and BMC of the total body (TB), lumbar spine (LS), total proximal femur (TPF) and forearm were determined using DXA (Hologic, QDR 1000-W). Structural properties of bone including BMD (g/cm²), cross sectional area (CSA, cm²) and section modulus (Z, cm³) of the narrow neck, intertrochanteric (IT) and shaft (S) regions of the TPF were assessed every 6-mo using the hip structural analysis program. Baseline differences between groups and 24-month change data were determined using one-way ANOVA and repeated measures ANCOVA, respectively. At baseline, groups were classified by %FAT: non-obese (%FAT<25, n=32) and obese (%FAT≥30, n=27). Although similar in maturation, obese females had significantly higher values for age (6.9 vs. 5.7 yrs), weight (32.1 vs. 21.3 kg), height (125.9 vs. 116.2 cm), FM (4.1 vs. 12.2 kg) and FFM (18.2 vs. 15.7 kg) compared to non-obese at baseline (p<0.05; η²>0.09). Over 24-mo, the obese gained more weight and FFM (p<0.01; η²>0.25) compared to non-obese. Baseline BMC, CSA and Z of all measured sites was significantly higher in the obese (p<0.05; η²>0.10) but after adjusting for age and height, differences between groups were only observed for TB BA and BMC (p<0.01; η²>0.11). 24-mo changes in TB BA and BMC, as well as forearm BA and S CSA were significantly greater in the obese (p<0.04; η²>0.06), however once corrected for FFM, these differences no longer remained, except for forearm BA (p=0.03; η²=0.05). Whether the changes in bone properties observed in obese vs. non-obese prepubertal females are sufficient to accommodate the observed weight gain is unknown. Future studies with site-specific estimates of bone material and structural properties in obese vs. non-obese children are warranted.

Disclosures: *N.K. Pollock, None.*

M022

Primary Human Osteoblasts Show Enhanced Differentiation upon Treatment with BMPs. W. A. Grasser, K. A. Riccardi*, V. M. Paralkar. CVMD Osteoporosis, Pfizer Global Research and Development, Groton, CT, USA.

Bone morphogenetic proteins (BMPs) are members of the transforming growth factor-beta (TGF- β) superfamily. They were initially identified by their ability to induce endochondral bone formation at ectopic sites which suggested an important role for these proteins in skeletogenesis. The differentiation of osteoblasts is regulated by various local factors in an autocrine and/or paracrine fashion, and a number of studies have shown that BMPs can have an effect on the recruitment, proliferation and differentiation of osteoblast progenitors. In addition, it has been demonstrated that BMPs can enhance the expression of markers of the mature osteoblast phenotype such as, alkaline phosphatase (AP), collagen synthesis, osteocalcin expression and the ability of the cells to form mineralized matrix. Studies with murine pluripotent stem cells have demonstrated an increased expression of osteoblastic phenotype upon treatment with BMPs. However, surprisingly little work has been done on the effects of BMPs on human cell systems. The clinical doses of BMP required to show bone healing are an order of magnitude greater than the doses observed in animal studies. Although various hypotheses for this discrepancy have been proposed our scientific understanding of this dose response remains poor. In this study, we wanted to develop a human cell culture system using primary human osteoblasts (HOB), characterize known markers of osteoblast expression and examine the effect of BMPs and in particular BMP-6 on these cell cultures. Treatment with rhBMP-6 accelerates cell differentiation as indicated by the formation of mineralized nodules by day 18 of culture versus 28 to 30 days in vehicle treated cultures. In addition, AP activity is dramatically increased beginning at Day 10 and is paralleled by a similar increase in the expression AP message as measured by qRT-PCR. The expression of BMP-6 message is down regulated in cultures that were treated with BMP-6 indicating the ability of BMP-6 to auto-regulate its own expression.

Disclosures: **W.A. Grasser, None.**

M023

In Vivo Imaging of Adenoviral vs. Lentiviral Gene Therapy in Two Bone Formation Models. B. T. Feeley¹, A. H. Conduah^{*1}, O. Sugiyama¹, N. Liu^{*1}, M. J. Jo^{*1}, I. S. Y. Chen^{*2}, J. R. Lieberman¹. ¹Orthopaedic Surgery, University of California, Los Angeles, Los Angeles, CA, USA, ²Dept of Microbiology, Immunology, Molecular Genetics and Medicine, UCLA AIDS Institute, University of California, Los Angeles, Los Angeles, CA, USA.

The clinical use of recombinant proteins and regional gene therapy are promising techniques to enhance bone formation in large bone defects that would be difficult to treat with allograft or autograft bone stock. The selection of the appropriate gene therapy strategy depends on the clinical scenario. We have previously demonstrated that lentiviral mediated delivery of BMP-2 produced robust bone formation *in vivo*. In this study, we compared the temporal expression patterns of adenoviral and lentiviral mediated gene therapy in two bone formation models using *in vivo* molecular imaging techniques. Rat bone marrow cells (RBMC) were co-transduced either lentiviral or adenoviral vectors containing the cDNAs for BMP-2 or luciferase, driven by the murine leukemia virus (MLV) promoter. *In vitro*, adenoviral expression of BMP-2 and luciferase in RBMCs peaked at 1 week, and was able to be detected by ELISA or luciferase assay, respectively, for 4 weeks after initial transduction. In contrast, lentiviral mediated expression of BMP-2 and luciferase was sustained in culture for 3 months. Luciferase activity correlated with BMP-2 expression *in vitro* ($R^2=0.83$). Using a cooled charged coupled device (CCD) camera, we were able to demonstrate prolonged *in vivo* gene expression in both a murine hindlimb muscle pouch and radial defect model. Adenoviral vectors expressed target gene (luciferase) expression for up to 21 days in both models, but lentiviral vectors expressed target gene expression for 3 months *in vivo* in both the hindlimb muscle pouch and radial defect model. Co-transduction with both the luciferase reporter gene and BMP-2 target gene did not affect BMP-2 production *in vitro*, or bone formation *in vivo*. In the radial defect model, 9/10 animals treated with Ad-BMP-2+Luc healed, and 9/10 animals treated with Lenti-BMP-2+Luc healed. There was no detectable difference in the amount of bone formed between the adenoviral and lentiviral groups with either histologic or radiographic analysis. These results suggest that lentiviral mediated delivery of BMP-2 can induce long term *in vitro* and *in vivo* gene expression, which may be beneficial when developing tissue engineering strategies to heal large segmental or cavitary bone defects. Our data also suggests that CCD imaging is a successful technique to follow *in vivo* gene therapy in bone formation models.

Disclosures: **B.T. Feeley, None.**

M024

C/EBP Homologous Protein (CHOP) Interacts with Cyclic AMP Responsive Element Modulator (CREM) and Enhances Bone Morphogenetic Protein (BMP)/Smad Signaling. R. C. Pereira, V. Deregowski, S. Rydzziel, E. Canalis. Research, Saint Francis Hospital and Medical Center, Hartford, CT, USA.

CCAAT/enhancer binding proteins (C/EBPs) regulate cell fate and gene regulation. C/EBP homologous protein (CHOP) forms heterodimers with classic C/EBPs and additional transcription factors, preventing their binding to target DNA sequences. In ST-2 cells, CHOP suppresses adipogenesis and induces osteoblastogenesis by sensitizing these cells to the effect of BMP-2 on Smad, but not on MAP kinase signaling. CHOP overexpression sensitizes a transiently transfected 12xSBE-Oc-pGL3 construct, containing 12 repeats of a

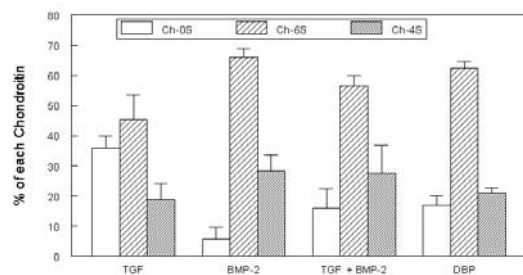
Smad binding site, to the effect of BMP-2, without modifying the phosphorylation of Smad 1/5/8. This suggests that indirect mechanisms are involved in the sensitization of the BMP-2 effect on transactivation. Accordingly, co-immunoprecipitation experiments and confocal microscopy failed to reveal direct interactions or co-localization of CHOP and Smad 1 after BMP-2 treatment. The effect of CHOP on BMP-2/Smad signaling did not require prolonged cellular exposure to CHOP, since acute co-transfection of a vector where CHOP was expressed under the control of the cytomegalovirus promoter enhanced the BMP-2 induced transactivation of the 12xSBE-Oc-pGL3 construct. However, the dimerization domain of CHOP was required since a CHOP dimerization mutant had no effect, also suggesting that CHOP acts indirectly, possibly by binding an inhibitor of transactivation. To test this possibility, we analyzed interactions and possible heterodimerization of CHOP with members of the cyclic AMP responsive element (CRE) binding protein (CREB)/activator of transcription (ATF) family of transcription factors, known to interact with CHOP and regulate transcription. Electrophoretic mobility shift assays of nuclei from CHOP overexpressing and vector transduced ST-2 cells, revealed that binding to a labeled CRE consensus sequence was decreased in CHOP overexpressing cells and supershift assays revealed that CRE modulator (CREM), but not ATF-1, ATF-3 or ATF-4 antibodies shifted the complex. To explore mechanisms involved, the expression and actions of CREM α , β , and γ were determined. Control and CHOP overexpressing cells expressed CREM α , β , and γ , and the level of expression increased as CHOP overexpressing cells differentiated in culture. In an initial co-transfection experiment with CREM α , β , and γ expression constructs, CREM β reduced the stimulatory effect of CHOP on the transactivation of 12xSBE-Oc-pGL3. In conclusion, CHOP enhances osteoblastic differentiation by sensitizing the BMP/Smad signaling pathway, and interactions with the transcriptional repressor CREM appear central to this effect.

Disclosures: **R.C. Pereira, None.**

M025

Similarity of Chondroinduction by Combined rhBMP-2/TGF β or Demineralized Bone *In Vitro*. J. Glowacki, S. Mizuno, S. Zhou. Orthopedic Surgery, Brigham and Women's Hospital, Boston, MA, USA.

Demineralized bone implants are widely used for skeletal repair and reconstruction. Demineralized bone powder (DBP) in a 3D porous collagen sponge chondro/osteoiduces target human dermal fibroblasts (hDFs) *in vitro*. Multiple pathways are signaled by DBP and they differ from those elicited by BMP-2. In this study, we tested the hypothesis that a combination of BMP-2 and TGF β 1 would approximate effects of DBP. Sponges were used either plain or with 3 mg DBP with 10^6 hDFs per sponge and cultured in DMEM with 1% heat-inactivated FBS. In one set of experiments, factors were added to the medium: 10 ng/ml TGF- β 1 and/or 100 ng/ml rhBMP-2. DBP, TGF β 1, and the combination of TGF β 1/BMP2 upregulated TGF β /Smad target genes (*TGF β 1*, *PAL-1*, *IGFBP3*) between 100 and 500%; as expected, BMP2 had little effect on those targets that are mediated through TGF β type I receptor (ALK-5). On the other hand, DBP and BMP2 upregulated the BMP/Smad target gene *ID3*. Cotreatment with a specific inhibitor of ALK-5 (SB431542, 10 μ M) antagonized the stimulation by DBP and TGF- β 1 on *TGF β 1*, *IGFBP3*, but not of BMP-2 on *ID3* gene expression. Thus, some of DBP's effects are mediated through TGF β /Smad signaling and some are mediated through BMP/Smad signaling. In another set of experiments, BMP-2 (6 μ g) and/or TGF β 1 (40 ng) were delivered in a square of absorbable collagen felt (identical to that used clinically) that was inserted into a collagen sponge for comparison with DBP-containing sponges. Sponges were cultured for 7 days for histological and biochemical analysis of chondroitin sulfate by fluorophore-assisted carbohydrate electrophoresis (FACE). Histological analysis showed metachromatic extracellular matrix (ECM) around cells in proximity to DBP and around cells within felt that contained the combination of rhBMP-2 and TGF β 1, and, to a lesser degree, that with only TGF β 1. FACE showed that sponges treated with DBP had the greatest content of Chondroitin 4- and 6-sulfate (Ch-4S and Ch-6S, 113 ± 18 ng, $p=0.023$). Cells treated with TGF produced more unsulfated (Ch-0S) than did the other groups. The cartilage-like distribution of Ch-0S, 4S, and 6S was similar for cells treated with DBP or the combination of BMP/TGF β (Figure). These data indicate that, although neither TGF β 1 nor BMP induced production of cartilage-specific ECM, a combination of TGF β 1 and BMP elicited effects in hDFs similar to those by DBP.



Disclosures: **J. Glowacki, None.**

M026

BMP3 Signals through SMAD2 in MC3T3 Cells. B. Sun^{*1}, J. Pretorius^{*2}, E. Valente^{*2}, D. L. Lacey¹, W. S. Simonet¹, W. G. Richards^{*1}. ¹Metabolic Disorders, Amgen, Thousand Oaks, CA, USA, ²Pathology, Amgen, Thousand Oaks, CA, USA.

BMP3 was first characterized as a protein with osteogenic activity isolated from bovine bone. However, this activity was called into question when BMP3 null mice were found to have increased bone mass. The cause of this apparent discrepancy is uncertain, but may be related to the complex biology of this molecule. In fact, even though BMP3 is a member of the TGF β family, analysis of a phylogenetic tree of this superfamily reveals that BMP3 does not group to the clade containing the osteogenic BMPs, but appears to constitute its own distantly related group along with BMP3b. To develop our understanding of this molecule and its involvement in bone biology, we studied the expression of BMP3 and the signaling pathways BMP3 utilizes in MC3T3.E1/C4 cells. BMP3 expression was studied by in situ hybridization in embryonic and adult mice. In embryonic bone, BMP3 was detected in perichondrium and mesenchymal condensations around developing bones, and in areas of ossification. In adult bone, BMP3 expression was detected in osteoblasts throughout bone including areas around the growth plate, in endosteal lining of cortical bone and in trabeculae of the epiphysis and diaphysis. To explore the signaling pathways used by BMP3 we first set out to replicate published data, which demonstrated that BMP3 could inhibit BMP2 induced osteogenic differentiation of W20 cells. We demonstrated a similar response in MC3T3.E1/C4 cells with conditioned medium containing BMP3 and with recombinant BMP3. This inhibitory response was only evident in the presence of BMP2, as inclusion of BMP3 alone in cultures of differentiating MC3T3 cells had no effect on the ability of these cells to produce the differentiation markers alkaline phosphatase and osteocalcin. We next addressed how BMP3 might engender this anti-osteogenic response. K. Lyons proposed several mechanisms to explain the observed anti-osteogenic effects of BMP3, including the involvement of SMAD signaling. We used phospho-SMAD specific antibodies to study SMAD signaling in MC3T3 cells treated with BMP3. In MC3T3 cells treated with BMP3 we were not able to detect phosphorylation of SMAD1, a BMP SMAD, but did detect phosphorylation of SMAD2, a TGF β SMAD. In addition, we demonstrated that BMP3 was capable of binding human activin receptor IIB and that BMP3 activated a TGF β reporter construct in C2C12 cells, but did not activate a BMP reporter construct in the same cell line. These data provide support for the hypothesis put forth by Lyons that the anti-osteogenic activity of BMP3 may result from the use of the TGF β /activin signaling pathway and potential sequestration of SMAD4 from, and potential inhibition of, the BMP osteogenic pathway.

Disclosures: **B. Sun**, None.

M027

LMP-1 Interacts with Smurf1 and Potentiates Cellular Responsiveness to BMP-2. S. Sangadala, Y. Liu, M. Viggeswarapu, S. D. Boden, L. Titus. Orthopaedics, Emory University, Decatur, GA, USA.

BMPs initiate osteogenic differentiation and maintenance of cell lineage while inhibiting myogenic and adipogenic differentiation pathways. The activity of BMPs is regulated through alteration in steady state levels of various key intracellular signaling proteins. LMP-1, an intracellular osteogenic factor, was observed to significantly increase the responsiveness of mesenchymal stem cells (MSCs) to BMP-2 by inducing bone nodule mineralization. Additional evidence of LMP-1/BMP-2 synergy was seen by induction of Dlx5 mRNA by overexpression of LMP-1 in BMP-2-treated MSCs. To determine the mode of action of LMP-1 we designed biochemical pull-down assays to identify key intracellular proteins that interact with LMP-1. Recombinant LMP-1 was labeled with SBED-biotin transfer agent and incubated with nuclear proteins. Biotin transfer to target interacting proteins was initiated by photo-activation. The linked proteins were de-coupled by reduction. Biotinylated target proteins were enriched, detected by western blots and identified by MALDI-TOF of in-gel tryptic digests of target proteins. Smad Ubiquitin Regulatory Factor 1 (Smurf1), was identified as key binding protein along with some cytoskeletal proteins. The identity of Smurf1 as binding protein, was verified based on molecular size (85 kDa), immunoreactivity with Smurf1 antibody and tryptic peptide mass profile. To determine if the interaction of Smurf1 occurs with endogenous LMP-1 we performed immunoprecipitations on nuclear extracts of mesenchymal stem cells using LMP-1-specific antibodies. The immunoprecipitates contained both Smurf1 and LMP-1 confirming that they co-associate in physiological conditions. To test our working hypothesis that LMP-1 potentiates BMP-2 response by protecting Smad1 from Smurf1-directed proteosomal degradation, we performed overexpression of LMP-1 in the presence or absence of BMP-2 treatment and determined the levels of phospho-Smad1. The level of phospho-Smad1 showed dramatic increase in cells overexpressing LMP-1 upon BMP-2 treatment. Further studies are underway to determine which domains of LMP-1 and Smurf1 are involved in binding interaction as well as the effect of their interaction on steady-state levels of other Smads targeted by Smurf1.

Disclosures: **S. Sangadala**, None.

M028

Desmoid Tumor with Ossification in Chest Wall: Possible Involvement of BAMBI Promoter Hypermethylation in Metaplastic Bone Formation. S. Kitazawa¹, R. Kitazawa¹, T. Kondo¹, K. Mori^{*1}, C. Obayashi^{*2}, T. Yamamoto^{*3}. ¹Division of Molecular Pathology, Kobe University Graduate School of Medicine, Kobe, Japan, ²Division of Diagnostic Pathology, Kobe University Graduate School of Medicine, Kobe, Japan, ³Department of Orthopaedic Surgery, Kobe University Graduate School of Medicine, Kobe, Japan.

Since the osteoporosis-pseudoglioma syndrome attributed to inactivating mutations in the Wnt receptor, LRP5, shows reduced bone mass, and conversely, since autosomal-dominant high bone mass traits attributed to activating mutations in LRP5 show increased bone mass, the classical Wnt/beta-catenin/LEF1 signaling pathway must play important roles in regulating bone density by modulating postnatal osteoblast proliferation. On the other hand, somatic mutations of the beta-catenin gene that result in the stabilization and accumulation of beta-catenin by escaping from ubiquitination, have been demonstrated as causative genetic alterations in desmoid-type fibromatosis (DF). DF, therefore, provides an in vivo constitutive active model for the classical Wnt/beta-catenin/LEF1 signaling pathway in mesenchymal cells. Here, we describe a sporadic case of DF with metaplastic ossification in the left anterolateral chest wall occurred in a 43-year-old man. Histopathological specimens were used for immunohistochemical, genetic and methylation studies. To explain the mechanism of metaplastic bone formation, we hypothesized that in the presence of active wnt signaling, mesenchymal cells transdifferentiate into an osteoblastic phenotype when additional events leading to the activation of BMP signaling occur either through the increased expression of BMPs, their receptors and intercellular signal transducers or the decreased expression of the inhibitors of BMP signaling. Immunohistochemically, the expression of BMP and activin membrane-bound inhibitor (BAMBI) was selectively diminished at the site of the ossifying focus, whereas that of BMP-2 and its receptor remained unchanged. We examined the methylation status of the BAMBI promoter by methylation-specific PCR, and observed CpG island hypermethylation in the promoter specifically in the microdissected samples taken from the ossifying focus, indicating that selective reduction of BAMBI expression is probably due to the selective hypermethylation of the BAMBI promoter region in the ossifying focus. Since both BMP and classical Wnt/beta-catenin/LEF1 signaling cooperatively and mutually induce differentiation of mesenchymal cells into osteoblastic cells and promote bone formation, the epigenetic event leading to the enhanced responsiveness to BMP signaling may play a crucial role in the formation of metaplastic bone.

Disclosures: **S. Kitazawa**, None.

M029

HSPGs Mediated BMP4 Signaling Is Disrupted in Fibrodysplasia Ossificans Progressiva Lymphoblastoid Cells. M. P. O'Connell^{*1}, P. C. Billings^{*1}, J. L. Fiori^{*1}, H. I. Roach^{*2}, E. M. Shore¹, F. S. Kaplan¹. ¹Orthopaedic Surgery, University of Pennsylvania, Philadelphia, PA, USA, ²University Orthopaedics, University of Southampton, Southampton, United Kingdom.

Fibrodysplasia ossificans progressiva (FOP), a rare autosomal dominant genetic disorder characterized by congenital malformations of the great toes and progressive heterotopic ossification of soft connective tissues, is associated with dysregulation of the bone morphogenetic protein (BMP) signaling pathway. Cell surface heparan sulfate proteoglycans (HSPGs), known as syndecans and glypicans, are ubiquitously expressed in almost every cell type and are capable of binding or affecting a range of molecules through interactions with their heparan sulfate side chains (HSSCs). BMP and their secreted antagonists have HSSC binding domains. We hypothesize that HSPGs play a role in modulating BMP4 signaling in FOP and control cells via interactions with BMP ligands and antagonists. Control and FOP lymphoblastoid cells (LCLs) were treated with heparinase III to specifically remove HSSCs, and with phosphatidylinositol-specific phospholipase C (PI-PLC), to remove GPI-linked core proteins (glypicans). Cells were subsequently treated with BMP4 and BMP signaling was monitored by following expression of the BMP early response genes ID1 and ID3 (inhibitors of DNA binding and differentiation) by real-time PCR. Treatment with PI-PLC had little if any effect on BMP signaling in control or FOP cells. In contrast, heparinase treatment resulted in a statistically significant reduction in expression of both ID1 and ID3 in BMP treated control LCLs but surprisingly not in BMP treated FOP cells. The HSSC binding domain on the BMP4 molecule resides in an independent region to the receptor binding site. Therefore, BMP4 could simultaneously bind to the BMP receptor type IA (BMPRIA) and cell surface HSPGs. We suggest that HSPGs act as ligand reservoirs for BMP4 that promote BMP signaling under normal conditions. Under conditions of receptor over-abundance, as in FOP cells, there is little or no contribution of HSPGs to BMP signaling. At present it is unknown if this effect is specific to one type of HSPG, to subtypes of HSPGs, or generalized to the entire population of HSSC containing molecules. Our data demonstrates that HSPG play an important role in BMP4 signaling but that role can be negated if a dysregulation exists in the signaling pathway, as in FOP.

Disclosures: **M.P. O'Connell**, None.

M030

Matrix Vesicles Are Carriers of Bone Morphogenetic Proteins (BMPs) and Non-Collagenous Matrix Proteins. N. N. Nahar^{*1}, L. R. Missana^{*2}, R. Garimella¹, S. E. Tague^{*1}, H. Clarke Anderson¹. ¹Department of Pathology, University of Kansas Medical Center, Kansas City, KS, USA, ²Oral Pathology, Tucuman University Dental School, Tucuman, Argentina.

A study was undertaken to confirm the presence of bone morphogenetic proteins (BMPs) 1 through 7 and non-collagenous matrix proteins, bone sialoprotein (BSP), osteopontin (OPN), osteocalcin (OC) and osteonectin (ON) in isolated matrix vesicles (MVs) of rat growth plate. Besides the well-defined role of MVs in the initiation of biomineralization in growth plate, developing bone, tendon and predentin, MVs of the growth plate could serve as carriers of morphogenetic information, such as BMPs. MVs thus could be involved in signaling uncommitted osteoprogenitor cells subjacent to the growth plate to undergo osseous differentiation. It is likely that MVs receive BMP proteins from the BMP-enriched cytoplasm of maturing chondrocytes of the growth plate during budding of the MVs into the matrix. BMPs carried in MVs would be released from the matrix at the base of the growth plate during cartilage resorption and vascularization. BMPs carried in MVs and released from the base of the growth plate could stimulate not only osteoblastic activity, but also osteoclastic resorption. MVs were isolated by differential ultracentrifugation from collagenase-digested rachitic rat tibial and femoral growth plate cartilage. The presence of BMPs 1-7, BSP, OPN, OC and ON was evaluated in the isolated MVs by western blot analysis. BMP-2 and BMP-4 were detected at the expected 18 KD as a monomeric molecular weight and BMP-6 appeared as two bands at an expected 15 and 18 KD level. BMP-3 was detected as single band at approximately 66 KD, which corresponds to a similar band of rhBMP-3. BMP-5 was identified as a dimer at 36 KD, a homodimer at 52 KD and another higher KD band that could be a homodimer with the mature protein at 70 KD. BMP-7 was detected at the expected 54 KD molecular weight with other bands that could represent a dimer at 36 KD, a pro-domain at 40 KD and a hemidimeric form at 70 KD, the latter consists of a mature dimer with a pro-domain. Immunoblots of BMP-1 showed the unprocessed precursor at approximately 111 KD and two splice variants were seen approximately at 79 KD and 34 KD. Non-collagenous proteins, BSP, OPN, OC and ON were detected at approximately 81 KD, 80 KD, 65 KD and 40 KD respectively. Thus our data confirmed the presence of BMP-1 through 7 and non-collagenous proteins, BSP, OPN, and OC and ON in isolated rat matrix vesicle. It is suggested that MVs may carry morphogenetic information, thus promoting differentiation of the lower growth plate and subjacent, newly forming bone. The non-collagenous matrix proteins in MVs could function to promote or regulate mineral-initiation by MVs.

Disclosures: N.N. Nahar, None.

M031

Prostaglandin E2 EP4 agonist (ONO-4819) Accelerates BMP-Induced Osteoblastic Differentiation via PKA Signaling. K. Nakagawa^{*}, Y. Ohta^{*}, Y. Imai, C. Nomura-Furuwatari^{*}, K. Takaoka. Department of Orthopaedic Surgery, Osaka City University Graduate School of Medicine, Osaka, Japan.

The anabolic effects of EP4 agonist (ONO-4819) on bone formation have been reported. In our previous *in vivo* study, we reported that ONO-4819 also accelerated BMP-induced ectopic new bone mass without changing systemic bone mass or density. However, the mechanism of ONO-4819 associated with BMP signaling is unknown. In this study, we attempted to clarify how ONO-4819 accelerates the BMP signaling in osteogenic cells in an *in vitro* system. **Materials and Methods:** Bone marrow derived stroma cells (ST2) with the capacity to differentiate into the osteoblastic lineage in response to exogenous BMP-2 (100ug/ml) stimulation were used. First, we examined the specificity of the EP4 agonist action towards BMP action by measuring the rate of change of differentiation markers, the change in Osterix expression by real-time RT-PCR analysis and alkaline phosphatase (ALP) activity in the presence or absence of BMP-2. Total RNA was extracted from the cells treated with BMP-2 and/or ONO-4819 for various periods of time and the expression levels of Osterix were assessed by real time RT-PCR. ALP activity was measured two days after the drugs were applied. To estimate the interaction between BMP signaling and PKA, we used the PKA inhibitor (H89) pre-treatment. Next, whether ONO-4819 accelerates or maintains the phosphorylation of regulatory Smads (Smad1/5/8) or not, we performed the western blot analysis using anti-phosphorylated Smad1/5/8 for the lysates from the cells treated with or without BMP-2 and/or ONO-4819. **Results:** Both ALP activity and Osterix expression in the ST2 cells were elevated significantly following BMP-2 treatment for a period of 48 hours. This elevation was further elevated by the addition of the EP4 agonist (10^{-9} - 10^{-5} M range). However, treatment of the cells with EP4 agonist alone for 48 hours did not alter the markers. The accelerated BMP action by the ONO-4819 was abolished by pre-treatment with PKA inhibitor, H89. Since levels of phosphorylated regulatory Smads (Smad1/5/8) were not changed by ONO-4819 in Western blot analysis using anti-phosphorylated Smad1/5/8, the accelerated BMP action by the EP4 agonist may be a result of cross-talk between the BMP (Smads) and PKA signaling pathways on the target genes of BMP at the transcriptional level. **Conclusion:** This study suggests that ONO-4819 accelerates BMP-induced osteoblastic differentiation of ST2 cells by enhancing the transcriptional activity of phosphorylated regulatory Smads in association with transcriptional factor(s) involved in the PKA signaling pathway on the target genes of BMP.

Disclosures: K. Nakagawa, None.

M032

Combination Treatment of rhBMP-2 and Bisphosphonate Stimulate Bone Formation and Inhibit Bone Resorption in the Transplanted Bone Allograft. Y. Kaji^{*}, S. Mori, T. Mashiba, T. Manabe^{*}, T. Akiyama^{*}. Orthopedic Surgery, Kagawa University, Kita-gun, Japan.

Recently, bone allografts have become very common in the field of orthopedic surgery. But the size of the graft is still limited if the blood supply is not preserved. To succeed bigger non vascularized bone allograft, stimulation of bone formation and inhibition of bone resorption in the grafted bone are needed. In this study we evaluated whether combination treatment of bone morphogenetic protein (BMP) and bisphosphonate effectively stimulates bone formation and inhibits bone resorption in bone allograft. Forty female Sprague-Dawley rats at 7 weeks of age were used as donors of bone allograft. Five mm thick bone discs were collected from mid-shaft of femora of donor rats and they were preserved in freezer (-80°C). At the time of bone graft surgery, saline (control), 5 microgram of rhBMP-2 (BM), 10^{-4} M of alendronate (AL), and mixture of rhBMP-2 and alendronate (BM+AL) were added on the bone discs. Fifteen microgram of heparin, which was recently found to stimulate the action of BMP, was also added on the bone discs in addition to BMP and alendronate (BM+AL+Hp). The discs were transplanted into the paravertebral muscles of forty male Wister rats at 7 weeks of age. Following bone labeling with calcein the bone discs were collected from recipients at 4 weeks after the transplantation surgery. Decalcified and undecalcified specimens were prepared for histomorphometry to evaluate the effect of BMP and alendronate on bone formation and bone resorption in the grafted bones. In the bone discs of control and AL group no remarkable bone formation and bone resorption were observed. On the other hand, significantly increased bone formation (increased labeled bone surface and volume of newly formed bone) was observed in the bone discs of BM group. However, in these discs bone resorption (the number of osteoclast and bone surface covered with osteoclasts) was also increased. In the bone discs of BM+AL group significantly increased bone formation and decreased bone resorption were observed. Heparin effectively stimulate the effect of BMP and the largest volume of newly formed bone was observed in the bone discs of BM+AL+Hp group. Our results suggests that combination treatment of BMP and bisphosphonate is very effective to preserve larger size of bone allograft. Addition of heparin effectively stimulate the effect of this treatment.

Disclosures: Y. Kaji, None.

M033

BMP-2 and Osteoporosis Associated Traits in 2,109 Young Adult and Elderly Women. E. Larzenius¹, M. Callreus¹, P. Gerdhem¹, K. Obrant¹, H. Luthman^{*2}, K. Åkesson¹. ¹Department of Clinical Sciences, Malmö, Clinical and Molecular Osteoporosis Research Unit, Malmö, Sweden, ²Medical and Genetics Unit, Malmö, Sweden.

Osteoporosis is a multifactorial disease with a strong genetic component. A candidate locus for regulation of osteoporosis has been identified on chromosome 20p12 by linkage analysis; a locus containing the gene for bone morphogenetic protein-2 (BMP-2). This multi-functional growth factor belongs to the transforming growth factor β superfamily and stimulates osteoblast differentiation and induces bone formation. Genetic variation at the BMP-2 locus has been reported linked and associated with osteoporosis and fracture before and after menopause in a recent report. The aim of this study was to investigate if allelic variation in the BMP-2 gene contributes to regulation of peak bone mass or postmenopausal bone mass in Swedish women. **Material and methods:** Four different single nucleotide polymorphism (SNP) in the BMP-2 gene region were genotyped in two randomly selected population-based cohorts; the PEAK-25 cohort of 1059 young adult women (age 25.5 \pm 0.2 yrs, BMI 23.0 \pm 3.8 kg/m²) and the Osteoporosis Prospective Risk Assessment study (OPRA) of elderly women (age 75.2 \pm 0.1 yrs, BMI 26.2 \pm 4.2 kg/m²). The primary phenotypes were bone mineral density (BMD) and quantitative calcaneus ultrasound (QUS). Previous fractures and lifestyles factors were also registered. The four SNPs were chosen in and around the BMP-2 gene; rs2373073 (SNP-2) is a rare missense S37A variant located in exon 2 and identified in the Icelandic and Danish populations, rs235767 (SNP-3) is located in intron 2, rs235710 (SNP-1) and rs235754 (SNP-4) are located 10 kb up-stream and 8 kb down-stream of the gene. **Result:** In the young women, QUS was the only phenotype consistently associated with the SNPs. SNP-1 and SNP-4 was nominally associated with two out of three calcaneus QUS parameters (p=0.017-0.032), using a multivariate regression model including body weight, height, smoking and years since menarche, the associations remained significant in SNP-1. These genotypes accounted for up to 1.6% of the population variance. Non of the SNPs were associated to QUS in elderly women. We could not confirm significant association with BMD of the S37A variant or of the allelic variation in any of the other SNPs in the BMP-2 region at the hip or spine in either population. Among elderly women 42% reported previous fracture, within this group, those homozygous for C in SNP-4 had significantly lower QUS values (p0.015-0.042). In summary, this study indicates that allelic variation of the BMP-2 gene may contribute to the genetic regulation of qualitative properties of bone and in particular of peak bone mass as measured with calcaneus QUS.

Disclosures: E. Larzenius, None.

M034

BMP Signaling in Bone Stimulates Osteoclastic Bone Resorption and Remodeling during Endochondral Bone Formation and Fracture Repair.

M. Okamoto*, J. Murai*, H. Yoshikawa, N. Tsumaki, Department of Orthopaedic Surgery, Osaka University Graduate School of Medicine, Suita, Japan.

Extensive studies have showed that bone morphogenetic proteins (BMPs) play important roles in skeletal patterning and postnatal bone maintenance. But it still remains obscure how BMPs are involved in endochondral bone development, which is the process residing between skeletal patterning and postnatal bone maintenance. This process is recapitulated during fracture healing after birth. BMP signals are regulated by a balance between BMPs and their antagonists including noggin. To clarify roles of BMP signaling in bone development, we here generated and analyzed transgenic mice expressing noggin or BMP4 in developing bone under the control of the 2.3-kb *Col1a1* promoter sequence which direct expression to immature osteoblasts. Overexpression of noggin in developing bone significantly inhibited osteoclastic bone resorption and caused increase in bone volume from 17.5 days postcoitus to 3 weeks after birth. Osteoblast numbers increased, but bone formation rates significantly decreased in noggin transgenic mice compared with the wild-type. Cortical bones of noggin transgenic tibiae were woven and frequently undergo fractures in spite of increased bone volume, suggesting mechanical weakness probably due to reduced remodeling. *Rankl* expression was not decreased. Co-culture experiments showed that osteoclastogenesis was reduced in co-cultures containing transgenic osteoblasts compared with those containing wild-type osteoblasts. This reduction in osteoclastogenesis *in vitro* was recovered by addition of recombinant BMP2, suggesting overexpressed noggin exerted its effects *via* down-regulating BMP signals. In parallel, overexpression of BMP4 in bone increased osteoclast number, causing severe bone loss at 16.5 and 18.5 days postcoitus. BMPs seemed to stimulate osteoclastogenesis directly. We also found that overexpression of BMP4 in cartilage expanded cartilage anlagen, leading to formation of thick bone. These phenomena were recapitulated in the process of fracture repair. After tibial fracture in mice, application of recombinant BMP2 at fracture sites 2 days after fracture produced a large callus, whereas application at 16 days after fracture caused transient callus resorption associated with an increase in the osteoclast number. Our results suggest that secreted BMPs in bone stimulate osteoclastic bone resorption and remodeling during endochondral bone development and fracture repair. BMP application to cartilage caused expansion of cartilage anlagen, resulting in increased volume of bone or callus. The present findings are useful for planning strategies for treating fractures using BMPs.

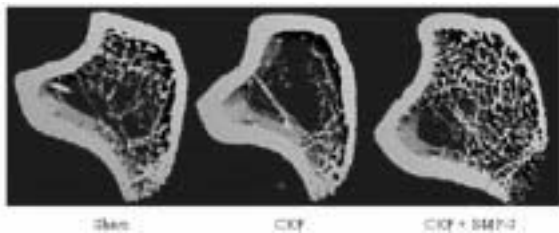
Disclosures: N. Tsumaki, None.

M035

Micro-CT Analysis of Trabecular Bone in a Rat Model of High-Turnover Renal Osteodystrophy: The Effects of Systemic Administration of BMP-7.

R. A. Dodds, D. Xu, X. Cui*, A. Hughes, J. Tullai*, P. Patel, F. X. Farrell, Growth Factors, Johnson&Johnson PRD, Raritan, NJ, USA.

BMP-7 (OP-1) is expressed highly in kidney during fetal development and in adult life. If the kidney experiences an acute injury, e.g., ischemia, BMP-7 mRNA levels decline in parallel with loss of renal function. Chronic renal failure (CKF) is a progressive disorder leading to end stage renal disease. Present treatments (ACE inhibitors) do not impact the deleterious effects of CKF, including renal osteodystrophy (RO). Skeletal abnormalities in patients, rats and mice with CKF include excessively increased bone turnover (² hyperparathyroidism), abnormal mineralization, and marrow fibrosis. In patients, this leads to fracture and extreme pain. This study evaluated the efficacy of BMP-7 in preventing RO in the rat CKF 5/6 nephrectomy model. Rats (400g) were nephrectomized (NPX): a left contra-lateral NPX was followed in two weeks by right total NPX. The upper and lower poles of the left kidney were removed in the first operation and the whole right kidney was then removed two weeks later. Sham surgery was the same procedure minus NPX. The rats received BMP-7 (100 ug/kg), or vehicle i.v., weekly, 5 weeks after the 2nd surgery, for 6 weeks, at which time the tibia were removed for micro-CT analysis. Briefly, BMP7 groups showed positive effects in inhibiting renal fibrosis, reducing mesangial area, tubular lumen dilation and interstitial edema. Furthermore, BMP-7 maintained normal blood pressure. The following structural parameters were assessed in the tibiae metaphyseal trabeculae: BV/TV, Tb.N, Tb.Th, Tb.Sp, trabecular connectivity and BMD. CKF resulted in a significant decrease in trabecular bone volume versus sham (50% decrease, $p < 0.05$), attributed to a decrease in Tb.N, but not Tb.Th. Tb.Sp was increased and BMD decreased (40% versus sham, $p < 0.05$) in the CKF tibia. Trabecular connectivity was dramatically decreased in the CKF rats bones (50% lower versus sham, $p < 0.05$). In the BMP-7 treated rats BV/TV and BMD were maintained at sham levels or dramatically increased ($p < 0.05$ versus CKF). As such, Tb.N and Tb.Sp were also equivalent to sham tibia. Trabecular connectivity was higher in the BMP-7 treated group (20% higher than CKF). In conclusion, BMP-7 prevented the disruption in bone integrity caused by renal failure.



Disclosures: R.A. Dodds, None.

M036

The Effects of Growth/Differentiation Factors-5, 6, and 7 on Mesenchymal Cell Condensation and Chondrogenesis. A. T. Boyce*, R. S. Tuan, NIAMS, NIH, Bethesda, MD, USA.

Growth/Differentiation Factor-5 (GDF-5), a member of the TGF-beta superfamily of bone morphogenic proteins, is required for limb mesenchymal cell condensation, joint formation, and chondrocyte maturation during skeletogenesis. In post-natal development, GDF-5 is expressed during the chondrogenic phase of endochondral fracture repair, recapitulating early developmental events. Brachypod (BP) mice have a functionally null mutation of the GDF-5 gene, causing an acromesomelic chondrodysplasia of the appendicular skeleton. GDF-5 is closely related to two additional GDFs: 6 and 7. While both GDF-6 and GDF-7 transcripts have been located in the developing bone, their functions have not been closely examined. Using limb bud micromass cultures from wild-type animals, we aim to determine whether GDF-5, 6, and 7 can accelerate mesenchymal cell condensation and chondrogenesis. Using limb bud micromass cultures from BP animals, we aim to determine whether GDF-5, 6, and 7 can rescue mesenchymal cell condensation and chondrogenesis. To quantify acceleration and rescue, we will use peanut agglutinin staining for condensation, alcian blue staining for chondrogenesis, and PCR for markers of maturation and differentiation. In addition, we are interested in the signaling cascade of the three GDFs in early limb bud development. While studies have identified the receptors GDF-5 can bind, none have examined the endogenous receptors and intracellular signaling components (SMADs) used in mesenchymal cell condensation and chondrogenesis. Using the limb bud micromass system, we will perform PCR and Western blotting to determine which receptors and SMADs are expressed and how their expressions and phosphorylation status are changed with time and addition of GDFs. We propose that GDF-5, 6, and 7 rescue the BP phenotype and accelerate wild-type condensation and differentiation, though the three GDFs may not use the same signaling cascade.

Disclosures: A.T. Boyce, None.

M037

Regulation of Differentiation and BMP Signaling by Twisted Gastrulation and Chordin in MC3T3-E1 Osteoblast-like Cells. R. Gopalakrishnan¹, O. Shimmi^{*2}, X. Jia^{*3}, A. E. Carlson^{*1}, L. Tervonen^{*1}, M. Jarcho^{*4}, M. B. O'Connor^{*2}, A. Petryk^{*4}.

¹Oral Sciences, University of Minnesota, Minneapolis, MN, USA, ²Genetics, Cell biology and Development, Howard Hughes Medical Institute University of Minnesota, Minneapolis, MN, USA, ³R&D Systems, Minneapolis, MN, USA, ⁴Pediatrics, University of Minnesota, Minneapolis, MN, USA.

Bone morphogenetic proteins (BMPs) are necessary for inducing osteoblast differentiation as well as for regulating and maintaining the differentiated state of committed osteoblasts. Twisted gastrulation (Tsg) and Chordin (Chd) are secreted proteins that regulate accessibility of BMP ligands to their receptors. Tsg has both anti-BMP and pro-BMP activity. Tsg antagonizes BMP signaling by forming ternary complexes with Chd and BMPs, thereby preventing BMPs from binding to their receptors. The pro-BMP activity is partly mediated by cleavage and degradation of Chd, which releases BMPs from ternary complexes. The roles of Tsg and Chd in osteoblast differentiation are not known. Therefore, using a well-characterized subclone of MC3T3-E1 cells, we investigated the roles of Tsg and Chd in osteoblast differentiation and mineralization. Our results show that Tsg and Chd are expressed in MC3T3-E1 osteoblast-like cells. While Tsg mRNA levels decrease during osteoblast differentiation, Chd levels are found to increase. Tsg and Chd proteins accumulate in the cell culture media as the osteoblasts differentiate. Further, Tsg and Chd treatment inhibits osteoblast mineralization in a dose-dependent manner. Evaluation of osteoblast differentiation markers revealed a dose-dependent reduction in alkaline phosphatase (ALP) activity following Tsg and Chd treatment. Osteocalcin (OCN) mRNA levels decreased following both Tsg and Chd treatment. To determine if the effects of Tsg and Chd on osteoblast differentiation are mediated by regulation of BMP signaling, we investigated the levels of phosphorylated Smad1 in MC3T3-E1 cells following treatment with Tsg and Chd. Both Tsg and Chd independently and in combination reduced pSmad1 levels in MC3T3-E1 cells treated with BMP4. Further, BMP2 partially reversed the inhibitory effects of Tsg and Chd on ALP activity. In summary, our results show that exogenous treatment with Tsg and Chd inhibits osteoblast differentiation and mineralization, and suggest that these effects could be partially mediated by regulation of BMP signaling.

Disclosures: R. Gopalakrishnan, None.

M038

Regulated BMP2 Gene Therapy for Bone Regeneration. J. Koh^{*1}, C. Ge^{*1}, Z. Wang^{*2}, P. Krebsbach^{*2}, R. T. Franceschi¹.

¹Periodontics, Prevention and Geriatrics, University of Michigan School of Dentistry, Ann Arbor, MI, USA, ²Biologic and Materials Sciences, University of Michigan School of Dentistry, Ann Arbor, MI, USA.

Adenoviruses expressing bone morphogenetic proteins (BMPs) have been extensively used as a gene therapy vectors for bone regeneration. These viruses induce bone formation and can partially heal calvarial and long bone critical size defects. However, because these vectors use a constitutively active viral promoter to drive BMP expression, they provide little control over the timing or level of BMP induction. Nevertheless, such control may be critical for successful bone regeneration. To begin exploring this issue, we developed and evaluated an inducible system for regulated synthesis of BMP2. Inducible BMP2 expression was achieved using a rapamycin (Rap)-inducible expression system (ARIAD

Pharmaceuticals). Rat BMP2 cDNA was cloned into a retrovirus containing a Rap-sensitive artificial promoter. BLK fibroblasts were transduced with this virus and a second vector encoding a 2-component Rap-binding factor to induce BMP2 expression. Stable cell lines were developed and tested for inducible BMP expression by ELISA. One clone (BLK-RapBMP2/23) was examined *in vitro* and *in vivo*. In the absence of rapamycin, cultured BLK-RapBMP2/23 cells produced undetectable BMP2. Rap treatment induced BMP2 expression in a dose-dependent manner (0.1-10 nM), and the expression was rapid (within 3-6 h) and readily reversible. To evaluate *in vivo* biological activity, BLK-RapBMP2/23 cells were suspended in a type I collagen hydrogel and implanted into subcutaneous sites or calvarial critical sized defect of syngeneic C57BL6 mice. In subcutaneous implants, a single i.p. injection of Rap induced BMP2 dose-dependently (0.1-3 mg/kg). The induction occurred within 24h and decayed to basal levels after 1 week. Alternate day Rap injections (1 mg/kg) induced subcutaneous ectopic bone formation and orthotopic bone regeneration from calvarial defects in mice containing BLK-RapBMP2/23 cell implants after 4-6 wks. In summary, we successfully developed a system for controlled expression of BMP2 using a rapamycin-inducible promoter. This system induces ectopic and orthotopic bone formation and should be extremely useful for identifying stages of bone healing that are most sensitive to BMP stimulation.

Disclosures: **J. Koh**, None.

M039

Osteoactivin Expression Is Regulated by BMP-2 through Smad-1 Signaling Pathway during Osteoblast Differentiation. **S. Abdelmagid^{*1}, T. A. Owen², S. N. Popoff¹, F. F. Safadi¹.** ¹Anatomy and Cell Biology, Temple University School of Medicine, Philadelphia, PA, USA; ²Cardiovascular and Metabolic Diseases, Pfizer Global Research and Development, Groton, CT, USA.

Our laboratory previously showed that osteoactivin (OA) is a secreted osteoblast-related glycoprotein and plays a distinct role in their differentiation and function. In this study, we examined whether the effect of BMP-2, a potent osteotrophic factor, can regulate OA expression using primary osteoblast cultures. Cultured osteoblasts were treated with different concentrations of BMP-2 and examined for OA expression. BMP-2 treatment caused a dose-dependent increase in OA expression with a maximum response at 50 ng/ml. In order to examine the regulatory effect of BMP-2 on OA expression during osteoblast development, osteoblast cultures treated with BMP-2 (50 ng/ml) caused an up-regulation of OA expression at all stages during osteoblast differentiation. We next examined whether OA is a downstream mediator of BMP-2 effect on osteoblast differentiation. OA anti-sense oligo-transfection was used to down regulate OA expression. Cells transfected with OA anti-sense oligonucleotide shows a reduction in OA expression associated with a decrease in alkaline phosphatase staining, nodule formation and mineralization compared to control, sense, transfected cultures. OA anti-sense oligo-transfected culture treated with BMP-2 shows re-induction of OA expression associated with a restoration of alkaline phosphatase staining, nodule formation and matrix mineralization. To examine whether the up-regulation of OA by BMP-2 is Smad-1 mediated, cultures were transfected with Smad-1 siRNA and treated with BMP-2. OA expression level was inhibited in Smad-1 siRNA transfected compared to non-silencing siRNA, transfected, control, cultures. Collectively, these data suggest a significant role for OA as a downstream mediator of BMP-2 effect in osteoblasts differentiation and BMP-2 regulates OA protein expression through Smad-1 signaling pathway.

Disclosures: **S. Abdelmagid**, None.

M040

Effects of Pulsed Electromagnetic Field (PEMF) and BMP-2 on Rat Primary Osteoblastic Cell Proliferation and Gene Expression. **N. Selvamurugan, S. Kwok^{*}, N. Partridge.** Physiology and Biophysics, UMDNJ-Robert Wood Johnson Medical School, Piscataway, NJ, USA.

Transforming growth factor- β (TGF- β) family members, including TGF- β s and bone morphogenetic proteins (BMPs), play important roles in directing fate decisions for mesenchymal stem cells. BMPs inhibit adipogenesis and myogenesis, but they strongly promote osteoblast differentiation. BMPs along with other growth factors or cytokines act synergistically to induce osteoblastic differentiation. The beneficial therapeutic effects of selected low energy, time varying pulsed electromagnetic fields (PEMFs) have been documented with increasing frequency to treat therapeutically resistant problems of the musculoskeletal system. PEMF promotes fracture healing in non-unions. Since PEMF has effects on bone formation *in vivo* and BMPs, in co-operation with other factors, have synergistic effects on bone formation, we hypothesized that a combined BMP-2 and PEMF stimulation would augment osteoblast proliferation and differentiation to a greater degree than treatment with either single stimulus. Hence, the objectives of this work were to determine the effect of BMP-2 and PEMF (Spinal-Stim) together or separately on osteoblastic cell proliferation, differentiation, and mineralization. We used normal rat osteoblastic cultures derived from postnatal day 1 rat calvariae. Every alternate day cells were treated with BMP-2 at different concentrations. The proliferative activity of cells was maximally increased at 25 ng/ml BMP-2 concentration at 7 days culture. Analysis of gene expression by real time RT-PCR from the cells in differentiation and mineralization phases showed that BMP-2 stimulated mRNA levels of alkaline phosphatase, type I collagen and osteocalcin. The effect of PEMF (1.5 Hz burst; 99 pulses per burst; 9/3 teslas/second amplitude; 6 h treatment, daily) on its own, or together with BMP-2 on rat osteoblastic cell proliferation, differentiation, and mineralization was determined. BMP-2 and PEMF had effects on proliferation of rat osteoblastic cells which were additive when both agents were combined. PEMF itself or together with BMP-2 increased only alkaline phosphatase mRNA expression and only during the differentiation phase. This effect was additive when both agents were combined. Hence, we suggest that a combined treatment of BMP-2 and

PEMF has additive effects on osteoblastic cell proliferation and early osteoblastic differentiation, and this additive effect is possibly mediated by different intracellular signaling pathways. Thus, a combined effect of BMP-2 and PEMF *in vitro* could be considered as groundwork for *in vivo* bone development that may support skeletal therapy.

Disclosures: **N. Selvamurugan**, Orthofix, Inc. 2.

M041

Fourier Transform Infrared Microscopic Analysis of Subchondral Sclerotic Lesion in Knee Osteoarthritis. **M. Sato^{*1}, N. Miyoshi^{*2}, H. Baba^{*1}.** ¹Orthopaedics and Rehabilitation Medicine, University of Fukui, Fukui, Japan, ²Pathology, University of Fukui, Fukui, Japan.

Introduction The subchondral bone has long been known to be sclerotic in osteoarthritis. Recently the turnover of bone mineral and collagen metabolism is increased several fold and further suggests that the subchondral bone plays a significant role in osteoarthritis. The biochemical and biomechanical properties of the subchondral bone are therefore of particular interest to elucidate the pathogenesis of osteoarthritis. **Study design** In the present study, we analyze the mineralization of subchondral sclerotic lesion in knee osteoarthritis by Fourier Transform infrared microspectroscopy (FTIRM). **Materials and methods** 10 OA knee joints were collected from elderly patients immediately after knee arthroplasty. Subchondral bone samples were isolated using a punch from distal medial femoral (MF), distal lateral femoral (LF), proximal medial tibial (MT) and proximal lateral tibial (LT) region. All samples were fixed and dehydrated and then, each of them were snap-frozen in liquid nitrogen and milled to a powder using a stainless steel mill. For IR micro-spectroscopic analysis, KBr pellets were prepared by mixing 10mg of bone powder with 500 mg of KBr in a mortar and pestle and pressing the pellet in a 13mm KBr pellet die. The spectra were recorded with FTIRM (model IRT-30; JASCO, Tokyo, Japan) coupled to a spectrometer (model 410M; JASCO, Tokyo, Japan) at a resolution of 4cm⁻¹, 200 scans. The mineral:matrix ratio was determined by integrating the area under the peak at phosphate vibration (900-1200 cm⁻¹) and Amide I \bar{A} (1725-1585 cm⁻¹) vibration in the FTIR spectrum. **Results** The mean mineral:matrix ratio of the medial sclerotic lesion (MF, 1.95 \bar{A} ±0.002, MT, 1.85 \bar{A} ±0.002) was significantly lower than the lateral region (LF, 2.45 \bar{A} ±0.002, LT, 2.50 \bar{A} ±0.017) of the subchondral bone. **Discussion** In this study, infrared data suggested the hypomineralization in the subchondral sclerotic lesion. The nucleation of mineralization requires the gap region within the precise organization of the collagen fiber. These structures are essential for the stability and strength of bone. In osteoarthritis, normal bone mineralization process might to be inhibited and the biochemical and biomechanical properties of subchondral bone might to be weakened.

Disclosures: **M. Sato**, None.

M042

Increase of Erythrocyte Ca and Mg with Age and Effect of Ca Supplementation. **T. Fujita¹, S. Ohgiani^{*2}, M. Ohue^{*1}, Y. Fujii^{*3}, A. Miyauchi^{*4}, Y. Takagi^{*1}.** ¹Medicine, Katsuragi Hospital, Kishiwada, Japan, ²Medicine, Imai Hospital, Osaka, Japan, ³Medicine, Calcium Research Institute, Kishiwada, Japan, ⁴Medicine, National Hospital System Hyogo Chuo Hospital, Hyogo, Japan.

Calcium (Ca) deficiency increases secretion of parathyroid hormone (PTH) Which paradoxically raises intracellular Ca interfering with signal transduction. Nevertheless, intracellular Ca has not been measured as frequently as its extracellular counterpart because of a sampling problem. Since erythrocytes are readily sampled as a representative cell mass, Ca in erythrocytes was measured along with magnesium (Mg), a commonly coexisting divalent cation, to assess its significance in systemic mineral metabolism. From 135 healthy male and female volunteers 2 ml blood samples were obtained with EDTA-2K anticoagulant and Ca content of the washed erythrocytes measured by atomic absorption spectroscopy. Both Ca (5~10 ppm, r= 0.195, p=0.0232) and Mg (30~75 ppm, r= 0.287, p=0.007) in erythrocytes significantly increased with advance in age. Neither erythrocyte Ca nor Mg showed significant gender difference. In 41, 12 and 13 of these subjects, 900mg, 300mg and 0mg /day active absorbable algal calcium (AAACa, Fujix) was supplemented respectively for 4 months. Erythrocyte Ca contents decreased by 1.13 (SE 0.22) ppm in A and by 0.24(SE 0.39) in B, but not in C with a highly significant difference between A and C (p<0.0001) and significant difference between A and B (p=0.0447). Ratio of erythrocyte Ca contents after/before supplementation in Group A was 75.1 (SE 2.3) % of that in the non-supplemented Group C (p= 0.0001), and that in Group B 86.6 (SE 4.4) % (p=0.0208). No significant changes occurred in erythrocyte Mg contents. The progressive increase in erythrocyte Ca content with age and its doseArelated decrease on supplementation with readily absorbable AAACa is compatible with a hypothesis of Ca deficiency and secondary hyperparathyroidism associated with aging and its reversal by effective Ca supplementation. Erythrocyte Ca measurement appears to be useful to evaluate the degree of Ca deficiency and efficacy of Ca supplementation.

Disclosures: **T. Fujita**, None.

M043

BrdU Tracking of Preosteoblasts in Formalin Fixed, Decalcified Regenerating Bone. E. C. Wahl^{*1}, J. Aronson^{*2}, R. A. Skinner^{*2}, C. K. Lumpkin². ¹Arkansas Children's Hospital Research Institute, Little Rock, AR, USA, ²Departments of Orthopedics and Pediatrics, University of Arkansas for Medical Sciences, Little Rock, AR, USA.

Distraction osteogenesis (DO) is a limb lengthening procedure that induces rapid bone formation by slowly stretching a surgically introduced fracture at a prescribed rate and rhythm. In order to track the pre-osteoblasts in the distraction gaps of rats, we utilized two types of immunohistochemical markers. The first was an injection of bromodeoxyuridine (BrdU), a thymidine analog, followed by immunohistochemical staining for BrdU positive nuclei. The second was the antibody against proliferating cell nuclear antigen (PCNA). Four male Sprague Dawley rats (350g) underwent standard DO surgery. External fixators were placed on the left tibiae and mid-diaphyseal tibial osteotomies were performed immediately following fixator placement. Distraction began one day after surgery at 0.2mm b.i.d. (0.4mm/day) for 12 days. On the twelfth day of distraction the rats were given an intraperitoneal injection of BrdU labeling reagent (1ml/100g). A rat was sacrificed 2, 24, 48, and 72 hours after the injection. At the time of sacrifice, the distracted tibiae were harvested and stored in neutral buffered formalin (NBF) until processed for histology. A small section of intestine from each rat was also collected as a positive BrdU control. After fixation in NBF, the tibiae were decalcified in 5% formic acid, dehydrated, and embedded in paraffin. Serial sections were then stained with either a mouse monoclonal antibody against PCNA (PC-10), a monoclonal antibody against BrdU, or a normal mouse IgG for negative control. A comparison of PCNA+ cells and H&E stained cells in serial sections at each time point demonstrated that the PCNA+ cells were located in the zone outlining the new osteoid columns and in the sinusoids between the columns. No PCNA+ cells were noted in the new microcolumns. A comparison of BrdU+ cells and H&E stained cells in serial sections at the 2 and 24 hour time points demonstrated that BrdU+ cells were also located outside the microcolumns. At the 48 hour time point, BrdU+ cells first appeared scattered throughout periosteal new bone, microcolumns, and cartilage. This same pattern was observed at the 72 hour time point, except that a greater majority of cells in the new columns were labeled. The results demonstrate for the first time that during DO at least a subset of the proliferating cells, juxtaposed to the newly developing osteoid column tips, can be "tracked" over a 48 -72 hour period, into the osteoid columns, confirming their identification as preosteoblasts.

Disclosures: C.K. Lumpkin, None.

M044

Comparative Analysis of Confocal and Light Microscopy for Detecting *In Vivo* Microdamage in Wild and Domesticated Animals. W. E. Anderson^{*1}, J. G. Skedros². ¹Univ. Utah Dept. Orthop. Surg., Salt Lake, UT, USA, ²UofU, SLC, UT, USA.

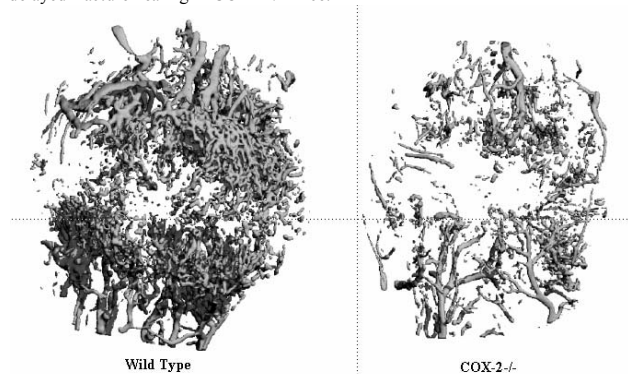
Microdamage (mdx) accumulation is believed to be important in the etiology of stress and fragility fractures. But detecting *in vivo* bone mdx is difficult. Confocal microscopy appears to be gaining popularity as the "gold standard" for detecting mdx because it is considered more sensitive than light microscopy. We tested this hypothesis using one calcaneus from each of 11 wild deer, 11 wild elk, 11 domesticated sheep, and 11 non-racing horses. In addition to examining entire bone sections, we also examined prevalent/predominant medial/lateral "shear" regions and caudal "tension" regions to see if these relatively more deleterious loading environments are associated with increased *in vivo* mdx when compared to cranial "compression" regions. 14mm-thick mid-diaphyseal segments were bulk stained in 1% basic fuchsin [Burr & Stafford 1990 Clin. Orthop.]. Two investigators, blinded to the hypotheses, rigorously examined three 100micron-thick slices/ bone at 10-40X using transmitted light and confocal microscopy for various forms of *in vivo* (fuchsin stained) mdx (linear microcracks, diffuse mdx, wispy mdx, and osteonal debonding). Confocal microscopy was conducted using a Nikon PCM-2000 with a green HeNe LASER (543nm wavelength excitation; 565 LP filter). Evaluation in light microscopy revealed 15 linear microcracks in 132 sections: nine in deer (4 bones), two in elk (1 bone), and four in horses (3 bones). In addition to confirming the presence of the 15 linear microcracks with light microscopy in the deer, elk, and horses, evaluation using confocal revealed 83 additional mdx entities (debonded, wispy, and diffuse), none of which could be detected with light microscopy. Frequencies of additional mdx entities included: deer (n=45; all bones), elk (n = 24; all bones), and horses (n=14; 9 bones). No mdx was detected in sheep calcanei using light or confocal microscopy. These results confirm the greater sensitivity of confocal microscopy. Higher levels of physical activity may explain why the wild animals exhibited significantly more mdx. Approximately 60% of mdx was concentrated in the caudal cortices where tensile strains are prevalent/predominant, possibly accounting for the high remodeling activity in this region. Confocal microscopy may help determine if bones subject to habitual bending incur similar regional variations in mdx prevalence and/or if these regional variations are minimized by regional adaptations (e.g., osteon densities, collagen orientation) that serve to "toughen" the bone. In turn, confocal microscopy may help determine how strain distributions might increase fracture propensity in some bones, especially with aging (e.g., proximal human femur).

Disclosures: W.E. Anderson, None.

M045

Assessment of Neovascularization in Fracture Healing of COX-2 *-/-* Mice Using Micro-Computed Tomography. C. Xie^{*1}, A. S. P. Lin^{*2}, E. M. Schwarz¹, R. E. Guldberg^{*2}, R. J. O'Keefe¹, X. Zhang¹. ¹Orthopaedics, University of Rochester Medical Center, Rochester, NY, USA, ²George W. Woodruff School of Mechanical Engineering, Georgia Institute of Technology, Atlanta, GA, USA.

Angiogenesis has been shown to play a key role in bone regeneration and fracture repair. We previously demonstrated that COX-2^{-/-} mice exhibited impaired fracture healing, as evidenced by significant delay in mesenchyme differentiation and cartilage mineralization. To further determine whether delayed mineralization in COX-2^{-/-} mice was associated with the deficiency in neovascularization, we used micro-computed tomography (Micro-CT) to examine the quantity and quality of vasculature in the fracture callus of COX-2^{-/-} mice and their wild type control mice. A mid-diaphyseal fracture was created via 3 point bending in mouse femur and subsequently stabilized by a metal pin placed in the intramedullary canal. MicroCT vascular imaging was obtained via perfusion of a lead chromate based contrast agent Microfil followed by complete decalcification. Segmentation was performed using software provided by Scanco to contour out the periosteal external callus and endosteal internal callus, excluding the cortex of the fractured femur. The three-dimensional reconstruction of microvasculature within fracture callus demonstrated a dramatic reduction of neovascularization in COX-2^{-/-} mice compared to the wild type control at day 14 post-fracture (Figure). Clusters of highly connected, closely spaced, and isotropically oriented small vessels were observed in wild type mice, but were almost absent in COX-2^{-/-} mice. Quantitative analyses demonstrated that the volume fraction of mineralization within fracture callus was reduced by 2.5 fold, whereas the total vessel volume fraction was reduced by 3.75 folds in COX-2^{-/-} mice (p<0.05, n=3). Accordingly, vessel separation was increased by 1.5 fold and the average thickness of the vessels was decreased by 25% in the knockouts (p<0.05). The dramatic difference seen between COX-2 knockout and wild type mice was the connectivity of the vessels. Wild type mice demonstrated about 25 fold higher connectivity than COX-2^{-/-} mice. Taken together, our data suggests that deficiency in angiogenesis may play a key role in delayed fracture healing in COX-2^{-/-} mice.



Disclosures: X. Zhang, None.

M046

Automated Volumetric Imaging of *In Vivo* Bone Formation Labels. G. J. Kazakia^{*1}, M. Singh^{*2}, W. Yao³, N. E. Lane⁴, T. M. Keaveny². ¹UC, San Francisco, CA, USA, ²UC, Berkeley, CA, USA, ³Stanford, Stanford, CA, USA, ⁴UC Davis, Sacramento, CA, USA.

In vivo administered fluorescent labels are indispensable in the study of bone metabolism. Standard histomorphometry - particularly in mineralized tissues - is technically challenging and labor intensive. Moreover, histomorphometric measures based on thin sections allow only 2D measures of the 3D structures of interest. With renewed interest in the role of bone quality in osteoporosis, the distinction between 2D and 3D measures of histological structures such as remodeling spaces and microdamage may be important. The goal of this work was to apply a novel technique for visualizing 3D distribution of fluorochrome labeled components within large biological specimens to the reconstruction of an *in vivo* administered bone formation label. This method is based on computer controlled milling technology and combines an arrayed imaging technique with fluorescence capabilities, thus enabling 3D fluorescence imaging of bone specimens of any size at high resolution (on the order of a few microns). Biological specimens containing fluorescent labels are embedded in an opaque resin and mounted onto the system for serial milling and imaging. After each milling pass, an imaging station excites the exposed fluorochromes and captures the emitted fluorescence through a series of filters. As an example, an *in vivo* calcein-labeled femur from a six month old female Sprague-Dawley rat was harvested and imaged. The proximal femur was fixed in 10% NBF, dehydrated, and embedded in opaque MMA. Autofluorescence was exploited to capture bone morphology using a UV excitation filter and a DAPI emission filter. Calcein fluorescence was imaged using a FITC filter set. Two 2x3 image arrays (one per filter set) were captured for each exposed surface. A 5 mm length was imaged using 680 slices at an in-plane resolution of 3 microns/pixel and an out-of-plane resolution of 8 microns. Two superimposed volumetric data sets were rendered for visualization - one representing bone morphology and a second representing bone formation zones. Spatial distribution of bone forming zones and their relation to local bone architecture were clearly distinguished and substructures such as an entire osteon (length 1.36 mm; mean diameter 129 microns) were isolated. Imaging time

ASBMR 27th Annual Meeting

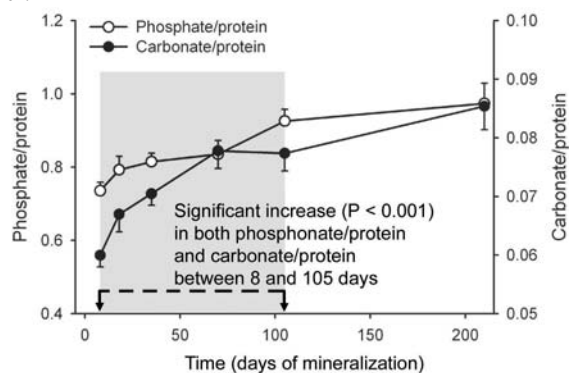
was approximately 20 h. However, the automated nature of the system greatly reduced operator time, requiring a total of 2 h (independent of total imaged volume). Use of this system is expected to provide unique *three-dimensional* data on structures such as osteons, remodeling cavities, mineralization distributions, remodeling surfaces, and microdamage, all having substantial relevance to studies in bone quality and osteoporosis.

Disclosures: *G.J. Kazakia, None.*

M047

How Long Does Secondary Mineralization of Osteonal Bone Take? R. K. Fuchs¹, M. R. Allen¹, M. E. Ruppel², L. M. Miller², D. B. Burr¹. ¹Anatomy and Cell Biology, Indiana University Medical School, Indianapolis, IN, USA, ²Brookhaven National Laboratory, National Synchrotron Light Source, Upton, NY, USA.

The time-course required for newly formed bone to achieve "complete" mineralization is unclear yet may be important to help understand how common anti-resorptive therapies for osteoporosis alter tissue mineralization. Our aim was to determine the time-course of secondary mineralization in normal cortical bone using synchrotron infrared (IR) microspectroscopy. Twelve 4-month old female New Zealand white rabbits were administered four different fluorochrome labels at various time points to identify sites of newly formed bone. Rabbits were sacrificed after 8, 18, 35, 70, 105, and 210 days of formation to determine the level of mineralization at labelled sites. Phosphate, carbonate, and collagen content of labeled osteons were measured from 4 μ m thick sections of tibial diaphysis using synchrotron Fourier transformed IR microspectroscopy (FTIRM). IR spectra were recorded using a Continuum IR microscope coupled to a Nicolet Magna 860 FTIR. Curve-fitting and area integrations were carried out on protein (Amide I: 1700-1600 cm^{-1}), carbonate (CO_3^{2-} : 905-825 cm^{-1}), and phosphate (PO_4^{3-} : 650-500 cm^{-1}) IR bands. Collagen cross-linking was studied as a ratio of 1660/1690 cm^{-1} . Because PO_4^{3-} is the most abundant anion in bone, overall mineralization was estimated by the ratio of PO_4^{3-} to protein. Results showed that the rate of increase of mineralization slowed to nearly zero by day 210, and did not change significantly between days 105 and 210, thus we assumed that mineralization was nearly complete by 210 days. After only 8 days, the level of mineralization was 76% of the value observed at day 210. Between days 8 and 105 the level of mineralization increased significantly, reaching 95% of its estimated final value by day 105 ($p < 0.001$, Fig. 1). Changes in CO_3^{2-} over time were similar to those seen for PO_4^{3-} . Mineral crystallinity and collagen cross-linking did not change significantly from days 8 to 210. Thus, changes in crystallinity and cross-linking either occur rapidly (< 8 days) or very slowly (longer than 210 days). Our findings demonstrate that newly formed osteonal bone continues to mineralize for approximately 3 months, by which time it has achieved 95% of its final value. The rate of mineralization slows asymptotically between 3 and 7 months of formation.



Disclosures: *R.K. Fuchs, Procter & Gamble Pharmaceuticals, Inc. 2.*

M048

Real Time Skeletal Metabolism Differences during and after Lactation Using Dynamic Micro-Positron Emission Tomography (MicroPET) Imaging. B. L. Anderson^{*1}, B. M. Bowman¹, J. Slater^{*2}, S. C. Miller¹.

¹Radiobiology, University of Utah, Salt Lake City, UT, USA, ²Loma Linda University, Loma Linda, CA, USA.

Lactation is a period of altered skeletal metabolism to provide the mineral requirements of milk production. During lactation, skeletal turnover is increased but dominated by bone resorption. After lactation there is a rapid transition or "reversal" to a profoundly anabolic period that reconstitutes the maternal skeleton. The purpose of this study was to determine the dynamic uptake of the bone-seeking ion [^{18}F] fluoride in different skeletal regions and to compare these results with histomorphometric indices of bone formation and resorption. ^{18}F is a bone seeking ion that either binds to bone tissue on the surface or as an ionic exchange with the hydroxyl groups of hydroxylapatite to form fluorapatite. Tomographic images with anatomic resolution can be obtained from the ^{18}F positron emission. Three groups of rats were studied: 1) Female rats at mid-lactation; 2) females rats at 18 hrs after weaning; and 3) non-mated, age-matched controls. ^{18}F at a (700 μCi) was injected into the tail vein at the beginning of image acquisition by microPET. Blood samples were taken 1 min after the ^{18}F injection and then every 5 minutes during the 70 minute scan. Fluoride activity was measured (gamma counter) in blood samples and individual bones. Dynamic images of the proximal tibia and lumbar vertebra (4-6) were reconstructed with 10 frames at 30 sec, 10 frames at 120 sec and 12 frames at 300 sec. From this, time-activity curves

were generated. The slowest rate of ^{18}F uptake was observed during mid-lactation; a period of excess bone resorption and bone loss. The fastest uptake of ^{18}F occurred in the early post-weaning period; a period of osteoclast apoptosis and commencement of mineral accumulation in the skeleton. The uptake of ^{18}F in the non-mated controls was intermediate with the other groups. As expected, relatively greater metabolic activity was observed in cancellous bone regions, particularly the metaphyseal spongiosa. This study first demonstrates the utility of using microPET to assess skeletal metabolism in a living animal. In this case, the changes in the rates of ^{18}F uptake can be correlated with the histomorphometric observations. This study also further demonstrates the profound differences in maternal mineral metabolism that occur during and immediately after lactation.

Disclosures: *B.L. Anderson, None.*

M049

Diesel Motor Oil Is an Effective Contrast Agent for Micro-CT Visualisation of Pre-Ossification Cartilage in the Mouse Fetal Limb. P. L. Salmon¹, M. Kmita^{*2}, D. Duboule^{*3}. ¹Skyscan, Aartselaar, Belgium, ²Frontiers in Genetics, University of Geneva, Geneva, Switzerland, ³Frontiers of Genetics, University of Geneva, Geneva, Switzerland.

The development of bones in the vertebrate fetus is an integral part of the development of segmented and articulated limbs. An important part of this development is the acquisition of proximal-to-distal patterning, and mutant mice have been employed to study the genetics of development of limb patterning (Duboule 2002). Development of pattern, sequence and symmetry are controlled by the highly conserved Hox genes. Two naturally occurring mutations, *Ulnaless* (Ul) and *Hypodactyly* (Hd), have proved useful in clarifying the respective roles of the HoxD and HoxA complex genes. To study developmental phenotypes of mice it is necessary to image the structure of bone at its first appearance in the fetus, both at the onset of calcification, and also importantly just before calcification. Such imaging should ideally be in 3 dimensions. Calcified bone can be imaged clearly in 3D by micro-CT since even low level calcification confers significantly higher x-ray absorption in bone compared to nonmineralised soft tissue. So newly calcifying bone is readily imaged by micro-CT. However pre-ossification cartilage in the developing mouse limb shows no x-ray contrast against surrounding soft tissue. Mineral oils were evaluated as contrast agent to facilitate micro-CT imaging of pre-ossification cartilage by conferring increased x-ray absorption selectively to pre-ossification cartilage. Of the oils evaluated diesel motor oil was found to be the most successful, providing sufficient contrast to allow spatial imaging of pre-ossification cartilage (see figure 1). It is possible that metals within the motor oil were sequestered by sulphur bridges within the glycosaminoglycans of cartilage.

Duboule D (2002) Making progress with limb models. *Nature* 418: 492-493.

Figure 1. Micro-CT cross-section images of a fetal mouse limb (ex-vivo) before (left) and after (right) immersion of the limb in diesel motor oil for one month. The oil immersion resulted in visualisation of pre-ossification cartilage rings representing the developing radius and ulna.

Disclosures: *P.L. Salmon, Skyscan 3.*

M050

LRP5 Regulation of Intrinsic Material Properties of Cortical Bone. G. E. Lopez Franco¹, R. Blank¹, B. L. McGuckin^{*2}, M. L. Johnson², D. M. Cullen², R. R. Recker², M. P. Akhter². ¹Endocrinology, University of Wisconsin Medical School, Madison, WI, USA, ²Medicine, Creighton University, Omaha, NE, USA.

The *LRP5*^{G171V} mutation (high bone mass [HBM]) is autosomal dominant and is responsible for high bone mass in human. Transgenic HBM mice harboring an expressing human *LRP5*^{G171V} construct show a similar phenotype with greater bone mass and strength than wild type mice as determined by whole bone testing. Whole bone quality, however, depend jointly on bone mass, architecture, and intrinsic bone tissue properties. To find if the HBM mutation affects tissue-level properties, we performed nanoindentation testing of fresh cortical bone from HBM mice and their nontransgenic (NTG) littermates. Femora from 17-week old (female, 8 mice/genotype) mice were polished with multiple grain diamond cloths and subjected to nanoindentation using a Triboscope (Hysitron, Minneapolis, MN) and a diamond Berkovich tip. A series of indentations in fused quartz were used to calibrate the area function and machine compliance. Approximately 10 indentations were made on the femoral mid-shaft anterior surface with a target force of either 3 or 9 mN at a constant loading rate of 400 mN/s, including a preliminary thermal drift rate correction limited to a maximum of 0.05 nm/s. The 50% to 95% of the unloading curves was used for calculation of elastic properties. The load-displacement data from each test were used to calculate reduced indentation modulus and hardness for bone tissue. The bone modulus was 48% greater in the HBM than the NTG mice (Table). The greater

modulus in the HBM agrees with the previously reported greater bone mass/density, strength, and bone ash content, but go beyond the prior findings in that nanoindentation allows modulus to be determined independent of specimen size and geometry. Our data show that the G171V mutation increases the cortical bone modulus in adult female mice, in addition to the mutation's effect on bone mass. However, the impact of G171V mutation on trabecular bone intrinsic properties remains unknown in both genders. Moreover, mechanical performance includes many aspects in addition to modulus and hardness, including ductility, viscoelasticity, and fatigue behavior. Therefore, additional work is needed to explore these additional biomechanical properties in HBM mice and fully explain the role of WNT signaling in regulating bone mass and strength.

Intrinsic material properties of cortical bone in mice		
	NTG	HBM
Modulus bone (GPa)	20.4 ± 5	30.2 ± 9.3 *
Hardness (GPa)	1.0 ± 0.4	1.1 ± 0.2

*P <0.05 as compared to NTG by Student's t test (mean ± SD)

Disclosures: **M.P. Akhter**, None.

M051

Effect of Image Noise and Partial Volume Averaging on QCT-Derived Femoral Neck Strength Indices. **M. Sode**¹, **J. Keyak**^{*2}, **T. Lang**¹. ¹Radiology, University of California, San Francisco, San Francisco, CA, USA, ²Orthopaedic Surgery, University of California, Irvine, Irvine, CA, USA.

The cortical thickness (CTh) can be as low as 0.5mm at some portions of the femoral neck, which is below the spatial resolution available for in vivo CT imaging. The resulting partial volume averaging (PVA) errors cause underestimation of cortical BMD and overestimation of CTh, but the effects of PVA errors on femoral neck strength estimates are not well understood. We carried out a computer simulation to understand the effect of PVA errors on the accuracy of strength estimates and the variation of these errors over the range of bone size and density values typical of postmenopausal women. In these simulations, a computer program generated femoral neck cross-sections consisting of 2 nearly concentric ellipses that were shifted slightly off-center along their common major axis. Our computer model allowed us to vary the CTh, trabecular BMD, and cross-sectional area (CSA). We varied superior CTh from 0.2-1.0 mm, inferior CTh from 3.0-5.0 mm, trabecular BMD from 50-150 mg/cm³ and CSA from 6-9 cm². To simulate CT imaging, the structures were blurred a spatial resolution of 2.0 mm FTWM, and Gaussian noise similar to noise of typical hip CT images was added to the images. We compared estimates of moments of inertia (Izz, Iyy, and Iyz), compressive and tensile stresses, and mean factor of safety (FOS) derived from the raw images (noBN) and the blurred, noisy images (BN). A bending moment 5.0 N was applied and FOS was calculated for each pixel as the strength/stress. The mean FOS calculated for the BN images consistently underestimated the true values. A similar trend was observed for the other parameters. This simulation provides an estimate of the magnitude and variability of accuracy errors introduced by PVA into CT-derived strength indices. Although they are lower, the calculated values are highly correlated with the true values. Further investigations will require use of realistic loading forces and cross-sectional shape models.

	Superior CTh [mm]	Inferior CTh [mm]	Trab BMD [mg/ cm ³]	CSA [cm ²]	NoBN FOS	BN FOS	%ΔFOS = (NoBNFOS - BNFOS)/ NoBNFOS
Osteoporotic	0.5	3.0	50	6.0	60.84	45.73	24.8%
Osteopenic	0.6	4.0	100	7.0	91.86	74.85	18.5%
Healthy	0.75	5.0	150	8.0	132.8	113.7	14.4%

Disclosures: **M. Sode**, None.

M052

Systematic Approach for Gene Screening within Discrete Compartments in the Growth Plate Using DNA Microarrays. **S. Nishimori**, **I. Paruch**^{*}, **H. M. Kronenberg**. Endocrine Unit and Harvard Medical School, Massachusetts General Hospital, Boston, MA, USA.

DNA microarrays are powerful tools for gene screening, but the murine growth plates are too small for straightforward microarray that requires high yield and high quality of total RNA. Here we report a systematic approach using the Affymetrix® GeneChip®, which can examine 45,000 putative genes on one chip. To investigate the molecular underpinnings of the conversion of round chondrocytes to flat columnar and then to hypertrophic chondrocytes, we attempted to dissect cells from the three distinct chondrocyte layers in the proximal tibiae from new born mice. We chose manual microdissection of fresh-frozen tissues under an inverted microscope rather than Laser Capture Microdissection, to obtain as much total RNA as possible, to minimize the needed rounds of RNA amplification. After collecting all the samples from the pups belonging to one litter, total RNA was isolated using an RNeasy Mini® column (Qiagen) with DNase I treatment. Using 20 tibiae, we dissected 200-260 sections for each layer, and could extract 2.7-4.8 µg of total RNA from each layer. Analysis of RNA by capillary electrophoresis using the Bioanalyzer® (Agilent Technologies) showed total RNAs with little degradation. We repeated these procedures with two other litters to prepare independent triplicate samples. After one round of amplification using T7dT primer in the Affymetrix® protocol, we could obtain sufficient complementary RNA probes (more than 15 µg for one chip). 9 Mouse Genome 430 2.0 Arrays showed us the similar average signal intensities, very low backgrounds, and consistency between parameters for normalizing intensities on each chip. Using the Rosetta Resolver® Gene Expression Data Analysis System (Rosetta Biosoftware), we screened differentially expressed genes in each layer as follows, 793 genes for Round(R)/Flat (F)>2.0, 646 genes for F/R>2.0, 1005 genes for Hyper (H)/R>2.0, 1247 genes for R/H>2.0, 532 genes for F/H>2.0, and 586 genes for H/F>2.0. To narrow the

list of candidate genes expressed preferentially in one layer or another, we performed real time (RT)-PCR for the second step of validation and *in situ* hybridization for the final step of validation. We found that signal intensities are as important as fold ratios, because genes with low signal intensities led to predictions sometimes not verified by RT-PCR. We are now picking up interesting genes which showed similar fold ratios in microarray and RT-PCR, for example, Nephroblastoma overexpressed gene (R/F/H=100/27/4), Carbonic anhydrase 3 (100/300/150), protease nexin I (R/F/H=100/200/400), etc. In summary, these procedures should prove useful for studying chondrocyte differentiation.

Disclosures: **S. Nishimori**, None.

M053

Osteoprotegerin Treatment Inhibits the Growth of Lytic Prostate Cancer Lesions in Bone. **J. M. Blair**¹, **L. A. Perryman**^{*2}, **H. Y. Pwint**^{*2}, **J. Leliott**^{*2}, **J. De Winter**^{*1}, **P. Russell**^{*2}, **C. R. Dunstan**¹, **M. J. Seibel**¹. ¹Bone Research Program, ANZAC Research Institute, Sydney, Australia, ²Oncology Research Centre, UNSW Clinical Medicine, Prince of Wales Hospital, Randwick NSW 2031, Sydney, Australia.

Prostate cancer (CaP) bone metastases, whilst typically osteoblastic, have a strong resorptive component. Therefore, we investigated whether osteoprotegerin (OPG) treatment inhibits tumour growth in a lytic CaP bone metastasis model. Male NOD-SCID mice aged 6-8 wks were injected with 4 x 10⁵ PC-3-EGFP cells into the right tibia. Serum samples and radiographs were taken at the start, middle and end of each study. Sera were analysed for mouseTRAP 5b levels. Harvested tibias were analysed by immunohistochemistry to detect human cytokeratins. Controls were age-matched non-injected and sham-injected mice. In study 1, mice were randomised for x3/wk treatment with vehicle or 1 mg/kg OPG starting at wk 0 (prophylaxis) or wk 2 (delayed treatment). In study 2, vehicle or 3 mg/kg OPG treatment x3/wk began at wks 1 (early), 0 (late) or 2 (delayed) (n=6-7 mice/ group): endpoint sera in study 2 were also analysed for osteocalcin levels. Osteolytic tumours were radiographically apparent in all vehicle-treated mice at wk 6. In study 1, OPG-treated mice had smaller osteolytic tumours and decreased serum mouseTRAP 5b levels in the prophylaxis group versus the vehicle-treated mice. In the delayed treatment arm, OPG treatment partially inhibited tumour growth and reduced serum mouseTRAP 5b levels when compared with vehicle control at wk 6. In study 2, early OPG mice had little evidence of tumor and had extended calcified growth plates; late OPG mice displayed little tumor growth; and, delayed OPG mice had small discrete tumors that did not breach the cortex. When compared with their respective vehicle controls, bone resorption was inhibited in early OPG mice (wk 1, p<0.0001; wk 2, p=0.0137; wk 6, p<0.0001), late OPG mice (wk 2, p<0.0001; wk 6, p=0.0002) and delayed OPG mice (wk 2, p=0.0210; wk 6, p<0.0001). Serum osteocalcin was significantly decreased in late and delayed OPG mice (p<0.0001 and p=0.0017, respectively) when compared with respective vehicle controls. All tumors were positive for anti-human pan-cytokeratin antibody. In conclusion, OPG treatment reduced bone resorption from the time treatment was initiated. Study 1 results suggested that low resorption levels were sufficient for PC-3-EGFP cells to establish and grow in bone, and that a higher OPG dose was required to inhibit PC-3-EGFP tumor growth in bone. Although low levels of bone resorption were still detected in study 2, 3 mg/kg OPG effectively inhibited prostate cancer induced osteolysis and tumor growth.

Disclosures: **C.R. Dunstan**, None.

M054

Functional and Anatomical Imaging Allows for More Sensitive Monitoring of Tumor Burden and Osteolysis in a Mouse Model of Breast Cancer Metastasis to Bone . **J. A. Sterling**, **B. Goins**^{*}, **B. Grubbs**^{*}, **M. Amurao**^{*}, **C. Zavaleta**^{*}, **A. Soundararajan**^{*}, **Z. Wang**^{*}, **W. Phillips**^{*}, **B. Ovajobi**, **G. Mundy**, **S. S. Padalecki**. UT Health Science Center, San Antonio, TX, USA.

The skeleton is the most common site of metastasis in breast cancer patients. We have hypothesized that once established in the skeleton, breast tumors induce a vicious cycle in which tumor produced factors stimulate bone resorption resulting in release of growth factors from bone further stimulating tumor growth and osteolysis. We have utilized a well-established mouse model of breast cancer metastasis to bone to identify molecular targets for the development of therapeutics. We have previously tested this hypothesis, monitoring bone metastases using standard radiography and bone histomorphometry. Osteolytic lesions are visible by radiography approximately 14-21 days after tumor cell inoculation via the left cardiac ventricle. Although tumors are well established at this time point, there are skeletal sites which cannot be visualized by radiography. Furthermore, it is not possible to monitor tumor burden in bone in living animals throughout the course of the experiment with these techniques. To better understand the relationship between tumor burden and osteolysis, we have used more sensitive techniques. In breast cancer patients, ¹⁸FDG PET scans and ^{99m}Tc-MDP SPECT are used to track tumor growth, bone metastases and response to therapy. We hypothesized that ¹⁸FDG MicroPET scans and ^{99m}Tc-MDP MicroSPECT with MicroCT anatomical co-registration would allow us to detect tumors at earlier time points, detect smaller bone metastases than by radiography alone, and more thoroughly test the vicious cycle hypothesis. Here, we present the first use of MicroPET, MicroSPECT/CT to track tumor burden and bone metastases in this model. Using this model, tumor in bone was detected as early as 7 days post tumor cell inoculation using ¹⁸FDG MicroPET, 7-days earlier than by radiography. In addition, ^{99m}Tc-MDP uptake was decreased in mice with more severe osteolytic lesions. Furthermore, we were able to detect osteolytic lesions by MicroCT that would otherwise have been undetectable by radiography because of their size and by histological methods because of their site. For example, multiple lesions in the scapula can be seen that were not visible by faxitron. These techniques are a better measure of tumor burden than traditional histologyallowing for monitoring of tumor burden throughout the course of metastasis. This approach will

enhance the utility of this model of as it will allow monitoring of changes in and correlations between tumor burden and osteolysis in mice bearing breast tumors with various manipulations.

Disclosures: **S.S. Padalecki**, None.

M055

⁴¹Ca Non-Invasively Identifies at High Sensitivity Skeletal Perturbations from Bisphosphonate Therapy and Metastatic Bone Disease. **D. J. Hillegonds***¹, **D. W. Burton***², **R. L. Fitzgerald***², **E. Denk***³, **T. R. Walczyk***³, **L. J. Deftos***², **J. S. Vogel***¹. ¹Lawrence Livermore National Laboratory, Livermore, CA, USA, ²San Diego Veterans Administration Healthcare System and University of California, San Diego, CA, USA, ³Swiss Federal Research Institute (ETH), Zurich, Switzerland.

The goal of this project is to develop ⁴¹Ca as a clinical tool for staging and monitoring skeletal tumor growth, assessing response to therapy, and detection of bone metastasis. We hypothesize that high precision assessment of bone turnover will enable improved clinical management in disorders affecting calcium metabolism. Following administration of a radiologically benign ⁴¹Ca dose, body-wide ⁴¹Ca/Ca quickly decreases as the tracer is cleared from small and fast calcium pools, concentrating in the skeleton, from which it is slowly re-released. Due to low natural abundance (<10⁻¹⁵), ⁴¹Ca remains above quantitation limits of accelerator mass spectrometry (AMS) for many years following a single <1ug dose. Low natural ⁴¹Ca/Ca variability (<10%) facilitates detection of small perturbations in bone turnover. We measured urinary ⁴¹Ca/Ca in 6 osteopenic postmenopausal women on weekly risedronate in a study conducted at ETH. Results show a consistent ⁴¹Ca/Ca decrease (53±9)% (mean±SD) from baseline that is significant at each post-intervention measurement, making ⁴¹Ca more sensitive than available biomarkers. We have also completed a preclinical study in 50 immunocompromised mice injected intratibially with a green fluorescent protein-expressing human prostate cancer cells (PC3-GFP) two weeks after an IP ⁴¹Ca dose. Five groups were treated monthly with vehicle or one of four bisphosphonates; six weeks later lesions were assessed via fluorimetry and X-rays. AMS analysis showed high correlation of ⁴¹Ca/Ca and serum PTHrP, [Ca²⁺], and fluorimetry; animals with low bone destruction (via X-ray) had significantly lower serum ⁴¹Ca/Ca. We have demonstrated that urinary ⁴¹Ca/Ca is consistently and significantly depressed from baseline with weekly risedronate in individual research subjects, making the ⁴¹Ca assay the most sensitive available marker of bone turnover. We have also shown that serum ⁴¹Ca/Ca identifies bone destruction and cancer proliferation in a preclinical model of metastatic prostate cancer.

Disclosures: **D.J. Hillegonds**, None.

M056

Skeletal Effect of Exemestane in Patients with Breast Cancer. **L. Banks***¹, **S. Girgis***¹, **R. Coleman***², **L. Porter***³, **G. Baffoe***¹, **D. Price***³, **E. Hall***³, **J. Bliss***³, **C. Coombes***¹. ¹Imperial College, London, United Kingdom, ²Weston Park Hospital, Sheffield, United Kingdom, ³Institute of Cancer Research, Sutton, United Kingdom.

Tamoxifen (T) preserves bone in post menopausal women with primary breast cancer but use of non-steroidal aromatase inhibitors (AI) can accelerate bone loss & increase fracture risk. Pre-treatment with T, coupled with possible anabolic effects of the steroidal AI exemestane (E) may lead to fewer adverse effects than up-front non-steroidal AI. In the IES, 4724 postmenopausal women with primary breast cancer, disease-free following 2-3 yrs T, were randomised to further T or E to complete a total of 5 yrs adjuvant endocrine therapy. We report results, up to 12 months, of the bone sub-protocol aimed to assess changes in bone density (BMD) & bone turnover during & after 2 yrs of stopping randomised treatment. 206 randomised IES patients (100E, 106T) with no evidence of osteoporosis or osteoporotic fracture, evaluable BMD measurements & not taking medication known to affect BMD participated in the bone sub-protocol. Lumbar spine & hip BMD measurements were assessed by dual-energy x-ray absorptiometry at pre-randomisation, 6 & 12 months. Serum & urine samples were collected pre & at randomisation, 3, 6, 9 & 12 months, for analysis of biochemical markers of bone turnover: urinary NTX & DPD, serum CTX, bone ALP, OC & PICP. At randomisation, the T & E groups were comparable with respect to patient demographics, BMD & bone markers. At 12 months a significant difference in the mean BMD percent change from randomisation was seen between the E & T groups (lumbar spine: -3.05% (95%CI: -4.09 to -2.01) p<0.0001; total hip: -1.56% (95% CI: -2.32 to -0.79) p=0.0001). Within the E group, a reduction was seen in lumbar spine & total hip BMD's [3.2 % (95% CI: 2.5 to 4.0) & 2.1% (1.6 to 2.7) respectively]. Significantly less change was seen within the T group [spine= -0.2% (-0.9 to 0.5), hip= -0.6% (-1.1 to -0.03)]. Difference in median % change of all bone markers from randomisation to each follow-up assessment was statistically significant between the E & T groups (p<0.0001, except for PICP p=0.002 at 3 months). At 12 months, there was a significant negative correlation between % change in lumbar spine BMD & % change in each of the bone markers (p<0.0001, except for CTX p=0.0002). Similar negative correlations were seen with total hip BMD (p<0.0001 for OC, p=0.0003 for CTX, p=0.001 for DPD, NTX & bone ALP, p=0.03 for PICP). In contrast to T, E has a significant effect on bone with BMD loss consistent with other AI's. Observed changes could be due to dual effects of T withdrawal & E treatment. Comparison of post treatment data will help elucidate this relationship.

Disclosures: **L. Banks**, None.

M057

Mevalonate Inhibition by Lipophilic Statin Induces Apoptosis in Human Prostatic Cancer Cells. **V. Thoreau***¹, **A. Kitzis***¹, **P. J. Marie***², **F. Debais***³. ¹LGCM CHU Poitiers and UMR 6187 CNRS, Poitiers, France, ²Inserm U 606, Lariboisiere Hospital, Paris, France, ³Department of Rheumatology, CHU, Poitiers, France.

Prostate cancer is the most common malignancy and a leading cause of male cancer deaths. Additionally, prostate cancer cells frequently metastasize to the bone marrow, resulting in significant mortality. Among possible mechanisms, dysregulation of apoptosis may play a role in the development of prostate cancer and metastatic process. Agents that promote malignant cell apoptosis may therefore help to develop new therapeutic strategies for prostate cancer. Inhibitors of 3-hydroxy-3-methylglutaryl coenzyme A (HMG-CoA) reductase were found to trigger apoptosis in soft tumor cells in vitro. In this study, we analysed the effects of a lipophilic statin (atorvastatin) and hydrophilic statin (pravastatin) (kindly provided by Bristol-Myers Squibb, USA) on apoptosis in androgen-independent human prostate cancer cells (PC3) and less-malignant, androgen-dependent LNCaP cells. Prostate cancer cells were treated with atorvastatin or pravastatin, at concentrations ranging from 0.1 to 100 µM. Apoptosis was determined by terminal deoxynucleotidyl transferase-mediated nick-end labeling (TUNEL) analysis, and annexin V binding and propidium iodide incorporation were analyzed with flow cytometry. Treatment with atorvastatin (10 µM) significantly increased by 50 % the number of TUNEL-positive prostatic cells (p <0.01) and the number of annexin V-positive apoptotic cells at 48 hours. Similar results were obtained with LNCaP cells. This pro-apoptotic effect occurred through stimulation of caspase-3 activity, as atorvastatin increased caspase-3 activity by about 50 % (p <0.001) at 48 hours. In contrast, no pro-apoptotic effect was observed with pravastatin on these cell lines. Pre-treatment with mevalonate prevented the effects of atorvastatin on apoptosis. Pre-treatment with geranylgeranylpyrophosphate (GGPP), but not farnesylpyrophosphate (FPP), also significantly decreased atorvastatin-induced apoptosis in PC3 cells. These results show that inhibition of mevalonate pathway by the lipophilic statin atorvastatin induces human prostatic cancer cell apoptosis by a mechanism involving caspase-3 activity. This suggests that some statins may be used for controlling prostate cancer cell growth and reduce progression to bone metastasis.

Disclosures: **F. Debais**, None.

M058

Msx2 Antagonizes Runx2 Regulation of Osteolytic Activity in Breast Cancer Cells. **G. L. Barnes***¹, **D. Buczak***¹, **J. Renz***¹, **A. Javed***², **J. B. Lian***², **G. S. Stein***², **L. C. Gerstenfeld***¹. ¹Orthopaedic Surgery, Boston University Medical Center, Boston, MA, USA, ²Cell Biology, University of Massachusetts Medical School, Worcester, MA, USA.

Recent studies from our laboratory have demonstrated that human breast cancer cells express the transcription factor Runx2, a central regulator of skeletal cell differentiation. We further showed that Runx2 regulated the ability of breast cancer cells to disrupt the normal balance of bone cell differentiation and the generation of osteolytic lesions in bone. One of the known co-regulatory proteins of Runx2 activity in osteoblasts is the Msx2 homeodomain factor. We have reported that in breast cancer cells Msx2 acts as a negative regulator of the expression of bone sialoprotein, a Runx2 regulated extracellular matrix molecule whose expression is highly correlated with skeletal metastasis in a number of cancers including breast, prostate and lung. The current studies examined the functional relationship between Runx2 and Msx2 in metastatic breast cancer cells. Highly aggressive MDA-MB-231 and LCC15-MB breast cancer cells express low to undetectable levels of Msx2 while low aggressive MCF-7 cells express high levels. This expression pattern is inversely correlated with both the aggressiveness of the individual cell lines and endogenous level of Runx2 expression. In addition, we found that when Runx2 function in MDA-MB-231 cells is disrupted by over-expression of a dominant negative mutant of Runx2 (C-terminal deletion of Runx2) Msx2 expression was markedly increased. In order to further analyze the function of Msx2 in breast cancer mediated osteolysis we have generated MDA-MB-231 based cell lines that over-express Msx2. Co-culture of these cells with bone derived marrow stromal cells (MSCs) demonstrated that over-expression of Msx2 partially rescues the imbalanced bone cell differentiation generated by breast cancer cells. Unlike control MDA-MB-231 cells, Msx2 over-expressing MDA-MB-231 cells do not inhibit osteoblast differentiation as determined by osteoblast associated mineralized nodule formation and the expression of the osteoblast marker genes. However, MSC co-cultured with Msx2 over-expressing MDA-MB-231 cells do express increased levels of the pro-osteoclastogenic cytokines RANKL, M-CSF and TNFα similar to control breast cancer cells. Taken together these data demonstrate a functional relationship between Runx2 and Msx2 in breast cancer cells and support the conclusion that Msx2 acts as a negative regulator of Runx2 functions involved in the generation of osteolytic lesions in bone.

Disclosures: **GL. Barnes**, None.

M059

The Runx2 Transcription Factor Supports Expression of Genes Coupled to the Invasive and Osteolytic Properties of Breast Cancer Cells. J. Pratap¹, A. Javed¹, G. L. Barnes², L. C. Gerstenfeld², M. Breen^{*1}, A. J. van Wijnen¹, J. L. Stein^{*1}, L. R. Languino^{*3}, G. S. Stein¹, J. B. Lian¹. ¹Department of Cell Biology and Cancer Center, University of Massachusetts Medical School, Worcester, MA, USA, ²Department of Orthopaedic Surgery, Boston University Medical Center, Boston, MA, USA, ³Department of Cancer Biology, University of Massachusetts Medical School and Cancer Center, Worcester, MA, USA.

Breast cancer (BC) cells metastasize to bone resulting in its destruction. Secreted factors from BC cells are known to disturb the balance between osteoblast and osteoclast activities, but the transcriptional mechanisms responsible for induction of factors that cause osteolytic lesions are poorly understood. We and others have demonstrated that Runx2 is upregulated in bone metastatic cancer cells compared to primary tumor cells. Here we addressed the role of Runx2 in the cancer cell by generating MDA-MB-231 BC cells stably expressing a Runx2 mutant (mRunx2) protein. Because mRunx2 protein blocks *in vivo* osteolytic activity of the parental MDA-MB-231 expressing wild type Runx2, we hypothesized that Runx2 contributes to cancer cell metastasis through expression of Runx target genes. Gene profiles of BC cells expressing wild type and mRunx2 revealed VEGF and several MMPs (matrix metalloproteinases) including MMP9, a key metastatic marker, are downregulated in the mRunx2 cells. We show here MMP9 is a novel Runx2 target gene by chromatin immunoprecipitation and EMSA studies and by loss of Runx2 mediated transcription after induction of a point mutation of a Runx site in the MMP promoter. Forced expression of Runx2 upregulates MMP9 promoter activity, indicating that Runx2 is a potent activator of the MMP9 gene. In addition, microarray data identified changes in expression of cytokines and integrins in the mRunx2 cells that suggests a less invasive and less osteolytic phenotype. To establish that Runx2 levels are related to metastasis, we performed Matrigel invasion assays. Cell invasion of the non-metastatic MCF-7 line was induced 3-fold upon Runx2 adenovirus mediated expression which also induced VEGF and MMP9. Depletion of Runx2 in metastatic MDA-MB-231 cells with siRNA results in significant decrease in endogenous MMP9 and other Runx2 target genes and decreases cell invasion by 65%. In conclusion, we identified MMP9 as a novel Runx2 target gene and demonstrated that Runx2 expression is directly correlated with invasive properties of bone metastatic breast cancer cells. These findings indicate that Runx2 plays an important role in modulating cancer cell invasion by regulating the expression of target genes implicated in bone metastases.

Disclosures: **J. Pratap**, None.

M060

The Effect of Bisphosphonates on Gene Expression: The GAPDH as a Housekeeping or a New Target Gene? F. Bertoldo^{*1}, M. Valenti^{*1}, L. Dalle Carbonare^{*1}, M. Zanatta^{*1}, S. Zenari^{*1}, Z. Carandante^{*1}, O. Vinante^{*2}, V. Lo Cascio¹. ¹Biomedical and Surgical Sciences, University of Verona, Verona, Italy, ²Oncologia Medica, Ospedale di Noale, Noale, Italy.

The employment of the RT-PCR method has been widely used for the analysis of gene expression in many systems, including tumor samples. The GAPDH (Glyceraldehyde-3-phosphate dehydrogenase) has been commonly considered as a constitutive housekeeping gene to normalize the specific gene expression. However the GAPDH has been shown to be upregulated in cancer. Bisphosphonates (BPs), synthetic analogs of pyrophosphate, are potent inhibitors of bone resorption and recently an antitumor effect has been shown *in vitro* and in animal models by inhibition of the mevalonate pathway. Furthermore BPs has been shown to modulate many gene expression not only in osteoclasts but also in cancer cells. The aim of this study was to evaluate GAPDH gene expression by real time RT-PCR (Applied Biosystems) in different breast (MCF-7 and T-47D) and prostate cancer cell lines (PC-3 and DU-145) lines (purchased from ATTC Rockville, MD, USA). treated with amino and non-amino bisphosphonates (clodronate, pamidronate, alendronate and zoledronate) to exclude, if any, effects of BPs on GAPD mRNA expression, and to explore the suitability of GAPDH as housekeeping gene in gene expression studies. Cells were treated for 48 h with BPs with doses of 10, 50 and 100 μ M. For each concentration three experiments were performed. The housekeeping gene B2M was used to normalized GAPDH mRNA expression. Our results show a significant dose-dependent downregulation of GAPDH gene expression after treatment of different cancer cells line with different amino-BPS. Zoledronate resulted the most powerful bisphosphonate, whereas Clodronate, a non-amino BP, exerted significant effect on GAPDH expression only with the highest concentration tested. In conclusion, the use of GAPDH as a control gene, in particular in studies investigating the effects of BPs on bone or cancer cells, should be inappropriate and RT-PCR data on the effects of BPs in cancer cell should be reviewed, utilizing a different house keeping gene, i.e. B2M. On the other hand, this gene could be considered as a novel target gene for BPs on cancer cells.

Disclosures: **F. Bertoldo**, None.

M061

p65 Subunit Is Essential for Osteoclastogenic Factors Expression in Breast Cancer Cells. C. Menaa, A. Abdoulaziz^{*}, S. Sprague. Medicine, Evanston Northwestern Healthcare, Evanston, IL, USA.

Bone metastases are a frequent complication in patients with advanced breast cancer (BC). This is related to the process by which tumor cells metastasize; that involves adhesion, migration, and induction of osteoclast (OC) formation. How tumor cells acquire these capacities and the mechanisms involved are not yet identified. However, it is known that tumor cells are the source of factors involved in bone metastasis, bone resorbing

factors (BF). Previous studies have highlighted the role of NF- κ B as potential signaling pathway critical for BC cell viability. Specifically, NF- κ B has been reported to be responsible for cell transformation, death resistance, and motility. In addition, constitutive activity of NF- κ B has been recorded in BC. During last year meeting we reported that NF- κ B activity is the key pathway involved in BC cells' capacity to secrete osteoclastogenic factors, a key element for bone metastasis. We also showed that I κ B kinase complex is involved in this process. Now, which subunits are involved in such activity and what triggers the I κ ks complex activity is yet to be analyzed. Five members of NF- κ B family have been described: p50/p105, p52/p100, Rel A (p65), Rel B and c-Rel. The classical complex involved into transcription activity is p65/p50 complex where only Rel bears transcription activity. Furthermore, previous studies demonstrated the abnormal nuclear translocation of RelA in cancer cells. Thus, the role of p65 in BF in BC cells was examined. Stable cell lines, MCF7 and MDA-MB-231, over-expressing p65 dominant negative where transactivation domain (c-terminal) was deleted (p65RHD) were developed. We found the absence of p65 activity blocks basal and activated NF- κ B as reported by luciferase reporter gene assay following TNF- α stimulation. Condition media harvested from these lines do not support OC formation compared to the WT type cells. The absence of BF factors was not related to a reduction into cell proliferation but rather a specific blockage BF expression. Further analysis in the upstream signaling pathway demonstrate that I κ ks complex is required for p65 translocation and transcription activity and more importantly the TAK/TAB complex is the module that regulates this complex and is involved into BF production by BC cells. In summary, we found that p65 subunit plays a key role into NF- κ B activity controlling BF production by BC cells. In conclusion, these data establish the role p65 subunit of the NF- κ B in bone metastasis in BC. Thus, RelA could be a suitable therapeutic target for bone destruction in BC.

Disclosures: **C. Menaa**, None.

M062

Estren Is Devoid of Proliferative Effects on Hormone-Dependent Human Breast and Prostate Cancer Cells and Counteracts the Mitogenic Effects of 17 β -Estradiol (E₂) or Dihydrotestosterone (DHT). P. Yang, S. Kousteni, S. C. Manolagas. Div. of Endocrinol., Center for Osteoporosis and Metabolic Bone Diseases, Central Arkansas Veterans Affairs Healthcare System, Univ. Arkansas Med. Sci., Little Rock, AR, USA.

It was reported earlier that, unlike E₂, 4-estren-3 α ,17 β -diol (estren) does not stimulate breast cancer cell proliferation. However, the potency of estren on a variety of kinase-mediated (nongenotropic) *in vitro* actions on bone cells is either similar or far greater than that of E₂ or DHT at equimolar concentrations. This is in spite of the fact that estren has 300-fold lower affinity for the estrogen receptor (ER) in conventional equilibrium binding assays, compared to E₂; and estren also binds to the androgen receptor (AR) with an affinity that is approximately 1/40 that of R1881 or 1/25 that of DHT. Because of reports suggesting that the effects of estren may result from its ability to activate classical genotropic actions of the ER and/or the AR, we have compared the effects of estren to those of E₂ or DHT on human breast and prostate cancer cell lines, respectively. Estren (10⁻¹² to 10⁻⁸ M), unlike E₂, had no effect on the proliferation of two ER positive breast cancer cell lines, MCF-7 and T47D. Moreover, when added to the cultures in the presence of the maximal mitogenic dose of E₂ (10⁻⁸ M), estren dose-dependently attenuated the proliferative effect of E₂. Consistent with the distinct biologic effect, whereas E₂ had a transient stimulatory effect, estren induced sustained ERK phosphorylation. Furthermore, whereas E₂ (10⁻⁸ M) induced the association of the p85 subunit of PI3K with the ER as well as the phosphorylation of the epidermal growth factor receptor (EGFR) and Akt, estren not only lacked these activities, but it opposed the E₂-induced changes. In difference to estren, DHT could not reverse the effect of E₂ on EGFR or PI3K/Akt phosphorylation. Likewise, in sharp difference from DHT or the androgenic metabolite 19-nortestosterone, estren (10⁻¹² to 10⁻⁸ M) not only did not affect the proliferation of the LNCaP prostate cancer cell line, but it antagonized the effects of DHT. We conclude that at least some of the effects of estren cannot be accounted for by classical genotropic actions through the ER or the AR. In addition, we propose that the distinct biologic profile of estren on hormone-dependent breast and prostate cancer cells may result from the activation of distinct signaling cascades that perhaps counteract those activated by classical ER or AR ligands, probably by recruiting distinct partners to the ER/kinase signalosomes.

Disclosures: **P. Yang**, None.

M063

Short- and Long-Term Precision of GE Lunar Prodigy and Hologic Delphi Scanners. T. N. Hangartner. BioMedical Imaging Laboratory, Wright State University, Dayton, OH, USA.

Whereas short-term precision is important in setting a lower bound on accuracy of a dual-energy absorptiometry instrument, long-term precision is particularly relevant in the assessment of follow-up scans done years later. The goal of this study was to determine the short- and long-term precision of GE Lunar Prodigy and Hologic Delphi scanners. As part of the daily quality assurance, a phantom containing four blocks of bone-like material, embedded in water-equivalent plastic and covering a density range from 0.45 to 2.9 g/cm² (Hologic units) was measured over a 3.5 year period. These BMD values span the range seen in images of common spine and hip scans. The plane areas of the blocks were evaluated by sub-region analysis on two GE Lunar Prodigy and two Hologic Delphi scanners. All scanners were stable over time periods between service events, and the data collected during these periods were used to calculate the short-term precision. For both Delphi scanners, the short-term precision was better than 0.6% for densities larger than 1 g/cm²; for the Prodigy scanners it was better than 0.7% for the two mid-sized blocks and 0.8% for the largest block. The precision error of the thinnest block was about 1.2% for all scanners. The long-term performance of all scanners was influenced by necessary recalibrations, as all scanners were moved to new locations during the observation period,

as well as regular scanner maintenance. The Delphi scanners showed no break points in the phantom data, only a very small but significant drift of 0.08% per year change in BMD. One of the Prodigy scanners showed changes between service events of -2.1%, -1.6%, -0.4%, -0.4% and 0.0%, resulting in a cumulative change of -4.5% compared to baseline. The other Prodigy scanner showed a +0.5% and a +1.0% change due to service events, resulting in a cumulative 1.5% change. Based on this small sample of scanners, the short-term precision is similar between Prodigy and Delphi scanners; however, the long-term precision is considerably worse for the Prodigy scanners.

Disclosures: **T.N. Hangartner**, Procter & Gamble Pharmaceuticals 2; Pfizer 2; Merck 2; Hologic 2.

M064

Imprecision of Whole Body DXA Measurements: Implications for Interpretation of within Person Changes in Fat, Lean and Bone Mass in Obese and Non-Obese Children. K. S. Wosje, B. Knipstein*, H. J. Kalkwarf. Division of Gen & Comm Peds, Children's Hospital Med Ctr, Cincinnati, OH, USA.

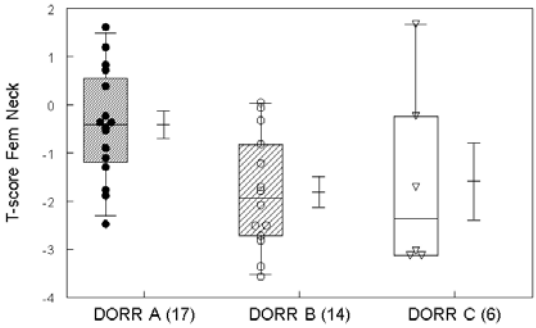
Supervision of children undergoing intervention to combat obesity requires clinicians to appropriately interpret within person data on changes in fat, lean and bone mass. Assumptions inherent to DXA measurement of body composition might lead to greater within person variance (imprecision due to instrument error) in obese than nonobese because of increased tissue thickness. We determined imprecision of whole body (WB) fat, lean and bone mass measurements in obese (n=32) and nonobese (n=34) children (6-19 y) using Hologic QDR 4500. We used the imprecision data to calculate the within person changes in fat, lean and bone mass that are necessary to ensure that those changes are unlikely to be a consequence of instrument error; these are termed least significant changes (LSC) and are expressed in absolute (kg) or relative (%) terms. Subjects received 2 WB DXA scans, with repositioning, and ht, wt, and abdominal thickness (abd thk) measurements. Imprecision was calculated as kg and % for fat, lean and bone mass by finding the root mean square average of within person SD (SD_w) for obese and nonobese. We calculated absolute and relative LSC values as 1.96*1.414*imprecision. We used linear regression to examine the association between SD_w (fat, lean or bone) and wt, fat mass, % fat, and abd thk. Obese and nonobese did not differ in age (12.7±3.2 y), ht (155±15 cm), or bone mass (2.0±0.6 kg). BMI %ile for age and sex was ≥96% for obese and 22-84% for nonobese. Expressed in kg, the LSC for fat and lean were 3.3 and 2.8 times higher, respectively, for obese [1.39 kg (fat), 1.30 kg (lean)] than nonobese [0.42 kg (fat), 0.47 kg (lean)]. Expressed as %, the LSC for fat was 1.5 times lower for obese (3.6%) than nonobese (5.2%), but the LSC for lean was 2.0 times higher for obese (2.6%) than nonobese (1.3%). Bone mass LSC values for obese and nonobese were 61 and 49 g, and 2.9% and 2.9%, respectively. There was a positive relationship between SD_w for fat mass and wt (R²=0.24), fat mass (R²=0.24), % fat (R²=0.13), and abd thk (R²=0.23) (all p<0.01). There was also a positive association between SD_w for lean mass and wt (R²=0.26), fat mass (R²=0.26), % fat (R²=0.17), and abd thk (R²=0.27) (all p<0.001). The positive association between SD_w for bone mass was significant for wt (R²=0.08), fat mass (R²=0.26), and abd thk (R²=0.08) (all p<0.05), but not % fat (R²=0.04, p=0.12). This study suggests that imprecision of DXA fat, lean and bone mass measurements increases with adiposity, but LSCs are low for both obese and nonobese. It is important to view imprecision in both absolute and relative terms. We speculate that body size of obese persons inhibits ideal positioning for WB DXA.

Disclosures: **K.S. Wosje**, None.

M065

Correlation of Plain Radiographic Indices of the Hip with Bone Mineral Density. J. Glowacki¹, A. P. Sah*¹, T. S. Thornhill*¹, M. S. LeBoff². ¹Orthopedic Surgery, Brigham and Women's Hospital, Boston, MA, USA, ²Medicine, Brigham and Women's Hospital, Boston, MA, USA.

The plain hip radiograph is one of the most widely used diagnostic tools in the orthopedic evaluation of hip pathology. T-scores by dual energy x-ray absorptiometry (DXA) and serum 25-hydroxyvitamin D levels were available from a previous study with postmenopausal osteoarthritic women presenting for total hip arthroplasty. We had previously reported that 25% of those subjects had occult osteoporosis by DXA and that 22% were vitamin D-deficient. The purpose of this study was to test the hypothesis that radiographic interpretation of osteoporosis by routine hip x-rays is correlated with bone mineral density. It was our aim to determine the relationships of T-score and serum level of 25-hydroxyvitamin D with radiographic parameters that assess bone geometry and structure at the hip. Pre-operative radiographs of postmenopausal women undergoing total hip arthroplasty for advanced osteoarthritis were studied. Radiographic parameters including Singh index, Dorr classification, canal-to-calcar ratio, and cortical thickness indices were measured and compared with T-score at the femoral neck and with serum vitamin D status. Pre-operative radiographs were available for 37 subjects and included 17 Dorr type A (funnel-shape canal), 14 type B, and 6 type C (stovepipe-shape canal) femurs. These three types showed significantly different canal-to-calcar ratios and cortical thickness indices (p<0.007). The median T-score at the femoral neck for type A bone (-0.415, p<0.02) was significantly higher than that of types B (-1.935) and C (-2.370) (Figure). Cortical thickness indices were correlated positively with T-score (p<0.005). Neither Singh grading nor canal-to-calcar ratios were correlated with T-score. With the numbers available, there was no relationship between vitamin D-deficiency and the radiographic parameters. DXA is not routinely performed prior to total hip arthroplasty, but was available for our study group of osteoarthritic women. Analysis of radiographic parameters of the hip and T-score at the femoral neck revealed several significant correlations. These radiographic measurements are easily obtainable from routine hip radiographs and provide information useful for diagnosis, treatment, pre-operative planning, and referral for DXA and osteoporosis management.



Disclosures: **J. Glowacki**, None.

M066

Estimated Volumetric Bone Mineral Density in a Rural Thai Men and Women: Khon Kaen Osteoporosis Study (KKOS). C. Pongchaiyakul*¹, T. V. Nguyen*², C. Foocharoen*³, R. Rajatanavin*⁴. ¹Division of Endocrinology, Department of Medicine, Faculty of Medicine, KKU, Thailand, ²Garvan Institute of Medical Research, Sydney, Australia, ³Division of Rheumatology, Department of Medicine, Faculty of Medicine, KKU, Thailand, ⁴Division of Endocrinology, Department of Medicine, Faculty of Medicine, MU, Thailand.

We examined the areal bone mineral density (aFNBMD) and volumetric bone mineral density at the femoral neck (vFNBMD) in rural Thai men and women. A total of 181 men and 255 women, between 20 and 84 years of age, living in rural areas of Khon Kaen province, were randomly selected. Areal FNBMD and estimated vFNBMD were determined using dual energy X-ray absorptiometry (DPX-IQ, GE Lunar Corp, Madison, WI). Men had a significantly higher aFNBMD than women, whereas the vFNBMD was similar regardless of sex. The peak for the aFNBMD vs. vFNBMD was observed between 20 and 29 vs. 30 and 39 years of age in men and women, respectively. The prevalence of osteoporosis in men and women using estimated vFNBMD vs. aFNBMD cut-offs was 19 and 14.2 vs. 11.8 and 26 percent, respectively. Prevalence increased with age. Volumetric BMD shows only small sex-correlated differences in bone density. Estimated volumetric BMD was more sensitive than areal BMD, when used to define the osteoporotic cut-offs in men, while it was less sensitive than areal BMD in women.

Disclosures: **C. Pongchaiyakul**, None.

M067

Fat Mass Measured by DXA and Risk of Cardiovascular Disease: Preliminary Results. S. R. Eis¹, S. A. Barros*², R. R. Machado*¹, B. Albergaria*¹, E. J. Moana*¹, J. C. Borges³. ¹CEDOES, Vitoria - ES, Brazil, ²LABIOM, UFES - Vitória (ES), Brazil, ³Universidade Católica de Brasília, Brasília, Brazil.

Cardiovascular disease (CVD) is one of the most important cause of death and morbidity around the world. In particular, body fat distribution has been shown to be an important predictor of risk of CVD. The details and the exact mechanism of how intra-abdominal obesity leads to these conditions is not completely known. Several studies have used DXA technology to provide a more direct measure of fat distribution than that provided by other methods such as anthropometric measurements. The purpose of the study was to evaluate the applicability of fat mass measured by DXA at the total body as well as the ratio between two standardized areas (Android and Gynoid) measured at the waist and the hip, respectively, as predictors of CVD. We evaluated 63 over weighted postmenopausal women with Body Mass Index (BMI) between 25 and 29.9, and divided into two groups as follows: (A)Disease group: 28 women (mean age 62.3 ± 2 and mean BMI 26.9 ±1.2) with recent diagnosis of coronary heart disease (CHD), established not more than 90 days before the evaluation date and (B)Control Group: 35 women (mean age 63.1 ±2 and mean BMI 26.0 ± 1.0) without such diagnosis. The study was approved by the local Ethics Committee and all subjects gave their written informed consent prior to their participation in this study. All women were submitted to a Total Body Densitometry scan, using a Prodigy (GE-Lunar, Madison USA) densitometer, and the scans were analyzed using the Encore® software version 9.15, 2005. A blood sample was collected and a biochemical panel was obtained from all subjects to evaluate other parameters related to the risk of cardiovascular disease. Table 1 summarizes the results for some of the measured parameters.

Group	Cholesterol(95%CI)	%Fat Mass Total Body (95%CI)	%Fat Mass Android Region (95%CI)	% Fat Mass Gynoid Region (95%CI)	A/G Ratio
A	223 (182-267)	44.1% (40.3-46.2)	45.9 (42.8-47.3)	40.2 (38.7-42.8)	1.14*
B	192 (176-215)**	40.2% (38.2-42.1)	39.5 (36.2-42.1)	42.1 (39.8-43.4)	0.93

** (p<0.05) * (p<0.02)

Cholesterol values were significantly higher in the CVD group vs. controls (p<0.05). There was no significant difference between the CVD and control groups for %fat at the total body, android, or gynoid regions. However, the Android/Gynoid Ratio as defined by DXA analysis was a significant predictor of CVD (p<0.02) in this group of overweight postmenopausal women. Further study is needed to confirm these results in larger groups and in different populations, as well as to determine the cutoff level that could perhaps identify increased risk of CVD.

Disclosures: **S.R. Eis**, GE Lunar 2.

M068

Recent Calcium Tablet Ingestion: Impact on Lumbar Spine Bone Mineral Density Measurement. D. Krueger¹, M. Checovich¹, D. Gemar¹, X. Wei^{*2}, N. Binkley¹. ¹University of Wisconsin Osteoporosis Clinical Research Program, Madison, WI, USA, ²Biostatistics and Medical Informatics, University of Wisconsin, Madison, WI, USA.

It is common for densitometry centers to require that patients abstain from ingesting calcium supplements prior to DXA examination to avoid interference with BMD measurement. However, it is not clear that this practice is important or necessary. This study assessed the impact of recent calcium supplement intake on lumbar spine BMD measurement and evaluated the frequency with which tablets are visualized on a DXA image. In this study, 36 subjects (3 male/33 female), mean age 66 years, received baseline and two subsequent spine scans using a GE-Lunar Prodigy densitometer. Subjects were randomly assigned to ingest one calcium tablet: Citracal (315 mg), OsCal (500 mg) or People's Choice (600 mg). Follow-up scans were performed 15 and 30 minutes after tablet ingestion. The three study groups were not different in age or BMI, however the L1-4 BMD was lower ($p < 0.05$) in the People's Choice group compared to the Citracal group. Specifically, the mean L1-4 T-score was -1.6, -1.1 and -0.1 in the Citracal, OsCal and People's Choice supplement groups respectively. The change in L1-4 BMD on repeat scans in this study was compared to the changes observed in a clinical precision dataset consisting of 30 patients scanned twice with repositioning between scans. In the clinical precision study, the least significant change (LSC) was 0.044 g/cm². In that set of 30 patients, the BMD change between scans differed from baseline by more than 0.044 g/cm² in 3 individuals. Similarly, in 3/36 subjects who ingested calcium tablets, L1-4 BMD changes greater than 0.044 g/cm² occurred at 15 minutes, only one of which persisted at 30 minutes. In an additional subject, the BMD differed by more than the LSC only at 30 minutes. Tablets were visualized on one or more scans in 47% (17/36) of subjects; in 38% at 15 minutes and 25% at 30 minutes. People's Choice calcium and OsCal were visualized in 66% of scans while Citracal did not appear in any scan. Visualization of calcium tablets was rarely associated with significant changes in BMD; in only a single instance was a significant BMD change demonstrated when a tablet was visualized. In conclusion, although calcium supplements are often visualized when DXA scans are performed soon after ingestion, they rarely affect measured BMD. It does not appear necessary to require abstinence from calcium supplement ingestion prior to DXA examination.

Disclosures: **D. Krueger**, None.

M069

Quantitative Assessment of Bone Tissue Mineralization with Polychromatic Micro-Computed Tomography. A. Burghard^{*1}, G. Kazakia^{*1}, A. Laib^{*2}, K. Saldanha^{*1}, S. Majumdar¹. ¹Radiology, University of California, San Francisco, San Francisco, CA, USA, ²Scanco Medical AG, Bassersdorf, Switzerland.

To date there is no consensus on the validity of calibrating polychromatic μ CT linear attenuation values to the degree of bone mineralization. The present study investigates short term reproducibility of phantom measurements, hydroxyapatite (HA) phantom sampling limitations, and the accuracy of calibrated mineral density measurements. Phantom and specimen measurements were made on a commercial μ CT system (μ CT-40, Scanco Medical). Custom beam hardening correction factors were determined using a 200 mg/cc HA wedge phantom imaged at 45, 55 and 70 kV. Density calibration of the reconstructed grayscale attenuation values was performed at each voltage setting using a phantom composed of 5 cylinders of HA-resin mixtures with mineral densities ranging from 0 to 800 mg/cc. Short term reproducibility was assessed by acquiring 5 sets of calibration data at each voltage. CV % was calculated for each cylinder at each energy level. To characterize sampling limitations due to phantom heterogeneity, the full length of the phantom was imaged at 70kV. Mean attenuation values were determined for the 800 mg/cc cylinder in 10 randomly placed regions with 6 different lengths ranging from 0.9 to 13 mm along the cylinder. RMS error was calculated for each length against the mean density of the full cylinder. The accuracy of mean mineral density measurements of bone tissue was assessed by comparison to ash density. Eight 8mm cylindrical cores of human vertebral bone were imaged at 70kV with a pixel size of 16 μ m. Mean mineral density was calculated from the grayscale of the bone phase. Tissue volume was determined for each sample using Archimedes' Principle prior to ashing at 600C for 48 hours. Ash density was correlated to mineral density determined by μ CT. The variation for repeat phantom scans ranged from 0.03% to 0.21%. In general, CV was highest at 70kV and lowest at 45kV. RMS error was found to decrease as the sampled length along the phantom increased. RMS error was generally higher in the low density cylinders (0.20-0.40% for 100, 200 mg/cc) and lower in the background and high density cylinders (0.04-0.20% for 0, 800 mg/cc). Mineral density in the vertebral cores ranged from 1.01 to 1.08 g/cc and was well correlated to ash density ($R = 0.85$). The proposed calibration technique was found to have a high level of precision over the short term, little error due to HA phantom granularity, and to accurately depict mean tissue mineralization. In the future, correlations will be extended to cover a wider range of tissue densities, anatomical sites, and species. Regular calibration measurements will be necessary to assess long term stability.

Disclosures: **A. Burghard**, None.

M070

The Effect of Dual Femur Scanning on Osteoporosis Diagnosis and Treatment Decision Making in Postmenopausal Women. R. E. Cole. Internal Medicine, Michigan State University College of Osteopathic Medicine, East Lansing, MI, USA.

The aim of this study was to determine: To what extent does a dual femur Bone Mineral Density (BMD) scan change osteoporosis diagnosis and treatment decision making over a single femur scan? Dual femur results from 313 postmenopausal women were evaluated for right/left T-score discordance at the femoral neck, trochanter, and total hip. Analysis determined the change in diagnosis and treatment classification for the spine measurement and dual femur measurements, as opposed to the spine and single femur measurement. Our results demonstrate when a dual femur scan is performed as opposed to a single femur scan, T-score differences between the contralateral hips result in a change to a more severe diagnosis or treatment category in 14.35% of subjects. We conclude that the dual femur BMD scan results in a change in diagnosis or treatment classification over a single femur scan in 1 in 7 subjects. This discrepancy is large enough to warrant consideration for performing a dual femur BMD scan on all postmenopausal women.

Disclosures: **R.E. Cole**, None.

M071

Development and Testing of a BMD Reporting Tool in a Tertiary Academic Centre. A. M. Cheung¹, H. McDonald-Blumer¹, L. Tile^{*1}, M. Kapral^{*1}, J. Pokovic^{*2}, H. Hu^{*1}, R. Ridout¹. ¹Osteoporosis Program and Department of Medicine, University Health Network and Mount Sinai Hospital, University of Toronto, Toronto, ON, Canada, ²Osteoporosis Program, University Health Network and Mount Sinai Hospital, Toronto, ON, Canada.

Despite recent ISCD guidelines for BMD reporting, the quality and usefulness of BMD reports are highly variable. The objective of our study is to develop and test a software model for BMD reporting based on ISCD guidelines and what referring physicians find useful. We reviewed the medical literature on risk factors for fractures in different populations and on the usefulness of various components in a BMD report. We then devised and tested an evidence-based software tool for BMD reporting. This software incorporates a simple clinical assessment that patients can complete by themselves, routine information obtained by the BMD technologist, validated fracture risk assessments based on a combination of risk factors and BMD where possible, and expert opinion of the reporting clinical densitometrist. The software tool was tested on a Hologic densitometer and the procedure was refined. The resulting MS Word document report gives the referring physician the information recommended by ISCD as well as quantitative estimations of 5-year, 10-year and lifetime fracture risks. Using this software tool as part of the reporting process does not require more time than routine review and reporting by the clinical densitometrist. This evidence-based software tool is useful for BMD reporting. It can be easily updated to incorporate new evidence on the relationship between BMD, risk factors and fracture risk as they emerge. Further testing and validation of this reporting software should be conducted at other academic centres.

Disclosures: **A.M. Cheung**, None.

M072

Age-Related Regional Changes in Body Composition and Bone Mass in Healthy Men. B. Oliveri, S. R. Mastaglia^{*}, C. Fernández^{*}, J. M. Deferrari^{*}, M. Seijo^{*}, A. Bagur^{*}. Sección Osteopatías Médicas, Hospital de Clínicas, Universidad de Buenos Aires, Buenos Aires, Argentina.

DXA methodology allows performing a precise assessment of bone mineral density (BMD) and the three compartments of body composition (BC): bone mineral content (BMC), fat and lean mass. These parameters are measured in a total body (TB) scan, and body subregions can be distinguished. This evaluation may have implications in clinical practice. Normal reference values are necessary to correctly evaluate changes in different diseases. The purposes of this study were to 1- Establish BMD reference values in healthy men at different decades of life (from the age of 20 to 79 years) 2- Analyze BMD and BC changes throughout the decades of life 3- Evaluate changes in the different subregions. The study population comprised 103 normal Caucasian male volunteers aged 20 to 79 years with a body mass index (BMI) between 20-30 g/m². BMD and BC (BMC, fat, %fat and lean mass) of TB and subregions (legs, arms, trunk, total spine and pelvis) were determined by DXA (LUNAR-DPX-L). The changes from 20-29 to 70-79 years were analyzed by ANOVA. Comparative data from 20-29 years and 70-79 years are shown. From 20-29 to 70-79 years there was a small decline of $\approx 4\%$ in TB BMD and subregions (arms, legs, trunk) (NS) and only pelvis and total spine BMD showed a significant diminution (10% and 6%; $p < 0.002$ and $p < 0.006$ respectively). TB BMC showed a 15% diminution ($p < 0.02$), with all subregion BMCs decreasing significantly from 13 to 23% ($p < 0.05$). TB lean mass also showed an 8% decline (56.5 vs 51.5 kg) ($0.1 < p < 0.05$) with only lean mass of the legs exhibiting a significant diminution (-15%) ($p < 0.001$). A progressive increase in BMI (24 ± 2.1 to 27 ± 2.0 g/cm²) ($p < 0.02$), percentage of fat ($18.8 \pm 5.6\%$ to $29.5 \pm 4.9\%$) ($p < 0.001$) and total fat mass (14.3 ± 5.7 to 21.6 ± 3.8) ($p < 0.003$), mainly due to a 5 kg (+73%) ($p < 0.0001$) increase in trunk fat mass, was observed throughout the decades of life. To conclude: 1-Reference values for TB and BMD of subregions and BC in healthy men were obtained for each decade of life. 2-Non significant changes in TB BMD, with a diminution in TB BMC, were observed with aging. 3- TB lean mass tended to decrease with aging, while BMI, TB fat mass and its percentage were found to increase. 3- Analysis of subregional BMD showed a diminution in total spine and pelvis and in all BMC subregions. 4.Evaluation of BC subregions showed a central increase in fat mass

(predominantly trunk) with peripheral lean mass (predominantly legs) tending to decrease. These changes in BC may have implications in the risk of cardiovascular and metabolic syndromes.

Disclosures: **B. Oliveri**, None.

M073

Bone Density and Geometry in Women With Osteopenia, Osteoporosis and Hip Fractures. **A. Bagur**, **M. Seijo***, **F. Solis***, **C. Mautalen***, **B. Oliveri***. Sección Osteopatías Médicas, Hospital de Clínicas, Universidad de Buenos Aires, Buenos Aires, Argentina.

Bone mineral density (BMD) and femur geometry are predictors of osteoporotic hip fractures (HF) (Osteoporos Int 5:167,1995). The aim of this study was to evaluate BMD and femur geometry of control women (C), patients with osteopenia (O), osteoporosis (OP) and HF. The study population comprised 75 C (age: 69.8 ± 5.2 years), 132 O (age: 70 ± 6.3 years), 48 OP (age 74.1 ± 6.3 years) and 13 with recent FC (age: 75.2 ± 8.8 years); BMD of the hip contralateral to HF was determined in the latter. BMD and femoral geometry were evaluated by DXA (Lunar Prodigy). BMD of femoral neck (FN), Ward triangle (W), trochanter (T), total femur (TF), upper FN (UFN) and lower FN (LFN) was determined. As regards geometry, hip axis length (HAL), cross sectional moment of inertia (CSMI), and cross sectional areas (CSA) of the femoral neck were evaluated. The following results were obtained (X ± 1SD):

	Controls	Osteopenia	Osteoporosis	Hip Fractures
Height	153.4 ± 0.06	152.9 ± 0.06	151.6 ± 0.06	156.1 ± 0.1***
Weight	71 ± 11.0	67.2 ± 10.1*	59.8 ± 10.1****	61 ± 11.15****
BMD FN	0.988 ± 0.09	0.771 ± 0.05****	0.642 ± 0.031****	0.688 ± 0.11****
BMD UFN	0.814 ± 0.11	0.614 ± 0.06****	0.497 ± 0.042****	0.507 ± 0.06****
BMD LFN	1.153 ± 0.10	0.924 ± 0.07****	0.781 ± 0.05****	0.865 ± 0.2****
BMD T	0.858 ± 0.09	0.687 ± 0.09****	0.669 ± 0.06****	0.55 ± 0.13****
BMD TF	1.046 ± 0.09	0.831 ± 0.09****	0.669 ± 0.06****	0.693 ± 0.14****
HAL	102.9 ± 6.15	102.07 ± 5.62	103.6 ± 4.92	110.2 ± 7.01***

p<0.01 ;***p<0.001; ****p<0.0001 versus control group
A greatest decrease ranging from 25 to 39% was observed in the upper femoral neck region. OP women presented decreased Height (151 ± 0.06 vs 156 ± 0.10 m, p<0.05) and HAL (103.6 ± 4.9 vs 110.2 ± 7.0 mm, p< 0.003) compared with HF. Our results show that: 1- Femur BMD decreased progressively in patients with O, OP and HF, compared with C. 2- The decrease was greatest at the level of the upper femoral neck, which is where the fracture may start. 3- Hip geometry allowed differentiating the fractured population from the osteoporotic population. 4- An index combining BMD and geometry may prove to be a useful predictor of hip fracture.

Disclosures: **A. Bagur**, None.

M074

Application of the National Osteoporosis Society Guidelines for Peripheral X-ray Absorptiometry Bone Densitometry Scanners (UK). **E. J. Harrison***, **H. Prow***, **J. E. Adams**. Clinical Radiology, ISBE, The University of Manchester, Manchester, United Kingdom.

In December 2004 the National Osteoporosis Society UK released guidelines for the use of peripheral dual energy X-ray absorptiometry (pDXA) scanners. These guidelines suggest a triage approach to classify patients into one of three groups: i) treatment recommended especially if accompanied with other risk factors ii) refer for axial DXA iii) no further action required if no low trauma fracture evident. To determine the thresholds for classification the document states that the upper triage threshold should be the peripheral T score below which 90% of osteoporotic subjects lie, and the lower triage threshold should be that above which 90% of non-osteoporotic subjects lie. The aim of this study was to determine threshold values for three peripheral devices (one pDXA and two quantitative ultrasound scanners (QUS)) and examine the degree of agreement in classification in the same group of subjects. The scanners used were the Pixi (GE Lunar) the CubaClinical (McCue) and the Achilles Insight (GE Lunar). One hundred and ninety seven female patients aged 55 to 70yrs had DXA of spine and hip and pDXA and QUS of the non-dominant calcaneum. Of these 63 patients were osteoporotic and 134 were normal using WHO criteria. The lower threshold T score value beneath which subjects should be treated (classification i) were -2.97 for Achilles, -2.28 for Cuba, -1.7 Pixi. The upper threshold T score value above which subjects required no more treatment (classification iii) were -1.64 Achilles, -1.25 Cuba, -0.4 Pixi. The classification of patients by the three devices was identical in 60% of patients. Using these thresholds on the Pixi 1.5% of osteoporotics would be missed and of the 23.4% treated 34.8% (8.1% of population) would be normal; on the Achilles 3.0% of osteoporotics would be missed and of 18.3% treated 36% (6.6% of population) would be normal; on the Cuba 3.0% of osteoporotics would be missed and of 17.3% treated 38.2% (6.6% of population) would be normal. In this study we have applied the NOS guidelines to three peripheral devices all of which scan the calcaneum. The agreement in classification between the three peripheral devices was only moderate and was at best 79% between the two QUS scanners. However the percentage of osteoporotic and normal patients placed in each classification by each peripheral scanner was similar. Using the threshold values determined for each scanner very few osteoporotics would be missed, however between 34.8 to 38.2% of those classed as requiring treatment were normal using the WHO criteria.

Disclosures: **E.J. Harrison**, None.

ASBMR 27th Annual Meeting

M075

Fracture Risk Assessment Model: Do Values Derived from Western Populations Apply to other Caucasians? **A. Arabi¹**, **H. Awada*²**, **R. Baddoura²**, **S. Haddad*³**, **N. J. Khoury*⁴**, **G. Ayoub*²**, **G. El-haji Fuleihan¹**.

¹Internal Medicine, American University of Beirut, Beirut, Lebanon, ²Rheumatology, Saint Joseph University, Beirut, Lebanon, ³Radiology, Saint Joseph University, Beirut, Lebanon, ⁴Diagnostic Radiology, American University of Beirut, Beirut, Lebanon.

Bone mineral density (BMD) using Dual-energy X-ray absorptiometry (DXA) is a powerful predictor of fractures. Estimates relating BMD to fracture risk have been expressed as RR/SD decrease in BMD, and most estimates were derived from large Western databases. The applicability of such estimates has not been validated in non-Western Caucasian populations. The aim of this study was to assess the ability of BMD measurements, to identify subjects with prevalent vertebral fractures, based on measurements at the hip or forearm in a local non-Western Caucasian population, and compare these estimates to those derived from Western counterparts¹⁻³. 460 subjects (301 women and 159 men), aged 65-85 years, were randomly recruited from a large metropolitan area. BMD at the hip and forearm were measured by DXA, using Hologic device. Lateral radiographs of the thoraco-lumbar spine were assessed using the semi-quantitative method of Genant (JBMR, 1993). Mild fractures were excluded. Age-adjusted Odds Ratio (OR) for vertebral fracture/SD decrease in BMD (hip or forearm) was derived by a logistic regression model using STATA version 7. 56 women (19%) and 18 men (12%) had at least one vertebral fracture.

Table. Age-Adjusted OR [95% CI] for vertebral fracture per SD decrease in non-Western Caucasian population using hip or forearm BMD, and comparison to estimates derived in Caucasians from Western countries.

Site	Local N=301women N=159 men	Western ¹ Metaanalyses women only	Western ² N=2067women N=317 men	Western ³ N=351women N=348 men
Total Hip (Women)	1.5 [1.1; 1.9]	1.8 [1.1; 2.7]	1.7 [1.5; 1.8]	2.4 [1.4; 2.1]
Distal Radius (Women)	1.5 [1.2; 1.8]	1.7 [1.4; 2.1]	-----	-----
Total Hip (Men)	1.7 [0.9; 3.1]	-----	1.4 [1.08; 1.7]	1.2 [0.9; 1.7]

¹ Marshall et al B Med J 1996 (based on 90.000 person years)

² Cauley et al, Osteoporos Int, 2004

³ Melton et al, JBMR, 1998

Our study suggests that the ability of BMD to predict prevalent vertebral fractures is the same in Caucasians whether from Western or non-Western countries, especially when using hip BMD. This has important implications regarding the applicability of using fracture risk assessment estimates in local populations using estimates derived from populations from Western countries.

Disclosures: **A. Arabi**, None.

M076

In Vivo and Ex Vivo Measurement of Skeletal Development in Non-Clinical Pediatric Studies in Rats. **I. A. Moreau***, **A. Varela**, **M. Sabourin***, **C. Chevrier***, **S. Barbeau***, **K. Robinson***, **J. Jolette***, **L. Chouinard**, **S. Y. Smith**. Charles River Laboratories Preclinical Services•CTBR, Senneville, PQ, Canada.

The aim of this study was to establish procedures for the evaluation of the effects of drugs in non-clinical pediatric studies on skeletal development in rats, the primary rodent species used in post-natal and juvenile studies. The techniques evaluated included radiography, DXA, pQCT, histology and histomorphometry. Litters of Sprague-Dawley CD (CD*[SD]IGS BR) rat pups were used ranging in age from 7 to 35 days. *In vivo* procedures were performed under isoflurane gas anesthesia. Medio-lateral and ventro-lateral radiographs were taken to measure the lengths of the femur, tibia and lumbar spine (L1-L6). The anatomical landmarks selected were reliable with coefficient of variation (CV%) on repeat measurements of the same animal up to 1.7% for males and females at 14 days of age. CV% between age groups ranged from 0.7% to 4.7% across all sites evaluated and were similar for males and females 14, 21, 28 and 35 days old. As expected, increases in bone length at each site with age were consistent with growth. In addition, radiographs allowed evaluation of morphological abnormalities. Peripheral QCT scanning was feasible and performed *in vivo* on pups as young as 7 days of age at the tibial proximal metaphysis and diaphysis, and provided information on the trabecular and cortical bone compartments and bone geometry. DXA scanning of the tibia of weanling rats 29 and 35 days of age was also feasible although manual bone mapping was necessary. Double staining of rat skeletal specimens at a range of ages from late gestation to weaning with Alizarin red S (for bone) and Alcian blue (for cartilage) allowed for confirmation of complete ossification of bones that were incompletely ossified or unossified when examined in fetuses, as well as the evaluation of cartilage. Histomorphometry measurements, including growth plate thickness in 35 day old rats, can be used to evaluate effects of drug treatment on bone mineralization, and provide structural and dynamic bone turnover variables for comparison among groups. This study demonstrates that conventional radiography, DXA and pQCT scanning, can be used *in vivo* to monitor skeletal growth at axial and appendicular sites. These data, combined with histology and histomorphometry evaluations, can provide a comprehensive assessment of the effects of a test agent on the developing skeleton.

Disclosures: **S.Y. Smith**, None.

M077

GE Lunar Prodigy DXA Accurately Predicts Skeleton Ash but not Fat and Lean Composition in Growing (1 to 60 kg) Pigs. D. K. Schneider*, T. D. Crenshaw. Animal Sciences, University of Wisconsin -Madison, Madison, WI, USA.

In earlier studies with neonatal pigs (J Bone Miner Res 11:S471) differences were observed between DXA measurements in live pigs and skeletal ash (ASH) determined following dissection of the entire skeleton. Bone mineral content (BMC) by DXA overestimated ASH. Technology for dual energy X-ray absorptiometry (DXA) has changed with introduction of improved detectors and scan modes in new models. Accuracy of the new instruments must be re-assessed. In preliminary work with neonatal pigs (1 to 6 kg) using the small animal scan mode for Prodigy (J Bone Miner Res 16:S459), ash was accurately predicted, but fat and lean composition was over-estimated. To further test accuracy of the GE Lunar Prodigy, 24 pigs ranging from 1.3 to 58.6 kg were scanned using various scan modes (Prodigy software version 8.10.027) across weight ranges. Pigs were killed then dissected to separate the skeleton, soft tissue and viscera contents. Each of the three fractions was ground and the water, fat, protein and ash contents were determined. Recovery of tissue weight following dissection and grinding was 95.5%. Calculation of the percentage of total body Ca recovered in skeletal tissue was 97.2%. Using the small animal (below 20 kg), adult standard (20 to 46 kg), and adult thick (above 46 kg) scan modes revealed a near perfect fit for DXA prediction of dissected skeletal ash (ash, $g = 3.34 + 1.001 \times \text{DXA BMC}$, $R^{2} = 0.999$), but inaccurate predictions of body fat (fat, $g = -11.8 + 1.89 \times \text{DXA Fat}$, $R^{2} = 0.978$) and body lean tissue (lean, $g = 373 + 0.834 \times \text{DXA Lean}$, $R^{2} = 0.99$). Correction equations are needed to adjust predictions of fat and lean composition if the small animal, adult standard, and adult thick scan modes are used at the designated weight ranges. Alternate modes (pediatric and adult thin modes) failed to accurately predict skeletal ash, fat, or lean. Therefore, correction equations are needed to accurately predict body composition if pediatric or adult thin scan modes must be used.

Disclosures: **T.D. Crenshaw**, None.

M078

Proximal Tibia Bone and Muscle Parameters Assessed by pQCT in Dialysis Patients with and without Fracture. C. Gordon¹, L. Beaumont^{*1}, S. Jamal². ¹Radiology, McMaster University, Hamilton, ON, Canada, ²St. Michael's Hospital, University of Toronto, Toronto, ON, Canada.

Introduction: Elevated levels of circulating parathyroid hormone (PTH) may be responsible for a reduction in the cortical bone mineral status in dialysis patients leading to an increased risk of fracture. In addition, the reduced mobility in these patients may result in muscle weakness that could also contribute to bone loss and an elevated fracture risk. Using peripheral quantitative computed tomography (pQCT), the aim of this study was to investigate whether there are differences in cortical bone density, bone geometry and muscle cross-sectional area and fat cross-sectional area in a group of dialysis patients with and without fracture. **Methods:** We studied a total of 43 men and women 50 years and older on maintenance hemodialysis for at least one year. Self reported low trauma or prevalent vertebral fractures assessed by morphometry were identified in 19 subjects. A timed six-minute walk was used to assess mobility in all subjects. Bone parameters and muscle cross-sectional area were measured at the proximal one-third tibia using a Stratec XCT 2000 pQCT scanner. A paired t-test was used to test statistical differences between the fracture and non-fracture subjects. **Results:** Dialysis subjects without fracture were able to walk twice the distance in six-minutes compared with those patients with fracture ($p < 0.0001$). pQCT measures showed a non-significant mean decrease in total bone mineral content (13%, $p = 0.06$), density (11%, $p = 0.1$) and area (3%, $p = 0.7$) between the fracture and non-fracture group. Significantly lower mean values for cortical content and area were noted in patients with fracture ($p < 0.04$). Modest, but significant reductions in geometrical parameters such as cortical area (21%, $p = 0.04$), cortical thickness (18%, $p = 0.04$), section modulus (24%, $p = 0.03$), and the axial strength strain index (26%, $p = 0.03$) were also noted for the fracture group. A 10% reduction in calf muscle cross-sectional area was also detected for the fracture group. This mean difference, however, was not statistically significant ($p = 0.2$). **Conclusion:** Despite a significant reduction in mobility, calf muscle area was not significantly different in dialysis patients with and without low trauma fractures. The modest but significant differences in cortical bone content and geometry detected between the fracture and non-fracture patients suggests that the increased fracture risk is primarily due to PTH imbalance. However, a timed walking test may also be a simple but effective indicator of increased fracture risk and underlying muscle weakness.

Disclosures: **C. Gordon**, Orthometrix Inc. 5.

M079

Multi-Modality Study of the Compositional and Mechanical Implications of Hypomineralization in a Rabbit Model of Osteomalacia. S. S. Anumula^{*1}, J. Magland^{*1}, H. Zhang^{*1}, H. Ong^{*1}, S. W. Wehrli^{*2}, F. W. Wehrli¹. ¹LSNI, Department of Radiology, University of Pennsylvania, Philadelphia, PA, USA, ²NMR Core Facility, Children's Hospital of Philadelphia, Philadelphia, PA, USA.

Water plays a pivotal role in the physiology and function of bone. Water serves as a medium for diffusion-mediated transport of molecules to and from osteocytes and is largely responsible for the bone's viscoelastic properties. Further, during mineralization, mineral crystals take the place of collagen surface-adsorbed water under volume retention. Here, we examine the hypotheses that (a) water content can be measured *in situ* by solid-

state proton NMR imaging, (b) that water is inversely related to mineral content, and (c) that the method is able to distinguish osteomalacic from normal bone. Hypomineralization was induced in a group of 5 rabbits (TR) using a previously developed protocol and the data compared with those of 5 control (CO) animals. ¹H images were acquired at 400 MHz from excised cortical bone by 3D ¹H solid-state imaging (SSI) of the tibia at a resolution of 183 μm . Porosity and degree of mineralization of bone (DMB) were measured by $\mu\text{-CT}$ at 16 μm resolution in the presence of calibration phantoms made of different concentrations of hydroxy apatite. Mechanical properties were measured as well using 3-point bending. Significantly higher water content was found by SSI in the TR group than in the CO group ($19.87 \pm 3.03\%$ vs. $16.61 \pm 2.22\%$; $p = 0.04$). This result parallels the higher porosity found for the TR group (1.94 ± 0.72 vs. $0.62 \pm 0.3\%$; $p = 0.003$), with positive correlations observed between bone water and porosity ($r^2 = 0.52$; $p = 0.02$). Conversely, DMB was lower in the TR group (1279.2 ± 25.68 vs. $1356.1 \pm 18.0 \text{ mg/cm}^3$; $p = 0.0003$). SSI-measured water content correlated negatively with DMB and with ash weight ($r^2 = 0.55$; $p = 0.01$ for the latter). Further, osteomalacic bone was mechanically impaired as indicated by reduced elastic modulus in N/mm^2 (522.10 ± 166.49 vs. 769.32 ± 231.5 ; $p = 0.05$) and ultimate strength (20.4 ± 3.34 vs. $28.3 \pm 3.21 \text{ N/mm}^2$; $p = 0.003$) relative to the control group. Finally, water content and mechanical quantities were inversely related to one another (ultimate strength; $r^2 = 0.49$; $p = 0.04$ and elastic modulus; $r^2 = 0.72$; $p = 0.004$). The data validate the above hypotheses and suggest that proton SSI of bone water can distinguish subtle differences in mineralization density and therefore may provide a new means for noninvasive assessment of DMB.

Disclosures: **S.S. Anumula**, None.

M080

Evaluation of a Contrast-Detail Phantom to Measure Image Quality of DXA Scanners Performing Vertebral Fracture Assessment. L. G. Jankowski¹, M. A. Costello^{*2}, S. B. Brov¹. ¹Center for Arthritis and Osteoporosis, Illinois Bone and Joint Institute, Morton Grove, IL, USA, ²Section of Endocrinology, University of Chicago Hospitals, Chicago, IL, USA.

While conventional radiographs are the current gold-standard for the detection of vertebral fractures, recent improvements in the image resolution of dual-x-ray absorptiometry (DXA) scanners have allowed their use to obtain low-dose images of the thoracolumbar spine for vertebral fracture assessment (VFA). Checks of system image resolution and contrast are not included in the quality assurance protocols provided by DXA manufacturers for these devices. We assessed whether a commercially available contrast-detail phantom designed for conventional radiography could be adapted for use with DXA scanners to monitor system imaging performance. A commercial radiographic contrast-detail phantom (CDRAD 2.0, Nijmegen St.Radboud, Netherlands) was scanned on a GE-Prodigy and Hologic Discovery SL DXA scanner. To simulate soft-tissue, the phantom was placed between two 4cm acrylic plates and images were acquired using the respective manufacturers' VFA acquisition modes, and analyzed using their standard display software. Standard computed digital radiographs (CR) were obtained in the same configuration for comparison. Images were evaluated under identical viewing conditions by two independent observers. Using the grading system provided by the phantom manufacturer, an inverse Image Quality Figures (IQF) was calculated for GE-Prodigy in dual energy (GE-DE) and single energy (GE-SE) display modes, and for the Hologic Discovery in standard (Hologic-IVA) and high-definition (Hologic HD) modes. This parameter is directly proportional to overall image quality. The mean IQF values for the two observers were 0.93, 0.24, 0.21, 0.91, and 0.94, for CR, GE-DE, GE-SE, Hologic IVA, and Hologic-HD phantom images respectively. The CDRAD 2.0 contrast-detail phantom can be adequately imaged and analyzed on DXA scanners performing VFA, and may have value in detecting image degradation of DXA systems over time if incorporated into DXA system quality control protocols. The Hologic IVA and IVA-HD scan modes delivered similar IQF values that were equal to digital computed radiography, and were four times better than GE Prodigy in either dual-energy or single energy imaging modes.

Disclosures: **L.G. Jankowski**, Aventis/Proctor & Gamble Pharmaceuticals 8.

M081

Changing Bone Densitometers in Clinical Practice: Effect on Precision Error. S. M. Hunt^{*}, J. C. Fertile^{*}. Martha Jefferson Hospital, Charlottesville, VA, USA.

Precision error in bone densitometry is directly related to the ability to monitor change in a patient's bone mineral density (BMD). Lower precision error reduces the least significant change (LSC), allowing a smaller measured change in BMD to be identified as biological rather than related to instrument variability. Precision error is influenced by the type of densitometer, the patient population, and by operator experience and training. Densitometry providers should determine their precision error after changes in densitometers or operators. Our hospital recently changed from using 3 Discovery systems to 3 Prodigy Advance systems. As part of the upgrade process, we evaluated the effect of changing densitometers on precision in our practice. A total of 35 subjects were scanned on one of three Discovery (Hologic) systems and on one of three Lunar Prodigy Advance (GE Healthcare) systems. Subjects were measured 3 times each, with repositioning between scans, at the spine (L1-L4) and femur on both densitometers. Average subject age was 61 ± 10 years; 30 women and 5 men participated. Fourteen subjects were scanned on scanner pair A (Discovery A + Prodigy A), 10 subjects on scanner pair B, and 11 subjects on scanner pair C. The clinic's technologists acquired and analyzed all the scans. BMD precision error was calculated as the root-mean-square standard deviation (RMS-SD) and coefficient of variation (RMS-%CV) for the repeated measurements. To directly compare the precision error between the devices, all Hologic values were converted to Lunar-equivalent BMD (1). The 4 technologists who worked with both Hologic and Lunar

systems had more experience using Hologic (>5 yrs, 3 yrs, 3 yrs, 3 yrs) than Lunar (< 4 months for all). The 1 technologist who worked only with Lunar systems had < 4 months experience. Precision data for each manufacturer were pooled. Discovery precision error was significantly higher (between 30% - 90%) at the spine (1.5% vs. 1.0%, p=0.011), femur neck (2.3% vs. 1.8%, p=0.024), and femur total (1.9% vs. 1.0%, p<0.0001) regions. There was no significant difference in precision at the trochanter region. We conclude that precision error with the Lunar Prodigy Advance densitometers was significantly lower compared to the Hologic Discovery, even when the technologists had less experience on the Lunar systems.

1. Lu et. al (2001) Osteoporos Int 12:438-444

	n	Prodigy Advance CV	Discovery CV	p
Spine L1-L4	34	1.0%	1.5%	0.011
Femur Neck	33	1.8%	2.3%	0.024
Femur Troch	33	1.5%	1.8%	0.060
Femur Total	35	1.0%	1.9%	< 0.0001
Femur Dual Total	26	0.6%		

Disclosures: **S.M. Hunt**, None.

M082

Changing from a Hologic to a Lunar Bone Densitometer: Effect on BMD and Precision Error. C. Albanese, R. Passariello*, M. Dante*. University of La Sapienza, Rome, Italy.

In a clinical osteoporosis practice today, patient management may involve comparison of bone mineral density (BMD) values obtained from different bone densitometers. The ability to identify a significant change in patient BMD obtained by two different densitometers is affected by two factors: how well the measurements between the different densitometers correlate and how large the precision error is. Lower precision error allows a smaller measured change in BMD to be identified as biological rather than related to instrument variability. Precision error is influenced by type of densitometer, patient population, and by operator experience and training. In our institution we recently introduced a Lunar Prodigy system while in the past measurements were performed on a Hologic QDR4500. We evaluated the effect of changing densitometers on precision and how well the measurements from these two densitometers correlate. A total of 42 women had bilateral femur scans on a QDR4500W (Hologic) system and a Lunar Prodigy (GE Healthcare) system. Subjects were measured twice on each system with repositioning between scans. Average subject age was 65 ± 7.5 years (50-80 yrs). Different technologists operated the Lunar and Hologic systems. BMD precision error was calculated as the root-mean-square standard deviation and coefficient of variation (CV) for the repeated measurements. To directly compare the precision error between the devices (1), all Hologic values were converted to Lunar-equivalent BMD. Only subjects with two measurements on both systems were included in the CV calculation. There was a strong correlation between QDR4500 and Prodigy total femur BMD values (r = 0.97). QDR4500 precision error at the total femur region was significantly higher than Prodigy precision error: left total femur (2.0% vs. 1.0%, p<0.0001), right total femur (1.4% vs. 0.9%, p<0.01). We conclude that BMD values between the Hologic QDR4500 and the Prodigy can be cross-calibrated. Precision error with the Lunar Prodigy densitometer was significantly lower at the total femur region compared to the Hologic QDR4500. This lower precision error with the new densitometer allows earlier detection of clinically relevant changes in patient BMD.

1. Lu et. al (2001) Osteoporos Int 12:438-444				
	n	Prodigy CV	QDR4500 CV	p
Left Total Femur	31	1.0%	2.0%	<0.0001
Right Total Femur	31	0.9%	1.4%	<0.01
Dual Total Femur	31	0.6%		

Disclosures: **C. Albanese**, None.

M083

A Call for Consensus Regarding Focal Structural Defects. K. E. Hansen, N. Binkley, D. Malone*, R. Christian, D. Krueger, N. Vallarta-Ast, R. Blank. Medicine, University of Wisconsin Osteoporosis Research Program & Clinical Center, Madison, WI, USA.

The International Society for Clinical Densitometry (ISCD) has published criteria by which to exclude vertebrae from lumbar spine densitometric analysis. Previously we reported that when applying these exclusion criteria there is only moderate agreement between interpreters, with poorest agreement regarding the identification of focal structural defects (FSD). To further investigate the utility of the ISCD vertebral body exclusion criteria, we assessed intra-observer reproducibility and specifically whether interpreters identify FSD consistently on two separate occasions. Five ISCD-certified physicians applied the ISCD vertebral exclusion criteria to 90 de-identified lumbar spine DXA printouts on two occasions at least four weeks apart, using a standardized worksheet to record exclusions and final T-scores. Three ISCD-certified technologists obtained the scans in a precision study; subjects included 64 women and 26 men with a mean age, weight, and L1-L4 T-score of 59.1 ± 9.3 years, 71.7 ± 13.8 kg and 0.1 ± 1.2, respectively. Interpreters had no access to their initial notes, when reviewing bone density studies on the second occasion. Resulting data were analyzed where appropriate with descriptive, Pearson's correlation coefficient, and kappa (κ) test statistics. Overall, intra-observer T-score reproducibility was excellent, with very high correlation coefficients (R=0.97-0.99) and small absolute differences in final lumbar spine T-score (range, 0.017 ± 0.126 to 0.140 ± 0.364) between paired analyses. With application of specific exclusion criteria, intra-observer κ were generally good or excellent, with over 60% of values falling between 0.6-1.0. In contrast, half of intra-observer κ values were <0.60 (moderate or fair) with application of the FSD exclusion criterion. Moving caudally from L1 to L4, all interpreters

excluded more vertebrae due to FSD. Notably, enormous inter-observer variability in vertebral body exclusion due to FSD was observed. For example, the five physicians excluded L4 on both occasions in 10, 21, 32, 50 and 78% of these scans. In conclusion, interpreters demonstrate high intra-observer T-score reproducibility when applying the ISCD exclusion criteria on two occasions at least four weeks apart. However, the definition of FSD varies greatly between observers and could potentially impact on patient diagnosis and treatment. Since FSD are a major source of lower inter-observer and intra-observer agreement, standardized definitions regarding what constitutes an FSD should in principle improve the quality and consistency of lumbar spine DXA interpretation.

Disclosures: **K.E. Hansen**, None.

M084

DXA Is Very Useful and Cost-Effective to Detect an Early Suspicious Osteolytic Bone Metastasis. I. Park¹, I. Lee^{*2}. ¹Orthopedic Surgery, Kyungpook University Hospital, Taegu, Republic of Korea, ²Endocrinology, Kyungpook University Hospital, Taegu, Republic of Korea.

The purpose of this study is to introduce the new clinical application of DXA as one of the useful methods to detect early suspicious osteolytic bone metastasis to prevent a pathologic fracture. At least 30 to 40% of bone mass should be decreased to differentiate an osteolytic bone lesion on plain radiographs. So, additional computed tomography(CT) or MRI and/or PET or bone scan should be necessary when bone metastasis is suspected, but plain radiographs failed to reveal it. Bone mineral density of 21 suspicious early bone metastasis were evaluated by a DXA(GE-Lunar Prodigy) to compare the BMD of both sides. Out of these 21 cases, 15 were confirmed with bone scan and/or MRI and/or PET/CT. Our results were as follows: First, DXA could detect an osteolysis of as low as 7 % of difference in BMD with comparison to the opposite normal control area. It is essential that region of interest should cover the entire osteolytic area. Second, DXA is more cost effective than MRI and/or PET/CT when a patient could not afford it. Third, on proximal femoral area where bone metastasis is very common, this method could be still effective even retrospectively with already acquired DXA data as long as both hip areas were checked.

Disclosures: **I. Park**, None.

M085

Low Levels of Knowledge, Confidence, and Self-Reported Use of Bone Density Testing among Family Medicine Residents. M. M. Luckey¹, S. Albert^{*2}, C. A. Berry^{*2}. ¹Saint Barnabas Osteoporosis and Metabolic Bone Disease Center, Mount Sinai Medical Center, Livingston, NJ, USA, ²Center for Health & Public Service Research, New York University School of Public Health, New York, NY, USA.

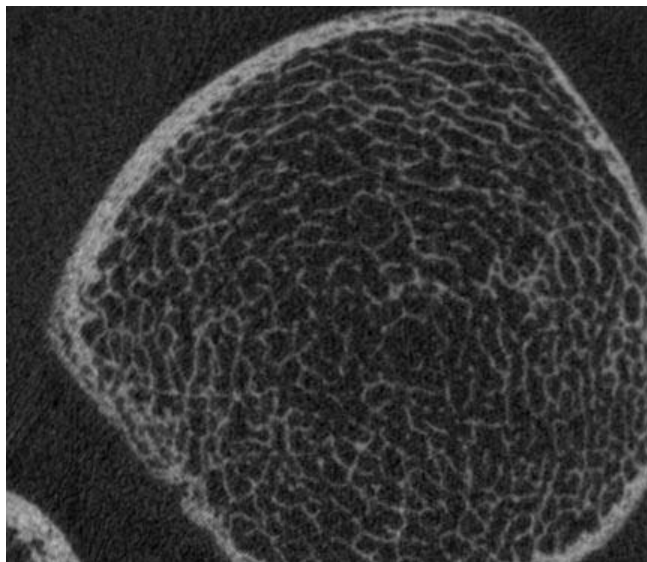
Despite the availability of evidence-based guidelines, simple diagnostic tests and effective therapy, less than one-third of patients with osteoporosis are identified or treated. Intervention by primary care providers will be required to change this number; however systematic training in osteoporosis is not routine in most postgraduate residency programs which could leave physicians without the confidence, knowledge and experience needed to make osteoporosis surveillance and treatment a routine part of primary care practice We sought to evaluate the levels of knowledge, confidence and bone density testing among Family Medicine residents attending thirty-one 1 and 1.5 day long *BetterBones* Osteoporosis Workshops provided by the Academy of Family Medicine Residency. Prior to the workshop residents completed a multiple-choice test of knowledge and a questionnaire regarding their current clinical practices, confidence in their ability to diagnosis and treat osteoporosis and the number of bone density tests ordered in the past 3 months. 717 Family Medicine residents (199 PGY2s; 487 PGY 3s and 30 fellows) from 256 residency training programs attended workshops between March 2003 and December 2004. Pre-workshop test scores of knowledge were low (58 ± 14%) and did not vary significantly by year of attendance at the workshop or by increasing PGY year. Only 20% of the 304participants queried expressed confidence in their knowledge and competence to diagnose and treat this disease. Among 561 residents seeing at least 20 women over age 50/ month (mean 56± 35 (SD)women/per month), 70% reported ordering ≤ 1 bone density test/ month and 25% had ordered no densitometry tests in the past 3 months . The calculated rate of bone density testing was <4% of women ≥ 50 years being tested. Higher levels of confidence, but not pre-workshop knowledge, were significantly correlated with self-reported bone density testing (Pearson r= 0.3, p<.001). These results indicate that intervention is required among family medicine residents to increase the appropriate detection of osteoporosis and that interventions that increase confidence may be particularly important.

Disclosures: **M.M. Luckey**, None.

M086

Bone Microarchitecture Evaluation *In Vivo* in Humans. M. A. Dambacher¹, M. Neff², H. Radspieler³, R. Rizzoli⁴, P. Delmas⁵, L. Qin⁶. ¹Metabolic Bone Diseases, Center for Osteoporosis, Zollikerberg, Switzerland, ²Bone Diseases, Center for Osteoporosis, Zürich, Switzerland, ³Center for Osteoporosis, München, Germany, ⁴Metabolic Bone Diseases, University Hospital Geneva, Geneva, Switzerland, ⁵Metabolic Bone Diseases, Hopital E. Herriot Lyon, Lyon, France, ⁶Orthopaedics and Traumatology, Chinese University, Hong Kong, China.

The non-invasive and quantitative/qualitative 3D bone structure analysis became available in humans with the help of high resolution pQCT (XtremeCT, Scanco Medical Ltd). The new high resolution pQCT enables the simultaneous acquisition of a stack of 100 tomograms with a maximal diameter of 126mm. The isotropic resolution is 120µm (10% MTF, isotropic voxel size 82µm). The tomograms are taken 7mm proximal from the endplate of the distal radius and/or 20mm of the distal tibia (see fig). The data acquisition time is about 3 minutes. The reproducibility is <±1% for structure elements. In praxi it is now routinely possible to quantify in vivo in humans the microarchitectural features as number of trabeculae, trabecular and cortical thickness, trabecular spacing and endosteal surface in addition to the volumetric BMD of trabecular and cortical bone. Such quantitative characterization will give better insight in pathogenesis and treatment of osteoporosis, as well as an improved individual fracture prediction.



Disclosures: M.A. Dambacher, None.

M087

Is there an Alternative to Basic Fuchsin Bulk Staining for the Assessment of Microcracks in Human Iliac Crest Bone Biopsies? B. Burt-Pichat*, M. E. Arlot, J. P. Roux*, P. J. Meunier, P. D. Delmas. INSERM unit 403, C. Bernard University, Lyon, France.

There is increasing interest in microcracks because 1/ they appear to trigger targeted remodelling; 2/ their accumulation in animal treated with high doses of bisphosphonates may lead to reduce bone toughness. Bulk staining with the fluorochrome on the bone specimen prior to embedding and sectioning is necessary to differentiate true microcracks from artefacts due to sectioning, but the most commonly used fluorochrome, basic fuchsin (BF), causes blurring and fading of tetracycline double labeling (TDL) performed in vivo before human iliac crest biopsies. The aim of this study was to validate another bulk staining that preserved TDL. Sixteen iliac crest biopsies taken in ewes after TDL were separated into two parts. One half was stained with the following fluorochromes: basic fuchsin in ethanol solution (BF), fluorescein, green calcein, blue calcein, alizarin complexon and xylenol orange, all either in ethanol- or water-based solution, either individually or in combination. Microcracks were analyzed on three 100 µm thick sections with both white light, epifluorescence and laser confocal microscopy, equipped with adequate filters. The other half biopsies were processed without bulk staining as control for TDL. In addition, all specimens were stained with Goldner's trichrome, solochrome cyanin R, toluidine blue and May-Grunwald Giemsa on 7 µm thick sections to analyze the quality of histomorphometric stainings. Finally, tests were performed on human iliac crest biopsies with TDL. The assessment of microcracks was similar in terms of number and length in sections stained with both BF and other fluorochromes either in ethanol or in water solution. With fluorochromes in water solution TDL was no more visible or blurred when compared to the one of the paired half biopsy. With fluorochromes in ethanol solution, TDL was similar to the labeling seen on the paired half biopsy, except for fluorescein that induced fading of TDL. For all fluorochromes, further stainings were of adequate quality for histomorphometry. Among all the analyzed fluorochromes calcein appears to yield the best results and was selected for microdamage bulk staining in human iliac crest biopsies. In conclusion bulk staining with calcein in ethanol solution 1/ stained microcracks

similarly to basic fuchsin, 2/ did not induce fading of TDL 3/ was visible in both epifluorescence and laser confocal microscopy 4/ preserved the quality of classical histomorphometric stainings.

Disclosures: B. Burt-Pichat, INSERM-Lilly contract 2.

M088

Hip Fracture Susceptibility in Elderly Men and Women Is Explained by Bone Instability Rather than by BMD. F. Rivadeneira¹, C. de Laet², T. J. Beck³, M. C. Zillikens⁴, J. J. Houwing⁴, A. Hofman¹, A. G. Uitterlinden¹, H. A. P. Pols¹. ¹Erasmus Medical Center, Rotterdam, The Netherlands, ²Scientific Institute of Public Health, Brussels, Belgium, ³Johns Hopkins University, Baltimore, MD, USA, ⁴LUMC, Leiden, The Netherlands.

Aim To elucidate what are the main structural properties of bone which determine the risk of hip fracture in elderly men and women. **Methods** This study is part of a large prospective population-based cohort including 147 incident hip fracture cases in 4806 individuals with hip structural analysis at baseline (mean follow-up 8.6 years). Narrow-neck BMD, bone width, cortical thickness, section modulus (index of bending strength) and buckling ratio (BR, a crude index of bone instability is the ratio of the distance from the center of mass to the estimated cortical thickness) were compared in relation to fracture using logistic regression together with areas under the ROC curve. Relative risks (hazard ratios from Cox regressions) of hip fracture per standard deviation were determined to model the one-year risk of fracture and the distribution of fractures across absolute parameter values. **Results** Hip fracture cases in both genders have lower BMD, thinner cortices, greater bone width, lower strength and higher instability (BR) (Table). Differences in BR (18-24%) are about two-fold those observed for BMD (11-13%). No significant difference is observed between the areas under the ROC curves of BMD (0.76) and BR (0.77). Risk at every level of BR is higher in women than men, while for BMD this increase in risk is only seen at very low BMD levels (Figure 1). Similarly, men have a greater risk of fracture at a given cortical thickness, while women have greater fracture risk at a given neck width. The interaction between neck width and cortical thickness is significant (p=0.01) in women and appears to be measured by the BR. In contrast to the displacement observed with BMD, fracture distribution appears to occur at the same absolute levels of bone instability (BR) in both men and women (Figure 2). **Conclusions** Even though buckling ratio does not offer additional predictive value over BMD, these findings suggest that bone instability (related to cortical thickness and bone width) plays a key role on local susceptibility to hip fracture. Further, a similar biomechanical instability threshold applies to both genders despite the known sexual dimorphism of bone.

TABLE. HIP GEOMETRY IN RELATION TO HIP FRACTURE

	MALES				FEMALES			
	HIP FRACTURE		P-value		HIP FRACTURE		P-value	
	Absent n=2025	Present n=41			Absent n=2740	Present n=106		
Age (years)	67.0 ± 0.17	73.2 ± 1.29	↑ 9.2%	<0.00001	67.6 ± 0.15	75.2 ± 0.77	↑ 11.3%	<0.00001
BMD (g/cm ³)	0.74 ± 0.00	0.66 ± 0.02	↓ 10.7%	0.0001	0.67 ± 0.00	0.59 ± 0.01	↓ 12.6%	<0.00001
Cortical thickness (cm)	0.14 ± 0.00	0.13 ± 0.00	↓ 11.2%	0.0002	0.13 ± 0.00	0.11 ± 0.00	↓ 13.0%	<0.00001
Bone width (cm)	3.45 ± 0.01	3.51 ± 0.04	↑ 1.9%	0.10	3.01 ± 0.00	3.08 ± 0.02	↑ 2.4%	0.002
Section modulus (cm ³)	1.39 ± 0.01	1.28 ± 0.05	↓ 7.7%	0.03	0.96 ± 0.00	0.88 ± 0.02	↓ 8.7%	0.0004
Buckling ratio	13.8 ± 0.1	16.3 ± 0.5	↑ 17.9%	<0.00001	13.5 ± 0.1	16.7 ± 0.3	↑ 23.8%	<0.00001

Estimates are (age-adjusted) means ± SEM measured at the narrow-neck region using HSA.

Figure 1. Absolute one-year fracture risk in individuals of age 70 years

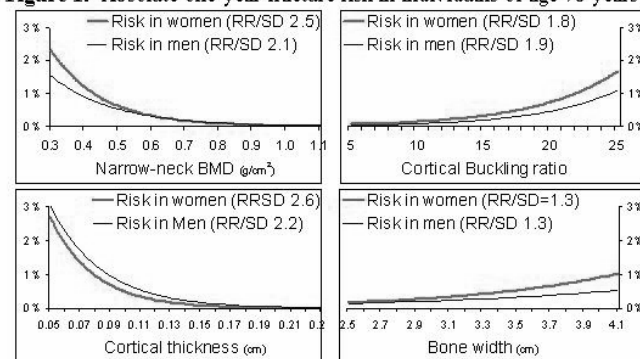
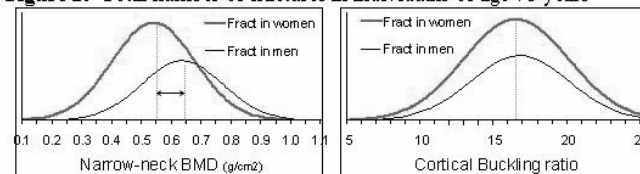


Figure 2. Total number of fractures in individuals of age 70 years



Disclosures: F. Rivadeneira, None.

M089

A Potential Method of Bone Viscoelasticity Measure *In Vivo*. Z. Bechor*¹, J. S. Merritt*², H. M. S. Davies³. Veterinary science, Melbourne University, Werribee, Victoria, Australia.

This study was designed to develop a method of measuring bone viscoelasticity in vivo. Biot's Poroelectric Theory predicts bone fluid flows as a result of a hydrostatic pressure gradient (1) and Biot's viscoelasticity theory predicts creep or stress relaxation due to fluid flow (1). Ultrasound speed (SOS; Sunlight, Equus, Tel-Aviv, Israel) was measured before (to provide a standard) and during applied hydrostatic pressure on a dorsomedial site on the first phalanx of the right and left forelimbs (RP1 and LP1) in five horses. In vivo hydrostatic pressure (undrained) was induced by elevating one forelimb, which increased intramedullary pressure and cortical hydrostatic pressure in the opposite forelimb (the weight bearing limb). In a previous study (2) it was observed in vitro that a reduction in SOS (drained condition) occurred when fluid flowed from a cut bone surface. The SOS measure was continued for 2-3 minutes and any delayed drop in SOS was recorded as a drained condition. The results showed a significant increase of 7% in the SOS on the right and 6.4% on the left (RP1, p = 0.02, SD +/- 32.5, LP1, p = 0.01, SD +/- 40.1) in the undrained condition compared with the standard. There was a delayed reduction in SOS of 62m/s on the right P1 in four horses, but these results were not significantly different from the standard (p=0.09, SD +/- 32.5). This viscoelastic test suggested that fluid pressure and fluid flow have an important role in the dorsomedial region of the cortical bone of P1 in horses. Our previous study (2) on the dorsal midshaft of the third metacarpal bone (MC3) showed a lower viscoelastic and higher elastic behaviour in response to hydrostatic pressure. Site morphology and microstructure differences such as porosity and dynamic changes in osteon dimensions might be reasons for differences between bone responses to hydrostatic pressure. In conclusion, this experiment demonstrated that a simple loading test like this may give site specific data on bone, poroelastic and viscoelastic properties. References: 1. P.M. Buechner, R.S. Lakes, C. Swan, R.A. Brand, 2001 A broadband viscoelastic spectroscopic study of bovine bone: implication for fluid flow. Annals of Biomedical Engineering, vol 29, pp 719-728. 2. Zafir Bechor, Jonathan Merritt, Helen MS Davies, 2005. Intracortical Third Metacarpal Bone Hydrostatic Pressure and Fluid Drainage effect on Ultrasound velocity. Accepted for 7th Fluid flow Workshop, NY, USA.

Disclosures: **Z. Bechor**, None.

M090

Three-Dimensional Microarchitecture of the New Bone Formation on the Prosthetic Implant: Reproducibility of Micro CT Assessment. Y. Jiang¹, J. Zhao¹, Y. H. An^{*2}. ¹Osteoporosis and Arthritis Research Group, University of California San Francisco, San Francisco, CA, USA, ²Orthopaedic Research Laboratory, Medical University of South Carolina, Charleston, SC, USA.

This study was designed to evaluate the precision of micro CT quantification of three-dimensional (3D) microarchitecture of the new bone formation inside the porous titanium prosthesis implanted in rabbits. Capturing true 3D bone micro architecture may improve our ability to understand the process of new bone formation on the surface of the implant, and to estimate the bone biomechanical properties in terms of fracture resistance as the mechanical competence of bone is a function of its apparent density and 3D distribution. Such changes can not be evaluated by 2D histological sections. We examined 20 titanium prosthesis implants in the distal femur of rabbits. The implants have different sizes of pore, and have different coating materials. The specimens were scanned using a Scanco micro CT with isotropic resolution of 20 µm. 3D structural parameters were directly measured without stereological model assumptions as in 2D histomorphometry. Values of 0 and 3 for the structure model index represent a perfect plate structure and an ideal cylindrical rod structure, respectively, while values ranging from 0 to 3 indicate a structure with both plates and rods of equal thickness, depending on the volume ratio of rods and plates. Round spheres have a structure model index of 4. Negative values indicate bone structure with concave surface as the Swiss cheese. Over 1 month later, the specimens were re-scanned and re-analyzed. The root mean square coefficient of variation of the 3D microstructural parameters of the newly formed bone was calculated as a measure of reproducibility. The results showed that the The root mean square coefficient of variation was 1.7% for bone volume fraction, 2.2% for connectivity density, 2.3% for structure model index, 1.4% for trabecular number, 3.1% for trabecular thickness, 0.8% for trabecular separation, 1.1% for degree of anisotropy. In conclusion, micro CT can reproducibly quantify 3D microarchitecture of the new bone formation inside the pores of the titanium prosthesis implants, which may find application in studying effects of different size of pores and different coating materials on osteogenesis.

Disclosures: **Y. Jiang**, None.

M091

Male Idiopathic Osteoporosis. Iliac Bone Biopsy Study by Micro-TC. M. Ciria¹, J. Blanch¹, L. Perez-Edo¹, M. Mariñoso^{*2}, D. Chappard³, S. Serrano^{*2}, J. Carbonell^{*1}, A. Diez-Perez⁴. ¹Rheumatology, Institut Municipal d'Assistència Sanitària, Barcelona, Spain, ²Pathology, Institut Municipal d'Assistència Sanitària, Barcelona, Spain, ³Rheumatology, University of Angers, Angers, France, ⁴Internal Medicine, Institut Municipal d'Assistència Sanitària, Barcelona, Spain.

There are few histomorphometric studies about male idiopathic osteoporosis (MIO). Our group found a decrease of osteoblasts and trabecular number in classic histomorphometric studies of iliac bone biopsies, showing a decreased formation levels

and a normal resorption levels. The aim of the present study is to examine the microarchitecture of cancellous bone with micro-TC techniques. We included 16 of 23 iliac bone biopsies performed in male with normocalciuric idiopathic osteoporosis, diagnosed by densitometric study. The control group included 11 age-matched, healthy men. Micro-TC study was performed with Microtomographie X-Skyscan. We studied bone volume / total volume (BV/TV), bone surface / bone volume (BS/BV), trabecular thickness (Tb.Th), trabecular separation (Tb.Sp), and trabecular number (Tb.N). Results: Bone volume / total volume, trabecular number and trabecular separation was lower in osteoporotic group than in control group. Tb.Th was similar in both groups (Table 1). Conclusions: In our sample, male normocalciuric idiopathic osteoporosis showed a low trabecular number and a high trabecular separation, with a maintenance of trabecular thickness. This findings differ of the postmenopausal osteoporosis.

	Micro-TC values		
	MIO	CONTROL	P
BV/TV	10.35 (0.03)	16.56 (0.05)	<0.05
BS/BV	22.36 (3.66)	20.66 (4.07)	NS
Tb.Th	0.1746 (0.03)	0.1831 (0.02)	NS
Tb.N	0.616 (0.14)	0.896 (0.25)	<0.05
Tb.Sp	1.53 (0.4)	1.02 (0.37)	<0.05

Disclosures: **M. Ciria**, None.

M092

Components of Micro-Architecture and Bone Density that Contribute to Biomechanical Characteristics of Bone. A Study in Ewe Femora. P. P. Geusens¹, Y. Jiang², J. Zhao^{*2}, S. Boonen³, M. Azria⁴. ¹Limburgs Universitair Centrum, Diepenbeek, Belgium & Department of Rheumatology, University Hospital, University of Maastricht, The Netherlands, Diepenbeek, Belgium, ²Osteoporosis and Arthritis Research Group, Department of Radiology, University of, San Francisco, CA, USA, ³Leuven University Center for Metabolic Bone Diseases and Division of Geriatric Medicine, K.U.Leuven, Leuven, Belgium, ⁴Novartis, Basel, Switzerland.

Many components of bone quality contribute to the different aspects of biomechanical competence of bone, including bone mineral density (BMD) and microarchitectural parameters. We analysed the correlation between biomechanical characteristics and measurements of BMD and microarchitecture in the femora of adult ewes. Methods. Twenty-eight middle aged (5-8 years old) ewes were part of a study of the effect of calcitonin on bone after ovariectomy (OVX) (JBMR, 2005:125). The animals were euthanized 6 months post-OVX. The femoral neck BMD was measured by dual x-ray absorptiometry (DXA). Compressive testing was performed on femoral trabecular cylinder cores of 8 mm in diameter and 10 mm in length with the axis of the cylinder aligned with the axis of the neck. Microarchitecture of femoral neck was examined with a magnetic resonance imager at 9.4 Tesla in axial, coronal, and sagittal planes at contralateral site. Uni- and multivariate analyses were performed between biomechanics, BMD and MR. Results. In univariate analysis, strength and stiffness were correlated with DXA and with several components of microarchitecture (Table). Toughness correlated with MR, but not with BMD. In a multivariate stepwise regression analysis, strength and stiffness correlated with BMD and TV/BV, while toughness was related to the mean length of the branches. Conclusions. Biomechanical characteristics show variable correlations with BMD and microarchitecture. These results indicate that microarchitecture of trabecular bone contributes significantly to its biomechanical characteristics, independent of BMD measured in the femoral neck.

	Uni- and multivariate correlations between biomechanics, BMD and MR analyses	
	Univariate analysis(R2)	Multivariate analysis (band R2)
DXA femoral neck	Strength/Stiffness/Toughness	Strength/Stiffness/Toughness
DXA femoral neck	.811***/.836***/ns	.588/ 1.090/ ns
MR:		
Trab. bone volume fraction (TV/BV)	.534***/.423**/.365**	.417/.225/ns
Trab. number (TbN)	.534***/.423**/.365**	ns/ns/ns
Trab. thickness (TbTh)	ns/ns/ns	ns/ns/ns
Trab. spacing (TbSp)	ns/ns/.212*	ns/ns/ns
Free ends	ns/ns/ns	ns/ns/ns
Nodes	.307**/.209*/.231*	ns/ns/ns
Branches	.393**/.333**/.352**	ns/ns/ns
Mean length of the branches	.271**/.164*/.484***	ns/ns/.695
*p<0.05, **p<0.01, ***p<0.001		R2: .887***/.901***/.484***
ns = not significant		

Disclosures: **P.P. Geusens**, Novartis 2.

M093

First Data of Forearm and Tibia Bone Micro Architecture in Young, Healthy Women, Using High Resolution 3DpQCT *In Vivo* . M. Backstroem^{*1}, G. Armbrrecht^{*1}, G. Beller^{*1}, J. Reeve², C. Alexandre³, R. Rizzoli⁴, A. Berthier^{*5}, L. Braak^{*5}, R. Binot^{*6}, B. Koller^{*7}, D. Felsenberg¹. ¹Zentrum für Muskel und Knochenforschung, Radiologie, Charité - Universitätsmedizin, Berlin, Germany, ²Department of Medicine and Institute of Public Health, Bone Research, University of Cambridge, Cambridge, United Kingdom, ³Faculte de Medicine, LBBTO, University of St. Etienne, Saint-Etienne, France, ⁴Division des maladies Osseuses, Department de Medicine Interne, Hopital cantonal Universitaire de Geneve, Geneva, Switzerland, ⁵Institut de Medecine et Physiologie Spatiale, Medes, Toulouse, France, ⁶European Space Agency, Noordwijk, Netherlands Antilles, ⁷Scanco Medical Ltd, Zürich, Switzerland.

At present, there are no normative data available for micro architectural parameters such as Bone Volume to Total Volume (BV/TV), Trabecular Number (Tb.N) and Trabecular Thickness (Tb.Th) of distal radius and tibia assessed using an *in vivo*, non invasive 3DpQCT with high resolution. Our aim was to assess first data and to investigate whether there are any differences between radius and tibia. Twelve women, aged 25-40 (mean 31,4±4,46) with BMI 18,9-23,0 (mean 20,99±1,45) were measured with a 3DpQCT with a nominal isotropic resolution of 100 µm (XtremeCT, Scanco Medical Ltd). A total scan length of 9 mm in axial direction, starting 9,5 mm and 22,5 mm proximal of the distal endplate in radius respective tibia, divided into 110 slices were simultaneously measured over a scan time of less than 3 minutes. Total effective dose were less than 5 µSv per scan. ANOVA was used for statistical evaluations. No significant differences were found between radius and tibia. To be sure that the age and BMI distribution mirrored the whole group, statistical analysis were carried out on 1) age groups 25-30 and 31-40 years old (6 subjects per group) and 2) BMI 18,9-21,0 and 21,1-23,0 (5 vs. 7 subjects per group). The parameters were first compared between the groups for radius and then for tibia, followed by a comparison of the parameters within the group but between radius and tibia. No significant differences were found. Hence, the group can be considered as homogenous and the reference data as a good reflection of the studied group.

Table 1: Mean values ± standard deviations for the entire group of young healthy women (25-40 years).

	RADIUS			TIBIA		
BV/TV	0,138	±	0,024	0,143	±	0,018
Tb.N	1,844	±	0,192	1,811	±	0,226
Tb.Th	0,075	±	0,010	0,080	±	0,008

Disclosures: **M. Backstroem**, None.

M094

Validation of Histomorphometric Indices in the Vertebral Spine of C57/BL Mice. S. Petersen^{*}, S. Syberg^{*}, N. R. Jorgensen. Osteoporosis Research Unit, Dep. of Clinical Biochemistry 339, Copenhagen University Hospital Hvidovre, Hvidovre, Denmark.

Bone histomorphometry is a widely used technique to determine bone formation, bone resorption, and other indices related to bone turnover. It is used in both human and animal samples, but only few methodological studies have described the optimal method to determine these parameters in mouse models. The aim of this study was therefore to establish and validate a standardized technique to measure indices of bone formative and resorptive activity, as well as cortical and trabecular thickness, and bone volume on bone slices of the vertebral lumbar spine from mice. Four-month old C57/BL mice were sacrificed, and lumbar spine was collected for histomorphometry. Sectioning and staining were performed according to standard methods. Fluorescent labeling for formative indices was performed 2 and 10 days prior to sacrifice. On each slide (5 for formative indices and 5 for all other indices), sections from 4-8 vertebrae (from L1 and down) were present. Mineralizing surface as percentage of bone surface (MS/BS, %), eroded surface as percentage of bone surface (ES/BS, %), bone volume in % of total volume (BV/TV, %), cortical thickness (C.Th, µm), and trabecular thickness (Tb.Th, µm), were determined. Further, mineral appositional rate (MAR, µm/day) and bone formation rate/V (BFR/BV, %/year) were also calculated. Ranges of the mean and coefficient of variation (CV%) are shown in table 1 for comparisons between the different vertebrae and within the vertebrae but between the different sections. No differences were found between the different sections. However, for most indices, differences between vertebrae were found, indicated by * in table 1. In conclusion, when measuring histomorphometric indices, it is important to determine these on specific lumbar vertebrae, when comparing with other animals, as there is a significant variation in most indices between the different vertebra. Table 1.

Index	Intervertebral comparison range	CV%	Intersection comparison range	CV%
MS/BS (%)	42.7-47.4*	1.7-5.2	43.6-46.5	4.8-5.9
ES/BS (%)	5.6-6.2	5.4-13.2	5.7-6.3	4.5-11.0
BV/TV (%)	17.7-32.3*	1.1-10.3	22.8-24.7	21.1-27.1
MAR (µm/day)	0.86-1.06*	3.6-11.3	0.92-0.98	6.2-13.9
BFR/BV (%/year)	0.565-0.884*	3.6-22.1	0.697-0.841	10.4-21.6
Tb.Th (µm)	31.0-37.4*	2.2-11.8	32.6-34.8	6.4-9.1
C.Th (µm)	95.6-126.2	4.6-11.2	109.4-115.3	5.3-13.4

Disclosures: **N.R. Jorgensen**, None.

M095

***In Vivo* Assessment of Trabecular Bone Structure in Human Vertebrae Using High Resolution Computed Tomography.** W. Timm^{*1}, C. Graeff^{*1}, J. Vilar^{*2}, T. N. Nickelsen³, T. Nicholson^{*3}, L. Lehmkuhl^{*4}, R. Barkmann^{*1}, C. C. Glüer¹. ¹Med. Physik, Klinik f. Diag. Radiologie, UK SH, Kiel, Germany, ²Dept. of Radiology, Hospital Dr. Peset, Valencia, Spain, ³Eli Lilly & Company, Windlesham, United Kingdom, ⁴Charité, Berlin, Germany.

The deficiencies of bone densitometry for monitoring osteoporosis treatment are well established. Here we introduce a method for *in vivo* structural analysis of trabecular bone at a central fracture site, the spine. In the Eurofors multi-center study, T-12 vertebrae were scanned with high resolution computed tomography (HRCT) in 67 osteoporotic women on Teriparatide treatment (20 µg per day). Measurements were repeated after 6 and 12 months. Microstructural variables were named analogous to standard histomorphometry nomenclature; a prefix “a” (for “apparent”) was added to indicate that variables are affected by the limits in spatial resolution (e.g. aBV/TV). The voxel size of the scans was 156 to 187µm in-plane and 300 to 500µm through-plane. All scans were calibrated and trabecular bone was segmented with a threshold of 250 mg/cm². The chosen threshold assured a continuous cortical shell, physiological aBV/TV values, and good separation of bone structure versus pseudo structure in soft tissue. Structural variables were calculated by StructuralInsight software developed in-house. Differences in spatial resolution of the different CT scanners used had a significant influence on measured structural variables (not affecting longitudinal analyses) and were compensated for. Structural information could be measured reproducibly: each variable was highly correlated with the same variable at the following visit (r²= 0.85 to 0.94). Long term precision errors for aBV/TV and aTb.N. were 12,5% and 11,2%, respectively, corresponding to monitoring time intervals of 1 and 1.2 years. Structural information was independent of BMD and BV/TV: For a given visit, structural variables were only weakly correlated with aBV/TV (r²= 0.06 to 0.24) or BMD (r²= 0.01 to 0.27), except for aTb.N, which was highly correlated to aBV/TV (r²= 0.95). Correlation between BMD and aBV/TV was r²= 0.27 at baseline. In multivariate correlation models, the best predictor for a structural variable in a return visit was the same variable at baseline (partial correlation rp²=0.65 to 0.86), compared to BMD at baseline (rp²= 0.04 to 0.21) and aBV/TV at baseline (rp²= 0.01 to 0.22). We conclude that structural analysis provides consistent information independent of BMD in spite of spatial resolution and image noise limits. This method allows to non-invasively study structural changes *in vivo* at one of the most relevant fracture sites requiring follow-up times in the individual patient of about 1 year.

Disclosures: **C. Graeff**, **Eli Lilly & Company** 2.

M096

Relationships between pQCT Indicators of Bone Mass, Mineral Density, Design and Strength in Forearms and Legs of Normal Men and Pre and Post MP Women. R. Capozza^{*1}, G. Cointry^{*2}, S. Ferretti^{*2}, S. Feldman^{*2}, N. Fracalossi^{*2}, L. Sarrio^{*2}, P. Reina^{*2}, M. Ferretti^{*2}, M. Ferullo^{*2}, G. Marchetti^{*2}, E. Roldan², J. Ferretti². ¹Scientific direction, GADOR S.A., Buenos aires, Argentina, ²Center for P-Ca Metabolism Studies (CEMFoC), Fac of Medicine, Natl Univ, Rosario, Argentina.

Aim. To describe the interrelationships between different bone properties and the muscle interaction with their biological determination. **Methods.** The associations between bone mass pQCT indicators (BMC, cortical area, trabecular density), design (CSMIs), mineral density (cortical vBMD) and strength (BSIs) and of muscle strength (CSA) in forearm (4 and 66% sites) and legs (4, 14, 38 and 66% sites) of 40 men, 60 pre MP women and 100 post MP women aged 25-85y were analyzed. **Results.** Indicators of bone mass, design and strength were higher in men than in pre MP women. Mass and strength (not design) indicators decayed significantly after MP. Cortical vBMD, higher in women than men, decayed more dramatically than other indicators after MP. *Distribution/mass* (MI/ CortCSA) and *distribution/quality* (MI/CortvBMD) curves showed that MIs tended to stabilize after MP, despite the bone mass reduction. The intracortical distribution of vBMD fell dramatically with a discontinuity of the areas of highest-density voxels (>1.0 cm⁻¹ attenuation threshold) after MP. The natural 1:1 and 1:1.5 proportionalities between trabecular and cortical BMC in 4% vs 14% and vs 38% leg sites respectively also decayed after MP. All bone indicators correlated with muscle area in both 66% sites showing a single, saturation relationship for men and pre MP women, and a lower slope for post MP women. **Interpretation.** Results suggest 1) Bone mass varies allometrically with body size and biomechanically with regional muscle strength in fertile individuals 2) Estrogen deficiency determines a loss of mass and especially mineralization (enhanced microporosity) of cortical bone, maintaining the diaphyseal design relatively stable, thus slowing the development of bone fragility 3) Bone *mechanostat* remains healthy (yet metabolically disturbed) after MP 4) Comparison of BMC between trabecular or cortical sites in the same individual allows detecting a faster deterioration of the former, as determined in "systemic" (primary or endocrine-metabolic) osteopenias 5) In practice a Z-scorization of the described natural relationships will provide suitable reference charts for original, biomechanical diagnosis of osteoporosis, and a differential diagnosis between "disuse" (with normal bone/muscle proportionality) and "systemic" (reduced bone/muscle proportionality and the trabecular/cortical bone mass ratio) osteopenias with differential therapeutic implications.

Disclosures: **E. Roldan**, None.

M097

Trabecular Bone Quality Evaluation By Using The Porous Mediums Connectivity Concept. A. C. A. Souza^{*1}, D. Barbieri^{*2}, R. Schneider^{*1}, W. L. Roque^{*3}. ¹Institute of Geriatrics, PUCRS University, Porto Alegre, Brazil, ²Dep of Bio Engineering, PUCRS University, Porto Alegre, Brazil, ³Department of Mathematics, Universidade Federal do RGS, Porto Alegre, Brazil.

The mechanical competence of trabecular bone is a function of both, bone mass and architecture. BMD is an important tool for osteoporosis diagnosis; however, it does not evaluate the bone structural and architectural quality. The modeling and visualization study of porous mediums in the trabecular bone, are very important for the comprehension of physical and geometrical properties. In general, the medium porosity is determined by visual calculation, based on the porous number counting that estimates the porous space percentage. The objective of this study is to develop a technique to identify the connectivity of the trabecular three-dimensional porous space by using the study of dissectors. A study of dissectors is a sequence of parallel tomographic images of thin slices with a separation L among surfaces took from a vertebral specimen. The porous are identified by using segmentation algorithms and their characteristics, as perimeter and area. The connectivity between porous of neighbor slices is identified in the orthogonal direction. The three-dimensional porous space connectivity is calculated by using the Euler-Poincaré volumetric characteristics technique. The final objective is to calculate an index that relates the number of isolated parts (N) to the number of connections in the porous space (C), and to the number of completely enclosed cavities (H). The Euler-Poincaré derived index reflects the trabecular structural and architectural quality. Seven cadaver collected vertebrae were scanned by Hologic 4500A DEXA and by a Siemens Somatom Plus CT. The vertebrae were scanned using resolution of 512 x 512 pixels, slices of 2.0 mm thickness. The images were segmented by an image processor software and the Euler-Poincaré derived index was calculated for every vertebra. Vertebrae 1 and 2 had BMD values compatible to osteoporosis and the Euler-Poincaré derived index confirmed low connectivity (low trabecular density and high porosity), revealing architectural deterioration. Vertebrae 3 and 4 had an osteopenic BMD values, however the index exhibited good trabecular connectivity, indicating good architectural structure. Vertebrae 5, 6 and 7 produced normal BMD values and the Euler-Poincaré derived index confirmed good trabecular structure. Despite vertebra 5 had lower BMD than 6 and 7, its trabecular connectivity index was better than 6 and 7. It can be concluded that trabecular porous connectivity evaluation provides important information for clinical decision related to bone structural quality, which is not seen through DEXA.

Disclosures: *A.C.A. Souza, None.*

M098

Improved Precision of Hip Structure Analysis Using Optimized Projection Images from Segmented 3D CT Scans of the Hip. J. K. Brown¹, Q. Qiao^{*2}, J. M. Weigert³, B. Khoo^{*4}, T. J. Beck². ¹Mindways Software Inc., Austin, TX, USA, ²Radiology, Johns Hopkins University, Baltimore, MD, USA, ³Radiology, Imaging Center of West Hartford, West Hartford, CT, USA, ⁴Med. Technology & Physics, Sir Charles Gairdner Hospital, Nedlands, Australia.

The hip structure analysis (HSA) method was developed to derive bone cross-sectional properties at certain locations in the proximal femur from 2D DXA data so that the bone mass data could be interpreted mechanically. A major limitation on HSA precision is that inconsistent femur position alters projected dimensions so that changes in time or differences between subjects cannot be distinguished from actual geometric differences. This is especially important in the measurement of cross-sectional moments of inertia (CSMI) and section moduli (Z) that are rotationally dependent in cross-sections that are not axially symmetric. CTXA™ (Mindways Software Inc.) is a commercial application that generates DXA-like projection data compatible with the HSA method from a 3D QCT data set. Whereas the projection view obtained from a DXA device is determined at the time of data acquisition, the CTXA™ projection view is done retrospectively during post-acquisition processing thus providing greater projection-view control than can be achieved in conventional DXA. We used paired CT scans from 24 adult subjects with repositioning between scans done at a single visit. Scans were acquired with a helical CT scanner (GE NX/i) at 100 mA, 120 kVp and a section spacing of 3 mm. CTXA images with pixel spacing of 0.7 mm in both directions were exported to the HSA program. Coefficients of variation were computed from data pairs and compared to average values from Hologic DXA scanners generated from paired scans with repositioning in a large clinical trial (Khoo B, et al, 2005 BONE In Press). Results are compared in the Table for the narrow-neck and shaft regions. For the shaft region only 15 subjects could be used due to shaft cut-off in some CTXA images. In this preliminary study precision by CTXA is considerably improved in all geometric parameters especially in CSMI and Z. It is likely that some further improvement can be obtained by optimizing the HSA algorithm and the CT scan protocol. The major advantage of higher precision is that research studies should be able to demonstrate significant geometric effects with smaller numbers of subjects than required for DXA.

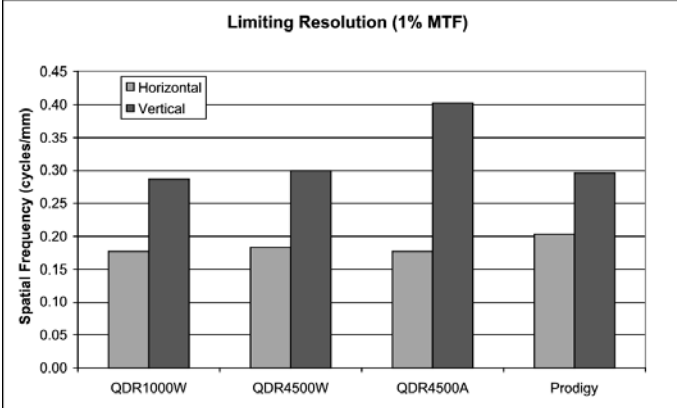
Region	Parameter	%CV	
		Hologic DXA Scanners	CTXA
Narrow-Neck	Bone Cross-Sectional Area	3.0%	0.9%
	Outer Diameter	2.3%	0.5%
	Cross-sectional Moment of Inertia	5.1%	1.9%
	Section Modulus	4.1%	1.4%
	Buckling Ratio	4.9%	1.6%
Shaft	Bone Cross-Sectional Area	2.4%	1.3%
	Outer Diameter	1.1%	0.4%
	Cross-sectional Moment of Inertia	3.7%	1.3%
	Section Modulus	3.0%	1.3%
	Buckling Ratio	3.4%	2.5%

Disclosures: *J.K. Brown, Mindways Software Inc. 4.*

M099

Image Resolution Properties of Conventional DXA Scanners and Implications for Measuring Structural Geometry. Q. Qiao^{*1}, B. Khoo^{*2}, R. I. Price², T. J. Beck¹. ¹Radiology, Johns Hopkins University, Baltimore, MD, USA, ²Sir Charles Gairdner Hospital, Nedlands, Australia.

Hip Structure Analysis (HSA) uses dimensional information from DXA scans in measuring cross-sectional geometry but scanner spatial resolution properties influence the ability to do so accurately. Because DXA scanner resolution is less important in BMD analysis, this has not been thoroughly evaluated. We measured the resolution of the Hologic QDR1000W, QDR4500A and QDR4500W, and the GE/Lunar Prodigy. An L-shaped copper foil was placed flat in a 20 cm thick stack of 1 cm thick tissue equivalent plastic and imaged with the DXA scanner. To evaluate effects of resolution on bone height above the tabletop, the copper foil was imaged after placing it between plastic layers in 1 cm increments from the bottom to the top of the stack. Using an oversampling method to eliminate aliasing, pixel distributions across the edge of the foil image were fitted to a sigmoid function and the first derivative was derived as the point-spread function (PSF). The modulation transfer function (MTF) was then determined from the Fourier transform of the normalized PSF. Resolution was evaluated separately in vertical (along table axis) and horizontal (across table) directions. The resolution limit was defined at the spatial frequency where the MTF fell to 1%. All scanners showed MTF asymmetry with better resolution in the vertical than horizontal direction; resolution was best for objects at the tabletop. Results measured at 10 cm above the tabletop (typical height of an adult femur in a hip DXA scan), are shown in the Figure. All scanners conformed reasonably well with theoretical resolutions based on scanner specifications. All four had comparable horizontal resolution, with a slight advantage for the GE/Lunar Prodigy. The main differences were in vertical resolution with the highest value in the QDR4500A. In practical terms, resolution differences between scanners are modest. The considerable MTF asymmetry means that blurring of bone margins is greater when the long axis of the bone is vertically oriented (edges blurred horizontally) than when oriented horizontally (edges blurred vertically). For ideal geometry measurements, the resolution should be closer to 1 line pair/mm and should not vary with orientation of the bone in the image. Current commercial DXA scanners are less than ideal in this respect.



Disclosures: *Q. Qiao, None.*

M100

Assessing Changes in Bone Structure and Strength of the Mid-femur in Children Using Magnetic Resonance Imaging. C. M. Modlesky¹, D. L. Johnson^{*1}, E. Miller^{*2}. ¹Department of Health, Nutrition and Exercise Sciences, University of Delaware, Newark, DE, USA, ²Department of Orthopaedics, Al duPont Hospital for Children, Wilmington, DE, USA.

Magnetic resonance imaging (MRI) has been used to assess the structure and strength of the mid-femur in adults and adolescents; however, these measurements have not been acquired in children. Furthermore, changes in these bone parameters during a typical intervention period have not been evaluated. The purpose of this study was to assess the changes in bone structure and strength of the mid-femur in typically developing children during a 9 month period using MRI. 10 children (5 girls and 5 boys) 8 to 11 years of age and within the 10th and 90th percentiles for height, weight and body mass index completed the study. Approximately 24 images (1 cm thick separated by 0.5 cm) of the entire femur were collected twice, 9 months apart, using a GE 1.5 T MRI (TR= 750, TE = 14, 1 NEX,

ASBMR 27th Annual Meeting

512 x 512 matrix, FOV = 20 cm). Images representing the middle third of the femur were identified and total bone volume, cortical bone volume, medullary volume, cross-sectional moment of inertia in the medial-lateral ($CSMI_{ml}$) and anterior-posterior ($CSMI_{ap}$) directions, section modulus in the medial-lateral (Z_{ml}) and anterior-posterior (Z_{ap}) directions, and polar moment of inertia (J) were assessed using a custom software program. There was a significant increase ($P < 0.05$) in total bone volume (13.0 %), cortical bone volume (12.2 %), medullary volume (14.4 %), $CSMI_{ml}$ (16.3 %), $CSMI_{ap}$ (20.0 %), Z_{ml} (10.1 %), Z_{ap} (16.1 %) and J (18.4 %). Furthermore, total bone volume, cortical bone volume, medullary volume, $CSMI_{ml}$, $CSMI_{ap}$, Z_{ml} , Z_{ap} and J measured at the original time point were strongly correlated with the same measures taken 9 months later ($r = 0.975$, 0.959, 0.984, 0.956, 0.931, 0.964, 0.966, and 0.949, respectively, $P < 0.05$). The findings suggest that measures of bone structure and strength of the mid-femur in typically developing children increase by approximately 10 % to 20 % during a 9 month period. Moreover, the assessment of the structure and strength of the mid-femur in children using MRI is very reliable.

Disclosures: **C.M. Modlesky**, None.

M101

Defining Cortical Bone by pQCT: *In Vitro* and *In Vivo* Accuracy of Bone Geometry. **S. Kontulainen**, **D. Liu***, **M. Jamieson***, **H. Macdonald***, **S. Manske***, **T. Oxland***, **H. McKay**. Orthopaedics, University of British Columbia, Vancouver, BC, Canada.

Peripheral quantitative computerized tomography (pQCT) is a relatively new technique to measure bone and to date there have been no validity studies or guidelines as to which modes and thresholds are the most accurate to analyse growing, mature or aging bone. The advantage of pQCT technology is its ability to measure the size, geometry and apparent volumetric density of a bone cross-section - all properties of bone that influence its mechanical integrity. Strength indices that estimate bone integrity are dependent on the measurements of total and cortical cross-sectional areas (ToA and CoA, respectively). Thus, accurate measurement of bone geometry is essential. Our first objective was to compare ToA and CoA values derived from several XCT-5.50 (Stratec) analysis protocols and MRI to histomorphometry *in vitro*. Our second objective was to determine the accuracy of different pQCT analysis protocols in healthy children by comparing *in vivo* pQCT results to MRI-derived ToA and CoA at the tibia. The overall goal of the study was to propose practical recommendations for pQCT analysis protocols that can be used to evaluate the growing skeleton in clinical practice and research. For *in vitro* accuracy, 18 human cadaver tibiae [donors' mean age 74 yrs (SD 6)] were measured with XCT-2000 and 1.5 Tesla MRI at 25% of the total length from the distal plateau. After scanning, histomorphometry from the same site was performed to obtain criterion ToA and CoA. For *in vivo* accuracy, 16 healthy girls [mean age 12.1 yrs (SD 0.5)] were measured with pQCT and MRI (criterion standard) at tibia 30% site. Several combinations of XCT analysis modes and thresholds (including manufacturer's defaults) were used to determine the most accurate protocol to represent the ToA and CoA criterion standards *in vitro* and *in vivo*. We determined the accuracy by calculating the %-difference between the criterion and measured value. For *in vitro* scans the most accurate measurement of ToA was obtained using CONTMODE 3 with an outer threshold of 169 mg/cm³ (-1.1%). The most accurate mode for CoA analysis was CORTMODE 4 with an inner threshold of 670 mg/cm³ (0.6%). For *in vivo*, ToA was analysed most accurately (-0.1%) when CONTMODE 1 was used with an outer threshold of 200 mg/cm³, and CoA (-0.2%) when CORTMODE 4 with an inner threshold of 480 mg/cm³ was used. Therefore, for paediatric bone, we recommend CONTMODE 1 with outer threshold 200 mg/cm³ to define ToA. For CoA measurements we recommend CORTMODE 4 with the outer threshold 200 mg/cm³ and inner threshold 480 mg/cm³. These analysis protocols are different from those recommended by the manufacturer (Stratec).

Disclosures: **S. Kontulainen**, None.

M102

Longitudinal Changes in 3D Microarchitecture of Paired Iliac Crest Bone Biopsies in Postmenopausal Women with Osteoporotic Vertebral Fracture. **J.J. Zhao**, **Y. Jiang**. Osteoporosis and Arthritis Research Group, University of California San Francisco, San Francisco, CA, USA.

This study was to compare true longitudinal postmenopausal osteoporotic changes in three-dimensional (3D) trabecular architecture, which may improve our ability to understand the pathophysiology of osteoporosis and other bone disorders, and to estimate bone biomechanical properties in terms of fracture resistance as the mechanical competence of trabecular bone is a function of its apparent density and 3D distribution. During aging and diseases such as osteoporosis, trabecular plates are perforated and connecting rods are dissolved, with a continuous shift from one structural type to the other, which can not be evaluated by 2D histological sections. In histomorphometry, there is debate about whether trabecular thinning occurs, or rather trabecular disappearance occurs with aging and/or menopause based on 2D sections using the parallel plate model. We examined 16 paired iliac crest bone biopsies (32 specimens), from 16 postmenopausal women with osteoporotic vertebral fractures and the hip/lumbar BMD at least 1 SD below the mean value in normal young women. The first biopsy was taken at age of 68 (± 7) yrs, 10 (± 9) yrs since menopause, while the second one 2 (± 0.5) years later. The subjects were not treated with anti-resorptive or anabolic agent for osteoporosis. The specimens were scanned using a Scanco micro CT with isotropic resolution of 17 μ m. 3D trabecular structural parameters were directly measured without stereological model assumption. Structure model index 0 represent an ideal plate structure and 3 represents rod structure. There was a significant change between paired bone biopsies in 3D trabecular bone volume fraction (14.8 \pm 1.3% vs. 11.3 \pm 0.8%, baseline vs. follow up), trabecular thickness (158 \pm 8 μ m vs. 142 \pm 6 μ m), structural model index (1.66 \pm 0.12 vs. 1.94 \pm 0.10), and

connectivity density (6.1 \pm 0.6 mm⁻³ vs. 4.9 \pm 0.5 mm⁻³). There was a trend of decreased 3D trabecular number, increased trabecular separation and degree of anisotropy, increased 3D cortical porosity, and decreased cortical thickness, in the follow up biopsies compared with baseline samples. Thus, 3D trabecular microstructure deteriorates in the iliac crest of postmenopausal osteoporotic women without active treatment. Trabecular thinning does occur and trabeculae shift from a plate-like structural type to a rod-like pattern, and become less connected.

Disclosures: **J.J. Zhao**, None.

M103

Genetic Markers for Ancestry Are Correlated with Bone Density and Size in African Americans. **C. M. Kammerer¹**, **J. R. Shaffer^{*1}**, **D. Reich^{*2}**, **E. Ziv^{*3}**, **D. C. Bauer^{*3}**, **J. Li^{*3}**, **A. B. Newman^{*1}**, **J. A. Cauley¹**, **T. B. Harris^{*4}**, **F. Tyllavsky^{*5}**, **J. M. Zmuda¹**. ¹U. Pittsburgh Graduate School of Public Health, Pittsburgh, PA, USA, ²Harvard Medical School, Boston, MA, USA, ³UCSF, San Francisco, CA, USA, ⁴National Institute on Aging, Bethesda, MD, USA, ⁵U. Tennessee Health Science Center, Memphis, TN, USA.

Bone density (BMD) and size (length) differ among ethnic groups and these differences may have a genetic basis. Recently, researchers have developed methods to map disease genes in admixed populations, e.g. African Americans (AA), which derive portions of their genomes from different ancestral groups. Admixture mapping depends on the extended linkage disequilibrium that is present in admixed populations. If the differences in BMD and related phenotypes among ethnic groups are due to differences in allele frequency at susceptibility genes, then individuals with low BMD will have increased ancestry from the population with lower BMD. We used data collected on 1794 European Americans (EA) and 1281 AA (52% women) from the Health Aging and Body Composition Study (ages 68 to 80 yrs). We first determined that, as expected, DEXA measurements of areal BMD of the hip, and computed tomography measurements of volumetric BMD of the spine were significantly higher among AA than EA. Although total height did not differ between groups, trunk length was significantly decreased and leg length was increased in AA compared to EA. Using genotype data on 45 ancestry informative markers, we performed model-based clustering methods to estimate the proportion of European ancestry (median = 0.18, range, 0.0 to 0.66) for each AA. After adjusting for significant demographic and lifestyle variables, we observed that an increased proportion of European ancestry was significantly associated with decreased areal femoral neck BMD ($r = -0.11$), volumetric total spine BMD ($r = -0.13$), and trabecular spine BMD ($r = -0.15$; $p < 0.01$ for all three traits). Although there was no relationship with total height, increased European ancestry was associated with increased trunk length ($r = 0.17$) and decreased leg length ($r = -0.17$, $p < 0.0001$ for both). Based on the mean differences between EA and AA, the relationship between admixture and BMD or body length was in the expected direction. Furthermore, the predicted differences in BMD between AAs who had 0% versus 100% European ancestry ranged from 0.76 to 0.88 standard deviations, similar to the reported mean BMD differences between African and European populations. These results demonstrate a novel relationship between degree of European ancestry and several skeletal measures. Use of ancestry informative markers in admixed populations has great potential to detect genes for BMD and related traits.

Disclosures: **C.M. Kammerer**, None.

M104

Identification of Mouse Chromosomes Influencing Bone Morphology and Composition. **H. Courtland¹**, **A. Hill^{*2}**, **J. Singer^{*3}**, **E. S. Lander^{*3}**, **J. H. Nadeau^{*2}**, **K. J. Jepsen¹**. ¹Orthopaedics, Mount Sinai School of Medicine, New York, NY, USA, ²Case Western Reserve University, Cleveland, OH, USA, ³MIT, Cambridge, MA, USA.

Research using inbred mice has demonstrated that three bone traits (area, moment of inertia, and ash content) explain 66-88% of inter-strain variability in fracture-related whole bone mechanical properties [1]. Given that the genetic determinants of these bone traits are poorly understood, we conducted a phenotypic analysis to map each trait to one or more chromosomes within the mouse genome. B6-i^a Chromosome Substitution Strains (CSSs) were used for this investigation. Each CSS is inbred and identical to the B6 host except that chromosome (i) is replaced with the corresponding intact chromosome from the A donor [2]. A total of 19 (17 autosomes, X, Y) CSSs were characterized in this study. Femurs from 14-16 week old (adult) B6 and B6-i^a mice (n=2-25 per group) were used in this analysis. Right femurs were taken for measurements of cortical area (CtAr) and moment of inertia (Jo) with analyses performed using IMAQ Vision Builder software. Left femurs were ashed at 600C for determination of ash content relative to wet weight. Significant differences in body weight-corrected mean trait values (as compared to host) were determined using genome-wide corrected multiple comparisons ($p < 0.004$) [2, 3]. This investigation revealed several strains with mean trait values significantly different from B6 indicating that substituted chromosomes in these strains harbor one or more QTLs for our measured bone traits. Male B6-(2, 4, X and Y)^a and female B6-16^a strains had mean ash content values that were smaller and larger than B6, respectively. CtAr mean values lower than B6 were found in male B6-(1, 9, 19, 14, 18, X and Y)^a and female B6-(2, 3, 10 and 12)^a while higher mean values were found in male B6-3^a and female B6-(6, 11 and 13)^a. Jo results were similar, though not identical, to those of CtAr with mean values lower than B6 in male B6-(1, 10, 14, 15, 16, 17 and X)^a and female B6-(2, 3, 12, 15 and 17)^a. Larger Jo values were found in male B6-3^a and female B6-(6 and 13)^a. Our results revealed only one significant chromosome substitution shared between male and female mice. Thus, genetic regulation of CtAr, Jo, and ash content appears to be sex-dependent. Although substitution of individual A chromosomes permitted B6 mice to gain one or more A phenotypes (small CtAr, small, Jo and large ash) [4], no single chromosome substitution

caused all three traits to manifest as an A phenotype. Instead, multiple chromosomes were found to independently regulate bone traits both positively and negatively depending on genetic background.

- [1] Jepsen *et al.* Mam Gen 2003
[2] Singer *et al.* Science 2004
[3] Belknap Mam Gen 2003
[4] Jepsen *et al.* JBMR 2001

Disclosures: **H. Courtland**, None.

M105

Single Chromosome Substitutions Regulate Mouse Bone Growth Patterns. **H. Courtland**¹, **A. Hill**^{*2}, **J. Singer**^{*3}, **E. S. Lander**^{*3}, **J. H. Nadeau**^{*2}, **K. J. Jepsen**¹. ¹Orthopaedics, Mount Sinai School of Medicine, New York, NY, USA, ²Case Western Reserve University, Cleveland, OH, USA, ³MIT, Cambridge, MA, USA.

Adult bone traits are the result of complex genetic variation in growth patterns. Two traits, cortical area (CtAr, tissue amount) and moment of inertia (Jo, tissue distribution), have distinct relationships to femur diameter and vary based on changes in the relative rate of expansion of the periosteal and endosteal surfaces. Thus, bones that are built differently can differ in Jo and/or CtAr and the ratio of these traits indicates differences in skeletal growth patterns. For example, B6 femurs have a greater Jo for a given CtAr than A/J (A) femurs [1] and this affords them a more robust (structurally efficient) skeleton. The goal of this study was to explore the genetic determinants of femur Jo/CtAr variation using mouse B6-i^A Chromosome Substitution Strains (CSSs). Each B6-i^A CSS is inbred and identical to a B6 host except that chromosome (i) is replaced with the corresponding intact chromosome from the A donor [2]. A total of 19 (17 autosomes, X, Y) CSSs were characterized in this study. Femurs from 14-16 week old (adult) B6 and B6-i^A mice (n=2-25 per group) were used in this analysis. Right femurs were taken for measurements of CtAr and Jo with analyses performed using IMAQ Vision Builder software. Significant differences in body weight-corrected mean Jo/CtAr values (as compared to host) were determined using genome-wide corrected multiple comparisons (p<0.004)[2,3]. This investigation revealed several strains with mean Jo/CtAr values significantly different from B6 indicating that substituted chromosomes harbor one or more QTLs influencing bone growth patterns. Jo/CtAr mean values lower than B6 (decreased structural efficiency) were found in male B6-(1, 2, 12, 14, 15, 17 and 18)^A and female B6-(4, 11, 12, 15 and 17)^A while higher mean values (increased structural efficiency) were found in male B6-3^A and female B6-(6, and 13)^A. Many chromosomal substitutions reduced the structural efficiency of the B6 host suggesting that A mice have one or more genes on multiple chromosomes significantly influencing the way bone is deposited during growth. However, only one substitution (B6-15^A) reduced structural efficiency completely to the A mean value, and since this was found only in male mice, genetic regulation of femur structural efficiency is likely sex-dependent. A-substitutions increasing structural efficiency beyond B6 may be a result of host-donor interactions that enhance existing B6 growth patterns through new favorable allelic interactions or a result of removing negative allelic regulation inherent in the mouse genome.

- [1] Price ASBMR Ann Meet 2002
[2] Singer *et al.* Science 2004
[3] Belknap Mam Gen 2003

Disclosures: **H. Courtland**, None.

M106

Biomechanical Differences between C3H and B6 Inbred Strains of Mice Depend on Geometric Differences, not on Material Differences. **G. H. van Lenthe**¹, **L. R. Donahue**², **R. Müller**¹. ¹Institute for Biomedical Engineering, ETH and University Zurich, Zurich, Switzerland, ²The Jackson Laboratories, Bar Harbor, ME, USA.

Thanks to recently developed genome-wide screening techniques major research efforts have been started to identify the genetic influence on components of bone strength, such as bone volume, bone geometry, and bone material properties. The gold standard to determine bone material properties is to estimate them from three-point bending tests, using Euler-Bernoulli beam theory. However, beam theory is only valid when certain conditions are met, e.g. constant cross section and large support width. Those conditions are not fully met for bones, hence, results can be inaccurate. The objective of this study was to assess whether deviations from beam idealizations affects outcomes of three-point bending tests; specifically, we assessed those effects for two commonly used mouse inbred strains C57BL/6J (B6) and C3H/HeJ (C3H). Fifteen femora of four-month old mice were µCT scanned using a 20 µm resolution. After reducing voxel size to 30 µm micro-finite element models were created that simulated a three-point bending test. Bones were tested in antero-posterior direction; distance between the supports was 5 mm. Assuming an arbitrary Young's modulus (E) of 5 GPa, the force necessary to obtain a prescribed displacement of the loader was calculated. Then, Young's modulus was estimated (E_{estim}) as if this test was a standard mechanical test, using the commonly used equation based on beam theory. Young's modulus was underestimated for all femora (Table 1), which was mostly caused by the fact that shearing displacements are not accounted for by beam-theory. Owing to their relatively thin cortex, underestimation was higher for B6 than for C3H caused by higher local deformation; furthermore, underestimation was higher for males than females.

	female	male
B6	35%	26%
C3H	61%	52%

Table 1: Estimated Young's modulus as percentage of true modulus (E_{estim}/E).

We conclude that Young's moduli as determined from three-point bending tests on murine femora are strongly underestimated. These effects are size-dependent, hence, are affected by sex and inbred strain. Applying our findings to reported data on B6 and C3H mice (with E ranging from 2.2 GPa for B6 males to 5.3 GPa for C3H females) indicate that these differences are not true differences, but that E ≈ 8.6 GPa for all B6 and C3H males and females; hence, reported differences for E can be explained solely by geometric effects.

Disclosures: **G.H. van Lenthe**, None.

M107

Allelic Imbalance in Human Osteoblasts: A Novel Experimental Tool to Extend Association Genetics into Functionality. **E. Grundberg**^{*1}, **T. Pastinen**^{*2}, **T. J. Hudson**^{*2}, **A. Kindmark**^{*1}, **O. Nilsson**^{*3}, **H. Brändström**^{*1}. ¹Department of Medical Sciences, Uppsala University, Uppsala, Sweden, ²Genome Quebec Innovation Centre, McGill University, Montreal, PQ, Canada, ³Department of Surgical Sciences, Uppsala University, Uppsala, Sweden.

Osteoporosis is considered as a complex polygenic disease involving interactions between multiple genes and the environment. Several approaches are currently being used to identify the genes underlying the disease. Genome-wide linkage studies and association studies, using single nucleotide polymorphisms (SNPs) in candidate genes are common strategies. However, most of the SNPs studied have no functional validation. A new approach for identification of regulatory SNPs has recently been described using quantitative detection of allele-specific transcripts. Allele ratios in RNA samples derived from heterozygous individuals are compared with the corresponding genomic DNA samples. Presence of a regulatory SNP will result in allelic imbalance, where a deviation from the 50:50 ratio between the two alleles is expected. The aim of this study was to investigate presence of allelic imbalance in three genes involved in sex hormone regulation of bone, the Estrogen receptor alpha (ERalpha), RIZ1 and CYP19 gene encoding aromatase. Deidentified trabecular bone samples were obtained from 70 donors undergoing bone graft procedures and the bone specimens were cultured until the cells that migrated from the bone reached confluency. RNA and DNA from each sample were isolated using standard procedures. For exclusion of low expressed candidate genes, microarray analysis was performed using total RNA from human trabecular bone cells hybridized to Affymetrix HG-U133A GeneChips. In average, assays for two publicly available SNPs located within coding regions in the genes were designed. Genotyping of the selected SNPs were performed using Fluorescence polarization-single base extension to allow quantitative detection of allele-specific transcripts. The method was successfully validated by analyzing an imprinted gene, MEST, and a gene previously reported to have allelic imbalance in lymphoblastoid cell lines, BTN3A2. None of the SNPs in the selected genes showed a statistically significant deviation from the 50:50 ratio and were considered not to have allelic imbalance. In conclusion, this screening tool using primary cultures of human trabecular bone cells will help us to identify regulatory polymorphisms in candidate genes for osteoporosis and thereby identify genes which contribute to the development of osteoporosis.

Disclosures: **E. Grundberg**, None.

M108

Genes Decrease Osteoporosis Risk also Decrease Risk of Obesity. **L. J. Zhao**^{*}, **Y. J. Liu**^{*}, **R. R. Recker**, **H. W. Deng**. Osteoporosis Research Center, Creighton University, Omaha, NE, USA.

It is widely known that increasing body weight (and thus higher risk to obesity) is associated with higher bone mineral density (BMD) (and thus lower risk to osteoporosis). This dogma has been widely held and creates an apparent dilemma since some molecular, cell developmental and intervention studies have suggested otherwise so that a decreasing risk in obesity may actually result in lower risk to osteoporosis. Therefore, we performed this large-scale quantitative genetic analysis to tackle this dilemma by asking the question: Do factors (particularly genes) that decrease osteoporosis risk tend to increase or decrease risk to obesity? Using DXA, we obtained measurements of bone mass, fat mass and lean mass, body weight, and information on age, sex, and life-style and medical history, on 4,489 Caucasians from 512 pedigrees. We evaluated the impact of shared genetic and environmental factors on bone mass, fat mass, lean mass, and BMI (body mass index) by analyzing genetic, environmental, and phenotypic correlations between them via uni- and bi-variate quantitative genetic analyses, with BMD *unadjusted* or *adjusted* for body weight. BMD is measured at spine, hip and distal forearm. Fat mass, lean mass, BMI, and BMD all have strong genetic determination, with heritability all >0.4 (p<0.001). When BMD is NOT adjusted for body weight, fat mass, lean mass and BMI are *positively* correlated (both genetically and environmentally) with BMD (p<0.001), consistent with the widely held dogma that increasing obesity risk (e.g., by increasing BMI and fat mass) tend to decrease risk to osteoporosis (by increasing BMD). However, interestingly, when BMD is adjusted for body weight, the genetic and environmental correlations between fat mass and BMD became *negative* (p<0.01). This result indicates that increasing fat mass (and thus obesity risk) is ACTUALLY associated with decreasing BMD (and thus increased risk to osteoporosis), IF the mechanic loading effect of body weight on BMD is adjusted. Our study, for the first time, may provide a solution to the dilemma by showing that, both genes and environmental factors that tend to decrease risk to osteoporosis (by increasing BMD) may also decrease risk to obesity (by decreasing fat mass) if the effect of mechanic loading on BMD due to body weight is adjusted for. Therefore, our study not only suggests that interventions through molecular pathways (based on discovered genes) and/or environmental or life-style modifications (such as nutritional supplements or exercises) tend to work favorably for the health care of both osteoporosis and obesity, but also re-assuring the effects of appropriate weight bearing, mechanical loading (and thus exercise) on a healthy skeletal system.

Disclosures: **L.J. Zhao**, None.

M109

Identification of Gender Specific Quantitative Trait Loci (QTL) for Trabecular and Cortical Bone in an F2-Intercross between GK and F344 Inbred Rat Strains. S. Lagerholm¹, K. Åkesson¹, H. Luthman^{*2}. ¹Department of Clinical Sciences, Malmö, Clinical and Molecular Osteoporosis Research Unit, Malmö, Sweden, ²Department of Clinical Sciences, Malmö, Medical Genetics Unit, Malmö, Sweden.

Genetic localization and identification of naturally occurring genetic variation (polymorphism) that regulate phenotypes, such as bone density in distinct trabecular and cortical compartments, allow penetration of the molecular pathophysiology of osteoporosis and development of new markers for the disease. Our primary aim was to identify chromosome regions genetically linked with peripheral quantitative computed tomography (pQCT) measures of trabecular and cortical bone quantity of tibia in (GKxF344)F2 rat intercross progeny. Material and methods: The GK rat is an established model for spontaneous multifactorial type-2 diabetes. Skeletal changes have been observed, making the rat well suited for studies of the association between osteoporosis and type-2 diabetes. F344 is a non-diabetic strain. The F2 progeny (121 male and 110 female rats) were genotyped for 181 genome-wide microsatellite markers at an average distance of 10 cM. For skeletal phenotypes, tibia was measured by pQCT at 7 months. Chromosomal location, order of markers, and the identification of QTLs were evaluated using MAPMAKER/QTL. Results: The observed difference of bone phenotypes in the F2-progeny between males and females, encouraged gender separated genetic linkage analyses to reduce non-genetic variance and optimize identification of gender specific QTLs. Three genome-wide significant QTLs (LOD ≥ 4.1) were identified in males (Chr 1, 7, and 15) and seven suggestive loci (LOD 2.8-4.0 on Chr 5, 6, 8, 10, 12, 14, and 17). In females, one significant QTL on Chr 18 was identified and eight suggestive loci were mapped on (Chr 1, 2, 3, 4, 7, 8, 10, and 12). The QTL on Chr 1 was linked with several cortical bone traits in both genders. The female specific locus on Chr 18 overlaps a QTL for insulin regulation, and the Chr 1, 7, and 10 loci overlap QTLs for body weight and glucose. Our results indicate that there are gender-gene interactions in the genetic regulation of trabecular and cortical bone quality. This study has expanded our knowledge about gender specific genetic regulation of bone traits, and despite the relatively small population, we are able to detect significant QTLs with significant impact on pQCT-phenotypes associated with bone quantity and quality. The results provide a platform for gene identification using congenic strains and advanced intercross populations generated between GK and F344.

Disclosures: **S. Lagerholm**, None.

M110

PTH1R Polymorphisms Influence BMD Variation through Effects on the Growing Skeleton. C. Vilarino-Guell^{*1}, P. Y. Woon^{*1}, L. J. Miles^{*1}, E. L. Duncan^{*1}, FAMOS Consortium^{*2}, ALSPAC Study^{*3}, C. D. Steer^{*3}, J. H. Tobias^{*1}, J. A. Wass^{*1}, M. A. Brown¹. ¹Botnar Research Centre, University of Oxford, Oxford, United Kingdom, ²OXAGEN, Abingdon, United Kingdom, ³Community Based Medicine, University of Bristol, Bristol, United Kingdom, ⁴Clinical Sciences at South Bristol, University of Bristol, Bristol, United Kingdom.

We sought to investigate whether polymorphisms in the *PTH1R* gene are associated with BMD in families in a subset of which we have previously demonstrated linkage of chromosome 3p21 with BMD, the region in which *PTH1R* is encoded. We also studied the effects of these polymorphisms in peak BMD in the Children in Focus subset (n=785, mean age 118 months) of the Avon Longitudinal Study of Parents and Children (ALSPAC). The *PTH1R* gene including its 14 exons, their exon-intron boundaries, and 1500 bp of its promoter region were screened for polymorphisms by dHPLC and sequencing in 36 osteoporotic cases. Eleven SNPs, one tetranucleotide repeat and one tetranucleotide deletion were identified. A cohort of 730 families, consisting of 1236 men (39%) and 1926 women (61%), ascertained with probands with low BMD ($z < -1.5$) was genotyped for the 5 most informative SNPs (minor allele frequency $> 5\%$). Total association between *PTH1R* polymorphisms and lumbar spine (LS), femoral neck (FN), and total hip (TH) raw BMD measures corrected for age, gender and height was tested using the program QTDT. In our osteoporosis families, a minor association was noted between LS BMD and alleles of a known functional tetranucleotide repeat (U4) in the *PTH1R* promoter region ($p=0.04$). Haplotypes composed of two to three markers consisting of combinations of SNPs rs4683301, rs724449, rs2242116 and rs1531137 were also associated with LS, FN and TH BMD ($p=0.04$ -0.008). This association was more pronounced in the youngest tertile of the population (age 16-44 years, $p=0.03$ -0.0007). Similar association was found for the ALSPAC cohort; two marker haplotypes of SNPs rs4683301 and rs724449 were associated with height ($p=0.008$), and total body less head BMD ($p=0.02$), corrected for age and gender. The strong positive association findings in our osteoporosis dataset support a role for genetic variation in *PTH1R* in population BMD. A significant role for this polymorphism in osteoporosis risk is further supported by previous data demonstrating that the same alleles of this polymorphism affect height, bone resorption and *PTH1R* transcription. The finding that the association of *PTH1R* with BMD was strongest in the youngest age tertile of the FAMOS families, and in the ALSPAC cohort, suggests a greater role for *PTH1R* variation in peak bone BMD than in bone loss in later life.

Disclosures: **M.A. Brown**, None.

M111

Idiopathic Osteoporosis in Men Is Familial and Sex Specific. E. S. Kurland¹, D. J. McMahon¹, J. S. Powell^{*1}, T. L. Colvin^{*1}, D. A. Greenberg^{*2}, J. P. Bilezikian^{*3}. ¹Department of Medicine, Columbia University, New York, NY, USA, ²Department of Statistical Genetics and Biostatistics, Columbia University, New York, NY, USA, ³Department of Medicine and Pharmacology, Columbia University, New York, NY, USA.

Many men with osteoporosis do not have a definable etiology and thus, are said to have idiopathic osteoporosis (IOM). To explore a possible genetic basis to IOM, we studied family members (FM) of 67 men. Eighty-one 1st degree relatives from 32 of these 67 probands (48%) were included. The mean age of the 67 probands was 49.4 ± 1.6 years (SEM) with mean lumbar spine (LS), femoral neck (FN) and 1/3 radius (RAD) Z-scores of -2.8 ± 0.1 , -1.5 ± 0.1 , -1.1 ± 0.2 respectively. Age and Z-scores did not differ significantly for the subset of 32 probands from whom the FM were recruited from the 35 probands whose FM were not studied. FM completed a questionnaire that included information on past medical, social history and medications. Identifiable secondary causes of osteoporosis were grounds for exclusion of FM. Bone mineral density (BMD) was measured at the LS, FN and RAD by DXA (Hologic or Lunar). Sex-specific reference databases were used for men and women. FM characteristics were as follows: 43 men (53%) and 38 women (47%) with mean ages of 44.6 ± 2.9 and 46.0 ± 3.0 yrs respectively (NS). Of the 81 FM, 38% were siblings [18 brothers (B), 13 sisters (S)], 26% parents [10 fathers (F) 11 mothers (M)] and 36% children [15 sons, 14 daughters (D)]. Age was comparable between males and females within these family subsets (NS). An average of 3 FM were recruited per proband (range 1-8). Mean Z-scores at the 3 sites measured were as follows for males compared with females: -1.5 ± 0.2 and -0.7 ± 0.2 , -0.6 ± 0.2 and -0.3 ± 0.2 , $+0.2 \pm 0.3$ and $+0.5 \pm 0.2$ for LS, FN and RAD respectively ($p < 0.05$ for LS comparison, unpaired t-test). BMD was most significantly different for sons as compared with D as follows: -2.0 ± 0.3 and -0.6 ± 0.3 , -0.7 ± 0.3 and $+0.1 \pm 0.2$, -0.2 ± 0.4 and $+0.6 \pm 0.2$ for LS, FN and RAD respectively ($p < 0.05$ at LS). For male relatives most severely affected (i.e., Z-score < -2.0), 47% of the sons (7/15) met this criterion at the LS in contrast to only 7% of D (1/14; $p < 0.02$ chi-square). For brothers, there was a trend at the LS, with 39% (7/18) affected as compared with only 8% (1/13) for S ($p=0.09$ chi-square). Parents (F and M) were affected to the same extent, 10% compared to 9%. These results suggest that IOM is familial, is not a sex-linked disorder- as father to son transmission occurs- but may be influenced by sex i.e. modified by the gender of the person expressing the genetic trait. Further family studies with particular emphasis on fathers, sons and brothers may help elucidate the genetic, hormonal and other factors that potentiate the expression of this disorder.

Disclosures: **E.S. Kurland**, None.

M112

Genetic Loci Influencing Age-Related Declines in Bone Quality. D. H. Lang¹, N. A. Sharkey¹, G. P. Vogler^{*2}, D. J. Vandenberg^{*2}, D. A. Blizard^{*3}, J. T. Stout^{*3}, G. E. McClearn^{*2}. ¹Kinesiology, Pennsylvania State University, University Park, PA, USA, ²Biobehavioral Health, Pennsylvania State University, University Park, PA, USA, ³Center for Developmental and Health Genetics, Pennsylvania State University, University Park, PA, USA.

This study was designed to increase our understanding of the genetic architecture responsible for age-related declines in bone quality. While peak bone mass has been shown to be a predictor of fracture risk it fails to completely explain the increased number of spontaneous fractures occurring in the aged population. Insight into the genetic regulation of the intrinsic material properties, material distribution, and bone architecture could provide new avenues for preventing increased fracture risk in aged individuals. The primary aim of this work was to identify quantitative trait loci (QTL) for age-related differences in skeletal measures of strength and architecture between 200 day and 800 day BXD recombinant inbred (RI) mouse strains. Three-point bending tests were used to assess the mechanical integrity of femora and tibiae and a shear test was performed on the femoral neck. Strain means were used in QTL analyses to search for chromosomal regions influencing skeletal phenotypes at 200 and 800 days of age. Additionally, the difference in RI strain means between 800 and 200 day skeletal phenotypes was used in QTL analyses to search for chromosomal regions influencing change in bone quality as a function of age. Of primary interest are the QTLs for phenotypes reflecting decrements in bone quality as a function of age. Therefore the QTL results from the sex-specific interval mapping analyses summarized in Table 1 only include those traits displaying age-related strain differences (middle column) and with LOD scores of 3.3 or greater in one of the three analyses described previously. The most interesting results are those on chromosomes 2, 3, 4, 5, and 9 where significant QTLs were identified for age-related differences, but were not identified in the specific 200 and 800 day analyses. The identification of QTLs for skeletal phenotypes at a distinct point in time does not necessarily indicate that the QTL is influencing age-related changes in bone quality. QTLs influencing a change in bone integrity as a function of age may be fundamentally more important in relation to osteoporosis and fracture risk in old age.

ASBMR 27th Annual Meeting

Table 1: QTL interval mapping results. *A-data adjusted for animal size, U-unadjusted, and B-both									
Chr.	Phenotypic Trait	*	Sex	200 Day BXD		800 - 200 Day Strain		800 Day BXD	
				RI Strain	Mean cM	Mean cM	Age Difference	RI Strain	Mean cM
					LOD				LOD
2	Femur Neck Ult. Load	A	M			23	3.3		
2	Femur Neck Ult. Load	U	M			27	4.6	51	2.3
3	Femur Head Diameter	B	M			34	3.7		
4	Femur Head Diameter	A	F			19	3.3		
4	Tibia Shaft Yield Disp.	A	F	59	1.9	58	4.2	36	1.6
5	Femur Shaft Stiffness	A	F			13	3.7		
9	Tibia % Water	A	M			13	3.3		
9	Femur Shaft Yield Disp.	A				26	3.3		
10	Femur Neck Ult. Work	A	F			2	3.0	2	4.0
11	Femur Shaft Ult. Work	U	F	26	2.4	26	3.4	26	2.2
12	Femur Epiphyseal Width	A	M			46	3.3	46	3.2
16	Femur Shaft Ult. Load	A	F	12	1.5	19	2.0	18	3.3
16	Femur Shaft Stiffness	B	F			16	4.1	16	3.8
16	Tibia Length	U	F			19	3.3		
16	Femur Shaft Ult. Work	B	F			21	4.0	21	4.1
18	Tibia Shaft Stiffness	U	M			49	2.1	49	3.3
20	Femur Shaft Ult. Disp.	U	F			27	2.1	30	3.5

Disclosures: **D.H. Lang**, None.

M113

Effect of Deficiency of L-Gulonolactone Oxidase on Mouse Gene Expression Profiling . **W. Gu¹, Y. Jiao^{*1}, J. Yan^{*1}, X. Li^{*2}, W. G. Beamer³.**
¹University of Tennessee Health Science Center, Memphis, TN, USA, ²University of Chicago, Chicago, IL, USA, ³The Jackson Laboratory, Bar Harbor, ME, USA.

Human species and guinea pigs are unable to synthesize ascorbic acid (Vitamin C) because of, unlike rodents, lack of the enzyme L-gulonolactone oxidase. Recently, we discovered a deletion, which includes all 12 exons in the gene for L-gulonolactone oxidase (LGO), from the spontaneous fractures (*sfx*) mouse, which is characterized by a spontaneous bone fracture seen around 6 weeks of age. However, it is not known if any other genetic elements also exist in the deleted region. To confirm the LGO is the only gene in the deleted region that causes the *sfx* disease, we have conducted an experiment to feed the *sfx* mice with Vitamin C and compare their phenotype with that of normal mice. We then conducted a study using microarray to analyze the impact of lacking of LGO on the gene expression of three tissues, Femur, kidney, and liver. Finally, we conducted semi-quantitative PCR to confirm selected genes from microarray analysis. Our study shows that although the size of the deletion on chromosome 14 is as large as 38 kb in *sfx* mice, it contains only the LGO gene. The *sfx* mice with Vitamin C in food grew at the same rate as their wild type littermates. On the aspect of gene expression profiles, we found that, in addition to the difference between normal and *sfx* mice, there were also differences among bone, kidney, and liver. Further comparison of the genes that differed by more than 2 of log2 values indicated that there were a small number of genes that change expression profiles in all of these three tissues, namely 11. While changes of expression profiles of 83 genes were the same between the liver and kidney, 30 were the same between the liver and bone and 44 between kidney and bone. The expression levels of five genes were further analyzed using semi-quantitative PCR. Among these five genes, expression of four of them was down regulated and one was up regulated. In addition, we found that one gene expressed only in bone. This gene also showed sex difference on its expression. It was down regulated in the male but not in the female mice. While the expression levels of other genes did not show the sex difference.

Disclosures: **W. Gu**, None.

M114

Hierarchical Clustering of Differentially Expressed Genes in Femoral Bone from Domestic and Wild Type Chickens Reveals Alterations of Specific Signalling Pathways. **C. L. Rubin^{*1}, P. Savolainen^{*2}, J. Lundeberg^{*2}, L. Andersson^{*3}, A. Kindmark¹.** ¹Dep. Med. Sciences, Metabolic Bone Diseases, Uppsala, Sweden, ²Dep. of Biotechnology, Royal Institute of Technology (RIT), Stockholm, Sweden, ³Dep. of Animal Breeding and Genetics, Swedish Univ. of Agricultural Sciences, Uppsala, Sweden.

With the aim of identifying differentially expressed genes, a global expression analysis of femoral bone RNA from individuals of two divergent lines of chicken was performed using cDNA-microarrays. Hierarchical clustering of the microarray data was performed to identify similarities in expression of differentially expressed genes. The domestic White Leghorn (WL) chicken and the wild ancestor, the Red Junglefowl (RJF) are separated by several thousand years of evolution. During domestication, selection in the WL for growth and egg-laying traits has resulted in profound phenotypic differences between the two lines. By performing Quantitative Trait Loci- (QTL) analyses of a WL and RJF intercross, we have previously identified genetic regions harbouring elements responsible for differences in several bone traits. Twenty individuals, (5 male and 5 female from each population) were sacrificed at 250 days of age (approved by local ethics committee). Femoral bones were snap frozen in liquid nitrogen and stored at -70°C. 20 µg of purified RNA from each individual and 20 µg reference RNA were subjected to cDNA synthesis and were labelled with either Cy3 or Cy5 in a dye swap manner, and were then hybridized onto the cDNA-microarray (developed at RIT and comprising 13000 putatively unique chicken clones). The raw fluorescence data was subjected to filtration, normalization and statistical tests in the software R. The Log2 transformed values of the ratio of fluorescence (sample/reference) for each individual were used as input files in the hierarchical

clustering, which was performed in the software Cluster. In the microarray analysis we identified 579 transcripts as differentially expressed between WL and RJ (measured by an empirical Bayesian approach, the B-test). Of the transcripts displaying differential expression, several belong to distinct signalling pathways and cluster together with a highly correlated pattern of expression, indicating that their expression is controlled by the same regulatory factors, possibly the genes or genetic elements responsible for the QTLs. Future plans include clustering of microarray data from different tissues of the same chicken individuals. This may reveal other affected signalling pathways or may add further information regarding the pathways identified in the analysis of bone tissue.

Disclosures: **C.L. Rubin**, None.

M115

The D727E Polymorphism of the Human Thyroid Stimulating Hormone Receptor Is Associated with Bone Mineral Density and Bone Loss in Women from the UK. **O. M. E. Albagha^{*1}, R. Natarajan^{*1}, D. M. Reid¹, S. H. Ralston².** ¹Medicine & Therapeutics, University of Aberdeen, Aberdeen, United Kingdom, ²Rheumatic Disease Unit, University of Edinburgh, Edinburgh, United Kingdom.

Genetic factors are important in the pathogenesis of osteoporosis and regulation of bone mass, but most genes responsible remain to be defined. Recent reports, using thyroid stimulating hormone receptor (TSHR) knockout mice, have shown that TSH exerts direct effects on bone cells through TSHR by inhibiting both osteoclastic bone resorption and osteoblastic bone formation (Abe *et al*, Cell 2003). *TSHR* null mice have severe osteoporosis at all skeletal sites and die by 10 weeks of age, whereas *TSHR*^{-/-} mice thrive normally but have pronounced osteoporosis and focal osteosclerosis. In this study, we investigated the role of *TSHR* gene as a candidate for regulation of bone mass by examining the association between a common polymorphism (D727E) of the *TSHR* gene and bone mineral density (BMD) in a population based study of ~1250 women randomly selected from Scotland who were followed-up for ~ 6 years. The D727E polymorphism was detected using PCR-direct DNA sequencing. BMD was measured using DXA. Genotype frequencies (D/D= 1078, D/E= 171, E/E= 8) were in Hardy-Weinberg equilibrium and were similar to those previously reported in white populations. We observed a significant association between D727E polymorphism and BMD, so that women having the D/D genotype had significantly reduced lumbar spine (LS) and femoral neck (FN) BMD (mean ± sem; LS= 0.999 ± 0.005; FN= 0.831 ± 0.004) compared to those without this genotype (LS= 1.028 ± 0.013, p=0.029; FN= 0.852 ± 0.009, p=0.036). The result remained significant after adjustment for confounding factors (age, body mass index, menopausal status and HRT use) using general linear model ANOVA (LS p-value=0.037; FN p-value=0.048). Analysis of D727E in relation to bone loss showed that annual rates of LS bone loss for women with D/D genotype were about 2 fold higher (-0.670 ± 0.036) than those without this genotype (-0.318 ± 0.103; p=0.0004) and the results remained significant after adjustment for confounding factors (p=0.003). A similar trend was observed for rates of FN bone loss but results were of borderline significance (unadjusted p= 0.04; adjusted p = 0.14). In conclusion, the work presented here is the first to report a significant association between polymorphisms of the human *TSHR* gene and BMD which suggest that allelic variation at the *TSHR* gene might be important for regulation of BMD in humans, raising the possibility that *TSHR* genotyping could be useful genetic marker for BMD and susceptibility to fractures. However, the exact mechanism by which this polymorphism affects BMD remains to be determined

Disclosures: **O.M.E. Albagha**, None.

M116

Variation in the PTH and PTHLH Genes, Serum PTH Levels and Bone Mineral Density in Elderly Women. **M. Tenne^{*}, P. Gerdhem, K. Obrant, H. Luthman^{*}, K. Åkesson.** Dept of Orthopaedics, Dept of Clinical Sciences, Malmö, Malmö, Sweden.

Parathyroid hormone (PTH) is a key regulator of calcium metabolism, whereas parathyroid hormone-like hormone (PTHLH) secretion has been observed in tumors, causing hypocalcaemia of malignancy, but it has also a physiological role during early bone growth. PTH and PTHLH act through the same receptor, the PTH/PTHLH receptor, a class B G-protein-coupled receptor. In addition, a second receptor the PTHR2 receptor has been identified. The physiological activity induced by PTH and PTHLH is depending on the N-terminal domain for ligand binding, where amino acid substitutions may have critical adverse effects on high-affinity ligand binding and biological activity. PTH hypersecretion induce bone resorption, whereas intermittent injection of PTH increase bone mass and is used for treatment of osteoporosis. To explore the effects of genetic variation in the PTH/PTHLH system, we have evaluated variations in genes for PTH and PTHLH in relation to osteoporosis associated traits in elderly women. The study group includes 1044 elderly women, all 75-yrs old, from the Malmö Osteoporosis Prospective Risk Assessment study (OPRA). They are extensively phenotyped: bone mineral density (BMD), quantitative calcaneus ultrasound, serum PTH, bone metabolic markers, fracture, health and life style, and followed for up to 8 years. Six polymorphic loci at the PTH locus on chromosome 11 were identified in the International HapMap Genotype Database, and three loci at the PTHLH locus on chromosome 12. The determined single nucleotide polymorphism (SNPs) allow for haplotype dissection of the gene to provide further inference of the locus. Of the PTH SNPs, two are located downstream, one in the intron and three upstream, while two PTHLH SNPs are located in the gene and one 2000 bp upstream. Two PTH SNPs were associated with serum PTH concentrations. Interestingly, homozygosity for the least frequent allele (TT) in same SNPs were associated with a history of previous fracture. One of the SNPs was associated with lower spinal BMD (p=0.007) at baseline, whereas no association was evident for the other measured sites, or for annual bone loss. We did not find any association between the analyzed polymorphisms of PTHLH and serum PTH or

ASBMR 27th Annual Meeting

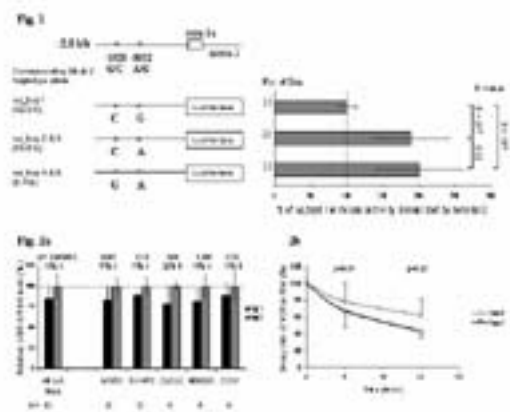
bone variables. The PTH system is of major importance for regulation of bone turnover particularly in the elderly. This is to our knowledge the first study evaluating variation in the PTH/PTHrP gene regions. Genetic analyses of this regulatory system by genotypes and haplotype dissection provide insights to the functional links between serum levels and the clinically significant end-points of bone mass and fracture in elderly women.

Disclosures: K. Åkesson, None.

M117

Regulatory Polymorphisms in the Vitamin D Receptor Gene Cause Reduced Expression. Y. Fang^{*}, A. Alesio^{*}, M. Jhamai^{*}, F. Rivadeneira¹, J. van Leeuwen¹, F. Jehan^{*}, H. Pols^{*}, A. Uitterlinden¹. ¹Internal Medicine, Erasmus Medical Center, Rotterdam, The Netherlands, ²Endocrinology, Bone & Development, Inserm U561, Hôpital Saint Vincent de Paul, Paris, France.

Introduction Vitamin D receptor (VDR) gene polymorphisms are associated with complex diseases, including osteoporosis, but with inconsistent results. We previously analysed LD haplotype blocks in Caucasians across the VDR gene, and found haplotype alleles of the promoter and 3' untranslated region (UTR) associated with increased fracture risk and decreased body height. To investigate the underlying mechanism, we performed functional experiments for individual polymorphisms and haplotypes in both the VDR promoter and 3'UTR areas. **Material & Methods** To examine promoter SNPs electrophoretic gel mobility shift assay (EMSA) were done using HEK293 or CaCo2 nuclear extracts, and luciferase reporter constructs were assayed in HEK293. We measured VDR mRNA level for the 3'UTR variations by transfecting constructs with VDR cDNA and the entire 3'UTR of either the hap_u1 (risk) allele or the hap_u2 (protective) allele in osteoblast cell lines MG63 and SV-HFO, and in HEK293, CaCo2 and COS1. mRNA stability was determined in MG63 at 0-8-24 h after inhibiting transcription. **Results** For the 1e/1a promoter we found that the "G" weaker binding (by EMSA) alleles at a known Cdx-2 site (1e-G-1739A) and a novel GATA binding site (1a-A-1012G) are both on the promoter risk ea_hap1 haplotype allele. We transfected reporter constructs containing 2 kb 1a-promoter sequence, and observed 53% lower expression of the risk ea_hap1 allele vs. ea_hap2 or 3 (Fig1, $p=5 \times 10^{-7}$, $n=51$ exp.). For the 3'UTR variants the normalized VDR mRNA level of hap_u1 was 15% lower for all cell lines combined with similar patterns in all individual cell lines (Fig2a, $p=2 \times 10^{-6}$, $n=53$). We observed a 30% faster mRNA decay of hap_u1 vs. hap_u2 in the MG63 (Fig2b, $p=0.02$, $n=9$). **Conclusion** We demonstrate *in vitro* that risk haplotypes in both the VDR promoter and the 3'UTR cause a modest reduction in mRNA level in potential target cells. We postulate these subtle functional effects to underlie the associations we reported for fracture and height, by resulting in a modestly reduced sensitivity for vitamin D signalling.



Disclosures: Y. Fang, None.

M118

Association Between Genetic Polymorphisms of Enzymes Involving Mevalonate Pathway (GGPS1, FDPS) and Therapeutic Response to Bisphosphonate. J. Choi^{*}, D. Kang^{*}, D. Kim^{*}, H. Song^{*}, S. Cho^{*}, S. Kim^{*}, J. Lee^{*}, Y. Chung^{*}, C. S. Shin^{*}. ¹Preventive Medicine, Seoul National University College of Medicine, Seoul, Republic of Korea, ²Internal Medicine, Dankook University College of Medicine, Cheon-An, Republic of Korea, ³Endocrinology and Metabolism, Ajou University School of Medicine, Suwon, Republic of Korea, ⁴Internal Medicine, Seoul National University College of Medicine, Seoul, Republic of Korea, ⁵DNA Link, Seoul, Republic of Korea.

Nitrogen containing bisphosphonates (N-BP) inhibit the enzymes of the mevalonate biosynthetic pathway including farnesyl pyrophosphate synthetase (FDPS) and geranylgeranyl diphosphate synthase (GGPS1), which result in inhibition of prenylation of small GTP-binding proteins in osteoclasts and disruption of the cytoskeleton. To investigate the relationship between FDPS and GGPS1 genetic polymorphisms and changes in BMD before and after N-BP treatment in Korean, 137 patients aged 32-82 years (60.4±10.23, mean±SD) were enrolled in this study. BMD at lumbar spine and femoral neck was measured by dual-energy X ray absorptiometry. PCR and direct sequencing were used to identify the polymorphisms of FDPS and GGPS1 in 48 healthy Korean; among five and eight SNPs screened, respectively, those of which the variant allele frequencies are more than 10% were selected (FDPS IVS1-98G>T, IVS9+66G>T and GGPS1 -8188A/

[Del] and IVS3-12~13T[Ins]). Genetic polymorphisms were determined by single base primer extension assay. The difference changes (%) of the BMD according to the genotypes of FDPS and GGPS1 were analyzed by Kruskal-Wallis test. The response of BMD at lumbar spine to N-BP significantly increased in subjects with GGPS1 -8188 A[Del] or IVS3-12~13 T[Ins] allele, respectively ($p=0.010$ and $p=0.007$); 9% changes of BMD at lumbar spine in subjects with GGPS1 variant allele (both -8188 A[Del] and IVS3-12~13T[Ins]) vs. only 5% with no variant allele of GGPS1. When we defined the non-responder group as subjects, who had BMD lost or unchanged after N-BP treatment, 14.1% of subjects were included. After adjustment for age, gender and initial BMD, the significant association remained between drug responsiveness and genetic polymorphisms of GGPS1 ($p=0.006$ and $p=0.015$, respectively). However, these associations were not found in the femoral neck BMD. No significant association was observed between BMD changes and FDPS polymorphisms.

Disclosures: J. Choi, None.

M119

Polymorphisms in the RANKL Gene Are Not Associated with Bone Mass or Risk of Osteoporotic Fractures. L. B. Husted, M. Carstens^{*}, L. Stenkjær^{*}, B. L. Langdahl. Endocrinology, Aarhus University Hospital, Aarhus Sygehus, Aarhus C, Denmark.

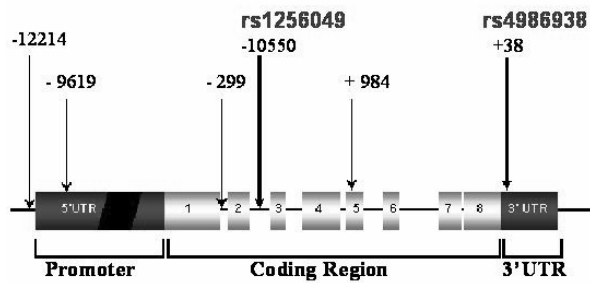
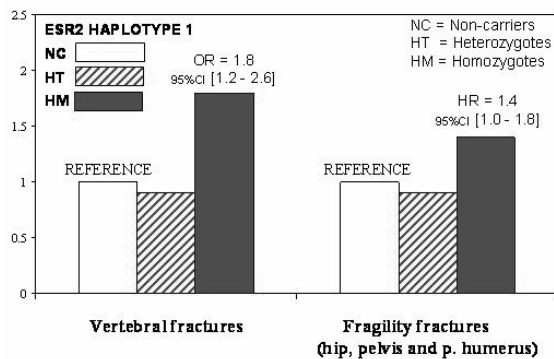
Interaction between receptor activator of nuclear factor-kappa B (RANK), RANK ligand (RANKL) and osteoprotegerin (OPG) controls recruitment and activity of osteoclasts. Genetic variant in these three genes are therefore possible contributors to the genetic background of osteoporosis. We have previously demonstrated that polymorphisms in the OPG gene are associated with changes in bone mass and risk of osteoporotic fractures. In this study we wanted to examine the RANKL gene for polymorphisms and the influence of such polymorphisms on bone mass and risk of osteoporotic fractures. We have examined the promoter (1128 basepairs upstream from the transcription initiation site) and the 5 exons for polymorphisms in 50 osteoporotic patients and 50 normal individuals using sequencing. We identified six polymorphisms: Three in the promoter: C-693-G, C-643-T and T-290-C, two in exon 1: C233-G and C252-T and one in intron 2: A513+14-G. The three promoter polymorphisms and C252-T were in almost complete linkage disequilibrium. C252-T is a conservative polymorphism, whereas C233-G is changing the 36th aminoacid from proline to arginine, however, this polymorphism was only found in 2% of the examined alleles. We examined the effect of T-290-C and A513+14-G on bone mass and risk of osteoporotic fractures in 720 osteoporotic patients and normal controls. The T-290-C polymorphism did not influence height and weight. In individuals with the TT, TC and CC genotypes BMD(1s) was 0.901 ± 0.175 g/cm², 0.901 ± 0.178 g/cm² and 0.898 ± 0.173 g/cm², respectively, ns. No differences in BMD at any of the hip sites were demonstrated. Furthermore, prevalence of the TT, TC and CC genotypes was 30.4%, 44.7% and 24.9% in patients with vertebral fractures, respectively, and 29.8%, 47.6% and 22.5% in normal controls, respectively, $\chi^2=0.60$, ns. Prevalence of the AA, AG and GG genotypes of the A513+14-G polymorphism was 71.7%, 25.0% and 3.3% in patients with vertebral fractures, respectively, and 67.3%, 30.2% and 2.5% in normal controls, respectively, $\chi^2=1.99$, ns. BMD(1s) was slightly reduced in the rare genotype, GG, 0.857 ± 0.236 g/cm² compared with 0.901 ± 0.176 g/cm² in the AA and 0.905 ± 0.167 g/cm² in the AG genotypes, however the difference did not reach significance. No differences were found between genotypes in BMD at the different hip sites, height and weight. In conclusion: We have found 6 polymorphisms in the RANKL gene. None of these are associated with bone mass and risk of osteoporotic fractures.

Disclosures: B.L. Langdahl, None.

M120

ESR2 Influences the Risk of Osteoporotic Fracture in Postmenopausal Women. M. C. Zillikens^{*}, F. Rivadeneira¹, J. van Meurs¹, T. Beck², J. Houwing^{*}, A. Hofman^{*}, J. van Leeuwen¹, C. van Duijn^{*}, H. A. Pols¹, A. Uitterlinden¹. ¹Erasmus Medical Center, Rotterdam, The Netherlands, ²Johns Hopkins University, Baltimore, MD, USA, ³LUMC, Leiden, The Netherlands.

Aim We examined the role of variants in the ESR2 gene (alone and in interaction with ESR1 and IGF1) in relation to the risk of osteoporotic fracture. **Methods** We studied six SNPs in the ESR2 gene (Fig 1) in a large population-based cohort of elderly men and women ($n=6343$). Results refer to the most frequent haplotype (haplotype 1) estimated from the intron 2 and 3'UTR SNPs. Interaction was studied with ESR1 (XbaI, PvuII haplotype 1) and IGF1 (CA_n promoter repeat). Outcomes included vertebral fracture (X-ray screening in 3469 individuals), incident non-vertebral fracture (mean follow-up 8.6 years), BMD and geometry from hip structural analysis (HSA). **Results** Female homozygous carriers (HM) of haplotype 1 in the ESR2 gene had increased risk of vertebral fracture (Fig 2). HM women had 1.1% ($p=0.06$) less vertebral area and 3.8% higher ($p=0.001$) buckling ratio (an index of bone instability). Non-carriers of haplotype 1 in either of the estrogen receptor genes (NC/NC) were the reference. Women homozygous carriers (HM) of ESR2 haplotype 1 and non-carriers (NC) of haplotype 1 in ESR1 (which have higher ER1 sensitivity-black bars) have 3.5 (95%CI 1.4 - 8.4) and 1.8 (95%CI 1.0 - 3.4) increased risk of vertebral (Fig 3) and fragility fracture (Fig 4); with p interaction = 0.06 and 0.10 for the risk of vertebral and fragility fracture, respectively. These interactions were stronger in women homozygous for the 192-bp allele of the IGF1 promoter polymorphism (p interaction = 0.002 and 0.01 for the risk of vertebral and fragility fracture, respectively) which have higher IGF-I levels. Similar gene interactions were observed for BMD and bone geometry (HSA). In men, no such effects were observed. **Conclusions** Presence of the ESR2 haplotype 1 (alone or in interaction with variants of ESR1 and IGF1) influences the risk of osteoporotic fracture in postmenopausal women.

Figure 1. Location of SNPs in the ESR2 gene**Figure 2. Risk of osteoporotic fracture by ESR2 haplotype 1**Disclosures: **M.C. Zillikens**, None.**M121**

Genetic Variation in Estrogen Receptor Alpha and Interleukin-6 Is Associated with Bone Mass Acquisition in Prepubertal Girls and Boys: Interaction with Calcium Supplements. **P. Pennisi**^{*1}, **T. Chevalley**², **D. Manen**^{*2}, **F. Herrmann**^{*2}, **M. Brandi**³, **R. Rizzoli**², **S. Ferrari**². ¹Dept. of Internal Medicine, University Hospital of Catania, Catania, Italy, ²Div. of Bone Diseases, Geneva University Hospital, Geneva, Switzerland, ³Dept. of Internal Medicine, University Hospital of Florence, Florence, Italy.

Estrogens regulate interleukin-6 (IL6) expression. Polymorphisms in estrogen receptor alpha (ESR1) and IL6 genes are associated with BMD, bone turnover and/or fracture risk in post-menopausal women. Whether genetic variation in ESR1 and IL6 plays a role on bone mass acquisition however remains unknown. We examined the association of ESR1-XbaI and IL6 -174 G>C polymorphisms with BMD and their interaction with calcium intake in 139 girls and 232 boys who received calcium supplements (800mg/d) or placebo for 1 yr. BMD at lumbar spine (LS), total hip (TH), femoral neck (FN), ultra distal (UR) and total radius (TR) was evaluated by DXA at baseline (mean age \pm SD, 7.6 \pm 0.4 yrs) and after 1 and 2 yrs (age, 9.9 \pm 0.5 yrs). Genotypes distribution was similar in both genders (rare alleles: ESR1 XX, 12%, IL6 CC, 15%). ESR1 genotypes were associated with BMD at most skeletal sites ($p=0.01-0.06$ adjusted for age, weight and height), with a borderline interaction with sex (Pinter \leq 0.09). Indeed, xx females had 2-6% higher BMD compared to Xx and/or XX (LS $p=0.04$ and $p=0.03$; FN $p=0.004$ and $p=0.05$; TH $p=0.009$ and ns; TR $p=0.005$ and ns at baseline and after 2 yrs, respectively), whereas males did not. ESR1 genotypes were not associated with BMD gain in absence of calcium supplements, but a significant interaction with calcium supplements occurred on hip (Pinter=0.03). Indeed, calcium supplements increased FN and TH BMD gain 2-3x above placebo among XX, but not among carriers of the x allele. At baseline, IL6 -174 genotypes were associated with BMD at LS (+4% in GG compared to CC and GC, $p=0.001$), but not at other skeletal sites, and without evidence of interaction with sex. After two years, this association became weaker ($p=0.05$), since GG from both genders had a 26% lower LS BMD gain during yr 2 in absence of calcium supplements ($p=0.01$ vs CC and GC, adjusted for age, pubertal stage, and changes in height and weight). Calcium supplements significantly increased TR and UR BMD gain in males and females ($p=0.006$ and $p=0.05$, respectively), without evidence of interaction with IL6 genotypes. In conclusions, ESR1-XbaI and IL6 promoter -174G>C polymorphisms are associated with BMD and BMD gain in prepubertal children. Whereas IL6 genetic variation appears to modulate bone mass acquisition at LS irrespective of sex and calcium intake, the broad influence of ESR1 genotypes on BMD was more prominent in females and may depend on the level of calcium intake.

Disclosures: **P. Pennisi**, None.**M122**

Two New Single Nucleotide Polymorphisms in the CYP19 Gene. Association with BMD in a Cohort of 256 Spanish Postmenopausal Women. **S. Balcells**^{*1}, **A. Enjuanes**^{*2}, **N. Garcia-Giralt**^{*2}, **A. Supervia**^{*3}, **X. Nogues**³, **S. Ruiz-Gaspa**^{*2}, **M. Bustamante**^{*1}, **L. Mellibovsky**^{*3}, **D. Grinberg**^{*1}, **A. Diez-Perez**³. ¹Genetics, University of Barcelona, Barcelona, Spain, ²IMIM, Barcelona, Spain, ³Hospital del Mar, Barcelona, Spain.

Background. Current evidence suggests that extragonadal estrogens play an important role in determining bone mineral density (BMD). Estrogen biosynthesis is catalyzed by the P450aromatase, encoded by the *CYP19* gene. An association analysis of promoter SNPs with BMD was conducted. **Materials and Methods.** Promoter regions of the *CYP19* gene were functionally explored by means of a luciferase reporter gene assay in MG-63 cells. Sequencing of relevant regions was performed to screen for new SNPs. Association analyses with BMD was carried out in a cohort of 256 Spanish postmenopausal women. **Results:** Promoter pII proved to be potent in driving transient luciferase expression in MG-63 cells. A region upstream of exon 1.6, including exon 1.6, was identified as containing repressor elements of promoter pII. In screening these *CYP19* promoter regions, two new SNPs (Aro1 and Aro2) located in exon 1.6 and promoter 1.6 respectively, were found. Aro1, but not Aro2, was associated with lumbar spine BMD in the cohort of Spanish postmenopausal women. Homozygotes AA (16% of the women) had significantly higher lumbar spine BMD as compared to GG or GA individuals ($p=0.029$). **Conclusions:** This study describes the Aro1 polymorphism, located in the exon 1.6 region upstream of the *CYP19* gene, which shows a previously undescribed association with lumbar spine BMD.

Disclosures: **D. Grinberg**, None.**M123**

Apolipoprotein E Genotype Is a Determinant of Serum Vitamin K, but not BMD, in Older Men and Women. **M. D. Crosier**¹, **M. K. Shea**^{*2}, **J. M. Ordovas**^{*2}, **C. M. Gundberg**³, **B. Dawson-Hughes**², **S. L. Booth**². ¹USDA Human Nutrition Research Center on Aging, Tufts University, Boston, MA, USA, ²Human Nutrition Research Center on Aging, Tufts University, Boston, MA, USA, ³Yale University, New Haven, CT, USA.

Apolipoprotein E (*APOE*) is a determinant of triglyceride-rich lipoprotein (TRL) clearance, and has a potential role in the regulation of bone formation. Vitamin K is a cofactor for the gamma-carboxylation of osteocalcin, and is carried by TRL. It has been proposed that *APOE*'s role in bone formation is mediated through the delivery of the fat-soluble vitamin K to osteoblasts. Cross-sectional associations of *APOE* with biochemical measures of vitamin K status [serum phyloquinone (vitamin K-1) and percent undercarboxylated osteocalcin (%ucOC)] were examined in 407 older men and women (mean age: 68y; 60% women) selected for low vitamin K intake (<100 μ g/day) as criteria for participation in a vitamin K clinical trial. All subjects had bone mineral density (BMD) of the hip, spine and total body measured by DXA. *APOE* was genotyped using a Taqman probe-based 5' nuclease assay. The distribution of the *APOE* genotypes were 3/3 263 (64.6%); 3/4 79 (19.4%); 2/3 47 (11.5%); 4/4 7 (7.1%) 2/4 11 (2.7%). All analyses were conducted at baseline, prior to randomization in the clinical trial. *APOE* genotype was significantly associated with serum phyloquinone concentrations ($p=0.04$), independent of serum triglycerides. Those with the E2/3 genotype had higher serum phyloquinone concentrations [mean (SD) 1.96 (2.65) nmol/L] compared to those with other genotypes (range of means: 0.94 to 1.17 nmol/L) ($p=0.02$). There was no association of *APOE* genotype with %ucOC or with BMD at any anatomical site. However, *APOE* genotype was associated with total osteocalcin concentrations ($p=0.001$); those with the E4/4 genotype had higher serum total osteocalcin concentrations [mean (SD) 12.6 (5.50) ng/mL] compared to those with other genotypes (range of means: 7.1-8.4 ng/ml). Limitations of this study are its cross-sectional design, small sample size and the potential for selection bias as these were primarily Caucasian individuals with low vitamin K intake. In conclusion, *APOE* genotype may be a non-dietary determinant of serum phyloquinone concentrations in older men and women. *APOE* genotype is also associated with serum concentrations of osteocalcin, which is a marker of bone formation, but not %ucOC, which is a marker of vitamin K status. The role of *APOE* genotype in the response of age-related bone loss to vitamin K supplementation needs to be determined.

Disclosures: **M.D. Crosier**, None.**M124**

Allelic Combinations of the CYP17 and CYP19 Genes: Skeletal and Hormonal Phenotypes. **N. Napoli**¹, **R. Del Fiacco**^{*1}, **S. Mumm**¹, **A. Fakhri**^{*2}, **G. B. Rini**^{*1}, **R. C. Villareal**¹. ¹Medicine, Washington University School of Medicine, St. Louis, MO, USA, ²Medicine, St. Lukes Hospital, St. Louis, MO, USA.

The T to C substitution in the promoter region of CYP17, and the G to A in Val⁸⁰ of CYP19, have been found to be associated with differences in the risk for osteoporosis. Since both genes coexist, it is likely that allelic combinations may predict bone density better than a particular allele of one gene alone. Our aim is to characterize the skeletal and hormonal phenotypes of the different allelic combinations of the T \rightarrow C (CYP 17) and the G \rightarrow A (CYP 19) base substitutions. One hundred seventy nine postmenopausal Caucasian women (mean age 64.09 \pm 0.6) participated in the study. Genotyping was performed by PYROSEQUENCING, serum estradiol (E₂) by ultrasensitive radioimmunoassay, sex-hormone-binding globulin by immunoradiometric assay and BMD by DEXA. For the CYP17, women with the C allele (TC+CC) had significantly lower spine BMD compared

ASBMR 27th Annual Meeting

to those with the TT genotype (0.924±0.01, 0.974±0.01, p=0.02). The same trend was observed for BMD of the proximal femur sites, but the differences were not significant. For the CYP 19, women with the A allele (GA+AA) have significantly lower BMD of the total femur (0.844±0.01, 0.896±0.01, p<0.01), femoral neck (0.701±0.01, 0.744±0.01, p=0.01) trochanter (0.642±0.01, 0.672±0.01, p=0.05) and intertrochanter (1.012±0.01, 1.0812±0.02, p=0.004) as compared to the GG genotype. There was no significant difference in BMD of the spine observed for this polymorphism. There were no significant differences in total and FEI among the variants of both polymorphisms, however, significant correlations between BMD in all regions of the proximal femur and FEI were observed among women carrying either the C (CYP17) or the A (CYP 19) allele (all p<0.01) as compared to no correlation between BMD at any site and estradiol levels in those without these alleles. Women with a combination of the C (CYP17) and the A (CYP19) alleles have the lowest BMD in the mainly trabecular regions of the spine (p=0.03), femoral neck (p=0.03), and trochanter (p=0.04) in comparison to other allelic combinations. There were no significant differences in the total E₂ and FEI among the different allelic combinations, however, significant stronger correlations were observed between BMD of the proximal femur and FEI in women carrying both alleles than either the C or the A allele alone. Our study indicated that the combined presence of the C (CYP 17) and the A (CYP 19) is associated with the worst bone density phenotype in both the spine and proximal femur. Our results also showed that BMD in these variants are more estrogen-dependent than other variants, and may be more sensitive to changes in circulating levels of estradiol than others.

Disclosures: **R.C. Villareal**, None.

M125

Postprandial Changes of Serum Fibroblast Growth Factor 23(FGF23) Levels on High Phosphate Diet in Healthy Men. **Y. Nishida***, **H. Yamanaka-Oikumura***, **Y. Taketani**, **T. Sato***, **K. Nashiki***, **H. Yamamoto**, **E. Takeda**. Clinical Nutrition, Health Biosciences, Tokushima, Japan.

Serum fibroblast growth factor 23 (FGF23) has been found as a novel phosphate (Pi) regulating hormone. Blood FGF23 levels are not only elevated in phosphate wasting disorders, but also are detectable in healthy individuals. Recent studies indicate that FGF23 may be implicated in the physiological regulation of Pi homeostasis in response to dietary Pi changes. To examine the postprandial changes of serum FGF23 levels, we performed a randomized crossover study loading meal with three different Pi amount in 8 healthy male volunteers (age 20-34). 1) P400; 400mg Pi provided as normal meal, 2) P800; 800mg Pi as normal meal and 400mg Pi supplement, 3) P1200; 1200mg Pi as normal meal and 800mg Pi supplement. Pi supplement was administered orally as a solution of neutral sodium and phosphate (mixture of Na₂HPO₄ and NaH₂PO₄). Calcium and other nutrients in each experimental meal were same (200mg of calcium per meal). Blood samples were collected at 0(12:00 a.m.), 0.5, 1, 1.5, 2, 3, 4, 6, and 8h following each meal, and serum concentrations of Pi, Ca, creatinine (CRE), 1,25(OH)₂D₃, intact-PTH, and intact-FGF23 were measured. Urine samples of after meals were also collected at 1-h intervals for 8h, and urinary concentrations of Pi, Ca, and CRE were measured. Serum intact-FGF23 was determined by the Human FGF23 ELISA kit (Kinos Inc., Tokyo, Japan). Urinary Pi excretion and serum Pi levels increased rapidly and dose-dependently (p<0.05). Urinary Ca excretion tended to decrease in response to phosphate loading but no change in serum levels of Ca and 1,25(OH)₂D₃. Serum intact-PTH levels in P1200 were significantly elevated at 1h and 4h compared with those of P400. Serum intact-FGF23 levels among all meals did not show any meaningful change until 6h. However, the mean serum intact-FGF23 level in P1200 at 8h increased by 29% than that of 0h, and was also significantly higher than that of P400 at 8h (P<0.05). In conclusion, postprandial serum intact-FGF23 levels were not affected immediately after single intake of high phosphate diet despite that of intact-PTH was rapidly increased.

Disclosures: **Y. Nishida**, None.

M126

FGF-23, FGF-7, sFRP-4, and MEPE Expression in Tumor Induced Osteomalacia. **M. A. Habra***¹, **S. E. HUANG***¹, **G. J. Cote***¹, **W. A. Murphy***², **R. L. Katz***³, **R. F. Gagel***¹, **M. J. Klein***¹, **A. O. Hoff***¹. ¹Department of Endocrine Neoplasia and Hormonal Disorders, The University of Texas, M.D.Anderson Cancer Center, Houston, TX, USA, ²Division of Diagnostic Imaging, The University of Texas, M.D.Anderson Cancer Center, Houston, TX, USA, ³Department of Pathology, The University of Texas, M.D.Anderson Cancer Center, Houston, TX, USA.

Tumor-induced osteomalacia (TIO) is a rare syndrome associated with the overproduction of fibroblast growth factor-23 (FGF23) by a variety of mesenchymal tumors. The role of other factors (matrix extracellular phosphoglycoprotein (MEPE), FGF-7 and secreted frizzled related protein 4 (sFRP-4)) in the development of TIO is unclear. The aims of the study is to evaluate serum FGF-23 levels before and after the resection of a tumor potentially causing TIO and to analyze the expression of FGF-23 and the other genes in TIO. Two patients with TIO and 6 healthy volunteers were studied. Patient 1 (84 year-old man), presented with myalgia, fatigue, and multiple fractures. After years of evaluation, an expanding soft tissue mass near the left tenth rib was discovered in an area that was previously thought a healed rib fracture. Phosphate abnormalities were corrected after the resection of the mass that was a hemangiopericytoma. Patient 2 (74 year-old man) continued to have clinical features of TIO after the resection of a left femur hemangiopericytoma and still requires vitamin-D and phosphate replacement. After IRB approval, we measured serum FGF-23 levels in the 2 patients with TIO and in 6 healthy controls using a two-site immunoassay for the FGF-23 C-terminus (Immutopics, San Clemente, CA). Mean serum FGF-23 was 24.7±14.4 RU/mL in volunteers, while patient 1

had serum FGF23 level of 2438 RU/mL prior to tumor resection that decreased to 26 RU/mL after surgery. Patient 2 with persistent TIO had serum FGF-23 level of 812 RU/mL. We used RT-PCR to study the expression of FGF-23, FGF-7, MEPE, and sFRP-4 in tumor tissue from patient 1 and control cell lines (HEK 293, HeLa, and U251). Tumor tissue expressed all 4 genes. While the expression of FGF-23 was limited to tumor tissue and a known positive control cell line (HEK 293), FGF-7 and sFRP-4 were expressed in the tumor and all cell lines. MEPE expression was identified in tumor tissue only. In summary, we confirmed the usefulness of measuring serum FGF-23 for diagnostic and follow-up purposes in TIO. We have also described TIO caused by a hemangiopericytoma expressing FGF-23 as well as FGF-7, MEPE and sFRP4. While this could suggest a potential association between several genes involved in phosphate metabolism, the expression of FGF-23 and MEPE appears to be more specific to tumor cells and thereby these two factors appear to be more significant for the development of TIO

Disclosures: **M.A. Habra**, None.

M127

Regulation of Fgf-23 Gene Expression in Bone by Dietary Phosphorus Is Independent of Phex Function . **F. Perwad***¹, **M. Y. H. Zhang***¹, **T. Yamashita***², **H. S. Tenenhouse***³, **A. A. Portale***¹. ¹Pediatrics, University of California San Francisco, San Francisco, CA, USA, ²Pharmaceutical Research Laboratories, Kirin Brewery Co. Ltd., Gunma, Japan, ³Pediatrics and Human Genetics, McGill University, Montreal, PQ, Canada.

X-linked hypophosphatemia in humans (XLH) and mice (*Hyp*) is caused by inactivating mutations in the *PHEX/Phex* gene and is characterized by hypophosphatemia due to renal phosphate (Pi) wasting, rickets, growth retardation, and inappropriately low renal production of 1,25(OH)₂D. Increased circulating FGF-23 is implicated in the pathogenesis of disordered Pi and vitamin D metabolism in XLH, but the mechanism whereby loss of PHEX function leads to increased serum FGF-23 concentrations is unknown. We have reported that in normal mice, dietary Pi intake regulates serum FGF-23 concentrations, and this effect is mediated by changes in serum Pi concentration. To determine whether serum FGF-23 concentration is regulated normally by dietary Pi in *Hyp*, we fed wild-type (WT) and *Hyp* mice diets with varying Pi content (0.02 to 1.65%) for 5 days. In WT mice, changes in dietary Pi intake from low (0.02%) to high (1.65%) induced a 7-fold increase in serum FGF-23 and a 3-fold increase in serum Pi concentrations. Serum FGF-23 concentrations varied directly and significantly with serum Pi concentrations across all diet groups (R=0.80, p<0.001). In *Hyp* mice, serum FGF-23 concentrations were 5- to 25-fold higher than those in WT mice, regardless of Pi intake. Nevertheless, serum FGF-23 levels in *Hyp* mice fed the 1.65% Pi diet were 3-fold higher than those in mice fed the 0.02% Pi diet (600 ± 284 vs 232 ± 99 pg/ml, respectively, p<0.01). In *Hyp*, the relationship between serum FGF-23 and Pi concentrations was direct and significant (R=0.60, p<0.001), similar to that observed in WT mice. To determine whether dietary Pi regulates serum FGF-23 concentrations by regulating *fgf-23* gene expression in bone, we fed WT and *Hyp* mice either 0.02% or 1% Pi diets, each for 5 days. In mice fed the 1% Pi diet, the abundance of *fgf-23* mRNA relative to that of GAPDH mRNA in calvaria was 30-fold higher in *Hyp* mice than in WT mice. Furthermore, feeding the 0.02% Pi diet induced an 85% suppression in *fgf-23* mRNA abundance in both WT and *Hyp* mice, compared with the abundance in each species fed the 1% Pi diet. The present data demonstrate that dietary Pi regulates serum FGF-23 concentration in both WT and *Hyp* mice, and suggest that changes in serum FGF-23 concentration reflect, at least in part, regulation of *fgf-23* gene expression in bone. The findings in *Hyp* mice provide evidence that regulation of FGF-23 gene expression in bone by dietary Pi is independent of PHEX function.

Disclosures: **F. Perwad**, None.

M128

Augmentation of Demineralized Bone Matrix by a Synthetic FGF-2 Mimetic. **X. Lin***¹, **P. O. Zamora***², **L. A. Pena***¹, **S. L. Campion***², **K. Takahashi***². ¹Medical, Brookhaven National Laboratory, Upton, NY, USA, ²BioSurface Engineering Technologies, Inc., College Park, MD, USA.

Demineralized bone matrix (DBM) is a bone graft material widely used in various orthopedic procedures. DBM contains bone morphogenetic proteins (BMPs) and other growth factors that are thought to be key to the ability of DBM to form new bone. However, the amounts of these growth factors are very low thus the osteoinductive potential of DBM is far from satisfactory in clinical settings. We recently described a synthetic peptide mimetic of FGF-2, designated F2A4-K-NS, which increased cell proliferation, cell migration, and angiogenesis, suggesting that it may have utility in bone repair. The purpose of this study is to evaluate whether this agonist mimetic could augment ectopic bone formation following subcutaneous implant of DBM in athymic rats. DBM (50 mg/implant) with and without F2A4-K-NS (20-, 100-, and 200 ng/implant) in a thermostable gel was injected s.c. on the backs of athymic rats. After 28 days the implant was explanted, fixed, and examined by X-ray analysis and by histological methods including von Kossa's staining. Examination of the implant sites did not reveal edema, necrosis, or tissue swelling on the underlying muscle or skin. The carrier (thermostable gel alone) explants showed only a small amount of radio-opacity examined by soft X-ray. The DBM explants exhibited radio-opacity with discrete foci with an overall density of 3.5 X10⁵ pixels/ROI. When the carrier contained DBM plus F2A4-K-NS, an increase in radio-opacity was clearly evident in all 3 dose groups (5.0, 5.3 and 4.6 X10⁵ pixels/ROI, respectively). A statistically significant increase in density was found for specimens in the 20- and 100 ng group. Micro-CT confirmed that when compared to either carrier only or DBM without peptide, the use of DBM plus F2A4-K-NS resulted in higher density and a larger physical size as indicated by a higher bone surface area. von Kossa's stain revealed that there was few calcium deposits in the carrier only samples. Inclusion of DBM in the carrier resulted in an increased amount of von Kossa's staining primary associated with the

DBM granules. When the carrier contained DBM plus F2A4-K-NS, the DBM granules were strongly positive for von Kossa's staining and the amount of staining was more uniformly distributed throughout the specimens. Quantitative analysis revealed that the relative amount of staining is higher in all F2A4-K-NS groups compared to DBM implants. A statistically significant increase in staining was found for specimens containing 100- and 200 ng when compared to the DBM alone group. **Conclusions:** The synthetic peptide F2A4-K-NS, a mimetic of FGF-2, augmented DBM-induced ectopic bone production in athymic animals.

Disclosures: **X. Lin**, Brookhaven National Laboratory 3.

M129

Fibroblast Growth Factor (FGF)-23 in Patients with Hypoparathyroidism: Its Role in Serum Phosphate Regulation. **H. Yamashita¹, Y. Yamazaki^{*2}, H. Hasegawa^{*2}, T. Yamashita^{*2}, S. Fukumoto³, T. Shigematsu^{*4}, J. J. Kazama^{*5}, M. Fukagawa⁶, S. Noguchi^{*1}.** ¹Surgery, Noguchi Thyroid Clinic, Beppu, Oita, Japan, ²Pharmaceutical Research Labs, KIRIN Brewery CO. LTD., Takasaki, Japan, ³Department of Internal Medicine, Tokyo University Hospital, Tokyo, Japan, ⁴Division of Nephrology, Tokyo-Jikeikai Medical School, Katsushika, Japan, ⁵Division of Clinical Nephrology and Rheumatology, Niigata University Graduate School of Medicine, Niigata, Japan, ⁶Division of Nephrology & Dialysis Center, Kobe University School of Medicine, Kobe, Japan.

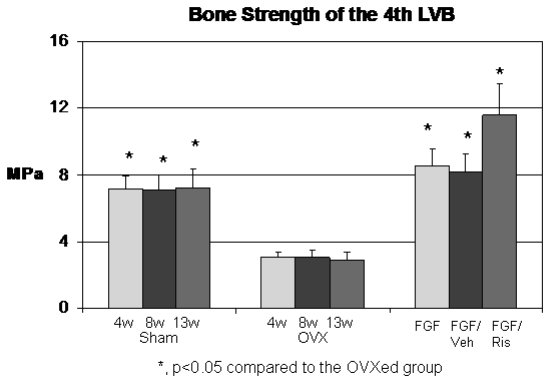
Hypoparathyroidism is a complication of thyroidectomy that causes hyperphosphatemia due to enhanced reabsorption of phosphate in the kidney by decreased parathyroid hormone (PTH) secretion and increased phosphate absorption from the alimentary tract induced active vitamin D administration. FGF-23 is a hormone-like factor that is thought to be important in phosphate homeostasis. However, the physiologic role of FGF-23 in hypoparathyroidism is not clear. We examined changes in serum levels of calcium, phosphate, intactPTH, and FGF-23 (normal range 10-50 ng/L) in 8 patients (7 women, 1 man, mean age 51 years) who developed transient hypoparathyroidism after thyroidectomy. We also examined serum levels of FGF-23, calcium, and phosphate in 14 patients (10 women and 4 men, mean age 50 years) with hypoparathyroidism which continued more than 1 year after thyroidectomy. Serum phosphate reached its peak level (6.1 ± 0.5 mg/dL) 2 or 3 days after development of hypoparathyroidism, followed by a peak in the serum FGF-23 level (87±39 ng/L). Serum levels of calcium, phosphate, and FGF-23 normalized after recovery of parathyroid function. The FGF-23 level was high (47±31 ng/L, range 20-133 ng/L) in stage of hypoparathyroidism. There was a significant positive correlation between serum phosphate and FGF-23 levels. Serum FGF-23 increased in patients with hypoparathyroidism and hyperphosphatemia and normalized along with normalized phosphate levels after recovery of parathyroid function. A significant positive correlation between serum phosphate and FGF-23 levels was identified, suggesting a possible feedback mechanism involving FGF-23 for the maintenance of serum phosphate homeostasis.

Disclosures: **H. Yamashita**, None.

M130

Restoration of Cancellous Bone Connectivity and Strength in Ovariectomized Mice Treated with Basic Fibroblast Growth Factor and Followed by an Anti-Resorptive Agent. **W. Yao¹, G. Balooch², R. Nalla^{*3}, J. Zhou^{*2}, Y. Jiang², T. Wronski⁴, N. Lane¹.** ¹Medicine, UCDMC, Sacramento, CA, USA, ²UCSF, San Francisco, CA, USA, ³Lawrence Berkeley National Laboratory, Berkeley, CA, USA, ⁴University of Florida, Gainesville, FL, USA.

The purpose of this study was to determine if bFGF and risedronate (Ris) would affect connectivity density (CD) and bone strength in OVXed mice. Six mos. Swiss-Webster mice were OVXed and left untreated for 4 wks. to develop cancellous osteopenia. Then were treated with bFGF (1 mg/kg, sc, 5x/wk) for 3 wks. At wks. 8, one group of bFGF-treated mice was sacrificed and the other two groups were switched to vehicle or Ris (5µg/kg, sc, 3x/wk) for 5 weeks. Endpoints evaluated included bone turnover markers by ELISA, distal femur architecture by uCT; bone formation by histomorphometry, and biomechanics of the 4th lumbar vertebrae (LVB). OVXed mice had significant reductions in BV/TV, CD, and bone strength, accompanied by elevated DPD/Cr, OC, MAR and BFR/BS (p<0.05). Treatment with bFGF resulted in higher BV/TV, Tb.N, CD, bone strength and higher bone turnover and bone formation in comparison to sham controls (p<0.05). Discontinuation of bFGF resulted in partial loss of gained BV/TV (50%) by 5 weeks with elevated DPD/Cr (40%) compared to the sham controls. However, BV/TV, Tb.N, CD, bone formation indices, and bone strength were still close to the sham levels. Treatment of OVXed mice with bFGF for 3 weeks followed by Ris sustained the elevated BV/TV, CD, and bone strength, which were almost double those of the sham control levels. DPD/Cr was 28% lower, whereas OC and BFR/BS were similar to sham controls after Ris administration. Thus, in osteopenic mice, bFGF treatment completely restored the lost bone mass and connectivity. However, the increment in distal femur BV/TV and CD gained by 3 weeks of bFGF treatment was partially lost after 5 weeks of treatment termination, whereas Ris maintained BV/TV and CD. Basic FGF treatment also increased bone strength by 195% in LVB compared to the OVXed group, the bone strength was sustained at least for 5 weeks after bFGF withdrawal; and Ris further increased bone strength by 41% compared to the bFGF-treated group. In conclusion, short-term bFGF administration restored trabecular bone mass, connectivity and bone strength and these parameters were maintained by Ris in osteopenic mice after withdrawal of bFGF treatment.



Disclosures: **W. Yao**, None.

M131

Dietary Phosphate Regulates Serum FGF-23 Concentrations in Healthy Men. **D. Antonucci¹, D. Sellmeyer¹, T. Yamashita^{*2}, A. Portale¹.** ¹University of California, San Francisco, CA, USA, ²Pharmaceutical Research Laboratories, Kirin Brewery Co. Ltd., Takasaki, Japan.

Phosphate (Pi) homeostasis is determined primarily by renal handling of Pi, which is regulated by dietary Pi intake, parathyroid hormone (PTH) and 1,25(OH)₂D. Recent evidence has accrued that fibroblast growth factor 23 (FGF-23), a circulating protein produced by osteogenic cells, also affects Pi homeostasis. States of excess FGF-23 are associated with hypophosphatemia due to renal Pi wasting, osteomalacia, and inappropriately low 1,25(OH)₂D concentrations. In contrast, FGF-23 gene ablation in mice is associated with increased serum Pi and 1,25(OH)₂D concentrations. An increase in dietary Pi intake increases urinary Pi excretion and decreases 1,25(OH)₂D production, whereas the converse occurs in response to dietary Pi restriction. To determine whether serum FGF-23 is regulated by dietary Pi and thereby might mediate the physiological response to changes in dietary Pi, we studied 13 healthy men during a 4-week dietary Pi intervention study. Throughout the study, all subjects consumed a diet that provided 500 mg of Pi per day (intakes are reported per 70 kg body weight). Calcium, sodium, potassium, magnesium and energy intakes were kept constant. Goal total oral Pi intake was achieved by supplementing the diet with a solution of neutral sodium and potassium Pi. The study had three diet periods, each of the same duration: 1) control Pi intake = 1,500 mg/day; 2) supplemented Pi intake = 2,300 mg/day; 3) restricted Pi intake = 625 mg/day, achieved by replacing the sodium and potassium Pi supplement with sodium and potassium chloride. Fasting blood and 24-hour urine samples were obtained on days 7-10 of each diet period. Serum FGF23 was measured by a sandwich ELISA that detects full-length FGF23 (Kainos Laboratories, Tokyo, Japan). As shown in the table, changes in dietary Pi induced significant changes in serum FGF-23 and 1,25(OH)₂D concentrations and in urinary Pi excretion.

Effect of changing dietary Pi on serum and urinary parameters (mean ± SD).			
Phosphorus intake	Serum		Urinary Excretion Phosphorus (mg/day)
	FGF-23 (pg/ml)	1,25(OH) ₂ D (pg/ml)	
Control (1500 mg/d)	28.9 ± 5.7	32 ± 9	1165 ± 293
Supplemented (2300 mg/d)	30.7 ± 8.7	29 ± 10	2069 ± 591 ^a
Restricted (625 mg/d)	19.6 ± 7.0 ^{ac}	40 ± 16 ^{ac}	593 ± 199 ^{ac}

Mean value differs from that during 1500 mg/day dietary Pi intake: ^aP < 0.001; ^bP < 0.05. Mean value differs from that during 2300 mg/day dietary Pi intake: ^cP < 0.001; ^dP < 0.05.

With restriction of dietary Pi to 625 mg/d, serum FGF-23 concentrations were significantly lower, and 1,25(OH)₂D significantly higher, than values on the control or supplemented Pi intakes. These data demonstrate that dietary Pi regulates serum FGF-23 concentrations in healthy men, and suggest that regulation of 1,25(OH)₂D production by dietary Pi is mediated, at least in part, by changes in circulating FGF-23.

Disclosures: **D. Antonucci**, None.

M132

Identification of Essential Molecule Responsible for Tissue Specific FGF23 Signaling. **I. Urakawa^{*1}, Y. Yamazaki^{*1}, T. Shimada^{*1}, K. Iijima^{*1}, H. Hasegawa^{*1}, J. Yasutake^{*1}, T. Fujita², S. Fukumoto², T. Yamashita¹.** ¹Pharmaceutical Research Laboratories, Kirin Brewery Co., Ltd., Takasaki Gunma, Japan, ²Department of Internal Medicine, The University of Tokyo Hospital, Tokyo, Japan.

The latest member of FGFs, FGF23, is a humoral factor that regulates renal phosphate reabsorption and metabolism of bioactive vitamin D. Although many FGFs show autocrine/paracrine effects, FGF23 is an endocrine factor, which is produced in bone and effects in kidney. Despite the unique activity of FGF23, either a special mechanism or molecules responsible for FGF23 signaling has been unclear. To elucidate the mechanism of FGF23 signaling, we searched early genes responsive to FGF23 in mice. Messenger RNA was purified from mouse kidneys one hour after FGF23 or vehicle administration and hybridized with a cDNA array including 2400 mouse cDNAs. As a result of that, we identified that mRNA abundance of early growth response gene-1 (Egr-1), which is known

ASBMR 27th Annual Meeting

as an immediate early response transcription factor, was increased within 30 minutes after FGF23 administration. Egr-1 expression is known to be downstream of ERK activation. In fact, we revealed that FGF23 induced ERK phosphorylation in mouse kidney within 10 minutes. Although the ERK phosphorylation and Egr-1 induction are ubiquitously equipped cellular mechanisms, these responses to FGF23 were observed only in kidney, pituitary and parathyroid glands, but not in other organs such as the heart, lung, liver and spleen. These findings indicated that FGF23 induced the activation of ERK followed by Egr-1 expression in these tissues probably through an FGF23 receptor specifically present in the kidney, pituitary gland, and parathyroid gland. To clarify the molecular mechanism responsible for the tissue-specificity, we purified a molecule that directly interacts with FGF23 from mouse renal homogenate. The tissue expression profile of this molecule corresponded to the tissue specificity of FGF23 signaling. Finally, FGF23 signaling was reproduced by the forced expression of this molecule in cells unresponsive to FGF23. These findings indicate that the molecule identified in this study constitutes a unique receptor for FGF23.

Disclosures: **I. Urakawa**, Kirin Brewery Co., Ltd. 3.

M133

Effect of Growth Hormone Replacement on FGF-23 and Phosphate Metabolism in Adult Growth Hormone Deficiency. **B. H. Durham**¹, **E. Joseph**^{*2}, **H. D. White**^{*2}, **A. M. Ahmad**^{*2}, **J. P. Vora**^{*2}, **W. D. Fraser**¹. ¹Clinical Chemistry, Royal Liverpool University Hospital, Liverpool, United Kingdom, ²Endocrinology, Royal Liverpool University Hospital, Liverpool, United Kingdom.

Renal tubular phosphate reabsorption, best expressed as the renal threshold for phosphate reabsorption in the proximal tubule [ratio of tubular maximal reabsorption of phosphate (TmPO4) to glomerular filtration rate (GFR) (TmPO4/GFR)] plays a predominant role in phosphate homeostasis. Serum phosphate concentrations increase following growth hormone replacement (GHR) in adult growth hormone deficiency (AGHD) with an increase in TmPO4/GFR. Fibroblast growth factor-23 (FGF-23) is a phosphate regulating peptide that decreases circulating phosphate concentrations by decreasing TmPO4/GFR and is regulated by circulating phosphate in a feed back mechanism. Twenty-one AGHD patients and 16 controls were consented to the study and compared at baseline. AGHD patients were randomly assigned to two groups. Group 1 (n = 11) were commenced on GH alone and group 2 (n = 10) were commenced on a daily dose of 1g of oral phosphate-Sandoz at 2200h as an adjunct to the GH. Patients were hospitalised at 0, 1 and 3 months for a period of 25-h and half-hourly blood and 3 hourly urine samples were collected for phosphate, 1,25(OH)2VitD, FGF-23 [C-terminal] and to calculate TmPO4/GFR. A higher FGF-23 concentration was associated with lower TmPO4/GFR, plasma phosphate and 1,25(OH)2VitD concentration in adult growth hormone deficient (AGHD) patients as compared to normal control subjects. Administration of GH alone increased TmPO4/GFR and 1,25(OH)2VitD by 1 month and plasma phosphate by 3 months. Adjunct phosphate supplementation increased plasma phosphate by 1 month with no change in TmPO4/GFR and 1,25(OH)2VitD. FGF-23 increased more rapidly (1 month compared to 3 months) and by a greater percentage with adjunct phosphate intake compared to GH alone. Inappropriately increased FGF-23 concentration may contribute to the phosphate depletion in untreated AGHD patients. FGF-23 increased with the increase in phosphate following GHR, but the net predominant effect of GH resulted in a positive phosphate balance possibly due to direct GH and IGF-1 effects. The more marked increase in FGF-23 following phosphate supplementation in addition to GH restricted the tubular reabsorption of phosphate and increase in 1,25(OH)2VitD concentration to maintain phosphate concentration within the normal range. GHR restores FGF-23 regulation by phosphate and FGF-23 has a role countering increasing phosphate concentration by altering the renal handling of phosphate and 1,25(OH)2VitD.

Disclosures: **B.H. Durham**, None.

M134

Analysis of FGF23 Production by Osteoblastic Cells Treated with 1,25-Dihydroxyvitamin D. **J. Yasutake**^{*1}, **T. Shimada**^{*1}, **Y. Yamazaki**^{*1}, **I. Urakawa**^{*1}, **K. Iijima**^{*1}, **H. Hasegawa**^{*1}, **T. Fujita**², **S. Fukumoto**², **T. Yamashita**¹. ¹Pharmaceutical Research Laboratories, KIRIN Brewery CO., LTD, Takasaki, Gunma, Japan, ²Department of Internal Medicine, The University of Tokyo Hospital, Tokyo, Japan.

FGF23 is a circulating polypeptide that plays an essential role in phosphate and vitamin D metabolism by controlling renal functions in a hormonal manner. Recent studies strongly suggested that cells in the osteoblast-lineage are major sources supplying circulating FGF23. Since both FGF23 transgenic mice and FGF23 null mice showed evident abnormality in bone, this molecule may serve as a local regulator of bone metabolism. On the other hand, recent studies also indicated that phosphate and 1,25-dihydroxyvitamin D (1,25D), the potential bone metabolism modulators, trigger the production of FGF23. To address the relationship between bone metabolism and FGF23, we investigated the mode of FGF23 production by osteoblastic cells in vitro. Mouse osteoblastic MC3T3-E1 cells were cultured with α MEM supplemented with 10% FBS to form a confluent monolayer on day 3 and allowed to differentiate by adding β -glycerophosphate and ascorbic acid. FGF23 mRNA abundance progressively increased up to day 24, but FGF23 protein concentrations in conditioned medium peaked by day 14. These findings suggest that the competency of FGF23 production seems to depend on a certain stage of differentiation. Then, we treated cells in various stages in this culture system with 1,25D for 72 hours and determined FGF23 concentrations in conditioned media. Treatment with 1,25D enhanced FGF23 concentration in conditioned media at every stage, while the maximum increase was

observed on day 6, suggesting that 1,25D-inducible FGF23 production is also dependent on a stage of cell differentiation. Interestingly, at this stage the 1,25D treated conditioned medium showed a 1.7-fold increase in phosphate concentration. To clarify the relationship between the alteration of phosphate metabolism and FGF23 production after treatment with 1,25D, time courses of changes in concentrations of phosphate and FGF23 in conditioned medium, phosphate transport activity, and FGF23 mRNA abundance were examined. Significant increases in FGF23 mRNA abundance and protein were observed after 12 and 24 hours, respectively. Phosphate transport activity decreased after 10 hours whereas phosphate concentration was not affected for 24 hours. These findings suggest that 1,25D and possibly local phosphate metabolism may be important in the regulation of FGF23 production by cells in a certain stage of osteoblast-lineage.

Disclosures: **J. Yasutake**, Kirin Brewery CO., LTD 3.

M135

Isolation and Culture of Chondrocytes from the Resting and Proliferating Zones of Developing Bovine Rib Growth Plate: Modulation of FGF-2 Binding by Perlecan. **J. R. Hassell**, **P. Govindraj**^{*}, **L. West**^{*}. Research, Shriners Hospitals for Children - Tampa, Tampa, FL, USA.

FGF-2 is a known regulator of chondrocyte proliferation in the developing growth plate. Perlecan is a heparan sulfate proteoglycan present in the growth plate and the perlecan null mouse shows reduced proliferation of the chondrocytes in the growth plate and defective endochondral ossification. The purpose of this study is to evaluate the effect of perlecan on the binding of FGF-2 to chondrocytes isolated from resting and proliferating zones of growth plates. Ribs were isolated from late second or early third trimester bovine fetuses, fractured at the bone/hypertrophic zone junction and growth plates serially sectioned into five, 1 mm sections. Slice 1, which contains chondrocytes from the hypertrophic zone was discarded and chondrocytes were isolated from each of slices 2 (lower proliferative), 3 (upper proliferative), 4 (intermediate) and 5 (resting) by sequential digestion with pronase followed by collagenase overnight and plated at 1×10^5 cells/cm² in serum free DMEM. Chondrocytes from slice 2 incorporated 4 - 8 fold more ³H-thymidine and chondrocytes from slice 3 incorporated 2 - 4 fold more ³H-thymidine as compared to chondrocytes from slices 4 and 5 over a 48h culture period. All chondrocytes incorporated ³⁵S₀₄ into a matrix associated with the cell layer and a soluble matrix in the medium. Western blots using an antiserum to perlecan showed perlecan to be in the matrix associated with the cell layer and in the matrix secreted into the culture medium. Based on digestion with chondroitinase ABC, the perlecan secreted into the medium contained more chondroitin sulfate than the cell layer perlecan. [¹²⁵I] FGF-2 bound to both the low affinity and high affinity receptors present in the cell layer. Competition studies show that cold FGF-2 had no effect on [¹²⁵I] FGF-2 binding to the low affinity receptor but reduced binding to the high affinity receptor by 55 - 75%. The addition of perlecan to the media, however, reduced [¹²⁵I] FGF-2 binding to both the low and high affinity receptor by ~60%. The results of these studies show that chondrocytes isolated from the resting and proliferating zones of the growth plate and plated in serum free DMEM retain their zone specific level of proliferation and produce a cell-associated matrix as well as soluble matrix containing perlecan. The results suggest that perlecan may serve as the low affinity receptor for FGF-2 and act to keep FGF-2 off the high affinity receptor.

Disclosures: **J.R. Hassell**, None.

M136

Bone Mineral Density in Active Female Adolescents with Stress Fracture. **K. J. Loud**¹, **L. J. Micheli**^{*2}, **S. K. Bristol**^{*3}, **S. B. Austin**^{*3}, **C. M. Gordon**⁴. ¹Adolescent & Sports Medicine, Children's Hospital Medical Center, Akron, OH, USA, ²Sports Medicine, Children's Hospital, Boston, MA, USA, ³Adolescent Medicine, Children's Hospital, Boston, MA, USA, ⁴Adolescent Medicine & Endocrinology, Children's Hospital, Boston, MA, USA.

The purpose of this study was to examine skeletal health among active female adolescents with a stress fracture, a potential marker of compromised bone quality. Otherwise healthy active females aged 13-22 years diagnosed with their first stress fracture by x-ray, bone scan, computed tomography, or magnetic resonance imaging at the sports medicine clinic of an urban tertiary care pediatric center were recruited. Subjects were enrolled prospectively and matched 2 controls per case. The project was approved by the local IRB. Height and weight were measured directly and information collected on physical activity, demographics, dietary intake, family history, medical history, and menstrual history by validated self-administered surveys. A-P areal bone mineral density (aBMD, g/cm²) was measured at the lumbar spine using an Hologic 4500 dual emission x-ray absorptiometry scanner. All analyses were conducted using STATA v8 statistical software, with conditional logistic regression modeling utilized to account for matching. Two-tailed p-values < 0.05 were considered significant. The mean age of the 144 participants was 16.1 ± 2.2 years. 97.9% (141) were Caucasian. 91.7% (121) were post-menarcheal, with mean age at menarche 13.0 ± 1.1 years. Two had an eating disorder. Mean daily intakes of calcium and vitamin D were 1103 ± 502 mg and 253 ± 159 IU, respectively. Cases had a marginally higher body mass index than controls (22.0 kg/m^2 vs. 21.1 kg/m^2 , p = 0.09). A family history of osteoporosis or osteopenia was significantly associated with stress fracture [odds ratio (OR) = 3.87, 95% confidence interval (CI): 1.50, 9.99], while family history of stress fracture, frequent fractures, or "brittle bones" was not (OR = 0.58, 95% CI: 0.16, 2.17). The spinal aBMD Z-score among the 36 participants with stress fracture was -0.11 (95% CI: $-0.46, 0.24$); cases with irregular menses (≤ 9 /year or amenorrhea ≥ 3 months) had a significantly lower spinal aBMD Z-score than those with regular menses (-0.85 vs. 0.10 , p = 0.02). In conclusion, this study demonstrates that BMD is compromised by menstrual irregularity and that active adolescent girls often consume inadequate quantities of calcium and vitamin D. Although subjects with stress fracture

demonstrated apparently normal spinal aBMD, the magnitude of the association between stress fracture and family history of osteopenia suggests that further investigations of intrinsic measures and genetic markers of bone quality are warranted in this population.

Disclosures: *C.M. Gordon, None.*

M137

Effects of Exercise Protocol and Equipment on Bone Formation

Stimulation. K. E. McAlpine¹, J. A. Tindall^{*2}. ¹Denver Research Institute, University of Denver, Evergreen, CO, USA, ²University of Colorado, Denver, CO, USA.

The purpose of this research was to evaluate the effectiveness of exercise protocol(s) utilizing resistance (composite) rods exercise equipment or free weights, to stimulate bone formation and bone resorption reduction. Subjects were paired for gender, age, height, weight, exercise experience, and fitness level. Three groups of paired participants were matched for inclusion into a free weight protocol, a composite rod protocol, or a control. This research utilized 2 treatments (free weight - treatment 1; composite rod - treatment 2) and 2 exercise protocols (same exercises in both treatments - protocol 1; modified exercises on the composite device - protocol 2). Protocol 2 involved a variety of modified exercises and physiological stimulation as a comparison between treatments. Subjects were selected in matched pairs and randomized; one participant from the paired match was placed into one of the first protocols (composite rod or free weight) and the second into the other. A third group, also with paired matches within the other groups, was utilized as a control for the composite rod equipment. Blood and urine bone biomarkers, total body fat composition, and DEXA scans of the hips and lumbar spine were performed prior to and at the end of the study for each participant. After a familiarization period of 2 weeks with the exercises and equipment, subjects began a 17 week, progressive load increase, exercise program. Each subject was required to take RDA recommendations for calcium and vitamin D and record their intake. Increases in osteocalcin (p=0.016) and reductions in serum and urine NTX were seen similarly in both protocols, but were significantly greater than the control group. Osteocalcin showed the greatest correlation (t test p=0.937) between the modified exercise protocol for the composite rod and the free weight exercise protocol. The use of the resistant rods in conjunction with protocol 2 provided similar stimulation for bone formation and reduction in bone resorption as protocol 1 using free weights. This research indicates that use of composite rod devices in conjunction with protocol 2 may provide a significant benefit for both the elderly and in microgravity situations where use of free weights may be more harmful, impractical, or impossible. The composite rod equipment could be utilized as suitable backup to the IRED and more complex future, long-term space travel, exercise devices. The composite rod equipment combined with the modified exercises, appears to provide equivalent results for bone formation as compared to free weights and therefore, is a more valuable backup mechanism than elastic bands currently used for space-travel exercise equipment failure.

Disclosures: *K.E. McAlpine, None.*

M138

Direct Loading in a Low Estrogen Environment in Prepubescent Female

Rats. V. R. Yingling, G. Taylor^{*}. Physical Education & Exercise Science, Brooklyn College (CUNY), Brooklyn, NY, USA.

The timing of puberty has emerged as an influential factor in the development of peak bone mass and strength. An increased age at puberty correlates with low bone mass in young women and an increased incidence of stress fractures. Low estrogen levels during bone development may decrease peak bone mass accrual in young adults by minimizing the mechanosensitivity of bone to physiologic loading. The purpose of this study was to determine if delayed puberty using gonadatropin-releasing hormone antagonist (GnRH-a) injections affects the response of cortical bone to compressive loading in female rats. Ten Sprague-Dawley rats (21 days of age) were randomly placed into 2 groups. The control group (C) established baseline data for compressive loading on the ulna. The low estrogen group (LE) was given GnRH-a injections (Cetrorelix) beginning at 25 days of age until sacrifice at 38 days. The right ulnae of both groups were loaded to approximately 4000 ustrain from day 32-36 using the following loading parameters; magnitude: 3.2 N, duration: 360 cycles/day, frequency: 2 Hz. Calcein injections (10 mg/kg) were given on days 29 and 36 and the rats were sacrificed on day 38. The right and left ulnae were dissected and prepared for histomorphometric analysis. The study was approved by the Institutional Animal Care and Use Committee at Brooklyn College (City University of New York). A delay in puberty resulted from the GnRH-a injections as confirmed by the delayed vaginal opening (3 of 5 animals never reached puberty during the protocol) and the decreased estradiol levels (18%) in the LE group. A significant increase in the total area perimeter (Ta.Pm) (4.51 %) and marrow perimeter (Ma.Pm) (26.31%) in the left ulna resulted in the LE group. There was no effect on mineralized surface (MS, %), mineral apposition rate (MAR, um/day) or bone formation rate (BFR, um/year) on the periosteal surface in either the left or right ulna of both the C or LE groups. On the endosteal surface, there was a decrease in BFR (32.84 %) in the LE group and compressive loading increased BFR in the C group, but had no effect in the LE group. This decrease in endocortical BFR in the LE group results in an increased Ma.Pm and loading does not stimulate bone formation at the endocortical surface. In summary, the GnRH-a injection protocol did suppress estradiol levels and delay puberty in the LE group; furthermore, BFR was suppressed at the endocortical surface. A delay in pubertal timing may affect bone's response to loading on the endosteal surface as evidenced by the lack of response in the LE group with an increased BFR in the C group. However, five days of loading did not affect periosteal BFR in either the C or LE groups suggesting that a longer loading protocol may be necessary.

Disclosures: *V.R. Yingling, None.*

M139

Body Fat Influences Bone Mass Mainly by Physical Loading - 2-Year

Longitudinal Study in Pubertal Girls. Q. Wang¹, P. Nicholson^{*1}, M. Alén^{*1}, H. Suominen¹, A. Koistinen^{*2}, H. Kröger^{*3}, S. Cheng¹. ¹Department of Health Sciences, University of Jyväskylä, 40014 Jyväskylä, Finland, ²Central Hospital of Central Finland, 40014 Jyväskylä, Finland, ³University of Kupio, Kupio, Finland.

Fat tissue affects bone mass (BM) by at least two independent mechanisms: physical loading and hormonal activity. Arms and legs are similarly exposed to genetic and endocrine makeup, nutrient intake, medication, and life-style factors such as smoking, while the effects of physical loading such as weight-bearing and muscular activity may be very different in these two bone sites. Therefore, investigating the relationship of BM of arm and leg with limb-matched lean mass (LM) and total body fat mass (FM) provides an indirect assessment of the physical loading effect of FM on BM. The study population consisted of 258 healthy girls, aged 10-13 years. BM, LM and FM were assessed by a dual-energy X-ray absorptiometry (GE Lunar Corp., Madison, WI USA) at baseline and after 2 years' follow-up. A multivariate hierarchical linear model was used to assess the relationship between total body FM and limb-matched LM-adjusted BM (BM/LM) of the upper and lower limbs. The results showed that BM/LM was similar (60 vs. 60g/kg) for arm and leg. The variation in BM explained by the limb-matched LM was also similar for the arm and leg (R²= 0.836 vs. 0.858). The correlation between leg BM/LM and total body FM was significantly higher than that between arm BM/LM and total body FM (r = 0.403 vs. 0.135, p<0.001). The change of total body FM (ΔFM) correlated with ΔBMC/ΔLM of the leg but not with that of the arm (r = 0.16 vs. -0.03). The results indicate that physical loading is the major mechanism by which FM affects BM.

Disclosures: *Q. Wang, None.*

M140

Strontium Ranelate Improves Intrinsic Bone Tissue Quality.

P. Amman^{*1}, L. Badoud^{*1}, S. Barrauld^{*1}, P. Chatelain², R. Rizzoli^{*1}. ¹Division of Bone Diseases, Department of Rehabilitation and Geriatrics, University Hospital, Geneva, Switzerland, ²Division Rhumatology, Institut de Recherches Internationales Servier, Courbevoie, France.

Strontium ranelate treatment improves bone mechanical properties. The increased energy to failure achieved with strontium ranelate is essentially due to an increase of plastic energy suggesting that bone formed under treatment can withstand greater deformation before fracture. In the hydroxyapatite crystal, Sr is concentrated in the hydrated crown at the surface of the mineral. To investigate whether strontium ranelate treatment could positively influence tissue quality, intrinsic bone tissue quality (elastic modulus, hardness and dissipated energy) was evaluated by nanoindentation test performed at the level of trabecular nodes and cortex under physiological or dry conditions in vertebrae of rats treated for 26 months with strontium ranelate at a daily dose of 0 (control) or 900 mg/kg (n=12 per group). Results are means±SEM, *p<0.05, **p<0.01, ***p<0.001 vs control by Student-t test. In intact vertebral body, strontium ranelate significantly increased vs control group ultimate strength (+23%, p<0.05), total energy (+71%, p<0.05), plastic energy (+143%, p<0.01). At the level of trabecular bone, strontium ranelate treatment resulted in significant increase of elastic modulus, hardness and dissipated energy vs control in physiological but not in dry condition. There is a less pronounced effect in cortex which might be related to the lower concentration of strontium achieved in cortical as compared to trabecular bone. The fact that this positive influence disappeared when bone samples were dried, suggests that the organic matrix might be implicated. By analogy with biomaterial or enamel treatment with cation, presence of strontium in bone could reduce the progression of microcrack in bone. By a step-way regression analysis, intrinsic bone tissue quality is predominant in predicting bone strength. These results show for the first time a direct action of strontium ranelate on bone tissue quality, which could explain part of the mechanism of action and the reduction in fracture risk in postmenopausal osteoporotic patients treated with strontium ranelate.

Bone Treatment	Cortical Control	Cortical strontium ranelate	Trabecular Control	Trabecular strontium ranelate
Elastic Modulus (GPa)	12.9±0.4	14.6±0.3**	12.4±0.3	14.2±0.4***
Hardness (mPa)	484±23	485±18	457±18	510±19*
Dissipated Energy (mN*nm)	3727±134	3944±102	3580±107	4159±117***

Disclosures: *P. Amman, SERVIER 5.*

M141

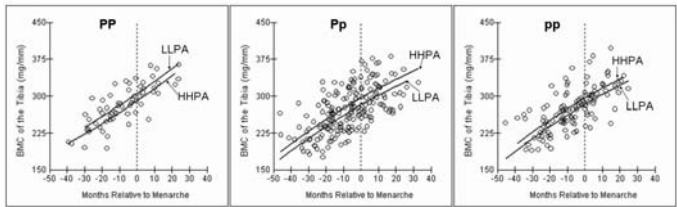
Exercise and Bone Growth during Puberty: Effects of Estrogen Receptor

α Polymorphism. S. Cheng¹, M. Suuriniemi^{*1}, H. Suominen¹, A. Mahonen^{*2}, H. Kröger², M. Alén^{*1}, T. CaLEX-study group^{*1}. ¹Univ. of Jyväskylä, Jyväskylä, Finland, ²Univ. of Kuopio, Kuopio, Finland.

Our previous cross-sectional data showed that physically active pre- and peri-pubertal girls (n=217) with a heterozygote *ERα* genotype (Pp) had significantly higher bone mass, density, and cortical thickness at loaded bone sites than their less active counterparts. The girls with homozygote genotypes did not seem to benefit from physical activity. To further explore this observation, we compared the girls with sustained high physical activity (HHPA, mean=4.3 hours/week during leisure time) to girls with low physical activity (LLPA, mean=1.7 hours/week) in a 4-year range when the girls underwent puberty within different *ERα* genotypes (PP, Pp, pp). Bone mineral content (BMC), areal density (aBMD), volumetric density (vBMD), cross-sectional area (CSA), cortical thickness (CTh), moment of resistance (SSI), and ultrasound attenuation (BUA) were assessed in whole body (WB),

ASBMR 27th Annual Meeting

femur neck (FN), lumbar spine (LS), distal radius (DR), tibia shaft (TS), and calcaneus (C) using different modalities. The girls in the HHPA group with Pp had significantly higher values of aBMD in the WB (p=.027), FN (p=.028) and LS (p=.026), and higher BMC in the FN (p=.008) and LS (p=.028), CSA (p=.033), BMC (p=.007), CTh (p=.005), SSI (p=.011) in the tibia, and BUA (p=.019) in the C at 24 months than the LLPA group with Pp. The HHPA group with pp also had higher BMC (p=.034) and BMD (p=.03) of the FN than the LLPA group with pp. When using a hierarchical multilevel regression model controlled for growth, the HHPA group with Pp tended to have consistently higher bone values throughout the menarche compared to the LLPA group (Fig). A similar trend was found in pp for some bone sites. As in our previous report, girls with a homozygote genotype PP did not benefit from high PA, while the benefit from PA was sustained in girls with a heterozygote genotype Pp. Furthermore, the *p* allele seems to be beneficial for bone growth while the *P* allele recessively impairs the osteostimulatory effect of physical activity.



Disclosures: **S. Cheng**, None.

M142

Maximum Rising Strength Is a Strong Predictor of Femoral Neck Bone Mineral Density in Healthy Women. **H. Blain**^{*1}, **L. Jaussent**^{*2}, **E. Thomas**³, **M. Picot**^{*2}, **J. Micallet**^{*4}, **C. Jeandel**^{*1}. ¹Department of Internal Medicine and Geriatrics, Centre Antonin Balmes, Montpellier, France, ²Department of Medical Informatics, University Hospital, Montpellier, France, ³Department of Rheumatology, University Hospital, Montpellier, France, ⁴Movement Analysis Laboratory, Propara Center, Montpellier, France.

Maximum knee extension strength (KES) is a strong predictor of femoral neck bone mineral density (FN BMD), but its measurement does not take into account other muscle forces of the lower limbs that are possibly involved in hip BMD maintenance. We recently developed an instrument for measuring maximum rising strength (MRS) by dynamometry and showed in 97 healthy subjects aged 23 to 90 years that the coefficient of variation of the mean of three peak values at 60° and 70° knee flexion of MRS measured in triplicate at three different occasions was 13.7%, close to that of KES (9.6%). The aim of the present study conducted in 249 other healthy women aged 18 to 76 years was to investigate whether MRS could be a better determinant of FN BMD (measured by DEXA) than KES. Using the Mann-Whitney U test, FN BMD was found to be correlated with age, height, weight, lean mass, MRS (p<0.001), and KES (p<0.01), and with physical activity performed during the last five years (measured using QUANTAP software) (p=0.05) but not with fat mass nor calcium intake. In multiple regression models, FN BMD was associated with age (OR=2.8 [CI,1.59-4.92]; p<0.001), weight (OR=0.37 [0.17-0.79]; p=0.001) and with MRS (OR=0.57 [0.35-0.93]; p<0.05) but not with KES. The present study shows that MRS is a stronger determinant of FN BMD than KES in healthy women, independent of their age, anthropometric features, and physical activity habits. These results suggest the interest of including assessment of MRS in screening programs for women who are at high risk of low FN BMD and suggest the possible interest of this instrument for lower limb strengthening and for increasing FN BMD in women at risk of fracture of the femoral neck bone.

Disclosures: **H. Blain**, None.

M143

Comparison of BMD, Percent Body Fat and Bone Turnover in Ultra-distance Runners and Sedentary Controls. **B. Cassim**^{*1}, **A. MacGregor**^{*2}, **M. Mars**^{*3}. ¹Department of Medicine, University of KwaZulu-Natal, Durban, South Africa, ²Department of Biomedical Science, Mangosuthu Techikon, Durban, South Africa, ³Department of Telehealth, University of KwaZulu-Natal, Durban, South Africa.

Women athletes who participate in vigorous physical activity are at risk to develop osteoporosis. This study was undertaken to compare the BMD, % body fat and biochemical markers of bone turnover in 55 premenopausal runners and 47 premenopausal sedentary healthy women and to determine the relationship between % body fat and BMD. BMD and % body fat were measured using the Hologic QDR 4500 densitometer. Commercial kits were used to measure urinary deoxypyridinoline crosslinks (DpD) and cross-linked N-telopeptides of type I collagen (NTx) and bone specific alkaline phosphatase (BALP) in the 55 runners and 18 controls and osteocalcin (OC) in 26 runners and 18 controls. The unpaired students t test and Pearson's correlation were used for statistical analysis. The runners were older than the control subjects (38.8 ± 4.7 yrs v 33.8 ± 6.3 yrs; p < 0.0001). Significant BMD and bone marker results are presented in the table. Runners had a significantly lower % body fat compared to controls (21.6 ± 5.7% v 38.2 ± 7%; p < 0.0001). In the controls, there was a significant correlation between % body fat and BMD at the total trunk (r = 0.61; p < 0.05), total hip (r = 0.81; p< 0.0001), femoral neck (r = 0.64; p< 0.05), trochanter (r = 0.71; p < 0.001) and intertrochanter region (r = 0.76; p< 0.001). In the runners there was a negative correlation between % body fat and

BMD at the total legs (r = -0.38; p < 0.05). This study confirms the site specific positive effects of exercise on BMD in eumenorrhoeic ultradistance runners and suggests that this is due to a decreased bone turnover. The low % body fat was not a risk factor for a low BMD in this cohort.

Comparison of BMD and Markers of Bone Turnover in Ultra-distance Runners and Sedentary Controls			
BMD g/cm ²	Runners(n = 55)	Controls(n = 47)	p Value
Total hip	0.935 ± 0.132	0.881 ± 0.125	<0.05
Neck	0.831 ± 0.127	0.785 ± 0.106	<0.05
Inter- trochanter	1.111 ± 0.172	1.036 ± 0.153	<0.05
Total arms	0.722 ± 0.050	0.923 ± 0.154	<0.0001
Total legs	1.126 ± 0.119	1.014 ± 0.080	<0.001
DpD (nM DpD/mM creatinine)	4.9 ± 1.9	6.3 ± 3.5	<0.05
Osteocalcin (nmol/L)	1.1 ± 0.5(n = 26)	2.0 ± 1.9	<0.05

Disclosures: **B. Cassim**, None.

M144

Improved Bone Strength in Women Following a 24-Week Total Body Periodized Resistance Training Program. **H. M. Isome**^{*1}, **B. C. Nindl**^{*1}, **R. Evans**¹, **M. Lester**^{*1}, **D. Catrambone**^{*1}, **L. Gotshalk**^{*2}, **W. J. Kraemer**^{*3}. ¹Military Performance Division, US Army Research Institute for Environmental Medicine, Natick, MA, USA, ²Health and Physical Education, University of Hawaii, Hilo, HI, USA, ³Kinesiology, University of Connecticut, Storrs, CT, USA.

This study evaluated the effects of 4 periodized resistance training programs on parameters of bone strength as measured by MRI. Seventy-nine untrained women (23.1±3.5y) were randomly assigned to: total body low repetition (TL) (3-8 RM, n=18), total body high repetition (TH) (8-12 RM, n=21), upper body low repetition (UL) (3-8 RM, n=21) and upper body high repetition (UH) (8-12 RM, n=19). All training was performed three times weekly for 24 weeks, with at least 24 hours of rest between sessions. Cross-sectional MRI images of the femur were taken before training (T1), at 12 weeks (T2), and after 24 weeks (T3) of training. Fifteen 10mm thick transaxial T1-weighted images were obtained at equal distances between the base of the femoral head and the distal end of the femur. Slice eight (mid-femur) was then analyzed using Scion Image v4.02 for Windows. Measures of bone strength included maximum second moment of area (I_{max}), minimum second moment of area (I_{min}), and polar second moment of area (J). Significant increases in femur strength were only observed in groups TH and TL. Increases were not evident at 12 weeks (T1-T2), but increased significantly from T2-T3 for I_{max} (1.5 and 1.5%), I_{min} (3.0 and 2.7%) and J (2.2 and 2.0%) in groups TH and TL, respectively (p<0.001). An overall increase in I_{max} (1.7 and 1.6%), I_{min} (3.2 and 3.0%) and J (2.3 and 2.2%) was observed in groups TH and TL, respectively, over the study period (p<0.001). No changes were observed in the UH or UL groups at any time point for any variable. We did not find significant differences between the TH and TL training groups. This study demonstrates that total body periodized resistance training significantly improves strength parameters of the femur, but may not be evident until after 12 weeks. Furthermore, adaptation in bone strength is localized to site specific areas that undergo repetitive loading associated with resistance training.

Disclosures: **H.M. Isome**, This project was supported by U.S. Army grant to Dr. William J. Kraemer, DAMD 17-95-5069. 3.

M145

Skeletal Biomechanics of the Florida Manatee. **K. B. Clifton**¹, **J. Yan**^{*2}, **J. J. Mecholsky**^{*2}, **R. L. Reep**^{*1}. ¹Physiological Sciences, University of Florida, Gainesville, FL, USA, ²Materials Science and Engineering, University of Florida, Gainesville, FL, USA.

Watercraft-related mortality of the Florida manatee, caused by propeller wounds or impact, accounts for 25% of all deaths from 1974-2004, and comprises 85% of human-related deaths. Reducing watercraft-related mortality is identified as a high priority in the manatee recovery plan. In order to establish safe boat speeds for manatee protection, an estimate of the forces required to fracture their bone is needed. A first step to improve the understanding of biological effects of boat strikes is to understand the material properties of manatee bone. This study investigated the material properties of manatee rib bone. Flexural strength, fracture toughness, Young's modulus, and work of fracture were measured for two size classes (subadults, adults) by sex. Parallepipeds were machined from ribs in the cranial, middle, and caudal body regions, and fractured in three-point bending. Fractographic analysis of fracture surfaces was used to calculate fracture toughness, and ultrasound was used to validate elastic modulus measurements. Mean flexural strength by animal ranged from 73-159 MPa, mean fracture toughness from 1.4-2.9 MPa·m^{1/2}, mean elastic modulus from 4-18 GPa, and mean work of fracture 3-6 MJ·m⁻³. In comparison, typical flexural strengths for human and bovine bone tested in 3-point bending are 209 MPa and 224 MPa, respectively. Toughness of human and bovine bone ranges from 2.2-6.3 MPa·m^{1/2}. Most variables were significantly different between sexes and age classes (p<0.05). Material properties increased with body size up to 265 cm total length, then leveled off or declined with increasing body size in the adults. Data indicate that manatee bone may be on average less strong and tough than other mammalian bone, which is consistent with their aquatic, shallow water habitat. Material properties are likely correlated to mineral content (67-70%), plexiform organization, and low remodeling rate.

Disclosures: **K.B. Clifton**, None.

M146

IGF-I Enhances Bone Recovery after 2 Weeks of Unloading. B. Boudignon*, P. Kurimoto*, S. Nishida, Y. Wang, H. Elalieh*, J. Cao, D. D. Bikle, B. P. Halloran. Endocrine unit, VAMC, San Francisco, CA, USA.

One of the most abundant growth factors in the bone, IGF-I is produced by bone cells, and stimulates osteoblast proliferation and bone formation. Studies show that IGF-I increases bone volume in normally loaded animals. However, during skeletal unloading induced by hindlimb elevation bone is resistant to the anabolic effects of IGF-I. In this context we wanted to know whether IGF-I could promote bone recovery during 2 weeks of reloading after a 2 week period hindlimb unloading, and if so whether the effects of IGF-I would be amplified by the reapplied load. Thirty six, 12 week old rats were divided into six groups; loaded (4 weeks), unloaded (4 weeks) and unloaded/reloaded (2/2 weeks), and treated with IGF-I infusion (2.5 mg/kg/d) or vehicle during the final two weeks. Cortical bone volume (tibia) was assessed at the time of reloading and before sacrifice. Tibial fat free weight, cortical BFR, and bone histomorphometry of the tibial metaphysis were assessed at the end of the experiment. Cortical bone volume did not change significantly during the four week experiment, a finding not surprising in such a short amount of time. However, tibial fat free weight was less in unloaded vehicle treated animals than in the loaded animals. Periosteal BFR decreased during unloading. During the 2 week recovery period in which skeletal loading was restored to normal, BFR in both the vehicle and IGF-I treated animals increased but the effect was greatly exaggerated in the animals treated with IGF-I. In IGF-I treated animals bone mass was restored more rapidly than in vehicle treated animals. These data show that unloading induces resistance to IGF-I, but that reloading after a period of skeletal unloading increases bone sensitivity to IGF-I. Thus IGF-I administration may be of benefit in treating patients following a period of immobilization when such patients are remobilized.

Disclosures: **B. Boudignon**, None.

M147

Mechanical Intervention Enhances Bone and Muscle in Young Women with Low Bone Density. V. Gilsanz¹, T. A. L. Wren¹, M. Sanchez^{*1}, C. Rubin². ¹Radiology & Orthopaedics, Childrens Hospital Los Angeles, Los Angeles, CA, USA, ²Biomedical Engineering, State University of New York, Stony Brook, NY, USA.

The purpose of this study was to determine whether high frequency, low magnitude mechanical stimulation can enhance bone and muscle in young women with low bone density. Cancellous density of the lumbar spine was measured by computed tomography (CT) in 150 healthy, sexually mature (Tanner 5) young women (age 16-21 yr) who had sustained a fracture. Those with the lowest density were divided into Intervention and Control groups (24 subjects per group). Those in the Intervention group were asked to stand on a vibrating platform (30 Hz vertical sinusoidal motion with 0.3g peak-to-peak acceleration) for 10 min every day for a year. CT images were obtained at the lumbar spine (L1-L3) and midshaft of the femur at baseline and 1-year. Cancellous bone density and area of the paraspinous musculature were measured from the vertebral images; cortical bone area and thigh muscle area were measured from the femoral images. The Intervention group showed greater increases in vertebral cancellous bone density and femur cortical bone area (Table). The Intervention group also showed greater increases in muscle area although statistical significance was obtained for the paraspinous musculature only (Table). These results demonstrate that a simple, non-pharmacological intervention can enhance bone properties in both the axial and appendicular skeleton of young women at risk for developing low peak bone mass and osteoporosis later in life. In addition, this is the first study to observe changes in muscle following low magnitude mechanical stimulation, suggesting that muscle activity may play an important role in mediating the bone response to the intervention. Low level mechanical stimulation appears to be a promising option for early intervention in those most likely to develop osteoporosis.

	Percentage change from baseline to 1-year, mean (SD)		
	Control % change	Intervention % change	p-value from t-test
Vertebral cancellous bone density	0.09 (4.54)	2.14 (4.93)	.065
Femur cortical bone area	1.09 (3.67)	3.35 (3.71)	.039
Paraspinous muscle area	0.51 (4.98)	5.38 (6.88)	.002
Thigh muscle area	2.17 (2.69)	3.63 (3.63)	.363

Disclosures: **T.A.L. Wren**, None.

M148

Playing Golf Is Associated with Increased Vertebral Bone Size and Mass in Post Menopausal Women. S. L. Bass¹, J. Cook^{*2}, K. Singleton^{*1}, J. Black^{*1}, R. Daly¹. ¹Centre for Physical Activity and Nutrition Research, Deakin University, Burwood, Australia, ²School of Physiotherapy, La Trob University, Bundoora, Australia.

A golf swing results in lateral bending that imparts shear, compressive and torsional strains on the spine. These forces, together with the rapid changes in the direction of their application and the intermittent nature of the game, create an ideal loading environment for an optimal osteogenic response. Thus we hypothesized that women who play regular golf would have greater lumbar spine bone traits than active controls. Forty-nine postmenopausal women aged 62.2 (95% CI: 60.3, 64.2) years who had been playing golf for 16.8 (12.8, 18.8) years were compared to 34 active controls aged 60.2 (58.0, 62.5) years matched for age, height, weight, age of menopause, years post menopause and prior use of

HRT. No subjects were currently using HRT. BMD, BMC and bone area were assessed by DXA. The degree of arthritis at the lumbar spine was quantified by an experienced radiologist from QCT scout scans.Lumbar spine BMD, BMC and bone area were 10%, 15% and 5% greater respectively in the golfers (table). The greater bone area was due to a 4% greater vertebral body width (not height). No differences in BMD were detected at total body or hip. There was no difference in the severity of arthritis between the golfers and controls; the lumbar spine of the majority of subjects was either normal or mildly arthritic.

Lumbar Spine (L1-L4)	Golfers (n=49)	Controls (n=34)
BMD (g/cm ²)	1.138 (1.099, 1.177)*	1.035 (0.977, 1.093)
BMC (g)	63.1 (60.0, 66.2)*	55.0 (50.8, 59.2)
Area (cm)	55.52 (53.98, 57.06) *	53.11 (51.39, 54.84)
Width (cm)	4.10 (4.02, 4.19) *	3.97 (3.88, 4.06)

[mean (95% CI)] *p<0.05

In summary, playing golf was associated with increased lumbar spine BMC, BMD and bone width. There was no evidence that playing golf was associated with increased incidence or severity of osteoarthritis. Thus the greater bone size and mass observed in the golfers is likely to be due to the load imparted by the swing. In conclusion, regular golf may be an ideal exercise for reducing the risk of low vertebral bone strength in postmenopausal women.

Disclosures: **S.L. Bass**, None.

M149

High Frequency Accelerations Attenuate Disuse-Induced Trabecular Bone Loss. R. A. Garman¹, L. R. Donahue², C. T. Rubin¹, S. Judex¹. ¹Biomedical Engineering, Stony Brook University, Stony Brook, NY, USA, ²The Jackson Laboratory, Bar Harbor, ME, USA.

High frequency low-level mechanical stimuli applied through whole-body vibrations to the weight bearing skeleton are anabolic. Administered by standing on a vibrating plate, these signals, while clinically promising, are limited by their reliance on weight bearing (standing on the plate may be difficult for the elderly, spinal cord injuries, etc.) and the skeletal sites responsive to the stimulus (only weight bearing bones of the lower and axial skeleton can be targeted). Recently, we demonstrated that high frequency accelerations, in the absence of weight bearing, are also anabolic in bone. This stimulus is based on subtle acceleratory motions that can be applied to specific segments of the skeleton and does not require external (e.g., weight bearing) or internal (e.g., muscle) forces. Here we hypothesized that high frequency accelerations can attenuate bone loss induced by mechanical unloading. The hindlimbs of ten adult female BALB/cByJ mice were unloaded for 3wk. Once a day for 20min, the left hindlimb was subjected to acceleratory motions (45Hz, 0.6g), while the right hindlimb served as a contralateral control. *In vivo* micro-computed tomography was used to describe the longitudinal changes in trabecular and cortical bone morphology for the metaphysis and epiphysis. Comparing the amount of bone loss between accelerated and contralateral (disuse-only) tibia within each mouse revealed that low-magnitude accelerations ameliorated metaphyseal trabecular bone loss, as the decrease in bone volume fraction was 29% greater in disuse-only tibiae than in accelerated tibiae (p<0.03). Trabecular bone micro-architecture responded similarly, as changes in trabecular number and trabecular separation were greater in disuse-only bones (Tb.N: -200%; Tb.Sp: +60%). However, accelerated tibiae experienced 73% greater bone loss in the metaphyseal cortex than disuse-only tibiae (p<0.02). In the epiphysis, there was no difference in the adaptive response of trabecular bone between tibiae, although accelerated tibiae displayed a greater increase in both periosteal (+120%, p<0.01) and endocortical areas (+250%, p<0.01) of the epiphyseal cortex, as compared to disuse-only tibiae. The results demonstrate that the application of accelerations can significantly alter the changes in bone morphology associated with unloading. These signals, unlike most loading regimes, are not based on deforming the skeleton and can be applied in the absence of weight bearing to specific sites of bone loss. Exploration of cellular activities responsible for the morphology changes will enable us to further elucidate bone's responsiveness to acceleratory motions.

Disclosures: **R.A. Garman**, None.

M150

Low-Level Mechanical Vibrations Enhance Bone Formation without Loss of Bone Quality in the Growing Skeleton. L. Xie^{*1}, B. Busa^{*1}, L. Donahue², C. Rubin¹, L. Miller³, S. Judex¹. ¹Biomedical engineering, Stony Brook University, Stony brook, NY, USA, ²The Jackson Laboratory, Bar Harbor, MN, USA, ³Brookhaven National Laboratory, Upton, NY, USA.

Extremely small magnitude, high-frequency, mechanical stimuli are capable of enhancing bone quantity and micro-architecture in the growing skeleton. Preliminary data indicate that these changes in bone morphology can be accounted for, at least in part, by a decrease in bone's *catabolic* activity. The hypothesis of this study was that, in addition to reduced osteoclastic activity, whole body vibrations (WBV) can concomitantly increase bone's *anabolic* activity in the growing mouse skeleton and that the chemical quality of mechanically stimulated bone is similar to that of normal bone. Eight-week old female BALB/cByJ mice were divided into three groups, baseline control (n=8), age-matched control (n=10), and WBV at 45Hz (0.3g) for 15min/d (n=10). Experimental mice were injected with calcein on day 15 and 20. After the 3-wk experimental protocol, 5-µm undecalcified frontal sections were analyzed for indices of bone formation and *in situ* chemical composition. Five spectra (12x12 µm) enclosed by double calcein labels on either side of endocortical surface of the metaphysis were analyzed by synchrotron infrared microspectroscopy (Brookhaven National Laboratory). *In vivo* strain gaging of two additional mice indicated that WBV induced strain oscillations of approximately ten microstrain on the periosteal surface of the proximal tibia. Comparisons between age-matched controls and vibrated mice indicated that superimposing the extremely low-level

mechanical signal on habitual activities for 15min/d increased bone's anabolic activity (BFR/BS) on the endocortical surface of the metaphysis by 30% ($p<0.05$). Chemical analyses revealed the newly formed bone (2-7d old) stimulated by WBV had similar bone properties as newly formed bone without WBV. There were no significant differences in bone mineral crystallinity, phosphate content, carbonate content, acid phosphate-to-total phosphate content, and mineral-to-matrix ratios. WBV, however, significantly decreased the collagen cross-linking ratios (1660/1690) in bone on endocortical surface ($p<0.05$), likely related to the increase in reducible cross-links of dihydroxylysinoxidation (DHLNL-1690). These data indicate that short durations of extremely low-levels of vibrations can enhance bone formation without loss of bone quality during skeletal growth. Considering their anabolic and anti-catabolic efficacy, these signal may be able to provide a non-pharmacological and safe means for increasing peak bone mass and decreasing the incidence of osteoporotic or stress fractures later in life.

Disclosures: **L. Xie, None.**

M151

Monitoring Load-Driven Fluid Flow Using Microparticles. M. Su*, P. Zhang*, Y. Huang*, H. Yokota. Anatomy and Cell Biology, Indiana University School of Medicine, Indianapolis, IN, USA.

Bone is a mechanosensitive tissue, and load-induced fluid flow in a porous bone matrix is considered a critical determinant in bone remodeling. The long-term objective is to characterize load-induced fluid flow in trabecular and cortical bones and evaluate the role of fluid flow in osteogenic potentials. The specific aim of the current study was to develop a novel method of monitoring load-induced fluid flow in a three-dimensional collagen matrix and bone samples *ex vivo* using microparticles. Two engineering goals were to develop a custom-made piezoelectric mechanical loader mountable to a fluorescence microscope (Nikon E600) and to image in real time a motion of microparticles on a surface of porous materials in response to well-controlled mechanical loading. The piezoelectric loader was constructed using a bimorph-type actuator (Megacera, Inc.). The actuator was driven by a piezoelectric driver (PZD700 M/S, TREK) and controlled by a BNC-2110 interface (National Instruments) with a custom-made MatLab program. Load-induced fluid flow was visualized through the motion of polystyrene microspheres and fluorescence nanoparticles (Polysciences, Inc.), ~ 0.5 to 3 μm in diameter. Time elapsed images were taken at varying intervals with a 10X objective lens, and the captured images were analyzed using MetaMorph software (Universal Imaging Co.). In order to examine the effects of matrix porosity, we deposited a varying amount of hydroxyapatite to type I collagen matrix (CollaCote, Sulzer Dental, Inc.). The matrix was soaked in a 500-mM CaCl_2 solution followed by a 500-mM Na_2HPO_4 solution for 15 min each. The matrix was then thoroughly rinsed in sterile water between immersions, and alternate immersion in CaCl_2 and Na_2HPO_4 solutions was repeated. In response to sinusoidal loads at 1-5 Hz, the motion of fluid flow inside the matrix was correlated to the distance from the neutral plane of the matrix (matrix center). Compared to fluid flow in the matrix with coarse pores (~ 100 μm in diameter), the flow amplitude and velocity were elevated in the matrix with fine pores (~ 20 μm in diameter) as well as in the matrix deposited with hydroxyapatite. On the surface of matrices as well as mouse femurs *ex vivo*, the microparticles moved vertical to the loading axis synchronous to the applied loads. No motion of the microspheres was observed in the matrix covered with collagen gel. In summary, the described microparticle-based visualization method is useful to investigate fluid flow in three-dimensional porous materials in response to mechanical loading.

Disclosures: **M. Su, None.**

M152

Loss of Half Runx2 Gene Dosage Specifically Exacerbates Reduction in Bone Formation Parameters Due to Unloading. R. Salingcarnboriboon¹, K. Tsuji¹, T. Komori², M. Noda¹. ¹Dept. of Molecular Pharmacology, Tokyo Medical and Dental University, Tokyo, Japan, ²Dept. of Developmental and Reconstructive Medicine, Division of Oral Cytology and Cell Biology, Nagasaki University Graduate School of Biomedical Sciences, Nagasaki, Japan.

Molecular mechanisms underlying reduction of bone formation in mechanical unloaded condition have not yet been fully understood. Runx2 has been suggested to be involved in mechanical signal *in vitro*. However, the roles of Runx2 in mechanical stimuli *in vivo* have not yet been known. The purpose of this paper is to examine the roles of Runx2 in unloading-induced bone loss *in vivo*. Tail-suspension induced significant loss of trabecular bone in wild type mice, whereas loss of half Runx2 gene dosage in Runx2 heterozygous knockout mice (Runx2^{+/-}) exacerbated trabecular bone loss. Furthermore, reduction of femoral cortical bone thickness and BMD were observed in Runx2^{+/-} mice after TS but not apparent in Wt mice. Heterozygous loss of Runx2 gene significantly suppressed the endosteal and periosteal mineral apposition rate (MAR) and bone formation rate (BFR) in the cortical bone to nearly undetectable levels after subjected to TS. Similarly, Runx2^{+/-} also exacerbated the suppression of MAR and BFR by TS in trabecular bone compartment. Runx2 and Osterix mRNA expression in cortical bone envelope was reduced significantly by TS in Wt mice. In contrast, Runx2 and Osterix gene in Runx2^{+/-} mice were not altered even after TS suggesting the presence of mechanism downstream to these molecules. Surprisingly, in Runx2^{+/-} mice Runx2 protein was down-regulated to nearly null level after TS. We further demonstrated that Cbl-b, the E3 ubiquitin ligase gene that has been reported to be up regulated after TS, bound directly to Runx2 and repressed transcriptional activity on 1.3 osteocalcin promoter suggesting the possible involvement of Cbl-b in degradation of Runx2 protein. These data indicated that Runx2 is a critical target of unloading stimuli to alter osteoblastic activity and bone formation.

Disclosures: **R. Salingcarnboriboon, None.**

M153

Differential Effect of Indomethacin on Cell Number and Alkaline Phosphatase Production during Osteogenesis *In Vitro*. W. J. Peterson¹, D. T. Yamaguchi². ¹Grecc 691/11g, VA Greater Los Angeles Healthcare System and UCLA School of Medicine, Los Angeles, CA, USA, ²Research Service 691/151, VA Greater Los Angeles Healthcare System and UCLA School of Medicine, Los Angeles, CA, USA.

Prostaglandins regulate bone formation. While it is known that osteoblasts go through distinct stages of proliferation and differentiation before mineralization, the intricate role that prostaglandins may play in this process under long term osteogenic conditions has not been established. Controversial results have been reported on prostaglandin activity, however, this may be due to differences in cell types and methods of assay used for study. Another source of controversy may be the phenotypic changes that occur during the developmental sequence of osteogenesis. Thus, osteoprogenitor cells undergo extensive proliferation before becoming differentiated osteoblasts. Once confluent, these cells continue their maturation, producing extracellular matrix proteins. It is possible that prostaglandins may affect either proliferation and/or differentiation at various intervals during the developmental process of bone formation. To test this hypothesis, we selected the MC3T3-E1 cell line because it is a well-known *in vitro* model that undergoes a developmental sequence of proliferation and differentiation similar to osteoblasts in primary cultures. Our approach to this study was to treat cultures with indomethacin to inactivate cyclooxygenase at various times after culture initiation. The effect of reduced prostaglandin synthesis and secretion on proliferation and differentiation was determined by assessing cell number and alkaline phosphatase production. Data are expressed as the mean \pm SE. The results show: (1) no effect of indomethacin concentration (4-64 μM) on cell number in cultures treated for 7 days; (2) maximal enhancement of alkaline phosphatase production (255% of control) per cell was observed using 64 μM of indomethacin in cultures treated for 7 days; (3) decreased cell number was first observed on day 10 in cultures treated with indomethacin for 12 days (61%, 55%, 33% of control on days 10, 11, and 12, respectively); (4) effects of indomethacin on cell number and alkaline phosphatase production are independent of exposure time; (5) indomethacin treatment enhanced the rate of alkaline phosphatase production per cell in cultures treated for 12 days (300% and 412% of control on days 11 and 12, respectively). These results suggest that prostaglandins may contribute to bone formation by regulating (1) the total number of osteoblasts per culture; (2) the proportion of osteoblasts undergoing differentiation and (3) the rate of alkaline phosphatase production per differentiated osteoblast.

Disclosures: **W.J. Peterson, None.**

M154

Inflammatory Kinins Synergistically Potentiate IL-1 β Induced Bone Resorption by a Mechanism Involving Increased Expressions of COX-2, mPGES-1, cPLA₂, and Prostaglandin Dependent Increased RANKL mRNA. A. B. Brechter, U. H. Lerner. Oral Cell Biology, Odontology, UMEÅ, Sweden.

The effects of a variety of kinins and kinin analogues on unstimulated and cytokine stimulated prostaglandin biosynthesis and on the expression of enzymes involved in arachidonic acid metabolism were studied in a human osteoblastic cell line, MG-63. In addition, the effects of kinins on cytokine induced prostaglandin biosynthesis and expression of molecules crucial for osteoclast differentiation was assessed in mouse calvarial bones. Co-treatment of MG-63 cells with BK and either interleukin-1 α (IL-1 α), IL-1 β or tumour necrosis factor- α (TNF- α) resulted in synergistic stimulation of prostaglandin E₂ (PGE₂) formation. The interactions were dependent on the concentrations of IL-1 β and TNF- α , as well as that of bradykinin (BK). IL-1 β induced PGE₂ formation was synergistically potentiated by several kinins and kinin analogues with affinity for BK B1 and B2 receptors and these interactions were specifically inhibited by B1 and B2 receptor antagonists. IL-1 β , TNF- α , BK B1 and B2 receptor agonists enhanced the expression of cyclooxygenase-2 (COX-2) mRNA. Co-stimulation resulted in synergistic potentiation of cytokine induced COX-2 mRNA and protein expression by BK B1 and B2 receptor activation. Membrane-associated PGE synthase-1 (mPGES-1) mRNA expression was upregulated by IL-1 α , a response that was synergistically potentiated by both BK and DALBK. Co-treatment with IL-1 α and either BK or DALBK resulted in a small enhancement of cPLA₂ mRNA, whereas COX-1 mRNA was unaffected. No synergistic interactions were observed in cells co-stimulated with kinins and either IL-6, IL-11, IL-17, OSM, LIF or TGF- β . In mouse calvariae, BK and DALBK synergistically potentiated IL-1 β induced PGE₂ formation, COX-2 mRNA, as well as receptor activator of NF- κB ligand (RANKL) mRNA. The synergistic effect on PGE₂ formation, was abolished by indomethacin, and the synergistic effect on RANKL was substantially inhibited by indomethacin. These results show that BK B1 and B2 receptors synergistically potentiate IL-1 β and TNF- α induced stimulation of prostaglandin biosynthesis in osteoblasts by a mechanism involving increased COX-2, mPGES-1 and cPLA₂ expression. The interactions also result in PGE₂-dependent enhanced expression of the osteoclast differentiation cytokine RANKL. These data explain the mechanism why kinins synergistically potentiate IL-1 β induced bone resorption in mouse calvariae.

Disclosures: **A.B. Brechter, None.**

M155

Effects of 1,25-Dihydroxyvitamin D₃ and 25-Hydroxyvitamin D₃ on Osteoblast Differentiation in Human Marrow Stromal Cell Cultures. J. Glowacki¹, S. M. Mueller^{*2}, J. S. Greenberger³, I. Bleiberg^{*4}, M. S. LeBoff⁵.

¹Orthopedic Surgery, Brigham and Women's Hospital, Boston, MA, USA, ²University Hospital, Zurich, Switzerland, ³Radiation Oncology, University of Pittsburgh, Pittsburgh, PA, USA, ⁴Sackler School of Medicine, Tel Aviv, Israel, ⁵Medicine, Brigham and Women's Hospital, Boston, MA, USA.

In vivo and *in vitro* studies indicate that a sub-population of bone marrow stromal cells has the potential to differentiate into osteoblasts. With alkaline phosphatase (AlkP) as an early indicator of osteoblastogenesis, we reported that there was a significant age-related decrease in osteoblast differentiation in marrow from men aged 38 to 80 years of age [J Cell Biochem 82:583, 2001]. We tested the hypothesis that both 1,25(OH)₂D₃ and 25-hydroxyvitamin D₃ (25OHD₃) stimulate osteoblastogenesis in marrow from elderly men and women. Bone marrow was obtained as discarded material from men and women undergoing total hip replacement for osteoarthritis. Low-density mononuclear cells were isolated and selected for adherence. Four thousand cells were cultured in each well of a 96-well plate with osteogenic supplements (10 nM dexamethasone, 5 mM β-glycerophosphate, 170 μM ascorbic phosphate). AlkP activity was measured after 6 days with the p-nitrophenol method with an ELISA plate reader. First, in a series of samples from 13 men (age range 27-79 years), 10 nM 1,25(OH)₂D₃ stimulated AlkP significantly in all samples (mean 164%), but with a significant decrease with age (r=-0.803, p=0.0009). Second, dose-response effects and comparison of 1,25(OH)₂D₃ and 25OHD₃ were studied with marrow stromal cells from elderly men and women (N= 17, 64-83 years). The 1,25(OH)₂D₃ stimulated 16 (94%), with peak stimulation between 1 and 10 nM 1,25(OH)₂D₃. Of the 9 samples with which comparisons were made, 7 (78%) were stimulated by 1,25(OH)₂D₃ and by 25OHD₃. There was equivalent stimulation by 1,25(OH)₂D₃ and 25OHD₃ in cells from 2 men and 1 woman. Thus, although there are differences in magnitude of stimulation, in peak dose, and in relative effects of vitamin D metabolites, normal marrow from elders shows osteoanabolic response to 1,25(OH)₂D₃ and by 25OHD₃. We speculate that vitamin D status of the subject may account for differences in *in vitro* behavior of marrow stromal cells. The vitamin D status of the subjects whose marrow was used in these studies was not determined, but in other work we reported that there was vitamin D-deficiency (serum 25OHD < 37.5 nmol/L) in 22% of 68 women admitted for total hip replacement for osteoarthritis from the same pool as those whose discarded marrow was used in this work. In addition, 4% had elevated serum parathyroid hormone (>6.8 pmol/L) [J Bone Joint Surg 85A: 2371, 2003].

Disclosures: **J. Glowacki**, None.

M156

Venous Ligation-Mediated Bone Adaptation Requires COX-2. H. Y. Stevens^{*}, D. R. Meays^{*}, J. Yeh^{*}, L. M. Bjursten^{*}, J. A. Frangos. La Jolla Bioengineering Institute, La Jolla, CA, USA.

Prostaglandins are local mediators of bone resorption and formation, known to be involved in bone's adaptive response to fluid shear stress (FSS). We have previously described a model of trabecular bone loss in hindlimb suspended mice and rats and demonstrated partial protection from osteopenia by ligation of the femoral vein. The increased FSS resulting from this ligation drove bone adaptation in the absence of mechanical loading. In this study we investigated the role of COX-2 in this adaptive response to FSS by use of *COX-2* knockout mice. Heterozygotic breeders (*COX-2* +/-) were generated from *COX-2* -/- males (B6; 129-Ptgs2^{tm1Jed}) and *COX-2* +/- females (B6; 129SF2/J). Female offspring were genotyped as *COX-2* knockout (KO); *COX-2* heterozygote (HET) and *COX-2* wild type (WT) at 4 weeks and recruited at 7 weeks. The proximal metaphysis of each femur was scanned *in vivo* by peripheral quantitative computed tomography (pQCT) and calcein administered. Six slices were recorded for the trochanteric region to assess initial volumetric bone mineral density (vBMD). On Day 2 the animals underwent venous ligation of a randomly-assigned femoral vein, with sham-operation of the contralateral limb and after 2 days' recovery, the mice were tail suspended for 10 days. On Day 14 femora were scanned *in vivo* by pQCT, xyleneol orange administered and the mice left to ambulate normally for 3 days before euthanasia (Day 17). Average percentage loss in trabecular vBMD was calculated for each bone. At the conclusion of the study, femora were embedded in glycol methacrylate for histomorphometric analysis. All animals lost comparable amounts of trabecular bone from sham limbs as a result of suspension. In WT mice, loss of trabecular BMD in the venous-ligated limb was significantly less than that of the sham-operated limb (ligated -33.9 ± 2.1 (% ± SEM); sham -38.9 ± 2.4, n = 9, p < 0.05); this effect, however, was not seen in KO (ligated -35.9 ± 2.9; sham -34.0 ± 3.1) or HET mice. Percentage gain in femoral periosteal circumference was greater in the ligated limb than in the sham limb for WT mice. KO and HET mice already possess femora of larger periosteal circumference than their WT littermates and ligation in these bones did not result in an increase in perimeter relative to sham. Histomorphometry on embedded KO femora revealed thinner cortices compared to WT and HET and less mineralizing perimeter compared to WT (total label). Therefore we propose that *COX-2* deficiency affects recruitment of osteoblasts along the endocortical surface. This is the first *in vivo* study to show that fluid-flow mediated bone adaptation, independent of mechanical strain, is *COX-2* dependent.

Disclosures: **H.Y. Stevens**, None.

M157

Dissolution of the Inorganic Phase of Bone Leads to Release of Calcium, which Has an Important Auto-Regulatory Role in Osteoclast Survival, and Affects the Coupling of Bone Formation to Bone Resorption. K. Henriksen¹, R. H. Nielsen^{*1}, M. G. Sørensen^{*1}, J. Gram^{*2}, S. Schaller^{*1}, J. Bollerslev³, M. A. Karsdal¹, T. J. Martin⁴. ¹Nordic Bioscience A/S, Herlev, Denmark, ²Ribe County Hospital, Esbjerg, Denmark, ³National University Hospital, Oslo, Norway, ⁴SVIMR, Melbourne, Australia.

Osteoclasts dissolve the inorganic phase of bone via acidification of the osteoclastic resorption lacunae by hydrochloric acid through the V-ATPase and the chloride channel CIC-7. Attenuated function of these results in osteopetrosis, characterized by increased osteoclast numbers, low or absent bone resorption and normal bone formation, suggesting that the coupling principle has been challenged. We investigated if the release of calcium during dissolution of the inorganic phase by the V-ATPase and CIC-7 is important for controlling osteoclast survival, bone resorption and for the coupling of bone formation to bone resorption *in vivo*. We used synthetic inhibitors of CIC-7 (NS5818/PB1), V-ATPase (bafilomycin A1), addition of calcium and the calcium channel antagonist Ryanodine in cultures of human osteoclasts on calcified and decalcified cortical bone slices, and the rat OVX model. NS5818 and bafilomycin dose-dependently inhibited bone resorption by mature osteoclasts, which inversely correlated to increases in the survival of calcitonin receptor positive multinuclear osteoclasts up to 300% at full inhibition. By comparison of osteoclast survival on normal bone slices to that of decalcified bone slices, inhibition of acidification led to increased survival only on normal bone, but not on decalcified bone. To specifically study the role of calcium in osteoclast survival, we used the calcium channel antagonist ryanodine and addition of calcium. We found that inhibition of calcium channels by ryanodine dose-dependently increased osteoclast survival up to 100% at 90 μM, and that calcium dose-dependently increased osteoclast apoptosis, with maximum effect at 40 mM. We used a potent CIC-7 inhibitor (PB1) *in vivo* in the OVX model (oral dosing 100 mg/kg/rat). Resorption was restored to sham levels, whereas bone formation was unchanged compared to OVX levels, as investigated by CTX-I and osteocalcin in serum. In conclusion, the release of calcium during acidification of the resorption lacuna, induces apoptosis of the osteoclasts, which controls the resorptive activity, thus forming a regulatory loop. Inhibition of osteoclastic bone resorption *in vivo* by blocking acidification does not lead to reduced bone formation in contrast to other anti-resorptive treatments. Thus, acidification attenuated osteoclasts that are non-resorbing may still be able to generate signals that are essential for bone formation.

Disclosures: **K. Henriksen**, None.

M158

Generation of Cell-Based Models for Studying Classical and Non-Classical ER Action in Osteoblastic Cells. A. Sanval, V. Rudnik^{*}, F. A. Sved, S. Khosla. Endocrinology Research, Mayo Clinic, Rochester, MN, USA.

Studies with female mice lacking classical ERE signaling of the Estrogen Receptor alpha (ER-α) have shown that these mice (ERα/NERKI) gained cortical bone following ovariectomy, and estradiol dose-dependently suppressed this increase; these changes were the opposite of those seen in wild type (WT) mice [JBMR vol. 19, suppl. 1 p S339, 2004]. These paradoxical effects of ovariectomy and estrogen on cortical bone in ERα/NERKI mice could be due to an alteration of the balance between classical (through EREs) and non-classical (through response elements other than EREs) signaling of ER-α in osteoblastic cells. To evaluate the effects of classical and non-classical signaling pathways in osteoblastic cells, we have sought to develop cell-based models using a human osteosarcoma cell line, U2OS, that is devoid of endogenous ERs. WT and NERKI mouse ER-α, cloned into the pcDNA3.1 vector, were used independently to transfect the U2OS cells. Neomycin-resistant colonies were isolated by ring cloning. The colonies were tested at the mRNA and also at the protein levels for the expression of the WT and the NERKI ER-α. One colony from each group that showed the expression of the respective proteins was tested in a functional assay with reporter plasmids containing either EREs or AP1 response elements. Our results showed that the clone containing the WT ER-α significantly upregulated luciferase activity from the ERE-luciferase reporter in response to estradiol treatment. ICI, when used alone, could not activate transcription of the luciferase reporter and abrogated the effects of estradiol. The clone containing the NERKI ER-α, on the other hand, failed to upregulate luciferase activity driven by an ERE in response to either estradiol or ICI alone or in conjunction with estradiol treatment, showing its inability to function through EREs, and hence, the classical pathway. Both NERKI and WT mER-α clones, however, activated the AP1-luciferase reporter in response to estradiol, indicating their abilities to act through the nonclassical pathway. Thus, we have generated cell-based model systems that can be used for dissecting the classical vs nonclassical ER pathways in osteoblastic cells at the molecular level.

Disclosures: **A. Sanval**, None.

M159

Hypoxia Induces PGE₂ and OPG Release from MC3T3-E1 Osteoblastic Cells. C. M. Lee, C. E. Yellowley. VM: APC, University of California, Davis, Davis, CA, USA.

It has been suggested that changes in regional oxygen tension may stimulate local bone cell activity and ultimately regulate bone maintenance and repair. Prostaglandin E₂ (PGE₂) is a potent regulator of bone remodeling exerting its effects on both osteoblast and osteoclast differentiation and activity. Osteoblasts regulate bone remodeling activity by expressing receptor activator of NF-κB ligand (RANKL) to induce, and osteoprotegerin

(OPG) to suppress osteoclastogenesis. In this study we examined the effect of lowering oxygen tension on levels of PGE₂, RANKL and OPG. Osteoblastic MC3T3-E1 cells were cultured in 2%, 5% or 21% oxygen. Conditioned media and whole cell lysates were collected at time points between 0 and 72 hours. RANKL protein levels were quantified by Western blot analysis. Media PGE₂ and OPG levels were quantified by ELISA. PGE₂ levels in media were markedly higher in cells cultured at 2% oxygen for 6 and 24 hours compared to cells cultured at 5 and 21% oxygen. OPG levels in cells grown in 2% oxygen were significantly increased at 24h compared to 5 and 21%. RANKL protein expression was not detectable by western blot analysis. Our data suggest that reduced oxygen tension significantly elevates PGE₂ and OPG release from MC3T3-E1 osteoblastic cells. Conditions inducing hypoxia in bone may include regional hypoxia at fracture sites and mechanical disuse. Since PGE₂, OPG and RANKL are involved in bone turnover, their modulation under hypoxic conditions may play a role in bone repair and remodeling under these conditions.

Disclosures: **C.M. Lee**, None.

M160

RUNX2 Potentiates, but Is not Required for, RANKL Expression in Mesenchymal Cells. **Q. Fu¹, W. Wang^{*2}, B. R. Olsen^{*2}, S. C. Manolagas¹, C. A. O'Brien¹.** ¹Endo/Metab, Center for Osteoporosis & Metabolic Bone Diseases, Central Arkansas Veterans Healthcare System, Univ. Arkansas for Med. Sciences, Little Rock, AR, USA, ²Department of Cell Biology, Harvard Medical School, Boston, MA, USA.

RANKL gene expression is limited primarily to bone and lymphocyte-containing tissues and stimulation of RANKL by osteoclastogenic hormones and cytokines is limited to cells of the mesenchymal lineage. However, the molecular basis of this cell type-specificity remains unknown. We have shown previously that cAMP-responsiveness of the murine RANKL gene is mediated in part by a distal enhancer, located 74 kb upstream from the transcription start site, which contains 2 cAMP response elements that are conserved among mammalian species. We now show that this enhancer also contains a potential RUNX2 binding site that is present in the RANKL gene of mammals and birds. Mutation of this binding site in the context of a luciferase reporter construct containing 120 kb of the murine RANKL 5-flanking region reduced basal and cAMP-stimulated RANKL transcriptional activity, suggesting that RUNX2 contributes to RANKL gene expression. RUNX2 binding to this sequence element was confirmed by gel shift assays using an anti-RUNX2 antibody. In addition, over-expression of RUNX2 in a stromal/osteoblastic cell line elevated the maximal cAMP-stimulation of the endogenous RANKL gene by 3-fold. However, expression of a dominant-negative version of RUNX2, consisting of the RUNX2 DNA-binding domain, did not suppress basal or cAMP-stimulated RANKL expression, but did suppress osteocalcin and bone sialoprotein expression. Conversely, expression of full-length RUNX2 in a hepatocyte cell line activated the endogenous osteocalcin and bone sialoprotein genes but did not activate either the endogenous RANKL gene or a stably integrated RANKL transgene. Moreover, dibutyl-AMP stimulated RANKL mRNA to the same extent in both wildtype and RUNX2-deficient mouse embryonic fibroblasts (MEFs). To determine whether other members of the RUNX family might participate in the control of RANKL in the absence of RUNX2, we quantified RUNX1 and RUNX3 mRNA in primary bone marrow stromal cells, a stromal/osteoblastic cell line, and MEFs. RUNX1 and RUNX3, as well as the non-DNA binding subunit Cbfb, were present in all three cell types. We conclude from these results that RUNX2, and perhaps RUNX1 or RUNX3, potentiate, but are not required for, RANKL expression in mesenchymal cells. Moreover, RUNX2 is not sufficient to confer RANKL expression in non-mesenchymal derived cells. Finally, these results suggest that although RUNX family members play a role in the cell type-specific expression of RANKL, additional factors are likely to be involved.

Disclosures: **C.A. O'Brien**, None.

M161

Prostaglandin E₂ Receptor (EP4) Agonist Stimulates Osteoblasts and Increases Bone Volume. **T. Ninomiya^{*1}, H. Nakamura², A. Hosoya^{*2}, Y. Arai^{*1}, N. Sahara^{*1}, K. Yamaguchi^{*3}, H. Oida^{*3}, H. Ozawa¹.** ¹Institute for Oral Science, Matsumoto Dental University, Nagano, Japan, ²Department of Oral Histology, Matsumoto Dental University, Nagano, Japan, ³Fukui Research Institute, ONO Pharmaceutical CO., LTD., Fukui, Japan.

Prostaglandin (PG) E₂ promotes bone resorption and bone formation. PGE₂ has four receptor subtypes which have been identified and cloned, designated as EP1, EP2, EP3, and EP4. EP4 receptor mediates PGE₂ induced osteoclasts differentiation in bone organ culture. On the other hand, it had reported that EP4 activation induced de novo bone formation within immobilized rats. However, the mechanism of bone formation induced by EP4 activation is not clarified. In this study, we investigated the mechanism of increased bone volume by EP4 activation using EP4 agonist treated rats. The effects of EP4 activation on bone structure and bone cell were evaluated by bone morphometric and histological analysis. Moreover, the measurement using in vivo μ CT was performed for investigating the effects of EP4 activation against a rat. Eighty male Sprague-Dawley rats aged 6 weeks were used in this experiment. EP4 agonist (ONO-4819, 10 μ g/kg BW) was subcutaneously injected into back two times a day at 8-h intervals for 5 weeks. The rats of control group received saline in the same way. Rats were fixed by 4% paraformaldehyde at 1, 3, 5, 7, 14, 21, 28, and 35th day after starting an injection of EP4 agonist. The left and right tibiae from each group obtained at each time point were used on the experiment of bone morphometric and histological analysis, respectively. Four rats (n=2) chosen from control and EP4 agonist group were subjected to analysis with in vivo μ CT (R_mCT, Rigaku, Tokyo) at each time point. On 1, 3, and 5th day, parameters of morphometric

analysis were did not show any difference between control and EP4 agonist group. However, bone volume and trabecular number of EP4 agonist group on 14th day increased approximately 1.16-fold compared with these of control group. In the experiments using in vivo μ CT, volume of bone formation on 21th day was higher than that of bone resorption. Moreover, histological data revealed that EP4 agonist induces activation of osteoblasts. These findings were associated with increase of bone volume morphometric findings. It was clearly that EP4 activation by EP4 agonist increased bone volume. Then, it was revealed that the methods using in vivo μ CT is available for evaluate a substantial effect to bone resorption or formation. This study suggests that EP4 agonist acts to osteoblasts and accelerates bone formation by activation of osteoblasts.

Disclosures: **T. Ninomiya**, None.

M162

Transforming Growth Factor Beta (TGF β) Stimulates CCL5/RANTES mRNA Expression and Secretion from Osteoblasts. **S. Yano¹, D. Kanuparthi^{*2}, S. Huang^{*2}, E. M. Brown², N. Chattopadhyay^{*2}.** ¹Endocrinology and Metabolism, Hematology/Oncology, Shimane University Faculty of Medicine, Shimane, Japan, ²Endocrinology, Diabetes and Hypertension, Brigham and Women's Hospital and Harvard Medical School, Boston, MA, USA.

TGF β is a cytokine released from bone matrix, which stimulates osteoblast (OB) proliferation and growth. CCL5/RANTES is a chemokine secreted from both OBs and osteoclasts; it regulates several functions of these cells by autocrine/paracrine modes of action. We show here that 1 to 10 ng/ml TGF β in a concentration-dependent manner induces RANTES secretion from mouse primary calvarial OBs and from the MC3T3-E1 OB cell line. Induction of RANTES secretion by 5 ng/ml TGF β is observed as early as 4 h, and is not suppressed by 5 mM actinomycin D, thereby suggesting that the effect of TGF β is exerted at a post-transcriptional level at this early time point. TGF β , however, increases the level of RANTES mRNA in an 18 h incubation with calvarial OBs and MC3T3-E1 cells, indicating that longer treatment increases RANTES mRNA expression. TGF β induces RANTES secretion from osteoblasts via the p38 MAP kinase pathway but not via the Src kinase pathway, as 10 mM SB203580 (a p38 MAPK inhibitor) abolished TGF β -induced RANTES secretion, while 300 nM PP-2 (Src kinase inhibitor) did not. Finally, 5 ng/ml TGF β produced rapid phosphorylation of p38 MAPK in MC3T3-E1 cells. Therefore, we conclude that TGF β induces RANTES mRNA and stimulates RANTES secretion from OBs, acting at least in part at a post-transcriptional level with the participation of the p38 MAPK pathway. Given that RANTES promotes the survival of OBs and enhances their chemotaxis (Yano, et al., Endocrinology 2005;146:2324-2335), it could participate in the mechanism through which osteoclastic bone resorption is coupled to subsequent osteoblastic renewal of bone.

Disclosures: **S. Yano**, None.

M163

Intraarticular Osteochondral Fracture-Induced Hemarthrosis Contains Osteoprogenitor Cells and Can Be a Useful Cell Source for Bone Regeneration. **T. Niikura^{*}, M. Miwa^{*}, Y. Sakai^{*}, S. Lee^{*}, R. Kuroda^{*}, T. Fujishiro^{*}, S. Kubo^{*}, M. Doita^{*}, M. Kurosaka^{*}.** Orthopaedic Surgery, Kobe University Graduate School of Medicine, Kobe, Japan.

Bone marrow stromal cells from the iliac bone are commonly used as a cell source at a clinical stage of bone regeneration therapy. However, there are drawbacks in their use, due to the invasiveness of bone marrow aspiration from a patient. Moreover, available cells from a single procedure are limited. Therefore, obtaining cells less invasively and investigating possible new cell sources are important goals. We hypothesized that an intraarticular osteochondral fracture-induced hemarthrosis is a potentially useful cell source, because it is likely it will contain osteoprogenitor cells from bone marrow that can be obtained in the absence of unnecessary invasion to the patient. Moreover, we can utilize a material which has been previously discarded as medical waste. Therefore we investigated whether the hemarthrosis-derived cells have the potential to differentiate into osteoblasts. We enrolled six patients suffering from osteochondral fractures of knee joints in this study. Patients were routinely treated with aspiration of the hemarthrosis, and then isolation and culture of the hemarthrosis-derived cells was conducted. Informed consent for participation in the study was obtained from all patients and the project was approved by the Ethics of Human Experiments of the Faculty of Medicine, Kobe University prior to start of the study. Mononuclear cells were harvested by density gradient centrifugations. After the expansion in the primary culture, we cultured these cells in a medium supplemented with dexamethasone, β -glycerophosphate, and ascorbic acid, or without them as control. The culture of these cells showed the formation of colonies of fibroblast-like spindle shape cells in the primary culture. The morphology of the treated cells appeared osteoblastic, cuboidal shape differing from the fibroblastic, spindle-like shape observed in the control. Matrix mineralization was observed only in the treated culture using alizarin red S staining. Moreover, alkaline phosphatase activity determined by the release of p-nitrophenol from p-nitrophenyl phosphate, and gene expressions of alkaline phosphatase, parathyroid hormone receptor, and osteopontin which were analyzed by RT-PCR were up-regulated in the treated culture compared with the control. Flowcytometry analysis of these cells showed positive for CD 29, 44, 105, 166, and negative for CD 14, 34, 45. Our results demonstrate that these cells contain osteoprogenitor cells, and are highly possibly derived from bone marrow, and are a useful cell source for bone regeneration.

Disclosures: **T. Niikura**, None.

M164

The Effect of Oxygen Diffusion Time on the Colony Formation and Proliferation of Human Connective Tissue Progenitor Cells in Primary Tissue Culture. S. M. Villarruel, R. Sinha*, C. A. Boehm*, J. Tao*, K. A. Powell*, G. F. Muschler. Biomedical Engineering, Cleveland Clinic Foundation, Cleveland, OH, USA.

Bone marrow (BM) contains a heterogeneous mixture connective tissue progenitors cells (CTPs), capable of forming one or more connective tissues. Understanding the effect pO₂ on CTP performance has important implications on in vitro assay and cell transplantation strategies. Oxygen can be toxic to cells through the generation of reactive oxygen species. Previously we showed that colony formation by CTPs increased at pO₂ of 7.6, 38, and 76 to mm Hg compared to pO₂ of 152 mmHg conventionally used for in vitro assays. This work investigates the effect of transient exposure to supraphysiological (152 mmHg) conditions during CTP culture. Conventional media preparation is supersaturated with atmospheric oxygen. To estimate the time necessary for atmospheric medium to reach steady state with lower pO₂, conditions following medium exchange a mathematical model of oxygen diffusion in tissue culture was developed using Ficks 2nd Law in 1D. This model predicted that 5 hours was necessary to achieve steady state with the lowest oxygen tension condition, P_{o2}= 7.6 mmHg. Pre-equilibration of medium to low pO₂ conditions prior to media exchange is a potentially important variable in assay of CTP performance. Iliac crest BM was harvested from 12 patients. Samples were cultured under osteoblastic conditions for six days. Cells were cultured in eight groups at one of four pO₂ levels (152, 76, 38, or 7.6 mmHg) using media that was either equilibrated at 152 mm Hg (control) or equilibrated at the appropriate lower pO₂. CTP cultures were assayed using imaging methods. A Quantix camera and motorized microscope controlled by Metamorph was used. Three-hundred individual 10x images were collected and montaged to create one full field of view image of each culture well. Quantitative characterization of individual CTP-derived colonies was performed. A total of 9,310 colonies containing 843,876 cells were assayed. Colony formation was 35% higher in lower oxygen levels when compared to 152 mmHg control. Treatment with pre-equilibrated media demonstrated greater colony forming efficiency at both 76 and 38 mmHg, suggesting that intermittent hyperoxia compromises CTP colony formation. Pre-equilibration did not have an effect on colony formation at 7.6 mmHg, suggesting a balance between hypoxia and transient hyperoxia. Proliferation rate among the colonies that were formed under each condition was not changed by pre-equilibration. Median cell density decreased with decreasing pO₂ in both groups. This work demonstrates that even short term exposure to hyperoxia using atmospheric pO₂ media reduces CTP colony forming efficiency.

Disclosures: **S.M. Villarruel**, None.

M165

Over-Potential of the Anabolic Actions of Specific Prostaglandin E EP4 Signaling by Osteopontin-Deficiency in Ovariectomized Mice. N. Kato¹, K. Kitahara^{*1}, S. R. Rittling^{*2}, D. T. Denhard^{*2}, H. Kurosawa^{*3}, M. Noda¹. ¹Molecular Pharmacology, 21st COE Program, Medical Research Institute, Tokyo Medical and Dental University, Tokyo, Japan, ²Cell Biology and Neuroscience, Rutgers University, Piscataway, NJ, USA, ³Orthopedics, Juntendo University, Tokyo, Japan.

In order to resume bone mass in severely osteopenic patients, anabolic actions of the agents have been sought. One of the possible agents is prostaglandin E EP4 receptor agonist (EP4A). However, such anabolic actions of EP4A should be further potentiated to obtain full recovery of bone mass. Osteopontin (OPN) was shown to modulate bone formation in vivo. Therefore, we examined at the molecular levels the effects of OPN-deficiency on the EP4 induced gene expression in osteoblasts and on bone formation in ovariectomized mice model. EP4A (ONO-AE1-329) was injected 3 times per day for 5 days a week for 4 weeks subcutaneously into the back of wild type (WT) or OPN deficient (OPN-KO) mice. Total RNA was extracted from the bone of each animals. The mRNA expression levels of the genes encoding proteins related to osteoblastic phenotypes were examined. EP4A treatment increased the expression levels of the OPN but not type 1 collagen (COL), ALP as well as upstream transcription factor gene, osterix, in WT. In contrast, expression levels of COL and ALP, and osterix were enhanced in OPN-KO mice after EP4A treatment. Thus, OPN is a specific target of the EP4 and is involved in suppression of EP4 activation. In order to examine the effects of OPN-deficiency on EP4 dependent activation of bone formation in osteopenic model, ovariectomy was conducted in WT and OPN-KO mice which were treated with either vehicle or EP4A. Ovariectomy suppressed the levels of bone volume in WT. EP4A enhanced bone mass in sham operated WT by about 20%, and resumed bone mass to reduce the suppression of bone mass levels by ovariectomy to reach up to 80% of the levels in sham operated group. OPN-deficiency did not alter the basal levels of bone volume and ovariectomy-induced bone loss was less than the levels observed in WT as reported previously. Strikingly, in OPN-KO mice, EP4A enhanced bone mass significantly up to 40% more than the bone mass level in OPN-KO mice treated with vehicle. In the presence of such over-enhanced bone mass, ovariectomy no longer alter the levels of bone volume. Thus, OPN-deficiency potentiated anabolic action of EP4 even in ovariectomized mice. Simultaneous suppression of bone resorption due to ovariectomy by OPN-KO could result in superinduction of bone volume compared to sham operated OPN-KO or sham operated WT. These data indicated the advantageous regimen of the cotreatment with EP4A and the antagonist against OPN of the bone loss due to ovariectomy.

Disclosures: **N. Kato**, None.

M166

Accelerating Fracture Healing by Manipulating Arachidonic Acid Metabolism. J. P. O'Connor, M. B. Manigrasso*. Orthopaedics, UMDNJ-New Jersey Medical School, Newark, NJ, USA.

Cyclooxygenases and lipoxygenases catalyze the conversion of arachidonic acid into prostaglandins and leukotrienes, respectively. These bioactive lipids participate in cell signaling events and are critical mediators of inflammation. We have previously shown that genetic or pharmacological ablation of cyclooxygenase-2 activity severely impairs fracture healing in rodents, indicating that inflammation or prostaglandin-mediated signaling events are essential for normal bone regeneration. Since arachidonic acid also is a lipoxygenase substrate, we hypothesized that loss of cyclooxygenase-2 activity would lead to increased levels of leukotrienes or a higher leukotriene to prostaglandin ratio during the inflammatory phase of fracture healing and that this altered level of leukotrienes could contribute to inhibition of bone regeneration. To test our hypothesis, fracture healing was assessed in mice genetically deficient for 5-lipoxygenase. Radiographs and histology indicated that fracture bridging occurred 2 weeks after fracture in mice lacking 5-lipoxygenase activity as compared to 3 weeks after fracture in wild-type control mice of identical genetic background and age. Torsional mechanical testing showed that after 4 weeks of healing, the material strength of the healing femurs from the 5-lipoxygenase deficient mice was approximately twice as strong as the controls (P < 0.001). The data support our hypothesis that excess leukotrienes impair fracture healing when cyclooxygenase activity is impaired. The data also indicate that pharmacological manipulation of arachidonic acid metabolism can be used to accelerate bone regeneration.

Disclosures: **J.P. O'Connor**, None.

M167

Gene Array Analysis of Connexin43 Null Osteoblasts. M. Watkins*, L. Screen*, B. Guillotin*, R. Civitelli. Bone and Mineral Diseases, Washington University in St. Louis, St. Louis, MO, USA.

Connexin43 (Cx43) is the major gap junction protein expressed by osteoblasts and osteocytes, and it is critically involved in bone formation. Mice genetically deficient of *Cx43* exhibit developmental abnormalities of the skeleton and impaired osteoblast function, attended by decreased expression of osteoblast genes, such as *osteocalcin* and $\alpha_1(I)$ collagen, and delayed mineralization in vitro. To further understand how Cx43 regulates osteoblast function, we performed a systematic analysis of gene expression profile of *Cx43* null osteoblasts compared to wild type cells using a gene array approach. Cells were isolated from the calvaria of newborn *Cx43* null and wild type littermates, and grown to confluence before RNA extraction. Cell extracts from 3 separate cell isolates from animals of 3 different litters were used individually. Total RNAs were dye labeled and hybridized to a 27kb mouse genomic cDNA array (Affimetrix Murine U74A chip). Genes whose expression was >4-fold different between *Cx43* null and wild type, consistently in all 3 experiments, were considered differentially expressed. Expression levels of 17% of the 12,326 genes were significantly down regulated in the Cx43 null samples compared to wild type; among these, *IGFBP-5*, *MMP12* and *Cxcl5*. Conversely, expression of only 2% of the assayed genes was significantly upregulated in Cx43 null osteoblasts compared to wild type osteoblasts, including *forkhead box-1* and *jun-b*. Differential gene expression was confirmed in a subset of these genes by real-time quantitative PCR. Osteoblast specific genes, including *Cbfa1*/*Runx2*, *alkaline phosphatase*, $\alpha_1(I)$ collagen and *osteocalcin* were analyzed by real-time quantitative PCR, and their expression profile was consistent with an immature osteoblastic phenotype in *Cx43* null calvarial cells, results entirely in agreement with the notion that lack of *Cx43* reduces the differentiation potential of osteoblastic cells. Data from this systematic analysis should be helpful in assessing the molecular mechanisms by which Cx43 modulates osteoblast differentiation and bone formation.

Disclosures: **M. Watkins**, None.

M168

Strong and Rapid Induction of Osteoblast Differentiation by Cbfa1/Til-1 Overexpression for Bone Tissue Engineering Applications. H. Kojima*, T. Uemura. Nanotechnology Research Institute, National Institute of Advanced Industrial Science and Technology(AIST), Tsukuba, Ibaraki, Japan.

Core binding factor alpha-1 (Cbfa1), known as an essential transcription factor for osteogenic lineage, has two major N-terminal isoforms: Pebp2alphaA and Til-1. To study the roles of these isoforms in bone regeneration, we applied an adenoviral vector carrying their genes to transduce primary osteoprogenitor cells in vitro and in vivo. Overexpression of the two isoforms induced rapid and marked osteoblast differentiation, with Til-1 being more effective in vitro, by examination of the alkaline phosphatase activity, calcium content, and Alizarin red staining. Til-1 overexpressing cells/porous biodegradable ceramic composites were transplanted into subcutaneous and bone defect sites in Fischer rats (cultured bone transplantation model) and markedly affected in vivo bone formation and osteoblast markers. The results demonstrated that the reconstitution of bone tissues, such as cortical bone and trabecular bone was accelerated by implantation of Til-1 overexpressing cells/porous biodegradable ceramic composites. Moreover, the new bone formation by Til-1 overexpression appeared to reflect replacement of new bone within the implant boundaries. To ascertain whether implanted Cbfa1 overexpressing cells could differentiate into osteogenic cells to create bone or whether it stimulated the surrounding recipient tissue to regenerate bone, implanted male donor cells were visualized by fluorescent in situ hybridization analysis. The proportion of implanted cells in the presumptive bone forming region was over 80% and did not change throughout from 3 days to 8 weeks after implantation. These findings suggested that the newly formed bone in the porous area of the scaffold is mostly produced by the implanted donor cells or their

derived cells, effectively by Til-1 overexpression. These in vitro and in vivo results suggested that the adenoviral vector encoding the Cbfa1 gene (Til-1) induced a rapid differentiation of osteoblasts in vitro and in vivo and could provide practical and instantaneous applications of bone tissue engineering to patients with skeletal defects.

Disclosures: **T. Uemura**, None.

M169

In Vitro Study of the Collagen and Osteocalcin Gene Expression in Osteoblasts of Patients with Postmenopausal Osteoporosis. S. Ruiz^{*1}, X. Nogués², A. Enjuanes^{*1}, J. C. Monllau^{*3}, E. Cáceres^{*3}, L. Mellibovsky^{*2}, J. Blanch⁴, I. Aymar^{*5}, A. Díez-Pérez². ¹URFOA, IMIM, Barcelona, Spain, ²Internal Medicine Department.URFOA, Hospital del Mar,IMIM,UAB, Barcelona, Spain, ³Orthopedic Department, Hospital del Mar,IMIM,UAB, Barcelona, Spain, ⁴Rheumatology department, Hospital del Mar,IMIM,UAB, Barcelona, Spain, ⁵URFOA, Hospital del Mar,IMIM,UAB, Barcelona, Spain.

In osteoporosis there is a negative balance between bone formation and resorption. This could be explained either by an intrinsic osteoblastic dysfunction or by abnormalities in their extrinsic regulatory elements. To further differentiate between both hypothesis *in vitro* studies of osteoblastic function at a cellular level are needed. *In vitro* measurements of Cbfa1 and BMP-2, implicated in the osteoblastic differentiation, and COL1A1 and osteocalcin gene expression, involved in the bone matrix deposition, were performed in a group of postmenopausal women with osteoporosis and in non osteoporotic controls. Twenty-one cases were included. Nine (age 74±6.3) were osteoporotic by BMD values (WHO criteria) and 12 were non-osteoporotic controls (age 69.7±5.8). Osteoblasts were cultured from trabecular bone of specimens obtained during total knee replacement surgery following the method described by Nacher et al (1). Cell lines were characterized by alkaline phosphatase activity and gene expression of osteocalcin. Cells were cultured in DMEM with 10% FCS for measurement of gene expression levels of Cbfa1, BMP-2, COL1A1 and osteocalcin. In the first subculture, and after synchronization, cells were incubated for 24 hours in basal conditions (0.1% BSA). Extraction of mRNA and reverse-transcriptase reaction (RT) were performed to obtain complementary DNA. Finally, gene expression was measured by real-time PCR. The different results are summarized in the table

	Cases (N=9)	Controls (N=12)	p (ANOVA)
Age	74 (6.3)	69.7 (5.8)	0.367
Lumbar spine BMD(g/cm ²)	0.917±0.130	1.066±0.240	0.004*
Femoral neck BMD(g/cm ²)	0.591±0.073	0.782±0.068	0.000*
Cbfa1 (AU)	2.13 (0.35)	2.24 (0.30)	0.810
BMP-2 (AU)	1.64 (0.32)	1.20 (0.20)	0.232
COL1A1 (AU)	1.29 (0.28)	2.29 (0.28)	0.049*
Osteocalcin (AU)	1.38 (0.15)	0.88 (0.17)	0.053

(*Significant effect, p<0.05. AU:Arbitrary Units)

Conclusions: In women with postmenopausal osteoporosis there is a significant decrease in the gene expression levels of type 1 collagen. This suggest an intrinsic osteoblastic defect that might result in a reduced bone matrix deposition and bone loss.

(1)Nacher M, Aubia J, Serrano S, Marinoso ML, Hernandez J, Bosch J, Díez A, Puig JM, Lloveras J. Bone Miner. Sep;26(3):231-43, 1994.

Disclosures: **S. Ruiz**, None.

M170

Runx2-Mediated Transcriptional Regulation of Osterix in Chondrocytes. Y. Nishio^{*}, Y. Wang^{*}, M. Paris^{*}, E. M. Schwarz, R. J. O'keefe, H. Drissi. Center for Musculoskeletal Research, University of Rochester, Rochester, NY, USA.

Osterix (Osx) and Runx2 are required mediators of skeletal development. Null mice for both proteins present abrogation of bone formation while their cartilage anlagen are fully formed. However, differences in cartilage terminal maturation between Osx and Runx2 knockout mice were reported. Using mouse limb bud-derived cells; we investigated the regulation of Osx in comparison to Runx2 in these progenitors undergoing chondrocyte hypertrophy between 2 and 16 days in culture. Both Osx and Runx2 mRNA are up-regulated throughout chondrocyte differentiation. Furthermore, BMP-2 induction of chondrocyte maturation is accompanied with up-regulation of both Osx and Runx2 transcripts between 4 and 16 days in culture. However, while TGF-beta which delays chondrocyte maturation has a very potent inhibitory effect on Runx2 mRNA at all time points, it only significantly inhibits Osx levels after 12 and 16 days in culture. Together these results suggest a possible temporal cooperative effect between these two factors during chondrocyte maturation. To further determine the transcriptional mechanisms underlying Osx expression, we isolated 2 kb 5' upstream region of the mouse Osx gene. Our 5'-RACE experiments determined a cap site for Osx mRNA at approximately -99 nucleotides upstream of the ATG. Sequence analysis of this TATA-less promoter shows several putative response elements for a variety of bone and cartilage related transcription factors including homeodomain proteins, Sox9, VDRE, SMAD binding elements, as well as zinc finger proteins including Runx and Sp motifs. Transfection of the osterix promoter driving the luciferase reporter gene into C3H10T1/2, ATDC-5 and MC3T3 cells shows a strong basal promoter activity between 0.5 and 2 kb. Further deletion mutant analyses show that the most proximal 0.8 kb of Osx promoter contains the highest activating domains while strong repressive domains were identified between 1.8 and 2kb. However, no significant tissue specificity between chondrocytes, osteblasts and embryonic fibroblasts was observed using these deletion constructs. Two putative Runx sites are overlapping between nt-713 and nt-698. Over-expression experiments indicate that Runx2 significantly transactivates the Osx promoter by at least 2 fold indicating that Osx is downstream of Runx2 in mesenchymal cells. Similarly, over-expression of Osx also

induces its promoter indicating a positive auto-regulation in these cells. Site directed mutagenesis is currently underway to further verify the regulation of Osx by itself and Runx2. Thus our results show for the first time a Runx-mediated pathway by which Osx is regulated in chondrocytes.

Disclosures: **Y. Nishio**, None.

M171

Development of an Osteoblast-Specific DNA Nuclear Targeting Sequence from the Human Type I Alpha 2 Procollagen Promoter for Development of Efficient Plasmid Expression Vectors. D. D. Strong¹, D. A. Dean^{*2}, T. A. Linkhart¹. ¹Research, Loma Linda VA Medical Center, Loma Linda, CA, USA, ²Medicine, Northwestern University, Chicago, IL, USA.

Translocation of plasmid DNA into the nucleus is an important rate-limiting step affecting transgene expression levels in non-dividing cells. Inclusion of a viral (SV40) DNA nuclear targeting sequence (DTS) in plasmid vectors enhances nuclear import efficiency and increases transgene delivery and expression *in vitro* and *in vivo*. Plasmid nuclear import involves cellular transcription factors that bind in the cytoplasm to the viral DTS and translocate the DNA by a nuclear localization signal (NLS) and α/β importin dependent process. To determine if osteoblast specific gene promoters contained transcription factor binding sequences that could enhance osteoblast specific plasmid nuclear targeting by a similar mechanism, a series of promoters from genes specifically and robustly expressed in osteoblasts (osteocalcin, collagen, BSP and Runx2) were cloned into the pGL3-reporter vector and microinjected into the cytoplasm of non-dividing cells. Nuclear import was monitored by *in situ* hybridization with a fluorescein-dUTP-labeled pGL3 vector probe. The plasmids were transfected into dividing osteoblasts, fibroblasts, and chondrocytes to determine promoter activity levels. Osteoblast specific promoter (luciferase) activity was normalized to β -gal activity expressed from the co-transfected pCMV β -gal vector. Each promoter tested demonstrated robust transcriptional activity in osteoblasts (ROS17/2.8) compared to the mouse osteocalcin (mOC) promoter (bp -1393 to +18), set at 100%: rat (r) Col1a1 (bp -2050 to +119) 300% > human (h) Runx2 (bp-345 to +8) 260%> hCol1a2 (bp -267 to +45) 247% hRunx2 (bp -2060 to +8) 240%> hCol1a1 (bp -290 to +172) 120% >hBSP (bp -1917 to +44) 120% >hOC (bp -345 to +28) 104%. By contrast, very low levels of activity were detected after transfection of chondrocytes, fibroblasts and marrow stromal cells. When tested for DNA nuclear import activity, only the hCol1a2 construct, the shortest of the promoters tested, showed nuclear import activity. Further, this DTS activity was osteoblast-specific and only occurred in human and rodent osteoblasts. Site-directed mutagenesis of putative transcription factor binding sites indicated that multiple response elements were required for osteoblast specific nuclear targeting. In conclusion, the hCol1a2 promoter contains a novel osteoblast-specific DTS that can be used for nonviral expression vector construction to increase transgene expression and increase the safety profile by specifically targeting osteoblasts in skeletal tissue with gene therapeutics.

Disclosures: **D.D. Strong**, None.

M172

Regulation of Gene Expression in U2OS Human Osteoblast-Like Cells by TGF β Inducible Early Gene-1. M. Subramaniam¹, J. R. Hawse¹, D. G. Monroe¹, K. Rasmussen^{*1}, M. Oursler², T. C. Spelsberg¹. ¹Biochemistry and Molecular Biology, Mayo Clinic, Rochester, MN, USA, ²Endocrine Research Unit, Mayo Clinic, Rochester, MN, USA.

TGF β inducible early gene-1 (TIEG) was originally identified in human osteoblasts as a primary response gene induced by TGF β . The TIEG gene encodes a 480 amino acid protein that contains three zinc fingers and belongs to the Krüppel-like family of transcription factors. TIEG is known to play a role in the regulation of gene expression, including Smad 2 and 7, and in the repression of cell proliferation. In order to understand the mechanisms by which TIEG mediates such cellular effects as TGF β signaling, cell proliferation and regulation of gene expression, it is essential to first identify those genes that are directly regulated by TIEG. We have created a doxycycline inducible TIEG human osteosarcoma cell line (U2OS) and have utilized microarray analysis to identify specific genes whose expression is altered in the presence of TIEG. U2OS-TIEG cells were treated with doxycycline for 24 hours and total RNA was isolated from control and doxycycline treated cells. Microarray analysis using human focus arrays (Affymetrix) identified 46 genes whose expression was either increased or decreased by 2-fold or greater levels in the presence of TIEG. Of these, 34 genes exhibited increased expression including the leptin receptor, a CCAAT-box-binding transcription factor, cell division cycle 2 and cyclin E2. Another 12 genes exhibited decreased expression in the presence of TIEG including chemokine ligand 1, an actin binding protein, L1 cell adhesion molecule and interestingly, TIEG itself. Confirmation of detected gene expression differences was carried out by semi-quantitative RT-PCR. Since a number of genes involved in the regulation of cell cycle exhibited altered expression levels and, since TIEG is known to play an important role in the regulation of cell proliferation, we sought to determine the effect of TIEG expression on osteoblast proliferation. TIEG expression resulted in a suppression of U2OS cell proliferation with a maximal decrease of 50% at 72 hours. Taken together, these data indicate that TIEG regulates the induction and repression of a number of genes involved in a wide variety of cellular processes and that TIEG expression also results in decreased U2OS cell proliferation.

Disclosures: **M. Subramaniam**, None.

M173

Activation of LEF/TCF- and Runx2- Dependent Transcription by MINT, the Msx2 Interacting Nuclear Matrix Target: Structure-Function Analysis. O. L. Sierra, S. Cheng, A. P. Loewy*, D. A. Towler. Dept of Medicine, Bone & Mineral Diseases, Washington University, St Louis, MO, USA.

MINT augments transcription from the osteocalcin FGF responsive element (OCFRE) via Runx2 activation domain 3. MINT co-localizes with the active form of PolII in the osteoblast nucleus, indicating that MINT functions as a nuclear scaffold for organizing osteoblast transcription. Spen - the Drosophila ortholog of MINT - is required for embryonic responses to Wingless- the Drosophila ortholog of Wnt1 and Wnt3a. Since canonical Wnt/catenin/LEF signaling is critical for osteoblast development, we assessed effects of MINT on LEF/TCF-dependent transcription. We studied signaling in 10T1/2 cells, an osteoprogenitor line that expresses endogenous MINT and responds to Wnt3a. Transient expression of full length MINT(1-3576) augments basal (5- to 12-fold) and Wnt3-stimulated (5-fold) transcription from a LEF/TCF responsive promoter - luciferase reporter, LEFLUC. By contrast, MINT(1-3576) has no effect on Smad-dependent transcription. MINT has 4 major domains: (1) the N-terminal RRM domain; (2) the Msx2 interacting MSXB /MID domain; (3) the Notch- inhibitory / RBP-J binding domain RAM7; and (4) the C-terminal SPOC domain (binds histone deacetylases / HDACs and mediates MINT homodimeric interactions). To better understand structural features of MINT that contribute to transactivation, we generated a series of MINT variants and assessed activity in transient co-transfection assays (nuclear localization signal in all variants). Like MINT(1-3576) and MINT(1-3237), MINT(1-2640) enhanced FGF2 activation of the OCFRE. However, MINT(1-2066) - lacking the MSXB/MID domain - could not augment OCFRE activity. LEFLUC activation was dependent upon MINT residues 2640-3237 (domain containing RAM7); although activating the OCFRE, MINT(1-2640) did not upregulate LEFLUC (suppressed activity). The spen C-terminal domain has been shown to function as dominant negative. Therefore, we generated EYFP-MINT(3101-3576), and studied actions of this nuclear putative dominant negative on OCFRE-LUC and LEF-LUC. EYFP-MINT(3101-3576) abrogated MINT(1-3576) activation of LEF-LUC and OCFRE-LUC. In summary, MINT enhances FGF2- and Wnt3a-dependent transcription, but has little if any direct effect on Smad-dependent transcription. The MINT MSXB/MID domain plays an important role in transcriptional activation of the OCFRE, while the MINT domain 2640 to 3237 containing RAM7 is required for LEFLUC activation. The MINT C-terminus regulates both activities. This suggests that overlapping yet distinct domains of MINT function to integrate nuclear responses to osteogenic transcription factors.

Disclosures: **O.L. Sierra, None.**

M174

The Activated Phospho-CREB Transcription Factor Stimulates BMP-2 Expression in Murine Osteoblast Cells; A Novel Mediator of PTH Action. J. R. Edwards*, M. Zhao, M. Qiao*, S. E. Harris*, G. R. Mundy. Cellular and Structural Biology, UTHSCSA, San Antonio, TX, USA.

Bone morphogenetic protein-2 (BMP-2) and parathyroid hormone (PTH) are known to be important anabolic factors in skeletal tissues. BMP-2 is a bone-derived growth regulatory factor capable of stimulating osteoblast differentiation from mesenchymal precursors and enhancing the activity of mature cells. Intermittent doses of PTH stimulate an increase in bone formation, but the mechanism of action by which this occurs remains largely unknown. PTH is known to activate protein kinase A (PKA) by stimulating cAMP. PKA can phosphorylate the cAMP response element binding protein (CREB), leading to nuclear translocation and gene transcription. Three putative CREB binding sites have been identified within the human BMP-2 promoter region, and in nerve cells, phospho-CREB has been shown to bind the BMP-2 gene. As PTH has been demonstrated to increase phospho-CREB, we investigated the possibility that the anabolic effects of PTH treatment are due to increased BMP-2 transcription and expression through CREB. To test this hypothesis, we used a reporter assay employing a luciferase tagged BMP-2 promoter sequence to assess the activity of the BMP-2 promoter within C2C12 and UMR106 cells. Transfected cells were treated with PTH (10, 50, 100nM), compounds reported to either prevent cAMP degradation (IBMX, 100µM) or inhibit PKA activity (KT-5720, 5µM), or transfected along with either active CREB cDNA or a vector control. RT- and Realtime-PCR was used to accurately assess expression of BMP-2 following treatments. Alkaline phosphatase levels were also determined in CREB transfected and PTH treated cells. CREB transfected UMR106 or C2C12 cells demonstrated up to x40 increase in BMP-2 promoter activity compared to vector controls. This effect was increased in CREB-transfected cultures treated with IBMX. Interestingly, a decrease in BMP-2 promoter activity was observed in samples treated with PKA inhibitor, KT-5720, following CREB transfection. PTH and IBMX treatment of serum-starved C2C12 cells also resulted in an increase in BMP-2 promoter activity compared to vehicle control, in the absence of active CREB cDNA. BMP-2 mRNA expression of CREB transfected cells was initially determined by RT-PCR. Realtime-PCR demonstrated increased BMP-2 expression in cells transfected with CREB. A small increase in alkaline phosphatase activity was also observed in CREB transfected cells compared to vector controls. Our study suggests that PTH stimulates BMP-2 expression in osteoblastic cell lines and this effect is mediated by PKA and CREB. This may be one of the mechanisms by which PTH induces osteoblast differentiation and causes an anabolic effect on bone.

Disclosures: **J.R. Edwards, None.**

M175

Runx2 Regulates Gene Expression of Aromatase a Terminal Enzyme Responsible for Estrogen Biosynthesis. J. Jeong*¹, H. Kim*¹, S. Kang*¹, S. Lee*¹, H. Kim*¹, E. Park¹, S. Kim¹, A. J. van Wijnen², J. L. Stein², J. B. Lian², G. S. Stein², J. Choi¹. ¹Biochemistry, Kyungpook National University, School of Medicine, Skeletal Diseases Genome Research Center, Daegu, Republic of Korea, ²Cell Biology, UMASS Medical School, Worcester, MA, USA.

Runx2 transcription factor is a critical regulator of osteoblast differentiation. Estrogen is another key regulator for bone growth, development and maintenance of adult bone health. Although both Runx2 and estrogen pathways are important in bone homeostasis, the relationship between Runx2 and genes responsible to the production of estrogen in bone has not been clearly understood. Here we show the evidence that aromatase, a terminal enzyme responsible for estrogen biosynthesis in mammals, is one of Runx2 downstream target genes. Aromatase has many tissue specific promoters. To see whether which promoters are active in bone cell lines, we performed RT-PCR using extracted RNA from human chondrosarcoma cell line A4 and osteosarcoma cell line HOS cells. Both cells revealed the activity of bone related promoters; promoter I.6 and promoter I.4. Next, to determine whether Runx2 regulates aromatase gene expression, we cloned promoter I.4 from human genomic DNA and the 0.8 kb Exon I.4 promoter sequence showed three Runx binding sites. In promoter luciferase assay, Runx2 increased aromatase gene promoter activity. In chromatin immunoprecipitation and gel mobility shift assay, endogenous Runx2 binds aromatase promoter. HeLa cells stably transfected with Runx2 expression vector showed higher expression of aromatase protein than that of empty vector stable cells, which was confirmed by western blot analysis. HeLa cells expressing Runx2 also produced estrogen much higher than that of control cells. However, progesterone production was not changed by Runx2 expression. Collectively, these results indicate that aromatase, a key peripheral estrogen production regulator, is one of Runx2 downstream target genes in bone cells.

Disclosures: **J. Choi, None.**

M176

Myeloid Elf-1 like Factor (MEF) Acts as a Repressor in Osteoblast Differentiation. Y. Kim*, B. Kim*, S. Lee*, W. Lee*, H. Ryoo, J. Cho. Biochemistry, School of Dentistry, Kyungpook National University, Daegu, Republic of Korea.

Runx and Ets family proteins control the expression of genes that are critical for biological processes such as proliferation, differentiation and cell death. Previous studies indicated that there are interactions between Runx and Ets family proteins and some of those interactions are important gene expressions and the cell differentiation. Myeloid elf-1 like factor (MEF) is a member of the Ets transcription factor family. In this study, we investigated the role of MEF in osteoblast differentiation. We observed that the expression of MEF suppresses the alkaline phosphatase activity induced by Runx2 and BMP-2 stimulation. We found that the MEF-mediated suppression of osteoblast differentiation is critically related with Runx2 regulation. First, MEF overexpression suppressed the positive effect of Runx2 on osteoblast differentiation probably through the downregulation of positive regulator, Dlx5, and the upregulation of negative regulator, Msx2 and Mab21. The notion is supported by our observations that MEF stimulated the transcription of Msx2 and Mab21 which have repressive function in BMP signaling pathway and suppressed the transcription of Dlx5. Second, we also found that Runx2 and MEF protein physically interact and make a complex, and the interaction is closely related with Runx2 binding to the cis-acting element, OSE2, in osteocalcin promoter. In addition, co-transfection of MEF almost completely diminished the induction of 6xOSE2-luciferase reporter activity by Runx2 transfection. Together our findings suggest that MEF functions as a negative regulator of osteoblast differentiation through functional regulation of Runx2 transcription factor by protein to protein interaction as well as transcriptional regulation on both activators and repressors for osteoblast differentiation.

Disclosures: **Y. Kim, None.**

M177

Expression of Dlx Genes During Osteoblast Differentiation. H. Li*¹, L. Kalajzic¹, S. Suriyapperuma*¹, D. Velonis*², M. S. Islam*¹, M. Mina*², A. C. Lichtler¹. ¹Genetics and Developmental Biology, University of Connecticut Health Center, Farmington, CT, USA, ²Pediatric Dentistry, University of Connecticut Health Center, Farmington, CT, USA.

We and others have shown that Dlx genes are important for osteoblast differentiation. Although Dlx5 single knock out mice display minimal long bone defects, and the Dlx5/6 double mutant embryos have a retarded ossification in both long bones and craniofacial bones, these mice still have significant bone formation. If Dlx genes are necessary for bone formation, then there must be redundant functions of Dlx genes. We believe a comprehensive study of the expression patterns and levels of all the Dlx genes is necessary. We did Q-PCR analysis by using Taqman probes to quantify the relative Dlx gene expression levels at day 2, 5, 7, 14, and 20 of primary mouse calvarial osteoblast cultures from day 5 neonatal pups. Since the amplification efficiencies of all the primers were close to 100%, a comparison of the ddCT value between Dlx genes will give the relative amount of gene expression at a particular time point. Our results show that Dlx4 is not significantly expressed at all the time points; Dlx1 and Dlx6 are slightly higher than Dlx4; Dlx2 is expressed at moderate levels, with highest level at day 2. Dlx5 and Dlx3 are the most highly expressed at all time points and both genes increased dramatically at later culture times. The Dlx3 message levels at day 20 were about 50 times higher than at day 5. Micro-

array and Q-PCR analysis were applied to study the *Dlx3* message level using RNA derived from FACS sorted calvarial cells at different stages from DMP-1-GFP, pOBCol3.6GFP or pOBCol2.3GFP transgenic mice. The *Dlx3* expression levels are about 800 to 2000 fold higher in DMP-1-GFP or 2.3 GFP positive cells from day 17 cultures, which correspond to highly differentiated cells, than Col3.6 GFP positive cells from day 7 cultures, which represent pre-osteoblasts. *In situ* hybridization of *Dlx3* in sections from developing chick calvaria and mandible, detected the *Dlx3* message in the condensing preosteogenic mesenchyme, the osteogenic cells in the periosteum covering the newly formed bone as well as in the osteogenic cells lining the bone marrow spaces in the more advanced stages of bone formation. These results are consistent with our previous studies as well as those of other laboratories that suggest that *Dlx3* may play an important role in regulating bone development. Because the knockout of the *Dlx3* gene is an embryonic lethal, its role in regulating osteoblast differentiation must be studied by creating an osteoblast specific knock out. Revealing the role of the *Dlx* family of genes in osteoblast differentiation will probably require creating combined knockouts of multiple genes.

Disclosures: **H. Li**, None.

M178

Titanium Particles Induce COX-2 through a NFkB Dependent Pathway in Fibroblast-Like Synoviocytes. X. Wei*, H. Drissi, X. Zhang, M. J. Zuscik, E. M. Schwarz, R. J. O'Keefe. Orthopaedics, University of Rochester, rochester, NY, USA.

Osteolysis is a major complication of joint replacement surgery and is related to wear debris particle mediated stimulation of biological pathways and effectors that result in bone resorption. An *in vivo* calvarial bone resorption model has shown that particles fail to stimulate osteolysis in a COX-2 *-/-* mice, but cause abundant bone resorption in wild type mice. Recent *in vitro* studies showed that titanium particles induce RANKL in fibroblast-like synoviocytes (FLS) through a COX2/PGE2 mediated mechanism, and that FLS expressed RANKL supports osteoclastogenesis. In this study, experiments were performed to examine the molecular mechanism involved in COX-2 gene induction. Titanium particles induced both COX-2 mRNA and protein levels in FLS. Luciferase reporter assays showed induction of the COX-2 promoter activity following stimulation with titanium particles. However, activation of the promoter was abolished when NFkB binding sites were mutated. Both Western blot, which demonstrated Ikb degradation, and EMSA, which showed gel retardation of an NFkB consensus oligonucleotide, confirmed activation of NFkB in FLS following titanium stimulation. Chromatin IP analysis was used to demonstrate association of NFkB to the native COX-2 promoter and demonstrated *in vivo* binding of NFkB (p65) to the endogenous COX-2 promoter region following treatment with titanium particles. The role of NFkB in the responsiveness of FLS cells to particles was further investigated in FLS cells stably expressing dominant negative Ikb (mlkB). Both induction of COX-2 by particles and interaction of p65 and COX-2 promoter were abolished in FLS cells expressing mlkB. Altogether the data support the hypothesis that COX2 gene activation by titanium particles in FLS is NFkB dependent. Since COX-2/PGE2 leads to RANKL induction in FLS cells, particle activation of NFkB is a critical target to prevent wear mediated osteolysis.

Disclosures: **X. Wei**, None.

M179

Cooperative Interactions between ATF4 and Runx2/Cbfa1 Stimulate Osteoblast-Specific Osteocalcin Gene Expression. G. Xiao¹, D. Jiang^{*1}, C. Ge^{*1}, Z. Zhao^{*1}, H. Bouls^{*1}, M. Phimpilai^{*1}, X. Yang^{*2}, G. Karsenty². ¹Periodontics/Prevention/Geriatrics, The University of Michigan, Ann Arbor, MI, USA, ²Molecular and Human Genetics, Baylor College of Medicine, Houston, TX, USA.

The role of ATF4 in osteoblast differentiation and bone formation was recently described using ATF4-deficient mice (Yang et al., Cell 117, 387-398, 2004). However, the mechanisms of ATF4 in bone cells are still not clear. In this study, we determined the molecular mechanisms through which ATF4 activates mouse osteocalcin (Ocn) gene 2 (mOG2) expression and mOG2 promoter activity. ATF4 increased levels of Ocn mRNA and mOG2 promoter activity in Runx2-containing osteoblasts but not in non-osteoblastic cells that lack detectable Runx2 protein. However, ATF4 increased Ocn mRNA and mOG2 promoter activity in non-osteoblastic cells when Runx2 was co-expressed. Mutational analysis of the OSE1 (ATF4-binding site) and the two OSE2s (Runx2-binding sites) in the 657-bp mOG2 promoter demonstrated that ATF4 and Runx2 activate Ocn via cooperative interactions with these sites. Pull-down assays showed that ATF4 and Runx2 physically interact in osteoblasts or when both factors were co-transfected in COS-7 cells. Regions within Runx2 responsible for ATF4 binding and activation were identified. This study is the first demonstration that cooperative interactions between ATF4 and Runx2/Cbfa1 stimulate osteoblast-specific Ocn expression and suggests that this regulation may represent a novel intramolecular mechanism regulating Runx2 activity and, thereby, osteoblast differentiation and bone formation.

Disclosures: **G. Xiao**, None.

M180

Mechanoinduction of FosB in Human Bone Marrow Stromal Cells. E. Hesse¹, M. Jagodzinski^{*1}, M. Wehmeier^{*2}, W. C. Horne³, R. Baron³. ¹Trauma Surgery, Hannover Medical School, Hannover, Germany, ²Clinical Chemistry, Hannover Medical School, Hannover, Germany, ³Orthopaedics & Rehabilitation, Yale University School of Medicine, New Haven, CT, USA.

Alternative splicing of the AP-1 family transcription factor FosB generates two truncated isoforms (Δ FosB and Δ 2 Δ FosB) that promote osteoblast differentiation and bone formation when over-expressed in mice. It was recently shown in a mouse model that FosB gene transcription is rapidly induced by mechanical stress applied both *in vivo* and *in vitro*. The aim of this study was to determine the effect of different mechanical strain patterns on FosB expression in human bone marrow stromal cells (hBMSC). hBMSCs were isolated from bone marrow aspirates obtained from seven healthy donors according standard protocols. The cell population was cultured in the presence of ascorbic acid, β -glycerophosphate and dexamethasone to induce osteoblast differentiation. At passage four, cells were plated on silicone dishes and subjected to cyclic mechanical strain (either 2% or 8% deformation, 1 Hz) for one, two or three periods of two hr on day one or for three 2 hr periods on day 4 or day 7, using a computer controlled uni-axial stretching device. Samples were treated independently. RNA was then extracted and FosB mRNA expression was measured by quantitative real-time RT-PCR and normalized to unstrained controls. Statistical analysis was done by ANOVA with pairwise comparison and Mann-Whitney test. FosB expression in samples subjected to mechanostimulation at the 8% strain level was significantly ($p < 0.05$) higher than the levels in matched 2% strain samples under all conditions. In day 1 samples, FosB expression increased progressively with the number of periods of 8% strain. Samples subjected to three periods of 8% strain on day 1, day 4 or day 7 had similar high expression levels. In the day 1 samples subjected to the 2% strain level, one and two periods of strain induced similar small increases in FosB expression, while the third period of strain induced a significant further increase. In contrast to the responses to 8% strain, the response to three periods of 2% strain increased with time in culture to day 4, then decreased to near-basal levels at day 7. Thus, we conclude that axial mechanostimulation induces FosB transcription in human mesenchymal osteoblast precursor cells in a cell-autonomous manner. The response varies with the absolute amount of strain, the number of strain events and, for low strain conditions, the number of days in culture. These data confirm the connection between mechanical strain and FosB expression, suggesting a role of FosB isoforms in mediating the effect of strain on bone formation in humans.

Disclosures: **W.C. Horne**, None.

M181

ATP6i, a Subunit of the Vacuolar Proton Pump, Is Expressed in Osteoblasts, but not Required for their Mineralization. A. F. Schilling, T. Linn^{*}, M. Gebauer^{*}, M. Priemel, J. M. Rueger^{*}, T. Schinke, M. Amling. Trauma Surgery, Hamburg University School of Medicine, Hamburg, Germany.

Approximately 50 % of the cases with autosomal recessive osteopetrosis are caused by mutations of the human ATP6i gene that encodes one subunit of the vacuolar proton pump (V-ATPase) necessary for osteoclastic bone resorption. In osteosclerotic oc/oc-mice a deletion within the murine ATP6i gene results in severe osteopetrosis associated with rickets. To analyze whether the mineralization defect observed in the oc/oc-mice is specific for impaired osteoclastic function, we first compared their phenotype with another mouse model of osteopetrosis, the c-src-deficient mice. Whereas the trabecular bone volume at the age of 2 weeks was strongly increased compared to wildtype littermates in both osteopetrotic models (BV/TV: 61.1 ± 4.2 % in oc/oc vs. 75.6 ± 5.1 % in c-src-/- vs. 15 ± 1.2 % in wildtype mice), the severe mineralization defects were specifically found in the oc/oc-mice (osteoid volume (OV/BV): 8.8 ± 0.8 % vs. 0.2 ± 0.1 % vs. 0.7 ± 0.2 %). So the osteomalacia is specific to ATP6i deficiency and independent of osteoclast dysfunction. Studying osteoblastic gene expression in the course of differentiation using an Affymetrix gene array we found that ATP6i was one of the genes that was strongly induced by mineralization of the cultures, thereby suggesting that ATP6i is required for bone mineralization in a cell-autonomous manner. To analyze this possibility we next assayed ATP6i expression by Northern Blotting. Although, we did find expression of ATP6i in mineralizing osteoblasts, we observed that the expression level was markedly lower compared to osteoclasts. This finding was confirmed by *in-situ* hybridization where ATP6i expression was readily detectable in osteoclasts, but virtually absent in osteoblasts as well as in growth plate chondrocytes. Most importantly however, when we analyzed primary osteoblasts derived from oc/oc-mice *ex vivo*, we found that they mineralized equally well as wildtype cultures. Taken together, these results suggest that the severe defects of bone mineralization in the absence of ATP6i are not caused by cell-autonomous defects of osteoclasts or osteoblasts. In contrast, it is most likely, that they are a solely a consequence of an impaired calcium homeostasis, since oc/oc-mice are hypocalcemic, unlike the c-src-deficient mice (6.5 ± 0.4 mg/dl vs. 9.3 ± 0.5 mg/dl vs. 9.2 ± 0.6 mg/dl).

Disclosures: **A.F. Schilling**, None.

M182

Jun B as a Key Mediator of PTHrP Actions on Cementoblasts. J. E. Berry^{*1}, E. L. Ealba^{*1}, N. S. Datta¹, G. J. Pettway^{*1}, E. Swanson^{*2}, M. J. Somerman², L. K. McCauley¹. ¹University of Michigan, Ann Arbor, MI, USA, ²University of Washington, Seattle, WA, USA.

The process of remodeling requires a balance of osteoclast and osteoblast function, and is mediated through OPG and RANKL. In the periodontium, this balance is also important for tooth eruption and protection from root resorption. The focus of this study was to determine the role of PTHrP in mediating cementoblast effects on this process. Assays revealed that immortalized murine cementoblasts express OPG and RANKL, and expression is altered by PTHrP in a similar manner as osteoblasts. PTHrP (0.1 μ M) treatment caused a 5-fold reduction in OPG and a 9-fold increase in RANKL, by ELISA. In parallel experiments, cementoblasts treated with PTHrP were evaluated by ELISA (nuclear isolates) and Northern blot for AP-1 transcription factors. The mRNA and protein of all Fos family members and JunB, but not c-Jun or JunD, were elevated. To further investigate the specific effects of JunB, cementoblasts were stably transfected with an expression plasmid containing full-length junB or a vector control plasmid. Untransfected cementoblasts and cells transfected with vector or junB were treated with vehicle or PTHrP. Cell lysates from untransfected and vector transfected cells showed a 4-fold decrease in OPG levels with PTHrP treatment, while junB transfectants had control levels of OPG less than the lowest level seen in treated control cells. OPG expression in the junB transfectants was not altered by addition of PTHrP, suggesting junB overexpression was mimicking a PTHrP down-regulated OPG state. Additionally, co-cultures with RAW cells indicated that junB transfectants were better able to support osteoclastogenesis than control cells, as evaluated by TRAP staining and enumeration. Investigation of downstream effects of JunB overexpression showed levels of BSP and osterix mRNA were dramatically reduced as compared to controls, and in vitro mineralization as measured by von Kossa staining was abolished, suggesting JunB restricts cementoblast differentiation. Western blot assay of cell cycle proteins showed an increase of cyclins D1 and A, indicating a shift in proliferation capacity of overexpressing cells. Control and JunB overexpressing cells implanted subcutaneously in nude mice also exhibited distinct differences, with JunB showing less mineralization and greater cell numbers. These data suggest that JunB plays a role in modulating osteoclastogenesis via OPG and restricting cementoblast maturation. Importantly, the fact that cementoblasts are very sensitive to PTHrP and JunB indicates that they may normally be responsible for limiting cementum remodeling, but can be induced to support odontoclastogenesis under certain circumstances.

Disclosures: **J.E. Berry, None.**

M183

T-box 3, a Transcription Factor, Is an Important Regulator of Osteoblast Proliferation. K. Govoni, J. Rung-Aroon^{*}, D. J. Baylink, S. Mohan. JLP VAMC and LLU, Loma Linda, CA, USA.

T-box (Tbx) genes are a family of transcription factors known to be involved in regulating several key developmental processes in various tissues. We identified Tbx3 as an acute growth hormone (GH) responsive gene using whole genome microarray analysis of RNA extracted from bones of GH-deficient (*lit/lit*) mice after a single injection of GH. Little is known about Tbx3, except that a mutation of Tbx3 results in human ulnar-mammary syndrome. In addition to the microarray data, we have found that Tbx3 expression is increased by GH, bone morphogenic protein-7, and Wnt3a in mouse osteoblast cells. Based on these data, we proposed the hypothesis that Tbx3 is an important regulator of osteoblast cell proliferation. To test this hypothesis, we used small interfering (si) RNA, to knock-down the expression of Tbx3 and evaluated the consequence on proliferation of MG63 human osteosarcoma cells. Using non-silencing Alexa Fluor 488-labeled control siRNA and transfection reagent (RNAiFect), we determined that with 300nM siRNA, our transfection efficiency was 60 to 70%. Using an alamarBlue assay, we determined that Tbx3 siRNA reduced osteoblast cell number 20 to 30% ($P < 0.01$). In addition, Tbx3 siRNA reduced serum-induced cell number by 30 to 40% ($P < 0.01$). No reduction in cell number was observed with transfection reagent alone or siRNA in the absence of transfection reagent. To determine if the effect of siRNA on cell number was due to decreased cell proliferation and not due to increased apoptosis, we measured DNA synthesis by determining [³H]thymidine incorporation into the cell, as well as, caspase activity, a measure of apoptosis. DNA synthesis decreased by 25 to 45% ($P < 0.01$) by Tbx3 siRNA in the presence of serum and no effect of siRNA was observed on caspase activity ($P > 0.1$). These data suggest that the decreased cell number, was due to inhibition of cell proliferation rather than induction of cell death. In conclusion, blocking Tbx3 expression inhibits both basal and serum-induced osteoblast cell proliferation, but does not induce cell death. Therefore, we predict that Tbx3 may be an important intracellular mediator of growth factor action on osteoblast proliferation.

Disclosures: **K. Govoni, None.**

M184

Twist Dimer Selection Regulates Cranial Suture Patterning and Fusion. J. Connerney^{*}, V. Andreeva^{*}, Y. Leshem^{*}, C. Muentener^{*}, M. Mercado^{*}, D. B. Spicer. Center for Molecular Medicine, Maine Medical Center Research Institute, Scarborough, ME, USA.

Haploinsufficiency of the basic-Helix-Loop-Helix (bHLH) transcription factor TWIST results in premature closure of the cranial sutures, termed craniosynostosis, however the mechanism underlying this defect is unclear. Here we have tested the hypothesis that the activity of Twist is dependent on its dimer partner and Twist dimer formation is

dynamically regulated in the cranial sutures. The cranial sutures are the growth centers separating the bones of the skull and are composed of two opposing osteogenic fronts and an intervening mesenchyme. Based upon the expression patterns of Twist and other HLH genes within the cranial sutures we hypothesized that Twist forms homodimers in the osteogenic fronts and Twist/E protein heterodimers in the mid-sutures. We have tested this hypothesis by determining if genes that are differentially regulated by these dimers are expressed in the predicted domains within the sutures. Our results support this hypothesis and importantly we have found that the Twist dimers differentially regulate the expression of mediators of the signaling pathways that regulate suture patency. Furthermore, Twist haploinsufficiency alters the ratio between these dimers, favoring an increase in homodimers, which results in an expansion of the osteogenic fronts and suture fusion. Finally, we are able to inhibit suture fusion in Twist +/- mice by promoting the formation of Twist/E protein heterodimers by either increasing E protein levels or decreasing the levels of the HLH inhibitor Id. Therefore, we have begun to provide a mechanistic understanding of craniosynostosis and have identified dimer partner selection as an important mediator of Twist function.

Disclosures: **D.B. Spicer, None.**

M185

Lef1 Overexpression Prevents Late Osteoblast Differentiation. R. A. Kahler¹, J. J. Westendorf². ¹Graduate Program in Microbiology, Immunology and Cancer Biology, University of Minnesota, Minneapolis, MN, USA, ²Department of Orthopaedic Surgery, University of Minnesota, Minneapolis, MN, USA.

Recent studies have shown that the Wnt signaling pathway is important for normal bone development and osteoblast function. Lef1 is a nuclear effector of the Wnt signaling pathway. Lef1 binds to and represses Runx2-mediated activity of the osteocalcin promoter. As osteoblast differentiation proceeds, Lef1 expression declines. These observations led to the hypothesis that Lef1 may repress the expression of late osteoblast differentiation genes and that the decline in Lef1 expression during differentiation is necessary to facilitate the upregulation of osteocalcin and other late differentiation genes. In order to study the biological role of Lef1 in osteoblast differentiation, we employed RNAi to reduce Lef1 expression in MC3T3 preosteoblasts. Stably Lef1-suppressed MC3T3 cells did not have any significant changes in proliferation or cell cycle. Differentiating Lef1-suppressed osteoblasts express differentiation markers, including alkaline phosphatase, osteocalcin and mineralization three to four days earlier than control cells. In order to determine what effect Lef1 overexpression would have on osteoblast differentiation, we have produced an MC3T3 cell line overexpressing Lef1. GFP expression via an internal ribosomal entry site was used to select Lef1 overexpressing cells as well as the empty vector control cells. Lef1 overexpression was confirmed using electrophoretic mobility shift assay as well as quantitative RT-PCR. Lef1 overexpression did not significantly alter cell proliferation. When induced to differentiate, Lef1 overexpressing cells have lower expression of the early differentiation marker alkaline phosphatase compared to control GFP cells and do not mineralize. Quantitative RT-PCR confirmed that expression of the late osteoblast differentiation genes, osteocalcin and bone sialoprotein, are delayed and decreased in Lef1 overexpressing cells compared to control cells. Runx2 levels, however, were not changed. These results suggest that Lef1 expression is regulated during osteoblast differentiation and that Lef1 expression must decrease in order to allow osteoblast differentiation to proceed.

Disclosures: **R.A. Kahler, None.**

M186

Large-Scale Proteomic and Microarray Analysis of Inorganic Phosphate Treated MC3T3-E1 Cells Reveals Dynamic Changes in Protein Regulation and Gene Expression. G. R. Beck¹, C. E. Camalier^{*1}, K. A. Conrads^{*1}, K. A. Simpson^{*1}, D. A. Lucas^{*2}, T. D. Veenstra^{*2}, T. P. Conrads^{*2}. ¹Center for Cancer Research, National Cancer Institute, Frederick, MD, USA, ²Laboratory of Proteomics and Analytical Technologies, SAIC-NCI, Frederick, MD, USA.

We have recently identified inorganic phosphate that is generated during osteoblast differentiation as an important signaling molecule necessary for pre-osteoblasts to reach a mineralization competent state. We have taken a systems approach to understanding the influences of inorganic phosphate on the process of differentiation and mineralization. To this end we have conducted microarray, proteomics, inhibitor and promoter studies on MC3T3-E1 cells treated with 10 mM inorganic phosphate for times ranging from 15 minutes to 24 hours. Our results reveal dynamic changes in signal transduction pathways, gene expression and protein levels starting within the first 15 minutes of exposure to elevated inorganic phosphate and extending through 24 hours. The products of the early phosphate responsive genes range in function from transcriptional activators to effectors of signaling pathways and include, among others members of the AP-1 transcription factor family. The increased expression of the majority of these immediate early genes, do not require protein synthesis and are ERK1/2 dependent. Ultimately changes in the cell phenotype are regulated by changes in both protein level and function. To evaluate downstream changes in the proteome in response to elevated phosphate we have used cleavable isotope-coded affinity tag (cICAT) labeling. This technique allows for the identification and determination of changes in relative abundance of thousands of proteins from cell lysate. A cICAT study of MC3T3-E1 cells treated with inorganic phosphate for 24 hours identified over 2500 proteins, 16% of which were altered by greater than 1.75 fold. A number of the identified phosphate-regulated proteins are involved in extracellular matrix function and cell metabolism. Taken together with the microarray studies the results suggest a role for inorganic phosphate as a signaling molecule capable of dynamically regulating gene expression and protein levels through discrete signaling networks. One

important effect on cell function and differentiation appears to be the regulation of the transition of the extracellular matrix from formation to maturation to mineralization. These studies not only begin to shed light on the mechanisms by which inorganic phosphate functions as a signaling molecule in osteoblast differentiation and mineralization but also demonstrate the power of large-scale systems analysis as an approach to understanding changes in cell function.

Disclosures: **G.R. Beck**, None.

M187

The Bone Phenotype of ICER Transgenic Mice Is not due to Alterations in ATF4 Expression. **T. K. Chandhoke**, **B. E. Kream**. Medicine, University of Connecticut Health Center, Farmington, CT, USA.

Inducible cAMP early repressor (ICER) is a member of the CREM transcription factor family and serves as a dominant negative regulator of cAMP-mediated transcription. ICER contains a basic leucine zipper (bZIP) region for DNA binding and dimerization. PTH has been shown to induce ICER expression potently and transiently in cultured osteoblasts and in calvariae *in vivo*. To establish the role of ICER in bone, we previously developed transgenic mice to overexpress ICER *in vivo* by cloning ICER cDNA with an N-terminal FLAG epitope downstream of a 3.6 kb fragment of the rat Col1a1 promoter (pOBCol3.6-ICER), targeting ICER overexpression broadly to cells of the osteoblast lineage. ICER transgenic mice showed reduced body size and weight, a dramatic reduction in trabecular bone parameters and disruption of cortical bone integrity. Femurs showed a marked reduction in osteocalcin (OC) expression while Col1a1 and bone sialoprotein (BSP) expression was less affected. *Ex vivo* analysis of osteogenic bone marrow stromal cell cultures showed reduced expression of Col1a1, BSP and OC as well as reduced mineralization. The aim of the present study was to determine whether the bone phenotype of ICER mice is due to alterations in ATF4 expression and/or function. *Atf4*-deficient mice display a distinct skeletal phenotype that resembles ICER transgenic mice in their reduction of trabecular bone volume, impaired osteoblast function and loss of OC expression *in vivo*. To examine whether ATF4 is in the ICER regulatory pathway, we examined ATF4 protein expression at days 14 and 21 in primary mouse calvarial osteoblasts (mCOB) cultured to confluence and then treated with ascorbate and β -glycerophosphate. Western blot analysis did not show a significant change in ATF4 protein expression, suggesting it may not be regulated by ICER. ATF4 has also been shown to post-translationally modify type I collagen synthesis. To determine if type I collagen protein synthesis was disrupted in ICER transgenic mice, reflecting an ATF4-like action, we examined collagen protein synthesis assessed by ^3H -proline incorporation into cultured neonatal mouse calvariae. There was no significant difference in percent collagen synthesis in ICER calvariae compared to WT. While these results suggest ATF4 expression is not affected by ICER, it is possible that ICER binds ATF4, a bZIP protein, and inhibits some of its osteoblast functions. Currently, co-immunoprecipitation experiments of ICER and ATF4 in mCOB cultures are being utilized to better understand the potential interaction of these two transcription factors. In addition, it is possible ICER binds to a variety of other bZIP transcription factors, disrupting their function.

Disclosures: **T.K. Chandhoke**, None.

M188

Transcription of the RUNX2/CBFA1 Gene Involves a SWI/SNF-Independent and BMP2-Enhanced Chromatin Remodeling at the P1 Promoter. **F. Cruzat**^{*1}, **A. Villagra**^{*1}, **J. Olate**^{*1}, **A. van Wijnen**², **J. Lian**², **G. Stein**², **J. Stein**^{*2}, **A. Imbalzano**^{*2}, **M. A. Montecino**¹. ¹Departamento de Bioquímica y Biología Molecular, Universidad de Concepción, Concepción, Chile, ²Department of Cell Biology, University of Massachusetts Medical School, Worcester, MA, USA.

The Runx2 transcription factor is essential for skeletal development as it up-regulates the expression of several bone-related genes. It has been indicated that the promoter P1 controls the expression of the Runx2-II isoform in osteoblastic cells. However, the specific molecular mechanisms involved in this tissue-specific regulation have not been definitively established. Changes in chromatin organization accompany transcriptional activity of eukaryotic genes. These chromatin-remodeling events can be mediated by the SWI/SNF complex, which alters chromatin structure in an ATP-dependent manner. Here, we have generated osteoblastic cell lines that inducibly express an ATPase-defective Brg1 catalytic subunit which forms inactive SWI/SNF complexes. The presence of these complexes result in inhibition of both expression and chromatin remodeling of bone-phenotypic markers expressed at late stages of osteoblast differentiation. In contrast, these inactive complexes neither affect RUNX2 transcription nor reduce chromatin remodeling at the P1 promoter, indicating that both processes are independent of SWI/SNF activity. Additionally, we find that the BMP2-dependent induction of Runx2 transcription in C2C12 myoblastic cells is accompanied by a significant enhancement in nuclease hypersensitivity at a highly specific region of the proximal P1 promoter, also in an SWI/SNF-independent manner. Together with previous results, our findings indicate that RUNX2 transcription requires a SWI/SNF-independent chromatin-remodeling event that sets the gene for transcription during early stages of development.

Disclosures: **F. Cruzat**, None.

M189

Ror2: A Novel Regulator of Osteoblast Differentiation. **J. Billiard**, **Y. Liu**^{*}, **R. A. Bhat**, **A. Mangine**^{*}, **R. A. Moran**^{*}, **L. M. Seestaller-Wehr**^{*}, **P. V. N. Bodine**. Women's Health Research Institute, Wyeth Research, Collegeville, PA, USA.

Ror2 is an orphan receptor tyrosine kinase with no signaling pathway identified. Mutations in the Ror2 gene cause severe skeletal defects in humans and mice. We have previously shown that Ror2 is expressed in human osteoblasts and is strongly regulated during differentiation being almost undetectable in pluripotent mesenchymal stem cells (hMSC) and increasing >30-fold after 21 days in osteogenic medium. We also showed that in late stages of differentiation, modeled by our collection of human conditionally immortalized osteoblastic (HOB) cell lines, Ror2 is highly expressed in committed proliferating pre-osteoblasts, but disappears in osteocytes. Thus Ror2 peaks in mid-stages of osteoblastic differentiation. Here we over-expressed Ror2 in cells that have the lowest endogenous levels of the receptor, undifferentiated hMSC and pre-osteocytes, and assessed its effects on markers of osteoblastic differentiation. We used adenoviral constructs to over-express Ror2, kinase-dead mutant Ror2KD, or β -galactosidase (β -gal) in hMSC and monitored matrix mineralization over 21 days in presence of ascorbic acid and β -glycerophosphate. Alizarin red histochemistry revealed that by day 9, Ror2-infected cells formed ~4 times more mineralized matrix than did the β -gal-infected controls. This effect was independent of the receptor kinase activity, since it was also observed in Ror2KD-infected cells. Infection with Ror2 or Ror2KD viruses also strongly promoted matrix mineralization in MC3T3-E1 murine osteoblast-like cells. Thus Ror2 expression increased formation of an extracellular matrix that undergoes mineralization, the ultimate phenotypic expression of an osteogenic tissue. Next, we stably transfected the HOB pre-osteocytic cell line with Ror2, Ror2KD, or empty vector and assessed alkaline phosphatase (AP) activity, osteocalcin secretion and apoptosis. In 3 independent clones, Ror2 over-expression inhibited AP activity by 80%, potentiated osteocalcin secretion by 3-fold and increased apoptosis by 1.6-fold. All these changes, including the fall in AP activity, are consistent with Ror2 promoting differentiation in late stages of human osteoblast formation. These changes were also observed in the Ror2KD line, but Ror2KD appeared less efficacious than the wild-type kinase in causing these effects. In summary, our studies identify Ror2 as a new regulator of osteoblast survival and differentiation, suggesting a novel role for this orphan receptor in bone formation.

Disclosures: **J. Billiard**, Wyeth Research 3.

M190

C/EBP α Isoforms Regulate Differentiation of Mesenchymal Stem Cells into Osteoblasts and Adipocytes. **M. Ueda**^{*}, **K. Hata**^{*}, **F. Ikeda**^{*}, **T. Matsubara**, **R. Nishimura**, **T. Yoneda**. Dept Biochem, Osaka Univ Grad Sch Dent, suite, Japan.

Osteoblasts and adipocytes share the common precursors of undifferentiated mesenchymal stem cells. The molecular mechanism that controls the commitment of the mesenchymal stem cells to osteoblasts and adipocytes are yet to be elucidated. Recent studies have shown that the transcription factor CCAAT/enhancer-binding protein (C/EBP) β and C/EBP δ promote not only adipogenesis but also osteoblastogenesis, suggesting the importance of C/EBP family proteins in the regulation of osteoblastogenesis as well as adipogenesis. Of note, C/EBP α , which is involved in the regulation of the late stages of adipocytic differentiation, is also shown to stimulate osteoblast differentiation. C/EBP α has two isoforms, namely p20 and p30, which completely or partially devoid of the transcription activation domain, respectively. Role of these two isoforms in mesenchymal cell differentiation is unknown. In the present study, we examined this using the C3H10T1/2 pluripotent mesenchymal cells. Western blot analyses showed that p20 and p30 are expressed in cells of osteoblast lineage. To examine whether p20 and p30 affect the differentiation of mesenchymal cells, cDNA of these molecules were overexpressed in C3H10T1/2 cells using an adenovirus system. P20 and p30 enhanced BMP2-induced osteoblastic differentiation of C3H10T1/2 cells, despite the fact that both isoforms have no transcription activation domain. To understand the molecular mechanism underlying this, interactions of p20 or p30 with Runx2 were examined. Overexpression of p20 or p30 dramatically enhanced Runx2-induced osteoblast differentiation. In contrast, p20 or p30 did not influence osterix-induced osteoblast differentiation. Consistent with these results, we found that p20 or p30 co-immunoprecipitated with Runx2. These results suggest that p20 and p30 control osteoblastogenesis in physical cooperation with Runx2. We next investigated the role of p20 and p30 in adipogenesis. Overexpression of C/EBP α induced adipocyte differentiation of C3H10T1/2 cells, whereas p20 or p30 showed no effects on adipogenesis. Of interest, overexpression of p20 or p30 inhibited adipogenesis induced by C/EBP α or C/EBP β / δ . In contrast, p20 or p30 did not affect the adipogenesis induced by PPAR γ , a critical transcription factor that regulates the late stages of adipogenesis. The results suggest that p20 or p30 specifically inhibits the C/EBP-induced adipogenesis in a dominant-negative fashion. In conclusion, our results suggest that C/EBP α isoform p20 and p30 are important transcription factors that control the direction of mesenchymal stem cell differentiation toward osteoblasts and adipocytes.

Disclosures: **M. Ueda**, None.

M191

Effects of IL-23 and IL-27, Newly Identified IL-12-Related Cytokines, on Osteoblasts and Osteoclasts. S. Kamiya^{*1}, K. Ono^{*1}, T. Ohwaki^{*2}, N. Morishima^{*2}, M. Asakawa^{*2}, T. Yoshimoto^{*2}, S. Wada^{*1}. ¹Clinical Sciences, Josai International University, Chiba, Japan, ²Intractable Immune System Disease Research Center, Tokyo Medical University, Tokyo, Japan.

Objective : Interleukin (IL)-23 and IL-27 is a novel IL-12 family member that plays a role in the regulation of T helper 1 differentiation. IL-27 induces proliferation and synergizes with IL-12 in interferon (IFN)-gamma production from naive CD4+ T cells, whereas IL-23 stimulates IFN-gamma production and proliferation in memory CD4+ T cells. Cytokines, such as IL-12 and IFN-gamma, are shown to be involved in bone metabolism, however the effects of IL-23 and 27 have not been fully clarified. In the present study, we have examined the effects of IL-23 and 27 on bone metabolism. Methods: Using primary calvarial osteoblasts (OB), derived from neonatal (0- to 2-day-old) ddY mice, the analysis of tyrosine phosphorylation of signal transducer and activator of transcription (STAT) 3 (Western blot), cell proliferation (WST-8 assay), alkaline phosphatase (ALP) activity (p-nitrophenylphosphate degradation assay), mineralization (von Kossa staining), and mRNA (ALP, type I procollagen, osteocalcin, and Runx2) expression (RT-PCR) in the presence or absence of IL-23 and 27 was investigated. We furthermore examined the effects of IL-23 and 27 on RANKL expression (flow cytometry) on OB and osteoclastogenesis (tartrate-resistant acid phosphatase staining) in the co-cultures of OB and bone marrow cells. We also compared the effects of IL-23 and 27 with those of IL-6/soluble IL-6R. Results: When OB were treated with IL-23 and 27 for 1h, tyrosine phosphorylation of STAT3 was clearly identified. However, neither IL-23 nor 27 affected OB proliferation, ALP activity, mineralization and OB specific mRNA expression as compared with those of control. These interleukins did not stimulate RANKL expression and osteoclastogenesis in co-cultures. Osteoclastogenesis induced by 1,25(OH)2D3 was neither affected by IL-23 nor 27. In contrast, IL-6 induced tyrosine phosphorylation of STAT3 in OB as well as IL23 and 27, but also increased ALP activity and its mRNA expression. IL-6 also inhibited mineralization at day 12-15 and induced RANKL expression. Osteoclastogenesis was also found to increase in co-culture system. There was a good correlation between osteoclastogenesis and RANKL expression on OB. Conclusions: IL-23 and 27 induced tyrosine phosphorylation of STAT3 in OB, but significant roles of the signaling have not been identified. We are now further investigating whether the modulation of intracellular signaling by IL-23 and 27 affects other cellular functions of OB, and the contribution of T cells to osteoclastogenesis in the presence of IL-23 and 27 as well.

Disclosures: **S. Kamiya**, None.

M192

DKK-1 Inhibits Differentiation of Primary Human Osteoblastic and MC3T3.E1 Cells in Culture. V. Shalhoub, J. Li^{*}, W. Qui^{*}, D. Martin^{*}, S. Simonet, D. Lacey, W. Richards. Metabolic Disorders, Amgen Inc, Thousand Oaks, CA, USA.

Mutations in LRP5, a component of the canonical Wnt signaling pathway, result in high and low bone phenotypes. Dkk-1 inhibits LRP signaling by bridging LRP and Kremen. Dkk/LRP is then endocytosed along with Kremen, thus interfering with the Wnt-induced interaction of frizzled with LRP. Recently, Dkk-1 over-expressing transgenic mice were shown to have decreased bone mass, supporting a role for DKK-1 as an inhibitor of LRP5 signaling in bone. Thus, the purpose of this study was to examine the direct effects of Dkk-1 on osteoblastic differentiation in culture. MC3T3.E1 cells are pre-determined osteoblastic cells. Over a period of 4 weeks in the presence of differentiation medium (50 ug/ml ascorbic acid and 10 mM beta-glycerol-phosphate), MC3T3.E1 cells up-regulate alkaline phosphatase (AP) and deposit mineral into their extra-cellular matrix. MC3T3.E1 cells were treated with murine Dkk-1 (0, 0.1, 1.0, 10, 100, 1000 ng/ml), initiated one day after plating, and every 48 hrs for three weeks. On days 2, 7, 15, 21, cells were stained for AP and mineral (von Kossa). In addition, AP activity, and calcium and protein accumulation were measured. In the presence of Dkk-1, AP and mineral were decreased in a time and dose dependent manner. For example, at 21 days, 54% and 72% decreases in calcium accumulation were observed with Dkk-1 treatment (1 and 100 ng/ml doses, respectively). Total cellular protein levels showed no differences with dose at any time. Primary adult human osteoblastic cells from femoral bone (41 year old donor), treated with Dkk-1 for 4 weeks similarly showed decreased mineral accumulation. Dkk-1 transcripts were found in the primary adult human osteoblastic cells, as well as adult human bone (39 year old donor). In conclusion, this study supports a role for Dkk-1 as a negative regulator of bone mass in osteoblastic cells in culture and in human bone.

Disclosures: **V. Shalhoub**, None.

M193

Increasing BMP Responsiveness in Human Mesenchymal Stem Cells *In Vitro* by Addition of the Osteoinductive LMP-1 Gene. M. Viggswarapu, M. Bargouti^{*}, M. Teklemariam^{*}, N. Baker^{*}, C. Rogers^{*}, L. Zhu^{*}, L. Titus, S. D. Boden. Orthopedics, Emory University, Decatur, GA, USA.

BMPs promote the differentiation of osteoprogenitor cells, and also induce osteogenesis in bone marrow stromal cells (MSCs) from rats and mice. However, compared to results with animal models, BMPs are relatively inefficient in inducing human MSCs to undergo osteogenesis, and are much less effective in promoting bone formation in human clinical trials. Previous studies indicated that, while human MSCs respond to Dex with elevated levels of the osteoblast marker alkaline phosphatase, most isolates of human MSCs fail to show alkaline phosphatase induction in response to BMP-2,-4 and -7. LIM Mineralization

Protein-1 (LMP-1) is an intracellular regulatory protein that can induce the expression of multiple BMPs and promote osteoblast differentiation *in vitro* and *in vivo*. The purpose of this study was: 1) To determine if LMP-1 can increase the responsiveness of human MSCs to BMP-2 as evidenced by increasing osteoblastic markers, and 2) To determine if LMP-1 can potentiate BMP-2 induction of mineralization by human MSC cultures. Human MSCs were expanded to passage 4 in the absence of Dex, seeded at 3x10⁴ cells/well in a six well plate in MSCBM media from Cambrex, and grown overnight. Some cells were infected for 30 min with Ad5/F35LMP-1 (5-10 pfu/cell) and grown for 72hrs with and without 100 ng/ml rhBMP-2. We used the chimeric adenoviral vector, Ad5/F35, which has been shown to transduce human hematopoietic stem cells and bone marrow hMSCs more effectively than Ad5 vectors. Treatment of cells with Ad5/F35LMP-1 (5-10 pfu/cell) plus 100 ng/ml rhBMP-2 dramatically induced mineralization observed by Alizarin red staining but neither rhBMP-2 nor LMP-1 alone induced mineralization in hMSCs on day 21. Similarly, neither BMP-2 nor LMP-1 alone increased alkaline phosphatase mRNA levels, but the alkaline phosphatase mRNA was increased 13 to 15-fold in cells treated simultaneously with both agents. BMP-2 alone increased the expression of the bone specific gene, osterix, 88 fold, but addition of BMP-2 to human MSCs overexpressing LMP-1 resulted in a synergistic 444 fold increase. Thus, concurrent exposure of human MSCs to LMP-1 enabled an ineffective dose of BMP-2 to facilitate bone formation. These data show that a non-responsive dose of BMP-2 co-administered with a non-osteoinductive dose of Ad5/F35LMP-1 resulted in a significant amount of mineralized bone formation in hMSC cultures. This key observation suggests that lower doses of rhBMP-2 can still have significant effects in the presence of genetically engineered cells.

Disclosures: **M. Viggswarapu**, None.

M194

Adherent Endotoxin Inhibits Spreading and Proliferation of Osteoblasts. J. L. Nalepka^{*}, E. M. Greenfield. Orthopaedics, CWRU, Cleveland, OH, USA.

We have previously shown that adherent endotoxin exists on the surfaces of orthopaedic implants sterilized, processed and packaged by a major implant manufacturer. In addition, early failure of certain lots of implant components has been associated with adherent endotoxin. The current study was designed to examine the effects of adherent endotoxin on attachment, spreading, proliferation and differentiation of osteoblasts. For this purpose, MC3T3-E1 preosteoblastic cells were cultured on titanium alloy (Ti) discs with high and low levels of adherent endotoxin. Adherent endotoxin did not affect cellular attachment assessed by measuring the DNA content of attached cells 15-60 minutes after plating. However, fluorescence microscopy of cells stained with phalloidin or CMdii showed that adherent endotoxin inhibited spreading. Thus, fewer cells spread on high endotoxin discs than on low endotoxin discs (6.2-fold and 4.3-fold less at 30 minutes and 24 hours respectively, $p < 0.02$). At 24 hours, large three dimensional aggregates containing 5-20 cells formed on high endotoxin discs. High endotoxin also completely blocked the 10-fold increase in cell number that occurs on low endotoxin discs between days 2 and 6. This is partially due to differences in proliferation since BrdU incorporation was 3.0-fold less on high endotoxin discs ($p < 0.0001$). In contrast, cell death assessed by measuring LDH release was not increased on high endotoxin discs. High endotoxin also significantly reduced total alkaline phosphatase activity on days 8-30 ($p < 0.05$). This is due to a decreased number of mature osteoblasts since alkaline phosphatase activity normalized to cell number was not affected. In conclusion, this study showed that adherent endotoxin inhibits spreading and proliferation of osteoblasts and thereby reduces the number of mature osteoblasts. These findings are consistent with the concept that adherent endotoxin impairs osseointegration *in vivo* and demonstrate that inhibition of cell spreading is the initial effect of adherent endotoxin.

Disclosures: **J.L. Nalepka**, None.

M195

Functional Responses of Osteoblastic Cells to Stimulation by Strontium. T. C. Brennan^{*1}, M. M. Muir^{*1}, A. D. Conigrave^{*2}, R. S. Mason¹. ¹School of Medical Sciences and Institute for Biomedical Research, University of Sydney, Sydney, Australia, ²School of Molecular and Microbial Sciences, University of Sydney, Sydney, Australia.

The divalent cation, strontium (Sr²⁺) has been shown to increase bone formation, decrease bone resorption and reduce the risk of fracture in postmenopausal women. The mechanisms underlying these actions of Sr²⁺ have not yet been elucidated. This study was aimed at evaluating some of the functional responses of the human osteoblast-like cell line, MG63, to stimulation by Sr²⁺. MG63 cells were cultured in DMEM supplemented with 10% FBS then adapted to serum-free medium for 24 hours before experimental treatments were added. The tested concentrations of Sr²⁺ were 0.01 to 1 mM in the presence of 1 mM Ca²⁺. Tritiated thymidine incorporation was used to measure the proliferative responses of the cells to Sr²⁺. Cell proliferation increased 2- to 3-fold as a function of increasing concentrations of Sr²⁺ ($p < 0.001$). The EC₅₀ was < 0.1 mM, well within the therapeutic range. Alkaline phosphatase activity also increased approximately 2-fold, but only at 1mM Sr²⁺ ($p < 0.001$). The differential expression of Receptor Activator of NFKB β -ligand (RANKL) and osteoprotegerin (OPG), which regulate osteoclast generation, was also observed using real-time PCR (RT-PCR). The RANKL:OPG mRNA expression ratio was more than halved by 0.1 and 1 mM Sr²⁺ ($p < 0.01$). The EC₅₀ for Sr²⁺ was < 0.1 mM. OPG protein concentrations, determined using ELISA, were significantly increased in the presence of Sr²⁺ ($p < 0.05$). Soluble RANKL protein (sRANKL) in culture supernatants was not detected. The effects of Sr²⁺ in this bone model were similar to those seen with 0.05mM of the calcium sensor agonist, gadolinium, in the presence of 1mM Ca²⁺. These data indicate that Sr²⁺, at pharmacologically relevant concentrations, is a potent regulator of bone cell function *in vitro* as well as *in vivo*. The molecular target for Sr²⁺ is not yet determined.

Disclosures: **T.C. Brennan**, None.

M196

Androgen Receptor Coordinates both Osteoblast Proliferation and Differentiation. H. Kang¹, M. Tsai^{*2}, C. Chang^{*3}, K. Huang^{*2}. ¹Graduate Institute of Clinical Medical Sciences, Chang Gung University/Chang Gung Memorial Hospital, Kaohsiung, Taiwan Republic of China, ²Center for Menopause and Reproductive Medicine Research, Chang Gung Memorial Hospital, Kaohsiung, Taiwan Republic of China, ³George Whipple Lab for Cancer Research, University of Rochester, Rochester, NY, USA.

Androgens have important effects on the human skeleton in both males and females. Hypogonadism in men is associated with increased bone turnover and bone loss, which is reversed after treatment with androgens. Clinical studies suggested that combined therapy of estrogens plus androgens might enhance bone mineral density and bone mass to a more significant degree than estrogen therapy alone in postmenopausal women. Our previous studies demonstrated that cancellous bone volumes are lower in the 8-week-old androgen receptor knockout (ARKO) mice than in both female and male wt littermates. These data indicate that AR is required for bone formation and osteoblast differentiation. To determine whether AR play a role in control of osteoblast proliferation, we compared proliferation rates of primary calvarial cells isolated from wild-type and ARKO embryos in the presence or absence of DHT treatment by MTT, BrdU incorporation and cell number counting assays. We also generated MC3T3-E1 cells in which over-expression of a stably integrated AR and knockdown expression of a stably AR siRNA to study the role of AR in osteoblastic cell growth. Our data showed that DHT accelerates cell growth of osteoblast cells in a time and dose dependent manner. AR-siRNA prevented DHT-induced Akt phosphorylation and ARKO osteoblast cell growth was slower than wild type osteoblasts. Fluorescence microscopy showed a distinct increase in immunostaining intensity in the nuclear interior after androgen treatment but no change in the subcellular distribution of Akt when the cells were pretreated with anti-androgen, hydroxylflutamide. In addition, androgen promotes mineralization of primary calvarial cells isolated from wild-type mice but not from ARKO mice. To further study the roles of AR on various differentiation stages of osteoblastic cells, the mRNA expression of AR, different stage bone marker genes and AR targeted genes from long-term wild-type and ARKO osteoblastic cell cultures with or without androgens, were quantified using real time PCR. Our data indicates that the role of AR on mineralization is dependent on the differentiation stage of the osteoblasts and the duration of androgen treatment. Together, these findings strongly suggest that the AR signaling is required for androgenic effects on bone metabolism, osteoblast proliferation and mineralization.

Disclosures: **H. Kang**, None.

M197

Functional Characterization of Wnt3-Fzd1 Chimera and its Role in the Differentiation of C3H10T1/2 Cells into Osteoblasts. R. A. Bhat, B. Stauffer^{*}, P. V. N. Bodine. Women's Health Research Institute, Wyeth Research, Collegeville, PA, USA.

Signaling through the canonical Wnt pathway has a dramatic effect on bone mass. It has been shown that the loss of function of the Wnt co-receptor, LRP5, in both humans and mice leads to decreased bone formation and bone mass, and gain of function mutations in this gene result in high bone mass, indicating the crucial role of Wnt/LRP signaling in bone formation. Wnts are secreted glyco/lipoproteins that interact with a membrane receptor complex composed of a Frizzled (Fzd) receptor and an LRP. Although 19 Wnt genes and 10 Fzd receptors have been identified so far, the specificity of the Wnt-frizzled interaction and the pathway that is stimulated by a specific ligand-receptor pair has not been fully addressed. The present study is focused on the development and validation of a Wnt3-Fzd1 chimera and its utility in the study of Wnt signaling in osteoblast differentiation. In U2OS osteosarcoma cells, the Wnt3-Fzd1 chimera activated a TCF-Luciferase reporter, and the fold induction was much higher than that obtained by Wnt3 cDNA alone. The deletion of the cytoplasmic tail of the Wnt3-Fzd1 chimera resulted in the loss of activation of canonical Wnt signaling. Point mutations in the PDZ domain in the cytoplasmic portion also resulted in the loss of Wnt signaling suggesting a critical role for the cytoplasmic region in Wnt signaling. Recombinant adenoviruses expressing the Wnt3-Fzd1 chimera and cytoplasmic tail deletion mutant were developed. The expression of the Wnt3-Fzd1 chimera up-regulated the TCF-Luciferase reporter, which was totally blocked by Dkk1 protein, suggesting the involvement of LRP in Wnt3-Fzd1 chimera signaling. To identify the role of Wnt signaling in osteoblast differentiation and maturation, murine C3H10T1/2 stromal cells were infected with adenovirus expressing the Wnt3-Fzd1 chimera or β -galactosidase (as a control for virus infection), and the cells were placed in osteogenic media. No increase in the alkaline phosphatase activity was observed between the uninfected and β -gal virus infected cells, suggesting that the virus infection per se had no effect on the differentiation of C3H10T1/2 cells. In Wnt3-Fzd1 chimera infected cells, the alkaline phosphatase activity increased as early as day 1, reached a peak on day 2, and decreased thereafter. The results indicate that canonical Wnt signaling driven by the Wnt3-Fzd1 chimera leads to the differentiation of C3H10T1/2 cells into the osteogenic pathway. The Wnt-Fzd chimera model has the potential to dissect the molecular mechanisms involved in the pluripotent stem cell commitment and differentiation into a cell type specific lineage.

Disclosures: **R.A. Bhat**, None.

M198

Gene Regulation in Adipogenic Transdifferentiation of Committed Osteoblasts. T. Schilling^{*1}, U. Nöth^{*2}, F. Jakob^{*1}, N. Schütze¹. ¹Molecular Orthopaedics, Orthopaedic Institute, Wuerzburg, Germany, ²Tissue Engineering, Orthopaedic Institute, Wuerzburg, Germany.

Diseases such as osteoporosis and osteonecrosis, may partly trace back to the age-related expansion of adipose tissue at the expense of osteogenic differentiation in human bone marrow. The molecular events of this adipogenic degeneration process are largely unknown. Recently, we established a cell culture system of human bone marrow-derived mesenchymal stem cells, in which the cells can be reprogrammed (transdifferentiated) during their differentiation from osteoblasts into adipocytes. After adipogenic transdifferentiation of committed osteoblasts (cells differentiated in osteogenic medium for 2 weeks), RT-PCR analysis displayed only adipogenic markers, but no osteogenic markers. To discover the fundamental molecular pathways of this reprogramming process at the level of global gene expression patterns, we performed an Affymetrix gene array analysis by comparing transdifferentiated adipocytes with committed osteoblasts. RNA was isolated 3 and 24 hours after the initiation of transdifferentiation (i. e. addition of adipogenic medium to committed osteoblasts) and compared with RNA from committed osteoblasts to identify potential control factors initiating the transdifferentiation process. The gene array analysis detected 248 regulated genes (signal log ratio at least 1.32, i. e. fold change at least 2.5, at one or both time points examined). Regulated gene products mainly belonged to the gene ontology classes of cell metabolism, cell signaling, transcription, development, and transport. The regulation pattern of 18 out of 22 selected genes (based on at least 4-fold regulation and functional potential; e. g. core promoter element binding protein, cysteine rich angiogenic inducer 61, kruppel like factor 4, and fatty acid binding protein 4) could be confirmed by semi-quantitative RT-PCR. Most of these gene products were also regulated in independent experiments. Our results show reproducible molecular changes associated with the transdifferentiation of mesenchymal stem cell-derived osteoblasts into adipocytes. Further investigation of selected gene products regarding their functions could reveal novel signaling processes initiating transdifferentiation or even acting as "molecular switches". Thus, novel targets could be detected for therapeutic applications in order to prevent adipogenic degeneration and to stimulate osteogenic differentiation.

Disclosures: **T. Schilling**, None.

M199

Interactive Network Construction and Pathway Analysis of Differentially Expressed Proteins at the Critical Cellular Events of Fracture Repair. H. Wang¹, J. T. Ryaby¹, R. Quigg^{*2}, X. Li^{*2}. ¹Research and Development, OrthoLogic Corp, Tempe, AZ, USA, ²Functional Genomics Facility, University of Chicago, Chicago, IL, USA.

Bone repair consists of inflammation, intramembranous ossification, chondrogenesis, endochondral ossification and remodeling. To better understand the translational regulation of these distinct but interrelated cellular events, we used the second generation of the BD Clontech™ Antibody Microarray to dissect and functionally characterize the differentially expressed proteins at each cellular event between intact and fractured rat femur. Genetic network analysis showed that proteins differentially expressed at a given cellular event tend to be physically or functionally correlated. Seventeen such interacting networks were established over five cellular events that were most frequently associated with cell cycle, cell death, cell-to-cell signaling and interaction, and cell growth and proliferation. Pathway analysis identified 18 molecular pathways that were significantly enriched during the bone repair process. Of those, ERK/MAPK, NF-kB, PDGF and T cell receptor signaling pathways were significant during three or more cellular events. The analysis revealed dynamic temporal expression patterns and cellular event-specific functions. The inflammation event at day 1 was characteristic of the molecular preparation initiating fracture repair. During this event, up-regulation of mitogenesis- and S phase-related proteins and down-regulation of meiosis-related proteins were prominently featured. Intramembranous ossification at day 4 was highlighted by down-regulation of the cell death-related proteins. Chondrogenesis at day 7 was molecularly most active; twelve molecular pathways were potentially active at this stage, including PDGF, VEGF, PPAR and P13K/AKT pathways. Endochondral ossification at day 14 was morphologically a key stage of generating permanent bone while molecularly exhibited a clear transition from the molecular/cellular function to the physiological system development/function. Osteoclast-mediated remodeling at day 28 was dominated by the integrin signaling pathway. The differential expression of representative proteins was confirmed by immunoblotting. The distinct changes in protein expression during these cellular events provide a molecular basis for developing cellular event-targeted therapeutic strategy to accelerate bone healing.

Disclosures: **J.T. Ryaby**, OrthoLogic Corp 1, 3.

M200

Anterior Cruciate Ligament Injury-Induced Hemarthrosis of the Knee as an Alternative Cell Source for Bone Regeneration. S. Lee, M. Miwa^{*}, Y. Sakai^{*}, R. Kuroda^{*}, T. Matsumoto, T. Niikura^{*}, M. Kurosaka^{*}. Department of Orthopaedic Surgery, Kobe University Graduate School of Medicine, Kobe, Japan.

The use of mesenchymal progenitor cells is promising for regenerative medicine. The most common source of such cells has been the bone marrow, although bone marrow procurement is an invasive procedure. In an attempt to searching for alternative sources of osteoprogenitor cells that could be obtained with minimal discomfort, we looked into

ASBMR 27th Annual Meeting

hemarthrosis caused by acute injuries of the anterior cruciate ligament (ACL) of the knee. The purpose of this study was to determine if cells derived from ACL injury-induced hemarthrosis could differentiate into osteoblast-lineage *in vitro*. Hemarthrosis was aspirated from the knee joint of 14 patients, 15-50 years of age, suffering from acute ACL injuries without intra-articular fractures. Mononuclear cells were isolated from the aspirated bloody joint fluids, which would otherwise be discarded, by density gradient separation, and cultured in α -MEM containing 10% FBS. The plastic adhering cells gave rise to colonies which first became visible around day 7 of culture as cells exhibited a fibroblast-like spindle shape, and the colonies eventually (by days 28) merged to form a uniform multicellular layer. At subconfluence, the adherent fibroblast-like cells were evaluated for cell surface marker expression using flow cytometry. The cells were consistently positive for CD29, CD44, CD105, and CD166, and were negative for CD14, CD34, and CD45, indicating these cells are not hematopoietic origin. Following treatment with osteogenic supplement, β -glycerophosphate, ascorbic acid, and dexamethasone or 1,25(OH) $_2$ D $_3$, the morphological transformation of the cells from spindle-like into cuboidal shapes was observed. Treatment of osteogenic supplement for 28 days resulted in a significant increase in activity of osteoblast-associated protein alkaline phosphatase (ALP) with maximum values attained on day 21 ($p < 0.001$, compared with that in the untreated cultures). Matrix mineralization was demonstrated on day 28 by Alizarin Red staining. RT-PCR analysis revealed that mRNA levels of osteoblast-related genes, ALP, osteocalcin, bone sialoprotein and osteopontin were up-regulated in the treated cultures. These results were similar to those observed in human bone marrow stromal cells from healthy volunteers. Taken together, our findings show that cells derived from ACL injury-induced hemarthrosis contain osteoprogenitor cells. 'Waste' ACL injury-induced hemarthrosis, which is easy to harvest with minimal invasion and discomfort, will be an alternative source for cell-based therapy such as augmentation of the tendon graft healing to bone in ACL reconstruction.

Disclosures: **S. Lee**, None.

M201

Suppressive Role of Regucalcin on Cell Differentiation and Mineralization in Osteoblastic MC3T3-E1 Cells. **M. Yamaguchi**, **M. Kobayashi***, **S. Uchiyama***. Laboratory of Endocrinology and Molecular Metabolism, Graduate School of Nutritional Sciences, University of Shizuoka, Shizuoka, Japan.

Regucalcin was discovered by Yamaguchi in 1978 years. This protein plays the multifunctional role as regulator in cell signaling system in many cells. Bone loss has been induced in regucalcin transgenic rats. Regucalcin has been shown to stimulate osteoclastic resorption *in vitro*. Furthermore, the role of regucalcin in the regulation of osteoblastic cell function was investigated. Osteoblastic MC3T3-E1 cells with subconfluent monolayers were cultured in a medium containing regucalcin (10-10 to 10-8 M) without fetal bovine serum (FBS). Regucalcin had no effect on osteoblastic cell proliferation. The results of RT-PCR analysis with specific primers showed that the expression of Runx2 and IGF-1 mRNAs in osteoblastic cells was significantly suppressed in the presence of regucalcin (10-10 or 10-9 M). TGF- β 1 mRNA levels were significantly enhanced by the 24 h-culture with regucalcin. Alpha 1(I) collagen and G3PDH mRNA levels were not significantly changed by culture with regucalcin. Alkaline phosphatase activity was significantly decreased in the lysate of cells cultured for 24 or 48 h with regucalcin (10-10 or 10-8 M). The expression of regucalcin in osteoblastic cells was demonstrated by RT-PCR and Western blot analysis. When regucalcin (10-7 M) was added into the enzyme reaction mixture containing the lysate of osteoblastic cells cultured in the absence of regucalcin, alkaline phosphatase activity was significantly decreased. Also, Ca $^{2+}$ /calmodulin-dependent nitric oxide (NO) synthase activity in the cell lysate was significantly decreased by addition of regucalcin (10-10 or 10-8 M) into the reaction mixture. The presence of anti-regucalcin monoclonal antibody (5 or 10 ng/ml) in the enzyme reaction mixture caused a significant increase in NO synthase activity in the cell lysate in the presence or absence of Ca $^{2+}$ /calmodulin, suggesting a role of endogenous regucalcin. When osteoblastic cells with subconfluency were cultured in the presence of regucalcin (10-10 or 10-9 M) for 18 days, the results with Alizarin red staining showed that the mineralization was markedly suppressed by culture with regucalcin. This study demonstrates that regucalcin regulates the function of osteoblastic cells, and that the protein suppresses cell differentiation and mineralization. This finding was a first time.

Disclosures: **M. Yamaguchi**, None.

M202

Dlk1/Pref-1 Maintains Self-Renewing Undifferentiated State of Human Mesenchymal Stem Cells by Upregulating Cytokine and Chemokine Gene Expression. **B. M. Abdallah***¹, **Q. Tan***², **J. Dahlgaard***², **M. Kassem**¹.

¹Endocrinology Dept., Odense University Hospital, Odense, Denmark,

²Department of Clinical Biochemistry and Genetics, Odense University Hospital, Odense, Denmark.

Dlk1/Pref-1 (delta like 1/pre-adipocyte factor 1) is a transmembrane protein belongs to the EGF-like homeotic proteins including Notch receptor and its ligands. We have previously shown that Dlk1 is a novel molecule that maintains the self-renewing undifferentiated state of human mesenchymal stem cells (hMSC) through inhibition of osteoblast and adipocyte differentiation (Abdallah BM, et. al., JBMR, 19:841-852, 2004). To investigate the molecular mechanisms underlying these effects, we identified the Dlk1-regulated genes in hMSC line over-expressing Dlk1 gene (hMSC-Dlk1) using DNA Microarray technology. Highly purified RNA from both control hMSC line (negative for Dlk1 expression) and hMSC-Dlk1 cells was subjected to gene chip analysis using the Affymetrix HG-U133A and this was followed by quantitative real-time PCR analysis.

Sixty nine genes were found to be significantly up-regulated (with > 3 folds) in hMSC-Dlk1 compared to control cell line. Interestingly, around 40% of these genes were annotated as pro-inflammatory cytokines including interleukins (IL) (e.g. IL-1 α , IL-1 β , IL-6); chemokines (e.g. IL8, CXCL-2,-3,-6, -11 and CCL20) and several other immune response factors (e.g. complement components 1 and 3). Real-time PCR analysis confirmed more than 90% of the DNA chip data. We have also found that the conditioned medium from hMSC-Dlk1 cell line (containing the secreted soluble active form of Dlk1) induced the same pattern of up-regulated cytokines and chemokines in either control hMSC line or normal hMSC lines obtained from several healthy donors. In addition, Dlk1 exerted synergistic effects on cytokine production e.g. IL-1, IL-6, IL-8, CCL20 and RANTES in presence of lipopolysaccharid [LPS (dose 1 and 100 ng/ml)] and upregulated their gene expression by 3, 6, 4.5, 7 and 3.8 folds respectively. In conclusion, the stimulatory effect of Dlk1 on cytokines expression by hMSC provides a novel mechanism by which Dlk1 exerts its inhibitory effect on hMSC osteoblast and adipocyte differentiation and consequently the maintenance of its self renewal capacity. Moreover, our findings suggest a new role for Dlk1 in the inflammatory and immune regulatory responses that need further investigations.

Disclosures: **B.M. Abdallah**, None.

M203

Oxysterols Enhance Osteoblast Differentiation *In Vitro* and Bone Healing *In Vivo*. **T. Aghaloo**¹, **C. Amantea***², **C. Cowan***³, **J. Richardson***², **B. Wu**³, **F. Parhami**², **S. Tetradis**¹. ¹School of Dentistry, Los Angeles, CA, USA, ²Geffen School of Medicine, Los Angeles, CA, USA, ³Bioengineering, UCLA, Los Angeles, CA, USA.

Anabolic agents that enhance bone formation are important for prevention and management of bone diseases. Oxysterols, naturally-occurring cholesterol oxidation products with multiple biologic activities, are made in part by cellular cytochrome P450 enzymes and autooxidation. We previously reported that continuous treatment of M2-10B4 (M2) mouse marrow stromal cells with specific oxysterol combinations induced osteogenic differentiation assessed by Runx2 protein expression and DNA binding activity, alkaline phosphatase (ALP) activity, osteocalcin (OCN) mRNA expression, and mineralization. Here, we investigated the ability of short term treatment of M2 cells with osteogenic oxysterols 22(S)-hydroxycholesterol + 20(S)-hydroxycholesterol (SS) to induce osteoblastic differentiation. We also explored the ability of these oxysterols to promote bone healing *in vivo*. M2 cells were treated with vehicle or 5 μ M SS for 0.5, 1, 2, 4, and 8 h. Oxysterols were removed, and cells allowed to differentiate in osteogenic medium (RPMI+5% FBS+50 μ g/ml asc +3 mM β -glycerophos). Osteogenic differentiation was assessed by ALP activity at 4 days, OCN mRNA expression at 8 days, and mineralization at 14 days. As little as 0.5 h SS treatment caused a 22-fold increase in ALP activity (Control: 5 ± 2 ; SS: 110 ± 3 units/mg protein \pm SD; $p < 0.001$). OCN mRNA expression and mineralization were significantly induced with only 4 h SS treatment by Northern and ⁴⁵Ca assays, respectively. Next, to explore the effects of osteogenic oxysterols *in vivo*, we utilized the established critical sized 5 mm rat calvarial defect model. Poly(lactic-co-glycolic acid) (PLGA) scaffolds alone or coated with 140 ng (low dose) and 1400 ng (high dose) oxysterol cocktail were implanted into the defects. Rats were sacrificed at 6 weeks and examined by μ CT (μ CT40, Scanco, PA). After scanning at medium resolution utilizing 55 kVp and 72 mA, 3D reconstructions were made, and the bone volume (BV; mm 3), total volume (TV; mm 3), and BV/TV ratio in the volume of interest (VOI; 5 mm defect) were measured. The PLGA scaffold alone showed slight bone healing (BV/TV = 0.17425). Low dose (BV/TV = 0.256933; $p < 0.05$) and high dose oxysterols (BV/TV = 0.259478; $p < 0.05$) significantly enhanced bone formation. Our results suggest that brief exposure to osteogenic oxysterols was sufficient to trigger events leading to osteoblastic cell formation. Oxysterols also induced 1.4-fold greater bone regeneration than control in a calvarial defect model. These *in vitro* and *in vivo* results identify oxysterols as anabolic agents with potential applications in bone healing.

Disclosures: **T. Aghaloo**, None.

M204

Regulation of the Differentiation of Mesenchymal Stem Cells by Retinoic Acid. **K. Hisada***¹, **K. Hata***¹, **H. Ikeda***¹, **T. Matsubara***¹, **F. Ichida***¹, **H. Yamamoto***¹, **H. Yatani***¹, **A. Yamaguchi***², **R. Nishimura***¹, **T. Yoneda***¹.

¹Biochem, Osaka Univ Grad Sch Dent, Suita, Japan, ²Pathol, Tokyo Medic and Dent Univ Grad Sch, Suita, Japan.

Previous studies have shown that retinoic acid (RA), a physiologically potent metabolite of vitamin A, stimulates osteoblastogenesis and inhibits adipogenesis. RA has been also shown to enhance BMP2-induced osteoblast differentiation, suggesting the interactions of RA with BMP2 are critical to the differentiation of mesenchymal stem cells. In the present study, we attempted to investigate the molecular mechanism by which RA promotes osteoblastogenesis and inhibits adipogenesis with a focus on the cross-talk between RA and BMP signaling. To approach this, we first determined the effects of RA on osteoblastogenesis using the pluripotent mesenchymal cell line C3H10T1/2 that differentiates to osteoblasts and adipocytes by BMP2 treatment. RA alone induced osteoblast differentiation by elevating alkaline phosphatase (ALP) activity. This action of RA was enhanced in the presence of BMP2. On the other hand, RA markedly inhibited BMP2-induced adipogenesis. To explore the relationship between RA and BMP2 signaling during osteoblast differentiation, we determined the interactions of RA receptor (RAR) propagation with BMP2 signaling molecule Smad1 and Smad4. RA increased Smad1- and Smad4-induced ALP activity in C3H10T1/2 cells. Treatment with RA also increased transcriptional activity of Smad1 and Smad4. Furthermore, immunoprecipitation experiments showed that RAR physically associated with Smad1 and Smad4. These results suggest that RA signaling functionally and physically interact with Smad, thereby up-

regulating the osteoblastogenic action of BMP2. To our surprise, RA did not influence the expression and function of Runx2. In addition, RA induced ALP activity in mesenchymal cells isolated from Runx2-deficient mice. Furthermore, RA had little effects on osteoblastogenic activity of osterix. We next studied the molecular mechanism by which RA inhibits adipocyte differentiation. Since transcription factors, C/EBP family and PPAR γ , play important roles in the regulation of adipogenesis, we examined the interactions of RA with these transcription factors. RA markedly inhibited the adipogenic action of C/EBP β and C/EBP β -induced PPAR γ expression. Furthermore, RA suppressed the adipogenesis induced by PPAR γ . In conclusion, our data suggest that RA stimulates osteoblastogenesis in cooperation with Smad but independent of Runx2 and osterix. RA inhibits adipogenesis through suppression of C/EBP β and PPAR γ . Thus, RA regulates the commitment of mesenchymal stem cell to osteoblasts and adipocytes at transcriptional levels.

Disclosures: **K. Hisada**, None.

M205

Regulation of Osteoblastic Differentiation by Recombinant Mouse

Amelogenin. M. Matsuzawa^{*1}, T. Sheu^{*2}, C. Huang^{*2}, R. Mroczek^{*2}, S. Kimoto^{*1}, H. Shinji^{*1}, S. Sato^{*1}, T. Kawase^{*1}, J. Puzas². ¹Kanagawa Dental College, Yokosuka, Japan, ²Orthopaedics, University of Rochester, Rochester, NY, USA.

Objectives: Amelogenins have been found to be abundant in enamel and have been reported to induce differentiation and mineralization in a variety of cells. However, the mechanism for regulation of this differentiation is not clear. The aim of this study was to characterize the effect of amelogenin on osteoblasts and periodontal ligament cells (PDL) and to identify possible proteins with which amelogenin can interact. **Methods:** To examine protein interactions of amelogenin, a phage display biopanning technique was used. In this experiment an osteoblast cDNA phage library, expressed in T7 phage, was used to bind a "bait" protein of interest. The bait protein was purified full-length mouse recombinant amelogenin (rM179). The recombinant amelogenin was immobilized on the bottom of a 96-well culture dish. The osteoblast cDNA phage library was exposed to amelogenin to test protein-protein interaction and specifically bound phage were then eluted. For the differentiation experiments purified rM179 protein was added to cultured PDL and ROS17/2.8 osteoblasts for 7 days. The mRNA expression of Runx2, type I collagen (COL1), bone sialoprotein, osteopontin, osteocalcin (OCN), osteonectin (ON), alkaline phosphatase (ALP), RANK ligand (RANKL), and osteoprotegerin (OPG) were quantitatively analyzed by RT-PCR. We also measured activation of the TGFbeta signaling pathway. **Results:** The DNA sequence that demonstrated one of the highest affinities for rM179 in the biopanning experiment was tissue inhibitor of metalloproteinase-2 (TIMP2). The physiological function of this association has been tested in a MMP functional assay. Exposure of amelogenin to osteoblasts increased mRNA for Runx2, COL1, ALP, and OCN. In the PDL cells, amelogenin increased RANKL mRNA levels whereas ON and OPG remained unchanged. Amelogenin was also found to activate TGFbeta signaling with a 4-fold increase. **Conclusion:** Amelogenin binds TIMP2 with very high affinity. This association may explain, in part, the mechanism by which degradation of the surrounding matrix by MMP's is a stimulus for osteoblast differentiation and nodule formation. Moreover, it appears that amelogenin can activate the TGFbeta signaling pathway without interaction with the TGFbeta receptor. Both effects would play a role in the regeneration of bone and periodontal ligament structures during development and/or during disease states.

Disclosures: **T. Sheu**, None.

M206

Overexpression of Wnt10b from the FABP4 Promoter in Mice Results in Increased Trabecular Bone Mass by Increasing Bone Formation and Mineralization. Y. L. Ma¹, Q. Q. Zeng^{*1}, C. N. Bennett², K. A. Longo^{*2}, W. S. Wright^{*2}, K. D. Hankenson³, O. A. MacDougald², G. Krishnan¹. ¹Endocrine Research, Eli Lilly and Company, Indianapolis, IN, USA, ²Molecular and Integrative Physiology, University of Michigan Medical School, Ann Arbor, MI, USA, ³Orthopedic Surgery, University of Michigan Medical School, Ann Arbor, MI, USA.

Activation of Wnt signaling by Wnt10b inhibits differentiation of preadipocytes and promotes osteogenesis in vivo (Bennett etc. *PNAS*; 102:9, 3324-29, 2005). To explore mechanisms whereby Wnt signaling increases osteogenesis, we used a metatarsal organ culture model to establish direct osteogenic action of Wnt10b. Treatment of metatarsals with conditioned media from Wnt10b overexpressing cells did not result in an increase in mineralization as visualized by light microscopy. In contrast, metatarsal organ co-culture with Wnt10b overexpressing cells yielded an increase in mineralization as visualized by light microscopy. Further, to establish the cellular mechanism of osteogenesis, we conducted histomorphometric analyses in 3 months old male FABP4-Wnt10b transgenic mice. At the distal femur, FABP4-Wnt10b mice showed increased trabecular area when compared to wild type littermate. Increased bone mass was the result of an increase in trabecular width and trabecular number, with a corresponding decrease in trabecular separation. Though there was no statistically significant difference in percent osteoblast surface, dynamic histomorphometric analyses revealed a significant increase in mineralizing surface (23%), mineral appositional rate (21%) and bone formation rate (50%) in the secondary spongiosa. Osteoclast number tended to decrease but the change did not reach statistical significance. Although no substantial changes were found in cortical bone of mid-femur at this age mice, a significant amount of marrow trabecular bone was seen in all the FABP4-Wnt10b mice, which was not seen in wild type mice. Our data confirm that Wnt signaling increases osteogenesis to promote bone formation and mineralization.

Disclosures: **Y.L. Ma**, Eli Lilly Company 3.

M207

From Human Marrow Mesenchymal Stem Cells to Bone, Fat, Neural Cells and Cartilage: An *In Vitro* Study. C. Shih, J. Shyu. Biology and Anatomy, National Defense Medical Center, Taipei, Taiwan Republic of China.

Mesenchymal stem cells (MSCs) are essential during development and its potential role in regenerative medicine is promising in the new future. In addition, current evidences suggested that the decrease in bone formation with age is associated with an imbalance between osteoblast and adipocyte differentiation from marrow MSCs. However, knowledge of phenotype characteristics of these MSCs and the controlling factors is relatively unknown. Thus, the aim of this study was to isolate, culture, and investigate the multiple potential of human bone marrow MSCs by density gradient separation method, CD marker selection, differentiation marker expression, bone colony formation, von Kossa stain, H&E stain, Safranin O stain, and light, phase contrast and fluorescent microscopy. MSCs, from human bone marrow, were isolated, purified, and expanded in DMEM medium. Appearance of cuboid-shaped osteoblastic cells, unmineralized, and mineralized colonies were noted 5, 10 and 14 days, respectively, after osteogenic induction. Histological sections showed mineralized matrix with lining osteoblasts and entrapped osteocytes. With adipogenic induction, small size lipid droplets began to appear within cytoplasm 4 days later. More and larger lipid droplets accumulation was noted 10 days after induction. After adding retinoid acid (RA) for 5 days, MAP2 positive cells were detected by immunocytochemical staining. GFAP positive cells were detected 12 days after neurogenic induction. Moreover, MSCs formed cartilage-like tissue using PLGA scaffold in a bioreactor about 2 weeks after chondrogenic induction. Much more cartilage matrix formation was noted 8 and 12 weeks in culture. The results of this study indicated human bone marrow CD 34⁺ MSCs could be isolated, cultured, and induced to undergo osteogenesis, adipogenesis, neurogenesis and chondrogenesis *in vitro*.

Disclosures: **C. Shih**, None.

M208

Dimethyl Sulfoxide Enhances Osteoblastic Differentiation of Murine Pre-Osteoblast Cells. W. M. W. Cheung, W. W. Ng^{*}, A. W. C. Kung. Department of Medicine and Research Centre of Heart, Brain, Hormone and Healthy Aging, The University of Hong Kong, Hong Kong, Hong Kong Special Administrative Region of China.

Dimethyl sulfoxide (DMSO) is the most effective solvent that mixes readily with most water-insoluble and water-soluble substances. Similar to retinoic acid, DMSO demonstrates diverse differentiation-inducing effects on many cell types, including leukemia cells, myoblasts and embryonic stem cells. Recently, it is demonstrated that the DMSO-induced differentiation of leukemia cells is mediated via the upregulation of the tumor suppressor PTEN, which leads to the decrease of Akt phosphorylation. Although DMSO serves as solvent for most ligand-receptor studies of bone formation, the effect of DMSO on bone formation remains obscure. In this study, the effect of DMSO on osteoblast differentiation and phenotype-specific gene expression was examined using murine preosteoblast MC3T3E1 clone 4 (MC) cells as model systems. At concentrations of 0.5-1%, DMSO enhanced the osteoblast differentiation of MC cells as demonstrated by Von Kossa staining. Using real-time RT-PCR, DMSO was shown to upregulate the expression of alkaline phosphatase and collagen type I α . To examine if DMSO acted on specific stage, osteogenic medium was supplemented with 1% DMSO transiently during osteoblast differentiation of MC cells. It was observed that maximum bone nodule formation was resulted when DMSO was supplemented at day 0-5 when compared with control. Expression of osteoblast-specific transcription factors, Runx2 and osterix, was upregulated during the differentiation process. DMSO treatment at day 5-10 or 10-15 resulted in no significant increase in bone nodule formation, suggesting that DMSO affects mainly the differentiation process but not the maturation, nor matrix mineralization process of osteoblast differentiation. While the expression of activated p42/p44 MAP kinases (MAPK) was downregulated, blockage of activated MAPK further enhanced the DMSO-mediated osteoblast differentiation. These data demonstrate that DMSO enhances osteoblast differentiation of MC cells by affecting the differentiation process via the inhibition of MAPK pathway.

Disclosures: **W.M.W. Cheung**, None.

M209

Fulvic Acid of Mumie Promotes Osteoblastic Differentiation in MC3T3-E1 Cells. E. Kim¹, J. Choi^{*2}, H. Jung^{*2}, I. Nam-Goong^{*3}, Y. Kim^{*1}. ¹Internal Medicine, Ulsan University Hospital, University of Ulsan, Ulsan, Republic of Korea, ²Biomedical Research Center, Ulsan University Hospital, Ulsan, Republic of Korea, ³Internal Medicine, Ulsan University Hospital, Ulsan, Republic of Korea.

Mumie is a semihard black resin formed by long-term humification and fulvic acid (MFA) from fractionated from crude Mumie is believed to have therapeutic properties and regeneration of bone tissue. **Purpose:** The purpose of this study was to investigate the effects of MFA on the osteoblastic differentiation in MC3T3-E1 cells. **Methods:** MC3T3-E1 cells were treated with different concentrations (100-1000 μ g/mL) of MFA in α -MEM medium for 1, 3, 6, 9, 12, 15, and 18 days. Cells incubated with simvastatin served as positive control or without MFA served as negative control. At the end of each incubation period, cells were harvested and alkaline phosphatase (ALP) activity was determined compared with control groups. Total mRNA was also extracted from MFA-treated cells and RT-PCR was performed to determine the mRNA levels of ALP and osteoprotegerin (OPG). **Results:** MFA enhanced ALP activity in a dose- and time-dependent pattern in

ASBMR 27th Annual Meeting

MC3T3-E1 cells. ALP activity was showed at relatively low doses (100 µg/mL) of MFA. ALP activity was highly elevated after culturing for 15 days in MFA-treated cells compared with positive control. It also significantly increased by MFA treatment from 9 to day 18 culture ($P < 0.01$) compared with negative control. RT-PCR analysis showed that MFA increased in the expression of ALP and OPG in MC3T3-E1 cells. **Conclusions:** This result indicates that MFA promotes osteoblastic differentiation, suggesting that it could be used for the treatment of bone metabolic disease such as osteoporosis.

Disclosures: **E. Kim**, None.

M210

The Stimulatory Effect of the Polyphenols in the Extract of Greens+™ Herbal Preparation on the Mineralized Bone Nodule Formation (MBNF) of SaOS-2 Cells Is Mediated via its Inhibitory Effect on the Intracellular Reactive Oxygen Species (iROS). **L. G. Rao¹, B. Balachandran^{*1}, A. V. Rao^{*2}.** ¹Medicine/Div Endocrinology & Metab, University of Toronto, St. Michael's Hospital, Toronto, ON, Canada, ²Department of Nutritional Sciences, University of Toronto, Toronto, ON, Canada.

Oxidative stress has been implicated in the pathophysiology of osteoporosis. Epidemiological studies associate polyphenol intake with increased bone mineral density. Polyphenols from plants have potent antioxidant properties. A commercially available herbal preparation, greens+™, is a good source of polyphenols. We studied the effects of the polyphenol extract of greens+™ on alkaline phosphatase activity (ALP) and MBNF in cultures of the human osteoblast cell line SaOS-2 and explored whether these effects involved iROS. The SaOS-2 cells were cultured in supplemented Ham's F-12 medium in the absence or presence of greens+™ extracts containing various concentrations of total polyphenol. Control cultures received the vehicle used to prepare Greens+™ extracts. Greens+™ extracts were added at day eight and at every medium change thereafter. At various time points, ALP was analyzed using the Lowry method and MBNF was analyzed by the von Kossa technique. To determine whether the polyphenol extracts inhibited iROS, the cells were incubated with varying concentrations of Greens+™ polyphenolic extracts at day 8 for 48 hours and the concentration of iROS analyzed by the 2',7'-dichlorofluorescein diacetate (2,7-DCFH-DA) fluorescent assay. To mimic oxidative stress condition, experiments were also carried out in the presence of hydrogen peroxide (H₂O₂). Our data showed that treatment of SaOS-2 cells with polyphenolic extracts of greens+™ resulted initially in a stimulation followed by inhibition of ALP and stimulation of mineralized bone nodule numbers and area ($p < 0.05$) in a time and dose-dependent manner. The polyphenolic extracts of Greens+™ significantly inhibited the endogenous production of iROS. Addition of H₂O₂ increased iROS in a time and dose-dependent manner ($p < 0.05$) that was inhibited dose-dependently by the polyphenolic greens+™ extract ($p < 0.05$). Similarly, varying concentrations of the polyphenol epicatechin, a major polyphenolic component of green tea, also inhibited the endogenous and H₂O₂-stimulated production of iROS, but to a lesser extent than the polyphenolic extract of Greens+™. In conclusion, our results showed that greens+™ extract influenced human osteoblasts differentiation and stimulated mineralization mediated by inhibition of iROS production. Our data suggests that greens+™ maybe an agent for the prevention of osteoporosis.

Disclosures: **L. G. Rao**, *ehn inc, Toronto, Canada 2.*

M211

Notch1 RAM Domain and Ankyrin Repeats Are Required for Notch Signaling and Action in Osteoblasts. **V. Deregowski, E. Gazzero, L. Priest*, S. Rydzziel, E. Canalis.** Research, Saint Francis Hospital and Medical Center, Hartford, CT, USA.

Notch receptors play a critical role in cell fate decisions and suppress osteoblast differentiation. The Notch receptor is a single pass transmembrane receptor activated by contact with membrane bound ligands Delta and Serrate/Jagged, which result in the proteolytic cleavage of the Notch receptor and the release of its intracellular domain (NICD). Notch interacts with members of the CBF1, Suppressor of Hairless, Lag-1/RBP-Jk (CSL) family of transcription factors, an interaction presumably mediated by the RBP-Jk associated module (RAM domain), that results in the activation of transcription. Deletion of the RAM domain results in loss of CSL induction in C2C12 cells, but the contribution of the ankyrin repeats, the second major component of the Notch gene, to this pathway is less clear. The purpose of this work was to determine the pathways responsible for inhibitory effects of Notch on osteoblastogenesis, and the contributions of the RAM domain and ankyrin repeats to this process. ST-2 stromal cells were transduced with retroviral vectors overexpressing NICD, or deletion mutants, lacking the RAM domain or the ankyrin repeats, under the control of the cytomegalovirus promoter. In an initial experiment, the expression of target and partner genes utilized for Notch signaling was examined by Northern blot analysis. Notch overexpression caused an increase in the RBP-Jk/CSL pathway-dependent hairy and E (spl) (HES)-1 transcripts, but did not change the expression of Deltex 1, 2 and 3, which are associated with activation of CSL-independent pathways. Confirming that Notch acts in osteoblastic cells by using the RBP-Jk/CSL pathway, acute co-transfection experiments revealed that NICD enhanced the transactivation of transiently transfected 12xCSL constructs containing 12 repeats of an RBP-Jk/CSL binding site directing luciferase expression. Removal of the RAM domain resulted in a partial loss, whereas removal of the ankyrin repeats resulted in total loss of 12xCSL activity, indicating that ankyrin repeats are at least as important in the induction of the CSL pathway as the RAM domain. Accordingly, deletion of ankyrin repeats resulted in loss of HES-1 transcript induction. NICD overexpression inhibited the effect of BMP-2 and of Wnt3a on alkaline phosphatase activity (APA), and deletion of the RAM domain or ankyrin repeats resulted in loss of the inhibitory effect on APA and on Wnt signaling, as evidenced by changes in Wnt induced secreted protein 1 transcript levels. In conclusion,

both the RAM domain and ankyrin repeats are required for Notch signaling through the RBP-Jk/CSL pathway, which appears responsible for the inhibitory effect of Notch on osteoblastogenesis.

Disclosures: **V. Deregowski**, None.

M212

Integrin Beta-1 Silencing Alters Osteoblast Response to Substrate Microtopography and 1,25(OH)₂D₃. **L. Wang¹, R. Olivares-Navarrete^{*1}, B. F. Bell^{*1}, G. Zhao^{*1}, M. Wieland^{*2}, D. L. Cochran^{*3}, B. D. Bovan¹, Z. Schwartz¹.** ¹Georgia Institute of Technology, Atlanta, GA, USA, ²Institut Straumann, Waldenburg, Switzerland, ³University of Texas Health Science Center at San Antonio, San Antonio, TX, USA.

Surface microroughness increases osteoblast differentiation and enhances responses of osteoblasts to 1,25(OH)₂D₃. Beta-1 integrin expression is increased in osteoblasts grown on Ti substrates with rough microarchitecture, and is regulated by 1,25(OH)₂D₃ in a surface-dependent manner, suggesting that beta-1 plays a role in mediating osteoblast response. Here, we silenced beta-1 expression in MG63 human osteoblast-like cells using small interfering RNA (siRNA) and examined response to surface microtopography and 1,25(OH)₂D₃. MG63 cells were transfected with plasmids containing beta-1 siRNA template as well as with control plasmids containing scrambled beta-1 sequences. Stably transfected cells were selected: MG63-B and MG63-BS, respectively. Beta-1 mRNA was reduced 65% in MG63-B cells but was unaffected in MG63-BS cells based on real time PCR analysis. Normal and transfected cells were grown on tissue culture plastic or Ti disks of different surface microtopographies: Ra < 0.6µm, Ra = 4-5µm, and Ra > 5µm. At harvest, alkaline phosphatase activity was measured in cell lysates and levels of osteocalcin, TGF-β1, PGE₂, and osteoprotegerin (OPG) in the conditioned media were measured by immunoassay. We compared beta-1 silencing in cells cultured on plastic with blocking integrin signaling using two different anti-beta-1 monoclonal antibodies. After initial attachment, antibodies were present throughout the 7-day culture. Beta-1 silenced MG63 cells cultured on plastic had reduced alkaline phosphatase activity and levels of osteocalcin, TGF-β1, PGE₂, and OPG in comparison with wild type or MG63-BS cells. Moreover, beta-1 silencing, but not the scrambled template, inhibited surface roughness effects on these parameters. 1,25(OH)₂D₃ increased alkaline phosphatase activity, and levels of osteocalcin, PGE₂, and OPG in wild type and MG63-BS cells and its effects were synergistic with those of the surface. However, effects of 1,25(OH)₂D₃ were partially inhibited by beta-1 silencing. Effects of beta-1 silencing differed from those of anti-beta-1 antibodies, which in turn, depended on the antibody used. These findings indicate that beta-1 functions in osteoblastic differentiation modulated by either surface microarchitecture or 1,25(OH)₂D₃, that beta-1 mediates, in part, the synergistic effects of surface roughness and 1,25(OH)₂D₃, and global reduction in beta-1 differs from selective inhibition of ligand binding.

Disclosures: **L. Wang**, None.

M213

Beta-Cryptoxanthin Stimulates Cell Differentiation and Mineralization in Osteoblastic MC3T3-E1 Cells. **S. Uchiyama*, M. Yamaguchi.** Laboratory of Endocrinology and Molecular Metabolism, University of Shizuoka, University of Shizuoka, Shizuoka, Japan.

Beta-cryptoxanthin (CRP), a kind of carotenoid, has been shown to stimulate bone formation and inhibit bone resorption in vitro. CRP can inhibit osteoclastogenesis in bone marrow culture system. Furthermore, the effect of CRP on cell differentiation and mineralization in osteoblastic MC3T3-E1 cells was investigated. Cells were cultured for 72 hours in an alpha-MEM containing 10% FBS, and the cells with subconfluency were changed to a medium containing either vehicle or CRP (10-8 to 10-6 M) without FBS. Cells were also cultured for 3 to 21 days. Gene expression in osteoblastic cells was determined using RT-PCR. Culture with CRP (10-7 or 10-6 M) for 3 days caused a significant increase in Runx2 type 1, Runx2 type 2, alpha 1 (I) collagen and alkaline phosphatase mRNA levels in osteoblastic cells. These increases were completely blocked in the presence of cycloheximide, an inhibitor of protein synthesis, or 5,6-dichloro-1-beta-D-ribofuranosylbenzimidazole, an inhibitor of transcriptional activity. Vitamin A (10-6 M) did not have a significant effect on Runx2 type 1 mRNA expression in the cells. The effect of CRP (10-6 M) in stimulating Runx2 type 1 and α1 (I) collagen mRNA levels, protein content and alkaline phosphatase activity in the cells was also seen in the presence of vitamin A (10-6 M), suggesting that the mode of CRP action differs from that of vitamin A. Prolonged culture with CRP (10-6 M) for 3-21 days caused a significant increase in cell number, DNA content, protein content and alkaline phosphatase activity in osteoblastic cells, suggesting that CRP stimulates cell proliferation and differentiation. Moreover, culture with CRP (10-7 or 10-6 M) for 5 to 21 days caused a remarkable increase in mineralization. This study demonstrates that beta-cryptoxanthin has a stimulatory effect on cell differentiation and mineralization due to enhancing gene expression of proteins which involve in bone formation, indicating that the carotenoid is an activator in osteoblastic bone formation.

Disclosures: **S. Uchiyama**, None.

M214

Particulate Wear Debris Alter Osteoclast Maturation through a COX-2 Dependent Mechanism. S. E. Prosser*, J. A. Struve, A. Palisch*, J. T. Ninomiya. Dept of Orthopaedics, Medical College of Wisconsin, Milwaukee, WI, USA.

Osteolysis and implant loosening remain the primary cause of implant failure following total joint arthroplasty. Although it is clear particulate debris play an important role in the process, the mechanisms involved in loosening remain complex. While the proteins RANKL and OPG are central in the maintenance of normal bone homeostasis, less is known about their function in osteolysis generated by particulate debris. More importantly, the intracellular signal transduction pathways involved in the activation of these proteins in response to particulate debris have not been fully characterized. We therefore hypothesized that regulation of the RANKL/OPG ration in response to particulate debris occurred through alterations in the gene expression and synthesis of cyclooxygenase-2(COX-2), a protein critical in the inflammatory response. We also hypothesized that inhibition of COX-2 activity would decrease the effects of particulate debris on the RANKL/OPG ratio, and subsequently result in a decrease in the maturation of osteoclast precursors. Titanium particles were added to osteoblasts in culture. Effects on COX-2 protein level were assessed by Western blots and prostaglandin secretion was determined by ELISA. Alterations in the gene expression of RANKL and OPG were determined by real-time PCR while OPG secretion was quantitated by ELISA. A specific inhibitor of COX-2, NS-398, was added 1 hour prior to addition of titanium and effects were determined as above. Cell lysates were collected and used to determine the effects on osteoclast maturation using a murine marrow cell assay. Addition of titanium particles to cells caused an increase in COX-2 protein levels at 2 and 6 hours and this corresponded to a 10-15 fold increase in secreted PGE₂ at 6 to 12 hours. COX-2 activity was blocked using the specific inhibitor NS-398 and this blocked PGE₂ secretion. The secretion and gene expression of OPG was increased in response to titanium but this increase was unaffected by the inhibition of COX-2. However, wear debris increased RANKL gene expression and this increase was reduced by the inhibition of COX-2. Whole cell lysates from osteoblasts incubated with wear debris increased osteoclast maturation and this effect was blocked by inhibition of COX-2. Taken together these findings demonstrate that titanium wear debris alter osteoclast maturation through a COX-2 dependent mechanism. In part, COX-2 altered the RANKL/OPG ratio by increasing RANKL gene expression rather than decreasing OPG secretion. This would also suggest that the COX-2 inhibitors which are widely used in the treatment of arthritis may also play a role in the prevention and regulation of osteolysis and implant loosening.

Disclosures: J.T. Ninomiya, None.

M215

Wear Debris Induces MCP-1 through COX-2 Dependent Pathway in Fibroblasts. J. T. Ninomiya, J. A. Struve. Dept of Orthopaedics, Medical College of Wisconsin, Milwaukee, WI, USA.

Aseptic loosening remains the primary cause of implant failure following total joint replacement. Wear debris from the loosening of orthopedic implants induces macrophage activation, pro-inflammatory cytokine release and osteoclast differentiation leading to osteolysis. Osteolytic membranes around failed total joint arthroplasties are infiltrated with macrophages, fibroblasts and giant cells as well as orthopaedic wear debris. Fibroblasts are known to secrete proinflammatory cytokines and degradative enzymes in response to wear debris. Recent studies show that fibroblasts also release monocyte chemoattractant protein-1 (MCP-1) in response to titanium and PMMA. MCP-1 is a chemokine that attracts monocytes and macrophages to sites of inflammation and has been found in membranes retrieved from failed total joint arthroplasties. Although we know fibroblasts produce MCP-1, the signaling mechanism by which MCP-1 is induced in fibroblasts is not clearly understood. Therefore we chose to investigate the particle induced signal transduction pathways that lead to increased MCP-1 production. Titanium particles were added to human foreskin fibroblasts in culture. Effects on COX-2 protein levels were assessed by Western blot and prostaglandin secretion was determined by ELISA. MCP-1 gene expression was determined by semiquantitative RT-PCR while protein was measured by ELISA. A specific inhibitor of COX-2 (NS-398) was added 1 hour prior to addition of titanium and effects were determined as above. Fibroblasts stimulated with titanium showed a dose dependent release of MCP-1 at 24 hours. At doses of 0.25 vol% and 0.5 vol%, titanium showed significant increases of MCP-1 over non-stimulated fibroblasts. Using a time course, a 0.5 vol% dose of titanium significantly increased MCP-1 protein at 12, 24 and 48 hours. With addition of a COX-2 inhibitor(NS-398), the MCP-1 level was reduced to control level at 24 hour and significantly reduced at 48 hours. MCP-1 gene expression is induced at 24 hours and the expression is reduced with the addition of the COX-2 inhibitor. PGE₂ protein was significantly induced by titanium and when the COX-2 inhibitor was added the protein levels were reduced to control amounts. Western blots show that titanium increases COX-2 protein levels and the addition of NS-398 blocks that induction. These findings suggest that MCP-1 induced by fibroblasts is modulated through the COX-2 pathway. Therefore, COX-2 inhibitors currently available may be useful in treating implant loosening due to wear debris induced osteolysis

Disclosures: J.T. Ninomiya, None.

M216

RNA Interference with Gq and G11 Proteins Suppresses Messenger RNA Expression of Osteoblast Functional Genes and Induces Changes in Cellular Morphology in Mouse Osteoblasts. A. Iida-Klein¹, D. S. Bischoff*², J. Zhu*², D. W. Dempster¹, T. J. Hahn², D. T. Yamaguchi². ¹Regional Bone Center, Helen Hayes Hospital, West Haverstraw, NY, USA, ²VA Greater Los Angeles Healthcare System, Los Angeles, CA, USA.

During bone remodeling, resting osteoblasts become activated upon receipt of external stimuli for bone formation and transform from a flat to a more cuboidal shape. In cardiac myocytes and platelets, guanine-nucleotide regulatory protein alpha q subunit (Gq) has been shown to play a role in cellular hypertrophy and cytoskeletal reorganization. We therefore hypothesized that Gq may play a role in regulation of cellular morphology and function in osteoblasts. Highly differentiated mouse calvarial MC4 osteoblasts were transfected with Gq and G11 siRNA at a 1:6 ratio of siRNA to liposome, and the temporal patterns of mRNA expression of Gq and G11 were examined by quantitative real time RT-PCR. Maximal Gq silencing at 90% (p<0.0001) was achieved by 24 hr, gradually decreasing to 67% (p<0.001) at 48 hr, and 42% (p<0.01) at 72 hr. Similarly, maximal G11 silencing at 95% (p<0.001) was achieved by 24 hr, but the silencing effect continued until 72 hrs. Gq silencing at the protein level was confirmed at 24 hr by significant suppression of Gq protein band density using western blot. Messenger RNA expression levels of three osteoblast-specific functional genes (core-binding factor alpha 1 [cbfa1], bone sialoprotein [BSP], and alkaline phosphatase [ALP]) were also measured by quantitative real time RT-PCR. Upon maximal Gq silencing at 24 hr, mRNA expression of cbfa1, BSP and ALP was suppressed by 70%, 92% and 52 % (all, p<0.01), respectively. Similar suppression of these osteoblast-specific genes was observed by maximal G11 silencing. In addition, osteoblast morphology was altered by Gq and G11 silencing, and the cells became flattened at 24 and 48 hr. The more cuboidal morphological phenotype was recovered over time. Thus, these results support our hypothesis that the Gq family of G proteins may play an important role in osteoblast function and cellular morphology.

Disclosures: A. Iida-Klein, None.

M217

Kremen 2 Is Required for Dkk1 Mediated Inhibition of LRP5/6-Wnt3a-TCF Signals in U2OS Osteoblast-Like Cells. B. M. Bhat¹, H. Lam*¹, V. E. Coleburn*¹, P. Yaworsky*², F. J. Bex¹. ¹Women's Health & Bone, Osteoporosis Group, Wyeth Research, Collegeville, PA, USA, ²Biological Technologies, Wyeth Research, Cambridge, MA, USA.

Recent analyses of LRP5 mutations in humans and mice have revealed the pivotal role LRP5 and Wnt-signaling play in bone metabolism. LRP5/6 and the secreted antagonist Dkk1 interact with recently identified single pass, transmembrane receptors Kremen1 (Krm1) and Kremen2 (Krm2) and synergistically inhibit the LRP5/6-Wnt-β Catenin signal. In addition, Kremens facilitate rapid endocytosis of LRP5/6 from the cell membrane and block LRP5/6-Wnt signaling. To investigate the functional role of Kremens we cloned Krm2 from U2OS cells and identified four splice variants. Analysis of these variants by Wnt-TCF assays in U2OS cells indicated that the variant lacking 44 C-terminal amino acids (aa) can enhance Dkk1 mediated inhibition, although the maximum effect was seen with the full length clone. Reports indicate that Krm2 activity is mediated by its interaction with the second cysteine-rich domain of Dkk1 and also that Krm2 can convert the LRP6-Wnt signal activator Dkk2 into an inhibitor in 293 cells. Recently, we have identified downstream deletion to the second cysteine-rich domain of Dkk1 that removes 21 C-terminal aa containing a putative N-glycosylation site, results in loss of its inhibitory function. To study whether Krm2 can alleviate the functional defect of Dkk1 deletion, co-transfection experiments were performed. They revealed that Krm2 could not reverse the lack of inhibitory function in the truncated Dkk1 and hence suggested that Krm2 requires this 21 aa region of Dkk1 to block LRP5-Wnt-TCF-signaling. To evaluate the functional importance of Krm2 in U2OS bone cells, we carried out Krm2 siRNA co-transfections with TCF reporters. In the absence of Wnt3a, a 2-3-fold increase in TCF activity as compared to the control siRNAs was observed. Thus, by inhibiting Krm2, a TCF signal is generated in bone cells presumably by releasing the Krm2-Dkk1 mediated suppression of the endogenous signal. In addition, when Krm2 siRNA was co-transfected with Wnt3a, there was a synergistic activation of the TCF signal. Moreover, Krm2 siRNA co-transfection with Dkk1 and Wnt3a abolished Dkk1 mediated inhibition (~95%) of Wnt-TCF signal in U2OS cells. These studies indicate the presence of functional endogenous Krm2 in U2OS bone cells as well as support the requirement of Krm2 for Dkk1 inhibitory function.

Disclosures: B.M. Bhat, None.

M218

Essential Roles of MAP Kinases p38 and ERK in the Activation of Osteoblastic Cells by Parathyroid Hormone. A. Rey*, D. Manen*, R. Rizzoli, S. Ferrari, J. Caverzasio. Service of Bone Diseases, Department of Rehabilitation and Geriatrics, University of Geneva, Switzerland.

Increased bone formation by PTH is mainly due to activation of osteoblastic cell differentiation (OBD), an effect largely mediated by the cAMP-Protein Kinase A (PKA) signaling pathway. The molecular mechanism by which PKA and/or the possible implication of other pathways in PTH-induced OBD are largely unknown. MAP kinases (MAPKs) have recently been shown to play a significant role in OBD. We thus investigated the role of MAPKs in the activation of osteoblastic cells by PTH. In early differentiated MC3T3-E1 cells, 10⁻⁷ M human PTH(1-34) (hPTH) enhanced alkaline

ASBMR 27th Annual Meeting

phosphatase (ALP) activity (8-10 fold) and doubled the production of osteocalcin (OC) after 24 h incubation. These effects were fully mimicked by 10 μ M forskolin (FSK). They were blunted by H89 (25 μ M) but not by Go6983 (10 μ M), which are specific inhibitors of PKA and PKC, respectively, confirming a major role of PKA in PTH-induced OBD. Activation of MAPKs by PTH in MC3T3-E1 cells was investigated using Western blot analysis. In confluent cells, hPTH enhanced p38 MAP kinase by 2.5 ± 0.3 fold ($p < 0.01$) at 2 h. This effect started after 1 h incubation, lasted about 2 hrs and was mimicked by 10 μ M FSK (3.5 ± 0.2 fold, $p < 0.001$). The stimulation of p38 by hPTH was completely blocked by 10 and 25 μ M H89 suggesting a PKA-dependent mechanism of activation. Associated with this effect, the stimulation of ALP induced by hPTH was dose-dependently (5-25 μ M) and completely inhibited by SB202190, a specific p38 inhibitor. This compound, however, did not influence PTH-induced cellular cAMP or OC production. As previously shown, PTH also enhanced ERK activity. However, preincubation of cells with 10 μ M of U0126, a selective inhibitor of ERK activation, significantly reduced OC production, but did not influence PTH stimulation of cAMP and ALP. Finally, a 5 week PTH(1-34) exposure significantly enhanced by 5-fold MC3T3-E1 matrix mineralization assessed as by alizarine red staining. This effect was markedly decreased ($> 80\%$) by the p38 (10 μ M) but not by the ERK inhibitor (10 μ M). In conclusion, these results describe for the first time that PTH can activate p38 in addition to ERK in osteoblastic cells and that this effect is mediated by a PKA-dependent mechanism. MAP kinases p38 and ERK are essential signaling pathways for PTH-induced osteoblastic differentiation. The p38 pathway plays a major role in enhanced ALP and matrix mineralization induced by PTH whereas ERK is rather implicated in changes of OC, strongly suggesting distinct signaling pathways downstream PKA in PTH-induced osteoblastic differentiation.

Disclosures: **J. Caverzasio**, None.

M219

Wnt 3a and a GSK3 β Inhibitor Differentially Regulate Wnt Pathway and Bone Formation Associated Genes in Primary Human Osteoblasts. L. V. Hale*, D. L. Halladay*, C. A. Frolik, B. A. Diserod*, C. M. Kelepouris*, Y. G. Yue*, J. Shou*, T. Wei*, T. Stewart*, A. Kumar*, L. Gelbert*, J. Onyia, P. Chen*, S. Huang*, R. J. S. Galvin. Lilly Research Laboratories, Eli Lilly and Company, Indianapolis, IN, USA.

Wnt glycoproteins comprise a highly conserved family of secreted lipid modified signaling molecules. These proteins regulate cell-to-cell interactions and are powerful regulators of cell proliferation and differentiation. The conventional (canonical) Wnt pathway involves proteins that directly participate in gene transcription and cell adhesion and has recently been implicated in bone formation. To further investigate the role of this pathway in bone formation, the effects of Wnt 3a and the GSK-3 β inhibitor, 603281-31-8, on human pre-osteoblasts (hOBs, L. X. Bi, Univ Texas Medical Branch) were evaluated in primary cell culture. The hOBs mineralize in the presence of β -glycerolphosphate, ascorbate, and dexamethasone producing a mineral identified by X-ray diffraction to be consistent with hydroxyapatite (HA). Both Wnt 3a conditioned medium (CM) and the GSK-3 β inhibitor enhance this mineralization to approximately the same magnitude in a dose-dependent manner. However, in contrast to inhibitor treated cells, at higher concentrations the Wnt 3a CM causes cell detachment. Microarray analysis of the treated hOBs followed by Taqman gene expression validation indicate that Wnt 3a CM and the GSK-3 β inhibitor similarly regulate expression of Axin2, DKK2, BMP4, osteomodulin (OMD), FZD8, ADAM19, as well as, a number of other genes not currently associated with bone. Fold-changes in gene expression seen with the inhibitor are much greater and often sustained longer than the fold-changes induced by Wnt 3a CM even though the genes are regulated in the same direction. Our data indicate that both Wnt 3a CM and the GSK-3 β inhibitor, 603281-31-8, are able to up-regulate HA accumulation in hOB cell culture. Likewise, they are both able to regulate specific genes linked to bone, as well as, a number of genes not currently thought to be connected to bone formation. However, the magnitude and timing of this regulation is different between the two treatments. Therefore, it is proposed that the GSK-3 β inhibitor bypasses some of the pathway regulatory steps that normally control the bone response to Wnt 3a.

Disclosures: **L.V. Hale**, Eli Lilly and Company 3.

M220

Further Indications for an Aantagonistic Role in LRP5-Mediated Wnt Signaling for Dickkopf1, Dickkopf3, Kremen1, and also Sclerostin. W. Balemans*, L. Van Wesenbeeck*, W. Van Hul. Dept. Medical Genetics, University of Antwerp, 2610 Antwerp, Belgium.

Wnt signaling plays an important role in many developmental processes and is regulated at multiple levels. Low density lipoprotein receptor-related protein 5 (LRP5), a co-receptor for Wnt proteins, activates canonical Wnt signaling, and is found to be associated with osteoporosis pseudoglioma syndrome (OPPG) and high bone density disorders. Extracellularly, Wnt signaling is modulated by a number of antagonists, including members of the Dickkopf (Dkk) and Kremen (Krm) families. Dkk1, Dkk2 and Dkk4 have been shown to bind LRP5/6. Whereas Dkk1, Dkk3 and Dkk4 inhibit Wnt signaling, Dkk2 can act as an activator or an inhibitor depending on the cellular context. The single transmembrane proteins Krm1 and Krm2 strongly cooperate with Dkk1, Dkk2 and Dkk4 to potentiate Dkk-mediated inhibition of Wnt signaling. Recently, sclerostin has been put forward as an additional candidate to modulate Wnt signaling. Loss of function of this protein causes sclerosteosis and van Buchem disease, two sclerosing bone dysplasias. Thus far, two studies suggested a modulatory effect of sclerostin on Wnt signaling. Although results from the first report postulated an indirect effect, a more recent study showed a direct inhibition of the Wnt pathway by binding of sclerostin to LRP5. In this study, the ability of Dkk1, Dkk3, Krm1 and sclerostin to modulate LRP5-mediated Wnt signaling was investigated using a TCF reporter based assay in HEK293T cells. Transient

transfection of a mouse Wnt1 expression construct slightly increased TCF-dependent transcriptional activation, which was further potentiated by co-expressing human LRP5. Co-transfection of increasing amounts of human Dkk1 and Dkk3 resulted in a dose-dependent decrease in LRP5-mediated Wnt signaling. Mouse Krm1 did not show a significant modulation of TCF transcriptional activity, however, when co-transfected with human Dkk1, a strong potentiation of Dkk1-mediated inhibition could be observed. Finally, a dose-dependent inhibition of LRP5-mediated Wnt signaling was also observed when transfecting mouse sclerostin. To conclude, our data confirmed antagonistic roles for Dkk1, Dkk3, Krm1, and also sclerostin on LRP5-mediated Wnt signaling. However, additional studies are necessary to find out whether sclerostin acts directly or indirectly on this pathway. In the past, molecular genetic and cell biology studies have already demonstrated important roles for LRP5, sclerostin and Dkk1 in bone tissue. Whereas no such functional roles have been found for Dkk3 and Krm1, molecular and cell biological experiments are currently ongoing in our lab to investigate this.

Disclosures: **W. Balemans**, None.

M221

Bisphosphonates Regulate Mediators of Cell Transduction in Osteoblasts. Q. Sun¹, R. W. Katz², J. P. Bilezikian¹. ¹Division of Endocrinology, College of Physicians and Surgeons, Columbia University, New York, NY, USA, ²Oral Medicine, College of Dentistry, New York University, New York, NY, USA.

Although bisphosphonates (BPs) have long been regarded to affect osteoclast actions primarily, recent studies have suggested that the osteoblast is also an important target. We previously reported that BPs suppress prenylation of small GTPases and stimulate total GTPase activity in osteoblasts (the UMR-106 cell line). In this study, we further describe the effects of BPs on Rho A, a member of the Rho family of GTPases in UMR-106 cells. Rho A prenylation was measured by immunoprecipitation after labeling with C14-mevalonate. Overnight exposure of cells to 0.1 mM risedronate (RIS) reduced Rho A prenylation by 61% below control levels. Under the same experimental conditions, exposure to alendronate (ALN) had a much smaller, 15% inhibitory effect (ALN vs RIS, $p < 0.001$). RIS stimulated GTPase activity to a greater extent than ALN: 156% vs 119% ($p < 0.05$). RIS also inhibited GTP binding to UMR 106 cells to a greater extent than ALN: 21% vs 10%. Under our experimental conditions, there was no translocation of Rho A from the cell membrane into cytosol. We conclude that in UMR 106 cells, BPs inhibit prenylation, stimulate GTPase activity, and inhibit GTP binding of Rho A, with RIS having a greater effect on these 3 processes than ALN. The results define further specific biochemical targets of BPs on osteoblasts and should help to elucidate molecular mechanisms of BP action in this newly recognized target cell.

Disclosures: **Q. Sun**, Alliance for Better Bone Health 2.

M222

Metabolic Acidosis-Induced Calcium Signals in Primary Osteoblasts. K. K. Frick, K. Nehrke*, N. S. Krieger, D. A. Bushinsky. Medicine/Nephrology Unit, University of Rochester, Rochester, NY, USA.

Compared to incubation in neutral pH medium, incubation of neonatal mouse calvariae in medium simulating physiologic metabolic acidosis (Met, reduced pH due to decreased $[\text{HCO}_3^-]$) induces a marked increase in net Ca efflux. In contrast, incubation in isohydric medium simulating respiratory acidosis (Resp, reduced pH due to increased Pco_2) has little effect on Ca flux. The Met-induced increase in net Ca efflux results from stimulation of osteoclastic resorption mediated through changes in osteoblastic activity. Met induces osteoblasts to increase COX-2 activity and expression of RANKL while simultaneously decreasing expression of type I collagen and alkaline phosphatase; again Resp has little effect on these parameters. The recent identification of G-protein-coupled proton sensing receptors (PSRs) provides a potential mechanism for transduction of an acidic extracellular pH into cellular responses. We have identified transcripts for the 4 known PSRs, OGR1, GPR4, TDAG8, and G2A, in total RNA isolated from cultured calvariae. To determine if one or more PSRs modulate Met-stimulated bone Ca efflux, we utilized the PSR inhibitor CuCl_2 (100 μ M) and found that it significantly inhibited Met-induced Ca efflux. Activation of PSRs appears to be coupled to increased inositol phosphate (OGR1) or cAMP (GPR4, TDAG8, possibly G2A) production. Using changes in intracellular Ca (Ca_i) as a surrogate for changes in inositol phosphate, we performed fluorescent imaging of fura-loaded primary osteoblasts grown on glass coverslips. The cells were analyzed in a closed chamber with entry and exit ports to facilitate rapid medium change at a fixed pH, Pco_2 , and $[\text{HCO}_3^-]$. Infusion of physiologic Met medium ($\text{pH} = 7.11$, $\text{Pco}_2 = 45$ mmHg, $[\text{HCO}_3^-] = 14$ mM) induced a marked, rapid, flow-independent, transient increase in Ca_i in individual cells. In contrast, infusion of Resp medium ($\text{pH} = 7.14$, $\text{Pco}_2 = 82$ mmHg, $[\text{HCO}_3^-] = 26$ mM) had no effect on Ca_i , even though the reduction in pH_i with Resp (as measured with BCECF) was at least as great as the reduction in pH_i with Met. These results indicate that a reduction in pH caused by a decrease in $[\text{HCO}_3^-]$ (Met) acts through a cell surface receptor, such as a PSR, to elicit Ca_i transients which may then modulate osteoblastic activity, implementing the subsequent increase in osteoclastic bone resorption. In contrast an equivalent reduction in pH caused by an increase in Pco_2 (Resp) did not elicit a Ca_i transient, indicating that the sensitivity of the PSR is modulated by $[\text{HCO}_3^-]$.

Disclosures: **K.K. Frick**, None.

M223

Notch1 Overexpression Inhibits Osteoblastogenesis by Suppressing Wnt/B-catenin but not BMP Signaling. V. Derogowski, E. Gazzero, L. Priest*, E. Canalis. Research, Saint Francis Hospital and Medical Center, Hartford, CT, USA.

Notch are transmembrane receptors that control cell fate decisions. Upon Delta or Jagged/Serrate ligand binding, Notch receptors undergo proteolytic cleavages leading to the release and nuclear translocation of the Notch intracellular domain (NICD), where it regulates transcription. ST-2 cells transduced with a retroviral vector overexpressing Notch 1 (NICD) under the control of a cytomegalovirus promoter exhibit impaired osteoblastogenesis. NICD overexpression inhibits the effect of bone morphogenetic protein (BMP)-2 and Wnt3a on markers of osteoblastogenesis, such as mineralized nodule formation and alkaline phosphatase activity (APA). To explore the mechanisms involved, we examined whether NICD overexpression modified BMP or Wnt signaling. BMP-2 induced the phosphorylation of Smad 1/5/8 and enhanced the transactivation of a transiently transfected BMP-responsive 12xSBE-Oc-pGL3 construct, containing 12 repeats of a Smad binding site directing luciferase expression, but NICD overexpression did not modify the level of phosphorylated Smad 1/5/8 or the transactivation of the 12xSBE construct in control or BMP-2 treated cells. BMP-2 had no significant effect on the phosphorylation of the mitogen activated protein (MAP) kinases ERK, p38 or JNK, and this was not changed by Notch. Since NICD overexpression prevented BMP-2 and Wnt induced osteoblastogenesis without altering BMP signaling, we examined whether Notch altered Wnt signaling. NICD overexpression decreased the activity of a Wnt/ β -catenin responsive construct, pTOPFLASH, containing multiple Tcf4/Lef1 binding sequences upstream of the luciferase gene. NICD overexpression also decreased the levels of β -catenin and transcripts of Wnt1 Induced Secreted Protein 1, a Wnt target gene involved in osteoblastogenesis. Transfection of a stable mutant β -catenin expression construct or the use of a Glycogen-Synthase Kinase 3 β (GSK 3 β) inhibitor (CHIR 99021), known to stabilize β -catenin by preventing its ubiquitination, partially rescued the inhibitory effect of Notch on Wnt signaling as determined by the transactivation of pTOPFLASH, despite a normalization of β -catenin levels by the GSK 3 β inhibitor. Accordingly, GSK 3 β inhibition only partially rescued the suppression of APA caused by Notch, indicating that restoration of β -catenin levels is not sufficient to rescue Wnt signaling and activity. In conclusion, Notch1 overexpression prevents BMP-2 and Wnt biological effects, without altering BMP signaling, indicating that Wnt signaling is required for osteoblastogenesis. Notch1 acts by reducing β -catenin levels and by alternate signals to suppress the Wnt/ β -catenin pathway.

Disclosures: **V. Derogowski**, None.

M224

Expression of Phosphodiesterase 4 Variants in Osteoblastic Cells. C. Nomura-Furuwatari*, Y. Ohta*, Y. Imai, K. Nakagawa*, K. Takaoka. Orthopaedic Surgery, Osaka City University Graduate School of Medicine, Osaka, Japan.

Bone formation is promoted with the treatments of BMPs and/or chemical compounds. Rolipram, a selective inhibitor of phosphodiesterase 4 (PDE4), is one of the chemical compounds promoting ossification in vivo. Four genes encoding PDE4 isoforms (PDE4A, PDE4B, PDE4C and PDE4D) are found in mammalian. Alternative splicing of PDE4 genes generates approximate 15 kinds of PDE4 variants. In order to identify active PDE4 variants in bone formation system, we investigated the expression of PDE4 variants in response to BMP treatment in osteoblastic cells. Expression of four PDE4 isoforms in osteoblastic cells was detected by RT-PCR. PDE4A and 4D were detectable in ST2, MC3T3-E1, C3H10T1/2 and primary-cultured calvarial osteoblast (PCO). PDE4A and PDE4D splicing variants in ST2 and PCO were identified by 5'-RACE method. PDE4A1, PDE4A10 and a novel variant of PDE4D were detected in ST2 cells. PDE4A10, PDE4D1, and the novel variant were detected in PCO. Previous reports indicated the induction of several variants with the increase of intracellular cAMP concentration. To examine the changes in the expression level of these variants with the treatment of BMP or cAMP, PCO was treated BMP4 and/or rolipram for 24 hours. Expression of PDE4A and 4D were quantified by real-time RT-PCR. PDE4D expression was increased 3 fold by the treatment of BMP4, 4 fold by rolipram, and 10 fold by both of BMP4 and rolipram respectively in compared to untreated cells. However, expression level of PDE4A showed no change with the treatment of BMP and/or rolipram. Real-time RT-PCR analysis showed that 4D1 was increased, but not in the novel variant. Induction of PDE4D1 by the elevation of intracellular cAMP concentration was also recognized in ST2, C2C12, MC3T3-E1 and C3H10T1/2. These results suggest that PDE4D1 is most important to control intracellular cAMP concentration in osteoblastic cells. Therapeutic potential of PDE4 inhibitors has been reported to cause some side-effects e.g. nausea and vomiting. Identification of PDE4 splicing variants expressing in bone formation is required for the development of compounds of lesser side-effects.

Disclosures: **C. Nomura-Furuwatari**, None.

M225

Roles for c-Abl in BMP Signaling, Id1 Expression, and Osteoblast Senescence. H. Kua*¹, Y. Hu*¹, X. Wang*¹, S. Boast*², S. Goff*², B. Li¹. ¹Institute of Molecular and Cell Biology, Singapore, Singapore, ²Columbia University, New York, NY, USA.

Mice lacking c-Abl exhibit a variety of complex phenotypes including retarded growth, premature death, lymphopenia and aging associated osteoporosis. Yet little is known on how c-Abl deficiency led to these abnormalities. We thus used the bone phenotypes to dissect the physiological function of c-Abl. Here we report that *c-Abl*^{-/-} osteoblasts showed reduced proliferation potential and they underwent premature senescence, manifested by increased expression of senescence associated β galactosidase and p16^{INKa}, without affecting the expression of p19/p53/p21. The elevated p16 expression in *c-Abl*^{-/-} osteoblasts was likely achieved by enhanced activation of ERKs (positive regulator) and down-regulation of Id1 (a negative regulator). c-Abl was found to positively regulate expression of Id1, a target gene of BMPs that are synthesized and secreted by osteoblasts, by modulating Smad1/5/8 phosphorylation, indicating a positive role for c-Abl in BMP signaling. In accordance, blockade of BMP actions by noggin/chordin resulted in a reduction of Id1, up-regulation of p16, and retarded growth in osteoblasts. This premature senescence of *c-Abl*^{-/-} osteoblasts could be rescued by c-Abl reconstitution or retroviral expression of Id1, and could be abrogated by p53 deficiency, but appeared to utilize a distinct mechanism from oxidative stress induced senescence. Our findings revealed novel roles for c-Abl in the BMP signaling pathway, Id1 induction, and osteoblast senescence. *c-Abl*^{-/-} mice present an animal model that links premature senescence of osteoblasts to aging associated osteoporosis.

Disclosures: **B. Li**, None.

M226

Characteristics of Circulating Mesenchymal Stem Cells in Fracture Non-Union Patients. C. Wan, Q. He*, M. McCaigue*, D. Marsh*, G. Li. Department of Trauma and Orthopaedic Surgery, Queen's University of Belfast, Belfast, United Kingdom.

The existence of peripheral blood derived mesenchymal stem cells (PB-MSCs) have been documented in adult human with low numbers. We have demonstrated previously that the number of PB-MSCs increased in the patients with fracture non-union. The present study was to compare the biological characteristics of the PB-MSCs from fracture non-union patients, with human bone marrow derived MSCs (BM-MSCs). 200 ml PB was collected from fracture non-union patients (n=9) and normal donors (n=8). Bone marrow from patients undergone hip replacement were used as controls. The mononuclear cells (MNCs) were isolated and cultured in α -MEM containing 15% FBS. The colony forming efficiency (CFE) of the PB-MNCs and BM-MNCs was calculated, and the phenotypes of PB-MSCs and BM-MSCs were compared using immunocytochemistry and flow cytometry methods. Their multipotent differentiation potentials into osteoblasts, chondrocytes, adipocytes, neurogenic and angiogenic cells were examined under specific inductive culture media. The in vivo osteogenic potential of PB-MSCs was examined by implanting the HA-TCP blocks seeded with PB-MSCs into the SCID mice for 12 weeks. After 28 days in culture, fibroblastic colonies were formed in the PB-MNCs cultures in 5 of 9 fracture non-union patients, with CFE ranging from 2.08-2.86 per 10⁶ MNCs. No fibroblastic colony was seen in PB-MNCs cultures of the 8 normal donors. Under flow cytometry examination, PB-MSCs and BM-MSCs were CD34 (low) and CD105+, but PB-MSCs were CD29-, CD44-, and ALP (low), whereas BM-MSCs were CD29+, CD44+, and ALP (high). Under specific differentiation inductions, the PB-MSCs differentiated into osteoblastic cells (ALP+, type I collagen+, osteocalcin+); chondrocytes (type II collagen+ and Alcian Blue nodules+); adipocytes (Oil red-O positive lipid accumulation). Neurogenic and endothelial differentiation of the PB-MSCs were also confirmed. For implantation study, newly formed woven bones were found in the biomaterials seeded with PB-MSCs, and they were positive for human osteocalcin immunostaining. This study indicated that there were more PB-MSCs in the peripheral circulation of the fracture non-union patients than that in the normal subjects. The PB-MSCs were clearly multi-potential cells, which had shared some common phenotypic markers with BM-MSCs, as well as many distinguishable makers from the BM-MSCs. The recruitment of the PB-MSCs through circulation might be a general phenomenon of systemic responses in many pathological conditions, such as fracture or wound healing and other systemic diseases. Further understanding the roles of PB-MSCs in diseases and repair may lead to novel therapeutic strategies.

Disclosures: **G. Li**, None.

M227

Immunity of Allogeneic Mesenchymal Stem Cells. X. Chen*¹, M. Armstrong*², G. Li¹. ¹Department of Trauma and Orthopaedic Surgery, Queen's University of Belfast, Belfast, United Kingdom, ²Department of Immunology, Queen's University of Belfast, Belfast, United Kingdom.

Interactions between T cells and mesenchymal stem cells (MSCs) demonstrated that MSCs possessed immuno-suppressive properties and were able to escape the host immune surveillance. The aim of this study was to examine the xenogeneic properties of rat mesenchymal stem cells (rMSCs) and their terminally differentiated cells upon contact with human lymphocytes and dendritic cells (DCs). Rat mononuclear cells (rMNCs) were harvested from adult GFP rat femur and cultured in DMEM at a concentration of 3 \times 10⁵ cells/cm² for 2-3 weeks. The attached primary rMSCs were passaged and subjected to adipogenic, chondrogenic and osteogenic media for further 13-28 days. The growth

ASBMR 27th Annual Meeting

kinetics of the rMSCs was assessed by BrdU incorporation and ELISA methods. Histology and immunocytochemistry (ICC) staining were used to confirm the phenotypes of differentiated rMSCs. The undifferentiated and differentiated rMSCs were seeded onto 96-well plates serving as target cells and human peripheral blood lymphocytes (hPBLs) as effector cells. The released lactate dehydrogenase (LDH) upon cell lysis was measured. A Dunn chamber chemotaxis analysis system was used to investigate the chemotactic potentials of rMSCs to human peripheral blood monocyte-derived DCs (hDCs). The migration of differentiated and undifferentiated rMSCs in the Dunn chamber system was tracked over a 10-hour period from the time-lapse images and statistically analysed. ICC and histology examinations confirmed the differentiation of rMSCs into osteoblasts, chondrocytes and adipocytes under induction media culture. The rate of cell proliferation was significantly reduced in rMSCs under chondrogenic induction. The chondrogenic MSCs had shown significant higher cyto-toxicity upon co-culture with hPBLs ($p=0.737$ VS positive control), while the other three test groups had low level of cyto-toxicity when compared with positive controls ($pMSCs=0.000$, $pAdi=0.000$, $pOsteo=0.001$). For Dunn chamber chemotaxis test, only chondrogenic rMSCs migrated towards to hDCs during 10h period (speed = $18.30 \pm 1.86 \mu\text{m/hr}$, $p < 0.0001$), while cell in the other groups showed random movements. The data indicated that among the three differentiated lineages, only chondrogenically differentiated MSCs were capable of interacting with DCs, and eliciting T cell-mediated cytotoxic immune responses in vitro. The adiogenic and osteogenic MSCs retain their immuno-suppressive properties as undifferentiated MSCs. Thus, allogeneic MSCs may be used to repair bone and soft tissue damages, but chondrogenically differentiated allogeneic MSCs may induce immune responses leading to their destruction.

Disclosures: **G. Li**, None.

M228

The Effect of Osteoactivin (OA) in Mesenchymal Stem Cell Differentiation. M. C. Rico, S. Salihoglu*, M. P. Hurley*, A. I. Nwaneshiudu*, S. N. Popoff, E. E. Safadi. Anatomy and Cell Biology, Temple University School of Medicine, Philadelphia, PA, USA.

Bone development is a complex process involving the expression of multiple genes coding for proteins that specifically induce the differentiation and activation of osteogenic cells. In particular, the differentiation of osteoblasts is a critical component requiring the expression of specific growth factors and regulatory proteins that control cell proliferation, differentiation and maturation. Among these proteins, osteoactivin (OA) has been implicated in osteoblast differentiation and function. Our laboratory previously showed that over-expression of OA in osteoblasts leads to an increase in their differentiation and function. In this study, we examined the effects of OA in mesenchymal stem cell (MSC) differentiation using the C2C12 and C3H10T1/2 MSC lines. OA was over-expressed in MSCs using a retroviral system. Osteoactivin protein expression was increased two-fold in over-expressing cells compared to Lac Z control cells for both C2C12 and C3H10T1/2. In addition, OA infection was compared to BMP-2 stimulation in the differentiation of MSCs. As expected, BMP-2 treatment alone of MSCs showed a moderate increase in the number of alkaline phosphatase (ALP) positive cells, increased in ALP cytoplasmic granule size and color intensity, indicating that BMP-2 was contributing to osteoblast differentiation. Furthermore, when MSCs were infected with an OA retrovirus, it showed an increase in the number of ALP positive cells in OA infected compared with uninfected cells. Moreover, OA infection showed even greater ALP staining when compared to BMP-2 stimulation. The most dramatic increase in the number of ALP positive cells were observed when MSCs were sequentially infected with OA retrovirus followed by BMP-2 stimulation. Interestingly, the C2C12 cells over-expressing OA showed a decrease in myocyte differentiation when compared to control cells. This was determined by visualization of contracting myocytes and staining for MF20, a marker for differentiating myoblasts. Using immunofluorescence staining, C3H10T1/2 OA over-expressing cells showed a dramatic increase in cell size and the formation of focal adhesion complexes. Overall, this data suggest that OA may play an important role in osteoblast differentiation from MSCs, possibly independently from BMP-2 stimulation. Future studies are required to determine the mechanism/s of action of OA in inducing MSCs commitment into osteoblasts.

Disclosures: **M.C. Rico**, None.

M229

Calcium Receptor Expression and the Effects of Different Extracellular Calcium Concentrations on VCAM+ Murine Bone Marrow Cells. T. Chen, L. Rodrigues*, W. Chang, D. Shoback. Endocrine Research Unit, VA Medical Center, San Francisco, CA, USA.

Previous studies have shown that cell populations derived from bone and bone marrow respond to exposure to different extracellular calcium concentrations ([Ca]_e). Changes in [Ca]_e have been implicated in the regulation of osteoblast proliferation and DNA synthesis, macrophage migration, osteoclast-mediated bone resorption, gene expression, and signal transduction. We previously showed that high [Ca]_e stimulated the formation of tartrate resistant alkaline phosphatase (TRAP)+ cells, TRAP activity, and the expression of TRAP-5b and calcitonin receptor mRNA in cultured murine bone marrow cells indicating enhanced development of osteoclasts in these marrow cultures. To determine whether high [Ca]_e were affecting gene expression globally and whether CaRs might mediate these effects, we isolated marrow from 6-week old male Black Swiss mice and sorted out bone marrow stromal cells (BMSCs) positive for CD106 or vascular cell adhesion molecule 1 (VCAM-1) by magnetic-activated cell sorting (MACS) using monoclonal antibodies to VCAM-1. We assessed the expression of the Ca receptor (CaR), VCAM-1 and the cell surface marker CD44 by confocal immunocytochemistry and changes in gene expression (osteopontin, OP; receptor activator of nuclear factor kappa B ligand, RANK-L; osteoprotegerin, OPG; type 1 collagen, coll 1) by real time quantitative PCR (qPCR). In

>80% of freshly isolated VCAM-1+ BMSCs, we observed strong cell-surface expression of CaRs that co-localized with the surface markers VCAM-1 and CD44. CaR immunoreactivity was also present in submembrane compartments. CaR expression persisted with culturing VCAM+ cells for 3 days at 1.8 mM Ca and co-localized with the surface marker CD44. qPCR was performed on RNA isolated from VCAM-1+ cells grown at different [Ca]_e for 7 days, and results were normalized to the mouse L19 gene (N=2 experiments in triplicate). OP mRNA increased at [Ca]_e of 1.7-, 5.0-, and 7.8-fold at 1.0, 3.0 and 6.0 mM Ca vs control cultures at 0.5 mM Ca. RANK-L RNA rose by 1.7-, 7.3- and 19-fold at 1.0, 3.0 and 6.0 mM Ca vs cultures grown at 0.5 mM Ca. There were no significant changes in OPG and coll 1 mRNA over the range of [Ca]_e tested. These studies indicate that CaR protein is expressed in VCAM-1+ BMSCs and that high [Ca]_e selectively regulate gene expression and in particular the expression of RANK-L mRNA, a surface molecule essential in the development and maintenance of function of bone-resorbing osteoclasts. These studies support a role for Ca generated locally in the bone microenvironment in the control of bone resorption. Studies are in progress to assess the role of CaRs in Ca-sensing by BMSCs.

Disclosures: **D. Shoback**, None.

M230

Quantitative Analysis of Bone Marrow, Fat, and Muscle as Sources of Human Connective Tissue Progenitors. C. Nakamoto*, C. Boehm*, D. Zamborsky*, H. Tao*, K. Powell*, G. F. Muschler. Biomedical Engineering, The Cleveland Clinic Foundation, Cleveland, OH, USA.

Adult musculoskeletal tissues contain heterogeneous populations of stem cells and progenitor cells (connective tissue progenitors, CTPs). The design of optimal methods for CTP targeting, harvest or processing for autogenous cell therapy requires characterization of the demographics of the CTP populations in normal tissues and their biological potential, which was the aim of this study. Bone marrow aspirates (BM), fat, and muscle tissue samples were obtained from 6 human subjects (age, 68–70). Fat and muscle tissue samples were minced and treated with collagenase type I and dispase. Cells from BM, fat, and muscle were counted and assayed for prevalence of CTPs using an established CTP colony formation assay. At day 6 cells were fixed and stained with DAPI. Fluorescent images of CTP cultures were acquired with a CCD camera. Quantitative characterization was performed on 3890 colonies (cell number, colony area) using a custom software. Fat and muscle samples (mean volume 3.1 ± 1.0 ml and 1.3 ± 0.6 ml, respectively) provided $10.6 \pm 11.3 \times 10^6$ cells/ml and $12.2 \pm 11.3 \times 10^6$ cells/ml, respectively, and a prevalence of 698 ± 1137 and 150 ± 152 CTPs/ 10^6 cells, respectively. In contrast, an average bone marrow aspirates provided $25 \pm 13 \times 10^6$ cells/ml with a prevalence of 45 ± 36 CTPs/ 10^6 cells. The concentration of nucleated cells in a BM aspirate sample was roughly a 2 fold higher than fat or muscle. However, the prevalence of CTPs among nucleated tissue-derived cells was the highest in fat (4 fold higher than muscle and 15 fold higher than BM). Furthermore, the overall concentration of CTPs was highest in fat (7400 CTPs/ml) compared to 1830 CTPs/ml in muscle and 1120 CTPs/ml in marrow aspirate). Colony size varied widely in all tissues, implying mean cycle times ranging from 17.9 to 32.8 hours. Fat-derived CTPs demonstrated lower mean proliferation rate, lower cell density in a colony than both muscle- and BM-derived cells. These data support the demographics of CTPs in marrow, fat, and muscle differs significantly. The biological potential of CTPs populations resident in these tissues also differs significantly, as manifest by differences in colony size and morphology (proliferation, migration and differentiation) under standardized conditions. Colony level analysis of CTPs is required to characterize the heterogeneity of tissue resident and tissue derived CTPs. Using morphometry and additional differentiation markers in vitro, to quantify subsets of tissue resident CTPs, this analysis can be a powerful tool for CTP population-based analysis.

Disclosures: **C. Nakamoto**, None.

M231

The Effects of the Angiogenic Inducer hCyr61 (CCN) on Human Bone Marrow-Derived Mesenchymal Stem Cells and the Endothelial Cell Line EAhy 926 - a Gene Expression Study. R. Wagemanns*, S. Jatzke*, E. Welzel*, U. Noeth*, F. Jakob*, N. Schuetze. Molecular Orthopaedics, Orthopaedic Institute, Wuerzburg, Germany.

The human cysteine rich protein 61 (hCYR61/CCN1) belongs to the CCN family of proteins which plays a role in fundamental cellular processes such as proliferation, differentiation and angiogenesis. Aim of the present study was to identify additional target cells for hCYR61 action in the bone microenvironment and to define the hCYR61 function at the level of gene expression profiling. Mesenchymal stem cells (MSCs) from human bone marrow were isolated from the femoral head obtained from patients undergoing total hip arthroplasty. Recombinant hCYR61 protein (rhCYR61) was purified from supernatants of baculovirus infected SF21 insect cells by affinity chromatography with protein G sepharose. Expanded MSCs and the endothelial cell line EAhy 926 were treated with rhCYR61 for various time points and concentrations. The proliferation of MSCs and EAhy 926 was determined photometrically using the WST-1 test. Total RNA was isolated and amplified according to standard procedures. The global gene expression pattern was performed with RNA from MSCs treated with rhCYR61 for 4 and 24 hours and with the EAhy 926 treated for 4 hours using the Affymetrix Chip HG-U133. Array analysis data were reevaluated by RT-PCR. MSCs and the endothelial cell line EAhy926 responded to the rhCYR61 treatment with an increase in proliferation rate of 30-100% in the concentration range of rhCYR61 between 0,5 and 1,5 $\mu\text{g/ml}$ cell culture medium. Array analysis of the MSCs identified rhCYR61-dependent gene products which represented transcription factors, growth factors and chemokines (25 candidates, 6 up, 9 down, cut off 2,5-fold regulation). Results indicate that human bone marrow-derived MSCs and endothelial cell line EAhy 926 are target cells for rhCYR61 function. The regulation

pattern of rhCYR61-dependent gene products strengthens the view that hCYR61 represents an integrator for signal transduction processes in cells within the human bone microenvironment. The extracellular signaling protein hCYR61 could represent an important control factor to enhance the stem cell pool. Together with its function in human osteoblasts and the role as an angiogenesis promoter the protein represents a candidate to coordinate tissue regeneration.

Disclosures: **R. Wagemanns**, None.

M232

Calcium Phosphate Surfaces Promote Osteogenic Differentiation of Mesenchymal Stem Cells. **P. Muller**^{*1}, **U. Bulnheim**^{*1}, **A. Diener**^{*1}, **F. Luthen**^{*1}, **B. Nebe**^{*1}, **K. Klinkenberg**^{*2}, **H. Neumann**^{*2}, **A. Liebold**^{*3}, **C. Stamm**^{*3}, **J. Rychly**⁴. ¹Department of Internal Medicine, University of Rostock, Rostock, Germany, ²DOT GmbH, Rostock, Germany, ³Department of Cardiac Surgery, University of Rostock, Rostock, Germany, ⁴Experimental Research Center, University of Rostock, Rostock, Germany.

Expansion and differentiation of mesenchymal stem cells on a scaffold in vitro which then can be implanted into bone represents a promising approach to regenerate bone after defects. We tested the effect of material surfaces on the differentiation of human mesenchymal stem cells. Mesenchymal stem cells were isolated from human bone marrow by cell adhesion to a purity of 95 % as tested by cell surface markers. After 14 days in expansion medium cells were seeded on a degradable xerogel composite (BONIT®matrix) composed of hydroxyapatite and β -tricalcium phosphate (XC), on hydroxyapatite coated titanium (HA) and on tissue culture plastics (TC) and cultured for further 14 days in osteoblastic differentiation medium containing glycerophosphate, ascorbic acid and dexamethasone. By staining of alkaline phosphatase (ALP) as a marker for differentiated osteoblasts we found that cells on XC and HA revealed a higher expression of ALP compared with cells on TC. We then further tested whether expansion medium is sufficient to differentiate stem cells to osteoblasts on the material surfaces. After 7 and 14 days in this medium we found a significant number of differentiated osteoblasts on XC and HA, whereas cells on TC remained negative for ALP. This result indicates that the material surfaces which contained calcium phosphate stimulate the differentiation of mesenchymal stem cells and suggests that characteristics of the material surfaces may replace the effects of components in the differentiation medium. Concerning cell characteristics that are related to cell adhesion we found a more compact cell morphology and a higher mobility of focal adhesions on calcium phosphate surfaces compared with tissue culture plastics. As a general mechanism that is probably involved in the switch from proliferation of mesenchymal stem cells to osteoblast differentiation we observed a translocation of the cell cycle inhibitor p21^{Cip/WAF1} from the nucleus on day 7 of the cell culture to the cytoplasm on day 21. Together, the results indicate that calcium phosphate surfaces promote osteogenic cell differentiation which is controlled by cell adhesion mechanisms. As a general mechanism of the switch from proliferation to osteoblast differentiation we propose an intracellular translocation of the protein p21^{Cip/WAF1}.

Disclosures: **J. Rychly**, None.

M233

Central Control of Bone Marrow Adipocyte Populations by Leptin. **M. Hamrick**¹, **M. Della-Fera**^{*2}, **D. Hartzell**^{*2}, **Y. Choi**^{*2}, **C. Baile**². ¹Medical College of Georgia, Augusta, GA, USA, ²University of Georgia, Athens, GA, USA.

Bone marrow adipogenesis is known to increase with age, and bone formation rate is inversely correlated with adipocyte number in bone biopsies of adult men and women. The negative impact of marrow adipogenesis on bone health is further indicated by the fact that women with osteoporosis have higher numbers of marrow adipocytes than those women with healthy bone. We have shown that leptin-deficient mice have low bone mass in the limb skeleton, and their limb bones also show increased bone marrow adipogenesis. We have also found that peripheral leptin treatment in leptin-deficient ob/ob mice reduces bone marrow adipocyte size and number, and that intracerebroventricular (icv) administration of leptin in rats causes adipose tissue in peripheral fat depots to undergo apoptosis in addition to activating lipolysis. We tested the hypothesis that leptin-induced reduction of bone marrow adipocyte number is mediated through a central, hypothalamic signaling pathway. Direct hypothalamic (ventromedial hypothalamus) injections of either vehicle (aCSF, 0.5 μ l/injection) or 0.5 μ g/day leptin (0.25 μ g/injection) were administered to male Sprague-Dawley rats (n=10 per group) twice daily for five days. The right tibia was cut across the proximal third of the shaft, decalcified in EDTA, embedded in paraffin, and sectioned at 5 μ m. Adipocytes were counted over a 0.10 mm² area and adipocyte density (N.At/Ma.Ar) expressed as the number of adipocytes per tissue area. Bone marrow was flushed from the right femur and a Beadlyte suspension array used to analyze adipocyte apoptosis in marrow samples using caspase-3 concentration as an apoptotic marker. Analysis of the proximal tibias from treated rats reveal that central (VMH) leptin administration significantly (P<.001) decreased adipocyte number by more than 50% in bone marrow. Analysis of caspase-3 concentration in bone marrow taken from the hindlimbs of control and treated rats reveals that leptin treatment significantly (P<.001) increased caspase-3 levels in bone marrow. Together, these data suggest that leptin regulates adipocyte apoptosis in bone marrow through a central, hypothalamic signaling pathway.

Disclosures: **M. Hamrick**, None.

M234

Osteoporosis and Impairment of Osteoblast Differentiation in Mouse Models of Accelerated Aging. **R. J. Pignolo**¹, **Y. Choi**^{*2}, **F. B. Johnson**^{*2}.

¹Department of Medicine, University of Pennsylvania, Philadelphia, PA, USA,

²Department of Pathology, University of Pennsylvania, Philadelphia, PA, USA.

Telomeres shorten with age in most human tissues, including bone, and because telomere shortening is a cause of cellular replicative senescence in cultured cells, including osteoblasts and mesenchymal stem cells (MSCs), we hypothesized that telomere shortening contributes to the aging of bone. Since laboratory strains of mice have telomeres that are 5-10 times longer than human telomeres, mice must lack telomerase for several generations (3-6, depending on genetic background) before telomeres become critically short and phenotypic defects can be easily detected. Osteoporosis is common in individuals with the Werner (WRN) premature aging syndrome. One of the targets of the WRN helicase is telomeric DNA and, given that mice have much longer telomeres than humans, murine telomeres never become short enough to elicit the "aging" phenotypes (in the absence of WRN) that occur in human cells. By combining the WRN mutation with the shortened telomeres of telomerase (TERC) knockout mice, synthetic defects in proliferative tissues have been observed. Here we demonstrate for the first time that deficiencies in genome maintenance molecules such as TERC and WRN, alone or in combination, cause a low bone mass phenotype (as measured by small animal DXA) and are the result of impairment in osteoblast differentiation and function. Markers of bone formation are reduced or absent in bone marrow-derived MSCs from WRN and TERC mutant mice while osteoclast differentiation is unchanged. We also show that bone marrow-derived MSCs from mutant mice have a reduced in vitro life span and display impaired osteogenic potential concomitant with characteristics of premature senescence. These data provide strong evidence that replicative aging of osteoblast precursors is an important mechanism of senile osteoporosis.

Disclosures: **R.J. Pignolo**, None.

M235

The Importance of Extracellular Matrix Components in the Culture and Differentiation of Adult Human Mesenchymal Stem Cells. **T. Helledie**^{*}, **C. Dombrowski**^{*}, **Z. Zhou**^{*}, **V. Nurcombe**^{*}, **S. Cool**. Stem and Tissue Repair, Institute of Molecular and Cell Biology, Singapore, Singapore.

In all tissues of the body there is a sub-population of adult stem cells. These multi-potential cells are recruited and activated to take part in tissue regeneration. Adult stem cells are a promising resource for therapy, but their numbers are low and they need propagation in vitro to be of therapeutic use. When these cells are cultured ex vivo it has proven difficult to recreate their natural microenvironment - "the niche". The niche is a sum of signals from interactions with the extracellular matrix (ECM) and neighboring cells, and the hormonal status in the microenvironment. In addition to the direct interaction with the stem cells, specific components of the ECM play key roles in the regulation and presentation of growth and adhesion factors, thus controlling intracellular signaling. By adding proteoglycan together with growth factors to the culture of bone marrow-derived adult human mesenchymal stem cells (hMSC), we have optimized the culture conditions for growth and differentiation of these cells. We have analyzed the effect of the proteoglycans on proliferation and differentiation of hMSC by using FACS analysis, CFU-F assays and differentiative staining. Knowledge of the interactions between proteoglycans, tissue-specific mitogens and other elements of the stem cell niche will ultimately lead to key discoveries in the use of ECM components for tissue engineering.

Disclosures: **S. Cool**, None.

M236

The Role of Stromal Derived Factor-1 Alpha in Bone Remodelling. **A. Zannettino**^{*}, **A. Kortesidis**^{*}, **A. Farrugia**^{*}, **S. Gronthos**. Division of Haematology, Institute of Medical and Veterinary Science, Adelaide, Australia.

The balance between bone formation and resorption is regulated by different cellular components within the bone marrow microenvironment. We surveyed a stromal cell cDNA library constructed from purified bone marrow stromal stem cells (BMSSC) in order to identify putative regulatory factors of bone turnover. Stromal derived factor-1 alpha (SDF-1) was one highly expressed gene found to be prevalent in uncommitted BMSSC. The chemokine, SDF-1 and its receptor, CXCR4 are involved with various functions such as mediating trafficking of cells between the bone marrow and peripheral blood. In the bone marrow, SDF-1 is expressed by endothelial cells, perivascular cells, some stromal elements in the marrow spaces and at the endosteal surfaces. We found that immature pre-osteogenic cells expressed greater levels of SDF-1 when compared with differentiated bone cells including osteoblasts, bone lining cells and osteocytes. Correspondingly, SDF-1 gene expression was rapidly down-regulated when BMSSC were cultured under osteoinductive conditions. Retrovirally transduced BMSSC, secreting high SDF-1 levels, displayed an enhanced ability to form ectopic bone in vivo and an increased capacity for cellular growth and survival in vitro. To examine the effect of SDF-1 on bone resorption, peripheral blood-derived osteoclast precursor cells were cultured under osteoclast-inductive conditions in the presence of recombinant human SDF-1. Our studies showed that SDF-1 mediated a measurable increase in both the number and the size of the resorption lacunae formed. The SDF-1 induced osteoclast activation correlated to an increase in the expression of a number of osteoclast associated genes including, RANKL, RANK, TRAP, matrix metalloprotease-9, Carbonic Anhydrase II, and Cathepsin K. In summary, our data suggest that SDF-1 plays a role in the maintenance and survival of immature BMSSC, and the recruitment and activation of osteoclast precursor cells.

Disclosures: **S. Gronthos**, None.

M237

Heparin Promotes Adipogenic Differentiation of Mesenchymal Precursors by Altering Cell-Extracellular Matrix Interactions. W. Luo*¹, M. S. Friedman*¹, C. N. Bennett*¹, O. A. MacDougald*², J. D. Miller*¹, K. D. Hankenson¹. ¹Orthopaedic Surgery, University of Michigan, Ann Arbor, MI, USA, ²Molecular and Integrative Physiology, University of Michigan, Ann Arbor, MI, USA.

A variety of growth factors have reciprocal effects on the osteoblast and adipocyte differentiation of marrow-derived mesenchymal progenitors. Recent work suggests that heparin has a positive affect on adipocyte differentiation, while, heparin negatively affects bone formation in vivo and osteoblast cell differentiation and function in vitro. In this study we have further explored the role of heparin in adipogenic induction of mesenchymal precursors. We have found that heparin is not sufficient to induce adipogenic induction of three different mesenchymal progenitors (immortalized murine marrow stromal cells, ST2 cells, or 3T3L1 preadipocytes), but heparin can potentiate adipogenic induction of these cells. Indeed, heparin is not sufficient to induce expression of the adipocyte transcription factors, PPAR- γ and C/EBP- α , nor the later stage adipocyte markers, LPL and FABP4, but heparin treatment in combination with standard adipogenic induction results in enhanced expression of these genes. This effect is dose and time dependent; heparin promotes adipogenic differentiation at concentrations greater than 0.1 microgram/ml when applied before day 3 of induction. The effect of heparin is independent of cell proliferation and cell density, and experiments with two different lipid-free conditions, serum-free and delipidated serum, indicate that heparin promotes adipogenesis independent of extracellular lipid or lipoprotein lipase activity. The effect of heparin is not due to its strong anionic charge because another anionic glycosaminoglycan, dextran, does not promote differentiation. Remarkably, short-term heparin treatment alters the morphology and adhesion characteristics of progenitor cells and longer treatment, in association with adipogenic induction, results in cell rounding and aggregation. In addition, heparin is able to counteract the negative effects of strong adhesive substrates, such as fibronectin, collagen and poly-L-lysine, on adipogenesis. We hypothesize that heparin promotes adipogenesis by disrupting cell-extracellular matrix interactions. This is consistent with recently published studies which suggest that cell rounding and subsequent inhibition of Rho signaling is required for adipogenesis, while Rho activation leads to osteoblasts formation.

Disclosures: **W. Luo, None.**

M238

Comparing Osteoprogenitor Source and Transplantation Protocols. L. Wang*, Y. Liu*, X. Jiang*, D. W. Rowe. Genetics and Developmental Biology, University of Connecticut Health Center, Farmington, CT, USA.

As interest in the therapeutic use of adult stem stems increases, it will become increasing difficult to judge which source of progenitor cells or transplantation protocol is optimal for engraftment and integration into host bone. Because the number of combinations that need to be evaluated will be large, a rapid and sensitive method will be required to identify promising strategies. We are utilizing bone restricted promoter-GFP constructs to distinguish between host and donor contribution to bone formation when progenitor cells are injected into the host marrow space. A comparison of transplantation of syngeneic C57Bl/6 donor -> recipient protocol with or without concomitant total body irradiation (TBI) and bone marrow transplantation (BMT) clearly showed greater engraftment when the endogenous bone is forced to recover from TBI. Thus the TBI/BMT protocol makes allogeneic transplantation a feasible method for engraftment evaluation and experience to date shows persistence of donor derived osteoblasts for at least 6 months. Comparison of various sources of progenitor cells indicate that freshly isolated calvarial digest cell exceed culture expanded calvarial cells, marrow stromal fibroblasts cultures grown either at low density or in the presence of FGF2 in their ability to engraft and make new bone matrix. Extended passaging or time in culture further reduced osteogenic differentiation. Freshly obtained calvarial cells also exceeded the ability of other progenitor cells to distribute widely throughout the marrow space. Adipose derived stromal cells and dermal fibroblast failed to show osteogenic activity. The possibility of inducing immune tolerance by systemic transplantation of new born mice was examined. While wide tissue distribution including bone and persistence of injected cells was observed, the engrafting cells were not osteogenic. Dermal fibroblasts exceeded osteoprogenitor cells derived from calvaria or marrow stromal in their ability to home to bone. To make these transplantation experiments more quantitative, protocols are being developed that use three colors of GFP to identify the host, reference donor and test donor cells. Similar to the competitive engraftment protocol used in the hematopoietic field, this approach not only relates the relative engraftments of the test versus a reference progenitor cell but can be used to assess intramarrow distribution and longevity. Developing standardized and quantitative methods for evaluating transplantation protocols and progenitor cell populations will be a requirement of federal licensing authorities and the reagent mice discussed here provide one avenue to meet this demand.

Disclosures: **L. Wang, None.**

M239

In Vivo Expansion and In Vitro Characterization of Pluripotent Adherent Stromal Cells in Mouse Adipose Tissue. Z. Huang¹, J. Bryvan*¹, H. Yu*¹, W. Horton², L. Sandell¹. ¹Orthopaedic Surgery, Washington University, St Louis, MO, USA, ²Oregon Health Sciences University, Portland, OR, USA.

Pluripotent adherent stromal cells (ASC) are a rare stem cell population that exists in the "niche" environment of many adult tissues. Scarcity of ASCs, immature in vitro culture condition and lack of unique cell surface markers hinder in vitro rapid expansion and purification of ASCs from transgenic and knockout mice. To address this, we investigated whether it was feasible to in vivo expand pluripotent adipose ASCs. 4 weeks old (4 wks) and 8 weeks old (8 wks) C57/B6 male mice were divided into 2 groups each and fed on normal diet (ND) and high fat diet (HFD) for approximately 2 and half months. Body weights were increased by 57%, 148%, 28% and 68% for mice on ND (4 wks), HFD (4 wks), ND (8 wks) and HFD (8 wks), respectively. Total fat weights (visceral and inguinal fat pads) were 0.88, 4.11, 0.60 and 3.60 grams for mice on ND (4 wks), HFD (4 wks), ND (8 wks) and HFD (8 wks), respectively. HFD increased total fat accumulation by 3.7 fold and 5.0 fold for mice (4 wks) and (8 wks), respectively. Adipose ASCs were isolated by collagenase digestion and attachment selection. They were fibroblast-like with no adipocyte present. Total cell numbers were 2.4×10^4 , 5.5×10^5 , 3.4×10^4 and 7.2×10^5 for mice on ND (4 wks), HFD (4 wks), ND (8 wks) and HFD (8 wks), respectively. HFD increased total ASCs by 22.5 fold and 20.0 fold for mice (4 wks) and (8 wks), respectively. Interestingly, ASCs per gram of fat were also increased by HFD, with 4.5 fold and 3.1 fold for mice (4 wks) and (8 wks), respectively. Pluripotency of adipose ASCs was tested for their ability to differentiate into three cell lineages, adipocytes, osteoblasts, and chondrocytes. Adipogenic differentiation was evident by intense Oil Red staining and increased RNA levels of CEBP α , Adipsin, and PPAR γ 1 and 2. Osteogenic differentiation was confirmed by increased nodule formation, Alizarin Red staining and increased RNA levels of alkaline phosphatase, osteopontin, and Runx2. Chondrogenic differentiation was confirmed by appearance of fluorescence in micromass culture using ASCs isolated from mice expressing EGFP under the type II-collagen promoter, and increased RNA levels of type II collagen, aggrecan, alkaline phosphatase and bone sialoprotein. Taken together, we have confirmed for the first time that mesenchymal ASC in adipose tissue can be expanded in vivo and have successfully established new methods to verify pluripotency of ASCs in vitro. Successful expansion and isolation of pluripotent ASCs in large quantity will facilitate further study of molecular mechanisms of mesenchymal cell differentiation in vitro using transgenic and knockout mice.

Disclosures: **Z. Huang, None.**

M240

Critical Requirement of JNK Activity for the Maintenance of Commitment to Osteoclasts. E. Chang*, J. Ha*, H. Huang*, H. Kim*, J. Ko. Cell and Developmental Biology, Seoul National Univ. College of Dentistry, Seoul, Republic of Korea.

Monocyte/macrophage lineage of hematopoietic cells serves as osteoclast precursors, which can further differentiate to mature osteoclast in microenvironment of bone. This precursor cells can differentiate to TRAP positive mononuclear pre fusion osteoclasts, which give rise to multinucleated osteoclasts in response to receptor activator of nuclear factor κ B (NF- κ B) ligand (RANKL). In this study, we found the mechanism by which JNK inhibition reverses the phenotype of mononuclear pre fusion osteoclasts into osteoclast precursors during RANKL-induced osteoclast differentiation. We show that JNK inhibition by SP600125 treatment specifically inhibits early stage of osteoclast differentiation but not late stage of it. The inhibitory effect of SP600125 down-regulated mRNA of various markers of osteoclasts and TNF receptor 1 (TNFR1), TNFR2, and RANK. Furthermore, pre fusion osteoclast cells treated with SP600125 for 24 h showed low expression of TNFR1, TNFR2, and RANK and high expression of macrophage antigen CD11b. Interestingly, cells in the presence of SP600125 showed higher phagocytic activity than pre fusion osteoclasts. Consistent with this, JNK inhibition repressed human peripheral monocyte derived osteoclast differentiation at the stage of pre-osteoclasts. We propose that JNK activity is required at the stage of pre fusion osteoclast differentiation into mature osteoclasts by maintaining their phenotype of osteoclast lineage.

Disclosures: **E. Chang, None.**

M241

Osteoclasts Prefer Old Bone. D. J. Leeming*¹, R. H. Nielsen*¹, I. Byrjalsen*¹, M. G. Sorensen*¹, C. Christiansen², T. J. Martin³, K. Henriksen¹, P. Qvist¹, M. A. Karsdal¹. ¹Nordic Bioscience, Herlev, Denmark, ²Center for Clinical and Basic Research, Ballerup, Denmark, ³SVIMR, Melbourne, Australia.

Osteoclasts resorb bone in order to repair micro cracks to maintain the quality of bone. How osteoclasts target old bone in order to sustain the quality of the skeleton by constant remodelling is currently not known. We investigated the hypothesis that old bones accumulate signals, which target the bone for remodelling by osteoclasts. Human osteoclasts were assessed for their ability to resorb bone, survive and differentiate on old versus young bone. Bovine cortical bone slices from 9-month-old calves and 8-year-old cows were used. The bones were assessed by measuring the amount of native form (α -CTX) and the age-modified form (β -CTX) of collagen type I. Monocytes were isolated from human peripheral blood using a CD14⁺ bead sorting system, seeded on young and old bone and cultured in the presence of 25ng/ml of M-CSF and RANKL in 10% serum for 21 days. Mature human osteoclasts were seeded on young and old bone and cultured for 5 days in 10% serum with 25ng/ml M-CSF and RANKL, followed by 48 hours in 0.1%

ASBMR 27th Annual Meeting

BSA. Subsequently, osteoclast numbers were investigated by counting of TRAP positive multinuclear cells and measurement of TRAP activity. Osteoclastic resorption was investigated by measurement of the β -CTX in the conditioned medium. Cortical bones slices from old cows contained 3 times lower alpha/beta ratios than that of young bones ($p < 0.01$). The formation of osteoclasts from osteoclast precursors cultured on young bone was more than 50% ($p < 0.001$) reduced compared to those formed on old bone, and osteoclastic resorption measured by β -CTX was 80% ($p < 0.001$) reduced on young bone compared to old bone. Mature osteoclasts were investigated by seeding already mature osteoclasts on young and old bone. Mature osteoclastic resorption was reduced 75% ($p < 0.001$) on young bone compared to that of old bone. By counting of cells on the bones, it was found that old bones had two times ($p < 0.01$) the number of multinuclear osteoclasts, whereas the number of mononuclear cells was two times higher on the young bone ($p < 0.01$). To ensure that the differences observed between young and old bone were not caused by individual differences in the bones and animals, we investigated bones from 14 different old cows and 4 young calves and found similar results. In summary, these data clearly show that old bones are more susceptible to bone resorption by osteoclasts than young bones, and that old bone support osteoclastogenesis better than that of young bone. Thus, the age of the bones might play an important role in controlling the amount of resorption, and thus play important roles in targeting osteoclasts to old bone in the remodelling process.

Disclosures: M.A. Karsdal, None.

M242

Overexpression of ADAM8 in Osteoclast Precursors Increases Osteoclast Formation and Decreases Trabecular Bone Volume *In Vivo*. V. Garcia Palacios¹, M. A. Subler^{*2}, H. Y. Chung¹, S. J. Choi¹, K. Patrene^{*1}, H. C. Blair³, J. J. Windle², G. D. Roodman⁴. ¹Medicine/Hem-Onc, University of Pittsburgh, Pittsburgh, PA, USA, ²Human Genetics, Virginia Commonwealth University, Richmond, VA, USA, ³Pathology, University of Pittsburgh, Pittsburgh, PA, USA, ⁴Medicine/Hem-Onc, University of Pittsburgh and VA Pittsburgh Healthcare System, Pittsburgh, PA, USA.

Members of the ADAM (A Disintegrin And Metalloprotease) family of proteins are Type I transmembrane proteins involved in cell proliferation, differentiation, migration, adhesion, fusion, and cell morphogenesis. They are composed of several homologous structural domains including metalloprotease, disintegrin, cysteine-rich, EGF-like, transmembrane and cytoplasmic domains. We reported that ADAM8 is the ADAM family member most highly expressed in OCL precursors and that blocking ADAM8 expression inhibits OCL formation. ADAM 8 also appears to have a role in immune function through its capacity to induce leukocyte migration and cell adhesion. ADAM8 is upregulated in particle-induced arthritis, suggesting that overexpression of ADAM8 plays a role in the bone destruction associated with this process. It is our hypothesis that ADAM8 may be associated with a variety of inflammatory arthritides, and it may mediate the bone destruction in these conditions. To test this hypothesis, we targeted ADAM8 to cells in the OCL lineage *in vivo* using the TRAP promoter to measure the effects of increased ADAM8 expression on OCL activity *in vivo*. Transgenic mice overexpressing ADAM8 formed twofold more multinucleated TRAP (+) cells in marrow cultures than control mouse cultures. Importantly, as these mice increased in age, their OCL formation capacity increased up to threefold as compared with the wild type littermates. Micro-computed tomography analysis of the fifth vertebrae from TRAP-ADAM8 mice showed that the trabecular bone fraction (bone area/total area; BA/Tar) was $40 \pm 7\%$, vs. $59 \pm 3.5\%$ for wild type mice. These data demonstrating that increased expression of ADAM8 targeted to OCLs results in enhanced OCL formation, increased OCL precursors *in vivo*, and decreased trabecular bone, support an important role for ADAM8 in OCL formation and are consistent with ADAM8 mediating bone destruction in inflammatory bone disease.

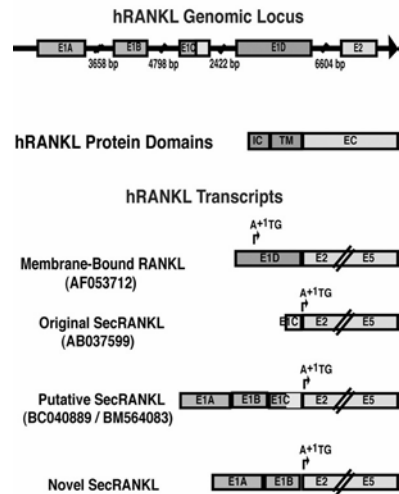
Disclosures: V. Garcia Palacios, None.

M243

The Expression of Novel Human RANKL mRNAs in Cell Types Associated with Inflammatory Bone Loss. N. C. Walsh¹, A. R. Pettit², C. A. Manning^{*1}, J. Wang¹, K. P. McHugh¹, E. M. Gravalles^{*1}. ¹Beth Israel Deaconess Medical Center, New England Baptist Bone and Joint Institute, Harvard Medical School, Boston, MA, USA, ²Institute for Molecular Bioscience, University of Queensland, Brisbane, Australia.

RANKL expression is requisite for osteoclastogenesis in physiologic bone remodeling and in inflammation-induced bone loss. This study characterizes the expression of RANKL mRNA splice variants in cell types known to be sources of RANKL in inflammation-induced bone loss. RANKL was described as a membrane-bound protein that can be cleaved to produce a functional soluble protein. Splice variants of the human RANKL (hRANKL) mRNA have also been described including one encoding a putative secreted form (AB037599, Fig 1). We have identified two EST sequences (BC040889, BM564083) in the hRANKL UniGene Cluster Hs.333791, that have additional sequence 5' of the original secreted RANKL mRNA. Genomic mapping shows that this additional sequence represents a 5' extension of the first exon of AB037599 (designated E1C) and includes 2 novel exons, designated E1A and E1B upstream of E1C (Fig 1). Expression of the BC040889 transcript was verified by RT-PCR from the human osteosarcoma cell line, Saos-2, the Jurkat T cell line and from primary T cells. We have also identified a novel splice variant of this sequence that lacks E1C. Importantly, the expression of both of these novel hRANKL mRNAs is upregulated by TNF- α or PTHrP in Saos-2, and by activation in Jurkat and primary T cells (CD3/CD28 or PMA/ionomycin). The longest open reading frame for both transcripts begins at E2, the start of the extracellular domain of the RANKL protein, indicating that these transcripts encode a putative secreted form of this protein.

Comparative genome analysis demonstrates the conservation of 1.8kb of sequence proximal to E1A, containing conserved binding sites for transcription factors implicated in inflammatory signaling. Preliminary studies indicate that this 1.8kb sequence acts as a basal promoter in transient transfection of Jurkat T cells and is inducible by PMA/ionomycin. This study is the first to identify the expression of mRNAs encoding a putative secreted form of hRANKL in cells known to express RANKL in inflammatory bone loss and highlights a novel regulatory region that may direct the expression of secreted hRANKL mRNAs in this setting.



Disclosures: N.C. Walsh, None.

M244

Cell Cycle Progression and Arrest in the Presence of RANKL Are Necessary for Osteoclastogenesis. T. Mizoguchi^{*1}, Y. Yamamoto^{*2}, T. Yamashita³, Y. Kobayashi¹, N. Udagawa³, M. Ito^{*1}, N. Takahashi⁴. ¹Institute for Oral Science, Matsumoto Dental Univ., Nagano, Japan, ²Aichi Gakuin Univ., Nagoya, Japan, ³Biochemistry, Matsumoto Dental Univ., Nagano, Japan, ⁴Graduate School of Oral Medicine, Matsumoto Dental Univ., Nagano, Japan.

Osteoclasts are terminally differentiated cells. We examined the role of cell cycle regulatory molecules in osteoclastogenesis. Mouse bone marrow macrophages (BMM ϕ) differentiated into osteoclasts in the presence of M-CSF and RANKL within 3 days. When hydroxyurea was added to BMM ϕ cultures at the beginning of the culture, both cell proliferation and osteoclast formation were inhibited. However, osteoclast formation was markedly enhanced, when hydroxyurea was added after culture for 1 day. These results suggest that cell cycle progression of BMM ϕ in the presence of RANKL is required for their differentiation into osteoclasts, and that the cell cycle arrest immediately after the proliferation enhances osteoclastic differentiation. These results were confirmed by the experiment of bromodeoxyuridine labeling. When the labeling was performed at the beginning of the culture in the presence of RANKL, all nuclei of osteoclasts were labeled. In contrast, when the labeling was performed after culture for 1 day and for 2 days in the presence of RANKL, 80% and 20% nuclei of osteoclasts, respectively, were labeled. This suggests that cell proliferation and cell cycle arrest occurs during osteoclast formation after stimulation of RANKL. A complex of cyclin and cyclin-dependent kinase (Cdk) drives the cell cycle. BMM ϕ expressed cyclins D1, D2, D3 and E1, and Cdks 2, 4 and 6. Expression of those proteins in BMM ϕ was decreased by the treatment with RANKL. The expression of cip/kip family proteins, p21^{cip1} and p27^{kip1}, both of which inhibit Cdk activity and induce cell cycle arrest, was examined in BMM ϕ . Expression of p27^{kip1} was up-regulated but that of p21^{cip1} was down-regulated in BMM ϕ treated with RANKL. This suggests that p27^{kip1} is involved in cell cycle arrest of RANKL-treated BMM ϕ . When BMM ϕ were co-transfected with cyclin D1 and Cdk 4 cDNAs, BMM ϕ proliferated and failed to differentiate into osteoclasts even in the presence of RANKL. In contrast, osteoclastic differentiation was accelerated in BMM ϕ transfected with p27^{kip1} cDNA. To elucidate whether RANKL-regulated cell cycle is specific for BMM ϕ or not, osteoblasts were transfected with RANK cDNA. RANKL activated p38, JNK and NF- κ B in osteoblasts expressing RANK, but failed to induce the cell cycle arrest. These results suggest that cell proliferation and cell cycle arrest immediately after the proliferation in osteoclast precursors in the presence of RANKL are required for their differentiation into osteoclasts.

Disclosures: T. Mizoguchi, None.

M245

Effects of Trichostatin A on Apoptosis and Differentiation of Osteoclasts. T. Yi^{*1}, J. Seo^{*1}, H. Kim^{*1}, S. Ko², J. Baek¹, G. Kim^{*1}, K. Woo^{*1}. ¹Dept. of Cell and Developmental Biology, Seoul National University, School of Dentistry, Seoul, Republic of Korea, ²Dept. of Pharmacology, Kangnung National University, School of Dentistry, Kangnung, Republic of Korea.

Histone deacetylase inhibitors (HDIs) are a new promising class of anticancer agents since they selectively inhibit the proliferation of tumor cells in culture and *in vivo* by inducing cell-cycle arrest, terminal differentiation, and/or apoptosis. Recently, some types of normal cells have been reported to be susceptible to HDIs. In this study, the effects of

ASBMR 27th Annual Meeting

Trichostatin A (TSA), one of HDIs, on osteoclasts were examined. TSA was continuously or transiently treated to mouse bone marrow macrophage/monocyte lineage cells during the differentiation into osteoclasts induced by M-CSF and RANKL. TSA (100 nM) increased the apoptosis of both preosteoclasts and mature osteoclasts, and activated the procaspases. TSA tended to affect to differentiation of osteoclast in a stage-specific manner. We also observed that TSA enhanced expressions of cyclin-dependent kinase inhibitors (p21waf1 and p15ink4b) and TRAIL/TRAIL R2, which are known to regulate the osteoclast differentiation. These findings indicate that osteoclast is one of susceptible cells to HDIs and imply that the precisely regulated acetylation might be involved in the osteoclastic differentiation.

Disclosures: **J. Seo, None.**

M246

Urokinase Receptor Is Involved in Bone Remodeling by Influencing Osteoclasts Resorption. **F. Furlan¹, N. Jorgensen², J. Jemsen^{*2}, A. Rubinacci^{*3}, E. Mrak^{*3}, M. Marezzana^{*3}, F. Blasi^{*1}.** ¹Molecular Genetics, University Vita-Salute, HSR, Milano, Italy, ²Endocrinology, Copenhagen University, Copenhagen, Denmark, ³Bone Metabolic Unit, HSR, Milano, Italy.

Urokinase receptor (uPAR) is actively involved in the regulation of important cell functions like adhesion and migration and it has been shown to interact with integrins. It has been previously shown that the major players of bone remodeling, osteoblasts (obs) and osteoclasts (ocs), produce urokinase (uPA) and express its receptor (uPAR). Moreover, The purpose of this study was to investigate the role of uPAR in bone remodeling. We analyzed the bone phenotype in uPAR-null female mice. The size of mutant mice was reduced as compared to normal animals, and in more details, there was a significant decrease in tibia length in mutant mice as compared to Wt. Bone mass analysis of uPAR Ko by peripheral quantitative computed tomography (pQCT), revealed an increase in bone mass with respect to wild type (p<0.02). The histomorphometric analysis of the tibia in uPAR Ko showed a reduction in the bone volume compared to wild type (more bone density but less bone volume) with a significant reduction in cortical thickness in Ko mice, and a reduction of resorbing surface in Ko bones compare to Wt. Moreover, mechanical tests showed a reduction in the capability to sustain a given load in uPAR Ko tibias as compared to tibias from wild type female animals (p<0.02). To explore the cellular basis of the bone defect in uPAR Ko mice, we cultured osteoblasts and osteoclasts in vitro. The results showed a proliferative advantage with no difference in apoptosis, and a higher susceptibility to matrix mineralization in uPAR Ko as compared to Wt obs. The production of proteins involved in the mineralization process, like alkaline phosphatase (ALP), was increased only during the first weeks of obs maturation. After 4 weeks, ALP was similar in both genotypes. RANKL expression on obs surface did not change between two different genotypes at different stages of differentiation. On the contrary the number of ocs formed in vitro using uPAR Ko monocytes was decreased compared to Wt. Moreover, we have found that uPAR co-localized with integrin b3 on ocs podosomes by confocal microscopy. Therefore, we would like to better understand the role of uPAR in ocs function by crossing uPAR Ko mice with integrin b3 ko mice. Experiments in order to investigate the downstream pathways in obs and ocs (AP1 family) are under current investigation. Together our preliminary data indicate that uPAR may play an important role in bone physiology by influencing osteoclasts function.

Disclosures: **F. Furlan, None.**

M247

MCP-1 Expression Correlates with Multinucleation of Human Osteoclasts. **C. J. Day*, S. R. J. Stephens*, M. S. Kim*, N. A. Morrison.** School of Medical Science, Griffith University, Gold Coast, Australia.

Osteoclasts are characterized as multinuclear cells positive for TRAP, calcitonin receptor (CTR), cathepsin K (CTSK) and NFATc1. MCP-1 is a CC chemokine that is induced by RANKL and suppressed by GM-CSF. In the absence of RANKL, treatment with MCP-1 and M-CSF results in multinucleated cells that are TRAP+ and express a range of osteoclast markers, including NFATc1, but do not resorb bone. In this study we examine the correlation between MCP-1 expression and multinucleation, using real time quantitative PCR to measure gene expression relative to RNA content rather than cell number. The role of different signalling pathways in human osteoclast differentiation were tested using antagonists: SB203580 (p38MAPK), U0126 (ERK1/2), rapamycin (mTOR), intracellular calcium regulators (IC-IBMECA) and NFATc1 inhibitors (cyclosporin A, CSA). In the mouse, SB203580 and CSA blocked osteoclast formation, while U0126 and rapamycin excited osteoclast formation. In contrast, in the human osteoclast system, only rapamycin permits multinuclear cell formation, while SB203580, U0126 and CSA block the formation of multinuclear cells. We sought another inhibitor of osteoclast formation based on our observation that the adenosine A3 receptor is induced by RANKL. Treatment with IC-IBMECA (an adenosine A3 agonist) inhibited the formation of multinuclear cells and also suppressed MCP-1 induction. RANKL induction of MCP-1 was abolished by those agents that blocked multinuclear cell formation (SB203580, U0126, CSA and IC-IBMECA) but MCP-1 induction was not affected by rapamycin. In stark contrast, the RANKL induction of TRAP and NFATc1 were not altered by any of these agents compared to the M-CSF and RANKL treated control, illustrating that TRAP and NFATc1 expression is not correlated with multinucleation. Although RANKL induction of TRAP and NFATc1 was not affected, the expression of CTR and CTSK showed differential effects when treated with osteoclast inhibitors. Treatment with SB203580 and IC-IBMECA resulted in down-regulation of CTSK. CTR expression in the presence of inhibitors was reduced with the exception of IC-IBMECA. Treatment with IC-IBMECA resulted in higher CTR expression than in control osteoclasts, suggesting an adenosine effect on CTR expression. The consistent outcome of the inhibitor experiments is that MCP-1 expression is highly correlated with multinucleation. Cells can be positive for TRAP and NFATc1 but are not

multinuclear unless MCP-1 expression is also present. This correlation is consistent with the observation that adding exogenous MCP-1 results in multinuclear polykaryons that are TRAP+, CTR+ and have high levels of NFATc1 but do not degrade bone.

Disclosures: **C.J. Day, None.**

M248

Truncation Mutants of RANKL within the TNF-Like Core Domain Inhibit RANKL-Induced Osteoclast Differentiation and Activation. **C. Wang^{*1}, J. W. Tan^{*1}, N. J. Pavlos^{*1}, J. M. Li^{*2}, J. Cornish², M. H. Zheng¹, J. Xu¹.** ¹Dept. of Orthopaedic Surgery, The University of Western Australia, Nedlands, Australia, ²Dept. of Medicine, University of Auckland, Auckland, New Zealand.

Receptor activator of NF- κ B ligand (RANKL) is a crucial factor necessary for osteoclast differentiation and activation. In this study we have examined the role of the TNF-like core domain of RANKL in osteoclast differentiation and activation. To this end, a series of truncation mutants of the TNF-like core domain of RANKL were expressed as GST-fusion proteins, and their biological activities assessed using a number of pro-osteoclastogenic systems. Osteoclastogenesis assays revealed that while GST-rRANKL (aa160-318) containing the full TNF-like core region strongly induced osteoclast formation, RANKL truncation mutants GST-rRANKL (aa239-318), (aa160-268), (aa160-291), (aa246-318) display significantly decreased osteoclastogenic activity. Consistently, the decrease in osteoclast number correlates with decreased TRACP activity and reduced calcitonin receptor and cathepsin K gene expression. Furthermore, competition studies revealed that all RANKL truncation mutants were capable of inhibiting RANKL (aa160-318)-induced osteoclast formation but with different efficacy, RANKL mutant (aa246-318) being the most potent. RANKL mutant (aa246-318) was also found to competitively decrease RANKL (aa160-318)-induced osteoclastic bone resorption *in vitro*. Interestingly, GST pull down studies reveal that all RANKL mutants have reduced binding affinity to RANK. In addition, all RANKL mutants display significant reduction in the activation of crucial osteoclastic signalling pathways including NF- κ B, ERK, JNKs and have decreased IKB α degradation as compared to the full-length protein. Together, our data indicate that RANKL mutants within the TNF-like core domain may act as competitive inhibitors of RANKL-induced osteoclast differentiation and activation and thus may offer potential therapeutic approaches to combat bone lytic disorders.

Disclosures: **C. Wang, None.**

M249

Characterization of the Osteoclast Precursors Committed by TRANCE. **A. Mochizuki^{*1}, M. Takami¹, T. Kawawa^{*2}, Y. Miyamoto¹, T. Suzawa¹, A. Yamada^{*1}, R. Suzumoto^{*3}, T. Sasaki³, A. Shiba^{*4}, R. Kamijo¹.** ¹Department of Biochemistry, School of Dentistry, Showa University, Tokyo, Japan, ²Department of Prosthodontics, School of Dentistry, Showa University, Tokyo, Japan, ³Department of Oral History, School of Dentistry, Showa University, Tokyo, Japan, ⁴Yomonkai Research Center, Tokyo, Japan.

Macrophages are capable to differentiate into osteoclasts in response to TRANCE (RANKL), indicating that TRANCE commits macrophages to be osteoclasts. To elucidate the mechanisms of this commitment, we determined when the macrophages are committed to be osteoclasts after TRANCE stimulation, and characterized the committed cells. Addition of TRANCE into the macrophage cultures induced osteoclast formation within 72h. When GM-CSF was added simultaneously with TRANCE, osteoclast formation was inhibited and dendritic cells were formed. However, GM-CSF could not inhibit osteoclast formation from macrophages pretreated with TRANCE for more than 24 h, suggesting that macrophages stimulated with TRANCE for 24 h are already committed to osteoclasts. TRAP activity of the committed cells was still as weak as fresh macrophages. Other inhibitory factors such as IL-4 and IFN- γ also failed to inhibit osteoclast differentiation from the committed cells. On the other hand, addition of OPG induced the cell death of the committed cells but not macrophages, suggesting that TRANCE is an essential factor for survival of committed cells. Interestingly, LPS and GM-CSF substituted for TRANCE and M-CSF, respectively to induce osteoclast formation from the committed cells. When zymosan particles were added to macrophage cultures, the macrophages incorporated the particles but never differentiated into osteoclasts by the stimulation with TRANCE. However, the committed cells incorporated zymosans and differentiated into osteoclasts by TRANCE stimulation. The zymosan particles were observed in the cytoplasm of bone resorbing osteoclasts by electron microscopic examination. Analysis of mRNA expression in the committed cells by RT-PCR revealed that committed cells express mRNAs typically expressed in macrophages as well as in osteoclasts. When macrophages were stimulated with LPS, intracellular signals were activated and TNF- α mRNA expression was strongly induced. In the committed cells, although the intracellular signals were activated, TNF- α mRNA expression level was significantly lower than macrophages. In conclusion, committed cells possess very unique characteristics that were different from macrophages and osteoclasts.

Disclosures: **A. Mochizuki, None.**

M250

Osteoclast Precursors Inhibit Osteoprotegerin Production by Osteoblasts during Mineralization. M. van Driel*, H. Jahr*, B. C. J. van der Eerden, C. J. Buurman*, M. Koedam*, A. G. Uitterlinden, H. A. P. Pols, J. P. T. van Leeuwen. Internal Medicine, Erasmus MC, Rotterdam, The Netherlands.

Osteoblasts play a pivotal role in bone metabolism as they are the bone forming cell while they also control bone resorption via regulation of osteoclast formation. Osteoblasts express the stimulator of osteoclast formation, RANKL, and its decoy receptor osteoprotegerin (OPG) and several factors have been shown to regulate RANKL and OPG production by osteoblasts of various origins. However, yet it is unknown whether there is a relation between the functional status (mineralization) of osteoblasts and their osteoclast supporting function, nor is it known whether in return osteoclasts can modify this osteoblast supporting function. To answer these questions we used a human osteoblast cell line (SV-HFO) that shows ongoing matrix production, has highest alkaline phosphatase activity around day 14 of culture and subsequently starts to mineralize the formed matrix. Osteoblasts were co-cultured with the osteoclast precursor cell line RAW264.7 in the presence of RANKL starting at day 9 (no mineralization; NM), day 16 (onset of mineralization; OM) or day 23 (fully mineralizing; FM) of osteoblast culture. Osteoclast formation was assessed at days 3, 5, 7 and 10 after start of co-culture. When RAW264.7 cells were seeded at the NM or OM stage within 5 days TRAP+ cells were formed which were shown to be functional by demineralization of calcified matrix formed. In contrast, when RAW264.7 cells were seeded at the FM stage up to 7 days no TRAP+ cells were detected and only a few TRAP+ cells appeared at day 10. Significance of osteoblast activity at the FM stage for inhibition of osteoclast formation was shown by using osteoblasts that were killed at day 23 by freeze thaw cycles. In this situation within 5 days after seeding RAW264.7 cells TRAP+ cells were formed. OPG measurement supported the observed inhibition of osteoclast formation as OPG production at the FM stage is about 10 fold higher than in the NM and OM stages, 519±77 and 51±10 pg/ml, respectively. This matched qPCR analyses that also demonstrated a progressive decrease in OPG/RANKL ratio during mineralization. Interestingly, co-culture with RAW264.7 cells resulted in a strong inhibition (80-85%) of OPG production by osteoblasts in the FM stage. In conclusion, the current study demonstrates that support of osteoclast formation is dependent on the osteoblasts functional status with osteoblast in the mineralizing stage being inhibitory for osteoclast formation. Moreover, the experiments show a novel feedback between osteoclasts and osteoblasts in which preosteoclasts down-regulate OPG production by osteoblasts thereby facilitating osteoclast formation.

Disclosures: *J.P.T. van Leeuwen, None.*

M251

The Effect of AZD0530, a Highly Selective Src Inhibitor, on Bone Turnover in Healthy Males. R. A. Hannon¹, G. Clack², A. Swaisland^{*2}, C. Churchman^{*2}, R. D. Finkelman³, R. Eastell¹. ¹Academic Unit of Bone Metabolism, University of Sheffield, Sheffield, United Kingdom, ²AstraZeneca, Macclesfield, United Kingdom, ³AstraZeneca Pharmaceuticals, Wilmington, DE, USA.

AZD0530 is a highly selective, dual-specific, orally available small molecule inhibitor of Src and Abl kinases. Src kinase plays an essential role in RANK-mediated osteoclast activation but may inhibit osteoblast activity. Abl may be required for normal osteoblast function. To examine the effect of AZD0530 on osteoclast and osteoblast activity we investigated changes in markers of bone turnover in response to AZD0530 treatment in a multiple ascending dose study in healthy male volunteers (ages 18-55 years). The study comprised placebo and 4 dose levels given to cohorts each of 12 volunteers. Volunteers in each cohort received a single dose of 60-250mg AZ0530 (n = 9) or placebo (n= 3) repeated, 7 or 10 days later, as multiple daily doses for 10 or 14 days. Serum and second morning urine were collected after an overnight fast prior to and 24 and 48 hours after the single dose and prior to and 24 and 48 hours after the final dose. Samples were collected at a follow-up visit 10-14 days after the last dose in the cohorts receiving the two highest doses. Markers of bone resorption measured were serum cross-linked C telopeptide of type I collagen (sCTX), urinary cross-linked N telopeptide (NTX), expressed as a ratio to urinary creatinine, and serum tartrate resistant acid phosphatase 5b (TRAP 5b). Markers of bone formation measured were procollagen serum type I N terminal propeptide (PINP) and bone specific alkaline phosphatase (Bone ALP).

Mean (95% CI) percentage changes from baseline in bone turnover markers 24 hours					
Dose	sCTX	uNTX/Cr	TRAP 5b	PINP	Bone ALP
ADZ0503					
	+17%	+5%	+9%	+17%	+3%
Placebo	(-7%,+49%)	(-23%,+44%)	(0%, +17%)	(-1%,+38%)	(-5%,+11%)
	-24%	-3%	+2%	+3%	+5%
60mg	(-41%,-1%)	(-32%,+37%)	(-7%, +11%)	(-14%,+24%)	(-4%,+15%)
	-55%	-39%	-13%	+23%	+10%
125mg	(-65%,-43%)	(-56%,-15%)	(-19%, -5%)	(+3%,+46%)	(+1%,+19%)
	-71%	-69%	-14%	+33%	-3%
185mg	(-77%,-63%)	(-78%, -56%)	(-21%, -6%)	(+11%, +58%)	(-11%,+5%)
	-88%	-67%	-11%	+13%	+9%
250mg	(-91%,-84%)	(-77%, -53%)	(-18%, -3%)	(-6%,+35%)	(0%, +19%)

Provisional PK-PD modeling suggests the relationship between AZD0530 plasma concentrations and CTX suppression is well described by an inhibitory sigmoid E-max model. Levels of sCTX and uNTX/Cr but not TRAP 5b appear to rise back rapidly towards baseline following cessation of dosing with the two highest doses. PINP tended to decrease after cessation of treatment, possibly reflecting the temporal difference in resorption and formation during bone remodelling. We conclude that suppression of Src kinase activity inhibits osteoclast-mediated bone resorption. The potential effect of Src inhibition on markers of bone formation warrants further investigation. AZD0530 may have therapeutic benefit in treating osteoclast-driven metastatic bone disease and osteoporosis.

Disclosures: *R.A. Hannon, AstraZeneca 2.*

M252

c-Jun Suppresses and JunB Enhances the Stimulation of Cathepsin K Promoter Activity by NFAT2 in RAW 264.7 Cells. B. R. Troen, A. F. Martinez*, M. Pang*, I. Fernandez*, W. Balkan*. Miami VAMC, Miller School of Medicine, University of Miami, Miami, FL, USA.

Receptor activator of NfκB ligand (RANKL) is a critical mediator of osteoclastogenesis and stimulates cathepsin K (CTSK) expression. However the regulation of CTSK expression is incompletely understood. Because RANKL treatment differentiates and activates osteoclasts via AP-1 and NFAT2, we have chosen to study the regulation of CTSK expression via AP-1 and NFAT2 in RAW 264.7 osteoclast precursor cells. Transfection analysis with CTSK promoter-luciferase plasmids unexpectedly demonstrated that c-jun inhibited CTSK promoter activity, whereas junB and a dominant negative c-jun (DN-c-jun) stimulated activity. Concurrent c-fos over-expression markedly enhanced the stimulation by junB. Surprisingly, both c-fos and a dominant negative c-fos (DN-c-fos) alone markedly suppressed CTSK promoter activity. Transfections with a minimal promoter-luciferase vector containing three tandem consensus AP-1 binding sites (3xAP-1-luc) exhibited the expected stimulation by c-fos and suppression of promoter activity by DN-c-jun and DN-c-fos. Interestingly, c-jun inhibited 3xAP-1 promoter activity. Over-expression of NFAT2 dramatically enhanced CTSK promoter activity. Deletion mutation analysis revealed that as few as 238 bp of the CTSK promoter exhibited a marked response to NFAT2. Mutation of a putative NFAT binding site 85 bp upstream of the transcription initiation site significantly reduced the response of the CTSK promoter to NFAT2. Since components of AP-1 have been shown to interact with NFAT2, we examined whether there are co-regulatory effects upon the CTSK promoter. Both junB and DN-c-jun acted synergistically with NFAT2 to dramatically stimulate CTSK promoter activity. In contrast, c-fos, c-jun, and DN-c-fos all suppressed the stimulation of CTSK promoter activity by NFAT2. Western blot analysis demonstrated that RANKL stimulated junB expression in a dose and time dependent manner. Therefore RANKL stimulates CTSK expression, at least in part, via junB in RAW cells, and both junB and DN-c-jun appear to stimulate CTSK promoter activity by facilitating the action of NFAT2. The apparent antagonism between c-jun and junB and the paradoxical effects of c-fos and DN-c-jun demonstrate that the regulation of CTSK transcription in RAW cells depends upon a critical balance between the components of AP-1 and NFAT2, which appear to act in a complex and, in some cases, unexpected manner. Direct binding assays will help to elucidate the essential protein-protein interactions that regulate transcription of the CTSK gene in response to RANKL.

Disclosures: *B.R. Troen, Procter & Gamble 2.*

M253

KR62776, a Novel PPAR-γ Agonist, Suppresses RANKL-Induced Osteoclast Differentiation through Inhibition of MAP Kinase Activation. J. Park^{*1}, J. Hong^{*1}, T. Kim^{*1}, J. Choi², M. Bae^{*3}, H. Cheon^{*3}, S. Kim⁴, E. Park⁵. ¹Skeletal Diseases Genome Research Center, Biomedical Institute, Kyungpook National University Hospital, Daegu, Republic of Korea, ²Department of Biochemistry, Kyungpook National University, Daegu, Republic of Korea, ³Medicinal Science Division, Korea Research Institute of Chemical Technology, Daejeon, Republic of Korea, ⁴Skeletal Diseases Genome Research Center, Kyungpook National University Hospital, Daegu, Republic of Korea, ⁵Cell and Developmental Biology, Biomedical Institute, Kyungpook National University Hospital, Daegu, Republic of Korea.

Peroxisome proliferator-activated receptor-γ (PPAR-γ) regulates the adipogenic differentiation at the expense of osteoblast differentiation, and inflammatory response pathways through inhibition of the mitogen-activated protein kinase (MAPK) pathways or the activation of the nuclear factor kappa B (NF-κB). Recently, thiazolidinedione class of anti-diabetic agents including troglitazone, pioglitazone, and rosiglitazone that activate PPAR-γ has also been implicated in regulation of osteoclast differentiation/function. We screened chemical library and identified KR62776 as a novel PPAR-γ agonist which has potential for treatment of Type 2 diabetes and obesity. In this study, we investigated the effects of KR62776 on osteoclast differentiation and function, and its influence on receptor activator of nuclear factor-κB ligand (RANKL)-induced early intracellular signaling pathways. KR62776 markedly decreased the differentiation of murine and human bone marrow mononuclear (BMM) cells and RAW264.7 cells into osteoclasts, as revealed by the reduced number of tartrate resistant acid phosphatase (TRAP)-positive multinucleated cells and decreased TRAP activity. KR62776 appears to have no cytotoxic effect on osteoclast precursors. Analysis of the mechanisms showed that KR62776 inhibited the RANKL-induced activation of p38 mitogen-activated protein kinase (p38MAPK) and c-Jun N-terminal kinase (JNK). Taken together, these results demonstrate that KR62776 has inhibitory activities on osteoclast differentiation through mechanisms involving inhibition of the RANKL-induced p38MAPK and JNK activation.

Disclosures: *E. Park, None.*

M254

c-Src Recruits SHIP to Podosomes in Osteoclasts, Leading to an Attenuation of Bone Resorption. K. Yogo¹, M. Mizutamari^{*1}, K. Mishima^{*1}, N. Ishida^{*1}, T. Sasaki^{*2}, T. Takeya^{*1}. ¹Graduate school of Biological Sciences, Nara Institute of Science and Technology, Ikoma, Japan, ²Department of Pathology and Immunology, Akita University School of Medicine, Akita, Japan.

c-Src plays an essential role in bone resorption by regulating cytoskeletal organization. Phosphatidylinositol 3'-kinase (PI3K) is one of the major downstream targets of c-Src and it has been reported that the Src/PI3K pathway is required for podosome assembly, motility and bone resorption in osteoclasts. Although SH2-containing 5'-inositol phosphatase (SHIP) has been known to antagonize PI3K pathway and act as a negative regulator in bone resorption, little is known about how SHIP activity is regulated or what molecule regulates the localization of SHIP in osteoclasts. In this study, we investigated the functional relationship between c-Src and SHIP in osteoclasts. First, we found that Src enhanced bone resorbing activity and was most effective in *ship*^{-/-} osteoclasts when assayed *in vitro*. Immunohistochemical analysis showed that SHIP appeared to localize to podosomes in osteoclasts and Src family kinase inhibitor PP1 or expressing dominant negative c-Src (K295M) impaired the localization. In addition, SHIP localized to focal adhesions in the presence of constitutively active form of c-Src (Y527F) in HeLa cells. These results suggest that the activity of c-Src is essential for the localization of SHIP to podosomes in osteoclast. Next, we examined the effect of direct association with c-Src on the localization of SHIP. We found that SHIP could bind to Src-SH3 domain through the P126-P129 region in the N-terminus, but the interaction was dispensable for the Src induced localization of SHIP in HeLa cells. Meanwhile, we identified p130^{Cas} and c-Cbl as novel SHIP-binding proteins in osteoclasts using co-immunoprecipitation with anti-SHIP antibody. The interactions appeared to be dependent on Src kinase activity and we found that Cas and c-Cbl associated with the SH2 domain of SHIP. Further, we investigated the role of the SHIP SH2 domain in bone resorption *in vitro* and found that SHIP lacking a functional SH2 domain could not rescue the hyper-bone resorbing activity of *ship*^{-/-} osteoclasts whereas wild-type SHIP could. Taken together, these results demonstrated that c-Src recruits SHIP to podosomes in a kinase activity-dependent manner in osteoclasts, and SHIP consequently functions in podosomes as a negative regulator of bone resorbing reactions activated by c-Src.

Disclosures: **K. Yogo, None.**

M255

Role of Protein Kinases C Signaling Pathway in the Effects of Strontium Ranelate on Osteoclasts. A. S. Lemaire-Hurtel^{*}, R. Mentaverri^{*}, A. Wattel^{*}, S. Kamel^{*}, M. Brazier. UMRO, Université de Picardie Jules Vernes, Amiens, France.

Strontium ranelate is a new anti-osteoporotic agent which has demonstrated its efficacy in reducing significantly the risk of vertebral and hip fracture in postmenopausal women. Strontium ranelate simultaneously stimulates bone formation and decreases bone resorption, which results in a rebalance of bone turnover in favor of bone formation. The intracellular signaling pathways involved in strontium ranelate effects are still under investigation. We and others have demonstrated that extracellular strontium (Sr) is a full agonist of the extracellular G-protein-coupled calcium-sensing receptor (CaR)¹ and that Sr inhibits bone resorption decreasing OCs recruitment, OCs activities and by increasing OCs apoptosis². We investigated intracellular signaling pathways which could be modulated by the CaR³ on both calcium (Ca)- and strontium ranelate-induced OCs apoptosis. Whereas phospholipase C was involved in the Sr- and Ca-induced OCs apoptosis, specific inhibitors of the IP₃-dependent signaling reduced by 50% the Ca-induced effects and failed to modulate the Sr-induced OCs apoptosis. These results suggested that strontium ranelate acts through different intracellular signaling pathways which might be diacylglycerol (DAG) and protein kinase C (PKC)-dependent. In the present study, purified mature OCs were cultured with PKC activators (OAG: analogous of DAG and phorbol esters: PMA, PDBu) in order to demonstrate the role of the DAG-PKC pathway in the OCs apoptosis. OCs apoptosis displayed a dose dependent increase in presence of these PKC activators: OAG (100µM), PMA (10µM) and PDBu (1mM). In a second time, OCs were cultured with strontium ranelate (24mM) or Ca in presence of non selective PKC inhibitors (calphostin C, staurosporine), or selective inhibitors of PKC isoforms (Gö-6976: inhibitor of conventional isoforms, and Ro-320432: inhibitor of α , β 1 and ϵ isoforms) versus strontium ranelate (24mM) or Ca alone. The presence of PKC inhibitors significantly reduced the strontium ranelate-induced OC apoptosis: $p < 0.01$ with calphostin C (1nM), $p < 0.001$ with staurosporin (1nM) and $p < 0.0001$ with both Gö-6976 (0.1nM) and Ro-320432 (1nM). Interestingly, such PKC inhibitors had no effect on the Ca-induced OCs apoptosis, confirming that intracellular pathways involved in strontium ranelate or Ca-induced OCs apoptosis were different. All together, our data indicate that strontium ranelate acts on OCs apoptosis through PKCs isoforms α and/or β 1, while Ca effects are IP₃ dependent.

¹ Quinn SJ, IOF 2004, Ost Int Suppl

² Mentaverri R, IOF 2004, Ost Int Suppl

³ Brown, ASBMR 5th Ed

Disclosures: **A.S. Lemaire-Hurtel, SERVIER 5.**

M256

Endotoxin Adherent to Orthopaedic Wear Particles Activates Toll-Like Receptor-4 (TLR-4)-Dependent Signaling Pathways without Inducing TLR Association with Lipid Rafts. M. A. Beidelschies^{*}, A. S. Islam^{*}, M. V. Smith^{*}, V. M. Goldberg^{*}, E. M. Greenfield. Orthopaedics, Case Western Reserve University and University Hospitals of Cleveland, Cleveland, OH, USA.

Aseptic loosening of orthopaedic implants is due to a cascade of events, including production of wear particles, and pro-inflammatory cytokines which stimulate osteoclast differentiation. We have shown that adherent endotoxin substantially increases the effects of the wear particles both in cell culture models and in the murine calvarial model. Moreover, these effects are dependent on TLR-4, the primary receptor for soluble LPS (the classical endotoxin produced by Gram-negative bacteria). We hypothesized that adherent endotoxin activates TLRs by mechanisms that differ from those used by soluble LPS. In support of this, wear particles did not induce TLR-4 or TLR-2 to associate with lipid rafts. In contrast, TLR-4 and TLR-2 associated with lipid rafts in response, respectively, to soluble LPS and soluble LTA (a major immunostimulatory molecule produced by Gram-positive bacteria). We further hypothesized that the intracellular signaling pathways induced by adherent endotoxin are similar to those induced by soluble LPS. We found that particles with adherent endotoxin rapidly induced NF- κ B p65 translocation to the nucleus, and stimulated phosphorylation of Akt and all three MAPK pathways (p38, ERK1/2, and JNK), while "endotoxin-free" particles induced substantially slower and weaker effects. Moreover, specific pathway inhibitors of ERK1/2 and PI3K/Akt blocked TNF production induced by particles with adherent endotoxin. Stimulation with wear particles increased Egr-1 expression, a transcription factor downstream of ERK1/2. Adherent endotoxin potentiated this expression and ERK1/2 pathway inhibitors blocked Egr-1 expression. p38 and JNK inhibitors did not block particle-induced TNF production. Specificity of the various inhibitors was demonstrated by showing that relatively inactive analogues did not mimic their effects and that their effects occurred at concentrations that were similar to those needed to block activation of their target pathways. The inhibitors did not block activation of related pathways and did not induce cytotoxicity. Overall, these results show that wear particles induce a signaling platform that is independent of lipid rafts. Furthermore, these results, taken together with those of other workers on NF- κ B, show that the NF- κ B, ERK1/2, and PI3K/Akt pathways act together to mediate production of TNF by endotoxin adherent to wear particles.

Disclosures: **M.A. Beidelschies, None.**

M257

The MEK/ERK Pathway Regulates Osteoclast Survival Through Regulation of Immediate Early Genes Egr1 and Egr2. E. W. Bradley¹, M. J. Oursler². ¹Graduate School, Mayo Clinic, Rochester, MN, USA, ²Endocrine Research Unit, Mayo Clinic, Rochester, MN, USA.

Reducing osteoclast numbers through targeting osteoclast survival pathways may provide future therapeutic targets to slow pathological bone loss and it is a goal of our research to define the signaling pathways regulating osteoclast survival. We have shown that chemical inhibition of MEK or protein synthesis inhibition leads to increased osteoclast apoptosis and we are focusing on discovering the mechanisms by which MEK promotes osteoclast survival. We therefore are seeking to identify downstream targets of MEK that support osteoclast survival. Using gene array technology coupled with Real Time PCR confirmation, we have identified two immediate early genes, Egr1 and Egr2, which function downstream of MEK in osteoclasts. Egr1 and Egr2 expression was inhibited by chemical inhibition of MEK1/2. Further, over-expression of constitutively active MEK1 leads to increased expression of Egr1 and Egr2. These data confirmed that Egr1 and Egr2 are downstream targets of the MEK/ERK pathway and studies were undertaken to explore the role of these early response genes in osteoclast survival. Over-expression of Nab2, the nuclear co-repressor for Egr1 and Egr2, led to an increase in osteoclast apoptosis. Since Nab2 blocks both Egr1 and Egr2, we wanted to determine the respective roles of these early response genes in osteoclast survival. Overexpression of Egr1 did not repress osteoclast apoptosis, leading to the conclusion that Egr2 is the downstream effector of MEK/ERK promotion of osteoclast survival. In order to determine whether Egr1 could replace Egr2 in supporting osteoclast survival, we chemically blocked MEK signaling and looked at the effect of Egr1 over-expression. Over-expression of Egr1 bypassed the effects of chemical inhibition of MEK 1/2 and led to decreased osteoclast apoptosis. In this study, Egr1 was capable of replacing Egr2 and promoting osteoclast survival. We conclude from these data that, although Egr1 is not the downstream effector of osteoclast survival, it can substitute for Egr2 when Egr2 expression is blocked by inhibiting MEK signaling. To determine whether additional targets were important in MEK-mediated support of osteoclast survival, we compared the impacts of MEK inhibition, Nab2 over-expression to inhibit Egr family members, and combined MEK and Nab2 over-expression on osteoclast survival. When compared to chemical inhibition of MEK1/2 alone, over-expression of Nab2 in combination with chemical inhibition of MEK1/2 did not further increase osteoclast apoptosis. These data support that MEK-mediated support of osteoclast survival is through increased expression of Egr family members.

Disclosures: **E.W. Bradley, None.**

M258

Overexpression of Leupaxin in Osteoclasts and Effects on Osteoclast Function. S. N. Sahu*, M. A. Khadeer*, G. Bai*, B. W. Robertson*, A. Gupta. Biomedical Sciences, University of Maryland, Baltimore, MD, USA.

Within the actin-rich podosomal complex in osteoclasts, several signaling molecules have been identified and characterized, which include structural proteins, protein tyrosine kinases, and regulators of the actin cytoskeleton. Leupaxin (LPXN), which belongs to the paxillin superfamily of adaptor proteins, has previously been identified as a component of the sealing zone in osteoclasts. LPXN bears ~37% identity to paxillin, and possesses multiple protein-protein interaction motifs such as repeated N-terminal leucine (L)- and aspartate (D)-rich sequences known as LD motifs, and C-terminal LIM (for Lin-11 Isl-1 Mec-3) domains. In osteoclasts, LPXN associates with a variety of proteins found in the sealing zone that include the protein tyrosine kinase Pyk2, the protein-tyrosine phosphatase-PEST (PTP-PEST), and regulators of the actin cytoskeleton. It was previously demonstrated that inhibition of LPXN expression resulted in reduced osteoclast resorptive activity. LPXN was previously cloned from a rabbit osteoclast cDNA library, and was found to be approximately 85% identical to the murine ortholog. A comparison of the amino acid sequences for the rabbit, human and murine orthologs of LPXN revealed that the second LD motif (LD2) was completely absent in the murine ortholog of LPXN, but which was highly conserved in both the human and rabbit orthologs. In the current study, we have examined the consequences of adenovirus-mediated overexpression of LPXN orthologs on murine osteoclast function. First, overexpression of the "endogenous" LPXN in murine osteoclasts (mLPXN) resulted in enhanced resorptive activity that was paralleled by an enhanced localization of key podosomal proteins at or near the sealing zone. However, when the rabbit ortholog of LPXN (rLPXN) was "ectopically" overexpressed in (murine) osteoclasts, an apparent "loss-of-function" resulted, which was paralleled by mis-localization of a similar repertoire of podosomal proteins. In order to determine a biochemical basis for our observations, a comparison of the amino acid sequences for both species orthologs was performed, which revealed the presence of a second leucine-aspartate (LD2)-rich protein-protein interaction domain, present only in rLPXN. Using GST-affinity precipitation, the LD2 motif present in rLPXN was found to bind Src. The ectopic overexpression of either the rLPXN or the LD2 domain resident in the rLPXN sequence, disrupted the normal localization of endogenous Src at the sealing zone in murine osteoclasts. In conclusion, we hypothesize that overexpression of rLPXN disrupts murine osteoclast function by causing a mis-localization of Src away from its normal distribution at the sealing zone.

Disclosures: **A. Gupta**, None.

M259

SHIP1 Regulates Osteoclastogenesis by Blockage of Proliferation of Osteoclast Precursors. P. Zhou¹, H. Kitaura¹, S. L. Teitelbaum¹, N. Namba^{*2}, C. D. Helgason^{*3}, R. K. Humphries^{*3}, G. Krystal^{*3}, F. P. Ross¹, S. Takeshita¹. ¹Pathology, Washington University, St Louis, MO, USA, ²Pediatrics, Okayama University, Okayama, Japan, ³Terry Fox Laboratory, BC Cancer Agency, Vancouver, BC, Canada.

SHIP1 is an SH2-containing inositol-5-phosphatase which negatively regulates phosphatidylinositol-3-kinase (PI3-K)-initiated signaling by dephosphorylating phosphatidylinositol-3, 4, 5-triphosphate. SHIP1 is essential for normal bone homeostasis, as knock out mice contain increased numbers of hyper-resorptive osteoclasts leading to osteoporosis. Here we characterize the mechanism by which SHIP1 negatively regulates osteoclast differentiation. We find that inhibition of M-CSF dependent osteoclast precursor proliferation by SHIP1 contributes to the ability of the lipid phosphatase to suppress osteoclastogenesis. SHIP1^{-/-} osteoclast precursors in the form of bone marrow macrophages are hyperproliferative, but not longer-lived, in response to M-CSF. This accelerated proliferation correlates with elevated accumulation of cyclins D1, D2 and D3, hyperphosphorylation of the tumor suppressor retinoblastoma protein (Rb) and accelerated down-regulation of p27, an inhibitor of cyclin-dependent kinases (CDKs). Our observation that M-CSF up-regulates cyclin D3 provides the first documentation of this fact. In the absence of SHIP1, M-CSF induced activation of Akt but not ERK is enhanced. Similarly, inhibition of PI3-K activity by the specific inhibitor, LY294002, abrogates M-CSF induced Akt activation, D-type cyclin expression and Rb phosphorylation. The PI3-K inhibitor also down-regulates p27 and dose dependently blocks osteoclast precursor proliferation, while not affecting cell viability. Reconstitution of SHIP1 expression in SHIP1^{-/-} osteoclast precursors via retrovirus corrects their enhanced Akt activation, proliferation and osteoclastogenesis. Retroviral expression of SHIP1 mutants lacking phosphatase activity, or the N-terminal SH2 domain or the C-terminal 163 amino acids in SHIP1^{-/-} osteoclast precursors fails to rescue enhanced osteoclastogenesis, documenting the requirement of these domains in SHIP1-regulated osteoclast precursor proliferation and osteoclastogenesis. Finally, osteoclastogenesis and peri-articular bone erosions are markedly increased in SHIP1^{-/-} mice with inflammatory arthritis, a condition characterized by increased M-CSF expression. The SHIP1-Akt pathway therefore suppresses bone loss in pathological states associated with excessive M-CSF.

Disclosures: **P. Zhou**, None.

M260

Gain and Loss Function Study Reveals that RGS10 Expressed Predominately in Osteoclast Is a Critical Mediator in [Ca²⁺]i Oscillations and Osteoclast Differentiation. S. Yang*, W. Chen*, Y. Li. Cytokine Biology, The Forsyth Institute, Harvard School of Dental Medicine, Boston, MA, USA.

It was reported that RANKL selectively evokes the [Ca²⁺]i oscillations that led to calcineurin-mediated activation of NFATc1, osteoclast specific gene expression and osteoclast terminal differentiation. However, the mechanism underlying how RANKL evokes [Ca²⁺]i oscillations is unknown. We hypothesized that related signaling proteins may be induced by RANKL and are involved in the RANKL-regulated [Ca²⁺]i oscillation-NFAT2 pathway. Using genome-wide Microarray screening to identify RANKL- inducible genes, we found that the mouse Regulator of G-protein Signaling 10 (RGS10) gene was predominately expressed in RANKL-induced osteoclast-like cells (OLCs). To characterize whether RGS10 is expressed in human osteoclast, Northern blotting and *in situ* hybridization were performed. The results proved that RGS10 is predominately expressed in human osteoclast. Previous reports indicate that "Regulators of G-protein signaling," or RGS proteins, play an important role in the regulation of [Ca²⁺]i oscillations in the immune, neural and cardiovascular systems. We hypothesize RGS10 may specifically regulate [Ca²⁺]i oscillations and lead to transcription and expression of osteoclast specific genes. To test the hypothesis, we used a gain and loss-function approach. Silencing of RGS10 expression using RNA interference (RNAi) blocked osteoclast terminal differentiation induced by RANKL. Our data further demonstrated that the failure of osteoclast terminal differentiation resulted from the absence of [Ca²⁺]i oscillations and lack of NFAT2 expression. Over-expression of RGS10 caused about 5% precursor cells to differentiate to TRAP+ mononuclear cells in absence of RANKL induction and largely increased the sensitivity to RANKL signaling in osteoclast differentiation. However, over-expression of RGS10 was unable to evoke [Ca²⁺]i oscillations without RANKL signaling, indicating RGS10 may cooperate with other factor(s) induced by RANKL to regulate [Ca²⁺]i oscillations and terminal differentiation of osteoclasts. These results thus reveal that RGS10 is involved in the RANKL evoking signaling pathway as a critical regulator of [Ca²⁺]i oscillations and is an essential factor for the terminal differentiation of osteoclasts induced by RANKL.

Disclosures: **S. Yang**, None.

M261

Stimulation of TREM2, A DAP12-associated Receptor, Leads to SHIP-1 Association with DAP12. J. A. Torchia^{*1}, S. C. Spusta^{*1}, W. E. Seaman^{*2}, W. G. Kerr^{*3}, M. C. Nakamura¹, M. B. Humphrey². ¹Dept. of Medicine, VA Medical Center and University of California, San Francisco, CA, USA, ²Dept. of Medicine and Microbiology/Immunology, VA Medical Center and University of California, San Francisco, CA, USA, ³Dept. of Interdisciplinary Oncology, University of South Florida and Moffitt Comprehensive Cancer Center, Tampa, FL, USA.

TREM2 (Triggering Receptor Expressed on Myeloid cells-2) and its signaling chain DAP12 are present in myeloid lineage cells including osteoclasts (OC). Deficiency of TREM2 and DAP12 are associated with abnormal OC development and function in humans and mouse. We have previously shown that TREM2-DAP12 stimulation leads to enhanced *in vitro* osteoclastogenesis and that *in vitro* mouse OC differentiation is dependent on DAP12 signals mediated through the ITAM motif in DAP12. To further define the signals stimulated by TREM2-DAP12, we transfected the preosteoclast cell line RAW264.7 with FLAG-tagged TREM2, FLAG-DAP12, or ITAM mutants of FLAG-DAP12, and determined proteins associated with DAP12 following FLAG-antibody ligation. Our studies reveal that FLAG crosslinking of FLAG-DAP12 or FLAG-TREM2 on RAW264.7 cells leads to enhanced association of SHIP-1 with the DAP12 adapter protein (at 20 and 40 min), which was not seen after ligation with isotype control Ab. The SHIP-1 association with DAP12 appeared to require an intact DAP12 cytoplasmic ITAM motif, as mutation of the both tyrosines within the ITAM decreased the SHIP-1 association observed with FLAG ligation in RAW264.7 cells expressing the Y65F/Y76F-FLAG-DAP12 mutant. SHIP-1 also co-precipitated with DAP12 in OC generated from C57BL/6 BMM and from OC generated with RAW264.7 cells treated with RANKL and MCSF. In RAW264.7 cells transduced with shRNAi for SHIP-1, we observed decreased SHIP-1 association with DAP12 using immunoprecipitation with DAP12 antibodies. We also evaluated TREM2 stimulation of SHIP-1 deficient OC precursors during osteoclastogenesis. Crosslinking with anti-TREM2 monoclonal Ab but not control Ab lead to a 4 fold increase in OC generated from SHIP-1^{-/-} BMM compared to wild type BMM. These results show a novel association of the DAP12 signaling adapter protein with SHIP-1 in both macrophages and OC. Association of SHIP-1 with ITAM motifs of other adapter proteins (CD3 chains) has been observed in other cell types. Stimulation of the DAP12-associated receptor TREM2 or DAP12 directly enhanced the association of SHIP-1 with DAP12, dependent on an intact ITAM motif. SHIP-1 has previously been shown to regulate osteoclastogenesis. Our study showing that in the absence of SHIP-1, TREM2-DAP12 crosslinking enhanced osteoclastogenesis suggests that SHIP-1 serves a role as an inhibitor of DAP12 signaling in OC.

Disclosures: **M.B. Humphrey**, Abbott Scholar in Rheumatology 2.

M262

IL-11 and IL-6 Stimulation of Osteoclast Formation Depends on STAT- but not ERK-mediated Pathways in Osteoblasts. J. M. W. Quinn¹, A. Nakamura^{*1}, B. J. Jenkins^{*2}, N. A. Sims³, M. Ernst^{*2}, T. J. Martin^{*1}, M. T. Gillespie¹. ¹Bone, Joint and Cancer Group, St. Vincent's Institute, Fitzroy, Australia, ²The Ludwig Institute for Cancer Research, Melbourne, Australia, ³Dept. of Medicine, The University of Melbourne, Fitzroy, Australia.

Cytokines acting through gp130, notably IL-11 and IL-6, play important roles in osteolysis. Both IL-11 and IL-6 stimulate RANKL production in osteoblasts (OB) and thereby trigger osteoclast formation in OB-haemopoietic cell co-cultures. Several osteolytic factors induce IL-11 in OB, which acts as an autocrine stimulus. The role of IL-6 is less clear but it is implicated in ovariectomy-induced bone loss. Two signaling pathways downstream of gp130 are known, involving STAT1/3 and SHP2/ras/ERK. Although dominant negative block of STAT3 in transfected UAMS-32 stromal cells reduces osteoclast formation in co-cultures, the roles of these pathways in OB has not been clarified. We employed cells from two knock-in mouse strains: gp130^{deltaSTAT/deltaSTAT} (d-STAT), which express truncated gp130 incapable of signalling via STAT1/3, and gp130^{Y757F/Y757F} (Y757F), which cannot signal via SHP2/ras/ERK. When bone marrow cells from these mice were stimulated by recombinant RANKL and M-CSF, d-STAT bone marrow formed similar numbers of osteoclasts to wild type (WT), while Y757F bone marrow yielded approximately two-fold more. IL-6 and IL-11 powerfully inhibited RANKL-stimulated osteoclast formation in Y757F bone marrow. In contrast, IL-11 had no effect on d-STAT and WT osteoclast formation, and IL-6 caused only a small reduction (<40%). Coculture of WT bone marrow cells with OB from WT, Y757F or heterozygous gp130^{deltaSTAT/+} mice resulted in formation of large numbers of osteoclasts in response to 1,25 dihydroxyvitamin-D3, IL-11 and IL-6, although for IL-6 the addition of IL-6 soluble receptor (IL-6sR) was required for maximal effects, as previously reported. In contrast, in cocultures using d-STAT OB, IL-11 and IL-6+IL-6sR caused no osteoclast differentiation, and the stimulus provided by 1,25 dihydroxyvitamin-D3 was greatly diminished, consistent with ablation of autocrine IL-11 action. Although gp130 ERK and STAT signals frequently oppose each other, ERK pathway blockade by PD98059 did not rescue osteoclast formation supported by d-STAT OB. We conclude that gp130 STAT1/3 signals in osteoclast progenitors can reduce osteoclast differentiation, but gp130 STAT1/3 signals in OB are essential for IL-6 and IL-11 dependent osteoclast formation in co-cultures.

Disclosures: **J.M.W. Quinn**, None.

M263

Rab3D Regulates a Novel Vesicular Trafficking Pathway that Is Required for Osteoclastic Bone Resorption. N. J. Pavlos^{*1}, J. Xu^{*2}, D. Riedel^{*3}, J. S. Yeoh^{*1}, S. L. Teitelbaum⁴, J. M. Papadimitriou^{*5}, R. Jahn^{*3}, F. P. Ross⁴, M. H. Zheng¹. ¹Dept. of Orthopaedic Surgery, The University of Western Australia, Nedlands, Australia, ²Dept. of Orthopaedic surgery, The University of Western Australia, Nedlands, Australia, ³Department of Neurobiology, Max Planck Institute for Biophysical Chemistry, Göttingen, Germany, ⁴Department of Pathology, Washington University School of Medicine, St Louis, MO, USA, ⁵Dept. of Pathology, The University of Western Australia, Nedlands, Australia.

Rab3 proteins are a subfamily of GTPases, known to mediate membrane transport in eukaryotic cells and play a role in exocytosis. Our data indicate that Rab3D is the major Rab3 species expressed in osteoclasts. To investigate the role of Rab3D in osteoclast physiology we examined the skeletal architecture of Rab3D-deficient mice and found an osteosclerotic phenotype. Although basal osteoclast number in null animals is normal the total eroded surface is significantly reduced, suggesting that the resorptive defect is due to attenuated osteoclast activity. Consistent with this hypothesis, ultra-structural analysis reveals that Rab3D^{-/-} osteoclasts exhibit irregular ruffled borders. Furthermore, while over-expression of wild-type, constitutively active or prenylation-deficient Rab3D has no significant effects, over-expression of GTP-binding deficient Rab3D impairs bone resorption *in vitro*. Finally, sub-cellular localisation studies reveal that, unlike wild-type or constitutively active Rab3D, which associate with a non-endosomal/lysosomal subset of post-trans-Golgi network (TGN) vesicles, inactive Rab3D localizes to the TGN and inhibits biogenesis of Rab3D-bearing vesicles. Collectively, our data suggest that Rab3D modulates a post-TGN trafficking step that is required for osteoclastic bone resorption.

Disclosures: **M.H. Zheng**, None.

M264

RAB3D-Dependent Vesicular Trafficking Is Mediated through its Interaction with TCTEX-1, a Light Chain of the Cytoplasmic DYnEIN Microtubule Motor Complex. J. Xu^{*1}, N. J. Pavlos^{*1}, A. Carrello^{*1}, K. Kroeger^{*2}, K. Ednet^{*2}, M. H. Zheng¹. ¹Dept. of Orthopaedic Surgery, The University of Western Australia, Nedlands, Australia, ²Western Australia Institute for Medical Research, The University of Western Australia, Nedlands, Australia.

Rab3D belongs to the family of small GTPases involved in the regulation of exocytosis. We have recently shown that Rab3D-deficient mice exhibit an osteosclerotic phenotype and that Rab3D is required for the maintenance of the osteoclastic resorptive organelle, namely the ruffled border membrane. Here, to further delineate the mechanism(s) underlying this phenomenon, we have employed a yeast two-hybrid system to identify potential Rab3D interacting proteins. Screening a mouse embryonic cDNA library, 5 clones (T18, -30, -37, -39 and -40) were positively identified which specifically interacted with the N-terminus of

Rab3D. Database searches identified these clones as mouse Tctex-1, a 14 kDa light chain of the multimeric cytoplasmic dynein motor complex. A specific interaction between Rab3D and Tctex-1 was confirmed by GST-pull down and co-localisation studies. Truncation analyses mapped the Tctex-1 binding site to the switch II/GTP-binding motif of Rab3D (amino acids 74-95). Consistently, bioluminescence resonance energy transfer (BRET) analysis demonstrated that Tctex-1 preferentially associated with the GTP-bound conformation form of Rab3D in live cells. When overexpressed, Flag-Tctex-1, GFP-dynaminin, or antisense-Tctex-1 disrupted the spatial distribution of Rab3D *in vivo*. Additionally, Rab3D-secretory granules localise to microtubules and are redistributed by nocodazole treatment into -COPI-positive Golgi mini-stacks in transfected COS-1 cells. These data lend support to the notion that Rab GTPases and molecular motor proteins act in concert to regulate directional membrane transport and furthermore suggest that Rab3D may functions to recruit and regulate the activity of cytoplasmic dynein Tctex-1, controlling the sorting and microtubule-dependent targeting of post-Golgi secretory granules to the ruffled border membrane during osteoclastic bone resorption.

Disclosures: **J. Xu**, None.

M265

The Role of Pyk2/Src in Calcitonin-induced Podosome Reassembly and Sealing Zone Detachment in Osteoclasts. J. Shyu, C. Shih, W. Lin*, H. Liu*. Biology and Anatomy, National Defense Medical Center, Taipei, Taiwan Republic of China.

Osteoclasts (OCs) are multinucleated, terminally differentiated cells which play an essential role in bone resorption. To resorb bone, OCs attach to extracellular matrix or the bone surface via specialized attachment structures called podosomes, which form a prominent F-actin-rich ring that is thought to correspond to the sealing zone of resorbing OCs. It had been showed that Pyk2/Src/Cbl complex is critical to the $\alpha_v\beta_3$ integrin-mediated signaling in podosome. The concept of outside-in and inside-out of integrin-mediated signaling has been elucidated in depth through the study of Pyk2/Src/Cbl complex. Calcitonin (CT) is a 32-amino acid polypeptide which inhibits OC motility, induces OC retraction, and disrupts the actin-ring structure of OCs. Thus it is reasonable to assume that the Pyk2/Src/Cbl complex in podosome could be the potential target for the CT-induced signaling. In isolated authentic rabbit OCs cultured on extracellular matrix-coated Petri dish, we previously showed that CT induced dephosphorylation and redistribution of Pyk2. The dephosphorylation of Pyk2 would be expected to prevent the formation of Pyk2/Src/Cbl complex and therefore inhibit OC motility and attachment. However, the effects of CT on Pyk2/Src/Cbl complex function and their distribution in OCs are not clear. We therefore investigated whether CT affects Pyk2/Src association and Src phosphorylation in OCs by using the immunoprecipitation and Western blot methods. The result showed that CT induced an increase of Src tyrosine phosphorylation and Pyk2/Src association. Using immunofluorescent confocal analysis, we showed that CT induces dephosphorylation of Pyk2 in the sealing zone and increase Src tyrosine phosphorylation and Pyk2/Src association in the central region of OCs. Further examination using specific Y416 and Y527 phosphorylation antibodies of Src showed that CT induced increase of Y416 but not Y527 phosphorylation. The increase of Y416 and decrease of Y527 phosphorylation were found in the central region of OCs after CT stimulation. In conclusions, CT may induce podosome reassembly and sealing zone detachment by decrease Pyk2 phosphorylation in the sealing zone and increase Y416 phosphorylation of Src and Pyk2/Src association in the central region of OCs.

Disclosures: **J. Shyu**, None.

M266

Regulation of Human Osteoclast Function by Redox and sRANKL-induced Intracellular ROS Production. J. M. Hodge*, N. Zimmerman*, L. A. Hodgson*, C. J. Aitken*, M. A. Chacksfield*, M. A. Kirkland*, G. C. Nicholson. Clinical and Biomedical Sciences, The University of Melbourne, Geelong, Victoria, Australia.

In animal models, reactive oxygen species (ROS) have been shown to activate osteoclasts and have been implicated as second messengers in RANKL-mediated osteoclastogenesis. The aim of this study was to investigate the role of ROS in the function of mature human osteoclasts. Osteoclasts were generated by culture of CFU-GM with human M-CSF and RANKL for 14 days. Modulation of resorbing capacity and survival were assessed in mature osteoclasts dissociated from the plastic substrate and re-cultured on dentine slices. Treatment with RANKL enhanced the survival of mature osteoclasts on dentine and was absolutely required for resorption. Resorption was further enhanced by the presence of both M-CSF and RANKL. Co-treatment with hydrogen peroxide (50µM) for 24 hours resulted in a 130% increase in osteoclast size and a 34% increase in resorption. In contrast, co-treatment with the thiol antioxidant N-acetylcysteine (NAC; 10 mM) reduced osteoclast size by 22% and number by 50%, and resorption was completely inhibited. When mature osteoclasts were RANKL- and serum-starved for 3 hours and then stimulated with RANKL (150 ng/mL) for 30 minutes, increased intracellular ROS-production was detected using fluorescence microscopy and the ROS-sensitive dye CM-H₂DCFDA. Pre-treatment with NAC blocked RANKL-induced intracellular ROS. Treatment with RANKL also stimulated a time-dependent increase in intracellular hydrogen peroxide, as measured using Amplex Red reagent, with peak accumulation at 10 minutes. Electrophoretic mobility shift assay demonstrated that pre-treatment of osteoclast precursors with hydrogen peroxide (10µM) for 16 hours resulted in increased RANKL-induced NF-κB activity, whereas pre-treatment with NAC (10mM) blocked this activity. Human osteoclast function is stimulated by ROS and inhibited by antioxidant quenching of ROS. Stimulation of osteoclast survival and resorbing activity by RANKL may be mediated by ligand-mediated intracellular ROS production.

Disclosures: **J.M. Hodge**, None.

M267

Impact of Increasing Overweight Prevalence on the Prevalence of Osteoporosis in Older US Women. A. Looker¹, K. Flegal^{*1}, L. J. Melton².
¹National Center for Health Statistics/CDC, Hyattsville, MD, USA, ²Mayo Clinic, Rochester, MN, USA.

The prevalence of overweight among older women in the United States has increased from 62 to 68% since the third National Health and Nutrition Examination Survey (NHANES III 1988-94) was conducted. Higher body mass index (BMI) is associated with higher bone mineral density (BMD), but the impact of the overweight increase on the prevalence of femur neck osteoporosis (FN OP) is not known. In the present study, we used osteoporosis data from NHANES III and overweight prevalence data from NHANES 1999-2002 to address this question in older women. The probability of FN OP for overweight (BMI>=25) vs normal weight women (BMI<25) was calculated using data for 3299 women ages 50+ years from NHANES III. FN OP was defined using T-scores based on 20-29 year old non-Hispanic white women; femoral bone density data were obtained using dual energy x-ray absorptiometry (Hologic QDR 1000). BMI was based on measured height and weight. In NHANES III, BMI was significantly related to femur neck BMD overall (r=0.47), and the prevalence of FN OP was significantly lower in overweight women than in normal weight women (10% vs 32%, respectively). The expected prevalence of FN OP given the higher current prevalence of overweight was then estimated by applying osteoporosis probabilities from NHANES III to the prevalence of overweight and normal weight for women ages 50+ years (n=2111) from NHANES 99-02. Given the current prevalence of overweight, the expected prevalence of FN OP in older women from NHANES 99-02 was only 1% lower than the prevalence observed in NHANES III (17% vs 18%, respectively). These results indicate that FN OP prevalence would be expected to decline by 0.22 units for every 1 unit increase in overweight prevalence. The estimated impact of overweight is likely small in part because the effect of increasing overweight is confined to a small proportion (e.g., 6%) of the total population of older women. Our results suggest overweight prevalence would need to increase to 91% (+23 units) among older women in order to lower FN OP prevalence by 5 units (-5%). In conclusion, although overweight is significantly related to bone density, the increasing prevalence of overweight among older US women appears unlikely to be accompanied by a significant reduction in osteoporosis prevalence.

Disclosures: **A. Looker**, None.

M268

Seasonal Importance on Vitamin D Deficiency in French Submariners. L. Bégot^{*1}, F. Labarthe^{*2}, N. Granger-Veyron^{*2}, E. Zérath^{*1}, X. Holy¹.
¹Integrated Physiology, IMASSA, Brétigny sur Orge, France, ²Health service, ESNLE, Brest, France.

The effects of total sunlight deprivation on vitamin D metabolism were studied in two 2-month French ballistic missile submarine patrols. One was with summer and the other with winter departure. Blood and urine samples were collected four times per patrol on 20 healthy male subjects: pre-patrol control and after 20, 41, and 58 days in the submarine at sea. Samples were frozen until analyses. No subject received sunlight or vitamin D supplementation during the 60-day patrols. Pre-patrol 25(OH)D values were normal for 75 % of submariners when departure was in summer and decreased thereafter during patrol (-41 % at the end of patrol). 20%, 4% and 0% of subjects had 25(OH)D levels above what is considered as normal value (32 ng/ml) after 20, 41 and 58 days respectively. Pre-patrol values of 25(OH)D were low (17.18 ± 1.11 ng/ml) at the occasion of winter departure and continued to decrease with patrol duration. 35% of submariners had values below 13 ng/ml considered as a deficiency level. 1,25(OH)2D was also significantly decreased during both patrols and the lowest values were observed at the end of the mission in the members of the winter patrol. A rapid decline in bone formation (total or bone ALP) and increase in bone resorption (ICTP and DPD) markers were observed at 20 days for both missions. Meanwhile serum pCO2 was found increased and blood pH decreased due to high ambient CO2 in the submarines atmosphere (0.7%) compared to 0.03% in normal air. Significant decrease in urinary excretion of calcium and slight increase in serum calcium were found from the 20th day. PTH was found decreased for both patrols. At the same time, change in urinary calcium levels associated with the increase in bone resorption could be consistent with a risk of nephrolithiasis development. The deficiency in vitamin D in subjects submitted to sunlight deprivation during submarine mission, and particularly for winter departure, could be consistent with a dietary supplementation. However, this kind of treatment should be discussed considering the risk for renal stone formation mainly due to the rise in intestinal absorption.

Disclosures: **L. Bégot**, None.

M269

Use of Vitamin D and Calcium Supplements in Women with Osteoporosis. P. Miller¹, Y. Chen², E. Barrett-Connor³, S. Brenneman^{*2}, E. Siris⁴.
¹Colorado Center for Bone Research, Lakewood, CO, USA, ²Outcomes Research and Management, Merck & Co., Inc, West Point, PA, USA, ³Department of Family and Preventive Medicine, University of California, San Diego, La Jolla, CA, USA, ⁴Metabolic Bone Disease Program, Columbia University Medical Center, New York, NY, USA.

Vitamin D and calcium are essential for the management of osteoporosis. We evaluated the utilization of vitamin D and calcium supplements and factors related to their use in women with osteoporosis or fracture in the National Osteoporosis Risk Assessment (NORA). NORA participants were postmenopausal women age >= 50 who had no prior

diagnosis of osteoporosis and no osteoporosis-specific treatment. Of 100,697 participants who responded to a follow-up survey around 3 years post baseline, 69,390 provided complete information on fractures, use of calcium, vitamin D, multivitamins and osteoporosis-specific medication. Descriptive analyses were stratified by multivitamin (MV) use (overall 65%) because MV generally provides some supplementation of calcium and vitamin D. MV usage was not affected by osteoporosis status, fracture or medication use. Logistic regression determined factors related to calcium and vitamin D use. Percent of women who reported calcium and vitamin D use stratified by MV use is shown in Table below for women who were on osteoporosis treatment, had a T-score <= -2.5, or had an incident fracture. Factors independently related to calcium use included younger age, higher education, good to excellent health, non-smoking, T-score <-1.0, osteoporosis medication use, MV use and ethnicity. Factors related to vitamin D were fracture since baseline, T-score <-1.0, osteoporosis medication use and MV use. We concluded that, in NORA, a smaller proportion of women reported taking vitamin D supplement compared to calcium supplement, even those being actively treated for osteoporosis. Vitamin D supplementation was less frequent in non-users of multivitamins compared to users of multivitamins. Efforts should be made to ensure adequate vitamin D supplementation in osteoporosis management

	Osteoporosis Treatment	Baseline T-score <= -2.5	Incident Fracture
MV users			
Calcium	86%	79%	78%
Vitamin D	47%	41%	39%
No MV users			
Calcium	64%	53%	44%
Vitamin D	27%	23%	19%

Disclosures: **P. Miller**, Procter & Gamble Pharmaceuticals, Aventis Pharmaceuticals, Roche Pharmaceuticals, Eli Lilly, Merck & Co., Novartis Pharmaceuticals, Pfizer Pharmaceuticals, Amgen 2; **Procter & Gamble Pharmaceuticals**, **Aventis Pharmaceuticals**, **Roche Pharmaceuticals**, **Eli Lilly**, **Merck & Co.**, **Novartis Pharmaceuticals**, **Pfizer Pharmaceuticals**, **Amgen**, **NPS** 5, 8.

M270

Antioxidant Defense System in Postmenopausal Women Residing in Endemic Fluorotic and Non Fluorotic Areas. S. Ravula^{*1}, C. V. Harinarayan², U. V. Prasad³, T. Ramalakshmi^{*3}, M. Vijayabhaskar^{*4}, E. G. T. V. Kumar^{*3}, R. Arunakumari^{*4}.
¹Biochemistry, University of Health sciences, Tirupati, India, ²Endocrinology & Metabolism, Sri Venkateswara Institute of Medical Sciences, Tirupati, India, ³Endocrinology & Metabolism, Sri Venkateswara Institute of Medical Sciences, Tirupati, India, ⁴Biochemistry, University of Health sciences, Tirupati, India.

To study the antioxidant defense system in postmenopausal women residing in fluorotic and non fluorotic areas. Twenty five post menopausal women (>10years menopause) (with mean age 57 years) residing in endemic fluorotic and non fluorotic villages (water fluoride >2ppm and <0.35ppm respectively) were studied for their dietary calcium (DC), phytates (DPH), urinary fluoride (UF), serum fluoride (SF), calcium (SCA), phosphorus (SPH), alkaline phosphatase (SAP), ntact parathormone (PTH), 25(OH)D (VIT D) levels, lipid per oxidation (MDA), glutathione - S- transferase (GST) and catalase (CAT) . The mean and standard deviation of these parameters are shown below:

	units	NON FLUROTICS		FLUROTICS	
		Mean	SD	MEAN	SD
UF	ppm	0.62	0.13	2.24	0.9*
SF	ppm	0.07	0.01	0.19	0.03*
DC	mg/day	288	36	255	19*
DPH	mg/day	152	15	169	15*
SCA	mg/dl	9.46	0.71	9.15	1.25
SPH	mg/dl	3.27	0.28	4.22	0.47*
SAP	KAU	5.61	1.11	8.64	1.82*
PTH	pg/ml	8.04	2.96	10.08	7.77
VITD	ng/ml	19.18	7.23	22.54	10.23
MDA	nmol/ml	2.79	0.35	3.82	0.35*
CATALASE	KU/gm Hb	54.37	23.37	42.99	19.22
GST	IU/L	65.5	26.89	40	18.22*

*p<0.0001 compared to controls
The dietary calcium was far below the RDA of the country. The vitamin D and PTH levels were comparable in both the villages. The antioxidant levels were significantly lower in women residing in fluorotic village. Women in non fluorotic village showed a strong positive correlation between catalase and PTH (r0.54;p<0.01) and negative correlation with SAP (r-0.52;p<0.008). In fluorotic villages MDA showed a negative correlation with SF (r-0.6;p<0.001) and positive correlation with DC (r 0.43; p<0.03). GST showed a negative correlation with PTH (r -0.42; p<0.04).For comparable age group, duration of menopause and vitamin D status, women residing in fluorotic area showed less antioxidant defense system and higher lipid per oxidation compared to the women residing in non fluorotic area. The poor antioxidant system could be attributed to high serum fluoride levels in these patients. The poor anti oxidant defense system could have a detrimental effect on bone mineral metabolism and mineralization

Disclosures: **S. Ravula**, None.

M271

Air Pollution and Bone Mineral Density. K. Alver*¹, A. J. Sogaard*¹, J. A. Falch*², P. Nafstad*³, H. E. Meyer³. ¹Division of Epidemiology, Norwegian Institute of Public Health, Oslo, Norway, ²Center of Endocrinology, Aker University Hospital, Oslo, Norway, ³Institute of General Practice and Community Medicine, University of Oslo, Oslo, Norway.

Higher fracture rates and more osteoporosis have been reported in urban compared to rural populations. Whether pollution can explain part of these differences is not known. Heavy metals, such as aluminium, cadmium and lead have been proposed as risk factors for osteoporosis because of the ability to be deposited in the skeleton, and an inhaled poisonous substance like tobacco smoking is established as a risk factor for osteoporosis and osteoporotic fractures. There is also indication that inflammatory processes, which might be affected by air pollution, might harm the skeleton. Pursuing this, the aim of this exploratory study was to investigate the association between indicators of air pollution and bone mineral density (BMD) in elderly Norwegian men. As part of the Oslo Health Study 2000-01, bone densitometry was performed in a sub-sample of 697 men aged 75/76 years with Dual Energy X-ray Absorptiometry (DXA). Air pollution was estimated by AIRQUIS, a model developed by The Norwegian Institute of Air Research. The model is based on information on emission, traffic counts, weather conditions, topography and measurements, and estimates daily levels of exposure for nitrogen dioxide (NO₂) and particles (PM₁₀ and PM_{2.5}). NO₂ and PM_{2.5} can be considered as indicators of traffic related air pollution. For PM₁₀ also other sources of emission like heating of dwellings and buildings will contribute to the exposure levels. Linking information from this model with information about each participant by the unique personal id-number produced estimates for air pollution exposure at the participants' home addresses. Regression analyses were used to study the association between indicators of air pollution (annual mean 1999) and BMD. Preliminary analysis showed a weak, but statistically significant, negative association between PM_{2.5} and total body BMD (b=-0.004, p=0.042). After adjusting for smoking status, education and body mass index, the association became significant with all three air pollution indicators (PM_{2.5}: b=-0.005, p=0.008; PM₁₀: b=-0.003, p=0.006; NO₂: b=-0.0007, p=0.028). The same pattern was also found for the association between total femur BMD and air pollution, although none of those associations were significant. In sum, we found a weak, but significant inverse association between indicators of air pollution and BMD. These initial findings warrant further investigation.

Disclosures: **K. Alver**, None.

M272

Intake of Vitamin D and Milk Was Associated with Increase in Muscle Mass and Decrease in Body Fat during Dieting in Young Women. T. Hirota¹, I. Kawasaki¹, H. Ikeda¹, T. Aoe¹, K. Hirota². ¹Research Laboratory, Tsuji Academy of Nutrition, Osaka-city, Japan, ²Obstetrics & Gynecology, Nissay Hospital, Osaka-city, Japan.

A diet-induced weight loss reduces bone mass and increases fracture risk later in life. However, unnecessary dieting is quite common among young slender women because of their slim images. Limited epidemiological and experimental data support the possibility that dietary calcium intake plays a role in body weight regulation. The objective was to assess the effect of dieting with or without milk supplementation on not only bone mineral density (BMD) but also fat and lean mass in normal weight young women. Furthermore the effect of vitamin D intake on change in lean and fat mass was also examined. Fifty one normal weight (body weight; 53.3±5.6 kg, body mass index; 21.05±1.63, 17.9~24.8) female students (aged 23.1±4.7 y) were engaged in dieting by decreasing in energy intake and increasing in physical exercise for 4 months. They were divided into 2 groups during dieting; one (n=28, milk group) was supplemented with milk (more than 200 ml/day) and the other (n=23, control group) was no supplement. We also observed subgroup of different intakes of vitamin D below or above average (4.7±3.4 µg/day). Vitamin D is not allowed to add to milk in our country. BMD (L2-4 and femoral neck), total body fat, and lean (muscle) mass were measured by DXA (GE Lunar, DPX) before and after dieting for 4 months. Nutritional intakes such as vitamin D and calcium were calculated from 3-day dietary record. Changes of body weight in all subjects during dieting were -0.71±2.05 kg (-6.7~4 kg; p<0.05) and those of BMD in L2-4 and femoral neck were -0.002 ±0.030 g/cm² (-0.055~-0.135 g/cm²) and -0.003±0.027 g/cm² (-0.068~-0.067 g/cm²), respectively. The changes of body fat and lean mass were -0.3±3.0 kg (-6.7~5.7 kg) and -0.4±2.4 kg (-5.2~5.8 kg), respectively. Any significant changes in BMD were not observed in all groups after moderate weight loss. However, higher reduction of body fat during dieting was observed in milk group (-0.8±2.8 kg), and further higher reduction was found in subgroup of milk with higher vitamin D (-2.7±2.2 kg; p<0.01) in comparison with control group (0.3±3.2 kg). Lean mass was found to be increased much more in milk with higher vitamin D subgroup (1.7±1.2 kg; p<0.01 versus -1.0±2.5 kg as control) during dieting. Intake of vitamin D was associated with the decrease in fat mass and increase in lean mass. Thus we suggest the decrease in lean mass as well as BMD by a diet-induced weight loss could be compensated by the increase intake of vitamin D and dairy product or calcium. It should be more important for elderly people who easily lose weight in order to prevent bone fracture.

Disclosures: **T. Hirota**, None.

M273

Underutilization of Calcium in an Osteoporotic Population. W. Y. Chow*¹, R. P. Heaney². ¹Health Outcomes, sanofi-aventis, Bridgewater, NJ, USA, ²Creighton University, Omaha, NE, USA.

The adequate intake of calcium is crucial for reducing bone loss, supporting osteoporosis treatments, and lowering risk of fractures in osteoporotic patients. Despite recommendations set forth by the National Osteoporosis Foundation and the Surgeon General's Report on Bone Health, consumption of dietary calcium remains low in patients with osteoporosis. According to the latest NHANES data, the median calcium intake in postmenopausal women is about 563 mg per day. The present study was undertaken to evaluate the utilization of calcium supplements in patients who are receiving anti-resorptive therapy. A cross-sectional study using the self-administered National Health and Wellness Survey was conducted by a healthcare consumer research company, Consumer Health Sciences (Princeton, NJ), in 2003 and 2004. Data on healthcare attitudes, behaviors, and over-the-counter (OTC) and prescriptive medication use were collected from a nationally representative sample of the US population. A total of 3420 osteoporotic patients were sampled from an internet panel and were stratified by education, gender, age and race. The patients included in the study (350 men and 3070 women) had a mean age of 61.5 years (range 18-65 years) and reported osteoporosis (physician-diagnosed) between 2003 and 2004. 997 patients (59.4%) and 947 patients (54.4%) indicated current use of a pharmacologic therapy for osteoporosis in 2003 and 2004, respectively. Of those treated with a bisphosphonate, 186 (36%) patients reported using an OTC calcium supplement in 2003; a similar proportion (33%; n=216) reported concomitant calcium supplement use in 2004. In the concomitant use cohort, the length of time over which patients reported using OTC calcium did not differ between 2003 and 2004 (85 months vs 92 months, P>0.05). Compliance with OTC calcium, measured by the number of days that patients used the supplement in the past month, decreased in 2004 compared with 2003 (-1.7 days; P<0.001). Calcium supplementation is underutilized in this osteoporotic population. Neither the proportion of calcium users nor compliance with calcium supplementation improved from 2003 to 2004. Efforts need to be made to ensure that every patient with osteoporosis receive at least the recommended daily intake of calcium.

Patient Characteristics			
	2003	2004	2003-2004
Number of Patients, n	1679	1741	3420
Women, n (%)	1504 (89)	1565 (90)	3070 (90)
Age, yrs (mean)	62	61	61.5
Number of Bisphosphonate Users	519	655	1174
Number of Bisphosphonate Users Who Take Calcium Supplements (%)	186 (36)	216 (33)	402 (34)
Reported No. of Days Taking Calcium Supplementation During Last Month, mean (SD)	29.5 (2.2)	27.8 (3.1)	28.6 (1.9)

Disclosures: **W.Y. Chow**, sanofi-aventis 3.

M274

Deficiency of Vitamin D and K Is Highly Prevalent in Patients with Hip Fracture. T. Nakano*¹, K. Tanaka², M. Yoshizawa*³, M. Kamao*⁴, N. Tsugawa*⁴, T. Okano⁴. ¹Orthopedics, Tamana Central Hospital, Tamana, Kumamoto, Japan, ²Food and Nutrition, Kyoto Women's University, Kyoto, Japan, ³Life and Environmental Sciences, Osaka Prefecture University, Osaka, Japan, ⁴Hygienic Sciences, Kobe Pharmaceutical University, Kobe, Japan.

The deficiency of vitamin D and K has been reported to be the risk factor for non-vertebral fracture. In this paper, we have measured plasma concentrations of vitamin D and K shortly after hip fracture to gain insight into the nutritional status of these patients at the time of the fracture. Seventy patients with hip fracture (17 males, 53 females; aged 84.2 +/- 7.3) were evaluated for their vitamin D and K status. In most patients, their blood samples were obtained within 24 hours after the fracture. Their plasma 25(OH)D and intact PTH levels were 13.3 +/- 8.2 (median; 12.2) ng/ml and 62.8 +/- 32.1 (median; 54.0) pg/ml, respectively. The plasma concentrations for phyloquinone, menaquinone-4 (MK4), and menaquinone-7 (MK-7) were 0.39 +/- 0.34 ng/ml (median 0.27), 0.06 +/- 0.11 (median; 0.05) ng/ml, and 1.67 +/- 2.34 (median; 0.82) ng/ml, respectively. Circulating level of undercarboxylated osteocalcin (ucOC), which represents vitamin K deficiency in the skeleton, was 4.85 +/- 4.03 (median; 3.29) ng/ml. Blood samples were also obtained from 22 age-matched nursing home residents adjacent to the hospital (5 males, 17 females; aged 85.4 +/- 6.9). Extremely low 25(OH)D concentration and high intact PTH levels suggest severe vitamin D deficiency. Low levels of PK and MK-7 together with high ucOC concentration indicate vitamin K deficiency in the skeleton. Since blood samples were obtained shortly after the fracture, above results are likely to represent the patients' nutritional status before fracture. Thus, most patients with hip fracture is in vitamin D- and K-deficient state, and these deficiencies are likely to predispose elderly people to fracture.

Disclosures: **T. Nakano**, None.

M275

High Prevalence of Vitamin D Inadequacy among Community Dwelling Post-Menopausal Women with Osteoporosis . P. Lips¹, J. Chandler², K. Lippuner^{*3}, E. Ragi^{*4}, J. Norquist^{*2}, P. Delmas^{*5}, D. Hosking⁶. ¹Vrije Universiteit Medical Center, Amsterdam, Netherlands Antilles, ²Merck Research Laboratories, Blue Bell, PA, USA, ³Osteoporosis Polyclinic University Hospital, Berne, Switzerland, ⁴Centro de Diag. e Pesq da Osteoporose do Espirito Santo Vitoria, -, Brazil, ⁵Hopital Edouard Herriot, Centre Prevention Osteoporose, Lyon, France, ⁶Nottingham City Hospital, David Evans Medical Research Centre, Nottingham, United Kingdom.

This study describes the distribution of serum 25-hydroxyvitamin D [25(OH)D] and the relationship with parathyroid hormone (PTH) levels among postmenopausal women with osteoporosis in various regions and across two seasons. A cohort of 2102 community-dwelling, postmenopausal women with osteoporosis from 18 countries [North, Central and Southern Europe, Middle East, Latin America, Asia and Pacific Rim] were recruited between May 2004 and April 2005. Serum 25(OH)D (Nichols Advantage competitive binding chemiluminescence immunoassay) and PTH were measured. Information on factors that could influence vitamin D status was obtained by patient questionnaire. Descriptive statistics were used to evaluate mean serum 25(OH)D and PTH levels by season and region and to estimate the frequency of vitamin D inadequacy defined as < 30 ng/ml. Mean age was 67.2 years, range 41 to 92, with 33% >70 years. 39% reported taking a vitamin D supplement >= 400 IU daily; 79% reported taking prescription medication for osteoporosis. Overall mean 25(OH)D was 27.2 ng/ml (SD=13.0, range 7-120). Overall prevalence of vitamin D inadequacy was 62%. Among women recruited during summer, prevalence of inadequacy was 61% and among those recruited during winter, prevalence was 65%. PTH values began to rise at 25(OH)D levels ≤ 30 ng/ml, supporting 30 ng/ml as the appropriate cutoff to define vitamin D inadequacy. Seasonal and regional distribution of vitamin D inadequacy is shown below:

Region	25(OH)D < 30 ng/ml (%)		
	Overall	Summer	Winter
Europe (n = 794)	54	52	58
Middle East (n = 314)	81	81	83
Asia* (n = 512)	70	63	81
Latin America* (n = 351)	53	57	51
Pacific Rim (n = 131)	62	71**	59
OVERALL (n=2102)	62	61	66

(*includes at least one equatorial country) (**complete data not yet available)
Results suggest that vitamin D inadequacy is widespread among women with osteoporosis across all continents. In this cross-sectional sample, the prevalence of vitamin D inadequacy is high regardless of latitude or season. Results underscore a need to improve physician and patient awareness of the importance of adequate vitamin D supplementation in postmenopausal women with osteoporosis.

Disclosures: **P. Lips**, *Eli Lilly 2, 5; Merck & Co. 2, 5; Aventis 2; Wyeth 2, 5.*

M276

Prevalence of Low Calcium Intake in Postmenopausal Osteoporotic Women: The Need for Supplementation. R. P. Heaney¹, S. Magowan², X. Zhou^{*2}, S. Boonen³. ¹Creighton University, Omaha, NE, USA, ²Procter & Gamble Pharmaceuticals, Mason, OH, USA, ³Leuven University, Leuven, Belgium.

Guidelines recommend that women over age 50 consume > 1200 mg/day of calcium. Calcium supplementation has been an integral part of all registration trials for osteoporosis since the Study of Osteoporotic Fractures (SOF), 1986-1988. The 1994 -1996 Continuing Survey of Food Intakes by Individuals (CSFII) reports over 90% of women, 50 years and older, consume less than the recommended level of 1200 mg/day of calcium in their diet. The objective of this analysis is to investigate the mean calcium daily intake and the prevalence of insufficient calcium intake among postmenopausal women based on 6 major osteoporosis Phase III trials conducted in the last 10 years. The percentage of women with daily baseline intakes below the minimum 1200 mg/day was calculated based on the reported mean and standard deviation of the average daily intakes from each trial. The aggregate baseline mean calcium intake was calculated from mean calcium daily and weighted for the number of patients enrolled in each trial. This analysis included 11,474 postmenopausal women with mean ages ranging from 53-71 years. The weighted mean calcium intake (all sources) for all 6 trials was 727 mg/day, which was slightly higher than the recently obtained 2004 NHANES data of 660 mg/day. The percent of postmenopausal women with insufficient calcium intake (below 1200 mg/day) was estimated to be 85.0%

(Table 1).

Table 1						
YEAR	STUDY	GROUP	NUMBER (patients)	MEAN AGE (years)	INTAKE MG (SD)	PERCENT < 1200 mg'
1995	Liberman et al.	All	994	63.0	738 (539)	80.4%
1996	FIT I	Treatment	1002	70.7	652 (417)	90.6%
		Placebo	1005	71	619 (397)	92.8%
		Treatment	452	53	910 (506)	71.7%
1998	EPIC	Treatment	445	54	971 (565)	65.7%
		Treatment	102	53	935 (594)	67.2%
		Placebo	461	53	889 (445)	75.8%
1998	FIT II	Treatment	2214	67.6	634 (405)	91.9%
		Placebo	2218	67.7	638 (395)	92.3%
		Treatment	316	68.2	907 (563)	69.9%
2000	PROOF	Treatment	316	69	911 (452)	73.9%
		Treatment	312	67.9	874 (480)	75.1%
		Placebo	311	68.2	979 (592)	64.6%
2001	Neer et al.	Treatment	444	69	786 (443)	82.5%
		Treatment	434	70	757 (449)	83.8%
		Placebo	448	69	762 (433)	84.4%
REVIEW	All STUDIES	All	11,474	66.3 yr	727 mg/d	85.0%

* calculation assumed a normal distribution with parameters
These data derived from the baseline assessments of major osteoporosis trials suggest that, despite increased public awareness, little has changed in the average daily calcium intake since SOF 1988 (714mg/day). Baseline calcium intake of patients is still approximately 500mg/day below the recommended daily amount. Postmenopausal osteoporotic women would benefit from a treatment regimen that includes calcium supplementation with their prescription medicine in order to maximize the fracture risk reduction benefits of osteoporosis therapy.

Disclosures: **R.P. Heaney**, *Merck 5, 8; GlaxoSmithKline 5.*

M277

The Influence of Lifestyle Factors on Bone Mineral Density at the Mid Radius Assessed Using pQCT. S. R. Pye^{*1}, K. A. Ward^{*2}, D. K. Roy^{*1}, C. M. Swarbrick^{*1}, J. E. Adams^{*2}, A. J. Silman^{*1}, T. W. O'Neill¹. ¹ARC Epidemiology Unit, The University of Manchester, Manchester, United Kingdom, ²Department of Imaging Science and Biomedical Engineering, The University of Manchester, Manchester, United Kingdom.

There are few data concerning the influence of lifestyle factors on bone mass and geometry assessed using peripheral quantitative computed tomography (pQCT). The aim of this analysis was to determine the influence of lifestyle factors on volumetric bone mineral density (vBMD) and total area (TA) at the mid radius in premenopausal women. 94 Caucasian women aged 26 to 36 years were recruited from population registers in Manchester (UK), and invited to attend for a lifestyle questionnaire which included questions concerning smoking, levels of regular physical activity (light, moderate, heavy, very heavy [scored 1-4]) and also duration of sports and physical exercise sufficient to produce sweating (per week: never, occasionally, < 1 hour, 1-2 hours, > 2 hours [scored 1-5]) during three age periods (11-17 years, 18-25 years and 26-35 years). For each of the physical activity variables, scores from each of the three age-periods were summed to provide an overall score, increasing values representing increasing activity. In addition, 69 (73%) subjects completed a 4-day food diary from which daily calcium intake was calculated. Height and weight were recorded. Volumetric BMD (vBMD) and total area (TA) were measured at the mid-shaft radius using pQCT (Stratec XCT 2000). Linear regression was used to explore the relationship between the pQCT parameters and putative risk factors with adjustments made for age, height and weight. The mean age of subjects was 31.4 years. Mean value for height was 1.6m, weight 72.8Kg and dietary calcium intake 787mg. 42% of subjects were current smokers. Mean vBMD was 1300.8mg/cm³ (SD=19.1) and TA 104.2mm² (SD=16.4). Compared to those in the lowest tertile of duration of physical exercise, those in the upper tertile (score > 11) had an increased vBMD (β coefficient 11.9; 95% CI 2.6, 21.2). There was, however, no association with TA (β coefficient -0.6; 95% CI -1.9, 0.7). Levels of regular physical activity, smoking and dietary calcium intake were not associated with either vBMD or TA. Increased duration of physical exercise is associated with an increase in vBMD though not TA at the mid radius in premenopausal women.

Disclosures: **T.W. O'Neill**, *None.*

M278

Risk Factors for Vitamin D Inadequacy among Women with Osteoporosis: An International Study. R. Rizzoli^{*1}, J. Eisman^{*2}, O. Ljunggren^{*3}, J. Chandler⁴, J. Norquist^{*4}, G. Krishnarajah^{*4}, S. Lim^{*5}. ¹Hopital Cantonal Universitaire de Geneve, Geneve, Switzerland, ²Garvan Institute of Medical Research, Sydney, Australia, ³Department of Medical Sciences, University Hospital, Uppsala, Sweden, ⁴Merck Research Laboratories, Blue Bell, PA, USA, ⁵Severance Hospital Department of Internal Medicine, Seoul, Republic of Korea.

This study determined risk factors for vitamin D inadequacy (25(OH)D <30 ng/ml) among postmenopausal women with osteoporosis in various regions of the world. A cohort of 2102 community-dwelling, postmenopausal women with osteoporosis from 18 countries [including Europe, Middle East, Latin America, Asia and Pacific Rim] were recruited. 1285 were recruited from May-October 2004 and 912 from December 2004 through April 2005. General health, education, sun exposure, skin reactivity, diet, recent travel to sunny climates, and vitamin D supplement use were collected by questionnaire. Other factors assessed included Body Mass Index (BMI), season, and latitude. Serum 25(OH)D (Nichols

Advantage) and PTH were measured at a single office visit. Multivariate logistic regression models estimated the odds ratios for vitamin D inadequacy for significant predictors. Mean age was 67.2 years, range 41 to 92. Overall mean 25(OH)D was 27.2 ng/ml (SD=13.0, range 7-120, median=25). PTH began to rise with total 25(OH)D < 30 ng/ml despite concerns of potential underestimation of 25(OH)D₂. Approximately 62% of women had vitamin D inadequacy. BMI >=30 kg/m², inadequate vitamin D supplementation, poor or fair health, and low sun exposure were significant predictors of vitamin D inadequacy. (Table) Countries with marked seasons had somewhat higher prevalence of vitamin D inadequacy than equatorial countries, but prevalence of inadequacy did not differ between summer and winter. Prevalence of vitamin D inadequacy ranged from 30% to 70% in equatorial countries and from 30% to nearly 100% in non-equatorial countries. These findings suggest a high prevalence of vitamin D inadequacy worldwide with modifiable factors of high body mass index, inadequate vitamin D supplementation, and low sun exposure. These results underscore a need to improve physician and patient awareness of the importance of adequate vitamin D supplementation in postmenopausal women with osteoporosis.

Risk Factor	Odds Ratios (95% CI) for Vitamin D inadequacy
BMI	
<=30 kg/m ²	Ref
>30 kg/m ²	2.1 (1.5,2.9)
Season	
Equatorial climate	Ref
Non-equatorial	2.3 (1.8, 2.9)
Vitamin D Suppl	
>= 400 IU daily	Ref
< 400 IU daily	2.0 (1.5,2.6)
no supplement	2.8 (2.2, 3.6)
General Health	
Excellent/Very Good	Ref
Good	1.3 (1.0, 1.7)
Fair/Poor	2.0 (1.5, 2.6)
Sun exposure index	0.96 (0.94,0.98)
Recent travel to sunny area	
Yes	Ref
No	1.5 (1.2,1.9)

Disclosures: **R. Rizzoli**, None.

M279

Population-Based Evidence that Serum 25(OH)D Levels below 80 nmol/L Reflect Vitamin D Deficiency. **J. M. Lappe, D. Travers-Gustafson***, **M. J. Barger-Lux***, **K. M. Davies***, **R. P. Heaney, R. R. Recker**. Osteoporosis Research Center, Creighton University, Omaha, NE, USA.

Optimal vitamin D nutrition is essential for skeletal health. Low levels of serum 25(OH)D and the concomitant decrease in serum calcium lead to an increase in serum parathyroid hormone (PTH). PTH increases mobilization of calcium from the skeleton that can cause and exacerbate osteoporosis. However, uncertainty exists regarding the optimum level of serum 25OHD, i.e. the level at which PTH stabilizes. Numerous studies suggest that 25(OH)D levels below 80 nmol/L are deficient. The purpose of this analysis is to evaluate the relationship between serum PTH and 25(OH)D in a randomly selected population-based sample of postmenopausal women. The analysis was conducted on data from 1179 white women randomly selected from the population of healthy postmenopausal women over 55 years of age in a nine-county farming area of Nebraska. Participants were enrolled into an intervention study of calcium and vitamin D. This report includes only data collected at baseline. Blood was drawn after a three-hour fast, and PTH and 25(OH)D were analyzed by RIA (Nichols Laboratories). Data were analyzed with SPSS Version 12.0 (SPSS Inc. Chicago). Persons with serum PTH above the 95th percentile of this population and those with serum calcium values in the highest quintile were excluded from the analysis since they most likely had primary and secondary hyperparathyroidism. Among the remaining subjects, the best fit for values of PTH and 25(OH)D was bilinear, and the point at which the curve flattened was approximately 80 nmol/L. Below this value, PTH dropped by 0.29 pg/ml per nmol/L of 25(OH)D increase. Above the cut-off, PTH was insensitive to 25(OH)D. Thus, findings from this population-based sample further support the existing evidence that values of 25(OH)D below 80 nmol/L are deficient.

Disclosures: **J.M. Lappe**, None.

M280

Increased Skin Pigmentation in β-Thalassemia Patients Does not Reduce UV-Mediated Vitamin D Synthesis. **R. Dresner-Pollak¹, C. D. Enk*², A. W. Goldfarb*³.** ¹Endocrinology, Hadassah - Hebrew University Medical Center, Jerusalem, Israel, ²Dermatology, Hadassah - Hebrew University Medical Center, Jerusalem, Israel, ³Hematology, Hadassah - Hebrew University Medical Center, Jerusalem, Israel.

Decreased serum 25-hydroxyvitamin D3 (25-OH-D) level has been reported in β-Thalassemia patients and may contribute to their bone disease (Dresner Pollak R, Br J Haematol 2000). Vitamin D3 is made by photoconversion of 7-dehydrocholesterol (7-DHC) in the skin to previtamin D3. Increased skin pigmentation has been shown to limit vitamin D3 synthesis because melanin competes with 7-DHC for the ultraviolet radiation (UVR). Increased skin pigmentation is a major clinical feature of severe β-Thalassemia, caused by both melanin and iron deposition. To study the effect of increased skin pigmentation on the production of vitamin D3 in β-Thalassemia we measured circulating 25-OH-D concentrations after exposure to a single standard dose of UVR. Minimal erythemal dose (MED mJ/cm2), defined as the lowest UVR sufficient to produce

perceptible erythema at 24 hours, was determined in 10 Thalassemia major patients and 10 healthy skin type-matched controls, using a xenon arc solar stimulator. In 4 Thalassemia patients and 4 healthy controls, serial blood samples were obtained for 8 days to determine the change in circulating 25-OH-D level by radioimmunoassay (Incstar) in response to a single total body exposure to 1 MED. Mean MED was significantly lower in Thalassemia patients (91.4 ±22.8 mJ/cm2) compared to controls (132.8±31.7 mJ/cm2, p<0.01), indicating the increased skin photosensitivity in Thalassemia patients possibly because of excess iron (Morliere P, Biochim Biophys Acta, 1997). Basal 25-OH-D concentration was significantly lower in Thalassemia patients compared to controls (10.5±6.0 ng/ml vs. 32±7.5 ng/ml, p<0.05). However, the increase in serum 25-OH-D over basal level in response to UVR was not significantly different between Thalassemia patients (44-80%) and controls (42-50%). Our findings suggest that vitamin D deficiency in β-Thalassemia patients cannot be attributed to increased skin pigmentation associated with decreased vitamin D production. Other explanations such as increased oxidation of vitamin D should be explored.

Disclosures: **R. Dresner-Pollak**, None.

M281

Characteristics of Men with Normal BMD and VFA-Detected Fractures. **N. Vallarta-Ast, S. Agrawal***, **D. Krueger, N. Binkley**. University of Wisconsin Osteoporosis Clinical Research Program, Madison, WI, USA.

Densitometric vertebral fracture assessment (VFA) is a useful technology to identify fracture in men. However, some men with VFA-identified fractures have normal BMD. Whether these men have “osteoporosis” is not clear. To begin characterizing such men, DXA studies, including VFA, of 827 male veterans referred for clinical bone mass measurement at the Middleton VAMC were reviewed. Of these men, 33 (4.0%) were identified who had grade 2 or 3 vertebral compression fractures using the Genant semiquantitative (SQ) system, but normal BMD at all three routinely imaged sites (L1-4 spine, proximal femur and one-third radius). Based upon history (including prior fracture, falls, medication and/or toxin use) obtained by the DXA technologist, these men were divided into three groups by inferring future fracture risk: high (prior low-trauma fracture, 17), low (prior high-trauma fracture, 7) and unknown (no prior known fracture, 9). Of those men with high or unknown presumed fracture risk, 77% (20/26) had historical risk factors contributing to skeletal fragility or a history of fracture with falling. The most common single fracture risk factor was chronic corticosteroid use (6/20), followed by other medications or toxins associated with bone loss (e.g., heparin, chemotherapeutics, alcohol abuse or anti-epileptics) in 11/20. An additional 6/20 related a history of frequent falls. Other noteworthy historical conditions included ulcerative colitis, hyperparathyroidism, chronic renal insufficiency and hypovitaminosis D. In only 6/26 were no fracture risk factors identified by history. Additionally, the spinal deformity index (SDI) was calculated for these men. SDI is the sum of the SQ grade for visualized vertebral bodies from T4-L4. By combining fracture number and severity, the SDI has recently been identified as predictor of future fracture risk in postmenopausal women. Mean SDI calculated for the fracture risk groups described above was 3.3, 2.0 and 2.7 in the high, low and unknown risk groups respectively. As such, a trend (p = 0.08) toward higher SDI was observed in men with prior low trauma fracture. In conclusion, medical history obtained by the DXA technologist identifies traumatic events and/or detects risk factors for fracture in the vast majority of men with normal BMD and VFA-identified fractures. Obviously, not all VFA-identified fractures are due to osteoporosis; however, medical history combined with SDI may help identify men at higher risk for future fracture. Finally, the high prevalence of secondary causes of bone loss suggests that a metabolic bone disease evaluation may be prudent in men with VFA-identified fractures in the presence of normal BMD

Disclosures: **N. Vallarta-Ast**, None.

M282

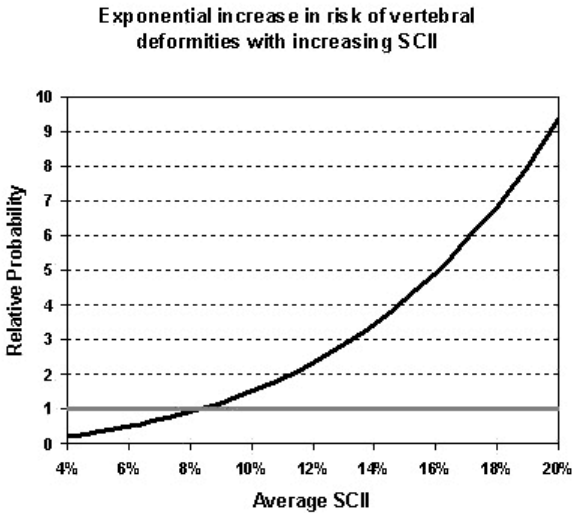
The Spinal Curvature Irregularity Index Predicts Vertebral Fractures: A Comparison with Spine and Femur BMD. **G. Maalouf¹, N. Schaaf*², R. Zebaze*³, N. Maalouf*⁴, J. Wehbe*¹, E. Seeman*³.** ¹St. George Hosp., Beirut, Lebanon, ²K.U., Leuven, Belgium, ³Departm. Endocrinology, Austin and Repatriation Med. Centre, Melbourne, Australia, ⁴Southwestern Med. Center, Dallas, TX, USA.

Vertebral fractures (VFs) are the most common consequence of osteoporosis. Diagnosing VFs from radiographs or DXA vertebral fracture assessment (VFA) images of thoracolumbar spine is an important tool in evaluation of osteoporosis. However, accurate diagnosis of VFs using these methods can be difficult. There is often no clear distinction between a structural failure and normal anatomic variation in anterior, middle and posterior height of the vertebrae. In this study we determined the capability of the Spinal Curvature Irregularity Index (SCII) to identify vertebral deformities. The SCII is the integrated average of the vertebral heights (VHs) over the thoracolumbar spine to give a quantitative estimate of the regularity of the spinal curvature (Zebaze,2004,JBMR). A large SCII is presumed to correlate with presence of vertebral deformities. We compared the capability of SCII in identifying vertebral deformities with that of spine and femur mineral density (BMD). VHs and spine and femur BMD values were obtained from VFA, AP-spine and femur DXA scans (Lunar Prodigy GE Healthcare) in 463 Lebanese women aged 20-89 yrs. ROC analysis and logistic regression was performed using Analyse-it and Minitab. SCII was cube root transformed for normality. T-test was used to compare average transformed SCII. The average SCII was significantly higher for subjects with one or more deformities (p<0.0001). SCII increases significantly with increasing numbers of vertebral deformities. The probability of having a deformity increases 2.1 times for every SD increase in SCII. ROC analysis shows that SCII is a better diagnostic tool for VFs than femur or spine BMD.

We conclude that the SCII clearly distinguishes between subjects with and without vertebral deformities. SCII is a superior predictor of vertebral deformity than is spine or femur BMD.

ROC Analysis: Area under the curve for identification of the presence of vertebral deformities			
Variable	Area	95% CI	p*
SCII	0.721	0.674, 0.768	<0.0001
Total Femur BMD	0.589	0.537, 0.640	0.0004
Femur Neck BMD	0.586	0.534, 0.637	0.0006
Femur Troch BMD	0.564	0.512, 0.617	0.0083
L1-L4 Spine BMD	0.542	0.489, 0.595	0.0612
L2-L4 Spine BMD	0.543	0.490, 0.596	0.0563

*Probability that there is no distinction between subjects with and without deformities



Disclosures: **G. Maalouf**, None.

M283

Combined Deterioration of Cancellous and Cortical Bone Structure and the Risk of Vertebral Fragility Fracture. **S. Qiu, S. Palnitkar*, D. Rao.** Bone & Mineral Research Lab, Henry Ford Health System, Detroit, MI, USA.

The effects of bone architectural deterioration on the risk of vertebral fracture have usually been studied by cancellous and cortical bone respectively. There is little information about the risk of vertebral fracture in subjects with both cancellous and cortical bone compromised. Iliac bone biopsies were performed in 144 postmenopausal white women, aged 50 to 73 years. Of them, 66 were non-fracture subjects and 78 suffered from non-traumatic vertebral fracture not just deformity. Conventional bone histomorphometry was conducted for all the subjects. In cancellous bone, the measurements included cancellous bone volume (BV/TV-Cn), trabecular thickness (Tb.Th), trabecular number (Tb.N) and trabecular separation (Tb.Sp), and in cortical bone, the cortical bone volume (BV/TV-Ct) and thickness (Ct.Th). The same measurements were also performed in 38 premenopausal women aged 20-49 years and a value of 1SD below the mean was used as the cutoff for determining the vertebral fracture risk. Logistic regression analysis demonstrated that Tb.N and Ct.Th were the most positive variables to affect the risk of vertebral fracture. The non-fracture postmenopausal women and fracture patients were separately divided into 4 groups depending on the level of Tb.N and Ct.Th: 1) normal Tb.N and Ct.Th; 2) low Tb.N but normal Ct.Th; 2) low Ct.Th but normal Tb.N and 4) low Tb.N and Ct.Th. Compared to the group with normal Tb.N and Ct.Th, the increase in the risk of vertebral fracture was similar in the groups with only low Tb.N (Odds ratio 3.29, 95% CI 1.14-9.45) and only low Ct.Th (Odds ratio 3.43, 95% CI 1.14-13.6). However, this risk increased to 27 fold (95% CI 7.63-95.2) in the group with low Tb.N and low Ct.Th. In non-fracture postmenopausal women, the prevalence of low Tb.N and Ct.Th was only 7.6% but in fracture patients the prevalence was 50%. Our study suggests that the combination of compromised cortical and cancellous bone structure confers a greater risk to vertebral fragility fracture, an observation that has hitherto been overlooked.

Disclosures: **S. Qiu**, None.

M284

Hip Fracture Incidence over a 10-Year Period: Reversal of a Secular Trend Related to a Specific Decrease of the Age-Adjusted Incidence in Institutional-Dwelling Elderly Women. **T. Chevalley¹, E. Guilley^{*2}, F. Herrmann^{*1}, P. Hoffmeyer^{*3}, C. H. Rapin^{*2}, R. Rizzoli¹.** ¹Service of Bone Diseases, Rehabilitation and Geriatrics, University Hospitals Geneva, Switzerland, ²Centre for Interdisciplinary Gerontology, University Hospitals Geneva, Switzerland, ³Service of Orthopaedic Surgery, University Hospitals Geneva, Switzerland.

Hip fracture in the elderly is the main burden of osteoporosis in terms of mortality, disability, impairment of quality of life and costs. On the other hand, there is an increase of age-adjusted hip fracture incidence (secular trend) in many studies. Long-term data on secular changes in women and men within a defined community are still scarce. We specifically examined from 1991 to 2000 the age distribution of patients with hip fracture, the secular changes in the incidence rates of hip fracture in women and men in a well defined community, and the influence of the residential status (institutional-dwelling or home-dwelling). All patients 60 years of age and older discharged with a diagnosis of a hip fracture (ICD-10 code: S72.0 and S72.1) were retrospectively identified from the computer records of the Geneva university hospital, which is receiving 95% of hip fracture occurring in a well defined area. From 1991 to 2000, 3951 hip fractures were recorded. This concerned 1409 institutional-dwelling women and 215 men and 1776 home-dwelling women and 551 men. Mean age (\pm SD) of women and men with hip fracture was 86.4 \pm 6.5 and 84.5 \pm 7.9 years in institutional-dwelling elderly, and 81.6 \pm 8.5 and 79.7 \pm 8.9 years in home-dwelling elderly (p<0.001). Over a 10-year period, mean age increased by +0.13 year per year (p=0.032) and by +0.14 year per year (p=0.038), in institutional-dwelling and home-dwelling elderly women, respectively. In men of the corresponding groups, mean age changes were +0.28 year (p=0.129) and -0.06 year (NS), respectively. The age-adjusted incidence rate of hip fractures, standardized to the 2000 Geneva population, decreased significantly by 1.3% per year in women (p=0.039) and remained unchanged in men (+0.5% per year, p=0.686). Among institutional-dwelling elderly women, hip fracture incidence decreased by 1.9% per year (p=0.044) whereas it remained stable (+0.0% per year, p=0.978) among home-dwelling women. In men, no significant change in hip fracture incidence occurred among institutional-dwelling (+1.0%, p=0.666) nor home-dwelling (+0.8% per year, p=0.565). In conclusion, despite an increase in the mean age of hip fractured women, the decrease in the age-adjusted incidence of hip fracture in institutional-dwelling elderly women was responsible for the significant decrease in age-adjusted incidence of hip fracture observed in women but not in men.

Disclosures: **T. Chevalley**, None.

M285

Renal Function and Risk of Hip and Vertebral Fractures among Older Women. **K. Ensrud¹, L. Lui², A. Ishani^{*1}, M. Shlipak^{*2}, B. Taylor¹, D. Antonucci^{*2}, K. Stone², S. Jamal³, M. Homan¹, S. Cummings².** ¹VAMC & U of MN, Minneapolis, MN, USA, ²UCSF & CPMC, San Francisco, CA, USA, ³U Toronto, Toronto, ON, Canada.

An increased rate of fractures has been observed in patients with end-stage renal disease, but the effect of less severe renal dysfunction on fracture risk is uncertain. To test the hypothesis that community-dwelling older women with impaired renal function are at increased risk of hip and vertebral fractures (fxs), we conducted a case-cohort study within the Study of Osteoporotic Fractures, a prospective cohort study of 9,704 women \geq 65 yrs. Baseline renal function in random samples of women who had fxs of 2 types since the baseline exam (149 with incident hip fx, 150 with incident vertebral fx) was compared with that in control women without incident fx of the specified type (376 & 293 controls for cases of hip and vertebral fx, respectively). Controls were drawn from a pool of 400 women randomly selected from the cohort regardless of fx status. We estimated the creatinine clearance (CrCl) in ml/min for each participant using the Cockcroft-Gault formula incorporating baseline age, gender, weight and serum creatinine; CrCl was classified by modified National Kidney Foundation criteria for chronic kidney disease. For the hip fx (vertebral fx) analyses, 46% (51%) had a CrCl \geq 60, 29% (29%) had a CrCl 45-59 and 25% (20%) had a CrCl <45. Fx cases were validated by x-ray reports (hip fx) and spine films taken at baseline & 3rd exam an average of 3.7 yrs later (vertebral fx). There was an independent, graded association between reduced renal function and the risk of hip fx; compared with women with normal renal function, those with moderate renal impairment had a 2.3-fold increase in risk. The relationship between renal function and vertebral fx was weaker in magnitude and did not reach significance. Further adjustment for health status, smoking, diabetes, prior fx and physical activity or substituting femoral neck or spine BMD for calcaneal BMD did not alter our results.

Renal Function	Relative Risk of Fx*	
	Hip Fx RH (95%CI)	Vertebral Fx OR (95% CI)
CrCl \geq 60 ml/min	1.0 (referent)	1.0 (referent)
CrCl 45-59 ml/min	1.6 (0.9-2.8)	1.1 (0.6-1.9)
CrCl < 45 ml/min	2.3 (1.2-4.7)	1.3 (0.6-2.8)

*adjusted for age, weight and calcaneal BMD

Older community-dwelling women with moderate renal dysfunction are at increased risk of hip fx. Our results in context of several studies reporting associations between chronic kidney disease and cardiovascular disease highlight the potential public health impact of chronic renal insufficiency.

Disclosures: **L. Lui**, None.

M286

Gender Specific BMD Profile in Norwegian Patients with Forearm Fractures. H. C. Gulseth^{*1}, C. G. Gjesdal², G. Haugeberg^{*3}. ¹Dept of Rheumatology, Betanien Hospital, Skien, Norway, ²Dept of Rheumatology, Haukeland University Hospital, Bergen, Norway, ³Dept of Rheumatology, Sorlandet Hospital, Kristiansand, Norway.

Osteoporotic fractures of the hip and spine are highly frequent in the Norwegian population. Several international studies have shown a relationship between osteoporosis and low impact forearm fractures in patients > 50 years. The main purpose of this study was to assess the prevalence of osteoporosis in Norwegian patients with low impact forearm fractures. Furthermore, we wanted to examine whether patient bone mineral density (BMD) for patients with low impact forearm fractures differed from the expected BMD for age. 640 patients aged > 50 years with low impact forearm fractures were included from three Norwegian Hospitals (Bergen n=272, Skien n=240 and Kristiansand n=128). The patients had hip and spine BMD measured according to the standard procedures with Lunar™ DXA equipment. Gender specific T and Z scores were extrapolated from the Lunar™ reference data. These reference data have previously been validated in a large scale Norwegian population study. A significant proportion of men and women with low impact wrist fractures had osteoporosis. The proportion was expectedly higher among female patients. Osteoporosis was defined as a T score below 2.5 SD in either hip or spine. 41% (n=554) of females had osteoporosis, of which 23% was in the hip and 31% in the spine. In the male patients, 28% (n= 84) had osteoporosis, 16% in the hip and 19% in the spine. In female patients the prevalence of osteoporosis increased with increasing age, but the same relationship was not observed in the male patients. Both men and women with low impact forearm fracture had a significantly lower BMD than expected from the Lunar™ reference data. Despite standardising for gender, age and weight, the mean Z score was significantly lower for men than for women. In the female patients the mean Z score (95% CI) in the hip was -0.43 (-0.50 to -0.35) and in the spine -0.19 (-0.31 to -0.07). In the male patients mean Z score (95% CI) in the hip was -0.73 (-0.98 to -0.48) and in the spine -0.64 (-0.10 to -0.29). The reason for this gender specific BMD profile in forearm fracture patients is unknown.

Age related prevalence of osteoporosis				
Age (Years)	50-59	60-69	70-79	80+
Women (n)	126	165	151	112
Osteoporosis hip (%)	8	9	32	53
Osteoporosis spine (%)	20	27	36	39
Men (n)	29	31	13	11
Osteoporosis hip (%)	7	23	8	27
Osteoporosis spine (%)	14	26	8	27

Disclosures: *H.C. Gulseth, None.*

M287

The Prevalence of Vertebral Fractures in Mexican Men over 50 Years. A Population-Based Study. P. Clark¹, M. Deleze², F. Cons-Molina³, J. Salmeron^{*4}, S. Ragi⁵, L. Palermo^{*6}, S. R. Cummings⁷. ¹Clinical Epidemiology Unit-Faculty of Medicine UNAM, IMSS, Mexico City, Mexico, ²Clinica de Osteoporosis, Puebla, Mexico, ³Unidad de Diagnostico de Osteoporosis, Mexicali, Mexico, ⁴Epidemiology & Health System Unit, IMSS, Morelos, Mexico, ⁵CEDOES, Vitoria, Brazil, ⁶Coordinating Center, University of California, San Francisco, CA, USA, ⁷SF Coordinating Center, CPMC Research Institute and UC San Francisco, San Francisco, CA, USA.

Osteoporosis in men has become a focus of research in the last decade in response to the increasing awareness of the health impact of this condition in males due to high mortality and economical impact. We reported recently that Mexican women have a high rate of vertebral fractures, similar to the results reported in the United States and some European countries. To date, no studies on the prevalence of vertebral fractures have been reported in Mexican men. Therefore, the aim of this study was to determine the prevalence of vertebral fractures in men 50 years and over in the City of Puebla, Mexico, following the same protocol used from our previous study in women. A stratified sample of 413 randomly selected men from Puebla, Mexico was surveyed in a face to face interview. A questionnaire was used to get information on demographics, osteoporosis risk factors and some life styles. BMD in two regions and lateral dorsal/lumbar X-rays were obtained in all cases in accordance with international protocols to be able to make cross-national comparisons. Digital morphometry was used to determine vertebral deformities by a modified Eastell criterion. The overall prevalence of vertebral fractures was 9.7 %. The prevalence increased with age having the highest prevalence in the older group as seen in the table. The prevalence of vertebral fractures in men is half of the prevalence estimated for women (19.5%). The higher prevalence in women starts at age 70 (18.6 % CI 10.7-26.6) while in men the higher prevalence starts a decade later. This pattern is similar with the patterns in other European countries and the USA. We conclude that vertebral fractures are more frequent in older age Mexican men, and these figures have to be taken into consideration by Mexican health authorities to plan future programs oriented to prevent and treat fragility fractures in men.

Age	Total N	Num of Fx	Prevalence and 95% CI
50-59	101	2	2.0 (-0.74-4.70)
60-69	103	8	7.8 (2.60-12.94)
70-79	106	8	7.5 (2.52-12.58)
> 80	103	22	21.4 (13.45-29.27)
Total	413	40	9.7 (6.83-12.54)

Disclosures: *P. Clark, None.*

M288

In Vivo 3 D Reconstruction of Human Vertebrae Using 3 Dimensional X-Ray Absorptiometry (3D-XA). S. Kolta¹, D. Mitton^{*2}, S. Quiligotti^{*2}, C. Ambrosi^{*2}, C. Roux¹, W. Skalli^{*2}. ¹Rheumatology, Cochin hospital, Paris, France, ²LBM, ENSAM, CNRS, Paris, France.

Lumbar spine BMD measured by DXA is an important risk factor for vertebral fracture. However, it is highly dependent on patient positioning and inter individual variations. Other parameters such as vertebral body size and shape independently affect its strength. Recent advances in stereoradiographic reconstruction techniques allow obtaining 3D bone geometry from landmarks identified on 2 radiographs and an a priori knowledge. The aim of our study was to evaluate the accuracy and precision of 3D reconstruction of human vertebrae using 2 perpendicular DXA scans both ex-vivo and in vivo. Sixteen human dried lumbar vertebrae were used to calculate the accuracy. They were scanned using a helical CT-scanner. The 3D reconstruction containing up to approximately 2000 points, were obtained using the SliceOmatic® software (accuracy ± 1 mm). DXA acquisitions of the vertebrae were performed using a standard Hologic QDR 4500 A device. The DXA scans were acquired in AP and lateral incidences. From both DXA images, anatomical landmarks were identified and 3D detailed models were reconstructed. The accuracy of 3D-XA reconstructions was evaluated in comparison with the CT-scan ones by superimposing the two models using geometrical transformations and a least square matching method. Results were expressed as point to surface distances. The AP and lateral views of the thoraco-lumbar spines (from T4 to L4) of 20 female patients, aged 61 ± 8 y, acquired by the imaging software on the same DXA device were used to calculate the precision. Their 3D reconstruction using the 3D-XA method was performed twice by 2 different observers. A set of geometric parameters including lateral, anterior and posterior vertebral body heights, superior, middle and inferior width and depth were calculated from 3D-XA reconstructions of 3 different observers for L1 - L4 vertebrae. Quantitative comparisons between the CT-scan reference reconstructions and the 3D-XA for the dried vertebrae yielded mean difference for the whole vertebrae of -0.2 ± 1.3 mm. Mean absolute value was 1.0 mm and 95% of errors < 2.6 mm. Maximal error reached 6.4 mm on the transverse process. The precision of the in vivo 3D reconstruction of the human vertebrae using the 3D-XA method showed a mean difference between the 2 observers of 0.4 ± 0.9 mm (2 RMS i.e. 95% of differences < 2.3 mm). Mean errors for geometric parameters calculated from 3D-XA ranged from 0.5 - 1.2 mm according to the parameter, (2 RMS 1.3 - 2.9 mm, < 9%) and maximal errors 1.9 - 4.7 mm (<16%). This pilot study shows that 3D-XA of human vertebrae is feasible in vivo using a standard DXA device allowing direct measurement of geometric parameters of the vertebrae.

Disclosures: *S. Kolta, None.*

M289

Fracture Risk Related to Selected Factors According to Site and External Cause of Injury. The 10-year Follow-Up Data of OSTPRE Study. R. J. Honkanen¹, M. T. Tuppurainen^{*2}, H. P. Kroger³. ¹Bone and Cartilage Research Unit, University of Kuopio, Kuopio, Finland, ²Gynaecology, Kuopio University Hospital, Kuopio, Finland, ³Surgery, Kuopio University Hospital, Kuopio, Finland.

The purpose was to find out differences in fracture risks according to site and external cause of fracture. The 10-year follow-up data of The Osteoporosis Risk Factor and Prevention (OSTPRE) Study cohort was used. The cohort was established in 1989 by selecting all women (N=14220) born in 1932-41 and resident in Kuopio Province, Finland. 11074 women responded to postal enquiries in 1989, 1994 and 1999. A total of 1915 women reported a follow-up fracture verified by patient record perusal. The effects of fracture history, smoking and nutritional calcium intake at baseline as well as hormone replacement therapy (HRT) during follow-up were studied as 3-category variables. In addition, a sum risk score (range 0-8) was formed out of these factors and was used as a 3-category (low, medium and high risk) variable in univariate and multivariate logistic regression. Considerable differences between fracture types and external cause categories were found (Table). The results imply that these factors apply better for osteoporotic fracture than other fracture risk estimation.

Table. Fracture risk related to selected factors according to site and external cause of fracture

Fracture site (No of women)	Smoking	Ca intake	HRT	Fracture history	Risk score§	Adjusted§ risk score
Forearm (736)		***	***	***	0.32***	0.31***
Non-forearm (1179)	***		**	***	0.43***	0.45***
Humerus (92)	*		**	*	0.17**	0.19**
Rib (159)	**			**	0.69	0.75
Spine (112)			*	***	0.31*	0.37*
Hip (35)				**	0.16**	0.19*
Tibia (68)			**	***	0.10***	0.11***
Ankle (381)	***		**	***	0.26***	0.28***
Total (1915)	**	**	***	***	0.35***	0.35***
External cause						
Fall on level (1352)	***	***	***	***	0.26***	0.26***
Fall, other (154)				**	0.40**	0.44*
Non-fall (654)				***	0.59**	0.58**
Bicycle (102)	*			***	0.32**	0.30**
Car crash (71)					3.89	4.00

*p<0.05, **p<0.01 ***p<0.001 §3-category sum score: low vs. high risk comparison (Odds Ratio). §Adjusted for baseline age, weight, height, No. of health disorders and leisure physical activity (N/Y)

Disclosures: *R.J. Honkanen, None.*

M290

Physical Activity and Fracture Risk in Older Men: A Prospective Study. K. L. Stone¹, S. R. Cummings¹, S. Harrison^{*1}, P. M. Cawthon¹, J. A. Cauley², K. E. Ensrud³, D. C. Bauer⁴, M. Stefanick^{*5}, B. Chan^{*6}, L. Marshall^{*6}, L. Lambert^{*6}, E. S. Orwoll⁶. ¹San Francisco Coordinating Center, San Francisco, CA, USA, ²University of Pittsburgh, Pittsburgh, PA, USA, ³University of Minnesota, Minneapolis, MN, USA, ⁴University of California, San Francisco, San Francisco, CA, USA, ⁵Stanford University, Palo Alto, CA, USA, ⁶Oregon Health Sciences University, Portland, OR, USA.

Prior studies suggest that increased physical activity in older adults may prevent falls and improve bone mineral density (BMD). Increased activity levels are associated with decreased risk of hip fracture in older women, but there is little data on this topic in men. Therefore we tested the association of physical activity and risk of non-spine and hip fractures in the Osteoporotic Fractures in Men (MrOS) study. During the MrOS baseline examination, 5995 men aged 65 and older were enrolled at six US clinic sites. Physical activity was assessed using the Physical Activity Scale for the Elderly (PASE). Activity levels were categorized as low (lowest quartile), medium (2nd or 3rd quartile) and high (upper quartile). Total hip BMD was assessed by DXA (Hologic QDR 4500W). Participants were contacted every four months by mail or phone to prospectively ascertain the occurrence of fractures. All fractures were confirmed by review of radiology reports. During a mean follow-up of 3.6 years, 256 men suffered non-spine fractures, and 46 had incident hip fractures. After adjustment for age and BMI, those with low activity levels had a 38% increased risk of non-spine fracture (Relative Hazard=1.38; 95% confidence interval 1.03 - 1.84) and 87% increased risk of hip fracture (RH=1.87; 0.98 - 3.57) compared to those with medium activity levels. Those with high activity levels did not differ significantly from those with medium activity levels. Controlling for smoking and alcohol, health status and comorbidities did not substantially alter the results, however increased risk of fracture among those with low activity levels (compared to medium activity) was attenuated after adjustment for hip BMD (RH=1.23; 95% CI 0.92-1.66 for non-spine fracture; RH=1.35; 95% CI 0.69-2.63 for hip fracture). When activity levels were classified according to type of activity (recreational, household chores, occupational), low levels of recreational activity were most strongly associated with risk of hip fracture (RH=2.87; 1.18 - 6.94). There were no apparent differences in non-spine fracture risk according to type of activity. In conclusion, older men with low activity levels are at increased risk of non-spine and hip fracture. This association is at least partly explained by low BMD. Low levels of recreational activity may be a stronger indicator of hip fracture risk.

Disclosures: **K.L. Stone**, None.

M291

Vitamin K Circulating Levels and Associations with Bone Metabolism in Healthy Japanese Women. N. Tsugawa^{*1}, M. Shiraki², Y. Suhara^{*1}, M. Kamao^{*1}, K. Tanaka³, T. Okano¹. ¹Hygienic Sciences, Kobe Pharmaceutical University, Kobe, Japan, ²Research Institute and Practice for Involuntional Diseases, Nagano, Japan, ³Nutrition, Kyoto Women's University, Kyoto, Japan.

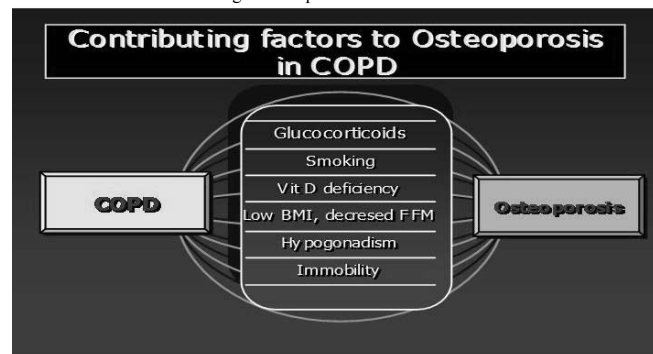
It is generally accepted that vitamin K deficiency is associated with low bone mineral density (BMD) and increased risk of bone fracture. Among the vitamin K homologues, phyloquinone (K₁), menaquinone-4 (MK-4) and menaquinone-7 (MK-7) are primarily observed in human plasma, however, the data are limited on their circulating levels and their associations with bone metabolism, or with γ -carboxylation of osteocalcin molecule. Our objectives were to measure circulating concentrations of K₁, MK-4, and MK-7 in Japanese women, and to elucidate whether each form of vitamin K has a significant association with bone metabolism. Healthy Japanese women (n=407), aged 30-88 yr (62.7±10.9 yr) were stratified by their age into three groups, the 30-49 yr (n=52), the 50-60 yr (n=219), and the 70~ yr (n=136) groups. Plasma K₁, MK-4, MK-7, undercarboxylated osteocalcin (ucOC; measured by the novel electro chemiluminescence immunoassay [ECLIA]), intact OC, Ca, P, bone-derived alkaline phosphatase activity (BAP), and urinary creatinine, N-terminal telopeptide (NTx), and deoxypyridinoline (DPD) were measured. As a result, K₁, MK-4, and MK-7 were detected in 100, 56.8, and 97.8 % of all subjects, respectively, and on average, MK-7 was highest and MK-4 was lowest among the three K vitamins in all age groups. K₁ and MK-7 correlated inversely with ucOC, but nutritional basal concentration of MK-4 had no associations with ucOC. Plasma K₁+MK-7 concentration required to minimize the ucOC concentration was less than 1.3 ng/mL in the 30-40 yr group, 4.7 ng/mL in the 50-69 yr group and more than 10.1 ng/mL in the eldest group. Bone metabolic markers did not correlate with vitamin K homologues concentrations except for relationship between K₁ and urinary DPD at 50-69 yr group and 70~ yr groups. As a conclusion, the certain role of ucOC remains unclear, however, if submaximal γ -carboxylation relates the prevention of fracture or bone mineral loss, circulating vitamin K concentrations in elderly people should be maintained higher than young people.

Disclosures: **Y. Suhara**, None.

M292

Skeletal Effects of Chronic Obstructive Pulmonary Disease: the EOLO Study. G. Crepaldi¹, S. Maggi^{*1}, S. Adami², D. de Feo³, S. Giannini⁴, S. Gonnelli⁵, G. Guglielmi^{*6}, G. Martini⁵, R. Nuti⁵. ¹CNR Aging Center, Padova, Italy, ²Rheumatology, Valeggio Hospital, Verona, Verona, Italy, ³Procter & Gamble, Rome, Italy, ⁴Internal Medicine, University of Padova, Padova, Italy, ⁵Internal Medicine, University of Siena, Siena, Italy, ⁶Radiology, Scientific Institute Hospital "CSS", San Giovanni Rotondo, Foggia, Italy.

The musculoskeletal system is frequently weakened by disabling pathologies like chronic obstructive pulmonary disease (COPD) and the factors involved in this association are multiple, as summarized in the following figure. Of particular concern is the fact that COPD patients are at higher risk for severe vertebral fractures, responsible for a lower lung function that leads to a worsening of the condition. A large, epidemiological study has been undertaken in order to assess the prevalence rates of osteoporosis and osteopenia in a random sample of patients referring to the outpatient pulmonary clinics in 100 centers in Italy (Evaluation of Obstructive Lung disease and Osteoporosis, E.O.L.O. Study for the EOLO Study Group). Each center is enrolling 80 patients, aged 50+ years, who are undergoing a routine assessment for COPD. After informed consent, their medical charts are reviewed and a complete evaluation for osteoporosis, including an interview and a bone ultrasound evaluation using the Achilles Express apparatus (Lunar Co, Madison, USA) are conducted. Subjects are excluded from the study for coexisting cancer, renal, hepatic, thyroid diseases, as well as for previous treatment with drugs affecting bone metabolism. The main objectives of the study are to define the prevalence rates of osteopenia and osteoporosis and of vertebral fractures and to compare them with data available in a population based study conducted in Italy in 2001 in the same centers (ESOPO). Secondary objectives are to evaluate the impact of the use of oral versus inhaled corticosteroids and of the duration of the COPD on the number and severity of vertebral fractures. A pilot and a feasibility studies have been conducted in January 2005, while the data collection phase began in February and is expected to last until July. Preliminary results will be available starting from September 2005.



Disclosures: **G. Crepaldi**, None.

M293

Impact of Early Osteoporosis Treatment on Subsequent Fracture Prevention Among Women With Clinical Vertebral Fracture. R. Lindsay¹, N. N. Borisov^{*2}, R. L. Sheer^{*2}, M. Steinbuch^{*2}. ¹Helen Hayes Hospital, West Haverstraw, NY, USA, ²Procter & Gamble Pharmaceuticals, Inc., Mason, OH, USA.

This study evaluated osteoporosis treatment use and its effect on prevention of subsequent fractures among women with a clinical vertebral fracture, utilizing an integrated administrative, medical and pharmacy claims database. A retrospective cohort study was conducted among women (aged 45+) with a new vertebral fracture verified with a diagnostic code and a record of radiologic exam, between July 1, 2000 and June 30, 2003. The cohort was followed for 12 months after the vertebral fracture to identify a subsequent fracture (vertebral and non-vertebral), osteoporosis treatment, and its subsequent fracture prevention effect. The following exclusion criteria were applied to the data: (1) in the 6 months period prior to the vertebral fracture, women with a record of previous (a) vertebral or non-vertebral fractures, (b) treatment with risedronate, alendronate, nasal calcitonin, or raloxifene, or (c) Paget's disease treatment, and (2) at any point of the study, women with a record of malignant neoplasm and/or trauma "E codes". A total of 7,233 women were identified with a new clinical vertebral fracture. The mean age was 73 years. Majority of the population (80%) did not receive any osteoporosis treatment (bisphosphonates or nasal calcitonin); 1,056 women (15%) received osteoporosis treatment within 90 days of their vertebral fracture (early-treatment cohort), and 358 women (5%) received treatment after 90 days of their vertebral fracture (late-treatment cohort). During the 1-year follow-up, 18% of untreated women experienced a subsequent fracture (vertebral or non-vertebral, n=1,039). Among women in the early-treatment cohort only 85 (8%) had a subsequent fracture (RR=0.51, p<0.01 compared to no treatment cohort), and in the late-treatment cohort, 76 (21%) had a subsequent fracture (RR=1.05, p=0.73 compared to no treatment cohort). Osteoporosis treatments were effective in their subsequent fracture prevention compared to no treatment as follows: risedronate (RR=0.30, p<0.01), alendronate (RR=0.47, p<0.01), and nasal calcitonin (RR=0.67, p=0.03). Among women aged 45+ years with a clinical vertebral fracture, the majority did not receive any osteoporosis treatment. Among those who received treatment, there was a significantly lower risk of developing a subsequent fracture. The early-treatment cohort trended toward fewer fractures compared to the late-treatment cohort. This suggests that a

fragility fracture demands immediate attention and rapid, effective treatment. Risedronate was observed to have a 70% reduction in the occurrence of subsequent fractures within 1 year of vertebral fracture.

Disclosures: N.N. Borisov, Procter & Gamble 1, 3.

M294

Adherence with Drug Therapy and Risk of Fracture among Women with Postmenopausal Osteoporosis. D. Weycker*¹, D. Macarios*², G. Oster*¹. ¹Policy Analysis Inc., Brookline, MA, USA, ²Amgen Inc., Thousand Oaks, CA, USA.

Osteoporosis drug therapy has been reported to prevent fracture in clinical trials. Little is known, however, about the relationship between adherence with such therapy and risk of fracture in clinical practice. A retrospective nested case-control design was employed. Data were obtained from a medical claims database containing information from over 30 US health plans on 15 million lives annually. Study subjects consisted of all women aged ≥ 45 years with postmenopausal osteoporosis (PMO) who initiated osteoporosis drug therapy (bisphosphonates, calcitonin, or raloxifene) between July 1998 and December 2003; those with secondary causes of osteoporosis were excluded. "Cases" consisted of all subjects who experienced an osteoporotic-related fracture between date of therapy initiation and end of observation period. "Controls" consisted of subjects who did not experience such a fracture during this period; they were matched to cases (1:1) based on age, drug therapy, therapy initiation date, and duration of follow-up (date of therapy initiation to date of fracture for cases). Adherence was measured based on number of therapy-days through end of follow-up. Conditional logistic regression was employed to examine relationship between adherence with osteoporosis drug therapy and odds of fracture, controlling for potential confounders. A total of 16,031 women with PMO initiated osteoporosis drug therapy; 724 (5%) experienced fracture following therapy initiation (mean duration of follow-up, 220 days). In multivariate logistic regression, odds of fracture were significantly lower for those with ≥ 180 (vs. < 30) days of therapy; odds did not differ for those with 30-179 (vs. < 30) days of therapy (Table). Among women with postmenopausal osteoporosis, poor adherence with osteoporosis drug therapy is associated with increased risk of fracture.

Parameter	Odds of fracture, by level of drug adherence			
	Unadjusted		Adjusted*	
	Odds Ratio	P-value	Odds Ratio	P-value
Number of Therapy-Days				
<30 (n=456)	1.00	--	1.00	--
30-89 (n=400)	0.86	0.39	0.93	0.72
90-179 (n=261)	0.89	0.57	0.92	0.73
180-359 (n=199)	0.53	0.01	0.52	0.02
≥ 360 (n=132)	0.57	0.05	0.53	0.05

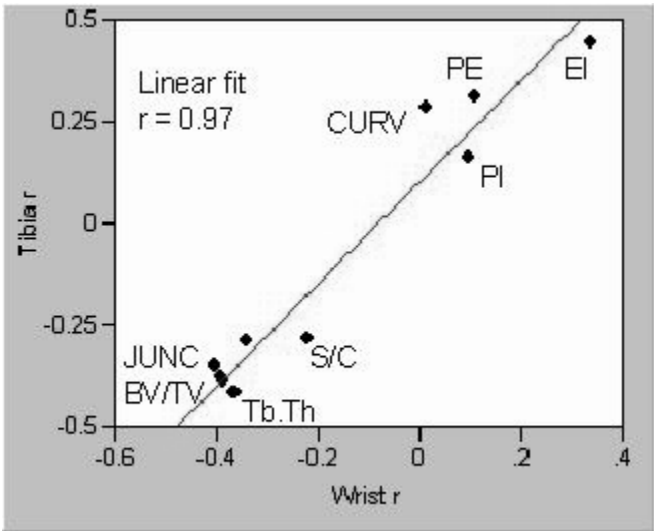
*Adjusted for history of fracture (pre-treatment), selected comorbidities, and use of selected medications.

Disclosures: D. Weycker, Amgen Inc. 5.

M295

Degree of Vertebral Deformities Is Associated with Topology of Trabecular Network Measured Noninvasively at Radius and Tibia Surrogate Sites. G. A. Ladinsky*, B. Vasilie*, A. Popescu*, M. Wald*, B. Zemel*, P. J. Snyder, L. Loh*, H. K. Song*, P. K. Saha*, A. Wright*, F. W. Wehrli. University of Pennsylvania, Philadelphia, PA, USA.

Bone loss after menopause is accompanied by architectural changes of trabecular bone (TB) that contribute independently to the bone's reduced mechanical competence. Until recently, however, there was no modality capable of assessing TB architecture noninvasively. In order to examine the hypothesis that TB network topology determines fracture resistance independent of BMD, we examined patients with varying degrees of vertebral deformity by means of the MRI-based virtual bone biopsy (VBB) conducted in the distal radius and distal tibia in women with age > 60 years and BMD T scores -2.5 ± 1.0 . Images were acquired at 1.5T and processed to yield bone volume fraction (BV/TV) maps with a final voxel size of $62 \times 62 \times 103 \mu m^3$. Vertebral deformities were assessed from mid-line sagittal MRIs (wedge, biconcavity and compression deformity) and a spinal deformity index (SDI) determined as the weighted sum of the three types of deformity. Digital topological analysis (DTA) was conducted on the skeletonized TB images (in which plates and rods are converted to surfaces and curves) and the voxel type (curve, surface, junction between fundamental types) determined. DTA voxel densities and TB thickness were determined as described previously and associations examined between these structural measures and SDI using single and multi-parameter regression models. Erosion index (EI, ratio of parameters expected to increase with osteoclastic resorption divided by those expected to decrease), density of voxels for curve-type trabeculae (C), and profile-edges (PE, essentially free ends) correlated positively with SDI while BV/TV, Tb.Th correlated negatively. Interestingly, there was no association between vertebral BMD by DEXA and SDI. Finally, the DTA parameters from both anatomic sites were found to be equally associated with vertebral deformity status as shown by a plot of the correlation coefficients for each parameter examined. The findings are in agreement with a less connected, more strut-like TB network paralleling increased susceptibility for vertebral deformity. (Sponsors: NIH RO1AR49553, T32DK07006)

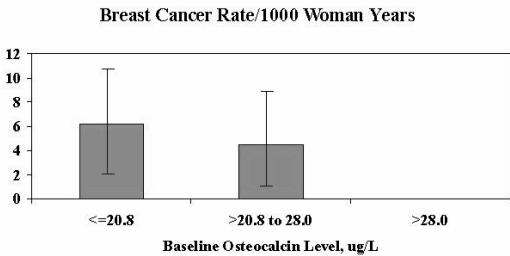


Disclosures: G.A. Ladinsky, Micro-MRI 4.

M296

Bone Turnover by Osteocalcin and Risks of Breast Cancer and Fracture: A Prospective Study. S. R. Cummings, T. Blackwell*. S.F. Coordinating Center, CPMC Research Institute and UC San Francisco, San Francisco, CA, USA.

Women with little or no estradiol (E2) tend to have high rates of bone remodeling and increased levels of osteocalcin (OC). Women with little or no E2 also have a substantially decreased risk of breast cancer. E2 is also synthesized by aromatase in both osteoblasts and breast tissue. We used the placebo group of the Multiple Outcomes of Raloxifene (MORE) trial to test the hypothesis that women with high OC levels have a decreased risk of breast cancer. We compared this association to the relationship of OC to risk of fracture. OC was measured at baseline (CIS Biointernational) in 913 postmenopausal women (mean age 67.5 years) with low BMD or osteoporosis. Serum E2 was measured by a double-antibody method (Covance). Incident breast cancer was confirmed by histopathology reports. Incident non-spine fractures were confirmed by radiographs and incident vertebral fractures by semiquantitative grading and morphometry of baseline and follow-up spine radiographs. After adjustment for age, OC level had no relationship to risk of non-spine (RH=1.10; 95%CI 0.88-1.38) or vertebral fracture (RR=1.13; 95%CI 0.86-1.47). Twelve incident breast cancer cases were confirmed during the 4-year trial. After adjustment for age, women with high OC ($> 28 \mu g/L$) had a lower risk (no cases) of breast cancer than did women with lower OC levels (P for trend = 0.027; Figure). Adjustment for baseline E2 did not attenuate this relationship. If confirmed by larger studies, OC may be a better marker of breast cancer than fracture risk.



Disclosures: S.R. Cummings, None.

M297

Factors Associated with the Ppresence of a Vertebral Fracture in a Population of Hip Fracture Patients. C. O Dwyer*¹, M. C. Casey*¹, M. Healy*¹, N. Maher*¹, C. Walsh*², J. B. Walsh¹. ¹Medicine for the Elderly, St James Hospital, Dublin, Ireland, ²Medical Statistics, Trinity College Dublin, Dublin, Ireland.

Introduction: All Hip fracture patients require a DXA scan to outrule Osteopenia or Osteoporosis and more recently lateral vertebral morphometric examination has been performed in conjunction with this investigation. We studied a group of hip fracture patients using both densitometry and bone biochemistry to identify any possible associations of vertebral fractures (Vfx) when they are present in hip fracture patients. Methods: 69 patients who presented with hip fracture had DEXA and lateral vertebral morphometry carried out. Osteoporosis was defined as T Score of < -2.5 at the hip or spine. All patients had serum bone markers performed within 48 hours of admission including

ASBMR 27th Annual Meeting

Osteocalcin (OC), C- telopeptide (CTx), Parathyroid Hormone(PTH) and 25(OH)vitamin D. Results: 19/69 (28%) had evidence of vertebral fracture on DEXA. Mean age was 77yrs in those without fracture and 81yrs in those with VFx. Those who had vertebral fracture had a mean weight of 50kg as apposed to those without 58kg (p<0.04). As expected the mean Femoral T score of those with vertebral fracture was -3.5 as apposed to -2.4 in those without (p<0.004).Likewise the mean Total Hip BMD mean was also lower in the VFx group (p<0.003). No significant differences were noted between the PTH levels in either group. There was a non significant trend towards mean osteocalcin and CTx values being lower in the vertebral fracture group. Conclusion: In those presenting with a hip fracture the presenceof a Vertebral fracture on DEXA scanning is associated with a significantly lower Hip BMD. However on assessment of bone markers ,although there was a trend to reduced bone turnover in this VFx group, this did not reach statistical significance and a larger study is required to assess these trends further.

Disclosures: M.C. Casey, None.

M298

Falls, Fractures and Health Status in Elderly Women Following Second Eye Cataract Surgery: A Randomised Controlled Trial. T. Masud¹, R. Harwood^{*1}, F. Osborne^{*2}, R. Gregson^{*}, A. Zaman^{*1}, A. Foss^{*1}. ¹Medicine, Nottingham City Hospital, Nottingham, United Kingdom, ²Ophthalmology, Queens Medical centre, Nottingham, United Kingdom.

We have previously shown that expedited first eye cataract surgery can significantly reduce fall rates and fractures (Harwood et al, BJ Ophthalmol 2005;89:53-9). Most cataracts in elderly people are bilateral. Some binocular functions, such as stereopsis, are associated with risk of falling. The aim of this follow up study was to determine if second eye cataract surgery can further reduce the risk of falling, and to measure associated health gains. 239 women aged over 70 years, with one un-operated cataract, were randomised to expedited (approximately 4 weeks) or routine (12 months wait) surgery. Falls were ascertained by diary, with follow up every 3 months. Health status including confidence (Tinetti Falls Efficacy Scale) and handicap (London Handicap Scale) was measured after 6 months. Visual function (especially stereopsis) improved in the operated group. Over 12 months follow-up, the rate of falling was reduced by 32% in the operated group (rate ratio 0.68, 95%CI 0.39-1.19; p=0.18). Confidence (mean diff 3.6 95%CI 0.9-6.2; p=0.008), and handicap (mean diff 4.4 95%CI=2.2-6.5; p<0.001) improved in the operated group compared with the control group. Five participants in the operated group had fractures (4%) compared to 2 (2%) in the control group (p=0.45). Second eye cataract surgery improves visual disability and general health and tended to reduce the rate of falling. The power of the study was not sufficient however to show any effect on fractures.

Disclosures: T. Masud, None.

M299

Bone Mineral Density in Myocardial Infarction Survivors. J. H. Magnus, D. Broussard^{*}. Tulane University Health Sciences Center, New Orleans, LA, USA.

Cardiovascular disease and osteoporosis have several common risk factors, and quite a few studies suggest a relationship. The objective of this study was to study cardiovascular disease risk factors and bone mineral density in subjects self-reporting previous myocardial infarction. This cross-sectional study used data from 1,393 white women and 1,309 white men aged 50-79 years who participated in the Third National Health and Nutrition Examination Survey (NHANES III) excluded those self reporting treated osteoporosis. Gender-specific mean BMD values for young adults were used to define osteoporosis and low BMD. The prevalences of osteoporosis and low BMD among those reporting a previous myocardial infarction were not significant when adjusting for age. Multiple logistic regression analysis revealed that self-reporting a previous myocardial infarction was significantly associated with low bone mineral density in men (odds ratio 1.68, [95% CI 1.14-2.47] $P=0.009$), but not in women, (odds ratio 1.63, [95% CI, 0.89 to 2.99] $P=0.12$). Age, cigarette smoking, physical inactivity and low body mass index were significantly associated with low BMD in both women and men and fasting glucose and HDL showed a slight protective effect. Previous fracture was strongly associated with low BMD in women (odds ratio 2.11, [95% CI, 1.13 to 3.93] $P=0.02$) as well as in men but the confidence intervals were very wide in men. We did however, not confirm earlier reports that stroke are associated with low BMD. These findings demonstrate that male survivors of myocardial infarction have low bone mineral density. Men surviving a heart attack should have their bone mineral density measured and osteoporosis prophylaxis if needed.

Disclosures: J.H. Magnus, None.

M300

Characteristics of Males Who Fracture: Comparison with Post-Menopausal Women. A. Stewart^{*}, J. Shotton^{*}, D. M. Reid. Osteoporosis Research Unit, University of Aberdeen, Aberdeen, United Kingdom.

Approximately 1 in 12 men and 1 in 3 women in the UK sustain a low trauma fracture over the age of 50 years. A low trauma fracture is often seen as an indicator of osteoporosis (OP). A local Fracture Liaison Service (FLS) has been in operation since 2003 and is offered to all men and women over the age of 60 years who sustain a low-trauma fracture. Patients are referred for bone mineral density (BMD) assessment by dual energy x-ray absorptiometry (DXA). A clinician reports all scans and suggests treatment, if required, to their primary care physician. To date 555 males have been referred to the FLS, of whom 369 (66.5%) were invited for a DXA scan (the remaining 186 were excluded by protocol),

and 275 (74.5% of those invited) have attended. The DXA scans were categorised according to WHO criteria. Of the men 41.6% had normal BMD at both sites, 37.1% had osteopenia at one or both sites, while only 21.3% had OP of at least one site. The DXA reports recorded the following options: invited to attend a Bone Clinic for further investigations; exclude secondary causes then treat with bisphosphonates if appropriate; bisphosphonate therapy; general lifestyle advice and other therapy, including calcium and vitamin D therapy. To compare we analysed the 871 females who attended for DXA scans. Only 5.1% of the males were referred for the Bone Clinic, 7.3% should have secondary causes excluded then treated with bisphosphonates, 9.5% should start bisphosphonates and 78.1% received general lifestyle advice. This compares to 7.2%, 9.2%, 20.6% and 63.0% respectively for females. The most common fracture site was the wrist for both males (25.4%) and females (43.4%). With regard risk factors 70% of the males had smoked (current and past), the mean units of alcohol consumed per week was 11.1 (SD 13.1), mean hours of exercise per week was 9.8 (SD 9.8), 63% indicated a previous fracture, 77.3% had had a fall in the last year, only 12% indicated a family history of OP, 16.3% had taken steroids and only 9.9% indicated taking some form of OP treatment. Significant differences (all $p < 0.01$) were found between genders only for smoking (females: 49.1%), mean alcohol units (females: 2.9 (SD 4.8)), mean hours of exercise (females: 6.3 (SD 8.7)), falls (females: 89.4%) and OP treatment (females: 46.7%). In conclusion, in comparison to women, the majority of men who fracture do not require OP treatment. Hence DXA scans could be targeted in a more efficient manner by eliminating those who may have had a high trauma fracture. Therefore this indicates that in a Fracture Liaison Service environment males may need to be dealt with in different ways to women to target services/treatment in the most effective way.

Disclosures: A. Stewart, None.

M301

Implications of a T-Score of -2.5 in Men Ages 50-65. R. A. Adler, C. S. Ryan^{*}, V. I. Petkov. Endocrinology, McGuire VAMC, Richmond, VA, USA.

DXA testing is best established for white postmenopausal women, but the meaning of a T-score of -2.5 in a man aged 50-65 is unclear. To help determine the clinical relevance of such a test, we retrospectively reviewed a convenience sample of 50 men ages 50-65 referred to a Metabolic Bone Clinic for osteoporosis. All the men had a T-score of the spine, hip, or distal 1/3 radius of -2.5 or worse. We determined why they had a bone mineral density test, final diagnoses, and risk factors for osteoporosis. Of the 50, 15 (30%) had a fracture (mostly minimal trauma) that led to a DXA test. Nine men were tested because of extensive exposure to oral glucocorticoids, and 2 had x-ray evidence of low bone mass. In addition, 4 had hypogonadism, 3 had multiple sclerosis, and 11 had chronic lung disease or asthma with use of oral or inhaled steroids. Our medical center has done screening studies in men, and 18 of 50 (36%) were identified by these studies, mostly using the OST screening tool. Thus, we reviewed risk factors and diagnoses uncovered in men found by screening projects. In 13 men who had DXA tests because of OST, 10 had low vitamin D levels. Hypogonadism was found in 2 and alcohol abuse in 2 others. Half of the men were smokers. Therefore, the meaning of a T-score of -2.5 in a man aged 50-65 should be viewed in the context of reasons for DXA testing. If there are good reasons for DXA testing, it is likely that the man is at risk for fracture. Indeed, of those men not found by screening tests, almost half (15/32) had a clinical fracture. The others had diagnoses or risk factors that made them susceptible to fracture. Those men whose osteoporosis was identified by screening tools also had demonstrable risk factors. We conclude that if a man aged 50-65 has a reason for DXA testing and has a T-score of -2.5 or worse, he should be considered at risk for fracture and should be treated. Until we have large studies determining 10 year fracture rates for men, evaluation and treatment are appropriate.

Disclosures: R.A. Adler, None.

M302

Men with Osteoporosis Discovered by the Osteoporosis Self-Assessment Tool (OST): Are They Different from other Men with Osteoporosis? V. I. Petkov, M. I. Williams^{*}, C. S. Ryan^{*}, R. A. Adler. Endocrinology, McGuire VAMC, Richmond, VA, USA.

The Osteoporosis Self-assessment Tool (OST) was developed as a screening instrument to determine the likelihood of low bone mineral density (BMD) by dual energy X-ray absorptiometry (DXA). The OST formula utilizes only two risk factors (age and weight) and stratifies the risk of osteoporosis into high, moderate and low. The purpose of this study is to determine the prevalence of risk factors, secondary causes, and laboratory abnormalities of bone and mineral metabolism in men diagnosed with osteoporosis (OP) as a result of OST screening (OST men) compared with other men with OP. We analyzed 160 consecutive men referred to a Metabolic Bone Clinic at a Veterans Affairs Medical Center (VAMC) between 7/02 and 7/04. OST was implemented as an electronic clinical reminder in the year 10/02 - 9/03. We reported previously that this intervention uncovered many men with OP. OP risk factors, conditions associated with secondary OP, and laboratory results were determined through retrospective chart review. OST men (N = 65) were older and tended to be shorter, with lower weight and bmi, and less exposure to drugs negatively affecting bone metabolism as compared to osteoporotic men (N= 95) who had BMD testing not related to screening studies. No difference in mean laboratory parameters was found (serum calcium and phosphorus, spot urine calcium to creatinine ratio, 25 OH vitamin D, PTH, sex hormones, thyroid function tests, serum creatinine, liver function tests, and alkaline phosphatase). In both groups, more than 2/3 were Caucasians, 80% used tobacco, 30% reported more than 2 drinks/day, more than half had sedentary lifestyle, 83% consumed < 1000 mg of calcium/day, and 43% < 400 IU of vitamin D. In both groups, about half reported a previous fracture, most due to minimal trauma. OST men had significantly lower prevalence of conditions associated with secondary OP (45% vs. 65%). At least one lab abnormality (most frequently vitamin D deficiency/insufficiency) was

present in 94% of OST men vs. 85% of the other men. The prevalence of OP risk factors was high in men diagnosed with OP due to OST screening and was similar to findings in other osteoporotic men.

Disclosures: *V.I. Petkov, None.*

M303

Bone Loss Associated with Post Gastrectomy in Japan. Y. Onoda^{*1}, K. Shiota^{*1}, K. Takaguchi^{*2}, T. Inaba^{*2}, K. Kita^{*2}, Y. Takei^{*3}, A. Satou^{*4}, M. Ando^{*5}, K. Kawamura^{*6}. ¹Department of Surgery, Kagawa Prefectural Central Hospital, Takamatsu, Japan, ²Department of Internal Medicine, Kagawa Prefectural Central Hospital, Takamatsu, Japan, ³Department of Orthopaedics, Ritsurin Hospital, Takamatsu, Japan, ⁴Department of Internal Medicine, Kagawa Prefectural Saiseikai Hospital, Takamatsu, Japan, ⁵Department of Internal Medicine, Mitoyo General Hospital, Toyohama, Japan, ⁶Department of Health, Kibi International University, Takahashi, Japan.

Partial or total gastrectomy due to peptic ulcer or stomach cancer has been an effective common operation but bone disorders sometimes occurs depending on the extent of the resection, and this will become our major concern after the gastrectomy. The objective of this study was to investigate the pathogenesis of bone disorders associated with postgastrectomy in elderly Japanese men. Fifty male patients (ranged from 48 to 82 years old) who received gastrectomy (PGX) at the *Kagawa Prefectural Central Hospital* were investigated. The PGX patients were examined their bone mineral density (BMD) with dual X-ray absorptiometry (QDR2000 or QDR4000, Toyo-Medic Inc.) at the lumbar spine. Osteoporosis or osteopenia were diagnosed according to their T-scores. The biological markers for bone metabolism and gastric endocrinal function, and existence of helicobacter pilori (HP) as a status of the remnant stomach were evaluated. Numbers of patients diagnosed as osteopenia and osteoporosis in PGX group were 9 (10.3%) and 5 (5.8%), respectively. BMD was significantly associated with the BMI and body weight in PGX group (p<0.005). BMD's were negatively associated with urinary NTX (r=-0.4321, p<0.005) and serum HDL levels (r=-0.4314, p<0.005). HP was positively correlated with BMD levels (r=0.373, p=0.011). On the other hand, urinary NTX levels were negatively associated with HP(r=-0.3990, p=0.007). Relatively high levels of i-PTH and 1,25(OH)₂D₃ were observed in several PGX patients, but this was not corresponded to the low serum Ca and the low BMD. No significant correlation was found between BMD and other biological markers for bone metabolism or gastric functions. No reduced serum level of vitamin D was observed in PGX group, and no apparent relationship was confirmed between BMD and impaired absorption of vitamin D due to gastrectomy. This study suggests that only low BMI will be a risk factor for low bone in PGX patients and that the bone loss in PGX patients who were diagnosed as osteopenia or osteoporosis was not attributed to the stimulated bone resorption. The further investigation or the longitudinal observation of these PGX patients should be carried in order to reveal the pathogenesis of bone loss in patients with lowered gastric function such as PGX.

Disclosures: *Y. Onoda, None.*

M304

Diabetes Status may Rule Out Bone Mineral Density Testing in Men but not in Women. D. L. Broussard^{*}, J. H. Magnus. Tulane University Health Sciences Center, New Orleans, LA, USA.

One of the greatest challenges for clinicians is to distinguish patients who should have BMD testing from those who are not likely to have low BMD. The purpose of this study was to explore whether diabetes status in older persons could be used to identify patients who do not require BMD testing. The relationship between diabetes and BMD was evaluated among the 4,915 African American, Mexican American, and white women and men aged 50-79 years who participated in the Third National Health and Nutrition Examination Survey (NHANES III) and did not self-report prior treatment for osteoporosis. Low BMD was classified as a total hip BMD of 1 SD or more below the young adult men BMD value. Race/ethnic and gender-specific mean BMD values for young adults were used to define low BMD. The prevalences of low BMD in subjects with and without diabetes were statistically significantly different when adjusted for age and race/ethnicity, but not when adjusting for body mass index. Multiple logistic regression analysis that controlled for several cardiovascular disease risk factors as well as osteoporosis risk factors revealed that diabetes was significantly associated with low BMD in men (odds ratio 0.72, [95% CI 0.54-0.94] *P*=0.02), but not in women, (odds ratio 0.80, [95% CI, 0.61 to 1.04] *P*=0.09). As expected, age, cigarette smoking, body mass index, and physical inactivity were independently associated with low BMD in both women and men. An interaction between diabetes and body mass index in this sample could not be established. The findings from this study suggest that bone density testing is probably not necessary for older diabetic men. However, the presence of diabetes should not exclude bone density testing in women. Even though it appears as though at least part of the relationship between diabetes and BMD acts through body mass index further research is needed to partition the individual influences of BMI and diabetes.

Disclosures: *D.L. Broussard, None.*

M305

The Risk of Non-Vertebral and Hip Fracture and Prevalent Falls in Older Men: The MrOS Study. B. K. S. Chan¹, L. M. Marshall¹, L. C. Lambert¹, J. A. Cauley², K. E. Ensrud³, E. S. Orwoll¹, S. R. Cummings⁴. ¹Endocrinology, Oregon Health & Science University, Portland, OR, USA, ²University of Pittsburgh, Pittsburgh, PA, USA, ³University of Minnesota, Minneapolis, MN, USA, ⁴CPMC Research Institute, San Francisco, CA, USA.

Falling is an important risk factor of non-vertebral fracture, particularly hip fracture. However, most previous reports of this association are from studies of older women or institutionalized adults. Therefore, we estimated the association of fall history on the incidence of non-vertebral and hip fractures in the MrOS cohort of community dwelling US men ages 65 years and older. 5,995 men completed baseline questionnaires. 96% of the men completed mid-study questionnaires (mean 2.0 years after baseline). Both questionnaires asked participants if they had fallen during the past 12 months, whether their fall resulted in an injury (including fracture, head injury, sprain or strain, bruising or bleeding, and other injury), and the number of times they had fallen. Fractures were reported on tri-annual questionnaires and confirmed from radiographs. Fracture follow-up was complete for 99% of the cohort. Mean follow-up was 3.7 years. Cox proportional hazards regression models were used to estimate hazard ratios (HR) for non-vertebral fracture and for hip fracture. Fall information was modeled as a time-dependent variable. Baseline information was updated by mid-study information, if available. We confirmed 256 non-vertebral fractures (11 per 1,000 person-years), including 46 hip fractures (2 per 1,000 person-years). 1,267 men (21%) reported a fall history at baseline (mean 1.8 falls per participant). 56% of these falls resulted in an injury. Similarly, 1,614 men (28%) reported a fall history at mid-study (mean 2.0 falls per participant). 55% of these falls resulted in an injury.

Outcome	Risk factor	HR	95% CI
Non-vertebral fracture*	Any prevalent fall	2.1	1.6, 2.7
	Injury from fall	2.3	1.7, 3.1
	No injury from fall	1.9	1.4, 2.7
	Per increase in number of falls	1.3	1.2, 1.4
	Any prevalent fall	1.8	1.0, 3.3
Hip fracture*	Injury from fall	2.2	1.1, 4.3
	No injury from fall	1.4	0.6, 3.2
	Per increase in number of falls	1.2	1.0, 1.5

* Adjusted for clinical site, age, and leg power measured by the Nottingham power rig

Older men who have fallen have twice the risk of non-vertebral and hip fractures as those who have not fallen. The risk from falls resulting in injury were greater, but not statistically greater, than the risk from falls with no injury. The increase of one fall was associated with a 30% non-vertebral fracture risk increase and a 20% hip fracture risk increase. These data are consistent with previous studies. Fall prevention may be important in preventing fractures in older men.

Disclosures: *B.K.S. Chan, None.*

M306

Risk Factors Associated with Osteoporosis in African-American U.S. Men Veterans. J. J. Shin^{*1}, E. Wininger^{*2}, C. Engelhart^{*1}, M. B. Zimering^{*1}. ¹Endocrinology, Dept of Veterans Affairs, Lyons, NJ, USA, ²Endocrinology, University of Medicine and Dentistry of New Jersey- New Jersey Medical School, Newark, NJ, USA.

Osteoporosis is a frequently missed diagnosis in the African-American population even in some men who have suffered fragility fractures. In a prior study in older white men veterans (n~ 600, mean age 69 yrs) five risk factors (age, body weight, emphysema, gastrectomy, two or more prior fractures) were each independently associated with femoral neck bone mineral density (FN-BMD). The aim of the current study was to test whether these or two additional risk factors (physical activity, stooped posture) correlated with BMD in ambulatory outpatient African- American men veterans (n =134, mean age 61 yrs) from New Jersey. African-American men had significantly (p<.0001) higher FN-BMD (0.875 ± .162) compared to white men (0.767 ± .131) g/cm². However, using NHANES III gender/ethnicity specific male normative data, the FN mean T-scores for African-American men were similar (-1.27 ± 1.04 vs -1.20 ± .96) to those in white men. The prevalence for FN osteoporosis (T≤ -2.5) was 7.6% and 10.5 % for whites and African-Americans, respectively. Lumbar spine (L1-L4) osteoporosis was apparent in a substantially higher proportion of younger African-American patients (15.7%) compared to older white men (6.3%). The overall prevalence of osteoporosis (lumbar spine or FN) among African-American patients was 19%. In univariate correlation analysis, body weight and occupational-related physical activity correlated significantly with both FN- and L1-L4 BMD. In multiple regression analyses, age (coeff -.0324; p <.0001) and body weight (coeff .0087; p<.001) correlated with FN-BMD; body weight (coeff .0154; p< .0001), and physical activity (coeff 0.514; p=.013) were independent predictors of L1-L4 BMD. Similar proportions of white (9.8%) and black (9%) men veterans reporting having suffered two or more prior fractures after the age of 40 yrs. Still there was no association between two or more prior fractures and osteoporosis in black men veterans. These results imply that aside from age and body weight, the same, self-reported risk factors associated with osteoporosis in white men did not predict osteoporosis in black men veterans. Body weight and (self-reported) physical activity were useful in devising a risk index [93% sensitivity and 50% specificity] for predicting spinal osteoporosis in black men veterans. The substantial prevalence of osteoporosis in African-American male veterans suggests that a risk index may be useful for identifying patients likely to benefit from BMD testing.

Disclosures: *J.J. Shin, None.*

M307

The Effects of Thiazide, NSAIDS, and Steroid Use on Bone Mineral Density in Men. B. Heaton*, E. A. Krall. Health Policy & Health Services Research, Boston University School of Dental Medicine, Boston, MA, USA.

Various medications have been shown to affect bone mineral density in men and women, particularly common medications used to treat ailments associated with aging such as hypertension, and inflammation. We examined associations between changes in bone mineral density and use of non-steroidal anti-inflammatory drugs (NSAIDS), thiazides, and corticosteroids in a cohort of men. Subjects were 361 men who have participated in the Normative Aging Study (NAS) since 1961 and enrolled in a bone density study from 1998 to 2003. Their ages ranged from 56 to 89 at baseline. Bone mineral density (BMD) was measured three times over a two-year period. Information on medication use, smoking status and dietary calcium intake was available from NAS study records. BMD measurement sites included total body (N=292), total forearm (N=294), femoral neck (N=273), and total femur (N=273). Data analysis was completed using ANOVA for repeated measures and proportional hazards regression. Potential confounders (cigarette use, calcium intake, age and body mass index) were included in the models. Seventy-two men used thiazides, 17 used steroids, and 40 used NSAIDS. Average durations of use for thiazides, steroids, and NSAIDS were 15, 8.9, and 8.9 years, respectively. Results showed a significant association of thiazide with increased BMD at the total forearm (p=0.02), and marginal significance at the total body (p=0.06), but no associations at the femoral neck and total femur. NSAIDS seemed to have a negative effect, with marginal significance, at the total body (p=.07), total forearm (p=.18) and total femur (p=.10). Femoral neck BMD was 3% lower among NSAIDS users compared to non-users but the difference was not statistically significant. However, for each year of use, NSAIDS users with normal femoral neck BMD at baseline were 1.3 times more likely to develop osteopenia or osteoporosis during follow-up (Hazards ratio=1.3, 95% confidence interval=1.1 to 1.4). Findings for steroids were not significant at any site, possibly due to the small number of steroid users. Much of the literature to date reporting on medication use and the effect on bone mineral density has been conducted in women or in populations with unique diseases or injuries to the bone. These results provide insight on the effects of three medications on bone mineral density in a population of men representative of the general population having controlled for potential confounding factors.

Disclosures: **B. Heaton**, None.

M308

Ethnic Differences in Bone Mineral Density And Vitamin D Status among Hispanic Men: Results From BACH/BONE. A. B. Araujo¹, M. F. Holick², T. C. Chen², J. Mathieu^{*2}, A. K. Turner², C. Link^{*1}, T. G. Travison^{*1}, J. B. McKinlay^{*1}. ¹New England Research Institutes, Watertown, MA, USA, ²School of Medicine, Boston University, Boston, MA, USA.

Data on race/ethnic differences in bone mineral density (BMD) and vitamin D status among men are relatively rare. A few studies have presented these data in Hispanic men. Despite the ethnic diversity of Hispanic populations, no study has provided estimates of BMD or vitamin D levels by ethnic background among Hispanic men. Our objective was to estimate ethnic differences in femoral neck areal BMD and 25-hydroxyvitamin D (25OHD) among 234 Hispanic men participating in the Boston Area Community Health/Bone (BACH/BONE) Survey, a population-based cross-sectional study of skeletal health in a racially/ethnically diverse sample of Boston men aged 30-79 y. Ethnicity was determined by self-report, classified as Puerto Rican (n=84, 36%), South American (n=44, 19%), Dominican (n=42, 18%), Central American (n=37, 16%), and Other (n=27, 12%). BMD (g/cm²) was measured with a Hologic QDR 4500W. Serum 25OHD was measured by competitive protein binding without prior chromatography. Mean age was 46.7±11.1 y. Mean femoral neck BMD was 0.870±0.935 g/cm². Mean 25OHD was 33.6±15.9 ng/ml. Age-adjusted mean femoral neck BMD was lowest among South American men (0.839 g/cm²). Relative to South American men, Dominican men had 7.1% higher BMD, followed by Puerto Rican (+5.4%), Central American (+3.1%), and Other (+1.7%) Hispanic men. Moreover, there was significant variation in the age-related decline in femoral neck BMD among the ethnic groups. South American men had the greatest decline (-0.76%/y), followed by Puerto Rican (-0.58%/y), Central American (-0.50%/y), Other (-0.28%/y), and Dominican (-0.03%/y) men. Differences persisted with adjustment for body composition and number of years since immigration. Age-adjusted mean 25OHD was lowest among Puerto Rican men (31.1 ng/ml). Relative to Puerto Rican men, South American men had 21.0% higher 25OHD, followed by Central American (+16.0%), Dominican (+12.2%), and Other (+4.1%) Hispanic men. There were no ethnic differences in the age-related change in 25OHD. In the first study to present estimates of BMD and 25OHD levels in Hispanic men by ethnic background, we show modest and relatively large differences in BMD and 25OHD, respectively. This suggests the possibility of differences in fracture risk and vitamin D insufficiency among Hispanic men, and highlights the importance of considering ethnic background in evaluations of skeletal health.

Disclosures: **A.B. Araujo**, None.

M309

Higher Serum 1,25-dihydroxy Vitamin D and 25-hydroxy Vitamin D Levels Are Associated with Better Physical Performance in Elderly Postmenopausal Women. P.B. Rapuri¹, J. C. Gallagher¹, L. Smith^{*2}. ¹Bone Metabolism, Creighton University, Omaha, NE, USA, ²Department of Preventive and Societal Medicine, University of Nebraska Medical Center, Omaha, NE, USA.

Vitamin D metabolites have been suggested to have a role in muscle strength, thereby affect the rate of falls in elderly women. An association between serum 25 hydroxy vitamin D (25OHD) and lower extremity function has been reported. There is no information on whether the active form of vitamin D, 1,25-dihydroxy vitamin D (1,25(OH)₂D₃) is associated with the measures of physical performance. In 489 elderly women, age range 65-77 years, we examined the association between serum 25OHD, 1,25(OH)₂D₃ or parathyroid hormone (PTH) and measures of physical performance of muscle strength at baseline. Timed rise (time to rise from a chair 3 times as quickly as possible), timed walk at normal speed a distance of 5 meters, grip strength (Hand Dynamometer in 90° of shoulder flexion) and exercise/activity score (PASE) were compared between quartiles of serum 25OHD, 1,25(OH)₂D₃ and PTH. The data were analyzed by analysis of covariance adjusting for age, BMI, calcium intake, caffeine intake and season was added to the 25OHD model. For serum 25OHD, women in the lowest quartile compared to higher quartiles were slower for the timed rise test, PASE score, timed walk normal and grip strength. Women with serum 25OHD levels < 31 ng/ml demonstrated worse physical performance. When the data was examined according to quartiles of serum 1,25(OH)₂D₃ similar results were found. Women in the lowest quartile compared to higher quartiles of 1,25(OH)₂D₃ were slower on timed rising, timed walk, grip strength and PASE scores, though statistical significance was observed only for grip strength. There was no significant association between serum PTH and physical performance measures. In conclusion, higher concentrations of serum 25OHD and 1,25(OH)₂D₃ are associated with better musculoskeletal function in the upper and lower extremities. 1,25(OH)₂D₃ which is the active form of vitamin D, rather than 25OHD, is probably playing the major role in muscle strength.

Physical Performance Measures Compared by Quartiles of 25OHD and 1,25(OH)2D3			
	Timed rise (sec)	Timed walk normal (sec)	Grip Strength (kg)
25OHD ng/ml			
Q1 5.7-24.5 (n=119)	9.6±0.40	5.1±0.10	24.6±0.40
Q2 24.6-31 (n=126)	8.7±0.26	4.9±0.10	25.1±0.41
Q3 31.1-37 (n=122)	8.4±0.29*	4.6±0.08*	25.0±0.43
Q4 37.1-87 (n=121)	8.4±0.25	4.9±0.11	25.4±0.37
1,25(OH)2D3 pg/ml			
Q1 16.2-28.6 (n=122)	9.5±0.35	5.0±0.12	24.2±0.45
Q2 28.7-33.9 (n=122)	8.5±0.24	4.9±0.08	25.0±0.38
Q3 34-39.1 (n=122)	8.3±0.27†	4.7±0.08†	25.8±0.40*
Q4 39.2-78 (n=121)	8.9±0.36	4.9±0.10	25.0±0.37

Data reported as unadjusted means±SEM. p values are derived from adjusted data. *p<0.05 and †p= 0.06 compared to quartile 1 using Tukey's post hoc multiple comparison test.

Disclosures: **P.B. Rapuri**, None.

M310

Family Physicians' Awareness of Key Osteoporosis Risk Factors and the Utilization of Bone Mineral Density (BMD) Testing Following a Multifaceted Osteoporosis Educational Intervention: Canadian Quality Circle (CQC) Pilot Project. A. Papaioannou¹, G. Ioannidis¹, B. Kvern^{*2}, A. Hodsman³, D. Johnstone^{*4}, C. Crowley⁴, J. D. Adachi¹. ¹McMaster University, Hamilton, ON, Canada, ²University of Manitoba, Winnipeg, MB, Canada, ³University of Western Ontario, London, ON, Canada, ⁴Procter and Gamble Pharmaceuticals, Toronto, ON, Canada.

The CQC project was developed to facilitate knowledge transfer and dissemination of the Canadian Osteoporosis Guidelines to family physicians. 52 family physicians (FPs) were recruited as members of 7 Quality Circles (QC). Members collected data on two separate occasions (wave 1, wave 2) for different patients via chart reviews and the completion of the data capture form on OP risk factors, diagnosis, and treatment. A total of 1505 and 1359 patient records were selected at random in waves 1 and 2, respectively. All patients were women 55 years of age and older. From wave 1, individual and QC data were collated in profiles and provided to the members. The QC's then met to discuss the profiles, identify and analyze barriers, recommend solutions, and participate in an OP problem based workshop. The primary focus of the workshop was to assess postmenopausal OP and risk factor identification. Wave 2 chart audit occurred after the intervention and was used to provide feedback on practice patterns. The current analyses examined physicians' perceived awareness of key risk factors (as described in the guidelines) including age (>65 yr), a prior fracture (hip, spine, or wrist), and family history of fracture, and the use of BMD testing in patients with key risk factors. The guidelines recommend that BMD testing should be conducted for all patients with key risk factors. Based on percentage and respective to wave 1 and wave 2, most FPs indicated that they were aware of their patients' key risk factors status for age (100%, 100%), hip fracture (98%, 100%), vertebral fracture (96%, 98%), and wrist fracture (96%, 100%). Fewer were aware of the status of their patients' family history of fracture (46%, 68%). A large proportion of these patients with key risk factors did not have a BMD test: age (36%, 28%), hip fracture (29%, 21%), vertebral fracture (24%, 18%), wrist fracture (19%, 15%), and family history of fracture (15%, 24%). In conclusion, most FPs were aware of their patients' key risk factors status other than family history of fracture. There was a disconnect between identification of high risk patients and requesting a BMD test for these patients. Future QC interventions should focus on bridging the gap between risk factor identification and further diagnostic work up (e.g., BMD) and if appropriate treatment initiation.

Disclosures: **A. Papaioannou**, Procter & Gamble 2, 5, 8; Merck 2; Sanofi-Aventis 5.

M311

Relationships between Falls, Spinal Mobility, and Muscle Strength in Patients with Osteoporosis. Y. Kasukawa, N. Miyakoshi, Y. Ishikawa*, M. Hongo, Y. Shimada*, E. Itoi. Department of Orthopedic Surgery, Akita University, Akita, Japan.

Falls and fall-related fractures are one of the important health problems in the elderly especially among those with osteoporosis. Multiple factors such as physical activity, body balance, and muscle strength of lower extremity have been considered as determinants of falls. We have recently demonstrated that decreased spinal mobility impairs the quality of life in patients with osteoporosis. According to these backgrounds, we hypothesized that the spinal mobility also could be a determinant of falls in these patients. To test this hypothesis, relationships between falls and spinal mobility, body balance, and muscle strength were evaluated in a total of 62 patients with osteoporosis (mean age, 71 years). All the participants had no neurological or other metabolic disorders except osteoporosis. They were divided into the fall group (n=26; 5 males and 21 females) that had histories of falls and/or fear of falling, or the non-fall group (n=36; 14 males and 22 females) that had no such episodes. The thoracic and lumbar kyphosis angles and range of motion (ROM) of the spine were measured in the upright position and at maximum flexion/extension with a computer-assisted device (Spinal Mouse®). The swaying and postural instability were evaluated using a computerized stabilometer (JK-101®). Grip strengths of bilateral hands were measured with a hand grip dynamometer. There were no significant differences in age, gender, height, body weight, and body mass index between the groups. The average grip strength of bilateral hands was 23% less in the fall group compared to the non-fall group (p<0.05). Lumbar spinal ROM was 29% less in the fall group than the non-fall group (p<0.05). However, no significant differences were observed between the groups in thoracic spinal ROM, total spinal ROM, and thoracic and lumbar kyphosis angles. The parameters reflecting the distance of body sway (the total and timed track length of the center of gravity, and the rectangular and total area covered by the track of the center of gravity) showed no significant differences between the groups. The results of the present study suggested that the decreased muscle strength and lumbar spinal mobility could be risk factors for falls in patients with osteoporosis.

Disclosures: **Y. Kasukawa, None.**

M312

An Age Related Decrease in Creatinine Clearance Is Associated with an Increase in Number of Falls in Untreated Women but not in Women Receiving Calcitriol. J. C. Gallagher¹, P. B. Rapuri¹, L. M. Smith*². ¹Bone Metabolism, Creighton University, Omaha, NE, USA, ²Department of Preventive and Societal Medicine, University of Nebraska Medical Center, Omaha, NE, USA.

An increase in the incidence of falls in the elderly is an important risk factor for fractures. An age related decrease in creatinine clearance (CrCl) and, a decrease in serum 1,25-dihydroxy vitamin D₃ (1,25(OH)₂D₃) with age may be risk factors which lead to falls in the elderly. In a double blind placebo controlled 3 year study designed to test the efficacy of calcitriol and estrogen in reversing bone loss in elderly women, we also collected prospectively data on falls. In the present study, we examined the effect of age related decline in renal function on fall incidence by comparing groups with a GFR < or >65 ml/min in untreated and treated women. The study population comprised of 489 normal elderly women aged 65-77 years randomized to 4 treatment groups, placebo (n=112), calcitriol (n=101) 0.25 mcg bid, conjugated equine estrogens (n=100) 0.625mg/d and calcitriol + estrogen (n=102). Data were analyzed using SAS statistical package. The cumulative number of falls were compared between groups in an intent to treat analysis for women with CrCl <65 ml/min and >65 ml/min. Using a Poisson regression model, CrCl was a statistically significant predictor of falls in the placebo group (p=0.05) but not in the estrogen or calcitriol groups. The mean cumulative number of falls per subject on placebo was 1.60 for CrCl <65 ml/min and 1.16 for CrCl >65 ml/min (p=0.05). In the calcitriol group the mean cumulative number of falls per subject was 0.89 for CrCl <65 ml/min and 0.88 for CrCl >65 ml/min (p=ns). In the estrogen group, the mean cumulative number of falls per subject was 1.14 for CrCl <65 ml/min and 1.26 for CrCl >65 ml/min (p=ns). For calcitriol + estrogen group, the mean cumulative number of falls per subject was 0.91 for CrCl <65 ml/min and 1.26 for CrCl >65 ml/min (p=ns). Comparing the groups with CrCl <65 ml/min, the odds of a fall were 1.8 (95% CI 1.2-2.8) times greater on placebo than on calcitriol, 1.79 (95% CI 1.2-2.6) greater compared to on calcitriol + estrogen and 1.4 (95% CI 0.9-2.1) greater compared to on estrogen only. There was a significant correlation (r=0.15, p<0.001) between serum 1,25(OH)₂D₃ and CrCl. The group with CrCl <65 ml/min had significantly lower (p<0.001) serum 1,25(OH)₂D₃ levels (33.4 ±0.69 vs 35.5 ±0.47 pg/ml) than women with CrCl >65 ml/min. In summary, untreated elderly women with a CrCl <65 ml/min had a highly significant increase in the number of falls whereas women treated with calcitriol had a significant reduction in the number of falls probably by increasing serum 1,25(OH)₂D₃ and improving muscle strength. ns=not significant

Disclosures: **J.C. Gallagher, Industry 2.**

M313

Postural Deformity and Postural Balance in Patients with Osteoporosis. Y. Ishikawa*, N. Miyakoshi, M. Hongo, Y. Kasukawa, S. Maekawa, H. Noguchi, Y. Shimada*, E. Itoi*. Orthopedic Surgery, Akita University School of Medicine, Akita, Japan.

Postural instability has been considered as a risk factor for falls and osteoporotic fractures. Previous studies demonstrated that several factors, such as neurological disorders, visual impairment, and muscle weakness had significant relationships with postural instability. In addition to these factors, postural deformity might also be a possible risk factor for postural instability and falls. The aim of this study, therefore, was to evaluate the influence of the postural deformity on postural balance in patients with osteoporosis. Sixty-one patients with osteoporosis (19 males and 42 females) with an average age of 74 years (range, 54-96 years) were included in this study. Their thoracic and lumbar kyphosis angles and the spinal inclination that reflected a forward bending posture were evaluated with a computer-assisted device (SpinalMouse®). The swaying and postural instability were evaluated using a computerized stabilometer (JK-101®) showing the following parameters: 1) timed track length; 2) enveloped area; 3) rectangular area; 4) deviation of lateral sway origin; 5) timed track length in lateral direction; 6) deviation of anteroposterior sway origin; and 7) timed track length in anteroposterior direction. The relationships between the parameters of postural deformity and postural balance were then analyzed using Pearson's correlation coefficients. No significant correlations were observed between all the parameters of postural balance and the thoracic kyphosis angle. However, all the parameters except two parameters indicating anteroposterior sways (deviation of anteroposterior sway origin and timed track length in anteroposterior direction) showed significant positive correlations with the lumbar kyphosis angle (p<0.05, r=0.263-0.456). Furthermore, all the parameters of postural balance showed significant positive correlations with the spinal inclination (p<0.05, r=0.395-0.664). These findings suggest that the lumbar kyphosis (but not thoracic kyphosis) which affects the spinal inclination and postural balance may be a risk factor for falls.

Disclosures: **Y. Ishikawa, None.**

M314

Repeated Measurements Analysis of Bone Fragility Risk Factors: First Results. G. Livshits*¹, I. Malkin*¹, G. Bigman*¹, E. Kobylansky*¹, M. J. H. Seibel². ¹Sackler Faculty of Medicine, Tel Aviv University, Israel, ²ANZAC Research Institute, Univ of Sydney, Sydney, Australia.

The contribution of genetic factors to inter-individual differences in the main components of bone strength, such as bone mineral density (BMD), bone size (BS) and bone geometry (BG) are presently well established. However, very little is known about the genetic effects on the rate and pattern of age related changes in these variables. The objective of the present study was to examine the contribution of putative genetic influences and life style factors (alcohol consumption, smoking and obesity) on the rate of change in BMD, BS, and BG in an ethnically homogeneous sample of Chuvasha families (Caucasians). The study was conducted on some 800 healthy individuals, of which 290 were measured twice after an interval of eight years. Computerized digital images of hand bones radiographs were examined for BMD, BS, and BG in all participating individuals. The studied phenotypes were not modified by HRT or any other continuous medical treatment. The family data were subjected to model fitting statistical-genetic analysis in order to find the most parsimonious and best fitting description of the above traits variation. The results showed that alcohol consumption and smoking did not significantly affect any of the studied bone traits. Age, sex and obesity significantly affected variation of the baseline levels of each of the traits, but did not contribute to the rate of their change after the effect on the baseline level was taken into account. Genetic effects were highly significant and prominent for baseline levels of all bone variables (but not their change) as expected. The rate of change in BS and BG depended very little on genetic factors (3 - 7% of the variation, p <0.06). However, the latter were highly significant (p<0.001) and strong, explaining 44% to 51% of the variation for changes of all examined BMD characteristics. The present analysis suggests that baseline variations in BMD and the rate of age related changes are likely influenced by different genetic sources.

Disclosures: **G. Livshits, None.**

M315

What Are the Most Common Risk Factors for Osteoporosis in Postmenopausal Spanish Women between 50-65 Years? C. Carbonel*¹, M. L. Rentero*², M. Romera³, S. FARO Group*⁴. ¹ABS Via Roma, Barcelona, Spain, ²Medical Department Lilly, Madrid, Spain, ³Hospitalet, U. Rheumatology, Barcelona, Spain, ⁴Primary Care, Centers, Spain.

To describe the prevalence of osteoporosis risk factors in a sample of postmenopausal women from 50 to 65 years old attended in Primary Care Centers in Spain. This is an observational, descriptive, cross-section study. 5000 women have participated in the study. They have been distributed in three age groups: 1906 women 50-55 years, 1378 women 56-59 years and 1615 women 60-65 years distributed between 96 centers of Primary Care Demographic, anthropometrical, osteoporosis and fracture risk factors were collected. Quantitative bone ultrasound scan was made to both the right and the left foot calcareous using Sahara equipment. Quantitative variables are described by the mean, median values and typical deviation, first and third quartile, and range (maximum and minimum values) are analyzed using ANOVA model. Qualitative variables are described by frequency and percentage and analyzed by Chi square test or, if non- applicable, by Fisher exact test. Confidence intervals of 95% are used. Baseline data: Menarche age: 12,87, menopausal

age: 48,49, number of children: 2,4, weight 69,7 +/- 11,8 Kg, Height 157cm, mean BMI is 28.3. Among the analyzed risk-factors 15.1% of women have had surgical menopause, 10.0% (490) are unable to stand up from a chair, 78.1% (3825) have never smoked, 10.3 % (505) have a history of fractures; forearm is the most frequent one. Decrease of height is 30.4% (1490). Intake of Calcium below 600 mg/day is 43.1% (2111).Drugs related with risk of osteoporosis and falls 35.1% (1718). Benzodiazepines are the most commonly used drugs in 22.7%. History of familial fractures is 22.3% (1094). Kyphosis 8,7% (916). Problems in her sensory perception that affect her ability to walk 7% (341). Other diseases affect the bone 11,9% (585). Number of hours per week the patients perform intentional physical activity 3,9 hours/per week, number of falls the patient sustained in the last year 22,8% (1119), observed loss weight greater than 10 % in the last ten years 8,1% (398). Risk factors of osteoporosis with more prevalence in Primary Care are modifiable factors, especially intake of calcium less than 600 mg/day. Drugs as benzodiazepine could be important. Decrease of height and history familial fractures are risk factors very frequently in the attention medical. It could be of great value to the physician the assessment of risk factors. It could mean a good way to approach osteoporosis diagnosis, to detect high-risk women and to evaluate the need of a DEXA measure.

Disclosures: C. Carbonel, Lilly, MSD , AVENTIS 6.

M316

Lack of Association between Subclinical Menstrual Irregularities and Changes in BMD in Healthy Pre-Menopausal Women. G. A. Hawker, M. French*, E. Waugh*, R. Ridout. University of Toronto, Toronto, ON, Canada.

The aim of this study was to examine the relationship between subclinical menstrual irregularities and changes in BMD among healthy pre-menopausal women. Caucasian women aged 20-40 years with regular menstrual cycles were recruited from the community to participate in a two-year prospective cohort study. We excluded women reporting use of oral contraceptives or other medication or illness known to affect bone metabolism or menstrual function. Physical activity, dietary factors and dietary restraint were assessed at 12-month intervals. BMD at the spine (L2-L4), total body and femoral neck (hip), and body composition were determined by DEXA. A single morning serum sample for estradiol and free testosterone was collected once during days 3-5 of one of the monitored cycles; morning saliva samples were collected daily for up to 12 cycles. Luteal phase length, progesterone levels, and ovulation were determined through urinary ovulation detection, salivary progesterone assays and menstrual diaries. The relationship between BMD change and each of menstrual cycle length, luteal phase length, mean and mid-luteal phase progesterone levels, % monitored cycles that were anovulatory, and serum estradiol and free testosterone were assessed separately for each site, before and after adjusting for age, body composition (% lean mass, weight, BMI), lifestyle factors (physical activity, smoking), dietary factors (calcium, vitamin D, dietary phytoestrogens), and dietary restraint, using linear regression. Of the 332 assessed at baseline, 194 completed the study and are included in this analysis. At baseline, mean age was 32.7 yrs (SD 4.7), mean BMI was 24.3 kg/m² (SD 4.7) and % lean mass was 66.25% (SD 9.5). Mean number of cycles monitored was 10.7 (1-14) with a mean cycle length of 28.8 days (23.6 - 55.2 days) and mean luteal phase length of 13.6 days (5.3 - 17.4 days); 22.3% of women experienced at least 1 anovulatory cycle. Mean changes in BMD at the spine, hip and total body were 0.02 gm/cm² (-0.11 - 0.12), 0.006 (-0.14 - 0.13), and 0.001 (-0.07 - 0.09), respectively. BMD changes at the spine were positively associated with estradiol and testosterone levels (p<0.02). At the hip, BMD changes were positively associated with estradiol levels and negatively with cycle length. These relationships held after adjusting for all other measures. At the total body, changes in BMD were associated with none of the menstrual cycle measures. In this prospective study of healthy pre-menopausal women, we could not confirm prior reports of an association between changes in BMD and sub-clinical menstrual irregularities in pre-menopausal women.

Disclosures: G.A. Hawker, None.

M317

Socioeconomic Variables and Fracture Risk: A Nationwide Register Study from Denmark. P. Vestergaard, L. Reinmark, L. Mosekilde. The Osteoporosis Clinic, Aarhus Amtssygehus, Aarhus, Denmark.

Purpose: To investigate the effects of income and other socioeconomic variables on fracture risk adjusted for disease related confounders. Methods: Case-control study where all subjects in Denmark with a fracture during the year 2000 (n=124,655) served as cases. From the general population three age- and gender matched subjects were selected as controls (n=373,962). Adjustment were made for income, living with someone vs. living alone, having a job vs. being out of work, education, co-morbidity (Charlson index), number of bed days in hospital, number of contacts to general practitioner, use of corticosteroids, prior fracture, and alcoholism. Results: Income was not associated with fracture risk upon adjustment for the other covariates. Living with someone was associated with a decreased risk of any fracture in all age. A higher education was associated with a decreased fracture risk in the age groups <60 years, but an increased fracture risk among subjects ≥60 years. Being at work was associated with a decreased hip fracture risk among subjects ≥40 years. Alcoholism and a prior fracture were significant predictors of fracture in all age groups. Conclusions: Income does not predict fracture risk in Denmark after adjustment for other social and comorbidity variables. This may signal neutralization of the effect by socio-economic compensation or that income was the product of underlying socio-economic variables.

Disclosures: P. Vestergaard, None.

M318

Prevalence of Osteoporosis-Associated Skeletal Pain at the Onset of Raloxifene Treatment: A Prospective Multicenter Observational Study in a Naturalistic Setting in Germany. S. Scharla¹, H. Oertel^{*2}, K. Helsberg^{*2}, F. Kessler^{*2}, F. Langer^{*2}, T. N. Nickelsen². ¹Practice for Internal Medicine and Endocrinology, Bad Reichenhall, Germany, ²Medical, Lilly Deutschland GmbH, Bad Homburg, Germany.

We assessed the prevalence and characteristics of osteoporosis-associated skeletal pain from the baseline data of a cohort of 3,299 postmenopausal women (mean age 68±9; BMI 25.5±3.9) with osteoporosis who were about to start treatment with the selective estrogen receptor modulator raloxifene in a naturalistic setting. Standardized data were collected by 810 office-based physicians in Germany. The frequency and intensity of pain during the 4 weeks preceding the baseline visit were also self-rated on a patient questionnaire that included a 100 mm VAS scale. The presence of osteoporosis was confirmed by low BMD (89.4%), documented fragility fractures (39.8%), or both. Also, 54.2% of patients had ≥1 clinical osteoporosis risk factor, and 58.1% had received prior drug treatment for osteoporosis. According to the physicians' documentation, 3,080 patients (93.4%) of the cohort experienced skeletal pain at baseline; the median prior duration of pain history was 3 years (>10 months in 75%). Back pain was reported by 85.1% of patients, 41.8% suffered from joint pain, and 32.5% from diffuse bone pain. 78.1% had frequent or permanent pain, and 56.4% required analgesics for skeletal pain. Of the 3,080 patients with pain, 2,864 (93.0%) also reported pain on the patient questionnaire. The mean intensity on the 100 mm VAS was 62.7 +/- 21.6 mm (median 66 mm; n=2,920). Despite the high prevalence of skeletal pain, only 1,313 patients (39.8%) had radiologically confirmed vertebral or clinical non-vertebral fragility fractures in the past (recent vertebral [≤6 months] 11.0%, old vertebral 22.9%, non-vertebral 18.9%). However, 83.5% of patients had x-ray findings indicating degenerative changes in the spine, (spondylosis, osteophytes, etc); while 21.7% had concomitant inflammatory or degenerative disease (rheumatoid arthritis, osteoarthritis, etc). Elevated bone markers were reported in 35.2% of patients with data (N=525). In summary, the prevalence of skeletal pain in this osteoporotic cohort was far higher than the prevalence of fragility fractures. Although our cohort may differ in some aspects from the general population of patients with postmenopausal osteoporosis (the imminent start of raloxifene treatment was a baseline characteristic of our cohort by definition), we conclude that skeletal pain is a major problem in osteoporosis patients with and without fractures. Thus, possible beneficial effects of osteoporosis medication on skeletal pain should be evaluated in more detail.

Disclosures: T.N. Nickelsen, H Oertel, K Helsberg, F Kessler, F Langer, T Nickelsen 3; S Scharla 5, 8.

M319

Screening Patients with Fragility Fracture: The Occurrence of Previously Undetected Disease, Particularly Endocrine Disease, Is Significant. G. P. R. Clunie¹, C. Parkinson^{*2}, S. Stephenson^{*1}. ¹Rheumatology, The Ipswich Hospital NHS Trust, Ipswich, United Kingdom, ²Endocrinology, The Ipswich Hospital NHS Trust, Ipswich, United Kingdom.

In October 2003 we started screening all patients with fragility fracture age 50-75y for osteoporosis, falls risk and underlying bone disease at our institution (National Health Service Hospital serving population of 320,000). In addition to identifying patients with osteoporosis, we prospectively sought to identify patients with previously undisclosed endocrine and other 'bone-relevant' conditions. All patients with a fragility fracture (any site) were initially screened with a DXA scan and biochemistry tests (urea [BUN], serum creatinine, electrolytes, CRP, immunoglobulins, thyroid and liver function tests, Bone Biochemistry, Testosterone and LH [men]) by a Nurse-led team. Abnormalities were discussed (with GPRC) and further blood, imaging and biopsy tests were organised if necessary under specialist medical supervision (GPRC and CP). In 18 months 870 (738 [85%] female) patients were seen, 96 (11%) of whom non-attended one or more visits. Of the 774 patients fully assessed 318 (41%) had distal forearm, 164 (21%) lower leg, 99 (13%) hip, 48 (6%) proximal humerus and 146 (19%) other fractures. Osteoporosis (fracture + any LSp vertebral, total hip or femoral neck BMD T score ≤-2.5) was diagnosed in 227/724 (31%) patients (DXA data was not available for 50). A bisphosphonate, HRT, raloxifene or strontium ranelate was recommended for 405/774 (52%) patients. We made 52 new (major) diagnoses in 45/774 (6%) patients (on average 1 new major diagnosis per 17 patients). Of these, 39 diagnoses were 'osteoporosis/fracture relevant', made in 35/774 (5%) patients (non or 2° osteoporosis causes of bone fragility). Diagnoses were classed as definite (27) or likely (12) - see table. New diagnoses of less relevance to bone were: hypothyroidism (10 patients), psoriatic arthritis (2 patients) and post-CVA epilepsy.

Condition	Diagnosis definite	Diagnosis likely
Primary Hyperparathyroid	11	1
Male Hypogonadism	3	5
Osteomalacia	4	4
Hyperthyroid disease	3	
Chronic alcohol excess	3	1
Excessive thyroxine	2	
Other (2)	Hypoparathyroid	Myeloma

This study illustrates the extent of (undisclosed) disease in patients 50-75y old (total 5-6%) presenting with fragility fracture to an orthopaedic service. Institutions implementing a 'fracture liaison' service should consider the likely burden of undiagnosed, particularly endocrine, disease in fracture patients over the age of 50y and should appropriate resources accordingly to support the service.

Disclosures: G.P.R. Clunie, None.

M320

Correlations between Vitamin D, Parathyroid Hormone, Urinary Calcium Excretion, Markers of Bone Turnover and Bone Density of Patients Referred to an Osteoporosis Center. P. M. Camacho¹, M. Girgis^{*2}, P. Sapountzi^{*1}, E. Holmes^{*3}, J. Sinacore^{*4}. ¹Endocrinology and Metabolism, Loyola University of Chicago, Maywood, IL, USA, ²Loyola University of Chicago, Maywood, IL, USA, ³Pathology, Loyola University of Chicago, Maywood, IL, USA, ⁴Department of Preventive Medicine, Loyola University of Chicago, Maywood, IL, USA.

Vitamin D deficiency is highly prevalent among patients with osteoporosis, leading to secondary hyperparathyroidism, decreased calcium absorption and poor response to therapy. Reports of assay variabilities have led to confusion about interpretation of 25 OHD levels. The primary aim of the study was to characterize the relationships between 25 OHD, 1-25 OHD, intact PTH, ionized calcium, phosphorus, 24 urine calcium excretion, bone specific alkaline phosphatase, urinary NTX/creatinine and bone density. We retrospectively analyzed clinical and laboratory data of 163 patients (143 female, 20 male; mean age 62.5 years) evaluated for low bone mass at Loyola University Osteoporosis and Metabolic Bone Disease Center. Patients were excluded if they were on vitamin D therapy or if they had primary hyperparathyroidism. 25-OHD was measured using Nichols chemiluminescent assay and intact PTH with Bayer Centaur assay. The strongest indirect relationship seen was between PTH and UrCa (r = -0.496, p<0.001). 25OHD showed a significant correlation with UrCa (r = 0.420, p<0.001), PTH (r = -0.215, p=0.014), BSAP (r = -0.288, p=0.010), and a trend with spine BMD (r = -0.156, p=0.071). Analysis of the subgroup with 25 OHD <=20 (26% of the group) showed that 25OHD correlated significantly with PTH (r = -0.354, p=0.027). The strong indirect correlation between PTH and UrCa (r = -0.540, p=0.021) remained in this group. 1,25OHD showed a trend associated with UrCa (r = 0.459, p=0.064) and spine BMD (r = -0.356, p=0.069). Ionized calcium, phosphorus or NTX/creatinine did not show significant correlations with PTH or Vit D levels. In an attempt to "define" vitamin D deficiency, we analyzed the 25 OHD threshold at which patients' PTH levels start to rise and UrCa start to decline. We found the difference between the means of PTH above and below a 25-OHD level of 30ng/ml to be significant. At 35ng/ml the significance was lost. The same 25 OHD level of 30ng/ml showed significant differences in the UrCa of patients with 25OHD above and below this threshold. This relationship was also significant at 35ng/ml and was lost at 40ng/ml. Our study showed that 25OHD weakly correlated with PTH. A level of 30 ng/ml appears to define vitamin D deficiency. This was seen in 48% of the population. Strong correlations seen with UrCa emphasized the importance of this test in the work-up of osteoporosis.

Disclosures: **P.M. Camacho, None.**

M321

Changes of Mineral/Matrix of Femoral Mid Shaft in Magnesium-Deficient Rats Treated with Vitamin K₂ or Alendronate. M. Kobayashi, K. Hara, Y. Akiyama. Department of Applied Drug Research, Tokyo, Japan.

As the improving effects of agents for osteoporosis on fracture can not be explained by the bone mineral content (BMC) alone, recent studies have reported bone quality as a factor involved in the effects. Previously, we found that rats fed low magnesium (Mg) diet reduced their bone mechanical property, that is, bone quality, without decreasing BMC (Bone 35, 2004). In this study, we compared the effects of a bone formation agent, vitamin K₂ (menatetrenone, K₂), and an anti-resorptive bisphosphonate, alendronate (ALN), using this model, and investigated the mechanism involved in the reduction of bone quality using Fourier transform infrared imaging (FTIRI). We divided 40 four-week-old male Wistar rats into 4 groups; the intact group, the low Mg-control group, the low Mg-K₂ group, and the low Mg-ALN group. Diet containing 90 mg/100 g of Mg was given to rats in the intact group, and diet containing 6 mg/100 g of Mg was given to rats in the three low Mg groups. K₂ was given to rats as a dietary supplement at 60mg/100g diet. ALN was subcutaneously administered at 200 µg/kg twice a week. After 8 weeks, the blood level of Mg and alkaline phosphatase activity in the low Mg-control group were lower than those in the intact group, and urinary deoxypyridinoline level (Dpd/Cr) was increased. The cortical (Ct) BMC and the Ct area for the femoral midshaft in the low Mg-control group were 110% of the values in the intact group. The maximum load and elastic modulus decreased to 81% and 50% of the values in the intact group, respectively. There was no significant difference in the Ct BMC between the low Mg-K₂ group and the low Mg-control group. However, the maximum load and elastic modulus in the low Mg-K₂ group were higher than the values in the low Mg-control group. In the low Mg-ALN group, the Dpd/Cr value was lower than that in the low Mg-control group, and the Ct BMC were higher. However, elastic modulus was similar between the two groups. The mineral/matrix (Min/Mat) ratio by FTIRI at the periosteum portion of inferior region of femoral midshaft increased to 140% of the value in the intact group. K₂ inhibited this change; however, ALN did not inhibit it. The changes in the Min/Mat ratio on FTIRI were correlated with the low Mg diet-related and drug administration-related changes in elastic modulus. Therefore, the Min/Mat ratio contributed to the changes in elastic modulus. These results suggest that K₂ improves the maximum load and elastic modulus by reducing the Min/Mat ratio, and that ALN increases the maximum load by increasing the BMC.

Disclosures: **M. Kobayashi, None.**

M322

Hip Bone Density Declines Following Gastric Bypass Surgery for Obesity Despite Stable Parathyroid Hormone and Vitamin D Levels. J. Fleischer¹, M. Bessler^{*2}, M. Johnson^{*1}, M. Della Badia^{*1}, N. Restuccia^{*2}, L. Olivero-Rivera^{*2}, D. J. McMahon^{*1}, S. J. Silverberg¹. ¹Medicine, Columbia University P & S, New York, NY, USA, ²Surgery, Columbia University P & S, New York, NY, USA.

Although bariatric surgery has become one of the most effective means to treat and prevent the complications of morbid obesity, there is growing concern that these procedures may be associated with adverse effects on skeletal health. Roux-en-Y Gastric Bypass (RYGB) is the most common procedure performed in the United States. Among the mechanisms by which RYGB could impact mineral metabolism are: vitamin D and calcium malabsorption and resultant secondary hyperparathyroidism; weight loss associated increases in bone turnover; and low serum 25-hydroxyvitamin D (25D) levels due to obesity itself. We therefore conducted a prospective observational study to investigate the impact of RYGB on skeletal metabolism. Data are available on the first 15 patients (3 men, 12 women). At baseline (± SEM) mean age was 46.3 yrs; BMI 47.9 ± 1.5 kg/m²; serum calcium (Ca) 9.1 ± 0.1 mg/dL. Mean 25D was at the low end of normal (21.5 ± 2.0 ng/mL; nl: 9-52) while PTH was at the upper end of normal (49 ± 5 pg/mL; nl: 10-65; 20% high). At 3 months, urinary calcium decreased (143 ± 21 to 73 ± 23 mg/24h; p<.005) and PTH trended upward (49 ± 5 to 56 ± 5 pg/mL; p= 0.1) despite marked increases in Ca and vitamin D supplements. After one year, patients lost 104 ± 5 lbs. According to surgical protocol, daily supplemental calcium intake increased from 432 ± 139 to 1501 ± 139 mg (p<.0001), while daily vitamin D increased from 413 ± 369 to 1694 ± 369 IU (p=0.01), with no significant change in serum Ca or 25D levels. Bone turnover markers increased significantly as early as 3 months after surgery, and by 12 months urinary NTx doubled (34 ± 4 to 68 ± 4 BCE/mmol Cr; p<.0001), while osteocalcin increased by a more modest 25% (4.1 ± .35 to 5.5 ± .35; p<.005). BMD declined at the total hip (-9.1. ± 2.0%, p<.005) and femoral neck (-11.5 ± 2.2%, p<0.0005), while lumbar spine and forearm BMD were stable. The decline in femoral neck BMD was associated with extent of weight loss (r=-.97, p<.002) but not with PTH or 25D levels. In summary, following RYGB, bone turnover rose rapidly and hip BMD declined. PTH and 25D remained stable with significant increases in calcium and vitamin D supplementation. In morbidly obese patients undergoing RYGB: 1) careful dosing of supplements may compensate for malabsorption; 2) decreased BMD may be due more to weight loss than to abnormal mineral metabolism. We conclude that pre-operative and ongoing assessment of mineral metabolism is a necessary adjunct to the care of these patients.

Disclosures: **J. Fleischer, None.**

M323

Vitamin D Deficiency and Hyperparathyroidism Despite High Caloric Intake in Morbid and Super Obese Patients. N. Sinha^{*1}, E. Stein^{*1}, G. Strain^{*2}, M. Gagner^{*2}, A. Pomp^{*2}, G. Dakin^{*2}, C. P. Sison^{*1}, R. Bockman³. ¹Endocrinology, Cornell University, New York, NY, USA, ²Surgery, NY Presbyterian Hospital, New York, NY, USA, ³Endocrinology, Hospital for Special Surgery, New York, NY, USA.

Vitamin D deficiency is extremely prevalent even in subjects with abundant caloric intake. Studies in patients presenting for bariatric surgery have demonstrated vitamin D (Vit D) deficiency and elevated parathyroid hormone (PTH) levels both prior to and following surgery. In our on-going prospective study, alterations in bone metabolism are studied in morbidly and super obese patients being evaluated for Roux-en-Y gastric bypass or biliopancreatic diversion with duodenal switch. At baseline and at various time points over 18 months post-operatively markers of bone turnover, calcitropic hormones and changes in bone density are followed. We specifically obtain anthropomorphic measurements, calcium, vit D and total caloric intake, serum calcium, 25-hydroxy vit D (25-OH VitD), intact PTH and urinary calcium, markers of bone formation, osteocalcin (OC) and bone-specific alkaline phosphatase (BSAP), and bone resorption, urine N-telopeptide (u-NTx) along with bone mineral density assessed by heel ultrasound, since the weight limit for standard densitometry is 300 pounds. To date, baseline data have been reviewed in 8 women and 7 men with mean body mass indices of 44 +/- 5 and 53 +/- 10 kg/m² respectively. Serum calcium, albumin and creatinine were within normal range. Bone relevant data are summarized in the table.

	Males				Females			
	Mean	S.D.	Min	Max	Mean	S.D.	Min	Max
Calcium Intake mg/day	1183	592	540	2077	476	354	36	1028
Caloric Intake kcal/day	3753	772	2793	4618	2549	193	2214	2685
Vit D Intake (IU/day)	361	269	25	777	123	95	10	289
PTH, intact (pg/ml)	102	43	37	151	99	87	24	247
25-OH Vit D (ng/mL)	15	6	8	24	19	6	9	25
u-NTx (nMBCE/mMCR)	29	14	9	46	30	17	13	62
OC (ng/mL)	8	5	2	12	6	3	1	9
BSAP (mcg/L)	14	11	6	26	19	4	12	23

Severe vitamin D deficiency (<10ng/mL) was found in 23% of patients. Vitamin D levels below 20 ng/mL were found in 69% of patients. All of our subjects had vitamin D levels below 30 ng/mL. We conclude that vitamin D deficiency and insufficiency are common in morbid and super obese patients. Despite extremely high caloric intake, careful dietary analysis revealed inadequate intake of both calcium and vitamin D reflecting poor nutritional choice and content. Women had significantly lower calcium intake when compared to men (p=0.03), with a trend toward lower vitamin D intake. The elevated PTH in the setting of prevalent vitamin D deficiency is reflective of secondary hyperparathyroidism in these patients. Despite PTH elevations markers of bone formation and resorption were not elevated and did not reflect a high bone turnover state.

Disclosures: **N. Sinha, None.**

M324

Is Vitamin-D Status More Important than Abundant Calcium Intake for Normal Calcium Homeostasis? G. Sigurdsson¹, L. Steingrimsdottir^{*2}, O. Gunnarsson^{*3}, O. S. Indridason^{*1}, L. Franzson^{*4}. ¹Department of Medicine, University Hospital, Reykjavik, Iceland, ²Public Health Institute of Iceland, Reykjavik, Iceland, ³Faculty of Medicine, University of Iceland, Reykjavik, Iceland, ⁴Clinical Chemistry, University Hospital, Reykjavik, Iceland.

The importance of adequate vitamin-D status and sufficient calcium intake is well recognized for optimum bone health. The interrelationship between calcium intake and vitamin-D status has not been addressed adequately in the past. The objective of this study was to evaluate the relative importance of high calcium intake and serum 25-hydroxy-vitamin-D (S-25(OH)D) for calcium homeostasis in healthy adults as determined by serum parathyroid hormone (S-PTH). The study group was a randomly selected population based group of men and women, age 35-85 years (n=2310). The calcium intake was assessed by a food frequency questionnaire and S-25(OH)D (RIA) and S-PTH (ECLIA) measured. The recruitment was evenly distributed through the whole year. Participation rate was 70% but after exclusion of those with diseases or medications affecting calcium metabolism 944 participants comprised the final study group. This was divided into three groups according to calcium intake (<800 mg, 800-1200 mg and >1200 mg/day) and other three groups according to S-25(OH)D values (<25, 25-45 and >45 nmol/l). The association between calcium intake, S-25(OH)D and S-PTH was assessed by ANCOVA and adjustment made for age, sex, smoking and body mass index. The lowest S-PTH values were observed in the groups with S-25(OH)D >45 nmol/l irrespective of calcium intake. When S-25(OH)D was 25-45 nmol/l, there was a significant increase in S-PTH, compared with S-25(OH)D > 45 nmol/l only when calcium intake was under 1200 mg/day. When S-25(OH)D was <25 nmol/l there was a significant increase in S-PTH in all calcium intake groups, compared with S-25(OH)D >45 nmol/l. At these low S-25(OH)D values there was a significant difference between calcium intake groups; those consuming >1200 mg/day had significantly lower S-PTH than those consuming <800 mg/day (p=0.02). These results indicate that adequate vitamin-D status with S-25(OH)D >45 nmol/l is sufficient to keep S-PTH in the ideal range even when calcium intake is below 800 mg/day. When S-25(OH)D is below 25 nmol/l high calcium intake >1200 mg/day does not prevent a significant rise in S-PTH even though it does significantly ameliorate the increase. Adequate vitamin-D status is crucial for calcium homeostasis and may reduce the requirements for calcium.

Disclosures: **G. Sigurdsson**, None.

M325

Dietary Restriction Alters Bone Density and Femoral Biomechanics in Aged Male Rats. J. Mardon^{*1}, A. Zangarelli^{*2}, S. Walrand^{*2}, Y. Boirie^{*2}, M. Davicco^{*1}, P. Lebecque^{*1}, M. Horcajada^{*1}, V. Coxam¹. ¹U3M, INRA, Saint Genès Champanelle, France, ²UMPE, INRA, Clermont-Ferrand, France.

Dietary restriction and more specifically caloric restriction are known to consistently extend lifespan of animals and significantly reduce age-associated disease and lesions. However, despite these beneficial aspects it may adversely affect bone physiology and mechanics. Thus, it could be considered as a factor risk in the development of osteoporosis. We investigated the effect of a five month dietary restriction in aged male rats on bone status and metabolism. Two groups of fifteen month-old Wistar male rats were examined in this study. Ten control animals were fed ad libitum with a standard diet. Another group of ten restricted rats was fed 40% less energy than controls. However, daily intakes of lipids, vitamins and minerals were the same in both groups. After five months of restriction, dietary-restricted animals showed a reduced body weight compared to controls as well as reduced leptin levels in plasma, suggesting a lower body fat mass, as well. Bone biomarkers assessment showed that osteocalcin concentrations did not vary among the two groups. However, urinary deoxypyridinoline levels significantly decreased. So, resorption was reduced with restriction. Femoral diameters and lengths were not affected by the diet. Femoral bone mineral density (BMD) was measured using dual energy X-ray absorptiometry (DEXA). Restricted animals exhibited lower total, metaphysal and diaphysal BMD than rats fed ad libitum. The assessment of biomechanical properties revealed a significant reduction in fracture load associated with restriction. Given that body weight is a major determinant of bone mass, BMD and biomechanical values were adjusted for this parameter. Normalization revealed that body weight reduction accounted for changes in fracture resistance, however it did not for changes in BMD: it was significantly higher for restricted animals. Those data demonstrated that, BMD and fracture load were adversely influenced by the decrease in the level of diet intake. Dietary restriction seemed to alter bone biomechanics proportionally to the way it affected body weight. This study suggests that dietary restriction is not without potential risk as lower BMD and biomechanic resistance are associated with increased risk of fractures.

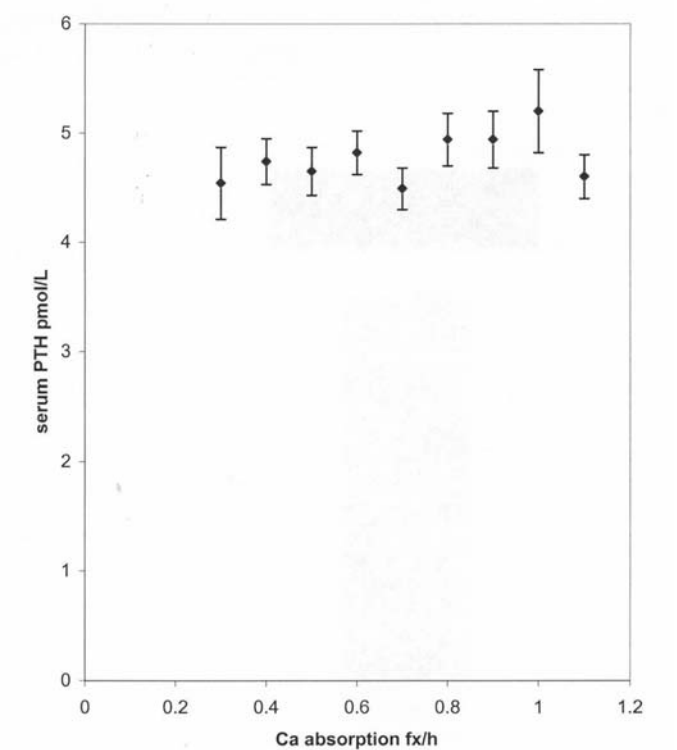
Disclosures: **J. Mardon**, None.

M326

What Is the Cause of Hyperparathyroidism in Vitamin D Deficiency? A. G. Need¹, M. Horowitz^{*2}, P. D. O'Loughlin^{*1}, P. S. Coates^{*1}, C. Nordin¹. ¹Clinical Biochemistry, Institute of Med and Vet Science, Adelaide, Australia, ²Medicine, Royal Adelaide Hospital, Adelaide, Australia.

Vitamin D deficiency causes a significant rise in serum parathyroid hormone (PTH), particularly when serum 25-hydroxyvitamin D (25(OH)D) levels fall below 40 nmol/L [1]. It is commonly claimed that this rise in PTH is caused by malabsorption of calcium as 25(OH)D levels fall but this, to our knowledge, has never been demonstrated. To test this hypothesis we have examined serum ionised calcium, calcium absorption, PTH and

25(OH)D, measured by previously described methods [1] in 1017 postmenopausal women attending our osteoporosis clinics. PTH was not related to calcium absorption (figure).



	COEFFICIENTS OF CORRELATION			
	PTH	Ca2+	Ca absorption	1,25(OH)2D
Ca2+	-0.139***			
Ca absorption	0.035	-0.012		
1,25(OH)2D	0.116***	-0.053	0.338***	
25(OH)D	-0.222***	0.027	0.092**	0.212***

Our data do not support the hypothesis that low calcium absorption due to low 25(OH)D stimulates PTH. There is a trend for a positive relation between 25(OH)D and ionised calcium which, although not statistically significant, suggests that the rise in PTH at low 25(OH)D levels is due to lack of the "calcemic action" of vitamin D as suggested by Carlsson and Lindquist [2].

1.Need et al, J Clin Endocr Metab 2004;89:1646-1649

2.Carlsson & Lindquist, Acta Physiol Scand 1955;35:53-55

Disclosures: **A.G. Need**, None.

M327

Influence of Soy Isoflavones Consumption on the Evolution of Bone Mass in Rat. J. Mardon^{*1}, J. Mathey^{*1}, C. Puel^{*1}, S. Kati-Coulibaly^{*2}, M. Davicco^{*1}, P. Lebecque^{*1}, M. Horcajada^{*1}, V. Coxam¹. ¹U3M, INRA, Saint Genès Champanelle, France, ²Laboratoire de Nutrition et Pharmacologie, UFR Biosciences, Abidjan, Cote d'Ivoire.

Research into human nutrition has led to an awareness of the health benefits that diet can offer by providing a complex array of naturally occurring bioactive molecules, such as phytoestrogens. Indeed, the bone-sparing effect of soy isoflavones (IF) has been demonstrated through epidemiological studies carried out in the Asian population. Nevertheless, there is no clear evidence if such a protection would result from a lifelong exposure. It is thus of the greatest interest to investigate the consequences of an early exposure. Sixty females Wistar rats were randomly divided into two groups (n=30). They were either fed a standard diet devoid of any soy proteins or the same food enriched with isoflavones (ADM, containing 348 mg of total IF (0.87 mg IF/g of diet). After an adaptation period of 30 days, they were allowed to mate and stayed on the same regimen during the whole gestation and lactation period. At weaning, female pups were allocated to 4 nutritional groups : within each experimental group, the animals were split into 2 groups fed either the standard (control diet) or the IF rich diet. At 2, 3, 6, 12, 18 and 24 months after birth, respectively, 10 animals in each group were intraperitoneally anesthetized with chloral hydrate. 48 h before death, the body composition was estimated by dual energy X-ray absorptiometry. On day -1, the 24 h urines were collected to assess deoxypyridinoline (DPD). Blood samples were collected to assess osteocalcin. Femurs were collected for mechanical testing and bone mineral density (BMD) measurement. Peak bone mass was achieved between 6 and 12 months. At 24 months, BMD was higher in perinatally exposed animals, whether exposure was followed or not after weaning. In the same way, femoral failure load during ageing was higher in the pups born from mothers exposed during pregnancy. In conclusion, the present experiment provides evidences for possible long-term outcomes after early exposure to phytoestrogens. We speculate that changes observed

in our experimental conditions may have occurred as a consequence of programming effects, like it is known for the endocrine and immune systems. Consequently, it must be ruled out that early programming events may be essential for the full protection.

Disclosures: **J. Mardon**, None.

M328

Dietary Onion Quercetin Inhibits Bone Loss in Ovariectomized Mice. M. Tsuji¹, H. Yamamoto¹, T. Sato¹, Y. Taketani¹, S. Kato², T. Inakuma^{*3}, E. Takeda¹. ¹Department of Clinical Nutrition, Institute of Health Biosciences, University of Tokushima, Tokushima, Japan, ²Institute of Molecular and Cellular Biosciences, University of Tokyo, Tokyo, Japan, ³Biogenics Research, Kagome Co., LTD., Tochigi, Japan.

Estrogen replacement therapy is indeed effective in preventing bone loss caused by menopause, but it is also accompanied by some adverse effects, such as uterine bleeding and breast cancer. This study was focused on development of nutraceuticals from onion extracts, to prevent and treat osteoporosis after menopause without any side effects. The effects of various onion extractions were tested by osteoclast formation assay using RAW264 mouse macrophage cells or primary bone marrow monocytes. Treatment with the liposoluble fraction extracted from raw onion, not baked or microwaved onion significantly reduced osteoclast numbers. HPLC analysis revealed that quercetin concentrations in each extracts were correlated with their preventive effects on osteoclast formation. Indeed, we elicited that quercetin, not rutin, inhibited the RANKL induced osteoclast formation in dose-dependent manner. Therefore, we investigated the effects of quercetin on bone loss in osteoporosis *in vivo*. Female C57BL/6J mice (9 weeks) were ovariectomized (OVX) or sham-operated (sham) as control. OVX mice were randomly allocated to three groups receiving a control diet (OVX) or diet with 0.25 % and 2.5% quercetin (LQ and HQ). Sham mice were given the same control diet. Following the 4-week experimental period, plasma concentration of total quercetin in LQ and HQ groups were 2.5µM and 7µM, respectively. Bone mineral density (BMD) and stress strain index (SSI) at lumbar spines L3 and femur bones were estimated by peripheral quantitative computed tomography (pQCT). Dietary quercetin, especially in HQ group, prevented the reduction of BMD and SSI in OVX mice. On the other hand, dietary quercetin did not induce estrogenic side effects in uterus. Furthermore, real-time PCR analysis revealed that the mRNA expression levels of TRPV6 (intestinal calcium transporter) were decreased by 40% in OVX mice when compared with sham mice, but not changed by dietary quercetin. These results suggest that quercetin is a potent inhibitor of osteoclastogenesis and dietary quercetin protect against bone loss in OVX mice.

Disclosures: **M. Tsuji**, None.

M329

Effects of Soluble Silicon Compound and Deep-Sea Water on Biochemical and Mechanical Properties of Bone and the Related Gene Expression in Mice. F. Maehira¹, Y. Jinuma^{*1}, Y. Eguchi^{*2}, I. Miyagi^{*1}. ¹Biometabolic Chemistry, Faculty of Medicine, University of the Ryukyus, Okinawa, Japan, ²Research Laboratory Center, Faculty of Medicine, University of the Ryukyus, Okinawa, Japan.

Silicon is an essential element for the formation of collagen and glycosaminoglycans in bone and cartilage. The silicon contents of seawater increases with increases of depth; 64 µM SiO₂ (1.8 ppm Si) in deep-sea water (DW) from 612-m in depth vs. 2.5 µM (0.07 ppm) in surface seawater (SW). The effects of DW on the bone metabolism were studied in comparison with sodium metasilicate (Si) and SW, in the cell culture and in the animal experiment using murine model of senile osteoporosis, SAMP6 and its control SAMR1. The additions of 10% DW from which NaCl was eliminated or 10 ppm Si as sodium metasilicate to the α-MEM medium exhibited the best cellular growth and the highest activities of ALP in MC3T3-E1 osteoblasts and TRAP in osteoclast-like cells compared with the medium control. The ⁴⁵CaCl₂ uptake was significantly enhanced in both MC3T3-E1 cells and osteoclast-like cells by the media containing 10% DW or 10ppm Si, as compared with the medium control. The enhancement of Ca uptake is beneficial to bone formation in osteoblasts and activates a transcription factor for terminal differentiation of osteoclasts. The results from the cell culture study indicated that DW and Si stimulates both osteoblastogenesis and osteoclastogenesis, i.e., bone turn-over. To investigate the effects of DW on the bone metabolism, weanling SAMP6 and SAMR1 were maintained for 6-months in the semisolid diet containing 39%of DW, SW from which NaCl was eliminated, and 200 ppm Si. Three-point bending tests indicated that DW increased the stiffness and the strength of bone, and the amount of energy absorbed in femurs of both strains R1 and P6 with greater increases in the former compared to the controls. The mRNA was extracted from the bone marrow of SAMR1 after the 6 month-experiment. The expressions of mRNA related to the bone metabolism were determined by RT-PCR, followed by real-time PCR. The mRNA expression of IL-11 and BMP-2, both of which stimulate the osteoblast development, and TGF-β which stimulates the expression of osteoclastogenesis inhibitory factor (OCIF), were significantly increased as well as type I procollagen mRNA. In addition, the expression of both OCIF and osteoclast differentiation factor (ODF) were elevated, resulting in the distinct increases of OCIF/ODF ratio. In conclusion, the results indicated that a soluble silicate and deep-sea water as its natural material stimulated the cell growth in both osteoblasts and osteoclasts in the cell culture, and promoted the bone metabolic turn-over in favor of the bone formation in the animal experiment.

Disclosures: **F. Maehira**, None.

M330

Celiac Disease and Vitamin D Status in Community-Dwelling Subjects with Hip Fractures. N. S. Kolatkar¹, J. Magaziner², W. Hawkes^{*2}, K. H. Mikulec³, N. A. Glass¹, M. S. LeBoff¹. ¹Skeletal Health and Osteoporosis Center, Division of Endocrinology, Diabetes, and Hypertension, Brigham and Women's Hospital, Boston, MA, USA, ²Department of Epidemiology and Preventive Medicine, University of Maryland, Baltimore, MD, USA, ³Division of Endocrinology, St. Luke's Hospital, Chesterfield, MO, USA.

Celiac disease is a reversible cause of low bone mass and vitamin D deficiency. However, the contribution of celiac disease to the high prevalence of vitamin D deficiency in patients with fragility fractures is unknown. Our group previously reported (LeBoff *et. al.* JAMA 1999) that elderly women with hip fractures have a greater prevalence of vitamin D deficiency compared with those admitted for elective joint replacement. To evaluate the contribution of celiac disease to vitamin D deficiency in women with hip fractures, we measured serum 25-hydroxyvitamin D [25(OH)D; DiaSorin RIA: normal 20-57 ng/ml] and tissue transglutaminase IgA (tTG-IgA; ELISA: normal <1 U) in 152 community-dwelling elderly women with hip fractures from Boston (n=30) and Baltimore (n=127), and 62 women admitted for elective joint replacement from Boston. In patients with normal tTG-IgA, serum total IgA (ELISA: normal 70-400 mg/dl) was determined and if low, tTG-IgG (ELISA: normal <20 U) was measured. Celiac disease was defined by tTG-IgA >7 U or tTG-IgG >26 U (sensitivity and specificity ≥ 95% for these methods). For the hip fracture patients, the age (mean ± SD) for the Boston and Baltimore cohorts was 77.9 ± 9.2 and 80.8 ± 7.9 years, and 91% and 96% were Caucasian, respectively. The (mean ± SD) age of patients admitted for elective joint replacement was 65.5 ± 9.2 years and 97% were Caucasian. Our findings follow:

	Hip Fracture Patients			Elective Joint Replacement
	Boston n=30	Baltimore n=127	Total n=157	Boston n=62
Median 25(OH)D (ng/ml)	13.0	14.4	14.1	21.3
Patients with celiac disease	1 (3.33%)	2 (1.57%)	3 (1.91%)	1 (1.61%)

The proportion with celiac disease in the combined hip fracture cohort was not significantly different from the elective joint replacement cohort despite a significantly lower median 25(OH)D level (14.1 v. 21.3 ng/ml, p<0.0001). While our study is limited by lack of biopsy confirmation, the prevalence of celiac disease observed in our hip fracture cohorts was slightly higher than reported in U.S. Caucasians (0.33-1.5%). To definitively determine if celiac disease contributes to the high prevalence of vitamin D deficiency in hip fracture patients, larger studies are warranted, as understanding this relationship may have important implications for fracture prevention and treatment.

Disclosures: **N.S. Kolatkar**, None.

M331

Lactose Intolerance and Skeletal Calcium Balance - Decreased Calcium Intake or Impaired Calcium Resorption? B. M. Obermayer-Pietsch^{*1}, M. Gugatschka^{*1}, A. Strele^{*2}, S. Reitter^{*1}, W. Plank^{*1}, A. Fahrleitner-Pammer¹, H. Dobnig¹, W. Goessler^{*3}, W. Renner^{*4}. ¹Department of Internal Medicine, Medical University, Graz, Austria, ²Center for Medical Research, Unit of Biostatistics, Medical University, Graz, Austria, ³Institute for Analytical Chemistry, Karl-Franzens University, Graz, Austria, ⁴Center for Medical Research, Medical University, Graz, Austria.

Lactose intolerance (LI) has been shown to reduce dairy intake in affected individuals due to intestinal lactase deficiency with consecutive lactose malabsorption, a condition affecting more than half of the human population. We recently reported on primary adult LI in postmenopausal women, defined by the LCT polymorphism, describing an association with reduced calcium supply, a decrease in bone mineral density and an increased number of nonvertebral fractures. However, it remains unclear, whether reduced bone mineral density in subjects with LI is a result of reduced calcium intake, impaired calcium absorption, or both. Out of the initial study, 133 women were reintevaluated according to their LCT genotype TT or CC. Seventy-three of them (genotypes TT n=41, CC n=32) were available for a conventional H₂ breath test and a simultaneous non-radioactive strontium absorption test that shows a close correlation to intestinal calcium absorption. Blood samples for glucose and strontium were drawn at baseline and 60 and 150 minutes after ingestion of 2.32 mmol strontium and 50 g lactose. Subjects with LI (LCT genotype CC, H₂ test positive) showed a 50% decrease in dairy calcium consumption. Serum strontium levels in CC subjects were comparable at baseline and after 60 minutes, however, differed significantly from TT subjects at 150 minutes following strontium and lactose administration (-45%, p<0.001). LI may thus not only reduce an individual's calcium intake in terms of dairy product consumption but also impair intestinal calcium absorption in the presence of lactose. Since lactose is a widespread ingredient of foods and medications, an additional decrease in calcium absorption could further contribute significantly to the risk of calcium imbalance and skeletal fragility in lactose intolerant subjects.

Disclosures: **B.M. Obermayer-Pietsch**, None.

M332

Bone Plays a Major Role in the Clearance of Triglyceride-Rich Lipoproteins from the Circulation in Mice. A. C. Niemeier^{*1}, D. Niedzielska^{*2}, U. Beisiegel^{*2}, W. R  ther^{*3}, J. Heeren^{*2}. ¹Dpt. of Orthopaedics and IBM II: Molecular Cell Biology, University Hospital Hamburg-Eppendorf, Hamburg, Germany, ²IBM II: Molecular Cell Biology, University Hospital Hamburg-Eppendorf, Hamburg, Germany, ³Dpt. of Orthopaedics, University Hospital Hamburg-Eppendorf, Hamburg, Germany.

Dietary lipids and lipophilic substances including lipophilic vitamins have important functions in bone metabolism. Triglyceride-rich lipoproteins (TRL) act as postprandial plasma carriers of dietary lipids and lipophilic vitamins and are responsible for their delivery to target organs. TRL uptake into the liver - as the central organ of lipoprotein metabolism - has been well characterized while the uptake process into peripheral organs is less well understood. No data are available on the uptake of TRL into mouse bone. Here, we investigated the uptake of TRL into murine bone in vivo. TRL were obtained from plasma of a hypertriglyceridemic patient as well as from a healthy normolipidemic proband and hydrolyzed in vitro by lipoprotein lipase (LPL) to obtain TRL-remnants (TRL-R), which represent the physiological ligand for lipoprotein receptors. TRL-R were labeled with Cy3-fluorescent dye and injected intravenously into C57Bl/6 (wild-type) animals. Immunodeficient SCID mice served as a control to exclude confounding immunological reactions against the human particles. Animals were systemically perfused at 20 and 60 minutes after injection. Organs were taken, processed for immunohistochemistry and confocal laser microscopy was performed. Of all organs analyzed (bone, liver, heart, skeletal muscle, kidney and spleen) highest amounts of fluorescence were detected in liver, bone marrow and kidney. After 20 minutes, uptake was observed into sinusoidal endothelial cells in liver and bone. Immunocounterstaining against the structural TRL-R component apolipoprotein E (apoE) proved that the signal was due to uptake of intact TRL-R particles in liver and bone. In contrast, kidney signals were found to be derived from free Cy3 dye. After 60 minutes, an apoE-associated signal translocation into underlying parenchymal cells was observed in liver and to a much lesser degree in bone, while Cy3 dye concomitantly dissociated from TRL-R and appeared in the urine. In conclusion, via this novel approach, we provide evidence that substantial amounts of TRL-R are cleared by murine bone marrow sinusoidal endothelial cells. This mechanism is likely to contribute to the physiological delivery of lipids and lipophilic vitamins to other bone cells. To better understand the fate of the particles after endothelial attachment, further investigations are currently being performed.

Disclosures: *A.C. Niemeier, None.*

M333

Possible Correlation of Vitamin D- and K-Deficiency and Bone Loss in Patients with Inflammatory Bowel Disease. K. Tanaka¹, Y. Nakanishi^{*1}, K. Shide^{*2}, H. Tsuiji^{*2}, H. Nakase^{*3}, T. Chiba^{*3}, M. Kamao^{*4}, N. Tsugawa^{*4}, M. Yoshizawa^{*5}, S. Kido^{*1}, T. Okano¹. ¹Food and Nutrition, Kyoto Women's University, Kyoto, Japan, ²Clinical Nutrition, Kyoto University Hospital, Kyoto, Japan, ³Gastroenterology, Kyoto University Hospital, Kyoto, Japan, ⁴Hygienic Sciences, Kobe Pharmaceutical University, Kobe, Japan, ⁵Life and Environmental Sciences, Osaka Prefecture University, Osaka, Japan.

Patients with inflammatory bowel disease (IBD) were evaluated for their bone mineral density (BMD) at lumbar spine, total hip, and radius using QDR-2000 (Hologic). Their plasma levels of 25-dihydroxy vitamin D; 25(OH)D, vitamin K (phyloquinone;PK, menaquinone 4;MK-4, menaquinone-7;MK-7), intact PTH, and indices of vitamin K deficiency (protein induced by vitamin K;PIVKA and undercarboxylated osteocalcin; ucOC) were measured. Their food intake was also evaluated. The subjects consisted of 26 patients with Crohn's disease (CD) and 25 patients with ulcerative colitis (UC). BMD, as expressed as age-adjusted Z value, was -1 to -2 SD, which was significantly lower in CD than in UC. Plasma concentration of 25(OH)D, PK, MK-4, and MK-7 was far below the reference value in Japanese population. Again they were lower in CD than in UC. Intact PTH level was significantly higher in CD than in UC. Plasma levels of 25(OH)D or PK correlated with BMDs. However, their food intake of vitamin D and K was far above the current requirement in Japan, and did not correlate with corresponding plasma levels. In contrast, their fat intake correlated with plasma concentration of vitamin D and K. Thus, severe malabsorption due to the inflammation in their intestine and restricted fat intake was strongly suspected. There was no significant difference in BMD between patients who were under glucocorticoid treatment and those who were not. Our results show that bone loss is an important clinical problem in IBD, and that nutritional factors are quite likely to be involved in its pathogenesis.

Disclosures: *K. Tanaka, None.*

M334

Vitamin D Status in Chronic Pancreatitis. P.L. Selby¹, A. J. Makin^{*2}, S. Gilfedder^{*2}, M. Davies¹, J. L. Berry¹. ¹Medicine, University of Manchester, Manchester, United Kingdom, ²Gastroenterology, Manchester Royal Infirmary, Manchester, United Kingdom.

In chronic pancreatitis there is an exocrine deficiency of pancreatic secretion resulting in the malabsorption of protein and fat. Vitamin D is an important fat-soluble vitamin which may be poorly absorbed under these circumstances resulting in potential skeletal problems for patients with chronic pancreatitis. Although some studies have suggested that patients with chronic pancreatitis do have an increased risk of vitamin D deficiency the

relationship with the severity of pancreatic exocrine deficiency is less well established. We have therefore sought to establish that relationship in a group of patients with chronic pancreatitis. 86 patients with chronic pancreatitis diagnosed by computed tomography or ERCP were studied. All had blood samples taken for measurement of vitamin D metabolites and parathyroid hormone. In addition, pancreatic exocrine secretion was measured using the PABA test which results in a pancreatic excretion index (PEI: normal value >0.7). The mean age was 49 (SD 14) years. There was exocrine pancreatic insufficiency with a mean PEI of 0.35 (95% confidence interval 0.30 - 0.41). Vitamin D levels were insufficient with mean 25OHD level of 9.0 ng/ml (following logarithmic transformation: 95% confidence interval 7.5 - 10.9). 1,25(OH)₂D was within normal limits with a geometric mean of 28.9pg/ml (95% confidence limit 25.7 - 32.5). 21 patients (24%) had 25OHD levels of <5 ng/ml thereby putting them at risk of osteomalacia. A further 36 (42%) of patients had 25OHD levels of between 5 and 15 ng/ml suggesting that their vitamin D status was inadequate for optimal bone health. Thus only 34% of patients with chronic pancreatitis had adequate vitamin D status. There was a significant correlation between log 25 OHD and PEI (r = 0.27, p = 0.03) and between log 25 OHD and log PTH (r = -0.41, p = 0.0006). These results indicate that vitamin D deficiency is an important problem in patients with chronic pancreatitis. It is associated with the presence of secondary hyperparathyroidism and is worsened by the degree of exocrine pancreatic damage. Attention should therefore be paid to vitamin D status and bone health in patients with chronic pancreatitis.

Disclosures: *P.L. Selby, None.*

M335

Does Soy Protein Supplementation Modulate Hematological Parameters in Postmenopausal Women? D. Y. Soung^{*1}, D. A. Khalil¹, A. Patade^{*1}, E. A. Lucas¹, B. J. Smith², L. Devareddy^{*1}, A. B. Arquitt^{*1}, B. H. Arjmandi¹.

¹Nutritional Sciences, Oklahoma State University, Stillwater, OK, USA, ²Department of Surgery, University of Oklahoma Health Sciences Center, Oklahoma City, OK, USA.

Despite the reported health benefits of soy isoflavones, there are concerns about their long-term use because ipriflavone, a synthetic isoflavone, has been shown to cause lymphocytopenia in postmenopausal women. Thus, the objective of this study was to investigate whether one year consumption of soy products (containing about 60 mg isoflavones) on a daily basis unfavorably alter hematological parameters in postmenopausal women not on hormone replacement therapy. Eighty-seven eligible postmenopausal women were randomly assigned to consume soy or control foods daily for one year. Following an overnight fast, venous blood was collected at baseline and at the end of the treatment period and analyzed for a complete blood count using an automated combined impedance-light focusing hematology counter (Pentra 120 Retic Hematology Instrument, ABX Diagnostics, Irvine, CA). The results are presented in the table below.

TABLE Effects of one year supplementation of soy or control foods on hematological parameters

Measures	Control (n=27)			Soy (n=35)		
	Baseline	Final	P values	Baseline	Final	P values
WBC(x10 ³ /mm ³)	5.91±0.31	5.91±0.32	0.9701	5.56±0.28	5.75±0.28	0.2884
LYM%	32.15±1.56	32.04±1.60	0.9300	33.55±1.41	32.94±1.42	0.9300
MON%	8.59±0.45	8.66±0.47	0.8900	9.78±0.41	8.63±0.42	0.0200*
NEU%	53.84±1.78	52.8±1.84	0.5270	51.06±1.6	52.10±1.62	0.4490
EOS%	3.22±0.32	3.40±0.33	0.5090	3.68±0.29	3.32±0.29	0.1430
BAS%	2.18±0.24	2.97±0.26	0.0017*	1.91±0.22	2.96±0.23	0.0006*
Hb (g/L)	137±2	137±2	0.7630	132±2	135±2	0.0364*
MCHC (g/L)	337±2	343±2	0.0212*	336±2	342±2	0.0126*
RDW (%)	13.22±0.24	14.00±0.25	0.0054*	13.27±0.22	13.83±0.22	0.0239*

Data represent least square mean ± SE. *Differences were considered significant at P value <0.05. WBC = white blood cells, LYM % = percentage of lymphocytes, MON % = percentage of monocytes, NEU % = percentage of neutrophil, EOS % = percentage of eosinophils, BAS % = percentage of basophils, Hb = hemoglobin, MCHC = mean corpuscular hemoglobin concentration, and RDW = red cell distribution width index. Our results indicate that consumption of 25g soy protein with 60 mg isoflavones daily for 1 year does not cause lymphocytopenia in postmenopausal women. However, the extent to which higher doses of isoflavones affect parameters, e.g. monocytes, basophils, and hemoglobin, and the interpretation of these findings needs further investigation.

Disclosures: *B.H. Arjmandi, None.*

M336

Varying Presentations of Vitamin D Deficiency Post Bariatric Surgery. M. Charitou^{*}, S. Weinerman, H. L. Katzeff^{*}. Medicine/Endocrinology, North Shore Long Island Jewish Health System, Lake Success, NY, USA.

Vitamin D deficiency as well as decreased BMD have been well described after bariatric surgery. Time to disease presentation is highly variable. We report a series of three cases of varying degrees of Vitamin D deficiency and bone loss. Case 1: D.S is a 53 yo female with a history of a 100 pound weight loss post bariatric surgery who originally presented in 1998 with an elevated PTH and a low-normal Ca found on routine PE. Her Vit D was modestly low at initial evaluation. At follow up 3 years later her Vit D was undetectable despite taking 400 IU/day. Her Vit D levels were difficult to normalize and despite being on Vit D 50,000 TIW and adequate calcium she was still deficient. At this point she was started on calcitriol.

ASBMR 27th Annual Meeting

Date	3/3/01	1/14/04	4/30/04	3/19/05
Vit D25/1,25	22/64	<7/	9/54	8/
PTH	90	93.6	83.6	69
Ca	8.5	8.3	8.1	8.6
BMD	7/01		5/04	
Spine	+0.97		+0.64	
Hip	+0.14		-0.3	
forearm	+1.08		+0.1	

Case 2: S.K is a 49 yo man with a history of biliopancreatic diversion 5 years prior who has lost 300 pounds over the first 2 years. Patients weight has been stable over the past 3 years however has had low 25 (OH) Vit D since his surgery. Despite being on daily supplementation of 1200 IU Vit D and twice weekly supplementation of Vit D 50,000 IU his 25 (OH) Vit D was still low. He was started on calcitriol.

Date	2/25/05	4/6/05
Vit D25/1,25	14	22
PTH		115
Ca	8.5	8.6
BMD	4/25/05	
Spine T score	-1.2	
Hip T score	-1.4	

Case 3:M.Z is a 60 year old female with a history of gastric bypass 2 years prior which resulted in a 140 pound weight loss. She was referred for evaluation of worsening BMD on oral bisphosphonate therapy. She was subsequently diagnosed with Vit D deficiency. She is currently taking Vit D 50,000 IU once weekly.

Date	1/31/05	4/13/05
Vit D25/1,25	13/45	23/64
PTH	47.5	97
Ca	8.6	8.5
BMD	5/03	12/04
Spine T score	-2.31	-3.0
Hip T score	+0.03	-0.53

Patients develop malabsorption through a variety of mechanisms after bariatric surgery. This can be so severe that despite high doses of Vit D they can still be deficient. These refractory cases may benefit from treatment with calcitriol or sunlight exposure.

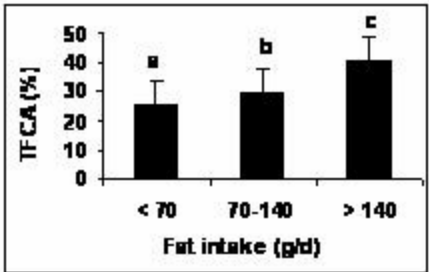
Disclosures: **M. Charitou**, None.

M337

Fat Intake Influences Calcium Absorption and Bone Mass. S. A. Shapses¹, C. S. Riedt^{*1}, R. E. Brolin^{*2}, M. P. Field^{*3}, R. M. Sherrell^{*3}. ¹Nutritional Sciences, Rutgers University, New Brunswick, NJ, USA, ²Surgery, Princeton Medical Center, Princeton, NJ, USA, ³IMCS, Rutgers University, New Brunswick, NJ, USA.

Calcium (Ca) absorption is influenced by dietary intake, yet to our knowledge no previous report has examined this relationship over a wide range of body weights. Our primary goal was to determine how macronutrients and Ca-regulating hormones influence Ca absorption and bone by examining women with variable nutrient intakes. In this study, 141 women (BMI: 23 - 74 kg/m², age: 24 - 75 years) were retrospectively examined for associations between true fractional calcium absorption (TFCA) and macronutrient intake, hormones, and bone mass. TFCA was measured by dual stable Ca isotope method (⁴²Ca and ⁴³Ca). Regional BMD and BMC was measured by DXA. Serum hormones included parathyroid hormone, estradiol, 1,25 dihydroxyvitamin D, 25-hydroxyvitamin D. Food intake was estimated using three day food records. In a stepwise regression model including age, body weight, hormones, dietary Ca and macronutrient intake, the largest independent predictor of TFCA was dietary fat intake (range 10 - 218 g/d) (**Table**). Fat intake together with age and serum PTH explained 31% of the variance in TFCA. TFCA differed in each tertile of fat intake (p < 0.0001), averaging 25.5 ± 7.6 %, 29.4 ± 9.0 % and 40.5 ± 8.2 % from lowest to highest tertile, respectively (**Figure**). The calories from fat (%) in each tertile was 30 ± 8 %, 38 ± 6 % and 50 ± 16 %. In addition, women in the middle compared to lowest tertile of fat intake had greater (p < 0.05) BMD and BMC at the femoral neck and trochanter, and greater ultradistal and 1/3 radius BMD and total body BMC, independent of body weight. TFCA was an independent predictor of BMD at all sites measured, explaining 2-8 % of the variance. These findings show that dietary fat intake is a primary predictor of TFCA in women, and intake in the lowest tertile (consuming < 70 g/d; ~ 30 % fat calories) results in lower TFCA and bone mass. The relationship between low fat diets and bone health requires further study.

N=141	Partial R ²	p-value
Dietary fat intake	0.2072	< 0.0001
Age	0.0619	0.0009
PTH	0.0354	0.0095



Disclosures: **S.A. Shapses**, None.

M338

Dietary Silicon Intake Is Associated with Bone Mineral Density in Premenopausal Women and Postmenopausal Women Taking HRT. H. M. Macdonald¹, A. E. Hardcastle^{*1}, R. Jugdaohsingh^{*2}, D. M. Reid¹, J. J. Powell^{*3}. ¹Medicine and Therapeutics, University of Aberdeen, Aberdeen, United Kingdom, ²GI Laboratory, Rayne Institute, St Thomas's Hospital, Lonodn, United Kingdom, ³MRC Human Nutrition Research, Cambridge, United Kingdom.

The relationship between intake of fruits and vegetables and bone health has been gaining interest recently. They may be beneficial because of their acid-balancing properties or because of other compoments they contain (vitamin C, folate, vitamin K, magnesium and anti-oxidants) that could plausibly affect bone health. Silicon, found in cereals, fruits and vegetables and some alcoholic beverages is an important mineral consituent of bone. Animal and cellular studies have indicated that silicon is involved in bone formation but there are few studies examining its role in humans. In the Framingham offSpring cohort association between dietary silicon and hip BMD was found for premenopausal women, less so for men, but not for postmenopausal women, suggesting a hormonal (estrogen) interaction. We examined whether silicon intake is associated with markers of bone health in perimenopausal women ± HRT in the UK . A total of 3199 women from APOSS underwent bone densitometry in 1990-3 (mean ± SD age: 48.5 ± 2.4 y) and again 6.3 ± 0.9 y later and completed a food frequency questionnaire. We found significant associations between energy adjusted silicon intake and BMD at hip (FN) (r=0.054 P=<0.01) and lumbar spine (LS) (r=0.036, P=0.04). After adjusting for menopausal status/ HRT use, age, weight, height, smoking, and physical activity level, dietary silicon accounted for 0.1% of the variation in FN BMD but the association at the spine was no longer significant. When menopausal groups were analysed separately the association between energy adjusted silicon intake and FN BMD, was significant for premenopausal women (n = 333) and current HRT users (n = 1170) only. There are many common food sources for silicon and other nutrients such as folate, potassium, fiber and vitamin C. The Pearson correlation values for the association of these nutrients with silicon (energy adjusted) were: 0.48 for potassium, 0.40 for folate, 0.55 for fiber, 0.57 for magnesium and 0.37 for vitamin C (P<0.001 for all associations). However when we tested each of these nutrients in the linear regression model, only magnesium was found to be a significant predictor of FN BMD. These data support the earlier findings of the Framingham study and additionally indicate that dietary silicon intake is positively associated with BMD in HRT-using post-menopausal women, adding further weight to a possible interaction between estrogen status and effects of silicon on bone.

Disclosures: **H.M. Macdonald**, None.

M339

Vitamin D Content in Body Fat and the Consequences of Bariatric Surgery on Vitamin D Status. T. C. Chen¹, D. Ingersoll^{*1}, Z. Lu^{*1}, J. Mathieu^{*1}, A. Forse^{*2}, M. F. Holick¹. ¹Vitamin D Research Laboratory, Boston University School of Medicine, Boston, MA, USA, ²Department of Surgery, Boston University School of Medicine, Boston, MA, USA.

We have previously documented that obesity is associated with vitamin D deficiency because whether coming from sun exposure or diet the vitamin D bioavailability is reduced by more than 50% in obese compared to non-obese adults. It has been assumed that vitamin D being fat-soluble was being sequestered in body fat. However to date there has been no report of the isolation of vitamin D from human body fat. We recruited 10 morbidly obese adults who were schedule for bariatric surgery. After obtaining informed consent and at the time of surgery we obtained abdominal fat. The abdominal fat was extracted for its lipid content and then saponified. It was prepurified on a straight phase Sep pak column followed by reverse phase and straight phase high performance liquid chromatography. Blood was collected before the surgery and at 3-month intervals after the surgery. The vitamin D content in human fat ranged between 4-320 ng/g of fat. The human fat contained both vitamin D₂ and vitamin D₃. To determine whether the mobilization of vitamin D from body fat after bariatric surgery could substantially raise blood levels of 25(OH)D we measured circulating concentrations of 25(OH)D at 3 month intervals after the surgery. There was no significant change in circulating concentrations of 25(OH)D in subjects that blood was collected from 3 and 6 months after the surgery. These results provide evidence that body fat sequesters vitamin D and this is the likely explanation for why obesity is associated with vitamin D deficiency. Furthermore, the mobilization of body fat after bariatric surgery has little effect on vitamin D status suggesting that as the fat is being mobilized that the vitamin D is being metabolized and excreted.

Disclosures: **T.C. Chen**, None.

M340

The Effects of Once-weekly Alendronate 70 mg on Bone Metabolism of Postmenopausal Women in Korea. H. Kim^{*1}, H. Shon^{*2}, J. Choi^{*2}, H. Lee^{*3}, E. Kim^{*4}, I. Park^{*5}, I. Park^{*6}, B. Kim^{*7}, I. Lee^{*7}. ¹Internal Medicine, Keimyung University Dongsan Medical Center, Daegu, Republic of Korea, ²Internal Medicine, Catholic University of Daegu, Daegu, Republic of Korea, ³Internal Medicine, Youngnam University, Daegu, Republic of Korea, ⁴Internal Medicine, Daegu Fatima Hospital, Daegu, Republic of Korea, ⁵Internal Medicine, Kyungpook National University, Orthopedic surgery, Republic of Korea, ⁶Obstetrics & gynecology, Kyungpook National University, Daegu, Republic of Korea, ⁷Internal Medicine, Kyungpook National University, Daegu, Republic of Korea.

Background: Once-weekly alendronate 70 mg is available for the treatment of postmenopausal osteoporosis. We performed a prospective study to evaluate the effect of once-weekly alendronate 70 mg on postmenopausal women with decreased bone mineral density (BMD). Methods: Participants had received once-weekly 70 mg dose of alendronate for twenty-four weeks with daily 1000 mg of calcium. BMD by dual energy X-ray absorptiometry was measured to assess the effects of once-weekly alendronate on bone at the first and last visit. The biochemical bone markers were measured after 12- and 24 week treatment. Results: The BMD at the lumbar spine (L1-4) and femoral neck were significantly increased after 24-week treatment by 7.116% and 2.029% respectively. The bone-specific alkaline phosphatase was decreased significantly after 12- and 24-week treatment by 15.5% and 21.1% respectively, and N-telopeptide crosslinks was decreased 22.8% and 18.9% respectively. The treatment was discontinued to one of the participants due to side effect. Overall, during the treatment, there were no significant side effect and laboratory abnormality. Conclusion: Once-weekly alendronate 70 mg significantly increased spine and femoral neck BMD and decreased biochemical marker of bone. The study proposes that alendronate 70 mg is effective and safe in preventing bone loss in postmenopausal women.

Disclosures: **H. Kim**, None.

M341

Effect of Risedronate on Bone Metabolism in Subacute Spinal Cord Injured Patients: Report of Two Cases. H. Kwak, S. Kim. Physical Medicine and Rehabilitation, Dong-A University College of Medicine, Busan, Republic of Korea.

Objective: To assess the effect of risedronate in subacute SCI patients. **Case 1:** For 6 months, 61-year-old spinal cord injured man with a L1 ASIA A (duration: 5 months) took a vitamin D 500 ng and calcium gluconate 1500 mg daily and risedronate 35mg weekly. In initial, his bone mineral density (BMD) was normal and serum osteocalcin (OC) level was borderline but urine deoxypyridinoline (u-DPD) level was markedly increased. After 6 months, u-DPD decreased about 46.5%. **Case 2:** For 8 months, 51-year-old spinal cord injured man with a C6 central cord syndrome ASIA D (duration: 3 months) took same medication and evaluation as case 1. In initial, BMD was -3.7 in lumbar spine, -2.2 in left femur and -2.0 in right femur. u-DPD level was markedly increased but serum OC level was normal. After 8 months, lumbar spine and femoral neck BMD were improved and u-DPD level became normalized. **Conclusion:** Risedronate show a preventive effect on bone loss in subacute SCI patients.

Disclosures: **H. Kwak**, None.

M342

Prophylactic Administration of Bisphosphonate during Gn-RH Agonist Therapy for Endometriosis. K. Aisaka, Y. Ikezuki^{*}, H. Uemura^{*}, V. Takame^{*}, S. Obata^{*}. Obstetrics & Gynecology, Hamada Hospital, Tokyo, Japan.

Objectives: Gn-RH agonist therapy is widely used for treatment of endometriosis. However, it is well known that there are some side effects due to too much suppress of plasma sex steroid hormone levels. Present study was performed to elucidate whether bisphosphonate administration could prevent bone loss during Gn-RH agonist therapy for endometriosis. Materials & Methods: Forty-nine patients of endometriosis who were undertaken Gn-RH agonist treatment (leuporelin, 1.88mg/4weeks) were subjected (Group A). They were administered bisphosphonate (risedronate 2.5mg/day) during Gn-RH agonist treatment for the prevention of bone loss. The bone mineral density (BMD) of the lumbar spine was examined by DXA method before, 6 and 12 months after the treatment. Urinary and plasma levels of the biomarkers of bone metabolism; urinary cross-linked N-telopeptides of type I collagen (NTX), for bone resorption marker, and plasma bone alkaline phosphatase (BAP), for bone formation marker were also measured in the same time to evaluate the effects of these medications. The same examinations were also done in 45 cases of endometriosis who were undertaken Gn-RH agonist treatment with estrogen progestogen (EP) preparations for the add back therapy (group B). All study had been done under the enough informed consent. Results: Percent changes of the BMD values of the group A increased significantly during the treatment compared to those in the group B (A vs. B, 6 months after: 1.34+/-0.67, 1.12+/-0.59, 12 months after: 1.41+/- 0.46, 1.19+/- 0.65%, p<0.05-0.02). Urinary NTX levels in the both groups decreased significantly on 6 months after the treatment compared to the previous values and there was also significant differences between group A and B after the treatment (before treatment, A vs. B: 42.6+/-12.0, 37.3+/-18.4, 6 months after: 19.0+/-9.5 vs. 29.5+/-10.1 nmolBCE/nmol cre., p<0.05). There was no significant change in plasma BAP levels between group A and B (before

treatment: 20.5+/-7.7 vs. 19.6+/-10.3, 6months: 18.2+/-9.5 vs. 22.4+/-13.0 U/l). Conclusion: From these results, it was concluded that there was a beneficial effect for the BMD values during Gn-RH agonist treatment using bisphosphonate (risedronate) administration. In addition, it was suggested that this method might be a standard regimen during Gn-RH agonist therapy for the patients who could not take EP preparations.

Disclosures: **K. Aisaka**, None.

M343

One-Year Treatment of Alendronate Increases Bone Area, Bone Mineral Density, Bone Mineral Content in Osteoporotic Japanese Women. S. Takata, N. Yasui^{*}, M. Takahashi^{*}, A. Abbaspour^{*}. Orthopedic Surgery, The University of Tokushima, Tokushima, Japan.

We studied the effects of one-year treatment of alendronate on bone area, bone mineral content (BMC) and bone mineral density (BMD) of whole body in osteoporotic Japanese women. Sixty-three women with primary osteoporosis, aged 55 to 79 years, were divided into two groups: women treated with alendronate for one year (5 mg/day; alendronate group, n=33) and women without treatment (control group, n=30). Bone area, BMC and BMD of whole body were measured using dual energy X-ray absorptiometry. The mean BMD of the 2nd to 4th lumbar vertebrae (L2-4BMD) of the alendronate and control groups were 107.4+/-5.0% and 100.0+/-6.1% compared to the respective pre-treatment levels, which was significantly different (p<0.0001). The percentage changes in whole body bone area of the alendronate and control groups were 102.5+/-4.0% and 99.4+/-2.8% compared to the respective pre-treatment levels, showing a significant difference (p=0.0006). The percentage changes in whole body BMC of the alendronate and control groups were 103.6+/-3.8% and 98.7+/-3.2% compared to the respective pre-treatment levels, showing a significant difference (p<0.0001). The percentage changes in whole body BMD of the alendronate and control groups were 101.0+/-2.0% and 99.5+/-1.8% compared to the respective pre-treatment levels, showing a significant difference (p=0.0033). The results showed that the percentage changes in bone area, BMC, BMD of the alendronate group were significantly greater than those of the control group, and suggest that one-year treatment of alendronate increases bone area, BMC and BMD.

Disclosures: **S. Takata**, None.

M344

Factors Influencing Adherence to Bisphosphonates for Osteoporosis. P. Thompson¹, C. Cooper², A. Carr^{*3}. ¹Rheumatology, Poole Hospital NHS Trust, Poole, United Kingdom, ²MRC Epidemiology Unit, University of Southampton, Southampton, United Kingdom, ³Clinimatrix, London, United Kingdom.

Non-adherence to bisphosphonate therapy is widely reported and clinically relevant but still common despite a once daily or weekly dosing regimen. This study was designed to identify factors influencing adherence to bisphosphonate therapy in the UK. Telephone interviews were conducted with 50 postmenopausal women aged over 50 with osteoporosis who had taken bisphosphonate therapy. A structured interview was conducted comprising: i) a validated questionnaire to collect detailed information about adherence (medication taking behaviours), patients' beliefs and expectations about osteoporosis and treatment (PHIT) ii) a utility-based rating scale to quantify patient preference and iii) an osteoporosis risk factor questionnaire. 48% of the women had sustained a previous fracture related to osteoporosis. 86% were currently taking bisphosphonates; 79% weekly and 21% daily. Non-adherence occurred with all bisphosphonates (19% of women took less than prescribed). Among the most frequently cited problems affecting adherence were: difficulty following the special instructions for taking bisphosphonates (46%); too frequent dosing (44%) and difficulty fitting treatment into daily routine (42%). Beliefs likely to influence adherence were prevalent; 54% of women were worried that if taken regularly the medication would stop working and 56% that they might become dependent upon bisphosphonates. 44% were worried about taking long-term medication. Expectations of treatment were conservative: 46% expected prevention of fractures. Patient preferences for different dosing frequencies were elicited on a utility-based rating scale (values 0-100 where 0 is worst health state imaginable, 100, best health state imaginable). 77% of women expressed a preference for taking bisphosphonates monthly rather than daily or weekly. Mean values for dosing frequency on the utility based rating scale were: daily 46.84 (SD 26.66), weekly 68.20 (SD 31.14), monthly 77.96 (SD 25.53). Monthly dosing in combination with a patient support programme was the most highly valued treatment option (mean value 81.36 SD 21.86). Non-adherence is a problem with bisphosphonate therapy. Reasons for non-adherence include: difficulty following the special instructions and frequency of dosing. These factors operate against a background of beliefs about tolerance and addiction to bisphosphonates, unease about long term medication and conservative expectations of treatment efficacy. These factors and beliefs need to be addressed if adherence, and therefore clinical outcomes, of bisphosphonate therapy are to be improved.

Disclosures: **P. Thompson**, Proctor & Gamble 5; Merck Sharp and Dohme 5; Roche Pharmaceuticals 5; GlaxoSmithKline 5.

M345

Change in Markers of Bone Turnover in Patients on High Dose Glucocorticoids Treated with Bisphosphonate. K. E. Naylor, R. Eastell. Academic Unit of Bone Metabolism, University of Sheffield, Sheffield, United Kingdom.

There has been concern that bone markers may be unsuitable for monitoring bisphosphonate therapy for glucocorticoid-induced osteoporosis because of the influence of underlying disease and changes in glucocorticoid dose on bone turnover marker variability. The aim of our study was to establish threshold values for the percentage change in biochemical markers, at a specificity of 90%, following risedronate treatment in patients treated with high dose glucocorticoids and postmenopausal women with low bone mass; this approach is a variant of the least significant change approach as it is based on the variability of bone turnover markers in the control group. Subjects were randomized to receive 5mg risedronate or placebo daily for 12 months. The study population consisted of 3 groups of patients. Patients initiating glucocorticoid treatment (prevention group RCP n=90), patients on established glucocorticoid treatment (treatment group RCT n= 120) and postmenopausal women (ROE) with low bone mass (T-score -2 or less, n=153). Bone turnover markers were measured at baseline and 6 months. The N-terminal telopeptide of type I collagen (NTX) was measured by Osteomark® ELISA (Ostex International, Seattle WA, USA). Bone alkaline phosphatase (BALP) was measured by IRMA, Tandem-R Ostase (Hybritech Inc., San Diego, CA, USA). A specificity of 90% for bone turnover marker change in the placebo group was used to determine the threshold. There was no significant difference between the baseline markers in the treatment and placebo groups for each study. Results for the baseline values and the percentage change in bone markers in the risedronate treated groups are shown in the table below.

Group	n	Baseline, mean (SE)	Threshold %	% change 6m
RCP NTX	47	66.5 (8.5)	-56.0	-49.4 (8.0)
RCT NTX	67	64.3 (5.5)	-56.3	-55.1 (3.8)
ROE NTX	79	66.7 (4.0)	-57.9	-49.9 (2.9)
RCP BALP	47	10.8 (0.5)	-50.7	-8.8 (6.2)
RCT BALP	67	11.3 (0.7)	-29.8	-20.1 (4.0)
ROE BALP	79	11.9 (0.5)	-44.4	-28.7 (3.0)

Biochemical markers of bone turnover can be used to monitor risedronate therapy in glucocorticoid treated patients. The least significant change thresholds and the mean changes in bone turnover markers are similar in patients treated with glucocorticoids and postmenopausal women with low bone density.

Disclosures: **K.E. Naylor**, Aventis 2; Procter & Gamble Pharmaceuticals 2.

M346

Large Proportions of Women with Postmenopausal Osteoporosis Respond to Once-Monthly Oral Ibandronate: 2-Year Results from MOBILE. R. R. Recker¹, M. Luckey^{*2}, J. A. Stakkestad^{*3}, R. Civitelli⁴, C. Hughes^{*5}, N. Mairon⁵, B. Bonvoisin⁵, C. Cooper⁶. ¹Creighton University, Omaha, NE, USA, ²Saint Barnabas Ambulatory Care Center, Livingston, NJ, USA, ³CECOR AS, Haugesund, Norway, ⁴Washington University School of Medicine, St Louis, MO, USA, ⁵F. Hoffmann-La Roche Ltd, Basel, Switzerland, ⁶MRC Epidemiology Resource Centre, University of Southampton, Southampton, United Kingdom.

In postmenopausal osteoporosis (PMO), bisphosphonate-induced increases in bone mineral density (BMD) and decreases in biochemical markers of bone turnover are significantly predictive for decreased fracture risk. In MOBILE, a randomized, double-blind, phase III study, once-monthly (50+50mg [single doses, consecutive days], 100mg [single day] and 150mg [single day]) and daily (2.5mg; active comparator) oral ibandronate (Boniva) regimens are being evaluated in 1,609 women (aged 55-80 years; ≥5 postmenopausal) with PMO (lumbar spine BMD T-score <-2.5 and ≥-5). All participants are receiving calcium (500mg) and vitamin D (400IU) supplements. To explore the likely antifracture benefit provided by the investigational regimens, the proportion of participants responding to treatment with increases in lumbar spine and/or total hip BMD ≥ baseline or ≥6% and ≥3%, respectively, and decreases in serum CTX (sCTX) of ≥50% or ≥70% was evaluated. As at 1 year, increases in lumbar spine and/or total hip BMD ≥ baseline or target values were observed in large proportions of participants at 2 years (**Table**). For all BMD endpoints, the proportion of responders was greatest with the 150mg regimen (p<0.05 vs daily; **Table**). Large proportions of patients also achieved clinically meaningful decreases in sCTX (**Table**). Again, the proportion of responders was largest with the 150mg dose (p<0.05 vs daily). In postmenopausal osteoporosis, these findings indicate that more women are likely to be responsive to once-monthly oral ibandronate than daily oral ibandronate, and that the 150mg dose provides additional treatment benefits.

Proportion (%) of participants responding to treatment with increases in BMD and decreases in sCTX				
	2.5mg daily	50/50mg monthly	100mg monthly	150mg monthly
LS BMD ≥baseline	86.4	87.8	87.8	93.5*
LS BMD ≥6% from baseline	35.4	41.2	45.3*	54.3*
TH BMD ≥baseline	78.4	83.2	88.8*	93.4*
TH BMD ≥3% from baseline	40.4	46.4	59.2*	65.1*
LS and TH BMD ≥baseline	70.5	75.3	79.3*	87.1*
sCTX ≥50% from baseline	65.6	60.9	63.5	78.7*
sCTX ≥70% from baseline	35.3	27.0	35.1	48.1*

LS = lumbar spine

TH = total hip

*p<0.05 vs 2.5mg

Disclosures: **R.R. Recker**, F. Hoffmann-La Roche Ltd 2, 5; GlaxoSmithKline 2, 5.

M347

Once-Monthly Oral Ibandronate Is at Least as Effective as Daily Oral Ibandronate in Postmenopausal Osteoporosis: 2-Year Findings from MOBILE. M. R. McClung¹, M. K. Drezner², J. Y. Reginster³, M. Bolognese⁴, C. Hughes^{*5}, N. Mairon⁵, B. Bonvoisin⁵, P. D. Delmas⁶. ¹Oregon Osteoporosis Center, Portland, OR, USA, ²University of Wisconsin, Madison, WI, USA, ³University of Liège, Liège, Belgium, ⁴Bethesda Health Research, Bethesda, MD, USA, ⁵F. Hoffmann-La Roche Ltd, Basel, Switzerland, ⁶Claude Bernard University and INSERM Research Unit 403, Lyon, France.

Therapeutic adherence with weekly oral bisphosphonates, while improved compared with daily dosing, remains suboptimal, compromising therapeutic outcomes in postmenopausal osteoporosis (PMO). Given the strong patient preference for less frequent bisphosphonate dosing schedules, it may be expected that further reducing the frequency of dosing (beyond weekly) could provide additional adherence benefits. Ibandronate (Boniva) is a potent, nitrogen-containing bisphosphonate with proven antifracture efficacy when administered orally, either continuously (daily) or intermittently with a dose-free interval of >2 months. In MOBILE, a randomized, double-blind, phase III study, the efficacy and safety of once-monthly oral ibandronate (50+50mg [single doses, consecutive days], 100mg [single day] and 150mg [single day]) is being compared with daily oral ibandronate (2.5mg; 3-year vertebral fracture risk reduction: 52%) in women (aged 55-80 years; ≥5 years postmenopausal) with PMO (lumbar spine BMD T-score <-2.5 and ≥-5). At 2 years, substantial increases in lumbar spine BMD were observed in the once-monthly and daily treatment arms: 5.3%, 5.6% and 6.6% in the 50+50mg, 100mg and 150mg groups, respectively, versus 5.0% in the daily group. As at 1 year, all once-monthly regimens were proven at least as effective as the daily regimen by non-inferiority analysis. The 150mg regimen continued to be statistically superior (p<0.001) to the daily regimen. Sizeable increases in proximal femur BMD (total hip, femoral neck and trochanter) were also observed in all treatment arms, with the greatest gains obtained with the 150mg regimen (all sites). While corroborating the outcome of the primary efficacy analysis, e.g. therapeutic equivalence of once-monthly oral ibandronate and daily oral ibandronate (for BMD endpoints), these 2-year findings also suggest that the 150mg regimen may provide greater therapeutic efficacy in PMO than the daily and 100mg regimens. This advantage may be reinforced by the improved adherence to therapy that may accompany the once-monthly dosing schedule.

Disclosures: **M.R. McClung**, F. Hoffmann-La Roche Ltd 2, 5; GlaxoSmithKline 2, 5.

M348

Effect of Pretreatment with Low-Dose Risedronate and/or Vitamin K2 on Early Cancellous Bone Loss after Ovariectomy in Rats. J. Iwamoto¹, T. Takeda^{*1}, C. L. Shen^{*2}, J. K. Yeh³. ¹Department of Sports Medicine, Keio University, Tokyo, Japan, ²Department of Pathology, Texas Tech University Health Science Center, Lubbock, TX, USA, ³Department of Medicine, Winthrop-University Hospital, Mineola, NY, USA.

The purpose of the present study was to examine the effect of pretreatment with low-dose risedronate and/or vitamin K2 on early cancellous bone loss induced by ovariectomy (OVX) in rats. Eighty female Sprague-Dawley rats, 4 months of age, were randomized by the stratified weight method into eight groups (n=10 in each group). Rats subjected to OVX, but not sham-operated rats, were treated with vehicle, risedronate, vitamin K2, or risedronate + vitamin K2 for 4 weeks before surgery, and the treatment was either discontinued (pretreatment groups) or continued after surgery (treatment continuation groups) for 2 weeks. Sham-operated rats were treated with vehicle throughout the experimental period. During the 4 weeks prior to surgery (pretreatment), risedronate and vitamin K2 (menatetrenone) were administered five times a week subcutaneously at the dose of 2.5µg/kg body weight and orally at the dose of 30 mg/kg body weight, respectively. During the 2 weeks after surgery (treatment continuation), risedronate and vitamin K2 were administered at the same doses, but only twice a week at the same doses. OVX decreased the bone volume/total tissue volume (BV/TV: 14.2±2.1[mean±SD]% vs. 17.8±1.9% in sham-controls, P<0.001) as a result of increased bone turnover. Both risedronate and vitamin K2 had an anti-resorptive effect on the cancellous bone. Treatment continuation with vitamin K2 (BV/TV: 16.1±1.8%), but not pretreatment (BV/TV: 14.4±1.9%), prevented the BV/TV loss. On the other hand, pretreatment with risedronate (BV/TV: 18.3±2.2%) prevented the BV/TV loss. Treatment continuation with risedronate alone increased BV/TV to beyond the values in controls (BV/TV: 21.2±2.7% vs. 17.8±1.9% in sham-controls, P<0.001). Furthermore, both pretreatment (BV/TV: 20.2±2.6%, P<0.05) and treatment continuation (BV/TV: 22.2±2.6%, P<0.001) with risedronate + vitamin K2 also increased the BV/TV to beyond the control values, with treatment continuation having a greater beneficial effect than pretreatment on the BV/TV and bone turnover. The present study demonstrates that pretreatment with low-dose risedronate had a beneficial effect on early cancellous bone loss after OVX in rats, and that treatment continuation with risedronate alone or risedronate in combination with vitamin K2 was effective at increasing cancellous bone mass, despite the reduced dosing frequency of the drugs.

Disclosures: **J. Iwamoto**, None.

M349

Intravenous Pamidronate for Pain Relief in Recent Osteoporotic Vertebral Compression Fracture. A Randomized, Double Blind, Controlled Study. T. Armingeat*, R. Brondino*, T. Pham*, V. Legré*, P. Lafforgue. Rheumatology, Hopital de la Conception, Marseille, France.

Introduction: We performed a randomized, double-blind, controlled clinical trial comparing intravenous pamidronate and placebo for pain relief in fresh osteoporotic vertebral compression fractures (VCF). **Patients and methods:** Patients were suffering of recent (40/100 mm) VCF due to osteoporosis. They were randomized to receive either infusions of placebo or intravenous pamidronate (30 mg) on 3 consecutive days (in all, pamidronate 90 mg). The main criterion of response was the diminution of standing pain on a 100 mm VAS scale at day 7. Other criteria were standing pain at day 3 and 30, supine pain at day 3, 7 and 30; Patient self-assessment of improvement, mobility index, and number of 20 % and 50 % responders (corresponding respectively to 20 and 50 % improvement in standing pain at day 7). Statistical analysis was made in intention to treat with non parametric tests. **Results:** 32 patients were enrolled in the study, 16 were allocated to placebo, and 16 to pamidronate. Pain was significantly decreased in both groups at day 7 (Placebo -23 mm; Pamidronate -42 mm). Difference of pain between group was -23.25 mm (IC [-42.3; -4.2], $p = 0.018$) at day 7, and -29 mm at day 30 ($p = 0.02$) in favor of pamidronate. **Responders 50 %:** There were 4 and 12 responders respectively in the placebo and in the pamidronate groups at day 7 (likelihood ratio: 8.372; $p = 0.004$). **Responders 20 %:** There were 9 and 14 responders respectively in the placebo and in the pamidronate groups at day 7 (likelihood ratio: 4.038; $p = 0.044$). Patient's self-assessment of improvement was 37 +/- 26 mm in the placebo group and 59 +/- 30 mm in the pamidronate group at day 7 ($p = 0.019$), and respectively 43 +/- 26 mm and 72 +/- 21 mm at day 30 ($p = 0.07$). Supine pain, Shöber index and finger ground distance showed no statistical difference between groups at day 7 and 30. No significant adverse reaction occurred. **Conclusion:** Pamidronate provides rapid and sustained pain relief in patients with acute painful osteoporotic VCF and is well tolerated. Its place within therapeutic armamentarium of painful fresh osteoporotic collapse has to be defined.

Disclosures: T. Armingeat, None.

M350

Safety and Tolerability of Intravenous Ibandronate Injections: DIVA 1-Year Analysis. M. K. Drezner¹, L. G. Ste-Marie², R. Nuti³, C. Benhamou⁴, C. Leigh^{*5}, P. Ward^{*5}, D. Masanaukaite^{*5}, E. M. Lewiecki⁶. ¹University of Wisconsin and GRECC, Madison, WI, USA, ²CHUM Hospital Saint-Luc, Montreal, PQ, Canada, ³University of Siena, Siena, Italy, ⁴IPROS-CHR, Orleans, France, ⁵F. Hoffmann-La Roche Ltd, Basel, Switzerland, ⁶New Mexico Clinical Research & Osteoporosis Center, Albuquerque, NM, USA.

Oral bisphosphonates are the treatment of choice for postmenopausal osteoporosis (PMO), but may be unsuitable or contraindicated for some women. Use of an intravenous (i.v.) bisphosphonate preparation could be advantageous for these patients. Ibandronate (Boniva) is a potent, nitrogen-containing bisphosphonate that can be administered as a rapid (15-30 seconds) i.v. injection with extended dosing intervals. To establish the optimal regimen, the efficacy and safety of 2mg q2mo and 3mg q3mo i.v. ibandronate injections is being compared with an established active comparator regimen (2.5mg daily oral ibandronate) in the ongoing DIVA study. In this double-blind, double-dummy, phase III study, a total of 1,395 women with PMO (aged 55-80 years; ≥ 5 years since menopause; lumbar spine [L2-L4] BMD T-score < -2.5 and ≥ -5.0) were randomized to one of three treatment arms, with all women receiving calcium (500mg) and vitamin D (400IU). Adverse events (AEs) were monitored throughout the study period. After 1 year, a similar overall incidence of adverse events (76-81%) and drug-related AEs (33-44%) was observed in the i.v. and oral treatment arms. The incidence of drug-related AEs leading to withdrawal was also low and similar (4.5-6.6%). A low and comparable incidence of drug-related serious AEs was observed ($< 1\%$ in all arms; $n = 7$). Flu-like illness, a combination of the investigator terms influenza-like illness and acute phase reaction, was reported with a slightly higher frequency in the i.v. arms (5.1% in the q2mo arm and 4.9% in the q3mo arm) than the daily arm (1.1%), but the overall incidence was low, with symptoms generally associated with the first injection only, mild to moderate in intensity and transient in nature. The incidence of clinical fractures observed across the treatment arms was similar. In summary, 2mg q2mo and 3mg q3mo i.v. ibandronate injections are well tolerated by postmenopausal women, and have a similar safety profile to an established daily oral ibandronate regimen that has previously shown tolerability similar to placebo. Thus, i.v. ibandronate injections are likely to be of utility for women who are unable to use oral bisphosphonates.

Disclosures: M.K. Drezner, F. Hoffmann-La Roche Ltd 2; GlaxoSmithKline 2.

M351

Potential Bone Mineral Binding Differences among Bisphosphonates Can Be Demonstrated by the Use of Hydroxyapatite Column Chromatography. M. A. Lawson^{*1}, J. T. Triffitt¹, F. H. Ebetino², B. L. Barnett^{*2}, R. J. Phipps^{*2}, R. M. Locklin^{*1}, R. G. G. Russell¹. ¹Nuffield Dept Orthopaedic Surgery, University of Oxford, Oxford, United Kingdom, ²New Drug Development, Procter & Gamble Pharmaceuticals, Mason, OH, USA.

Bisphosphonates (BPs) are the most widely used class of antiresorptive agents for the treatment of metabolic bone diseases, and are known to bind strongly to bone mineral. There is a growing appreciation that small but potentially important differences exist among the BPs, not only in their relative potencies but also in their duration of action. Our

recent studies (Nancollas et al, Bone, in press) suggest that unexpected differences in mineral binding affinities contribute both to potency and to reversibility of action. In order to study the differences in mineral binding that may relate more directly to the retention and diffusion through bone of BPs, and other phosphate-containing compounds, we have developed a method based on FPLC, using hydroxyapatite columns (3 x 25 mm) to which phosphate-containing compounds can adsorb and be eluted by using increasing phosphate buffer concentrations (1-1000mM) at pH 6.8. The individual compounds emerge as discrete peaks detectable by UV absorbance and/or mass spectrometry. Under the conditions used the retention times (RT) (mins; mean \pm SEM) for the BPs were 22.0 \pm 0.1 for zoledronate, compared with the faster elution of 16.16 \pm 1.17 for risidronate, and 7.33 \pm 0.08 for NE10790, a risidronate analogue in which one of the phosphate groups is replaced by a carboxyl group. These elution patterns were reproducible and the RTs statistically different ($p < 0.05$). The known importance of the OH group at the C-1 position was verified in observed faster elution of the risidronate analog (13.16 \pm 0.6) lacking this C-1 OH group and also for the 2-pyridyl analog of risidronate (18.6 \pm 0.3 vs 14.4 \pm 0.5 with or without the C-1 OH group respectively). These results confirm that differences in hydroxyapatite-binding affinities are an important feature of BPs, and indicate that the side chains contribute to mineral binding affinities in addition to the P-C-P backbone. Indeed, modeling studies indicate that the N atoms in the BP side chains can co-ordinate with OH groups in HAP with bonding efficiencies related to their overall binding affinity. The differences among BPs in binding to HAP may go some way to explain the variations in retention and persistence of effects of BPs observed in animal studies as well as in clinical studies.

Disclosures: M.A. Lawson, Graham Russell 2, 5.

M352

An International Comparison of the Impact of Dosing Frequency on Adherence with Bisphosphonate Therapy among Postmenopausal Women in the UK and Germany. N. O. Lynch^{*1}, M. Walker^{*2}, W. Cowell^{*2}, N. Suppapanva^{*3}, T. Hammerschmidt^{*4}, U. Rigney^{*1}. ¹GlaxoSmithKline, Greenford, United Kingdom, ²Roche Ltd, Welwyn, United Kingdom, ³GlaxoSmithKline, Collegeville, PA, USA, ⁴GlaxoSmithKline, Munich, Germany.

While high adherence (medication compliance and treatment persistence) to bisphosphonate (BP) therapies is necessary to maximize benefit, patients often omit doses or discontinue treatment for a variety of reasons. The objective of this study was to quantify adherence with daily and weekly BP regimens for postmenopausal osteoporosis (PMO), and compare findings in the UK and Germany. Mediplus databases in the UK (~2.5 million patients, 600 GPs) and Germany (~1.5 million patients, 500 GPs) (Jan 2001-Jan 2005) were used to identify postmenopausal women (≥ 50 years) newly-prescribed (no BP prescription for ≥ 12 [UK] or ≥ 6 [Germany] months prior to index prescription) a once-weekly (OW; alendronate 70mg [UK, Germany], risidronate 35mg [UK]) or once-daily (OD; alendronate 10mg, risidronate 5mg [UK]) BP. The OW and OD cohorts were followed for 12 months from the date of index prescription. Medication possession ratio (MPR) was used to estimate compliance. Persistence was calculated as the number of days from the initial prescription to the date of discontinuation of therapy. The number of women identified was 5,962 from the UK and 288 from Germany (UK: OW = 5,102, OD = 860; Germany: OW = 144, OD = 144). Mean age was 73 years in both the UK and Germany. MPR for the combined study cohort was 63.3% in the UK and 44.7% in Germany. However, in both countries OW users had a significantly higher MPR than OD users (UK: 70.3 vs 56.3%; Germany: 51.7 vs 37.7%; $p < 0.0001$). Overall, average treatment persistence during the 12-month follow-up period was 207 days in the UK and 189 days in Germany. However, a significantly longer time to discontinuation was observed for OW users (UK: 228 days; Germany: 227 days) compared to OD users (UK: 186 days; Germany: 172 days; $p < 0.0001$). At the end of 12 months in the UK, 43.6% of women on the OW regimen and 33.3% of women on the OD regimen had persisted with therapy. For Germany, the results were similar, with 46.5% of women still on the OW regimen and 27.8% on the OD regimen 12 months after BP initiation. Women with PMO prescribed a OW BP regimen had significantly higher rates of compliance and longer persistence compared with those taking a OD regimen. However, rates for both regimens were suboptimal. Results were consistent across both countries, indicating that a less frequent BP dosing regimen increases adherence. Continued development of more convenient regimens and health care initiatives to enhance adherence are needed to maximize the therapeutic potential of bisphosphonates.

Disclosures: N.O. Lynch, GlaxoSmithKline 3.

M353

The Effect of a Once-Weekly Tablet Containing Alendronate and Vitamin D₃ for the Treatment of Osteoporosis. P. T. Lips¹, R. R. Recker², C. J. Rosen³, H. Bone⁴, H. W. Minne⁵, G. Callahan^{*6}, A. Lamotta^{*6}, W. He^{*6}, A. Santora⁶. ¹Department of Endocrinology, Vrije University Medical Center, Amsterdam, The Netherlands, ²Osteoporosis Research Center, Creighton University, Omaha, NE, USA, ³Maine Center for Osteoporosis Research, St. Joseph Hospital, Bangor, ME, USA, ⁴Michigan Bone and Mineral Clinic, Detroit, MI, USA, ⁵Metabolic Bone Disease, Clinic Der Furstenhof, Bad Pyrmont, Germany, ⁶Merck Research Laboratories, Merck & Co., Inc., Rahway, NJ, USA.

Vitamin D is an integral part of effective osteoporosis therapy, but many osteoporosis patients have inadequate vitamin D and fail to recognize the need for supplementation. This study evaluated the efficacy, safety, and tolerability of a once weekly tablet containing 70 mg alendronate (ALN) and 2800 IU cholecalciferol (D) in osteoporosis patients. This

was a 15-week, randomized, double-blind, multi-center, controlled study in winter/early spring. Patients with baseline serum 25OHD <9 ng/mL were excluded. Postmenopausal women and men with osteoporosis (T≤-2.5) were randomized to once-weekly ALN with 2800 IU D (ALN+D; n=357) or ALN alone (n=351). Patients were instructed to avoid sunlight and not take vitamin D supplements. Serum 25OHD - the primary efficacy endpoint - and urinary N-telopeptides of type I collagen (NTx) were measured at Weeks 0, 5, 10, and 15. Safety and tolerability were assessed by a clinical review of adverse experiences (AEs). Serum 25OHD averaged 22 ng/mL at baseline and declined in the ALN only group, but was 26% higher in the ALN+D group at Week 15 vs ALN alone; mean 25OHD levels at Week 15 were 23.1 and 18.4 ng/mL, respectively (p<0.001). Thus, ALN+D reduced the risk of 25OHD deficiency (<9 ng/mL) vs ALN alone by 91% at Week 15 [1% vs 13% incidence, respectively; RR, 0.09 (p<0.001)] and reduced the risk of 25OHD <15 ng/mL by 64% [11% vs 32%, respectively; RR, 0.36 (p<0.001)]. Reductions in NTx were similar in both groups. The overall incidence of clinical AEs was not significantly different between treatment groups. Hypercalciuria (ie, >25% increase in 24-hour urine calcium excretion from baseline and urine calcium excretion value > ULN) was rare, and occurred at the same incidence in both treatment groups (n=7 per group). There were no cases of hypercalcemia. The serum 25OHD distributions in this study are not representative of all osteoporosis patients because the study excluded 25OHD <9 ng/ml and limited vitamin D from either sunlight or other supplements. However, even under these restrictive conditions, a once weekly tablet containing ALN and cholecalciferol improved vitamin D status, greatly reducing the risk of deficiency, with antiresorptive efficacy and a safety and tolerability profile similar to that of ALN alone.

Disclosures: **P.T. Lips**, Merck & Co., Inc. 2, 5; *Eli Lilly and Co.* 2, 5; *Aventis* 2; *Wyeth* 2, 5.

M354

Comparison of Alendronate and Raloxifene to Prevent Bone Loss when Estrogen Therapy Is Discontinued in Postmenopausal Women. M. R. McClung¹, M. Omizo¹, E. Mossman^{*1}, D. Conn^{*1}, L. Cole^{*1}, P. Workman^{*1}, E. Chen^{*2}, A. E. de Papp², M. Kocher^{*3}, N. Watts². ¹Oregon Osteoporosis Center, Portland, OR, USA, ²Merck & Co., Inc., West Point, PA, USA, ³University of Cincinnati Bone Health and Osteoporosis Center, Cincinnati, OH, USA.

Estrogen prevents bone loss after menopause, but is no longer recommended for long term use solely for the prevention of bone loss. When women discontinue estrogen treatment, bone loss occurs, and some women are candidates for alternative treatments to prevent that loss of bone mass. Raloxifene and alendronate are both approved for the treatment and prevention of postmenopausal osteoporosis. This study compared the ability of these two treatment options to prevent bone loss in women who recently discontinued estrogen therapy. Postmenopausal women who were within 6 months of discontinuing estrogen therapy were randomly assigned to receive alendronate 70 mg weekly (n=61) or raloxifene 60 mg daily (n=63) with double placebo. Daily intakes of calcium and vitamin D were at least 1000 mg and at least 400 IU, respectively. BMD of the PA lumbar spine (LS) and total hip were measured at baseline, 6 and 12 months. Urinary N-telopeptide (NTX-u) was measured at baseline, 3 and 12 months. No differences were noted between treatment groups in these baseline characteristics: mean age (59.2 years); mean years since menopause (10.8); mean LS BMD (T-score -0.9), NTX-u (55.9 nmol/mmol) or mean months since stopping estrogen therapy (2.9). At 12 months, compared with baseline, statistically significant increases in BMD at the LS and total hip and a reduction of NTX-u were seen with alendronate treatment. In subjects who received raloxifene, a significant decrease occurred in LS BMD, but no change was noted in total hip BMD or NTX-u. The differences between groups in BMD and NTX-u were significantly different (p<0.001) at each time point. The proportion of women who experienced a decrease of LS BMD of at least 3% at 12 months was greater in subjects who received raloxifene (32.8%) than who took alendronate (1.8%). Both drugs were well tolerated. There were no differences between treatment groups in the incidence of upper GI adverse experiences or vasomotor symptoms. Alendronate was more effective than raloxifene in preventing bone loss and reducing bone resorption in postmenopausal women who recently discontinued estrogen therapy.

Treatment Group	Percent Change from Baseline at 12 Months (Least Square Mean (95% CI))		
	PA Lumbar Spine BMD	Total Hip BMD	NTX-u
Alendronate	+2.3 (1.5, 3.1)	+1.1 (0.5, 1.6)	-48.2 (-55.2, -40.0)
Raloxifene	-1.4 (-2.1, -0.6)	-0.5 (-1.0, 0.1)	-3.1 (-16.6, 12.5)

Disclosures: **M.R. McClung**, Merck & Co., Inc. 2.

M355

Does Alendronate Reduce the Risk of Non-Vertebral Fracture in Women without Vertebral Fracture who Have Osteopenia and a History of Non-Vertebral Fracture? The Fracture Intervention Trial (FIT). K. M. Ryder^{*1}, D. C. Bauer², A. J. Bush^{*3}, S. Satterfield^{*3}, L. Palermo^{*2}, A. Schwartz^{*2}, A. Feldstein^{*4}, K. Ensrud⁵, S. R. Cummings⁶. ¹Int Med, UTHSC, Memphis, TN, USA, ²PSG, UCSF, San Francisco, CA, USA, ³Prev Med, UTHSC, Memphis, TN, USA, ⁴CHR, Kaiser Permanente, Portland, OR, USA, ⁵Int Med, VAMC, Minneapolis, MN, USA, ⁶PSG, UCSF, CPMC Res Inst, San Francisco, CA, USA.

There is controversy about treatment of postmenopausal women with 'osteopenia.' Guidelines recommend treating women without existing vertebral fracture (VFX) who have T-scores below -1.5 if they also have a history of a postmenopausal non-vertebral fracture (non-VFX). However, the effectiveness of bisphosphonates on the risk of subsequent non-VFX in these women is not known. Among 2705 women in FIT without prevalent VFX with a FN T-score from -1.6 to -2.5, 880 reported any non-VFX after age 45. ALN

substantially reduced the risk of non-VFX in women with a T-score ≤ -2.5, regardless of Fx history. However, treatment did not significantly reduce the risk of non-VFX in women with a FN T-score > -2.5, including no reduction in risk among those with a prior non-VFX (Table). Relative risk (95% C.I.) of non-VFX in women without VFX assigned to ALN, compared to placebo.

FN T-score	History of non-VFX	No history of non-VFX
Above -2.5 (n=2705)	1.3 (0.9, 1.8)	1.0 (0.8, 1.4)
≤ -2.5 (n=1727)	0.7 (0.6, 0.95)	0.6 (0.4, 0.9)

Among women without existing VFX and with a FN T-score between -1.5 and -2.5, ALN has been shown to reduce the risk of VFX; however treatment does not reduce the risk of non-VFX, even among those with a history of non-VFX fracture. Among women with a non-VFX, measurement of FN BMD identifies a subgroup (T ≤ -2.5) whose risk of non-VFX will be reduced by ALN.

Disclosures: **K.M. Ryder**, Eli Lilly 2.

M356

Hip and Nonspine Fracture Risk Reductions Differ among Antiresorptive Agents. Evidence from Randomized Controlled Trials. U. A. Liberman¹, P. Geusens², M. C. Hochberg³, A. Chattopadhyay^{*4}, P. D. Ross⁴. ¹Tel Aviv University, Petah-Tikva, Israel, ²Limburg University & University of Maastricht, Diepenbeek, Belgium, ³University of Maryland, Baltimore, MD, USA, ⁴Merck Research Laboratories, Rahway, NJ, USA.

A number of antiresorptive agents reduce the risk of vertebral fractures (fx), but few have shown consistent effects on hip and other nonspine fx. Meta-analysis provides a more precise estimate than individual trials when results are consistent across pooled trials. Earlier meta-analyses summarized the results for vertebral and nonspine fx.¹ New data have emerged for hormone therapy (HT),^{2,3} alendronate (ALN),⁴ risendronate (RIS),⁵ and ibandronate (IBN).⁶ We surveyed recent reports of randomized, placebo-controlled trials with nonspine and/or hip fx, and used meta-analysis where appropriate to test for heterogeneity and derive pooled estimates. With RIS (n=12958), the relative risk (RR) reduction was 27% for nonspine fx (RR=0.73; 95% CI= 0.61, 0.87)¹ and 26% for hip fx (RR=0.74; 0.58, 0.94); there was no significant interaction of treatment and age >80. With ALN, heterogeneity existed; doses >5 mg/d were significantly more effective. The RR reduction with ALN >5 mg (n=3723) was 49% for nonspine fx (RR=0.51; 0.38, 0.69).¹ The hip fx RR reduction was 55%; (RR=0.45; 0.29, 0.72) when osteoporotic women in FIT (ALN 5 mg in years 1-2) were included (n=6804),⁴ and 55% (RR=0.45; 0.18, 1.13) for doses >5 mg (n=3723).¹ With HT (n= 27347,^{2,3} not limited to osteoporotic patients), risk was reduced by 36% for hip fx (RR=0.64; 0.49, 0.84) and 25% for nonspine fx (RR=0.75; 0.70, 0.81). For IBN, there was no consistent evidence of hip or nonspine fx risk reduction. The incidence of nonspine fx in the largest IBN trial (n=2946) was 9.2%, 8.9% and 8.2% in the 2.5 mg/d, intermittent dosing (240 mg every 3 mo), and placebo groups, respectively.⁶ A post-hoc subgroup analysis reported a significant interaction between treatment and BMD with a nonspine fx RR reduction of 69% with daily 2.5 mg (but not intermittent dosing) among only those women with T-scores <-3.0 and prior vertebral fx.⁶ The magnitude of effect on hip fx appears to be similar to that for nonspine fx for each drug, but differs among drugs. Based on current data, ALN reduces the risk of hip and nonspine fx by 49-55%, HT by 25-36%, and RIS by 26-27%. There is insufficient and/or inconsistent evidence of an effect on these fx for ibandronate,⁶ calcitonin,¹ and raloxifene.¹

¹Cranney et al. Endocr Rev 2002;23:570-8. ²Cauley et al. JAMA 2003;290:1729-38. ³Women's Health Initiative JAMA 2004;291:1701-12. ⁴Papapoulos Osteoporos Int 2004;doi:10.1007/s00198-004-1725-z. ⁵McClung et al. NEJM 2001;344:333-40. ⁶Chesnut et al. JBMR 2004;19:1241-9.

Disclosures: **U.A. Liberman**, Merck 8.

M357

Persistence and Compliance with Bisphosphonate Therapy among Postmenopausal Osteoporotic Women: A Comparison between Daily and Weekly Regimens. K. F. Huybrechts^{*1}, K. J. Ishak^{*2}, I. Proskorovsky^{*2}, J. J. Caro^{*1}. ¹Caro Research Institute, Concord, MA, USA, ²Caro Research Institute, Montreal, PQ, Canada.

The purpose of this analysis was to compare the level of persistence and compliance among postmenopausal osteoporotic women treated with daily or weekly bisphosphonates in actual practice. Data were obtained from a managed care database which comprises claims and eligibility records for over ten million lives covered under various public and private benefit plans in the United States. The study cohort included women with a diagnosis of osteoporosis (ICD-9 code 733.0) followed by at least one prescription for alendronate 10mg once daily, alendronate 70mg once weekly, risendronate 5mg once daily, or risendronate 35mg once weekly between January 1, 2001 and June 30, 2002. The first prescription for either one of these medications was considered the index prescription. Non-persistence was defined as a gap of >30 days between two subsequent prescriptions. Time to non-persistence was defined as the time from the index prescription to the start of the gap in medication availability. Compliance was measured using the medication possession ratio (MPR), defined as number of days during which the patient had medication available within follow-up time considered, divided by the follow-up time. Analyses were conducted using a continuous as well as a categorical (<80%, ≥80%) definition of compliance. Outcomes were compared between daily and weekly regimens. Patients who switched from a daily to a weekly regimen during the course of their follow-up were censored at the time of the switch. Of the 2,905 new users identified based on a 6-month run-in window, 31% had an index prescription for a daily regimen, 69% for a weekly regimen. After 6 months, 46.7% of women on the once-weekly regimen and 41.9%

ASBMR 27th Annual Meeting

of women on the once daily regimen persisted with their therapies. At 12 months, the respective percentages were 27.7% and 18.9%. Longer persistence was thus observed for once-weekly (median:146 days) when compared to the once-daily users (median:120 days), but the differences were not statistically significant. At 12 months, once-weekly users had a significantly higher MPR than the once-daily users (53.7% vs. 46.9%, $P=0.0022$). Similarly, the proportion of highly compliant patients ($\geq 80\%$) was 23% for the daily versus 32% for the weekly regimen ($P=0.0025$). Although higher rates of compliance and longer persistence are observed for the weekly compared to the daily regimen, rates for both regimens are suboptimal, and the social, clinical and economic implications of such behavior are known to be substantial. Until compliance is improved, we will continue to fail in meeting an important public health goal.

Disclosures: **K.F. Huybrechts**, Novartis Pharma AG 5.

M358

Alendronate Effects on Histomorphometric Parameters: Is There Evidence for Over-Suppression of Turnover? **R. R. Recker**. Osteoporosis Research Center, Creighton University, Omaha, NE, USA.

Alendronate (ALN) is a potent antiresorptive agent that decreases bone remodeling primarily through inhibition of osteoclast activity. Decreased bone resorption is prompt, robust, and sustainable through at least ten years of continued treatment. Because remodeling is essential for maintenance of skeletal integrity, it is important to examine whether treatment with ALN might impair this function. Studies that reported histomorphometric analyses of specimens following ALN treatment were reviewed. Iliac crest biopsies obtained after up to 10 years of ALN treatment^{1,2} showed normal quality lamellar bone, with no evidence of impaired mineralization. Double-labeling, a clear indicator of active bone formation, was present in all specimens. Men and women with glucocorticoid-induced osteoporosis who were treated with ALN for one year had normal mineral apposition rates (MAR), although 3 biopsies failed to show tetracycline label⁴. In another study, ovariectomized baboons were treated with ALN for 2 years, after which biopsies were obtained from both the iliac crest and the lumbar spine³. Double label was present in all specimens, and the MAR was similar to that seen in non-ovariectomized animals. In studies of high-dose (5-6 times usual clinical dose) ALN in dogs, no evidence of impaired mineralization was seen, and the MAR was similar to that of control animals^{5,6}. Further, in a study of pre- and post-fracture treatment with very high dose ALN (10 times usual clinical dose), label was present in all specimens, with no difference in MAR⁷. No evidence of over-suppression of bone turnover, as assessed by histomorphometry of specimens from participants in clinical trials of up to 10 years' duration, has been associated with the use of ALN in postmenopausal osteoporosis. Animal studies, in which much higher doses of ALN were used, confirm the safety of ALN. Although an increase in microcrack density of cortical bone has been reported by some authors, higher microcrack density has been associated with increased bone strength⁸.

¹Recker R, et al. Curr Med Res Opin 2005

²Recker R, et al. ASBMR 2004

³Balena R, et al. J Clin Invest 1993

⁴Chavassieux PM, et al. J Bone Miner Res 2000

⁵Mashiba T, et al. J Bone Miner Res 2000

⁶Ding M, et al. Calcif Tissue Int 2003

⁷Peter CP, et al. J Orthop Res 1996

⁸Sobelman OS, et al. J Biomech 2004

Disclosures: **R.R. Recker**, Eli Lilly 2, 5; GSK 2, 5; Merck & Co 2, 5; Novartis 2, 5.

M359

Rationale and Design of the MOTION Study (Monthly Oral Therapy with Ibandronate for Osteoporosis Intervention). **F. Cosman**¹, **M. R. McClung**², **C. J. Rosen**³, **S. Epstein**⁴, **V. Devas**^{*5}, **B. El Azzouzi**^{*6}, **B. Bonvoisin**⁷, **J. Zanchetta**⁷, **C. Cooper**⁸, **P. D. Delmas**⁹. ¹Helen Hayes Hospital, West Haverstraw, NY, USA, ²Oregon Osteoporosis Center, Portland, OR, USA, ³Maine Center for Osteoporosis, Bangor, ME, USA, ⁴Mount Sinai School of Medicine, New York, NY, USA, ⁵GlaxoSmithKline, Collegeville, PA, USA, ⁶F. Hoffmann-La Roche Ltd, Basel, Switzerland, ⁷Centro de Osteopatis Medica, Buenos Aires, Argentina, ⁸MRC Epidemiology Resource Centre, University of Southampton, Southampton, United Kingdom, ⁹Claude Bernard University and INSERM Research Unit 403, Lyon, France.

Active comparator studies are an accepted means for establishing the relative efficacy and safety of alternative treatment options. However, as clinical endpoints are often difficult to use (especially in chronic disease), comparison of validated surrogate markers is an accepted alternative. In light of its predictive value for fracture risk reduction within the class of bisphosphonates, the surrogate marker of change (%) in bone mineral density (BMD) has been used to establish the relative efficacy of weekly oral bisphosphonates in postmenopausal osteoporosis (PMO).¹ A similar comparative study (MOTION) is ongoing to compare the efficacy of once-monthly oral ibandronate, a potent, nitrogen-containing bisphosphonate with proven antifracture efficacy with extended dosing intervals, with weekly oral alendronate. In MOTION, a randomized, double-blind, double-dummy study, close to 1,900 women (55-84 years, ≥ 5 years postmenopause) with PMO (lumbar spine [L2-L4] BMD T-score <-2.5 and ≥ -5.0) will receive either 150mg once-monthly oral ibandronate or 70mg weekly oral alendronate for 1 year. To maintain blinding, participants will also receive once-monthly or weekly oral placebo, plus daily calcium (500-1,500mg) and vitamin D (400IU). The co-primary study endpoints are change (%) from baseline in lumbar spine and total hip BMD at 1 year. Subsequent non-inferiority tests will explore the comparable efficacy of the once-monthly and weekly oral regimens (non-inferiority margin: 1.14% and 0.87%, respectively). Secondary endpoints include change (%) in hip

trochanter BMD at 1 year and the biochemical marker of bone turnover sCTX in a subset of patients (30%) at day 7 and months 3, 6 and 12. Adverse events will be monitored throughout the study. Clinical vertebral and non-vertebral fractures will also be assessed, and their respective rates compared. In summary, MOTION will explore the relative efficacy and safety of once-monthly oral ibandronate and weekly oral alendronate. Data from the MOTION study will further assist physicians in identifying the most appropriate treatment option in PMO.

1. Rosen C, et al. J Bone Miner Res 2005;20:141-51.

Disclosures: **F. Cosman**, F. Hoffmann-La Roche Ltd 2; GlaxoSmithKline 2.

M360

Current Treatment of Osteoporosis: Rationale for Inclusion of Vitamin D. **S. Epstein**. Medicine and Geriatrics, Mount Sinai School of Medicine, New York, NY, USA.

At present, oral bisphosphonates are the most widely used pharmacologic treatment for osteoporosis. Guidelines for their use stress the importance of concomitant use of calcium and vitamin D if dietary sources are inadequate. Low levels of vitamin D are associated with development of secondary hyperparathyroidism, increased bone turnover, and loss of bone. Clinical trials of new drugs typically provide both calcium and vitamin D to all participants, in order to optimize treatment effects. Review of recommended serum vitamin D levels, estimates of prevalence of vitamin D insufficiency, and current treatment patterns and needs of patients with osteoporosis was performed. General consensus has evolved to suggest that serum vitamin D levels should be high enough to minimize serum parathyroid hormone (~ 30 ng/ml; 75 nmol/L)¹. However the exact level at which this impacts on bone health has not been fully established. Vitamin D insufficiency has been reported in many studies of older adults². Further, two recent parallel studies, one conducted in the United States and the other in 18 countries around the world, reported that 52% and 58%, respectively, of patients with osteoporosis, many of whom were receiving treatment, had levels <30 ng/ml (75 nmol/L)^{3,4}. Adequate nutrition, including vitamin D, is recognized as essential to skeletal health. Frank deficiency is associated, in the child, with rickets and, in the adult, with osteomalacia; insufficiency with secondary hyperparathyroidism. In addition, vitamin D has an important role (amongst others) in neuromuscular function, balance, and sway, all of which may, through an effect on risk of falling, contribute to fracture risk. A number of observational studies have reported a high prevalence of low levels of vitamin D in such subjects. Guidelines for the management of osteoporosis recommend both calcium and vitamin D supplementation, in addition to treatment with bone-specific agents. Two recent large epidemiologic studies have confirmed the widespread prevalence of low serum 25-(OH)D levels in women with osteoporosis, including women receiving definitive treatment with anti-resorptive agents. Inclusion of vitamin D with the weekly dose of bisphosphonate will insure that patients receive the minimum recommended amount of vitamin D, helping to prevent deficiency in these women without compromising the absorption of either agent.

1. Dawson-Hughes B, et al. Osteoporos Int 2005;doi:10.1007/s00198-005-1867-7

2. Lips P. Endocr Rev 2001;22:477-501

3. Holick MF, et al. J Clin Endocrinol Metab 2005;doi:10.1210/jc.2004-2364

4. Hosking D, et al. Osteoporos Int 2005;16(Suppl 3)S50

Disclosures: **S. Epstein**, Merck 2, 5, 8; Roche-GSK 5, 8; Novartis 5, 8.

M361

Cost-Effectiveness of Bisphosphonate Therapies for Women with Postmenopausal Osteoporosis: Implications of Improved Persistence with Ibandronate. **B. Ettinger**^{*1}, **S. R. Earnshaw**^{*2}, **C. N. Graham**^{*2}, **M. M. Amonkar**^{*3}, **R. W. Baran**^{*4}. ¹UCSF, San Francisco, CA, USA, ²RTI Health Solutions, Research Triangle Park, NC, USA, ³GlaxoSmithKline, Collegeville, PA, USA, ⁴Roche Laboratories, Nutley, NJ, USA.

Several studies have shown improved persistence with weekly bisphosphonate (BP) dosing compared to daily dosing yet $>50\%$ of patients on the weekly regimen discontinue therapy within a year¹. Ibandronate, a monthly-administered oral BP, provides an opportunity to further improve persistence, a parameter not well modeled in previous analyses on the cost-effectiveness (CE) of osteoporosis therapy. We developed a Markov model to estimate the CE of BP treatment for women with established osteoporosis. The model, based on a 10 year time horizon and 3-year length of therapy, evaluated CE of three BPs: ibandronate, alendronate, and risedronate. Vertebral, hip and wrist fracture efficacy were assigned a class effect as estimated by the literature². Persistence with weekly therapy was referenced to rates reported for natural populations³ receiving weekly BPs (36% year 1, 24% years 2 and 3) and to an absolute 15% improved persistence (51% year 1, 39% years 2 and 3) for ibandronate. The analysis population was post-menopausal women aged ≥ 50 years with prevalent radiologic vertebral deformity and hip BMD T-score ≤ -2.5 . Yearly drug cost was referenced to wholesale acquisition cost for each BP. Direct health resource costs for fracture states were estimated from published literature and discounted at a 3% yearly rate⁴. All costs were reported in 2004 US\$. More fractures/1000 patients were avoided (vs. no treatment) with ibandronate (126) than with alendronate (87) or risedronate (87) resulting in lower fracture care costs/patient (\$6,159, \$6,448, and \$6,448, respectively). Drug costs/patient increased from \$759 with alendronate and \$737 with risedronate to \$1,059 under conditions of improved persistence with ibandronate. The incremental cost/fracture avoided (vs. no treatment) was lower with ibandronate (\$1,018) compared to alendronate (\$1,360) and risedronate (\$1,111). Sensitivity analyses show improved outcomes with greater baseline fracture risk. A small improvement in persistence with BP therapy augments the benefit realized in patient populations. These benefits include fewer fractures for patients without a significant increase in cost to payers. Increased drug costs due to increased persistence are largely offset by reduced fracture care costs.

1. Cramer JA, et al. J Bone Miner Res 2004;19 (Suppl. 1):S448

2. Kanis JA, et al. Health Technology Assessment 2002: Vol. 6:29
3. Utilization with bisphosphonate therapy: Ingenix II. Data on file - Roche.
4. Eddy DM, et al. Osteo Int 1998; Suppl 4:S7-S80.

Disclosures: **B. Ettinger**, Roche 5.

M362

Persistence With Bisphosphonate Therapy and Fracture Risk in Postmenopausal Women in a Managed Care Environment. D. Gold¹, F. Cosman², J. Frytak^{*3}, R. Baran^{*4}, M. Amonkar^{*5}, B. Martin^{*6}. ¹Duke Univ Med Ctr, Durham, NC, USA, ²Helen Hayes Hosp, West Haverstraw, NY, USA, ³i3 Magnifi, Eden Prairie, MN, USA, ⁴Roche Laboratories, Nutley, NJ, USA, ⁵GlaxoSmithKline, Collegeville, PA, USA, ⁶Univ of Arkansas for Med Sciences, Little Rock, AR, USA.

Oral bisphosphonates (BP) are the standard of care for postmenopausal osteoporosis (PMO). Current daily and weekly BP regimens are associated with poor persistence with therapy, which may affect clinical outcomes such as fracture. The purpose of this study was to investigate the correlation between persistence with BP therapy and claims diagnoses of fracture events using long-term managed care claims data. A retrospective analysis of claims data from a large health care plan affiliated with i3 Magnifi examined the relationship between persistence with BP therapy and fracture risk. Women, ≥45 yrs of age, who initiated new alendronate therapy and met other inclusion criteria (no Paget's disease, HIV, cancer or drug-induced osteoporosis) were considered for analysis. Patients with 24 months of follow-up were stratified into persistent (>6 months on therapy) and nonpersistent (<6 months on therapy) cohorts. Non-persistence was defined as a >30-day gap in medication supply. Osteoporosis-related fractures were identified through specified ICD-9 database codes. The risk for an osteoporosis-related fracture diagnosis was assessed using a Cox-proportional hazards model. A total of 4769 women were assigned to either persistent (n=2029) or nonpersistent (n=2740) cohorts. The persistent cohort had a 6-month persistence rate of 42.5%. During the follow-up period a total of 214 subjects had a claim with a diagnosis of fracture--79 (3.9%) in the persistent cohort and 135 (4.9%) in the nonpersistent cohort. Women in the persistent cohort had a 26% lower risk of a diagnosis of fracture during the follow-up period than those in the nonpersistent cohort (HR=0.739, P=0.047). Women age 45-54 yrs (n=1936, HR = 0.412, P=0.0001) and 55-64 yrs (n=2294, HR = 0.524, P=0.0015) experienced a lower risk of fracture compared to women 65 yrs and older (n=539). The greatest increase in risk of fracture during the follow-up period was observed in women with a fracture claim during the 6-month baseline period prior to initiating therapy (HR=10.846, P<0.0001). This analysis of medication usage among women initiating BP therapy for PMO in a managed care setting confirms that persistence with current therapeutic regimens is suboptimal and is associated with a risk of osteoporosis-related fracture. Strategies to improve persistence, such as simplified and less-frequent dosing, should be adopted and will likely provide greater treatment benefit with respect to protection against fractures.

Disclosures: **D. Gold**, GlaxoSmithKline 5; Roche 5.

M363

Illustrating Drug Utilization Associated with the Weekly Oral Bisphosphonates for Osteoporosis Using the Drug-O-Gram. K. Kahler^{*}, M. A. Omar^{*}, D. Gause^{*}. Novartis Pharmaceuticals Corporation, East Hanover, NJ, USA.

Drug utilization patterns over time are commonly presented as persistency rates for longitudinally collected data. These analyses require the use of specific criteria regarding gaps between refills to categorize patients as still persistent with therapy. While this is valuable, another tool that allows a more liberal assessment of drug use is the Drug-O-Gram, which incorporates the many possible patterns of drug use that may occur within a follow-up period. The objective of this study was to use a visually friendly approach, the Drug-O-Gram, to illustrate the amounts and patterns of drug use in patients with osteoporosis. This was a retrospective analysis of MarketScan, a secondary medical and pharmacy claims database. We studied female osteoporosis patients in Medicare risk-managed care plans, newly treated with the once-weekly forms of the oral bisphosphonates (OB) alendronate and risedronate. Patients were selected based on a diagnosis of osteoporosis in 2002, and with first osteoporosis drug use occurring anytime between 7/1/2002 and 12/31/2002. The date of each prescription fill of the OB and the amount of drug dispensed for each fill was used to ascertain which of the following 365 days of the year each patient had drug available with them for consumption. The Drug-O-Gram was then created to plot the percentage of patients with drug available on each day. This was done separately for patients who had started on alendronate or risedronate. Alendronate (n = 4,029) and risedronate (n = 2,550) patients were included in the analysis. The Drug-O-Gram plots showed a sharp decline in drug use in the initial months following start of therapy, followed by a gradual but consistent decline for the remainder of the year. The pattern was similar for patients in both the alendronate and risedronate groups. The Drug-O-Gram plots suggest declining drug use associated with the weekly dosing regimens of both alendronate and risedronate. Osteoporosis is a chronic condition that necessitates patients to continue with their therapies in order to obtain adequate fracture risk reduction. Newer treatment approaches that help to promote longer exposure to drug therapy are clearly needed.

Disclosures: **K. Kahler**, Novartis Pharmaceuticals Corporation 3.

M364

Treatment of Postmenopausal Osteoporosis with Oral Ibandronate Reduces Activation Frequency to Healthy Premenopausal Levels. R. R. Recker, K. M. Davies^{*}, M. J. Barger-Lux^{*}. Osteoporosis Research Center, Creighton University, Omaha, NE, USA.

The anti-fracture efficacy of oral ibandronate has been demonstrated in a large, multinational, double-blind, placebo-controlled, 3-year fracture-prevention study (the BONE Trial). However concerns remain as to whether over-suppression of bone turnover might occur in the course of such treatment. As part of the BONE Trial, transilial bone biopsies were obtained, in either month 22 or 34 of treatment, from a subset of subjects from each of the three treatment groups: placebo; continuous oral daily ibandronate (2.5mg/day); intermittent oral ibandronate (20mg every other day for 12 doses every 3 months). All participants, including those in the placebo group, received calcium 500 mg/d and vitamin D 400 IU/d. Here we compare a key measure of bone turnover - activation frequency (Ac.f) - in these subjects with Ac.f in transilial biopsies from other groups of women. All measurements of Ac.f were carried out in our histomorphometry laboratory. The table summarizes these data and the results of non-parametric tests of difference.

Activation Frequency, #/yr	n	Median	Inter-quartile range
Subjects in the BONE Trial, at least 5 yr postmenopausal, ages 55-80			
Placebo, ibandronate study	33	0.22*	0.11 - 0.39
Continuous ibandronate	33	0.10	0.04 - 0.20
Intermittent ibandronate	31	0.13	0.08 - 0.20
Subjects in other studies			
Premenopausal, healthy, >age 46	51	0.13	0.06 - 0.20
1 yr postmenopausal, healthy, age 55	51	0.24*	0.15 - 0.41
Postmenopausal, healthy, age 60	34	0.37**	0.22 - 0.66
Postmenopausal, osteoporosis, age 67	89	0.42**	0.29 - 0.72

*P<0.05 compared to premenopausal, continuous ibandronate, and intermittent ibandronate

**P<0.05 compared to 1 yr postmenopausal and to placebo

As the table indicates, both continuous and intermittent treatment with oral ibandronate yielded values for Ac.f that were equivalent to those in healthy premenopausal women; in the placebo group, values for Ac.f were similar to those in healthy women 1 year after menopause. We conclude that these dose regimens of ibandronate - which result in fracture reduction - do not over-suppress bone remodelling, given that the values for Ac.f are not different from those in healthy premenopausal women.

Disclosures: **R.R. Recker**, Roche 2, 5; Merck 2, 5; Lilly 2, 5; Procter & Gamble 2, 5.

M365

Effect of 10 Years of Alendronate on the Risk of Non-Spine Fracture. A Novel Approach to Modeling Long-Term Effects of Treatments. S. Cummings¹, C. Shinoff^{*1}, L. Palermo^{*2}, D. Sellmeyer¹, C. McCulloch^{*3}, K. Ensrud⁴. ¹CPMC Research Institute, UCSF, S.F. Coordinating Center, San Francisco, CA, USA, ²UCSF, S.F. Coordinating Center, San Francisco, CA, USA, ³UCSF, Epidemiol and Biostat, San Francisco, CA, USA, ⁴U. Minnesota, Minneapolis, MN, USA.

There have been no 10 year placebo-controlled trials of the effect of bisphosphonates on fracture risk, this must be estimated from shorter placebo-controlled trials. The Fracture Intervention Trial (FIT) randomized 6,459 postmenopausal women to alendronate (ALN) or placebo (PBO). The trial (and PBO group) stopped after about 4 years. 1,099 of the FIT participants, all of whom had taken alendronate for 5 years, volunteered to continue in a 5 year extension (FLEX) and were randomly assigned to take 5 more years of ALN (10 yr total) or placebo (5 yr ALN then 5 yr PBO). Women who continued into FLEX had different characteristics than other women in FIT, so comparisons of rates of fractures in the FIT placebo group to the rates in the women who received 10 years of alendronate in FIT + FLEX would be biased. To avoid this bias, we developed a method to project the risk of fracture during 10 years of placebo. For every woman assigned to 10 years of alendronate in FLEX, we created a "virtual twin" with identical characteristics at FIT baseline; together comprising a virtual placebo group. The model projects the future risk of fracture in each virtual twin from the rate observed in the FIT placebo group, adjusted for the characteristics of the twin. We developed the model using baseline data and rates of fracture observed in a randomly selected half of the FIT placebo group and compared these to observed rates during FIT in the other half. We estimated an 18.6% cumulative incidence of fractures vs. 18.3% observed. Using the estimated placebo rates and observed rates for the treated group, we projected a 27% decreased risk of non-spine fractures vs. the 28% reduction observed during FIT. In the model, alendronate reduced the rate of non-spine fractures 27% during the first 5 years but continued treatment with alendronate did not reduce the risk of non-spine fractures during the next 5 years (R.R. = 1.0; 95% CI: 0.77, 1.23). Our analyses indicate that, among women resembling participants in FIT, alendronate reduces the risk of non-spine fracture during the first 4 to 5 years of treatment but beyond this period does not reduce the age-related increase in risk of non-spine fractures that occurs without treatment. This method may allow estimates of the long-term effectiveness of treatments tested in short-term placebo-controlled trials with long term extension of treatment groups.

Disclosures: **C. Shinoff**, None.

M366

Effect of Concomitant Statin Therapy in Bisphosphonate Treated Patients with Osteoporosis. J. L. Guyer*, M. I. Williams*, V. I. Petkov, R. A. Adler. Endocrinology and Bone Metabolism, McGuire VA Medical Center, Richmond, VA, USA.

Bisphosphonates, commonly used in osteoporosis treatment, work by inhibiting an enzyme in the mevalonate pathway which is required for the production of isoprenoids necessary for osteoclastic function. HMG-CoA reductase inhibitors (statins), used in the treatment of hypercholesterolemia, also interfere with the mevalonate pathway by inhibiting its first step. It is therefore thought that statins may also have an effect on bone resorption with some recent studies showing an increase in bone mineral density (BMD) and decrease in fracture risk. Our goal was to determine if the combination of a statin and bisphosphonate provides an additive, synergistic or no benefit over bisphosphonate treatment alone. Medical and BMD records of patients who had at least 2 BMD tests and received bisphosphonate therapy from a single Veterans Affairs Medical Center for at least 12 months between January 1995 and January 2003 were reviewed. Patients were divided into two groups; one with concurrent statin use, the other without. The change in bone mineral density at the spine and total hip was compared by student t-test. ANCOVA was used to adjust for covariates and differences between groups. Patients treated with both drugs (N = 115) were heavier and received a greater number of concomitant medications than patients treated with bisphosphonate only (N = 90). Age, gender and race distribution were similar. A significantly smaller proportion of patients died in the statin group (7% vs 21%). The average exposure to statins was 47 months, and to bisphosphonates: 43 months for statin users and 38 months for bisphosphonate only users. There was a non-significant trend toward greater increase in BMD at the spine and total hip in patients receiving both drugs. In the spine, the total percent change in BMD was 7.2% vs. 5.7% (p-value 0.058); per year of BMD follow-up 2.6% vs. 2.2%. In the total hip, the total percent change was 2.3% vs 1.1% (p-value 0.071); per year 0.8% vs 0.3%. However, when adjusted for differences in weight, length of bisphosphonate exposure and BMD follow-up, these differences become less prominent. Statins probably do not add any benefit toward increase in BMD over bisphosphonate treatment alone.

Disclosures: **J.L. Guyer**, None.

M367

Risedronate Demonstrates Antifracture Efficacy over a Range of Baseline BMD Levels. R. Lindsay¹, S. Magowan², I. Barton^{*3}, D. Felsenberg⁴, J. D. Adachi⁵. ¹Helen Hayes Hospital, West Haverstraw, NY, USA, ²P&G Pharmaceuticals, Mason, OH, USA, ³P&G Pharmaceuticals, Egham, United Kingdom, ⁴Univ Hospital Benjamin Franklin, Berlin, Germany, ⁵McMaster University, Hamilton, ON, Canada.

Baseline BMD level and risk factors are important considerations in the decision to initiate osteoporotic therapy. The WHO commentary on the threshold for intervention is not the same as the diagnostic threshold for osteoporosis. Currently, there is little available information concerning the efficacy of osteoporotic therapies over a range of baseline T-scores. This study investigates the fragility fracture efficacy (vertebral and nonvertebral) of risedronate 5 mg/day in postmenopausal women over 4 ranges of femoral neck (FN) T-scores. This analysis included 2575 postmenopausal women from 4 phase III trials: VERT MN & NA, BMD MN & NA. Women were randomized to receive placebo or risedronate and treated for up to 3 years. Subjects were stratified into 4 subgroups based on level of baseline FN T-score. Fractures included in the analysis were vertebral and nonvertebral (composite of 6 sites). The fracture incidence and relative risk reduction for each baseline BMD range are summarized for each subgroup. In the four BMD strata, fracture incidence in the placebo group increased with decreasing baseline BMD values, potentially confounded by increasing age and an increased percentage of patients with prevalent vertebral fractures (PVF). Risedronate, however, demonstrated significant anti-fracture efficacy in postmenopausal women, regardless of baseline level T-score ranges (Table 1). Treatment by T-score interaction was p = 0.653. Although baseline BMD is an important predictor of fracture risk, Risedronate's demonstrated efficacy against fragility fractures appears to be independent of baseline BMD level.

Table 1: Osteoporotic Fracture Incidence in Placebo and Risedronate Patients with Baseline FN T-score Data < -1.5 (VERT-MN & NA, BMD-MN & NA)

Baseline score	T- N	Mean Age	Percent PVF	Placebo Incidence	Risedronate Incidence	Hazard Ratio	P value
≤ -1.5 to > -2.0	609	67	63.1%	20%	14%	0.58	<0.05
≤ -2.0 to > -2.5	822	68	68.7%	27%	19%	0.63	<0.01
≤ -2.5 to > -3.0	682	69	78.4%	36%	26%	0.61	<0.005
< -3.0	462	71	87.7%	46%	27%	0.44	<0.001

Disclosures: **R. Lindsay**, None.

M368

Alendronate Improved Bone Mineral Density in Patients with Juvenile Osteoporosis. P. Madyastha*, W. Ries, B. Hollis, F. Reed*, L. Key. Pediatrics, Medical University of South Carolina, Charleston, SC, USA.

The current study was designed to evaluate the safety and efficacy of therapy with alendronate (Fosamax), vitamin D, and calcium in treating juvenile osteoporosis. Ten children (age 6-13 years) with multiple fractures and osteoporosis [Z score ≤-2 SD based on bone mineral density (BMD) by dual energy x-ray absorptiometry (DEXA)] were treated with alendronate for 12 months. The BMD of the lumbar spine and hip (total hip, trochanter, and femoral neck) and markers of bone turnover, (serum bone-specific alkaline

phosphatase and urinary N-telopeptide), mineral apposition rates (MAR) and micro-architecture of the iliac crest were followed to evaluate the safety of 12 months of alendronate administration. Alendronate therapy resulted in an improved Z-score for BMD measurements at 6 months and 12 months of therapy in assessments of both the spine and hip. There were no new fractures during the treatment period. Bone biopsy showed normal lamellar structure without mineralization defects and normal bone apposition rates. Normal or improved growth was observed in all patients. Alendronate therapy is safe and effective when used to increase the bone density of children with osteoporosis and two or more fractures.

Disclosures: **P. Madyastha**, None.

M369

Use of Upfront Loading Doses of Bisphosphonates: Novel Method to Advance the Beneficial Effects of Bisphosphonates on Enhancing Fracture Reduction. S. J. Wimalawansa. Medicine, Robert Wood Johnson Medical School, New Brunswick, NJ, USA.

Introduction: Bisphosphonates are efficacious in enhancing BMD and decreasing fracture rates. However, the absorption of oral bisphosphonates is usually poor (<1%). Therefore, it may take about a year to get adequate amount of the bisphosphonate into bone, to be effective in fracture reduction. Rationale: We hypothesized that if adequate amount of the bisphosphonate gets into bones earlier in the course of a treatment, then one should see a rapid response and enhance the beneficial effects on BMD and fracture reduction. Method: We have examined the effectiveness of loading doses of oral and intravenous bisphosphonates on BMD in comparison with the standard doses of same agents. We have compared the effects of loading doses of alendronate, risedronate and pamidronate with their standard recommended doses for osteoporosis over a one-year period. Results: A statistically significant increase of BMD was observed in both oral and intravenously administered agents with in 3-6 months (with the biomarker changes within first 4 weeks), in comparison to 6 months with standard therapy. There was no statistical difference between the responses observed with alendronate and risedronate (Tables 1 and 2).

Table 1: Comparison of BMD increases with conventional and loading doses of risedronate

Increase in spinal BMD	Standard dose	Loading dose
3 months	+0.4%	+1.5%
6 months	+2.2%	+4.0%
12 months	+4.3%	+5.6%

Table 2: Comparison of BMD increases with conventional and loading doses of alendronate

Increase in spinal BMD	Standard dose	Loading dose
3 months	+0.4%	+1.2%
6 months	+1.1%	+3.6%
12 months	+4.5%	+5.8%

Conclusion: If the fracture efficacy of an anti-resorptive drug depends on the rapidity of the reduction of bone turnover and enhancement of the BMD, then this new approach of administration of bisphosphonates should significantly enhance the fracture reduction efficacy of bisphosphonates, especially for patients with fragility fractures. This novel approach of administering bisphosphonates should be cost-effective in prevention of fractures in high-risk patients, particularly beneficial for those patients with high bone turnover and who has been diagnosed with established osteoporosis.

Disclosures: **S.J. Wimalawansa**, Better Bone Health 5; Lilly 8; Roche 8.

M370

Prolonged Hypocalcemia from Intravenous Zoledronic Acid: An Unusual Case. S. A. Talwar, J. F. Aloia. Endocrinology, Winthrop-University Hospital, Mineola, NY, USA.

A healthy 60 year-old white lady was enrolled in an osteoporosis prevention trial using intravenous bisphosphonate (zoledronic acid) at our center. Her past medical history included asthma, hypothyroidism, gastroesophageal reflux disease, anxiety disorder and significant surgical history included spinal surgery at L4-L5 for disc herniation, cholecystectomy and thyroidectomy for goiter at age 19. She was medically stable on medications that included Synthroid 112 mcg/d, Advair, singulair, albuterol prn, protonix 40mg once a day, Paxil 40mg daily, calcium and vitamin D supplements (1000-1200 mg/d) and a multivitamin supplement. She had a normal screening physical exam and laboratory assessment. The screening bone density revealed osteopenia at Lumbar spine (0.922 g/cm²) and total femur (0.835 g/cm²). Her screening labs revealed an H/H: 13.5/38, BUN/Cr: 19/ 0.7, S. Ca: 8.7 mg/dl, P: 4.1 mg/dl, Alb: 4.5 g/dl, Total protein: 7.2 g/dl, Mg: 2.3 mg/dl, Creatinine clearance : 100 ml/min, 25-OHD: 18.3 ng/ml (=45.75 nmol/L), TSH: 0.34mIU/ml A week after the patient was randomized in study, she developed symptoms of tiredness, perioral tingling and numbness, tingling in her hands. There was no evidence of Chvostek or Trousseau's sign. Serum calcium was found to be low (results below). She was advised to increase calcium supplement to a total of 2400 mg/d along with vitamin D 1000 IU/d. Her symptoms resolved with this intervention, however, the biochemical hypocalcemia persisted more than 3 months after the incident with slow improvement. Additional work up revealed a concomitant elevated phosphorus and an inappropriately low serum parathyroid hormone when serum calcium was low confirming inability of parathyroid gland to compensate for the biochemical abnormality.

ASBMR 27th Annual Meeting

Labs	Baseline	2 weeks	4 weeks	6 weeks	8 weeks	15 weeks
S. Ca	8.7	6.4	6.8	7.3	7.6	8.0
S. P	4.1		6.1	4.9	4.4	4.9
S. Albumin	4.5	4.3	4.5	4.0	4.2	4.2
S. Mg	2.3		2.3	2.1		1.9
PTH		37 (N-terminal)			27 (Intact)	
S. 25-OHD	18.3				13.2	
S. TSH	0.3	0.236			0.666	
S. 1,25-OHD					19.3 pg/ml (15.9-55.6)	
24 hour urine Calcium					288 mg/d	

Conclusion: History of previous thyroidectomy could result in incipient hypoparathyroidism that can manifest acutely when challenged. Use of bisphosphonates in patients with prior thyroidectomy should be accompanied by evaluation of serum calcium a week after the drug administration to avoid a fatal medication related adverse event.

Disclosures: S.A. Talwar, None.

M371

Compliance with Osteoporosis Medications among 40,000 Medicare Beneficiaries. D. H. Solomon¹, J. Avorn^{*1}, J. N. Katz^{*2}, J. S. Finkelstein³, J. Polinski^{*1}, M. Arnold^{*4}, M. A. Brookhart^{*1}. ¹Division of Pharmacoepidemiology, Brigham and Women's Hospital, Boston, MA, USA, ²Division of Rheumatology, Brigham and Women's Hospital, Boston, MA, USA, ³Endocrine Unit, Massachusetts General Hospital, Boston, MA, USA, ⁴Boston University School of Public Health, Boston, MA, USA.

Background: Long-term compliance with pharmacologic treatments for many asymptomatic conditions has been found to be sub-optimal, but little is known about compliance with medications used for osteoporosis. We assessed the level and determinants of compliance with drugs prescribed for osteoporosis. **Methods:** We conducted a retrospective cohort study using health care claims data from US Medicare and filled prescriptions from a state pharmaceutical benefits program. The study included 40,002 persons aged 65 or older who filled at least one prescription for a medication used for osteoporosis (alendronate, calcitonin, hormone replacement therapy, raloxifene, or risedronate) between 1996 and 2002. The outcome of interest was sub-optimal medication compliance, defined as less than 67% of days covered during a 60-day period. Other analyses examined the time until the first 120-day period without filling a prescription for an osteoporosis medication. **Results:** One year after initiating treatment for osteoporosis, 45% of patients went 120 days without filling any prescriptions for osteoporosis treatment. Five years after initiation, 52% of patients were not continuing to fill prescriptions for any osteoporosis drug. Several characteristics independently predicted sub-optimal compliance (described above): male gender, older age, more comorbid conditions, more non-osteoporosis medications prescribed, lack of testing for bone mineral density (BMD) before and/or after initiating a medication, and no fracture before and/or after initiating a medication. After controlling for these patient characteristics, patients begun on raloxifene were less likely to have sub-optimal compliance than those begun on a bisphosphonate; conversely, those started on HRT or calcitonin were more likely to have sub-optimal compliance. However, models adjusted for significant patient variables explained only 6% of the variation in compliance. **Conclusions:** Nearly half of the patients we studied had stopped pharmacologic treatment for osteoporosis within one year of initiation. While several patient characteristics were significantly correlated with sub-optimal medication compliance, patient variables explained little of the variation. Further studies are needed to better define factors contributing to non-compliance so that effective interventions can be developed.

Disclosures: D.H. Solomon, Merck 2; Procter & Gamble 2.

M372

A Randomized Controlled Trial of Mailed Osteoporosis Education to Older Adults: Survey Results. D. H. Solomon¹, J. Avorn^{*1}, J. Polinski^{*1}, M. Arnold^{*2}, J. S. Finkelstein³, A. Licari^{*1}, C. Canning^{*1}, S. Gauthier^{*4}, J. N. Katz^{*5}. ¹Division of Pharmacoepidemiology, Brigham and Women's Hospital, Boston, MA, USA, ²Boston University School of Public Health, Boston, MA, USA, ³Endocrine Unit, Massachusetts General Hospital, Boston, MA, USA, ⁴Arthritis Foundation, Newton, MA, USA, ⁵Division of Rheumatology, Brigham and Women's Hospital, Boston, MA, USA.

Purpose: To assess the effect of a mailed educational intervention on older adults' knowledge, attitudes, and preventive behaviors regarding osteoporosis. **Methods:** We conducted a public health trial in 31,715 Medicare beneficiaries from Pennsylvania who participated in a drug benefits program for low-moderate income elderly. All women over 65, and all men and women with a history of fracture or chronic oral glucocorticoid use were included. Approximately half of the participants were randomly selected to receive 2 mailings aimed at improving knowledge of osteoporosis and enhancing preventive activities, such as using calcium and vitamin D, reducing fall risks in the home, obtaining a BMD test, and taking medications when necessary. We surveyed a sample of intervention and control subjects to determine the effects of the intervention on knowledge, attitudes, self-efficacy (confidence in one's ability to perform a specific behavior), and behavior regarding osteoporosis prevention and treatment. **Results:** Six hundred randomly selected participants in the intervention and an equal number in the control group were invited to participate. 15 had died and 636 of the remaining 1185 (54%) completed the survey. Respondents and non-respondents did not differ significantly with respect to measured sociodemographic factors. All scales had good reliability (Cronbach's alphas > 0.7). Knowledge of osteoporosis was relatively strong and not different between intervention

(mean = 62% correct responses) and control subjects (mean = 64%; p = 0.5). Perceived susceptibility to osteoporosis was high and similar across groups (p = 0.6). Self-efficacy for participating in osteoporosis prevention and treatment was very good in both the intervention (mean = 4.5, maximum = 5) and control groups (mean = 4.4, p = 0.3). On average, subjects in the intervention group reported participating in 3.1 of 6 preventive osteoporosis activities compared with 3.0 in the control group (p = 0.3). **Conclusions:** A mailed educational intervention for osteoporosis was not associated with better knowledge, higher perceived susceptibility, more self-efficacy, or performance of preventive behaviors among the at-risk older adults that we studied. More intensive patient interventions may be required to bring about changes that lead to reduced fractures.

Disclosures: D.H. Solomon, Merck 2; Procter & Gamble 2.

M373

Baseline Clinical Characteristics of Postmenopausal Women with Osteoporosis and an Inadequate Clinical Response to AntiOsteoporosis Drugs in the Observational Study of Severe Osteoporosis (OSSO): The French Cohort. P. Fardellone¹, I. Jamonneau^{*2}, S. Liu-Léage^{*2}, S. Tcherny^{*2}. ¹CHRU, Amiens, France, ²Lilly France, Suresnes, France.

The OSSO study is a 12 month prospective, observational study conducted in six European countries. Participants are postmenopausal women with osteoporosis and an inadequate clinical response to approved antiosteoporosis drug, defined as: (i) the presence of a new clinical fragility fracture despite prescription of any antiosteoporosis drug for at least 12 months before the fracture (index fracture cohort), and/or (ii) discontinuation of any antiosteoporosis drug due to compliance problems and/or side effects (compliance cohort). OSSO aims to evaluate changes in health-related quality of life (HRQoL), resource utilisation and risk factors associated with incident fractures. 418 women with a mean age of 71.4±8.9 years were enrolled in France. 196 women (46.9%) were recruited in the index fracture cohort, 222 (53.1%) women in the compliance cohort. The patients characteristics for both groups are presented in the table. The index fracture patients by comparison with the compliance patients were older, more glucocorticoids (GC) past users and had more fractures history. The vertebral fractures represented 46% of these fractures in the index fracture and 40% in the second group. Both groups had a low BMD at the different sites. In the index fracture group, the last clinical fragility fractures occurred despite an antiosteoporosis administrated treatment for at least 12 months, were mainly located at the spine (56.4%). Alendronate was the most commonly discontinued osteoporosis medication (31.5%) followed by risedronate (18.3%), hormone replacement therapy [HRT] (14.5%), raloxifene (13.6%), etidronate (12%), estrogen replacement therapy (5.7%). Gastrointestinal problems were the main reason for discontinuing alendronate (63.4%) and risedronate (46.4%), hot flushes for raloxifene discontinuation (26.8%). Discontinuation due to non compliance was the highest for HRT (42.2%). In conclusion, the baseline clinical characteristics of postmenopausal women with osteoporosis and an inadequate clinical response to antiosteoporosis drugs indicate that they have numerous risk factors for subsequent fracture, especially in the index fracture cohort at the highest risk for fractures.

	Patients Characteristics		p value
	Index Fracture n= 196	Compliance Side effects n= 222	
Age (years)	73.4±8.2	69.6±9.1	<.001
BMI(kg/m ²)	24.5±4.2	24.6±4.1	ns
Maternal hip fracture (%)	11.7	14.6	ns
Past GC use (%)	17.9	9	.008
			<.001
Prevalent fractures history (%)	81*	64	* not including the last clinical fracture
Lumbar Tscore	-3	-2.9	ns
Total Hip Tscore	-2.4	-2.4	ns

Disclosures: P. Fardellone, None.

M374

Nasal Salmon Calcitonin Reverses Post-Fracture Bone Loss in the Distal Radius Fractures and Retains its Mechanical Properties as Assessed with Peripheral Tomography (pQCT). G. P. Lyritis, P. Boscainos^{*}, P. Giannoulis^{*}, P. Raptou^{*}, A. Galanos^{*}, G. Kiniklis^{*}. Laboratory for the Research of Musculoskeletal System, Athens, Greece.

Fracture of the distal forearm is a common incident that has been attributed to post-menopausal bone loss. A post-fracture decrease of bone mineral density has been described, but a limited number of authors have clinically investigated the orthopaedic indications of calcitonin in post-fracture disease. The purpose of this study is to examine the effect of salmon calcitonin on early post-fracture decrease of BMD and the mechanical parameters. 54 post-menopausal women with unilateral forearm fracture (28 patients receiving 200 IU daily salmon nasal spray (Miacalcic, Novartis) and 26 patients receiving matched placebo) started treatment immediately after the fracture for a period of 3 months. All patients were randomly assigned in the treatment groups. Fracture was immobilized after reduction with a plastic cast (ScotchCast Plus, 3M) allowing repeated bone measurements without an interference to the precision of the measurements. pQCT measurements (Stratec 2000) of the fractured as well as the intact forearm were made 2-3 days after the fracture and at 10, 45 and 90 days after fracture. All measurements were made at 10mm (ROI 1), 20mm (ROI 2) and 40mm (ROI 3) from a reference line placed at the most proximal point of the distal radioulnar joint. Parameters assessed were the BMD of cortical and cancellous bone, and Strength Strain Index at all directions. Statistical analysis included ANOVA for measuring percentile difference from baseline BMD and ANCOVA with initial measurements for confirmation of ANOVA results. A statistically

significant difference in favor of the calcitonin treated group was shown at the end of the third month of treatment in total density (p=0.05), total area (p=0.05), and cortical thickness (p=0.038) in the fracture arm at ROI 1. At the level of ROI 2 in the fractured arm it was found a protective effect in trabecular content (p=0.044), cortical content (p=0.044), cortical thickness (p=0.038), cortical area (p=0.05), SSI_x (p=0.033) and SSI_p (p=0.041). It is interesting that women receiving calcitonin showed an additional protective effect in the non-fractured arm in bone content of ROI 1 (trabecular content p=0.035, total area=0.053), in bone content (trabecular content p=0.05, cortical density p=0.031) and mechanical properties (SSI_x p=0.06) in ROI 2 and in cortical content (p=0.05) and cortical area (p=0.06) of ROI 3. In conclusion after a wrist fracture immediate daily administration of nasal salmon for a period of 3 months has a beneficial protective effect in bone content and bone strength, as assessed by peripheral tomography.

Disclosures: *G.P. Lyritis, None.*

M375

Compliance and Effect of Bone Protective Treatment in Elderly Females: 5 Year Follow-Up Study. *S. M. Doherty, S. A. Steel, A. Goodby**. Centre for Metabolic Bone Disease, Hull and East Yorkshire Hospitals NHS Trust, Hull, United Kingdom.

We carried out a study to compare the logistical feasibility of undertaking diagnosis, risk assessment and treatment of osteoporosis among the young elderly (70 to 75 years) female population in a hospital (Group I) and primary care based settings (Group II). Of 695 females invited to participate, 491 (71%) attended. As part of this study the subjects underwent bone mineral density (BMD) of spine and hip (Group I only) and broad band ultrasound attenuation (BUA) of the heel. Data was collected on medical, drug and social factors thought to influence bone strength and fracture risk. Subjects were considered at increased risk of fragility fracture if T-score for spine or hip was below -2.5 (Group I) or if BUA was below 60 dB/MHz. These were randomised to bone protective treatment in the form of HRT, Bisphosphonates or Calcium and Vitamin D supplementation. The study pre-dates the change in recommendations regarding HRT. After 5 years, subjects were invited to attend the hospital for a follow-up visit that included BMD of spine and hip, BUA of heel. Data was collected on acceptance of and compliance with treatment and adherence to lifestyle and dietary advice. Falls and fractures since the previous visit were recorded. 379 subjects (77%) were invited to attend for follow-up bone densitometry. 112 subjects (23%) were not recalled - 53 (11%) had died, 53 (11%) had left their practice and 6 (1.2%) were not recalled for other reasons. Of 261 attending for follow-up, 110 had been defined osteoporotic and randomised to bone protective treatment. 96 (87%) were commenced on treatment and 57 (52%) remained on treatment at 5 years, 11 having changed treatment during the follow-up period (Table 1).

	Calcium+Vit D	HRT	Bisphosphonate
Randomised	41	32	36
	53	12	28
Prescribed	(12 from HRT group 2 from Bisph group)	(7 not prescribed)	(1 from HRT group 2 from Ca+D group 6 not prescribed)
Continued	34	2	10
Discontinued and on no treatment	15	7	14
Changed	4 to Bisph	2 to Ca+D 1 to Bisph	4 to Ca+D

There were 30 patients suffering incident fragility fractures: 17 defined osteoporotic (10 who were on treatment and 7 not on treatment) and 13 non-osteoporotic. **Conclusion** Osteoporosis screening of females aged 70 to 75 years identifies 1/3rd as being osteoporotic. General Practitioners are willing to prescribe and patients willing to accept bone protective treatment, particularly Calcium and Bisphosphonates. After 5 years, 52% of those defined at risk in our population were compliant with some form of bone protective treatment.

Disclosures: *S.M. Doherty, None.*

M376

A Study Comparing Primary Care and Specialty Physicians' Approach to Diagnosis and Treatment of Osteoporosis. *T. A. Karas*¹, C. Leman*², J. Sinacore*², P. Camacho¹*. ¹Endocrinology, Loyola University Medical Center, Maywood, IL, USA, ²Statistics, Loyola University Medical Center, Maywood, IL, USA.

Objective: The objective of the study is to analyze the approach to screening, diagnosis and treatment of osteoporosis among physicians in various specialties, demographic locations, and practice settings who evaluate and treat patients at high risk for osteoporosis. Design Setting: Analysis of a cross-sectional survey developed to assess the practice of osteoporosis screening, diagnosis and treatment. Aims: To compare the approach to screening, diagnosis, and treatment of osteoporosis among six groups of physicians. To determine if gender, years in practice, and practice setting affects screening, diagnosis and treatment of osteoporosis within each group of specialists. Results: One hundred twenty-two surveys were returned electronically including 27 from geriatrics, 25 from endocrine, 23 from obstetrics/gynecology, 20 from rheumatology, 19 from primary care and 8 from orthopedics. In screening for osteoporosis, 94% of the physicians surveyed would order DXA for a patient with 2 or more risk factors. The three risk factors most likely to initiate DXA scanning were height loss (93%), chronic prednisone use (89%) and menopause (86.6%). Low testosterone (60%) and vertebral deformities (74%) in an elderly male were the risk factors least likely to instigate DXA. Endocrinologists and rheumatologists were more likely to order DXA given any risk factor or patient scenario as compared to the other specialties, while orthopedic surgeons were least likely. Rheumatologists were most likely

to initiate treatment in patients followed by endocrinologists, geriatricians, primary care physicians and obstetrician/gynecologists. Alendronate and Risedronate were deemed the most efficacious treatments by >98% of all physicians while calcium/vitamin D and calcitonin were thought to be the least efficacious. In general, patients were more likely to be screened, diagnosed and treated for osteoporosis by female physicians practicing in urban, academic settings who had been in practice >6 years. Conclusions: Osteoporosis is a common disease that is underdiagnosed and undertreated despite published guidelines. The results of this survey teach us where to focus educational efforts to improve prevention and treatment of osteoporosis.

Disclosures: *T.A. Karas, None.*

M377

Magnitude of Change in BMD and Bone Turnover Markers after Cessation of Risedronate Treatment: Biological Effect or Statistical Phenomenon? *D. Kendler¹, N. B. Watts², X. Zhou*³, S. T. Harris⁴, A. Grauer³*. ¹St. Vincent's Hospital, Vancouver, BC, Canada, ²University of Cincinnati, Cincinnati, OH, USA, ³P&G Pharmaceuticals, Mason, OH, USA, ⁴UCSF, San Francisco, CA, USA.

Surrogate markers such as bone mineral density (BMD) and bone turnover markers (BTM) are important predictors of fracture risk in untreated subjects. Their predictive value after treatment cessation is unknown as are patient characteristics predicting post-therapy changes in those surrogates. The 4th year of the VERT-NA study provided patients who had received risedronate 5 mg daily (N=398) during the first 3 years and the original placebo group (N=361) with 1000 mg calcium and 500 IU vitamin D (if levels were low) during the discontinuation year (yr 3-4). Patients previously treated with risedronate showed an increase in NTX and a decrease in BMD in the discontinuation year. This analysis used stepwise linear regression model selection to investigate potential predictors of the magnitude of surrogate marker change after treatment cessation, including age, years since menopause and percent change in BMD and BTM over the original 3year treatment. The model showed, that greater BMD loss in the discontinuation year was associated with greater BMD gains in the initial 3 years of treatment (p<0.001 for LS, FN). Greater increases in NTX and BSAP after therapy cessation were also associated with more pronounced BTM suppression at the end of the 3-year treatment (p<0.001 for NTX, p=0.002 for BSAP). This inverse relationship was also observed in the control group. Age and years since menopause were not significantly associated with BMD or BTM percent changes during year 4 (p>0.2). Previously reported findings from this study have demonstrated that patients previously on risedronate for 3 years maintained a significant 47% reduction of vertebral fracture risk in the discontinuation year, despite significant increases in NTX and BSAP and significant declines in BMD. We conclude that patients return toward pretreatment BMD and BTM after discontinuing risedronate. Patient characteristics predictive of this change could not be determined. However, the magnitude of BMD and BTM changes 1-year after discontinuation are inversely related to the changes observed during the 3 years on treatment. As the same phenomenon was also evident in the placebo group, this is most likely consistent with a regression to the mean phenomenon. Following these surrogates in the year after risedronate cessation is therefore of limited predictive value for evaluation of individual patient's short-term fracture risk.

Disclosures: *D. Kendler, Wyeth, NPS, Johnson & Johnson, Zelos, Takeda 2; Merck, Pfizer, Novartis, Lilly 2, 5; Servier 5.*

M378

Utilization and Correlates of Osteoporosis Treatment in Postmenopausal Women: Observations from the National Osteoporosis Risk Assessment (NORA). *E. S. Siris¹, P. D. Miller², E. Barrett-Connor³, S. Sajjan*⁴, T. W. Weiss¹, Y. Chen¹*. ¹Toni Stabile Osteoporosis Center, Columbia University Medical Center, New York, NY, USA, ²Colorado Center for Bone Research, Lakewood, CO, USA, ³Dept. of Family and Preventive Medicine, Univ. of California, San Diego, CA, USA, ⁴Outcomes Research, Merck & Co., Inc., West Point, PA, USA.

Guidelines exist for the use of pharmacological agents to prevent bone loss and fracture. However, clinical gaps in osteoporosis treatment persist. We evaluated the utilization and correlates of osteoporosis treatment within one year of a bone mineral density (BMD) test using data from women in the National Osteoporosis Risk Assessment (NORA). Participants in NORA were postmenopausal women, >= 50 years old, had no prior diagnosis of osteoporosis, and were not on osteoporosis-specific treatment at the time of enrollment. Both participants and their physicians received education on osteoporosis and its management and treatment at enrollment. Current analysis included 32,383 women at increased risk for fracture (T-score < -2.0 or T-score < -1.5 with at least one risk factor) who reported osteoporosis treatment (alendronate, calcitonin, or raloxifene; risedronate was not yet available) status at the time of the one-year follow-up (5/1999-6/2000). New hormone therapy (HT) use, reported at follow-up, was not included in the primary analysis since it was not known if HT was specifically prescribed for osteoporosis. However, HT was included in sensitivity analyses. Correlates for osteoporosis treatment were selected based on logistic regression stepwise selection procedure. Among the 32,383 women at increased risk for fracture, 13,588 women (42%) reported being on osteoporosis treatment approximately one year after the BMD test. In multivariate analysis the following factors were associated with increased odds for treatment: a lower T-score, speaking to a doctor about risk of osteoporosis during follow-up, BMD testing during follow-up, lower body mass index, age between 60 and 79 years, and Asian ethnicity. In contrast, current smoking at baseline, current HT use at baseline, and African American ethnicity were associated with a decreased odds of treatment. Including new HT to the analysis increased the treatment rate to 62%; correlates for treatment did change significantly. In conclusion,

despite physician and patient education on osteoporosis, we found that less than one-half of NORA women who were at increased risk for fracture reported receiving treatment. Significant opportunity exists to improve care for women at high risk who should receive treatment to prevent fracture.

Disclosures: **E.S. Siris**, Merck & Co., Inc 2, 5, 8; Proctor & Gamble 5; Eli Lilly 5, 8; Amgen, Novartis, Pfizer 5.

M379

A Comparison of Self-Report and Pharmacy Data for Current Use of Anti-Osteoporotic Medications. **J. R. Curtis**¹, **A. O. Westfall**^{*2}, **J. J. Allison**^{*3}, **A. Freeman**^{*4}, **K. G. Saag**¹. ¹Division of Rheumatology, University of Alabama at Birmingham, Birmingham, AL, USA, ²Department of Biostatistics, University of Alabama Birmingham, Birmingham, AL, USA, ³Division of Preventive Medicine, University of Alabama Birmingham, Birmingham, AL, USA, ⁴Aetna Integrated Informatics, Blue Bell, PA, USA.

Purpose Pharmacy data is commonly used to assess population-based quality of care. Often used as a gold standard, pharmacy data may over or under-report **actual** drug use and has not been previously compared with self-report for osteoporosis medications (O-Rx). We examined agreement (Kappa), positive/negative predictive value (PPV/NPV), sensitivity (Se), specificity (Sp), and discordance between pharmacy data and self-reported current use of O-Rx among glucocorticoid (GC) users at risk for osteoporosis. **Methods** We mailed a questionnaire on current use of O-Rx to 6,282 chronic GC users (60+ days) with pharmacy benefits enrolled in a national managed care plan. Survey results were compared to 2.5 yrs of preceding pharmacy data. ROC curves examined Se/Sp of various pharmacy fill windows. Multivariable logistic regression identified factors associated with discordance between self-reported current bisphosphonate (BP) use and filled BP Rx. **Results** Respondents (n=2,363) were mean age 53 (SD=14) yrs, 70% women, 78% Caucasian, 55% employed, 61% college educated. Comparing pharmacy fills within 180 days of the survey to self-reported current O-Rx use (gold standard), the K (\pm 95% CI); PPV, NPV, Se, and Sp of the pharmacy data was: Alendronate (n=327): 0.80 (0.76,0.84); 93%, 96%, 74%, 99.1% Risedronate (n=142): 0.78 (0.72,0.84); 91%, 98%, 70%, 99.5% Calcitonin (n=63): 0.64 (0.53,0.75); 78%; 99%; 56%; 99.5% Raloxifene (n=31): 0.70 (0.56,0.83); 77%, 99.5%, 65%, 99.7% Area under the ROC was 0.96 (alendronate) and 0.92 (risedronate). Among self-reported current BP users, >90% filled a BP Rx at least once in the previous 2.5 yrs; the Se/Sp of pharmacy data was maximized using a \leq 180 day fill window. Factors associated with lack of pharmacy data confirmation included non-Caucasian ethnicity (OR 1.7, 95%CI 1.0-2.9) and income $<$ \$20,000 (OR 1.7,0.9-3.3). **Conclusion** Among chronic GC users, agreement between self-report and pharmacy data for O-Rx was good. In contrast to under-reporting commonly observed in validation studies for other drugs that compare self-reported **past** use with pharmacy data, under-reporting of **current** O-Rx was rare. A 6 month pharmacy fill window failed to identify >25% of self-reported current bisphosphonate users. Self-report of current O-Rx is a good surrogate if pharmacy data are unavailable; longer pharmacy fill windows are needed in studies relying on pharmacy data to assess quality of care.

Disclosures: **J.R. Curtis**, None.

M380

Impact of Depressive Symptoms on Treatment Adherence and Study Compliance in a Trial on Osteopenia and Osteoporosis in Elderly Postmenopausal Women. **H. Boerst**^{*}, **O. Bock**, **M. Kalbow**^{*}, **D. Felsenberg**. Centre for Muscle and Bone Research, Charité - Campus Benjamin Franklin, Berlin, Germany.

Long-term adherence with oral bisphosphonates is required for optimal and sustained therapeutic outcome in clinical practice. Study compliance is also a factor of general interest in clinical trials on osteoporosis. The aim of this study was to evaluate the impact of depressive symptoms in elderly postmenopausal women with osteopenia or osteoporosis on their adherence to oral bisphosphonate treatment and on study compliance. Data of 175 postmenopausal osteopenic and osteoporotic women, mean age (SD) 73.6 (3.8) years, participating in an investigator initiated trial with alendronate 70 mg weekly and calcium 500 mg daily in postmenopausal osteopenia and osteoporosis were analysed. The trial was conducted after institutional review board approval and in accordance with the Declaration of Helsinki. Depressive symptoms were evaluated at baseline by the Beck Depression Inventory (BDI), a validated and most widely used self-rating scale for measuring depression. Treatment adherence ($>$ 80% of alendronate taken) and study compliance were assessed one year after baseline. The overall drop-out rate was 13.1 %. BDI mean value (SD) was 8.4 (5.2) in adherent and compliant patients and 12.6 (7.1) in drop-out patients. The drop-out rate in patients with pathological BDI values (\geq 18, equivalent to 2 SD above normal mean) was 43.7% and fourfold and therefore significantly higher than in patients with BDI $<$ 18 ($p < 0.001$). There was no significant difference in drop-out rates between patients with normal BDI ($<$ 12) and borderline BDI (12-17, equivalent to 1 - 2 SD above normal mean): 9.3% and 13.3% respectively. Depressive symptoms have a major impact on treatment adherence and study compliance in osteopenic and osteoporotic elderly women. Our data suggest the usefulness of a depression assessment, e.g. using BDI self-rating scale, before initiating antiresorptive treatment in osteoporotic elderly women, especially before recruiting these patients for clinical trials, in order to enhance treatment adherence and to improve study compliance. Furthermore, patients with depression should be identified to ensure their adequate treatment and to improve their overall quality of life.

Disclosures: **O. Bock**, None.

M381

Effects of Animal Rights Activism and the Women's Health Initiative Findings on the Well-Being of Mares Used in Premarin Production. **E. J. B. Murray**^{*}. GRECC/Medicine, VAGLAHS/University of California, Los Angeles, Sepulveda/Los Angeles, CA, USA.

The purpose of this study was to determine the effects of animal rights activism and the reduced use of **Premarin** (pregnant mares' urine) on the welfare of horses used in the PMU (pregnant mares' urine) industry. On-line database and web searches were conducted to assess equine management practices and estimate the effects of truncating the high-dose estrogen and progestin arm of the Women's Health Initiative (WHI) trial and falling Premarin sales on the number of horses in the industry. At the height of Premarin production in 2002, there were approximately 437 PMU ranches in the prairie provinces of Canada (Alberta, Manitoba, and Saskatchewan) and N. Dakota with at least 36,000 mares in production. The gross revenue to ranchers was about \$2,000 to \$2,500/mare. NAERIC (the North American Equine Ranching Information Council) estimates that there are now 122 PMU ranches in Canada and N. Dakota, with $<$ 12,000 broodmares in production. In the early decades of PMU production, animal rights activists reported serious deficiencies, including unclean housing; improperly fitted urine collection devices; inadequate nutrition, veterinary care, and exercise; and severe water rationing. Government, animal welfare organization, and industry investigations from the 1960s to the 1990s led to the development of the "Recommended Code of Practice for the Care and Handling of Horses in PMU Operations," which established voluntary, self-regulated guidelines for shelter, access to water and food, companionship, diagnosis and treatment of abnormal behavior, injury, and disease, and emergency planning. No serious incidents involving PMU ranches have been reported to SPCAs in Canada for about 5 years. While conditions improved for mares, over-production of foals remained a serious problem. An estimated 15,000 PMU foals were sold to feedlots and slaughterhouses each year for as little as \$350/horse. NAERIC was created in 1995 to assist ranchers in breeding and marketing high-quality foals that could be sold as performance/companion stock. By 2002, 2/3 of the improved foals were sold for use in equine activities, rather than for food consumption. The severe decline in the Premarin market created a crisis, with horses selling for as little as \$50-\$100 at auction. In 2004, the industry agreed to help pay for transportation, Coggins testing, and health certification for displaced PMU mares/foals adopted in N. America. Horses are still available, with registered pregnant mares selling for about \$650-\$1,700 through on-line adoption agencies. Available strains include warm-bloods, quarter/paint horses, Appaloosas, any of several draft breeds, and mixes of these breeds.

Disclosures: **E.J.B. Murray**, None.

M382

Implementation of a Community-Based Post-Fracture Care Model: 'Behind the Break'. **S. Jaglal**¹, **E. Bogoch**^{*2}, **D. Brooks**^{*1}, **J. Carroll**^{*3}, **G. Hawker**⁴, **L. Jaakkimainen**^{*5}, **H. Kreder**^{*6}, **M. Zwarenstein**^{*7}. ¹Rehabilitation Science, University of Toronto, Toronto, ON, Canada, ²Surgery, St. Michael's Hospital, Toronto, ON, Canada, ³Family Medicine, Mount Sinai Hospital, Toronto, ON, Canada, ⁴Osteoporosis Research Program, Sunnybrook and Women's College Health Sciences Center, Toronto, ON, Canada, ⁵Family Practice, Sunnybrook and Women's College Health Sciences Center, Toronto, ON, Canada, ⁶Surgery, Sunnybrook and Women's College Health Sciences Center, Toronto, ON, Canada, ⁷Institute for Clinical Evaluative Sciences, Toronto, ON, Canada.

The purpose of this project was to implement a local resource-based post-fracture care model to facilitate continuity of care from the hospital where the fracture is first treated, to the primary care setting for osteoporosis investigation and management. This is the first phase of a research project to evaluate a model in four communities in Ontario, Canada. This project used participatory action research methodology. Communities with a shortage of family physicians, a sufficient volume of fracture and access to a bone density machine were invited to submit a letter of interest. Funding was provided to each hospital to hire a local site coordinator to assist with implementation. Dissemination strategies targeted health care professionals in the hospital and community and fracture patients. To facilitate health care professional education a toolkit was developed. To raise awareness among fracture patients, tear off pads, bookmarks and booklets were disseminated within the hospital and community. Strategies to increase awareness included presentations, one-on-one meetings with hospital staff and a quarterly project newsletter. Each site conducted 18 to 21 meetings and 3 to 9 presentations with hospital staff, management and community health care professionals and organizations. In addition, newspaper, radio and television media promoted key messages. Approximately 515 toolkits were disseminated through seven workshops with rehabilitation therapists and one-on-one educational outreach with family physicians (n=95) and other community-based health care professionals. Seventy-two percent of family physicians received educational outreach visits between February and April, 2005. These visits ranged in length from 5 to 30 minutes. Preliminary findings indicate that the materials were well received and that the program is a worthwhile initiative. For successful implementation, it is important that the hospital and surrounding community take ownership of the osteoporosis initiative. This will ensure that the project reflects local resources, meets the needs of the community and will facilitate buy-in of local health care professionals.

Disclosures: **S. Jaglal**, None.

M383

Reduction of Pain and Fracture Incidence after Kyphoplasty of Chronically Painful Vertebral Fractures: 1-Year Outcomes of a Prospective Controlled Trial of Patients with Primary Osteoporosis. I. Grafe^{*1}, K. Da Fonseca^{*2}, J. Hillmeier^{*2}, P. Meeder^{*2}, M. Libicher^{*3}, G. Noeldge^{*3}, P. Nawroth^{*1}, C. Kasperk¹. ¹Internal Medicine I, Endocrinology, University of Heidelberg, Heidelberg, Germany, ²Orthopedic Surgery, University of Heidelberg, Heidelberg, Germany, ³Radiology, University of Heidelberg, Heidelberg, Germany.

Kyphoplasty has been shown to reduced pain and improve mobility in patients with chronically painful osteoporotic vertebral fractures. Since improvement of spinal biomechanics by restoration of vertebral morphology may affect fracture incidence, long term clinical benefit and thereby cost-effectiveness, we assessed occurrence of new vertebral fractures and clinical parameters one year after kyphoplasty compared to a conservatively treated control group in a prospective study. 60 patients with osteoporotic vertebral fractures due to primary osteoporosis were included: 40 patients were treated with kyphoplasty, 20 served as controls. All patients received standard medical treatment. Morphological characteristics, new vertebral fractures, pain (visual analog scale), physical function (EVOS score) (range 0-100 each) and back-pain-related doctor visits were assessed 12 months after kyphoplasty. There were significantly less patients with new vertebral fractures of the thoracic and lumbar spine after 12-months in the kyphoplasty group (P=0.0084). Pain scores improved from 26.2 to 44.4 in the kyphoplasty group and changed from 33.6 to 34.3 in the control group (P=0.008). Kyphoplasty treated patients required a mean of 5.3 compared to 11.6 back-pain-related doctor visits/patient in the control group during 12 months follow-up (p=0.006). Kyphoplasty as an addition to medical treatment and when performed in appropriately selected patients by an interdisciplinary team persistently improves pain and reduces occurrence of new vertebral fractures and health care utilization for at least 12 months in individuals with primary osteoporosis.

Disclosures: **I. Grafe**, None.

M384

Lasofixifene Phase 2 and Phase 3 Clinical Trial Design and Strategy. A. Lee¹, D. Radecki¹, K. Wolter¹, J. Proulx¹, M. Buonanno^{*1}, V. Dillon^{*1}, T. Houck^{*1}, M. Orri^{*2}, W. Day³. ¹Pfizer Global Research and Development, New London, CT, USA, ²Pfizer Global Research and Development, Sandwich, United Kingdom, ³Pfizer Global Research and Development, La Jolla, CA, USA.

Lasofixifene, a next-generation selective estrogen receptor modulator (SERM), demonstrated estrogen agonist effects on bone and lipids, and estrogen antagonist effects on the breast and uterus in pre-clinical models.* The Phase 2 and Phase 3 clinical development program for lasofixifene (Phase 2-3) is described in this overview. Early stage safety and efficacy of lasofixifene was evaluated in 3 Phase 2 multiple dose studies conducted in young healthy postmenopausal women. Lasofixifene was studied over a 600-fold dose range of 0.17 mg/d to 10 mg/d using 9 doses of lasofixifene and 2 active comparators (Prempro and Evista). The studies ranged from 1 to 2 years. Lasofixifene clinical effects were consistent with the preclinical models and demonstrated consistent increases in lumbar spine BMD (2%-4%) and reductions in LDL-C (15%-20%). Dose modeling from Phase 2 allowed selection of doses for Phase 3 development. The Phase 3 program includes studies conducted in postmenopausal women with either osteopenia or osteoporosis. Two identical, double-blind, placebo-controlled 2-year studies (OPAL) to support an application for the prevention of postmenopausal osteoporosis have been completed. These studies were conducted using lasofixifene 0.5 mg/d, 0.25 mg/d (anticipated lowest fully-effective dose) and 0.025 mg/d (ED₅₀, 50% of effective dose). An ongoing fracture trial (PEARL) is being conducted with 2 doses of lasofixifene (0.25 mg/d and 0.5 mg/d) and a comparative trial (CORAL) is being conducted with 0.25 mg/d compared to Evista. The basic study design inclusion and exclusion criteria and primary and secondary endpoints will be outlined.

*Ke, Hua Zhu, Paralkar, Vishwas M, Grasser, William A, et al. Effects of CP-336,156, a new nonsteroidal estrogen agonist/antagonist, on bone, serum cholesterol, uterus, and body composition in rat models. *Endocrinology*: 1998; 139:2068-76.

Disclosures: **A. Lee**, Pfizer 3.

M385

Lasofixifene Phase 2 Dose Response Analysis in Postmenopausal Women. W. Day¹, J. Martel^{*2}, A. Lee². ¹Pfizer Global Research and Development, San Diego, CA, USA, ²Pfizer Global Research and Development, Groton, CT, USA.

Lasofixifene is a next-generation selective estrogen receptor modulator (SERM) that prevents bone loss and affects the estrogen receptor differently in various tissues. During dose selection for the Phase 3 program, efficacy results from Phase 2 trials were analyzed to identify the lowest dose providing a maximal response for increasing bone mineral density (BMD) or lowering lipids (LDL-C) in postmenopausal women. Results of the dose modeling were also correlated with the safety data to provide assurances of a positive benefit:risk profile. Lasofixifene dose selection utilized data from three active and/or placebo controlled Phase 2 trials. The trials were 1 to 2 years and spanned a 600-fold dose range (9 dose levels; 0.017 mg/d to 10 mg/d). An E_{MAX} model was fit to the data for lumbar spine BMD (LS-BMD), total hip BMD (TH-BMD), and LDL-C data to generate dose-response curves. Maximal placebo-adjusted treatment effects were obtained and were used

to derive ED₉₀ (90% maximum effect dose), and ED₅₀ (50% of the maximal effect dose). Dose selection was based on, *inter alia*, the estimate of ED₅₀ for various efficacy endpoints. A *Responders Analysis* was also utilized. It estimated lasofixifene treatment effect on the probability for a positive outcome. Subjects were classified as strong, moderate or non-responders and were differentiated on the basis of LS-BMD, TH-BMD and LDL-C responses. The E_{MAX} model estimated the maximal placebo-adjusted treatment effects for the respective endpoints: LS-BMD, TH-BMD, and LDL-C, to be 1.6%, 1.4% and -17.3%. The theoretical doses predicted to achieve an ED₉₀ were 0.19, 0.38, 0.18 mg/day, respectively. Although the E_{MAX} data suggested that the dose response in LS might be more sensitive than LDL-C and TH responses, the *Responders Analysis* suggested that maximal efficacy occurred with a dose of 0.25 mg/d and was associated with the occurrence of both LDL and BMD responses in a subject. *Responders Analysis* confirmed the ED₅₀ dose of 0.025 mg/d as a low effect dose. Safety evaluations were also considered in the modeling; however, there were too few events to establish a dose response relationship for selected class related adverse events (DVTs, uterine or breast cancers and uterine prolapse). Moreover, there was no apparent evidence of a dose-related toleration effect on hot flushes or leg cramps over the dose range. The overall results of the dose selection analyses suggested that the lowest dose necessary to achieve a fully efficacious response on total hip BMD, lumbar spine BMD and LDL-C is 0.25 mg/d.

Disclosures: **W. Day**, Pfizer 3.

M386

Multi-Disciplinary Group Education Increases Persistence with Pharmacological Treatment in Osteoporosis - Interim Analysis from a Randomised Trial. D. Nielsen^{*1}, J. Ryg^{*1}, N. Nissen^{*1}, L. Stilgren^{*1}, W. Nielsen^{*2}, B. Dahl-Andersen^{*2}, B. Knold^{*1}, A. R. Madsen^{*1}, K. Brixen¹.

¹Endocrinology, Odense University Hospital, Odense, Denmark,

²Physiotherapy, Odense University Hospital, Odense, Denmark.

Persistence with pharmacological therapy in osteoporosis is often low in clinical settings. Group education increases patients' knowledge, however, the effect of such programs on adherence with therapy remains to be demonstrated. We hypothesized that persistence with pharmacological treatment may be increased by a multi-disciplinary systematic group education program in patients with osteoporosis. This preliminary analysis comprised 280 patients (250 women and 30 men) aged 64 [47 to 81] years, recently diagnosed with osteoporosis. Participants were randomized to either the "school" (n=146) or "control" group (n=134). In the school group, patients attended classes for four days during 4 weeks. Each class had 8-12 participants. Teaching performed by nurses, physiotherapists, dieticians, and doctors covered "facts on osteoporosis", "fractures and pain", "diet", "preventive measures", "balance and exercise", and "medical treatment". Participants in the school group also received programmed telephone calls four times during 4 months and an invitation for a follow-up meeting after 12 months. The control group received standard care. DEXA was performed in all participants after 12 and 24 months. Persistence with pharmacological treatment was assessed using a self administered questionnaire at study entry and after 3, 12, and 24 months. Eighty-eight percent of the patients had started bisphosphonates, 10% raloxifen, and 1% teriparatide. Five and 7 patients were excluded from the control and school groups, respectively, since no specific pharmacological therapy was initiated. At the time of the interim analysis 229, 166, and 61 patients had completed at least 3, 12, or 24-months of follow-up, respectively. During the study, 8 patients (7%) in the control group and 1 patient (1%) in the school group stopped treatment prematurely and persistence with therapy was significantly higher (p<0.02) in the school group compared with controls (Kaplan-Meier). The persistence in both groups, however, was much higher (93-99 % at 24 months) compared with previous studies in clinical cohorts. This suggests that the participants in our study were more motivated than patients in an ordinary clinical setting. This, however, only underscores the significance of our finding in the intervention group. We conclude that a multi-disciplinary group education program increases the persistence with pharmacological therapy significantly in patients with osteoporosis.

Disclosures: **D. Nielsen**, Eli Lilly 2; Merck, Sharpe and Dohme 2; Aventis 2; Servier 2.

M387

Effect of an Information-Based Intervention on the Management of Minimal and Moderate Trauma Fractures: A Randomized Study. D. Bliuc^{*}, J. A. Eisman, J. R. Center. Bone and Mineral Program, Garvan Institute of Medical Research, St Vincent's Hospital, University of New South Wales, Sydney, Australia.

Despite the high risk for subsequent fracture following an initial osteoporotic fracture, the majority of subjects with fragility fractures receive no treatment for osteoporosis. This study aimed to firstly determine whether an information-based intervention could change post-fracture management of osteoporosis, and secondly define participant- and doctor-related barriers to osteoporosis management. Consecutive fracture patients (n=198) from the outpatient fracture clinic at St Vincent's Hospital, Sydney were interviewed over a 15 month period (February 2002-July 2003). Fracture risk factors, prior investigation and treatment for osteoporosis were collected at baseline. Participants were initially contacted after 3 months. Those not investigated or treated were randomized to either a personalized letter or the same letter plus a free BMD offer. Final follow-up was obtained after another 6 months. Less than 20% of participants had a primary care physician follow-up three months after the fracture, leaving 159 who were randomized to a personalized letter (n=79) and a personalized letter plus free BMD (n=80). Significantly more people were investigated for osteoporosis in the letter plus BMD offer group (38% vs. 7%; p=0.001), but treatment rates were very low in both groups (< 6%). Of those tested, 66% had low bone density, but only 24% were recommended therapy. Among the few individuals 36

ASBMR 27th Annual Meeting

(23%) who contacted their primary care physician, only 9 (25%) were recommended treatment. Independent predictors for management outcome were age over 50 for a primary care physician follow-up, female gender for having a BMD test, and having had a BMD test for treatment. Belief that their fracture was osteoporotic, although uncommon (12%) was the only independent predictor of having a BMD test, of primary care physician follow-up and of receiving treatment. In this study, an information-based intervention led to a modest increase in the proportion of people investigated for osteoporosis, however there was no significant effect on treatment rates. However, belief that their fracture was related to osteoporosis was the most consistent factor related to better management. Being female and over the age of 50 were independent predictors for follow-up and subsequent treatment. This randomized study demonstrates major patient and doctor-related barriers to effective osteoporosis management.

Disclosures: **D. Bliuc**, None.

M388

Baseline Clinical Characteristics of Postmenopausal Women with Osteoporosis and an Inadequate Clinical Response to Osteoporosis Drugs in the Observational Study of Severe Osteoporosis (OSSO). D. Sykes^{*1}, C. Cooper², S. Adami³, P. Fardellone^{*4}, F. Jakob^{*5}, J. Melo-Gomes^{*6}, E. Martin-Mola^{*7}, T. Nicholson^{*1}, N. Thalassinou^{*8}, D. Torgerson^{*9}, F. Marin¹. ¹Eli Lilly, Windlesham, United Kingdom, ²MRC Environmental Epidemiology Unit, Southampton General Hospital, Southampton, United Kingdom, ³University of Verona, Verona, Italy, ⁴Hospital Nord, Amiens, France, ⁵Julius-Maximilians Universität, Würzburg, Germany, ⁶Servimed, Lisbon, Portugal, ⁷Hospital La Paz, Madrid, Spain, ⁸Evangelismos General Hospital, Athens, Greece, ⁹University of York, York, United Kingdom.

OSSO is a 12-month, prospective, observational study conducted in six European countries. Participants are postmenopausal women with osteoporosis and an inadequate clinical response to osteoporosis drugs defined as: (i) the presence of a new clinical fragility fracture despite prescription of any approved osteoporosis drug for at least 12 months before the fracture (index fracture cohort), and/or (ii) discontinuation of any approved osteoporosis drug due to compliance problems and/or side effects (compliance/side effect cohort). Patients who satisfied both criteria were analysed according to the first event. Data collected at baseline included patient demographics, medical and osteoporosis history, risk factors for osteoporosis and falls, medication use, disease status, HRQoL and medical resource utilisation. At baseline, the distribution by country of the 2314 women (mean (SD) age 70.2 (9.0) yrs, mean (SD) BMI 25.8 (4.4) kg/m²) was: Germany (36%), Spain (18%), France (18%), UK (15%), Greece (11%) and Portugal (2%). Overall, (1309) 57% of patients were in the index fracture cohort and (1005) 43% in the compliance/side effect cohort. A significantly higher proportion of the index fracture cohort had a history of previous fractures (excluding index fracture) (73.8%) than the compliance/side effect cohort (59.9%, P<0.001). Mean BMD T-scores at the LS and FN were lower in the index fracture cohort than in the compliance/side effect cohort (-3.2 vs -3.1 for LS, P=0.005; -2.7 vs -2.5 for FN, P=0.039). Of the ARs discontinued alendronate was cited most commonly (37.2%), followed by risendronate (18.3%). Gastrointestinal problems were the main reason for discontinuing alendronate (62.7%) and risendronate (62.2%). Non-compliance was the most commonly cited reason for discontinuation for calcitonin (27.4%) and HRT (24.1%). 27% of participants had concurrent diseases, most commonly RA (10.4%) and COPD (6.7%). In conclusion, the baseline data indicate these patients have numerous risk factors for subsequent fracture, especially those in the index fracture cohort.

Disclosures: **F. Marin**, Employee 3.

M389

Generalized and Local Bone Loss in Patients with Rheumatoid Arthritis Treated with Infliximab. M. Vis¹, E. Haavardsholm^{*2}, G. Haugeberg^{*2}, A. Voskuyl^{*1}, T. Uhlig^{*2}, B. Dijkman¹, A. Woolf³, T. Kvien^{*2}, W. Lems¹. ¹VU university medical center, Amsterdam, The Netherlands, ²Diakonhjemmet Hospital, Oslo, Norway, ³Royal Cornwall Hospital, Truro, United Kingdom.

Object The aim of the present study was to assess in a large cohort of RA patients the effect of infliximab on generalized and local bone loss. **Methods** Patients with RA, 92 from Amsterdam and 10 from Oslo, who were treated with infliximab during one year were included. All patients had active RA at the start of treatment. Disease activity was measured before every infusion by the disease activity score of 28 joints (DAS-28). The BMD of the spine (n=102) and hip (n=89) measured by DEXA and hand (n=53) measured by DXR was determined before the start of treatment and after one year of treatment with infliximab. **Results** The patient group consisted of middle aged (mean age 53 years), mainly female, patients (83%). The median (range) disease duration was 8 (1 to 49) years, twenty-five (25%) patients used prednisone (median dose 7.5 mg). According to the EULAR response criteria 40 patients had a good response, 43 patients a reasonable response and 19 patient had a non response at 1 year. During treatment with infliximab the BMD of the vertebral spine and hip did not change. In contrast, BMD of the hand decreased significantly by 0.004 g/cm³ (-0.8 percent) during the year (p < 0.05). The group of non and reasonable responders were taken together (n=62) and compared to the good responders (n=40). In the good responder group BMD at all sites showed a more favourable change than in the group of non and reasonable responders. This difference was

statistically significant different for the hip. (Table 1) **Discussion** The main conclusions of the present study are that 1-year treatment with infliximab arrests generalized bone loss in RA patients, but does not stop the localized bone loss at the hands.

Table 1			
	Non / reasonable response	Good response	P
BMD vertebral-spine (%-change))	-0.574 (5.02)	0.74 (5.3)	NS
BMD total hip (%-change)	-0.68 (3.8)	0.77 (3.4)	P < 0.05
BMD hand (%-change)	-1.2 (2.6)	-0.63 (2.3)	NS

Disclosures: **M. Vis**, None.

M390

Orally Administered ANABU™ (GlcNBu) Protects Joint Surfaces in Streptococcal Cell Wall Antigen (SCW)-Induced Arthritis in Lewis Rats. T. P. Anastassiades¹, M. Grynepas², J. Carran^{*1}, X. Wang^{*2}, A. Cherian^{*2}.

¹Medicine, Rheumatology, Queen's University, Kingston, ON, Canada, ²Mount Sinai Hospital, Toronto, ON, Canada.

In previous work we had shown that GlcNBu (N-butyryl glucosamine) decreases the inflammation of SCW arthritis and increases BMD in this model. This investigation explores the effects of GlcNBu on bone loss. Chronic SCW arthritis was induced in female rats by a single IP injection. The Groups studied were: (a) no arthritis, no treatment; (b) arthritis, no treatment; (c) arthritis, GlcNBu 20mg/kg/day; (d) arthritis, GlcNBu 200mg/kg/day. The removed left tibiae were scanned using micro computed tomography to qualitatively and quantitatively measure the GlcNBu dosage effects on bone architecture. Isosurfaces generated from the scans show progressively less bone erosion with increasing dosages of GlcNBu.(Figure). Trabecular bone volume, number and thickness, and subchondral plate thickness increased with GlcNBu dosage, so that Group (d) was similar to Group (a). Significant increases occurred predominantly in the lateral epiphysis and the metaphysis of the high dose group. The structure model index values decreased significantly (p=0.030) in the metaphysis from the untreated SCW-induced group to the high dose group, indicating a less rod-like trabecular structure. Strut analysis showed a significant increase (p =0.034) in the length of node to node struts from the untreated SCW-induced group to the high dose group on the medial side of the proximal epiphysis. The Results indicate a dose-dependent increase in bone connectivity. The metaphyseal bone structure changes suggest that GlcNBu functions systemically. Comparison of the isosurfaces and the architectural parameters studied in this investigation demonstrate that GlcNBu effectively protects bone from further erosion in this model of chronic inflammatory arthritis.

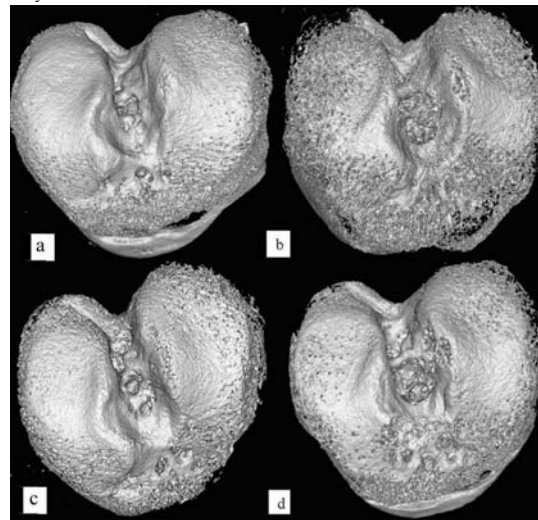


Figure: Isosurfaces of proximal rat tibia (a) No arthritis, no treatment; (b) arthritis, no treatment; (c) arthritis + low dose GlcNBu; (d) arthritis + high dose GlcNBu.

Disclosures: **T.P. Anastassiades**, Anacoti Ltd: US Patent issued for ANABU and arthritis treatment; submitted for utility of ANABU for Osteoporosis 4.

M391

Barriers and Facilitators to Osteoporosis Medication Adherence: Patient Perceptions and Strategies. A. Papaioannou¹, A. Pathak^{*1}, K. Nair^{*2}, S. Burns^{*2}, E. Lau^{*2}, L. Dolovich^{*2}, A. Sawka¹, C. Kennedy¹, J. D. Adachi¹.

¹McMaster University, Hamilton, ON, Canada, ²Centre for Evaluation of Medicines, Hamilton, ON, Canada.

Medication non-adherence is a common problem that may lead to treatment failure and undesired clinical outcomes. Adherence with osteoporosis medication ranges from 8% to 70%. Despite the importance of medication adherence for fracture prevention, few studies have examined the implications of this from the patients' perspective. The purpose of this study was to explore barriers and facilitators of osteoporosis medication adherence and to explore adherence strategies from the patient's perspective. Participants were community dwelling, post-menopausal women (mean age = 71 years, SD 8.2) taking medication for osteoporosis treatment or prevention. Twenty-nine participants were recruited from family

medicine/specialist practices and community pharmacies. The mean length of time on osteoporosis medication was 2.9 years (SD 2.7). 38% had a previous fragility fracture, and 66% had drug plan coverage. Five focus groups of approximately 6 patients were conducted using a semi-structured interview guide. Participants were asked 9 open-ended questions regarding the importance of adherence, reasons for non-adherence, and their perceptions of different adherence strategies. Group sessions were digitally recorded, transcribed verbatim, and independently coded by two team members to identify common themes. An operational codebook was developed based on current literature and the emerging themes. QSR NVIVO software was used to organize the data. Common barriers included: denial about the condition; not realizing the seriousness; belief that lifestyle modifications are enough; fear/experience of side effects; feeling over-medicated; and feeling that healthcare providers did not provide enough medication-related information or monitoring of progress. Facilitators included: being informed and taking responsibility; perceiving benefits outweigh the risks; belief in the value of delaying the onset of osteoporosis; desire to avoid fractures, shrinking, stooping; planning ahead/daily routines; trust in the doctor's expertise; tracking BMD improvements; and receiving credible/accessible information and follow-up from healthcare providers. Key aspects relevant to osteoporosis medications were the challenges of special administration requirements (i.e. timing with food and other meds, not lying down afterwards) and a preference for once weekly vs. once daily regimens. In conclusion, many adherence factors were modifiable and healthcare providers should consider ongoing medication-related discussions with patients regarding concerns and strategies.

Disclosures: **A. Papaioannou**, None.

M392

Development of a Bone and Cartilage Stimulatory Peptide (BCSP™) with Bone Targeting Properties. **D. R. Sindrey¹, P. T. Biessels^{*1}, R. R. Simon^{*1}, M. R. Doschak^{*2}, H. Uludag².** ¹Millenium Biologix Corp., Mississauga, ON, Canada, ²Department of Chemical and Materials Engineering, University of Alberta, Edmonton, AB, Canada.

We have previously reported the discovery of a novel osteogenic peptide that in animal models has shown promise for the treatment of osteoporosis and as a bone stimulating agent for fracture healing. One of the difficulties in developing small molecule peptides for therapeutic use resides in their inherent short half-lives. An ideal agent would be one that could target bone, or in the case of fracture healing be retained within synthetic bone graft substitute materials. To address this issue we synthesized a number of peptide analogs of BCSP-1 with various C-terminal modifications designed to impart affinity to Skelite™, a resorbable BGS. 5 BCSP derivatives were synthesized and screened in vitro for their affinity to Skelite. Briefly, 5mm Skelite granules were incubated in a 1 mM solution of peptide in 70% methanol for 4 hrs, the amount of peptide bound to the scaffold was then assessed by measuring the final concentration in solution by HPLC analysis. The results tabulated below show that the BCSP-21 had the highest affinity for Skelite. In comparison to BCSP-1 where 95% of the protein remained in solution, only 5% of BCSP-21 remained in solution after the 4 hr incubation period.

Peptide	C-terminal modification	% Bound to Skelite
BCSP-1	-	4.5%
BCSP-21	-pSer-pSer-pSer-Glu-Glu	95.0%
BCSP-21b	-pSer	6.8%
BCSP-21c	-Glu-Glu-Glu-Glu	17.6%
BCSP-21d	-Gla-Gly-Gla-Glu	6.4%
BCSP-21e	-Gla-Glu	7.5%

pSer (phosphoserine); Gla (gamma-carboxyglutamic acid)

The binding affinity of BCSP-1 for Skelite was further explored through radiokinetic studies in vivo. 4 x 4mm porous Skelite scaffolds were coated with I-125 labeled BCSP-1 (1 mg) or BCSP-21 (1.2 mg) and implanted subcutaneously into the abdominal region of S.D rats. The amount of radioactivity was then assessed on days 1,2,4,7, and 10. As predicted in vitro, BCSP-1 showed almost no binding activity to Skelite with less than 1% of the original radioactivity remaining after 24hrs of implantation. Subsequent time-points show a logarithmic decrease in radioactivity over time, with approximately 0.1% of the peptide remaining at day 10. BCSP-21 however, showed a significant affinity for the implant retaining up to 15% of the starting radioactivity at day one and a gradual loss thereafter with up to 3% bound at day 10. The results of these studies indicate that pSer modification of BCSP-1 is an effective means to localize biologically active small peptides to hydroxyapatite-like surfaces and may represent a novel agent for the treatment of osteoporosis and/or fracture healing.

Disclosures: **D.R. Sindrey**, Millenium Biologix Corp 1, 3.

M393

Short Term Effects of Estrogen, Tamoxifen and Raloxifene on Bone Density and Bone Turnover. **M. Baz Hecht, J. W. Nieves, V. Shen, R. Lindsay, F. Cosman.** Clinical Research/Regional Bone Centers, Helen Hayes Hospital, West Haverstraw, NY, USA.

Estrogen, tamoxifen and raloxifene are all known to have beneficial effects on the skeleton, however the relative effects of these agents have not been compared in a head to head trial. This randomized placebo controlled study compared the effects of these three treatments vs. placebo on bone mineral density (BMD) and bone turnover in 94 postmenopausal women, mean age 55.7 years, mean 5.7 years from menopause. After baseline measurements of bone mass, and blood and urine sampling, women were randomly assigned to receive oral estrogen (conjugated equine estrogen 0.625 mg; n=23), tamoxifen 20 mg (n=24), raloxifene 60 mg (n=24) or placebo (n=23) daily for 6 months. Markers of calcium homeostasis [serum ionized calcium, phosphorus, 1,25-dihydroxyvitamin D (1,25(OH)₂D) and intact PTH], bone formation [serum osteocalcin

(OC), propeptide of Type I procollagen (P1CP) and bone specific alkaline phosphatase (BSAP)], bone resorption [crosslinked N-telopeptide of type I collagen (NTX)] and lumbar spine and hip BMD were measured at baseline and at 6 months of treatment. A subset of 45 patients also had body composition measurements. After 6 months, serum ionized calcium decreased with all 3 active therapies (greatest decline for estrogen, 1.7%; raloxifene 1.2%, p<0.02, 0.3% tamoxifen, NS). Serum intact PTH increased with all 3 active treatments (17%, 29% and 39% for estrogen, raloxifene and tamoxifen respectively, all p<0.01). Serum phosphorus decreased with estrogen and tamoxifen (9%, p<0.09 and 14%, p<0.007, respectively). 1,25(OH)₂D increased with estrogen (24%, p<0.07), but not with the other agents. Bone turnover markers decreased with all three treatments, however only the effects of estrogen and tamoxifen were significant compared to baseline values and to placebo. OC decreased 15% (p<0.004) and 27% (p<0.0001), BSAP decreased 21% (p<0.0001) and 25% (p<0.0001) and NTX decreased 10% (p<0.0002) and 17% (p<0.0003) with estrogen and tamoxifen respectively. P1CP decreased 17% with estrogen (p<0.001). Lumbar spine BMD and total body mineral content increased significantly only with estrogen at this time point (2.1%, p<0.02 and 1.3%, p<0.03, respectively). Total hip BMD increased with tamoxifen 1.2% (p<0.03) and with estrogen 0.7% (p=0.11). Total body fat was not affected by any of these agents. Six months treatment of non-osteoporotic women with estrogen and tamoxifen benefits the skeleton, producing decreases in bone turnover and increases in BMD, while raloxifene is a weaker antiresorptive agent, with effects of lower magnitude over this short time period.

Disclosures: **M. Baz Hecht**, None.

M394

Skeletal Effects of Bazedoxifene Acetate (BZA) in Ovariectomized Mice and Comparison of BZA's Effects with Raloxifene (RAL) and Lasofoxifene (LAS) in Intact Mice. **Y. P. Kharode, P. D. Green*, C. L. Milligan*, P. V. N. Bodine, F. J. Bex, B. S. Komm.** WHRI/Bone Metabolism, Wyeth Reserach, Collegeville, PA, USA.

Bazedoxifene acetate (BZA) is a novel, selective estrogen receptor modulator (SERM) that prevents osteopenia and reduces serum cholesterol without uterotrophic effects. We conducted studies to evaluate the effects of oral administration of BZA in ovariectomized (ovx) and intact female C57BL6 mice. Ten week-old ovx mice were administered BZA daily (0.1 mg/kg, 0.3 mg/kg, 1.0 mg/kg, 3.0 mg/kg, 10 mg/kg) or vehicle for sixty days. A group of sham-operated mice served as controls. OvX + vehicle resulted in significant bone loss in comparison to sham (392±8 mg/cm³ vs.479±8 mg/cm³ and 93±5 mg/cm³ vs.149±5 mg/cm³ for total and trabecular densities, respectively). Post-treatment total (466 to 502 mg/cm³) and trabecular vBMD (121 to 136 mg/cm³) measured by pQCT significantly increased in all treatment groups compared to the ovx +vehicle group. Uterine weight in ovx +vehicle group (16±1mg) was significantly lower than that for sham group (65±5 mg, p<0.01), but with the exception of the BZA, 0.1mg/kg group (25±1mg) was not different from any of the BZA groups (ranged 15 to 19 mg). In a similar study, 0.3 mg/kg/day, po ethinyl estradiol (EE) significantly increased total and trabecular densities and uterine weight compared to the ovx +vehicle group. To evaluate and compare the effects of BZA with raloxifene (RAL) and lasofoxifene (LAS) in an estrogen-replete setting, 10-week old ovary intact mice were treated with 3 mg/kg/day, po for 30 days. EE (0.3 mg/kg/day, po) served as a control. Post-treatment femoral evaluation revealed that, compared to the vehicle group, all treatment groups had significant accrual of trabecular bone as judged by pQCT and µCT analysis. BZA, RAL and LAS, significantly decreased while EE significantly increased the serum cholesterol. Uterine weights were lower in the BZA group (BZA, 46±1 mg, p<0.05 vs vehicle, 68±5 mg; RAL, 64±3 mg; LAS, 53±2 mg) and were significantly higher in EE group (198± 12 mg) compared to the vehicle group. Our results indicate that in C57BL mice, BZA prevented ovx-induced osteopenia without causing uterine stimulation. In ovary-intact mice, BZA, RAL and LAS produced accrual of bone, and significantly reduced serum cholesterol, but only BZA exhibited anti-estrogenic effects on the uterus. The mechanisms that are responsible for the ability of a SERM to increase bone mass in intact mice may be osteogenic but further work is needed to determine this. In conclusion, BZA is a novel SERM with tissue selective effects that may offer selective skeletal protection without uterine stimulation under quite different physiologic conditions.

Disclosures: **Y.P. Kharode**, Wyeth 3.

M395

Differential Effects of 5α-Dihydrotestosterone (DHT) and a Novel Selective Androgen Receptor Modulator (SARM) on Prostate and Bone in Intact and Orchidectomized (ORX) Male Rats. **H. Z. Ke, D. T. Crawford*, H. Qi*, H. A. Simmons, M. Li, T. A. Brown, D. D. Thompson, X. N. Wang*, E. D. Salter*, J. P. O'Malley*, C. T. Salatto*, R. J. Hill*, B. A. Lefker*, K. O. Cameron*.** Pfizer Global R & D, Groton, CT, USA.

SARMs have been hypothesized to have beneficial effects on bone without causing prostate hypertrophy in men. CE590 is a newly identified SARM that selectively binds to the androgen receptor (AR) with an IC50 of 16 nM, and acts as a receptor agonist in AR-transfected C2C12 cells with an EC50 of 0.4 nM. The purpose of this study was to compare the different effects of CE590 and DHT on prostate and bone in intact and ORX rats. Male SD rats at 11 months of age were sham or ORX. Both sham and ORX rats were treated with CE590 at 30 mg/kg, twice daily by oral gavage or DHT at 8 mg/kg by s.c. injection for 8 weeks. Levitor ani weight increased significantly after treatment with CE590 or DHT in both sham and ORX rats, indicating that both CE590 and DHT act as an AR agonists on levitor ani regardless of endogenous androgen levels. Compared with sham controls, prostate weight decreased significantly by 26% in sham rats treated with CE590, while it increased significantly by 66% in sham rats treated with DHT, indicating CE590

ASBMR 27th Annual Meeting

acts as an AR antagonist while DHT acts as an AR agonist on prostate in intact rats. Although prostate weight in ORX rats treated with CE590 was significantly higher than that in ORX controls, it was still much lower than sham controls. However, prostate weight in ORX rats treated with DHT was significantly higher than that in sham or ORX controls. These data indicate that CE590 has much less of an effect on prostate than DHT in ORX rats. PQCT analysis of distal femoral metaphysis showed that DHT significantly decreased total bone content (-6%), total bone density (-8%) and trabecular density (-9%), while CE590 had no significant effect on these parameters in sham rats compared with sham controls, indicating DHT acts as an AR antagonist on bone while CE590 had no effects in intact male rats. Treatment with CE590 in ORX rats for 8 weeks completely prevented ORX-induced decreases in trabecular content, trabecular density, cortical content, cortical area and cortical thickness. However, DHT had no significant bone effect in ORX rats at the dose administered. Trabecular bone histomorphometry analysis showed that CE590 prevented ORX-induced increases in bone resorption and bone turnover. In summary, CE590 decreased prostate weight and had no significant effect on bone while DHT increased prostate weight but decreased bone density in intact male rats. In ORX rats, CE590 protected against bone loss and DHT had no effect on bone. These results suggest that SARMs have potentials for management of osteoporosis in men with lower gonadal function.

Disclosures: **H.Z. Ke**, Pfizer Inc. 1, 3.

M396

Lasofoxifene Protects against Ovariectomy-Induced Deterioration in Bone Microarchitecture and Geometry in Rats. H. Qi*, D. T. Crawford*, H. A. Simmons, T. A. Brown, D. D. Thompson, H. Z. Ke. Pfizer Global R &D, Groton, CT, USA.

We have previously reported that lasofoxifene (Laso), a new selective estrogen receptor modulator, currently in clinical development for management of osteoporosis, prevents ovariectomy (OVX)-induced bone loss and preserves bone strength in rats. However, the effect of Laso on bone microarchitecture and geometry has not been previously characterized in OVX rats. In this study, S-D female rats at 13 weeks of age were OVX and treated orally with Laso at 0.01, 0.05 or 0.25 mg/kg/d, or 17 α -ethynylestradiol (EE) at 0.03 mg/kg/d for 8 weeks. Micro-CT and PQCT analysis were performed on the distal femoral metaphysis. OVX for 8 weeks induced a significant decrease in total volumetric density (TVD), total volumetric content (TVC), trabecular bone volume (BV/TV), thickness (TbTh), number (TbN), connectivity density (ConnD) and cross sectional moment of inertia (CSMI), and a significant increase in structure model index (SMI), bone surface to volume ratio (BS/BV), trabecular pattern factor (TbPF) and endocortical circumference (EndoC). These data indicate that OVX induced significant loss in trabecular and endocortical bone and deteriorated bone microarchitecture and geometry. Compared with OVX controls, OVX rats treated with Laso at all dose levels had significantly higher TVD, TVC, BV/TV (114% -128%), indicating Laso protects against bone loss in OVX rats. OVX rats treated with Laso at all dose levels had significantly higher TbTh and TbN, and significantly lower SMI (35% - 40%), BS/BV (18% - 23%), indicating Laso preserves plate-like trabeculae and protects against OVX-induced trabecular deterioration. Significantly higher ConnD (93% - 121%) and significantly lower TbPF (52% - 62%) in OVX rats treated with Laso signifies Laso preserves the surface connectivity of trabeculae. Significantly higher CSMI and significantly lower EndoC in OVX rats treated with Laso revealed that Laso preserved the geometrical properties of bone. Histomorphometry analysis of trabecular bone confirmed that Laso decreased osteoclast number, osteoclast surface and bone turnover rate. Efficacy observed in all above parameters did not differ among 3 dose groups for Laso. The protective effects found in Laso treatment were similar to those observed with EE in OVX rats. In summary, Laso at a dose as low as 0.01 mg/kg/d significantly protected against OVX-induced trabecular bone loss and deteriorations in bone microarchitecture and geometrical properties. The protective effects of Laso on bone strength in OVX rats as reported previously may stem from its protective effects on bone mass, bone turnover, microarchitecture and geometry.

Disclosures: **H. Qi**, Pfizer Inc 1, 3.

M397

Effects of Raloxifene on Bone Mineral Density and Biochemical Markers of Bone Remodeling in Postmenopausal Women Pre-treated with Raloxifene or Alendronate for One Year. J. Brown¹, K. W. Ng², G. Toss³, C. Zhou^{*4}, M. Wong⁴, M. W. Draper⁴. ¹Le Centre Hospitalier Universitaire de Quebec Pavilion Chul, Sainte-Foy, PQ, Canada, ²University of Melbourne, Melbourne, Australia, ³University Hospital, Linkoping, Sweden, ⁴Lilly Research Laboratories, Indianapolis, IN, USA.

As several antiresorptive agents with differing mechanisms of action are now available to prevent and/or treat postmenopausal osteoporosis, transitions from one therapy to another often occur in clinical practice. In postmenopausal women (≤ 75 years of age, femoral neck BMD T-score < -2.0), the effects of treatment with placebo (PL), raloxifene 60 mg/d (RLX), alendronate 10 mg/d (ALN), or RLX+ALN on bone mineral density (BMD) and biochemical markers of bone remodeling after one year have been studied and previously reported [JCEM 87(2002):985-92]. After the initial year of therapy in this study, women in each of the 4 treatment groups were re-randomized to either PL or RLX, and treated for an additional year. This new report summarizes the second-year BMD and bone marker results for those women who had been randomized to RLX or ALN in the first year (RLX-PL, n= 34; RLX-RLX, n=35; ALN-PL, n=35; ALN-RLX, n=30). All women received elemental calcium 500 mg/d and vitamin D 400-600 IU/d supplements throughout the entire 2-year study. Lumbar spine, femoral neck, and total hip BMD were measured by DXA at baseline and at 6-month intervals. Biochemical markers of bone remodeling were

measured at 0, 1, 6, 12, and 24 months. The Table shows the difference in mean percent change in BMD and bone markers in RLX versus PL from the end of year 1 to the end of year 2.

Variable	RLX in Year 1	ALN in Year 1
Lumbar Spine BMD	1.49*	2.02*
Femoral Neck BMD	1.46	1.17
Total Hip BMD	2.43*	1.63*
Osteocalcin	-38.1*	-39.3*
Bone-Specific Alkaline Phosphatase (BSAP)	-18.4*	-33.7*
N-Telopeptide	-60.3	-68.9
C-Telopeptide	-173.3*	-58.7

* p<0.05 between RLX and PL

In women treated with either RLX or ALN in year 1 (Table), RLX treatment in year 2 produced significant increases in lumbar spine and total hip BMD compared with PL. Irrespective of the therapy given in year 1, markers of bone remodeling in year 2 were lower in the RLX group compared with PL. Significant differences between the PL and RLX groups were seen for osteocalcin and BSAP in women given either RLX or ALN in year 1, but for C-telopeptide, these were seen only in women treated with RLX in year 1. In conclusion, RLX treatment exerts positive effects on BMD and biochemical markers of bone remodeling, compared with PL, regardless of prior treatment with either RLX or ALN.

Disclosures: **J. Brown**, Eli Lilly 2, 5, 8; Merck 2, 5, 8.

M398

Prevalence of Osteoporosis-Associated Skeletal Pain and its Further Course Following Initiation of Raloxifene Treatment: A Prospective Multicenter 6-Month Observational Study in a Naturalistic Setting. S. Scharla¹, H. Oertel^{*2}, K. Helsberg^{*2}, F. Kessler^{*2}, F. Langer^{*2}, T. N. Nickelsen². ¹Practice for Internal Medicine and Endocrinology, Bad Reichenhall, Germany, ²Medical, Lilly Deutschland GmbH, Bad Homburg, Germany.

In this 6-month observational study we assessed the prevalence of osteoporosis-associated skeletal pain and its course during treatment with the selective estrogen receptor modulator raloxifene in a naturalistic setting. 810 office-based physicians in Germany documented clinical, diagnostic, and pain data of 3,299 female patients with postmenopausal osteoporosis at baseline, after approx. 6 weeks and 6 months of treatment, or at premature treatment discontinuation. At each visit, the presence or absence of back, joint, and diffuse bone pain, as well as sleep quality and the use of analgesics were assessed. In addition, frequency and intensity of pain during the 4 weeks preceding each assessment were self-rated on a patient questionnaire using a 100 mm visual analogue scale (VAS). According to the physician documentation, 93.4% of 3,299 patients (mean age 67.6 \pm 9.3 years, 89.4% with reduced BMD, 39.8% with ≥ 1 confirmed fragility fracture) had skeletal pain at baseline, which had been preexisting for >10 months in 75%. 85.1% of patients had back pain, 41.8% joint pain and 32.5% diffuse bone pain. After 6 months, pain intensity (VAS) had decreased in 89% of patients and increased in 9.4%. The mean decrease in pain intensity (VAS) was -42% (95% CI -40%:-44%; p<0.0001; N=2,491). Need for analgesics and sleep quality improved in parallel. Subgroup analyses revealed relevant decreases in pain intensity after 6 months of raloxifene treatment in all subgroups assessed, including patients with pre-baseline pain for >6 months and regardless of the presence or absence of prior fractures (Table). The resulting hypothesis that raloxifene may exert a pain-alleviating effect in women with osteoporosis requires confirmation in a randomized, placebo-controlled trial.

Pain intensity (100 mm VAS, mean +/-SD)				
Patient Characteristics	N	Baseline [mm]	% Change	95%CI
Any old or recent (<6 months) fractures	1020	68.6 \pm 19.5	-43	-40;-46
Neither old nor recent fractures	1297	59.4 \pm 21.3	-42	-39;-44
Degenerative and/or inflammatory disease only	1050	60.9 \pm 20.6	-41	-39;-44
Fractures in absence of degen. and inflamm. dis.	46	69.4 \pm 22.7	-57	-50;-63
Preexisting pain (PEP) \leq 4 weeks	29	73.5 \pm 20.4	-54	42;-65
PEP > 4 weeks but \leq 6 months	304	63.4 \pm 21.3	-50	-46;-54
PEP > 6 months	1465	64.7 \pm 19.8	-43	-40;-45

Disclosures: **T.N. Nickelsen**, H Oertel, K Helsberg, F Kessler, F Langer, T Nickelsen 3; S Scharla 5, 8.

M399

Progestins with No Glucocorticoid Activity May Be a Better Choice for Hormone Replacement Therapy to Achieve More Beneficial Effects on Bone Metabolism. Y. Ishida, T. Taguchi^{*}. Department of Orthopaedic Surgery, Yamaguchi University School of Medicine, Yamaguchi, Japan.

A number of studies suggest that progestagens may have beneficial effects on bone metabolism. C21 Progestin medroxyprogesterone acetate (MPA) is one of the most commonly prescribed progestins for hormone replacement therapy (HRT). However, there appear to be that MPA with significant glucocorticoid (GC) activity may decrease bone density. We have previously argued that bone loss associated with MPA administration is caused by decreased osteoblast differentiation as a result of MPA occupying the GC receptor since increasing GC receptor occupancy beyond that reached at normal (= optimal) GC concentrations attenuates osteoblast differentiation. This randomized controlled trial was conducted to test the hypothesis that progestins with no GC activity, e.g. C19 progestin norethisterone (NET), may be a better choice for HRT to achieve more beneficial effects on bone metabolism. A total of 91 postmenopausal women aged 50-75 with osteoporosis were randomly allocated into three groups: 1) HRT-MPA (conjugated estrogen 0.625 mg/day plus MPA 2.5 mg/day); 2) HRT-NET (conjugated estrogen 0.625

mg/day plus NET 5 mg/day); or 3) control (no treatment). Thoracic and lumbar spine radiographs and bone mineral density (BMD) at distal 1/3 radius were assessed at baseline and at every 6 months during the 2-year study period, along with markers of bone turnover [serum bone specific alkaline phosphatase (BAP) and urinary N-telopeptide of type I collagen (NTX)]. Mean changes in BMD relative to baseline after the 2-year treatment in HRT-MPA, HRT-NET, and control was 1.6%, 2.7%, and -2.6%, respectively. Interestingly, the rate of increase in BMD in HRT-NET was significantly greater than that in HRT-MPA (p=0.01). The incidence of new vertebral fractures during the 2-year treatment was 13% (4/31) in HRT-MPA, 7% (2/29) in HRT-NET, and 27% (8/30) in control. There were significant decreases in BAP from baseline after the 2-year treatment in HRT-MPA (-23.8%, P<0.01) and HRT-NET (-19.2%, P<0.01) (4.6% difference, P=0.4). In control, no significant changes in BAP were found as compared with baseline. A significant reduction in NTX was seen in HRT-MPA (-45.4%, P<0.001) and HRT-NET (-47.9%, P<0.001) (2.5% difference, P=0.6), while no significant changes were found in control. We conclude that progestins with no GC activity may be a better choice for the HRT treatment to achieve more beneficial effects on bone metabolism than progestins with GC activity.

Disclosures: **Y. Ishida**, None.

M400

Effects of Raloxifene Treatment during One Year on OPG-RANK Ligand System in Postmenopausal Osteoporosis. **D. Fernández-García^{*1}, P. Mezquita-Raya^{*2}, R. Reyes-García^{*1}, M. de la Higuera^{*1}, G. Alonso^{*1}, A. Martín García^{*3}, M. Ruiz-Requena^{*4}, M. Muñoz -Torres¹.** ¹Bone Metabolism Unit. Endocrinology Division, San Cecilio Hospital, Granada, Spain, ²Endocrinology Division, Torrecárdenas Hospital, Almería, Spain, ³Nuclear Medicine Division, San Cecilio Hospital, Granada, Spain, ⁴Biochemistry Division, San Cecilio Hospital, Granada, Spain.

Previous in vitro studies suggest that the antiresorptive effect of raloxifene (a selective estrogen receptor modulator) might be mediated by changes in several cytokines involved in the bone remodelling process. In this context, the OPG-RANKL system is considered a key component in the osteoclastogenesis regulation. However, the long term effects of this treatment are not adequately established in osteoporotic patients. To determine the effects of raloxifene treatment on serum concentrations of OPG, RANKL, biochemical markers of bone turnover and BMD in untreated women with postmenopausal osteoporosis, we selected 47 postmenopausal women (mean age 63±7 years) with densitometric criteria of osteoporosis (T-score ≤-2.5 SD). We determined at baseline, 3, 6 and 12 months anthropometric parameters, biochemical markers of bone turnover, serum levels of OPG (OPG ELISA, BIO-MEDICA-GRUPPE Wien, Austria), RANKL (sRANKL ELISA BIO-MEDICA-GRUPPE Wien, Austria) and BMD (DXA; Hologic QDR 4500) in lumbar spine (LS) femoral neck (FN) and total hip was measured basal and 12 months after raloxifene (60 mg/day) treatment. BMD in LS increased significantly (2.5%) at the 12th month of treatment (p=0.031). The biochemical markers of bone turnover (total alkaline phosphatase, bone alkaline phosphatase, osteocalcin, TRAP, urine CTX) decreased significantly from the third month of treatment. Serum levels of OPG decreased at the third month of treatment (p = 0.001) and returned to basal levels at 6th and 12th month. Change of OPG levels between baseline and third month was related to the decrease of CTX between the same study point (r=0.33; p<0.05). There were a high percentage of undetectable serum RANKL levels (>60%) in all visits. The mean serum values of RANKL were significantly different between basal and 12 months (p<0.05). The treatment with raloxifene in osteoporotic postmenopausal women leads to a initial decrease in serum levels of OPG and changes in RANKL serum levels that might be attributed to the inhibitor effect on bone remodelling as anticatabolic drug.

Disclosures: **D. Fernández-García**, None.

M401

Osteocyte Survival Is Affected by Raloxifene Treatment. **H. W. van Essen^{*1}, P. J. Holzmann^{*1}, R. Blankenstein^{*2}, P. Lips¹, N. Bravenboer¹.** ¹Endocrinology, VU Medical Center, Amsterdam, The Netherlands, ²Clinical Chemistry, VU Medical Center, Amsterdam, The Netherlands.

Increased osteocyte apoptosis, as the result of oestrogen deficiency, could play a role in the decrease of bone mass and bone strength seen in postmenopausal osteoporosis. We investigated whether raloxifene treatment of postmenopausal women affects osteocyte survival. In a substudy from the MORE¹ trial trans-iliac bone biopsies were taken from 24 women at baseline and after two years of treatment with either placebo or raloxifene. Goldner staining and tetracycline labelling were performed to evaluate static and dynamic histomorphometry. Immunohistochemical detection of cleaved caspase-3 was performed to visualize apoptosis. In the trabecular bone total osteocytes, positively stained osteocytes and empty lacunae were counted. Percent positive cells and percent empty lacunae were calculated. Differences between baseline and follow-up were tested with Wilcoxon paired t-test, treatment effect was tested with Mann-Whitney sign-rank test and association between osteocyte apoptosis and histomorphometrical indices were analysed with linear regression. There was no difference in percentage positive osteocytes between baseline and follow-up biopsies in both the placebo and the raloxifene groups. The percentage empty lacunae increased significantly in the placebo group (9.17 ± 2.30 vs 11.30 ± 1.43; p = 0.019), but not in the raloxifene group. There was no difference in percent change between the placebo and raloxifene groups. At baseline there was a negative association between bone remodelling indices and the percentage of positive osteocytes (BFR/BV: slope = -0.148; p = 0.008, ES/BS: slope = -0.628; p = 0.082). In the placebo group the change in bone remodelling in two years was negatively associated with the change in percent positive osteocytes (BFR/BV: slope = -1.915; p = 0.038, ES/BS: slope = -0.802; p = 0.085). In the raloxifene group this association was not observed. Analysis of the regression lines

showed that the association between the change in percent positive osteocytes and the change in BFR/BV was significantly different in the raloxifene group compared to the placebo group (p = 0.045). The negative association of osteocyte apoptosis with bone remodelling indicates that a high bone remodelling quickly removes apoptotic osteocytes. This association is still intact after two years in the placebo group, but is lost in the raloxifene group. This suggests that raloxifene treatment has an effect on osteocyte survival but that direct measurement of apoptosis was unable to reveal this. Possibly the groups were too small to detect such a difference.

¹Ott, S.M J Bone Miner Res, 2002;17:341-348

Disclosures: **H.W. van Essen**, None.

M402

Effect of DHT (5-alpha-dihydrotestosterone) on Body Composition and Cortical Bone of the Adult Female Estrogen Deficient, Osteopenic Rat. **T. Cusick, S. Harada, D. Kimmel.** Merck & Co., West Point, PA, USA.

Elderly individuals may have increased osteoporotic fracture risk due to both low bone mass and increased frailty. Androgens may not only stimulate bone formation and increase bone mass, but also improve muscle mass. The purpose is to study the effects of DHT on cortical bone and body composition of adult, estrogen deficient, osteopenic rats. Female rats (N=76) were ovariectomized (age 14wks) and became osteopenic for 10 weeks. Rats (38/grp) were treated subcutaneously daily with vehicle (Veh) or 3mg/kg DHT. Whole body lean and fat mass (LBM & FBM) were measured monthly (EchoMRI-700; Echo Medical Systems; Houston, TX). After 17 weeks, 24 rats of each group were necropsied after in-life double calcein labeling. Treatment was halted and the remainder were necropsied 15 weeks later. Central femur BMD and BMC (bone mineral density and content) were measured (DXA; Hologic 4500). Periosteal mineralizing surface (pMS/BS), total periosteal area (TPA), marrow cavity area (MCA), and cortical area (Ct.Ar) were measured on 100µm non-decalcified central femur cross-sections. T-test of means, comparing Veh and DHT at each time (*P<.02; **P<.001), was executed.

Variable	Veh17wk	DHT17wk	Veh32wk	DHT32wk
BMD (mg/cm ³)	214±10	224±12*	222±13	226±20
BMC (mg)	118±11	128±10*	120±14	133±15*
MS/BS (%)	48.1±20.5	56.6±22.0*	41.6±12.8	37.1±17.6
TPA (mm ²)	9.94±1.02	10.26±0.80	9.74±0.86	11.09±0.83*
MCA (mm ²)	3.38±0.56	3.31±0.47	3.48±0.39	3.85±0.64
Ct.Ar (mm ²)	6.56±0.56	6.95±0.57*	6.37±0.53	7.25±0.67*

LBM became significantly greater in DHT than in Veh rats after 4wks (+4.1%*) and remained so during active treatment (+11.7%** @ 17wks). FBM was also less with DHT (-16% @4wks; -28% @17wks). pMS/BS is elevated by 3mg/kg/d DHT at 3.5wks (data not shown). BMD, BMC, pMS/BS, and Ct.Ar were greater with DHT after 17wks. DHT-related LBM/FBM and pMS/BS effects dissipated, but BMC, TPA, and Ct.Ar remained significantly greater after recovery. **Conclusion:** Body composition becomes leaner with DHT treatment, at the same time when periosteal bone formation is stimulated. These changes in LBM/FBM and pMS/BS precede increased cortical bone mass. Though body composition and bone formation return to normal after recovery, increased total periosteal and cortical area persist, suggesting that androgens improve cortical bone macroarchitecture in a way that increases cross-sectional moment of inertia, indicating permanent improvements in mechanical strength of cortical bone.

Disclosures: **T. Cusick**, Merck & Co. 3.

M403

[Leu²⁷]cyclo(Glu²²-Lys²⁶) hPTH 1-31NH₂ Potently Preserves Bone Structure after Ovariectomy by Effectively Inhibiting Bone Resorption. **H. Shen^{*}, S. Maclean^{*}, V. Ross^{*}, C. Allen^{*}, A. Burns^{*}, G. E. Willick^{*}, J. F. Whitfield, G. A. Candeliere.** Institute of Biological Sciences, National Research Council of Canada, Ottawa, ON, Canada.

The parathyroid hormone (PTH) analogs hPTH-(1-31)-NH₂ (OSN), [Leu²⁷] cyclo (Glu²²-Lys²⁶) hPTH-(1-31)-NH₂ (OSC) and hPTH-(1-34)-NH₂ (FTA) show differences in receptor affinity and signaling, which suggests differences in bone-anabolic mechanism. PTH analog treatment increased serum osteocalcin and femoral trabecular thickness equally in sham and ovariectomized (OVX) rats, but unequally caused larger effects on bone volume, marrow space, and node-to-termini ratio in OVX. This indicates that all PTH analogs stimulated bone formation and inhibited the breakdown of the trabecular lattice after OVX. PTH analogs were injected daily into OVX rats at doses of 6, 10 and 20 nmoles/kg of body weight. FTA and OSC stimulated serum osteocalcin and increased trabecular thickness equally, whereas OSN was less potent. The FTA-induced changes in bone volume, node:termini ratio, and marrow space plateaued between 10 and 20 nmoles/kg of body weight. The changes induced by OSC, particularly the reduction of marrow space, continued to increase in this dose-range. Thus, OSC at 20 nmoles/kg of body weight was significantly more potent than FTA at preventing trabecular lattice breakdown and marrow space expansion in OVX rats, probably by effectively inhibiting osteoclasts. Cellular and kinetic indices showed that all PTH analogs significantly increased mineralizing surfaces and bone formation rate, but not osteoblast surface density or mineral apposition rate. Only, FTA and OSC significantly increased the reduction in osteoclast surface density and eroded space that normally occurs late after OVX. Therefore, PTH analogs stimulated osteoblast lineage cells at a non-mineralizing transitional stage and inhibited mature osteoclasts. In rat calvaria organ and cell cultures, and bone marrow co-culture models, intermittent pulsing with PTH analogs (10nM) showed that OSC, but not the other peptides, significantly increased parietal bone thickness and reduced calvaria eroded space, reduced TRAP stain intensity and increased the rate of bone nodule formation. RT-PCR also showed that the PTH analogs stimulated the expression of osteoblast differentiation markers, but reduced osteoclast markers, and

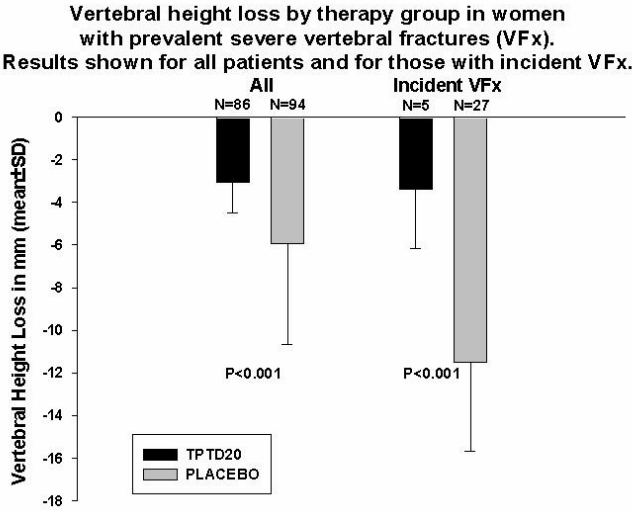
lowered the RANKL:OPG ratio. These results show that these primary in vitro systems can reproduce the cellular mechanisms underlying PTH analog actions in vivo. In conclusion, this study indicates that FTA, OSN and OSC drive committed osteoblast lineage cells toward bone-making, and OSC is the most effective osteoclast inhibitor that potently preserves bone structure after OVX.

Disclosures: **GA. Candelieri**, Zelos Therapeutics 2.

M404

Teriparatide Reduces Vertebral Height Loss in Women With Osteoporosis and Severe Prevalent Vertebral Fractures. **H. K. Genant**¹, **S. Prevrhal**², **G. G. Crans**³, **E. V. Glass**³, **J. H. Krege**³. ¹UCSF-OARG and Synarc Inc., San Francisco, CA, USA, ²UCSF-OARG, San Francisco, CA, USA, ³Eli Lilly and Company, Indianapolis, IN, USA.

In the Fracture Prevention Trial, a randomized, placebo-controlled study of 1637 postmenopausal women with osteoporosis, teriparatide [rhPTH (1-34)] increased bone mineral density and reduced fracture risk (Neer 2001). Prevalent and incident vertebral fractures were defined using a visual semi-quantitative method (Genant 1993). To assess the effects of teriparatide on preservation of vertebral height, we assessed quantitative morphometry (QM) of baseline and study endpoint spine radiographs from teriparatide 20 mcg/day (TPTD20, N=95) and placebo (N=86) treated patients with prevalent severe vertebral fractures. An investigator blinded to patient group assignment determined anterior, middle, and posterior heights for each T4-L4 vertebra. For each patient, the difference in vertebral height (mm) from baseline to study endpoint was measured by QM at 3 locations (anterior, midpoint, and posterior) for each vertebra (L1-L4 and T4-T12). The outcome measure for each patient was the maximum height loss among all these height differences. Treatment group means, of the maximum height loss, were compared using a two-sided t-test at significance level 0.05. Vertebral height loss in the TPTD20 group was significantly reduced versus placebo (Figure, t-test P<0.001). In women with new vertebral fractures, height loss of fractured vertebrae in the TPTD20 group was significantly reduced versus placebo group, -3.4 mm versus -11.5 mm, respectively (Figure, P<0.001). In summary, teriparatide reduced vertebral height loss and fracture-associated vertebral height loss versus placebo.



Disclosures: **H.K. Genant**, Eli Lilly and Company, Wyeth, GSK, Roche, Amgen, Novartis, NPS, P&G, Aventis 5.

M405

The Cost-Effectiveness of Parathyroid Hormone and Alendronate in High-Risk Osteoporotic Women. **H. Liu**^{*1}, **K. Michaud**^{*2}, **S. Nayak**^{*3}, **D. B. Karpf**^{*4}, **D. K. Owens**^{*3}, **A. M. Garber**^{*3}. ¹Endocrinology & Metabolism and Center for Primary Care and Outcomes Research, Stanford University, Stanford, CA, USA, ²Center for Primary Care and Outcomes Research, Stanford University, Stanford, CA, USA, ³Veterans Affairs Palo Alto Healthcare System and Center for Primary Care and Outcomes Research, Stanford University, Palo Alto, CA, USA, ⁴Endocrinology & Metabolism, Stanford University, Stanford, CA, USA.

Osteoporosis is a common and costly disease. Parathyroid hormone [1-34] (PTH) is a promising new agent for the treatment of osteoporosis although its cost-effectiveness is unknown. The purpose of our study was to evaluate the cost-effectiveness of PTH-based treatment strategies compared to the current market leader, alendronate, for the first-line treatment of high-risk postmenopausal osteoporosis. We developed a microsimulation incorporating fracture-type and individual risk to compare placebo vitamin D and calcium sufficiency to three treatment strategies: life-long alendronate (ALN), two years of PTH (PTH-Alone), and two years of PTH followed by life-long alendronate (PTH->ALN). We used studies identified in a search of MEDLINE and U.S. data sources whenever possible. Long-term anti-fracture efficacy for PTH and alendronate was extrapolated from available data. Our reference population was treatment-naïve 70-year old osteoporotic Caucasian

women with pre-existing vertebral fracture. We employed a lifetime horizon and societal perspective. Our primary outcome was cost per quality-adjusted life-year (QALY) gained. We discounted costs and QALYs at a 3% annual rate. In our reference case, the incremental cost-effectiveness ratio (ICER) was \$42,000/QALY for ALN and \$92,000/QALY for PTH->ALN. PTH-Alone was dominated and did not appear on the cost-effectiveness frontier even if its anti-fracture efficacy was assumed to persist for 20 years after cessation of PTH. In scenario analysis, PTH->ALN was consistently less cost-effective than ALN; under reference case assumptions for ALN, PTH->ALN would be less cost-effective than ALN even if PTH->ALN could reduce fracture rates to zero percent. Our results were sensitive to the cost of medication. If the cost of PTH was reduced by 50%, PTH->ALN would be more cost-effective than ALN; if the cost of alendronate was reduced by 75%, ALN would be cost-saving. The cost-effectiveness of PTH-Alone is inferior to ALN and PTH->ALN. While PTH->ALN is less cost-effective than ALN, significant reductions in the cost of PTH could substantially improve the cost-effectiveness of this treatment strategy.

Disclosures: **H. Liu**, None.

M406

Baseline Characteristics of Subjects Enrolled during the First 18 Months of DANCE: Direct Assessment of Non-Vertebral Fractures in Community Experience. **D. T. Gold**^{*1}, **W. Shergv**^{*2}, **P. Chen**^{*3}, **D. A. Misurski**^{*3}, **R. B. Wagman**³. ¹Department of Psychology, Duke University Medical Center, Durham, NC, USA, ²School of Medicine, University of Alabama, Huntsville, AL, USA, ³Eli Lilly and Company, Indianapolis, IN, USA.

The randomized placebo-controlled clinical trial experience may differ from community practice. When recombinant teriparatide (TPTD) studies were initiated, therapeutic options for osteoporosis were limited. DANCE examines the long-term effectiveness, safety, and tolerability of TPTD in a large diverse patient population, including subjects with co-morbidities, severe osteoporosis, and/or prior osteoporosis therapy. About 4000 men and women will ultimately participate in this prospective observational trial. They will receive TPTD 20 mcg/day for up to 24 months and will be followed for another 24 months. All aspects of patient care, including diagnostic and therapeutic interventions, will be conducted by study physicians. As of February 1, 2005, 1148 subjects enrolled. Baseline demographics and those of the TPTD clinical trial populations are provided (Table). Age and lumbar spine (LS) BMD values were similar to the clinical trials. 836 subjects had ≥ 1 prior fractures. There were a total of 522 prior non-vertebral fragility fractures in 257 subjects. The most common were: ribs (19.0%), foot/toes (13.6%), hip (12.5%). A total of 522 prior vertebral fragility fractures were documented in 244 subjects. The most common were: L1 (14.2%), T12 (13.6%), T7 (10.0%). 424/522 (81.2%) of prevalent vertebral fragility fractures were associated with back pain. 88.3% of subjects received prior osteoporosis therapy [bisphosphonates (79.1%), hormone replacement (26.1%), calcitonin (23.8%), raloxifene, (15.7%)]. 21.8% received both hormone replacement and bisphosphonates. 941/1144 (82.3%) had ≥ 1 active medical conditions including: corrective lenses (57.2%), hypertension (35.9%), pulmonary disease (17.1%), rheumatoid arthritis (11.9%). 217/1147 (18.9%) had a history ≥ 1 cancers including: breast (6.8%), skin (6.2%), colon (1.4%), uterine (1.2%), ovarian (0.9%). Further examination of this heterogeneous population will provide information about the TPTD clinical experience, facilitating an evidence-based approach to patient management.

	Baseline Subject Demographics		
	DANCE (18 months) mean ± SD (n = 1146)	Fracture Prevention Trial ¹ mean ± SD (n = 1637)	Orwoll et al. ² mean ± SD (n = 437)
Age (Women)	69.5 ± 11.5 (n = 1023)	69.5 ± 7.0	/
Age (Men)	65.9 ± 12.7 (n = 123)	/	58.7 ± 13.0
Caucasian	92.9%	98.7%	99.1%
LS BMD (g/cm ²)			
Women	0.77 ± 0.15 (n = 742)	0.82 ± 0.17	/
Men	0.80 ± 0.17 (n = 74)	/	0.87 ± 0.14
Smoking	14.2%	17.0%	29.7%
Alcohol	28.8%	37.3%	30.0%
Caffeine	81.9%	84.3%	87.9%

¹Neer et al. N Engl J Med 2001;344:1434-41. ²Orwoll et al. J Bone Miner Res 2003;18:9-17.

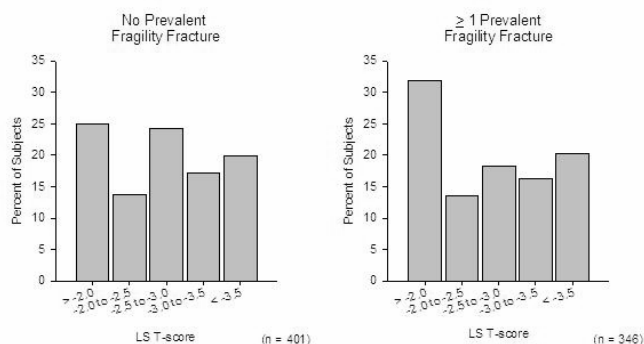
Disclosures: **D.T. Gold**, Eli Lilly, Procter and Gamble, Aventis, Novartis, Kyphon, GSK, Roche 5.

M407

Rationale and Evidence for Initiating Teriparatide Therapy: Interim Results from DANCE. **S. L. Silverman**¹, **P. D. Miller**², **N. B. Watts**³, **P. Chen**^{*4}, **D. A. Misurski**^{*4}, **R. B. Wagman**⁴. ¹Division of Rheumatology, Cedars Sinai Medical Center, Beverly Hills, CA, USA, ²Department of Medicine, Colorado Center for Bone Research, Lakewood, CO, USA, ³Bone Health and Osteoporosis Center, University of Cincinnati, Cincinnati, OH, USA, ⁴Eli Lilly and Company, Indianapolis, IN, USA.

Recombinant teriparatide (TPTD) efficacy has been demonstrated in clinical trials, but experiences in community practice may differ. The Direct Assessment of Non-vertebral Fracture in Community Experience (DANCE) study is a prospective observational study examining the long-term effectiveness, safety, and tolerability of TPTD in a large heterogeneous population in the community setting. To better understand the rationale and evidence used to initiate TPTD, we reviewed baseline fracture status, baseline BMD T-scores, and a physician questionnaire for 1148 subjects at 89 sites enrolled in DANCE by

February 1, 2005. Physicians specializing in endocrinology, rheumatology, or internal medicine and those demonstrating an interest in osteoporosis have been invited. As of February 1, 2005, 1 to 50 subjects have been enrolled by any single site. Subjects invited were prescribed TPTD 20 mcg/day by their physician during routine practice. 257 subjects had prior non-vertebral fragility fractures (522 total non-vertebral fragility fractures), while 244 subjects had prior vertebral fragility fractures (522 total vertebral fragility fractures). Mean lumbar spine (LS) BMD T-score was -2.6 (n=817) and mean femoral neck BMD T-score was -2.5 (n=798). Distributions of LS T-scores, stratified by presence/absence of prevalent fragility fracture are shown (graph). When physicians were queried regarding reasons for TPTD initiation, 84.2% of subjects were felt to have multiple fracture risk factors; of these, 63.1% were believed to have very low BMD, 38.5% had previous osteoporotic fracture, 19.3% sustained a new osteoporotic fracture, and 12.6% cited height loss. Of the 71.4% of subjects who initiated TPTD because of failure on previous osteoporosis therapies, 42.6% had a decline in BMD, 20.4% had fractured while on other osteoporosis therapy, and 14.2% had no change in BMD. Several factors, in addition to BMD, seemed important in the decision to initiate TPTD therapy. Continued collection of data will help elucidate the rationale and level of evidence used when initiating TPTD therapy.



Disclosures: **S.L. Silverman**, Eli Lilly 2, 5.

M408

Bone Marker Changes in One Month Treatment with Teriparatide (LY 333334) Injections (rDNA origin) in Men and Post-Menopausal Women with Severe Osteoporosis. **A. Acosta**¹, **M. Rivas**¹, **K. Roman**^{*2}. ¹PRSA Medical, Eli Lilly and Company, San Juan, Puerto Rico, ²External Assessor, Eli Lilly and Company, San Juan, Puerto Rico.

There is evidence about calcium metabolism & fracture incidence variations across ethnic groups and geographic regions (Melton&Cooper 2001, Laudarle 1997, Bryan 2003). Overall weighted prevalence of osteoporosis among Puerto Rican postmenopausal women without vertebral fracture was 29% (95CI 25.4, 34.4%) in a population-based study (Haddock 2004). However, bone metabolism changes in response to osteoporosis treatment has not been studied in the Puerto Rican population. To answer this question, a prospective, multi-center, cohort, randomized trial of 60 severely osteoporotic patients was conducted in 10 specialty outpatient clinics primarily to evaluate bone metabolism marker changes (resorption and formation) after one month of treatment with 20 mcg of teriparatide. A secondary objective was to identify these patients' osteoporosis risk factors by using the Millennium One-Minute Osteoporosis Risk-Test. All patients received approximately 1000mg/day of elemental calcium and 400 to 1200 IU/day of vitamin D. A total of 57 patients were entered: 96% women and 4% men. Average age for all patients was 70 years, CI 95% (68,73). Fifty percent or more of the patients in this cohort had the following risk factors for osteoporosis: menopause before age 45 and a history of low impact fracture, 67.4% reported 1.2 inches lost in height. Forty-five (79%) patients received at least one dose of study drug; 41 (72%) completed the study. Two patients were discontinued early from the study by the investigators due to non-serious adverse events. A paired *t*-test was performed in order to evaluate P1CP changes after one month of teriparatide treatment. The average difference in P1CP levels was 40 ug/L, CI 95% (23.6, 57.1), (p=0.001). Adjusting for previous use of bisphosphonates and after a one-month washout period, statistically significant differences were observed between baseline and final P1CP values using a random effect model (p=0.000). The relationship between bisphosphonate use and P1CP values was not statistically significant (p = 0.30). The average difference in NTx levels was 0.20 nmol BCE/L, CI 95% (-1.16, 1.6), (p=0.76). In conclusion, statistically significant increase of a bone formation marker, P1CP, but no change of a bone resorption marker, NTx, were observed in severely osteoporotic Puerto Rican patients after one month of treatment with teriparatide and a one-month bisphosphonate washout period. NTx changes may not have been observed because of the relatively short bisphosphonate washout period or suggest an anabolic window effect.

Disclosures: **A. Acosta**, Eli Lilly and Company 3.

M409

Ostabolin-CTM: A Novel Parathyroid Hormone Analogue Uncouples Bone Turnover in Monkeys Treated for 1-Year. **J. Jolette**^{*1}, **S. Y. Smith**¹, **I. A. Moreau**^{*1}, **C. H. Turner**², **J. Mayer**^{*1}, **B. Rushton**^{*3}, **P. Morley**^{*4}. ¹Charles River Laboratories Preclinical Services•CTBR, Senneville, PQ, Canada, ²Indiana University, Indianapolis, IN, USA, ³Zelos, Stevenage, United Kingdom, ⁴Zelos Therapeutics, Ottawa, ON, Canada.

Ostabolin-CTM (Leu²⁷, Cyclo[Glu²²Lys²⁶]-hPTH[1-31]amide), a novel parathyroid hormone (PTH) analogue being developed for the treatment of osteoporosis, was administered daily by subcutaneous injection to gonad-intact cynomolgus monkeys (4/sex/group) at dose levels of 0, 2, 10 and 25 µg/kg for 52 weeks to evaluate toxicity. Monkeys were 30 to 40 months of age (2.3-3.5 kg) at treatment start. Blood and urine samples were collected to measure biochemical markers of bone turnover and tibiae were retained for histomorphometry following labeling with calcein green 15 and 5 days prior to euthanasia. Ostabolin-CTM was well tolerated with no hypercalcemia observed in blood samples collected at Weeks 13, 26 or 39 or 52, approximately 24 hours post-dose. Bone turnover markers indicated a dual effect of Ostabolin-CTM since significant increases in the bone formation marker osteocalcin and significant decreases in the bone resorption marker C-telopeptide were observed. Another bone resorption marker, urinary DPD, did not differ from controls. In addition, bone mass, as measured by DXA and pQCT, was increased at the lumbar spine, femur and tibia. Changes in vertebral BMD translated into significant increases in bone strength. Ostabolin-CTM substantially increased osseous accretion in the cancellous and endocortical bone compartments of the proximal tibia at all doses. Tibial cancellous bone volume increased by more than 50% in all Ostabolin-CTM-treated groups compared to controls and in the tibial mid-diaphysis, increases in cortical width and relative cortical area with concurrent decreases in medullary area were observed. Only minor increases in cortical porosity were observed at the two highest dose levels. The increase in bone mass appeared to be related to increases in bone formation and decreases in bone resorption as measured by a significant reduction in osteoclast surface. In conclusion, the results of this study are consistent with the anticipated anabolic effects of Ostabolin-CTM as a PTH analogue. However, increases in indices of bone formation were associated with decreases in indices of bone resorption (decreased bone resorption markers and decreased osteoclast surface area), consistent with the uncoupling of these events. To summarize, Ostabolin-CTM increased bone formation activity and reduced bone resorption in skeletally immature monkeys. This combination of anabolic and anti-catabolic actions may have significant therapeutic value in the treatment of osteoporosis.

Disclosures: **P. Morley**, None.

M410

What Percent of Women with Postmenopausal Osteoporosis Experience an Increase in Lumbar Spine BMD Following 18-Months of Teriparatide Treatment? **J. C. Gallagher**^{*1}, **C. J. Rosen**², **P. Chen**^{*3}, **D. A. Misurski**^{*3}, **R. Marcus**³. ¹Bone Metabolism Unit, Creighton University Medical Center, Omaha, NE, USA, ²Maine Center for Osteoporosis Research and Education, St. Joseph Hospital, Bangor, ME, USA, ³Eli Lilly and Company, Indianapolis, IN, USA.

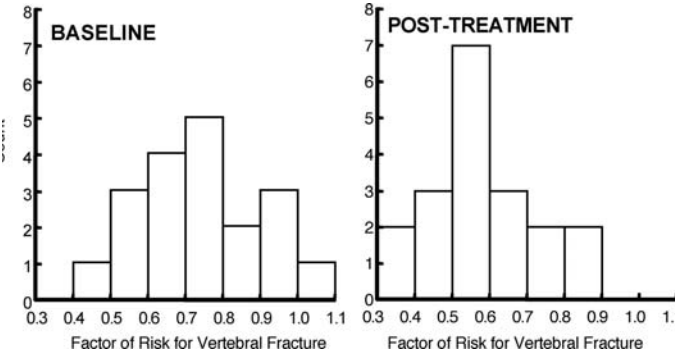
Physicians frequently ask what BMD responses can be expected in their teriparatide-treated patients. We therefore determined the BMD response rate, defined as the proportion of women with postmenopausal osteoporosis (PMO) whose lumbar spine (LS) BMD responses after 18 months of TPTD met or equaled the least significant change (LSC), in two randomized controlled trials. The first involved teriparatide 20 mcg/day (TPTD20) and 40 mcg/day (TPTD40) (Neer et al. *N Engl J Med* 2001). The second trial involved TPTD20 (McClung et al. 2005 (in press)). Subjects in both trials had minimal prior exposure to bisphosphonates and all received supplemental calcium and vitamin D. We assumed the DXA index of precision to be 1%, giving an LSC value of 3%. Only women who had LS BMD measurements at all specified time points through 18 months were included in this analysis. For the commercially available TPTD20 dose, 91% (118/129) of women achieved an increase in LS BMD ≥ 3% at 18 months. Of the 11 who did not, 3 had actually responded at 12 months. For TPTD40, 94% (118/125) achieved the 3% criterion at 18 months. Of the 7 who did not, 1 had responded at 12 months. There were no significant differences in the percent of women who responded to TPTD20 and TPTD40 at either 12 or 18 months. In the second trial, 94% (64/68) of women receiving TPTD20 had a LS BMD increase ≥ 3% at 18 months. 2 of the 4 patients who did not respond to TPTD20 at 18 months had responded at 12 months. Examination of baseline characteristics for women who were "non-responders" to TPTD showed no significant differences in age, baseline BMD, vitamin D status, or renal function compared to "responders". In addition, 73% (16/22) of BMD non-responders showed robust increases in the bone formation marker Procollagen Type I N-Propeptide (PINP) at 3 months, emphasizing the limitation of relying exclusively on BMD to identify responders. This analysis demonstrates that over 90% of treatment-compliant women with PMO and minimal prior bisphosphonate exposure have a LS BMD response to TPTD.

Disclosures: **R. Marcus**, Eli Lilly and Company 3.

M411

Combining Biomechanical Measures of Vertebral Strength with Estimates of Spinal Loading to Assess the Effects of Osteoporosis Therapies on Vertebral Fracture: A Pilot Study in PaTH. M. L. Bouxsein¹, D. M. Black², J. Muller^{*1}, J. Bilezikian³, S. Greenspan⁴, K. Ensrud⁵, L. Palermo^{*2}, P. M. Crawford^{*6}, C. J. Rosen⁷, T. M. Keaveny⁶. ¹BIDMC, Boston, MA, USA, ²UCSF, San Francisco, CA, USA, ³Columbia Univ., New York, NY, USA, ⁴Univ of Pittsburgh, Pittsburgh, PA, USA, ⁵Univ of Minnesota, Minneapolis, MN, USA, ⁶ON Diagnostics, Berkeley, CA, USA, ⁷MECORE, Bangor, ME, USA.

Osteoporosis therapies reduce vertebral fracture risk to a greater extent than are predicted based on changes in areal BMD (aBMD). One explanation for this discrepancy is that aBMD measurements do not adequately reflect effect of treatment on bone strength. An alternative, but complementary explanation is that changes in BMD alone do not reflect the relationship between skeletal loading and bone strength that ultimately determines the probability of fracture. Introduced by Hayes et al (1991), the ‘factor of risk’ approach proposed the ratio of approach load to whole bone strength as a method for fracture risk assessment. To explore the clinical utility of this biomechanically-based fracture risk assessment in the context of osteoporosis treatment, we conducted a pilot study in 19 randomly selected postmenopausal women from the PaTH study who were treated for 1 yr with PTH(1-84) 100 mcg sq daily plus calcium and vit D. QCT-based finite element models were used to measure lumbar vertebral strength before and after treatment. A biomechanical model of the spine was used to estimate the subject-specific compressive load on the lumbar vertebrae during forward flexion with 10 kg in the hands. The factor of risk for vertebral fracture (Φ) was computed as the ratio of spinal load to vertebral strength where theoretically, fracture occurs when $\Phi > 1$. **Results:** Following treatment the distribution of Φ shifted towards lower values (ie. to the left), indicating a reduced risk for vertebral fracture (Figure). The mean values, SD and range of Φ were 0.73 ± 0.16 (0.48-1.05) and 0.58 ± 0.15 (0.33 - 0.83), pre- and post-treatment, respectively. Defining high fracture risk when $\Phi > 0.90$, 4 of 19 (21%) subjects were at high risk for fracture at baseline, whereas none were after treatment. In summary, this pilot study demonstrates the potential utility of an approach that combines biomechanical measures of bone strength with estimates of skeletal loading to assess the effects of osteoporosis therapies on fracture risk.



Disclosures: **M.L. Bouxsein**, None.

M412

Early Change in Bone Turnover Following Teriparatide (RhPTH 1-34) in the Eurofors Study: Influence of Prior Therapy and Association with BMD Change at One Year. A. Blumsohn¹, K. Brixen^{*2}, G. Sigurdsson^{*3}, F. Marin^{*4}, P. Ochs^{*4}, S. Liu-Leage^{*4}, A. Graebe^{*4}, R. Eastell¹. ¹University of Sheffield, Sheffield, United Kingdom, ²Dept of Endocrinology, Universitetshospital, Odense, Denmark, ³Landspítalinn University Hospital, Reykjavik, Iceland, ⁴Eli Lilly & Company, Windlesham, United Kingdom.

We examined the performance of three markers of bone formation following teriparatide. EUROFORS is an ongoing randomized prospective study of teriparatide in postmenopausal osteoporosis with or without prior antiresorptive (AR) therapy. During year one patients received open-label teriparatide (20 µg/d) with Ca (500 mg/d) and Vitamin D (400-800 IU/d). Participants were pre-defined as osteoporosis treatment-naïve (Group 1), or with adequate clinical response (Group 2) or inadequate response (Group 3) to prior AR therapy. 87.7% of patients with AR exposure used a bisphosphonate for a mean 33.5±30.7SD months. Markers of bone formation included serum procollagen I N-terminal Propeptide (PINP; Roche Diagnostics), bone specific alkaline phosphatase (BAP; Beckman Coulter Inc) and total alkaline phosphatase (TAP) at baseline, 1 month and 6 months of teriparatide. An additional sample was collected between 3-14 days of the 6 month visit in 82 women to determine repeat-test precision of assessment on teriparatide. The proportionate increases (mean,SEM) from baseline are tabulated by subgroup.

Group (N)	1 (182)	2 (177)	3 (398)
Pre Rx PINP ug/L	55.2±2.5	35.1±2.0	33.9±1.3
PINP %Δ1m	103±9	167±18	166±9
PINP %Δ6m	252±22	620±66	609±34
BAP %Δ1m	16.7±2.8	22.5±2.6	26.3±1.9
BAP %Δ6m	61.4±5.2	97.5±9.4	108.3±5.4
TAP %Δ1m	6.5±1.8	8.7±1.8	9.4±1.1
TAP %Δ6m	24.4±2.6	34.6±4.0	37.9±2.2

PINP showed by far the largest change in response to therapy. Individuals with prior AR had lower baseline values for each marker, but response after 6 months of teriparatide was not blunted. The absolute value of each marker on therapy at 6 months was independent of prior therapy (ANOVA all P>0.7). The repeat test CV of the three markers on therapy were similar (CV% nested ANOVA; PINP=9.9%; BAP=6.8%; Total AP=7.0%). The signal to noise ratio (%Response/CV%) was largest for PINP (S/N=53, 14 and 5 for PINP, BAP and TAP respectively at 6 months for all groups). Indices of bone formation or change in formation were only modestly predictive of change in BMD at the spine or total hip at 1 year. We conclude that PINP is likely to be the most sensitive marker to detect response to therapy. The response of bone formation markers in patients on teriparatide does not appear to be adversely influenced by prior antiresorptive therapy.

Disclosures: **A. Blumsohn**, Eli Lilly & Company 2.

M413

Structural Analysis of Vertebral Trabecular Bone Structure Allows to Assess the Effect of Teriparatide Treatment Independently of BMD. C. Graeff^{*1}, W. Timm^{*1}, J. Farrerons^{*2}, T. N. Nickelsen³, E. Blind⁴, J. Kekow^{*5}, R. Mörcke^{*6}, S. Boonen^{*7}, M. Audran^{*8}, C. C. Glüer¹. ¹Med. Physik, Klinik f. Diag. Radiologie, UK SH, Kiel, Germany, ²Hospital Santa Creu I Sant Pau, Barcelona, Spain, ³Eli Lilly & Company Europe, Bad Homburg, Germany, ⁴Med. Universitätsklinik, Würzburg, Germany, ⁵Fachkrankenhaus Rheumatologie, Vogelsang, Germany, ⁶Endokrinolog. Praxis, Magdeburg, Germany, ⁷University of Leuven, Leuven, Belgium, ⁸Centre Hospitalier Universitaire, Angers, France.

We have developed a method based on High Resolution Computed Tomography (HRCT) for following treatment-induced changes in bone structure in the vertebrae in vivo¹. Here we demonstrate that the effect of teriparatide (TPTD) treatment over one year can be measured at a central fracture site, the T-12 vertebrae. In the Eurofors study, osteoporotic women received 20 µg/d of TPTD over one year. Prior to study start most patients had received antiresorptive treatment, and a large fraction of them had not showed adequate response to this treatment. A third group had not received such treatment. HRCT scans were conducted at baseline, 6 and 12 months. Microstructural variables were named analogous to standard histomorphometry nomenclature; a prefix ‘a’ (for ‘apparent’) was added to indicate that variables are affected by the limits in spatial resolution (e.g. aBV/TV). Complete structural data were available for 67 patients aged 69.4 ± 6.8 years, and BMD of L1-3 was measured by QCT in 59 patients. All measured structural variables showed significant (p<0.0001) improvements under TPTD, see table. Increases were consistently larger during the first 6 months of treatment. TPTD response did not differ among the three pre-study treatment groups. Changes in structure and BMD over 6 months correlated with r²= 0.18 to 0.25, over 12 months with r²= 0.3 to 0.5. Compared to BMD the increases in aBV/TV (normalized to standard deviations at baseline) were larger at 6 months (p = 0.003) and 12 months (p = 0.001).

Variable	Baseline	Increase over 6 months		Increase over 12 months	
		[SD baseline]	[%]	[SD baseline]	[%]
aBV/TV	0.10 ± 0.05	0.35 ± 0.40	20.8%	0.55 ± 0.63	34.3%
aTb.N	0.36 ± 0.16 1/mm	0.27 ± 0.36	16.5%	0.40 ± 0.52	25.8%
aTb.Th	0.29 ± 0.04 mm	0.27 ± 0.34	4.0%	0.41 ± 0.50	6.2%
aTb.Sp	2.72 ± 1.24 mm	-0.12 ± 0.19	-9.5%	-0.17 ± 0.31	-13.9%
BMD	51.2 ± 19.1 mg/cm ³	0.20 ± 0.47	10.4%	0.38 ± 0.48	16.8%

Baseline results and increases in SD of baseline under TPTD treatment (mean±SD) TPTD treatment effects on bone structure can be monitored non-invasively. For aBV/TV treatment response is larger than for BMD, especially in the early phase of the treatment.

¹ W. Timm et al.: ‘In Vivo Measurement of Trabecular Bone Structure in Human Vertebrae Using HRCT’; this meeting

Disclosures: **C. Graeff**, Eli Lilly & Company 2.

M414

The Effect of Teriparatide Treatment on Quantitative Ultrasound in Women with Established Osteoporosis. S. Gonnelli, G. Martini, C. Caffarelli*, S. Salvadori*, A. Montagnani*, A. Cadiri*, R. Nuti. Department Internal Medicine, University of Siena, Siena, Italy.

Since BMD measurement by DXA does not seem able to register all the changes induced in bone by Teriparatide [hPTH (1-34)] and may give misleading results there is a pressing need to explore the utility of other diagnostic modalities in the non-invasive assessment of the effects of Teriparatide on bone. This study aimed to determine whether Teriparatide influences Quantitative Ultrasound (QUS) parameters and to compare the changes of QUS with that of BMD. Fifty-two postmenopausal women (aged 70.9 ± 8.1 years) with established osteoporosis under treatment with antiresorptive drugs for at least 12 months were studied. The patients, after a 1-month run-in phase during which they received only daily supplements of calcium(1000 mg) and vitamin D (400 IU), were randomly assigned to either once daily 20 µg Teriparatide (FORSTEO, Eli Lilly and Co) s.c. injection (n=26) or to continue the previous antiresorptive treatment (n=26). Here we report the 10 month interim results. At baseline and at 2-month intervals we measured QUS at calcaneus, by Achilles-GE, Lunar (speed of sound: SoS, broadband ultrasound attenuation: BUA and Stiffness: S), at phalanges, by Bone Profiler-IGEA (amplitude dependent speed of sound: AD-SoS, bone transmission time: BTT, fast wave amplitude: FWA) and BMD at right hand (BMD-H) by DXA-GE Lunar. BMD at lumbar spine and at femur (GE Lunar) was measured on a 6 monthly basis. Teriparatide significantly reduced BMD-H at month 4 (-2.2%, p<0.01) and at month 6 (-3.9%, p< 0.001) thereafter BMD-H returned progressively to basal values. In the Teriparatide group AD-SoS showed significant change only at month 4 (-1.7%, p<0.05) whereas BTT decreased significantly

ASBMR 27th Annual Meeting

($p < 0.01$) at all time points and FWA increased at month 6 (13%) at month 8 (12,7%) and at month 10 (6%). At month 6 the changes in BTT and BMD were significantly ($p < 0.05$) correlated. The patients treated with antiresorptives did not show any significant changes in QUS at phalanges and BMD-H. At month 10 the changes in S was similar in patients treated with Teriparatide and in those treated with antiresorptive drugs (2.1 % vs 1.5%). The changes in BMD-LS at month 6 were significantly ($p < 0.01$) higher in the Teriparatide group (5.6% vs 0.7%). In conclusion Teriparatide determined a notable, even though transient, decrease in BMD-H and differently influenced diverse ultrasound signal parameters (e.g. FWA increase and BTT decrease). This suggests that some QUS parameters (e.g. FWA/BTT ratio) could represent a potential instrument in monitoring bone response to Teriparatide in osteoporotic patients.

Disclosures: **S. Gonnelli**, None.

M415

Treatment of Osteopenic Rhesus Monkeys with Parathyroid Hormone 1-84 for 16 Months Improves Vertebral Trabecular Bone Quantity and Quality. **I. A. Moreau**^{*1}, **S. Y. Smith**¹, **R. E. Guldberg**², **C. H. Turner**³, **M. K. Newman**^{*4}, **J. Fox**⁴. ¹Charles River Laboratories Preclinical Services•CTBR, Senneville, PQ, Canada, ²Georgia Institute of Technology, Atlanta, GA, USA, ³Wyeth University, Indianapolis, IN, USA, ⁴NPS Pharmaceuticals, Salt Lake City, UT, USA.

Densitometry, histomorphometry and biomechanical studies have shown that daily treatment of osteopenic rhesus monkeys with parathyroid hormone 1-84 (PTH) increased vertebral bone density and significantly improved biomechanical competency by stimulating new bone formation. To assess local mechanisms of altered function, PTH-induced changes in trabecular architecture in thoracic vertebrae were evaluated by micro-computed tomography (μ CT). T10 vertebrae from Sham and ovariectomized (OVX) controls, and OVX animals treated with PTH at 5, 10 or 25 μ g/kg/day (8 to 10 animals/group) were scanned (VivaCT 40, Scanco). Results were compared with indices of bone strength from compression testing of T11/T12 vertebral cores. Relative to OVX controls, all PTH-treated groups demonstrated increased bone volume fraction (BV/TV) with associated increases in trabecular number (Tb.N), thickness (Tb.Th) and connectivity (Conn.D). Increasing the dose from 10 to 25 μ g/kg/day caused further increases in Tb.N and Conn.D, but not BV/TV or Tb.Th. However, a 39% improvement of yield stress in T11/T12 cores from the 10 g/kg/day group was reduced to 29% in animals given 25 μ g/kg/day. This apparent reversal in strength may be due, in part, to increased bone turnover, activation frequency and osteoid synthesis. The dose-related decrease in the structural model index (SMI) in the 5 and 10 g/kg/day groups was also partially reversed with high dose PTH, possibly contributing to the reversal in strength at this dose. A decrease in SMI is consistent with tunneling of thickened trabeculae as the mechanism to increase Tb.N, and modification of architecture from a rod-like to more plate-like structure. High dose PTH in this monkey study uniquely showed that higher bone turnover rates were not associated with further increases in BV/TV, but were associated with increased Conn.D and partial reversal of effects on SMI and bone strength. Treatment at 25 μ g/kg/day increased bone turnover resulting in a greater proportion of newly mineralizing bone that may have lower strength. Data for monkeys treated with PTH at 5 or 10 μ g/kg/day are consistent with human iliac crest biopsy data where higher bone formation with trabecular tunneling also resulted in increased Conn.D and a decrease in SMI (ASBMR 2005). This study demonstrates that PTH treatment improves biomechanical integrity by altering both the quantity and quality of trabecular bone in a dose-dependent manner.

Disclosures: **J. Fox**, None.

M416

The Effect of Teriparatide on Bone Remodeling Is not Related to Serum Levels of Osteoprotegerin and RANKL. **G. Martini**, **S. Gonnelli**, **B. Franci**^{*}, **M. Campagna**^{*}, **A. Avanzati**^{*}, **S. Salvadori**^{*}, **L. Gennari**, **R. Valenti**, **C. Caffarelli**^{*}, **B. Luciani**^{*}, **R. Nuti**. Department of Internal Medicine, University of Siena, Siena, Italy.

In vitro studies indicate that parathyroid hormone (PTH) decreases osteoprotegerin (OPG) secretion by the osteoblasts and increases RANKL production. Studies in healthy men have shown a negative correlation between endogenous PTH and serum OPG; moreover a decrease of serum OPG with an increase of serum RANKL have been reported by an interventional study where postmenopausal women with glucocorticoid osteoporosis were treated with intermittent injections of PTH. The aim of this study is to evaluate the behaviour of serum OPG and RANKL in women with established postmenopausal osteoporosis treated for six months with teriparatide (20 μ g/die). We enrolled 21 women (aged 71.5 ± 7.8 years) with one or more vertebral fractures and a T-score at densitometric examination of lumbar spine or proximal femur lower than -2.5. Patients on treatment were included in the study after a three months wash-out period. As control group, we studied 15 age-matched women. A blood sample was drawn from each patient at baseline and after two, four and six months from the beginning of teriparatide administration. Bone turnover was evaluated by: specific bone alkaline phosphatase (BSAP), osteocalcin (BGP), and intact N-terminal propeptide of type I procollagen (PINP) as markers of bone formation; C-telopeptides of Type-I collagen (CTX) as markers of bone resorption. Serum OPG and RANKL were assessed using a sandwich enzyme immunoassay (Osteoprotegerin and RANKL, Biomedica, Austria). Precision intra and interassay was lower than 10%. Basal values of bone markers, serum OPG and RANKL in treated patients and control group did not differ significantly. No correlations were found between bone markers and serum OPG and RANKL at baseline. Patients on teriparatide treatment showed a significant increase in both formation and resorption markers. The increase of BGP and PINP resulted statistically significant after two months, while the increase of CTX became significant

after four months. The highest values of all markers were found at sixth months. Serum OPG and RANKL levels did not change significantly, though they showed a tendency to increase. OPG peaked at fourth month, while the highest value of RANKL was found at sixth month. These data confirm that teriparatide stimulates bone formation by activating osteoblast function which leads, later, to osteoclast activation. Serum OPG and RANKL do not appear to be involved in parathyroid action on bone.

Disclosures: **G. Martini**, None.

M417

Evidence that the Cellular Mechanisms Responsible for the Anabolic Effect of Intermittent PTH Are Different in Murine Cancellous and Periosteal Bone. **A. A. Ali**, **C. A. O'Brien**, **I. Gubrij**, **R. A. Wynne**^{*}, **A. M. Parfitt**, **R. S. Weinstein**, **S. C. Manolagas**, **R. L. Jilka**. Div. Endo/Metab, Center for Osteoporosis and Metabolic Bone Diseases, Central Arkansas Veterans Healthcare System, University of Arkansas for Medical Sciences, Little Rock, AR, USA.

Intermittent administration of PTH to animals and humans stimulates bone formation on both cancellous and periosteal bone surfaces, but the underlying mechanisms are unclear. Intermittent PTH increases the number of osteoblasts on murine cancellous bone, at least in part, by attenuating their apoptosis (from a prevalence of ~12% to ~4% by ISEL labeling). To investigate the role of lining cell activation, we generated mice expressing thymidine kinase (tk) in cells of the osteoblast lineage under the control of the 3.6-kb fragment of the collagen promoter (Col3.6-tk mice). Immunolabeling indicated expression of the transgene in cancellous and periosteal bone cells. Consistent with earlier evidence for an osteoblast lifespan of ~10 days in murine cancellous bone, daily administration of ganciclovir (8 mg/kg) to 4-5 month old Col3.6-tk mice caused a gradual loss of cancellous osteoblasts over a 2 week period as they died naturally by apoptosis or became osteocytes, but could not be replaced by replicating progenitors. Lining cells were unaffected as determined by immunostaining for tk and the osteoblast lineage marker N-cadherin. Nevertheless, daily injections of 100 ng/g PTH(1-34) (along with ganciclovir) for an additional 2 weeks failed to stimulate bone formation in cancellous bone. Moreover, reactivation of the available lining cells to become osteoblasts did not occur. We now report that the prevalence of osteoblast apoptosis in periosteal bone is ~10-fold lower than in cancellous bone. Moreover, osteoblast number and bone formation rate (BFR) on the periosteal bone surface were unaffected by 2 weeks of ganciclovir administration to Col3.6-tk mice. Administration of PTH for an additional 2 weeks failed to stimulate periosteal bone formation in contrast to the 3-4-fold increase in BFR at this site in PTH-treated mice not given ganciclovir. These findings indicate that osteoblast lifespan in periosteal bone is much longer than in cancellous bone, reducing the potential importance of reduced apoptosis in the anabolic effect of PTH at this site. Moreover, maintenance of periosteal osteoblast number over a 4 week period is not as dependent on replacement by replicating progenitors as it is in cancellous bone. Hence, the anabolic effect of intermittent PTH on periosteal bone must involve actions of PTH on osteoblast progenitors that result in increased replication or differentiation, attenuation of their apoptosis, or a combination of these effects.

Disclosures: **A.A. Ali**, None.

M418

Oral Administration of ANABU™ (GlcNBu) to Ovariectomized (OVX) Rats Increases Bone Mineral Density (BMD), Long Bone Growth and Modulates Gene Expression in the Liver. **T. P. Anastassiades**, **X. Yang**^{*}, **J. Carran**^{*}, **K. Rees-Milton**^{*}, **D. Wainman**^{*}. Medicine, Rheumatology, Queen's University, Kingston, ON, Canada.

In previous studies, we had shown increased BMD in the long bones of an inflammatory arthritis model in the rat, by feeding GlcNBu (N-butylryl glucosamine). The aim of this study is to determine if oral administration of GlcNBu affects BMD, bone growth and gene expression in the non-OVX and the OVX-rat model. Female Sprague Dawley rats were randomized into four Groups (8 animals each). In addition to their normal diet, the animals were fed on a daily basis (once a day), with either of GlcNBu 200 mg/kg, or an equimolar amount of glucose (Glc) for 6 months. Groups 1, 2, 3 and 4 were, respectively: Glc-fed, non-OVX, (Control); GlcNBu-fed, non-OVX; Glc-fed, OVX; GlcNBu-fed, OVX. The BMD and body composition was measured by DXA (Hologic 4500, small animal software) every 2 months. At sacrifice (6 months), femurs were removed for physical measurements. The total RNA from the liver was extracted (RNeasy Kit, Qiagen) and gene expression was assessed by microarray (rat 8K gene, fluorescent Cy3 and Cy5), with Group 1 serving as the control for each of Groups 2-4. The Results showed that there was increased length of femurs for Group 4 vs 3 and in femoral wet weights (trends), as well as for Group 2 vs 1 (Figure). As expected, OVX led to increased body mass. The BMD of Group 4 femoral heads were higher than Group 3. Total body mineral content + lean body mass was also highest in Group 4. By microarray (all compared to Group 1), the number of regulated genes (> 2-fold) in the liver were: Group 2, 13; Group 3, 40; Group 4, 57. A small number of genes were highly regulated only in Group 3. We conclude that oral administration of GlcNBu results in enhanced growth and increased BMD of femurs in the OVX rat. The microarray analysis (rat 8K gene chip) showed that a number of genes in the liver were remarkably regulated by GlcNBu. Comparisons of the 4 experimental Groups suggest that GlcNBu feeding selectively regulates some genes post-ovariectomy. Since some of the selectively up-regulated genes in Group 4 encode for circulating protein growth factors, we speculate that this may constitute a mechanism of action for the effects of GlcNBu on bone.

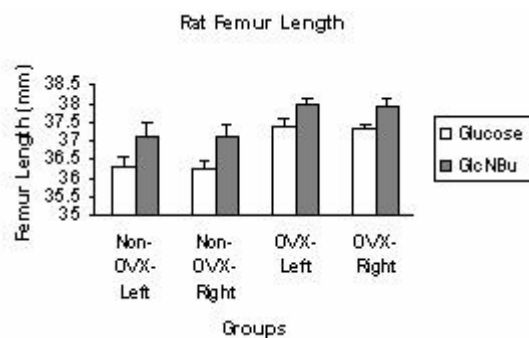


Fig. Effect of GlcNBu on Femoral Length (OVX and Controls)

Disclosures: **T.P. Anastasiades**, Anacoti Ltd: Patent submitted for utility of ANABU for Osteoporosis 4.

M419

A Non-Prostanoid EP4 Receptor Selective Prostaglandin E₂ Agonist Restores Bone Mass and Strength in Aged Ovariectomized (OVX) Rats. H. Z. Ke¹, D. T. Crawford¹, H. Qi¹, H. A. Simmons¹, T. A. Owen¹, V. M. Paralkar¹, M. Li¹, L. C. Pan¹, B. Lu¹, W. A. Grasser¹, T. A. Brown¹, K. O. Cameron¹, B. A. Lefker¹, P. DaSilva-Jordine¹, D. O. Scott¹, W. S. S. Jee², D. D. Thompson¹. ¹Pfizer Global R & D, Groton, CT, USA, ²Univ. of Utah, Salt Lake City, UT, USA.

We reported that knockout of EP4 receptor led to low bone mass in mice. The purpose of this study was to determine whether a newly discovered, non-prostanoid EP4 receptor selective agonist, CP432, could produce bone anabolic effects in aged OVX rats with established osteopenia. CP432 binds to the EP4 receptor with an IC₅₀ of 8 nM, while does not bind to other prostanoid receptors. CP432 stimulates the EP4 receptor to initiate signaling by the cAMP pathway with an EC₅₀ value of 0.6 nM. CP432 at 0.3, 1 or 3 mg/kg/d was given for 6 weeks by s.c injection to 12-month-old rats that had been OVX for 8.5 months. Total femoral bone mineral density (TF-BMD) by DEXA increased significantly by 8%, 20% and 20% in OVX rats treated with CP432 at 0.3, 1 and 3 mg/kg/d, respectively, as compared with OVX controls. TF-BMD did not differ in OVX rats treated with CP432 compared with sham controls. Trabecular bone histomorphometry of the 3rd lumbar vertebral body showed that CP432 completely restored trabecular bone volume back to the levels of sham controls, accompanied with an increase in trabecular thickness and trabecular number. Compared with OVX controls, a dose-dependent decrease in osteoclast number (-52 to -62%) and osteoclast surface and a dose-dependent increase in mineralizing surface, mineral apposition rate and bone formation rate-tissue reference (+42% to +130%) were found in OVX rats treated with CP432. CP432 at 1 and 3 mg/kg/d significantly increased total tissue area (+18% to +30%) and cortical bone area (+17% to +30%) in the tibial shafts compared with both sham and OVX controls. At these doses, CP432 significantly increased periosteal and endocortical bone formation and significantly decreased endocortical bone resorption. CP432 at all doses significantly and dose-dependently increased ultimate strength in lumbar vertebral body (+17 to +53%) compared with both sham and OVX controls. At 1 and 3 mg/kg/d, CP432 significantly increased maximal load in three point bending test of femoral shaft (+11% to +44%) compared with both sham and OVX controls. In summary, CP432 completely restored trabecular bone mass and strength to levels equal to sham controls, and restored cortical bone mass and strength to the levels greater than sham controls in established osteopenic, aged OVX rats by stimulating bone formation and inhibiting bone resorption on trabecular and cortical surfaces. These results suggest that EP4 receptor selective agonists have therapeutic potentials for osteoporosis.

Disclosures: **H.Z. Ke**, Pfizer Inc 1, 3.

M420

Development of Polymeric Drug Delivery Systems that Can Differentially Target Bone Formation and Resorption Surfaces. D. Wang¹, S. C. Miller², B. L. Anderson², M. Sima³, P. Kopeckova³, J. Kopecek³. ¹Pharmaceutical Sciences, University of Nebraska Medical Center, Omaha, NE, USA, ²Radiobiology Division, University of Utah, Salt Lake City, UT, USA, ³Pharmaceutics and Pharmaceutical Chemistry/CCCD, University of Utah, Salt Lake City, UT, USA.

The targeting of therapeutic agents to the skeleton and its different functional surfaces remains a particular challenge. Achieving this may enhance the efficacy of various drugs while reducing systemic side effects. Biocompatible water-soluble polymers provide a platform to attach various targeting moieties and drugs. The purpose of this study was to determine the ability of recently developed bone-targeting polymeric delivery systems to differentially recognize bone resorption or formation surfaces. For this, two bone-targeting moieties were compared; a bisphosphonate (Alendronate, Alen) and D-aspartic acid octapeptide (D-Asp₈). N-(2-hydroxypropyl)methacrylamide (HPMA) copolymers containing D-Asp₈ or Alen were synthesized via free radical copolymerization or polymer-analogous reaction. Fluorescein isothiocyanate (FITC) was attached to the polymers to served as a drug surrogate and a fluorescence detection probe. The delivery systems were administered (iv) to young male balb/c mice and female rats that had been ovariectomized (Ovx) for 3 months. Forty-eight hours prior to polymer injection, tetracycline was given as

a marker for active bone mineralization. Bones were collected 24 hours after the polymer injection and undecalcified sections were prepared for evaluation by fluorescence microscopy. The Alen-containing delivery system was found to extensively label bone surfaces with particular uptake on bone formation sites (TC labeled). However, the D-Asp₈-containing delivery system had a preferential uptake for resorption surfaces. When the fluorochrome patterns were compared with subsequent histological analyses, D-Asp₈-containing delivery system uptake sites were authentic resorption surfaces covered by osteoclasts. These findings demonstrate the preferential skeletal uptake of the novel delivery systems and differential uptake on formation and resorption surfaces using a bisphosphonate or D-aspartic acid octapeptide as targeting moieties. Many therapeutic agents may be attached to these delivery platforms via tissue specific releasing mechanisms (structures that are sensitive to cathepsin K, low pH, etc). The application of this novel technology may greatly enhance the delivery of promising new or established therapeutic agents to the affected sites for a variety of skeletal diseases, including osteoporosis and cancer bone metastases, and subsequently improve their efficacy and safety profile.

Disclosures: **D. Wang**, None.

M421

β-Antagonists Effects on Bone Architecture and Bone Cell Activity in the Tibia of Ovariectomized Rats. N. Bonnet¹, H. Beaupied¹, N. Laroche², L. Vico², E. Dolleaux¹, L. Benhamou¹, D. Courteix¹. ¹U658 Inserm & ATOSEP, Orleans, France, ²E0366 Inserm LBTO, St Etienne, France.

β-antagonists have been suggested to induce therapeutical effects on bone, but their effects on bone properties remain controversial. The aim of this study was to assess the effects of propranolol on both the trabecular/cortical bone architecture and biomechanical properties of the tibia. Sixty 6-month old Wistar female rats were divided into 5 groups. During 10 weeks SC daily injections were performed: 14 Sham rats and 14 ovariectomized (OVX) rats receiving normal saline (placebo), 42 OVX rats receiving propranolol (PRO: 100µg/kg/day n=14; 5mg/kg/day n=14; 20mg/kg/day n=14). Cortical and trabecular microarchitectural parameters were assessed by 3D microtomography. Propranolol effects were analysed by sequential Bone Mineral Density measurements (BMD, QDR1000W). Histomorphometry was performed on the proximal metaphysis. Mechanical properties were measured using three-point bending tests. On the tibia, propranolol 5mg and 100µg had significant higher BMD than placebo whereas propranolol 20mg and placebo groups had significant lower BMD compared to Sham. Compared to baseline, placebo rats displayed a lower BV/TV (-54.7%, p<0.001) whereas propranolol 100µg treatment lowered bone loss (BV/TV of -8.6%). Propranolol 100µg group had a higher Tb.Th (6.81%, p<0.001), Tb.N (46.15%, p<0.001), and a lower SMI (-54.0%, p<0.01) than placebo. Animals treated with propranolol 20mg did not differ from placebo group. The groups treated with propranolol 5mg had the same effect as propranolol 100µg except for the Tb.Th. In cortical bone of the mid-diaphysis, propranolol 100µg group had a significant higher cortical width (6.0%, p<0.01), lower cortical pore number (-52.4%, p<0.01) and cortical porosity (-63.63%, p<0.01) compared to placebo. Ultimate force was significantly higher only in Sham (92.56 N) and propranolol 100µg (94.12 N) groups compared to propranolol 20mg (p<0.01). Histomorphometric bone cell activities are shown in Table 1. These results point out the preventive effects of β-antagonists on the trabecular/cortical microarchitecture and bone marrow adiposity, suggesting a potential therapy in post menopausal women.

Table 1: Histomorphometric parameters of the proximal tibia of ovariectomized rats

	Oc.BS (%)	MAR (µm/day)	MS/BS (%)	N.At (/mm ²)
SHAM	4.78 ± 0.76 ^{a,c,d}	2.63 ± 0.08 ^{a,d,e}	0.12 ± 0.01 ^{a,c,d,e}	731 ± 21.60 ^{a,c}
OVX	12.84 ± 1.20 ^{b,c,e}	2.80 ± 0.12 ^{c,d,e}	0.31 ± 0.01 ^{b,d,e}	2034 ± 71.65 ^{b,d,e}
OVX PRO 20mg	16.10 ± 1.33 ^{a,b,d,e}	3.97 ± 0.08 ^{a,b}	0.29 ± 0.02 ^{b,d,e}	2018 ± 63.88 ^{b,d,e}
OVX PRO 5mg	10.60 ± 1.02 ^{b,c,e}	3.59 ± 0.20 ^{a,b,e}	0.23 ± 0.01 ^{a,b,c}	618 ± 75.25 ^{a,c}
OVX PRO 100µg	6.90 ± 0.41 ^{a,c,d}	4.37 ± 0.13 ^{a,b,d}	0.21 ± 0.02 ^{a,b,c}	869 ± 46.29 ^{a,c}

a: significant vs OVX, b significant vs SHAM, c significant vs OVX PRO 20mg, d significant vs OVX PRO 5, e significant vs OVX PRO 100µg, p<0.05.

Disclosures: **N. Bonnet**, None.

M422

Central Regulation of Cortical Bone: Opposing Effects of Y2 Receptor and Leptin Pathways. P. A. Baldock¹, S. Allison¹, A. Sainsbury², R. Enriquez¹, H. Herzog², E. Gardiner³, J. A. Eisman¹. ¹Bone and Mineral Research Program, Garvan Institute of Medical Research, Sydney, NSW, Australia, ²Neurobiology Program, Garvan Institute of Medical Research, Sydney, NSW, Australia, ³School of Medicine, University of Queensland, Brisbane, Qld, Australia.

The hypothalamus is known to modulate potent bone anabolic signals. Y2 receptor knockout [Y2R KO] and leptin deficient [ob/ob] mice display increased bone volume and osteoblast activity in cancellous bone. As cortical bone plays a major role in bone strength, we examined the effects of these two major pathways on cortical bone and osteoblast activity. Male, 16 week old wild type [wt], Y2R KO, ob/ob and Y2R/ob knockout mice were examined in groups of 5-8 animals. In addition, conditional hypothalamic Y2R knockout was conducted at 11 weeks of age with collection at 16 weeks. Cortical bone was examined by DXA [BMC mg, BMD mg/cm²] in isolated whole femora, in mid shaft and in distal thirds and histologically at the femoral mid-shaft cross section. Osteoblast activity was measured by mineral apposition rate [µm/d] in sagittal sections following dual tetracycline labelling. In Y2R KO, femoral shaft and distal BMC was significantly greater than wild type, consistent with greater cortical area and thickness. In ob/ob, despite significantly greater body weight, cortical area and thickness in the femoral shaft was

reduced compared to wild type and Y2R KO also for shaft and distal BMC compared to Y2R KO. In the Y2R/ob cross, despite shaft BMC being reduced compared to Y2R KO, shaft cortical area and thickness and distal BMC were similar to wild type levels. Due to comparable changes in BMC and bone area, BMD did not differ between groups at either site. Endocortical osteoblast activity was similar in Y2R KO and Y2R/ob and greater than in wt and ob/ob. Increased cortical osteoblast activity was also observed 5 weeks after hypothalamic ablation of Y2R in adult mice compared to controls (0.23 ±0.01 vs 0.17 ±0.02, p<0.05).

	wt	Y2R KO	ob/ob	Y2R/ob
Body weight (g)	26.7 ± 4	29.8 ± 1	52.4 ± 4 a b	47.3 ± 5 a b
Shaft BMC (mg)	7.8 ± 1	8.8 ± 1a	6.7 ± 1 b	6.6 ± 1 b
Shaft Cortical Area (mm ²)	0.9 ± 0.03	1.1 ± 0.04 a	0.7 ± 0.06 a b	0.9 ± 0.02 b
Shaft Cortical Thickness (µm)	191 ± 6	221 ± 7a	151 ± 13 a b	175 ± 7 b
Distal BMC (mg)	10 ± 1	12 ± 1a	9 ± 1 b	11 ± 1
Distal Endocortical MAR (µm/d)	0.21 ± 0.03	0.31 ± 0.03 a	0.24 ± 0.01b	0.32 ± 0.01a c

a p< 0.05 vs wt, b p< 0.05 vs Y2R KO, c p<0.05 ob/ob vs Y2R/ob. Therefore, the Y2 receptor pathway represents an adult-inducible stimulator of cortical as well as cancellous bone formation. Y2R deficiency increased BMC and osteoblast activity in Y2R/ob mice, in part counteracting the leptin-deficient reduction in cortical bone. These data clearly delineate opposing effects of Y2R and leptin pathways on cortical bone.

Disclosures: **P.A. Baldock**, None.

M423

Low-Dose Strontium Increased the Formation of New Lamellar Bone at the Periosteal Surface, with Normal Mechanical Competence. H. Oxlund, J. S. Thomsen*, T. T. Andreassen. Dept of Connective Tissue Biology, University of Aarhus, Inst of Anatomy, Aarhus, Denmark.

Low-dose strontium (Sr) has been shown to possess bone anabolic properties. In the present study the effects of Sr chloride on tibia cortical bone of intact and ovariectomised (OVX) rats were studied. Seventy-five Wistar female rats, 6 months old, were allocated to five groups: 1. Baseline control, 2. Sham operated group, 3. OVX, 4. Sr, 5. OVX + Sr group. Sr chloride, 4 mmol/day, was given in the drinking water for 140 days. The rats were injected with Alizarin Red 7 days after start of the experiment, and calcein 14 days and tetracycline 4 days before killing by exsanguination. The mechanical properties of the tibia diaphysis were studied by a 3-point-bending test. No differences were found in the stress, stiffness and deflection parameters between the groups. Mid-diaphyseal transverse sections were cut and dynamic histomorphometry was performed on the basis of the fluorochrome labels. The periosteal bone formation rate (BFR) was increased (P=0.01) in the Sr group (0.74 ± 0.13, mean ± SEM) compared with the control group (0.53 ± 0.09 µm³ x 10³/day). The periosteal BFR was increased (P=0.001) in the OVX group (1.74 ± 0.20 m³ x 10³/day) compared with the sham group (0.53 ± 0.09 µm³ x 10³/day). Likewise, the periosteal BFR was increased (P=0.02) in the OVX + Sr group (2.47 ± 0.21 m³ x 10³/day) compared with the OVX group. Sr did not increase the mid-diaphyseal endocortical bone formation. In conclusion, low-dose Sr given perorally increased the periosteal bone formation, but did not stimulate endocortical bone formation. The new cortical bone exhibited a normal lamellar structure, and the mechanical competence of the cortical bone seemed to be preserved.

Disclosures: **H. Oxlund**, None.

M424

Strontium Ranelate Effects on Osteoblasts: A Potential Role of Endogenous Prostaglandins. S. Choudhary¹, C. Alander*¹, P. Halbout*², L. Raisz¹, C. Pilbeam¹. ¹UConn Center for Osteoporosis, University of Connecticut Health Center, Farmington, CT, USA, ²Groupe Servier, Courbevoie Cedex, France.

Strontium ranelate is a new anti-osteoporotic treatment with a dual effect on bone formation and bone resorption. Previous studies have shown that strontium can increase prostaglandin (PG) production in osteoblasts by increasing the expression of the inducible cyclooxygenase (COX)-2. The present study was designed to assess the role of endogenous PG production in the anabolic response to strontium ranelate. Bone marrow stromal cells (MSC) from 7 to 8 wk old mice and primary calvarial osteoblast (POB) cells from neonatal mice were cultured under differentiating conditions for 10-14 d. Strontium was tested at 1 and 3 mM, mixed with ranelic acid at 10 and 30 µM, respectively, in order to reflect the ratio found in the human plasma of patients after dosing. Measurements included bone alkaline phosphatase (ALP) activity, normalized to total protein, and alizarin red staining for mineralization. In MSC cultures, continuous treatment with strontium ranelate (3 mM Sr²⁺) for 10 and 14 d significantly increased ALP activity by 92% (p<0.01) and 63% (p<0.01), respectively, as well as mineralization. In the presence of NS-398 (0.1 µM), a selective inhibitor of COX-2 activity, there was no significant increase in ALP activity with strontium ranelate in MSC cultures. When MSC cultures were treated with strontium ranelate for varying intervals (first 3, first 7 or last 7 d) during 14 d of culture, treatment for the first 7 d with strontium ranelate (1 and 3 mM Sr²⁺) increased ALP activity by 69% (p<0.05) and 110% (p<0.01), respectively. Cumulative PGE₂ levels in MSC cultures measured after a 7 d treatment with strontium ranelate (1 and 3 mM Sr²⁺) were respectively elevated 2.4-fold (p<0.01) and 11.0-fold (p<0.01). NS-398 blocked all significant increases in PGE₂ production. In POB cells cultured for 14 d, treatment with strontium ranelate (3 mM Sr²⁺) for 0-3, 0-7, or 0-14 d of culture significantly increased ALP activity by 186% (p<0.01), 95% (p<0.05) and 92% (p<0.05), respectively. NS-398 also inhibited the increase in ALP activity in this system (preliminary data). To summarize, strontium ranelate stimulated the anabolic response of MSC and POB as shown by the increased ALP activity and mineralization in both models, which was coupled to an endogenous PG

production. We conclude that the ability of strontium ranelate to stimulate endogenous PG production represents one attractive hypothesis to support the beneficial effect of strontium ranelate on bone formation.

Disclosures: **S. Choudhary**, Servier, Courbevoie Cedex, France 2.

M425

A Peptide Derived from Chemokine CXCL7 Stimulates Bone Formation and Increases BMD in OVX Rats. S. A. F. Peel, G. O. Ramirez-Yañez*, D. Squires*, L. T. Malek. Osteopharm Inc, Oakville, ON, Canada.

It was previously reported that a fragment of the human CXC chemokine neutrophil activating peptide-2 (NAP-2, CXCL7) stimulated bone mineral apposition in rats (Tam 2004, US Pat.No. 6,693,081). The purpose of this study was to determine whether the modified 8 amino acid peptide Ac-TTSGIHPK-amide derived from CXCL7 (OSB) would increase bone formation in ovariectomized (OVX) rats. Virgin SD rats were OVX or sham operated at 23 weeks of age and placed into groups (N=12) on the basis of DEXA measurements of bone and body composition. Eight weeks after surgery the rats in 3 groups received injections for 5 days a week of PBS (sham and OVX groups) or OSB (300 nmoles/kg) in PBS. Changes in bone were monitored monthly by DEXA (regional and whole body) and bimonthly by pQCT. After 26 weeks of treatment the rats were sacrificed, serum samples were collected for biomarker analysis and bones were collected for terminal analysis by pQCT or fixed for histology. Rats treated with OSB had significantly increased whole body BMC and BMD compared to OVX control by DEXA (p<0.03). Terminal analysis of the lumbar spine (L3) by pQCT demonstrated that OSB significantly increased total BMC and BMD (p<0.02) and cortical area and BMC (p<0.006) relative to the OVX control. For tibia and femur, the OSB treated group had significantly higher trabecular BMC and BMD (p<0.03) at metaphyseal sites, and higher cortical area and BMC (p<0.04) at diaphyseal sites. The OSB group had significantly higher total BMC and BMD (p<0.03) at the femoral neck than the OVX control. Analysis of blood samples for markers of collagen degradation showed no differences between OVX and OSB treated animals. Samples analyzed for osteocalcin showed an increase with OSB treatment that neared significance (p = 0.09). Based on these results we conclude that OSB stimulates bone formation and increases BMD in OVX rats. These results suggest that OSB may be efficacious as bone anabolic drugs for the treatment of osteoporosis.

Disclosures: **S.A.F. Peel**, Osteopharm Inc 3.

M426

Novel Peptides Stimulate Bone Formation *In Vitro* and *In Vivo*. G. O. Ramirez-Yañez*, S. A. F. Peel, D. Squires*, L. T. Malek. Osteopharm Inc, Oakville, ON, Canada.

The novel peptide OSA was derived from the sequence of a cDNA clone in a fetal human liver library. A series of structurally related 10 amino acid peptides were developed based on the active region of the original peptide (Tam 2004 patent WO2004/050701). The aim of the present study was to test the efficacy of these novel peptides in bone formation. Neonatal rat calvaria (3-5 days old) were either treated with OSA peptides (10⁻⁹ M), or IGF-1 (50 ng/ml) or left untreated. Mineralization and matrix synthesis were evaluated based on incorporation of ⁴⁵Ca and ³H-proline. Calvaria treated with OSA peptides had a significantly higher incorporation of ⁴⁵Ca and ³H-proline compared with the untreated control (p<0.05), similar to the IGF-1-treated calvaria. Virgin SD rats were OVX or sham operated at 23 weeks of age and placed into groups (N=12) on the basis of DEXA measurements of bone and body composition. Eight weeks after surgery the rats received injections for 5 days a week of PBS (sham and OVX groups) or 1 of 3 OSA peptides (117M, 153M or 155M; 300 nmoles/kg) in PBS. Changes in bone were monitored monthly by DEXA (regional and whole body) and bimonthly by pQCT. After 26 weeks of treatment the rats were sacrificed, serum samples were collected for biomarker analysis and bones were collected for terminal analysis by pQCT or fixed for histology. OSA treated rats showed significant increases in whole body BMC and BMD after 3 and 6 months of treatment as compared with the OVX control (p<0.05). Terminal pQCT analysis indicated that rats treated with one OSA peptide analog (155M) had significantly higher trabecular BMD at lumbar vertebrae (p<0.05) and at metaphyseal sites in the tibia (p<0.007) and femur (p<0.03) than the OVX rats treated with vehicle. Total BMD of the femoral neck was significantly higher (p<0.04) in the group treated with OSA 155M than in the OVX control. Serum samples tested for markers of bone resorption (RatLaps) or formation (osteocalcin) showed no significant differences between the groups, possibly due to the large variations observed within each group. These results demonstrate that OSA peptides stimulate bone formation *in vitro* and *in vivo*. Further these peptides may be useful in the treatment of osteoporosis.

Disclosures: **G.O. Ramirez-Yañez**, Osteopharm Inc 3.

M427

Characterization of Osteogenic Oxysterols and their Molecular Mechanism(s) of Action. J. A. Richardson*¹, C. M. Amantea*¹, K. Nguyen*², M. E. Jung*², T. J. Hahn¹, F. Parhami¹. ¹Medicine, UCLA, Los Angeles, CA, USA, ²Chemistry, UCLA, Los Angeles, CA, USA.

Identification of anabolic agents that enhance bone formation is critical for the better management of bone fractures and osteoporosis. We previously reported that specific oxysterol compounds, products of cholesterol oxidation, used in combination have potent osteogenic properties when administered to osteoprogenitor cells *in vitro* and to neonatal mouse calvarial organ cultures *ex vivo*. The oxysterol combinations with osteogenic

activity consisted of 22(R)- or 22(S)-hydroxycholesterol with 20(S)-hydroxycholesterol (RS and SS, respectively). Recently we found that the oxysterol 20S, when used alone at doses of 5-15 μ M in cultures of marrow stromal cells, M2-10B4 (M2), induced the formation of mature osteoblastic cells demonstrated by the induction of alkaline phosphatase (ALP) activity, Runx2 DNA binding and protein expression, osteocalcin (OCN) mRNA expression, and mineralization. Pre-treatment or co-treatment of cells with 22S or 22R oxysterols greatly enhanced the osteogenic effects of 20S suggesting that 22S and 22R prime the osteoprogenitor cells for better responsiveness to 20S. We have identified other oxysterols with osteogenic properties when used alone or in combination with 22R or 22S. These newly identified oxysterols are 5-cholesten-3 β , 20 α -diol 3-acetate, 24(S),25-epoxycholesterol, 24(S)-hydroxycholesterol (also known as cerebrosterol), and 26-hydroxycholesterol, all of which induced the markers of osteogenic differentiation in M2 cells. In contrast, 4 β -hydroxycholesterol and 7 α -hydroxycholesterol did not have osteogenic properties suggesting that the carbon side chain of the sterols and the position of the hydroxyl groups are important characteristics of the osteogenic sterols. Structurally similar molecules to oxysterols, estren, estrone, and β -estradiol, which do not have the carbon side chain and have differences in the position and number of their double bonds, did not have any osteogenic properties. Pretreatment of M2 cells with the hedgehog signaling inhibitor, cyclopamine (1-10 μ M), significantly inhibited SS-induced ALP activity, Runx2 protein and OCN mRNA expression, and mineralization. In addition, pretreatment of cells with the inhibitor of Wnt signaling, DKK-1 (1 μ g/ml), significantly inhibited SS-induced ALP activity, OCN expression and mineralization but not Runx2 protein expression. These results suggest that the oxysterol-induced osteogenic differentiation of cells is mediated through hedgehog- and Wnt-dependent mechanisms. Oxysterols form a new class of osteoinductive agents that may be useful in the enhancement of local and/or systemic bone formation.

Disclosures: **F. Parhami**, None.

M428

Systemic Administration of Thyroid Stimulating Hormone (TSH) Prevents and Restores Bone Loss in Rats Following Ovariectomy. K. T. Sampath¹, P. Simic^{*2}, R. Sendak¹, N. Draca^{*2}, S. Schiavi^{*1}, J. McPherson^{*1}, S. Vukicevic². ¹Genzyme Corporation, Framingham, MA, USA, ²Laboratory for Mineralized Tissues, Zagreb Medical School, Zagreb, Croatia.

Thyroid stimulating hormone (TSH) affects bone remodeling as demonstrated by reduced bone mass in TSH receptor knockout mice (Abe E, et al Cell, 115: 130-140, 2003) and in post-menopausal euthyroid patients following single administration of human TSH (Mazzioti G, et al., JBMR 20: 480-486, 2005). In the present study, we examined whether the systemic administration of TSH could prevent and restore bone loss in an osteoporosis animal model. Female SD rats were ovariectomized (OVX) at 6 months and the TSH therapy was started immediately (prevention mode), and 3 months following OVX (restoration mode). Animals were divided into six groups (12 rats/group): (1) Sham, (2) Ovariectomized (OVX), (3) OVX + TSH (low dose), (4) OVX + TSH (medium dose), (5) OVX + TSH (high dose) and (6) OVX + 17- β estradiol. Recombinant human TSH (Thyrogen®) (0.7, 7.0 and 70 μ g/rat) or rat pituitary-derived native TSH (0.01, 0.1, 0.3, 1, 3 and 10 μ g per rat) were administered i.p., three times per week. The whole body, lumbar spine and hind limbs bone mineral density (BMD) were measured at 2 week intervals in vivo, following 8-16 weeks of therapy. Results show that TSH significantly increased BMD at all measured sites both in the prevention and restoration mode. Doses of 0.1 and 0.3 μ g/rat of TSH significantly increased the BMD of the hind limbs whereas the dose of 0.01 μ g/rat of TSH did not have an effect on BMD. High doses of human and rat TSH had lesser effect on BMD. Ex vivo BMD values of excised femur, tibia and lumbar spine confirmed the in vivo measurements. Compared to OVX, OVX plus TSH increased cortical thickness of femurs by 14.5% as measured by pQCT, and increased BV/TV by 163%, trabecular thickness by 21.1% and trabecular number by 125% as determined by μ CT analyses. Serum biochemical analyses suggest that TSH suppresses the ovariectomy-induced bone turnover by decreasing osteocalcin and C-telopeptide levels to sham values. Importantly, low TSH doses had no effect on serum T3 and T4 values, suggesting TSH at these levels may have a direct effect on bone without affecting the thyroid axis. In vitro studies demonstrate that TSH inhibits RANKL induced-osteoclast formation, osteoclast-mediated resorption, promotes osteoblast differentiation and provides protection against apoptosis in osteoblast enriched cultures. These results demonstrate for the first time that systemically administered TSH can suppress high bone turnover following ovariectomy and exert both anti-resorptive and anabolic effects on bone remodeling, resulting in both prevention and restoration of bone loss in aged OVX rats.

Disclosures: **S. Vukicevic**, None.

M429

Characterization of Bone and Cartilage Stimulating Peptide Derived from the Collagen Type I Alpha I Chain. D. Sindrey, E. Plawinski^{*}, R. R. Simon^{*}, J. Auluck^{*}, J. Terryberry^{*}. Millenium Biologix Corp, Mississauga, ON, Canada.

We have previously reported on the bone stimulating effects of Bone and Cartilage Stimulating Peptides for the treatment of bone trauma and other bone diseases like osteoporosis. Originally extracted from bovine bone as BCSS (Bone Cell Stimulating Substance, Clark I. et al 1988) we have demonstrated through extensive purification and structure function studies, one of the active components as being a fragment of procollagen 1A1 1156-1174. Purification of BCSS bovine extracts by RP-LC, ion exchange and size exclusion chromatography, identified an active collagen fragment that was confirmed by identification from digests of collagen Type I. Several overlapping candidate peptides ranging from a 4mer to 16mer were synthesized with different N and C terminal truncations and/or additions to optimize biological activity in a rat tibia model of bone

formation. No ectopic bone formation was noted in any of the animals. Histologically, the change in bone size was a result of periosteal bone proliferation and was peptide related. A noticeable intra-medullary bone proliferation was also seen in rats treated with the most active peptides and was considered peptide-related as it was not observed in any rats treated with carrier or Saline. Typical increases in local BMD were 10-12% above controls with peptides as small 450 kD. In vitro testing demonstrated two basic cellular responses in rat calvaria cells of increased proliferation and differentiation as seen by the 3 fold increase in WST assay; a 36% increase in the number of bone nodules and a 71% increase in bone area formed in calvaria cultures. These data corresponded well with observations in vivo of a rapidly proliferating periosteum and its subsequent mineralization. Bioactivity was sequence dependent and resided in two novel and complimentary sequence motifs in the BCSP-1 molecule. The synthesis of these molecules by solid phase peptide chemistry and their subsequent testing in a rat tibia model of bone formation validated the collagen origin of the original BCSS bovine extracted material. The actions of BCSP peptides on cell interactions in osteogenesis demonstrated specificity toward bone cells present in the periosteum as noted by the absence of heterotopic or ectopic bone formation. The rapid onset of the stimulatory effect and the absences of ectopic bone formation make the BCSP peptides a potent site-specific candidate for the treatment of bone fracture and trauma. Osteoinductive BCSP is currently in development for the treatment of local bone repair and systemic treatment of various skeletal diseases.

Disclosures: **D. Sindrey**, Millenium Biologix 1, 3.

M430

Retrovirus-Mediated Gene Transfer of RANK-Fc Ameliorates Bone Resorption in Ovariectomized Mice. D. Kim^{*1}, S. Her^{*2}, S. Cho^{*2}, S. Kim², S. Kim^{*2}, C. S. Shin². ¹Department of Internal Medicine, Dankook University College of Medicine, Cheon-An, Republic of Korea, ²Department of Internal Medicine, Seoul National University College of Medicine, Seoul, Republic of Korea.

Postmenopausal osteoporosis is characterized by increased bone resorption due to estrogen deficiency. RANK-Fc, a fusion protein that specifically blocks RANKL binding to RANK, has been known to be efficient and well-tolerated in animal models of osteoporosis. Here we show that cell-based gene therapy with RANK-Fc effectively prevented bone loss in ovariectomized (OVX) mice. Twenty-four young adult female C57B mice were used and repeated intraperitoneal injection of mesenchymal stem cells (MSCs) transduced with retrovirus was performed as follows: (1) Sham-operated mice (SHAM, n=6) (2) OVX mice treated with PBS (OVX-P, n=6) (3) OVX mice injected with MSCs cells transduced with control retrovirus (OVX-GFP, n=6) (4) OVX mice injected with MSCs transduced with RANK-Fc (OVX-RANK-Fc, n=6). Cellular expression of RANK-Fc was confirmed by Western blot analysis of cell lysates and conditioned medium, and also by ELISA for the mice serum. Measurement of BMD by dual energy x-ray absorptiometry (PIXImus) revealed that OVX-RANK-Fc group showed significantly higher BMD (p<0.05) than either the OVX-P group or OVX-GFP group after 8 weeks. The expression of GFP, which is co-expressed with RANK-Fc was observed in the liver, spleen, and intra-abdominal fat of mice but not in femur or freshly isolated bone marrow. Our results suggest that expression of RANK-Fc by genetically modified MSCs may be a feasible option for ameliorating the OVX-induced bone loss.

Disclosures: **D. Kim**, None.

M431

Lumbar Spinal Mobility and Back Extensor Strength Are Important Factors for Quality of Life in Patients with Osteoporosis. N. Miyakoshi, M. Hongo, S. Maekawa, Y. Ishikawa^{*}, Y. Shimada^{*}, E. Itoi^{*}. Orthopedic Surgery, Akita University School of Medicine, Akita, Japan.

We have recently demonstrated that quality of life (QOL) in patients with osteoporosis is affected by the total spinal mobility and that the back extensor strength is the most significant contributor to the total spinal mobility. However, how much thoracic and lumbar spinal mobilities affect QOL has not been clarified. In this study, we evaluated the relation between QOL and thoracic and lumbar spinal mobilities and their related factors in patients with osteoporosis. A total of 174 postmenopausal women with osteoporosis aged over 50 years (mean, 68 years) were included in this study. Their QOL was evaluated using the Japanese Osteoporosis QOL Questionnaire (JOQOL) proposed by the Japanese Society for Bone and Mineral Research. JOQOL contains six domains with higher scores indicating higher levels of QOL. Bone mineral density (BMD) of the lumbar spine, proximal femur, and whole body were measured with dual-energy X-ray absorptiometry. The kyphosis angle and range of motion (ROM) of thoracic and lumbar spine were measured in the upright position and at maximum flexion/extension with a computer-assisted device (SpinalMouse®). The number of vertebral fractures was evaluated with lateral radiographs of the spine. Bilateral grip strengths and isometric back extensor strength were evaluated with dynamometers. JOQOL showed significant correlation (p<0.05) with age (r=-0.303), back extensor strength (r=0.455), grip strengths of dominant and non-dominant hands (r=0.273 and r=0.255, respectively), number of vertebral fractures (r=-0.282), BMDs of proximal femur and whole body (r=0.200 and r=0.157, respectively), lumbar kyphosis angle (r=-0.296), and lumbar spinal ROM (r=0.345). Among these factors, the multiple regression analysis revealed that the back extensor strength and lumbar spinal ROM were the significant contributors to the JOQOL. We conclude that back extensor strength and lumbar spinal mobility (but not thoracic mobility) are the important factors for QOL in patients with postmenopausal osteoporosis.

Disclosures: **N. Miyakoshi**, None.

M432

Calcium Phosphate versus Polymethylmethacrylate - A Prospective, Randomized, Clinical Trial of Percutaneous Balloon Kyphoplasty. T. R. Blatter^{*1}, A. Weckbach^{*2}. ¹Trauma & Reconstructive Surgery, Leipzig University, Leipzig, Germany, ²Trauma Surgery, Wuerzburg University, Wuerzburg, Germany.

In kyphoplasty and vertebroplasty, polymethylmethacrylate (PMMA) currently represents the standard augmentation material. It is characterized, however, by a lack of osteointegration and its limited biocompatibility. This prospective, randomized trial investigated the feasibility of calcium phosphate (CaP) for augmentation of osteoporotic vertebral body fractures by means of percutaneous balloon kyphoplasty in comparison to PMMA. Inclusion criteria were osteoporotic fractures of vertebral bodies in the thorocolumbar spine, patient age ≥ 65 years, and fracture age ≤ 4 months. Exclusion criteria were tumor lesions and additional posterior instrumentation. A total of 60 osteoporotic vertebral body fractures in 56 patients were included. CaP and PMMA were randomly applied in 30 cases each. All 60 fractures were classified type A (acc. to Magerl et al.). Of these, 19 were classified type A3. 52/56 patients experienced p.op. pain relief (2.1 ± 1.9 to 8.2 ± 1.5 on a Visual Analogue Scale from 0 "worst" to 10 "best"). Endplate angles were restored by $6.2^\circ \pm 2.9$ on average. For both parameters (pain relief and restoration of endplate angle), no statistically significant difference was found between the groups. Cement-specific complications were vascular embolism using PMMA (n=2); subtotal "cement-washout" using CaP (n=1); and substantial loss of correction on radiographs 6 weeks p.op. due to cement failure in all fractures type A3, if CaP had been applied (n=9). There was no case of cement failure, when PMMA had been used. Currently in kyphoplasty, a routine use of CaP cannot be recommended. Due to its minor resistance to bending, extension, and shear forces compared to PMMA, there is a high risk for cement failure and subsequent loss of correction in the well defined clinical setting of osteoporotic vertebral body fractures type A3.

Disclosures: **T.R. Blatter**, *Kyphon* 5.

M433

Health-Related Quality of Life in Postmenopausal Women with Osteoporosis and an Inadequate Response to Anti-Osteoporosis Medication: Baseline Results of the French Cohort from the Observational Study of Severe Osteoporosis (OSSO). P. Fardellone¹, I. Jamonneau^{*2}, A. Alfonsi^{*2}, S. Liu-Léage^{*2}. ¹CHRU, Amiens, France, ²Lilly France, Suresnes, France.

Osteoporosis-related fractures can cause pain, physical impairment and loss of functional ability, thereby significantly impairing patient quality of life. However, the impact of an inadequate response to anti-osteoporosis treatment, especially on patient quality of life, is not well understood. The Observational Study of Severe Osteoporosis (OSSO) is a 12-month, European, prospective, observational study of postmenopausal women with osteoporosis and an inadequate response to anti-osteoporosis therapy, defined as: (i) the presence of a new fragility fracture (vertebral or non-vertebral) despite prescription of any approved anti-osteoporosis therapy for at least 12 months before the fracture, and/or (ii) discontinuation of any approved anti-osteoporosis therapy due to compliance problems and/or side effects. The primary objective of OSSO is to evaluate changes in health-related quality of life (HRQoL). A total of 418 women enrolled in France were included in the baseline analysis: 196 (46.90%) in the index fracture cohort and 222 (53.10%) in the compliance/side effect cohort, a less severe patients' group based upon the patients characteristics. HRQoL was assessed using the osteoporosis disease-specific QUALEFFO questionnaire (Lips et al, Osteoporos Int 1999). At baseline, the mean (SD) total QUALEFFO score for the OSSO French population (n= 418) was 42.7 (18.8), and the mean (SD) scores for the five domains were: pain 46.2 (27.4), physical function 33.0 (23.0), social function 56.9 (25.9), general health 62.7 (20.7) and mental function 42.4 (19.2). The mean total QUALEFFO score was significantly higher in the index fracture cohort than in the compliance/side effect cohort (47 vs 38.8, $P<0.001$). Similarly, the scores for each of the five domains were significantly higher in the index fracture cohort. In the subgroup of index patients who sustained a vertebral fracture a few months before enrolment in the study, the mean total QUALEFFO score was higher and respectively 55.4 (17) in those with a lumbar vertebral fracture, 53.1 (15.8) with a thoracic vertebral fracture, 49.4 (15) with a lumbar and thoracic vertebral fracture. In conclusion, there is a clear impairment of quality of life at baseline in the French postmenopausal women with osteoporosis taking part in the OSSO study. The impairment is more pronounced in the index group as it was the most severe group with a higher proportion of patients with multiple fractures history. The vertebral fracture worsens the quality of life.

Disclosures: **P. Fardellone**, *None*.

M434

Health-Related Quality of Life in Postmenopausal Women with Osteoporosis and an Inadequate Response to Anti-Resorptive Medication: Baseline Results from the Observational Study of Severe Osteoporosis (OSSO). D. Sykes^{*1}, C. Cooper², S. Adami³, P. Fardellone^{*4}, F. Jakob^{*5}, J. Melo-Gomes^{*6}, E. Martin-Mola⁷, T. Nicholson^{*1}, N. Thalassinou^{*8}, D. Torgerson^{*9}, F. Marin¹. ¹Eli Lilly, Windlesham, United Kingdom, ²MRC Environmental Epidemiology Unit, Southampton, United Kingdom, ³University of Verona, Verona, Italy, ⁴Hospital Nord, Amiens, France, ⁵Julius-Maximilians University, Wurzburg, Germany, ⁶Servimed, Lisbon, Portugal, ⁷Hospital La Paz, Madrid, Spain, ⁸Evangelismos General Hospital, Athens, Greece, ⁹University of York, York, United Kingdom.

Osteoporosis-related fractures can cause pain, physical impairment and loss of functional ability, thereby adversely affecting HRQoL. However, the impact of an inadequate response to osteoporosis treatment, especially on HRQoL, is not well understood. OSSO is a 12-month, European, prospective, observational study of postmenopausal women with osteoporosis and an inadequate response to anti-resorptive therapy, defined as: (i) the presence of a new fragility fracture despite prescription of any approved anti-resorptive therapy for at least 12 months before the fracture, and/or (ii) discontinuation of any approved anti-resorptive therapy due to compliance problems and/or side effects. Patients who satisfied both criteria were analysed according to the first event. The primary objective of OSSO is to evaluate changes in HRQoL. 2314 women were included in the baseline analysis: 1309 (57%) in the index fracture cohort and 1005 (43%) in the compliance/side effect cohort. HRQoL was assessed using QUALEFFO. Each domain score and the total QUALEFFO score are expressed on a scale from 0 to 100, with 0 corresponding to the best HRQoL. At baseline, the mean (SD) total QUALEFFO score for completers (n=2279) was 46.9 (18.6), and the mean (SD) scores for the five domains were: pain 52.4 (26.5), physical function 39.0 (22.9), social function 56.7 (25.5), general health 68.9 (20.9) and mental function 44.7 (18.0). The mean total QUALEFFO score was significantly higher in the index fracture cohort than in the compliance/side effect cohort (49 vs 44, $P<0.001$). Similarly, the scores for each of the five domains were significantly higher in the index fracture cohort. The mean total QUALEFFO scores varied across the participating countries, ranging from 42.7 in France to 50.7 in Germany. The median total QUALEFFO score of the OSSO population (47.0) is higher than that reported previously in control subjects (20.3) and osteoporosis patients with vertebral fracture (35.3) (Lips et al, Osteoporos Int 1999). In conclusion, there is a clear impairment of HRQoL at baseline in the postmenopausal women with osteoporosis taking part in OSSO.

Disclosures: **F. Marin**, *Employee* 3.

M435

BALTO I: Women Treated for Osteoporosis Rate Preference and Convenience for Once-Monthly Ibandronate versus Once-Weekly Alendronate. R. Emkey¹, N. Binkley², L. Seidman³, C. Rosen⁴. ¹Reading Hospital, Reading, PA, USA, ²Institute on Aging, University of Wisconsin-Madison, Madison, WI, USA, ³Philadelphia Women's Research, Philadelphia, PA, USA, ⁴Saint Joseph Hospital, Bangor, ME, USA.

Adherence to oral bisphosphonate therapy for osteoporosis treatment is suboptimal. Whereas prior studies have evaluated the impact of treatment adherence on outcomes such as fracture risk and bone mineral density, few have investigated patient-reported preferences for available dosing regimens. The purpose of the BALTO I study was to evaluate patient reports of preference and convenience for once-monthly ibandronate versus once-weekly alendronate. Women with PMO (n=342) were enrolled in a 6-month, prospective, randomized, open-label, 2-sequence, 2-period, crossover study (BALTO I) which examined their preferences for once-monthly oral ibandronate (150 mg) or once-weekly oral alendronate (70 mg). In sequence A (n=170) patients received once-monthly ibandronate for 3 calendar months followed by once-weekly alendronate for 12 weeks. In sequence B (n=172), the 2 treatment periods were reversed. There was no washout period between the 2 treatment regimens. Subjects completed a self-administered questionnaire at the final study visit during which they were asked to rate preference and convenience for monthly ibandronate and weekly alendronate. The intent-to-treat population (n=298) included women who received at least one dose of each study medication and completed the preference question. The majority of women preferred the once-monthly ibandronate treatment regimen and found it more convenient than once-weekly alendronate. Of those women expressing a preference (n=276), 71.4% preferred monthly ibandronate while 28.6% preferred weekly alendronate. Of subjects reporting on convenience (n=264), 74.6% found the monthly ibandronate dose more convenient compared with 25.4% who found weekly alendronate more convenient. Significantly more women with PMO preferred monthly ibandronate therapy and found it more convenient when compared with once-weekly alendronate. These findings suggest that once-monthly ibandronate treatment may be associated with improved medication adherence.

Disclosures: **R. Emkey**, *None*.

M436

Genetic, Clinical and Cellular Analysis of Forty-Seven Osteopetrotic Patients. A. Del Fattore*, B. Peruzzi*, C. Di Giacinto, A. Cappariello*, D. Fortunati*, M. Iacobini*, M. Luciani*, E. Lanino*, C. Messina*, S. Cesaro*, H. Fryssira*, P. Grabowski*, R. P. Kapur*, H. K. Datta*, A. Taranta*, S. Migliaccio*, M. Longo, A. Teti. Experimental Medicine, University of L'Aquila, L'Aquila, Italy.

Osteopetrosis (OP), a genetic bone disease characterized by osteoclast failure, is classified in three forms: infantile malignant Autosomal Recessive OP (ARO), Intermediate autosomal Recessive OP (IRO), and Autosomal Dominant OP (ADO) I and II. Among 47 patients admitted to this study, 19 were diagnosed with ARO, 1 with IRO and 27 with ADOII. Five ARO patients had known ATP6i gene mutations, 1 had a novel mutation (delC8807 DNA) and 3 were negative. Fourteen ADOII patients bore heterozygous mutations of the C1CN7 gene and 6 were negative, suggesting additional genes are also involved in this form. Identical C1CN7 mutations associated with variable severity, with no apparent correlation with gene polymorphism. Most ADOII patients showed decreased bone ALP but increased osteocalcin, and all patients had elevated TRAcP. Increased ALP was instead observed in ARO patients, so we examined whether osteoblasts were affected in iliac crest biopsies. Ob.S/BS was increased in 3 cases and near the max normal value in 2. Four patients showed increased serum PTH independently of Ob.S/BS status, suggesting no correlation between the two events. Most patients had elevated osteoclasts, except three with no osteoclasts, suggesting a defect in osteoclastogenesis. Bone marrow transplantation in the latter patients was without effect, consisting with a microenvironmental defect. In vitro, osteoclasts from patients generally showed no significant changes in formation rate, morphology or intracellular acidification. However, we observed altered adhesion to substrate and podosome formation in an IRO patient, and increased motility in three ADOII patients. As expected, the ADOII and ARO osteoclasts degraded bone matrix significantly less than controls, but bone resorption by ARO osteoclasts was not abolished. To test whether residual resorption activity could rely on the Na⁺/H⁺ antiport, control osteoclasts were treated with 75 nM of the H-ATPase inhibitor Bafilomycin, which reduced resorption to the ARO level, and 50 microM of the Na⁺/H⁺ antiport inhibitor EIPA. Pit formation was eliminated, without cytological alteration of osteoclast, which suggests an important physiological role for the antiport in the residual bone resorption in ARO. Extracellular acidification increased pit formation both in controls (>2fold) and in patients (~2fold in ADOII and ~3fold in ARO), providing a rationale for new therapies based on pH and Na⁺/H⁺ antiport manipulation.

M437

Fibrous Dysplasia: Pain Prevalence Increases with Age but Is not Due to an Increase in Bone Disease. M. H. Kelly*¹, B. A. Brillante*¹, X. Cineceros*², S. Guirguis*³, M. T. Collins*⁴. ¹Nursing and Patient Care Services, National Institutes of Health, Bethesda, MD, USA, ²Henry M. Jackson Foundation for the Advancement of Military Medicine, Rockville, MD, USA, ³Wooten High School, Bethesda, MD, USA, ⁴Craniofacial and Skeletal Diseases Branch, National Institute of Dental and Craniofacial Research, National Institutes of Health, Bethesda, MD, USA.

Fibrous Dysplasia (FD) is a congenital, non-heritable skeletal disorder in which normal bone and bone marrow are replaced by fibro-osseous tissue. Skeletal abnormalities associated with FD include pain, bowing, fractures and limb length discrepancy. We observed that pain appeared to be a more frequent complaint in adults than children, and that this difference did not appear to be attributable to the development of new FD lesions. To test if these observations were true, we assessed the differences in the prevalence of pain and the number and location of FD lesions in a cohort of children and adults with FD. A population of 33 children and 43 adults was studied. Radioisotopic bone scans were used to identify the sites of skeletal involvement. The self report Brief Pain Inventory was used to determine overall pain and which FD sites were painful. The following measures were assessed: 1) pain prevalence in adults and children, 2) pain distribution, 3) distribution of skeletal lesions, 4) differences in the distribution of skeletal lesions between adult and pediatric patients. The data confirmed that pain is a common feature of FD, reported by 67% of the population, and that pain is more common in adults than children (children 45%, adults 83%, p<.0005). The lower extremities were the sites most likely to be painful (children 56%, adults 89%, p=.005). The sites most commonly involved with FD were the head (children 94%, adults 86%, p=NS) and lower extremities (children 97%, adults 86%, p=NS). FD lesions were found less frequently in upper extremities, (children 88%, adults 62%, p<.05), ribs (children 64%, adults 71%, p=NS) and the spine (children 45%, adults 71%, p<.05). The spine was the only site at which there was a significant increase in FD involvement over time, but this site did not appear to be a significant source of overall pain morbidity. FD is more commonly associated with pain in adults than in children. The reason for this is not clear, as fractures are more common in children and the occurrence of new lesions (other than in the spine) is not a significant feature of aging. Parents and practitioners should be cognizant of the high prevalence of pain and treat it appropriately. The mechanism of bone pain in FD, its increase in adulthood, and the apparent ability of bisphosphonates to relieve pain are unknown and represent an area which warrants further investigation.

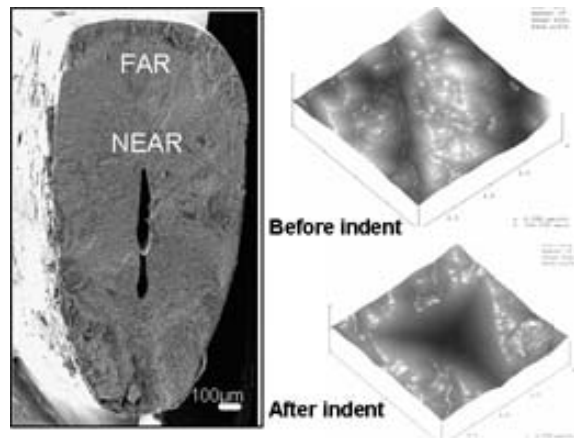
Disclosures: **M.H. Kelly**, None.

M438

Mechanical Consequences of the *Col1a2*^{oim} Mutation in Mouse Dentin. G. E. Lopez Franco¹, D. Stone^{*2}, A. Huang^{*3}, N. Pleshko Camacho³, R. D. Blank¹. ¹Medicine, University of Wisconsin-Madison, Madison, WI, USA, ²Materials Science and Engineering, University of Wisconsin-Madison, Madison, WI, USA, ³Research Division, Hospital for Special Surgery, New York, NY, USA.

Mice harboring the *Col1a2*^{oim} mutation (*oim*) express dentinogenesis imperfecta (DI). As we have described before, both *oim/oim* and *oim/+* mice display a reduction in the density and regularity of dentinal tubules in the matrix adjacent to the pulp. It is not yet clear what the mechanical consequences of the *oim* mutation in dentin are. Moreover, dentin's maturity varies with distance from the pulp, with the dentin farther from the pulp deposited earlier than that closer to the pulp. In order to compare the effect of *Col1a2* genotype and position on mechanical properties, we compared Young's modulus (E) and hardness (H) of dentin at different locations (near and far from the pulp chamber) in the three *Col1a2* genotypes. Upper incisors fractured at the junction epithelium were polished prior to testing. Nanoindentation was performed by using a TriboScope and a diamond Berkovich tip at 3000μN following experimental calibration with a fused quartz standard. Data were analyzed by the Oliver and Pharr method and groups compared by 2 factor ANOVA. E and H data are summarized in the table below. We found that dentin was harder and stiffer far from the pulp (P < 0.001). We believe that this reflects the effect of dentin maturity. The effect of genotype on E and H is also significant (P = 0.003), but there is not a clear-cut mutant allele dosage effect. For E, the effect of genotype was statistically significant at both locations, whereas on H, it was only significant near the pulp (interaction P < 0.001). Near the pulp, the presence of two mutant alleles caused dentin to be harder and stiffer. Far from the pulp, heterozygosity for the *oim* mutation led to the greatest E and H. These data suggest that the effect of α2(I) content on dentin mechanics depends on matrix maturity.

Position	E (GPa) ± sd		H (GPa) ± sd	
	Far	Near	Far	Near
+/+	22.5 ± 3.1	19.4 ± 4.8	1.5 ± 0.4	0.6 ± 0.1
+/ <i>oim</i>	37.1 ± 4.3	17.9 ± 3.3	2.2 ± 1.2	0.5 ± 0.1
<i>oim/oim</i>	28.7 ± 6.9	26.2 ± 3.2	1.6 ± 0.6	0.9 ± 0.1



Disclosures: **G.E. Lopez Franco**, None.

M439

GNAS mRNAs from the Paternally-Inherited Allele Are Decreased in Progressive Osseous Heteroplasia (POH), a Human Disorder of Ectopic Ossification. M. Xu*, F. S. Kaplan, E. M. Shore. Orthopaedic Surgery, University of Pennsylvania, Philadelphia, PA, USA.

Progressive osseous heteroplasia (POH) is an autosomal dominant disorder of extensive dermal ossification during childhood followed by progressive and disabling bone formation within skin, skeletal muscle, and deep connective tissue. POH is a rare condition, with most cases arising as a spontaneous mutation. However, in each of the few families that show inheritance of POH, transmission is from fathers. Heterozygous inactivating mutations of *GNAS* have been found in both familial and sporadic cases of POH. In all cases of POH examined, *GNAS* mutations consistently occur on the paternally-inherited allele. The *GNAS* gene is transcriptionally complex, initiating mRNA synthesis from multiple promoters and unique first exons that splice into common exons 2-13. The most abundant product of the *GNAS* gene is Gsα mRNA, which is biallelically expressed in most tissues. The *GNAS* mutations in most patient cell lines produce an unstable mRNA, and levels of Gsα mRNA and protein are reduced. Unlike Gsα mRNA, other *GNAS* transcripts are synthesized from only one of the two alleles. The *GNAS*-Nesp55 transcript is only expressed from the maternally-inherited allele, and the *GNAS*-XLαs and *GNAS*-1A transcripts are paternally expressed. We used quantitative RT-PCR to examine *GNAS* transcript levels in lymphocyte cell lines from POH patients and controls. While the Nesp55 mRNA is expressed at similar levels in patients and controls, POH cells express the XLαs and 1A mRNAs at reduced levels. These data suggest that the clinical expression of *GNAS* inactivating mutations in POH patients is not solely dependent on the level of Gsα expression but may be influenced by the expression levels of other *GNAS* transcripts.

Disclosures: **E.M. Shore**, None.

M440

Fibrodysplasia Ossificans Progressiva: Middle-Age Onset with Poor Response to Aggressive Immunosuppressive Therapy. S. J. DiMartino^{*1}, E. F. DiCarlo^{*1}, A. L. Boskey¹, M. P. Whyte². ¹Hospital for Special Surgery-Weill Medical College, Cornell University, New York, NY, USA, ²Division of Bone and Mineral Diseases, Washington University School of Medicine, St. Louis, MO, USA.

Fibrodysplasia ossificans progressiva (FOP) is a rare, genetic disorder characterized by ectopic bone formation and congenital malformation of the great toes. The gene defect is unknown and there is no established medical treatment. Early lesions of heterotopic bone present over the neck, spine, or shoulder as painful nodules that are warm, erythematous, and tender. Histology shows proliferating fibroblasts with sparse inflammatory cells. Within a few months, the lesions ossify by an endochondral process. Most patients first develop ossification before 15 years of age (mean onset 3 - 5 years). We report a middle-age woman with FOP who first developed ectopic ossification at age 47 years. Symptoms began with progressive pain, redness, warmth, and swelling over a scapula. CT showed asymmetric thickening of the muscles and fascial planes, but no ectopic bone formation. Biopsy revealed proliferating fibroblasts with scattered inflammatory cells. Prednisone, 60 mg daily, was started for a suspected inflammatory fasciitis. Symptoms initially improved, but returned during steroid taper - now involving several regions over the posterior thorax, flank, and chest. Despite high dose corticosteroids, immunosuppressive agents, and alendronate early in the course of this ossification, ectopic bone deposition progressed rapidly. She had the typical hallux valgus deformity of FOP. Methylprednisone (24 mg BID), methotrexate (maximum dose: 25 mg weekly), and alendronate (35 mg weekly) appeared to improve symptoms. Subsequently, however, these worsened, and methotrexate was discontinued due to non-efficacy (total time of treatment: 14 weeks). While continuing high dose steroids and alendronate, she developed new, larger lesions during trials of azathioprine (maximum dose: 125 mg daily, total time of treatment: 10 weeks) and mycophenolate mofetil (maximum dose: 1 g BID, total time of treatment: 10 weeks). CT 13 months after onset of symptoms showed many regions of ectopic bone involving the fascial planes of the thoracic, abdominal, and pelvic walls. Our patient demonstrates that FOP may present well into adulthood when progression may seem inexplicably rapid despite early intervention with high dose steroid, immunosuppressive, and bisphosphonate therapy. It is important to recognize an adult-onset presentation for FOP because early diagnosis can help avoid harmful procedures (e.g. biopsy or surgical excision typically exacerbates the disorder) and unnecessary treatment.

Disclosures: **S.J. DiMartino**, None.

M441

High-Normal Bone Mass in a Child with Insulin-Resistance Syndrome (Rabson-Mendenhall) despite Severe IGF-I, IGF-II and IGFBP-3 Deficiency. J. L. Fowlkes, H. N. Coleman^{*}, R. C. Bunn^{*}, K. M. Thrallkill. Pediatrics, UAMS and ACHRI, Little Rock, AR, USA.

Rabson-Mendenhall syndrome is a rare genetic disorder characterized by severe insulin resistance due to defects in signaling through the insulin receptor (IR). Phenotypically, these individuals display characteristic features including premature and dysplastic dentition, coarse facial features, lack of subcutaneous fat, acanthosis nigricans, enlarged genitalia, hypertrichosis, paradoxical hypoglycemia with postprandial hyperglycemia, and circulating insulin levels which have been reported to be as high as 1000 times normal. Investigations of the growth hormone (GH) - insulin-like growth factor (IGF) axis in this individual, revealed severe deficiencies in IGF-I, IGF-II and IGFBP-3, and hyperinsulinemia (see Table). Thus, it was anticipated that this child would have severe bone deficits, as has been described in other clinical scenarios where the IGF axis is similarly perturbed (e.g. growth hormone resistance syndrome, IGF-I deletion). While long-bone studies revealed no gross malformations (with the exception of short 4th metacarpals) and the bone age was delayed at -2.0 STD, DEXA scanning revealed a total body bone density Z-score of +2.0 (800 gm/m²), suggesting an overall high-normal BMD for age. We propose a mechanism by which supra-normal concentrations of insulin may substitute for the actions of IGFs in bone formation by signaling through the IGF-I receptor.

Age (months)	GH (ng/ml)	IGF-I (ng/ml)	IGF-II (ng/ml)	IGFBP-1	IGFBP-3 (mg/L)	Insulin (uU/ml)
24	<0.3 (<0.7-6)	<10	<10 (334-642)	177* (10-500)	0.10 (1.4-3.0)	3590 (1.5-20.5)
27	2.8		43	275** 154***		
32	2.1	17 (31-160)	50		0.4	70** 909***
37	3.8	11 (45-230)	80		0.3	151.5**
40	<0.3	45	80		0.3	190**
47	1.6	41	58	107**	0.1 (1.4-6.0)	570**
98		<0.6 (88-474)	<10	183** (30-1000)	0.3 (2.1-4.2)	178** (4-27)

*random; **fasting; ***post-prandial; () = normal range for age

Disclosures: **J.L. Fowlkes**, None.

M442

Hypophosphatasia: Misleading *In Utero* Presentation for the Childhood and Odonto Forms. D. Wenkert¹, W. H. McAlister^{*2}, J. H. Hersh^{*3}, S. Mumm⁴, M. P. Whyte¹. ¹Center for Metabolic Bone Disease and Molecular Research, Shriners Hospitals for Children, St. Louis, MO, USA, ²Mallinckrodt Institute of Radiology, Washington University School of Medicine, St. Louis, MO, USA, ³Weisskopf Center for the Evaluation of Children - Department of Pediatrics, University of Louisville, Louisville, KY, USA, ⁴Division of Bone and Mineral Diseases, Washington University School of Medicine, St. Louis, MO, USA.

Hypophosphatasia (HPP) is a rare, heritable rickets/osteomalacia featuring deficient activity of the “tissue nonspecific” isoenzyme of alkaline phosphatase (TNSALP) from deactivating mutation of the *TNSALP* gene. We warn that skeletal deformity *in utero* may not imply a severe outcome. Patients assessed with severe skeletal findings on fetal ultrasound (u/s) from 3 separate families were referred with mild bone disease *ex utero*. Abortion had been discussed for each. These 3 boys, described below, and 5 previously reported girls distinguish “benign prenatal HPP” (BP-HPP) from “perinatal” HPP, a typically lethal, autosomal recessive form of HPP which also manifests *in utero*. The 3 mothers carry different *TNSALP* missense mutations. At birth, each boy had mild limb bowing and shortening and then manifested delayed walking and early tooth loss. *Family 1*: Fetal u/s of 2 pregnancies to a mother with “childhood” HPP (C-HPP) showed severe “skeletal bowing” and demineralization. The 1st was terminated. The 2nd produced a boy with C-HPP. He, his mother, and the aborted fetus each carried a single *TNSALP* mutation (A1133T; Asp361Val). *Family 2*: Fetal u/s showed oligohydramnios, small size, and “extremity fractures” interpreted as OI. By age 3 years, long bone bowing had spontaneously improved. Developmental delay, failure to thrive, and cataracts were unexplained. X-rays showed no rickets (“Odonto-HPP”). The subsequent pregnancy, w/o oligohydramnios, showed no u/s abnormalities. The patient, mother, and sibling each carried a single *TNSALP* mutation (G188T; Gly46Val). *Family 3*: Fetal u/s of a boy with C-HPP showed *in utero* bowing and dwarfism. He had 2 *TNSALP* mutations (G526A; Ala159Thr and A881C; Asp277Ala). In each of these BP-HPP families, with either autosomal dominant or recessive inheritance, mothers carried a *TNSALP* mutation. The BP-HPP skeleton seems to improve during the 3rd trimester of pregnancy. Thus, BP-HPP must be considered when prenatal u/s shows fractures or bowing. Analysis of fetal or parental *TNSALP* would identify possible BP-HPP. A single mutation in the fetus or only 1 parent would suggest this outcome. With two *TNSALP* mutations, normal chest size, adequate skull mineralization, or presence of *in utero* packing may help distinguish BP-HPP from severe perinatal, but not infantile, forms of HPP.

Disclosures: **D. Wenkert**, None.

M443

Deactivating Germline Mutations in LEMD3 Cause Osteopoikilosis and Buschke-Ollendorff Syndrome, but not Melorheostosis. S. Mumm¹, X. Zhang^{*1}, W. H. McAlister^{*2}, D. Wenkert³, M. P. Whyte³. ¹Division of Bone and Mineral Diseases, Washington University School of Medicine, St. Louis, MO, USA, ²Mallinckrodt Institute of Radiology, Washington University School of Medicine, St. Louis, MO, USA, ³Center for Metabolic Bone Disease and Molecular Research, Shriners Hospitals for Children, St. Louis, MO, USA.

In 2004, heterozygous loss-of-function mutations in the LEMD3 gene (also called MAN1), which encodes an inner nuclear membrane protein, were shown to be a cause of osteopoikilosis (a benign, autosomal dominant, skeletal dysplasia featuring multiple hyperostotic lesions symmetrically throughout the skeleton) and Buschke-Ollendorff syndrome (BOS) (a benign, autosomal dominant disorder combining osteopoikilosis with disseminated connective tissue nevi). In some of these families, unusually large areas of dense bone were called “melorheostosis” which typically refers to a troublesome sporadic skeletal dysostosis characterized by asymmetrical “flowing hyperostosis” of the cortex of long bones often with overlying soft tissue abnormalities. Others had previously proposed that melorheostosis results from a second, post-zygotic, somatic mutation in the putative osteopoikilosis gene. We investigated patients representing 9 separate families with sclerosing bone disorders where LEMD3 represented a candidate gene abnormality: 1 osteopoikilosis, 2 BOS, 2 melorheostosis, 1 reported with both osteopoikilosis and melorheostosis, and 3 additional patients with other bone dysplasias including 1 mixed-sclerosing-bone dystrophy, 1 osteomesopyknosis, and 1 polycystic osteosclerosis with hypercalcemia. Genomic DNA, isolated from blood lymphocytes, was amplified by PCR and sequenced for all the coding exons and adjacent splice site regions for the LEMD3 gene. We did not study melorheostosis lesional tissue. A heterozygous nonsense mutation (T1433A, Leu478Stop) was found in exon 1 for the osteopoikilosis patient, and a heterozygous nonsense mutation (exon 1, C1323A, Tyr441Stop) and another heterozygous mutation (insertion or deletion in exon 1) were found in the 2 BOS patients. Likewise, a heterozygous nonsense mutation (C1963T, Arg655 Stop) in exon 7 was detected for the patient with osteopoikilosis and “melorheostosis”. However, no LEMD3 mutations were detected for any other patient, including the 2 patients with classic melorheostosis. We conclude that osteopoikilosis and BOS are caused by heterozygous deactivating LEMD3 mutations, however, melorheostosis remains of unknown etiology.

Disclosures: **S. Mumm**, None.

M444

Metabolic Bone Disease in Patients Presenting Short Bowel Syndrome. R. Javier*¹, A. Ledit*², J. Reimund*², J. Kuntz*¹. ¹Rheumatology, Universitary Hospital, Strasbourg, France, ²Hepatogastroenterology, Universitary Hospital, Strasbourg, France.

Despite its pathophysiology remains incompletely understood, metabolic bone disease (MBD) is a frequent complication of home parenteral nutrition (HPN) needed by short bowel syndrome (SBS). Patients with SBS not needing HPN may also be at risk for developing bone complications. Therefore, we analyse bone status in SBS patients without HPN and compared them to HPN patients trying to identify some favouring factors in each group. AIMS & methods : Fourteen SBS patients (mean age 53 years, 25-80) which do not need HPN have been compared to 18 HPN (mean age 57 years, 17-79).The mean duration of HPN was 40 months. Clinical symptoms were recorded as well as laboratory parameters including markers of bone metabolism, hormonal, inflammatory and nutritional status, radiological studies and bone mineral density (BMD) measured by dual absorptiometry. Statistics used non parametric tests. Results : In HPN group, bone pain was present in 11 patients (61 %) and 4 (22 %) had a fracture (mostly vertebral fractures). In SBS without HPN group, 4 experienced bone pain (29 %) and 1 had a vertebral fracture. Clinical nutritional status and nutritional proteins were normal and comparable in both groups. In both groups, BMD was decreased : in HPN group, no patient had normal BMD, 10/18 (56 %)were osteoporotic (T score <- 2.5) and 8/18 (44%) were osteopenic (-2,5< T score<-1) compared with respectively 5/14 (36%) and 8/14 (57%) in SBS without HPN group (difference not statistically significative). In HPN group, BMD was negatively correlated to duration of SBS (mean duration of SBS :72 months ,6-240 months) and orosomucoid suggesting that a long duration of malnutrition combined with persistent and unexplained inflammation can be deleterious for bone status. In SBS without HPN, BMD was associated with low body mass index, low 25OH vit D3, low serum albumin, vitamine A and IGF-1 concentrations. Conclusion : Most SBS patients with and without HPN had metabolic bone disease often with pain and fractures. In SBS without HPN patients, MBD seems to be related to subclinical malnutrition. This was not the case in HPN patients in whom no particular favouring factor could be identified. Therefore, we recommend to assess systematically bone status in SBS patients with and without HPN also in those having an apparently normal nutritional status. Attention must be given to 25OH vit D3 levels

Disclosures: **R. Javier**, None.

M445

Cytokine-Mediated Osteoclastogenesis: A Possible Mechanism for Excess Bone Loss in Postmenopausal HIV Infected Women. M. T. Yin*¹, L. Laurence*², J. M. Fakruddin*², D. Irani*³, J. F. Dobkin*¹, E. Shane³. ¹Infectious Diseases, Columbia University, NY, NY, USA, ²Laboratory for AIDS Virus Research, Weill Medical College of Cornell University, NY, NY, USA, ³Endocrinology, Columbia University, NY, NY, USA.

Low bone density (BMD) is a complication of HIV/AIDS and may be accelerated by certain types of antiretroviral (ARV) therapy. Excess bone loss may be related to HIV-associated upregulation of bone resorbing cytokines (TNF- α , RANKL) or to direct effects of ARVs on osteoclasts (OC). We have reported that ritonavir (RTV), at concentrations (1-5 μ M) found in HIV+ patients, increases osteoclastogenesis in vitro, likely by facilitating downstream RANKL signaling mechanisms. To investigate the pathogenesis of the bone loss, we measured serum bone turnover markers and cytokines, and BMD by DXA in 51 HIV+ and 31 HIV- postmenopausal (PM) women of similar age and ethnicity. We also compared OC differentiation from subject's peripheral blood mononuclear cells, cultured in the presence of their own sera (Autologous Serum-induced OC Induction or AOI assay). Serum osteocalcin, N-telopeptide (NTX), RANKL, TNF- α and AOI were significantly higher and total hip (TH) BMD lower in HIV+ PM women (Table). Bone alkaline phosphatase (BAP) was significantly higher (42.3 \pm 22 v 32.9 \pm 8, p=0.04) and spine (LS) BMD lower (0.856 \pm 0.14 v 0.968 \pm 0.16, p=0.02) among HIV+ PM women currently receiving ARVs (N=40) than not. Women on RTV (N=8) had higher serum osteocalcin (10.5 \pm 3 v 7.4 \pm 6, p=0.03), TNF- α , (115.2 \pm 28 v 50.7 \pm 26, p<0.001) and AOI (1.81 \pm 0.3 v 1.22 \pm 0.2, p=0.01) than HIV+ women not on RTV. AOI and TNF- α levels were positively correlated (r=0.61, p<0.001). In summary, serum bone-resorbing cytokines are higher in HIV+ than HIV- PM women and associated with lower BMD and increased OC induction *in vitro*. RTV is associated with higher serum TNF- α , osteocalcin, and OC activity. We conclude that HIV infection is associated with greater propensity for osteoclastogenesis, which may be mediated by TNF- α and RANKL and further increased by RTV. Such conditions may favor excess bone loss in HIV+ PM women.

Table. Biochemical indices and BMD in HIV+ and HIV- PM women, Mean \pm SD

	HIV+	HIV-	P values
BAP	40.4 \pm 20 ng/ml	34.4 \pm 16	0.16
Osteocalcin	7.6 \pm 4 ng/ml	5.9 \pm 2	0.01
NTX	23.3 \pm 11 nm/l	17.2 \pm 6	0.002
RANKL	49.1 \pm 29 pg/ml	27.7 \pm 20	0.03
TNF- α	62.7 \pm 37 pg/ml	10.3 \pm 8	<0.001
AOI	1.34 \pm 0.3 OD	1.19 \pm 0.1	0.03
TH BMD	0.845 \pm 0.15 g/cm ²	0.917 \pm 0.13	0.03

Disclosures: **M. T. Yin**, None.

M446

Comparing Risk Factors for Hip and Knee Osteoarthritis in Japan and Britain. N. Yoshimura¹, H. Oka*¹, H. Kawaguchi², K. Nakamura², C. Cooper³. ¹Department of Joint Disease Research, Graduate School of Medicine, the University of Tokyo, Tokyo, Japan, ²Department of Orthopaedic Surgery, Faculty of Medicine, the University of Tokyo, Tokyo, Japan, ³MRC Epidemiology Resource Centre, University of Southampton, Southampton General Hospital, Southampton, United Kingdom.

Osteoarthritis (OA) is a frequent course of pain and disability in both Japan and Britain, however, there is little comparative study of the hip and knee OA among different ethnic groups. We therefore performed parallel case-control studies of hip and knee OA in Britain and Japan, with the objective of exploring differences in the risk factors profile between the two countries. In each country, we selected representative population samples (Japan: Wakayama, Arita, Sennan; Britain: Portsmouth and North Staffordshire). A case register was established in each district whereby the orthopaedic surgeons recorded all men and women aged 45 years and over, who were listed for hip/knee arthroplasty. For each case, a control of the same sex, age (to within three years) was selected randomly from the list of resident registrations of the same city where the case lived. Cases and controls completed a structured interviewer-administered risk factor questionnaire. One hundred and fourteen in hip OA (11 men and 103 women) and 138 (37 men and 101 women) in knee OA completed the study in Japan. In the hip study, there was a statistically significant association between occupational lifting and OA, such that regular lifting of 25 kg in the individual's first job (OR=3.0, 95% CI 1.1-8.4) was associated with an increased risk of hip OA. In the British study of hip OA, independent risk factors included obesity, previous hip injury, the presence of Heberden's nodes, and occupational lifting. In the Japanese knee study, the heaviest weight in the past (OR 2.9, 95% CI 1.2-7.1), previous knee injury (OR 4.1, 95% CI 1.9-8.9), and total working period (OR 1.03, 95% CI 1.01-1.06) represented independent factors associated with knee OA after controlling for other risk factors. In the British study for knee OA, independent risk factors included obesity, previous knee injury, the presence of Heberden's nodes, and occupational kneeling/squatting. These data suggest that obesity, previous injury and occupational factors are risk factors for knee OA in Britain and Japan. The data provide a marked contrast with hip OA, which was associated with obesity in Britain, but not in Japan.

Disclosures: **N. Yoshimura**, None.

M447

Defective Implant Osseointegration under Protein Undernutrition: Reversal by PTH or Pamidronate. R. Dayer*, R. Rizzoli, P. Ammann. Department of rehabilitation and geriatrics, Division of bone diseases, Geneva, Switzerland.

Protein deficiency is highly prevalent among patients in orthopedic wards. We previously demonstrated that isocaloric low protein intake impairs titanium implant osseointegration in rats, with a decreased strength needed to loose the implant and altered bone microarchitecture in the implant vicinity. This is associated with decreased bone formation and increased bone resorption. Whether stimulator of bone formation or inhibitor of bone resorption could improve titanium implant osseointegration under protein undernutrition conditions is not known. We measured the resistance to pull-out of 1 mm diameter titanium rods implanted into proximal tibia of 10 month-old female rats receiving a normal (n=27) or isocaloric low protein diet (n=27). After 2 weeks on either diet, the implants were inserted, and the rats received PTH (1-34) (40 μ g/kg, 5/7 days), pamidronate (0.1mgP/kg, 5/28 days) or the corresponding vehicles for 8 weeks. Then, the tibias were removed for microtomographic histomorphometry. For pull-out strength resistance to implant pull-out was tested by recording the maximal force necessary to completely loose the implant. All results are expressed as means \pm SEM. Significance of difference was evaluated with an analysis of variance (* vs 15% casein, ° vs 2.5% casein). Pull-out strength was significantly lower in rats fed an isocaloric low protein diet compared with control rats. PTH and pamidronate markedly increased pull-out strength in animal fed a normal or a low protein diet; the effect of PTH being of higher magnitude. The PTH- or pamidronate increase in pull-out strength were associated with significant changes of trabecular bone volume, trabecular number and thickness, connectivity and bone contact Index in the vicinity of the implant. A structure model index (SMI) analysis revealed a significant shift to a more plate-like pattern in the rats treated with PTH or pamidronate, irrespective of the diets. We confirm that isocaloric low protein intake reduces the osseointegration of titanium implant. Treatments with PTH or pamidronate prevent the deleterious effect of protein undernutrition and even markedly improve the implant osseointegration. These results indicate potential problems of prosthetic replacement in protein undernourished patients and suggest some systemic treatments to prevent them.

	Pull-out strength Casein normal	Pull-out strength Casein low	BV/TV Casein normal	BV/TV Casein low
control	31.3 \pm 2.7	22.1 \pm 2.0 *	0.20 \pm 0.02	0.11 \pm 0.01 *
pamidronate	52.8 \pm 4.6 *	43.0 \pm 3.0 **	0.44 \pm 0.03 *	0.36 \pm 0.02 **
PTH 1-34	93.5 \pm 3.9 *	100.4 \pm 7.8 **	0.47 \pm 0.03 *	0.47 \pm 0.05 **

Disclosures: **R. Dayer**, None.

M448

Bone Density and Vitamin D Status in Men and Women with Lower Extremity Stress Fractures. N. A. Glass^{*1}, T. Martin^{*2}, M. Walcott^{*1}, J. Glowacki², M. S. LeBoff¹. ¹Endocrine, Brigham and Women's Hospital, Boston, MA, USA, ²Orthopedics, Brigham and Women's Hospital, Boston, MA, USA.

Stress fractures, which account for 10% of all sports injuries, are caused by repetitive strain that exceeds the compensatory threshold of bone. Vitamin D deficiency can lead to low bone density, and if severe, rickets or osteomalacia, with associated skeletal abnormalities such as pseudofractures or stress fractures. Data on the vitamin D status of otherwise healthy adults with stress fractures are limited. This study was designed to determine the bone health and prevalence of vitamin D deficiency in otherwise healthy adults with stress fractures. We enrolled 25 men and women between the ages of 18-40 years, 11 with stress fractures of the lower extremity (Fx) and 14 without stress fractures (NFx.) All subjects were screened for secondary causes of low bone mass. Bone mineral density (BMD) and body composition were measured by dual x-ray absorptiometry (DXA). Lab evaluations for 25 (OH) vitamin D (DiaSorin RIA, Stillwater, MN; normal 20-57 ng/ml), and n-telopeptides (NTX) were completed. Heights and weights were obtained and body mass index (BMI) was calculated.

Variable	Fracture (mean±SD)	Control (mean±SD)	p value
BMD Spine (g/cm ²)	0.969±0.022	1.079±0.022	0.002
BMD Femoral Neck (g/cm ²)	0.826±0.024	0.959±0.032	0.005
BMD Trochanter (g/cm ²)	0.694±0.024	0.801±0.027	0.009
BMD Total Hip (g/cm ²)	0.948±0.034	1.067±0.031	0.018
BMD Whole Body (g/cm ²)	1.138±0.020	1.185±0.019	0.120
25(OH)D ng/ml (median, range)	34.82, (11.85-76.68)	32.94, (13.22-63.16)	0.395
NTX nmol/mmol Cr (median, range)	51.50, (25-109)	37.00, (5-123)	0.426

There was an equal distribution of men and women in each group, and the groups did not differ in age (Fx=26.2±2.2, NFx= 21.8±2.5, p=0.087,) BMI (Fx=21.8±0.92, NFx=22.3±0.41, p= 0.603,) percent body fat (Fx=21.2±2.4, NFx=19.8±2.1, p=0.664 ,) or weight (Fx=64.1±3.26, NFx=67.9±2.06, p=0.310.) Men and women with stress fractures had low BMD of the hip and spine with normal vitamin D levels compared with controls. With the numbers available, there were no significant differences in vitamin D status or NTX levels between groups. With continued enrollment, the lack of differences in vitamin D levels between groups will be tested. In conclusion, men and women with stress fractures of the lower extremity have significantly lower BMD of the hip and of the spine compared with controls.

Disclosures: **N.A. Glass**, None.

M449

Mechanism of Bone Formation in Non-Hereditary Heterotopic Ossification. K. L. Foley^{*1}, N. Hebel^{a*2}, R. K. Suda^{*1}, M. Keenan^{*2}, R. J. Pignolo¹. ¹Department of Medicine, University of Pennsylvania, Philadelphia, PA, USA, ²Department of Orthopaedic Surgery, University of Pennsylvania, Philadelphia, PA, USA.

In postnatal life, new bone formation is normally restricted to regeneration of osseous tissue at sites of fracture. However, heterotopic ossification, or the formation of bone outside the normal skeleton, can occur within muscular, adipose, or non-muscle fibrous connective tissue. Ectopic bone formation is the only example of complete recapitulation of an organ system, replete with hard tissue, vascular, and marrow elements. Non-hereditary heterotopic ossification (NHOO) may occur after musculoskeletal trauma, following CNS injury, with certain arthropathies, or following injury or surgery that is often sustained in the context of age-related pathology. Histological development of heterotopic ossification has not been adequately described. We performed a histological analysis of 20 bone specimens from 17 patients with NHOO secondary to common precipitating conditions, including traumatic brain injury, spinal cord injury, trauma without neurologic injury, and total hip or knee arthroplasty. All bone specimens revealed normal endochondral osteogenesis at heterotopic sites. In order of sequence progression, the histological stages of NHOO lesion formation are: (1) perivascular lymphocytic infiltration, (2) lymphocytic migration into soft tissue, (3) reactive fibroproliferation, (4) neovascularity, (5) cartilage formation, and (6) endochondral bone formation. This study establishes the predominant histopathological findings associated with NHOO and can serve as a basis for elucidation of candidate gene(s) in the pathogenesis of this disorder.

Disclosures: **R.J. Pignolo**, None.

M450

Fluoride in Bottled Teas. M. P. Whyte. Division of Bone and Mineral Diseases, Washington University School of Medicine, St. Louis, MO, USA.

In January 2005, we reported skeletal fluorosis (SF) in an otherwise healthy, middle-age, American woman who consumed inordinate amounts of double-strength *instant* tea throughout her adult life. Although SF is rare in the U.S., it is common in Asia when inferior quality, F⁻ rich, “brick” tea is consumed. SF causes axial skeletal pain and ligament ossification. There is no established treatment. At that time, we found that the fluoride (F⁻) concentration in beverages made regular strength in distilled water using several U.S. commercial instant tea mixes exceeded FDA limits (1.4-2.4 ppm) for bottled water and beverages, and for one preparation of one brand the EPA limit (4.0 ppm) for drinking water. We cautioned that SF could result from long-term consumption of excessive amounts of some *instant* teas. Here, the F⁻ content is reported for commercial, ready-to-drink, *bottled*, liquid teas purchased from a supermarket and assayed, once again, using

“ion-specific electrode with known additions” methodology (*Table*). We find (single examination of 11 individual bottled teas) 4 of 11 were at, or exceeded, FDA limits for F⁻ in bottled beverages. Tea drinking remains popular in the U.S. and increasingly is suggested to promote health. Intake of at least 10 mg F⁻ daily for 10 yrs seems necessary for “preclinical SF”, i.e. the “no-observed-adverse-effect level” for adults. EPA National Primary Drinking Water Regulations stipulate a maximum F⁻ of 4.0 ppm, i.e., the lowest effect level for crippling SF of 20 mg/d with continuous exposure for at least 20 years. Accordingly, the Public Health Service regulates community water fluoridation stipulating optimum levels 0.7 -1.2 ppm depending on average air temperature. Preference for commercial drinks is diminishing per capita consumption of tap water. Our concern is that SF may result from prolonged drinking of excessive amounts of some teas. Our findings call for better understanding of amounts and systemic effects of F⁻ in teas.

Preparation	Product	F ⁻ (ppm or mg/L)		
		Laboratory 1	Laboratory 2	Mean±
1	Lipton Original Iced Tea	3.5	3.4	3.4
2	Nestle Iced Tea	2.9	2.8	2.8
3	Arizona Diet Green Tea with Ginseng	1.4	1.4	1.4
4	“ Iced Tea with Lemon	1.7	1.8	1.7
5	“ No Carb Green Tea	1.3	1.3	1.3
6	“ Iced Tea with Ginseng	1.8	1.8	1.8
7	“ Fox Stress Herbal Iced	2.3	2.3	2.3
8	Sweet Leaf Herbal	0.9	1.0	0.9
9	“ Green	3.3	3.1	3.2
10	“ Sweet	4.2	4.0	4.1
11	Snapple Iced Tea	1.0	1.0	1.0

‡ Mean of the four determinations (duplicate in both laboratories).

Disclosures: **M.P. Whyte**, None.

M451

Osteoporosis, Dental Status and Disability in an Elderly Population of Northeastern Italy. E. Musacchio^{*1}, E. Perissinotto^{*2}, P. Binotto^{*3}, L. Sartori¹, F. Silva-Netto^{*1}, S. Zambon^{*1}, M. Corti^{*4}, E. Manzato^{*1}, G. Baggio^{*5}, G. Crepaldi⁶. ¹Medical & Surgical Sciences, University of Padova, Padova, Italy, ²Environmental Medicine & Public Health, University of Padova, Padova, Italy, ³University of Padova, Padova, Italy, ⁴ULSS n.16, Padova, Italy, ⁵Medicina Generale, Padova Hospital, Padova, Italy, ⁶Aging Branch, CNR, Padova, Italy.

The diagnosis of osteoporosis and the evaluation of fracture risk are currently based on bone mass assessment. X-ray evaluation of dental arches has been suggested as a reasonable alternative to densitometry. The risk factors for osteoporosis include risk factors associated with periodontal disease and related tooth loss. Moreover, dental impairment *per se* is a risk factor for the progression to disability. To evaluate the usefulness of dental status assessment for identifying subjects at risk of low bone mass and disability, we studied 3,099 elderly (age 76.8±8.7) participating in the PRO.V.A., a large epidemiological study carried out in Northeastern Italy. All subjects underwent home interview and clinical visit with oral examination and physical performance measures. Ultrasonographic assessment of bone mass as well as biochemical determination of bone parameters were performed. The mean number of residual teeth was 7.3 (M 7.9, F 6.9) while the prevalence of edentulism was 43.7%, increased with age and was more pronounced in the females. Prostheses of both arches were largely used (78.7%), yet 17.6% of the edentulous subjects did not wear any artificial denture. Difficulty at chewing food was reported by 47.4% and at swallowing by 14.0% of the total population. Residual teeth number showed significant correlations with instrumental and biochemical parameters as well as with functional indexes such as grip strength, knee extension and ADL disability. Logistic regression analysis adjusted on age and vit. D levels demonstrated a significant association between high teeth number and bone mass (O.R. 1.6; 95% CI 1.2-2.1). Subjects with conserved dentures and without osteoporosis had less disability and depression but low residual teeth number alone identified a larger proportion of impaired subjects compared to the presence of osteoporosis alone. In particular, in the oldest class of age (85+ yrs), disability was reported by 55.7% of the subjects but only by 29% of those with more than 20 teeth and the same results were found in the case of previous falls (40.8% vs 24.7%). Our data demonstrate that oral disorders could have significant effects on frailty and disability markers in the elderly. Moreover, the correlations with bone remodelling and instrumental parameters suggest a possible clinical use of dental evaluation, at least in epidemiological studies.

Disclosures: **E. Musacchio**, None.

M452

Regional Changes in Body Composition 3 Months to 30 Years after Traumatic Spinal Cord Injury (SCI): Results of a Cross Sectional Study in 100 Paraplegic Men. C. Senn^{*1}, O. Franta^{*1}, A. W. E. Popp¹, D. Michel^{*2}, H. Knecht^{*2}, R. Perrelet^{*1}, G. Zaech^{*2}, K. Lippuner¹. ¹University Hospital of Berne, Osteoporosis Policlinic, Berne, Switzerland, ²Swiss Paraplegic Center, Nottwil, Switzerland.

It has been shown earlier that paraplegia induces severe and sustained infralesional cortical and trabecular bone loss (Osteoporosis Int 2004; 15:180-9). However, little is known on the long-term changes in body composition (lean mass, fat mass and bone mass) at the supra- and infralesional levels. The aim of the study was to document the long-term supralesional (arms) and infralesional (legs) changes in body composition with time since SCI in paraplegic men. One hundred paraplegic men (age 18-60ys) with complete motor posttraumatic medullary lesion T1-L3 and total motor and total or partial sensory loss (Frankel stage A or B) since 3 months to 30 years were included in this cross-sectional study. Body composition was assessed on whole body scans performed by DXA (Hologic QDR 4500A™). Total mass (TM), lean mass (LM), fat mass (FM), and bone mass (BM) of arms and legs were determined and expressed as grams. In addition, the ratios of LM/TM,

FM/TM, and BM/TM were calculated in percent. The influence of time since SCI on these parameters was then tested using logarithmic regression analysis. Means \pm SD of the relative distribution of tissues in arms and legs are shown in the table.

	Supralesional (arms)	Infralesional (legs)
LM/TM (%)	78.9 \pm 6.5	64.6 \pm 10.2
FM/TM (%)	16.5 \pm 6.8	32.3 \pm 10.6
BM/TM (%)	4.6 \pm 0.6	3.1 \pm 0.8

With time since SCI, TM, LM, FM, and BM of the arms increased ($r^2=0.3$, $p<0.0001$; $r^2=0.2$, $p<0.0001$; $r^2=0.1$, $p<0.01$ and $r^2=0.1$, $p<0.01$, resp.). A non significant trend towards a decrease in LM/TM was accompanied by a non-significant trend towards an increase in FM/TM with time since SCI (both $p<0.1$), while BM/TM was significantly reduced ($r^2=0.15$, $p<0.0001$). In the legs, TM, and LM did not change significantly with time since SCI, while FM increased ($r^2=0.1$, $p<0.05$) and BM dramatically decreased ($r^2=0.4$, $p<0.0001$). Furthermore, with time since SCI, LM/TM, and BM/TM decreased ($r^2=0.1$, $p<0.05$, and $r^2=0.5$, $p<0.0001$, resp.), whereas FM/TM increased ($r^2=0.1$, $p<0.01$). In paraplegic men, 3 months up to 30 years post SCI, total, lean, fat, and bone mass increase with time since SCI in the arms, possibly as a result of intensive physical training and use of the arms. In the legs, total mass remains unchanged, bone mass is lost extensively, while lean mass is partly substituted by fat mass.

Disclosures: **C. Senn**, None.

M453

Improved Biocompatibility of Niobium-Containing Titanium Alloys with Respect to Macrophage Activation and Inflammatory Osteolysis. **K. A. Rider**^{*1}, **C. J. Boehlert**^{*2}, **L. M. Flick**¹. ¹Biology, Alfred University, Alfred, NY, USA, ²Chemical Engineering and Materials Science, Michigan State University, Lansing, MI, USA.

Biocompatibility of implant materials is a critical issue in the design and success of any orthopaedic implant. In this study, the biocompatibility of two vanadium-free Ti-Al-Nb alloys, Ti-15Al-33Nb and Ti-21Al-29Nb, was tested and compared to that for commercially pure titanium (CP Ti) and alumina ceramic (Al₂O₃). Previous work in this area has shown that CP Ti induces significant inflammatory osteolysis while alumina ceramic has been described as biologically inert. Biocompatibility was assayed using in vitro cell culture techniques to examine macrophage-mediated phagocytosis and production of inflammatory cytokines. In addition, particles of each material were used in a small-animal model of wear debris-induced osteolysis to measure the osteolytic response and to assess the degree of T-cell infiltration. RAW 264.7 cells phagocytosed all types of particles readily and did not experience a loss of viability as a result. High levels of TNF α were produced in response to the CP Ti particles after only 24 hours but not in cultures with either niobium alloy or the alumina ceramic particles. In vivo, substantial osteolysis was observed 10 days post particle implantation with the CP Ti and alumina particles but not with either alloy. The osteolysis correlated with an extensive T-cell infiltrate in the CP Ti group but not the Al₂O₃ animals. The results showed that there was no significant difference in the biocompatibility of the two alloys compared to each other. However, despite equivalent phagocytosis by the macrophage cell line, the amount of TNF α and osteolysis was reduced in response to the alloys compared to commercially pure titanium. In addition, the immune system appears to discriminate between the alloys and the CP Ti, as immunohistochemistry demonstrated reduced staining for T-cells in the soft tissue surrounding the implanted particles in the alloy-treated groups but not the CP Ti animals. These results suggest that these alloys would be potentially useful for orthopaedic applications due to their improved biocompatibility.

Disclosures: **L.M. Flick**, New York State Office of Science, Technology and Academic Research (NYSTAR) 2.

M454

Metabolic Bone Disease as a Result of Pregnancy and or Famine in an Ancient Egyptian Mummy. **J. Denton**, **A. R. David**^{*}. KNH Centre for Biomedical and Forensic Studies in Egyptology, University of Manchester, Manchester, United Kingdom.

Skeletal remains of ancient cultures are often the only human remains useful for examination. External osteometric measurement is a commonly practiced method of examination but it is limited in its application. Much more scientific information can be obtained by the histological examination of soft tissues and skeletal remains. The KNH centre at Manchester University houses the International Human Mummy Tissue Bank, some of the Nubian specimens from this collection were used in this study. All femurs were assessed using osteometric parameters to be female. Trephine samples were taken from the lateral femoral condyles of 10 of the Nubian Mummies. The samples were decalcified in EDTA and LR White acrylic resin embedded. Sections 5 micron thick was stained by Toluidine blue. Histological examination of the femoral condyle from one of the Nubian mummies showed the presence normal lamellar bone in the centre of most of the trabeculae. The surface of this normal bone showed evidence of extensive osteoclastic resorption. On cessation of the resorption there was a period of new bone formation, following a prolonged apposition of new bone the cycle of osteoclastic resorption was repeated involving the new woven bone and extending down to and through the old normal lamellar bone. However, this time there was no period of subsequent new bone formation and it can be assumed that death of the individual stopped this continuing cycle. In addition to the altered function of the bone there was marked osteopenia. Pregnancy and lactation are both causes of cyclic osteoclastic resorption with subsequent new bone formation.

Concurrent poor nutrition will exacerbate the osteoclasia and have an influence on the properties of the new bone formation in the healing phase. The remaining nine bone specimens were unremarkable.

Disclosures: **J. Denton**, None.

M455

Vancomycin Covalently Bound to Ti6Al4V Pins Eradicates Bacterial Colonization. **V. Antoci**^{*1}, **B. Jose**^{*2}, **N. Hickok**^{*1}, **E. Wickstrom**^{*2}, **A. Zeiger**^{*2}, **I. M. Shapiro**¹, **J. Parvizi**^{*1}, **C. S. Adams**¹. ¹Orthopaedic Surgery, Thomas Jefferson University, Philadelphia, PA, USA, ²Biochemistry, Thomas Jefferson University, Philadelphia, PA, USA.

Despite immense improvements, periprosthetic infection continues to compromise the success of joint arthroplasty. We have developed a novel method to covalently tether vancomycin to metal (Ti powder and Ti6Al4V pins) surfaces using solid phase peptide synthesis. The reaction efficiency was monitored suggesting that vancomycin was present in saturating concentrations on both the powder and pins. Based on immunohistochemical staining, vancomycin was evenly distributed over the surface of the Ti powder and Ti6Al4V pins, while controls exhibited no staining. To determine bactericidal activity, quantitative culture of *S. aureus* was performed after 30, 60, 90, and 120 min static incubation at 37° C, and followed by serial dilution plating. Table 1 reports the normalized colony counts from this experiment (* = significantly different from Ti). The vancomycin-tethered Ti powder reduced colony formation by 75% at 1 h and 88% at 2 h when compared to Ti control. Viability of adherent bacteria on vancomycin-tethered Ti6Al4V pins was determined by confocal laser microscopy (Olympus Fluoview 300) after staining using the Live/Dead BacLight Viability Kit (Molecular Probes). Based on the Live/Dead assay, *S. aureus* readily adhered to control surfaces, emitting extensive green fluorescence (green = live and red = dead bacteria). In contrast, *S. aureus* attachment was nearly abolished on vancomycin-tethered surfaces (powder and pins). When either surface that had been previously exposed to *S. aureus* were washed, re-challenged and analyzed, the vancomycin-tethered surfaces retained their ability to kill *S. aureus*. Our surface modification shows potent antibacterial activity able to actively eradicate bacteria on the surfaces while showing long term stability resistant to physical stress. This technology is likely to provide the answer for the manufacturing of targeted implants that can be self-protective against periprosthetic infection and may remedy the shortcomings of the current antibiotic delivery methods including unpredictable elution kinetics, lack of long-term activity, and inactivation of antibiotics by methylmethacrylate cement.

Table 1. Ti-tethered vancomycin inhibits proliferation of *S. aureus*.

	30 min	60 min	90 min	120 min
Ti	100.00	140.84	128.80	100.52
VAN-Ti	39.41	34.08	22.90	11.72

Disclosures: **C.S. Adams**, None.

M456

RAGE Null Mice Exhibit Enhanced Bone Turnover. **K. H. Ding**¹, **Z. Z. Wang**^{*2}, **Z. Deng**^{*2}, **M. W. Hamrick**^{*3}, **P. P. Nawroth**^{*4}, **J. X. She**^{*2}, **D. M. Stern**^{*5}, **C. M. Isles**⁶, **Q. S. Mi**^{*2}. ¹Medicine, Medical College of Georgia, Augusta, GA, USA, ²Center for Biotechnology and Genomic Medicine, Medical College of Georgia, Augusta, GA, USA, ³Cellular Biology, Medical College of Georgia, Augusta, GA, USA, ⁴Medicine and Neurology, University of Heidelberg, Heidelberg, Germany, ⁵Medical College of Georgia, Augusta, GA, USA, ⁶Medicine and Orthopedic Surgery, Medical College of Georgia and the Augusta VA Hospital, Augusta, GA, USA.

To test the hypothesis that activation of RAGE (Receptor for Advanced Glycation End products) contributes to normal bone turnover, we examined RAGE knockout mice on bone densitometry (DEXA), bone imagine (X-ray), bone biomechanics, and blood serum biochemistry. Compared to age-matched 1- and 3-month-old male C57Bl/6J controls, RAGE-/- mice exhibited a significant increase in bone density in whole body, spine, and right femur measured PIXImus (Whole body: 1 M: wild-type: .0290 \pm .0015; RAGE-/-: .0327 \pm .0005, $P < .001$; 3 M: wild-type: .0474 \pm .0016; RAGE-/-: .0509 \pm .0023, $P < .001$; Spine: 1 M: wild-type: .0311 \pm .0031; RAGE-/-: .0348 \pm .0011, $P < .01$; 3 M: wild-type: .0531 \pm .0035; RAGE-/-: .0550 \pm .0043, $P > .05$; Right femur: 1 M: wild-type: .0324 \pm .0023; RAGE-/-: .0387 \pm .0011, $P < .001$; 3 M: wild-type: .0649 \pm .0036; RAGE-/-: .0700 \pm .0043, $P < .01$; Data are Means \pm SD, g/cm², n=9-15). Consistent with these bone density data, RAGE-/- mice also had significantly lower levels of bone breakdown marker pyridinoline (1 M: wild-type: 1.95 \pm .2; RAGE-/-: 1.71 \pm .2, $P < .05$; 3 M: wild-type: 2.20 \pm .3; RAGE-/-: 1.72 \pm .3, $P < .01$, nmol/L, n= 9-15) and a significant decrease in IL-6 level at 3-month old (wild-type: 11.62 \pm 5.6; RAGE-/-: 6.34 \pm 3.1, $P < .05$), although there are no significant changes between these two group animals at age 1- and 3-month old in blood serum alkaline phosphatase, calcium, and glucose. Biomechanics study reveled that RAGE-/- mice at 3-month-old had a significant increase in energy to break point (wild-type: .004 \pm .001; RAGE-/-: .007 \pm .002, $P < .01$), in strain at user break (wild-type: .0071 \pm .014; RAGE-/-: .093 \pm .020, $P < .05$), in displacement at user break (wild-type: .477 \pm .060; RAGE-/-: .610 \pm .125, $P < .01$), and in modulus of toughness (wild-type: .152 \pm .032; RAGE-/-: .212 \pm .058, $P < .05$). Together, these data suggest that RAGE plays an important role in normal bone turnover, it may inhibit bone breakdown and/or stimulate bone formation. To our knowledge, this is the first evidence to show RAGE's role in bone *in vivo*.

Disclosures: **K.H. Ding**, None.

M457

Three-Year Treatment with Intravenous Pamidronate in a Woman with Hepatitis C Associated Osteosclerosis. S. Ortolani, S. Vai^{*}, R. Cherubini^{*}, S. Saraifoger^{*}. Centre for Metabolic Bone Disease, Istituto Auxologico Italiano, Milan, Italy.

Hepatitis C-associated osteosclerosis (HCAO) is an impressive example of acquired diffuse osteosclerosis in adults firstly described in 1992. Only twelve cases have been reported since then and we presented at 2002 ASBMR meeting the first HCAO case from Europe, with 1 year follow-up without treatment. She was a 65-yr-old woman, with hepatitis C virus infection from blood transfusion more than 13 years earlier, referred to us in January 2001 for severe pain of thighs, legs and upper arms and significant walking disability, requiring high doses of analgesics. Diagnosis of HCAO was based on marked and diffuse cortical and trabecular osteosclerosis involving all the skeleton except the cranium, with high remodeling osteosclerosis but lamellar bone texture at bone biopsy. Biochemical markers of bone turnover were 4 to 20 times the upper normal limits and DXA bone mineral density at different skeletal sites ranged from +1.7 to +5.3 T-score. After 1 year without treatment bone density increased by 15.0% at lumbar spine and 10.2% at total hip. We report now a three-year follow-up of intermittent intravenous pamidronate treatment. The rationale for using a potent bisphosphonate was based on the assumption that reducing the number of remodeling cycles could result in a lower rate of bone gain. Intravenous pamidronate (45 mg every other month) was administered for 3 year associated with oral calcium 1.2 g/day and calcitriol 0.5 mcg/day. Clinical improvement of bone pain was observed starting from the first pamidronate infusion and was maintained. All the bone turnover markers (serum total AP and OC, urine NTx) decreased slowly but continuously during the whole 3-year treatment. Bone density at different skeletal sites markedly increased during the first year of pamidronate treatment, with changes even larger than those observed during the previous 1-year non treatment period: +18.5% at lumbar spine and +15.5% at total hip. During the two following years of pamidronate treatment the yearly rate of gain in bone density was less than half the rate recorded during the first treatment year: + 7.0% at lumbar spine and +6.9% at total hip. This case indicates that pamidronate, after the expected early increase in bone density due to remodeling space contraction, is able to slow down but not to prevent further bone gain in HCAO. This behavior supports the concept that pamidronate reduces the number of active BMUs, while the balance at BMU level remains positive. We also hypothesize that the addition of corticosteroid to bisphosphonate treatment could reverse bone gain in HCAO.

Disclosures: **S. Ortolani**, Novartis 2.

M458

Alterations in the Mechanical Properties of Bone due to Type II Diabetes. H. A. Hogan¹, B. A. Vyvial^{*1}, J. D. Alcorn^{*1}, J. M. Swift^{*2}, R. D. Prisby^{*2}, S. A. Bloomfield², M. D. Delp^{*2}. ¹Mechanical Engineering, Texas A&M University, College Station, TX, USA, ²Health and Kinesiology, Texas A&M University, College Station, TX, USA.

The purpose of this study was to investigate the effects of Type II diabetes on cortical bone properties using the Zucker Diabetic Fatty (ZDF) rat animal model. Age-matched groups of ZDF and lean controls (CON) were terminated at 3 developmental stages: pre-diabetes (7wks) with normal serum glucose (GLU) and high serum insulin (INS); acute diabetes (13 wks) when both GLU and INS are high; and chronic diabetes (20 wks), with normal INS and high GLU. Mechanical properties of the femur were measured by 3-point bending tests to characterize mid-diaphyseal cortical bone. As animal age increased and the effects of diabetes become more pronounced, cortical bone properties were lower than in CON rats. More specifically, whole-bone, or extrinsic properties, were affected more than tissue material properties. For example, the bone stiffness was 17% lower for ZDF vs. CON at 13 wks and 22% lower at 20 wks, yet the tissue elastic modulus was 22% lower at 13 wks but not significantly different at 20 wks. The ultimate (or maximum) breaking force was not different at 13 wks but 19% lower at 20 wks. In contrast, the tissue ultimate stress was not different at 13 or 20 wks. The greater effects of diabetes at the whole bone level can be attributed largely to smaller cross-sectional geometry for ZDF, particularly at 20 wks in which case the cross-sectional moment of inertia was 20% lower. Toughness was quantified by taking the energy absorbed from yield to ultimate load and normalizing it by the total energy absorbed to ultimate. This normalized post-yield energy should be indicative of material tissue toughness. The resulting post-yield energy values were not significantly different at either 13 or 20 wks, but the trend suggests more brittle behavior for the ZDF animals (means were 7% lower at 13 wks and 20% lower at 20 wks). The reductions in mechanical properties observed in this study may be associated with alterations in blood flow caused by Type II diabetes, as others have observed [Prisby et al., FASEB J. 47(4): 286, 2004].

Disclosures: **H.A. Hogan**, None.

M459

Ectopic Secretion of Parathyroid Hormone (PTH) by Thymus Epithelium Cells. M. P. Garcia^{*1}, M. H. D'Adamo^{*1}, A. D. Jaen^{*2}, M. R. Barbich^{*1}, L. S. Algranati^{*3}, E. Mazzaro^{*4}, P. F. Argibay^{*1}, L. C. Plantalech⁵. ¹Instituto de Ciencias Basicas y Medicina Experimental, Hospital Italiano, Buenos Aires, Argentina, ²Pathology, Hospital Italiano, Buenos Aires, Argentina, ³Nephrology, Hospital Italiano, Buenos Aires, Argentina, ⁴Surgery, Hospital Italiano, Buenos Aires, Argentina, ⁵Endocrinology, Hospital Italiano, Buenos Aires, Argentina.

Introduction: Supernumerary and ectopic thymus localization of parathyroid glands are a common finding in uremic hyperparathyroidism (HPTu). A hypothesis sustained that ectopic localization of parathyroids are vestiges of a common development of the thymus and the parathyroids. In other hand we hypothesized that equal embryologic cell could involutedly to primitive stadium and secrete others hormones (PTH) with an appropriate stimulus. Objective: to demonstrate PTH secretion by thymus epithelial cells in pathological circumstances. Material And Methods: Thymus epithelial cells and parathyroid intratymic adenoma obtained by surgical resection of a patient with renal transplant and HPTu, were fractionated for fixation and tissue culture (only thymus cells) in a regular medium. Conventional histology, Immunohistochemistry for PTH and TUNEL assay were performed in the fixed tissue. The presence of PTH was evaluated by radio-immune assay (RIA middle molecular fraction n v: 20-100pg/ml) in the culture medium of thymus and human fibroblast culture (control). Results: PTH hormone was detected in the culture medium from the thymus tissue (0hs: 85 pg/ml, 24 hs:251pg /ml, 96 hs: 106 pg/ml) Those values contrasts with the PTH levels from human fibroblasts culture medium (PTH range: 25 - 40 pg/ml). Conventional cells (epithelium and lymphocyte) was observed in the patient's thymus. Positive immunohistochemistry for PTH was verified only in the parathyroid tissue and in the thymus epithelial cells of the patients, and did not seen in control thymus. No apoptosis was detected by TUNNEL assay in any tissues. Conclusion: Our preliminary data suggests that under pathological conditions, epithelial cells from the thymus could secrete spontaneously PTH hormone, suggesting a common origin among parathyroid glands and the thymus. New molecular biology and functional studies are in development to research the origin and the conditions that induce the PTH production by thymic cells.

Disclosures: **L.C. Plantalech**, None.

M460

Perifusion Analysis of PTH Secretion from Normal and Pathological Human Parathyroid Cells. A. D. Conigrave^{*1}, H. Mun^{*1}, L. Delbridge^{*2}.

¹School of MMB, University of Sydney, University of Sydney, NSW, Australia,

²Department of Surgery, Royal North Shore Hospital, St Leonards, NSW, Australia.

We have developed a perifusion technique for the analysis of PTH secretion from cells prepared from small samples of normal and pathological human parathyroid tissue. All tissue samples were obtained according to ethics guidelines established by the Northern Sydney Area Health Service of NSW, Australia. Cells were prepared from one or more small tissue pieces (1-2 mm³) using a modification of a standard collagenase/DNase method (Brown et al., Am. J. Med. 71, 565-570; 1981) taking care to remove the digested tissue from the protease-rich medium and resuspend it in fresh albumin-containing medium prior to trituration. After release of the cells in variably sized clumps by trituration, they were recovered by centrifugation (100 g, 2 min). In this way, yields of around 40,000 high quality cells were obtained from single samples of normal parathyroid tissue and up to 1 million cells or more were obtained from samples of pathological human parathyroid tissue. A yield of 40,000 cells was sufficient to detect intact human PTH secretion from 1 mL bed volume columns of sephadex perifused at a rate of 1.5 mL min⁻¹ with 37 °C equilibrated physiological saline solutions containing 1 mg mL⁻¹ albumin as a carrier for PTH. Samples were processed using a high throughput intact PTH autoanalyzer (Immulite 2000). PTH secretion rates from perifused cells were found to respond to variations in the concentrations of two recognised activators of the extracellular Ca²⁺-sensing receptor: Ca²⁺ and L-amino acids (Conigrave et al., J. Biol. Chem. 279, 38151-38159; 2004). The IC₅₀ for extracellular Ca²⁺ was approximately 1.1 mM in normal cells and was variably elevated in cells prepared from samples of adenomatous tissue. Typically, high extracellular Ca²⁺ concentrations (> 1.4 mM) maximally suppressed PTH secretion from normal parathyroid cells by 80-90%. Brown et al. (Endocrinology 116, 1123-1132; 1985) previously described a method for the perifusion of bovine parathyroid cells. The current results indicate that the perifusion technique can also be used reliably for the analysis of acute changes in PTH secretion from small samples of human parathyroid tissue.

Disclosures: **A.D. Conigrave**, None.

M461

Bone Microarchitecture in Mild Primary Hyperparathyroidism. L. Dalle Carbonare^{*1}, P. Ballanti^{*2}, F. Bertoldo^{*1}, S. Giannini³, M. Valenti^{*1}, M. Zanatta^{*1}, S. Zenari^{*1}, G. Realdi^{*3}, V. Lo Cascio¹. ¹Dpt. of Biomedical and Surgical Sciences, Medicina Interna D, Verona, Italy, ²Dpt. of Experimental Medicine and Pathology, Section of Pathology, Roma, Italy, ³Dpt. of Medical and Surgical Sciences, Clinica Medica I, Padova, Italy.

Primary hyperparathyroidism (PHPT) is a common endocrine disease and the high levels of parathyroid hormone cause demineralization of bone and increased risk of fracture. On the other hand, the effect of mild PHPT on bone structure is more ambiguous. Aim of this study was to evaluate the effect of PHPT on cancellous bone volume, structure and microarchitecture in the Italian population. Twelve transiliac biopsy specimens taken in untreated postmenopausal women aged 67±2 years with primary hyperparathyroidism were compared with 14 biopsies taken in normal women aged 71±1 years. None of the women presented any other disorder affecting bone metabolism. In these samples we evaluated the direct and indirect histomorphometric parameters of bone microarchitecture using an image analysis system consisting of an epifluorescent microscope (Leica DMR) connected to an analogic 3 CCD camera (Sony DXC 390P) and a computer equipped with a specific software for histomorphometric analyses. Preliminary results on the first 8 samples of each group showed no significant differences between PHPT patients and controls in cancellous bone volume, trabecular thickness and number. Connectivity parameters were higher in PHPT patients than in controls. The results of strut analysis are reported in the table.

	PHPT	Controls	P
Total Skeletonized Length (µm)	13834±2129	8844±313	<0.05
NodeNumber/Tissue Volume (#/mm2)	4.22±1.39	2.02±0.20	=0.05
NodetoNode Length/Total Skeletonized Length (%)	36.99±6.50	22.63±3.52	<0.05
NodetoTermini Number	25.91±5.83	11.73±1.61	<0.05
Node/Termini	0.68±0.13	0.59±0.16	NS

Indirect parameters of microarchitecture (Trabecular Bone Pattern Factor, Marrow Star Volume and Fractal Dimension) were similar in the two groups. In conclusion, preliminary histomorphometric data showed that cancellous bone volume is preserved in the PHPT women, and microarchitecture seemed to be better than in normal women.

Disclosures: **L. Dalle Carbonare**, None.

M462

Genetic Testing In Familial Isolated Hyperparathyroidism. F. Cetani¹, E. Pardi^{*1}, S. Borsari^{*1}, E. Ambrogini^{*1}, M. Lemmi^{*1}, E. Vignali¹, A. Picone^{*1}, G. Viccica^{*1}, S. Mariotti^{*2}, L. Dejana^{*2}, P. Miccoli^{*3}, A. Pinchera^{*1}, C. Marcocci¹. ¹Endocrinology and Metabolism, University of Pisa, Pisa, Italy, ²Endocrinology, University of Cagliari, Cagliari, Italy, ³Surgery, University of Pisa, Pisa, Italy.

Primary hyperparathyroidism is usually a sporadic disorder, but in a minority of cases (<10%) occurs as part of hereditary syndromes, including multiple endocrine neoplasia types 1 and 2A (MEN1 and MEN2A), hyperparathyroidism-jaw tumor syndrome (HPT-JT), familial hypocalciuric hypercalcemia (FHH), and familial isolated hyperparathyroidism (FIHP). Four of these syndromes have a well recognized molecular etiology, while it is still unclear whether FIHP is an incomplete expression of these syndromic forms or a distinct genetic entity. Indeed, although the majority of FIHP cases have currently unrecognized causes, some FIHP kindreds have been associated with mutant MEN1, HRPT2 and calcium-sensing receptor (CASR) genotypes. In this study we report the results of *MEN1*, *CASR*, and *HRPT2* gene sequencing of 13 subjects with FIHP belonging to 6 unrelated families (A, B, C, D, E and F). The clinical diagnosis of FIHP was based on the absence of typical MEN1 or HPT-JT manifestations. Genomic DNA was isolated from tumor samples and peripheral leukocytes. Highly polymorphic microsatellite loci located within *HRPT2* gene and flanking *MEN1* gene were PCR amplified and examined for loss of heterozygosity. Four of the 6 probands of the FIHP families were found to have germ line mutations in the *MEN1* gene. These consisted of a missense mutation in exon 9 (D418H) in family A, an acceptor splice site mutation in intron 4 (IVS4-9G>A, producing an aberrant splicing of mRNA that would result in prematurely truncated protein) in family B, a new intronic deletion of two bases located 20 nucleotides upstream exon 5 (IVS4-20delCT), in family C, and a splice donor site in intron 1 (IVS1+1 G>A) in family E. The *MEN1* mutations were also found in all affected family members. No mutation was identified in *MEN1* and *HRPT2* genes in the probands of family D and F. LOH analyses at *MEN1* and *HRPT2* loci revealed no evidence of allelic loss in any of the parathyroid tumors studied. In summary, 4 of the 6 FIHP kindreds showed a germline mutation of *MEN1* gene, while no molecular defect could be identified in the remaining 2 families. Our confirm that a substantial proportion of FIHP families represent a phenotypic variant of MEN1 syndrome.

Disclosures: **F. Cetani**, None.

M463

TGF α /EGFR Induction Is Essential for Low Ca-induced Parathyroid Hyperplasia in Early Kidney Disease in Rats. T. Sato^{*}, I. Gonzalez-Suarez^{*}, J. Yang^{*}, E. Slatopolsky, A. S. Dusso. Internal Medicine/Renal, Washington University, St. Louis, MO, USA.

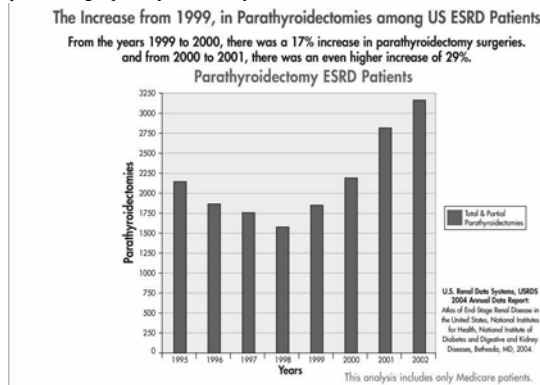
Persistent hypocalcemia is the most powerful stimulus for parathyroid hyperplasia. Since enhanced parathyroid expression of transforming growth factor- α (TGF α) and its receptor, the epidermal growth factor receptor (EGFR), was identified as the main contributor to high P-induced parathyroid hyperplasia in kidney disease, the present studies assessed the contribution of TGF α /EGFR-driven growth to the severe parathyroid cell growth induced by kidney disease and low dietary calcium (Ca). 5/6 nephrectomized rats were fed either a low (0.1% Ca) or a high Ca (2 % Ca) diet to further aggravate or completely block the mitogenic signals triggered by the onset of kidney disease, respectively, for one week. Rats fed low dietary Ca also received either vehicle or Erlotinib, a potent and highly specific inhibitor of EGFR-tyrosine kinase, which catalyzes a mandatory step for TGF α activation of the EGFR. A 3.7-fold increase in parathyroid cell proliferation, as measured by the number of nuclei staining positive for PCNA or Ki67, was induced by kidney disease and low Ca-intake compared to that observed in 5/6 nephrectomized rats fed the high Ca diet. The increase in parathyroid cell proliferation in the 5/6 nephrectomized rats fed the low Ca diet coincided with simultaneous 3-fold increases in parathyroid TGF α and EGFR content. Importantly, suppression of TGF α /EGFR-signaling, through intraperitoneal daily doses of 6 mg of Erlotinib/kg body weight, not only prevented parathyroid hyperplasia but also low Ca-induced increases in parathyroid TGF α with an efficacy comparable to that of the high Ca diet. We conclude that TGF α induction of its own expression and EGFR-driven growth constitutes the main pathogenic mechanism for the severe parathyroid hyperplasia induced by low dietary Ca in early experimental kidney disease.

Disclosures: **T. Sato**, None.

M464

Unexplained 4 Year Increase in Parathyroidectomies in the United States. T. L. Cantor. President, Scantibodies Laboratory, Inc., Santee, CA, USA.

Since the mid 1990's there has been an increase in the use of vitamin D sterol analogs to accomplish a "medical parathyroidectomy" for ESRD (end stage renal disease) patients. The overall expectation was that there would be a subsequent decrease in the number of parathyroidectomies among ESRD patients. Therefore, the USRDS (US Renal Data Services) database on parathyroidectomies was examined for its most recent rate of parathyroidectomies among Medicare beneficiaries to see if this expectation was, indeed, realized. From 1995 through 1998 the number of parathyroidectomies declined steadily among the Medicare ESRD patients in the US as expected. However, in 1999 the trend changed, with an increasing number of parathyroidectomies. This trend has persisted through 2001 (the latest data available). From 1999 to 2000 there was a 17% increase in parathyroidectomies and from 2000 to 2001 there was a 29% increase in parathyroidectomies. For 2002 there was a further increase in parathyroidectomies. K/DOQI (National Kidney Foundation's Kidney Disease Outcome Quality Initiative) guideline 14 states that "parathyroidectomy should be recommended in patients with severe hyperparathyroidism (serum levels of intact PTH >800 pgm/ml)." Therefore, the predominant intact PTH assay used should be examined for any changes that might explain this increase in parathyroidectomies. Meanwhile, this data indicates a reason for caution before prescribing a parathyroidectomy.



Disclosures: **T.L. Cantor**, Scantibodies 4.

M465

Cortical PQCT Measures Are Associated with Fractures in Dialysis Patients. S. A. Jamal¹, C. Gordon², D. C. Bauer³. ¹Medicine, University of Toronto, Toronto, ON, Canada, ²Radiology, McMaster University, Hamilton, ON, Canada, ³S.F. Coordinating Center, CPMC Research Institute, and UC San Francisco, San Francisco, CA, USA.

Fractures are common in hemodialysis (HD) patients yet DXA of the hip and spine are not associated with fractures in this group. One explanation is that HD patients have a selective decrease in volumetric cortical bone density, not identified by standard DXA

testing. We used peripheral quantitative computed tomography (pQCT) of the distal radius to examine associations between volumetric cortical and trabecular densities and fracture in 36 men and 16 women, 50 years and older, on HD for at least one year. We inquired about low trauma fractures since starting HD and confirmed self reported fractures by review of radiology reports. Prevalent vertebral fractures were identified by morphometry. pQCT measurements were taken of the non-dominant radius using the Stratec XCT 2000. At 4% of the ulna length we assessed volumetric trabecular density (mg/cm^3), and at 20% we assessed volumetric cortical density (mg/cm^3), total area (mm^2), cortical area (mm^2), and cortical thickness (mm). We used logistic regression analyses to examine the relationship between fracture (prevalent vertebral and/or self-reported non-spine) and each of the pQCT measures described above. Results are adjusted for age, weight and gender and reported as Odds Ratios (OR) per standard deviation decrease in the independent variable. The mean (\pm SD) age was 65.9 ± 8.9 years, the mean weight was 72.9 ± 15.2 kg and most (35 of 52 subjects) were Caucasian. The mean PTH was 33.8 pmol/L ($12.6 - 57.2$). Of the 52 subjects 27 subjects had either a prevalent vertebral fracture or low trauma fracture since starting dialysis. The mean trabecular density was $159.7 \pm 60.6 \text{ cm}^3$, cortical density $1119.7 \pm 72.9 \text{ cm}^3$, total area $320.1 \pm 121.3 \text{ mm}^2$, cortical area $66.4 \pm 22.8 \text{ mm}^2$ and cortical thickness $1.8 \pm 0.6 \text{ mm}$. There was no association between fractures and trabecular density (OR = 1.2; 95% Confidence Interval (CI): 0.43 to 1.7) or total area (OR = 1.1; 95% CI: 0.49 to 1.7). A decrease in cortical density was associated with an increased odds of fracture (OR = 15.7; 95% CI: 2.9 to 83.9), as was a decrease in cortical area (OR = 3.0; 95% CI: 1.3 to 7.2), and a decrease in cortical thickness (OR= 3.3; 95% CI: 1.4 to 7.8). Serum PTH was inversely correlated ($r = 0.6$) with cortical density but was not associated with fractures. Cortical, but not trabecular parameters are associated with fractures in HD patients. These findings may explain the lack of association between fracture and DXA measured at the hip and spine. Further studies are needed to determine the relationship between PTH and other determinants of cortical bone density and fracture in HD patients.

Disclosures: **S.A. Jamal**, None.

M466

Skeletal Resistance to Parathyroid Hormone Induced by Uremic Toxins Causes Adynamic Bone Disease in Chronic Renal Failure. **Y. Iwasaki¹, H. Yamato², T. Nii-Kohn³, M. Fukagawa³.** ¹Health Sciences, Oita University of Nursing and Health Sciences, Oita, Japan, ²Development, Kureha Special Laboratory Co, Ltd., Fukushima, Japan, ³Nephrology & Dialysis center, School of Medicine, Kobe University, Kobe, Japan.

Adynamic bone disease (ABD), which is characterized by reduced bone formation and resorption, has become an increasingly common manifestation of bone abnormalities in patients with end-stage renal failure. It has been recognized that skeletal resistance to parathyroid hormone (PTH) underlies the pathogenesis of ABD; however, the mechanisms of such resistance remain unclear. To elucidate the pathogenesis of ABD under uremic condition, we established a rat model simulating low turnover bone disease secondary to renal failure, using thyroparathyroidectomy (TPTx) and partial nephrectomy (Nx). TPTx-Nx rats were infused physiological doses PTH and injected thyroid hormone. We analyzed bone histomorphometric parameters and demonstrated gene expression using semi-quantitative RT-PCR. In TPTx-Nx rats, reduced bone formation was observed, which was ameliorated by pharmacological dose intermittent PTH injection in dose dependent manner. The expression of parathyroid/parathyroid-related peptide (PTH/PTHrP) receptor and alkaline phosphatase (ALP) genes was reduced significantly in TPTx-Nx compared with TPTx rats. Since reduction of bone formation was dependent on the degree of renal dysfunction, we evaluated whether the uremic toxin, which accumulated in blood with development of chronic renal insufficiency, influenced bone metabolic turnover. Although many uremic toxin was known, we focused on indoxyl sulfate (IS), which is known uremic toxin, and measured serum concentration of IS in our model. IS accumulated in the serum was dependent on renal dysfunction. Treatment with oral charcoal absorbent (Kremezin, Kureha Chem. Ind, Japan) not only reduced serum IS concentration, but also reversed the decreased bone formation. In addition, IS suppressed the production of cAMP stimulated by PTH treatment in mouse primary osteoblastic cells with dose dependency in vitro. IS also increased oxidative stress and inhibited cell proliferation in a dose dependent manner. In these cells, expression of organic anion transporter-3, which mediates cellular uptake of indoxyl sulfate, was also confirmed. Our data suggest that the accumulation of uremic toxins might cause dysfunction of osteoblastic cell and lead to decreasing response to PTH. Skeletal resistance to PTH may induce, at least in part, by accumulation of uremic toxins including IS.

Disclosures: **Y. Iwasaki**, None.

M467

CSF-1R in the Pathogenesis of Osteoporosis in Idiopathic Hypercalciuria. **R. Pramanik¹, J. Asplin^{*1}, C. Lindeman^{*1}, S. Donahue^{*1}, S. Sprague^{*2}, M. Favus³, E. Coe^{*3}.** ¹Litholink Corporation, Chicago, IL, USA, ²Evanston Northwestern Healthcare, Northwestern University, Evanston, IL, USA, ³University of Chicago, Chicago, IL, USA.

Idiopathic hypercalciuria (IH) is a state of excess urine calcium excretion with normal serum calcium, in the absence of other known mineral disorders. IH is the most common metabolic abnormality found in kidney stone patients. Many kidney stone patients with IH have low bone mineral density (BMD) and epidemiologic studies show an increased risk of fracture in stone formers. Excess urine calcium may be from intestinal calcium hyperabsorption and bone resorption. Low BMD in IH is thought to be due to excessive osteoclastic bone resorption, but the underlying molecular mechanisms which drive high osteoclastic bone dissolution are unknown. Differentiation of peripheral blood monocytes (PBMs) into functional osteoclasts can be demonstrated in vitro in the presence of

macrophage colony stimulating factor (M-CSF) and soluble RANKL. The M-CSF receptor (CSF-1R) is necessary for osteoclast differentiation and is expressed in the PBM. Therefore, we have investigated the potential role of PBM CSF-1R in the urinary calcium excretion in stone forming IH probands, family members and non-stone forming normocalcemic subjects. The protocol was approved by an institutional review board. IH was defined as 24-h urine calcium excretion greater than 250 mg and 300 mg, for women and men respectively, while on a non-restricted diet. PBMs were isolated using Dynabeads conjugated with CD14 monoclonal antibody and CSF-1R levels measured by quantitative Western blotting. Cellular total protein from THP-1 monocytic cells was used to create a standard curve. Each microgram of THP-1 cell lysate protein was assigned an arbitrary value of 50 units of CSF-1R since the actual amount was not known. Serum M-CSF levels were measured using a commercial ELISA kit. PBM from stone forming IH patients had higher levels of CSF-1R, 38.27 ± 1.14 unit/microgram vs. 18.28 ± 0.81 unit/microgram (\pm SE, $n=23$, $p=0.04$). CSF-1R levels were positively correlated with the 24-h urine Ca excretion ($R^2 = 0.26$ and $p=0.01$). Although serum M-CSF levels were not different between stone formers and non-stone formers, serum M-CSF levels were positively correlated with the urine calcium excretion ($R^2 = 0.19$, $p=0.03$). However, serum MCSF levels and PBM CSF-1R levels were not correlated. The results suggest that higher levels of CSF-1R in the PBMs of IH patients may mediate their increased differentiation to mature osteoclasts, resulting in increased bone resorption and bone loss.

Disclosures: **R. Pramanik**, None.

M468

High Rate of Hypogonadism and Vitamin D Insufficiency in Males on Dialysis. **U. Gruntmanis¹, B. Leach^{*2}, C. V. Odvina³, J. E. Zerwekh³, K. Sakhaee^{*3}.** ¹Endocrinology, UT Southwestern Medical Center and Dallas VA Medical Center, Dallas, TX, USA, ²UT Southwestern Medical School, Dallas, TX, USA, ³Center for Mineral Metabolism and Clinical Research, UT Southwestern Medical Center, Dallas, TX, USA.

It has been recently postulated, that in dialysis patients not only 1,25 dihydroxy vitamin D but low 25 hydroxy vitamin D contributes to elevated PTH levels. Frequency of hypogonadism has not been well studied in dialysis dependent men. In this study our goal was to determine frequency of vitamin D insufficiency/deficiency and hypogonadism in dialysis dependent men. We screened 67 dialysis dependent men as part of a double blind prospective controlled trial of testosterone replacement and its role on bone mineral density in this population. Data presented here are from screening visit only. We screened 45 African American, 14 Hispanic and 8 Caucasian men. All patients who did not have history of hormone sensitive cancer, sleep apnea, drug or alcohol use, elevated prostate specific antigen, intact PTH level above 600pg/ml, were medically stable, and did not have glucocorticoid use in last three months were invited for a screening visit. Levels of intact PTH, calcium, phosphorus, 25 hydroxy vitamin D, 1,25 dihydroxyvitamin D, total testosterone, estradiol, bone specific alkaline phosphatase and tartrate-resistant acid phosphatase-5b were measured in morning fasting blood sample. In our study population, median age was 52 and length of dialysis was 22 months. Median 25 hydroxy vitamin D level was 23ng/dl. 66.6% of men had 25 hydroxy vitamin D levels below 25ng/ml and 5.2% below 10ng/ml. Levels were not statistically different between racial groups. 38.8% of men had testosterone level below 300ng/dl. Estradiol level was low (below 20pg/ml) in 15.2% of men. Median bone specific alkaline phosphatase (BAP) and intact PTH levels were 21.5 U/L and 170pg/ml, respectively. There was positive correlation between intact PTH and BAP levels ($p=0.03$). There were no other statistically significant correlations between any measured parameters. We conclude that vitamin D deficiency and hypogonadism are common in men on dialysis.

Disclosures: **U. Gruntmanis**, None.

M469

Impact of Parathyroidectomy on the Morphology and the Number of Osteocyte in Hemodialysis Patients with Secondary Hyperparathyroidism. **A. Yajima¹, H. E. Takahashi², Y. Ogawa^{*3}, T. Inou^{*1}, O. Otsubo^{*1}, S. Yagi^{*1}, K. Otsubo^{*1}, Y. Tominaga^{*4}.** ¹Nephrology, Towa Hospital, Tokyo, Japan, ²Niigata University of Health and Welfare, Niigata, Japan, ³Urology, University of the Ryukyus, Okinawa, Japan, ⁴Surgery, Nagoya Second Red Cross Hospital, Nagoya, Japan.

Purpose: Basic Multicellular Unit (BMU) with osteoid seam is considered to be a newly formed bone, and the other bone is an older one. Life-cycle of osteocyte was divided into the two groups, namely, the presence or the absence of osteocyte in lacunar. We compared these two stages of osteocytes in BMU or in an older bone by assessing the differences of the morphology and the number of osteocyte early after parathyroidectomy with immediate autotransplantation (parathyroidectomy) for secondary hyperparathyroidism. Methods: The patients were 14 hemodialysis patients with secondary hyperparathyroidism treated by parathyroidectomy, and the mean age of the patients was 57.3 years and serum intact PTH was 1225.8 pg/ml . In addition, iliac bone biopsies were performed before and at 3-9 weeks after parathyroidectomy. Bone histomorphometric analysis was also performed to measure the primary parameters including (1) Bone volume (BV), (2) Bone volume of BMU with osteoid seam (BV_{BMU}), (3) Number of osteocyte (N.Ot), and (4) Number of empty lacunar (N.Empty Lc) and the derived indices including (1) Number of osteocyte per BV_{BMU} ($\text{N.Ot}/\text{BV}_{\text{BMU}}$), (2) Number of osteocyte in bone exclusive of BMU with osteoid seam ($\text{N.Ot}/\text{BV}-\text{BV}_{\text{BMU}}$), (3) Number of empty lacunar ($\text{N.Empty Lc}/\text{BV}$). Results: (1) $\text{N.Ot}/\text{BV}_{\text{BMU}}$ significantly decreased from 355.5 ± 103.5 to $249.7 \pm 91.9 \text{ N/mm}^2$ ($p<0.01$), (2) $\text{N.Ot}/(\text{BV}-\text{BV}_{\text{BMU}})$ also decreased from 176.4 ± 46.3 to $150.0 \pm 53.0 \text{ N/mm}^2$ ($p<0.01$), (3) $\text{N.Empty Lc}/\text{BV}$ significantly increased from 12.1 ± 8.2 to $38.7 \pm 15.9 \text{ N/mm}^2$. Conclusions: It was considered that the number of osteocyte in BMU and bone exclusive

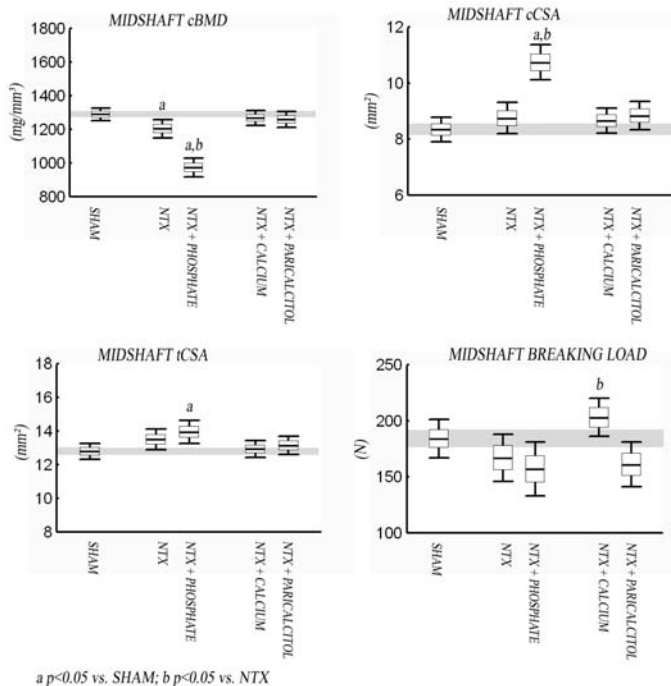
of BMU with osteoid seam were decreased by an abrupt declination of serum PTH levels. An increase of N.Empty Lc/BV was thought to be caused by an enhanced apoptosis of osteocyte after parathyroidectomy.

Disclosures: **A. Yajima**, None.

M470

Renal Failure Aggravated by Extensive Phosphate-Loading - An Ultimate Test for the Bone Mechanostat. **J. Jokihäärä**, **I. Pajamäki**, **T. Vuohelainen***, **P. Kööbi***, **P. Jolma***, **J. Kalliovalkama***, **P. Kannus***, **H. Sievänen***, **I. Porsti***, **T. L. N. Järvinen**. University of Tampere, Tampere, Finland.

A built-in system called the Mechanostat adapts the strength of bones to incident loading through changes in the mineral mass and geometry. Should it be of evolutionary origin, we hypothesized that it maintained the mechanical integrity of bones even under the extreme metabolic challenge of end-stage renal failure and phosphate overload. Accordingly, 67 eight-week old male rats were randomized and subjected to 5/6 nephrectomy (NTX) or sham-operation. After a 15-wk period of disease progression, the NTX'd rats were assigned to receive either normal chow (NTX), chow with excessive phosphate (NTX+P), chow containing phosphate-binding calcium salts (NTX+Ca), or normal chow and parenteral injections of non-calcemic vitamin-D analog (paricalcitol, NTX+Pari) for the subsequent 12 wks. At the end of this 27-wk experiment, a comprehensive structural analysis of the femoral midshaft was performed (pQCT scanning and mechanical testing). In both the NTX and NTX+P groups, there was an approximately 50% mortality rate (7/13 survived in both groups), whereas in the NTX+Ca and NTX+Pari groups 9/13 and 11/13 survived, respectively. Dramatic increases were found in the PTH values in both the NTX and NTX+P groups (1173 ± 978 and 3620 ± 675 , respectively) compared to 99 ± 53 in the Sham-operated. However, the Ca²⁺-supplementation effectively suppressed the PTH levels (4 ± 2), while the PTH was clearly increased in the NTX+Pari group (620 ± 762). These dramatic changes resulted in a NTX-induced decrease in the volumetric bone density (cBMD) of the femoral midshaft (-7%, $p < 0.05$ vs. Sham), an effect that was further aggravated by phosphate-loading (-25%, $p = 0.000$ vs. Sham; -19%, $p = 0.000$ vs. NTX). However, despite these dramatic reductions in bone mass, the structural strength of the midshaft was maintained in both NTX and NTX+P groups by an apparent compensatory increase in the cortical cross-sectional area (cCSA) (+29%, $p = 0.000$ vs. Sham; +23%, $p = 0.000$ vs. NTX). In conclusion, the preservation of the structural strength of femoral midshaft - even under these extreme circumstances of end-stage renal failure and severe phosphate-loading (e.g., a 40-fold increase in plasma PTH) - quite persuasively suggests that the bone Mechanostat remains functional till the very end of animal life.



Disclosures: **J. Jokihäärä**, None.

M471

Fibroblast Growth Factor 23 and Bone Mineral Density in Normal and Patients with End Stage Renal Disease. **S. B. Hong**¹, **E. Kim**^{*1}, **M. Nam**^{*1}, **W. Park**¹, **B. Lee**^{*2}, **Y. Kim**^{*1}. ¹Internal medicine, Inha University, Incheon, Republic of Korea, ²Gynecology, Inha University, Incheon, Republic of Korea.

Introduction: In addition to parathyroid hormone and vitamin D, phosphate-regulating factor, phosphatonins have been shown to be associated with the hypophosphatemic rickets(XLH) and autosomal dominant hypophosphatemic rickets(ADHR). Fibroblast growth factor 23(FGF23), circulating phosphaturic factor increased in ADHR, tumor induced osteomalacia(TIO) and end stage renal disease(ESRD). However, the role of FGF23 in pathologic condition is not yet clear. We investigated association of FGF23 and phosphate regulation in patients with ESRD. **Methods:** Fasting serum FGF23 levels and serum biochemical parameters were measured using a human FGF23 (C-terminal) ELISA assay in 62 subjects with hyperphosphatemic subjects with ESRD and 10 age-matched controls. Bone mineral density, percent body fat and intact PTH and 25(OH)D3 were measured. **Results:** FGF23 (RU/ml) concentrations were higher in patients with ESRD ($p < 0.001$). Serum phosphorus levels were not correlated with FGF23, but have positive correlation with serum BUN($r = 0.644$, $p < 0.01$) and creatinine($r = 0.628$, $p < 0.01$). Intact PTH and 25OH D3 had no association with BMD of femur and neck. **Conclusion;** These findings suggest that FGF23 and serum phosphorus are independently regulated and have little role in bone metabolism in patients with ESRD.

Disclosures: **S.B. Hong**, None.

M472

Evaluation of 25(OH) Vitamin D Serum Levels in Uremic Patients in Hemodialysis (HD). **A. L. Negri**^{*1}, **E. Del Valle**^{*1}, **E. Fradinger**^{*2}, **J. R. Zanchetta**¹. ¹Nephrology, Instituto de Investigaciones Metabólicas, Buenos Aires, Argentina, ²Instituto de Investigaciones Metabólicas, Buenos Aires, Argentina.

Little is known about the magnitude of vitamin D deficiency in patients with stage 5 Chronic Kidney Disease (CKD). Thus we evaluated serum 25(OH) vitamin D levels in 84 stable patients in chronic HD (41 months) of both sexes, with a mean age 58.9 ± 16.6 years, during the month of September (end of winter in the Southern hemisphere). 25(OH) vitamin D serum levels were measured by RIA (Diasorin Stillwater, Minesotta,USA; Interassay CV <15%). Intact PTH was measured by an automated method (Elecsys). We also determined serum albumin, creatinine, PCR and BMI as nutritional parameters and Functional capacity (FC) according to Karnofsky index. We considered adequate vitamin D levels those >30 ng/ml; vitamin D insufficiency 30 to 10 ng/ml and vitamin D deficiency <10 ng/ml. We found vitamin D insufficiency in 64.2% of the patients and vitamin D deficiency in 11.9%. There was no correlation between 25(OH) vitamin D serum levels and serum iPTH levels ($r = 0.08$) or age ($r = 0.14$), but there was a positive correlation with serum albumin ($r = 0.22$) and with creatinine ($r = 0.38$). Patients with FC 1-2 (n:70, 83.3%) had a significantly higher 25 OH D serum levels compared with patients FC 3-4 (n:14, 16.6 %): 25.9 vs 17.1 ng/ml ($P = 0.03$). These data indicate that vitamin D insufficiency/deficiency is highly prevalent in patients stage 5 CKD on dialysis (76.1%) at the end of winter and it seems to be related to poorer nutrition and worse functional class.

Disclosures: **A.L. Negri**, None.

M473

Nano SIMS as an Analytical Tool for Trace Metal Detection in Bone from Patients Receiving Long Term Haemodialysis. **J. Denton**¹, **F. Hillion**^{*2}, **F. Horreard**^{*2}, **A. G. Cox**³. ¹Laboratory Medicine, University of Manchester, Manchester, United Kingdom, ²CAMECA, Paris, France, ³Centre Analytical Sciences, University of Sheffield, Sheffield, United Kingdom.

The purpose of this study is to investigate the potential of the NanoSIMS 50 instrument in the identification of trace elements in bone at an ultrastructural level coupled with high sensitivity to parts per billion levels of the test element. Quantitative bulk analysis of bone by solution ICP-MS is of limited usefulness in the understanding of the biological processes underlying the possible accumulation of the element. In order to identify and spatially resolve the elements present at the cellular level it is necessary to use complex ion or other beam techniques. The NanoSIMS 50 instrument offers this ability to map ions in mineralised tissues at extremely low concentrations <1ppm with a spatial resolution of between 50 and 500 nm depending on the size of the square ion beam used. Samples of trabecular bone derived from a trans-iliac biopsy from an end stage renal failure patient treated by haemodialysis and receiving lanthanum carbonate as a phosphate binder were used as a test specimen. A sample of trabecular bone from a haemodialysis treated renal patient receiving aluminium hydroxide as a phosphate binder was used as control. The specimen was ethanol fixed and Araldite CY 212 embedded. A block 10mm diameter and 100 micron thick was taken by diamond blade, polished by diamond abrasion techniques and gold coated. Using a 400 X 400 nm primary O- beam areas 40x40micron were examined by raster mapping. There was a discrete deposition of lanthanum highly localised at the surface of the test bone, 2 micron in depth and no detected lanthanum other than natural background within the deeper matrix when compared to the control specimen.

Disclosures: **J. Denton**, None.

M474

Laser Ablation -Inductively Coupled Plasma - Mass Spectrometry as an Analytical Tool for Trace Metal Analysis in Bone from Renal Haemodialysis Patients. A. G. Cox¹, J. Denton². ¹Centre Analytical Sciences, University of Sheffield, Sheffield, United Kingdom, ²Laboratory Medicine, University of Manchester, Manchester, United Kingdom.

The purpose of this study is to investigate the potential use of Laser Ablation -Inductively Coupled Plasma - Mass Spectrometry (LA-ICP-MS) as a technique for the identification of metals in bone at ultra trace concentrations in the sub parts per billion range linked to a spatial resolution capability of < 5 micron. Samples of bones from an end stage renal failure patients treated by haemodialysis and receiving lanthanum carbonate as a phosphate binder were used as test specimens and samples from haemodialysis patients receiving aluminium hydroxide as a phosphate binder were used as controls. Analytical calibration standards were prepared by adding known lanthanum concentrations to co-precipitating calcium phosphate solutions and drying the resulting precipitate. The bone specimens were ethanol fixed and LR White embedded for subsequent bone histomorphometry. The analytical calibration pellets were processed in an identical manner. Using a 4 micron diameter laser beam to provide high resolution analysis both samples and standards were examined. There was a discrete deposition of lanthanum highly localised at the surface of the bone and occasional localisations of the metal deep within bone at areas thought to be reversal lines. Lanthanum concentrations deep within the bone matrix were no different to endogenous lanthanum concentrations found in the control group treated with aluminium. When the data was compared to the analytical calibration standards the maximum localised concentrations in the test specimens was shown to be in the low parts per billion range indicating the presence of lanthanum but at a very low concentrations.

Disclosures: **A.G Cox**, None.

M475

25-Hydroxyvitamin D₃ Suppresses PTH Synthesis and Secretion by Cultured Bovine Parathyroid Cells: Potential Role for Autocrine 1,25-Dihydroxyvitamin D₃. C. S. Ritter^{*1}, H. J. Armbrecht², E. Slatopolsky¹, A. J. Brown¹. ¹Renal Division, Washington University Medical School, Saint Louis, MO, USA, ²Biochemistry, Saint Louis University, Saint Louis, MO, USA.

Reduction of parathyroid hormone (PTH) levels by 1,25-dihydroxyvitamin D₃ [1,25(OH)₂D₃] is believed to function as part of an endocrine feedback loop. PTH enhances the renal conversion of 25-hydroxyvitamin D₃ to 1,25(OH)₂D₃ by the 1 α -hydroxylase, and 1,25(OH)₂D₃, acting through the vitamin D receptor (VDR) of the parathyroid glands reduces PTH gene transcription. However, PTH levels are known to correlate better with 25(OH)D₃ than 1,25(OH)₂D₃. The recent discovery of 1 α -hydroxylase mRNA and protein in parathyroid tissue suggests the possibility of an autocrine action of locally-produced 1,25(OH)₂D₃, but this has not been demonstrated. In the present study we demonstrated 1 α -hydroxylase activity in parathyroid cells by incubating with 25(OH)D₃ (10⁻⁶ M) and measuring 1,25(OH)₂D₃ secreted into the medium using a RIA (IDS Inc., Fountain Hills, AZ). The presence of 1 α -hydroxylase was confirmed by immunohistochemistry of parathyroid cells using an antibody raised against a C-terminal peptide of the human 1 α -hydroxylase. Incubation with 25(OH)D₃ (10⁻⁶ M) for 72 h reduced PTH secretion by 54 \pm 23 % (p = 0.012) and PTH mRNA by 57 \pm 6%; these decreases are comparable to the maximal suppression by 1,25(OH)₂D₃ in this system. In summary, 25(OH)D₃ can act directly on parathyroid cells to reduce PTH secretion and synthesis. Parathyroid cells appear to be capable of metabolizing 25(OH)D₃ to 1 α -hydroxylated metabolites, but whether this activation is required for the suppressive effects of 25(OH)D₃ remains to be determined.

Disclosures: **C.S. Ritter**, None.

M476

Prevalence of Vitamin D Insufficiency and Osteoporosis in Patients with Severe Chronic Liver Disease and Liver Transplantation. M. Rodriguez-Garcia^{*1}, C. Gomez¹, L. G. Dieguez^{*2}, M. Rodriguez^{*2}, M. Naves^{*1}, A. Rodriguez-Rebollar^{*1}, M. T. Fernandez-Coto^{*3}, J. B. Cannata-Andia¹. ¹Bone and Mineral Research Unit. Instituto Reina Sofia de Investigacion., HUCA, Oviedo, Spain, ²Gastroenterology, HUCA, Oviedo, Spain, ³Biochemistry, HUCA, Oviedo, Spain.

Bone loss and vertebral fractures (Vt Fx) are common complications after liver transplantation (Tx); both pre- and post-transplant factors may be implicated in its pathogenesis. This study aimed to compare relevant bone markers, such as vitamin D status, bone mass and Vt Fx in patients with severe chronic liver diseases waiting for liver Tx (Pre-Tx group), with patients after the first year of liver Tx (Post-Tx group). Forty patients who received a liver Tx in the previous year (mean time of Tx 9 \pm 3 months) were compared with 38 patients with chronic liver disease waiting for liver Tx. For both groups, the study included measurement of fasting serum biochemical markers [25-OH D₃, 1-25 (OH) D₃, iPTH, Ca, P, alkaline phosphatase and others], bone mineral density (BMD) at lumbar spine and hip (Hologic QDR-1000) and X-ray evaluation of thoracic and lumbar spine. Other demographic, anthropometric and relevant clinical data were also registered. A population-based cohort of the same geographical area, age and gender was also used as a comparator (n=309). The prevalence of Vt Fx was 25% in pre-Tx, 29% post Tx and 15.7% in the general population. In pre-Tx patients, the rate of Vt Fx did not differ between sexes. By contrast, post-Tx women suffered a significantly higher rate of Vt Fx (42.1%) compared with post-Tx males (8.3%) and also with women of the general population (18.7%, p<0.05). At total hip, densitometric osteoporosis (WHO criteria) in pre-Tx women was higher (28.6%) compared with men (10.3%). Also at the total hip, BMD was

significantly lower in Pre-Tx patients having Vt Fx (Z-score -1.78 \pm 0.45 vs 0.17 \pm 1.32, p<0.005). By contrast there were no differences at any site in the Post-Tx group. The mean 25 (OH) D₃ serum levels in pre-Tx patients were low (18 \pm 12 ng/ml) although similar to post-Tx patients (18 \pm 9.4 ng/ml) and general population (19 \pm 10 ng/ml). However, there was more prevalence of severe deficiency (< 10 ng/mL) in the pre-Tx patients (34.5%) compared with post-Tx (23.8%) and general population (21.5%). In addition, in pre-Tx women, a significant positive relationship was found between 25 (OH) D₃ and 1.25 (OH)₂ D₃(r=0.83, p<0.05). In summary, severe chronic liver disease is associated with low bone mass, a high rate of Vt Fx and lower 25 (OH) D₃ serum levels even before the liver transplantation. Although several other factors may be involved, an adequate vitamin D supplementation is mandatory to reducing bone abnormalities in chronic liver disease.

Disclosures: **M. Rodriguez-Garcia**, None.

M477

Alendronate Treatment in Long-Term Liver or Cardiac Transplanted Osteoporotic Patients. G. Martinez^{*1}, L. Gil-Fraguas^{*2}, E. Jodar¹, A. Escalona^{*1}, A. Moreno^{*3}, E. Garcia^{*1}, E. Moreno^{*3}, M. Gómez^{*4}, F. Hawkins¹. ¹Endocrinology Service, University Hospital 12 de Octubre, Madrid, Spain, ²Rehabilitation Service, University Hospital 12 de Octubre, Madrid, Spain, ³Digestive Surgery Dpt, University Hospital 12 de Octubre, Madrid, Spain, ⁴Cardiology Service, University Hospital 12 de Octubre, Madrid, Spain.

Background: early institution of therapy may prevent bone loss after transplantation (Tx). However, the best therapeutic option in long-term transplanted patients with osteoporosis has not been defined yet. Our **aim** was to investigate the effects of alendronate on bone mineral density in long-term Tx patients with osteoporosis. **Patients and Methods:** Forty-four patients (17 liver and 27 cardiac recipients), mean age 56 y., with densitometric osteoporosis (T-score < -2.5) more than 2 years after Tx were treated with alendronate (70 mg p.o. once weekly) and minimum of 1000 mg of calcium and 400 IU vitamin D₃ daily p.o.. Mean time since Tx was similar in both groups (56 months in liver recipients, 52 months in cardiac Tx patients). In liver recipients immunosuppressive therapy included tacrolimus in 65% and Cyclosporine A in 35% of patients, but none was receiving corticosteroids at the time of study. In cardiac recipients > 90% of patients was on prednisone treatment (mean dose 5.7 mg/day, mean accumulate dose 11505 mg). BMD changes were assessed after one year of treatment at lumbar spine and hip (DXA, Hologic QDR 4500). **Results:** In liver recipients mean lumbar BMD increase was + 8.1 \pm 7.1%, whereas mean total hip BMD increased +3.8 \pm 4.3% , femoral neck BMD increased +3.3 \pm 6.9% and trochanteric BMD increased +7.3 \pm 6.0 % . In contrast, BMD responses in cardiac recipients were less impressive; mean lumbar BMD increase was +2.1 \pm 3.6%, mean total hip BMD -1.1 \pm 6.4%, and femoral neck BMD increased +1.2 \pm 4.6%. Treatment was well tolerated in all the patients. **Conclusion:** Weekly oral alendronate plus calcium and vitamin D₃ is an effective treatment in long-term Tx-related osteoporosis, particularly in liver recipients. Concomitant immunosuppressive drugs used could influence the response to the antiresorptive treatment in these patients.

Disclosures: **G. Martinez**, None.

M478

Evolution of Bone Density after Heart Transplantation: Influence of Anti-Resorptive Therapy. L. Gil-Fraguas^{*1}, E. Jodar², G. Martinez^{*2}, M. A. Escalona^{*2}, J. Vara^{*1}, E. Robles^{*1}, F. Hawkins². ¹Rehabilitation, University Hospital 12 de Octubre, Madrid, Spain, ²Endocrinology, University Hospital 12 de Octubre, Madrid, Spain.

Osteoporosis and osteoporotic fractures are common complications after heart transplantation. The purpose of this study was to evaluate the effects of antiresorptive therapy (calcium and vitamin D [CaVD], calcitonin [CT], etidronate [ETN] or alendronate [ALN]) at standard doses in the evolution of bone mineral density (BMD) in heart transplant recipients. **Patients and Methods:** We studied 216 patients (aged [mean (SD)] 54(10) years, 85% males, BMI 24.25(3.25) kg/m²) undergoing heart transplantation. BMD was assessed by DXA (Hologic 4500) in lumbar spine (LS) and total femur (TF) sites at baseline, 6, 12 and 24 months. Patients with normal BMD at baseline were placed in CaVD group and served as controls, the rest of the patients were random allocated in CT, ALN or ETN group. 152 patients had 24 months of follow-up. The statistical analysis included the following tests: Scheffe, Manova and Wilks' Lambda. **Results:** As expected, baseline LS and TF BMD (gr/cm²) was higher in CaVD group (LS/TF: 0.973(0.114)/ 0.925(0.129), respectively; p<0.05) without significant differences among the rest of the groups (LS/TF: CT: 0.873(0.157)/ 0.820(0.116); ETN: 0.882(0.121)/ 0.893(0.121); ALN: 0.884(0.147)/ 0.832(0.109)). The changes in BMD (%) are showed in the table:

Group/Site	6 Mo	12 Mo	24 Mo
CaVD LS	-3.34(5.55)	-3.97(5.65)	-3.07(7.0)
CaVD TF	-1.66(3.71)	-3.41(4.06)	-3.15(3.89)
CT LS	-4.3(6.4)	-4.94(5.26)	-0.93(6.39)
CT TF	-3.85(5.83)	-4.85(6.10)	-3.59(5.87)
ETN LS	-5.27(4.85)	-5.42(5.66)	-1.87(6.22)
ETN TF	-3.67(5.55)	-5.54(4.97)	-4.65(5.46)
ALN LS	0.53(5.16)	0.79(5.17)*	4.90(8.42)*
ALN TF	-0.39(4.0)*	-0.63(4.14)*	-0.46(5.16)*

*p<0.001 vs any other group.

Conclusions: According to other studies, heart transplantation produces a high bone loss with a recovery phase beginning 6 (LS) to 12 (TF) months after the procedure. Alendronate is associated with lower bone loss at femoral neck and even with a relative increase in lumbar spine bone density.

Disclosures: **E. Jodar**, None.

M479

Cyclosporine A Increases Growth but Leads to Secondary Hyperparathyroidism in Young Rats. C. P. Sanchez, Y. He*. Pediatrics, University of Wisconsin Medical School, Madison, WI, USA.

Cyclosporine A (CsA) is a potent and frequently used immunosuppressive agent in the maintenance of renal allograft. A decline in bone mass has been reported with CsA therapy, but its effect on growth has not been evaluated. Thus, 38 male weanling Sprague-Dawley rats were randomly divided into 3 groups: Control (N=13), Pred (N=6) and CsA (N=13). Half of the animals from each group were treated for 2 weeks and the remaining animals received treatment for 4 weeks. Prednisone was given at 3 mg/kg/day, CsA at 10 mg/kg/day and Control animals received saline at the same volume by gavage route. The animals underwent cardiac perfusion with 4% PFA/PBS at the time of sacrifice. Blood was obtained for serum calcium, phosphorus, creatinine and intact PTH. The proximal tibia was collected for growth plate morphometry and immunohistochemistry studies. Change in body weight, body length and tibial length measurements were obtained at the end of the study period (Table 1).

Parameters	Two weeks			Four weeks		
	CsA, N=6	Pred, N=6	Control ,N=6	CsA, N=7	Pred, N=6	Control, N=7
Delta Weight, gm	78 ± 3	70 ± 8	73 ± 8	156 ± 5	150 ± 9	159 ± 4
Delta length, cm	9.3 ± 0.7*	8.3 ± 0.4	8.5 ± 0.5	15 ± 0.5	15 ± 0.8	16 ± 0.9**
Tibial Length, cm	3.3 ± 0.05*	3.1 ± 0.05	3.1 ± 0.1	3.6 ± 0.09	3.5 ± 0.08	3.7 ± 0.06**
Intact PTH, pg/ml	76 ± 10	84 ± 20	56 ± 20	220 ± 50	172 ± 23	99 ± 25**
Serum Calcium, mg/dl	9.8 ± 1.0	9.4 ± 1.0	10 ± 0.4	10 ± 0.5	10 ± 0.3	10 ± 0.2
Serum Phosphorus, mg/dl	11 ± 0.5	12 ± 0.3	12 ± 0.5	11 ± 0.5	11 ± 0.3	11 ± 0.7

*p<0.02 vs Pred, Control; **p<0.01 vs CsA, Pred
After 2 weeks, CsA increased bone growth in the proximal tibia (using tetracycline labeling); 275±75 um/day versus 154±53 um/day and 120±20 um/day in Control and Pred groups, p<0.01. At the end of 4 weeks, bone growth declined in both CsA and Pred groups compared to Control, 220±50 um/day and 150±43 um/day versus 313±70 um/day, respectively, p<0.04. The width of the growth plate cartilage did not differ in all groups. Histochemical staining for TRAP did not change, however, RANKL expression in the chondro-osseous junction increased in the CsA group compared to Control, 0.5±0.06 and 0.3±0.02, p<0.02. The increase in bone growth during CsA therapy may in part be due to an increase in chondroclastic resorption. The mechanisms that may lead to the development of secondary hyperparathyroidism with prolonged therapy need further investigation.

Disclosures: **C.P. Sanchez**, None.

M480

Body Composition and Serum IGF-1, IGFBP- 3 and Leptin in Children before and after Liver Transplantation. E. Karczmarewicz*¹, J. Pawowska*², E. Skorupa*¹, E. Krykiewicz*¹, H. Matusik*¹, H. Ismail*³, J. Ryko*², J. Jankowska*², M. Teisseyre*², P. Kaliciski*³, J. Lukaszkiwicz*⁴, J. Socha*², R. Lorenc*¹. ¹Department of Biochemistry and Experimental Medicine, The Children's Memorial Health Institute, Warsaw, Poland, ²Department of Gastroenterology, Hepatology and Immunology, The Children's Memorial Health Institute, Warsaw, Poland, ³Department of Pediatric Surgery and Transplantation, The Children's Memorial Health Institute, Warsaw, Poland, ⁴Department of Biochemistry, Medical Academy Warsaw, Pharmacy Faculty, Warsaw, Poland.

The aim of the study was to investigate body composition and serum IGF-1, IGFBP-3 and leptin in children qualified for liver transplantation (Ltx) before Ltx and during 6, 9, 12 months after transplantation. 24 children aged 1.3-5 years before performed living related liver transplantation were enrolled into the study. Serum levels of IGF-1, IGFBP-3 and leptin were determined by automated and manual immunoassays. Body composition (total body bone mineral content -TBBMC, lean mass, fat mass) were determined using densitometric measurement (Lunar - DPX). All patients were supplemented with 25(OH)D (1-2 µg/kg body weight). After transplantation immunosuppressive treatment was introduced with tacrolimus (to keep the serum level 8-19 ng/dl) and prednisone (0.1 mg/kg body weight). Statistical tests were considered significant with a *p* value 0.05 or less. Before Ltx serum IGF-1 and IGFBP-3 as well as TBBMC were significantly decreased in comparison to control values (10-60 vs. 17-248 ng/ml, 200-680 vs. 1300-2078 ng/ml, 49 - 268 vs. 110-308 g for IGF-1, IGFBP-3 and TBBMC respectively). Content of lean mass (6342-10167 vs. 4811-9846 g) and fat mass (719-2266 vs. 517-1959 g) in cholestatic children are comparable with those of age matched control group. After Ltx IGF-1 and IGFBP-3 significantly increased, reaching values of healthy control group (IGF-1: 99-300 vs. 88-747 ng/ml, IGFBP-3: 1895-3545 vs. 1433-2059 ng/ml). This increase is observed as early as 1-6 months after Ltx, and it is stable during 18 months of observation. Serum leptin level is stable and comparable to control values after Ltx (0.7-10.2 vs. 0.4-5.5 ng/ml). The rates of changes in body composition in children after Ltx were compared to changes in healthy children: lean body mass - 40% decrease, fat body mass - 20% increase, BMC - not significantly different. Successful transplantation in cholestatic children, despite normalization of IGF-1, IGFBP-3, and leptin, does not induce acceleration in BMC growth rate. It indicates that children after Ltx will not normalize their bone mineral content (BMC) before puberty.

Disclosures: **E. Karczmarewicz**, None.

M481

Bone Mineral Density after Renal Transplantation in Adolescents. M. Matsuda-Abedini*¹, J. Shepherd*², R. Mathias*¹, E. von Scheven*¹, A. A. Portale*¹. ¹Pediatrics, University of California, San Francisco, San Francisco, CA, USA, ²Radiology, University of California, San Francisco, San Francisco, CA, USA.

Loss of bone mineral occurs after renal transplantation in children, but the magnitude and duration of loss are unclear. Most studies to date have employed AP DXA of the lumbar spine to assess areal BMD (aBMD), but this technique is confounded by changes in skeletal size and maturation during growth, limiting its use in cross-sectional studies of growth-retarded patients. Serial measurements of aBMD might overcome this problem by comparing subjects to themselves. The shortcomings of planar densitometry might also be circumvented by measuring volumetric BMD (vBMD), using AP combined with lateral DXA (latvoldXA) or quantitative computed tomography (QCT). The objectives of the current prospective study were to: 1) determine the magnitude of decrease in BMD after renal transplantation in adolescents, and 2) compare aBMD and two estimates of vBMD, latvoldXA and QCT. We measured BMD of the lumbar spine in 20 ethnically diverse renal transplant recipients (11M), aged 16 ± 2.9 years (SD), at time of transplant and 9 and 18 months afterwards. Immunosuppression included corticosteroids in all patients; cumulative corticosteroid dose at 9 months was 92 ± 32 mg/kg. aBMD of the lumbar spine was determined by AP DXA (Hologic), and vBMD was determined by lumbar latvoldXA and QCT (GE 9800 Quick Scanner). To date, 18 subjects completed the 9 month visit and 10 subjects the 18 month visit. At transplant, aBMD z-score determined for chronologic age and gender (Hologic QDR-Delphi/A research reference data) was 0.06 ± 1.02. At 9 months post-transplant, aBMD decreased by 4.9 ± 10%, and the z-score decreased by 0.68 ± 0.73 (p<0.001). At 18 months, aBMD z-scores remained below baseline by 0.63 ± 0.8. vBMD determined by latvoldXA at 9 months post-transplant decreased slightly, 3.9 ± 11.6%, but not significantly, with little further change at 18 months. By contrast, vBMD determined by QCT decreased by 12.8 ± 16% (p<0.01) at 9 months and 14.4 ± 21% at 18 months. The correlation between latvoldXA and QCT was 0.6 (p<0.001). Bland-Altman comparison of paired measurements by these two methods revealed a mean difference of 0.036 g/cm³ (95% CI: 0.026 to 0.046), with wide limits of agreement (-0.03 to 0.10). These data show that lumbar BMD decreases significantly in the first 9 months after renal transplantation in adolescents and remains decreased at 18 months post-transplant. The magnitude of loss in BMD is substantially underestimated by both AP and latvoldXA compared with that determined by QCT. The poor correlation between latvoldXA and QCT and the large limits of agreement do not support using the two methods interchangeably.

Disclosures: **M. Matsuda-Abedini**, None.

M482

Normal Circulating Levels of C-PTH Fragments in Parathyroidectomized (PTX) Rats during the IV Infusion of hPTH(1-84) over 48 h. M. Usatii*¹, J. H. Brossard*¹, L. Rousseau*¹, J. R. Lavigne*², R. J. Zahradnik*², P. D'Amour*¹. ¹Department of Medicine, Centre de recherche du CHUM, Hôpital Saint-Luc, Montréal, PQ, Canada, ²Immutopics Int., San Clemente, CA, USA.

The contribution of hPTH(1-84) peripheral metabolism to circulating C-PTH fragments remains quantitatively uncertain. Early studies were performed in pentobarbital anesthetized animals with impaired hepatic blood flow, hPTH(1-84) clearance and probably C-PTH fragments formation (D'Amour et al., JBMR 11:1075, 1996). We have reevaluated C-PTH fragments formation in non anesthetized PTX rats infused IV over 48 h with hPTH(1-84). Groups of 8 rats, maintained on a normal chow diet supplemented with 1% Ca gluconate in drinking water, were PTX and implanted SC, one week later, with an osmotic minipump which delivered hPTH(1-84) IV at 0.12 or 0.24 nmol/kg/h or vehicle alone. Rats were sacrificed at 48 h by exsanguination through the abdominal aorta. Circulating PTH molecular were separated by HPLC. Serum and HPLC fractions were assayed with Bio-Intact (BI), Intact (I) and Carboxyl (C) human (h) or rat (r) PTH ELISAs (Immutopics Int. San Clemente, CA). Molecular forms identified by the hPTH assays were quantitated by planimetry. Results are means ± SD. Sham-vehicle rats had a mean Ca⁺⁺ of 1.24 ± 0.03 mmol/L with mean PTH levels of 4.99 ± 1.29 (rBI), 15.33 ± 4.03 (rI) and 16.52 ± 8.44 pmol/L (rC) while PTX-vehicle rats a Ca⁺⁺ of 0.98 ± 0.07 mmol/L (p <0.001) with undetectable rPTH levels (p <0.001). hPTH(1-84), 0.12 nmol/kg/h increased Ca⁺⁺ to 1.11 ± 0.09 mmol/L (p < 0.001) and hPTH levels to 22.4 ± 13 (hBI), 30.5 ± 16.8 (hI), and 71 ± 35 pmol/L (hC) while 0.24 nmol/kg/h increased Ca⁺⁺ to 1.33 ± 0.07 mmol/L (p < 0.001) and hPTH levels to 46 ± 26 (hBI), 51 ± 34 (hI) and 208 ± 110 pmol/L (hC). HPLC fractionation disclosed 14.4% of hPTH(1-84) with the lower infusion rate and 11.8% with the higher. N-PTH was 1.3 and 1.1%, non-(1-84) PTH 2.7 and 2.9% and smaller C-PTH fragments 81 and 84% during the same infusions. This composition is very similar to the one of a normocalcemic individual and suggests a major contribution of peripheral metabolism to C-PTH fragments formation. Peripheral metabolism appears as important as parathyroid gland secretion in the generation of circulating C-PTH fragments. Our study may even suggest a reciprocal control between both processes since a normal pattern of circulating PTH was observed during hPTH(1-84) infusions. These results will be useful to design experiments on PTH fragments biological effects in PTX rats. This work was made possible by grants from Canadian Institutes of Health Research (CIHR) (MOP-7643) and NPS Pharmaceuticals.

Disclosures: **P. D'Amour**, NPS Pharmaceuticals 2.

M483

Measurement of PTH-Induced ERK and Akt Activation and Phosphorylation of Downstream Targets Using Phosphospecific Antibody Cell-Based ELISAs (PACE). C. K. Vance*, J. A. Cole. Biology, University of Memphis, Memphis, TN, USA.

Growth factor and G protein-coupled receptor signaling converge on ERK and Akt (or PKB) to regulate proliferation, differentiation and cell survival. Recent studies have shown that PTH-induced ERK and Akt activation may involve cAMP, PKC, Ca^{2+} and/or EGF receptor transactivation but most techniques used to identify pathways involved in PTH signaling are low throughput and labor-intensive. We modified the PACE protocol described by (Versteeg *et al*, *Biochem. J.* 350:717) to rapidly assay ERK and Akt and identify substrate molecules. Antibody selectivity was determined by treating 3T3 fibroblasts, renal LLC-PK, and renalOK cells with EGF± the PI3K inhibitor wortmannin (to confirm Akt activation) or PMA ± the MEK inhibitor PD98059 (to confirm ERK activation). Cells were fixed in 4% formaldehyde, blocked in 10% FBS and primary (polyclonal anti-pS⁴⁷³Akt or monoclonal pT²⁰³pY²⁰⁴ERK) and secondary antibodies (HRP-coupled goat anti-mouse- and goat anti-rabbit IgG, respectively) were titrated. EGF-stimulated wortmannin-sensitive Akt activity and PMA-induced PD98059-sensitive ERK activity were detected in each cell line. In OK cells, PACE assays of PTH-, EGF-, cAMP- and phorbol ester-mediated ERK and Akt activation produced results identical to those of immune complex assays and/or Western blotting. Downstream signaling molecules were identified by assaying the phosphorylation state of the non-receptor tyrosine kinases Pyk2 (anti-pY⁴⁰²Pyk) and Src (anti-pY⁵²⁷Src), the Akt substrates BAD (anti-pS¹³BAD) and GSK (anti-pS²¹⁹GSKα/β), the ERK-activating MEK1/2 (anti-pS^{217/221}) and the ERK substrate p90RSK (anti-pT⁵⁷³p90RSK). EGF and PTH caused time- and dose-dependent phosphorylation of Src, BAD, GSK, MEK and p90RSK. Although pPyk2 was detected, neither EGF nor PTH changed its phosphorylation state. These data demonstrate that the PACE assay is readily adaptable to a variety of cell lines. In addition, this assay can be used to rapidly identify the signaling pathways leading to Akt and ERK activation as well as the phosphorylation state of downstream signaling molecules. Finally, PACE should allow for the rapid identification of the phosphorylation state of any molecule for which a phosphospecific antibody is available.

Disclosures: J.A. Cole, None.

M484

Dynamics of PTH Secretion in Normal Individuals. Differences Related to 3 Generations of PTH Assay. P. D'Amour¹, A. Rákel^{*1}, J. H. Brossard¹, L. Rousseau^{*1}, T. Cantor². ¹Department of Medicine, Centre de recherche du CHUM, Hôpital Saint-Luc, Montreal, PQ, Canada, ²Scantibodies Laboratory Inc., Santee, CA, USA.

The parathyroid function of 8 normal individuals was studied with 3 different generations of PTH assay to seek better quantitative information on the composition and control of circulating PTH molecular forms by ionized calcium (Ca^{++}). Eight volunteers, 4 males and 4 females, were infused with $CaCl_2$ and Na citrate over 2 h, one week apart, to modulate Ca^{++} by ± 0.2 mmol/L. A cyclase activating (CA) PTH IRMA with a 1-4 epitope which recognizes hPTH(1-84) and N-PTH, a total (T) PTH IRMA with a 12-18 epitope which recognizes hPTH(1-84) and non-(1-84) PTH and a carboxyl-terminal (C) RIA which reacts mainly with small C-PTH fragments, were used to measure PTH in serum and in HPLC fractions. Circulating PTH molecular forms present in serum at various Ca^{++} concentrations were separated by HPLC, revealed by the various PTH assays and quantitated by planimetry using results of the most appropriate assay for each molecular form. A 4 parameters sigmoidal mathematical model was used to analyze the parathyroid function measured with each assay as well as the evolution of various PTH fragments/PTH(1-84) ratios. Results are means \pm SD. Stimulated ($CA = 7.37 \pm 1.65$; $T = 8.60 \pm 1.91$; $C = 14.06 \pm 3.29$ pmol/L) and non suppressible ($CA = 0.52 \pm 0.18$; $T = 0.75 \pm 0.22$; $C = 4.28 \pm 1.50$ pmol/L) PTH values were highest in the C-PTH assay ($p < 0.001$) while slope and set point values did not differ among assays. PTH fragments/PTH(1-84) ratio values going from hypo to hypercalcemia were highest for the C/CA ratio (1.92 ± 0.29 to 9.75 ± 3.98) and the C/T ratio (1.69 ± 0.23 to 6.11 ± 1.33) and much lower for the T/CA ratio (1.15 ± 0.04 to 1.86 ± 0.73 ; $p < 0.01$). The set point of each ratio modulation by Ca^{++} (1.26 ± 0.11 to 1.29 ± 0.03) was higher than the set point of PTH secretion by Ca^{++} (1.21 ± 0.02 to 1.22 ± 0.02 ; $p < 0.001$). A planimetric evaluation of HPLC profiles disclosed that hPTH(1-84) represented only 4.1, 16.5 and 31.2% of circulating PTH in hypercalcemia, normocalcemia and hypocalcemia respectively. Similar values were 1.1, 2.7 and 6% for N-PTH, 6.8, 7.8 and 8.3% for non-(1-84) PTH and 88.1, 73.1 and 54.4% for smaller C-PTH fragments. These results confirm that the bulk of circulating PTH is made of smaller C-PTH in all circumstances, hPTH(1-84) representing at most 31% of circulating PTH. N-PTH and non-(1-84) PTH represent at most 15% of circulating PTH. These values will be useful to design in vivo and in vitro experimental to study the role of PTH(1-84) and PTH fragments in PTH physiopathology. Work supported by grant MOP-7643 from Canadian Institutes of Health Research (CIHR).

Disclosures: J.H. Brossard, None.

M485

Stimulation of Cyclic AMP/PKA Signaling Induces the Activation of Canonical Wnt Pathway in Osteoblastic Cells. A. Suzuki^{*1}, T. Michigami¹, T. Kubota^{*1}, K. Ozono². ¹Department of Environmental Medicine, Osaka Medical Center and Research Institute for Maternal and Child Health, Osaka, Japan, ²Department of Pediatrics, Osaka University Graduate School of Medicine, Osaka, Japan.

Although it is well known that intermittent administration of parathyroid hormone (PTH) stimulates bone formation, the underlying molecular mechanisms are not fully understood. Since accumulating evidences have indicated the critical roles of Wnt/LRP signaling pathway in bone formation, it is reasonable to hypothesize that Wnt/LRP pathway might mediate the anabolic effect of PTH on bone. Therefore, in the current study, we have investigated the effect of stimulation of cyclic AMP (cAMP)/PKA signaling, one of the signaling pathways downstream PTH, on the canonical Wnt signaling pathway. To address this issue, we utilized a human osteoblastic cell line SaOS-2. In the reporter assays using a T-cell Factor (TCF)-reporter plasmid Super(8x)TOPflash and a control plasmid phRL-TK, treatment with 5-50 μ M forskolin, an activator for adenylyl cyclase, induced TCF-dependent transactivation in a dose-dependent manner. The relative reporter activity of Super(8x)TOPflash reached maximum in 5 hours and began to decline at the 12-hour time point. As to the intracellular cAMP content determined by ELISA, it peaked within 1 hour and then decreased by the treatment with forskolin. A western blot analysis demonstrated the intracellular accumulation of β -catenin by treatment with forskolin, suggesting that the stimulation of cAMP/PKA signaling induced the activation of canonical Wnt pathway. We next examined the effect of the simultaneous treatment with Wnt3a and forskolin on the TCF-dependent transactivation using Super(8x)TOPflash. Wnt3a was prepared as the conditioned media obtained from L cells expressing Wnt3a. Wnt3a induced the TCF-dependent reporter activity in a dose-dependent manner as expected. Of note, treatment with both Wnt3a and forskolin synergistically increased the reporter activity. Finally, we performed RT-PCR analyses to examine the effects of forskolin on the expression of the molecules involved in Wnt/LRP signaling pathway, and found that the expression of dkkopf-1 (DKK-1), which acts as an antagonist of Wnt/LRP signaling, was markedly decreased by treatment with forskolin. Pretreatment with PKA inhibitor H89 abolished the down-regulation of DKK-1 expression by forskolin, confirming that PKA is involved. Taken together, these results strongly suggest that there might be a crosstalk between cAMP/PKA signaling and Wnt/LRP pathway, and that Wnt/LRP pathway might be involved in bone formation induced by PTH.

Disclosures: A. Suzuki, None.

M486

Regulation of Rheumatoid Fibroblast-Like Synoviocyte Apoptosis: A Role for Adrenomedullin-Calcitonin Receptor-Like Receptor Pathway. B. Uzan^{*1}, J. M. Launay^{*2}, J. M. Garel^{*1}, R. Champy^{*1}, H. K. Ea^{*1}, M. Cressent^{*1}, E. Lioté^{*1}. ¹Hospital Lariboisière, INSERM 606, Paris, France, ²Hospital Lariboisière, IFR 139, Paris, France.

Pathogenesis of rheumatoid arthritis is incompletely understood: defective fibroblast-like synoviocyte (FLS) apoptosis and increased cell proliferation have been considered. A Fas apoptosis signaling defective pathway and the expression of mutant p53 tumor suppressor gene are the two current mechanisms for defective RA FLS apoptosis. Adrenomedullin (ADM) is a 52-amino acid peptide with angiogenic, anabolic and anti-apoptotic properties. ADM binds to plasma membrane receptors composed of calcitonin receptor-like receptor (CRLR), coupled to adenylate cyclase (AC)-protein kinase A (PKA), and receptor activity modifying protein (RAMP) type 2 or 3. To date, only ADM has been detected at high concentrations in RA plasma, synovial fluid and tissues compared to osteoarthritis (OA). In this first study, we investigated ADM, CRLR and RAMP mRNA and protein expression in RA and OA cultured FLS, as well as its functional role in regulating FLS-induced apoptosis. ADM, PAM (peptidylglycine a-monooxygenase, its activating enzyme), and receptor CRLR, RAMPs, mRNA, and CRLR protein expressions were evaluated in RA and OA FLS by RT-PCR and Western blotting, respectively. Under ADM stimulation, CRLR-coupled AC activity was measured in RA FLS cell lysates, and RA FLS serum-free and TNF- α -induced apoptosis was evaluated by caspase-3 (Cas-3) activity and MTT assays. Cultured RA and OA FLS constitutively expressed ADM, PAM, and RAMP 2 and 3 mRNAs. By contrast, CRLR mRNA expression was up-regulated in RA FLS compared to OA FLS, and only RA-FLS expressed various detectable CRLR protein expression in all cultured samples. The ADM receptor, CRLR, was functional since increased cAMP was measured in cell lysates after ADM stimulation. An early stimulation was achieved at low ADM concentration (10-10M). ADM inhibited the combined (e.g., serum privation and TNF- α stimulation)-induced RA FLS apoptosis in a dose-dependent manner as assessed by Cas-3 expression and MTT viability assay. The anti-apoptotic effect of ADM on RA-FLS was related to AC activation and cAMP production, since these effects were inhibited by the pretreatment with H-89, a protein kinase A inhibitor, and mimicked by forskolin. This study has shown for the first time that: 1) ADM and activating enzyme mRNAs are expressed in FLS, 2) CRLR, its receptor, is functionally expressed by RA-FLS. The expression of the receptor in RA-FLS is consistent with the evidence that its endogenous ligand, ADM, may influence cell apoptosis and contribute to the defective apoptotic process in RA synovium.

Disclosures: B. Uzan, None.

M487

Temporal Dependence of PTH (1-34) for Anabolic Actions in an Osteoregeneration Model. G. J. Pettway*¹, C. L. Wei*², L. K. McCauley².¹Biomedical Engineering, University of Michigan, Ann Arbor, MI, USA,²Periodontics/Prevention/Geriatrics, University of Michigan, Ann Arbor, MI, USA.

Parathyroid hormone (PTH) is currently the only anabolic agent in clinical use for the treatment of osteoporosis, but the mechanisms of its anabolic actions are still unclear. In this study, an innovative osteoregeneration model was used to investigate the temporal effects of intermittent PTH treatment on tissue engineered bone. Ectopic ossicles containing cortical and trabecular bone and a hematopoietic marrow were generated from implanted bone marrow stromal cells (BMSCs). Three weeks of PTH (40µg/kg/day) or vehicle treatment were initiated 1 day (group 1), 1wk (group 2), 2wks (group 3), or 3wks (group 4) after implanting BMSCs. Calcein flurochrome was administered to mice 10 and 3 days prior to sacrifice. Microradiographic and histomorphometric analyses of plastic embedded tetrachrome stained ossicle sections revealed an anabolic response in all PTH-treated ossicles, regardless of when treatment was initiated. Flurochrome labeling also revealed an increase in bone formation in PTH versus vehicle treated ossicles in all groups. However, the anabolic response to PTH was the most pronounced in ossicles where treatment was initiated 1wk after cell implantation (group 2). A qualitative increase in tartrate resistance acid phosphatase (TRAP) positive cells was observed in PTH-treated ossicles in this group. In addition, qRT-PCR revealed a 2-fold increase in RANKL mRNA expression in ossicles treated with PTH for 1wk initiated 1wk after implanting cells, suggesting that PTH stimulates osteoclastic activity in early stages of ossicle development. Other early events of PTH action in 1wk and 2wk old ossicles were also evaluated. Osteocalcin (OCN) mRNA was low in 1wk old ossicles and increased significantly at 2wks, suggesting that PTH targets cells at the stage of transition from pre-osteoblasts to mature matrix producing osteoblasts. These data indicate that anabolic actions of PTH in tissue engineered ossicles are temporally dependent on the differentiation of implanted BMSCs and suggest that cells such as osteoclastic cells may also contribute to PTH anabolic actions.

Disclosures: **G.J. Pettway**, None.

M488

PTHrP Induces Smurf2 and Inhibits TGF-Beta Signaling in Growth Plate Chondrocytes. M. Herceg*, M. Mulcahey*, K. Kim*, Q. Wu, E. M. Schwarz, J. E. Puzas, R. J. O'Keefe, H. Drissi, M. J. Zuscik, R. N. Rosier. Orthopaedics, University of Rochester, Rochester, NY, USA.

Parathyroid hormone related peptide (PTHrP) and transforming growth factor-beta (TGF-beta) are potent inhibitors of chondrocyte maturation. The influence of these factors is critical for normal phenotypic behavior of chondrocytes in the articular surface and in the growth plate, evidenced by accelerated chondrocyte maturation in mouse models of reduced TGF-beta or PTHrP signaling. Furthermore, it is established in growth plate chondrocytes (GPCs) that TGF-beta induces PTHrP expression, indicating that there is cross-talk between these pathways leading to enhanced inhibitory effects of TGF-beta on the maturational program. Since inhibition of terminal differentiation in GPCs is the result of an interaction between these two pathways, a strong signal must be required to induce these cells to ultimately reach the hypertrophic stage, a required step during normal endochondral ossification. Recently, we have discovered that PTHrP induces Smurf2, an E3 ubiquitin ligase that targets the type I TGF-beta receptor and phospho-Smad2 for degradation in the proteasome. Based on this, we hypothesize that PTHrP induction of Smurf2 expression, leading to inhibition of the TGF-beta signaling cascade, ultimately allows GPCs to overcome the maturational inhibition exerted by both TGF-beta and PTHrP. Confirming induction of Smurf2 expression/function, treatment of GPCs with PTHrP i) up-regulates Smurf2 mRNA as measured by real time RT-PCR and ii) decreases TGF-beta-induced signaling on the P3TP-luciferase reporter. To elucidate the mechanism behind this effect of PTHrP on TGF-beta signaling, we performed western blots to assess type I TGF-beta receptor and phospho-Smad2 protein levels in cells treated with PTHrP. Consistent with our hypothesis, PTHrP mimics Smurf2 by strongly inducing degradation of both of these substrates. Use of RNA interference (RNAi) to knock-down Smurf2 expression was then performed to directly determine the role of Smurf2 in these effects of PTHrP. After confirming successful knockdown of the Smurf2 mRNA (70%), western Blot analysis showed that in the presence of a Smurf2 RNAi-oligo retrovirus, the effect of PTHrP on type I TGF-beta receptor and phospho-Smad2 levels was abrogated. These findings support our hypothesis that through an induction of Smurf2, PTHrP can turn off TGF-beta signaling, which should lead to down-regulation of PTHrP and removal of the two main roadblocks to terminal maturation in GPCs. This signaling interplay represents a novel regulatory paradigm that may be critical for maintenance of the temporal progression of chondrocyte hypertrophy during skeletal development and repair processes.

Disclosures: **M.J. Zuscik**, None.

M489

Cortical Bone Effects of PTH or Alendronate in Senile and Severely Osteopenic Ovariectomized Rats. Y. L. Ma, A. Schmidt*, R. Cain*, Q. Q. Zeng, J. Oskins*, H. U. Bryant, M. Sato. Lilly Research Labs, Indianapolis, IN, USA.

Intact or ovariectomized (Ovx) rats at about 19 months of age were treated with hPTH (1-38) (10 (Ovx only), 30µg/kg/d sc) or alendronate (ABP 28µg/kg twice weekly sc) during the latter 4 months of life. Ovx rats were severely osteopenic, having been ovariectomized at 6 months of age and allowed to lose bone for 13 months before initiating treatment. Cortical bone effects of PTH or ABP were evaluated in femora or tibia by QCT, biomechanics, and histomorphometry. Evaluation of body weight- as a measure of normal loading- showed a 12% reduction for PTH but not ABP relative to intact controls; no differences in body weight were observed between Ovx rat groups. In intact animals, load to failure analyses showed that PTH 30µg/kg increased midshaft strength by 15% and femoral neck strength by 14% relative to intact controls, whereas ABP had no effect on midshaft or femoral neck strength in intact animals. In Ovx rats, PTH dose dependently increased midshaft strength (20% and 34%) and femoral neck strength (25% and 23%) over Ovx controls. Strength parameters were restored by PTH to the level of age-matched Sham controls. For both intact and Ovx rats, PTH strength benefits resulted from significant increases in midshaft BMD (11 to 21%), midshaft BMC (10 to 22%), cortical area (7% to 16%), cortical thickness (11% to 21%), and periosteal bone formation rate (330% to 370%). In aged ovariectomized rats, ABP had no effect on midshaft strength or femoral neck strength. ABP had no effect on midshaft BMD, BMC, cortical area, or periosteal bone formation rate relative to respective intact or Ovx controls. Therefore, the ABP effects on bone formation activity in cortical bone were unlike the ABP cancellous bone effects (vertebra) where bone formation activity were markedly reduced, BFR/BS, by -79% and -75% relative to intact and Ovx controls, respectively. Nevertheless, the data taken together showed that PTH was superior to ABP in enhancing strength, increasing bone mass, and improving the spatial architecture of cortical bone sites such as the diaphysis and proximal femur in senile intact and in aged, severely osteopenic rats, even towards the end of their lifespan.

Disclosures: **M. Sato**, Eli Lilly & Co. 3.

M490

Parathyroid Hormone Stimulation of Syndecan-4 in Osteoblastic Cells. L. J. Raggatt¹, L. Qin², S. Cool³, V. Nurcombe^{*3}, N. Partridge². ¹Institute for Molecular Bioscience, University of Queensland, Brisbane, QLD, Australia, ²Department of Physiology and Biophysics, UMDNJ-Robert Wood Johnson Medical School, Piscataway, NJ, USA, ³Institute of Molecular and Cellular Biology, Proteos, Singapore.

Syndecan-4 is a membrane bound heparan sulphate proteoglycan that binds a number of growth factors, cytokines, proteases and cell adhesion molecules. The expression of the syndecan core proteins and their specific heparan sulphate attachments occurs in cell-, tissue- and developmentally specific patterns. In a screen to identify novel PTH regulated genes using cDNA microarray technology, we identified that syndecan-4 expression is increased in osteoblastic UMR-106-01 cells in response to parathyroid hormone (rPTH 1-34). Confirmation of these data using real time RT-PCR showed that steady state levels of syndecan-4 mRNA increased by 2 h, peaked at 4 h (4 fold) and had diminished by 12 h. The influence of PTH was restricted to syndecan-4 as the mRNA expression of the other members of the syndecan family were unchanged after PTH treatment of UMR 106-01 cells. The cAMP analogue 8Br-cAMP and the PKA activator PMA were used to investigate which of these classical PTH signal transduction pathways regulate expression of syndecan-4. The cAMP analogue 8Br-cAMP mimicked the PTH induction of syndecan-4 suggesting that the cAMP signal transduction pathway is utilized by PTH to regulate expression of the syndecan-4 gene. In contrast, PMA, which activates the PKC pathway, did not stimulate syndecan-4 mRNA expression. Cycloheximide did not affect expression of syndecan-4 mRNA in response to PTH treatment suggesting that the increase in steady state mRNA levels was due to transcriptional activation of the gene and did not require de novo protein synthesis. Interestingly regulation of syndecan-4 in osteoblastic cells also occurred in response to the pro-osteoclastic agents vitamin D₃ and PGE₂ suggesting syndecan-4 may have a broader role in bone biology. To confirm the in vivo significance of the PTH regulation of syndecan-4, 4 week old Sprague-Dawley rats were injected subcutaneously with vehicle (0.9% saline solution) or hPTH(1-38) (8 µg/100 g). The primary spongiosa was removed from the distal femur 0.5, 1, 4, or 8 h after injection and RNA harvested. A very rapid increase in syndecan-4 expression occurred at 0.5 h post injection, peaked at 2 h (10 fold) and had returned to base line by 4 h post injection. Taken together these data show that PTH can regulate the expression of syndecan-4 in osteoblastic cells and we therefore propose that syndecan-4 may act as a co-receptor for growth factors and cytokines in the anabolic bone response to PTH.

Disclosures: **L.J. Raggatt**, None.

M491

Parathyroid Hormone 1-34 Enhances Titanium Implant Osseointegration and Peri-Implant Bone Parameters in Rat Tibial Model of Low Density Trabecular Bone: A Micro CT Analysis. Y. Gabet^{*1}, D. Kohavi^{*2}, J. Levy^{*3}, R. DiMarchi^{*3}, M. Chorev^{*4}, R. Müller⁵, I. Bab¹. ¹Bone Laboratory, The Hebrew University of Jerusalem, Jerusalem, Israel, ²Dental Implantology Center, Hebrew University-Hadassah School of Dental Medicine, Jerusalem, Israel, ³Department of Chemistry, Indiana University, Bloomington, IN, USA, ⁴Laboratory for Translational Research, Harvard Medical School, Cambridge, MA, USA, ⁵Swiss Federal Institute of Technology (ETH) and University of Zürich, Jerusalem, Switzerland.

The use of endosseous titanium implants in dentistry and orthopaedic surgery has been the standard of care for several decades. However, implantation in low density bone has a poor prognosis and experimental studies show delayed implant integration following gonadectomy-induced bone loss. Intermittently administered parathyroid hormone 1-34 [iaPTH(1-34)] is the leading bone anabolic therapy, reversing bone loss and enhancing fracture healing. Hence, the aim of the present study was to assess whether iaPTH(1-34) stimulates the integration of titanium implants in low density bone. Threaded titanium implants, 0.9 mm in diameter, were inserted horizontally into the proximal tibial metaphysis of 5 months old rats, 7 weeks after orchietomy. Treatment with PTH(1-34), at 5, 25 and 75 µg/Kg/day commenced immediately thereafter and lasted for 8 weeks. Thereafter, the implantation site was subjected to a quantitative micro CT analysis. The specimens were scanned at 15 µm resolution using maximal energy and integration time to minimize artifacts resulting from the highly radio-opaque metal implant. Osseointegration was calculated as the percent implant surface in contact with bone (%OI) quantified as the ratio of "bone"-to-total voxels in contact with the implant. In addition, we measured in the peri-implant bone the trabecular bone volume density (BV/TV), trabecular number (Tb.N), trabecular thickness (Tb.Th) and connectivity density (Conn.D). Using a curve-fit analysis all parameters were corrected for variation in implant position to compensate for the growth plate-diaphyseal decreasing gradient in trabecular bone content. iaPTH(1-34) stimulated all of these parameters dose-dependently. The maximal enhancement of the %OI, BV/TV, Tb.N, Tb.Th and Conn.D was 154%, 263%, 142%, 150% and 200%, respectively. There were no significant differences between the 25 and 75 µg/Kg doses, other than in the case of Tb.Th that was significantly higher at 75 µg/Kg. These findings suggest that iaPTH(1-34) effectively enhances implant anchorage in low density trabecular bone and demonstrate the feasibility of improving the clinical prognosis of endosseous implantation in the osteoporotic skeleton.

Disclosures: **Y. Gabet**, None.

M492

The Stimulation of Amphiregulin Expression in Osteoblastic Cells by Parathyroid Hormone Requires the Protein Kinase A and cAMP Response Element-Binding Protein Signaling Pathway. L. Qin, N. C. Partridge. Physiology and Biophysics, UMDNJ-Robert Wood Johnson Medical School, Piscataway, NJ, USA.

Parathyroid hormone (PTH), an anabolic and catabolic agent for bone metabolism, has profound effects on gene expression in the osteoblast. Recently, we identified that amphiregulin (AR), an epidermal growth factor (EGF)-like ligand, is induced by PTH as an immediate early gene. AR has important roles in bone metabolism: stimulating preosteoblast proliferation while inhibiting osteoblast differentiation. We hypothesized that one mechanism of PTH's anabolic action is to increase AR expression resulting in expansion of the number of bone marrow stromal stem cells and their derived osteoblast progenitors. In the present report, we studied the signaling pathway PTH uses to regulate AR expression in osteoblastic cells. Only PTH (1-34, activates both PKA and PKC) and PTH (1-31, activates PKA), but not PTH (13-34, activates PKC) were able to stimulate AR mRNA levels in UMR 106-01 cells by real-time RT-PCR. In the presence of the PKA inhibitor H89, but not in the presence of the PKC inhibitor GF109203X, PTH(1-34) lost its ability to induce AR expression. The cAMP analog, 8-Br-cAMP, strongly stimulated AR expression. Injection of rats with PTH (1-38, activates both PKA and PKC) or PTH(1-31), but not PTH (3-34, activates PKC), highly and transiently stimulated AR mRNA levels in the osteoblast-rich femoral metaphyseal primary spongiosa. These results demonstrated that PTH regulates AR in a cAMP-PKA-dependent manner both *in vitro* and *in vivo*. Alignment of human, mouse and rat AR promoters revealed a highly conserved cAMP-response element (CRE) just upstream of a TATA box. In UMR 106-01 cells, Western blots demonstrated that after PTH treatment the phosphorylation of CRE-binding protein (CREB) peaked at 45 min, preceding the peak of AR mRNA synthesis (60 min). Moreover, luciferase reporter assays using human AR promoter-luciferase constructs revealed that the binding of phosphorylated CREB to the CRE site in the AR promoter plays an important role in basal, PTH-induced and prostaglandin E₂ (PGE₂)-induced AR expression in osteoblastic cells. Mutation of this CRE site resulted in a significantly lower basal AR promoter expression and a much lower PTH and PGE₂ responsiveness of the AR promoter. Co-transfection with a dominant-negative CREB (KCREB) along with AR promoter constructs completely eliminated the PTH and PGE₂ stimulation of the AR promoter. In summary, our data suggest that PTH-induced AR mRNA expression in osteoblastic cells is mediated primarily through cAMP-PKA-CREB signaling.

Disclosures: **L. Qin**, None.

M493

Interference with Connexin43 Function Attenuates Parathyroid Hormone Regulation of the Rat Osteocalcin Promoter. A. De Marzo^{*1}, J. P. Stains², R. Civitelli¹. ¹Bone and Mineral Diseases, Washington University in St. Louis, St. Louis, MO, USA, ²University of Maryland Sch. Med., Baltimore, MD, USA.

Interference with connexin43 (Cx43) decreases PTH stimulation of cAMP production and osteoblast differentiation *in vitro*; and we find that the osteoanabolic effect of PTH *in vivo* is also attenuated in mice with conditional deficiency of osteoblast Cx43. Using the osteocalcin (OC) gene as a model, we explored the molecular bases of Cx43 modulation of PTH action in osteoblasts. Exposure of ROS 17/2.8 cells to 10⁻⁸ M PTH (1-34) for 16-24 hours induced a ~ 6.8 fold stimulation of OC mRNA accumulation, measured by real time PCR. By contrast, in ROS 17/2.8 cells stably expressing chicken connexin45 (cCx45), which interferes with Cx43 function, PTH treatment induced only a ~1.4 fold increase of OC mRNA. We then studied gap junction sensitivity of OC gene transcription in response to PTH, and transiently co-transfected ROS 17/2.8 cells with cCx45 and a series of 5' deleted rat OC promoter-luciferase reporter constructs (OCLUC). Treatment (16-24h) of cells with PTH induced a ~1.8 fold increase in -637OCLUC and -199OCLUC promoter activities, confirming that proximal regions of the OC promoter are PTH responsive. Importantly, cCx45 overexpression decreased both basal and PTH-stimulated -199OCLUC activity by 60 and 70 percent, respectively. Further, a -92OCLUC reporter, which spans a known CT-rich element and OSE1, still retained PTH responsiveness, though to a lesser degree than the -199OCLUC; and overexpression of cCx45 repressed the PTH response of this fragment by 80%. Deletion of the previously characterized gap junction responsive CT element from this construct (-92ΔCTOCLUC) did not affect PTH responsiveness in cells transfected with empty vector, although PTH response was abrogated when cCx45 was co-transfected with -92ΔCTOCLUC, suggesting that OSE1 activation by PTH (but not basal activity) is gap junction sensitive. Accordingly, cCx45 co-transfection abolished PTH stimulated activity from a heterologous promoter-reporter construct containing 6 copies of OSE1 (1.5 vs. 1.0 fold stimulation), whereas a CTLUC construct was insensitive to PTH, although it was down-regulated by cCx45. In contrast, co-transfection cCx45 actually synergized with PTH or forskolin in activating a non canonical cAMP response region present in the proximal OC promoter (ROCR), and a canonical cAMP response element (CRE). Thus, the ability of cCx45 to attenuate PTH effect on osteocalcin transcription mediated through OSE1 seems to be independent of ROCRR and CRE. However, the net effect on OC gene transcription and the signals converging on OSE1 during PTH stimulation are modulated by changes in Cx43 function.

Disclosures: **A. De Marzo**, None.

M494

Cross-Linking of Modified PTH(1-15) Antagonist Analogs to the Juxtamembrane Portion of the PTH/PTHrP Receptor. R. C. Gensure¹, T. Dean^{*2}, T. J. Gardella². ¹Pediatrics, Ochsner Clinic Foundation, New Orleans, LA, USA, ²Endocrine Unit, Massachusetts General Hospital, Boston, MA, USA.

We recently described a new class of conformationally constrained, N-terminal PTH fragment analogs that bind exclusively to the juxtamembrane (J) domain region of the PTH/PTHrP receptor and function as competitive antagonists (Shimizu, et. al., J Biol Chem., 2005). These PTH(1-15) analogs contain multiple, affinity-enhancing substitutions, together the *p*-benzoyl-L-phenylalanine (Bpa) substitution at position 2, which blocks receptor activation and renders the ligand photoreactive. To explore whether these N-terminal PTH antagonists occupy the same receptor-binding site as that used by the N-terminal portion of the unmodified intact ligand, we covalently cross-linked [Deg¹³, Bpa², Gln¹⁰, Ala¹², Har¹¹, Trp¹⁴, Tyr¹⁵]PTH(1-15)NH₂ to the receptor and mapped the site of photo-insertion. Parallel studies were performed with [Ac³, c¹, Bpa², Aib³, Gln¹⁰, Ala¹², Har¹¹, Trp¹⁴, Tyr¹⁵]PTH(1-15)NH₂. Both of these antagonists cross-linked to the receptor segment Phe⁴¹⁵(TM6)-Met⁴⁴¹(third extracellular loop). Cyanogen bromide failed to cleave the cross-linked complexes at Met⁴²⁵, and mutation of this methionine to Ala reduced cross-linking efficiency of each peptide, suggesting that cross-linking occurred at or near Met⁴²⁵. This same receptor residue is the cross-linking site identified previously by us and others for the intact antagonists [Bpa²]PTH(1-34) and [Bpa²]PTHrP(1-36), as well as the agonist [Bpa¹]PTH(1-34). We thus conclude that the modified PTH(1-15) scaffold occupies approximately the same space in the J domain-binding pocket as does the N-terminal residues of unmodified PTH(1-34) and PTHrP(1-36) ligands. This same binding pocket appears to be used by the N-terminal residues of both agonist and position 2-modified antagonist analogs of both PTH and PTHrP, and is therefore likely to play a critical role in receptor activation. Further studies with additional PTH ligands, including J domain-selective agonist and antagonists, may yield additional information regarding the configuration of this binding pocket and thus facilitate the design of new PTH/PTHrP receptor agonists and antagonist ligands.

Disclosures: **R.C. Gensure**, None.

M495

Receptor-Like Binding Activity for Non-Amino Terminal PTHrP. R. H. Hastings^{*1}, D. W. Burton², J. J. Grzesiak^{*3}, M. Bouvet³, L. J. Deftos².

¹Anesthesiology, Veterans Administration San Diego Healthcare System (VASDHS) and University of California, San Diego, San Diego, CA, USA, ²Medicine, VASDHS and UCSD, San Diego, CA, USA, ³Surgery, VASDHS and UCSD, San Diego, CA, USA.

The most widely studied effects of PTHrP have been of its amino terminus, which signals through the PTH/PTHrP type 1 receptor that it shares with PTH. However, there is accumulating and compelling evidence that non-amino terminal peptides of PTHrP, generated through processing of the native isoforms, can also exert biological effects that include growth regulation and tumor progression. Some actions of these various PTHrP domains are exerted at the cell surface and presumably result from activation of cell-surface receptors, likely G-protein coupled. The nature of the non-amino terminal PTHrP receptor(s) is unknown, but preliminary data regarding the effects of different PTHrP moieties on important cell functions such as proliferation and apoptosis open the possibility of novel PTHrP receptors in many cell types. In this study, we measured the specific binding of radiolabeled PTHrP38-94 to isolated plasma membranes from prostate cancer cells (DU 145, LNCaP and PC-3) and lung type II epithelia cells (RLE and MB 48) using a 96-well plate filtration system for receptor-ligand interactions. Non-specific binding was measured in the presence of 5 μ M unlabeled peptide. Unlabeled PTHrP38-94 and 67-94 peptides displaced binding of the labeled peptide to the cell membranes, with 38-94 being more effective than 67-94. The competitive displacement curves appeared to be rectangular hyperbolas, with saturable binding and IC50 values of 50-100 nM for displacement of the radioligand in the cell lines, similar for those reported for the carboxyl-terminal PTH receptors (Divieti et al. Endo 146:1863-70, 2005). Conversely, PTHrP1-34 and 140-173 peptides did not displace the midmolecule PTHrP radiolabeled peptide using the same concentration range. Saturable dose response curves within physiologic concentration ranges of peptide suggest the existence of PTHrP midmolecule receptor-like binding proteins in prostate cancer and alveolar type II derived cell membranes.

Disclosures: **D.W. Burton**, None.

M496

A Novel Member of the Calcitonin Gene-related Peptide Family, Calcitonin Receptor-stimulating Peptide, Inhibits Osteoclastogenesis. H. Hagiwara¹, M. Notoya^{*2}, R. Arai^{*2}, T. Katafuchi^{*3}, N. Minamino^{*3}.

¹Dept. of Biomedical Engineering, Tooin University of Yokohama, Yokohama, Japan, ²Dept. of Biosciences and Biotechnology, Tokyo Institute of Technology, Yokohama, Japan, ³Dept. of Pharmacology, National Cardiovascular Center Research Institute, Osaka, Japan.

We isolated a novel peptide, calcitonin receptor-stimulating peptide (CRSP), from porcine brain and the administration of this peptide into rats induced a transient decrease in the plasma calcium concentration. Therefore, we investigated the effects of CRSP on osteoclastogenesis. Osteoclast-like cells were formed from spleen cells or bone marrow cells by a combination of the receptor activator of nuclear factor- κ B ligand (RANKL) and macrophage colony-stimulating factor (M-CSF). CRSP dose-dependently inhibited the formation of multinuclear osteoclast-like cells with expression of CT receptor. CT receptor inhibitor antagonized in part inhibition of osteoclast formation by CRSP. Furthermore, CRSP destroyed the actin ring that is a typical index of osteoclast activity, and this inhibitory action was due to signal pathways of protein kinase A. Our findings indicate that CRSP inhibits osteoclastogenesis *via* the inhibition of the formation and the activity of osteoclastic cells. The inhibitory effects of CRSP on osteoclast metabolism were similar degree to those of calcitonin. CRSP might provide a clue to the development of tools useful in the prevention and treatment of osteoporosis.

Disclosures: **H. Hagiwara**, None.

M497

PTHrP Gene-Driven lacZ Expression in Chondrocytes and Bone Cells. X. Chen¹, B. E. Dreyer^{*1}, V. Hammond^{*2}, W. M. Philbrick^{*1}, A. E. Broadus¹.

¹Department of Medicine, Endocrine Division, Yale University, New Haven, CT, USA, ²Florey Institute, University of Melbourne, Parkville, Australia.

We have created CD-1 mice with an allelic lacZ-PTHrP gene insertion. Based on the elimination of PTHrP instability sequences in the 3' end of the construct and the sensitivity of lacZ methods, we guesstimate that the system provides a 5-to10-fold increase in PTHrP detectability at most sites. Here, we focus on sites relevant to bone. First, we studied chondrocyte (C) lacZ expression from development through adulthood. LacZ expression was polarized at the proximal and distal ends of C condensations. This polarization was maintained in subarticular locations after the formation of the primary ossification center. Two populations of lacZ-expressing Cs appeared with formation of the secondary center: one was a subarticular layer one to several cells deep just at the articular surface and the second a layer 4 to 6 cells deep at the junction of the resting and proliferative zones at the top of the C columns. These sites were maintained through adulthood. The perichondrium was strongly lacZ-positive around the costal cartilage but not elsewhere. Second, we expected to identify lacZ-expressing osteoblasts but have thus far not detected such cells in the primary bone collar, primary spongiosa, trabeculae or periosteum. Third, we identified strong lacZ expression in the periosteum and in fibrous tendon insertion sites, with weaker expression at fibrocartilagenous sites. In simple periosteum of only two fibroblast-like cell layers, lacZ was expressed in the peripheral layer; at osteochondral junctions there was an

abrupt transition from lacZ-positive periosteal to lacZ-negative cells at the margin of a synovial joint space. Fibrous tendon insertions comprise so-called bony sites, at which a cord-like tendon inserts into bone at an acute angle, and so-called periosteal sites, at which a layer of periostum joins muscle to bone over a large surface area. LacZ was strongly expressed at both such sites in a layer of cells that lay between the muscle cells and the internal bone cells. This localization was suggestive of both putative force induction of PTHrP and putative paracrine PTHrP function, and we speculate that PTHrP in these locations might be associated with periosteal bone accretion during growth and/or in response to mechanical force and also in the tethering of muscle insertions to bone.

Disclosures: **X. Chen**, None.

M498

Brain, Breast and Bone Circuit: Interactions of Prolactin, PTHrP and Calcitonin during Lactation. J. P. Woodrow¹, A. O. Hoff², R. F. Gagel², C. S. Kovacs¹.

¹Memorial University of Newfoundland, St. John's, NF, Canada,

²University of Texas MD Anderson Cancer Center, Houston, TX, USA.

PTHrP is abundantly expressed by lactating mammary tissue, from which it reaches the maternal circulation to upregulate bone resorption and thereby provide calcium to milk. In addition to PTHrP, lactating mammary tissue expresses the calcium receptor (CaR), calcitonin (CT), CT receptor (CTR), VDR, and 1-alpha-hydroxylase (1 α). Prolactin and CaR both regulate mammary PTHrP expression; in turn, CT inhibits prolactin by direct actions on pituitary lactotrophs. Furthermore, CT has recently been shown to regulate bone metabolism during lactation: *Ct*-null mice lost twice as much trabecular bone mineral content during lactation as wt siblings, and the loss was normalized by daily sc treatment with CT but not by vehicle or CGRP. The present studies were designed to examine if PTHrP is upregulated in mammary tissue of *Ct*-null mice, and to determine if local or systemic factors might explain any alteration in PTHrP expression. *Ct* null mice and wt sisters were mated to the same *Ct*+/- males, and followed through full 70 day cycles of pregnancy, lactation and recovery. Time points included non-pregnant (baseline), late pregnancy/early lactation (peak) and late lactation (trough). Serum and plasma were collected by cardiac puncture. Mammary tissue was surgically excised, snap-frozen, and then RNA was extracted. Real time quantitative RT-PCR was performed in triplicate using the ABI Prism 7000 Sequence Detection System. mRNAs included PTHrP, 1 α , VDR, CTR, CaR, and the epithelial calcium transporters (CaT1 and CaT2/ ECAC). Serum prolactin was measured using a murine prolactin RIA developed by the National Hormone Peptide Program. PTHrP mRNA was upregulated in *Ct*-null versus wt by a fold increase of 3.28 ± 0.09 (SD) at the trough point ($p < 0.01$). No differences between *Ct*-null and wt were observed for 1 α , VDR or CaR, whereas CTR, CaT1 and CaT2 were not detectable. Mean serum prolactin [ng/ml] was elevated in *Ct*-null at each time point vs wt: 64.8 vs 23.2 [baseline], 251.6 vs 173.0 [peak], and 44.8 vs 29.0 [trough] ($p < 0.02$ by ANOVA). *Ct*-null mice have enhanced bone resorption during lactation that is not simply due to loss of the inhibitory effect of CT on osteoclasts. PTHrP expression is increased in mammary tissue of *Ct*-nulls, which in turn should further augment bone resorption. Increased PTHrP expression may result from loss of local actions of CT within mammary tissue and within the pituitary. In conclusion, mammary expression of PTHrP is enhanced during lactation in the absence of calcitonin, revealing a physiological loop through which brain and breast control bone during lactation.

Disclosures: **J.P. Woodrow**, None.

M499

Regulation of Granulocyte-Macrophage Colony-Stimulating Factor Receptor Beta in the CT/CGRP Null Mouse. A. O. Hoff, E. Huang^{*}, G. J. Cote, R. F. Gagel.

Endocrine Neoplasia & Hormonal Disorders, University of Texas M.D. Anderson Cancer Center, Houston, TX, USA.

There is evolving evidence that interleukin 3 (IL3) plays an important role in the differentiation of osteoclasts. Absence of IL3 in marrow cultures causes differentiation of monocytic hematopoietic precursors toward an osteoclast lineage; addition of IL3 reverses this effect, leading to macrophage differentiation (*J Immunol* 171:142, 2003; *J Biol Chem* 280:11759, 2005). In an attempt to better understand why PTH stimulates greater bone resorption and calcemic response in the CT/CGRP null mouse, we performed gene microarray analysis of RNA from bone marrow of CT/CGRP KO and WT animals. The RNA was obtained by perfusing the marrow cavity of long bones with a lysis buffer. Samples obtained from 3 WT and 3 KO animals were analyzed by gene microarray analysis using the Affymetrix Gene Chip Mouse Genome 430 2.0 Array. Fifty-three genes were found to be differentially expressed as defined by a greater than 2-fold change and 2722 genes had a greater than 1.5-fold change (both $p < 0.05$). When this gene set was analyzed using the Ingenuity Pathways Analysis™ application, we identified greater than a 2-fold increase in colony stimulating factor 2 receptor β 1 and β 2 (CSF2RB1 and CSF2RB2) gene expression, the receptors for IL-3, IL-5 or GM-CSF. In addition, there was increased expression of several downstream signaling proteins. IL-3 expression was decreased (-1.55 fold; $p < 0.05$). Prior studies indicate that regulation of this receptor system is important in delineation of the osteoclast phenotype. The finding that the receptor system is upregulated and IL-3 downregulated in the marrow of CT/CGRP KO mice with a greater calcemic response to PTH suggests that CT or CGRP, either directly or indirectly, regulates this receptor system.

Disclosures: **A.O. Hoff**, None.

M500

EBP50 Regulates PTH1R-mediated Effects on Vascular Smooth Muscle Cell Proliferation. L. Zhang*, C. A. Syme*, A. Bisello. Department of Medicine, University of Pittsburgh, Pittsburgh, PA, USA.

The parathyroid hormone (PTH) type 1 receptor (PTH1R) and its ligands PTH and PTHrP play diverse and important roles in the pathophysiology and pharmacology of the vascular system. The signaling activities of the PTH1R are remarkably cell-specific, and, indeed, the cellular responses of "classical" PTH targets (osteoblasts and kidney cells) are fundamentally different from those of vascular smooth muscle cells (VSMC). In particular, while PTH and PTHrP typically stimulate MAPK activity and proliferation in bone and kidney cells (where the PTH1R signals through both Gs and Gq proteins), they potently inhibit VSMC proliferation (where only Gs coupling occurs). Recent evidence shows that ezrin-binding protein 50 kDa (EBP50), also known as NHERF1, contributes to signaling specificity and trafficking of the PTH1R. We found that in vascular tissue EBP50 was expressed predominantly by the endothelial cells, whereas extremely low levels were detected in VSMC. In clonal A10 VSMC, PTH(1-34) and PTHrP(1-36) stimulated cAMP formation in a regulated fashion: both receptor desensitization and resensitization occurred. Stimulation with 100 nM PTHrP(1-36) induced membrane clustering and partial internalization of the PTH1R-GFP within 5 min. After 15 min virtually all of the membrane receptor was internalized. Stimulation of A10 cells maintained in 1% serum with 100 nM PTH(1-34) or PTHrP(1-36) led to a significant reduction (approx. 35%) of cell proliferation (determined by ³H-Thymidine incorporation). In similarly prepared A10 cells, inhibition of the ERK1/2 pathway by 10 μ M PD98059 caused a 33 \pm 2% reduction in ³H-Thymidine incorporation. Inhibition of PI3K by 20 μ M LY294002 resulted in a 75 \pm 2% reduction in DNA synthesis, indicating that both ERK1/2 and PI3K contribute to VSMC proliferation. Consistent with these observations, PTHrP(1-36) inhibited phosphorylation of ERK1/2 and PKB both in A10 and primary VSMC. Moreover, PTHrP rapidly (5 min) decreased the nuclear staining of phosphorylated ERK1/2. Expression of EBP50 in A10 cells (either transiently or stably) affected neither the cAMP activity of the PTH1R nor its ability to internalize upon agonist occupancy. However, EBP50 expression reduced the anti-proliferative effect of PTHrP such that no differences in thymidine incorporation were observed upon treatment with PTHrP. In summary, these data indicate that cAMP-mediated inhibition of ERK1/2 and PI3K activity occurs in VSMC in response to PTH1R agonists, resulting in inhibition of cell proliferation. In addition, the expression level of EBP50 in VSMC determines the mitogenic responses to PTH1R stimulation.

Disclosures: **A. Bisello**, None.

M501

Novel Ligands for Analysis of Carboxyl-PTH Receptors in Bone Cells.

S. Banerjee*, G. Suliman*, H. Jüppner, F. R. Bringham, P. Divieti. Endocrine Unit,

Massachusetts General Hospital, Boston, MA, USA.

The major secreted form of parathyroid hormone is intact PTH (1-84), although various N-terminally truncated fragments (Carboxy-terminal PTH; CPTH) are present in the blood stream as well. These CPTH fragments are either secreted from the parathyroid glands or released following proteolysis of the intact hormone in the peripheral organs. A physiological role of these CPTH fragments is suggested by the fact that their secretion is regulated by serum calcium and by evidence of biological responses to CPTH peptides in vivo and in vitro. In this study, we have characterized 4 synthetic CPTH peptides for binding to the osteocytic cell line OC59 (PTH1R-null murine osteocytic cells) and ROS17/2.8 to assess their utility in identifying and cloning PTH receptors from these cell lines. The peptides used were [Tyr34]hPTH(23-84) \pm benzylphenylalanine (Bpa) at position 24 and [Tyr34]hPTH(24-84) \pm Bpa at position 26 to facilitate photoaffinity crosslinking of the receptor during subsequent purification attempts. All peptides were C-terminally biotinylated at 84. The function of these synthetic peptides was addressed by analyzing specific binding of 125I-radiolabeled peptides, in the absence vs. presence of homologous nonradioactive peptide(s), to intact cells or isolated plasma membranes. For the whole cell binding, the IC50 values for all the peptides tested were found to be in the range of 20-40 nM, as previously reported, whereas a higher value was seen with membranes. Both whole cells and membranes were incubated with 125I-labeled Bpa-containing peptide and photoaffinity crosslinking was carried out using high wavelength UV radiation for 15-20 minutes, followed by lysis in SDS-PAGE sample buffer and electrophoresis. Upon autoradiography, ~220 kDa and ~80 kDa bands were found and hypothesized to be putative CPTH receptors. Alternatively, western blot analysis was carried out with Streptavidin-HRP, and identical bands were detected. Partial purification of the CPTH receptor(s) was attempted using immobilized hPTH antibody-agarose matrix or immobilized streptavidin matrix, or a combination of both. Surprisingly, upon 2-step purification, only the ~80 kDa protein could be purified, implying that the ~220 kDa protein is likely a transient aggregate. This was further verified by guanidium hydrochloride treatment of the electroeluted ~220 kDa band, which was seen to resolve into ~80 kDa protein. On preliminary characterization, the ~80 kDa protein was found to exhibit a slightly acidic pI and most likely to be non-glycosylated. Further analysis by high-resolution 2D electrophoresis is ongoing to attempt isolation of the CPTH and subsequent identification by mass spectrometry.

Disclosures: **S. Banerjee**, None.

M502

Type 1 Parathyroid Hormone Receptor Nuclear Trafficking: Association of PTH1R with Karyopherin Alpha2 and Beta1. B. W. Pickard*, A. B. Hodsmann, L. J. Fraher, P. H. Watson. Medicine, University of Western Ontario, London, ON, Canada.

Advances in the study of GPCRs have revealed that several members of the Class A Rhodopsin like receptors demonstrate the ability to translocate to the nucleus, in addition to their traditional membrane bound signalling properties. Previous studies in our laboratory have shown that the PTH1R, a class B Secretin like GPCR, appears in the nucleus of target cells. Proteins, such as PTH1R, destined for the nucleus or nuclear envelope contain intrinsic nuclear localization signals (NLS) which specify their ultimate destination. Many receptors and ligands are targeted to the nucleus through the interaction of their NLS with proteins of the karyopherin family and it is likely that PTH1R transport is also regulated by the karyopherins. The purpose of this study is to demonstrate the interaction of PTH1R with the karyopherins. Using immunoprecipitation and affinity chromatography we show that the PTH1R forms a complex with both karyopherin alpha2 and beta1. Total cell protein from random cycling wild type MC3T3-E1 and ROS 17/2.8 cells were immunoprecipitated with antibodies for PTH1R, karyopherin alpha2 or karyopherin beta1. When the immunoprecipitates were separated and subsequently exposed to biotinylated PTH (1-84) a single band was present on the gel at 66.3 kDa corresponding to the PTH1R. To confirm the interaction between PTH1R and both karyopherin alpha2 and beta1 the complex was purified from total cell protein using a PTH linked affinity chromatography column. PTH1R was purified from wild type random cycling ROS 17/2.8 and MC3T3-E1 cells. Using an anti-karyopherin alpha2 antibody, western blots detected karyopherin alpha2 at 58 kDa in the sample. Also, using an anti-karyopherin beta1 antibody western blots detected karyopherin beta1 at 94 kDa. These results indicate that the karyopherins were associated with the PTH1R at the time of the purification. In random cycling wild type SaOS-2 and MC3T3-E1 cells immunofluorescence demonstrated that the PTH1R was detected in the nucleus. Both karyopherin alpha2 and beta1 can be detected in the nucleus as well as in the cytoplasm. The overlay of the immunofluorescent images demonstrates the spatial overlap of the three proteins consistently within the cell in areas such as the nucleus. Examination of the z-sections obtained from deconvolution microscopy revealed that the nuclear PTH1R and karyopherins were localized to the nucleoplasm. Our interest in PTH1R lies in the fact that the mechanism of action of the anabolic response of bone to intermittent PTH therapy is not well understood. The nuclear trafficking of the PTH1R provides a new avenue of investigation into the pleiotropic actions of PTH.

Disclosures: **B.W. Pickard**, None.

M503

Expression of a PTH1R-GFP Construct in F1 PTH1R-Null Osteoblasts: Restoration of cAMP Responsiveness to PTH(1-34). E. K. Patterson*¹, P. H. Watson¹, A. B. Hodsmann¹, G. N. Hendy², L. Canaff^{*2}, P. A. Divieti³, L. J. Fraher¹. ¹Medicine, University of Western Ontario, London, ON, Canada, ²Medicine, McGill University, Montreal, PQ, Canada, ³Endocrine Unit, Mass General, Harvard University, Boston, MA, USA.

Previous immunocytochemical studies in our laboratory demonstrated the unexpected result that the Type I Parathyroid Hormone Receptor (PTH1R) is apparently able to localize to the nucleus of cells in the gut, ovary, testes, liver and kidney in the rat. Further studies in the clonal cell line MC3T3-E1, demonstrated that this localization to the nucleus occurs in a cell-cycle dependent manner, moving into the nucleus just before S-phase. An analysis of the amino acid sequence of all available PTH1Rs revealed a putative NLS of the bipartite type first described in nucleoplasmin. We have been employing various PTH1R constructs tagged with green fluorescent protein (GFP) to determine the mechanism of import of the PTH1R. The purpose of this study is to demonstrate that our GFP tagged PTH1R constructs are capable of restoring cAMP signaling in PTH1R knock-out cells, and that the fusion protein appears in the expected location in the plasma membrane as a preliminary step to further studies of nuclear trafficking of the PTH1R. The PTH1R construct used for these studies represents amino acids 1 to 577 of the mature peptide with a C-terminal GFP tag. F1 osteoblast cells were cultured in 24-well plates for 24 hours prior to transfection in alpha-MEM with 10% FBS. F1 cells were transiently transfected with a PTH1R-GFP plasmid using Lipofectamine 2000, according to the manufacturer's protocol and transfection reagent alone was used as a control. Twenty-four hours post-transfection, cultures were treated with various concentrations of PTH(1-34) for 15 minutes and the resulting cAMP response per well measured. While control cells showed no response to PTH, the transfected F1 cells demonstrated a dose-dependent increase in cAMP from 20 fmol/well to 800 fmol/well at a PTH concentration of 1x10⁻⁸ M. Localization of fusion protein constructs was determined 24 and 48 hours post-transfection using fluorescence microscopy showing cells to have strong signal in the plasma membrane. These results demonstrate that our fusion protein construct is able to restore cAMP responsiveness to PTH in F1 cells and the fusion protein is also properly inserted into the plasma membrane.

Disclosures: **E.K. Patterson**, None.

M504

NHERF1/EBP50 and NHERF2/E3KARP Regulate PTH1R Endocytosis.

W. B. Sneddon¹, B. Wang^{*1}, P. A. Friedman². ¹Dept. of Pharmacology, University of Pittsburgh School of Medicine, Pittsburgh, PA, USA, ²Depts. of Pharmacology and of Medicine, University of Pittsburgh School of Medicine, Pittsburgh, PA, USA.

Parathyroid hormone (PTH) is the principal regulator of extracellular calcium homeostasis. Its effects on kidney and bone are mediated by the Type 1 PTH receptor (PTH1R). The PTH1R is internalized in a cell- and ligand-specific manner in PTH target cells. In kidney distal tubule (DT) cells and some bone cell lines (e.g. ROS17/2.8), both the agonist PTH(1-34) and the antagonist PTH(7-34) induce PTH1R internalization. Progressive truncation of PTH fragments from N terminus positions 1-7 leads to reduced cyclic AMP formation and increased PTH1R internalization in DT cells. We also demonstrated that the Na/H exchanger regulatory factor (NHERF1:EBP50) blocks PTH1R endocytosis by antagonist PTH fragments. Mahon et al reported that both NHERF1 and NHERF2 (E3KARP) bind to the PTH1R through an atypical C-terminal PDZ-binding domain. We hypothesized that NHERF1 and NHERF2 are functionally redundant and are able to substitute for one another. We further hypothesized that truncation of PTH(7-34) from its N terminus impairs its ability to induce PTH1R internalization in the absence of NHERF. PTH1R internalization was measured by real-time confocal fluorescence microscopy of mouse DT cells stably expressing 10⁶ EGFP-tagged PTH1R/cell. PTH(7-34), (8-34) and (9-34) internalized the PTH1R 65%, 47% and 44%, respectively. PTH1R endocytosis was abolished in the presence of either NHERF1 or NHERF2. Neither PTH(10-34) nor PTH(7-31) internalized the PTH1R. We, therefore, conclude that positions 1-9 and 32-34 of PTH are required for induction of PTH1R internalization in the absence of NHERF. We additionally conclude that NHERF1 and 2 are functionally equivalent in terms of their ability to inhibit PTH1R internalization by antagonist PTH fragments. NHERF1 and 2 are expressed in mouse proximal but not distal renal tubules. The magnitude and pattern of NHERF1 and 2 expression may, therefore, have important implications for understanding PTH1R function in kidney and bone in states of calcium wasting and aging.

Disclosures: P.A. Friedman, None.

M505

PTH1R Activation of ERK Requires Transactivation of the Epidermal Growth Factor Receptor. **W. B. Sneddon¹, Y. Yang^{*1}, P. A. Friedman².** ¹Dept. of Pharmacology, University of Pittsburgh School of Medicine, Pittsburgh, PA, USA, ²Depts. of Pharmacology and of Medicine, University of Pittsburgh School of Medicine, Pittsburgh, PA, USA.

The Type 1 PTH receptor (PTH1R) activates multiple signaling pathways, including mitogen-activated protein kinase (MAPK, ERK), in a cell- and ligand-specific manner. In previous work we showed that PTH stimulated ERK1 and ERK2 in kidney distal tubule cells. Blockade of ERK1/2 inhibited PTH-stimulated calcium transport. There is evidence that some G protein-coupled receptors, such as the β_2 adrenergic receptor, transactivate the Epidermal Growth Factor Receptor (EGFR) and that this is required for activation of ERK1/2. In the present work we examine the role of EGFR in ERK1/2 activation by PTH. ERK1/2 activation was measured by phosphospecific immunoblotting. Results were normalized to total ERK1/2. In distal tubule kidney cells expressing 10⁶ PTH receptors/cell (D1 cells), PTH(1-34) (100 nM) stimulated ERK2 phosphorylation 4-6-fold after 10 min. This was blocked completely by the EGFR inhibitor, AG1478 (1 μ M) but not by the Platelet Derived Growth Factor Receptor inhibitor, AG1295 (25 μ M). One mechanism whereby a GPCR can transactivate the EGFR is by metalloprotease cleavage of membrane-bound HB-EGF, a potent EGFR ligand. We examined this mechanism by first activating the PTH1R in D1 cells and then applying the conditioned media to HEK293 cells, which do not express the PTH1R. Conditioned media from PTH(1-34)-treated D1 cells activated ERK1/2 3-4 fold in HEK293 cells. AG1478, when applied to HEK293 cells, completely inhibited transactivation of ERK1/2 by the conditioned media. PTH(1-34) (100nM), when applied directly to HEK293 cells, had no effect. This indicates that the conditioned media from the D1 cells contains a factor that activates ERK1/2 in HEK293 cells in an EGFR-dependent manner. HB-EGF (1 ng/ml) directly activated ERK1/2 in HEK293 cells. Pretreatment of the D1 cells with the matrix metalloprotease inhibitor GM-6001 (10 μ M) abolished the transactivation of ERK1/2 by PTH in HEK293 cells. We, therefore, conclude that ERK1/2 activation in distal kidney cells by PTH(1-34) requires PTH1R activation of a metalloprotease that leads to cleavage of HB-EGF and transactivation of the EGFR.

Disclosures: W.B. Sneddon, None.

M506

The Role of the PTH Receptor C Terminus and Pertussis Toxin-Sensitive G Proteins on MAP Kinase Activation. **Y. Yang^{*1}, W. B. Sneddon¹, B. Wang^{*1}, P. A. Friedman².** ¹Dept. of Pharmacology, University of Pittsburgh School of Medicine, Pittsburgh, PA, USA, ²Depts. of Pharmacology and of Medicine, University of Pittsburgh School of Medicine, Pittsburgh, PA, USA.

The Type 1 PTH receptor (PTH1R) activates multiple signaling pathways, including mitogen-activated protein kinase (MAPK, ERK), in a cell- and ligand-specific manner. In previous work we showed that PTH stimulated ERK1 and ERK2 (ERK1/2) in kidney distal tubule cells. Blockade of ERK1/2 inhibited PTH-stimulated calcium transport. In the present study we examine the role of pertussis toxin (PTX)-sensitive G proteins in ERK1/2 activation by PTH. ERK1/2 activation was measured by phosphospecific immunoblotting. Results were normalized to total ERK. In distal tubule kidney cells expressing 10⁶ PTH

receptors/cell (D1 cells), PTH(1-34) (100 nM) stimulated ERK2 phosphorylation 4-6-fold after 10 min. No consistent change of ERK1 was noted. ERK2 activation was blocked by overnight pre-treatment with PTX. A dominant negative minigene for G α_{i13} blocked both basal and PTH-stimulated ERK1/2 activation in D1 cells. We then characterized the role of the C terminus of the PTH1R in PTX-sensitive ERK1/2 activation by PTH. We used HEK293 for these studies because they do not express endogenous PTH1Rs. Cells were transiently transfected with either the wild type PTH1R (ETVM), a PTH1R where the C-terminal methionine was mutated to alanine (ETVA), or a PTH1R truncated at position 480 lacking most of the C terminus distal to transmembrane domain 7 (480stop). Transfections were optimized such that receptor expression was equivalent as determined by PTH1R immunoblotting. PTH(1-34) (100 nM) stimulated ERK1/2 by the ETVM, ETVA and 480-stop PTH1Rs 21-fold, 27-fold and 57-fold, respectively. Overnight pre-treatment with PTX inhibited PTH(1-34)-stimulated ERK1/2 by the ETVM and 480-stop PTH1Rs by 60%. In contrast, PTX abolished ERK1/2 activation by the ETVA PTH1R. The M-A mutation at the C terminus (a PDZ recognition motif) of the PTH1R abrogates the interaction between the PTH1R and the sodium proton exchanger regulatory factor (NHERF1). It is not known if NHERF plays a role in PTH1R activation of ERK1/2. These data suggest that mutation of the PDZ-interaction motif of the PTH1R may interfere with a NHERF-dependent pathway for ERK1/2 activation. Furthermore, the 2-fold increase in ERK1/2 stimulation by the truncated 480stop PTH1R over the wild type ETVM PTH1R suggests a modulatory role for the C terminus. We conclude from these experiments that there are multiple signaling pathways for PTH-stimulated ERK1/2 activation and that PTH1R-mediated stimulation of the PTX-sensitive G protein G $_i$ is a key mediator of this process.

Disclosures: P.A. Friedman, None.

M507

PTH/PTHrP Receptor Phosphorylation Regulates PTH Activation of ERK1/2 MAP Kinases and Gene Expression. **H. A. Tawfeek^{*}, A. B. Abou-Samra.** Endocrine Unit, Massachusetts General Hospital, Boston, MA, USA.

PTH activates ERK1/2 MAP kinases in renal and osteoblastic cells. The regulatory mechanisms involved in PTH activation of ERK1/2 have not been elucidated. The goal of the current study was therefore to examine the role of PTH/PTHrP receptor phosphorylation in regulation of ERK1/2 response. The effects of PTH on ERK1/2 activation were examined in LLC PK-1 renal tubular cells stably expressing a wild type (WT-PPR cells) or a phosphorylation-deficient (PD-PPR cells) mutant PTH/PTHrP receptor. ERK1/2 activation was assessed by immuno-blot analysis, using anti-phospho-(active) ERK1/2 antibody. The data demonstrated that PTH activation of ERK1/2 in the PD-PPR cells was similar to that in the WT-PPR cells during early time points (0-40 min). In the WT-PPR cells treatment with PTH for longer time periods (60-120 min) resulted in down-regulation of ERK1/2 activation response; ERK1/2 activity returned to basal levels at 60 min and decreased below basal levels at 90-120 min. Interestingly, in contrast to the WT-PPR cells, the PD-PPR cells exhibited sustained activation of ERK1/2 in response to PTH treatment. ERK1/2 activity in the PD-PPR cells remained elevated over basal at 60-90 min and returned to basal levels at 120 min of PTH treatment. We further examined whether the effects of PTH on ERK1/2 activation in the PD-PPR cells modulate gene expression. Strikingly, PTH treatment caused higher expression of c-fos gene in the PD-PPR cells than in the WT-PPR. The effects of PTH on c-fos gene expression in the WT- and PD-PPR cells were attenuated by U0126, a specific ERK1/2 pathway inhibitor. It has been shown that β -arrestin2 recruitment is involved in ERK1/2 nuclear translocation; the effects of PTH on β -arrestin2 translocation were therefore examined in the WT- and PD-PPR cells stably expressing green fluorescent protein (GFP)-tagged β -arrestin2. Compared to the WT-PPR cells, PTH treatment caused a weak β -arrestin2 translocation in the PD-PPR cells. This finding suggests a possible role for β -arrestin2 in the effects of PTH/PTHrP receptor phosphorylation on ERK1/2 regulation. Altogether, these data suggest that PTH/PTHrP receptor phosphorylation, via its regulatory role in PTH activation of ERK1/2 MAP kinases, influences gene expression.

Disclosures: H.A. Tawfeek, None.

M508

The Use of Mixture-Based Combinatorial Libraries for the Development of Novel Calcitonin and/or Parathyroid Hormone Analogues. **R. Houghten.** Torrey Pines Institute for Molecular Studies, San Diego, CA, USA.

The approaches and concepts that encompass combinatorial chemistry represent a paradigm shift in drug discovery and basic research. Viewed initially as a curiosity by the pharmaceutical industry, combinatorial chemistry approaches are now recognized as essential drug discovery tools that decrease the time taken for discovery and increase the throughput of chemical screening by as much as 1000-fold. Although the use of mixture-based synthetic combinatorial libraries was one of the first approaches presented, its inherent strengths are only recently being recognized. Numerous mixture-based libraries of peptides, peptidomimetics and heterocycles have been synthesized and deconvoluted using the positional scanning approach. Mixture-based library approaches for drug discovery and vaccine development will be discussed. The results presented demonstrate that combinatorial mixture synthesis and screening can play a vital role in the discovery of new leads for a variety of targets, ranging from antimicrobial and to new calcitonin and/or parathyroid hormone analogues.

Disclosures: R. Houghten, None.

M509

A Methionine Scan of Region [168-176] of the Parathyroid Hormone Receptor 1 - The “Magnet Effect”. A. Wittelsberger¹, B. E. Thomas^{*1}, D. F. Mierke^{*2}, M. Rosenblatt¹. ¹Department of Physiology, Tufts University School of Medicine, Boston, MA, USA, ²Department of Chemistry and Molecular Pharmacology, Brown University, Providence, RI, USA.

Parathyroid hormone (PTH) 1-34 contains two α -helical domains associated with specific functions: the N-terminal helix is required for activation of its G protein-coupled receptor, and the C-terminal helix is mainly responsible for receptor binding. We recently focused on the role of the mid-domain of PTH. From photoaffinity-crosslinking studies, we found that a *p*-benzoylphenylalanine (Bpa) residue at either position 11 or 21 crosslinked to the same receptor region [165-176]. We now present a “methionine scan” of receptor region [168-176]. This region has amphipathic helical character (see Figure), and is expected to lie on top of the membrane [1]. The two ligands, [Bpa¹¹]-PTH and [Bpa²¹]-PTH, were crosslinked to the mutant receptors [S168M]-, [E169M]-, [V171M]-, [K172M]-, [F173M]-, [L174M]-, and [N176M]PTH^{R1}, transiently expressed on Cos-7 cells. The ligand-receptor conjugates were then isolated, digested with endoglycosidase F and cyanogen bromide, and analyzed by SDS-PAGE. A band similar in size to free ligand was obtained for the whole range of mutants when crosslinked to Bpa¹¹-PTH, and for [S168M]-up to mutant [L174M]PTH^{R1} when crosslinked to Bpa²¹-PTH. Such a ligand fragment (ligand + CH₂SCN) is generated by crosslinking to the methyl group of methionine [2]. We conclude that the reactivity of Bpa towards methionine is significantly increased compared to other residues. We call this the “Magnet Effect” of methionine. Outside the above-mentioned range, i.e. with receptor mutant [V183M], we do not observe the characteristic band with either Bpa¹¹-PTH or Bpa²¹-PTH. Hence, crosslinking contact points can be shifted by the presence of methionine in a receptor domain.



[1] Pellegrini, M., et al., Biochemistry 37:12737, 1998.
[2] Kage, R., et al., J. Biol. Chem. 271:25797, 1996.

Disclosures: *A. Wittelsberger, None.*

M510

Optimizing Vitamin D Nutrition in Healthy Adults. M. R. Patel^{*}, S. A. Talwar, J. F. Aloia, S. Pollack^{*}, J. Yeh. Bone Mineral Research Center, Winthrop-University Hospital, Mineola, NY, USA.

Purpose: While there is emerging consensus that the optimal serum 25-hydroxyvitamin D (25-OHD) level is 80 nmol/L, the adequate daily intake of vitamin D₃ to achieve this level is unknown in a multiethnic population. Methods: We are reporting preliminary data on 16 black (8 active, 8 placebo) and 46 white (24 active, 22 placebo) subjects enrolled in an ongoing randomized placebo-controlled study of vitamin D₃ dosing in healthy subjects with suboptimal 25-OHD. Those with chronic medical conditions, morbid obesity, disorders of bone metabolism, or those taking medications known to interfere with bone or vitamin D metabolism were excluded. Subjects were randomized 1:1 to vitamin D₃ or placebo. The dose was based on initial 25-OHD level. For 25-OHD <50 nmol/L, subjects were given 100 μ g/d, and for 25-OHD between 50-80 nmol/L, subjects were given 50 μ g/d. Fasting urine and serum calcium were measured at each visit. 25-OHD was measured by RIA using the DiaSorin assay. Dietary intake of vitamin D and calcium were estimated using 3-day diet logs. We are reporting data after 8 weeks of supplementation. Results: There were no baseline differences between active and placebo subjects. Basal weight and BMI were significantly higher in blacks than whites. Vitamin D intake was similar in all groups. 7/8 blacks and 10/24 whites had basal 25-OHD <50 nmol/L and were started on 100 μ g/d of vitamin D₃. The remaining active subjects were started on 50 μ g/d. After 8 weeks of either 50 or 100 μ g of vitamin D₃ supplementation, the achieved serum 25-OHD level was 81.7 and 73.8 nmol/L for whites and blacks, respectively (See Table). 25-OHD did not change significantly from baseline for placebo subjects. 25% of blacks and 54% of whites achieved the optimal 25-OHD level. 6/8 active black subjects and 11/24 active white subjects require additional daily vitamin D₃ supplementation. Serum calcium and fasting urine Ca/Cr did not change significantly from baseline and was not different from placebo. No adverse events were reported. Conclusion: If the goal is to achieve 25-OHD >80 nmol/L for the majority of people, we would recommend >50 μ g/day for whites and

>100 μ g/day for blacks during the winter. As seasonal influence on 25-OHD is less in blacks, they may require >100 μ g/day for most of the year. The dose-response to oral vitamin D₃ supplementation appears similar between blacks and whites.

Parameter	Response to vitamin D3 supplementation		P value (blacks vs. whites)
	Blacks Mean (SE) n=16	White Mean(SE) n=46	
Weight (lbs)	161.7 (7.4)	146.6 (4.3)	0.085
BMI (kg/m ²)	27.1 (0.9)	23.9 (0.5)	0.003
% Body Fat	32.2 (2.09)	28.7 (1.19)	0.156
Basal 25-OHD (nmol/L)	35.5 (4.9)	53.2 (2.8)	0.002
Active Placebo	32.8 (4.9)	59.8 (2.9)	<0.001
8wk 25-OHD (nmol/L)			
Active	73.8 (5.4)	81.73 (3.0)	0.270
Placebo	40.6 (5.4)	58.15 (3.2)	0.007
Change in 25-OHD (nmol/L)			
Active	38.3 (6.1)	28.45 (3.4)	0.169
Placebo	7.84 (6.1)	-1.69 (3.7)	0.191
Change in 25-OHD/ μ g/d (nmol/L/ μ g/d)			
Active	0.39 (0.05)	0.38 (0.05)	0.970

Disclosures: *M.R. Patel, None.*

M511

Effect of Caffeine on Vitamin D Receptor Expression and Estrogen Receptor Transcriptional Responses in Osteoblast Cells. P. B. Rapuri¹, J. C. Gallagher¹, Z. Nawaz^{*2}. ¹Bone Metabolism, Creighton University, Omaha, NE, USA, ²Department of Biochemistry and Molecular Biology, University of Miami School of Medicine, Miami, FL, USA.

Of the various risk factors contributing to osteoporosis, dietary/lifestyle factors are important. In a clinical study we reported that women with caffeine intakes >300mg/d had higher bone loss and women with one particular variant (tt) of vitamin D receptor (VDR) are at a greater risk for this deleterious effect of caffeine. However, the mechanism of how caffeine effects bone metabolism is not clear. Both estrogen and 1,25-dihydroxy vitamin D₃ (1,25(OH)₂D₃) play a critical role in regulating bone metabolism. The receptors for both these hormones, VDR and estrogen receptor (both ER α and ER β) have been demonstrated in osteoblasts and they belong to the same superfamily of nuclear hormone receptors. We hypothesized that caffeine may effect the ER and VDR expression, transcriptional activity and estrogen and 1,25(OH)₂D₃ mediated actions in bone. We therefore examined the effect of different doses of caffeine (0.2, 0.5, 1.0 and 10 mM) on endogenous and 1,25(OH)₂D₃ induced VDR protein expression in osteoblast-like cells, U2-OS. We also tested the effect of different doses of caffeine on ER α transcriptional responses in U2-OS cells. In U2-OS cells testing the effect of caffeine on VDR, caffeine treatment resulted in appearance of a higher molecular weight band (probably phosphorylated form of VDR) whose intensity increased with increasing dose of caffeine. In cells treated with 10 mM caffeine the higher molecular weight band was the only prominent band visible. Caffeine also dose dependently decreased the 1,25(OH)₂D₃ induced VDR expression by about 50 to 70% at doses of 1 and 10 mM respectively. The effect of caffeine on ER α transcriptional responses was tested using transient transfection assays in U2-OS cells. U2-OS cells were transfected with ER α and ERE linked to luciferase reporter gene. Cells were treated with different doses of caffeine alone or different doses of caffeine + estradiol and luciferase activity was determined in cell lysates. Caffeine at highest dose tested decreased ER α basal transcriptional activity and dose dependently decreased the estrogen stimulated ER α transcriptional activity. At a dose of 10 mM caffeine, estrogen stimulated transcriptional activity of ER α was decreased by about 60%. Our results suggest that caffeine effects the endogenous and 1,25(OH)₂D₃ stimulated VDR expression in osteoblast cells. We also demonstrated that caffeine effects the basal and estrogen stimulated ER α transactivation in osteoblast cells.

Disclosures: *P.B. Rapuri, None.*

M512

Effects of PTH and 1 α ,25(OH)₂-Vitamin D₃ on JNK and P38 MAPK in Rat Intestinal Cells. N. Buzzi^{*}, V. Gonzalez Pardo^{*}, R. Boland^{*}, A. Russo de Boland^{*}. Biologia, Bioquímica & Farmacia, Universidad Nacional del Sur, Bahia Blanca, Argentina.

We have previously demonstrated that parathyroid hormone (PTH) and the steroid hormone 1 α ,25(OH)₂-vitamin D₃ [1 α ,25(OH)₂D₃] activate the cytosolic tyrosine kinase c-Src in rat intestinal cells (enterocytes), which, in turn, participates in the phosphorylation and activation of the MAP kinases ERK1 and ERK2. In the present study we examined whether these hormones are able to stimulate other members of the MAP kinases family. Our results show that, 1 α ,25(OH)₂D₃ induces the phosphorylation and activation of p38 MAPK in rat enterocytes. This effect was time and dose-dependent, with maximal stimulation at 2 min (+3 fold) and 1 nM. Opposite to the steroid hormone, PTH decreases, within 15 to 30 min, the basal phosphorylation and activity of p38 MAPK. 1 α ,25(OH)₂D₃-dependent p38 phosphorylation was suppressed by SB 203580, a selective inhibitor of p38 MAPK. Ca²⁺ chelation with EGTA, inhibition of c-Src- family tyrosine kinase with PP1 or protein kinase A (PKA) inhibition with Rp-cAMP, attenuated hormone effects. Stimulation of rat enterocytes with 1 α ,25(OH)₂D₃ (1 nM) or PTH (10 nM) also resulted in the phosphorylation and activation of c-jun N-terminal protein kinases (JNK 1/2). The effect of either hormone on JNK 1/2 was transient, peaking at 1min (+200%) and 2 min (+300%) for 1 α ,25(OH)₂D₃ and PTH, respectively. Incubation of enterocytes with 1 α ,25(OH)₂D₃ was followed by a rapid induction of c-Fos expression (+1 fold, 5 min) which was blocked by SB 203580 and partially suppressed by the ERK1/2 inhibitor, PD 98059, while incubation

with PTH did not alter the levels of the oncoprotein. Collectively, these data suggest that PTH and $1\alpha,25(\text{OH})_2\text{D}_3$ differentially regulate p38 MAPK and JNK1/2 in rat intestinal cells and that p38 MAPK has a central role in $1\alpha,25(\text{OH})_2\text{D}_3$ -induction of the oncoprotein c-Fos.

Disclosures: **A. Russo de Boland**, None.

M513

MAP KINASES p38 and JNK Are Activated by the Steroid Hormone $1\alpha,25(\text{OH})_2\text{D}_3$ in the C2C12 Muscle Cell Line. **C. Buitrago***, **A. C. Ronda***, **A. Russo de Boland***, **R. Boland***. Biología, Bioquímica & Farmacia, Universidad Nacional del Sur, Bahía Blanca, Argentina.

In chick skeletal muscle cell primary cultures we previously demonstrated that $1\alpha,25(\text{OH})_2\text{D}_3$ -vitamin D_3 [$1\alpha,25(\text{OH})_2\text{D}_3$], the hormonally active form of vitamin D_3 , increases the phosphorylation and activity of the extracellular signal-regulated mitogen-activated protein (MAP) kinase isoforms ERK1 and ERK2, their subsequent translocation to the nucleus and involvement in DNA synthesis stimulation. In this study we show that other members of the MAP kinase superfamily are also activated by the hormone. Using the muscle cell line C2C12 we found that $1\alpha,25(\text{OH})_2\text{D}_3$ within 1 min phosphorylates and increases the activity of p38 MAPK. The immediately upstream kinases MKK3/MKK6 were also phosphorylated by the hormone suggesting their participation in p38 activation. $1\alpha,25(\text{OH})_2\text{D}_3$ was able to dephosphorylate/activate the ubiquitous cytosolic tyrosine kinase c-Src in C2C12 cells and studies with specific inhibitors imply that Src participates in hormone induced-p38 activation. Of relevance, $1\alpha,25(\text{OH})_2\text{D}_3$ induced in the C2C12 line the stimulation of MAPKAP-kinase 2 and subsequent phosphorylation of HSP27 in a p38 kinase activation-dependent manner. Treatment with the p38 inhibitor, SB203580, blocked p38 phosphorylation caused by the hormone and inhibit the phosphorylation of its downstream substrates. $1\alpha,25(\text{OH})_2\text{D}_3$ also promotes the phosphorylation of c-jun N-terminal protein kinases (JNK 1/2), the response is fast (0.5-1 min.) and maximal phosphorylation of the enzyme is observed at physiological doses of $1\alpha,25(\text{OH})_2\text{D}_3$ (1 nM). The relative contribution of ERK-1/2, p38 and JNK-1/2 and their interrelationships in hormonal regulation of muscle cell proliferation and differentiation remain to be established.

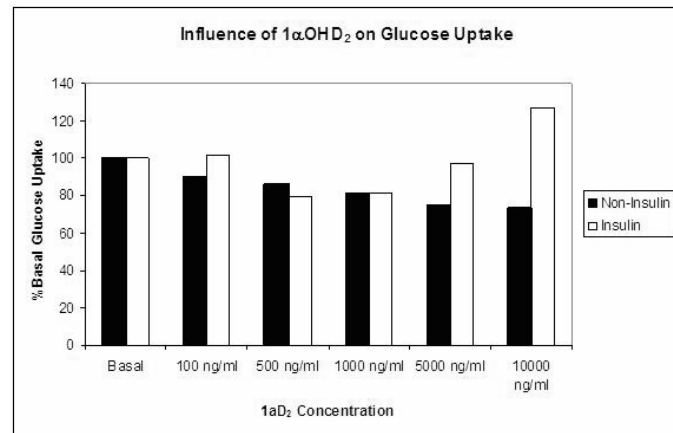
Disclosures: **R. Boland**, None.

M514

Influence of $1\alpha\text{OH}$ Vitamin D_2 on Insulin and PPAR γ Mediated Glucose Transport. **N. Fleming***¹, **C. Corley-Mastick***¹, **R. S. Fredericks***².

¹Biochemistry, University of Nevada Reno, Reno, NV, USA, ²Endocrine Associates, Reno, NV, USA.

Glucose transport and its subsequent processing within 3T3L-1 adipocytes provides insight to fundamental processes of cellular signaling. We are particularly interested in the effects of $1\alpha\text{D}_2$ as differentiated from 1-25 αD_3 as interactants with insulin stimulated and PPAR γ driven processing. It is possible that $1\alpha\text{D}_2$ has intracellular signaling capabilities mediated non-genomically. We have observed that 2-deoxyglucose uptake mediated by insulin can be suppressed by either $1\alpha\text{D}_2$ or 1-25 D_3 in a dose dependent manner. These effects are reversed by rosiglitazone, a PPAR γ agonist, and are associated with accelerated triglyceride production. The effect of $1\alpha\text{D}_2$ in the absence of insulin or rosiglitazone reveals a u-shaped response suggesting a reversal mechanism mediated by the induction of 24-hydroxylase consistent with known effects of a membrane receptor as a mediator of direct actions of $1\alpha\text{D}_2$. The data supports an integrated model which includes the scaffolding protein MNAR as the modulator for insulin induced glucose uptake under the influence of both $1\alpha\text{D}_2$ and 1-25 D_3 providing a drive for selection of 1 hydroxylation as a down stream signal of glucose oxidation independent of 25 hydroxylation. Both membrane and nuclear actions are mediated through the VDR, with those of $1\alpha\text{D}_2$ restricted to MNAR. 25 hydroxylation has evolved as an effect which is downstream of PPAR γ to provide nuclear selective action of 1α hydroxylated Vitamin D . Subsequent influences of both membrane and nuclear activity on energy partitioning should be applicable to explanation of Vitamin D influence on cell behavior including cell differentiation, immune regulation, phosphate transport via MARRS, and the endocrine role of 1-25 D_3 as a systemic signal.



Disclosures: **N. Fleming**, None.

M515

Identification and Characterization of Vitamin D Response Elements in Human and Mouse Epithelial Calcium Channel-2 Genes. **J. Lu***¹, **K. R. Stayrook***¹, **X. Bu***¹, **B. Khalifa***¹, **T. Wei***¹, **C. A. Frolik***¹, **T. P. Burris***¹, **Z. Zhang***², **J. C. Fleet***², **S. Nagpal***¹. ¹Lilly Research Laboratories, Eli Lilly & Company, Indianapolis, IN, USA, ²Dept. of Foods and Nutrition, Purdue University, West Lafayette, IN, USA.

1,25-dihydroxyvitamin D_3 [$1,25-(\text{OH})_2\text{D}_3$] plays a pivotal role in calcium homeostasis and bone mineralization by facilitating intestinal calcium absorption. $1,25-(\text{OH})_2\text{D}_3$ increases calcium absorption from gut by inducing the duodenal expression of epithelial calcium channel-2 (ECaC2). Here, we describe the molecular mechanism involved in $1,25-(\text{OH})_2\text{D}_3$ -mediated regulation of ECaC2 expression, and identify functional vitamin D response elements (VDREs) in the promoter regions of human and mouse ECaC2 genes. We show that VDR and retinoid X receptor (RXR) heterodimers bind *in vitro* to these VDRE sequences. In transactivation assays, human and mouse ECaC2 VDREs when coupled to a heterologous minimum promoter, exhibited $1,25-(\text{OH})_2\text{D}_3$ -dependent transcriptional activation. Further, chromatin immunoprecipitation assays demonstrate $1,25-(\text{OH})_2\text{D}_3$ -dependent recruitment of RXR-VDR heterodimers to the human ECaC2 VDRE in intestinal cells. We also demonstrate that the rat ECaC2 gene does not contain any putative VDREs in the 5kb upstream region and its expression is also not induced by the VDR ligand in a rat duodenal cell line that shows $1,25-(\text{OH})_2\text{D}_3$ -dependent induction of other vitamin D -responsive genes including calbindin-9k. Finally, *in vivo* $1,25-(\text{OH})_2\text{D}_3$ was less efficacious in rat in inducing the expression ECaC2 than mouse duodenum, indicating species context-dependent regulation of ECaC2 expression by vitamin D .

Disclosures: **J. Lu**, None.

M516

Gender- and Tissue-Specific Effects of 1,25-Dihydroxyvitamin D and EB1089 in Intestine and Bone of Mature Rats. **S. Karmakar***¹, **R. Narayanan***¹, **D. S. Perrien***², **L. J. Suva***², **N. L. Weigel***¹, **C. L. Smith***¹.

¹Molecular & Cellular Biology, Baylor College of Medicine, Houston, TX, USA, ²Orthopaedic Surgery, University of Arkansas for Medical Sciences, Little Rock, AR, USA.

Use of the natural vitamin D receptor (VDR) ligand, 1,25-dihydroxyvitamin D (1,25-D) as a bone protective agent is restricted by hypercalcemia, prompting the development of vitamin D analogs such as EB1089 that are less calcemic than 1,25-D. In our previous studies of male rats, 1,25-D more effectively attenuated disuse-induced osteoporosis than EB1089. Conversely, studies in female rats demonstrated that the same dosage of EB1089 prevented disuse-induced osteoporosis, while 1,25-D was ineffective. Based on these previous results, a direct comparison of the effects of EB1089 and 1,25-D on male and virgin female Sprague-Dawley rats was initiated. Animals were obtained at 4 months of age, and fed a diet containing 1% calcium, 0.5% phosphorus and 1000 IU/kg vitamin D for two months prior to study initiation. At 6-months of age, male and female rats were each divided into groups (n=8), that received either vehicle (80% polypropylene/20% 0.05 M sodium phosphate), 0.03 $\mu\text{g/day/kg}$ BW 1,25-D or 0.3 $\mu\text{g/day/kg}$ BW EB1089 (Leo Pharmaceuticals) via Alzet mini-osmotic pump. Serum calcium measurements at the experiment conclusion confirmed that neither 1,25-D or EB1089 induced hypercalcemia in male or female rats. After 28 d of treatment, animals were euthanized, and the left proximal tibia excised for *ex vivo* evaluation by micro-computed tomography (μCT). A 33% increase in bone volume/total volume ($p<0.05$) was observed in EB1089 female rats in comparison to vehicle controls, and a corresponding 18% decrease in bone surface/bone volume ($p<0.05$) indicated a positive response, consistent with the 62% decrease in the structure model index signifying increased mechanical strength. No significant changes in μCT values for 1,25-D-treated females were found, nor were differences observed for either treatment group of male rats. Both VDR agonists induced comparable expression of the VDR target genes, 1α -hydroxylase and 24-hydroxylase in the kidneys of male and female rats. However, significant decreases of PTH levels were observed only in EB1089 treated females (71%, $p<0.05$) and 1,25-D treated males (50%, $p<0.05$). Expression of the calbindin D_{9k} calcium transporter was significantly increased in the duodenum of EB1089, but not 1,25-D treated females, while the converse was observed for male rats. The ability of EB1089 to increase calbindin D_{9k} and suppress PTH levels in female but not male rats suggests that enhanced calcium transport in the female intestine may contribute to the improved efficacy of EB1089 in the female *versus* male skeleton.

Disclosures: **S. Karmakar**, None.

M517

Plasma 24,25-Dihydroxyvitamin D and Urinary 25-Hydroxyvitamin D Binding Activity of Black and White Female Adolescents. **M. Thierry-Palmer***¹, **V. Henderson***¹, **R. El Hammali***¹, **S. Cephas***¹, **C. Palacios***², **B. R. Martin***², **C. M. Weaver***². ¹Biochemistry, Morehouse School of Medicine, Atlanta, GA, USA, ²Foods and Nutrition, Purdue University, West Lafayette, IN, USA.

African Americans have been demonstrated to have significantly lower mean plasma 25-hydroxyvitamin D (25-OHD) concentrations, compared with Caucasian Americans in reports based on the Third National Health and Nutrition Examination Survey. We tested the hypothesis that plasma 24,25-dihydroxyvitamin D (24,25-(OH) $_2\text{D}$) concentrations would be lower in black female adolescents than in white female adolescents, because of greater sensitivity of the vitamin D endocrine system of black adolescents to salt. Plasma 24, 25(OH) $_2\text{D}$ concentration, urinary vitamin D metabolite content, and urinary 25-OHD

ASBMR 27th Annual Meeting

binding activity were determined for 11 black and 10 white female adolescents (11-15 years old), who were participants in a dietary study that involved three-week low salt (1.3 g, 56 mmol/24 hr sodium) and three-week high salt (3.86 g, 168 mmol/24 hr sodium) intake in a randomized, crossover design. Plasma 24,25-(OH)₂D concentrations of the white female adolescents were significantly higher than that of the black female adolescents ($P < 0.001$). Plasma 24,25-(OH)₂D concentrations of five black adolescents (45%) and three white adolescents (33%) at week 3 of high salt intake were approximately half the values at week 3 of low salt intake. Urinary 25-OHD binding activities of these "responders" were approximately doubled at week 3 of high salt intake. Urinary 25-OHD binding activities of the black adolescents, but not the white adolescents, were directly correlated with urinary sodium ($r = 0.57$, $P = 0.009$, $n = 10$). Urinary 25-OHD binding activities of the adolescents were variable (0 - 1.8 nmol/h), and the means did not significantly differ between black and white adolescents. White adolescents had higher mean urinary vitamin D metabolite content than black adolescents at week 2 ($P < 0.05$), perhaps because of higher vitamin D metabolite concentrations in plasma. We conclude that lower plasma 24,25-(OH)₂D concentrations of the black female adolescents, compared with the white female adolescents, can not be explained by difference in urinary loss of vitamin D metabolites.

Disclosures: **M. Thierry-Palmer**, None.

M518

A Role for Substrate 25-hydroxyvitamin D in Post-Translational Targeting of the Vitamin D 24-Hydroxylase to Mitochondria. **S. Ren, L. Nguyen***, J. S. Adams. The Burns and Allen Research Institute and Division of Endocrinology, Cedars-Sinai Medical Center and David Geffen School of Medicine at UCLA, Los Angeles, CA, USA.

The vitamin D-24-hydroxylase (CYP24) gene product requires post-translational transport to the inner mitochondrial membrane in order to access key co-factors and achieve functional capacity. Like most mitochondrial proteins encoded by nuclear genes, mitochondrial import of CYP24 gene product is directed by an N-terminal, mitochondrial targeting sequence. We have previously shown (J Biol Chem, Papers in Press, March 23, 2005, M414522200) that naturally occurring splice-variants of the CYP24 will encode substrate binding isoforms of the 24-hydroxylase that lack mitochondrial import potential and hence catalytic capability. On the other hand, factors other than the presence of an N-terminal targeting sequence, which promotes mitochondrial importation of the vitamin D hydroxylases, are not well understood. Here we investigated the potential for 24-hydroxylase substrates 25-hydroxyvitamin D (25-D) and 1, 25-dihydroxyvitamin D (1, 25-D) to alter the distribution of the 24-hydroxylase between the cytoplasmic and mitochondrial compartments of the cell. Chick myelomonocytic HD-11 cells were pre-incubated without (vehicle alone) or with 200 nM 1, 25-D and/or 25-D before obtaining whole cell or mitochondrial protein extracts for Western blot analysis and total cellular RNA for quantitation of CYP24 gene expression. Western blots were probed with anti-chick 24-hydroxylase and anti-grp75 antibody; grp75 is a resident mitochondrial chaperone protein and used here to control the loading of mitochondrial extract. CYP24 gene expression increased > 10-fold ($p < 0.01$) and 24-hydroxylase protein level increased to 2.3-fold ($p < 0.05$) in whole cell extracts of 1, 25-D-treated compared to vehicle-treated HD-11 cells. However, there was no increase in the mitochondrial content of 24-hydroxylase after exposure to 1, 25-D alone. When the HD-11 cells were pretreated with 1, 25-D to induce CYP24 gene expression and then exposed to substrate 25-D or vehicle for 3 hr, whole cell 24-hydroxylase levels remained constant, but 24-hydroxylase protein was significantly ($p < 0.01$) redistributed to mitochondria. Redistribution of the 24-hydroxylase to the mitochondrial compartment could be detected as early as 30 min after exposure of the cell to substrate 25-D. These data suggest that extra-mitochondrial interaction of the 24-hydroxylase with substrate 25-D, but not 1, 25-D, facilitates mitochondrial importation of the CYP24 gene product and the subsequent synthesis of 24, 25-dihydroxyvitamin D.

Disclosures: **S. Ren**, None.

M519

Substrate-Mediated Mitochondrial Localization of the 25-Hydroxyvitamin D-1-Hydroxylase. **S. Wu, L. Nguyen***, J. S. Adams. Burns and Allen Research Institute and the Division of Endocrinology, Cedars-Sinai Medical Center, David Geffen School of Medicine at UCLA, Los Angeles, CA, USA.

The CYP27B1 gene product is responsible for the synthesis of the active vitamin D metabolite, 1,25-dihydroxyvitamin D (1,25-D; calcitriol) from substrate 25-hydroxyvitamin D (25-D; calcidiol). Synthetic activity of this cytochrome P₄₅₀-monooxygenase requires its transfer from the cytoplasm to the inner mitochondrial membrane, the site of residence of crucial enzyme co-factors. This translocation process for the 1-hydroxylase is facilitated, in part, by the presence of an N-terminal mitochondrial targeting sequence encoded by the first exon of the CYP27B1 gene. We have previously reported (J Bone Miner Res, 19:S202, 2004) that overexpression of an N-terminally-truncated 1-hydroxylase, devoid of its mitochondrial localization signal, significantly decreased 1,25-D synthesis in CYP27B1-expressing HKC-8 human kidney cells. These results suggested that the N-terminally-truncated 1-hydroxylase served as a dominant-negative inhibitor of hormone synthesis by competitively binding substrate 25-D in the cell cytoplasm. These data also suggested that the interaction of enzyme and substrate might 1) occur extramitochondrially and 2) modulate synthesis of product 1,25-D by controlling the transfer of the 1-hydroxylase from cytoplasm to mitochondria. CYP27B1 specific primers and anti-1-hydroxylase antibody were used to quantitate CYP27B1 mRNA and mitochondrial 1-hydroxylase content by RT-PCR and Western blot analysis, respectively, in human HKC-8 and mouse TCMK-1 kidney cells before and after exposure to 0.2 to 200 nM 25-D substrate. Incubation with 25-D led to a significant dose- and time-dependent increase in the mitochondrial content of 1-hydroxylase protein without a change in

CYP27B1 transcript expression in these cells; 120 minutes post 25-D exposure, mitochondrial enzyme content was increased 5-fold above basal levels ($p < 0.001$). Mitochondrial localization of the 1-hydroxylase was blocked and cytoplasmic 25-D content increased significantly ($p < 0.02$) by stable overexpression of an exon-1-deficient construct, explaining the previously-observed dominant-negative action of this N-terminally-truncated 1-hydroxylase. We conclude that mitochondrial localization and subsequent enzymatic synthesis of 1,25-D can be promoted by interaction of the 1-hydroxylase with substrate 25-D in the cell cytoplasm; events that can be blocked by altering the N-terminal targeting sequence of the 1-hydroxylase.

Disclosures: **S. Wu**, None.

M520

Age-Related Changes of the Expression Level of CYP2R1 in Growing Male Mice. **M. Kamao***¹, **M. Shimomukai***¹, **N. Kubodera***, **T. Okano***.

¹Department of Hygienic Sciences, Kobe Pharmaceutical University, Kobe, Japan, ²Chugai Pharmaceutical Co., Ltd., Gotemba, Japan.

Purpose: Vitamin D must be hydroxylated at C-25 and C-1 α positions before acquiring its full activity. It has been reported that at least six cytochrome P450 (CYP), namely CYP2C11, CYP2D25, CYP2R1, CYP2J3, CYP3A4 and CYP27A1 are involved in the C-25 hydroxylation step of vitamin D. Although, mitochondrial CYP27A1 used to be regarded as a physiologically important C-25 hydroxylase, CYP2R1 is thought to play a substantial role due to the absence of sex and species differences and catalytic ability toward both vitamin D₂ and D₃. However, the basic properties of CYP2R1 including age-related changes of expression level have not been fully characterized. In the present study, we examined and compared the changes of CYP2R1 mRNA expression with those of the other metabolic enzymes of vitamin D, CYP27A1, CYP27B1 (C-1 α hydroxylase) and CYP24 (C-24 hydroxylase) in growing mice. Materials and Methods: Male C57BL/6 mice were fed regular rodent chow. The liver, kidney and testis were taken from mice aged 0, 2, 3 and 7 weeks old. The mRNA levels of CYP2R1, CYP27A1, CYP27B1 and CYP24 were measured by real time RT-PCR. Results: The mRNA expression levels of both CYP2R1 and CYP27A1 in the liver increased until 7 weeks after birth. The plasma levels of 25-hydroxyvitamin D were gradually increased from 3 to 7 weeks after birth in association with the mRNA levels of CYP2R1 and CYP27A1. On the other hand, there was no change in the mRNA levels of both CYP27B1 and CYP24 in the kidney from 3 to 7 weeks old. The expression of CYP2R1 mRNA was similar to or even higher in the testis than in the liver and increased until 7 weeks after birth. Conclusion: These results suggest that CYP2R1 as well as an already-known enzyme, CYP27A1 might be a nutritionally-important vitamin D C-25 hydroxylase for the regulation of calcium metabolism in growing mice. Moreover, CYP2R1 in the testis is likely to play a role in maturation of male mice.

Disclosures: **M. Kamao**, None.

M521

Parathyroid Hormone and Calcitonin Increase Protein Levels of the Renal Vitamin D 1alpha-Hydroxylase Cytochrome P450 (CYP27B1) in Renal Tubular Cells. **H. J. Armbricht, M. A. Boltz***. Geriatric Center (11G-JB), St. Louis VA Medical Center, Saint Louis, MO, USA.

Previous studies have shown that a number of factors regulate CYP27B1 mRNA levels in renal tubular cells, but there have been few studies on the regulation of CYP27B1 protein. We have developed and characterized a polyclonal antibody against a C-terminal synthetic peptide that recognizes both mouse and pig CYP27B1 protein on Western blots. To study the regulation of the protein, we have used the AOK-B50 renal cell line. This is the porcine proximal tubule LLC-PK1 cell line stably transfected with opossum PTH receptors. PTH treatment resulted in a large increase in a single band of 53,000 molecular weight, as evidenced by Western blotting. This band disappeared when the antisera was pre-absorbed with synthetic peptide. PTH (100 nM) rapidly increased CYP27B1 protein levels 3-4 fold by 6 hours with a peak at 24 hours and levels still elevated at 48 hours. On the other hand, PTH treatment resulted in only a transient increase in CYP27B1 mRNA levels that peaked at 4 hours and was largely gone by 24 hours. In dose response studies, PTH increased CYP27B1 protein levels at concentrations as low as 1 nM. By using cycloheximide to block translation, the half life of the CYP27B1 protein was estimated to be 6 hours. CT (100 nM) treatment for 6 hours increased CYP27B1 protein to levels comparable to those seen with PTH. With regard to mechanisms, CYP27B1 protein levels were markedly stimulated by forskolin and 8-bromo-cAMP but not by phorbol esters. This suggests that the action of PTH and CT may be via a cAMP-mediated pathway. Preincubation with 1,25(OH)₂D (100 nM) for 16 hours did not decrease the stimulatory effect of PTH on CYP27B1 protein. These studies demonstrate that in this cell line PTH produces a transient increase in CYP27B1 mRNA followed by a sustained increase in CYP27B1 protein via a cAMP-mediated pathway. Since the CYP27B1 protein normally has a short half life, the factors responsible for this sustained increase remain to be elucidated.

Disclosures: **H.J. Armbricht**, None.

M522

Elevated Expression of the Vitamin D Nuclear Receptor and of the 25-Hydroxyvitamin D 1 α -Hydroxylase in Colorectal Hepatic Metastases. C. Demers^{*1}, P. M. Huet^{*1}, J. Bolduc^{*1}, M. Bilodeau^{*1}, D. Ménard^{*2}, R. Lapointe^{*3}, A. Roy^{*3}, R. Létourneau^{*3}, M. Gascon-Barré¹. ¹Centre de recherche, Hôpital St-Luc, CHUM, Montreal, PQ, Canada, ²Anatomie et Biologie cellulaire, Université de Sherbrooke, Sherbrooke, PQ, Canada, ³Chirurgie, Hôpital St-Luc, CHUM, Montreal, PQ, Canada.

Colorectal carcinoma are among the most common causes of cancer death while vitamin D(D) and its hormone 1,25(OH)₂D have been shown to decrease tumour growth and prolong survival. To exert its bioactivity, D must be captured by tumour cells containing the D activating enzymes and express the 1,25(OH)₂D receptor (VDR_n). While fairly differentiated primary colon cancer cells express both the VDR_n and D-1 α -hydroxylase, no report has yet identified their presence in extracolonic metastases. The study aimed at investigating whether colorectal hepatic metastases process the cellular effectors necessary to respond to D. **Methods:** The study was carried out in 19 subjects bearing colorectal hepatic metastases who underwent liver resection. Samples of tumoral and adjacent normal livers were evaluated for the presence of the VDR_n, the D 1 α -(CYP27B1) and 25-(CYP27A1) hydroxylases. Normal adult kidneys, foetal intestines and hepatic tumours of non-colorectal origin were used as controls. **Results:** Compared to adjacent normal liver tissue, VDR_n mRNA and protein levels were markedly increased in colorectal hepatic metastases (14 and 10 fold respectively compared to normal liver tissue) and comparable to that of normal human kidneys. Similarly, CYP27B1 was significantly increased in hepatic colorectal hepatic metastases (4 and 2 fold for mRNA and protein respectively) with expression levels comparable to that of the normal human foetal intestine. In contrast, hepatic lesions of other origin expressed both VDR_n and CYP27B1 at a level comparable to normal liver tissue. CYP27A1 was also found in colorectal hepatic metastases albeit at levels lower than in the normal liver but at levels similar to that of the normal kidney or of hepatic non-colorectal tumour specimens. **Interpretation:** The study illustrates that colorectal hepatic metastases possess the enzyme machinery necessary for D anabolism and express VDR_n indicating that they stand to respond to D or the hormone 1,25(OH)₂D. These observations thus suggest that the maintenance of an optimal D status may be an important preventive factor following resection of malignant colorectal tumours. They also provide a rationale for the use of 1,25(OH)₂D or its analogs as adjuvant therapy for non-resectable colorectal hepatic metastases.

Disclosures: **C. Demers**, Leo Research Foundation 2.

M523

Tandem Construct and Recombinant Stable Expression of Vitamin D C-1 α (CYP27B1) and C-24 (CYP24) Hydroxylase Fusion Products with Their Cofactors Adrenodoxin and Adrenodoxin Reductase. E. Kim^{*}, R. Oyesanya^{*}, C. Wong^{*}, C. Chakaran^{*}, M. J. Beckman^{*}. Biochemistry, Virginia Commonwealth University, Richmond, VA, USA.

The 25-hydroxyvitamin D 1 α -hydroxylase (CYP27B1) and the 25-hydroxyvitamin D₃-24-hydroxylase (CYP24), are enzymes that regulate, activity and catabolism of 1,25-dihydroxyvitamin D₃ (1,25(OH)₂D₃), respectively. Both enzymes require adrenodoxin (AdX) and adrenodoxin reductase (AR), generic electron transport proteins for all mitochondrial forms of cytochrome P450, for enzyme activity. In the this study, a recombinant DNA assembly of CYP27B1 fused with AR and AdX in tandem and CYP24 fused with AR and AdX in tandem were engineered. Each tandem construct was cloned into the pIZT insect cell vector bearing zeocin resistance. The resulting pIZT-1 α -AR-AdX and pIZT-24-AR-AdX constructs were transfected in the presence of insectin plus into *Spodoptera frugiperda* (*Sf-9* insect cells). To isolate stable lines, monolayers of *Sf-9* cells were grown for 24 h and washed with PBS before treatment with zeocin (500 μ g/ml) in serum-free insect cell medium. Individual colonies, obtained at 3-4 weeks were expanded in a 6-well plate in the zeocin selection medium. *Sf-9* cells with stable P450 activity and product formation were confirmed by growth of cells in the presence of iron (Fe) via IronMax 100 (IM-100) containing media and conversion of [³H]-25-OH-D₃ to 1 α - and 24-hydroxylated side-chain products. Previously, cholesterol side-chain cleavage enzyme (P450_{sc}) and vitamin D 25-hydroxylase (CYP 27) have successfully been fused with AR and AdX and shown to be fully functional in transfection experiments. Therefore, these recombinant plasmids were made in order to establish new stable transfectant P450 systems for study in insect cells. These new systems will provide novel *in vitro* models to allow further detailed investigation of the function of the enzymes as well as the metabolism of vitamin D and its analogs.

Disclosures: **M. J. Beckman**, None.

M524

Isolation and Identification of 3-epi Vitamin D3: A Novel Metabolite of Vitamin D3. G. Wang^{*1}, G. T. Palmore^{*1}, C. Ceailles^{*2}, P. Vouras^{*2}, R. Ray^{*3}, R. Horst⁴, G. S. Reddy⁵. ¹Engineering, Brown University, Providence, RI, USA, ²Chemistry, Northeastern University, Boston, MA, USA, ³Boston University, Boston, MA, USA, ⁴National Animal Disease Center, Ames, IA, USA, ⁵Chemistry, Brown University, Providence, RI, USA.

Since our original demonstration of the metabolism of 1,25(OH)₂D₃ into 1,25(OH)₂-3-epi-D₃ in human keratinocytes, there have been several reports indicating that epimerization of the 3 hydroxyl group of vitamin D compounds is a common metabolic process. Recent studies reported the metabolism of 25OHD₃ and 24, 25(OH)₂D₃ into their respective C-3 epimers, indicating that the presence of 1 hydroxyl group is not necessary

for the 3-epimerization of vitamin D compounds. In our most recent study, we also reported the metabolism of 1OHD₃, a non 25-hydroxylated vitamin D₃ compound into its 3 epimer. From these studies, it became obvious that the presence of neither 1 hydroxyl group nor 25 hydroxyl group is required for C-3-epimerization of vitamin D compounds, and that vitamin D₃ itself can be 3 epimerized. To provide direct proof of the metabolism of vitamin D₃ into its C-3 epimer we studied the metabolism of vitamin D₃ in the human hepatocellular carcinoma (Hep G2) cell line, which is known to express the C-3 epimerization pathway. We noted the conversion of vitamin D₃ into a new metabolite, the identity of which was established to be 3 epi vitamin D₃ by its comigration with synthetic 3-epi vitamin D₃ standard in two different HPLC systems and GC/MS analysis. Furthermore, we also isolated 3 epi vitamin D₃ from the serum of vitamin D₃ intoxicated rats. Thus for the first time we show that vitamin D₃ itself can be metabolized into its C-3 epimer both *in vitro* and *in vivo*.

Disclosures: **G. Wang**, None.

M525

Importance Of Ruling Out Osteoid Osteoma In Hip Pain Syndrome. R. Mastaglia^{*1}, G. Aguilar^{*2}, B. Oliveri^{*1}. ¹Sección Osteopatías Médicas, Hospital de Clínicas, Universidad de Buenos Aires, Buenos Aires, Argentina, ²Servicio de Diagnóstico por Imágenes, Universidad de Buenos Aires, Buenos Aires, Argentina.

Hip pain is a frequent presenting complaint in the clinical practice. Osteoid osteoma must be considered a likely diagnosis in young patients presenting chronic unspecific pain in this area. A 29 year -old Caucasian man was seen in the clinic offices due to pain in the right groin. Onset of pain was two years prior to consultation, and it increased with exercise. The patient had interrupted his usual sports practice (Rugby) due to progressively increasing pain. He had not traveled or been exposed to infectious disease. He had no antecedents of fever, trauma, or other musculoskeletal pain. The pain was dull and aching, was not associated with any specific activity or time of day, and decreased with anti-inflammatory drugs (AINES). On physical examination, he appeared to be a healthy man. He reported tenderness in the groin and right upper thigh but no palpable mass or inguinal lymphadenopathy was found. Abduction and internal and external rotation of the right hip caused slight pain. A traumatologist who evaluated the patient two years previously indicated magnetic resonance imaging (MRI) of the right leg. Sequence T2 -weighting showed bone edema in the right femoral neck characterised by hyperintense signal in cancellous bone, without alteration in the femoral head. Diagnosis at the time was "transient osteoporosis". Avascular necrosis of the hip was ruled out. Further MRI studies were performed for follow-up. The second MRI showed persistence of cancellous bone edema without alteration in the femoral head despite time. Routine and mineral laboratory, bone densitometry and spine X-rays were normal. Pelvic radiography revealed slight bone sclerosis with thickening of the medial cortex at the level of the right femoral neck. The Computed Tomography scan revealed a lucent lesion (nidus) in close contact with the medial cortex of the femoral neck, which presents reactive sclerosis and thickening. "Osteoid osteoma " was diagnosed. Choice therapy is complete excision of the nidus. Osteoid osteoma is one of the most frequent and characteristic bone tumor lesions. The typical symptom is permanent pain, and symptom severity increases peaking at night. In the case of our patient, clinical presentation was not typical and diagnosis was possible because the physician strongly suspected it to be osteoid osteoma. Thus, image diagnosis studies other than x-rays must be performed, allowing correct diagnosis of "Osteoid osteoma" in a young person presenting bone pain.

Disclosures: **S.R. Mastaglia**, None.

VITAMIN D WORKING GROUP

WG1

Fgf-23 and Vitamin D Interactions In Vivo. D. Sitara¹, R. St-Arnaud², R. G. Erben³, M. S. Razzaque^{*1}, B. Lanske¹. ¹Oral & Developmental Biology, Harvard School of Dental Medicine, Boston, MA, USA, ²Genetics Unit, Shriners Hospital, Montreal, PQ, Canada, ³Dept. of Natural Sciences, University of Veterinary Medicine, Vienna, Austria.

FGF-23 has been identified as the circulating phosphaturic factor associated with renal phosphate wasting leading to rickets and osteomalacia, as found in patients with autosomal dominant hypophosphatemic rickets, oncogenic osteomalacia, and X-linked hypophosphatemia. We recently reported the generation of Fgf-23 null animals resulting in a phenotype including growth retardation, severe hyperphosphatemia, increased serum ALP activity and 1,25(OH)2D3 concentrations, abnormal bone mineralization, and tissue calcifications. A similar phenotype has been reported in patients with familial tumor calcinosis, caused by inactivating mutations in the FGF-23 gene. In the current study we studied the expression of Fgf-23 postnatally by lacZ staining of various adult tissues of Hyp/Fgf-23^{+/+} and Hyp/Fgf-23^{-/-} mice, and were able to detect strong signals in all bones. We also investigated whether part of the abnormal Fgf-23 null phenotype is due to the increased 1,25(OH)2D3 levels. Thus, we established a new mouse model in which we eliminated vitamin D dependent mechanisms in Fgf-23 null mice by generating double mutant animals which were deficient for both Fgf-23 and 1 α (OH)ase, the enzyme that converts the inactive form of vitamin D to the active form. Our data demonstrate for the first time that deleting the 1 α hydroxylase gene from Fgf-23 null mice reverses the severe hypersphosphatemia to hypophosphatemia, suggesting that regulation of phosphate homeostasis by Fgf-23 is at least partly vitamin D-dependent. In addition to the biochemical measurements, we performed routine histological analysis and analyzed the mineralization pattern of the long bones of Fgf-23^{-/-}, 1 α (OH)ase^{-/-}, and Fgf-23^{-/-}/1 α (OH)ase^{-/-} double mutant animals, by von Kossa staining on methylmetacrylate sections and Alizarin Red S staining on full body skeletons. Our findings suggest that Fgf-23^{-/-}/1 α (OH)ase^{-/-} double mutant mice resemble the phenotype of 1 α (OH)ase^{-/-} single knock-out animals as they exhibit ricketic appearance such as a wider growth plate with an expansion of hypertrophic chondrocytes, and a decrease in mineral deposition. Alizarin staining of all compound mutant skeletal elements clearly illustrated that the abnormal nodule formation previously observed in many Fgf-23 null bones had completely disappeared indicating that 1,25(OH)2D3 must have caused these features. We are currently measuring proliferation and apoptosis rates and are evaluating the expression of skeletal marker genes by in situ hybridization.

WG2

1,25(OH)2D3 Induces Rapid Response in Growth Plate Chondrocytes and Osteoblasts through Its Membrane-Associated Binding Protein, ERp60. L. Wang, R. A. Chaudhri^{*}, K. L. Wong^{*}, Z. Schwartz, B. D. Boyan. Georgia Institute of Technology, Atlanta, GA, USA.

Steroid hormones act via traditional nuclear receptor mechanisms, as well as rapid non-genomic pathways by activating membrane associated protein kinases. 1,25-dihydroxyvitamin D3 [1,25] activates the PKC α signaling pathway in prehypertrophic and upper hypertrophic zone (growth zone) growth plate chondrocytes via activation of phospholipase A2 (PLA2), cyclooxygenase-1 (Cox) and PLC. Factors that upregulate responsiveness to 1,25 in growth plate chondrocytes increase expression of PLA2 activating protein (PLAA), suggesting that it links ERp60 to PLA2. Antibodies to the N-terminal amino acid sequence of ERp60 (Ab100), a 1,25 binding protein present in chondrocyte and osteoblast plasma membranes, block the signaling cascade. Growth zone chondrocytes from VDR^{-/-} mice also respond to 1,25 with a rapid increase in PKC via the same PLC-dependent mechanism. To better understand the role of ERp60, we examined its tissue distribution in the tibial growth plate of VDR^{-/-} mice using immunohistochemistry and compared this to PLAA; we determined its subcellular localization and relationship to the caveolar scaffolding protein caveolin-1 and to the nVDR by confocal microscopy of rat growth zone cells; we assessed the relative contributions of the N and C terminals to the overall mechanism; and we examined response to 1,25 in osteoblast-like ROS 17/2.8 cells (stable) after silencing ERp60 expression with siRNA. Immunohistochemistry using Ab100 showed that ERp60 and PLAA were limited to the prehypertrophic and upper hypertrophic cell zones of the growth plate and to the metaphyseal osteoblasts, both of which are responsive to 1,25. Immunostain was absent from the resting zone, which lacks a rapid PKC response. ERp60 and caveolin-1 were present in the plasma membrane whereas the nVDR was primarily in the nuclei of growth zone cells. Ab100 and Ab101 (generated to the C-terminus of ERp60) both blocked PLC and PKC activation and downstream biological responses, suggesting that both termini are involved in the mechanism. Compared to scrambled siRNA treated cells, Erp60 siRNA significantly decreased the effect of 1,25 on PKC activity in ROS 17/2.8 cells. Additional studies showed that activation of PKC in ROS 17/2.8 cells was via PLC and Cox. In conclusion, 1,25 binding protein ERp60 and PLAA are present in 1,25-responsive chondrocytes and osteoblasts in vivo and in vitro, ERp60 and Cav-1 are present in the plasma membrane, and rapid PKC signaling requires functional activation of ERp60 signaling via PLC and COX.

POST TRANSPLANTATION AND BONE DISEASE WORKING GROUP

WG3

Management of Metabolic Bone Disease in the Kidney Transplant Recipient: Practice Patterns in 2005 and Recommendations for Therapy. Paul J. Scheel Jr., M.D., Department of Medicine, Johns Hopkins Medical Institute, Baltimore, Maryland, USA.

Patients who undergo renal transplant are at high risk of several forms of metabolic bone disease and subsequent fractures following kidney transplant. This increase risk can be attributed to the multiple metabolic derangements that occur during the various stages of chronic kidney disease (CKD) leading up to the transplant and the skeletal toxic effects of medication used post transplant to prevent allograft rejection. Patients with CKD who progress to ESRD are known to have histologic evidence of both high and low turnover bone disease. High turnover bone disease is secondary to decreased production of 1:25 OH vitamin D from the failing kidney and subsequent hyperparathyroidism (HPT). Depending on the length of time HPT is present and the type of, and duration of therapy, this elevated level of PTH may or may not regress to normal levels following the transplant. Low turnover or adynamic bone disease has been attributed to Aluminum containing phosphate binders, deposition of beta 2 microglobulin, over treatment with vitamin D compounds, nutritional defects associated with ESRD and in patients who were treated with peritoneal dialysis. Other metabolic problems associated with CKD that affect skeletal health prior to transplant include hypogonadism, chronic acidosis, and in hemodialysis patients, chronic exposure to Heparin. Patients who receive a kidney transplant therefore enter transplantation with significant bone disease of varying histology. Following a successful transplant there is resolution of many of these metabolic derangements that are attributed to a failing kidney. There are however new insults that affect skeletal health. The agents used to prevent allograft rejection; glucocorticoids and calcineurin inhibitors have both been shown to decrease bone mineral density (BMD). This demineralization occurs primarily during the periods of high corticosteroid use and is associated with increased fracture risk. Additional insults that occur post transplant include hypophosphatemia, metabolic acidosis and in some persistent hyperparathyroidism associated either with decreased vitamin D or secondary to persistent HPT. Therapies aimed at reducing post transplant bone demineralization and fracture include: minimizing glucocorticoid use and rapid taper to < 10 mg in patients with stable renal function, monitoring and replacement of 25- OH and 1:25 OH vitamin D deficient patients, adequate dietary calcium intake, the use of bisphosphonates, especially in the first six month post transplant, and recognition and treatment of persistent CKD and associated complications.

WG4

Treatment of Bone Loss after Renal Transplantation in Children: Alfacalcidol versus Calcitonin Therapy. A. A. M. El-husseini. Nephrology, Mansoura Urology and Nephrology Center, Mansoura, Egypt.

Background. Osteoporosis is a well-known complication of renal transplantation in children. We conducted a randomized trial comparing alfacalcidol with calcitonin for the treatment of bone loss. Methods. Among 59 young patients who received live related renal transplant and were subjected to dual energy x-ray absorptiometry (DEXA), 30 patients had low bone mineral density (BMD) (z-score < -1) were enrolled onto the study. Their mean age at time of transplantation was 13.5 ± 3.4 years and the mean duration after transplantation was 46 ± 32 months. Patients with low BMD were randomized into two equal homogeneous groups: group 1 received daily alfacalcidol 0.25 microg by mouth and group 2 received 200 IU /day nasal spray calcitonin. Every patient in both groups received daily 500-mg calcium carbonate supplements. Parameters of bone metabolism (intact parathyroid hormone, serum osteocalcin and urinary deoxypyridinoline) and BMD were assessed before and after the study period. Estimates of bone loss and the incidence of fractures among untreated patients were obtained from a reference group of 15 prospectively recruited patients who received renal transplants within the same period as the intervention groups. Results. At one year, the BMD at the lumbar spine had increased from -2.3 to -0.5 in the alfacalcidol group and from -2.3 to -1.0 in the calcitonin group while it was decrease from -2.2 to -2.5 in the reference group. Incidence of vertebral fractures did not differ significantly among the groups (13.3 percent in the calcitriol group, 6.7 percent in the calcitonin and the reference groups). Serum intact parathyroid hormone level decreased significantly in the alfacalcidol group compared with the calcitonin group ($P = 0.042$). Apart from transient hypercalcemia in 1 patient in the alfacalcidol group, no other significant adverse effects were noted. Conclusion. This study suggested the value of alfacalcidol and calcitonin agents in the treatment of osteopenia and osteoporosis in young renal transplant recipients. These therapies were safe, tolerable, simple to administer and potentially applicable to other renal transplant patients.

WG5

Prevalence of Vitamin D Insufficiency and Osteoporosis in Patients with Severe Chronic Liver Disease and Liver Transplantation. M. Rodriguez-Garcia*, C. Gomez¹, L. G. Dieguez*², M. Rodriguez*², M. Naves*¹, A. Rodriguez-Rebollar*¹, M. T. Fernandez-Coto*³, J. B. Cannata-Andia¹. ¹Bone and Mineral Research Unit. Instituto Reina Sofia de Investigacion., HUCA, Oviedo, Spain, ²Gastroenterology, HUCA, Oviedo, Spain, ³Biochemistry, HUCA, Oviedo, Spain.

Bone loss and vertebral fractures (Vt Fx) are common complications after liver transplantation (Tx); both pre- and post-transplant factors may be implicated in its pathogenesis. This study aimed to compare relevant bone markers, such as vitamin D status, bone mass and Vt Fx in patients with severe chronic liver diseases waiting for liver Tx (Pre-Tx group), with patients after the first year of liver Tx (Post-Tx group). Forty patients who received a liver Tx in the previous year (mean time of Tx 9 ± 3 months) were compared with 38 patients with chronic liver disease waiting for liver Tx. For both groups, the study included measurement of fasting serum biochemical markers [25-OH D3, 1-25 (OH) D3, iPTH, Ca, P, alkaline phosphatase and others], bone mineral density (BMD) at lumbar spine and hip (Hologic QDR-1000) and X-ray evaluation of thoracic and lumbar spine. Other demographic, anthropometric and relevant clinical data were also registered. A population-based cohort of the same geographical area, age and gender was also used as a comparator (n=309). The prevalence of Vt Fx was 25% in pre-Tx, 29% post Tx and 15.7% in the general population. In pre-Tx patients, the rate of Vt Fx did not differ between sexes. By contrast, post-Tx women suffered a significantly higher rate of Vt Fx (42.1%) compared with post-Tx males (8.3%) and also with women of the general population (18.7%, $p < 0.05$). At total hip, densitometric osteoporosis (WHO criteria) in pre-Tx women was higher (28.6%) compared with men (10.3%). Also at the total hip, BMD was significantly lower in Pre-Tx patients having Vt Fx (Z-score -1.78 ± 0.45 vs 0.17 ± 1.32 , $p < 0.005$). By contrast there were no differences at any site in the Post-Tx group. The mean 25 (OH) D3 serum levels in pre-Tx patients were low (18 ± 12 ng/ml) although similar to post-Tx patients (18 ± 9.4 ng/ml) and general population (19 ± 10 ng/ml). However, there was more prevalence of severe deficiency (< 10 ng/mL) in the pre-Tx patients (34.5%) compared with post-Tx (23.8%) and general population (21.5%). In addition, in pre-Tx women, a significant positive relationship was found between 25 (OH) D3 and 1.25 (OH)2 D3 ($r = 0.83$, $p < 0.05$). In summary, severe chronic liver disease is associated with low bone mass, a high rate of Vt Fx and lower 25 (OH) D3 serum levels even before the liver transplantation. Although several other factors may be involved, an adequate vitamin D supplementation is mandatory to reducing bone abnormalities in chronic liver disease.

WG6

Alendronate Treatment in Long-Term Liver or Cardiac Transplanted Osteoporotic Patients. G. Martínez*¹, L. Gil-Fraguas*², E. Jódar¹, A. Escalona*¹, A. Moreno*³, E. García*¹, E. Moreno*³, M. Gómez*⁴, F. Hawkins¹. ¹Endocrinology Service, University Hospital 12 de Octubre, Madrid, Spain, ²Rehabilitation Service, University Hospital 12 de Octubre, Madrid, Spain, ³Digestive Surgery Dpt, University Hospital 12 de Octubre, Madrid, Spain, ⁴Cardiology Service, University Hospital 12 de Octubre, Madrid, Spain.

Background: early institution of therapy may prevent bone loss after transplantation (Tx). However, the best therapeutic option in long-term transplanted patients with osteoporosis has not been defined yet. Our aim was to investigate the effects of alendronate on bone mineral density in long-term Tx patients with osteoporosis. Patients and Methods: Forty-four patients (17 liver and 27 cardiac recipients), mean age 56 y., with densitometric osteoporosis (T-score < -2.5) more than 2 years after Tx were treated with alendronate (70 mg p.o. once weekly) and minimum of 1000 mg of calcium and 400 IU vitamin D3 daily p.o.. Mean time since Tx was similar in both groups (56 months in liver recipients, 52 months in cardiac Tx patients). In liver recipients immunosuppressive therapy included tacrolimus in 65% and Cyclosporine A in 35% of patients, but none was receiving corticosteroids at the time of study. In cardiac recipients > 90% of patients was on prednisone treatment (mean dose 5.7 mg/day, mean accumulate dose 11505 mg). BMD changes were assessed after one year of treatment at lumbar spine and hip (DXA, Hologic QDR 4500). Results: In liver recipients mean lumbar BMD increase was $+8.1 \pm 7.1\%$, whereas mean total hip BMD increased $+3.8 \pm 4.3\%$, femoral neck BMD increased $+3.3 \pm 6.9\%$ and trochanteric BMD increased $+7.3 \pm 6.0\%$. In contrast, BMD responses in cardiac recipients were less impressive; mean lumbar BMD increase was $+2.1 \pm 3.6\%$, mean total hip BMD $-1.1 \pm 6.4\%$, and femoral neck BMD increased $+1.2 \pm 4.6\%$. Treatment was well tolerated in all the patients. Conclusion: Weekly oral alendronate plus calcium and vitamin D3 is an effective treatment in long-term Tx-related osteoporosis, particularly in liver recipients. Concomitant immunosuppressive drugs used could influence the response to the antiresorptive treatment in these patients.

WG7

Evolution of Bone Density after Heart Transplantation: Influence of Anti-Resorptive Therapy. L. Gil-Fraguas*¹, E. Jodar², G. Martinez*¹, M. A. Escalona*², J. Vara*¹, E. Robles*¹, F. Hawkins². ¹Rehabilitation, University Hospital 12 de Octubre, Madrid, Spain, ²Endocrinology, University Hospital 12 de Octubre, Madrid, Spain.

Osteoporosis and osteoporotic fractures are common complications after heart transplantation. The purpose of this study was to evaluate the effects of antiresorptive therapy (calcium and vitamin D [CaVD], calcitonin [CT], etidronate [ETN] or alendronate [ALN]) at standard doses in the evolution of bone mineral density (BMD) in heart transplant recipients. Patients and Methods: We studied 216 patients (aged [mean (SD)] 54(10) years, 85% males, BMI 24.25(3.25) kg/m²) undergoing heart transplantation. BMD was assessed by DXA (Hologic 4500) in lumbar spine (LS) and total femur (TF) sites at baseline, 6, 12 and 24 months. Patients with normal BMD at baseline were placed in CaVD group and served as controls, the rest of the patients were random allocated in CT, ALN or ETN group. 152 patients had 24 months of follow-up. The statistical analysis included the following tests: Scheffe, Manova and Wilks' Lambda. Results: As expected, baseline LS and TF BMD (gr/cm²) was higher in CaVD group (LS/TF: 0.973(0,114)/ 0.925(0,129), respectively; p<0.05) without significant differences among the rest of the groups (LS/TF: CT: 0.873(0,157)/ 0.820(0,116); ETN: 0.882(0,121)/ 0.893(0,121); ALN: 0.884(0,147)/ 0.832(0,109)). The changes in BMD (%) are showed in the table:

Group/Site	6 Mo	12 Mo	24 Mo
CaVD LS	-3,34(5,55)	-3,97(5,65)	-3,07(7,0)
CaVD TF	-1,66(3,71)	-3,41(4,06)	-3,15(3,89)
CT LS	-4,3(6,4)	-4,94(5,26)	-0,93(6,39)
CT TF	-3,85(5,83)	-4,85(6,10)	-3,59(5,87)
ETN LS	-5,27(4,85)	-5,42(5,66)	-1,87(6,22)
ETN TF	-3,67(5,55)	-5,54(4,97)	-4,65(5,46)
ALN LS	0,53(5,16)	0,79(5,17)*	4,90(8,42)*
ALN TF	-0,39(4,0)*	-0,63(4,14)*	-0,46(5,16)*

*p<0.001 vs any other group.

Conclusions: According to other studies, heart transplantation produces a high bone loss with a recovery phase beginning 6 (LS) to 12 (TF) months after the procedure. Alendronate is associated with lower bone loss at femoral neck and even with a relative increase in lumbar spine bone density.

WG8

Bone Mineral Density after Renal Transplantation in Adolescents. M. Matsuda-Abedini*¹, J. Shepherd*², R. Mathias*¹, E. von Scheven¹, A. A. Portale¹. ¹Pediatrics, University of California, San Francisco, San Francisco, CA, USA, ²Radiology, University of California, San Francisco, San Francisco, CA, USA.

Loss of bone mineral occurs after renal transplantation in children, but the magnitude and duration of loss are unclear. Most studies to date have employed AP DXA of the lumbar spine to assess areal BMD (aBMD), but this technique is confounded by changes in skeletal size and maturation during growth, limiting its use in cross-sectional studies of growth-retarded patients. Serial measurements of aBMD might overcome this problem by comparing subjects to themselves. The shortcomings of planar densitometry might also be circumvented by measuring volumetric BMD (vBMD), using AP combined with lateral DXA (latvolDXA) or quantitative computed tomography (QCT). The objectives of the current prospective study were to: 1) determine the magnitude of decrease in BMD after renal transplantation in adolescents, and 2) compare aBMD and two estimates of vBMD, latvolDXA and QCT. We measured BMD of the lumbar spine in 20 ethnically diverse renal transplant recipients (11M), aged 16 ± 2.9 years (SD), at time of transplant and 9 and 18 months afterwards. Immunosuppression included corticosteroids in all patients; cumulative corticosteroid dose at 9 months was 92 ± 32 mg/kg. aBMD of the lumbar spine was determined by AP DXA (Hologic), and vBMD was determined by lumbar latvolDXA and QCT (GE 9800 Quick Scanner). To date, 18 subjects completed the 9 month visit and 10 subjects the 18 month visit. At transplant, aBMD z-score determined for chronologic age and gender (Hologic QDR-Delphi/A research reference data) was 0.06 ± 1.02. At 9 months post-transplant, aBMD decreased by 4.9 ± 10%, and the z-score decreased by 0.68 ± 0.73 (p<0.001). At 18 months, aBMD z-scores remained below baseline by 0.63 ± 0.8. vBMD determined by latvolDXA at 9 months post-transplant decreased slightly, 3.9 ± 11.6%, but not significantly, with little further change at 18 months. By contrast, vBMD determined by QCT decreased by 12.8 ± 16% (p<0.01) at 9 months and 14.4 ± 21% at 18 months. The correlation between latvolDXA and QCT was 0.6 (p<0.001). Bland-Altman comparison of paired measurements by these two methods revealed a mean difference of 0.036 g/cm³ (95% CI: 0.026 to 0.046), with wide limits of agreement (-0.03 to 0.10). These data show that lumbar BMD decreases significantly in the first 9 months after renal transplantation in adolescents and remains decreased at 18 months post-transplant. The magnitude of loss in BMD is substantially underestimated by both AP and latvolDXA compared with that determined by QCT. The poor correlation between latvolDXA and QCT and the large limits of agreement do not support using the two methods interchangeably.

Numeric**3T3L1 preadipocytes**, M237**A****AAE581**, 1179, SU270, SU447. SEE ALSO*Cathepsin K inhibitor(s)***AC-100 (Dentonin)**, F461, SA461, SU214**Acceleratory motion, high frequency**

Disuse-induced trabecular bone loss and, M149

Acid, dietary, F306, SA306, SU429**Acidosis**, 1148. SEE ALSO *Metabolic acidosis***Actin**, 1145, SU222, SU298**Actin ring**, M496**Activating transcription factor 3 (ATF3)**, SA164**Activating transcription factor 4 (ATF4)**, M179, M187**Activator protein 1 (AP-1)**, F258, SA258**Acumen Explorer (laser-scanning fluorescence microplate cytometer)**, SU281**Adenosine 5'-triphosphate (ATP)**

Fluid flow-induced human MSCs proliferation and, SU217

Adenosine receptor

Expression in MC3T3 E1 cells, SU260

Adenoviral gene therapy*In vivo* imaging in two bone formation models, M023**Adherent stromal cells (ASC)**

Pluripotent, M239

Adipocytes, 1114, 1184, M198, M233**Adipogenesis (adipocyte differentiation)**

Alendronate combined with vitamin D and inhibition of, F412, SA412

Androgen receptor and, 1198

C/EBP α isoforms and, M190

Enhancement in BMSCs lacking VDR, F496, SA496

GILZ-mediated inhibition of, F513, SA513

Glucocorticoid signaling inhibition by overexpression of 11 β -HSD2 in mature osteoblasts and, F507, SA507

Heparin effects on, M237

PPAR γ 2 control of regulatory pathways for, SU242PPAR γ 2 effects in diabetes mellitus, type 1 and, F399, SA399

Retinoic acid and, M204

Adiponectin, 1047, SU205**Adipose tissue**. SEE ALSO *Fat tissue*

Leptin effects on cortical bone size in non-weight-bearing bone in young men and, 1046

Loss of ER α signaling via EREs, differential effects on total body vs. marrow, F511, SA511Mouse, *in vivo* expansion and *in vitro* characterization of pluripotent adherent stromal cells from, M239**A disintegrin and metalloproteinase 8 (ADAM8)**, M242**A disintegrin and metalloproteinase 10 (ADAM10)**, 1188**A disintegrin and metalloproteinase with thrombospondin**, SU048**Adolescents**

Anorexia nervosa and bone cross-sectional geometry in, SA473

BMD after kidney transplantation in, M481, WG8

BMD determinants in female, SA001

Discontinuation of pamidronate for osteogenesis imperfecta and, 1088

Fractures as osteoporosis risk, 1136

HIV-infected, oral cholecalciferol effects on serum levels of 25(OH)D in, SU476

IGF-I and bone remodeling in girls with type 1 diabetes, SA469

Adolescents (Cont'd)

Leptin effects on adipose tissue and cortical bone size in non-weight-bearing bone in, 1046

Menstrual irregularity and low BMD in female runners, SU356

Orthopedic complications in overweight, F472, SA472

Peak bone growth and weight in Japanese, M010

Physical activity and BMD in Japanese, M012

Plasma 24,25(OH) $_2$ D and urinary 25(OH)D binding activity of black and white female, M517

Polycystic ovary syndrome and low bone resorption in obese, SU474

SNPs in VDR promoter and growth in female, SA495

Stress fractures and BMD in active female, M136

Vitamin D status and calcium absorption on range of calcium intakes in black and white, M007

Adrenal adenoma

Serum OPG levels and, SA371

AdrenalectomyBone histomorphometric change in leptin deficient Ob/Ob mice with γ 2-MSH administration and, SU027**Adrenal hyperplasia, congenital**, SA471 **β -Adrenergic blockers**, F176, F345, SA176, SA345 **β -Adrenergic receptor**, F397, SA397 **β -Adrenergic receptor-1 (ADR β 1)**, SU381 **β -Adrenergic receptor-2 (ADR β 2)**, 1040, SU381**Adrenocorticotrophic hormone (ACTH)**, SU291**Adrenodoxin**, M523**Adrenodoxin reductase**, M523**Adrenomedullin-calcitonin receptor-like pathway**, M486**Adult growth hormone deficiency**, M133**Advanced glycation end products (AGEs)**, SU075**African Americans**, M103, M306. SEE ALSO *Blacks***African heritage**, F112, SA112. SEE ALSO *Blacks***AFX signaling pathway**, 1068**Aged**. SEE ALSO *Age factors*; *Aging*

Accuracy of self-report of fractures, SU334

Bone instability and hip fracture risk in, M088

Bone loss, weight fluctuation and mortality risk in, SU343

Community-dwelling, vitamin D deficiency and fracture risk in, F351, SA351

Daily, weekly, or monthly protocols to reach desired serum concentration of 25(OH)D for, SU428

Dental status, osteoporosis and disability in Italy, M451

80 and over, serum levels of OPG and RANKL in, SU004

Fall risk and type 2 diabetes in, F347, SA347

Frailty and bone turnover rates predicts mortality in, 1133

Frailty and risk of falls and fracture in women, SU335

Optimal serum 25(OH) $_2$ D levels for, F349, SA349

Osteoporosis epidemiology and treatment in Americans, SU359

Randomized, controlled trial of mailed osteoporosis education to, M372

Sex hormones levels and fall risk in community-dwelling, 1041

Smoking and decreased physical performance in women, SA304

VDR gene polymorphism and falls in, SA501

Without osteoporosis, fall-related factors and fracture risk in, SU344

Age factors. SEE ALSO *Aged*; *Aging*

Adipogenic transdifferentiation of committed osteoblasts, M198

Angiogenic response after ischemic necrosis of femoral head, SA136

Baseline BMD, genetics, and rate of changes related to, M314

BMD predictor in Asian men and women, SU003

Bone marrow stromal cells responsiveness to IGF-I and, SU012

Bone microstructure at wrist and, 1075

Calcium and magnesium in erythrocytes and, M042

Caspase-2 deficiency, bone resorption and, 1141

Cortical bone porosity, predicting 3D structure at human, anterior femoral mid-shaft and, SU016

Creatinine clearance and falls in women not treated with calcitriol, M312

CYP2R1 expression in growing mice and, M520

DMPA effect on bone remodeling markers and, SU156

Fracture frequency in patients over 50 in a Mexico City trauma hospital, SU326

Fracture risk assessment using T-scores and, F293, SA293

Human bone marrow stromal cell responses to PTH and, M004

Incident fractures in glucocorticoid-induced osteoporosis and, SA368

Iron and free radical accumulation in bone, SU450

Mineral metabolism and bone turnover markers in 461 Chinese, M001

Old bone as target for osteoclasts in bone resorption, M241

Short-term and long-term absolute fracture risk by BMD and, 1138

Spinal BMD changes and accumulated bone loss rate in Korean women, SU001

Age, Gene/Environment Susceptibility (AGES)-Reykjavik Study, SU334**Aggrecan**, SU048, SU088**Aging**. SEE ALSO *Aged*; *Age factors*

BMD and bone turnover in women associated with, SU006

Bone strength and BMD loss in spine and hindlimb of mice and, SU019

Changes in serum levels of OPG and RANKL and, SU004

Homocysteine modification of bone matrix proteins and, SU074

QTL influencing declines in bone quality related to, M112

ROS effects on bone and, F401, SA401

Sex differences in cortical bone mineralization in fibular shaft and, SU015

Sex hormone-binding globulin as negative independent BMD predictor for

Swedish men and, SU524

TGF- β 1 expression decreases and, SA162**Aging (animal models)**, 1140, M325, M489, SU384**Air pollution, BMD and**, M271**Akp2**, 1031**Akt**, 1068, M483**Akt1**, 1139**Ald1a2**, SU247**Alendronate**

Anabolic effect on bone through MSCs differentiation by, F412, SA412

BMD in men with prostate cancer treated with androgen-deprivation therapy and, SU121

Bone alkaline phosphatase *versus* total alkaline phosphatase and, SU141

Bone formation targeting by, M420

Key Word Index

ASBMR 27th Annual Meeting

Alendronate (Cont'd)

Bone loss in men with prostate cancer treated with androgen-deprivation therapy and, F381, SA381

Bone mineral/matrix changes in magnesium-deficient rats treated with, M321

Bone remodeling and histomorphometric patterns with, M358

Bone remodeling and microdamage accumulation with postmenopausal osteoporosis clinical doses of, 1081

Cortical bone effects in senile and severely osteopenic ovariectomized rats of, M489

Cost-effectiveness of PTH in high-risk osteoporotic women and, M405

Discontinuation, bone loss prediction with increased bone resorption after, F406, SA406

Discontinuation, in children with fracturing osteoporosis, bone status and, SU401

Discontinuation of long-term, change in bone turnover markers after, SU400

Drug-O-Gram of weekly doses illustrating utilization of, M363

Femoral neck bone loss in postmenopausal women with breast cancer after tamoxifen withdrawal and, SU108

Fracture risk reduction effects and, F425, SA425

Hip and nonvertebral fracture risk and, M356

Juvenile osteoporosis effects of, M368

Long-term liver or cardiac transplanted osteoporotic patients and, M477, WG6

Micro-CT of cortical and trabecular bone of transilial biopsy treated with, SU393

Monitoring, clinical performance of six TRAP assays for, SU147

Nonvertebral fracture risk for women without vertebral fracture with osteopenia and nonvertebral fracture history and, M355

Once-monthly ibandronate 150 mg treatment *versus* once-weekly 70 mg treatment with, M359

Once-weekly 35 mg treatment and BMD in Japanese osteoporosis patients, SU389

Once-weekly 70 mg treatment and bone metabolism of postmenopausal Korean women, M340

Once-weekly 70 mg treatment *versus* 10 mg once daily in osteopenia associated with primary biliary cirrhosis, SU392

One-year treatment effects in osteoporotic Japanese women, M343

Osteogenesis imperfecta type I treatment with weekly, SA443

Patient preferences for once-monthly ibandronate *versus* once-weekly, M435

PBMCs from patients with rheumatoid arthritis responses to, SU493

Periosteal and endocortical bone formation in ilium of osteoporotic women, F414, SA414

Periosteal bone formation in adult female ilium and, 1221

Persistence and adherence to, among chronic glucocorticoid users, SU390

PTH rechallenge one year after first PTH course and long-term, 1079

Raloxifene for bone loss prevention after estrogen therapy discontinuation in postmenopausal women *versus*, M354

RhBMP-2 effects on bone allografts and, M032

Risedronate effects on BMD and bone resorption in osteoporosis *versus*, SU395

Serum level cathepsin K changes in postmenopausal women treated with, SU274

Alendronate (Cont'd)

Upfront loading doses of, M369

Use of bone turnover markers to select osteopenic postmenopausal women for, SU151

Vitamin D insufficiency and impairment of postmenopausal osteoporosis treatment with, SU462

In vitro effects on apoptosis and death of macrophage-like cells and, SU299

Withdrawal in ovariectomized rats and cancellous bone remodeling, SA415

Women with impaired renal function and, SA413

Alendronate plus vitamin D₃

Once-weekly, M353

Alfacalcidol

Therapeutic uses of, SU457, SU458, WG4

Alkaline phosphatase

Alendronate effects on bone *versus* total, SU141

BMPs and primary human osteoblasts' differentiation, M022

Correlation between serum and salivary concentrations of, SU157

Hypophosphatasia and tissue nonspecific isoenzyme of, M442

Indomethacin and rate of production during osteogenesis of, M153

Pueraria thunbergiana enhancement of, SU233

Alveolar bones, SA082

Amelogenin, M205

Amenorrhea, M013, SU434. SEE ALSO *Menstruation*

AMG 162, SU304, SU446, SU453, SU455

Amino acids

Aromatic *versus* branched-chain, SU508

Phosphorylated, SA272

4-(2-Aminoethyl)-benzenesulfonyl fluoride hydrochloride (AEBSF), F023, SA023

Amish Family Osteoporosis Study, SU178

Amphiregulin, M492

ANABU (N-butyl glucosamine), M390, M418

Androgen-deprivation therapy, F381, SA329, SA381, SU121

Androgen receptor

Androgen action on cortical bone surfaces and, F515, SA515

BMP signaling effects on β -catenin and signaling by, SU117

Body fat, adipogenesis, osteoblast differentiation and, 1198

Genetic evidence of function in osteoclasts of, F509, SA509

Inactivation in mineralizing osteoblasts of, 1097

Inhibition of prostate cancer cell growth by Smad1 as co-repressor induced by PDF/BMP of, F129, SA129

Osteoblast proliferation, differentiation and, M196

Androgens

In premenopausal women, aging effects on, SU002

5 α -Androstane-3 β ,17 β -diol (3 β Adiol), urinary, SU522

Angiotensin-converting enzyme (ACE) inhibitors, SA296

Animal rights activism, M381

Ankyrin repeats

Notch signaling and action in osteoblasts and, M211

Annexin II receptor

Cloning and characterization of, F275, SA275

Anorexia nervosa, SA402, SA473. SEE ALSO *Eating disorders*

Antiepileptic drugs

Predictors of BMD in patients on, SA449

Antigens

Immune response, SU275

Antioxidants

Water fluoridation, postmenopausal women and, M270

Apolipoprotein A1 (ApoA1)

VDR antagonist ZK 191784 and gene expression by, SA517

Apolipoprotein E (APOE), M123

Apoptosis

Bovine articular chondrocytes, basic calcium phosphate crystals and, SU032

Caspase3 control in osteoblasts and osteoclasts of, SA189

Glucocorticoid-induced, MCP-3 and, SA285

Homocysteine in human BMSCs and, SU226

HSP60-induced, via ROS-mediated mitochondrial pathway and p38 activation in osteoblast-lineage cells, SU227

Osteoblastic activity in C3H/HeJ mice *versus* C57BL/6J mice and, SU229

Osteocalcin-A20 chimeric gene protection of osteoblasts from, SA193

In rheumatoid fibroblast-like synoviocytes, regulation of, M486

Smad4-induced, by inducing Bim alternative splicing as ER- α cofactor, 1117

Trichostatin A-induced, in osteoclasts, M245

Unloading and osteocyte *versus* osteoblast, 1092

Apyrase

Effect on ATP and fluid flow-induced proliferation of human MSCs, SU217

Aquaporin 9

Osteoclast differentiation and, SU278

Arachidonic acid

Metabolism manipulation, bone regeneration and, M166

Aromatase, M175, SU521, SU526, SU527

β -Arrestin, SA480

Arrestins, F397, SA397

Arthritis, 1196, M390, SU041, SU488. SEE ALSO *Osteoarthritis; Rheumatoid arthritis*

Asians, M003, SU003. SEE ALSO *specific ancestry groups*

D-Aspartic acid octapeptide (D-Asp₈), M420

ATDC5 cells, SU072, SU088

Atherosclerosis

Osteoporosis, abdominal aorta calcification and, SA337

Atorvastatin, M057, SU018

ATP6i

Expression in osteoblasts, M181

Atrasentan plus zoledronic acid

For prostate cancer metastasis to bone, 1213

Avon Longitudinal Study of Parents and Children (ALSPAC), SA299

AZD0530

Bone turnover in males and, M251

B

Back extensor strength, M431, SU439

Balance, postural, M313, SU444

BALB/c-MC cells, SU107. SEE ALSO *Breast cancer cells*

BALTO I study, M435

Bariatric surgery, M322, M336, M339

Basel Osteoporosis Study, SU166

Basic fibroblast growth factor (bFGF), M130, SA137, SU202, SU209

Bazedoxifene acetate (BZA), M394, SA431

Bcl-2, F142, F194, SA142, SA194

Bcl-2, F192, SA192

Bending motion, cyclic

Cartilage *versus* bone formation and, SU092

BetterBones Workshop, M085, SU321

Betula platyphylla var. japonica, SU056

Bim slicing

Smad4-induced apoptosis and, 1117

ASBMR 27th Annual Meeting

Key Word Index

Biom mineralization foci (BMF), F023, SA019, SA023

Biopsy

Iliac crest, F435, M087, M091, M102, SA435
MRI-based virtual bone, 1055, M295
Transilial, F414, SA414, SU393

Bioreactors

Cell cultures in, SU245, SU249

Bisphosphonates. SEE ALSO *Alendronate*;

Etidronate; *Ibandronate*; *Pamidronate*;
Risedronate; *Zoledronic acid*

Adherence, dosing frequency for
postmenopausal osteoporosis and,
M352

Adherence, factors influencing, M344

Adherence, fracture risk reduction in
postmenopausal women and, SU403

Adherence, nonvertebral osteoporotic fractures
and, SU417

Adherence of postmenopausal women with
osteoporosis to weekly *versus* daily,
SU397

Aromatase inhibition and BMD in mice and,
SU526

Bone mineral binding differences among, M351

Bone turnover markers in glucocorticoid-
induced osteoporosis and, M345

Calcium supplementation purchases by users of,
SU422

Cbfa1/Runx2 overexpressing mice for
evaluating efficacy of, SU399

Cell transduction mediators in osteoblasts and,
M221

Chronic dosing in rats, bone anabolic response
to PTH and, F220, SA220

Computer model of hydroxyapatite binding
affinities of, SU306

Daily or weekly adherence by French women
with osteoporosis, SU416

Daily supply of dietary calcium by women with
postmenopausal osteoporosis on,
SU398

Dietary calcium intake with early
postmenopausal osteoporosis, SU419

Drug-O-Gram illustrating utilization of weekly,
M363

Farnesyl diphosphate synthase crystal structure
and molecular interactions with, F408,
SA408

FDPS genetic polymorphism and therapeutic
response to, M118, SA121

GAPDH gene expression and, M060

GGPSI genetic polymorphism and therapeutic
response to, M118

Intravenous, effects after discontinuation in
children, SU396

Intravenous, osteonecrosis of jaw and, 1218

Literature-based meta-analysis relating BMD
increases and fracture risk reduction
with early suppression of bone turnover
markers, F404, SA404

Nitrogen-containing, purinergic receptor
signaling and, SU257

OPG delivery and retention to bone after
conjugation with, SU454

Osteogenesis imperfecta in children, site-
specific bone responses with, SU482

PBMCs from patients with rheumatoid arthritis
responses to, SU493

Periosteal osteoblast activity in rat femur and
tibia, SA409

Persistence and compliance with daily *versus*
weekly, M357

Persistence with ibandronate and cost-
effectiveness for postmenopausal
osteoporosis of, M361

Persistent usage of, hospitalization risk
reduction for osteoporosis fractures
and, SU388

Primary bone tumor cells *in vitro* and, SU094

Bisphosphonates. SEE ALSO *Alendronate*;

Etidronate; *Ibandronate*; *Pamidronate*;
Risedronate; *Zoledronic acid* (Cont'd)

Prophylactic administration during Gn-RH
agonist therapy for endometriosis,
M342

PTH effect in ovariectomized rats and humans
versus effect of, SU411

Resorbing osteoclasts and availability to non-
resorbing cells of, SU309

Statin therapy in osteoporosis patients
concurrent with, M366

UMR-106 cells' cultural milieu and effects of,
SU240

Upfront loading doses of, M369

Vitamin D, rationale for inclusion in current
osteoporosis treatment with, M360

In vitro effects on apoptosis and death of
macrophage-like cells and, SU299

Blacks, F474, M510, M517, SA474. SEE ALSO
African Americans; *African heritage*

Blomstrand lethal chondrodysplasia (BLC),
1086, SA488

Blood. SEE ALSO *Peripheral blood mononuclear
cells*

Calcification of elastic lamellae of devitalized
rat aortas incubated in, SA026

Daily, weekly, or monthly protocols to reach
desired concentration for elderly of
25(OH)D in, SU428

Early response of OPG from zoledronic acid
treatment in, SU206

Isolation and identification of factors inhibiting
myogenesis and inducing osteoblast
differentiation, SA161

Multipotent skeletal stem cells in, SU031

TRACP 5b stability in human samples, SU162

Bmx, SA276

Body composition

Age-related regional changes in healthy men,
M072

Assessment of total percentage of fat from spine
and femur DXA measurements in
Chinese, SU127

Bone loss and incident vertebral fractures in
women over 50 and changes in, SU358

Bone mass in adults and, SU320

Calcium supplementation in Korean
postmenopausal women and, SA422

Cycling exercise effects on, SU440

DHT in adult female estrogen-deficient,
osteopenic rat and, M402

GE Lunar Prodigy densitometry measurement
precision, SU132

GE Lunar Prodigy DXA prediction of fat and
lean composition in pigs, M077

HIV treatment and changes in, SU136

Lean *versus* fat mass as predictor of peak BMC
and BMD in mice on high-fat diet,
M006

Leptin, BMD, and fat *versus* lean mass, SU314

Multi-ethnic older men, F338, SA338

Reference values in normal Chinese women,
SU131

Serum IGF-I, IGFBP-3, and leptin levels in
children before and after liver
transplantation, M480

Sex-specific role of lean mass in femoral neck
BMD in parent-offspring pairs, SA115

Spinal cord injury and changes to, M452

Body fat. SEE ALSO *Adipose tissue*; *Fat tissue*

Androgen receptor and, 1198

Assessment of total percentage from spine and
femur DXA measurements in Chinese
of, SU127

Bone properties in prepubertal females and,
M021

DXA measurement of, M067

Body fat. SEE ALSO *Adipose tissue*; *Fat tissue*
(Cont'd)

Loss of ER α signaling via EREs, differential
effects on total body vs. marrow fat
and, F511, SA511

Physical loading and bone mass influences of,
M139

Vitamin D and milk intake by dieting young
women and, M272

Vitamin D content in, M339

Body height, F009, SA006, SA009. SEE ALSO
Height loss; *Skeletal growth*

Body size, SU016, SU485. SEE ALSO *Bone size*

Body weight. SEE ALSO *Body fat*; *Obesity*;
Overweight; *Weight loss*

BMD in women and, SU360

BMD predictor in Asian men and women,
SU003

Bone loss and incident vertebral fractures in
women over 50 and changes in, SU358

Fluctuation, mortality risk in elderly and,
SU343

Genetic factors in estrogen synthesis, activity
on peak bone mass and, SU184

Obesity and femoral neck structural strength in
women relative to, F179, SA179

Osteoporosis prevalence in older US women
and, M267

Peak bone growth in Japanese adolescents and,
M010

Very low birth, bone mass at lumbar spine in
young adults and, 1132

Whole body DXA of obese subjects treated with
carnitine and loss of, SU125

Bone acidic glycoprotein-75 (BAG-75), F023,
SA023

Bone allografts, M032. SEE ALSO *Transplantation*

Bone and cartilage stimulating peptides (BCSP),
M392, M429, SU263

Bone architecture. SEE ALSO *Bone geometry*; *Bone
microarchitecture*

Arrestins selective regulation of adrenergic
agonist effects on, F397, SA397

Biomechanical properties in two mice strains
and, SU193

Bone biomechanical properties in human
vertebrae and, SU084

Electromagnetic field treatment effects on
degeneration by hexa-chlorobenzene
of, SU065

HCN2 ion channels and regulation of, F039,
SA039

Hip structural analysis with segmented 3D CT
scans, M098

Human mandible, assessment of mechanical
significance by remodeling simulation
of, SU085

Leptin receptor and, 1108

Loading influences on, SU363

Loading modalities influence on non-weight
bearing and weight-bearing, SA178

Longitudinal assessment in women, SA359

Peripheral trabecular bone measurement in
osteopenic women with and without
fractures, F360, SA360

Propranolol effects on bone cell activity in
ovariectomized rat tibias and, M421

Trabecular, RANKL inhibition in female mice
and, SU452

Bone biomechanical properties

Aged male rats on caloric restriction and, M325

Body size, regional muscle strength, estrogen
status in women and, M096

Bone architecture in two mice strains and,
SU193

Bone microarchitecture and bone density
components of, M092

Cortical and trabecular architecture
contributions in human vertebrae to,
SU084

Key Word Index

ASBMR 27th Annual Meeting

Bone biomechanical properties (Cont'd)

- Cross section geometry of femoral neck and, F079, SA079
- Diabetes mellitus, type 2 and, M458
- Estrogen withdrawal, sensitivity to loading and, F181, SA181
- Finite element modeling of bone removal changes in, SU086
- Florida manatee, M145
- Orchidectomized rats treated with two doses of risedronate and, SA378
- PTH(1-84) treatment in osteopenic rhesus monkeys and, M415
- Soy isoflavones diet in rats and, M327
- Three-point bending of rat femoral midshaft in mediolateral plane for testing, SA184

Bone cancer, SA248. SEE ALSO *Bone metastasis*

Bone composition

- Mouse chromosomes influencing, M104

Bone diseases. SEE ALSO *specific diseases*

- TGF- β regulation of mechanical properties and composition of bone matrix and, SA163

Bone formation. SEE ALSO *Bone tissue*

engineering; Distraction osteogenesis; Fracture healing

- N-Acetylcysteine and, SA223
- Adipogenesis inhibition and, F513, SA513
- Adiponectin regulation of, 1047
- Automated volumetric imaging of *in vivo* labels for, M046
- BMP-stimulated, sclerostin inhibition of, 1029
- Bone and cartilage stimulating peptides derived from Col1a1 and, M429
- Bone resorption, caspase3 and, SA189
- Caf1 suppression of, F014, SA014
- Calcium release at dissolution of inorganic phase of bone and, M157
- Calcium/vitamin D₃ and low dose oral silicon and, SA421
- Cathepsin K inhibitor compound A in ovariectomized cynomolgus monkeys and, SU276
- Caveolin-1 deficiency and, F450, SA450
- Cbfb and Runx2-BMP signaling in, 1014
- CD34+ cells, 1066
- CD40 ligand and, F370, SA370
- Cortical, SB-462795 in ovariectomized cynomolgus monkeys and, F236, SA236
- Cyclic *versus* daily PTH and, 1180
- Disruption of Dkk-LRP5/6 interaction and, 1062
- Dkk proteins and, 1001
- DMP1 regulation of, 1111
- Ectopic, in response to BMP2 *versus* DBM, SA015
- Endochondral, BMP signaling stimulation of bone resorption and remodeling during, M034
- Endochondral, B-Raf kinase and, SU038
- Endochondral, CNP/GC-B system regulation of, F028, SA028
- Endochondral, 1,25(OH)₂D₃ suppression of, SA494
- Endochondral, Ihh signaling and Wnt/ β -catenin signaling in, 1003
- Endochondral, TGF- β signaling in, SA157
- Endochondral, transient receptor potential vanilloid 4 and, SU040
- Endochondral, *Trps1* transcriptional repressor role in, 1032
- Endochondral, Wdr5 interaction with Ihh and Wnt signaling pathways during, F041, SA041
- Endothelin-1 regulation of osteoblast secretion of paracrine regulators and, SU261
- Engrailed-1 pleiotropic functions in, 1185

Bone formation. SEE ALSO *Bone tissue*

engineering; Distraction osteogenesis; Fracture healing (Cont'd)

- Exercise protocols and equipment effects on, M137
- Extracellular matrix genes expression in demineralized bone-mediated, SU237
- GSK3 inhibitor 603281-8 and PTH actions in, F437, SA437
- HB954 expression in osteoblasts and, F199, SA199
- High fat/diabetogenic effects in congenic mouse with altered osteoblast differentiation on, 1035
- Hoxa-10 regulation of, 1013
- HSD2 overexpression and, SU520
- HSP60-induced apoptosis and p38 activation in osteoblast-lineage cells and, SU227
- IGF-1 in aged-mouse model, M005
- Inhibition by activated T lymphocytes, interferon- γ mediation of, F131, SA131
- Inhibition, transgenic expression of human Bcl-2 with osteoblast differentiation and, F194, SA194
- Leptin deficient Ob/Ob mice with adrenalectomy, γ -MSH administration and, SU027
- LMP-1 interaction with Smurf1 and cellular responsiveness to BMP-2 in, M027
- Metaplastic, BAMBI promoter hypermethylation and, M028
- Micro CT of bone implants and, M090
- Modified 8 amino acid peptide Ac-TTSGIHPK-amide derived from CXCL7 stimulation in ovariectomized rats of, M425
- Nell-1 induced, SU204
- Nf1* expression in osteoblasts and, 1051
- In non-hereditary heterotropic ossification, M449
- OSA peptide *in vitro* and *in vivo* stimulation of, M426
- OST-PTP and, SA040
- Overexpression of PAPP-A and, SA146
- Oxysterols and, M203, M427
- P2X7 receptor and, SU253
- Parietal, odd-skipped related 2 and, F208, SA208
- Periosteal, AAE581 in non-human primates and, 1179
- Periosteal and endocortical, in osteoporotic women treated with alendronate, F414, SA414
- Periosteal, endocortical, and trabecular envelopes of adult female ilium, SU368
- Periosteal, estrogen status and alendronate effects in adult female ilium and, 1221
- Periosteal, RANKL inhibition in orchiectomized rats and, 1226
- Periostin-like-factor and, SU077
- PGE₂ receptor subtype EP₄ receptor agonist and acceleration of, M161
- PKA and BMP signaling during, SU235
- PlexinD1 and patterning of, 1209
- Polymeric drug delivery systems targeting, M420
- Polyphenol extract from dried plum and, SU246
- Polyphenols from Greens+ herbal preparation and, M210
- Protein kinase C δ and Wnt-induced, SU268
- rhBMP-2 effects in biodegradable scaffold, SA018
- RhTGF β 2 effect in rat femur titanium implant model, SA159
- Ror2 and, M189
- Runx2 transcriptional repression by SOX9 during, 1017
- Seasonal vitamin D deficiency in French submarine patrols and, M268

Bone formation. SEE ALSO *Bone tissue*

engineering; Distraction osteogenesis; Fracture healing (Cont'd)

- Secondary mineralization in normal cortical bone, M047
 - Signaling selective PTH(1-34) analogs and, F481, SA481
 - Soluble silicon and seawater effects on, M329
 - TGF β 2 receptor and, F160, SA160
 - TSH in aged, ovariectomized rats and, M428
 - VEGF overexpression and aberrant, 1151
 - Vibration for mechanical stimulation of bone and, SU445
 - In vitro* indomethacin effects on cell number and AP production during, M153
 - In vivo* imaging of adenoviral *versus* lentiviral gene therapy models of, M023
 - Wnt signaling and increases in, M206
 - ZFP 521 overexpression and, 1183
- Bone geometry**. SEE ALSO *Bone architecture; Bone microarchitecture*
- β -Adrenergic blockers influences on, F345, SA345
 - Biomechanical differences between C57Bl/6 mice, C57Bl/6 mice and, M106
 - Bone strength of cancellous bone and, SA363
 - Changes in proximal femur in young female gymnasts, M020
 - Changes in proximal femur throughout life, SA087
 - Cross section of femoral neck, F079, SA079
 - Ethnic diversity in older men of, 1135
 - Femur, parity influence on, SU140
 - Gene search for femoral neck cross-sectional, 1211
 - Hip, genome-wide linkage of, SU175
 - Hip, hip fractures and, SU339
 - Hip, hormone interventions and, SA430
 - Image resolution properties of DXA scanners and measurement of, M099
 - Lasofloxifene protection against ovariectomy-induced deterioration of, M396
 - Oral contraceptive use in young women and, F353, SA353
 - Skeletal growth and, 1127
 - Spaceflight, long-duration, recovery after, 1172
 - Tennis-playing at distal radius and, SA186
 - In vivo* and *in vitro* accuracy measured by pQCT, M101
 - In vivo* reconstruction of human vertebrae with 3D-X-ray absorptiometry, M288
- Bone implants**. SEE ALSO *Titanium implants*
- Micro CT of new bone formation on, M090
 - Osteoblast activity inhibition from adherent endotoxin on, M194
 - In vitro* chondrointroduction by rhBMP-2/TGF β or demineralized bone powder, M025
- Bone loss**. SEE ALSO *Bone loss, inflammatory; Disuse osteopenia; Osteopenia; Osteoporosis*
- Age-related, PPAR- γ -activating oxidized lipids from Alox15 in mice and, 1140
 - Age-related spinal BMD changes in Korean women and accumulated, SU001
 - Alfacalcidol *versus* calcitonin therapy after renal transplantation in children for, SU457, WG4
 - AR inactivation in mineralizing osteoblasts and trabecular, 1097
 - Biliary cirrhosis in Japanese women and, SU315
 - In children, SU480
 - CHOP overexpression and, F206, SA206
 - Chronic mild stress in mice and, SU377
 - CIZ action in mechanical and estrogenic signaling in disuse and ovariectomy-induced, F174, SA174
 - Continuous PTH treatment and upregulation of T cells localization to bone surface, 1049

Bone loss. SEE ALSO *Bone loss, inflammatory; Disuse osteopenia; Osteopenia; Osteoporosis* (Cont'd)

Coronary artery disease in aged rat model and chronic inflammation-induced, SU384
Darglitazone treatment and, SA394
Dietary quercetin in ovariectomized mice and inhibition of, M328
Docosahexaenoic acid *versus* eicosapentaenoic acid in ovariectomized mice and, SA132
Finite element analysis of bone biomechanical properties after, SU086
Gastrectomy in Japanese and, M303
Genetic effects in peri- and postmenopausal women, SA113
Glucocorticoid-induced, CD40 ligand and, F370, SA370
In inflammatory bowel disease, vitamin D and vitamin K deficiencies and, M333
Infliximab treatment for rheumatoid arthritis and, M389
Lactating IL-1R1-/- mice, in femur but not spine, SU212
Longitudinal, population-based study of trabecular bone in young adult women and men, 1010
Mexican American heritability of change of BMD and, F100, SA100
Mortality risk in elderly and, SU343
In older men who drink milk fortified with calcium and vitamin D₃ and, F419, SA419
Ovariectomy in cathepsin K knockout mice and, F234, SA234
Ovariectomy in cathepsin K knockout mice and MMP inhibitor attenuation of, SA233
Ovariectomy-induced systemic, sclerostin-neutralizing monoclonal antibody effects on, 1082
Ovariectomy induced, thymic T cells output and, 1115
Phenolic compounds in safflower seeds and ovariectomy-induced, SA514
PPAR γ 2 effects in diabetes mellitus, type 1 and, F399, SA399
Prediction over 5 years after alendronate discontinuation, F406, SA406
Rate in perimenopausal women, ER β gene polymorphisms and, SU005
Self-rated health status, forearm BMD and, SA300
Sevelamer hydrochloride in aged ovariectomized rats and, SU431
Smoking, estrogen deficiency and, SA200
Spinal cord injury in mice and, SA448
TSH in aged, ovariectomized rats and, M428
TSHR D727E polymorphism in women from UK and, M115
Unloading-induced, ventromedial hypothalamus mediation of, F393, SA393
Vibration for mechanical stimulation of bone and, SU445

Bone loss, inflammatory. SEE ALSO *Osteoarthritis; Rheumatoid arthritis*
Expression of RANKL mRNAs in cell types associated with, M243**Bone markers**

Age-dependent changes in mineral metabolism in 461 Chinese, M001
Antiresorptive therapy compliance by postmenopausal osteoporotic patients and short-term monitoring of, SU409
Baseline, predicting 2-yr. change in BMD in systemic lupus erythematosus with, SU490
Bisphosphonates for glucocorticoid-induced osteoporosis and, M345

Bone markers (Cont'd)

Bone architecture in women and, SA359
Clinical performance of six TRAP assays and, SU147
Correlation between serum and salivary concentrations of, SU157
Discontinuation of long-term alendronate and changes in, SU400
Discontinuation of long-term oral low-dose hormone replacement therapy and, SU143
DMPA effect on, SU156
Early implant performance correlating bonding strength with titanium implants and bone, SA045
Ethnic differences in bone metabolism, fracture risk, SU372
Fracture effects in daily clinical practice on, SU155
Homocysteine serum levels and, SA328
Infliximab effects in rheumatoid arthritis on, SU495
Lasofloxifene effects in postmenopausal women on, F429, SA429
Literature-based meta-analysis of bisphosphonates relating BMD increases and fracture risk reduction with early suppression of, F404, SA404
Lycopene consumption in postmenopausal women and, SA308
Mathematical model of bone remodeling in rats, predictions of PTH(1-34) dose response by, SA484
Men with celiac disease, idiopathic vertebral fracture and, SA383
Mortality in frail elderly and, 1133
Nonvertebral fracture prediction and, SA350
Once-monthly oral ibandronate in postmenopausal osteoporosis and, SU410
Osteoarthritis, SU153
Oxidative stress markers and, F391, SA391
Postmenopausal osteoporotic women compared to premenopausal reference range, SU159
Postmenopausal women with accelerated bone turnover and, SA298
Post-parathyroidectomy bone mass changes predictions and, SU469
Raloxifene and osteoporosis pretreatment for one year in postmenopausal women, M397
Raloxifene effects in postmenopausal Korean women with osteoporosis, SA424
Reference range in premenopausal oral contraceptive users and nonusers, SU158
Risedronate discontinuation and magnitude of change in, M377
SELDI-TOF mass spectrometry diagnosis of postmenopausal osteoporosis, SU150
Teriparatide treatment for severe osteoporosis, one month treatment and changes in, M408
TRAP 5b, number of osteoclasts in human osteoclast culture, SU303
rTSH and, SU378
Ultra long distance female runners *versus* sedentary women, M143
Vitamin D and calcium treatment for low-energy fractures and, SU459

Bone marrow

Chronic monitoring in rats of telemetered intramedullary pressure, SA059
Leptin and adipocyte populations in, M233
Monoclonal gammopathies and dendritic cells in, SA061
Osteoclastogenesis and microenvironment of multiple myeloma, SU201

Bone marrow (Cont'd)

Quantitative analysis of, as source for connective tissue progenitors, M230

Bone marrow cells

Postmenopausal women, estradiol and *in vitro* osteoclastogenesis, RANKL expression in, F374, SA374

Rat, *in vitro* osteogenic response to bFGF and BMP-2, SU202

Bone marrow macrophages (BMM ϕ)

BMSCs modulation of contributions to TNF α -induced osteoclastogenesis *in vivo* by, F247, SA247

Cell cycle progression and arrest for RANKL-induced osteoclastogenesis in, M244

Bone marrow mononuclear cells (BMMNC), SA259, SU249**Bone marrow sinusoidal endothelial cells, M332**
Bone marrow stromal cells (BMSCs)

Aging and responsiveness to IGF-I through down-regulation of IGF-I signaling pathways by, SU012

Col1 mRNA expression in osteoblast lineage cells *versus*, 1044

Human, 1,25(OH)₂D₃ and 25(OH)D₃ effects on osteoblastogenesis, M155

Human, age-related PTH responses in, M004

Human, connective tissue growth factor and attachment onto hydroxyapatite scaffold *in vivo* by, SU062

Human, homocysteine and apoptosis via ROS-mediated mitochondrial pathway in, SU226

Human, mechanical strain and FosB expression in, M180

Human, statins and differentiation into osteoblasts of, SU234

Intracellular fate of plasmid DNA and non-viral carriers in, SU215

Lacking VDR, adipogenesis enhancement in, F496, SA496

Modulation of macrophages and T-cells contributions to TNF α -induced osteoclastogenesis *in vivo*, F247, SA247

Murine, heparin effects on adipogenesis in, M237

Murine, inhibin A effects not mediated by FSH and LH in, SU250

ONO-4819 and BMP-induced differentiation via PKA signaling in, M031

Rabbit model, NaOH and osteogenesis on PLGA scaffolds of, SU058

Regulation of thrombospondin-2 expression during differentiation of, SA038

Stromal derived factor-1 α role in, M236

Temporal dependence on PTH(1-34) for anabolic actions in, M487

3-dimensional matrices for *in vitro* study of, SA219

VCAM-1 positive, calcium receptor expression and, M229

Bone mass. SEE ALSO *Bone mass, peak; Bone size*

Age-related regional changes in healthy men, M072

Age, sex, growth variables in healthy children and acquisition of, M011

Akt1 and maintenance of, 1139

AMG 162 in cynomolgus monkeys and, SU453

AMG 162 pharmacokinetics after subcutaneous dosing in postmenopausal women, SU446

Arrestins selective regulation of adrenergic agonist effects on, F397, SA397

Bazedoxifene acetate in ovariectomized cynomolgus monkey and, SA431

Beta blockers for cardiovascular disease and, 1040

Key Word Index

ASBMR 27th Annual Meeting

Bone mass. SEE ALSO *Bone mass, peak; Bone size* (Cont'd)

Birthsize, adult size and body composition effects on, SU320
 Body size, regional muscle strength, estrogen status in women and, M096
 Brain natriuretic peptide and, SU379
 β -Catenin haploinsufficiency and reduced, F229, SA229
 Chinese American women with osteoporosis and, SU129
 Circulating OPG levels and COL1A1 polymorphism in postmenopausal women and, SU374
 CP432 restoration in aged ovariectomized rats, M419
 Diphtheria toxin receptor expression in osteoblasts, osteocytes and, F289, SA289
 ER α signaling via EREs in male mice and, 1142
 ER β gene polymorphisms in men and women and determination of, SU186
 Fat intake and, M337
 Gene on congenic (alcohol preferring or non-preferring) rat chromosome 4 affecting, F110, SA110
 GGHRV12, GGSRV02, GHRHV10 and, SA119
 G-protein coupled receptor kinases and, F225, SA225
 Growth- and age-related deficits in women with low volumetric BMD, SU316
 HCN2 ion channels and regulation of, F039, SA039
 Intermittent PTH effects in ovariectomized rats on, SA436
 Leptin gene therapy effects on weight loss in female rats and cancellous, 1048
 Loading influences on, SU363
 LRP6 in *ringelschwanz* mutant mice and acquisition of, 1181
 Mx2, canonical Wnt signals and, 1004
 Newborns, genetic and maternal determinants at humerus in, M016
 Oral contraceptive use in young women and, F353, SA353
 PGE₂ receptor subtype EP₄ receptor agonist and, M161
 Physical loading and body fat influences on, M139
 Pre- and postmenopausal women, 10-year follow-up study, SU009
 Rac-2—reduced osteoclast function and increased, F270, SA270
 RANKL effects in mice on, SA357
 Receptor for advanced glycation end products and regulation of, SA271
 Response to D-galactose, sex differences in, SU365
 Runx2 with deleted or expanded QA domain and, F214, SA214
 SB-462795 in ovariectomized cynomolgus monkeys and, SA235
 Serum homocysteine levels in postmenopausal women and, SU373
 Social position in pregnancy and childhood, SA299
 Soy isoflavones diet in rats and, M327
 Trabecular, global knockdown of calcitonin receptor in young female mice and, 1161
 Treatment of adults with endogenous Cushing's syndrome and, SA369
 Very low birth weight effects at lumbar spine in young adults of, 1132
 ZFP 521 overexpression and, 1183

Bone mass, peak

After childhood acute lymphoblastic leukemia, SU477
Akp2 regulation in mice of, 1031

Bone mass, peak (Cont'd)

C-864T polymorphism in LRP5 and, SU191
 Consolidation determinants in young women, M015
 Cx43-/floxOCN^{Cre} mice lacking connexin43 and, F286, SA286
 Genetic and gender regulation in congenic strains for mouse distal chromosome 1 of, F114, SA114
 Genetic factors related to estrogen synthesis and activity on, SU184
 LRP5 gene polymorphism in men and, SU189
Bone matrix. SEE ALSO *Matrix calcification*
 Histological analysis of warfarin-treated rats and, SU023
 Homocysteine modification of, SU074
 Mapping calcium, phosphorus, and magnesium, in klotho mouse mineralization of, SU025
 Mineralization suppression with adenovirus-mediated FGF23 overexpression, SA139
 QTL on mouse chromosome 12, bone nanoindentation regulation by, SU182
 Raman spectroscopy of bone mineral crystallinity in, SA284
 Solid bone of rat imaging using water and fat suppressed proton magnetic resonance imaging, SU145
 TGF- β regulation of mechanical properties and composition of, SA163
Bone metastasis. SEE ALSO *Breast cancer metastasis to bone; Prostate cancer metastasis to bone*
 Bone resorption sites and, F072, SA072
 α -CTx as indicator for, F074, SA074, SU116
 DXA for detection of early osteolytic, M084
 Hepatocyte growth factor role in, SU107
 Osteoclastic function in microenvironment of extracellular matrices in, SU271
 PGE₂ EP₄ receptor and osteolysis action in, F062, SA062
 Renal cell carcinoma, MMP regulation of TGF- β in, F156, SA156
 Renal cell carcinoma, TGF- β stimulation of IL-6, PDGF-AA, and VEGF in, 1126
 Tumor expression of RANKL and BMPs influences lung cancer, F135, SA135
 Zoledronic acid and PTH(1-34) combination after radiation therapy for, SU112

Bone microarchitecture. SEE ALSO *Bone architecture; Bone geometry*

β -Adrenergic blockers influences on, F345, SA345
 Biomechanical properties of trabecular bone in femoral neck and, M092
 Evaluation *in vivo* in humans, M086
 Of forearm and tibia in young healthy women, M093
 Fructo-oligosaccharides and soy isoflavones effects on, SU432
 Genetic diversity intrinsic to fracture healing and, SA101
 Idiopathic osteoporosis in premenopausal women and, SU361
 Intermittent PTH effects in ovariectomized rats on, SA436
 Lasofoxifene protection against ovariectomy-induced deterioration of, M396
 Mild primary hyperparathyroidism and, M461
 Osteogenesis imperfecta and variability in, SA441
 Of pre- and postmenopausal trabecular bone, F358, SA358
 Radiation therapy and, SA398
 Strontium salts effects in rats on, SU028

Bone microarchitecture. SEE ALSO *Bone architecture; Bone geometry* (Cont'd)

3D, longitudinal changes in iliac crest bone biopsies in postmenopausal women with osteoporotic vertebral fractures, M102
 2D lateral spine radiographs of vertebral trabecular, SA091
 Vertebral, multidetector row computed tomography of, F362, SA362
Bone mineral content (BMC)
 Age, sex, growth variables in healthy children, M011
 Alendronate treatment for one-year in osteoporotic Japanese women and, M343
 Bone size in children and, SU126
 Of children's heads relative to total body values for, M019
 Lean *versus* fat mass as predictor in mice on high-fat diet of peak, M006
 Pre- and postmenopausal women, 10-year follow-up study, SU009
 Rats with testicular torsion, detorsion, and orchiectomy, SA382
Bone mineral density (BMD)
 ACE inhibitor use in older Chinese and, SA296
 β -Adrenergic blockers influences on, F345, SA345
 African American genetic markers for ancestry and, M103
 Aged male rats on caloric restriction and, M325
 Age-related loss in spine and hindlimb of mice, bone strength and, SU019
 Aging in women and changes in, SU006
 Air pollution and, M271
 Alendronate treatment for one-year in osteoporotic Japanese women and, M343
 Alendronate treatment once-weekly in osteoporosis patients and, SU389
 Alendronate *versus* risedronate for osteoporosis and, SU395
 AMG 162 and increases in, SU304
 Anorexia nervosa, serum OPG levels and, SA402
 Antiepileptic drugs and patients on, SA449
 Baseline, 2-yr. change in BMD in systemic lupus erythematosus and, SU490, SU492, SU494
 Baseline, risedronate's antifracture efficacy and, M367
 Bone strength in glucocorticoid-induced osteoporosis *versus*, 1197
 N-Butyryl glucosamine effects in ovariectomized rats on, M418
 CAST chromosome 1 QTL and, F102, SA102
 Chondrocyte-specific disruption of IGF-1 in mice and, 1152
 COX-2 inhibitors effect on, 1076
 Cx43-/floxOCN^{Cre} mice lacking connexin43 and, F286, SA286
 Decreased, increased cholesterol levels in women aged 65 years and older, SU130
 Depression in postmenopausal Korean women and, SU350
 Diabetes status and testing in men and women, M304
 Distribution in premenopausal women with idiopathic osteoporosis, 1175
 DXA measurements, calcium supplements and, M068
 Endometriosis treatment with DMPA-SC 104 *versus* leuprolide acetate and, SU517
 Erythropoietin in elderly men and, SA303
 Estimated volumetric, in rural Thai men and women, M066
 Evolution in young premenopausal women with idiopathic osteoporosis, SU421

Bone mineral density (BMD) (Cont'd)

Family physicians testing, M310
Farnesyl diphosphate synthase in elderly women and, SU185
In female adolescents, determinants of, SA001
Femoral neck, sex-specific role of lean mass in parent-offspring pairs of, SA115
Femoral neck trabecular and cortical volumetric correlates of, 1073
Forearm, self-rated health status, bone loss and, SA300
Fracture risk categorization and, 1037
Fracture risks in Hispanics and, M308
Fragility fractures during risedronate treatment and changes in, SA405, SA407
Gender-specific profile, forearm fractures and, M286
Genetic epistasis and genomic regions identified for, SU179
Genetic influences on age-related changes in, M314
Genomic variation in Wnt10b of men and, F341, SA341
Glucocorticoid action on osteoclasts and reductions in, F367, SA367
Hip fractures and, SU339
Hip, in multi-ethnic older men, F338, SA338
Hip, in premenopausal women, aging effects on, SU002
HIV-positive women and, SU347
Hormone replacement therapy discontinuation and, SU143
Human, PPAR γ gene polymorphisms and, SU194
Hypertension, PTH levels and, SU507
Hypoparathyroidism and distribution of, SU470
IL-1 system gene polymorphism effects after HRT in postmenopausal women on, SU183
Intravenous ibandronate for postmenopausal osteoporosis and, SU413
Inulin *versus* fructo-oligosaccharides enhancement in rats of, SA420
Lasofoxifene effects in postmenopausal women on, F429, SA429
Leptin, fat mass, lean mass and, SU314
Lifestyle factors and pQCT assessment at mid-radius of, M277
Low, absence of BMP-2 and, 1025
Low volumetric in women, growth- and age-related bone mass deficits and, SU316
Lumbar, and raloxifene in postmenopausal Korean women with osteoporosis, SA424
Lumbar, in Korean women with and without metabolic syndrome, SA400
Lumbar, women with postmenopausal osteoporosis treated with teriparatide and, M410
Measurement in older women, fracture prediction and, 1057
Measurement, osteoporosis prevalence and, SU313
Menstrual irregularities in high school runners and, SU356
Menstrual subclinical irregularities in premenopausal women and, M316
Men with celiac disease, idiopathic vertebral fracture and, SA383
Men with untreated Graves' disease and, SU375
Mexican Americans and, F100, SA100, SU195
Microdamage accumulation in postmenopausal women and, F356, SA356
Mid-shaft of human femur, bone turnover and, SA049
Modified 8 amino acid peptide Ac-TTSGIHPK-amide derived from CXCL7 increases in ovariectomized rats of, M425
Myocardial infarction survivors, M299

Bone mineral density (BMD) (Cont'd)

OPG promoter polymorphism in older women, fracture risk and, 1039
Orange pulp or juice diet for orchidectomized rats and, SU013
Osteoporosis management and access to testing, SU312
Overweight but not obesity in women and, SU360
Oxidative stress markers and, F391, SA391
Patients with fractures, SA295
Peak, admixture mapping, SU176
Peak, lean *versus* fat mass as predictor in mice on high-fat diet of, M006
Polychromatic micro-computed tomography of, M069
Postmenopausal women with accelerated bone turnover and, SA298
Prediction over 15 years, incident vertebral fractures and, F297, SA297
PTH1R phosphorylation and anabolic effect of intermittent PTH administration on, 1159
Raloxifene and osteoporosis pretreatment for one year in postmenopausal women and, M397
In rats with testicular torsion, detorsion, and orchiectomy, SA382
Relatives of individuals with osteogenesis imperfecta and, 1089
Reporting tool development and testing, M071
Risedronate discontinuation and magnitude of change in, M377
Risedronate, vitamin D, or vitamin K effects in Japanese osteoporosis patients on, SU408
Serotonin, long-term administration and, SU213
Serum leptin and adiponectin concentrations in Korean postmenopausal women, SU211
Sex differences in bone size in children and, SU318
Sex hormone-binding globulin as negative independent predictor for elderly Swedish men of, SU524
Sex steroids as predictor in elderly Swedish men of, SA510
Short-term and long-term absolute fracture risk by age and, 1138
Short-term effects of estrogen, tamoxifen, and raloxifene on, M393
Site-discordance of osteoporosis categorization in menopausal women using, F077, SA077
Site-specific fracture risk differences among older osteoporotic women and, F325, SA325
Skeletal growth and, 1127
Sox4, osteoblast regulation and, SU232
Spaceflight, long-duration, recovery after, 1172
Stress fractures of lower extremity and, M448
Teriparatide treatment for 12 months in postmenopausal osteoporosis and, SA432
Teriparatide treatment for osteoporosis in women and, 1223
Thiazide, NSAIDs, and steroids use by men and, M307
Thyroxine treatment for thyroid carcinoma and, SA390
Total body, GE Lunar Prodigy densitometry measurement precision, SU132
T-scores of -2.5 in men ages 50–65, M301
Valproic acid in juvenile Sprague-Dawley rats and, SA302
Vertebral fractures, monoclonal gammopathy of undetermined significance, and lumbar, SA392
Vertebral fractures with COPD and, SA342

Bone mineral density (BMD) (Cont'd)

Vitamin D and calcium treatment for low-energy fractures and, SU459
Vitamin K₁ intake in perimenopausal women and, SU423
Vitamin K in postmenopausal women and, SU425
Volumetric, ethnic diversity in older men of, 1135
Whole body and hip, in older Americans, dietary acid and, F306, SA306
Young male monkeys treated with SB-462795 and, F232, SA232

Bone mineralization. SEE ALSO

Hypomineralization; Matrix calcification

Bone turnover at mid-shaft in human femur and, SA049
Cortical, aging and sex differences in fibula, SU015
Cortical, secondary mineralization in, M047
Fibronectin control of, 1054
In klothe mouse, mapping calcium, phosphorus, and magnesium in, SU025
MEPE-ASARM peptide-associated defects in X-linked hypophosphatemia of, 1163
Polychromatic micro-computed tomography assessment of, M069
Of rachitic growth plate despite calcium deprivation leading to hypocalcemia, SU024
Recovery from dietary calcium deficiency in pigs of, SU017

Bone morphogenetic protein-2 (BMP-2)

Absence of, skeletal growth, development and, 1025
Activation of β -catenin signaling in osteoblasts by, SA226
Bone regeneration and regulated gene therapy with, M038
 β -Catenin recruitment to Smad-containing complexes by, 1109
Dishevelled-Smad1 interaction links Wnt/ β -catenin signaling in osteoblast progenitors with signaling by, F133, SA133
Ectopic bone formation in response to DBM *versus*, SA015
Gli2 signaling molecule and effects on chondrocytes of, 1154
LMP-1 and human MSCs' responsiveness to, M193
LMP-1 synergy with, M027
Osteoactivin expression regulation through Smad-1 signaling during osteoblast differentiation by, M039
Osteoporosis-associated traits in women and, M033
P300 regulation of Id1 gene promoter and, SA201
PEMF and, effects on osteoblastic cell proliferation, gene expression, M040
Phospho-CREB transcription factor and expression in murine osteoblasts of, M174
PI 3K and MAPK signal relay in statin-induced expression of, F227, SA227
Recombinant human, alendronate effects on bone allografts and, M032
Recombinant human, and bone formation in biodegradable scaffold, SA018
Runx2 and osteogenic activity by, 1015
Runx2/Cbfa1 gene transcription and, M188
Runx2-Smad physical association and bone formation induced by, 1030
T3, insulin and redifferentiation of dedifferentiated chondrocytes and, SA034
Tendon formation induced by manipulation in MSCs of, SU061

Key Word Index

Bone morphogenetic protein-2 (BMP-2) (Cont'd)
3-dimensional matrices for *in vitro* study of MSCs and, SA219

In vitro osteogenic response of rat bone marrow cells to, SU202

Bone morphogenetic protein-3 (BMP-3)
Signaling through SMAD2 in MC3T3 cells, M026

Bone morphogenetic protein-4 (BMP-4)
Blood serum, osteoblast differentiation and myogenesis inhibition by, SA161
HSPGs mediation of signaling in fibrodysplasia ossificans progressiva lymphoblastoid cells and, M029
Postnatal role in osteoblast function and bone quality for, 1026

Bone morphogenetic protein-6 (BMP-6)
Bone restoration in aged osteoporotic rats and ovariectomized knockout mice, 1027
Primary human osteoblasts' differentiation and, M022

Bone morphogenetic protein-7 (BMP-7)
Androgen receptor signaling effects on β -catenin and signaling by, SU117
Calcification stimulated in VSMC by, F021, SA021
Renal osteodystrophy and, M035
Vascular calcification and renal osteodystrophy treated with, F016, SA016

Bone morphogenetic protein and activin membrane-bound inhibitor (BAMBI)
Metaplastic bone formation and, M028

Bone morphogenetic proteins (BMPs)
Bone remodeling during endochondral bone formation and fracture repair stimulated by, M034
Cbfb in bone formation and, 1014
ColX gene expression in prehypertrophic chondrocytes and retinoid stimulation of signaling by, 1022
Dlx5 transcription factor and cooperative interaction of Runx2 with, F012, SA012

Inhibition, osteolytic metastatic prostate cancer tumor formation and, SA069

Matrix vesicles as carriers of, M030

Metastatic lung cancer in bone and tumor expression of, F135, SA135

Molecular dissection in fibrodysplasia ossificans progressiva lymphoblastoid cells of signaling by, SA011

Notch1 overexpression, inhibition of osteoblastogenesis and signaling by, M223

ONO-4819 and bone marrow stromal cells differentiation via PKA signaling induced by, M031

Osteoblast senescence, c-Abl and signaling by, M225

Osteosclerosis from GATA-1 expression impairment and BMPs expression and of BMP receptors, SA013

PKA signaling during osteogenic differentiation of hMSCs and, SU235

Primary human osteoblast differentiation and, M022

PTHrP signaling during mammary gland development and signaling by, 1157

SARA β regulation of gene expression in xenopus and human osteoblast differentiation induced by, 1028

Schnurri-2 activation of bone remodeling by coupling to, 1052

SOST expression in calvaria organ culture and, SU209

Suppression of Smad6 expression by pentoxifyline and cAMP treatment of, SA017

WISP-1 splice variants and possible relationship with signaling by, SU081

Bone morphogenetic protein/Smad signaling

CHOP interaction with CREM and, M024

Bone morphogenetic proteins receptor 1A (*Bmpr1a*), 1034

Bone pain. SEE *Pain, skeletal*

Bone quality. SEE ALSO *Microdamage accumulation*

Accretion in developing murine skeleton, M018

Genetic loci influencing age-related declines in, M112

Hypoparathyroidism and, SU465

Strontium ranelate and, M140

Targeted deletion of BMP4 in adult mice and, 1026

Vibration-enhanced bone formation in skeletal growth and, M150

Bone regeneration. SEE ALSO *Fracture healing*

Anterior cruciate ligament-induced hemarthrosis of knee as cell source for, M200

Biological effects of self-setting α -tricalcium phosphate on dental implants and, SU057

Bromodeoxyuridine and preosteoblast tracking in, M043

Cbfa1/Til-1 overexpression, M168

Human bone-marrow derived MSCs, migration in response to cue for, 1065

Hydroxyapatite and polylactic acid plate in rats and, SU068

Intermittent PTH in normal and ovariectomized rats, F433, SA433

Intraarticular osteochondral fracture-induced hemarthrosis and, M163

Mustang gene promoter in, SA042

Nell-1 induced, SU204

Regulated BMP2 gene therapy for, M038

TM promotion of chondrogenesis and, SU033

Type I diabetes rat model, osteoactivin and, SU251

Bone remodeling

Adiponectin and, SU205

Aging in women and, SU006

Akt1 and maintenance of, 1139

Alendronate and histomorphometric patterns in, M358

Aromatic *versus* branched-chain amino acid effects on, SU508

AZD0530 in healthy men and, M251

Cancellous, alendronate or risedronate withdrawal in ovariectomized rats and, SA415

Candidate gene on chromosome 10 affecting serum IGF-I, BMD and, 1212

Children with Crohn disease and, SA477

Comparison of risedronate, vitamin D, or vitamin K in Japanese osteoporosis patients on, SU408

Cyclin D1 promoter transcriptional activation by PTHrP and, SA195

Dynamic muscle contraction, interstitial fluid flow and, F185, SA185

Early change after teriparatide in, M412

Formation of T cell niches at resorption sites after ovariectomy and, F395, SA395

FSHR deficiency in female mice and, SA516

Hyperhomocysteinemia restoration by folate therapy and, SU380

Hypoparathyroidism and PTH improvement of, SU467

Idiopathic osteoporosis in premenopausal women and, SU361

IGF-I in adolescent girls with type 1 diabetes and, SA469

Leptin effects in rodents and sheep on, SU210

Mid-shaft of human femur, mineralization and, SA049

Oral ibandronate and activation frequency of, M364

Bone remodeling (Cont'd)

Placental growth factor regulation of, F253, SA253

Prostate cancer bone metastasis, mechanism of, SU049

RAGE null mice and enhanced, M456

Rat cycle, mathematical model predicting bone marker response to PTH(1-34) dosing, SA484

Schnurri-2 coupling to BMP and RANKL and activation of, 1052

Serum homocysteine levels in postmenopausal women and, SU373

Simulation for assessing mechanical significance of mandibular bone structure, SU085

Stromal derived factor-1 α role in, M236

Strontium ranelate in postmenopausal osteoporosis and, 1084

Teriparatide effects on, M416

TIEG role in, SU010

Treatment of adults with endogenous Cushing's syndrome and, SA369

Urokinase receptor role in, M246

Vitamin K in postmenopausal women and, SU425

Bone remodeling markers. SEE *Bone markers*

Bone resorption

AAE581 prevention after oral treatment in rat, monkey and, SU270

Alendronate *versus* risedronate for osteoporosis and, SU395

AMG 162 and suppression of, SU304

Anisotropic, in human cortical bone, SU310

Attenuation of, c-Src recruitment of SHIP to podosomes in osteoclasts and, M254

Bisphosphonates availability to non-resorbing cells of mineralized tissues, SU309

Bone formation, caspase3 and, SA189

Bone loss prediction over 5 years after alendronate discontinuation and, F406, SA406

Calcitriol effects against, PTH secretion suppression and, F520, SA520

Calcium release at dissolution of inorganic phase of bone and, M157

Calcium-sensing receptor mediation of strontium ranelate effects on, SU511

Caspase-2 deficiency and age-associated increase in, 1141

Cathepsin K siRNA transfection inhibits in primary human osteoclasts of, SU307

CD40 ligand and, F370, SA370

Cortactin-induced actin assembly and, SA245

CTX/TRACP 5b ratio as index for, SU290

Estrogen-regulated, calcium channel antagonists and, SU014

FSH regulation of, F376, SA376

Gene therapy with RANK-Fc in ovariectomized mice and, M430

High serum concentrations of low-density-lipoprotein and, SU239

IL-1 β -induced, kinins and, M154

Impaired Csk recruitment into lipid rafts from decreased Cbp expression and, 1146

Index (CTX/TRACP 5b) as useful tool in rat orchidectomy model, SU161

Integrin-linked kinase inactivation and inhibition of, 1147

LIF *versus* OSM stimulation of, SU208

Lipopolysaccharide and phenytoin suppression, PGE₂ production in, SU301

Low levels of, polycystic ovary syndrome in obese adolescents and, SU474

LRP6 in *ringelschwanz* mutant mice and, 1181

Lycopene consumption and biomarkers in postmenopausal women for, SA308

Modulation of osteoclast activity by advanced glycation end products and, SU075

Bone resorption (Cont'd)

Nf1 expression in osteoblasts and, 1051
 Nocturnal, GLP-2 in postmenopausal women and, 1225
 Old bone as target for osteoclasts in, M241
 p38 MAPK mediation of metabolic acidosis-induced, SU258
 Phosphothreonine, phosphotyrosine and, SA272
 Polymeric drug delivery systems targeting, M420
 PTH radioisotope OSC after ovariectomy and, M403
 Rab3D mediated by Tctex-1 and vesicular trafficking during, M264
 Rab3D regulation of vesicular trafficking pathway in, M263
 Risedronate reduction in two weeks of, SU407
 Rosuvastatin inhibition of, SU308
 SB-462795 inhibition of cathepsin K and *in vitro* and *in vivo* inhibition of, SA231
 Seasonal vitamin D deficiency in French submarine patrols and, M268
 Short-term effects of estrogen, tamoxifen, and raloxifene on, M393
 Skeletal colonization by tumor cells and sites of, F072, SA072
 Suppression by cathepsin K inhibitor compound A in ovariectomized cynomolgus monkeys, SU276
 T cells activation and IFN γ effects on, F387, SA387
 Thyroxine treatment for thyroid carcinoma and, SA390
 Urinary tritiated tetracycline assessment of ovariectomy stabilization and diet effects in rats on, SU011
 Young male monkeys treated with SB-462795 and, F232, SA232
 Zinc supplementation and, SA416
 Zoledronic acid, single intravenous dose, effects after 18 months of, SU164

Bone resorption markers. SEE *Bone markers*

Bone Safety Evaluation, balance domain validation, SU444

Bone size. SEE ALSO *Bone mass*

African American genetic markers for ancestry and, M103
 BMC in children and, SU126
 CAST chromosome 1 QTL and, F102, SA102
 Caveolin-1 and, 1182
 Chondrocyte-specific disruption of IGF-1 in mice and, 1152
 Diet in ovariectomized ER α receptor knockout mice and, SU418
 Linkage and association of 14 genetic loci with, SA111
 Loading influences on, SU363
 Loss of sex-specific differences in leptin knockout mice, SA508
 Paternal, neonatal bone mineral accrual and, F002, SA002
 Serum homocysteine levels in postmenopausal women and, SU373
 Sex differences in BMD in children and, SU318
 Sex steroids as predictor in elderly Swedish men of, SA510

Bone strength

Age-related loss in spine and hindlimb of mice, BMD and, SU019
 AMG 162 in cynomolgus monkeys and, SU453
 Bazedoxifene acetate in ovariectomized cynomolgus monkey and, SA431
 BMD in glucocorticoid-induced osteoporosis *versus*, 1197
 Cortical, directional sensitivity of rodent long bones to collagen denaturation, SU093
 CP432 restoration in aged ovariectomized rats, M419

Bone strength (Cont'd)

Diphtheria toxin receptor expression in osteoblasts, osteocytes and, F289, SA289
 Femoral neck, estrogen as determinant in elderly men of, SA384
 Femoral neck, QCT-derived indices, partial volume averaging errors and, M051
 Genetic architecture in weight-bearing *versus* non-weight-bearing bones and, F112, SA112
 HCN2 ion channels and regulation of, F039, SA039
 Leptin receptor and, 1108
 Microstructural finite element analysis of mouse model, SA109
 Orange pulp or juice diet for orchidectomized rats and, SU013
 Physical activity, dietary calcium in older women and, SA310
 RANKL effects in mice on, SA357
 RANKL inhibition in rats overexpressing secreted OPG transgene and, SU451
 Remodeling cavities and stress risers in cancellous bone and, SA363
 Skeletal growth and, 1127
 Total body periodized resistance training program in women and, M144
 Vertebral, PTH and, 1056
 Vertebral, spinal loading population-based study and, 1074
 Young male monkeys treated with SB-462795 and, F232, SA232

Bone tissue engineering

Calcium phosphate and osteogenic differentiation of MSCs, M232
 Cbfa1/Til-1 overexpression for, M168
 Extracellular matrix in hMSCs culture and differentiation for, M235
 LMP-1 and human MSCs' responsiveness to BMP-2 for, M193
 Nell-1 induced bone formation, fusion, and regeneration for, SU204
 Osteogenic capacity of embryonic stem cells, SU053
 Temporal dependence on PTH(1-34) for anabolic actions in, M487

Bone turnover. SEE *Bone remodeling*

Bone turnover markers. SEE *Bone markers*

Bone viscoelastic properties

In vivo measurement of, M089

Bone volume. SEE *Bone mass*

Boston Area Community Health/Bone (BACH/BONE), M308**Bovine bone substrates**

Human osteoclast cultures of, SU289

B-Raf kinase

Endochondral bone development and, SU038

Bread fortified with 125 mcg of vitamin D₃, SU427

Breast cancer. SEE ALSO *Breast cancer metastasis to bone*

Alendronate and femoral neck bone loss in postmenopausal women after discontinuation of tamoxifen for, SU108

Exemestane, skeletal effects of, M056

Ibandronate administration and dosage with radiation therapy for, SA075

Osteocalcin levels and risk for, M296

Osteocyte stimulation of chemotaxis and invasiveness of, SU111

Osteopontin and bone and lung metastases in, 1214

Breast cancer antiestrogen resistance 1 (BCAR1)

Nongenomic estrogen signaling regulating osteoclast formation via, F505, SA505

Breast cancer-associated gene 3 (BCA3)

Rac-1 interaction in osteoclasts with, SU269

Breast cancer cells. SEE ALSO *BALB/c-MC cells;*

MDA-MB-231 breast cancer cells

Bone metastasizing, TGF- β 1 regulation of ATF3 in, SA164

Estren effects on, M062

Gli2 and TGF- β stimulation of PTHrP expression in, F066, SA066

Msx2 negative regulation Runx2 of osteolysis in, M058

p65 subunit of NF- κ B in bone metastasis by, M061

PTHrP regulation of Dkks' expression in, 1219

Runx2 and gene expression by invasive and osteolytic, M059

Breast cancer metastasis to bone

Biological pathways of ICTP and CTx in, SU148

Differential gene expression of metastasis-related genes in, SA071

E-selection expression on vascular endothelial cells in, SU120

Functional and anatomical imaging for tumor burden and osteolysis monitoring in mice, M054

Hypoxia and HIF-1 α expression in, 1007

Ibandronate *versus* zoledronic acid for, SA073

Measuring α -CTx for early detection of, SU116

Osteolysis mechanism in, SU123

RANKL influence on malignant activities of, SA067

SD-208 in mouse model and, 1216

Serum biochemical markers associated with, SU146

Broadband ultrasound attenuation (BUA). SEE ALSO *Ultrasound*

Map of heel, SA098

Bromodeoxyuridine (BrdU)

Preosteoblast tracking in regenerating bone and, M043

Btk

Regulatory role in osteoclast differentiation, SA276

Buschke-Ollendorff syndrome

Deactivating germline mutations in LEMD3 (MAN1) and, M443

N-Butyryl glucosamine

Effects on long bones, BMD, and gene expression in liver, M418
 Streptococcal cell wall-induced arthritis in Lewis rats and, M390

C**C2C12 (MSC) cells**

BMP2 and Runx2/Cbfa1 gene transcription in, M188

1 α ,25(OH) $_2$ D $_3$ activation of p38 MAPK and JNK in, M513

17 β -Estradiol binding proteins expression and subcellular localization in, SU518

LSN509010 and Runx2 mRNA expression in, F202, SA202

Mustang gene promoter in, SA042

Osteoactivin and differentiation of, M228

Phospho-CREB transcription factor and BMP-2 expression in, M174

C3H10T1/2 (MSC) cells

HDAC inhibitor induced differentiation of, SA205

LSN509010 and Runx2 mRNA expression in, F202, SA202

Osteoactivin and differentiation of, M228

Rap1 activation and differentiation of, F218, SA218

Wnt3-Fzd1 chimera and differentiation of, M197

C3H/HeJ mice

Bone biomechanical properties and architecture in, SU193

Key Word Index

ASBMR 27th Annual Meeting

C3H/HeJ mice (Cont'd)

Bone geometry differences between C57Bl/6 mice and, M106
Osteoblastic activity in C57Bl/6J mice *versus*, SU229

C6 cells

Runx2 modulation of RANKL expression in, SA209

C19 progestin norethisterone (NET)

Hormone replacement therapy *versus*, M399

C57Bl/6 cells

GFP and transplantation protocols comparison using, M238

C57Bl/6J–C3H/HeJ intercross mice

QTL for mechanoresponsive BMD and bone size in, F183, SA183

C57Bl/6J mice

ENU mutant with higher BMD, F106, SA106
Osteoblastic activity in C3H/HeJ mice *versus*, SU229

C57Bl/6 mice

Age factors, CYP2R1 expression in growing, M520
Bone geometry differences between C57Bl/6 mice and, M106
sFRP3 overexpression and bone metabolism in, SU256
Triglyceride-rich lipoprotein clearance in, bone and, M332
Validation of vertebral spine histomorphometric indices of, M094

C57Bl/6 x 129 COX-2 mice, CD-1 COX-2 mice *versus*, SA482**CAAT/enhancer-binding proteins (C/EBP) homologous protein (CHOP)**

BMP/Smad enhanced signaling and CREM interaction with, M024
Overexpression, osteopenia and, F206, SA206

c-Abl

BMP signaling, Id1 expression, osteoblast senescence and, M225

N-Cadherin/cadherin-11

Osteoblastogenesis and, 1063

Caffeine

Effect on VDR and ER in osteoblast cells, M511

Calcein in ethanol solution

For iliac crest biopsy, M087

Calcidiol

Long-term treatment of hypovitaminosis D with cholecalciferol *versus*, SU461

Calcitonin

Alfacalcidol therapy after renal transplantation in children for bone loss *versus*, SU457, WG4
Collagen-induced arthritis and, SU041
CYP27B1 and levels in renal tubular cells of, M521
Mixture-based combinatorial (chemical) libraries for development of, M508
Nasal salmon, bone content and strength after distal radius fractures and, M374
Oral salmon, morning and evening dosing, food intake and bioavailability and efficacy of evening dose of, SA417
Osteoclast formation, gene expression and, SU288
Physiologic function of, in genetically modified mouse models, 1162
PTHrP, prolactin interactions during lactation with, M498
Pyk2/Src role in podosome reassembly and sealing zone detachment in osteoclasts induced by, M265
Rapid osteoclast apoptosis at end of lactation in maternal skeleton and, SU300
 α -Calcitonin gene-related peptide (CGRP)
Mice deficient with, 1162

Calcitonin receptor

Acumen Explorer quantitation in differentiating osteoclast cultures of, SU281
Global knock-down of, trabecular bone volume in young female mice and, 1161

Calcitonin receptor-stimulating peptide (CRSP)

Osteoclastogenesis inhibition by, M496

Calcitriol. SEE ALSO Cholecalciferol

Age-related creatinine clearance decreases and falls in women not treated with, M312
PTH secretion in rats and antiresorptive effects of, F520, SA520

Calcium. SEE ALSO Vitamin D plus calcium

Bone matrix mineralization in klotho mouse, mapping of, SU025
Fat intake and absorption of, M337
Homeostasis measures, 2-yr. change in systemic lupus erythematosus and, SU492
Lactose intolerance and intestinal absorption of, M331
Measurements in erythrocytes of magnesium and, M042
Metabolic acidosis-induced signals, in osteoblasts, M222
Phytoestrogens and intestinal absorption of, SA423
Reduced forearm BMD in postmenopausal women and urinary loss of, SU385
Release at dissolution of inorganic phase of bone, bone formation, bone resorption and, M157
Vitamin D deficiency and urinary excretion of, M320

⁴¹Calcium

Accelerator mass spectrometry to monitor metabolism in end stage renal disease of, SU165
Staging and monitoring skeletal tumor growth with, M055

Calcium-binding proteins

Inulin *versus* fructo-oligosaccharides and mucosal levels in rats of, SA420

Calcium channel antagonists

Estrogen-regulated bone resorption and, SU014

Calcium, dietary

Aromatic *versus* branched-chain amino acid effects on excretion and absorption of, SU508
Bone strength in older women and, SA310
Calcium homeostasis and vitamin D status *versus*, M324
Daily supply in women with postmenopausal osteoporosis on bisphosphonate therapy, SU398
Early postmenopausal osteoporosis and, SU419
Lactose intolerance and, M331
Osteoporosis and, M273
Postmenopausal osteoporotic women, M276
Skeletal growth recovery from deficiency in pigs of, SU017
Vitamin D status and calcium absorption in black and white adolescents and range of, M007

Calcium ion

Extracellular regulation of PTH release, caveolin-1 and cytoskeleton role in, SU497
Extracellular regulation of VDR level in human kidney proximal cells, SU515
Motility initiation in osteoclasts and signals by, SA241
Osteoblast activity prediction with rest-inserted loading induced oscillations of, SU218
Post-parathyroidectomy bone mass changes predictions and, SU469
PTH-enhanced response to mechanical stimulation in osteoblasts and PKC-induced cytoskeleton rearrangement, SA173

Calcium ion (Cont'd)

PTH secretion dynamics in normal individuals using, M484
RSG10 regulation of oscillations in RANKL-induced osteoclast differentiation, M260

Calcium ion/calmodulin-dependent protein kinase 1 β (CaM kinase 1 β)

mRNA expression in growth plate chondrocytes and metaphyseal osteoblasts, SU046

Calcium ion/calmodulin-dependent protein kinase II (CaM kinase II)

Phosphorylation of Ets2 in mechanotransduction pathway of cranial morphogenesis, SA055

Calcium ion-sensing receptor

Alternatively-spliced, extracellular, in growth plate chondrocytes, SU510

Calcium phosphate

Basic, apoptosis in bovine articular chondrocytes and crystals of, SU032
Osteogenic differentiation of MSCs, M232
Percutaneous balloon kyphoplasty using PMMA *versus*, M432

Calcium receptor

VCAM-1 in bone marrow cells and expression of, M229

Calcium-sensing receptor (CASR)

Aromatic *versus* branched-chain amino acid effects on calcium excretion, absorption, bone turnover and, SU508
Calcium transport into milk and, F486, SA486
Dimerization in endoplasmic reticulum, SA487
Expression of extracellular domain in insect cells of, SU512
Genetic determinants of bone size and, SA111
Haplotype polymorphisms, renal stone phenotype in primary hyperparathyroidism and, F122, SA122
IL-6 transcriptional upregulation via elements in gene promoters of, SU514
In osteoblasts, identification of, SU516
Physiological relevance of Venus flytrap module and mutation in, SA485
Ser⁸²⁰Phe mutation in Italian family with autosomal dominant hypocalcemia, SA118
Strontium ranelate effects on osteoclasts and, SU511

Calcium supplementation

Bisphosphonate users purchases of, SU422
BMD in postmenopausal women and CDX-2 polymorphism and VDR start codon association with, SU192
BMD in young premenopausal women with idiopathic osteoporosis and, SU421
Body composition and fat distribution in obese Korean postmenopausal women and, SA422
Calcium and magnesium in erythrocytes and, M042
Effects in elite gymnasts *versus* school children, SA008
Genetic variation in ER α and IL-6, bone mass acquisition in children and, M121
Lumbar spine BMD measurements and, M068
Women with osteoporosis, M269

Calmodulin-dependent protein kinase II γ (CaMKII γ)

Osteoclastogenesis regulation via RANK signaling modulation, SU284

 α -Calmodulin kinase II (α -CaMKII)

Osteosarcoma cell cycle progression and, SU100

Caloric restriction. SEE ALSO Dietary restraint

BMD and biomechanical effects in aged male rats of, M325

Calpain

- Cytoskeletal rearrangement in osteoclasts and, SA241
- RANKL-supported osteoclastogenesis and, SA263

Canadian Multicentre Osteoporosis Study (CaMOS), SA097**Canadian Quality Circles (CQC) Projects, M310, SU386, SU387****Cancellous bone**

- Cellular mechanisms for anabolic effect of intermittent PTH in, M417
- Connectivity and strength in ovariectomized mice treated with bFGF and risedronate, M130
- Decreased osteocyte density in idiopathic osteoporosis in men, SA379
- Leptin gene therapy effects on weight loss and bone mass in female rats, 1048
- Remodeling cavities and stress risers in, SA363
- Risedronate and/or vitamin K₂ pretreatment effect in ovariectomized rats on early loss of, M348
- Skeletal loading effects during post-lactation recovery on, SA182

Cancer. SEE ALSO *Bone metastasis*

- α -CTx as indicator for bone metastasis in, F074, SA074
- Therapeutic applications of 25-OHD₃ in, 1202
- Treatment in children, bone accretion elongation and metabolic activity studies and, M014

Cardiac cachexia

- Hyperaldosteronism and osteopenia in, SU349

Cardiotrophin-1 (CT-1)

- Osteoclast formation and function regulation by, 1190

Cardiovascular calcification. SEE ALSO *Vascular calcification*

- Osteoporosis and, SU022

Cardiovascular calcification (animal models)

- Atorvastatin and, SU018

Cardiovascular disease

- Bone mass and beta blockers for, 1040
- Brain natriuretic peptide and, SU379
- Chronic inflammation-induced bone loss in aged rat model and, SU384
- DXA measurement of body fat mass and, M067

Carnitine

- Fat mass loss in obese subjects treated with, SU125

Cartilage

- Aberrant bone formation and VEGF overexpression in, 1151
- Abnormal development with TGF- β 1 receptor deficiencies in mice, 1192
- Auricular, CTGF/CCN2 reinforces molecular phenotype *in vitro*, SU034
- Hypoxia promotion of matrix synthesis and suppression of terminal differentiation via HDAC4 in, 1024
- Pre-ossification, diesel motor oil as contrast agent for micro-CT visualization of mouse fetal limb, M049
- Risedronate effects on metabolism in osteoarthritis, SU030
- Tamoxifen inducible Cre transgenic mouse and temporal control of gene deletion in, 1153

Cartilage, articular

- Betula platyphylla* var. *japonica* inhibition of IL-1 α -induced effects in rabbits on, SU056
- PGE₂ subtype EP₂ agonist and growth of, SA029

Cartilage defects, small volume

- Targeted *in vivo* MRI measurements of knee, SU043

Cartilage repair

- Mechanobiological regulation of molecular expression and tissue phenotype in, SU092

Cartilage tissue engineering

- T3, BMP-2, and insulin in redifferentiation of dedifferentiated chondrocytes, SA034

Cas-interacting zinc finger protein (CIZ)

- Mechanical and estrogenic signaling in disuse and ovariectomy-induced bone loss, F174, SA174

Caspase2 deficiency

- Age-associated increase in bone resorption and, 1141

Caspase3

- Bone metabolism and, SA189
- RANKL-induced osteoclast differentiation and, SU292

CAST chromosome 1 QTL

- BMD loci and bone size locus of, F102, SA102

CAST/EiJ mice, SA105**Cataracts, M298, SU050** **β -Catenin.** SEE ALSO *Wnt/ β -catenin signaling*

- BMP-2 activation of signaling in osteoblasts by, SA226
- Bone mass and haploinsufficiency of, F229, SA229
- Convergence of androgen receptor and BMP signaling pathways on, SU117
- Growth plate chondrocyte differentiation, maturation and BMP signaling induced by, 1110
- NFAT signaling in osteoblasts, SA228
- Recruitment by BMP-2 to Smad-containing complexes from Tcf/Lef-dependent transcriptional machinery, 1109
- TRAIL and TNF α regulation of osteocyte-osteon structure by removal of gap junctions via proteasomal degradation with probable downstream signaling by, SA217

Cathepsin K

- Deficient mice, pycnodysostosis features and, SU277, SU456
- Growth plate matrix structure and deficiency of, SA022
- MMPs and compensation for osteoclast loss in activity of, SA237
- Osteoclastic activity and serum levels of, SU142
- Prostate cancer growth in bone and, SU113
- Repeatability, intra-subject and postprandial variability in serum measurements, SU144
- Serum level changes in postmenopausal women treated with alendronate, SU274
- siRNA transfection inhibits bone resorption in primary human osteoclasts, SU307
- TRAP regulation in osteoclasts and, SU272
- Cathepsin K inhibitor(s).** SEE ALSO *AAE581; SB-462795*
- Compound A in ovariectomized cynomolgus monkeys, SU276
- Safety, effects on bone resorption markers, and pharmacokinetics in healthy subjects of, SU447

Cathepsin K promoter

- c-Jun suppression and JunB enhancement by NFAT2 in RAW 264.7 cells of, M252

Caucasians. SEE ALSO *Whites*

- Fracture risk values from Western populations application to other, M075
- Hip strength and femoral neck length in Chinese *versus*, SU364

Caveolin-1 (Cav-1)

- Bone size and, 1182
- 1 α ,25 OH₂D₃ regulation of growth plate and, SU045

Caveolin-1 (Cav-1) (Cont'd)

- Extracellular calcium ion-regulated PTH release and role of cytoskeleton and, SU497
- Sexually dimorphic changes in bone phenotype with deficiency of, F450, SA450

CBA/H mice, SU193**Cbfa1/Runx2 overexpressing mice, SU399****Cbl**

- Downregulation of osteoclast activity by, F279, SA279
- Fibronectin-dependent osteoblast detachment, apoptosis and, F190, SA190

CCAAT/enhancer-binding protein α (C/EBP α)

- p20 and p30 isoforms, MSC differentiation and, M190

CCAAT/enhancer-binding protein β (C/EBP β)

- 24(OH)ase transcription and, 1204
- SWI/SNF chromatin remodeling complexes, transcriptional regulation of 24(OH)ase and, 1201

CCAAT/enhancer-binding proteins (C/EBPs)

- Osteogenesis, odontogenesis and transcription factors of, F210, SA210

CCL5 protein

- TGF β stimulation of mRNA expression and secretion in osteoblasts of, M162

CCN genes

- Expression and regulation in murine osteoblasts of, SA126

CCR4-associated factor 1 (Caf1)

- Expression in chondrocytes, ovaries, brain and suppression of BMP-induced bone formation, mineral apposition rate and, F014, SA014

CD14⁺ monocytes

- SDF-1 promotion of circulation by, 1071

CD24

- Expression in intervertebral disks, SU054

CD34⁺ cells

- Bone healing and, 1066

CD40 ligand

- Glucocorticoid-induced bone loss and, F370, SA370

CD44

- OPN interaction with in osteolysis mechanism in breast cancer metastasis, SU123

Cdc25C-associated kinase 1 (C-TAK1)

- MITF interaction with during osteoclast differentiation, SA281

CDX-2 polymorphism

- VDR start codon and calcium supplementation effect on BMD in postmenopausal women, SU192

CE590

- Effects on prostate and bone in intact and orchidectomized rats of DHT *versus*, M395

Celiac disease

- BMD and bone markers in men with idiopathic vertebral fracture and, SA383
- DiGeorge syndrome, hypocalcemia as presenting feature in, SA468
- Vitamin D status in community-dwelling people with hip fractures and, M330

Cell Track cell-scanning system

- For expression cloning of carboxyl-terminal PTH receptor, SA492

Cementoblasts

- JunB mediation of PTHrP action on, M182
- MAPK and GSK signaling in mechanical responses to fluid shear stress by, SU220
- Ultrasound stimulation and *in vitro* proliferation, metabolism of, SU063

Cementum-derived cells

- Human, SU082

Centrifugation

- Density gradient, of human MSCs for isolation and culture *in vitro*, M207

Key Word Index

ASBMR 27th Annual Meeting

Cerebral palsy

Pamidronate for osteoporosis in children with, SU394

c-Fos

NF- κ B and osteoclastogenesis mediated by, SA255

Chemokines

Dlk1/Pref-1 effects on human MSCs and, M202

Chicory oligofructose

Inulin enhancement of BMD and mucosal levels of calcium binding proteins in rats *versus*, SA420

Children. SEE ALSO *Girls; Infants; Osteogenesis imperfecta; Puberty; Skeletal growth*

Adult BMC and physical activity in, 1012

Age, sex, growth variables and BMC, BMD acquisition in healthy, M011

Alendronate treatment of osteoporosis in, M368

Alfacalcidol *versus* calcitonin therapy for bone loss after renal transplantation in, SU457, WG4

Assessing changes in femoral bone structure and strength using MRI, M100

BMC and bone size variables in, SU126

Body composition and serum IGF-I, IGFBP-3, and leptin levels with liver transplantation, M480

Bone loss causes in, SU480

Bone status assessment with Lunar pediatric total body software, SU481

Bone ultrasound in infants *versus*, SU167

Burned, growth hormone as anabolic agent in, SU475

Calcium supplementation, genetic variation in ER α and IL-6, and bone mass acquisition in, M121

Calcium supplementation in elite gymnasts *versus*, SA008

With cerebral palsy, pamidronate for osteoporosis in, SU394

Congenital adrenal hyperplasia and BMD in, SA471

Crohn disease and bone turnover in, SA477

Dietary intake and bone health in, SU353

Forearm fractures, radiologic evaluation for, M017

Fractures as osteoporosis risk, 1136

With fracturing osteoporosis, alendronate discontinuation and bone status in, SU401

Fragility fractures in, and reduced BMD at forearm and hip, higher % body fat, 1130

Gender differences in long bones shape in, SU319

HIV-infected, oral cholecalciferol effects on serum levels of 25(OH)D in, SU476

Insulin-resistance syndrome and high-normal bone mass in, M441

Intravenous bisphosphonates effects after discontinuation in, SU396

Mexico City Invest in Your Bones program for, SA010

With nephrotic syndrome, glucocorticoids effects in, 1060

Obese, whole body DXA imprecision in measuring body composition changes in, M064

Orthopedic complications in overweight, F472, SA472

Physical activity and BMD in Japanese, M012

Physical activity and nutritional effects on fitness and bone mineral acquisition with acute lymphoblastic leukemia in, SU473

Radiation therapy effects on bone architecture, SA398

Sex differences in bone size and BMD in, SU318

Children. SEE ALSO *Girls; Infants; Osteogenesis imperfecta; Puberty; Skeletal growth* (Cont'd)

Skeletal growth and hip fracture prediction in late adulthood, 1058

T cells and bone metabolism in Crohn disease of, SU478

Total body BMC, head BMC and, M019

Chinese

Age-dependent changes in mineral metabolism and bone remodeling markers in, M001

BMD and ACE inhibitor use in older, SA296

Body composition reference values in normal women, SU131

Body fat assessment of total percentage from spine and femur DXA measurements in, SU127

Hip strength and femoral neck length in Caucasians *versus*, SU364

Chinese American, bone mass determinants and osteoporosis in women, SU129**ChMIL**

Soluble, hypovascularity of tendon and, SA054

Cholecalciferol. SEE ALSO *Calcitriol*

Long-term treatment of hypovitaminosis D with calcidiol *versus*, SU461

Oral, effects on serum levels of 25(OH)D in HIV-infected children and adolescents, SU476

Cholesterol

Increased, and decreased BMD in women aged 65 years and older, SU130

Chondrocytes

Articular, gene expression of passaged human, SA043

Articular, PGE₂ subtype EP₂ agonist and growth of, SA029

Articular, Wnt signaling in human and bovine, SA031

Bovine articular, basic calcium phosphate crystals and apoptosis in, SU032

B-Raf and PTHrP-induced proliferation of, SU038

Caf1 expression in, F014, SA014

Canonical Wnt signaling and differentiation of, 1064

Canonical Wnt signaling and hypertrophy mediation through Runx2, 1020

In developing bovine rib growth plate, FGF2 binding modulation by perlecan in, M135

1,25(OH)₂D₃ binding protein ERp60 and, SA500, WG2

Dlx2 stimulation of maturation *in vitro* and *in vivo*, 1155

Dysplasias of, 1033, 1086, SA488, SU064

Epiphyseal, aggrecan synthesis and turnover by ADAMTS proteases and, SU048

Expression of osteoclastogenesis-related molecules in, SU036

Gene expression, canonical Wnt signaling and Twist 1 repression of, SU199

Human, genistein reduction of proinflammatory molecules in, SU044

Hypertrophic, *Col10a1* distal element tissue-specific expression in, F030, SA030

Hypertrophic, culture to study physiological death of, SU039

Hypertrophic, large latent complex of TGF β produced by, SA155

IL-1 β -induced death mediated by iNOS and NADPH oxidase, SA037

Prehypertrophic, ColX gene expression and retinoid stimulation by BMP signaling and direct transcriptional activation in, 1022

PTH inhibition of ERK1/2 in, SU042

PTHrP gene-driven LacZ expression in, M497

Chondrocytes (Cont'd)

Runx2-mediated transcriptional regulation of osterix in, M170

Wnt/ β -catenin signaling in maturation of, F048, SA048

Chondrogenesis (chondrocyte differentiation)

Canonical Wnt signaling and Twist 1 repression of, SU199

β -Catenin-induced BMP signaling for, 1110

Gene screening within discrete compartments of growth plate and, M052

Genes expression induced by loading and, F057, SA057

Genes regulated by extracellular inorganic phosphate in, SU051

Growth/differentiation factors 5, 6, 7 effects on, M036

IGF-I effects on, SA151

Immunity of allogenic MSCs differentiated by, M227

Precursors to, SU031

RGS proteins role in regulation of, SU037

Runx1, 2, or 3 regulation of, F032, SA032

S100A1, S100B inhibition of hypertrophic, 1006

SHP2 mutations in Noonan syndrome and disorganized, 1085

Ski acceleration of hypertrophic, SA175

Sox9 expression regulation by TIP39/PTHR2 signaling and inhibition of, SA490

TGF- β signaling in early limb, SA157

TM, in *Sox9*-independent manner without inducing hypertrophy, SU033

Transient receptor potential vanilloid 4 and, SU040

Wnt/ β -catenin signaling and Wnt3a roles in, 1019

Wnt signaling in sFRP1 null mouse and, 1021

Chondrosarcoma

Hedgehog pathway-inhibitor and proliferation of, SU101

Hip, teriparatide for osteoporosis and, SU505

Chordin

Twisted gastrulation protein and regulation of osteoblast differentiation and BMP signaling by, M037

Chordoma

CD24 expression in intervertebral disks and, SU054

Chromatin

Estrogen-dependent remodeling *in vivo* at CIITA, 1143

Vitamin D and estrogen hormone-specific modifiers recruitment to, F518, SA518

Chromosome 4

Genes affecting alcohol preference and bone mass in congenic rats on, F110, SA110

Chromosome 10

Candidate gene affecting serum IGF-I, BMD, and bone remodeling on, 1212

Chromosomes 20q11-13

Femoral neck bone geometry and, 1211

B6-i^A Chromosome substitution strain mice, M104, M105**Chronic lung disease of prematurity, SA475****Chronic obstructive pulmonary disease (COPD)**

Skeletal effects, M292

Vertebral fractures in, SA342

CIMC-4 cells, SU216**Cinacalcet**

End stage renal disease, changes in intact PTH, PTH(1-84)/PTH(7-84) and calcium x phosphate product after 5 months on, SU506

Hypocalciuric hypercalcemia with recurrent pancreatitis and, SU509

Tumor-induced osteomalacia management with, SA454

c-Jun

Suppression of cathepsin K promoter activity by NFAT2 in RAW 264.7 cells, M252

Climbing exercise

Trabecular bone turnover in ovariectomized mice and, F172, SA172

Clinical practice guidelines

CQC Pilot Project for Care of Patients at Risk for Osteoporosis, SU387

Clinical Test of Sensory Interaction and Balance, Modified (mCTSIB), SU444**Clinical trials**

Depressive symptoms, treatment adherence and study compliance in, M380

Lasofexifene phase 2 and phase 3 design and strategy, M384

Modeling long-term treatment effects in, M365

Cloning, molecular

Cell Track (cell-scanning system) of carboxyl-terminal PTH receptor, SA492

Coatbridge Disease Management Programme, United Kingdom, SU330**Cocaine and amphetamine regulated transcript (CART)**

Behavioral change in GIP receptor knockout mice and, SA050

Col1a2^{oim} mice, M438**Collagen type I**

Calcification of elastic lamellae of devitalized rat aortas incubated in serum and, SA026

Compressive biomechanical properties of human lumbar vertebrae and advanced glycation end products of, SA058

Fibronectin images of role in assembly of, SU073

Gene expression in postmenopausal osteoporosis and, M169

Pueraria thumbergiana enhancement of, SU233

Collagen type I 3.6 promoter

GFP expression in osteoclast lineage and, F266, SA266

Collagen type I α 1

Characterization of bone and cartilage stimulating peptides derived from, M429

Gene polymorphism and BMD variations in Polish men, SA123

Genetics and remaining lifetime fracture risk, SU342

Polymorphism and serum OPG levels, bone mass in postmenopausal women and, SU374

mRNA expression in BMSCs *versus* osteoblast lineage cells, 1044

Sp1 polymorphism, BMD and fracture associated with, 1210

Collagen type II

Mechanical stress in differentiated ATDC5 cells and upregulation of, SU088

Collagen type X

Gene expression in prehypertrophic chondrocytes and retinoid stimulation by BMP signaling and direct transcriptional activation, 1022

Mechanical stress in differentiated ATDC5 cells and upregulation of, SU088

Collagen type X 10a1 distal promoter element

Tissue specific expression in hypertrophic chondrocytes *in vivo*, F030, SA030

Collagen type XI α 2

Osteoblast-specific DNA nuclear targeting and, M171

Collagen(s)

Crtap protein and prolyl 3-hydroxylation of fibrillar, F053, SA053

Spectromicroscopy of oxidative damage to, SU020

Collagen(s) (Cont'd)

Thermal denaturation of, directional sensitivity of rodent long bones cortical strength to, SU093

Collagenase 3

Large latent complex of TGF β produced by hypertrophic chondrocytes and, SA155

Metastatic melanoma cells and osteoblast interaction induction of, SA063

Collagen cross links, vitamin B₆ and vitamin K₂ effects in diabetic WBN/Kob rats on, SU420**Colle's fractures**

Bone microarchitecture in hip fractures *versus*, 1178

Colony-stimulating factor-1 (Csf-1)

Growth plate dysplasia and, SU036

Colorectal cancer

Elevated VDR α and 1,25(OH) $_2$ D in hepatic metastasis of, M522

Combinatorial (chemical) libraries

Mixture-based, for calcitonin and/or PTH analogues, M508

Community-based post-fracture care model, M382**Community-dwelling people. SEE ALSO**

Institutional-dwelling people

Celiac disease, vitamin D status and hip fractures in, M330

Kidney function and fracture risk in older women, M285

Sex hormones levels and fall risk in, 1041

Vitamin D deficiency and fracture risk in, F351, SA351

Vitamin D deficiency and functional changes in lower extremities after hip fractures in women, SU337

Vitamin D deficiency in postmenopausal women with osteoporosis, M275

Competitive protein binding assay (CPBA)

Serum levels of 25(OH) $_2$ D $_2$ and 25(OH) $_2$ D $_3$ from patients treated with pharmacological doses of vitamin D $_2$, SA523

Computerized dynamic posturography-sensory organization test (CDP-SOT), SU444**Computer models. SEE ALSO Mathematical models**

Clinical assessment of vertebral deformations, F321, SA321

Hydroxyapatite binding affinities of bisphosphonates, SU306

Computer software

BMD reporting tool development and testing, M071

Gene admixture mapping, SU176

Image processor, for trabecular bone evaluation using porous mediums connectivity concept, M097

Connective tissue growth factor (CTGF). SEE ALSO CCN genes

Downstream mediation of TGF- β 1-induced MSC condensation, SU035

Endothelin-1 regulation of osteoblast secretion of, bone formation and, SU261

hBMS cell attachment onto hydroxyapatite scaffold *in vivo* and, SU062

Connective tissue growth factor (CTGF)/CCN2

Auricular cartilage molecular phenotype *in vitro* and, SU034

Connective tissue growth factor-derived peptide (CTGF-P)

Osteoblast adhesion, spreading, differentiation and, SU078

Connective tissue progenitor cells

Oxygen diffusion time and colony formation, proliferation of, M164

Quantitative analysis of bone marrow, fat, muscle as sources of, M230

Connective tissue progenitor cells (Cont'd)

Wnt signaling and, SU255

Connexin43

Cx43-/floxOCN^{Cre} mice lacking, bone accrual and peak bone mass in, F286, SA286

Gene array analysis of osteoblasts deficient of, M167

Osteoblast response to treatment with FGF2, IGF1 and, SU265

PTH osteoanabolic action *in vivo* and, 1228

PTH regulation of rat osteocalcin promoter and, M493

Connexin43 gap junctions

Responsiveness of HIG-82 cells to IL-1 β and, SU069

Contraceptives, oral

Bone mass and geometry influence in young women on, F353, SA353

Endurance training effects on bone mass, geometry in young women on, SU352

Reference range for bone turnover markers in premenopausal users and nonusers, SU158

Copenhagen School Child Intervention Study (CoSCIS), SU318**Core binding factor α -1 (Cbf α 1)**

Til-1 (N-terminal isoform) overexpression for tissue engineering, M168

Core binding factor β (Cbf β)

BMP/Runx2 signaling in bone formation and, 1014

Cortactin

Actin assembly at sealing zone of osteoclasts and, SA245

Cortical bone

Acquisition, circulating IGF-I and, 1193

Adipose tissue and bone size in non-weight-bearing bone in young men, leptin and, 1046

Alendronate effects in postmenopausal osteoporotic women on, SU393

Androgen receptor and androgen action on surfaces of, F515, SA515

Anisotropic resorption by osteoclasts of, SU310

DHT in adult female estrogen-deficient, osteopenic rat and, M402

Femur, prediction by QCT of ultimate stress in, SU089

Fractures in dialysis patients and pQCT of, M465

Gender-specific QTL in F2-intercross of GK and F344 inbred rats, M109

Glucocorticoid-induced osteoporosis and structure of, F086, SA086

Low-dose strontium and formation of, M423

LRP5 regulation of intrinsic material properties of, M050

MRI of distal radius in postmenopausal women, SA083

Neuromuscular degenerative disease devastation of, SU371

Porosity, predicting 3D structure at human, anterior femoral mid-shaft, SU016

PTH(1-84) effects at hip, 1083

PTH or alendronate effects in senile and severely osteopenic ovariectomized rats on, M489

RANKL inhibition in orchietomized rats and geometry of, 1226

Secondary mineralization in, M047

Serotonin, long-term administration and, SU213

Sex differences in mouse response to nerve damage and, SU362

Skeletal and sexual maturation effects in peripheral skeleton of, F004, SA004

T-lymphocytes and post-ovariectomy loss of, SA375

Vertebral strength assessment role of, F088, SA088

Key Word Index

Cortical bone (Cont'd)

Y2 receptor, leptin pathways and regulation of, M422

Corticosteroids

BMD in 5-8 year olds treated for chronic lung disease of prematurity with, SA475
BMD in men and, M307

COS-7 cells

Mustang gene promoter in, SA042

Coumadin. SEE ALSO *Warfarin*

Osteoporosis and, SA344

CP432

Bone mass and strength restoration in aged ovariectomized rats, M419

CP-533,536

Fracture healing in canine model of oblique tibial osteotomy and, SU200

CpG

Mouse RANKL gene transcription and methylation of promoter of, SA203

CpG-oligodeoxynucleotides

IL-12 mediation of anti-osteoclastogenic effect by, F251, SA251

Cranial neural crest cells

TGF- β regulation of proliferation and differentiation during frontal bone development of, F222, SA222

Craniofacial skeleton

Cooperative signaling by FGF1 and FGF2 in development of, I195

Craniosynostosis

Octacalcium phosphate in, SA003
Twist dimer selection and mediation of, M184

Cranium

CaM kinase II phosphorylation of Ets2 in mechanotransduction pathway of morphogenesis, SA055

C-reactive protein

Fracture risk in postmenopausal women and, F319, SA319

Creatinine clearance

Age-related decreases and falls in women not treated with calcitriol, M312
Bone quality in elderly men, muscle strength and, SU008

Crohn disease

Bone turnover in children with, SA477
T cell activation in pediatric, SU478

Crtap protein

Prolyl 3-hydroxylation of fibrillar collagens and, F053, SA053

 β -Cryptoxanthin

Osteoblast differentiation, mineralization and, M213

c-Src

G β proteins in PTH-induced signal transduction in rat intestinal cells and, SA478
Inhibition and decreased breast cancer-induced lethality and metastasis incidence in nude mice, F068, SA068
 α , β ₃-Integrin signaling of cytoskeletal organization in osteoclasts and, F244, SA244
Recruitment of SHIP to podosomes in osteoclasts leading to bone resorption attenuation, M254

C-terminal c-Src kinase binding protein (Cbp)

Impaired recruitment of Csk into lipid rafts from decreased expression of, increased bone resorption and, I146

C-terminal c-Src kinase (Csk)

Impaired recruitment into lipid rafts from decreased Cbp expression, increased bone resorption and, I146

CTXA scanning device

Hip structure analysis with segmented 3D scans, M098

C-type natriuretic peptide/guanylyl cyclase B (CNP/GC-B) system

Endochondral ossification regulation by, F028, SA028

Cushing's syndrome

Bone mass, remodeling after treatment for, SA369

Serum OPG levels and, SA371

CXC chemokines

ELR⁺ motif in human MSCs, dexamethasone and, SU203

CXCL7

Modified 8 amino acid peptide Ac-TTSGIHPK-amide derived from, bone formation stimulation and BMD increases in ovariectomized rats and, M425

Cyclic AMP

Enhancement of BMP action through suppression of Smad6 expression by pentoxifyline and, SA017
PTH(1-34) responsiveness to, M503

Cyclic AMP/PKA signaling

Activation of canonical Wnt pathway in osteoblastic cells and, M485
Amphiregulin expression in osteoblastic cells by PTH, M492

Cyclic AMP response element binding protein (CREB). SEE ALSO *Phospho-CREB transcription factor*

FGF2 and phosphorylation in osteoblasts of, F142, SA142

Cyclic AMP response element modulator (CREM)

BMP/Smad enhanced signaling and CHOP interaction with, M024

Cyclic GMP protein kinase I (PKG I)

Calcium and calpain-dependent cytoskeletal rearrangement in osteoclasts and, SA241

Cyclin D1 promoter

Transcriptional activation by PTHrP, SA195

Cyclin-dependent kinase 4

Runx2 switching in osteoblast differentiation and, I016

Cyclin-dependent kinase 6

Runx2 switching in osteoblast differentiation and, I016

Cyclists, nutritional evaluation and body composition of, SU440**Cyclooxygenase-2 (COX-2)**

Fluid flow regulation of the 3'-untranslated region in MC3T3 E1 cells of, SA169
Fluid shear stress in osteoblasts, NFAT regulation of expression of, SU224
Fracture healing, arachidonic acid metabolism manipulation and, M166
Knockout mice, genetic background effects on phenotype of, SA482
Neovascularization assessment of fracture healing using micro-computed tomography in mice deficient in, M045
Particulate wear debris, osteoclast maturation and, M214
R-FB effects on inhibition of IGFBP-6 transcription mediated by, SA145
Titanium particles induced, NF- κ B-dependent pathway in fibroblast-like synoviocytes and, M178
Venous ligation-mediated bone adaptation and, M156
Wear debris induced MCP-1 in fibroblasts and, M215

Cyclooxygenase-2 (COX-2) inhibitors

BMD and, I076

Cyclosporine A

Bone growth in rats, secondary hyperparathyroidism and, M479

CYP2R1

Age-related changes in expression level in growing mice of, M520

CYP17

Skeletal and hormonal phenotypes and allelic combinations of, M124

CYP19

BMD in postmenopausal women and new single nucleotide polymorphisms in, M122
Skeletal and hormonal phenotypes and allelic combinations of, M124

CYP24

Expression with adrenodoxin and adrenodoxin reductase, M523

Cyp26a1

Retinoic acid inhibition, osteoblast differentiation and, SU247

CYP27B1

Expression with adrenodoxin and adrenodoxin reductase, M523
PTH and calcitonin increase protein levels in renal tubular cells of, M521

Cysteine rich protein 61/cryptococcal crooked neck 1 protein (CYR61/CCN1)

In hMSCs and EAh9 926 cells, M231

Cysteine rich protein 61 (CYR61). SEE ALSO

CCN genes
Endothelin-1 regulation of osteoblast secretion of, bone formation and, SU261

Cytokines

Dlk1/Pref-1 effects on human MSCs and, M202
11 β -HSD1 activity in osteoblasts and, F365, SA365

Cytosine deaminase (CD)/5 fluorocytosine (5FC)

Bone cancer treatment regulated by TRAP promoter in mice transgenic for, SA248

Cytoskeleton, osteocyte

C-PTHR regulation through calcium influx-dependent mechanisms of, SA493

D**D6S440 dinucleotide CA repeat polymorphism of ER α ,** SU188**DAPI2,** M261**Darglitazone**

Bone surface specific effect in mice, SA394

Decision making, BMD scan, SU317**(23S)-25-Dehydro-1 α -hydroxyvitamin D₃-26,23-lactone (TEI-9647)**

VDR and RANKL-induced osteoclast formation blockage by, SA497

(23S)-25-Dehydro-26,33-lactone (MK) side chain of 1,25D/VDR antagonist

Molecular mechanism of, SA503

Dehydroepiandrosterone (DHEA)

supplementation, SU424

Delta-like 1/pre-adipocyte factor 1 (Dlk1/Pref-1)

Human MSCs and, M202

Demineralized bone matrices (DBM), M128, SA015, SU237**Demineralized bone powder (DBP),** M025, SA153**Demographics**

DANCE clinical trial on teriparatide treatment for osteoporosis, M406
Hip fractures among elderly women and, F327, SA327
Men with hip fractures, SA339

Dendritic cells, SA061, SU275**Dendritic cell-specific transmembrane protein (DC-STAMP)**

Cell-cell fusion during osteoclastogenesis regulated by Ap-1, NFAT and, F258, SA258

Osteoclast fusion mediated via C-terminus domain of, SU282

ASBMR 27th Annual Meeting

Key Word Index

Denmark

Socioeconomic factors and fracture risk in, M317

Densitometers

Changing machines in clinical practice, precision error and, M081, M082
Contrast-detail phantom evaluation in, M080
Cross-calibration of pencil-beam and fan-beam, SU138

Densitometry

Family practice residents orders for, M085
Focal structural defects, ISCD call for consensus on, M083
Heel and hip bone, in postmenopausal women with hip fractures, SA292
Peripheral, for hip fracture risk screening, SU137
Short- and long-term precision of GE Lunar Prodigy *versus* Hologic Delphi scanners, M063
Vertebral fracture assessment, F313, M281, SA313

Dental implants

Biological effects of self-setting α -tricalcium phosphate and, SU057

Dental status

Mandibular BMD measurement correlation with clinical findings of, SA082
Osteoporosis and disability in elderly people in Italy, M451

Dentin

AC-100 and formation in direct and indirect pulp capping models in beagles of, F461, SA461

Mechanical consequences of *Colla2^{oim}* mutation in, M438

P20C/EBP β and dysplasia in, F210, SA210

Dentin matrix protein 1 (DMP1)

Gene expression in osteocytes with local strain, 1093
Mechanically induced expression in osteocytes of, F168, SA168
Osteomalacia and osteocyte lacuno-canalicular system abnormalities rescue, 1111

Dephosphorylation

Postmitotic, Runx2 control in proliferating osteoblasts by, SU228

Depot-medroxyprogesterone acetate (DMPA)

Bone remodeling markers and, SU156
Leuprolide acetate in treatment of endometriosis and, SU517

Depression, M380, SU350, SU377**Desmoid tumor with chest wall ossification**

BAMBI promoter hypermethylation in, M028

Dexamethasone

ELR⁺ CXC chemokines in human MSCs and, SU203
Endothelial cells and MSCs differentiation induced by, SA213

 Δ FosB

Fat accumulation in adipocytes of mice overexpressing, 1114

Diabetes, M304, SU329, SU420**Diabetes mellitus, type 1**

IGF-I and bone remodeling in adolescent girls with, SA469
PPAR γ 2 and bone adiposity and loss in, F399, SA399
Rat model, osteoactivin and alveolar bone regeneration in, SU251

Diabetes mellitus, type 2

Alterations in mechanical properties of bone and, M458
Bone loss and darglitazone treatment for, SA394
Fall risk in older adults with, F347, SA347
Risk factors for falls and fractures in older women with, SU355

Dialysis. SEE ALSO *Hemodialysis*

Hypogonadism and vitamin D insufficiency in men on, M468

Diasorin radioimmunoassay

LS-MS/MS measurement of 25(OH)D *versus*, SA527
Vitamin D assay with, SA526

Dickkopf 1 (Dkk-1) protein

Binding to cells overexpressing LRP5 in radioactive binding assay, Kremen-2 and MesD effects on, SA128
Bone formation and compounds disrupting LRP5/6 interaction with, 1062
Endothelin-1 regulation of osteoblast secretion of, bone formation and, SU261
Kremen 2 and inhibition of LRP5/6-Wnt3a-TCF signals in U2OS osteoblast-like cells by, M217
Myeloma bone disease and, 1124, 1125
Osteoblastic differentiation and, M192
Overexpression in osteoblasts, intermittent PTH treatment in mice and, 1191
PTH-mediated activation of canonical Wnt signaling in bone and, 1002
Temporal expression in embryonic, growing, and adult mouse bone by, SA130
Wnt/ β -catenin signaling in chondrogenesis and, 1019

Dickkopf (Dkk) proteins

Osteoblast function and bone formation *in vitro* and *in vivo*, 1001
PTHrP regulation of expression in breast cancer cell lines of, 1219

Diesel motor oil

As contrast agent for micro-CT visualization of pre-ossification cartilage in mouse fetal limb, M049

Diet. SEE ALSO *Food intake; Nutrition*

Bone health in children and, SU353

Dietary restraint. SEE ALSO *Caloric restriction*

Subclinical ovulatory disturbances and BMD in premenopausal women and, SU348

Dietary supplements

Daily calcium intake with osteoporosis, M273
Low calcium intake in postmenopausal osteoporotic women and, M276
Milk basic protein and bone metabolism in healthy menopausal women, SU426
Optimal vitamin D levels in healthy adults, M510
Vitamin D and calcium in women with osteoporosis, M269

DiGeorge syndrome

Hypocalcemia, celiac disease and, SA468

Digital topological analysis (DTA)

Trabecular network at radius and tibia, degree of vertebral deformities and, M295

5 α -Dihydrotestosterone (DHT)

Body composition and cortical bone in adult female estrogen-deficient, osteopenic rat, M402
Effects on prostate and bone in intact and orchidectomized rats of CE590 *versus*, M395
Skeletal growth in SAMP6 mouse model and, SU525

1 α ,25 Dihydroxyvitamin -3-epi-D₃, isolation and identification of, M524**1,25 Dihydroxyvitamin D**

FGF23 regulation by, SA456
Free, calculation of using vitamin D binding protein capacity measurements, SA522
Gender- and tissue-specific effects in intestine and bone of mature rats of, M516
Serum levels in Norwegians and Pakistanis living in Oslo, Norway, SA346

24,25 Dihydroxyvitamin D

Plasma, in black and white female adolescents, binding activity of, M517

1,25 Dihydroxyvitamin D₃

Biological potency in ligands of, SA521
FGF23 production by osteoblasts treated with, M134
 β_1 -Integrin silencing and osteoblast response to, M212
Osteoblast differentiation in human marrow stromal cultures and, M155
Physical performance in elderly postmenopausal women and, M309
Recruitment to chromatin, F518, SA518
Regulation of FGF23 gene transcription in osteoblasts and, SA144
Skeletal anabolic effects and mineral ion homeostasis in 1 α -hydroxylase and PTH null mice and, 1203
Vascular invasion in long bone development during embryonal period and, SA494
In vivo FGF23 functions dependent on, 1164
In vivo FGF23 interactions with, WG1

1 α ,25 Dihydroxyvitamin D₃

Activation of p38 MAPK and JNK in C2C12 cells by, M513
Caveolae and Cav-1 for regulation of growth plate by, SU045
JNK and p38 MAPK in rat intestinal cells and, M512
Osteoclast formation supported by chondrocytes expressing RANKL and, 1067
Wnt pathway effects on osteoblast differentiation, proliferation and, SA221

1,25 Dihydroxyvitamin D₃ binding protein ERp60

Rapid response in growth plate chondrocytes and osteoblasts from, SA500, WG2

1,25 Dihydroxyvitamin D₃/vitamin D receptor system

PTH catabolic effect but not anabolic effect and, 1099

Dimethyl sulfoxide (DMSO)

Osteoblast differentiation, gene expression and, M208

Diphenylhydantoin (DPH)

Lipopolysaccharide suppression in bone resorption of, SU301

Diphtheria toxin receptor

Reduced bone mass, strength and expression in osteoblasts and osteocytes of, F289, SA289

Direct Assessment of Non-Vertebral Fractures in Community Experience (DANCE), M406, M407, SA438**Dishevelled 1 (Dvl-1)**

Wnt/ β -catenin signaling–BMP-2 signaling in osteoblast progenitors and Smad1 interaction with, F133, SA133

Distraction osteogenesis

Bromodeoxyuridine and preosteoblast tracking in bone regeneration, M043
IGF-1 and new bone formation in, M005
OPN deficient mice with delayed healing during, SU080

Disuse osteopenia. SEE ALSO *Unloading*

Baseline bone morphology, cell activity and degree of, SA165
QTL determining degree of, SU174
Trabecular, high frequency accelerations and, M149

DIVA study, F410, M350, SA410, SU412, SU413***Dlx2***

Murine chondrocyte maturation *in vitro*, *in vivo* and, 1155

Dlx5

Osteoblast differentiation in transgenic mice and, 1186

Key Word Index

Dlx5 transcription factor

BMPs and Runx2 cooperative interactions and, F012, SA012

Dlx genes

Expression in osteoblast differentiation, M177

DNA-dependent protein kinase (DNA-PKs)

Nuclear hormone receptors interaction for nVDRE-mediated transcriptional inhibition of PTHrP gene with, 1119

DNA microarrays. SEE *Gene chip analysis***DNA nuclear targeting sequence (DTS)**

Osteoblast-specific, M171

Docosahexaenoic acid (DHA)

Bone loss in ovariectomized mice by eicosapentaenoic acid *versus*, SA132

Drug design

VDR structure, function and, 1120

Drug-O-Gram

Illustrating drug utilization with weekly oral bisphosphonates using, M363

Dual energy X-ray absorptiometry (DEXA)

Cortical bone loss assessment using Mechanical Response Tissue Analyzer *versus* QUS and, SU133

Referrals of high risk patients by neurologists and orthopedic surgeons for, SA294

Dual X-ray absorptiometry (DXA)

Assessment of total body % fat from spine and femur measurements in Chinese, SU127

Bone size and density in children with Turner syndrome prior to growth hormone therapy, SU483

Calcium supplements and lumbar spine BMD measurements with, M068

Cardiovascular disease risk and fat mass measured by, M067

Contrast-detail phantom evaluation in, M080

Conventional, image resolution properties' implications for structural geometry measurements with, M099

Cross-calibration of pencil-beam and fan-beam, SU138

Detection of early osteolytic bone metastasis, M084

Dual femur scanning for antiresorptive therapy monitoring, SU135

Evaluation of systemic use of glucocorticoids in primary health care, SA372

Femur geometry, changes throughout life in, SA087

Hip fractures with vertebral fracture present, M297

Local *versus* international reference standards for, F081, SA081

Peripheral, National Osteoporosis Society guidelines and, M074

Repeatability and sensitivity of vertebral morphometry studies with Norland scanner, SU124

Risk-equivalent cutoff levels based on total femur, SU139

Single *versus* dual femur monitoring with, SA076

Skeletal recovery after long-duration spaceflight predicted by, 1171

Total body composition changes with HIV treatment, SU136

T-scores of -2.5 in men ages 50–65, M301

Usefulness for skeletal mass assessment in older women, SA352

Whole body, of fat mass loss in obese subjects treated with carnitine, SU125

Whole body, within person changes in body composition, M064

Z-scores risk-equivalents for other techniques and, 1176

Dynamin

Dynamin GTPase- and Src-dependent regulation of Pyk2 phosphorylation in osteoclasts and, 1150

E

E11

Osteoblast differentiation into osteocytes and, SA287

E297D (CASR activating mutation)

Venus flytrap module and, SA485

EAhy 926 (endothelial) cells

HCYR61 effects on, M231

Early B cell factor-1 (EBF-1)

Osteoblast, adipocyte development and, 1184

Early growth response protein 1 (Egr1)

FGF23 signaling and, M132

MEK/ERK pathway regulation of osteoclast survival and, M257

Early growth response protein 2 (Egr2)

MEK/ERK pathway regulation of osteoclast survival and, M257

Eating disorders. SEE ALSO *Anorexia nervosa*

Bone mass change in physically active young females and, M013

EB1089 (vitamin D analog)

Gender- and tissue-specific effects in intestine and bone of mature rats and, M516

ECOSAP Study, F093, SA092, SA093**Egyptian mummy**

Metabolic bone disease in, M454

Eicosapentaenoic acid (EPA)

Bone loss in ovariectomized mice by docosahexaenoic acid *versus*, SA132

Elastin expression

CTGF/CN2 reinforcing auricular cartilage molecular phenotype *in vitro* and, SU034

Elderly people. SEE *Aging***Electromagnetic field (EMF) treatment**

Halogenated hydrocarbons effects on bone structure and, SU065

Embryonic development

Kidney, MGP and vitronectin co-localization in, SA052

Meckel's cartilage, gp130-mediated signaling in, SU066

Embryonic stem cells. SEE ALSO *Mesenchymal stem cells; Stem cells*

Testing osteogenic capacity *in vivo*, SU053

Enamel matrix derivative

OPG production in human osteoblasts and, SA134

Endocrine system diseases

FGF23 biochemical mechanisms of action and, 1104

Screening patients with fragility fractures and previously undetected, M319

Endometriosis

BMD evaluation after treatment with promegestone plus placebo or estradiol for, SA426

Prophylactic bisphosphonates during GnRH agonist therapy for, M342

Treatment with DMPA-SC 104 *versus* leuprolide acetate, bone effects of, SU517

Endoplasmic reticulum stress

Ascorbic acid protection of osteoblasts from, SU266

Multiple myeloma and, SU105

Endothelial cells

MSC differentiation into osteoblasts and, SA213

Endothelin-1

Regulation of osteoblast secretion of paracrine regulators, bone formation and, SU261

Endothelin-A receptor (*Ednra*) mutant mice, SU070**Endotoxin, adherent**

Activation of TLR-4-dependent signaling without inducing TLR association with lipid rafts by, M256

On bone implants, osteoblast activity inhibition and, M194

End stage renal disease (ESRD)

Adynamic bone disease misdiagnosis by using intact PTH assay *versus* PTH(1-84) assay for, SU501

⁴¹Ca and accelerator mass spectrometry to monitor calcium metabolism in, SU165

Changes in intact PTH, PTH(1-84)/PTH(7-84) and calcium x phosphate product after 5 months on cinacalcet, SU506

FGF23 and BMD in healthy people and patients with, M471

Engrailed-1 (En1)

Pleiotropic functions in bone formation, 1185

Enhanced green fluorescent protein (EGFP). SEE ALSO *Green fluorescent protein*

Osteogenic capacity of embryonic stem cells and, SU053

Enterochromaffin (ECL) cells

PTHrP as candidate for hormone derived from gastric, SA396

ENU (N-Ethyl-N-nitrosourea) mutagenesis program, F104, F106, SA104, SA106**Enzyme-linked immunosorbent assay (ELISA)**

Cathepsin K serum measurements, SU144

Ntx validation in cynomolgus monkey with, SU152

EphrinB2 activation by RANK-c-Fos-NFAT cascade in osteoclast formation, SU287**Epidemiologic Study on the Prevalence of Osteoporosis (ESOPO)**, F301, SA301**Epidermal growth factor receptor (EGFR)**

PTH1R activation of ERK and transactivation of, M505

Signaling inhibition, lung squamous cell carcinoma-associated humoral hypercalcemia of malignancy and, 1215

Epidermal nevus syndrome

FGF23, *GNAS1* and skeletal histology evaluation in, SA452

Epigallocatechin gallate deficiency

Inhibitory effect on titanium particle-induced TNF- α release and, SU197

Epithelial calcium channel-2 genes

Identification and characterization, in human and mouse, M515

Epithelial cells, human

HDAC inhibitor-induced TCF/LEF-driven luciferase in, SA205

PTH ectopic secretion by thymus, M459

EPOLOS Study, SA123**Errors.** SEE *Partial volume averaging errors; Precision error***Erythrocytes**

Calcium measurements in, M042

Erythropoietin

BMD in elderly men and, SA303

E-selectin

Expression in breast cancer metastasis, SU120

ESR1 gene polymorphism

BMD variations in Polish men and, SA123

ESR2

Osteoporotic fracture risk in postmenopausal women and, M120

Estradiol

BMD evaluation after endometriosis treatment with promegestone and, SA426

Determinants of serum levels in males, SU521

Gene expression regulation in osteoclast cytoskeleton by, SU523

ASBMR 27th Annual Meeting

Key Word Index

Estradiol (Cont'd)

- Hepatic IGF-I gene expression in growth hormone resistant mice, JAK-STAT pathway activation and, 1199
- Male skeletal sensitivity to PTH and, 1107
- In vitro* osteoclastogenesis and RANKL expression in bone marrow of postmenopausal women and, F374, SA374

17 β -Estradiol

- Recruitment to chromatin, F518, SA518

17 β -Estradiol binding proteins

- Expression and subcellular localization in C2C12 (MSC) cells, SU518

Estren

- Effects on human breast cancer and prostate cancer cell lines, M062

Estrogen(s)

- Bone cells' birth and apoptosis in mice in which ER α cannot interact with DNA and, 1098
- Bone mechanosensitivity to loading and withdrawal of, F181, SA181
- Calcium channel antagonists and bone resorption regulated by, SU014
- Chromatin remodeling *in vivo* at CIITA dependent on, 1143
- Genetic factors in synthesis, activity on peak bone mass and, SU184
- Idiopathic male osteoporosis, leptin levels and, SA385
- Nongenomic signaling in osteoclastogenesis, BCAR1 and, F505, SA505
- Rapid osteoclast apoptosis at end of lactation in maternal skeleton and, SU300
- ROS effects on bone and age-related deficiency of, F401, SA401
- Runx2 regulation of aromatase gene expression and synthesis of, M175
- Short-term effects on BMD and bone resorption, M393
- Smoking and bone response to deficiency of, SA200
- Structural simulation of osteoporosis type I and type II induced by deficiency of, SA348

Estrogen receptor

- Caffeine effect and transcriptional response in osteoblast cells of, M511
- Models for classical and non-classical action in osteoblastic cells by, M158

Estrogen receptor α

- Calcium supplementation, bone mass acquisition in children and genetic variation in, M121
- Elimination of signaling via EREs, osteopenia and bone mass acquisition deficits in male mice, 1142
- Loss of signaling via EREs, differential effects on total body vs. marrow fat and, F511, SA511
- Low BMD and osteoporotic fracture risk with dinucleotide CA repeat polymorphisms in, SU188
- Osteocyte mechanotransduction and, 1116
- Raloxifene treatment and expression in bone by, SA504
- RBBP1 and suppression of osteoblast proliferation by, 1200
- Smad4-induced apoptosis by inducing Bim alternative splicing as cofactor of, 1117

Estrogen receptor α coactivator RIZ1

- BMD in elderly men and deletion polymorphism in, SU187

Estrogen receptor β

- Gene polymorphisms and bone loss rate in perimenopausal women, SU005
- Gene polymorphisms predict osteoporosis risks in men and women, SU186
- Genetic determinants of bone size and, SA111

Estrogen receptor β (Cont'd)

- Mechanotransduction role of, 1091
- Osteocyte mechanotransduction and, 1116
- TIEG regulation by estrogen in human osteoblasts and, SA506

Estrogen receptor β agonist LSN500307

- Pharmacologic actions in ovariectomized rats, SA427

Estrogen response elements (EREs)

- Loss of ER α signaling via, differential effects on total body vs. marrow fat and, F511, SA511

Ethnic/racial group differences

- Admixture of African American genetic markers for ancestry, M103
- BMC and bone parameters in early pubertal girls, M003
- BMD and vitamin D status among Hispanic men, M308
- BMD scan decision making and, SU317
- Hip BMD and body composition in older men, F338, SA338
- Markers of bone metabolism and fracture risk, SU372
- Osteoporosis fractures and costs in USA by, F317, SA317
- Serum levels of 1,25(OH)₂D in Norwegians and Pakistanis living in Oslo, Norway, SA346
- Volumetric BMD and bone geometry in older men and, 1135

Etidronate

- In vitro* effects on apoptosis and death of macrophage-like cells and, SU299

Ets2

- CaM kinase II phosphorylation in mechanotransduction pathway of cranial morphogenesis, SA055

EUROFORS Study, M095, M412, M413, SA432**European OPTIFORD Study**, SU427**Evaluation of Obstructive Lung Disease and Osteoporosis (EOLO)**, M292**Evista/Alendronate Comparison (EVA) Trial**, F425, SA425**Ewing's sarcoma**, SU094**Exemestane**

- Skeletal effects in breast cancer patients, M056

Exercise. SEE ALSO *Physical activity; Physical fitness; Resistance training; specific sports*

- Acquisition of BMD in young Japanese women and, M009
- Equipment and protocols effects on bone formation, M137
- Growing children and bone mineral accrual due to, 1011, F187, SA187
- Oral contraceptives and endurance training effects on bone mass, geometry in young women, SU352
- Osteoporosis patient quality of life and low-intensity back, SU439
- Skeletal growth during puberty and, M141

Extracellular matrix. SEE ALSO *Matrix calcification*

- Fibronectin regulation of assembly of, 1054
- Genes expression in demineralized bone-mediated osteogenic differentiation, SU237
- hMSCs culture, differentiation and, M235
- Images of assembly and reorganization in living osteoblasts of, SU073
- Osteoclastic function in bone metastasis microenvironment of, SU271
- 3-dimensional matrices for *in vitro* study of MSCs and, SA219

Extracellular matrix proteins, non-collagenous

- Matrix vesicles as carriers of, M030

Extracellular signal-regulated kinase 1/2 (ERK1/2)

- C-PTH and pertussis toxin-sensitive G proteins role in activation of, M506
- EGFR transactivation and PTH1R activation of, M505
- Endochondral ossification and, 1023
- MCP-1-induced TRAP+ multinuclear cells in osteoclast differentiation and, F249, SA249
- MMP-13 expression regulated by ROS in ATDC5 cells and, SU072
- PTH1R and activation by G protein and β -arrestin of, SA480
- PTH inhibition in chondrocytes of, SU042
- PTH/PTHrP phosphorylation and PTH activation of, M507
- PTH receptor activation via G β -c-Src tyrosine kinase to phosphorylation of, SA478
- PTH receptor and NHERF1 switching of, 1160
- Statin-induced BMP-2 expression and osteoblast differentiation and PI 3 K-induced activation of, F227, SA227

Extracellular signal-regulated kinase (ERK)

- FGF23 signaling and, M132
- Measurement of PTH-induced, using phosphospecific antibody cell-based ELISAs, M483
- PTH activation of osteoblasts and, M218

Ezrin

- PTH-mediated downregulation of NaPi-IIa in opossum kidney cells and, F479, SA479

Ezrin-binding protein 50 (EBP50)

- PTH1R-mediated effects on vascular smooth muscle cell proliferation and, M500

Ezrin, radixin, and moesin (ERM) proteins

- Osteoclast migration and PIP2 regulation of, SA273

F**F2A4-K-NS**

- DBM augmentation and, M128

Fall risk

- Diabetes type 2 in older women and, SU355
- Frailty in older women and, SU335
- Knee bend test for monitoring, SU433
- Older adults with diabetes, type 2, F347, SA347
- Patients with fragility fractures and, SU351
- Second cataract surgery in elderly women and, M298
- Sex hormones levels in community-dwelling older persons and, 1041

Falls

- Age-related decrease in creatinine clearance in women not treated with calcitriol, M312
- Nonvertebral and hip fracture risk in older men and, M305
- Personal history predicts non-spinal fracture but not spinal fracture, SU338
- Spinal mobility, muscle strength in osteoporosis and, M311
- VDR gene polymorphism in elderly and, SA501

Family medicine, *BetterBones Workshop* use in, SU321**Family physicians**. SEE ALSO *Physicians*

- Awareness of osteoporosis risk factors and BMD testing by, M310
- Osteoporosis medication prescriptions by, SU386
- Referral patterns for men to osteoporosis scanning service by, SA340

Fan-beam DXA

- Cross-calibration with pencil-beam DXA, SU138

Key Word Index

ASBMR 27th Annual Meeting

Farnesyl diphosphate synthase (FDPS)

- BMD in elderly women and, SU185
- Crystal structure and molecular interactions with nitrogen-containing bisphosphonates, F408, SA408
- Genetic polymorphisms, bisphosphonates therapeutic response and, M118
- Intron 1 polymorphism (A/C), as bisphosphonate therapy marker, SA121
- Rat bone anabolic response to PTH after chronic bisphosphonates and, F220, SA220

Fat, dietary

- Bone acquisition in congenic mouse with altered osteoblast differentiation and diabetogenic or high levels of, 1035
- Calcium absorption, bone mass influences of, M337

Fat tissue. SEE ALSO *Adipose tissue*

- Arrestins selective regulation of adrenergic agonist effects on, F397, SA397
- Mice overexpressing Δ FosB, accumulation in adipocytes of, 1114
- Quantitative analysis of, as source for connective tissue progenitors, M230
- Whole body DXA of obese subjects treated with carnitine and loss of, SU125

Femoral head

- Bone geometry, genome-wide linkage of, SU175
- Ibandronate intra-osseously administered in infarcted, F476, SA476
- Ischemic necrosis of, aging and angiogenic response after, SA136
- Ischemic necrosis of, RANKL inhibition of femoral head deformity in immature pigs after, 1128

Femoral neck

- Cross section geometry of, F079, SA079
- Estrogen as determinant in elderly men of strength of, SA384
- Fracture incidence in Okinawa, Japan, SA326
- Fracture prediction, total hip BMD *versus* DXA at, 1009
- Gene search for cross-sectional geometry of, 1211
- Heritable anthropometric factors for familial association in BMD of, SA115
- Image noise and partial volume averaging on QCT-derived strength indices, M051
- Length in Chinese *versus* Caucasians, hip strength and, SU364
- Maximum rising strength as BMD predictor in healthy women of, M142
- Obesity and structural strength in women of, F179, SA179
- Trabecular and cortical volumetric BMD correlates of, 1073
- Trabecular bone microarchitecture and biomechanical characteristics of, M092

Femur

- Age, body size role in predicting 3D structure of cortical porosity at human anterior mid-shaft, SU016
- Antiresorptive therapy monitoring with dual DXA scanning of, SU135
- Assessing changes in children of bone structure and strength using MRI, M100
- Changes in young female gymnasts in geometry of, M020
- Changes throughout life in geometry of, SA087
- Chromosome X QTL influence on geometry, bending strength in mice of, SA107
- Densitometry adjustment for body size in healthy German children of, SU485
- Effect of dual scanning on osteoporosis diagnosis and treatment decision making in postmenopausal women, M070

Femur (Cont'd)

- Estradiol therapy in mouse with congenital aromatase deficiency and width/length of, SU527
- Genetic and gender regulation of BMD and size in congenic strains for mouse distal chromosome 1 of, F114, SA114
- Hip fracture prediction using automated structural measurements of proximal femur in pelvic radiographs, F090, SA090
- Human, mineralization and bone turnover at mid-shaft of, SA049
- Murine, functional and morphological phenotyping of, SA109
- Osteoclast genetic variability and 3D spatial distribution in inbred mice, F262, SA262
- Osteocytes in hindlimb-suspended mouse, hypoxia and, 1173
- Parity and geometry of, SU140
- Prediction by QCT of ultimate stress in cortical bone of, SU089
- Signaling pathways in hierarchical clustering of differentially expressed genes from chickens, M114
- Single *versus* dual DXA monitoring of, SA076
- Solid bone matrix of rat imaging using water and fat suppressed proton magnetic resonance imaging, SU145
- Three-point bending in mediolateral plane for testing biomechanical properties in rats, SA184

Fetal osteoblastic cells, human

- Comparative *in vivo* study of long-term growth dynamics in bioreactor *versus* in tissue-culture grade polystyrene, SU245

Fetuin

- Laser capture microscopy-captured biomineralization foci and, SA019

FHL2

- Inhibition of activated osteoclast in TRAF6-dependent manner by, SA278

Fibrillin 1

- In tight skin mutation mice, F046, SA046

Fibroblast growth factor 1 (FGF1)

- Bone formation and mass in osteoglyphonic dysplasia and, F138, SA138
- Craniofacial development and cooperative signaling with FGF2 by, 1195

Fibroblast growth factor 2 (FGF2)

- Cbl-mediated ubiquitination of α 5 integrin mediation of fibronectin-dependent osteoblast detachment, apoptosis induced by activation of, F190, SA190
- Connexin43 and osteoblast response to treatment with, SU265
- Craniofacial development and cooperative signaling with FGF1 by, 1195
- Perlecan modulation of binding to chondrocytes in developing growth plate by, M135
- PTH induction of Bcl2, CREB phosphorylation, Runx2 nuclear accumulation in osteoblasts and, F142, SA142
- Synthetic mimetic of, DBM augmentation and, M128

Fibroblast growth factor 7 (FGF7)

- Expression in tumor-induced osteomalacia, M126

Fibroblast growth factor 23 (FGF23)

- Biochemical mechanisms of endocrine action, 1104
- BMD in healthy people and patients with end stage renal disease and, M471
- Characterization of knockout mice deficient in VDR and, F140, SA140
- Dietary phosphate regulation in healthy men of, M131
- 1,25(OH)₂D regulation of, SA456

Fibroblast growth factor 23 (FGF23) (Cont'd)

- Epidermal nevus syndrome with focal bone defects and hypophosphatemic rickets and, SA452
- Expression in tumor-induced osteomalacia, M126
- Familial tumoral calcinosis and mutants of, F442, SA442
- First *versus* second generation assays with dietary phosphate of changes in serum, SA143
- Growth hormone replacement effects in adult growth hormone deficiency and, M133
- High phosphate diet in healthy men and postprandial changes in, M125
- Identification of molecule responsible for tissue specific signaling by, M132
- Overexpression causing secondary hyperparathyroidism, reduced 25-(OH)₂D₃-1 α -hydroxylase activity and, F453, SA453
- PHEX/Phex* function and regulation by dietary phosphorus of gene expression in bone of, M127
- Phosphate depletion and hypophosphatemia regulation of, F459, SA459
- Phosphate homeostasis in untreated Graves' disease regulated by, SA451
- Plasma cell dyscrasias and serum levels of, SA060
- Production in osteoblasts treated with 1,25(OH)₂D₃, M134
- Serum phosphate regulation in patients with hypoparathyroidism and, M129
- Structural survey of, 1165
- Suppression of osteoblast development and matrix mineralization with adenovirus-mediated overexpression of, SA139
- Tumoral calcinosis with hyperphosphatemia and gene mutation in, F444, SA141, SA444
- Tumor-induced osteomalacia and measurements of, SA460
- Vitamin D₃ but not PTH regulation gene transcription in osteoblasts of, SA144
- Vitamin D dependent functions *in vivo* of, 1164
- Vitamin D interactions *in vivo* with, WG1
- Fibroblast growth factor binding protein 1 (FGFBP1)**
- BMD in Mexican Americans and, SU195
- Fibroblast-like synoviocytes**
- Rheumatoid arthritis and apoptosis regulation in, M486
- Fibroblasts**
- Wear debris induced MCP-1 and COX-2 dependent pathway in, M215
- Fibrodysplasia ossificans progressiva**
- Middle-age onset, immunosuppressive therapy and, M440
- Fibrodysplasia ossificans progressiva lymphoblastoid cells**
- HSPGs mediation of BMP4 signaling disrupted in, M029
- Molecular dissection of BMP signaling pathways in control of, SA011
- Fibronectin (FN)**
- Assembly and reorganization imaged in living osteoblasts, SU073
- Expression in MSCs, CTGF regulation of, SU035
- Mineralization control by, 1054
- Fibrous dysplasia**
- Age-related pain prevalence increases in, M437
- Periostin expression in, SA216
- Fibrous tendon insertion sites**
- PTHrP gene-driven LacZ expression in, M497
- Fibula**
- Aging and sex differences in cortical bone mineralization in, SU015

ASBMR 27th Annual Meeting

Key Word Index

Fidgetin-like 1

Osteoblast proliferation, differentiation and apoptosis and, SU236

Finite element analysis

Bone removal changes in biomechanical properties, SU086
Mapping load environment in histological sections of bone surrounding titanium implants, SA056

First Nations Bone Health Study (Canadian Aborigines), SU327, SU328, SU329, SU372**Flagellin**

Osteoclast formation and, M002

Flavopiridol

Inhibition of osteoblasts and osteoclasts, SU305

Fluid flow/fluid shear stress

ATP and human MSCs proliferation induced by, SU217
Canonical Wnt pathway, BMP signaling and osteoblast proliferation induced by, SU219
COX-2 and venous ligation-mediated bone adaptation to, M156
Modeling in Haversian bone, SU091
Monitoring with microparticles, M151
NFAT regulation of COX-2 expression in osteoblasts, SU224
P2Y purinergic receptors expression in bone-related cells and response to, SA177
Regulation of the 3'-untranslated region of cyclooxygenase-2 in MC3T3 E1 cells by, SA169
Runx2 regulation in MC3T3 E1 cells with intensity-dependent, SU225

Fluoresceinated dextran tracers

Imaging vascular routes for *in vivo* delivery to murine growth plate, SA033

Fluorescence imaging, 3D volumetric

Automated imaging of *in vivo* bone formation labels, M046

Fluorescent activated cell sorting (FACS)

Osteoclastic mitochondrial mass and potentials quantification using, SU293

Fluoridation, water

Antioxidant status of postmenopausal women and, M270

[¹⁸F]-Fluoride positron imaging spectrometry ([¹⁸F]-fluoride PET)

Metastatic osteolytic, osteoblastic, and mixed lesions in prostate cancer model, SU115

[¹⁸F]-Fluorodeoxyglucose positron imaging spectrometry ([¹⁸F]FDG-PET)

Metastatic osteolytic, osteoblastic, and mixed lesions in prostate cancer model, SU115

Tumor burden and osteolysis monitoring in breast cancer bone metastasis mouse model, M054

Tumor burden imaging in 5TGM1 mouse model, SU098

Fluorosis

Skeletal, bottled teas and, M450

Fluoxetine

Stimulation of osteoclastic activity by, SA047

Follicle-stimulating hormone (FSH)

Bone anabolic effects of inhibin A and, SU250
Bone resorption and, F376, SA376
Hypogonadism-induced osteoporosis and bone mass regulation by, 1043

Osteoclast formation, survival and, 1100

Follicle-stimulating hormone receptor (FSHR)

Osteoporotic phenotype with deficiency in female mice of, SA516

Food intake

Evening dose of oral salmon calcitonin and, SA417

Forearm. SEE ALSO *Colle's fractures; Wrist*

Fractures, children undergoing radiological evaluation for, M017

Fractures, gender-specific BMD profile and, M286

High resolution 3DpQCT study of bone microarchitecture in healthy, young women, M093

Lifestyle factors and pQCT assessment of BMD in, M277

Structural and density changes after injury to, SU369

Urinary calcium loss and reduced BMD in postmenopausal women, SU385

Forskolin/PTH

Selective VDR DNA binding to OPN gene promoter induced by, 1120

FosB, human

Mechanical strain and expression in hBMSCs by, M180

Fra1 protein

Prenatal osteosclerosis and, SA211

Fracture healing. SEE ALSO *Bone regeneration*

Absence of BMP-2 and impaired, 1025

Arachidonic acid metabolism manipulation and, M166

BMP signaling stimulation of bone resorption and remodeling during, M034

CD34+ cells and, 1066

CP-533,536 effects in canine model of oblique tibial osteotomy, SU200

Differential protein expression analysis of, M199

Genetic diversity of skeletal ontogeny and, SA101

Local bone formation using lovastatin microbead scaffolds, SU029

Lysophosphatidic acid and osteoblast migration during, SA124

Mechanobiological regulation of molecular expression and tissue phenotype in, SU092

Neovascularization assessment in COX-2-/- mice using micro-computed tomography, M045

Osteofornin acceleration in rats of, SU198

Osteoporosis treatment in home health care settings, SA354

Oxysterols and, M203

PB-MSCs and, M226

mPGES-1 contribution to, F125, SA125

PTH mediation of early stem cell recruitment during, F483, SA483

Fracture history

BMD predictor in Asian men and women, SU003

Fracture Index

Validation in population-based sample of Swiss elderly women using QUS device, SU168

Fracture Intervention Trial (FIT), M355, M365, SA413, SU141**Fracture Intervention Trial (FIT) Long-Term Extension (FLEX),** F406, M365, SA406, SU400**Fracture prediction**

BMD measurement in older women and, 1057

In elderly Swedish men, prior osteoporosis-related fractures, sex steroids and, SA510

Elderly without osteoporosis, fall-related factors and, SU344

Hip, socioeconomic factors in California 1996–2000 and, SA311

Long-term, of incident vertebral fractures, 1038

Nonvertebral, assessment tool for postmenopausal women, SU357

Nonvertebral, heel bone ultrasound and resorption markers for, SA350

Fracture prediction (Cont'd)

Over 15 years, BMD and incident vertebral fractures, F297, SA297

Personal fall history, and non-spinal *versus* spinal, SU338

Skeletal growth during infancy and childhood or hip fracture in late adulthood, 1058

Total hip BMD *versus* DXA at femoral neck for, 1009

Vertebral, COPD and, SA342

Fracture risk

Adherence to bisphosphonates therapy by postmenopausal women and, SU403

Adherence with drug therapy for postmenopausal osteoporosis and, M294

Age- and dose-dependent hormone replacement therapy effects on, 1227

Age factors and T-scores for assessment of, F293, SA293

BMD reporting software tool development and testing, M071

Bone architecture in women and, SA359

Bone instability in elderly and, M088

Breast cancer risk and, M296

Collα1 genotypes and remaining lifetime, SU342

Community-dwelling older people with vitamin D deficiency and, F351, SA351

C-reactive protein levels in postmenopausal women and, F319, SA319

Diabetes type 2 in older women and, SU355

DXA assessment using local *versus* international reference standards for, F081, SA081

ERα D6S440 dinucleotide CA repeat polymorphism and, SU188

ESR2 influence in postmenopausal women on, M120

Ethnic differences in markers of bone metabolism and, SU372

Fall-related factors in elderly without osteoporosis and, SU344

Falls in older men and, M305

Frailty in older women and, SU335

Hip, differential effects of hormone therapy, alendronate, risedronate, and ibandronate, M356

Hip, plasma vitamin B12 in elderly and, F309, SA309

Hip, population screening with peripheral densitometry and questionnaire, SU137

Hip, prevalent radiographic vertebral fractures after 10 years of follow-up and, F315, SA315

Hip, prior non-spine fractures after 10 years of follow-up and, F315, SA315

HIV-positive women and, SU347

IGFBP-2 in elderly men and osteoporotic, 1137

Inhaled steroids and, SA364

Kidney function in older women and, M285

Life expectancy changes in Ireland and, SU332

Literature-based meta-analysis of bisphosphonates relating early suppression of bone turnover markers to, F404, SA404

Long term effects of randomized controlled trial on osteoporosis screening on, 1042

LRP6 variants in elderly men and, F120, SA120

Medical risk factors in Canadian Aboriginal people and, SU329

Neuromuscular function in older men and, SA343

Nonvertebral, alendronate for women without vertebral fracture with osteopenia and nonvertebral fracture history, M355

Nonvertebral, composite measures of, SA411

Nonvertebral, differential effects of hormone therapy, alendronate, risedronate, and ibandronate, M356

Key Word Index

Fracture risk (Cont'd)

- Nonvertebral, prediction with calcaneal ultrasound, F093, SA093
 - Norwegian Medicine Agency osteoporosis treatment guidelines for wrist fractures and, SU333
 - OPG promoter polymorphism in older women and, 1039
 - Physical activity in older men and, M290
 - Postmenopausal women between 50–65 years, factors for osteoporotic, M315
 - Postmenopausal women in managed care, persistence with bisphosphonate therapy and, M362
 - Quality of life for women with osteoporosis and, SU354
 - Related to selected factors according to site and external cause, M289
 - Risk-equivalent cutoff levels based on total femur DXA, SU139
 - Runx2 glutamine repeat mutations and, 1059
 - Second cataract surgery in elderly women and, M298
 - Socioeconomic variables and, M317
 - Systemic lupus erythematosus and, SU487
 - Teriparatide treatment for osteoporosis in women and, 1223
 - Upfront loading doses of bisphosphonates and, M369
 - Vertebral, deterioration of cancellous and cortical bone structure and, M283
 - Vertebral, multidetector row computed tomography for *in vivo* analysis of, F362, SA362
 - Vitamin K₁ intake in perimenopausal women and, SU423
 - Western populations values application to other Caucasians, M075
 - WHO risk categorization in menopausal women and ten-year absolute fracture risk, 1037
 - Wrist fractures in postmenopausal women and, SU340
- Fractures.** SEE ALSO *Colle's fractures; Fractures, fragility; Hip fractures; Vertebral fractures; Wrist fractures*
- Accuracy of self-report in older people of, SU334
 - BMD in patients with, SA295
 - Bone turnover markers in daily clinical practice, SU155
 - Community-based care model after, M382
 - Frequency in patients over 50 in a Mexico City trauma hospital, SU326
 - Homocysteine serum levels and, SA328
 - Incident, in glucocorticoid-induced osteoporosis, age factors and, SA368
 - Lack of osteoporosis care following, SU336
 - Low-energy, BMD and bone markers with vitamin D and calcium treatment for, SU459
 - In men *versus* postmenopausal women, M300
 - Men with prostate cancer, SA329
 - Non-union, peripheral blood derived MSCs characteristics in, M226
 - Nonvertebral osteoporotic, adherence to bisphosphonate therapy and, SU417
 - In older women, VDR translation start site polymorphism and, F323, SA323
 - Osteoporotic, incidence projections by skeletal site in USA, 1078
 - Osteoporotic, kyphoplasty and reduction in, M383
 - Osteoporotic, persistent usage of bisphosphonates and hospitalization risk reduction for, SU388
 - Osteoporotic, RANKL gene polymorphisms and, M119

- Fractures.** SEE ALSO *Colle's fractures; Fractures, fragility; Hip fractures; Vertebral fractures; Wrist fractures* (Cont'd)
- In postmenopausal women, histomorphometric indicators of microdamage accumulation, F356, SA356
 - During puberty, implications in old age, 1131
 - Refracture rates and mortality, F331, SA331
 - Rib, as marker of osteoporosis and mortality, SU322
 - Spontaneous, absence of BMP-2 and, 1025
 - Spontaneous, mouse model of, 1045
 - Standard risk factor audit *versus* targeting fragility, SU331
 - Stroke and subsequent rates of, F334, SA334
 - In young women, mechanical stimulation of bone and muscle after, M147
- Fractures, fragility**
- In children, reduced BMD at forearm and hip, higher % body fat and, 1130
 - Hip, age factors and, SU376
 - Improved care with osteoporosis education after, SU325
 - Inadequate clinical response to therapy or discontinuation of therapy and new, M388
 - Information-based intervention and management of, M387
 - In men, *LRP5* genetic polymorphisms and, SA336
 - Nonvertebral, vitamin D deficiency in Scottish adults and, SA318
 - Osteoporosis and fall risk with, SU351
 - Osteoporosis care pathways for hospital patients with, SA312
 - Postmenopausal, prevalence of, SU330
 - Recognizing Osteoporosis and its Consequences in Quebec and, SA335
 - Risedronate efficacy over range of baseline BMD levels with, M367
 - During risedronate treatment, BMD changes and, SA405, SA407
 - Screening patients with previously undetected disease and, M319
 - Vertebral, deterioration of cancellous and cortical bone structure and risk of, M283

Framingham Osteoporosis Study, 1040, F309, SA309, SU175

Free radicals

- Age-associated accumulation in bone, SU450

Frizzled (Fzd) receptor 1

- In Wnt3-Fzd1 chimera, M197

Frontal bone

- TGF- β regulation of cranial neural crest cells proliferation and differentiation during development of, F222, SA222

Fructo-oligosaccharides

- Additive effects of soy isoflavones and, SU432
- Inulin enhancement of BMD and mucosal levels of calcium binding proteins in rats *versus*, SA420

Fuchsin dyes staining in iliac crest biopsy

- Alternative to, M087

Fulvic acid of Mumie

- Osteoblast differentiation and, M209

G

G11 protein

- Osteoblast cellular morphology, function and RNA interference with, M216

D-Galactose

- Sex differences in bone tissue response to, SU365

Gamma-glutamyl carboxylase (GGCX)

- Vitamin K-dependent activity of vitamin K compounds in liver, bone and, SA198

ASBMR 27th Annual Meeting

Gap junction signaling for RANKL-induced osteoclastogenesis, SA283**Gastrectomy**

- Bone loss in Japanese after, M303

Gastrocalcin

- PTHrP as candidate for, SA396

G β proteins

- c-Src tyrosine kinase in PTH-induced signal transduction in rat intestinal cells and, SA478

Geelong Osteoporosis Study, F319, SA319**GE Lunar Prodigy densitometers**

- Precision of total body BMD and body composition using, SU132
- Prediction of fat and lean composition in pigs, M077
- Short- and long-term precision of Hologic Delphi scanners *versus*, M063
- Total Body software, body size adjustments of, SU481
- Total Body software, performance in preterm infants and newborns, SU484

Gene chip analysis. SEE ALSO *Microarray analysis*

- Dlk1/Pref-1 effects on human MSCs, M202
- Gene screening within discrete compartments of growth plate using, M052

Gene expression

- Chondrocyte differentiation regulated by extracellular inorganic phosphate and, SU051
- micRNA binding sites in osteonectin 3' untranslated region, SU079
- Passaged human articular chondrocytes, SA043
- PTH-PTHrP phosphorylation regulating PTH activation of ERK1/2 and, M507
- RANKL mRNAs in cell types associated with inflammatory bone loss, M243
- Regulation in U2OS osteoblast-like cells by TIEG, M172
- Signatures of MLO-Y4 osteocyte cell model, SA291
- TNF-induced oscillatory and combinatorial NF- κ B binding to DNA and, SA254

General Practice Research Database (GPRD)

- Stroke and subsequent fracture rates, F334, SA334

Gene therapy

- Bone regeneration and regulated BMP2, M038
- Intracellular fate of plasmid DNA and non-viral carriers in bone marrow stromal cells and, SU215
- Osteoblast-specific DNA nuclear targeting for, M171

Genetic epistasis

- Genomic regions identified for BMD considering, SU179

Genetic materials

- Decreasing obesity risk and osteoporosis risk with use of, M108

Genetic predisposition to disease

- Idiopathic osteoporosis in men, M111

Genetics

- Baseline BMD, rate of age-related changes and, M314

Genistein

- Reduction of proinflammatory molecules in human chondrocytes by, SU044

GENOMOS study, 1210**Genotype-by-parity**

- Effects on BMD in pedigreed baboons, SU177

Geranylgeranyl diphosphate synthase (GGPS1)

- Genetic polymorphisms, response to bisphosphonates and, M118

Ginger

- Action on rheumatoid arthritis by phenolic compound extracts from, SU489

ASBMR 27th Annual Meeting

Key Word Index

Girls. SEE ALSO *Children*

- Bone mass accrual modulation by IGF-I and muscle mass in pubertal, F007, SA007
- Chinese postmenarcheal, total body and forearm bone mass determinants in, SA005
- Effects on 24-months of gymnastics training on insulin-like growth factors in prepubertal, SA150
- Multisite QUS precision and normative data for Caucasian, SA095
- Prepubertal, body fat and bone properties in, M021

GIUMO Study, SA364**Gla proteins**

- Bone matrix in warfarin-treated rats and, SU023

Gli2 signaling molecule

- BMP-2 and PTHrP expression in growth plate and, 1154
- TGF- β stimulation of PTHrP expression in breast cancer cells and, F066, SA066

Globin activator of transcription (GATA-1)

- BMP and receptors expression in bone marrow of mice deficient with, SA013

Glucagon-like peptide 2 receptor (GLP-2)

- Nocturnal bone resorption in postmenopausal women and, 1225

Glucagon-like polypeptide 2 receptor (GLP2R)

- Expression in circulating peripheral blood cells, SU382

Glucocorticoid-induced leucine zipper (GILZ)

- Inhibition of adipocyte differentiation mediated by, F513, SA513

Glucocorticoid receptor

- 24(OH)ase transcription and, 1204
- Localization in osteoblasts, glucocorticoid-induced osteoporosis and, 1101

Glucocorticoids. SEE ALSO *Osteoporosis, glucocorticoid-induced; Progestins with no glucocorticoid activity*

- Bone formation, HSD2 overexpression and, SU520
- Children with nephrotic syndrome and, 1060
- 11 β -HSD1 activity in osteoblasts and, F365, SA365
- Mouse osteoprotegerin gene expression regulation by, SU519
- Osteoclast life span, bone density and, F367, SA367
- Persistence and adherence to alendronate and risedronate among chronic users of, SU390
- Primary- and secondary-prophylaxis to systemic use in primary health care of, SA372
- Risedronate and PTH effects in mouse model of osteoporosis induced by, SU067

Glucosamine. SEE *N-Butyryl glucosamine***Glucose-dependent insulinotropic peptide (GIP) receptors**

- Mouse behavior and deficiency of, SA050
- Osteoclastic activity inhibited by, SA269

Glucose transport

- 1 α -(OH) D₂ influence on insulin and PPAR γ mediated, M514

Glv-1

- Cataract and nephrotic syndrome in transgenic rats overexpressing, SU050

Glyceraldehyde-3-phosphate dehydrogenase (GAPDH)

- Bisphosphonates effect on gene expression by, M060

Glycogen synthase kinase 3 α / β inhibitor 603281-8

- PTH anabolic actions in bone and, F437, SA437

Glycogen synthase kinase 3 β (GSK-3 β)

- Inhibitor (603281-31-8) of, and bone response to Wnt 3a, M219
- Mechanical response by cementoblasts to fluid shear stress and, SU220

Glycosaminoglycan (GAG)

- Betula platyphylla* var. *japonica* and activity in rabbit articular cartilage of, SU056

Glypicans

- BMP4 signaling disrupted in fibrodysplasia ossificans progressiva lymphoblastoid cells mediated by, M029

GNAS

- Progressive osseous heteroplasia and expression of, M439
- Pseudohypoparathyroidism type-1b variants and mutations of, 1036

GNAS1

- Epidermal nevus syndrome with focal bone defects and hypophosphatemic rickets and, SA452

Golfing

- Vertebral bone size and mass in postmenopausal women, M148

Gonadotropin-releasing hormone agonist therapy

- Prophylactic bisphosphonates during endometriosis treatment with, M342

Gothenburg Osteoporosis and Obesity Determinants (GOOD) study, 1129, F009, SA006, SA009, SU522**gp130 cytokines**

- Osteoclast formation and function regulation by, 1190

G-protein coupled receptor kinases

- Enhanced bone mass in mice lacking, F225, SA225

G proteins. SEE ALSO *Guanine-nucleotide regulatory protein α q*

- hXL α_s , as component of, F491, SA491
- Pertussis toxin-sensitive, ERK 1/2 activation role of, M506
- PTH1R and activation of ERK1/2 by β -arrestin and, SA480

Granulocyte-macrophage colony-stimulating factor (GM-CSF)

- IL-12 and IL-18 in skeletal development and signaling by, SA250
- Regulation of beta receptor gene expression in CT/GRP null mouse, M499

Graves' disease, untreated, SA451, SU375**Green fluorescent protein (GFP).** SEE ALSO

- Enhanced green fluorescent protein*
- Col3.6 promoter and expression in osteoclastic lineage by, F266, SA266
- Osteoprogenitor source and transplantation protocols comparison and, M238
- PTH1R tagged by, in F1 PTH1R-null osteoblasts, cAMP responsiveness to PTH(1-34) and, M503
- PTH action on osteoblast cultures expressing stage-specific, SA191

Greens plus herbal preparation

- Mineralized bone nodule formation in SaOS-2 cells and polyphenols from, M210

Growth. SEE *Skeletal growth***Growth/differentiation factors 5, 6, 7**

- Mesenchymal stem cells condensation and chondrogenesis and, M036

Growth hormone

- Burned children and anabolic effects of, SU475
- Direct action in osteoblasts, Cre/Lox disruption in IGF-1 receptor and, 1194
- Replacement of and FGF23, phosphate metabolism in adult growth hormone deficiency, M133
- T-box 3, osteoblast proliferation and, M183

Growth hormone/insulin-like growth hormone 1 deficiency mouse model, SU181**Growth hormone receptor**

- Bone mass and single nucleotide polymorphisms of, SA119

Growth hormone receptor (Cont'd)

- Estradiol recovery of hepatic IGF-I gene expression through JAK-STAT pathway and, 1199

Growth hormone releasing hormone gene

- Bone mass and single nucleotide polymorphisms of, SA119

Growth hormone secretagogue receptor

- Bone mass and single nucleotide polymorphisms of, SA119

Growth plate. SEE ALSO *Skeletal growth*

- β -Catenin-induced BMP signaling for chondrocyte differentiation, maturation in, 1110
- Cathepsin K deficiency and matrix structure of, SA022
- Caveolae and Cav-1 for 1 α ,25 OH₂D₃ regulation of, SU045
- Expression of osteoclastogenesis-related molecules in, SU036
- Gene screening within discrete compartments of, M052
- IGF signaling in early regeneration after irradiation of, SA152
- Murine, imaging vascular routes for *in vivo* delivery of fluoresceinated tracers to, SA033
- Rat, Ihh and PTHrP expression during recovery of growth retardation in, SA036
- Rickets and mineralization of, despite calcium deprivation leading to hypocalcemia, SU024

Growth plate chondrocytes

- Alternatively-spliced, extracellular calcium ion-sensing receptor in, SU510
- CaM kinase 1 β mRNA expression in, SU046
- Ossification regulation by CNP/GC-B system, F028, SA028
- PTHrP induces Smurf2 and inhibits TGF β signaling in, M488

GST-rRANKL mutants

- Inhibition of RANKL-induced osteoclast differentiation and activation by, M248

Guanine-nucleotide regulatory protein α q (Gq).SEE ALSO *G proteins*

- Osteoblast cellular morphology, function and RNA interference with, M216

Guanylyl cyclase. SEE ALSO *C-type natriuretic peptide/guanylyl cyclase B system*

- Calcium and calpain-dependent cytoskeletal rearrangement in osteoclasts and, SA241

Guinea pig model for circulating multipotential skeletal stem cells, SU031**L-Gulonolactone oxidase**

- Mouse gene expression profiling and deficiency of, M113

Gulonolactone oxidase (GULO) gene

- Vitamin C deficiency, spontaneous fractures and, 1045

Gymnasts

- Bone geometry changes in proximal femur of young female, M020
- Calcium supplementation for, SA008
- 24-months of training effects on insulin-like growth factors in prepubertal female, SA150

H**HB954**

- Expression in bone, F199, SA199

Health beliefs

- Cognitive representations by first degree relatives of osteoporosis patients and, SU346

Key Word Index

ASBMR 27th Annual Meeting

Health care costs

- Improved persistence with ibandronate once-monthly and, M361
- Osteoporosis fractures by race/ethnicity and gender in USA, F317, SA317
- Paget's disease treatment in privately insured population, SA466
- Projections for osteoporosis fractures by skeletal site in USA, 1078
- Provision of hip protectors to Ontario nursing home residents and, SU435
- PTH and alendronate in high-risk osteoporotic women, M405
- Risedronate *versus* strontium ranelate treatment for postmenopausal osteoporosis in Germany, SA403
- Use of bone turnover markers to select osteopenic postmenopausal women for alendronate therapy and, SU151
- Vertebral fractures, first year after, SA330

Health care systems

- Community-based post-fracture care model, M382
- Lack of osteoporosis care following fractures and, SU336

Health status

- Forearm BMD, bone loss and self-rated, SA300
- Non-persistence during daily therapy and, SU402

Health Study of Nord-Trøndelag (HUNT), Norway, SA300**Hearing loss**

- Osteoporosis of ossicle in mice and, SU007

Heart transplantation

- Alendronate treatment for osteoporosis associated with, M477, WG6
- BMD evolution after, antiresorptive therapy and, M478, WG7

Heat shock protein 60 (HSP60)

- Apoptosis via ROS-mediated mitochondrial pathway and p38 activation in osteoblast-lineage cells induced by, SU227

Heat shock protein 90/heat shock protein 47 (Hsp90/Hsp47)

- Bisphosphonates and expression in osteoblasts of, SU257

Hedgehog. SEE ALSO *Indian hedgehog*

- Oxysterol-induced osteogenic differentiation and, M427
- Signaling and proliferation of osteosarcomas and chondrosarcomas, SU101

Heel. SEE ALSO *Ultrasound, calcaneal quantitative*

- Scanning confocal ultrasound for quantitative prediction of bone density and strength in, SU173

Height loss

- Historical, vertebral fractures' detection using, SA320
- Teriparatide effects in osteoporotic women with severe prevalent vertebral fractures on, M404
- Vertebral deformity over one year and, SA314

HeLa cells

- Mustang gene promoter in, SA042

Hemarthrosis

- Bone regeneration and, M163, M200

Hemodialysis. SEE ALSO *Dialysis*

- Cortical bone measurements with pQCT and fractures with, M465
- 25(OH)D serum levels with uremia and, M472
- Parathyroidectomy with secondary hyperparathyroidism, osteocyte morphology/number and, M469
- pQCT of bone and muscle parameters with and without fractures, M078
- Tools for trace metal detection in bone with, M473, M474

Heparan sulfate proteoglycans (HSPGs)

- BMP4 signaling disrupted in fibrodysplasia ossificans progressiva lymphoblastoid cells and, M029

Heparin

- Adipogenic differentiation of mesenchymal progenitors and, M237

Heparin binding EGF-like growth factor

- Reduced bone mass, strength and expression in osteoblasts and osteocytes of, F289, SA289

Hepatitis C-associated osteosclerosis

- Intravenous pamidronate for, M457

Hepatocellular carcinoma (Hep G2) cells, M524**Hepatocyte growth factor (HGF)**

- Bone metastasis of mouse breast cancer cells and, SU107

Hexa-chlorobenzene (HCB)

- Electromagnetic field treatment and bone structure degeneration by, SU065

HIG-82 cells (rabbit synovial fibroblast), SU069**High performance liquid chromatographic (HPLC) assay, SA523****High resolution computed tomography. SEE**

ALSO *Quantitative computed tomography*

- Vertebral trabecular bone structure analysis, teriparatide treatment assessment with, M413

In vivo assessment of human vertebral

trabecular bone with, M095

High temperature factor A1 (HtrA1)

- Mineralized matrix deposition by osteoblasts and, SA025

Hip. SEE ALSO *Femoral head; Femoral neck; Hip structure analysis*

- Bariatric surgery and BMD declines despite stable PTH and vitamin D levels in, M322

- Hormone interventions and geometric structure of, SA430

- Mandibular index correlation with BMD of, SA089

- Osteoarthritis, risk factors in Japan *versus* Britain, M446

- Pain, osteoid sarcoma and, M525

- Plain radiographic indices correlation with BMD, M065

- Structural analysis, genome-wide linkage of geometry in, SU175

- Total BMD *versus* DXA at femoral neck as fracture risk predictor, 1009

Hip fractures

- Bayesian random effects model for pooling hip protector use to decrease, SU436

- Bone density and geometry in women with, M073

- Bone microarchitecture in Colle's fractures *versus*, 1178

- Celiac disease and vitamin D status in community-dwelling people with, M330

- Demographics among elderly women and, F327, SA327

- Demographics, length of stay, and mortality for men with, SA339

- Femoral neck fracture incidence in Okinawa, Japan, SA326

- Fragility, age factors and, SU376

- Heel and hip bone densitometry in postmenopausal women with, SA292

- Incidence and outcomes in Quebec, Canada, SU341

- Institutional-dwelling elderly women over 10 years, M284

- Life expectancy changes in Ireland and risk for, SU332

- Mandatory osteoporosis consultation in patients with, SU345

- Osteoporotic, serum CTx levels in, SU154

Hip fractures (Cont'd)

- Physical fitness and nutrition in elderly women and, SA332

- Plasma vitamin B12 in elderly and risk of, F309, SA309

- Prediction in elderly women using clinical factors and QUS, F096, SA096

- Prediction using automated structural measurements of proximal femur in pelvic radiographs, F090, SA090

- Prevention in Japanese aged-care facilities with increased hip protector use, SU441

- Reduced volumetric BMD and geometric properties with, SU339

- Socioeconomic factors in California 1996–2000 as predictor of, SA311

- Susceptibility in elderly, bone instability and, M088

- Time trends in mortality after, 1077

- Vertebral fractures and DXA scans of, M297

- Vitamin D and vitamin K deficiency in, M274

- Vitamin D deficiency and lower extremity functional changes in women and, SU337

Hip protectors

- Bayesian random effects model for pooling hip fracture outcomes and, SU436

- Economic implications of providing Ontario nursing home residents with, SU435

- Hip fracture prevention in Japanese aged-care facilities with increased use of, SU441

Hip structure analysis (HSA)

- Conventional DXA scanners image resolution properties and implications for measuring, M099

- Segmented 3D CT scans for, M098

Hispanics, M003, M308**Histomorphometry**

- Alendronate and bone remodeling patterns, M358

- Automated volumetric imaging of *in vivo* labels for bone formation, M046

- Microdamage accumulation indicators in postmenopausal women, F356, SA356

- Validation of vertebral spine indices of C57Bl/6 mice, M094

Histone deacetylase 4 (HDAC4)

- Hypoxia suppression of cartilage matrix terminal differentiation via, 1024

Histone deacetylase inhibitors (HDIs)

- Osteoclast apoptosis, differentiation and, M245

- Rheumatoid arthritis management and, SA027

- TCF/LEF-drive luciferase induced by, SA205

Histone deacetylases

- Runx2, osteoblast maturation and, F204, SA204

HIV

- BMD and fracture risk in women, SU347

- Cytokine-mediated osteoclastogenesis in postmenopausal women with, M445

- Oral cholecalciferol effect on serum levels of 25(OH)D in children and adolescents infected with, SU476

- Total body composition changes with treatment for, SU136

Hologic densitometers

- Automated computer-aided detection of vertebral fractures, SA324

- Short- and long-term precision of GE Lunar Prodigy scanners *versus* Delphi, M063

Home health care

- For osteoporosis treatment, SA354

Homocysteine

- Apoptosis via ROS-mediated mitochondrial pathway in human BMSCs, SU226

- Bone markers and serum levels of, SA328

- Bone matrix proteins modification by, SU074

- Serum levels in postmenopausal women, bone mass, bone turnover and, SU373

- Systemic lupus erythematosus and, SU487

Horizon Pivotal Fracture Trial with Zoledronic Acid, SA314

Hormone replacement therapy (HRT)

Age- and dose-dependent effects on fracture risk, 1227

Dietary silicon and BMD in premenopausal and postmenopausal women on, M338

Discontinuation of long-term oral low-dose, SU143

Hip and nonvertebral fracture risk and, M356
IL-1 system gene polymorphism effects on BMD in postmenopausal Korean women and, SU183

PTH(1-84) safety and efficacy in postmenopausal osteoporotic women on, 1080

Horses

Reduced use of Premarin and welfare of, M381

Hospitalization

Osteoporotic fractures, persistent usage of bisphosphonates and reduction in, SU388

Hospitals

Osteoporosis care pathways for patients with fragility fractures in, SA312

Hospitals, trauma

Fracture frequency in patients over 50 in Mexico City, SU326

Hoxa-10

Runx2 activation and osteogenesis regulation by, 1013

Hrk-deficient mice

Ovariectomy effects on bone quality in, SA103

Human bone substrates

Human osteoclast cultures of, SU289

Humerus

Genetic and maternal determinants of bone mass in newborns at, M016

Humoral hypercalcemia of malignancy

Lung squamous cell carcinoma-associated, EGFR signaling inhibition and, 1215

Hyaluronan

Suppression of IL-1 β action on rheumatoid synovial fibroblasts via ICAM-1, SU071

Hydrogen peroxide

RANKL-induced osteoclast differentiation and, SU292

Hydrostatic pressure

In vivo measurement of bone viscoelastic properties and, M089

Hydroxyapatite

Computer model of bisphosphonates binding affinities to, SU306

Monitoring load-driven fluid flow using microparticles and, M151

Hydroxyapatite column chromatography

Bone mineral binding differences among bisphosphonates using, M351

Hydroxyapatite scaffold

Bone augmentation with polylactic acid plate and, SU068

Connective tissue growth factor and hBMSC *in vivo* attachment onto, SU062

Mechanical strain caused by ultrasound and bone formation in, SU090

24-Hydroxylase (24(OH)ase)

Substrate 25-(OH)₂D role in post-translational targeting to mitochondria of, M518

Hydroxyl ions

One-dimensional ³¹P-¹H spectroscopy of, SU059

[^{99m}Tc]-Hydroxymethylene diphosphonate single photon emission computed tomography (MDP-SPECT/CT)

Tumor burden and osteolysis monitoring in breast cancer bone metastasis mouse model, M054

[^{99m}Tc]-Hydroxymethylene diphosphonate single photon emission computed tomography (MDP-SPECT/CT) (Cont'd)

Tumor burden imaging in 5TGM1 mouse model, SU098

11 β -Hydroxysteroid dehydrogenase type 1 (HSD1)

Inflammatory cytokines and glucocorticoids effects on, F365, SA365

Hydroxysteroid dehydrogenase type 2 (HSD2)

Overexpression, calvarial development in transgenic mice and, SU520

11 β -Hydroxysteroid dehydrogenase type 2 (HSD2)

Glucocorticoid signaling inhibition by overexpression of, F507, SA507

25-Hydroxyvitamin D

Assay variations and status of, SA526

Clinical relevance of fractioning into 25(OH)D₂ and 25(OH)D₃, F524, SA524

Daily, weekly, or monthly protocols to reach desired serum concentration for elderly of, SU428

Diasorin radioimmunoassay *versus* LC-MS/MS for measurement of, SA527

Health-related quality of life in postmenopausal osteopenic women and serum levels of, SU463

Optimal serum levels for older people, F349, SA349

Physical performance in elderly postmenopausal women and, M309

Plain hip radiographic indices correlation with BMD and serum levels of, M065

Substrate, role in post-translation targeting of 24-hydroxylase to mitochondria and, M518

Ultraviolet B effects on serum levels in humans of, SA519

Uremic patients in hemodialysis and serum levels of, M472

Urinary, in black and white female adolescents, binding activity of, M517

Vitamin D deficiency and serum levels of, M279

25-Hydroxyvitamin D-1 α -hydroxylase

Abnormal renal phosphate transport in *hyp*-mice and, 1205

25-Hydroxyvitamin D-1-hydroxylase

Colorectal hepatic metastasis and levels of, M522

Substrate mediated mitochondrial localization of, M519

25-Hydroxyvitamin D₂

Serum level comparisons of patients treated with pharmacological doses of vitamin D₂, SA523

1 α -Hydroxyvitamin D₂

Influence on insulin and PPAR γ -mediated glucose transport, M514

1 α ,25-Hydroxyvitamin D₂-vitamin D₃/VDR genomic antagonists

Elucidation of molecular mechanism of antagonism by (23S)-25-dehydro-26,33-lactone (MK) side chain of, SA503

1,25-Hydroxyvitamin D₃

Epithelial calcium channel-2 genes expression regulated by, M515

19-nor-1,25-Hydroxyvitamin D₃

Prostate cancer treatment using analogs of, SU110

25-Hydroxyvitamin D₃

Optimal supplementation in healthy adults, M510

Osteoblast differentiation in human marrow stromal cultures and, M155

25-Hydroxyvitamin D₃ (Cont'd)

Serum level comparisons of patients treated with pharmacological doses of vitamin D₂, SA523

Suppression of PTH synthesis and secretion by cultured bovine parathyroid cells, M475

Therapeutic cancer applications for, 1202

25-Hydroxyvitamin D₃-1 α -hydroxylase

Cancer cells growth and siRNA against, 1202

Secondary hyperparathyroidism from FGF23 overexpression and reductions in, F453, SA453

25-Hydroxyvitamin D₃ 24-hydroxylase (24(OH)ase)

Substrate 25-(OH)₂D role in post-translational targeting to mitochondria of, M518

SWI/SNF chromatin remodeling complexes and VDR-C/EPB β in transcriptional regulation of, 1201

Transcription regulation by glucocorticoids, 1204

Hyperaldosteronism

Osteopenia in cardiac cachexia and, SU349

Hypercalcemia

Hypocalciuric, with recurrent pancreatitis, cinacalcet and, SU509

Induced by 1 α ,25(OH)₂D₃ analogs in osteopetrotic (op/op) mice *versus* osteoclast-absent c-fos deficient mice, F260, SA260

Severe, thyrotoxicosis and, SU471

Hypercalcemia (animal models)

Hypomagnesemia, hypokalemia, and hyperphosphatemia in horses and, SU513

Hypercalcemia, familial hypocalciuric

Physiological relevance of Venus flytrap module in CASR and, SA485

Hypercalciuria, idiopathic

CSF-1R in osteoporosis pathogenesis in, M467

Hyperhomocysteinemia

Restoration by folate therapy, uncoupled bone remodeling in, SU380

Hyperkyphosis. SEE ALSO Kyphosis

Heritability of, SU180

Hyperostosis frontalis interna

Elevated bone turnover markers in patient on teriparatide and, SA434

Hyperoxia

Connective tissue progenitor cells' formation, proliferation and, M164

Hyperparathyroidism. SEE ALSO

Parathyroidectomy

Accuracy differences of sestamibi scanning between severe and mild, SU468

Familial isolated, genetic testing in, M462

Vitamin D deficiency and, M326

Vitamin D deficiency in morbid and super obese patients, M323

Hyperparathyroidism, primary

Bone microarchitecture in mild cases of, M461

CASR haplotype polymorphisms and renal stone phenotype of, F122, SA122

Epidemiology in Rochester, MN 1993–2001, SU464

Mutational analysis of PTH 3' untranslated region in, SU472

Parathyroidectomy and asymptomatic, 1167

Vitamin D depletion prevalence among subjects seeking advice about management of, 1168

Vitamin D ratio in separating familial hypocalciuric hyperparathyroidism from, SU479

Hyperparathyroidism, secondary

Cyclosporine A treatment in rats, skeletal growth and, M479

Key Word Index

Hyperparathyroidism, secondary (Cont'd)

Reduced 25-(OH)₂D₃-1 α -hydroxylase activity and FGF23 overexpression causing, F453, SA453

Hyperpolarization-activated and cyclic nucleotide gated nonselective cation channels-2 (HCN2)

Bone architecture, strength and, F039, SA039

Hypertension

BMD and PTH levels in, SU507

Hypocalcemia

Autosomal dominant, physiological relevance of Venus flytrap module in CASR and, SA485

CaR Ser⁸²⁰Phe mutation in Italian family with hypertension and autosomal dominant, SA118

DiGeorge syndrome, celiac disease and, SA468

Mineralization of rachitic growth plate despite calcium deprivation leading to, SU024

Zoledronic acid and prolonged, M370

Hypogonadism

FSH regulation of bone mass and osteoporosis due to, 1043

Hypomineralization. SEE ALSO *Mineral apposition rate*

Rabbit model of osteomalacia, study of compositional and mechanical implications of, M079

Hypoparathyroidism

Bone mineral density distribution in, SU470

Bone quality and, SU465

FGF23 and serum phosphate regulation in patients with, M129

Markedly elevated BMD in elderly man with, SU466

PTH improvement of bone turnover in, SU467

Hypophosphatasia

Adult, teriparatide treatment for, F457, SA457

Benign prenatal and odonto forms, M442

Infantile, homozygosity for TNSALP mutation C1348T causing variably lethal outcome in blacks, F474, SA474

Infantile, transplantation using bone fragments and cultured osteoblasts, 1166

Hypophosphatemia

In DMP1 null mouse, MEPE overexpression in osteocytes of, SA462

FGF23 regulation by phosphate depletion and, F459, SA459

Hypophosphatemia, X-linked

Altered mRNA expression of membrane transporters in, SA458

MEPE-ASARM peptide-associated mineralization defects in, 1163

PHEX/Phex mutation in osteoblasts and, 1105

Hypothalamus, ventromedial

Central nervous system control of unloading-induced bone loss and, F393, SA393

Hypothyroidism, latent

Heel QUS in postmenopausal Japanese women and, SA361

Hypovitaminosis D

Long-term treatment of, SU461

Hypoxia

Cartilage matrix synthesis via p38 MAPK and suppression of terminal differentiation via HDAC4, 1024

Expression, osteolytic bone metastases in breast cancer and, 1007

Femoral osteocytes in hindlimb-suspended mouse and, 1173

PGE₂ and OPG release from MC3T3-E1 cells and, M159

Hypoxia-inducible factor 1 α

Decreased osteoblastogenesis of hMSCs in model microgravity by upregulation of NOS2 and, SA171

Hypoxia-inducible factor 1 α (Cont'd)

Expression, osteolytic bone metastases in breast cancer and, 1007

I

Ibandronate

Administration and dosage with radiation therapy for breast cancer, SA075

Bone resorption markers in postmenopausal osteoporosis and once-monthly oral, SU410

Daily *versus* once-monthly, for postmenopausal osteoporosis, M347

Hip and nonvertebral fracture risk and, M356

Intra-osseously administered in infarcted femoral head, F476, SA476

Intravenous, BMD in postmenopausal osteoporosis and, SU413

Intravenous, efficacy in postmenopausal osteoporosis, F410, SA410

Intravenous, renal tolerability of, SU412

Intravenous, safety and tolerability of, M350

Nonvertebral fracture risk reduction by, SA411

Once-monthly, cost-effectiveness of, M361

Once-monthly, for postmenopausal osteoporosis, M346, SU415

Once-weekly 70 mg alendronate treatment *versus* once-monthly 150 mg treatment with, M359

Oral, bone remodeling activation frequency and, M364

Oral, breast cancer bone metastasis reduction with, SA073

Patient preferences for once-weekly alendronate *versus* once-monthly, M435

Primary bone tumor cells *in vitro* and, SU094

ICTP biological pathway in breast cancer bone metastasis, SU148**Id1 gene**

Osteoblast senescence, c-Abl and expression of, M225

Id1 gene promoter

p300 and regulation of, SA201

IkB kinase- γ (NEMO)

Cytokine-induced osteoclastogenesis and, F282, SA282

Ilium

Adult female, bone formation in periosteal, endocortical, and trabecular envelopes of, SU368

Alendronate influence on periosteal and endocortical bone formation in osteoporotic women, F414, SA414

Immunity

Of allogenic mesenchymal stem cells, M227

Indian hedgehog (*Ihh*). SEE ALSO *Hedgehog*

BMP-2 and PTHrP expression in growth plate and, 1154

Postnatal chondrocyte-specific deletion of, F035, SA035

PTH inhibition of ERK1/2 in chondrocytes and, SU042

Rat growth plate during recovery of growth retardation and expression of, SA036

Wdr5 interaction during endochondral bone formation with signaling by, F041, SA041

Wnt/ β -catenin signaling in endochondral bone formation, synovial joint development and signaling by, 1003

Indomethacin

Osteoblast cell number, AP production during osteogenesis and, M153

Inducible cAMP early repressor (ICER)

Osteoblast functions, ATF4 expression and, M187

Infants. SEE ALSO *Children*

Birthsize effect on bone mass, SU320

Bone ultrasound in children *versus*, SU167

Hypophosphatasia, transplantation of bone fragments and cultured osteoblasts in, 1166

Lunar Total Body software performance in preterm, SU484

Skeletal growth and hip fracture prediction in late adulthood, 1058

Infants, newborn

Genetic and maternal determinants of bone mass at humerus, M016

Lunar Total Body software performance in, SU484

Paternal bone size and bone mineral accrual in, F002, SA002

Inflammatory bowel disease

Vitamin D and vitamin K deficiencies and bone loss in, M333

Infliximab

Bone loss in patients with rheumatoid arthritis treated with, M389

Bone turnover markers in rheumatoid arthritis patients treated with, SU495

Influenza infection

RANK-Fc and host immune resistance to, SU448

Inhalation therapy

Safety assessments, SU128

Inhibin A

FSH, LH effects on bone marrow cells, and anabolic effects of, SU250

Overexpression and bone *versus* muscle loss in hindlimb-suspended mice, 1169

In silico virtual screening

Finding compounds disrupting Dkk-LRP5/6 and, 1062

Institutional-dwelling people. SEE ALSO

Community-dwelling people

Bayesian random effects model for pooling hip protector use to decrease hip fractures in, SU436

Hip fractures among elderly women over 10 years, M284

Insulin

BMP-2, T3 and redifferentiation of dedifferentiated chondrocytes and, SA034

1 α -(OH) D₂ influence on, M514

Insulin-like growth factors

Effects on 24-months of gymnastics training in prepubertal females on, SA150

Overexpression of PAPP-A and, SA146

Signaling in growth plate early regeneration after irradiation, SA152

Insulin-like growth factor I (IGF-I)

Aging and bone marrow stromal cells responsiveness to, SU012

Bone density, bone size in mice, and chondrocyte-specific disruption of, 1152

Bone mass accrual modulation in pubertal girls by muscle mass and, F007, SA007

Bone recovery after 2 weeks of unloading and, M146

Bone turnover in adolescent girls with type 1 diabetes and, SA469

Candidate gene on chromosome 10 affecting bone turnover, BMD and, 1212

Chondrogenic differentiation of mouse bone marrow-derived MSCs and, SA151

Circulating, during peak bone acquisition, 1193

Connexin43 and osteoblast response to treatment with, SU265

Estradiol recovery of hepatic gene expression in growth hormone resistant mice of, 1199

Insulin-like growth factor I (IGF-I) (Cont'd)

Estradiol therapy in mouse with congenital aromatase deficiency and serum levels of, SU527

β 3 Integrin recruitment and, SU262

New bone formation in aged-mouse model, M005

Osteoclastogenesis regulation and signaling by, SA147

Rabson-Mendenhall syndrome in child with high-normal bone mass and deficiency in, M441

Reloading after unloading and restored responsiveness of, SU221

Signaling, PAPP-A deletion effects on murine skeleton and, F149, SA149

Zinc supplementation and response to protein supplements by, SA416

Insulin-like growth factor I (IGF-I) receptor

Growth hormone direct action in osteoblasts and Cre/Lox disruption of, 1194

Insulin-like growth factor II (IGFII)

Rabson-Mendenhall syndrome in child with high-normal bone mass and deficiency in, M441

Insulin-like growth factor binding protein 2 (IGFBP-2)

Osteoporotic fracture risk in elderly men and, 1137

Insulin-like growth factor binding protein 3 (IGFBP-3)

Rabson-Mendenhall syndrome in child with high-normal bone mass and deficiency in, M441

Insulin-like growth factor binding protein 6 (IGFBP-6)

Non-canonical Wnt 11 transcriptional suppression of, SA148

R-FB effects on COX-2-mediated inhibition of transcription by, SA145

Insulin-resistance (Rabson-Mendenhall) syndrome

High-normal bone mass in child with severe IGF-I, IGF-II, and IGFBP-3 deficiency, M441

 $\alpha_v\beta_1$ -Integrin

Osteoclast activity and signaling by, SA243

 $\alpha_v\beta_3$ -Integrin

Syk role in signaling cytoskeletal organization in osteoclasts by, F244, SA244

 $\alpha 5$ Integrin

Fibronectin-dependent osteoblast detachment, apoptosis induced by FGFR-2 activation, F190, SA190

Mechanosensory role in hemichannel opening for prostaglandin release with mechanical stress, 1095

 β_1 -Integrin

Osteoblast response to substrate microtopography and 1,25(OH)₂D₃ and silencing of, M212

 β 3 Integrin

IGF-1 signaling in osteoblasts and, SU262

NFATc1 mediation of RANKL-induced osteoclast differentiation and, SA257

Integrin-linked kinase (ILK)

Bone resorption and inactivation of, 1147

Intercellular adhesion molecule-1 (ICAM-1)

Hyaluronan suppression of IL-1 β action on rheumatoid synovial fibroblasts via, SU071

Interferon α

Myelopoiesis in SLE-associated non-erosive inflammatory arthritis and, SU488

Interferon β signaling

2-ME mediated osteosarcoma cell death and, SU097

Interferon β /Stat1 signaling

RANKL-induced iNOS/NO as negative feedback inhibitor during osteoclastogenesis and, 1070

Interferon γ

Bone formation inhibition by activated T lymphocytes mediated by, F131, SA131

IL-12 and IL-18 in skeletal development and signaling by, SA250

Inhibition of CXCR4 and chemotactic recruitment of osteoclast precursors by SDF-1 suppressed by, SA265

Osteoclastogenesis and, SU279

Regulation of osteoclast inhibitory peptide-1 gene promoter, SU311

T cell activation and bone resorption effects *in vivo* by, F387, SA387

Interleukin-1 β

Bone resorption induced by, kinins and, M154

Chondrocyte death induced by, SA037

Connexin43 gap junctions and responsiveness of HIG-82 cells to, SU069

Interleukin-1 receptor 1

Bone loss in femur but not spine of lactating mice deficient in, SU212

Interleukin-1 system gene polymorphism

BMD change after HRT in postmenopausal Korean women and, SU183

Interleukin-3

Osteoclastogenesis inhibition by irreversible down-regulation of RANK expression by, SA268

Interleukin-4

STAT-6 dependent pathway for osteoclastogenesis inhibition by, SU207

Interleukin-6

Calcium supplementation, bone mass acquisition in children and genetic variation in, M121

Endothelin-1 regulation of osteoblast secretion of, bone formation and, SU261

LIF *versus* OSM and mRNA expression of, SU208

Pagetic-like osteoclasts formation and, 1207

STAT-mediated pathways in osteoblasts, osteoclast formation and, M262

Stunted skeletal growth and altered bone phenotype in transgenic mice overexpressing, F470, SA470

TGF- β stimulation in renal cell carcinoma bone metastasis of, 1126

Transcription of CASR via elements in both P1 and P2 promoters, SU514

Interleukin-7

Ovariectomy-induced bone loss and, 1115

Rescue of bone phenotype of IL-7 KO mice with osteoblast-specific overexpression of, 1189

Interleukin-11

STAT-mediated pathways in osteoblasts, osteoclast formation and, M262

Interleukin-12

Anti-osteoclastogenic effect of CpG-oligodeoxynucleotides, F251, SA251

IFN γ and GM-CSF signaling and skeletal developmental role of, SA250

Interleukin-13

STAT-6 dependent pathway for osteoclastogenesis inhibition by, SU207

Interleukin-18

IFN γ and GM-CSF signaling and skeletal developmental role of, SA250

Interleukin-23

Effects on osteoblasts and osteoclasts, M191

Interleukin-27

Effects on osteoblasts and osteoclasts, M191

International Society for Clinical Densitometry (ISCD)

Call for consensus on focal structural defects, M083

Intervertebral disks. SEE ALSO *Vertebrae, lumbar*

CD24 expression in, SU054

Degeneration of, Runx2 and, F032, SA032, SU055

Intracellular junctions

Osteoblast differentiation and phosphatidylinositol 3-kinase signaling activation at, SA230

Intramedullary pressure

Chronic monitoring in rats of telemetered, SA059

Inulin

Fructo-oligosaccharides enhancement of BMD and mucosal levels of calcium binding proteins in rats *versus*, SA420

Ipriflavone

Hematological patterns in postmenopausal women and, M335

Iron

Age-associated accumulation in bone, SU450

Ischemic necrosis of femoral head

Aging and angiogenic response after, SA136

RANKL inhibition of femoral head deformity in immature pigs after, 1128

Isotope-coded affinity tags (ICAT)

Proteomic study of osteoblast differentiation, SU283

Italians, F301, SA117, SA118, SA301, SA322

J

J77.1 macrophage-like cells, SU299

J774 macrophages

Co-cultured with rabbit osteoclasts, uptake of fluorescent alendronate analogue in, SU309

Jagged1

Induced in UMR 106-01 cells, effectiveness of PTH(1-84) *versus* PTH(1-34) for, SU503

PKA activation and PTH regulation of osteoblastic, F197, SA197

PTH regulation of Notch signaling during osteoblast maturation and, 1113

JAK-STAT pathway

Estradiol recovery of hepatic IGF-I gene expression in growth hormone-resistant mice through, 1199

Jansen-type metaphyseal chondrodysplasia, SA488**Japanese**

Alendronate treatment once-weekly and BMD in osteoporosis patients, SU389

Bone loss after gastrectomy in, M303

Bone loss and biliary cirrhosis in women, SU315

Circulating vitamin K and bone metabolism in healthy women, M291

Femoral neck fracture incidence in Okinawa, SA326

Latent hypothyroidism and heel quantitative ultrasound in postmenopausal women, SA361

Vertebral fracture risk prediction by radiographic absorptiometry and QUS in women, SA078

Jun activation binding protein 1 (Jab1)

TGF β /BMP signaling and, F154, SA154

JunB

Enhancement of cathepsin K promoter activity by NFAT2 in RAW 264.7 cells, M252

PTHrP actions on cementoblasts and, M182

Key Word Index

ASBMR 27th Annual Meeting

Jun N-terminal kinase (JNK)

1 α ,25(OH)₂D₃ activation of, in C2C12 muscle cells, M513
KR62776 suppression of RANKL-induced osteoclast differentiation by inhibiting activation of, M253
PGE₂ signaling pathway and, SA196
Prefusion osteoclast differentiation stage and, M240

c-Jun N-terminal protein kinases (JNK1/2)

PTH and 1 α ,25(OH)₃ differential regulation on rat intestinal cells of, M512

K

Karyopherin α 2 and β 1

PTH1R association with, M502

Kat2J.Nek1-/- mice

Skeletal defects in growing bone of, apoptosis in skeletal tissues in, 1156

Khon Kaen Osteoporosis Study (KKOS), Thailand, M066

Kidney

Extracellular calcium ion concentration and regulation of VDR level in cells of human, SU515
Intravenous ibandronate and safety in, SU412
PTH and calcitonin effects on CYP27B1 levels in tubular cells of, M521
Risedronate safety over wide range of serum concentrations in, SU406

Kidney disease, experimental

TGF α /EGFR induction for low calcium-induced parathyroid hyperplasia in rats, M463

Kidney failure

BMP-7 for osteodystrophy in, M035
Phosphate loading, bone mechanostat system and, M470

Kidney failure, chronic

Skeletal resistance to PTH induced by uremic toxins in, M466

Kidney function

Alendronate in women with impaired, SA413
Hip and vertebral fracture risk among older women and, M285

Kidney transplantation

Alfacalcidol *versus* calcitonin therapy in children for bone loss after, SU457, WG4
BMD in adolescents after, M481, WG8
Metabolic bone disease management, WG3

Kininogen

Paget's disease and, SA467

Kinins

IL-1 β -induced bone resorption and, M154

Knee bend test

Fall risk and, SU433

Knees

Bone formation enhancement in mouse tibia with frequency-dependent loading of, SA180
Osteoarthritis and subchondral sclerotic lesion in, M041
Osteoarthritis, risk factors in Japan *versus* Britain of, M446
PAPSS2 deficiency and premature degenerative joint disease of, SU047
Targeted *in vivo* MRI measurements of small cartilage defect volumes in, SU043

Knockin mice

Col10a1 N617K mutation, 1033
Gp130 δ Σ TAT/ δ Σ TAT, M262
PTHrP(1-84), 1050

Knockout mice

Androgen receptor, F509, F515, M196, SA509, SA515
BMP-6, 1027
Bmpr1a, 1034

Knockout mice (Cont'd)

c-Abl^{-/-}, M225
Calcium ion-sensing receptor, SU510
Cardiotrophin-1, 1190
Cartilage-specific conditional for TGF- β -receptor type I, 1192
 β -Catenin, F229, SA229
Cathepsin K, F234, SA022, SA233, SA234, SU277, SU456
Cav-1, 1182
Caveolin-1, F450, SA450
Connexin43, M167
COX-2, M045, SA482
Crtap protein, F053, SA053
Csf-1, SU036
CT/CGRP, M499
Cx43-/-floxOCN^{Cte}, F286, SA286
DC-STAMP, SU282
dkk1, 1001
DMP1, SA462
Double conditional *Fgfr1/Fgfr2*, 1195
EBF-1, 1184
ER α receptor, SU418
FGF23/VDR, F140, SA140
FSHR, SA516
Glucose-dependent insulinotropic receptor, SA050
gpl30^{-/-}, SU066
G-protein coupled receptor kinases, F225, SA225
Growth hormone receptor, 1199
Growth plate proteoglycans, SA022
HB954, F199, SA199
Hrk, SA103
1 α -Hydroxylase, 1099, 1203
Hypercholesterolemic LDLR^{-/-}, SU018
Ihh, F035, SA035
IL-1R1^{-/-} mice, SU212
IL-7, 1189
 α_v -Integrin, SA243
Integrin-linked kinase, 1147
Interferon γ receptor, SU279
Klotho, SU025
Leptin, SA508
5-Lipoxygenase, M166
Mitf^{A^{GA-9}}/*Mitf*^{A^{GA-9}}, SU294
Ncad^{+/-}/Cad11^{-/-}, 1063
Nf1, 1051
NF- κ B p50/p52, SA255
OPG^{-/-}, SU007
Osteoblast-selective androgen receptor, 1097
Osteocalcin, F051, SA051
Osteopontin, SU302
OST-PTP, SA040
Oxidized LDL receptor (SR-A), F242, SA242
P2X7 receptor, SU253
PAPP-A, F149, SA149
PAPSS2 (brachymorph), SU047
Placental growth factor, F253, SA253
PTH, 1203
Rab3D, M263, M264
Rac-2, F270, SA270
RANK, SA256
RANKL, SU491
Rgs2^{-/-}, SU037
Sca-1, SU370
sFRP1, 1021
Telomerase, M234
TIEG, SU010
TRAP, SU275
TRPV4, SU040
Urokinase receptor, M246
VDR, 1099, SA494

Koreans

Age-related spinal BMD changes and accumulated bone loss rate in women, SU001

Koreans (Cont'd)

Alendronate 70 mg once-weekly treatment and bone metabolism of postmenopausal women, M340
Body composition, fat distribution with calcium supplementation in obese postmenopausal women, SA422
Depression and BMD in postmenopausal women, SU350
IL-1 system gene polymorphism effects after HRT on BMD in postmenopausal women, SU183
Lumbar BMD, in women with and without metabolic syndrome, SA400
Raloxifene effects on lumbar BMD and bone markers in postmenopausal women with osteoporosis, SA424
Serum leptin and adiponectin concentrations and BMD in postmenopausal women, SU211

KR62776

Suppression of RANKL-induced osteoclast differentiation by inhibition of MAPK activation, M253

Kremen 2

Binding of DKK1 to cells overexpressing LRP5 in radioactive binding assay and, SA128
Dkk1-mediated inhibition of LRP5/6-Wnt3a-TCF signals in U2OS osteoblast-like cells, M217

Kyphoplasty

Percutaneous balloon, calcium phosphate *versus* PMMA for, M432

Kyphoscoliosis

Crtap protein loss and, F053, SA053

Kyphosis. SEE ALSO Hyperkyphosis

Lumbar, postural balance, osteoporosis and, M313
Thoracic, weighted kypho-orthosis program for, SU438

L

Lactation

Bone loss in femur but not spine of IL-1R1^{-/-} mice and, SU212
Bone mass recovery after weaning in mice, 1087
Calcium transport into milk for, F486, SA486
Prolactin, PTHrP, and calcitonin interactions during, M498
Rapid osteoclast apoptosis in maternal skeleton at end of, SU300
Real-time skeletal metabolism difference during and after, M048
Skeletal loading effects on cancellous bone during recovery after, SA182

Lactoferrin

LRP5 and anti-apoptotic effect in osteoblasts of, SU230

Lactose intolerance

Intestinal calcium absorption and, M331

LacZ

PTHrP gene-driven expression in chondrocytes and bone cells of, M497

Lamellar bone

Low-dose strontium and formation at periosteal surface of, M423

Laser ablation-inductively coupled plasma-mass spectrometry

Trace metal detection in bone for hemodialysis patients, M474

Laser capture microscopy

Of biomineralization foci for proteomic analysis, SA019

ASBMR 27th Annual Meeting

Key Word Index

Lasofloxifene (LAS)

- BMD and bone turnover markers in postmenopausal women with low or normal BMD and, F429, SA429
- Extraskeletal effects on postmenopausal women, SA428
- Ovariectomy-induced deterioration of bone microarchitecture and geometry in rats and, M396
- Phase 2 and phase 3 clinical trial design and strategy, M384
- Phase 2 dose response analysis in postmenopausal women, M385
- Skeletal effects in intact mice of bazedoxifene acetate *versus*, M394

Legg-Calve-Perthes disease

- Ibandronate intra-osseously administered in femoral head and, F476, SA476

Length of stay

- For men with hip fractures, SA339

Lentiviral gene therapy

- In vivo* imaging in two bone formation models of adenoviral gene therapy *versus*, M023

Leptin

- Adipose tissue and cortical bone size in non-weight-bearing bone in young men and, 1046
- Behavioral change in GIP receptor knockout mice and, SA050
- BMD in Korean postmenopausal women, adiponectin and serum levels of, SU211
- Bone formation inhibition and bone mass control in rodents and sheep, SU210
- Bone marrow adipocyte populations and, M233
- Cortical bone regulation and signaling by, M422
- Effects on weight reduction and cancellous bone mass in female rats, 1048
- Fat mass, lean mass, BMD and, SU314
- Idiopathic male osteoporosis, estrogen levels and, SA385
- Sex-specific bone size difference in knockout mice, SA508

Leptin receptor

- Bone structure and strength influences of, 1108

Leukemia, acute lymphoblastic

- Peak bone mass after childhood case of, SU477
- Physical activity and nutritional effects on fitness and bone mineral acquisition of children with, SU473
- Vitamin D deficiency with, SU096

Leukemia inhibitory factor receptor (LIFR)

- Bone resorption, RANKL and IL-6 mRNA expression, STAT3 activation and, SU208

Leupaxin

- Overexpression in osteoclasts, M258

Leuprolide acetate

- DMPA-SC 104 in treatment of endometriosis, effects on bone *versus*, SU517

Leuprorelin

- BMD evaluation after endometriosis treatment with estradiol and, SA426

Life expectancy changes. SEE ALSO *Mortality*

- Hip fracture risk in Ireland and, SU332

Ligaments

- Integrin $\alpha 7$ and resistance to mechanical stress-induced mineralization by, SA024

LIM mineralization protein-1 (LMP-1)

- BMP-2 responsiveness in human MSCs and, M193
- Interaction with Smurf1 and cellular responsiveness to BMP-2 enhanced by, M027

Lipid rafts, cellular membrane

- Adherent endotoxin TLR-4 activation without inducing TLR association with, M256
- V-ATPase-containing, and ruffled membrane formation in osteoclasts, SU296

Lipopolysaccharide

- Phenytion suppression and PGE₂ production in bone resorption and, SU301

Lipoprotein, low-density (LDL)

- High serum concentrations, increased bone resorption, osteoblast maturation inhibition and, SU239
- Lasofloxifene phase 2 dose response analysis in postmenopausal women and, M385

Lipoprotein, oxidized low-density (LDL) receptor

- Osteopetrosis and, F242, SA242

Lipoprotein-related protein-5/6 (LRP5/6)

- Kremen 2 and Dkk1-mediated inhibition of Wnt3a-TCF signals in U2OS osteoblast-like cells and, M217
- Temporal expression in embryonic, growing, and adult mouse bone by, SA130

Lipoprotein-related protein-5 (LRP5)

- Autosomal dominant type I osteopetrosis mutations of, osteoblast support of osteoclastogenesis and, 1206
- Bone formation and compounds disrupting Dkk interaction with, 1062
- Genetic determinants of bone size and, SA111
- Genetic polymorphisms influence on BMD in men, SA336
- Kremen-2 and MesD effects on Dkk-1 binding to cells overexpressing, SA128
- Lactoferrin anti-apoptotic effect in osteoblasts and, SU230
- Mutation in OPPG affecting bone accrual and eye development, SA439
- Osteoporosis-pseudoglioma syndrome and, SA099
- Peak bone mass and C-864T polymorphism in, SU191
- Peak bone mass in men and gene polymorphism of, SU189
- Regulation of intrinsic material properties of cortical bone by, M050
- Spinal osteoarthritis and Q89R polymorphism in postmenopausal women and, SU190
- Wnt3-Fzd1 chimera signaling and, M197
- Wnt signaling and sclerostin binding to, M220

Lipoprotein-related protein-6 (LRP6)

- Bone formation and compounds disrupting Dkk interaction with, 1062
- Bone resorption, bone mass acquisition in *ringelschwanz* mutant mice and, 1181
- Variants, fracture risk in elderly men and, F120, SA120

Lipoproteins, triglyceride-rich

- In mice, bone role in clearance of, M332

5-Lipoxygenase

- COX-2 activity ablation, fracture healing and, M166

Liquid chromatography-mass spectrometry (LC-MS)

- Vitamin D assay with, SA526

Liquid chromatography-tandem mass spectrometry (LS-MS/MS)

- Diasorin radioimmunoassay of 25(OH)D *versus*, SA527
- 25(OH)D immunoassays using, F524, SA524

Lithium chloride

- Wnt pathway effects on osteoblast differentiation, proliferation and, SA221

Liver

- N-Butyryl glucosamine effects in ovariectomized rats on gene expression in, M418
- OPG gene expression of patients with biliary cirrhosis in, SA388
- C-telopeptide, PINP and metabolism of, SU149

Liver cirrhosis, biliary

- Alendronate once-weekly 70 mg treatment *versus* 10 mg once daily in osteopenia associated with, SU392
- Bone loss in Japanese women and, SU315
- OPG gene expression in liver of patients with, SA388

Liver transplantation

- Alendronate treatment for osteoporosis associated with, M477, WG6
- Body composition and serum IGF-I, IGFBP-3, and leptin levels in children before and after, M480
- Vitamin D insufficiency and osteoporosis in, M476, WG5

Loading. SEE ALSO *Hydrostatic pressure*

- Body fat influences on bone mass and, M139
- Bone architecture *versus* bone mass influences of, SU363
- Cyclic, NMDA receptors and bone cellular potentiation from, 1094
- DMP1 and MEPE expression in osteocytes and, F168, SA168
- Estrogen receptor β role in response to, 1091
- Estrogen withdrawal and bone mechanosensitivity to, F181, SA181
- Expression of mechanosensitive, prochondrogenic genes, F057, SA057
- Frequency-dependent bone formation enhancement in mouse tibia, SA180
- Microarray analysis of molecular mechanisms in rat bone of, SU223
- Modulation of RANKL, OPG expression in MC3T3.E1 cells and, SA167
- Non-weight bearing and weight-bearing bone structure and types of, SA178
- Osteoblast activity prediction by Ca²⁺ oscillations induced by rest-inserted, SU218
- Prepubescent female rats with low estrogen and, M138
- QTL in C57BL/6J-C3H/Hej intercross mice for BMD and bone size responsive to, F183, SA183
- Skeletal growth benefits, 1170
- Skeletal loading effects on cancellous bone during post-lactation recovery, SA182
- Spinal, assessment of osteoporosis therapies efficacy using estimates of, M411
- Spinal, vertebral strength population-based study and, 1074
- 3D model of DMP1 gene expression in osteocytes with, 1093

Long bones

- Bmpr1a* age-dependent role in development of, 1034
- N-Butyryl glucosamine effects in ovariectomized rats on, M418
- 1,25(OH)₂D₃ regulation of vascular invasion during embryonal development of, SA494
- Directional sensitivity of rodent cortical strength to collagen denaturation in, SU093
- Gender differences in children, SU319
- Longitudinal Aging Study Amsterdam (LASA),** 1134, F349, SA349
- Lovastatin,** SU029, SU234

Lower extremities

- Functional changes after hip fractures in women, vitamin D deficiency and, SU337
- Maximum rising strength as predictor of femoral neck BMD in healthy women, M142

LSN500307

- Pharmacologic actions in ovariectomized rats, SA427

Key Word Index

ASBMR 27th Annual Meeting

Lumbar spine

- DXA measurements of BMD, calcium supplements and, M068
- Quality of life with osteoporosis and mobility of, M431
- Very low birth weight effects on bone mass in young adults at, I132

Lunar pediatric total body software. SEE *GE Lunar Prodigy densitometers***Lung cancer**

- Expression of RANKL and BMPs influences bone metastasis of, F135, SA135

Lung squamous cell carcinoma

- Humoral hypercalcemia of malignancy in mouse model of, EGFR signaling inhibition and, I215

Lung type II epithelial cells

- Non-amino terminal PTHrP receptor-like binding activity in, M495

Lupus erythematosus, systemic

- Baseline BMD and bone turnover markers predict 2-yr. change in BMD in, SU490
- Baseline BMD and calcium homeostasis measures with 2-yr. change in BMD in, SU492
- Homocysteine level, BMD, and fracture risk in, SU487
- Interferon α effects on myelopoiesis non-erosive inflammatory arthritis associated with, SU488
- Serum OPG, RANKL, and 2-yr. change in BMD in, SU494

Luteinizing hormone (LH), bone anabolic effects of inhibin A and, SU250**Lycopene, dietary**

- Biomarkers of oxidative stress and bone resorption in postmenopausal women and, SA308

Lymphocytopenia

- Soy protein supplementation in postmenopausal women and, M335

Lymphoid enhancer-binding factor 1 (Lef1)

- Overexpression, late osteoblast differentiation and, M185

Lymphoid enhancer-binding factor (Lef)/T cell factor (TCF)

- β -Catenin recruitment by BMP-2 to Smad-containing complexes from transcriptional machinery of, I109
- Transcription activation by MINT, M173

Lysin-63 (K-63)-linked polyubiquitin chains

- E3 ligase activity of TRAF6 required for RANK-induced osteoclastogenesis and, I069

Lysophosphatidic acid

- MC3T3-E1 cells' motility and, SA124

M**Macrophage-colony stimulating factor receptor (CSF-1R)**

- Osteoporosis pathogenesis in idiopathic hypercalciuria and, M467

Macrophage inflammatory protein 1 (MIP-1)

- Multiple myeloma cell-derived, dendritic cells actions of, SU102

Macrophage-like cells

- Bisphosphonates *in vitro* effects on apoptosis and death of, SU299

Macrophages

- Cell-cell fusion, DC-STAMP expression during, F258, SA258

Magnesium

- Alendronate or vitamin K₂ treatment and bone mineral/matrix changes in rats deficient of, M321
- Bone matrix mineralization in klothe mouse, mapping of, SU025

Magnetic resonance imaging

- Assessing changes in children of femoral bone structure and strength using, M100
- Targeted *in vivo* measurements of small cartilage defect volumes in knee joints, SU043

Magnetic resonance imaging, high resolution

- Distal radius in postmenopausal women to assess cortical bone, SA083

Magnetic resonance T₂ relaxation time

- Trabecular bone structure assessment and, SA085

Mammary glands

- PTHrP and BMP signaling interactions during development of, I157

MAN1 germline mutations

- Osteopoikilosis, Buschke-Ollendorff syndrome and, M443

Managed care

- Health care costs in first year after vertebral fractures, SA330
- Persistence with bisphosphonate therapy and fracture risk in postmenopausal women in, M362

Manatee, Florida

- Skeletal biomechanics of, M145

Mandible

- Assessment of mechanical significance of structure by remodeling simulation, SU085
- BMD measurement and dental clinical findings, SA082
- gp130-mediated signaling in development of, SU066
- P20C/EBP β and reduced alveolar bone mass in, F210, SA210

Mandibular index

- Correlation with hip and spine BMD, SA089

Marfan syndrome

- Tight skin mutation mice skeletal phenotype and, F046, SA046

Mast cells

- Osteopenia development in ovariectomized mice deficient in, F389, SA389

Mathematical models. SEE ALSO *Computer models*

- Osteoporosis type I and type II from estrogen deficiency, SA348
- Predictions of bone marker response to PTH(1-34) dosing in rats, SA484

Matrix Assisted Laser Desorption Ionization - Time of Flight (MALDI-TOF)

- Proteomic study of osteoblast differentiation, SU283

Matrix calcification. SEE ALSO *Extracellular matrix*

- HtrA1 regulation of mineralized matrix deposition by osteoblasts in, SA025

Matrix extracellular phosphoglycoprotein (MEPE). SEE ALSO *MEPE-ASARM peptide*

- Expression in tumor-induced osteomalacia, M126

- Mechanically induced expression in osteocytes of, F168, SA168

- Overexpression in DMP1 null mouse, SA462

Matrix gla protein (MGP)

- C-terminal binding with vitronectin, SA052

Matrix metalloproteinase-1 (MMP-1)

- Hyaluronan suppression of IL-1 β action via ICAM-1 on rheumatoid synovial fibroblasts and, SU071

Matrix metalloproteinase-3 (MMP-3)

- Hyaluronan suppression of IL-1 β action via ICAM-1 on rheumatoid synovial fibroblasts and, SU071

Matrix metalloproteinase-13

- Expression regulated by ROS in ATDC5 cells, SU072

Matrix metalloproteinases

- Betula platyphylla* var. *japonica* and activity in rabbit articular cartilage of, SU056
- Compensation for cathepsin K activity loss in osteoclast function and, SA237
- Prinomastat as inhibitor of, SA233
- TGF- β regulation in renal cell carcinoma bone metastasis by, F156, SA156

Matrix proteins

- AC-100 and new bone formation by cell binding to, SU214

Matrix vesicles

- BMPs and non-collagenous matrix proteins carried by, M030

MC3T3.E1/C4 (clone 4 murine) cells

- BMP-3 signaling through Smad2 in, M026
- Differentiation, dimethyl sulfoxide enhancement of, M208

MC3T3.E1 cells

- Adenosine receptor expression in, SU260
- Androgen receptor and proliferation, differentiation of, M196
- Canonical Wnt signals and Mx2 pro-osteogenic actions in, I004
- β -Cryptoxanthin stimulation of cell differentiation, mineralization of, M213
- Dkk-1 and differentiation of, M192
- Expression of rate-limiting enzyme for serotonin synthesis by, SA386
- Fidgetin-like 1 effects on proliferation, differentiation and apoptosis of, SU236
- Fluid flow regulation of the 3'-untranslated region of cyclooxygenase-2 in, SA169
- Fulvic acid of Mumie and differentiation of, M209
- Hypoxia-induced PGE₂ and OPG release from, M159
- Lef1 overexpression, and late differentiation of, M185
- Lysophosphatidic acid and motility of, SA124
- MAPK and TNF inhibition of differentiation by, SU241
- Mechanical loading alteration of RANKL, OPG expression in, SA167
- Mustang gene promoter in, SA042
- NaOH and osteogenesis on PLGA scaffolds of, SU058
- NFAT regulation of COX-2 expression with fluid shear stress in, SU224
- Phosphatidylinositol 3-kinase signaling activation at intracellular junctions and differentiation of, SA230
- Polycystin-1 and *Runx2* promoter activity in, I061
- Polyphenol extract from dried plum and nodule formation in, SU246
- Proteomic and microarray analysis of inorganic phosphate treated, M186
- Regucalcin and differentiation, mineralization of, M201
- Regulation of osteoblast differentiation and BMP signaling by twisted gastrulation protein and chordin in, M037
- Resistin expression and regulation in, SA252
- Ror2 and matrix mineralization in, M189
- Shear intensity-dependent regulation of Runx2 in, SU225

MDA-MB-231 breast cancer cells, SA065, SU123**Measles virus nucleocapsid protein**

- TNF- α -induced osteoclast differentiation and, F464, SA464

Mechanical Response Tissue Analyzer (MRTA)

- Cortical bone loss assessment using DEXA and QUS *versus*, SU133

Mechanical strain. SEE *Stress, mechanical*

ASBMR 27th Annual Meeting

Key Word Index

Mechanostat system

Renal failure aggravated by phosphate loading, M470

Meckel's cartilage

Embryonic, gp130-mediated signaling in morphogenesis of, SU066

Medicare beneficiaries

Osteoporosis medications compliance among, M371

MEK/ERK pathway

Eg21, Egr2 and osteoclast survival regulation by, M257

2-Melanocyte-stimulating hormone (2-MSH)

Bone histomorphometric change in leptin deficient Ob/Ob mice with adrenalectomy and, SU027

Melanoma

Metastatic, collagenase 3 induced by osteoblast interaction with, SA063

Melorheostosis

Deactivating germline mutations in LEMD3 (MAN1) and, M443

Membrane-type 1 matrix metalloproteinase (MT1-MMP)

RANKL shedding activity and, 1188

Men

African American veterans, osteoporosis risks in, M306

Age-related regional changes in body composition and bone mass, M072

AZD0530 effect on bone remodeling in healthy, M251

BMD and bone markers with idiopathic vertebral fracture and celiac disease, SA383

BMD and thiazide, NSAIDs, and steroids use by, M307

BMD in myocardial infarction survivors, M299

Bone marker changes with one month teriparatide treatment for severe osteoporosis, M408

Demographics, length of stay, and mortality with hip fractures, SA339

Determinants of aromatase expression and serum estradiol levels in, SU521

Elderly, bone quality in, creatinine clearance, muscle strength and, SU008

Elderly, ER α coactivator RIZ1 deletion polymorphism and BMD of, SU187

Elderly, erythropoietin and BMD in, SA303

Elderly, estrogen as determinant of femoral neck bone strength in, SA384

Elderly, IGFBP-2 and osteoporotic fracture risk in, 1137

Elderly, LRP6 variants and fracture risk in, F120, SA120

Elderly Swedish, SHBG as negative independent BMD predictor in, SU524

Elderly Swedish, SHBG TAAAA repeat polymorphism and hormone levels and BMD in, SA512

Estrogen and leptin levels with idiopathic osteoporosis in, SA385

Ethnic diversity in volumetric BMD and bone geometry of, 1135

Fractures in postmenopausal women *versus* fractures in, M300

Healthy, dietary phosphate regulation of FGF23 in, M131

Hypogonadism and vitamin D insufficiency with dialysis, M468

Laboratory testing and for diagnosis osteoporosis, SA380

LRP5 gene polymorphism and peak bone mass in, SU189

LRP5 genetic variants influence BMD in, SA336

Mexicans over 50 years, vertebral fracture prevalence in, M287

Men (Cont'd)

Nonvertebral and hip fracture risk with falls by, M305

Normal BMD and fractures detected with densitometric vertebral fracture assessment in, M281

Older, hip BMD and body composition in multi-ethnic, F338, SA338

Older, neuromuscular function and fracture risk in, SA343

Older, physical activity and fracture risk in, M290

Osteoporosis Self-assessment Tool and, M302

Polish, VDR, COL1A1, ESR gene polymorphisms and BMD variations in, SA123

Referral patterns to osteoporosis scanning service by family practitioners, SA340

Short-term and long-term absolute fracture risk by BMD and age, 1138

Skeletal effects of milk fortified with calcium and vitamin D₃, F419, SA419

Spinal cord injuries and mechanical properties of tibia in, SA377

Testosterone and estradiol effects on skeletal sensitivity to PTH in, 1107

T-scores of -2.5 in ages 50-65, M301

Untreated Graves' disease, BMD in, SU375

Wnt10b and bone density in, F341, SA341

Young adult, senile osteoporosis differences with osteoporosis in, SU367

Young adult, trabecular bone loss in, 1010

Young adult, urinary 3 β Adiol as BMD predictor in, SU522

Menaquinone-4 (MK-4)

Vitamin K-dependent gamma-glutamyl carboxylase activity of vitamin K compounds in liver, bone and, SA198

Menatetrenone (MK-4). SEE ALSO Vitamin K₂

Osteoclast formation inhibition and osteoclast precursor cell differentiation inhibition and, SU280

Menopausal women. SEE ALSO Women

Milk basic protein supplementation and bone metabolism in, SU426

Site-discordance of osteoporosis categorization in, F077, SA077

Ten-year absolute fracture risk and WHO risk categorization in, 1037

Menstruation. SEE ALSO Amenorrhea

Dietary restraint in premenopausal women, BMD, and subclinical disturbances in, SU348

Irregularity and low BMD in high school runners, SU356

Subclinical irregularities in premenopausal women, BMD changes and, M316

MEPE-ASARM peptide. SEE ALSO Matrix

extracellular phosphoglycoprotein

Mineralization defects in X-linked hypophosphatemia and, 1163

MesD

Binding of DKK1 to cells overexpressing LRP5 in radioactive binding assay and, SA128

Mesenchymal stem cells (MSCs). SEE ALSO

Embryonic stem cells; Stem cells

Alendronate and differentiation of, F412, SA412

Allogenic, immunity of, M227

Bone marrow-derived, IGF-I effects on chondrogenic differentiation of, SA151

Bone regeneration, anterior cruciate ligament-induced hemarthrosis of knee as source for, M200

Calcium phosphate and osteogenic differentiation of, M232

Canonical Wnt signaling and osteoblast or chondrocyte differentiation from, 1064

Mesenchymal stem cells (MSCs). SEE ALSO

Embryonic stem cells; Stem cells (Cont'd)

Canonical Wnt signals and Msx2 pro-osteogenic actions in, 1004

Circulating, non-union fractures and, M226

CTGF role in downstream mediation of TGF- β 1-induced condensation and regulation of FN, Sox9 expression in, SU035

Differentiation, C/EBP α isoforms and, M190

ELR⁺ CXC chemokines in human, dexamethasone and, SU203

Endothelial cells and differentiation into osteoblasts by, SA213

Growth/differentiation factors 5, 6, 7 effects on condensation of, M036

Human, ATP and fluid flow-induced proliferation of, SU217

Human, bone-marrow derived, extracellular matrix and, M235

Human bone marrow-derived, hCYR61 effects on, M231

Human, bone-marrow derived, migration in response to fracture regeneration cue by, 1065

Human, decreased osteoblastogenesis in microgravity model by, SA171

Human, Dlk1/Pref-1 effects, M202

Human, isolation and culture *in vitro*, M207

Human, LMP-1 and BMP-2 responsiveness in, M193

Human, PKA and BMP signaling during osteogenic differentiation of, SU235

Murine model of commitment and differentiation, SU052

Osteoactivin and differentiation of, M228

Osteogenic effects in aged ovariectomized rats of bFGF and prior intra-arterial injection of, SA137

PPAR γ 2 and regulation of differentiation by, SU242

Retinoic acid and differentiation of, M204

Runx2 and RANKL expression in, M160

Tendon formation induced by manipulation of Smad8 and BMP2 in, SU061

ZIP1 overexpression and initiation of osteogenic lineage from, 1112

Metabolic acidosis. SEE ALSO Acidosis

Calcium signaling in osteoblasts and, M222

p38 MAPK mediation of prostaglandin synthesis and bone resorption by, SU258

Metabolic bone disease

In ancient Egyptian mummy, pregnancy and/or famine and, M454

Kidney transplantation recipients, management in, WG3

Short bowel syndrome and, M444

Metabolic processes

Osteoblast gene expression and differentiation, SU243

Metabolic syndrome

Lumbar BMD, in Korean women with and without, SA400

Metaphyseal chondrodysplasia type Schmid (MCDS)

Knockin mouse model for *Col10a1* N617K mutation associated with, 1033

Metformin

Osteoblast growth and differentiation induced by, SU196

Methionine

Scan of PTHR1 region [168-176], M509

2-Methoxyestradiol (2-ME)

Interferon signaling and osteosarcoma cell death mediated by, SU097

Methylmethacrylate

Vertebral compression fractures and injections of, SA333

Key Word Index

ASBMR 27th Annual Meeting

Mevalonate

Inhibition by atorvastatin, apoptosis in human prostate cancer cells and, M057

Mexican Americans

FGFBP1 and BMD in, SU195
Heritability of BMD in, F100, SA100

Mexicans

Vertebral fracture prevalence in men over 50 years, M287

MG63 osteoblast-like cells, M195, SU263**MHC class II transactivator protein (CIITA)**

Estrogen-dependent chromatin remodeling *in vivo* at, I143

Microarray analysis. SEE ALSO *Gene chip analysis; Gene expression*

Connexin43 null osteoblasts, M167
Differential gene expression in oral squamous cell carcinoma, SU106
Differential protein expression during fracture healing, M199
Estradiol regulation of gene expression in osteoclast cytoskeleton, SU523
Gene expression signatures of MLO-Y4 osteocyte cell model, SA291
Inorganic phosphate treated MC3T3 E1 cells, M186
Molecular mechanisms of mechanical loading in rat bone, SU223

Micro-computed tomography. SEE ALSO

Quantitative computed tomography
Bone integrity with BMP-7 treatment of renal failure, M035
Cortical and trabecular bone of transilial biopsy treated with alendronate, SU393
Male idiopathic osteoporosis study of iliac crest biopsy, M091
Neovascularization assessment in fracture healing of COX-2-/- mice, M045
3D-microarchitecture descriptors correlation with texture analysis of X-ray radiographs, SU366
3D-microarchitecture of new bone formation on prosthetic implants, M090

Micro-computed tomography, high resolution

Cortical shell role in vertebral strength assessment, F088, SA088

Micro-computed tomography, polychromatic

Bone tissue mineralization assessment, M069

Microdamage accumulation

Confocal *versus* light microscopy for *in vivo* detection in wild and domesticated animals, M044
Diffuse *versus* linear microcracks, bone quality and, SA188
Histomorphometric indicators in postmenopausal women of, F356, SA356

Microgravity, modeled

Decreased osteoblastogenesis of hMSCs by upregulation of NOS2 and HIF-1 α , SA171
RhoA activity downregulation and actin cytoskeletal disruption in, SU222

Microphthalmia-associated transcription factor (MITF)

C-TAK1 interaction with during osteoclast differentiation, SA281
Osteoclast differentiation, bone development and, SU294

Micro-positron emission tomography

Imaging real-time skeletal metabolism difference during and after lactation, M048

Microscopy, confocal *versus* light

In vivo microdamage accumulation detection in wild and domesticated animals, M044

Microscopy, light

Osteogenesis imperfecta bone structure, SA441

Microscopy, multiphoton

Imaging vascular routes for *in vivo* delivery of fluoresceinated tracers to murine growth plate, SA033

Microspectroscopy, synchrotron infrared

Secondary mineralization in cortical bone, M047

Microstructural finite element analysis

Functional and morphological phenotyping of murine femora and, SA109

Microtubules

Runx2 association with, nucleo-cytoplasmic shuttling and, F212, SA212

Milk basic protein (MBP) supplementation

Bone metabolism in health menopausal women and, SU426

Milk, dietary

Fortified with calcium and vitamin D₃, skeletal effects on older men and, F419, SA419
Muscle mass and body fat in dieting young women and, M272

Mineral apposition rate (MAR). SEE ALSO

Hypomineralization
Alendronate therapy and, M358
Bisphosphonates *in vivo* effects on periosteal surfaces of, SA409
Caf1 suppression of, F014, SA014

Mitochondria

Importation of CYP24 and synthesis of 24,25-(OH)₂D, M518
Substrate mediated localization of 25-hydroxyvitamin D-1-hydroxylase in, M519

Mitogen-activated protein kinase kinase 6 EE (MKK6EE)

Endochondral ossification and, I023

Mitogen-activated protein kinase kinase 6 (MKK6)

p38 MAPK signaling, osteoclast survival and induced by, SA274

Mitogen-activated protein kinase (MAPK)

KR62776 suppression of RANKL-induced osteoclast differentiation by inhibiting activation of, M253
Mechanical response by cementoblasts to fluid shear stress and, SU220
TNF inhibition of osteoblast differentiation and, SU241

MLO-A5 cells, SA287**MLO-Y4 cells**, I061, SA285, SA287, SA291, SA386**MOBILE study**, M346, M347**Monoclonal gammopathies**

Bone marrow dendritic cells and, SA061

Monoclonal gammopathy of undetermined significance (MGUS)

Vertebral fractures and, SA392

Monocyte chemoattractant protein-1 (MCP-1)

COX-2 pathway, wear debris and, M215
ERK1/2 dependent stage in osteoclast differentiation and, F249, SA249
Multinucleation of human osteoclasts and expression of, M247

Osteoclast precursor recruitment by PTH-stimulated osteoblastic expression of, I149

Monocyte chemoattractant protein-3 (MCP-3)

Glucocorticoid-induced apoptosis and, SA285

Monocyte chemotactic protein-1

PTH stimulation of osteoblastic expression, I149

Monthly Oral Therapy with Ibandronate for Osteoporosis Intervention (MOTION) Study, M359**Mortality.** SEE ALSO *Life expectancy changes*

Bone loss, weight fluctuation in elderly and risk of, SU343
Bone turnover in frail elderly and, I133

Mortality. SEE ALSO *Life expectancy changes*

(Cont'd)

Calcaneal QUS in postmenopausal women and, SA092

Men with hip fractures, SA339

Osteoporosis refracture rates and, F331, SA331

Rib fracture as marker in osteoporotic men and women of, SU322

Time trends after hip fracture for, I077

Mother of pearl resorption

In vivo and *in vitro* studies of osteoclasts and, SA240

MRL/MpJ mice, SA105**Msx2**

Bone mass, canonical Wnt signals and, I004
Runx2 regulation of osteolysis in breast cancer cells and, M058

Msx2-interacting-nuclear-matrix-target (MINT) protein

Activation of LEF/TCF- and Runx2-dependent transcription by, M173

Multidetector row computed tomography

In vivo analysis of vertebral microstructure for fracture risk evaluation, F362, SA362

Multiple endocrine neoplasia type 1 (MEN1)

Familial isolated hyperparathyroidism and, M462
Gene expression by ribozymes and siRNAs in cultured cells, SA108

Multiple myeloma. SEE ALSO *Myeloma bone disease*

MIP-1 derived from, actions on dendritic cells in, SU102

Osteoclastogenesis and bone marrow microenvironment in, SU201

p62^{ZIP} expression, RANKL and TNF- α effects in osteoclast formation and, I217

Plasma cell-specific unfolded protein response in, SU103

Proteasomal capacity and ER stress in, SU105
RANKL, OPG, PTHrP, and OCIL expression in, SU095

γ δ T cells targeting of bone marrow microenvironment of, I123

Multislice computed tomography

Radiographs of osteoporotic vertebral fractures *versus* sagittal CT reformations with, SU324

Mumie, fulvic acid of

Osteoblast differentiation and, M209

Muscle dynamics

Interstitial fluid flow and bone remodeling and, F185, SA185

Muscle mass

Bone mass accrual modulation in pubertal girls by IGF-I and, F007, SA007
Skeletal, DXA usefulness for assessment in older women of, SA352
Vitamin D and milk intake by dieting young women and, M272

Muscle performance

Fracture risk in older men and, SA343
Smoking, elderly women and decreased, SA304
Vitamin D deficiency and, I134

Muscle RING finger protein 1 (MuRF1)

Unloading-induced bone loss and, I174

Muscle strength

Bone mass pQCT indicators and, M096
Bone quality in elderly men, creatinine clearance and, SU008
Spinal mobility, falls in osteoporosis and, M311

Muscle tissue

Quantitative analysis of, as source for connective tissue progenitors, M230

Mustang gene promoter

Identification and characterization of, SA042

Myeloid elf-1 like factor (MEF)

Repressor in osteoblast differentiation, M176

ASBMR 27th Annual Meeting

Key Word Index

Myeloma bone disease. SEE ALSO *Multiple myeloma*
Dkk1 inhibition and osteoblast activity, bone formation, and tumor growth inhibition in, 1125
Dkk1 modulation of osteoclastogenesis, bone resorption and, 1124
Tumor burden imaging in 5TGM1 mouse model of, SU098

Myeloma cells
Bone marrow microenvironment and TRAIL-induced apoptosis of, SA064
SERMs-induced apoptosis of, SU104

Myelomeningocele
BMD in patients with, SA445

Myocardial infarction
BMD in survivors of, M299

Myosin IIA, nonmuscle
Suppression in differentiating osteoclast cultures affects cell adherence and multinucleation, SA239

N

N-acetylcysteine (NAC)
Bone formation and, SA223

NanoSIMS, M473

National Health and Nutrition Examination Surveys, SU130, SU313

National Health and Wellness Survey (NHWS), SU359

National Osteoporosis Risk Assessment (NORA), M269, M378, SU340

Natriuretic peptide
Brain, skeletal effects of, SU379

Natriuretic peptide, C-type. SEE *C-type natriuretic peptide/guanylyl cyclase B system*

Nek1 protein kinase, 1156

Nell-1 (protein strongly expressed in neural tissues and containing EGF-like domains, type 1), SU204

Nemo-like kinase (NLK), SU259

Nephrotic syndrome, 1060, SU050

Nerve damage
Sex differences in mouse response to, SU362

NET (C19 progestin norethisterone)
HRT *versus*, M399

Neural crest cells, SU070

Neurofibromin (Nf1)
Osteoblastic expression of, 1051

Neurologists
Referrals of high risk patients for DEXA exam by, SA294

Neuromuscular degenerative disease (mouse model), SU371

Neuromuscular function
Knee-bends for fall risk monitoring, SU433

Neutrophil activating peptide-2 (NAP-2). SEE *CXCL7*

Nichols Advantage assays, SA523, SA526, SU502, SU504

Nicotinamide-adenine dinucleotide phosphate oxidase, SA037

Nitric oxide synthase 2, SA171

Nitric oxide synthase, inducible (iNOS), 1070, SA037

N-methyl-D-aspartate receptors, 1094

Nonsteroidal anti-inflammatory drugs (NSAIDs), M307, SA145

Noonan syndrome, 1085

Norland scanner, SU124

Northern California Kaiser-Permanente patients
Stroke and subsequent fracture rates, F334, SA334

Norwegian Medicine Agency
Application of osteoporosis treatment guidelines for wrist fracture patients, SU333

Notch1, M223

Notch 1 RBP-Jk associated module (RAM domain), M211

Notch signaling, 1113

N-terminal polyglutamine-alanine domain, F214, SA214

Nuclear factor activated T cells 1 (NFAT1), SA255

Nuclear factor activated T cells 2 (NFAT2), M252, SA255

Nuclear factor activated T cells c1 (NFATc1), M247, SA257, SA267, SU287

Nuclear factor activated T cells (NFAT), 1148, F258, SA228, SA258, SU224

Nuclear factor-κ B (NF-κB)
CFos/NFAT1- or 2 mediated osteoclastogenesis and, SA255
Expression in TNF-induced osteoclastogenesis *in vitro*, 1196
p65 subunit of, bone metastasis by breast cancer cells and, M061
RANKL-induced iNOS/NO as negative feedback inhibitor during osteoclastogenesis and signaling by, 1070
Titanium particles induce COX-2 through pathway in fibroblast-like synoviocytes dependent on, M178
TNF-induced oscillatory and combinatorial binding to DNA by, SA254
ZIP1 zinc transporter overexpression and binding activity in osteoclasts by, SU297

Nuclear factor-κ B (NF-κB) p65 subunit, F264, SA264

Nuclear hormone receptors, 1119

Nucleus pulposus (NP), SU054

Nursing home residents, SU427, SU435, SU441, SU460. SEE ALSO *Community-dwelling people; Institutional-dwelling people*

Nutrient delivery, SA290

Nutrition, M009, SA332, SU440. SEE ALSO *Diet*

O

O-1 (small molecule stimulator of OPG), SU449

O-2 (small molecule stimulator of OPG), SU449

Ob.CASR (calcium-sensing receptor in osteoblasts), identification of, SU516

Obesity. SEE ALSO *Body weight; Overweight*
Calcium supplementation in Korean postmenopausal women and, SA422
Femoral neck structural strength in women and, F179, SA179
Genetic and environmental factors decreasing osteoporosis risk and risk of, M108
Morbid and super, vitamin D deficiency and hyperparathyroidism in, M323
Polycystic ovary syndrome and low bone resorption in adolescents, SU474
Quality of life and weight loss in patients with osteoarthritis and, SA044
Whole body DXA imprecision in measuring body composition changes in children, M064

Observational Study on Severe Osteoporosis (OSSO), M388, M434, SU354
French cohort, M373, M433

OC59 (PTH1R-null murine osteocytic cells), M501

Octacalcium phosphate (OCP)
Mouse sutures during normal development and craniosynostosis and, SA003

Odd-skipped related 2 (Osr2) parietal bone formation and, F208, SA208

Odense Androgen Study, SU189

Oligonucleotide trapping
Identification of VDRE binding proteins and transcription factors by, SA498

Omega-3 fatty acids
p38-MAPK pathway and vascular calcification inhibition by, SA224

Oncostatin M receptor (OSMR)
Bone resorption, RANKL and IL-6 mRNA expression, STAT3 activation and, SU208

ONO-4819
BMP-induced osteoblast differentiation via PKA signaling and, M031

Orange pulp or juice
Bone homeostasis in orchidectomized rat model of osteoporosis and, SU013

Orchidectomy (animal models)
Bone biomechanical properties in rats treated with two doses of risedronate, SA378
CE590 *versus* DHT effects on, M395
Orange pulp or juice and bone homeostasis in, SU013
RANKL inhibition and cortical bone geometry in rats after, 1226
Rats, ratio of osteoclast activity/osteoclast number as parameter in, SU161

Orthopedic surgeons
Referrals of high risk patients for DEXA exam by, SA294

Orthosilicic acid
Choline-stabilized, calcium/vitamin D₃ effect on bone formation with, SA421

OSA peptide
Bone formation *in vitro* and *in vivo* stimulated by, M426

OSB peptide
Derived from CXCL7 and increased BMD in ovariectomized rats, M425

OSE2-Luciferase reporter gene
Runx2-dependent reporter gene activation, osteocalcin induction, and bone loss *in vivo*, SA207

Oslo Health Study, SA346

Ossicles, auditory
Osteoporosis and hearing loss in mice, SU007

Ossification
Non-hereditary heterotropic, bone formation in, M449

Ostabolin-C. SEE ALSO *[Leu²⁷]cyclo(Glu²²-Lys²⁶) human Parathyroid hormone 1-31NH₂*
Bone turnover in monkeys with osteoporosis, M409

Osteoactivin-derived (OA-D) peptides
Osteoblast adhesion, spreading, migration, differentiation and, SU076

Osteoactivin (OA)
Alveolar bone regeneration in diabetic rat model, SU251
Expression regulation by BMP-2 through Smad-1 signaling during osteoblast differentiation, M039
MSC differentiation and, M228

Osteoarthritis. SEE ALSO *Arthritis; Rheumatoid arthritis*
Absence of BMP-2 and, 1025
Biomarker in, SU153
Connexin43 gap junctions and responsiveness to IL-1β in, SU069
Hip and knee, risk factors in Japan *versus* Britain, M446
Molecular basis for heritable forms of, F116, SA116
mPGES-1 and pathogenesis of, F125, SA125
Phospho-Smad3 degradation and cartilage-specific overexpression of Smurf2 induced, 1005
Quality of life and weight loss in obese patients with, SA044

Key Word Index

ASBMR 27th Annual Meeting

Osteoarthritis. SEE ALSO *Arthritis; Rheumatoid arthritis* (Cont'd)

Risedronate effects on pain and cartilage metabolism in, SU030
 Senescence-accelerated mouse models for temporomandibular joint, SA355
 Spinal, Q89R polymorphism in LRP5 in postmenopausal Japanese women and, SU190
 Subchondral sclerotic lesion in knee, M041
 TGF- β 1 expression increased in, SA162
 Vertebral fractures and radiological signs in postmenopausal women of, SA316

Osteoarthritis, inflammatory (animal models)
 Glucosamine effects on long bones, BMD, and gene expression in liver, M418**Osteoblast differentiation (osteoblastogenesis).**SEE ALSO *Osteoblasts*

Adipogenic transdifferentiation and, M198
 Amelogenin (recombinant mouse) regulation of, M205
 Androgen receptor and, 1198
 Androgen receptor and proliferation and, M196
 BMP-4 in blood serum and, SA161
 BMP-7, human aortic vascular smooth muscle cells and, F021, SA021
 BMPs and primary human osteoblasts, M022
 N-Cadherin/cadherin-11 deleterious effects on, 1063
 Canonical Wnt signaling and, 1064
 C/EBP α isoforms and, M190
 CTGF-P stimulation of, SU078
 1,25(OH) $_2$ D $_3$ and 25(OH)D $_3$ effects in human bone marrow stromal cells, M155
 1 α ,25 (OH) $_2$ D $_3$ and Wnt pathway effects on, SA221
 Dimethyl sulfoxide enhancement, M208
 Dkk-1 and primary human osteoblasts, M192
 Dkk proteins and, 1001
Dlx5 in transgenic mice and, 1186
Dlx genes expression in, M177
 Engrailed-1 modulation of, 1185
 Estrogens control in mice in which ER α cannot interact with DNA and, 1098
 Glucocorticoid signaling inhibition by overexpression of 11 β -HSD2 and inhibition of, F507, SA507
 MAPK and TNF inhibition of, SU241
 Metabolic regulation of, SU243
 Mouse models of accelerated aging and, M234
 Myeloid elf-1 like factor repression in, M176
 Non-canonical Wnt 11 transcriptional suppression of IGFBP-6 and, SA148
 Notch1 overexpression and inhibition of, M223
 Notch signaling and action in, M211
 Osteoactivin-derived peptides and, SU076
 Osteoactivin expression regulation by BMP-2 through Smad-1 signaling during, M039
 Osteoformin *in vitro* stimulation of, SU198
 Oxandrolone stimulation of, SU060
 Palmitoylation and, SU231
 Periostin-like-factor and, SU077
 Phosphatidylinositol 3-kinase signaling activation at intracellular junctions and differentiation of, SA230
 PPAR γ 2 control of regulatory pathways for, SU242
 PTH action on stage-specific GFP expressing osteoblast cultures, SA191
 Rap1 activation and, F218, SA218
 Regucalcin and, M201
 Retinoic acid and, M204
 Retinoid signaling pathway regulation of, SU247
 RhoA downregulation and actin cytoskeletal disruption in modeled microgravity and, SU222
 Rho-ROCK pathway in, SU244

Osteoblast differentiation (osteoblastogenesis).SEE ALSO *Osteoblasts* (Cont'd)

rRNA gene expression for, Runx2 transcription factor and, 1053
 Runx2 cell cycle regulation and, SU248
 Runx2 domains required for, 1015
 Runx2 switching in, 1016
 SARA β regulation of BMP-induced gene expression in xenopus and human, 1028
 Transgenic expression of human Bcl-2 with bone formation inhibition and, F194, SA194
 TSP2 expression regulation during, SA038
 Vitamin C and ATP synthesis in, 1045
 WISP-1 splice variants and differently regulation of BMP-induced, SU081

Osteoblasts. SEE ALSO *CIMC-4 cells; MC3T3.E1 cells; U2OS osteoblast-like cells; UMR-106-01 cells; UMR-106 cells*

Adherent endotoxin on bone implants and, M194
 Apoptosis due to unloading, mechanism of action for, 1092
 Ascorbic acid protection from endoplasmic reticulum stress of, SU266
 ATF4 expression in ICER transgenic mice and, M187
Bcl-2 and anabolic action of PTH in, F192, SA192
 Bisphosphonates and cell transduction mediators in, M221
 Bisphosphonates *in vivo* effects on, SA409
 BMP-2 activation of β -catenin signaling in, SA226
 BMP2 and PEMF effects on, M040
 Ca $^{2+}$ oscillations induced by rest-inserted loading, and prediction of activity by, SU218
 c-Abl and senescence in, M225
 Calcium-sensing receptor in, identification of, SU516
 CaM kinase 1 β mRNA expression in, SU046
 Canonical Wnt pathway, BMP signaling and fluid shear stress-induced proliferation of, SU219
 β -Catenin and NFAT signaling in, SA228
 CHOP overexpression and inhibition of, F206, SA206
 Cola1 mRNA expression in BMSCs *versus*, 1044
 Collagenase 3 induced by metastatic melanoma cells interaction with, SA063
 Connexin43 and growth factors actions on, SU265
 Connexin43 and PTH anabolic action *in vivo* on, 1228
 Connexin43 deficient, gene array analysis of, M167
 CTGF-P stimulation of adhesion, spreading by, SU078
 Cytokines and glucocorticoids effects on 11 β -HSD1 activity in, F365, SA365
 Development suppression with adenovirus-mediated FGF23 overexpression, SA139
 1,25(OH) $_2$ D $_3$ binding protein Erp60 and, SA500, WG2
 1,25(OH) $_2$ D $_3$ treatment and FGF23 production in, M134
 DMP1 regulation of bone mineralization and, 1111
 EBF-1 and development of, 1184
 Farnesyl diphosphate synthase in, anabolic response to PTH after chronic bisphosphonates and, F220, SA220
 FGF2 and PTH induction of Bcl2, CREB phosphorylation, and Runx2 nuclear accumulation in, F142, SA142

Osteoblasts. SEE ALSO *CIMC-4 cells; MC3T3.E1 cells; U2OS osteoblast-like cells; UMR-106-01 cells; UMR-106 cells* (Cont'd)

Fibronectin-dependent detachment, apoptosis mediated by Cbl-mediated ubiquitination of α 5 integrin, F190, SA190
 Flavopiridol inhibition of, SU305
 Genetic basis for osteoporosis and allelic imbalance in, M107
 Glucocorticoid-induced osteoporosis and glucocorticoid receptor localization in, 1101
 Growth hormone direct action in, IGF-1R and, 1194
 Histone deacetylases and maturation of, F204, SA204
 HtrA1 regulation of mineralized matrix deposition by, SA025
 Human, enamel matrix derivative and OPG production in, SA134
 Human, ER β regulation of TIEG by estrogen in, SA506
 IL-6 and IL-11 dependent osteoclast formation and STAT1/3 signaling in, M262
 IL-23 and IL-27 effects on, M191
 β 3 Integrin and IGF-1 signaling in, SU262
 β 1-Integrin silencing and response to substrate microtopography and 1,25(OH) $_2$ D $_3$ by, M212
 LRP5 and lactoferrin anti-apoptotic effect in, SU230
 Maturation inhibition, high serum concentrations of low-density-lipoprotein and, SU239
 Metabolic acidosis-induced calcium signals in, M222
 Metabolic regulation of gene expression and differentiation, SU243
 Metformin and growth, differentiation of, SU196
 Molecular phenotyping of osteoblastic lineage cells lines using TaqMan Low Density Arrays, SA215
 Murine, CCN genes expression and regulation in, SA126
 Murine, Dkk-1 overexpression and intermittent PTH treatment of, 1191
 Murine, MSCs commitment and differentiation into, SU052
 Nuclear extracts, interaction with Runx2 P2 promoter alleles, 1208
 Osteoactivin-derived peptides and function of, SU076
 Osteocalcin-A20 chimeric gene protection from apoptosis, SA193
 Osteoclastogenesis role of, SA147
 Osteoclast precursors inhibit OPG production by, M250
 Oxytocin and estrogen mediation of activity by, 1102
 p38 MAPK and ERK roles in PTH activation of, M218
 Phosphodiesterase 4 variants expressed in, M224
 PKC-induced cytoskeleton rearrangement in PTH-enhanced calcium ion response to mechanical stimulation in, SA173
 Primary cultured mouse calvarial, N-acetylcysteine and, SA223
 Primary response genes expression regulation by intermittent *versus* continuous PTH, SU499
 Progesterone inactivation in human, SA373
 Prostate cancer cells interaction during bone metastasis with, SU119
 Protein expression patterns in proteomic comparison to osteocytes of, SA288

Osteoblasts. SEE ALSO *CIMC-4 cells*; *MC3T3.E1 cells*; *U2OS osteoblast-like cells*; *UMR-106-01 cells*; *UMR-106 cells* (Cont'd)

PSA and metastatic prostate cancer response by, SU118

PTH-dependent modulation of Jagged1, PKA activation and, F197, SA197

PTH regulation of Notch signaling during maturation of, 1113

RBBP1 and ER α -specific suppression of proliferation by, 1200

Reloading after unloading and restored proliferation of, SU221

Resistin expression and regulation in, SA252

RNA interference with Gq and G11 proteins and cellular morphology and function of, M216

Runx2 cell cycle regulation and proliferation, growth of, SU248

Runx2 in, compounds activating, SA207

Schnurri-2 coupling to BMP and RANKL and activation of, 1052

Small molecule stimulators of OPG from, SU449

Sox4 and regulation of, SU232

Strontium ranelate effects on, M424

Targeted overexpression of IL-7 in, and rescue of bone phenotype of IL-7 KO mice, 1189

T-box 3, growth hormone and proliferation of, M183

TGF β stimulation of CCL5/RANTES mRNA expression and secretion in, M162

TNF effects on BMP signaling in, 1018

VDR subcellular trafficking regulation in, 1118

Vitamin D₃ regulation of FGF23 gene transcription in, SA144

Wnt3a and GSK-3 β inhibitor differential regulation of, M219

Wnts, bone metastasis of prostate cancer cells and, F070, SA070

X-linked hypophosphatemia and *PHEX/Phex* mutation in, 1105

Zinc uptake in, 1112

Osteoblast-specific DNA nuclear targeting, M171

Osteocalcin-A20 chimeric gene
Osteoblast apoptosis inhibition by, SA193

Osteocalcin, N-terminal fragment
Roche Elecsys 2010 immunoanalyzer assay of, SU163

Osteocalcin (OCN)
ATF4 interaction with Runx2/Cbfa1 and osteoblast-specific gene expression by, M179

Bone loss induced by ovariectomy in warfarin-treated rats and, SU021

Breast cancer risk and levels of, M296

Gene expression in postmenopausal osteoporosis and, M169

OSE2 activity, bone loss *in vivo* and, SA207

Premenopausal women, aging effects on, SU002

Pueraria thunbergiana enhancement of, SU233

Sensory responses and, F051, SA051

Vitamin K in postmenopausal women and undercarboxylated, SU425

Osteocalcin promoter
Connexin43 function and regulation by PTH in rat model by, M493

Osteoclast-absent c-fos deficient mice, F260, SA260

Osteoclast inhibitory lectins (OCILs)
Expression in multiple myeloma, SU095

Osteoclast inhibitory peptide-1 (OIP-1/hSca) gene promoter
Interferon γ regulation of, SU311

Osteoclastogenesis (osteoclast differentiation)
ACTH and maturation of, SU291

Acumen Explorer quantitation of calcitonin receptor-positive cells in, SU281

Aquaporin 9 and, SU278

BCAR1 and nongenomic estrogen signaling regulating, F505, SA505

Bmx and Btk regulatory roles in, SA276

In bone marrow of postmenopausal women, estradiol therapy and, F374, SA374

Calcitonin effects on, SU288

Calcitonin receptor-stimulating peptide and inhibition of, M496

Calpain and RANKL-supported, SA263

CaMKII γ and regulation via RANK signaling modulation of, SU284

Caspase 3 and hydrogen peroxide in RANKL-induced, SU292

Cbp expression in osteoclasts and RANKL-induced, 1146

Cell-cell fusion in, DC-STAMP expression during, F258, SA258

C-TAK1 interaction with MITF during, SA281

Cytokine-mediated, HIV in postmenopausal women and, M445

1 α ,25 (OH)₂D₃ and chondrocyte expression of RANKL, 1067

Engrailed-1 regulation of, 1185

EphrinB2 as transcriptional target gene of NFATc1 during, SU287

Estrogens control in mice in which ER α cannot interact with DNA and, 1098

FSH enhancement of, 1100

Gap junction channels mediate signals for RANKL-induced, SA283

IGF-1 signaling and regulation of, SA147

IL-3 inhibition of by irreversible down-regulation of RANK expression, SA268

IL-4 and IL-13 inhibition of, SU207

Induced by 1 α ,25(OH)₂D₃ analogs in osteopetrotic (op/op) mice *versus* osteoclast-absent c-fos deficient mice, F260, SA260

Interferon γ and regulation of, SU279

JNK and perfusion stage of, M240

K63-linked polyubiquitin chains catalyzed by E3 ligase TRAF6 required for RANK signaling and, 1069

KR62776 suppression by MAPK activation inhibition by RANKL-induced, M253

MCP-1-induced TRAP+ multinuclear cells in, F249, SA249

MITF requirement for, SU294

MK-4 inhibition of, SU280

Multiple myeloma bone marrow microenvironment and, SU201

NEMO inhibition of, F282, SA282

NFATc1 mediation of RANKL induction of β 3 integrin in, SA257

NF- κ B p50/p52 expression and cFos/NFAT1- or 2 mediated, SA255

Nonmuscle myosin IIA and cell adherence, multinucleation of, SA239

OPG inhibition by glucocorticoids and, SU519

RANKL and cell cycle progression, arrest and, M244

RANKL expression in osteoblasts and flagellin stimulation of, M002

RANKL-induced iNOS/NO as negative feedback inhibitor during, 1070

RANKL-induced, NF κ B p65 subunit and, F264, SA264

RANKL-induced, SDF-1 and, 1071

RANKL truncation mutants inhibition of RANKL-induced, M248

Rap1 activation and negative regulation of, F218, SA218

Osteoclastogenesis (osteoclast differentiation) (Cont'd)

RGS10 regulation of [Ca²⁺]_i oscillations in RANKL-induced, M260

Risedronate inhibition in PBMC in postmenopausal osteoporosis from, SU414

SHIP1 blockage of osteoclast precursor proliferation and regulation of, M259

Sphingosine kinase in RANKL-induced, SU286

TIEG expression in osteoclast precursors and suppression of, SU285

TNF α -induced, bone marrow stromal cells modulation of contributions by macrophages and T cells *in vivo* to, F247, SA247

TNF α -induced, measles virus nucleocapsid protein and, F464, SA464

TNF-induced *in vitro*, NF- κ B expression and, 1196

TRAF6 signaling strength and, SA261

Trichostatin A effects in, M245

VDR or RANKL-induced, TEI-9647 blockage of, SA497

Osteoclast precursors
ADAM8 overexpression, osteoclast formation and, M242

Calcitonin effects on, SU288

Committed by TRANCE, characterization of, M249

Interferon γ regulation of OIP-1/hSca gene promoter in, SU311

MK-4 enhancement of animobisphosphonates inhibition of cell differentiation by, SU280

OPG production by osteoblasts during mineralization inhibited by, M250

Osteoblast expression of MCP-1 stimulated by PTH to recruit, 1149

Osteoclast differentiation suppression by TIEG expression in, SU285

Pagetic-like osteoclasts formation, and IL-6 and TAF η -17 expression in, 1207

SDF-1 promotion of circulation by, 1071

SHIP1 blockage of proliferation by, osteoclastogenesis regulation and, M259

TNF inhibition of SDF-1 and mobilization of, 1072

TSH and differential expression of TNF- α in, SA246

Osteoclasts. SEE ALSO *Sealing zone of osteoclasts*
Advanced glycation end products and activity of, SU075

Androgen receptor function in, genetic evidence of, F509, SA509

Anisotropic human cortical bone resorption by, SU310

Annexin II receptor cloning and characterization and study of, F275, SA275

Apoptosis at end of lactation in maternal skeleton and, SU300

Autocrine/paracrine action of platelet-activating factor receptor on, F127, SA127

Calcium ion signaling and motility in, SA241

Calcium-sensing receptor and strontium ranelate effects on, SU511

Cardiotrophin-1 regulation of formation and function by, 1190

Cathepsin K as TRAP regulator in, SU272

Cbl downregulation of tyrosine kinases and decreased activity in, F279, SA279

Col3.6 promoter and GFP expression in, F266, SA266

COX-2 mechanism for maturation of, particulate wear debris and, M214

CTX/TRACP 5b ratio as resorption index, SU290

Key Word Index

ASBMR 27th Annual Meeting

Osteoclasts. SEE ALSO *Sealing zone of osteoclasts* (Cont'd)

Cytoskeleton regulation by a Syk, Src and $\alpha_v\beta_3$ -integrin complex, F244, SA244
 Dynamin GTPase- and Src-dependent regulation of Pyk2 phosphorylation in, 1150
 Estradiol regulation of gene expression in cytoskeleton of, SU523
 Extracellular acidification action on OGR1 and, 1148
 Extracellular matrices' microenvironment function of, SU271
 Flavopiridol inhibition of, SU305
 Fluoxetine stimulation of activity by, SA047
 FSH enhancement of survival of, 1100
 FSH regulation of, F376, SA376
 Fusion mediated via DC-STAMP C-terminus domain, SU282
 Genetic variability and 3D spatial distribution in inbred mice femurs, F262, SA262
 GIP receptors and nutrient-induced inhibition of bone breakdown by, SA269
 Glucocorticoid action on, F367, SA367
 Human cultures of, comparison of human and bovine substrates in, SU289
 IL-12 mediation of CpG-oligodeoxynucleotides and, F251, SA251
 IL-23 and IL-27 effects on, M191
 $\alpha_v\beta_1$ -Integrin signaling and, SA243
 Leupaxin overexpression in and effects on function of, M258
 MEK/ERK pathway regulation of survival of, M257
 Mitochondrial mass correlation to morphology and function of, SU293
 MMPs and compensation for cathepsin K activity loss in function of, SA237
 Molecular aspects of polyphosphoinositides in migration of, SA273
 Mother of pearl resorption, *in vivo* and *in vitro* studies, SA240
 In multiple myeloma, p62^{ZIP} expression, RANKL and TNF- α effects on formation of, 1217
 Old bone as target for, M241
 Oxytocin and estrogen mediation of activity by, 1102
 p38 MAPK signaling and MKK-6-induced survival of, SA274
 Pagetic-like, formation of, 1207
 PFQEP³⁶⁹⁻³⁷³ activation of Akt and AFX and survival of, 1068
 PKC signaling and strontium ranelate effects on, M255
 Primary human, cathepsin K siRNA transfection inhibition of bone resorption in, SU307
 Pycnodysostosis, cathepsin K deficiency, and survival of, SU277, SU456
 Rac-1 interaction with BCA3 in, SU269
 Rac-2 and reduced resorptive activity by, F270, SA270
 RANK deficiency in the hematopoietic compartment and development of, SA256
 RANKL induction of NFATc1 in, SA267
 Receptor for advanced glycation end products and regulation of, SA271
 Redox and sRANKL-induced intracellular ROS production and functional regulation of, M266
 Resistin expression and regulation in, SA252
 Schnurri-2 coupling to BMP and RANKL and activation of, 1052
 SHIP-1 and inhibition of DAP12 signaling in, M261
 TGF- β activation of Smad independent signaling and survival of, SA280

Osteoclasts. SEE ALSO *Sealing zone of osteoclasts* (Cont'd)

Tropomyosin isoforms and attachment structures of, SA238
 TSH and differential expression of TNF- α in, SA246
 Urokinase receptor and function of, M246
 V-ATPases and ruffled membranes in, SU296, SU298
 VDR subcellular trafficking regulation in, 1118
 ZIP1 zinc transporter expression in, SU297

Osteocyte lacunae

Raman spectroscopy of bone mineral crystallinity in, SA284

Osteocyte-osteon structure

TRAIL and TNF α regulation by removal of gap junctions, SA217

Osteocytes

Apoptosis due to unloading, mechanism of action for, 1092
 Breast cancer chemotaxis and invasiveness, stimulation by, SU111
 CD40 ligand and survival of, F370, SA370
 C-PTHrP regulation of cytoskeleton through calcium influx-dependent mechanisms, SA493
 E11 function in, SA287
 ER α and ER β role in mechanotransduction of, 1116
 Idiopathic osteoporosis in men and, SA379
 Parathyroidectomy in hemodialysis patients with secondary hyperparathyroidism and, M469
 Protein expression patterns in proteomic comparison to osteoblasts of, SA288
 Raloxifene and survival of, M401
 3D model of local strain and DMP1 gene expression in, 1093

Osteoformin

Acceleration of fresh fracture repair in rats, SU198

Osteogenesis imperfecta

BMD in relatives of individuals with, 1089
 Pamidronate and metaphyseal modeling in children with, F440, SA440
 Pamidronate discontinuation effects in children and adolescents with, 1088
 Pamidronate for children with, 1090
 Site-specific bone responses to bisphosphonates therapy, SU482
 Type I treatment with weekly alendronate, SA443
 Variable bone structure in, SA441
 Zoledronic acid for, safety and efficacy of, SA447

Osteoglophonic dysplasia

FGFR1 role in bone formation and mass in, F138, SA138

Osteohealth Audit, United Kingdom, SU331**Osteoid sarcoma**

Hip pain syndrome and, M525

Osteomalacia (animal models)

MEPE overexpression in osteocytes of, SA462
 Rabbit, compositional and mechanical implications of hypomineralization in, M079

Osteomalacia, tumor-induced

Cinacalcet management of, SA454
 FGF23, FGF7, sFRP-4, and MEPE expression in, M126
 FGF23 measurements in, SA460

Osteonecrosis of the jaw

Intravenous bisphosphonates and, 1218

Osteonectin

micRNA binding sites in 3' untranslated region, SU079

Osteons, secondary

Surface area/volume relationships in equine radii, SA290

Osteopenia. SEE ALSO *Bone loss; Disuse osteopenia*

Alendronate once-weekly 70 mg treatment *versus* 10 mg once daily for primary biliary cirrhosis-associated, SU392
 Bone density and geometry in women with, M073
 Bone turnover and DHEA supplementation in postmenopausal women with, SU424
 COPD and, M292
 ER α signaling via EREs in male mice and, 1142
 Health-related quality of life and 25(OH)D serum levels in postmenopausal women with, SU463
 Hyperaldoosteronism in cardiac cachexia and, SU349
 Kypho-orthosis program for thoracic kyphosis in, SU438
 Ovariectomized mice deficient in mast cells and development of, F389, SA389
 Potassium citrate neutralization of acidogenic Western diet and BMD in postmenopausal women with, SU429
 Targeted deletion of BMP4 in adult mice and, 1026
 Vertebral trabecular bone quality and PTH(1-84) treatment in rhesus monkeys with, M415

Osteopetrosis

Autosomal dominant type I, LRP5 mutations and osteoblast support of osteoclastogenesis in, 1206
 Autosomal dominant type II, determination of carrier status in, F446, SA446
 Autosomal recessive, ATP6i expression in osteoblasts and, M181
 Autosomal recessive, PLEKHM1 gene and, 1103
 Genetic, clinical, and cellular analysis of, M436
 Oxidized LDL receptor (SR-A) knockout mice, F242, SA242

Osteopetrotic (op/op) mice, F260, SA260**Osteopoikilosis**

Deactivating germline mutations in LEMD3 (MAN1) and, M443

Osteopontin

Bone and lung metastases in breast cancer and, 1214
 CD44 interaction with in osteolysis mechanism in breast cancer metastasis, SU123
 Deficiency in ovariectomized mice, over-potentialization of anabolic actions of EP4A signaling in, M165
 Delayed healing during distraction osteogenesis and deficiency of, SU080
 Gene promoter, PTH/forskolin induced VDR DNA binding to, 1120
Pueraria thunbergiana enhancement of, SU233
 Wear-debris induced osteolysis and deficiency of, SU302

Osteoporosis. SEE ALSO *Osteoporosis (animal models); Osteoporosis, glucocorticoid-induced; Osteoporosis, male; Osteoporosis, postmenopausal*

Abdominal aorta calcification and, SA337
 Access to BMD testing and management of, SU312
 Adherence to bisphosphonates for, M344
 Adherence to medications for, patient perceptions and strategies with, M391
 Alendronate plus vitamin D₃ once-weekly for, M353
 Allelic imbalance in human osteoblasts and genetic basis for, M107
 Anti-osteoporosis medication and long term effects of randomized controlled trial screening for, 1042
 BMD screening in fracture patients for, SA295

Osteoporosis. SEE ALSO *Osteoporosis (animal models); Osteoporosis, glucocorticoid-induced; Osteoporosis, male; Osteoporosis, postmenopausal* (Cont'd)

Bone density and geometry in women with, M073

Bone Safety Evaluation balance domain validation and, SU444

Cardiovascular calcification and, SU022

Care pathways for hospitalized patients with fragility fractures, SA312

Chinese American women, SU129

Chondrosarcoma of right hip and teriparatide for, SU505

COL1A1 Sp1 polymorphism as genetic marker of, I210

COPD and, M292

Coumadin patients and, SA344

Daily calcium intake and, M273

Daily or weekly bisphosphonates adherence by French women with, SU416

Dental status and disability in elderly people in Italy, M451

Early treatment and subsequent fracture prevention, M293

Education mailed to older adults on, randomized, controlled trial of, M372

Epidemiology and treatment in elderly Americans, SU359

ER β gene polymorphisms and risks in men and women for, SU186

Estrogen deficiency-induced type I and type II, structural simulation of, SA348

Fall risk in patients with fragility fractures from, SU351

Falls, spinal mobility, and muscle strength in, M311

Family physicians awareness of risk factors of, M310

Family physicians prescriptions of medications for, SU386

Fracture risk and quality of life conditions for women with, SU354

Fractures and costs by race/ethnicity and gender in USA, F317, SA317

Fractures in childhood and adolescence as risk factor for, I136

Health beliefs and cognitive representations by first degree relatives of, SU346

Hypogonadism-induced, FSH regulation of bone mass and, I043

Identifying patients by using standard risk factor audits or targeting fragility fractures, SU331

Idiopathic, bone remodeling and bone microarchitecture in premenopausal women with, SU361

Idiopathic, in premenopausal women, BMD distribution and, I175

Idiopathic, young premenopausal women on calcium and vitamin D supplements, BMD evolution in, SU421

Improved care with post-fracture education for, SU325

Incidence and cost projections for fractures by skeletal site in US, I078

Juvenile, alendronate effects on BMD in, M368

Kypho-orthosis program for thoracic kyphosis in, SU438

Mandatory consultation with low intensity hip fracture patients about, SU345

Medicare beneficiaries' compliance with medications for, M371

Nonvertebral fracture risk in women with, composite measures of, SA411

Normative calcaneal ultrasound data in Italians, F301, SA301

Obesity risk and genetic, environmental factors decreasing, M108

Postural deformity and balance in, M313

Osteoporosis. SEE ALSO *Osteoporosis (animal models); Osteoporosis, glucocorticoid-induced; Osteoporosis, male; Osteoporosis, postmenopausal* (Cont'd)

Prevalence and diagnosis of, SU313

PTH rechallenge one year after first PTH course, long-term alendronate and, I079

Quality of life, lumbar spinal mobility, back extensor strength and, M431

Quantitative ultrasound evaluation of teriparatide treatment in women with, M414

Raloxifene treatment and skeletal pain associated with, M318, M398

Refracture rates and mortality, F331, SA331

Rheumatoid arthritis and screening for, SU486

Rib fracture as marker in men and women of, SU322

Self-report *versus* pharmacy data for current use of medications for, M379

Senile, differences with young adult osteoporosis, SU367

Severe, bone marker changes with one month teriparatide treatment in men and postmenopausal women, M408

Site-discordance of categorization in menopausal women for, F077, SA077

Statin therapy and bisphosphonate therapy in, M366

Therapeutic efficacy assessment using spinal loading estimates and vertebral strength measures, M411

Transplantation-related, alendronate treatment for, M477

Treatment in home health care settings, SA354

T-score precision and diagnosis of, SU134

Vitamin D deficiency and correlations with PTH, urinary calcium, bone turnover markers, and BMD in, M320

Vitamin D deficiency risk factors for women with, M278

Vitamin D insufficiency in liver disease and liver transplantation patients and, M476, WG5

Vitamin D, rationale for inclusion in current treatment for, M360

Young adult, differences with senile osteoporosis, SU367

Osteoporosis (animal models)

Accelerated aging and, M234

Alendronate and risendronate at clinical doses and bone remodeling, microdamage accumulation in, I081

Atorvastatin and, SU018

BMP-6 restoration of bone in aged rats with, I027

Crtp protein loss and, F053, SA053

Cyclic *versus* daily PTH and, I180

Glucocorticoid-induced mouse model, risendronate and PTH effects in, SU067

Hearing loss in mice and, SU007

Ostabin-C effects on bone turnover in monkeys treated for one year, M409

Placental growth factor regulation of bone remodeling in, F253, SA253

Platelet-activating factor deficiency and prevention of osteoporosis in ovariectomized mice, F127, SA127

PTH(1-34) and titanium implant osteointegration in low density rat tibial model of trabecular bone, M491

Sca-1, as age-dependent phenotype, SU370

Senile, temporomandibular joint status in, SA355

Osteoporosis, glucocorticoid-induced

Age factors and rate of incident fractures in, SA368

Bisphosphonates effects on bone turnover markers in, M345

Osteoporosis, glucocorticoid-induced (Cont'd)

Endogenous PTH and pathogenesis of, SA366

Glucocorticoid action on osteoclasts and, F367, SA367

Glucocorticoid receptor in osteoblasts and, I101

Mechanism of disparity between bone density and strength in, I197

Trabecular and cortical bone structure in, F086, SA086

Osteoporosis, male

Family practitioner referrals to scanning service for, SA340

Idiopathic, estrogen and leptin levels in, SA385

Idiopathic, familial and sex-specific nature of, M111

Idiopathic, iliac crest biopsy study with micro-CT of, M091

Laboratory testing and diagnosis of, SA380

LRP5 genetic polymorphisms and, SA336

Oral risendronate for, SU404

Osteocyte density from iliac cancellous bone biopsy and, SA379

Risendronate therapy and new vertebral fracture risk reduction in, SU391

Osteoporosis, postmenopausal. SEE ALSO *Postmenopausal women*

Adherence to daily *versus* weekly bisphosphonates, M357, SU397

Adherence with drug therapy and fracture risk in, M294

Alendronate once-weekly *versus* ibandronate once-monthly, patient preferences for, M435

Alfacalcidol *versus* vitamin D plus calcium effects on spinal BMD in, SU458

Antiresorptive therapy compliance by short-term monitoring of bone turnover markers in, SU409

Antiresorptive therapy monitoring with dual femur DXA scanning, SU135

Bisphosphonates dosing frequency, adherence and, M352

Cathepsin K serum levels, osteoclastic activity and, SU142

Collagen and osteocalcin gene expression in osteoblasts, M169

Compliance and effect of bone protective treatment in, M375

Depressive symptoms, treatment adherence and, M380

Dietary calcium intake by women on bisphosphonates for, SU398

Dietary calcium intake with early, SU419

Fractures after discontinuation of therapy for, M388

Health-related quality of life and discontinuation of therapy for, M434

Health-related quality of life and inadequate clinical response to therapy for, M433, M434

Ibandronate daily *versus* once-monthly for, M347

Ibandronate once-monthly for, M346, SU415

Ibandronate, once-monthly oral, and bone resorption markers in, SU410

Ibandronate once-monthly *versus* alendronate once-weekly, patient preferences for, M435

Inadequate clinical response to therapy for, M373, M388

Intravenous ibandronate and BMD gains in, SU413

Intravenous ibandronate efficacy in, F410, SA410

Intravenous ibandronate for, renal tolerability of, SU412

Intravenous ibandronate safety and tolerability in, M350

Oral ibandronate and bone remodeling activation frequency in, M364

Key Word Index

ASBMR 27th Annual Meeting

Osteoporosis, postmenopausal. SEE ALSO

Postmenopausal women (Cont'd)
Prevalence, increasing overweight in US and, M267
PTH(1-84) safety and efficacy with hormone replacement therapy in, 1080
PTH/PTHrH system genetic variations and, M116
Raloxifene effects on lumbar BMD and bone markers in Koreans, SA424
Raloxifene treatment for one year and OPG-RANKL ligand system, M400
Risedronate, early intervention with, SU407
Risedronate inhibition of osteoclastogenesis from PBMCs in, SU414
Risedronate safety over wide range of serum concentrations in, SU405
Risedronate *versus* strontium ranelate for, clinical benefits and cost savings of, SA403
SELDI-TOF mass spectrometry diagnosis of, SU150
Strontium ranelate effects on bone remodeling and bone safety in, 1084
Teriparatide treatment for, lumbar spine BMD response after, M410
Treatment utilization and correlates in, M378
Vitamin D insufficiency impairment and alendronate treatment for, SU462

Osteoporosis-pseudoglioma syndrome (OPPG)

Bone accrual, eye development and LRP5 mutation in, SA439
LRP5 and, SA099

Osteoporosis Risk Factor and Prevention (OSTPRE) Study, M289, SA418**Osteoporosis Self-assessment Tool (OST)**

Men diagnosed with osteoporosis and, M302

Osteoporotic Fractures in Men Study, 1073**Osteoprotegerin-Fc (OPG-Fc)**

Anti-osteoclast activity of RANK-Fc inhibition of RANKL *versus* RANKL inhibition by, SU448
Antitumor efficacy in osteolytic metastases models, SA065

Osteoprotegerin (OPG)

Bone loss, immune status in arthritic rats and RANKL inhibition of, SU295
Bone remodeling in hyperhomocysteinemia restoration by folate therapy and, SU380
Brain natriuretic peptide and serum levels of, SU379
Cushing's syndrome and serum levels of, SA371
Delivery and retention to bone after conjugation with bisphosphonate, SU454
Enamel matrix derivative and production in human osteoblasts of, SA134
Expression in multiple myeloma, SU095
Expression in rheumatoid arthritis, SU491
Extreme longevity and serum levels of, SU004
Gene expression in liver of patients with biliary cirrhosis, SA388
Glucocorticoid regulation of gene expression by, SU519
Hypoxia-induced release from MC3T3-E1 cells, M159
IL-4 and IL-13 inhibition of osteoclastogenesis by increasing, SU207
Mechanical loading alteration of expression in MC3T3-E1 cells of, SA167
Osteoclast precursors inhibit osteoblast production of, M250
Promoter polymorphism, hip fracture risk in older women and, 1039
RANKL, 2-yr. change in BMD in systemic lupus erythematosus and serum levels of, SU494

Osteoprotegerin (OPG) (Cont'd)

RANKL inhibition and bone strength in rats overexpressing secreted transgene of, SU451
Serum levels and COLIA1 polymorphism in healthy postmenopausal women, SU374
Serum levels in anorexia nervosa of, SA402
Small molecule stimulators of, SU449
Teriparatide effects on bone remodeling and, M416
rTSH and serum levels of, SU378
Tumor growth inhibition in lytic prostate cancer lesion in bone and, M053
Zoledronic acid treatment and early plasma levels response from, SU206

Osteoprotegerin-receptor activator of NFκB ligand (OPG-RANKL) ligand system

Raloxifene treatment for postmenopausal osteoporosis and, M400

Osteosarcoma, 1220, SU094, SU097, SU100, SU101**Osteosclerosis**, M457, SA013, SA211**Osteotesticular protein tyrosine phosphatase (OST-PTP)**

Skeletal development and, SA040

Osteotomy. SEE *Bone regeneration***Osterix (Oss)**

Endothelial cells and MSC differentiation into osteoblasts, SA213
Runx2-mediated transcriptional regulation in chondrocytes, M170

Ovarian cancer G protein-coupled receptor 1 (OGR1)

Osteoclast survival and extracellular acidification action on, 1148

Ovariectomy (animal models)

AAE581 in non-human primates against bone loss induced by, 1179
AAE581 prevention of bone resorption after oral treatment in rat, SU270
β-Adrenergic receptor-1 and -2 signaling and bone loss after, SU381
Alendronate or risedronate withdrawal and cancellous bone turnover in, SA415
Aromatase inhibition effects on BMD in mice *versus*, SU526
Bazedoxifene acetate and bone loss in cynomolgus monkey, SA431
Bisphosphonate and PTH effect on trabecular bone in, SU411
BMP-6 restoration of trabecular bone in BMP-6 knockout mice, 1027
Bone loss from oxidative stress through T cell activation in, 1144
Bone loss in by docosahexaenoic acid *versus* eicosapentaenoic acid in, SA132
Bone size in ERα receptor knockout mice and, SU418
Cancellous bone connectivity and strength in mice treated with bFGF and risedronate, M130
Cathepsin K knockout mice and bone loss after, F234, SA234
CIZ action in mechanical and estrogenic signaling in bone loss induced by, F174, SA174
Climbing exercise and trabecular bone turnover in mice, F172, SA172
Cortical bone effects of PTH or alendronate in severely osteopenic rats, M489
Cortical bone-forming effects of SB-462795 in cynomolgus monkeys, F236, SA236
CP432 restoration of bone mass and strength in aged rats, M419
Dietary onion quercetin inhibition of bone loss in, M328
ERβ agonist pharmacologic actions in rats, SA427

Ovariectomy (animal models) (Cont'd)

Formation of T cell niches at resorption surfaces, F395, SA395
Gene therapy with RANK-Fc and bone resorption in mice, M430
HSP60-induced apoptosis and p38 activation in osteoblast-lineage cells in rats, SU227
Intermittent PTH effects on bone mass and bone microarchitecture in rats, SA436
Intermittent PTH for cancellous bone regeneration in rats, F433, SA433
Lasofloxifene protection against skeletal deterioration from, M396
MMP inhibitor in cathepsin K knockout mice and bone loss after, SA233
Modified 8 amino acid peptide Ac-TTSGIHPK-amide derived from CXCL7 stimulation of bone formation and BMD in rats, M425
MSCs, prior intra-arterial injection of, and osteogenic effects of bFGF in aged rats, SA137
OPN-deficiency in mice, over-potential of anabolic actions of EP4A signaling by, M165
Osteocalcin in warfarin-treated rats and bone loss induced by, SU021
Osteopenia development in mast cell deficient mice, F389, SA389
Phenolic compounds in safflower seeds and bone loss in, SA514
Platelet-activating factor deficiency and prevention of osteoporosis in, F127, SA127
Propranolol effects on bone architecture and bone cell activity of rat tibias, M421
PTH radioisotope OSC after, M403
Risedronate and/or vitamin K₂ pretreatment effect on early cancellous bone loss in rats after, M348
Rosuvastatin prevention of bone loss in, SU308
SB-462795 prevention of bone mass loss in cynomolgus monkeys, SA235
Sclerostin-neutralizing monoclonal antibody effects on systemic bone loss in, 1082
Sevelamer and bone loss in aged rats, SU431
Skeletal effects of bazedoxifene acetate in mice, M394
Thymic T cell activity and bone loss induced by, 1115
Trabecular bone mass in T-lymphocyte deficient mice and, SA375
TSH and bone loss prevention, bone restoration in aged rats, M428

Overweight. SEE ALSO *Body weight*

Children and adolescents, orthopedic complications in, F472, SA472

Oxandrolone

Osteoblast differentiation and, SU060

Oxygen diffusion time

Connective tissue progenitor cells' formation, proliferation and, M164

Oxysterols

Bone regeneration and, M203
Molecular mechanism(s) of action, M427

Oxytocin

Estrogen mediation of bone cell activity and, 1102

P**P2X7 receptor**

Bone formation and, SU253

P2Y purinergic receptors

Fluid flow-induced expression in human bone-related cells and, SA177
Signaling activation by bisphosphonates, SU257

p16^{INK4a}

C-terminal region of PTHrP regulation of, 1050

P20C/EBP β

Reduced alveolar bone mass in mandible, dentin dysplasia and, F210, SA210

p21^{Cip/WAF1}

Calcium phosphate and osteogenic differentiation of MSCs, M232

p27^{kip1}

Nuclear targeting of PTHrP and cellular proliferation by, 1158

p38 MAPK

1 α ,25(OH)₂D₃ activation of, in C2C12 muscle cells, M513

Endochondral ossification and, 1023

Hypoxia promotion of cartilage matrix synthesis via, 1024

KR62776 suppression of RANKL-induced osteoclast differentiation by inhibiting activation of, M253

MMP-13 expression regulated by ROS in ATDC5 cells and, SU072

Parathyroid hormone activation of osteoblasts and, M218

PGE₂ signaling pathway and, SA196

Prostaglandin synthesis and bone resorption by metabolic acidosis mediated by, SU258

PTH and 1 α ,25(OH)₂ differential regulation on rat intestinal cells of, M512

Signaling, molecular dissection of BMP signaling in fibrodysplasia ossificans progressiva lymphoblastoid cells and, SA011

Signaling, osteoclast survival and, SA274

Vascular calcification inhibition by omega-3 fatty acids and, SA224

p42/44 MAP kinases

Dimethyl sulfoxide enhancement of osteoblast differentiation and, M208

Inhibition, osteosarcoma cell apoptosis and, 1220

p62^{np} expression

RANKL and TNF- α effects in osteoclast formation in multiple myeloma and, 1217

p300

Id1 promoter activity regulation and, SA201

Paget's disease

Cathepsin K serum levels, osteoclastic activity and, SU142

Economic evaluation of long term zoledronic acid *versus* risedronate for, SA465

Kininogen (elevated serum high molecular weight) in, SA467

Treatment costs in privately insured population, SA466

Zoledronic acid for, single 4mg infusion of, SA463

Pain, skeletal

Back response to 12 months treatment with teriparatide in postmenopausal osteoporosis and, SA432

Fibrous dysplasia, age-related increases in, M437

Intravenous pamidronate in recent osteoporotic vertebral compression fracture for, M349

Kyphoplasty and reduction in, M383

Osteoid sarcome of hip and, M525

Raloxifene and osteoporosis-associated, M318, M398

TRPV1 role in cancer-associated, 1121

Paired related homeobox 1 protein (Prx-1)

Appendicular skeleton and calvaria defects with TGF β 2 receptor deletion in cells expressing, F160, SA160

Palmitoylation

Osteoblast differentiation and, SU231

Pamidronate

Discontinuation effects in children and adolescents with osteogenesis imperfecta, 1088

Hepatitis C-associated osteosclerosis, intravenous application of, M457

Intravenous, for pain relief in recent osteoporotic vertebral compression fracture, M349

Metaphyseal modeling in children with osteogenesis imperfecta, F440, SA440

MK-4 enhancement of inhibition of osteoclast precursor cell differentiation by, SU280

Osteogenesis imperfecta treatment in children with, 1090

Osteoporosis in children with cerebral palsy and, SU394

Titanium implant osteointegration under protein undernutrition and, M447

In vitro effects on apoptosis and death of macrophage-like cells and, SU299

Pancreatitis, chronic, M334**Parathyroid cells, cultured bovine, M475****Parathyroidectomy, 1167, M464, M469, SU469.**

SEE ALSO *Hyperparathyroidism*

Parathyroidectomy (animal models), M482**[Leu²⁷]cyclo(Glu²²-Lys²⁶) human Parathyroid hormone 1-31NH₂ (PTH analog), M403.**

SEE ALSO *Ostabin-C*

Parathyroid hormone(1-34). SEE ALSO***Teriparatide***

Bone formation and signaling selective analogs of, F481, SA481

Bone regeneration model and temporal dependence for anabolic actions on, M487

Cross-linking to juxtamembrane portion of PTH/PTHrP with antagonist analogs of, M494

Jagged1 mRNA induced in UMR 106-01 cells by, SU503

Mathematical remodeling cycle model for predicting bone marker response to dosing in rats of, SA484

Rechallenge one year after first PTH course, long-term alendronate and, 1079

Spine fusion and fusion mass volume and treatment with, SU496

Titanium implant osteointegration in low density trabecular rat tibial model, M491

Zoledronic acid combination with, after radiation therapy for bone metastasis, SU112

Parathyroid hormone(1-38), F437, SA437**Parathyroid hormone(1-84)**

Cortical and trabecular bone at hip and, 1083

First vertebral fracture prevention in postmenopausal women with low bone mass using, 1222

Human, infusion over 48 hours and circulating C-PTH fragment levels in parathyroidectomized rats, M482

Jagged1 mRNA induced in UMR 106-01 cells by, SU503

Safety and efficacy with hormone therapy in postmenopausal osteoporotic women, 1080

Secretion dynamics in normal individuals, M484

Trabecular bone architecture in postmenopausal osteoporotic women treated with, F435, SA435

Vertebral trabecular bone quality in osteopenic rhesus monkeys and treatment with, M415

Parathyroid hormone(22-31), F489, SA489**Parathyroid hormone/forskolin, 1120****Parathyroid hormone/parathyroid hormone-like hormone (PTH/PTHrP) system**

Genetic variation in, M116

Parathyroid hormone/parathyroid hormone-related peptide receptor (PTH-PTHrP), 1086, M494, M507, SA488**Parathyroid hormone/parathyroid hormone-related protein receptor (PTH/PTHrP), SA480****Parathyroid hormone (PTH)**

Aging, human bone marrow stromal cell responses and, M004

Antiresorptive effects of calcitriol and, F520, SA520

Bcl-2 and anabolic action in bone of, F192, SA192

Calcemic response and GM-CSF receptor beta regulation of gene expression in CT/ CGRP null mouse, M499

Canonical Wnt signaling activation in bone, Dkk1 and, 1002

Caveolin-1 and cytoskeleton role in extracellular calcium ion regulated release of, SU497

Connexin43 and osteoanabolic action *in vivo*, 1228

Connexin43 function and regulation of rat osteocalcin promoter by, M493

Continuous treatment and bone loss through upregulated T cells localization to bone surfaces, 1049

Continuous treatment, gene expression regulation by intermittent *versus*, SU499

Cortical bone effects in senile and severely osteopenic ovariectomized rats of, M489

Cost-effectiveness of alendronate in high-risk osteoporotic women and, M405

Cyclic *versus* daily dosage, bone formation in murine lumbar vertebrae and, 1180

CYP27B1 and levels in renal tubular cells of, M521

Differential effect in ovariectomized rats and humans of bisphosphonates and, SU411

1,25(OH)₂D₃/VDR system and catabolic but not anabolic effect of, 1099

Early stem cell recruitment during fracture repair and, F483, SA483

Ectopic secretion by thymus epithelial cells of, M459

G β proteins and c-Src tyrosine kinase in signal transduction in rat intestinal cells induced by, SA478

Glucocorticoid-induced osteoporosis in mouse model and, SU067

25(OH)D₃ suppression of synthesis and secretion by cultured bovine parathyroid cells of, M475

Hypertension, BMD and levels of, SU507

Increased vertebral strength and, 1056

Intact, adynamic bone disease misdiagnosis in ESRD with assay of, SU501

Intact, changes in Nichols Advantage assay of, SU502

Intact, changes in Nichols Bio-Intact PTH assay, SU504

Intermittent treatment, bone mass and bone microarchitecture in ovariectomized rats, SA436

Intermittent treatment, cellular mechanisms for anabolic effect in murine cancellous and periosteal bone, M417

Intermittent treatment, Dkk-1 overexpression in murine osteoblasts and, 1191

Intermittent treatment, for cancellous bone regeneration in normal and

ovariectomized rats, F433, SA433

Key Word Index

ASBMR 27th Annual Meeting

Parathyroid hormone (PTH) (Cont'd)

- Intermittent treatment, gene expression regulation by continuous treatment *versus*, SU499
- Intermittent treatment, PTH1R and anabolic response of bone to, 1159
- Intermittent treatment, PTH1R and mechanism of action of anabolic response of bone to, M502
- JNK and p38 MAPK in rat intestinal cells and, M512
- Mixture-based combinatorial (chemical) libraries for development of analogs of, M508
- Mutational analysis of 3' untranslated region in primary hyperparathyroidism of, SU472
- Notch signaling regulation during osteoblast maturation and, 1113
- Osteoblast cultures expressing stage-specific GFP and, SA191
- Osteoblastic Jagged1 increases through PKA activation by, F197, SA197
- p38 MAPK and ERK roles in osteoblast activation by, M218
- Pathogenesis of glucocorticoid-induced osteoporosis and, SA366
- Perfusion analysis of secretion from normal and pathological human parathyroid tissue, M460
- PKC-induced cytoskeleton rearrangement in response to mechanical stimulation in osteoblasts enhanced by, SA173
- Post-parathyroidectomy bone mass changes predictions and, SU469
- Rat bone anabolic response after chronic bisphosphonates to, F220, SA220
- Regulation of FGF23 gene transcription in osteoblasts and, SA144
- Secretion dynamics in normal individuals, M484
- Serum levels of carboxyl fragments in parathyroidectomized rats and hPTH infusion over 48 hours, M482
- Skeletal anabolic effects and mineral ion homeostasis in 1 α -hydroxylase and PTH null mice and, 1203
- Skeletal resistance in chronic renal failure to, M466
- Structure-activity relationship study of analogs modified in position 5, SU498
- Syndecan-4 stimulation in osteoblastic cells by, M490
- Testosterone and estradiol effects on male skeletal sensitivity to, 1107
- Titanium implant osteointegration under protein undernutrition and, M447
- Vitamin D deficiency and, M320
- Vitamin D plus calcium dosing regimens and secretion in women over 65 of, SA418

Parathyroid hormone receptor, 1160, F170, SA170

Parathyroid hormone receptor 1 (PTH1R), M110, M509, SU498

Parathyroid hormone receptor 2 (PTH2R), SU498

Parathyroid hormone receptor 2/ tuberoinfundibular peptide, SA490

Parathyroid hormone receptor, carboxyl-terminal, M501, M506, SA492, SA493

Parathyroid hormone-related peptide, carboxyl-terminal, 1050

Parathyroid hormone-related peptide (PTHrP)

- BMP signaling during mammary gland development and signaling by, 1157
- Calcitonin, prolactin interactions during lactation with, M498
- As candidate for stomach-derived ECL-cell hormone, SA396

Parathyroid hormone-related peptide (PTHrP) (Cont'd)

- DNA-PK–nuclear hormone receptors and nVDRE-mediated transcriptional inhibition of, 1119
- Expression in multiple myeloma, SU095
- Gli2 signaling molecule and effects on chondrocytes of, 1154
- JunB mediation of action on cementoblasts by, M182
- Non-amino terminal, receptor-like binding activity for, M495
- Peptides derived from, and osteoblast-stimulating factors expression in prostate cancer cells of, SU114
- Prostate cells and peptides derived without amino termini from, SU109
- Rat growth plate during recovery of growth retardation and expression of, SA036
- Smurf2 induced and TGF β signaling inhibited in growth plate chondrocytes by, M488
- Transcriptional activation of cyclin D1 promoter by, SA195

Parathyroid hormone-related protein (PTHrP), 1158

Parathyroid hormone-Sp1–nuclear factor-Y_{DIST} DNA element, SA502

Parathyroid hormone type 1 receptor (PTH1R)

- EGFR transactivation and ERK1/2 activation by, M505
- Ezrin-binding protein 50 regulation of vascular smooth muscle cells proliferation mediated by, M500
- GFP-tagged, expression in F1 PTH1R-null osteoblasts, M503
- Karyopherin α 2 and β 1 and, M502
- NHERF1/EBP50 and NHERF2/E3KARP regulation of endocytosis in, M504
- Phenylalanine-34 of PTH and internalization by NHERF1 regulation of, F489, SA489
- Phosphorylation-deficient, increased PTH anabolic effects in mouse model expressing, 1159

Parathyroid tissue

- Perfusion analysis of PTH secretion from normal and pathological, M460

Parity, SU140, SU177

Partial volume averaging errors

- QCT-derived femoral neck strength indices and, M051

Particulate wear debris. SEE *Wear debris*

Patient compliance (adherence)

- With alendronate and risendronate treatment among chronic users of glucocorticoids, SU390
- Bisphosphonates dosing frequency for postmenopausal osteoporosis and, M352
- Bisphosphonates for osteoporosis and, M344
- Bisphosphonates, nonvertebral osteoporotic fracture risk and, SU417
- Daily or weekly bisphosphonates in French women with osteoporosis and, SU416
- Daily *versus* weekly bisphosphonates and, M357
- Depressive symptoms in postmenopausal osteoporosis and, M380
- With drug therapy for postmenopausal osteoporosis, fracture risk and, M294
- Fracture risk reduction in postmenopausal women with bisphosphonates, SU403
- Health status and health-related quality of life effects on, SU402
- Ibandronate once-monthly and, M361
- New fragility fractures after osteoporosis therapy discontinuation and, M388
- With osteoporosis medications among Medicare beneficiaries, M371
- With osteoporosis medications, patient perceptions and strategies for, M391

Patient compliance (adherence) (Cont'd)

- With pharmacological treatment in osteoporosis, patient education and, M386
- By postmenopausal women in managed care on bisphosphonate therapy, M362
- By postmenopausal women with osteoporosis to weekly *versus* daily bisphosphonates, SU397
- Self-report *versus* pharmacy data of anti-osteoporotic medications on, M379
- Short-term monitoring of bone turnover markers in postmenopausal osteoporotic women on antiresorptive therapy and, SU409
- With teriparatide, factors associated with, SA438

Patient education

- BetterBones Workshop*, SU321
- Multilingual, BMD scan decision making and, SU317
- Persistence with pharmacological treatment in osteoporosis and, M386
- Post-fracture osteoporosis care and, SU325
- Post-fracture osteoporosis management and, M387
- Randomized, controlled trial of mailed osteoporosis education to older adults, M372

PC3 prostate cancer cells, F070, SA065, SA070. SEE ALSO *Prostate cancer cells*

PDL-L2 (periodontal ligament) cells, SA024

Pediatric Osteoporosis Prevention Study, 1011, F187, SA187

Pencil-beam DXA

- Cross-calibration with fan-beam DXA, SU138

Pentosidine

- Compressive biomechanical properties of human lumbar vertebrae and, SA058

Pentoxifyline (PeTx)

- BMP action and, SA017

Perfusion analysis

- PTH secretion from normal and pathological human parathyroid tissue, M460

Perimenopausal women, SA113, SU005, SU423

Periodontal ligament, M205, SA216, SU083

Periosteal bone

- Cellular mechanisms for anabolic effect of intermittent PTH in, M417

Periosteum

- PTHrP gene-driven LacZ expression in, M497

Periostin

- Expression in normal tissue and fibrous dysplasia, SA216

Periostin-like-factor (PLF), SU077

Peripheral blood derived MSCs

- In non-union fractures, M226

Peripheral blood mononuclear cells (PBMCs), F249, SA249, SA259, SU382, SU414, SU493

Peripheral dual X-ray absorptiometry (pDXA), M074

Peripheral quantitative computed tomography (pQCT)

- Bone and muscle parameters in dialysis patients with and without fractures, M078
- Defining cortical bone in adolescents and cadavers by, M101
- Fractures in dialysis patients and cortical bone measurements with, M465
- Lifestyle factors and assessment of BMD in mid-radius with, M277
- 3D, trabecular architecture measurement in osteopenic women with and without fractures, F360, SA360
- Tibia, spinal cord injury and, SA080

Peripheral quantitative computed tomography (pQCT), high resolution

Bone microarchitecture evaluation *in vivo* in humans, M086
3D, bone microarchitecture evaluation of hip fractures and Colle's fractures, 1178
3D, forearm and tibia microarchitecture in young healthy women, M093

Perlecan

FGF-2 binding in chondrocytes and, M135

Peroxisome proliferator-activated receptor γ 2 (PPAR γ 2)

Bone adiposity and loss in type 1 diabetes and, F399, SA399
Osteoblast, adipocyte differentiation and, SU242

Peroxisome proliferator-activated receptor γ (PPAR γ)

BMD in humans and polymorphisms in, SU194
Bone loss and age-related Alox5 activation of lipid peroxidation products of, 1140
1 α -(OH) D_2 influence on glucose transport mediated by, M514
Transactivation, nemo-like kinase suppression of, SU259

PFQEP³⁶⁹⁻³⁷³

Osteoclast survival by activation of Akt and AFX by, 1068

pH

TRAP activity and, SU273

Phenytoin

Lipopolysaccharide suppression in bone resorption of, SU301

PHEX/Phex gene, 1105, M127**Phosphate**

FGF23 regulation by hypophosphatemia and depletion of, F459, SA459
FGF23 regulation in untreated Graves' disease of homeostasis of, SA451
Renal 1,25(OH) $_2$ D production in *hyp*-mice and renal transport of, 1205

Phosphate, dietary

FGF23, postprandial changes in healthy men and, M125
First *versus* second generation assays of blood FGF-23 changes with, SA143
Hormonal responses to alterations in, SU500
Serum FGF23 concentrations in healthy men and, M131

Phosphate, extracellular inorganic, SU051**Phosphate, serum**

FGF-23 in patients with hypoparathyroidism and regulation of, M129
Growth hormone replacement effects on metabolism in adult growth hormone deficiency of, M133
Post-parathyroidectomy bone mass changes predictions and, SU469

Phosphatidylcholine, SU267**Phosphatidylethanolamine**, SU267**Phosphatidylinositol 3-kinase (PI 3 K)**, F227, SA227**Phosphatidylinositol 3 kinase (PI3K)-Akt signaling**, SU264**Phosphatidylinositol 3-kinase signaling**, SA230**Phosphatidylinositol 4,5-diphosphate (PIP2)**, SA273**Phosphoadenosine-phosphosulfate synthetase 2 (PAPSS2)**, SU047**Phospho-CREB transcription factor**, M174**Phosphodiesterase 4**

Variants expressed in osteoblasts, M224

Phospholipase A $_2$ activating protein (PLAA)

In growth plate chondrocytes and osteoblasts, SA500, WG2

Phospholipase D hydrolysis

Of phosphatidylethanolamine and phosphatidylcholine after PTH treatment of UMR-106 cells, SU267

Phosphorus

Bone matrix mineralization in klotho mouse, mapping of, SU025

Phosphorus, dietary, PHEX/Phex actions on FGF-23 and, M127**Phosphorylation, mitotic**

Runx2 control in proliferating osteoblasts by, SU228

Phosphospecific antibody cell-based ELISAs (PACE)

Measurement of PTH-induced ERK, Akt activation, or phosphorylation of downstream targets using, M483

Phosphothreonine

Bone resorption and, SA272

Phosphotyrosine

Bone resorption and, SA272

Phylloquinone-4 (PK)

Vitamin K-dependent gamma-glutamyl carboxylase activity of vitamin K compounds in liver, bone and, SA198

Physical activity. SEE ALSO *Exercise*

Adult BMC and childhood, 1012
BMD in Japanese children and adolescents and, M012
Bone strength in older women and, SA310
Fracture risk in older men and, M290
Mechanical vs. metabolic effect on BMD self-reported by postmenopausal women, SU437
pQCT assessment of BMD at mid-radius and, M277

Physical fitness

Hip fractures in elderly women and, SA332

Physicians. SEE ALSO *Family physicians*

Lack of osteoporosis care following fractures and, SU336

Osteoporosis diagnosis and treatment by primary care *versus* specialty, M376

Post-fracture osteoporosis management by, M387

Referrals of high risk patients for DEXA exam by, SA294

Phytoestrogens, SA423. SEE ALSO *Soy isoflavones*; *Soy protein***Pinctada margaritifera**

Osteoclasts and nacre from, SA240

Placebos

Non-persistence during daily therapy and, SU402

Placental carrier transporter gene (PMCA3), 1008**Placental growth factor (PIGF)**

Bone remodeling and, F253, SA253

Plasma cell dyscrasias

Serum FGF23 and, SA060

Plasma cells

In multiple myeloma, SU103

Plasma membrane calcium ATPase 2 (PMCA2), F486, SA486**Platelet-activating factor (PAF) receptor**, F127, SA127**Platelet-derived growth factor (PDGF)**, 1126, SU209**PLEKHM1 gene**

Autosomal recessive osteopetrosis and, 1103

PlexinD1

Skeletal patterning of bone development and, 1209

Plum, dried, SU246, SU430**Podosomes in osteoclasts**, 1145, M254, M265**Polycystic ovary syndrome**, SU474**Polycystin-1**

Mechanosensor promotion of Runx2 and, 1061

Poly-glutamic acid stretch

Targeting and immobilization of bioactive peptides on mineralized tooth matrices using, SU082

Poly(lactic acid (PLA) plate

Bone augmentation with hydroxyapatite and, SU068

Poly(lactic acid-polyglycolic acid copolymer (PLGA) scaffold, M207, SU029, SU058**Polymerase chain reaction, real-time**

Molecular phenotyping of osteoblastic lineage cells lines using TaqMan Low Density Arrays, SA215

Polymethylmethacrylate (PMMA), M432**Polyphenols**

Nodule formation and, M210, SU246

Polyphosphoinositides

Osteoclast migration and, SA273

Poly(propylene fumarate) (PPF) scaffold, SA018**Porous mediums connectivity concept**, M097**Portuguese people**, SU169, SU170**Postmenopausal women**. SEE ALSO *Osteoporosis, postmenopausal*

Aged 50–65 years, risk factors for osteoporosis fracture in, M315

Alendronate effects on periosteal bone formation in adult female ilium in, 1221

Alendronate therapy, use of bone turnover markers for selection of, SU151

AMG 162 and bone mass increases in, SU455

AMG 162 pharmacokinetics after subcutaneous dosing in, SU446

Assessment tool for nonvertebral fracture risk prediction in, SU357

BMD measurement and fracture prediction in, 1057

BMD, serum leptin and adiponectin concentrations in, SU211

BMD with accelerated bone turnover in, SA298

Bone marker changes with one month teriparatide treatment for severe osteoporosis, M408

Bone mass and BMC changes over 10 years among, SU009

Bone protective treatment for osteoporosis, compliance with and effect of, M375

Bone turnover and DHEA supplementation in osteopenic, SU424

Cataract surgery, second, fall and fracture risk after, M298

CDX-2 polymorphism and VDR start codon association with calcium supplementation effect on BMD in, SU192

Community-dwelling osteoporotic, vitamin D deficiency in, M275

C-reactive protein levels and fracture risk in, F319, SA319

CYP19, new single nucleotide polymorphisms in, and BMD in, M122

Diabetes type 2 and risk factors for falls and fractures by, SU355

Dual femur scanning on osteoporosis diagnosis and treatment decision making in, M070

Elderly, serum 1,25(OH) $_2$ D and 25(OH)D levels association with physical performance in, M309

ESR2 influence on osteoporotic fracture risk in, M120

Estrogen therapy discontinuation, alendronate *versus* raloxifene to prevent bone loss in, M354

Fracture risk and bone architecture in, SA359

Fractures in men *versus* fractures in, M300

Fragility fracture prevalence in, SU330

FSH enhancement of osteoclast formation and survival, 1100

Genetic effects on bone loss in, SA113

GLP-2 and nocturnal bone resorption in, 1225

Golfing effects on vertebral bone size and mass in, M148

Key Word Index

Postmenopausal women. SEE ALSO *Osteoporosis, postmenopausal* (Cont'd)
Healthy, circulating OPG levels, COLIA1 polymorphism, and bone mass in, SU374
Hip fractures, heel and hip bone densitometry in, SA292
Histomorphometric indicators of microdamage accumulation in, F356, SA356
Hormone replacement therapy and dietary silicon effects on BMD in, M338
Japanese, latent hypothyroidism and heel quantitative ultrasound in, SA361
Korean, alendronate 70 mg once-weekly treatment and bone metabolism of, M340
Korean, BMD and depression in, SU350
Korean obese, body composition and fat distribution with calcium supplementation in, SA422
Lasofoxifene effects on BMD and bone turnover markers in, F429, SA429
Lasofoxifene extraskelatal effects on, SA428
Lasofoxifene phase 2 dose response analysis in, M385
With low bone mass, first vertebral fracture prevention using PTH(1-84) in, 1222
Lycopene consumption and biomarkers of oxidative stress and bone resorption in, SA308
In managed care, persistence with bisphosphonate therapy and fracture risk in, M362
Mortality and calcaneal ultrasound in, SA092
Osteoporotic, bone turnover markers in, SU159
Osteoporotic, low calcium intake in, M276
Osteoporotic vertebral fractures and longitudinal changes in 3D microarchitecture of paired iliac crest bone biopsies in, M102
Raloxifene effects as osteoporosis pretreatment for one year in, M397
Raloxifene treatment and ER α expression in bone of, SA504
Self-reported physical activity by, mechanical vs. metabolic effect on BMD in, SU437
Serum homocysteine levels and bone mass, bone turnover, and bone size in, SU373
Serum level cathepsin K changes and alendronate treatment in, SU274
Soy protein supplementation and hematological patterns in, M335
Spinal osteoarthritis and Q89R polymorphism in LRP5 of, SU190
Spinal radiography indications in, 1224
Trabecular bone architecture changes with menopause, F358, SA358
Trabecular bone architecture one-year changes using MRI-based virtual bone biopsy of, 1055
Urinary calcium loss and reduced forearm BMD in, SU385
VDR translation start site polymorphism and fractures in, F323, SA323
Vertebral fractures and radiological signs of osteoarthritis in, SA316
Vitamin D deficiency and serum 25(OH)D levels, M279
Vitamin K and undercarboxylated osteocalcin, bone turnover or density in, SU425
Water fluoridation, antioxidant status and, M270
Wrist fractures and subsequent hip, spine, rib, and wrist or forearm fractures in, SU340
Posture, M313. SEE ALSO *Kyphosis*
Potassium citrate
Neutralization of acidogenic Western diet with, BMD in postmenopausal osteopenic women and, SU429

Precision error
Clinical diagnosis and, M081, M082, SU134
Prednisolone
Calcitonin and, SU041
Pregnancy
Social position, bone mass in childhood and, SA299
Pregnancy-associated plasma protein A (PAPP-A), F149, SA146, SA149
Premarin
Welfare of horses and reduced use of, M381
Premenopausal women
Alendronate effects on periosteal bone formation in ilium of, 1221
Androgens, osteocalcin and hip bone density in, SU002
BMD evolution and idiopathic osteoporosis in, SU421
Bone mass and BMC changes over 10 years among, SU009
Dietary restraint, subclinical ovulatory disturbances and BMD in, SU348
Dietary silicon and hormone replacement therapy effects on BMD in, M338
Fracture risk and bone architecture in, SA359
Healthy, subclinical menstrual irregularities and BMD changes in, M316
With idiopathic osteoporosis, BMD distribution and, 1175
With idiopathic osteoporosis, bone remodeling and bone microarchitecture in, SU361
Reference range for bone turnover markers compared to postmenopausal osteoporotic women, SU159
Reference range for bone turnover markers in oral contraceptive users and nonusers, SU158
Senile osteoporosis *versus* osteoporosis in, SU367
Trabecular bone architecture changes after menopause, F358, SA358
Primary care physicians
Osteoporosis care and, M376
Prinomastat
Bone loss after ovariectomy in cathepsin K knockout mice and, SA233
Procollagen type I N-terminal peptide (PINP), SU149, SU160
Progesterone
Inactivation in human osteoblasts, SA373
Progestin medroxyprogesterone acetate (MPA), M399
Progestins with no glucocorticoid activity
HRT *versus*, M399
Progressive osseous heteroplasia, M439
Prolactin
PTHrP, calcitonin interactions during lactation with, M498
Promegestone
BMD evaluation after endometriosis treatment with estradiol and, SA426
Propranolol
Effects on bone architecture and bone cell activity of ovariectomized rat tibias, M421
Prostaglandin E₁ synthase
Microsomal (mPGES-1), fracture healing, osteoarthritis effects of, F125, SA125
Prostaglandin E₂, M159, SA196, SU214, SU258, SU301
Prostaglandin E₂ receptor subtype EP₂ receptor, SA029
Prostaglandin E₂ receptor subtype EP₂ receptor agonist, SU200
Prostaglandin E₂ receptor subtype EP₄ receptor, F062, SA062
Prostaglandin E₂ receptor subtype EP₄ receptor agonist, M031, M161, M165. SEE ALSO *CP432*
Prostaglandins, M153, M424, SA482

Prostate, CE590 versus DHT effects on, M395
Prostate cancer, F381, SA329, SA381, SU110, SU121. SEE ALSO *Prostate cancer metastasis to bone*
Prostate cancer cells. SEE ALSO *PC3 prostate cancer cells*
Bone metastasis pathways for osteoblasts interaction with, SU119
Estren effects on, M062
Mevalonate inhibition by lipophilic statin and apoptosis in human, M057
Non-amino terminal PTHrP receptor-like binding activity in, M495
PTHrP-derived peptides' regulation of osteoblast-stimulating factors expression by, SU114
PTHrP-derived peptides without amino termini from, SU109
Smad1, as androgen receptor co-repressor induced by prostate-derived factor, inhibition of, F129, SA129
Prostate cancer metastasis to bone
Bone remodeling mechanisms in, SU049
Cathepsin K inhibition and, SU113
Gene expression associated with, SU122
Measuring α -CTx for early detection of, SU116
OPG inhibition of tumor growth in, M053
PSA and osteoblastic response in, SU118
Ras activation and, 1122
In vivo imaging of osteolytic lesions, SA069
Zoledronic acid and atrasentan treatment for, 1213
Prostate-specific antigen (PSA), SU118
Protease inhibitors, 1163
Proteasome inhibitors, SU103, SU105
Protein kinase A, F197, SA197, SU235, SU260. SEE ALSO *Cyclic AMP/PKA signaling*
Protein kinase C, 1148, M255, SA173
Protein kinase C δ , SU268
Proteoglycans, M235
Proteomics
Bone biomineralization foci, SA019
Comparison of osteoblasts and osteocytes show protein expression patterns, SA288
Inorganic phosphate treated MC3T3 E1 cells analysis, M186
Osteoblast differentiation, SU283
Pseudohypoparathyroidism type-Ib, 1036
PTH and Alendronate Study (PaTH), 1056
Puberty
Delayed, loading and bone formation in female rats, M138
Ethnic/racial group differences in BMC and bone parameters in girls, M003
Exercise and bone growth during, M141
Fractures in, implications in old age and, 1131
Growth spurt age and final height determinants in young Swedish men, SA006
Male growth spurt age and trabecular and cortical BMD in young adults, 1129
Total body and forum bone mass determinants in Chinese postmenarcheal girls, SA005
Pueraria thunbergiana
Osteoblast differentiation and, SU233
Pulsed electromagnetic fields (PEMFs), M040
Pycnodysostosis, SU277, SU456
Pyk2, 1150
Pyk2/Src, M265

Q

QRT 2000 (quantitative real-time ultrasound machine), SU172
Quality of life, M431, SA044, SU439, SU443
Quality of life, health-related, M433, M434, SU402, SU463

Quantitative computed tomography (QCT). SEE ALSO *High resolution computed tomography; Micro-computed tomography; Multislice computed tomography; Peripheral quantitative computed tomography*

Bone size and density in children with Turner syndrome prior to growth hormone therapy, SU483

Forearm structural and density changes after injury, SU369

Long-term *in vivo* scanning of nasal turbinates in cynomolgus monkeys, SU128

Prediction of ultimate stress in femoral cortical bone by, SU089

Spinal loading and vertebral strength population-based study, 1074

Quantitative evaluation, SU281. SEE ALSO *Ultrasound, quantitative*

Quantitative real time polymerase chain reaction (QRT-PCR), SU052

Quantitative trait loci

BMD and bone size using cross of MRL and CAST inbred mice strains, SA105

BMD in Amish men, SU178

Bone and body composition phenotypes in GH/IGF-I deficiency mouse model, SU181

Chromosome X, influence on femoral geometry and bending strength in mice, SA107

Disuse osteopenia identification, SU174

Gender-specific, for trabecular and cortical bone in F2-intercross of GK and F344 inbred rats, M109

Influences on age-related bone quality declines, M112

Mechanoresponsive BMD and bone size, F183, SA183

On mouse chromosome 12, bone nanoindentation regulation by, SU182

Quebec, Canada

Hip fractures incidence and outcomes in, SU341

Quercetin, dietary (onion extract), M328

Questionnaires

Fragility fracture prevalence in postmenopausal women, SU330

Hip fracture screening, SU137

Self-administered bone-specific physical activity, SU437

R

Rab3D

Vesicular trafficking in bone resorption and, M263, M264

Rabson-Mendenhall (insulin-resistance) syndrome, M441

Rac-1

BCA3 interaction in osteoclasts with, SU269

Rac-2

Reduced osteoclast function, increased bone mass and, F270, SA270

Radiation therapy (radiotherapy), SA075, SA152, SA398

Radiographic absorptiometry, SA078

Radiographs/radiography. SEE ALSO *X-rays*
Childhood forearm fracture evaluation with, M017

Detection of osteoporotic vertebral fractures with sagittal CT reformations *versus*, SU324

Hologic densitometer automated computer-aided detection of vertebral fractures *versus* conventional, SA324

Plain hip, correlation with BMD, M065

Spinal, indications in postmenopausal women, 1224

2D lateral spine, of vertebral trabecular microstructure, SA091

Radiologists

Visual recognition of vertebral compression deformities by, SU328

Radius, distal. SEE ALSO *Colle's fractures; Wrist; Wrist fractures*

MRI in postmenopausal women to assess cortical bone, SA083

Tennis-playing and bone geometry at, SA186

Raloxifene (RAS)

Alendronate after estrogen therapy discontinuation in postmenopausal women *versus*, M354

Bazedoxifene acetate in intact mice *versus*, M394

BMD and bone remodeling markers in postmenopausal women pre-treated for one year with, M397

ER α expression in bone and, SA504

Fracture risk reduction effects and, F425, SA425

Lumbar BMD and bone markers in postmenopausal Korean women with osteoporosis, SA424

OPG-RANKL ligand system in postmenopausal osteoporosis and, M400

Osteocyte survival and, M401

Osteoporosis-associated skeletal pain and, M318, M398

Short-term effects on BMD and bone resorption, M393

Raman spectroscopy, SA284

RANTES (regulated on activation, normal T expressed and secreted)

In osteoblasts, M162

Rap1

Bone metabolism regulation and, F218, SA218

Ras

Prostate cancer metastasis to bone and, 1122

H-Ras-GTPase

Mechanical inhibition of RANKL regulated by, F166, SA166

RAW 264.7 cells, M252, SA252, SU197, SU291

RCJ3.15 (chondrogenic) cells, SA042

Reactive oxygen species (ROS), F401, M266, SA401, SU072, SU272, SU273

Receptor activator of NF κ B Fc (RANK-Fc), M430, SU448

Receptor activator of NF κ B ligand (RANKL).

SEE ALSO *Osteoprotegerin-receptor activator of NF κ B ligand system*

Bone loss, immune status in arthritic rats and OPG inhibition by, SU295

Bone remodeling in hyperhomocysteinemia restoration by folate therapy and, SU380

Bone resorption, BMD and AMG 162 inhibition of, SU304

Calpain and osteoclastogenesis supported by, SA263

Cbp expression in osteoclasts and osteoclastogenesis induced by, 1146

Cortical and trabecular bone mass and strength in mice and, SA357

Expression at erosion sites in rheumatoid arthritis, SU491

Expression in bone marrow of postmenopausal women, estradiol therapy and, F374, SA374

Expression in mesenchymal cells, Runx2 and, M160

Expression in multiple myeloma, SU095

Expression in oral squamous cell carcinoma, SU099

Expression in osteoblasts and flagellin stimulation of osteoclastogenesis, M002

Extreme longevity and serum levels of, SU004

Gap junction channels mediate signals for osteoclastogenesis induced by, SA283

Gene polymorphisms of, M119

Receptor activator of NF κ B ligand (RANKL).

SEE ALSO *Osteoprotegerin-receptor activator of NF κ B ligand system* (Cont'd)

Gene transcription suppressed by CpG methylation of its promoter region, SA203

IL-4 and IL-13 inhibition of osteoclastogenesis by decreasing, SU207

Induction of NFATc1 in osteoclasts and, SA267

Inflammatory bone loss and secreted mRNAs in, M243

Inhibition, bone strength in rats overexpressing secreted OPG transgene, SU451

Inhibition, cortical bone geometry in orchiectomized rats and, 1226

Inhibition, femoral head deformity after ischemic necrosis of femoral head in immature pigs and, 1128

Inhibition, osteolytic metastatic prostate cancer tumor formation and, SA069

Inhibition, trabecular architecture in female mice and, SU452

iNOS/NO as negative feedback inhibitor during osteoclastogenesis induced by, 1070

LIF *versus* OSM and mRNA expression of, SU208

Malignant activities of metastatic breast cancer cells and, SA067

Mechanical inhibition regulated by H-Ras-GTPase, F166, SA166

Mechanical loading alteration of expression in MC3T3-E1 cells of, SA167

Metastatic lung cancer in bone and tumor expression of, F135, SA135

NFATc1 targets β 3 integrin in osteoclast differentiation induced by, SA257

OPG, 2-yr. change in BMD in systemic lupus erythematosus and serum levels of, SU494

OPG inhibition by glucocorticoids and stimulation of, SU519

Osteoclastogenesis and 1 α ,25(OH) $_2$ D $_3$ mediated chondrocyte expression of, 1067

Osteoclastogenesis, cell cycle progression, arrest and, M244

RANK expression in TNF-induced joint erosion and inflammation *in vivo* and, 1196

Regulation of osteoclast function by redox and intracellular ROS production by, M266

RGS10 regulation of [Ca $^{2+}$] $_i$ oscillations in RANKL-induced osteoclast differentiation and, M260

Runx2 expression and, SA209

Schnurri-2 activation of bone remodeling by coupling to, 1052

Shedding activity, MT1-MMP and ADAM10 in, 1188

Sphingosine kinase in osteoclastogenesis induced by, SU286

Teriparatide effects on bone remodeling and, M416

Truncation mutants of as inhibitors of osteoclast differentiation and activation induced by, M248

rTSH and serum levels of, SU378

Receptor activator of NF κ B (RANK)

Bone remodeling in hyperhomocysteinemia restoration by folate therapy and, SU380

CaMKII γ and osteoblastogenesis regulation via signaling by, SU284

E3 ligase activity of TRAF6 required for signaling and programming osteoclast progenitors by, 1069

Expression in normal and malignant haemopoietic cells, SA259

Expression in rheumatoid arthritis, SU491

FHL2 attenuation of TRAF6-mediated signaling by, SA278

Key Word Index

ASBMR 27th Annual Meeting

Receptor activator of NFκB (RANK) (Cont'd)
IL-3 inhibition osteoclastogenesis by irreversible down-regulation of expression by, SA268
IL-4 and IL-13 inhibition of osteoclastogenesis by decreasing, SU207
Osteoclast development and deficiency in the hematopoietic compartment of, SA256
RANKL expression in TNF-induced joint erosion and inflammation *in vivo* and, 1196
Receptor for advanced glycation end products (RAGE), M456, SA271
Recognizing Osteoporosis and its Consequences in Quebec (ROCQ), SA335
Redox
Regulation of osteoclast function by, M266
Regucalcin
MC3T3-E1 cells differentiation, mineralization and, M201
Regulator of G-protein signaling 2 (RGS2)
Mechanical stress of human periodontal ligament cells and, SU083
Regulator of G-protein signaling 10 (RGS10)
[Ca²⁺]_i oscillations regulation by, M260
Regulator of G-protein signaling (RGS) proteins
Chondrocyte differentiation and, SU037
Renal cell carcinoma bone metastasis, 1126, F156, SA156
RepliCell Bioreactor System, SU249
Residency, family practice
Bone density testing usage in, M085
Resistance training, M144, SU442. SEE ALSO *Exercise*
Resistin
In osteoblasts and osteoclasts, SA252
Retinoblastoma-binding protein 1 (RBBP1)
ERα-specific suppression of, 1200
Retinoic acid
MSCs differentiation and, M204
Retinoic acid receptor signaling
Osteoblast differentiation and, SU247
Retinoids
ColX gene expression in prehypertrophic chondrocytes and, 1022
Retinoid X receptor (RXRα)
Phosphorylation of, F499, SA499
R-FB
COX-2-mediated inhibition of IGFBP-6 transcription and, SA145
RGD integrin binding motif
Bioactive peptides on mineralized tooth matrices and, SU082
Rheumatoid arthritis, M389, SU486, SU491, SU493, SU495. SEE ALSO *Arthritis; Osteoarthritis*
Apoptosis regulation in fibroblast-like synoviocytes, M486
Rheumatoid arthritis (animal models), SA027, SU295, SU489
Rheumatoid synovial fibroblasts
Hyaluronan suppression of IL-1β action via ICAM-1 on, SU071
RhoA
Modeled microgravity and downregulation of, SU222
RhoA GTPase
Inhibition, osteosarcoma cell apoptosis and, 1220
Rho-associated kinase 1 and 2 (ROCK1 and 2)
In primary osteoblasts, SU244
RhoE
Mechanical stress of human periodontal ligament cells and, SU083
Rho GTPases
Expression in primary osteoblasts, SU244
Rib fractures, SU322
Ribosomal RNA gene expression
Runx2 transcription factor and, 1053
Rickets (animal models), SU024

Rickets, hereditary hypophosphatemic with hypercalciuria, 1106
Rickets, hypophosphatemic, SA452
ringelschwanz mutant mice, 1181
Risedronate (RIS)
Alendronate effects on BMD and bone resorption in osteoporosis *versus*, SU395
Baseline BMD and anti-fracture efficacy of, M367
BMD changes and fragility fractures during treatment with, SA405, SA407
Bone biomechanical properties in orchidectomized rats treated with two doses of, SA378
Bone metabolism in subacute spinal cord injured patients, M341
Bone remodeling, microdamage accumulation with postmenopausal osteoporosis, 1081
Bone resorption reduction in two weeks, SU407
Cancellous bone connectivity and strength in ovariectomized mice treated with bFGF and, M130
Cell transduction mediators in osteoblasts and, M221
Comparison of vitamin D or vitamin K in Japanese osteoporosis patients to treatment with, SU408
Discontinuation in ovariectomized rats, cancellous bone remodeling and, SA415
Discontinuation, magnitude of change in BMD and bone turnover markers, M377
Economic evaluation of long term zoledronic acid for Paget's disease *versus*, SA465
Glucocorticoid-induced osteoporosis in mouse model and, SU067
Health care costs for postmenopausal osteoporosis in Germany *versus* strontium ranelate, SA403
Hip and nonvertebral fracture risk and, M356
Illustrating drug utilization using Drug-O-Gram of weekly, M363
Inhibition of osteoclastogenesis from peripheral blood mononuclear cells in postmenopausal osteoporosis, SU414
New vertebral fracture risk reduction in men with osteoporosis, SU391
Oral, for men with osteoporosis, SU404
Pain and cartilage metabolism in osteoarthritis and, SU030
Persistence and adherence to, among chronic glucocorticoid users, SU390
Pretreatment effect on cancellous bone loss after ovariectomy in rats with or without vitamin K₂, M348
Renal clearance over wide range of serum concentrations of, SU406
Safety over wide range of serum concentrations in postmenopausal osteoporosis, SU405
Upfront loading doses of, M369
In vitro effects on apoptosis and death of macrophage-like cells and, SU299
RNA, small interfering
Cathepsin K transfection in human osteoclasts and, SU307
Roche Elecsys 2010 immunoanalyzer, SU160, SU163
Root resorption
Ultrasound stimulation of cementoblasts and, SU063
Ror2
Osteoblast regulation differentiation and, M189
ROS17/2.8 cells, M501, SA386
Rosuvastatin, SU308
Rowers
Skeletal homeostasis in runners *versus*, SU087

Ruffled membranes of osteoclasts, V-ATPases and, SU296, SU298
Runners/running, M143, SU087, SU356, SU434
Run domain factor 1 (Runx1)
Chondrocyte differentiation and, F032, SA032
Run domain factor 2/core binding α factor 1 (Runx2/Cbfa1), M179
Run domain factor 2/core binding α factor 1 (Runx2/Cbfa1) gene P1 promoter, M188
Run domain factor 2 P2 promoter alleles, 1208
Run domain factor 2 (Runx2)
Aromatase gene expression regulation by, M175
Association with microtubules, nucleocytoplasmic shuttling and, F212, SA212
Bone formation reduction due to unloading and loss of half gene dosage of, M152
Canonical Wnt signaling and chondrocyte hypertrophy mediation through, 1020
Cbfb in bone formation and, 1014
Cdk6 and Cdk4 switching in osteoblast differentiation and, 1016
Cell cycle regulation, osteoblast proliferation, growth, differentiation and, SU248
Chondrocyte differentiation and, F032, SA032
Compounds activating, bone loss *in vivo* and, SA207
Control in proliferating osteoblasts of, SU228
C terminus deletion, abrogation of osteogenic function by, 1030
Degeneration of canine intervertebral disc and enhanced, SU055
Dlx5 transcription factor and cooperative interaction of BMPs with, F012, SA012
Domains for osteoblast differentiation, 1015
FGF2 and nuclear accumulation in osteoblasts of, F142, SA142
Glutamine repeat mutations influencing BMD and fracture, 1059
Histone deacetylases and, F204, SA204
Hoxa-10 activation of, 1013
LSN509010 and mRNA expression of, F202, SA202
Msx2 negative regulation of osteolysis in breast cancer cells by, M058
Myeloid elf-1 like factor repression in osteoblast differentiation and, M176
N-terminal polyglutamine-alanine domain, functional study of, F214, SA214
Osteolysis in breast cancer cells, gene expression and, M059
Osterix transcriptional regulation in chondrocytes by, M170
RANKL expression in mesenchymal cells and, M160
RANKL gene expression and, SA209
Ribosomal RNA gene expression and, 1053
Shear intensity-dependent regulation in MC3T3 E1 cells of, SU225
Smurf1-mediated degradation of, 1187
TNF effects on Smurf1 E3 ligase in osteoblasts and, 1018
Transcription activation by MINT, M173
Transcriptional repression by SOX9 during skeletogenesis, 1017
Run domain factor 2 (Runx2) promoter, 1061
Run domain factor 3 (Runx3), F032, SA032

S

S100A1 (SOX trio target molecule), chondrocytes activity and, 1006
S100B (SOX trio target molecule), chondrocytes activity and, 1006
Safflower seeds
Bone loss in ovariectomized rats and, SA514
SaOS-2 cells, M210, M485, SA205, SU233, SU263

SB-462795. SEE ALSO *Cathepsin K inhibitor(s)*

Bone resorption, BMD, and bone strength in young male monkeys and, F232, SA232

Bone resorption inhibition with cathepsin K inhibition by, SA231

Cortical bone-forming effects in ovariectomized cynomolgus monkeys of, F236, SA236

Prevention of bone mass loss in ovariectomized cynomolgus monkeys by, SA235

SBC-5 (lung cancer metastasis) cells, SU271**Scanning small angle X-ray scattering (sSAXS),** SU028**Scantibodies Laboratory, PTH assays,** SU504**Scavenger receptor, class A (SR-A)**

Osteopetrosis and, F242, SA242

Schnurri-2 (Shn-2)

Coupling in bone remodeling to BMP and RANKL, 1052

Sclerostin-neutralizing monoclonal antibody

Ovariectomy-induced systemic bone loss and, 1082

Sclerostin (SOST)

Expression regulation by osteotropic factors in calvaria organ culture, SU209

Wnt signaling and binding to LRP5 by, M220

Wnt signaling and inhibition of BMP-stimulated bone formation by, 1029

SD-208

Breast cancer bone metastasis in mouse model and, 1216

Sealing zone of osteoclasts

Cortactin role in actin assembly at, SA245

Leupaxin overexpression in osteoclasts and Src localization at, M258

Nacre from *Pinctada margaritifera* and, SA240

Nonmuscle myosin IIA and, SA239

Pyk2/Src role in calcitonin-induced detachment of, M265

Seawater

Biochemical and mechanical properties of bone and, M329

Secreted frizzled-related protein 3 (SFRP3)

Overexpression, bone metabolism and, SU256

Secreted frizzled-related protein 3 (SFRP3),

mouse, SU252

Secreted frizzled-related protein 4 (SFRP4)

Expression in tumor-induced osteomalacia, M126

Na⁺Pi IIA co-transporter in proximal tubule cells and, SA455

Secreted placental alkaline phosphatase (SEAP)

RANKL shedding assay system using plasmids encoding, 1188

Secreted protein acidic and rich in cysteine. SEE *Osteonectin***Selective androgen receptor modulators**

(SARMs). SEE *5 α -Dihydrotestosterone*

Selective estrogen receptor modulators

(SERMs). SEE ALSO *Bazedoxifene acetate*; *Lasofloxifene*

Myeloma cell apoptosis and, SU104

Reduction of proinflammatory molecules in human chondrocytes by, SU044

Selective serotonin uptake inhibitors (SSRIs)

Osteoclastic activity stimulated by, SA047

Senescence-accelerated mouse models, SA355**Senescence-accelerated (SAMP6) mouse model,** M329, SU525**Sensory responses**

Osteocalcin null mutant mice and altered, F051, SA051

Serine protease

Activation of BAG-75 and mineral nucleation within biomineralization foci, F023, SA023

Serotonin, SA386, SU213**Sevelamer hydrochloride**

Bone loss in ovariectomized rats and, SU431

Sex differences

Androgen receptor, cortical bone modeling and, F515, SA515

BMD profiles in Norwegian patients with forearm fractures, M286

Bone microstructure at wrist and, 1075

Bone response to D-galactose, SU365

Bone size and BMD, SU318

Bone size in leptin knockout mice, loss of, SA508

Cortical bone mineralization in fibular shaft in aged and, SU015

Diabetes status and BMD testing, M304

1,25(OH)₂D and EB1089 effects in intestine and bone of mature rats, M516

Genetic regulation of bone in congenic strains for mouse distal chromosome 1 and, F114, SA114

Long bones' shape in children, SU319

Mouse chromosomes influencing bone growth patterns, M105

Mouse chromosomes influencing bone morphology, composition and, M104

Nerve damage responses of mice, SU362

Osteoporosis fractures and costs in USA by, F317, SA317

Vertebral fracture detection by physical examination and, SU323

Sex hormone-binding globulin (SHBG), SA512, SU524**Sex hormones/steroids**

Fall risk in community-dwelling older persons and, 1041

Predictors of BMD, bone size and prior osteoporosis-related fractures in elderly Swedish men, SA510

SH2-containing 5'-inositol phosphatase 1 (SHIP1)

Negative regulation of osteoclast differentiation by, M259

TREM2 stimulation leads to DAP12 association with, M261

SH2-containing 5'-inositol phosphatase (SHIP)

Bone resorption attenuation, and c-Src recruitment to podosomes in osteoclasts of, M254

Sheep

Leptin and bone formation inhibition and bone mass control in, SU210

Short bowel syndrome

Metabolic bone disease in, M444

Shoulder

Calcific deposits of, SA020

SHP2 mutations

Disorganized chondrogenesis and, 1085

Silicon

Dietary, BMD in premenopausal and postmenopausal women on HRT and, M338

Dietary, calcium/vitamin D₃ effect on bone turnover and BMD with, SA421

Soluble, biochemical and mechanical properties of bone and, M329

Simvastatin

hBMSCs' differentiation into osteoblasts *in vitro* and, SU234

Single-nucleotide polymorphisms (SNPs)

Of BMP-2, osteoporosis-associated traits in women and, M033

VDR promoter and growth in female adolescents, SA495

Skeletal ash, DXA prediction in pigs of, M077**Skeletal growth (development).** SEE ALSO *Body height*

Age factors, CYP2R1 expression in mice and, M520

Androgen action in SAMP6 mouse model and, SU525

Skeletal growth (development). SEE ALSO *Body height* (Cont'd)

Androgen action on cortical bone surfaces and, F515, SA515

Body composition effects on bone mass and, SU320

Bone accretion elongation and metabolic activity in rat during, M014

Bone geometry, density, and strength determinants in, 1127

Bone quantity and quality accretion in murine, M018

Chromosome substitutions regulate mouse patterns of, M105

Cyclosporine A treatment in rats, secondary hyperparathyroidism and, M479

Defects in Kat2J/Nek1-/- mice, 1156

1,25-(OH)₂D₃ and PTH anabolic effects in 1 α -hydroxylase and PTH null mice and, 1203

Exercise during puberty and, M141

Infancy and childhood, hip fracture risk prediction and, 1058

Intra-uterine, PMCA3 expression and, 1008

Mechanical loading benefits to health and, 1170

Paternal bone size and neonatal, F002, SA002

Peak, weight in Japanese adolescents and, M010

PTHR1 polymorphisms influence BMD variation through, M110

Recovery from dietary calcium deficiency in pigs, SU017

Retardation with deletion of mid- and carboxyl-regions of PTHrP, 1050

School curriculum-based exercise and, 1011, F187, SA187

SNPs in VDR promoter in female adolescents and, SA495

Stunted, altered bone phenotype in IL-6 transgenic mice and, F470, SA470

Temporal expression of LRP5/6, Dkk-1, and other Wnt-signaling components in, SA130

Trabecular and cortical BMD in young adult men, and age at pubertal spurt in, 1129

Vibration-enhanced bone formation and bone quality in, M150

In vivo and *ex vivo* measurement in nonclinical pediatric studies in rats of, M076

Skelite

Bone-targeting bone and cartilage stimulating peptide and, M392

Skin color

Ultraviolet B effects on serum levels 25(OH)D in humans and, SA519

UV-mediated vitamin D synthesis and β -Thalassemia changes in, M280

Ski, TGF- β signaling, hypertrophic differentiation in chondrocytes and, SA175**Smad1,** F129, F133, M039, SA129, SA133**Smad2,** M026**Smad3,** 1005**Smad4,** 1117, F154, SA154**Smad6,** 1187, SA017**Smad8,** SU061**Smad anchor for receptor activation- β (SARA β),** 1028**Smad-independent signaling,** SA280**Smad-interacting domain (SMID),** 1030**Smad ubiquitin regulatory factor 1 (Smurf1),** 1187, M027**Smad ubiquitin regulatory factor 1 (Smurf1) E3 ligase,** 1018**Smad ubiquitin regulatory factor 2 (Smurf2),** 1005, M488**Smoking,** M277, SA200, SA304**Social position**

Pregnancy, and bone mass in childhood, SA299

Key Word Index

Socioeconomic factors

- Fracture risk in Denmark and, M317
- Hip fracture prediction in California 1996–2000 and, SA311
- Mexico City Invest in Your Bones program and, SA010

Sodium-dependent phosphate transporter

- Intracellular signaling in rat aortic smooth muscle cells of vasopressin-induced, SU026

Sodium-dependent phosphate transporter, type IIa (NaPi-IIa)

- Ezrin and PTH-mediated downregulation in opossum kidney cells of, F479, SA479
- SFRP4 actions in proximal tubule cells on, SA455

Sodium-dependent phosphate transporter, type IIc (NaPi-IIc)

- Homozygous loss-of-function mutation and renal phosphate-wasting, 1106

Sodium-dependent phosphate transporter, type III (Pit-1)

- Cataract and nephrotic syndrome in transgenic rats overexpressing, SU050

Sodium/hydrogen exchanger regulatory factor type 1 (NHERF1:EBP50)

- Extracellular signal-regulated kinase signaling by PTH receptor and, 1160
- Phenylalanine-34 of PTH and regulation of PTH1R internalization by, F489, SA489
- PTH1R endocytosis regulation and, M504

Sodium-hydrogen exchanger regulatory factor type 2 (NHERF2:E3KARP)

- PTH1R endocytosis regulation and, M504

Sodium hydroxide

- Osteogenesis on PLGA scaffolds and, SU058

Sox4

- Osteoblast regulation and, SU232

Sox9

- Expression in MSCs, CTGF regulation of, SU035
- TIP39/PTHR2 signaling inhibition of chondrogenesis by regulation of, SA490

SOX9 (Sox9)

- Runx2 transcriptional repression during skeletogenesis and, 1017
- TM promotion of chondrogenesis and, SU033

Soy isoflavones, M327, SU432. SEE ALSO

Phytoestrogens

Soy protein, M335, SU418**SPA-1-/- osteoclast-like cells**, F218, SA218**Spaceflight, long-duration**, 1171, 1172**Specialty physicians**

- Osteoporosis diagnosis and treatment by, M376

Spectrometry

- ⁴¹Ca and accelerator mass, calcium metabolism monitoring in ESRD, SU165
- Tandem LC-Mass (LC-MS/MS), of vitamin D₂ therapy effects, SA523

Spectromicroscopy

- Of oxidative damage to collagen, SU020

Spectroscopy

- Fourier transform infrared, of subchondral sclerotic lesion in knee osteoarthritis, M041
- One-dimensional ³¹P-¹H, of hydroxyl ions in bone mineral, SU059

Sphingosin-1-phosphate (S1P)

- RANKL-induced osteoclastogenesis and, SU286

Sphingosine kinase (SPHK)

- RANKL-induced osteoclastogenesis and, SU286

Spinal cord injuries, M341, M452, SA080, SA377, SA448**Spinal curvature irregularity index**

- Vertebral fracture prediction with, M282, SA322

Spinal mobility

- Falls, muscle strength in osteoporosis and, M311

Spine

- Anteroposterior view, vertebral fracture assessment and, F084, SA084
- Mandibular index correlation with BMD of, SA089

Spine fusion

- PTH effects on, SU496

Spinomed active orthosis, SU443**Spinomed orthosis**, SU443**Spondyloepimetaphyseal dysplasia**

- PAPSS2 mutation and, SU047

Spondyloepiphyseal dysplasia type Kimberley (SEDK)

- Molecular basis of, F116, SA116

Spontaneous fractures (sfx) mouse, M113**Sprague-Dawley rats**, F057, SA057, SA302, SU202, SU300**Squamous cell carcinoma**

- Oral, SU099, SU106

Src

- Actin dynamics and turnover in osteoclast podosomes and, 1145
- Leupaxin overexpression in osteoclasts and, M258

Src/ERK signaling

- Osteoblast survival, osteoclast apoptosis and formation suppression and, SU264

ST2 cells, M237, SA209, SU259**STAT1/3**

- Signaling in osteoblasts, IL-6 and IL-11 dependent osteoclast formation and, M262

STAT3 protein

- LIF *versus* OSM and activation of, SU208

STAT6

- IL-4 and IL-13 inhibition of osteoclastogenesis and, SU207

Statins, F227, M366, SA227, SU234. SEE ALSO

specific Statins

Staurosporine

- Chondrocyte death and, SU039

Stem cell antigen-1 (Sca-1/:y6A)

- Null mice as age-dependent osteoporotic phenotype, SU370

Stem cells. SEE ALSO *Embryonic stem cells;*

Mesenchymal stem cells

- Circulating human organ, immune recognition and control of, SU254
- Circulating multipotential skeletal, SU031
- PTH recruitment during fracture repair of, F483, SA483
- Therapy, immune recognition and control of circulating human organ stem cells consequences for, SU254
- Therapy, osteoprogenitor source and transplantation protocols comparison for, M238

Steroids, inhaled

- Effects on BMD and fracture risk with, SA364

Strain, mechanical. SEE *Stress, mechanical***Stress, chronic mild**

- Depression and bone loss in mice with, SU377

Stress fractures, M136, M448**Stress, mechanical**

- Bone formation, resorption regulation in cultured osteoblasts by, SU216
- Confocal *versus* light microscopy for *in vivo* microdamage accumulation detection in wild and domesticated animals, M044
- Differentiated ATDC5 cells up-regulate type II, X collagen and aggrecan transcripts in response to, SU088
- FosB expression in hBMSCs and, M180

Stress, mechanical (Cont'd)

- Integrin α 7 and ligament resistance to mineralization induced by, SA024
- α 5 Integrin role in hemichannel opening for prostaglandin release due to, 1095
- Periostin expression in mesenchymal tissues and, SA216
- PKC-induced cytoskeleton rearrangement in PTH-enhanced calcium ion response in osteoblasts to, SA173
- RhoE and RGS2 in response of human periodontal ligament cells to, SU083
- Signaling in transgenic mice expressing osteoblast-specific PTH/PTHrP receptor, PTH receptor signaling and, F170, SA170

Stress, oxidative, 1144, F391, SA308, SA391, SU020**Stroke**

- Fracture rates after, F334, SA334

Stromal derived factor-1 α (SDF-1 α), bone remodeling and, M236**Stromal derived factor-1 (SDF-1)**

- Chemotactic recruitment of osteoclast precursors by, SA265
- TNF promotion of osteoclast precursor mobilization through inhibition of, 1072
- Transendothelial migration of circulating CD14⁺ monocytes and osteoclast precursors, 1071

Strontium

- Functional responses of osteoblastic cells to, M195
- Low-dose, lamellar bone formation at periosteal surface and, M423

Strontium ranelate

- Bone remodeling and bone safety in postmenopausal osteoporosis, 1084
- Bone resorption, calcium-sensing receptor and, SU511
- Health care costs for postmenopausal osteoporosis treatment in Germany *versus* risedronate, SA403
- Intrinsic bone tissue quality and, M140
- Osteoblasts and, M424
- PKC signaling pathways and osteoclast apoptosis induced by, M255

Strontium salts

- Bone ultrastructure in rats and, SU028

Study of Osteoporotic Fractures (SOF)

- Automated structural measurements of proximal femur in pelvic radiographs, hip fracture prediction and, F090, SA090
- Hyperkyphosis, heritability of, SU180
- Long-term prediction of incident vertebral fractures, 1038
- OPG promoter polymorphism in older women and fracture risk, 1039
- Radiographic vertebral fractures, prior non-spine fractures and hip fracture risk after 10 years, F315, SA315
- Site-specific fracture risk differences among older osteoporotic women, F325, SA325
- Stroke and subsequent fracture rates, F334, SA334

Submarine patrols

- French, seasonal vitamin D deficiency in, M268

Substance abuse

- Fracture risk in Canadian Aboriginal people and, SU329

Sun exposure

- Inadequate vitamin D status despite, 1177

Sunlight OmniSense Multisite Ultrasound

- Precision and normative data for Caucasian girls, SA095
- Vertebral deformity assessment and, SA097

Surface enhanced laser desorption ionization time-of-flight (SELDI-TOF) mass spectrometry

Biomarkers for osteoporosis diagnosis using, SU150

Osteoarthritis biomarker research, SU153

Surface microtopography

β_1 -Integrin silencing and osteoblast response to, M212

SW480 conditioned media

Wnt signaling and connective tissue progenitor cells colony formation, proliferation in, SU255

Swedish National Registry

Stroke and subsequent fracture rates, F334, SA334

SWI/SNF chromatin remodeling complexes

Runx2/Cbfa1 gene transcription and, M188
VDR-C/EPB β in transcriptional regulation of 24(OH)ase and, 1201

Swiss Evaluation of the Methods of the Osteoporotic Fracture (SEMOF),

SA332, SU168

Swiss Evaluation of the Methods of the Osteoporotic Fracture (SEMOF) plus French cohort (EPIDOS),

F096, SA096

Syk kinase

α , β_3 -Integrin signaling of cytoskeletal organization in osteoclasts and, F244, SA244

Syndecan-4

PTH stimulation in osteoblastic cells of, M490

Syndecans

BMP4 signaling disrupted in fibrodysplasia ossificans progressiva lymphoblastoid cells mediated by, M029

Synovial joints

Formation of, Ihh signaling and Wnt/ β -catenin signaling in, 1003

Induction of, Wnt/ β -catenin signaling in, F048, SA048

T**TAF_{II}-17**

Pagetic-like osteoclasts formation and, 1207

Tamoxifen

Discontinuation, SU108

Postnatal chondrocyte-specific *Ihh* deletion using, F035, SA035

Short-term effects on BMD and bone resorption, M393

Tamoxifen inducible Cre transgenic mouse,

1153

TaqMan Low Density Arrays,

SA215

Tartrate resistant acid phosphatase 5b (TRAP 5b or TRACP 5b)

Human osteoclast culture activity and number of osteoclasts, SU303

As marker of osteoclast number, SU161

Measurement of human osteoclast cultures, CTx ratio to, SU290

Stability in human serum samples, SU162

Tartrate resistant acid phosphatase positive mononuclear prefusion osteoclasts

JNK activity and maintenance of commitment to, M240

Tartrate resistant acid phosphatase positive multinucleated osteoclasts (TRAP+ MuOCL)

ADAM8 overexpression and osteoclast formation, M242

MCP-1 expression and, M247

Osteoclast differentiation and MCP-1-induced, F249, SA249

Tartrate resistant acid phosphatase (TRAP or TRACP)

Antigen presentation by dendritic cells and, SU275

Tartrate resistant acid phosphatase (TRAP or TRACP) (Cont'd)

Cathepsin K as regulator in osteoclasts of, SU272

Clinical performance of six assays for, SU147

Trypsin-cleavage and ROS generating activity of, SU273

Tartrate resistant acid phosphatase (TRAP) promoter

Bone cancer treatment in mice transgenic for cytosine deaminase regulated by, SA248

T-box 3

Growth hormone, osteoblast proliferation and, M183

T cell factor (TCF). SEE ALSO *Lymphoid enhancer-binding factor/T cell factor*

Kremen 2 and Dkk1-mediated inhibition of Wnt3a-LRP5/6 signals in U2OS

osteoblast-like cells and, M217

T cells

Allogenic mesenchymal stem cells and, M227

Bone marrow stromal cells modulation of contributions to TNF α -induced osteoclastogenesis *in vivo* by, F247, SA247

Bone metabolism in pediatric Crohn disease and, SU478

Bone resorption at specific bone sites after ovariectomy and, F395, SA395

IFN γ effects on bone resorption and activation of, F387, SA387

IFN γ mediation of bone formation inhibition by activated, F131, SA131

Localization to bone surfaces from continuous PTH treatment, bone loss and, 1049

Oxidative stress and estrogen deficiency-induced bone loss through activation of, 1144

Post-ovariectomy trabecular and cortical bone loss and, SA375

 $\gamma\delta$ T cells

Targeting myeloma bone marrow microenvironment by, 1123

Tctex-1

Rab3D-dependent vesicular trafficking in bone resorption and, M264

Teas, bottled

Fluoride in, M450

Technetium Tc 99m sestamibi

Differences in accuracy in severe or mild hyperparathyroidism, SU468

Tec kinases

Regulatory roles in osteoclast differentiation, SA276

TEI-9647 ((2S)-25-dehydro-1 α -hydroxyvitamin D₃-26,23-lactone)

VDR and RANKL-induced osteoclast formation blockage by, SA497

Telomerase

Knockout mouse model with osteoporosis and osteoblast differentiation impairment, M234

 α -C-Telopeptide (α -CTx)

Sensitivity to metastatic bone disease with, F074, SA074, SU116

 β -C-Telopeptide (CTx)

Osteoporosis treatment and serum levels of, SU160

C-Telopeptide (CTx)

Biological pathway in breast cancer bone metastasis, SU148

Lack of hepatic metabolism of, SU149

As marker of osteoclast activity, SU161

Measurement of human osteoclast cultures, TRAP 5b ratio to, SU290

Serum levels with vertebral and hip fractures, osteoporosis and, SU154

Serum *versus* salivary concentrations, SU157

N-Telopeptide (NTx)

Validation in cynomolgus monkey, SU152

Temperature, room

Axial transmission ultrasound bone measurements and, SA094

Temporomandibular joint osteoarthritis

Senescence-accelerated mouse models for, SA355

Tendinitis

Calcifying, of shoulder, SA020

Tendon, SA054, SU061**Tennis-playing**

Bone geometry at distal radius and, SA186

Teriparatide. SEE ALSO *Parathyroid hormone(1-34)*

Adult hypophosphatasia treated with, F457, SA457

BMD and back pain response to 12 months treatment for postmenopausal

osteoporosis with, SA432

BMD change and fracture risk reduction in osteoporotic women treated with, 1223

Bone marker changes with one month treatment of men and women with severe osteoporosis, M408

Bone remodeling effects of, M416

Chondrosarcoma of right hip and, SU505

DANCE clinical trial on osteoporosis treated with, M406

DANCE clinical trial on rationale, evidence for initiating therapy with, M407

Early change in bone turnover after, M412

Hyperostosis frontalis interna, and elevated bone turnover markers in patient on, SA434

Lumbar spine BMD response in women with postmenopausal osteoporosis treated with, M410

Quantitative ultrasound in women with well-established osteoporosis and treatment with, M414

Vertebral height in osteoporotic women with severe prevalent vertebral fractures and, M404

Vertebral trabecular bone structure analysis with high resolution computed tomography, M413

Testicles, rat

BMD and BMC with torsion, detorsion, or removal of, SA382

Testosterone

Male skeletal sensitivity to PTH and, 1107

Tetracycline, tritiated (³H-TC)

Diet effects on bone resorption in ovariectomized rats and, SU011

Tetramethyl thiuram disulfide (thiram)

Tibial dyschondroplasia in chickens induced by, SU064

Tg-4x300 founder mice,

F030, SA030

Thailand

Estimated volumetric BMD in rural men and women, M066

 β -Thalassemia

UV-mediated vitamin D synthesis and skin pigmentation changes in, M280

Thiazide

BMD in men and, M307

Thiazolidinedione drugs

Bone surface specific effect in mice, SA394

Thienoindazole derivative small compound T-198946 (TM),

SU033

3D volumetric fluorescence imaging

Automated imaging of *in vivo* bone formation labels, M046

3D X-ray absorptiometry

In vivo reconstruction of human vertebrae with, M288

3T3L1 preadipocytes

Heparin effects on adipogenesis in, M237

Key Word Index

Thrombospondin-2 (TSP2)

Marrow stromal cell differentiation and expression of, SA038

Thymus epithelial cells

Ectopic PTH secretion by, M459

Thyroid carcinoma

BMD changes and bone turnover with thyroxine treatment for, SA390

Thyroid hormone (T3)

BMP-2, insulin and redifferentiation of dedifferentiated chondrocytes by, SA034

Thyroid-stimulating hormone receptor/thyrotropin (TSHR), M115**Thyroid-stimulating hormone/thyrotropin (TSH)**

Bone formation in aged, ovariectomized rats and, M428

Bone remodeling markers and, SU378

Differential TNF α expression in osteoclasts, osteoclast progenitors and, SA246

Thyrotoxicosis

Severe hypercalcemia due to, SU471

Tibia

Bone formation enhancement with frequency-dependent loading of mouse knee, SA180

Dyschondroplasia in chickens of, SU064

High resolution 3DpQCT study of bone microarchitecture in healthy, young women, M093

Men with spinal cord injuries and mechanical properties of, SA377

Spinal cord injuries and pQCT at, SA080

Tight skin (Tsk) mutation mice

Skeletal phenotype, F046, SA046

Til-1 (Cbfal N-terminal isoform)

Overexpression for tissue engineering, M168

Tissue-culture grade polystyrene

Growth dynamics of human fetal osteoblastic cells in bioreactor *versus* in, SU245

Tissue engineering. SEE Bone tissue engineering; Cartilage tissue engineering**Tissue inhibitor of metalloproteinase-2 (TIMP2)**

Amelogenin (recombinant mouse) binding and, M205

Tissue-nonspecific isoenzyme of alkaline phosphatase (TNSALP) (C1348T)

Infantile hypophosphatasia causing variably lethal outcome in blacks with homozygosity for, F474, SA474

Titanium implants

Biocompatibility of niobium alloys, M453

Defective osteointegration under protein undernutrition, M447

Early implant performance bone markers correlating bonding strength with bone and, SA045

Finite element analysis for mapping load environment in histological sections of bone surrounding, SA056

PTH(1-34) and osteointegration in low density rat tibial model of trabecular bone, M491

Rat femur model, rhTGF β 2 effect in, SA159

Vancomycin for periprosthetic infection with, M455

Titanium particles

COX-2 gene induction through NF- κ B-dependent pathway in fibroblast-like synoviocytes, M178

TNF- α release induced by, SU197

TMC-33 cells, 1155**Tobago Family Study, F112, SA112****Toll-like receptor 4 (TLR-4)-dependent signaling, M256****Toll-like receptor 9, F251, SA251****Tomography. SEE High resolution computed tomography; Micro-computed tomography; Micro-positron emission tomography; Multidetector row computed tomography; Multislice computed tomography; Peripheral quantitative computed tomography; Quantitative computed tomography****Trabecular bone**

Acquisition, circulating IGF-I and, 1193

ADAM8 overexpression and, M242

Alendronate effects in postmenopausal osteoporotic women on, SU393

Architecture in early postmenopausal women, MRI-based virtual bone biopsy of one-year changes in, 1055

Architecture in female mice, RANKL inhibition and, SU452

AR inactivation in mineralizing osteoblasts and loss of, 1097

Assessment with magnetic resonance T₂ relaxation time, SA085

Bone surface topology mapping, and quality assessment of, SU171

Evaluation using porous mediums connectivity concept, M097

Gender-specific QTL in F2-intercross of GK and F344 inbred rats, M109

Global knockdown of calcitonin receptor in young female mice and volume of, 1161

Glucocorticoid-induced osteoporosis and structure of, F086, SA086

Immobilization and sensory neuropeptide signaling at post-junctional level in, SU383

Improvements in postmenopausal osteoporotic women treated with PTH(1-84), F435, SA435

Loss in young adult women and men, 1010

Low density, PTH(1-34) and titanium implant osteointegration in, M491

Neuromuscular degenerative disease devastation of, SU371

Pre- and postmenopausal structure, F358, SA358

PTH(1-84) effects at hip, 1083

Restoration in ovariectomized BMP-6 knockout mice by BMP-6, 1027

Skeletal and sexual maturation effects in peripheral skeleton, F004, SA004

3D-pQCT measurement in osteopenic women with and without fractures, F360, SA360

T-lymphocytes and post-ovariectomy loss of, SA375

Vertebral deformity, degree of, and microarchitecture of, M295

Vertebral microstructure, 2D lateral spine radiographs of, SA091

Vertebral microstructure, high resolution CT assessment of, M095, M413

Transforming growth factor α /epidermal growth factor receptor

Calcium-induced parathyroid hyperplasia in early kidney disease in rats and, M463

Transforming growth factor β

Amelogenin (recombinant mouse) and signaling by, M205

Bone matrix mechanical properties, composition and signaling by, SA163

CCL5/RANTES mRNA expression and secretion from osteoblasts and, M162

Chondrocyte death and, SU039

Cranial neural crest cells proliferation and development during frontal bone development and, F222, SA222

ASBMR 27th Annual Meeting

Transforming growth factor β (Cont'd)

Elevation of CXCR4 and chemotactic recruitment of osteoclast precursors by SDF-1 enhanced by, SA265

Fibronectin regulation of incorporation into bone matrix of, 1054

Gli2 and stimulation of PTHrP expression in breast cancer cells by, F066, SA066

Large latent complex of, produced by hypertrophic chondrocytes, SA155

MMP regulation in renal cell carcinoma bone metastasis of, F156, SA156

Osteoclast survival and activation of Smad independent signaling by, SA280

PTHrP inhibited of signaling in growth plate chondrocytes by, M488

Renal cell carcinoma bone metastasis, IL-6, PDGF-AA, VEGF stimulation by, 1126

Signaling in early limb chondrogenesis by, SA157

Ski inhibits signaling by, SA175

Suppression of PPAR γ transactivation in MSCs and, SU259

Tight skin mutation mice skeletal phenotype and, F046, SA046

In vitro chondrointroduction by rhBMP-2 and, M025

Transforming growth factor β 1

Osteoblastic expression in osteoarthritic patients and the elderly of, SA162

Regulation of ATF-3 and its target genes in bone metastasizing breast cancer cells, SA164

Regulation of SOST expression in calvaria organ culture by, SU209

Transforming growth factor β 1 receptor, 1192**Transforming growth factor β 2, SA159****Transforming growth factor β 2 receptor, F160, SA160****Transforming growth factor β /BMP signaling, F154, SA154****Transforming growth factor β inducible early gene-1 (TIEG), M172, SA158, SA506, SU010, SU285****Transforming growth factor β /Smad signaling, SA153****Transgenic animals**

Mice, C57B1/6 OPN-/-, SU080

Mice, cartilage specific *Dlx2*, 1155

Mice, Cbfa1/Runx2 overexpressing, SU399

Mice, CHOP expression in osteoblast function, F206, SA206

Mice, Col2a1Cre-TM, 1153

Mice, Col3.6GFP/Col2.3ATK, F266, SA266

Mice, cytosine deaminase, SA248

Mice, diphtheria toxin receptor, F289, SA289

Mice, *Dlx5* regulation of osteoblast differentiation in, 1186

Mice, dominant negative Osr2, F208, SA208

Mice, expressing osteoblast-specific constitutively active PTH/PTHrP receptor, F170, SA170

Mice, Fra1 protein and prenatal osteosclerosis in, SA211

Mice, HSD2 overexpression and calvarial development in, SU520

Mice, ICER, M187

Mice, *LRP5*^{G171V}, M050

Mice, mandibular phenotype of p20C/EBP β , F210, SA210

Mice, MKK6EE, 1023

Mice, overexpressing PAPP-A, SA146

Mice, pOBCol3.6GFP and PTH actions on osteoblast proliferation and apoptosis, SA191

Mice, Runx2 with deleted or expanded QA domain, F214, SA214

Mice, SFRP3, SU252

Mice, sFRP3, SU256

ASBMR 27th Annual Meeting

Key Word Index

Transgenic animals (Cont'd)

Mice, ZFP 521 overexpression, 1183
Rats, Pit-1, SU050

Transglutaminase (TG) substrate

Bioactive peptides on mineralized tooth
matrices and, SU082

Trans-Golgi network

Rab3D regulation of vesicular trafficking
pathway in bone resorption after, M263

**Transient receptor potential vanilloid 1
(TRPV1)**

Cancer-associated bone pain and, 1121

**Transient receptor potential vanilloid 4
(TRPV4)**, 1096, SU040**Transplantation.** SEE ALSO *Bone allografts*; *Heart
transplantation*; *Kidney transplantation*;
Liver transplantation

Bone fragments and cultured osteoblasts in
infantile hypophosphatasia, 1166

GFP and comparison of osteoprogenitor source
and protocols for, M238

Immune recognition and control of circulating
human organ stem cells consequences
for, SU254

**Treatment of Osteoporosis with PTH (TOP)
study**, 1083, 1222, F435, SA435 **α -Tricalcium phosphate, self-setting**

Osteogenesis with dental implant placement
and, SU057

***Trichoplusia ni* (High Five) insect cells**, SU512**Trichostatin A**

Osteoclast apoptosis, differentiation and, M245

**Triggering receptor expressed on myeloid cells-2
(TREM2)**, M261**Triglyceride-rich lipoproteins in mice**

Bone role in clearance of, M332

Triiodothyronine

Chondrocyte death and, SU039

Tropomyosin

Isoforms localize to distinct microfilament
populations in osteoclasts, SA238

***Trps1* transcriptional repressor**

Endochondral bone formation and, 1032

Trypsin

ROS generating activity of TRAP and cleavage
of, SU273

T-scores, F293, M074, M301, SA293, SU134,
SU139. SEE ALSO *Z-scores***Tuberoinfundibular peptide 39/parathyroid
hormone receptor 2 (TIP39/PTHR2)
signaling**, SA490**Tumoral calcinosis**

FGF23 gene mutation and, F442, F444, SA141,
SA442, SA444

Tumor necrosis factor

Bone formation inhibition, 1018
MAPK and osteoblast differentiation inhibition
by, SU241

Oscillatory and combinatorial binding of NF- κ B
to DNA by, SA254

Osteoclast precursor mobilization promoted by
inhibition of SDF-1, 1072

Tumor necrosis factor- α

Bone marrow stromal cells modulation of
contributions by macrophages and T
cells *in vivo* to osteoclastogenesis
induced by, F247, SA247

Canonical Wnt signaling inhibition by, SU238
Human osteocyte-osteon structure regulation
by, SA217

Titanium particle-induced release of, inhibitory
effect of epigallocatechin gallate
deficiency through inhibition of MAPK
and AP-1/NF- κ B on, SU197

TSH and differential expression in osteoclasts,
osteoclast progenitors of, SA246

**Tumor necrosis factor receptor-associated
factor-2 (TRAF2)**, F277, SA277**Tumor necrosis factor receptor-associated
factor-5 (TRAF5)**, F277, SA277**Tumor necrosis factor receptor-associated**

factor-6 (TRAF6), 1069, F277, SA261,
SA277, SA278

Tumor necrosis factor-related activation

induced cytokine, M249, SA261

Tumor necrosis factor-related apoptosis-

inducing ligand, SA064, SA217

Tumor suppressor genes

C-terminal region of PTHrP regulation of, 1050

Turmeric

Action on rheumatoid arthritis by phenolic
compound extracts from, SU489

Turner syndrome, SU483**Twist1**, SU199**Twisted gastrulation protein (Tsg)**, M037**Twist/Twist**

Cranium regeneration and, M184, SU070

Tyrosine kinases

Cbl-decreased osteoclast activity and, F279,
SA279

U

U2OS osteoblast-like cells, M158, M172, M217,
M511**U-33/ γ 2 cells**, SU242**Ultrasound**

Cementoblast *in vitro* proliferation and
metabolism and, SU063

Differences between infants and children in
bone, SU167

Low-intensity pulsed, new bone formation and,
SU090

Ultrasound, axial transmission

Room temperature and measurements at
extremities, SA094

Ultrasound, calcaneal quantitative

BUA map of heel, SA098

Latent hypothyroidism in Japanese
postmenopausal women and, SA361

Mortality in postmenopausal women and,
SA092

Nonvertebral fracture prediction and, SA350
Nonvertebral fracture risk prediction with,
F093, SA093

Normative data in Italians, F301, SA301
Normative data in Portuguese, SU169

Ultrasound, quantitative (QUS)

Cortical bone loss assessment using Mechanical
Response Tissue Analyzer *versus*
DEXA and, SU133

Dietary intake and bone health in children,
SU353

Fracture Index validation in population-based
sample of Swiss elderly women using,
SU168

Hip fracture prediction in elderly women using
clinical factors and, F096, SA096

Portuguese adults, SU170

Teriparatide treatment in women with well-
established osteoporosis and, M414

VDR gene polymorphism in geographically
isolated women and, SA117

Vertebral fracture risk prediction in Japanese
women by radiographic absorptiometry
and, SA078

Vertebral fracture risk prediction using, SU166

Ultrasound, quantitative real-time

Description of *QRT 2000* device, SU172

Ultrasound, scanning confocal

Bone surface topology mapping, trabecular
bone quality assessment and, SU171

Quantitative prediction of bone density and
strength in human heel using, SU173

Ultrasound, Sunlight OmniSense Multisite

Precision and normative data for Caucasian
girls, SA095

Vertebral deformity assessment and, SA097

Ultraviolet B

Effects on serum 25(OH)D in humans, SA519
Variable responses to, inadequate vitamin D
status and, 1177

UMR-106-01 cells, M490, M492, SU503**UMR-106 cells**, M174, SA386, SU240, SU267**United Kingdom Vitamin D External Quality****Assessment Scheme (DEQAS)**

On storage conditions for vitamin D

metabolites, SA525

Unloading. SEE ALSO *Disuse osteopenia*

Bone formation reduction and loss of half
Runx2 gene dosage in, M152

Central nervous system control of bone loss
from, ventromedial hypothalamus and,
F393, SA393

CIZ action in mechanical and estrogenic
signaling in bone loss induced by,
F174, SA174

IGF-I and bone recovery after two weeks of,
M146

Inhibin A overexpression and bone *versus*
muscle loss in mice, 1169

Leptin *versus* β -blockers mitigation of bone loss
due to, F176, SA176

MuRF1 and bone loss induced by, 1174

Osteocyte *versus* osteoblast apoptosis and, 1092
Polyphenol compounds in dried plum and bone
recovery after, SU430

Reloading after, osteoblast proliferation, IGF-I
responsiveness and, SU221

Sensory neuropeptide signaling at bone in post-
junctional level and, SU383

TRPV4 mediation of bone loss due to, 1096

Urban-rural difference

Air pollution, BMD and, M271

Vitamin D insufficiency in South India, SA305

Urokinase receptor, role in bone remodeling,

M246

V

Vacuolar H⁺-ATPases (V-ATPases)

Lipid raft transport to ruffled membranes of
osteoclasts and, SU296

Vacuolar H⁺-ATPases (V-ATPases) subunit B

Actin-binding activity of, SU298

Valproic acid

BMD in juvenile Sprague-Dawley rats and,
SA302

Vancomycin

Periprosthetic infection and, M455

Vascular calcification. SEE ALSO *Cardiovascular
calcification*

Abdominal aorta, osteoporosis and, SA337
Chronic kidney disease stimulation of, BMP-7
action in skeletal deposition of
phosphate and, F016, SA016

Elastic lamellae of devitalized rat aortas
incubated in serum and, SA026

Inhibition by omega-3 fatty acids via p38
MAPK pathway, SA224

Osteoporosis and, SU022

**Vascular cell adhesion molecule 1 (VCAM-1), in
BMSCs, calcium receptor expression
and**, M229**Vascular endothelial growth factor**

Aberrant bone formation in mice
overexpressing isoforms in cartilage of,
1151

Pueraria thunbergiana enhancement of, SU233
TGF- β stimulation in renal cell carcinoma bone
metastasis of, 1126

Vascular smooth muscle cells (VSMC), 1158,
M500**Vascular smooth muscle cells (VSMC), human
aortic**, F021, SA021**Vascular smooth muscle cells (VSMC), rat
aortic**, SU026

Key Word Index

ASBMR 27th Annual Meeting

Vasculogenesis

CD34+ cells and, 1066

Vasopressin

Intracellular signaling mechanism of Na-dependent phosphate transport activity and, SU026

Venus flytrap module

CASR mutation and physiological relevance of, SA485

Vertebrae, lumbar. SEE ALSO *Intervertebral disks*

Pentosidine and compressive biomechanical properties of, SA058

Vertebral (compression) deformities

In Canadian Aboriginal women, SU327

Computerized model for clinical assessment of, F321, SA321

Degree of, association with topology of trabecular network and, M295

Height loss over one year and, SA314

Multisite ultrasound and, SA097

Prediction with spinal curvature irregularity index, M282

Sensitivity for visual recognition of, SU328

Vertebral compression fractures. SEE ALSO

Vertebral fractures

Intravenous pamidronate for pain relief in recent osteoporotic, M349

Vertebroplasty patient characteristics, SA333

Vertebral fracture assessment, densitometric

AP spine view for reliability and accuracy of, F084, SA084

Contrast-detail phantom evaluation in, M080

Hologic automated computer-aided, SA324

Indications for densitometry patients, F313, SA313

Local *versus* international reference standards and, F081, SA081

Men with normal BMD and fractures detected with, M281

Repeatability and sensitivity with Norland scanner of, SU124

Vertebral fractures

BMD prediction over 15 years of incident, F297, SA297

Bone architecture and, SU084

COPD and, M292, SA342

Deterioration of cancellous and cortical bone structure and risk of, M283

DXA scans of hip fractures and, M297

Early osteoporosis treatment and prevention of subsequent, M293

Historical height loss and detection of, SA320

Incident, long-term prediction of, 1038

Kyphoplasty and reduction in osteoporotic, M383

Lumbar BMD, monoclonal gammopathy of undetermined significance and, SA392

Medical resource utilization and costs in first year after, SA330

New incident, alendronate *versus* risedronate for, SU395

Osteoporotic, and longitudinal changes in 3D microarchitecture of paired iliac crest bone biopsies in postmenopausal women, M102

Osteoporotic, radiographs *versus* sagittal CT reformations for detection of, SU324

Osteoporotic, serum CTx levels in, SU154

Osteoporotic, *Spinomed* and *Spinomed active* orthosis use after, SU443

Prediction with spinal curvature irregularity index, M282, SA322

Prevalence in Mexican men over 50 years, M287

Prevention in postmenopausal women with low bone mass using PTH(1-84) of first, 1222

Radiographic, prior non-spine fractures and hip fracture risk after 10 years of follow-up, F315, SA315

Vertebral fractures (Cont'd)

Radiological signs of osteoarthritis in postmenopausal women and, SA316

Risedronate therapy and risk reduction in male osteoporosis for new, SU391

Risk prediction by QUS in postmenopausal women, SU166

Risk prediction by radiographic absorptiometry and QUS in Japanese women, SA078

Sex differences in detection by physical examination of, SU323

Spinal radiography indications in postmenopausal women, 1224

Teriparatide effects on vertebral height in osteoporotic women with severe prevalent, M404

Vertebral geometry. SEE ALSO *Bone geometry*

In vivo reconstruction with 3D-X-ray absorptiometry of, M288

Vertebral strength. 1074, F088, M411, SA088.

SEE ALSO *Bone strength*

Vertebroplasty

Patient characteristics, SA333

Veterans

Osteoporosis risks in African American men, M306

Vibration. M147, M150, SU442, SU445**Vitamin A**

β -Cryptoxanthin effects on osteoblast differentiation, mineralization *versus*, M213

Vitamin B₆

Bone mechanical properties and collagen cross-links in diabetic WBN/Kob rats and, SU420

Vitamin B₁₂

Hip fracture risk in elderly and plasma levels of, F309, SA309

Vitamin C

Deficiency, gulonolactone oxidase gene, spontaneous fractures and, 1045

Osteoblast protection from endoplasmic reticulum stress by, SU266

Vitamin D. SEE ALSO *Vitamin D plus calcium; specific analogs and derivative forms*

Alendronate inhibition of bone marrow adipogenesis when combined with, F412, SA412

Assay variations and status of, SA526

Bariatric surgery consequences on status of, M339

Bone health in female Army recruits and, SA307

Calcium homeostasis and calcium intake *versus* status of, M324

Celiac disease and hip fractures in community-dwelling people and, M330

Chronic pancreatitis and, M334

Comparison of risedronate or vitamin K in Japanese osteoporosis patients to treatment with, SU408

CpG methylation of its promoter and RANKL gene activation suppression by, SA203

Deficiency, acute lymphoblastic leukemia and, SU096

Deficiency, bone loss in inflammatory bowel disease and, M333

Deficiency, community-dwelling postmenopausal women with osteoporosis and, M275

Deficiency, fracture risk in community-dwelling older people and, F351, SA351

Deficiency, hip fractures and, M274

Deficiency, hip fractures and lower extremity functional changes in women and, SU337

Deficiency, hyperparathyroidism and, M326

Deficiency, hyperparathyroidism in morbid and super obese patients and, M323

Vitamin D. SEE ALSO *Vitamin D plus calcium; specific analogs and derivative forms* (Cont'd)

Deficiency, in people seeking advice on managing primary hyperparathyroidism, 1168

Deficiency, neuromuscular performance and, 1134

Deficiency, non vertebral fragility fractures in Scottish adults and, SA318

Deficiency, risk factors for women with osteoporosis and, M278

Deficiency, serum 25(OH)D levels and, M279

Deficiency, varying presentations after bariatric surgery of, M336

Dietary, muscle mass and body fat in dieting young women and, M272

Fracture risks in Hispanics, M308

Inadequacy, abundant sun exposure and, 1177

Inadequacy, impairment of alendronate treatment of postmenopausal osteoporosis and, SU462

Inadequacy in nursing home residents, rapid correction of, SU460

Insufficiency in liver disease and liver transplantation patients, M476, WG5

Insufficiency in South India rural and urban people, SA305

Rationale for inclusion in current treatment for osteoporosis, M360

Seasonal deficiency in French submarine patrols, M268

Serum levels required for maintenance and buildup of bone in young Japanese women, M008

Supplements, BMD evolution in young premenopausal women with idiopathic osteoporosis and, SU421

Supplements in women with osteoporosis, M269

β -Thalassemia skin pigmentation changes and UV-mediated synthesis of, M280

Vitamin D₃. SEE ALSO *Alendronate plus vitamin D₃*

Regulation of SOST expression in calvaria organ culture by, SU209

Safety and BMD effects for Romanian nursing home residents of bread fortified with 125 mcg of, SU427

Vitamin D binding protein

Measurement of capacity of, free 1,25(OH)₂D and, SA522

Vitamin D metabolites

Storage conditions and measurement of, SA525

Vitamin D nuclear receptor (VDR_n)

Colorectal hepatic metastasis and levels of, M522

Vitamin D plus calcium

Alfacalcidol effects on spinal BMD in postmenopausal osteoporosis *versus*, SU458

BMD evolution after heart transplantation and, M478, WG7

Dosing regimens and PTH secretion in women over 65, SA418

Effects on bone markers and BMD after low-energy fractures, SU459

Low dose oral silicon as adjunct to bone formation by, SA421

Prophylaxis for systemic use of glucocorticoids in primary health care, SA372

Vitamin D ratio

Separating familial hypocalciuric hyperparathyroidism from primary hyperparathyroidism and, SU479

Vitamin D receptor. SEE ALSO *1,25*

Dihydroxyvitamin D₃/vitamin D receptor system

Adipogenesis enhancement in BMSCs lacking, F496, SA496

Vitamin D receptor. SEE ALSO *I,25**Dihydroxyvitamin D₃/vitamin D receptor system* (Cont'd)

ApoA1 gene expression regulation by antagonist ZK 191784 of, SA517

Biological potency and affinity of vitamin D ligands to, SA521

Caffeine effect and expression in osteoblast cells of, M511

Characterization of knockout mice deficient in FGF23 and, F140, SA140

Extracellular calcium ion concentration and regulation in human kidney cells of, SU515

Gene polymorphism and BMD variations in Polish men, SA123

Gene polymorphism and falls in elderly, SA501

Gene polymorphism and QUS in geographically isolated women, SA117

Heterodimer binding to human PTH Sp1/nuclear factor Y_{DIST} DNA element, SA502

24(OH)ase transcription and, 1204

Regulatory polymorphisms cause reduced signaling by, M117

Retinoid X receptor phosphorylation and prevention of vitamin D-dependent nucleocytoplasmic trafficking, F499, SA499

Subcellular trafficking regulation, 1118

SWI/SNF chromatin remodeling complexes, transcriptional regulation of 24(OH)ase and, 1201

Translation start site polymorphism and fractures in older women, F323, SA323

Vitamin D receptor 1a promoter

Growth in female adolescents and SNPs in, SA495

Vitamin D receptor start codon

CDX-2 polymorphism and calcium supplementation effect on BMD in postmenopausal women, SU192

Vitamin D response element

In human and mouse epithelial calcium channel-2 genes, M515

Vitamin D response element binding proteins

Oligonucleotide trapping for identification of, SA498

Vitamin K

APOE genotype is determinant of serum levels in elderly of, M123

Bone metabolism in healthy Japanese women and serum levels of, M291

Comparison of risedronate or vitamin D in Japanese osteoporosis patients to treatment with, SU408

Deficiency, bone loss in inflammatory bowel disease and, M333

Deficiency, hip fractures and, M274

Gamma-glutamyl carboxylase activity of vitamin K compounds in liver, bone dependent on, SA198

Undercarboxylated osteocalcin, bone turnover or density in postmenopausal N. American women, SU425

Vitamin K₁, dietary

BMD and fracture risk in perimenopausal women and, SU423

Vitamin K₂. SEE ALSO *Menatetrenone*

Bone mechanical properties and collagen cross-links in diabetic WBN/Kob rats and, SU420

Bone mineral/matrix changes in magnesium-deficient rats treated with, M321

Vitronectin

C-terminal of matrix gla protein binding with, SA052

W**Warfarin**, SA344, SU021, SU023**Water and fat suppressed proton magnetic resonance imaging (WASPI)**, SU145**Wdr5**

Endochondral bone formation and, F041, SA041

Weaning

Bone mass recovery in mice and, 1087

Wear debris, M214, M215, SU302**Weight loss.** SEE ALSO *Body weight*

Bone loss and incident vertebral fractures in women over 50 and, SU358

Leptin gene therapy effects on cancellous bone mass in female rats and, 1048

Quality of life in obese patients with osteoarthritis and, SA044

Werner premature aging syndrome

Mouse model with osteoporosis and osteoblast differentiation impairment, M234

Whites. SEE ALSO *Caucasians*

BMC and bone parameters in early pubertal girls, M003

Optimal vitamin D supplementation in healthy adults, M510

Plasma 24,25(OH)₂D and urinary 25(OH)D binding activity in black female adolescents *versus*, M517**Wnt3a**

Glycogen synthase GSK3β inhibitor and bone response to, M219

Kremen 2 and Dkk1-mediated inhibition of LRP5/6-TCF signals in U2OS osteoblast-like cells and, M217

P300 regulation of Id1 gene promoter and, SA201

Wnt3-Fzd1 chimera

C3H10T1/2 cells differentiation and, M197

Wnt10b

Bone density in multiethnic sample of men and, F341, SA341

Wnt 11

Non-canonical transcriptional suppression of IGFBP-6 by, SA148

Wnt/β-catenin signaling

Dishevelled-Smad1 interaction links BMP signaling in osteoblast progenitors with, F133, SA133

Dual role in chondrogenesis, 1019

Human and bovine articular chondrocytes and, SA031

Ihh signaling in endochondral bone formation, synovial joint development and, 1003

Notch1 overexpression, inhibition of osteoblastogenesis and, M223

Role in synovial joint induction and chondrocyte maturation, F048, SA048

Wnt-induced secreted protein 1 (WISP-1)

Splice variants and possible relationship with BMP signaling, SU081

Wnt-induced secreted proteins (WISP) 1, 2, and 3

Expression and regulation in murine osteoblasts of, SA126

Wnt signaling

Bone formation increases and, M206

Bone mass, Msx2 and, 1004

Canonical, BMP signaling in mediating fluid shear stress-induced osteoblast proliferation and, SU219

Canonical, cAMP/PKA signaling activation in osteoblastic cells of, M485

Canonical, chondrocyte hypertrophy mediation through Runx2, 1020

Canonical, chondrogenesis and chondrocyte gene expression repression and, SU199

Canonical, Dkk1 and PTH-mediated activation of, 1002

Wnt signaling (Cont'd)

Canonical, osteoblast or chondrocyte differentiation and, 1064

Canonical, TNF-α inhibition of, SU238

Chondrogenesis in sFRP1 null mouse and, 1021

Connective tissue progenitor cells colony formation, proliferation and, SU255

1α,25 (OH)₂D₃ effects on osteoblast differentiation, proliferation and, SA221

Inhibition by sclerostin binding to LRP5, M220

Lef1 overexpression, late osteoblast differentiation and, M185

Oxysterol-induced osteogenic differentiation and, M427

Promotion of osteoblast survival, osteoclast apoptosis and formation suppression by, SU264

Protein kinase Cδ and osteogenesis induced by, SU268

Sclerostin inhibition of BMP-stimulated bone formation by antagonizing, 1029

Suppression of PPARγ transactivation in MSCs and, SU259

Temporal expression in embryonic, growing, and adult mouse bone by components of, SA130

TGFβ/Smad signaling and demineralized bone powder activation in human dermal fibroblasts of, SA153

Wdr5 interaction during endochondral bone formation with, F041, SA041

Wnts, osteoblastic bone metastases in prostate cancer cells through, F070, SA070**Women.** SEE ALSO *Contraceptives, oral;**Menopausal women; Osteoporosis, postmenopausal; Perimenopausal women; Postmenopausal women; Premenopausal women*BMD, %body fat, and bone turnover in ultra-long distance runners *versus* sedentary, M143

BMP2 and osteoporosis-associated traits in, M033

Body composition reference values in normal Chinese, SU131

Bone formation in periosteal, endocortical, and trabecular envelopes of adult ilium, SU368

Elderly, farnesyl diphosphate synthase and BMD in, SU185

Elderly, hip fractures among, F327, SA327

Elderly, institutional-dwelling, hip fractures over 10 years among, M284

Growth- and age-related bone mass deficits with low volumetric BMD in, SU316

Healthy Japanese, circulating vitamin K and bone metabolism in, M291

HIV-positive, BMD and fracture risk in, SU347

Inhaled steroids and fracture risk in, SA364

Japanese, biliary cirrhosis and bone loss in, SU315

Lumbar BMD with and without metabolic syndrome, SA400

Older osteoporotic, site-specific fracture risk differences among, F325, SA325

Older US, overweight, and osteoporosis prevalence in, M267

Physically active young, eating disorders, amenorrhea and bone mass change in, M013

Short-term and long-term absolute fracture risk by BMD and age, 1138

Vitamin D deficiency risk factors for osteoporotic, M278

Young adult, trabecular bone loss in, 1010

Young, dieting, vitamin D and milk intake by, M272

Key Word Index

Women. SEE ALSO *Contraceptives, oral;*
Menopausal women; Osteoporosis,
postmenopausal; Perimenopausal women;
Postmenopausal women; Premenopausal
women (Cont'd)
Young, peak bone mass consolidation,
determinants in, M015
Young, serum vitamin D levels required for
maintenance and buildup of bone in,
M008
Women's Health Initiative, M381
Hormone Trials, SA430
Observational Study, F179, SA179
Wrist. SEE ALSO *Radius, distal*
Gender, age and bone microstructure at, 1075
Wrist fractures, M374, SU333, SU340

X

XLa₁, human, F491, SA491
X-ray absorptiometry. SEE *Dual energy X-ray*
absorptiometry; Dual X-ray
absorptiometry; 3D X-ray absorptiometry
X-rays, M049, SA089, SA372, SU366. SEE ALSO
Radiographs/radiography

Y

Y2 receptor
Cortical bone regulation, signaling and, M422
Yeast-2-hybrid analysis, SA158

Z

Zinc finger protein 521 (ZFP 521), 1183
Zinc supplementation, SA416
ZIP1, 1112
ZIP1 zinc transporter, SU297
ZK 191784, SA517
Zoledronic acid
For children with osteogenesis imperfecta,
safety and efficacy of, SA447
Combination with atrasentan for prostate cancer
metastasis to bone, 1213
Early response of circulating osteoprotegerin
with, SU206
Economic evaluation of long term risedronate
for Paget's disease *versus*, SA465
Intravenous, bone turnover at 18 months after
single dose of, SU164
Intravenous, breast cancer bone metastasis
reduction with, SA073
For Paget's disease, single 4mg infusion of,
SA463
Prolonged hypocalcemia from, M370
PTH(1-34) combination after radiation therapy
for bone metastasis, SU112
In vitro effects on apoptosis and death of
macrophage-like cells and, SU299
Z-scores, 1176, F293, M096, SA293, SU139. SEE
ALSO *T-scores*

Author Index

A		Alander, C.	M424	Annunziata, K.	SU359	Aymar, I.	M169
		Alapatt, M.	SA101	Ansbacher, R.	SU002	Ayoub, G.	F081, M075, SA081
Aakula, S.	1065, F160, SA151, SA160	Alaql, Z. S.	SU080	Anthony, M. S.	SU313	Azria, M.	M092
		Alatalo, S. L.	SU147, SU272, SU273	Antoci, V.	M455	Azuma, Y.	F509, SA054, SA509
Aaronson, S.	F070, SA070	Alayli, G.	SA085	Antonucci, D.	M131, M285		
Abbaspour, A.	M343	Albagha, O. M. E.	M115	Anumula, S. S.	M079		
Abbott, T.	SU403, SU417	Albanese, C.	M082, SU125	Aoe, S.	SU426		
Abdoud, S. L.	1156	Albergaria, B.	M067	Aoe, T.	M272		
Abdallah, B. M.	M202	Albert, S.	M085, SU321	Aoyagi, K.	SA078	Bab, I.	M491, SU377
Abdelmagid, S.	M039	Albertsson Wikland, K.	SU481	Aoyama, T.	SA029	Baba, H.	M041
Abdouelaziz, A.	F264, M061, SA264	Alcorn, J. D.	M458	Appleton, C. Thomas George	SU037	Babbar, R.	SU129
Abe, E.	SA246	Alen, M.	F007, M139, M141, SA007	Arabi, A.	F081, M075, SA081	Bachrach, L.	SA001
Abe, M.	1123, SU070, SU102	Alesio, A.	M117	Arabian, A.	1147	Bacic, D.	SA455
Abe, Y.	SA078, SU277	Alexander, R. V.	SU498	Arai, H.	F028, F479, SA028, SA479	Backstroem, M.	M093
Abedin, M.	SA224	Alexandersen, P.	1225	Arai, M.	SU110	Baddoura, R.	F081, M075, SA081
Abi Fadel, M.	SA439	Alexandre, C.	1178, M093	Arai, R.	M496	Badenhop-Stevens, N. E.	1130
Abou-Samra, A.	1159, M507	Alfonsi, A.	M433	Arai, T.	SA082	Badoud, I.	M140
Abrahamsen, B.	SU189, SU469	Algranati, L. Salomon	M459	Arai, Y.	M161, SU123	Bae, J.	1015, 1030
Abrams, E.	SU476	Alhava, E. Matti.	SA418	Arakaki, H.	SA326	Bae, M.	M253
Abu-Amer, Y.	F282, SA282	Alhborg, H.	1138	Araki, N.	1024	Bae, S.	SA044
Abu-Zahra, H.	1106, F444, SA444	Ali, A. A.	M417	Arango-Hisijara, I.	SU076, SU078	Bae, T.	SA424
Acan, B.	SU215	Ali, S. M.	SU438	Araujo, A. B.	1077, M308	Bae, Y.	SA514
Achenbach, S. J.	SU464	Ali, Z.	SU047	Ardeshipour, L.	1087	Baek, J.	M245
Achyutharao, R.	1205	Alimov, A. P.	SA502	Arendell, L.	SA352, SA430	Baek, J. H.	SA223
Ackerman, J. L.	SU059, SU145	Alini, M.	SA213, SU210, SU234	Arends, R. J.	SU411	Baek, K.	F176, F391, SA176, SA391
Ackerman, K. E.	SU087, SU434	Alkhodair, K.	SU039	Argibay, P. F.	M459	Baek, Y. Hyeon	SU056, SU233
Ackert-Bicknell, C.	1035, F114, SA114, SU242	Allaart, R.	SU486	Arias, A.	SA324	Baffoe, G.	M056
		Allan, A. L.	SA067	Arizona, H.	SU389	Bafico, A.	F070, SA070
Acosta, A.	M408	Allanore, Y.	SA439	Arjmandi, B. H.	M335, SU044, SU246, SU430, SU432	Bagegni, N.	SU418
Adachi, J. D.	M310, M367, M391, SA097, SA405, SU325, SU386, SU387, SU435, SU436	Allasino, B.	SA371	Arlot, M.	SU393	Baggio, G.	M451
		Allbery, S.	SU394	Arlot, M. E.	1084, M087, SA058, SU084	Bagur, A.	M072, M073
Adami, S.	F301, M292, M388, M434, SA301, SU415	Allen, C.	M403	Arlt, W.	SA373	Baheiraai, A.	SU317
		Allen, M. J.	SU112	Armas, L. Anne Graeff	SA519	Bakra, P.	F057, SA057
Adams, C. S.	M455	Allen, M. R.	1081, M047	Armbricht, G.	1224, M093	Bai, G.	1112, M258, SU297
Adams, D. J.	1189, F046, F210, SA046, SA210, SA482, SU093	Allison, J. J.	M379, SU390	Armbrecht, H. J.	M475, M521	Bai, S.	SA278
		Allison, S.	M422	Armbrecht, T.	M349	Bai, X.	F453, SA453
Adams, G.	SA089	Allistion, T.	SA163	Armingeat, T.	SA065	Baik, H. Woon	SA400
Adams, J. Elizabeth.	M074, M277, SA008, SA475	Almageor, O.	SU490, SU492, SU494	Armstrong, A.	SA065	Baile, C.	M233, SA050
		Aloia, J. F.	M370, M510, SU027	Armstrong, M.	M227	Baile, C. A.	SA150
Adams, J. S.	F046, F210, F475, F518, M518, M519 SA454, SA518	Alon, U. S.	SU396	Arnold, C.	F090, SA089, SA090, SA091, SU043	Bailey, D. A.	1012
Adams, M. F.	F088, SA088	Alonso, G.	M400, SU274, SU374	Arnold, A.	SU472	Bailey, M.	SU275
Adams, S. L.	1022	ALSPAC Study	M110	Arnold, M.	M371, M372	Bajayo, A.	SU377
Adamu, S.	SA357, SU295, SU304	Altmann, E.	SU270	Aronson, J.	M043	Bajwa, A.	SU515
Adamus, A.	1218	Altundag, K.	1218	Aropuu, S.	SU402	Baker, B. L.	SU503
Adler, R. A.	M301, M302, M366, SA380	Alvarez, G.	SA200	Arpad, S. Moshe	SU476	Baker, N.	M193
		Alvarez, L.	SA388, SU392	Arqueros, P.	F093, SA093	Bakulin, A. V.	1171
Adler-Wailes, D.	F472, SA472	Álvarez-Álvarez, P. Luis	SA316	Arquitt, A. Bender	M335	Balachandran, B.	M210
Adrian, C.	1225	Alver, K.	M271	Arrington, S. A.	SU112	Balcells, S.	1210, M122
Afzal, F.	1030	Amadio, P.	SU010	Arslanian, S.	SU474	Baldock, P. A.	M422
Agas, D.	F142, SA142	Amano, A.	F208, SA208	Arunakumari, R.	M270	Balemans, W.	M220
Aggounne, T. K.	SU160	Amano, H.	SA189, SA246	Arwady, A. L.	SU401	Balkan, W.	M252
Aghaloo, T.	M203, SU204	Amantea, C.	M203, M427	Arzaga, R. R.	1048	Ballanti, P.	F470, M461, SA470
Agrawal, S.	M281, SU460	Amato, I.	M004	Asahara, T.	1066	Balooch, G.	F370, M130, SA163, SA370, SU067
Agüero, R. G.	SA324	Ambekar, A.	SU324	Asakawa, M.	M191	Balooch, M.	SA163, SU067
Aguila, H. L.	1189, F266, F374, SA256, SA266, SA374	Ambrogini, E.	1167, M462	Asano, J.	SU102	Bamji, M.	SU476
		Ambrosi, C.	M288	Asawa, Y.	SA034	Banchereau, J.	SU488
Aguirre, J.	1092, 1116, F286, SA286	Amcheslavsky, A.	F251, SA251	Ashley, L. A.	SU014	Bandeira, C.	SU468
Aharon, R.	SU278	Amedei, A.	SA118, SA121, SA141	Aso, Y.	F032, SA032	Bandeira, F.	SU468
Ahlborg, H.	1011, F187, SA187	Amerling, R.	SU506	Asou, Y.	SU055, SU302	Bandyopadhyay, A.	1025
Ahlborg, H. G.	F327, SA327, SA329	Amizuka, N.	SA488, SU023, SU025, SU040, SU057, SU068, SU107, SU271	Aspelund, T.	SU334	Banerjee, S.	F444, M501, SA444
Ahmad, A. M.	M133			Aspenberg, P.	F057, SA057	Banks, L.	M056
Ahmed, Y.	SU039	Amling, M.	1101, 1162, M181, SU210	Asplin, J.	M467	Banu, J.	SA132
Ahn, B.	SU373	Amman, P.	M140	Astrand, J.	F057, SA057, SA295	Bar-Shavit, Z.	F251, SA251, SU278
Ahn, C.	SA422	Ammann, P.	M447, SA416, SU050	Asuncion, F.	SA357	Baran, D.	SU526
Ahn, J.	SA040	Amonkar, M.	M362, M361	Asuncion, F.	SU295, SU304	Baran, R.	M362
Ahn, K. Jeung	SA400	Amurao, M.	M054	Aswad, R. A.	SU035, SU251	Baran, R. W.	M361
Ahn, S.	SU252	An, J.	SU236	Aswani, S.	SU214	Baranci, M.	SA335
Aisaka, K.	M342	An, K. N.	SU010	Athavale, S.	F476, SA476	Barbazán, C.	SU354
Aitken, C. J.	M266	An, Y. H.	M090	Atkins, G. J.	SA259	Barbe, M. F.	SU035
Akaike, T.	SA037	Anastassiades, T. P.	M390, M418	Atkinson, E. J.	1010, 1074, 1075, SU464	Barbeau, S.	M076
Akatsu, T.	SU107	Andersen, L.	SU318	Atkinson, J.	SU453	Barbich, M. Rosa	M459
Akel, N. S.	1169, SU250	Andersen, M.	SU189	Aubenger, P.	1220	Barbieri, D.	M097, SU445
Åkesson, K.	M033, M109, M116, SA328	Andersen, B. L.	M048, M420	Aubin, J. E.	SA139, SA196	Barbutto, N.	1079
		Anderson, C.	1026	Audran, M.	M413, SA061, SA432	Barden, H. S.	SU131, SU134, SU135, SU136
Akhter, M. P.	F358, M050, SA200, SA358	Anderson, G.	SU201	Aukrust, P.	SU380	Bare, S.	F414, SA414, SU368
Akinsanya, K. O.	SU498	Anderson, J.	SA243, SU201	Auluck, J.	M429, SU263	Bare, S. J.	1221
Akira, S.	F125, SA125	Anderson, K.	SA071	Ausili, E.	M011	Bare, S. P.	F358, SA358
Akiyama, K.	SU062	Anderson, S.	SA421	Ausk, B. J.	SU218	Barger-Lux, M. Janet	M279, M364, SA519
Akiyama, T.	M032	Anderson, W. E.	M044, SA290	Austin, S. Bryn	M136		
Akiyama, Y.	M321, SU021, SU023	Andersson, L.	M114	Avanzati, A.	M416, SU378, SU379	Bargouti, M.	M193
Akune, T.	1047	Andersson, N.	SA396	Avorn, J.	M371, M372	Barisic-Dujmovic, T.	F046, F266, SA046, SA266
Akuta, T.	SA037	Ando, M.	M303, SU315	Awad, H.	SU488		
Akyol, Y.	SA085	Andreassen, T. Torp	M423	Awada, H.	F081, M075, SA081	Bariteau, J. T.	M014
Al, M.	SA465	Andreeva, V.	M184	Awadallah, A.	SU249	Barker, D. J. P.	1058
Al-Shoha, A.	SA463	Angeli, A.	SA371	Axell, A. Maree.	1161	Barkmann, R.	M095
Alam, I.	1108, F110, SA110	Angelucci, A.	F068, SA068	Aya-Ay, J.	F476, SA476	Barlogie, B.	1125
				Ayers, D.	1021	Barnes, G. L.	F483, M058, M059, SA484

Author Index

ASBMR 27th Annual Meeting

Barnett, B. L.	M351, SU306	Bellido, T.	1092, 1116, F286, F289, F401, SA286, SA289, SA401, SU019, SU264	Bizot, J.	SU193	Booth, S. L.	M123
Baron, R.	1001, 1019, 1114, 1145, 1150, 1183, F279, M180, SA027, SA279	Bellin, B. J.	SA158	Bjursten, L. M.	M156	Borah, B.	SU086
Barr, C.	SU403, SU417	Benasciutti, E.	1143, SU103	Black, C.	F404, SA404	Borba, V. Z. C.	SU164
Barr, C. E.	SA411	Benhamou, C.	M350, SA186	Black, D.	F325, SA325	Bord, S.	SU280
Barr, R. J.	1042	Benhamou, L.	F345, M421, SA345, SU193	Black, D. E.	SA411	Borel, O.	SU316
Barrack, M.	SU356	Benito, A.	SA103	Black, D. M.	1056, F406, M411, SA083, SA314, SA406, SU400	Borge, M.	SA092
Barragan, L.	SA288	Benito, P.	SU137	Black, E. C.	F202, SA202, SA205	Borges, J. C.	M067
Barragan-Adjemian, C.	SA287	Bennett, C. N.	M206, M237	Black, J.	M148	Borisov, N. N.	M293, SA330
Barrauld, S.	M140	Bensamoun, S. F.	SU010	Blackwell, T.	1073, M296	Borke, J. L.	SA055, SA056
Barrero, M.	SU093	Benson, D. M.	1051	Blain, H.	M142, SA115	Borovecki, F.	1027, SU200
Barrett-Connor, E.	1073, 1135, F338, M269, M378, SA338, SU340	Benton, H. P.	SU089	Blaine, T. A.	SA263	Borsari, S.	M462
Barron, J.	SU355	Bergot, C.	SU073	Blair, A.	SU431	Borysenko, C. W.	SA217
Barros, H.	SU169, SU170	Bergström, B.	1106, F444, SA444	Blair, H. C.	1043, 1100, F376, F505, M242, SA217, SA241, SA243, SA376, SA505	Boscainos, P.	M374
Barros, S. Amaury	M067	Bergwitz, C.	SA240	Blake, G. M.	SA053	Boskey, A. L.	M440, SA022, SU465
Barsony, J.	1118	Berlanga, E.	SU461	Blanch, J.	M091, M169, SA379, SU137	Botolin, S.	F399, SA399
Bartkiewicz, M.	1191	Bernardo, Y.	SA463	Blanco, A.	SU196	Boudignon, B.	M146, SU012, SU221
Bartl, C.	SA020	Berndt, T.	SA455, SU500	Blank, R.	M050, M083	Bouillon, R.	1067, 1151, 1199, F253, F515, SA253, SA515, SU525
Bartl, R.	SA020	Berner, H. S.	SU205	Blank, R. D.	M438, SU020	Boulos, P.	SU435, SU436
Barton, I.	M367, SA405, SU405, SU406	Bernstein, C. N.	SU372	Blankenstein, M. A.	SU223	Bouls, H.	M179
Barton, I. P.	SA407	Berry, C.	SU321	Blankenstein, R.	M401	Boulukos, K.	1001
Basillais, A.	SU193	Berry, C. A.	M085	Blasi, F.	M246	Boumah, C.	1113
Basle, M. F.	SA061, SA378, SU299, SU366	Berry, J. E.	M182	Blatter, T. R.	M432	Bounoutas, G. Steven	1159
Basoglu, T.	SA382	Berry, J. L.	M334, SA525	Bleiberg, I.	M155	Bours, V.	SU104
Bass, S.	F419, SA419	Berthier, A.	M093	Blenk, T.	1224	Boushey, C.	M003
Bass, S. L.	M148	Bertin, T. K.	F053, SA053	Blind, E.	M413	Bousson, V.	SU089
Bassford, T.	F179, SA179, SA352, SA430	Bertoldo, F.	F122, M060, M461, SA122	Bliss, J.	M056	Boutroy, S.	F360, SA360
Bastepe, M.	1036, F491, SA491	Bertolino, S. V.	SU440	Blisc, D.	M387	Bouvard, D.	F190, SA190
Bastianelli, E.	SA027	Bertossi, E.	SA445	Blizard, D. A.	M112	Bouvet, M.	M495
Bataille, R.	SA061	Bertrand, G.	1086	Blizotes, M. M.	SA386	Bouvet, S.	1220
Bateman, T. A.	SA357, SA398, SU362	Besenbacher, F.	SU028	Bloomfield, S. A.	F176, M458, SA176	Bouxsein, M.	1025, 1035, 1193, F481, SA481
Battista, C.	F122, SA122	Bessette, L.	SA335	Blotman, F.	SA115	Bouxsein, M. L.	1074, 1097, F360, Z F397, M411, SA058, SA360, SA397, SU084, SU294, SU381
Batum, L.	SU189	Bessler, M.	M322	Blumenkrantz, G.	F086, SA086	Bowe, E. A.	1094
Bauer, D. C.	1073, F090, F406, M103, M290, M355, M465, SA090, SA406, SA413, SU141, SU151, SU400	Betschart, C.	SU270	Blumsohn, A.	M412, SU358	Bowman, B. M.	M048, SU300
Bauer, J. S.	SU324	Bevelock, L. M.	1113	Boast, S.	M225	Bowman, P.	SU335
Bauer, R. L.	F100, SA100, SU195	Bex, F. J.	M217, M394, SA128	Boban, I.	F046, F266, SA046, SA266	Box, J.	F319, SA319
Baugh, M.	SU290	Bezouglaia, O.	SU499	Bock, O.	M380, SA095	Boyan, B. D.	1182, F450, M212, SA450, SA500, SU045
Bauss, F.	F476, SA476	Bhalla, A. K.	M015	Bockman, R.	M323	Boyce, A. T.	M036
Baxter-Jones, A. D. G.	1012	Bhan, A.	1168	Boden, S. D.	M027, M193	Boyce, B.	1196, SA255
Baylink, D. J.	1045, 1152, F102, F104, F106, F183, M183, SA102, SA104, SA105, SA106, SA146, SA183, SA508	Bhat, B. M.	M217, SA128	Bodic, F.	SU366	Boyce, B. Francis	1018, 1072, F053, SA053
Baylink, D. J.	SU219, SU229	Bhat, R. A.	M189, M197	Bodine, P. V. N.	1021, M189, M197, M394	Boyce, R.	F232, SA232
Baz Hecht, M.	M393	Bhattacharya, A.	SA132	Body, J.	SA073, SA075	Braak, L.	M093
Beamer, W.	1035, 1212, SA105, SU181	Bhattacharya, R. K.	SA098	Boehlert, C. J.	M453	Brackett, D. J.	SU384
Beamer, W. G.	F102, F114, M113, SA102, SA114, SU182	Bhattacharya, S. K.	SU349	Boehm, C.	M230, SU255	Bradbury, B. D.	SU313
Bean, J.	M017	Bi, L. X.	SU060, SU198	Boehm, C. A.	M164	Bradley, E. W.	M257
Beary, J.	SU406	Bian, H.	SA136	Boeke, A. J. P.	1134	Bradshaw, M. P.	SU422
Beattie, K.	SU435, SU436	Bian, J.	SA333	Boerst, H.	M380	Brady, S.	F472, SA472
Beaulieu, M.	SA335	Bianchi, D.	M017	Bogado, C. E.	1083	Brain, J.	1212
Beaumont, L.	M078	Bianchi, E.	F397, SA397	Boghossian, S.	1048	Branco, J.	SU169, SU170
Beaupied, H.	M421, SU193	Bianchi, G.	SU458	Bogoch, E.	M382	Brandberg, J.	SU521
Bechor, Z.	M089	Biber, J.	SA455	Boileau, C.	SA439	Brandi, M.	M121, SA108, SA121
Beck, G. R.	M186	Bicakci, U.	SA382	Boireau, P.	SU254	Brandi, M. L.	1210, SA117, SA118, SA141, SU458
Beck, T.	M120, SA352, SA430	Bicho, M.	SU507	Boirie, Y.	M325	Brändström, H.	M107, SU187
Beck, T. J.	F179, M020, M021, M088, M098, M099, SA150, SA179, SA310, A384, SA473, SU175	Bieber, B.	SU243	Boivin, G.	1090	Brankin, E.	SU330, SU331
Beckman, M. J.	M523, SU515	Bielez, B.	SA455	Boland, R.	M512, M513, SA478, SU518	Branstetter, D.	SU448
Bédouet, L.	SA240	Biessels, P. T.	M392	Bolduc, J.	M522	Brass, L. M.	1077
Beek van, H.	SU223	Bigliani, L. U.	SA263	Bollag, W.	SA050	Braun, M.	M007
Beers, A. E.	SA517	Bigman, G.	M314	Bollerslev, J.	1206, M157, SA369, SU380	Bravenboer, N.	M401, SA504, SU223
Begerow, B.	SU443	Bijsterbosch, J.	SU486	Bolognese, M.	F410, M347, SA410, SA428	Brazier, M.	M255, SA240, SU511
Bégot, L.	M268	Bikle, D.	SU510	Bolon, B.	1082, SU451	Brazin, A.	SA165
Behloul, H.	SU341	Bikle, D. D.	M146, SA147, SU221, SU262	Boltz, M. A.	M521	Brebene, A.	SA246
Behnam, K.	SA015	Bilezikian, J.	M411	Bone, H.	F429, M353, SA429, SU159	Brecht, A. B.	M154
Behringer, R. R.	1152	Bilezikian, J. P.	1056, M111, M221, SA385, SU129, SU130, SU164, SU240, SU465, SU467, SU470	Bone, H. G.	1222	Breedveld, F.	SU486
Beidelschies, M. A.	M256	Bilinski, P.	SA123	Bonewald, L.	1061, 1093, 1111, F370, SA284, SA287, SA288, SA370	Breen, M.	M059
Beier, F.	SU037	Billard, J.	M189	Bonjour, J.	1136	Brennan, I.	SU332
Beighton, P.	F116, F138, SA116, SA138	Billings, P. C.	M029, SA011	Bonnet, N.	F345, M421, SA345, SU193	Brennan, K.	F507, SA507, SU520
Beischel, J. A.	SU489	Bilodeau, M.	M522	Bonvoisin, B.	M346, M347, M359, SU410, SU415	Brennan, T. C.	M195
Beisiegel, U.	M332	Binkley, N.	1177, M068, M083, M281, M435, SU425, SU460	Booker, T.	1185	Brenneman, S.	M269
Belisle, K. J.	SA527	Binkley, N. C.	SA526	Boonen, S.	1199, F515, M092, M276, M413, SA515, SU404, SU405, SU406, SU525	Bride, F.	SU444
Belknap, J. K.	1031, SA107	Binot, R.	M093	Bonewald, L. F.	1033, SA025	Bridges, J. F.	SA337
Bell, B. F.	M212	Binotto, P.	M451	Bonjour, J.	1136	Briesacher, B.	SA466
Beller, G.	M093	Birkedal, H.	SU028	Bonnet, N.	F345, M421, SA345, SU193	Briffa, N. K.	SA310
		Birmingham, J.	F232, SA232	Bonjour, J.	1136	Briggs, D.	SA333
		Bischoff, D. S.	M216, SU203	Bonnet, N.	F345, M421, SA345, SU193	Briggs, M. D.	1033
		Bischoff-Ferrari, H. A.	1041, SA501	Bonjour, J.	1136	Brillante, B. A.	M437
		Bisello, A.	M500	Bonjour, J.	1136	Bringas, Jr, P.	F222, SA222
		Bishop, J. E.	SA503	Bonjour, J.	1136	Bringhurst, F. R.	1002, F481, M501, SA143, SA481
		Biv, N.	SU257	Bonjour, J.	1136	Brink, P. R.	SU351
		Bizios, R.	SU310	Bonjour, J.	1136	Briot, K.	SA426, SU357

(Key: 1001-1228 = Oral, F = Friday Plenary poster, SA = Saturday poster, SU = Sunday poster, M = Monday poster, WG = Working Group Abstract)

ASBMR 27th Annual Meeting

Author Index

Bristol, S. K.	M136	Burnett, S. M.	SA143	Cao, X.	1028, 1117, F057, F129,	Chan, B. K. S.	1135, M305
Brixen, K.	M386, M412, SU189,	Burnham, J. M.	1060		F133, F154, F513,	Chan, C.	SU133
	SU469	Burns, A.	M403		SA057, SA129, SA133,	Chan, G.	SU167
Broadus, A. E.	M497	Burns, S.	M391	Capanna, R.	SA154, SA513	Chan, H.	1019
Brochier, G.	SA378	Burns, T. L.	M019	Capozza, R.	SA141	Chan, H. Yun	SA027
Brod, M.	SA438	Burr, D. B.	1081, F138, F356, M047,		M096	Chan, V.	SA111, SU005, SU186,
Brolin, R. E.	M337		SA138, SA356, SA415	Cappariello, A.	M436		SU191
Bromberg, I.	SU428	Burra, S.	1095	Capriotti, C. A.	F234, SA233, SA234	Chan, W. Si	SA026
Brondino, R.	M349	Burris, L. L.	SU281	Caradonna, P.	M011	Chandhoke, T. K.	M187
Bronson, S.	SU052	Burris, T. P.	M515	Carandante, Z.	M060	Chandler, J.	M275, M278
Bronson, S. K.	SU053	Burrows, M.	SU126	Carbonel, C.	M315	Chandler, R.	F160, SA160
Bronze, M. S.	SU384	Burt-Pichat, B.	1084, M087	Carbonell, J.	M091, SA379	Chandraratna, R. A.	SU247
Brooke-Wavell, K.	SA094	Burton, D. W.	M055, M495, SU109,	Carbonell, S.	SA141	Chang, C.	1028, M196
Brookhart, M. Alan	M371, SU312		SU114	Carbonell Sala, S.	SA121	Chang, E.	M240
Brooks, D.	M382	Burton, D. W.	SU165	Cardoso-Landa, L.	1043, 1100	Chang, M.	SU334
Brorson, S. H.	SU046	Busa, B.	M150	Carey, A. H.	1210	Chang, S.	SA263, SU449
Brorson, S. Henning	SU232	Bush, A. J.	M355	Carlos, A. S.	1031	Chang, W.	M229, SU510
Brossard, J. H.	M482, M484	Bushinsky, D. A.	M222, SU258	Carlson, A. E.	M037	Chappard, C.	SA186
Brot, C.	SU423	Bushnell, T.	1072	Carlson, T. H.	SU160, SU163	Chappard, D.	M091, SA061, SA378,
Broussard, D.	M299	Bustamante, M.	M122	Carmeliet, G.	1067, 1151, F253,		SU299, SU366
Broussard, D. L.	M304	Butters, R. R.	SU497		SA253	Chappell, R.	SU425
Brown, A. J.	M475	Button, C.	SU369	Carmeliet, P.	F253, SA253	Chariot, A.	SU104
Brown, D. L.	SU014	Buurman, C. J.	M250	Caro, J. J.	M357	Charitou, M.	M336
Brown, E. M.	M162, SU497, SU511	Buxton, E. C.	SA147, SU221	Carossino, A.	SA108	Charles, P.	SU423
Brown, I.	SU108	Buzzi, N.	M512	Carpio, I.	SA316	Charlesworth, D.	SU402
Brown, J.	1037, M397	Byrjalsen, I.	1225, F074, M241,	Carr, A.	M344	Charlton-Kachigian, N.	1004
Brown, J. Keenan	M098		SA074, SA417, SU116	Carr, L. G.	F110, SA110	Chatelain, P.	M140
Brown, J. P.	SA097, A335, SA407,	Byun, D.	SU211	Carran, J.	M390, M418	Chattopadhyay, A.	M356
	SA448	Byun, J.	SU236, SU256	Carrello, A.	M264	Chattopadhyay, N.	M162, SU511
				Carroll, J.	M382	Chatzioannou, A.	SU115
Brown, L. G.	SU117, SU118, SU122			Carstens, M.	M119	Chaudhary, L.	F016, SA016
Brown, M.	F419, SA419			Carvalho, R. S.	SU080	Chaudhri, R. A.	SA500
Brown, M. A.	M110, SA336			Casado, E.	SA342, SU461	Chavassieux, P.	1090, SU393
Brown, T. A.	M395, M396, M419,	Caballeria, L.	SA388, SU392	Cascio, P.	SU105	Checovich, M.	M068, SU425
	SA394	Cabanillas, M. E.	SU096	Casey, M. Casey	M297	Chehade, M.	SU153
Brownbill, R. A.	SU360, SU385	Cabra, A.	SA010	Cassim, B.	M143	Chellaiah, M. A.	SA273
Browner, W.	1039	Cáceres, E.	M169	Castagnola, P.	F053, SA053	Chelsler, D. A.	SU145
Broy, S. B.	M080	Cachizumba, M. O.	SA324	Castaldoni, A.	SA447	Chen, A.	SU038
Brubaker, K. D.	SU117	Cadiri, A.	M016, M414	Castermans, E.	SU104	Chen, C.	1133, SA195
Bruder, J.	F100, SA100, SU195	Caffarelli, C.	M414, M416	Castillo, A. B.	1170	Chen, D.	1005, 1018, 1110, 1155, 1187,
Bruder, J. M.	SU121	Cahall, D.	SU404	Castro, J. A.	SA092		SA226
Bruel, H.	SA485	Cahill, R.	1166	Castro, L.	SA087	Chen, E.	M354, SA526, SU158,
Bruggers, C.	SU473	Cain, R.	M489	Castro, V.	SU196		SU159
Brun, M. B.	SA092	Cain, R. L.	SA427	Catala-Lehnen, P.	1162	Chen, F.	SU127, SU131, SU132
Brunden, K.	SU516	Caira, F.	SU018	Catrambone, D.	M144	Chen, G.	SU489
Brunell, R.	F429, SA429	Caire, G.	SA352	Cattley, R.	1082	Chen, H.	1117
Bruner, A.	SA001	Calabrò, A.	M016, SU379	Caudarella, R.	SU458	Chen, H.	F518
Brunner, F.	SU419	Caldas, G.	SU468	Cauley, J.	1038, 1073, F179, F306,	Chen, H.	SA050
Brünning, C.	SU101	Calex-Study Group	M141		F425, SA179, SA306,	Chen, H.	SA518
Bruno, M.	SA324	Calis, K.	F472, SA472		SA343, SA352, SA425,	Chen, I. S. Y.	M023
Bruzoni, M.	SU394	Callahan, G.	M353		SA430, SU335	Chen, J.	SA278
Bruzzaniti, A.	1150	Callander, N.	SU201			Chen, J. Ren	SA055
Bryan, J.	M239	Callon, K. E.	SU230			Chen, K.	SA427
Bryant, B. Ann	SA337	Callreus, M.	M033			Chen, M.	1110, 1187, SA226
Bryant, H. U.	F437, M489, SA427,	Calomme, M. R.	SA421			Chen, P.	1223, M219, M406, M407,
	SA437	Calvet, J.	1061				M410
Bryant, T.	SA354	Calvi, L.	F170, SA170				SA438
Bu, S. Young.	SU384	Calvi, L. Maria	F197, SA197	Caulfield, M. P.	SU158	Chen, P.	1054, SU073
Bu, X.	M515	Camacho, P.	M376	Caverzasio, J.	M218, SU050	Chen, Q.	SU131, SU132
Buckendahl, P.	F051, SA051	Camacho, P. M.	M320	Cawthon, P.	SU335	Chen, R.	SU298
Buckle, C.	SU095	Camalier, C. E.	M186	Cawthon, P. Mannen	M290	Chen, S.	M229, SU510
Buckley, C. D.	F365, SA365	Camerino, C.	1102	Ceailles, C.	M524	Chen, T.	M308, M339, SA253,
Bucovic, D.	SA390	Cameron, I.	1133	Cenci, S.	1143, SU103, SU105	Chen, T. C.	SU110
Buczak, D.	M058	Cameron, K. O.	M395, M419	Center, J. R.	1137, 1138, M387,		
Buford, W. L.	SU060, SU198				SA329, SU342, SU343,		
Bugaresti, J.	SA080	Caminis, J.	SA314		SU344	Chen, W.	M260, SU277
Buhl, T.	SA207, SU270	Camozzi, V.	SA445	Cephas, S.	M517	Chen, X.	1140
Buinewicz, A.	SU158	Campagna, M.	M416	Cepollaro, C.	SA117	Chen, X.	M227
Buitrago, C.	M513, SU166	Campagna, M. Stella	SU378	Cerda, D.	SU392	Chen, X.	M497
Bukata, S. V.	SU496	Campagna, S.	SU379	Cervo, E.	M016	Chen, X.	SA219
Bula, C. M.	SA503	Campion, S. L.	M128	Cesaro, S.	M436	Chen, Y.	1017
Buljan-Culej, J.	1027	Canaff, L.	M503	Cetani, F.	1167, M462	Chen, Y.	1156
Bullock, H. A.	F202, SA202	Canaff, L.	SA487	Cha, B.	SA422	Chen, Y.	F030
Bulnheim, U.	M232	Canaff, L.	SU514	Chabadel, A.	SA240	Chen, Y.	F053, F214
Bunegin, M.	1214	Canalis, E.	F206, M024,	Chabanel, D.	SA332	Chen, Y.	M269, M378
Bünger, M. H.	SU028		M211, M223, SA126, SA206	Chaboteaux, C.	SA075	Chen, Y.	SA030
Bunker, C. H.	F112, F338, F341,	Candeliere, G. A.	M403	Chacksfield, M. A.	M266	Chen, Y.	SA053, SA214
	SA112, SA338, SA341	Canfield, A. E.	SA025	Chadha, A. B.	SU490, SU492, SU494	Chen, Y.	SU131, SU132
	M005, M441	Canhao, H.	SU169, SU170	Chadwick, R.	1045	Chen, Y.	SU312, SU340
Bunn, R. Clay	M384	Cannata-Andia, J. B.	M426, SU322	Chai, S. Ching	SU432	Chen, Z.	F179, SA179, SA352, SA430
Buonanno, M.	M016	Canning, C.	M372	Chai, Y.	F222, SA222	Cheng, S.	1004
Burckhardt, P.	SA332, SA350	Cannone, V.	SA117	Chakarun, C.	M523	Cheng, S.	1131, F007, M139, M141
Burde, D.	SU347	Cantor, T.	M484, M464, SU501,	Chaki, O.	SA298	Cheng, S.	M173
Burge, R.	1078, F317, SA317		SU502, SU504, SU506	Chakravarty, S.	1216	Cheng, S.	SA007
Burge, R. T.	SA403	Canturk, F.	SA085, SA382	Chalberg, C.	SU109, SU114	Cheng, Z.	SU510
Burghardt, A.	M069, SU221	Cao, J.	M146	Chambers, A. F.	SA067	Cheon, H.	M253
Burke, G. N.	SU135	Cao, J. J.	SU012	Chambon, P.	F509, SA509	Cheong, J. M. K.	SU011
Burke, P. K.	SU135			Champy, R.	M486	Cherian, A.	M390
Burke, S.	SU431			Chan, A.	1151	Cherian, P. P.	1095
				Chan, B.	M290, SA343	Chernova, T.	SU480

(Key: 1001-1228 = Oral, F = Friday Plenary poster, SA = Saturday poster, SU = Sunday poster, M = Monday poster, WG = Working Group Abstract)

Author Index

ASBMR 27th Annual Meeting

Chernova, T. O.	SU136	Clairmont, A.	1130	Corey, E.	1213, SU113, SU117,	Czech-Kowalska, J.	SU484
Cherubini, R.	M457	Clark, E. M.	SA299, SU319	SU118, SU122	SU118, SU122	Czerwinski, E.	SA123
Chest, V.	F106, SA106	Clark, G.	SA290	Coriolano, A. Teixeira	SU468	Czirok, A.	1054, SU073
Cheung, A.	SU133	Clark, P.	M287	Corley- Mastick, C.	M514		
Cheung, A. M.	M071, SU463	Clark, S. H.	F046, F266, SA046,	Cormier, C.	SA439		
Cheung, C. Lung	SU191		SA266	Cornish, J.	M248, SU230		
Cheung, W. M. W.	M208, SU186	Clarke, A. F.	SU039	Cornuz, J.	F096, SA096, SA332,	D'Adamo, M. Horacio	M459
Chevalley, T.	1136, M121, M284	Clarke, I.	SU210		SA350	D'Agruma, L.	F122, SA122
Chevrier, C.	M076, SU128	Clarke Anderson, H.	M030, SA013	Corti, M.	M451	d'Alésio, A.	SA495
Chew, C. S.	SA055	Clarkson, A.	SA060	Cortizo, A. Maria	SU196	D'Amelio, P.	SU414
Chhokar, V. S.	SU349	Clemens, T. L.	1105, 1194, F133,	Coschigano, K.	1199	D'Amour, P.	M482, M484
Chiang, J.	SU129		SA133	Cosenza, M. E.	SU453	D'Angelo, M.	SA155
Chiba, K.	SU054	Clement, J. G.	SA049, SU016	Cosman, F.	1079, 1180, M013,	D'Erasmo, E.	SA322, SA392, SU458
Chiba, T.	M333	Clément-Lacroix, P.	1001, SA027		M359, M362, M393	D'Silva, N.	SU099
Chihara, K.	F444, SA366, SA444	Cliffe, J.	SU402	Costa, L.	SU169, SU170	Da Fonseca, K.	M383
Chikazu, D.	1016	Clifton, K. B.	M145	Costa-Guda, J.	SU472	Dacquin, R.	SA040
Chikuda, H.	1016	Clifton-Bligh, P.	SA060	Costan, A.	SU427	Dahl-Andersen, B.	M386
Chin, H.	1186	Clifton-Bligh, R. J.	SA060	Costello, M. A.	M080	Dahlgaard, J.	M202
Chiodini, I.	F122, SA122	Clines, G. A.	SU261	Costin, G.	SU483	Dai, G.	SU145
Chirgwin, J. M.	SU261	Clohisy, D.	SA248	Cote, G. J.	M126, M499	Dai, J.	SU113
Chiu, H.	SU182	Close, P.	SU104	Cotte, F. Emery	SU416	Dai, S.	F282, SA282
Chiu, M. Wan. Sze	1161	Clouthier, D. E.	SU070	Coudert, A.	SU244	Daida, Y. Goh	1177
Chiusaroli, R.	F481, SA481	Clowes, J. A.	SU382	Coughlin, S.	SU394	Daigo, Y.	SA355
Cho, J.	M176	Clunie, G. P. R.	M319	Coupey, S.	SA001	Dakin, G.	M323
Cho, S.	M118, M430	Coates, P. S.	M326	Courteix, D.	F345, M421, SA186,	Dal Canto, N.	M016, SU367
Cho, S.	SA514	Cochran, D. L.	M212		SA345, SU193	Dalkin, A.	SA460
Cho, S.	SU449	Cockerham, S.	SA427	Courtland, H.	M104, M105	Dalla-Bona, D. A.	SU063
Cho, Y. Mee	1215	Coe, F.	M467	Coustry, F.	1023	Dallal, G.	SU508
Chock, M.	1122	Coenegrachts, L.	F253, SA253	Cowan, C.	M203	Dallas, M. Robert	1054, SU111
Choi, D. Young	SU056	Cohen, A.	SU108	Cowan, C. M.	SU204	Dallas, S. L.	1054, SA025, SU073, SU111
Choi, H.	SU001	Cohen, A. J.	1022	Cowan, L.	SU448	Dalle Carbonare, L.	M060, M461
Choi, H.	SU373	Cohen, D. Rachel	SU325	Cowell, C. T.	SA005	Daly, M.	SU332
Choi, J.	M118	Cohen, R.	1107	Cowell, W.	M352	Daly, R.	M148
Choi, J.	M175	Cohen, S. B.	SU455	Cox, A. G.	M473, M474	Daly, R. M.	F419, SA419
Choi, J.	M209	Cohen-Solal, M. E.	SU523	Cox, G. A.	SU371	Dambacher, M. A.	M086, SU419
Choi, J.	M253	Cointry, G.	M096	Cox, K.	1025	Damron, T. A.	M014, SA152, SU112
Choi, J.	M340	Colaianne, G.	1102	Cox, T. M.	SU275	Dang, Q.	SA477
Choi, J.	SA514, SU197	Cole, D.	F122, SA122	Coxam, V.	M325, M327	Danikas, A.	SU244
Choi, J.	SU248	Cole, J. A.	M483	Coxon, F. P.	SU309	Danks, L.	SA276
Choi, J. W.	SU066	Cole, L.	M354	Coyle, L.	SA060	Dann, P. R.	1087, 1157
Choi, J. Y.	SU066	Cole, R. E.	M070	Craig, T.	SA455, SU512	Dante, M.	M082
Choi, J. Yong	SU226, SU227	Cole, W. G.	SA099	Crane, M.	F404, SA404	Danti, M.	SU125
Choi, S.	SA514	Coleburn, V. E.	M217	Crane, N. J.	SA003	Daragon, A.	SU495
Choi, S. Jin	M242, SA243	Coleman, H. N.	M441	Cranmer, P.	SU453	Dare, L.	SA231
Choi, W.	SA044	Coleman, I. M.	SU049, SU122	Cranney, A.	SU435, SU436	Darnay, B.	SA278
Choi, Y.	M233	Coleman, R.	M056	Crans, G. G.	M404	Darnay, B. G.	1069, F277, SA277
Choi, Y.	M234, SA261, SA375	Colgan, G.	SU396	Crawford, D. T.	M395, M396, M419	DaSilva-Jordine, P.	M419
Choi, Y.	SU183	Coll, M.	SU137	Crawford, G.	1045	Data, N. S.	F192, SA192
Chorev, M.	M491, SU498	Collin-Osdoby, P. A.	1070, 1071,	Crawford, P. M.	M411	Datta, H. K.	M436
Chou, S.	F222, SA222		SA265	Crawford, R. P.	1056	Datta, N. S.	M182, SA195
Chou, Y.	SU204	Collins, E. S.	SA308	Crenshaw, T. D.	M077, SU017	Davey, R. A.	1097, 1161
Choudhary, S.	M424, SA482	Collins, J.	SU430	Crepaldi, G.	F301, M292, M451,	Davico, M.	M325, M327
Chouinard, L.	M076, SA431	Collins, J. K.	SU246		SA301	David, A. R.	M454
Chow, W. Y.	M273	Collins, M. T.	M437, SA454, SA456	Crespo, V.	SA436	David, S.	SU058
Christakos, S.	1201, 1204	Collins, W. C. J.	SU447	Cressent, M.	M486	Davidson, M.	SA428, SU130
Christensen, C.	SU304	Colucci, S.	1102	Cretet, V.	SU146	Davie, M. W. J.	SA383
Christensen, S. Engkjaer	SU479	Colussi, G.	SA460	Cristallini, S.	SU509	Davies, B. A.	SA158
Christian, R.	M083	Colvin, T. L.	M111	Crockett, J. C.	SU308	Davies, H. Margaret Sarah	M089,
Christiansen, C.	1080, F074, F321, M241,	Combs, S. G.	SU014	Cromer, B.	SA001		SU039
	SA074, SA321, SA417,	Comeaux, S.	1107	Crosier, M. D.	M123	Davies, K. M.	F358, SA358
	SU116, SU149, SU410	Compston, J. Elizabeth	SU280	Crotti, T. N.	SA257	Davies, K. Michael	M279, M364
Christianson, C. A.	F197, SA197	Conaway, H. H.	SU207	Croucher, P. I.	SA064, SU095	Davies, M.	M334, SA525
Christoffersen, H.	SU376	Condon, K.	F138, SA138	Crowley, C.	M310, SU386, SU387	Davies, R.	F404, SA404
Chu, K.	F446, SA446	Conduah, A.	F135, SA135	Crozier, S. R.	1008, F002, SA002	Davis, C. M.	SA177
Chu, W. Jing.	M001	Conduah, A. H.	M023, SA069	Cruzat, F.	M188	Davis, E. I.	SA508
Chun, Y. P.	F192, SA192	Conigrave, A. D.	M195, M460	Csermus, V.	SU377	Davis, P. M.	SU478
Chung, D.	1228	Conn, D.	M354	Cui, L.	SU365	Davis, S. I.	1104, 1165, F138, SA138
Chung, H.	SU174	Connemey, J.	M184	Cui, X.	M035	Davis, S. S.	F442, SA442
Chung, H. Y.	M242	Connor, J. R.	F199, SA199	Cullen, D. M.	M050, SA200	Davis, T.	F404, SA404
Chung, U.	1006, 1014, 1016	Conover, C. A.	F149, SA149	Cullen, M. J.	F442, SA442	Davis, W.	SU345
Chung, U.	1047	Conrads, K. A.	M186	Cumming, R.	1133	Davison, K. Shawn	SA097, SA335
Chung, U.	1139, SA034, SU033	Conrads, T. P.	M186	Cumming, S.	SU003	Dawson-Hughes, B.	1041, 1078,
Chung, W.	SU129	Cons-Molina, F.	M287	Cummings, S.	F325, F429, M285,		F317, M123, SA317,
Chung, Y.	1045	Conzelman, M.	SA501		M365, SA325, SA343,		SU422, SU508
Chung, Y.	M118, SU252	Cook, J.	M148		SA429, SU335	Day, C. J.	1208, F249, M247,
Chung, Y.	SU256	Cool, S.	M235, M490	Cummings, S. R.	1038, 1039, 1057,		SA249, SU307
Chung, Y. Suk	1152	Coombe, D.	SU091		F090, F297, F323, F334,	Day, I. N. M.	SA119
Churchill, G.	SU242	Coombes, C.	M056		F347, M287, M290, M296,	Day, T. F.	1064, F048, SA048
Churchman, C.	M251	Coombs, H. F.	F114, SA114		M305, M355, SA090, SA297,	Day, W.	M384, M385
Chyttil, A.	F160, SA160	Cooper, C.	1008, 1058, F002, F334,		SA323, SA334, SA347, SA413	Dayer, R.	M447
Cianferrotti, L.	1167, F496, SA496		M015, M344, M346, M359,	Cupples, L. A.	1040, SU175, SU194	De Benedetti, F.	F470, SA470
Cignarelli, M.	F122, SA122		M388, M434, M446, SA002,	Cupples, L. Adrienne	F309, SA309	de Boer, J.	SU235
Cillessen, A. H. N.	SU385		SA119, SA334	Curl, W.	SA050	de Bruijne, M.	F321, SA321
Cineceros, X.	M437	Cooper, D. M. L.	SU016, SU047	Currier, B. L.	SA018	De Camilli, P.	1145
Ciria, M.	M091, SA379, SU137	Cooper, J. A.	SA245	Curtis, J. R.	M379, SA354, SU390	de Crombrughe, B.	1023
Cisneros, F. A.	SU326	Cooper, M. S.	F365, SA365, SA373	Cusick, T.	M402	de Eccher, G.	SA445
Civitelli, R.	1063, 1109, 1228, M167,	Cope, J.	SA333	Cusumano, G.	SA117	de Feo, D.	F301, M292, SA301,
	M346, M493, SU265, SU412	Corbin, T. J.	SU451	Cutler, C.	SA454		SU257
Clack, G.	M251			Cutler, C. M.	SA456		

(Key: 1001-1228 = Oral, F = Friday Plenary poster, SA = Saturday poster, SU = Sunday poster, M = Monday poster, WG = Working Group Abstract)

ASBMR 27th Annual Meeting

Author Index

De Gendt, K.	F515, SA515	Devas, V.	F404, M359, SA404	Dovio, A.	SA371	Einhorn, T. A.	F483, SA015, SA101,
De Geronimo, S.	F122, SA122	Devine, A.	SA310	Dow, E.	F437, SA437		SA136, SA483, SU080, SU092
de la Figuera, E.	SA092	Devlin, H.	SU251	Downs, T.	SU109	Eiriksdottir, G.	SU334
de la Higuera, M.	M400, SU374	Devogelaer, J. Pierre	SA420	Doxsey, S. J.	F212, SA212	Eis, S. R.	M067
de la Piedra, C.	SA436	Deyhim, F.	SU013	Drab, M.	1182	Eisenman, P. A.	SA182
de Laet, C.	M088	Dhawan, P.	1201, 1204	Draca, N.	M428, SU431	Eisman, J.	M278
De Leenheer, E.	SU095	Di Bella, S.	SU414	Draman, M. S.	F442, SA442	Eisman, J. A.	1137, 1138, M387,
de Leval, L.	SU104	Di Benedetto, A.	1063, 1102	Draper, M. W.	M397		M422, SA221, SA329, SU317,
De Marzo, A.	M493	Di Fede, G.	SA117	Dresner-Pollak, R.	M280		SU342, SU343, SU344
De Paola, V.	M016, SU367, SU378,	Di Giacinto, C.	F068, F470, M436,	Dreyer, B. E.	M497	Ekema, G.	SU516
	SU379		SA068, SA470	Drezner, M. K.	1105, 1177, 1205,	Eksarko, P.	SU487, SU494
de Papp, A. E.	M354, SA526, SU158,	Di Gregorio, S.	SA087, SU140,		1222, F459, M347, M350, SA459	El Azzouzi, B.	M359
	SU159		SU484	Drigo, P.	SA445	El Hammali, R.	M517
De Rekeneire, N.	F347, SA347	Di Munno, O.	F301, SA301	Drissi, H.	1020, 1110, 1155, M170,	El Hasnaoui, A.	SU416
de Stasio, G.	SU020	Diab, T.	SA188		M178, M488, SU488	El-Difrawy, S.	SA492
de Vernejoul, M.	SU399, SU523	Diacinti, D.	SA322, SA392	Drobney, E.	SA460	El-Hajji Fuleihan, G.	M075, SA449
De Villafranca, L.	SA010	Diaz-Curiel, M.	SA436	Drummond, F.	SU332	El-Hajjifuleihan, G.	F081, SA081
de Villier, W. J. S.	F242, SA242	Diaz-López, J. B.	SU322	Duan, J.	SA050	El-Husseini, A. A. M.	SU457
de Vries Bouwstra, J.	SU486	Dib, L.	SA449	Duan, Y.	SU316, SU364	Elalieh, H.	M146, SU221
de Winter, J.	M053, SU467	DiCarlo, E. F.	M440	Duarte, D. Jacinto	SU507	ElAlieh, H. Z.	SA147
Deal, C. L.	F457, SA457	Dick, W.	SA501	Dubanett, S.	F135, SA135	Elefteriou, F.	1051
Dean, D. A.	M171	Didelot, N.	F190, SA190	Dube, M. G.	1048	Elgin, F.	1017
Dean, T.	F491, M494, SA491	Didier, H.	SU166	Duboeuf, F.	SA058, SA359, SU084	Elkins, M.	SA333
Debacquer, D.	SA384	Diegues, L. G.	M476	Duboule, D.	M049	Ellingsen, J. Eirik	SA045
Debiasi, F.	M057, SU495	Diener, A.	M232	Duchemin, L.	SU089	Elvins, D.	M015
DeBold, C. Rowan	F084, SA084	Dieter, E.	SU445	Ducher, G.	SA186	Emami, K. H.	SU117
Deckelbaum, R. A.	1185	Díez-Pérez, A.	F093, M091, M122,	Ducy, P.	F202, SA202	Emeson, R. B.	1162
Dedhar, S.	1147		M169, SA093, SA379	Dufresne, T. E.	SU086	Emkey, R.	M435, SU413, SU415
Deferrari, J. M.	M072	DiGirolamo, D. James	1194, F133,	Dugar, S.	1216	Emmerson, A. J. B.	SA475
Defetos, L.	SU109		SA133	Dukas, L. C.	SU008	Empert, J.	SU444
Defetos, L. J.	M055, M495, SU114,	Dijkmans, B.	M389, SU486	Duncan, E. L.	M110	Engbersen, A.	SA465
	SU165	Dillon, D. A.	SU014	Duncan, R. L.	SA173, SU220	Engelhart, C.	M306
Deiana, L.	M462	Dillon, V.	M384	Dunford, J. E.	F408, SA408	Engelke, J.	SU425, SU460
Del Fattore, A.	F470, M436, SA470	DiMarchi, R.	M491	Dunham, K.	SU052	Engelson, E.	SU476
Del Fiocco, R.	M124, SA322	DiMartino, S. J.	M440	Dunlop, D. D.	SU490, SU492, SU494	Engler, T.	F437, SA437
Del Monte, F.	SA121	DiMeglio, L. A.	1089, M007, SA468,	Dunn, N.	F102, SA102	Enjuanes, A.	M122, M169, SA388
del Pino, J.	SA316		SU482	Dunstan, C. R.	F507, M053, SA507,	Enk, C. D.	M280
Del Rio, L.	SA087, SU484		SU351		SU142, SU144, SU520	Enomoto, F.	SU462
Del Rio, L. Miguel	SU140	Dinant, G.	M456, SA050	Duplat, D.	SA240	Enriquez, R.	M422
Del Valle, E.	M472	Dinulescu, D. C.	1031, SA107	Dupont-Versteegden, E.	1169	Ensrud, K.	1038, F325, M285, M355,
del Villar, V.	SA316	Dion, N.	SA036, SU024	Dupuis, J.	1040, SU194		M365, M411, SA325,
Delahunty, K.	1212, F114, SA114	Dionysiotis, Y.	SA377	Duque, G.	F412, SA412		SA343, SA413, SU335
Delany, A. M.	SU079	Diren, B.	SA085	Durham, B. H.	M133	Ensrud, K. E.	1073, 1135, F297,
Delattre, O.	SA240	Disarò, B.	SA445	Durmus, D.	SA085		F315, F323, M290, M305,
Delbridge, L.	M460	Diseroad, B. A.	M219	Durosier, C.	F096, SA096		SA297, SA315, SA323, SU151
Deleze, M.	M287	Divakara, V. P.	SU073	Dusevich, V.	1054, SU073	Epstein, S.	M359
Della Badia, M.	M322	DiVasta, A. D.	SA473	Dusso, A. S.	M463	Epstein, S.	M360
Della-Fera, M.	M233, SA050	Divieti, P.	M501, SA492, SA493	Dwyer, D.	SU295	Erben, R.	F353, SA353
Delmas, P.	1009, 1084, F429,	Divieti, P. A.	M503	Dyer, A. R.	SU487	Erben, R. G.	1164, F520, SA520
	M086, M275, SA429, SU141	Dixon, S. Jeffirey	1148, SU253	Dziegiel, M. Hanefeld	SA237	Eriksen, C. Grith	SA162
Delmas, P. D.	1223, F360, M087,	Do, N. Nam	SA055, SA056			Eriksson, A.	SA510, SA512, SU524
	M347, M359, SA058,	Dobkin, J. F.	M445			Eriksson, J. G.	1058
	SA359, SA360, SU075,	Dobnig, H.	F356, M331, SA356			Erkens, J. E.	SU388
	SU084, SU316	Dobritz, M.	SU324			Ernst, M.	M262
Delp, M. D.	M458	Dobrzanska, A.	SU484	Ea, H. Komg.	M486, SU032	Escaig, F.	SU254
Delsignore, R.	SA134, SU004	Docherty, E.	F199, SA199	Ealba, E. L.	M182	Escalante, C.	SU096
DeMarco, J. E.	SU053	Dodds, R. A.	M035	Eamshaw, S. R.	M361	Escalona, A.	M477
Demay, M. B.	F041, F496, SA041,	Dodge, D. A.	SA427	Eastell, R.	1132, 1224, F079, M251,	Escalona, M. Angeles	M478
	SA496	Doecke, J.	1059		M345, M412, SA079,	Escara-Wilke, J.	SU113
deMelo, N.	SA428	Doecke, J. D.	1208		SU139, SU156, SU358, SU382	Esfandiari, E.	SU275
Demer, L. L.	SA224	Doherty, S. M.	M375	Eastvold, M.	SA527	Eshleman, A.	SA386
Demers, C.	M522	Doi, K.	SU375	Ebeling, P. R.	SA336	Eskildsen, P. Claes	SU459
Demissie, S.	1040, SU175, SU194	Doita, M.	M163	Eberhardt, C.	SU094	Eskridge, T.	1168
DeMoss, D. L.	SU014	Dolleans, E.	M421	Eberle, P.	SU061	Essmyer, K.	F474, SA474
Dempster, D.	1175, SU361	Dolovich, L.	M391	Ebetino, F. H. F408, M351, SA408,	SU306,	Eswaran, S. K.	F088, SA088
Dempster, D. W.	1180, F435, M216,	Dombrowski, C.	M235		SU309	Ettinger, B.	M361, SU336
	A435, SU465, SU467, SU470	Donahue, H. J.	SA177, SU217,		SU182	Ettinger, M. P.	1222
Denegre, J.	1035		SU283		SU324	Evans, G. L.	F389, SA389
Deng, H. Wen	1211, M108, SU179	Donahue, L.	1045, M018, M150,	Econs, M. J.	1108, F138, F446,	Evans, H.	1172
Deng, Z.	M456		SU174, SU181		SA138, SA446, SA460, SU176	Evans, H. J.	1171
Denhardt, D. T.	M165	Donahue, L. R.	1035, F114, M106,	Edderkaoui, B.	F102, SA102, SA105	Evans, J. F.	SU027
Denhardt, D. T.	SU302		M149, SA109, SA114, SA165	Edenberg, H. J.	1108	Evans, M. J.	SU275
Denk, E.	M055	Donahue, S.	M467	Ederveen, A. G. H.	SU411	Evans, R.	M144
Dennis, J. E.	SU249	Dong, S.	SA157	Edmonson, M.	SU359	Evans, S.	SA383
Dennison, E. M.	1008, F002, SA002,	Dong, Y.	1020, 1110	Ednet, K.	M264	Evdokiou, A.	SA259
	SA119	Donohue, J. Michael	SA248	Edwards, J. R.	M174	Ewing, S.	SU335
Denson, K.	SU384	Donovan, M.	SU129, SU361	Edwards, K.	SU356	Eyre, D. R.	F053, SA053
Denton, J.	M454, M473, M474	Donovan, M. A.	1175	Ee, R.	1019	Ezura, Y.	1052, 1096, 1209
Deregowski, V.	M024, M211, M223	Donsante, C.	1063	Eelloo, J. A.	SA475		
Derksen, S.	SU329	Doody, S. L.	SA182	Egan, C.	SU312		
Derynck, R.	SA163	Dorado, G.	SU374	Egermann, M.	SU210		
Deschênes, C.	SA036, SU024	Dorst, A.	SU391	Eghbali-Fatourech, G. Z.	1044	Fabbro, D.	F068, SA068
Desranleau, S.	SU152	Doschak, M. R.	M392, SU454	Eguchi, Y.	M329	Faber, H.	SU391
Desrouleaux, K.	1218	Dossa, T.	1147	Ehrlich, D.	SA492	Faber, P.	SU516
destaing, o.	1145	Doucet, M.	1126, F156, SA156	Eichenberger Gilmore, J. M.	M019	Faccio, R.	SA245
deTakats, D.	SU402	Dougall, W.	SA065	Eick, J. David	1111	Fagerlund, K. M.	SU147, SU272,
Devados, R.	1030	Dougall, W. C.	F135, SA135, SU448	Eiken, P.	SU423		SU273
Devareddy, L.	M335, SU044, SU432	Doupe, M.	SU327, SU328, SU372			Fahrleitner-Pammer, A.	M331

(Key: 1001-1228 = Oral, F = Friday Plenary poster, SA = Saturday poster, SU = Sunday poster, M = Monday poster, WG = Working Group Abstract)

ASBMR 27th Annual Meeting

Author Index

Girgis, S.	M056	Graeff, C.	M095, M413	Guirguis, S.	M437	Hanley, D. A.	1222, SA097, SU435,
Gjesdal, C. Gram	M286, SU333	Grafe, I.	M383	Guise, T. A.	1213, 1216, SU261,		SU436
Glackin, C.	SA148	Graham, C. N.	M361		SU526	Hannan, M. T.	F309, SA309
Glass, E. V.	M404	Graham, J.	SA333	Guive, M.	F370, SA370	Hanning, C.	F199, SA199
Glass, N.	SU087, SU434	Graham, L.	SU059	Gujral, R.	SA050	Hannon, R. A.	M251, SU206, SU358
Glass, N. A.	M330, M448	Gram, J.	1206, M157	Guldborg, R. E.	F450, M045, M415,	Hans, D.	F096, SA096
Glatt, V.	1097	Grandchamp, B.	1086		SA450, SU045	Hansen, K. E.	M083
Gleghorn, L. J.	F116, SA116	Granger-Veyron, N.	M268	Gulseth, H. Christian	M286, SU333	Hansen, S. Eiberg	SU318
Glezer, S.	SU387	Granhholm, S.	SU288	Gunaratna, N. S.	SU011	Hansen, T. P. K.	SU028
Glimcher, M. J.	SU059, SU145	Grano, M.	1102	Gunawardene, S.	SA143	Haque, T.	SU202
Glorieux, F.	1088, F440, SA440	Grant, C. S.	SU464	Gundberg, C. M.	1184, M123	Hara, K.	M321, SU021, SU023
Glowacki, J.	M004, M025, M065,	Grant, M.	SA487	Gunnarsson, O.	M324	Hara, T.	1123
	M155, M448, SA153,	Grant, S.	SU444	Günther, C.	SU407, SU409	Hara, Y.	SU055
	SA312, SU337	Grasser, W. A.	M022, M419	Günther, O.	SU407, SU409	Harada, A.	M008, M009, SU006
Gluer, C.	1009	Grassi, F.	1049, 1144, F395, SA395	Günther, S.	SU407, SU409	Harada, S.	M402
Glüer, C. C.	1176, 1224, M095,	Gratacòs, J.	SA342, SU461	Guntur, A. R.	SA230	Harada, Y.	SU055
	M413, SU139	Grauer, A.	M377	Guo, D.	1026, SA287, SA288, SA291	Hardcastle, A. E.	M338
Gluhak-Heinrich, J.	1093, F168,	Gravallese, E. M.	M243, SU491	Guo, J.	1002, F481, SA481	Hardy, R.	F365, SA365
	SA168, SA285, SA462	Green, J. R.	SU270	Guo, K.	F408, SA408	Harel, Z.	SA001
Gocek, J.	SU018	Green, M.	1030	Guo, R.	1018, 1072	Harfe, B. D.	1025
Godang, K.	SA369	Green, P. D.	M394	Guo, T.	SU383	Harke, J. M.	SU425
Godfrey, K. M.	1008, F002, SA002	Green, S.	SA430	Guo, X.	1064, F048, SA048	Harkness, M.	SA318
Goekoop-Ruiterman, Y.	SU486	Greenberg, D. A.	M111	Guo, Y. Fang	SU179	Haro, H.	SU055
Goel, P.	1130	Greenberger, J. S.	M155	Gupta, A.	1112, 1124, F088, M258,	Harpavat, M.	SA477
Goellner, J.	SU019	Greenfield, D. M.	SU358		SA088, SA363, SU098, SU297	Harrington, J. J.	SU516
Goellner, J. J.	1197, F289, SA289	Greenfield, E. M.	F166, M194,	Gurzov, E.	SU244	Harris, M.	1026
Goemaere, S. J. A. G.	SA384		M256, SA166, SU216	Gustafsson, B. I.	SA047, SU213	Harris, M. A.	SA291, SA462
Goessler, W.	M331	Greenfield, H.	SA005	Guthrie, J.	SA288, SU111	Harris, M. B.	SA312
Goettig, S.	SU094, SU101	Greenfield, J. R.	SU142, SU144	Gutierrez, G.	SU029	Harris, S.	1093, SA288
Goettsch, W. Gerrit	SU388	Greenspan, S.	1056, M411, SA477	Gutierrez, S.	1015, 1030	Harris, S.	SU403, SU417
Goetz, R.	1104	Greenspan, S. L.	1222, F381, SA098,	Gutierrez, Y.	F138, SA138	Harris, S. E.	1026, 1154, 1157,
Goff, S.	M225		SA381, SU185, SU474	Guyer, J. L.	M366		F168, M174, SA168,
Going, S.	F179, SA179, SA352	Greenwald, K. E.	SA344				SA285, SA291, SA462
Going, S. B.	M003	Greeves, J. Patricia	SA307			Harris, S. S.	SU508
Goins, B.	1141, M054, SU098	Gregson, R.	M298			Harris, S. T.	M377
Gold, D.	M362, M406	Grey, A. B.	SU230	Ha, E.	1130	Harris, T.	F306, SA306, SU334
Gold, M.	SA001	Gridley, D. S.	SA398	Ha, H.	M002	Harris, T. B.	F347, M103, SA347
Goldberg, V. M.	M256	Griffin, T. L.	SU165	Ha, J.	M240	Harrison, E. J.	M074
Golden, E. B.	1022	Grigoriadis, A. E.	SA216, SU244	Haaland, D. Allan	SU325	Harrison, J.	1163
Goldfarb, A. W.	M280	Grimaldi, A.	SU414	Haapalahti, J.	SU143	Harrison, J. R.	F210, SA210
Goldman, H. M.	SA049	Grinberg, D.	M122	Haas, M. J.	SA517	Harrison, S.	M290
Goldring, S. R.	SA257, SU491	Grisanti, M.	1226, SU304	Haavardsholm, E.	M389	Hartard, M.	F353, SA353, SU352,
Goll, J.	SA098	Grisanti, M. S.	SU451, SU452	Habash, D. L.	SA423		SU442
Goltry, K.	SU249	Griz, L.	SU468	Haberland, M.	1162	Hartl, F. C.	SU166
Goltzman, D.	1050, 1076, 1099,	Grizzle, W.	1117	Habermeyer, P.	SA020	Hartmann, B.	1225
	1203, F453, SA453,	Grönfeldt, V.	SU318	Habra, M. Amir	M126	Hartsfield, J. K.	F138, SA138
	SA488, SA490, SA516	Gronowicz, G.	F194, SA194	Haddad, S.	SA081, M075, SA081	Hartzell, D.	M233
Gómez, A.	SA342, SU461	Gronthos, S.	M236	Hadfield, K. D.	SA025	Haruyama, N.	1192
Gomez, C.	M476	Groot, M.	SA465	Hadjiargyrou, M.	SA042	Harvey, N. C. W.	1008, F002, SA002
Gómez, M.	M477	Gross, G.	SU061, SU086	Haenscheid, H.	SU433	Harwood, R.	M298
Gomez, S.	SA436	Gross, T.	1182, SA333	Hagger, G.	F199, SA199	Hase, H.	SA246
Gómez-Alonso, C.	SU322	Gross, T. S.	SU218	Hagiwara, H.	M496	Hasegawa, H.	F140, M129, M132,
Gómez-Martín, F.	F093, SA093	Grosschedl, R.	1184	Hahn, J.	SU122		M134, SA140
Gomi, N.	SU015	Grøsvik, K.	SA252	Hahn, T. J.	M216, M427	Hasegawa, K.	SA494
Gonçalves, S.	SA324	Grovas, L.	SU394	Haigh, J. J.	1151	Hashimoto, J.	SA386
Gong, J.	SU127	Grove, M. R.	SU336	Haigh, K.	1151	Hashimoto, N.	1214
Gong, Y.	SU298	Grubbs, B.	1141, F066, M054,	Håkanson, R.	SA396	Hashimoto, T.	1123, SU102
Gonnelli, S.	M016, M292, M414,		SA066, SU098	Halbout, P.	M424	Hassan, M. Q.	1013, SU248
	M416	Gruber, B.	SU173	Hale, L. V.	M219, SA205	Hassell, J. R.	M135
González, I.	SU137	Grundberg, E.	M107, SU187	Hall, C. L.	F070, SA070	Hasselstrom, H.	SU318
González, M. R.	SA092	Gruntmans, U.	M468	Hall, D. B.	M020, SA150	Hastings, R. H.	M495
Gonzalez Pardo, V.	M512	Grynpas, M.	M390, SU133, SA103,	Hall, E.	M056	Hasty, K. A.	SU349
González-Macias, J.	F093, SA092,		SU370	Hall, S. L.	SA145	Hata, K.	1146, M190, M204
	SA093, SA402, SU184	Grzesiak, J. J.	M495	Halladay, D. L.	F437, M219, SA205,	Hatayama, A.	SU276
Gonzalez-Suarez, I.	M463	Grzesik, W.	SU082		SA437	Hattori, T.	SU034
Goodby, A.	M375	Gu, J.	SU005	Halleen, J. M.	SU147, SU161,	Haug, E.	SA346
Gopalakrishnan, R.	M037	Gu, S.	1095		SU162, SU272, SU273,	Haugeberg, G.	M286, M389, SU333
Gorai, I.	SA298	Gu, W.	M113, SU182		SU289, SU290, SU303	Hausler, K. D.	1219
Gordon, C.	M078, M465, SA080	Gu, Y.	SA177	Halleux, C.	SA207, SA215	Havenith, G.	SA094
Gordon, C. M.	M136, SA471, SA473	Guanabens, N.	SA388, SU392,	Hallgrimsson, B.	SU016, SU047	Havill, L. M.	SU177
Gordon, N.	SU336		SU421	Halloran, B. P.	M146, SA147,	Hawker, G.	M382
Gori, F.	F041, SA041	Guardia, G.	SA463		SU012, SU221	Hawker, G. A.	M316, SU348
Goribar, A. F.	SA010	Guarneri, V.	1218, F122, SA122	Halse, J.	SU413	Hawkes, W.	M330, SU337
Gorski, J. P.	F023, SA019, SA023	Guaydier-Souquières, G.	SA495	Hamel, L.	SU366	Hawkins, F.	M477, M478
Goshen, I.	SU377	Gubago, L.	SU093	Hamilton, N.	SU091	Hawse, J. R.	1200, M172, SA158,
Goto, M.	SA161	Gubrij, I.	M417	Hamilton, S. Anne.	SA398		SA506, SU010, SU285
Goto, Y.	SA355	Gückel, C.	SU166	Hammerschmidt, T.	M352	Hay, E.	1220
Gotshalk, L.	M144	Gudnason, V.	SU334	Hammond, V.	M497	Hayakawa, N.	SA361, SU026
Goulet, G. C.	SU091	Guenou, H.	F190, SA190	Hamrick, M.	M006, M233	Hayman, A. R.	SU275
Govindraj, P.	M135	Guerrero, T.	F093, SA093	Hamrick, M. W.	M456	He, B.	1050
Govoni, K.	M183	Guertin, P. A.	SA448	Han, J.	F391, SA391	He, J.	SA193, SU192
Govoni, K. E.	1152	Gugatschka, M.	M331	Han, K.	SU286	He, Q.	M226
Gowen, M.	SA231	Guggenbuhl, P.	SU366	Han, L.	1098, F401, SA401, SU264	He, W.	M353
Gozzini, A.	SA117, SA141	Guglielmi, G.	M292	Han, S.	SU154	He, Y.	M479
Grabenstein, T.	SA215	Guido, V.	SU174, SU181	Haney, C.	SU396	Healy, D. R.	SA394
Grabowski, P.	M436	Guillemin, F.	SA115	Hangartner, T. N.	M063	Healy, E. M.	SA302
Gracious, B. L.	SA302	Guilley, E.	M284	Hankenson, K.	F057, SA057	Healy, M.	M297
Graebe, A.	M412	Guillotin, B.	M167	Hankenson, K. D.	M206, M237, SA038	Heaney, J. D.	SU053

(Key: 1001-1228 = Oral, F = Friday Plenary poster, SA = Saturday poster, SU = Sunday poster, M = Monday poster, WG = Working Group Abstract)

Author Index

ASBMR 27th Annual Meeting

Heaney, R. P.	M273, M276, M279, SA519	Hirota, T.	M272	Houghten, R.	M508	Imai, Y.	M031, M224, SA017
Heaton, B.	M307	Hirsinunmmi, R.	SU161	Houwing, J.	M088, M120	Imamovic, A.	1040, SU194
Hebela, N.	M449	Hisada, K.	M204	Hovhannisyan, H.	SU248	Imamura, S.	SA361, SU026
Heeren, J.	M332	Hitz, M. F.	SU459	Hoving, J.	SU155	Imbalzano, A.	M188
Hefferan, T. E.	SA018	Hochberg, M.	1057, SA413, SU335	Howard, K. M.	1060	Imbriaco, R.	SA118
Hegde, P.	F199, SA199	Hochberg, M. C.	1038, 1039, F297, F323, F406, M356, SA297, SA323, SA406, SU159	Howard, L.	SU430	Imel, E.	F138, SA138
Hegedüs, L.	SU469	Hodge, J. M.	M266	Howard, T. D.	F358, SA358	Imel, E. A.	SA460
Hegeman, J.	SU155	Hodgson, L. A.	M266	Hrgovic, Z.	SA390	Inaba, T.	M303, SU315
Heickendorff, L.	SU479	Hodsman, A.	M310, SU386, SU387	Hrovat, M.	SU145	Inada, M.	F062, SA062, SA063
Heikkinen, J.	SU143	Hodsman, A. Bryan	M502, M503	Hruska, K. A.	F016, F021, SA016, SA021	Inagaki, K.	SA361, SU026, SU301
Heinonen, A.	SA178, SU339	Høegh-Andersen, P.	1206	Hsu, W.	SU115	Inakuma, T.	M328
Heldt, K.	SU394	Hoff, A. O.	1218, M126, M498, M499, SU096	Hsu, Y.	1212	Indridason, O. Skuli	M324
Helgason, C. D.	M259	Hoffman, S.	F199, SA199	Hu, C. Yong	SA027	Ingersoll, D.	M339
Helledie, T.	M235	Hoffman, S. J.	F234, SA233, SA234	Hu, H.	M071, SU463	Ingold, P.	F220, SA220
Heller, H. J.	SA460	Hoffmann, A.	SU061	Hu, W.	SU215	Inkson, C. Anne	SU081
Hellingman, A. A.	SU320	Hoffmann, K.	1226	Hu, Y.	M225	Inou, T.	M469
Hellqvist, Å.	1129, SA006	Hoffmann, O.	SU305	Huang, A.	M438	Inoue, D.	1123, SU102
Helsberg, K.	M318, M398	Hoffmeyer, P.	M284	Huang, C.	M205	Inoue, S.	SU190
Helvering, L. M.	F202, SA202	Hofman, A.	F120, M088, M120, SA120	Huang, D. C.	1202, F499, SA499	Inouye, K.	SU110
Henderson, J. E.	1185	Hofmann, F. B.	F039, SA039	Huang, E.	M499	Inskip, H. M.	1008, F002, SA002
Henderson, V.	M517	Hofstaetter, J. Gerhard	1175	Huang, H.	M240, SU298	Insogna, K.	1191, F270, SU269
Hendrix, S.	SU130	Hogan, B.	1026	Huang, H. Ping	SA027	Insogna, K. L.	M001
Hendy, G. N.	1099, 1203, F491, M503, SA487, SA491, SU514	Hogan, H. A.	M458	Huang, J.	F154, SA154	Ioannidis, G.	M310, SA097, SU386, SU387
Henriksen, D. B.	1225	Hoiseth, A.	F293, SA293	Huang, K.	M196	Ioannidis, J. P. A.	1210
Henriksen, K.	1206, M157, M241, SA237	Hokken-Koelega, A. C. S.	SU320	Huang, S.	M162	Iqbal, J.	1043, 1100, F376, SA254, SA376
Henriksson, M.	SU477	Holen, I.	SU206	Huang, S.	M219	Irani, D.	M445
Henry, M. J.	F319, SA319, SU364	Holick, M. F.	M308, M339, SA523, SA526, SU110	Huang, W.	SU058	Ireland, D. C.	SU280
Hens, J. R.	1157	Holländer, R.	SU166	Huang, Y.	M151, SU225	Irie, N.	SU287
Henschler, R.	SU094, SU101	Holliday, L.	SU298	Huang, Z.	M239	Irwin, R.	SU243
Her, S.	M430	Holliday, L. Shannon	SA238, SU296	Huang, S. Eileen	M126	Isaia, G.	F301, SA301, SU458
Herath, C. S. K.	SU293	Hollis, B.	M368	Huard, J.	SA069	Isaia, G. Carlo	SU414
Herault, Y.	SU193	Holmegaard, S. Nistrup	SU376	Hudson, M.	SU341	Isaksson, A.	SA328
Herber, M.	F520, SA520	Holmes, C.	SU370	Hudson, T. J.	M107	Isales, C. M.	M006, M456, SA050, SU291
Herceg, M.	M488	Holmes, E.	M320	Huet, P. Michel	M522	Ish-Shalom, S.	SU428
Herings, R. M. C.	SU388	Holmes, J. A.	SA294	Huff, G. R.	SU064	Ishak, K. J.	M357
Herman, B. A.	1141	Holst, J. Juul.	1225	Huff, W. E.	SU064	Ishani, A.	M285, SA413
Hermann, A. Pernille	SU423	Holven, K.	SU380	Huffman, N. Tennille	F023, SA019, SA023	Ishibashi, O.	SA024
Hernandez, C. J.	SA363	Holvik, K.	SA346	Hughes, A.	M035, SU308	Ishida, K.	SU058
Hernández, J. Luis.	SA402	Holy, X.	M268	Hughes, C.	F410, M346, M347, SA410, SU410, SU413	Ishida, N.	M254
Herndon, D. N.	SU060, SU475	Holzmann, P.	SA504	Huh, J. Eun	SU056, SU233	Ishida, Y.	M399
Herold, D. A.	SU165	Holzmann, P. J.	M401	Hulter, H. N.	SU429	Ishihara, H.	SU270
Herrmann, F.	M121, M284	Homan, M.	M285	Humphrey, M. B.	M261	Ishihara, Y.	SU301
Hersh, J. H.	M442	Honasoge, M.	1168	Humphries, R. K.	M259	Ishii, S.	1052, F127, SA127
Hershey, C. L.	SU294	Hong, H.	SU086	Hung, I. H.	1195	Ishijima, M.	1192, SU462
Herskovitz, R. M.	1060	Hong, J.	M253, SU197	Hunt, S. M.	M081	Ishikawa, I.	F014, SA014
Hertweck, P.	SA001	Hong, S.	SU022, SU493	Hurd, J.	SU181	Ishikawa, M.	1066
Herzog, H.	M422	Hong, S. B.	M471, SU154	Hurley, M. M.	F142, SA142	Ishikawa, Y.	M311, M313, M431
Hess, P.	F090, SA090, SA091, SU043	Hongo, M.	M311, M313, M431, SU439	Hurley, M. P.	M228	Ishizuka, S.	SA497, SA503
Hesse, E.	M180	Honjo, T.	1217, F464, SA464	Hurst, I.	SU298	Islam, A. S.	M256
Hesslein, D. G. T.	1184	Honkanen, R.	SA418	Hurwitz, S.	SU087, SU337	Islam, M. Saiful	M177
Hewer, T.	SA292	Honkanen, R. J.	M289	Husted, L. Bjerre	M119, SA162	Ismail, H.	M480
Hewison, M.	F365, F518, SA365, SA373, SA518	Honsawek, S.	SU237	Huston, A.	SU201	Isoda, R.	SU277
Heymsfield, S.	SA352, SA430	Hoogendorn, E. H.	SA460	Huybrechts, K. F.	M357	Isome, H. M.	M144
Hiasa, M.	SU102	Hoopes, J.	SA290	Hwang, S. M.	SA231, SA484	Itabashi, A.	SU426
Hickok, N.	M455	Hooshmand, S.	SU044, SU246	Hyams, J. S.	SU478	Ito, H.	SU055, SU071
Hide, K.	SA082	Hoppman, N.	SU195	Hyer, S.	SU355	Ito, M.	F362, M244, SA362, SU007, SU239
Higano, C. S.	SU049, SU122	Horazdovsky, B. F.	SA158	Hyun, B.	F086, SA083, SA086	Ito, S.	SU110
Higashio, K.	SA161	Horcajada, M.	M325, M327			Ito, Y.	F222, SA222
Higgins, L. S.	1216	Horii, M.	1066			Itoh, M.	SA361, SU026, SU050
Hikiji, H.	F127, SA127	Horizonzo, H.	SA326, SU088			Itoi, E.	F433, M311, M313, M431, SA433, SU439
Hikita, A.	1188	Horlait, S.	SU357			Itokawa, T.	F270, SU269
Hill, A.	M104, M105	Horlick, M.	SU476			Itzstein, C.	F279, SA279
Hill, J.	1168	Horne, W.	1114, 1145, 1150, F279, SA279			Ivaska, K.	SA328
Hill, R. J.	M395	Horne, W. C.	1183, M180			Iwai, T.	SU090
Hillegonds, D. J.	M055, SU165	Horowitz, M.	M326			Iwamoto, J.	M348
Hillier, T.	1038, F297, SA297	Horowitz, M. C.	1184, SA013			Iwaniec, U. T.	1048, SA137
Hillier, T. A.	1039, 1057, F323, SA323	Horreard, F.	M473			Iwasaki, H.	1066
Hillion, F.	M473	Horst, R.	M524			Iwasaki, Y.	M466
Hillmeier, J.	M383	Horst, R. L.	1202, SU064			Iwata, H.	SU408
Hilton, M. J.	1153	Hortobagyi, G. N.	1218			Iwata, K.	1081, SA409
Hindson, D.	F262, SA262	Horton, J. A.	M014, SA152			Izquierdo, M.	SU244
Hino, K.	F174, F393, SA174, SA393	Horton, L.	1035, F114, SA114				
Hirabayashi, M.	SU050	Horton, W.	M239, SA033				
Hiraga, T.	1007, 1121, F218, SA218, SU123	Horton, W. A.	SA151				
Hirahara, F.	SA298	Horwood, N. J.	SA250, SA276				
Hirai, H.	F174, SA174	Hoshi, K.	1016, 1047, SA034				
Hiraki, A.	1214	Hosking, D.	M275, SU159				
Hiramitsu, T.	SU071	Hosogane, N.	F258, SA258, SU054				
Hirao, M.	1024	Hosoi, T.	SU190				
Hirasawa, G.	SU527	Hosoya, A.	M161, SU123				
Hirasawa, H.	SU239	Hou, X. Wei	SA055, SA056				
Hirota, K.	1007, M272	Houck, K. A.	F202, SA202				
		Houck, T.	M384				

(Key: 1001-1228 = Oral, F = Friday Plenary poster, SA = Saturday poster, SU = Sunday poster, M = Monday poster, WG = Working Group Abstract)

ASBMR 27th Annual Meeting

Author Index

Jacquel, A.	1220	Jo, O. D.	1163	Kamekura, S.	F125, SA125	Kawai, M.	1085
Jacques, P. F.	F309, SA309	Jódar, E.	M477, M478	Kamel, S.	M255, SA240, SU511	Kawai, N.	SU063
Jacquin, C.	F266, SA256, SA266	Joe, A.	SU108	Kamijo, R.	M249, SA037, SA161	Kawai, S.	F208, SA208
Jaeger, W.	SU305	Johansson, A.	SA283, SU207	Kamimura, T.	SA054	Kawamoto, A.	1066
Jaen, A. del Valle	M459	Johansson, H.	1009	Kamiya, N.	1034	Kawamura, K.	M303, SU315
Jaglal, S.	M382	Johnell, O.	1009, F327, F334, SA303, SA327, SA334, SA510, SA512, SU187, SU524	Kamiya, S.	M191, SU107	Kawamura, N.	1139
Jagodzinski, M.	M180			Kamkar, L. Lili	SU246	Kawasaki, I.	M272
Jahn, R.	M263			Kammerer, C. M.	F100, F112, M103, SA100, SA112, SU195	Kawase, T.	M205
Jahnukainen, K.	SU477	Johnson, D. L.	M100	Kanaan, R. A.	SU035, SU078	Kawashima, H.	SA024
Jahr, H.	M250	Johnson, F. Brad	M234	Kanaya, F.	SA326, SU088	Kawawa, T.	M249
Jain, A.	SA456	Johnson, M.	M322, SU108, SU424	Kanazawa, H.	1195	Kayasuga, R.	SU276
Jain, J.	SU517	Johnson, M. L.	M050	Kanda, T.	1209	Kazakia, G.	M069
Jakob, F.	M198, M231, M388, M434	Johnston, S. Claiborne	F334, SA334	Kane, R. L.	SU151	Kazakia, G. J.	M046
Jakobsson, J.	SU522	Johnstone, D.	M310, SU386, SU387	Kaneki, H.	1018	Kazama, J. James	M129
Jalava, T.	SU402	Jokihaara, J.	F181, M470, SA181	Kaneko, H.	F374, SA374	Ke, H. Z.	M395, M396, M419, SA394, SU253
Jamal, S.	M078, M285	Jolad, S. D.	SU489	Kaneko, R.	SU050	Keaveney, T. M.	SA363
Jamal, S. A.	M465, SA413	Jolette, J.	M076	Kang, D.	M118	Keaveny, T. M.	1056, F088, M046, M411, SA088
James, C. G.	SU037	Jolette, J.	M409	Kang, H.	M196	Keenan, M.	M449
Jamieson, D.	SA526	Jolette, J.	SA431	Kang, M.	F391, M002SA391	Keinan-Adamsky, K.	SU061
Jamieson, D. P.	SA523	Jolette, J.	SU128	Kang, S.	M175, SA451	Kekow, J.	M413
Jamieson, M.	M101	Jolma, P.	M470	Kanis, J. A.	1009, SU402	Kelepouris, C. M.	M219
Jamonneau, I.	M373, M433	Jones, A.	SU363	Kannus, P.	F181, M470, SA178, SA181, SU009	Keljo, D.	SA477
Jan, S.	SU312	Jones, C. D.	F202, SA202	Kansagor, J. Nan	1031, SA107	Keller, B.	F030, SA030
Janckila, A. J.	SU147, SU273	Jones, J.	SA065, SU448	Kantarjian, H. M.	SU096	Keller, E.	SU113
Janeiro, C.	SU310	Jonsson, B. Y.	SU334	Kanuparthi, D.	M162	Keller, E. T.	F070, SA070
Jankowska, J.	M480	Joo, I.	SA424	Kanzaki, S.	SU007	Keller, H.	SU209
Jankowski, L. G.	M080	Jorgensen, N.	M246	Kapadia, R.	SU199	Kelling, D. G.	SA523
Jansen, D.	1065	Jorgensen, N. R.	M094, SA372	Kaplan, F. S.	M029	Kelly, K.	1122
Janz, K. F.	M019	Jose, B.	M455	Kaplan, F. S.	M439	Kelly, M. H.	M437, SA454, SA456
Jarcho, M.	M037	Joseph, F.	M133	Kaplan, F. S.	SA011	Kendler, D.	F425, M377, SA425
Jarrett, J. C.	SU119	Joseph, L.	1076	Kapner, A.	SU407, SU409	Kendler, D. L.	SU410
Järvinen, T. L. N.	F181, M470, SA181, SA184	Josse, R. G.	SA308	Kapoor, A.	1045	Kennedy, C.	M391, SU325
Jatzke, S.	M231	Jouanny, P.	SA115	Kapral, M.	M071	Kenner, G. H.	SU450
Jausse, I.	M142	Journe, F.	SA075	Kapur, R. P.	M436	Kerr, W. G.	M261
Javaid, M. K.	1008, 1058, F002, SA002	Judex, S.	M018, M149, M150, SA165, SU173, SU174, SU371	Kapur, S.	SU219	Kerry, S.	SU355
Javed, A.	1015, 1030, F212, M058, M059, SA212, SU228	Jueppner, H.	SA143	Karaplis, A.	SA488	Kesavan, C.	F183, SA183
Javier, R.	M444	Jugdaohsingh, R.	M338, SA421	Karaplis, A. C.	1050, 1203, F453, SA453, SA490, SA516	Kessler, C.	SU079
Jaworski, M.	SA123	Juhász, A.	SU065	Karas, T. Anya	M376	Kessler, F.	M318, M398
Jean, S.	SA335, SA448	Juillet, F.	SU146	Karasik, D.	1040, SU175, SU194	Key, L.	M368
Jeandel, C.	M142, SA115	Jun, J. Hye	SA223	Karczmarewicz, E.	M480, SA123	Key, L. L.	SU279
Jee, B.	SU183	Jung, H.	M209	Karin, N. J.	SA124	Key Jr, L. L.	SU311
Jee, W. S. S.	M419	Jung, M. E.	M427	Karlsson, M.	1011, F187, SA187	Keyak, J.	M051
Jeffcoat, M.	SA089	Jung, Y.	SA514	Karlsson, M. K.	F327, SA327, SU318	Khadeer, M. Abdul	1112, M258, SU297
Jehan, F.	M117	Jüppner, H.	1036, 1106, F444, F491, M501, SA444, SA490, SA491, SA492, SA493	Karlsson, S.	1192	Khalidi, N.	SU325
Jehle, S.	SA495			Karmakar, S.	M516	Khalifa, B.	M515
Jehle, S.	SU429	Jurdic, P.	SA240	Karmin, J. A.	SA167, SA263, SU224	Khalil, D. Agha	M335, SU432
Jeker, H.	SU209	Juriscicova, A.	SA103	Karner, I.	SA390	Khan, A. D.	SA340
Jemsen, J.	M246			Karperien, M.	1029	Khan, A. Sultan	SA094
Jemtland, R.	SA369, SU046, SU232			Karpf, D. B.	M405	Khan, T. S.	SU370
Jen, H.	SA320, SU323			Karsdal, M. A.	1206, M157, M241, SA237	Kharode, Y. P.	M394
Jenkins, B. J.	M262	Kaabeche, K.	F190, SA190	Karsenty, G.	1051, F032, F202, M179, SA032, SA040, SA202	Khoo, B.	M098, M099, SA310
Jennings, S.	SU150	Kacena, M. A.	SA013	Kartsogiannis, V.	SU095	Khosla, M.	SU466
Jensen, E. D.	F204, SA204	Kadler, K. E.	1033	Kasahara, Y.	SA054	Khosla, S.	1010, 1044, 1074, 1075, 1142, 1200, F511, M158, SA348, SA506, SA511, SU150, SU382, SU464
Jensen, J. Beck	SU459	Kado, D. M.	SU180	Kashima, T.	SA216	Khouri, N. J.	F081, M075, SA081
Jeong, J.	M175	Kadono, Y.	SA261, SA375	Kasperk, C.	M383	Kido, S.	1123, M333, SU102
Jeong, J. U.	SA231	Kadowaki, T.	1047, 1139	Kassem, M.	M202, SA460	Kiefe, C. I.	SU390
Jepsen, K. J.	F262, M104, M105, SA101SA262, SU456	Kafri, N.	SU346	Kasukawa, Y.	F433, M311, M313, SA433	Kiel, D. P.	1040, F309, SA309, SU175, SU194
Jerome, C.	1179, F232, F236, SA232, SA235, SA236, SU270	Kagan, R.	SU158	Katafuchi, M.	SA355	Kifor, I.	SU497
Jespersen, J.	SU149	Kahan, A.	SA439	Katafuchi, T.	M496	Kifor, O.	SU497
Jhamai, M.	F120, M117, SA120	Kahler, K.	M363	Katagiri, M.	1016	Kii, I.	SA216
Jia, D.	1197, F367, SA367	Kahler, K. H.	SU359	Katagiri, T.	SA161, SA201	Kiklevich, V.	F461, SA461
Jia, X.	M037, SU383	Kajantie, E.	1058	Kati-Coulibaly, S.	M327	Kikuchi, M.	SU085
Jiang, D.	M179, SU266	Kaji, H.	F444, SA366, SA444	Kato, N.	M165, SU302	Kim, B.	M176
Jiang, G.	SU358	Kaji, Y.	M032, SU015	Kato, S.	F509, M328, SA494, SA509, SU110, SU259	Kim, B.	M340
Jiang, H.	SA180	Kakar, S.	F483, SA101, SA483	Katselnik, D.	SU121	Kim, B.	SU001
Jiang, J.	SU298	Kakikawa, T.	SU389	Katz, J. N.	M371, M372	Kim, B.	SU373
Jiang, J. X.	1095	Kakita, A.	SU026	Katz, R. L.	M126	Kim, C.	SU211
Jiang, X.	F048, M238, SA048	Kakizawa, H.	SA361, SU026	Katz, R. W.	M221, SU240	Kim, D.	M118, M430
Jiang, Y.	M090	Kaku, M.	SU298	Katzeff, H. L.	M336	Kim, D.	SA167, SA263
Jiang, Y.	M092, M102, M130	Kalajzic, I.	M177	Kaufman, J.	SA384	Kim, D.	SA422, SA451
Jiao, F.	SU182	Kalbow, M.	M380	Kaufman, J. J.	SU172	Kim, D.	SU056
Jiao, Y.	M113, SU182	Kaldate, R.	F404, SA404	Kaufman, R. J.	SU266	Kim, D.	SU224
Jie, L.	SA456	Kalebic, T.	SU146, SU148	Kaufman, S.	1226	Kim, D.	SU236
Jilka, R.	F401, SA401, SU019	Kaliciski, P.	M480	Kaur, K.	F365, SA365, SA373	Kim, D.	SU252
Jilka, R. L.	1140, F289, M417, SA219, SA289	Kalinowski, J.	1189, SU212	Kavanagh, K.	F408, SA408	Kim, D. Jae	SU226, SU227
Jin, J.	SA514	Kalkwarf, H.	F004, SA004	Kawada, N.	SU276	Kim, D. Yoon	SU233
Jin, L.	SA111	Kalkwarf, H. J.	M017, M064	Kawaguchi, A.	SU085	Kim, E.	M209
Jirik, F. R.	SU047	Kalla, S. E.	SA217, SA241	Kawaguchi, H.	1006, 1014, 1016, 1047, 1139, F125, M446, SA034, SA125, SU033	Kim, E.	M340
Jo, H.	1182, F166, F450, SA166, SA450, SU045	Kallinen, M.	SU339	Kawahara-Baccus, T.	1177	Kim, E.	M471
Jo, M.	SU115	Kallio, P. J.	SU161				M523
Jo, M. J.	M023	Kalliovalkama, J.	M470				SU154
		Kalra, S. P.	1048				
		Kamao, M.	M274, M291, M333, M520				

(Key: 1001-1228 = Oral, F = Friday Plenary poster, SA = Saturday poster, SU = Sunday poster, M = Monday poster, WG = Working Group Abstract)

Author Index

ASBMR 27th Annual Meeting

Kim, G.	M245	Kizaka-Kondoh, S.	1007	Kousteni, S.	1098, 1116, F401,	Kurasawa, K.	SA298
Kim, G. S.	SA223	Kjobli, E.	SA252	M062, SA401, SU019, SU264		Kurihara, N.	1207, 1217, F275, F464,
Kim, G. Su	SU226, SU227	Klaushofer, K.	1175	Kovacs, C. S.	M498		SA275, SA464, SA497
Kim, H.	1128	Klaushofer, K.	SU470	Koyama, T.	SU426	Kurimoto, P.	M146, SU221
Kim, H.	F247, SA247	Kleerekoper, M.	SU002	Kozai, K.	SA196	Kurimoto, P. S.	SU012
Kim, H.	F391, SA391	Klein, G. L.	SU060, SU475	Kozlow, W.	SU526	Kurland, E. S.	M111, SA385
Kim, H.	F476, SA476	Klein, M.	1218	Kraemer, W. J.	M144	Kuroda, R.	1066, M163, M200
Kim, H.	M002	Klein, M. J.	M126	Kraenzlin, C.	SU144	Kuroda, T.	M008, M009, SU006
Kim, H.	M002	Klein, R. Frederick	1031, SA107	Kraenzlin, M.	SA350, SU166	Kurosaka, M.	1066, M163, M200
Kim, H.	M175	Kleinmond, C.	F353, SA353, SU352,	Kraenzlin, M. E.	SU142	Kurosawa, H.	1052, M165, SU462
Kim, H.	M175		SU442	Krahn, J.	SU372	Kurth, A. A.	SA403, SU094, SU101
Kim, H.	M240	Klinkenberg, K.	M232	Krakow, D.	1017	Kuznetsov, S. A.	SU031
Kim, H.	M245	Klobucar, A.	SA390	Krall, E. A.	M307	Kvalheim, G.	SU205
Kim, H.	M340	Kmita, M.	M049	Krane, S. M.	SA063	Kvern, B.	M310, SU386, SU387
Kim, H.	SA136	Knaack, D.	SA015	Krapf, R.	SU429	Kvien, T.	M389
Kim, H.	SU286	Knackstedt, M.	SU363	Kream, B.	1026, 1212, F229, SA229	Kwak, H.	M002, M341, SU350
Kim, H.	SU286	Kñallesvsky, A.	SA324	Kream, B. E.	1097, M187	Kwok, S.	M040, SA164
Kim, H. Jin	SA400	Knapp, S.	F408, SA408	Krebsbach, P.	M038	Kwok, T.	SA296, SU003
Kim, I.	SA514	Knecht, H.	M452	Kreder, H.	M382	Kwon, S.	SU493
Kim, J.	SU183	Kneissel, M.	SU209	Kreeftenberg, H.	SU155		
Kim, J. T.	SU066	Knight, C. B.	SU106	Krege, J. H.	1223, M404		
Kim, J. Young	SA400	Knipstein, B.	M064	Kreikemeier, R.	SU394		
Kim, K.	1005	Knold, B.	M386	Kreisel, T.	SU377	Labarthe, F.	M268
Kim, K.	M488, SA175	Ko, H.	SU082	Kremer, R.	1202, F499, SA499	Labat, M.	SU254
Kim, K.	SA422	Ko, J.	M240	Krenak, L.	SU115	Lacey, D.	M192
Kim, K.	SU373	Ko, S.	M245, SA285, SU111, SU449	Krenning, E. P.	SU320	Lacey, D. L.	1082
Kim, M. S.	F249, M247, SA249	Koay, M. Audrey	SA336	Kriauciunas, A.	SU281	Lacey, D. L.	M026, SA130
Kim, S.	1120	Kobayashi, M.	M201, M321, SU021,	Krieg, M.	SA332, SA350, SU166,	LaCroix, A.	F179, SA179, SA352,
Kim, S.	M118		SU023		SU168		SA430
Kim, S.	M175, M253	Kobayashi, S.	SU441	Krieg, M. A.	F096, SA096	Ladinsky, G. A.	1055, M295
Kim, S.	M341	Kobayashi, T.	1034, SU395	Krieger, N. S.	M222, SU258	Lafforgue, P.	M349
Kim, S.	M430	Kobayashi, Y.	M244, SA274	Krishnan, G.	F202	Lafuma, A.	SU416
Kim, S.	M430	Kobyliansky, E.	M314	Krishnan, G.	M206	Lagerholm, S.	M109
Kim, S.	SA514	Kocher, M.	M354	Krishnan, G.	SA202, SA427	Lai, B.	SU005
Kim, S.	SU183	Koczon-Jaremkko, B.	SA375	Krishnarajah, G.	M278	Lai, B. M. H.	SU186
Kim, S.	SU197	Kodaira, K.	SA161	Kriss, M.	1071	Lai, B. Ming Hei	SU188, SU191
Kim, S.	SU211	Koedam, M.	M250	Kristijan, K.	SA466	Lai, J. S.	SU118
Kim, S.	SU236	Koerts, K.	SU155	Kristo, C.	SA369	Lai, L. Pui.	SU042
Kim, S.	SU350	Kogaki, S.	1085	Kroeger, K.	M264	Laib, A.	M069
Kim, S.	SU373	Koh, J.	M038	Kröger, H.	1131, M139, M141	Laing, E. M.	M020, M021, SA150
Kim, S.	SU449	Koh, J. Min	SU226, SU227	Kröger, H. Johannes	SA418	Lam, H.	F185, M217, SA185
Kim, S. Y.	SU066	Kohavi, D.	M491	Kroger, H. P.	M289	Lambert, L.	M290
Kim, S. Yoon.	SU226, SU227	Kohler, T.	SA109	Kronenberg, H. M.	1002, 1034, F170,	Lambert, L. C.	M305
Kim, T.	M253, SU197	Kohlwey, L.	SU443		M052, SA170, SU038	Lamolle, S.	SA045
Kim, T. S.	SU122	Kohn, C. W.	SU513	Krueger, D.	1177, M068, M083,	Lamothe, B.	1069
Kim, Y.	M176	Kohn, S.	SU298		M281, SU425, SU460	Lamotta, A.	M353
Kim, Y.	M209	Koide, M.	SU301	Kruk, M.	SA123	Lamy, O.	SU168
Kim, Y.	M471	Koike, T.	SA017, SU441	Krumdieck, C.	SU074	Lancaster, E. A.	SU430
Kim, Y.	SA354	Koistinen, A.	M139	Krumholz, H. M.	1077	Land, C.	1088, F440, SA440
Kim, Y.	SA451	Koizumi, M.	F074, SA074, SU116	Kruse, H. P.	SU413	Lander, E. S.	M104, M105
Kim, Y.	SU154	Kojima, H.	M168	Krykiewicz, E.	M480	Landis, B.	1065
Kim, Y.	SU211	Kojima, T.	SA488, SU068	Krystal, G.	M259	Landoll, J. D.	1130
Kim, Y.	SU449	Kokubu, C.	1181	Ku, S.	SU183	Lane, J. A.	SU496
Kim, Y. Kwang	F051, SA051	Kolatkhar, N.	SA312, M330	Kua, H.	M225	Lane, N.	F086, F370, M130, SA086
Kimata, M.	SU051	Koller, B.	M093	Kubo, S.	M163	Lane, N.	SA370
Kimmel, D.	1221, F414, M402,	Koller, D. L.	1108, SU176	Kubodera, N.	M520	Lane, N. E.	M046, SU067
	SA414, SU368, SU393	Kolta, S.	M288, SA426	Kuboki, T.	SU034, SU062	Lang, D. Hammer	M112
Kimoto, S.	M205	Koltz, P. F.	1215	Kubota, S.	SU034	Lang, P.	SA089
Kimura, A.	F032, SA032	Komarova, S. V.	1148	Kubota, T.	1181, M485	Lang, T.	M051
Kindblom, J. M.	1129, SA006	Komatsu, Y.	F028, SA028, SU375	Kucharski, C.	SU202, SU215	Lang, T. F.	1135, 1172, SU467
Kindle, L.	1071	Kometani, M.	SU270	Kucharski, C. Maria	SU454	Langdahl, B.	F410, SA410, SU028
Kindmark, A.	M107, M114, SU187	Kominsky, S.	1126	Kuchuk, N.	F351, SA351	Langdahl, B. L.	1210, M119, SA162
King, A.	F317, SA317	Kominsky, S. L.	F156, SA156	Kudo, A.	SA216	Langer, F.	M318, M398
King, A. B.	1078	Komm, B.	SA431	Kudo, I.	SA326	Langhammer, A.	SA300
Kingery, W. S.	SU383	Komm, B. S.	1021, M394	Kudo, H.	F125, SA125	Langman, C. B.	SU401, SU490,
Kiniklis, G.	M374, SA377	Komori, H.	SU055	Kugai, N.	SU107		SU492
Kinnaert, E.	SA075	Komori, T.	1014, M152	Kugimiya, F.	1014, 1139, SU033	Languino, L. R.	M059
Kinney, J.	F370, SA370	Komulainen, M. Helena	SA418	Kujala, U.	F007, SA007	Lanino, E.	M436
Kinney, J. H.	SU067	Kondo, H.	1096, 1174	Kukuljan, S.	F419, SA419	Lankford, J.	SA284
Kipersztok, S.	SU517	Kondo, S.	SA054	Kulak, C. A. M.	SU164	Lanske, B.	1164, F035, SA035
Kirby, H.	1082	Kondo, T.	M028, SA203, SA209,	Kullessa, H.	1026	Lantz, R. Clark	SU489
Kirchbichler, A.	SU352		SU519	Kulkarni, A. B.	1192	Laor, T.	M017
Kirilov, M.	1101	Konger, R. L.	1215	Kulkarni, N. H.	F437, SA437	LaPlante, K.	SU258
Kirkland, M. A.	M266	Konno, N.	SU395	Kulkarni, P. M.	F425, SA425	Lapointe, R.	M522
Kirkwood, K. L.	SU099	Kontulainen, S.	M101	Kumar, A.	F437, M219, SA437	Laporte, S.	F499, SA499
Kishikawa, K.	SU276	Kontulainen, S. A.	1127	Kumar, E. G. T. V.	M270	Lappe, J. M.	F358, M279, SA358
Kita, K.	M303	Kööbi, P.	M470	Kumar, R.	F459, SA200, SA455,	Laredo, J.	SU089
Kita, K.	SU315	Kopchick, J. J.	1199		SA459, SA498, SU500, SU512	Laroche, N.	M421
Kitahara, K.	1052, M165, SU462	Kopecek, J.	M420	Kumar, S.	F199, F232, F234, F236,	Larrosa, M.	SA342, SU461
Kitase, Y.	SA285	Kopeckova, P.	M420		SA199, SA231, SA232, SA233,	Larson, E. A.	1031, SA107
Kitaura, H.	F244, F247, M259,	Korlagunta, K.	SU432		SA234, SA235, SA236	Larsson, T. E. M.	1165, F138, F442,
	SA244, SA247, SA278	Kortesidis, A.	M236	Kumar, T. R.	1043, 1100		SA138, SA442
Kitazawa, R.	M028, SA203, SA209,	Kostakis, P.	SA259	Kumar, U.	SA487	Larzenius, E.	M033
	SU519	Kostenuik, P.	1082, 1128, 1226, SA357,	Kume, M.	M008, M009, SU006	Lascau, V.	SU024
Kitazawa, S.	M028, SA203, SA209,		SU295, SU304, SU451, SU452, SU453	Kung, A.	SA111, SU005	Lascau-Coman, V.	SA036
	SU519	Koszewski, N. J.	SA502	Kung, A. W. C.	M208, SU186,	Lassova, L.	1022
Kittaka, A.	SU110	Kotadiya, P.	SA238, SA239		SU188, SU191	László, K.	SU234
Kitzis, A.	M057	Kotha, S.	1093, 1111	Kuntz, J.	M444	Lattmann, R.	SA207, SU270
Kiviranta, I.	SU339	Kotowicz, M. A.	F319, SA319	Kuperwasser, C.	SA071		

(Key: 1001-1228 = Oral, F = Friday Plenary poster, SA = Saturday poster, SU = Sunday poster, M = Monday poster, WG = Working Group Abstract)

ASBMR 27th Annual Meeting

Author Index

Lau, A. G.	SA357	Lee, W.	SA514	Li, X.	1113, 1149	Liu, H.	M405
Lau, E.	M391, SU003	Lee, Z.	M002	Li, X.	1226, F204, SA204	Liu, J. Chang	SU124
Lau, H.	SA111	Leeming, D.	F074, SA074, SU116,	Li, X.	M113, M199	Liu, L.	M005
Lau, K. H. W.	SA508, SU219		M241	Li, X.	SU304, SU451, SU452	Liu, L.	SA246
Lau, K. Hing William	SU229	Leet, A.	SU031	Li, Y.	M260	Liu, L.	SU130
Launay, J. Marie.	M486	Lefker, B. A.	M395, M419	Li, Y.	SA217	Liu, M.	1002
Launer, L.	SU334	Lefkowitz, R. J.	SA480	Li, Y.	SA394	Liu, M.	F437, SA437
Laurence, J.	M445	LeGates, J.	SU076	Li, Y. Ping	SU277	Liu, M.	SU099
Laurie, D.	SA522	Legrand, E.	SA378	Lian, J.	M188	Liu, N.	M023, SA069
Laviano, A.	SU125	Legrand, O.	Su138	Lian, J. B.	1013, 1015, 1021, 1030,	Liu, N. Q.	F135, SA135
Lavigne, J. R.	M482	Legré, V.	M349		1053, F212, M058, M059, M175,	Liu, P.	1062
Law, B.	1158	Lehesjoki, A. E.	SA099		SA212, SU228, SU248	Liu, S.	1026, SA144
Lawson, A.	1082	Lehmann, T.	SA217	Liang, B.	SA029	Liu, W.	1068
Lawson, M. A.	M351	Lehmkuhl, L.	M095	Liang, P.	F199, F234, SA199, SA233,	Liu, X.	1051
Lazarenko, O.	SU242	Leigh, C.	M350, SU412		SA234	Liu, X.	1194
Lazaretti-Castro, M.	SA447	Leininger, R.	SU214	Liberman, U. A.	M356	Liu, X.	SU245
Lazarov, M.	F461, SA461, SU214	Leliott, J.	M053	Libicher, M.	M383	Liu, Y.	1019
Lazell, R.	SU476	Lemaçon, A.	SA495	Libouban, H.	SA378	Liu, Y.	M027
Le Bihan, E.	SA115	Lemaire-Hurtel, A. S.	M255, SU511	Licari, A.	M372	Liu, Y.	M189
le Henanff, A.	SU495	Leman, C.	M376	Lichinitser, M.	SA073	Liu, Y.	M238, SA191
Leach, B.	M468	Lemineur, G.	F345, SA345	Lichtenberg, S.	SA020	Liu, Y.	F244, SA244
Leal, J.	SA065	Lemmi, M.	M462	Lichtler, A.	1026	Liu, Y.	SU455
Leary, E. Teng	SU160, SU163	Lems, W.	M389	Lichtler, A. C.	1186, F138, F229,	Liu, Y. Jun	M108
Lebecque, P.	M325, M327	Lems, W. F.	SU486		M177, SA138, SA229	Liu, Z.	F133, SA133
LeBlanc, A.	1172	Lengner, C. J.	1021	Lichtman, J. H.	1077	Liu-Léage, S.	M373, M412, M433
LeBlanc, A. D.	1171	Lenox, M.	SA033	Lie, A.	SA283, SU207	Livi, R.	SA118
LeBoff, M.	F179, SA179, SA352,	Lensmeyer, G.	1177	Lieberman, J. R.	F135, M023,	Livingston-Carr, J.	SA302
	SA430	Lentzsch, S.	SU201		SA069, SA135, SU115	Livshits, G.	M314
LeBoff, M. S.	M065, M155, M330,	Leof, E. B.	SA280	Liebold, A.	M232	Lix, L. L.	SU329
	M448, SA312, SA473, SU087,	Leonard, M.	F004, SA004	Liese, S.	1162	Ljunggren, O.	M278, SA303, SA510,
	SU337, SU434	Leonard, M. B.	1060	Liew, S.	F090, SA089, SA090,		SA512, SU187, SU524
Lebovitz, J.	F264, SA264	Leoncini, G.	SA118		SA091, SU043	Lloyd, N. E.	SU503
Lecka-Czernik, B.	SU242	Leong, W.	SU231	Liew, Y. Ying	SA027	Lo Cascio, V.	M060, M461
Leder, B. Z.	1107	Lepescheux, L.	SA027	Lightfoot, S. A.	SU384	Locklin, R. M.	M351, SA064
Ledit, A.	M444	Leppänen, O.	F181, SA181, SA184	Lightwood, D.	1082	Loewy, A. P.	1004, M173
Lee, A.	M384, M385	Lerer, T.	SU478	Lilleeng, S. E.	SA300	Loh, L.	M295
Lee, B.	1017, 1032, F030, F053,	Lerner, G.	SU394	Lim, G. C.	SA434, SU466	Lohman, T.	F179, SA179, SA352,
	F214, SA030, SA053, SA214	Lerner, M. R.	SU384	Lim, J.	SA224		SA430
Lee, B.	M471	Lerner, U. H.	SU288, M154, SU207,	Lim, S.	M278	Lokshin, A.	SU201
Lee, B.	SU154		SU208	Lim, S.	SA422, SA451, SU236,	Lombas, C.	SA324
Lee, B. J.	SU371	LeRoith, D.	1193		SU252, SU256	Long, C.	SU290
Lee, B. S.	SA238, SA239	Leroy, C.	SA485	Lim, Y.	SA226	Long, F.	1153, SU268
Lee, C.	SA044	Leshem, Y.	M184	Lim, Y. B.	1005	Long, R. K.	SA147, SU221, SU262
Lee, C.	SU487, SU490, SU492,	Leslie, W. D.	1037, F077, SA077,	Lima, F.	SU069, SU265	Longo, K. A.	M206
	SU494		SU327, SU328, SU329, SU372	Lin, A. S. P.	M045	Longo, M.	M436
Lee, C. M.	M159	Lespesailles, E.	SU193, F345, SA345	Lin, H. Shu	SA027	Longobardi, L.	1065, F160, SA151,
Lee, D.	SU001	Lester, M.	M144	Lin, S.	SU127, SU131, SU132		SA160
Lee, D.	SU183	Létourneau, R.	M522	Lin, W.	M265	Lonn, L.	SU521
Lee, D.	SU373	Letuchy, E. M.	M019	Lin, W.	SU171, SU173	Looker, A.	M267
Lee, F. Y.	SA167, SA263	Leung, P.	SU003	Lin, X.	M128	Loomis, C. A.	1185
Lee, F. Y.	SU224	Levasseur, R.	SA439	Lin, X.	SU131	Loomis, R. M.	M014
Lee, H.	1107	Levenson, A. S.	SU119	Lin, Y.	SU353	Lopez, E.	SA240
Lee, H.	M340	Levine, A. L.	SU513	Lin, Y. Ling	SU294	Lopez Franco, G. E.	M050, M438,
Lee, H.	SA044	Levy, J.	M491	Lin, Z.	SA043		SU020
Lee, H.	SA167, SA263	Levy, M.	SU185	Lindberg, M.	SU524	López-Bernus, A.	SA316
Lee, H.	SA422	Levy, S. M.	M019	Lindeman, C.	M467	Lorch, G.	1215
Lee, H.	SU224	Lewiecki, E. Michael	F425, M350, SA425,	Linden, C.	1011, F187, SA187	Loredo-Osti, J. C.	1106
Lee, I.	M084		SU415, SU455	Lindsay, J. R.	SA456	Lorenc, R.	1210, M480, SU484,
Lee, I.	M340	Lewiecki, M.	F429, SA429	Lindsay, R.	1079, 1180, M013,		SA123
Lee, J.	M002	Lewinski, A.	SA123		M293, M367, M393, SA405	Lorentzon, M.	1046, 1129, F009, SA006,
Lee, J.	M118	Lewis, C. E.	1135, F179, F338,	Lindsey, D.	SU383		SA009, SA510, SA512, SU521, SU522
Lee, J.	F306, SA306		SA179, SA338, SA352, SA430	Ling, J.	SA284	Lorenzo, J.	1212
Lee, J.	SU256	Lewis, R.	1008	Linglart, A.	1036	Lorenzo, J. A.	1184, 1189, F374, SA256,
Lee, J. Dong	SU056, SU233	Lewis, R. D.	M020, M021, SA150	Linglart, A.	F491, SA491		SA374, SA375, SU212
Lee, K.	SA320	Li, A.	SU174	Linhardt, R. J.	1104	Lorraine, J.	F425, SA425
Lee, K.	F374, SA374	Li, B.	M225	Link, C.	M308	Løseth, O. Petter	SU046
Lee, K.	F391, SA391	Li, B.	F704, SA074	Link, T. M.	SU324	Lotinun, S.	F389, SA389
Lee, K.	SU211	Li, B.	SU231	Linkhart, T. A.	M171, SA145, SA148	Loud, K. J.	M136
Lee, K.	SU252	Li, C. Y.	SU456	Linn, T.	M181	Louie, M.	SU130
Lee, K.	SU323	Li, E.	SU277	Lioté, F.	M486, SU032	Lovett, J.	F313, SA313
Lee, K. Ho	SA400	Li, F.	SU099	Lippuner, K.	M275, M452	Lovitch, D.	F023, SA023
Lee, O. Sun	SU226, SU227	Li, G.	M226, M227	Lips, P.	1134, F349, F351, M275,	Lowe, V.	1098
Lee, S.	1066	Li, H.	1186, M177		M401, SA349, SA351,	Löwik, C. W. G. M.	1029
Lee, S.	1189	Li, J.	1039		SA504, SU223	Lozano, C.	SU354
Lee, S.	M163	Li, J.	1108	Lips, P. T.	M353	Lozano-Tonkin, C.	SA402
Lee, S.	M175	Li, J.	M103	Listrat, A.	F190, SA190	Lu, B.	M419
Lee, S.	M176	Li, J.	M192	Litscher, S.	SU020	Lu, C.	F154, SA154
Lee, S.	M200	Li, J.	SA130	Little, C. B.	SU048	Lu, G.	F275, SA275
Lee, S.	SA167	Li, J.	F356, SA356	Little, W.	M018	Lu, J.	M515
Lee, S.	SA223	Li, J. M.	M248	Litvin, J.	SU077	Lu, L.	SA018
Lee, S.	SA451	Li, M.	M395, M419	Litwack-Harrison, S.	F325, SA325	Lu, S. S.	1180
Lee, S.	SU224	Li, M.	SA394	Liu, C.	SA042	Lu, X.	SU238, SU241
Lee, S.	SU236	Li, M.	SU023, SU040, SU107,	Liu, D.	M101	Lu, Y.	1111
Lee, S.	SU286		SU271	Liu, D.	SU220	Lu, Y.	1172
Lee, S. Keun	1152	Li, P.	1196	Liu, G.	SA034	Lu, Y.	SU113
Lee, S. Kyeong	SA256, SA375	Li, Q. N.	1117	Liu, G.	SU129	Lu, Z.	M339
Lee, S. Kyu	SA400	Li, X.	1028	Liu, G.	SU450	Luca, V.	SU427
Lee, W.	M176	Li, X.	1062	Liu, H.	M265	Lucani, B.	M416, SU378, SU379

(Key: 1001-1228 = Oral, F = Friday Plenary poster, SA = Saturday poster, SU = Sunday poster, M = Monday poster, WG = Working Group Abstract)

Author Index

ASBMR 27th Annual Meeting

Lucas, C.	SA426	Maekawa, S.	F433, M313, M431, SA433	Marín, F.	F093, M388, M412, M434, SA092, SA093, SA432	Mavroeidi, A.	SU437
Lucas, D. A.	M186					Maye, P.	F229, SA229
Lucas, E. A.	M335, SU044, SU246, SU430, SU432	Maes, C.	1067, 1151	Marini, F.	SA108, SA121	Mayer, J.	M409, SU152
Luciani, M.	M436	Magaziner, J.	M330, SU337	Mariñoso, M.	M091, SA379	Mayer, U.	SA024
Luckey, M.	M346	Maggi, S.	F301, M292, SA301	Mariotti, S.	M462	Mazzaro, E.	M459
Luckey, M. M.	M085, SU321	Magland, J.	M079	Marquis, R. W.	SA231	Mazzuoli, G.	SA322
Ludwig, A.	F039, SA039	Magne, N.	SA075	Marriott, T. B.	I222	Mbalaviele, G.	1063, 1109
Lui, L.	F297, F323, M285, SA297	Magni, C.	SA186	Mars, M.	M143	McAlister, W. H.	1166, M442, M443, SA452
Lui, L.	F315, SA315	Magno, C. L.	F249, SA249	Marsh, D.	M226		
Lui, L.	SA323	Magnus, J. H.	M299, M304	Marshall, G. W.	SA163	McAlpine, K. E.	M137
Lui, L. Yung	I039	Magosch, P.	SA020	Marshall, L.	M290, SA343	McBride, D. J.	SU178, SU195
Luisetto, G.	SA445, SU458	Magowan, S.	M276, M367, SA405, SA407, SU405, SU406	Marshall, L. M.	1135, F338, M305, SA338	McCabe, G. M.	M003
Luk, K.	SA111					McCabe, G. P.	M007, SU011
Lukaacs, J. L.	SU002	Magyar, C. E.	SU499	Marshall, S. J.	SA163	McCabe, J.	SU304, SU451
Lukaszkievicz, J.	M480, SA123	Mahajan, S. Suhas	SU432	Marshall, T. A.	M019	McCabe, L. D.	M003
Lumeng, L.	F110, SA110	Mahaney, M. C.	SU177	Martel, J.	M385	McCabe, L. R.	F399, SA399, SU243
Lumpkin, C. K.	M005, M043	Mahboubi, S.	F004, SA004	Martineti, V.	M362	McCaigie, M.	M226
Luna, S.	SA436	Maher, N.	M297	Martin, B. R.	M007, M517	McCarthy, A. Desmond	SU196
Lund, M. T.	F321, SA321	Mahllos, J.	I061	Martin, D.	M192	McCarthy, M.	F194, SA194
Lund, R.	SA519	Mahon, M. J.	F491, SA491	Martin, P.	I001	McCauley, L. K.	F192
Lundberg, P.	SU207, SU288	Mahonen, A.	F007, M141, SA007	Martin, R.	I008	McCauley, L. K.	M182, M487, SA192, SA195
Lundblad, J. R.	I031	Mailhot, G.	SA036, SU024, SU036	Martin, S. W.	SU446		
Lundeberg, J.	M114	Maimous, E. G.	SU060, SU198	Martin, T.	1190, M448	McClain, D.	SA469
Lundgren, I.	SU207	Mairon, N.	M346, M347, SU410, SU415	Martin, T. J.	F437, M157, M241, M262, SA437, SU095	McClearn, G. E.	M112
Luo, G.	SU172	Maiti, A.	SU515	Martín Forero, E.	SU354	McClintock, C.	1089, SU482
Luo, H. Mei	SU365	Majeska, R. J.	F072, SA072	Martin Garcia, A.	M400	McCloskey, E.	SU402
Luo, W.	M237	Majima, T.	SU375	Martín Mola, E.	SU354, M388, M434	McCloskey, E. V.	1009, F079, SA079
Luong-Nguyen, N.	SA215	Majithia, A.	I185	Martineti, V.	SA121	McClung, M.	F429, SA429
Luque-Recio, F.	SU374	Majumdar, S.	F086, M069, SA083, SA086, SU221, SU324	Martinez, A.	SU421	McClung, M. R.	M347, M354, M359
Luthen, F.	M232			Martinez, A. F.	M252	McCrea, J. D.	SA292
Luthman, H.	M033, M109, M116	Mak, K.	I003	Martinez, G.	M477, M478	McCulloch, C.	M365
Luttrell, L. M.	SA480	Makhijani, N. S.	SU203	Martinez, J.	SA402	McDaniel, L.	I075
Lutz, W.	SA498	Makin, A. J.	M334	Martinez de Osaba, M.	SA388, SU421	McDonald, J. M.	SA171, SA228, SU100, SU222
Luzi, E.	SA108	Makitie, O.	SA099, SU477			McDonald-Blumer, H.	M071
Luzzi, V.	SU160	Makovey, J.	SA113	Martínez-Hernández, P.	SA316	McGuckin, B. L.	F358, M050, SA358
Ly, C.	SU095	Makuch, L. A.	SU120	Martini, G.	M016, M292, M414, M416, SU367, SU378, SU379	McGuinness, A.	SU332
Lyles, K. W.	F334, SA334	Malaise, M.	SU104			McGunagle, D.	SA333
Lynch, C. M.	SA248	Malavolta, N.	F122, SA122	Martinen, E.	SA099	McGurk, C.	SU402
Lynch, N. O.	M352, SU388	Malek, L. T.	M425, M426	Marucco, A.	SA445	McHugh, K. P.	M243, SA257
Lyngstadaas, S.	SA252, SA045, SU205	Malkin, I.	M314	Maruyama, S.	SA024	McKay, H.	M101
		Mallet, E.	SA485	Maruyama, T.	F062, SA062	McKay, H. A.	I127
Lynn, H.	SA296	Mallmin, H.	SU187	Marvin-Bivens, C.	I035	McKee, M. D.	SA462
Lyrítis, G. P.	M374	Malluche, H. H.	F242, SA242, SA502	Masanauskaitė, D.	F410, M350, SA410, SU412, SU413	McKenna, B.	SA492
Lyrítis, G. Panagiotis	SA377, SU471					McKenna, C.	I213
Lyssy, A.	SA403	Malone, D.	M083	Masarachia, P. J.	SU393	McKenna, C. R.	I216
		Malouf, D.	F262, SA262	Mascarenhas, L.	F138, SA138	McKenna, R.	SU526
		Manabe, T.	M032, SU015	Mascarenhas, M. R. G.	SU507	McKinlay, J. B.	M308
		Mancini, L.	SU041	Mashiba, T.	M032, SU015	McKinney, K.	SU494
		Mandadi, K.	SU013	Masi, L.	SA108, SA117, SA118, SA121, SA141	McLaughlin, M. Kathleen	SU163
		Mandel, D. R.	SA294			McLean, R. R.	F309, SA309
		Manen, D.	F397, M121, M218, SA397	Masinde, G.	SA105	McLellan, A. R.	F331, SA331
				Mason, R. S.	M195, SA060	McMahon, D.	SU129, SU361, SU476
		Maness, N. O.	SU430	Mason-Savas, A.	SU036	McMahon, D. J.	M111, M322, SA385, SU108
		Mangine, A.	M189	Massari, F. E.	SA324		
		Mango, A.	I083	Massin, P.	SU299	McManus, J. F.	1097, 1161
		Manicourt, D. H.	SA420	Mastaglia, S. R.	M072	McMichael, B.	SA238, SA239
		Manigrasso, M. B.	M166	Masud, T.	M298	McNaught, T.	SU167
		Manivet, P.	SU523	Masunari, N.	SU338	McPherson, J.	M428
		Manjubala, I.	I175	Masuyama, R.	I067	McQuillian, C.	SA318
		Mankani, M. H.	SU031	Matemba, S.	SA283	Meada, N.	SA196
		Mann, E.	SU347	Mathew, S.	F016, F021, SA016, SA021	Meays, D. R.	1173, M156, SA059
		Mann, K. A.	SU112			Mecholsky, J. J.	M145
		Manning, C.	SU491	Mathey, J.	M327	Medich, D. L.	SA098
		Manning, C. A.	M243	Mathian, A.	SU488	Mediratta, A.	SU129
		Manolagas, S.	I092, I098, 1116, 1140, 1197, F286, F289, F367, F401, M062, M160, M417, SA219, SA286, SA289, SA367, SA401, SU019, SU264	Mathias, R.	M481	Meeder, P.	M383
				Mathieu, J.	M308, M339, SA523	Mehrotra, M.	SA169
				Mathisen, A. L.	I083	Meier, C.	1137, SU142, SU144
				Matkovic, V.	1130, M003	Meinhardt, U.	SU142, SU144
				Matsubara, T.	1146, M190, M204	Mellibovsky, L.	M122, M169
				Matsuda, A.	SA024	Mello, M. Tulio	SU440
				Matsuda-Abadini, M.	M481	Mellström, D.	1046, 1129, F009, SA006, SA009, SA303, SA510, SA512, SU187, SU522, SU524
				Matsumoto, A. M.	I198		
				Matsumoto, K.	SU107	Melo-Gomes, J.	M388, M434
				Matsumoto, N.	I163	Melton, L. J.	1009, 1010, 1074, 1075, M267, SU151, SU464
				Matsumoto, T.	1066, 1123, F509, M200, SA361, SA509, SU026, SU102	Melton, III, L. Joseph	SA348
						Melton, M.	SU159
				Matsuo, K.	F258, SA211, SA255, SA258, SU007, SU287	Même, S.	SA186
						Men, P.	SU450
				Matsusaki, T.	SA029	Menaa, C.	F264, M061, SA264
				Matsuura, M.	SU324	Ménard, D.	M522
				Matsuyama, M.	SU050, M205	Menéndez-Arango, J.	SA402
				Matteo, J. J.	SA128	Menn, S.	SU175
				Mattioli, P. M.	SA155	Menon, Y.	SU345
				Mattiuzzi, G. N.	SU096	Mentaverri, R.	M255, SU511, SU511
						Menzies, D.	I086
				Matusik, H.	M480	Merabet, Z.	SA058, SU084
				Mautalen, C.	M073		

(Key: 1001-1228 = Oral, F = Friday Plenary poster, SA = Saturday poster, SU = Sunday poster, M = Monday poster, WG = Working Group Abstract)

ASBMR 27th Annual Meeting

Author Index

Mercado, M.	M184	Missana, L. R.	M030	Moreau, I. A.	F435, M076, M409,	Murai, J.	M034, SU090
Merle, B.	SU075	Missbach, M.	1179, SU270	M415, SA435, SU128		Murakami, M.	F125, SA125
Merlotti, D.	M016, SU367, SU379	Misurski, D. A.	1223, M406, M407,	Moreau, M.	SA378, SU299	Murakami, S.	1023
Merritt, J. Simon	M089		M410	Morello, R.	F053, SA053	Murasawa, S.	1066
Merville, M.	SU104	Mitchell, B. D.	F100, SA100, SU178,	Moreno, A.	M477	Muratore, M.	SU458
Mesenbrink, P.	SA314		SU195	Moreno, E.	M477	Muratori, F.	F470, SA470
Messina, C.	M436	Mitchell, C.	SU330, SU331	Moreno, L. D.	SU133	Murer, H.	SA455
Metge, C. J.	SU327, SU328, SU329	Mitchell, J.	SU042	Morgan, D.	SU384	Murphy, A.	1216
Metge, C. Jane.	SU372	Mitsuhashi, H.	SA054	Morgan, E. F.	SU092	Murphy, S.	SA281
Metzger, D.	F509, SA509	Mitton, D.	M288, SU089	Morgan, K.	1106	Murphy, T. C.	F166, SA166, SU216
Meunier, P. J.	1084, 1090, F096,	Miwa, M.	M163, M200	Morgan-Bagley, S.	1128	Murphy, W. A.	M126
	M087, SA096	Miyabara, Y.	M008, M009, SU006	Mori, H.	SU276	Murray, E. J. B.	M381
Meury, T. R.	SA213, SU234	Miyagi, I.	M329	Mori, K.	M028, SA203, SA209	Murray, M. A.	SA469
Meyer, H. E.	M271, SA346	Miyakoshi, N.	F433, M311, M313,	Mori, S.	M032, SU015	Murray, T. M.	SA308
Meyer, M. H.	SA458		M431, SA433, SU439	Mori, T.	F172, SA172	Murrills, R. J.	SA128
Meyer, R. A.	SA458	Miyamoto, T.	F258, SA258, SU054,	Mörické, R.	M413	Musacchio, E.	M451
Meyers, V. E.	SA171, SU222		SU072, SU282, SU287	Morii, H.	SA082	Muscarella, L.	F122, SA122
Mezaki, Y.	SU259	Miyamoto, Y.	M249, SA037	Morin, S. N.	SU341	Muschler, G. F.	M164, M230, SU255
Mezghrani, A.	SU105	Miyasaka, N.	1096	Morinobu, M.	F174, SA174	Muser, J.	SU429
Mezquita-Raya, P.	M400, SU274,	Miyata, H.	SU239	Morishima, N.	M191	Muzzin, P.	SU381
	SU374	Miyatake, H.	SU315	Morissey, C.	SU049	Myoui, A.	1024, SU090
Mi, Q. Sheng.	M456	Miyauchi, A.	F444, M042, SA444,	Morita, A.	M010, M012		
Miao, D.	1050, 1099, 1203, F453,		SU030	Morita, K.	F258, SA258, SU054,		
	SA453, SA516	Miyauchi, M.	SU063		SU072, SU282		
Micallef, J.	M142	Miyaura, C.	F062, SA062, SA063	Moriyama, K.	SU083	N'Cho, M.	F437, SA437
miccoli, p.	1167, M462	Miyoshi, N.	M041	Morley, P.	M409	Nabizadeh, F.	SU129
Michalska, D.	F356, SA356	Mizoguchi, F.	1096	Moro, L.	SU257	Nadeau, J. H.	M104, M105
Michalsky, D.	F356, SA356	Mizoguchi, T.	M244	Moroi, R.	SU277	Nadella, K. S.	1215
Michaud, K.	M405	Mizuno, A.	1096, SU040	Morony, S.	1226, SA357, SU304,	Nafstad, P.	M271
Michel, D.	M452	Mizuno, S.	M025		SU451	Naganathan, V.	SA113
Micheli, L. J.	M136	Mizutamari, M.	M254	Morris, H. A.	1097	Naganawa, T.	F142, SA142
Michigami, T.	1181, M485, SU051	Mizwicki, M. T.	SA503	Morris, H. Arthur	1161	Nagao, S.	SU050
Micsenyi, A.	SA217	Moana, E. J.	M067	Morris, M. D.	SA003	Nagaraja, H. N.	SA423
Middleton, S.	SU295	Mobley, S. L.	1130	Morrison, A.	F199, SA199	Nagata, K.	SU389
Middleton-Hardie, C.	F461, SA461,	Mocanu, V.	SU427	Morrison, N. A.	1059, 1208,	Nagata, M.	SA361
	SU214	Mochizuki, A.	M249		F249, M247, SA249, SU307	Nagpal, S.	M515
Midura, R. J.	F023, SA023	Modlesky, C. M.	M020, M021,	Morrissey, C.	SU122	Nagy, A.	1151
Mierke, D. F.	M509, SU498		M100, SA150	Mortlock, D.	F160, SA160	Nagy, T. R.	F242, SA242
Miesse, A. M.	SU362	Modrowski, D.	1220	Morvan, F.	1001, 1183	Nahar, N. Nazmun	M030
Migliaccio, S.	M436	Moedder, U. I. L.	F511, SA511	Mosekilde, L.	1227, M317, SU423,	Nair, K.	M391
Mikati, M. A.	SA449	Moelgaard, A.	SA417		SU479	Naka, H.	M010, M012
Mikkola, T.	SU339	Moeller, G.	SU419	Moses, A. M.	SA434, SU466	Nakadate, M.	SU057
Mikulec, K. Hanser	M330	Moens, P.	1103	Moses, H.	1065, F160, SA160	Nakagawa, K.	M031, M224
Mikumo, M.	SU006	Moermans, K.	1067	Mosher, D. F.	1054	Nakagawa, K.	SA198
Milanesi, L.	SU518	Moffett, A.	SA428	Mossman, E.	M354	Nakajima, S.	1181
Miles, L. J.	M110	Moffett, S. P.	1039, F323, F341,	Mouthon, G.	SU254	Nakamichi, Y.	F260, F509, SA260, SA509
Milet, C.	SA240		SA323, SA341	Móvère, S.	1199	Nakamoto, C.	M230
Milewicz, A.	SA123	Mogensen, B.	SU334	Móvère Skrtic, S.	1046, SA396,	Nakamoto, T.	F174, SA174
Miller, F.	M100	Mohammad, K.	SU526		SU521	Nakamura, A.	F479
Miller, J.	SA038	Mohammad, K. S.	1213, 1216,	Moyer-Mileur, L. J.	SA469, SU473	Nakamura, A.	M262
Miller, J. D.	M237		SU261	Mrak, E.	M246	Nakamura, A.	SA479
Miller, L.	M018, M150	Mohammadi, M.	1104	Mroczek, R.	M205	Nakamura, H.	F260, M161, SA260, SU123
Miller, L. M.	M047	Mohan, S.	1045, 1152, F102, F104,	Mucioño, L. M.	SU326	Nakamura, K.	1006, 1014, 1016, 1047,
Miller, M.	1107		F106, F183, M183, SA102,	Mudano, A. S.	SA333		1139, 1188, F125, M446,
Miller, M.	SA284		SA104, SA105, SA106,	Muedner, C.	1162		SA034, SA125, SU033
Miller, P.	M269, SA405, SU340,		SA146, SA148, SA183, SA508	Mueller, D.	SU324	Nakamura, M.	F260, SA260
	SU405, SU406	Mok, J.	SU211	Mueller, S. M.	M155	Nakamura, M. C.	M261
Miller, P. D.	1222, 1223, M378,	Moll, C.	SA352	Muentener, C.	M184	Nakamura, T.	1192
	M407, SA407, SU410	Moll, C.	SU421	Mughal, M. Zulf	SA008	Nakamura, T.	F014
Miller, R.	SA065	Möller, G.	SU398, SU407	Mughal, M. Z.	SA475	Nakamura, T.	F172
Miller, R. E.	SU448	Molloy, M. G.	SU332	Muir, M. M.	M195	Nakamura, T.	F509
Miller, S.	F429, SA429	Monegal, A.	SA388, SU392, SU421	Mujeeb, K. A.	F212, SA212	Nakamura, T.	SA014
Miller, S. C.	M048, M420, SA182,	Monga, S. P.	SA217	Mukherjee, A.	1194	Nakamura, T.	SA029
	SU300, SU450	Monjo, M.	SA045, SA252	Mulcahey, M.	M488	Nakamura, T.	SA172
Miller, T. A.	SU058	Monllau, J. Carlos	M169	Mullaney, S.	SU165	Nakamura, T.	SA509, SU071
Milligan, C. L.	M394	Monroe, D. G.	1200, M172, SA506	Mullen, C.	SU158	Nakamura, T.	SU107
Milner, R.	SU347	Montagnani, A.	M016, M414	Muller, J.	1074, M411	Nakamura, T.	SU190, SU239, SU389
Mina, M.	F210, M177, SA210	Montecino, M.	SU248	Muller, J. M.	SA278	Nakanishi, Y.	M333
Minagawa, A.	SA201	Montecino, M. A.	M188	Muller, P.	M232	Nakanishi, Y.	SU276
Minamino, N.	M496	Montemurro, G.	1102	Müller, R.	M106, M491, SA109,	Nakano, T.	M274
Minamizaki, T.	SA196	Montero, J. J.	F093, SA093		SU361, SU465	Nakao, K.	F028, SA028
Minas, K.	SU485	Montero, M.	SA436	Mulloy, A.	SA050	Nakao, K.	SU034
Minck, D.	SA431	Montrose-Rafizadeh, C.	SA427	Mumm, S.	1166, F474, M124, M442,	Nakao, K.	SU375
Minelli, R.	SU004	Moon, K.	SU154		M443, SA452, SA474	Nakase, H.	M333
Minematsu, H.	SU224	Moon, S.	SU183	Mun, H.	M460	Nakashima, A.	SA201
Minisola, S.	F122, SA122, SA322,	Mooney, S. D.	F442, SA442	Mundo, J.	SU421	Nakashima, K.	1052, 1096, 1209, F393,
	SA392	Moonga, B. S.	1043, 1100, F376,	Mundt, C. A.	1012		SA393
Minne, H.	SA432		SA376	Mundy, G.	1124, 1141, 1154, F066,	Nakatsuru, Y.	F028, SA028
Minne, H. W.	M353, SU443	Mooradian, A. D.	SA517		M054, M174, SA066, SU029, SU098	Nakayama, T.	SA029
Minnion, J.	F199, SA199	Moore, A.	1082	Muneta, T.	SU302	Nakayama, Y.	SA054
Mirams, M.	SA060, SU039	Moore, A. J.	1097, 1161	Munivez, E.	1017	Nakura, N.	F172, SA172
Mirch, M.	F472, SA472	Moore, F. D.	SU497	Munns, C.	1088	Nalepka, J. L.	M194
Mirosa, D.	SA250	Moore, K.	SA137	Muñoz, E.	SU354	Nalla, R.	F370, M130, SA370
Mirwald, R. L.	1012	Moore, T. L.	F202, SA202	Munoz, F.	F360, SA359, SA360	Nalla, R. K.	SA163
Mishima, K.	M254	Moosgaard, B.	SU479	Muñoz -Torres, M.	M400, SU274,	Nalla, R. K.	SU067
Mishina, Y.	1034	Moran, R. A.	M189		SU374	Nam, M.	M471, SU154
Mison, A.	1213	Moravits, D.	SA284	Munro, R.	SU330, SU331	Nam-Goong, I.	M209
Mison, A. P.	1216			Munsey, T. G.	1031, SA107	Namba, N.	1085

(Key: 1001-1228 = Oral, F = Friday Plenary poster, SA = Saturday poster, SU = Sunday poster, M = Monday poster, WG = Working Group Abstract)

Author Index

ASBMR 27th Annual Meeting

Namba, N.	M259	Niehrs, C.	1001	Nyman, J. A.	SU151	Olivares-Navarrete, R.	M212
Namiki, M.	SA161	Nielsen, B. Rubek	SA372	Nzeusseu Toukap, A.	SA420	Oliveri, B.	M072, M073
Nanes, M. S.	F166, SA166, SU216, SU238, SU241	Nielsen, D.	M386			Olivero-Rivera, L.	M322
Napierala, D.	1032, F030, SA030	Nielsen, M.	F321, SA321			Olivier, S.	SU104
Napoli, N.	M124, SA117	Nielsen, M.	SU046			Olmos, J. M.	SA402
Narayanan, R.	M516	Nielsen, R. H.	M157, M241, SA237			Olmsted-Davis, E.	SA040
Narla, R.	1015	Nielsen, T. Leo	SU189			Olsen, B. R.	M160
Narusawa, K.	SU190	Nielsen, W.	M386			Olsen, H. Juhl	SA162
Nashiki, K.	F479, M125, SA479	Niemeier, A. Claudius	M332			Olson, D. A.	1031, SA107
Nashimoto, M.	SA201	Nieto, I.	F093, SA093			Olczynski, W. P.	F410, SA097, SA410
Naski, M. C.	SA230, SU199	Nieuwenhuijzen-Kruseman, A. C.	SU351			Omar, M.	SA466
Nasser, P.	SA101	Nieves, J. W.	1079, M013, M393			Omar, M. A.	M363, SU359
Natarajan, R.	M115	Niewolna, M.	1213			Ominsky, M.	1082, 1226, SU295, SU304
Natt, F.	SA207	Niewolna, M.	1216			Ominsky, M. S.	SU451, SU452, SU453
Naval, E.	SA342	Niewolna, N.	SU526			Omizo, M.	M354
Naveh-Many, T.	SU472	Nifuji, A.	F393, SA393			Ong, H.	M079
Naves, M.	M476, SU322	Niger, C.	SU069, SU265			Ono, K.	M191, SU107
Navon, G.	SU061	Nii-Kohno, T.	M466			Ono, M.	SU062
Nawaz, Z.	M511	Niida, S.	SA189			Ono, N.	F170, SA170
Nawroth, P.	M383	Niikura, T.	M163, M200			Ono, Y.	SA361, SU026, SU050
Nawroth, P. P.	M456	Nikander, R.	SA178			Onoda, Y.	M303, SU315
Nayak, S.	M405	Nilsson, O.	M107			Onoe, Y.	M008, M009, SU006
Naylor, K. E.	M345	Nilsson, S.	1129, SA006			Onyia, J.	M219
Nazarian, A.	SU145	Nilsson-Ehle, H.	SA303			onyia, J. E.	F437, SA437
Neal, A.	SA333	Nindl, B. C.	M144			Oono, K.	F140, SA140
Neale, S.	SU153	Ninomiya, J. T.	M214, M215			Ophoff, J.	SU525
Nebe, B.	M232	Ninomiya, K.	F258, SA258, SU054, SU072			Opotowsky, A.	SU129
Need, A. G.	M326	Ninomiya, T.	F260, M161, SA260, SU123			Oppermann, U.	F408, SA408
Neff, L.	1114, 1150, 1183, F279, SA279	Nishida, S.	M146, SA147, SU221, SU262			Orav, J. E.	1041
Neff, M.	M086	Nishida, T.	SU062			Ordovas, J. M.	M123
Neff, M.	SU419	Nishida, Y.	M125			Orgee, J.	SU402
Negri, A. L.	M472	Nishimori, S.	M052			Oriente, P.	SU458
Negron, A.	F461, SA461	Nishimoto, M.	SA052			Orimo, H.	F362, SA362
Nehrke, K.	M222	Nishimoto, S. K.	SA052			Orito, Y.	SU441
Nell, D.	1126, F156, SA156	Nishimura, H.	1066			Orlic, I.	1027
Nelson, A.	SA001	Nishimura, R.	1146, M190, M204, SA255			Ornitz, D. M.	1104
Nelson, A. E.	SA060	Nishio, Y.	M170			Ornitz, D. M.	1195
Nelson, D.	SA001	Nishiwaki, T.	SA211			Orri, M.	M384
Nelson, D.	SA430	Nishiwaki-Yasuda, K.	SA361, SU026, SU050			Orsi, A.	SU105
Nelson, D. A.	F179, SA179, SA352	Nishiyama, T.	SA216			Ortolani, S.	M457, SU458
Nelson, J. B.	F381, SA381	Nissen, N.	M386			Orwoll, D.	SA466
Nelson, P. S.	SU049, SU122	Nissen, P. H.	SU479			Orwoll, E.	SA303, SA343, SA510, SA512, SU003, SU187, SU524
Nenseter, M.	SU380	Nissen-Meyer, L. Sophie H.	SU046			Orwoll, E. S.	1031, 1073, 1135, F338, M290., M305, SA107, SA338, SU404
Ness, A. R.	SA299	Nissen-Meyer, L. Sofie H.	SU232			Orzechowski, L.	F185, SA185
Nestlerode, C. S.	F341, SA341	Niu, Q. T.	SU027			Osborne, F.	M298
Neumann, H.	M232	Niu, T.	1212			Osdoby, P. A.	1070, 1071, SA265
Neville, M. C.	F486, SA486	Niu, Z.	1022			Ose, L.	SU380
Nevitt, M.	1038	Niyibizi, C.	SU052			Oshima, H.	SA368
Nevitt, M. C.	F315, F347, SA315, SA347	Noale, M.	F301, SA301			Oskins, J.	M489, SA427
New, S. A.	SA008	Noda, M.	1052, 1096, 1174, 1209, F014, F170, F174, F393, M152, M165, SA014, SA170, SA174, SA393, SU025, SU302			Osmond, C.	1058
Newitt, D. C.	F086, SA083, SA086	Noeldge, G.	M383			Oster, G.	M294, SU397
Newman, A. B.	M103	Noeth, U.	M231			Oteo, Á.	SU354
Newman, D. E.	SU177	Nofroni, I.	SA392			Otsubo, K.	M469
Newman, M. K.	1083, F435, M415, SA435	Noguchi, H.	F433, M313, SA433			Otsubo, O.	M469
Newton, J.	SA146	Noguchi, S.	M129			Ott, S. M.	SU049
Nezu, Y.	SU055	Noguchi, T.	SU301			Ouchi, Y.	SU190
Ng, K. Wah	M397, SU095	Nogues, X.	1210, M122, M169			Oudheusden, H. Van	SU411
Ng, M.	SA111	Nomura, C.	SA017			Oursler, M.	M172, SA158, SA506, SU010, SU285
Ng, M. Y. M.	SU186	Nomura, S.	SU057			Oursler, M. Jo	M257, SA280
Ng, W. W.	M208	Nomura-Furuwatari, C.	M031, M224			Outwater, E.	F179, SA179, SA352, SA430
Ng, W. Wai Sun	SU191	Nonaka, K.	SA082			Owan, I.	SA326, SU088
Nguemo-Djioemetio, J.	SU305	Nooka, A.	1218			Owen, C.	SU370
Nguyen, H.	SU304	Nordin, C.	M326			Owen, T. A.	M039, M419, SU035
Nguyen, K.	M427	Norjavaara, E.	1129, SA006			Owens, D. K.	M405
Nguyen, L.	F518, M518, M519, SA518	Norman, A. W.	SA503			Oxland, T.	M101
Nguyen, M.	F035, SA035	Norman, B.	SA427			Oxlund, H.	M423, SU028
Nguyen, N. D.	1138, SA329, SU314, SU342, SU343, SU344	Norquist, J.	M275, M278			Oyajobi, B.	M054
Nguyen, T. V.	1137, 1138, M066, SA113, SA329, SU142, SU144, SU314, SU317, SU342, SU343, SU344	Nöth, U.	M198			Oyajobi, B. O.	1124, 1154, F066, SA066, SU098
Nguyen-Yamamoto, L.	F499, SA499	Notini, A. J.	1097			Oyamada, A.	1066
Nicasi, A.	SU509	Notini, A. Jane.	1161			Oyarzo-Somoza, J. N.	SU489
Nicholas, S.	F179, SA179, SA352, SA430	Notomi, T.	F039, SA039			Oyesanya, R.	M523
Nichols, J.	SU356	Notoya, M.	M496			Oz, O. K.	SU527
Nicholson, G. C.	1059, 1208, F319, M266, SA319	Novack, D. Veis	F247, SA247, SA278			Ozaki, S.	1123, SU102
Nicholson, P.	M139	Novak, A.	SU388			Ozawa, H.	F260, M161, SA260, SU123
Nicholson, T.	M095, M388, M434, SA432	Novotny, R.	1177, M003			Ozdemir, J.	F032, SA032
Nickel, E. D.	SU014	Nowson, C.	F419, SA419			Ozono, K.	1085, 1181, M485, SU051
Nickelsen, T. N.	M095, M318, M398, M413, SA432	Nozaka, K.	F433, SA433				
Nickerson, J. A.	1053	Nozawa, M.	SU462				
Nicks, K. M.	SU250	Nunez, G.	SA103				
Nicolella, D.	1111, SA284	Nurcombe, V.	M235, M490				
Nie, S.	1028	Nurzenski, M. K.	SA310				
Niedzielska, D.	M332	Nuti, R.	M016, M292, M350, M414, M416, SU367, SU378, SU379, SU458				
Niehaus, M.	SU453	Nwaneshiudu, A. I.	M228				

(Key: 1001-1228 = Oral, F = Friday Plenary poster, SA = Saturday poster, SU = Sunday poster, M = Monday poster, WG = Working Group Abstract)

ASBMR 27th Annual Meeting

Author Index

Padmanabhan, V.	SU002	Patel, S.	SU355	Phipps, R. J.	M351	Pratap, J.	1015, 1053, M059, SU248
Page, K.	1049, 1144, F387, F395, SA387, SA395	Paterson, A.	SA111	Pi, M.	SU516	Preisinger, E.	SU352
Pagel, C. N.	SU039	Pathak, A.	M391	Picard, S.	SA448	Pretorius, J.	M026, SA130
Pajamäki, I.	F181, M470, SA181	Patil, B. S.	SU013	Pickard, B. Warren	M502	Prevhal, S.	M404
Pajevic, P.	F481, SA481	Patrene, K.	M242, SA243	Picone, A.	1167, M462	Preziosa, I.	SU125
Palacios, C.	M517	Patrick, A. L.	F112, F338, F341, SA112, SA338, SA341	Picot, M.	M142	Price, C.	F262, SA101, SA262
Palazzuoli, A.	SU379	Patterson, E. Kenneth	M503	Pidasheva, S.	SA487	Price, D.	M056
Palermo, L.	1038	Pavlos, N. J.	M248, M263, M264	Piemonte, S.	SA392	Price, H.	SU401, SU490, SU492
Palermo, L.	1056	Pavo, I.	F356, SA356	Pieper, K. A.	SA527	Price, P. A.	SA026
Palermo, L.	F297, F406, M287, M355, M365, M411, SA297, SA406	Pawowska, J.	M480	Pierroz, D.	F397, SA397	Price, R. I.	M099, SA310
Palermo, L.	SU141	Paz-Filho, G. J.	SU164	Pierroz, D. D.	SU381	Prié, D.	1086
Palermo, L.	SU180, SU400	Peachy, H.	1055	Pignolo, R. J.	M234, M449	Priemel, M.	1101, 1162, M181, SU210
Palisch, A.	M214	Peacock, M.	1089, M007, SA460, SU176, SU482	Pijpers, E.	SU351	Priest, L.	M211, M223
Palmore, G. Tayhas	M524	Pearman, A. Terrece	SU503	Pike, J. W.	1120, SA267, SA521	Primeaux, S.	SU201
Palmqvist, P.	SU207	Pearson, L. H.	SU336	Pilbeam, C.	M424, SA169	Primhak, R.	1132
Palnitkar, S.	M283	Pecaut, M. J.	SA398	Pilbeam, C. C.	SA482	Prince, C.	SU074
Palomares, K. T. S.	SA015, SU092	Peck, A.	SA385	Pillai, G.	SU447	Prince, R.	1059
Pan, L. C.	M419, SA394	Pedersen, J. Skov	SU028	Pilli, T.	SU378	Prince, R. L.	SA310
Pan, W.	SA248	Pedersen, M. E.	SU046, SU232	Pilote, L.	SU341	Prior, H. J.	SU329
Pan, W.	SU353	Pederson, L.	SU285	Pinchera, A.	1167, M462	Prior, J. C.	SU347
Panda, D.	SA490	Pedrazzoni, M.	SA134, SU004	Pines, A.	SU257	Prior, K.	F266, SA266
Pandolfo, M. Concetta	SA117	Pedula, K. L.	1057	Pingsterhaus, J. M.	1004	Prisby, R. D.	M458
Pang, M.	M252	Peel, N. F.	SU156, SU358	Pinheiro, M. Medeiros	SU440	Procopio, E.	SA118
Pantschenko, A. G.	F194, SA194	Peel, S. A. F.	M425, M426	Pinho, S.	1001	Proskorovsky, I.	M357
Panupinthu, N.	SU253	Pelled, G.	SU061	Pinto, D. Santos.	SU507	Prosser, S. E.	M214
Papachristou, D. J.	1043, 1100, F376, SA376	Pelletier, V.	SA036	Pioda, G.	SU509	Proulx, J.	F429, M384, SA428, SA429
Papadimitriou, J. M.	M263	Peltz, G.	1039, F323, SA323	Piovesan, A.	F122, SA122	Provot, S.	SU038
Papadimitropoulos, E. A.	SU435, SU436	Pena, L. A.	M128	Pirri, M.	SA175	Prow, H.	M074
Papaioannou, A.	M310, M391, SU325, SU386, SU387, SU435, SU436	Pendleton, C. M.	SU014	Pisprasert, V.	SU314	Prufer, K.	1118
Papapoulos, S.	SA411	Peng, X.	1204	Pitukcheewanont, P.	F138, SA138, SA460, SU483	Przybelski, R.	SU460
Papapoulos, S. E.	1029	Peng, Y.	1043, 1100	Plank, W.	M331	Psarelis, S.	SU471
Parada, L.	1051	Peng, Y.	F376	Plantalech, L. Carmen	M459	Puel, C.	M327
Paralkar, V. M.	M022, M419, SU200	Peng, Y.	SA246	Plawinski, E.	M429	Punyanyia, M.	SA352
Pardi, E.	M462	Peng, Y.	SA376	Pleshko Camacho, N.	M438	Purswani, M.	SU476
Pardo, C. E.	SU017	Pennella, A.	SU369	Plotkin, H.	SU394	Puutio, J. P.	SU477
Pares, A.	SA388, SU392	Penning, F.	SU388	Plotkin, L.	1092, 1116, F286, SA286	Puzas, E.	SA302
Parfitt, A.	1092, SU019	Pennington, C.	M006	Plotkin, L. I.	F289, SA289	Puzas, J.	M205
Parfitt, A. M.	1197, F367, M417, SA367	Pennisi, P.	M121	Plouffe, L.	F425, SA425	Puzas, J. E.	1005, M488
Parhami, F.	M203, M427	Penteado, V. Santos Rocha	SU440	Pludowski, P.	SU484	Pwint, H. Y.	M053
Parikh, N.	1168	Pepe, J.	SA392	Pluijm, S. M. F.	F349, F351, SA349, SA351	Pye, S. R.	M277
Paris, M.	M170	Pereira, R. C.	F206, M024, SA206	Poblenz, A. T.	F277, SA277		
Parisi, M. S.	SA126	Pereverzev, A.	1148	Pockwinse, S. M.	F212, SA212		
Park, D.	SA224	Pérez Cano, R.	SU354	Pocock, N. A.	SU317	Qi, H.	M395
Park, D. Suk	SU056, SU233	Perez-Edo, L.	M091, SA379, SU137	Pognonec, P.	1001	Qi, H.	M396
Park, E.	M175	Peris, P.	SA388, SU392, SU421	Pogoda, P.	SU210	Qi, H.	M419
Park, E.	M253, SU197	Perissinotto, E.	M451	Pohorecky, L. A.	F051, SA051	Qian, W.	1049
Park, E. K.	SU066	Perkins, V.	1082	Pokovic, J.	M071	Qian, W.	1115
Park, E. Kyun	SU226, SU227	Perlman, S.	1166	Polinski, J.	M371, M372, SU312	Qian, W.	1144
Park, H.	SU211	Perrelet, R.	M452	Polivy, J.	SU348	Qian, W.	F387
Park, I.	M084	Perretti, M.	SU041	Pollack, S.	M510	Qian, W.	F395
Park, I.	M340	Perrien, D. S.	1169, M516, SU250	Pollin, T. I.	SU178	Qian, W.	SA387
Park, I.	M340	Perry, S.	F306, SA306	Pollock, N. K.	M021	Qian, W.	SA395
Park, I.	SA514	Perryman, L. A.	M053	Pols, H.	F120, M117, SA120	Qiao, M.	1154, M174
Park, J.	M253, SU197	Persson, E.	SU207, SU208	Pols, H. A.	1210, M120	Qiao, Q.	M098, M099
Park, K. Seo	SA400	Peruzzi, B.	1103, M436	Pols, H. A. P.	M088, M250	Qin, L.	1149, M086, M490, M492
Park, R.	SA514	Perwad, F.	M127	Pomp, A.	M323	Qin, X.	SA146
Park, S.	SA451	Pescarmona, G. Piero	SU414	Pongchaiyakul, C.	M066, SU314	Qin, Y.	F185, SA185
Park, S.	SA451	Peters, D. M.	1054	Ponnappakkam, T.	SA443	Qin, Y.	SA193
Park, S.	SA451, SU236	Petersen, K.	SU149	Pons, F.	SU392, SU421	Qin, Y.	SU171
Park, S.	SU236	Petersen, S.	M094	Pope, R. M.	SU487, SU494	Qin, Y.	SU173
Park, S.	SU256	Peterson, C. A.	SU418	Pope, S.	F306, SA306	Qin, Y.	SU192
Park, W.	M471, SU493	Peterson, J. M.	1075	Popescu, A.	M295	Qiu, S.	M283
Park-Sarge, O. K.	SA502	Peterson, M. C.	SU446	Popescu, A. M.	1055	Qiu, T.	F129, SA129
Parker, A.	F030, SA030	Peterson, W. J.	M153	Popescu, V.	SA003	Qu, Y.	F425, SA425
Parker, R. A.	F381, SA381	Petit, J. Luc	SA036, SU024	Popoff, S. N.	M039, M228, SU035, SU076, SU078, SU251	Quarles, L.	1026
Parker, R. A.	SU185	Petit, M. A.	1127	Popp, A. W. E.	M452	Quarles, L.	1061
Parkinson, C.	M319	Petkov, V. I.	M301, M302, M366, SA380	Porsti, I.	M470	Quarles, L. Darryl	SA144, SU516
Paro, R.	F470, SA470, SU046, SU232	Petrel, C.	SA485	Portale, A.	M131	Quesada, J. Manuel	SU374
Partanen, J. M.	1195	Petri, A.	SU065	Portale, A. A.	M127, M481	Qui, W.	M192
Partridge, N.	1149, M040, M490	Petropoulou, K.	SA377	Portegijs, E.	SU339	Quigg, R.	M199
Partridge, N. C.	1113, M492, SA164	Petrusci, M. Teresa	SA392	Porter, L.	M056	Quilgotti, S.	M288
Paruch, J.	M052, SU038	Petruschke, R. A.	SA526, SU159	Portero, N.	1084	Quinet, R.	SU345, SU505
Parvizi, J.	M455	Petryk, A.	M037	Pothion, S.	SU193	Quinkler, M.	SA373
Pasco, J. A.	F319, SA319	Pettersson, K.	SA328	Potter, L.	SA484	Quinn, J. M. W.	1190, M262, SA250
Pasquale, M. K.	SA403	Pettit, A. R.	M243, SU491	Potts, J.	SA493	Quinn, S. J.	SU497
Pasqualetto, E.	SU105	Petto, H.	F356, SA356	Pourmand, E.	SA022	Qvist, P.	F074, M241, SA074, SU116, SU149
Passariello, R.	M082, SU125	Pettway, G. J.	M182	Powell, D.	SA383, SA383		
Passeri, G.	SA134, SU004	Pettway, G. J.	M487	Powell, J. J.	M338, SA421		
Pastinen, T.	M107	Pfeifer, M.	SU443	Powell, J. S.	M111		
Paszty, C.	1082, SA130	Pham, T.	M349	Powell, K.	M230, SU255	R.Parthasarathy, P.	SA305
Patade, A.	M335	Philbrick, W.	1183	Powell, K. A.	M164	R.Surendranath, C.	SA305
Patano, N.	1102	Philbrick, W. M.	M497	Powers, M.	F461, SA461	Rackoff, P.	SA460
Patel, M.	SU312	Phillips, W.	M054, SU098	Poynton, A.	SU496	Radács, M.	SU065
Patel, M. R.	M510	Phimphilai, M.	F012, M179, SA012	Pramanik, R.	M467		
Patel, P.	M035	Phipps, R.	1081, SU086, SU399				

(Key: 1001-1228 = Oral, F = Friday Plenary poster, SA = Saturday poster, SU = Sunday poster, M = Monday poster, WG = Working Group Abstract)

Author Index

ASBMR 27th Annual Meeting

Radecki, D.	F429, M384, SA428, SA429	Rehage, M.	SA146	M278, M284, M447, SA096, SA397, SA416, SU050, SU381	Rowe, D.	F229, SA229
Radspieler, H.	M086	Rehm, S.	F232, SA232	Roach, H. I.	Rowe, D. W.	M238, SA191
Ragage, J.	I086	Reich, D.	M103	Robbie Ryan, M.	Rowe, G. Cameron	I114
Raggatt, L. J.	M490	Reid, D. M.	1042, 1210, 1224, F410, M115, M300, M338, SA410, SU139, SU437	Roberts, S. A.	Rowe, P. S. N.	1163, SA462
Ragi, E.	M275	Reid, I. R.	SU230	Robertson, B. W.	Rowell, L.	SU415
Ragi, S.	M287	Reijnders, C. Maria Alida	SU223	Robinson, B.	Roy, A.	M522
Rahman, M. Mizanur	SA132	Reilly, G.	F039, SA039	Robinson, B. Gregory	Roy, D. K.	M277
Rahnert, J.	F166, SA166	Reimund, J.	M444	Robinson, K.	Roy, S. K.	SU447
Rahner, J. A.	SU216	Reina, P.	M096	Robinson, L. J.	Roy-Chaudhury, A.	M017
Raisz, L.	M424	Reinhold, M. I.	SU199	Robinson, M.	Ruat, M.	SA485
Raisz, L. G.	F374, SA374, SA482	Reinholt, F. P.	SU046, SU232	Robles, E.	Rubin, C.	M018, M147, M150, SA165, SU173, SU174, SU371
Rajamannan, N. M.	SU018	Reiss, M.	SA164	Robling, A. G.	Rubin, C. L.	M114
Rajani, R.	F057, SA057	Reiter, E.	SA480	Roca, H.	Rubin, C. T.	M149
Rajatanavin, R.	M066	Reith, W.	I143	Roddie, C.	Rubin, J.	1182, F166, F450, SA166, SA450, SU216, SU238, SU241
Rajgopal, A.	F212, SA212, SU228	Reitter, S.	M331	Rodriguez, S.	Rubin, M. R.	SU424, SU465, SU467, SU470
Rajpar, M. Helen	I033	Reitz, R. E.	SU158	Rodriguez-Garcia, A.	Rubiacchi, A.	M246
Räkel, A.	M484	Rejnmark, L.	1227, M317, SU423	Rodriguez-Garcia, M.	Rucci, N.	F068, F470, SA068, SA470
Rakos, R.	SU255	Ren, S.	M518	Rodriguez, L.	Ruchala, P.	SU498
Ralston, S. H.	1059, 1210, M115	Renner, W.	M331	Rodriguez, M.	Rudkin, G. H.	SU058
Ramalakshmi, T.	M270, SA305	Renshaw, K.	SU249	Rodriguez, S.	Rudnik, V.	M158
Ramberg, J.	SU143	Rentero, M. Luz	M315	Rodriguez-Garcia, A.	Rueger, J. Maria	1162, M181, SU210
Ramesar, R.	F116, SA116	Renz, J.	M058	Rodriguez-Garcia, M.	Ruffato, E.	SU105
Ramirex-Yañez, G. O.	M425, M426	Reponen, J. J.	SU161	Rodriguez-Rebollar, A.	Ruffieux, C.	F096, SA096
Ramiro, M.	SA087	Reseland, J.	SA252	Rodriguez-Roca, G.	Ruffieux, D.	SA332
Ramnaraine, M.	SA248	Reseland, J. E.	SU205	Rogers, C.	Ruffing, J.	M013
Ramos, R.	SU354	Resnick, H. E.	F347, SA347	Rogers, J.	Ruiz, S.	M169
Ramsey-Goldman, R.	SU487, SU490, SU492, SU494	Resnick, N. M.	F381, SA381	Rogers, M. J.	Ruiz Requena, M. Estrella	SU374
Rane, A.	SU522	Restuccia, N.	M322	Rognan, D.	Ruiz-Gaspa, S.	M122
Ransjö, M.	SA283	Rey, A.	M218	Rohira, A.	Ruiz-Requena, M.	M400, SU274
Rao, A. Venketeshwer	M210	Rey, C.	SU032	Rohner, D.	Rummeny, E. J.	SU324
Rao, A. V.	SA308	Reyes, J. M.	SU076	Roldan, E.	Rundle, C. H.	SA508
Rao, D.	I168	Reyes-Garcia, R.	M400, SU274	Romagnoli, E.	Rung-Aroon, J.	M183
Rao, D.	M283	Rhee, Y.	SA422, SA451, SU236, SU252, SU256	Roman, K.	Ruppel, M. E.	M047
Rao, D.	SA463	Rhew, E. Y.	SU487, SU494	Roman-Roman, S.	Rushton, B.	M409
Rao, H.	SA243	Rhim, J. S.	I202	Romanello, M.	Russell, J. M.	SU260
Rao, L. G.	M210, SA308	Rho, J.	SU182	Romera, M.	Russell, P.	M053
Rao, S.	SA467	Riancho, J. A.	SU184	Romeu, J.	Russell, R. Graham	F408, M351, SA064, SA408, SU306
Raossanal, C.	SU089	Ribeiro, E.	SA447	Ronda, A. Carolina	Russo de Boland, A.	M512, M513, SA478, SU518
Rapin, C. Henri	M284	Riccardi, K. Andrew	M022	Rongish, B. J.	Rüther, W.	M332
Raptou, P.	M374, SA377	Rich, L.	I021	Rongish, B. J.	Ryzko, J.	M480
Rapuri, P. B.	M309, M312, M511, SA304	Richards, J. Brent	I076	Roodman, G. D.	Ryaby, J.	SU043
Rasi, S.	SU162	Richards, W.	M192		Ryaby, J. T.	M199
Rasmussen, H.	SU508	Richards, W. G.	M026, SA130		Ryan, C. Shiloh	M301, M302, SA380
Rasmussen, K.	M172, SA506	Richardson, D.	SU106		Ryan, L. E.	SA423
Rath, N. C.	SU064	Richardson, J.	M203		Ryan, M.	I049
Rauch, F.	1088, F440, SA440	Richardson, J. A.	M427		Ryan, Z.	SU512
Rauh, M.	SU356	Richardson, T. I.	SA427		Rychly, J.	M232
Ravanti, L.	SU161	Rickard, D.	F199, SA199, SA484		Ryder, K. A.	F306, SA306
Ravaux, P.	SU495	Rico, M. C.	M228, SU035, SU251		Ryder, K. M.	M355
Ravi, D.	SU245	Riddle, R. C.	SU217		Rydziel, S.	M024, M211, SA126
Ravula, S.	M270	Rider, K. A.	M453		Ryg, J.	M386
Rawadi, G.	1001, 1019, SA027	Ridout, R.	M071, M316		Ryoo, H.	M176
Ray, G. T.	SU336	Riedel, D.	M263		Ryu, J.	SU286
Ray, M. R.	SA067	Riedt, C. S.	M337			
Ray, R.	M524, SA523	Ries, W.	M368, SU279			
Raz, B.	SU428	Ries, W. L.	SU311			
Razzaque, M. S.	I164	Riesen, W.	SA350			
Reading, I.	M015	Rigante, D.	M011			
Realdi, G.	M461	Riggs, B. L.	1010, 1074, 1075			
Reame, N. Elizabeth	SU002	Rigney, U.	M352			
Reaney, L.	SU402	Riis, B. J.	SA417			
Rebmann, A.	F220, SA220	Riley, D.	I156			
Recchia, I.	F068, SA068	Ringe, J. D.	SU391, SU398			
Recker, R.	1221, F414, F425, F429, SA414, SA425, SA429, SU368, SU393	Ringelheim, J.	SA471			
		Rini, G. Batista	M124, SA117			
Recker, R. R.	1211, F358, F435, M050, M108, M279, M346, M353, M358, M364, SA358, SA435, SU179, SU412, SU413	Rios, H.	SA462			
		Rios, H. F.	I111			
		Rios, R.	SU013			
		Rissanen, J.	SU272, SU303			
		Rissanen, J. P.	SU161, SU289, SU290			
Recker, S.	1221, F414, SA414, SU368	Risteli, J.	SU143			
Recknor, C.	F425, SA425, SU444	Ritchie, R. O.	SA163			
Reddy, G. Satyanarayana	M524	Ritchlin, C.	SU488			
Reddy, S. V.	F275, SA275	Ritter, C. S.	M475			
Reddy, S. V.	SA467	Rittling, S. R.	M165, SA164, SU302			
Reddy, S. V.	SU279	Rivadeneira, F.	M088, M117, M120			
Reddy, S. V.	SU311	Rivas, D.	F412, SA412			
Reddy, V.	SA463	Rivas, M.	M408			
Reece, A.	F331, SA331	Rivera, M. F.	SA137			
Reed, F.	M368	Riviere, P. J.	SU498			
Reep, R. L.	M145	Rizzo, J. R.	I057			
Rees-Milton, K.	M418	Rizzoli, R.	1136, F096, F397, M086, M093, M121, M140, M218, SA205			
Reeve, J.	1210, M093					
Reginster, J. Y.	M347					
Regmi, A.	SA205					

(Key: 1001-1228 = Oral, F = Friday Plenary poster, SA = Saturday poster, SU = Sunday poster, M = Monday poster, WG = Working Group Abstract)

ASBMR 27th Annual Meeting

Author Index

Saito, M.	SU420	Savage, T.	F210, SA210	Seibel, M.	1133	Shigemoto, M.	SU375
Saito, T.	1006	Savaiano, D. A.	M003	Seibel, M. J.	1137, F507, M053, SA507, SU142, SU144, SU164, SU467, SU520	Shih, C.	M207, M265
Sajjan, S.	M378, SU340	Savolainen, P.	M114			Shih, M.	F461, SA461
Sakai, A.	F172, SA172, SU239	Sawa, M.	SU462			Shih, M. S.	SU214
Sakai, N.	1181	Sawada, N.	F479, SA479	Seibel, M. J. H.	M314	Shih, R. N. J.	1163
Sakai, Y.	M163, M200	Sawaya, R.	SA449	Seidman, L.	M435	Shim, S.	F391, SA391
Sakaki, T.	SU110	Sawka, A.	M391	Seijo, M.	M072, M073	Shimada, T.	F140, M132, M134, SA140
Sakamoto, Y.	SU462	Sawka, A. M.	SU435, SU436	Seiki, M.	1188		
Sakari-Rantala, R.	SU339	Saxon, L. K.	1091	Seino, Y.	SA494	Shimada, Y.	M311, M313, M431, SU439
Sakhaee, K.	M468	Sayegh, G.	1218	Sekiguchi, S.	SA361, SU026, SU050		
Saku, T.	SA024	Sazonova, N. I.	SU136	Sekimoto, E.	SU102	Shimazaki, M.	SA216
Sakurai, T.	1121	Schaaf, N.	M282, SA322	Selby, P. L.	M334	Shimazu, K.	SA216
Salamon, E. A.	SU327, SU328, SU372	Schacht, E.	SU008	Selby, P. Leslie	SA525	Shimer, K.	SA151
		Schaffler, M.	1093	Selhub, J.	F309, SA309	Shimer, K. S.	1065, F160, SA160
Salatto, C. T.	M395	Schaffler, M. B.	1043, 1100, F072, SA072, SU456	Selim, A.	SA155, SA492	Shimizu, M.	F260, SA260, SU071
Salazar, V.	1109			Selim, A. A.	SA493	Shimizu, S.	SU302
Saldanha, K.	M069	Schaller, S.	1206, M157, SA237	Selinger, C. I.	SU307	Shimizu, T.	F127, SA127, SU389
Saleh, H.	1190	Scharla, S.	M318, M398, SU442	Sellmeyer, D.	M131, M365	Shimmi, O.	M037
Saless, N.	SU020	Schatz, D. G.	1184	Sellmeyer, D. E.	F306, F347, SA306, SA347	Shimomukai, M.	M520
Salganik, T.	SU428	Scheibel, S.	SU504			Shimomura, J.	SA488
Salihoglu, S.	M228	Scheinfeld, V. L.	SA155	Selmer, R.	SA346	Shimooka, S.	SA488
Salingcarboriboon, R.	M152	Schell, B.	SU444	Selvamurugan, N.	M040, SA164	Shin, C. Soo	M118, M430
Salmeron, J.	M287	Scher, J.	SU463	SEMOF-Group	SA332	Shin, H. I.	SU066
Salmon, P. L.	M049	Schett, G.	SU295	Sena, K.	SA159	Shin, J.	SU493
Salo, P. T.	SU047	Schiavi, S.	M428, SA455	Sendak, R.	M428	Shin, J. J.	M306
Saloranta, P.	SU162	Schibel, S.	SU502	Senn, C.	M452	Shinar, H.	SU061
Salter, E. D.	M395	Schilling, A. F.	1101, 1162, M181, SU210	Seo, H.	SA157	Shindou, H.	F127, SA127
Salvadori, S.	M414, M416, SU378			Seo, J.	M245	Shinji, H.	M205
Sam, K.	1032	Schilling, T.	M198	Serebro, L.	SU345	Shinoda, Y.	1047
Samadfam, R.	1099	Schimmoller, F.	1216	Sereika, S. M.	SA098	Shinoff, C.	M365
Sambrook, P.	1133, SA113	Schinke, T.	1162, M181	Serra, R.	SA157	Shinoff, C. Woo	F334, SA334
Samelson, E. J.	F309, SA309	Schipani, E.	1002, F170, F481, SA170, SA481	Serrano, S.	M091, SA379	Shinomiya, K.	F032, SA032, SU055, SU302
Sampaio, A. Vinicius	SU247			Seton, M.	SA466		
Sampath, K. T.	M428, SU431	Schlaffler, M. B.	SA022	Sevenet, N.	SU523	Shiota, K.	M303
Samuel, W.	SA296	Schmidt, A.	M489	Sferrazza, C.	SA117	Shipman, C.	1124
Sanchez, C. P.	M479	Schmidt, J. A.	SA527	Shackelford, L. C.	1171	Shipman, C. M.	SA064
Sanchez, M.	M147	Schneider, D. K.	M077, SU017	Shaffer, J. R.	F100, M103, SA100	Shiraki, M.	M291, SU190, SU389
Sanchez, S.	SA091	Schneider, E.	SU210	Shahab, S.	SU061	Shitaye, H.	SA038
Sanchez, T. Victor	SU124	Schneider, H. G.	F319, SA319	Shaker, J.	SA460	Shivdasani, R. A.	1032
Sánchez-Navarro, J.	SA316	Schneider, P.	SU433	Shalhoub, V.	M192	Shlipak, M.	M285
Sandell, L.	M239	Schneider, R.	M097, SU445	Sham, P.	SA111	Shoback, D.	M229, SU510
Sandy, J. D.	SU048	Schnell, J. C.	SU210	Sham, P. C.	SU186	Shockley, K.	SU242
Sangadala, S.	M027	Schoeller, M.	SA076	Shan, J.	SU197	Shogren, K. Lynn	SU097
Sanjay, A.	1145, F279, SA279	Schoenherr, M.	SU094	Shanahan, F.	SU332	Shohami, E.	SU377
Sanson, P.	SA134, SU004	Schofield, P. J.	SU404	Shane, E.	1175, M445, SU361, SU465, SU467, SU470, SU476	Shon, H.	M340
Santana, M. G.	SU440	Schoonmaker, J. E.	SU112			Shore, E. M.	M029, M439, SA011
Santini, D.	SU206	Schoor van, N. M.	1134	Shao, J.	1004	Shorr, R. I.	F347, SA347
Santora, A.	M353, SU389, SU393	Schott, A. M.	F096, SA096	Shao, J. Z.	SU277	Short, W. H.	SU369
Santora, A. C.	F406, SA406, SU400	Schousboe, J.	F325, SA325	Shapiro, F.	SA441	Shortkroff, S.	SA031
Santos de Araujo, R. M.	SU083	Schousboe, J. T.	F084, F315, SA084, SA315, SU151	Shapiro, I. M.	M455, SU292	Shotton, J.	M300
Sany, J.	SU495			Shapses, S. A.	M337	Shotwell, M.	SU444
Sanyal, A.	M158	Schroeder, B.	SU394	Sharkey, N. Allen	M112	Shou, J.	F437, M219, SA437
Sapountzi, P.	M320	Schroeder, T. M.	F204, SA204	Sharp, C.	SA383	Shuldiner, A. R.	SU178
Saraifoger, S.	M457	Schteingart, C.	SU498	Sharrow, A. C.	1043, 1100, F376, F505, SA217, SA241, SA376, SA505	Shulman, D.	SA460
Saraiva, G.	SA447	Schuetz, G.	1101			Shultz, K.	1035, SU181
Sarasa, D.	SA436	Schuetze, N.	M231	Shaughnessy, J. D.	1125	Shultz, K. L.	F102, F114, SA102, SA114
Sarge, K. D.	SA502	Schuit, F.	1199				
Sargent, M.	SU372	Schule, R.	SA278	She, J. Xiong	M456	Shyu, J.	M207, M265
Sarrio, L.	M096	Schultis, H. W.	SU407, SU409	Shea, J. E.	SA182	Sibonga, J. D.	1171
Sartori, L.	M451	Schurman, L.	SU196	Shea, M. Kyla	M123	Sicari, B. M.	1158
Sasaki, S.	M008, M009	Schütze, N.	M198	Sheer, R.	SA330	Siddappa, R.	SU235
Sasaki, T.	F222, M249, M254, SA222	Schwartz, A.	F406, M355, SA406, F347, SA347, SU400	Sheer, R. L.	M293	Sidney, S.	F334, SA334
		Schwartz, A. V.		Shelton, R. S.	1197	Siegal, G. P.	SU100
Satcher, R. L.	SU119			Shen, C. Li	M348	Siegel, E.	SU150, SU153
Satia, J. A.	SU313	Schwartz, Z.	1182, F450, M212, SA450, SA500, SU045	Shen, H.	1211, M403	Sierra, O. L.	M173
Sato, H.	SA355			Shen, Q.	1201	Sievänen, H.	F181, M470, SA178, SA181, SA184, SU009
Sato, M.	F202	Schwarz, E.	1155, 1196	Shen, R.	1187		
Sato, M.	F260	Schwarz, E. M.	1005, 1020, 1072, M045, M170, M178, M488, SU488	Shen, V.	M393, SU451	Siffert, R. S.	SU172
Sato, M.	F356			Shen, X.	F129, F513, SA129, SA513	Siggeirsdottir, K.	SU334
Sato, M.	M041			Shen, Y.	SU252	Sigurdsson, G.	M324, M412, SA432, SU334
Sato, M.	M489	Schwarz, P.	SA372	Sheng, M. H. C.	SU229		
Sato, M.	SA202	Scillitani, A.	F122, SA122	Shepherd, J.	F004, M481, SA004	Siimes, M. A.	SU477
Sato, M.	SA260	Scott, D.	SA354	Sheppard, D.	SA243	Sijanovic, S.	SA390
Sato, M.	SA356	Scott, D. O.	M419	Shergy, W.	M406	Silbert, L. J.	F072, SA072
Sato, M.	SA427	Scott, P. L.	SA294	Sherrard, D. J.	SU475	Silkman, L.	SA101
Sato, N.	F260, SA260	Screen, J.	M167	Sherrill, R. M.	M337	Siller-Jackson, A. J.	1095
Sato, N.	SU301	Seales, E. C.	SU222	Sherrill, D.	F179, SA179, SA352, SA430	Silman, A. J.	M277
Sato, S.	F032	Seaman, W. E.	M261			Silva, A.	SU038
Sato, S.	M205	Sebald, E.	1017	Sheu, T.	M205	Silva-Netto, F.	M451
Sato, S.	SA032	Sebald, W.	SU202	Sheu, Y.	F338, SA338	Silve, C.	1086, SA485
Sato, T.	F509	Sebastian, A.	F306, SA306	Shevde, N. K.	1120, SA267, SA521	Silveira, F. D.	SA324
Sato, T.	M125, M328	Secreto, F. J.	1200, SA506	Shi, W.	1028	Silver, J.	SU472
Sato, T.	M463	Sedlinsky, C.	SU196	Shi, X.	F513, SA513	Silver, P.	SU336
Sato, T.	SA509	Seeman, E.	M282	Shi, Y.	SA148, SA221	Silverberg, S. J.	M322, SU108, SU424, SU465, SU470
Sato, Y.	M010, M012	Seeman, E.	SU316, SU363, SU364	Shiba, A.	M249	Silverman, S.	SU403, SU410, SU417
Satou, A.	M303, SU315	Seerattan, R. A.	SU047	Shibata, H.	1123	Silverman, S. L.	M407, SA311, SA339
Satterfield, S.	M355	Seestaller-Wehr, L. M.	M189	Shide, K.	M333		
Saunders, T.	SU453	Segal, E.	SU428	Shigematsu, T.	M129		

(Key: 1001-1228 = Oral, F = Friday Plenary poster, SA = Saturday poster, SU = Sunday poster, M = Monday poster, WG = Working Group Abstract)

Author Index

ASBMR 27th Annual Meeting

Sima, M.	M420	Solomon, D.	1078, F317, SA317	Steingrimsdottir, L.	M324	Sun, Q.	M221, SU240
Simic, P.	1027, M428, SU431	Solomon, D. H.	M371, M372, SU312	Stenglein, E. A.	SA324	Sung, H.	1171
Siminoski, K.	1037, SA320, SU323	Solyom, A. M.	SU489	Stenkjær, L.	M119	Sung, H.	SU449
Simmons, H. A.	M395, M396, M419, SA394	Soma, K.	F170, SA170	Stepan, J. J.	F356, SA356	Suominen, H.	1131, M139, M141
Simoes, E.	SA432	Somerman, M. J.	M182	Stephens, A.	1059, 1208	Supervia, A.	M122
Simon, J.	SA330	Sommer, S.	SU500	Stephens, P.	1082	Suppapanya, N.	M352
Simon, J.	SA428	Son, J.	SU373	Stephens, S. R. J.	F249, M247, SA249	Suriyapperuma, S.	M177
Simon, R. R.	M392, M429	Song, H.	M118, SU252		M319	Susa, M.	F068
Simonelli, C.	SA076	Song, H. Kwon	1055, M295	Stephenson, S.		Susa, M.	F220
Simonet, S.	M192	Song, J.	SU082	Sterling, J. A.	1154, F066, M054, SA066	Susa, M.	SA068, SA207, SA215
Simonet, W. Scott	1082, M026, SA130	Song, J. J.	SU035		M456	Susa, M.	SA220
	SU126	Song, M.	SA223	Stern, D. M.	SU267, SU284	Susa, M.	SU270
Simpson, D.	SU527	Sonoyama, W.	SU062	Stern, P. H.	1173, M156, SA059	Susanto, E.	1019
Simpson, E. R.	1133	Soo, C.	SU204	Stevens, H. Y.	1042, M300	Sutter, B.	SU138
Simpson, J.	M186	Sørensen, M. G.	M157, M241, SA237	Stewart, A.	SU437	Suttie, J.	SU425
Simpson, K. A.	1190, M262, SA250	Sorenson, S. M.	SA290	Stewart, A. D.	1158	Suuriniemi, M.	1131, M141
Sims, N. A.	1148, SU253	Sorimachi, H.	1174	Stewart, A. F.	SU463	Suutari, S.	SU289, SU290
Sims, S. M.	M320	Sornay-Rendu, E.	SA359	Stewart, B.	SA060	Suva, L.	SU526
Sinacore, J.	M376	Sosa, M.	SA364	Stewart, I. Joyce	SU048	Suva, L. J.	1169, M516
Sinacore, J.	SU438, SU439	Soshi, S.	SU420	Stewart, M.	F365, SA365, SA373	Suva, L. John	SU150
Sinaki, M.	M429	Sosnoski, D. M.	SU120	Stewart, P. M.	1092, 1140, F286, SA286, SU019	Suva, L. J.	SU153
Sindrey, D.	M392, SU263	Soundararajan, A.	1141, M054	Stewart, S.	F437, M219, SA437	Suzawa, M.	SU259
Sindrey, D. R.	M104, M105	Soung, D. Yu	M335, SU044, SU246, SU432	Stewart, T.	M386	Suzawa, T.	M249, SA037
Singer, J.	1045	Souza, A. C. A.	M097, SU445	Stilgren, L.	SU469	Suzuki, A.	1181, M485
Singh, A.	1156	Spaczynski, M.	SA123	Stilgren, L. S.	SU427	Suzuki, A.	SA361, SU026, SU050
Singh, A. T. K.	SU267	Spadaro, J. A.	SU369, SU466	Stitt, P. A.	F425, SA425	Suzuki, H.	SU025
Singh, M.	M046	Spady, M.	SU345	Stock, J. L.	SU018	Suzuki, M.	1096, SU040, SU301
Singh, R.	F481, SA481, SU500	Spady, M. C.	SU505	Stock, S.	1117	Suzuki, R.	1139
Singh, R. J.	F524, SA524, SA527	Spagnoli, A.	1065, F160, SA151, SA160	Stockard, C.	1067	Suzuki, T.	F258, SA258, SU054, SU072
Singh, S.	F277, SA277	Spector, E. R.	1171	Stockmans, I.	SU275	Suzumoto, R.	M249
Singleton, K.	M148	Spector, T.	1080	Stokes, C. R.	SU295	Swaissland, A.	M251
Sinha, N.	M323	Spector, T. D.	SA421	Stolina, M.	M438	Swaminathan, R.	SA421
Sinha, R.	M164	Spelsberg, T. C.	1200, M172, SA158, SA506, SU010, SU018, SU285	Stone, D.	F325, M285, SA325, SU335	Swanson, C.	SU521
Sinigaglia, L.	F301, SA301	Spevak, L.	SA022	Stone, K.	1039, 1057, 1073, F323, M290, SA323	Swanson, E.	M182
Sipilä, S.	F007, SA007, SU339	Spica, E.	F470, SA470	Stone, K. L.	1141	Swarbrick, C. M.	M277
Sipos, A.	F429, M269, SA429, SU340, SU403, SU417	Spicer, D. B.	M184	Story, B.	SU446	Swift, J. M.	M458
Siris, E.	SU403, SU417	Spies, S.	SU487, SU490, SU492, SU494	Stouch, B. J.	SU115	Swinnen, J.	F515, SA515
Siris, E. S.	M378	Spilsbury, H.	F319, SA319	Stout, D.	M112	Syberg, S.	M094
Sison, C. P.	M323	Sprague, E.	1095	Stout, J. T.	M323	Syddall, H. E.	SA119
Sitara, D.	1164	Sprague, S.	F264, M061, M467, SA264	Strain, G.	SA152	Syed, F. A.	1142, F511, M158, SA511
Sitia, R.	SU103, SU105	Spurney, R. F.	F225, SA225, SA480	Strauss, J. A.	SU178	Sykes, D.	M388, M434
Sivakumar, P.	1054, SU073	Spusta, S. C.	M261	Streeten, E. A.	M331	Sylvester, F.	F131, SA131
Skalli, W.	M288, SU089	Squire, M. E.	SA165	Strele, A.	1101	Sylvester, F. A.	SU478
Skedros, J. G.	M044, SA290	Squires, D.	M425, M426	Stride, B.	1102	Syme, C. A.	M500
Skerjanec, A.	SU447	Sridhar, S.	SU291	Strippoli, M.	SA148	Syversen, U.	SA047, SA252, SU205, SU213
Skerry, T. M.	1094, F039, SA039	Srinivasan, S.	SU218, SU311	Strohbach, C.	M171, SA145, SA148	Szejnfeld, V. Lucia	SU440
Skinner, R. A.	M480	Srivastava, A.	F104, F106, SA104, \ SA106, SA508	Strong, D. D.	F347, SA347	Szulc, P.	SA359
Skorupa, E.	SU155		SU396	Strotmeyer, E. S.	F232, F234, F236, SA231, SA232, SA234, SA235, SA236, SA484	Szulc, P.	SU316
Slaets, J.	SU473	Srivastava, T.	1147, 1164	Stroup, G.	SA236, SA484	Szymczyk, K. H.	SU292
Slater, H.	M048	St-Arnaud, R.	F206, SA206	Stroup, G. B.	SA233		
Slater, J.	M463, M475	Stadmeyer, L.	SA501	Struve, J. A.	M214, M215		
Slatopolsky, E.	F222, SA222	Stachelin, H. B.	SA001	Studer, A.	SU209	Tabakovic, A.	SU245
Slavkin, H. C.	SU112	Stager, M.	SU008	Stumpf, U. Cordula	SU094	Tabin, C.	1025
Sledz, T.	SU424	Stähelin, H. B.	M493, SU069, SU265	Stunes, A. Kamilla	SU205	Tabruyn, S.	SU104
Sliney, J.	SU320	Stains, J. P.	M346	Stunes, K.	SA047, SA252, SU213	Tachikawa, K.	SU051
Slingerland, A. S.	SU017	Stakkestad, J. A.	M232	Su, H.	1050	Tada, M.	SU441
Smiltneek, A. J.	F349, F351, SA349, SA351	Stamm, C.	SU370	Su, M.	M151, SA180, SU225	Tae, H.	F391, SA391
Smit, J. H.	M335, SU384, SU430	Stanford, W. L.	SU283	Subler, M. A.	M242	Tagawa, M.	SU055
Smith, B. J.	M516	Stanley, B. A.	F262, SA262	Subramaniam, M.	1200, M172, SA158, SA506, SU010, SU018, SU285	Tagil, M.	F057, SA057, SA295
Smith, C. L.	1132	Stapleton, S.	SA101			Taguchi, T.	M399
Smith, C. M.	1182, F206, SA206	Stapleton, S. N.	M197	Suda, R. K.	M449	Tague, L.	M017
Smith, D.	SU114	Stauffer, B.	M515	Suda, T.	F258, SA161, SA258, SU054, SU072, SU282, SU287	Tague, S.	SA013
Smith, K. C.	M309	Stayrook, K. R.	F435, M350, SA036, SA335, SA435, SU024	Sudre, L.	SA025	Tague, S. E.	M030
Smith, L.	M312, SA304	Ste-Marie, L. G.	1216	Sueiras-Diaz, J.	SU498	Takada, I.	SU259
Smith, L. M.	M256	Stebbins, E. G.	M375	Sugama, R.	SA017, SU441	Takada, Y.	SU426
Smith, M. V.	SU349	Steel, S. A.	SA003	Sugimoto, T.	F444, SA366, SA444	Takagi, C.	SU375
Smith, R. A.	F202, SA202	Steenhuis, P.	M110	Sugiyama, O.	M023	Takagi, H.	SU408
Smith, R. C.	F435, M076, M409, M415, SA431, SA435, U128, SU152, SU453	Stefanick, M.	M290	Suh, C.	SU183	Takagi, T.	1052
Smith, S. Y.	SA250	Stefanick, M. L.	1135, F338, SA338	Suh, K.	SU211	Takagi, Y.	M042, SU030
	SU248	Stein, E.	M323	Suhara, Y.	M291	Takaguchi, K.	M303, SU315
Smyth, M. J.	1160, F489, M504, M505, M506, SA489	Stein, G.	M188	Sukhu, B.	SA103	Takahashi, A.	SU085
Sneddon, W. B.	SU145	Stein, G. S.	1013, 1015, 1021, 1030, 1053, F212, M058, M059, M175, SA212, SU228, SU248	Suliman, G.	M501, SA493	Takahashi, H.	SU050
Snyder, B. D.	1055, M295			Sullivan, J.	SU258, SU304	Takahashi, H. Eimei	M469
Snyder, P. J.	F446, SA446	Stein, J.	M188	Sumner, D. R.	SA159	Takahashi, K.	1085, M128, SA189
Snyder, R.	SA162	Stein, J. L.	1013, 1015, 1021, 1030, 1053, F212, M059, M175, SA212, SU228, SU248	Sun, B.	M026	Takahashi, M.	M343
Soballe, K.	SU301	Steinbeck, M. J.	SU292	Sun, B. H.	1191	Takahashi, N.	F260, M244, SA260, SA274
Sobue, T.	M480	Steinbuch, M.	M293, SA330	Sun, B. Hua	M001	Takahashi, Y.	SA054
Socha, J.	SA099	Steines, D.	F090, SA089, SA090, SA091, SU043	Sun, C.	1028	Takaishi, H.	SU072
Sochett, E. B.	M051			Sun, L.	1043, 1068, 1100, 1102	Takaishi, Y.	SA082
Sode, M.	M271, SA346			Sun, L. Z.	F376, SA376	Takaiwa, M.	1105, 1205, F459, SA459
Sogaard, A. Johanne	SU246			Sun, Q.	F066, SA066	Takaku, H.	SA201
Soliman, A.	M073				1108	Takame, V.	M342
Solis, F.							

(Key: 1001-1228 = Oral, F = Friday Plenary poster, SA = Saturday poster, SU = Sunday poster, M = Monday poster, WG = Working Group Abstract)

ASBMR 27th Annual Meeting

Author Index

Takami, M.	M249, SA037	Teitelbaum, S. L.	F244, F247, M259, SA244, SA247, SA278, SA452, M263	Topol, L.	F048, SA048	Uetani, M.	F362, SA362
Takane, K. K.	1158			Torab-Parhiz, A.	SU174	Uhlig, T.	M389
Takaoka, K.	M031, M224, SA017, SU441	Teklemariam, M.	M193	Torchia, J. A.	M261	Uitterlinden, A.	F120, M117, M120, SA120
Takata, S.	M343	Telera, A. Rita	SU004	Torgerson, D.	M388, M434		
Takata, T.	SU063	Tell, G.	SU257	Torgerson, D. J.	1042	Uitterlinden, A. G.	1210, M088, M250, SA123
Takato, T.	1014, 1016, F127, SA034, SA127, SU033	Tempos, K.	SU471	Toribio, R. E.	1215, SU513	Uludag, H.	M392, SU202, SU215, SU454
Takeda, E.	F479, M125, M328, SA479	ten Broeke, R.	SU351	Torigoe, K.	1192	Underhill, T. Michael	SU247
Takeda, M.	SA082	ten Dijke, P.	1029	Toriyama, K.	SU270	Underwood, J.	1053
Takeda, S.	1174, F032, SA032, SU055	ten Duis, H.	SU155	Torner, J. C.	M019	Urakawa, I.	F140, M132, M134, SA140
Takeda, T.	M348, SU085	Tenenhouse, H. S.	1106, M127	Torreken, S.	1067, F253, SA253	Urano, T.	SU190
Takei, Y.	M303, SU315	Tenne, M.	M116	Torto, R.	1048	Urata, M. M.	F222, SA222
Takeshita, S.	F247, M259, SA247	Teno, N.	SU270	Toss, G.	M397	Urushino, N.	SU110
Taketani, Y.	F479, M125, M328, SA479	Teoh, N. N.	SA137	Tosteson, A.	1078, F317, SA317	Usadel, K.	SA390
		Teplyuk, N.	SU248	Tosteson, A. N. A.	SA348, SU336	Usatii, M.	M482
		Terryberry, J.	M429	Toth, B.	1218	Usui, M.	1052, F014, SA014
		Terryberry, J. W.	SU263	Towler, D. A.	1004, M173	Usui, T.	SU190
		Tervonen, L.	M037	Toyama, Y.	F258, F374, SA211, SA258, SA374, SU054, SU072, SU282	Utian, W. H.	F425, SA425
Takeuchi, K.	SU271	Terwedow, H.	1212			Uusi-Rasi, K.	SU009
Takeuchi, Y.	1047	Terzolo, M.	SA371	Toye, K.	SA384	Uzan, B.	M486, SU032
Takeya, T.	M254	Tesfai, J.	SA508	Toyoda, H.	SU441		
Takeyama, K.	SU110	Teti, A.	1103, F068, F470, M436, SA068, SA470, SU046, SU232	Tracy, J. K.	SU335		
Takezawa, S.	SU259			Tran, D.	SU091		
Takigawa, M.	SU034, SU062	Tetradis, S.	M203, SU499	Tran, K.	SA146		
Takita, M.	F062, SA062, SA063	Tezuka, K.	SU085	Travers, R.	1088		
Takizawa, F.	SA024	Thabane, L.	SU435, SU436	Travers-Gustafson, D.	M279	V	
Talwar, S. A.	M370, M510	Thaden, J. J.	1140	Travison, T. G.	M308	V Prasad, U.	M270
Tamai, N.	1024	Thalassin, N.	M388, M434	Tremblay, G. B.	1148	V. Harinarayan, C.	M270, SA305
Tamaki, J.	M010, M012	The GIUMO Study	SA364	Trent, K. D.	SU014	V.L.N.Srinivasarao, P.	SA305
Tamayo, J. A.	SA010	Theiler, R.	SA501, SU166	Triffitt, J. T.	M351	V.Prasad, U.	SA305
Tamburstuen, M.	SA252	Theim, K.	F472, SA472	Troen, B. R.	M252	Väänänen, H. Kalervo	SU147, SU272, SU273, SU303
Tamburstuen, M. V.	SU205	Thierry-Palmer, M.	M517	Troiano, N.	1191, F270	Vaananen, K.	SA328
Tamma, R.	1102	Thomas, A. M.	SU527	Tronche, F.	1101	Vääräniemi, J.	SU272
Tamone, C.	SU414	Thomas, B. E.	M509, SU498	Trovas, G.	SA377, SU471	Vaheri, R.	SU143
Tamura, C.	SA201	Thomas, C. David L.	SA049, SU016	Trovero, F.	SU193	Vai, S.	M457
Tamura, N.	F028, SA028	Thomas, D. A.	SU096	True, L. D.	SU049, SU122	Valcourt, U.	SU075
Tan, H. L.	1226, SU304, SU451, SU452	Thomas, E.	M142	Trueblood, E.	SA065	Valdimarsson, S.	SU481
		Thomas, T.	1178, SU495	Truppo, C.	SU312	Valente, E.	M026
Tan, J. W.	M248	Thomasius, F. Eva	SU442	Tsai, M.	M196	Valenti, M.	M060, M461
Tan, Q.	M202	Thommesen, L.	SA047, SA252, SU205, SU213	Tsai, Y. Lin	SU175	Valenti, R.	M416, SU378, SU379
Tanaka, E.	SU063		M395, M396, M419, SU200	Tsakalagos, N.	SU471	Valero, C.	SA402, SU184
Tanaka, H.	1085	Thompson, D. D.		Tsomaia, N.	SU498	Valiente, M.	SA316
Tanaka, H.	F459, SA459			Tsuchida, T.	SU395	Valkusz, Z.	SU065
Tanaka, H.	SA494	Thompson, J.	SU512	Tsugawa, N.	M008, M274, M291, M333	Vallarta-Ast, N.	M083, M281
Tanaka, I.	SA368	Thompson, K.	SU309			Valleggi, F.	SU379
Tanaka, K.	M274, M291, M333	Thompson, P.	M344	Tsuji, H.	M333	van Bezooijen, R. L.	1029
Tanaka, M.	SU276	Thompson, R.	F057, SA057	Tsuji, K.	1025, M152	van Blitterswijk, C.	SU235
Tanaka, S.	1188, SA274	Thomsen, J. Skovhus	M423	Tsuji, M.	M328	van der Eerden, B. C. J.	M250
Tanaka, S.	SU239	Thoreau, V.	M057	Tsukamoto, K.	1199	van der Horst, G.	1029
Tanaka, S. M.	SA180	Thorngren, K. G.	SA295	Tsumaki, N.	1024, M034, SU090	van der Veer, E.	SU155
Tanaka, T.	SU420	Thornhill, M.	SU106	Tsuruga, E.	SA467, SU311	van Driel, M.	M250
Tanaka, Y.	SU102	Thornhill, T. S.	M065	Tsutsui, M.	SU239	van Duijn, C.	M120
Tander, B.	SA382	Thornton, D. J.	1033	Tsutsumi, R.	SU110	van Essen, H. W.	M401
Tander, B.	SA382	Thorsten, S.	SU210	Tsuzuki, T.	SA355	van Helden, S. H.	SU351
Tang, T.	SA224	Thraillkill, K. M.	M005, M441	Tu, C.	SU510	Van Herck, E.	SU525
Tang, W.	SA144	Tieder, M.	1106	Tu, S.	SU109, SU114, SU353	Van Houtte, P.	SA075
Tang, Y.	F133, F154, SA133, SA154	Tile, L.	M071	Tu, X.	SU268	Van Hul, E.	1103
Taniguchi, T.	SU389	Timm, W.	M095, M413	Tuan, R. S.	M036	Van Hul, W.	1103, M220
Tanini, A.	SA117, SA118, SA121, SA141	Timmermann, B. N.	SU489	Tuck, A. B.	SA067	van Leeuwen, H.	SA047, SU213
		Timmermans, J.	1103	Tuckermann, J.	1101	van Leeuwen, J.	F120, M117, M120, SA120
Tanko, L.	F074, SA074, SU116	Tindall, J. A.	M137	Tullai, J.	M035	van Leeuwen, J. P. T.	M250
Tankó, L. B.	F321, SA321, SA417, SU412	Ting, K.	SU204	Tuppurainen, M. T.	M289, SA418	van Lenthe, G. Hendrik	M106, SA109
		Tintut, Y.	SA224	Turégano, M.	SA092		
Tanne, K.	SA139, SU063	Titus, L.	M027, M193	Turgeman, G.	SU061	Van Loan, M. D.	M003
Tanner, S. J.	F149, SA149	Tjulandin, S.	SA073	Turner, A. K.	M308	Van Lommel, L.	1199
Tanofsky-Kraff, M.	F472, SA472	Toba, Y.	SU426	Turner, C. H.	1091, 1108, 1170, F110, F168, M409, M415, SA110, SA168, SA431	Van Looveren, R.	F253, SA253
Tao, H.	M230	Tobe, K.	1139			van Meurs, J.	F120, M120, SA120
Tao, J.	M164, SU255	Tobias, J. H.	M110, SU319			van Nieuwpoort, J.	SU155
Taranta, A.	M436	Tobias, J. R.	SA299	Turner, R. T.	F389, SA389, SU097	van Schoor, N. M.	1210, F349, F351, SA349, SA351
Tare, R.	1013	Tobin, F.	SA484	Tweed, K.	SU355		
Tatarczuch, L.	SU039	Tognarini, I.	SA108	Tylavsky, F.	M103	van Staa, T. P.	F334, SA334
Tawfeek, H.	1159	Toguchida, J.	SA029	Tylavsky, F. A.	F306, SA306	Van Wesenbeeck, L.	1103, M220
Tawfeek, H. A. W.	M507	Tojeiro, S.	SA092	Tyndall, A.	SU166	van Wijnen, A.	M188
Taxel, P.	F374, SA374	Tokita, A.	SU462			van Wijnen, A. J.	1013, 1030, 1053, F212, M059, 175, SA212, SU228, SU248
Taylor, A. F.	SU217, SU283	Tokumoto, A.	SU501				
Taylor, B.	F325, M285, SA325	Tokutomi, K.	SA355	U		van't Hof, R. J.	SU308
Taylor, B. C.	1039, F315, SA315	Toledo, D.	SU354	Ubriani, K. R.	1158	Vance, C. Kim.	M483
Taylor, E. D.	F472, SA472	Tomaszek, T.	SA231	Uchida, S.	SU389	Vanden Berghe, D. A.	SA421
Taylor, G.	M138	Tometsko, M.	SA065	Uchiyama, S.	M201, M213	Vandenbergh, D. J.	M112
Taylor, K.	SA290	Tomin, E. Andrew	SU496	Uchiyama, Y.	SA298	Vandenbulcke, K.	SU480, SU481, SU484
Taylor, P.	1008, F002, SA002	Tominaga, M.	1121	Udagawa, N.	F260, M244, SA260, SA274	Vandenput, L.	SU522
Taylor, T.	1045	Tominaga, Y.	M469			Vanderkerken, K.	SU095
Tcherny, S.	M373	Tomlinson, G.	SU463	Ueda, A.	F218, SA218	Vanderschuere, D.	1199, F515, SA515, SU525
Tebben, P.	SA455	Tomomitsu, T.	SU389	Ueda, M.	M190	Vanegas, S. M.	SA137
Tehrani, S.	SA245	Tomoyasu, A.	SA161	Ueland, T.	SA369, SU380		
Teisseyre, M.	M480	Tong, K.	SA314	Uematsu, S.	F125, SA125		
		Tonini, G.	SU206	Uemura, H.	M342		
		Toombs, A. S.	1198	Uemura, T.	M168		

(Key: 1001-1228 = Oral, F = Friday Plenary poster, SA = Saturday poster, SU = Sunday poster, M = Monday poster, WG = Working Group Abstract)

Author Index

ASBMR 27th Annual Meeting

Vanek, C.	1031, SA107	Vukicevic, S.	1027, M428, SU200,	Wang, Z.	M038	West, L.	M135
VanHouten, J. N.	1087, F486,		SU431	Wang, Z.	M054	West, T. V.	SU385
	SA486, SU212	Vuohelainen, T.	M470	Wang, Z.	SA179, SA352, SA430	Westbrook, I.	SA047, SU213
Vanness, D. J.	SA348	Vyas, K.	1092, 1116, F286, SA286	Wang, Z.	SU098	Westendorf, J. J.	F204, M185, SA204
VanOrden, R.	SU473	Vyskocil, V.	SU412	Wang, Z. Z.	M456	Westfall, A. O.	M379, SU390
Vanpottelbergh, I.	SA384	Vyvial, B. A.	M458	Ward, C.	SA060	Westmore, M.	F356, SA356
Vara, J.	M478			Ward, K. A.	M277, SA008, SA475	Weycker, D.	M294, SU397
Varbanov, A.	SU357			Ward, L. M.	SA460	Weynand, L. S.	SU127, SU134
Varela, A.	F435, M076, SA435,			Ward, P.	F410, M350, SA410,	Wheeler, V.	F112, SA112
	SU128, SU453				SU412, SU413	Wheeler, V. W.	F338, F341, SA338,
Vargas-Voracek, R.	F090, SA090,	Waarsing, E.	SA047	Ward, Y.	1122		SA341
	SA091, SU043	Waarsing, E.	SU213	Warden, S. J.	1170	Whelan, B. R.	SU332
Varghese, S.	F131, SA131	Wacker, W. K.	SU127, SU134	Warmington, K.	1082, SU304	White, H. D.	M133
Varkey, M.	SU202	Wada, H.	SA054	Warmington, K. S.	SU451, SU452	White, K. E.	1104, 1165, F138, F442,
Varret, M.	SA439	Wada, S.	M191, SU107	Warren, A.	1098, SU264		SA138, SA442
Vashishth, D.	SA188, SU310	Wada, Y.	SU085	Warren-Ulanch, J. G.	SU474	White-Greenwald, M.	SA344
Vasilic, B.	1055, M295	Wadhwa, S.	SU081	Warshawski, R.	SA320, SU323	Whitfield, J. F.	M403
Vasko-Moser, J.	SA484, F234,	Wafu, W. S.	SA434	Warzecha, J.	SU101	Whitson, H. E.	F334, SA334
	SA231, SA233, SA234	Wagemanns, R.	M231	Wass, J. A.	M110	Whyte, M. P.	1166, F457, F474, M440,
Vazquez, I.	SU392	Wagenmakers, L.	SU155	Watanabe, S.	SU054		M442, M443, M450,
Veber, D. F.	SA231	Wagman, R. B.	M406, M407	Watanabe, T.	F509, SA509		SA452, SA457, SA474
Veenstra, T. D.	M186	Wagman, R. B.	SA438	Waterhouse, K. M.	SU396	Wicherts, I. S.	1134
Velonis, D.	M177	Wagner, C.	SA455	Watkins, M.	M167	Wick, B. Christine	SU398
Venkatachalam, S.	M015	Wagner, J. M.	F381, SA381	Watson, C. A.	F199, SA199	Wickes, C. K.	SA307
Venken, K.	1199, F515, SA515,	Wagoner, W. J.	1031	Watson, M.	SU230	Wickstrom, E.	M455
	SU525	Wahl, E. C.	M005, M043	Watson, P. H.	M502, M503	Wideman, C.	1124, SU098
Veno, P. A.	SU111	Wahlberg, L.	SU162	Wattel, A.	M255	Widlund, H. R.	SU294
Ventura, M.	SA371	Wainman, D.	M418	Watts, N.	M354	Wieland, M.	M212
Verbruggen, N.	SU159	Wakabayashi, H.	1121	Watts, N. B.	M377, M407, SA405,	Wilkes, M. C.	SA280
Vered, I.	SU346	Wakisaka, S.	1121		SA407	Willemsen, G.	SU155
Vergara, S.	SU298	Walcott, M.	M448, SU087	Waugh, E.	M316	Williams, J. P.	F242, SA242
Verhoeven, G.	F515, SA515	Walcott, M. E.	SU434	Waugh, E. J.	SU348	Williams, M. I.	M302, M366
Vescovini, R.	SA134, SU004	Walczyk, T. R.	M055	Weaver, C. M.	M003, M007, M517,	Williams, P.	1214
Vesga, J.	SU354	Wald, M.	M295		SU011	Williams, R.	SA033
Vessella, R.	1213	Waldman, S.	SU133	Webb, C.	M006	Williams, W.	F404, SA404
Vessella, R. L.	SU049, SU117,	Waldum, H.	SA047, SU213	Weber, J. M.	F197, SA197	Williamson, M. K.	SA026
	SU118, SU122	Wales, J.	1132	Weber, K.	1126, F156	Willick, G.	SU112
Vestergaard, P.	1227, M317, SU423,	Walker, M.	M352	Weber, K.	F520	Willick, G. E.	M403
	SU479	Wallis, G.	F116, SA116	Weber, K.	SA156	Willing, M. C.	M019
Vettenranta, K.	SU477	Wallis, G. A.	SA025	Weber, K.	SA520	Wilson, A.	SA344
Viala, J.	SA186	Walrand, S.	M325	Weber, K. T.	SU349	Wilson, A. R.	M020, M021, SA150
Vibert, M.	1086	Walrant-Debray, O.	SA495	Webster, W. Kirk	1069	Wilson, K. E.	F084, SA084
Vicicca, G.	1167, M462	Walsh, C.	M297	Weckbach, A.	M432	Wimalawansa, S. J.	M369, SU293
Vico, L.	1178, M421	Walsh, J. B.	M297	Wehbe, J.	M282	Windahl, S. H.	SA006
Vidal, S.	SU421	Walsh, J. Susan	SU156	Wehmeier, K. R.	SA517	Winder, S.	SU167
Viertomies, L. R.	SU477	Walsh, N. C.	M243, SU491	Wehmeier, M.	M180	Windle, J. J.	1217, F464, M242,
Vieth, R.	SU427, SU428, SU463	Wan, C.	M226	Wehrli, F. W.	1055, M079, M295		SA464
Viggeswarapu, M.	M027, M193	Wan, M.	1117	Wehrli, S. W.	M079	Winer, K.	F004, SA004, SA456
Vignali, E.	1167, M462	Wan, M.	F154, SA154	Wei, C. L.	M487	Wing, N.	SU121
Viguet-Carrin, S.	SA058	Wang, B.	1160, M504, M506	Wei, S.	1068, F247, SA247	Wininger, E.	M306
Vijayabhaskar, M.	M270	Wang, C.	M248	Wei, T.	F437, M219, M515, SA437	Winkel, A.	SU061
Vila, J.	F093, SA092, SA093	Wang, C. Leo	1186	Wei, T.	SU383	Wintermantel, T.	1101
Vilar, J.	M095	Wang, D.	M420	Wei, X.	M068	Wiren, K.	SA386
Vilarino-Guell, C.	M110	Wang, G.	M524	Wei, X.	M178	Wiren, K. M.	1198
Villa, A.	1103	Wang, H.	M199	Weidenfeld, J.	SU377	Wirsching, J.	SU209
Villagra, A.	M188	Wang, H.	SA139	Weigel, N. L.	M516	Wise, L. M.	SA103
Villareal, R. C.	M124	Wang, J.	1028	Weigert, J. M.	M098	Wiseman, M.	F353, SA353, SU352,
Villarreal, A.	SU013	Wang, J.	M243	Weiler, H. A.	SU327, SU328, SU372		SU442
Villarruel, S.	SU255	Wang, J. Mei	SU119	Weinans, H.	SA047, SU213	Wiseman, R. W.	SU243
Villarruel, S. M.	M164	Wang, L.	SU124	Weinerman, S.	M336	Wittelsberger, A.	M509, SU498
Vinante, O.	M060	Wang, L.	1182	Weinstein, L. S.	SA456	Wittert, G.	SU153
Vinberg, N.	SU149	Wang, L.	F225	Weinstein, R.	1092, F286, F401,	Wlodarska, A.	SU082
Vincent, C.	SA259	Wang, L.	F450, M212, M238		SA286, SA401, SU019	Wolfinbarger, L.	SU237
Vincenzi, B.	SU206	Wang, L.	SA450, SA500, SU045	Weinstein, R. S.	1140, 1197, F289,	Woll, N. L.	SU052, SU053
Virdi, A. S.	SA159	Wang, N.	1117		F367, M417, SA289, SA367	Wolter, K.	F429, M384, SA428,
Virji, M.	F376, SA376	Wang, N.	F154, SA154	Weir, P.	F232, SA232		SA429
Vis, M.	M389	Wang, Q.	M139	Weiss, T.	SU312	Wong, C.	M523
Visser, A.	1029	Wang, R.	F007, SA007	Weiss, T. W.	M378	Wong, D. H.	1216
Vittinghoff, E.	F347, SA347	Wang, S.	1068	Weissenbacher, E. R.	F353, SA353,	Wong, J.	1078, F317, SA317
Vivarelli, M.	F470, SA470	Wang, W.	M160		SU352, SU442	Wong, K.	1182, F450, SA450, SU045
Vogel, J. S.	M055, SU165	Wang, X.	F112	Weitzmann, M. N.	1115, F387, F395,	Wong, K. L.	SA500
Vogler, E. A.	SU245	Wang, X.	M225		SA387, SA395	Wong, M.	M397
Vogler, G. P.	M112	Wang, X.	M390	Weitzmann, N.	1049	Woo, J.	SU003
Voide, R.	SA109	Wang, X.	SA112	Wells, A.	SA217	Woo, K.	M245
Vokes, T. J.	F313, SA313	Wang, X.	SA508	Welsman, J. Racheal	SU126	Woo, K. Mi.	SA223
von Scheven, E.	M481	Wang, X.	SU316	Welty, F.	SA428	Wood, D.	SA043
Voorzanger-Rousselot, N.	SU146,	Wang, X.	SU364	Welzel, F.	M231	Wood Steiman, P.	SU327, SU328, SU372
	SU148	Wang, X. N.	M395	Wenderoth, D.	SU404	Woodrow, J. P.	M498
Vora, J. P.	M133	Wang, Y.	1023	Wendling, D.	SU495	Woodruff, K.	1156
Voskuyl, A.	M389	Wang, Y.	1077	Wenkert, D.	M442, M443, SA452	Woodworth, T. G.	SU447
Voss, A.	1162	Wang, Y.	1194	Wergedal, J. E.	1045, 1152, F102,	Woolf, A.	M389
Votta, B.	SA484	Wang, Y.	M146		F106, F183, SA102,	Woon, P. Y.	M110
Vouros, P.	M524	Wang, Y.	M170		SA105, SA106, SA146,	Woong Hwan, C.	SU022
Voznesensky, O.	SA169	Wang, Y.	SA147		SA183, SA508	Workman, P.	M354
Voznesensky, O. S.	SA482	Wang, Y.	SA152	Wergedal, J. E.	SU229	Worsfold, M.	SA383
Vuille, R.	SA207	Wang, Y.	SA191	Wermers, R. A.	SU464	Worthing, A.	1218
Vuillemin, A.	SA115	Wang, Y.	SU221	Werner, P.	SU346	Wosje, K. S.	M064
Vujevich, K. T.	SA098	Wang, Z.	F179	Weryha, G.	SU138	Woznica, I.	SU498
				Wessner, L. L.	SU261	Wraae, K.	SU189

(Key: 1001-1228 = Oral, F = Friday Plenary poster, SA = Saturday poster, SU = Sunday poster, M = Monday poster, WG = Working Group Abstract)

ASBMR 27th Annual Meeting

Author Index

Wren, T. A. L.	M147	Yamaguchi, T.	SA211, SA366	Yaworsky, P. J.	SA128	Zbranca, E.	SU427
Wright, A.	M295	Yamakawa, K.	F125, SA125	Ye, L.	1034, 1111	Zebaze, R.	M282
Wright, A. C.	1055	Yamaki, M.	SU123	Yeh, J.	M156	Zebaze, R. M.	SU363
Wright, H.	SA019	Yamamoto, H.	F174, F393	Yeh, J.	M510	Zeiger, A.	M455
Wright, J. E. Irene	SU454	Yamamoto, H.	F479, M125	Yeh, J. K.	M348, SU027	Zeldin, S.	SU425
Wright, N.	F179, SA179, SA352, SA430	Yamamoto, H.	M204	Yellowley, C. E.	M159	Zella, L. A.	SA521
		Yamamoto, H.	M328	Yeo, H.	SA228	Zemel, B.	1055, F004, M295, SA004
Wright, N. P.	1132	Yamamoto, H.	SA174, SA393	Yeoh, J. SG.	M263	Zemel, B. S.	1060
Wright, W. S.	M206	Yamamoto, H.	SA479	Yerges, L. M.	F341, SA341	Zenari, S.	M060, M461
Wronski, T.	M130	Yamamoto, R.	SA139	Yeung, S.	SA336	Zeng, Q. Q.	M206, M489, SA427
Wronski, T. J.	1048, SA137	Yamamoto, T.	F014	Yi, T.	M245	Zeng, Y.	SU198
Wu, B.	M203, SU204	Yamamoto, T.	M028	Yin, J.	1122	Zeni, S. N.	SU140, SU157
Wu, C.	SU160, SU163	Yamamoto, T.	SA014	Yin, M. T.	M445	Zérath, E.	M268
Wu, D.	1062	Yamamoto, Y.	M244	Yingling, V. R.	M138	Zerbini, C.	F429, SA429
Wu, G.	F179, SA179, SA352, SA430	Yamana, K.	1207	Yirmiya, R.	SU377	Zernicke, R.	SU091
Wu, J. J.	1191	Yamana, K.	SA054	Ylipahkala, H.	SU147, SU272, SU273, SU303	Zernicke, R. Fredrick	SU454
Wu, L.	1117	Yamanaka, M.	SU462			Zerwekh, J. E.	M468
Wu, M.	1183	Yamanaka, Y.	SA054	Ylönen, S.	SU289, SU290	Zhan, F.	1125
Wu, Q.	1005, M488, SA175	Yamanaka-Okumura, H.	M125	Yogiashi, Y.	SU259	Zhang, A.	SA523
Wu, S.	M519	Yamano, E.	SU063	Yogo, K.	M254	Zhang, F.	1104
Wu, T.	SU365	Yamashita, D. S.	F236, SA231, SA235, SA236	Yokota, H.	M151, SA180, SU225	Zhang, H.	M079
Wu, T. Te	SA055		M129	Yoneda, T.	1007, 1121, 1146, 1214, F208, F218, M190, M204, SA208, SA218, SU123	Zhang, H. Ying	M001
Wu, X.	1049	Yamashita, H.	F192, SA192			Zhang, J.	1026
Wu, X.	F408, SA408	Yamashita, J.	F140, M127, M129, M131, M132, M134, M244, SA140, SA274	Yoo, M.	SU056, SU211	Zhang, J.	1183
Wu, Y.	SU059, SU145	Yamashita, T.	M466	Yoo, M. Chul	SU232	Zhang, J.	SA173
Wu, Z.	SA484		SA298	Yoshida, M.	M009, SU006	Zhang, J.	SA314
Wynne, R. A.	1140	Yamato, H.	SA366	Yoshida, Y.	1209	Zhang, J.	SU113
Wynne, R. A.	M417	Yamauchi, H.	F140, M129, M132, M134, SA140	Yoshie, H.	SA024	Zhang, J. Ping	1157
Wynnycky, C.	SU133	Yamauchi, M.	SA449	Yoshikata, R.	M008, M009, SU006	Zhang, L.	M500
Wysolmerski, J. J.	1087, 1157, F486, SA486, SU212	Yamazaki, Y.	M113, M145	Yoshikawa, H.	1024, M034, SU090	Zhang, L.	SU284
	SA239		SU050	Yoshikawa, H.	SA139, SA196	Zhang, M.	SU097
Wysolmerski, R. B.	F131, SA131, SU478	Yamout, B.	1110, SA226	Yoshiko, Y.	M191	Zhang, M. Y. H.	M127
Wynga, N.		Yan, J.	1188	Yoshimoto, T.	F509, SA509	Zhang, N.	SA065
		Yan, K.	1163	Yoshimura, K.	M446	Zhang, P.	M151, SA180
		Yan, Y.	1163	Yoshimura, N.	SU301	Zhang, Q.	1072
		Yana, I.	1163	Yoshinari, N.	M274, M333	Zhang, Q.	1196
Xi, Y.	1184	Yanagawa, N.	1163	Yoshizawa, M.	SA024	Zhang, Q.	SA005
Xia, Q.	F185, SA185, SU171, SU173	Yang, D.	F481, SA481	Yoshizawa, T.	SA177	Zhang, R.	1023
Xia, Y.	M179, SU266	Yang, H. Ru	SU233	You, J.	1053, F212, SA212, SU228, SU248	Zhang, S.	1061
Xiao, G.	SU382	Yang, J.	1028	Young, D. W.	SU081	Zhang, S.	1111
Xiao, J.	F142, SA142	Yang, J.	M463		SU252	Zhang, S.	SA462
Xiao, L.	SU179	Yang, J.	SA167	Young, M. F.	SU252	Zhang, W.	F194, SA194
Xiao, P.	1061	Yang, L.	F079, SA079	Yu, E.	1045, F183	Zhang, X.	1198
Xiao, Z.	M045	Yang, P.	M062	Yu, H.	M239	Zhang, X.	M045, M178
Xie, C.	SA050	Yang, Q.	SU131, SU132	Yu, H.	SA105, SA183	Zhang, X.	M443
Xie, D.	M150	Yang, S.	M260, SU277	Yu, J. C.	SA055	Zhang, X.	SA386
Xie, Y.	1111	Yang, S.	SU279, SU311	Yu, K.	1195, SU269	Zhang, X.	SU204
Xie, Y.	SA462	Yang, W.	1026, F168, SA168, SA291	Yu, X.	1070	Zhang, Y.	1062
Xing, L.	1018	Yang, W.	SA462	Yu, X.	1104, 1165, F138, SA138	Zhang, Y.	1141
Xing, L.	1072, 1196	Yang, X.	1049	Yu, X.	SA265	Zhang, Y.	1155
Xing, L.	SA255	Yang, X.	1053	Yuan, B.	1105, 1205, F459, SA459	Zhang, Y.	SU127, SU131
Xing, Y.	1205	Yang, X.	F387	Yuan, Y. Y.	SA357	Zhang, Y. Z.	SU283
Xing, Z.	SU349	Yang, X.	M179	Yue, Y. G.	M219	Zhang, Y. Z.	SU279
Xiong, D. Hai	1211	Yang, X.	M418			Zhang, Z.	1043
Xu, D.	M035	Yang, X.	SA387			Zhang, Z.	1045
Xu, H.	SU127	Yang, X.	SU248			Zhang, Z.	1100
Xu, J.	M248, M263, M264, SA043	Yang, X. Fang	1202			Zhang, Z.	F376
Xu, L.	1140	Yang, Y.	1003, 1064	Zack, D. J.	SU295, SU455	Zhang, Z.	M515
Xu, M.	M439	Yang, Y.	1160	Zaech, G.	M452	Zhang, Z.	SA193
Xu, M.	SA482	Yang, Y.	F048	Zahradnik, R. J.	M482	Zhang, Z.	SA376
Xu, S.	SU174	Yang, Y.	M505, M506	Zaidi, M.	1043, 1100, 1102, F376, SA254, SA376	Zhang, Z.	SU192
Xu, X.	1212	Yang, Y.	SA048	Zaidi, S.	1043, 1100, F376, SA376	Zhao, C.	SU287
Xue, J.	F505, SA505	Yang, Y.	SA516	Zaidi, S. K.	1030	Zhao, G.	M212
Xue, Y.	1203	Yang, Z.	1019	Zajac, J. D.	1097, 161	Zhao, H.	SA278
		Yang, Z.	SU502, SU504	Zakem, J.	SU345, SU505	Zhao, J.	1054
		Yano, F.	1014, 1016, SU033	Zallone, A.	1043, 1100, 1102	Zhao, J.	M090
		Yano, S.	M162, SA366	Zaman, A.	M298	Zhao, J.	M092
		Yanovski, J. A.	F472, SA472	Zambon, S.	M451	Zhao, J.	SA288
Yaccoby, S.	1125	Yao, C.	SU284	Zamborsky, D.	M230	Zhao, J.	SU111
Yaden, B. C.	SA427	Yao, G. Q.	1191	Zamor, P. O.	M128	Zhao, J. J.	M102
Yagi, M.	F258, SA258, SU054, SU072, SU282	Yao, H.	F450, SA450, SU045	Zanatta, M.	M060, M461	Zhao, L. J.	M108
		Yao, W.	F370, M046, M130, SA370, SU067, SU383	Zanchetta, J.	F429, M359, SA429	Zhao, M.	1154, F066, M174, SA066
Yagi, S.	M469	Yao, Z.	1072, 1196, SA255, SU113	Zanchetta, J. R.	1083, 1222, M472, SA324	Zhao, R.	F007, SA007
Yahiro, Y.	SU337	Yaroslavskiy, B. B.	1043, 1100, F376, SA241, SA376			Zhao, W.	SU383
Yajima, A.	M469		F028, SA028	Zanchetta, M. B.	SA324	Zhao, Z.	M179, SU266
Yakar, S.	1193	Yasoda, A.	SU071	Zanetti, A.	SU429	Zheng, H.	1070
Yam, L. T.	SU147	Yasuda, T.	SA037	Zangarelli, A.	M325	Zheng, J.	1062
Yamada, A.	M249, SA037	Yasuhara, R.	M343	Zannettino, A.	M236	Zheng, M. H.	M248, M263, M264
Yamada, H.	SU276	Yasui, N.	F140, M132, M134, SA140	Zannettino, A. C. W.	SA259	Zheng, M. Hao	SA043
Yamada, S.	SA189	Yasutake, J.	SA018, SU097	Zarrabettia, A. L.	SU184	Zheng, Q.	1017, 1032, F030, SA030
Yamada, S.	SU408		M204	Zarrabettia, M. T.	SU184	Zheng, Y.	F507, SA507, SU520
Yamada, Y.	1192	Yates, K. E.	SA031	Zavaleta, C.	M054	Zhong, Q.	SA050, SU291
Yamaguchi, A.	M204, SA209, SU519	Yatani, H.	SA337	Zavaleta, C.	SU098	Zhou, C.	M397
Yamaguchi, D. T.	M153, M216, SU058, SU203	Yatani, H.	SA031	Zayzafoon, A.	SU100	Zhou, G.	1017, 1032, F030, F214, SA030, SA214
		Yatani, H.	SA031	Zayzafoon, M.	SA171, SA228, SU100, SU222	Zhou, H.	1043, 1100
Yamaguchi, K.	M161	Yatani, H.	SA031			Zhou, H.	F376, F507, SA376
Yamaguchi, M.	1047	Yatani, H.	SA031			Zhou, H.	SA507, SU095
Yamaguchi, M.	M201, M213	Yatani, H.	SA031				

(Key: 1001-1228 = Oral, F = Friday Plenary poster, SA = Saturday poster, SU = Sunday poster, M = Monday poster, WG = Working Group Abstract)

Author Index

Zhou, H.	SU361, SU465
Zhou, H.	SU520
Zhou, J.	M130
Zhou, J.	SA144
Zhou, P.	F247, M259, SA247
Zhou, Q.	SU127, SU131
Zhou, S.	1184, M004, M025, SA153
Zhou, T.	SU231
Zhou, X.	M276
Zhou, X.	M377
Zhou, Z.	M235, SU283
Zhu, A.	SU230
Zhu, J.	M216
Zhu, J. Hua	SU203
Zhu, K.	SA005
Zhu, L.	1043, 1100
Zhu, L.	M193
Zhu, L. L.	F376, SA376
Zhu, M.	F270
Zhu, S.	SU077
Zilberman, Y.	SU061
Zillikens, M. Carola	M088, M120
Zimering, M.	SA460
Zimering, M. B.	M306
Zimmerman, N.	M266
Zimmermann, J.	SU113, SU146, SU148
Zingmond, D.	SA311, SA339
Zion, M.	1079, M013
Zipfel, W.	SA033
Ziv, E.	M103
Zmierczak, H.	SA384
Zmuda, J. M.	1039, 1073, 1135, F112, F323, F338, F341, M103, SA112, SA323, SA338, SA341
Zou, W.	F244, SA244
Zouch, M.	1178
Zuo, J.	SU296, SU298
Zuscik, M.	1005, 1155, M178, M488, SA175
Zwarenstein, M.	M382